TRANSACTIONS

OF THE

AMERICAN SOCIETY

OF

CIVIL ENGINEERS

(INSTITUTED 1852)

VOLUME 118

1953

NEW YORK
PUBLISHED BY THE SOCIETY

1953

NOTE.—The Society is not responsible for any statement made or opinion expressed in its publications.

CONTENTS

PAPERS AND DISCUSSIONS

(Alphabetical Indexes Begin on Page 1283)

No.		Page
2534	**CONTROL OF EMBANKMENT MATERIAL BY LABORATORY TESTING**	
	By F. C. Walker and W. G. Holtz	1
	Discussion:	
	By George F. Sowers	26
	D. P. Krynine	29
	D. F. Glynn	33
	F. C. Walker and W. G. Holtz	35
2535	**LAKE MICHIGAN EROSION STUDIES**	
	By John R. Hardin and William H. Booth, Jr.	39
	Discussion:	
	By Thomas B. Casey	51
	Charles E. Lee	55
	John R. Hardin and William H. Booth, Jr.	59
2536	**GRAPHICAL SOLUTION OF HYDRAULIC PROBLEMS**	
	By Kenneth E. Sorensen	61
2537	**FINAL FOUNDATION TREATMENT AT HOOVER DAM**	
	By A. Warren Simonds	78
	Discussion:	
	By James B. Hays	100
	V. L. Minear	101
	Byram W. Steele	103
	William H. McAlpine	104
	Fred H. Lippold	105
	O. E. Boggess	106
	H. Cambefort	107
	A. Warren Simonds	109
2538	**INFLUENCE LINES BY CORRECTIONS TO AN ASSUMED SHAPE**	
	By James P. Michalos and Edward N. Wilson	113
2539	**THIN-WALLED MEMBERS IN COMBINED TORSION AND FLEXURE**	
	By Warner Lansing	128
2540	**FLOCCULATION PHENOMENA IN TURBID WATER CLARIFICATION**	
	By W. F. Langelier, Harvey F. Ludwig, and Russell G. Ludwig	147
2541	**UNDERGROUND CORROSION OF PIPING**	
	By R. A. Brannon	165
	Discussion:	
	By Lyle R. Sheppard	177
	R. A. Brannon	177
2542	**ANALYSIS OF GROUND-WATER LOWERING ADJACENT TO OPEN WATER**	
	By Stuart B. Avery, Jr.	178
	Discussion:	
	By Matthew I. Rorabaugh	194
	S. J. Johnson	199
	Howard P. Hall	204

No.		Page
2543	RESEARCH IN WATER SPREADING	
	By Dean C. Muckel	209
2544	UTILIZATION OF UNDERGROUND STORAGE RESERVOIRS	
	By Harvey O. Banks	220
2545	THE ALLEGHENY CONFERENCE—PLANNING IN ACTION	
	By Park H. Martin	235
	Discussion:	
	By Louis P. Blum	243
	Park H. Martin	244
2546	DIVERSIONS FROM ALLUVIAL STREAMS	
	By C. P. Lindner	245
	Discussion:	
	By T. Blench	270
	Serge Leliavsky	272
	A. R. Thomas	276
	D. C. Bondurant	278
	C. P. Lindner	282
2547	THE DEVELOPMENT OF STRESSES IN SHASTA DAM	
	By J. M. Raphael	289
	Discussion:	
	By Ross M. Riegel	310
	Roy W. Carlson	310
	J. Laginha Serafim	311
	A. D. Ross	313
	J. A. Hanson	315
	A. Warren Simonds	316
	J. M. Raphael	317
2548	INDUSTRIAL WASTE TREATMENT IN IOWA	
	By Paul Bolton	322
2549	TORSION OF PLATE GIRDERS	
	By F. K. Chang and Bruce G. Johnston	337
	Discussion:	
	By Arthur P. Jentoft, Richard W. Mayo, and E. Russell Johnston	383
	F. K. Chang and Bruce G. Johnston	396
2550	THE DELAWARE MEMORIAL BRIDGE: A SYMPOSIUM	397
	PLANNING AND CONSTRUCTION	
	By Homer R. Seely	398
	DESIGN PROBLEMS	
	By Charles H. Clarahan, Jr., and Elmer K. Timby	411
2551	A NAVIGATION CHANNEL TO VICTORIA, TEX.	
	By Albert B. Davis, Jr.	420
2552	RATE OF CHANGE OF GRADE PER STATION	
	By Clarence J. Brownell	437
	Discussion:	
	By T. F. Hickerson	457
	Robert T. Howe	457
	E. N. Prouty	459
	C. J. Brownell	456

No. Page

2553 VARIATION OF WIND VELOCITY AND GUSTS WITH HEIGHT
By R. H. Sherlock 463

Discussion:
By W. Watters Pagon 489
Irving A. Singer and Maynard E. Smith 491
Percy H. Thomas and M. H. Fresen 494
Robert A. McCormick 498
Edward Cohen 499
R. H. Sherlock 500

2554 IRRIGATION WATER RIGHTS IN THE HUMID AREAS
By Howard T. Critchlow 509

Discussion:
By Harold E. Gray 515
Howard T. Critchlow 516

2555 HORIZONTALLY CURVED BOX BEAMS
By Charles E. Cutts 517

Discussion:
By A. George Mallis 535
DeForest A. Matteson, Jr. 535
Charles E. Cutts 541

2556 ENGINEERING ASPECTS OF WATER WAVES: A SYMPOSIUM 545
SURFACE WATER WAVE THEORIES
By Martin A. Mason 546

CHARACTERISTICS OF THE SOLITARY WAVE
By James W. Daily and Samuel C. Stephan, Jr. 575

LONG-PERIOD WAVES OR SURGES IN HARBORS
By John H. Carr 588

Discussion:
By John S. McNown 604
B. W. Wilson 609
John H. Carr 615

ENGINEERING ASPECTS OF DIFFRACTION AND REFRACTION
By J. W. Johnson 617

Discussion:
By M. E. Stelzriede 649
J. W. Johnson 651

WAVE FORCES ON BREAKWATERS
By Robert Y. Hudson 653

Discussion:
By Kenneth B. Kaplan 675
R. G. Hennes and C. E. Leonoff 676
Robert Y. Hudson 684

2557 STRESSES IN DEEP BEAMS
By Li Chow, Harry D. Conway, and George Winter 686

Discussion:
By Arturo M. Guzmán and Cesar J. Luisoni 703
William A. Conwell 704
Harry D. Conway and George Winter 707

2558 THE VALUE AND ADMINISTRATION OF A ZONING PLAN
By Huber Earl Smutz 709

Discussion:
By Henry Horowitz 722
Huber Earl Smutz 722

No.		Page
2559	ANALYSIS OF ARCH DAMS OF VARIABLE THICKNESS	
	By W. A. Perkins	725
	Discussion:	
	By Alfred L. Parme	754
	L. J. Mensch	757
	Fairfax D. Kirn and Gurmukh S. Sarkaria	758
	A. C. Josephs	763
	George E. Goodall	764
	W. A. Perkins	766
2560	TORSION OF I-TYPE AND H-TYPE BEAMS	
	By John E. Goldberg	771
	Discussion:	
	By Kurt H. Gerstle	791
	John E. Goldberg	792
2561	STEADY-STATE FORCED VIBRATION OF CONTINUOUS FRAMES	
	By C. T. G. Looney	794
	Discussion:	
	By E. F. Masur	815
	A. S. Veletsos	817
	William A. Conwell	820
	C. T. Looney	822
2562	TOPOGRAPHIC MAPPING IN KENTUCKY	
	By Phil M. Miles	829
	Discussion:	
	By Herbert Milwit	837
2563	EAST ST. LOUIS VETERANS MEMORIAL BRIDGE	
	By A. L. R. Sanders	838
	Discussion:	
	By W. H. Jameson	845
	Joseph Sorkin	846
	A. L. R. Sanders	848
2564	BANK STABILIZATION BY REVETMENTS AND DIKES	
	By Raymond H. Haas and Harvill E. Weller	849
	Discussion:	
	By Harrison V. Pittman	861
	E. R. de la Sayette	865
	Serge Leliavsky	866
2565	RICE IRRIGATION IN LOUISIANA	
	By E. E. Shutts	871
	Discussion:	
	By Lloyd E. Meyers, Jr.	885
	E. E. Shutts	886
2566	DEVELOPMENT OF A FLOOD-CONTROL PLAN FOR HOUSTON, TEX.	
	By Ellsworth I. Davis	888
2567	CHARACTERISTICS OF FIXED-DISPERSION CONE VALVES	
	By Rex A. Elder and Gale B. Dougherty	907
	Discussion:	
	By Edwin W. Murphy	928
	Rodolfo E. Ballester	930
	T. T. Siao	932
	Verne Gongwer	937
	Rex A. Elder and Gale B. Dougherty	943

No. Page

2568 METHOD FOR MAKING HIGHWAY SOIL SURVEYS
By K. B. Woods 946

Discussion:
By George F. Sowers 956
K. B. Woods 960

2569 ELECTRICAL ANALOGIES AND ELECTRONIC COMPUTORS: A SYMPOSIUM
SURGE AND WATER HAMMER PROBLEMS
By Henry M. Paynter 962

Discussion:
By E. B. Strowger 990
George R. Rich 992
Donald R. F. Harleman and Edward N. Rein 995
Henry M. Paynter 1004

APPLICATION TO AN HYDRAULIC PROBLEM
By R. E. Golver, D. J. Hebert, and C. R. Daum 1010

Discussion:
By J. van Veen 1017
W. Douglas Baines 1020
T. Blench 1024
R. E. Glover, D. J. Hebert, and C. R. Daum 1025

APPLICATION TO STREAM-FLOW ROUTING
By Max A. Kohler 1028

Discussion:
By Alfred J. Cooper 1039
C. O. Clark 1042
Max A. Kohler 1044

HYDRODYNAMIC PROBLEMS IN THREE DIMENSIONS
By P. G. Hubbard and S. C. Ling 1046

PIPE NETWORKS STUDIED BY NONLINEAR RESISTORS
By Malcolm S. McIlroy 1055

Discussion:
By Charles L. Barker 1066
Malcolm S. McIlroy 1067

2570 EFFECT OF ENTRANCE CONDITIONS ON DIFFUSER FLOW
By J. M. Robertson and Donald Ross 1068

Discussion:
By Steponas Kolupaila 1092
Arthur L. Collins 1092
R. M. Olson 1092
J. M. Robertson and Donald Ross 1094

2571 UNCONFINED GROUND-WATER FLOW TO MULTIPLE WELLS
By Vaughn E. Hansen 1098

Discussion:
By Ahmed Shukry 1116
Carl Rohwer 1120
David K. Todd and Lloyd C. Fowler 1121
Vaughn E. Hansen 1126

No.		Page
2572	**FIELD STUDY OF A SHEET-PILE BULKHEAD**	
	By C. Martin Duke	1131
	Discussion:	
	By Gregory P. Tschebotarioff	1157
	Walter C. Boyer	1163
	Paul Baumann	1167
	S. Packshaw	1169
	W. F. Way	1172
	J. Owen Lake	1173
	K. Terzaghi	1175
	D. P. Krynine	1182
	Trent R. Dames and David C. Liu	1187
	Roy W. Carlson	1188
	C. Martin Duke	1190
2573	**FLEXURE OF DOUBLE CANTILEVER BEAMS**	
	By F. E. Wolosewick	1197
	Discussion:	
	By Lu-Shien Hu	1208
	Lewis Schneider	1210
	Ray W. Clough	1212
	William A. Conwell	1215
	F. E. Wolosewick	1219
2574	**REVIEW OF FLOOD FREQUENCY METHODS: FINAL REPORT OF THE SUBCOMMITTEE OF THE JOINT DIVISION COMMITTEE ON FLOODS**	1220

(The President's Annual Address normally found at the end of the annual *Transactions*, this year, was included as Paper No. 2577 in the *Centennial Transactions*.)

MEMOIRS OF DECEASED MEMBERS

Past-President

Franklin Thomas 1231

Other Members

Frank Rea Allen 1232
George Douglas Andrews 1233
David Maurice Berry 1235
Alexander Bonnyman 1236
Charles Frederick Capes 1236
Charles Stuart Clark 1237
Walter William Colpitts 1238
Ralph Stephenson Corlew 1240
George Thomas Dean 1241
Frank Holliday Derby 1242
John Ralph Dobbin 1242
John North Edy 1243
Joseph Wilton Ellms 1244
Edmund Burke Feldman 1245
Edwin Clifford Finley 1247
Glenn Frederick Finner 1248
Joseph Watson Gross 1248
Marvin Furr Hartsfield 1249
William Sherman Hewett 1250
George Percival Holland 1252
Clement John Howard 1252
George William Howson 1253
William Henry Hunt 1255
George Washington Kelly 1255
Clyde Charles Kennedy 1256
Karl Quill Kirk 1258
Alphonsus Paul McBrady 1258
Donald Hull McCreery 1259
Andrew Jackson McKenzie 1260
John Owen Miller 1261
Franz Martin Misch 1262
John Earl Morelock 1263
Charles Frederick Parker 1264
William Allen Poe 1265
Fremont Emerson Roper 1266
Royal Upson St. John 1268
Philip Tustin Samuel 1267
William Hatfield Sears 1269
George David Shannahan 1270
Josiah Roscoe Sharp 1270
Joseph Wagoner Sheppard 1271
John Dolson Slye 1272
John Godfrey Spielman 1273
John Edward Stirling Thorpe 1274
Eugene True Thurston, Jr. 1275
George Neville Wheat 1276
Robert Lewis Wing 1277
Walter Ferrell Winton 1278
Clement Tehle Wiskocil 1279
William Clayton Witt, Jr. 1280
Byrle Burton Womble 1281

PAPERS AND REPORTS OF COMMITTEES PUBLISHED NOVEMBER, 1952-NOVEMBER, 1953, INCLUSIVE, AS ASCE PROCEEDINGS-SEPARATES, NOS. 157 TO 334, ACCEPTED FOR FUTURE PUBLICATION IN TRANSACTIONS, BUT NOT INCLUDED IN VOL. 118

No.		*Proceedings-Separates*
157	RADIAL IMPACT ON AN ELASTICALLY SUPPORTED RING By Edward Wenk, Jr.	November, 1952
160	ICE PRESSURE AGAINST DAMS: STUDIES OF THE EFFECTS OF TEMPERATURE VARIATIONS By Bertil Löfquist	December, 1952
161	ICE PRESSURE AGAINST DAMS: SOME INVESTIGATIONS IN CANADA By A. D. Hogg	December, 1952
162	ICE PRESSURE AGAINST DAMS: EXPERIMENTAL INVESTIGATIONS BY THE BUREAU OF RECLAMATION By G. E. Monfore	December, 1952
165	DESIGN CURVES FOR ANCHORED STEEL SHEET PILING By Walter C. Boyer and Henry M. Lummis, III	January, 1953
166	THE DESIGN OF FLEXIBLE BULKHEADS By James R. Ayers and R. C. Stokes	January, 1953
167	SEWAGE DISPOSAL IN TIDAL ESTUARIES By Alexander N. Diachishin, Seth G. Hess, and William T. Ingram	January, 1953
168	SPECIAL DESIGN FEATURES OF THE YORKTOWN BRIDGE By Maurice N. Quade	January, 1953
169	RATING CURVES FOR FLOW OVER DRUM GATES By Joseph N. Bradley	February, 1953
170	RAPID COMPUTATION OF FLEXURAL CONSTANTS By Thomas G. Morrison	February, 1953
171	UNIFIED MASS-TRANSPORTATION SYSTEM FOR NEW YORK By William Reid	February, 1953
172	AERONAUTICAL CHARTING AND MAPPING By Charles A. Schanck	February, 1953
173	ELECTRONIC DEVICES IN AIR TRANSPORT By F. B. Lee	February, 1953
174	ZONING MAPS FOR AIRPORTS By Benjamin Everett Beavin, Sr.	February, 1953
175	DESIGN OF SIDE WALLS IN CHUTES AND SPILLWAYS By D. B. Gumensky	February, 1953
177	EARTHQUAKE STRESSES IN SHEAR BUILDINGS By M. G. Salvadori	March, 1953
178	RAINFALL STUDIES USING RAIN-GAGE NETWORKS AND RADAR By H. E. Hudson, Jr., G. E. Stout, and F. A. Huff	March, 1953
179	STIFFNESS CHARTS FOR GUSSETED MEMBERS UNDER AXIAL LOAD By John E. Goldberg	March, 1953
180	A DIRECT STEP METHOD FOR COMPUTING WATER-SURFACE PROFILES By Arthur A. Ezra	March, 1953

No.		Proceedings-Separates
181	SLACKWATER IMPROVEMENT OF THE COLUMBIA RIVER By O. E. Walsh	April, 1953
182	HIPPED PLATE ANALYSIS, CONSIDERING JOINT DISPLACEMENTS By Ibrahim Gaafar	April, 1953
183	GROUP LOADINGS APPLIED TO THE ANALYSIS OF FRAMES By I. F. Morrison	April, 1953
184	DAM MODIFICATIONS CHECKED BY HYDRAULIC MODELS By E. S. Harrison and Carl E. Kindsvater	April, 1953
185	NONELASTIC BEHAVIOR OF BRIDGES UNDER IMPULSIVE LOADS By S. J. Fraenkel and L. E. Grinter	April, 1953
186	SETTLING RATE OF SUSPENSIONS IN SOLIDS CONTACT UNITS By A. A. Kalinske	April, 1953
187	THE EQUIVALENT RECTANGLE IN PRESTRESSED CONCRETE DESIGN By John J. Peebles	April, 1953
188	LAMINAR TO TURBULENT FLOW IN A WIDE OPEN CHANNEL By W. M. Owen	April, 1953
189	SNOW HYDROLOGY FOR MULTIPLE-PURPOSE RESERVOIRS By Herbert S. Riesbol	May, 1953
190	ANALYSIS OF CORRECTIVE ACTIONS FOR HIGHWAY LANDSLIDES By R. F. Baker	May, 1953
191	THE ENGINEER'S ROLE IN METROPOLITAN TRAFFIC PLANNING By Lloyd Braff	May, 1953
192	RELIEF WELL SYSTEMS FOR DAMS AND LEVEES By W. J. Turnbull and C. I. Mansur	May, 1953
193	VELOCITY MEASUREMENTS OF AIR-WATER MIXTURES By Lorenz G. Straub, John M. Killen, and Owen P. Lamb	May, 1953
194	CITY PLANNING TECHNIQUES By Russell H. Riley	June, 1953
195	SPECIAL PROCEDURES FOR PAVEMENT DESIGN By L. A. Palmer	June, 1953
196	RECENT AIRPORT DESIGN AND DEVELOPMENT By Philip A. Hahn	June, 1953
197	FRICTION FACTORS FOR TURBULENT FLOW IN PIPES By Edward F. Wilsey	June, 1953
198	LIVE LOADING FOR LONG-SPAN HIGHWAY BRIDGES By R. J. Ivy, T. V. Lin, Stewart Mitchell, N. C. Raab, V. J. Richey, and C. F. Scheffey	June, 1953
199	PLATES WITH BOUNDARY CONDITIONS OF ELASTIC SUPPORT By S. J. Fuchs	June, 1953
201	WIND LOADS ON TRUSS BRIDGES By John M. Biggs	July, 1953
245	THE AMPLIFICATION OF STRESS IN FLEXIBLE STEEL ARCHES By Robert S. Rowe	August, 1953

No.		Proceedings-Separates
249	A METHOD FOR CALCULATING STRESSES IN RIGID FRAME CORNERS By Harvey C. Olander	August, 1953
251	ANALYSIS OF CONTINUOUS COMPOSITE STEEL AND CONCRETE BEAMS By John Sherman	August, 1953
257	PUTTING A SEWAGE TREATMENT PLANT INTO OPERATION By Benjamin Benas	August, 1953
260	REVENUE BOND FINANCING FOR AIRPORT IMPROVEMENTS By James C. Buckley	September, 1953
261	NUMERICAL ANALYSIS OF CONTINUOUS FRAMES IN SPACE By James Michalos	September, 1953
262	ANCHORED BULKHEADS By Karl Terzaghi	September, 1953
263	BRIDGES ON WEST VIRGINIA TURNPIKE By Elmer K. Timby	September, 1953
265	PRESTRESSED CONCRETE GIRDERS, MANHATTANVILLE COLLEGE, PURCHASE, N. Y. By Curzon Dobell	September, 1953
266	PROGRESS IN PRESTRESSED CONCRETE CONSTRUCTION By J. F. Jelley	September, 1953
267	ALGAE RESPONSIBLE FOR ODOR AND TASTE IN PUBLIC WATER SUPPLIES By George J. Turre	September, 1953
268	ROCKY MOUNTAIN MASS CONCRETE OPERATIONS By George P. McIndoe	September, 1953
269	GRANBY PUMPING PLANT FOUNDATIONS AND DESIGN By W. R. Judd and W. H. Wolf	September, 1953
270	CONSTRUCTION OF GRANBY PUMPING PLANT By R. J. Willson	September, 1953
273	CHARTS FOR DESIGNING AIR CHAMBERS FOR PUMP DISCHARGE LINES By W. E. Evans and C. C. Crawford	September, 1953
274	ANALYSIS OF WATER HAMMER BY CHARACTERISTICS By C. A. M. Gray	September, 1953
275	WAVE-WASH CONTROL ON MISSISSIPPI RIVER LEVEES By Rudolf Hertzberg	September, 1953
276	HIGHWAY BRIDGES ON DEEP FOUNDATIONS By Louis Duclos	September, 1953
280	PROGRESS REPORT ON STUDIES ON THE DESIGN OF STABLE CHANNELS BY THE BUREAU OF RECLAMATION By E. W. Lane	September, 1953
281	THE DEVELOPMENT OF THE TURBULENT BOUNDARY LAYER ON STEEP SLOPES By William J. Bauer	September, 1953

No.		*Proceedings-Separates*
289	**OFFSHORE PETROLEUM INSTALLATIONS** By Jack S. Toler	September, 1953
298	**JOINT TRANSLATION BY CANTILEVER MOMENT DISTRIBUTION** By L. E. Grinter and C. H. Tsao	October, 1953
320	**PEAK DISCHARGE FOR HIGHWAY DRAINAGE DESIGN** By Carl F. Izzard	October, 1953
321	**ERECTION OF THE MAIN RIVER SPAN, PASSAIC RIVER CROSSING, NEW JERSEY TURNPIKE** By Jonathan Jones	November, 1953
322	**DESIGN OF FRAMES BY RELAXATION OF YIELD-HINGES** By J. Morley English	November, 1953
329	**AN INTERSTATE ROUTE AND ITS URBAN CONNECTIONS** By D. W. Ormsbee	November, 1953
331	**DEFLECTION OF LAMINATED BEAMS** By L. G. Clark	November, 1953
332	**POST-BUCKLING STRENGTH OF REDUNDANT TRUSSES** By E. F. Masur	November, 1953
334	**LATERAL BUCKLING OF CHANNELS AND Z-BEAMS** By H. N. Hill	November, 1953

ERRATA

Transactions Vol. 117—1952

Page xiii, delete the number, title, and publication date for *Proceedings-Separate No. 133*.

Page 32, line 3, should read: "(1 hectare = 2.47104 acres)."

Page 250, line 14, change "skelton" to "skeleton."

Page 407, line 4, following Fig. 4, "three distinct transitions ***" should read "two distinct transitions ***."

Page 577, the last word on the fourth line from the top of the page should read "structural."

Page 835, third line from the bottom of the page, change "explained" to "expanded."

Page 902, in the caption of Fig. 23, change the symbol ψ to the symbol ϕ.

Page 1376, under the subject heading, "Structural Analysis," the cross-reference should be: "*see* Equations; Structures, Theory of."

Page 1380, under the subject heading, "Surveys and Surveying, Geodetic," the author of "National Geodesy—***" is Leo P. Colbert.

Page 1385, under the subject heading, "Turbulence," the first discusser of the paper entitled "Turbulent Transfer***" is Emmett M. Laursen.

Transactions Vol. 118—1953

Pages 272 through pages 275, the name, "Leliavsky," should be substituted for "Bey" in the running head.

Pages 776 and 777, in Eq. 14*a*, the first fraction on the right side should read $-\frac{E\,b^2\,h}{16}$; Eq. 14*b*, should read $(\tau_{zz})_b = -\frac{E\,b^2\,h}{16}$, etc.; and in Eq. 15, the first fraction on the right side should read $-\frac{E\,t^2_f\,z}{8}$.

Page 1125, Fig. 15, the incorrect plotting of points should be corrected to agree with the values on page 1124, Table 1.

AMERICAN SOCIETY OF CIVIL ENGINEERS
Founded November 5, 1852
TRANSACTIONS

Paper No. 2534

CONTROL OF EMBANKMENT MATERIAL BY LABORATORY TESTING

By F. C. Walker[1] and W. G. Holtz,[2] Members, ASCE

With Discussion by Messrs. George F. Sowers, D. P. Krynine, D. F. Glynn, and F. C. Walker and W. G. Holtz

Synopsis

The United States Bureau of Reclamation (USBR) laboratory has established procedures for standardizing the testing of material to be used in embankments of earth dam structures. This paper describes these tests and their applications, and their correlation with field data.

Compaction testing has been developed from the procedures established by R. R. Proctor, M. ASCE. The test has been slightly modified, and laboratory methods of determining the compaction effect of sheepsfoot rollers are described. The effect of rock present in the soil mixture is analyzed, and compaction testing of pervious materials is also considered. The laboratory tests led to the development of efficient compaction equipment and procedures for field use.

It is difficult to correlate data from permeability tests made in the laboratory with results of field tests. The conditions of these tests are outlined, and their merit is analyzed. These tests have resulted in the development of a theory of pore pressure that is valuable in appraising the characteristics of a given embankment material. The pore pressure principle is discussed, and the basic equations used in the determination of pore pressure are listed.

Consolidation and settlement tests can be carried out in the laboratory, and by using adjustments of the basic tests, it is possible to secure good correlation with field data.

Development of the triaxial shear test has produced a valuable tool in the analysis of soil samples. The apparatus and procedure of these tests is outlined, as well as modifications made necessary by pore pressure considerations.

Note.—Published in December, 1951, as *Proceedings-Separate 108*. Positions and titles given are those in effect when the paper or discussion was received for publication.

[1] Head, Earth Dams Section, Bureau of Reclamation, U. S. Dept. of the Interior, Denver, Colo.

[2] Head, Earth Laboratory Section, Bureau of Reclamation, U. S. Dept. of the Interior, Denver, Colo.

The stability of an earth structure is dependent to a great extent on the moisture conditions at the time of placing. The theory of limiting moisture content is discussed, and it is related to the field control of moisture in embankments. The effect of pore pressure and rock content is analyzed, and several typical examples are cited.

Introduction

Within the field of soil mechanics there are several closely related but nevertheless distinct fields of endeavor, each of which has its own set of problems for which individual solutions have been developed. In the past few years, there has been a growing awareness that these individual solutions cannot be directly applied to related fields of endeavor even though they contain many useful ideas. In this field the USBR is primarily concerned with hydraulic structures such as large earth dams, and irrigation works, and to a lesser extent with nonhydraulic structures. As a result, the highest development of certain qualities of the soil that are largely incidental for other fields of endeavor has been found necessary. The observations reported in this paper and the solutions that have been developed should be considered as information that may aid in the solution of related problems but not as established procedures to be adopted without question.

In the development of designs for earth dams and irrigation canals, the primary emphasis of the USBR has been directed toward the retention of water. In the past it has been emphasized to the exclusion, or at least subordination, of other requirements. Actually, absolute imperviousness cannot be achieved and its relative value must be weighed against other equally important considerations. Therefore, any dam or canal embankment must not only have sufficient watertightness to serve the purpose for which it is intended, but also the structure must be stable within itself, and it must hold its form with time—that is, consolidation and settlement should remain within tolerable bounds for the life of the structure. Beyond these requirements are provisions for the utilization of modern construction equipment and procedures and the simplification of operation and maintenance.

What, then, are the characteristics of a soil that is suitable? The permeability of the soil under the condition of use must be known as well as its strength and how much it will change under load with the passing of time. The workability and durability of the soil in the structure are also important factors. There are laboratory tests available whereby values of permeability, stability, and consolidation may be determined for a given soil sample. There are no direct means available for defining workability or durability, but there are numerous index tests suitable for this purpose. Many investigators have been endeavoring to correlate tests such as grain size, density, plasticity index, penetration resistance, and others, with performance. Certain advantages of such tests in indicating cheaply the relative properties of a soil are recognized, but no way has been discovered in which these values might be applied to the development of a rational design, except by purely empirical procedures.

This paper does not concern itself with the evaluation of these abstract characteristics. The laboratory procedures described herein are presented only in brief form, as they are described in detail elsewhere.[3]

All design theories require that a soil be homogeneous and isotropic. Those familiar with soils in practice know that there is considerable variation in the properties of the various samples tested for control purposes. The extent of these variations for different kinds of materials under normal construction control is under study, and the effect of these variations upon the performance of a given design is also of interest. In order to secure a valid comparison, the same standards of control have been maintained for all earth dams constructed since 1941. These dams, representing more than 30 separate fills, have been built of a great variety of materials under an extreme variety of construction conditions. These fills range from structures 40 ft high to some which are 450 ft high, and the volume of the structures range from 100,000 cu yd to 10,000,000 cu yd. The results of the numerous control tests have shown that a considerable spread must be tolerated, but it is possible to keep within pre-established limits, and, in some respects, the behavior of the completed structure can be predicted. There is also reason to believe that if it is possible to perform sufficient laboratory tests to establish reliable averages, these averages, properly interpreted, provide valid values for use in design analyses.

COMPACTION TESTING

Adaptation of the Proctor Test.—When the USBR first established a laboratory for the study and control of soils to be used in earth embankments, the findings of Mr. Proctor[4] were used as a basis. Except for minor modifications, the tests used to establish compaction, penetration resistance, permeability, and consolidation performance standards are the basic tests still used. Proctor's original laboratory tests were performed on minus ¼-in. soil fractions (parts of the sample that pass a ¼-in. sieve). The soil was compacted into a mold in three layers, each layer being tamped by "25 firm 12-inch strokes using a rammer of 5½-pound weight with a striking area two inches in diameter." The mold used was "about 4 inches in diameter by 5 inches high" and had a 1/20-cu-ft capacity. Mr. Proctor determined that a compaction cylinder of less than 1/20-cu-ft volume gave density and needle data that could not be correlated properly with field compaction by sheepsfoot rolling. Compaction tests made in 1/30-cu-ft molds, that have been widely used as a standard, generally have been found to provide slightly higher maximum density, slightly lower optimum moisture, and slightly higher penetration values than those found under field conditions because the material is more confined. In order to standardize the compaction test for USBR purposes, standards were adopted after considerable independent laboratory and field study. These standards include: (1) a 1/20-cu-ft cylinder (about 4¼ in. inside diameter by 6 in. long); (2) a 5½-lb hammer, with 2-in.-diameter tamping foot; (3) Hammer

[3] "Earth Manual," Bureau of Reclamation, U. S. Dept. of the Interior, Appendix, Denver Federal Center, Denver, Colo.

[4] "Fundamental Principles of Soil Compaction," by R. R. Proctor, *Engineering News-Record*, Vol. 111 1933, p. 245.

blow secured by 18-in. free drop; and (4) 25 blows on each of three 2-in. compacted layers.

The laboratory study established that the 18-in. free-fall drop of the hammer was approximately equal to the 12-in. firm stroke specified by Mr. Proctor. Penetration tests were made in the manner originally specified. An impact machine for making the standard compaction test by mechanical means has been fabricated, but the machine is used only for research purposes. It has been found that the manual test is satisfactory for all practical purposes, and the manual equipment can be readily handled in the field as well as in the laboratory.

Laboratory Analysis of Sheepsfoot Roller Compaction.—The standard laboratory impact procedure for establishing compaction characteristics had been questioned by some engineers who believed it did not give data comparable to those obtained on actual embankment using sheepsfoot rollers. Therefore, large-scale compaction tests using the sheepsfoot principle were undertaken in the laboratory in 1936. The equipment used is shown in Fig. 1. Essentially, this machine consists of a hydraulic jack and an adjustable platform containing a pressure capsule for measuring the compacting forces. The adjustable platform allows the compaction of samples of various thicknesses. The compaction cylinder assembly consists of three parts—the base, the main cylinder, and a removable upper collar. The main cylinder is about 12 in. in diameter and 12 in. deep with a 0.75-cu-ft capacity. The removable collar is 9 in. long. The specimens were placed in three 6-in. compacted layers, after which the collar and top layer were removed and the density determined on the bottom layers. The compaction test was made on several materials containing up to 10% rock particles ranging in size from ¼ to 1½ in. Various moisture conditions were investigated as well as various conditions of coverage and knob pressures to develop moisture-density relations for the various compaction conditions. The results and implications of these tests will be discussed in detail in following paragraphs. However, as a matter of standards, it was found that the sheepsfoot compaction test gave data comparable to those obtained by the standard laboratory impact tests, and, therefore, it was felt that the standard (impact) test should be used for embankment materials, investigations, and embankment control.

FIG. 1.—COMPACTION TEST APPARATUS

Theoretical Density of Rock and Soil Mixtures.—The standard laboratory compaction tests are conducted on the soil fraction of the total material.

This is assumed to be the portion of a sample that passes through No. 4 sieve. If the total material contains rock particles (particles larger than those passing the No. 4 sieve), the theoretical density of the total material can be computed from the formula:

$$D_t = \frac{1}{\frac{P}{D_r} + \frac{1-P}{D_s}} \qquad (1)$$

in which D_t is the dry density of soil and rock; D_s is the dry density of soil fraction as compacted; D_r is the dry density of rock fraction (specific gravity times 62.4); and P is the percentage of rock (expressed as a decimal). There are, however, physical limits to this method of calculation as shown by the example in Fig. 2. This figure shows graphically the effect on density of soil and rock fractions varying from $P = 0\%$ to $P = 100\%$ of the total material. The theoretical formula is valid only if the dry weight of rock per unit volume of the total material does not exceed the unit weight of the rock particles (generally taken as the dry rodded unit weight). If a material contains more than about 70% rock particles by weight of the total material, the relations as determined by the theoretical formula do not apply. Actually, this percentage varies from about 65% to 75%, depending upon the gradation, shape, and other like characteristics of the rock particles. The percentage of rock particles that a total material can contain without exceeding the physical limitations of the formula is called the theoretical upper limit of percentage of rock. This is shown by graphical presentation in Fig. 2. In this figure, the curve ABCD is the theoretical density curve (D_t) for total material (in pounds per cubic foot) as computed from the formula. The weight of rock (W_r) and the weight of soil (W_s) in pounds per cubic foot of total compacted material, are shown as

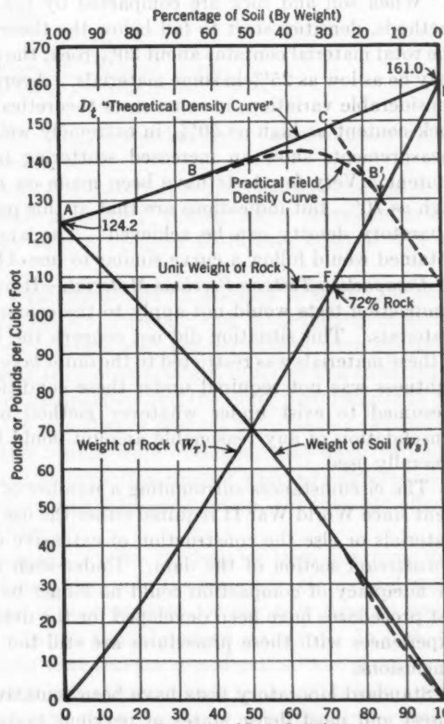

FIG. 2.—LIMITATION OF THE THEORETICAL DENSITY FORMULA

continuous heavy curves which cross below the theoretical density curve. In this case the unit weight of the rock particles alone was found by laboratory experiments to be 108.0 lb per cu ft, and the maximum compacted dry density of the soil fraction (D_s) was 124.2 lb per cu ft (specific gravity = 2.68). Similarly, the density of the rock fraction was 161.0 lb per cu ft (specific gravity = 2.53). Since the unit weight of rock particles cannot exceed 108.0 lb per cu ft, the total material cannot contain more than 72% rock, if the rock voids are filled with compacted soil. The weight of rock (W_r) curve must then take the shape OFE. If this particular material contains more than 72% rock and if the gradation is maintained as the total material is compacted, the theoretical density will be reduced in accordance with curve CE and the curve ABCE becomes the limiting theoretical density curve for this material.

When soil and rock are compacted by field methods, or even laboratory methods, densities start to fall below the theoretical laboratory density when the total material contains about 30% rock, the percentage causing interference may be as low as 25% in some materials. Averages from several projects show considerable variation; in some cases theoretical densities were maintained for rock content as high as 50%, in extremely well-graded material. Individual measurements show an increased scattering in the zone beyond 40% rock content. Very few tests have been made on materials with rock content as high as 70%, but indications are that at this point 85% to 90% of theoretical laboratory density can be achieved. The average of the densities actually obtained would follow a curve similar to line ABB′E in Fig. 2.

Compaction Tests on Pervious Material.—It was recognized that the standard compaction tests would not apply to the coarse-grained noncohesive pervious materials. This situation did not concern the USBR greatly because the use of these materials was restricted to the outer layers of an embankment. Watertightness was not required under these conditions, satisfactory stability was presumed to exist under whatever method of compaction was used, and consolidation of any reasonable amount could be tolerated in the thin zones generally used.

The circumstances surrounding a number of dam sites chosen for development since World War II required either the use of very large zones of pervious materials or else the construction of extensive drainage blankets beneath the downstream section of the dam. Under such circumstances it was felt that the adequacy of compaction could no longer be left to chance. Accordingly, test procedures have been developed for the determination of relative density. Experiences with these procedures are still too limited to merit drawing any conclusions.

Standard laboratory tests have been tentatively adopted to determine the loosest and most dense states of pervious materials. The loosest density is determined by placing the dry granular soil in a prescribed manner with a hand scoop in a 0.1, 0.5, or 1.0-cu ft mold (depending on the maximum size of the particles) until the mold is filled to overflowing. The poured material is struck off with a straight edge, and the weight and density of the soil is determined. The highest density of the soil is determined for sands by compacting the granular soil in 1-in. layers, at optimum moisture, into the standard 1/20-

cu ft compaction cylinder using a compaction hammer having a 3½-in. diameter foot and a 10-lb drop weight. Fifty well-distributed blows of the drop hammer, falling 18 in. are applied to each layer. Vibration is used if this procedure produces densities equal to or greater than those obtained by the impact method or if gravel sizes are present; 0.5 or 1.0 cu ft cylinders are used for testing these coarser materials. The relative density (D_R), expressed as a percentage, is computed by the following equation:

$$D_R = \frac{e_{max} - e}{e_{max} - e_{min}} \times 100 \ldots\ldots\ldots\ldots (2)$$

in which e is the in-place void ratio; e_{max} is the void ratio at loosest state; and e_{min} is the void ratio at most compact state. For convenient field use, the foregoing equation may be written:

$$D_R = \frac{D_{max}(D - D_{min})}{D(D_{max} - D_{min})} \times 100 \ldots\ldots\ldots\ldots (3)$$

in which D is the in-place density; D_{max} is the density in most compact state; and D_{min} is the density in loosest state.

The field control for these pervious materials is specified to obtain at least 70% relative density. Although laboratory studies have been conducted, tests and field observations are still in progress to further confirm this requirement.

Design of Field Compaction Equipment.—In an attempt to secure the compaction standards first outlined by Mr. Proctor[4] and subsequently modified for USBR practice,[5] continuously larger and heavier rollers were specified. Test sections of various types were tried in an attempt to arrive at a comparison between the standard laboratory compaction and the roller performance in the field with indifferent success. It was always possible to achieve a fair degree of comparison, but many erratic results were obtained, that have variously been ascribed to lack of sufficient construction control, excessive differences in the conditions between laboratory and field compaction, confinement effects, and influence of oversize materials.

USBR engineers finally designed a roller far heavier than anything then available. This roller was so heavy that only the largest tractors could pull it successfully. With such rollers it was possible for the first time to secure consistently compaction equivalent to the laboratory standard. In fact, the first reports were so encouraging that serious consideration was given to increasing this standard. Fortunately, no changes were made, so the information being gathered is still referred to the same standard.[5] Wartime interruptions with the resulting changes in construction practices and economics, and the loss of personnel with the prerequisite technical skill, have all contributed to a reduction in the quality of compaction control that was being achieved in the first postwar years. Therefore, the safety margin of compacting ability

[5] "Earth Manual," Bureau of Reclamation, U. S. Dept. of the Interior, Chapter VII, Denver Federal Center, Denver, Colo.

available in this roller has been extremely valuable. The result is that the type of compaction sought since 1936 is finally being successfully achieved but only with specific types of soil and only if reasonably good construction practice is followed.

The laboratory compaction tests with sheepsfoot type tampers, described previously, provide some interesting information on the comparison of laboratory and field data. The standard USBR roller provides knob pressures up to 490 lb per sq in. when fully ballasted with sand and water, as based on a total roller weight of 41,500 lb acting on 5% of 240 knobs, each with a 7.07-sq in. area. With the basic 12-roller passes usually specified, this roller provides a theoretical coverage of 70%, when the knobs are not worn, or 62% when the knobs are worn the maximum allowable amount.

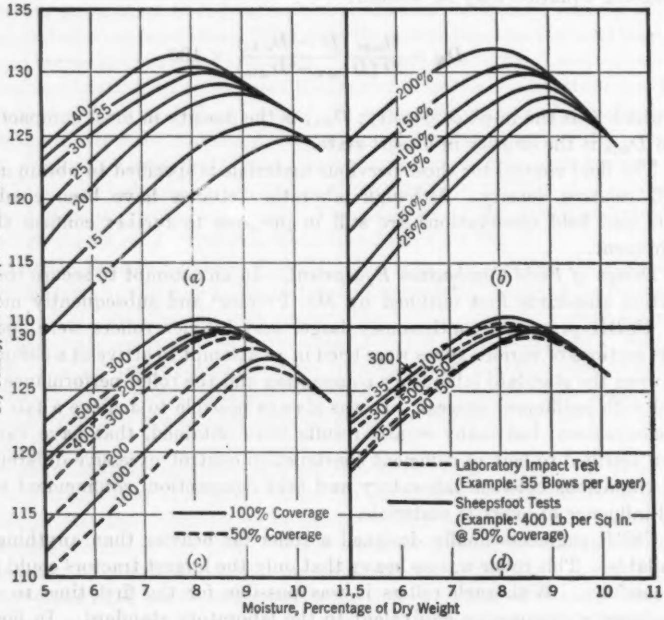

FIG. 3.—COMPARISON OF RESULTS OF COMPACTION STUDIES

Laboratory Standards for Compaction Tests.—By comparing the curves in Fig. 3, based on Platte River embankment material studies, it can be seen that the compaction characteristics for the sheepsfoot and impact compaction tests are quite similar. With 200 lb per sq in. knob pressures, a sheepsfoot roller coverage of about 80% is required to equal the results obtained by the laboratory standard impact test. Likewise, at 50% coverage, knob pressures of 350 to 400 lb per sq in. are required to equal the results obtained by the

laboratory standard test. On the basis of this information, about 29 blows per layer in the laboratory compaction cylinder are required to equal the sheepsfoot results under maximum knob pressures, and 50% coverage or 35 to 40 blows per layer are required under maximum knob pressures and 70% coverage. Recognizing some loss of efficiency in field compaction, it has been estimated that laboratory compaction of 30 to 35 blows per layer gives compaction values similar to field roller compaction under maximum knob pressures and 70% coverage. For this reason, 33 blows per layer laboratory impact compaction is often used as a control for moisture limit tests and other detailed laboratory tests. It should be noted, however, that the difference in density and moisture relations obtained by the 25 blows per layer commonly used in laboratory compaction tests and in field control or the 33 blows per layer laboratory standard is relatively small, and the former test is quite satisfactory for design and control work.

There is no one best way to compact all kinds of materials. Instead, the USBR has tried to determine the need for compaction of any soil in accordance with the purpose it is to serve. Some granular coarse-grained soils could be compacted as well, or better, simply by the passage of a large tractor as they were with tractor and roller. Decreasing densities must be accepted with increased percentages of coarse material in otherwise well-graded mixtures. No evidence has been found that so-called over-compaction, first referred to by the late Theodore T. Knappen,[6] M. ASCE, is a matter of concern. The expansive properties of bentonitic clays are recognized, but this type of material is normally avoided in the construction of earth dam embankments. Slight expansion of samples compacted in the laboratory has been noted when the load was removed after the samples had been loaded and saturated. There has been some evidence that the upper layers of a highly compacted fill demonstrate a slight rebound, but it is believed that the benefits of high compaction far exceed the disadvantages that such behavior may produce. There are, in fact, some who infer that the kind of compaction required by the USBR is inadequate.[7]

With the increase in compactive effort in the field it was found advisable to decrease the moisture used for compaction as determined by laboratory tests. Although the original intention was to reduce the opportunity for development of high pore pressure, this change also brought the moisture content closer to the optimum for the roller, avoided the danger of having soft fills when slight excesses of moisture occurred, and provided a greater margin of acceptable moisture limits for satisfactory compaction. The difficulties experienced with fill construction in 1930, when the puddle fill philosophy still dominated the picture instead of the practices used for embankment construction today, emphasize the need for dry firm fills obtainable only with heavy compactors and limited moisture.

If the idea is accepted that the various performance characteristics of a given soil can be defined within reasonable limits if the density and moisture

[6] "Calculation of the Stability of Earth Dams," by Theodore T. Knappen, *Transactions*, Second Congress on Large Dams, Vol. IV, 1936, p. 505.

[7] "Laboratory Soil Compaction Methods, Penetration Resistance Measurements, and the Indicated Saturated Penetration Resistance," by R. R. Proctor, *Proceedings*, Second International Conference on Soil Mechanics and Foundation Eng., Vol. V, 1948, p. 242.

content are established, then laboratory performance and field performance may reasonably be comparable since experience shows that within established limits these conditions can be duplicated.

Permeability Tests

Development of Standard Technique.—Laboratory permeability tests of embankment materials are performed on the minus No. 4 fraction of the soil, using specimens 8 in. in diameter by 3 in. deep. The soils are compacted in steel cylinders at optimum moisture and maximum laboratory density in three equal layers, following the procedures originally outlined by Mr. Proctor but somewhat modified by the USBR. If the material will undoubtedly show a moderate permeability rate, greater than 1.0 ft per yr the modification consists of using a loading standard equivalent to 20 ft of fill, assuming that this will give a conservative value of permeability for the equivalent section of the embankment. If, however, the material to be tested is one in which the permeability is very low, the practice of using a loading equivalent to 100 ft of fill has been adopted as giving a more reliable indication of the character of the soil. If, upon further consideration, it is found necessary to use such material for the impervious section of a major dam, the permeability and consolidation characteristics throughout the entire range of loading are then examined.

In 1940 it was found necessary to consider for use in an embankment a soil that consisted of a mixture of about 50% gravel and 50% clay. Previous experience of the USBR led to the belief that in such a case the characteristics of the fine-grained portion would control the character of the mixture. In about this range of gradation the USBR standards of compaction would be attained only with great difficulty, if at all. It was deemed desirable, therefore, to test the complete material instead of only the minus No. 4 size, so a testing procedure was devised for such materials. When materials containing a considerable proportion (about 25%) of particles larger than No. 4 size (those retained on a No. 4 sieve) are tested, large steel permeability cylinders 20 in. in diameter by 9 in. deep are used. The maximum particle size for this test is limited to 3 in. In this test the material is compacted in three equal layers, at laboratory optimum moisture for the mixture at the density anticipated for the field compaction operation. Loads are applied to both large and small specimens through springs, and facilities are available for consolidation measurements.

Permeability tests on undisturbed fine-grained soils are made on cylindrical specimens, 3½ in. in diameter by 3 in. to 9 in. long. These specimens are placed in rubber sleeves, and the sleeves are attached to perforated end plates. The specimen and container assembly is placed in a pressure chamber and surrounded by water. A pressure slightly in excess of the percolating water pressure is applied to the chamber to hold the sleeve tightly against the specimen. Relatively air-free or de-aired water is permeated through the specimen by gravity or pressure flow until a constant rate is obtained. In all cases the test conditions are selected to duplicate the actual field conditions as closely as possible.

Field Tests.—The idea has been advanced that flow through soils followed a certain pattern.[8] Laboratory tests on sand models and electrical analogies provided a means for determining the flow lines for a given design, and the La Place equation provided a means of evaluating the loss through the designed section. To prove the reliability of these interpretations, wells were sunk into some of our older dams to locate the position of the uppermost (or phreatic) flow line. Assuming that bedrock provided the lowermost flow line and also that the quantity of water passing the dam could be determined, it would then be possible to check the permeability of the materials in a dam.

It soon became evident that the water levels measured in these wells did not correspond to any preconceived ideas for the location of the line of saturation. It seemed that with the low permeabilities of the surrounding soil in the embankment, these wells acted either as reservoirs or drains, and some other method would have to be devised that did not require a supply of water from the embankment. Subsequently, pressure cells that met this requirement were installed. Although it is now believed that the pressures revealed by these cells were reliable, when the cells remained operative, the information that would enable a check of laboratory permeability tests was not obtained. Permeability no longer seems important in connection with embankments since material having a permeability so low that loss through the embankment is economically negligible has always been available for the core of the dam. If, in actual construction, field permeabilities are a hundred times as great as in the laboratory, losses through the usual embankment would still be unimportant.

Foundation permeabilities have been even more difficult to correlate with laboratory measurements. This must be expected, for it is virtually impossible to reproduce either field conditions in the laboratory or exercise laboratory control in the field. If field and laboratory tests show results of the same order of magnitude, excellent correlation is considered to have been achieved. Nevertheless, many surprisingly accurate estimates of leakage into foundation excavations have been made from rather questionable data combined with judgment and experience. Although attempts to check laboratory permeability in the field have been unsuccessful so far, they have been instrumental in disclosing a phenomenon of embankment behavior whose importance in large embankments far exceeds any permeability considerations. This is the development of the pore pressure concept.

The Pore Pressure Concept

Background of the Theory.—The significance of pore pressure and its effect on the stability of a soil mass was recognized by F. F. Smith, J. H. A. Brahtz, and L. W. Hamilton of the USBR during the early part of 1936. It was the result of an effort to rationalize observations made during field permeability testing and to interpret laboratory shear tests. The concept of pore pressure and its effect on the stability of a soil mass was not new in soil mechanics at that time. There were numerous references to the phenomenon by other

[8] "Seepage Through Dams," by Arthur Casagrande, *Journal*, New England Water Works Assn., Vol. 51, 1937, p. 131.

authorities, including the writings of Karl Terzaghi,[9] Hon. M. ASCE. However, detailed descriptions of the phenomenon, as well as supporting data, were seldom given. To obtain the data necessary to support the concept, a testing program that eventually consisted of numerous shear and pore pressure tests was undertaken by Mr. Hamilton in cooperation with Messrs. Brahtz and Smith. The preliminary findings of this program were published in 1939.[10] Since that time considerable additional research work had been carried out, although this work was later curtailed to some extent during World War II and the post-war years because of personnel limitations and heavy construction work programs. Later research work of the USBR in this field has not been published, but the results of actual pore pressure measurements in earth dams constructed by the USBR were contained in an article prepared for the Second International Conference on Soil Mechanics and Foundation Engineering.[11]

Theoretical Derivation.—Pore pressure, as defined for the purposes of this paper, is the internal hydrostatic pressure or the pressure in the pore fluid of a soil mass. Pore pressure develops in a soil mass as consolidation from loading takes place. As the shearing strength of soil due to frictional resistance depends on the contact pressures between the soil grains, loss of strength takes place as pore pressure develops, since pore pressure reduces the particle contact pressures. This simple relationship can be expressed as follows:

$$f = \bar{f} + u \qquad (4)$$

in which f is the total stress (or fill load); $\bar{f}$ is the effective stress (grain to grain pressure causing consolidation); and u is the pore pressure. The loading of a soil mass produces a volume change that must be accompanied by either a corresponding extrusion or a compression of the pore fluid. Thus, if the soil is of low permeability, compression of the pore fluid will result. A soil mass is made up of solid soil particles, water, and air, and the pore fluid is defined as the water and air components of the mass. Within the normal range of pressures encountered, both the soil particles and water are practically incompressible. Therefore, the volume change occurs as a compression of the air, and pore pressures are produced even though the voids are not filled with water. The magnitude of the pore pressures developed in a soil mass is therefore dependent upon: (*a*) the compressibility of the pore fluid; (*b*) the volume change of the mass under given loads; and (*c*) the permeability of the mass and the surrounding material.

The pore pressure resulting from the consolidation of a soil mass can be computed by the following equations

$$u_e = u_a \left(\frac{V_a + h\,V_w}{V'_a + h\,V_w} - 1 \right) \qquad (5a)$$

or

$$u_e = \frac{u_a\,\delta V}{V_a + h\,V_w - \delta V} \qquad (5b)$$

[9] "Principles of Soil Mechanics," by Charles Terzaghi, *Engineering News-Record,* Vol. 95, 1925, p. 1029.

[10] "The Effects of Internal Hydrostatic Pressure on the Shearing Strength of Soils," by L. W. Hamilton, *Proceedings,* A.S.T.M., Vol. 39, 1939, p. 1100.

[11] "Ten Years of Pore Pressure Measurements," by W. W. Daehn and F. C. Walker, *Proceedings,* Second International Conference on Soil Mechanics and Foundation Eng., Vol. III, 1948, p. 245.

in which u_e is the pore pressure after consolidation (gage pressure); u_a is the initial pore pressure (usually considered as absolute atmospheric pressure); V_a is the initial volume of free air in the soil mass (percentage of initial volume); V'_a is the consolidated volume of free air in the soil mass (percentage of initial volume); $\delta V = V_a - V'_a$ which is the volume change caused by consolidation (percentage of initial volume); V_w is the volume of water in soil mass (percentage of total initial volume); and h is the capacity of water to dissolve air as derived from Henry's law (approximately 0.02).

Eq. 5*a*[11] is similar to Eq. 5*b*, but is expressed in a slightly different manner more convenient to use.[12] Both equations are based on Boyle's law for compressibility of gasses and Henry's law for the solubility of air in water at constant temperature. In using these equations for computing pore pressures, the assumption is made that, if a soil containing air, water, and solids is loaded without permitting drainage, it will consolidate; and the consolidation occurs as a volume change in the air content. The air will not only develop pressure according to Boyle's law, but it will dissolve in water according to Henry's law by a weight proportional to the pressure and the volume of water present.

This method is used to estimate pore pressures in earth dam structures, and good correlations with actual field and laboratory measurements have been obtained.

Consolidation and Settlement Tests

In order to distinguish between consolidation and settlement, as applied to embankments and foundations, the change in volume of an embankment is referred to as consolidation, and the same process in a foundation is referred to as settlement.

In 1938 the USBR began the installation of telescoping pipe apparatus[5,12] in the major dams built under its jurisdiction. With this apparatus it is possible to measure the foundation settlement at the point where the apparatus is installed and also to measure the consolidation in any increment of the embankment bracketed by crossarms. It is also possible to correlate consolidation with time and load. Attempts have been made to measure fill consolidations to accuracies approaching 0.001 ft, but the measurements were found to be so erratic that no use could be made of this refinement. Therefore, measurements have been restored to the former standard of 0.01 ft. Individual measurements deviate quite widely from the average; but in cases in which a continuous record is established either with time or depth, it is possible to draw an average performance curve that may be expected to approximate the true conditions.

Laboratory consolidation tests on fine-grained soils are conducted in fixed ring consolidometers on specimens 4¼ in. in diameter by 1¼ in. high. For foundation soils specimens taken at the site are cut to fit the consolidometer rings, and for tests on embankment soils the materials to be tested are compacted into the container at anticipated field moisture and density conditions. The loadings, conditions of saturation, and other factors used during the test are dependent on the problem to be studied and on the anticipated field conditions. When embankment materials containing more than 25% rock

[12] "Estimating Construction Pore Pressures in Rolled Earth Dams," by J. W. Hilf, *Proceedings*, Second International Conference on Soil Mechanics and Foundation Eng., Vol. III, 1948, p. 234.

particles are to be tested, the 20-in. diameter percolation-settlement cylinders are used.

Some of the first attempts to correlate field and laboratory data showed an extremely wide divergence. When laboratory tests of an embankment material showed potential consolidation in the neighborhood of 9%, field measurements showed less than 2% consolidation. It was evident that some adjustment was required. The laboratory tests were performed on samples limited to a minus No. 4 size, whereas the material used in the fill contained material up to 3 in. in size and the plus No. 4 material comprised 30% to 70% of the total. Assuming that the coarse-grained fraction did not contribute to the measured consolidation, it was possible to reduce the discrepancy between field and laboratory observations by about one half. It was also noted that quite high pore pressures were being measured in this embankment. These pressures would act to reduce the effective consolidating load and would not be present in the small laboratory samples as drainage was provided. By making this adjustment it was found that close agreement between laboratory tests and field observations could be obtained on the basis of averages.[13]

Based on settlement and consolidation records obtained to date, there is reason to believe that the camber (that is, the slight longitudinal hump, placed on a dam during construction) will compensate for about 100 years of consolidation and settlement, assuming an exponential time-consolidation relationship. In a properly compacted dam, the determination of potential settlement from laboratory tests thus becomes relatively unimportant. On the other hand, as higher and higher dams are built, the consideration of pore pressure as a force tending to destroy stability becomes very important. It is, therefore, assumed that the laboratory field relationship on consolidation is valid, enabling the use of laboratory tests to determine the magnitude of pore pressure to be anticipated in the fill under various placement conditions.

Shear Tests

Testing Conditions.—All shear testing is carried out by the triaxial test method. Various size specimens are used, depending upon the type of samples submitted and the problem to be investigated. Specimens varying in size from $1\frac{3}{8}$ in. in diameter by $2\frac{3}{4}$ in. high to $3\frac{1}{2}$ in. in diameter by 9 in. high are generally used. The smallest specimens are used for foundation materials since several specimens can be cut from the same horizon of a 6-in.-diameter core. These specimens are always used when testing impervious clays since the short specimen allows more rapid equalization of pore pressure throughout the specimen and thus provides a reasonable testing period. The larger specimens are generally used for testing remolded embankment materials. These specimens are more suitable for this type of work because it is difficult to mold a small specimen to a uniform density condition. The laboratory control specified for companion shear specimens of this type is 0.5 lb per cu ft density and 0.1% moisture content.

---

[13] "The Use of the Maximum Principal Stress Ratio as the Failure Criterion in Evaluating Triaxial Shear Tests on Earth Materials," by W. G. Holtz, *Proceedings*, A. S. T. M., Vol. 47, 1947, p. 1067.

The triaxial shear tests are usually conducted on sealed specimens with pore pressure measurements being taken at the ends of the specimens throughout the test. The shear values reported are based on effective pressures and represent the shear characteristics of the materials at zero pore pressure conditions. Preconsolidation prior to shear testing with or without drainage is performed if required by the data to be assembled. When tests are required on foundation specimens that are thoroughly saturated, unconfined compression tests are made to determine the approximate cohesion of the material. The shear tests described are conducted on the soil fraction of the material. The need for triaxial tests on materials containing rock particles is recognized, and equipment is being designed for conducting shear tests on materials containing up to 3-in. size particles. (Equipment for testing coarse-grained soils in specimens up to 9-in. diameter × 22-in. length is now in use.)

During the earlier stages of the USBR laboratory (1933 to 1936), direct shear tests were conducted to determine cohesion and friction values since it was recognized that the stress conditions induced by the direct shear test were not comparable to the stress conditions induced in an actual structure. Specimens that varied in size from 8 to 144 sq in. of shearing area were used. The larger specimens were used to test materials containing rock particles up to 1½ in. in size. It was noted in these particular tests that there was no change in the shear values of materials containing up to 10% rock particles over the shear for the soil fraction that contained no particles larger than No. 4 size.

Effect of Pore Pressure.—In an effort to interpret shear test data and find the explanation of the variations caused by different test procedures and moisture-density conditions, the pore-pressure concept was developed. This led to the principle of approaching the soil stability problem from the viewpoint of pore pressure. As research proceeded, it became evident that pore pressure could be neglected only when volume changes were so controlled that the pore fluid would drain from the specimen at the same rate as the volume change took place. When materials of low permeability were tested, it was found that the time required for testing was increased to such an extent as to make the test practically impossible.

One of the first indications of the effect of pore pressure was the fact that direct shear test results on soils that were not free-draining did not give a straight-line relation between the normal applied load and the corresponding shearing resistance. For the lower normal loads the consolidation of the mass was small; consequently, the compression of the pore fluid was so negligible that the pore pressure was relatively ineffective in reducing particle contact pressures. As the normal loads were increased and the consolidation of the mass became greater, the pore pressure increased and a resulting loss of effective particle contact pressure took place. Thus, the plot of applied normal load against shearing strength is a curve having its greatest slope at the lower loads and a lesser slope at the higher loads. This is also true when the moisture content of the mass is increased, the shearing strength becoming less as the water content is increased (or the air content decreased) because the pore fluid is less compressible and builds up to greater amounts under load.

Laboratory test specimens are subjected to stress under considerably different conditions than may prevail in the prototype when pore pressure is present. For example, the laboratory specimen is tested in a matter of hours, whereas the loading process in the prototype may extend over several years. Drainage conditions are also entirely different. In such circumstances it would be futile to attempt to use the results of laboratory shear tests without pore pressure correction in the design of a large earth dam with any expectation of a similar behavior in the prototype.

It was necessary, therefore, to select a shear test and to perfect testing techniques that would provide the control desired. Methods and equipment of measuring pore pressure during the test had to be developed so the true shearing strength of the material could be determined. The triaxial shear test was considered excellent for this purpose because drainage could be controlled and pore pressure measurements taken.

The Triaxial Shear Test.—A great deal of effort was expended on the development of equipment and techniques for determining the true shear characteristics of a soil mass by the triaxial shear test method. From these developments it has been found that a straight-line relationship between effective normal load and the corresponding shear resistance generally exists up to the condition of complete saturation for remolded soils. This is true provided the line of limiting shear resistance is constructed on the basis of effective stresses, and the stresses are determined at the actual time of failure of the specimen. The point of maximum principal stress ratio, which corresponds closely to the point of minimum volume, is used as the failure criterion.[13] Many investigators do not believe that clay soils exhibit true frictional resistance, but the results of many triaxial tests on numerous remolded soils by the USBR seems to indicate a general straight-line relationship, providing effective stresses and the proper failure criterion are used. This principle is illustrated in Fig. 4. The numbers at the ends of the curves in Fig. 4 denote the applied lateral pressure, and the vertical lines indicate the point of maximum stress ratio. It is recognized that the straight-line relationship between normal load and shear resistance does not hold for all types of soils and conditions in the lower load range. For example, natural loess soils of low density do not develop normal shear characteristics until some normal load is applied that will break down the natural loose structure and bring the particles into contact. In this case, a definite break occurs in the line of limiting shear resistance at that loading, after which the line becomes one of normal constant slope.

A three-dimensional (consolidation-pore pressure-permeability) test was developed to study volume change against pore pressure of remolded and undisturbed soils under load. The test is also well adapted for determining the permeability of undisturbed soils as previously mentioned. In this test, cylindrical soil specimens in rubber sleeves are sealed to perforated metal end plates and are subjected to chamber pressures only, and the relation between volume change and pore pressure is studied under sealed and drained conditions. Excellent correlations between computed pore pressures and pore pressures measured during the test have been obtained.

Limiting Moisture Concept and Modified Control Based on Laboratory Studies

Since the development of modern practices for controlling moisture and compaction in the construction of rolled-earth dams, common field control procedures have been based on the principle that the most desirable condition for the placement of earth materials in embankments is the condition corresponding to the peak point of the moisture density curve. This trend in construction control was based on the theory that materials so placed would provide a fill of minimum permeability, minimum consolidation, minimum water content when saturated, and maximum ultimate stability. For practical reasons, limits for moisture control generally have been based on moisture content corresponding to some percentage of the laboratory maximum density as determined from the density-moisture curve. The concept is extremely broad and illustrative of the tendency to generalize about the performance of a soil mass without giving full consideration to all the factors involved in placing and loading the mass.

The effect of pore pressure on stability assumes increased importance as the placement moisture content is increased, as the fill loads become large, and the permeability of the materials used becomes small. The magnitude of these pore pressures has been actually observed through laboratory and field observations[12] as well as computed on the basis of rational formulas.[13] It was, therefore, considered necessary to reduce construction pore pressures by reducing the placement moisture content as much as possible. It is also well known that a soil mass that is placed at too low a moisture content will consolidate upon saturation. The amount of consolidation is dependent on the placement moisture, the consolidation characteristics of the soil, and the final load conditions.

The USBR believed that the laboratory could furnish an important guide for rolled-fill construction by the establishment of suitable moisture control limits so that neither high pore pressures nor excessive consolidation would result during or after construction. The consolidation test was used primarily for determining these limits. The laboratory tests used and the methods for determining the placement moisture limits have been described in detail elsewhere[14] and will be referred to only briefly in this paper.

Moisture Content Limits.—The lower limit is defined as the lowest placement moisture content at which saturation will have no effect on consolidation under the fill load being considered. The data for determining the limiting moisture contents are presented in terms of dry density, placement moisture, and applied pressures, as shown in Fig. 5. The sample used as a basis for the curves in Fig. 5 was a lean silty clay material with a specific gravity of 2.67 and composed of 24.7% clay size (− 0.005 mm). The four solid lines that were drawn through the unsaturated, consolidated dry densities obtained at each placement moisture condition provide the consolidated dry density versus placement moisture curves for each respective load condition, before consolidation, when drainage is permitted. Similarly, the four dashed lines that were drawn

[14] "The Determination of Limits for the Control of Placement Moisture in High Rolled-Earth Dams," by W. G. Holtz, *Proceedings*, A.S.T.M., Vol. 48, 1948, p. 1240.

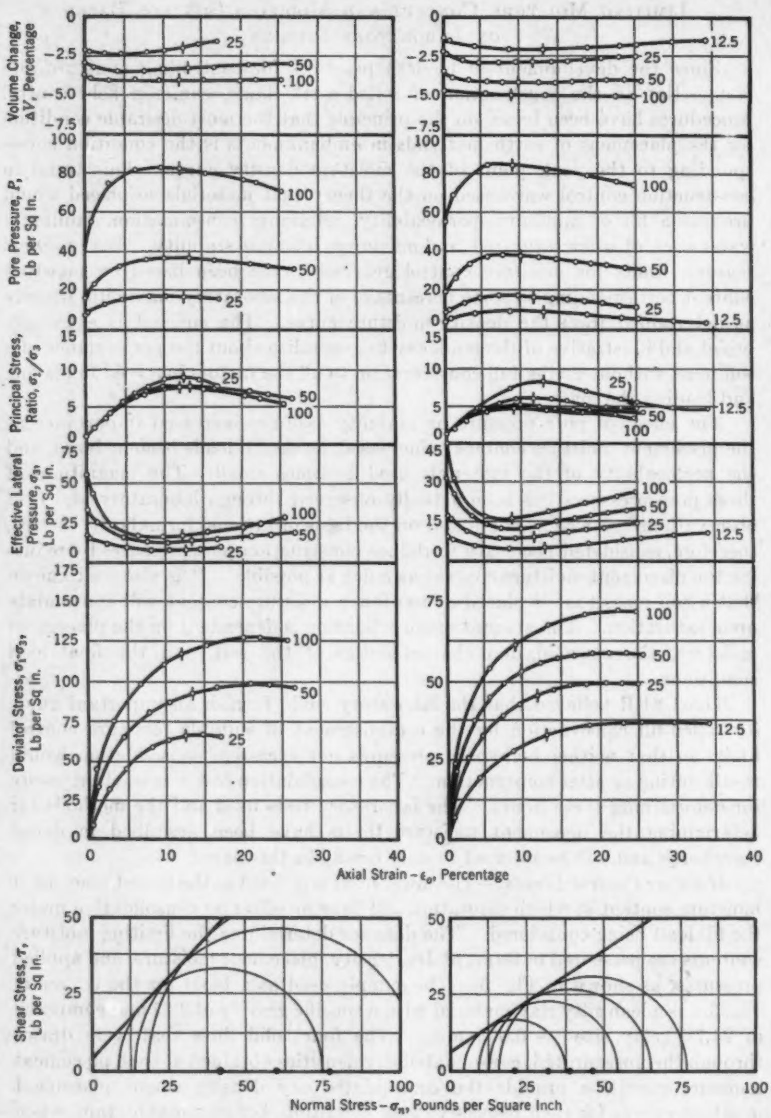

(a) TEST 7–T
SAMPLE 3RX-43
SAND WITH CLAY BINDER

(b) TEST 13–T
SAMPLE OOT-8
CLAY, LEAN SILTY

Fig. 4.—Triaxial Shear

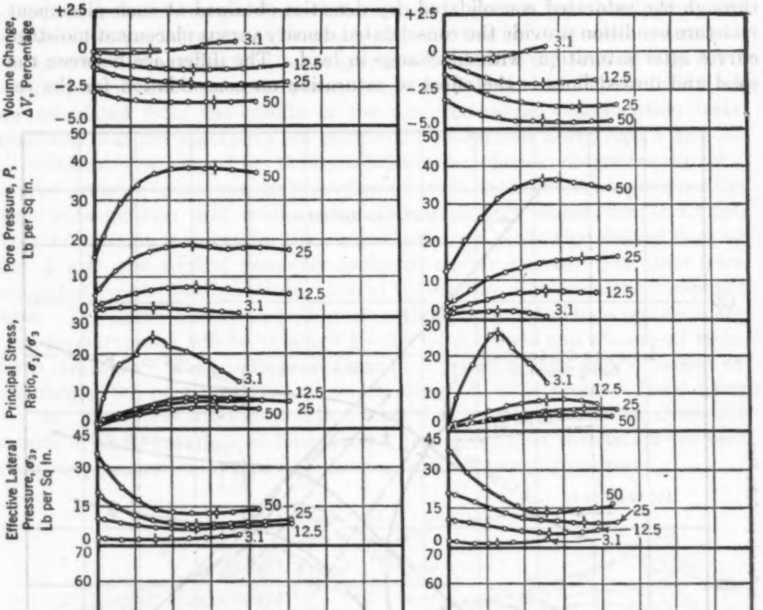

(c) TEST 19—T
SAMPLE ATX-3
CLAY MODERATE TO HIGH PLASTICITY

(d) TEST 20—T
SAMPLE ATX-1
CLAY VERY PLASTIC AND VERY COMPRESSIBLE

TESTS ON TYPICAL MATERIALS

through the saturated consolidated dry densities obtained at each placement moisture condition provide the consolidated density versus placement moisture curves after saturation, without change in load. The difference between the solid and dotted lines is the effect of saturation on consolidation for the re-

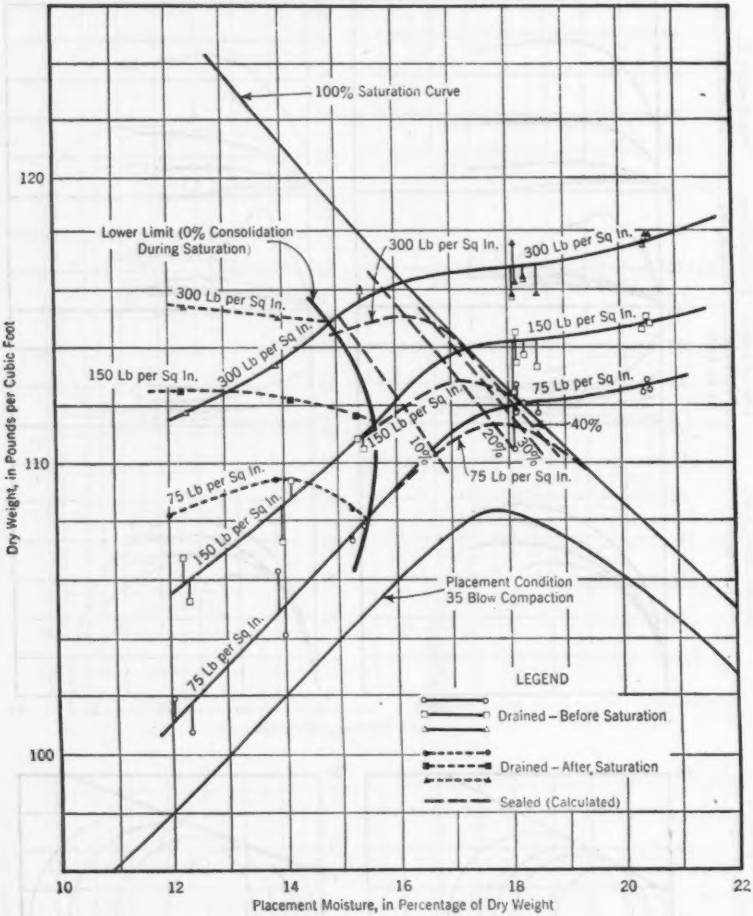

FIG. 5.—LIMITING MOISTURE CURVES

spective loads applied. The intersection of these two lines gives the placement condition at which no additional consolidation will occur upon saturation.

The upper limit is defined as the highest placement moisture content that can be tolerated without producing serious construction pore pressures tending

to reduce the safety factor of the embankment to an unacceptable degree. As practical limitations make it necessary to vary this limit in various parts of the structure, the upper limits are given as heavy dashed lines in Fig. 5 for several pore pressure values in percentage of total load. The upper limit lines are calculated from the results of the one-dimensional consolidation tests, assuming that the specimens are completely sealed and using Eqs. 4 and 5*b*. Calculations were made from the consolidation test data to determine the total applied pressure (pore pressure plus effective pressure) necessary to produce the same consolidation that would occur if the soil were sealed from drainage. This information is shown for the various pressures as the thin dashed lines on Fig. 5 with the applied pressures indicated on the curves. The lines were computed for the total pressures desired by interpolation from the computed data. The heavy dashed lines that cross these thin dashed lines represent the pore pressures that will be obtained for the fill pressures and placement moistures indicated. The positions of these pore pressure lines were obtained by calculating the pore pressures at points along the total pressure lines, using Eq. 5*b*. Pore pressure-consolidation tests that have been used to check the results of these calculations have shown extremely good correlation between the pore pressures computed and those actually obtained from tests.

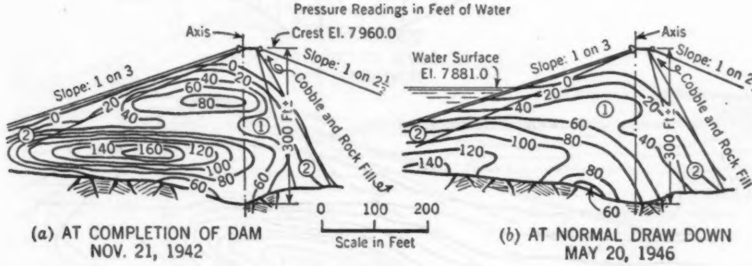

FIG. 6.—PORE PRESSURES IN GREEN MOUNTAIN DAM

Modification of Criteria.—The criteria given were developed for tests on fine-grained impervious soils containing no rock particles. It was recognized that these concepts would have to be modified when considering impervious soils containing greater than about 25% rock. Large-scale consolidation tests were undertaken, therefore, to study these soils from one project in which this type of material was used.[15] These tests, although probably too expensive and lengthy to be standardized for all borrow materials containing a considerable proportion of rock, provided information that can be applied to other soil and rock mixtures. Briefly, it was found that the probability of high pore pressure decreases as the rock content is increased, because the consolidation of the total material is restricted by the increase in rock content. This restriction of consolidation is greater than can be accounted for by the solid rock volume

[15] "The Effect of Rock Content and Placement Density on Consolidation and Related Pore Pressure in Embankment Construction," by H. J. Gibbs, *Proceedings*, A.S.T.M., Vol. 50, 1950, p. 1343.

displacing the compressible fine soil fraction and thus indicates the effect of particle interference. It was further found that for a given type of grain size distribution curve, 3-in. maximum size material showed less consolidation and the same or less pore pressure than 1-in. maximum size material. This was caused mainly by the corresponding increase in rock content. However, for equal total rock content, the 3-in. maximum size material showed greater consolidation and greater pore pressure than the 1-in. maximum size material. This was attributed to the fact that the 3-in. maximum size provided a better graded material, more adaptable to dense arrangement of particles, than did the 1-in. maximum size.

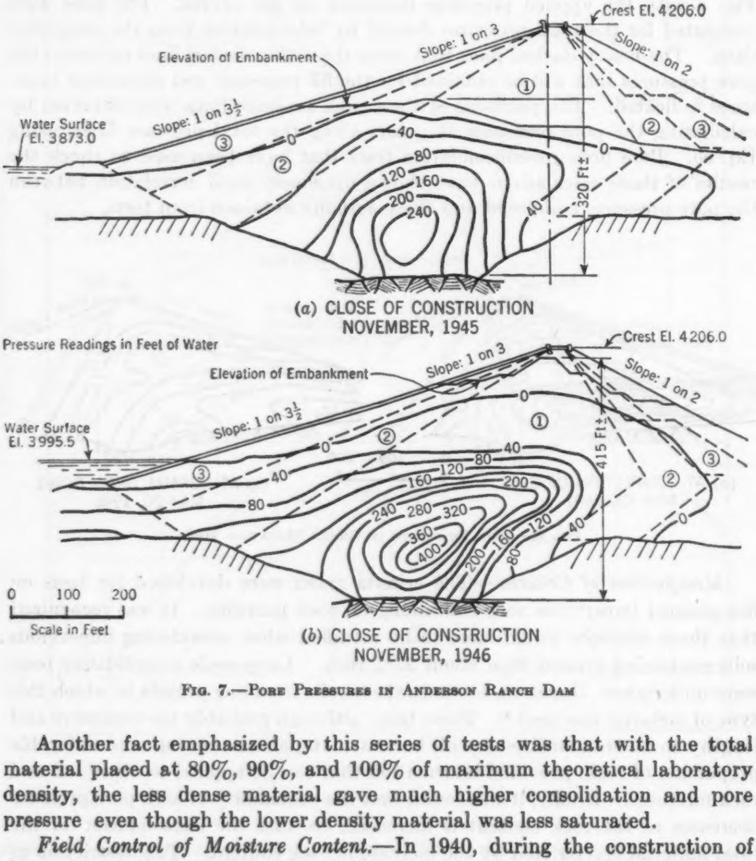

Fig. 7.—Pore Pressures in Anderson Ranch Dam

Another fact emphasized by this series of tests was that with the total material placed at 80%, 90%, and 100% of maximum theoretical laboratory density, the less dense material gave much higher consolidation and pore pressure even though the lower density material was less saturated.

Field Control of Moisture Content.—In 1940, during the construction of Green Mountain Dam (Blue River, Colo.), a structure more than 300 ft high, it was observed that much higher pore pressures were being developed than had been anticipated on the basis of the knowledge then existent. In some

instances these pressures amounted to 65% of the superimposed fill. The pore pressures, when the fill was completed, are shown on Fig. 6. Fortunately the construction season was limited to the summer months. This allowed some pore pressure dissipation during the winter months. The soil used was a clayey, glacial till that contained about 40% rock fragments larger than No. 4 screen. Abnormally high densities, that in some cases were as high as 150 lb per cu ft, were reported, with the average dry density of a great many tests being 136 lb per cu ft. Placement moisture approximated the laboratory optimum.

As a result of this experience, laboratory studies were initiated to find a means for alleviating these high pressures. The limiting moisture concept was the result. Limited tests indicated that, if field compaction using the rollers as specified by the USBR were performed at a moisture content about 2% dry of the laboratory optimum, a very material reduction in pore pressure would be possible. Immediately following World War II a number of dams were started, but, because of the limited time available, it was impossible to complete limiting moisture tests, and therefore, the above general criterion was adopted for control.

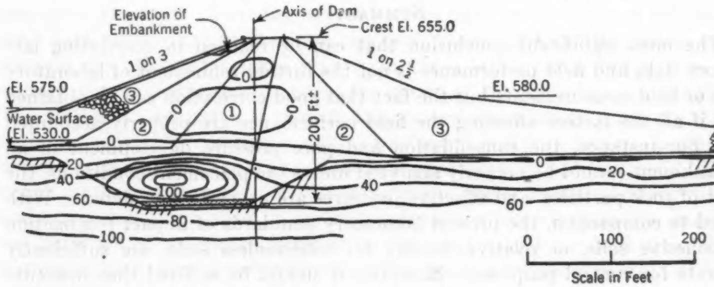

FIG. 8.—PORE PRESSURES IN DAVIS DAM, APRIL 21, 1949

The efforts were only partly successful, not because of any defect in the concept but because it was difficult to overcome the entrenched policy of requiring compaction at laboratory optimum moisture and the recommendation by many authorities that compaction at conditions more moist than optimum should be used. In the construction of Anderson Ranch Dam near Mountain Home, Idaho, moisture control approximated laboratory optimum in the lower, more critical areas and the pore pressures developed in the central part of the dam were 80% to 100% of the values predicted for such conditions. The upper part, in which drier placement conditions were attained, shows very little pore pressure. The pore pressure condition at two stages of construction is shown on Fig. 7. In the Horsetooth Reservoir dams near Fort Collins, Colo., and at Jackson Gulch Dam near Moncos, Colo., it was necessary to use soils that would have developed very high pore pressures if compacted at laboratory optimum moisture. Limiting moisture tests were used for control,

and the resultant pore pressures are insignificant. In the cutoff trench at Davis Dam near Kingman, Ariz., materials were used that had not been analyzed for pore pressure. Tests made prior to World War II and before limiting moisture control was inaugurated indicated that it would be difficult to achieve a high impermeability and that pore pressure probably would not be a problem. The first placements were made using material with a water content greater than optimum. By the time the first pore pressure measurements could be made, there was about 50 ft of fill over the pressure cells located in this material. As additional fill was placed, there was a corresponding increase in pore pressure, showing that the pore fluid carried all the additional load of the dam. Corrective measures had been instituted by this time, and the pore pressures in the remainder of the fill are small as can be seen in Fig. 8 This figure also shows what can be done if limiting moisture control is followed. It has been observed, after a material is compressed to the point where the contained moisture completely saturates the material, that any additional load is carried entirely by the pore water. In some soils this condition has been developed with very small loads (less than 10 lb per sq in.), and in many soils it is attained at between 100 and 200 lb per sq in. when optimum moisture is used for compaction.

Summary

The most significant conclusion that can be reached in correlating laboratory data and field performance is not the further refinement of laboratory tests or field measurements but the fact that good correlation can be obtained only if all the factors affecting the field performance are properly accounted for. For instance, the consolidation and pore pressure development of an embankment cannot be properly analyzed unless the placement conditions, the effect of rock particles, and effective pressures are properly considered. With regard to compaction, the present laboratory standards of impact compaction for cohesive soils, or relative density for cohesionless soils, are sufficiently accurate for control purposes. However, it should be realized that moisture and density requirements established by this control must be modified when necessary to conform to the actual density-moisture-compactive effort data obtained from rolling operations in the field at the start of each dam construction operation. From a design standpoint, the results obtained from the standard impact compaction tests are conservative.

One of the greatest needs in studying embankment materials from a laboratory standpoint is for tests of compaction, permeability, consolidation, pore pressure, and shear on soils containing rock particles. This phase of laboratory testing has been neglected because of the length of time and the expensive equipment usually required for these tests. The USBR has tried to fill in a few gaps in this particular phase of testing by development of the large sheepsfoot compaction tests and large-scale permeability and consolidation tests. A research program to study the permeability and consolidation characteristics of several types of soil containing varying amounts of rock particles between the No. 4 and 3-in. size will also produce valuable data. The study of the shear characteristics of such embankment materials has been

particularly neglected, and triaxial equipment has been designed by the USBR for such a study.

On the basis of information available to date (1951), the following tentative conclusions on earth materials containing rock particles have been reached. With a rock content between about zero and $\frac{1}{3}$, the total material behaves very similarly to the soil fraction having particles smaller than the No. 4 size. When the total material contains between about $\frac{1}{3}$ to $\frac{2}{3}$ rock particles, there is theoretically sufficient soil to fill the rock voids, but this may not be true from the practical standpoint of placing the material because as the amount of rock is increased the particle interference is also increased. In this case, increasing rock content may cause an increase in permeability, a decrease in consolidation, and probably an increase in effective shear resistance. Above about $\frac{2}{3}$ rock content in the total material there is insufficient soil to fill the voids by any compaction method, and the material takes on the characteristics of a gravelly or rock-particle material. Permeability in such material will always be relatively high, consolidation relatively low, and frictional resistance should be relatively high.

Any program for correlating laboratory data and field performance should emphasize facilities for collecting measurements for checking the field performance of a structure. Too often structures are built on the basis of laboratory data, and all thought of checking the performance is forgotten unless some unusual condition later takes place. In these latter cases, initial data are usually not available, and a complete study of the situation is impossible. The USBR is attempting to remedy this general situation on those structures under its control by not only installing settlement and pore pressure measuring devices in its earth dams as it has done in the past, but, in addition, establishing bench marks or settlement measuring devices in power plants, pumping plants, and canal structures, with proper initial condition records to enable checking the behavior of structures founded on soil that may have been treated, or untreated, and constructed with or without piles or any combination of these conditions.

DISCUSSION

GEORGE F. SOWERS,[16] A.M. ASCE.—The embankment soil-testing program of the USBR has been well presented in this paper. All too often such comprehensive studies are presented to the profession piece by piece with no integrated summary of the entire work.

Under the heading, "Compaction Testing: Adaptation of the Proctor Test," the authors state that compaction tests made in 1/20-cu-ft molds do not result in the same maximum density and optimum moisture as in the 1/30-cu-ft mold. How much, specifically, are the differences, and do they materially exceed the variations in these same properties that occur when different but apparently identical samples of the soil (from different parts of a borrow pit) are tested? It seems unfortunate that a 1/20-cu-ft cylinder was selected unless the authors have specific data to show that the compaction data found with this mold more closely represent field compaction. Most other laboratories use the 1/30-cu-ft mold of the American Society for Testing Materials (ASTM) or the 6-in. California Bearing Ratio mold.

The authors state that the sheepsfoot compaction data were found to be comparable to the data obtained by the standard laboratory tests. How are these compared, since one represents static pressure and the other dynamic tamping? The writer has made a brief study which compared the two on the basis of "compactive effort," which is the work expended during the compaction process. The work done in dynamic compaction was computed from the height-of-fall and the weight of the hammer. The work of static compaction was found by measuring the pressure variation and the deformation and plotting a work diagram. The results of tests on a slightly plastic silt of relatively low compressibility indicated that static compaction produced dry densities 10% higher than dynamic compaction when the energy expended during the compaction was identical. Tests comparing field compaction with laboratory dynamic compaction (by the United States Waterways Experiment Station at Vicksburg, Miss.) indicate that, sometimes, the respective dynamic and static compaction curves are not even the same shape.

Although the authors do not specifically so state, the testing program they describe is apparently a part of a much larger program of improving the design of the USBR earth dams. As such, its purpose is necessarily to improve existing techniques of testing and field control, and to verify them by field observations. The value of such work—particularly of the verification by field observations—cannot be overestimated. There is a limit, however, to the value of improving what has been done. Often it may be useful to re-evaluate the present methods to see if a different approach might also be better.

The construction of a fill—whether it be an embankment for an earth dam or highway, a fill for a floor slab, or a subgrade for an airfield—is a manu-

[16] Associate Prof. of Civ. Eng., Georgia Inst. of Technology, Atlanta, Ga.; and Cons. Soils Engr., Law-Barrow Agee Lab. Inc., Atlanta, Ga.

facturing process. The objective is to obtain a product that will perform satisfactorily, and at a minimum cost.

At least three approaches to this objective are possible: (1) Construct the fill according to arbitrary standards of soil compaction and embankment design. (2) Construct the fill according to an arbitrary standard of soil compaction but design the embankment on the basis of the physical properties of the compacted soil. (3) Determine the physical properties of the soil under different assumed construction procedures and select the construction procedure that results in the most economical design.

Unfortunately, the first approach is the most widely used. The arbitrary standards of compaction adopted (such as, "The soil shall be compacted to a density equal to 95% of the standard Proctor method") are based on some empirical relationships between compaction and performance. However, in any particular job there is no assurance that the specified compaction is either enough to produce a satisfactory fill or that it is not far more than necessary. The design of the embankment is based on past designs, no attention being paid to the properties of the compacted fill. It is not surprising that many embankments settle or fail and that others cost too much.

The second approach is essentially that described by the authors. An arbitrary standard of soil compaction is established, based on past experience with the soils and structures involved. This standard is usually the result of trial and error rather than any rational and systematic program of determining just how much compaction is necessary.

The design of the structure with this approach is not based purely on tradition as it is in the first. Instead, the physical properties of the soil (such as strength, compressibility, and permeability) are determined by laboratory tests on the soil compacted according to the standard. These properties are used to modify the traditional designs so that the structure will be adequately safe

TABLE 1.—PHYSICAL PROPERTIES OF COMPACTED SOILS

Property	Relative Importance[a]			Factors Influencing the Properties[a]		
	Dams	Fills	Sub-grades	Soil composition	Moisture content	Density
(1)	(2)	(3)	(4)	(5)	(6)	(7)
Strength	1	2	1	1	1	1
Changes in strength	1	2	1	1	1	3
Compressibility	1	1	2	1	2	1
Changes in compressibility	1	1	2	3	1	3
Swelling and shrinking	2	2	1	1	1	3
Permeability	1	3	1–3	1	3	2
Capillary potential	3	2	1	1	3	2

[a] Numbers listed indicate degrees of influence or importance: 1 = primary; 2 = secondary; and 3 = little or none.

and as economical as possible. Of course there is always the danger that the laboratory tests will not be representative of field conditions; therefore, the verification of the test results by studies of the performance of the full-sized structure is essential. The authors have properly emphasized this phase of

their work, and their report that consolidation and pore-pressure predictions show good correlation with field measurements and that permeability estimates do not—is a valuable contribution.

The third approach is the logical successor to the second. If it is recognized that the design of the structure should be based on the physical properties of the compacted soil, it logically follows that the degree of compaction required is that which produces a satisfactory embankment at a minimum cost. Such an approach will result eventually in the most economical designs, but its development will require considerably more study regarding the physical properties of compacted soils and the factors that influence them.

The soil mechanics laboratory of the School of Civil Engineering at the Georgia Institute of Technology, at Atlanta, has been engaged in a study of compacted soils since 1950. The first step was to list those physical properties which are important in different phases of soil construction and to establish (on the basis of present soil theories) the factors that influence those properties. A tentative list of such properties and their influencing factors is given in Table 1. In this table, "soil composition" includes grain size, shape, and mineralogy.

Basically, the physical properties that affect the design are soil composition, density, and moisture. Of these, the first offers the least possibility of control at the present time except in the case of subgrades. The designer is forced to use local materials because of the high cost of transporting large quantities of soil, and this ordinarily limits him to a relatively narrow choice. In the future, soil modification or stabilization by use of chemicals or cementing materials may be practical, but this is too expensive at the present time, except for subgrades.

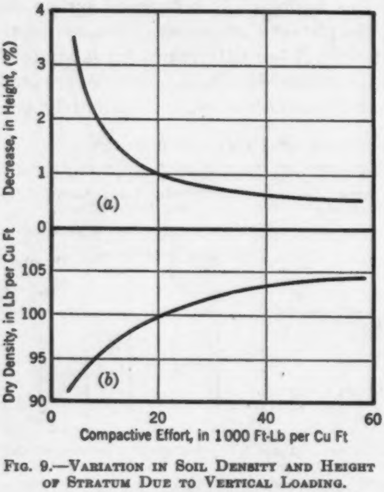

FIG. 9.—VARIATION IN SOIL DENSITY AND HEIGHT OF STRATUM DUE TO VERTICAL LOADING.

Density and moisture content offer wider possibilities of control. The cost of controlling moisture does not vary much whether the percentage of moisture required is high or low. The control of density costs money, however, and so the economical design for a given type of soil results when the cost of obtaining additional density is equal to the savings in design and construction costs due to that additional density.

For any one method of compaction, the cost of obtaining density is roughly proportional to the compactive effort employed. The cost will be different for different methods, however, because some are more efficient than others. For example, vibration at the natural frequency of the soil is very efficient for compacting sands, but of little or no value in plastic clays.

The variation of density and of the properties that depend on density is not directly proportional to the compactive effort. Fig. 9 shows that the rate of improvement of the soil properties becomes progressively smaller as the compactive effort increases for a given moisture content. The sample was micaceous silt of relatively low compressibility, compacted at 16% moisture. The vertical effective pressure was increased from 0 lb per sq ft to 4,000 lb per sq ft. Moisture content was approximately the optimum for the modified method of the American Association of State Highway Officials. Families of such curves showing the effect of moisture content and effort can be developed for any of the physical properties of interest in any particular job. With the aid of such data the designer should be able to select the compaction that will produce the most economical design.

D. P. Krynine,[17] M. ASCE.—Wide laboratory practice of the USBR is clearly defined in this paper. Its reading may open new avenues of thought to both practical engineers and laboratory workers, but also may inspire some doubts. The writer wishes to comment on certain items of the paper and to ask some questions.

Density of Rock and Soil Mixture.—In the case of an artificially compacted fill Eq. 1 gives exaggerated results for all values of P, which is the percentage of the material retained on a No. 4 sieve ("rock"). This formula was derived under the assumption that rock in a compacted rock-soil mixture acts as displacer only; but in reality rock material interferes with the compaction of the matrix, which is the material passing through the No. 4 sieve. Eq. 1 gives correct values of the density of a rock-soil mixture, however, if density D_o is substituted for D_s, the maximum laboratory density of the matrix of the mixture. Symbol D_o would represent the density of the matrix as controlled by the overall dry density of the mixture D_t, the dry density of rock fraction D_r, and the per-

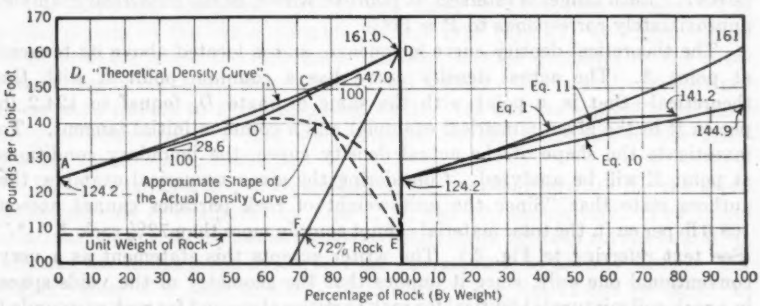

Fig. 10.—Actual Density Curve

Fig. 11.—Comparison of Different Density Curves for a Given Rock-Soil Material

centage of rocks P expressed as decimals. If D_r equals 161 lb per cu ft as in the numerical example, density D_o would be

$$D_o = D_t \frac{1 - P}{1 - 0.0062\, D_t\, P} \quad \text{(6)}$$

[17] Cons. Engr., San Francisco, Calif.

Formulas such as Eq. 6 apply to all natural reasonably compact rock-soil mixtures—that is, excluding loose gravel deposits, decomposed granite, or other particle material. Formulas such as Eq. 6 also mean, in general, that it is impossible to prepare a rock-soil mixture of a density D_t as given by Eq. 1, if it is at the same time required to maintain the maximum laboratory density D_s of the matrix.

Between points A and D in Fig. 10, Eq. 1 represents a flat hyperbolic curve. For convenience in comparison, letters designating analogous points in Fig. 10 and in Fig. 2 are the same, the former being a modification of the latter. By differentiating Eq. 1, the slopes of a tangent to that curve may be found:

$$\frac{dD_t}{dP} = \frac{\frac{1}{D_s} - \frac{1}{D_r}}{\left(\frac{P}{D_r} + \frac{1-P}{D_s}\right)^2} \ldots\ldots\ldots\ldots\ldots\ldots (7)$$

Placing $P = 0$ in Eq. 7, the slope of the tangent to curve 1 at point A may be computed thus:

$$\left(\frac{dD_t}{dP}\right)_{P=0} = D_s\left(1 - \frac{D_s}{D_r}\right) \ldots\ldots\ldots\ldots\ldots\ldots (8)$$

It should be borne in mind that, since a slope is expressed by an abstract number, the value given by Eq. 8 should be divided by 100 lb per cu ft. Noting that in both Figs. 2 and 10 the vertical and horizontal scales are equal, the slope of the tangent to the theoretical density curve at point A for the given numerical example is 0.286. In an analogous sense, placing $P = 1$ in Eq. 7, the slope of the tangent to the theoretical density curve at point D would be 0.47. Both tangents intersect at point O, which, in the numerical example, approximately corresponds to $P = 56\%$.

The theoretical density curve is concave, and is located above its tangent at point A. The actual density curve has a common point A with the theoretical—that is, a point with the same ordinate D_s (equal to 124.2 lb per cu ft in the given numerical example) and a common initial tangent. To investigate the shape of the actual density curve, the boundary conditions at point E will be analyzed. Considering the given numerical example, the authors state that "Since the unit weight of rock particles cannot exceed 108.0 lb per cu ft, the total material cannot contain more than 72% rock * * *." (See text referring to Fig. 2.) The writer accepts this statement as a very conventional one only, since it implies that the geometry of the voids space in a rock-soil mixture is identical for rock particles alone and for rock surrounded by the matrix, which in a general case cannot be proved. For the purposes of this discussion this is not important, however, since it is necessary only to have some point E roughly at the position shown in Fig. 2 or Fig. 10 toward which the curve slopes down. In fact, the value of P corresponding to point E cannot increase. Algebraically, this fact should be expressed thus:

$$(dP)_{P=1} = 0 \ldots\ldots\ldots\ldots\ldots\ldots (9a)$$

or

$$\left(\frac{dD_t}{dP}\right)_{P=1} = -\infty \ldots\ldots\ldots\ldots\ldots\ldots\ldots\ldots(9b)$$

Eq. 9*b* means that the tangent to the actual density curve at point E is vertical. Since this is so, the actual density curve is convex (Fig. 10). It cannot be located above the tangent AO, but may be close to that tangent. In Fig. 10 the curve in question deviates from the direction of the tangent at point O after which density D_t must reach its maximum value. On both sides of the maximum the actual density curve should be rather flat, the values of density being practically constant within a certain range (between 60% and 70% of rock in the given numerical case). A simplified method of computing the actual density of the rock-soil mixture D_t may be as follows: Up to the value of $P = 0.6$,

$$D_t = D_s\left[1 + P\left(1 - \frac{D_s}{D_r}\right)\right] \ldots\ldots\ldots\ldots\ldots\ldots(10)$$

in which P is expressed in decimals. From $P = 0.6$ through $P = 0.8$ the value of D_t may be considered practically constant.

Other attempts have been made to correct the so-called "theoretical" curve expressed by Eq. 1. For instance, the Civil Aeronautics Administration[18] (CAA) expresses the density of rock-soil mixtures for runway base and sub-base materials according to Eq. 11,

$$D_t = (1 - P)\, D_s + 0.9\, P\, D_r \ldots\ldots\ldots\ldots\ldots\ldots(11)$$

In this case, correction is made by decreasing the value of D_r instead of D_s which, of course, is immaterial so far as the numerical result is concerned if the correction coefficient (0.9 in this case) is adequately chosen. The writer objects to the use of formulas of this type (Eq. 11) for higher values of P, however, since the differences between vertical ordinates of the theoretical density curve and those of the actual density curve in such cases are not linear with respect to P (as suggested by Eq. 11) but are expressed by more involved functions of P and are controlled by the properties of the interparticle space in rock material.

Fig. 11 compares the dry densities of the rock-soil mixture for the given numerical case as computed by Eqs. 1, 11, and 10, respectively. The values of actual density D_t are located probably somewhere between curves 11 and 10, whereas the values given by curve 1 are exaggerated, as already stated. For higher values of P close to 100%, neither Eq. 1 nor Eq. 11 can be used. In deriving Eq. 10, the writer did not even attempt to go as far as $P = 90\%$ or better, since such mixtures, generally, are loose and cannot be considered as compacted material.

Over-Compaction.—Failures of earth structures generally occur as a result of combined action of several causes, one of which is predominant. In the absence of secondary causes this predominant cause alone in many cases

[18] "Standard Specifications for Construction of Airports," Office of Airports, Civ. Aeronautics Administration, Washington, D. C., January, 1948, p. 571.

may not produce failure. In the opinion of the writer, this is true in the case of over-compaction that may often take place but remains unnoticed except for some extraordinary cases such as that reported in 1936 by the late Mr. Knappen,[6] Again, over-compaction may cause residual stresses of various magnitudes, and only the strongest ones are capable of causing considerable displacements in the compacted mass. Also, the direction of least resistance along which the over-compacted material may move is usually upward; and a motion in this direction may simply pass without being recorded. The writer has no data pertaining to over-compaction of fills at his disposal; but he is aware of two failures of retaining walls which, in his opinion, were caused predominantly by over-compaction of the backfill. In one of these cases the backfill of a typical reinforced concrete wall was compacted with pneumatic rammers in the afternoon. The next morning the top of the wall was found out of position and the reinforcement had failed in tension.

When material for a compacted fill is studied, it is important to determine whether or not it has expansive properties, especially in highway and runway engineering and in the case of footings to be built on artificial fill or otherwise. The expansion pressure apparatus used by the California Division of Highways[19] is a device in which the compacted soil specimen is confined under a perforated disk covered with water. The pressure exerted by the soil at the point of incipient expansion is measured by a device similar to a proving ring. A pressure of 0.5 lb per sq in. requires only 0.001-in. movement in order to register on the gage; therefore, the pressure is measured at virtually constant volume. The final expansion pressure is recorded after the specimen has been in the device for 24 hours. An Oakland (Calif.) laboratory that has performed a considerable number of expansion measurements reports that most local soils show increasing expansion pressure as compaction is increased. In other words, the denser an expandable material is, the larger will be its expansive tendency. In an example taken at random, a material compacted in the laboratory to dry densities of 118.1 lb per cu ft, 119.8 lb per cu ft, and 122.2 lb per cu ft when saturated showed expansion pressure of 141 lb per sq ft, 282 lb per sq ft, and 496 lb per sq ft, respectively. The Atterberg limits of the given material were—liquid limit, 34%; plastic limit, 23%; and the plasticity index, 11%. Presumably, such records require further study and interpretation, but in any case they can be considered as a preliminary evidence in favor of the possibility of over-compaction.

Pore Pressure.—The authors ably state (see under the heading, "The Pore Pressure Concept: Theoretical Derivation") that "Pore pressure develops in a soil mass as consolidation from loading takes place." Only a few words need to be added to this statement. Pore pressure also develops when pore fluid is brought into contact with a large hydraulic head that may be produced by an insignificant quantity of fluid. Such is the well-known phenomenon of liquefaction of saturated deposits as brought to the attention of the profession by Arthur Casagrande, M. ASCE, as early as 1936.[20] Such is also the case of

[19] "The Factors Underlying the Rational Design of Pavements," by F. N. Hveem and R. M. Carmany, *Proceedings*, Highway Research Board, National Research Council, Washington, D. C., Vol. 28, 1948, p. 132.

[20] "Characteristics of Cohesionless Soils Affecting the Stability of Slopes and Earth Fills," by Arthur Casagrande, *Journal*, Boston Soc. of Civ. Engrs. Vol. 23, 1936.

numerous slides after rains in hilly countries when a saturated mantle, 3 ft to 4 ft thick, slides. In this case sliding is caused by a considerable decrease (or even vanishing) of normal pressure which holds the mantle against the body of impervious hill that otherwise remains intact. Slides of this kind occur in different earth materials, not necessarily silts. The bouncing of earth material during fill construction, sometimes observed in soils with considerable sand content, probably is also explained by air pressure in the voids. This phenomenon (often alarming for inexperienced inspectors on the job) passes within a few days.

Questions.—Much attention has been paid in engineering literature to the concept of critical voids ratio (or critical density), especially in textbooks. The writer has never had the opportunity or necessity to use this concept except when he was teaching classes in soil mechanics. In the paper, the critical voids ratio is not mentioned. How does this concept fit in the general picture of the USBR activities?

Reverting to the subject of pore pressure and particularly to Henry's law, the writer would like to know whether this law is applicable to capillary moisture or to free water only.

Scope of the Paper.—The writer believes that this fine paper will be useful to builders of fills of all kinds. The paper would be still more useful had the authors strongly stressed the necessity of examining not only the material for the fill itself but also the material and conditions under the planned fill, which unfortunately are sometimes neglected with disastrous results.

D. F. Glynn,[21] A.M. ASCE.—This comprehensive summary of the current USBR practice for applying experimental soils studies to the design and construction of major earth fill dams is an extremely important addition to soil mechanics data. The presentation is particularly timely because of the conflicting views held regarding the importance of pore pressures to shear resistance.

The authors have suggested that certain details of their conclusions may require modification to suit local conditions. Experience during investigations for, and present construction of, the Upper Yarra Dam in Australia have shown that in some cases the effect of the local conditions may be more important than the basis for the general practice. In illustrating this point, it may be noted that the Upper Yarra Dam is a 290-ft earth and rock dam founded directly on sandstone and siltstone rock. All the rock fill and the major part of the earth fill are being obtained from this base rock. After rolling the softer parts the resultant earth fill is a stony loam with 25-blow optimum conditions of about 110 lb per cu ft and 17%. The climate is a West Coast type, with an annual rainfall of from 40 in. to 60 in., and little or no snow. Even after prolonged rain, borrow material can be dug from the undisturbed condition at about optimum moisture content.

Under these conditions, the selection of moisture content limits is being dictated by construction considerations rather than on the basis of a guide

[21] Superv. Engr., Soils and Hydr. Testing, Melbourne and Metropolitan Board of Works, Melbourne, Australia.

such as in Fig. 5. For two reasons the fill must be compacted at about optimum conditions instead of the drier state suggested by the authors. First, when the fill is compacted drier than 1% or 2% below optimum moisture content, it is impracticable to obtain consistent densities comparable with optimum values. Instead, the fill behaves more like the granular coarse-grained soils recommended for tractor compaction. Second, the humid climate prevents any effective drying of materials except during the three or four summer months. Thus, fill must be placed at not drier than the average moisture content of the borrow material in place. It is further questioned whether this somewhat wetter placing is always as dangerous as shown in Figs. 6, 7, and 8. It is believed that these conditions may not be serious with some less compressible types of materials. The evidence of Deer Creek Dam[11] in Utah would seem to support this view.

Although the USBR pattern roller has been adopted as standard, it has not proved as satisfactory as indicated in Fig. 3. On the fill at Upper Yarra Dam, it is barely able to reach the equivalent of the 25-blow laboratory compaction standard. To improve the densities and to assist in shedding rain from the bank, the procedure has been changed. Each layer is now spread to a 12-in. depth. This is rolled with twelve passes of the fully ballasted USBR roller. The loose surface is then finished with four passes of a grooved roller weighing about 8,500 lb per ft of width. This grooved roller is a special experimental unit assembled from the units used in the construction of Silvan Dam in Australia, during the early 1930's.[22] This combination has decreased the total of spreading and rolling costs, has shed rain better, and has provided densities at least 2% to 4% better than the USBR roller alone. This experience suggests that it may be advantageous to consider whether new roller techniques are not needed.

Eqs. 5, adopted for the computation of pore pressures, are extremely useful in determining the pore pressures to be expected for any given consolidation. It should be recognized, however, that the accuracy of this prediction depends on a specific gravity test of the soil. This test seems simple, but minor variations in procedure cause significant changes in the values. For example, the boiling of the water and soil prior to the evacuation increased the measured specific gravities of a soil from 2.68 to 2.72. It is thus suggested that the more direct expression of the triaxial compression tests results[23] provides a better basis for design assumptions. In this case the pore pressures measured in specimens at failure are related to the total maximum principal stresses. These results are the limiting pore pressures, and they require some reduction to allow for factors such as smaller consolidation, dissipation of pore pressures, and increased rock percentages. Although either basis for predicting the pore pressures requires correction to make them suitable for use in design analysis, the triaxial compression results have the merit of being a more direct and positive measurement.

---

[22] "The Construction of Silvan Dam, Melbourne Water Supply," by A. E. Kelso, *Proceedings*, Inst. of C. E., London, England, 1937, p. 403.

[23] "Triaxial Compression Testing of Soils," by D. F. Glynn, *Proceedings*, Conference on the Shear Characteristics of Soils, Melbourne Univ., Melbourne, Australia, June, 1952.

The authors' discussions and conclusions regarding the effect on the properties of a soil caused by the addition of rock were of the greatest value. They did not mention whether any attempts had been made to test samples composed wholly of rock fragments, or what basis was used to predict the shear resistances of rock fill. In the absence of any positive information, triaxial compression tests were performed on loosely compacted samples of Upper Yarra Dam rock fragments. These varied in size from about $\frac{3}{16}$ in. to $\frac{1}{2}$ in. As such, of course, they did not develop pore pressures. The puncturing of the rubber envelope during the test made their performance very difficult. However, after a fairly comprehensive series of tests it was established that the values of the cohesion parameter were all zero and the friction parameter was between 0.8 and 0.9. The lower value was accepted as a probable minimum suitably adjusted to serve as a basis for stability analysis of the rock fill. Do the authors propose to use the large USBR triaxial apparatus for rock fill studies?

Finally, it is desired to express appreciation to the authors for their most valuable service in making available this very well considered assembly of field, laboratory, and office experience.

F. C. Walker[24] and W. G. Holtz,[25] Members, ASCE.—Answers to Mr. Sowers' questions follow: A suite of thirteen samples from Falcon Dam on the Rio Grande was tested in 1949, according to the ASTM standard in a 1/30-cu-ft cylinder and the USBR standard in a 1/20-cu-ft cylinder. The compactive effort was the same per unit volume in all tests. The maximum densities by the ASTM method averaged 1.7 lb higher than the average of the USBR tests. Maximum densities were attained at a moisture content 0.5% higher in the USBR tests than by ASTM procedure. Mr. Proctor has reported similar differences. Values for any one type of test by different operators may vary approximately 1 lb per cu ft, but will be erratic, whereas the smaller ASTM cylinder produced consistently higher values.

The writers discussed the reason for the adoption of the 1/20-cu-ft compaction cylinder. The cylinder adopted is the same as the original and present Proctor mold, and many feel that it should have been adopted as an ASTM and Highway Research Board (HRB) standard rather than the 1/30-cu-ft mold.

There are several variables that may be changed—both in dynamic and static compaction procedures—which materially influence the results, although the energy input is the same. Originally, the laboratory test result was considered to be the desirable objective, and field compaction procedures were modified over a period of time until equivalent results were obtained. Subsequently, performance records have shown that the laboratory test result does not define the most desirable objective. Therefore, it is now used as a reference point for defining the deviation required for field compaction control. A change in characteristics can be controlled better by modifying established relations between the field and laboratory than by developing new procedures.

In practice, all three of the approaches described by Mr. Sowers are used in the development of a design. For minor structures, the arbitrary standard

[24] Head, Earth Dams Section, Bureau of Reclamation, U. S. Dept. of the Interior, Denver, Colo.
[25] Head, Earth Materials Lab., Bureau of Reclamation, U. S. Dept. of the Interior, Denver, Colo.

approach is used although the characteristics for a specified degree of compaction are checked if not reasonably well known. When construction requires the use of soils whose characteristics are well understood, the second approach is most commonly used. When the nature of the soils is not well understood and where foundation conditions are unusual, the third method of approach is the one used in the development of the design. It is not uncommon for all three approaches to be used in various parts of a single structure. When the third procedure is used, it is essential of course, that there be a program of follow-up observations to check whether the field conditions are actually comparable to the laboratory assumptions.

The writers cannot agree entirely with the relative importance Mr. Sowers has assigned to factors influencing the soils properties. They have found permeability to be markedly influenced by moisture content used during compaction, and swelling and shrinking characteristics are quite clearly a function of the density achieved by compaction.

There is generally a widespread misconception of the cost of achieving density through compaction. The cost of securing the compaction that the USBR has required varies between 2¢ and 4¢ per cu yd. On the other hand, securing satisfactory moisture control has been extremely variable. Occasionally a satisfactory moisture content naturally exists in the borrow pit, in which case the cost for moisture control is very small. More frequently, moisture either must be added or removed from the materials before they can be compacted satisfactorily. In some instances, extensive drying operations have been required; in others, water has had to be transported for several miles in order to be applied to the borrow pit so that satisfactory moisture conditions could be achieved. Situations can be visualized in which it will be more practicable to construct a fill with material having inferior moisture control and a larger section to compensate than to minimize the volume of material used in the embankment.

Sufficient compactive effort should be used in the construction of water-retaining structures so that a high degree of uniformity is achieved. For this purpose, it is advisable to operate well up onto the flatter parts of the compactive effort dry-density curve, because of variations in compactive effort that are commonly experienced during practice. Expensive testing and inspection are thereby held to a minimum.

Mr. Krynine has further emphasized the properties that the writers wished to demonstrate. It is not practicable to achieve the high degree of densification that theoretical formulas would indicate due to particle interference as rock content increases. Even on a theoretical basis, Eq. 1 is not valid at percentages greater than about that indicated by point B. The value $P = 1$ should be thought of as a limit line for the part B′E of the curve in Fig. 2 and there appears to be no reason why the curve should be parallel to the vertical limit $P = 1$. It does not appear to the writers that the curve B′E approaches a vertical at some small increment away from $P = 1$ as, say, $P = 0.99$. By actual computation it can be seen that it would be impossible to obtain densities indicated by Mr. Krynine's OE-curve (Fig. 10), say, at $P = 0.9$ (90% rock). Curve OE shows the weight of total material to be 130 lb per cu ft at this point. The

weight of the rock would then have to be 117 lb. From actual test, as indicated by point E or line FE, the weight of rock cannot exceed 108 lb. If lines CE or BB'E are used, the weight of rock will never exceed the maximum—108 lb. There seems to be no reason why a true density curve should follow a tangent line AC, Fig. 10, which is purely mathematical. The true curve for any particular material is dependent upon the gradation and shapes of the rock particles in terms of interference offered. Because of the reduction in density that is achieved when rock content appreciably exceeds 50%, the USBR is not allowing materials to be placed in the impervious sections of dam embankments which contain a greater proportion of rock particles than 50%. In some instances, the USBR has, with a small increase in compactive effort, been able to obtain densities indicated by Eq. 1 with rock contents as high as 40%. Eq. 11, therefore, establishes a density requirement of a lower degree than is practicable to obtain within the normal working range.

Mr. Krynine asks how the critical voids ratio concept fits into the picture of USBR activities. During the design of some of its dams, the critical voids ratio condition was extensively considered and numerous laboratory tests were made. The writers' present definition of critical density, and the concept involved in its use, vary somewhat from those originally advanced by Mr. Casagrande. In performing triaxial shear tests for determining a critical density, the tests are made on saturated specimens which are sealed after initial consolidation, and the pore pressure is measured throughout the shear tests. Of course, tests are made on several specimens under different placement density and lateral pressure conditions. A maximum allowable pore pressure value (say, 10% or 20% of the applied lateral pressure) consistent with the design is selected. If the pore pressure development for a given set of density and pressure conditions does not exceed this allowable maximum at any time during the test, the soil is considered to be compacted above critical density for that structure and under the conditions assumed. It has been observed that most sands compacted to 70% relative density are above critical density. This relative density can usually be obtained without difficulty by water and heavy tractor compaction in dam construction.

Mr. Krynine also asks whether Henry's law is applicable to capillary moisture or the free water only, in the determination of pore pressures. There seems to be no reason why Henry's law should not be equally applicable to capillary moisture as to other free water. In the range where only capillary moisture exists in an embankment, pore pressure (in USBR experience) has not been of any consequence.

As Mr. Glynn states, it is always necessary to modify general principles to suit local conditions, particularly when high dams are being constructed of materials for which there is limited experience record. Until quite recently, the USBR has been able to avoid the use of residual soils and disintegrated rock in the construction of earth dams. However, since the preparation of the referenced paper,[11] construction of several dams has been initiated wherein it was necessary to utilize such materials. In one instance, there was sufficient breakdown during the process of compaction so that optimum moisture requirement had to be increased about 4% over that indicated when the earth-fill

material was tested in order to produce a satisfactory final product. It is probable that the increase in moisture requirement which Mr. Glynn experiences at the Upper Yarra Dam may be due to similar causes. Tests made in the USBR laboratory on a sample of material from one of the proposed borrow pits for Upper Yarra Dam showed extreme breakdown during compaction and shear.

The writers question whether the compaction procedure that Mr. Glynn is using is the best achievable procedure. There is always danger of developing a highly stratified fill when thick layers are used or when one type of compaction is used for the deeper part of the lift and another method of compaction for the superficial part of each lift. A preferable procedure would be to use a thinner lift—say, about 8 in. and to work the heavy grooved roller and the sheepsfoot roller in tandem so that the rock crushed by the action of the heavy grooved roller could be compacted into the matrix by the sheepsfoot roller. It is obviously desirable to secure the greatest breakdown practicable in utilizing disintegrated rock.

In addition, the writers have used the measurements of pore pressures obtained from triaxial tests as a basis for determining pore pressures that might be found in an actual structure. There are, however, many factors in the procedure used for measuring pore pressures in laboratory samples which may produce erroneous results. Other investigators have found the results of direct measurements to be so unreliable that they hesitate to use them.

The USBR has not investigated the strength characteristics of rock fragments sufficiently to warrant an opinion. Data secured from the measurement of the angle of repose on talus and gravel slopes have been used as a basis for design in structures where rock fragments or cobbles have been used. This procedure is considered to be on the conservative side, since excavation into talus or gravel deposits commonly stands, at least temporarily, on steeper slopes. The large trixial testing equipment mentioned in the paper has been completed and research tests on gravelly soils are continuing. Specimens 9 in. in diameter by 22 in. long are being tested. From this work, it is hoped to obtain a better understanding of the shear characteristics of coarse-grained soils.

The work of the USBR is largely confined to the arid western area of the United States and primarily to those areas at higher elevations within that region. Before a comprehensive appraisal of this situation may be said to exist, there should be additional information on the utilization of the plastic soils more commonly found in the eastern part of the United States and also experiences in the utilization of tropical soils, as well as additional experiences concerning the uses of residual soils and disintegrated rock. The comments of the discussers have served to introduce some experiences in this area.

AMERICAN SOCIETY OF CIVIL ENGINEERS
Founded November 5, 1852

TRANSACTIONS

Paper No. 2535

LAKE MICHIGAN EROSION STUDIES

BY JOHN R. HARDIN,[1] M. ASCE, AND
WILLIAM H. BOOTH, JR.,[2] A. M. ASCE

WITH DISCUSSION BY MESSRS. THOMAS B. CASEY, CHARLES E. LEE, AND JOHN R. HARDIN AND WILLIAM H. BOOTH, JR.

SYNOPSIS

The State of Illinois, acting through the Division of Waterways, has become increasingly concerned with the erosion problem of Lake Michigan within the state limits. As a result, the state requested a cooperative beach erosion control study to determine the best plan of improvement for stabilizing the shore line. This paper deals with the erosion conditions, prior corrective actions, and structures, and describes the protective measures that have been recommended.

INTRODUCTION

A cooperative study of the erosion of the shores of Lake Michigan in the Chicago area was completed by the Corps of Engineers (United States Army) and the State of Illinois in 1950. The problems encountered and the considered judgments of the cooperating agencies as to corrective measures required are believed to be of interest to other engineers facing similar problems. The problem involved not only the protection of existing property, but also the solution of a pressing social need for more recreation facilities for the people of Chicago. Although the economics of the improvements and the sharing of cost are important features of the study, this paper is devoted only to the general problem of shore erosion and protection.

The shore lines of the Great Lakes have changed continually for thousands of years. Before the time of written history, these changes were primarily of glacial nature. Within historic times, Lake Michigan has been eroding its western shore from the vicinity of Green Bay, Wis., southward to the vicinity of 55th Street in Chicago. The main physical forces that are responsible for this erosion are wind, wave, and current action. The principal direct agent in producing the erosion is wave action that breaks down and stirs up the material.

NOTE.—Published in February, 1952, as *Proceedings-Separate No. 115*. Positions and titles given are those in effect when the paper was received for publication.

[1] Div. Engr., Colonel, Corps of Engrs., U. S. Dept. of the Army, Chicago, Ill.

[2] Engr., Office, Chf. of Engrs., Washington, D.C.

The eroded material moves generally southward, until it reaches the vicinity of 55th Street, where accretion begins to balance erosion. At the south end of the lake, the eroded material enters a natural collecting ground, forming beaches and the famous sand dunes of Indiana.

These changes in the shore line and beaches did not disturb, to any great extent, the forefathers who settled along the lake shores. If the beach was washed away by storm waves or by currents, the early settler merely built another cabin, of easily obtained native materials, a few hundred feet further inland and went about his business.

However, the solution of the problem resulting from beach erosion and changes in shore line is not that simple in the twentieth century. Quite literally, billions of dollars' worth of property fronts on the lake along the Illinois shore line. There are thirteen cities and villages, two military reservations, and thousands of commercial, industrial, residential, and recreational properties along the 58 miles of shore line within the state of Illinois.

Since man began to build structures and modify the shore line, the natural processes have been disturbed at various points so that numerous local exceptions may be made to the foregoing erosional and depositional trends. Outstanding examples of these exceptions are the areas of accretion found north of artificial structures, such as the harbor structures at Waukegan and Wilmette, and the bulkhead projection north of Foster Avenue in Chicago. Another example is the general absence of the appreciable littoral drift south of Foster Avenue. Thus, it may be said that the problem of shore line protection against erosion is a problem created or aggravated by civilization.

Physiographic Sections

A detailed examination of the Illinois shore line of Lake Michigan indicates that, for purposes of erosion control, this shore line may be logically divided into sections based upon both the natural and artificial features. The four divisions adopted for the purposes of this study are as indicated in Fig. 1. These divisions are: (1) Northern lake plain section; (2) lake border moraine section; (3) southern lake plain section; and (4) the artificial fill section.

(1) *Northern Lake Plain Section.*—This section of the shore extends from the Wisconsin-Illinois state line (actually from Kenosha, Wis.) to Waukegan Harbor. It is an eroding section of the shore, except north of the Waukegan Harbor structures that form an inpounding area for the natural shore drift moving southward. This general section of the shore is little developed, except at Winthrop Harbor, Zion, and Waukegan. The Lake is fronted by a relatively low plain with old beach ridges and dunes, and the erosion taking place represents essentially a recapture of the ancient glacial lake deposits by the present lake.

(2) *Lake Border Moraine Section.*—This section of the shore extends from the south side of Waukegan Harbor to the jetty at Wilmette Harbor. Here the shore consists of bluffs having heights as much as 90 ft above lake levels. A beach, with a maximum width of 200 ft and an average width of 75 ft land-

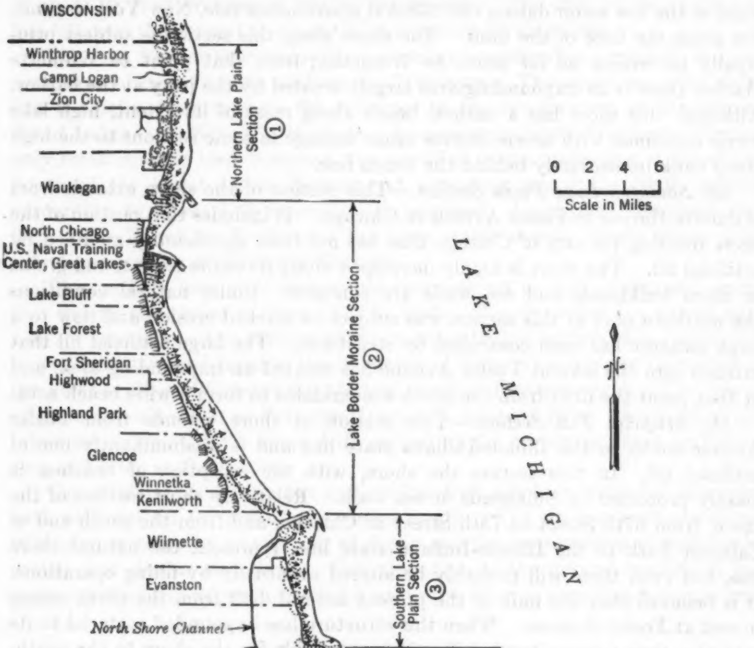

FIG. 1.—BEACH PROCESSES AND LITTORAL DRIFT ON THE ILLINOIS SHORE OF LAKE MICHIGAN

ward of the low water datum (El. 578.5 ft above mean tide, New York datum), lies along the base of the bluff. The shore along this section is subject principally to erosion as far south as Winnetka; from that point to Wilmette Harbor there is an impounding area largely created by the jetty at the harbor. Although this shore has a natural beach along most of its extent, high lake levels combined with severe storms cause damage in some sections to the high steep bank immediately behind the beach line.

(3) *Southern Lake Plain Section.*—This section of the shore extends from Wilmette Harbor to Foster Avenue in Chicago. It includes that portion of the shore fronting the city of Chicago that has not been significantly modified by artificial fill. The shore is highly developed along its entire extent, and groins or short bulkheads and sea walls are common. Under natural conditions the northern part of this section was subject to marked erosion and now to a large measure has been controlled by structures. The large artificial fill that extends into the lake at Foster Avenue has created an impounding area, and at that point the drift from the north accumulates to form a wide beach area.

(4) *Artificial Fill Section.*—This section of shore extends from Foster Avenue south to the Illinois-Indiana state line and is predominantly one of artificial fill. In this section the shore, with the exception of beaches, is mainly protected by bulkheads or sea walls. Relatively short reaches of the shore, from 67th Street to 75th Street in Chicago, and from the south end of Calumet Park to the Illinois-Indiana state line, represent the natural shore line, but even these will probably be altered eventually by filling operations. It is believed that the bulk of the present natural drift from the north comes to rest at Foster Avenue. When this structure has impounded material to its capacity, then some natural drift will be available for the shore to the south. The impoverishment of the drift by the Foster Avenue impounding area, combined with the great depth of water in front of the filled land to the south, has resulted in marked changes in the natural shore line trends and in the conditions of shore drift. As a consequence, reliance for bathing beaches has been largely shifted to the creation of artificially nourished beach areas along this section of shore line.

Shore Line Changes

The data on shore line changes are available for four periods: 1872–1873, 1909–1911, 1937–1938, and 1946–1947. It was difficult to make a definite comparison of this data since the first two periods were taken from old surveys. The data for the third period were obtained from aerial photographs and a field survey made by the State of Illinois, and the data for the fourth period were obtained from a survey made specifically for the erosion study. The changes in the shore line were analyzed within the framework of the four sections of the shore line previously described.

The northern lake plain section is generally characterized by erosion of the shore line during the entire period, except that portion immediately above the Waukegan Harbor breakwater. The data indicate that the average annual rate of recession of the shore line ranges from about 10 ft at the Wisconsin-Illinois state line to about 1 ft at the Illinois Beach State Park, with accretion

of about 28 ft at Waukegan Harbor breakwater. The offshore depth change has followed the general trend of the changes in the shore line.

The lake border moraine section contains considerable variation in local conditions of shore line and offshore depth changes. The condition of the shore line is chiefly dependent on the influence of the breakwaters at Waukegan, Great Lakes, and Wilmette Harbors. Immediately below Waukegan Harbor only small changes have occurred, as a result of riprap protection of the shore. South of the Great Lakes Harbor and extending into Lake Bluff, erosion amounting to about 4 ft annually has occurred. In general, the shore line from Lake Forest to Kenilworth has been stable during recent years, with accretion occuring at Wilmette Harbor.

The southern lake plain section has been subject to both erosion and accretion during the period of from 1872 to 1946. The shore line has varied only 1 or 2 ft annually. The offshore depth contours in this section have, in general, moved lakeward and considerable amounts of material have been deposited in the areas south of Wilmette Harbor and north of Foster Avenue. The heavy offshore deposit south of Wilmette Harbor is believed to be the result of the lakeward diversion of the shore drift, caused by the projecting shore conformation and jetty at the harbor.

The artificial fill section has a shore line that has been extended lakeward with artificial fill for almost the entire length. The fill has been stabilized in a large measure by the placing of riprap and the construction of bulkheads, groins, and similar structures. This alteration of the natural conditions has made it difficult to determine whether natural erosion or accretion has occurred.

Factors Affecting Erosion

Waves and Currents.—Of all the movements of the lake water, waves are the most significant in considering shore protection. Most waves are generated by the action of wind upon the water surface, and their direction and magnitude generally depend upon the direction and intensity of the wind. The action of the wave against the shore induces an alongshore current that moves material. High lake levels allow the waves to reach farther inland for this erosive action while low lake levels may reduce depths of water over offshore bars so that favorable wave action may carry material from the bars to the beaches.

No special observations were made to determine the strength of the shore currents along the Illinois shore, but some data were obtained from the Department of Geology, Northwestern University, on current observations at Evanston, Ill. These observations covered a period of 18 months and indicated that when currents were present, the prevailing movement is southward about 65% of the time, and northward about 35% of the time. The southward-moving currents generally had higher velocities than those moving north, with maximum observed values near shore of about 3.5 ft per sec southward. The velocity of the currents was determined by observing floats in the zone just outside the breaking waves. The stronger southward-moving currents develop a greater drift of sand in that direction, which is in conformity with the observed accumulation of sand on the north side of existing structures.

Littoral Drift.—The estimated annual rates of shore drift along the Illinois shore are as follows:

Section	Drift, in cubic yards
Northern lake plain	90,000
Lake border moraine	57,000
Southern lake plain	40,000
Artificial fill	Negligible

Protective Structures.—It appears that, in the past, local judgment has generally determined the method or methods to be used in improving and stabilizing the shore line. As a result, wide differences in the character, planning, and design of structures are evident. Some have been effective, and others have been useless. A large number and variety of structures, many dating prior to 1900, have been constructed in an effort to retard erosion and to maintain a beach. Most of those constructed of wood as a basic material are now completely disintegrated, or so badly in need of repair as to make them ineffective. Other old types, especially concrete or steel bulkheads, have held up very well and continue to provide effective protection. High lake stages have again put emphasis on shore protection and, as a consequence, a number of new structures, groins in particular, have been constructed.

There are many types of protective structures in use along the Illinois shore line. The predominant types are: (*a*) Solid groins; (*b*) permeable groins; (*c*) breakwaters or jetties; (*d*) hooked piers; (*e*) submerged breakwaters; (*f*) bulkheads and sea walls; and (*g*) riprap revetment.

(*a*) Solid Groins.—Solid groins have been the most widely used structures for stabilizing the shore line and creating beaches. They are as numerous as all other protective structures combined, and comprise more than three-fourths of all beach building types. They have been built most extensively in the lake border moraine section where the littoral drift is generally adequate to build and maintain a beach.

The height of the groins has been observed to have considerable effect on their functioning. Those that have heights not exceeding 3 or 4 ft above low water datum have retained material on their north side and yet have permitted some material to be carried over the top so that beaches are found on both sides. The higher groins, that have prevented the flow of drift over them, have starved the beach "downdrift," resulting in a saw-toothed configuration in the shore line. Long groins (exceeding 250 ft in length) interrupt the drift and also produce the saw-toothed effect especially if the groins are comparatively high. It has been noted that short groins (less than 100 ft in length) have been outflanked unless the landward end has been protected by a bulkhead or riprap to prevent erosion. Solid groins of any type can function successfully only in so far as the supply of material is adequate for the maintenance of the beach.

(*b*) Permeable Groins.—Permeable groins of a patented type are comparatively new to the Chicago area, and almost all of this type have been built since 1938. They were developed on the theory that structures with increasing permeability from the bottom to the top and from the shore end lakeward would impound sufficient material to stabilize the shore line, create a beach of

equal width on both sides of the structure, and pass enough drift to avoid starving the beach "downdrift." Generally, the groins have been constructed of precast concrete members, built in crib fashion to the desired height and length, and usually topped with a concrete deck slab. The high costs of these reinforced concrete structures, however, have led to the use of permeable steel groins. These latter groins are constructed of solid steel sheet piling with an extensive series of holes or slots cut in the web.

An examination of the beaches in the Chicago area indicates that the permeable type of groins does pass enough material to avoid starving the shore "downdrift." However, there is evidence to indicate that in many cases they do not retain sufficient material to hold a protective beach, especially where there is a small amount of littoral drift.

The effectiveness of the groin in retaining material is increased by a reduction in permeability. This has been accomplished by the use of the steel sheet pile permeable groins, in which the permeable area has been greatly reduced and is limited to the upper portions of the offshore end of the groins. The tops of these groins are stepped down toward the lakeward end. This type of permeable groin approaches the concept of the low sloping impermeable groin.

(*c*) Breakwaters or Jetties.—Breakwaters are similar in construction to the solid groins, but are larger in cross section, heavier in construction, and greater in length. They are intended primarily as navigation improvements, and, as such, are located chiefly at the harbor entrances. Because of their length, they affect the movement of material along the shore to the extent that all, or a major portion, of the littoral drift is impounded. A large fill is thus accreted on the north side of the breakwater, as has previously been mentioned for the harbors at Waukegan and Wilmette, although the beaches to the south are starved. Studies of some of the harbors indicate progressive shoaling in the offshore zone on the south side, probably caused by the trailing bars near the outer end of the breakwater, or possibly by temporary reversal of littoral drift.

(*d*) Hooked Piers.—These structures are designed to retain material and prevent its further movement from the area of entrapment or placement. The hook feature gives a pleasing appearance, and was designed to provide additional impounding capacity without constructing the outer end of the pier in deep water. The structure at Loyola Park (Chicago, Ill.) is 800 ft long with the outer end built at an angle of 45° toward the north, and the pier at Montrose Avenue is 2,420 ft long with its outer end curved in the shape of a question mark. The pier at North Avenue is similar to that at Montrose Avenue. These piers, about 7 to 8 ft above low water datum, have been very effective in intercepting drift or retaining artificial fill. Other structures have been used in conjunction with piers to assist in retaining the material in place. Groins have been constructed north of the pier at Loyola Park, and groins and a submerged breakwater are part of the system assisting the pier at North Avenue. No other structures have been erected to assist the pier at Montrose Avenue. The structure at Loyola Park has intercepted the shore drift and

created beach to a line predicted at the time of construction, and the groins have effectively slowed down the transport of the impounded material. The structures at North Avenue have retained 75% of the placed material over a period of 5 years, the lost material probably escaping around the end of the pier.

(*e*) Submerged Breakwaters.—There are four submerged breakwaters in the study area, all within the city limits of Chicago. They are located offshore, across concave sections of the shore line, and are constructed either of steel piling or of rubble mound. They are constructed parallel to the shore line in water depths of 13 to 20 ft and located approximately 500 ft offshore. The top elevations of the breakwaters vary from 2 to 6 ft below low water datum. The primary function of submerged breakwaters is the retention of filled material landward, without creating a landlocked pond. The tops of fills placed at the submerged breakwaters were generally from 3 to 5 ft below the tops of the submerged structures. In so far as can be determined, the breakwaters have retarded direct offshore movement of the filled material, although some scouring along the landward and lakeward sides of the vertical steel piling breakwaters has been noted. In addition to their function of retaining the sand fill, they were designed to act as a baffle in breaking up the waves crossing the structure. Obviously, the reduction in wave energy shoreward of the submerged breakwater reduces the movement of fill material on the beach.

(*f*) Bulkheads and Sea Walls.—These structures are essentially walls built parallel to the shore line to limit the shoreward movement of the waterline, to protect the shore from wave action, and to retain backfill in place along the shore. They do not protect the beach but under severe storm conditions may promote erosion of the beach fronting them as a result of scour from wave action. Sea walls differ from bulkheads primarily in size and in type of material used for construction. The sea walls in the study area are massive structures built of square-cut limestone blocks each weighing 5 to 15 tons. Bulkheads, used as protection along this section of shore, are constructed of steel sheet piling, concrete, timber piling, or of timber piling cribs filled with stone. Sea walls have been built most extensively within the city limits of Chicago, where considerable Park District property has been protected by that method. Well-constructed bulkheads have proved effective in protecting the shore from erosion, except during unusual storms. The sea walls in Chicago have prevented erosion practically at all times, although water from breaking waves has caused some delay to traffic on adjacent highways where walls are not of sufficient height.

(*g*) Riprap Revetment.—Two types of stone riprap shore protection have been used, differing primarily in the way the material is placed, and the foundation upon which it rests. Dumped riprap, ranging from construction material debris to 20-ton capstones, has been used as a protective measure in almost every community along the lake. Industries, in particular, utilize that method extensively. Objection to dumped riprap is that it is not as pleasing in appearance as placed riprap. Placed riprap is much less common than dumped riprap, but where it has been used, principally by the Chicago Park District, it is found to be quite effective and very serviceable.

Ice Conditions.—The ice conditions along the shore line of Lake Michigan are to be considered in studying the erosion problem. During average years, ice usually starts to form along the Illinois shore of Lake Michigan about the middle of December. Generally, the initial ice sheet attains a thickness of 6 to 8 in. and extends for some distance lakeward. This initial condition does not remain unchanged, but is usually followed by upheavals as a result of storms and wave action, with the consequent formation of ice hummocks and windrows along the shore. The ice becomes honeycombed and weakened about the middle of March, forming into moving fields and windrows. The ice field drifts in all directions, depending upon the direction of the wind. During severe winters, shifting ice fields, forced ashore by strong winds, often are piled to heights up to 20 ft, and offshore windrows form to the same heights or even higher. During January, 1948, ice was piled as much as 15 ft above the water surface and extended 50 to 100 ft behind the sea walls and bulkheads in Chicago. These huge ice masses, piled on the shore, do not, in general, cause damage to beaches or riprap and may provide additional protection against damage from storm waves. These masses, however, may cause damage to other protective structures, because of the tremendous load superimposed thereby, and, in some cases, individual members of structures may be bent or broken when the waves undercut the base of the ice. Floating ice has damaged many timber structures by abrasive action.

Recommended Improvements

The State of Illinois, acting through the Division of Waterways, held three public hearings in 1947 to ascertain the views of local officials, property owners, and interested persons with reference to the problems in their areas and the plan of improvement desired. The public hearings were limited to discussion of the improvement to public property, and no views were obtained from private property owners other than in a general way. The views obtained were given careful consideration in developing the plan of improvement.

As previously mentioned the shore line has been divided into four sections: 1. The northern plain; 2. the lake moraine; 3. the southern plain; and 4. the artificial fill.

1. *Northern Plain Section.*—As stated previously, this section of shore line is eroding in the northern part of the area. In general, erosion caused by wave attack of the unprotected shore may be reduced by building a beach of suitable profile to dissipate the wave energy. This is considered one of the best methods of protection, especially if the supply of sand transported by littoral currents is sufficient to maintain the beach. The rate of drift in this section is moderately heavy when compared with the sections south of Waukegan. The construction of impermeable groins in this area would impound material for the desired protection and provide a beach for recreational use. The width of the beach desired would control the length of the groins to be constructed. A typical section of the proposed shore improvements is indicated in Fig. 2. This design is based upon retaining sufficient drift to achieve the desired results, yet allowing a portion of the sand to move downdrift to nourish other areas.

If groins were constructed along the entire reach, the littoral drift would be absorbed or discontinued and might result in erosion to the south. The number of groins constructed per year should be governed by the amount of littoral drift traveling along the section under consideration.

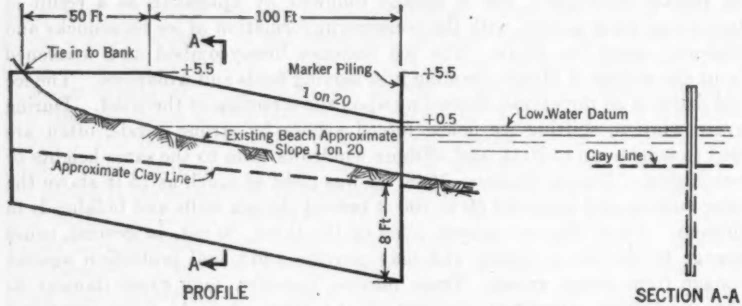

Fig. 2.—Sheet Steel Piling Groin for Northern Lake Plain Section

2. *Lake Border Moraine Section.*—This section of shore is developed for the most part as a residential area of fine homes. The shore line has been generally stabilized by the construction of protective works, although some sections in the northern part are subject to erosion. The rate of drift varies from lean in the north to moderate in the south. The enlargement of the beaches in the northern part of the section would be dependent upon artificial fill.

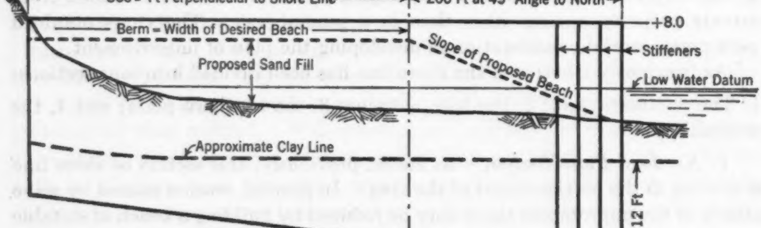

Fig. 3.—Steel Jetty, Southern Lake Plain Section

The type of shore improvement for this section is the same as that proposed for the northern lake plain section, except that the sloping section of the groin is 1 on 30, which conforms to the natural beach slope in this region. Such a slope increases the over-all length of the groin to 200 ft. The number of groins constructed per year should be determined by the method indicated for the northern plain section.

3. *Southern Plain Section.*—This section of shore line is highly developed for parks and residences. The northern zone is subject to erosion, but this erosion has been controlled by protective structures such as riprap and bulkheads. The rate of drift varies, being heavier in the southern zone. A typical section of the proposed improvement for providing additional beach area and protection is indicated in Fig. 3. The length of the jetty would depend upon the area of beach desired. Sand fill may be pumped in, if the requirements for the beach will not be satisfied by natural accretion processes. Protection and enlargement of the beach areas could also be provided by the construction of a system of groins and artificial fill, but since the length of public property along the shore line is limited, the jetty type of construction is recommended to improve and provide the needed beach areas.

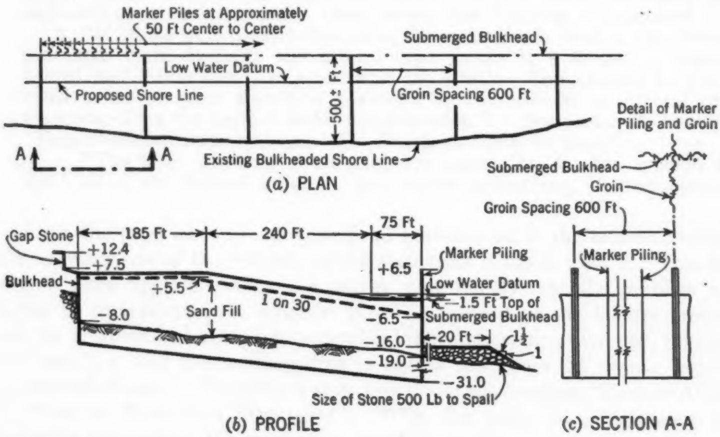

FIG. 4.—SUBMERGED OFFSHORE STEEL BULKHEAD AND STEEL GROINS FOR ARTIFICIAL FILL SECTION

4. *Artificial Fill Section.*—The bulkheads in this section have stabilized the shore line, and the development of beaches has depended upon artificial fill because of the lack of littoral drift. The urgent problem is the construction of adequate beaches for the dense urban population. Based upon a peak load attendance of about 8% of the population, and allowing 75 sq ft per person (generally accepted as the area desired for recreation), the beach area required for Chicago would be 22,800,000 sq ft. Existing beaches in the Chicago area total 9,216,000 sq ft, leaving a deficit in beach area of 13,584,000 sq ft. The only portion of the shore line available for development of additional recreational beaches in Chicago lies lakeward of the existing sea wall. This necessitates the construction of beaches in relatively deep water. The Park District of Chicago believes that, ultimately, the entire Chicago lake front may be required for beach purposes to meet the demand for recreation. The typical proposed improvements for this section would consist of a sand fill retained by a steel sheet piling submerged breakwater, a steel sheet piling pier, and steel sheet

piling impermeable intermediate groins to retard the migration of the sand. The proposed construction is indicated in Fig. 4.

Summary

From the description of protective works, it is apparent that the problems of arresting shore line erosion involve many geological and engineering considerations. The proposed solutions discussed call for the gradual building of new beaches to provide protection for the shore line, as well as recreation for the neighboring population. If beaches are not desired, or if they are considered too expensive to provide protection against wave action, then the next best method to prevent erosion of the shore appears to be the use of some means of direct armoring, such as by bulkheads or riprap revetment.

DISCUSSION

THOMAS B. CASEY,[3] M. ASCE.—Three of the points developed in the paper are believed worthy of further mention, both with respect to the basic and fundamental importance of the facts stated and with regard to studies currently in progress on the problems involved. These three items, listed in reverse order from that in the paper for convenience in discussion, are as follows:

a. "From the description of the protective works, it is apparent that the problems of arresting shore line erosion involve many geological and engineering considerations." (See under the heading, "Summary.")

b. "If groins were constructed along the entire reach [that is, the Northern Lake Plain Section], the littoral drift would be absorbed or discontinued and might result in erosion to the south. The number of groins constructed per year should be governed by the amount of littoral drift traveling along the section under consideration." (See under the heading, "Recommended Improvements: 1. Northern Plain Section.")

c. "The main physical forces that are responsible for this erosion are wind, wave, and current action." (See under the heading, "Introduction.")

Even the most cursory and superficial examination of the erosion problem will convince one of the validity of the statement made in item *a*. This fact is even more apparent when one delves more deeply into the problem and begins to comprehend the number, type, and extent of the factors present, and the complex and often unpredictable interrelationships involved, together with the fact that the primary erosive agents are forces of nature beyond the control of man. The authors state (see under the heading, "Factors Affecting Erosion: Protective Structures") "***in the past, local judgment has generally determined the method or methods to be used in improving and stabilizing the shore line." There is no question but that this has been the case and that this is largely the reason for the further conclusion, "Some [methods] have been effective, and others have been useless." These efforts cannot be strongly condemned, however, because an adequate knowledge of the nature and extent of the engineering and geological problems involved was not available, and necessity dictated that design proceed on the basis of available information. Not only in the past has this been the case, but even at the present time the knowledge of the fundamental characteristics of the basic elements involved in the erosion problem is wholly deficient. Therefore, present-day efforts at shore protection on Lake Michigan are still based largely on judgment, and although there are undoubtedly many factors and relationships analogous to all beach erosion problems, the solution of each requires separate study and evaluation. Thus, the problems on Lake Michigan cannot be solved simply by an analogy with problems on the Pacific coast; they require a study and knowledge of the several factors as they exist on Lake

[3] Chf. Engr., Div. of Waterways, Dept. of Public Works and Bldgs., State of Illinois, Springfield, Ill.

Michigan. Thus it is that serious deficiencies in basic data do exist and that, until these have been corrected, efforts at protection must continue on a basis of individual ingenuity and judgment.

The matters presented by the authors under item *b* immediately raise questions about which deficiencies in basic information exist. Disregarding, for the moment, the physical forces that the groin system must withstand, and neglecting entirely the important and interesting legal questions inherent in the recommendation that the number of groins constructed per year should be governed by the amount of littoral drift traveling along the reach under consideration, one is concerned, necessarily, with a number of questions relative to the basic characteristics of the littoral drift itself as a prerequisite to the design of the groin system. In other words, the successful solution of a beach erosion problem, like any other engineering problem, is predicated on the definition of the physical conditions causing the problem. In so far as shore erosion is concerned, and with particular reference to the littoral drift, Martin A. Mason,[4] M. ASCE, has propounded three questions which, if answered, serve to define the causative physical conditions: What are the sources and character of the beach material? What are the rates of supply and loss of material to and from the problem area? What is the manner of movement of material from the source to the beach and from the beach to other areas?

Prior to the surveys and studies conducted by the Chicago District, Corps of Engineers (in the course of the preparation of the cooperative beach erosion report on the Illinois shore of Lake Michigan), virtually nothing had been done in that state toward any comprehensive and integrated study of these several factors. It is apparent that one such survey of these complex and erratic factors is inadequate to serve as a basis for well-founded conclusions relative thereto, and that studies must be conducted systematically over a period of years before definite trends and patterns can be established.

In recognition of the need for such a coordinated and systematic study, the State of Illinois initiated a program in 1950 which has as its primary objective the more precise definition of the causative conditions as set forth in the foregoing three questions. These studies, as presently programmed, entail the following features with respect to the littoral drift:

1. Periodic soundings on selected ranges;
2. The taking of bottom surface samples on the sounding ranges at frequent intervals;
3. Cross sectioning and sampling of the beaches and bluffs at selected locations;
4. Measurement of shore erosion or accretion by actual field survey and study of aerial photographs;
5. Detailed study of the effect of various storms on the trap efficiency of selected existing groins of various types; and
6. Laboratory analysis of samples for grain size and heavy mineral, magnetic mineral, and carbonate content.

[4] "Method of Solution of Shore Problems," by Martin A. Mason, *Bulletin*, Beach Erosion Board, Washington, D. C., January, 1948.

These procedures, together with others that may be developed in the course of the studies, must be applied over a period of time sufficient to cover a variety of conditions of lake stage—storm direction, duration and intensities, and seasonal changes—to provide a clear picture of the characteristics of the littoral drift along these shores. This study will then enable the engineer to determine the most feasible and economical method of providing remedial measures and to predict with a reasonable degree of accuracy the adequacy of the measures toward achieving the desired protection, and their effect on other reaches of shore.

Of the three major physical forces stated in item *c*, neither wind nor currents, by themselves, are considered to have any major status as erosive agents on these shores. Beyond doubt, the primary erosive agent is wind-generated waves which, in deep water, generally vary both in magnitude and direction with the intensity and direction of the generating wind. Here again, the engineer responsible for the design of protective measures is confronted with a deficiency in basic knowledge. Waves are not only the principal erosive agent, but also are responsible for the transport of beach material, in that the littoral current is primarily the long-shore component of the wave impinging upon the shore. In addition, the major forces which the protective works must be capable of withstanding structually are wave forces.

The effectiveness of wave attack in shore erosion varies not only with the magnitude and direction of the deep-water waves but with the configuration of the shallow near-shore bottom (refraction effect), the stage of the lake, the topography and character of the material of which the shore is composed, and the character and extent of existing shore protection works. Of these several factors, all except the first are generally susceptible of evaluation by ordinary and well-known methods of field survey, and observation and data thereon can be had without undue difficulty. The real deficiency exists in accurate information on the remaining and most important factor—that is, the magnitude and direction of the deep-water waves.

In order to overcome this basic deficiency, the current program of beach erosion studies includes the observation of deep-water wave characteristics, lake stage, and wind direction, duration, and intensity. Each of these factors possesses points of major interest, and, indeed, lake stage is a favorite topic of conversation along the shores of the Great Lakes at the present time (1952) due to the generally prevailing high-stage cycle. It is considered expedient here, however, to mention only a few points of interest on these matters.

Observations of lake stages are being made (1952) at the Wilson Avenue Waterworks Intake Crib of the City of Chicago, located some 3 miles offshore, and at the Waukegan Waterworks, at Waukegan Harbor, for sounding and sampling operations and to study lake level changes at these locations in comparison with those at other gaging points. These stage changes include not only the normal fluctuation of the average elevation of the lake, but those shorter fluctuations caused by wind setup and changes in barometric pressure—all of which have an important bearing on the effectiveness of wave attack on the shores.

Continuous observations of wind direction, intensity, and duration are made at the same sites. These observations are particularly important because wind is the generating agent for the waves and, in that sense, may be the real cause of shore erosion on Lake Michigan. Furthermore, observation of wind direction is important because no satisfactory method for determining wave direction directly has yet been derived, and it is necessary to assume that deep-water wave direction varies generally with wind direction. It is also of interest to note that an analysis of the data thus far obtained substantiates the findings reported by the late John R. Freeman[5] (Past-President, ASCE) in 1926, that wind velocities observed at points out in the lake are often materially greater than those observed at United States Weather Bureau stations on shore. Thus, records from shore stations cannot be relied upon to give a true picture of storm intensities on the lakes.

TABLE 1.—STORM OF NOVEMBER 5 TO 8, 1951, LAKE MICHIGAN AT WILSON AVENUE INTAKE CRIB, CHICAGO, ILL.

Date (November, 1951)	Central Standard Time[a]	Lake stage (mean tide at New York, N. Y.)	WIND		WAVES		
			Direction[b]	Velocity[c]	Time[d] (sec)	Height, in Feet	
						Average[e]	Maximum[f]
(1)	(2)	(3)	(4)	(5)	(6)	(7)	(8)
5	11:30 p.m.	581.05	118	16	...	...	...
6	11:25 a.m.	581.62	87	33	5.81	5.02	7.75
6	11:26 p.m.	582.10	50	34	7.42	5.58	9.35
7	11:26 a.m.	582.35	353	44	9.17	6.05	8.57
7	11:27 p.m.	582.05	322	20	8.84	4.19	6.00
8	11:27 a.m.	581.35	275	18	7.14	1.68	2.99

[a] Period of analysis generally extends 15 min beyond indicated time. [b] Wind direction expressed as azimuth measured clockwise from north. [c] Wind velocity in miles per hour. [d] Average period of well-defined series of highest waves recorded. [e] Average height of ⅓ highest waves observed during period of analysis. [f] Highest single wave observed.

In order to obtain data on deep-water wave characteristics, a Mark IX Wave Recorder was established at the Wilson Avenue Waterworks Intake Crib in 1951, and a similar unit is scheduled for installation off Waukegan Harbor in 1952. Data from these gages, which are generally operative only for the period from May to November of each year because of the danger of losing instruments from ice action during the winter months, will provide reliable information as to the period and height of deep-water waves, from which other characteristics may be deduced from derived relationships.

In condensed form, Table 1 contains data taken from recording instruments at the Wilson Avenue Waterworks Intake Crib for the storm of November 5 to 8, 1951, and will serve to give some indication as to the type and extent of data being obtained.

In conclusion, the statement of the authors that "***the problems of arresting shore line erosion involve many geological and engineering considera-

[5] "Regulation of the Great Lakes and Effect of Diversion," by John R. Freeman, Chicago San. Dist., Chicago, Ill., October, 1926.

tions" is here repeated for the sake of emphasis. Most shore erosion control works are admittedly costly, and experience has shown that the construction of such works without a knowledge of the characteristics of the factors involved often not only fails to achieve the desired purpose, but indeed may prove to aggravate conditions in the problem area and elsewhere—all with a consequent heavy financial loss to the owner. Few will deny that adequate knowledge of these factors is lacking and that the studies necessary to define them, even over a relatively limited shore line such as that of Illinois, are far beyond the scope of the engineer engaged in designing protective measures at a particular site. The task must then devolve upon an organization whose scope extends beyond the limitations of the individual or the political subdivision.

The report upon which the paper is based constituted the first step along those lines in Illinois.

CHARLES E. LEE,[6] A.M. ASCE.—The paper under discussion deals with the Lake Michigan shore line and the attending remedies for erosion, considering average lake levels. The writer will discuss, in general terms, the high lake levels, and the feasibility of the proposed plans for providing adequate protection during the rare-frequency, long-term fluctuation of the lake level—basing his discussion on the Fort Sheridan (Illinois) observations.

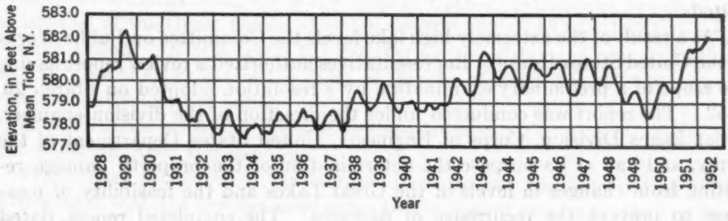

FIG. 5.—MEAN ELEVATION OF LAKE MICHIGAN

The timeliness of the paper was shown expressly by a survey of damage to the Lake Michigan shore line occurring between the spring of 1951 and the spring of 1952. There was a higher rate of damage during that time than was ever recorded before. This damage could be related directly to the increase in development of the shore line properties and to the existing high level of the Great Lakes which caused inundation of greater area and greater depths of water at structures and at the toe of the bluffs. This high lake level, of course, permitted waves to propagate farther inland and caused waves of greater height to act on the structures and on the easily eroded bluffs.

The level of Lake Michigan fluctuates (in addition to temporary fluctuations such as seiches and lake setup) simultaneously in two separate patterns, one an annual variation and the other a long-term variation (see Fig. 5).

The annual variation of the lake level may be related to the seasonal pattern of the precipitational runoff. The low extreme of the curve is usually reached

[6] Hydr. Engr., Great Lakes Div., Corps of Engrs., Chicago, Ill.

during February, following the period of least runoff. As the thaw and spring rains begin, the curve rises until a peak is reached in the late summer months of July or August. The irregular long-term variation in lake level must also be related to precipitation, but experience shows that the long-term peak lake level does not occur during the same year as peak rainfall. The long-term variation was high in 1952, as might be expected, since an analysis of records of precipitation on the Great Lakes drainage basin shows an ascending trend for the 16-year period, 1934–1950, and downward since that time, but still above average. The monthly mean elevation of Lake Michigan for July, 1952, was 582.66 ft above mean tide at New York, the highest monthly mean elevation attained since 1887. Gage readings for the early part of August, 1952, indicated a slight increase in stage. However, it was hoped that the seasonal crest would be reached during that month and that the stage would begin its normal seasonal decline. The highest one-month average level of record (from 1860 to 1952), was elevation 583.68, and occurred in June, 1886.

The damage that occurred in the spring of 1952 was intensified by the fact that the lake level did not descend, as is normal, during the winter of 1951-1952 (see Fig. 5). This phenomenon occurred only once previously during the 92-year period of record (fall to spring of 1928–1929). The high stages persisting through the seasonal period in which wind storms occur most frequently, and abetted by the resulting wind tides and seiches, permitted the high wind waves to proceed such a distance inland that extreme damage resulted.

As a result of the extremely high lake levels the Committee on Public Works of the United States House of Representatives authorized a review report having the scope of a preliminary examination by a resolution adopted on March 26, 1952. The report was conducted under the direction of the division engineer, Great Lakes Division, Corps of Engineers, United States Department of the Army, and had as its purpose the determination of the property damage resulting from changes in levels of the Great Lakes and the feasibility of measures to prevent the recurrence of damages. The completed report, dated June 9, 1952 (hereinafter referred to as the "Corps of Engineers' report"), was submitted to the chief of engineers. The authorized scope of the report, with the attending limitations of funds and time, did not permit sufficient study to determine specific designs or make other than general recommendations. However, it was recommended that a comprehensive study of survey scope be made to determine:

1. The feasibility of a plan of regulation of the levels of the Great Lakes that will best serve the interests of all water uses, including the reduction of damages to shore properties, the use of the Great Lakes for navigation, and the use of the storage and outflows from the Great Lakes for power development; and

2. The advisability of adopting local-protection flood-control projects for areas along the shores of the Great Lakes and tributary streams that are subject to inundation as a result of fluctuations in the levels of the lakes, where such projects are found to be feasible and economically justified.

3. Also recommended were (*a*) a plan for coordinated shore protection by state and local governments, (*b*) shore protection measures by individual local property owners, and (*c*) the enactment of state and local legislation controlling shore line construction.

(*a*) A coordinated plan for the protection of shores and shore properties against the action of waves and currents was recommended for development by each of the states, or political subdivisions thereof, for their shores fronting the Great Lakes. Federal participation in these studies and the protection of publicly owned property would be governed by the provisions of Public Law No. 520, 71st Congress, approved July 3, 1930, and Public Law No. 727, 79th Congress, approved August 13, 1946.

(*b*) It was recommended that individual owners of properties bordering the Great Lakes provide such permanent or temporary protection for their properties from the action of waves and currents as is found by them to be warranted. Where feasible, the protection provided should be integrated into a comprehensive plan for a contained beach segment.

(*c*) States and political subdivisions of states adjoining the Great Lakes were advised to give consideration to the enactment of appropriate laws to control construction in areas subject to wave attack or shore line recession, and in the flood plain of the Great Lakes.

The Corps of Engineers' report also disclosed that damages in the sum of $61,252,900 occurred along the 5,479 miles of United States shore line (including islands) of the Great Lakes, of which $49,970,750 could be related directly to wave action. Of this total, $11,288,000 worth of damage occurred along the 108 miles of shore line in the State of Illinois, of which $11,097,700 may be related directly to wave action.

In accordance with the division engineer's recommendation, a survey report was authorized and prepared.

Preliminary estimates of the increase in shore line recession during 1951, as compared with the average rates given by the author (see under the heading, "Shore Line Changes"), have been made for (1) the Northern Lake Plain Section, (2) the Lake Border Moraine Section, and (3) the Southern Lake Plain and Artificial Fill Sections.

(1) *Northern Lake Plain Section.*—An increase of 500% is estimated for the vicinity of Winthrop Harbor and Illinois Beach State Park. The average increase throughout the entire section is about 300%.

(2) *Lake Border Moraine Section.*—An increase of more than 200% is estimated over the entire section—with a much larger rate in parts of Wilmette and Fort Sheridan.

(3) *Southern Lake Plain and Artificial Fill Sections.*—It is estimated that the recession rate increased approximately 75% during 1951.

Because of this increased erosion and other damage, some construction was required to prevent the complete destruction of property or irreparable damage. The construction, in general, was of protective walls, groins, or combinations of both. The writer knows of no detailed data concerning the effec-

tiveness of the new construction, except for the case that follows: In April, 1951, a contract was let for the construction of ten groins on the United States Army Reservation of Fort Sheridan, in the Lake Border Moraine Section (a total of twenty-one were recommended for the entire reservation). Five of these groins, spaced from 300 ft to 400 ft apart, were constructed during the period of May through August, 1951, according to the design described by the author (see under the heading,"Recommended Improvements"). The remaining five groins covered by the aforementioned contract were scheduled for construction during the summer and fall of 1952. However, during a summer storm, the downdrift end groin was outflanked and the impounded beach was lost. Because of this loss and because of construction difficulties at high lake stages, the construction of the five additional groins, to their entire length, did not appear feasible. It was decided that the inner portions of the groins (the length that could be accomplished by land plant) would be constructed during the fall of 1952, and the remainder in the spring of 1953. From August to December, 1951, a series of monthly soundings was taken to determine the effectiveness of the groins in impounding the beach material that traveled along the shore (ice prevented sounding during the winter months). There were two lines of soundings for each groin—one immediately updrift of the groin, and one midway between the groins. The lines extended from the toe of the bluff to the 6-ft depth contour (referred to low water datum for Lake Michigan, which is about 4.2 ft below the July, 1952, lake level). The surveys indicated that a slight accretion had occurred between the shore line and the 6-ft depth contour, opposite the five constructed groins. The accretion shoreward of the shore line was negligible, except at the two most northerly (updrift) groins.

Surveys of the area made in April and May, 1952, after the ice had melted, revealed further accretion at these five groins. Specifically, it was indicated that there was some loss of material updrift of the first groin (numbering consecutively from north to south or updrift to downdrift), but that an extensive gain had occurred in the area between that and the penultimate groin; some loss was revealed between the penultimate and end groins; and erosion had taken place downdrift of the end groin. Therefore, it may be concluded that the three updrift groins were filled to the extent that an appreciable volume of material was flowing around the outer ends of, and over, the groins, but that a condition of slight deprivation existed below the fourth groin. A preliminary estimate of quantities showed a total gain of more than 12,000 cu yd during the period from December, 1951, to May, 1952. The rate of impoundment during this five-month period leads to the conclusion that reasonable protection would be afforded the area protected by the ten groins, and that a normal material balance would be restored in from 3 years to 4 years from the time of initial construction, if conditions remained favorable to accretive action.

The observed action of these groins over a short period was gratifying, as observations at other successful groins have revealed that a flattening of the offshore gradient preceded shore line and onshore accretion. Another example of the groins reacting according to design was the fact that at the updrift

groins the excess material passed over the groins, providing nourishment for the immediate downdrift side, which is usually most vulnerable to erosion. However, some erosion was noted in the vicinity of the most southerly groin, indicating a paucity of material in movement downdrift of the penultimate groin. In this regard, more consideration might be given to the desirability of further limiting the number of groins that should be constructed during any one season of average lake levels.

It is considered that the indications of successful action of the Fort Sheridan groins present considerable verification of the efficacy of the design presented by the author, for the Northern Lake Plain and the Lake Border Moraine sections. Proper limits should be placed on the amount of construction per year. It is believed that the groin design will provide adequate protection during periods of extremely high lake levels as well as during average lake levels.

John R. Hardin,[7] M. ASCE, and William H. Booth, Jr.,[8] A. M. ASCE.—Valuable additions to the subject of erosion have been provided by Messsrs. Casey and Lee. It is gratifying to know that the State of Illinois has initiated a program for collecting basic data on the erosional forces along the Illinois shore line of Lake Michigan. It is hoped that other agencies will plan similar programs of this nature to be applied to the other Great Lakes. It is also gratifying to read, in Mr. Lee's discussion, that the groin system recently constructed at Fort Sheridan is performing as originally contemplated.

In the past, the protection of shore line against erosion has engaged far too little professional interest among engineers, in spite of the fact that the need for remedial works has become increasingly apparent. The study of shore erosion forces is in its infancy (1952); however, a considerable amount of detailed technical information is available describing the effect of wave action on beaches and concerning related problems. In spite of the advances made, much remains to be learned, and the existing (1952) scientific knowledge of shore erosion forces has not been satisfactorily disseminated through the engineering profession.

Littoral drift is an important consideration in providing protection along the coast. The quantity of drift can be evaluated by the volume of material trapped by shore structures, either natural or man-made, and from knowledge of the rate of depletion of sources of supply—for example, the erosion of bluffs or headlands. Each man-made structure extending into the water will have an effect on the erosional or dispositional forces, thereby causing changes in the immediate area. If several groins are constructed in a physiographic unit, the volume of impoundment might be sufficient to trap most or all of the littoral drift for several years, depending on the quantity of drift traveling in the area. It is agreed that studies over a period of years would indicate more clearly the trend in the volume of material traveling along the shore, but the emergency need for protection will not permit such investigations. The data pertaining to the Illinois shore line can be used to great advantage in planning the remedial measures.

---

[7] Asst. Chf. of Engrs., Office of Chf. of Engrs., Corps of Engrs., Washington, D. C.

[8] Engr., Office of Chf. of Engrs., Washington, D. C.

The writers would like to elaborate on the statement, made in their paper (see under the heading, "Introduction") and referred to by Mr. Casey, that "The main physical forces that are responsible for this erosion are wind, waves, and current action." Under the section entitled "Factors Affecting Erosion," the three forces are described. The dominant force is the wind-generated wave. The theory of the formation and growth of wind waves, as developed by H. U. Sverdrup and W. H. Munk of the Scripps Institution of Oceanography, University of California, at La Jolla, takes into consideration wind speed, wind duration, and fetch, and relates these variables to wave length, period, and velocity. Wave forecasts by the Sverdrup-Munk relationship have been shown by comparative observation to approximate natural conditions reasonably well. The offshore waves seldom travel in a direction perpendicular or parallel to the shore, but usually approach the shore at some intermediate angle. As the waves reach shoaling water having a depth of half the wave length, their characteristics (excepting the wave period) are modified. In particular, the velocity of advance is reduced and the wave length is shortened. This bottom effect causes a so-called refraction or bending of the wave in a direction such that the crest of the wave tends to conform to the bottom contours. The amount of these changes may be determined by the construction of "refraction diagrams." A refraction diagram may be considered to be a map showing the wave crests at a given time, or the successive positions of a particular wave crest as it moves shoreward. Crests several wave lengths apart are sufficient to show the bending of the waves. Such diagrams will indicate the direction of the alongshore component. Waves breaking at an angle to the beach produce a current that moves parallel to the beach; this is known as the littoral current. The effect of waves on a sand beach is especially pronounced at the breaker line, where large quantities of sand are thrown into suspension. The direction of wave approach causes the littoral current that carries suspended sand along the shore. Therefore, the main physical forces for the area under discussion are wind, waves, and currents.

AMERICAN SOCIETY OF CIVIL ENGINEERS
Founded November 5, 1852

TRANSACTIONS

Paper No. 2536

GRAPHICAL SOLUTION OF HYDRAULIC PROBLEMS

By Kenneth E. Sorensen,[1] J. M. ASCE

Synopsis

The graphical solution of first order differential equations provides a simple and flexible means of solving several common and important problems in the field of hydraulics.

The method of graphical solution is developed and applied to problems involving reservoir flood routing, water power studies, the tracing of water surface curves in nonuniform channel flow, and the determination of water surface variation in surge tanks. Several examples are presented and solved.

The method of extending the graphical solution to second order differential equations is also explained.

Introduction

Several common and important problems in the field of hydraulics require the solution of a differential equation of the first order in the form

$$d\frac{f_1(y)}{dx} + f_2(y) = f_3(x) \qquad \text{(1)}$$

in which x is the independent variable and y is the dependent variable. A graphical solution of this equation is possible if the functions $f_1(y)$, $f_2(y)$, and $f_3(x)$, and the values of x_1 and y_1 at some one point are known. Eq. 1 may be approximated as

$$\Delta f_1(y) = f_1(y_2) - f_1(y_1) = [f_3(x) - f_2(y)]\,\Delta x \qquad \text{(2)}$$

Furthermore, if the assumption is made that

$$f_2(y) = \tfrac{1}{2}\,[f_2(y_2) + f_2(y_1)] \qquad \text{(3)}$$

Note.—Published in February, 1952, as *Proceedings-Separate No. 116*. Positions and titles given are those in effect when the paper was received for publication.

[1] Structural Engr., Harza Eng. Co., Chicago, Ill.

and that $f_3(\bar{x})$ is the mean value of $f_3(x)$ between points (x_1, y_1) and (x_2, y_2) then

$$f_1(y_2) - f_1(y_1) = [f_3(\bar{x}) - f_2(y_1)]\frac{\Delta x}{2} + [f_3(\bar{x}) - f_2(y_2)]\frac{\Delta x}{2} \quad \ldots\ldots(4)$$

Fig. 1 demonstrates a graphical method for solving Eq. 4. Curve 1 is plotted with $f_1(y)$ as ordinates and $f_2(y)$ as abscissas. Line 2 is then drawn vertically at a distance from the origin equal to $f_3(\bar{x})$. If, from point y_1 on

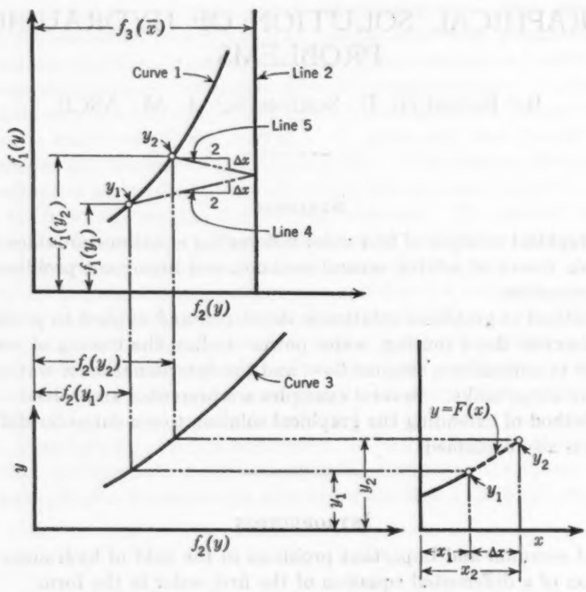

FIG. 1.—GRAPHICAL SOLUTION OF A FIRST ORDER DIFFERENTIAL EQUATION

curve 1, line 4 is drawn at slope $\frac{\Delta x}{2}$ to intersect line 2, and if from that intersection line 5 is drawn at slope $-\frac{\Delta x}{2}$ to intersect curve 1 at y_2, then

$$f_1(y_2) - f_1(y_1) = [f_3(\bar{x}) - f_2(y_1)]\frac{\Delta x}{2} + [f_3(\bar{x}) - f_2(y_2)]\frac{\Delta x}{2} \quad \ldots\ldots(5)$$

which is identical to Eq. 4. To permit a plot of $y = f(x)$, curve 3 is drawn with y as ordinates and $f_2(y)$ as abscissas. By projecting from curve 1 through curve 3, each new value of y_2 obtained may be plotted opposite the corresponding value of x. Once y_2 has been established, it then serves as y_1 for the next interval Δx, and the graphical process is repeated.

Applications to Hydraulics

A number of problems encountered in the field of hydraulics may be conveniently solved by the foregoing method. Examples of such problems are flood routing for reservoirs, water power studies, nonuniform flow in channels, and surge tank studies.

Reservoir Flood Routing.—The equation for reservoir flood routing is

$$\frac{dC}{dT} = I - Q \quad (6)$$

in which C = reservoir volume = $f_1(h)$ (h equals the reservoir elevation); I = inflow = $f_3(T)$ (T equals the time); and Q = outflow = $f_2(h)$; so that

$$\frac{df_1(h)}{dT} + f_2(h) = f_3(T) \quad (7)$$

This equation is in the same form as Eq. 1.

Fig. 2(a) shows the graphical solution of Eqs. 6 and 7. Curve 1 is plotted with coordinates Q and C and curve 3 is plotted with coordinates h and C (reservoir volume curve). Both h and Q can be plotted as functions of time as the graphical solution progresses. As $f_3(t) = I$, it is convenient to plot the inflow hydrograph to the same scale as Q. Then, line 2 can be drawn by projecting horizontally from the average value of I for each period ΔT.

If wedge storage is to be considered and its quantity is known, a family of curves may be drawn for curve 1, each labeled with the appropriate value of I. Then, as shown in Fig. 2(b), the curve corresponding to I_1 is used for the initial point (h_1), and the curve corresponding to I_2 is used for the final point (h_2). However, curve 1, corresponding to zero wedge storage, must be used for projecting to curve 3 in obtaining the plot of h against time.

Water Power Studies.—Closely allied to reservoir flood routing is the water power study involving determination of reservoir drawdown required to maintain constant power output of a plant under varying conditions of reservoir inflow. The equation for power is

$$P_h = Q f'_2(h) \quad (8a)$$

or

$$Q = f_2(h, P_h) \quad (8b)$$

in which Q is the discharge through the turbines, P_h is the horse power, and f_2 (h, P_h) is a function of reservoir elevation that includes the effect of tailwater rise and the hydraulic and mechanical efficiency.

If $f_2(h, P_h)$ is substituted for $f_2(h)$ in Eq. 7, then the method described for Fig. 2 will permit a plot of reservoir elevation against time for any specific power output.

Nonuniform Flow in Channels.—Bernoulli's theorem for flow in channels (Fig. 3(a)) may be expressed

$$\frac{dE}{dL} + S = 0 \quad (9)$$

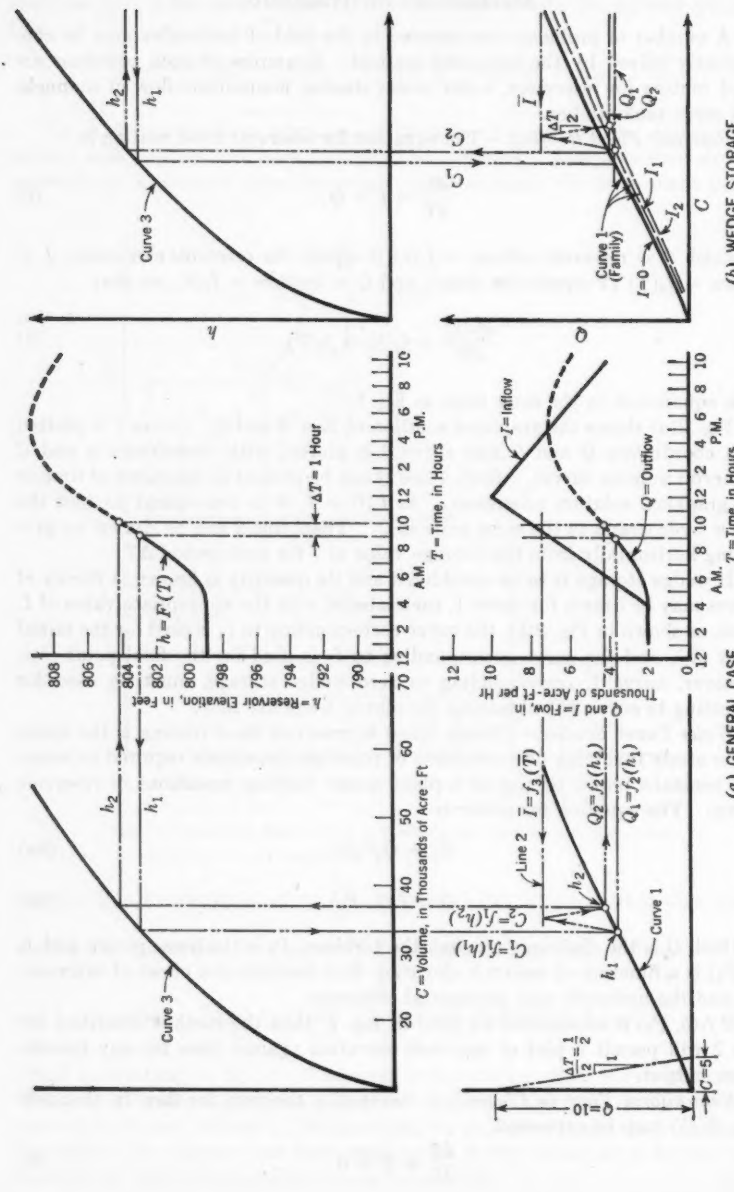

FIG. 2.—GRAPHICAL SOLUTION OF RESERVOIR FLOOD ROUTING

in which E = total energy $= D + \frac{V^2}{2\,g} - S_o L$; D is the depth of water; V is the velocity; S_o = bottom slope $= f_3(L)$; L is the length of reach measured along the channel bottom; and S = friction slope $= f_2(D)$. If Q is constant, $D + \frac{V^2}{2\,g} = f_1(D)$, and Eq. 9 then takes the form

$$\frac{df_1(D)}{dL} + f_2(D) = f_3(L) \ldots\ldots\ldots\ldots\ldots\ldots (10)$$

In the case of certain symmetrical artificial channels, such as those shown in Fig. 3(*b*), it is desirable to alter Eq. 10 somewhat. In accordance with gener-

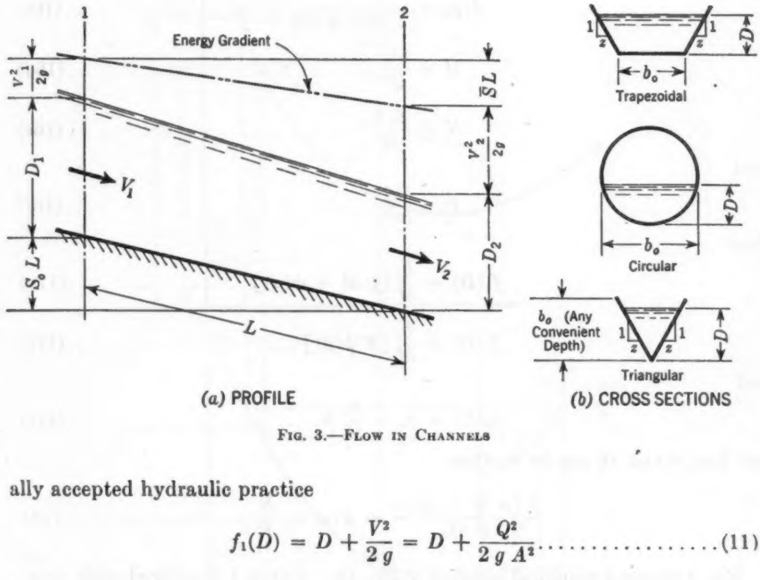

(*a*) PROFILE (*b*) CROSS SECTIONS

FIG. 3.—FLOW IN CHANNELS

ally accepted hydraulic practice

$$f_1(D) = D + \frac{V^2}{2\,g} = D + \frac{Q^2}{2\,g\,A^2} \ldots\ldots\ldots\ldots\ldots\ldots (11)$$

in which A = the area $= a\,b_o^2$ (b_o is as defined in Fig. 3(*b*)) and

$$f_2(D) = S = \frac{Q^2\,n^2}{2.2082\,A^2\,R^{4/3}} \ldots\ldots\ldots\ldots\ldots\ldots (12)$$

in which n = the coefficient of roughness, and R = the hydraulic radius $= r\,b_o$. Letting

$$a = F_1\left(\frac{D}{b_o}\right) \ldots\ldots\ldots\ldots\ldots\ldots (13)$$

and

$$r = F_2\left(\frac{D}{b_o}\right) \ldots\ldots\ldots\ldots\ldots\ldots (14)$$

then

$$f_1(D) = b_o \frac{D}{b_o} + \frac{Q^2}{2\,g\,a^2\,b^4_o} \ldots\ldots\ldots\ldots\ldots\ldots (15a)$$

and

$$f_2(D) = \frac{Q^2\,n^2}{2.2082\,a^2\,r^{4/3}\,(b_o)^{16/3}} \ldots\ldots\ldots\ldots\ldots\ldots (15b)$$

Furthermore, if

$$\rho = \frac{D}{b_o} \ldots\ldots\ldots\ldots\ldots\ldots (16a)$$

$$\phi(\rho) = \frac{1}{2\,g\,a^2} \ldots\ldots\ldots\ldots\ldots\ldots (16b)$$

$$\psi(\rho) = \frac{1}{2.2082\,a^2\,r^{4/3}} \ldots\ldots\ldots\ldots\ldots\ldots (16c)$$

$$M = \frac{b^5_o}{Q^2} \ldots\ldots\ldots\ldots\ldots\ldots (16d)$$

$$N = \frac{S_o\,b^4_o}{Q^2} \ldots\ldots\ldots\ldots\ldots\ldots (16e)$$

and

$$P = \frac{n^2}{b^{4/3}_o} \ldots\ldots\ldots\ldots\ldots\ldots (16f)$$

then

$$f_1(D) = \frac{b_o}{M}[\rho\,M + \phi(\rho)] \ldots\ldots\ldots\ldots\ldots\ldots (17a)$$

$$f_2(D) = \frac{b_o}{M}[P\,\psi(\rho)] \ldots\ldots\ldots\ldots\ldots\ldots (17b)$$

and

$$f_3(L) = S_o = \frac{b_o}{M} N \ldots\ldots\ldots\ldots\ldots\ldots (17c)$$

and Eqs. 9 and 10 can be written

$$\frac{d\,[\rho\,M + \phi(\rho)]}{P\,dL} + \psi(\rho) = \frac{N}{P} \ldots\ldots\ldots\ldots\ldots\ldots (18)$$

Fig. 4 shows a graphical solution of Eq. 18. Curve 1 is plotted with ordinates of $\rho\,M + \phi(\rho)$ and abscissas of $\psi(\rho)$. Line 2 is drawn at a distance $\frac{N}{P}$ from the origin. Curve 3 is drawn with ordinates of ρ (or D) and with abscissas of $\psi(\rho)$. Lines 4 and 5 are drawn at slopes $\frac{P\,\Delta L}{2}$ in the process of the graphical solution.

Certain characteristics of Eq. 18 and Fig. 4 are worthy of mention:

1. The functions $\phi(\rho)$ and $\psi(\rho)$ are functions of channel shape only.
2. Curve 1 is dependent on the factors of channel shape, Q and b_o, only.
3. Distance $\frac{N}{P}$ is dependent on the values of Q, b_o, S_o, and n, only.

4. The slope $\frac{P\,\Delta L}{2}$ is dependent on the factors b_o, n, and ΔL, only.

5. The low point of curve 1 occurs at the value of $\rho_c = \frac{D_c}{b_o}$ in which D_c is the critical depth of the channel for flow Q.

6. The intersection of line 2 with curve 1 coincides with the value of $\rho_o = \frac{D_o}{b_o}$, in which D_o is the depth of channel at which uniform flow occurs.

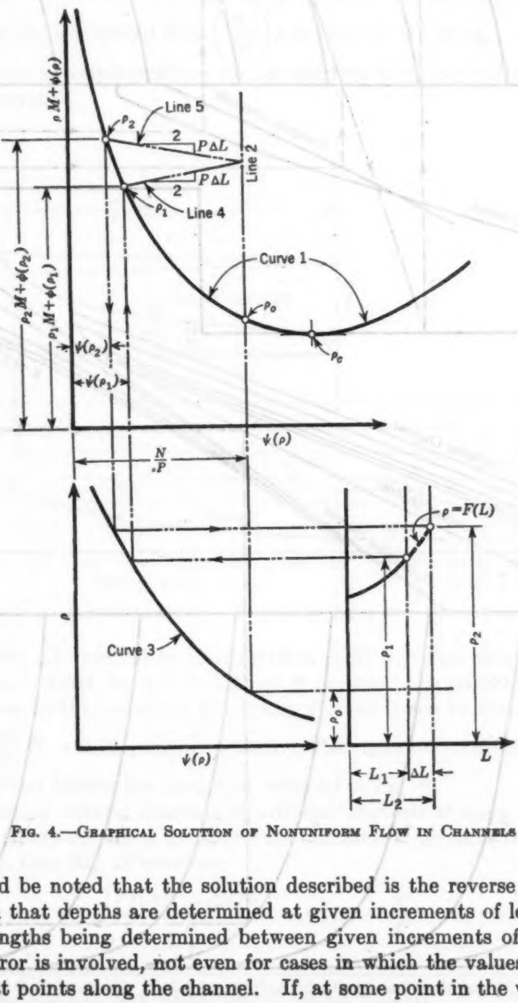

FIG. 4.—GRAPHICAL SOLUTION OF NONUNIFORM FLOW IN CHANNELS

It should be noted that the solution described is the reverse of the usual methods, in that depths are determined at given increments of length, rather than the lengths being determined between given increments of depth. No trial and error is involved, not even for cases in which the values of S_o and n may vary at points along the channel. If, at some point in the water surface

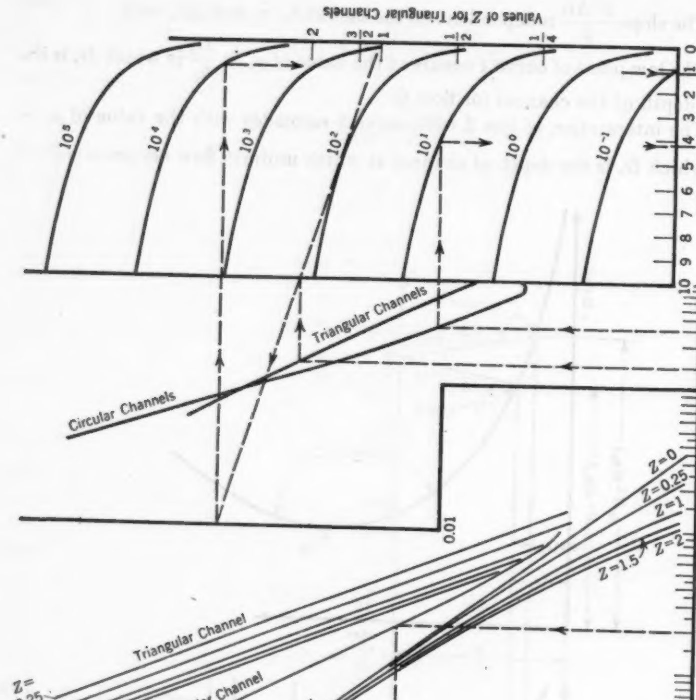

FIG. 5.—CHART FOR DETERMINING VALUES OF $\phi(\rho)$ AND $\psi(\rho)$

plot, it is desired to change the increment of length (ΔL) being used, only the slopes of lines 4 and 5 are affected. The smaller the value of ΔL chosen, the more accurate the solution becomes, particularly in regions in which the curvature of curve 1 is sharp.

Values of $\phi(\rho)$ for the channels shown in Fig. 3(*b*) can be obtained from Fig. 5. The values of $\psi(\rho)$ for circular and triangular channels can also be obtained from Fig. 5. Values of $\psi(\rho)$ for rectangular and trapezoidal channels can be obtained from the "Handbook of Hydraulics" by Horace W. King,[3] M. ASCE, as $\psi(\rho)$ of Eq. 18, is identical with $\left(\frac{1}{K'}\right)$,[2] as used by Mr. King.

Fig. 6 shows a sample problem for the solution of a backwater curve in a rectangular channel.

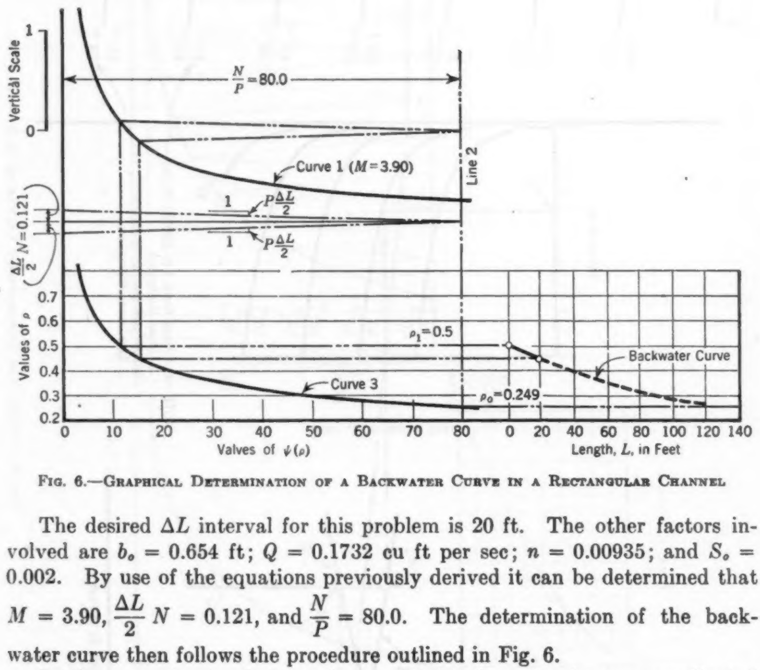

FIG. 6.—GRAPHICAL DETERMINATION OF A BACKWATER CURVE IN A RECTANGULAR CHANNEL

The desired ΔL interval for this problem is 20 ft. The other factors involved are $b_o = 0.654$ ft; $Q = 0.1732$ cu ft per sec; $n = 0.00935$; and $S_o = 0.002$. By use of the equations previously derived it can be determined that $M = 3.90$, $\frac{\Delta L}{2} N = 0.121$, and $\frac{N}{P} = 80.0$. The determination of the backwater curve then follows the procedure outlined in Fig. 6.

In the case of natural channels or artificial channels of more complicated section, it is more convenient to express the functions in terms of D rather than ρ. If $b_o = 1$, then Eq. 18 becomes

$$\frac{d\,[D\,M' + \Phi(D)]}{d\,\frac{P'}{L}} + \Psi(D) = \frac{N'}{P'} \qquad (19)$$

[3] "Handbook of Hydraulics for the Solution of Hydraulic Problems," by Horace W. King, McGraw-Hill Book Co., Inc., New York, N. Y., 3d Ed., 1939, pp. 341–356, Table 114.

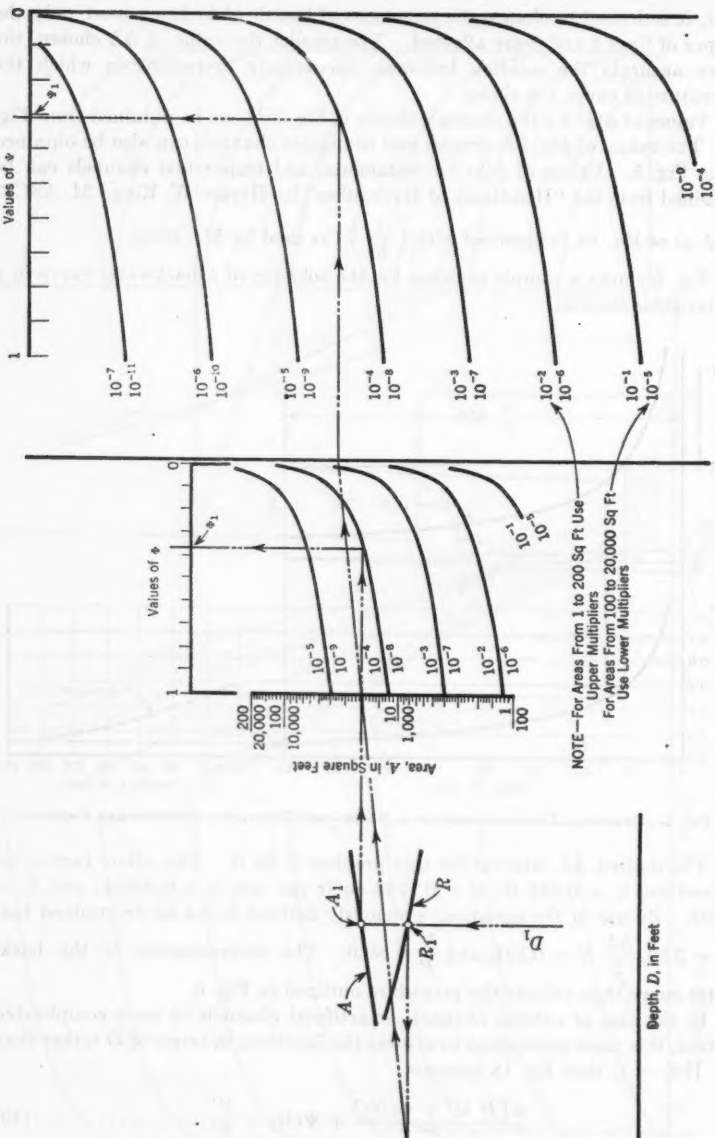

FIG. 7.—CHART FOR DETERMINING VALUES OF $\Phi(D)$ AND $\Psi(D)$

in which

$$\Phi(D) = \frac{1}{2\,g\,A^2} \qquad (20a)$$

$$\Psi(D) = \frac{1}{2.2082\,A^2\,R^{4/3}} \qquad (20b)$$

$$M' = \frac{1}{Q^2} \qquad (20c)$$

$$N' = \frac{S_o}{Q^2} \qquad (20d)$$

$$P' = n^2 \qquad (20e)$$

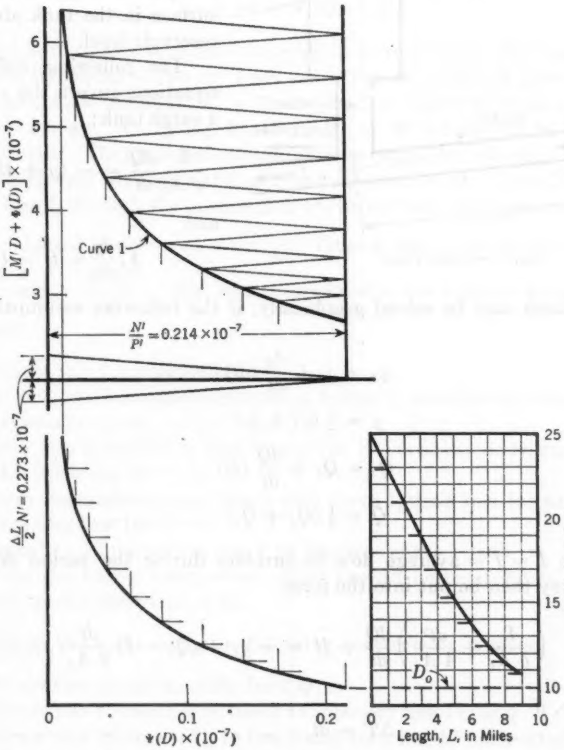

FIG. 8.—GRAPHICAL DETERMINATION OF A BACKWATER CURVE FOR A TRAPEZOIDAL CHANNEL

The graphical solution of Eq. 19 is then the same as that for Eq. 18. Values of $\Phi(D)$ and $\Psi(D)$ can be calculated directly, or the chart of Fig. 7 may be used. Fig. 8 shows the graphical solution of a backwater curve in a trapezoidal channel for which curves 1 and 3 were plotted from the functions obtained from Fig. 7.

The factors for this channel are: $Z = 1$; $b_o = 100$ ft; $Q = 6220$ cu ft per sec; $n = 0.022$; $S_o = 0.0004$; and $D_1 = 25$ ft.

Surge Tanks.—A typical surge tank arrangement is depicted in Fig. 9. The letter symbols used in that figure are as follows: Q is the flow in the conduit; A_c is the conduit area; L is the conduit length; A_t is the tank area; I is the flow to the turbine; H_c is the total head loss in the conduit; H_r is the total head loss in the riser; $H = H_c + H_r$ = the total head loss; and y is the height of the water surface in the tank above the reservoir level.

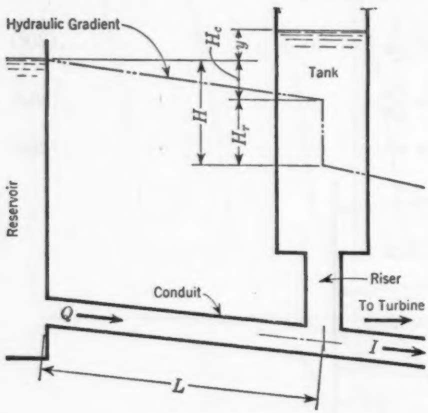

FIG. 9.—SURGE TANK

The following differential equations govern the action of a surge tank;

$$\frac{L}{g\,A_c}\frac{dQ}{dt} = -\,(y + H)\,..\,(21)$$

and

$$A_t\frac{dy}{dt} = Q - I\,...\,(22)$$

These equations may be solved graphically, if the following assumptions are made:

$$y_2 = y_1 + \frac{dy}{dt}\,(dt)\,\ldots\ldots\ldots\ldots\,(23a)$$

$$y = \tfrac{1}{2}\,(y_1 + y_2)\,\ldots\ldots\ldots\ldots\,(23b)$$

$$Q_2 = Q_1 + \frac{dQ}{dt}\,(dt)\,\ldots\ldots\ldots\ldots\,(23c)$$

$$Q = \tfrac{1}{2}\,(Q_1 + Q_2)\,\ldots\ldots\ldots\ldots\,(23d)$$

Also assume $I = \bar{I}$ = average flow to turbines during the period dt. Eqs. 21 and 22 may then be put into the form

$$\left(\frac{L}{g\,A_c} + \frac{dt^2}{4\,A_t}\right)\frac{dQ}{dt} + H = -\,y_1 - (Q_1 - \bar{I})\,\frac{dt}{2\,A_t}\,\ldots\ldots\,(24)$$

Furthermore, if

$$\Delta T = dt\,\ldots\ldots\ldots\ldots\,(25a)$$

$$M = \frac{1}{\dfrac{L}{g\,A_c} + \dfrac{\Delta T^2}{4\,A_t}}\,\ldots\ldots\ldots\ldots\,(25b)$$

and

$$N = \frac{\Delta T}{2\,A_t}\,\ldots\ldots\ldots\ldots\,(25c)$$

then

$$\frac{dQ}{M\,dt} + H = -y_1 - N(Q_1 - \bar{I}) \qquad (26)$$

and

$$y_2 = y_1 + N(Q_1 - \bar{I}) + N(Q_2 - \bar{I}) \qquad (27)$$

Eq. 26 is similar in form to Eq. 1 and can be solved in a similar manner.

For the specific problem of instantaneous and complete reject of load by the turbine $\bar{I} = 0$ and Eqs. 26 and 27 become

$$\frac{dQ}{Mdt} + H = -y_1 - NQ_1 \qquad (28)$$

and

$$y_2 = y_1 + N(Q_1 + Q_2) \qquad (29)$$

The surge tank in this problem is subject to instantaneous shutdown from an initial flow (Q) equal to 760 cu ft per sec. The other factors pertinent to the problem are: $A_t = 228$ sq ft; $A_c = 78.4$ sq ft; $L = 450$ ft; $H = 31.1 \times 10^{-6}\,Q^2$; and $\Delta T = 2.5$ sec. Using Eq. 25, the value of M is found to be 5.41 and N equals 0.00546. The graphical solution of these equations is shown in Fig. 10(a). Curve 1 is plotted with ordinates of Q and abscissas of H. Line 2 is drawn at slope of 1 on 1 through the intersection of the vertical axis with reservoir level ($y = 0$). Line 3 is drawn at slope $\frac{1}{N}$. Lines 4 and 5 are drawn with slopes $+\frac{M\,\Delta T}{2}$ and $-\frac{M\,\Delta T}{2}$. If y_1 and Q_1 are known, the value of Q_2 can be found as follows:

a. Project line 6 horizontally from Q_1;

b. Project line 7 horizontally from y_1 to line 2, and line 8 vertically to the horizontal axis;

c. Draw line 9 parallel to line 3, and line 10 vertically downward from the intersection with line 6;

d. From the intersection of line 6 with curve 1, draw line 11 parallel to line 4 until reaching line 10;

e. Draw line 12 parallel to line 5 to intersect curve 1; and

f. From the above intersection, draw line 13 horizontally to the end of period ΔT, giving the value of Q_2.

To obtain the value of y_2, the following construction is made:

(1) Draw line 14 horizontally from Q_2;

(2) Draw line 15 parallel to line 3 to intersect line 14; and

(3) Draw line 16 vertically to line 2 and draw line 17 horizontally to end of period ΔT, giving y_2.

The foregoing steps are then repeated for the next interval ΔT, using new values of y_1 and Q_1.

In cases of gradual reject or acceptance of load by the turbines, Eqs. 26 and 27 must be satisfied. If I is not equal to zero, then H becomes a function of I

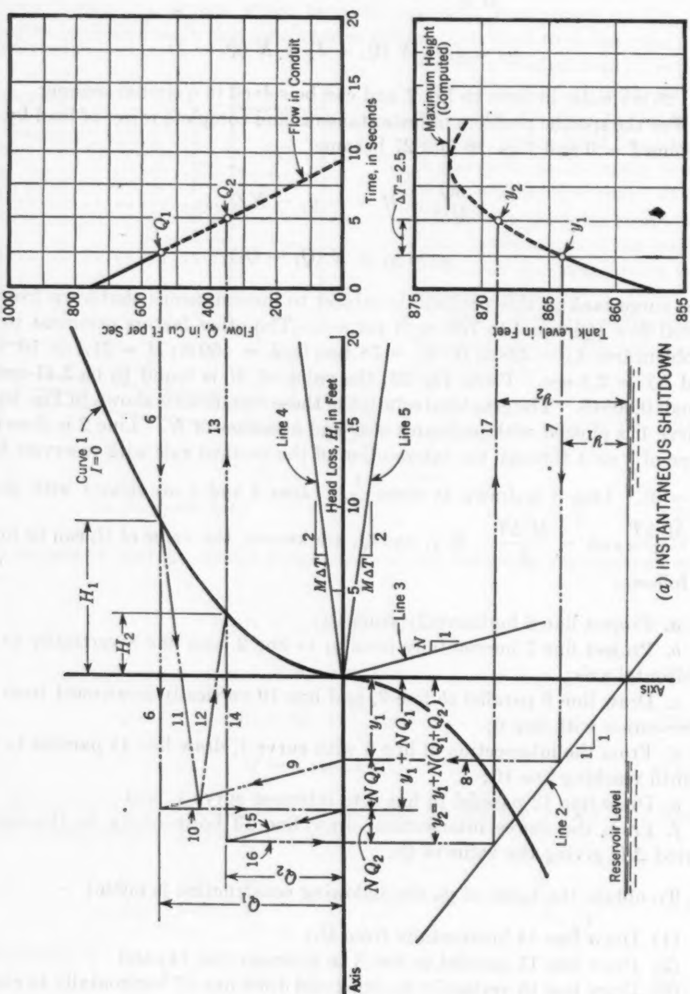

(a) INSTANTANEOUS SHUTDOWN

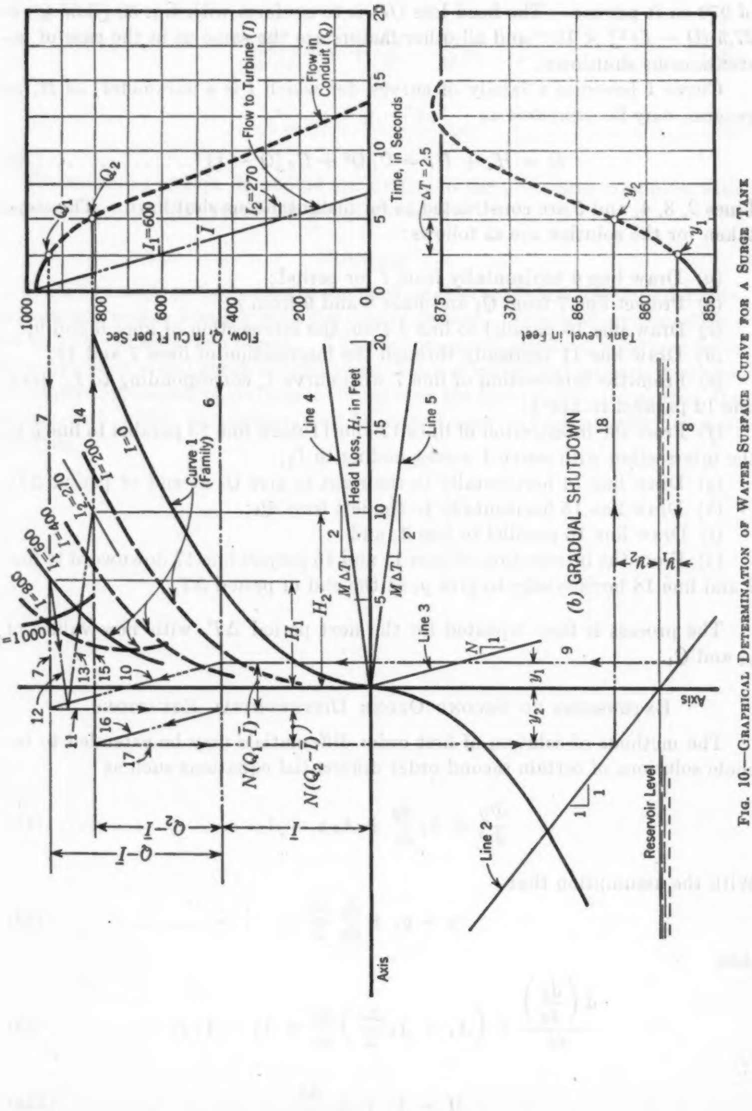

FIG. 10.—GRAPHICAL DETERMINATION OF WATER SURFACE CURVE FOR A SURGE TANK

as well as of Q, and the problem is similar to that of flood routing wherein wedge storage is considered. The solution is as shown in Fig. 10(b). In this case, the turbine shuts down gradually, in a period of 7 sec, from an initial flow (Q) of 970 cu ft per sec. The head loss (H) is to conform with Eq. 30 [$3.55\,Q^2 + 27.5\,(Q - I)^2$] $\times 10^{-6}$ and all other factors are the same as in the case of instantaneous shutdown.

Curve 1 becomes a family of curves, for which I is a parameter, as H, in general, may be expressed as

$$H = H_e + H_r = C_1\,Q^2 + C_2\,(Q - I)^2 \quad \text{(30)}$$

Lines 2, 3, 4, and 5 are constructed as for instantaneous shutdown. The steps taken for the solution are as follows:

(a) Draw line 6 horizontally from $\bar{I}$ for period;
(b) Project line 7 from Q_1 and lines 8 and 9 from y_1;
(c) Draw line 10 parallel to line 3 from the intersection of lines 6 and 9;
(d) Draw line 11 vertically through the intersection of lines 7 and 10;
(e) From the intersection of line 7 with curve 1, corresponding to I_1, draw line 12 parallel to line 4;
(f) From the intersection of lines 12 and 11 draw line 13 parallel to line 5 to the intersection with curve 1 corresponding to I_2;
(g) Draw line 14 horizontally to the right to give Q_2 at end of period ΔT;
(h) Draw line 15 horizontally to the left from Q_2;
(i) Draw line 16 parallel to line 3; and
(j) From the intersection of lines 11 and 16 project line 17 downward to line 2 and line 18 horizontally to give y_2 at the end of period ΔT.

The process is then repeated for the next period ΔT, with new values of y_1 and Q_1.

Extensions to Second Order Differential Equations

The methods of solution of first order differentials may be extended to include solutions of certain second order differential equations such as

$$\frac{d^2y}{dx^2} + A_1\frac{dy}{dx} + A_2\,y = A_3 \quad \text{(31)}$$

With the assumption that

$$y = y_1 + \frac{dy}{dx}\frac{\Delta x}{2} \quad \text{(32)}$$

then

$$\frac{d\left(\dfrac{dy}{dx}\right)}{dx} + \left(A_1 + A_2\frac{\Delta x}{2}\right)\frac{dy}{dx} = A_3 - A_2\,y_1 \quad \text{(33)}$$

If

$$M = A_1 + A_2\frac{\Delta x}{2} \quad \text{(34a)}$$

and

$$\psi = \frac{dy}{dx} = \frac{\psi_1 + \psi_2}{2} \quad \text{(34b)}$$

then

$$\frac{d\psi}{M\,dx} = \psi + \frac{A_3}{M} - \frac{A_2}{M} y_1 \quad \text{(35)}$$

and

$$y_2 = y_1 + \frac{\psi_1 + \psi_2}{2} \Delta x \quad \text{(36)}$$

The solutions of Eqs. 35 and 36 are similar to the preceding examples, with the simplification that curve 1 is a straight line.

Summary

Most hydraulic problems are of such nature that graphical solutions can give an accuracy well in keeping with the results desired. Trial and error solutions can be avoided as shown herein. The advantages of graphical solutions lie in the continuous visual check against gross errors of individual numerical values, the simple mechanical operations involved once the basic curves are plotted, the facility with which parameters may be varied, and the adaptability to spot checking.

AMERICAN SOCIETY OF CIVIL ENGINEERS

Founded November 5, 1852

TRANSACTIONS

Paper No. 2537

FINAL FOUNDATION TREATMENT AT HOOVER DAM

By A. Warren Simonds,[1] M. ASCE

With Discussion by Messrs. James B. Hays, V. L. Minear, Byram W. Steele, William H. McAlpine, Fred H. Lippold, O. E. Boggess, H. Cambefort, and A. Warren Simonds

Synopsis

In the design of Hoover Dam, the Bureau of Reclamation (USBR) of the United States Department of the Interior found it necessary to give careful consideration to certain features that were not subject to an exact mathematical analysis. The treatment of the foundation was one of those matters that involved a design based largely on experience and precedent. Because of the height of the structure and the resulting increase in pressure caused by the exceedingly high head, there was no established antecedent that would furnish a suitable comparison for the foundation treatment. However, pressure grouting was anticipated to reduce seepage, to eliminate uplift pressure in the foundation beneath the dam and appurtenant structures, and to correct defects in the bedrock. In addition to the grouting treatment, a drainage system downstream from the grouted area was considered essential. This paper describes the problems encountered in designing the treatment of the foundation, the conditions that developed after the reservoir had filled, and the corrective measures that were undertaken to make foundation conditions agree with the original design assumptions.

Introduction

Hoover Dam is located on the Nevada-Arizona boundary near Las Vegas, Nev., in a deep gorge formed by the Colorado River. The plan of the dam and its appurtenant structures is shown in Fig. 1. It is a concrete-arched gravity structure having a maximum height of 726 ft above the foundation rock, a maximum base thickness of 660 ft, and a crest length of 1,244 ft. The volume of concrete in the dam is 3,251,137 cu yd. Two spillways of the

Note.—Published in December, 1951, as *Proceedings-Separate No. 109.* Positions and titles given are those in effect when the paper or discussion was received for publication.

[1] Engr., Bureau of Reclamation, U. S. Dept. of the Interior, Denver, Colo.

side-channel type, equipped with drum gates, are provided to insure against any possibility of the dam being overtopped by flood discharges. These spillways are located on the abutments a short distance upstream from the dam and discharge into inclined tunnels 50 ft in diameter, driven through the abutments. The power plant is located in the canyon downstream from the dam and consists of 3 sections—the 2 wings housing the power units located on each side of the canyon, and a central section housing the machine shop, dispatcher's room, and offices, situated above the downstream toe of the dam. Water is conveyed to the power units by means of two tunnels (referred to as the upper and lower penstock tunnels) through each abutment.

The canyon in which Hoover Dam is located is known as the Black Canyon of the Colorado River. Before construction excavation was begun, this canyon varied in width from 250 to 500 ft at normal river surface and was from 1,000 to 1,500 ft deep. Excavation of the overburden disclosed that the river had cut a narrow gorge, about 50 ft deep, in the bottom of the canyon.

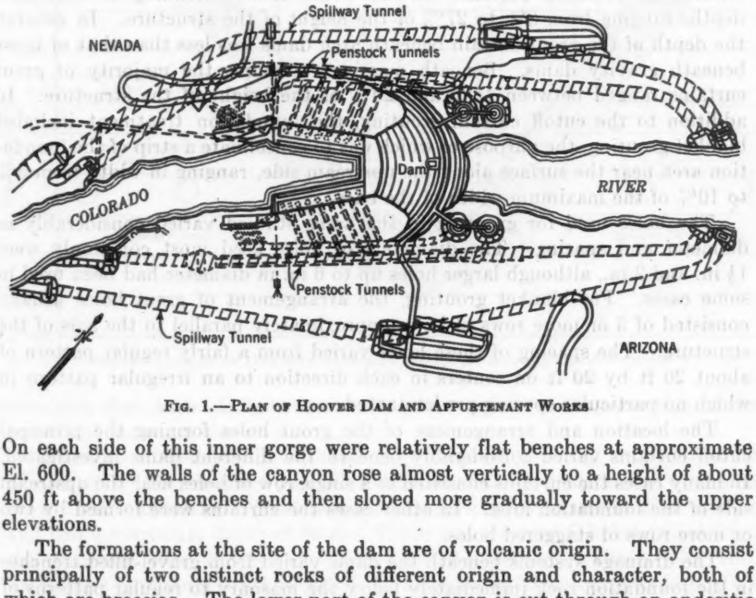

FIG. 1.—PLAN OF HOOVER DAM AND APPURTENANT WORKS

On each side of this inner gorge were relatively flat benches at approximate El. 600. The walls of the canyon rose almost vertically to a height of about 450 ft above the benches and then sloped more gradually toward the upper elevations.

The formations at the site of the dam are of volcanic origin. They consist principally of two distinct rocks of different origin and character, both of which are breccias. The lower part of the canyon is cut through an andesitic tuff-breccia that is a dark red, firmly cemented sedimentary breccia. The upper part of the canyon is formed of a light-colored latite flow breccia. The contact between the two breccias is tight and almost indiscernible in places. Although there is an extensive pattern of faulting in the vicinity of the dam, the structure is located on a massive block between 2 well-defined faults. A zone of minor faulting passes through the Nevada abutment, beneath the dam, between El. 840 and El. 940. The formation is characterized by springs of warm alkaline water in the vicinity of the dam.

Sources of Design Information for Foundation Treatment.—Prior to making the actual plans for foundation treatment, an extensive search into the field of pressure grouting was made. Questions involving methods, procedures, grout mixes, and equipment were studied, and laboratory investigations were made to furnish additional information. The principal design problems that were considered were: (*a*) The extent to which the foundation treatment would be necessary; (*b*) the size and spacing of grout holes; (*c*) the location of the cutoff curtain; and (*d*) the location and depth of the drainage curtain.

To aid in solving these problems, a comprehensive study was made of the foundation treatment of 50 of the highest masonry dams. Of this group of dams, those having heights ranging from 300 to 400 ft were selected as the most favorable sources of information on foundation treatment of high dams. This group was comprised of dams that had been constructed by private organizations as well as government agencies.

The investigation revealed that the foundation treatment consisted of forming grout cutoff curtains beneath these dams, extending to maximum depths ranging from 8% to 27% of the height of the structure. In general, the depth of the grout curtain beneath arch dams was less than that of those beneath gravity dams. Beneath massive structures the majority of grout curtains ranged between 15% and 20% of the height of the structure. In addition to the cutoff curtain grouting, the foundation treatment included blanket grouting, the purpose of which was to consolidate a strip of the foundation area near the surface along the upstream side, ranging in width from 5% to 10% of the maximum width of the base.

The holes used for grouting in the dams studied varied considerably in diameter and spacing. The diameters of holes used most commonly were 1½ in. and 2 in., although larger holes up to 6 in. in diameter had been used in some cases. For blanket grouting, the arrangement of grout holes usually consisted of 3 or more rows of holes approximately parallel to the axis of the structure. The spacing of these holes varied from a fairly regular pattern of about 20 ft by 20 ft on centers in each direction to an irregular pattern in which no particular spacing predominated.

The location and arrangement of the grout holes forming the principal cutoff curtains varied considerably beneath the different dams investigated. In many cases the curtains consisted of a single row of holes near the upstream side of the foundation area. In other cases the curtains were formed by two or more rows of staggered holes.

The drainage systems beneath the dams varied from gravel-filled trenches in the foundation rock immediately below the masonry to regular patterns of drainage holes drilled into the bed rock slightly downstream from the grouted cutoff curtain. For the highest dam studied (405 ft), the maximum depth of the drainage holes was 40 ft—about one third the depth of the grout curtain or one tenth the height of the structure.

Original Foundation Treatment at Hoover Dam.—The original foundation treatment consisted of a program of grouting and drainage. In the grouting program three classes of holes were used, designated according to location, depth, and range of pressures. The classes were: A holes that formed the

cutoff curtain and were grouted at high pressure; B holes for blanket grouting that provided a general consolidation of the surface rock and sealed near-surface seams at low pressure; and C holes that were drilled from the upstream edge of the base, inclined in a downstream direction and grouted at intermediate to high pressures. The blanket grouting was done from the surface of the foundation rock prior to placing concrete. The original plans for the C-hole grouting provided for this work to be done after the A-hole grouting and the drilling of the drainage holes had been completed, in order to test the water-tightness of the A- and B-hole grouting and to effect a final seal of the foundation rock. As actually performed, the program was altered to permit the commencement of water storage at an early date. The C-hole grouting was begun after 11 alternate A holes at the lowest elevation had been completed, and the grouting of the holes of both series was continued simultaneously, with the

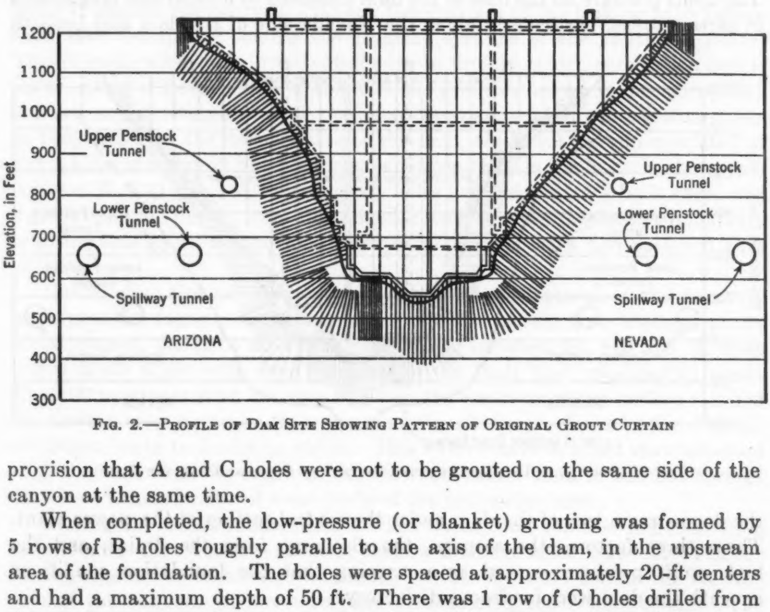

FIG. 2.—PROFILE OF DAM SITE SHOWING PATTERN OF ORIGINAL GROUT CURTAIN

provision that A and C holes were not to be grouted on the same side of the canyon at the same time.

When completed, the low-pressure (or blanket) grouting was formed by 5 rows of B holes roughly parallel to the axis of the dam, in the upstream area of the foundation. The holes were spaced at approximately 20-ft centers and had a maximum depth of 50 ft. There was 1 row of C holes drilled from the upstream edge of the dam, spaced at 10-ft centers. These holes were drilled to a maximum depth of 125 ft. The main cutoff curtain was formed by the A holes that were drilled and grouted from a foundation gallery located along the plane of the axis of the dam and immediately above the bed rock.

The A holes forming the curtain grouting were drilled to depths of 150 ft, or about 21% of the height of the dam, across the lower part of the canyon. These holes were spaced at 5-ft centers and the depth of 150 ft was maintained to El. 675. Above this elevation the depth of the holes was decreased uniformly to 100 ft at El. 1200. These holes were inclined 15° upstream from the axis of the dam. The pattern of this series of holes is shown in Fig. 2.

The drainage system was constructed by drilling holes from the foundation gallery. Beneath the lower part of the dam the holes were drilled vertically. At the bottom of each abutment they were fanned (as shown in Fig. 3) until at El. 700 the holes were approximately horizontal. The remaining holes except for the section in the Arizona abutment above El. 1100 were drilled with a slight upward slope so as to drain freely into the gutters of the galleries. The holes varied in depth from a maximum of 102 ft at the lowest part of the canyon to a minimum of 20 ft near El. 1200.

Undesirable Conditions Developed.—During the initial filling of the reservoir, particularly during the years 1937 and 1938, troublesome seepage developed into the penstock tunnels and also through the abutments as a result of the exceedingly high head of water. Water from the foundation drainage system entered the galleries of the dam in excessive quantities in some locations. The uplift pressure on the base of the dam increased to undesirable magnitudes in certain areas, particularly along the Nevada side of the dam and beneath

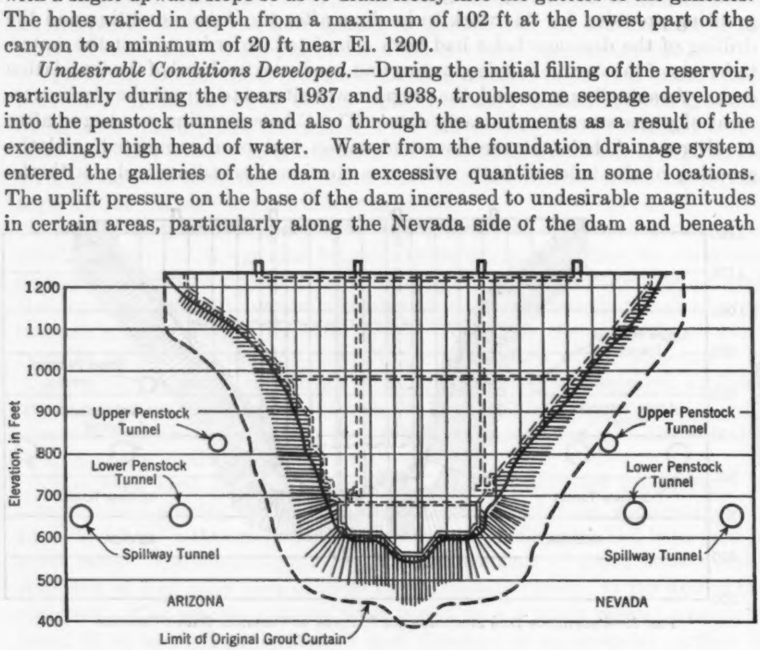

FIG. 3.—PROFILE OF DAM SITE SHOWING PATTERN OF ORIGINAL DRAINAGE SYSTEM

the downstream tow of the dam under the central section of the power plant. These three factors—the seepage, the discharge from the drains, and the high uplift pressure—served as a warning that the foundation conditions beneath the dam were far from satisfactory.

These difficulties were apparently the result of insufficient grouting prior to filling the reservoir. However, in planning the original scheme of foundation treatment it was realized that additional grouting would probably be necessary at some future time, so when these undesirable conditions developed they were not altogether unexpected.

Inadequacy of Original Grouting.—In the original grouting program several complications developed that impaired the effectiveness of the desired watertight barrier in the foundation and abutments of the dam. The complications consisted of leaks of grout into the abutment joints (described in the following sections) and difficulties resulting from geologic features of the site. The

first of these factors could be remedied mechanically but the second required study, exploration, and the development of equipment and methods.

The mass concrete at Hoover Dam had been placed in blocks that were bounded by radial and circumferential joints, After the concrete had been placed and artifically cooled to a predetermined temperature distribution, the contraction joints between the blocks were grouted to make the structure monolithic. A specially designed joint between the concrete and the rock had been constructed at each abutment. These joints had not been grouted prior to filling the reservoir because it was contemplated that additional tightening of the dam against the abutments would be necessary at some future time, after the structure had deflected downstream under water load.

At the time the A-hole grouting was in progress, grout leaked from some of the holes into the abutment joints. Because of the inaccessability of the leaks, it became necessary to abandon the grouting of the leaking holes rather than take the risk of fouling the grouting systems of the abutment joints. This procedure left gaps in the cutoff curtain through which percolation developed. On the Nevada side of the dam the grout curtain was formed by 191 A holes, and of this number 33 holes had been abandoned while grouting was in progress. On the Arizona side of the dam, the grout curtain consisted of 202 A holes of which 21 holes had been abandoned. On the Nevada abutment, between El. 840 and 940, several grout holes had penetrated a fault zone, and 4 grout holes in this area were abandoned, chiefly because of excessive quantities of grout that had been injected into them. Minor leaks had occurred at 3 of these holes.

Contributing Geologic Features.—Several geologic features at the dam site were possible sources of seepage and uplift pressure. Two distinct minor faults crossed the right abutment of the dam between El. 840 and El. 940. These faults apparently were branches of the fault that appeared at about El. 1100 upstream from the dam. When the reservoir water surface reached the faulted area upstream from the dam, the abutment drains in the Nevada abutment began to discharge water. This water was cool, a fact that indicated that the water had its origin in the reservoir rather than in the hot springs that were characteristic of some parts of the foundation area.

During the construction period, when excavation for the dam had been completed in the river channel area, shallow drainage holes were located in the inner gorge of the excavation and along the bench at El. 600 on the Nevada side of the canyon, wherever seepage or shattered zones were found. The flow from these holes (usually warm water) was piped to the drainage gallery at about El. 555. Later, when the dam was practically finished, an attempt was made to grout these holes. The grouting was ineffective due to a premature set of the cement, and the pipe headers, to which the holes had been connected, were plugged. Subsequently, the flow from the warm springs apparently filled the zones of close shearing beneath the dam, thereby causing excessive uplift pressure to develop. The location of the shear zones is shown in Fig. 4.

Another geologic feature that had caused considerable speculation was the presence of manganese seams in the foundation rock. These seams were known locally as "mud" seams because of the dark color of the drill cuttings

as compared to the normal reddish brown color of the andesitic cuttings. These seams varied in thickness from a fraction of an inch to several inches. Grout holes frequently crossed the seams, particularly along the axis of the dam beneath the galleries at El. 553 and El. 603. Because of the soft nature

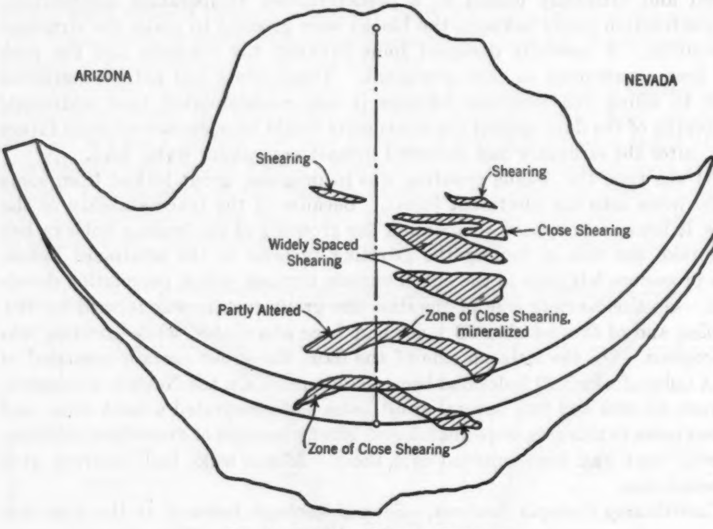

FIG. 4.—SHEARING ZONES IN FOUNDATION

of the manganese in the seams it was difficult to obtain good cores of this material, but one of the better specimens of core showing the manganese seam is shown in Fig. 5.

Purpose of Additional Grouting and Drainage Program.—The purpose of the program of additional grouting and drainage was to correct the undesirable foundation conditions. The specific results that were to be accomplished are as follows:

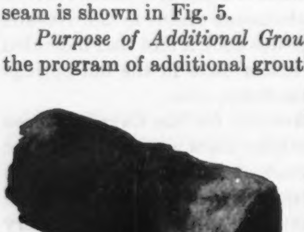

FIG. 5.—MANGANESE SEAM IN CORE DRILLED FROM FOUNDATION OF HOOVER DAM

(*1*) To reduce the uplift pressure acting on the base of the dam, particularly in the area at the downstream toe beneath the central section of the powerhouse;

(*2*) To reduce the seepage through the abutments, especially behind the Nevada and Arizona wings of the powerhouse;

(*3*) To eliminate the seepage of hot alkaline water through the concrete lining of the lower Nevada penstock tunnel. This seepage water was injurious to the protective paint of the penstock; and

(*4*) To eliminate the seepage of cold water into the upper Nevada penstock tunnel and both Arizona penstock tunnels.

Extent of Foundation Treatment.—The grouting consisted of an additional cutoff curtain with an entirely new and deeper system of A holes. This curtain was formed by utilizing the original drain holes of the dam that were drilled to such depths as the foundation conditions required. The area in the Nevada abutment, beneath the intake towers and the Nevada spillway tunnel, was grouted. The grout curtain was extended into the Nevada abutment from the original A-hole system beneath the dam 600 ft to the right of the Nevada spillway tunnel. The voids behind the concrete lining and the surrounding rock of the lower Nevada penstock tunnel were regrouted, starting at the tunnel plug and extending downstream for a distance of about 300 ft. An area in the Arizona abutment between the left wing of the powerhouse and the Arizona spillway tunnel was also grouted.

An entirely new drainage system was formed by drilling from the grouting-and-drainage gallery into the foundation and abutments downstream from the new system of grout holes. A number of drain holes were drilled beneath the central section of the powerhouse at the downstream toe of the dam, and a series of drain holes was drilled from the Nevada penstock tunnel through the hot spring area in the abutment downstream from the dam, behind the right wing of the powerhouse. A series of drains was also drilled downstream from the grout curtain that extended into the Nevada abutment. This series was drilled from a construction adit extending from the powerhouse to the Nevada spillway tunnel.

This program involved the injection of 251,115 sacks of cement into the foundation and abutments of Hoover Dam under difficult and severe conditions. There was a total of 298,383 linear ft of drilling of which 34,115 ft were for drainage purposes. The remainder was for grouting and included the drilling of additional grout holes, the redrilling of hardened grout from holes for deeper stages, reaming holes, and the miscellaneous drilling necessary for the grouting program.

Conditions Necessitating Additional Grouting

The conditions that developed at Hoover Dam, as the reservoir filled, were far from ideal. The initial filling was accompanied by the appearance of seepage in prominent places at the dam site. A wet area developed at a conspicuous place on the Nevada canyon wall above the powerhouse roof, at about El. 800. The flow was not great, but it presented an unsightly appearance because of its location. The most troublesome seepage developed in the lower elevations of the canyon, behind the wings of the powerhouse and in the areas adjacent to the 50-ft diameter tunnels. The seepage behind the powerhouse increased until it became necessary to excavate small trenches in the floors of the lower galleries of the powerhouse to serve as drains for the accumulated water.

Seepage into the penstock tunnels was another undesirable condition. The concrete in the arches of the tunnel lining had been placed by pneumatic methods and the quality of this concrete was somewhat variable. Some areas were extremely porous, and the alkaline water from the warm spring seeped through, dripped on the penstocks, and destroyed the paint. An attempt to

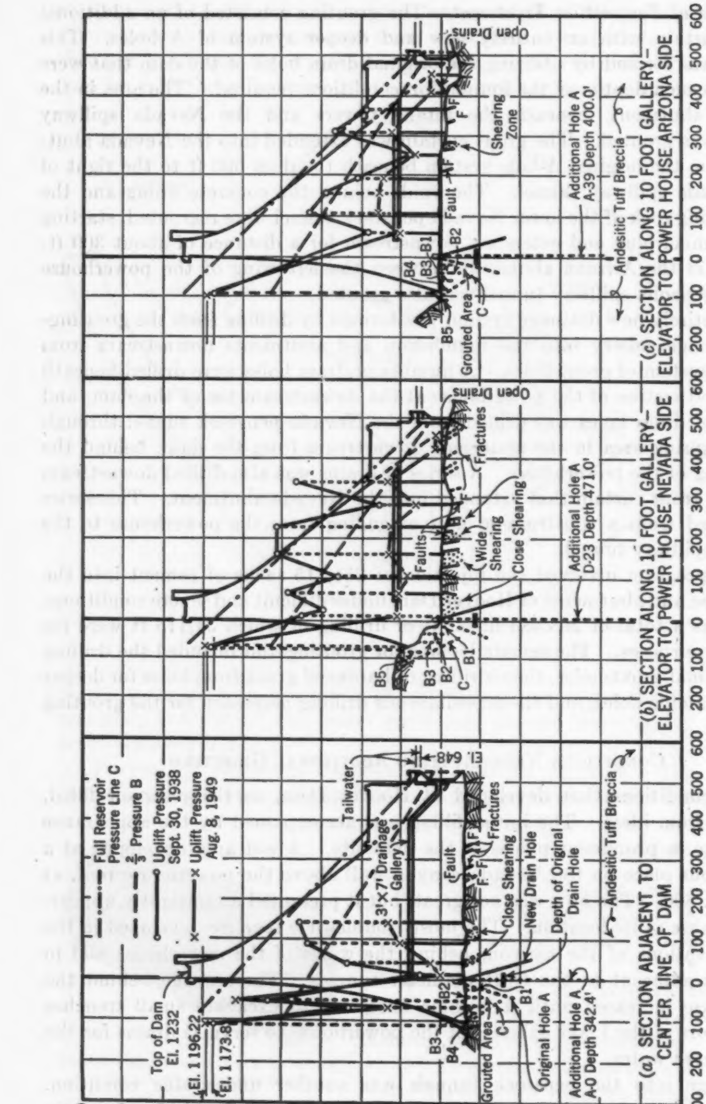

Fig. 6.—Uplift Pressure Gradients

protect the paint had been made by installing metal troughs beneath the leaks and conveying the water to systems of pipe headers. However, during certain seasons of the year the humidity arising from the seepage water condensed and formed moisture on the metal, and the periods of wetting and drying caused deterioration of the paint and extensive corrosion as soon as the protective coating of paint had been penetrated. The expense involved in maintaining the outlet and penstock paint jobs was an item of considerable importance.

Increase in Uplift Pressure on Base of Dam.—The increasing uplift pressure on the base of the dam was of gravest concern to the engineers responsible for the safety of the structure. The measurements of uplift pressure were obtained from 4 lines of pipes installed for this purpose. There were 7 pipes along the Nevada bench, 6 pipes adjacent to the line of centers, 7 pipes along the Arizona bench, and 4 pipes in the upper circumferential drainage gallery. Semi-monthly measurements were started August 12, 1935, and continued until December 15, 1946. After that date they were made at monthly intervals. Uplift pressure measurements were also made at some drains from 1935 to 1937 to supplement the information obtained from the regular uplift pressure pipes.

In the design of Hoover Dam, the following assumptions relative to uplift pressure were used in making the stress analysis:

> "Uplift pressure intensities were assumed to vary as a straight line from full reservoir pressure at the upstream face to zero or tailwater pressure at the downstream face.
>
> "At planes of contact between the dam and canyon rock, uplift pressures were assumed to be effective over two-thirds the area."[2]

The maximum uplift pressures at the base of the dam just prior to the time that the additional grouting was started are shown in Figs. 6 and 7. The two-thirds full pressure line (B) and the full reservoir pressure line (C) are shown also in these figures. The worst condition of uplift pressure occurred along the Nevada abutment at line B, in which the magnitude of pressure exceeded that of the full reservoir pressure line (C). At the time of this measurement (September 30, 1938) the reservoir water surface was at El. 1178.8. It had been noted that the ratio of the uplift pressures to the reservoir pressures had been increasing after each annual rise in reservoir level, and it was considered essential to correct this undesirable condition.

Plans and Preparation for Corrective Measures.—The chief complication to any proposed remedial measure was the ungrouted abutment joints that had been provided for contact grouting between the concrete of the dam and rock abutments. Grouting these joints would effectively seal the areas in which grout had leaked when the A-hole grouting was in progress, but this grouting could not be done until after the dam had deflected downstream under water load. The results of precise surveys made in 1938 by triangulation indicated that the structure had deflected downstream about $\frac{1}{2}$ in. As soon as this fact had been determined, the 2 abutment joints were grouted. This

[2] "Boulder Canyon Project," *Technical Investigations Bulletin 4*, Bureau of Reclamation, U. S. Dept. of the Interior, Denver, Colo., Final Reports, Part V, p. 66.

resulted in stopping several noticeable leaks that appeared at the junction of the downstream face of the dam and the abutments, and also stopped the serious seepage into the lower galleries of the Nevada wing of the powerhouse.

The increasing intensity of the uplift pressures near the downstream toe of the dam, particularly beneath the central section of the power plant, was considered to be the most serious situation that had developed. Plans were made to start the remedial measures while the abutment joint grouting was in progress. A line of drainage holes was to be drilled through the concrete

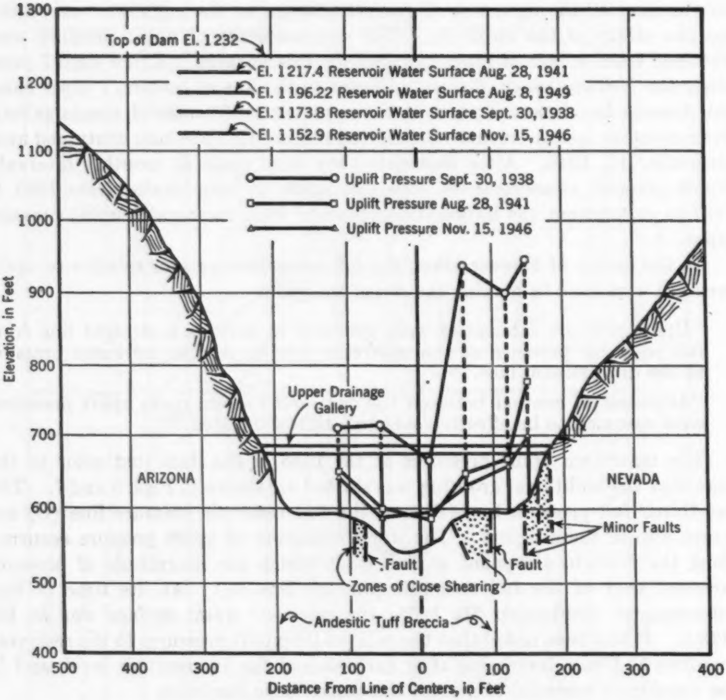

FIG. 7.—UPLIFT PRESSURE GRADIENT IN DEVELOPED SECTION ALONG CENTER LINE OF UPPER DRAINAGE GALLERY

of the dam into the foundation rock in the area of the high uplift pressure. Actually 2 rows of holes were drilled for this purpose, one row being vertical and the other dipping upstream at an angle of 45°. The holes were drilled from one of the lower galleries in the powerhouse (at El. 616) that would permit any intercepted flow to drain into the lowest sump by gravity. Several of these drains discharged large flows of warm water.

In attempting to plan an effective program for additional grouting, consideration was given to regrouting areas in the foundation in which grouting

had been abandoned before completion. Because of the increasing amount of seepage that was developing in widespread areas, the effectiveness of the original grouting was problematical, and it was realized that the available information on existing foundation conditions was inadequate. Therefore, a systematic exploration of the foundation was started by drilling BX-size core holes, in an attempt to find where defects in the foundation rock existed. Based on the results of the exploratory drilling, a plan was developed to form an additional grout curtain downstream from the row of A holes. The additional cutoff curtain was to extend deeper into the foundation than the original cutoff curtain.

Exploratory drilling revealed also that the original grout curtain extended an insufficient distance laterally into both abutments. The indications were that the area in the Nevada abutment between the dam and the spillway structure required consolidation by grouting. There was a particularly porous zone in the abutment on the reservoir side of the Nevada spillway.

As a result of this exploratory drilling, it was planned to continue the new cutoff curtain into each abutment and to form a deeper curtain along the reservoir side of the Nevada spillway. After this grouting had been accomplished, it was further planned to drill additional drain holes downstream from the new grout curtain.

Method of Grouting and Material Used

At the start of the program of additional grouting, considerable experimentation was required to determine a suitable procedure that would not increase the uplift pressure on the base of the dam. The first holes drilled from the grout and drainage gallery at El. 553 developed flows of water that provided sufficient drainage, in some cases, to reduce the uplift pressure slightly. When grouting operations started, the uplift pressure would increase. Continual vigilance on the part of the engineers directing the grouting was required to keep a high uplift pressure from developing and yet accomplish an effective job of grouting. It was realized that single-stage grouting of a deep hole that crossed several water-bearing seams was not the most efficient practice, but this was done until a suitable method combining stage and packer grouting could be developed.

As soon as the grouting work became organized, a systematic procedure of stage grouting was used. In areas in which open seams were crossed (as determined by the flow of water into the hole), it was customary to drill slightly beyond the seam and then grout. After allowing the grout to set for approximately 16 hours, the hardened grout was drilled from the hole. The condition of the grout determined the type of bit used in opening the hole and, whenever possible, borium sawtooth bits were used to save wear on the diamond bits.

In holes in which flows of water from 200 to 300 gal per min were encountered, experimental grouting with packers was tried. The first packers did not prove successful because of the difficulty in seating them against the flow of water in holes of nonuniform diameter. Stage grouting was resorted to, and the holes were grouted in successive stages by starting at the top of

the hole and then working progressively downward. Later, a satisfactory packer and a method for inserting it against large flows of water was developed.[3]

Cement Used.—An entirely satisfactory cement, suitable for foundation grouting, had not been developed during the construction period at Hoover Dam. Standard Portland cement had been used successfully in areas free from hot alkaline water, but when grouting in the warm spring areas, this type of cement was unsatisfactory. When it came in contact with the hot alkaline water, a flash set would occur and the grout pumps would stall as the pumping pressure built up without forcing any grout into the foundation. The high temperature was presumed to be a contributing cause of this trouble, consequently, several attempts were made to cool the area surrounding the grout holes in the foundation by pumping cool water into the holes prior to grouting. This procedure was not successful, apparently because an insufficient amount of water had been pumped into the grout holes, and premature stiffening of cement continued to occur. The exact cause of this difficulty was not determined. However, the suspicion continued to be prevalent that either the temperature of the water or the contact of the cement with the alkaline salts—or possibly the combination of the two—might have been contributing factors to this trouble.

The first step in an attempt to obtain a satisfactory grouting cement was the use of an oil well-type grouting cement that had been found successful in grouting areas in which hot salt water had been encountered in oil fields. Unfortunately, these cements were ground fairly coarse, as compared with later practices in manufacturing standard and modified cements. The average specific surfaces ranged from 1,100 to 1,400 sq cm per gram for cements of this type manufactured in the west coast area. However, a special grind of oil well cement that was finer than usual was obtained. This cement had an average specific surface of 1,865 sq cm per gram, or about the same as that of the standard Portland cements obtainable.

The oil well cement had some very desirable characteristics for grouting, but it was not completely satisfactory. It contained a small percentage of the usual dark-colored particles of unground clinker that had a tendency to settle out from the rest of the grout when the thin mixes were pumped through long supply lines. This coarse material had always been undesirable for injecting into holes in tight ground.

While the field forces were occupied in the elimination of coarse material in the cement, laboratory investigations were being made to find a finely ground cement with the characteristics of oil well cement. It was found that by adding a commercial retarder, composed of calcium salt of lignin sulphonic acid and triethanolamine, to the modified cement, a resulting product was obtained that had the desirable characteristics and was more finely ground than the oil well cement. This product was used in grouting throughout most of the foundation area in which warm water was encountered.

Grouting Program

Preliminary Work.—The first step in the grouting program was a check of the inspector's daily reports of the grouting activities of the construction period.

[3] "Header Assembly Permits Grouting Against High Hydrostatic Pressures," by George T. Evans, *Civil Engineering*, Vol. 19, June, 1949, p. 48.

The locations in which groups of grout had been abandoned indicated areas in which additional grouting appeared desirable. A group of 9 of the original Nevada A holes that penetrated the zone of minor faulting between El. 840 and El. 940 in the area bearing cold water were opened and redrilled to depths of 150 ft, and an attempt was made to regrout them. This grouting was not entirely satisfactory, since only small quantities of cement, ranging from 2 to 7 sacks per hole, could be injected. The seams in the rock surrounding these holes had been closed, apparently by the original grouting, so it was felt that the additional grouting would be more effective if new holes were used.

Foundation Conditions Encountered.—While the grout crew was attempting to regrout the Nevada A holes between El. 840 and El. 940, unexpected developments were encountered by the drill crew working in the foundation gallery at El. 553. The original drainage plan that had been followed during construction between axis stations 5+46 and 8+04 was to drill alternate drain holes on 10-ft centers to maximum depths of 100 ft, as shown in Fig. 3. In order to relieve the high uplift pressure and to explore the foundation area, intermediate holes were drilled along the row of drains. This drilling disclosed the presence of manganese seams extending across the foundation beneath the river channel at El. 525. Lenses of broken rock were found at lower elevations, and flows of water were encountered, indicating the presence of open cracks or seams.

Steps were immediately taken to correct these defects in the foundation. It was decided to convert all of the original drain holes into a new line of A holes that would form an additional cutoff curtain, and later drill a new drainage system downstream from this second grout curtain. The procedure planned was to wash the soft manganese material from the seams in the foundation using the group of 3 holes at a time to prevent having too large an area of the foundation beneath the 726-ft high dam unsupported. Grouting with packers was tried in this area, but it was unsuccessful because of excessive interconnections between holes, through cracks and seams in the foundation rock.

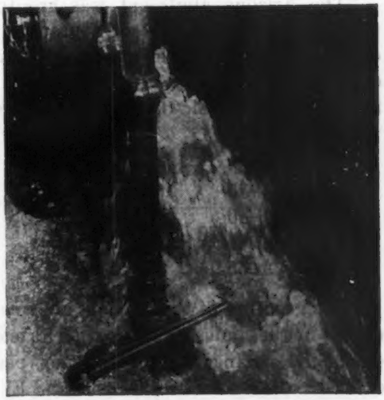

Fig. 8.—Flow of Water From Foundation Grout Hole

As the drilling progressed, areas of broken rock shear zones, lenses of uncemented volcanic sand, and open seams that produced large flows of water, such as that shown in Fig. 8, were encountered. Each hole had individual characteristics, and every sack of cement injected benefited the foundation. The policy adopted was to drill the new grout holes deep enough to assure that one "run" of drilling (approximately the length of drilling necessary to fill a 5-ft core barrel) was in good sound rock. This was determined by an examination of

the core from the hole. As the drilling was carried on with 3 shifts per day, different men were responsible for determining if the bottom of the hole was in good sound rock. This personal factor, together with the natural irregularities of the foundation conditions, resulted in considerable variation in the depth of holes in the new grout curtain.

The resulting grout curtain is shown in Fig. 9. The deepest hole was hole D-23 on the Nevada side of the river channel. This hole was one of the most important holes drilled. Its final depth was 479.8 ft, and 322 sacks of cement were used in grouting it. At a depth of 420 to 450 ft it penetrated a shear zone that was the apparent source of the uplift pressure over the greater part of the base of the dam. Although the quantity of cement used in grouting was not great, it had a widespread effect in reducing the uplift pressure. Over 5,000 sacks of cement were injected in this immediate area before the program was completed, and this resulted in a material reduction of the uplift pressure.

As the grouting progressed, it was found that fairly deep holes were necessary. The method of closures was adopted as the optimum method of procedure. In this method, the primary holes were drilled and grouted at fairly wide spacing. The next holes were drilled and grouted halfway between the primary holes, and this procedure continued until the amount of grout used indicated that the foundation was tight. When unusual conditions indicated that additional holes were desirable, they were drilled as needed.

The Arizona abutment was grouted in a fairly uniform manner. The primary holes took the most grout, and subsequent holes required smaller quantities of grout as the abutment grew progressively tighter. The maximum quantity of cement injected in 1 hole in the Arizona abutment was 8,258 sacks in hole A-124 at El. 1000. Other holes that took large quantities of cement were as follows:

Hole	Sacks of cement	Hole	Sacks of cement
A-35	1,817	A-100	1,927
A-40	4,882	A-106	3,598
A-46	3,368	A-129	1,486
A-55	3,585	A-138	2,235

The grouting of the Nevada abutment was complicated by the presence of cracks in the andesitic geological formation. The first grouting in this area, completed during the construction period, indicated the presence of fairly extensive cracks between El. 800 and El. 1000. In exploring this area by core drilling, several cores, showing cracks up to 2 in. wide well filled with grout, were found. Although during the construction period over 13,000 sacks of cement had been injected in this area, during this period seepage appeared on the canyon wall above the roof and behind the Nevada wing of the powerhouse. Because of the unsightly appearance of this seepage, considerable effort was exerted to dry up the wet area above the roof. Although the quantity of grout injected in this area was fairly small, it was necessary to drill about 20 holes before the path of the seepage was intercepted.

Blanket Grouting of the Upstream End of the Nevada Penstock Tunnel.—During the construction of the lower Nevada penstock tunnel, a faulted zone

was encountered about 150 ft downstream from the tunnel plug. No major seams were crossed in this area. The disturbance consisted of a maze of smaller cracks that crossed the tunnel at an angle of about 45° with the axis, in plan. This area had been grouted during the construction period using both low-pressure and high-pressure methods. The low-pressure grouting was for the purpose of filling voids back of the lining caused by an overbreakage of the abutment rock, and the high-pressure grouting sealed the rock around the tunnel bore and also formed 2 cutoff rings around the tunnel at the plug section.

The porous concrete through which the seepage entered the tunnel covered such an extensive area that it was decided to regrout the upper end of the tunnel for a distance of about 300 ft immediately downstream from the plug. This was done by laying out patterns of holes at intervals of 20 ft along the axis of the tunnel. Each pattern consisted of 7 holes, sloping upward, above the horizontal diameter of the tunnel. The patterns were laid out with the

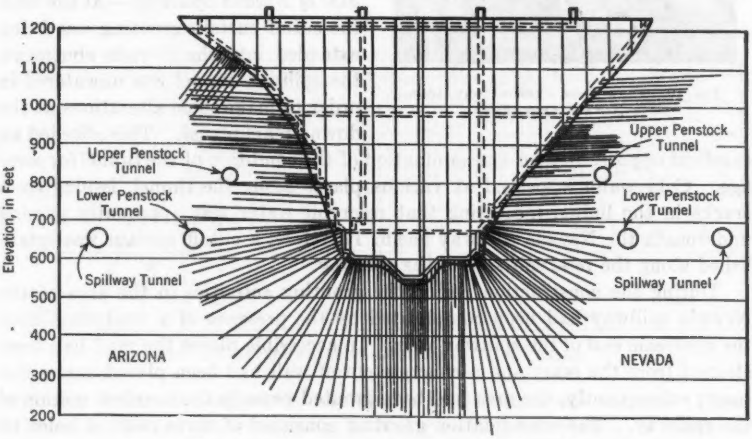

FIG. 9.—PROFILE OF DAM SITE SHOWING ADDITIONAL GROUT CURTAIN

intention of intersecting as many seams as possible; consequently, the holes on the river side of the tunnel were drilled pointing upstream and the holes on the abutment side pointing downstream.

In drilling holes in this area, cracks that produced large flows of water were penetrated at considerable depth. In order to dry up the wet areas in the tunnel, it was necessary to drill holes ranging in depth from 100 to 250 ft. The most effective procedure was to drill the deep holes and grout in stages, using packers and fairly high pressures. A total of 142 holes was drilled to an aggregate depth of 17,767 ft, and the amount of cement used in grouting this area was 6,589 sacks.

As the program progressed, it became necessary to extend the grout curtain deeper into the Nevada abutment. Deep holes were drilled, first from the Nevada penstock tunnel and then from the spillway tunnel. When drilling to the right of the spillway tunnel, cracks were found that yielded great flows

of water, up to 450 gal per min from a BX-size hole. Fig. 10 illustrates the flow encountered in a hole that had been grouted in stages to a depth of 178 ft. This flow was encountered in drilling 14 ft further. Over 56,000 sacks of cement were used in grouting this area.

Before the grouting was completed in this area, core holes were drilled for test purposes and for additional exploration of the abutment. Films of grout as thick as $1\frac{1}{4}$ in. were found in the cracks in the water-bearing area. Only a small quantity of seepage was obtained from the holes drilled through the grouted areas after the grouting was completed, indicating that the grouting program had been effective.

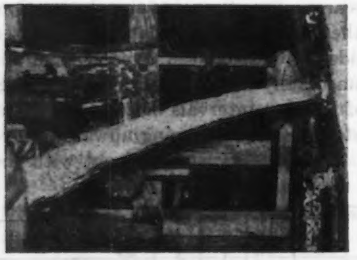

Fig. 10.—Flow From Exploratory Hole in Nevada Abutment

Curtain Grouting Along Reservoir Side of Nevada Spillway.—At the time the cutoff curtain grouting was being extended into the Nevada abutment, the spillway tunnel was unwatered in order to make some alterations at the downstream portal. This afforded an excellent opportunity for an examination of the condition of the tunnel for seepage. Cold water appeared at various places along the tunnel, issuing from cracks in the lining, indicating that reservoir water was apparently passing underneath the Nevada spillway basin. Therefore, a cutoff curtain was established along the reservoir side of the spillway.

During the construction period the grouting activities in the area of the Nevada spillway had been complicated by the presence of a mud seam near the upstream end of the spillway weir. In accessible places the mud had been cleaned from the seam and a concrete cutoff wall had been placed across the seam; subsequently, the area had been grouted beneath the overflow section of the spillway. The consolidation grouting consisted of three rows of holes 18 ft apart, the holes being spaced 20 ft on centers. The cutoff curtain consisted of a line of holes spaced 10 ft on centers, drilled along the reservoir side of the weir section to a maximum depth of 50 ft.

The additional cutoff curtain was placed along the upstream edge of the spillway section. At the time this grouting was done, the reservoir water covered most of the area. A casing was cemented into shallow holes in the foundation rock, and all drilling and grouting was performed through the casing. Detection of underwater grout leaks from the surface of the foundation rock was made by using a water scope, and leaks of this type were effectively sealed by manipulating the grout mix.

The additional cutoff curtain consisted of holes drilled approximately 10 ft on centers as shown in Fig. 11. The holes were drilled in a fan-shaped pattern at the upstream end of the spillway structure in order to extend the grout curtain into the abutment and were approximately vertical throughout the length of the structure. At the downstream end, the holes were inclined in a

downstream direction to connect with the main grout curtain of the dam between the penstock and spillway tunnels.

Drainage Program

As previously described, the first additional drains were drilled through the downstream toe of the dam from the gallery at El. 616 in the central section of the powerhouse, to relieve the uplift pressure acting over the downstream area of the base. As soon as this drilling had been effected, additional holes and grouting were organized in a systematic procedure. The work of drilling drainage holes was alternated with the drilling of grout holes in order to provide continuous employment for the drill crews.

New Drains Drilled From the Foundation Gallery.—As soon as all the additional grouting in a group of 6 or more holes of the new cutoff curtain beneath the dam had been completed by utilizing holes that were

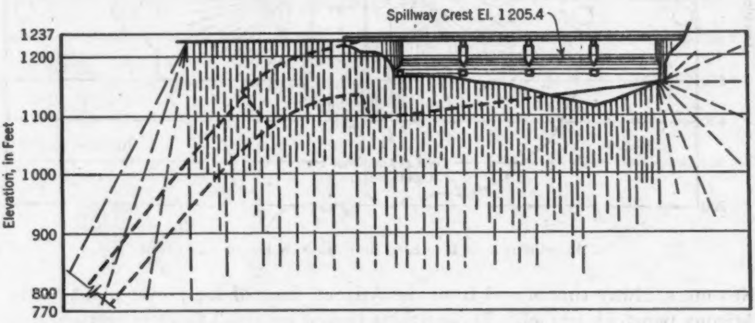

Fig. 11.—Nevada Spillway—Additional Grout Curtain

originally drains, drilling of the new drains in that area was started. These holes were arranged as shown in Fig. 12 and were drilled to maximum depths of 250 ft. The general plan was to drill these holes pointing downstream at an angle of 15° with the plane of the axis of the dam, and these new drains were drilled EX size.

At the beginning of the drainage program, the new drains were drilled to depths that produced a notable effect in the uplift pressure gages. By experimentation it was found that in the original river gorge, holes 170 ft deep drilled on 5-ft centers were effective. A spacing of 10 ft on centers was used across both benches at El. 600, and the holes were drilled slightly deeper in areas in which core drilling indicated defective rock.

The vertical shafts in which the spiral stairways were located were not designed to accommodate a diamond drill rig. Although the stair treads could be uncoupled and swung to one side to provide access to the gutter in which the drains were located, the center post did not afford sufficient clearance for setting up a diamond drill in the shaft. Additional drains, therefore, were not drilled from the shafts, but patterns of drain holes were laid out from the inclined stairways above and below the shafts to serve the abutment area,

and the holes were drilled from locations in which there was sufficient working space.

Additional drains were drilled in both abutments, downstream from the areas served by the curtain grouting. The drilling was done from the construction adits that extended from the Nevada wing of the power plant to the

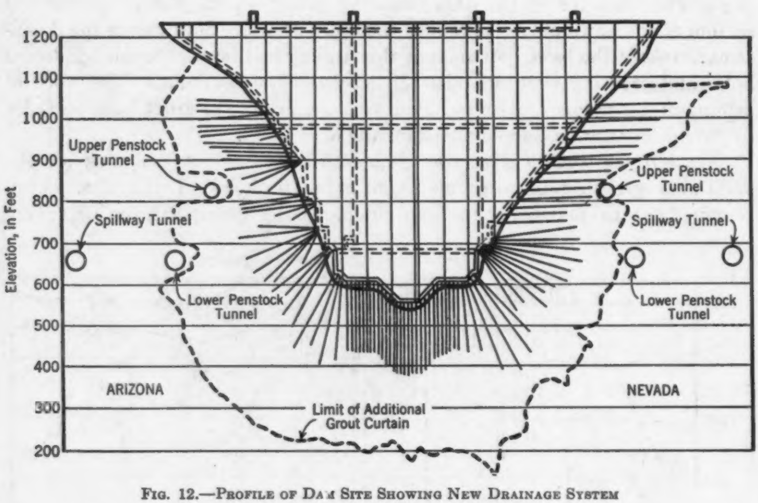

FIG. 12.—PROFILE OF DAM SITE SHOWING NEW DRAINAGE SYSTEM

Nevada spillway tunnel and from the Arizona wing of the power plant to the Arizona penstock tunnel. These drains picked up small flows of seepage that had passed the grout curtain and were effective in drying up wet areas on the canyon walls behind the back walls of the wing sections of the power plant.

RESULTS OF PROGRAM OF ADDITIONAL GROUTING AND DRAINAGE

Reduction in Uplift Pressure.—One of the most significant results of the program of additional grouting and drainage was the lowering of the uplift pressure on the base of the dam to considerably less than that used in the assumptions on which the design was based. Curves showing the uplift pressure before the work started in the fall of 1938 and the pressure that occurred during the high water period of 1949 are shown in Figs. 6 and 7. The pressure observed at set A along the line of centers of the dam is now considerably less than one half the magnitude of the pressure that occurred during the fall of 1938. The observed pressure at set B along the gallery at El. 705 on the Nevada side of the dam is about one third of the magnitude of the pressure that occurred during the fall of 1938. At set C, along the El. 705 gallery on the Arizona side of the dam, the observed pressure is now about one half that observed in 1938. The only zone beneath the base of the dam in which the uplift pressure may be greater than the two-thirds pressure line (B) is upstream from the grout curtain, an area in which there is no provision for

measuring uplift pressures. The uplift pressure at the downstream toe of the dam beneath the central section of the powerhouse has been reduced until it is no longer of any concern.

Reduction in Discharge from Drains and Seepage Water.—During the season of 1938, prior to starting the additional grouting, the seepage water entering the galleries from the foundation drainage system was in excess of 200 gal per min. Shortly after this program had been started, when a number of deep drains had been drilled to relieve the uplift pressure and very little grouting had been done, flows from the drains increased to over 2,000 gal per min. As the grouting progressed, the discharge from the drains decreased until it is now (1950) about 135 gal per min.

Prior to the grouting program, seepage water found its way into some of the construction grouting galleries that were not equipped with drainage systems. As the seepage water accumulated, it was customary to dip up this water in buckets and carry it out by hand. In 1935, a maximum of 95 buckets of water per week was removed from the galleries. As a result of the drying up of the abutments due to grouting, this seepage entering the galleries has been eliminated.

The drainage water from the abutment area that could be measured was that which entered the penstock tunnels. The bulk of the seepage found its way into the lower Nevada penstock tunnel, and a nominal volume of seepage entered the other tunnels. Before the grouting program was started, 3 pumps with a total capacity of 3,300 gal per min were used for pumping the seepage from the lower Nevada penstock tunnel, and weir measurements indicated that a maximum of 2,660 gal per min was pumped. This flow was reduced until the entire volume could be handled by a small eductor, and the pumps were removed from the tunnel.

Reduction in Maintenance Costs.—Prior to the additional grouting and drainage program, an item of major concern and expense was the protection of the penstocks and other metal work in the tunnels from the corrosive effect of the excessive seepage entering through the construction joints and porous concrete in the arches of the tunnels. This condition was especially bad in the lower Nevada and lower Arizona penstock tunnels. During the years 1939 and 1940 the services of from 4 to 5 pipe fitters with helpers were normally required to install and maintain metal troughs and other protective devices in the arches of the penstock tunnels. As the program progressed, less work was required; by 1946, the labor requirement had diminished until the work could be accomplished by the part time services of 1 pipe fitter and helper, and at present this work is no longer necessary. Repainting the penstocks to protect the metal cost $29,979.18 in 1939, but by 1946, the requirement for painting was only $5,894.16. The cost of pumping the seepage water from the tunnels amounted to $11,270.34 in 1939, but by 1946, this item was $5,861.68, and since 1946 there has been a further reduction in maintenance costs.

Cost of Grouting and Drainage Program

The entire program of foundation treatment at Hoover Dam extended over a period of years in which a wide variation of costs occurred. The work

was started in the pre-World War II period and extended through the duration of the war and into the post-war period. In order to make a fair comparison of the cost of this work, Table 1 was prepared to show the cost of foundation grouting and drainage of masonry dams constructed during the period from 1931 to 1947. The dates of the last cost reported used in compiling these data are included to show the approximate time that the work was completed.

In Table 1 the cost of the grouting and drainage is expressed in a percentage of the total cost of the structures only, and the cost of the respective appurtenant works of these dams is not considered. In general, the cost of foundation treatment ranges between 1% and 2%. In the case of the Owyhee Dam (in Oregon), an extensive program of grouting was necessary because of structural defects in the foundation. For this reason, the cost of the foundation grouting and drainage amounted to 4.97% of the cost of the dam. The Marshall Ford Dam (in Texas) was built in two stages, each of which required grouting and

TABLE 1.—COST IN DOLLARS OF FOUNDATION GROUTING AND DRAINAGE OF CONCRETE DAMS CONSTRUCTED BY THE USBR, 1927–1947

Dam	State	Total cost of dam	Volume of concrete (cu yd)	Foundation Grouting and Drainage		Date of cost report
				Cost	Percentage of total cost	
(1)	(2)	(3)	(4)	(5)	(6)	(7)
Gibson	Mont.	2,388,000	161,173	29,000	1.21	April, 1931
Deadwood	Idaho	1,359,000	55,463	13,000	0.96	June, 1931
Owyhee	Ore.	6,728,000	488,113	334,000	4.97	May, 1938
Seminoe	Wyo.	7,083,000	173,127	138,000	1.95	Aug., 1941
Parker	Ariz.-Calif.	4,695,000	290,640	48,000	1.03	Nov., 1942
Grand Coulee	Wash.	112,990,000	10,181,742	1,460,000	1.29	Dec., 1942
Marshall Ford	Tex.	23,395,000	1,838,167	572,000	2.46	May, 1947
Shasta	Calif.	74,567,000	6,353,227	676,000	0.91	May, 1947
Hoover	Ariz.-Nev.	77,549,000	3,251,137	1,840,000	2.38	July, 1947
Friant	Calif.	18,636,000	2,030,736	267,000	1.43	Dec., 1947

drainage. The result of this two-fold treatment was to bring the cost of grouting and drainage to 2.46%. The cost of the foundation grouting and drainage program at Hoover Dam amounted to $1,840,000, or only 2.37% of the cost of the dam.

SUMMARY AND CONCLUSIONS

The original plan for the foundation treatment at Hoover Dam by grouting and drainage, based on the satisfactory foundation treatment of 50 of the highest dams in service at that time, was not sufficient for the structure because of the exceedingly high pressure developed after the reservoir filled. The inadequacy of the treatment was indicated by seepage into the tunnels, seepage through the abutments, and excessive uplift pressure on the base of the dam. Geological defects in the andesitic formation comprising the foundation and abutments complicated these undesirable conditions and made additional treatment necessary.

To prevent seepage and to reduce uplift pressure, the depth of the grout curtain beneath the maximum section of the dam should have been about

300 ft (equivalent to 41% of the height of the dam) instead of the 21% used in the original design.

To render effective aid in controlling the uplift pressure on the base of the dam, the depth of the drain holes beneath the maximum section should have been about 200 ft (equivalent to 28% of the height of the dam) instead of the 14% used in the design.

To correct geological defects in the foundation and abutments, a program of washing and grouting inadequate areas was necessary. This part of the program was based on conditions uncovered by exploratory drilling.

For effective grouting, it was found that a combination of stage (or successive) grouting, with packer grouting was best. For packer grouting, drill holes from 1½ in. to 2 in. in diameter were necessary. The spacing of the holes varied with the conditions encountered, but in general, the spacing ranged from 5 to 20 ft measured along the foundation gallery.

The grouting procedure required the use of extremely thin grout mixtures and pressures as high as could be safely maintained without displacing the foundation rock. In general, the grout mixture used in the final grouting was thinner and the pressures somewhat lower than those used in the original grouting. The water cement ratio of the grout mixture used in the original program ranged from 7:1, measured by volume, for tight holes to 1:1 for holes in which leaks developed. The maximum pressures used were generally about 750 lb per sq in., although in a few holes pressures as high as 1,000 lb per sq in. were used. In the program of final treatment, the water-to-cement ratios usually ranged from 15:1 to 5:1, although in areas of tight rock the initial injections of grout occasionally consisted of 20:1 mixtures. Grout mixtures of these consistencies were generally pumped with pressures ranging from 550 to 600 lb per sq in. The use of a commercial retarder for the grout mixtures was advantageous in areas of hot alkaline water.

At the conclusion of the program of final foundation treatment, it was evident that by means of a judicious program of grouting and drainage, the seepage through the abutments can be practically eliminated, and the uplift pressure on the base of the dam can be controlled adequately and maintained at a value materially less than that used in the design assumptions.

DISCUSSION

JAMES B. HAYS,[4] M. ASCE.—The writer was fortunate enough to be familiar with the field work during the early stages of grouting under the base of Hoover Dam. The treatment of the sides in canyon walls was done later. Although it is easy to criticize afterward, the writer thought in his own mind, at the time, that the abutment grouting should have been extended to meet a ring-grouted cutoff curtain in each of the tunnels. If this had been done, each of the tunnels should have been grouted solidly all around for their full length upstream from the main curtain. Downstream from the main cutoff curtain, drain holes would have been included. Such treatment might have taken care of a large part of the leakage that developed later. However, it would not have solved all the problems. The right abutment was the source of a hot water supply that undoubtedly would have been affected by the reservoir when filled.

The drainage wells in the dam immediately downstream from the grout curtain were probably mostly in the grouted zone and not in the open rock where they should be to relieve upward pressure. The paper indicates this and explains how the problem was corrected. It has long been the writer's opinion, since the completion of Hoover Dam, that, in many cases, a general all-over drainage system is desirable under high concrete dams. Special attention must be given to drainage of known faults, seams, joints, or other water-carrying zones.

Some interesting facts concerning the effects of high-pressure grouting at Hoover Dam came to the writer's attention. The lower system of contraction joints had been grouted to about 200 ft from the base of the dam, using pressures limited to about 50 lb per sq in. The joints had copper seals to divide the work into 50-ft lifts and into two sections upstream and downstream. There was also a seal at the bottom just above the rock. The high-pressure foundation grout broke through the bottom seal and followed up the contraction joints that had already been grouted, for a considerable height.

The upstream toe of the dam had a shelf of concrete, or spread footing, projecting over the rock. At one point, where it was about 10 ft thick, the high-pressure grouting of a C-hole actually split the concrete. The author could possibly elaborate on this phase and give the correct data.

The grouting system provided for the abutments was neither protected by seals nor divided into sections, as were the contraction joints. Hence, there was difficulty in keeping the grouting pipes and tubes from being plugged when leakage developed from the foundation. It is understandable why the decision was made at the time to limit the foundation grouting on the abutment to avoid plugging the abutment contact grouting. Present hindsight judgment suggests that low-pressure consolidation grouting over the abutments would

---

[4] Chf. Engr., Kenney Dam, Nechako, B. C., Canada (British Columbia International Eng. Co. of Vancouver, B. C., Canada).

have corrected this. In the case of Hoover Dam, it would have been a difficult job due to the steepness of the walls. After the concrete was in place, the high-pressure grouting could have been completed. The drainage holes would have had to be deep enough to penetrate well behind the consolidated zone and at the same time well outside the high-pressure grout curtain.

The author's description of the re-grouting and re-drainage work is quite clear to one who was familiar with the general geology of the dam site, and furnishes answers to practically all the questions that would arise. The conditions are different at all dam sites. Each location is a problem in itself. Grouting is usually started from a basic pattern. As the work proceeds, a day by day study of the "take" or results determines whether additional work is needed or not. The geology must be studied as thoroughly as possible in order to produce the desired results.

The Hoover Dam experience, as well as that of some other dams, reveals the fact that the foundation treatment problem is frequently a much larger problem than is ordinarily visualized.

In some types of dams a certain amount of controlled leakage that will not harm the structure is permissible. Flood-control dams would fall in this category. In others, where the value of water is high, the allowable leakage is small. However, in all cases, the leakage should be handled through an adequate drainage system.

V. L. Minear,[5] M. ASCE.—This is a unique and valuable paper. It is unique, in that where the average paper glosses over or ignores mistakes, this paper points to certain rather serious errors in design and construction procedure, together with the measures taken to correct them. It thus offers a valuable opportunity to examine some of the present-day practices in the light of experience in the USBR over a period of twenty years on this dam.

Hoover Dam was designed and constructed when "***the available information on existing foundation conditions was inadequate." During the years that have elapsed, the science of engineering geology has made great strides in the field of foundation exploration. This has taken much of the guesswork out of foundation grouting and drainage. Modern practice consists of a program whereby the original grouting design, based upon the general information obtained during preliminary investigations, is modified in accordance with information which becomes available as construction progresses. Thus, after the site has been dewatered and the foundation rock exposed by stripping, the surface is cleaned meticulously so that surface manifestation of subsurface defects can be seen, measured, mapped, and studied. Thereafter, grout holes are drilled into the rock from end to end of the dam at close intervals along the cutoff. These holes are then pressure tested, pressure washed, and pressure grouted under the strictest control and with a complete record kept of the behavior of the foundation under known conditions. Moreover, it is common practice to put down additional core drilled exploratory holes in questionable areas. It has been found that, if these data are collected and

[5] Engr. (Foundations), Office of the Chf. of Engrs., U. S. Dept. of the Army, Washington, D. C.

analyzed as they become available, any engineering geologist who is "worth his salt" will have a detailed knowledge of subsurface conditions and will be in a position to give valuable advice to the construction forces. This goes far in eliminating the necessity for making important decisions on a trial-and-error basis. The employment of a competent full-time resident geologist costs money, but it has been found to be cheaper and more satisfactory than making "***a systematic exploration of the foundation*** by drilling BX-size core holes, in an attempt to find where defects in the foundation rock existed" (see under the heading, "Plans and Preparation for Corrective Measures") under completed dams showing signs of distress.

"The increasing uplift pressure on the base of the dam was of gravest concern to the engineers responsible for the safety of the structure." (See under the heading, "Increase in Uplift Pressure on Base of Dam.") Dams are being built, even today (1952), without provisions for making observations on the pressure acting on their bases. Uplift is an important consideration in the design of dams, yet actually little is known concerning how it develops, its intensities, and how and where it acts. Consequently, arbitrary assumptions are used in design. These easily can be in error in any specific case due to unknown or partly understood subsurface conditions, faulty grouting, the leaching out of an originally tight curtain, or the clogging of drain holes as time passes. The forces actually acting at any given time are the ones that are of real importance. These forces are easily and cheaply determined, and their magnitude compared with design assumptions, by installing and reading uplift gages, as described by Kenneth B. Keener,[6] M. ASCE. By means of the gages, ample warning is given so that remedial measures can be taken in time, should that become desirable. Had the USBR failed to install such gages in Hoover Dam and failed to make systematic reading thereon, the dangerous condition which developed might not have become known until possibly too late. The author states (see under the heading, "Inadequacy of Original Grouting"):

> "Because of the inaccessability of the leaks it became necessary to abandon the grouting of the leaking holes rather than take the risk of fouling the grouting systems of the abutment joints. This procedure left gaps in the cutoff curtain through which percolation developed."

It is not unusual to see present-day design showing gravel drains located in close proximity to areas which are to be pressure grouted. Pressure grouting, properly done, searches out any openings existing nearby and fills them with grout. Consequently, when grouting is begun, it frequently happens that hole after hole breaks into the drains. It is common practice under such conditions to thicken the grout and wash out the drains. The former is an euphemism for "kill the hole," and the latter is easier said than done. The result too often is that neither an effective drainage system nor a grout curtain is provided. Scheduling construction operations so that grouting precedes the placement of gravel, or substituting drain holes drilled after the grouting is finished, avoids this difficulty.

[6] "Uplift Pressures in Concrete Dams," by Kenneth B. Keener, *Transactions*, ASCE, Vol. 116, 1951, p. 1218.

Under the heading, "Inadequacy of Original Grouting," the author states:

> "On the Nevada abutment * * * several grout holes had penetrated a fault zone, and 4 grout holes in this area were abandoned, chiefly because of excessive quantities of grout that had been injected into them."

The treatment that should be given a hole that takes an exceptionally large quantity of grout is debatable. It is the writer's opinion that foundation problems should be solved at the time of construction, and, moreover, that abandoning or deliberately choking a hole which penetrates a leaking zone is no solution of the problem. It merely postpones the "evil day." Grouting, to stop leakage or to reduce uplift after the dam is in service, is a most discouraging experience. The rock generally is so saturated with water that the grout travels widely and there is no way to prevent it. Furthermore, not only does the flowing water carry away much of the grout, but there is also a tendency to build up a barrier near the toe, in the very area where free drainage is most desirable. This behavior makes grouting beneath a dam with full reservoir a hazardous undertaking unless uplift gages are available to serve as guides to changes in the distribution and intensities of uplift which accompany grout injection. These changes can be rapid and of alarming proportions. Because of the possibility of these and other serious consequences, it is felt that engineers should have more valid reasons for abandoning a hole than some preconceived notion of the amount of grout that it should take. This is not to say that the endless pouring of neat cement down a hole is advocated. When the formation is such that large grout "takes" are anticipated, specifications should provide for the use of fillers such as sand, bentonite, rock flour, flyash, or even clay, in preference to simply abandoning the hole and hoping for the best.

In effect, this paper is a case history of the progress made in the "art" of pressure grouting during the period elapsed since 1930. As such, it merits the closest study by those engineers interested in the design and construction of this highly specialized work.

BYRAM W. STEELE,[7] A. M. ASCE.—The entire program of foundation treatment for Hoover Dam is summarized in this paper in a way that should be very helpful in the foundation treatment of future dams regardless of size.

During the construction period it is not always possible to complete a finished program of foundation grout treatment. This fact should be obvious, but if it is, it is ignored in most cases; and, likewise, in most cases adequate provision for future grouting is not made at the time the construction of the dam is nearing completion.

Hoover Dam is a "near ideal" in regard to the manner in which foundation investigation and treatment were handled over a long period of years. This class of work is not readily accomplished by contracts because of the many elements of uncertainty that are continually arising which demand changes in procedure not readily made under contract specifications.[8] Foundation investigation and the later foundation treatment should be done by force account,

---

[7] Cons. Engr., Arlington, Va.

[8] "Treatment of Foundations for Large Dams by Grouting Methods," by A. W. Simonds, Fred H. Lippold and R. E. Keim, *Transactions*, ASCE, Vol. 116, 1951, p. 548.

rather than by contract, and it should be done by engineers who are familiar with conditions at the site of the work during construction. There are relatively few dam projects of any magnitude that cannot afford a drilling and grouting unit specially designed for this type of work, and a crew of experienced men to operate it until foundation treatment has been satisfactorily completed.

There is another phase of the grouting problem that is worthy of careful consideration. It is the necessity for the services of an experienced geologist in the early stages of the investigation and also during the grouting operations. A geologist who has had considerable experience in dam foundation treatment can contribute much to the success of the job by virtue of his knowledge of geological formations. Such knowledge is not usually possessed by civil engineers.

The writer would like to suggest that foundation treatment for future dams of any magnitude be set up on a force account basis rather than on a contract basis, and also that experienced foundation engineers be employed early in the pre-construction stage and then retained until all post-construction foundation treatment has been completed. In too many instances the foundation treatment is handled by inexperienced men with such equipment as is available on the job, with the result that effective treatment is not accomplished.

Last but not least, there is no easier way to waste time and money than by pumping cement grout into a hole in the ground without adequate checks on where the grout is going and whether it is doing any good. Here is where the geologist's knowledge of foundation formations is valuable. It can be used to excellent advantage in planning a well-coordinated program for all phases of the drilling and grouting; and it will be valuable later, when interpreting the diamond-drill cores of a few typical areas to see whether the penetration of grout anticipated has been accomplished, and whether the grout in the cracks and crevices is dense and impervious, or porous and chalky.

William H. McAlpine,[9] Hon. M. ASCE.—A frank and quite complete description is presented of the many problems connected with grouting and the foundation treatment required to reduce uplift pressures and leakage of the dam to reasonably safe proportions. It should be very helpful to the many engineers and geologists engaged in the design and construction of dams on rock foundations, especially the higher dams on the poorer rocks. It may be regarded as a sequel to papers by other authors.[10,3,6]

The author does not indicate what uplift assumptions were made in the design of the dam, but it is quite evident that the depths of grout curtain and drainage wells were quite inadequate for the character of the foundation and height of the Hoover Dam. Since the construction of this dam was first begun, there has been a great impetus in the construction of many high dams by government agencies who employ large engineering organizations including specialists and outside consultants, from time to time. As a result, there has

---

[9] Chf. Engr., Office of the Chf. of Engrs., U. S. Dept. of the Army, Washington, D. C.

[10] "Correction of Reservoir Leakage at Great Falls Dam," by A. H. Weber, *Transactions*, ASCE, Vol. 116, 1951, p. 31.

been a decided advance in the "art" of subsurface explorations and foundation treatment, including grouting and drainage. Nevertheless, a carefully planned foundation treatment frequently must be modified during construction because of conditions not fully disclosed by the borings.

Finally, it seems possible that the knowledge to be gained from the uplift observations made on numerous dams may lead to some economy in design.

FRED H. LIPPOLD,[11] M. ASCE.—The problems and complications involved in an adequate treatment of the foundation of a high masonry dam are presented admirably in this paper. No "rule of thumb" method can be used in designing a foundation grouting and drainage treatment program; each foundation has its individual problems that can, and do, vary as much as the individual geologic formations at different sites. Minor faulting and zones of shearing at different locations would have affected, materially, the grouting program at Hoover Dam. The paper also shows the desirability of a thorough foundation treatment program during initial construction to alleviate the probability of additional treatment at some later date.

Of particular interest to the writer was the number of holes that were abandoned during the initial grouting program. It is realized that even under ideal conditions it is occasionally necessary to abandon grouting any hole because of excess leakage, but the percentage at Hoover Dam seems high. Subsequent inability to regrout the zone by reopening the same hole would tend to prove the theory that the most effective way to grout any open zone or seam is through the first hole connecting to it. Although there may be a limit to the volume of cement that should be injected into any one hole, the total is indeterminate unless it is known exactly where the grout is going. Certainly such a limit would be high. Adjacent holes just a few feet away often miss the seam or intersect it where it is tight, with the net result that an excessive amount of drilling is required to complete the job.

Much was learned about both the design and technique of foundation treatment at Hoover Dam, and on more recent construction the initial treatment is far more complete. However, due to peculiar geologic conditions it could still be necessary to perform some additional work after a dam is in operation. Based on this realization, pipes for grouting are usually spaced at 5-ft centers along the foundation gallery even though it is contemplated that such close spacing may not be required by the method of closures during the initial construction. The unused pipes can be used for additional treatment if softening of seams, foundation deflection, or some other latent foundation defects appear after the reservoir is filled.

It is seldom, if ever, possible to create a grout curtain that will not allow a small amount of percolation. The drainage holes are designed to pick up these flows and relieve the uplift pressure. However, the drainage holes (like grout holes) can fail to intersect seams or can cross them where they are locally tight. Where flow from foundation drains is not high, additional drainage holes often effectively reduce the uplift at a nominal cost. This method of uplift relief has

[11] Engr., Bureau of Reclamation, U. S. Dept. of the Interior, Denver, Colo.

been used on two USBR dams of medium height in recent years. The great difference in cost dictates that this method should be studied thoroughly before an extensive supplemental grouting program is begun. Where seepage flows are high (such as they were at Hoover Dam) additional grouting is called for, but in addition the supplemental drainage-hole pattern was probably much more effective than the original one.

The paper also shows the need of extensive foundation treatment in the case of an extremely high dam even where the foundation is relatively good. A less competent foundation might not have been susceptible to successful treatment by pressure-grouting methods alone. The quantity of water flowing from some of the holes effectively shows that when cutoff drifts or shafts may be required, they must be built before the reservoir is filled. The problems of pressure grouting a foundation under full reservoir head are complex, as well as costly. There must have been many difficult problems in performing the actual operation. It is gratifying to know, however, that even under such adverse conditions, pressure grouting and drainage were capable (although admittedly costly) of relieving the undesirable conditions.

O. E. Boggess[12].—An excellent presentation of factual data on foundation problems at Hoover Dam and their ultimate solution is contained in this paper. The necessity for extensive additional grouting, as outlined by the author, demonstrates the importance of a thorough job of foundation treatment during construction. The regrouting of the foundation of a dam, particularly a high dam, after the reservoir has filled and the dam is in operation, presents a difficult and expensive operation. As engineer in charge of the work at the site, the writer observed first hand the problems encountered during the regrouting of Hoover Dam.

Many of the holes carried large flows of water under high pressure (150 lb per sq in. to 200 lb per sq in.). This condition made drilling much more difficult and hazardous than usual. In addition to slowing down the drilling speed, the threat that drill rods would become free and plunge out of the hole under the heavy flow and high pressure was always present.

In one instance, during the drilling of a horizontal hole, a slip of a wrench caused 400 ft of drill rods to come out of the hole as if they had been shot out of a cannon. Fortunately, the only casualty was a mangled mass of drill rods. Only experienced and seasoned drillers were used on this work.

The problem of unobserved grout leaks into the reservoir did not prove serious at Hoover Dam. The tendency of the grout to follow the line of least resistance in a downstream direction was often noted by an increase in the uplift pressure gages throughout the dam. The direction of the grout travel and the extent of the area being grouted was well indicated by the action of the uplift gages. In most instances where the uplift gages showed an increase in pressure during grouting, the readings decreased to somewhat below the original reading after the hole was completed. The back pressure at the collar of the hole was checked periodically during grouting. When back pressure was near reservoir head at the elevation of the hole and remained stationary, it was

[12] Engr., Bureau of Reclamation, U. S. Dept. of the Interior, Denver, Colo.

suspected that grout was leaking into the reservoir. As a final determination, air was forced into the hole and the reservoir surface was watched for air bubbles. If air bubbles showed through the reservoir, the grout mixture was gradually thickened until the hole sealed off. It is believed that very little grout was lost through leaks into the reservoir.

Relatively thin grout mixtures were used in the regrouting at Hoover Dam. After experimenting with various mixes, it was found that even holes that accepted water freely would plug prematurely after a few sacks had been injected unless a starting mixture of thin grout was used. In leaks that were observed a considerable distance from the hole, it was often noted that the water-cement ratio (w/c) of the grout at the leak was much lower than that of the grout being injected. This indicated that the water was being forced out of the grout as it traveled through the rock. Since this condition existed after the reservoir filled and the foundation rock had become saturated, it would appear that even thinner mixes would be necessary during construction when the foundation rock was comparatively dry. The author mentions hole A-124 in the Arizona abutment that accepted a total of 8,258 sacks. This hole was started with a w/c of 10:1. During the injection of the first 100 sacks the w/c was gradually reduced to 6:1. Several attempts were made to reduce the w/c to 5:1 as the grouting progressed, but each time the hole showed signs of tightening up and the w/c was changed back to 6:1. The grouting of this hole had a widespread effect in drying up the Arizona abutment, particularly in the upper penstock tunnel.

There were many interesting problems during the course of the operation but by continued efforts they were overcome and in retrospect appear minor. The final result is proof of the effectiveness of the program, and the foundation conditions must have been materially improved.

H. Cambefort[13].—This extremely interesting paper illustrates how an initial deficiency in tightness and drainage of the foundation has been successfully remedied.

The French engineer who specializes in this kind of work, and is accustomed to foundations of dams consisting of cracked limestone, is astonished to discover that the depth of the cutoff curtain of Hoover dam was determined by a statistical study of the depths of grout curtains established at other dams, and that a reconnaissance of the foundation was made only for corrective purposes. Such a method may be justifiable for dams on rivers whose bed is alluvial, but not for large dams founded on rock. In this case, the subterranean water circulates in the cracks or joints of the rocks at great depths, causing uplift pressures or high leakage flow.

The science of geology provides no means of determining the depth to which grout should be forced. Only an investigation by core drilling with clear water and water testing, as the hole is deepened, can be accepted as precise. These water tests are performed by placing a cap below a test section of about 5 m (16.4 ft) in the foundation drill hole. Clear water is pumped into this section. A manometer indicates the pressure, and a meter indicates the volume of water

[13] Civ. Engr., School of Bridges and Highways, Prof. of Soil Mechanics, School of Public Works, Paris, France.

injected during a fixed time—in general, equal to 10 min. The unit pressures are progressively increased up to 2, 4, 6, 8, . . . kg per sq cm, for example, and the tests must be completed in decreasing the pressures in the same sequence—8, 6, 4, 2 kg per sq cm.

The flow curve, plotted as a function of the pressure, provides ample indications of any cracking in the rock. Eventually, it leads to the evaluation of the coefficient of permeability of a pulverulent soil which is equivalent to the broken rock. Thus, the extent of the leakage can be computed from the leakage itself.

When the water test of a section is finished, the cement is injected, thus providing a way to interpret the subsequent tests; and, at the same time, the procedure assists in determining the magnitude of cement absorption necessary to tighten the broken rock mass.

Experience indicates that it is uesless to inject grout into rock in which the absorption, in the course of tests, is not more than 1 liter per min per m (0.08 United States gal per min per ft of hole) under a pressure of 10 kg per sq cm (142 lb per sq in.)—the test lasting 10 min. The equivalent coefficient of permeability is of the order of 10^{-7} m per sec (3.28×10^{-7} ft per sec). These criteria have been established by Maurice Lugeon,[14] in relation to dams more than 30 m (98.4 ft) high. For lower dams, one can be content with 0 maximum of 3 liters per min per m (0.24 United States gal per min per ft of hole). Criteria such as these, which eliminate all personal factors, are certainly better than those that consist merely of obtaining a core sample of sound rock 1.50 m (4.92 ft) long. The fixed injections are always made on sections or stages about 5 m (16.4 ft) long to avoid the sedimentation of cement which occurs in longer sections and which seals the entrance to the cracks before they can be grouted. Such injections can be made as the drilling advances, from top to bottom; they can be made in reverse order, from bottom to top, which plainly separates the operation of drilling from that of grouting.

Before beginning the injection, a brief test of water pressure is made to clean the cracks and to determine the proportions of the grout to be used at the outset. During the injection, if the pressure does not increase, the engineer increases the proportions of the grout progressively (that is, he reduces the water-cement ratio).

The very large cracks are closed quickly with a mixture of cement, clay, silicate of sodium and water, which is a thixotropic mixture and is intended not to penetrate very far. Thereafter, ordinary cement grouting is completed. The cleaning of cracks as practiced at Hoover Dam sometimes yields good results, but not always. Finally, the spacing of the injection bore holes (grout holes) is determined by a preliminary test involving two or three bore holes with a control hole in the center. The variations in the quantities of cement injected supply an index of the modification required of the spacing selected for the test.

These procedures (used in France for several decades) utilize the same principles as those used in the United States, but they differ in details as stated herein.

---

[14] "Barrages et géologie," by Maurice Lugeon, Dunod, Paris, France, 1933, p. 87.

A. WARREN SIMONDS,[15] M. ASCE.—The question that so often arises in grouting the foundations of dams—whether the program of treatment, as designed, will be adequate, inadequate, or more than adequate—is raised indirectly by Mr. Hays. The most opportune time for providing adequate treatment of the foundation is during the construction period. However, one cannot be sure of the adequacy of the foundation treatment until after the reservoir has filled and seepage or leaks begin to develop. If the curtain grouting at Hoover Dam had been extended during construction to meet the ring-grouted cutoffs in each of the tunnels (as mentioned by Mr. Hays), the foundation conditions would have been improved, but it is probable that some additional work would have been required later.

As Mr. Hays points out, the drainage holes should be placed a sufficient distance downstream from the grout curtain to penetrate ungrouted rock. After the small seams in the rock have been partly blocked by grout, holes drilled in such an area are rarely as efficient for drainage purposes as those drilled in ungrouted rock. When the high uplift pressures were first noticed, an attempt was made to control this pressure by drainage only. A few holes were drilled in strategic places to lower the uplift pressure, but the discharge from them was so great that it taxed the capacity of the sump pumps within the dam. It was then decided to proceed with the additional grouting in order to reduce the flow of water through the foundation. The drainage holes drilled subsequent to the grouting program were effective in reducing the uplift pressure with only a nominal discharge.

The occasionally-observed travel of grout over long distances was always an item of concern to the engineers in charge of the grouting at Hoover Dam. The travel of grout into the contraction joints did not recur during the program of additional grouting. However, grout did travel extensively through the abutments at times. While holes were being grouted in the Arizona abutment in the area between El. 800 and El. 900, grout leaked from cracks in the concrete lining of the lower penstock tunnel throughout a wet area over 400 ft long in the arch of the tunnel. This grouting resulted in drying a large part of the wet area. While another hole in this same area was being grouted, grout leaked into the tunnel about 200 ft below the hole. This leak was sealed, and the grout traveled upward and broke out through the highway, crossing the dam a short distance beyond the abutment.

Mr. Hays also mentions the possibility of cracking concrete by grout pressure in holes drilled through concrete, as was experienced while grouting beneath the upstream toe of the dam. As a result of this experience, it became standard practice to encase all such holes prior to grouting. The USBR later adopted a practice of eliminating the casing and setting a packer in the grout hole in the foundation rock immediately beneath the concrete, thereby preventing the pressure of the grout from acting on the concrete. Satisfactory grout packers had not been developed at the time Hoover Dam was constructed.

Messrs. Hays, Minear, Steele, and Lippold emphasize the necessity of obtaining reliable geologic information. In the construction of large dams, where a large expenditure of money is involved, the full-time services of a

[15] Engr., Bureau of Reclamation, U.S. Dept. of the Interior, Denver, Colo.

competent engineering geologist is desirable. However, some underground exploration of the foundation by core drilling is necessary to supplement the geological observations at the surface. In many cases it is the underground conditions not readily discernible at the surface that are the sources of trouble.

Mr. Minear emphasizes the value of uplift pressure indicators at the base of the dam. This relatively inexpensive equipment has proved of great value for giving warning of undesirable conditions not only during the initial filling, but throughout the life of the reservoir. The installation at Hoover Dam proved to be worth many times its cost during the period of grouting operations, because it was the only means of indicating exactly what conditions were developing as the grouting progressed.

Mr. Minear also calls attention to difficulties that arise when drainage systems are installed in areas where grout leaks may possibly develop. Grout leaks into drains frequently result in impairing the efficiency of the drains or, occasionally, even in rendering them worthless. If no provisions for protection of the drains are made at the time of construction, water may be introduced into them during the period of grouting and, if necessary, held under pressure, or the drains may be flushed at frequent intervals. However, as soon as grout has found its way into a drain, it is likely that its efficiency will never be as great as before it was contaminated.

Regrouting a dam foundation to stop leaks and control uplift pressure can be a most discouraging procedure at times, as Mr. Minear emphasizes. If an open passageway is the source of leakage, it should be plugged adequately when a connection for grouting has been established. Stopping the grouting before the passageway is effectually sealed usually invites future trouble. In view of the possibility of the flow of water carrying the cement grout to the downstream area of the foundation and establishing a cutoff in the wrong place, the following precautions were taken. Before starting the program of additional grouting, a series of drain holes was drilled into the foundation below the downstream toe of the dam from one of the lower galleries in the central section of the power house. The discharge from these drains was checked frequently for indications of grout, but none appeared. This procedure, together with observations of uplift pressure, served to indicate any change taking place in the foundation beneath the dam.

Mr. Steele mentions the value of doing foundation investigation and treatment by force account rather than by contract. The flexibility of procedure provided by a force account crew was advantageous on many occasions when unforseen developments made additional exploration necessary. The ability to continue grouting on a "slow" hole as long as it was felt desirable contributed to better control of the grouting operations. This eliminated such trickery as opening and closing the blow-off valve of the grout supply line under pressure to "slug off" a grout hole, altering pressure gages to show erroneous readings, and mixing the grout insufficiently in order to plug an unprofitable hole with thick grout.

Mr. McAlpine's discussion indicates that the uplift assumptions used in the design of the dam were not clear as stated by the writer. The magnitude of the uplift pressure was assumed to vary as a straight line from full reservoir

pressure at the upstream face to zero or tailwater pressure at the downstream face. On the three sections of the dam in Fig. 6, this gradient is shown as "Full Reservoir Pressure Line C." It was further assumed in the design of the dam that the uplift pressures were effective over two thirds of the area of the base. It is realized that the question of the area over which the uplift pressure is effective is subject to a diversity of opinion.[6] The gradient shown in Fig. 6 as "¾ Pressure B" was used as a warning gradient. When the uplift pressure at a section reached values lying above this line, plans were begun for correcting this condition. Before the additional grouting commenced, however, the uplift pressure exceeded the full reservoir gradient used in the design. The areas of excessive uplift pressure were along the Nevada side of the dam and beneath the downstream toe of the dam under the central section of the power plant.

Mr. Lippold's discussion is a valuable addition to the paper in that it emphasizes the effect of local geological conditions on uplift pressures and upon leakage through the foundation. His comments relative to thorough foundation treatment during the initial construction period, as compared with additional treatment at some later date, are reasonable. He emphasizes the fact that the purpose of the grouting program is to control seepage beneath the dam and that of the drainage program is to relieve pressure.

Mr. Boggess comments on the complex problems encountered in regrouting the foundation of a high dam under full reservoir pressure. The difficulties encountered in drilling grout holes that produced large flows of water under pressure are well described. He also explains the use of the uplift pressure gages when grouting with full reservoir pressure against the dam. His discussion emphasizes the necessity of using relatively thin grout mixes in regrouting the foundation rock and cites a typical example of the behavior of grout holes under variations of grout mixes.

It is interesting to note from Mr. Cambefort's discussion that the grouting procedures used in France are based on the same principles as are those used in the United States, but that the two vary somewhat in details. In regard to determining the depth of grout holes used in the original grouting of the foundation of Hoover Dam, the investigation of the foundation treatment of fifty high dams was a study to determine what precedent, if any, existed in the case of extremely high structures. This study was supplemented by field investigations consisting of core drilling twenty-two holes and driving two test tunnels. Information thus obtained was the basis for deciding upon the maximum depth of 150 ft for the original cutoff curtain holes.

The method of precise water testing of sections of an individual hole can serve to determine the depth of that hole in most cases. However, in designing a dam, dependence on water tests only is not advisable. If there are definite geological defects beyond the effective range of the water tests, they should be investigated by a competent geologist, and plans should be made for adequate treatment. In the final grouting at Hoover Dam, the section of the grout holes used for determining the depth of the hole in most cases would meet the criteria for permeability set forth by Mr. Cambefort.

There is considerable difference between grouting a limestone foundation that is full of large cracks and a foundation of igneous origin, such as the andesitic breccia at Hoover Dam. In the former case, there is merit in using a grout mixture of cement, clay, sodium silicate, and water intended not to penetrate beyond the foundation area of the dam. In the case of the andesitic formation at Hoover Dam that was subjected to extremely high reservoir pressure, it was necessary to use a thin grout of neat cement and to force it far into the foundation and abutments, at times, to effect an adequate stoppage of leaks. It is gratifying to have the details of the procedures used in France available for comparison with those used in the United States.

AMERICAN SOCIETY OF CIVIL ENGINEERS
Founded November 5, 1852

TRANSACTIONS

Paper No. 2538

INFLUENCE LINES BY CORRECTIONS TO AN ASSUMED SHAPE

By James P. Michalos,[1] A. M. ASCE, and Edward N. Wilson,[2] J. M. ASCE

Synopsis

An analytical procedure is presented for obtaining influence lines for continuous structures by successive numerical corrections to an assumed shape. The structure may have any variation in cross section and may or may not be subject to sidesway. Any degree of precision is possible.

Introduction

In the design and analysis of continuous structures, influence lines are virtually essential. The usual method of constructing influence diagrams is by computing influence values for different positions of a unit load applied to the structure. This is rather tedious work, and the method is not particularly suitable to quick approximations which may be adequate for design purposes.

A procedure is presented in this paper for determining influence lines for any continuous girder or rigid frame by successively correcting an assumed shape. It can be used to obtain approximate influence lines for preliminary design or to obtain precise influence lines for final design and analysis. Certain factors related to those used in moment distribution[3] are employed, as are certain values generally available in tabular or graphical form. The procedure is based on two concepts:

1. The Müller-Breslau influence line theorem[4]; and
2. A concept by which the influence line for a continuous structure is obtained by adding corrections to an influence line obtained by neglecting continuity.

Note.—Published in April, 1952, as *Proceedings-Separate No. 124*. Positions and titles given are those in effect when the paper was received for publication.

[1] Associate Prof. of Civ. Eng., Iowa State College, Ames, Iowa.

[2] Structural Engr., Fruin-Colnon Contracting Co., St. Louis, Mo.

[3] "Analysis of Continuous Frames by Distributing Fixed-End Moments," by Hardy Cross, *Transactions*, ASCE, Vol. 96, 1932, p. 1.

[4] "Die Graphische Statik der Bankonstruktionen," by H. Müller-Breslau, 5th Ed., Vol. 2, Part 1, A. Kroner, Stuttgart, Germany, 1922.

The procedure involves an assumption of a statically possible solution. Such an assumption introduces errors in the geometry which are then adjusted, to any required precision, by successive corrections.

General Procedure

A powerful means for visualizing the shape of any influence line results from a principle stated by H. Müller-Breslau.[4] From this principle it follows that, if a unit deformation corresponding to the particular function—such as moment, shear, or reaction—under consideration is produced, the deflected structure draws its own influence line. By means of this concept influence lines may be quickly sketched. However, to obtain quantitative results it is necessary to evaluate individual ordinates to the line. This is usually done by computing the value of the particular function under consideration for different positions of a unit load.

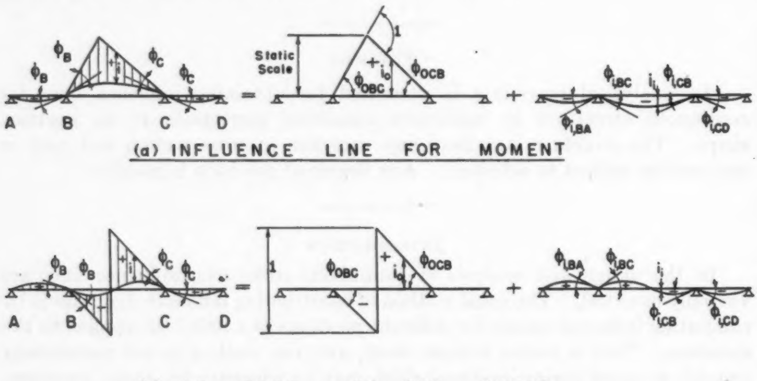

Fig. 1.—Influence Lines by Combining an Assumed Solution and a Correction

A quantitative scale can be obtained by constructing the influence diagram in two steps. First, the structure is considered cut so that it becomes statically determinate, and the influence line is drawn for the statically determinate span. Ordinates to this line can be determined exactly by computations of statics or from a consideration of the geometry of the bent line resulting from the application of a unit deformation. Secondly, correction deformations necessary to restore continuity are applied. If the deflected load line resulting from these correction deformations is superimposed on the statical influence line, an influence diagram for the continuous structure is obtained. Superposition to obtain influence lines, using computed influence ordinates, has been demonstrated elsewhere.[5]

Fig. 1 shows influence lines obtained in two steps. A solution which satisfies statics is assumed; but this assumption involves errors in the geometry, and a

[5] "Continuous Frames of Reinforced Concrete," by Hardy Cross and N. D. Morgan, John Wiley & Sons, Inc., New York, N. Y., 1932, pp. 249–252.

correction pattern is added such that the requirements of continuity are also satisfied. End slopes, ϕ, and ordinates, i, are obtained from

$$\phi = \phi_o + \phi_i \qquad (1a)$$

and

$$i = i_o + i_i \qquad (1b)$$

The subscripts o and i are associated with the assumed and the correction values, respectively. The angles will be considered positive when they are measured clockwise from the original position of the load line. The ordinates will be considered positive when they are on one side of the original position of the load line and negative when they are on the other side.

In Fig. 1 the unbalanced angle of the assumed static solution splits into the final angle and the correction angle. Thus, to restore continuity it is necessary to rotate the cut ends through a total relative angle equal to the angle of the assumed solution. In other words, the arithmetic sum of the correction angles at a joint is always known. The magnitude of the individual correction angles will depend on the relative flexibilities of the adjacent parts of the structure. By splitting the unbalanced angles, as best as one can, in proportion to the relative flexibilities, fairly accurate results are possible. To obtain precise results it is necessary to determine the correction angles and the corresponding displacements precisely. In what follows, first a method is presented for determining the correction angles to any desired accuracy, and then a method is presented for obtaining correction ordinates to a precision of the same order as that of the angles.

Determination of Correction Angles.—The method of moment distribution for determining moments at the joints of continuous structures is universally known. Since end slopes and moments are related, angle distribution has been proposed for use in analyzing continuous structures.[6] In addition, an angle distribution procedure has been used to construct an influence line for a beam of constant moment of inertia.[7]

In this section a perfectly general distribution method is presented for determining correction angles, ϕ_i. The structure is considered cut at all supports, and the correction angles are obtained by successively distributing unbalanced angles. Unbalanced angles are distributed in proportion to relative flexibilities, F, and each distributed angle induces an angle, called the carry-over angle, at the far end of the member. The carry-over angles are determined by multiplying the distributed angles by angle carry-over factors, $\mathcal{C}$.

Suppose that a discontinuity, ϕ_o, is introduced by member AO at joint O of the frame in Fig. 2. To restore continuity at the joint, member AO and the remainder of the frame as a whole must be rotated relative to each other until the discontinuity is removed, that is, until all members framing into joint O have the same slope, ϕ. The stiffnesses, K, in Fig. 2 represent the moment necessary to rotate a member through a unit angle, the far end being hinged or fixed, as the case may be. For example, K_{OA} is the moment necessary to

[6] "Analysis of Continuous Frames by Balancing Angle Changes," by L. E. Grinter, *Transactions*, ASCE, Vol. 102, 1937, p. 1020.

[7] "Determining Influence Lines by Balancing Angle Changes," by L. E. Grinter, *Engineering News-Record*, Vol. 121, 1938, p. 443.

rotate member OA through a unit angle at joint O, end A being hinged, as shown. Flexibility is defined as the rotation per unit moment, or I/K. An unbalanced angle ϕ_o at joint O, Fig. 2, is distributed among the members of the joint as follows: ϕ_{iOA} to the member introducing the discontinuity, and ϕ to all other members. Since the sum of the moments at joint O must equal zero,

$$K_{OA}(\phi_o - \phi) = (K_{OB} + K_{OC} + K_{OD})\,\phi \qquad (2)$$

from which

$$\phi = \frac{F_{OBCD}}{F_{OA} + F_{OBCD}}\,\phi_o \qquad (3)$$

Also in Fig. 2

$$\phi_{i\,OA} = -(\phi_o - \phi) = -\frac{F_{OA}}{F_{OA} + F_{OBCD}}\,\phi_o \qquad (4)$$

In Eqs. 2, 3, and 4, $F_{OA} = \frac{1}{K_{OA}}$ expresses the flexibility of member OA at end O; and $F_{OBCD} = \frac{1}{K_{OB} + K_{OC} + K_{OD}}$ defines the group flexibility of members OB, OC, and OD.

In distributing angles, joints are considered free to rotate, and it is necessary to modify the usual tabulated values of stiffness (end fixed) by multiplying such values by $(1 - C_{AB}\,C_{BA})$, in which C_{AB} and C_{BA} are moment carry-over factors from end A to end B and from end B to end A of a member, respectively. Values of stiffness, far end fixed, and of moment carry-over factors are generally available.[8]

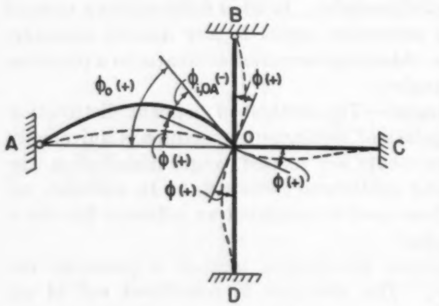

FIG. 2.—DISTRIBUTION OF AN UNBALANCED ANGLE

It can be shown that the angle carry-over factor, $\mathcal{C}_{BA}$, from end B to end A of any member is always numerically equal, but opposite in sign, to the moment carry-over factor, C_{AB}, from end A to end B. That is,

$$\mathcal{C}_{BA} = -C_{AB} \qquad (5)$$

Table 1 illustrates the method of determining correction angles in the general case of a continuous beam with a variable moment of inertia. Table 1(*a*) contains the constants used in distributing angles, and the moment distribution constants from which they were computed. Attention is called to the fact that a modified stiffness (stiffness, end hinged) was not used for member CD, in Col. 4. The distribution procedure is simplified if end D is considered fixed, as it actually is. If a modified stiffness were used for CD, it would be necessary to restore the angle at D to zero after each carry-over.

[8] "Handbook of Frame Constants," Portland Cement Assn., Chicago, Ill., 1947.

Inasmuch as only two members meet at each joint, the correction angles to be distributed are directly proportional to the flexibilities of the individual members.

The actual distribution of unbalanced angles is shown in Table 1(*b*). Angle distribution factors are indicated in boxes above the joints, and angle carry-over factors are written above arrows indicating the direction of the carry-over.

TABLE 1.—Correction Angles, Continuous Beam with Variable Moment of Inertia

(*a*) Distribution Constants

Member	Moment Distribution Constants			Constants for Distributing Angles		
	Moment carry-over	Relative Stiffness: Fixed end	Relative Stiffness: Hinged end	Angle carry-over	Relative flexibility	Distribution factor
(1)	(2)	(3)	(4)	(5)	(6)	(7)
AB	0.879	0.162	...	...	...	...
BA	0.418	0.341	0.216	−0.879	4.63	0.514
BC	0.711	0.400	0.227	−0.609	4.40	0.486
CB	0.609	0.467	0.265	−0.711	3.77	0.483
CD	0.907	0.248	...	...	4.03	0.517
DC	0.562	0.400	...	...	...	...

(*b*) Distribution of Unbalanced Angles

(b)

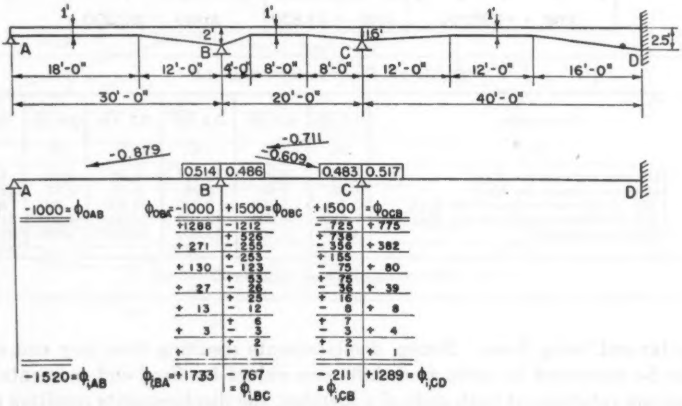

For purposes of illustration, unbalanced angles of − 1,000 at each end of member AB and + 1,500 at each end of span BC have been assumed. These values have been underscored twice to separate them from the successive corrections. Signs are determined automatically. As previously explained, angles are considered positive when they are measured clockwise from the original position. The distribution to the member introducing the unbalanced

angle is opposite in sign to that angle, whereas the distribution to the other member (or members) is of the same sign as the unbalanced angle. Because end A is hinged, no carry-over would be made from end A to end B. Consequently, it is not necessary to make intermediate carry-overs from B to A.

Determination of Correction Ordinates.—Consider an influence line for a fixed-end moment. The ordinates to such an influence line, for members of various shapes, can be found in many available tables and charts,[8] but from the Müller-Breslau principle, these ordinates are displacements of the load line that result from the application of a unit rotation at the end of the member,

TABLE 2.—ORDINATES OF THE DEFLECTED LOAD LINE WHEN END ANGLES ARE KNOWN

(a) DEFLECTION ORDINATES FROM END ANGLES

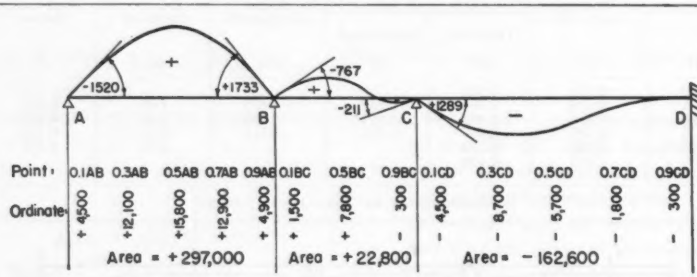

(b) DETAIL COMPUTATIONS, SPAN AB

Description (1)	$0.1\ \overline{AB}$ (2)	$0.3\ \overline{AB}$ (3)	$0.5\ \overline{AB}$ (4)	$0.7\ \overline{AB}$ (5)	$0.9\ \overline{AB}$ (6)	Area (7)
Influence ordinate for M_{AB}[a]	2.32	3.63	2.44	0.85	0.07	54.6
Influence ordinate for M_{BA}[a]	0.56	3.81	6.98	6.70	2.77	123.7
1,520 × influence ordinates for M_{AB}	3,520	5,500	3,700	1,300	100	83,000
1,733 × influence ordinates for M_{BA}	980	6,600	12,100	11,600	4,800	214,000
Deflection ordinate	4,500	12,100	15,800	12,900	4,900	297,000

[a] Their values are available in various publications.

the far end being fixed. Hence, displacements resulting from any end angle may be computed by ratio from influence values for fixed-end moments. If there are rotations at both ends of a member, the displacements resulting from each end angle can be computed separately and combined to obtain the actual displacement. Similarly, areas under the deflected line may be computed by multiplying the tabulated fixed-end moment for a unit uniform load by the actual end angles. For the special case of members of constant moment of inertia, ordinates to the influence line for fixed-end moment at an end A may be determined readily by means of the expression:

$$i = a\, b^2\, L \tag{6}$$

in which L is the length of the member; $a\,L$ is the distance from end A to the section considered; and $b\,L$ is the distance from the section considered to the opposite end of member. The area under such an influence line is $L^2/12$.

Table 2 illustrates the computation of ordinates to the deflected load line when the end angles are known. The beam is that of Table 1. Detail computations are shown in Table 2(b) for span AB. At each point the ordinate to

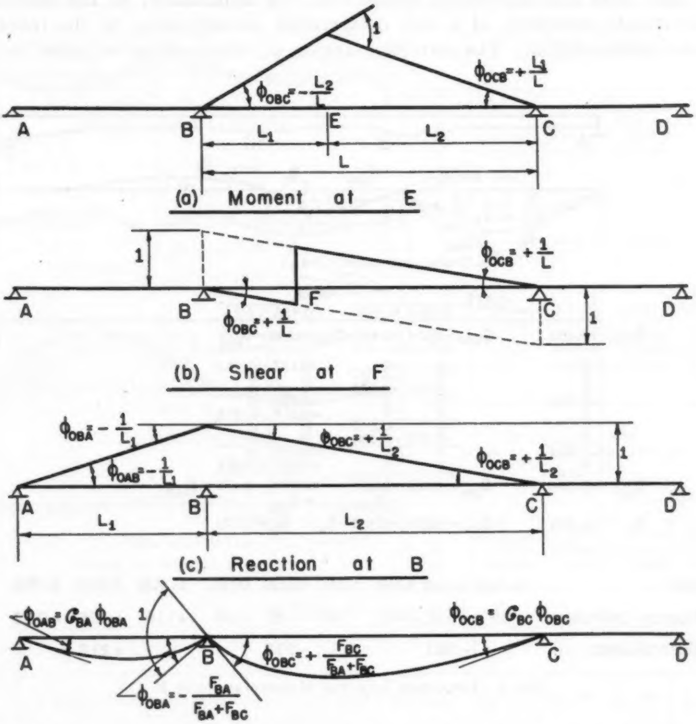

FIG. 3.—STATIC INFLUENCE LINES

the deflected load line is obtained by ratio from the values for fixed-end moments at ends A and B. The latter values are readily available in various publications. In span BC the rotation at end C produces displacements opposite to those produced by the rotation at end B. As a result, ordinates and areas are computed as the numerical difference of those found for rotations at ends B and C separately.

Influence Lines For Continuous Beams

In this section the step-by-step procedure, as applied to continuous beams, is outlined, and several numerical examples are presented.

The first step is to consider the structure cut at the supports. Next draw the influence line for the statically determinate structure and obtain the unbalanced angles, ϕ_o, at the joints. These angles can be determined readily by substitution in the expressions shown on the statical influence lines in Fig. 3. In each case the expressions result from the application, to the statically determinate structure, of a unit deformation corresponding to the function under consideration. The correction angles, ϕ_i, which are to be added to the

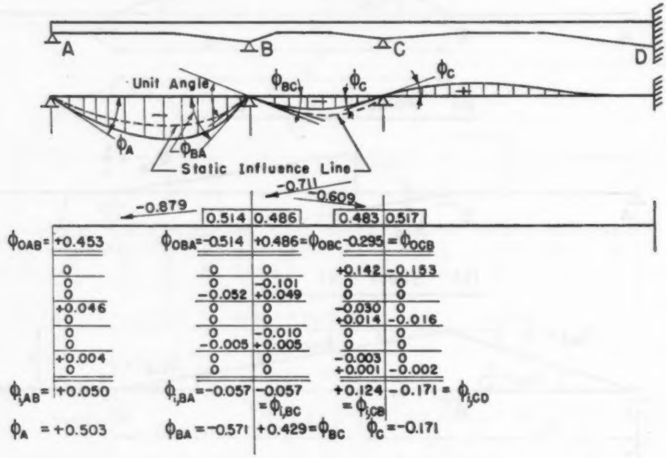

Point	0.3AB	0.5AB	0.7AB	0.3BC	0.5BC	07BC	0.3CD	0.5CD	0.7CD
Influence Ordinate	-3.97	-5.22	-4.27	-1.89	-1.85	-1.16	+1.14	+0.76	+0.23
Influence Area		-98.1			-23.9			+21.6	

Fig. 4.—Influence Line for Moment at Point B

unbalanced angles are then computed, to any desired accuracy, as in Table 1. With the correction angles known, the correction influence ordinates, i_i, are computed and added to the static influence ordinates, i_o, to obtain the influence ordinates for the continuous beam.

Table 3 and Fig. 4 show influence lines for moment, shear, and reaction in the same continuous beam as that in Table 1. In each case the correction angles and ordinates were determined as in Tables 1(*b*) and 2. Areas under the influence line in each span were determined as explained in the previous section and illustrated in Table 2. In the influence line for shear at point E (values in Table 3, Col. 4), it is of particular interest to note that the original unbalanced angles at points B and C (ϕ_{OBC} and ϕ_{OCB}) will be the same for all

TABLE 3.—INFLUENCE LINES FOR CONTINUOUS BEAMS WITH VARIABLE MOMENT OF INERTIA

Influence line (1)

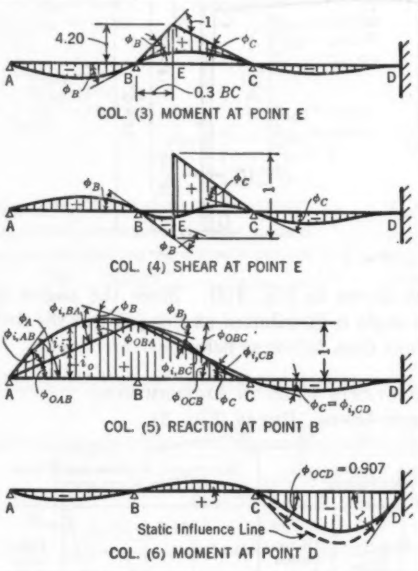

Joint (2)	Point E: Moment (3)	Point E: Shear (4)	Reaction point B (5)	Moment point D (6)
(a) Unbalanced Angles ϕ_o (That Is, ϕ_{OAB}, ϕ_{OBA}, Etc.)				
AB	...	...	−0.0333	...
BA	...	...	−0.0333	...
BC	−0.700	+0.0500	+0.0500	...
CB	+0.300	+0.0500	+0.0500	...
CD	...	...	...	+0.907
DC	...	...	...	−1.000
(b) Correction Angles ϕ_i (That Is, $\phi_{i\,AB}$, $\phi_{i\,BA}$, Etc.)				
AB	+0.301	−0.0338	−0.0507	+0.157
BA	−0.342	+0.0385	+0.0577	−0.179
BC	+0.358	−0.0115	−0.0256	−0.179
CB	−0.246	−0.0127	−0.0070	+0.386
CD	+0.054	+0.0373	+0.0430	−0.521
DC	0	0	0	0
(c) Final Angles (That Is, ϕ_D, ϕ_C, ϕ_B, and ϕ_A, Respectively)				
D	0	0	0	−1.000
C	+0.054	+0.0373	+0.0430	+0.386
B	−0.342	+0.0385	+0.0244	−0.179
A	+0.301	−0.0338	−0.0840	+0.157

(d) Influence Ordinates

Column[a]	Span A to B: 0.3 $\overline{AB}$	0.5 $\overline{AB}$	0.7 $\overline{AB}$	Area[b]	Span B to C: 0.3 $\overline{BC}$	0.5 $\overline{BC}$	0.7 $\overline{BC}$	Area[b]	Span C to D: 0.3 $\overline{CD}$	0.5 $\overline{CD}$	0.7 $\overline{CD}$	Area[b]
3	−2.40	−3.12	−2.55	−58.6	+2.50	+1.14	+0.45	+18.1	−0.36	− 0.25	−0.07	− 6.8
4	+0.27	+0.35	+0.29	+ 6.58	−0.08[c]	+0.50	+0.08[c]	+ 4.00	−0.25	− 0.17	−0.05	− 4.70
5	+0.70	+1.02	+1.13	+24.90	+0.79	+0.56	+0.30	+10.76	−0.29	− 0.19	−0.06	− 5.42
6	−1.25	−1.63	−1.33	−30.80	+1.16	+1.77	+1.64	+22.2	−6.71	−11.07	−9.86	−262.8

[a] Column numbers on Tables (*a*), (*b*), and (*c*). [b] Influence area. [c] These are the shear influence ordinates for 0.1 $\overline{BC}$ and 0.9 $\overline{BC}$.

shear influence lines in span BC. As a result, the correction angles and ordinates are identical for all shear influence lines. In the influence line for moment at D (values in Table 3, Col. 6) the required unit deformation at point D is automatically retained during the distribution of angles. These influence ordinates are obtained directly from the final angles. In Fig. 4, the unit

angular deformation introduced at point B, with ends A and C free to rotate, is split between spans AB and BC in the manner indicated in Fig. 3(*d*). The values thus obtained—0.514 to BA and + 0.486 to BC—are the only ones that satisfy statics. The unbalanced angles at points A and C also have been

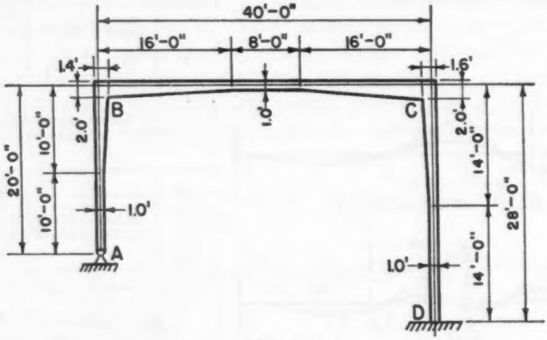

FIG. 5

determined from the relationships shown in Fig. 3(*d*). Since the angles at joint B are already balanced, zero angle is distributed at this joint in the first cycle. Carry-overs and distributions then follow as before.

TABLE 4.—FRAME CONSTANTS USED IN DETERMINING PRECISE INFLUENCE LINES (REFER FIG. 5)

Member	Moment Distribution Constants[a]			Angle Distribution Constants[b]			Influence Values for Fixed-End Moments[a]			
	Carry-over factor	Relative Stiffness		Carry-over factor	Flexibility	Distribution factor	Points[c]			Influence area
		Fixed end	Hinged end				0.3 *L*	0.5 *L*	0.7 *L*	
(1)	(2)	(3)	(4)	(5)	(6)	(7)	(8)	(9)	(10)	(11)
AB	0.697	0.222	...	...	...	...	2.69	2.06	0.90	28.72
BA	0.434	0.356	0.248	−0.697	4.03	0.41	1.86	3.55	3.62	43.16
BC	0.720	0.357	0.172	−0.720	5.95	0.59	7.96	6.80	2.60	167.36
CB	0.720	0.357	0.172	−0.720	5.95	0.65	2.60	6.80	7.96	167.36
CD	0.413	0.314	...	−0.788	3.18	0.35	5.46	5.48	3.02	52.7
DC	0.788	0.165	0.111	−0.413	...	...	1.07	2.63	3.62	93.3

[a] These values are generally available. [b] These are derived values. [c] *L* denotes any corresponding member shown in Col. (1).

INFLUENCE LINES FOR RIGID FRAMES

As with continuous girders, influence lines for rigid frames are obtained by adding a correction pattern to a static influence line. In general, however, this correction pattern must be adjusted for sidesway induced in the frame.

Fig. 5 shows an unsymmetrical frame, hinged at one end and fixed at the other. The constants necessary for determining the correction angles are

shown in Table 4. Influence values for fixed-end moment, used in computing the ordinates and areas of the correction patterns, are included also. The moment distribution constants and the influence values for fixed-end moments

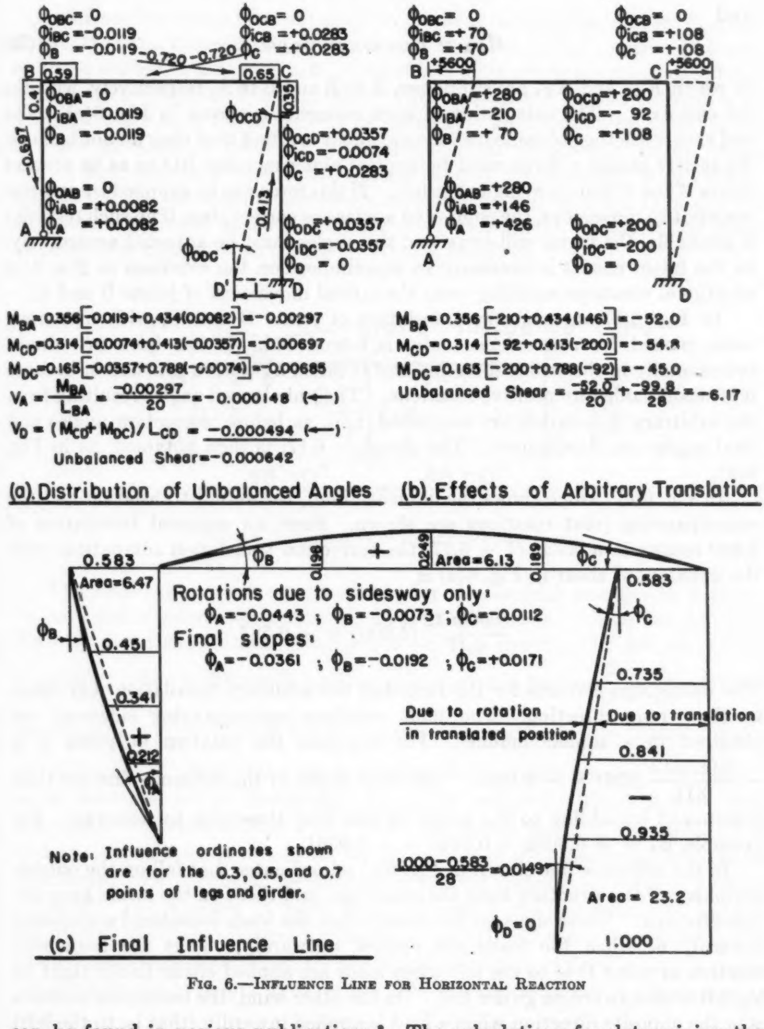

Fig. 6.—Influence Line for Horizontal Reaction

can be found in various publications.[8] The calculations for determining the influence line for horizontal reaction at point D are shown in Fig. 6. In Fig. 6(*a*) the static influence line is shown dashed, and the numerical values of the original unbalanced angles, the correction angles, and the final angles are given.

It can be shown that in any member, AB, subjected to rotations ϕ_A and ϕ_B at its ends A and B, respectively,

$$M_{AB} = K_{AB}\,(\phi_A + C_{AB}\,\phi_B) \quad \text{(7a)}$$

and

$$M_{BA} = K_{BA}\,(\phi_B + C_{BA}\,\phi_A) \quad \text{(7b)}$$

in which K_{AB} and K_{BA} are stiffnesses, A to B and B to A, respectively, with the far end fixed. The calculation of such moments is shown in Fig. 6(*a*). The end shears are then obtained, as shown, and it is found that they do not balance. To satisfy statics a force must be applied along member BC so as to prevent joints B and C from moving to the left. If this force can be supplied by external restraint to movement, the computed angles are correct; but, if no such restraint is available, the frame will sway and the angles must be adjusted accordingly. In the latter case it is necessary to superimpose on the rotations in Fig. 6(*a*) additional rotations resulting from the lateral movement of joints B and C.

In Fig. 6(*b*) an arbitrary translation of joints B and C, with numerical value picked for convenience only, is introduced. It has been introduced intentionally in the wrong direction and is called a positive translation because it is accompanied by positive rotations. The unbalanced angles resulting from the arbitrary translation are computed, and, as before, correction angles and final angles are determined. The shear, − 6.17, is then obtained, as in Fig. 6(*a*).

In Fig. 6(*c*) (which shows the influence line), the actual translation and the accompanying joint rotations are shown. Since an assumed translation of 5,600 results in a shear of − 6.17, the correction translation compatible with the unbalanced shear in Fig. 6(*a*) is

$$-\frac{0.000642}{6.17}\,(5{,}600) = -\,0.583.$$

The minus sign corrects for the fact that the arbitrary translation was taken in the wrong direction. The joint rotations accompanying sidesway are obtained in a similar manner. For example, the rotation at point A is $-\dfrac{0.000642}{6.17}\,(426) = -\,0.0443$. The final slopes of the influence line are then determined by adding to the angles in Fig. 6(*a*) those due to sidesway. For example, $\phi_A = +\,0.0082 - 0.0443 = -\,0.0361$.

In the influence line shown in Fig. 6(*c*) all ordinates that fall on the outside periphery of the structure have the same sign, and those on the inside have the opposite sign. These signs are consistent when the loads considered are applied inwardly or when the loads are applied outwardly. Thus the horizontal reaction at point D is to the left when loads are applied either to the right on leg AB or downward on girder BC. On the other hand, the horizontal reaction is in the opposite direction when a load is applied inwardly (that is, to the left) on leg CD. The influence ordinates along the legs were determined by adding the ordinates due to translation only to those due to rotation in the translated position. The values of the end angles required to compute that increment of

an influence ordinate due to rotation in the translated position can be determined readily by means of the final end slopes and translations. For example, at point C the angle is $0.0171 - \frac{1.000 - 0.583}{28} = 0.0022$.

Influence lines have been obtained for moment in the girder and for moment at end D of the frame in Fig. 5 but are not included in this paper. The procedure is similar to that of Fig. 6. The effects of an arbitrary translation have already been determined in Fig. 6(*b*). These results are used in correcting all other influence lines for the effects of sidesway. In determining an influence line for moment at point D, after the original unbalanced angles ($\phi_{ODC} = -1.000$; and $\phi_{OCD} = +0.413$) are distributed, the moment, M_{ODC}, necessary to impose the original unit deformation (rotation) at point D of the cut structure is included in computing the shear at point D. That is, the shear at point D is computed as $(M_{ODC} + M_{DC} + M_{CD})/28$.

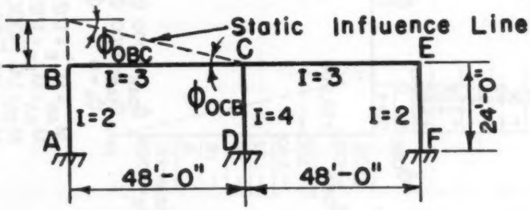

FIG. 7.—PROPERTIES OF A TWO-SPAN RIGID FRAME

The final influence line presented is for the vertical reaction in a three-legged bent of prismatic members. Properties of such a frame are shown in Fig. 7. Relative stiffness (hinged-end for the girders; but for the actual fixed-end condition of the columns) were computed as follows: $\frac{3}{4} \times \frac{3}{48} = 0.0468$ for the girders; $\frac{2}{24} = 0.0833$ for the outside columns; and $\frac{4}{24} = 0.1667$ for the interior column. Since there are more than two members framing into joint C, more than one set of distribution factors is required. These factors were computed by means of Eqs. 3 and 4 and are shown boxed in Fig. 8(*a*). The first number in the box represents the percentage of the unbalanced angle to be distributed to a particular member when the unbalance is introduced by that member. The number in parenthesis represents the percentage to be distributed to all other members framing into joint C. Because the flexibilities of the columns were determined for the actual condition of fixed ends, no angles are carried over to points A, D, or F. The unbalanced shear is determined as before.

In Fig. 8(*b*) the shear due to an arbitrary translation of + 24,000 is determined. The actual translation of the column tops is $\frac{0.000116}{26.9} \times 24{,}000$

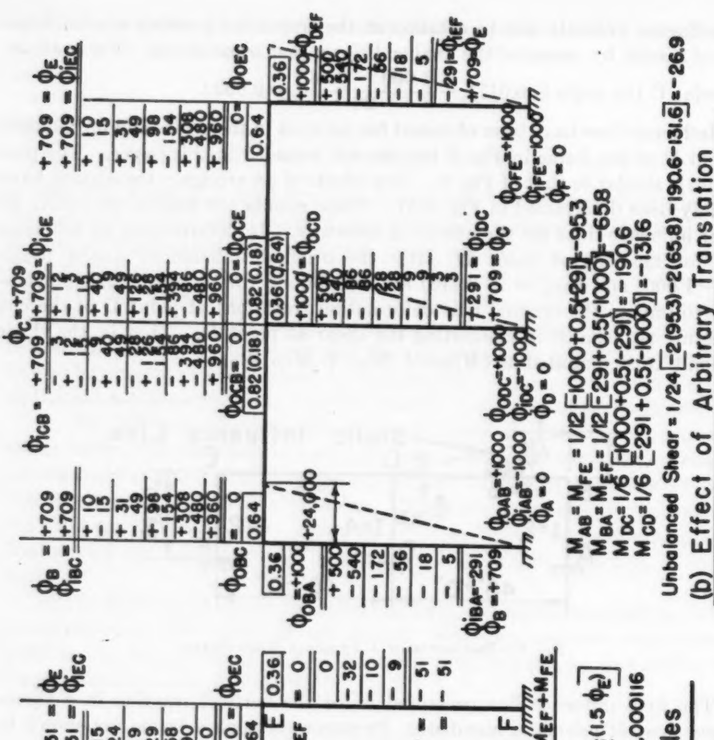

FIG. 8.—DISTRIBUTION PROCEDURE, INFLUENCE LINE FOR VERTICAL REACTION AT POINT A

$= 0.1035$; and the angles caused by the translation are (at points B, C, and E) $+ 709 \times \dfrac{0.1035}{24{,}000} = + 0.0031$. Before translation, the same angles were: At point B, $\dfrac{+ 575}{48{,}000} = + 0.0120$; at point C, $\dfrac{+ 263}{48{,}000} = + 0.0055$; and, at point E, $\dfrac{- 51}{48{,}000} = - 0.0011$. The final angles are: $\phi_B = + 0.0120 + 0.0031 = + 0.0151$; $\phi_C = + 0.0055 + 0.0031 = + 0.0086$; and $\phi_E = - 0.0011 + 0.0031 = + 0.0020$. The influence line is shown in Fig. 9. The sign

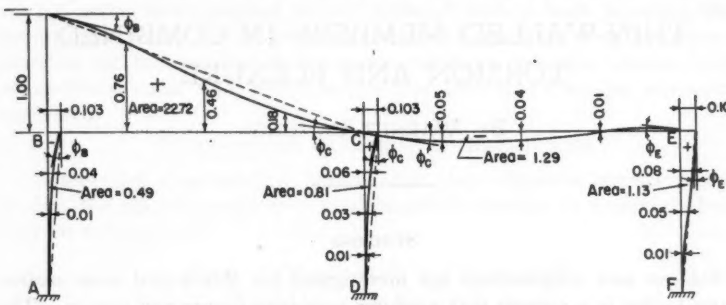

FIG. 9.—INFLUENCE LINE FOR VERTICAL REACTION AT POINT A

convention used for ordinates is the same as that explained in connection with Fig. 6(*c*). The leg CD has been considered an outside member of circuit ABCD. As before, the correction influence ordinates, i_i, have been obtained by ratio from the ordinates to influence lines for fixed-end moment.

OTHER APPLICATIONS

The procedure described in this paper can be used to obtain preliminary influence lines for the design of continuous trusses. The trusses may be treated as continuous beams, with or without variation in moment of inertia, and influence lines may be determined for moment at the supports. By means of these influence lines, influence diagrams may then be obtained for stress in the various members.

If desired, the procedure can also be used to determine displacements in continuous beams and frames. The ends of all members are considered cut, and the deflections and end rotations of all loaded members are determined. Then correction angles and ordinates are computed and combined with the angles and ordinates of the assumed static solution to obtain the true deflected structure.

CONCLUDING REMARKS

A procedure has been presented for obtaining influence lines, to any desired precision, directly from a consideration of geometry. The structure for which influence lines are desired may have members of constant or variable moment of inertia and may or may not be subject to sidesway. In addition to enabling one to determine precise influence values, the procedure readily lends itself to the development of judgment and a sense of scale.

AMERICAN SOCIETY OF CIVIL ENGINEERS
Founded November 5, 1852

TRANSACTIONS

Paper No. 2539

THIN-WALLED MEMBERS IN COMBINED TORSION AND FLEXURE

By Warner Lansing[1]

Synopsis

Stresses and deformations are investigated for thin-walled open section beams loaded in a manner that produces combined flexure and torsion. The analysis is based on the fundamental equations given by J. N. Goodier. It is shown that the expression for rotations of cross sections is analogous to the equation of equilibrium for a laterally loaded tie rod and, because of the analogy, approximate solutions are available in important practical cases, the accuracy of which may be easily estimated.

The analysis is illustrated by considering briefly the behavior of channels loaded by transverse forces acting in the plane of the web. A comparison with test results shows reasonable agreement, and design procedures for braced channels have been suggested in agreement with this work.[2] In the rapidly expanding field of light-gage steel construction, members of this type are frequently used in a manner to which this analysis applies directly.

While lateral buckling problems are not stressed in this paper, it is incidentally shown that critical loads may be easily obtained as limiting cases of eccentric loading.

Introduction

The stability of thin-walled open section bars of arbitrary shape submitted to end thrust has been thoroughly investigated during the past several

Note.—Published in March, 1952, as *Proceedings-Separate No. 119.* Positions and titles given are those in effect when the paper was received for publication.

[1] Formerly instructor in Eng. Mechanics, Cornell Univ., Ithaca, N. Y.; Presently in Eng. Dept., Grumman Aircraft Eng. Corp., Bethpage, N. Y.

[2] "Performance of Laterally Loaded Channel Beams," by G. Winter, W. Lansing, and R. B. McCalley. *Research, Engineering Structure Supplement*, Academic Press, Inc., New York, N. Y., 1949, p. 49.

decades.[3,4,5] The original theory has been extended[6,7] to include the more general problem of such bars under thrust, bending, and twisting. In all this work the determination of buckling loads has been emphasized.

There are many uses for thin-walled open sections bars, however, that result in definite rotational deflections and related secondary stresses from the very beginning of loading. Examples are the channel and the Z-section used as beams, that is, loaded by transverse forces in the plane of the web. Twist occurs from the start in the former case because the loads are not applied through the shear center and, in the case of the Z-section, because the loads are not acting in a principal plane. Although critical loads represent theoretical upper limits for the performance of such members, it is necessary in practical use to determine their stresses, rotations, and other design factors at subcritical loads. It is with this type of problem that this paper is primarily concerned.

The General Equations of Equilibrium

Considering a prismatical bar of open, but otherwise arbitrary, cross section, the general equations of equilibrium for loading by transverse forces may be written[7] as

$$M_\xi = -E\,I_x\,v'' = M_x + \beta\,M_y - u'\,M_z \qquad \text{(1a)}$$

$$M_\eta = E\,I_y\,u'' = -\beta\,M_x + M_y - v'\,M_z \qquad \text{(1b)}$$

$$M_\zeta = \left[G\,C + \frac{M_\xi\,K_1}{I_x} - \frac{M_\eta\,K_2}{I_y}\right]\beta' - E\,\Gamma\,\beta''' = u'\,M_x + v'\,M_y + M_z \qquad \text{(1c)}$$

in which E is Young's modulus of elasticity; G is the shear modulus of elasticity; the location of the fixed coordinate system x, y, and z, with shear center at the origin and x and y parallel to the principal centroidal axes, is shown in Fig. 1; ξ, η, and ζ are the corresponding displaced cross-sectional axes; u and v are the displacements of the shear center of any section in the x and y directions, respectively; and β is the rotation of the section about the shear center. One, two, or more primes refer to the first, second, and so on, derivatives with respect to z.

The resultant of the force system acting on the part of the member to the right of any section may be represented by a force vector applied at the displaced shear center of the section, plus a resultant moment. Then, following the right-hand screw convention, M_x, M_y, and M_z are the components of the

---

[3] "Torsion and Buckling of Open Sections," by H. Wagner, *Technical Memorandum No. 807*, National Advisory Committee for Aeronautics, Govt. Printing Office, Washington, D. C., October, 1936.

[4] "Torsion and Buckling of Open Sections," by H. Wagner and W. Pretschner, *Technical Memorandum No. 784*, National Advisory Committee for Aeronautics, Govt. Printing Office, Washington, D. C., January, 1936.

[5] "Twisting Failure of Centrally Loaded Open-Section Columns in the Elastic Range," by Robert Kappus, *Technical Memorandum No. 851*, National Advisory Committee for Aeronautics, Govt. Printing Office, Washington, D. C., March, 1938.

[6] "The Buckling of Compressed Bars by Torsion and Flexure," by J. N. Goodier, *Bulletin No. 27*, Cornell Univ. Eng. Experiment Station, Ithaca, N. Y., December, 1941.

[7] "Flexural-Torsional Buckling of Bars of Open Section," by J. N. Goodier, *Bulletin No. 28*, Cornell Univ. Eng. Experiment Station, Ithaca, N. Y., January, 1942.

latter parallel to the x, y, and z axes, whereas M_ξ, M_η, and M_ζ represent the moment resolved into ξ, η, and ζ components.

As for the geometrical properties of the cross section, I_x and I_y are the usual principal moments of inertia, and C is the torsional constant. (For constant thickness t, C is very closely $\frac{1}{3} s\, t^3$, in which s is the developed length of the center line.) The symbol Γ is the warping constant and its calculation is covered in standard texts on aircraft structural analysis[8,9,10] and will not be discussed here. (However, a formula for determining Γ for a channel section is given later.) Finally,

$$K_1 = \int_A (y - y_e)\,(x^2 + y^2)\,dA \qquad (2a)$$

and

$$K_2 = \int_A (x - x_e)\,(x^2 + y^2)\,dA \qquad (2b)$$

in which x_e and y_e are the coordinates of the centroid of the section, and A is its area. The terms in Eq. 1c involving K_1 and K_2 represent the contribution to the internal twisting moment of the ordinary bending fiber stress (σ_b) which may be written

$$\sigma_b = \frac{M_\xi\,(y - y_e)}{I_x} - \frac{M_\eta\,(x - x_e)}{I_y} \qquad (3)$$

The analogous effect in bars under uniform axial compression (P) results in the term $-P\,\rho^2\,\beta'$, in which ρ is the radius of gyration of the section taken about the shear center.

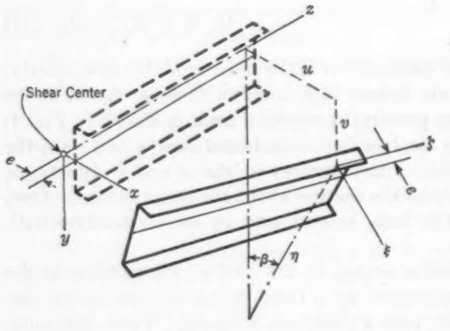

Fig. 1

In deriving Eq. 1 for use in stability problems, that is, for infinitesimal displacements, Mr. Goodier used first-order approximations for the direction cosines between x, y, z, and ξ, η, and ζ. It would appear that the expressions will also be sufficiently accurate for determining finite deformations and the accompanying stresses under stable conditions, provided the limitations on beam deflections of the ordinary engineering beam theory are observed, and rotations of cross sections are held to a maximum of, say, 5°.

[8] "Airplane Structural Analysis and Design," by Ernest E. Sechler and Louis G. Dunn, John Wiley & Sons, Inc., New York, N. Y., 1942.

[9] "Airplane St ructures," by A. S. Niles and J. S. Newell, John Wiley & Sons, Inc., New York, N. Y., Vol. 2, 3d Ed., 1943.

[10] "Fundamentals of Aircraft Structures," by Millard V. Barton, Prentice-Hall, Inc., New York, N. Y., 1948.

The Tie Rod Analogy.—Eq. 1c may be written

$$E\,\Gamma\,\beta''' - T\,\beta' = -\,u'\,M_x - v'\,M_y - M_z \qquad (4)$$

in which $T = G\,C + M_\xi\,K_1/I_x - M_\eta\,K_2/I_y$. In this form, provided T is constant, Eq. 4 is mathematically identical to the equation of equilibrium of the laterally loaded tie rod. The warping rigidity of the thin-walled open section beam ($E\,\Gamma$) represents the flexural rigidity of the tie rod; β represents the deflection of the tie rod; T represents the tie rod's axial force; and the term $-\,u'\,M_x - v'\,M_y - M_z$ represents the shear in the tie rod caused by the transverse load. In the case of the tie rod, the following is a familiar technique for obtaining an approximate solution.[11] The problem is first solved with only the transverse loads acting, the axial force being set equal to zero. The deflections are then corrected by multiplying by a factor $\left[1 + \frac{T}{T_{cr}}\right]^{-1}$, in which T_{cr} is the Euler buckling load. Bending moments in the tie rod $E\,\Gamma\,\beta''$ are corrected by adding a term $T\,\beta$. If T is actually variable instead of constant, conservative estimates may be made for it.

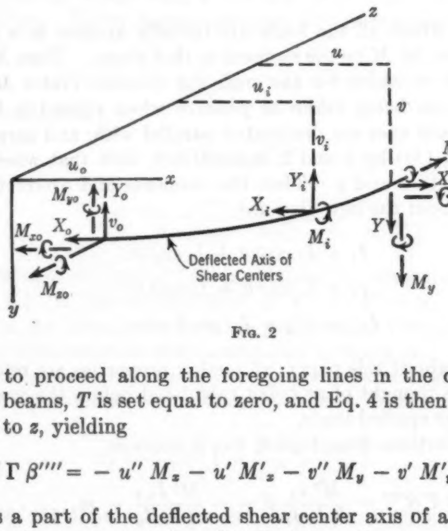

FIG. 2

In order to proceed along the foregoing lines in the case of thin-walled open section beams, T is set equal to zero, and Eq. 4 is then differentiated once with respect to z, yielding

$$E\,\Gamma\,\beta'''' = -\,u''\,M_x - u'\,M'_x - v''\,M_y - v'\,M'_y - M'_z \qquad (5)$$

Fig. 2 shows a part of the deflected shear center axis of a beam, acted upon by various loads, concentrated or distributed as the case may be. It is seen that in the interval from z to $z + dz$, the increase in M_z is

$$-\,Y\,(u'\,dz) + X\,(v'\,dz) + m_z\,dz$$

in which m_z is the intensity of the moment of a distributed load about the shear center axis, if such is present, and X and Y are the components of the

[11] "Strength of Materials," by S. Timoshenko, D. Van Nostrand Co., Inc., New York, N. Y., Vol. 2, 2d Ed., 1941, p. 49.

ordinary beam shear in the x and y directions. Now,

$$M'_x = Y \qquad \text{(6a)}$$

$$M'_y = -X \qquad \text{(6b)}$$

and

$$M'_z = -u'\,Y + v'\,X + m_z \qquad \text{(6c)}$$

Substituting in Eq. 5,

$$E\,\Gamma\,\beta'''' = -u''\,M_x - v''\,M_y - m_z \qquad \text{(7)}$$

In what follows, it is assumed that it is permissible to neglect the terms in M_z in Eqs. 1a and 1b. This can be shown to be legitimate for I-beams, Z-sections, and channels loaded by transverse forces in the plane of the web.[12] The simplified expressions of Eqs. 1a and 1b may now be used to eliminate the terms u'' and v'' from Eq. 7, yielding

$$E\,\Gamma\,\beta'''' - \frac{I_x\,M_x^2 + I_y\,M_y^2}{E\,I_x\,I_y}\,\beta = -\frac{M_x\,M_y\,(I_x - I_y)}{E\,I_x\,I_y} - m_z \qquad \text{(8)}$$

In the case in which all the loads are initially applied in a plane that is parallel to the z axis, let M be the moment in that plane. Then $M_x = M\cos\theta$ and $M_y = M\sin\theta$, in which θ is the angle the moment vector M makes with the x axis, clockwise, being taken as positive when viewed in the positive z direction. New fixed axes are designated parallel with, and perpendicular to, the moment vector (M) by 1 and 2, respectively, such that when $\theta = 0$, axes 1 and 2 coincide with x and y. Then the moments and product of inertia of the cross section about the new axes are

$$I_1 = I_x\cos^2\theta + I_y\sin^2\theta \qquad \text{(9a)}$$

$$I_2 = I_x\sin^2\theta + I_y\cos^2\theta \qquad \text{(9b)}$$

$$I_{1,2} = (I_x - I_y)\sin\theta\cos\theta \qquad \text{(9c)}$$

Here and throughout this paper, all section properties are referred to fixed axes, and are to be thought of as being calculated before the various sections are displaced by the applied loads.

With the substitutions from Eqs. 9, Eq. 8 becomes

$$E\,\Gamma\,\beta'''' - \frac{M^2\,I_1}{E\,I_x\,I_y}\,\beta = -\frac{M^2\,I_{1,2}}{E\,I_x\,I_y} - m_z \qquad \text{(10)}$$

It will be noted that, for sections with point symmetry, $K_1 = K_2 = 0$, and T in Eq. 4 is a constant, namely, $G\,C$. Under these conditions T could have been used explicitly in the subsequent work with no additional complications, yielding an additional term $-\,G\,C\,\beta''$ on the left of Eq. 10. With the latter included in Eq. 10, the equations of equilibrium for the lateral

[12] "Stresses in Thin Walled Open Section Beams Due to Combined Torsion and Flexure," by W. Lansing, thesis presented to Cornell University, at Ithaca, N. Y., in 1949, in partial fulfilment for the degree of Doctor of Philosophy.

stability of I-beams obtained by S. Timoshenko[13] are contained as special cases.

If M is constant, such as in loading by end couples, the solution of Eq. 10 presents no problem. On the other hand, if M varies with z, as it will for loading by transverse forces, an exact solution is very difficult, and approximate methods must be employed.

The homogeneous equation associated with Eq. 10, that is,

$$E\,\Gamma\,\beta'''' - \frac{M^2 I_1}{E\,I_x\,I_y}\,\beta = 0 \qquad (11)$$

is the well-known differential equation for the whirling speed of a rotating shaft. The iteration method of A. Stodola,[14] used in connection with this problem, is thus suggested.

Example: Channel Simply Supported at the Ends, Loaded at the Middle

Deflection Analysis.—For the specific case of a simply supported channel of length $2\,l$, and depth $2\,h$, subject to a single concentrated load $2\,P$, applied at midspan at the top of the web, $\theta = 0$ and $M = P\,(l - z)$, $m_z = 0$. The origin is at midspan. Under these conditions Eq. 10 reduces to

$$E\,\Gamma\,\beta'''' - \frac{P^2\,l^2}{E\,I_y}\left(1 - \frac{z}{l}\right)^2 \beta = 0 \qquad (12)$$

The boundary conditions are

$$\beta(l) = \beta'(0) = \beta''(l) = 0 \qquad (13a)$$

and

$$\beta'''(0) = \frac{P\,[e + h\,\beta(0)]}{E\,\Gamma} \qquad (13b)$$

The indicated value of the term $\beta'''(0)$ is obtained by using the left and middle expressions of Eq. 1c and noting that at $z = 0$, $\beta' = 0$, and $M_\zeta = -P\,[e + h\,\beta(0)]$. In the latter, the term $\sin \beta(0)$ has been replaced by the term $\beta(0)$ and e is the distance from the shear center to the web.

Following the method of Mr. Stodola, an expression satisfying the boundary conditions for β, but arbitrary otherwise, should now be substituted in Eq. 12:

$$\beta_1 = \beta_1(0)\left[1 - \frac{6}{5}\frac{z^2}{l^2} + \frac{1}{5}\frac{z^4}{l^4}\right] \qquad (14)$$

This equation has the appropriate general shape of a single half-wave, and the fact that it does not satisfy one of the boundary conditions, namely, Eq. 13b, is of no practical importance. Now,

$$\frac{E^2\,\Gamma\,I_y}{P^2\,l^2}\,\beta''''_2 = \beta_1(0)\left[1 - \frac{6}{5}\frac{z^2}{l^2} + \frac{1}{5}\frac{z^4}{l^4}\right]\left(1 - \frac{z}{l}\right)^2 \qquad (15)$$

---

13 "Theory of Elastic Stability," by S. Timoshenko, McGraw-Hill Book Co., Inc., New York, N. Y., 1st Ed.,1936, Chapter 5, pp. 239–286.

14 "Mathematical Methods in Engineering," by Theodore von Kármán and Maurice A. Biot, McGraw-Hill Book Co., Inc., New York, N. Y., 1st Ed., 1940.

The subscripts 1 and 2 are to identify, respectively, the assumed and derived functions for β.

By direct integration,

$$\frac{E^2\,\Gamma\,I_y}{P^2\,l^3}\,\beta'''_2 = \beta_1(0)\left[\frac{z}{l} - \frac{z^2}{l^2} - \frac{1}{15}\frac{z^3}{l^3} + \frac{3}{5}\frac{z^4}{l^4} - \frac{1}{5}\frac{z^5}{l^5} - \frac{1}{15}\frac{z^6}{l^6} + \frac{1}{35}\frac{z^7}{l^7}\right] + C_1 \qquad (16)$$

in which C_1 is the constant of integration. From Eq. 13*b*, it can be seen that

$$C_1 = \frac{E\,I_y\,h}{P\,l^3}\,\beta_2(0) + \frac{E\,I_y\,e}{P\,l^3} \qquad (17)$$

Integrating a second time and using the third boundary condition of Eq. 13*a* yields

$$\frac{E^2\,\Gamma\,I_y}{P^2\,l^4}\,\beta''_2 = \beta_1(0)\left[-\frac{323}{1400} + \frac{1}{2}\frac{z^2}{l^2} - \frac{1}{3}\frac{z^3}{l^3} - \frac{1}{60}\frac{z^4}{l^4} + \frac{3}{25}\frac{z^5}{l^5} - \frac{1}{30}\frac{z^6}{l^6} - \frac{1}{105}\frac{z^7}{l^7} + \frac{1}{280}\frac{z^8}{l^8}\right] + \left[\frac{E\,I_y\,h}{P\,l^3}\,\beta_2(0) + \frac{E\,I_y\,e}{P\,l^3}\right]\left[\frac{z}{l} - 1\right] \qquad (18)$$

In a similar way, two more integrations give

$$\frac{E^2\,\Gamma\,I_y}{P^2\,l^6}\,\beta_2 = \beta_1(0)\left[\frac{6709}{79{,}600} - \frac{323}{2800}\frac{z^2}{l^2} + \frac{1}{24}\frac{z^4}{l^4} - \frac{1}{60}\frac{z^5}{l^5} - \frac{1}{1800}\frac{z^6}{l^6} + \frac{1}{350}\frac{z^7}{l^7} - \frac{1}{1680}\frac{z^8}{l^8} - \frac{1}{7560}\frac{z^9}{l^9} + \frac{1}{25{,}200}\frac{z^{10}}{l^{10}}\right] + \left[\frac{E\,I_y\,h}{P\,l^3}\,\beta_2(0) + \frac{E\,I_y\,e}{P\,l^3}\right]\left[\frac{1}{3} - \frac{1}{2}\frac{z^2}{l^2} + \frac{1}{6}\frac{z^3}{l^3}\right] \qquad (19)$$

Before proceeding further, it is desirable to introduce the maximum fiber stress caused by elementary beam action, $\bar{\sigma} = P\,l\,h/I_x$. Then, the three dimensionless constants of Eq. 19 involving sectional properties can be expressed as

$$\frac{E^2\,\Gamma\,I_y}{P^2\,l^6} = \frac{I_y\,\Gamma\,h^2\,E^2}{I^2_x\,l^4\,\bar{\sigma}^2} = \frac{1}{\alpha} \qquad (20a)$$

$$\frac{E\,I_y\,h}{P\,l^3} = \frac{h^2\,I_y\,E}{l^2\,I_x\,\bar{\sigma}} = \gamma \qquad (20b)$$

and

$$\frac{E\,I_y\,e}{P\,l^3} = \frac{h\,e\,I_y\,E}{l^2\,I_x\,\bar{\sigma}} = \delta \qquad (20c)$$

From the discussion of the tie rod analogy, it is understood that, for the conjugate tie rod, the right-hand side of Eq. 15 is proportional to a distributed lateral load. In order to obtain the approximately correct rotations for this

problem, accordingly the right-hand side of Eq. 19 is multiplied by the factor

$$\nu = \left[1 + \frac{T}{T_{cr}}\right]^{-1} \qquad (21)$$

in which T is as defined previously. In the resulting equation, $\beta_1(0)$ is set equal to $\beta_2(0)$; dropping the subscripts and employing Eq. 20, at midspan ($z = 0$),

$$\frac{1}{\alpha}\,\beta(0) = \nu\left\{\beta(0)\,\frac{6709}{75{,}600} + \beta(0)\,\frac{\gamma}{3} + \frac{\delta}{3}\right\} \qquad (22)$$

Solving for $\beta(0)$ gives

$$\beta(0) = \frac{\nu\,\alpha\,\dfrac{\delta}{3}}{1 - \nu\,\alpha\left[\dfrac{6709}{75{,}600} + \dfrac{\gamma}{3}\right]} \qquad (23)$$

The iterative process need be carried no further, as this expression is already sufficiently accurate for engineering use.

Limiting Case of Eccentric Loading.—Eq. 23 is also valid for the rotation at midspan of a simply supported I-beam loaded by a central force at the top flange at a distance e from the plane of the web. The point of application of the force may be shifted to the centroid by allowing e and h in Eq. 13*b* to shrink to zero. This in turn requires that γ and δ go to zero in Eq. 23. Thus, $\beta(0)$ can be different from zero only if

$$1 - \nu\,\alpha\,\frac{6709}{75{,}600} = 0 \qquad (24)$$

An exact solution of this lateral buckling problem for I-beams has been obtained by Mr. Timoshenko,[13] and thus a comparison will give an estimate of the accuracy of the approximate method.

Referring to the discussion on the tie rod analogy, T_{cr} for this problem is the "Euler load" associated with the equation $E\,\Gamma\,\beta''' + G\,C\,\beta' = 0$. The boundary conditions given in Eq. 13, with the change previously discussed (that is, $\beta'''(0) = 0$), are equivalent to those of a simply supported column of length $2\,l$. Hence,

$$T_{cr} = \frac{\pi^2\,E\,\Gamma}{4\,l^2} \qquad (25)$$

and

$$\nu = \left[1 + \frac{G\,C\,4\,l^2}{E\,\Gamma\,\pi^2}\right]^{-1} \qquad (26)$$

Using Eq. 26 and the expression for α from Eq. 20*a*, and letting $P = Q/2$, $l = L/2$, and $a^2 = G\,C/E\,\Gamma$, Eq. 24 may be solved for Q_{cr} to give

$$Q_{cr} = \frac{m\,\sqrt{E\,I_y\,G\,C}}{L^2} \qquad (27)$$

in which $m = 17.11\,\sqrt{1 + \dfrac{\pi^2}{a^2\,L^2}}$.

Written in this form the equation is identical to the Timoshenko solution. Comparing m for the same range of values of $a^2 L^2$ as given by Mr. Timoshenko[15] the difference was never found to exceed 0.5%. The approximate solution is thus satisfactory in practical applications.

Stress Distribution in Loaded Channel.—Returning to the channel problem, the following simplified way of visualizing the stress distribution was indicated by George Winter, M. ASCE, in an unpublished research report. The displacement of the midspan section may be considered as proceeding in the successive stages depicted in Fig. 3. The section, then, is thought of as being first displaced downward in simple translation. The stresses induced would be those of the ordinary beam theory and are indicated in character by the appropriate signs at the corners of the section, minus signs denoting compression and plus signs tension.

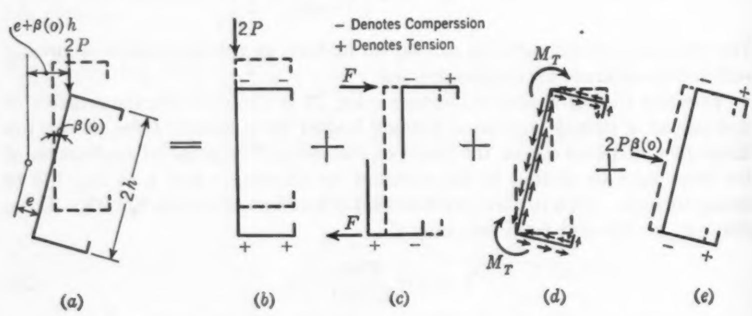

FIG. 3.—STRESS DISTRIBUTION IN A CHANNEL SUBJECTED TO TORSION AND FLEXURE

Next, the channel is considered as cut and the two halves displaced much like two individual beams, resulting in the appropriate indicated corner stresses. To fit the two halves together, they are next rotated about their individual shear centers, giving rise only to shear stresses of the ordinary St. Venant character. In this inclined position, finally, the component of the vertical load parallel to the major axis causes additional bending about the minor axis, with its corresponding normal stresses. This picture is not an exact one but is discussed only to indicate the general type of the resulting stress distribution; it is shown in another paper[2] that this simplified concept, somewhat modified, leads directly to an entirely satisfactory approximate analysis for design purposes. It is evident that, under such a stress distribution, cross sections are distorted out of their original planes. For this reason, the stresses associated, in particular, with the second displacement stage (Fig. 3(*c*)) are generally known as warping stresses.

The stresses of the first and last displacement stages (Fig. 3(*b*) and 3(*e*)) are of course represented by σ_b, Eq. 3. A more precise definition of the warping

[15] "Theory of Elastic Stability," by S. Timoshenko, McGraw-Hill Book Co., New York, N. Y., 1st Ed., 1936, p. 267, Table 22.

stresses is provided by the expression,

$$\sigma_s = E\,\beta''\,(w_1 - \bar{w}_1) \qquad (28)$$

first stated by H. Wagner[3,4] for thin-walled open section bars in nonuniform torsion. The quantity $w_1 - \bar{w}_1$ is the warping displacement, for unit twist, measured from a plane normal to the ζ axis and containing the centroid of the warped surface of the cross section. The term $w_1 - \bar{w}_1$ is a section property; Fig. 4 shows its variation along the mean line of a channel with lips. The ordinates of the points in Fig. 4 are defined as follows:

$$W_1 = h\,e \qquad (29a)$$

$$W_2 = h\,(e - b) \qquad (29b)$$

$$W_3 = h\,(e - b) - (e + b)\,d \qquad (29c)$$

The formula for the warping constant Γ in this case is

$$\Gamma = \frac{2\,t}{3}\left[(h + e)\,W^2_1 + (b - e)\,W^2_2 + d\,(W^2_2 + W_2\,W_3 + W^2_3)\right] \qquad (30)$$

At any section the stress σ_s is seen to be distributed in a manner proportional to $w_1 - \bar{w}_1$. Comparing Fig. 4 with the stress distribution that accompanies the second displacement stage, Fig. 3(c), the two are seen to be rather similar, the difference consisting in linear variations of stress in the web and lips according to the Wagner theory, as contrasted with the constant values of the approximate method. A slight modification of the latter accounts satisfactorily for this difference. The conclusion, reached by a study of Fig. 3, that the maximum fiber stress occurs in compression at the upper junction of web and flange, is thus confirmed by the more exact theory. Evaluating σ_b and σ_s at this point and adding,

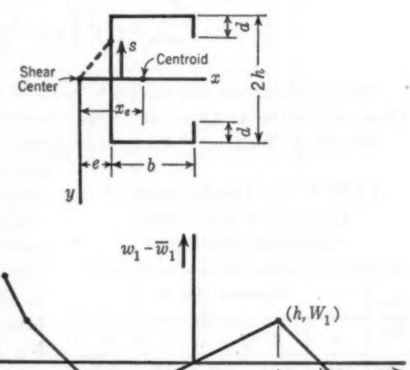

FIG. 4.—VARIATION OF WARPING DISPLACEMENT ALONG THE MEAN LINE OF A CHANNEL

$$\sigma_{\max} = -\,\bar{\sigma}\left(1 + \frac{S_x}{S_y}\beta(0)\right) + E\,\beta''(0)\,W_1 \qquad (31)$$

in which $S_x = I_x/h$, $S_y = I_y/(x_c - e)$ ($x_c - e$ is the distance from the mid-plane of the web to the centroid), and W_1 is the value of $w_1 - \bar{w}_1$ for the point

in question, as given in Fig. 4. In Eq. 23 $\beta(0)$ is expressed and $\beta''(0)$ is obtained by setting $z = 0$ in Eq. 18 and adding a term $\frac{T}{E\,\Gamma}\beta(0)$. The analogous step in tie rod problems consists of adding to the term $E\,\Gamma\,\beta''$ (the "bending moment" due to transverse loads only) the "moment of the axial load," $T\,\beta$, as discussed previously. Thus,

$$\beta''(0) = -\frac{\alpha}{l^2}\left[\delta + \beta(0)\left(\frac{323}{1400} + \gamma\right)\right] + \beta(0)\frac{T}{E\,\Gamma} \quad \text{.......(32)}$$

In this problem as $M_\eta = M\,\beta$, T may be written as

$$T = G\,C\left[1 - \frac{I_z\,K_2}{I_y\,h}\,\frac{\bar{\sigma}}{G\,C}\left(1 - \frac{z}{l}\right)\beta\right] \quad \text{.............(33)}$$

(K_1 vanishes for reasons of symmetry.) It is seen that the value of T varies along the bar, having a maximum value at the supports

$$T_{\max} = G\,C \quad \text{........................(34a)}$$

and a minimum value at midspan

$$T_{\min} = G\,C\left(1 - \frac{I_z\,K_2}{I_y\,h}\,\frac{\bar{\sigma}}{G\,C}\beta(0)\right) \quad \text{..............(34b)}$$

Two calculations are made, in each of which T is assumed to be constant. These will serve as upper and lower bounds for the true answer.

Results of Numerical Analyses.—Analyses have been made for four channel sections that appear to represent the extremes for the commercially available shapes as commonly listed.[16] The dimensions of these sections are given in Table 1 referred to the typical section in Fig. 5. The results for the most unfavorable of these sections, namely, No. 3, are shown in Fig. 5. The usual criterion for design purposes would stipulate that the carrying capacity of the member is reached when yielding starts in the most highly stressed fiber. For a beam with no tendency to twist, this means, as usual, that the maximum fiber stress $\left(\bar{\sigma} = \frac{P\,l\,h}{I_z}\right)$ becomes equal to the yield point. In a channel, however, this fiber stress corresponds only to the first of the four displacements (Fig. 3(*b*)) and is augmented at the most highly stressed point (upper left corner) by the additional stresses represented by the $\beta(0)$ and $\beta''(0)$ terms on the right-hand side of Eq. 31.

TABLE 1.—DIMENSIONS IN INCHES OF ANALYZED CHANNEL SECTIONS

Section No.	Dimension (Fig. 5)				
	D	B	d	t	R
1	12.0	3.50	1.0	0.135	3/16
2	12.0	3.50	0.7	0.075	3/32
3	3.0	1.75	0.7	0.105	3/16
4	3.0	1.75	0.4	0.048	3/32

[16] "Light Gage Steel Design Manual," Am. Iron and Steel Inst., New York, N. Y., 1949.

To assess the reduced efficiency of a channel section as compared to a similar section prevented from twisting, it is simplest to plot against the span length that simple bending stress $\bar{\sigma} = \frac{P\,l\,h}{I_x}$ that will result in yield stress at the most unfavorable fiber. This information has been plotted in Fig. 5 for a yield point of 33,000 lb per sq in. for mild structural steel ($E = 30 \times 10^6$ lb per sq in.). In the same figure is shown the angle of rotation $\beta(0)$ that exists when yielding begins in the upper left corner.

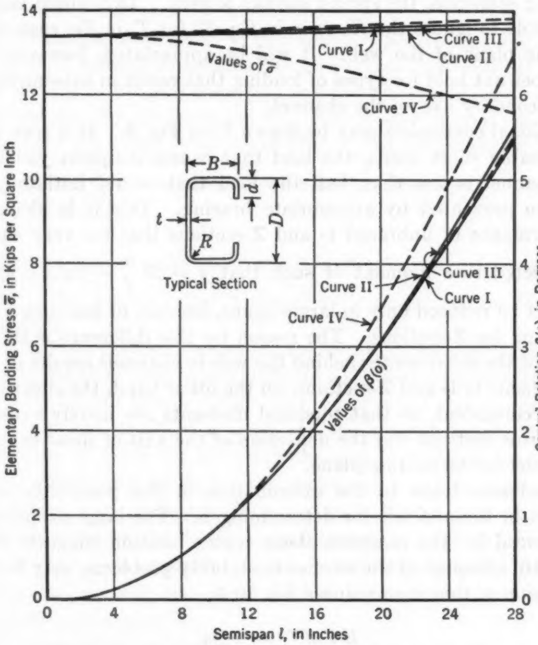

FIG. 5.—ANALYSIS RESULTS FOR CHANNEL SECTION NUMBER 3

The curves designated I are based upon an assumed constant value of $T = G\,C$, and $T_{cr} = \frac{\pi^2 E\,\Gamma}{4\,l^2}$. This would be quite proper if the problem at hand were a question of lateral stability. In that case $\beta(0)$ would be very small, and from Eq. 34 $T_{\max} = T_{\min} = G\,C$. The problem presently being investigated is different in that the eccentrically applied central force causes rotation from the very beginning of loading. Thus for $\beta(0)$ equal to a maximum value of, say, 5°, $\bar{\sigma}$ from curve I is 13,800 lb per sq in. and using these figures plus $G = 11.5 \times 10^6$ lb per sq in. (mild steel), $T_{\min}$ is 0.89 $T_{\max}$. The term T being analogous to the axial force in tie rods, which of course tends to

reduce deflections and bending moments, the curves marked I are seen to be unconservative, and may be considered an upper bound for the correct curves. A lower bound may be obtained based upon a T equal to the T_{min} of Eq. 34*b*, into which values of $\bar{\sigma}$ and $\beta(0)$ are substituted from curves I.

Curves designated II have been plotted on this basis. The two bounds are sufficiently close together that the position between them of the curves representing the exact solution is immaterial for engineering purposes. Indeed, for the semispan $l = 28$ in., for which $\beta(0)$ is approximately $5\frac{1}{2}°$ by either of the two curves, the ordinates to the two $\bar{\sigma}$ curves differ by less than 2%, and for decreasing semispan, the spread shrinks to zero. This would indicate that it is permissible to ignore the K_2 term in Eq. 33 for T, in the case of channels loaded in the plane of the web. It will be appreciated, however, that this statement does not hold for types of loading that result in substantial bending about the secondary axis of the channel.

An additional conclusion may be drawn from Fig. 5. It is seen that, even for impracticably short spans, the load that causes incipient yielding in the unbraced channel is less than half the load that would initiate yielding if twisting were prevented by appropriate bracing. This is in sharp contrast to the performance of unbraced I- and Z-sections that for very short spans, can be subjected to a moment M such that $\bar{\sigma} = M \frac{h}{I}$ = yield point, and in which $\bar{\sigma}$ must be reduced only in larger spans, because of buckling for I-beams and of twisting for Z-sections. The reason for this difference is the fact that the location of the shear center behind the web in channels results in a primary twisting moment; in I- and Z-sections, on the other hand, the shear center and centroid are coincident, so that torsional moments are merely caused by the rotation of cross sections and the deflection of the axis of shear centers out of a plane parallel to the loading plane.

This conclusion leads to the examination of the possibility of another simplification in the analysis for determining β. The large primary twisting moment induced by the eccentric shear center location suggests that the β term in Eq. 10, although of the essence in stability problems, may be negligible here. Omission of this term reduces Eq. 10 to

$$E\,\Gamma\,\beta'''' = -m_z \qquad (35)$$

and using $T = G\,C$, yields expressions that plot as the dashed curves III of Fig. 5. These should be compared with curves I, which are different only in that the β term has been included. Since the curves practically coincide, this approximation is clearly permissible.

It may be somewhat surprising to note that the efficiency of this channel increases slightly with increasing span. It would seem more natural to observe a decrease in efficiency caused by the secondary effects associated with the central rotation. This and certain other effects can best be explained by a qualitative argument based upon Fig. 3. Consider the channel to be loaded by a force $2\,P$ that varies inversely with the span $2\,l$, so that the elementary bending stress $\bar{\sigma}$ remains constant. Under these conditions the principal part

of the torsional moment, $P\,e$, varies inversely as l. Then the central rotation angle $\beta(0)$, if it were dependent only upon the torsional rigidity of the channel (the action depicted in Fig. 3(*d*)), would be of constant magnitude $\frac{P\,e\,l}{G\,C}$.

On the other hand, if the deformation were to depend only on the action of Fig. 3(*c*) an entirely different situation would prevail. Then, each half of the section performs as if it were a simple beam acted upon by the force

$$F = 2\,P\,[e + \beta(0)\,h]\frac{1}{2\,h} \qquad (36)$$

Since the location of the load F on this fictitious horizontal beam, and its span, are identical to those for the channel as a whole (for vertical bending), the resulting horizontal bending moments and the corresponding stresses shown in Fig. 3(*c*) are directly proportional to those caused by vertical bending, Fig. 3(*b*), except for the minor influence of $\beta(0)$. The central deflection of the half-beam, $\delta = \frac{F\,(2\,l)^3}{48\,E\left(\frac{I_y}{2}\right)}$, is related to the central rotation $\beta(0)$ by the formula $\beta(0) = \delta/h$ and again neglecting secondary effects, $\beta(0) = \frac{P\,e\,l^3}{3\,E\,I_y\,h^2}$. For this action then, the central rotation would vary as the square of the span, $P\,l$ being constant.

It follows from the two expressions for $\beta(0)$ that, for a given section, for very short spans, the channel is much stiffer in differential bending (Fig. 3(*c*)) than it is in the St. Venant torsion (Fig. 3(*d*)), while if the span is made sufficiently large, the opposite situation is true. In the case of section 3 (the stockiest of the sections of Table 1), for which the curves of Fig. 5 are plotted, as the semispan l goes from 0 to 28 in., the performance passes from the differential bending regime into an intermediate one in which an appreciable part of the torsional load is carried by the St. Venant torsion. Thus, as l increases, more of the total stress σ_{max} is available as primary bending stress $\bar{\sigma}$. The nonlinearity of the torsional moment because of the influence of $\beta(0)$ diminishes this effect, but does not quite cancel it.

In the cases of the other three channels listed in Table 1, the performance is predominantly in the differential bending regime, and the $\bar{\sigma}$ curves drop off with increasing span. As an example of the behavior of such relatively thinner sections, Fig. 6 gives the corresponding information for section 1.

In order to evaluate this effect quantitatively, the dashed lines designated curve IV in Fig. 5 are plotted. They are based upon Eq. 35, and differ from curve III only in that the tie rod correction is omitted; that is, the value of T is taken equal to zero. This is equivalent to assuming the torsional rigidity, $G\,C$, to be zero. For the section of Fig. 5, the results are rather conservative when compared with curves III. In the case of each of the other three sections, the curves III and IV all lie much closer together, and have spreads between the $\bar{\sigma}$ curves of less than $4\frac{1}{2}\%$ for $\beta(0)$ equal to approximately 5° (see Fig. 6).

Whether or not the torsional rigidity plays a significant role may be determined by the size of the parameter $\nu = \left[1 + \frac{G\,C}{E\,\Gamma}\frac{4\,l^2}{\pi^2}\right]^{-1}$. The ratio $\frac{G\,C}{E\,\Gamma}\frac{4\,l^2}{\pi^2}$ is a measure of the relative stiffnesses of the channel in the St. Venant torsion and in differential bending. This follows from the two expressions previously given for $\beta(0)$, when it is understood that $I_y\,h^2$ is merely an approximation

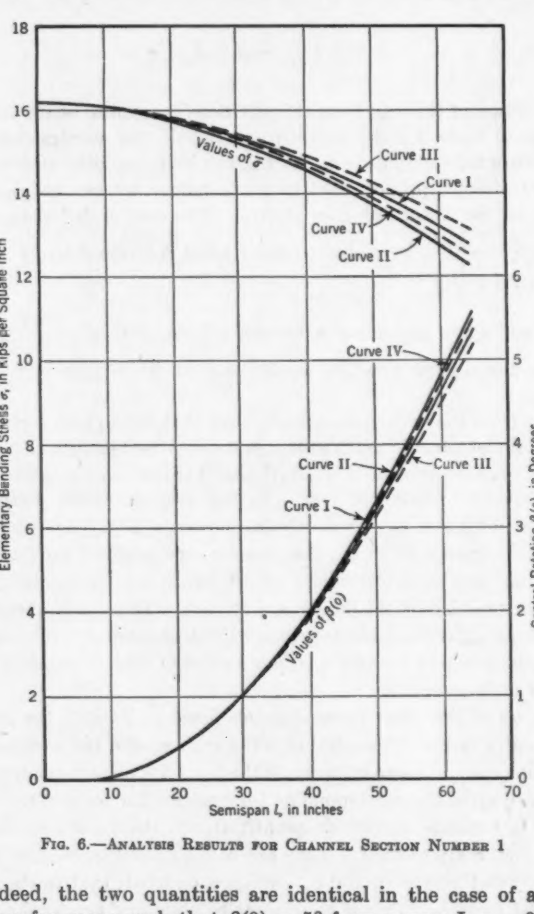

FIG. 6.—ANALYSIS RESULTS FOR CHANNEL SECTION NUMBER 1

for Γ. Indeed, the two quantities are identical in the case of an I-section. Evaluating ν for spans such that $\beta(0) = 5°$ from curves I, $\nu = 0.920$, 0.973, 0.734, and 0.927 for sections 1 through 4, respectively. It is seen that for $0.9 < \nu < 1$, the effect of the $G\,C$ term on $\beta(0)$ is very minor. For smaller values of ν, such as 0.734 for section 3, the increase in carrying capacity because of the torsional rigidity becomes significant.

Braced Channels

Solution for Intermediate Bracing.—The action of intermediate bracing is now easily visualized. It prevents horizontal displacement of the fictitious half-beams at the points of bracing; consequently, these half-beams are converted from simple beams of span length equal to that of the entire channel to continuous beams with individual spans equal to the distance between braces. If, for example, the braces were applied at the third points of the span, the half-beam would perform as the continuous beam shown in Fig. 7 when loaded by the force F as given by Eq. 36. The resulting maximum horizontal bending moment on the half-beam and the corresponding stresses of Fig. 3(b) are less than one quarter of those obtained without bracing, as can be verified easily by continuous beam analysis.

The tie rod correction for braced channels can always be neglected without noticeable error because of the reduced equivalent span. For example, in the case of bracing at the third points discussed above, the ratio T/T_{cr} is one ninth of the value without braces. A reduction of this magnitude will certainly move ν extremely close to unity.

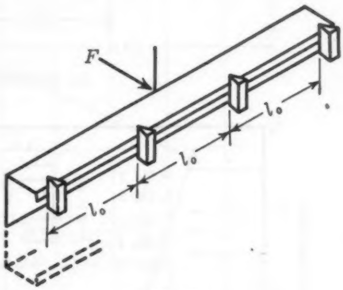

Fig. 7

The procedure, then, in braced channel problems, is based upon Eq. 35. Drawing upon the analogy between it and the equation for an ordinary beam, solutions are effected by any of the usual beam theory methods. Warping stresses are thereafter obtained from Eq. 28.

Tests.—Tests on braced channels have been performed by Mr. Winter and R. B. McCalley (J. M. ASCE) as one phase of an extensive research project on light-gage steel structures sponsored at Cornell University (Ithaca, N. Y.) by the American Iron and Steel Institute.[2] A brief summary of some of the results is presented here for completeness.

Seven different types of thin-walled channels were tested. Their depths ranged from 4 in. to 8 in., the widths from 2.5 in. to 4 in., and the thicknesses from 0.060 in. to 0.151 in., whereas the lips were about $\frac{3}{4}$ in. for all sections. Loads were applied through multiple ball bearings and knife edges to allow lateral and rotational motion as free from frictional constraint as was possible to achieve in a hydraulic testing machine. Analyses were made for the channels braced as in Fig. 8(a).

The measured and computed stresses are shown in Fig. 8(b) for that channel for which the agreement between experimental and theoretical values was least satisfactory. It is seen that the points of highest stress are the junctures of web and flange, with the stress being slightly larger at the upper one of these two points. These maximum stresses will govern practical design. The theoretical values are seen to agree with those from tests within about 5%.

Agreement is seen to be quite satisfactory also for station 4 in Fig. 8(*b*) but is rather far off for station 2. It should be noted that, in thin-walled members loaded in flexure, the cross sections were distorted out of their original shape to a degree that depends upon the width and thickness of the flanges and the depth

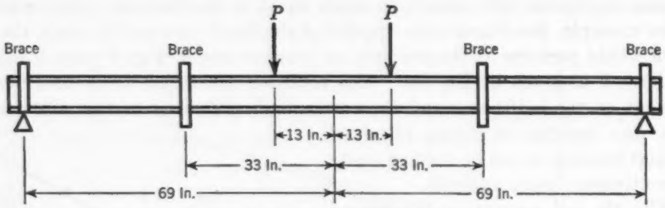

(*a*) BRACING OF TEST CHANNEL

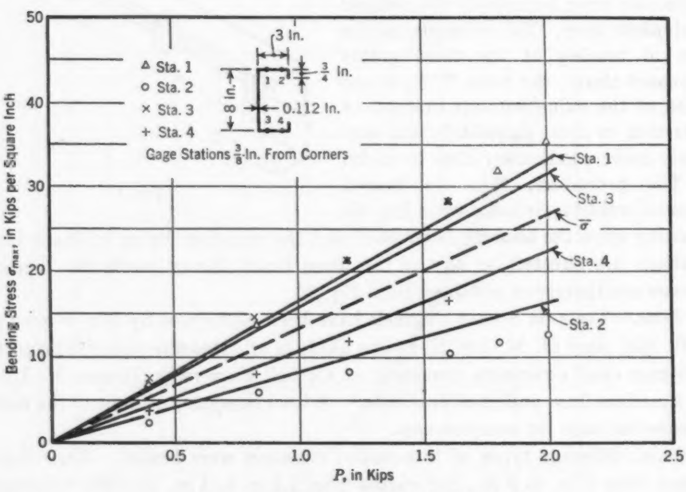

(*b*) MEASURED AND COMPUTED STRESSES FOR LEAST SATISFACTORY TEST CHANNEL

FIG. 8.—ANALYSIS OF BRACED CHANNEL

of the member.[17,18] This distortion, although small in practical terms, is likely to affect the distribution of the longitudinal stresses over the section, a factor that is not accounted for in the analysis.

[17] "Stress Distribution in and Equivalent Width of Flanges of Wide, Thin Wall Steel Beams," by G. Winter, *Technical Note No. 784*, National Advisory Committee for Aeronautics, Govt. Printing Office, Washington, D. C., November, 1940.

[18] "Performance of Thin Steel Compression Flanges," by George Winter, Third Congress of the International Assn. for Bridge and Structural Eng. Preliminary Publications, Liège, France, September, 1948, p. 137.

SIMPLY SUPPORTED Z-BEAMS

Eq. 10 has also been solved for simply supported **Z**-beams loaded in the plane of the web.[12] The particular loads considered were end couples, central force, and uniformly distributed load. Eq. 14 was again used for β, leading to the same type of calculations as described herein for the channel.

The counterpart of curves I of Fig. 6 is given in Fig. 9 for the **Z**-section that has the same cross-sectional dimensions as those of channel section No. 1, except that the flanges are turned in opposite directions. However, the loading

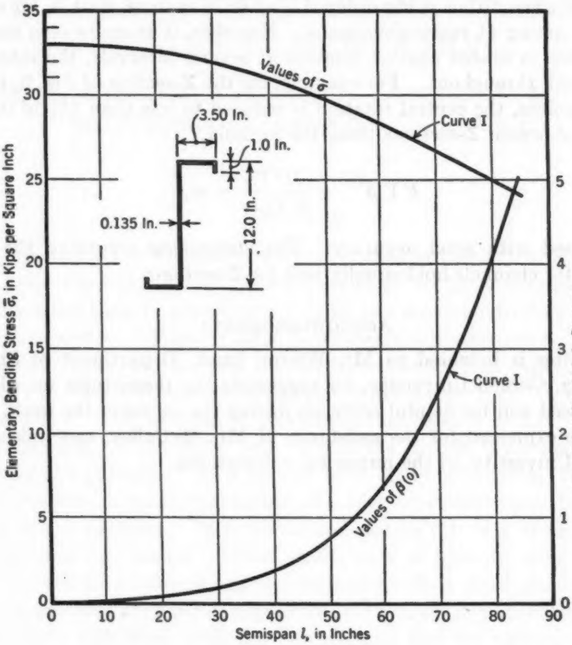

FIG. 9.—ANALYSIS RESULTS FOR Z-SECTION

is by end couples, as this results in larger secondary stresses and deflections than either of the other two types of loading systems for which analyses were made. The maximum stress again occurs at the upper junction of web and flange, although the stress at the extremity of the upper flange lip is only slightly smaller when $\beta(0)$ is of the order of 5°. It is seen that for very small spans the **Z**-section may be subjected to a moment (M) such that $\bar{\sigma} = \dfrac{M\,h\,I_z}{I_x\,I_y}$ = yield point. As the semispan l increases, $\bar{\sigma}$ drops off, and for $l = 85$ in. (for which $\beta(0)$ is 5°), $\bar{\sigma} = 24{,}100$ lb per sq in., or about 0.73 σ_{max}.

In order to determine whether the β term in Eq. 10 may be neglected in **Z**-beam problems, that equation is best written as

$$E\,\Gamma\,\beta'''' = \frac{M^2\,I_1}{E\,I_x\,I_y}\left(\frac{I_{12}}{I_1} - \beta\right) - m_z \ldots\ldots\ldots\ldots\ldots (37)$$

In the case of a **Z**-section loaded by end couples, with the origin at midspan, $\beta(l) = \beta'(0) = \beta''(l) = \beta'''(0) = 0$, $m_z = 0$, and, clearly, β can be replaced by zero only if it is small compared with I_{12}/I_1. Since the latter ranges from -0.218 to -0.614 for the sections available commercially,[16] this step is not permissible when $\beta(0)$ is of the order of 5° (0.0873 radian), that is, for unbraced **Z**-sections acting at reasonable spans. However, it is easily seen that, when the **Z**-section is braced against rotation at several intervals, the rotation will be very small throughout. For example, for the **Z**-section of Fig. 9, braced at the third points, the central rotation is reduced to less than 1% of its former value. For braced **Z**-sections then, the formula,

$$E\,\Gamma\,\beta'''' = \frac{M^2\,I_{12}}{E\,I_x\,I_y} - m_z \ldots\ldots\ldots\ldots\ldots\ldots\ldots (38)$$

may be used with good accuracy. The statements regarding the tie rod correction for channels hold equally well for **Z**-sections.

ACKNOWLEDGMENTS

The writer is indebted to Mr. Winter, head, Department of Structural Engineering, Cornell University, for suggesting the thesis topic on which this paper is based and for helpful criticism during the course of the work. Gratitude is also expressed for the assistance of Mr. McCalley, research associate at Cornell University, in the numerical calculations.

AMERICAN SOCIETY OF CIVIL ENGINEERS

Founded November 5, 1852

TRANSACTIONS

Paper No. 2540

FLOCCULATION PHENOMENA IN TURBID WATER CLARIFICATION

By W. F. Langelier,[1] Harvey F. Ludwig,[2] A. M. ASCE, and Russell G. Ludwig,[3] J. M. ASCE

Synopsis

Inorganic turbidity in natural waters consists principally of clay particles derived from the soil. These particles range up to 5μ in diameter, but the particles smaller than 1μ are the most stable and are of controlling importance in rapid flocculation. These smaller particles are characterized by, and derive their stability from, an electrical double layer surrounding each particle, the outer layer of which comprises exchangeable cations such as Na^+, K^+, Ca^{++}, Mg^{++}, and H^+. The addition of polyvalent cations such as Al^{+++}, Fe^{+++}, or other coagulants, to the water will repress the double layer and lower the stability of the particles. At a critical level of destabilization, the particles begin to coalesce, forming aggregates, at a rate dependent upon the exchange capacity of the particles. In most natural waters this rate of aggregation is slow, and some mechanical binding agent, such as hydrous aluminum oxide, is also required to accelerate aggregation and to effect rapid clarification. In practice, a properly adjusted dosage of a single hydrolyzing coagulant chemical, such as alum, will effect both the destabilizing and the mechanical binding actions.

Optimum flocculation represents the attainment of a complex equilibrium in which many variables are involved, including turbidity, particle size distribution, exchange capacity, pH, and alkalinity. Alkalinities above and below optimum result in excessive and insufficient production of binder material, respectively. Smaller clay colloids of less than 1μ size are necessary for stabilizing the hydrous oxide particles through mutual coagulation, and for

Note.—Published in February, 1952, as *Proceedings-Separate No. 118*. Positions and titles given are those in effect when the paper was received for publication.

[1] Prof. of San. Eng., University of California, Berkeley, Calif.

[2] Senior San. Engr., U. S. Public Health Service, Office of the Surgeon General, Washington, D. C.

[3] Cons. San. Engr., Ludwig Brothers, Engrs., Pasadena, Calif.

inducing agglomeration of other large particles present. Larger particles of 1 to 5μ size are needed to serve as building units, to form compact and dense flocs. If the water is initially deficient in colloids, its flocculation behavior may be improved by the addition of bentonites, activated silica, or other negatively charged colloidal material.

Introduction

Flocculation, as employed in the clarification of turbid water, has been the subject of many excellent papers extending over many years. Some of the most widely quoted of these[4,5,6,7,8] have dealt principally with the behavior of various coagulants as affected by the chemical properties of the water, but without particular consideration of the character of the dispersed phase. The authors have previously described results of flocculation experiments conducted with dilute suspensions prepared from known types of clays.[9] This paper briefly reviews the conclusions drawn therefrom and includes additional data amplifying the concepts previously developed.

In the earlier paper it was concluded that the rapid flocculation of turbid water with alum normally comprises two distinct reactions, one involving partial destabilization of turbidity particles by aluminum ions through ion exchange, the other involving formation of a hydrous oxide gel, resulting from the hydrolysis of the coagulant that serves as an agglomerating agent or binder material. In the treatment of most waters, a properly adjusted dosage of a hydrolyzing coagulant, such as an aluminum or ferric salt, will satisfy both demands economically, but in some cases, a preadjustment of buffer capacity and pH may improve performance and reduce cost by the alteration of the relative proportions of coagulant entering into the two basic reactions. In this concept, the phenomenon of mutual coagulation, which assumes the formation of positively charged hydrous oxide particles, is believed to be of secondary importance. Mutual coagulation may assist in bringing about the destabilization of turbidity particles and may aid the agglomerating action by facilitating the rapid agglomeration of newly forming hydrous oxide particles, but mutual coagulation is not essential to either process. Support of this belief is furnished by data showing that as the exchange capacity of the suspension increases above a critical limit, rapid flocculation and clarification are effected through the use of chemicals that do not hydrolyze to form insoluble hydroxides.

---

[4] "Coagulation of Water with Alum by Prolonged Agitation," by W. F. Langelier, *Engineering News-Record*, Vol. 86, 1921, p. 924.

[5] "An Experimental Study of the Relation of Hydrogen Ion Concentrations to the Formation of Floc in Alum Solutions," by Emery J. Theriault and W. Mansfield Clark, *Public Health Reports*, U. S. Public Health Service, Washington, D. C., Vol. 38, 1923, p. 181.

[6] "Alumina Floc—X-Ray Diffraction Study," by Henry B. Weiser, W. O. Milligan, and W. R. Purcell, *Industrial and Engineering Chemistry*, Vol. 32, 1940, p. 1487.

[7] "Effect of Salts on the Rate of Coagulation and the Optimum Precipitation of Alum Floc," by Ben H. Peterson and Edward Bartow, *Industrial and Engineering Chemistry*, Vol. 20, 1928, p. 51.

[8] "Formation of Floc by Aluminum Sulfate," by Edward Bartow, A. P. Black, and Owen Rice, *Industrial and Engineering Chemistry*, Vol. 25, 1933, p. 811.

[9] "Mechanism of Flocculation in the Clarification of Turbid Waters," by W. F. Langelier and H. F. Ludwig, *Journal*, Am. Water Works Assn., Vol. 41, 1949, p. 163.

Two equivalent representations of this concept of flocculation are shown in Fig. 1. For an ordinary water, the turbidity of which exhibits a relatively low exchange capacity, there are two possible flocculation zones: (1) Primary or normal flocculation; and (2) secondary or high-range flocculation. In normal flocculation the added coagulant is involved simultaneously in both an exchange and a hydrolysis reaction. In secondary flocculation, that is, in the presence of an excess of coagulant, destabilization and flocculation are brought about solely by the high concentration of active cations (Al^{+++} and H^+ ions). Fig. 1 shows that as the exchange capacity of the turbidity increases progressively, the zone of normal flocculation moves to the right and becomes increasingly wider. At the same time, the onset of secondary flocculation occurs in the presence of correspondingly less coagulant. At and above a certain critical exchange capacity, the two flocculation zones merge. At still higher exchange capacities,

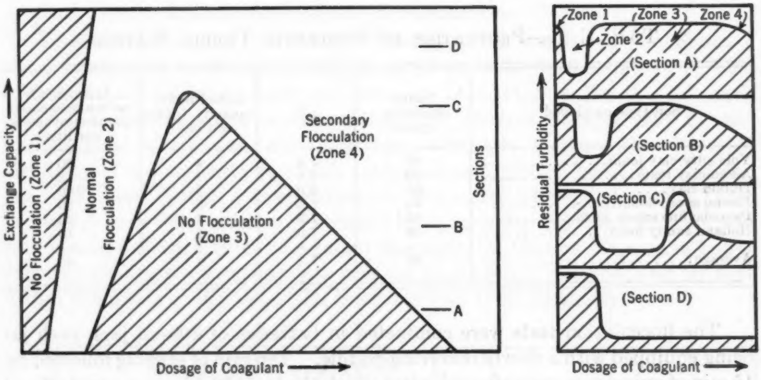

(*a*) GRAPHICAL REPRESENTATION OF FLOCCULATION PHENOMENA AS RELATED TO EXCHANGE CAPACITY

(*b*) SAME DATA SHOWING TURBIDITY REDUCTIONS

FIG. 1.—FLOCCULATION PHENOMENON RELATED TO EXCHANGE CAPACITY AND TURBIDITY REDUCTION

secondary flocculation supercedes the primary type, and excellent flocculation and clarification occur in the absence of hydrolysis. The exchange capacity of a given water can be increased by the addition of negatively charged colloids, as, for example, activated silica, bentonite, and various other materials. For waters of less than optimum turbidity or exchange capacity, the addition of such substances may greatly improve flocculation and clarification within the primary or normal range. The added particles, through their capacity to agglomerate rapidly when destabilized, promote the agglomeration of all of the suspended particles present. Also, the added particles may furnish buffer capacity that is valuable in the event that the chemical alkalinity of the system is low. In addition, as will be discussed later, these negatively charged colloids may be helpful in improving the density of the flocs.

Experimental Procedure

In Table 1 are given the properties of synthetic turbid waters prepared from six different representative types of soils. These suspensions were made by dispersing the original soil mass in distilled water and then allowing the suspension to settle for 24 hr, after which a proper depth of supernatant was siphoned off to include only particles of approximately 1.40μ (1μ = 0.001 mm) diameter or less. The resulting turbidities ranged from 45 to 63 ppm. In this approximate range of turbidity, the separate effects of the different flocculation variables are accentuated. In Table 1, the initial buffer capacity is the acid titre of the suspension and is the result of exchange adsorption of hydrogen ions by the clay particles. Exchange capacity is a property of the suspension obtained by multiplying the weight of the suspended particles (obtained by evaporation) by their exchange or saturation capacities as measured by the standard acetate procedure employed in soil technology.

TABLE 1.—Properties of Synthetic Turbid Waters

Soil type employed	Initial turbidity (ppm)	pH	Initial buffer capacity (ppm) as $CaCO_3$	Approximate exchange capacity (milliequivalents per liter)
Yolo silty clay loam	60	7.0	4	80
Aiken clay loam	62	7.0	4	15
Dublin clay	60	6.9	3	100
Fresno sandy loam	45	7.3	5	50
Panoche fine sandy loam	62	7.3	4	20
Holland sandy loam	58	7.0	4	10
Average	58	7.1	4	45

The flocculation tests were conducted in batteries of 200-ml jars, each jar being equipped with a slowly revolving paddle. Ten min of stirring followed by 15 min of quiescence were allowed, after which the top 100 ml was poured off and reserved for turbidity and pH measurement. The test data also included several other criteria, such as the floc quality, the time of floc formation, the rate of floc settling, and the size and quality of floc. Almost invariably, however, it was found that the turbidity reduction alone constituted an adequate criterion of optimum flocculation, for, in order to secure a low residual turbidity, each of the other factors had also to be at, or near, its respective optimum condition.

Five series of flocculation tests, employing alum as a coagulant, were undertaken for each of the six synthetic waters. In addition, two series of tests were made to study other pertinent factors. The test series are listed in the following tabulation:

Test series	Description
I	Varying concentrations of $NaHCO_3$, to indicate effects of bicarbonate alkalinity.
II	Varying concentrations of either NaOH or $Ca(OH)_2$, for adjustment of pH and buffer capacity.
III	Varying concentrations of either NaCl or Na_2SO_4, for anion or salinity effects.

Test series	Description
IV	Varying concentrations of sodium hexametaphosphate and sodium versenate, as examples of sequestering or chelating agents.
V	Varying concentrations of various surface active agents.
VI	Tests to determine the relative behavior of various hydrolyzing coagulants, such as aluminum sulfate, aluminum chloride, ferric chloride, ferric sulfate, thorium nitrate, and lanthanum chloride.
VII	Tests to study turbidity particle size distribution as related to coagulant demand.

In all tests following Series I, the samples were buffered with 0.5 milliequivalents per liter of $NaHCO_3$. This concentration of buffer or alkalinity was found to be the optimum, for the range of turbidities studied, for distinguishing the separate effects of the other variables.

Interpretation of Experimental Data

Effect of Bicarbonate Alkalinity.—The pertinent results of the Series I tests, which were made with $NaHCO_3$ added as buffer in amounts of 0, 0.20, 0.50, and 1.00 milliequivalents per liter, are illustrated in Fig. 2. For each water the plotted points represent the most efficient dosages (D_e) for the various total alkalinities (B). This total alkalinity includes the titratable alkalinity of the turbidity particles. Also, at each plotted point is shown the final pH-value (pH_e) corresponding to the most efficient dosage. These curves are seen to be a series of straight lines, showing: (*a*) That different soil suspensions exhibit different coagulant demands; (*b*) that an increase in buffer capacity results in a proportionate increase in coagulant demand; and (*c*) that within the limits of the tests, pH_e increases with total alkalinity.

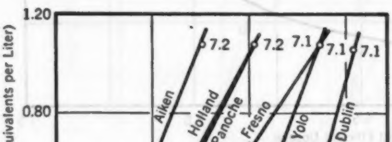

FIG. 2—COAGULANT DEMAND OF SOIL SUSPENSIONS IN WATERS OF VARYING TOTAL ALKALINITY

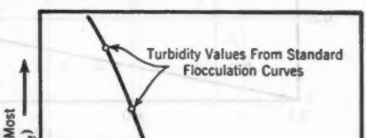

FIG. 3.—OPTIMUM FLOCCULATION CONDITIONS FOR A GIVEN WATER

If, for a given suspension, the various values of total alkalinity are plotted against the corresponding residual turbidities (T_e) at the most efficient dosage, a curve of the type shown by Fig. 3 is obtained. An examination of this curve permits selection of the minimum value of total alkalinity at which good

clarification occurs, and beyond which the resulting improvement in clarification is small, compared with the increase in coagulant that will be required to obtain this clarification. This alkalinity may properly be termed the optimum alkalinity (B_o) because it represents the greatest turbidity reduction obtainable commensurate with an economical coagulant dosage. The pH_e-value associated with this optimum value may be termed the optimum pH for that water, pH_o, and the most efficient dosage at that alkalinity the optimum dosage (D_o). For the six suspensions studied, the optimum alkalinity was from 0.5 to 0.8 milliequivalents per liter in every case, and the corresponding optimum pH-values varied between the narrow limits of 7.0 to 7.2.

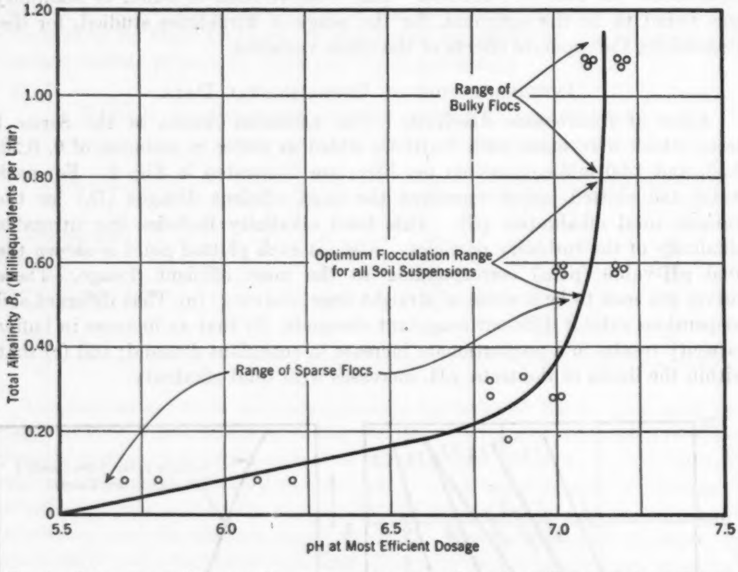

FIG. 4.—RELATIONSHIP BETWEEN TOTAL ALKALINITY AND pH AT MOST EFFICIENT ALUM DOSAGE

Fig. 4 has been plotted to show a typical variation in values of pH_e with increasing bicarbonate alkalinity. From this curve it is interesting to note that the value of pH_e increases with total alkalinity until it reaches a maximum of about 7.1. This relationship indicates that alkalinity in excess of optimum results in the waste of an equivalent amount of coagulant. In the treatment of waters of this type, it may be advantageous to neutralize a portion of the alkalinity with a strong acid prior to the addition of coagulant.[4] A probable explanation of this phenomenon may lie in the fact that in the presence of hydroxyl ions, the added aluminum ions form soluble complexes. Thus, when the initial pH is greater than optimum, the alum first added to the water would not form hydrous oxide but instead would combine with OH^- ions to form complex aluminate anions, liberating hydrogen ions. The continued removal of

OH^- will eventually lower the pH to the optimum, at which point a further addition of alum effects the normal reactions. Since at this point most of the complex cations would be converted to hydrous oxide, the resulting floc is bulky.

Referring again to Fig. 2, it will be noted that, although all of the suspensions have about the same initial turbidity and alkalinity and have approximately the same pH_e- and B_e-values, they exhibit variable coagulant demands. At a constant alkalinity of 0.5 milliequivalents per liter, the coagulant demands vary from about 4.5 ppm to 13.5 ppm. A comparison of the D_e-values with the exchange capacities for the various suspensions shows that, in general,

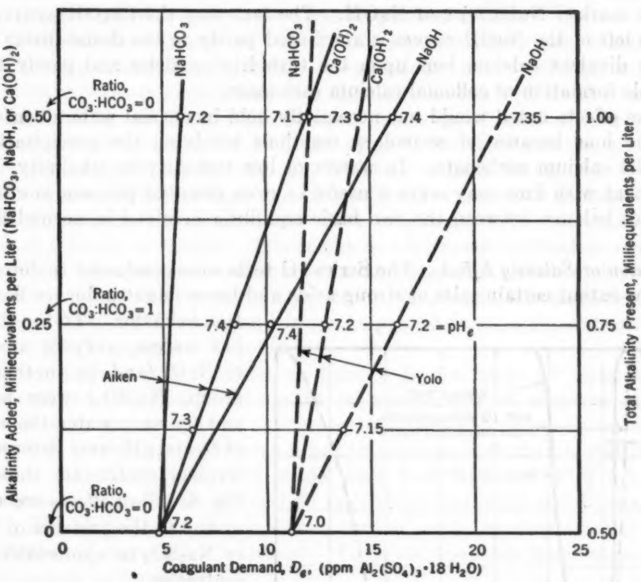

FIG. 5.—EFFECT OF CO_3 — HCO_3 RATIO ON ALUM DEMAND AT CONSTANT TOTAL ALKALINITY

values of D_e increase in an amount equal to the exchange capacity, indicating that greater amounts of Al^{+++} ions are needed for destabilizing the particles of greater exchange capacity. The lack of an absolutely consistent relationship between the values for D_e and the exchange capacity is probably, in part, the result of the variation in size distribution of the turbidity particles. The Series VII studies, discussed subsequently, were undertaken to investigate this factor.

Adjustment of pH and Buffer Capacity.—The Series II tests were made to determine the effect on alum coagulant demand of variable ratios of carbonate and bicarbonate alkalinity. For this purpose, varying increments of either sodium or calcium hydroxide were added to the bicarbonate suspensions.

The results for suspensions of two clay types that are typical are shown in Fig. 5. The curves in this figure indicate that the coagulant demand for a given total alkalinity increases as the ratio of carbonate to bicarbonate increases. The reason for this is apparent, when it is noted that efficient coagulation under the conditions of the test procedure occurs only upon the addition of sufficient alum to lower the pH to an approximately constant value of from 7.1 to 7.2. The amount of alum (or acid) required for this purpose is a function of both total alkalinity and buffer capacity; that is, the amount depends upon the types of alkalinity present and the buffer properties of these types in the pH-range considered. The separate effects of total alkalinity and of buffer capacity in the region above pH 7.2 are indicated by the relative slopes of the curves marked $NaHCO_3$ and NaOH. The fact that the $Ca(OH)_2$-curves fall to the left of the NaOH-curves is attributed partly to the destabilizing effect of the divalent calcium ions upon the turbidity particles and partly to the possible formation of colloidal calcium carbonate.

The effects noted would not necessarily hold in normal waters containing calcium ions because of secondary reactions involving the precipitation of colloidal calcium carbonate. In waters of low turbidity or alkalinity, a pretreatment with lime may serve a useful or even essential purpose in effecting a better balance between the two basic equilibria involved in normal flocculation.

Anion or Salinity Effect.—The Series III tests were conducted to determine to what extent certain salts of strong acids and bases might influence flocculation behavior. To the six turbid waters, varying amounts of NaCl (and, in another test group, Na_2SO_4) were added, and for each water the values of D_e and pH_e were determined. Typical results are shown in Fig. 6. Two effects are noted as due to the presence of NaCl or Na_2SO_4 in appreciable concentration:

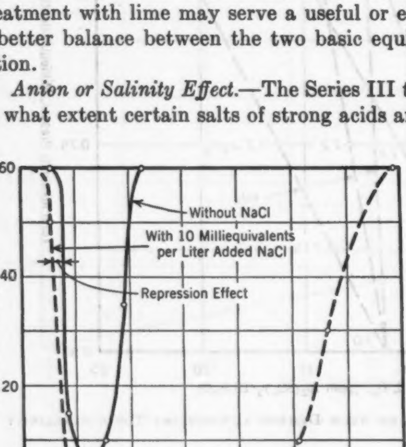

FIG. 6.—EFFECT OF SODIUM CHLORIDE ON ALUM DEMAND AND RESIDUAL TURBIDITY

1. The Na^+ ions exert a slight destabilizing effect, as illustrated by the slight decrease in coagulant demand. This phenomenon is in agreement with colloid theory and may be attributed to a repression, rather than an exchange effect caused by the high concentration of cations in the water medium surrounding the negatively-charged suspended clay particles.

2. The zone or range of effective clarification is appreciably widened. This effect is similar to that obtained by increasing the buffer capacity of the

system, but must be due to a different cause. The phenomenon has been noted and discussed by B. H. Peterson and Edward Bartow,[7] M. ASCE, and by Mr. Bartow, A. P. Black, and Owen Rice.[8]

Another observation made in this series of tests was that large dosages of either NaCl or Na_2SO_4, beginning at roughly 400 ppm, had a detrimental or dispersing effect on floc formation, resulting in a fine, slow-settling floc. Similar results have been observed in attempts to flocculate turbid sea water. H. T. S. Britton[10] notes that the chloride ion has a dispersing action on hydrous oxide micelles, and through peptization tends to prevent their formation. In the studies mentioned in this paper, however, similar phenomena occurred in the presence of either chloride or sulfate. A more likely explanation is that suggested by the work of Henry Bassett and Reginald Durrant.[11]

In discussing their "emulsoid" theory of hydrous oxides, these researchers report that the hydrous oxide micelle is, essentially, a very viscous or glassy liquid, with or without a crystalline core, that is separated from the surrounding water medium by an electric double layer made up of fixed cations and of oscillating counter anions. In addition, some of the fixed cations, and with them their accompanying anions, may infiltrate or pass through the particle surface into the viscous medium and so modify its composition from an initial, essentially hydrous aluminum oxide to a combination of this oxide with aluminum chloride or sulfate. The degree to which such infiltration occurs is a mass action phenomenon, so that when a large amount of a salt such as NaCl or Na_2SO_4 is added to the system, many of the resulting cations and anions pass into the micelle, until eventually it no longer exists as a separate mass of hydrous oxide but passes into solution.

Effect of Sequestering or Chelating Agents.—In the Series IV tests, sodium metaphosphate and sodium versenate (a sodium salt of ethylene digmine tetracedic acid) were employed as representative sequestering or chelating substances that, in practice, have been noted to interfere with normal flocculation behavior. The data from tests made with Yolo suspensions of 0.5 milliequivalents per liter alkalinity and 60 ppm initial turbidity are illustrated in Fig. 7. The alum dosage (D_e) increases linearly as the concentration of metaphosphate or of versenate is increased. For metaphosphate the relationship is approximately as follows:

$$D_e = 4.86\,C + 11.2 \qquad (1)$$

in which C is the concentration of sodium metaphosphate in ppm and D_e is in ppm of $Al_2(SO_4)_3 \cdot 18\,H_2O$. Thus, at an alkalinity of about 0.5 milliequivalents per liter, the presence of a unit weight of metaphosphate requires an increase in alum dosage of almost five units, if the flocculation results are to be satisfactory. It is significant, however, that the quality of the flocs produced at most efficient dosage progressively decreases as the concentration of metaphosphate increases. Furthermore, at metaphosphate concentrations of 5 ppm or more, normal alum flocculation could not be obtained, regardless of the amount of alum added.

[10] "Hydrogen Ions," by H. T. S. Britton, Chapman & Hall, Ltd., London, England, 1932.

[11] "Equilibria and Changes in Metal Hydroxide Sols," by Henry Bassett and Reginald G. Durrant, *Journal*, The Chemical Soc., London, England, 1942, p. 277.

The specific manner in which the metaphosphate causes this effect cannot be positively ascertained with the data at hand. The metaphosphate, through its sequestering properties, could conceivably interfere with both the destabilizing phase and the binder-agglomeration phase of the flocculation process. Mr. Bassett and Mr. Durrant[11] note that metaphosphates may partly prevent the hydrolysis of aluminum and ferric salts, and, also, that the hydrous oxide that does form will be peptized or dispersed. The observed data are readily explained by the application of this information; thus, metaphosphate inhibits the formation of proper binder, sequesters the polyvalent cations, and probably

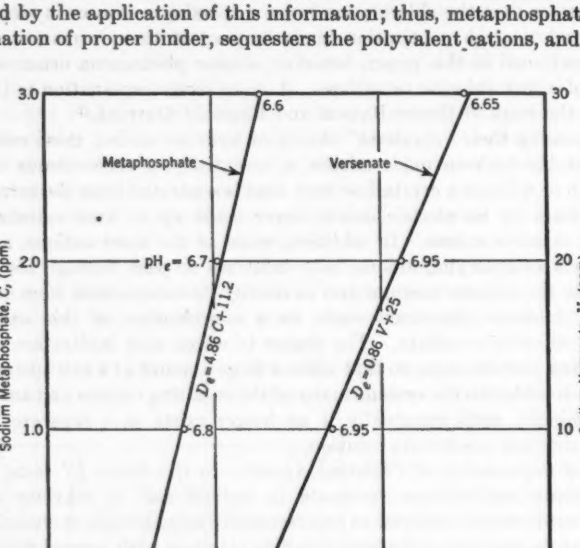

FIG. 7.—EFFECT OF SEQUESTERING AGENTS ON ALUM FLOCCULATION

also tends to peptize the clay turbidity particles and increase their resistance to destabilization. At low concentrations of metaphosphate, the first two of these adverse effects may be overcome simply by increasing the coagulant dosage to provide the necessary excess alum over that amount inactivated by the metaphosphate; but, even so, the peptization of the clay particles results in an inferior floc. At high concentrations of metaphosphate, the peptization of the clay particles may be so complete that no dosage of alum can affect their agglomeration.

It is interesting to note that the effect of metaphosphate on flocculation can scarcely be attributed to the formation of complex sodium-aluminum-phosphate anions in stoichiometric proportions.[12] For stoichiometric sequestration, the

[12] "Sequestration, Dispersion, and Dilatancy—Lecture Demonstrations," by T. H. Daugherty, *Journal of Chemical Education*, Vol. 25, 1948, p. 482.

amount of metaphosphate needed to sequester 1 milliequivalent per liter of Al^{+++} would be of a magnitude of from 100 to 200 ppm, whereas only 22.8 ppm are actually required. A possible explanation is that the metaphosphate consists of chains of molecules, the chains being of various lengths and intertwined so that the amount of aluminum ions sequestered by the metaphosphate molecule $(NaPO_3)_n$ could be much greater than indicated by the stoichiometric relationships. Another possible explanation assumes the formation of Werner complexes, in which a metaphosphate anion replaces one or more of the aqua groups attached to the hydrated Al^{+++} ion.

The results obtained with sodium versenate were similar to those obtained with metaphosphate, except that more versenate than metaphosphate is required to produce the same results. Also, it was possible to effect flocculation in the presence of as much as 170 ppm versenate, simply by adding sufficient alum, and the linear relationship extended over the entire 0 to 170 ppm range.

Effect of Surface Active Agents.—The Series V tests involved the effects of a number of the synthetic surface active agents on the flocculation of Yolo type suspensions. In recent years, these agents have come into wide use both in the home and in industry. One of the common properties of these substances is their ability to disperse colloidal particles, and in this action they achieve the opposite of flocculation or deflocculation. The various agents investigated included representatives of the anionic, cationic, and nonionic groups. As was anticipated, the results obtained varied widely for different agents. Of the anionics, Santamerse No. 1, an alkylarylsulfonate that is typical of the type of synthetic surface active agent now being produced in greatest quantities, was added in concentrations up to 50 ppm, and had no effect whatever on the flocculation phenomena. Similarly Sterox SE, a nonionic polyoxyethylene thioester, in concentrations up to 0.06% by volume, had no noticeable effect. However, Sterox CD, another nonionic, in a concentration by volume of 0.004%, caused the complete dispersion of a system that otherwise would have produced an excellent floc. Triton NE, a liquid nonionic polyoxyethylene ester, when added in concentrations by volume up to 2.0%, had only a slight effect on flocculation phenomena, in that it caused a slight increase in residual turbidity obtained with the same dosage of coagulant. Another anionic agent, TDA, interfered very much with normal flocculation behavior. A concentration of 0.005% by volume increased the coagulant demand of the test suspension from 25 ppm alum to 50 ppm, and a concentration of 0.01% by volume increased the coagulant demand to 100 ppm. In both instances, the residual turbidity at most efficient dosage increased considerably. Kreelon 4G, an anionic alkylarylsulfonate, showed no effect on flocculation behavior in concentrations up to 17 ppm but at this, and higher, concentrations effected increasing floc dispersion, reaching complete dispersion at 40 ppm. However, by increasing the alum dosage from its initial value of 25 ppm to 30 ppm, the dispersive action was completely overcome, and, in fact, the resulting flocs were of greatly increased size and density.

Tests were also made with one cationic agent, Hyamine 1622-CRYS, a quaternary compound. Additions of this compound up to 15 ppm did not influence the flocculation behavior, but a dosage of 20 ppm effected complete

dispersion of a system that otherwise would have developed a good floc. Also, increasing the alum dosage from its initial demand value of 25 ppm to dosages as high as 100 ppm did not overcome the dispersion effect. The dispersion effect of cationics might be expected to interfere in sewage treatment processes involving flocculation, except that the cationics are not compatible with the anionics, which are manufactured and employed in far greater amounts.

TABLE 2.—FLOCCULATION DATA EMPLOYING

Coagulant	Chemical formula	SYNTHETIC Yolo			Aiken			Dublin		
		Dosage in milli-equiva-lents per liter	In terms of alum[a]	pH_e	Dosage in milli-equiva-lents per liter	In terms of alum[a]	pH_e	Dosage in milli-equiva-lents per liter	In terms of alum[a]	pH_e
Alum	$Al_2(SO_4)_3 \cdot 18\ H_2O$	0.100	1.00	7.0	0.043	1.00	7.2	0.123	1.00	7.0
Aluminum chloride	$AlCl_3 \cdot 6\ H_2O$	0.100	1.00	7.0	0.046	1.07	7.2	0.131	1.07	6.9
Ferric chloride	$FeCl_3 \cdot 6\ H_2O$	0.230	2.30	6.7	0.150	3.48	6.8	0.220	1.79	6.6
Ferric sulfate	$Fe_2(SO_4)_3 \cdot 9\ H_2O$	0.290	2.90	6.5	0.150	3.48	6.8	0.260	2.11	6.6
Lanthanum chloride	$LaCl_3 \cdot 7\ H_2O$	0.100	1.00	7.2	0.100	2.32	7.15	0.200	1.63	6.9
Thorium nitrate	$Th(NO_3)_4 \cdot 4\ H_2O$	0.300	3.00	6.6	0.150	3.48	6.8	0.200	1.63	6.7

[a] Weight of coagulant required as compared with alum.

Relative Behavior of Various Hydrolyzing Coagulants.—The Series VI tests were made to compare in detail the relative flocculating efficiencies of various salts that hydrolyze to form an insoluble hydrous oxide binder material. For each of the salts or coagulants employed, the most efficient dosage, D_e, was determined for each of the six waters, buffered with 0.5 milliequivalents per liter $NaHCO_3$. The required coagulant dosages in milliequivalents per liter are given in Table 2.

The conclusions drawn from these data are as follows:

a. Aluminum chloride dosages are about 15% greater than those required with alum, but otherwise the phenomena are similar. The difference is attributed to the composition of the hydrous oxide micelles as affected by Cl^- and $SO_4^=$ ions. Mr. Britton[10] notes that the formation of visible hydrous oxide micelles from a solution of any hydrolyzing salt, when alkali is progressively added, is preceded by a period of formation of colloidal or "soluble" particles too small to be seen or to be effective. The presence of the Cl^- ion, either from the use of aluminum chloride or from the water medium, has a dispersing effect that promotes and prolongs the formation of inactive hydrous oxide and so decreases the efficiency of the coagulant. This effect has been described by Lewis B. Miller.[13]

b. Under the conditions of the tests, ferric chloride was more efficient than ferric sulfate, but both were much less efficient than alum on an equivalent basis.

[13] "A Study of the Effects of Anions Upon the Properties of 'Alum Floc,'" by Lewis B. Miller, *Public Health Reports*, U. S. Public Health Service, Washington, D. C., Vol. 40, 1925, p. 351.

c. Inasmuch as Fe^{+++} and Al^{+++} ions are regarded by colloid chemists as being approximately equal in their effect in the destabilization of clays,[14] it is concluded that hydrous ferric oxide binder is much less efficient than hydrous aluminum oxide binder, with approximately three times as much being required. Correspondingly, the pH_e-values obtained with the iron salts are lower than those obtained with the aluminum salts, by about 0.35 pH-units. However, it should be noted again that the tests were conducted under conditions favorable for alum flocculation, and for waters of different character, the efficiency of the iron salts might compare more favorably.

VARIOUS HYDROLYZING ELECTROLYTES

TURBID WATER DESIGNATION											
Fresno			Panoche			Holland			Average		
Dosage in milli-equiva-lents per liter	In terms of alum[a]	pH_e	Dosage in milli-equiva-lents per liter	In terms of alum[a]	pH_e	Dosage in milli-equiva-lents per liter	In terms of alum[a]	pH_e	Dosage in milli-equiva-lents per liter	In terms of alum[a]	pH_e
0.085	1.00	7.0	0.062	1.00	7.2	0.062	1.00	7.2	...	1.00	7.10
0.110	1.29	7.0	0.077	1.24	7.1	0.077	1.24	7.0	...	1.15	7.03
0.190	2.23	6.8	0.140	2.26	6.8	0.140	2.26	6.7	...	2.39	6.72
0.220	2.59	6.7	0.140	2.26	6.8	0.140	2.26	6.7	...	2.60	6.68
0.100	1.18	7.2	0.100	1.61	7.2	0.075	1.21	7.1	...	1.49	7.12
0.250	2.94	6.7	0.150	2.42	6.9	0.200	3.23	6.7	...	2.78	6.73

d. With lanthanum chloride as coagulant, the residual turbidities obtained at most efficient dosages are considerably higher than with iron and aluminum salts. The flocs produced were small and of poor quality. The La^{+++} ions are undoubtedly effective for destabilization, but apparently not enough binder material of good quality can form to be really effective. The poor performance of lanthanum may be attributed to the greater solubility of lanthanum hydrous oxide at ordinary pH-values. As shown by Mr. Britton, appreciable quantities of lanthanum hydrous oxide form only at a pH of 8.4 or greater.

e. Thorium nitrate is an effective and very rapid flocculating agent. In all tests it yielded extraordinarily large flocs. The turbidity reductions effected at most efficient dosage were considerably better than with any other coagulant. These excellent results may be attributed to a combination of a very powerful destabilizing agent, Th^{++++}, together with an excellent hydrous oxide binder. Mr. Britton notes that visible thorium hydrous oxide particles begin to form at pH-values as low as 3.5.

f. Considering each of the six salts tested, the pH_e-values are lower, as would be expected, in proportion to increased requirements for binder demand. However, the turbidity reductions effected at the most efficient dosage are somewhat greater in proportion to this increase in binder demand. Thus, to produce an effective hydrous iron oxide binder requires three times more ferric than

[14] "Properties of Colloids," by Hans Jenny, Stanford University, Stanford, Calif., 1938.

aluminum salt, but the clarification effected by the iron salts is consistently better to a small but noticeable degree. Similarly, to produce an effective hydrous thorium oxide binder requires about 3.7 times as much thorium salt as alum, but the resulting clarification is even better than that produced by the iron salts.

Effect of Particle Size.—An important variable in coagulant demand is the fineness of the particles that comprise the turbidity. In order to investigate

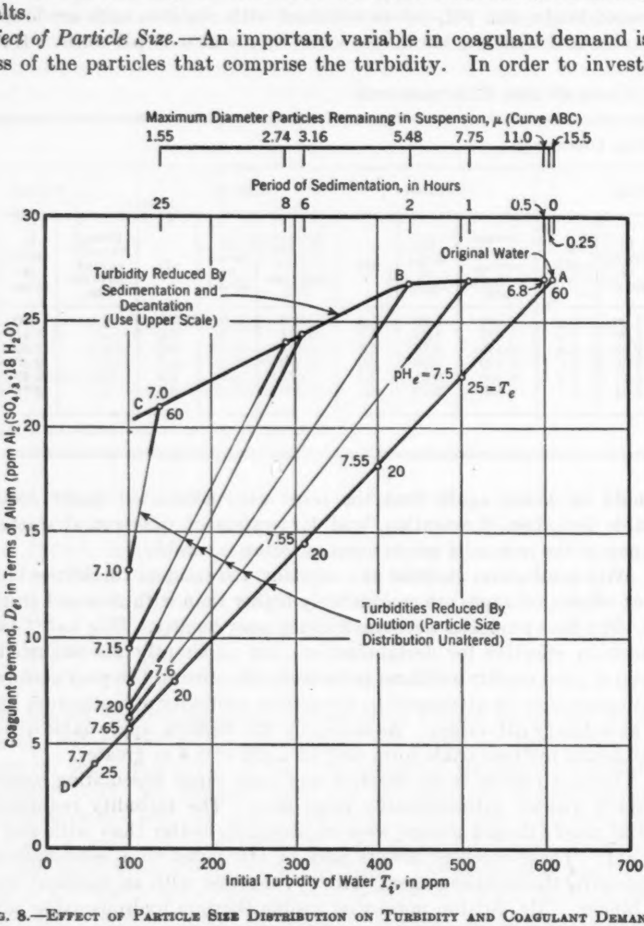

FIG. 8.—EFFECT OF PARTICLE SIZE DISTRIBUTION ON TURBIDITY AND COAGULANT DEMAND

the effect of varying particle size distribution, a stock suspension was prepared by dispersing Yolo silty clay loam in distilled water to a concentration of 1,000 ppm. This water had an initial turbidity of 610 ppm. Alum flocculation tests were made to determine its coagulant demand and also the coagulant demand of various dilutions of the stock suspension down to 10%, or 61 ppm, in each case in the presence of 0.5 milliequivalents per liter of $NaHCO_3$.

Other batches of the stock suspension were prepared and allowed to remain quiescent for varying periods of time, ranging from 15 min to 25 hr. Following the designated periods of settling, the top or supernatant 20 cm of each suspension was drawn off, and its coagulant demand similarly determined. In addition, coagulant demand tests were made of each of the settled waters after dilution to obtain uniform turbidities of 100 ppm. The results of these tests are plotted in Figs. 8 and 9.

The upper curve (ABC) of Fig. 8, with scales read from the top, shows the change in coagulant demand for varying turbidities obtained by plain settling and decantation. In the range AB there is practically no decrease in coagulant demand, indicating that particles greater than about 5μ diameter exert little, if any effect. It was noted in making the tests in this range that some of the particles were not incorporated into the flocs but settled rapidly to the bottom of the test jar. In the range BC no separation of particles was noted, but the coagulant demand decreased from 27 ppm to 21 ppm as a result of the absence of particles of diameters from about 5μ down to about 1.5μ. The coagulant demand at point C may be considered as comprising an exchange demand plus a binder demand. Soil technologists have shown that practically all the exchange capacity of a clay suspension is associated with particles smaller than 1.5μ diameter. Therefore, the exchange demand may be considered practically constant between points B and C, and the decrease in coagulant demand with decreasing turbidity must be the result of a lower binder demand This would be expected since the particles of 1.5–5μ size are incorporated into the floc.

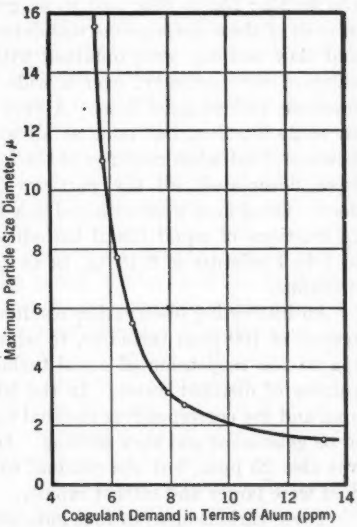

Fig. 9.—Effect of Particle Size on Coagulant Demand with a Constant Turbidity of 100 ppm Using Yolo Suspension

The lower curve (AD) of Fig. 8 shows that the coagulant demand of the diluted stock suspensions, wherein the particle size distribution remains unaltered, decreases in almost direct proportion to the decrease in turbidity. The intermediate curves have similar significance. These straight-line relationships indicate that dilution decreases both the exchange and binder demands in equal proportion.

The plotted points on a vertical line of Fig. 8 representing a constant turbidity of 100 ppm, show the variation in coagulant demand caused by differences in particle size distribution. In Fig. 9 these data have been replotted to show maximum particle size diameters. It will be noted that the coagulant

demand increases progressively as the percentage of smaller particles becomes greater, and that the rate of increase is very great when the particles present are predominantly of a diameter less than 2μ.

To gain additional information concerning the relationship between coagulant demand and particle size distribution, and also to confirm the results described, a suspension of the Yolo silty clay loam was fractionated by means of repeated subsidence and decantation. On the basis of Stoke's law computations, the suspension was separated into groups containing only particles of the following diameters: 0 to 1μ; 1μ to 2μ; 2μ to 5μ; 5μ to 15μ; 15μ to 25μ; 25μ to 60μ; and those greater than 60μ. The coagulant demand of each of these suspensions was determined. Good flocs, although gelatinous and slow settling, were obtained with the 0 to 1μ fraction, regardless of the value of the turbidity, over a wide range. Surprisingly, none of the other fractions yielded good flocs. A very few sparse flocs were obtained with the 1μ to 2μ fraction, but none at all with the coarser fractions. It was noted, however, that when mixtures of the finest fraction and various coarser fractions were flocculated, all the particles present were readily incorporated into flocs. Good flocs were obtained in a 1 to 1 mixture of the 0 to 1μ and the 1μ to 2μ fractions of equal initial turbidity. Similar results were obtained in a 2 to 1 to 1 mixture of 0 to 1μ, 1μ to 2μ, and 2μ to 5μ fractions of equal initial turbidity.

An interesting observation resulted from the alum flocculation of a 0 to 1μ system of 100 ppm turbidity, to which had been added 25% by volume of a 15μ to 25μ suspension of equal turbidity, as compared with adding 25% by volume of distilled water. In the latter case, the coagulant demand was 25 ppm and the corresponding residual turbidity 35 ppm, and the flocs were noted to be gelatinous and slow settling. In the former case, the coagulant demand was also 25 ppm, but the residual turbidity was reduced to 10 ppm and the flocs were larger and settled rapidly.

These various observations indicate the role of particle size in alum flocculation. The effective alum flocculation of a turbid water requires, in addition to suitable pH and alkalinity, turbidity particles both finer and coarser than approximately 1μ diameter. The smaller particles possess colloidal properties, and some of these are needed for neutralizing positive charges formed on the hydrous oxide binder particles (mutual coagulation). The aggregation of the colloidal turbidity particles, which results when they are destabilized by a suitable polyvalent cation, appears to induce agglomeration of the larger non-colloidal particles. This agglomerating action facilitates subsequent floc formation by the hydrous oxide binder material. The particles greater than 1μ serve as suitable structural units for building up dense rapidly settling flocs, in the same manner in which larger aggregates are graded with smaller aggregates in the making of dense concrete. The practice of adding powdered limestone as a coagulant aid in reactor-type flocculation units is an application of this principle.

If, in any given water, there is a shortage of either the finer or coarser particles, the addition of the missing material will result in more efficient flocculation and clarification. If the turbidity of a given water contains a

proper distribution with respect to both types of particles, the addition of either will increase the coagulant demand without improvement in clarification. Particles that are too large to be taken up by the flocs exert no effect on coagulant demand nor on flocculation behavior.

Summary and Conclusions

Inorganic turbidity in natural waters consists principally of clay particles derived from the soil. Those particles may range up to 5μ in diameter, but it is the less than 1μ colloidal fraction that is most stable and of controlling importance in rapid flocculation. Such colloids are characterized by, and derive their stability from, an electrical double layer surrounding each particle, comprising fixed inner negative charges balanced by various adsorbed cations (Na^+, K^+, Ca^{++}, Mg^{++}, or H^+) that diffuse into the surrounding water medium. Other cations present in the dispersion medium may enter into ion exchange reactions with the initially adsorbed cations, in accordance with the law of mass action and with the relative exchange adsorbabilities of the various cations. The addition of polyvalent cations to the system will repress the double layer and thus lower the stability of the particles, until a point is reached at which the particles begin to coalesce very slowly to form aggregates. Such aggregates will settle out over a long period of time, but the clarification effected by short-period settling comparable to plant practice will be negligible. Destabilization to a greater degree will increase the rate of coalescence, until finally a visible reduction in turbidity will be possible with short settling periods. The rate of coalescence at any degree of destabilization will be greater for particles having adsorbed cations that are initially Na^+ or K^+ rather than Ca^{++}, Mg^{++}, or H^+. A more important factor affecting the rate of agglomeration is the total exchange capacity of the turbidity particles; that is, the total concentration of adsorbed or exchangeable cations in the system. In waters of very high exchange capacities, exceeding certain critical limits, the agglomeration following destabilization will be very rapid, resulting in large flocs and rapid clarification. Any electrolyte yielding active cations (polyvalent or H^+ cations) will produce this effect, and the presence of a hydrolyzing coagulant, such as an aluminum and iron salt, is not required. Under these conditions the rapid agglomeration of the destabilized colloidal particles also induces the agglomeration of larger noncolloidal particles that may be present. Mutual coagulation is not involved in this type of flocculation.

Most natural waters contain less than critical concentrations of exchange capacity, and for these waters the aggregates that form following destabilization are too small for rapid settling. In order to effect a rapid clarification of normal waters, it is necessary that a suitable agglomerating agent or binder material be present, which will bind the various small aggregates into large and rapidly settling flocs. In practice, a properly adjusted dosage of a single hydrolyzing coagulant chemical, such as an aluminum or ferric salt, will effect both actions. In alum flocculation a portion of the Al^{+++} ions is effective in destabilizing the turbidity particles, and the remainder of the ions, through hydrolysis, form insoluble hydrous oxide binder material. The dosage of alum needed for the destabilization process will equal the exchange capacity of the system, and

essentially all of the initially absorbed cations will be replaced by Al^{+++}. The hydrous oxide required will depend upon the concentration and particle size distribution of the turbidity.

Optimum flocculation represents the attainment of a very complex equilibrium in which many variables are involved. Thus, for a given water there will be interrelated optima of conditions such as turbidity, particle size distribution, exchange capacity, pH, and alkalinity, at which proper amounts of destabilizing ions and also of hydrous oxide are produced with a minimum total coagulant dosage. Alkalinities in excess of optimum result in the waste of an equivalent amount of coagulant through production of excess binder material. At alkalinities less than optimum, not enough hydrous oxide can be produced to satisfy the binder demand of the particles. Also, for optimum flocculation, the water must contain a suitable number of colloidal clay particles of a size less than 1μ and a sufficient number of larger particles of sizes from 1μ to about 5μ. All of the exchange demand is associated with the less than 1μ fraction, but both fractions influence the binder demand. The smaller clay particles are necessary for stabilizing the hydrous oxide particles through mutual coagulation, and, also, their agglomeration following destabilization will induce agglomeration of other suspended particles present. The larger clay particles serve as building units to permit the formation of compact, dense flocs. If the water contains more of either type of particle than is needed for optimum results, the coagulant demand will be increased without corresponding benefit. If the water is initially deficient in colloids, its flocculation behavior may be improved by the addition of bentonite or other clay colloids of high exchange capacity, activated silica, or other negatively charged colloidal material. The addition of bentonites or other colloidal clays may also be helpful in providing buffer capacity to a water initially low in bicarbonate alkalinity.

Detergency, in a sense, is the opposite of flocculation, and the presence of detergents or surface active agents inhibits flocculation in varying degrees. They may peptize the turbidity particles, increasing their stability and thus inhibiting flocculation or preventing it altogether. Sequestering agents, such as hexametaphosphate, may similarly peptize the turbidity particles and, in addition, may inactivate an amount of coagulant equivalent to the number of active cations sequestered.

AMERICAN SOCIETY OF CIVIL ENGINEERS

Founded November 5, 1852

TRANSACTIONS

Paper No. 2541

UNDERGROUND CORROSION OF PIPING

By R. A. Brannon[1]

With Discussion by Messrs. Lyle R. Sheppard, and R. A. Brannon

Synopsis

The corrosion of the outside surfaces of underground metallic piping is an electrolytic phenomenon dependent on the presence at the pipe surface of water containing dissolved salts or gases. This corrosion is always associated with the flow of electric current from metal to solution and from solution to pipe. There is little difference in the rate at which metals usually employed for pipe fabricating corrode underground. It does not seem likely that metals having inherent corrosion resisting properties will be developed and made available in the quantities and at the low prices required.

The electrolytic nature of corrosion suggests two methods of corrosion control: (1) The prevention of contact between the pipe and the soil water by means of protective coating and (2) the use of electric currents to counteract the currents associated with corrosion. Satisfactory and effective protective coatings are available, and cathodic protection, which utilizes electric current, is being more and more widely used to control corrosion. By judicious uses of either, or both, of these methods, almost any desired degree of corrosion control can be achieved.

The large number of variable factors that must be evaluated in each corrosion control problem gives rise to a need for engineers with specialized knowledge of the principles and techniques of corrosion control. There is a large and growing group of corrosion engineers who are acquiring more and more of this knowledge.

The success with which it is now possible to control the corrosion of underground piping may indicate a need for a re-examination of earlier studies on which the selection of materials for such piping was based.

Note.—Published in May, 1952, as *Proceedings-Separate No. 130*. Positions and titles given are those in effect when the paper or the discussion was received for publication.

[1] Supervising Corrosion Engr., Humble Pipe Line Co., Houston, Tex.

Introduction

This discussion of the subject of underground corrosion of piping will be based on the writer's experience in the industry of transporting liquid petroleum by pipe lines, and his association with others in this industry and the related industry of transporting petroleum gas by pipe lines. Although the underground piping systems with which members of the ASCE are concerned may differ in many respects from those in the oil and gas industries, it is likely that many of the corrosion problems are common to all of them. This paper will be limited to the corrosion of the outside of metal piping buried in soil.

Nature of Underground Corrosion

The corrosion of metals buried in soil results from electrolytic action between the metals and the moisture present in the soil. The moisture contains dissolved salts and gases (principally oxygen) and serves as the electrolyte in this electrolytic action. Since moisture is usually present in varying amounts, and this moisture contains varying amounts of dissolved matter, there is an infinite variety in the rate of corrosion of buried metals and in the pattern that the corrosion takes. Electrolytic corrosion is always associated with a flow of electric current. This current flows from the metal into the electrolyte (in this case the soil water) at the points at which the metal is corroding, thence through the soil water to other points on the metal surface and back into the metal. The circuit is completed by the flow of the current through the metal back to the points of discharge. The areas of metal at which current is discharged from the metal to the electrolyte are known as anodic areas, and the metal areas at which current is collected from the electrolyte are known as cathodic areas. At anodic areas, iron is oxidized from the metallic state to ferrous ions that pass into solution in the electrolyte, while at the cathodic areas, a chemically-equivalent amount of ionic hydrogen is reduced to the gaseous state and plated out on the metal surfaces. There is a definite relation between the quantity of iron which goes from the metallic state into solution and the amount of current in the electrolytic circuit. One ampere passing from metallic iron into an electrolyte for a period of one year will result in 20 lb of iron being changed from the metallic to the ionic, or soluble, state. Conversely, the corrosion of 20 lb of metallic iron will result in the generation of the equivalent of 1 ampere-year of current.

Normally, the anodic areas are quite small in comparison with the cathodic areas. It is this characteristic of electrolytic corrosion that makes it so important to owners and operators of underground piping systems. In few cases would the metal loss resulting from corrosion be of economic importance if the loss were uniformly distributed over the entire surface area. It is this concentration of the metal loss at the small anodic areas that results in the familiar pitting of the metal. These pits frequently develop at such rates as to result in the early penetration of the pipe walls.

The question, "Why do some areas of underground pipe surfaces become anodic while others become cathodic?" can only be answered by stating that the causes can be infinite in number and variety. Some of the more common causes are as follows: Variations in the concentration of dissolved salts in the

soil water; variations in the amount of oxygen dissolved in the soil water; variations in the condition of the pipe; and contact with other metals or substances such as carbon and cinders. Survey methods have been developed that may be used to predict with good accuracy the corrosiveness of soils on piping systems to be buried in them. Other methods are available for determining whether a piping system that has already been installed is corroding, and where the corrosion is taking place. The consideration of these methods is beyond the scope of this paper.

The knowledge that corrosion of underground piping systems is electrolytic in nature—that is, dependent upon the presence at the metal surface of soil water—and that such corrosion is always associated with a flow of electric current, is of practical value because it suggests methods of controlling the corrosion.

Methods of Corrosion Control

Methods of Construction Other Than Burial in Soil.—Although there is a trend toward the installation of piping above the ground in the petroleum industry, the vast majority of the pipe is still installed underground. There seems to be little likelihood that the practice of burying water supply and sewage lines will be changed to any significant degree. Overhead stream crossings are fairly common in all types of piping systems, and corrosion control is one of the reasons for using this method of construction. This method of control is quite important in those cases in which it is applicable, but can only be used in a tiny fraction of the total amount of pipe in service. The installation of piping in conduits, with provisions for draining soil water away from the pipe, or other special construction, might be applicable in certain situations but is not usually practical for extensive piping systems.

In general, it may be stated that there is no satisfactory method of constructing extensive piping systems except by burying them underground. Exceptions to this rule are found in the case of pipe lines constructed in sparsely settled areas.

Selection of Materials of Construction.—A method of reducing the corrosion rate that naturally suggests itself to many people is that of selecting a material that is inherently resistant to corrosion. One of the principal reasons for the almost universal use of vitrified-clay pipe or concrete pipe for main sewage lines is the resistance of these materials to corrosion. The success with which certain piping materials can withstand atmospheric and other common corrosion enviroments naturally leads to the assumption that a metal can be found or produced that will satisfactorily withstand soil corrosion.

The present prospects that such a metal will be found are not encouraging. Investigations conducted by the National Bureau of Standards, Underground Corrosion Section,[2,3] have indicated that there is no significant difference in the rate of corrosion of metals commonly used in making pipe, when buried in soil. This rate applies to cast iron, wrought iron, steel (both Bessemer and open hearth), and iron or steel alloyed with small amounts of such metals as copper,

[2] "Underground Corrosion," *Circular C 450*, National Bureau of Standards, U.S. Dept. of Commerce, Washington, D.C., 1945, pp. 241–244.

[3] "Soil Corrosion and Pipe Line Protection," by Scott Ewing, Am. Gas Assn., New York, N. Y., 1938, pp. 33–44.

nickel, and chromium. A significant reduction in the corrosion rate was observed only when the alloying elements were greatly increased, as exemplified by stainless steels such as those containing 18% chromium and 8% nickel. It is obvious, of course, that alloys such as these are not available in the quantities required for underground piping and that their cost is too high to consider them seriously for such use.

Cast-iron pipe has a long record of successful and satisfactory use under many conditions in the water supply and sewage handling fields. In so far as soil corrosion is concerned, one of the principal reasons for this success is that, being a much cheaper material on a weight basis than other metallic pipe materials, such as steel or wrought iron, the pipe is usually made with relatively thick wall sections. These thick walls allow a considerable amount of corrosion to take place before failure occurs and instances are on record in which the graphite remaining after all the iron had corroded out had continued to give satisfactory service.

Copper pipe is now being widely used in service lines from water mains to the facilities of small consumers, such as home owners and small businesses. Copper pipe has many advantages as compared with pipe made of other materials, in addition to its excellent corrosion resistance. It should be remembered, however, that copper, being a metal that is more noble than iron, will form a galvanic couple with iron and may cause the corrosion of the iron in the vicinity of the contact between the two metals. Since the amount of copper pipe is usually quite small in comparison with the amount of iron pipe to which it is connected, the amount of corrosion resulting from such installations is negligible in most cases. There is a possibility, however, that an increasing use of copper pipe in conjunction with iron pipe may lead to the corrosion of the iron pipe which will be of economic importance. It should also be remembered that the copper pipe is protected from corrosion to some extent because of its connection to the iron pipe and its corrosion resistance may not be so good if it is used in sufficient quantities, or if it is electrically insulated from all buried iron structures.

The subject of selection of materials of construction as a means of corrosion control may be summarized by stating that there is no appreciable difference in the underground corrosion rate of metals commonly used in large quantities for making pipe. Pipe made of cast iron has certain advantages with regard to corrosion resistance, principally because of its structure and, to some extent, because of other factors such as silicon content and the nature of the corrosion products. These other factors are complicated and variable in nature and were not discussed. Piping made of higher priced material such as copper is used in limited amounts in some cases, such as for domestic service lines, in which the cost of the pipe material is not a major factor in the over-all cost of the installation.

Preventing Contact Between the Pipe and the Corrosive Agent by Protective Coatings.—The corrosion of underground piping is an electrolytic phenomenon, therefore, it is necessary that soil moisture be in contact with the surface of the pipe in order for corrosion to occur. It would seem to be a relatively simple

matter to apply a paint or coating that would keep the moisture from contact with the pipe.

Experience with iron and steel structures above ground had shown that certain paints were effective to a satisfactory degree in preventing atmospheric corrosion. When these paints were used on underground piping, it was found that the exposure conditions were vastly different. Under atmospheric conditions the painted surface would be alternately wet and dry. Even porous coatings would resist moisture for considerable periods, and corrosion caused by moisture reaching the metal would stop when the surface became dry again. The soluble ferrous iron would be oxidized almost immediately to insoluble ferric oxide that would tend to plug the pores in the coating and to cover any exposed metal with dense corrosion products that were very nearly waterproof. Underground, the soil moisture was continuously present in varying concentrations so that there was little opportunity for the drying of the paint film. Under many conditions, the soil water was anaerobic, or free of dissolved oxygen, so that the soluble ferrous iron could migrate considerable distances away from the pipe before it was oxidized. Under such conditions, protective films or coatings of corrosion products were not formed.

It soon became apparent to early operators of underground piping systems that paints that dry by evaporation of solvents are not well suited for the prevention of underground corrosion in those areas where such corrosion is really severe. Evaporation of the solvent left pores in the paint film that allowed water to pass through to the metal, with the result that the pitting rate was not seriously reduced by the application of the paint. These operators then turned to the application of bituminous coatings, such as asphalt and coal tar, which were heated and applied in a molten state. These coatings set to various degrees of hardness upon cooling and many of them were satisfactory in their resistance to the absorption of soil moisture and maintained this property for long periods of time. These coatings usually consisted of a priming coat made up of the bitumen dissolved in a solvent. This primer, being quite thin and free flowing at the time of application, penetrated the irregularities in the pipe surface and, after drying, served as a bonding agent between the pipe and the hot bitumen.

The early destruction of many of these coatings led to the discovery that the principal cause of failure was the physical action of the soil. This action, given the name, "soil stress," results when the soil shrinks and swells with changes in moisture content and during the settling period while the loose backfill over and around the pipe is being consolidated to its normal consistency. These stresses are of considerable magnitude and are exerted over long periods of time so that the bituminous coatings, which are susceptible to cold-flow, are readily distorted and penetrated. Early attempts to overcome the effects of soil stress consisted of adding fillers to the bituminous coatings, thus increasing their resistance to cold-flow. These hardened enamels provided some improvement in coating service, but it soon became apparent that additional reinforcement and shielding were required in many cases.

There are two principal requirements that a protective coating must meet. The first is that it shall be waterproof and prevent soil moisture from coming

into contact with the pipe. Owing to the obvious difficulties involved in inspecting, repairing, and recoating underground piping, this property must be maintained for long periods of time and preferably for the service life of the installation. The second is that the coating shall be able to resist soil stress to such a degree that it will not readily be penetrated to the metal at any point. It has been determined that this soil-stress action is not limited to the period of backfill settling but that it persists as long as there are changes in the moisture content of the soil that cause corresponding changes in the specific volumes of the soil.

Metal Coatings.—The use of coatings of metals more noble and more resistant to corrosion than iron, such as copper, tin, or nickel, as protection for iron pipe has not been successful because the cost of these metals limits to a few thousandths of an inch the thickness of the coating that can be applied. These thin coatings are easily broken mechanically, and the underlying iron becomes anodic to the coating at the points of coating failure with the result that the pipe is rapidly pitted, and early failure results. The metals that are baser than iron, such as zinc and cadmium, are more effective as coatings for pipe.

Zinc-coated, or galvanized, pipe is widely used in service lines and for other installations in which small diameter pipe is necessary. The galvanized pipe gives longer service than bare iron or steel pipe because the zinc is usually attacked at a lower rate than iron, and after the zinc has corroded in some areas it continues to provide protection to the exposed iron by galvanic action. In some areas galvanized pipe does not provide satisfactory length of service and additional methods of corrosion control are needed. The life of the zinc coating is likely to be greatly reduced because of galvanic action, if the small service lines are connected directly to large uncoated iron mains. The same action might result from the connection of galvanized pipe to buried copper pipe. The electrical insulation from each other of pipes having different metals exposed to the soil should be considered.

Cadmium coatings, which are usually applied to iron or steel by the electroplating process, are approximately equivalent to zinc coatings in effectiveness. They are several times as expensive, however, and are not of commercial importance as pipe coatings.

Such metals as magnesium and aluminum would be suitable as coatings for iron from the standpoint of their galvanic action, but they have not been used for this purpose. Advantage is being taken of their galvanic action to provide cathodic protection to iron and steel pipes.

Paints.—As a general rule, paints are not effective for corrosion protection for underground piping because most of them are not waterproof for long periods of submersion; and, because they are relatively thin, they are readily penetrated by stones, clods of earth, and soil stress. There are locations, however, in which paints, such as the bitumen-in-solvent type, provide economical and satisfactory corrosion control. In these cases, the soil is usually sandy and does not exhibit soil-stress effects. The soil is also likely to be dry most of the time. Instances are on record in which bare pipe corroded rapidly in such soils, although parallel lines painted with asphalt solution were not at-

tacked. Other factors may have also influenced the corrosion rates, but considerable benefit from the paint coating was indicated.

Pipe manufacturers realize that the rusting of pipe in transit and in storage prior to use will detract from the appearance of the pipe and sometimes result in damage. Clear lacquer or other paints is frequently applied to steel pipe to prevent this rusting. Since the removal of these mill-applied paints is usually regarded as necessary before the application of additional protective coatings, it is general practice to order pipe without them.

Bituminous Coatings.—The most widely used coating materials for preventing corrosion of underground piping are bituminous enamels applied in the molten state over primers prepared from corresponding materials. The enamels are nearly always reinforced by having a mat of glass fibers imbedded in them, or shielded by an outer wrap of asbestos felt, or both.

As mentioned previously, the bituminous coating materials have been modified during manufacture to increase their resistance to cold-flow. There are factors that limit this modification, however, because hardness and brittleness go together and the coating must remain flexible enough at low atmospheric temperatures to permit handling of the pipe during the remaining construction operations without cracking the coating. Special enamels have been developed that remain sufficiently flexible to prevent cracking at low temperatures and that still exhibit satisfactory resistance to cold-flow. These are sometimes referred to as modified or plasticized enamels.

The use of glass fibers as reinforcing materials is fairly new. Several trial uses had been made prior to 1945, but since that time their use has become quite general. When imbedded in the enamel coating, the glass fibers, possessing tremendous strength in relation to their size, act as a reinforcement. This gives added resistance to shattering that might occur as the result of blows received during construction operations and to cold-flow that might result from the steady, long applied forces of soil stress.

Asbestos felt, saturated with asphalt or coal tar to match the bituminous enamel, has been used as a part of pipe line coatings for many years. The felt is wrapped over the enamel, usually while the enamel is still hot, so that the two materials are fused together. The felt acts to extend the areas on which pressures from rocks, clods, and soil stress act, so that the unit stress on the enamel is reduced and distortion is thereby reduced.

There have been attempts, with some success, to make pipe-coating shields of other materials, such as glass fibers. Rag or paper base felts were used in the beginning as pipe coating shields, but their use declined rapidly when experience showed that they were readily attacked and destroyed by soil bacteria and when the need for a long lasting shield to resist soil stress beyond the initial backfill settling period was demonstrated.

The selection of the coating structure to be used, as well as the selection of the component parts of the coating, is based on a consideration of many factors, including—known or predicted severity of the corrosive action; degree of soil stress action to be expected; cost of materials and application; length of service expected of the coating; the possible use of alternate or auxiliary methods of

corrosion control such as cathodic protection; and consequences of failure of the piping system. The coating structures in which bituminous materials are utilized, and some of the factors affecting their performance will now be described briefly.

Primer and enamel coatings without reinforcements or shields are not widely used because they offer little resistance to soil stress, and the additional cost of a reinforcement or shield is small compared with the total cost of the coating. The added strength of the coating is much greater than the added cost. Primer, enamel, and asbestos felt is a coating structure that is very widely used. It has adequate waterproofing and soil-stress resisting properties to give satisfactory service under a wide range of conditions. Application methods have been developed that make possible the installation of this type of coating at costs that are comparable to costs of simpler and less effective coatings.

Primer, enamel, and glass fiber reinforcement is a coating structure that came into use during a period when there was an insufficient quantity of asbestos felt on the market to meet the needs of industry. This structure is still favored by some engineers and is being rather widely used. The glass fiber material is considerably lower in cost than asbestos felt, and this probably accounts for a large part of its popularity. An outside wrap of kraft paper is frequently used with this coating structure to provide heat reflection during construction operations, greater toughness to resist damage from handling operations, and a measure of shielding effect during the period of backfill settling.

Primer, enamel, glass fiber reinforcement and asbestos felt is a fairly complex structure that may be used for one or more reasons. The value and cost of the installation may be such that the extra cost of the more effective coating may be readily justified, the pipe line may be located in an area in which its failure would be especially expensive or hazardous and extra effort should be made to prevent corrosion failures, or the soil may be unusually corrosive or exhibit unusual soil-stress effects. The use of this coating structure is quite common on major construction projects.

Mastics are coatings composed of graded sand, limestone dust, asbestos fiber, and a bituminous binder. These coatings are heated for application and are installed on primed pipe. Special equipment has been developed for application by extruding the mastic around the pipe. Upon cooling, a very hard coating is formed that has exceptionally good resistance to soil stress and moisture penetration. These coatings are usually quite thick in comparison to other coatings, and experience has shown them to be very effective in preventing corrosion. The mastics have several disadvantages, such as requiring great quantities and weights of materials, leading to considerable materials-handling costs either before or after the application of the coating to the pipe, specialized equipment not generally available to the industry is required for application, and special skills are required in the patching and repairing of the coating. Even considering these handicaps, it is possible under some circumstances to obtain mastic coatings at prices that are competitive with prices of other coatings.

Tapes saturated with bitumen are available for wrapping pipe. By heating the tapes during and after application, fairly homogeneous coatings can be obtained. The unit costs of coatings made from these tapes are quite high, and they are intended for use at locations in which small amounts of coating are to be applied and the unit application cost of other type coatings would be extremely high.

The preparation of the metal surface of the pipe is just as important for the proper functioning of a pipe protective coating as for any paint coating. Although great improvements have been made in the equipment available for cleaning pipe, there are some conditions under which it is extremely difficult to achieve a satisfactory job of metal surface preparation. Used pipe that is rough and pitted is especially hard to clean, and conditions sometimes exist in the field making the complete removal of moisture from the surface of the pipe practically impossible. In cases in which the pipe is at a lower temperature than the surrounding air, there is a danger that moisture will be present on the pipe surface. Probably the best cleaning jobs are accomplished by heating the pipe to a temperature several degrees above atmospheric, sandblasting or shot blasting the pipe for removal of scale, rust, and other foreign matter, and then priming the pipe while it is still at a temperature above atmospheric.

The use of proper application techniques and proper materials—handling techniques—is especially important in the case of pipe line coatings. Once the lines are buried, an inspection of the coatings to detect flaws becomes quite difficult, and the repair of the coatings becomes so costly as to be impractical in most cases.

Several companies specialize in the application of protective coatings to pipe in plants set up at pipe mills or at conveniently located shipping points. Semiportable plants are sometimes set up at rail heads, or other points at which the pipe can be routed through the plants as it is moved to points of use. Each length of pipe is coated, leaving a few inches of bare pipe at each end for jointing. Such plants have certain advantages compared with field operations—shelter can be provided to protect the operations from the weather; it is a comparatively simple matter to provide for heating the pipe; heavier, more substantial and, in some cases, more effective equipment can be used; the pipe can be rotated for both cleaning and coating operations, permitting better inspection and control of these operations; and the ability to offer steady employment at one location may lead to more efficient work on the part of the application crews.

Equipment and methods have been developed for efficient and effective application of protective coatings in the field. The method of installation in which the coating is applied to the pipe in one continuous operation after the pipe has been joined, usually by welding, has certain advantages over the plant method of coating individual lengths of pipe and then coating the joints after the pipe has been welded into the line. Each method of coating application has advantages or objections, depending upon the conditions of the situation under which the pipe line is to be constructed. In some cases these conditions make the advantages of one or the other so obvious that the selection of the method is easy. In other cases, the conditions may be such as to make

the selection of method dependent upon the personal preference of the engineer or other person responsible for the selection.

Regardless of the method employed, it should always be recognized that a proper application of protective coatings requires considerable skill and experience on the part of the operators and inspectors. The best of materials will be of little value if they are not properly applied.

Concrete Coatings.—Concrete coatings applied directly to steel pipe have been used to some extent. The concrete was usually applied to a thickness of 1.5 in. or more by using either removable forms or wooden forms that were left in place, or by pouring the concrete into the ditch after the pipe had been placed, with spacers to hold the pipe in position. These coatings were effective in preventing corrosion when properly applied, but have not been widely used because of the high cost and the low rate at which they can be applied.

There has been a considerable use of concrete coatings over bituminous coatings for special applications. These coatings have been applied by forming in molds or by cement guns or variations. They are usually applied for the dual purpose of providing a rigid outside shield, and providing weight to prevent large diameter pipes carrying light materials (such as natural gas) from floating in marshy areas.

Grease Type Coatings.—Considerable use has been made, and some is still being made, of coatings formulated from petroleum greases. These relatively soft coatings sometimes exhibit remarkable resistance to soil stress. They have a tendency to absorb moisture, however, and their electrical conductance is usually high. The trend has been to incorporate harder and higher melting point materials into these coatings so that they approach the bituminous coatings in physical properties.

Plastic Tapes.—The successful use of plastic insulating tapes in the electrical field led to their development as protective coatings for pipes. Although the use of these tapes is limited, because of high material cost, to wrapping of field joints in plant or factory-applied coatings and to the coating of small amounts of pipe at individual locations, there is a possibility that the convenience and low labor cost of their application will lead to their wider use. The effectiveness of the coatings has not been fully determined, but they should prove satisfactory in this respect.

Other Coatings.—Certain other coatings have been proposed and some of them have been used to some extent. Vitreous enamels have been tried and found to be effective but are subject to cracking and are high in cost. Thermosetting resin coatings are very effective when properly applied but are too high in cost for all except a few uses. No doubt other coatings have been tried and it is certain that any new coating that meets the requirement of being waterproof and is able to withstand the effects of soil stress for long periods of time will receive consideration from the designers and operators of underground piping systems.

Cathodic Protection.—The second method of corrosion control suggested by the electrolytic nature of corrosion is that of controlling the electric currents that are always associated with this corrosion. Since corrosion occurs at the anodic areas at which the current leaves the pipe, it should be possible to pre-

vent current from leaving the pipe at any point and thus prevent corrosion. This can be done effectively and economically in many cases and widespread and evergrowing use is being made of the method.

Briefly, cathodic protection of underground pipe consists of connecting the negative side of a direct current source to the pipe line and the positive side to a buried structure of steel, cast iron, carbon, or graphite, called a ground bed. The electrolytic portion of the electrical circuit is from the ground bed, through the soil water to the pipe. The remainder of the circuit is through metallic conductors. The ground bed is consumed by the iron or carbon going into solution at the points at which the current enters the soil. Chemically equivalent quantities of hydrogen are plated out of the soil water onto the pipe being protected. The hydrogen plated out on the pipe tends to insulate the pipe from the soil water and to oppose the flow of additional current. The current then seeks other points of entry, so the entire pipe surface tends to collect current uniformly at all points. The local electrolytic cells are neutralized and corrosion is prevented or reduced. The effect of cathodic protection is to transfer the corrosion from the pipe where it causes damage to the ground bed where the damage can be tolerated.

While the theory of cathodic protection is simple, an endless variety of problems is encountered in the practical application of it. The amount of current required for protecting unit areas of metal, for instance, varies widely depending upon the electrical resistivity of the protective coating on the pipe, the degree to which oxidizing agents remove the hydrogen that is deposited on the pipe, and the nature of the salts dissolved in the soil water.

Protective coatings have a tremendous effect upon the amount of current required for protection. Some well-coated lines require only a few milliamperes per mile of pipe, although similar uncoated or poorly coated lines may require a hundred or more amperes per mile. In some cases, the complete cathodic protection of a piping system is not feasible because of the high power costs involved.

The commonly used sources of power for cathodic protection are rectifiers for converting alternating current to direct current, direct-current generators, and galvanic anodes made of magnesium, aluminum, or zinc. The galvanic anodes serve as both ground bed and power source and are used up in the process of generating power.

Since electric currents flowing in the soil always chose the paths of least resistance, they hop onto any metallic conductor going their way and ride it as far as they can. These conductors may be other pipe lines, telephone, telegraph or power cables, or any other elongated buried structure. If the current must leave the structure through an electrolytic rather than a metallic conductor to complete its circuit, the structure will likely be damaged by corrosion. This characteristic of electrolytic currents makes necessary the cooperation of all owners of underground structures within the areas influenced by cathodic protection installations. This is particularly true in urban areas in which the underground networks of pipes and cables of the various utilities are practically interlaced. Through proper cooperation, all damage can be

prevented and all participants can benefit from the application of cathodic protection.

The Corrosion Engineer

The scope of this paper, coupled with the fact that most of the points mentioned could be discussed at much greater length and the knowledge that each problem presents many variables that must be evaluated, should lead to the conclusion that specialists are needed in the field of corrosion control. There is a large group of these specialists called corrosion engineers. The field is already so broad that few individuals are expert in all phases, and considerable specialization has taken place in which a particular engineer's skill is confined largely to one phase, such as cathodic protection.

Many corrosion engineers need additional training and experience. The growing awareness throughout industry of the cost of corrosion losses is leading to increasing demands for competent corrosion engineers to help control this cost. There can be no doubt that the demand will bring forth both the training and the men.

Degree of Control Attainable

For new underground piping systems it is now possible to state with confidence that, for all practical purposes, soil corrosion can be completely controlled at reasonable costs. This achievement is of tremendous importance to the industries involved and to the national economy, since it means that extra metal thickness does not have to be provided as a corrosion allowance. It may be that piping systems of interest to sanitary engineers can now be constructed of steel pipe, with its excellent properties of strength, toughness, flexibility, and ease of construction, instead of the weak, bulky, and fragile materials used in the past.

It is often possible to arrest partly, or completely, the corrosion of existing systems by the application of cathodic protection. Even in cases in which the power requirements for cathodic protection are high, it is usually more economical to apply cathodic protection than to replace, repair, or recoat the piping systems. The ability to keep existing systems in operation is also of tremendous economic importance to the industry involved and to the United States as a whole.

DISCUSSION

LYLE R. SHEPPARD.[4]—The subject of this paper is covered very well by Mr. Brannon. However, the writer would further stress the importance of utilizing the experiences of others in corrosion mitigation because it has become such a specialized field.

Also, it is felt that the author should present some of the reasons for the greater interest in underground corrosion of pipes. Among these reasons are the following representing conditions existing in 1952:

1. A greater variety and larger volumes of products are being transported by pipe lines;
2. The increased operating pressure used in pipe lines constitutes a greater hazard;
3. Deeper burial in unleached (and thus more corrosive) soils to minimize partly safety hazards has become the practice;
4. The need for continued pipe line service has increased because of the dependence on them, rather than on other means of transportation;
5. The percentage of oil storage volume in service has decreased in comparison with the volume transported by pipe lines, more oil going immediately into process;
6. There is a trend toward the use of thinner pipe to conserve steel and to decrease construction and investment costs;
7. The value of the transported products has increased;
8. The property damage due to leaks has become more costly; and
9. The costs of pipe line replacements, both in materials and labor, have increased.

R. A. BRANNON.[5]—The author agrees that the additions suggested by Mr. Sheppard are appropriate. Although each of the items he lists could be discussed at greater length, it is believed that the mention Mr. Sheppard has made of them is sufficient to indicate the reasons for the greater interests in underground corrosion of pipes.

---

[4] Senior Chemist, Shell Pipe Line Corp., Houston, Tex.

[5] Supervising Corrosion Engr., Humble Pipe Line Co., Houston, Tex.

AMERICAN SOCIETY OF CIVIL ENGINEERS

Founded November 5, 1852

TRANSACTIONS

Paper No. 2542

ANALYSIS OF GROUND-WATER LOWERING ADJACENT TO OPEN WATER

By Stuart B. Avery, Jr.[1]

With Discussion by Messrs. Matthew I. Rorabaugh, S. J. Johnson and Howard P. Hall

Synopsis

In the construction of foundations for structures adjacent to open bodies of water, it is frequently necessary to lower the ground water by a system of wells. In such operations, it is highly desirable to know in advance the pumping capacity required to maintain the drawdown at particular elevations during normal and high water stages. This information can usually be obtained with the aid of pumping tests and mathematical analyses.

The purpose of this paper is to present formulas and graphs for the analysis of ground-water lowering and to demonstrate the use of such formulas and graphs. These mathematical relationships were developed for the purpose of determining pumping capacities required for dewatering a powerhouse site adjacent to a river.

Two sets of formulas have been derived; one for determining the relation between required pumping capacity and the drawdown at the center of a well installation, the other for determining the relation between the drawdown at the center of the well installation and the drawdown at any other point. With these formulas it is possible to determine:

(1) The rate of pumping required to maintain any desired drawdown with various arrangements of wells; and

(2) The change in rate of pumping required for any change in drawdown, arrangement of wells, or water stage.

In order to simplify the analysis, well installations have been considered to be circular, rather than having the usual square or rectangular arrangement.

Note.—Published in December, 1951, as *Proceedings-Separate No. 106*. Positions and titles given are those in effect when the paper or the discussion was received for publication.

[1] Lecturer on Foundation Eng., Harvard Univ. Cons. Eng., Cambridge, Mass.

Derivation of Formulas

Basic Formula and Assumptions.—Phillip Forchheimer[2] has derived (by the method of images) a general equation for the drawdown due to pumping from a series of wells adjacent to an open body of water with a straight shore line. This condition is shown in Fig. 1. The Forchheimer equation is

$$z^2 = H^2 - \frac{1}{\pi k}\left(q_1 \log_e \frac{S_1}{R_1} + q_2 \log_e \frac{S_2}{R_2} + \cdots + q_n \log_e \frac{S_n}{R_n}\right) \ldots\ldots (1)$$

in which z is the height of water surface above impervious boundary; H is the height of water surface above impervious boundary prior to pumping; k is the effective coefficient of permeability; $q_1, q_2, \ldots q_n$ is the rate of pumping

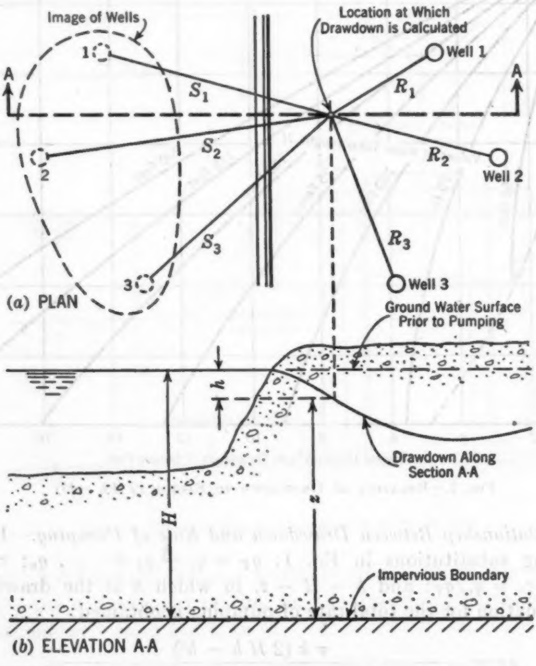

Fig. 1.—Series of Wells Adjacent to Open Water

from wells 1, 2, . . . n, respectively; $S_1, S_2, \ldots S_n$ is the distance from location at which drawdown is calculated to the image of wells 1, 2, . . . n, respectively; and $R_1, R_2, \ldots R_n$ is the distance from location at which drawdown is calculated to wells 1, 2, . . . n, respectively. This equation is based on six assumptions:

[2] "Hydraulik," by Phillip Forchheimer, B. G. Teubner, Leipzig and Berlin, Germany, 1930, pp. 82–90.

(*a*) The validity of J. Dupuit's assumptions that, for small inclinations of the free surface of a gravity flow system, the flow is horizontal and the velocity is proportional to the slope of the free surface[3];

(*b*) The existence of a steady flow condition;

(*c*) The existence of a horizontal impervious boundary at depth H below the open water surface;

(*d*) A homogeneous and isotropic character for the pervious stratum;

(*e*) Horizontal ground-water surface prior to pumping; and

(*f*) Pervious well casings penetrating to the impervious boundary.

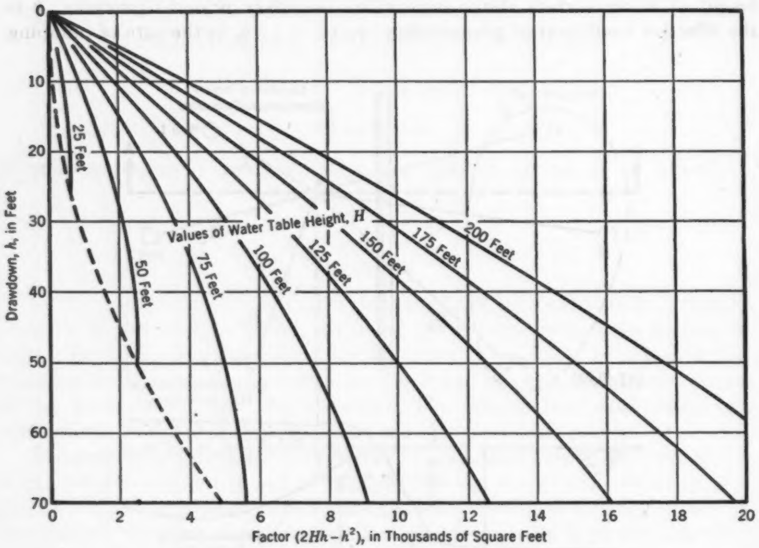

FIG. 2.—RELATION OF DRAWDOWN TO FACTOR ($2\,H\,h - h^2$)

Basic Relationship Between Drawdown and Rate of Pumping.—By making the following substitutions in Eq. 1: $q_T = q_1 + q_2 + \ldots q_n$; $c_1 = q_1/q_T$, $c_2 = q_2/q_T$, $c_n = q_n/q_T$; and $h = H - z$, in which h is the drawdown; the following equation for the total rate of pumping is obtained:

$$q_T = \frac{\pi\,k\,(2\,H\,h - h^2)}{\left(c_1 \log_e \frac{S_1}{R_1} + c_2 \log_e \frac{S_2}{R_2} + \cdots + c_n \log_e \frac{S_n}{R_n}\right)} \qquad (2)$$

From this equation it is seen that for any arrangement of wells adjacent to open water, the total rate of pumping (q_T) is directly proportional to ($2\,H\,h - h^2$); and, when the drawdown ratio $\left(\frac{h}{H}\right)$ is small, the rate of pump-

[3] "Etudes théoriques et pratiques sur le mouvement des eaux," by J. Dupuit, 2d Ed., Paris, France, 1863.

ing (q_T) is almost directly proportional to the drawdown (h). This relationship is shown in Fig. 2, which facilitates estimating the value of q_T for various values of h when the value of q_T is known from observation for one value of h, provided that the ratios $c_1, c_2, \ldots c_n$ remain constant.

Drawdown at the Center of One Ring of Wells.—Fig. 3 shows a single ring of wells. This ring has a radius of r_1 with its center a distance p from the shore line. It is assumed that the total discharge is uniformly distributed along the ring among an infinite number of wells.

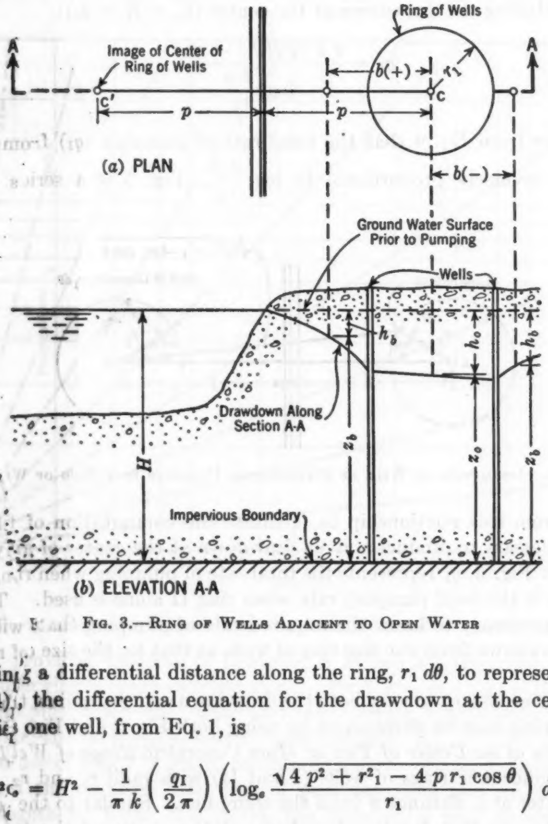

Fig. 3.—Ring of Wells Adjacent to Open Water

Assuming a differential distance along the ring, $r_1\,d\theta$, to represent one well (see Fig. 4), the differential equation for the drawdown at the center of the ring for this one well, from Eq. 1, is

$$z^2_o = H^2 - \frac{1}{\pi k}\left(\frac{q_I}{2\pi}\right)\left(\log_e \frac{\sqrt{4p^2 + r^2_1 - 4pr_1\cos\theta}}{r_1}\right) d\theta \ldots\ldots (3)$$

in which z_o is the height of water surface at the center of the ring above impervious boundary, q_I is the total rate of pumping from all wells in ring I, assuming no other wells are being pumped, and θ is the polar angle at the center of ring I, measured clockwise from a normal to the shore line to any point on the ring.

To obtain the effect produced by an infinite number of wells in a ring, the differential term in Eq. 3 is integrated from 0 to 2π. This integration results in the equation of the drawdown surface at the center:

$$z^2_o = H^2 - \frac{1}{\pi k}\left(\frac{q_I}{2\pi}\right)\int_o^{2\pi} \log_e \frac{\sqrt{4p^2 + r^2_1 - 4pr_1\cos\theta}}{r_1}\, d\theta \quad (4)$$

or

$$z^2_o = H^2 - \frac{q_I}{\pi k}\log_e \frac{2p}{r_1} \quad (5)$$

or, by introducing the drawdown at the center ($h_o = H - z_o$):

$$q_I = \frac{\pi k\,(2Hh_o - h^2_o)}{\log_e \dfrac{2p}{r_1}} \quad (6)$$

It follows from Eq. 6 that the total rate of pumping (q_I) from a ring of wells, I, is inversely proportional to $\log_e \frac{2p}{r_1}$. Fig. 5 is a series of curves

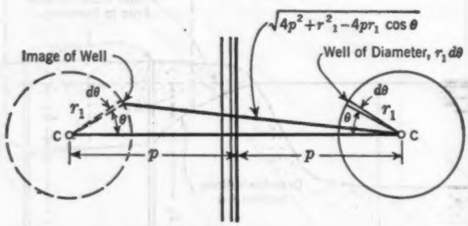

FIG. 4.—ASSUMPTION OF WELL OF DIFFERENTIAL DIAMETER IN A RING OF WELLS

computed from this relationship to facilitate the computation of the rate of pumping necessary to produce a given drawdown at the center of any size ring of wells. In Fig. 5, q_I represents the total rate of pumping when ring I only is used and q_{II} is the total pumping rate when ring II alone is used. To use the curves it is necessary to know the required rate of pumping that will produce the same drawdown from one size ring of wells as that for the size of ring under study.

When it is necessary to vary both the drawdown and the radius, the required rate of pumping may be determined by using both Fig. 2 and Fig. 5.

Drawdown at the Center of Two or More Concentric Rings of Wells.—Fig. 6 shows two concentric rings of wells (I and II) with radii r_1 and r_2, having a common center at a distance p from the shore line. Similar to the derivation of Eq. 4, the equation for the drawdown at the center of the two rings is obtained

$$z^2_o = H^2 - \frac{\bar{q}_I}{\pi k}\log_e \frac{2p}{r_1} - \frac{\bar{q}_{II}}{\pi k}\log_e \frac{2p}{r_2} \quad (7)$$

in which $\bar{q}_I$ and $\bar{q}_{II}$ are the total rates of pumping from rings I and II, respect-

ively. By substituting $q_T = \bar{q}_I + \bar{q}_{II}$, $C_I = \bar{q}_I/q_T$, and $H - h_o = z_o$—

$$q_T = \frac{\pi\, k\, (2\, H\, h_o - h^2_o)}{\log_e \dfrac{2\, p}{r_2} - C_I \log_e \dfrac{r_1}{r_2}} \qquad (8)$$

This equation shows that for two rings of wells, the total rate of pumping, q_T, is inversely proportional to $\left(\log_e \dfrac{2\, p}{r_2} - C_I \log_e \dfrac{r_1}{r_2}\right)$. From this relationship it is possible to determine, for any desired value of the ratio C_I, the total rate of pumping (q_T) required from two concentric rings of wells to produce a given

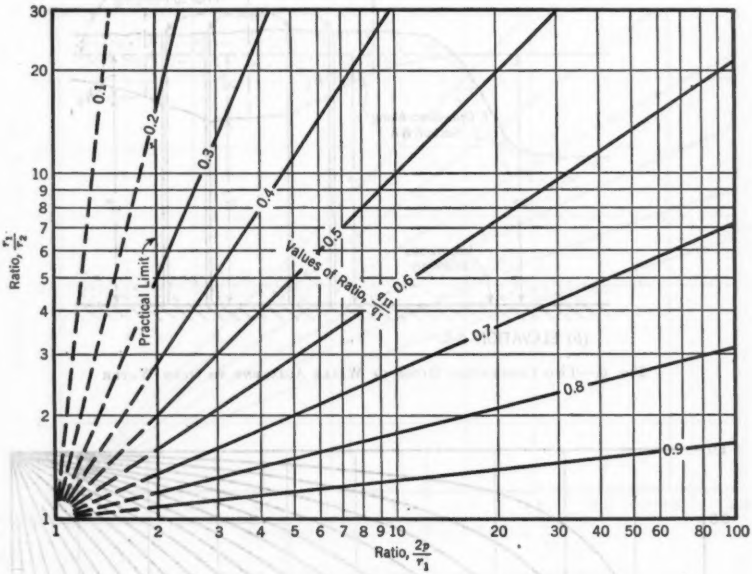

FIG. 5.—ESTIMATION OF PUMPING RATE FOR WELLS IN RINGS OF VARIOUS RADIUS

drawdown, provided the rate of pumping is known for the same drawdown when the outer ring is being pumped alone. First, if q_I and q_{II} are the required rates of pumping when the outer and inner rings, respectively, are being pumped alone, the ratio q_{II}/q_I may be obtained from Fig. 5. The second step requires the use of Fig. 7, a graph containing a series of curves facilitating the estimation of the required total rate of pumping from two concentric rings operating together. From this figure, the ratio q_T/q_I may be obtained for various values of the ratios q_{II}/q_I and C_I.

The general equation for the total rate of pumping for n concentric rings of wells is

$$q_T = \frac{\pi\, k\, (2\, \mathrm{H}\, h_o - h^2_o)}{C_I \log_e \dfrac{2\, p}{r_1} + C_{II} \log_e \dfrac{2\, p}{r_2} + \cdots + C_n \log_e \dfrac{2\, p}{r_n}} \qquad (9)$$

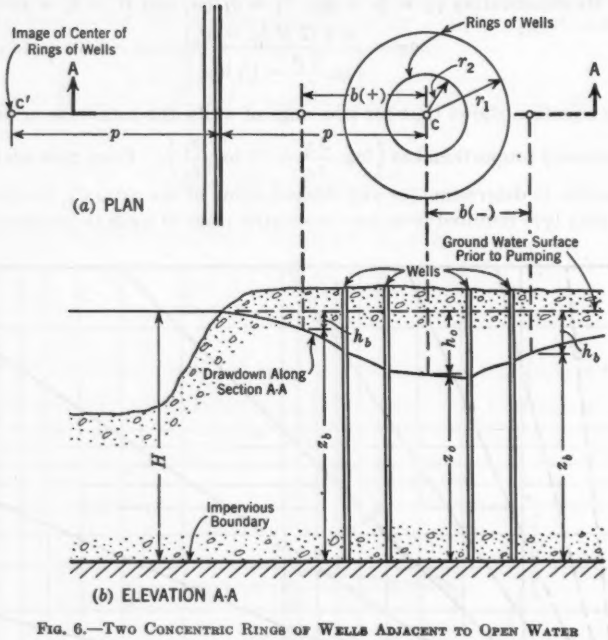

FIG. 6.—TWO CONCENTRIC RINGS OF WELLS ADJACENT TO OPEN WATER

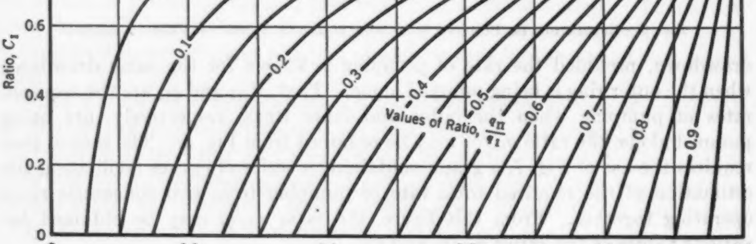

FIG. 7.—ESTIMATION OF PUMPING RATE FOR TWO CONCENTRIC RINGS OF WELLS OPERATING TOGETHER

in which $C_n = q_n/q_T$. From this equation it is seen that the total rate of pumping is inversely proportional to $\left(C_{\text{I}} \log_e \frac{2p}{r_1} + C_{\text{II}} \log_e \frac{2p}{r_2} + \cdots + C_n \log_e \frac{2p}{r_n}\right)$. For any specific cases involving more than two rings it may be helpful to prepare graphs similar to Fig. 5 and Fig. 7.

Effect of a Rise or Fall in Water Stage on the Rate of Pumping.—It is often desired to maintain a constant drawdown, despite fluctuations in the level of adjacent open water. Where such fluctuations are of very short duration, their

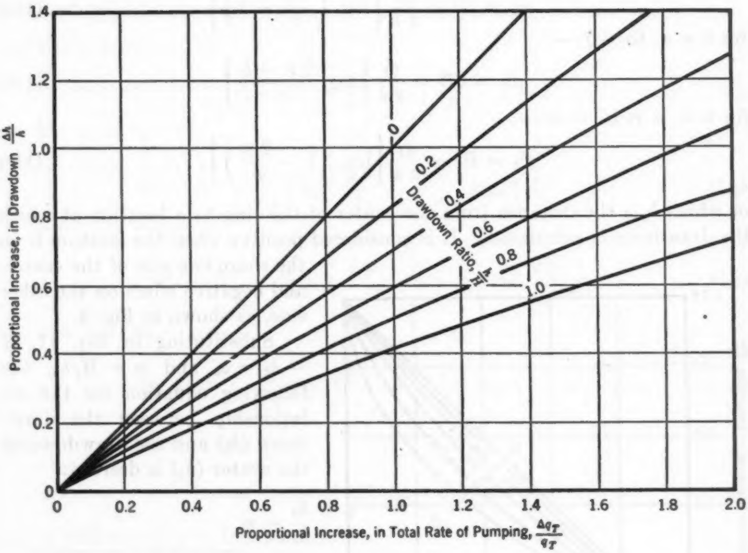

FIG. 8.—EFFECT OF RISE OF WATER STAGE ON PUMPING RATE

effect on the drawdown may be negligible. However, when a rise or fall in the open water level lasts long enough to establish a new steady condition of flow, a change is required in the total rate of pumping if the ground-water surface at a desired point is to remain unchanged.

If the rise or fall in open water level (ΔH) equals the change in drawdown (ΔH) and $H' = H + \Delta H$, $h' = h + \Delta h$, Δq_T is the change in total rate of pumping due to change in open water level, $q'_T = q_T + \Delta q_T$, $w = H/h$ and drawdown ratio $= h/H$, the change in the rate (Δq_T) may be expressed by the following equation, derived from Eq. 2

$$\frac{\Delta q_T}{q_T} = \frac{\Delta h}{h}\left[1 + \frac{\frac{\Delta h}{h} + 1}{2w - 1}\right] \qquad (10)$$

Figs. 8 and 9 represent graphical solutions of Eq. 10 for rising and falling water stages, respectively. When the drawdown ratio is small, the rate of change in the pumping rate is approximately proportional to the rate of change in the drawdown, whereas for higher drawdown ratios, the rate of change in the pumping rate is larger than the rate of change in the drawdown.

Drawdown Curve for a Single Ring of Wells.—Following the procedure used in deriving Eq. 5, the equation for the drawdown surface along a line through the center of the ring and perpendicular to the shore line is obtained:

for $b = p$ to r_1—

$$z^2_b = H^2 - \frac{q_1}{\pi k}\left[\log_e\left(\frac{2p}{b} - 1\right)\right] \quad \text{(11a)}$$

for $b = r_1$ to $-r_1$—

$$z^2_b = H^2 - \frac{q_1}{\pi k}\left[\log_e \frac{2p - b}{r_1}\right] \quad \text{(11b)}$$

for $b = -r_1$ to $-\infty$—

$$z^2_b = H^2 - \frac{q_1}{\pi k}\left[\log_e\left(1 - \frac{2p}{b}\right)\right] \quad \text{(11c)}$$

in which b is the distance from the center of the ring to a location at which the drawdown is calculated. It is considered positive when the location is on the shore line side of the center, and negative when on the other side, as shown in Fig. 3.

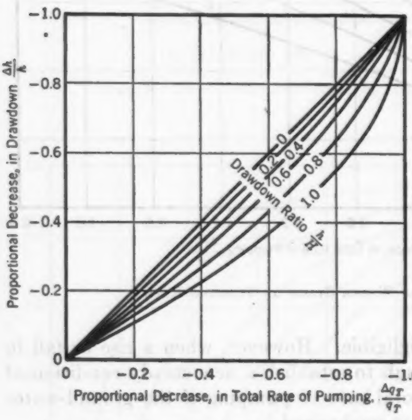

Fig. 9.—Effect of Fall of Water Stage on Pumping Rate

Substituting in Eq. 11, $H - h_b = z_b$ and $w = H/h_o$, the following equation for the relationship between the drawdown (h_b) and the drawdown at the center (h_o) is derived:

$$\frac{h_b}{h_o} = w - \sqrt{w^2 - (2w - 1)\frac{Z}{\log_e 2p}} \quad \text{(12)}$$

in which:

for $b = p$ to r_1—

$$Z = \log_e\left(\frac{2p}{b} - 1\right) \quad \text{(13a)}$$

for $b = r_1$ to $-r_1$—

$$Z = \log_e \frac{2p - b}{r_1} \quad \text{(13b)}$$

for $b = -r_1$ to $-\infty$—

$$Z = \log_e 1 - \frac{2p}{b} \quad \text{(13c)}$$

For the case in which the ring consists of a series of wells so widely spaced that they can no longer be considered to form a continuous ring of wells, Eq. 13 may be evaluated by letting

$$Z = \sum_{1}^{n} \frac{1}{n} \log_e \frac{S_n}{R_n} \qquad (14)$$

For an explanation of symbols, see Fig. 1.

Drawdown Curve for Two Concentric Rings of Wells.—In a manner similar to that used in the derivation of Eq. 11, the equation is derived for the drawdown surface along a line through the center of two concentric rings and perpendicular to the shore line:

for $b = p$ to r_1—

$$z^2_b = H^2 - \frac{q_T}{\pi k} \log_e \left(\frac{2p}{b} - 1 \right) \qquad (15a)$$

for $b = r_1$ to r_2—

$$z^2_b = H^2 - \frac{\bar{q}_{\mathrm{I}}}{\pi k} \log_e \frac{2p - b}{r_1} - \frac{\bar{q}_{\mathrm{II}}}{\pi k} \log_e \left(\frac{2p}{b} - 1 \right) \qquad (15b)$$

for $b = r_2$ to $-r_2$—

$$z^2_b = H^2 - \frac{\bar{q}_{\mathrm{I}}}{\pi k} \log_e \frac{2p - b}{r_1} - \frac{\bar{q}_{\mathrm{II}}}{\pi k} \log_e \frac{2p - b}{r_2} \qquad (15c)$$

for $b = -r_2$ to $-r_1$—

$$z^2_b = H^2 - \frac{\bar{q}_{\mathrm{I}}}{\pi k} \log_e \frac{2p - b}{r_1} - \frac{\bar{q}_{\mathrm{II}}}{\pi k} \log_e \left(1 - \frac{2p}{b} \right) \qquad (15d)$$

for $b = -r_1$ to $-\infty$—

$$z^2_b = H^2 - \frac{q_T}{\pi k} \log_e \left(1 - \frac{2p}{b} \right) \qquad (15e)$$

From this equation it follows that

$$\frac{h_b}{h_o} = w - \sqrt{w^2 - (2w - 1) \frac{Z}{\log_e \frac{2p}{r_2} - C_{\mathrm{I}} \log_e \frac{r_1}{r_2}}} \qquad (16)$$

in which:

for $b = p$ to r_1—

$$Z = \log_e \left(\frac{2p}{b} - 1 \right) \qquad (17a)$$

for $b = r_1$ to r_2—

$$Z = \log_e \left(\frac{2p}{b} - 1 \right) - C_{\mathrm{I}} \log_e \frac{r_1}{b} \qquad (17b)$$

for $b = r_2$ to $-r_2$—

$$Z = \log_e \frac{2p - b}{r_2} - C_{\mathrm{I}} \log_e \frac{r_1}{r_2} \qquad (17c)$$

for $b = -r_2$ to $-r_1$—

$$Z = \log_e\left(1 - \frac{2p}{b}\right) - C_{\mathrm{I}} \log_e \frac{-r_1}{b} \quad \text{(17d)}$$

for $b = -r_1$ to $-\infty$—

$$Z = \log_e\left(1 - \frac{2p}{b}\right) \quad \text{(17e)}$$

In order to determine the drawdown for any point at a distance y from the center of the rings and a distance x from the image point of the center, the same general equation (Eq. 16) applies except for the values of Z that are:

for $y = 0$ to r_2—

$$Z = \log_e \frac{x}{r_2} - C_{\mathrm{I}} \log_e \frac{r_1}{r_2}$$

for $y = r_2$ to r_1—

$$Z = \log_e \frac{x}{y} - C_{\mathrm{I}} \log_e \frac{r_1}{y} \quad \text{(17f)}$$

for $y = r_1$ to ∞—

$$Z = \log_e \frac{x}{y}$$

Within the inner ring, the drawdown is independent of the distance from the center of the rings (y). Consequently, contour lines of the ground-water surface within this ring are arcs of circles with a common center at the image point of the center of the well system.

Nonconcentric Rings of Wells with Their Centers on a Line Perpendicular to the Shore Line.—It is sometimes necessary to dewater two separate areas that have their centers on a line perpendicular to the shore line, as shown in Fig. 10. Replacing the actual shape of the well installations by circles, the ratio between the drawdowns at the centers of the two rings may be expressed

$$\frac{h_{bo}}{h_{ao}} = w_a - \sqrt{w_a^2 - (2w_a - 1)\left[\frac{\log_e\left(\frac{2p}{f} - 1\right) + C_{b/a}\log_e \frac{2(p-f)}{r_b}}{\log_e \frac{2p}{r_a} + C_{b/a}\log_e\left(\frac{2p}{f} - 1\right)}\right]} \quad \text{(18)}$$

in which ring b is between ring a and the shore line, $w_a = H/h_{ao}$, $C_{b/a} = \bar{q}_b/\bar{q}_a$, $\bar{q}_a$ is the rate of pumping from ring a, $\bar{q}_b$ is the rate of pumping from ring b, p is the distance from the center of ring a to the shore line, and f is the distance between the centers of rings a and b; or, solving for $C_{b/a}$:

$$C_{b/a} = \frac{(1 - 2w_a)\log_e\left(\frac{2p}{f} - 1\right) - \frac{h_{bo}}{h_{ao}}\left(\frac{h_{bo}}{h_{ao}} - 2w_a\right)\log_e \frac{2p}{r_a}}{\frac{h_{bo}}{h_{ao}}\left(\frac{h_{bo}}{h_{ao}} - 2w_a\right)\log_e\left(\frac{2p}{f} - 1\right) - (1 - 2w_a)\log_e \frac{2(p-f)}{r_b}} \quad \text{(19)}$$

The ratio of the drawdown at any point outside the two rings to the drawdown

at the center of ring a is:

$$\frac{h}{h_{ao}} = w_a - \sqrt{w^2_a - (2\,w_a - 1)\left[\frac{\log_e \dfrac{x_a}{y_a} + C_{b/a} \log_e \dfrac{x_b}{y_b}}{\log_e \dfrac{2\,p}{r_a} + C_{b/a} \log_e \left(\dfrac{2\,p}{f} - 1\right)}\right]} \quad ..(20)$$

in which x_a and x_b are the distance from the location at which the drawdown is being calculated to the image point of the center of rings a and b, respectively, and y_a and y_b are the distance to the center of rings a and b, respectively.

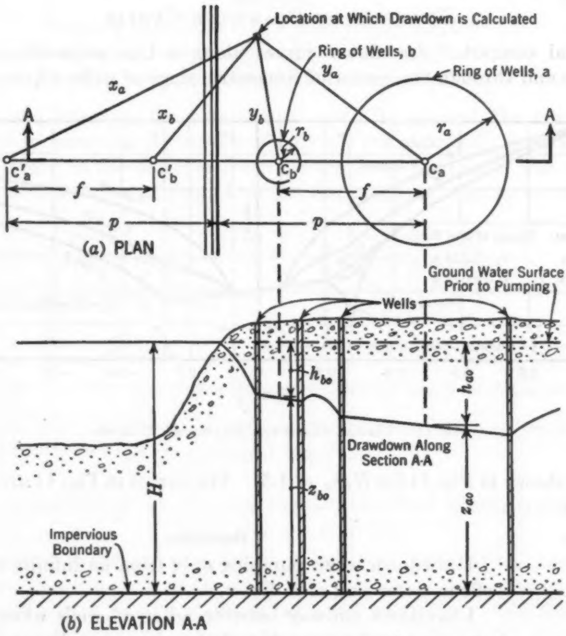

FIG. 10.—TWO NONCONCENTRIC RINGS OF WELLS ADJACENT TO OPEN WATER

In the course of his studies, the writer found it necessary to solve the following problem: Ring a has been in operation and the required drawdown (h_{ao}) and the rate (q_a) have been obtained, when pumping from ring a alone. It is desired to install a ring b in order to obtain a drawdown h_{bo} at its center. The required rate of pumping ($\bar{q}_b$) for this ring can be determined by the following procedure:

1. Solve Eq. 19 for $C_{b/a}$.
2. Solve the following equation for $\bar{q}_a$, the rate required for ring a when

ring b is also in operation:

$$\bar{q}_a = \frac{q_a}{1 + C_{b/a}\dfrac{\log_e\left(\dfrac{2p}{f} - 1\right)}{\log_e \dfrac{2p}{r_a}}} \quad \ldots\ldots\ldots\ldots\ldots\ldots\ldots (21)$$

3. $\bar{q}_b = C_{b/a}\,\bar{q}_a$.

The rate of pumping for other arrangements of nonconcentric rings of wells may be determined also by deriving equations similar to those given.

Examples of Drawdown Curves

Typical computed drawdown curves along a line perpendicular to the shore line and through the center of concentric rings of wells adjacent to open

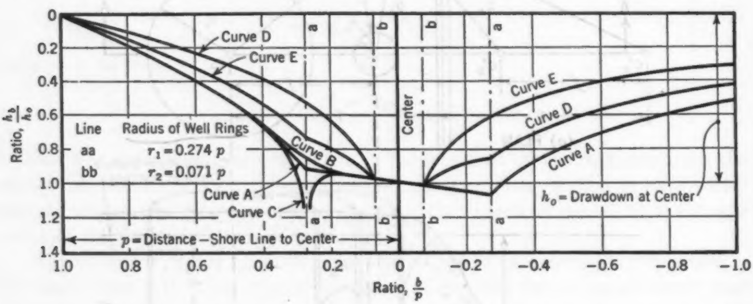

Fig. 11.—Typical Computed Drawdown Curves

water are shown in Fig. 11 for $H/h_o = 4.5$. The curves in Fig. 11 are identified as follows:

Curve	Description
A	Drawdown when pumping only from an infinite number of wells in outer ring of radius r_1
B	Drawdown midway between adjacent wells when pumping from six equally spaced wells in ring of radius r_1 (see Fig. 12 (*a*))
C	Drawdown directly through two wells when pumping from six equally spaced wells in a ring of radius r_1 (see Fig. 12 (*b*))
D	Drawdown when pumping $\frac{1}{3}$ from an infinite number of wells in inner ring of radius r_2 and $\frac{2}{3}$ from an infinite number of wells in outer ring of radius r_1,
E	Drawdown when pumping only from an infinite number of wells in inner ring of radius r_2

The computed drawdown within the inner ring in all cases is practically a plane surface, with a slight dip away from the shore line.

When a single ring consists of a small number of wells only, the drawdown curve in the vicinity of the ring varies from the plane surface. Note in Fig. 11 that midway between adjacent wells the drawdown, Curve B, is higher than the drawdown, Curve A, for a continuous ring of wells; whereas in the vicinity of the well the drawdown, Curve C, is lower. As the number of wells in the ring is increased, the drawdown at the well and midway between adjacent wells (Curves C and B respectively), approaches the drawdown curve for an infinite number of wells in the ring (Curve A).

Assuming the same drawdown at the center, the relative rates of pumping required to produce the drawdown curves, A, D, and E, are as follows:

Curve	Description	Relative rate of pumping
A	Pumping only from ring I with radius 0.274 p	1.00 q_I
D	Pumping $\frac{2}{3}$ from ring I and $\frac{1}{3}$ from ring II	0.81 q_I
E	Pumping only from ring II with radius 0.071 p	0.60 q_I

The foregoing rates are for a particular case. In general, the ratio between these rates of pumping is dependent only on the following: (1) Ratio of the radius of ring I to the distance from the center of the ring to the shore line; (2) Ratio of the radius of ring II to the distance from the center of the ring to the shore line; and (3) Ratio between the rates of pumping from each ring of wells, when they are being pumped together.

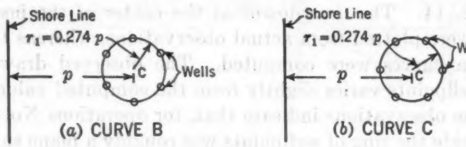

FIG. 12.—WELL LAYOUT FOR DRAWDOWN CURVES B AND C IN FIGURE 11

ANALYSIS OF AN ACTUAL INSTALLATION OF WELLPOINTS ADJACENT TO A RIVER

The writer made an analysis of a wellpoint installation, consisting of three stages of wellpoints, as shown in Fig. 13(a), that were used to dewater a power house site on sand and gravel adjacent to a river. The first stage of wellpoints consisted of 148 points at an average spacing of 5 ft. In the second stage there were 215 points at an average spacing of 3 ft, and the third stage had 67 points at an average spacing of 3 ft. For purposes of analysis, the roughly square arrangements of wellpoints were assumed circular as shown in Fig. 13(b), with a common center and each circle enclosing approximately the same area as the approximate square it replaces.

Since no pumping tests were made at this site prior to the installation of the first stage of wellpoints, no analysis was made until after the first stage had been placed in operation. This stage, for convenience, is called operation No. 1. Operation No. 2 consists of pumping only from the second stage of wellpoints, and operation No. 3 is pumping $\frac{2}{3}$ of the total rate from the second stage and $\frac{1}{3}$ from the third stage. Observations made on each pumping

operation were used to compute in advance the rate of pumping required for the succeeding operation. The computed rates varied from the actual measured rates by 4% for operation No. 2 and 14% for operation No. 3. The effective coefficient of permeability computed from the three operations is given in Table 1.

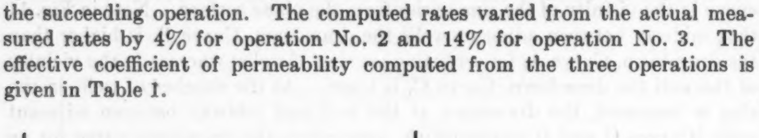

FIG. 13.—WELLPOINT INSTALLATION ADJACENT TO RIVER

The drawdown curves normal to the river for the three pumping operations are shown in Fig. 14. The drawdowns at the center of the installation and the river stages were plotted from actual observations, whereas the remainder of the drawdown curves were computed. The observed drawdown in the vicinity of the wellpoints varies slightly from the computed value as shown in the figure. These observations indicate that, for operations No. 1 and No. 2, the drawdown inside the ring of wellpoints was roughly a plane surface dipping slightly toward the river rather than away from the river as indicated in the analysis. The difference is probably due to the fact that the pumps for all stages were connected to the headers on the river side of the installation and, consequently, because of larger friction losses in the headers, the yield from the wellpoints on the land side was not so large as that from the wellpoints on the river side. Corrections could be made in the computations of drawdown for uniform variations of this type in the rate of pumping, if the variations were considered large enough to justify the additional computations.

TABLE 1.—EXAMPLE OF WELLPOINT INSTALLATION

Operation number	Effective coefficient of permeability (ft per min)	Rates of Pumping (gal per min) Measured	Computed	Error (%)
1	0.092	2578	....	....
2	0.096	4407	4210	− 4
3	0.083	4546	5180	+14

The drawdown during operation No. 3, at a point approximately 500 ft from the wellpoint installation, was computed to be within a fraction of a foot of the actual observed drawdown at this point.

In anticipation of flood stages in the river, curves for this site showing the rates of pumping required to maintain various drawdowns for various river stages were prepared. These curves, computed on the assumption of a steady flow condition, indicated that the rate of increase in the pumping rate would be

about proportional to the rate of increase in the drawdown caused by the rise in the river stage. Observations made during flood stages prior to pumping indicated that it takes about a week for the full effect of a rise in the river stage to be reflected in the ground water at this site. Consequently, the river stage would have to remain constant for this same length of time before a condition of steady flow is reached.

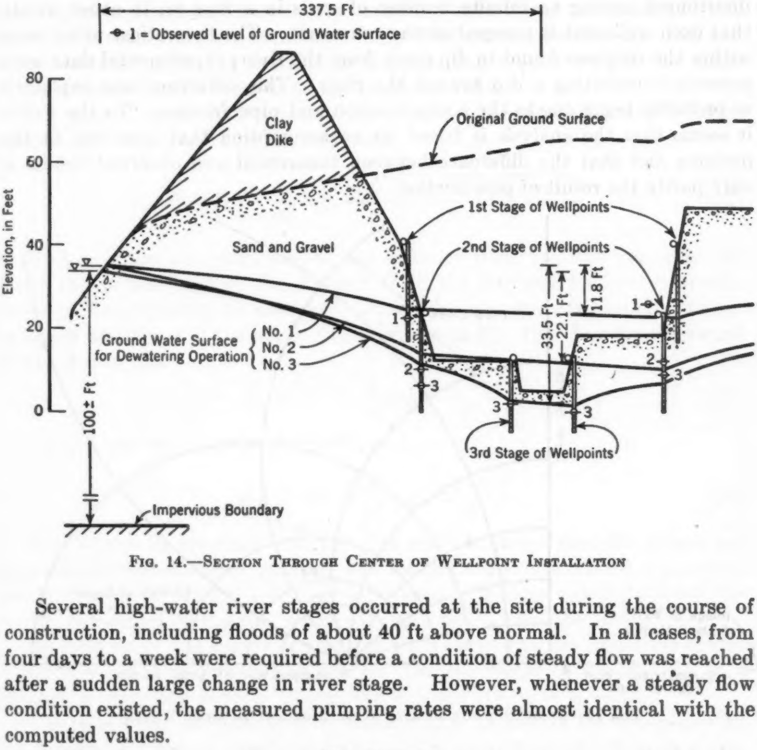

FIG. 14.—SECTION THROUGH CENTER OF WELLPOINT INSTALLATION

Several high-water river stages occurred at the site during the course of construction, including floods of about 40 ft above normal. In all cases, from four days to a week were required before a condition of steady flow was reached after a sudden large change in river stage. However, whenever a steady flow condition existed, the measured pumping rates were almost identical with the computed values.

CONCLUSION

Many simplifications are required in the assumptions upon which this analysis is based, in order that simple, workable formulas can be derived. Consequently, errors up to 10% or 15% are to be expected in estimates of rates of pumping and drawdowns. The writer, however, believes that computed estimates within these limits are desirable on all large well installations.

ACKNOWLEDGMENT

The writer is indebted to Mr. José Corso, J. M. ASCE, who checked the derivation of all the formulas, and to A. Casagrande, M. ASCE, for numerous suggestions and encouragement.

DISCUSSION

MATTHEW I. RORABAUGH,[4] A. M. ASCE.—An orderly analysis of ground-water lowering adjacent to open water is presented in this paper, the entire analysis being based on the assumption that the total discharge is uniformly distributed among an infinite number of wells in a ring or, in other words, that each wellpoint is pumped at the same rate. The theoretical water level within the ring was found to dip away from the river; experimental data were presented indicating a dip toward the river. This difference was explained as probably being due to the pump location and pipe friction. To the writer it seems that the analysis is based on an assumption that does not fit the problem and that the difference between theoretical and observed results is only partly the result of pipe friction.

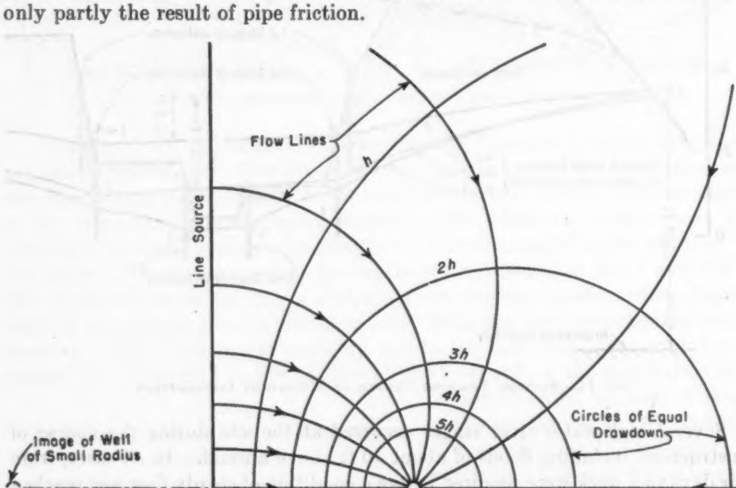

FIG. 15.—FLOW NET FOR PUMPED WELL ADJACENT TO OPEN WATER

In practice, a suction pump is connected to a line or ring of wellpoints. The system is one of constant drawdown at all points on the ring, not uniformly distributed pumping. An analysis based on constant drawdown will be consistent with the field installation and will produce a solution that fits the problem—that is, it is presumed that the excavation is level and that a horizontal, rather than a dipping, water level is desired.

Fig. 15 shows a flow net for the case of a pumping well of very small diameter located near a surface source of water. The flow lines are arcs of circles having their centers on the line source. The lines of equal drawdown are nonconcentric circles having their centers on a line normal to the line source.

[4] Dist. Engr., Ground Water Branch, U. S. Geological Survey, Louisville, Ky.

The theory and equations for this system (for the artesian case) have been published by Morris Muskat[5] and C. E. Jacob.[6]

This system is readily adaptable to the problem of a ring pumped at constant drawdown. All that must be done is to place the ring on one of the circles of equal drawdown rather than concentric with the hydraulic center of the system. Pumping from the ring will not be uniformly distributed, being greater on the riverward side where gradients are steeper and stream lines are more dense, and less on the landward side where gradients are less steep and stream lines are less dense. The flow pattern outside the ring will be the same for pumping the ring as for pumping a small well at the same rate, if the small well is located at the hydraulic center.

The drawdown at any point in the field for the case of a small-radius pumped well is expressed by the equation,

$$z^2 = H^2 - \frac{q}{\pi k} \log_e \frac{\sqrt{4\,a^2 + r^2 - 4\,a\,r\cos\theta}}{r} \qquad (22)$$

in which q is the pumping rate; a, the distance from the line source to the center of the well; and r, the distance from the pumped well (or hydraulic center of flow system) to any point at which drawdown is desired. Other terms are as defined in the paper and as shown in Fig. 16. For the riverward profile, $\theta = 0$, and

$$z^2_d = H^2 - \frac{q}{\pi k} \log_e \frac{2\,a - d}{d} \qquad (23)$$ ✓

For the landward profile, $\theta = 180°$, and

$$z^2_{d'} = H^2 - \frac{q}{\pi k} \log_e \frac{2\,a + d'}{d'} \qquad (24)$$ ✓

Eqs. 23 and 24 are similar to Eqs. 11a and 11c except that the former are for a single small-diameter pumped well located a distance a from the source, whereas the latter are for a ring being pumped at a uniformly distributed discharge, the center of the ring being at a distance p from the source.

The location of the center of the ring with respect to the hydraulic center of the flow net is determined as follows: Let the center of the ring be at a distance p from the source. Then, the eccentricity, e, is $p - a$.

The term e can be evaluated by writing Eqs. 23 and 24 for two points on the specified profiles at locations diametrically opposite each other on a ring of radius r_1; thus, in Eq. 23, $d = r_1 - e$; in Eq. 24, $d' = r_1 + e$. Since the drawdown is the same at all points on the ring, the log terms of these two equations are equal. From this relationship,

$$e = p - \sqrt{p^2 - r^2_1} \qquad (25)$$

Since $e = p - a$, then

$$a = \sqrt{p^2 - r^2_1} \qquad (26)$$

[5] "The Flow of Homogeneous Fluids Through Porous Media," by Morris Muskat, McGraw-Hill Book Co., Inc., New York, N. Y., 1937 p. 175.

[6] "Engineering Hydraulics," Ed. by Hunter Rouse ("Flow of Ground Water," by C. E. Jacob, Chapter 5), John Wiley & Sons., Inc., New York, N. Y., 1950, p. 345.

Thus, if the location of the center of the ring, p, and the radius of the ring, r_1, are known, the location of the hydraulic center a is determined. Knowing a, the profiles on the riverward and landward sides are computed from Eqs. 23 and 24.

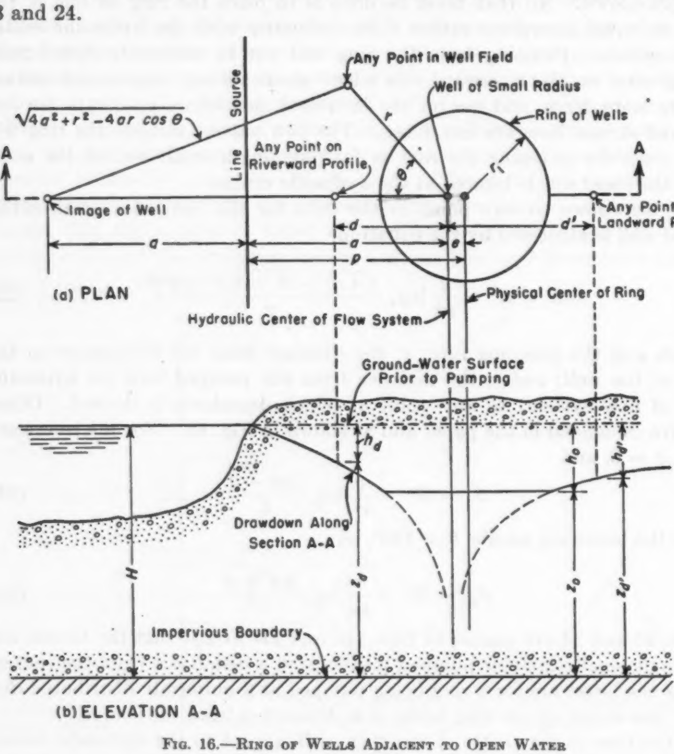

FIG. 16.—RING OF WELLS ADJACENT TO OPEN WATER

The equation for discharge for a given drawdown at any point on the ring or any point within the ring is determined from Eq. 23 or Eq. 24 by substituting $d = r_1 - e$; $d' = r_1 + e$; $e = p - \sqrt{p^2 - r^2_1}$; $a = \sqrt{p^2 - r^2_1}$; $z_d = z_d' = z_o$; $h_d = h_d' = h_o$; and $z_o = H - h_o$; thus—

$$q = \frac{\pi k (2 H h_o - h^2_o)}{\log_e \dfrac{p + \sqrt{p^2 - r^2_1}}{r_1}} \quad \ldots\ldots\ldots\ldots\ldots\ldots (27)$$

Eq. 27 is similar to Eq. 6 except that eccentricity is included. For a single well or a very small ring, when r_1 is small relative to p, the log term approaches $\frac{2p}{r_1}$ as in Eq. 6.

The significance of the constant drawdown approach is demonstrated in Fig. 17, which shows profile A, Fig. 11, and the solution for the same case by the constant drawdown method. Note that the constant drawdown solution produces a horizontal profile within the ring which is consistent with the results desired and is consistent with the field condition of a group of wellpoints connected to the same pump. It should be emphasized that, for this partic-

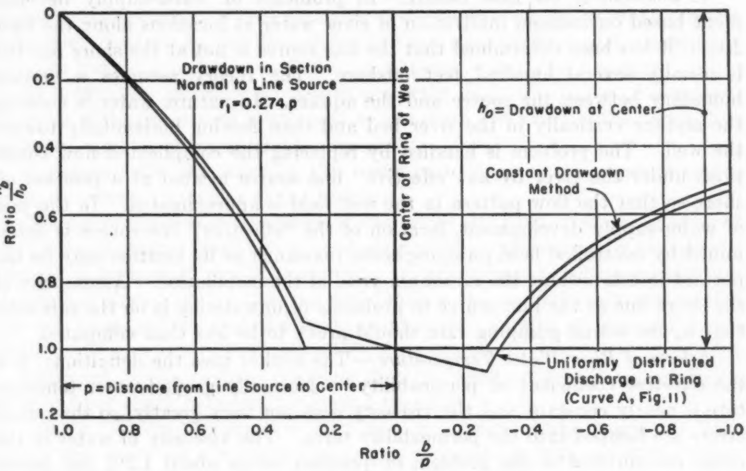

FIG. 17.—DRAWDOWN CURVES BY TWO METHODS

ular case, the eccentricity is small, so that the discharge required to produce the same center drawdown, as determined by Eq. 27, is only about 1.0% larger than that determined from Eq. 6.

The discharge as computed by the two methods differs only in the log term. The discharge required to produce the same center drawdown for the constant drawdown method will be larger than that by the uniformly distributed discharge method by the ratio $\dfrac{\log \dfrac{2\,p}{r_1}}{\log \dfrac{p + \sqrt{p^2 - r_1^2}}{r_1}}$. As r_1 approaches p (that is, for excavations very close to the surface source) this ratio will become large; for $p = r$, the ring becomes tangent to the source, and both methods break down since this condition would infer direct pumping from the surface source.

The differences in the profiles outside the ring will become larger as r_1 approaches p, as shown by comparing Eqs. 11*a* and 11*c* with Eqs. 23 and 24. For the constant drawdown method, as the ratio r_1/p is made larger the eccentricity is increased, a becomes smaller (the hydraulic center moves riverward), and the riverward profile becomes steeper. The profiles outside the ring based on Eqs. 11*a* and 11*c* are independent of r_1 so that changing r_1 does not alter the profiles.

This discussion has been limited to the problem of a single ring; but the criticism of the basic assumption of a ring having equal distribution of discharge rather than a ring of constant drawdown applies to all the variations covered in the paper.

Two other points might be mentioned briefly: (1) The location of the line source and (2) the effects of river-water temperature.

1. *Location of the Line Source.*—In problems of water-supply development based on induced infiltration of river water at locations along the Ohio River, it has been determined that the line source is not at the shore line but is usually several hundred feet offshore. The theory assumes a vertical boundary between the source and the aquifer. In nature, water is entering the aquifer vertically in the river bed and then flowing horizontally toward the well. The problem is handled by replacing the complicated flow conditions under the river by an "effective" line source located at a position off shore so that the flow pattern in the well field is approximated. In the case of water-supply development, location of the "effective" line source is determined by controlled field pumping tests, inasmuch as its location may be important in establishing the minimum yield of the installation. Assumption of the shore line as the line source in problems of unwatering is on the safe side; that is, the actual pumping rate should prove to be less than computed.

Effects of River-Water Temperature.—The author uses the definition: "*k* is the effective coefficient of permeability." Normally ground-water temperature is nearly constant and the viscosity does not vary greatly, so that small errors are lumped into the permeability term. The viscosity of water in the range encountered in the problem in question varies about 1.5% per degree Fahrenheit; thus a rise of 1° F will increase flow rates about 1.5%. The temperature of the surface source becomes an important item in the problem if unwatering is continued over a long time. As an example of the range involved, Ohio River water varies in temperature from 32° to about 85° during the year. Continued pumping near the river induces water of varying temperature to enter the aquifer and flow to the point of pumping. The problem becomes complicated as river water mixes with ground water of a different temperature, heat exchange occurs between the water and sand, and flow rates at each point adjust themselves to the temperature prevailing at that point. The distance from the river is an important item. Detailed records at an installation at Louisville, Ky., for the period from 1945 to 1951 show a range in temperature from 47° to 64° for the discharged water. Statistical analysis shows the flow rate for a condition of constant river level and constant pumping level to vary from 85% to 115% of the average value. In the case of unwatering over a long period, the pumping rate might vary as much as 30% or 40% between summer and winter. Also, this factor will cause variations in the pumping distribution in the ring—in the summer, discharge from wellpoints on the riverward side will increase and in the winter, discharge on the riverward side will decrease. Perhaps Mr. Avery can furnish information as to how long pumping continued in his example, what seasons it covered, whether temperatures of discharged water were recorded, and

whether any differences in pumping rate or water level were noted which would be related to the temperature variable.

Inasmuch as the temperature variable was neglected in the analysis, the six assumptions given at the beginning of the paper should be increased to seven by adding (*g*) The river temperature and groundwater temperature are equal and do not change during the pumping period.

The conclusion that errors as great as 10% to 15% are to be expected might be questioned. Where pumping tests have been run to evaluate the "effective" distance to the line source and the permeability, and where temperature has been included in the computations, water supplies based on induced infiltration generally have been predicted with this degree of accuracy. However, if the line source is assumed as the shore line and the temperature is neglected, greater errors should be expected.

Summary.—On the basis of the assumptions made, the paper presents a sound, orderly treatment of the problem.

The assumption that discharge is uniformly distributed in the ring does not fit the problem, inasmuch as a sloping profile is produced by the theory whereas a horizontal profile is desired. Analysis based on the assumption of constant drawdown at the ring will produce the desired horizontal profile and will be consistent with the field operation of pumping at constant drawdown.

Observed results confirm the view that the constant drawdown approach gives a closer check between theory and practice.

Effects of river temperature were not considered in the analysis. Neglecting this item may introduce errors of as much as 30% or 40%. This item alone is considerably larger than the 10% to 15% limit of error assumed by the author.

S. J. Johnson,[7] A. M. ASCE.—The dearth of information on the engineering aspects of ground-water lowering for construction purposes and the need for such information combine to make this paper one of unusual timeliness and importance. In the United States, ground-water lowering for construction purposes has been all too often resorted to as an expediency when in trouble or used without recognition of its possibilities and limitations. The practical aspects of ground-water lowering operations are of primary importance and an impressive quantity of working knowledge is available. However, the theoretical aspects have not been developed simultaneously with the practical aspects, even though theoretical considerations can supplement field experience to advantage and can also form a logical framework for the acquisition and organization of practical knowledge and experience. Publication of this paper, reviewing some of the available theoretical methods, is therefore of significant value. It is unfortunate that the scope could not have been extended to include a complete review of ground-water lowering theory.

It would have been of some interest and importance if the author had reviewed the status of the available knowledge on ground-water lowering methods

[7] Chf., Embankment and Foundation Branch, Waterways Experiment Station, Corps of Engrs., U. S. Dept. of the Army, Vicksburg, Miss.

of analysis. The writer's understanding of this subject is as follows: The equation for gravity flow to a single well, which depends on the validity of the Darcy law,[8] was formulated by Mr. Dupuit in 1863,[3] as was stated by the author. Before 1900, Mr. Forchheimer developed the equations for flow to groups of wells and used the method of images to develop equations for the flow to wells supplied by a line source.[9,10] The formulas for practically all cases of the flow of water to either well or wellpoint systems (either single or multiple stage with the wells arranged in a line, rectangle, or circle) were presented prior to 1930. For example, the first edition of the book by W. Kyrieleis[11] on ground-water lowering by pumping from wells was published in 1913 and presented most of the equations needed for calculating the effect of pumping from wells. The second edition, by Mr. Kyrieleis and W. Sichardt, was published in 1930. Other references are those by H. Weber[12] and Mr. Sichardt[13]; the latter contains formulas for multiple-stage well systems supplied by a circular source. Unfortunately, practically none of the available theory is found in American engineering literature. Additional investigations are needed to develop further certain theoretical considerations, but the available theory is sufficient for many practical applications. Therefore, the significance of this paper is readily apparent.

The Dupuit assumptions have been subjected to much criticism and many have questioned the usefulness of the theoretical methods for estimating drawdown which are based upon it, although its usefulness for satisfactorily estimating the quantity of flow has been acknowledged. Mr. Casagrande has pointed out that the Dupuit assumptions are satisfactory if the slope of the lowered water surface is not too great. This has been confirmed through model tests by H. E. Babbitt, M. ASCE, and D. H. Caldwell,[14] A. M. ASCE, in relaxation solutions by Shih-Te Yang,[15] and by the model tests and relaxation studies of H. P. Hall.[16] Although extensive data are not available, it appears that the Dupuit assumptions do not involve an excessive error in the estimated drawdown at a distance beyond from ten to fifteen well diameters from the center of the well. Consequently, it can be assumed that the Dupuit-Forchheimer theory for steady-state gravity flow to well systems is valid for ordinary requirements in estimating the quantity of flow and the lowered ground-water level, except that the computed values of the lowered ground-water level near

[8] "Les fontaines publiques de la Ville de Dijon," by H. Darcy, Dijon, France, 1856.

[9] "Über die Ergiebigkeit von Brunnenanlagen und Sicherschlitzen," by Ph. Forchheimer, *Zeitschrift des Architekten und Ingenieuren Vereins zu Hannover*, Vol. 32, 1886.

[10] "Grundwasserspiegel bei Brunnenanlagen," by Ph. Forchheimer, *Zeitschrift des oesterrlichischen Ingenieur und Architekten-Vereins*, Vol. 50, 1898.

[11] "Grundwasserabsenkung bei Fundierungsarbeiten," by W. Kyrieleis, Julius Springer, Berlin, Germany, 1928.

[12] "Die Reichweite von Grundwasserabsenkungen mittles Rohrbrunnen," by H. Weber, Julius Springer, Berlin, Germany, 1928.

[13] "Das Fassungsvermögen von Rohrbrunnen und seine Bedeutung für die Grundwasserabsenkung insbesondere für grössere Absenkungstiefen," by W. Sichardt, Julius Springer, Berlin, Germany, 1928.

[14] "The Free Surface Around, and Interference Between, Gravity Wells," by H. E. Babbitt and D. H. Caldwell, *Bulletin No. 30*, Univ. of Illinois, Urbana, Ill., Jan 7, 1948.

[15] "Seepage Toward a Well Analyzed by the Relaxation Method," by Shih-Te Yang, thesis presented to Harvard University, in Cambridge, Mass., in 1949, in partial fulfilment of the requirements for the degree of Doctor of Philosophy.

[16] "Investigation of Steady Flow Towards a Gravity Well," by H. P. Hall, thesis presented to Harvard University, in Cambridge, Mass., in 1950, in partial fulfilment of the requirements for the degree of Doctor of Philosophy.

the wells will be considerably too low. However, this does not affect the practical usefulness of the theory, since it is the lowering at a distance from the wells—as at the center of an excavation—that is the practical interest.

The author's procedure in developing Eq. 3 is not clear and the resulting effect is that his mathematics appear to be incorrect. Apparently, this is because of his desire to conserve space, but the reader cannot readily supply the missing steps. The author assumes for simplicity that there are an infinite number of wells in Eq. 3 and loses the reader in proceeding to Eq. 4. For equal well discharges, Eq. 1 becomes:

$$H^2 - z^2_o = \frac{q}{\pi k}\left[\sum_{i=1}^{i=n} \log_e S_i - \sum_{i=1}^{i=n} \log_e R_i\right] \qquad (28)$$

in which $i = 1, 2, \cdots n$. For wells of diameter $r_1\, d\theta$ so close that they touch, the number of wells, n, equals $2\pi \frac{r_1}{r_1\, d\theta}$ or $n = \frac{2\pi}{d\theta}$ so that the flow per well becomes $\frac{Q\, d\theta}{2\pi}$, in which Q is the total flow from the system. Thus, introducing the expression for $S_i = \sqrt{4 p^2 + r^2_1 - 4 p r_1 \cos\theta}$, Eq. 28 becomes

$$H^2 - z^2_o = \frac{Q}{\pi k} \times \left[\frac{d\theta}{2\pi}\sum \log_e S_i - \frac{d\theta}{\pi}\sum \log_e R_i\right] \qquad (29)$$

An evaluation of $\sum \log_e S_i\, d\theta$ is the integration referred to in Eq. 4, which results in Eq. 5.

The writer has found it convenient to express the terms in the brackets in Eq. 28 in the forms of dimensionless expressions and graphs for a finite number of wells. If Q is the total well flow, Eq. 28 may be expressed as

$$H^2 - z^2_o = \frac{Q}{n\pi k}\left[\sum_{i=1}^{i=n} \log_e \frac{S_i}{R_i}\right] \qquad (30)$$

which becomes, for a circular well arrangement, since $\sum_{i=1}^{i=n} \log_e R_i = n \log_e r_1$

$$H^2 - z^2_o = \frac{Q}{\pi k}\left[\frac{1}{n}\sum_{i=1}^{i=n} \log_e S_i - \log_e r_1\right] \qquad (31)$$

Using the notations from Fig. 4,

$$S_i = \left[r^2_1 + (2p)^2 - 4 r_1 p \cos(i-1)\frac{2\pi}{n}\right]^{\frac{1}{2}}$$

or

$$S_i = r_1\left[1 + 4\left(\frac{p}{r_1}\right)^2 - 4\left(\frac{p}{r_1}\right)\cos(i-1)\frac{2\pi}{n}\right]^{\frac{1}{2}} \qquad (32)$$

and

$$\log_e S_i = \log_e r_1 + \frac{1}{2}\log_e\left[1 + 4\left(\frac{p}{r_1}\right)^2 - 4\left(\frac{p}{r_1}\right)\cos(i-1)\frac{2\pi}{n}\right] \qquad (33)$$

The summation $\frac{1}{n}\sum_{i=1}^{i=n} \log_e S_i$ now can be expressed in dimensionless form and plots of it can therefore be simply prepared. Eq. 31 thus becomes

$$\left.\begin{aligned} H^2 - z^2{}_o &= \frac{Q}{\pi k}\left[\log_e r_1 + L - \log_e r_1\right] \\ \text{or} \qquad H^2 - z^2{}_o &= \frac{Q\,L}{\pi k} \end{aligned}\right\} \ldots (34)$$

where

$$L = \frac{1}{2\,n}\sum_{i=1}^{i=n} \log_e\left[1 + 4\left(\frac{p}{r_1}\right)^2 - 4\,\frac{p}{r_1}\cos\,(i-1)\,\frac{2\,\pi}{n}\right] \ldots\ldots (35)$$

The value of L is plotted in Fig. 18 for various values of p/r_1 and different numbers of wells. The flow per well is assumed to be the same for all wells. It can be seen that L is only slightly dependent on the number of wells used. Therefore, the expression, $L = \log_e 2\,p/r_1$, as given (in effect) by the author in Eq. 5, may be used regardless of the number of wells when p/r_1 is greater than about 2, and for a moderate number of wells when p/r_1 is less than 2.

The equation for the lowered water surface in the wells, when a limited number of wells is used, can be obtained simply and is of interest. If the distance from the impervious layer to the water surface in the well is denoted by z_w, it is apparent from Eq. 1 that for a circular arrangement of wells with an equal flow per well

$$H^2 - z^2{}_w = \frac{Q}{\pi k}\left[\frac{1}{n}\sum_{i=1}^{i=n} \log_e S_i - \frac{1}{n}\sum_{i=1}^{i=n} \log_e R_i\right] \ldots\ldots\ldots (36)$$

It is apparent that $\frac{1}{n}\sum_{i=1}^{i=n} \log_e S_i$ can be obtained from the previous evaluation of this summation by simply letting $2\,p$ equal the distance from the well at which the drawdown is desired to the center of the imaginary well system, which distance may be called $2\,p'$. For most well systems the value of the summation can be approximated by $\log_e r_1 + \log_e \frac{2\,p'}{r_1}$. Mr. Sichardt explains that

$$\frac{1}{n}\sum_{i=1}^{i=n} \log_e R_i = \log_e r_1 - \frac{1}{n}\log_e \frac{r_1}{n\,r_w} \ldots\ldots\ldots\ldots\ldots (37)$$

in which r_w is the well radius.[18] It follows that the evaluation of the water in the well may be found from the equation,

$$H_e^2 - z^2{}_w = \frac{Q}{\pi k}\left[\log_e \frac{2\,p'}{r_1} + \frac{1}{n}\log_e \frac{r_1}{n\,r_w}\right] \ldots\ldots\ldots\ldots (38)$$

The author limits his discussion to circular well arrangements. If a rectangular system of wells or wellpoints is used, it may be converted into an equivalent circular system having an enclosed area equal to the area of the

rectangle, or the rectangular system can be analyzed by using the graph prepared by Mr. Weber.[12] The writer has found it convenient also to prepare dimensionless graphs of $\sum \log_e S_i$ and $\sum \log_e R_i$ for lines of wells. These graphs also can be used to find the lowering at any point when using a rectangular area.

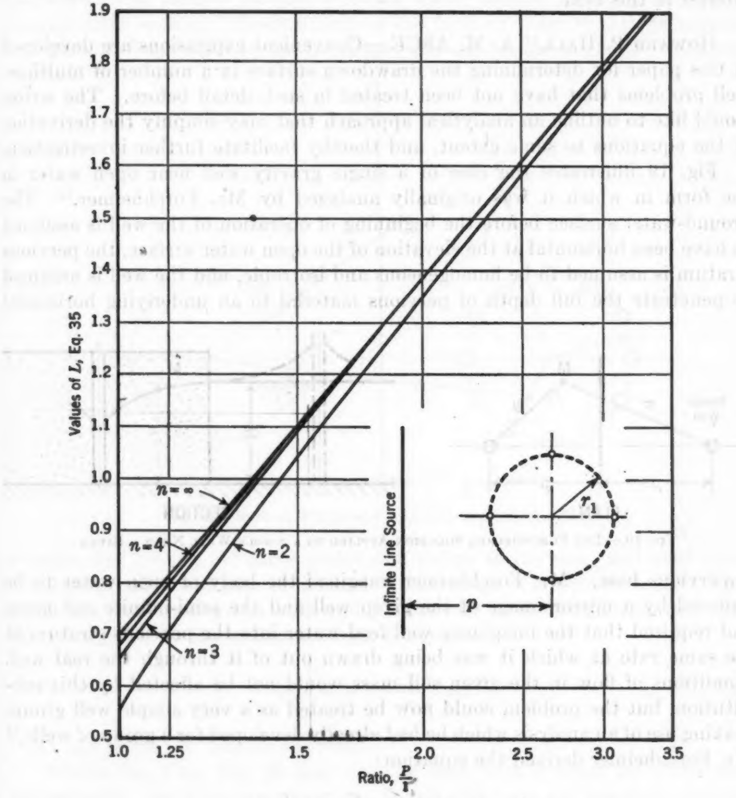

FIG. 18.—CIRCULAR SYSTEM WITH INFINITE LINE SOURCE

The example given by the author is particularly interesting because it demonstrates an engineering approach to a ground-water lowering operation. Unfortunately, there are only a limited number of cases where such an approach is actually used. The author did not indicate how he treated the fact that the wells only partly penetrate the previous stratum. This is a practical feature of considerable importance. He apparently assumed that the wells completely penetrated the pervious stratum, which is a different assumption from that sometimes made. The author's viewpoint on this phase would be appreciated. The length and spacing of the wellpoints are pertinent and should, perhaps, be indicated.

In conclusion, the writer wishes to emphasize his belief in the substantial significance of this paper and in the practicability of applying this approach. At present, only a few engineers have been applying in practice the available theory for ground-water lowering. It is hoped that the paper will stimulate interest in this field.

HOWARD P. HALL,[17] A. M. ASCE.—Convenient expressions are developed in this paper for determining the drawdown surface in a number of multiple-well problems that have not been treated in such detail before. The writer would like to outline an analytical approach that may simplify the derivation of the equations to some extent, and thereby facilitate further investigation.

Fig. 19 illustrates the case of a single gravity well near open water in the form in which it was originally analyzed by Mr. Forchheimer.[18] The ground-water surface before the beginning of operation of the well is assumed to have been horizontal at the elevation of the open water surface, the pervious stratum is assumed to be homogeneous and isotropic, and the well is assumed to penetrate the full depth of pervious material to an underlying horizontal

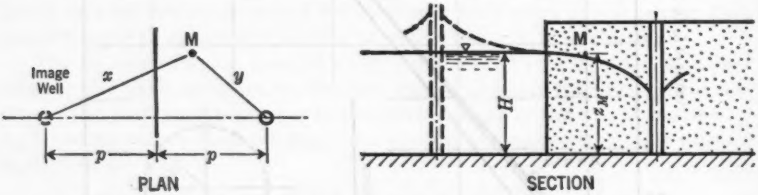

FIG. 19.—THE FORCHHEIMER SOLUTION APPLIED TO A SINGLE WELL NEAR A RIVER

impervious base. Mr. Forchheimer imagined the body of open water to be replaced by a mirror image of the given well and the semi-infinite soil mass, and required that the imaginary well feed water into the pervious stratum at the same rate at which it was being drawn out of it through the real well. Conditions of flow in the given soil mass would not be affected by this substitution, but the problem could now be treated as a very simple well group. Making use of an analysis which he had already developed for a group of wells,[19] Mr. Forchheimer derived the equation:

$$z^2 = H^2 - \frac{q}{\pi\, k} \log_e \frac{x}{y} \quad \text{.....................} (39)$$

in which z is the elevation of an arbitrary point on the free surface, measured from the impervious base; H is the elevation of original ground-water surface, measured from the impervious base; q is the rate of flow from the imaginary well to the given well; k is the coefficient of permeability of the pervious stratum; and x, y are the distances from the arbitrary point to the imaginary well and given well, respectively.

[17] Asst. Prof. of Civ. Eng., Northwestern Univ., Evanston, Ill.

[18] "Grundwasserspiegel bei Brunnenanlagen," by Ph. Forchheimer, *Zeitschrift des oesterreichischen Ingenieur und Architekten-Vereins*, Vol. 50, 1898, pp. 629–648.

[19] "Uber die Ergiebigkeit von Brunnenanlagen und Sicherschlitzen," by Ph. Forchheimer, *Zeitschrift des Architekten und Ingenieuren Vereins zu Hannover*, Vol. 32, 1886, pp. 539–564.

Referring now to the problem in the paper, let Fig. 20 represent a typical arrangement of a number of wells in a circle having a radius r_1 and a center at a distance p from open water. Eq. 4 and Eq. 11 have been derived with such an arrangement in mind, but with the well group idealized as a ring composed of an infinite number of small wells—that is, as a well having an annular cross section. Examination of the form of these equations suggests that the problem might be analyzed by replacing the given ring of wells with

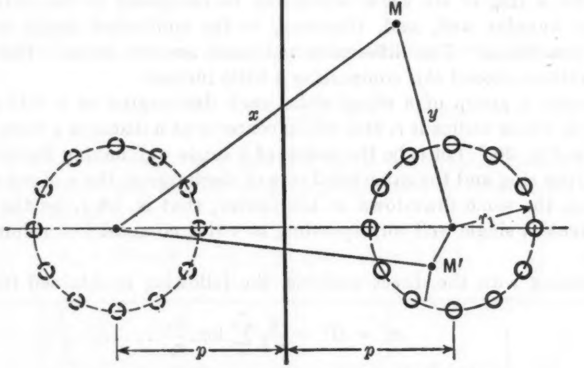

FIG. 20.—RING OF WELLS AND AN EQUIVALENT SINGLE WELL

a single well having the same center and radius as the ring, and discharging at a rate equal to the sum of the rates of discharge of the given wells. Thus, if n is the number of given wells and q is the rate of discharge from each well, Eq. 39, applied to this substitute well, becomes—

$$z^2_M = H^2 - \frac{n\,q}{\pi\,k} \log_e \frac{x}{y} \quad \text{(40)}$$

—for any point, M, outside the ring.

Within the ring, Eq. 39 may also be used, but it must be noted that, theoretically, the drawdown contours within this area are concentric circular arcs whose center is the center of the image ring. (The original analysis superposed the drawdown of the given well upon the negative drawdown of the image well.) Thus, the elevation of the drawdown surface at any point within the ring is the same as that of a point on the ring circumference at the same distance from the image center. Eq. 39 for a point, M′ (Fig. 20) within the ring may therefore be written:

$$z^2_{M'} = H^2 - \frac{n\,q}{\pi\,k} \log_e \frac{x}{r_1} \quad \text{(41)}$$

A comparison of Eqs. 40 and 41 with Eqs. 11 shows that they are the same. It should be noted that the introduction of the idea of an equivalent single

well does not reduce the time and labor required for computing numerical results since the equations are the same, but the derivation is somewhat simpler since the analytical procedure is reduced to the direct application of one equation.

The foregoing discussion indicates only that the equivalent single well may be substituted for a well of annular cross section without loss of theoretical accuracy. It is also of importance to know to what extent the number of wells can be reduced and the radius of ring increased in relation to p (Fig. 20) before the device loses its theoretical validity. Fig. 11 contains drawdown curves for a ring of six wells, which can be compared to the curve for the idealized annular well, and, therefore, to the equivalent single well, under similar conditions. The differences indicated are not large. The following considerations extend this comparison a little further.

Consider a group of n equal wells, each discharging at a rate q, located on a circle whose radius is r_1 and whose center is at a distance p from the shore line, as in Fig. 20. Let r_e be the radius of a single well having the same center as the given ring and the same total rate of discharge as the n given wells, and producing the same drawdown at the center; that is, let r_e be the radius of the equivalent single well corresponding to a ring composed of a finite number of wells.

Beginning with the direct analysis, the following is obtained from Eq. 1:

$$z^2_o = H^2 - \frac{q}{\pi k} \sum_1^n \log_e \frac{x_n}{r_1} \quad \text{.................... (42)}$$

in which z_o is the elevation of the free surface at the center of the ring, and x_n is the distance from the center of the ring to the image of the nth well.

An analysis of the same case by the equivalent single well gives

$$z^2_o = H^2 - \frac{n\,q}{\pi k} \log_e \frac{2\,p}{r_e} \quad \text{.................... (43)}$$

If the drawdown at the center is to be the same, it follows that

$$n \log_e \frac{2\,p}{r_e} = \sum_1^n \log_e \frac{x_n}{r_1} \quad \text{.................... (44)}$$

or

$$\left(\frac{2\,p}{r_e}\right)^n = \frac{x_1, x_2, \cdots, x_n}{(r_1)^n} \quad \text{.................... (45)}$$

and

$$\frac{r_e}{r_1} = \frac{2\,p}{\sqrt[n]{x_1, x_2, \cdots, x_n}} \quad \text{.................... (46)}$$

Eq. 46 is a convenient form in which to compare the radius of the equivalent single well to the radius of the given ring of wells. If p is large in relation to r_1, it follows that $x_1 \approx x_2 \approx \cdots \approx x_n \approx 2\,p$, and the ratio reduces to unity, as would be expected. As r_1 approaches the magnitude of p, the corresponding changes in the ratio are insignificant until the circumference of the ring of wells comes very close to the shore line. For example, in the case of a ring

of as few as four wells located at the quarter points, the radius of the equivalent single well is less than 1% different from the ring radius until p becomes less than $1.125\,r_1$. Consequently, it appears that, from the point of view of drawdown at the center, the equivalent single well is an acceptable analytical device in most cases.

The differences at the circumference of the ring are the greatest, as Fig. 11 indicates. Eq. 1 applied to a point on the circumference of the ring may be written

$$H^2 - z^2 = \frac{q}{\pi k} \sum_1^n \log_e \frac{x_n}{y_n} \qquad (47a)$$

The corresponding expression using the equivalent single well becomes

$$H^2 - z^2 = \frac{n\,q}{\pi k} \log_e \frac{x}{r_1} \qquad (47b)$$

In cases where the drawdown is assumed to be not greater than $0.2\,H$, Mr. Casagrande recommends the following approximation as introducing an error of not more than 10%:

$$H^2 - z^2 = (H + z)(H - z) \approx 2\,H\,h \qquad (47c)$$

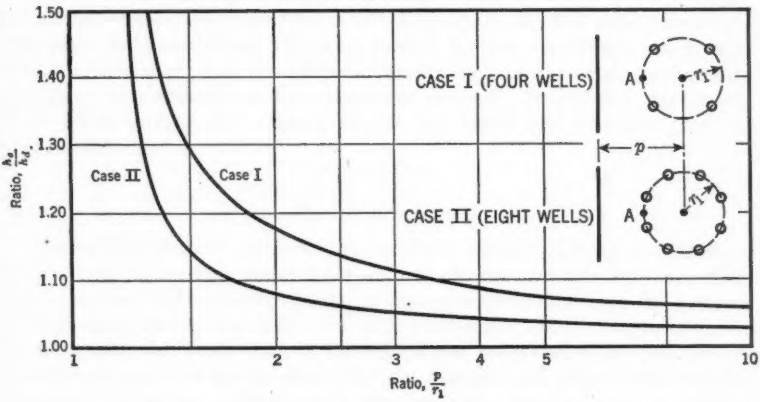

FIG. 21.—RATIO $\frac{p}{r_1}$ VERSUS $\frac{h'_e}{h_d}$ AT POINT A

in which h is the drawdown $= H - z$. If Eq. 47b is divided by Eq. 47a with this approximation introduced, the resulting equation expresses the ratio of drawdowns computed by the two methods:

$$\frac{h_e}{h_d} = \frac{\log_e \left(\dfrac{x}{r_1}\right)^n}{\log_e \dfrac{x_1, x_2, \cdots, x_n}{y_1, y_2, \cdots, y_n}} \qquad (48)$$

in which h_e is the drawdown determined by use of the equivalent single well and h_d is the drawdown determined by summation of the contributions of individual wells.

Eq. 48 provides the basis for the curves of Fig. 21. A ring of four wells and one of eight are considered separately. Each group is arranged so that the point on the ring circumference which is nearest the shore line is also midway between two wells. Thus, point A corresponds to the largest discrepancy between the equivalent single well solution and the conventional summation for a given number and location of wells. In view of the fact that these differences are localized, as the six-well drawdown curve of Fig. 11 indicates, it appears from Fig. 21 that, even at the ring circumference, the equivalent single well is reasonably reliable in most cases.

AMERICAN SOCIETY OF CIVIL ENGINEERS

Founded November 5, 1852

TRANSACTIONS

Paper No. 2543

RESEARCH IN WATER SPREADING

By Dean C. Muckel[1]

Synopsis

To determine the factors affecting the rate of recharge of ground water by means of spreading basins, a program of research and field experimentation was carried on in the San Joaquin Valley, in California. The results of this research are reported in this paper.

Early studies had determined the percolation characteristics of undisturbed and disturbed soils, and the research of this program checked these characteristics under field conditions. In order to vary the test conditions, two groups of ponds were used, and the effect of factors such as chemical, mechanical, vegetative, and operational conditions was studied. In addition, treatment of the basin surface with organic matter was tested and found to produce good results.

Introduction

The method of water conservation known as water spreading is defined as the practice of diverting water from natural stream channels and spreading it over porous lands, thereby giving it opportunity to sink into the ground and eventually become a part of the main ground-water body. The term water spreading has also been used in some localities to describe the practice of diverting stream flow during flash floods to pasture and other lands for the purpose of irrigation. Although the two spreading systems may be similar in design, their purposes are definitely different. As used in this paper, the term is applied only to the practice of diverting for replenishment of the underground water supplies. Such spreading is used in areas in which pumping from wells is a major means of obtaining water.

Spreading for replenishment of the ground-water supplies involves much greater quantities of water than those required for irrigation. Water is applied to areas in such quantities and for such long periods of time that the

Note.—Published in December, 1951, as *Proceedings-Separate No. 111.* Positions and titles given are those in effect when the paper was received for publication.

[1] Engr., Div. of Irrig. and Water Conservation, Soil Conservation Service, U. S. Dept. of Agri., Pomona, Calif.

amount of water retained in the root zone is negligible. The purpose of such application is to stimulate percolation, to replenish the ground-water supplies, and to raise the water table, whereas in irrigation, an adequate application consists of a few inches per irrigation, or 2 to 4 ft per yr. In spreading for replenishment of ground water, several acre-ft per acre of water may be put into the ground in a single day.

The need for water spreading has been apparent in many localities for many years, and it is of growing importance in others. Pumping from wells has long been the principal source of water in parts of the semiarid West, and since 1930 the demand for water has increased greatly as more land has been brought under irrigation, and domestic and industrial uses have been expanded. Other areas throughout the United States have reported increases in the draft on ground-water supplies. More efficient pumping equipment, improved well-drilling methods, and a wider distribution of power have accounted for some of the increase. In the East and Middle West, these drafts on the ground water have occurred from demands for domestic, industrial, and other uses, such as air conditioning.

Water spreading was first attempted on a large scale in the south coastal basin of California because conditions there lent themselves well to this type of conservation, and the need for water was great. Areas suitable for spreading exist at the mouths of the many canyons where they debouch from the mountains. The streams have built up relatively steep debris cones by dropping their loads of boulders, gravel, and sands as they strike the flatter slopes of the valleys. Because of the coarse material of which these cones are composed, the lands are not particularly suitable for cultivation and are, in general, classed as waste land. Those areas are porous and have high rates of infiltration and, consequently, are well adapted to water spreading. Spreading has also been contemplated for the recharging of ground-water supplies in other areas. In the San Joaquin Valley, spreading of flood waters is a part of the Central Valley Water Plan and is also contemplated by local water storage districts. In fact, the North Kern Water Storage District on the Kern River Delta near Bakersfield, Calif., has withheld a large area of valuable agricultural land from cultivation for the purpose of spreading and recharging the ground-water supplies within its boundaries. Natural spreading areas consisting of waste land and composed of porous soils are practically nonexistent in those parts of the San Joaquin Valley needing replenishment and, therefore, spreading must be done on the finer textured soils such as sandy loams and fine sandy loams.

RESEARCH PROJECTS

The research work reported in this paper deals with water spreading in the San Joaquin Valley. The problem here was to obtain and maintain a satisfactory percolation rate, whereas on the gravel cones of southern California, the problem was primarily one of construction and maintenance.

Early Studies.—Tests started in 1936 showed that the percolation rate decreased below the limit of practicability when water was applied continuously to an undisturbed soil for extended periods. A search of the literature showed that considerable experimental work was being done at that time on the problem

of infiltration, but in nearly all cases, the experiments were made in connection with the infiltration of rainfall or irrigation water. Consequently, the water was applied for short runs only. In spreading, water may be applied continuously for weeks or even months at a time.

Typical percolation rate curves are shown in Fig. 1. The curve representing undisturbed soils indicates that after a short shutdown, the curve repeats itself but at a lesser rate. On the basis of work done in the laboratory with

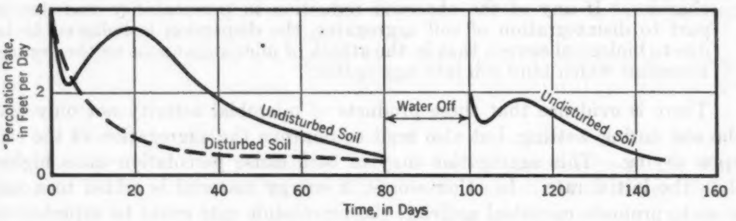

FIG. 1.—TYPICAL PERCOLATION RATE CURVES

soil cores,[2] the S-shaped percolation rate curve was explained as follows:

"a. The initial decrease in permeability or infiltration rate is believed to be caused by dispersion and swelling of the soil particles. This is much more pronounced in some soils than others.

"b. The increase in permeability following the initial decrease accompanies the elimination of entrapped air from the soil. This air is slowly dissolved in the water passing through the soil.

"c. The gradual decrease in permeability that follows is due primarily to biological activity in the soil."

The typical percolation rate curve for soil plowed or otherwise disturbed prior to spreading is also given in Fig. 1. In this case, the rate of percolation is apparently controlled at or near the soil surface, and the rate of the entrance of water into the soil is less than the rate at which the water would move through the soil profile. Therefore, the entrapped air influence is not effective. Technically, at least a portion of this curve probably represents infiltration rate rather than percolation rate.

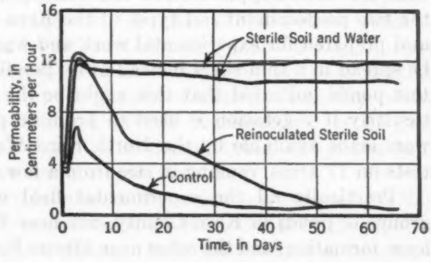

FIG. 2.—PERMEABILITY-TIME CURVES FOR EXETER SANDY LOAM UNDER PROLONGED SUBMERGENCE

The explanation of the S-shaped curve was substantiated later by permeability tests with sterile soil and water. In Fig. 2, note that the permeability

[2] "Effect of Entrapped Air Upon the Permeability of Soils," by J. E. Christiansen, *Soil Science*, Vol. 58, No. 5, November, 1944.

of sterile soil and water was maintained at approximately the maximum rate, although the control operated under ordinary unsterile conditions followed the typical curve of Fig. 1. The conclusions from this experiment were:

> "Sterile permeability tests conducted to determine the cause of decrease permeability under prolonged submergence gave no evidence of soil aggregate breakdown due to purely physical causes. The reduced permeability appears to be due entirely to microbial sealing. The soil pores probably become clogged with the products of growth, cells, slimes or polysaccharides. If any of the observed reduction in permeability was due in part to disintegration of soil aggregates, the dispersion is believed to be due to biological causes, that is, the attack of microorganisms on the organic materials which bind soil into aggregates."

There is evidence that these products of microbial activity not only seal the soil during wetting, but also tend to improve the aggregation of the soil upon drying. This aggregation may in turn cause percolation rates higher than the initial rate. In other words, if energy material is added to a soil so as to promote microbial activity, the percolation rate could be expected to decrease rapidly but upon drying, followed by the reapplication of water, the percolation could be expected to be at a higher rate than the initial run. This action has occurred on field test ponds and will be discussed later.

The San Joaquin Valley Project.—The research program described in this paper has concentrated on checking some of the foregoing conclusions under field conditions and developing some practical method of maintaining the peak rates or stimulating percolation during the entire run. The sterilization of soil and water is, of course, an impossibility under field conditions.

An intensive series of field experiments was started in 1944. A group of 9 test ponds, originally started in 1936 by the North Kern Water Storage District, was put into operation, and 37 others were constructed. Fifteen of these ponds were in isolated locations along the approximate line of the Friant-Kern Canal. These ponds were located on different soil types and served from different water supplies. The remaining ponds were located in two groups on the two predominant soil types of the Kern area. A 6-acre tract was leveled and prepared for experimental work and was so laid out that the water could be spread in a thin sheet instead of by ponding. Results of some of the small test ponds indicated that this might be the proper method of spreading, particularly if vegetation is used to promote percolation. In addition, records were made available by the North Kern Water Storage District of spreading tests on 17 areas, ranging in size from a few acres to over 50 acres.

Practically all the experimental field work has been confined to two groups of ponds in Kern County, one near Wasco, located on Hesperia sandy loam formation, and the other near Minter Field, located on Exeter sandy loam. By confining the tests to these groups, the differences in quality of the water supplying the ponds, soils, and other factors have been eliminated to a large extent, and various treatments of soil and water can be tried and compared with control ponds. It should be borne in mind that these small test ponds are intended to give only relative rates between different soil and water treatments, and the percolation rates are not necessarily applicable to large-scale spreading areas.

Treatment of Test Ponds

The test ponds were subjected to a variety of treatments. These included different cultural treatments, mulches, various grasses, chemical treatments, and different methods of operating with alternate wet and dry periods and shallow, deep, and fluctuating water depths. The effects of all treatments were checked against the rates obtained from undisturbed control ponds. Some of the experiments were not considered practical on a large scale but were of an academic nature, though important in the search for a practical solution of the percolation problem.

The field treatments attempted fall under one of five general classes: (*a*) Chemical; (*b*) mechanical; (*c*) vegetative; (*d*) operational procedures; and (*e*) addition of organic matter.

(*a*) *Chemical.*—The immediate concern in connection with the effect of chemical treatment on percolation rates is the characteristics of the water supply. Ordinarily, in water spreading there is no choice of water, but its suitability for spreading should be examined as far as available knowledge permits. Considerable information exists as to the effects of certain types of water on the percolation rates consequent to irrigation, and these effects, in general, are believed to apply to spreading.

It is common knowledge that hard water is more conducive to rapid infiltration than soft water. Water that is relatively high in calcium and magnesium is called hard, and water low in these elements is called soft. Ordinarily, water analyzing below 30 ppm of calcium and magnesium is considered soft, from 30 to 60 ppm fairly hard, and above 60 ppm hard.

Sodium is another element known to affect the movement of water into or through a soil. Its importance lies not so much in the quantity present, but in its relation to the elements calcium and magnesium. The sodium percentage, calculated by dividing the quantity of sodium by the sum of the quantities of calcium, magnesium, sodium, and potassium (all in equivalents per million), is the usual way to classify the quality of water for irrigation with respect to the sodium effect on the soil. A water of high sodium percentage tends to deflocculate the colloidal soil particles and, consequently, hinders the movement of water. As is the case with hardness, no inflexible distinction can be drawn between a good and a poor quality of water. Generally, water in which the sodium percentage is above 65% is considered to be of poor quality, between 50% and 65% the quality is questionable, and below 50% it is satisfactory both for irrigation and for spreading.

The waters that are of primary interest in this study are those of the San Joaquin River, to be delivered through the Friant-Kern Canal of the Central Valley Project, and that of the Kern River. Both have water of low total salt content. The conductance of Friant-Kern Canal water is less than 10. The sodium percentage of 38.4 is considered to be satisfactory for spread g, but the water definitely falls into the class of a soft water with respect to calcium carbonate and, therefore, is not of the best quality from a water-spreading point of view. Kern River water has a conductance of about 25. The hardness is fair, being around 50 ppm. The sodium percentage varies considerably from maximums of 70 to minimums of about 30 and averages

about 50. Surface storage is proposed for Kern River, and it is not known what effect, if any, this storage will have on the water quality.

For the isolated ponds along the line of the Friant-Kern Canal, the waters used for testing differed materially. Some of these waters were classed as good and some as unsatisfactory. At one pond, the soil was a loamy sand and from all appearances should have taken water at a rapid rate. However, the water supply was wholly unsatisfactory, as the sodium percentage was 96 and the hardness 12.7 ppm. As a result, the percolation rate decreased to only a few hundreths of a foot per day after a few weeks' application of water. The variation in the quality of the water supplying these isolated ponds was one reason for their discontinuance.

In view of the known effects of water quality on percolation rates, several experiments were made at the Minter Field and Wasco test ponds to determine the effect and practicability of undertaking soil or water treatment to lower the sodium percentage or to raise the hardness. Applications of gypsum ($CaSO_4$) and calcium chloride ($CaCl_2$) were beneficial and increased percolation rates, but only temporarily. Fig. 3 illustrates the results obtained by the use of gypsum and calcium chloride.

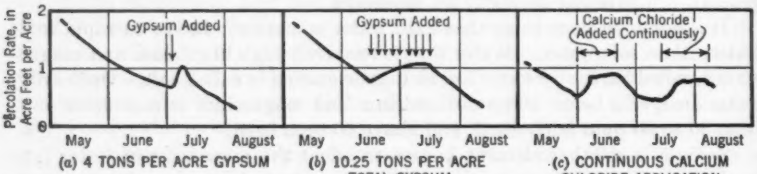

FIG. 3.—EFFECT OF TREATMENT ON PERCOLATION RATE

Other chemical tests included the application of lime to increase the water hardness and copper sulphate for algae control. Some of these tests were not conclusive in so far as their intended purposes were concerned. No tests were made to determine whether or not the soil or water was affected by the addition of the chemicals since the result was read only in the effect on the percolation rate.

(*b*) *Mechanical.*—The treatments classed as mechanical involved the spading of the soil, the removal of the top soil, the raking or scraping of the soil surface, the sinking of auger holes backfilled with gravel, and the covering of a pond with a tar-papered roof to exclude sunlight.

Sod removal, with and without spading, was found to be detrimental to percolation. Spading or plowing alone prior to the application of water appears to be beneficial at the Wasco Ponds, but is of questionable value at Minter Field. After a prolonged period of spreading, initial percolation rates could be recovered only by allowing the soil to dry and then breaking it up by spading or plowing.

Raking or scraping off the top ¼ in. or ½ in. of soil surface apparently had no effect. During nearly all spreading runs, numerous bubbles (air or other gas) were noted on the soil surface. The removal of these bubbles by daily

raking had no apparent effect. There are several theories as to what these bubbles contain, how they are formed, and what their effect on percolation might be, but, unfortunately, there has been no opportunity to investigate them thoroughly. One sample was analyzed as air, although other casual inspections indicated carbon dioxide and marsh gas. It is entirely possible, and perhaps probable, that the bubbles contain entirely different gases at the start of a run and at the end, which might be six months later. The bubbles seem to be more numerous on some days and in some ponds than on other days and in other ponds. The presence of these bubbles may or may not play an important part in the study of the soil microbiology.

Evidence obtained in the laboratory on soil cores and in the field with tensiometers shows that the percolation rate decrease is caused by changes that take place at the soil surface and in the topsoil containing, among other things, organic matter. Auger holes were drilled and backfilled with gravel to by-pass the surface soil. This treatment apparently has some merit as beneficial results were obtained at Minter Field. The effects at Wasco are questionable. This is to be expected, as a sand stratum exists at Minter Field that is penetrated by the auger holes. The soil is more uniform, and no such sand stratum exists at the Wasco ponds.

Because prior research[2] had indicated that the rates during an early part of the spreading run were affected by air entrapped in the soil, an attempt was made to hasten its removal. Four auger holes were drilled to a depth of 20 ft in a test pond. The holes were backfilled with gravel to within 1 ft of the surface, and this last foot was filled with tamped earth. Vents, consisting of ¾-in. pipe, extended from the gravel fill above the water surface. The treatment was not effective. A 1944 report[3] also found that it was not possible to drive all the air from the soil by slowly saturating the soil column from the bottom upward or by applying water at the top. The air entrapped in the soil was removed by being dissolved in the water passing through the soil. If this conclusion is correct, the use of vents with auger holes was, of course, doomed to failure.

As a further test of algae control, one pond was covered with a tar-papered roof so as to exclude all sunlight. No effect was noted on the percolation rates.

(c) *Vegetative.*—Trials with vegetation were made for two purposes: (1) To increase or maintain percolation rates; and (2) to find a grass or plant that would survive on water-spreading areas and to provide a cash or forage crop.

Due to the high cost of spreading, it is highly desirable to derive some productive use from the land other than spreading. The best possibility is believed to be the raising of hay or grazing crops. The conditions to be met by a grass or another plant in the San Joaquin Valley are severe. Spreading will normally occur in the late winter and spring months, although in wet years the period might be prolonged considerably. In drought years there will not only be no water to spread, but no water available to irrigate the grasses or plants to sustain them on a spreading area. Normally, there will be drought periods of several months each year, extending through the summer and fall. The

[3] "Effect of Microorganisms on Permeability of Soil Under Prolonged Submergence," by L. E. Allison, *Soil Science*, Vol. 63, No. 6, June, 1947.

grass or plant desired is, therefore, one that will grow under several months of constant wetting, survive the long, hot, dry summers, and provide a hay or forage crop. In order to avoid artificial reseeding, perennial plants or those that reseed or grow voluntarily are desirable.

Several grasses and other plants were tried. These were, in general, native to the area and grew under the conditions set forth above. Highly pestiferous plants, such as Johnson grass (Sorghum halepense), were not considered. Bermuda grass appears to have the greatest possibility. It grew luxuriantly under prolonged wetting, provided the tops were not submerged, but died under total submergence. Bermuda grass survived long drought periods and, furthermore, is considered a good grass for grazing lands. There is evidence that after it had become well established it improved the ability of the soil to take water.

Paragrass also grew luxuriantly under spreading conditions, but its value as a forage crop is not definitely known. A very dense growth was obtained, but apparently it does not withstand freezing temperatures, as the tops froze back to the soil or water surface each winter. Volunteer growth appeared in the following spring, however.

Dallis grass (considered a pest in some parts of the valley owing to its tendency to grow in irrigation ditches), Rhodes grass, rye grasses, salt grass, Sudan grass, and bluestem were all tried, but none appeared to have the possibilities of Bermuda grass. Bermuda grass, considered a pest or weed in cultivated crops, is quite common throughout the San Joaquin Valley. Its value as a pasture, however, renders it satisfactory on a spreading area. In fact, any other grass planted on a spreading area would apparently have a difficult time to escape being crowded out by Bermuda grass.

Button willow shrubs (baccharis glutinosa) were planted and grown successfully in two ponds, but no effect on the percolation rate could be noted. As far as is known, they have little forage or other value. They were found growing wild on the large spreading areas of southern California.

Alfalfa failed on soil wet continuously for a 10-day period and then dried 10 days, and the rate of percolation was not benefited by its use.

(*d*) *Operational Procedures.*—Under this classification are included the experiments with different depths of water, different lengths of drying periods between runs, the cessation of water application before the percolation rate reaches a minimum, and the desilting of the water supply.

As would be expected, the percolation rate varies directly with changes in the depth of water or head during a spreading run. However, if a spreading run is started and maintained at a shallow depth (0.2 or 0.3 ft) throughout a run, the percolation rates tend to be higher and maintain themselves better than when the water is applied at depths of 1 or 2 ft. This variation may be caused by differences in sunlight reaching the soil, temperature, or other factors. It is also well established by these tests that certain plant growths will thrive with the shallow depths of water, whereas they are drowned out under the greater depths.

The effect of interruptions of spreading apparently depend largely on the degree of drying that takes place in the topsoil. Short interruptions (of a

few days or less) usually have only a temporary effect on the percolation rate, and after a few days, the rates appear to return to what would have been expected had no interruptions occurred. It is believed that air entering the soil during a short interruption in spreading causes the temporary changes in percolation rate upon restarting.

Interruptions of such duration that the topsoil dries usually cause an increase in percolation rates, and in some cases, have resulted in a rate recovery equal to the initial rate. Usually, however, the rates during the second run were somewhat smaller than the initial rates, although the shapes of the curve were similar, as previously mentioned and illustrated in Fig. 1. Soil samples were taken during all off periods, and the degree of drying of the top 6 in. of soil was recorded. Tests were made to determine the effect of drying the soil to a 10% soil moisture content, as compared with a 5% soil moisture, but other uncontrolled factors made it impossible to draw any definite conclusions. The field capacity of the top 6 in. of soil at Wasco is approximately 11.5% and the wilting point 5.5%. At Minter Field, the field capacity is 8.7% and the wilting point 3.3%. During the summer, the surface soil dries rapidly, and percentages of 10 or lower can be obtained in a relatively short time (two or three weeks). During the winter months, showers and cool foggy weather usually prevent the top soil from drying below 10% at any time.

A desilting of the water at Minter Field was attempted by passing the water from one pond through another pond to allow settling. No effect on the percolation rate was noted. Tests to determine whether or not the water was actually desilted were not made, so the results are inconclusive.

(*e*) *Addition of Organic Matter.*—The addition of organic matter was tested on several ponds. In some cases, the results were remarkable, and percolation rates were increased several times over the rate obtained on undisturbed soils. Of all the materials applied, cotton gin waste was found to give the best results. Alfalfa hay applied at the rate of 5 or 10 tons per acre gave temporarily beneficial results. Barley, Sudan grass, Paragrass, and Dallis grass that were grown to maturity and then spaded under or cut and allowed to lie on the ground, gave indications of being beneficial in some cases, but the results were insignificant in most instances. Cornstalks at field run, spaded under with and without ammonium sulphate, were tried. The cornstalks applied with ammonium sulphate resulted in a high peak percolation rate, but the high rates were of short duration, and a fairly rapid decline in rate followed the peak. Barnyard manure applied at 8 tons per acre had no noticeable effect on the percolation rate.

Cotton gin waste, consisting of boll hulls, leaves, stems, a few seeds, and a small amount of lint resulted in substantially increased percolation rates in every trial. Unfortunately, no measurement of the amount of material when first applied was made, other than to record it as a 6-in. layer. Three different methods of application were tested: (1) The waste in a trial was added to the soil surface or merely added to a pond during spreading operations; (2) the material was spaded under, then kept moist for 30 days by frequent irrigations or continual submergence. At the end of the 30-day period the soil was permitted to dry to 10% moisture or less before the spreading. This

30-day moist or wet period was called an incubation period that is believed to start or hasten the process of decomposition; and (3) the cotton gin waste was spaded under immediately prior to spreading.

In the first and third methods, the results were highly beneficial, but the effect was delayed for several weeks or more before it became apparent. By the second method (spading the gin waste material into the soil and then giving a 30-day incubation period, followed by a drying-out period before spreading), increased percolation rates were obtained almost immediately.

In addition to the increased percolation rates, the long-lasting effect of an application of cotton gin refuse is of prime importance. Applications made in 1946 were still apparently highly effective in 1950. It is true that percolation rates fluctuate from high peaks and decline to relatively low rates, but in every case in which the gin refuse had been previously applied, high percolation rates were recovered upon drying and spading. The rates during spreading reached peaks of 14 ft per day, leveled off at 4 to 5 ft per day, and declined to a few hundreths of a foot per day after a run of several weeks (Fig. 4).

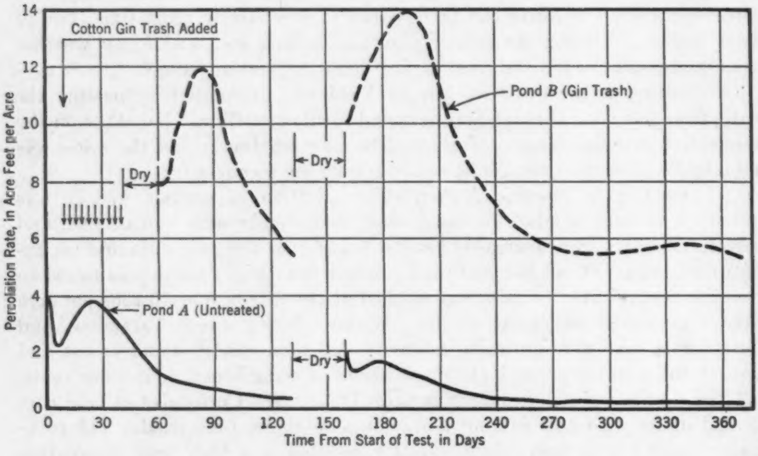

FIG. 4.—EFFECT OF COTTON GIN TRASH ON PERCOLATION RATE

The behavior of the gin-trash treated ponds ties in closely with experiments that demonstrated in the laboratory that microbiological activity causes the decrease in percolation rates under prolonged submergence.[4] The gin trash provides food for the soil microorganisms, or perhaps food for certain types of organisms. The residues left during the decomposition of the gin trash cause a rapid sealing of the soil, but in turn tend to improve the soil aggregation and upon drying, the percolation rates are improved materially.

[4] "Report for 1944 Laboratory Phases of Cooperative Water Spreading Study," by J. E. Christiansen and O. C. Magistad, U. S. D. A., Regional Salinity Laboratory, Bureau of Plant Industry, Soils and Agri. Eng., Washington, D. C., 1944.

LABORATORY WORK

There are many phases of the water-spreading problem that cannot be worked out under field conditions. A pond may respond to a certain treatment, but the reason for such response cannot be determined without laboratory investigation. Because of the outstanding results obtained in the field with cotton gin trash, the laboratory work is important in that phase of treatment. While gin trash is available in the San Joaquin Valley, it is at present expensive to apply to large areas. Also, spreading is needed in other areas in which gin trash is not available, and it is felt that if more information is obtained on why this treatment promotes percolation, it will be possible to assist in those areas. The feeling is that the gin-trash treatment is possibly a very important and significant solution to the problem of percolation under prolonged wetting.

ACKNOWLEDGMENT

Agencies participating in this study are: North Kern Water Storage District; Bureau of Reclamation, United States Department of the Interior; Arvin-Edison Water Storage District; Rubidoux Laboratory and Regional Salinity Laboratory, Bureau of Plant Industry; California Division of Water Resources; Madera Irrigation District; and the Division of Irrigation and Water Conservation, Soil Conservation Service (Research, United States Department of Agriculture).

AMERICAN SOCIETY OF CIVIL ENGINEERS

Founded November 5, 1852

TRANSACTIONS

Paper No. 2544

UTILIZATION OF UNDERGROUND STORAGE RESERVOIRS

By Harvey O. Banks,[1] A. M. ASCE

Synopsis

The scope of this paper is limited to the consideration of planned utilization of the water storage capacity available in the unconsolidated tertiary and quaternary alluviums of stream valleys, interior valleys, and coastal plains, with particular reference to conditions in Southern California. The objective of such utilization is to achieve maximum salvage at minimum cost of that portion of the water supply that now wastes to the ocean or is lost through evaporation and consumptive use by natural vegetation. To accomplish this salvage, it will often be necessary during dry periods deliberately to draw down the water table in the ground-water basin much farther than it would otherwise fall, in order to create storage capacity.

The development of commercial supplies from ground water for irrigation, municipal, and other uses has caused a certain degree of involuntary utilization of underground storage, and the extent of such utilization, with consequent salvage, will increase as further development of ground-water supplies proceeds. Numerous artificial recharge, or spreading, projects have been initiated, but the net effect of many of these has been limited to keeping the water table slightly higher in dry years than it would have been otherwise. The ground-water basins would have filled during wet periods from natural percolation without spreading. No deliberate attempt has been made during drought periods to create additional underground capacity to be filled by water salvaged during later wet periods. Carefully planned utilization of the immense potential storage capacity available in the alluviums with ground-water basins operated in a manner somewhat analogous to surface reservoirs can frequently achieve a much greater salvage.

In some instances, only planned operation of the ground-water basin is required to produce ample conservation to meet the need for additional water. In other cases, the construction of relatively small surface reservoirs to act as regulatory storage that increases stream-bed percolation and arti-

Note.—Published in January, 1952, as *Proceedings-Separate No. 114*. Positions and titles given are those in effect when the paper was received for publication.

[1] Cons. Engr., Los Angeles, Calif.

ficial recharge thus will be operated in conjunction with underground storage to achieve maximum conservation necessary. In general, costs for underground storage should be far less than for the equivalent amount of salvage obtained by construction and operation of surface reservoirs alone. Few surface reservoir sites of large capacity, high yield, and low cost are still unused. Properly operated, there are no evaporation losses from most underground reservoirs, but, generally speaking, water must be pumped from them for use, thus adding to the final cost. However, this is not often a major item in the economic comparison of underground storage versus surface storage alone.

To obtain the full conservation of available water supplies at a reasonable cost will require the extensive utilization of underground storage, as will the large scale reclamation of sewage. Thorough investigation of the hydrology of the ground-water basins must precede development and utilization. To create storage capacity and to supply adjacent areas of deficiency, the exportation of pumped water from ground-water basins of large potential capacity and with ample tributary inflow may be required. A change in the location and pattern of pumping may be indicated.

Owners of overlying land and others having prior rights in the ground-water basins often object to the utilization of underground storage when an additional lowering of water table during dry periods, causing increased pumping costs, is necessary. Complex physical, engineering, financial, and legal problems are involved.

Introduction

There is a regrettable tendency during drought periods to regard any drop in the water table of ground-water basins as a danger sign, without pausing to consider that the supply of water to the water table at such times is below average and that such a drop, in some instances, may be actually beneficial in salvaging wasteful consumptive use and in providing space for storage of later surplus waters. The ideal situation in the minds of many is to keep ground-water basins as nearly full as possible at all times, and large expenditures have sometimes been made for that purpose. The net result has frequently been a slight saving of pumping costs and a large waste of water that could have been used to good advantage elsewhere in areas of deficiency.

Hydrology

An excellent treatise on the hydrology of ground-water basins has been given by Harold Conkling,[2] M. ASCE. The subject will be treated here only in sufficient detail to serve as a background for the discussion of utilization of underground storage.

General Hydrologic Equation.—The various elements involving supply to, and disposal from, a ground-water unit, including the overlying surface,

[2] "Utilization of Ground-Water Storage in Stream System Development," by Harold Conkling, *Transactions*, ASCE, Vol. 111, 1946, p. 275.

are related in accordance with the following equation:

$$Q_i + P + U_i + I_i = Q_o + U_o + C + I_o + \Delta S \ldots\ldots\ldots (1)$$

in which Q_i is the surface inflow; P is the precipitation on the surface; U_i is the amount of underflow entering the unit; I_i is the artificial importation of water or sewage; Q_o is the surface outflow; U_o is the amount of underflow leaving the unit; C is the consumptive use (evapo-transpiration loss); I_o is the artificial exportation of water or sewage; and ΔS is the change in storage.

The change in storage as used in this equation includes not only that occurring beneath the water table (surface of the saturated alluvium), but also that within the root zone and between the root zone and the water table, over the period of time considered.

All the elements of supply and disposal (with the possible exception of precipitation) are, or can be, affected to some degree by man's activities.

Supply to the Water Table.—The sum of the following items, corrected for any change in storage as previously defined is the aggregate amount of water reaching the water table: percolation from precipitation; stream-bed percolation; artificial recharge through spreading grounds and diffusion wells; underflow into the ground-water unit; return flow from irrigation; return flow from cesspools and septic tanks; and leakage from water mains. In many ground-water basins, the opportunity for stream-bed percolation is limited by a high ground-water table.

As previously stated, each of these items is affected by artificial development and culture. To illustrate: In a natural state the average percolation of precipitation is comparatively small because the type and density of natural vegetation that becomes established consume nearly all of the average rainfall. When irrigated culture is substituted for natural vegetation, the percolation of precipitation tends to increase because the initial soil moisture deficiency at the onset of the rainy season is decreased. The regulation of runoff may increase stream-bed percolation and allow greater artificial recharge. The regulation from a portion of the watershed allows a greater proportion of the runoff from other areas to percolate or be spread. Stream-bed percolation may be entirely or partially cut off by the construction of lined flood control channels.

If the ground-water basin has a large capacity, enabling it to be drawn down without any danger of deficiency and, as is sometimes the case, if it will fill from natural percolation during wet periods, there is little benefit to be obtained from artificial recharging, other than that of keeping the water table slightly higher during dry periods. Very little over-all conservation is achieved. It must also be emphasized that if spreading is beneficial, the true salvage obtained is the difference between the amount of water spread and the amount that would have percolated naturally if allowed to remain in the stream channel.

Disposal from the Water Table.—Water reaching the water table is disposed of by means of the following items: Artificial extractions; underflow out of the ground-water unit; effluent seepage (or rising water); consumptive

use by natural or artificial vegetation, deriving its water supply directly from the water table; artificial drainage; and change in storage beneath the water table.

The elevation of the water table affects the magnitude of underflow, effluent seepage, drainage, and consumptive use. In cases in which underflow, drainage, and effluent seepage serve as sources of supply to lower basins, no over-all salvage can be attained by decreasing these items through a lowering of the water table in a basin. However, if there are areas of natural water-consuming vegetation that feed directly on the water table, considerable salvage sometimes can be achieved by such lowering. Increasing artificial extractions and exporting the water to other areas of deficiency may accomplish the desired result.

Some ground water must be allowed to escape from the basin in order to prevent a gradual build-up of dissolved salts to undesirable concentrations. Disposal from the water table must equal the supply to it. If the net change in storage over a complete cycle of dry and wet periods is negative, then the basin is overdrawn with respect to the historic conditions of supply.

Safe Yields.—Safe yield may be defined as the average annual rate of artificial extraction from a ground-water basin which will not:

a. Exceed the difference between the average annual supply to the waste water table as defined previously and the average annual disposal from the water table by underflow, effluent seepage, drainage, and direct consumptive use;

b. Lower the water table sufficiently to permit intrusion of sea water or other water of undesirable quality or to prevent sufficient flow through the basin to maintain proper balance of dissolved salts;

c. Lower the water table beyond the economic limit for cost of pumping; or

d. Interfere with prior rights of others in adjacent ground-water basins.

It is apparent from this line of reasoning that safe yield is not a unique nor a fixed value. It is also obvious that the water table must be lowered somewhat below that for natural conditions in order that there may be a safe yield, since safe yield represents, in part, salvage from natural processes of disposal by underflow, effluent seepage, and direct consumptive use. This salvage can be achieved only be lowering the water table. A lowering of the water table may increase the stream-bed percolation and provide more space for storage of surplus water in wet years. The value of safe yield is dependent, then, other factors remaining the same, upon the assumption that is made as to the average elevation of the water table to be maintained. With extractions limited to safe yield, the water table will fluctuate around this average more or less in accordance with the sequence of wet and dry years. Safe yield changes in magnitude as cultural activities and developments alter the supply to the water table and disposal therefrom. Methods of determining safe yield have been adequately treated.[2,3]

[3] "Report of Referee," by Harold Conkling, George B. Gleason, and Elmer C. Marliave, ***Raymond Basin Area Reference***, Vol. 1, Div. of Water Resources, Dept. of Public Works, State of California, 1943 (City of Pasadena vs City of Alhambra, et al, No. Pasadena C-1323).

Storage Capacity.—For the utilization of underground storage, the storage capacity available must be estimated from average specific yield, area, and the depth to which the basin may be dewatered below the highest allowable water table. The limitations on maximum depth to which a basin can be unwatered have been discussed previously.

In confined (or pressure) aquifers there is some small change in storage in the aquifer itself and some leakage from the confining strata as pressure is decreased. Storage capacity in such aquifers is not available for utilization unless it is possible to draw the piezometric level down below the top of the aquifer so that a free water table results.

Project for Ventura County, California

General Description of the Area and its Hydrology.—Three river systems (Ventura River, Santa Clara River, and Calleguas Creek) drain most of Ventura County, plus a considerable area in Los Angeles County (in California) lying to the east, as shown by Fig.1. For purposes of this paper, only those

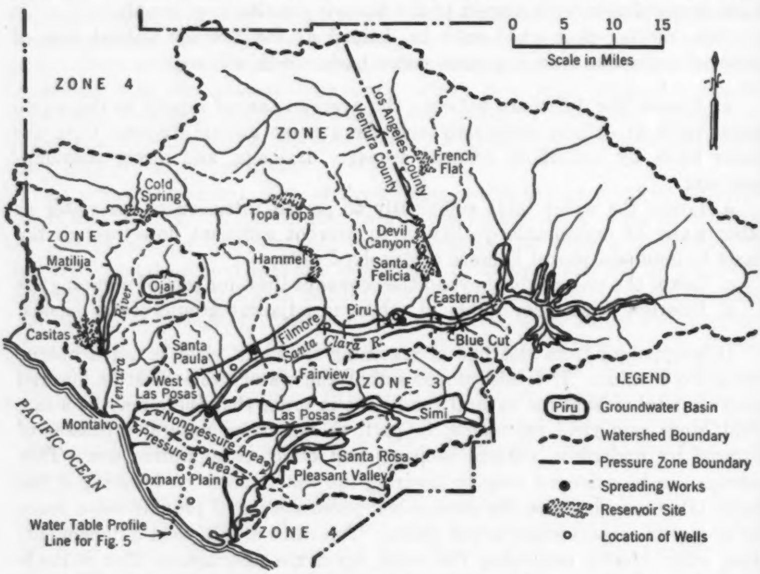

Fig. 1.—Ground-Water Basins in Ventura County, California

portions of Ventura County drained by or supplied by the Santa Clara River will be considered. The river and its tributaries, Sespe Creek and Piru Creek, are the only sources from which significant amounts of new water may be made available by conservation measures to supply the coastal plain and areas to the south of the Santa Clara River Valley.

Ground water is extensively produced from alluvial deposits that range in thickness from 100 ft or less up to several thousand feet. Lateral con-

strictions and other natural impediments to the movement of ground water divide the area into hydrologic units, or ground-water basins. These basins are delineated in Fig. 1. Eastern Basin, lying mostly in Los Angeles County, will not be further considered in this paper.

South and southwest of the pressure line that runs east and southeast from Ventura to the mountains on the south side of Pleasant Valley, in California (as shown in Fig. 1), the ground-water aquifers are overlain and confined by a relatively impermeable cap of clay and fine-grained silty deposits having considerable thickness. The bottom of this confining member is some distance below sea level in all parts of the plain. Water in these aquifers is under pressure and has produced numerous artesian or flowing wells.

Inland from the pressure line, there are no extensive confining members, and free water-table conditions exist. Montalvo Basin acts as the forebay area, or storage reservoir, from which ground water moves into the pressure aquifers of the coastal plain. The Santa Clara River System thus supplies not only its own valley but all of the coastal plain including the western portion of Pleasant Valley. If the severe overdraft existing in the nonpressure portion of Pleasant Valley were supplied, and if sufficient additional water could be imported and spread, it is possible that this area could also act as a forebay area to partly supply the pressure aquifers of the southerly portion of the coastal plain.

The total average annual surface inflow to Santa Clara River in Ventura County is estimated at about 230,000 acre-ft, of which nearly 40% is contrib-

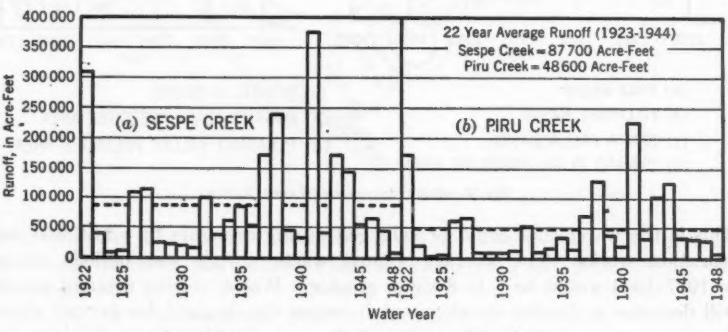

FIG. 2.—ANNUAL RUNOFF IN SESPE AND PIRU CREEKS

uted by Sespe Creek and about 20% by Piru Creek. The extreme variation in annual runoff and the more or less cyclic character of the supply is shown by the hydrograph (Fig. 2). Annual runoff in Sespe Creek has varied from a minimum of 9% of average flow to a maximum of 430% of average. Inflow during wet periods is much more than sufficient to fill all ground-water basins along the river.

Two spreading areas are in use at the present time (December, 1951)—one near Piru, Calif., with a capacity of 75 cu ft per sec and the other near Saticoy, Calif., with a capacity of 145 cu ft per sec.

A drought similar to the one that occurred from 1923 to 1936, inclusive, has been used as the critical period in studies for the project. Combined average annual runoff in Sespe and Piry Creeks during this period was 54% of the long-term mean.

It is estimated that the average annual waste to the ocean in the Santa Clara River, with present culture and existing conservation works, would be 36,000 acre-ft for a drought period similar to that of 1923–1936. Of this total, 24,000 acre-ft would be from Sespe Creek and 3,000 acre ft from Piru Creek.

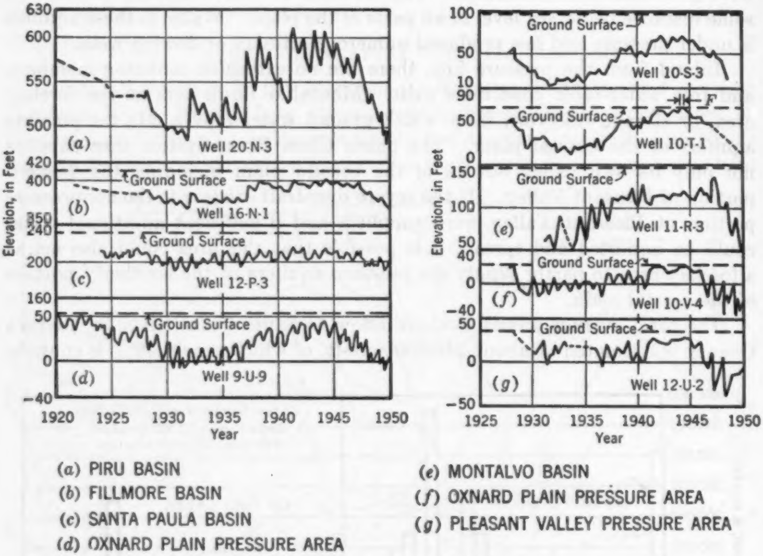

FIG. 3.—FLUCTUATION OF WATER TABLE

This is the water that could be salvaged during droughts by additional conservation works. The average annual waste during wet periods similar to 1937–1944 would be 7 to 8 times greater. Waste during drought periods will decrease as further development increases the demand for ground water, thereby causing a greater lowering of the water table in the Fillmore and Santa Paula Basins (in California). This lowering will give greater opportunity for stream-bed percolation, and the net conservation efficiency of any surface reservoirs that may be built will tend to decrease. Fluctuations of water table at wells in basins supplied by Santa Clara River are shown in Fig. 3. Although wide fluctuations are shown for Piru Basin, it is believed that there can be no overdraft there because of the ample depth of saturated alluvium remaining below the low point that has been, or may be, reached by the water table and the fact that the basin will always fill during wet periods. Fluctuations of the water table in all basins above Saticoy, will tend to increase because of increased demand, but there is no danger of overdraft. The con-

struction and operation of surface reservoirs on tributary streams will keep these basins full, unless they are utilized as underground storage reservoirs.

Over much of the coastal plain, the water (or piezometric level) is now below sea level, as shown by Figs. 4 and 5, and evidence indicates that sea

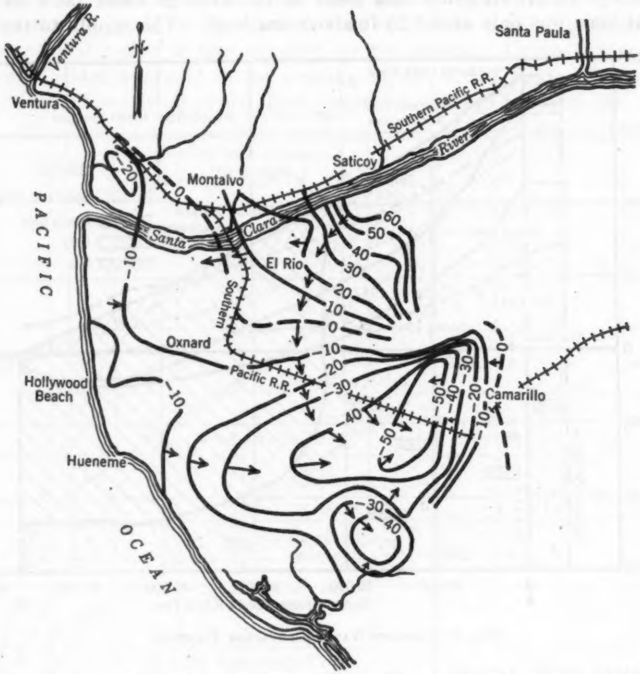

FIG. 4.—GROUND-WATER CONDITIONS ON OXNARD PLAIN IN APRIL, 1949

water intrusion has already advanced inland to some extent. The ground-water conditions on the Oxnard Plain in April, 1949, are indicated by the following table:

Elevation in feet below sea level	Area, in acres
0	55,500
−10	38,900
−20	21,600
−30	15,900
−40	7,000
−50	1,500

As indicated by the profile across the plain for spring, 1947 (Fig. 5), the transmissibility of the pressure aquifers is insufficient to meet the demand even with the Montalvo Basin (the forebay area) nearly full, unless a steep hydraulic

gradient is produced by drawing the piezometric level below sea level in distant portions on the plain.

Available storage capacity in the Montalvo Basin is about 80,000 acre-ft above the record low point reached in 1931. It is believed that the basin should not be drawn below this point as the average water table elevation at that time was only about 25 ft above sea level. The supply to the Mon-

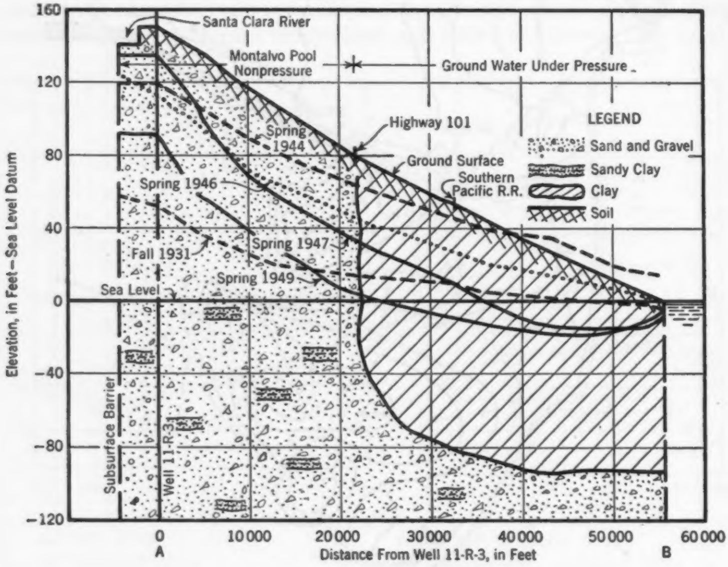

FIG. 5.—GROUND-WATER ELEVATION PROFILES

talvo Basin from the Santa Clara River during drought periods, without upstream regulation, is about 34,000 acre-ft per yr, whereas total demand on the basin is 61,000 acre-ft per yr (1950). As cultural development proceeds, the supply to the Montalvo Basin will decrease, and the demand on it will increase, thus aggravating the situation unless remedial measures are undertaken.

The problem, then, is to supply sufficient supplemental water to the coastal plain to maintain the piezometric surface above sea level at all times, or to maintain a ground-water ridge along the coast. Studies indicate that an average of 27,000 acre-ft should be provided annually by the initial project during drought periods, and that the need for new water may rise to an ultimate of 53,000 acre-ft per year.

Yield and Cost of Surface Reservoirs.—Feasible reservoir sites capable of salvaging significant amounts of water exist only on Sespe and Piru Creeks. The three most likely sites—Cold Spring and Topa Topa on Sespe Creek and Devil Canyon on Piru Creek—will be described in this paper. The capacity of Cold Spring Reservoir is limited to about 40,000 acre-ft unless several

miles of highway on extremely mountainous terrain are relocated. This is usually a very expensive undertaking.

Curves of annual yield for these reservoirs are given in Fig. 6. Curve A in each case represents yield that might be obtained from the reservoirs if all present downstream rights, other than gravity rights diverting directly from the stream, could be disregarded; that is, if there were no utilization of the ground water that is now supplied by the stream. Curve B represents new water added annually to the existing supply of the Santa Clara River system during the critical period, from runoff available at the dam site. This

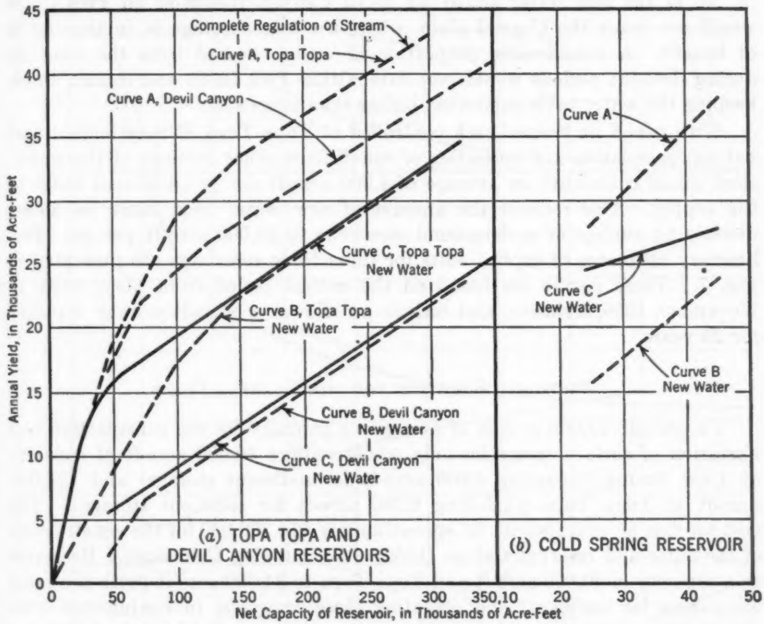

FIG. 6.—CAPACITY-YIELD CURVES FOR SURFACE RESERVOIRS

presumes the reservoir to be operated in a conventional manner with more or less uniform annual release in the regimen of demand, without regard to any planned utilization of ground water. Some of this new water for smaller capacities would be from the percolation of spill. Curve C represents new water that would be added with the reservoir operated in conjunction with underground storage. Water stored in the reservoir would be released as soon and as fast as it could be stored underground. Diversion from the release for immediate use would be made whenever possible, but the regimen of release would not be related to such use but rather to the capacity of the stream bed and spreading grounds to absorb the water. Other water would be spread first, when available, in order to achieve maximum salvage. Wells would be installed and water pumped as needed from the underground to supply

areas of deficiency distant from the underground reservoir. Under this latter plan of operation, surface reservoirs act merely as regulatory storage to enable the runoff to percolate naturally or artificially, but the true storage reservoir is underground.

As previously stated, as cultural development proceeds, the amount of new water that will be added by reservoirs to the supply that would otherwise exist will progressively decrease. Evaporation and prior gravity rights were deducted in calculations for all curves of Fig. 6. Curves B and C are based on the critical period from May, 1923, to November, 1936, inclusive.

All of the new water added by Devil Canyon Reservoir on Piru Creek would not reach the Coastal plain, where the true shortage is, in time to be of benefit. A considerable proportion of water released from the reservoir during drought periods would percolate within Piru Basin and remain there, keeping the water table somewhat higher than otherwise.

With runoff on Sespe Creek controlled at Topa Topa, it is estimated that natural percolation and spreading of runoff from other portions of the watershed would contribute an average of 4,000 acre-ft per yr additional water to the supply. This reduces the amount of new water that must be added directly by surface or underground reservoirs to 23,000 acre-ft per yr. Preliminary estimates of capital costs for these three reservoirs are presented in Fig. 7. These curves are based on the critical period from May, 1923, to November, 1936, inclusive, and include an allowance for silt storage capacity for 25 years.

Proposed Solution for the Coastal Plain

To provide 23,000 acre-ft of new water annually by the construction and operation of surface reservoirs only would require 40,000 acre-ft of capacity at Cold Spring (including 4,000 acre-ft for sediment storage) and 125,000 acre-ft at Topa Topa (including 6,000 acre-ft for sediment storage). The cost for this program would be approximately $14,300,000 for the construction of the dams and reservoirs alone (1950). By building Cold Spring Reservoir to a capacity of 40,000 acre-ft and Topa Topa to 34,000 acre-ft (with the same allowances for sediment) and operating these reservoirs in conjunction with the 80,000 acre-ft of underground storage capacity available in the Montalvo Basin (assumed to be full at beginning if the critical period), the cost of construction of surface reservoirs could be reduced to $7,600,000 (1950). This is the project that is proposed for construction.

To this latter cost should be added the cost of drilling and equipping the 6 or 8 wells necessary and the cost of pumping water from Montalvo Basin. These wells need not be more than 250 to 300 ft deep, and the pumping lift would not be more than 150 ft. While these additional costs have not been definitely estimated, it is apparent that they would be far less than the $6,700,000 saving over the cost of construction of the surface reservoirs. Not all of the water put into Montalvo Basin would need to be pumped, since some would be distributed through the underground aquifers leading out from the basin.

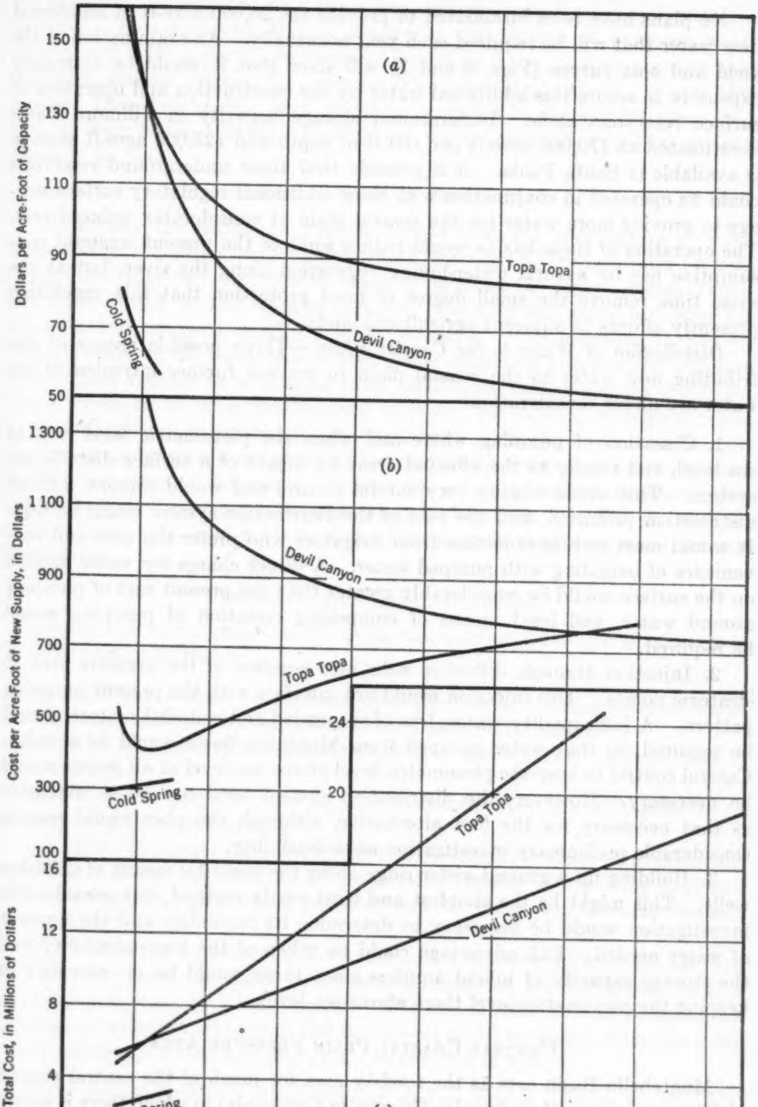

FIG. 7.—COST OF SURFACE RESERVOIRS (1950)

No plans have been formulated to provide the 26,000 acre-ft of additional new water that will be required each year eventually. An examination of the yield and cost curves (Figs. 6 and 7) will show that it would be extremely expensive to secure this additional water by the construction and operation of surface reservoirs alone. Underground storage capacity in Fillmore Basin is estimated at 170,000 acre-ft per 100 ft of depth and 125,000 acre-ft storage is available in Santa Paula. It is possible that these underground reservoirs could be operated in conjunction with some additional regulatory surface storage to provide more water for the coastal plain at considerably reduced cost. The operation of these basins would reduce some of the present wasteful consumptive use by natural water-loving vegetation along the river, but at the same time remove the small degree of flood protection that this vegetation presently affords to adjacent agricultural lands.

Distribution of Water to the Coastal Plain.—Three possible means of distributing new water to the coastal plain to prevent further intrusion of sea water are under consideration:

1. Cessation of pumping where and when the piezometric level falls to sea level, and supply to the affected areas by means of a surface distribution system. This would require very careful control and would present difficult distribution problems, and the cost of the distribution system would be high. It would meet serious objection from irrigators who prefer the ease and convenience of irrigating with pumped water. A direct charge for water applied on the surface would be considerably greater than the present cost of pumping ground water, and legal means of compelling cessation of pumping would be required.

2. Injection through diffusion wells into aquifers of the pressure area at strategic points. This injection would not interfere with the present pumping pattern. A high quality water, free of suspended and colloidal matter, would be required, so that water pumped from Montalvo Basin would be suitable. Careful control to keep the piezometric level above sea level at all points would be necessary. However, the distribution system need not be so extensive as that necessary for the first alternative, although the plan would require considerable preliminary investigation as to feasibility.

3. Building up a ground-water ridge along the coast by means of diffusion wells. This might be the simplest and least costly method, but considerable investigation would be necessary to determine its feasibility and the amount of water needed. Full advantage could be taken of the transmissibility and the storage capacity of inland aquifers since there would be no necessity of keeping the piezometric level there above sea level.

Central Coastal Plain Pressure Area

Montebello Basin acts as the forebay area for much of the central coastal plain pressure area (Los Angeles County, in California) in which there is severe overdraft and sea water intrusion. It has been estimated that, with cultural conditions as of 1945, by pulling the water table in Montebello Basin down an additional 50 ft during dry periods (thus creating storage space to be filled during subsequent wet periods), an average of about 15,000 acre-ft of water

per year could be salvaged from the waste, using existing storage and spreading facilities. To accomplish this, a change in the pattern of pumping would be required, with a partial cessation of pumping from pressure aquifers near the coast and an increase in pumping from Montebello Basin. Water thus pumped from the forebay area would be supplied to the coastal areas by a surface distribution system. Further sea water intrusion would be at least partially halted.

Reclamation of Sewage

To achieve the maximum possible benefit from the reclamation of water from sewage, the utilization of underground reservoirs will be necessary for both storage and dilution. In the west basin, lying along the coast between Venice and Long Beach in Los Angeles County, extensive sea water intrusion has occurred, and pumping greatly exceeds recharge. It is proposed to add reclaimed water to the basin in this area, using spreading grounds and diffusion wells. This appears to be cheaper than possible alternative sources of supply. There seems to be little justification, however, for adding reclaimed water to an underground basin that is not overdrawn, unless the basin is to be operated as an underground reservoir with water pumped therefrom and exported to adjacent areas of deficiency. Otherwise, as stated before, the only result is to maintain the water table somewhat higher than it would be were no water added. A careful analysis of the hydrology in each case must precede development.

Financial and Legal Problems

Among the many problems involved, the following five are considered to be of primary importance:

(1) How can control be retained over the sale and distribution of water that has been salvaged by operation of an underground reservoir?

(2) Who will receive the benefit of such a conservation program and to what extent?

(3) Who is to pay the costs for conservation? How are such costs to be allocated and in what amounts?

(4) How can a legal right be attained to operate an underground reservoir, particularly if exportation is to be increased? Owners of overlying land and others having land rights would probably seek to enjoin such increase through court action

(5) Where it is necessary to lower the water table to achieve salvage, are present users from the basin to be recompensed for the additional cost of pumping, and, if so, by what amount? The incremental cost of pumping an acre-foot of water an additional 100 ft is about $1.70 for power only, assuming a plant efficiency of 60% and energy at one cent per KWH.

These similar problems are perplexing, and no simple solution is apparent. Present rights in the ground water can be determined by the adjudication procedure and these rights used as a basis for the determination of benefits and damages. This is rather lengthy and expensive, but has been used with success in ground-water problems in Southern California.

Summary

The planned utilization and operation of underground storage offer the most economic means of conservation of waste waters in many areas. In Ventura County many millions of dollars can be saved by such utilization combined with regulatory surface storage, as compared to the use of surface storage only. For sewage reclamation, underground reservoirs must be used for dilution and storage in most instances.

Utilization of underground storage is by no means a simple matter, and a thorough hydrologic investigation is necessary.

AMERICAN SOCIETY OF CIVIL ENGINEERS
Founded November 5, 1852

TRANSACTIONS

Paper No. 2545

THE ALLEGHENY CONFERENCE—PLANNING IN ACTION

By Park H. Martin,[1] M. ASCE

With Discussion by Messrs. Louis P. Blum and Park H. Martin

Synopsis

Since 1943, the Allegheny Conference on Community Development has been developing and backing a plan of municipal improvement for the greater Pittsburgh (Pa.) area. This paper outlines the aims of the organization and its method of cooperation with existing planning bodies.

Among the many civic improvements credited to the Conference are a successful smoke abatement program, highway and bridge development, planning for stream pollution abatement, and alleviation of parking congestion in the city. In addition, the Conference has been active in the redevelopment of Pittsburgh's Golden Triangle district.

Introduction

Purpose.—The Allegheny Conference on Community Development (hereafter called the Conference) is an incorporated civic agency, privately financed, designed to do a job of research and planning in Allegheny County, Pennsylvania, to the end that an over-all community development program might be created, and by educational means to secure public support for such a program. Formed in the spring of 1943, the Conference first produced tangible results in the early part of 1945. Citizen committees, composed of persons qualified to deal with the particular phase of the program under study, were appointed. In some instances in which local, qualified agencies existed, they were asked to undertake specific studies; in other instances, studies have been carried on by the Conference staff. Consultants have been called in as needed.

Scope of Program.—As a result of the studies, the Conference developed a community development program that included recommendations on the following major items: smoke control; flood control; highways and bridges;

Note.—Published in May, 1952, as *Proceedings-Separate No. 131*. Positions and titles given are those in effect when the paper or the discussion was received for publication.

[1] Executive Director, Allegheny Conference on Community Development, Pittsburgh, Pa.

airport expansion; stream pollution abatement; refuse disposal; recreation; housing; redevelopment of blighted areas; parking facilities; Point Park; better subdivision control; enabling legislation conferring broader powers on the State Department of Highways, the City of Pittsburgh and County of Allegheny; and mass transportation.

Concurrent with these studies, the staff conference completed reports[2,3,4,5,6,7,8] on subjects of community interest as well as studies concerning the economics of the area.

As the various studies were completed and approved by the Conference executive committee, they were released to the public. This was accomplished by published reports, newspaper releases, radio programs, and public talks before civic groups and service clubs. An average of over 100 talks a year are made by members of the Conference staff to various groups. Before public release was made of specific recommendations on any subject, particularly when such recommendations affect a public body, conferences were held with the responsible public officials, explaining the recommendations and the reasons behind them. The same policy was followed with the public press. By observing this practice, not once since 1945 has there been a serious difference either with responsible public officials or any one of the three major daily newspapers in the region.

Accomplishments

The avowed purpose of the Conference has been to present a comprehensive nonpartisan civic program for the betterment of Pittsburgh and Allegheny County. When other civic or public planning bodies have been involved, the Conference has been careful to work with and secure agreement with those agencies.

The program presented for parking relief was the only one that a public or private agency seriously objected to. The Pittsburgh Real Estate Board and individual parking lot operators ineffectively opposed the recommended program. An impressive list of accomplishments can be credited to the Conference. Some of the major ones are listed in this section.

Smoke Abatement.—This project is considered the keystone of the Conference program. In appraising what has been accomplished on this subject, the background of Pittsburgh must be considered. Traditionally, Pittsburgh had been known as the "smoky city"—a city of heavy industry; a city in the heart of a great bituminous coal area; a city that from its founding had depended upon soft coal as its main source of fuel and power; a city traversed by deep valleys in which are located major trunk-line railroads and upon whose rivers plowed the coal burning towboats.

In 1941, Pittsburgh had enacted a modern smoke control ordinance.

[2] "Population Trends in Southwestern Pennsylvania," by Bertrand J. Black, *Allegheny Conference Digest*, Vol. 1, No. 2, December, 1945.

[3] "Living Costs in Pittsburgh Compared with Other Cities," by Lawrence R. Guild, *ibid.*

[4] "Climates in Competition," by Elizabeth Sellers, *ibid.*, Vol. 1, No. 3, April, 1946.

[5] "River Stages and Flood Map," by C. K. Harvey, *ibid.*, Vol. 1, No. 2, December, 1945

[6] "Pittsburgh's Resources: Bituminous Coal," by Lawrence R.Guild, *ibid.*, Vol. 1, No. 3, April, 1946.

[7] "Housing Survey of Pittsburgh & Allegheny County," by Max Nurnberg, July, 1946.

[8] "A Housing Program for Pittsburgh and Allegheny County," by Max Nurnberg, January, 1949.

However, with the advent of World War II, no major attempt was made to enforce it, nor was any serious enforcement attempted until October 1, 1946. At that time the Conference spearheaded the fight to have the ordinance enforced. By action of City Council on October 1, 1946, the ordinance was made effective as far as all users of solid fuels, except one- and two-family homes, and they were to come under its terms on October 1, 1947.

The results have been dramatic. Five heating seasons have passed without one of the old-time smoggy days. According to the records of the Bureau of Smoke Control, the average dust fall in Pittsburgh has been reduced from 60 tons per sq mile per month in 1938 to 50 tons per sq mile per month in 1950. Considering that there always is a large amount of dust and dirt other than pollution from combustible materials in the air of any city, the reduction resulting from smoke control is far greater than would appear from the dust fall report. The Pittsburgh United States Weather Bureau records show 701 hr of moderate smoke in 1945, and only 393 hr in 1950. In 1945, there were 226 hr of heavy smoke, but this had been reduced to 56 hr in 1950. The beneficial results of the smoke control program have been reflected in the favorable attitude of the average Pittsburgh resident to the Conference program.

Flood Control.—In 1936, Pittsburgh, along with many other cities in the Ohio Valley, suffered greatly from a disastrous flood. As a result of the widespread damage and destruction caused by the flood, the federal government instituted a program for the construction of a series of flood control dams at the head waters of the Allegheny and Monongahela Rivers. Six of these dams have been completed as of 1951, and the seventh and most important (Conemaugh) will be completed in 1952. Had these seven dams been in existence in 1936, the crest of that flood at the "Point" (confluence of rivers) in Pittsburgh would have been reduced 10.3 ft and no water would have flooded the Triangle.

Highways and Bridges.—For some time, the two major official planning bodies in Allegheny County, the City and County Planning Commissions, had proposed a new east-west arterial highway through Pittsburgh and Allegheny County. Designed as a limited access highway, its cost was far beyond the ability of the city and county to finance. It was recognized locally that if the project were to be built, it would have to be undertaken by the Commonwealth of Pennsylvania. Submitted to the state as early as 1938, the project had received favorable consideration, but no positive steps were taken towards its construction until the fall of 1945. In October of that year, because of the insistence of several of the sponsors of the Conference, the governor announced that the state would build the project, as well as a state park at the point. Just nine months later, in July of 1946, construction was started on the first section of the highway. The project, named the Penn-Lincoln Highway, is 25 miles in length, 9.5 miles of which are east of the Triangle, and is estimated to cost about $90,000,000 (or approximately $4,000,000 per mile). As of June, 1951, over $50,000,000 had been spent or was under contract on 17 miles of the total length.

In addition to its major role in getting the project underway, the Conference has played an important part in acting as coordinator between the state and the local public officials and planning bodies. Financed mainly by the commonwealth and allotment of portions of normal federal grants, the highway has received local assistance in the amounts of $1,000,000 from the City of Pittsburgh and $5,000,000 from Allegheny County, as well as direct construction of 2.5 miles of four-lane divided highway by the County of Allegheny at a cost of over $3,000,000.

The divided highway is four lanes in width except for the first four miles east of the Triangle that are six lanes wide. Design features of the road are low grades, one tunnel 3700 ft long, eight major bridges, numerous smaller bridges, and fifteen complete or partial interchanges. The Penn-Lincoln Highway skirts the edge of the Pittsburgh Triangle with interchanges provided at each end. On the east, the highway is the major connection between Pittsburgh and the western extension of the Pennsylvania Turnpike.

Concurrent with the construction of the Penn-Lincoln Highway, three major river bridges have been constructed across the Monongahela River and one on the Allegheny River. One of these, known as the Elizabeth Bridge on U.S. Route No. 51, has been constructed by the state at a cost of $6,500,000. The other two, the George Rankin Bridge and the Dravesburg Bridge, were completed by Allegheny County at a cost of $8,500,000 each. The New Kensington-Tarentum Bridge, a state project, was built at a cost of $4,500,000.

Greater Pittsburgh Airport.—During World War II, the federal government offered to build a modern landing field in Allegheny County if the county would provide the land. The county accepted the offer and purchased 1500 acres of land west of Pittsburgh, at which location the field has been built at a cost of $5,000,000. Since the termination of the war, the county has constructed one of the largest and most modern terminals in the country. The buildings and facilities represent a county investment of over $23,000,000. The Conference was a factor in securing public backing for provision of funds for the airport construction. Located 13.5 miles west of the Triangle, the field will be served by the Penn-Lincoln Highway and is not more than 20 min driving time from the central business district of Pittsburgh.

Stream Pollution Abatement.—In 1945, the Commonwealth of Pennsylvania instituted a program of stream purification. Approximately 90 municipalities in Allegheny County, that were polluting the waters of the state, received notice to prepare plans and specifications for the construction of sewage disposal facilities. After study of the problem, the Conference Committee on Stream Pollution Abatement recommended that the situation could best be handled on a county-wide basis, by one agency, and recommended the creation of a County Sanitary Authority. Subsequently, after public hearings, the Board of County Commissioners created an Allegheny County Sanitary Authority. Over 60 municipalities, including the City of Pittsburgh, have since entered into an agreement with the authority for the design of a system of collector sewers and a disposal plant. This phase of the work should be finished early in 1952, and the treatment project, estimated to cost from $50,000,000 to $60,000,000, will then be ready for construction.

The Pittsburgh Package.—Not a project in itself, but rather a series of legislative measures found necessary and advantageous in providing ways and means for the carrying on of the Pittsburgh Program, the "Pittsburgh Package" epitomizes one of the steps taken to rescue planning from futility in that city. As a result of Conference studies and in order to fill gaps in the powers of the city, county, and state to undertake steps considered essential to the success of the program, the Conference, in conjunction with the Pittsburgh Regional Planning Association and the Pennsylvania Economy League, developed a series of ten legislative measures for presentation to the State Legislature in 1947–1948. Passage of eight of the ten measures and approval by the governor resulted, among other things, in relieving the city of liability for consequential damage on the Penn-Lincoln Highway. It also authorized the city to create a Department of Parks and Recreation, thus elevating this important city function to its proper status. The city was also empowered to create a public parking authority, and the county was empowered to build and operate refuse disposal plants and to control the emission of smoke from railroad engines.

In addition to initiating construction on the Penn-Lincoln Parkway within the city limits, a Department of Parks and Recreation has been created and has already embarked on its parks and recreation program. The county has passed a comprehensive smoke control ordinance that is now effective as far as all users of solid fuels are concerned, with the exception of one- and two-family homes, which will come under its terms in 1953.

Public Parking Authority.—For its initial program, the Parking Authority has chosen to erect four facilities, with two others to follow shortly after their completion. The four initial units provide 2700 car spaces and are expected to cost $9,000,000 including land and incidental expenses. Of open-deck type construction, they are essentially facilities for short-time parkers. The sites were selected after careful engineering studies of parking demand. Initial financing was by loans made by the City of Pittsburgh, amounting to $250,000, and later a private loan of $2,500,000 from a pool of 8 Pittsburgh banks. The authority plans to finance the entire operation by the sale of revenue bonds that will in no way pledge the credit of the city. The city has, however, pledged its parking meter receipts, which are well over $100,000, annually to the Parking Authority as security for its loans. In the middle of 1951, the initial four sites had been acquired, the demolition of existing buildings was taking place, and construction plans and specifications were completed.

Point Park.—The Allegheny and Monongahela Rivers converge at an angle of about 50° to form the Ohio River. The land lying between the two rivers extending from their confluence east about one mile, comprising 330 acres, is known as the Golden Triangle, the central business district of Pittsburgh. The 36 acres included in the western end of the Triangle comprise the new State Point Park. This site is one of the most historic tracts of land in America. At this location, the French built Fort Duquesne, which they later blew up upon the approach of the British and Colonial forces under General Forbes. Fort Pitt was then erected by the British. Many historians believe that the question of whether the United States would be an English- or French-speaking nation was settled here.

At the time of the Governor's announcement, in October, 1945, of his intention to build a State Park at the Point, the area was a run-down blighted commercial area. Criss-crossed by surface and elevated railroad tracks, occupied by a large freight house, obsolete loft buildings and other commercial buildings and parking lots, it was an area rapidly declining in value, with many tax delinquent properties.

The entire 36 acres of land, excepting streets and alleys, has since been acquired by the state at a cost of $7,500,000, and all buildings in the area have been razed. Plans for the treatment of the park area have been concurred in by the state and all interested local, civic, and governmental units. The Allegheny Conference has been a major factor in bringing this project to its advanced status. Immediately following the Governor's announcement, the secretary of the State Department of Forests and Waters asked the Conference to represent his department in preparation of the land plan and coordination of the various interested groups. This the Conference has done.

One of the major problems involved has been the agreement on plans for a major traffic interchange between the new Penn-Lincoln Highway and the Ohio River Boulevard. This interchange, cutting across the park area, has been laid out to the satisfaction of all concerned. Part of the adopted plan requires the demolition of two major river bridges at the Point, with the erection of two new ones as part of the interchange plan. As part of the solution of the problem, the old freight warehouse has been replaced by the Pennsylvania Railroad at a site beyond the central business district, at a cost of $4,500,000.

The Gateway Redevelopment Project.—The 23 acres of the Golden Triangle immediately adjoining the new Point Park was an area similar to the Point Park area—blighted, declining in value, with no prospect of rehabilitation if left to its own resources. During the winter of 1946, following the Point Park announcement, the Conference, after considerable study, decided to campaign for the redevelopment of the area. A committee of the Conference went to New York City, N. Y., and met with Thomas I. Parkinson, president of the Equitable Life Assurance Society, and presented a plan in which the Equitable would act as redeveloper. At the request of the Conference, on November 18, 1946, the City of Pittsburgh established a redevelopment authority. It was not until February 14, 1950, however, that the Equitable and the Urban Redevelopment Authority signed the formal contract for the project. This is the first major commercial redevelopment project that has been successfully undertaken in the United States.

By late 1950, the major portion of the 23 acres had been cleared of old buildings and the Equitable had two 20-story structures and one 24-story office building under construction. This phase of the project is estimated to cost more than $30,000,000. The land plan being followed is unique; there are wide, open spaces between buildings with generous malls and walks through the grounds giving the effect of carrying the Point Park through the Gateway Project.

Jones and Laughlin Project.—Another major project the Urban Redevelopment Authority has successfully undertaken is the redevelopment of a blighted

area upstream from the Point and across the Monongahela River. This area, 125 acres in extent, was assembled by the redevelopment authority, with Jones and Laughlin Steel Corporation acting as the redeveloper for the expansion of its industrial plant. Well along in construction by the middle of 1950, this project is estimated to cost $72,000,000.

The Redevelopment Authority is advancing plans for a housing redevelopment project in a blighted area known as the Hill District of Pittsburgh. As soon as a sufficient reservoir of low-cost relocation housing has been developed to house displaced persons, it is planned to initiate this project.

Golden Triangle Projects.—Four other major projects have been undertaken to improve the Golden Triangle. They are private ventures, financed entirely by private funds, and it is probably safe to say that none of these projects would be underway had there been no successful community development program.

The first of these projects is the new 41-story Mellon-Steel Building that will house the Mellon National Bank and Trust Company and the main offices of the United States Steel Corporation. Substantially completed in 1951, this project is costing some $30,000,000. One block removed from the Mellon-Steel Building, the Aluminum Company of America has a 30-story office building costing $12,000,000. The block between these two buildings has been acquired by the City of Pittsburgh for a public park. This was made possible by a gift of $4,000,000 by certain Pittsburgh foundations to the city for that purpose. The city intends to lease the underground rights to the parking authority for the construction of a 5-story underground short-time parking facility. As planned, this project will provide about 950 car spaces.

One block removed from the parking area, a 14-story downtown apartment-hotel building is being constructed, and one block farther away a second downtown apartment building, 16 stories in height, has been erected. These two buildings are estimated to cost a total of $12,000,000.

The Golden Triangle and Assessed Valuations

Of the 330 acres comprising the Golden Triangle, 70 acres are occupied by streets and alleys, leaving 260 acres of land for business and commercial use. Of these 260 acres, approximately 75 acres are in the process of redevelopment.

In 1936, the assessed valuations of the City of Pittsburgh for taxable purposes reached the all-time high of $1,211,867,000. By 1947, this valuation had declined about 20.4% to $961,000,000. During this period of time, the percentage of loss in assessed valuation in the Triangle was 27%, with the decadent areas at the Point showing a much higher percentage loss.

Since 1947, the downward trend in valuation has been reversed in the city as a whole, until in 1951, the assessed valuation reached $1,017,885,000, an increase of about 6% over the low of 1947. In the Triangle, excluding the construction outlined in this paper, the increase has been about 10%. The value of the new construction, including a number of minor projects not mentioned, is approximately $90,000,000. When this new construction goes on the tax books, the assessed valuation of the Triangle will be greatly increased.

It is interesting to note the trends in movement of people in and out of the Triangle. The figures of the Bureau of Traffiic Planning of Pittsburgh show that in 1927, on an average business day, 297,000 people entered the Triangle. By 1942 this figure had fallen to 247,000 persons, by 1946, it had risen to 255,000, and as of 1950, it had reached an all-time high of 308,000 persons. Although it is difficult to analyze the reasons for these changes, in some measure, it is believed that the Community Improvement Program has been in part responsible.

One may well ask the question, "Has all that has transpired in Pittsburgh meshed in with the Master Guiding Plan of the City Planning Commission?" The answer generally is yes. There have been times, not in respect to the general plan, but rather as to certain aspects of some particular project, that there have been minor differences of opinion, but these differences have been ironed out.

To those who ask how so much has been accomplished in such a short space of time, it can be pointed out that it has been accomplished by enlightened leadership on the part of business, civic, and elected officials. No single group by itself could have brought all this about, but with every group working together much has been accomplished.

DISCUSSION

Louis P. Blum,[9] M. ASCE.—The history of flood prevention in Pittsburgh by the construction of a series of flood control dams is reviewed by Mr. Martin. It is pertinent to trace the history of this idea from its original conception.

After the disastrous flood of 1907, the Pittsburgh Flood Commission was formed to study local floods and suggest the proper solution to the problem. The chairman of this commission was H. J. Heinz, a leading merchant. An engineering committee was formed under the chairmanship of E. K. Morse, M. ASCE, consisting of George S. Davison and Morris Knowles (Honorary Members, ASCE), and Paul Didier, Emil Swenson, W. G. Wilkins (Members, ASCE), and Julian Kennedy, a member of the American Society of Mechanical Engineers. George M. Lehman, M. ASCE, executive engineer on the commission, made extensive surveys of flood damage and established high water marks within the Allegheny, Monongehela, Ohio, and Youghiogheny river basins. Its voluminous report, issued in 1912, and based on extensive surveys, contained a wealth of engineering data on floods (Report of Flood Commission of Pittsburgh, Pa., to Pittsburgh Chamber of Commerce, 1911). Although the commission recommended walls for local protection, their main recommendation was the construction of a system of flood-regulating reservoirs in the headwaters of the Allegheny, Monongahela, and Youghiogheny rivers. This engineering report is believed to have been the pioneer of American proposals for the harnessing of river floods. Preliminary designs of proposed reservoirs, based on the actual topography, were published in the report.

The solution was regarded as visionary and impractical. Engineering comment was extremely critical. Nevertheless, the flood commission remained in existence for several years, defending and publicizing its conclusions and predicting future floods of greater magnitude. The army engineers, the Pittsburgh civil authorities, and the public placed little faith in the possibility of a recurrence of flood disaster. However, on March 17, 1936, the largest flood in Pittsburgh history was recorded. Renewed investigation by the army engineers resulted in the recommendation of a system of flood-regulating reservoirs in the same general localities and of the same general design as those of the original flood commission report. Considering the limited time and resources of the commission, its conclusions coincided closely with the later reports, upon which construction was based, and have proved highly successful. This is typical engineering achievement—an idea is evolved, further investigation follows, and then actual construction is the result.

Now that Pittsburgh is nearly free from flood menace, the joint achievement and meritorious cooperation of the Pittsburgh Flood Commission, the army engineers, and the Allegheny Conference can be recorded.

---

[9] Retired, Pittsburgh, Pa.

PARK H. MARTIN,[10] M. ASCE.—The discussion by Louis P. Blum, M. ASCE, is historically correct. It pays tribute to members of the ASCE who were prominent in a bygone generation. Probably the outstanding impression that one would get from the discussion is to the effect that most public works projects, particularly those of great magnitude such as the flood control program for the Pittsburgh district, are the result of the thinking and efforts of a number of people over a long period of time.

To those in the city planning field, it is apparent that this same impression is true in connection with most important city improvement projects. The work of the Allegheny Conference may also be said to fall in this category. Many national magazines and papers have dramatized the developments brought about by the Pittsburgh development program during the past seven years. Whether this has been overemphasized depends upon one's viewpoint. Those who are connected with the program are aware that its success cannot be attributed to any one person or to any one group. Most of the projects have had years of thought and planning by numerous people, but it has remained for the Allegheny Conference to bring the planning to fruition. It is believed that the example set in Pittsburgh has had a beneficial effect on other American cities and has brought to city planning the public understanding that it has not had before.

It seems appropriate to close with a comment on Mr. Blum, who discussed a phase of this paper. He recently passed away, leaving behind an honorable record of integrity and professional skill.

[10] Executive Director, Allegheny Conference on Community Development, Pittsburgh, Pa.

AMERICAN SOCIETY OF CIVIL ENGINEERS
Founded November 5, 1852
TRANSACTIONS

Paper No. 2546

DIVERSIONS FROM ALLUVIAL STREAMS

By C. P. Lindner,[1] M. ASCE

With Discussion by Messrs. T. Blench, Serge Leliavsky, A. R. Thomas, D. C. Bondurant, and C. P. Lindner

Synopsis

The hydraulic effects of diversions and their withdrawal of sediment from alluvial streams are discussed in this paper. In order that a clear understanding of the influence of diversion may be had, characteristics of the flood hydrograph and of the stage-discharge relation are described. Factors influencing the diversion of bed load and the variation in the quantity of diversion with the angle of diversion are developed and supported by an analysis of model experiments. A conception of the balanced stream is presented to explain the effect of diversion on the river and diversion channels, and items to be considered in planning the diversion entrance are given. The use of the principles and factors of this paper will aid in arriving at a reasonable appraisal of the results to be expected from diversion, but model experimentation is the best medium for securing results upon which a high degree of dependence can be placed.

Hydraulics of Diversions

Effect on Discharge with Storage Area Above the Diversion.—When a diversion is located a short distance below an extensive valley storage area, the rate at which water is withdrawn from the main stream is not the net reduction in river discharge immediately below the diversion, for an increase in peak discharge is likely to result from operation. To demonstrate this effect synthetic discharge-storage relationships were prepared in which the increments of storage per unit change in discharge were quite large. These relationships were used with appropriate rating curves to route a hypothetical flood past a diversion floodway. The results of the routing are shown in Fig. 1. For the hypothetical flood the inflow to the stream reach attained a maximum rate of 1,800,000 cu ft per sec. Thus, the natural storage, with the floodway not operating, reduced the peak inflow by about 450,000 cu ft per sec. With the floodway operating,

Note.—Published in January, 1952, as *Proceedings-Separate No. 112*. Positions and titles given are those in effect when the paper or the discussion was received for publication.

[1] Chf. Engr., South Atlantic Div., Corps of Engrs., U. S. Dept. of the Army, Atlanta, Ga.

valley storage reduced the same peak inflow by about 360,000 cu ft per sec. Approximately 90,000 cu ft per sec, then, was the lost storage effect or the increase in discharge caused by operation of the floodway. This is emphasized further in Fig. 1, which shows the discharge in the floodway to be slightly under 230,000 cu ft per sec and the net reduction in river discharge to be about 140,000

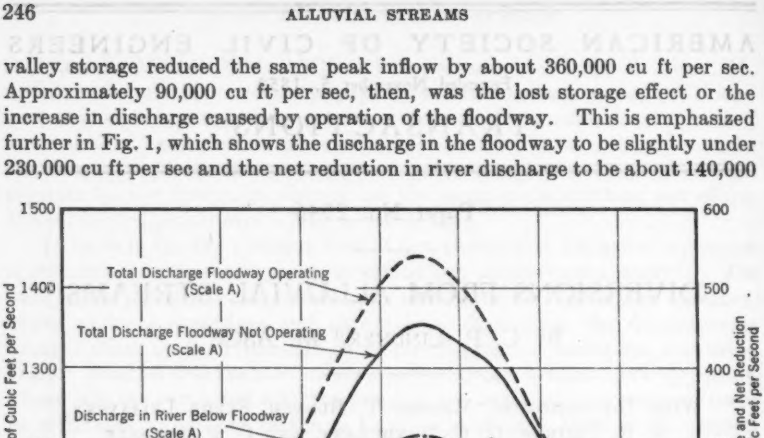

FIG. 1.—OPERATION OF FLOODWAY DOWNSTREAM FROM LARGE STORAGE AREA

cu ft per sec. About 39% of the water withdrawn by the floodway was required to compensate for the lessened natural storage effect caused by floodway operation.

Care must be exercised in the operation of a diversion with a controlled inlet. If the control works are opened abruptly, the total discharge rates will be increased by virtue of the withdrawal from valley storage until sufficient time has elapsed to permit the attainment of channel slopes that are normal with the diversion operating. For many years it was thought that a cutoff (which may be considered a re-entrant diversion) would increase stages downstream about as much as it reduced them upstream. This belief was either inspired or supported by the observation of a cutoff on the Mississippi River that occurred quickly at high stages. Discharges and stages were promptly increased below, which was natural since the rapid lowering of stages above the cutoff withdrew water that was in detention storage. The same results will follow the sudden opening of a diversion at high stages.

Effect on Discharge With Storage Area Below the Diversion.—With the diversion located just above a large natural storage area, the loss in effectiveness downstream may also be serious, for the net reduction immediately below the diversion is greater than at points farther downstream. To illustrate: In one case it

was assumed that the next reach below the diversion had the same storage and discharge characteristics as the reach above, for which Fig. 1 was prepared. Through this reach were routed the flows shown in Fig. 1 for the total discharge with the floodway not operating, and for discharge in the river below the floodway, the flows remaining in the river after floodway withdrawals. Peak discharges were found to be 1,182,000 cu ft per sec with the floodway not operating and 1,097,000 cu ft per sec with the floodway operating. The difference of 85,000 cu ft per sec is the effect of the diversion at the lower end of the next reach downstream. Since the net reduction immediately below the diversion was about 140,000 cu ft per sec, the reduction was diminished about 39% in the next downstream reach.

Modification of Water Surface Slope.—

Flood-Wave Flow Characteristics.—It is well recognized that a diversion increases the water surface slope in the main channel upstream. The effect of a diversion on the slope downstream has been given little attention. An understanding of flow characteristics is necessary for a complete realization

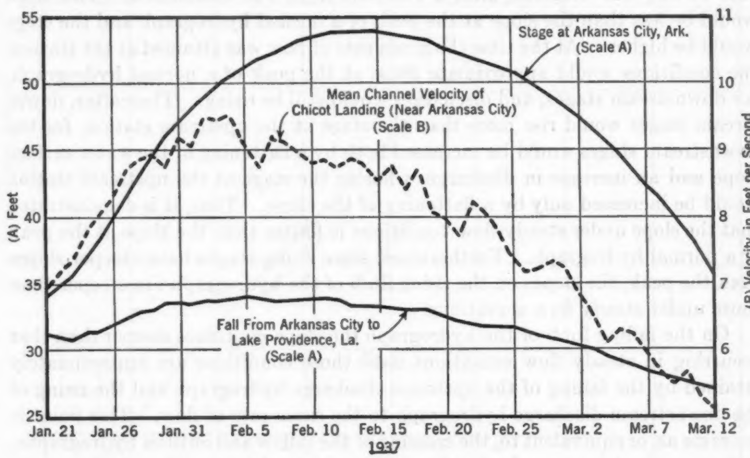

FIG. 2.—MISSISSIPPI RIVER—1937 FLOOD

of the effect on downstream slopes. In Fig. 2, the stage hydrograph and the mean channel velocities of the 1937 flood in the Mississippi River at Arkansas City, Ark., have been plotted as has the fall from Arkansas City downstream to Lake Providence, La. This fall is indicative of the river slope below Arkansas City. The slope on the rising limb of the hydrograph is steeper than at corresponding stages on the falling limb. As a result, the velocities are greater on the rising limb, and it follows that the discharge for any given stage is greater also. The maximum discharge rate may occur before the crest stage when the slope is still greater than at the crest.

The steeper slope on the rising limb of the hydrograph is caused by the fact that the rise at any point precedes the rise at a point below. The difference is

increased by valley storage which lengthens the time lag and reduces the stage at the downstream point by lessening the rate of flow at the crest and on the rising limb of the hydrograph. On the falling limb of the hydrograph, reverse conditions prevail. At the instant of crest, the water surface downstream is still rising, thus lessening the slope. The reduction in slope continues as the stage downstream rises to crest and then falls less in each coinciding period of time than does the stage at the point upstream to which the hydrograph applies. The reduction is augmented by the withdrawal of water from valley storage below the gaging station. This increases rates of discharge at downstream points and causes high stages there to persist.

Flood-Wave and Steady-Flow Slopes Compared.—At peak stage, the slope is greater than it would be if the flow that occurred at that stage continued sufficiently long to create steady-flow conditions. Under the latter conditions, all points are at stages corresponding to the same flow. Thus, if the discharge were to rise to a given quantity and then continue at that rate for an indefinite period, the stage at any station would continue to rise slightly after the given rate of flow was attained, until a constant slope was established. This slope would be less than the slope at the peak of a normal hydrograph and the stage would be higher. At the time the given rate of flow was attained at the station, the conditions would approximate those at the peak of a normal hydrograph, for downstream stages, and discharges would still be rising. Thereafter, downstream stages would rise more than the stage at the upstream station, for the downstream stages would be increased both by a flattening of the water surface slope and an increase in discharge, whereas the stage at the upstream station would be increased only by a flattening of the slope. Thus, it is demonstrated that the slope under steady-flow conditions is flatter than the slope at the peak of a normal hydrograph. Furthermore, since rising stages have steeper slopes than the peak, the slopes on the rising limb of the hydrograph are steeper than those under steady flow conditions.

On the falling limb of the hydrograph the slope continues steeper than that occurring in steady flow conditions until those conditions are approximately attained by the falling of the upstream discharge hydrograph and the rising of the downstream discharge hydrograph to the same rate of flow. This point is the same as, or equivalent to, the crossing of the inflow and outflow hydrographs, well recognized in river hydraulics as the peak of the outflow hydrograph. Thereafter, the upstream hydrograph will fall faster than the downstream hydrograph, and slopes at and below the upstream station will be flatter than those occurring in steady-flow conditions. When the equality of discharge rates at 2 points is used to approximate steady-flow conditions, the length of the reach between the points should be so limited that the contained storage can be related to the stage or discharge at the downstream point. In addition, the reach should be long enough to prevent changes below the reach from affecting stages at the upstream end of the reach. There should also be no material inflow within the reach, or intermediate inflow should be removed by analytical adjustment. In the case of a reach so selected, at the time the discharges at the head and foot of the reach are equal, the flows at intermediate points should

be equal to the flows at the ends of the reach. Accordingly, substantially steady-flow conditions exist.

The Stage-Discharge Relation.—Because higher slopes and velocities exist on the rising limb of a flood wave than at equal stages on the falling limb, the stage-discharge relation (or rating curve) takes the form of a loop. Fig. 3 is an

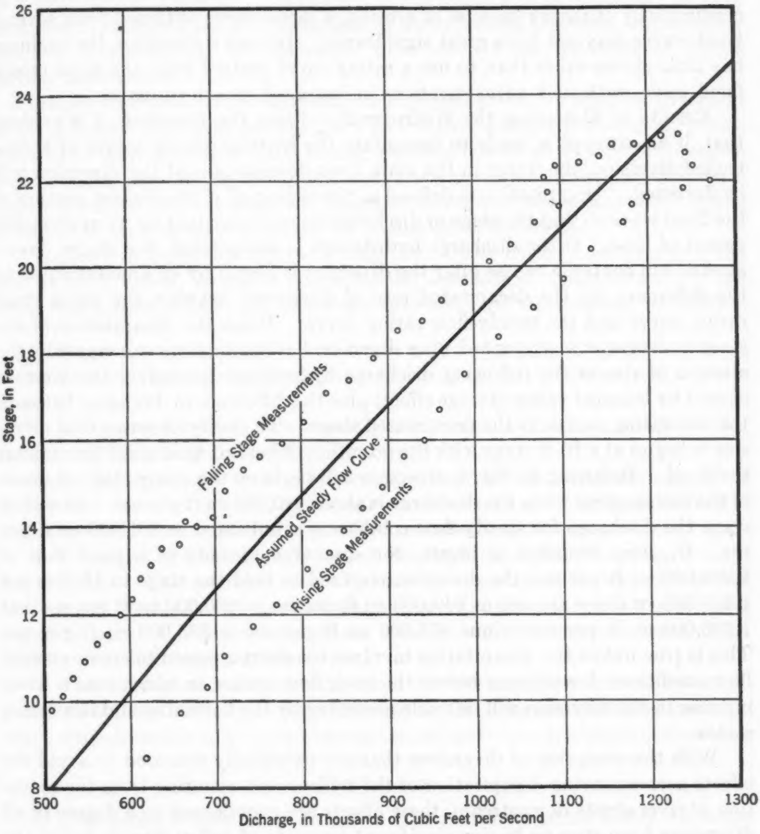

FIG. 3.—EXAMPLE OF STAGE-DISCHARGE RELATIONS, MISSISSIPPI RIVER

example. The mean rating curve, drawn as an average between the rising and falling segments of the loop, does not necessarily represent steady-flow conditions. If the rise of the flood is rapid and the fall is slow, discharges taken from the mean rating curve will be higher than those for steady-flow conditions. The reverse will be true if the rise is slow and the fall is rapid. In the absence of other changes, a composite mean rating curve obtained from many flood waves should approximate a steady-flow rating curve.[1] Care should be exercised,

however, in passing the curve through the top of each flood loop. If the point near the top of each loop is selected in accordance with the suggestions contained in the preceding paragraph, these points should approximately represent steady-flow conditions. These points may be expected to lie toward the falling stage side of the loop from the peak stage unless the maximum flow was of sufficient duration to establish steady-flow conditions. Since an alluvial stream is continuously changing because of erosion, a mean curve obtained from several flood waves may not have great significance. In such a situation, the engineer has little choice other than to use a rating curve plotted from the most recent flood wave, with such adjustments as he has good reason to make.

Results of Flattening the Hydrograph.—From the foregoing, it is evident that, if an attempt is made to decapitate the hydrograph by means of a controlled diversion, the slopes in the main river downstream of the diversion will be flattened. Decapitation is defined as the slicing off of the highest portion of the flood wave so that the stage or discharge remains constant for an appreciable period of time. If the discharge hydrograph is decapitated, the stages downstream will continue to rise after the diversion is begun by an amount equal to the difference (at the decapitated rate of discharge) between the rising stage rating curve and the steady-flow rating curve. When the decapitation of the stage hydrograph is attempted, once diversion has begun, it must increase by the amount of rise of the inflowing discharge hydrograph (including the increase caused by lessened valley storage effect) plus the difference in discharge between the two rating curves at the decapitated stage. To clarify: Assume that diversion is begun at a 16-ft stage with the intention of holding that stage throughout the flood. Referring to Fig. 3, diversion will begin on the rising stage segment of the rating curve when the discharge is about 940,000 cu ft per sec. At a 16-ft stage the discharge for steady-flow conditions is indicated as 865,000 cu ft per sec. If, after diversion is begun, the discharge ascends to a peak flow of 1,200,000 cu ft per sec, the diversion required to hold the stage to 16 ft is not 1,200,000 cu ft per sec minus 940,000 cu ft per sec = 260,000 cu ft per sec, but 1,200,000 cu ft per sec minus 865,000 cu ft per sec = 335,000 cu ft per sec. This is true unless the decapitation involves too short a period to create steady-flow conditions downstream before the peak flow occurs, in which case a lesser increase in the diversion will be made necessary by the flattening of downstream slopes.

With the exception of diversions that are specifically operated to avoid the effects accompanying decapitation of the hydrograph resulting from the reduction of river slopes downstream, these effects are experienced to a degree in all diversions from streams having significant amounts of valley storage below the diversion, whether or not the diversions are controlled. This follows from the fact that diversions generally flatten the hydrograph.

Stage Reduction.—Above and below a diversion, stages in the main stream are reduced. Above the diversion, slopes are steepened, and the reduction in stage diminishes in accordance with backwater principles. Below the diversion, slopes usually are flattened, thus increasing the stage required to transmit flows and reducing the effectiveness of diversion in terms of stage lowering. In addition, if there is appreciable valley storage above the diversion, the maximum

rates of flow immediately above the head of the diversion are increased so that stages neither above nor below the diversion are lowered in magnitude corresponding to the rate at which water is withdrawn. Furthermore, with a substantial amount of valley storage below the diversion, the lowering of stages downstream diminishes with distance from the diversion. It should be remembered also that increments of discharge per foot change in stage usually increase in a downstream direction. Thus, even in the absence of other factors tending to diminish stage lowerings, a reduction of water surface elevation immediately below a diversion may be equivalent to a much lesser reduction at points farther downstream.

Velocity Changes.—Velocities may be expected to be modified by diversion in accordance with the slope changes. In the river above the diversion, velocities will be increased with the increase, growing less in an upstream direction and reaching zero at the first point above the diversion drawdown influence. Below the diversion, velocities will generally be reduced because of the lowering of the crest rates of discharge and the flattening of the slopes.

Summary of Hydraulic Effects of Diversion.—The hydraulic effects and the results of diversion, assuming consequential amounts of valley storage in the main steam both above and below the diversion, are summarized as follows:

1. Stages are lowered above and below a diversion;
2. Velocities are increased upstream and reduced downstream from a diversion;
3. Valley storage effect is reduced upstream from a diversion, and the maximum rate of discharge is thereby increased;
4. By flattening the hydrograph, a diversion reduces valley storage effect in the main river downstream resulting in the loss of a part of the peak discharge and stage reduction that normally would be caused by storage;
5. When the hydrograph is flattened, steady-flow conditions are approached downstream. This increases stages by causing coincidence or near coincidence of the peak discharge and peak stage, and also by causing crest or near crest stages to occur at downstream points when points above are at crest stage, thereby reducing water surface slopes.
6. The diminished valley storage effect downstream from a diversion (mentioned above) further reduces slopes by causing the stage and discharge reducing effect of the diversion to be progressively less effective in a downstream direction.

Operation

If a diversion is open at all times, so that it will withdraw water whenever the stage in the main stream exceeds the elevation of the bottom of the diversion, the flood hydrograph will be flattened roughly in proportion to the amount the peak stage is reduced, but it will not be decapitated. The valley storage effect in reducing flood peak discharge will be diminished both upstream and downstream from the diversion but will not be eliminated, for the normal shape of the hydrograph is retained even though its amplitude is reduced. If the hydrograph, as modified by the diversion, passes through sizable storage areas downstream, its peak flow and discharge rates are so affected by that storage

that (barring additional tributary inflow) the peak flow continues to reduce. This reduction is not as great as it would be if the flood were unmodified by the diversion of water. Accordingly, as a modified flood wave continues downstream through an accumulatively increasing amount of valley and channel storage, the peak reduction diminishes. This situation can be contrasted with the situation in which the hydrograph is decapitated by the operation of a control structure. In the latter instance there is a greater increase in discharge because of the elimination of upstream storage, for water can go into storage at that point only through tilting of the water surface. This is so because the stage at the lower end of the reach where the diversion is located is fixed or approximately fixed. As the flows represented by the decapitated hydrograph pass downstream through large storage areas, the rising limb of the hydrograph continues to be reduced by valley storage and the falling limb increased. The flat top is reduced in extent more and more until eventually a rounded hydrograph is formed once more. From the point of diversion to the nearest point downstream where the hydrograph no longer has a flat top, the peak discharge is constant; that is, the peak discharge is not reduced by the valley storage. In this stretch, the entire reduction in peak flow of the natural flood wave, unmodified by the operation of the diversion, is the amount that the peak-flow reduction caused by the diversion diminishes. Let R_u denote the reduction in peak flow of the natural flood wave before modification under the operation of the diversion; let R_s denote the reduction in peak flow of the flood wave modified by diversion; and, let R_d denote the reduction caused by the diversion immediately below it. Then $R_d + R_s - R_u$ is the net reduction caused by the diversion, but in the stretch in which the hydrograph is decapitated, $R_s = 0$. Accordingly, the reduction in peak flow and stage accomplished by the diversion will diminish faster in a downstream direction if the hydrograph is decapitated, than if the diversion is operated to produce a normally shaped hydrograph. A diversion that is open at all times will produce such a hydrograph.

Decapitation of the hydrograph to produce a wide, flat crest can be accomplished only with a controlled inlet. If the purpose of the diversion is to reduce flood heights, decapitation should be avoided by judicious operational procedure. This is advisable unless there is little valley and channel storage above the diversion, within the range of its influence, or below the diversion to the location where flood height reductions are desired.

The harmful effects of excessive flattening of the hydrograph can probably best be avoided by providing no control structure, but where a structure is necessary, these effects can be mitigated by operating the structure so as to pass a flood wave of approximately normal shape. This can be achieved in the most practicable way by passing water through the structure relatively early on the rising stage of the hydrograph and paralleling as nearly as possible the stage hydrograph that would occur without diversion. For instance, if it is required that the controlled stage in the river not exceed 16 ft, and if it is predicted that the peak stage without diversion would rise to 19 ft, operation should begin as soon as possible, and the rates at which water is withdrawn should be equivalent to 3 ft on the gage. Of course, if there is excess diversion capacity and no objection to using it, there should be no hesitancy in drawing

the stage below 16 ft simply because this action would flatten the hydrograph. The closest approach to eliminating the unfavorable results of flattening of the hydrograph can be made in reaches with constant storage increments per foot of stage. An example of such a reach would be one completely bounded laterally by levees or steep escarpments.

Withdrawal of Sediment by Diversion

Suspended Sediment.—Experiments conducted at the United States Waterways Experiment Station,[2] at Vicksburg, Miss., showed that when loess was the transported sediment, the division of the material between the stream and the branch was very nearly in proportion to the water distribution. Since loess is an extremely fine material, it may be concluded that most of it was carried in suspension. Table 1 summarizes the results of experiments at Iowa State College,[3]

TABLE 1.—Percentage of Total Sediment Passing Through a Branching Arm for Various Sediment Sizes[a]

Test number	Slope of channel	Percentage of flow in branch	Size of Sieve								
			¾ Inch	4	10	20	40	60	80	100	200
1	0.0182	49.1	91.2	84.8	76.1	72.3	68.8	59.6	50.7	49.8	48.1
			186	173	155	147	140	121	103	101	98
2	0.0214	27.8	64.3	60.1	57.2	55.5	42.1	34.1	32.3	28.2	21.0
			231	216	206	200	151	123	116	101	76
3[b]	0.0214	25.6	61.3	58.4	55.2	47.3	40.6	33.2	30.0	26.4	19.9
			239	228	216	185	159	130	117	103	78
4	0.0346	14.8	24.6	22.7	20.0	19.1	18.8	18.4	18.1	17.8	16.5
			166	153	135	129	127	124	122	120	111

[a] The first line of values for each test is the percentage of the total sediment of the indicated sieve size passing through the branch. The second line of values is the ratio of that percentage to the percentage of total flow in the branch. [b] Outlet flow was retarded by perforated plates.

at Ames, and lends a measure of support to this indication that suspended sediment divides in proportion to water distribution. In these tests the slopes were steep and except for Test No. 3, the outlets were free fall. Both channels were rectangular with dimensions 6 in. by 5 in., and the branching channel diverged 30° from the main channel. Slopes of all arms of channels were equal, but the actual relation of the surface slopes could not be determined from the test reports. The 100-mesh material in three of the tests divided almost exactly in proportion to the division of flow. The 200-mesh material divided approximately in proportion to flow in Test No. 1, and, for all practical purposes, behaved similarly in Test No. 4. In this latter test, the difference in percentage of flow and percentage of 200-mesh material passing into the branch channel was only 1.7. However, the variation in division of the 200-mesh material in the various tests does not appear to be consistent with variations for other sizes. Channel sizes were small, and slopes were steep, so it may have been difficult

[2] "Movement of Bed Load in a Forked Flume," by Herbert D. Vogel, *Civil Engineering*, Vol. 4, February, 1934, p. 73.

[3] "Stream Sedimentation in a Divided Channel," by Albert Guy Dancy, thesis presented to Iowa State College, Ames, Iowa, in 1947, in partial fulfilment of the requirements for the degree of Master of Science.

to obtain a natural distribution of the finer material in the channel above the diversion.

It has been concluded[4] that fine materials in transportation are distributed comparatively uniformly throughout the river cross section. In connection with the mechanics of the withdrawal of water by a diversion, this conclusion supports the concept that suspended sediment, as differentiated from bed load, divides at a diversion approximately in direct proportion to the division of water quantities.

Bed Load.—

Variation with Diversion Discharge.—Herbert D. Vogel, M. ASCE,[2] reported results of test runs using Red River sand. In these tests, the rates of discharge in the main channel above the branch were held practically constant. Both channels were 2 ft wide and rectangular in section, and the angle of bifurcation was 30°. The results are summarized in the following tabulation:

Flow in branch channel as percentage of total flow	Deposits in branch channel as percentage of total deposits
65.0	85.1
49.4	75.9
48.8	75.2
34.9	63.6
30.2	45.3
29.9	51.3
24.2	37.1
23.3	38.2
15.9	17.9

Sand traps were not provided so sand carried beyond the ends of the flumes was lost. Later experiments indicated that sand was carried past the end of a branch channel before it reached the end of the main channel; such loss, if accounted for, would cause the percentages of material carried by the branch channel to be larger than the percentages of total deposits listed above. Red River sand is rather fine, so that some sand may have been carried in suspension. Sand in suspension would divide approximately in proportion to the division of water quantities. Therefore, if such sand actually were deposited below the bifurcation, the percentages of deposits in the branch channel also were reduced (because of the material in suspension) below what would have been recorded had the material been transported entirely as bed load. Such deposition appears possible, for later experiments indicated that slopes below the bifurcation were flattened by diversion. Since the slope in the main channel is smallest near and below the point of diversion, any deposition of suspended sediment that might have occurred was greatest in the main channel. Unbalanced deposition of this nature also would lower the percentage of deposits in the branch channel.

Variation with Particle Size.—Later experiments[2] utilized flumes of semicircular cross section, with bottoms as before on the same horizontal plane.

[4] "Study of Materials in Suspension, Mississippi River," *Technical Memorandum No. 122-1*, U. S. Waterways Experiment Station, Vicksburg, Miss., 1939.

The main channel had a 2-ft radius and the side channel a 1-ft radius. Sand traps were provided to make possible runs that were continuous over long periods of time. The approximate average results were

Type of sediment	Discharge in side channel as percentage of total discharge	Sediment entering side channel as percentage of total sediment
Red River sand	38	52
Polk Creek sand	36	65

These results do not confirm the results of the preliminary tests (and possibly rightfully not because of the different character of the channels and the altered test conditions). Since the Polk Creek sand was coarser than the Red River sand, the results do indicate that a greater percentage of coarser materials will pass into a side channel than is the case with finer materials. It is probable that a portion of the finer material becomes suspended or is in a partially suspended state, in which the grains are driven high in the water stream. However, this does not explain the difference in the diversion of coarse and finer materials, both of which have sufficient particle size to travel as bed load. Experiments conducted at Iowa State College[3] emphasize the need for further explanation of this phenomenon. The results of these tests are shown in Table 1. In addition to indicating in a general way the effect of changing the percentage of flow in the branching arm, Table 1 reveals that, without exception, as the particle size of the sediment is reduced, the percentage of the size diverted is also reduced. Particles of the ⅜-in. and No. 4 sieve size should normally be transported as bed load by rolling, sliding, or saltation with small vertical amplitude. Yet a lesser percentage of the No. 4 size particles was diverted than of the ⅜-in. size. An unsuccessful attempt was made to explain this phenomenon on the basis that the larger sized particles, having less surface area exposed to the action of the current per unit weight of the particle, travel more slowly along the bed and, therefore, could be deflected more easily. The greater percentage of diversion of the coarser particles shown by these tests appears to conflict with discussions and demonstrations by A. Schoklitsch[5] of sorting in bends.

Conditions of the Iowa State College experiments may have influenced the results in such a way as to cause the distribution in accordance with particle size as shown in Table 1. With the slopes rather steep, it is possible that all sizes were carried more or less in suspension, but proportionately more of the larger sizes were able to settle into the bottom area near the head of the branch channel. It is believed that near the bottom of the channel the component of velocity in the direction of the main channel downstream is relatively low and the component in the direction of the side channel relatively high. Thus, the distribution of particle sizes would occur as shown by Table 1, because the particles suspended at higher elevations in the stream would divide in accordance with the division of the water at each level. In the demonstrations conducted by Mr. Schoklitsch, as in natural river bends, conditions were not such as would cause the degree of unbalance of velocity components that in all likelihood occurs at the

[5] "Hydraulic Structures," by A. Schoklitsch (translated by Samuel Schulits), A.S.M.E., New York, N. Y., 1937.

head of a branch channel, especially a branch channel in a flume that has a relatively large cross section with respect to that of the main flume. Further investigation is needed to determine whether a diversion from a natural stream will withdraw a greater proportion of coarse than of fine materials and to furnish a convincing explanation of the distribution of particle size that occurs. Application of test results to natural streams is fraught with hazards unless conditions are in accordance with correct scale ratios or the mechanics of all observed phenomena is understood.

Channel Slopes and Effect of Slopes on Bed-Load Diversion.—In the article by Colonel Vogel[2] two other points are mentioned that may be useful in developing a theory pertaining to the relatively large amount of bed load diverted by channels branching from flumes or from natural streams, when the branch is so located as to facilitate withdrawal of bed load. First, a series of experiments in which water surface profiles were recorded indicated that slopes were flattened in the main flume near the head of the branch channel and also downstream therefrom. The second point is expressed by the following observation made as a result of experiments conducted at Cornell University, Ithaca, N. Y., and is quoted from the article by Colonel Vogel.[6]

> "For tests of short duration (6 hr) the percentage of bed load deposited in the side flume increased with an increase in slope throughout the flume. Such increase in slope was obtained by lowering the tailgates of the two flumes."

Angle of Diversion.—Experiments have been made at the Karlsruhe hydraulic laboratory to determine the amount of sedimentary material diverted by channels branching from a straight channel at various angles.[7] The following tabulation summarizes the results of these tests for sharp edges at the point of branching:

Angle of diversion from straight channel	Percentage of sediment in diversion	Percentage of sediment in straight channel below diversion
30	97.3	2.7
60	96.2	3.8
90	90.5	9.5
120	87.5	12.5
150	92.0	8.0

In these experiments the channels were rectangular, and the diversion channel and the main channel below the point of diversion were the same size as the main channel above the point of diversion. The width was 0.656 ft, and the bottom slope was 0.003. The evidence available indicates that the sediment used was sand. With the low slopes used it is probable that practically all the sediment moved along the bed. At the point of diversion the volume of flow was divided equally between the two channels.

[6] "Movement of Bed Load in a Forked Flume," by Herbert D. Vogel. *Civil Engineering*, Vol. 4, February, 1934, p. 77.

[7] "Hydraulic Laboratory Practice," ed. by John R. Freeman (translation), A.S.M.E., New York, N. Y., 1929.

In experiments at the United States Waterways Experiment Station using a model of a Mississippi River bend,[8] tests were made to determine the effect of the angle of diversion on the amount of bed load withdrawn. Three angles between the diversion and current were used: 45°, 90°, and 135°. Diversion site No. 1, as shown in Fig. 4, was selected for the tests, since the greatest amount of sand was withdrawn in model runs of a 40-ft river stage at this location. The 45° and 135° diversions were bent at the bank line and con-

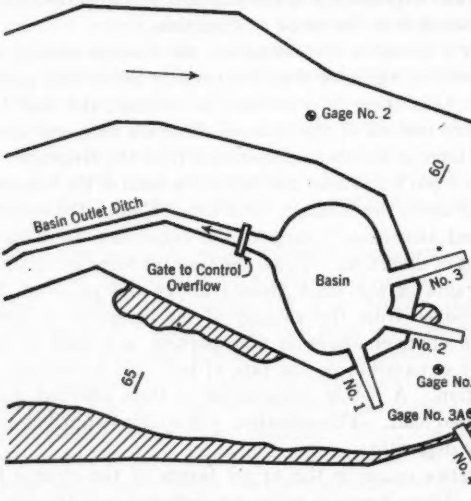

FIG. 4.—LOCATION OF DIVERSIONS IN MODEL STUDY OF BED-LOAD MOVEMENT

tinued at those angles into the river. Landward of the bank line, all diversions were approximately at right angles to the river channel. In the prototype the diversion channel dimensions were equivalent to widths of 300 ft and depths of 30 ft below the 40-ft stage at which these tests were run. The results are summarized as follows:

Angle of diversion in degrees	Percentage of bed load diverted
45	97
90	80
135	85

Although the experimental conditions were considerably different from those at the Karlsruhe laboratory, the results appear to give a qualitative check, especially with respect to the variation with angle of diversion. Although the percentages of bed load diverted seem to confirm the Karlsruhe results, it should be remembered that these diversions were excavated through

[8] "Model Study of the Movement of Bed Material Around Bends and Through Diversion Channels," *Technical Memorandum No. 3-1*, U. S. Waterways Experiment Station, Vicksburg, Miss. (unpublished).

the point bar at a location that had been found to be most favorable for the diversion of bed load. At other locations the percentages of diverted bed load would have been less.

Factors Influencing Diversion of Bed Load.—Analysis of the experiments described has led to the identification of factors that cause a branch channel to carry proportionately more bed load from a flume—and from a river when conditions are right for the purpose—than the water diverted. These factors furnish at least a partial explanation of the changes in the proportions of bed load diverted with variation in the angle of diversion.

Immediately after a diversion is constructed, the average velocity upstream from the point of diversion is greater than the velocity below that point. This is caused by the fact that there is more area to conduct the flow below the point of diversion, since instead of one channel there are two, and one of these channels usually is as large as the channel upstream from the diversion. The low slopes observed in the main flume near and below the head of the branch channel (mentioned previously under the heading, "Bed Load: Channel Slopes and Effect of Slopes on Bed-Load Diversion") support the conclusion that the velocity changes near the point of diversion. Thus, the tractive force is rather abruptly reduced below the value in the main stream above the point of diversion. Material cannot be moved from the vicinity of the diversion as fast as it is moved in, unless the channel above is transporting bed load at less than capacity. Under any circumstances the rate of bed-load movement slows at the point of bifurcation. A better opportunity is thus afforded the branch channel to withdraw bed load. This situation will continue until channel sizes have been reduced by deposition.

The highest velocities occur in the upper layers of the stream from 0.6 depth to the surface. These layers of water are deflected into the side channel with greater difficulty than the lower layers that have less velocity. Accordingly, a large portion of the water that flows down the straight channel below the junction is derived from the upper layers of the stream which do not carry bed load. A relatively dead water area results, so far as flow down the straight channel is concerned, near the bottom of the stream in the junction area. With the top water flowing down the straight channel there is little opportunity for the bed load to move in that direction, and a substantial portion of the water in the branch channel must be derived from the lower layers of water in the main channel. These layers transmit the bed load, and a large proportion of of this load is moved into the branch channel.

Even if the head of the branch channel is in a pool in which no appreciable differences in movement from top to bottom exist, it appears that the normal vertical velocity curve might not be established in the branch channel for the distance required to accelerate the water from no velocity in the pool to the velocity permitted by the slope and the frictional resistance in the branch channel. It might be expected, then, that the ratio between velocities near the bottom and upper layer velocities would be greater at the entrance to a branch channel than at other locations. This would encourage the diversion of bed load into the branch channel.

It should be noted that the conditions of tests described resulted in a greater slope in the branching channel than in the straight channel below. In the Karlsruhe laboratory tests, the same amount of water was drawn into each channel. Since the velocity was directed down the main channel, in order to compensate for the difference in velocity head, additional slope in the branch channel was needed. Thus, as the two channels were of equal size in the tests, the tractive force near the head of the branch channel exceeded that in the straight channel below the fork. Therefore, the diversion of a greater amount of sediment into the branch channel was promoted, and this will be the case whenever a similar condition exists. Attention is invited to observation made under the heading, "Bed Load: Channel Slopes and Effect of Slopes on Bed-Load Diversion," relative to the effect of increased flume slopes, substantiating the conclusions just reached. As the flume slopes increased, the velocities increased, and, accordingly, for any given rate of diversion, the slope in the branch channel necessarily increased more to compensate for the velocity head directed downstream and for the greater difficulty of turning the higher velocity jets into the branch flume.

Another factor probably enters into the diversion of bed load. It is best appreciated by an examination of a branching channel that departs from the main channel with a small angle. A side channel that diverges from the straight channel at 30°, for example, will have a tendency to create a meander pattern upstream from the bifurcation. The material moving on the stream bed will then tend to adopt a path with respect to the meander pattern similar to that shown in Fig. 5. The bed load will pass toward the inside of the bend at the upstream side of the branch channel. Thus, it is drawn to the head of the branch channel and moves into that channel with the diverted water. In the case of exceedingly sharp bends, the normal pattern is disrupted, and deposition does not occur on the convex point. Accordingly, for high angles of diversion it may be expected that the meander effect will not assist in the diversion of bed load. It should be noted that a bendway which is an element of a meander pattern is in itself of the nature of a diversion. The first section of the stream that moves around the point or convex side of the bendway is diverted from the main stream, and each jet that moves around the bend successively outward from the point is diverted from the stream that is still continuing toward the concave side of the bend. Thus, a bendway is a continuous succession of diversions. Each deflected jet will transport bed load in accordance with the effect on it of factors influencing bed-load diversion and with the amount of material presented for diversion. Therefore, the meander pattern effect is not an elemental factor affecting bed-load diversion but is a complex of other factors. However, since these factors operate within the meander to cause its peculiar pattern of bed-load movement and again act separately with respect to a branching channel, the meander pattern may be viewed as a separate factor in relation to bed-load movement into a branching channel.

If material is moving along the bed of a stream with a noticeable velocity, its diversion is affected by the magnitude of the angle through which the material must be turned. It is manifestly diverted through a small angle with greater ease and less force than is required for a large angle. For small

diversion angles the approaching particles have a component velocity in the direction of the branch channel, whereas for a 90° diversion the entire movement of each particle into the branch channel must be created by the diversion forces. For still larger angles a component of the movement down the main stream must be overcome as well. However, if the material comes to rest before it is drawn into the branch channel, the angularity factor just described will be nonexistent.

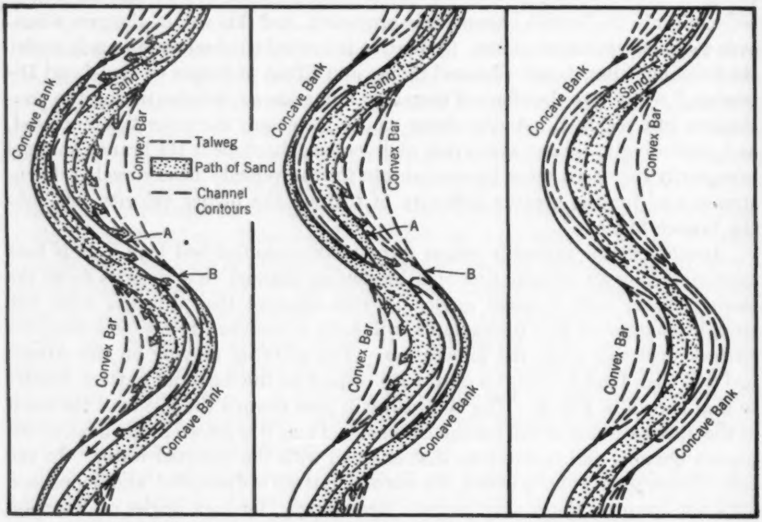

FIG. 5.—PATHS OF SAND TRAVEL IN MEANDERING RIVERS

A summary of the factors that influence the diversion of bed load is given at this point for convenience of reference:

a. The velocity factor or the reduction in velocity at the bifurcation;

b. The velocity in the branch channel. The velocity must be sufficient to transport the sediment presented;

c. Differential velocity effect;

d. The vertical velocity effect;

e. The slope factor which depends upon the relative slopes in the main channel and in the branch channel;

f. Meander pattern created by branch channel; and

g. Angularity factor.

With the exception of factor *b* which was not mentioned previously, these factors were discussed in preceding paragraphs in the order listed.

Additional Factors Affecting Bed-Load Diversion in Natural Streams.—Previously, it has been implied that in natural streams the amount of bed

load withdrawn depends on the point in a river bend at which the entrance to a diversion is located. Evidence has been furnished which shows the path of sand travel in an alluvial stream.[9] Fig. 5 is reproduced from this study. When banks erode rapidly, the material from the caving bank moves downstream and deposits on the next point bar on the same side of the river. This is also true when banks erode with difficulty, but in this case, the bed load also moves from the point opposite the caving bank and crosses the thread of the stream in the general vicinity of the crossing to the point bar below. Some of the material that reaches this point bar is deposited there, and a portion passes downstream, again crossing the thread of the stream to the next point bar. For this condition to exist, material must be entering from above the reach at a faster rate than the banks are caving in the reach under consideration. If this material is entering at the same rate as the banks are caving, sand will not move from point bar to point bar across the thread of the stream. In this case, the distribution and path of the bed load will be similar to that described for rapidly eroding banks. Thus, the references to rapid erosion, and other comparable terms are relative only and do not apply simply to rate of bank erosion. Rather, the terms represent relations between rates of bank erosion and amounts of bed load carried in from points above the reach. Generally, it may be said that the material moving from above cannot be less than that caved from the bank below, for the latter will eventually accommodate itself to the amount of material deposited on the point opposite. Fig. 5 also shows that in reaches in which there is no erosion, bed load entering the head of the reach passes through from point bar to point bar, swinging away from the concave bank in each instance.

To minimize the withdrawal of bed load, a diversion should be located, if practicable, in a reach in which there is no erosion. This alone will not insure a low rate of withdrawal, for, in addition, the entrance to the diversion should be in the concave bank an appreciable distance below the next upstream point bar in order that it will be as far as practicable from the path of sand travel. In reaches in which the banks are eroding, there is little movement along the bank between points A and B in Fig. 5. This section of bank, however, is very close to and just below the next upstream point bar. If the entrance to a diversion is located there, it is possible that the diversion might be capable of influencing the path of the sand and of withdrawing material from the altered path or from the convex bar above. Therefore, it appears that the best point of diversion, to minimize withdrawal of bed load, is near point B or a short distance downstream where bank caving is still small. The optimum location can be determined only through study of the actual stream, but model tests will furnish valuable assistance.

Though proximity to the sand path and exposure to a source of bed load are major considerations affecting the movement of bed load into a diversion, once the exposure has been established other factors that have been discussed become of prime importance. Considerable mention has been made of the effect of the angle between the main channel and the diversion channel. Fig. 5 shows

[9] "A Laboratory Study of the Meandering of Alluvial Rivers," by J. F. Friedkin, U. S. Waterways Experiment Station, Vicksburg, Miss., May, 1945.

that in meandering streams, the path of the bed load does not follow the thread of the stream. Accordingly, the angle between the channel and the bed load path must be taken into account in planning a diversion. For example, if the angle between the diversion and the bed load were less than the angle between the channel and the diversion, the effect of the angularity and the differential and vertical velocity factors will be augmented, with no change in the impact of the other factors. Thus, the proportion of the bed load withdrawn will probably be larger than if the angles were the same. If, instead, a lesser angle exists between the channel and the diversion than between the latter and the bed-load path, the proportion of the bed load withdrawn probably will be diminished.

The conclusions drawn with respect to the effect of the location of diversion in a river bend were substantiated by other tests conducted at the Waterways Experiment Station.[8] In these tests, diversions were located in a reproduced Mississippi River bendway at four points, as shown in Fig. 4. The diversions were approximately at right angles to the river channel, with two exceptions that have been mentioned previously in the discussion of angle of diversion. Runs were made at two water surface elevations, one corresponding to a 40-ft prototype stage and the other to a 20-ft stage. In both instances, diversion channel areas 30 ft deep by 300 ft wide were available below the water surface at diversions Nos. 1, 2, and 3. Diversion No. 4 was cut to thalweg depth. The amounts of flow withdrawn were needed to produce velocities sufficient to move bed load into and through the diversions. Test results showing the effect on bed-load withdrawal of the location of a diversion in a river bend are shown in Table 2. For each run at a given stage the same amount of water was diverted as for all other runs at that stage.

TABLE 2.—TESTS SHOWING THE EFFECT ON BED-LOAD WITHDRAWAL OF THE LOCATION OF A DIVERSION IN A RIVER BEND

Diversion operating	Forty-foot stage	Twenty-foot stage
WATER[a]	10%	20%
No. 1[b]	80%	....[c]
No. 2[b]	75%	89%
No. 3[b]	20%	87%
No. 4[b]	0	0

[a] Percentage of water withdrawn. [b] Percentage of bed load withdrawn with Diversion No. 1, etc., operating. [c] Not tested.

The concave bank could not erode because it was constructed of concrete. Had this bank been of friable material, it is likely that some of the material that would have caved from the bank above Diversion No. 4 would have been withdrawn by that diversion. The small amount of material withdrawn by Diversion No. 3 during the 40-ft stage tests is indicative of the importance of the proximity of the sand path to the diversion entrance. The bed load did not concentrate on the bar side until it reached the vicinity of Diversion No. 2. A large portion of the bed load was far out in the channel from Diversion No. 3, so that it could not be deflected into the diversion. By prior runs without diversions, it was ascertained that the bed load concentrated on the bar (or convex) side of the bend further upstream for the 20-ft stage than for the 40-ft stage. A comparison of the withdrawals through Diversions No. 2 and No. 3 confirms this observation. The explanation probably lies in the fact that for

lower stages, the velocities are generally lower. The stream can be turned around bends with greater ease when velocities are lower, and, hence, there is more deflection in the upstream portion of the bend. In a natural stream, the stage and slope vary continuously, and, as a result, the bed-load path and the points at which maximum and minimum withdrawal of sediment through diversion would occur also change continuously. This fact should be taken into account in planning diversions from natural streams.

In many diversions the bottom of the branch channel may be at a considerably higher elevation than the bottom of the main channel. Assuming both banks to be steep and the velocities to be of such magnitude that bars of appreciable vertical height cannot build, the bed load will travel along the bottom of the main channel, and the side channel will of necessity derive its water from comparatively high layers of the main stream. Under these conditions, little bed load will be diverted. Should the diversion quantities be large, it is probable that a bar will build near the head of the diversion because of the change in velocity and transporting capacity there. If the bar is raised to a level within the range of influence of the diversion, the latter will then withdraw bed load, and the proportion withdrawn will increase with the continued elevation of the bar. In predicting consequences of this nature to be expected from a high-level diversion, the relative amount of diverted water and the location of the bed-load path must be considered.

An Adjusted or Balanced Stream

When the bed load, slope, quantity of water, and channel size are adjusted so that point bars build at the same rate as opposing banks cave, the stream is considered in this paper as being in balance. The condition can best be understood in the instance of a stream having freely erodible banks and bed. The channel is a relatively continuous series of reversing bends. In each bend the concave bank caves, and a bar, known as a point bar, builds on the convex bank opposite. The material caved from the concave bank is deposited on the next downstream point bar that is on the same side of the stream as the bank from which the material caved. This tends to constrict the channel, but to compensate for the constriction the concave bank caves across the river from the point bar on which the deposit occurred. When the caving and deposition process is such that the average cross-sectional area does not change materially except for changes that must accompany alterations in shape to maintain transporting capacity, the stream may be said to be in balance. Banks will cave, and bars will build at compensating rates. However, as bends lengthen or are eliminated by cutoffs, the elements that must be adjusted to attain the condition of balance are changed. It is doubtful, therefore, that an alluvial stream is ever quite in balance. The growth of a long bend, for example, can flatten slopes upstream, and, consequently, for a short time, erosion above and the material delivered to the point bars in the bend are reduced. Erosion in the bendway continues, enlarging the channel and lessening the slope and velocity. This action reduces erosion in the bendway, and, as a result of the diminishing amount of bed load reaching the next bar downstream, a similar reaction occurs there and so on down the river. The flattening of slopes down-

stream causes slopes above the bendway in question to increase once more. In turn, this causes a whole series of counterreactions tending toward the re-establishment of the original conditions. The foregoing assists in partial visualization of the continual changes taking place. The realization of this fluid condition and the knowledge that erodibility varies from place to place furnish an understanding of the serpentine movements of an alluvial stream. There is no true balance since the condition viewed as balance presupposes a condition of change.

The only differences between a stream with freely erodible bed and banks and a stream with bed and banks that are more difficult to erode are variations of degree and time. If a large amount of material is delivered to a reach that is not readily erodible, slopes and channel dimensions will be established so that part of the material is transported downstream past the point bars. The amount deposited on the point bars will be the amount sufficient to compensate for the scour on the opposite bank. It can easily be seen that in a reach in which the bed and banks are practically nonerodible, the material delivered will deposit only in sufficient amount to create the necessary transporting capacity. Thereafter, material delivered will be carried through the reach.

Effect of Diversion on River Channel

Effect Above the Diversion.—Since the stage is reduced at the point of diversion, the slope of the water surface upstream is increased. This effect may be either permanent or temporary depending on the erodibility of the bed and banks upstream. If the banks are relatively resistant to erosion and the bed is easily erodible, the channel will deepen. The slope will gradually flatten immediately upstream from the diversion while the slope further upstream will steepen. With this progressive erosion of the bed, stage reduction caused by the diversion will extend farther and farther upstream. The extent of this reduction influence depends on the ability of the bed to support a steeper slope than the river had before the diversion was made. Resistant areas in the river bed will have a great effect on the extent of diversion influence or at least will delay its upstream movement. Except for the existence of resistant areas and the possibility of the bed supporting slightly increased slopes, no limit can be visualized under the conditions assumed, unless the diversion and the river below it are incapable of transporting the bed load carried to the point of diversion. In this case, the building up of the river and the diversion will limit, at least temporarily, the upstream effect of the diversion by lessening the stage reduction.

If the bed and banks upstream from the diversion are easily erodible, a deepening of the channel probably will still occur but only temporarily, for bank caving will be accelerated. The bank caving will operate to lengthen the channel and thereby reduce the slope. In this instance, also, the effect of the diversion on the river above may be reduced by the inability of the diversion and the river below the diversion to carry away the added bed load resulting from the accelerated bank caving.

Effect Below Diversion When Bed and Banks Are Resistant.—Should the banks and bed of the river channel below the diversion be highly resistant to

erosion, the diversion may have little effect on that channel except over a long period of years, and the material carried past the diversion may pass downstream without consequence. If the bed load is lessened more than the transporting capacity of the river, there may be a depression of the water surface elevations in addition to that attributable to lowered discharge, because the channel section formerly occupied by bed load will, after diversion, be occupied partly by water. It should be remembered, however, that the channel was carved to its existing size and shape through the interaction of varying the discharge rates, the slope, and the bed load. The regimen will have been disturbed by the diversion so that the process of adjustment will be activated. To visualize the interaction of these features, first assume that the stream before diversion was transporting bed load to the limit of its capacity, and that the diversion reduces the discharge but does not change the amount of bed load delivered to the channel downstream. The transporting power of the stream will have been reduced so that deposits will occur in the channel. These deposits may manifest themselves both as a general filling of the bed and in the formation of bars that reduce the cross section of the channel to conform to the changed discharge rates. The slope is increased by the reduction in cross section, and as the slope increases, the transporting power of the stream increases until eventually it is able to transport the material delivered to it. The filling should be most rapid in the first reach below the diversion and gradually work downstream.

Now assume that the bed load is diverted without reduction in downstream discharge. This is a hypothetical condition that could be induced only through an increase in the discharge above the diversion in amounts equal to the water diverted. Presupposing a balance below the diversion before its construction or occurrence, at the existing slopes the stream will easily be able to transport the material that passes the diversion. Because of the reduced quantity of bed material, stages and slopes will probably be lowered slightly, but since the bed and banks are resistant, no other changes should be evident for many years. Slowly, however, the stream will erode its channel so that eventually it creates for itself a channel area and slope that is in balance with the bed material transported.

With a decrease in the water quantity below the diversion, the bed tends to build, and bars tend to form so that the slope is increased; and with the bed load decreased, the bed tends to scour and the slope tends to diminish. With both water quantity and bed load decreased, the course of action will be determined by the change that is predominant. From preceding discussion, it appears that unless the diversion is located with respect to river bars, bends, and sediment path, in such a manner as to withdraw a minor portion of the bed load, the transported material will be reduced disproportionately to the reduction in discharge. Thus, the channel below the diversion should transport the bed material carried past it without filling, and there should be a long-time trend toward scour. Before the conclusion can be drawn that a disproportionate amount of the bed load will be diverted, however, the locations of the bed, bar, and paths of sediment near the entrance to the diversion at all stages should be studied. It should be remembered that the configuration of the

stream changes in its cycle from high water to low water, so that although the diversion may withdraw a large part of the bed load at one phase of the hydrograph, it may withdraw a much lesser proportion at another phase.

Effect Below Diversion When the Bed Is Erodible and Banks Are Resistant.—The preceding discussion applies equally well to channels with erodible beds and to those with erodible banks. There are some minor variations, however. In a channel with erodible bed but resistant banks, a reduction in the discharge without a corresponding reduction in bed load will reproduce almost exactly the action that was described for the nonerodible channel. Bars will enlarge, and the bottom will elevate to produce a slope capable of transporting the bed load with the lesser volume of water. If the bed load is reduced without proportionate reduction in discharge, and if a balance between transporting capacity and bed load originally existed, the bed of the stream just below the diversion will start scouring immediately. If, in the first reach or two below the diversion, sufficient material is placed in motion to replace the material withdrawn by the diversion, the channel farther downstream will experience no effect from the diversion for some time. The scour in the upper section will reduce the slope, and the capacity to erode and move material in that section. Thus, the stream enters reaches farther and farther downstream with unsatisfied transporting capacity. As a result, the scour of the bed proceeds in a downstream direction. This differs somewhat from the stream with bed and banks that are difficult to erode. At no location will the latter have its transporting capacity satisfied, so slow erosion may occur simultaneously throughout the entire stretch of the stream below the diversion.

Effect Below Diversion When Bed and Banks Are Erodible.—Should the condition be such that both the bed and banks below a diversion are eroded with relative ease, a reduction in discharge without a reduction in bed load will probably result in a retardation of the bank caving for a period except at points that are not well accommodated to the curvature appropriate for the reduced flow. The bed will rise, and bars will grow rapidly until the slope has been increased to an extent that will enable the stream to transport the bed material being delivered to it. Filling and bar building will proceed in a downstream direction, as the bed load will be deposited first in the reach immediately below the diversion. It is at this point that the effect of reduced transporting capacity is first felt. This reach will fill and increase its slope rapidly. As soon as filling has proceeded sufficiently, bank scour will be accelerated. Material will be carried to and perhaps beyond the next point bar, and the cycle is repeated there and continues downstream. The lag in the downstream direction occurs only in the beginning of the cycle. No cycle is completed before activity in the next bend or reach begins. The net result is that the slope of the entire stream below the diversion is increased, and the cross-sectional area is modified until there is a balance between bank caving and material deposition. Thereafter, if the banks erode with the necessary ease, the amount of material caved from the banks should be about the same as it was prior to diversion, since there was assumed to be no change in the amount of bed load moved and presumably deposited on point bars which must be compensated for by scouring of the opposite bank.

In the case of the hypothesis that the bed load is reduced by the diversion but the amount of water below the diversion is not changed, the initial action when both bed and banks are easily erodible will be much the same as the case in which only the bed was erodible. The bed and banks of the first reach below the diversion will scour and supply bed load to the next and succeeding reaches. As scour occurs in the first reach below the diversion, the cross section there is enlarged, and the slope and velocity are reduced. The rate of erosion diminishes so that sufficient material is not supplied to the next downstream reach to maintain its balance. The bed and banks of the next reach begin to scour and so on throughout the whole stretch of the river below the diversion, or of that part that has erodible bed and banks. Eventually, the cross-sectional area is increased, and the slope is reduced to reach a balance between transporting capacity and the amount of material moved as roughly represented by the amount passing the diversion. Thereafter, the river below the diversion will act as a balanced stream flowing through erodible material. To a great extent, the material passing the diversion will be deposited on the next point bar, and bank caving and meandering should proceed at a rate that will compensate for this deposition. Since the amount of material passing the diversion was assumed to be less than before diversion, even though the condition of no reduction in discharge was imposed, bank caving should be retarded. It should be noted, however, that velocities were reduced, and banks that may be considered freely erodible at one velocity may not be so freely erodible at a lower velocity. Accordingly, some of the bed load carried past the diversion may not be deposited on the next point bar but may be carried farther down the channel in the manner represented by the central diagram of Fig. 5. The result of this action would be a further reduction in the rate of bank caving.

In the case of an actual diversion in which bed load is withdrawn in disproportionately large amounts in relation to the quantity of water diverted, the flattening of the slopes below the diversion will reduce stages at its entrance, thereby lessening the amounts diverted and increasing the slopes and bank caving upstream. These results will tend to cause more bed load to pass below the diversion entrance. Thus, the flattening of the slopes below the diversion is partly resisted by the effects that it causes; however, the rates of accelerated bank caving above the diversion are gradually reduced as the steepened slopes are extended farther and farther upstream. Finally, a balance is reached in which the slope and rate of erosion below the diversion are less than before commencement of diversion, but greater than were the caving upstream from the diversion not accelerated and the amount of diversion not reduced by the lowered stages resulting from the flattened slopes downstream.

Action in the Diversion Channel

The action in the diversion channel is no different from that in any stream channel. If the diversion has been so located that it withdraws a large proportion of the bed load, its slope, cross section, and the amount of water diverted must be adequate to transport the material, or filling in the diversion channel will occur. The filling will reduce the water and bed load entering the diversion and thus raise stages at the head of the diversion. This increases the slope

in the diversion unless the stage increase is prevented by the enlargement of the main stream below the diversion. If the slope is increased in this manner and the bed load is reduced sufficiently to enable the discharge in the diversion to transport the bed load withdrawn from the main stream, a condition of quasi balance will eventually be created similar to the balance in an alluvial stream as previously discussed. Bends will form if the banks are erodible, and the diversion will act as a normal stream in an alluvial bed. However, the slope increase is limited by the stage in the main stream that existed before the diversion was made. In fact, if scour occurs in the main channel below the diversion, the limit of slope increase will be still lower. The attainment of this limit requires the complete closure of the diversion. Thus, an explanation may be offered for the closure of natural outlets in the past. When sufficient slope cannot be attained to transport the material deposited at, and carried into, the head of the diversion, its channel will fill, with a large amount of the material deposited near the head of the diversion in the form of a bar. At high water this bar may be elevated so that the succeeding low water will be below the crest of the bar, and no water will be diverted at that time. When the river stage again exceeds the crest elevation of the bar, a large amount of material will be carried over the bar for a brief period, widening it and further reducing the flow and transporting capacity across the bar and in the rest of the diversion channel. As a result, the bar will continue to be elevated. Eventually, its crest will be topped only by high stages. This is the probable action that takes place when a high bar forms across the entrance to the old bendway channel at the head of a cutoff.

For a diversion designed and located to withdraw a minimum of bed load, the action will be the same as discussed above for the river below the diversion with a disproportionate decrease in bed load. With easily erodible bed and banks, scouring will occur in the diversion channel immediately below the entrance. This will increase the flow into the diversion which in turn will increase the rate of scour, unless the withdrawn bed load is increased in proportion to the increase in discharge. The scour will proceed in a downstream direction, enlarging the entire diversion. The diversion will continue to enlarge until: (1) Sufficient material is drawn from the main stream to inhibit further enlargement; (2) a delta of sufficient length to reduce velocities below scouring magnitudes is built out from the outlet of the diversion; or (3) a portion of the diversion develops a braided channel to an extent capable of increasing stages and reducing velocities so that discharge increase is stopped, and scouring velocities no longer exist.

A diversion constructed with a slope greater than that required to carry the bed load delivered to it will act in a manner similar to the diversion that extracts a relatively small amount of bed load from the main stream. It will scour its bed and banks, and, if compensating factors such as increase in bed load or delta building do not develop rapidly enough, the main stream may adopt the diversion for its ultimate course. This situation is illustrated by a cutoff across a narrow neck of a bendway that quickly becomes the main channel.

Planning the Diversion Entrance

Should there be a choice in locating the diversion entrance, many of the factors discussed above will affect that choice as well as the layout of the diversion. Four of the major considerations are:

(a) *Relation to the Point at Which Reduced Stage is Desired.*—If the purpose of the diversion is the reduction of flood stages, it appears preferable to locate the diversion above the stretch in which the stage reduction is desired, unless this location places a large storage area within the range of drawdown influence.

(b) *Increase in Velocity.*—The entrance to a diversion should be located upstream from the stretch in which an increase in velocity is undesirable, either from the standpoint of navigation or of acceleration of bank caving. If an upstream location of the diversion's entrance is not practicable, it should then be located as far downstream as possible.

(c) *The Angle of Diversion.*—The angles between the entrance to the diversion, the main stream, and the bed-load path will affect the amount of bed load withdrawn.

(d) *The Site at Which the Diversion Leaves the River Channel.*—The amount of bed load withdrawn will depend on the point at which the diversion is made from a river channel. A diversion entrance cut through a bar or located near the bed-load path will withdraw a large amount of material. One located far from the bed-load path will withdraw little material.

Conclusions

Each diversion contemplated from an alluvial stream must be given intensive study. Effects have been sufficiently discussed in this paper to permit an estimate of the results to be expected if all necessary factual data are obtained. Though a diversion from an alluvial stream cannot be designed to accomplish desired results with the exactness of other engineering design, thorough analysis will produce a design that will approach the ends desired and will remove many of the uncertainties. A qualitative analysis may be possible, but a quantitative analysis is apparently still beyond the capabilities of present scientific knowledge. Quantitative predictions involving the time factor can be approached only by statistical study of past occurrences and by model experimentation. The latter is costly and difficult. It is almost an impossible task to reproduce to scale all the conditions found in a natural stream. However, at the present time model experiments offer the most promising method of securing a quantitative approximation of results in which confidence can be reposed. Continued study by the engineering profession may yet bring forth a thoroughly scientific approach.

DISCUSSION

T. Blench,[10] M. ASCE.—Valuable features of this interesting paper include the following:

1. A quantitative example of the effect of storage in producing the well-known difference between rising-stage and falling-stage river rating curves;
2. A nonmathematical discussion of unsteady flow; and
3. A qualitative discussion of the interconnection of water and sediment diversion, and their effects on regime.

The phenomenon of item 1 is often attributed to sediment movement only. The example shows that it can be explained entirely by capacity effect. It also shows that the relieving effect of a floodway may be much less than the floodway discharge. However, there is no statement of the volume of storage assumed, and no statement as to whether it would correspond to a lake (implying no sediment downstream), to the spill of a plains river at high stage, or to the capacity of an incised river. Would the author kindly elucidate?

Item 2 should be valuable because the intractability of the differential equations tends to drive engineers away from the subject. Their fear is unfortunate, for mathematics answers "how much," but common sense and perseverance answer "how" and, often, "approximately how much."

Item 3 quotes exhaustive and good American information. Experience gained in India can confirm and extend the information from America. The movement of coarser bed sediment to the inside of a curve must have been forced on the attention of oriental inundation canal builders from time immemorial, and the writer has found that illiterate cultivators on Indian canals know about it. The phenomenon is the basis of action of all sediment-excluding devices for canals, and has been examined in models and verified from prototypes by Sir Claude Inglis,[11] M. ASCE. Perhaps its most striking use was the construction of a curved approach to the Sukkur Barrage, on the Indus River in Sind, Pakistan, on Sir Claude's recommendation, to cause coarse bed sediment to deflect away from the canal heads and over the barrage. The writer can confirm that the coarser grades of bed material are more susceptible to the differentiating action of curvature of flow, so that excluders for very coarse sand and fine gravel can be 100% efficient, whereas for 0.20-mm sand they cannot be expected to achieve much; the reason presumably lies in the different settlement velocity laws. Experience in India also indicates that the size of the bed sediment is a major factor in determining regime slope, whereas the suspended load is of little importance.

---

[10] Cons. Engr. and Associate Prof. of Civ. Eng., Univ. of Alberta, Edmonton, Albta., Canada.

[11] "The Behaviour and Control of Rivers and Canals," by Sir Claude Inglis, *Research Publication No. 13*, Central Waterpower Irrig. and Nav. Research Station, Govt. of India, Poona, Bombay, India, 1949, Chapter 6.

The writer would modify the author's conclusion that "* * * model experiments offer the most promising method of securing a quantitative approximation of results in which confidence may be reposed." Bed material in models is often quite unlike that of the prototype; investigators probably never make any attempt to show the difference in bed material between parent and offtakes and are handicapped by the fact that the bed-load charge cannot be measured in the prototype. Such models cannot deal with regime developments arising from sediment differentiation into offtakes, as so ably discussed by the author; for answering questions about rate of development of sediment phenomena the models must be equally unreliable. They would improve if devised to take cognizance of the sediment behavior of the prototype (assuming that the scale is large enough to keep in the proper range of behavior). This fact requires that they should be used along with scientific analysis of the prototypes, requiring patient field investigation. For scientific field analysis, there is a need for a basis of theory, which is provided at present by regime theory.[12,13] Consequently, the writer would state the requisites of a proper investigation to be (*a*) models, (*b*) field observation, and (*c*) theory applied to field and model results.

Generally, all three are required to reinforce one another, but items (*b*) and (*c*) combined should render item (*a*) unimportant in many cases, whereas

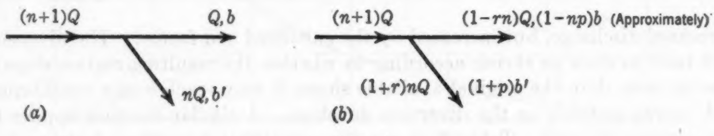

FIG. 6

item (*a*) alone is of little value without the others. Of course, this view refers to the use of models for the problems under discussion, not for problems of a quite different type.

In the writer's experience, theory has been found to fit river data very well where special circumstances have allowed it to be checked. For example, the distribution of bed sediment size between parent and diversion, after regime has been attained, fits with discharges and slopes according to regime theory; the size of assisted cutoff (for a meander) that will develop itself when opened is given reasonably by theory. The following problem should indicate what theory can do, why the author's appreciation of the factors controlling behavior is so important, and why models should be devised to work in terms of those factors if their present status is to be improved; the problem was suggested to the writer by the Atchafalaya Diversion, as described by Leo M. Odom,[14] M. ASCE.

Fig. 6 (*a*) shows a parent channel of dominant discharge $(n + 1)Q$ splitting into a diversion of dominant discharge $n\,Q$ and a residue of Q. Because of the

[12] "Hydraulics of Sediment Bearing Canals and Rivers," by T. Blench, 1951 (available from author).

[13] "Civil Engineering Reference Books," by E. H. Probst and J. Comrie, Butterworth's, London, England, 1951 (Chapter on "Canals, Channels and Rivers").

[14] "Atchafalaya Diversion and Its Effect on the Mississippi River," by Leo O. Odom, *Transactions*, ASCE, Vol. 116, 1951, p. 503.

approach conditions to the diversion, its bed factor is b' whereas that of the residue is b. The system is in regime. Fig. 6 (b) shows the conditions just after engineers have developed the diversion to take discharge of fractional amount r in excess of the previous amount, and have altered the approach conditions into the diversion, so that the bed factor there exceeds the previous one by a fraction p. What will happen?

The answer, qualitatively and very briefly, assuming that p and r are positive, is that the regime slope of the diversion will be reduced by the

TABLE 3.—INITIAL PERCENTAGE INCREASE IN REGIME SLOPE, FOR $n = 30\%$

Values of p	(a) Percentage increase of regime slope in diversion after excavating and altering approach conditions				(b) Corresponding increase in the residue's regime slope			
	Values of r, the fractional flow in excess of the previous amount:							
	1.0	0.5	0.25	0	1.0	0.5	0.25	0
0.0	$-16\frac{2}{3}$	$-8\frac{1}{3}$	$-4\frac{1}{6}$	0	+5	$+2\frac{1}{2}$	$+1\frac{1}{4}$	0
0.1	$-8\frac{1}{3}$	0	$+4\frac{1}{6}$	$+8\frac{1}{3}$	$+2\frac{1}{2}$	0	$-1\frac{1}{4}$	$-2\frac{1}{2}$
0.2	0	$+8\frac{1}{3}$	$+12\frac{1}{2}$	$+26\frac{2}{3}$	0	$-2\frac{1}{2}$	$-3\frac{3}{4}$	−5

increased discharge, but increased by the enhanced bed factor. The diversion will tend to grow or shrink according to whether the resulting regime slope is less or more than the original available slope; it may reach a new equilibrium if b' grows suitably as the diversion develops. A similar solution applies to the residue channel. Table 3 shows the quantitative answers from regime theory, and would direct an investigator to observe the proper site data and to make a suitable model.

SERGE LELIAVSKY,[15] M. ASCE.—The problem of the withdrawal of sediment from alluvial rivers into side channels is ably discussed in this paper. Apart from its general importance, it is of specific interest to irrigation engineers in connection with headwork design because the volume of heavy sediment which is deviated from the parent channel into a distributory or main canal determines to a large extent the operational maintenance expenditure of an irrigation system. If one realizes that the annual cost of canal clearances in the budget of the Egyptian Irrigation Service is measured in millions of pounds, it will be obvious that the problem under consideration must be a matter of deep concern to those in charge of these works.

In particular, within the last decade, a new approach to this problem has been initiated by a group of designers led by Abdel Azim Ismail Bey,[16] Director General of Reservoirs. They center their attention on the local asymmetry of the flow pattern at the intake of the siding. The importance of this pattern lies in its adverse effect on the efficiency of the defensive devices

[15] Cons. Engr., Cairo, Egypt.

[16] "Treatment of Heavy Silt in Canals," by Adbel Azim Ismail Bey. Report to the Second International Technical Congress, Cairo, Egypt, 1949.

commonly used to reduce the part of the bed load taken by the side channel, such as the various types of sand screens, sills, and weirs.

As a main parameter of the asymmetry of the flow, the analyst usually takes the angle between the parent channel and the diversion, which is termed the "angle of twist" by the new school (apparently the "angle of diversion" according to the author's nomenclature).

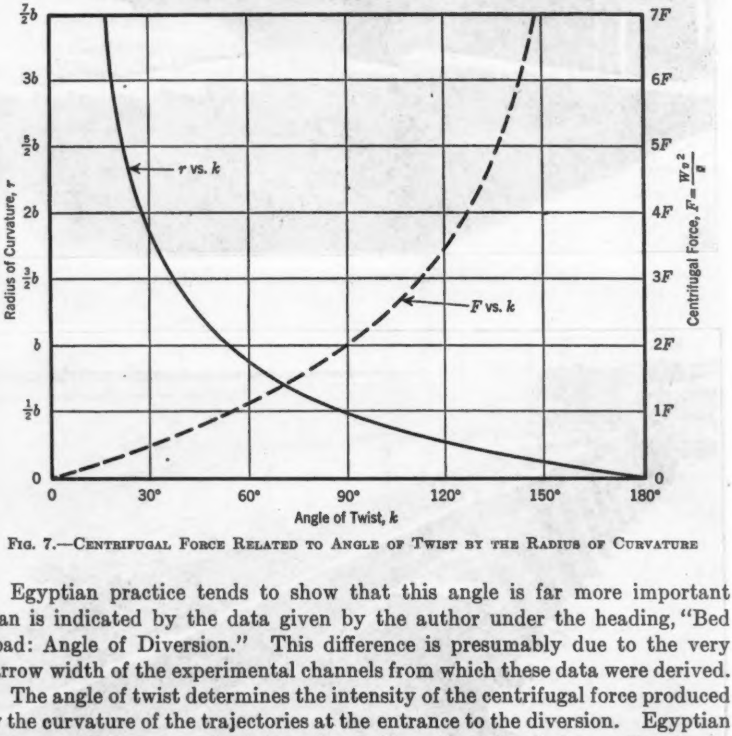

FIG. 7.—CENTRIFUGAL FORCE RELATED TO ANGLE OF TWIST BY THE RADIUS OF CURVATURE

Egyptian practice tends to show that this angle is far more important than is indicated by the data given by the author under the heading, "Bed Load: Angle of Diversion." This difference is presumably due to the very narrow width of the experimental channels from which these data were derived.

The angle of twist determines the intensity of the centrifugal force produced by the curvature of the trajectories at the entrance to the diversion. Egyptian engineers of the new school therefore believe that the division of sediment between the main and secondary channels is a function of this angle. Fig. 7 is a tentative diagram giving the average radius of curvature in terms of b, the bed width of the diversion, and as a function of the angle of twist. In the expression for centrifugal force, W is the weight, v is the velocity, and g is the acceleration produced by gravity. The chart was prepared by the writer from theory, experiments, and observations.

The centrifugal forces constitute the main local factor governing the behavior of the sediment at the entrance to the diversion. The difference between the centrifugal force at the surface and that at bed level produces a helicoidal flow pattern in which the heavily silt-laden filaments of the water in the main channel rise to the surface, entraining their charge of coarse bed load

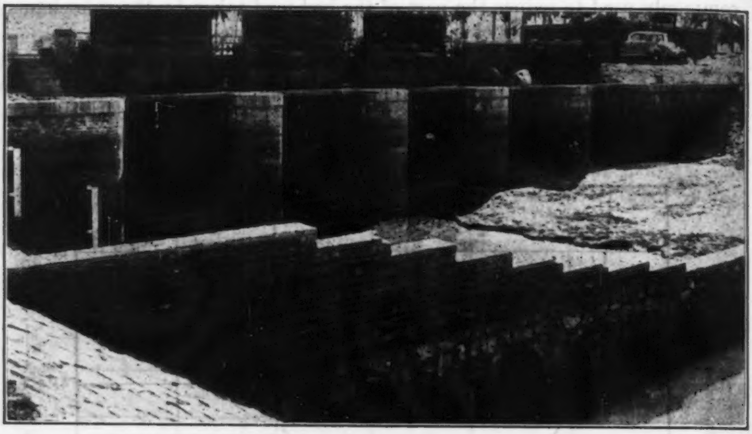

FIG. 8.—SAND SCREEN WITH SLOPING SILL AT ABOU-EL-AHDAR

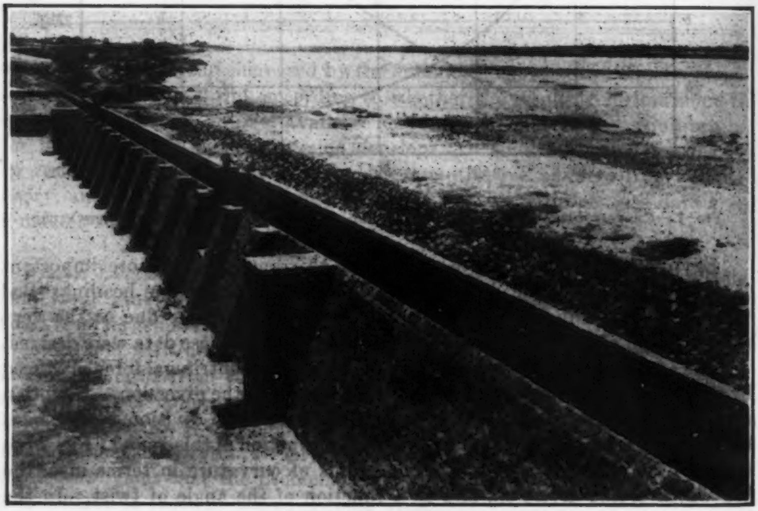

FIG. 9.—HEAD REGULATOR OF KELABIA CANAL, WITH A DISCHARGE OF ABOUT 8,500,000 CUBIC METERS PER DAY (ABOUT 12,507,000 CU FT PER HR)

into the diversion over the sill of the sand screen. When there is no sand screen, the same three-dimensional mixing effect, by upsetting the pattern of sediment distribution typical of straight channels, increases the volume of the coarse bed load being deviated into the siding. For this reason, the angle of twist may play a more important part than would appear from the paper.

The individual links in the logical chain which led to this conclusion have been either confirmed theoretically or verified by model tests at the Delta Barrage Laboratory in Egypt. Characteristically, the final proof of this chain is believed to be supplied by the consistently satisfactory performance works designed on the angle-of-twist principle. In fact, in order to fight asymmetry of flow, the screen itself must be asymmetrical; that is, the sill of the sand screen must not be made level but should be on a slope determined by the angle of twist.

Fig. 8 illustrates one of the earliest designs prepared according to this idea. The steep slope of the rigid sill of the permanent sand screen should be noted. This design decreased the silt deposits in the controlled canal, but was not fully satisfactory, as evidenced by the bank or shoal that is seen to have formed

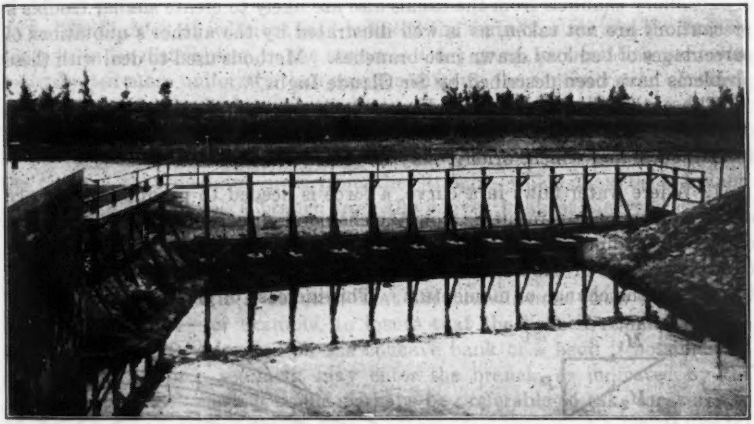

FIG. 10.—SAND SCREEN WITH UPRIGHTS FOR FLUSH BOARDS, AT BAHR TIRA CANAL; DISCHARGE ABOUT 2,500,000 CUBIC METERS PER DAY (ABOUT 3,700,000 CU FT PER HR)

on the upstream side of the entrance. Such a shoal (and its counterpart, the scour hole on the downstream side of the entrance) is the result of the helicoidal flow pattern, and, therefore, increases with the angle of twist, if its effect is not counteracted by a properly designed sloping sand screen. It is usually symptomatic of heavy silt deposits in the canal.

Further ameliorations of the idea were as follows: (*a*) The sloped sill was extended over the entire width of the weir so that the sill slope approximated more closely that of the surface of the vortex as shown in Fig. 9, and (*b*) the level of the sand screen was made adjustable, depending on the changes of water level in the parent channel. A design embodying these improvements is shown in Fig. 10. The sand screen in this case is provided with metal uprights designed to carry flush boards. When in operating position, the tops of the flush boards are arranged step-wise, in accordance with the calculated slope.

The saving in clearances caused by these advancements in screen design is sufficiently great to confirm the angle-of-twist theory.

A rather curious point about this theory is that it must have been felt intuitively by the ancient Arab engineers, who were in charge of Egyptian irrigation for more than a thousand years, because they always tended to place their intakes at the concave bank of the Nile (as suggested by the author) but with the axis of the diversion tangent to that of the river. The angle of twist was thus reduced to nearly zero. From this standpoint, the layout of diversion No. 4 in Fig. 4 is definitely an anomaly.

A. R. Thomas,[17] M. ASCE.—The tendency of branch channels to draw excessive bed load has for many years been a problem in India, where irrigation canals are supplied by diversion of water from alluvial rivers. Canals which draw water at points unfavorably located with respect to the curvature of the parent river quickly lose capacity through the deposit of sand or silt. Offtakes of subsidiary channels from the canals also are likely to create similar trouble if precautions are not taken, as is well illustrated by the author's quotations of percentages of bed load drawn into branches. Methods used to deal with these problems have been described by Sir Claude Inglis.[18]

The author has given several possible causes for the excessive bed load drawn into branches. In the writer's opinion there is one explanation which is fundamental and which, briefly, may be stated as follows:

1. Where water flows in a curve, a force is needed to produce the change of momentum of flow resulting from the change in direction of flow. In a river or curved channel, the water level rises toward the outer concave bank, the transverse slope of the surface representing the increase of pressure required to produce the change of momentum. This increase of pressure is uniform on

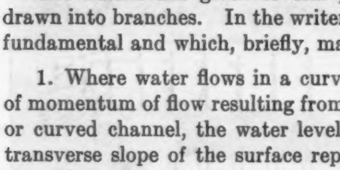

Fig. 11.—Vector Diagrams (M_1 = Initial Momentum, M_2 = Deflected Momentum, P = Lateral Force Due to Transverse Pressure Gradient, Equal in Each Case)

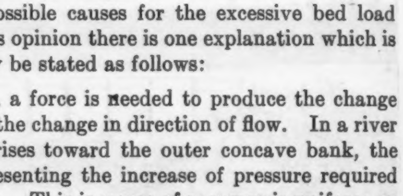

Fig. 12.—Diagrammatic Plan, Showing Flow Lines (Surface———Bed— — —)

any vertical; that is, at any point in plan the pressure increase is the same in the water near the surface as in the water vertically beneath. The forward velocity of flow is greater at the surface, however, than near the bed so that, with the same force acting on each, due to the same pressure gradient, the flow at the bed is deflected more than the flow at the surface, as will be clear from Fig. 11, showing vector diagrams of change of momentum of small

---

[17] Res. Engr., Stewart, Sviridov & Oliver, Queenstown, Union of South Africa.

[18] "The Behaviour and Control of Rivers and Canals," by Sir Claude Inglis, *Research Publication No. 13*, Central Waterpower Irrig. and Nav. Research Station, Govt. of India, Poona, Bombay, India, 1949.

imaginary prisms of water at the surface and bed. The difference between the angles is reduced by the interchange of momentum due to turbulence and by bed friction; but the general result is that the mean curvature of surface flow in plan is less than the mean curvature of the channel, whereas the mean curvature of bed flow is greater, as shown in Fig. 12, producing the well-known feature of cross flow at bends and surface water diving at the concave bank.

2. Similar action occurs at a branch. If the main channel is straight and the branch is at an angle to it, the flow entering the branch is curved and the slower-moving bed water will be deflected more sharply toward the branch channel than the surface water, with the result that the branch draws a larger proportion of bed water. If the branch begins on the concave bank of a curved channel, however, so that the flow is deflected less in entering the branch than in following the main channel, the branch will draw a larger proportion of surface water.

3. The division of sediment load between the main channel and the branch depends on its distribution in the stream. On a given vertical, fine sediment is distributed more uniformly than coarse sediment, the concentration of which increases toward the bed. The tendency, therefore, is for the fine sediment to be distributed in proportion to the ratio of the discharges and the coarse sediment (including the bed load) to be drawn in excessive proportion into the channel that deviates most from the straight, which may be a branch from a straight channel, a branch from the convex bank of a curved channel (as shown by the author in discussing the data relating to Fig. 4), or the main channel, if the branch is from the concave bank.

It follows that, if it is required that the branch must draw a minimum of coarse sediment—for example, to insure that the branch remains open—the branch should be located on the concave bank of a bend if possible. If this bank is eroding, sediment may enter the branch, as indicated by the author, but in such cases it would perhaps be preferable to take measures to prevent the bank erosion rather than to locate the branch at a less favorable point.

In India, Sir Claude developed the possibilities of using the curvature of flow to control sediment load and used this method in several cases. The most spectacular was perhaps at the diversion of the Mithrao Canal from the Eastern Nara River in Sind, where the angle of the diversion was acute and the canal was drawing excessive coarse sediment. After a series of model experiments, in which the directions of flow of surface, mid-depth, and bed water were clearly seen, the old diversion was closed, a bend was formed in the river, and a new approach channel (with a diversion on the concave bank) was provided for the Mithrao. The remedy was so effective that a canal with a diversion from the river downstream began to draw excessive sediment, and further measures had to be taken to increase the proportion of sediment drawn by the Mithrao.

It is to be noted that the control of sediment load by the curvature of flow requires a "normal" velocity distribution decreasing from a maximum at the surface to a minimum at the bed. If the velocity is equalized by a contraction of

the channel immediately upstream from the diversion, excessive turbulence, or other cause, or if the sediment distribution is equalized, the sediment load will be divided in nearer proportion to the discharge. Models provide an excellent qualitative indication of what is likely to occur in the prototype, but as curvature effects are usually exaggerated in vertically exaggerated models, the effect of scales must be considered in judging the results.

D. C. BONDURANT,[19] A. M. ASCE.—The author's presentation of the withdrawal of sediment by diversion focuses attention on a phenomenon which is too frequently neglected in the planning of diversion systems. In distinguishing so sharply between bed load and suspended load, however, he has tended to obscure an important phase of the action. His description of the nature of the phenomenon would have been strengthened by greater emphasis on the role of the slower currents in the lower levels of the flow.

In his statement that Red River sand is rather fine, so that some sand may have been carried in suspension, the author infers that only fine sands may be carried in suspension. He proceeds from this inference to the statement that sand in suspension would divide approximately in proportion to the division of water quantities. This is in line with his prior concept that suspended load, as differentiated from bed load, divides at a diversion approximately in direct proportion to the division of water quantities. Actually, the suspension may contain sand ranging in size from fine to coarse. These sands are ordinarily found in greater quantities near the bed of the stream, with the concentration decreasing toward the surface. As noted by the author, the slower currents near the bed are the more easily diverted, and since the concentration of suspended sands is greater at that level, the suspension also contributes to the imbalance of the diversion.

The distribution of suspended sediments in a stream is a function of the size of sediments, turbulence of the flow, and material available. Materials in the size range of silts and clays, which settle in water in accordance with Stokes' law, are normally found to be evenly distributed throughout the flow. The finer sands may be fairly well distributed, but will be found in somewhat greater quantities near the bed. With the increasing size of the particle, the distribution becomes more unbalanced, and the proportion found at the lower levels of the suspension increases. With the increasing turbulence of the flow, the distribution of the sands in suspension becomes more even. At some stages of the flow, material that normally travels in the form of dunes along the bed is swept into semisuspension, traveling as a fluid mass near the bed.

The distribution of sand-size sediments, as measured in the Missouri River near Omaha, Nebr., on October 18, 1951, is shown in Fig. 13, together with the velocity distributions and the bed material distributions determined with each series of measurements. These distributions (which are typical of a large number observed) were made from a boat anchored in a straight reach of open river which was relatively free from extraneous influences. Measurements were made at the depths shown on the velocity curve, velocities being observed

[19] Head, Sediment Section, Missouri River Div., Corps of Engrs., U. S. Dept. of the Army, Omaha, Nebr.

with a Price type current meter and sediment being sampled with a point-integrating (P-46) sampler.[20] Bed material samples were obtained at each vertical with a BM-48 (clamshell type) sampler which samples only the top 2 in. of the bed. The two verticals shown were measured on the same day at different points on the same cross section, and the two are presented to illustrate the variation of the distribution of sediments with the variation in turbulence of the flow. The measured data, plotted logarithmically by size fractions, fol-

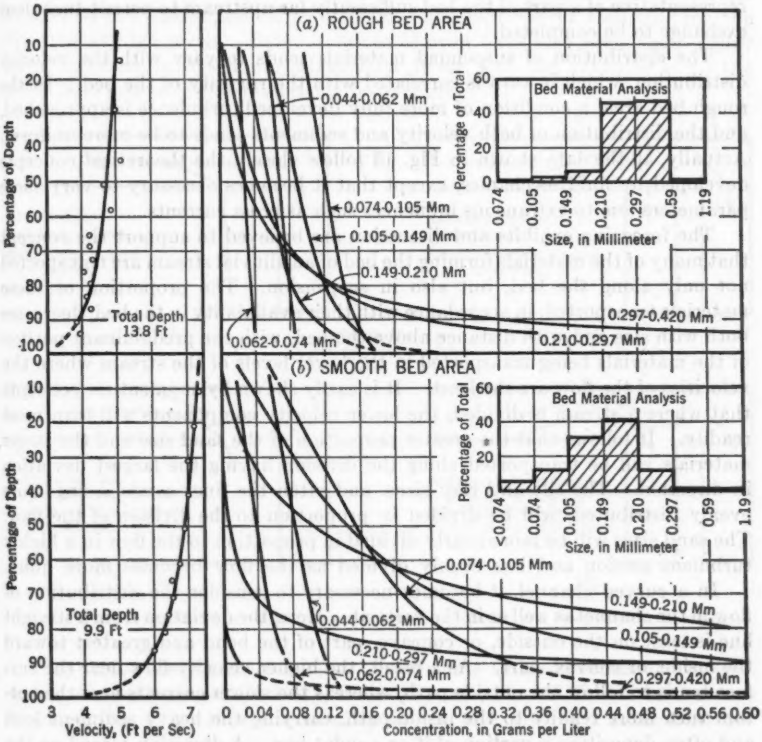

FIG. 13.—DISTRIBUTION OF SEDIMENT AND VELOCITY, MISSOURI RIVER AT OMAHA, NEBR.

lowed very closely a straight-line plot which was extended to obtain the concentrations below the lowest points measured (dashed parts of the curves). In the examples presented, materials finer than 0.044 mm are not shown.

It will be noted that the concentrations of the larger sand sizes increase as the bed is approached, and that this proportionate increase is greater as the size of the particle increases. There is also a distinct correlation between

[20] "Measurement and Analysis of Suspended Sediment Loads in Streams," by Martin E. Nelson and Paul C. Benedict, *Transactions*, ASCE, Vol. 116, 1951, p. 910, Fig. 11.

the predominant sizes of the sand-size material in suspension and the predominant sizes of the bed material. This latter correlation is emphasized when it is noted that it exists in both the examples shown, although the predominating sizes are at variance between the two. It is suggested that the bed samples are each representative of a fairly extensive bed area, rather than of a point, since each vertical was selected so as to be in an area of similar bed characteristics sufficiently extensive to permit the suspension to be representative. It is anticipated that the distribution of the sediment in any vertical would be representative of a part of the bed sufficiently far upstream to permit turbulent exchange to be completed.

The distribution of suspended materials tends to vary with the velocity distribution, which in turn is correlated with the rugosity of the bed. In the rough bed area, a condition of more fully developed turbulence is approached, and the distribution of both velocity and sediments tends to be more uniform. Actually, all the data shown in Fig. 13 follow closely the theoretical concepts developed by fluid mechanics, except that it becomes necessary to vary some parameters due to extraneous influences such as cross currents.

The foregoing exhibits and discussion are believed to support the concept that many of the materials forming the bed of an alluvial stream are transported not only along the bed, but also in suspension. The proportion of these materials transported, in accordance with their availability in the bed, decreases both with size and with distance above the bed, with the predominant portion of the materials being transported in the lower levels of the stream where the velocities of the flow are the least. It is easily shown by momentum concepts that where a stream is divided, the lower velocity components will turn most readily. It follows that the greater proportion of the sand size and the larger materials will be transported along the division having the largest deviation in direction. The silt and clay sizes, and often the finer sands, being more evenly distributed, will be divided in proportion to the division of the flow. The sand sizes will be more nearly divided in proportion to the flow in a highly turbulent section and less evenly divided as the flow becomes more quiet.

In a curved channel, it becomes necessary to consider the distribution of flow in the channel as well as in the vertical. Here, the deviation from a straight line is least on the outside, or concave, part of the bend and greatest toward the inside, or convex, part. As a result, the higher velocity flow near the surface tends to follow the outside path, whereas the slower currents near the bottom turn more readily to the inside path, carrying the heavy sediment load and often depositing a portion of it as a point bar. A diversion placed on the outside of a bend would have little opportunity to receive the coarser sediments even though it diverts the slower currents in the adjacent vertical. A diversion placed on the inside of the bend should receive a very high proportion of the sediment.

In a diversion having a minor take-off angle, the proportion of sediment diverted should be more nearly equivalent to the proportion of water diverted, since momentum forces would not be so predominant. With greater angles of diversion, however, it is doubtful that the degree of turn would affect the division of sediment radically until a point was reached at which the direction

of flow was almost reversed. In this latter instance it might be anticipated that the flow regimen could be so changed locally that more of the sediment would be carried past the diversion.

In respect to diversions in which the bottom is considerably higher than the bottom of the channel, the author states that the diversion will of necessity derive its waters from the higher levels of the stream, and that little bed load will be diverted. In so far as the material traveling along the bed is concerned, he may be essentially correct. Large volumes of sand deposited on farm lands flooded by the Kansas and Missouri rivers indicate, however, that sand may be diverted at high levels. Large volumes of sand have also been noted below levee crevasses on the lower Mississippi River, but the evidence as to the immediate source of this material is inconclusive.

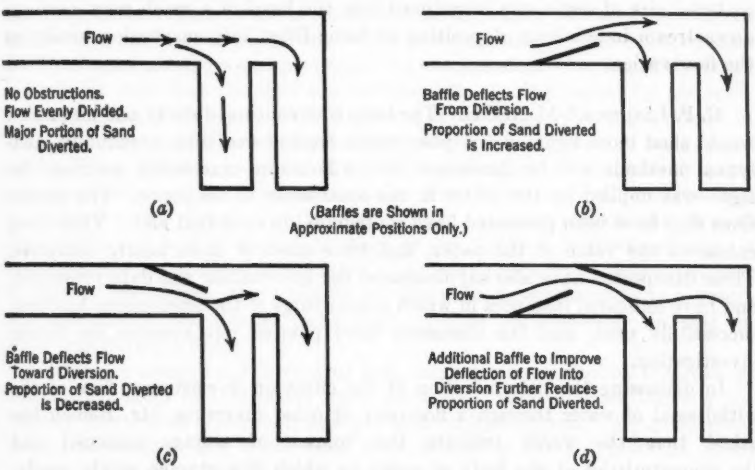

FIG. 14.—SAND BED FLUME WITH DIVERSION CHANNEL TO ILLUSTRATE DIVERSION OF SEDIMENTS

For demonstrating the diversion of sediments to his students at the University of California, at Berkeley, H. A. Einstein, M. ASCE, has used a very simple device (Fig. 13(*a*)), consisting simply of a diversion take-off at 90° and approximately equal division of flow. The student measures the quantities of sand transported, finding that the proportion diverted is much higher than the proportion of water. He is then asked to place deflectors in such a manner as to reverse the proportions of sediment, and on the first trial he usually tries to deflect the current from the diversion (Fig. 13(*b*)), which results in an even higher proportion of sediment diverted. It is only after the deflectors are so placed that the current is deflected into the diversion (Fig. 13(*c*)) that he finds the lesser part of the sediment being diverted. The least diversion of sediment occurs with two or more baffles arranged so that the current flows almost directly into the diversion outlet (Fig. 13(*d*)).

In describing an adjusted or balanced stream, the authór states that material caved from a concave bank is deposited on the next downstream point bar that is on the same side of the stream as the bank from which the material is caved. This is indeed a statement that will be strongly supported by many river engineers and one which is largely derived from the experiments of J. F. Friedkin.[9] It is essentially correct in so far as the material moving along the bed, which is the basis of Captain Friedkin's studies, is concerned. It is also correct that caving and deposition through a reach must be equal if the reach remains in balance. It cannot be postulated, however, that bed material in suspension will not be carried through long reaches, or that the availability of sand size material in transport at any point is dependent upon the caving of a bend or bends upstream. Even in a stream having fixed banks, the bed-material size of sediments introduced into the head of a reach may continue downstream indefinitely, depositing or being lifted into suspension locally as the flow varies.

C. P. LINDNER,[21] M. ASCE.—The hope that continued study and discussion would shed more light on the phenomena treated—so that, eventually, analytical methods will be developed that will assure reasonably accurate design—was implied by the writer in the conclusions to his paper. The discussions that have been presented have contributed toward that end. They have enhanced the value of the paper, and have made it more nearly complete. These discussions have also supplemented the information and data presented, and have indicated instances in which a knowledge of the phenomena has been successfully used, and the discussers have pointed out avenues for future investigation.

In discussing the determination of the effect on downstream flow of the withdrawal of water through a floodway or other diversion, Mr. Blench has asked that the writer indicate the volume of storage assumed and the characteristics of the body of water to which this storage would apply. The storage in the reach for a given elevation at the outflow point changes when the floodway operates. Even if the storage were related to the water surface elevation at the midpoint of the reach, the fact that a sloping stream was used with an unequal distribution of water surface area along its path would cause the storage for any elevation with the floodway operating to be different from the storage for the same elevation with the floodway not operating. It is believed that little purpose would be served by utilizing space to present 2 stage-storage or discharge-storage curves that do not apply to any specific river reach. The storage areas used varied with outflow stage from about 1,000,000 acres to 2,000,000 acres. This would correspond to a large reach on the Mississippi River, probably including a backwater area. Such reaches are used regularly with excellent results in routing flows through that stream.

As an example that may serve to relate quantities and effects in the readers'

[21] Chf. Engr., South Atlantic Div., Corps of Engrs., U. S. Dept. of the Army, Atlanta, Ga.

minds, the Bonnet Carré Spillway (Louisiana) and the reach of the Mississippi River from Red River Landing (Louisiana) to Bonnet Carré may be cited. In this reach, the river is closely confined by levees, or by levees and natural escarpments, so that overbank storage areas are extremely small. In fact, the storage in the reach is about one tenth that of the reach assumed in the paper. The inflow to the reach may attain a peak of 1,500,000 cu ft per sec, a rate only 300,000 cu ft per sec less than that used in the paper. The Bonnet Carré Spillway, at the foot of the reach, was designed to withdraw 250,000 cu ft per sec. This rate is comparable to the rate of withdrawal by the floodway cited in the paper. The stage at the foot of the reach is lowered a maximum of about 3 ft. This stage lowering gradually diminishes in an upstream direction, so that there is little or no effect at Red River Landing, the head of the reach. Thus, a wedge of storage is eliminated by the operation of the Bonnet Carré Spillway. This wedge is small because the entire volume of storage in the reach is not large in proportion to the flow quantities. Moreover, because the eliminated storage is wedge-shaped, the average stage lowering in the reach is probably only approximately one half the 3-ft lowering caused by the spillway at the foot of the reach. If the spillway is opened early on the approach of the flood, this decrease in stage is attained gradually over a period of two or three weeks. When it is remembered that the reach is bounded on both sides by levees and escarpments so that when water reaches these limits, the area for all practical purposes does not change with increase in stage, it can be realized that storage increments per foot of change in stage or per 1,000-cu-ft-per-sec change in discharge are not modified appreciably by spillway operation. Without change in storage increments, there can be no alteration in discharge. As a result, the operation of the Bonnet Carré Spillway does not noticeably increase the discharge during a flood.

From the foregoing it is evident that there are many factors that can influence the effect of a diversion upon discharge. Among them, but not previously mentioned, is the sharpness of the flood hydrograph. A rapidly rising flood, rather than one which rises more slowly, is affected more by valley storage. Therefore, the elimination of storage by reducing storage increments will increase the discharge of a flash type of flood more than that of a less "flashy" flood. Each case must be analyzed separately. However, if conditions correspond to those of the example presented in the paper (see under the heading, "Hydraulics of Diversions")—that is, although all scales and quantities are changed, if they are changed proportionately—the relative effects will be the same. The example in the paper emphasizes the fact that the withdrawal of water by a diversion does not necessarily reduce the flow downstream by the amount diverted. This fact applies to small streams as well as to large ones where there is a comparatively appreciable amount of valley storage within the influence of diversion drawdown. It has only minor application to incised streams because storage is small and storage increments on such streams do not increase noticeably with stage.

In general, the writer concurs with Mr. Blench's remarks regarding model experimentation. In the conclusions to the paper it was stated:

"* * * at the present time model experiments offer the most promising method of securing a quantitative approximation of results in which confidence can be reposed."

The phrase, "at the present time," was intended to carry its literal meaning. There was no implication that model experimentation would always remain as the most promising method. In fact, because of the cost and time involved in model studies, it is hoped that less costly and more exact and expeditious methods will be developed.

A proper investigation, as Mr. Blench asserts, includes (*a*) models, (*b*) field observation, and (*c*) theory applied to field and model results. However, the writer is inclined to place field observations first, with theory applied to those investigations, before undertaking a model study, unless it is believed that the latter will aid in guiding the field observations, which is often the situation. In that case, the model study and field observations should proceed more or less concurrently. In almost every instance, a model test of a natural stream requires a large number of field data before the model can be designed and constructed and the test can proceed.

The regime theory seems to offer promise for dependable analytical solutions in the future. However, the various factors are as yet difficult to appraise accurately, and at least one of the three basic equations[22] should be reduced to curves for expeditious solution. Referring to Table 3, the slope changes considerably with p, the change in the bed factor. It would be difficult to choose p accurately for any diversion modification, especially in view of the selection of bed and near-bed sediment that may be practiced by the diversion. For example, if the diversion before modification withdraws most or all of the coarse fractions of the sediment, the modification (assuming the sediment withdrawal to be increased thereby) must accomplish the increase through withdrawal of finer fractions. This will change the bed factor and make the selection of the value of p difficult. The foregoing is not meant to detract from the value of the regime theory nor to suggest that it is not now useful. On the contrary, it would seem to have great potentialities. However, it does offer the opportunity for further development. The probability of inaccuracy in choosing regime theory factors emphasizes the desirability of verifying, with a model study, designs of costly works based on that theory, or on the experience of the designing engineer. Such verification furnishes comfort and confidence to the designer.

Mr. Leliavsky has suggested that the writer did not sufficiently stress the importance of the concept of the angle of diversion or the angle of twist. There was no intention to minimize its importance. It was the variation of sediment withdrawal with the angle of twist that prompted the writer to seek an explanation and led to the conception of the factors influencing bed-load diversion. Most of these factors operate because of the angle of diversion and vary with it. The differential velocity effect, the meander pattern created by the branch channel, and the angularity factor are all intimately connected with the centrifugal force mentioned by Mr. Leliavsky. It may also be conceived that the

[22] "Regime Theory for Self-Formed Sediment-Bearing Channels," by Thomas Blench, *Transactions* ASCE, Vol. 117, 1952, p. 383.

centrifugal force influences somewhat the vertical velocity effect and the slope factor. Thus, it seems that much more emphasis was placed on the angle of diversion in the paper than is evident.

The paper implies the importance of the angle of diversion by stating that these factors furnish at least a partial explanation of the changes in proportions of bed load diverted with variation in the angle of diversion. All factors may operate together, but the relative importance of each changes as the angle is modified. To illustrate—assume that the diversion channel carries the same quantity of water as the main channel below the point of diversion. Then, for small diversion angles, the water is deflected into the branch channel with relative ease so that the differential velocity, vertical velocity, and slope factors have little influence, but the meander pattern and the angularity factor are favorable for the diversion of bed load. As the angle between the straight channel and the branch channel becomes greater, the differential velocity, vertical velocity, and slope effects increase, but the meander and angularity influences become less favorable. It is doubted that the angularity factor changes much for angles greater than 90°, but the meander pattern effect, even though reducing, may persist for angles of diversion that are somewhat greater. The differential and vertical velocity influences increase to a maximum at an angle of 90°, or slightly greater, and probably remain rather constant for greater angles. As long as the same amount of water is diverted into the branch channel, the effect of the slope factor will grow with increasing angles, and the velocity factor will be equally operative at all diversion angles.

Mr. Leliavsky stated that Fig. 7 was prepared by him from theory, experiments, and observations. It appears that only the curve for radius of curvature is directly based on experiment and observations. The curve for centrifugal force is derived from the radius of curvature curve by assuming that $1\,F = \frac{W\,v^2}{g\,b}$. Thus, where the radius is $\frac{1}{2}\,b$, the centrifugal force is $2\,F$, etc. This being the case, Fig. 7 would be clearer if b were added to the denominator of the right-hand side of the equation that designates the scale for centrifugal force.

Mr. Leliavsky would do the engineering profession, especially in the United States, an additional service if he were to submit the data upon which his radius of curvature curve was founded, together with its derivation. An explanation of his method of determining the profile of the vortex that establishes the slope of the sand screen would be of great value, also. It is possible that the profile of the vortex can be approximated from the radius of curvature and centrifugal force curves by assuming that the difference in centrifugal force from the inside to the outside of the bend is balanced by the superelevation of the water surface, but there will be velocity differences in an actual case, for which compensation must be made. Theoretical development supported by experimental data and field observations would be helpful.

Mr. Thomas has presented a clear and perhaps more fundamental explanation of the effect of curvature than was given in the paper. He treats the same forces as discussed by Mr. Leliavsky in somewhat different terms. Both refer to differences in momentum, centrifugal force, or velocity from top to

bottom of the stream. As mentioned in the remarks concerning the discussion of Mr. Leliavsky, factors outlined in the paper depend upon this difference. It does explain to a considerable extent why a diversion, when located so as to be exposed to the sediment path, will withdraw a disproportionately large amount. However, the variation of sediment withdrawal with change in the angle of diversion cannot be explained solely on difference in velocity, nor will this difference cause a diversion to withdraw sediment if that diversion is not exposed to the path or to a source of sediment. For these reasons, the writer found it necessary to develop a breakdown into the factors influencing diversion of sediment.

Mr. Thomas has cited a very outstanding instance of the reduction in diversion of sediment that can be accomplished by proper location of the entrance. Such examples add convincing support to the paper.

Referring to Mr. Bondurant's discussion, the writer realized that it is difficult to differentiate or fix a fine line of demarcation between bed load and suspended load. Certainly, it was not intended that the term "bed load" should apply only to material moving on the bed of the stream. Rather, for want of a better term, it was used to describe material moving with heavy concentrations in the lower levels of the stream. A studied reading of the descriptions of the factors influencing diversion of bed load will indicate this.

By his statement that Red River sand is rather fine, so that some sand may have been carried in suspension, the writer did not intend to infer that only fine sands are carried in suspension. However, fine particles can be driven higher in the stream with less energy than coarser particles of the same specific gravity unless, of course, the specific gravity is less than 1.0. The writer referred to a publication[4] with which it must be presumed that the writer was familiar, and in which it is shown that sand is carried in suspension even to the top levels in the Mississippi River. It shows, also, that the greatest concentration occurs in the lower levels of the stream, usually in about the lower 10 ft. Above this level, the sand distribution is relatively uniform with depth. This high concentration of the coarser particles near the bottom is to be expected because the rate of change of velocity—and hence probably the turbulence transfer—is greatest in the lower levels of the stream. The Mississippi River measurements indicated that the concentration of silt sizes was nearly uniform from top to bottom.

Mr. Bondurant has presented very valuable and enlightening data in Fig. 13, showing the vertical distribution in the stream of various fractions of the sand. These are the only data with such a complete breakdown that have come to the attention of the writer. Of course, the curves apply to the sites where the data were obtained and cannot be used elsewhere except for purposes of drawing general conclusions and to serve as a guide for similar investigations. The data will probably change with velocity, with character of the bed, with curvature, with total solids, and with amounts of the various fractions. One set of curves has been designated "Rough Bed Area" and the other "Smooth Bed Area." As pointed out by Mr. Bondurant, the "Rough Bed Area" shows a more uniform distribution of sediment with depth than the "Smooth Bed Area." This is to be expected with conditions being identical. However, the con-

ditions are not the same, but may contain compensating influences. For example, the rates of change of velocities are greater at the "Smooth Bed Area" location. This condition would tend to produce more turbulence transfer and appears to be an anomaly because the greater turbulence (and turbulence transfer) would normally be expected where there is a rough bed. However, where the roughness is considerable, it may tend to equalize velocities by producing a large amount of turbulence that results in intimate mixing of water from various levels. Possibly this can be explained, also, by the difference in velocities, and by the fact that the effect of roughness may be relative, depending on the velocity. Despite the lesser velocities and the rates of change of velocity at the "Rough Bed Area" location, the coarser particles are projected higher in the stream than in the "Smooth Bed Area." This may not be caused entirely by the difference in the nature of the beds. The "Smooth Bed Area" appears to have had a larger amount of total solids, especially in the intermediate sizes, and only a small amount of the larger sizes of sand. This high concentration of solids, especially in the lower levels, may have offered a resistance to the projection of the larger sizes upward. Both sets of curves show that materials in suspension above points at five tenths of the depth or six tenths of the depth are distributed relatively uniformly, that the finer fractions have comparatively uniform concentrations from top to bottom of the stream, and that concentrations of coarser particles increase enormously with depth in the lower levels. It is believed that these differences would be accentuated in a deeper stream.

Mr. Bondurant properly has pointed out that material carried in a stream may be transported for long distances and not deposited on the next point bar downstream. This was mentioned in the paper (see under the heading, "Withdrawal of Sediment by Diversion") and reference was made to Mr. Friedkin's experiments. The writer observed Mr. Friedkin's experiments many times and often discussed them with him. Therefore, the fact that the material moved along the bed either in close contact therewith, or by saltation, can be rather authoritatively confirmed. However, the discussion of this item in the paper was not restricted to material moving on the bed, nor was it intended to imply that all the material from a caving bank would deposit on the next point bar when it was asserted (see under the heading, "Withdrawal of Sediment by Diversion"): "* * * the material from the caving bank moves downstream and deposits on the next point bar on the same side of the river." Obviously, some of the material will be in a highly suspended state and other portions of it will remain suspended at high levels for a sufficient time to by-pass the next point bar. The material that is deposited on a point bar can be either that which moves along the bed or that which is carried in suspension (especially in the lower layers) and can come to rest because of slackened velocities in the vicinity of the bar. For completeness (as suggested by Mr. Bondurant), the paper should have mentioned that suspended sediment, even if that sediment is sand, can be carried for long distances without permanent or temporary deposition. It is believed that the first clause of Mr. Bondurant's last sentence should be modified to read, "Even in a stream having erodible banks * * *." In a stream having fixed banks, the bed material introduced at

the head of a reach may be expected to continue downstream unless it is so coarse or heavy that the currents cannot move it.

The writer feels that the discussions of his paper have been outstanding and is properly grateful to each of the discussers. The ideas they have contributed, the examples cited, and the data presented may assure that the paper will be of value to the profession.

AMERICAN SOCIETY OF CIVIL ENGINEERS

Founded November 5, 1852

TRANSACTIONS

Paper No. 2547

THE DEVELOPMENT OF STRESSES IN SHASTA DAM

By J. M. Raphael,[1] A. M. ASCE

With Discussion by Messrs. Ross M. Riegel, Roy W. Carlson, J. Laginha Serafim, A. D. Ross, J. A. Hanson, A. Warren Simonds, and J. M. Raphael

Synopsis

In accordance with the practice adopted at many other major dams constructed by the Bureau of Reclamation (USBR), United States Department of the Interior, and by other agencies, strain meters and other instruments were embedded in Shasta Dam, in California, during construction to give continued assurance of structural integrity and to furnish data leading to future refinements in design and analytical methods of stress analysis. Determination of stress from long-time strain measurements in concrete, which creeps under load, is an involved process, and the method of analysis is presented herein to aid in evaluating the stress observations. Stresses were determined near the base of the spillway in Shasta Dam, and the relation of observed stress to construction procedures is discussed. Data are presented in the form of graphs showing year-by-year development of stress. Vertical stress distribution is unusual since the maximum compressive stress occurs near the center of the base. A wide variation in stress at the exposed face is shown. Horizontal normal stress appears to be omnidirectional, and shear stress is much like that predicted in nonlinear stress analyses. Principal stresses lie very close to the transverse plane and show gradual progression in inclination from upstream to downstream face. Near the toe, the second principal stress is tension. The general shape of the vertical stress distribution curve appears to be established by the weights of the individual blocks at the time the contraction joints at the base of the dam were grouted. Resultants lie generally in the region bounded by the upper one-third line and the center of the base. Stresses are generally low, and the dam appears amply stable.

Note.—Published in February, 1952, as *Proceedings-Separate No. 117*. Positions and titles given are those in effect when the paper or discussion was received for publication.

[1] Head, Structural Behavior Group, Bureau of Reclamation, U. S. Dept. of the Interior, Denver, Colo.

Introduction

Ever since 1926, when USBR participated with the ASCE in the Arch Dam Investigation conducted by the Joint Committee of Founder Societies,[2,3,4] this bureau has made detailed measurements of the structural behavior of its major dams to give continued assurance of structural safety and to furnish data leading to refinements in design. Measurements have been made of stress, strain, volume change, temperature, uplift, pore pressure, deflections, joint opening, cracking, seismic action, and foundation deformations. Although in some cases stress in concrete dams has been measured directly with stress meters, the greatest reliance has been placed on the stress computed from strain meter measurements in dams. The development of suitable meters for reliable measurement of long-time volume change in concrete has been gradual, culminating in 1934 in the elastic-wire strain meter developed by Roy W. Carlson, A. M. ASCE, of the University of California, at Berkeley. Paralleling the development of the meter itself, there was development of a suitable method for converting strain in concrete, which creeps under load, to the stresses that caused the deformations. The method departs somewhat from the simple relationships obtained for elastic materials, and is presented herein in sufficient detail so that the reader can evaluate the reliability of the stress distribution curves presented by the writer.

This paper is limited in scope to a presentation of the stresses found at the base of the spillway section of Shasta Dam. An attempt is made to draw conclusions regarding the behavior of gravity dams in general from observation of the structural behavior of Shasta Dam, from the beginning of construction in 1940 until May, 1947. Altogether, in the complete studies, observations were summarized from 1,200 instruments embedded in the dam, at 224 strain gage stations on its surface, numerous precise level and traverse surveys in and around the dam, and the various laboratory and field tests necessary to establish the properties of the concrete in the foundation material. Analysis of the heterogeneous mass of data provided consistent evidence that cannot fail to assure designers of the continuing safety of the dam and that cannot fail to provide an important adjunct to the design of future dams of greater height and mass.

Shasta Dam

Shasta Dam is the largest structure of the Central Valley Project, on the Sacramento River, about 11 miles north of Redding, Calif. The dam impounds a 487-ft-deep reservoir having a capacity of 4,493,000 acre-ft. The principal tributaries to Shasta Reservoir are the Sacramento, Pit, and McCloud rivers, draining an area of 6,600 miles and having an average annual discharge of 5,200,000 acre-ft. The spillway of the dam is controlled by three 110-ft by 28-ft drum gates and has a maximum capacity of 200,000 cu ft per sec.

---

[2] "Arch Dam Investigation," Vol. I, by the Committee on Arch Dam Investigation, The Engineering Foundation, *Proceedings*, ASCE, Vol. LIV, 1928, p. 1, Part 3.

[3] "Arch Dam Investigation," Vol. II, by the Committee on Arch Dam Investigation, Sub-Committee on Model Tests, The Engineering Foundation, 1934.

[4] "Arch Dam Investigation," Vol. III, final report of the Committee on Arch Dam Investigation, The Engineering Foundation (manuscript copy), 1933.

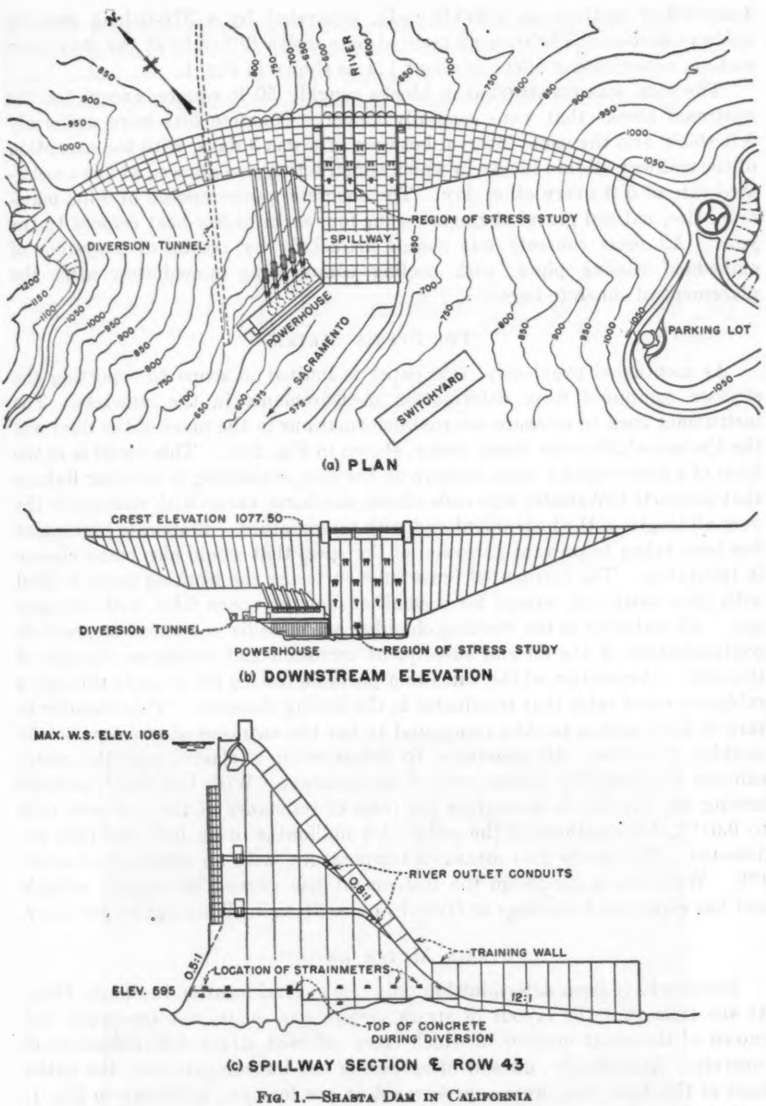

Fig. 1.—Shasta Dam in California

Fig. 1 shows the dam plan, elevation, and a spillway section taken at the center line of Row 43. Shasta Dam is a curved-gravity, mass-concrete dam, 3,460 ft long, 602 ft high with a maximum base width of 568 ft. It contains 6,230,000 cu yd of concrete. Its alinement is unusual, consisting of two curved

nonoverflow sections on 2,500-ft radii, separated by a 375-ft-long straight spillway section. The over-all ratio of base width to height at the maximum section, not counting fillets, is about 1:1 as shown in Fig. 1.

The dam was constructed in blocks roughly 50 ft square, except for the upstream blocks that were generally longer. Concrete lifts were uniformly 5 ft thick, and the usual interval between lifts was 3 days, with the exception of the spillway closure blocks in which construction was allowed at the accelerated rate of 5 ft every other day. The concrete was composed of 6-in., maximum size, natural gravel aggregate using four sacks of low-heat cement to the yard. All mass concrete was cooled artificially by means of a system of embedded cooling pipes, with cooling commencing immediately after the placement of concrete began.

The Strain Meter

As mentioned previously, this paper is limited in scope to reporting the stresses computed from deformation measurements in the concrete. The instrument used to measure internal deformations in the mass of the dam was the Carlson elastic-wire strain meter, shown in Fig. 2(*a*). This meter is in the form of a long cylinder with anchors on the end, containing a four-bar linkage that supports two elastic wire coils whose resistance varies with changes in the over-all length of the instrument and with temperature. Elaborate precaution has been taken to prevent corrosion of the wires that would also cause change in resistance. The corrugated brass tube enclosing the working parts is filled with pure castor oil, except for a small cushioning space filled with nitrogen gas. All materials in the working chamber are metallic or ceramic to preclude contamination of the oil and subsequent corrosion and resistance changes of the wire. Connection of the wires to a portable testing set is made through a rubber-covered cable that terminates in the sealing chamber. This chamber in turn is filled with a tar-like compound to bar the entrance of moisture to the working chamber. All resistance to deformation is elastic, and the meter exhibits no hysteresis under cyclical deformation. With the usual portable testing set, capable of measuring the ratio of resistance of the two wire coils to 0.01%, deformations of the order of 4 millionths of an inch per inch are detected. The meter also measures temperature, with an accuracy of about 1°F. With this same design the instrument has proved thoroughly reliable and has given good readings at Grand Coulee Dam, in Washington, for 12 yr.

Strain Meter Layout

Stresses have been determined in only one general location in Shasta Dam. At the time that the layout of strain meters was made, not too much was known of the exact manner in which creep affected strain determinations in concrete. Accordingly, instead of spreading the instruments over the entire mass of the dam, they were concentrated at one location, as shown in Fig. 1, so that the maximum amount of corroborative information might be obtained to aid in the evaluation of the effect of creep. Groups of meters were embedded at nine general locations throughout the width of the dam at El. 600 in Row 43. These strain meters were arranged in clusters of nine each, with pairs of

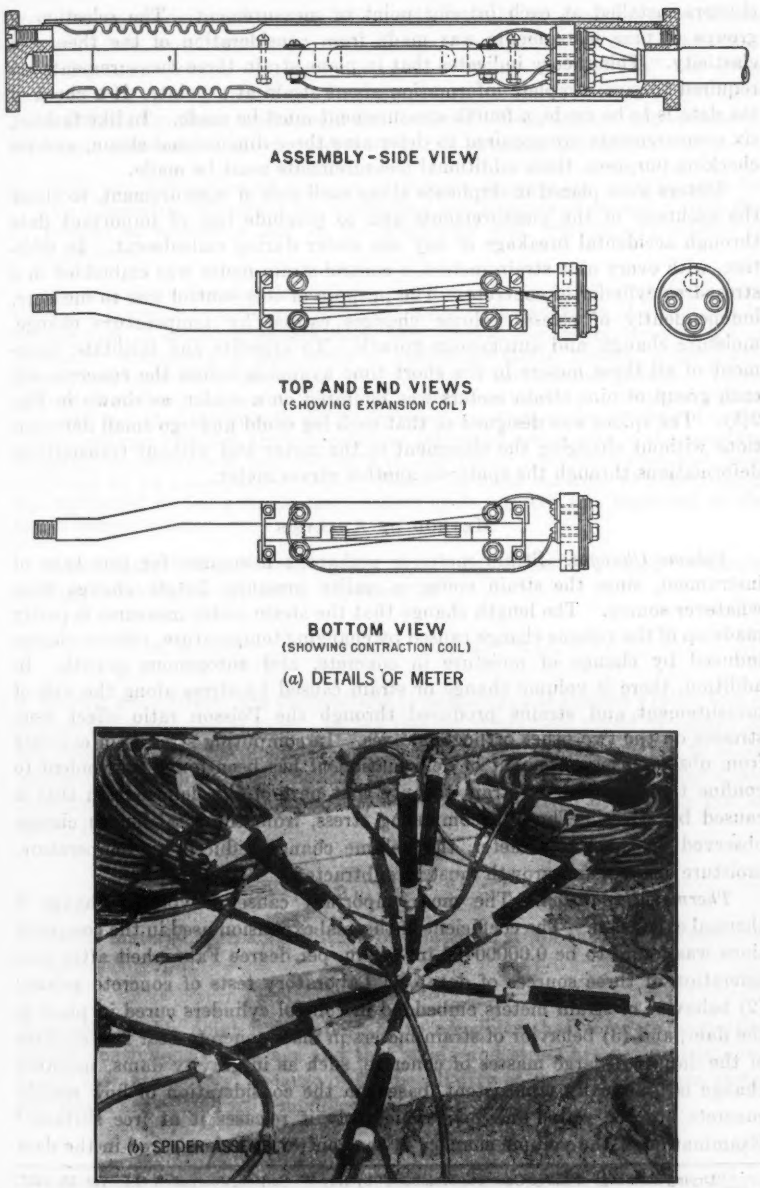

FIG. 2.—ELASTIC-WIRE STRAIN METER

clusters installed at each interior point of measurement. The selection of groups of nine instruments was made from consideration of the theory of elasticity. This theory indicates that in plane strain three measurements are required to give complete information about strain at a point. If a check of the data is to be made, a fourth measurement must be made. In like fashion, six measurements are required to determine three-dimensional strain, and for checking purposes, three additional measurements must be made.

Meters were placed in duplicate along each axis of measurement, to check the accuracy of the measurements and to preclude loss of important data through accidental breakage of any one meter during embedment. In addition, with every nine strain meters, a control strain meter was embedded in a stress-free cylinder of concrete. The purpose of this control was to measure, independently of stress, volume changes caused by temperature change, moisture change, and autogenous growth. To expedite and facilitate placement of all these meters in the short time available before the concrete set, each group of nine strain meters was mounted on a spider, as shown in Fig. 2(*b*). The spider was designed so that each leg could undergo small deformations without changing the alinement of the meter and without transmitting deformations through the spider to another strain meter.

Method of Analysis

Volume Changes.—Strain meter is perhaps a misnomer for this type of instrument, since the strain meter in reality measures length change from whatever source. The length change that the strain meter measures is partly made up of the volume change caused by changing temperature, volume change induced by change of moisture in concrete, and autogenous growth. In addition, there is volume change or strain caused by stress along the axis of measurement and strains produced through the Poisson ratio effect from stresses on the two other orthogonal axes. In computing stresses in concrete from observed measurement of deformation, it has been found convenient to confine the definition of strain to only that part of the deformation that is caused by stress. Thus, in computing stress, from the total length change observed on the strain meter, the volume change induced by temperature, moisture change, and growth must be subtracted.

Thermal Expansion.—The most important cause of volume change is thermal expansion. The coefficient of thermal expansion used in the computations was found to be 0.00000485 in. per in. per degree Fahrenheit after consideration of three sources of data: (1) Laboratory tests of concrete prisms; (2) behavior of strain meters embedded in control cylinders cured in place in the dam; and (3) behavior of strain meters in mass concrete near free surfaces of the dam. In large masses of concrete, such as in gravity dams, moisture change is practically nonexistent, based on the consideration of how readily concrete absorbs water and how reluctantly it releases it at free surfaces.[5] Examination of the volume changes in the control cylinders cured in the dam

[5] "Drying Shrinkage of Large Concrete Members," by Roy W. Carlson, *Journal*, A.C.I., Vol. 33, 1937, p. 327.

disclosed no evidence of volume change that could be ascribed to moisture change; hence, no allowance for such change was made in the computations.

Autogenous Growth.—Autogenous volume change or "growth" has been detected in Tygart Dam (West Virginia), Norris Dam (Tennessee), Hiwassee Dam (North Carolina), and Grand Coulee Dam (Washington), and in laboratory tests of several types of concrete. It has been stated that:

> "The primary causes of autogenous volume changes are considered to be the volumetric changes in the crystalline constituents of cement during the process of hydration and in the gelatinous and crystalline products of hydration."[6]

Growth characteristics are different for different types of cements and for the same types of cement from different mills. Observations of structures in service and of sealed cylinders show that growth can be either positive or negative. Examination was made of embedded strain meters, control cylinders, and laboratory specimens for evidences of autogenous growth. These showed that there were some slight evidences of autogenous growth of Shasta concrete, but that the growth definitely was a function of the number of cycles of temperature to which the concrete was subjected, being zero in the constant temperature specimens, and 0.000048 in. per in. in specimens that had been subjected to 14 temperature cycles. Since the mass concrete of Shasta Dam was subjected to but a single temperature cycle, growth was neglected in the strain computation.

Theoretical Derivation.—In elastic materials, stress is related to strain through Hooke's law, generally expressed as

$$\sigma_x = \frac{E}{(1+\mu)(1-2\mu)}\left[(1-\mu)\,\epsilon_x + \mu\,(\epsilon_y + \epsilon_z)\right]\ldots\ldots\ldots(1)$$

in which σ is the stress; E is the modulus of elasticity; μ is Poisson's ratio; and x, y, z are three orthogonal axes. In like fashion, it has been found expedient, in computing the stresses along the axis of any particular strain meter, to allow for the strain induced by the Poisson ratio effect by adding a part of the strain measured by the orthogonal meters, using a modification of Hooke's law as shown in Eq. 2.

$$\epsilon'_x = \frac{1}{(1+\mu)(1-2\mu)}\left[(1-\mu)\,\epsilon_x + \mu\,(\epsilon_y + \epsilon_z)\right]\ldots\ldots\ldots(2)$$

In elastic material, stress would then be related to strain through the modulus of elasticity.

$$\sigma_x = E\,\epsilon'_x\ldots\ldots\ldots\ldots\ldots\ldots\ldots\ldots\ldots\ldots(3)$$

However, at this point it is important to recognize that concrete properties change continuously with age and that strain and stress are not proportional except instantaneously, because of the peculiarity of creep. Therefore, stress and strain are related by a modified equation:

$$\sigma_x = E'\,\epsilon'_x\ldots\ldots\ldots\ldots\ldots\ldots\ldots\ldots\ldots\ldots(4)$$

[6] "Autogenous Volume Changes of Concrete," by Harmer E. Davis, *Proceedings*, ASTM, Vol. 40, 1940, p. 1103.

which simply states that stress and strain are related through an effective modulus of elasticity, E'. Determination of the effective modulus of elasticity involves the determination of the laws governing the continued deformation of concrete under sustained loading, termed "creep."[7]

Creep.—Creep is measured experimentally by subjecting sealed specimens to sustained loading. Some of the 48 cylinders tested for Shasta Dam have been loaded as much as 10 yr. From these and other tests, the nature of creep was determined to be susceptible to mathematical analysis and prediction, through the following general properties:

1. Creep is a delayed elastic deformation involving no changes corresponding to crystalline breakdown or slip, and is not the plastic flow of a viscous solid;
2. At working stress, creep is proportional to stress, but when stress approaches the ultimate strength of concrete, creep increases much more rapidly than stress;
3. When the effect of age on changing the properties of concrete is taken into account, all creep is recoverable;
4. Creep is independent of sign, and bears the same proportion to either positive or negative stress; and
5. The principle of superposition applies to creep.

When laboratory data were examined, it was seen that age affected creep in a dual role: Creep is proportional to duration of loading, and inversely proportional to the age at which the load is first applied. A logarithmic curve of the form:

$$\epsilon = \frac{1}{E} + f\,(K) \log_e (t + 1) \qquad (5)$$

was fitted to the experimental data for Shasta Dam creep specimens. Eq. 5 defines a three-dimensional plot, called the creep surface, that has as variables the total strain, age at time of loading, and duration of loading. The general appearance of the creep surface for Shasta Dam low-heat cement concrete is shown in Fig. 3. On the left-hand axis is plotted K, the age of the concrete when it is first loaded. The right-hand axis is t, the duration of loading, or the time that has elapsed after loading was first performed. Plotted vertically is ϵ, the total deformation. The first term in Eq. 5 is the instantaneous deformation, or the amount of deformation that takes place immediately on the application of load. The second term shows the continuing deformation with time. For instance, to follow along the highest point on the curve, it is found that for a loading of 1 lb per sq in. applied at the age of 2 days, concrete will be instantaneously deformed slightly more than 0.000001 in. per in. As time passes, with the loading of 1 lb per sq in. maintained, the concrete will continue to deform, until at the end of about 3 yr the total deformation is almost three times as much as the instantaneous deformation. It is well known, of course, that concrete hardens with age, and this fact is reflected in

[7] "A New Aspect of Creep in Concrete and Its Application to Design," by Douglas McHenry, *Proceedings*, ASTM, Vol. 43, 1943, p. 1069.

the creep surface. For loading at later ages, the instantaneous deformation is smaller than the earlier deformation, and the rate of creep is correspondingly less. It is this fact that has made analysis of strain meter readings so difficult in the past.

Computation Procedure.—A step-by-step computation has been used to determine stress from the strain curve. The computation is illustrated in Fig. 4. The smoothly curved full line at the top of Fig. 4 is the given strain curve.

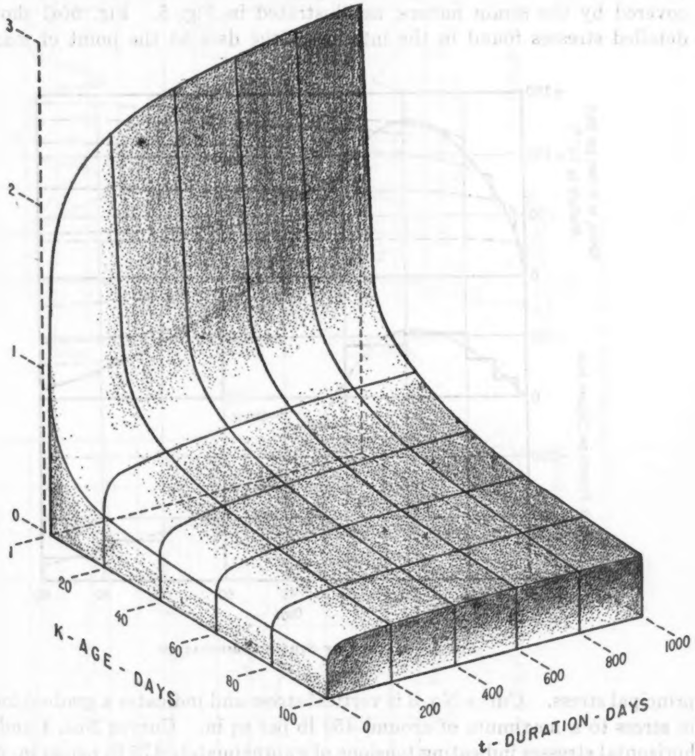

Fig. 3.—Creep Surface for Low-Heat Cement Concrete at Shasta Dam

For a short interval, a stress is applied so that the instantaneous strain plus the creeping strain resulting from this increment of stress closely approximates the given strain curve for that interval, as shown in the dotted strain curve. To the original increment of stress, another is added, so that its instantaneous strain curve plus creeping strain (when added to the previous curve of creep from the original stress) also crosses the given strain curve, and so on. When necessary, negative stress increments are subtracted from the previous total

stresses, resulting in negative instantaneous strain plus negative creep subtracted from the previous total creep strain, as shown in Fig. 4. The stepped curve of increments of stress is connected by a smooth line that represents the required stress history corresponding to the given strain history.

Stresses

Point Stresses in Interior of Dam.—Using the foregoing system of stress computations, stresses were found at each point of measurement for each direction covered by the strain meters, as illustrated in Fig. 5. Fig. 5(*a*) shows the detailed stresses found in the interior of the dam at the point of maximum

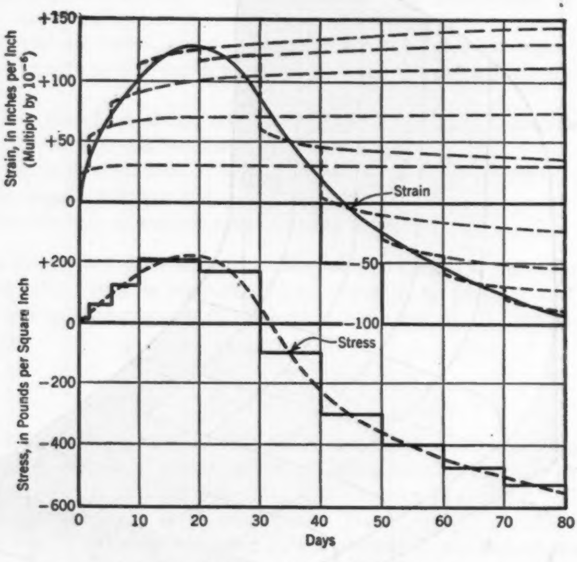

Fig. 4.—Method of Stress Computation

principal stress. Curve No. 3 is vertical stress and indicates a gradual increase in stress to a maximum of around 450 lb per sq in. Curves Nos. 1 and 2 are horizontal stresses indicating tensions of approximately 175 lb per sq in. during early ages. The lowest curve of Fig. 5(*a*) shows the temperatures observed at this location, indicating the early temperature rise, a quick drop from primary cooling, a slow increase caused by continued hydration of cement, a period of secondary cooling during the summer of 1943, immediately preceding the grouting of the joints, and a slow continued rise of about 7° F since that time.

Fig. 5(*b*) shows the stresses measured 2 ft in from the downstream face. In Fig. 5(*b*), Curve No. 3 represents stresses normal to the surface and 2 ft from the face of the dam. All the other curves represent stresses in various

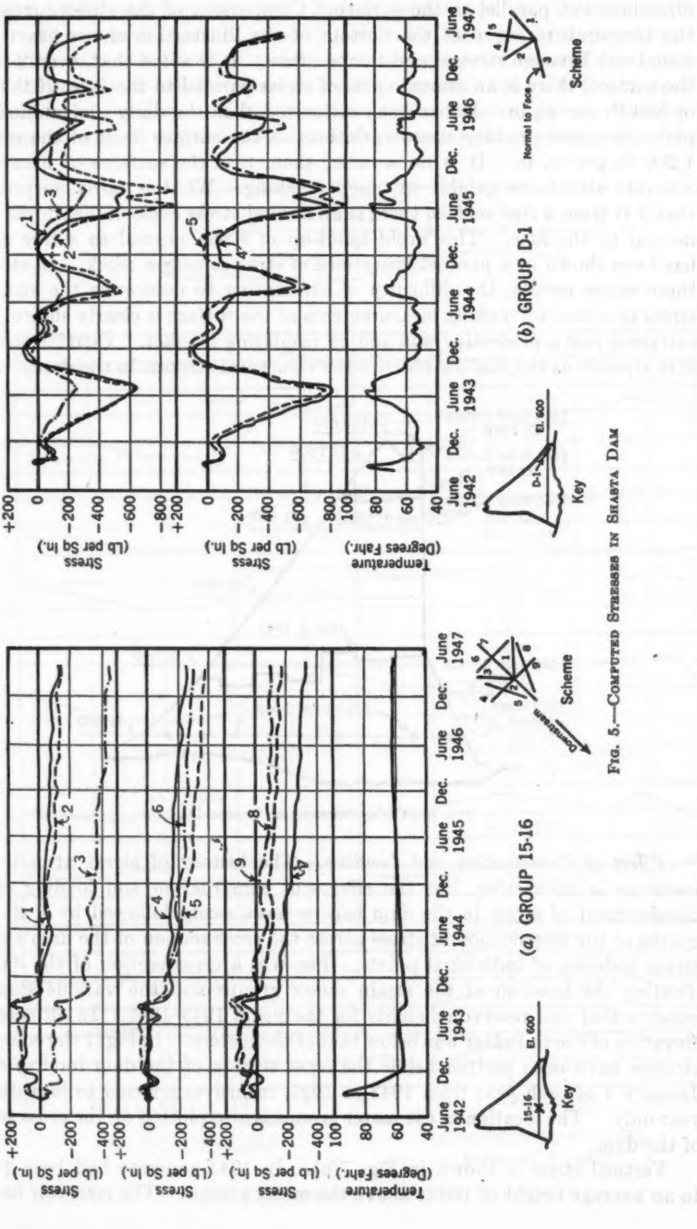

FIG. 5.—COMPUTED STRESSES IN SHASTA DAM

directions but parallel to the surface. Comparison of the stress curves with the temperature curve at the bottom of the illustration shows exact correspondence between stresses and temperature. It is noted that, even 2 ft from the surface, there is an annual cycle of stress parallel to the face, of the order of 800 lb per sq in. It has been estimated that the daily and annual temperature cycles produce stress variations at the surface itself of the order of 1,200 lb per sq in. It is no wonder, then, that the surfaces of many large concrete structures exhibit so much cracking. What is fairly surprising is that 2 ft from a free surface there is an annual stress cycle of 300 lb per sq in. normal to the face. This rapid build-up of stress normal to a free surface has been shown in a photoelastic study of stresses near a crack. In studying these stress results, the difficulty of attempting to determine the structural stress in a dam by making measurements at the surface is clearly shown. The surface is just a protective skin and an insulating blanket. Variable temperature stresses at the surface obscure the structural stresses in the dam.

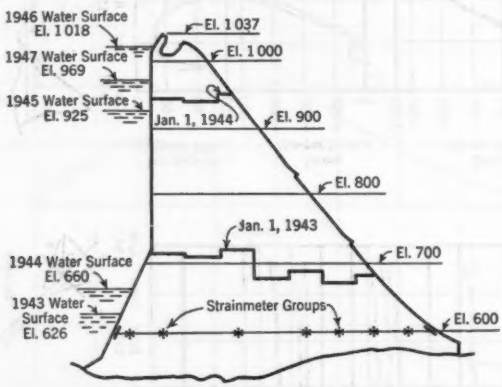

Fig. 6.—Cross Section of Shasta Dam

Effect of Construction and Loading.—The history of stress at individual locations is interesting, but the effects of construction and loading on the development of stress in the dam can be more easily followed by a study of curves of the distribution of stress across the cross section of the dam than by stress histories of individual points. Fig. 6 is a cross section of the dam indicating the location of the strain meter groups and the various stages of construction and reservoir heights for the years 1943–1946. In all cases the elevation of the tailwater was below that of the meters. In Fig. 7 the computed stresses have been plotted below the cross section of the dam for five dates, January 1 of each year from 1943 to 1947, inclusive, referred to hereafter by year only. The location of the meter groups is also plotted on the cross section of the dam.

Vertical stress is shown in Fig. 7(*a*). In 1943 concrete had been placed to an average height of 100 ft above the meter groups. The reservoir had not

yet begun to fill, and there was only 26 ft of head above the elevation of the meters. The observed vertical stress at this time averaged only 40 lb per sq in. In 1944 the dam was almost completed, but the reservoir was still low. Observed vertical stress had increased to a maximum of around 300 lb per sq in. at the center of the dam. In 1945 the dam was completed, and the reservoir had risen to 325 ft of head above the elevation of the instruments. The

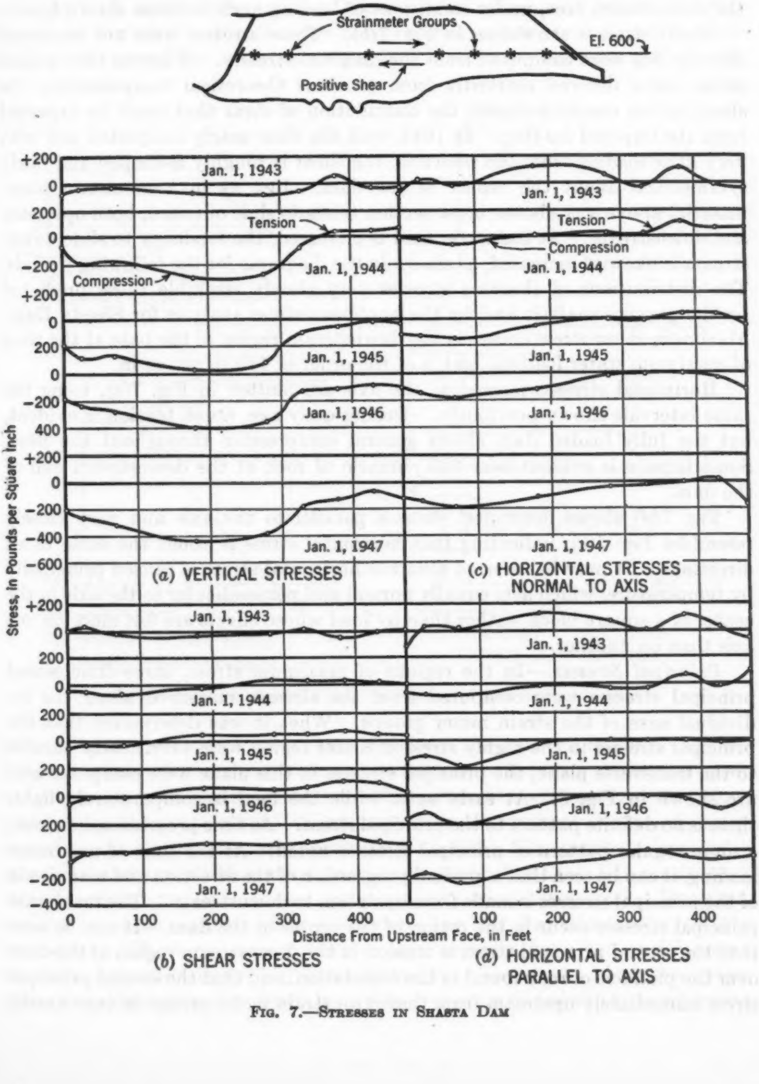

Fig. 7.—Stresses in Shasta Dam

characteristic stress distribution was well established by that time, and maximum stress was found near the center of the dam. In general, stress increased from compression at the upstream face to a maximum slightly downstream from the center of the dam, then fell off rather rapidly and continued with a fairly low value of compression to the downstream face. This distribution is in contrast with the usual assumption that stress increases in some manner from low compression at the upstream face to a great deal higher compression near the downstream face, under conditions of loading such as those shown herein.

Shear stresses are shown in Fig. 7(*b*). These stresses were not measured directly but were computed from the diagonal stresses. Whereas the vertical stress curve differed markedly from previous theoretical computations, the shear curves resemble closely the distribution of shear that could be expected from the imposed loading. In 1944, with the dam nearly completed and with very little loading from the reservoir, the shear is roughly S-shaped and fairly symmetrical about the center of the dam. Just as in a mountain mass, material above any chosen cross section tends to slide outward, both upstream and downstream. As the water load is increased, the tendency to slide downstream is likewise increased, as shown in the diagrams for the following periods. The distributions of shearing stresses very closely resemble those predicted by the gravity analysis and by the nonlinear stress analysis for Shasta Dam. Maximum shear stress occurs in the downstream region of the base at the time of maximum water loading, and is of the order of 110 lb per sq in.

Horizontal stresses normal to the axis are plotted in Fig. 7(*c*), using the same intervals shown previously. During early age, much tension is evident, but the fully loaded dam shows general compression throughout the base. Some tension is evident near the pinnacle of rock at the downstream end of the dam.

Fig. 7(*d*) shows horizontal stresses parallel to the axis and very closely resembles Fig. 7(*c*), indicating that horizontal stress is about the same in all directions. It may be inferred that the horizontal stress is caused principally by temperature, which acts equally normal and perpendicular to the axis in the center of a square block, rather than by load whose effects are felt more on one axis than on another.

Principal Stresses.—In the regions of maximum stress, three-dimensional principal stresses were computed from the stresses measured along the individual axes of the strain meter groups. When it was determined that the principal stresses in the highly stressed center region were very nearly parallel to the transverse plane, the principal stresses in this plane were computed and are shown in Fig. 8. At early ages, while the load is comparatively light, there is no definite pattern to the principal stress. As time progresses, however, a more regular pattern of principal stress is noted. At the time of maximum loading, it can be seen that a gradual progression of the direction and magnitude of the principal stresses is made from upstream to downstream. The maximum principal stresses occur in the region of the center of the dam. It can be seen that the second principal stress is tension in the downstream region of the dam over the pinnacle of rock found in the foundation, and that the second principal stress immediately upstream from these two strain meter groups is very nearly

zero. Tension has been suspected to be present in attenuated fillets at the downstream face of the dam and is unmistakably indicated herein. It might be inferred from the observed tensions that load should be brought more directly into the foundation by increasing the slope of the downstream face in order to ameliorate this condition.

Comparison of Stress and Load.—In all of the stress diagrams discussed, the stresses have been plotted exactly as computed, and no attempt has been made to force equilibrium between the observed stress distribution and the known external load. Fig. 9 shows how well the stresses actually do balance the known external load. In each case, in this series of diagrams, the full line

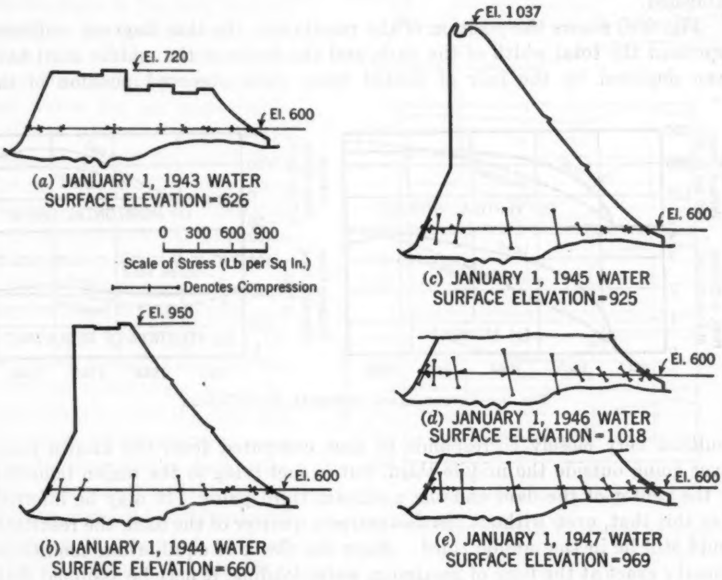

FIG. 8.—PRINCIPAL STRESSES IN A TRANSVERSE PLANE IN SHASTA DAM

labeled "load" refers to values computed from the external loading, and the dotted line labeled "reaction" refers to values computed from the strain meter measurements. In checking the vertical stresses, the average load was computed from the total weight of concrete plus the vertical weight of water acting on the sloped upstream face above El. 600. The reaction diagram is merely an average of the vertical stresses shown in Fig. 7(*a*). It can be seen that at early age reaction does not increase nearly as rapidly as load. However, at the time of maximum loading of the dam, the two diagrams are very nearly in balance. These early discrepancies may actually have occurred because of partial support of Row 43 by Rows 42 and 44. The row in which the meters were embedded was constructed from 4 to 8 months ahead of the neighboring

rows. It is quite possible that, since Row 43 was completely cooled while the other rows were yet expanding, the neighboring rows may have taken part of the load of Row 43 that would normally have been observed in the strain meters.

The moments of the load and reaction computed about the upstream face are shown in Fig. 9(*b*) and exhibit about the same discrepancies as do the vertical stress diagrams. The observed average horizontal shear shown in Fig. 9(*c*) at all times is less than what might be expected from the known load, from which it may be inferred that a residual shearing stress exists due to some local condition of temperature. In separate studies, the variation of horizontal stress and shear throughout a 5-ft lift of concrete has been established.

Fig. 9(*d*) shows the position of the resultants. In this diagram, ordinates represent the total width of the dam, and the limits of the middle third have been depicted by the pair of dotted lines. The observed position of the

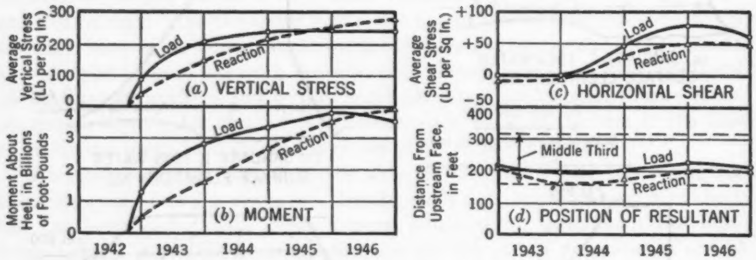

FIG. 9.—EXTERNAL AND INTERNAL LOAD CHECKS

resultant very closely corresponds to that computed from the known load, never going outside the middle third, but in fact lying in the region bounded by the center of the dam and the upstream third point. It may be inferred from this that, even without the downstream quarter of the dam, the resultant would still lie in the middle third. Since the check of equilibrium conditions is nearly exact at the time of maximum water loading, it may be assumed that equilibrium does exist under conditions of cantilever loading and, as a corollary, that very little water load is supported by arch action. This corroborates the designers' assumptions that the arching of Shasta Dam is too slight to be of appreciable structural value but merely serves to allow the dam to follow the configuration of the site.

Analysis of Vertical Stress.—Referring again to the discrepancies evident in the vertical stress diagram and the moment diagrams, it is interesting to note the minor modifications made to Fig. 7(*a*) when equilibrium is forced between the reaction and the load. Fig. 10 shows the vertical stress distribution for Fig. 7(*a*) corrected so that vertical equilibrium and moment equilibrium have been achieved. Correction was made by adding to the curve of observed vertical stresses a uniformly varying correction that would make $\Sigma V = 0$ and $\Sigma M = 0$. The chief difference between the observed and corrected stress

diagrams is that the questionable tension that formerly was shown in the downstream region of the 1944 stress distribution has now disappeared entirely. In general, the appearance of the stress distribution diagram is unchanged. As before, vertical stress increases from some moderate compression at the upstream face to a maximum value near the center of the dam, thence falling off rapidly to a uniformly low stress in the downstream quarter of the dam.

It must be recognized of course, that as of 1947 the reservoir had not reached the maximum water surface elevation of 1065, the top of the open drum gate. A foot increase in depth at the top of the reservoir puts much more stress on the dam than a corresponding increase at a lower level. Shasta Dam is the only dam in which, to the best knowledge of the writer, vertical stresses have been observed to be of such a low value for an appreciable distance near the downstream face. It should be noted that this is likewise the only dam having an extensive upstream projection at the lower elevations in the dam. This may provide a clue to a manner in which it may be possible to gain economy in design of gravity dams. By providing a loading shelf for the weight of water to rest on at the lower elevations in the dam and shaving a corresponding amount from the downstream face of the dam, equivalent stability, more uniform stressing, and increased economy is provided without essential change in stability. Photoelastic studies made in the laboratories of the USBR tend to check this hypothesis.

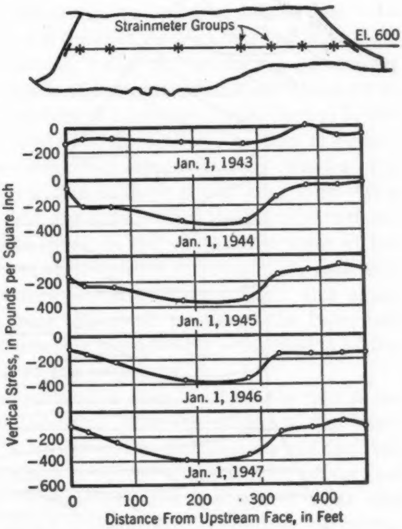

FIG. 10.—VERTICAL STRESSES CORRECTED TO BALANCE KNOWN LOADS

Temperature conditions were examined to see if these would account for the unaccustomed appearance of the vertical stress distribution diagrams. In studies of strain meter measurements in naturally cooled gravity dams, extensive transfer of stress from the interior to the outer boundaries of the dam has been noted, as the center of the mass cools slowly to final stable temperature. Typically, interior vertical stresses in Tygart, Norris, and Hiwassee dams are reported very close to zero instead of the 50 to 200 lb per sq in. that might be expected, and stress near the outer face was correspondingly increased to maintain equilibrium. Conversely, if the center of Shasta Dam had warmed up to a much greater degree than the outer regions, the core might be expected to be supporting more than its usual share of the load, with consequent diminu-

tion of stress near the outer boundaries. Could observed maximum stresses at the center of Shasta Dam have been caused by a temperature rise at this location?

Concrete in large masses continues to hydrate for many years after it has been placed. In Fig. 5(*a*) a long-time rise in temperature lasting at least 4 yr is evident following the period of final cooling. At Hoover Dam, in Washington, equilibrium conditions appear to have been reached in 1949 as the temperature rose steadily but slowly since 1934. If the temperature rise was

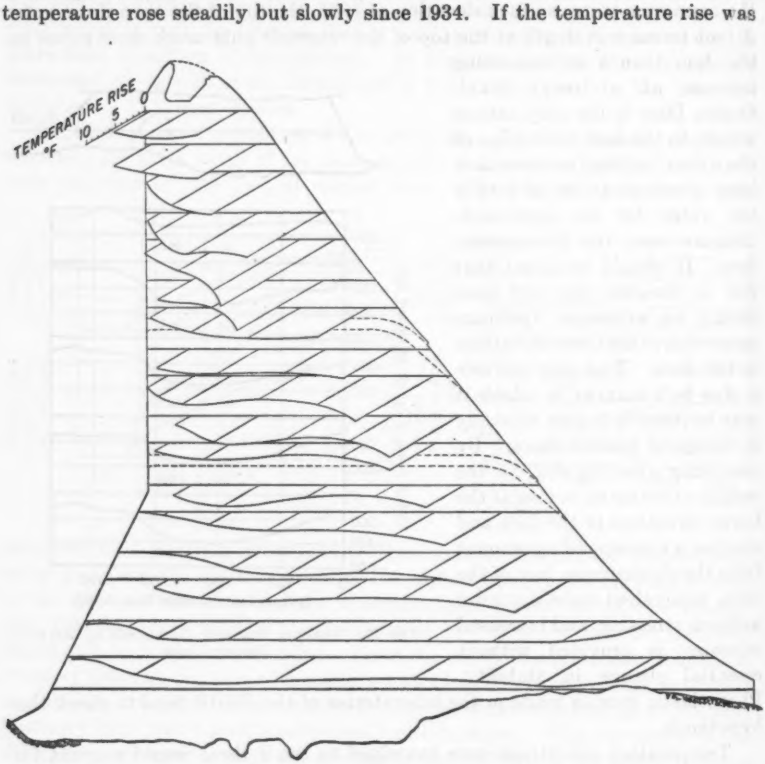

FIG. 11.—TEMPERATURE RISE AFTER FINAL COOLING AT SHASTA DAM

confined to the center of the dam by the blanketing effect of the outer layers of concrete, while the outer layers remained stable in temperature because of closer proximity to the relatively stable cyclical air temperature, the center might be expected to expand more than the outside, and it might be deduced that the center of the dam would bear more than its share of the load, with consequent higher compression. To produce the observed distribution of stress, the distribution of temperature rise would have to bear a close resemblance to the stress diagram. Fig. 11 shows the temperature rise following final cooling at various

elevations in the dam. For each elevation, the actual temperature rise is plotted outward from the dam, the width of the shelf being proportional to the temperature rise. It can be seen that, near the regions in which the strain meters were placed, temperature rise was nearly uniform across the cross section of the dam. Since the curve of distribution of temperature rise of the base bears no resemblance to the stress distribution, explanation must be found elsewhere for the increased compression at the center portions of the dam.

Advanced stress analyses of concrete gravity dams have not been particularly helpful in explaining the observed distribution of vertical stress at the base of Shasta Dam. For high dams, it has been the practice of the USBR to make a nonlinear stress analysis for the maximum cantilever of the dam. In this analysis, the dam and a portion of the foundation are analyzed as a single unit composed of a homogeneous material, using the analogy between the stress system of a plate loaded in the plane of the plate, and the deflections of a plate of the same shape bent under a system of boundary forces normal to the plate. The nonlinear stress analysis made for the spillway section of Shasta Dam[8] shows a stress distribution that resembles somewhat that found at the upstream portion of the dam. However, the analysis shows very high stress near the downstream face of the dam, that was not found in the actual structure.

In another study[9] consideration was given to the effect on stresses at the base of a gravity dam of differences between rigidity of foundation rock and dam concrete. For the relative rigidities found in Shasta Dam, this again gave maximum compressive stresses near the upper center of the base, but stresses at the heel were tensile, and there was considerable compression at the toe. These conditions were not found in the prototype.

O. C. Zienkiewicz[10] has determined vertical stresses in which the maximum stress under dead load plus live load occurred near the center of the base, with minimum stresses near the faces. However, this distribution was dictated by water loading, since dead loading alone produces a distribution of vertical stress resembling the Levy triangle. This is just the opposite of what was noted in the prototype, in which the shape of the stress distribution curve was established by dead load.

Photoelastic studies[11] have given good correlation between predicted and observed stress distributions. Dead load stresses in these studies were very nearly the same as those reported in this paper, and the water load gave equivalent modifications to the dead load stresses.

Since dead load is so predominantly responsible for the shape of the vertical stress distribution curve and since the dam was cut up into small segments by the method of construction, analysis was made to see what the dead load stress distribution might be if all loads went directly downward to the founda-

---

[8] "Determination of Nonlinear Stress Distribution in Maximum Spillway Section of Shasta Dam," by Sidney D. Larson, *Technical Memorandum No. 606*, Bureau of Reclamation, U. S. Dept. of the Interior, Denver, Colo., 1940.

[9] "Effect of the Relative Foundation Rigidity on the Stresses in a Gravity Dam with Application to the Grand Coulee Dam," by I. K. Silverman, C. N. Zangar, J. E. Soehrens, and J. H. A. Brahtz, *Technical Memorandum No. 494*, Bureau of Reclamation, U. S. Dept. of the Interior, Denver, Colo., 1935.

[10] "The Stress Distribution in Gravity Dams," by O. C. Zienkiewicz, *Journal*, Inst. of C. E., Vol. 27, 1946–1947, p. 224.

[11] "Photoelastic Analysis of Stresses at Elevation 600—Shasta Dam Spillway Section," *Photoelastic Report No. 11*, Bureau of Reclamation, U. S. Dept. of the Interior, Denver, Colo., 1949.

tion, instead of being distributed, as is commonly assumed in most elastic analyses. Fig. 12 shows the appearance of the dam at the time the longitudinal joints in the vicinity of the strain meter installation were grouted. Immediately below this diagram, there is plotted, as the dashed curve, the distribution of stress computed for each separate block in the dam. Associated with this is the balanced observed stress for the same data plotted as a full line. It can be seen that at this period, that represented very nearly the entire dead load of the dam with practically no water loading, there was very close correspondence between the two diagrams with the exception of the end points that are greatly modified by surface temperature. The weight and moment of the remaining concrete load and the maximum water load were then distributed over the entire base, since this now has been welded into a whole by grouting, resulting in the lower dotted diagram of this figure. As before, the balanced observed vertical stress distribution is plotted as the full line. It can be seen that correspondence is very close for both diagrams, indicating a tendency for dead load to be supported by the foundation directly beneath, instead of being distributed over the entire base.

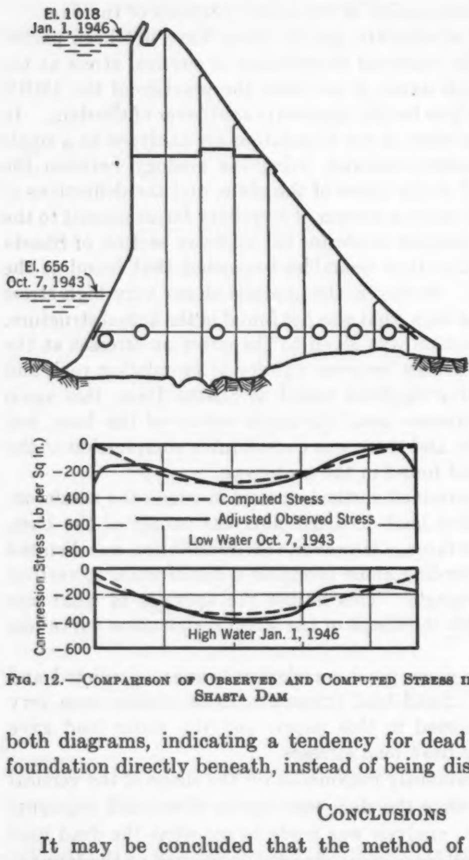

FIG. 12.—COMPARISON OF OBSERVED AND COMPUTED STRESS IN SHASTA DAM

CONCLUSIONS

It may be concluded that the method of determining stress from the strains measured in the interior of concrete dams can be considered reliable. The rather unusual stress distribution at the base of Shasta Dam appears to be consistent with the shape of the dam and its method of construction. Construction techniques and temperature change have a greater influence on stresses in gravity dams than the water load. The low magnitude of the actual stresses in the dam gives ample assurance of structural safety. The measured results cited herein provide source data for the design and analysis of large concrete dams.

ACKNOWLEDGMENT

The results presented in this paper represent the combined efforts of many individuals and are by no means the sole efforts of the writer. The instruments, without which the work would have been impossible, were devised and manufactured by Roy W. Carlson. Laboratory tests were supervised and analyzed by USBR engineers Douglas McHenry (M. ASCE) and J. A. Hanson, who also devised and elaborated the method of stress computation. Following completion of the installations in the dam, crews of technicians, headed in turn by engineers I. E. Houk, Jr. (J. M. ASCE), G. Tarleton, and the late J. A. Moore, patiently observed, recorded, and analyzed the data. Detailed computations were under the direct supervision of C. L. Townsend. Other men, too numerous to mention, aided in all steps of the investigation. The writer, under the general direction of Kenneth B. Keener (M. ASCE), head, Dams Branch, USBR, laid out the program, supervised the installation, and analyzed the results. Acknowledgment should also be made of the contributions of Tennessee Valley Authority (TVA) and United States Engineer Department (USED) engineers in the continued development of the analysis of strain measurements.

DISCUSSION

Ross M. Riegel,[12] M. ASCE.—A major conclusion of the paper is that actual stresses in large dams are profoundly affected by the construction procedures pursued. For example, when longitudinal joints in a high dam are grouted, conditions as they exist at that time tend to be "locked up" and to remain despite the subsequent effects of the application of water load. Two illustrations may be cited. If a dam is built in two successive vertical stages, as was the case at Shasta Dam and at Fontana Dam in North Carolina, the "locking up" feature applies to the first stage. If the several blocks in a transverse section are not carried upward more or less simultaneously, stresses due to differential shrinkage and temperature effects may be similarly locked.

The process of design should consider the effects of the procedure of construction, and, if necessary, place appropriate restrictions on that procedure to the end that the behavior of the finished structure as to stresses will be that which the designers intended and expected.

A further conclusion to be drawn from the paper is that Shasta Dam is unnecessarily heavy in section. It is the writer's understanding that the heavy section was adopted to secure a high shear-friction factor at the foundation level. If so, it might be reasonably questioned whether conservatism in this respect was not on the excessive side.

Roy W. Carlson,[13] A.M. ASCE.—The analysis of stresses in Shasta Dam, as presented in this paper, is perhaps the first published account of stresses determined in a service dam from measurements of internal length changes. A remarkable fact is that the stresses so determined were confirmed in many ways: (1) All strain meters were in duplicate and good checks were shown by the duplicate meters; (2) an extra strain meter was installed in each plane and provided a satisfactory check on the dilatation at each station; (3) the average of vertical stresses as indicated by the analysis checked the known vertical loads at various ages reasonably close; (4) the moment indicated by the pattern of vertical stresses checked the known overturning moments at various ages; and (5) the directions of principal stresses varied in a consistent and reasonable manner from upstream to downstream face. Thus, it was established that the stresses shown by Mr. Raphael were reliable and accurate to a degree sufficient for engineering purposes.

Having determined the stresses at the base of Shasta Dam, it appears that economies can be achieved in gravity dams. An examination of Fig. 10 shows that very little stress developed near the downstream portion of the dam at any time. It is indicated that about 25% of the dam could have been removed from the region of the downstream face without changing the be-

[12] Cons. Engr., Gibbs and Hill, Inc., New York, N. Y.
[13] Cons. Engr., Berkeley, Calif.

havior in any significant way. Gravity dams are made extravagantly thick, partly because an unreasonably large allowance is made for uplift pressure, and partly because engineers add greatly to allow for uncertainties. The Shasta analysis shows that such a dam could be made much thinner with safety, and that there need be very little uncertainty in the degree of safety when suitable measurements are made.

The question of uplift pressure has been studied actively in recent years and the subject need not be discussed herein. The writer's purpose instead is to call attention to Mr. Raphael's brilliant work in determining stresses in a service dam and to suggest the value of this accomplishment. Its value to future dams promises to be great; also, Mr. Raphael's service in revealing the action and safety of Shasta Dam is of immediate value. More emphasis could well be placed on providing a continuous check on the safety of important dams, now that Mr. Raphael has demonstrated how it can be done.

J. Laginha Serafim,[14] A. M. ASCE.—The information given by the author constitutes one of the most valuable contributions to the knowledge of the structural behavior of mass-concrete dams presented since the 1930's In fact the total stresses caused by all kinds of loadings, developed in Shasta Dam from the beginning of construction, were determined by a rational method.

Analysis of the data furnished by the gages embedded in concrete had not been presented before, although such instruments have been in use for more than twenty years at major American and European dams. The writer believes that this success of the analysis was aided by the fact that Carlson strain gages were used and a better knowledge of concrete was obtained.

However, in the method of stress determination used at Shasta Dam[15] there are some difficulties, namely: (1) The computations are too laborious; (2) the method requires a perfect knowledge of the volume changes caused by influences other than stress; (3) it provides little accuracy, since the theory of creep of concrete is only approximate; and (4) it requires laboratory testing of a large number of concrete specimens, cured under conditions of temperature and humidity like those of the concrete in the dam.

The coefficient of thermal expansion used for the computations was determined both from measurements made on laboratory specimens and from measurements made in the structure itself, the autogenous growth of concrete being neglected. In fact, the coefficient of thermal expansion of concrete is not constant. Moreover, if the data furnished by gages placed near the surface are considered in determining its magnitude, the results will not be very reliable, especially if the gages are placed near the downstream face of the dam, where both capillarity[16] and shrinkage phenomena occur. The use of concrete prisms (located in the interior of the dam) for the purpose of control measurements involves the risk of humidity changes in the chamber separating the prisms

---

[14] Head, Dams Studies Section, Lab. of Civ. Eng., Structural Branch, Lisbon, Portugal.

[15] "Determination of Stresses from Measurements in Concrete Dams," by J. M. Raphael, Third Congress on Large Dams, R-54, Stockholm, Sweden, 1948.

[16] "Beanspruchung von Gewichtsstaumauern durch das strömende Sickerwasser," by K. Terzaghi, *Die Bautechnik*, Vol. 12, 1934, p. 379.

from the dam concrete, in which case the prisms might be subject to conditions different from those of the mass concrete. This fact has been recognized in making similar measurements at Portuguese dams. The Laboratório de Engenharia Civil, Ministério das Obras Publicas, in Lisbon, Portugal, uses the arrangement illustrated by Fig. 13, which has the following advantages: The concrete that encloses the gages is (1) integral with the mass concrete; (2) free to undergo changes in length; and (3) protected against the air in the chamber by copper foil. Such an arrangement eliminates the difficulties in the determination of volume changes.

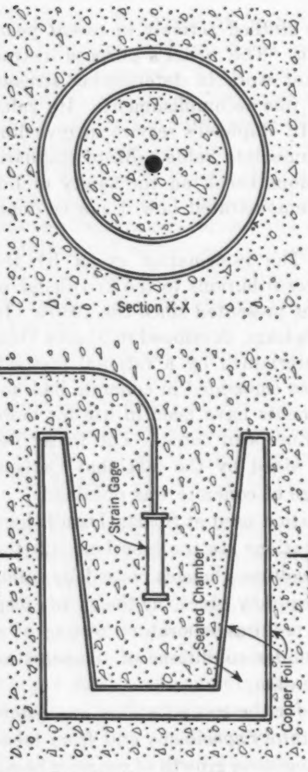

Fig. 13.—Null-Stress Meter

The influence of creep remains the most difficult problem to be solved in determining the stresses from strain measurements in mass concrete. Creep of concrete, as well as any other mechanical properties of concrete, cannot be determined without a dispersion of the results, even when the determinations are made at the same time on prisms of the same concrete cast on the same date. Creep is not entirely proportional to stress, not even for low stresses, and it is probably affected by the three-dimensional state of stress. In addition, it is affected by temperature and humidity conditions; the slow penetration of the water into the pores of concrete in hydraulic structures is a process that depends on many variables.

All these facts must be taken into account in laboratory testing. This requires a large number of different tests.

The author found that the stresses in the center of the dam are higher than those near the faces. This suggests the following explanation:

In a number of tests in tunnels, it has been found that the deformability of large rock masses is always greater than that of concrete, even after grouting (which no doubt decreases deformability). In like manner, the foundation rock of Shasta Dam may be more deformable than the concrete; this would account for the unusual stress distribution.

The differences between reaction and external loadings, illustrated in Fig. 9, were ascribed to the partial support of Row 43 exerted by Row 42 and Row

44. However, it is also possible that such differences are ascribable to the deficiencies inherent in the method, in which case information would be available concerning the accuracy it provides. A full explanation of the accuracy of the method would greatly increase the value of the author's paper. Although in a gravity dam like Shasta, it is possible for the final check of stresses to be made statically by comparing the reaction with the external loads, the writer does not actually know how such a check could be made in the case of an arch dam.

The writer questions conclusions with regard to the possible savings in gravity dams. Before it becomes possible to consider saving concrete in gravity dams having the usual cross sections, a full and detailed explanation of the determined stresses (including temperature stresses) will be required. For instance, models might be tested in which the foundation rock could be faithfully reproduced. In a gravity dam, the factor of safety against overturning is much lower than the usual safety factors encountered in structural engineering. On the other hand, the author fails to state whether the pore pressure in the concrete, and the uplift in the foundations, have reached their maximum values, corresponding to the steady state.

Because of its value, this study by Mr. Raphael deserves to be completed, with any available measurements of deflections, joint opening, temperature, pore pressure, and other factors influencing the stresses, so as to give a more complete picture of the structural behavior of the dam.

A. D. Ross[17].—Admiration and the closest study are due this paper because it is the result of a determined attempt to obtain the actual stresses in a major structure. Analytical studies and tests of materials and models can give much useful information; but knowledge of the behavior of the actual structure is the ultimate objective and it is both stimulating and encouraging to have these satisfactory records covering a long period.

The postulation of the creep surface is a reasonable approach to the problem and it is clearly of the correct general form for the three variables to which it relates. Thus, if—by careful control—the analyst eliminates the differences in creep caused by the water-cement ratio, the class of cement, the mineral character and grading of the aggregate, the ambient humidity, and other significant factors, a sufficient number of tests under constant sustained stress will define the creep surface for a particular concrete, but will not solve the problem of varying stress. This leads to a consideration of the effective modulus in Eq. 4. For the condition of constant stress, this equation is obviously correct and it is probably adequate for practical purposes when the stress is varying slightly and gradually—as, for example in the relaxation of prestressed concrete. It is less satisfactory, however, when the stress varies markedly and rapidly, and particularly when there is a reversal of stress. The equation is based on the assumption that the stress, σ_x, at any time, t, is uniquely determined by the effective modulus E', and the total strain ϵ'_x. However, it is possible to have two identical concretes exhibiting, at the same instant, the same total strain while carrying quite different stresses. This will happen if the stress histories

[17] Prof. of Civ. Eng., King's College, Univ. of London, London, England.

prior to that instant have been different. In other words (taking an extreme example), assume that two identical specimens have been maintained under a tensile stress of 100 lb per sq in. and a compressing stress of 1,000 lb per sq in. After (say) 3 months, the stress in the first is also raised to 1,000 lb per sq in. in compression. The total strains in the two specimens will never be the same although Eq. 4 suggests that at all times after 3 months the strains would be identical.

The writer appreciates that the semi-graphical construction in Fig. 4 is designed to deal with this difficulty, but does it really take into account the previous stress history? For example, between (say) 30 days and 40 days in Fig. 4 it would be incorrect to estimate increments of elastic strains plus creep strains from the creep surface for $K = 30$ days and $t = 0$ days to $t = 10$ days because these are appropriate only to concrete, that is, 30 days old and previously unloaded. To explain it less scientifically, much of the potential creep can be "squeezed out" of concrete if it is stressed early in its existence. The writer has made a mathematical analysis[18] that takes into account a variable stress history; but the problem is intrinsically a difficult one and the writer cannot claim that it is more than an approximation (and then only for unidirectional stress) because the equations neglect the effects of aging. Doubtless the construction of Fig. 4 resulted from the assumptions that the principle of superposition was applicable to the problem and that creep was wholly recoverable. Although these assumptions might apply to a very mature concrete, it seems unlikely that they can be true early in its existence.

Additional questions with regard to the computation of stresses also arose. Were the laboratory tests for the basic creep data conducted under uniaxial or triaxial conditions; and were the ambient conditions normal atmospheric or were they comparable with those of the interior of the dam? These questions seem important because creep appears to be due primarily to colloidal seepage and it is well known that the ambient humidity is a most influential factor in the question of creep. Incidentally, this condition would lead to the expectation of a greater creep—and therefore a reduction in stress—near the exposed downstream face of the dam. Also, it would be interesting to learn how the Poisson effect was handled in the computations. For short-period loading, concrete behaves very much like an elastic material with a relatively low value of the Poisson ratio, but was the Poisson effect considered in any way when computing creep strains? The writer's studies of concrete under various states of plane combined stresses suggest that the creep in the direction of one principal stress is quite independent of the creep along the orthogonal axis; that is, the Poisson ratio for creep strain seems to be zero. Finally, it is of interest to inquire whether any difficulties with zero drift of the strain gages were encountered—in view of the long period of service.

The effects that some of these uncertainties would have on the computed stresses are problematical, although they might help to explain the discrepancies between load and reaction that are noticeable at the end of 1943 in Fig. 9. In view of the complexity of the problem, close agreement between load and

[18] "Creep and Shrinkage in Plain, Reinforced and Prestressed Concrete," by A. D. Ross, *Journal*, Inst. of C. E., Vol. 21, No. 1, 1943, p. 38.

reaction throughout 4 yr could scarcely be expected and the author is to be congratulated on this paper, which, by the frank presentation of data derived from a variety of methods, must give much reassurance to designers.

J. A. HANSON[19].—The factual information on actual stresses developed in a structure, as reported by Mr. Raphael, should be studied by all designers of large concrete dams. In the limited space available, the author could not present the background of the creep theory as used by the USBR. This discussion describes in brief the laboratory studies, made by the writer and others, that substantiate the author's method for analyzing the effect of creep on stresses in Shasta Dam.

The problem of creep in structural behavior investigations of mass concrete involves approximations. In the writer's opinion, these approximations are no larger and of no more importance than similar assumptions made in the theory of elasticity as applied to concrete. At best, concrete is only a "statistically" homogeneous and isotropic material and, as Mr. McHenry states,[7] "It is almost axiomatic that when dealing with concrete any thought of high precision must be dropped at the outset." Such a situation does not preclude the application of either creep or elastic theory to concrete, but indicates a practical limit to profitable refinements of structural analysis.

The theory of creep in concrete as used by the USBR is represented by Eq. 5 and Fig. 4, and is simply a theory of "delayed" elasticity. As such, it requires superpostition of time effects and direct proportionality of creep to stress within the working range. Two of the creep-testing programs in the Engineering Laboratories (USBR) were designed to check these specific items for mass concrete. Superposition of time effects is easily and rigidly checked by comparison of measured and computed creep recovery. This computation, of course, must take the aging characteristics of concrete into account. In one of the programs, the computed recovery was from 100% to 120% of that measured and, in the other program, greater than 80%. Proportionality of creep to stress has been shown indirectly by the recovery measurements and was also demonstrated directly by loading similar test specimens in pairs so that the stress intensity of one was twice that of the other. These pairs of loadings were applied to specimens of four different ages, up to 90 days. In each case, the magnitude of creep from the higher load was twice that from the lower load within the normal dispersion of the data.

The interior of a large mass of concrete must retain the original moisture content, and this condition is duplicated in the laboratory by sealing the specimens in waterproof jackets. Several tests have shown that sufficient precision for determining stress from measured strain may be maintained even though the temperature effect on creep is neglected. In these tests, the sealed concrete was subjected to loads that maintained constant length or a particular strain history while undergoing a typical mass-concrete temperature cycle. Two such tests were reported by Mr. McHenry.[7] Stresses were com-

---

[19] Structural Research Engr., Eng. Labs., Bureau of Reclamation, U.S. Dept. of the Interior, Denver, Colo.

puted from the strain data by the step procedure described by the author, using constant-temperature creep functions. The agreement between measured and computed stress was good in all cases, indicating that, although temperature effect on creep may be of interest from a research viewpoint, it is not of great importance in structural behavior studies of large dams.

The aging characteristic of the particular concrete is the most important single factor affecting creep and instantaneous strain. It is not necessary that a large number of specimens be tested when determining the effect of age on the creep function for a particular structure. The routine program at the Engineering Laboratories consists of a total of only ten specimens of 6-in. diameters. Duplicate specimens are loaded to constant stress at ages of 2 days, 28 days, and 365 days. Single specimens are loaded at ages of 7 days and 90 days and two specimens function as free controls. As a check on the extrapolated creep function, the 7-day and 90-day specimens are unloaded at 1 yr, allowed to recover to age 5 yr, and then reloaded.

Measurements of recovery and creep from different load intensities have validated the principles of superposition and stress proportionality in the creep theory. The laboratory comparison of the computed and measured stresses and the separate check of equilibrium between the stress distribution and the applied loads in the structure have demonstrated that reliable values of existing stresses can be determined even though minor influences on the creep of concrete are neglected.

A. Warren Simonds,[20] M. ASCE.—The distribution of stress within a massive concrete dam has been a problem of concern to designers for many years. It has long been recognized that, in analyzing a dam section, the assumption of linear variation of stress distribution was not correct. Consequently, numerous attempts have been made to evaluate existing conditions more closely, following three general methods: (1) Mathematical analysis, (2) model analogies, and (3) analyses based on observations made with instruments embedded within the mass of the structure. Mr. Raphael has made use of method (3) in his evaluation of stresses in Shasta Dam. This investigation, made with an improved type of strain gage, has resulted in a thorough and complete evaluation of the stresses that substantiates the theory of nonlinear stress distribution along the base of the dam.

From a study of the stress diagrams, it is apparent that the method of construction has a profound effect on the distribution of stress along the base of the structure. The fact that block construction was used at Shasta Dam and that the joints between the blocks were not grouted until after a considerable height of concrete above the foundation had been placed and cooled undoubtedly contributed to the shape of the stress curves shown in the paper. If Shasta Dam had been built using long monolithic blocks extending from the upstream to the downstream face (a practice now discontinued in building very large dams), and if the concrete had been cooled to different temperature conditions, the resulting pattern of stress distribution would have been

[20] Engr., Bureau of Reclamation, U.S. Dept. of the Interior, Denver, Colo.

changed materially. In such a case, stresses much higher than those given by the author might have developed under similar loading conditions.

The strain measurements show that the effects of temperature variation on the concrete in the area near the surface range through a fairly large cycle (see Fig. 5(*b*)). Although the annual change in the interior of the mass concrete may be small, the daily variation at the surface may account for the extensive patterns of shallow cracks that are frequently observed on exposed areas. Annual variations in the stress cycle of the order of 800 lb per sq in. to 1,200 lb per sq in. are sufficient to cause cracks to develop.

Information that should be of interest to designers is the diagram showing the results of the author's computations of three-dimensional principal stresses from the stresses measured along the individual axes of the strainmeter groups (see Fig. 8). The appearance of tension among the second principal stresses is noted particularly in the vicinity of a rock pinnacle in the foundation. This tension may be the cause of cracks in the concrete which are observed frequently near irregularities in the foundation or abutments.

It is of considerable interest to note, in Fig. 7, the development of stress as the dam was built and as the reservoir filled. A condition little realized by most designers is emphasized—namely, that the construction procedure and temperature changes have greater influence on stresses in gravity dams than does the water load.

Most gravity dams are designed with a reasonable factor of safety based on a maximum condition of loading. Frequently, the assumed maximum loading is obtained by combining a series of loads or conditions that are likely to subject the structure to the highest allowable stress. Although it is assumed that the structure may be subjected to the most severe load conditions at one particular time, it is possible (but not probable) that this condition actually will occur. The stresses shown on the diagrams presented by the author are the results of observations made when the dam was subjected to only a fraction of the load assumed for design purposes. It will be interesting to observe the stresses that develop in Shasta Dam when it is subjected to a more severe condition of loading—one that presumably resembles more nearly the loading condition assumed in the design.

J. M. Raphael,[21] A. M. ASCE.—The interest shown in this paper, evidenced by the commendatory remarks, by the questions raised by the criticisms made, and by the supplemental data presented, is gratifying to the writer.

Mr. Riegel has assumed correctly that the heavy cross section of Shasta Dam was dictated by stability requirements, using conservative assumptions for the shear-friction factors.[22] In answer to Mr. Riegel's question as to whether conservatism in this respect was not on the excessive side, the USBR design criteria have been reviewed and restated as a result of studies made on actual dams. Designs that have since been planned for construction reflect the new criteria and design concepts in their generally leaner outlines.

---

[21] Head, Structural Behavior Group, Bureau of Reclamation, U. S. Dept. of the Interior, Denver, Colo.

[22] "The Design of Shasta Dam," by Kenneth B. Keener, *Civil Engineering*, July, 1943, p. 317.

Mr. Carlson also discusses the economy of the structure, pointing out that, from the standpoint of stress distribution, approximately 25% of the dam could have been removed from the region of the downstream face without changing the behavior significantly. In this connection, Mr. Simonds' remarks serve as a timely reminder that the dam has never experienced the maximum stresses for which it was designed. Maximum high water was not reached until May, 1952. Prior to the present writing (1952), no earthquake has occurred near the structure that would cause the accelerations for which it was designed. Similarly, uplift pressures have been only a fraction of the design pressure, attesting to the efficiency of the grout barrier and the drainage system. However, in a gravity dam, it is not usually the stress distribution or the magnitude of stress but rather the stability factor that controls the design.

Mr. Serafim comments that, in the method of stress determination used at Shasta Dam, the computations are too laborious. This is all too true of the method in use at the time of the Shasta Dam analysis. However, since that time several improvements have been made in the computation methods of the USBR. The most important of these improvements was the successful use of punched-card machines to do the actual work. By using the machines and a

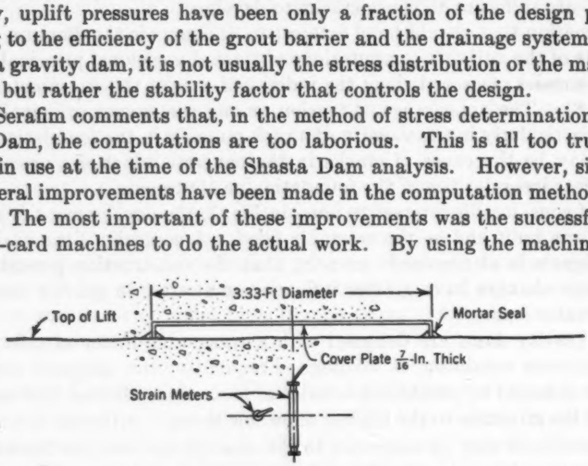

FIG. 14.—UNSTRESSED STRAIN METER DETAIL

more streamlined computation method, the analytical process has been accelerated sufficiently so that stresses now can be determined shortly after the field data are obtained. As an example, the USBR has been able to follow the actual development of stress in the base of Hungry Horse Dam, in Montana, as concrete was placed and the reservoir rose. Results from this and other major USBR dams should be available for study after 1953.

When Mr. Serafim states that the coefficient of expansion of concrete is not constant, he is perhaps placing too much emphasis on early-age behavior. The USBR has found some evidence indicating an early high value of the coefficient of expansion, which drops rapidly to a constant normal value within the first day. However, this condition is a phenomenon of the chemical expansion of the cement in the concrete during the first heating cycle, and is not applicable thereafter. The coefficient of expansion varies slightly with age. To put it in its proper perspective, the coefficient of expansion of various types of concrete ranges through a few millionths of an inch per inch per degree Fahrenheit, from 4×10^{-6} in. per in. per degree Fahrenheit to 7×10^{-6} in. per in. per degree Fahrenheit. Observed variation of any concrete with temperature varies by about one ten-millionth of an inch per inch and the variation with age is still less. The magnitude of stress error introduced by ignoring the variation with tem-

perature for a concrete in which the temperature range is about 30°F is less than 10 lb per sq in.—with correspondingly less error introduced by ignoring the effect of age. In any case, considering the length of the record involved in dam measurements and the general low values of stress the first day, the USBR has neglected this effect in its analysis.

Mr. Serafim's suggestion to make control measurements for the coefficient of expansion and the growth at points remote from the surface is good, as is the scheme he uses to embed the strain gage in mass concrete. Similar considerations led the USBR to the installation shown in Fig. 14, which was used at two recent dams. In these dams the vertical meter near the top of the lift measures, in effect, the coefficient of expansion—with possibly some contri-

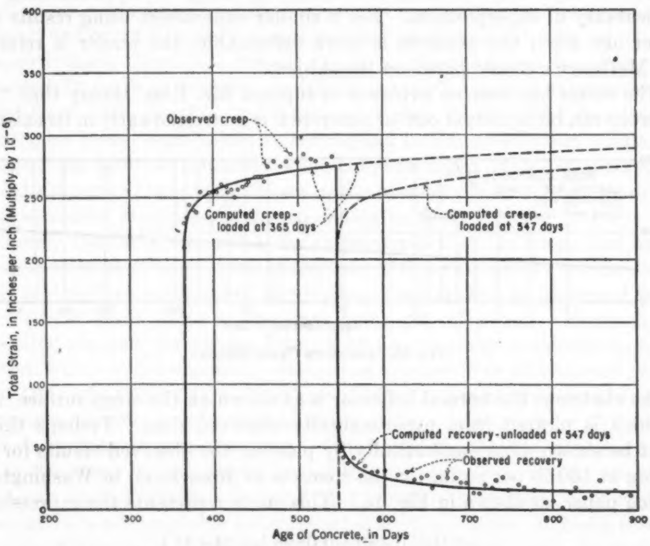

FIG. 15.—RECOVERY PREDICTED FROM CREEP CURVES, USING THE PRINCIPLE OF SUPERPOSITION

bution, through Poisson's ratio, of a fraction of the horizontal strain. The latter is evaluated separately by the horizontal strain meter. In this respect, Mr. Serafim's installation is superior; there can be no side effects if the copper container is flexible enough.

Mr. Serafim's remark that the deformability of large rock masses is always greater than that of concrete is thought-provoking, to say the least. In attempting to gage the effect of foundation rigidity on the stresses in Shasta Dam, the writer used the results of bearing tests made directly on the foundation rock. These tests indicated that the modulus of elasticity of the foundation rock was four to five times that of the concrete of the dam. It is understood that Mr. Serafim's tests utilize bearing areas almost ten times as large as those used at Shasta Dam and may reveal facts not shown in USBR tests.

Also, in Mr. Serafim's tests, the actual bearing is accomplished by a steel capsule rather than by the mortar patch and rigid plate used by the USBR.

Most of Mr. Ross' objections to the method of computing stress from a varying strain history hinge on the validity of the principle of superposition. Perhaps the results of an experiment made to test this principle will answer his objections. Fig. 15 shows the observations of a sealed cylinder of Shasta Dam concrete loaded at 1 yr with a constant load of 500 lb per sq in., and unloaded at $1\frac{1}{2}$ yr. The circled points are actual observations. The smooth lines are taken from the creep surface. The part of the curve representing recovery is plotted as the difference between the curves of 1-yr loading and $1\frac{1}{2}$-yr loading. It can be seen that the observed data follow very closely the theoretical lines derived using the commonly accepted understanding of the applicability of superposition. For a similar experiment using results at any earlier age when the concrete is more deformable, the reader is referred to Mr. McHenry's classic paper on the subject.[7]

The writer has seen no evidence to support Mr. Ross' theory that "potential creep can be 'squeezed out' of concrete if it is stressed early in its existence."

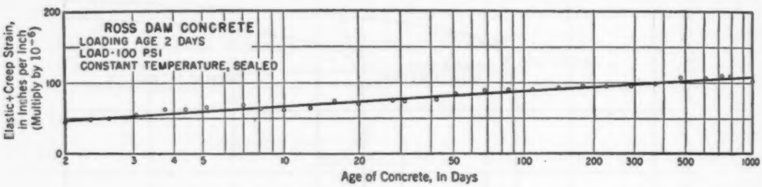

FIG. 16.—SPECIMEN CREEP RECORD

On the contrary, the normal behavior is as shown on the creep surface, in Fig. 3, which is plotted from experimentally observed data. Perhaps this fact might be shown more emphatically by plotting the observed results for 2-day loading at 100 lb per sq in. for the concrete at Ross Dam, in Washington, on semilog paper, as shown in Fig. 16. This curve represents the expression:

$$\epsilon = 100[0.480 + 0.0898 \log_e(t+1)].$$

Fig. 16 shows that, at the end of 1,000 days, there was no evidence that creep had been squeezed out of the concrete.

In one series of tests, run especially to find the effect of creep on the Poisson ratio, it was found that the range of values for the Poisson ratio for concrete loaded at a particular age was very narrow—for example, between 0.15 and 0.17. At the same time, it was found that the range of the variation of the Poisson ratio with age at first loading was much larger, of the order of between 0.12 and 0.19. This variation was used in the analysis of strain meter data for the dam. It was not found that the Poisson ratio for any age of loading was zero, as suggested by Mr. Ross. However, these were all uniaxial tests; no tests of creep under triaxial conditions have been made by the USBR. Indeed, the writer is not aware of any published results of triaxial creep tests. This field might be fruitful for further study.

Mr. Hanson elaborates on tests and controls used by him to establish the creep properties of Shasta Dam concrete. It is considered that the number of specimens used to establish the creep properties of a particular concrete is quite modest as compared, for instance, to the number of cylinders used to control the strength of concrete being used in a dam. As the creep properties of concrete gain in importance to designers of concrete structures, tests of creep will become more common, and more information will become available. Mr. Hanson's array of tests might well form the nucleus of a standard test for creep in concrete.

Mr. Simonds, one of the pioneers of model dam testing, shows the place of this prototype investigation among the three general methods for investigating the distribution of stress within a massive concrete dam. Each method has its limitations. Mathematical studies usually are limited by the necessity of expressing body and boundary forces in some mathematical form which may only approximate actual conditions. Load applications and boundary conditions usually must be modified greatly in models for ease in fabrication and manipulation. Mr. Serafim has indicated a step in the right direction by modifying his model foundations to correspond to the actual state. Although prototype tests indicate faithfully what happens in the actual structure, it is difficult to separate the several causes in the over-all effect. When more data become available, multiple correlation should be used.

Probably the most important design principle that can be gained from a study of the distribution of stress at the base of Shasta Dam is that the dimensions of a structure constructed like Shasta Dam cannot be increased indefinitely without some parts of the dam going out of action. However, the results cited are only for Shasta Dam; they do not really constitute sufficient data from which to draw general conclusions applicable to all concrete gravity dams. Only when many dams have been studied in this manner can the special conditions applicable to the individual dams be separated from the general laws that apply to all concrete dams. It is hoped that by the stimulus of this example the many investigations known to be underway in the Americas and Europe can be brought to successful and fruitful conclusions, and that the results can be made available for correlative studies. From inquiries received from dam designers in England, France, Portugal, India, and Australia, as well as from other agencies in the United States, it is believed that this paper is but the forerunner of many more after investigations now (1952) contemplated are completed. If this wealth of material becomes available, the paper will have served its purpose.

AMERICAN SOCIETY OF CIVIL ENGINEERS
Founded November 5, 1852

TRANSACTIONS

Paper No. 2548

INDUSTRIAL WASTE TREATMENT IN IOWA

By Paul Bolton[1]

Synopsis

Ranking first in the United States as an agricultural producer, Iowa also has a large and thriving manufacturing industry. This paper deals with the major sources of industrial pollution of the waters within the state, and the measures taken to reduce this pollution.

Data as to the volume of waste expected, the strength of the waste, and recommended treatment are given for the major industries in Iowa. The paper includes descriptions of the problems encountered in the treatment of wastes from packing houses, locker plants, dairy processing plants, canneries, rendering plants, beet sugar refineries, soybean processing plants, plating shops, and a number of minor industries in the state.

Introduction

Scope.—A paper dealing with industrial waste treatment in Iowa should be prefaced by an explanation of the scope of the subject and the difficulties encountered in obtaining a datum from which to work so that a realistic picture of the over-all problem is given. The subject provides a broad field of discussion, ranging from the establishment that the industrial waste problem exists to the details of specific types or methods of treatment fitted for a particular local situation.

In order to narrow the field of discussion to a comprehensible scope it has been approached from the standpoint of establishing at least three points: First, that a problem does exist, along with an idea of its magnitude; second, that available methods of treatment have cut deep inroads into the promiscuous discharge of untreated wastes to the intra-state streams; and, third, that an extensive problem of stream pollution still exists that must be corrected.

Preparation of an estimate of the situation for a discussion on any of the three points requires a great volume of information which is not readily available.

Note.—Published in September, 1952, as *Proceedings-Separate No. 149*. Positions and titles given are those in effect when the paper was received for publication.

[1] Associate Director, Div. of Public Health Eng., State Dept. of Health, Des Moines, Iowa.

However, through the cooperation of official agencies, industries that have been surveyed by consulting engineers, and the Iowa State Department of Health, and because of the availability of published reports, reliable estimates of the volume of the industrial wastes contributed by the major sources of pollution have been developed.

Sources of Waste.—Although Iowa is considered primarily an agricultural state, the dollar value of manufactured products is as high as, or higher than, the farm income. The estimated value of manufactured products for 1950 was $2,500,000,000 as compared to the 1949 cash farm income of $2,040,530,000. Although it is conceded that Iowa ranks first nationally as an agricultural state, it is probably not realized that it also has 3,856 manufacturing establishments located in 600 cities and towns.

Limitations.—Prior to establishing a datum predicated on the volume of waste to be treated, any evaluation of the industrial waste problem within the state should be commensurate with the provisions of the Iowa Stream and Lake Pollution Law. Until July 4, 1951, the power vested in the Iowa State Department of Health, permitting studies to determine ways and means of eliminating or of controlling the extent of pollution of the waters in or bordering on the state, did not apply to the lower 5,000 ft of any stream flowing into a river at a place where such river forms a part of the boundary line of the state. Therefore any evaluation should exclude the wastes discharged into the Mississippi River, the Missouri River, and the Big Sioux River—and wastes discharged as close as 5,000 ft from such rivers.

Treatment of Packing House Wastes

Magnitude of Waste.—Meat packing is one of the principal sources of pollution in the state. The published receipts of meat processed show that Iowa led the nation in 1949 with 4,148,000,000 lb of live weight. Although this is only 11½% of the "kill" in the nation, it represents a sizable industrial waste problem both as to volume and constituents.

Utilizing the 1949 published receipts of livestock at public yards, an estimate of the disposition to packers can be established without reference to any individual plant. The processing of all types of animals within the state represents a flow of waste of approximately 20,400,000 gal per day. Deducting the quantity discharged into those waters in or within 5,000 ft of the border streams, this amounts to a flow of 17,800,000 gal per day which is under the jurisdiction of the stream and lake pollution law. In terms of untreated wastes, and based on biochemical oxygen demand (B.O.D.), the volume processed would represent 155,000 lb for the entire kill, or 136,000 lb per day discharged into intra-state waters. These values are based on working days and do not represent the maximum volumes during periods of maximum kill. Of the quantity discharged into the intra-state streams, approximately 70% is treated in privately-owned plants or in combination with domestic sewage in municipally-owned treatment plants. Only one major packer located on an intra-state stream remains without some degree of treatment.

A review of the information available on the expected contributions of waste from the packing industry presents an interesting study. F. W. Mohlman[2] in a study of 14 Chicago (Ill.) packing plants, and 2 plants outside Chicago, determined the quantities listed in Table 1. A few results from the files of the Iowa State Department of Health are also given. On the subject of packing house wastes, R. W. Bates[3] states that good packing house control makes it possible to maintain a value of 2½ lb of B.O.D., per equivalent hog, in the raw screened effluent of a killing plant. This value corresponds to 20 lb per ton of live weight.

Handling of Packing House Waste.—The reporting of B.O.D. and volumes of packing house wastes should not be misconstrued to mean that these analyses are all that are needed to design a treatment plant adequately. The suspended solids content (which may range from well below 50% of the B.O.D. to values exceeding it) is extremely important in computing the volume of solids to be handled. The grease content should also be a guide to the necessity of grease

TABLE 1.—RECORD OF PACKING HOUSE WASTES

Description	Reported by F. W. Mohlman[a]					Iowa State Dept. of Health		
	Hogs	Cattle	Mixed kill	Mixed kill	Mixed kill	Mixed kill	Beef[b]	Hogs[b]
Number of plants averaged	four	four	six	one	one	...	...	...
Average water used[c]	4,275	3,225	4,633	4,080	4,900	3,690	1,700	424
Biochemical oxygen demand[d]	28.0	28.5	29.9	17.8	43.1	15.75	7.89	8.00

[a] The first three columns refer to packing plants in Chicago, Ill., and the fourth and fifth columns, to packing plants outside the city. [b] Water loss and B.O.D. for these plants are given in units per animal. [c] Except as noted in the last two columns, these values refer to the average gallons of water used, per ton of live weight processed. [d] Except as noted in the last two columns, these values refer to pounds of the biochemical oxygen demand, per ton of live weight processed.

removal units. The presence of each of these items can be affected materially by the operations within the plant itself. Efficient recovery of grease and nitrogenous materials as a by-product, and for treatment purposes, may eliminate the necessity of grease removal equipment in the treatment process and reduce clarifier sizes if little of the material is settleable.

It is usually much cheaper, when practicable, to handle waste materials in the dry, semi-dry, or separate form rather than diluted with water for removal from the immediate premises. The latter course involves installing expensive treatment facilities to remove the waste from the water-carried system. The handling of paunch contents in the semi-dry state, the conscientious collection of all blood, and the prevention of carry-overs from cookers are examples of practices that help reduce the volume of pollutional material.

A good research and recovery program is a vital part of any plant or industry program to reduce the quantity of waste, to facilitate treatment,

[2] "Packing House Industry," by F. W. Mohlman, *Industrial and Engineering Chemistry*, May, 1947, pp. 637–641.

[3] "A Discussion of Packing Plant Waste Disposal," by R. W. Bates, Annual Meeting of the Iowa Sewage Works Assn., 1948 (unpublished).

and, in many instances, to increase income from the sale of recoverable products, or to reduce the losses in the processing of the raw material.

Examples of Packing House Waste Treatment.—One of the first plants installed exclusively for the treatment of packing house wastes was constructed because of an acute stream pollution condition in one of the smaller streams of the state. An activated-sludge plant was installed in the early 1920's to treat the wastes. Although the plant was increased in size soon after installation, it was later abandoned in favor of biological filters because of the difficulties encountered in the operation and control of the activated sludge, and the sludge disposal problem.

The two-stage biological filtration plant was constructed in 1928. The units utilized are as follows: Flocculator, pre-settling tank, primary clarifier, primary filter, intermediate clarifier, equalizing tank, final filter, and final clarifier.

One of the unusual units in the plant is the primary filter. This is a rectangular trickling filter 3 ft deep. The filter is equipped for backwashing to eliminate the clogging that would be expected in a unit that operates at a load reaching 16,500 lb of B.O.D. per acre-ft, and with a water loading of only 5,000,000 gal per acre per day to 8,500,000 gal per acre per day. The filter has proved its value in the treatment at this plant since it removes approximately 55% of the applied load.

The second-stage filter, 7½ ft deep, is also quite heavily loaded from a B.O.D. standpoint: One computation indicates a loading of 1,100 lb per acre-ft, although much higher loadings have been reported. This plant produces an effluent of less than 50 ppm of B.O.D. most of the time.

Another type of treatment is practiced at Waterloo, Iowa, where the effluent of the packing house grease removal units and fine screens is treated through the municipally-owned plant. The packing house wastes are pumped directly into pretreatment units without mixing with the domestic wastes. The pretreatment installation consists of grit removal and grease removal units, a primary clarifier, and roughing filters. The effluent of the roughing filters can be mixed with the raw domestic wastes or with the domestic wastes following treatment in the detritors and grease removal and flocculation units. The combined wastes are then treated through primary clarifiers, conventional biological filters, and final clarifiers.

The roughing filters for the packing house waste are 6 ft deep and operate at B.O.D. loads of from 5,000 to 9,300 lb per acre-ft. No recirculation is employed on these units and the water loading is considerably less than the high-rate range. A limited number of results indicates a removal of from 48% to 56% through the roughing filters, and an over-all pretreatment plant removal of from 77% to 82%. The B.O.D. of the raw packing house waste, as received at the treatment plant, ranges from 1,000 ppm to 2,000 ppm.

The second-stage filters that receive the combined pretreated load and the city clarified waste are 7½ ft deep. These filters operated at loads ranging from 600–800 lb of B.O.D. per acre-ft to 1,800–2,400 lb per acre-ft, depending on the contribution of the industrial establishments. The results on these filters, in combination with the final clarifiers, indicate removals of from 75% to

88%. It should be noted that the remarkable removals through the filters are accompanied by a corresponding degree of supervision to prevent ponding and clogging.

A review of the 1950 reports indicates a final effluent with B.O.D. ranging from 18 ppm to 72 ppm in February to 18 ppm to 34 ppm in July. These results follow the pattern of loading on the treatment facilities. The plant is heavily overloaded and expansion is needed.

In Iowa most of the plants treating packing house wastes combined with municipal wastes employ two-stage biological filters, especially where the packing house waste is the "tail that wags the dog." Exceptions to the two-stage filter process are Cedar Rapids, Des Moines, and Marshalltown. At Cedar Rapids and Des Moines single-stage filters are used and at Marshalltown the activated sludge process.

Activated sludge at Marshalltown has been successful as far as treatment is concerned but has required considerable operation. The dilution of the packing house wastes with sizable quantities of other wastes may be one of the contributing factors to the success of the process. Mr. Mohlman attributes the success attained in treating the Chicago packing house load at the southwest treatment works, by the activated-sludge process, to the fact that considerable dilution with other wastes is available.

Filter Design.—In passing from a discussion of packing house waste to other wastes it should be emphasized that the filter loads quoted are higher than would normally be used in design, particularly on second-stage filters. Relatively deep filters at lower loadings are less susceptible to an immediate deterioration of effluent resulting from sudden increases in applied strengths, and can generally be relied on for a more stable effluent because of better nitrification. Of course, there are other factors to be considered in filter design.

Treatment of Locker Plant Waste

Another waste resulting from the killing of animals (and similar in some characteristics to packing house wastes) is the effluent from locker plants. According to the Iowa State Department of Agriculture, 686 locker plants are registered and licensed. Of this number, approximately 3.6% are situated where the waste would discharge into border streams. A sufficient number of plants have been surveyed to give a representative cross section of the wastes involved.

Characteristics of the Waste.—The estimates of the B.O.D. of this industry are based on good housekeeping within the "killing" plants. This includes the exclusion of parts of animals, meat, hair, and the contents of the intestines from the sewers, the collection of all blood, and squeegeeing of floors and tables prior to the washdown of equipment. The offal of the killing process, in most instances, is collected and processed by by-products companies.

The wastes discharged into the streams in the interior of the state from this source are estimated at 1,048,000 gal and 12,300 lb of B.O.D. per day. Approximately 43% is discharged into treatment plants and the remainder is untreated. Of the waste reported as treated, approximately 10% is discharged

into septic tanks without further treatment and therefore the effectiveness of the treatment provided is questionable.

Treatment Problems.—The small size of the locker plants, as a general rule, complicates the treatment of the wastes. Two or three of the small establishments have installed septic tanks, followed by subsurface absorption fields, in an effort to remedy the immediate problem. The septic tanks and soil absorption systems were both leniently designed. The first such unit was installed on a trial basis and about a year later was reported as still functioning satisfactorily; a very limited number have been built with no further word from the owners. This type of treatment and disposal system is not recommended but is mentioned because of the results attained. The problem of the small locker plant that must treat its own waste should be studied by the industry itself.

The discharge of these wastes in appreciable quantities into municipal sewerage systems with sand filters usually causes considerable difficulty. If good housekeeping is practiced in the plant, very little of the waste will settle; therefore, the treatment is largely dependent on the secondary facilities. In the removal of this organic matter, sand filters clog frequently and require drying and skimming.

Treatment of Dairy Industry Wastes

Magnitude of Problem.—The waste contributed by the dairy industry is of considerable magnitude, as can be deduced from the volume of dairy products produced in 1949. The Iowa Crop and Reporting Service has revealed that the whole milk equivalent of manufactured dairy products totaled 4,414,000,000 lb. The products manufactured by the dairy industry vary widely and produce wastes with a wide range of strength and constituents. The wastes from butter manufacturing will vary in B.O.D. content from 500 ppm–600 ppm to as high as from 1,500 ppm–5,000 ppm. These findings are quoted on the basis of a good program of waste prevention in the creamery and the collection of all buttermilk and spillage without discharge into the sewer system. The ease with which these values are increased as a result of spills or poor operating conditions is readily evident when the B.O.D. of the products handled is known. Whole milk has a 5-day B.O.D. of approximately 102,000 ppm; skim milk, 73,000 ppm; buttermilk, 64,000 ppm; and the whey from cheese plants, 32,000 ppm. In other words, small quantities of these wastes have a sudden impact on treatment facilities.

A report of the Waste Disposal Task Committee of the Dairy Industry Committee strongly stresses the role of waste prevention in waste treatment. The committee reports that good operation methods can keep the waste loss in receiving operations at less than 0.35%.

The manufactured products are the bases of estimates of the status of industrial wastes since, of the 5,921,000,000 lb of milk produced on the farm, only 2% is used for retail sales to consumers. According to the 1949 report of the Iowa Department of Agriculture, there are 390 creameries, 831 skim milk stations, 23 central churning plants, and 30 cheese factories within the state.

It is estimated that the manufacturing processes of the dairy industry produce 3,393,000 gal of waste and 37,549 lb of B.O.D. per day. These values are based on the estimated number of working days and do not include seasons of maximum production. The quantity produced in the interior of the state, in accordance with the coverage of the stream and lake pollution law, reduces this waste to 3,040,000 gal and 33,300 lb of B.O.D. A cross section of this industry, based on creamery wastes disposition, indicates that approximately 49% of the waste goes into private sewer lines without treatment, 14% discharges into private sewer lines with treatment, 13% into municipal sewers without treatment, and 24% into municipal sewers with treatment.

The volume discharged into private sewer lines with treatment should be viewed with caution. In most instances, this consists of septic tank treatment only, which has not proved effective for the adequate reduction of dairy wastes even as primary treatment.

Treatment Procedures.—Milk wastes consist largely of organic solids, fat, milk sugars, and protein in the form of casein. The breakdown of the milk sugars into acids, primarily lactic acid, and the development of lethal levels injurious to biological life in the treatment processes, indicate that milk wastes should be treated while fresh, and treatment should be under aerobic conditions. Max Levine, in research work at the Iowa Engineering Experiment Station (Iowa State College, at Ames) showed that the production of ammonia in the treatment of protein wastes practically ceased when appreciable quantities of milk wastes were added.[4] At the same time, the acidity materially increased, retarding the action of the ammonia forming organisms.

W. E. Galligan and Mr. Levine proved[5] that dairy wastes were amenable to biological filtration in their studies of milk waste treatment in the late 1920's and early 1930's. Filters loaded in the standard rate range of from 375 to 600 lb per acre-ft per day (or from 1,120 lb to 1,640 lb for the 8 hr of operation) reduced the raw waste (from 480 ppm–1,240 ppm of B.O.D. to 30 ppm–60 ppm of B.O.D.) in the final effluent. Approximately 95% removal was effected when using a quartzite rock from 1 in. to 2½ in. in size. Such plants were installed at two creameries and the results quoted are from one of the plants under operating conditions.

With the introduction of the high-rate filter, many of the dairy industries desire to use them for the treatment of wastes because of the economy of installation compared to standard rate filters; but there is not a sufficient accumulation of results on high-rate filters to determine a reliable expected removal through these units.

H. A. Triebler and H. G. Harding of the National Dairy Research Laboratories also reported[6] a lack of results in their discussion of dairy industry wastes. From a review of all types of treatment available they reported that one-stage or two-stage trickling filters of the high-rate recirculating type appear to be

[4] "Fundamentals in the Purification of Creamery Wastes," by Max Levine, *Bulletin 77*, Eng. Extension Dept., Iowa State College, Ames, Iowa, Vol. XXIV, No. 20, October 14, 1925.

[5] "Purification of Creamery Waste on Filters at Two Iowa Creameries," by W. E. Galligan and Max Levine, *Bulletin 115*, Iowa Eng. Experiment Station, Iowa State College, Ames, Iowa, Vol. XXXII, No. 44, April 4, 1934.

[6] "Dairy Industry," by H. A. Triebler and H. G. Harding, *Industrial and Engineering Chemistry*, May, 1947, pp. 608–613.

preferred in the dairy waste field, depending on the degree of treatment required. This preference was attributed to relatively low initial and operation costs and to the fact that these units are fairly foolproof and immune to disturbances resulting from occasional overloading.

One filter installation in Iowa reduced the B.O.D. of dairy waste from 2,290 ppm to 970 ppm or 58%. The filter load was 1,920 lb of B.O.D. per acre-ft for the 10-hr daytime period of treatment plant operation, based on the settled applied waste, or 4,560 lb of B.O.D. per acre-ft for the total applied, whereas the hydraulic load was only one third of that considered to be in the high-rate range. These results were from a single composite. Changes were made in the operation of the plant, and the water loading on the filter was increased to 20,000,000 gal per acre per day. A plant study gives the following data: The raw waste had a B.O.D. of 7,500 ppm and the final effluent, 400 ppm for a 94.7% removal. Although processing in the dairy plant ceases at about 2:00 p.m., the treatment plant runs continuously. The waste is cycled through the filter until 5:30 a.m. and then a sufficient amount is diverted to the final settling compartment and the receiving ditch so that, by the time the processing starts, the holding basin receiving the raw waste is drawn down sufficiently to hold the day's flow. The filter effluent returns to the raw sewage holding basin and is continuously aerated by compressed air.

Processes are available, therefore, for treating milk wastes separately but, because of the high cost of constructing standard rate filters and an insufficient amount of operating data to forecast the efficiency of high-rate filters adequately, the need for further study is evident.

Combined Treatment.—The treating of large quantities of milk wastes combined with domestic wastes has presented problems. The formation of acids through the breakdown of milk sugars has eliminated the use of Imhoff tanks as primary treatment units because of the interference with digestion, and accompanying foaming. In some instances in which Imhoff tanks are used, the creamery waste, after adequate grease and grit removal, has been carried to the treatment plant site and discharged directly into the filter. This by-passing of the primary units has eliminated interference with their operation.

Treatment of Cannery Wastes

The canning industry (including only the plants limited to vegetable canning) produces a large quantity of waste, in season, which is high in B.O.D. and the industry is noted for its use of copious quantities of water. The waste putrefies quite rapidly if not treated and emits obnoxious odors, giving rise to nuisance conditions.

Waste.—A resumé of the size of the vegetable canning industry located in the interior of the state gives a close approximation of the volume and disposition of its wastes. The total waste from the industry is approximately 4,178,000 gal per average day of operation, of which 2,848,000 gal is produced in the interior of the state. The estimate is based on polluted wastes only, and does not include cooling water used in those plants in which separation is practiced. The total B.O.D. contained in the 2,848,000 gal of waste is estimated to be 80,200 lb. The waste varies in strength in accordance with

each individual plant, the product canned, and the volume of water in which the waste is carried. Selecting random results from the files, the B.O.D. strength of composite samples of the waste varies from 1,400 ppm to 4,000 ppm. Stack wastes, resulting from corn canning, will be as high as 32,000 ppm in B.O.D. and, if mixed with the processing wastes, raises the organic content substantially.

The wastes produced in the interior of the state can be further broken down into 167,000 gal per day lagooned, 1,780,000 gal irrigated, 653,000 gal discharged into municipal treatment plants, and 279,000 gal untreated.

In most instances, canning plants are located in small communities near the source of the raw products. The tremendous seasonal load disrupts local sewage treatment facilities, not designed for the additional waste, to the extent that little effective treatment is accomplished. This condition, plus severe conditions of stream pollution, necessitated either the provision of additional treatment units or the development of other methods of disposal.

Methods of Treatment.—Lagooning was tried at a number of places and some lagoons are still in use. Difficulties with some lagoons developed because of odor nuisances. The breakdown of the organic matter in the lagoons emits objectionable odors, requiring careful isolation of the ponds, or chemical treatment. Odors can be inhibited through the use of sodium nitrate in sufficient quantities to satisfy approximately 20% of the B.O.D. Lagoons must also be located carefully to secure the proper type of subsoil and to prevent seepage into coarse gravel and subsequent discharge into streams without sufficient filtration.

Because of the difficulties or objections anticipated with other methods of treatment or disposal, irrigation in shallow trenches was tried in 1934 and 1936. The only pretreatment was screening of the wastes with fine mesh screens. This waste was pumped into irrigation trenches approximately 24 in. wide at the top, 15 in. wide at the bottom, and from 9 in. to 18 in. deep. The ridges between the furrows were from 3 ft to 3½ ft wide. It was learned that, if the trench bottoms were maintained level for the full length, and if no trench was reused until after dewatering and drying, a relatively small acreage would dispose of the wastes from a sizable canning plant. The objectionable odors of lagooning were also avoided by this method.

An irrigation field must be located where the soils are of such a substance and texture that they will readily absorb the wastes, and the field must be properly supervised to function satisfactorily. Two of the fields studied have disposed of approximately 100,000 gal to 150,000 gal of waste per acre per day.

Treatment of Rendernig Wastes

The rendering industry has presented a particular problem in the disposal and treatment of wastes because of the isolated locations of the manufacturing plants. This requires private treatment facilities and, in most locations, a good degree of treatment because of the nature of the waste.

Magnitude of the Problem.—The use of barometric condensers for cooker control materially increases the quantity of wastes involved and the size of treatment plant required. The entrained organic matter in the barometric

condenser water or the quantity carried over from the cookers through normal or careless operation is generally sufficient to necessitate treatment. In an attempt to reduce the volume of waste requiring treatment, the industry has been encouraged for years to utilize vacuum pumps for the control of cookers. At first this suggestion was resisted because of the fear of insufficient quality control on the products. Only in recent years has the use of vacuum pumps in this area been utilized for such purposes. The cooling water for condensing the discharge of vacuum pumps can be divorced entirely from pollutional material and, at the same time, is available for dilution of the treatment plant effluent.

The 72 plants registered in the State of Iowa are widely scattered and in only two or three locations is all the waste discharged into municipal systems with treatment plants. One or two other plants are so located, but only part of the waste discharges into the municipal sewers. Some of the plants are equipped with septic tanks but, for the purposes of estimating the volume of treated wastes, these plants are not included since, in most locations, they do not provide adequate treatment. The total waste discharged from the industry is estimated to be 4,680,000 gal and 18,000 lb of B.O.D. per day. Approximately 3.5% is discharged into municipal systems and treated and another 10% is credited with treatment in privately-owned plants.

Methods of Treatment.—A treatment plant, consisting of a high-rate backwash type, aerated filter was installed to treat the wastes from one of the rendering plants. The filter was arranged for recirculation, the filter effluent being returned to the recirculation pump sump. The solids were to be collected on the filter, backwashed into the settling tank, and, after settling, lagooned for disposal. The filter medium was $\frac{5}{16}$-in. by $\frac{9}{16}$-in. anthracite. Forced draft filter ventilation was included in the design. The outlet from the plant was through the wet well for the pump discharging into the anthracite filter.

After a 3-week or 4-week period of operation, observations were made on the effluent. The plant effluent had a soapy, whitish-gray appearance. Analyses of the waste by a commercial firm indicated a reduction of 61% in B.O.D. and 51% in suspended solids. The raw waste contained 166 ppm suspended solids and 370 ppm of B.O.D., and the final effluent contained 81 ppm suspended solids and 144 ppm of B.O.D.

Later observations indicated an effluent of the same appearance as previously noted, and grab samples collected after backwashing the filter showed no reduction in B.O.D. between the settling tank effluent and the final effluent. These samples were collected at an inopportune time but represented the strength of waste discharged by the plant after backwashing. The grid for aerating the filter was not in use at the time the grab samples were collected.

A different type of disposal system was constructed at another rendering plant. This treatment plant consisted of a grease trap for the collection of floating material and settleable solids, followed by a subsurface filter absorption system. The settling tank was too small for effective settling. The filter absorption system consisted of a large pit filled to a 4-ft depth with from 1 in. to 4 in. of washed rock. Distribution was accomplished by laying farm-tile lines on $4\frac{1}{2}$-ft centers longitudinally over the rock. The joints in the tile were

covered with burlap and a layer of from 18 in. to 24 in. of clay. This installation operated for approximately two years before the filter absorption system clogged. The management, however, feels that it has been sufficiently successful, and they are planning to install a second such system with larger units.

In 1947 a plant of the separate sludge, high-rate filter type was installed to treat the wastes from one plant prior to discharge into a practically dry run. The wastes had been causing gross pollution in the receiving ditch and were creating an odor problem. The plant was installed and designed to treat the wastes from the unloading room, cooker room, hasher, and washer, and also the sanitary wastes of the employees. A study of the barometric condenser wastes had indicated that the B.O.D. was sufficiently low to be controlled by chlorination. Soon after operations were started it was found that the barometric condenser waste was not being controlled by the available chlorinator, particularly when the material for processing was received in a bad state of decomposition.

After a number of meetings of the plant officials, the consulting engineer, and the Iowa State Department of Health, it was decided to install vacuum pumps and surface condensers to reduce the volume of polluted waste so that it could all be discharged into the treatment plant. A blower was installed to produce suction from the top of the old chlorine contact tanks and maintain a vacuum on the cookers. The cooling water was sprayed on the outside of the contact tanks to condense all the waste possible from the cookers. The condensed wastes are discharged into the treatment plant. The blower discharges the noncondensable gases into the fire box of the gas-fired plant boiler. The cooling water is collected without contact with polluting material and directed to the treatment plant outfall line for dilution of the treatment plant effluent.

This change-over immediately reduced the loadings on the plant. In addition to the 10,000,000-gal-per-acre-per-day filter, 8 ft deep, with a straight-line clarifier ahead of it, a nonmechanical, conical, final clarifier was installed following it, and an open-sludge digester with sludge beds for the disposal of the removed solids. Recirculation is accomplished through the primary clarifier.

Three studies of this plant have been made. Composite samples of the effluent indicated the B.O.D. to be 40 ppm and 43 ppm during periods when the average load of fresh material was being processed and 160 ppm during a period of heavy production of partly decomposed material. The recirculation ratio varies from 5 to approximately 14. The computed filter loading, based on total applied, was 0.134 lb per sq ft per day, when the effluent had a B.O.D. of 43 ppm.

The treatment of reducing plant waste is in the research and development stage, and more experience on plant-scale applications is necessary to determine the suitability of the available processes in regard to permissible plant loadings to produce a required effluent.

Treatment of Other Industrial Wastes

Beet Sugar Processing.—A large sugar processing firm located on a relatively small stream has controlled its wastes for a number of years by ponding.

The wastes consist principally of beet wheel water, battery and pulp press water, lime flume water, and Steffen's waste water. All the wastes, amounting to approximately 3,000,000 gal per day, are discharged into the ponds. Some of the wastes are later reclaimed but approximately 2,500,000 gal per day are stored for release into the river during periods of high runoff in the spring. The strength of these wastes can be judged by the beet flume water which contains from 350 ppm to 500 ppm of B.O.D., or higher, if spoiled beets are used. The pulp water contains a B.O.D. of from 700 ppm to 900 ppm and the Steffen's waste has a B.O.D. of 3,000 ppm. The Steffen's waste, amounting to a sizable volume, is one of the wastes now reclaimed. The lime flume water is lagooned separately for lime reclaiming. In the spring, the release of the water to the receiving stream is controlled by the analyses of the ponded waste and the volume of flow in the stream. Curves were developed based on the flow in the stream, the temperature of the stream water, the strength of the waste released from the ponds, and the apportionment of the allowable oxygen available for use in the stream water among the various users in the area. This control arrangement has prevented heavy pollutional conditions in the receiving stream since the implementation of the procedures.

Poultry Industry.—The size of the poultry industry can be estimated from the 1947 production figures. The total production was 48,198,000 head, of which 2,565,000 were turkeys. Ninety-one plants are listed as processing poultry, some of which have a capacity of several thousand birds per day. Poultry packing wastes are amenable to treatment by biological filtration. Poultry dressing establishments are usually located with access to municipal sewers and the wastes are treated in combination with municipal sewage. The strength of these wastes varies from 300 ppm to 1,000 ppm of B.O.D., depending on the efficiency of blood collection and the method of handling battery manure.

Soybean Processing.—Soybean processing in Iowa is a sizable industry. The plants may be of the expeller type but, in general, extraction is used for the removal of the oil from the beans. The use of hexane in the extraction process adds the danger of explosion or fire, if accidents occur, and appreciable quantities of the solvent escape to the sewer or treatment processes. Where the wastes were discharged into sewers and were well diluted, no difficulty was reported in the treatment. It is imperative that escape-proof units be provided between the plant and the sewer system to prevent, positively, the admission of hexane into the sewerage system. Trichlorethylene is a noninflammable solvent but is not widely used. It does eliminate the explosive or fire hazard, however.

At isolated plants without treatment facilities, most of the treatment has been within the plant in the form of recovery. Better hexane recovery methods have been employed, as well as recovery of the soybean meal. Only a limited amount of information is available on strengths; however, the data available indicate that the B.O.D. can be reduced from approximately 300 ppm to 100 ppm by improved recovery processes.

Although it is known that the hexane carry-over can be quite readily volatilized out of the waste, no other data relative to treatment are available. It is a problem that will require study to develop suitable processes of treatment.

Plating Industry.—In Iowa, the plating industry has grown in connection with the manufacture of farm machinery, household appliances, and heavy machinery, until its wastes are developing into a problem. The use of cyanide in plating as well as such heavy metals as chromium, cadmium, copper, and others adds to the list of industrial wastes that must be controlled. These wastes, in sufficient quantities to be a hazard to the stream, usually come from spills, dumping of contaminated tanks, and similar sources, rather than from a constant discharge into the sewer. Some of the industries are becoming so large, however, that the carry-over on parts removed from the plating tanks is approaching the allowable limit. Volumes have been written on oxidation, reduction, neutralization, and disposal of these wastes as a result of continuing research. The use of chlorine for the oxidation of cyanides is recognized, but the first plant scale application is just now under construction in Iowa.

In smaller installations, the use of holding tanks to collect plating wastes (if accidental spills occur or substandard tanks must be discarded) should not be overlooked. The contents of the holding tank can then be drained off over a long period of time or oxidized or reduced and then bled at a slow rate. If large quantities of sewage are available for dilution, it may be possible to reduce the concentration through controlled discharge and dilution to below any hazardous degree of concentration.

Manufactured Gas.—Gas plant wastes from the production of manufactured gas represent a sporadic problem. Although such installations have decreased in number because of the shipping or piping of gas into the state, a sufficient number are still operating to classify the waste as a problem. Such installations are usually located in large centers of population, and with careful primary treatment units can reduce the phenolic and mulch content to such a level and quantity that it can be mixed with domestic sewage without injurious effects on the treatment processes. Good reclamation procedures and reuse of water within the plant can reduce the quantity of waste and its constituents materially. Amply designed separators with scum and sludge removal facilities can be used for removal of the mulch that either floats or settles with a reduction in temperature. This material can then be salvaged for use in by-products. Further treatment of the clarifier separator effluent (by replaceable coke or similar filters) may be required. Within the writer's experience, these principles, properly applied and controlled, have permitted treatment of gas plant wastes with large volumes of municipal sewage.

Oily Wastes.—Oil wastes are a problem in some streams and sewers because of the servicing of railroad motive power and the use of cutting oils and coolants in the manufacture of farm machinery and heavy equipment. Oils and greases of the usual type can be removed by the use of gravity separators or clarifiers. The use of emulsions, however, further complicates the problem. Most large users of cutting oils or solvents process the oils for reuse; but the residue and volume rejected must be treated prior to discharge into the streams. The emulsions can usually be broken by depressing the potential of hyrogen (pH) by the use of alum or acids and, after skimming and settling, the pH-value can be raised with lime and further removal effected by settling.

Sugar Processing.—An experience with ion exchange for the purification of sugar products should be mentioned as a matter of interest, to show how complications can occur in the disposal or treatment of wastes. The waste from this industry was lagooned for disposal and this operation was reasonably satisfactory until the regeneration waste of the ion exchangers was added. The exchangers were regenerated by sulfuric acid. After a reasonable period of time, to allow good digestion to become established, the resulting odor of hydrogen sulfide could be detected for considerable distances. A change to hydrochloric acid in the regeneration process eliminated the odor problem.

Miscellaneous Waste Problems.—The wastes from the manufacture of starch and its allied products, alcohol, furfural, paper, and beverages (including beer) are all found within the boundaries of the State of Iowa. Some of these industries are beyond the control of the stream pollution law and for others treatment is provided.

The wastes produced in some of the new types of industries include flouro-silicate wastes from the manufacture of phosphate fertilizers, arsenic, and other compounds from the production of biologicals and the wastes from the manufacture of insecticides. These wastes contain complicated organic compounds, treatment of which requires research, time, and effort.

The effect of such wastes can be realized, however, when it is considered that two of the worst fish kills in recent years have occurred as a result of the discharge of an insecticide into a sewer system equipped with treatment, and of a change in the type of raw waste discharged into a stream because of a toxic preservative used to prevent mold formation in food containers. These intermittent occurrences can be more damaging to fish and other aquatic life than the continuous discharge of improperly treated sewage or wastes. The suddenness of their effect prohibits migration of the biological life and traps them below the outlets into the streams.

Conclusion

The three points presented at the beginning of this paper have been established. An industrial waste problem does exist in Iowa although known processes and methods of treatment have controlled a large proportion of it. There is much work to be done from the standpoint of the installation of new facilities and the expansion or replacement of those in existence. This will require not only the united effort of all official agencies but also the wholehearted cooperation of all industries. It should be remembered that, although anyone engaged in the profession of sanitary or public health engineering (whether publicly or privately employed) stands ready, willing, and eager to be of assistance, it is still largely industry's own problem to analyze wastes and develop methods of treatment.

Acknowledgment

At the annual meeting of the Iowa Engineering Society at Des Moines on January 23, 1951, a paper entitled "Status of Industrial Treatment in Iowa" was presented by the writer.[7] The present paper has some modifications

[7] "Status of Industrial Waste Treatment in Iowa," by Paul Bolton, *The Exponent*, Iowa Eng. Soc., April, 1951.

of the former work, adapted to the requirements of the Society for purposes of encouraging widespread discussion on a general plane.

The task of studying the official reports from the several agencies of the various levels of government was notably lessened by the assistance of the persons charged with the promulgation of the reports. This cooperation was the only means of establishing the factual information necessary for a basis of the paper. This assistance was sincerely appreciated.

Deep gratitude for the information taken from both published and unpublished reports as referenced and those studied but not drawn upon is also expressed.

Also acknowledged is the assistance of several of the engineers of the Iowa State Department of Health who helped assemble the information into summary form for the final presentation.

AMERICAN SOCIETY OF CIVIL ENGINEERS
Founded November 5, 1852

TRANSACTIONS

Paper No. 2549

TORSION OF PLATE GIRDERS

BY F. K. CHANG,[1] J. M. ASCE AND BRUCE G. JOHNSTON,[2] M. ASCE

WITH DISCUSSION BY MESSRS. ARTHUR P. JENTOFT, RICHARD W. MAYO, AND E. RUSSELL JOHNSTON, JR.; AND F. K. CHANG AND BRUCE G. JOHNSTON

SYNOPSIS

Analytical and experimental research was undertaken at Lehigh University, Bethlehem, Pa., to determine the stress distribution, stiffness, and strength of bolted, riveted, and welded plate girders under uniform twisting moment. Seventy-two tests were made on fifteen different specimens. Eleven of the specimens were finally tested into the plastic range.

Except for initial pilot tests of small specimens, all tests were made on the 2,000,000 in.-lb torsion testing machine[3] especially built for this program of research. Test variables included the number of cover plates, the rivet pitch, variable tension in bolts, and a variety of girder cross-section sizes up to 4 ft in depth, with or without stiffeners.

Formulas are proposed for calculating rivet or bolt pitch and size of welds for the bolted, riveted, and welded plate girders, or, when rivet pitch or weld size are given, the torsional stiffness and strength can be predicted.

INTRODUCTION

General.—In the design of an open section such as an I-beam, bending is of primary importance and the problem of torsion, if it exists at all, is usually secondary. If torsional loads are of primary concern, a closed box or tube section is generally used.

A knowledge of the torsional behavior of built-up I-section girders is expecially necessary in problems involving lateral buckling, as corroborated by recent investigators in this field. Karl de Vries, M. ASCE, states "Torsion formulas for plate girders do not seem to be available * * *."[4] George Winter,

NOTE.—Published in April, 1952, as *Proceedings-Separate No. 125.* Positions and titles given are those in effect when the paper or discussion was received for publication.

[1] Formerly Research Asst., Dept. of Civ. Eng. and Mechanics, Lehigh Univ., Bethlehem, Pa.; now with the Pennsylvania State Dept. of Highways, Harrisburg, Pa.

[2] Prof. of Structural Eng., Univ. of Michigan, Ann Arbor, Mich.; formerly Director of Fritz Eng. Laboratory, Lehigh Univ., Bethlehem, Pa.

[3] "A Torsion Testing Machine of 2,000,000 Inch-Pound Capacity," by F. K. Chang, K. Endre Knudsen, and B. G. Johnston, *Bulletin No. 160*, A.S.T.M., September, 1949, p. 49.

[4] "Strength of Beams as Determined by Lateral Buckling," by Karl de Vries, *Transactions*, ASCE, Vol. 112, 1947, p. 1245.

M. ASCE, in a similar paper comments, "The amount of experimental evidence on the torsional behavior of built-up members cannot yet be regarded as sufficient."[5]

The general mathematical treatment of the torsion problem was first made by Saint-Venant[6] in 1855. He also presented particular solutions for constant twisting moment applied to shafts of various cross sections. His solution for the rectangle is directly applicable to the plate girder, which consists principally of an assemblage of narrow rectangles.

Summary of Torsion Theory.—The development of the general torsion theory[6,7] is not within the scope of this paper. In the case of a straight shaft of uniform, circular cross section, the relationship between torsional moment (M) and angle of twist per unit length (θ) is given by

$$M = J\,G\,\theta \qquad (1)$$

in which G is the modulus of elasticity in shear, and J is the polar moment of inertia. In the case of the circular section, plane cross sections before twist remain plane after twist and the resultant shear stress at any point is proportional to the distance from the central axis of the shaft. Neither of these assumptions will hold for the noncircular sections, but the relationship given by Eq. 1 may then be modified to

$$M = K\,G\,\theta \qquad (2)$$

in which K is defined as a torsion constant[8] determined by the shape and dimensions of the cross section. S. Timoshenko[7,9] uses the notation C as equal to $K\,G$, in which C is termed the "torsional rigidity" of the particular section.

In the case of the narrow rectangle having a width w, more than 3 times the thickness t, the solution by Saint-Venant reduces to

$$K = \frac{w\,t^3}{3} - 0.21\,t^4 \qquad (3)$$

In the case of the circular shaft the resultant shear stress τ is given by

$$\tau = \frac{M\,r}{J} \qquad (4)$$

in which r is the radial distance from the central axis of the shaft.

For a rectangular plate the resultant shear stress in the cross section will be parallel in direction to the wide side and will be proportional in magnitude to the normal distance from the middle plane, except near the narrow edges. Away from the narrow edges, at the surface of the broad sides, the maximum shear stress in the narrow rectangle is closely approximated by

$$\tau_{max} = \frac{M\,t}{K} \qquad (5)$$

[5] "Strength of Slender Beams," by George Winter, *Transactions*, ASCE, Vol. 109, 1944, p. 1321.

[6] "Résistance des Corps Solides," by M. Navier, 3rd Ed., 1864, as edited by Saint-Venant.

[7] "Theory of Elasticity," by S. Timoshenko, McGraw-Hill Book Co., Inc., New York, N. Y., 1934.

[8] "Structural Beams in Torsion," by Inge Lyse and B. G. Johnston, *Transactions*, ASCE, Vol. 101, 1936, p. 857.

[9] "Strength of Materials," by S. Timoshenko, D. Van Nostrand Co., New York, N. Y., 2d Ed., Vol. 2, 1941.

The maximum shear stress parallel with the narrow surface at the ends of the section is always less in magnitude than the maximum stress in the broad sides; hence Eq. 5 gives the maximum stress in the section.[8] When w is more than four times t, as in the case of most components of structural sections, the error in Eq. 3 is negligible.

There have been many investigations of torsion problems, few of which treat the subject of built-up girders, the primary concern of this paper.

The torsion of rolled structural I-beam and wide flange sections has been the subject of an earlier investigation.[8] Formulas were developed for evaluating the torsional constant (K) for rolled sections, but the application of these formulas to built-up members, such as riveted, bolted, or welded plate girders was open to question. The various components of a built-up member may act together as an equivalent solid section, or, if not joined, may act separately. The torsional stiffnesses evaluated for these extreme assumptions will be very different. In some practical cases, the equivalent solid section torsion constant (the measure of torsional stiffness) is as much as 15 times as large as the value of K for separate action. In order to determine the magnitude of K for built-up sections, an extensive experimental investigation was considered necessary. I. E. Madsen,[10] M. ASCE, has made a study showing that the torsional constants of small models of riveted and welded built-up I-beams are somewhat less than those of the equivalent solid section.

Because small size specimens with cold driven rivets were used in the tests conducted by Mr. Madsen, the object of the investigation reported on in this paper was to test larger girders and to make an extensive study of the various factors such as pitch of rivets and bolts, size of weld, tension in bolts, and the presence of stiffeners, that might affect the torsional behavior of built-up members.

Built-up Plates

The rectangular section composed of built-up plates will be discussed first because these units are the basic component of the built-up plate girder.

If a stack of n plates, each of equal thickness t, is bolted or riveted together and transmits a torsional moment, the range of behavior will be between that of a solid piece with the thickness $n\,t$ as one extreme and that of n plates twisted separately as the other. The torsional constant of a plate varies as the cube of its thickness. Therefore, built-up plates with equivalent solid section behavior are much stronger and stiffer than built-up plates with separate action. With n as the number of plates, the ratio of the moment of the solid piece to the moment of the stack of separate plates equals n for the same maximum resultant shear stress. For the same angle of twist, the ratio of moments becomes equal to n^2.

For example, a stack of 4 plates, riveted together, will twist 16 times more and be stressed 4 times more if its plates act separately than if it behaves as an equivalent solid section. In actual cases, the built-up plates behave somewhere between these two extremes, depending principally on the pitch, tightness, and

[10] "Report of Crane Girder Tests," by I. E. Madsen, *Iron and Steel Engineer*, November, 1941.

location of gage lines of bolts or rivets. This intermediate behavior will be termed integral behavior in this paper.

Slip Between Different Components.—The different components of the built-up plate will slip longitudinally with respect to each other during twist if loosely bolted together. If this slip can be prevented, integral behavior, as previously defined, will be obtained. The longitudinal slip between plates (assuming no interaction) may be considered as arising from two causes: (1) The slip caused by the longitudinal warping of each individual cross section (independent of the location of the center of twist); and (2) the longitudinal displacements resulting from rigid body rotations. These factors are dependent on the location of the center of twist and an arbitrary location of zero displacement. The shearing stress distribution in the component rectangular sections is independent of the second type of displacement.

Longitudinal warping of the individual cross section may be closely approximated for the narrow rectangular shape of thickness t and width w. At section x-x in Fig. 1(a), a short distance from the narrow edge, the resultant shear will

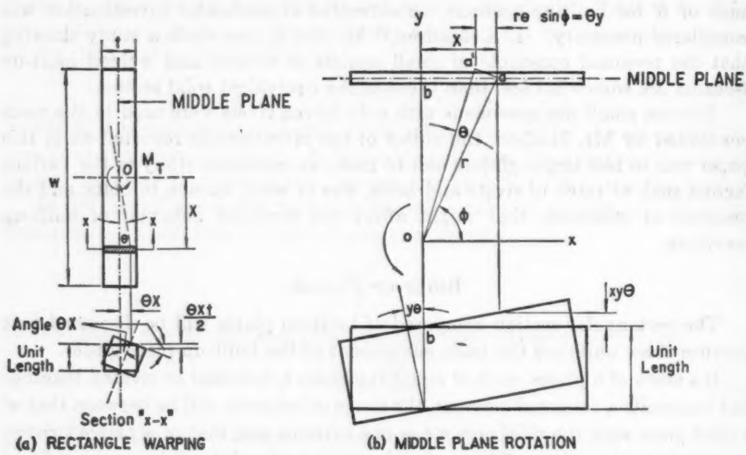

Fig. 1.—Longitudinal Displacement

act nearly parallel to the wide side of the rectangle and the component of shear stress acting parallel to the plane x-x will be of negligible magnitude. Hence, if a unit length of section is twisted through the angle θ, with the center of twist at 0, section x-x must rotate as a rigid body through angle $\theta\,x$. For small angles of twist there will be negligible longitudinal displacement of the middle plane of the rectangle, except for regions very near the narrow edges. Hence, there will be longitudinal warping displacements equal in magnitude to $\theta\,x\,t/2$ at the surface of the wide face. Near the narrow edges this simple relationship will no longer be valid and a more rigorous approach is required for precise evaluation.[6] Nevertheless, the warping displacement at the extreme corners will be

closely approximated for the very narrow rectangle by letting $x = w/2$ and, therefore, will equal approximately $\theta\, w\, t/4$.

The longitudinal displacements, when the center of twist is not at the centroidal axis but at any location 0 as shown in Fig. 1(*b*) is next considered. Assume that point b does not move longitudinally and let r be the distance from point 0 to any point a in the middle of the plane of the rectangle. The angle between r and x is denoted ϕ. During the twist θ per unit length, any point a will be displaced transversely a distance $r\,\theta$ to point a′ and the component of this displacement in the middle plane of the rectangle will be $r\,\theta \sin \phi = y\,\theta =$ a constant. Since there is zero shear stress in the middle plane of the rectangle (except near the narrow edges) constant lateral displacement equal to $y\,\theta$ can take place in this plane only by rotation through angle $y\,\theta$, as shown in Fig. 1(*b*). This rotation results in longitudinal displacements of magnitude $x\,y\,\theta$ in the middle plane relative to point b.

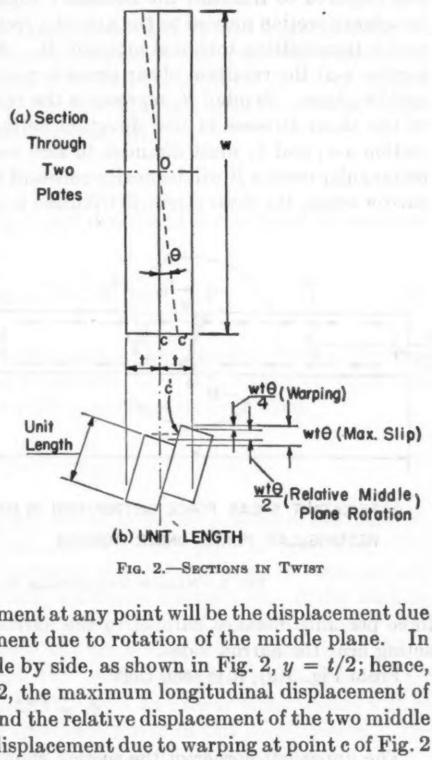

Fig. 2.—Sections in Twist

The total longitudinal displacement at any point will be the displacement due to warping added to the displacement due to rotation of the middle plane. In the case of 2 rectangular plates side by side, as shown in Fig. 2, $y = t/2$; hence, at the narrow edge where $x = w/2$, the maximum longitudinal displacement of the middle plane $x\,y\,\theta = \theta\,w\,t/4$ and the relative displacement of the two middle planes is $\theta\,w\,t/2$. If the relative displacement due to warping at point c of Fig. 2 is added to the displacement just obtained for the middle planes, the amount of total slip between the two plates can be determined.

$$\text{Slip} = \frac{\theta\, w\, t}{2} + \frac{\theta\, w\, t}{2} = \theta\, w\, t \quad \ldots\ldots\ldots\ldots\ldots\ldots (6)$$

This expression applies to any number of plates as long as they are of the same thickness. If the plates are of different thickness, the term t in Eq. 6 should be the average thickness of the two adjacent plates in question.

Pitch of Rivets or Bolts to Develop Integral Action.—If it were possible to eliminate the relative slipping of the several plates when bolted or riveted together, the assemblage of plates would then act integrally. The required shearing forces transmitted by the interfaces between such plates would have to be

furnished in large part by friction developed as a result of the clamping action of the bolts or rivets.

A study of the approximate stress distribution within a solid rectangular section under torsion will permit the determination of the pitch and bolt or rivet size required to transmit the necessary shear forces. Fig. 3(*a*) represents an imaginary section normal to the axis of a rectangular bar of width w and thickness t, transmitting torsional moment M. Away from the narrow sides (as at section a-a) the resultant shear stress is proportional to the distance from the middle plane. Symbol S_1 represents the resultant shear force per unit width of the shear stresses in one direction acting over one half the thickness at section a-a; and S_1 must diminish to zero near the narrow edges but in a thin rectangular section it will be nearly constant over most of the width. Near the narrow edges, the shear stress distribution is complex, but the average resultant

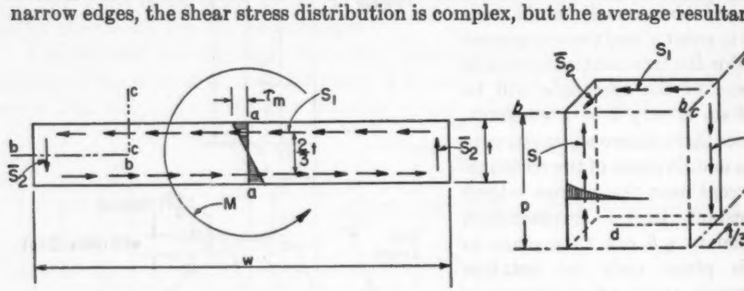

(a) RESULTANT SHEAR FORCE DISTRIBUTION IN NARROW RECTANGULAR PLATE UNDER TORSION

(b) FREE BODY DIAGRAM OF CORNER SEGMENT

Fig. 3.—Narrow Rectangular Plate Under Torsion

force per unit distance parallel to the narrow side is represented by force $\bar{S}_2$ acting near the narrow sides.

From Fig. 3(*a*), it is seen that

$$S_1 = \frac{\tau_m t}{4} \qquad (7)$$

The upper left corner of the section shown in Fig. 3(*a*) is now isolated by longitudinal sections along lines b-b and c-c, as shown in Fig. 3(*b*). From the equivalence of shear stresses acting on planes that are 90° apart, longitudinal shear resultants of magnitude S_1 per unit length must act along section c-c. In the isolated corner section, equilibrium of forces in the longitudinal direction requires that the shear stress resultant along the middle plane section through line b-b also have an intensity S_1 per unit length.

One half of the resultant torsional couple is supplied by the forces S_1 and the other half is supplied by the forces $\bar{S}_2$ as will be shown. In Fig. 3(*b*), summing the moments about axis d-d

$$\frac{\bar{S}_2\, t\, p}{2} = \frac{S_1\, p\, t}{3} \qquad (8a)$$

or

$$\bar{S}_2 = \tfrac{2}{3} S_1 \qquad (8b)$$

The torque supplied by S_2 is seen to be a little less than $S_2\,w\,t$ and that supplied by the distributed S_1 forces is a little less than $\frac{2\,S_1\,w\,t}{3}$. Hence, introducing the relationship $S_2 = \frac{2}{3}S_1$, it is seen that the torques supplied by S_1 and S_2 are at least approximately equal.

The rectangular section can be assumed to be split into 2 plates along its middle plane (b-b of Fig. 3(a)) and the 2 portions bolted or riveted together at the narrow edges using bolt pitch p. The distributed forces S_1 in the middle plane section through line b-b, over distance p, might then be assumed to be replaced by a concentrated rivet or bolt shear (R).

$$R = S_1\,p \qquad (9)$$

Substituting S_1 from Eq. 7 into Eq. 9 and denoting the combined thickness of the two plates by T,

$$R = \frac{\tau_m\,T\,p}{4} \qquad (10)$$

The given thickness T and pitch p determine a definite ratio between the rivet shear R and the maximum torsional shear stress τ_m. If p_r is the rivet pitch that will produce rivet slip R' and shear yield τ_y at the same time, then

$$p_r = \frac{4\,R'}{\tau_y\,T} \qquad (11)$$

If the pitch is greater than p_r rivet slip will occur before yielding of the material. If the pitch is less than p_r, the material will yield prior to rivet slip. The initial linear relationship between torsional moment and angle of twist per unit length will be limited by slip or yield, whichever occurs first. If the working allowable values of rivet shear stress imply identical factors of safety with respect to slip and yield, respectively, the pitch to produce these values simultaneously will be p_r as given by Eq. 11. Although these factors of safety are usually not equal, the accepted allowable rivet and shear stress values will be used in discussing the design of the specimens tested in this investigation. The rivet pitch for balanced design in pure torsion will be assumed as:

$$p_r = \frac{4\,R_w}{\tau_w\,T} \qquad (12)$$

in which R_w is the allowable single shear value of the rivet, and τ_w is the permissible shear stress for the material. The effective rivet or bolt clamping distance along the length of the plate must be evaluated to assure that the distributed shear force S_1, acting along the middle plane section through line b-b within the rivet or bolt pitch will be replaced by the rivet or bolt shear. The solution of the problem of a rectangular strip loaded on opposite sides by two opposed forces acting in the same line and normal to the surface shows that the compression in the middle plane falls away rapidly and changes to tension at a distance from the line of action of the forces slightly greater than half the plate

thickness.[11] The problem under consideration is somewhat different since it involves three-dimensional effects rather than two-dimensional and since no tension can be developed between the plates. However, it seems reasonable to assume that the effective clamping distance per rivet is equal to the sum of the diameter of the rivet (or bolt) head (A) and the over-all thickness of the assembly (T). Therefore, the rivet or bolt pitch should not be larger than a critical value ($A + T$) or, denoting this critical pitch by p',

$$p' = A + T \ldots\ldots\ldots\ldots\ldots\ldots\ldots\ldots (13)$$

The effect of making p larger than p' will be treated in a later section.

When there are more than 2 plates, Eqs. 10, 11, and 12 still apply since the force per unit length (S_1) to be transmitted between the 2 plates nearest the

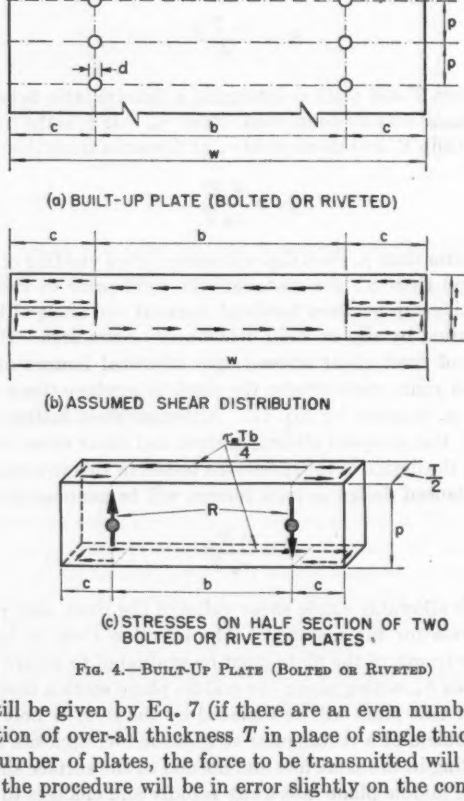

(a) BUILT-UP PLATE (BOLTED OR RIVETED)

(b) ASSUMED SHEAR DISTRIBUTION

(c) STRESSES ON HALF SECTION OF TWO BOLTED OR RIVETED PLATES

FIG. 4.—BUILT-UP PLATE (BOLTED OR RIVETED)

center will still be given by Eq. 7 (if there are an even number of plates) with the substitution of over-all thickness T in place of single thickness t. If there are an odd number of plates, the force to be transmitted will be somewhat less than S_1 and the procedure will be in error slightly on the conservative side.

[11] "Theory of Elasticity," by S. Timoshenko, McGraw-Hill Book Co., Inc., New York, N. Y., 1934, p. 49.

Evaluation of the Torsion Constant.—When several plates are riveted or bolted together, as shown in Fig. 4, the outer rows of rivets or bolts may be too far from the edges of the plates to produce the pressure required to develop sufficient friction near the edges to replace the longitudinal S_1 forces.

Mr. de Vries[4] assumed that the assemblage between the outer rows of rivets or bolts acts as a solid section, and beyond the line of the assumed solid section, only the contribution of the individual plates would be counted upon. This assumption, as shown in Fig. 4(*b*), seems reasonable, simple, and on the conservative side. The integral action torsion constant (K_I) can be obtained by modifying Eq. 3 according to the foregoing assumptions. Using the notation in Fig. 5, the torsion constant for *n*-plates of equal thickness is

$$K_I = \frac{b\,T^3}{3} + \frac{n\,2\,c\,t^3}{3} - 0.21\,T^4 \qquad (14a)$$

or, if the edge effect is neglected,

$$K_I = \frac{b\,T^3}{3} + \frac{n\,2\,c\,t^3}{3} \qquad (14b)$$

If the plates are not of equal thickness, the second term in Eqs. 14*a* and 14*b* should be changed to $\frac{2}{3}c\,\frac{\sum t^3}{n}$.

Based on the assumed stress distribution in Fig. 4(*b*), the rivet pitch formula may be derived directly from the equilibrium of moments acting on the half section of a combination of 2 bolted or riveted plates having pitch length *p*, as shown in Fig. 4(*c*). The resultant shear stress on 1 plate, over length *b*, as previously demonstrated will be $\frac{\tau_m\,T\,b}{4}$. This stress develops a couple about a line normal to the plate interface. This couple is equal to $\frac{\tau_m\,T\,b\,p}{4}$ and is opposed by the couple produced by rivet shear *R* with moment arm *b*. Equating the two couples:

$$p = \frac{4\,R}{\tau_m\,T} \qquad (15)$$

This equation is identical with Eq. 11 as previously derived.

When more than 2 plates of equal thickness are bolted or riveted together, as shown in Fig. 5, the single shear force on the rivets at the center plane of the combined unit will be the same as in the case of 2 plates (provided the total number of plates is even) and Eq. 11 for rivet pitch will be unchanged. If there are an odd number of plates of equal thickness, the interface between the central plate and the adjacent plate will not be at the center of the stack and Eq. 11 will be slightly too conservative—the error being about 11% for the case of 3 plates and 4% for

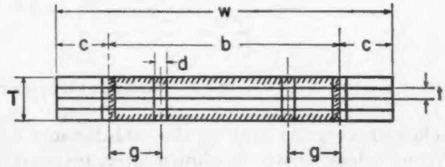

Fig. 5.—Bolted or Riveted Plates

5 plates. In the interest of simplification, for actual design it seems desirable to neglect this discrepancy.

If there are 4 rows of rivets, as shown in Fig. 5, it might be presumed that the two inner rows would not be as effective as the outer rows. Possibly the rivet value of the inner rows should be discounted slightly, or solid section

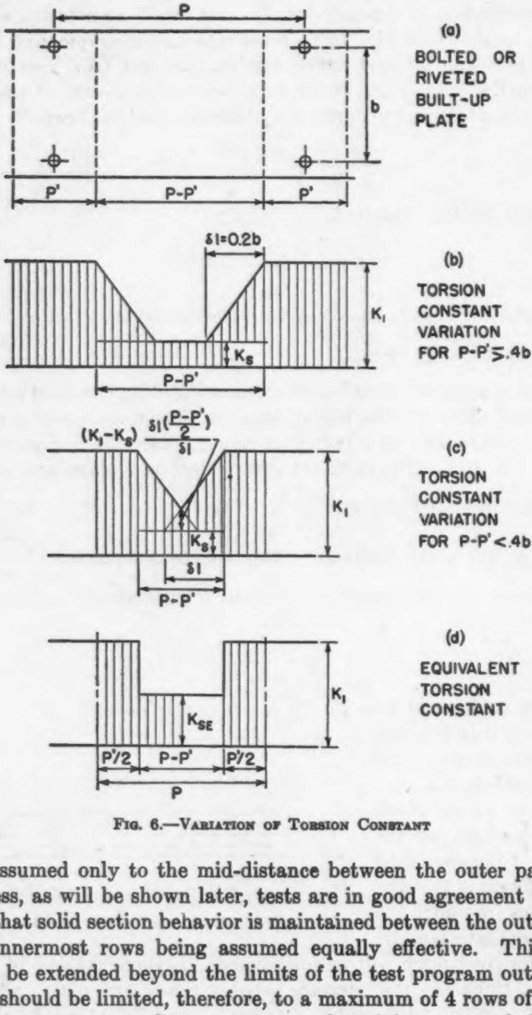

FIG. 6.—VARIATION OF TORSION CONSTANT

behavior assumed only to the mid-distance between the outer pairs of rows. Nevertheless, as will be shown later, tests are in good agreement with the assumption that solid section behavior is maintained between the outermost rows with the innermost rows being assumed equally effective. This procedure should not be extended beyond the limits of the test program outlined in this paper and should be limited, therefore, to a maximum of 4 rows of rivets, with the inner rows as near to the outer ones as the minimum permissible gage (g) will allow.

Loosely bolted together or not bolted or riveted at all, n-plates would act separately and the torsional constant for separate action would be

$$K_s = n \frac{w\,t^3}{3} \qquad (16)$$

If the pitch is larger than the critical pitch (p', Eq. 13), there will be a tendency for the plates to develop separate action in the spaces between the rivet lines. This question also arises in the case of a welded girder having intermittent welds to connect the component parts, in which case no clamping effect should be assumed between the welds and p' is simply the intermittent weld length.

In Fig. 6(a), along the clamped portion (p'), the integral torsion constant (K_I) will be used. Along the portion ($p - p'$) each plate will be assumed to act separately with both ends partially restrained. By ends are meant the dashed lines in Fig. 6(a), at which location integral action is assumed to begin in the riveted or bolted region. For a solid rectangular plate with middle cross section remaining plane during twist, Mr. Timoshenko[12] found that the decrease of ϕ (total angle of twist), resulting from the local constraint is the same as that decrease corresponding to the diminution of the length by the quantity $\delta\, l$; $\delta\, l$ is independent of the length and varies in value from 0.212 w to 0.195 w, according to the ratio of w to t. The problem of this paper is somewhat different since, although partially restrained, the ends of the component parts do not remain completely plane, but have approximately the same degree of warping as the equivalent solid section. However, as approximation, the transition between K_I and K_S will be assumed as shown in Fig. 6, thereby compensating for the partial restraint effect.

In view of the approximations involved, the value of $\delta\, l$ in the present case will be assumed as 0.2 b. The equivalent torsional constant along the length ($p - p'$) will be

$$K_{SE} = \frac{\delta l\, K_I + (p - p' - \delta l)\, K_S}{p - p'} = \frac{0.2\, b\, K_I + (p - p' - 0.2\, b)\, K_S}{p - p'} \qquad (17a)$$

for $p - p' \gtrless 0.4\, b$.

If $p - p'$ is smaller than 0.4 b, the torsion constant will be assumed to vary as shown in Fig. 6(c) and the equivalent torsion constant will be

$$K_{SE} = \frac{\frac{p - p'}{2} K_S + \left[0.4\, b - \frac{(p - p')}{2}\right] K_I}{0.4\, b} \qquad (17b)$$

for $p - p' < 0.4\, b$.

The over-all effective torsion constant K_{eff} along the length p can be found by use of Fig. 6(d). By use of Eq. 2,

$$\phi_1 = \frac{M\, p'}{K_I\, G} \qquad (18a)$$

---

[12] "On the Torsion of a Prism One of the Cross-Sections of which Remains Plane," by S. Timoshenko, *Proceedings*, London Mathematical Society, Vol. 20, 1922, p. 389.

and

$$\phi_2 = \frac{M\,(p - p')}{K_{SE}\,G} \quad \ldots\ldots\ldots\ldots\ldots\ldots\ldots (18b)$$

Then,

$$\phi_p = \phi_1 + \phi_2 = \frac{M\,p'}{K_I\,G} + \frac{M\,(p - p')}{K_{SE}\,G} \ldots\ldots\ldots\ldots\ldots (19)$$

in which ϕ_p is the total angle of twist over the length p; ϕ_1 is the total angle of twist over the length p'; and ϕ_2 is the total angle of twist over the length $(p - p')$. The average twist per unit length (θ_{aver}) will be

$$\theta_{\text{aver}} = \frac{M}{P\,G}\left[\left(\frac{1}{K_I} - \frac{1}{K_{SE}}\right)p' + \frac{p}{K_{SE}}\right] \ldots\ldots\ldots (20)$$

since

$$K_{\text{eff}} = \frac{M}{G\,\theta_{\text{aver}}} \ldots\ldots\ldots\ldots\ldots\ldots\ldots\ldots\ldots (21)$$

Therefore,

$$K_{\text{eff}} = \frac{K_{SE}}{1 - \left(1 - \dfrac{K_{SE}}{K_I}\right)\dfrac{p'}{p}} \ldots\ldots\ldots\ldots\ldots\ldots (22)$$

If p is greater than p', the force distribution shown in Fig. 4(c) is valid only over the distance p', wherein integral behavior is assumed, and the maximum shear stress in this region, for a given rivet stress R is, from Eq. 10,

$$\tau_I = \frac{4\,R}{p'\,T} \ldots\ldots\ldots\ldots\ldots\ldots\ldots\ldots\ldots\ldots (23)$$

If the rivet pitch exceeds p', the calculation of maximum shear stress must also be modified outside of the clamped region in riveted or bolted members, or between intermittent welds in welded members. Within the clamped or welded zone the maximum shear stress may be assumed as

$$\tau_I = \frac{M\,T}{K_I} \ldots\ldots\ldots\ldots\ldots\ldots\ldots\ldots\ldots\ldots (24a)$$

If the term $(p - p')$ is greater than 0.4 b, completely separate action midway between rivets or welds implies that the maximum shear stress at this location is

$$\tau_S = \frac{M\,t}{K_S} \ldots\ldots\ldots\ldots\ldots\ldots\ldots\ldots\ldots\ldots (24b)$$

If the plates are not all of the same thickness, t should be taken as the thickest of the individual plates.

If the term $(p - p')$ is less than 0.4 b the maximum shear stress will be intermediate between τ_I and τ_S. Assuming a linear relationship,

$$\tau_{IS} = M\left[\frac{T}{K_I}\left(1 - \left(\frac{p - p'}{0.4\,b}\right)\right) + \frac{t}{K_S}\left(\frac{p - p'}{0.4\,b}\right)\right] \ldots\ldots (24c)$$

Eqs. 24 are advanced tentatively in the belief that they will give conservative strength estimates. Insufficient stress measurements were made regarding the change in stress along the length of the girder to investigate this item in detail.

Effect of Transverse Holes and Stress Concentration.—If a plate containing several open holes is twisted, there will be localized stress concentrations near the holes. In the elastic range these stresses can be computed approximately by available formulas.[13] If the plate is one of several comprising a built-up bolted or riveted girder, the clamping action of the bolts and rivets, as well as the stress carried through the rivet heads by plate friction, will alter the local stress condition and tend to eliminate the effect of the hole. Furthermore, as in the case of bending of plate girders, initial local yielding in the steel will permit stress redistribution and the holes therefore will have little effect upon the general behavior of the member as a whole.

In the tests to be reported on, as a limiting case, some of the plate assemblages were tested with zero or nearly zero bolt tension. In such cases, the holes would have their maximum effect on the torsional stiffness. It was found that a reduced effective width gave good agreement with test results. The reduced effective width is the average width of a solid plate of identical thickness that has the same net volume of material as is in the actual plate with holes deducted. For example, in the case of a plate of width w, having n rows of holes of diameter d and pitch p, the effective width would be

$$w_{eff} = w - \frac{n \pi d^2}{4 p} \qquad (25)$$

Bolted, Riveted, and Welded Plate Girders

When bolted, riveted, or welded plate girders are twisted, slip between different parts may occur as in the case of built-up plate sections. Therefore, the fabricated girders may not be the equivalent of solid sections, either in stiffness or strength. However, if sufficient rivets, or bolts having adequate tension, or adequate welds are used, it is possible to hold the slippage to a minimum and develop integral behavior intermediate between complete solid section and separate behavior.

Slip Between Different Components.—The maximum slip between different components of fabricated plate girders, if the bolts or rivets are loose, is of comparable magnitude to the slip between any 2 plates of similar size, as given previously by Eq. 6. In a girder of I-section, if there are 2 or more cover plates, the maximum slip between any 2 cover plates would be given directly by Eq. 6. In the case of an angle connecting flange to web of a riveted plate girder, the longitudinal displacement of the middle plane of the angle is determined by the integrated effect of the friction of the component parts adjacent to it. The determination of such slip on the basis of arbitrary hypotheses will not be discussed in this paper as it is of academic interest and the obvious objective in design is to eliminate as much slip as possible by means of bolts, rivets, or welds.

[13] "Strength of Materials," by S. Timoshenko, D. Van Nostrand Co., New York, N. Y., Vol. 2, 2d Ed., 1941, p. 317.

Evaluation of Torsion Constant.—The torsion constant (K) may be determined for rolled sections by standard formulas and procedures.[8] In studying the test results of built-up girders, it is of interest to compute K values for the two extreme conditions of equivalent solid section behavior and separate action behavior, between which the actual integral behavior will lie.

The procedure used in this paper for built-up girders parallels that previously described for the case of built-up plates. Fig. 7 indicates the nomenclature

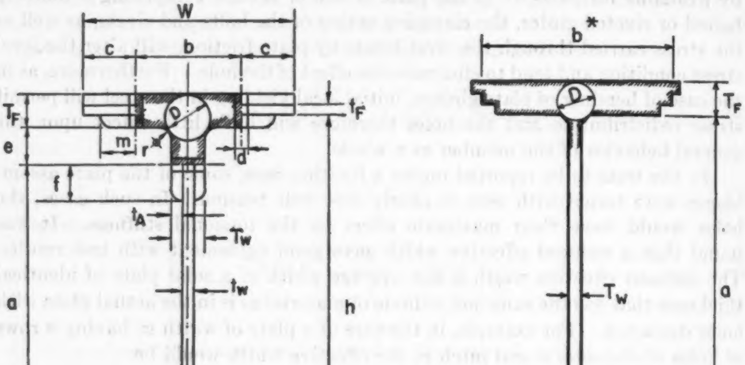

FIG. 7.—NOTATION FOR BUILT-UP GIRDERS

for girder sections. The effective flange width assumed as solid section is the same as that previously discussed in the case of an assemblage of plates, as shown by the shaded areas in Fig. 7.

As noted in the case of the single rectangular plate (Eq. 14*a*), there is an edge loss (a negative term) in the equation for the torsion constant. As the

ratio of width to thickness increases, this edge loss factor becomes a relatively small item and may be neglected without serious error. When 2 or more rectangles are joined together to form a T-section or I-section, the torsion constant may be obtained by summing the contributions of the separate rectangles, using Eqs. 14*a* or 14*b*, but there is an additional contribution at the juncture or junctures of the various parts that has been called the hump effect.[8] This effect may be evaluated as a function of D^4 (Fig. 7). For the rolled section there is some justification for including both the edge loss and hump effects in evaluating the torsion constant, as was done for the rolled I- and WF-shapes,[8,14] even though these effects tend to offset each other. For riveted or bolted girders however, the uncertainty as to the clamping action of the bolts or rivets makes such refinements unjustifiable. It is also desirable to have as simple a formula as will give an approximation satisfactory for design purposes. This is more important in the case of the plate girder than for the rolled section as in the latter instance sizes are standardized and tables[14] of *K*-values are available. In view of these facts both the hump and edge effects will be neglected in this analysis. Referring to Fig. 7(*a*) and letting *n* equal the number of cover plates in each flange, the torsion constant will be

$$K_I = \tfrac{2}{3} b\, T^3_F + \tfrac{1}{3} e\, T^3_w + \frac{n\, 4\, c\, t^3_F}{3} + \frac{4\,(m+f)\, t^3_A}{3} + \tfrac{1}{3} a\, t^3_w \ldots (26)$$

If the different parts act separately, the torsion constant, neglecting edge effects will be

$$K_S = \tfrac{1}{3}\left[2\, n\, w\, t^3_F + h\, t^3_w + 4\left(f + e + m + \frac{(b - t_w)}{2}\right) t^3_A\right] \ldots (27)$$

For welded girders (Fig. 7(*b*)) the integral torsion constant can be derived in a similar manner

$$K_I = \tfrac{2}{3} b\, T^3_F + \tfrac{1}{3} a\, t^3_w \ldots\ldots\ldots\ldots\ldots\ldots (28)$$

If the different parts acted separately, with *n* plates in each flange, the separate action torsion constant (K_S) neglecting the edge effects would be

$$K_S = \frac{2\, n\, b\, t^3_F}{3} + \tfrac{1}{3} a\, t^3_w \ldots\ldots\ldots\ldots\ldots\ldots (29)$$

Rivet or bolt pitch (p_r) may be determined by Eqs. 11 or 12, as developed for the case of built-up plates. Then, the pitch required in the flange to simultaneously develop allowable working rivet shear (R_w) and maximum shear stress due to torsion (τ_m) will be

$$p_r\ (\text{flange}) = \frac{4\, R_w}{\tau_w\, T_F} \ldots\ldots\ldots\ldots\ldots (30a)$$

if the permissible shear stress is 12 kips per sq in., Eq. 30*a* becomes

$$p_r\ (\text{flange}) = \frac{R_w}{3\, T_F} \ldots\ldots\ldots\ldots\ldots (30b)$$

with the clamping distance requirement (Eq. 13) that p' (flange) $= A + T_F$.

[14] "Torsional Stresses in Structural Beams," *Booklet S-57*, Bethlehem Steel Company, 1950.

The maximum torsional shear stress in the vertical legs of the angles that connect the web plate to the flange will be less than that in the flanges by the factor T_w/T_F, hence the pitch required in these legs is

$$p_r\,(\text{web}) = \frac{4\,R_w}{\tau\,(\text{web})\,T_w} = \frac{4\,T_F\,R_w}{\tau_m\,T^2_w}\ldots\ldots\ldots\ldots\ldots(31a)$$

Again, if the permissible shear stress is 12 kips per sq in.,

$$p_r\,(\text{web}) = \frac{T_F\,R_w}{3\,T^2_w}\ldots\ldots\ldots\ldots\ldots\ldots\ldots\ldots(31b)$$

with the clamping distance requirement that p' (web) $= A + T_w$.

If the rivet or bolt pitch is larger than the critical value p', the torsion constant should be reduced. Eqs. 17*a*, 17*b*, and 22 for built-up plate case can be applied.

No tests were made in combined bending and torsion. Presumably, in combined bending and torsion, the rivet shear produced by torsion, as given by Eq. 10, could be combined with the rivet shear produced by the over-all shear resultant of the vertical loads. The combined rivet shear should not exceed the permissible rivet value.

For welded plate girders, the sizes of welds should be such as to sustain the maximum shearing stress developed in the welds for solid section behavior. For example, if the size of welds to connect the flange cover plates is desired, a study of the free body diagram of Fig. 3(*b*) will indicate that the strength of the welds required is S_1 lb per linear in. which equals $\frac{\tau_m\,T_F}{4}$ lb per linear in. by Eq. 7. If a weld of the size $\frac{S}{8}$ in. is assumed to have an allowable strength of 1.2 S kips per in., corresponding to a shear stress of 13.6 kips per sq in. through the minimum weld section, the size of weld can then be determined by finding

$$S = \frac{\tau_m\,T_F}{4.8}\ldots\ldots\ldots\ldots\ldots\ldots\ldots\ldots\ldots\ldots(32a)$$

For maximum shear stress due to torsion of $\tau_m = 12$ kips per sq in.

$$S = 2.5\,T_F\ldots\ldots\ldots\ldots\ldots\ldots\ldots\ldots\ldots\ldots(32b)$$

The required size of weld is $\frac{S}{8}$ in. If welds connecting the various cover plates are intermittent rather than continuous, Eqs. 17*a* or 17*b* and Eq. 22 may be applied to approximate the effective loss in torsional rigidity, in which case p is the weld spacing and p' is the length of weld.

Strength.—In a rolled section under torsion, the critical shearing stress will occur along the outer surface of the beam and along the fillets where the material is thickest. In built-up structural members, the maximum shear stress may occur somewhere else, especially around the rivet or bolt heads. However, neglecting these local stresses, the approximate shear stress can be determined by Eq. 5, with the proper value of total thickness T substituted for the plate thickness t.

The shearing stress is a function of the thickness of the material and the maximum stress in the flange (τ_F) and in web (τ_w) will be approximately

$$\tau_F = \frac{M\,T_F}{K} \qquad (33a)$$

$$\tau_w = \frac{M\,T_w}{K} \qquad (33b)$$

provided the bolt or rivet pitch is less than p' for longitudinal continuity or in case of a welded girder that welds are continuous.

If the pitch exceeds p', or if intermittent welds are used in a welded girder, the maximum shear stress in the flange will occur midway between the lines of rivets or betweeen the intermittent welds, as the case may be, and may be computed by Eq. 24. This equation probably gives too conservative an approximation of the strength but the problem will be an unusual one because continuous welds should be used if torsional strength is important.

A plate girder of I-beam shape will not be desirable if torsional loads are the primary design factor. The usual need for torsional information will be in connection with lateral instability, when the torsional and lateral bending stiffnesses are of primary concern, and in cases in which the load on the girder primarily causes bending but eccentric application also causes torsion. In lateral instability, the only stress due to torsion at loads below the critical, will be those unpredictable amounts of stress caused by unavoidable eccentricities in load and the maximum shear stress to be expected is considerably less than 12 kips per sq in. Eqs. 30*b* and 31*b* provide an unduly severe rivet pitch requirement in such a case and should be modified by introducing in Eq. 10 the value of τ_m as required by the actual situation. In combined bending and torsion, as stated before, the rivet pitch would need to be determined so as to transmit properly the combined shear caused by both bending and torsion.

Illustrative Calculation

To illustrate the application of the foregoing equations, the plate girder sections, shown in Fig. 8, of riveted and welded members, respectively, will be used as examples. The numerical results will not agree exactly with those reported in comparison with actual tests as the latter are based on measured dimensions of specimens whereas the following examples will make use of the nominal dimensions.

Illustrative Example: Riveted Plate Girder.—Using the notation of Fig. 7(*a*), the following dimensions are obtained from Fig. 8(*a*):

Symbol	Length in inches	Symbol	Length in inches
a	39.00	t_A	0.625
b	10.00	t_F	0.625
c	2.00	t_W	0.500
d	0.875	T_W	1.750
e	4.125	T_F	1.850
f	1.250		
h	48.50		

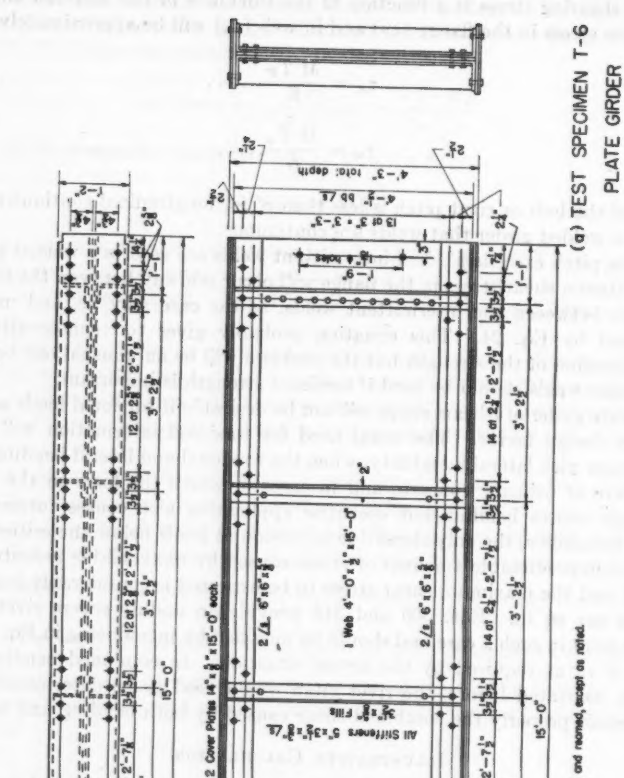

(a) TEST SPECIMEN T-6
PLATE GIRDER

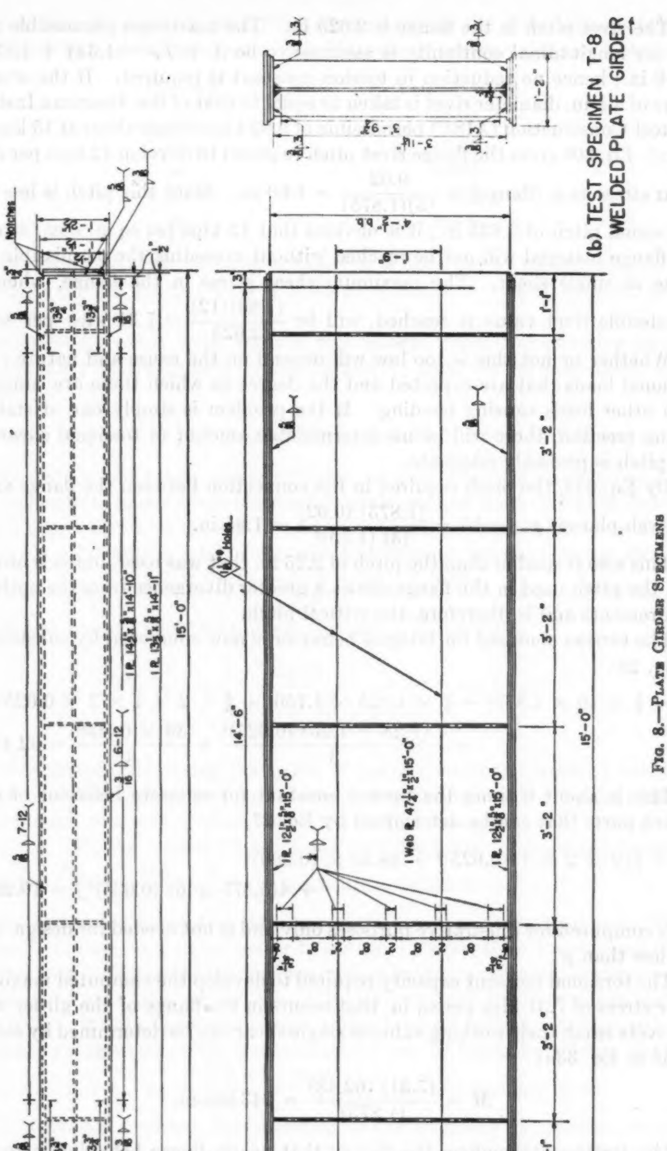

FIG. 8.—PLATE GIRDER SPECIMENS

The rivet pitch in the flange is 2.625 in. The maximum permissible pitch (p') for longitudinal continuity is assumed to be $A + T_F = 1.344 + 1.875 = 3.219$ in.; hence no reduction in torsion constant is required. If the working value of a $\frac{7}{8}$-in. diameter rivet is taken as equal to that of the American Institute of Steel Construction (AISC) permissible of 9.02 kips (single shear at 15 kips per sq in.), Eq. 30*b* gives the flange rivet pitch required to develop 12 kips per sq in. shear stress as p_r (flange) $= \dfrac{9.02}{(3)(1.875)} = 1.60$ in. Since this pitch is less than the actual pitch of 2.625 in., it is obvious that 12 kips per sq in. shear stress in the flange material will not be reached without exceeding the permissible rivet value in single shear. The maximum shear stress in the flange, when the permissible rivet value is reached, will be $\dfrac{(1.60)(12)}{2.625} = 7.31$ kips per sq in.

Whether or not this is too low will depend on the cause and nature of the torsional loads that are expected and the degree to which these are combined with other loads causing bending. If the problem is simply one of stability during erection, there will be no determinable amount of torsional shear and the pitch is probably adequate.

By Eq. 31*b*, the pitch required in the connection between the flange angles and web plate is p_r (web) $= \dfrac{(1.875)\ (0.02)}{(3)\ (1.75)^2} = 1.85$ in.

This also is smaller than the pitch of 2.25 in. that was used, but it is obvious that the pitch used in the flange shows a greater divergence from the optimum requirements and is, therefore, the critical pitch.

The torsion constant for integral behavior is now computed by substitution in Eq. 26:

$$K_I = \tfrac{2}{3} \times 10 \times 1.875^3 + \tfrac{2}{3} \times 4.125 \times 1.750^3 + \tfrac{1}{3} \times 2 \times 4 \times 2 \times 0.625^3 + \frac{4\ (1.25 + 1.25)\ (0.625)^3}{3} + \frac{39 \times 0.500^3}{3} = 62.43 \text{ in.}^4$$

This is about 6 times the torsion constant for separate behavior of component parts that can be determined by Eq. 27.

$$K_S = \tfrac{1}{3}[2 \times 2 \times 14(0.625)^3 + 48.50 \times (0.500)^3 + 4(5.375 + 6)\ (0.625)^3] = 10.28 \text{ in.}^4$$

K_S is computed for illustrative purposes only and is not needed for design when p is less than p'.

The torsional moment capacity required to develop the computed maximum shear stress of 7.31 kips per sq in. that occurs in the flange of the girder when the rivets reach their working value in single shear can be determined by solving for M in Eq. 33*a*:

$$M = \frac{(7.31)\ (62.43)}{(1.875)} = 243 \text{ kip-in.}$$

The test results confirm the theory that nearly-linear behavior in torsion will be obtained up to torsional moments greater than the computed value of 243 kip-in.

Illustrative Example: Welded Plate Girder.—Using the dimensions obtained from Fig. 8(*b*), and the notation of Fig. 7(*b*), the following values are obtained:

Dimension	Length in inches
a	47.25
b_{aver}	13.50
t_F	0.625
T_F	1.875
t_W	0.500

The torsion constant for integral behavior is obtained by substitution of the foregoing values in Eq. 28: $K_I = \frac{2}{3} \times 13.50 \times 1.875^3 + \frac{1}{3} \times 47.25 \times 0.500^3 = 61.29$ in.^{4}

Intermittent welds were used in this girder; hence the effective torsion constant must be determined by Eq. 22, and K_S must also be determined using Eq. 29:

$$K_S = \tfrac{2}{3} \times 3 \times 13.5 \times 0.625^3 + \tfrac{1}{3} \times 47.25 \times 0.500^3 = 8.56 \text{ in.}^4$$

The distance center to center of welds, or weld pitch (p) is 12 in., and the average length of flange cover plate welds equivalent to rivet clamping distance (p') is 6.5 in. The term $(p - p') = 5.5$ in. This is greater than $0.4\,b = 5.4$ in., hence, Eq. 17*a* applies and the equivalent torsion constant along distance $(p - p')$ is: $K_{SE} = \dfrac{2.7 \times 61.29 + (5.5 - 2.7) \times 8.56}{5.5} = 34.45$ in.^{4} Then, by Eq. 22, the average effective torsion constant is determined,

$$K_{\text{eff}} = \frac{34.45}{1 - \left(1 - \dfrac{34.45}{61.29}\right) \times \dfrac{6.5}{12}} = 45.16 \text{ in.}^4$$

This example illustrates the value of using continuous welds if torsional rigidity of welded girders is of importance. Continuity would effect an increase in the torsion constant of more than 35% in this example.

By Eq. 32*b*, the required continuous fillet weld size for balanced torsional strength is $\dfrac{2.5 \times 1.875}{8} = \dfrac{5}{8}$ in. to the nearest eighth inch.

The fillet welds connecting the edges of the two top cover plates are of 3/16-in. size, 6 in. long, and 12 in. center to center. Hence, they do not meet these requirements. The welds will be assumed as having a permissible shear value (in kips per linear inch) of $1.2\,S = (1.2)\,(1.5)$; and S is the weld size in eighths of an inch. Within the welded zone, where integral behavior is assumed, the maximum shear stress in the flange material can be found by solving Eq. 32*a* for the value of τ_m: $\tau_m = \dfrac{4.8\,S}{T_F} = \dfrac{(4.8)\,(1.5)}{1.875} = 3.84$ kips per sq in.

The torsional moment corresponding to the foregoing flange shear stress is found by solving Eq. 24*a* for the value of M; $M = \dfrac{\tau_m K_I}{T_F} = \dfrac{(3.84)\,(61.29)}{1.875}$ $= 125.5$ kip-in.

TABLE 1.—Test Program

Designation (1)	Description (2)	Rivet or Bolt: Pitch (in.) (3)	Rivet or Bolt: Gage lines (4)	Bolt torque[a] (ft-lb) (5)
	(a) Built-Up Plates P-1, 6-In. by ½-In. Plates (See Fig. 9(a))			
	Single Plate—			
P-1-1	No holes	....	....	....
P-1-2	With holes	4½	....	....
	Two Plates			
P-1-3	Bolted together	4½	....	0
P-1-4	Bolted together	4½	....	30
P-1-5	Bolted together	4½	....	70
P-1-6	Bolted together	4½	....	130
P-1-7	Bolted together	4½	....	170
	Four Plates			
P-1-8	No holes	....	....	....
P-1-9	With holes	4½	....	....
P-1-10	Bolted together	4½	....	190
P-1-11	With holes	2¼	....	....
P-1-12	Bolted together	2¼	....	40
P-1-13	Bolted together	2¼	....	100
P-1-14	Bolted together	2¼	....	150
P-1-15	Bolted together	2¼	....	190
P-1-16	Riveted together	2¼	....	....(P)
	(b) Built-Up Plates P-2, 20-In. by ½-In. Plates (See Fig. 9(b))			
	Single Plate—			
P-2-1	No holes	....	....	....(P)
P-2-2	With holes	2¼ (staggered)	....	....
	Two Plates			
P-2-3	Bolted together	2¼ (staggered)	Four outer lines	0
P-2-4	Bolted together	2¼ (staggered)	Four outer lines	150
P-2-5	Bolted together	2¼ (staggered)	Four outer lines	300
P-2-6	Bolted together	2¼ (staggered)	Four inner lines	300
P-2-7	Bolted together	6¾ (center)[b] 2¼ (ends)[b]	Four inner lines	300
P-2-8	Bolted together	6¾ (staggered)	Four inner lines	300
	Four Plates—			
P-2-9	Bolted together	2¼ (staggered)	Four outer lines	0
P-2-10	Bolted together	2¼ (staggered)	Four outer lines	15
P-2-11	Bolted together	2¼ (staggered)	Four outer lines	150
P-2-12	Bolted together	2¼ (staggered)	Four outer lines	300
P-2-13	Bolted together	2¼ (staggered)	Four inner lines	150
P-2-14	Bolted together	2¼ (staggered)	Four inner lines	300
P-2-15	Bolted together	6¾ (center)[b] 2¼ (ends)[b]	Four inner lines	300
P-2-16	Bolted together	6¾ (staggered)	Four inner lines	300
P-2-17	Bolted together	2¼ (staggered)	Four inner lines	5
P-2-18	Bolted together	2¼ (staggered)	Four inner lines	0
P-2-19	Riveted together	2¼ (staggered)	Four inner lines	....(P)
	(c) 20-In. Built-Up Bolted Plate Girder, T-1A; No Cover Plate (See Fig. 9(c))			
T-1A-1	Bolted	2¾	....	0
T-1A-2	Bolted	2¾	....	100
T-1A-3	Bolted	2¾	....	200
T-1A-4	Bolted	2¾	....	300
T-1A-5	Bolted	5½	....	300
T-1A-6	Bolted	8¼	....	300
T-1A-7	Bolted	8¼ (center) 5½ (ends)	....	300
T-1A-8	Bolted	5½ (center) 2¾ (ends)	....	300

[a] Specimens all tested in the elastic range except those designated "(P)" which were also tested in the

TABLE 1.—(CONTINUED)

Designation (1)	Description (2)	Rivet or Bolt: Pitch (in.) (3)	Rivet or Bolt: Gage lines (4)	Bolt torque[a] (ft-lb) (5)
(d) 20-In. Built-Up Bolted Plate Girder, T-2A; One Cover Plate (See Fig. 9(c))				
T-2A-1	Bolted	$2\frac{3}{4}$	....	15
T-2A-2	Bolted	$2\frac{3}{4}$	....	150
T-2A-3	Bolted	$2\frac{3}{4}$	....	300
T-2A-4	Bolted	$5\frac{1}{2}$ (center) $2\frac{3}{4}$ (ends)	....	300
T-2A-5	Bolted	$8\frac{1}{4}$ (flange) $5\frac{1}{2}$ (web)	....	300
7-2A-6	Bolted	$8\frac{1}{4}$	....	300
(e) 20-In. Built-Up Bolted Plate Girder, T-3A; Two Cover Plates (See Fig. 9(c))				
T-3A-1	Bolted	$2\frac{3}{4}$	....	100
T-3A-2	Bolted	$2\frac{3}{4}$	....	300(P)
(f) 20-In. Built-Up Bolted Plate Girder, T-5A; Three Cover Plates (See Fig. 9(c))				
T-5A-1	Bolted	$2\frac{3}{4}$	....	30
T-5A-2	Bolted	$2\frac{3}{4}$	....	150
T-5A-3	Bolted	$2\frac{3}{4}$	....	300
T-5A-4	Bolted	$2\frac{3}{4}$ (web) $8\frac{1}{4}$ (flange[c])	....	300
T-5A-5	Bolted	$2\frac{3}{4}$ (web) $8\frac{1}{4}$ (flange)	....	300
(g) 50-In. Built-Up Bolted Plate Girder, T-6A (See Fig. 8(a))				
T-6A-1	Bolted, no stiffeners	See Fig. 8(a)	....	100
T-6A-2	Bolted, no stiffeners	See Fig. 8(a)	....	300
T-6A-3	Bolted, with stiffeners	See Fig. 8(a)	....	100
T-6A-4	Bolted, with stiffeners	See Fig. 8(a)	....	300
(h) 20-In. Built-Up Riveted Plate Girder, T-B-1 (See Fig. 9(c))				
T-1B-1	Riveted	See Fig. 9(c)	....	....(P)
T-2B-1	Riveted	See Fig. 9(c)	....	....(P)
T-4B-1	Riveted	See Fig. 9(c)	....	....(P)
T-5B-1	Riveted	See Fig. 9(c)	....	....(P)
(i) 50-In. Built-Up Riveted Plate Girder, T-6B-1 (See Fig. 8(a))				
T-6B-1	Riveted, with stiffeners	See Fig. 8(a)	....	....(P)
(j) 20-In. Welded Plate Girder, T-7 (See Fig. 9(d))				
T-7-1	Welded, no cover plate	....	....	....
T-7-2	Welded, one cover plate	....	....	....(P)
(k) 50-In. Welded Plate Girder, T-8 (See Fig. 8(b))				
T-8-A1	No cover plate and no stiffener	....	....	....
T-8-A2	Stiffeners but no cover plate	....	....	....
T-8-B2	Two cover plates, with stiffeners	....	....	....(P)
Rolled Section T-9; 18WF77 (See Bethlehem Manual of Steel Construction)				
T-9	Rolled Section	....	....	....(P)

Plastic Range. [b] Staggered. [c] At the mid-third section of the flange.

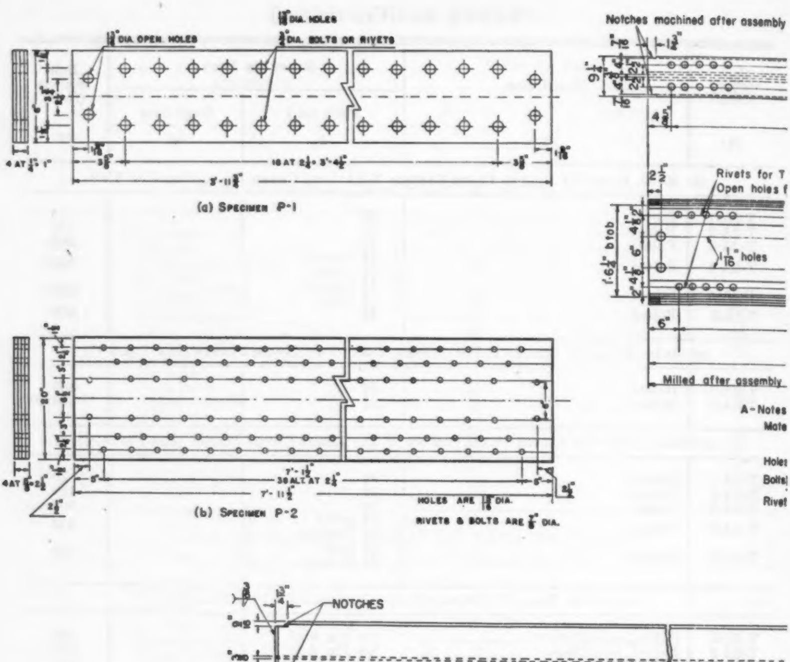

13/16" DIA. OPEN HOLES
13/16" DIA. HOLES
3/4" DIA. BOLTS OR RIVETS
16 AT 2 1/4 = 3'-4 1/2"
(a) SPECIMEN P-1
30 ALT. AT 2 1/4"
HOLES ARE 15/16" DIA.
RIVETS & BOLTS ARE 7/8" DIA.
(b) SPECIMEN P-2
Notches machined after assembly
Rivets for T
Open holes f
1 1/16" holes
Milled after assembly
A-Notes
Mate
Holes
Bolts
Rivet
NOTCHES
6-12
14'-8"
14'-9"
1 PL 8 1/2" x 1/2" x 14'-8"
1 PL 9 1/2" x 5/8" x 14'-9"
1 Web PL 17 1/4" x 3/8" x 14'-9"
1 PL 9 1/2" x 5/8" x 14'-9"
1 PL 8 1/2" x 1/2" x 14'-8"
14'-4"
14'-9"

FIG. 9.—TEST

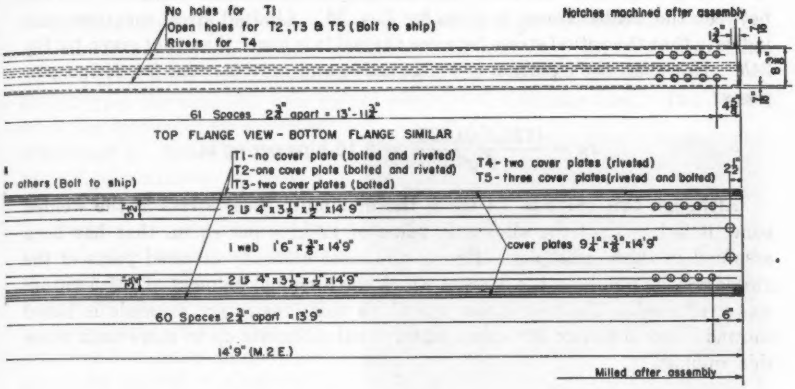

rial: Structural carbon steel ASTM-A7. All plates of one thickness to be made from the same rolling. The materials for the angles and plates must have nearly the same physical properties.

: 15/16" ϕ, subpunched and reamed, except as noted.

. 7/8" ϕ, high strength, yield point 70,000 psi. minimum, with hexagonal nuts.

s. 7/8" ϕ, report the temperature of the rivets when driven and the manner of driving.

(c) TEST SPECIMENS – T1, T2, T3, T4, and T5. (one each) – BUILT UP I BEAMS

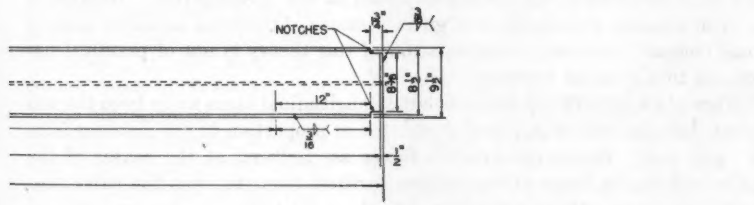

(d) TEST SPECIMEN T-7
WELDED PLATE GIRDER

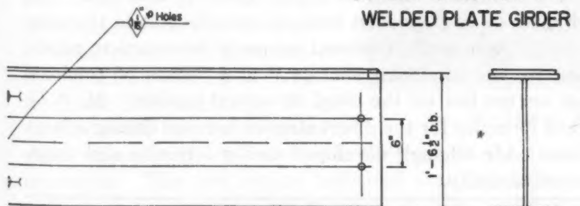

SPECIMENS

Since p' is greater than 0.4 b, the maximum shear stress in the flange, midway between the welded zones, is given by Eqs. 24. Limited stress measurements indicate that the actual stress between the welds is lower than that given by Eq. 24b. However, the equation is conservative and may be used for design purposes:

$$\tau_S = \frac{(125.5)(0.625)}{8.56} = 9.16 \text{ kips per sq in.}$$

Although this value is 2.4 times the maximum shear stress in the welded zone, it is less than the allowable value of 12 kips per sq in. that has been assumed in these examples. Hence, the most critically stressed parts of the girder are the welds, on the basis of which the torsional moment of 125.5 kip-in. was evaluated. The test girder on which this illustrative example is based showed linear behavior for values of torsional moments up to more than twice this amount.

Torsional Behavior Above the Elastic Range

If the torsional moment exceeds the value causing initial yielding of the material, there is a gradual increase of the yielded zone and the amount of twist per unit increment of torsional moment progressively increases. The elastic-plastic behavior of structural members in torsion has been treated by others,[15,16,17] usually on the basis of no strain-hardening. Mr. Chang has discussed the plastic behavior of the specimens tested in this investigation. Because of the great twisting deformations of girder sections at torsional moments causing initial inelastic behavior, a presentation of this theory is not of practical importance to the design engineer.

When the angle of twist becomes large, longitudinal fibers away from the axis of twist become helices and tend to shorten in proportion to the distance from the twist axis. Hence compressive forces are induced at the center of the section and tensile forces at the sections farthest removed from the twist axis. The tensile forces, acting at the largest angle to the twist axis, have a torsional component about the axis of twist resisting the applied torsional moment. The effect is negligible for small twist angles but becomes considerable in the early stages of plastic yielding. As a result, torsional moments for complete plastic yielding, as computed by the sandheap analogy,[15] give values of torsional moment strength that are too low for the usual structural section. M. S. G. Cullimore [18] has derived formulas for the direct stresses induced during a large twist of I-beam sections. Mr. Chang[19] developed similar formulas and measured these stresses experimentally.

[15] "Plasticity," by A. Nadai, McGraw-Hill Book Co., Inc., New York, N. Y., 1931.

[16] "The Torsion of Solid and Hollow Prisms in the Elastic and Plastic Range by Relaxation Methods," by F. S. Shaw, *Report 11*, Australian Council for Aeronautics, November, 1944.

[17] "On Torsion of Plastic Bars," by F. G. Hodge, Jr., *Journal of Applied Mechanics*, Vol. 16, No. 4, December, 1949, p. 399.

[18] "The Shortening Effect—A Non-linear Feature of Pure Torsion," by M. S. G. Cullimore, *Engineering Structures-Research Engineering Structures Supplement*, Colston Papers, Academic Press, New York, N. Y., 1949.

[19] "Torsion of Built-Up Structural Members," by F. K. Chang, thesis presented to Lehigh University, Bethlehem, Pa., in 1950, in partial fulfilment of the requirements for the degree of Doctor of Philosophy.

TEST PROGRAM, SPECIMENS, AND TEST APPARATUS

As the scale factor in bolted, riveted, and welded girders may be important, experimental work on full-size specimens was necessary to verify formulas. Table 1 gives a list of the specimens tested in the complete test program. For bolted types the variables were bolt tension, pitch, and gage lines. The details of all the specimens are shown in Figs. 8 and 9. Space limitations permit presentation of only a part of the test results.

FIG. 10.—TORSION TESTING MACHINE

Design of Specimens.—In general, the specimens tested were not specifically designed for torsion, but rather were intended to have proportions that are common for plate girders designed for normal vertical loads that cause bending in the plane of the maximum moment of inertia. Nearly minimum bolt or rivet pitch was used in many cases, but tests were also made with alternate lines of bolts removed. A detailed analysis of the predicted torsional properties of all the various specimen combinations that were tested and are as listed in Table 1 is not within the scope of this paper. However, the results of many such analyses are shown by the plotted theoretical torque-twist curves in the graphical presentation of test results. The procedure of analysis has been outlined in detail in the two illustrative examples that were based on test specimens T6B and T8B.

The AISC allowable single shear value for rivets was used in the analysis of both the riveted and bolted specimens. The test results indicated that the high tensile strength bolts used, when tightened to 300 ft-lb torque, very nearly simulated the behavior of rivets in the elastic range and in the early stages of yielding.

Specimens P1 and P2 were used to study the behavior of built-up plates. These plates simulate the flange of a heavy girder, from which most of the girder's stiffness and strength in torsion is derived.

With one exception (Test T3A2), the bolted girders were tested only in the elastic range, in order to study the effect of various combinations of plates,

rivet pitch, and line and row spacing to the best advantage. Then, after the bolted tests, the specimens were riveted in the shop and returned to the lab for final testing to failure.

Although the rivet pitch in specimens P1, P2, and T1 to T6 is in many cases less than that required for full torsional strength, the pitch is usually adequate or nearly adequate to provide longitudinal continuity. In such a case full torsional rigidity should be obtained at low torsional loads but general inelastic behavior due to slip, yield, or both, will start at lower levels than for a balanced design.

The rivets were driven using a 50-ton bull riveter with a pressure of 100-lb gage. The rivets were at a temperature of 1650° F (cherry red) when driven and the approximate driving time was 0.05 min per rivet.

The 2 welded girders (specimens T7 and T8) had welds ample for shear stresses that would result from vertical loads causing bending. As shown in the illustrative example, these specimens were underdesigned in strength and longitudinal continuity when tested for pure torsion.

Test Apparatus.—The torsion testing machine, as shown in Fig. 10, was designed and constructed especially for this project and has been described elsewhere.[3] The torque is applied to the specimen by an end plate attached to an 88-in diameter rotating head that is turned by means of a 4-in. by $\frac{1}{4}$-in. flat wire rope, using an old standard model testing machine as the power source. To measure the applied torque accurately, calibrated aluminum torque tubes of various capacity, mounted with SR-4 gages, are inserted at one end of the stationary head. The stationary head, in turn, while resisting the applied torque, rests on rollers that permit longitudinal movement when the specimen shortens during the twist.

Measurements of deformation were made by the means listed in the following tabulation:

Measurement	Apparatus
Strain	SR-4 gages
Angle of twist	Level bars
Variation in length during twist	Ames dials
Slip between different components	Whittemore gages

Adjustable-level bar seats were placed at several stations along the length of each girder. The difference of tilt angle between 2 level bar stations, divided by the distance between them, gives the angle of twist per unit length.

In all tests reported herein, approximately free-end conditions were obtained. Torque is applied by end fixture plates as shown in Fig. 10. The ends are free to warp, except for friction forces that are small in proportion to the forces required to fully restrain the section against warping. Local end-effects caused by the manner of application of the torque taper off very rapidly. The center portion of the girder, therefore, was assumed to be in a state of uniform torsion.

Test Results

Physical Tests of Materials in Test Specimens.—The tensile properties of every part of each specimen were determined. In general, the material met the

American Society for Testing Materials (ASTM) specification requirements for A-7 steel for bridges or buildings. In computing theoretical twists per unit length per unit torsional moment, a representative value of shear modulus (G) was taken as 11,450 kips per sq in., to correspond with a value of $E = 29{,}500$ kips per sq in. and Poisson's ratio value of 0.29.

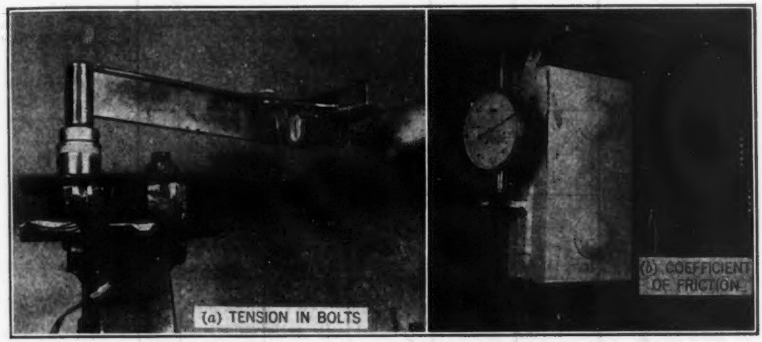

FIG. 11.—BOLT AND RIVET TESTS

Bolt and Rivet Tests.—The tension in the bolts was determined as a function of applied bolt torque by mounting SR-4 strain gages on the shank of bolts in the manner shown in Fig. 11(*a*). By this means, the strain in the bolt can be measured and the tensile force developed in the bolt can be computed for various applied torques. A curve typical of these test results is shown in Fig. 12. Then, the effective coefficient of friction between the plates or between the bolt head, nut, or washer and plate was determined by using a set-up similar to that shown in Fig. 11(*b*) for a riveted specimen. This coefficient depends on the quantity, composition, and the condition of dryness of the paint, the roughness of the surface, and other such factors. For ordinary unpainted structural steel, an average value of 0.25 was obtained for the coefficient of friction. The test results are summarized in Table 2.

TABLE 2.—EFFECTIVE COEFFICIENT OF FRICTION FOR BOLTED SPECIMENS

Torque applied (ft-lb)	Unit stress (lb per sq in.)	Total stress (lb)	Average load, to start slip[a] (lb)	Effective coefficients of friction
100	17,000	10,000	5,100	0.25
200	35,000	21,000	10,900	0.26
300	50,000	30,000	16,900	0.28

[a] Double shear bolt value for friction.

Tests were made to determine the values of coefficients of friction for rivets in single shear for conditions typical of those used in manufacturing the test specimens. The test results for the various conditions of equipment, air pressure, temperature, and driving time are summarized in Table 3. These

specimens allowed 0.5-in. slip before coming to bearing, thus differentiating clearly between the effects of friction and bearing resistance.

Plate Specimens.—These were a preliminary to girder tests and only a representative selection of test results are presented in this paper.

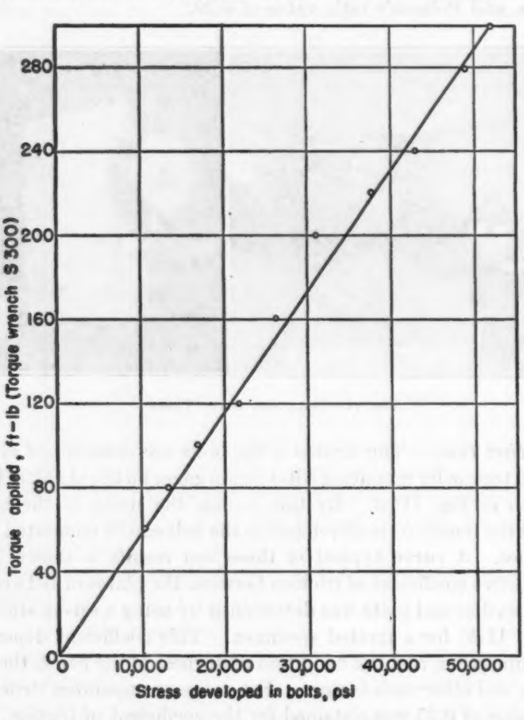

FIG. 12.—TYPICAL TORQUE-TENSION CURVE FOR ¾-INCH HIGH STRENGTH BOLTS

The 6-in. × ¼-in. plates (specimen P1, Fig. 9(*b*)) were pilot tests in a standard 24,000 in.-lb torsion testing machine. All other specimens were tested by using the 2,000,000 in.-lb machine. In the tests there were 2 rows of bolts, ¾ in. diameter at 2¼ in. center to center. The effect of bolt tension on both the strength and stiffness of a stack of 4 plates is shown in Fig. 13, with the curve for riveting included for comparison. The test result for 2 plates bolted together is almost identical to that of the 4-plate case.

Four 20-in. × ⅝-in. plates (specimen P2, Fig. 9(*b*)) bolted together were twisted in the elastic range only. The effects of bolt torque and gage line location are shown in Fig. 14(*a*). The longitudinal slip between plates during twist was also measured, and was found to depend largely on the bolt torque. The longitudinal slippage between loosely bolted plates checked very well with theoretical curves as determined by Eq. 6.

Four plates riveted together were tested to complete failure. The torque-twist and torque-slip curves of the test are shown in Fig. 14(*b*). Strain lines appeared on the rivet heads at 240,000 in.-lb torque, on the plate near the rivet heads at 301,000 in.-lb, and in the portion between the two outer rows of rivets at 326,500 in.-lb.

TABLE 3.—Results of Tests on Rivets for Specimen T6

Test number	Driving equipment	Air pressure (lb per sq in.)	Approximate rivet temperature (degrees Fahrenheit)	Approximate driving time (min)	Load at start of slip[a] (lb)
S1a	Bull riveter[b]	100	1650[c]	0.05	32,000(T6)
S1b	Bull riveter	100	1650[c]	0.05	20,000(T1 to T5)
S2	Hand gun	100	1650[c]	0.05	19,000
S3	Bull riveter[b]	80	1650[c]	0.05	20,000
S4	Bull riveter[b]	100	1900[d]	0.05	30,500
S5	Bull riveter[b]	100	1650[c]	0.25	35,000

[a] Double shear value. [b] 50 ton model. [c] Cherry red. [d] Bright cherry red.

Rolled Section (*Specimen T9*).—One rolled section was tested in order to compare its characteristics with the bolted, riveted, and welded types and to correlate this program with earlier investigation.[8] The test results were shown to be in good agreement with this former research. The torque-twist curve is shown in Fig. 15(*a*). Strain lines first appeared along the fillets at 75,000 in.-lb

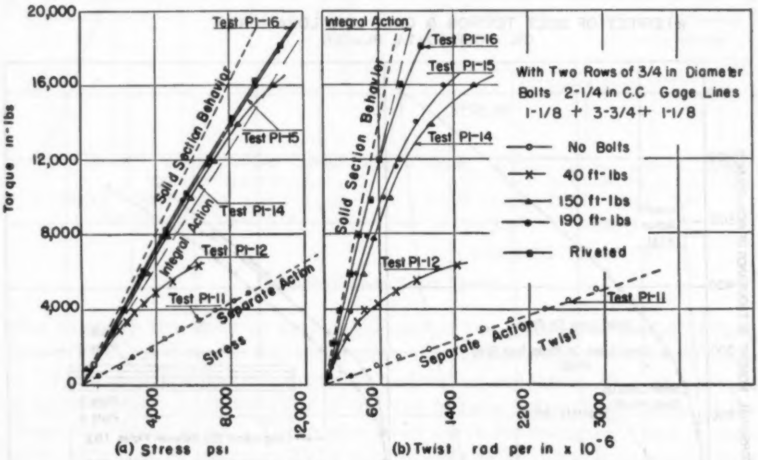

Fig. 13.—Test Results for 4 Plates Bolted Together

where stress concentrations occurred due to the sharp curvature of the fillet. At 86,000 in.-lb strain lines appeared along the center line of the flange where the largest inscribed circle touches the boundary. The moment for the completely plastic state, assuming no strain-hardening, is also shown, but it is noted

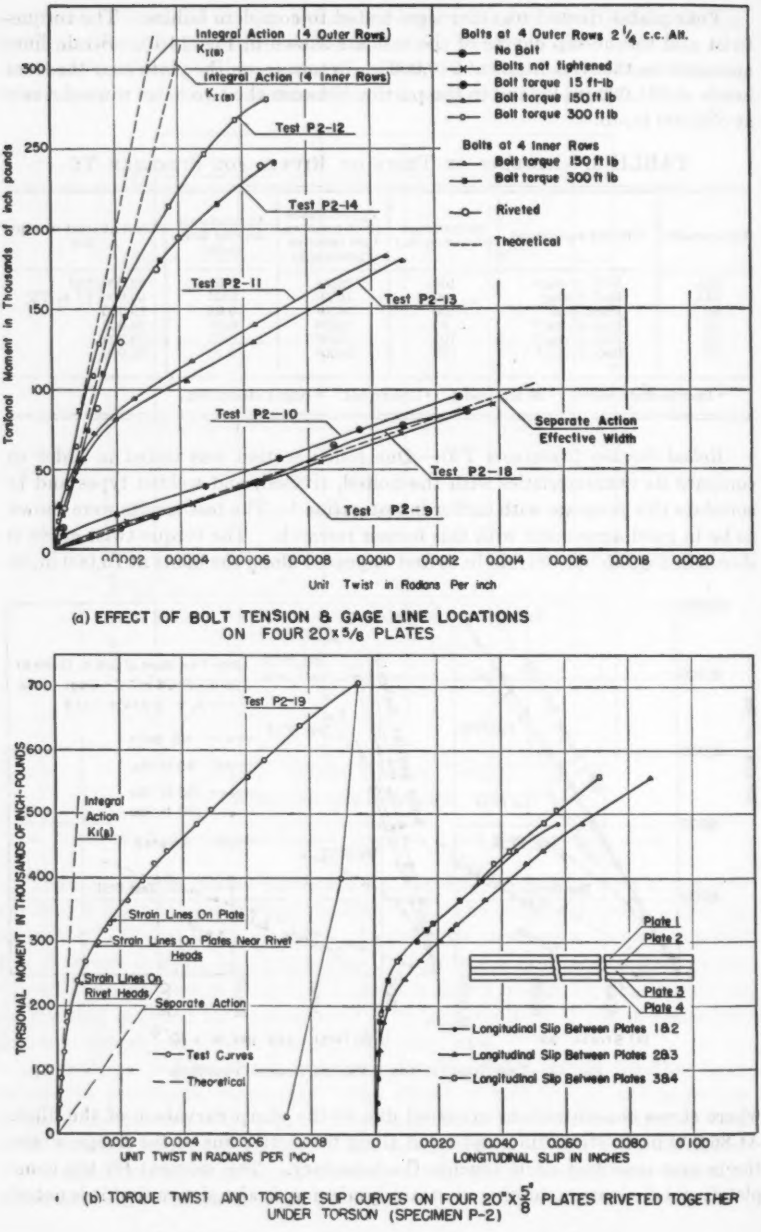

(a) EFFECT OF BOLT TENSION & GAGE LINE LOCATIONS ON FOUR 20 × 5/8 PLATES

(b) TORQUE TWIST AND TORQUE SLIP CURVES ON FOUR 20" × 5/8" PLATES RIVETED TOGETHER UNDER TORSION (SPECIMEN P-2)

Fig. 14.—Characteristic Curves for Assembly of 4 Plates

that even at low unit twist angle the beam offers a much higher torsional resistance caused by the development of longitudinal normal stresses.[19]

Bolted Plate Girders.—All bolted specimens except T3 were tested in the elastic range only. Different bolt pitches and bolt torques were used in these

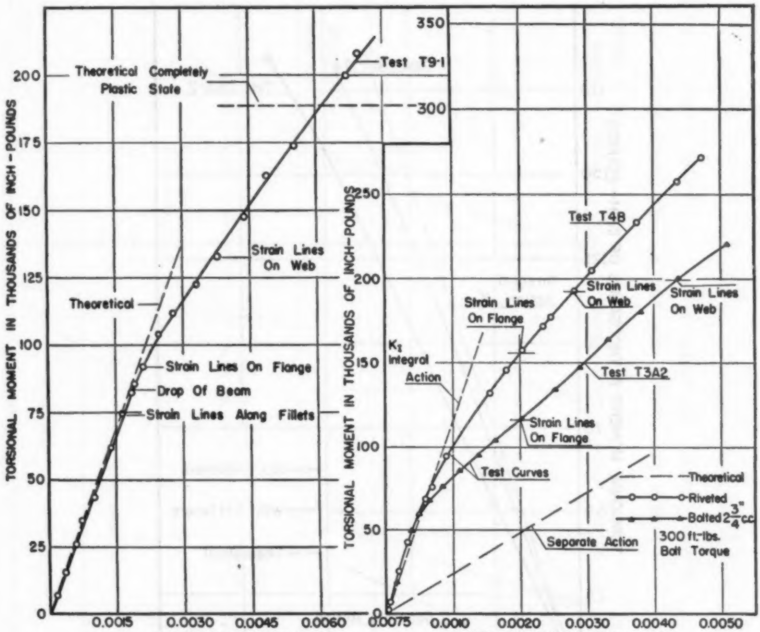

(a) TORQUE - TWIST CURVE FOR ROLLED SECTION (SPECIMEN T 9)

(b) 23 TORQUE TWIST CURVE FOR 20" X 9" GIRDERS (SPECIMENS T3 AND T4)

FIG. 15.—TORQUE-TWIST CURVES

tests to study the effect of various factors on the stiffness of bolted girders. In test T3A2, as shown in Fig. 15(*b*), strain lines appeared around the bolt heads at 117,000 in.-lb and on both the flange and web at 210,000 in.-lb. At a torque of about 340,000 in.-lb buckling of the web became noticeable because of the flange shortening effect. The torque-twist curve for specimen T3A2 is compared with that of specimen T4B1 that has the same dimensions except that beam T4B1 is riveted instead of bolted. It may be noticed that the bolted (300 ft-lb bolt torque) and riveted specimens behave more or less the same in the lower load range, but the riveted specimens were relatively stronger in the inelastic range, after initial slip.

In order to accurately determine the torsion constant (K) of this and other test specimens, the elastic range torque-twist curves were drawn to a larger

scale than that of Fig. 15(*b*). From Eq. 2, *K* is defined as the slope of the torque-twist curve (in the elastic range) divided by *G*.

The effect of stiffeners on bolted girders was also studied in the test of specimen T6. The test results are plotted in Fig. 16. The shearing stress

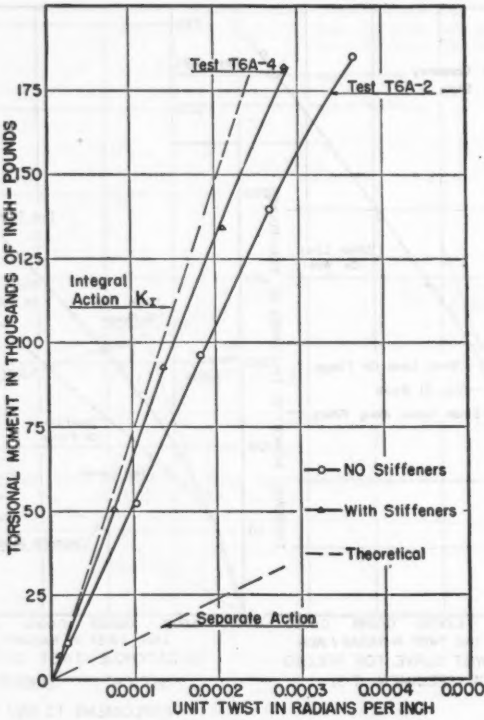

FIG. 16.—EFFECT OF STIFFENERS

distribution in the bolted specimens was similar to that shown by the riveted girders.

Riveted Plate Girders.—Riveted plate girders 20 in. deep were tested to failure. The torque-twist curve for test T1B (with no cover plates) is shown in Fig. 17(*a*). The torque-twist curve for beam T2B (one cover plate) is shown in Fig. 17(*b*). Strain lines first appeared on the flange near the rivet heads at a load of 111,000 in.-lb. At 202,500 in.-lb strain lines started to appear on the web.

The torque-twist curve beam of T4B (with two cover plates) is plotted in Fig. 15(*b*) in comparison with that of a similar bolted girder. The sequence of appearance of strain lines on specimen T4B was similar to that of specimen T2B.

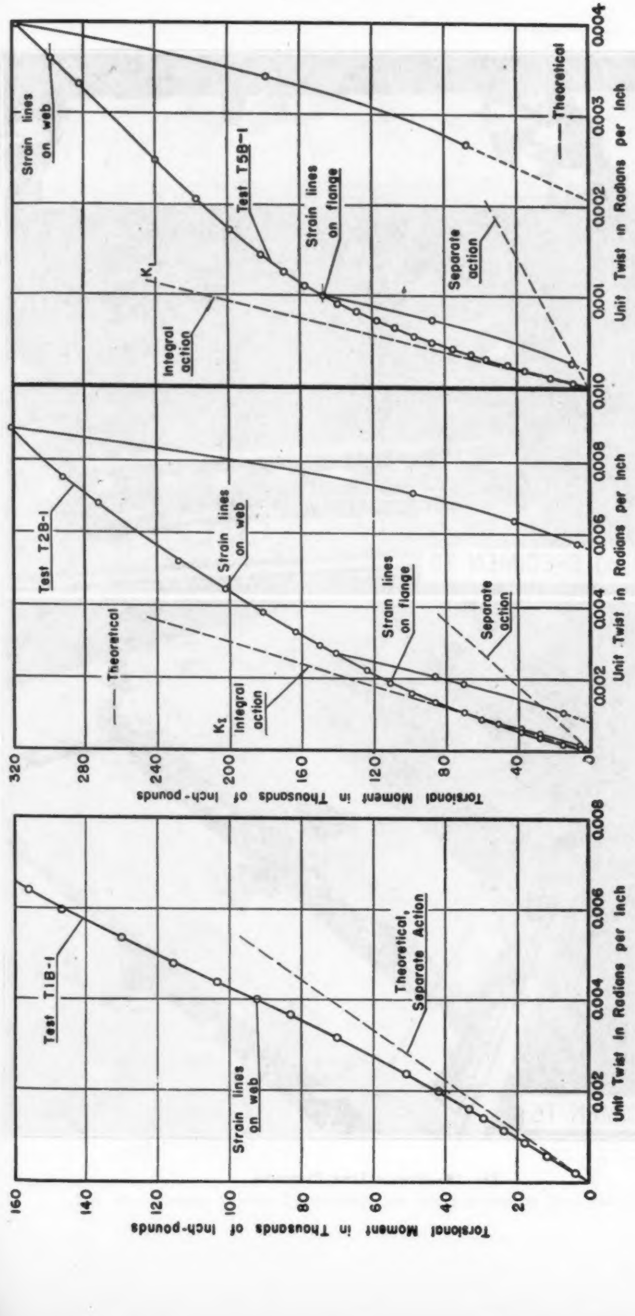

(a) TORQUE TWIST CURVES FOR 20" x 9" RIVETED GIRDER, (SPECIMEN T-1)

(b) TORQUE-TWIST CURVES FOR 20" x 9" RIVETED GIRDER (SPECIMEN T-2)

(c) TORQUE-TWIST CURVES FOR 20" x 9", RIVETED GIRDER (SPECIMEN T-5)

FIG. 17.—TORQUE-TWIST CURVES FOR RIVETED GIRDERS

FIG. 18.—STRAIN LINE PATTERNS

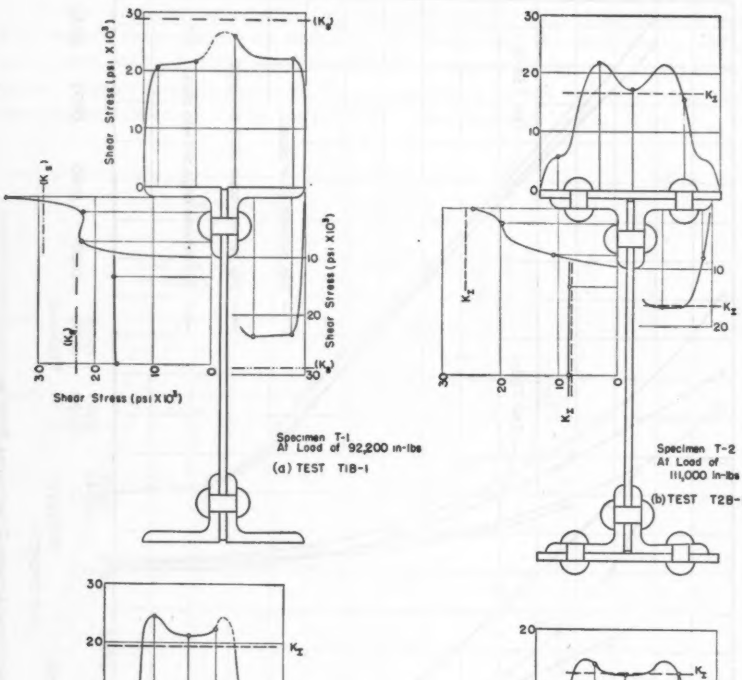

FIG. 19.—RIVETED GIRDER DISTRIBUTION OF SHEAR STRESS IN KIPS PER SQUARE INCH

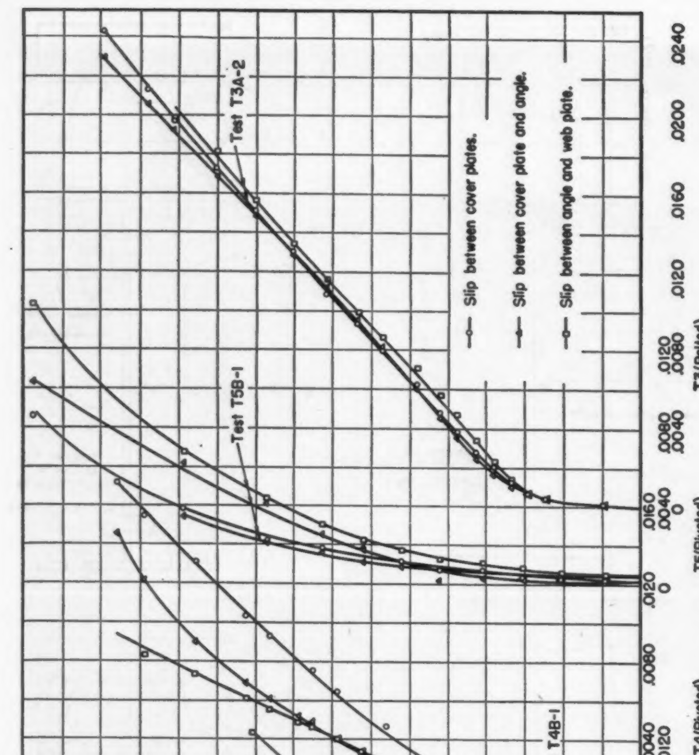

FIG. 20.—VARIATION OF LONGITUDINAL SLIP WITH APPLIED TORQUE FOR RIVETED AND BOLTED GIRDERS

As with all other bolted and riveted specimens, the first strain lines in test T5B (with 3 cover plates) appeared on the flange near the rivet heads. At a load of 240,200 in.-lb the strain lines started to appear on the rivet heads themselves. Strain lines as shown in Fig. 18 appeared on the web when the load reached 298,000 in.-lb. The torque-twist curve is shown in Fig. 17(*c*).

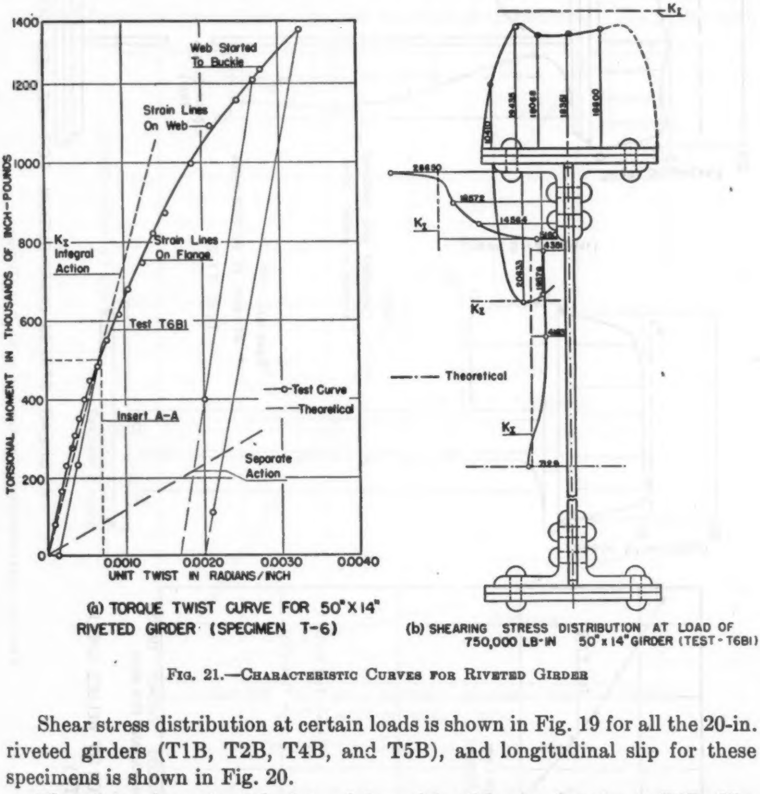

(a) TORQUE TWIST CURVE FOR 50"X14" RIVETED GIRDER (SPECIMEN T-6)

(b) SHEARING STRESS DISTRIBUTION AT LOAD OF 750,000 LB-IN 50"x14" GIRDER (TEST-T6BI)

FIG. 21.—CHARACTERISTIC CURVES FOR RIVETED GIRDER

Shear stress distribution at certain loads is shown in Fig. 19 for all the 20-in. riveted girders (T1B, T2B, T4B, and T5B), and longitudinal slip for these specimens is shown in Fig. 20.

The 50-in. deep riveted plate girder with stiffeners (specimen T6B, Fig. 8(*a*)) was tested to failure. The torque-twist curve is shown in Fig. 21(*a*). The first strain line appeared at the flange near the rivet heads at 750,000 in.-lb and then progressed along the flange between the two rows of rivets. This behavior agrees with the assumption made in evaluating the integral action torsion constant—that the portion between rivet lines acts as a solid section. Fig. 18(*b*) shows the strain line pattern after twist when a maximum load of 1,340,000 in.-lb had been applied to the specimen. The strain lines on the web indicate the buckling that occurred. Fig. 21(*b*) shows the shear stress distribution at 750,000 in.-lb torque.

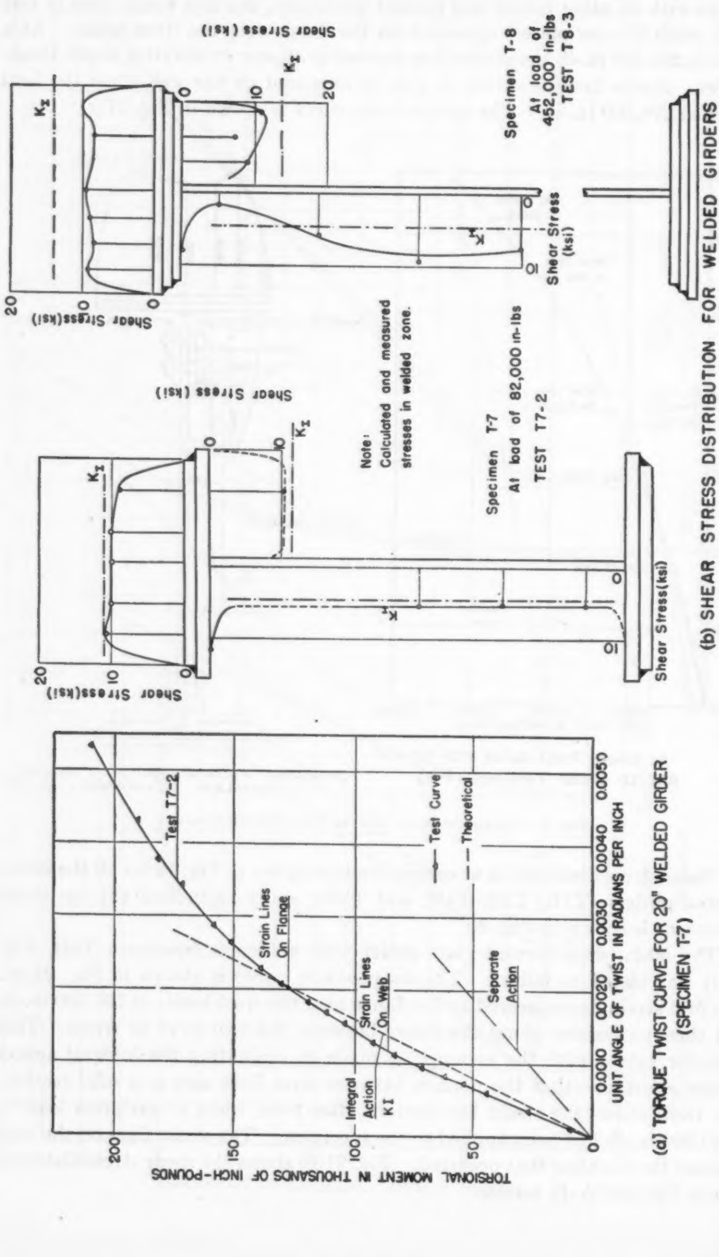

FIG. 22.—CHARACTERISTIC CURVES FOR A WELDED GIRDER

Welded Girders.—The 20-in. welded girder (specimen T7-2, Fig. 14(*a*)) was first tested in the elastic range with no cover plate, then tested to destruction with one cover plate on each flange. Fig. 22(*a*) is the torque-twist curve for the latter test. The shear stress distribution at 82,000 in.-lb is shown in Fig. 22(*b*).

A 50-in. welded plate girder with no cover plate (specimen T8-3, Fig. 8(*b*)) was first tested in the elastic range with and without stiffeners. The girder with

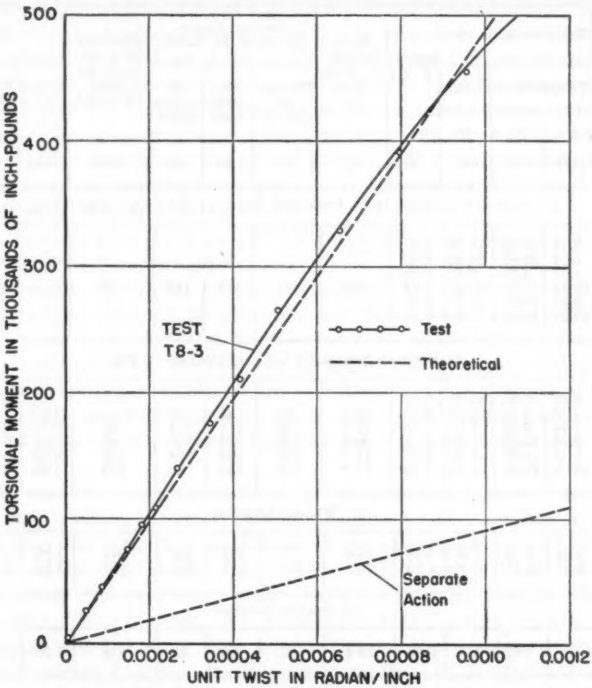

FIG. 23.—TORQUE-TWIST CURVE FOR WELDED GIRDER

web stiffeners and also two cover plates added to each flange was then tested to failure. The torque-twist curve is shown in Fig. 23. Good agreement is noted between the theoretical value of K (K_{eff} as determined by Eq. 22) and the test results. The maximum torque applied was 940,000 in.-lb. At 519,000 in.-lb strain lines first appeared along the inward side of the flange and at 639,000 in.-lb torque, strain lines appeared on both the flange and the web. The buckling of the web became very apparent at a torque of 710,000 in.-lb and at 930,000 in.-lb torque the welds connecting the cover plates started to break, with a corresponding rapid increase in angle of twist.

The shear stress distribution at 452,000 in.-lb for a location within the zone of the intermittent welds is shown in Fig. 22(*b*). The flange stresses in this

section are lower than the theoretical although the web stresses are higher, indicating the possibility that in this region of the girder the shape of the section was not being maintained and the flanges were twisting less than the web. Several shear stress measurements were made between the intermittent welds,

TABLE 4.—Summary of Test Program and Comparison with Theoretical Values

Test number	Torsion Constant[a] Theoretical K_S	Torsion Constant[a] Theoretical K_I	Torsion Constant[a] Test K	Ratio K/K_I	Shear stress τ_y[b] (kips per sq in.)	Initial Yield Moment (In.-Kips) Theoretical (Eq. 5)[c]	Initial Yield Moment (In.-Kips) By strain lines	Initial Yield Moment (In.-Kips) By strain gages	Moment[d] at a proportional limit (in.-kips)	Ratio Col. 8/Col. 7	Ratio Col. 9/Col. 7	Ratio Col. 10/Col. 7
(1)	(2)	(3)	(4)	(5)	(6)	(7)	(8)	(9)	(10)	(11)	(12)	(13)
(a) Bolted Specimens (¾-In. Diameter Bolts at 300 Ft-Lb Bolt Torque)												
P2-5	3.13	11.28	10.70	0.95	....	....	....	....	....	....	....	....
P2-12	6.27	85.60	83.80	0.98	....	....	....	....	....	....	....	....
T2A-3	1.94	5.75	7.42	1.29	....	....	....	....	....	....	....	....
T3A-2	2.28	10.36	10.65	1.03	20.9	174	117	118	60	0.67	0.68	0.35
T5A-3	2.43	18.65	15.43	0.83	....	....	....	....	....	....	....	....
T6A-4	10.22	64.92	59.60	0.92	....	....	....	....	....	....	....	....
(b) Riveted Specimens (¾-In. Diameter Rivets)												
P2-19	6.27	67.25	61.10	0.91	....	....	....	....	....	....	....	....
T1B-1	1.56	1.56	1.86	1.19	20.7	65	82	70	....	1.26	1.08	....
T2B-1	1.94	5.75	6.61	1.15	21.1	140	111	124	56	0.79	0.89	0.40
T4B-1	2.28	10.36	12.20	1.18	20.8	173	158	157	60	0.91	0.91	0.35
T5B-1	2.43	18.65	17.40	0.93	21.1	242	168	198	100	0.69	0.82	0.41
T6B-1	10.22	64.92	73.10	1.13	21.7	738	750	750	530	1.02	1.02	0.72
(c) Welded Girders												
T7B-1	2.34	5.40	6.35	1.18	19.8	77	138	138	100	1.79	1.79	1.30
T8B-1	8.01	42.47[e]	43.40	1.02	20.5	266	519	581	480	1.95	2.18	1.80
(d) Rolled Section												
T9-1	....	4.01[f]	3.83	0.96	19.4	86	86	86	98	1.00	1.00	1.14

[a] Computed values based on measured dimensions. [b] $\tau_y = 0.58\,\sigma_y$ in which σ_y is based on actual tensile tests. [c] $M_y = \frac{K\,\tau_y}{T}$. [d] Moment at 0.00006 radians per in. permanent set. [e] K_{eff} by Eq. 22. [f] Includes hump and end-loss effects.

but not exactly at the midway point. These stresses averaged about 1.5 times the stress in the welded zone. The approximate stress midway between welds, by the tentatively proposed Eq. 24, would be 2.4 times the stress in the welded zone.

Discussion of Test Results

Stiffness of Built-Up Plates and Plate Girders.—In Table 4, the torsion constants obtained by test are compared with the values computed by use of the proposed torsion constant formulas. The equations for K_I, neglecting both

the hump and edge effects, give reasonably good agreement with test results in both the bolted and riveted cases. For specimen T1B, K_S (separate action) is the same as K_I (integral action) because this girder is without cover plate and has only one row of rivets connecting the flange and the web.

For the *riveted or welded girders* (Table 4, Col. 4) the value of K determined by test was never more than 9% less than that determined by formula.

Strength of Built-Up Plates and Plate Girders.—For structural members used in common practice, a unit twist of approximately 0.00006 radians per in. might be allowable. The torsional moments that will cause a permanent set of this value are tabulated in Col. 10, Table 4, thereby defining the approximate range of linear behavior and affording an arbitrary basis of strength comparison.

In the riveted and bolted girder tests the torque-twist curves start to bend before the value of τ_{max} reaches the yield point in pure shear. The reverse is true for the rolled section and the welded girders. The torque-twist curves for unloading are nearly straight lines, approximately parallel to the initial straight portion of the torque-twist curve.

Col. 6, Table 4, gives the shear yield of the material as calculated from tensile coupon tests for the various specimens.

By using Eq. 5 and the coupon strength of the material, the torsional moment at initial yield can be predicted and these moments for all the plate girders are listed in Table 4, Col. 7. The moments at the initial yield, as indicated by strain lines (Col. 8) and by strain gages (Col. 9) are also tabulated for comparison. Cols. 11 and 12 show the relationship of these moments to those predicted by the tensile coupon tests and Eq. 5. The initial yield torsional moments as determined by strain lines and strain gages are similar in most of the tests.

Col. 10 lists the torsional moment at an arbitrary degree of permanent twist (0.00006 radians per in.) By examination of Col. 13 it is seen that for bolted and riveted girders, this amount of set develops at 35 to 72% of the theoretical moment for initial yield. This set is caused by two factors: (1) The rivet or bolt pitch used was usually greater than that required by Eq. 11; and (2) the working value of rivets, as permitted by AISC, is very close to the rivet loads that cause initial slip. Cols. 11 and 12 show that (omitting test T1B-1) actual yield occurred at moment loads varying from 67 to 102% of that predicted by Eq. 5 with early rivet or bolt slip undoubtedly being a contributing factor to the shear stresses that were higher than predicted. Test T1B-1 showed different behavior from the other riveted or bolted specimens. The slope of the torque-twist curve in this test increased initially with an increase of moment. Apparently, behavior is initially very nearly that of separate action, as assumed, but the interfaces between flange angles and web plate may develop greater friction because of binding as twist develops, thus approaching partial integral behavior.

The welded girders exhibited quite different behavior from the riveted or bolted specimens. The calculated values of moment at initial yield are based on separate action, because of the fact that the welds are intermittent and spaced at a distance of more than 0.4 b apart. This is probably an over-conservative approximation. Better agreement between theory and test would probably

have been obtained had fully continuous welds been used and these should be required if maximum available torsional strength is required. The behavior of these welded girders, underdesigned as they were for torsion, shows their marked superiority in this respect to similar riveted girders.

The rolled section exhibited excellent agreement between theory and test, as might be expected, since in this case integral behavior is inherent in this section and not a characteristic that is approximately brought about by rivets or welds. Similar agreement should be obtained for welded girders with fully continuous welds of adequate strength interconnecting the edges of all cover plates.

For the shear stress distribution on the surface of the flange and web, the integral torsion constant (K_I), used in Eq. 5, neglecting both the hump and edge effects, is in fairly good agreement with test results.

The testing program emphasized the factors that affect the torsional behavior of built-up structural members. The most important of these are: (*a*) The tension in the bolts; (*b*) the method of driving rivets; (*c*) the bolt or rivet gage line location; (*d*) the pitch of the bolts or rivets; and (*e*) the presence of stiffeners.

(*a*) *Tension in Bolts.*—From Table 2, it is seen that the bolt tension directly affects the bolt values in friction, which in turn are required to supply the longitudinal shearing stresses over the length p in the interface. Slip between different components will occur if the resultant of the latter stresses is greater than the bolt value in friction. Therefore, in a given design, the tension in the bolts will determine at what torsional moment appreciable slip will occur and the corresponding point of departure from straight-line relationship in the torque-twist curve.

(*b*) *Method of Driving Rivets.*—The rivet value in friction varies with the method of driving. If this value is too low, slip may occur early. Test results indicate that the $\frac{7}{8}$-in. rivets, driven by ordinary shop practice, correspond to $\frac{7}{8}$-in. high strength bolts, without washers, tightened to 300 ft-lb bolt torque.

(*c*) *Gage Line Locations of Bolts and Rivets.*—In evaluating the integral action torsion constant, the assemblage is assumed to act as an equivalent solid section between the outer rows of rivets or bolts. This assumption agrees very well with the test results. Therefore, the gage line location of bolts and rivets affects both the strength and stiffness of built-up members. If possible, the rivet (or bolt) lines should be located near the edge of the built-up member in order to obtain a torsionally stronger and stiffer member.

(*d*) *Pitch of Rivets or Bolts.*—The effect of rivet and bolt pitch on the stiffness and strength of built-up structural members has been approximately evaluated. If the pitch is larger than $p' = A + T$ (the pitch required for longitudinal continuity), the torsional constant (K) will be reduced according to Eqs. 17 and 22 and the maximum shear stress will be increased in comparison with full integral behavior. Likewise, the torsion constant is reduced and the shear stress raised if intermittent welds are used in welded girders.

(*e*) *Stiffeners.*—Stiffeners have little effect on the strength and stiffness of built-up members under uniform torsion in the elastic range. The riveted girders with stiffeners are somewhat stiffer than those without stiffeners. The

effect of stiffeners on welded girders is not appreciable. An important function of stiffeners is to tie the flange and web together in deep girders to assure that the flange and the web will twist through the same angle. In other words, the stiffeners serve to maintain the shape of the cross section, an important function at points of torsional load application.

Summary

Equations for evaluating the torsion constant of built-up plates and plate girders are developed and illustrative examples presented. Eqs. 14, 26, and 28, for built-up plates, riveted and bolted plate girders, and welded plate girders, respectively, are recommended for practical design purposes.

The pitch of rivets or bolts affects both the stiffness and strength of built-up structural members in torsion. For strength, the pitch should be designed by using Eqs. 11 and 12 and for longitudinal continuity the pitch should not be greater than $p' = A + T$. If a pitch greater than p' is used, the torsion constant should be determined by Eqs. 17 and 22 and shear stress computed by Eq. 24. The reduced strength and stiffness of welded girders with intermittent welds may be evaluated in a manner similar to that for riveted girders having a pitch greater than p', the effective clamping distance, which in this case corresponds to the length of the individual weld.

The typical shear stress distributions in bolted and riveted plate girders under torsion are shown in Figs. 19, 21, and 22. The maximum shear stress in the girder sections tested occurs in the fillet between flange and web. The next highest stress occurs in the flange near the rivet (or bolt) head. The stress concentrations in the fillets have little effect on the over-all torsional behavior. Eq. 5 is in good agreement with measured shear stresses in the flange and web away from the fillets.

The slip between different components of the built-up members under torsion is discussed. Eq. 6 determines the extent of slip between the corners of loosely bolted built-up plates. The tightness of bolts or the method of driving rivets determines at what torsional moment slip will occur and at what point the torque-twist curve will depart from the straight line relationship.

Stiffeners in deep riveted plate girders increase the torsional stiffness somewhat and may be required in deep girders to maintain the shape of the cross section.

Acknowledgment

This project was carried out in the Fritz Engineering Laboratory of the Lehigh University's Department of Civil Engineering and Mechanics, which is under the chairmanship of W. J. Eney. Facilities for the program were made available as well as the assistance of Paul Kaar, Kenneth Harpel, and other staff members.

The building of the special torsion testing machine required for this program received additional financing through the support of the Institute of Research of Lehigh University together with aid from the Pennsylvania State Department of Highways in cooperation with the United States Bureau of Public Roads. The program itself received major additional financing by the Research Corpor-

ation of New York City, N. Y., and the Lehigh Structural Steel Company, the latter firm having donated most of the test specimens. The Sub-committee on Torsion of the ASCE Applied Mechanics Committee aided in planning and guiding the test program.

This paper is based on a complete report of the test program that was prepared by Mr. Chang as a thesis in partial fulfilment of requirements for a doctorate degree at Lehigh University in 1950. The title of this thesis is "Torsion of Built-up Structural Members" and it is available on loan from the university.

DISCUSSION

ARTHUR P. JENTOFT,[20] RICHARD W. MAYO,[21] AND E. RUSSELL JOHNSTON, JR.,[22] JUNIOR MEMBERS, ASCE.—The design procedure proposed by Messrs. Chang and Johnston has made available for the first time a reliable practical approach to the determination of the torsional properties of built-up sections. Using the authors' procedure and the same machine, the torsional properties of two built-up riveted column sections were investigated. The results of this investigation are included in this discussion.

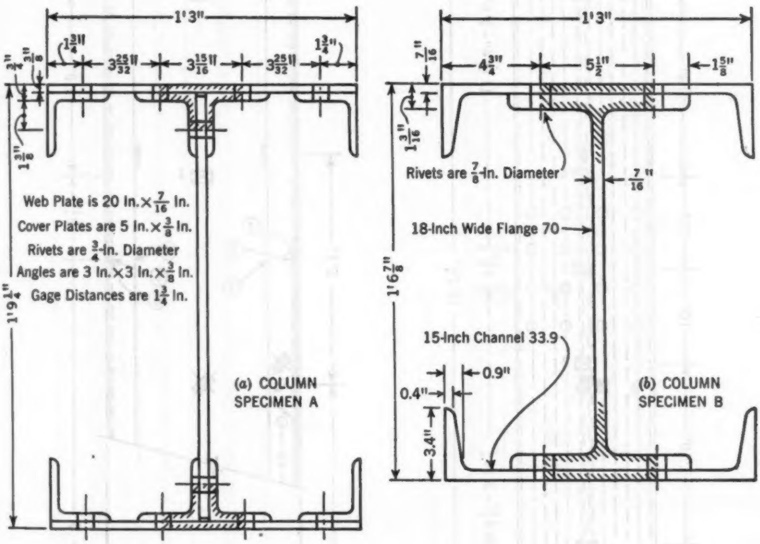

FIG. 24.—CROSS SECTIONS OF TEST SPECIMENS

Fig. 24 shows cross sections of the columns. One section was built up entirely of plates and angles, and will be designated here as Column Specimen A. The other section was composed of a wide-flange beam with channels covering the flanges, and will be referred to as Column Specimen B.

The investigation included the calculation of the stiffness, critical stresses, and strength of each of the built-up sections following the procedure suggested by Messrs. Chang and Johnston, and the testing of the two columns to determine

[20] Structural Designer, Jackson & Moreland Engrs., Boston, Mass.
[21] Structural Designer, David Taylor Model Basin, Washington, D. C.
[22] Asst. Prof. of Civ. Eng., Lehigh Univ., Bethlehem, Pa.

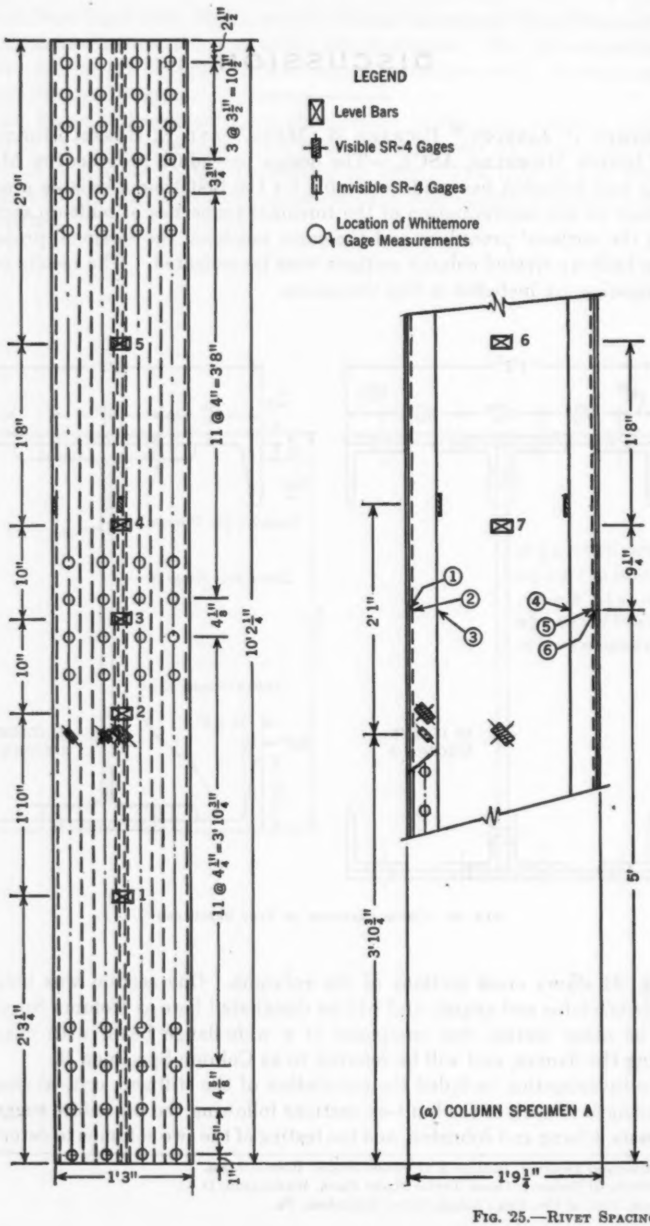

FIG. 25.—RIVET SPACING, AND

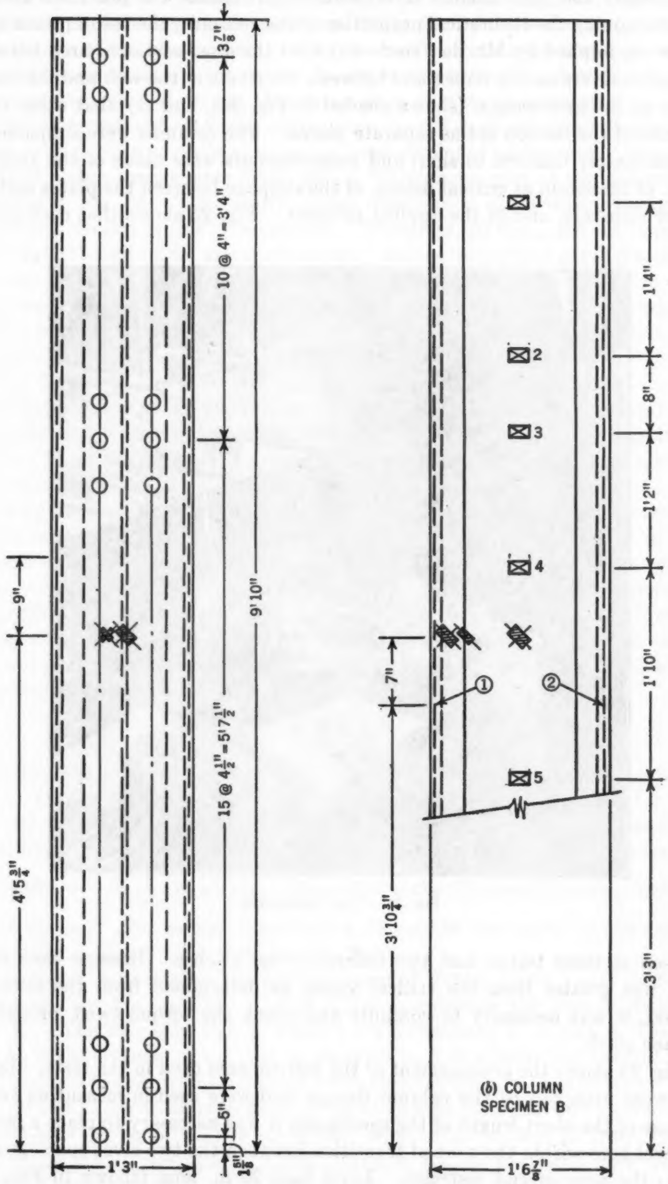

(b) COLUMN SPECIMEN B

AND LEVELS

how closely the experimental data would approximate the predicted results. In determining the theoretical properties of the columns, the assumptions were made—as implied by Mr. de Vries[4]—(a) that the cross-sectional area between the inside rivets on the flange and between the rivets in the web and the flange forms an integral section (shown shaded in Fig. 24), and (b) that other components of the section act as separate pieces. The columns were subjected to approximately uniform torsion; and measurements were made of the angle of twist, of the strain at critical points, of the slippage between the plates and adjacent members, and of the applied moment. Fig. 25 shows that each of the

Fig. 26.—Test Apparatus

built-up sections tested had two different rivet pitches. Because each rivet pitch was greater than the critical value, as determined from the authors' method, it was necessary to compute and check the torque twist properties for each pitch.

Fig. 26 shows the arrangement of the instruments used in the tests. Level bars were attached to the column flanges and were used in measuring twist. Because of the short length of the specimens, it was necessary to place a few of the level bars within the zone of transition between the two rivet spacings and within the zone of end restraint. Level bars 20 in. long (shown in Fig. 26)

were used in the elastic range, and 3-in. bars were used in the post-elastic range. The locations of the level bars are shown in Fig. 25. A level bar was placed at each change of the rivet spacing in an attempt to determine the transitional effect from one section to the next. In one case, a pair of check-level bars was placed on the web. However, these extra bars were found unnecessary.

The measurement of stress distribution by SR-4 strain gages (located as shown in Fig. 25) was made at only one cross section of each beam. Measurements of plate slippage were made with a Whittemore gage at the one section indicated in Fig. 25. The shearing stress distribution in the elastic range was of primary interest in this investigation. Therefore, all the gages were applied at 45° to the longitudinal axis of the beam. Some longitudinal gages remaining from the previous column tests on these specimens were still in sufficiently good condition to provide qualitative information. A strain-coat of whitewash was applied prior to the testing, for the purpose of determining the location and direction of strain lines, and the load at which they would occur.

The first step in the procedure of the tests was to apply a third of the calculated moment of initial yield and then to release this load. The column was then reloaded with approximately two thirds of this moment and again released. Finally, the loading was continued past the value of the moment causing initial yield into the plastic range.

Computation of Torsional Properties.—The procedure followed in determining the torsional properties was essentially that used by the authors. Col. 2 of Table 5 shows that the rivet pitches of these sections were found to be critical in all cases; hence, K_{eff}-values were required. Although the corrections for hump effect and end resistant were included in the evaluation of the stiffnesses of the columns, it is agreed that these terms are negligible in most cases, and in fact will partly cancel each other. The stiffness values determined in Table 6 come from the expression,

$$K = \Sigma \tfrac{1}{3}\, b\, t^3 - \Sigma\, V\, t^4 + \Sigma\, \alpha\, D^4 \dots\dots\dots\dots\dots\dots (34)$$

in which K is the stiffness or torsion constant, b is the developed length (see Fig. 7), t is the thickness of each component of the section, V is 0.105 for each free end, and D is the diameter of the largest circle that can be inscribed in a connection of two rectangles. The value of α is given by the expression, $\alpha = 0.094 + 0.07 \dfrac{r}{T_F}$, in which r is the radius of the fillet and T_F is the thickness of the flange.[23] For column Specimen A, D may be computed by the expression: $D(2\, r + T_F) = (T_F + r^2) + (r + T_{w/4})$.

Values of constants for the computations of Tables 5 and 6 may be found by use of Figs. 7(*a*) and 24. Col. 3, Table 5, indicates the proper choice of Eqs. 17. The values in Col. 5, Table 6 are determined from Col. 4, Table 5, and K_o is the stiffness of the part of the cross section outside the integral area.

To obtain the allowable flange and web-shear stresses, p_r is determined from Eqs. 30 and 31 for an allowed shear stress of 12 kips per sq in. and an R_w-value of 9.02 kips per sq in. Thus p_r (flange) equals 4.01 in. and p_r (web) equals

[23] "Structural Beams in Torsion," by Inge Lyse and B. G. Johnston, *Transactions*, ASCE, Vol. 101, 1936, p. 862.

1.605 in. for Column Specimen A. For Column Specimen B, p_r is 2.51 in. Because the web pitch of Column Specimen A deviates further from optimum requirements than does the flange pitch, it is used in finding the web shear which in turn determines the maximum allowable torsional moment, M.

TABLE 5.—COMPUTATION OF K FOR THE INTEGRAL SECTION[a]

Actual pitch, P, in inches (1)	$p' = A + T_F$, in inches (2)	$p - p'$, in inches (3)	K_I, in inches[4] (4)	K_S, in inches[4] (5)	K_{SE}, in inches[4] (6)	K_{eff}, in inches[4] (7)
COLUMN SPECIMEN A						
4.00 (Flange)	$2.00 < p$	$2.00 > 0.4b$	1.108	0.238	0.604	0.782
4.00 (Web)	$2.44 < p$	$1.56 < 0.4b$[b]	1.530	0.173	0.86	1.170
4.25 (Flange)	$2.00 < p$	$2.25 > 0.4b$	1.108	0.238	0.568	0.738
4.25 (Web)	$2.44 < p$	$1.81 > 0.4b$[b]	1.530	0.173	0.764	1.071
COLUMN SPECIMEN B						
4.00	$2.588 < p$	$1.41 < 0.4b$	5.60	1.790	4.39	5.10
4.50	$2.588 < p$	$1.91 < 0.4b$	5.60	1.790	3.95	4.75

[a] Shaded area in Fig. 1. [b] Value of b assumed to be the same as for the flange.

In the part of Specimen A having 4-in. pitch, $\tau_{max} = \frac{1.605}{4}\,12 = 4.81$ kips per sq in., and Eq. 24*b* yields $M = \frac{1.953\,(4.81)}{0.437} = 21.50$ kip-in. In the part having 4.25-in. pitch, $\tau_{max} = 4.53$ kips per sq in. and $M = 20.25$ kip-in.

TABLE 6.—COMPUTATION OF K FOR THE AREA OUTSIDE THE INTEGRAL SECTION

Description (1)	α (2)	Diameter, D, in inches (3)	Stiffness,[a] K, in inches[4] (4)	ΣK_I, in inches[4] (5)	$K_e = K - \Sigma K_I$, in inches[4] (6)
Column Specimen A:					
Flange angles	0.152	0.56	0.465		
Web and cover plates	0.123	1.346	3.936		
Total			4.401	2.638	1.76
Column Specimen B[b]	0.124	1.39	9.44	5.60	3.84

[a] Computed using Eq. 34. [b] Hump and end effects for the channel are negligible.

In the part of Specimen B having 4-in. pitch, $\tau_{max} = 7.53$ kips per sq in. and Eq. 24*c* yields $M = 58.30$ kip-in. In the part having 4.50-in. pitch, $\tau_{max} = 6.69$ kips per sq in. and $M = 50.79$ kip-in.

Test Results.—Fig. 27 shows Specimen A after testing. The brackets shown are those used with the 3-in. level bars. In general, the test results confirmed

the predicted properties of the two built-up sections as determined by the calculations. However, in some respects certain results are not completely explained by the theoretical analysis.

TABLE 7.—COMPUTATION OF K_{eff}—VALUES FOR ENTIRE SECTION

Description	Column Specimen A		Column Specimen B	
	Pitch = 4.00 in.	Pitch = 4.25 in.	Pitch = 4.00 in.	Pitch = 4.50 in.
K_e[a]	1.76	1.76	3.84	3.84
K_{eff} of Int. Area[b]	1.95	1.81	5.10	4.75
Total K_{eff}	3.71	3.57	8.94	8.59

[a] From Table 6. [b] From Table 5.

FIG. 27.—COLUMN SPECIMEN A AFTER TESTING

The first column tested was built up entirely of plates and angles. The torsional rigidity constant K was determined analytically for each of the 2 rivet pitches of this column. The values of K_{eff} were 3.57 in.[4] and 3.71 in.[4] for the 4.25-in. and the 4-in. rivet pitches, respectively. Curves in Figs. 28

and 29, relating plotted angle of twist to moment for this beam, show that the calculated K constants were very close to the actual conditions up to the point of initial yield. The legend for Fig. 28 is the same as that for Fig. 27. However, in the plastic range, where the K-value would be expected to decrease, the curves show an increase in stiffness of the member. This increase of stiffness continued until the web of the beam began to buckle. The high stiffness during the plastic range for this flexible column may have been caused partly by the moment produced by the increase in longitudinal forces as the twisting moment increased. It can be seen from Figs. 28 and 29 that the effect of the two rivet pitches is not great and that the K constant is nearly the same for all portions of the beam.

The second beam tested was composed of a wide-flange beam and 2 channels acting as cover plates. The constants K_{eff} calculated for this beam were 8.59

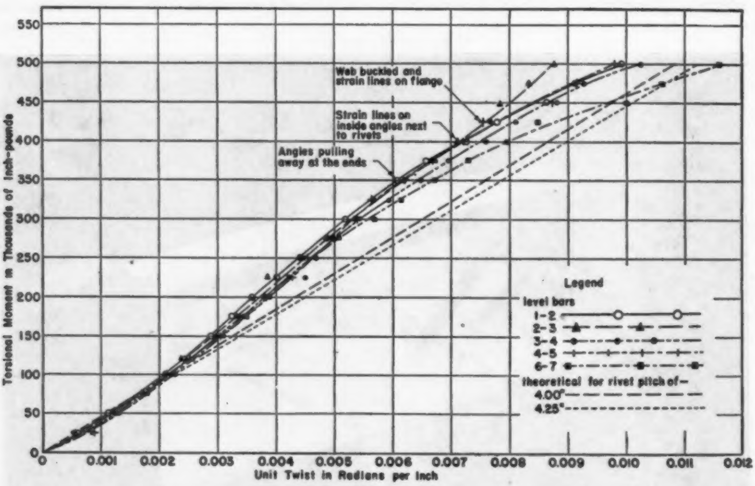

FIG. 28.—TORQUE-TWIST RELATIONSHIPS FOR COLUMN SPECIMEN A

in.[4] and 8.94 in.[4] for the 4.50-in. and 4-in. rivet pitches, respectively. From the curves of Fig. 30 it can be seen that these values were very close to actual conditions up to the initial yield, after which the actual stiffness decreased slowly for the remainder of the test. In the plastic range this beam behaved more as expected than did the previous beam. However, this beam was of thicker material and was not as flexible.

Fig. 31 shows how the actual K-values varied with respect to moment throughout the test for each of the beams. The plotted points in Fig. 10 are average stiffnesses for the 2 sections. For Specimen B there was a gradual decrease in K as the moment increased. The results for the other specimen indicated an increase in K until the web began to buckle, after which this K-value decreased also.

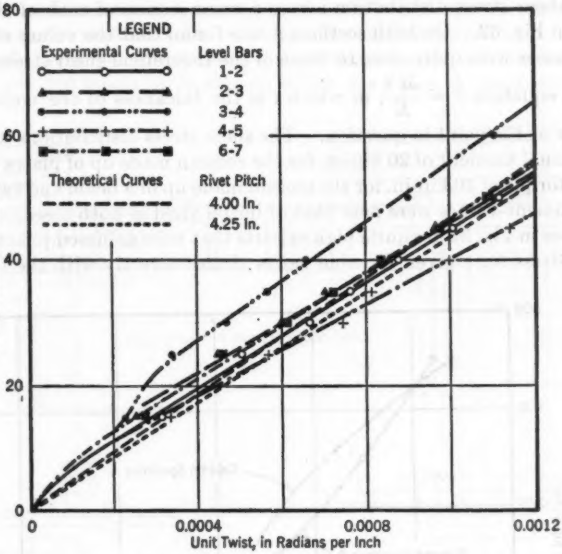

Fig. 29.—Torque-Twist Relationships for Column Specimen A in Part of the Elastic Range

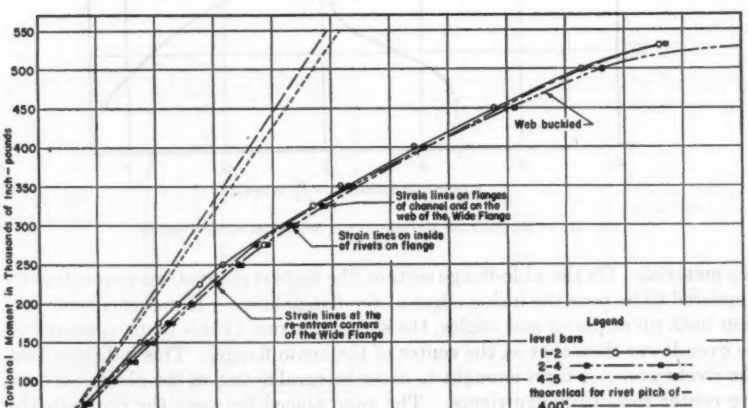

Fig. 30.—Torque-Twist Relationships for Column Specimen B

The shear stress distribution across a cross section of each of the beams is plotted in Fig. 32. On both sections it was found that the values of the actual shear stresses were quite close to those of the theoretical shear stresses as found from the equation $\tau = \frac{M\,t}{K}$, in which t is the thickness of the material acting integrally at the point in question. The shear stress distributions were plotted at a torsional moment of 20 kip-in. for the column made up of plates and angles, and at a torque of 40 kip-in. for the section made up of a beam and two channels. These moment-values were near that of initial yield in both cases. The shearing stresses in Fig. 32 are quite high in parts that were assumed to act integrally, and the stress for a given K-value varies almost directly with the thickness of

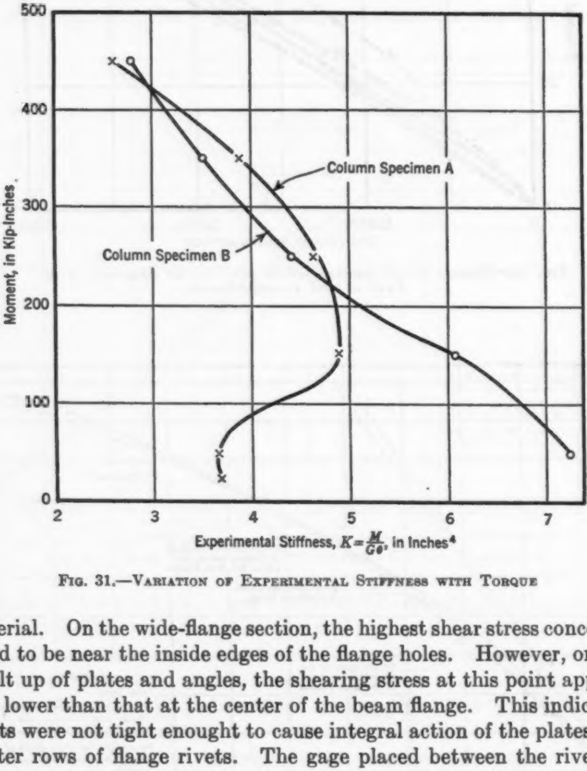

FIG. 31.—VARIATION OF EXPERIMENTAL STIFFNESS WITH TORQUE

the material. On the wide-flange section, the highest shear stress concentration appeared to be near the inside edges of the flange holes. However, on the section built up of plates and angles, the shearing stress at this point appeared to be even lower than that at the center of the beam flange. This indicates that the rivets were not tight enought to cause integral action of the plates between the center rows of flange rivets. The gage placed between the rivets in the outside row on the flange indicated a stress somewhat higher than the stress produced by separate action. Therefore, it seems probable that these rivets caused enough friction between the plates to result in somewhat better than separate action of the outside portions of these plates. More gages would be needed as checks to make the shear stresses at these points more reliable. In

general, the experimental shear stresses of both beams agreed fairly closely with the calculated shear stresses based on the usual assumptions.

In Fig. 33, the longitudinal stress distribution was plotted for moments of 250 kip-in. and 500 kip-in for Specimen B and Specimen A, respectively. In

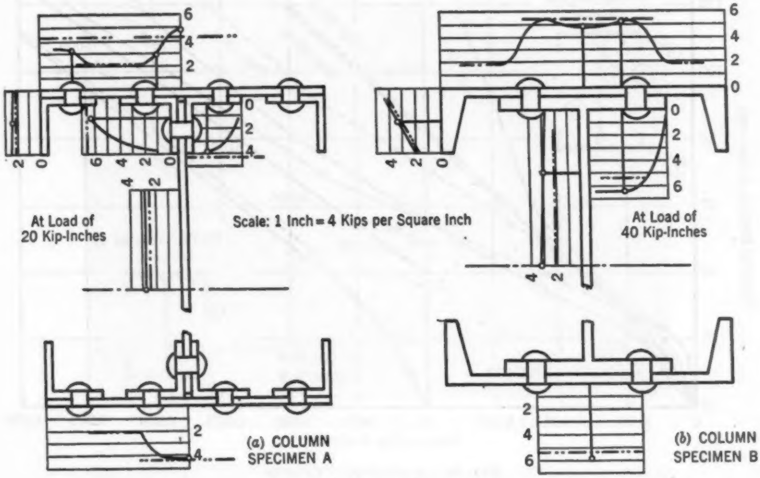

Fig. 32.—Shear Stresses

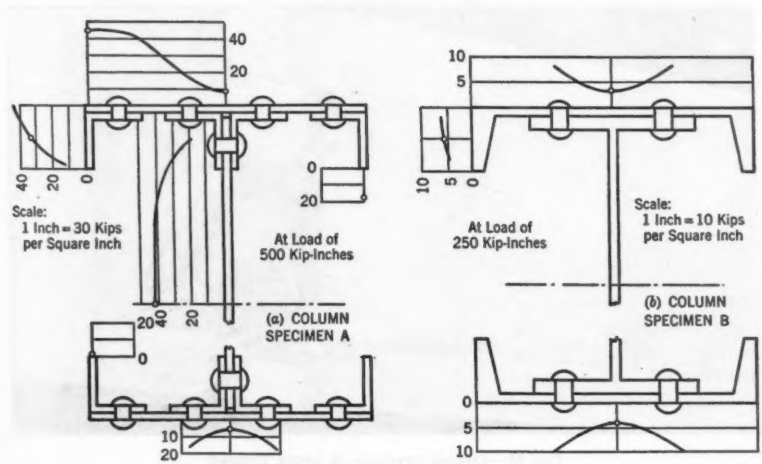

Fig. 33.—Longitudinal Stresses

both tests, insufficient longitudinal gages were applied to give representative longitudinal stress distributions, and the effect was that of having only local longitudinal stresses determined accurately.

No computations were made for the extent of slip that could be expected to occur between various components of either of the beams during the torsion test. However, most of the curves plotted in Fig. 34 for slip of adjacent mem-

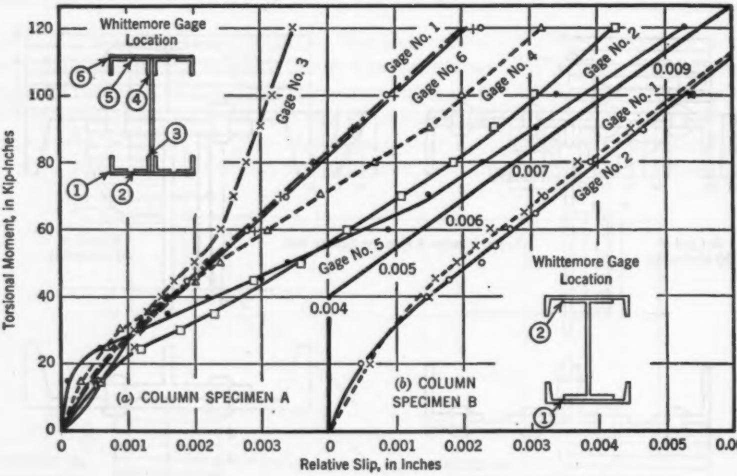

Fig. 34.—Torque-Slip Curves

Fig. 35.—Column Specimen B After Testing

bers with respect to moment were reasonable, and in most cases the extent of slip increased more rapidly as larger moments were applied.

Fig. 29, shown previously, is a general view of Column Specimen A after testing. The strain lines caused by buckling may be seen along the web of the

member. These occurred at intervals of approximately the width of the web plate.

The strain lines due to buckling in Column Specimen B may be seen in Fig. 35. The strain line pattern near a re-entrant corner of the wide-flange beam in

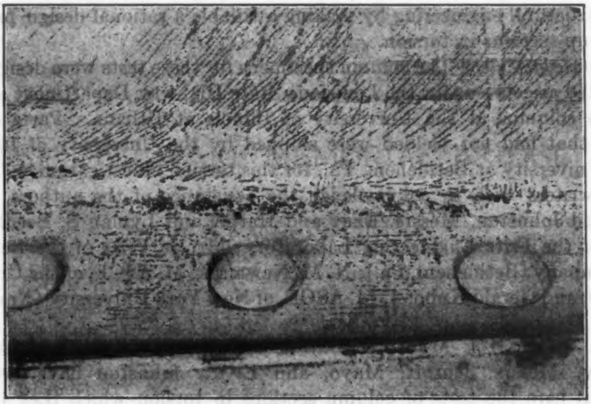

FIG. 36.—STRAIN LINE PATTERN, FILLET OF WIDE-FLANGE BEAM

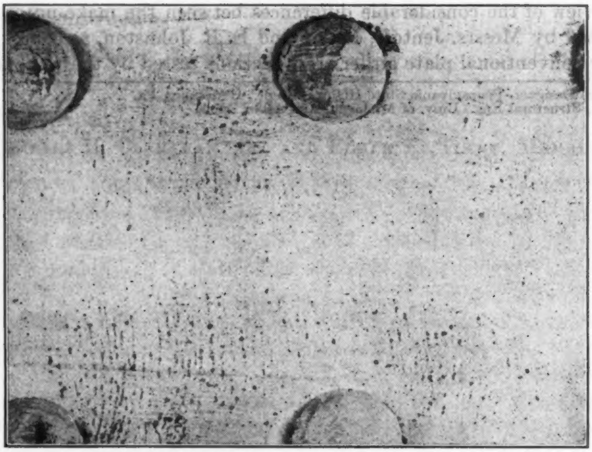

FIG. 37.—STRAIN LINE PATTERN ON CHANNEL

this column is pictured in Fig. 36. The fillet runs horizontally across the middle of the view. Fig. 37 shows the strain line pattern on the channel that forms the cover plate of Specimen B.

Conclusions.—The various assumptions proposed by the authors to make possible the determination of the properties of built-up riveted girders apply

satisfactorily to columns of somewhat different cross section than the girders used in the authors' tests. Considering the very large difference between the properties of such sections when acting entirely integrally and when acting separately, it is believed that the authors' assumptions give remarkably good results. This paper undoubtedly makes an important contribution to the field of structural engineering by making available a rational design procedure for built-up sections in torsion.

Acknowledgments.—The column specimens for these tests were designed and constructed as columns for the Louisiana State Highway Department and were tested as columns at the University of Illinois at Urbana. Parts of these columns that had not yielded were shipped by the University of Illinois to Lehigh University at Bethlehem, Pa., for this torsion investigation.

The writers wish to acknowledge the assistance of the authors, Messrs. Chang and Johnston, Messrs. Eney and Harpel and Lyman S. Beedle, A.M. ASCE, of the Fritz Engineering Laboratory; Mr. de Vries of the Bethlehem Steel Company (Bethlehem, Pa.); N. M. Newmark, M. ASCE, of the University of Illinois; and Gerald Kubo, A. M. ASCE, of New York University (New York).

F. K. CHANG,[24] J. M. ASCE, AND BRUCE G. JOHNSTON,[25] M. ASCE.—Evidently, Messrs. Jentoft, Mayo, and E. R. Johnston have performed with great care the tests of column sections in torsion which they have described in their discussion. Their contribution and corroboration are greatly appreciated by the writers of this paper. This corroboration is especially gratifying in view of the considerable differences between the make-up of the sections tested by Messrs. Jentoft, Mayo, and E. R. Johnston, as compared with the more conventional plate girder cross sections tested by the writers.

[24] Bridge Designer, Pennsylvania State Highway Dept., Harrisburg, Pa.
[25] Prof., Structural Eng., Univ. of Michigan, Ann Arbor, Mich.

AMERICAN SOCIETY OF CIVIL ENGINEERS
Founded November 5, 1852
TRANSACTIONS

Paper No. 2550

THE DELAWARE MEMORIAL BRIDGE

A SYMPOSIUM

	PAGE
Planning and Construction By Homer R. Seely, M. ASCE	398
Design Problems By Charles H. Clarahan, Jr., and Elmer K. Timby, Members, ASCE	411

AMERICAN SOCIETY OF CIVIL ENGINEERS

Founded November 5, 1852

TRANSACTIONS

THE DELAWARE MEMORIAL BRIDGE: PLANNING AND CONSTRUCTION

By Homer R. Seely,[1] M. ASCE

Synopsis

All phases of the planning and construction of the Delaware Memorial Bridge, sixth longest suspension bridge in the world, spanning the Delaware River below Wilmington, Del., are described in this paper. The writer, project engineer on the bridge construction, describes the history and financing of the span and then details the various steps in erection.

Sinking of caissons for the river piers and anchorages is briefly described, followed by a comprehensive treatment of superstructure erection techniques. Erection of suspended footwalks for cable construction and the essential steps of cable spinning are given in detail. The paper also describes erection of the suspended steelwork and the placing of the concrete pavement.

Introduction

History.—For more than 50 years the ever-increasing demand for vehicular crossings on inland waterways of the United States generally has been met, even in some cases where the ultimate traffic does not justify their construction.

One notable exception to this general rule was the crossing of the Delaware River between Delaware and New Jersey, south of Wilmington. At this location the need had been served since 1925 with diminishing success by the Pennsville-New Castle Ferry. Traffic lines, miles in length, waiting to cross the river on holiday weekends were common and on July 1, 1950, it was reported that a delay of 6 hr was suffered by some of the motorists, creating conditions requiring emergency aid from the police.

Although there had been proposals advanced by private interests to construct a crossing, nothing materialized until the State of Delaware, by legislation in 1939, directed the State Highway Department to investigate the legal,

Note.—Published in July, 1952, as *Proceedings-Separate No. 137.* Positions and titles given are those in effect when the paper was received for publication.

[1] Project Eng., Howard, Needles, Tammen & Bergendoff, Wilmington, Del.

engineering, and financial problems involved in constructing a crossing. These studies were completed and a report submitted in 1941. Although consideration was given to establishing some form of a bi-state organization with New Jersey, it was determined that this was not necessary since Delaware could undertake the construction alone. This was largely the result of the outcome of a boundary dispute starting back in the colonial days, whereby the line between the present states of Delaware and New Jersey, within a 12-mile radius of New Castle, Del., was finally decreed by the Supreme Court to lie along the low-water mark on the New Jersey side of the river.

Legislation and Financing.—In 1945, immediately following World War II, the Delaware Legislature authorized the State Highway Department to construct, operate, and maintain a river crossing and to defray its cost by an issue of revenue bonds in an amount not to exceed $25,000,000.

An Act of Congress, passed in 1946, granted the state a franchise for a bridge meeting the requirements of the War and Navy departments. Enabling legislation also was passed by the State of New Jersey approving Delaware's proposal to construct a bridge and agreeing to accept title to such property and, if necessary, condemn such property within its boundaries as might be needed for the bridge approach.

The application for a War Department permit was made on August 27, 1946, and this was granted on March 15, 1947. The permit stipulated a horizontal clearance of 2,000 ft between fender lines measured normal to the channel and an underclearance of 175 ft above mean high water for a channel width of 1,500 ft, thus requiring the construction of a bridge having a center span of 2,150 ft, the sixth longest in the world. The site selected is about 3 miles south of Wilmington at which point the river narrows from Delaware Bay.

The legislation was amended to establish the Delaware Crossing Division of the Highway Department and to authorize an increased bond issue of $40,000,000. The bonds were sold at a slight premium in June, 1948, carrying an interest rate of 4%. It had been planned to construct a six-lane bridge with highway connections extending from the du Pont Highway (Route 13) in Delaware to Route 44 in New Jersey. However, after taking bids for the tower and anchorage piers in January, 1948, it was evident that only a four-lane structure could be built and a contract for the construction of the piers on this basis was consummated in July, 1948. As bids for the remaining work were received, the continued rise in construction costs made it evident that there would not be sufficient funds to construct the highway approach on the Delaware side beyond New Castle Road, the first highway paralleling the river. The construction of the highway extending from this point westward to Route 13, including an interchange at either end, was then advanced by the state as a federal aid project. Costs continued to mount and in order to complete the bridge it finally became necessary to secure more funds. The State Legislature in its 1951 session authorized an additional bond issue of $3,900,000, part of which, however, is to be used to reimburse the state for the highway extension. Legislation was also passed at this session providing for a further bond issue to cover the cost of acquiring the ferry, which is an obligation of the Trust Inden-

ture. This extension in the amount of $2,500,000 was passed at a recent special session of the Legislature.

At the time of the initial studies in 1941, it was estimated that about 4,606,000 vehicles would cross the bridge in 1952, assuming that it would be open for traffic in 1944. In 1948 when the bonds were sold, this estimate was scaled downward to 3,817,000, reflecting the recession resulting from World War II. However, the rapidly mounting ferry traffic prior to the bridge opening on August 16, 1951, clearly justified rescaling the 1952 estimate to 5,130,000 vehicles, increasing to 7,677,000 by 1960. During the first six months of operation, the actual traffic totaled over 2,590,000 vehicles, with an average toll of approximately 83 cents. At this rate, amortization of the entire cost of the bridge is assured before 1970.

Main Piers

Horizontal and Vertical Control.—Immediately after the contract for the main piers had been signed, steps were taken to establish the triangulation system required to locate the piers. The bridge center line had been arbitrarily located for the earlier studies and a preliminary triangulation system set up for locating the borings, to a large degree making use of the existing monuments of the Corps of Engineers, United States Department of the Army. The principal base line of the final system was laid out along a tangent section of a branch freight line of the Pennsylvania Railroad on the Delaware side, which line essentially parallels the river at this point. The base line was 6,547,222 ft in length. A check line 5,401,634 ft in length was laid out on the New Jersey side running through a high tension transformer station of the Deepwater Power Plant. The measurement of this line was accordingly somewhat precarious. The base line measurements were made by setting braced stakes at 100-ft stations with set scribe marks on copper plates fastened to the top of the stakes. Six sets of measurements were made of each line, rotating the personnel in the various positions to obtain an independent check. The average of four sets was used in each case, resulting in maximum variations of 0.017 ft and 0.045 ft, respectively.

Timber towers approximately 30 ft in height were required at each of the four primary stations in order to obtain clear lines of sight. Double towers were constructed, an inner tower for supporting the instrument surrounded by an independent tower and platform for the observers. The instrument was used with a trivet resting on a heavy bent steel plate securely bolted to the tower legs. It was centered by transit plumbing from the monument below. Observations were started with a 20-sec transit, but progress was slow because of the poor atmospheric conditions that existed much of the time. Accordingly, a theodolite, reading to 0.1 sec was acquired, materially speeding the remaining observations as well as those required during the sinking of the caissons. Two stations of the Corps of Engineers' network were tied into the system to simplify the proper location of the piers in relation to the center line of channel. The system also included two secondary stations to facilitate the pier location and to serve as controls during construction.

The Corps of Engineers' datum was used for vertical control, being established by a bench mark on the wall of the Deepwater Power Plant. Initially, water levels were used for the river and Delaware land piers but before final grades were set on any of these piers, sufficient work had been completed in the river so that it was possible to establish differential levels across the river.

Land Piers.—The construction of the piers has already been described at some length.[2,3] However, a brief description of the work will be included in this paper.

The approach piers are all founded on wood piles, driven to "practical refusal" (deemed to be to a bearing capacity of 35 tons). The footings of the New Jersey land piers were constructed in open excavations in which the ground-water level was lowered with well points. Jets were used in driving the piles to aid penetration through a firm layer of material overlaying the stratum in which refusal was obtained. The concrete was mixed at the site, with ingredients being delivered by rail.

On the Delaware side, the footings of the land piers were constructed in sheeted excavations extending through the land fill that had been previously placed over the marsh mud extending some 2,000 ft inland from the shoreline.

The sheeting consisted of timber panels inserted between the flanges of steel H-beams driven at predetermined locations around the pier footings, and braced at ground level with timber wales. In some cases, cross-struts were required to reinforce the wales and in a few cases additional bracing was installed at the bottom of the excavation. The most noteworthy feature of this operation was the general absence of water seepage through the marsh mud, which meant that very little pumping of the excavations was necessary. The shafts of piers W6 to W24, inclusive, were constructed with only three form units, two of which were progressively shortened at the bottom for piers W13 to W24, inclusive, and the lower pour of piers W6 to W12, inclusive. This necessitated pours up to nearly 30 ft in height. The concrete was mixed in a central mixing plant and trucked to the site.

River Piers.—The river approach piers were constructed by the conventional cofferdam method. Underwater steam hammers were used to drive the piles so as to reduce the length of cutoffs, for which no payment allowance was made. In order to obtain adequate penetration, the piles were fitted with steel shoes. Steel spud beams were used as leads for positioning and driving both vertical and batter piles. Upon completion of pile driving, the cofferdams were sealed with 5 ft of tremie concrete deposited on a 2-ft layer of sand placed upon the mud bottom. The balance of the pier construction was carried on in the open air. The pier bases were faced with granite above El.-5.0.

The two tower piers and the west anchorage pier were constructed with open dredged caissons founded on layers of compact clay. The tower caissons were about 69 ft by 116 ft in size with four rows of seven dredge wells, each 15 ft in diameter. The east caisson was founded at El. −115.6 and the west caisson at El. −86.9. The material under the sloping surfaces of the caisson

[2] "Mammoth Tremie Seal Poured in 7½-Day Continuous Operation," by Carl H. Cotter, *Civil Engineering*, November, 1950, p. 29.

[3] "Forty-Million-Dollar Suspension Bridge to Link Delaware and New Jersey," by Homer R. Seely, *ibid.*, November, 1949, p. 40.

walls and between the wells was loosened with water jets and removed with air lifts. The tower caissons were tremie sealed in a single operation to a plane 15 ft above the cutting edges. The two inside rows of wells were capped at El. +5 within the pier bases, which were faced with granite from El. −5 to the top of the base at El. +20. Buttresses between the outside wells extend from El. −6 down to El. −30, at which plane these wells were capped.

Anchorage Piers.—The caisson for the west anchorage pier was about 95 ft wide and 221 ft long and contained five rows of twelve dredge wells also 15 ft in diameter. This caisson was founded at El. −92.7 and sealed in three sections, the three westerly transverse rows of wells being cleaned and sealed first, followed in turn by the three easterly rows and then the six center rows. Care had to be taken not to dislodge the material under the cross-walls separating these areas until after the end sections had been sealed to prevent the tremie concrete from flowing prematurely into the center section. The easterly row of wells were capped at El. −20 to form a setback at this level, the remaining wells being capped at El. +5. A cofferdam extension to the caisson was used to construct an overhang at the west end. Granite facing was installed from El. −5 to the top of the pier at El. +15.

The cutting edges of the caissons were assembled at the Camden plant of the New York Shipbuilding Company. Welded construction was used throughout. Sheet pile sand islands were used to hold the caissons in position upstream and downstream, and steel pile dolphins in the other directions. Daily checks were made on the position and plumbness of the caissons during all stages of sinking and each was founded well within the tolerances set up in the specifications that permitted a maximum horizontal variation of 9 in. for the tower piers and 18 in. for the anchorage piers, and a maximum variance from plumb of 9 in. per 100 ft of height.

Because of the short supply of plate steel, the east anchorage pier was constructed within a cofferdam about 99 ft by 225 ft in plan dimensions. After pre-dredging the river bed to El. −40, four units of welded steel bracing, weighing approximately 140 tons each, were successively lowered into their correct locations and supported on steel spud piles driven to below founding depth. The sheet piling was driven to refusal also well below the founding depth. The material within the cofferdam was dredged to a stratum of compact sand that existed at an average elevation of −68.5 ft and cleaned with an air lift. The cofferdam was sealed with 32 ft of concrete. This was placed in a continuous operation lasting about 7½ days, and required the mixing and placing of about 27,000 cu yd of concrete. The concrete was deposited in four passes of 8 ft each starting and ending at the east end. Air lifts were used toward the end of each layer to remove the accumulation of soft material that was pushed ahead of the tremie concrete. The cofferdam was pumped out at the end of 7 days and the balance of the pier constructed in the open air. Cellular construction was used, as was the case for the west anchorage.

No special steps were taken for controlling the temperature of the tremie concrete during the period of curing, other than reducing the cement content from 6½ to 5 bags per cu yd. As soon as possible after dewatering the cofferdam, five core holes 24 ft deep were drilled in the concrete and water temperatures

in these holes determined at three depths varying from about 2 ft to 22 ft. The difference in temperature at these depths generally was about 10° F. On September 14, 1949, 23 days after completing the seal, the maximum temperature observed was 142°. The rate of cooling at this stage was about 1° per day, decreasing to about 0.35° per day on November 10, 1949, on which date the observations had to be discontinued.

Concrete Handling.—The concrete for all the river piers was mixed in two floating mixer plants; one containing two mixers with 1-yd capacity, was generally used on the approach piers, and the other containing two mixers with 2-yd capacity, for the large piers. Both plants, however, placed the tremie seal of the east anchorage pier. Wherever possible, the concrete was deposited directly in the forms through chutes and elephant trunks. Bottom-dump buckets were used for the balance of the placement. Cement was shipped in bulk and transferred to barges at the Pigeon Point Terminal of the Reading Railroad, about one-half mile north of the bridge site. The aggregates were delivered by barge from their source approximately 30 miles up the river. During the placing of the east anchorage seal, five barge loads of aggregate were held in reserve to guard against delivery failures that, however, did not materialize.

Anchorages

The construction of the anchorage blocks followed immediately the completion of the foundation piers. This work included the erection and embedment of 900 tons of structural steel forming the anchors for the main cables. The outstanding feature of this construction was the heights to which the concrete was placed with the floating derricks; the buttresses supporting the cable saddles reached to El. +158. About 23,200 cu yd of concrete were required for each anchorage block. Allowances of approximately 10 in. were made in the heights of the anchorage blocks to compensate for settlement. Since sealing the piers, periodical surveys disclose that the settlement of the east anchorage has been about 3 in. and the west anchorage about 3.5 in.

Approach Superstructure

General.—Erection of the bridge superstructure began on February 15, 1950, at the west abutment, and on March 14 at the east abutment. The steel for the west approach was delivered over a specially constructed railroad siding built along the right of way to the river edge. On the New Jersey side, use was made of the relocated track leading to the Deepwater Power Plant, from which a siding had been extended to the river by the pier contractor. The steelwork for placement over the water was shipped to the Wilmington Marine Terminal, at which point it was reloaded on steel barges for delivery to the bridge site.

The trusses, girders, floorbeams, and stringers were fabricated at Ambridge, Pa., and the balance of the steel consisting principally of the brackets, sidewalk and fascia units, and center median curbs, at Trenton, N. J. About 14,900 tons of steel were required for both approaches.

Approach Span Erection.—The continuous girder spans were erected by crawler cranes working on the ground. The truss spans were erected on falsework bents by the cantilever method, using single boom travelers working on the deck. Falsework bents located at the $\frac{1}{6}$-, $\frac{1}{3}$-, and $\frac{2}{3}$-span panel points were used for the first span and a single bent at the $\frac{2}{3}$ point for each of the remaining four spans. After erection of each of these spans was completed, the offshore end was jacked up sufficiently to release the falsework bent. The top chords, which had temporarily been made continuous with the previous span were then cut, blocking was removed from between the ends of the bottom chords, and the span lowered into its final position on the pier. Erection of the approach spans was substantially completed by December 1, 1950. The travelers were then left in place to dismantle the cable spinning equipment at the anchorages.

Towers

General.—The erection of the main towers was started immediately upon completion of the piers, the first steel for the west tower being set on March 17, 1950, and for the east tower on April 26. Each tower consists of two cellular T-section legs connected at the top (El. +437) and just below the roadway with flat-arched portal struts. The tower legs are each battered about 2 ft in their height.

The west tower was fabricated at Ambridge, and the east tower at Gary, Ind. The steel for both towers was shipped to the Wilmington Marine Terminal, thence on barges to the bridge site.

The tower legs were fabricated in thirteen tiers varying in height from 23 ft for the base tier to 40 ft for the tier opposite the lower portal. The height of the tiers below the floor level was increased 8 in. to allow for pier settlement. Generally each tier was divided into three units. The base tier, however, was fabricated in five units and the tier at the lower portal in four units. The heaviest single unit weighed about 54 tons.

Tower Erection.—The bearing areas on the piers had been ground with a carborundum-belt grinding machine to within 0.007-ft variation from a true plane. Just prior to setting the base sections, a thin layer of neat Portland cement was screeded over the bearing area. The steelwork is positively connected to the piers by use of 16 pairs of (6 by 6 by $\frac{3}{4}$ in.) angles for each leg, extending down through sleeves to I-beams embedded in the pier. These angles were spaced to project up into eight of the outside tower cells adjacent to the web plates. Hydraulic jacks resting on the base slabs and pressing up on diaphragm plates inserted between the outstanding legs of the angles were used to induce tensile stresses of 18,000 lb per sq in. in the angles. While maintaining this tension, holes were drilled in the tower webs and the connections riveted. The spaces remaining inside the sleeves were then filled with cement grout.

The first two tiers of both towers were set with a floating derrick which also erected the creeper travelers used to hoist the balance of the tower steelwork. After erecting two tiers, the travelers were, successively, jumped with block and falls and reconnected each time near the top of the tower legs. The

connections were made through 6-in.-diameter pins inserted into steel brackets bolted to the tower sections. As the tower legs are battered, the brackets were provided with adjustable connections to maintain the same relative spacing. Intermediate guide brackets were also installed to keep the travelers upright during the periods of jumping. Temporary cross-struts were placed at El. +307 to stiffen and space the tower legs.

Platforms entirely encircling the tower legs were used for heating the rivets that were projected to the various locations inside the tower legs and portals by pneumatic rivet passers. Cage elevators gave easy access to the roadway level, the temporary cross-struts, and the tower tops, from which points ladders extended up or down to the platforms. The cable saddles were set on brackets on the shore side of the towers in order to place them at the points of balanced free cables. Tower deflections of about 2 ft would otherwise have been required.

The erection of the west tower was completed on August 16, 1950, and the east tower on August 23, 1950. Approximately 4,100 tons of steel were required for each tower.

Cable Spinning

Preparation.—During the latter stages of tower erection, preparations for cable spinning had been started at the anchorages. As has been the practice on the majority of suspension bridges previously constructed, the footbridges were supported on lengths of suspender rope. Four ropes were used for each footbridge that extended from anchorage to tower and tower to tower. These ropes were first laid on the bed of the river and then hoisted to their connections at the towers. The decking for the footbridges consisted of chain link wire fencing stretched across 6-in. by 8-in. timbers spaced about 10 ft center to center and attached to the underside of the ropes. The footbridges were stiffened by the usual arched rope system, making temporary use of the permanent handropes. Cross-bridges were erected at the center and quarter points of the main span. The tramway hauling ropes were carried on steel sheave frames over the saddles and timber bents at about 200-ft intervals along the footbridges. The hauling ropes were driven by two diesel engines, one located at each anchorage. The engines were synchronized by selsyn motor controls to operate in unison with a single control. Electrically controlled clutches were also used, making it possible to stop movement of the hauling ropes from various points throughout the length of the footbridges.

Spinning Procedure.—Actual spinning alternated from one cable to the other, so upon completion of each set of strands, the hauling ropes were interchanged at each drive machine. Twin spinning wheels were used on each part of the ropes so that in full production four loops or eight wires were laid for each trip of the wheels. Leading from the reels, the cable wires were run over the top of a compensating sheave tower with loops inside, in which weighted floating sheaves fluctuated up and down depending upon the relative speeds of the wire reels and the spinning wheels. In their lower positions the floating sheaves actuated brake bands on the reels, thus slowing them or stopping them entirely whenever the spinning wheels stopped.

The cables consisted of nineteen strands of 436 wires each, built initially to a hexagonal cross section with three strands on a side. Approximately 3,360 tons (or 12,725 miles) of wire were required for the two cables. No. 6 cold-drawn, hot-dipped galvanized wire was used in lengths of about 3,000 ft, and spliced with threaded sleeve couplings. The wire was manufactured, spliced, and reeled at Trenton and trucked to the Marine Terminal for transfer to the anchorages by barge.

The cable strands were spun directly in the saddles that were machined to the circular cross section of the cables. In order to maintain the wires of each strand in their correct relative position, temporary separators and wood blocks were inserted at intervals throughout the lengths of the saddles. For the first layer, these separators consisted of pieces of cable wire inserted in holes drilled in the saddle troughs. The order of spinning was as follows: (*a*) Strands Nos. 1, 2, and 3 forming the bottom layer; (*b*) strands Nos. 4, 5, 6, and 7 occupying the second layer; (*c*) strand No. 10 located at the center of the cable; (*d*) strands Nos. 8, 9, 11, and 12 completing the third layer; (e) strands Nos. 13, 14, 15, and 16 forming the fourth layer; and (*f*) strands Nos. 17, 18, and 19 forming the top layer. When spinning the groups of three strands, only one loop of wire was pulled out each trip from the one anchorage for the middle strand of the group. The center strand (No. 10) was spun by handling it as two strands and pulling single wire loops from each anchorage with each trip of the wheels. Thus, this strand was formed by four endless lengths of wire instead of two, as for each of the other strands. Upon completion, each strand was compacted and seized at approximately 10-ft intervals with thin metal bands.

Each individual wire was adjusted in each span to hang at the predetermined sag as measured by guide wires initially set by survey instruments. Each completed strand was again adjusted to its correct sag in each span, the first strand being set by instruments and the following in proper relation to the first. Observations for the strand adjustments were made in the early morning or on cloudy days, when all the wire would be more nearly at the same temperature. After the first set, the strand adjustments always consisted of lengthening the strands at the anchorages and slipping them through the saddles to lower them to their correct position in each of the three spans since each set was spun high in each span in order to clear the adjusted strands below. This lengthening was done with a two-part wire rope tackle containing a 60-ton hydraulic pulling jack in one part. This tackle arrangement released the tension in the strand connecting bar, thus permitting the removal of the required number of shims from the adjustable pin connections of these bars to the embedded bars.

Wire spinning started on October 26, 1950, and was completed on January 16, 1951. During this time there was an unusual amount of windy weather, resulting in the loss of 26 working days. The spinning operation was normally on a two-shift basis.

Suspended Spans

Finishing of Cables.—On completion of cable spinning, the equipment at the anchorages was dismantled by the approach travelers. The guy derricks

that had been used in handling the wire reels were re-assembled on the tower portals for erection of the first panels of suspended steelwork and the assembly and disassembly of the suspended span travelers. However, at these locations, steel struts bolted to the tower legs were used in place of guys.

The cables were compacted with the usual device consisting of six hydraulic jacks radially mounted in a steel frame encircling the cable, with each jack actuating a segment of a circular shoe. The compactors were applied at 2-ft to 3-ft intervals, progressing in both directions from the tower tops, and a temporary wire seizing was applied at each point of compaction.

Cable compaction was followed immediately by placement of cable bands and suspenders. The suspenders were all measured while under dead load tension, cut and socketed at Trenton, and trucked to the Marine Terminal for delivery by barge. Overhead trolley lines, formed from the two parts of the hauling ropes, were used to transport the cable bands and shorter suspenders from the tower tops. The long suspenders were hoisted directly from reels mounted on the barges, using a single part hoist rope clipped at intervals to one leg of the suspender rope.

The cable band bolts were tightened with torque wrenches. Extensometer measurements, made on at least two bolts in each band, served as a check on the wrenches. The tightening was repeated as the steel was erected and again just prior to the wrapping of the cables.

The cables were wrapped in the usual manner with No. 8 galvanized annealed wire. This work was done by a machine consisting of a ring that surrounded the cable and was supported on a saddle that slid along the cable. The ring was rotated by an electric motor. Three spools of wrapping wire were mounted on the ring, and the wire unwound as the ring was rotated. The wires were led in tension over and under guides to lie side by side on the cable. As this operation was done prior to the cables reaching full dead load stress, the wire tension was increased considerably above the 300 lb as specified. At each cable band the wrapping terminates in recesses machined in the ends of the band.

After the wire ends were secured, the recesses were caulked with lead wool. Red lead paste was applied to the cable just prior to wrapping. Three coats of paint then completed the cable work.

Erection of Steel.—The suspended span steelwork, fabricated at Ambridge and Trenton, was all shipped to the Marine Terminal, where a large amount of subassembly and riveting was completed prior to delivery to the bridge site. The floorbeam trusses were completely assembled and riveted and the stiffening trusses were assembled and riveted in double panel units, with the exception of the four center panels of the main span and two end panels of the side spans that had to be erected in individual pieces.

The steelwork erected on the first pass of the travelers, begining at the towers, consisted of the stiffening trusses, floorbeams, top and bottom laterals, inspection walkway, and two lines of stringers. As the profile curvature of the erected steelwork in the earlier stages of this pass was just the reverse of its final curvature, unusual methods were adopted by the contractor to connect the stiffening truss units. Each of the bottom chord splices could have been left

unconnected, which would have made it difficult to develop lateral stiffness to resist movement from wind. Connecting the bottom chords however, in effect, made the forward suspenders too short, so in order to attach them, the stiffening trusses had to be lifted up (or in reality the main cables pulled down) sufficiently to slip the suspender sockets under their seat angle connections. This was done with blocks and falls, the upper block being connected to a shorter pair of suspenders, temporarily placed over the main cable for this purpose, and the lower block connected to the top of the bottom chord of the stiffening truss. The reverse curvature, however, was too great to permit this treatment for every stage, so at two points in each side of the main span and at one point in the side spans, the bottom chords and laterals were temporarily left unconnected. Wire ropes were used at these points to maintain continuity of the lateral system.

The truss members in the four center panels of the main span and the two end panels of the side spans were erected individually. The closure of the stiffening trusses offered no difficulty as, being discontinuous at the towers, their relative positions were easily adjusted to match the closing members. Erection started on February 16, 1951, and closure of the center span was accomplished on April 22, 1951, with the side spans being completed during the following week. The travelers then retraced their way back to the towers, setting the remainder of the steelwork. As the dead load was added, the tower tops were jacked shoreward under the cable saddles in four increments to their normal positions, after which holes were drilled and the permanent bolts placed. About 7,800 tons of steel were required for the suspended spans.

Roadway Paving

The two roadways, each 24 ft wide, were constructed of reinforced concrete with the riding surfaces pitched to the side and center curbs. The formwork was extremely simple. Cross-timbers resting on the bottom flanges of the stringers supported longitudinal timbers adjacent to the stringers. These in turn carried an upper set of cross-timbers framed at either end to the bevel of the haunches adjacent to the stringers. These timbers were forced up against the underside of the stringer flanges, wooden wedges being used to adjust them to the correct plane. Plywood decking completed the formwork. Only a nominal amount of nailing of the plywood was required to hold it in contact with the cross-timbers, which in turn were toe-nailed to the longitudinal timbers below. Joints in the plywood were sealed with adhesive tape. Thus, the erection and stripping of the forms were done with a minimum of damage, permitting several reuses of the form material. Stripping of the approach roadway forms was done from traveling platforms under the deck steelwork, supported by two lines of hangers and inverted I-beam trolleys that engaged longitudinal beams attached to the top surface of the platforms. The hangers and trolleys were progressively shifted ahead as the platform moved forward. Scaffolding supported on wire ropes was used for stripping the forms for the suspended spans.

The roadways were poured full width and finished with standard highway screed machines. These units ran on rails formed by 4-in. H-beams bolted

with flanges vertical to the tops of the curbs, thus bridging the numerous rivet heads at these locations.

The concrete was mixed at central mixing plants and trucked to the bridge deck. Here it was discharged into motor buggies that operated on timber runways placed over the walkways and outer edge of the roadways. Pouring always began at the far end of each panel and progressed toward the point of supply. As the dumping platform moved ahead, the sections of the runway overhanging the curb had to be removed to clear the screed machine. Only a small amount of longitudinal screeding and floating by hand following the machine-finishing was required to produce a satisfactory surface. Brooming and spraying with curing compound completed the paving operation.

The placement of the concrete on the suspended spans was carefully scheduled to introduce the load as uniformly as possible and prevent excessive distortions of the steelwork. This was done in four passes, progressing in each case, from east to west. The roadway slabs on the suspended spans are divided into panels by transverse stress joints spaced about 104 ft apart. For each pass, generally every fourth panel was poured. In the two roadways these also were staggered by one panel, so that the forms could be quickly shifted laterally from one roadway to the other with no cutting The first pass started about 200 ft west of the east tower, and the second pass at the east anchorage. The forms were left in place for 7 days in lieu of curing the underside of the slab. To speed up the operation, sufficient material was made available to form one complete roadway from anchorage to anchorage. All concrete for the suspended span and anchorage roadways was delivered to the west anchorage.

Completion of Anchorage

During the period of erecting the suspended steelwork and placing the concrete deck, the balance of the anchorage concrete was poured. This work had to be coordinated with the addition of the dead load to the cables so as to avoid excessive soil pressures at the rear of the anchorage piers. Approximately 7,250 cu yd of concrete were required to complete each anchorage. On the Delaware side, this concrete also was mixed at a central mixing plant and delivered by truck to the site at deck level, at which point it was distributed by conventional methods, including pumping. On the New Jersey side the operation was essentially similar. Here, however, the concrete was largely mixed at the site, with dry batches delivered by truck.

Conclusion

The bridge was opened for traffic on August 16, 1951, about 2 years and 6 months from the beginning of construction in February, 1949. However, considerable work remains to be done. This work consists of principally of the remainder of the painting, the installation of the electrical system, and the construction of the tower pier fenders. The fenders will be cantilevered from the piers, connected to steel struts that were inbedded in the concrete. (The contracts awarded in the course of bridge construction and the contractors are listed in Table 1, with approximate costs.)

TABLE 1.—CONTRACTS AWARDED FOR CONSTRUCTION OF THE DELAWARE MEMORIAL BRIDGE (BELOW WILMINGTON, DEL.)

Contract No.	Description	Contractor	Estimated cost
1	Borings	Sprague and Henwood, Inc.	$ 33,206
2	Tower piers and anchorage foundations	Merritt-Chapman & Scott Corp., New York, N. Y.	11,615,407
3A	Approach river piers	Merritt-Chapman & Scott Corp., New York, N. Y.	1,223,797
3B	West approach land piers	Conduit and Foundation Corp., Philadelphia, Pa.	582,106
3C	East approach land piers	Lewis and Bowman, Inc., Goldsboro, N. C.	861,558
3D	Anchorage blocks	Merritt-Chapman & Scott Corp., New York, N. Y.	1,856,946
4	Towers and suspended steelwork	American Bridge Co., Philadelphia, Pa.	6,106,000
5	Cables and suspenders	American Bridge Co., Philadelphia, Pa.	2,311,985
6	Approach superstructure steelwork	American Bridge Co., Philadelphia, Pa.	5,383,294
7A	Anchorage tops	Lewis and Bowman, Inc., Goldsboro, N. C.	1,132,550
7B	Concrete deck	The Whiting-Turner Contracting Co., Baltimore, Md.	1,043,329
8	Field painting	Buffalo Sheeting & Painting Co., Buffalo, N. Y.	338,324
9	Fenders	Merritt-Chapman & Scott Corp., New York, N. Y.	298,880
10	Electrical installation	Garrett Miller & Co., Wilmington, Del.	249,133
11	Tower elevators	Otis Elevator Co., Philadelphia, Pa.	32,985
12	East approach grading	Henry C. Eastburn & Son, Newark, Del.	55,126
13	East approach paving	Newark Construction Co., Newark, Del.	243,368
14	West approach grading	Henry C. Eastburn & Son, Newark, Del.	148,294
15	West approach paving	James Julian, Elsmere, Del.	322,602
16	Pennsylvania Railroad Overpass	Conduit and Foundation Corp., Philadelphia, Pa.	194,455
17	Front range light structure	Thomas Earle and Sons, Inc., Philadelphia, Pa.	57,004
18	New Castle Interchange ramps	....	211,400
19	Administration Bldg. and toll booths, etc.	Cantera Construction Co., Wilmingron, Del.	366,197
20	Maintenance Bldg. and additional toll facilities	....	107,000
21	West approach embankment	Citro and Sons, Inc., Wilmington, Del.	21,965
22	Planting operations	David Bachtle, Mendenhall, Pa.	26,408

ACKNOWLEDGMENT

The firm of Howard, Needles, Tammen & Bergendoff was the engineer, and O. H. Ammann, M. ASCE, and the firm of Moran, Proctor, Freeman and Mueser, acted as consultants. A. Gordon Lorimer was the consulting architect, and the writer was the project engineer.

The director of the project, representing the State of Delaware was W. A. McWilliams, M. ASCE, former chief engineer of the State Highway Department. He was preceded by W. W. Mack, who had also served as chief engineer of the department, and by Gen. Eugene Reybold (retired), M. ASCE, former chief of the Corps of Engineers.

AMERICAN SOCIETY OF CIVIL ENGINEERS

Founded November 5, 1852

TRANSACTIONS

THE DELAWARE MEMORIAL BRIDGE: DESIGN PROBLEMS

BY CHARLES H. CLARAHAN, JR.,[1] AND ELMER K. TIMBY,[2] MEMBERS, ASCE

SYNOPSIS

The Delaware Memorial Bridge, at the southern end of the New Jersey Turnpike, is 10,756 ft long, including a major suspension span with girder and truss approaches. Specifications governing the design of the bridge elements are derived and discussed in this paper.

Subsurface conditions governing pier design are described, and settlement problems that required solution are introduced. The authors stress the need for extensive research in suspension bridge design to foster economy and safety in construction.

PRELIMINARY DESIGN

General Description.—The Delaware Memorial Bridge crosses the Delaware River between Deepwater, N. J., and a point in Delaware south of Wilmington. It supports two 24-ft roadways for a length of 10,756 ft. The sixth longest suspension bridge that has been built to date (1952) comprises about three eighths of that length. The approaches include ten deck truss spans 336.5 ft long and 3,460 ft of continuous deck girder spans, each 116.7 ft or 93.3 ft long. The two 24-ft roadways are separated by a 3-ft-wide median strip with a stepped curb, and 3-ft-wide safety walks are provided on either side, giving a width between railings of 57 ft on the approach spans. The safety walks on the suspended spans are 3.7 ft wide. The funds available for the project were limited. Although it is conservative in every respect, the design necessarily had to be economical as well.

Design Criteria.—The design of a conservative suspension bridge that is economical as well, today, must depend on the designer's judgment of what is conservative. He has no generally-accepted and well-defined basis of design to guide

NOTE.—Published in August, 1952, as *Proceedings-Separate No. 147.* Positions and titles given are those in effect when the paper was received for publication.

[1] Chf. Designer, Howard, Needles, Tammen & Bergendoff, Cons. Engrs., New York, N. Y.

[2] Partner, Howard, Needles, Tammen & Bergendoff, Cons. Engrs., New York, N. Y.

him in the quantitative requirements for several important characteristics. Relatively few suspension bridges have been built with a span of more than a quarter of a mile and no one knows whether those bridges are overdesigned or underdesigned.

The behavior of the original Tacoma Narrows Bridge, in the State of Washington, and several bridges designed at the same time have indicated that plate girders are not desirable for the stiffening elements of long suspension bridges. The failure of the Tacoma Narrows Bridge demonstrated that too little was known as to how stiff a stiffening system should be. Wind load has shown itself to be a dynamic factor in design but there are no known means of translating the air movements at a given locality into the characteristics that a bridge must embody. Something is known about this and related problems, but sufficient research is not available to establish new rules of design for large suspension bridges.

The net result is that adequate bridges can be designed, but there is not enough reliable information available to justify highly refined studies of ultimate economy. Economy is an important factor for the simple reason that a small percentage of a large construction cost is an appreciable sum of money; but, the first and most important factor is adequacy.

Most suspension bridge designers agree that a prime requisite for a conservative design is a double lateral system that, properly proportioned, will eliminate torsional deflections of the suspended structure of sufficient magnitude to harm the structure or to cause concern among the users of the bridge. In addition, the structure should be wide enough to prevent undesirable lateral deflections and should have sufficient vertical stiffness to prevent undesirable vertical deflections. There are no rigid standards to determine with precision what lateral or vertical deflections are undesirable, except by a study of the behavior of existing bridges.

It would be desirable for a bridge to have inherent aerodynamic stability. However, a double lateral system, properly proportioned and with a reasonable distance between the two planes of laterals, can provide torsional rigidity sufficient to prevent the resonance that would otherwise make a suspended span aerodynamically unsafe.

Early in the studies of the basic features of the suspended structure of the Delaware Memorial Bridge, the use of two planes of laterals was established as a necessary requirement. The required spacing of the stiffening trusses and cables to provide the desired width of roadway was 61 ft. The ratio of span to width is 35, which is about three quarters of the same ratio for the Golden Gate Bridge in San Francisco, Calif. There was no reason to be further concerned about the width of the bridge.

Considerable thought was given to the depth of the stiffening trusses. A minimum chord of about 70-sq-in. effective gross area was considered satisfactory for transverse wind loads. The shape of the chord section was largely determined by the width of the truss verticals. The connections of the suspenders to the verticals of the stiffening trusses required the use of a 21-in.-wide flange beam for the vertical. The problem then became one of determining the vertical spacing of the chords. A study of other suspension bridges seemed

to provide the only answer. Most of the long suspension bridges have only one plane of laterals and, therefore, their behavior in wind should be less satisfactory than with two planes of laterals. However, it was decided that this advantage would be largely discounted and kept as an additional factor of safety. A comparison of the vertical stiffness of numerous suspension bridges and their behavior in high winds indicated that this bridge, which has a weight of about 11,200 lb per ft, should have a moment of inertia of about 28,000 in.^{2}-ft^2 in two trusses. This rigidity is considered the minimum for a similar bridge with one plane of laterals, but it is believed to be amply conservative for a bridge with two planes of laterals. To obtain a moment of inertia of about 14,000 in.^{2}-ft^2 per truss with chord areas of 70 sq in. required a depth of 20 ft, which also provided satisfactory spacing between the two planes of laterals.

From architectural and economical considerations it was desirable to place the top chord of the stiffening truss above the sidewalk. This location permitted a reduction in the elevation of the roadway above the water, a decrease in length of the approaches, and a decrease in the width of the structure, since the top chord functions as part of the railing. The side elevation of the structure presents a cleaner appearance, eliminating the interference of a heavy railing with a functional truss. However, the top lateral system is necessarily eccentric to the top chord, which produced complications in design and erection of the bridge but not in its functioning.

Floor System.—With some of the main features of the suspended structure thus determined, it became possible to study the floor in greater detail. Several panel lengths were evaluated. Since the maximum spacing of suspenders was considered to be about 50 ft, the most economical panel length for the floor was found to be half that distance. The panel length finally adopted was a little less than 26 ft.

Considerable attention was directed to the material to be used in the floor. It is impossible to be certain what exact relationship exists between the weight of a given suspension bridge and the required rigidity of the stiffening trusses, but there is reason to believe that a relationship exists. Certainly a study of the behavior of existing suspension bridges in high winds seems to indicate such a relationship. Some attention was given to the use of a lightweight roadway slab, but a 7-in. reinforced concrete slab of conventional design was finally selected as providing the best surface. The increase in weight over that of a lightweight floor was considered to be of some benefit and the extra cost resulting from this weight was partly offset by the reduction in cost of the roadway slab as compared with lightweight floors. The median strip, with its stepped curb, would have been very heavy in concrete, and, therefore, was made of steel. The sidewalk, which is only an emergency and maintenance walk, is built of heavy grating to facilitate snow removal and reduce weight. The steel curbs are open.

It is customary to use expansion joints at frequent intervals in the floor system of suspension bridges to reduce the longitudinal bending in the floor beams because of changes in the length of the stiffening truss chords caused by changes in stress. Studies of these bending stresses indicated that a spacing

of 104 ft was satisfactory between these joints. Because of the frequency of the joints, the stringers are placed on top of the floor beam and designed for continuous action over four spans. Such a design eliminates the undesirable stresses produced in a continuous floor slab when the stringers frame into the floor beams as simple spans.

The floor beams were studied as trusses and as plate girders with brackets or sway bracing to the bottom lateral system. The trussed floor beams proved slightly more expensive but were adopted because they have less wind area, they have smaller deflections, and they provide very stiff cross frames for the torsion-resisting structure.

Logically, the top laterals were made the depth of the top chord of the floor beams. The bottom laterals and the bottom chord of the floor beam were made the depth of the bottom chord of the stiffening truss.

The preliminary selection of the depth and chord area of the stiffening trusses has been discussed. It was desired to use I-sections for the diagonals and the use of one and two diagonals per panel was studied. For reasons of economy, it was decided to use only one diagonal. A single diagonal also somewhat reduces the apparent depth of the truss and facilitates maintenance.

Cable Design.—The cable sag ratio of the center span was made one tenth. An increase in sag would have produced a more flexible structure and a decrease in sag would have increased the size and cost of the anchorages. The normal sag ratio of one tenth is a desirable compromise.

With a tentative design for the stiffening trusses, the maximum chord stresses from live load were determined by the Hardesty-Wessman method of approximations[3] and the stresses resulting from wind on the center span were determined using the approximation procedure[4] introduced by E. L. Pavlo, M. ASCE. These approximate methods are quite satisfactory for preliminary designs, although it would be desirable to have the Hardesty-Wessman approximations extended to include the maximum shears. These approximations indicated that carbon steel would be satisfactory for the center-span trusses but that the greater part of the side spans had excessive unit stresses for carbon steel and slightly thicker silicon steel sections were required.

The towers are similar to those adopted for the Bronx-Whitestone Bridge, in New York, N. Y. The simplicity of their design is ideal for bridges of this size. It is possible that some slight saving could be obtained with fully-braced towers but the expenditure of a moderate additional sum to eliminate diagonal bracing seems fully warranted.

Final Design

Specifications.—The final design of the suspension bridge was based on the following design specifications (in general, which followed the determinations just described, referring to the 1944 official specifications of the American Association of State Highway Officials—AASHO):

[3] "Preliminary Design of Suspension Bridges," by Shortridge Hardesty and Harold E. Wessman, *Transactions*, ASCE, Vol. 104, 1939, p. 579.

[4] Discussion by E. L. Pavlo of "Suspension Bridges under the Action of Lateral Forces," by Leon S. Moisseiff and Frederick Lienhard, *ibid.*, Vol. 98, 1933, p. 1107.

Live Load.—For the approaches and the floor of main spans, H20-S16 loads were specified. Stiffening trusses, cables, towers, and anchorages were designed for a load of 2,250 lb per lin ft of bridge.

Exposed Areas for Determining Wind Loads.—The exposed area for application of transverse wind loads was considered to be the area of the structure as seen in side elevation plus the area of the leeward truss, railings, suspenders, cables and hand ropes, and leeward tower columns except the parts shielded by the floor system. The exposed area of all ropes and cables was taken as two thirds of the projected area based on the gross diameter.

The exposed area for the application of longitudinal wind loads was considered to be one half of the area of all truss members, floor beams, laterals, sway bracing, stringer diaphragms, suspenders, and railing posts as seen in cross sections of the suspended structure, and the entire area of towers as seen in elevation.

Wind Pressures.—The wind pressures on the exposed area were assumed as moving loads of the following intensities: (*a*) 30 lb per sq ft on the suspended spans and (*b*) 35 lb per sq ft on the towers, cables, and suspenders.

Wind Loads, Quartering Winds.—In considering quartering winds, the assumed simultaneous effect was based on seven tenths of the computed transverse wind load plus seven tenths of the computed longitudinal wind load.

Temperature Changes.—Two stipulations involving temperature changes were: (1) For stresses resulting from temperature changes, a drop in temperature of 58° F (from 68° F to 10° F) or a rise in temperature of 42° F (from 68° F to 110° F); and (2) For movements caused by temperature, a drop of 78° F or a rise of 62° F.

Normal Unit Stresses.—Normal unit stresses were as required by AASHO.

Allowable Unit Stresses.—Normal unit stresses were specified for the floor system. For the stiffening trusses, allowable stresses of 1.1 times the combined normal unit stresses for dead load, settlement, temperature, and live load were used, as well as 1.25 times the normal unit stresses for dead load, settlement, temperature, and wind combined. For laterals, allowable stresses of 1.25 times the combined normal unit stresses for dead load, settlement, temperature, and live load were used. The allowable stresses for the towers were the normal unit stresses for dead load, settlement, temperature, and live load combined, or 1.25 times the normal unit stresses for dead load, settlement, temperature, and wind combined. For bending in two directions, the allowable unit stresses in compression were increased in the lower quarter of the tower to vary uniformly from the allowable unit stress in compression of normal or 1.25 times the normal unit stress at a point one quarter of the height of the tower above the base plate to the allowable stress in tension of normal or 1.25 times normal unit stress at the top of the base plate.

Some specifications for suspension bridges have included combinations of live load with one half of the wind load—and full wind load with one-half live load at higher unit stresses, but in this case it was considered preferable to design for only a heavy live load or a high wind at moderate unit stresses.

Since there is a great reduction in highway live loads during storms, it is deemed unnecessary to combine live load with high winds.

Computations.—The detailed calculations were largely conventional. Live-load stresses in the stiffening trusses were computed by the deflection theory. The stresses in the side-span trusses were also computed, for loadings over the entire span, by simultaneous equations to determine the effect of having the anchorage saddle set back 32 ft from the truss support. Wind stresses were determined by simultaneous equations following the Moisseiff-Lienhard analysis.[5] Stresses caused by longitudinal deflections of the tower were found by successive approximations of the deflection. Transverse wind stresses in the towers were computed by a modification of the slope deflection method to introduce the effect of eccentricities caused by deflections, in a manner similar to the method of analysis developed for the Golden Gate Bridge towers.

Foundation Conditions

Subsoil Characteristics.—At this location, rock is several hundred feet below the surface. The upper portion of the ground consists of deposited strata of sand, gravel, and mud to varying depths of less than 100 ft. Below these deposits are the firmly compacted beds of clay, sand, and gravel of the Cretaceous, Tertiary, and Quarternary ages, with nearly horizontal stratifications, previously compacted by much higher loadings than exist at the time construction was started. For estimating the bearing values of these lower soils, the angle of internal friction was assumed to be 32°, which is well below the average values obtained from direct shear tests.

Foundation Details.—The east anchorage is founded at about El.-70 on a thin layer of compact varved sand, clay, and silt over compact gray sand. The west anchorage, founded at El.-96, is on a thick bed of varved clay, silty sand, and lignite except for the southeast corner, which is carried on medium to fine gray sand. The site was crossed by an erosion gulley running diagonally across the foundation. The depth of the gulley extended to approximately El.-87, nearly 50 ft outside the anchorage. The west tower pier landed on hard red and gray clay at El.-87 and the east tower pier on similar material at El.-115.

In general, foundation pressures are moderate, giving factors of safety of at least two, except temporarily under the rear of the anchorages during erection conditions and under the tower piers during wind loadings. In these two cases, the factor of safety was reduced to 1.8.

Settlement.—Naturally, with weight concentrations of the magnitude of these foundations, rather large settlements could be expected, as the loads imposed on the materials described changed during erection and will continue to change until conditions of equilibrium are re-established. The computed settlements reach ultimate values as high as 1 ft. The design provided that the computed increments of settlements after cable spinning began were to be closely equal for all the piers. To compensate for the settlements, a band of concrete 8 in. high was added at the base of the upper part of the anchorage and

[5] "Suspension Bridges under the Action of Lateral Forces," by Leon S. Moisseiff and Frederick Lienhard, *Transactions*, ASCE, Vol. 98, 1933, p. 1080.

the tower below the roadway level was increased 8 in. in height. The calculated settlements showed a probable rotation of the anchorage saddle toward the towers, which would produce a deflection of the towers toward the channel. Because of these settlements, the design longitudinal deflections of the towers were increased by 0.25 ft in either direction as the probable range of field errors in securing design dimensions and by an additional deflection of 0.2 ft toward the channel to allow for the effects of computed settlements.

The anchorages tilted toward the shore during their construction, as predicted because of heavier soil pressures under the rear of the anchorages. To obtain the design dimensions, the anchorages were built to the plane of the top of the anchorage caissons instead of to a horizontal plane. From the computed settlements, it was predicted that the anchorage saddles would be located 2 in. farther from the towers than the design dimension at the time of starting cable spinning. Measurement of this distance at the time cable spinning began confirmed this prediction closely.

If the calculated settlements are accurate, the bridge will be at its design elevation about 2 years after it is completed and will ultimately be about 2 in. low. During the last year of construction, however, the increments of settlement were about 50% of the calculated settlements and the bridge is now expected to remain slightly higher than design elevations. Because of the unusual foundation conditions for a bridge of this magnitude, the settlements are recorded every month and are studied carefully. To date (1952), there has been no reason to suspect that the design of the piers is not completely satisfactory and conservative in all respects.

Design Details.—The tower piers are simple in design. The caisson is larger than the pier top because of soil conditions, giving the cross section the appearance of a milk bottle.

The anchorage was developed gradually through a series of studies to develop an economical, conservative design. The first studies were made with the eyebars arranged in seven vertical rows, which gave a wide anchor block. In the development process it became apparent that a narrower anchorage block, with the eyebars arranged in five vertical rows, was better adapted to the final shape of the anchorage. In general, the top part of the anchorage at the rear consists of two anchor blocks of concrete surrounding the two anchor chains, a heavy wall connecting the blocks, and two masses of concrete over the anchor blocks. The resultant of the weight of this concrete and the load on the anchor chain is a horizontal load on two large girders in the vertical plane of the cables that extend to the high columns at the front of the anchorage. These columns support both the saddles at the turning point of the cables and the reactions for the side spans. The front faces of these columns are sloped, in order to keep the resultant loads well inside the columns. The upper part of the anchorage, as described previously, rests on a 10-ft slab of concrete that is heavily reinforced. The lower part developed gradually during design, changing from two or three caissons into a single unit believed to have the largest area of any caisson in use up to that time. Bidding plans were developed for two caissons and one caisson. The single caisson proved slightly cheaper.

Approaches

Numerous studies were made to develop an economical design of pleasing appearance for the approaches. These studies were conventional and similar to the studies made for any long bridge. Some minor possible savings were rejected to eliminate a multiplicity of span lengths and depths of structure.

Design specifications were practically the same as those of the AASHO (1944) with the exception of the omission of the combinations of live load and 30-lb wind, which seemed unjustified for girder and truss bridges carrying four lanes of traffic. Ordinarily the combination does not govern the design in such cases and only increases the time required to make a design.

The median strip and safety walks were designed to carry the standard truck wheels at 50% over the normal allowable unit stresses. The curb was designed for a lateral load of 1,000 lb per lin ft, or a concentrated lateral load of 6,000 lb. The lower part of the railing was designed to carry a concentrated lateral load of 10,000 lb applied to 2 ft above the sidewalk.

These loads on the sidewalk, median strip, curb, and railing are much higher than the AASHO specifications but were believed to be essential for a bridge of this size.

Model Tests

As usual, studies during the design of this bridge re-emphasized the need for more exact design criteria. Properly proved theoretical methods would make it possible to eliminate that part of the safety factor required by lack of specific information on structural requirements. With the intention of adding slightly to the knowledge in this field, a research program was sponsored by the designers at Princeton University, at Princeton, N. J., to study the problem of torsional rigidity and stress distribution in the suspended structure of a suspension bridge. The final design of the Delaware Memorial Bridge was used as the prototype and a nearly exact model of twelve panels at one-twelfth scale was built. The members were built up with continuous welds and spot welds and the connections were made with machine screws and nuts tightened with a torque wrench.

Although the tests and theoretical calculations are planned to extend over several years, tests have already been made with a single lateral system (the top lateral system of the prototype) and with a double lateral system. The tests were made by applying a static torque at each end of the model with all forces vertical. The torsional deflection with a double lateral system was found to be only 5% of the deflection with a single lateral system. For this loading the structure is statically determinate to the same degree as a simple-span truss in which secondary stresses are ignored. The stresses in all laterals are equal and can be found by equating the forces on a single-vertical truss. The truss is subjected to a torque (in a longitudinal direction) composed of two equal and opposite vertical forces, one at each end. This torque is resisted by an equal and opposite torque composed of horizontal forces having an arm equal to the distance between centers of the laterals. The horizontal force is the sum of the components of one plane of the laterals parallel to the truss. As previously mentioned, the stresses in all laterals are equal. The stresses

in the vertical truss are those caused by the applied forces at the ends of the truss and the components of the laterals. The test data of the model closely checked the theoretical calculations of the stresses and deflections.

Much more work is necessary to develop a simple method of computing the torsional stresses in a suspension bridge. In these model tests the corners of the model were free to deflect vertically and horizontally. In a suspension bridge there are restraints that always prevent vertical motion and sometimes horizontal motion at one end of a span. In addition, the cable also acts to produce restraints at the suspender points. The effect of these restraints must be determined.

The tests on the model have confirmed the belief that a second plane of laterals greatly increases the torsional strength of the suspended structure. Much work remains to be done on this one phase of the design problem. Other phases require similar detailed attention. The writers are of the opinion that: (1) The development and confirmation of the necessary criteria can only be accomplished through a well-planned program of research extending over several years; (2) such development and confirmation are economically sound subjects for research; (3) much more needs to be known about wind-load characteristics at particular sites; and (4) large-scale models of suspended structures, towers, and topography should form a part of the program.

Conclusion

In summary, it can be stated that the Delaware Memorial Bridge is designed conservatively and is stable and adequate to resist all probable loads. If additional reliable criteria had been available to the designers, it might have been possible to achieve some slight economies with assurance that safety would not thereby be impaired. Until such time as well-established criteria are available, designs based on past satsifactory performance are mandatory for major suspension bridges.

Acknowledgment

The bridge was designed by the firm of Howard, Needles, Tammen & Bergendoff. The consulting staff consisted of A. Gordon Lorimer, architect; Moran, Proctor, Freeman, and Mueser, consultants on foundations; and O. H. Ammann, M. ASCE, consultant on suspension spans.

AMERICAN SOCIETY OF CIVIL ENGINEERS

Founded November 5, 1852

TRANSACTIONS

Paper No. 2551

A NAVIGATION CHANNEL TO VICTORIA, TEX.

By Albert B. Davis, Jr.[1]

Synopsis

The navigation channel to Victoria, Tex., will provide a channel for barge transportation as a feeder or tributary channel to the Gulf Intracoastal Waterway. The engineering problems involved are those of location and design of the channel and appurtenant facilities. Separate plans are presented for a sea-level canal and for a lock canal. Comparison of the two plans on a cost basis favors the sea-level plan and, because of the inadequate water supply for operation of a lock canal, it is concluded that the sea-level canal is preferable for a navigation channel to Victoria. The conclusions presented in this paper are those of the writer and do not necessarily represent the views of the Corps of Engineers, United States Department of the Army.

Introduction

The federal Guadalupe River Project for a navigation channel to Victoria is an example of the tributary or feeder channels of the Gulf Intracoastal Waterway on the Texas Gulf Coast. These feeder channels extend inland about as far as it is practicable to carry a tide-water or sea-level canal. The problems that are encountered in locating and designing the channel to Victoria were generally similar to the problems encountered on the initial extension of navigation upstream from the coastal waters.

The Guadalupe River, one of the larger streams in Texas, has a drainage area of about 10,200 sq miles, including the San Antinio River, its principal tributary, which empties into the Guadalupe River 11 miles above its mouth and has a drainage area of about 4,200 sq miles. The drainage area of the Guadalupe, exclusive of the San Antonio River, is about 6,000 sq miles. The Guadalupe River empties through Mission Lake and Guadalupe Bay into San Antonio Bay (one of the larger coastal bays on the Texas coast) which is separated from the Gulf of Mexico by Matagorda Island, an off-shore bar formation.

Note.—Published in October, 1952, as *Proceedings-Separate No. 154*. Positions and titles given are those in effect when the paper was received for publication.

[1] Chf., Planning and Reports Branch, Galveston Dist., Corps of Engrs., U. S. Dept. of the Army, Galveston, Tex.

Connection between San Antonio Bay and the Gulf of Mexico is indirect through several small bays to a permanent pass on the north and an intermittent pass on the south. The main channel of the Gulf Intracoastal Waterway extends along the mainland shore of the small coastal bays and across the lower end of San Antonio Bay. The vicinity of the project channel is shown in Fig. 1.

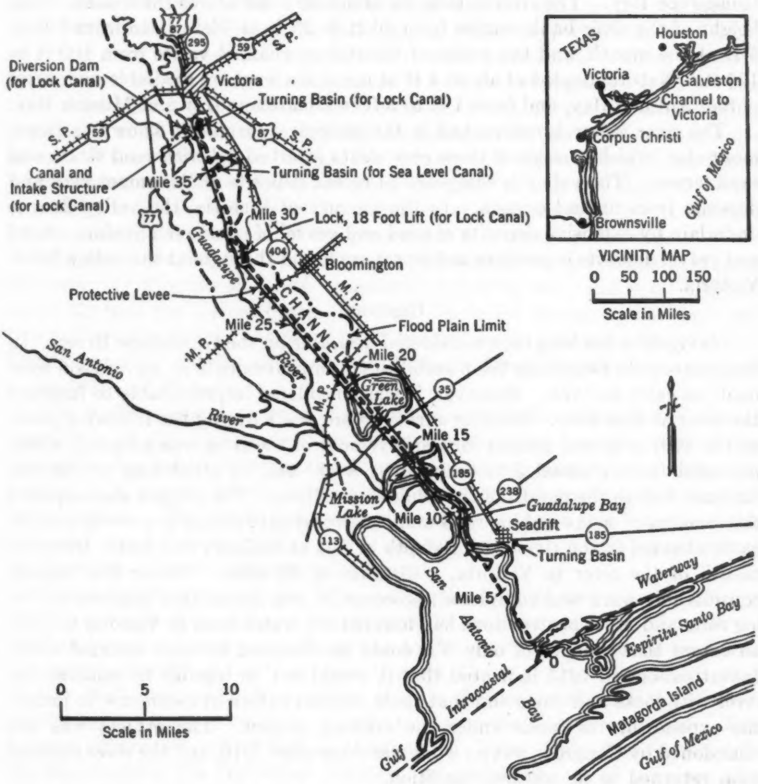

FIG. 1.—CHANNEL TO VICTORIA, TEX.

The City of Victoria is on the left bank of the Guadalupe River, 52 miles above its mouth and about 40 miles on an air line from the Gulf Intracoastal Waterway at the lower end of San Antonio Bay. The town of Seadrift, Tex., lies on the northeast shore of San Antonio Bay about 7 miles from the Intracoastal Waterway and about 5 miles from the mouth of the Guadalupe River.

The valley of the Guadalupe River below Victoria is well defined by bordering bluffs. The elevation of the general land surface slopes at a uniform rate about 65 ft above mean sea level in the vicinity of Victoria to 25 ft at the mouth

of the river, 10 ft in the vicinity of Seadrift, and 1 ft or 2 ft adjacent to the Intracoastal Waterway. The river valley is entrenched in this land surface, and has surface elevations of about 55 ft at Victoria and 1 ft or 2 ft near the mouth of the river. The river channel meanders through the valley with bed elevations of 30 ft at Victoria, decreasing to −18 ft just above the delta at River Mile 4, rising to −10 ft at the mouth and 1 ft on the bar at its mouth in Guadalupe Bay. The river is tidal for about 25 miles above the mouth. The height of the river banks varies from 20 ft to 25 ft at Victoria to from 3 ft to 5 ft at the mouth, and the width of the stream channel varies from 100 ft to 175 ft. Natural depths of about 4 ft at mean sea level are available over most of San Antonio Bay, and from 1 ft to 3 ft in Guadalupe Bay and Mission Bay.

The river valley is entrenched in the geological formation known as Beaumont clay, which consists of thick clay strata interbedded with sand strata and sand lenses. The valley is composed of recent deposits of Beaumont clay and deposits from upland erosion. In the vicinity of Victoria, the valley floor is underlain by extensive deposits of sand and gravel of commercial value. Sand and gravel deposits in pockets and lenses are found throughout the valley below Victoria.

History

Navigation has long been considered desirable on the Guadalupe River. In fact, surveys to determine the possibilities of improvements for navigation were made as early as 1875. However, it was considered impracticable to improve the river at that time. Further surveys were made during the following years and in 1907 a federal project for improvement of the river was adopted, which provided for a channel 5 ft deep, 40 ft wide, and 16 miles long across San Antonio Bay to the mouth of the Guadalupe River. The project also required the removal of snags and log rafts and the dredging of shoals to provide a navigable channel in the river with a depth of 5 ft at ordinary low water from the mouth of the river to Victoria, a distance of 52 miles. Under this project considerable work was completed; however, it was found that removal of the log rafts and other obstructions had lowered the water level at Victoria to such an extent that a depth of only 3 ft could be obtained by open channel work. Investigations in 1915 indicated that it would not be feasible to canalize the river with locks and dams and that there was not sufficient commerce to justify the expenditure of funds under the existing project. The project was not abandoned by Congress, but no work was done after 1916, and the river channel soon returned to its natural condition.

A comprehensive report on the possibilities of navigation on the Guadalupe River was made in 1935 and a plan for improvement of the river to Victoria was proposed which provided for three low-lift locks and dams in the natural river channel. It was found, however, that the probable benefits to commerce would not be sufficient to justify the improvement at that time.

The next investigation of the river for navigation purposes was made in 1938. The report on that investigation favored improvement for navigation and resulted in the existing project which was authorized by Congress in the River and Harbor Act of March 2, 1945, in accordance with the reports printed in *House Document No. 247*, 76th Congress, 1st session.

Project Plan

The plan recommended in the project document report (*House Document No. 247*, 76th Congress, 1st session) for improvement of the Guadalupe River provides for a channel 9 ft deep and 100 ft wide, extending from the Gulf Intracoastal Waterway, by way of Seadrift, to a point on the Guadalupe River 3 miles above Victoria. The channel dimensions were selected to conform to those of the main channel of the Intracoastal Waterway, which, at that time, were 9 ft deep at mean low tide by 100 ft wide on bottom. (Mean low tide datum used by the Corps of Engineers is 1 ft below mean sea level.) The authorized plan provides for a lateral canal with two navigation locks having a total lift of 36 ft. It was proposed to install hydropower generating units at each of the locks and to protect the channel and adjacent land from floods by constructing a protection levee along the river side of the channel. Subsequently, in a favorable report, construction of a harbor of refuge at Seadrift was recommended as a part of the project for a channel to Victoria.

The recommended plan was authorized subject to the provisions that local interests: (1) Furnish all lands, easements, rights of way, and spoil disposal areas; (2) hold the United States free from claims for damages from construction and maintenance of the project; (3) bear all costs of required bridge modification; and (4) provide adequate terminal facilities including turning basins at Seadrift and Victoria.

The studies made during the course of the investigations that led to recommendation of the project were to determine the most feasible route for a navigable channel to Victoria and to develop the adequacy of the water resources of the river for the operation of the proposed navigation locks and power plants. The investigation also developed the costs and benefits of the proposed channel to show its economic measure and the advisability of federal construction of the navigation improvement.

The authorized project provides for the location of the channel inshore along the bay section and as a lateral canal in the river section. The inshore location from the Intracoastal Waterway to the mouth of the Guadalupe River follows the practice of the Galveston District, Corps of Engineers, of locating shallow-draft channels inshore rather than in the open waters of the shallow coastal bays, whenever feasible, in order to reduce the maintenance cost. The lower maintenance cost of inshore locations has been amply demonstrated in the experience of the Galveston District. Above the mouth of the river, the route lies in the left flood plain of the river, following generally the channels of several sloughs that meander down the flood plain. The channel enters the river immediately downstream from Victoria at the proposed site of the Victoria turning basin. The lateral channel route was selected instead of a natural river channel route because it would:

a. Avoid the deleterious effects of frequent flooding in the lower valley and the consequent interruptions to traffic;
b. Be about 9 miles shorter;
c. Require one less lock and two less dams,
d. Involve a substantially lower first cost;

e. Require materially smaller costs for maintenance and operation;
f. Afford flood protection to a considerable area of the natural flood plain; and
g. Provide opportunity to drain considerable area of poorly drained land in the protected area.

Water supply studies made during the investigations indicated an ample supply for operating the locks and for generating sufficient electric power to justify the installation of hydroelectric generators at the two dams. The minimum flow of record is 150 cu ft per sec.

Following authorization of the present project in 1945, funds were made available for detailed planning of the improvement. Field surveys were made to furnish a topographic map with a 1-ft contour interval of a 2,000-ft strip along the route of the lateral navigation canal. At the same time, borings were made along the route of the canal to obtain knowledge about the subsurface materials.

In the interval following the project report, development of a rice irrigation system and location of an industrial plant on the lower Guadalupe River, both dependent on the river flow for water supply, were started. The appropriation of water for these activities raised the question of the adequacy of the water resources for operation of a lock canal. Accordingly, it was decided to include consideration of a sea-level canal in the detailed planning studies.

The planning studies covered the determination of the following:

1. The most feasible alinement for a lock canal and a sea-level canal from the standpoint of cost and navigation requirements;
2. Details of the appurtenant features of a lock canal and of a sea-level canal;
3. The adequacy of the water resources of the region to supply agricultural, industrial, and navigation demands; and
4. The most feasible plan for a navigation channel to Victoria.

Channel Alinement

At the beginning of the planning studies to determine the channel location and alinement, reconsideration was given to a lateral canal as compared to a canal in the natural river channel. This study showed that the advantages of the lateral canal in lowering first cost and maintenance cost and in affording a more dependable and safer channel for navigation were sufficient to discard any further consideration of improving the natural river channel to provide navigation to Victoria. Consideration also was given to the feasibility of locating a lock in the vicinity of Guadalupe Bay and locating the canal on the high bordering bluff from that point to Victoria. This location avoided some of the difficulties encountered in placing the channel in the flood plain, but the considerably higher cost of rights of way and the high severance damages involved made this location impracticable and it was not studied further. The most feasible location for the lateral navigation channel is in the left flood plain. The alinement of the channel is the same for either a lock canal or a sea-level canal.

Locating the channel route along the northeast side of San Antonio and Guadalupe bays, and Mission Lake, offered no particular difficulty, although several different alinements were studied. The selected route is on a straight line from the junction with the Intracoastal Waterway to the upper end of San Antonio Bay. This route avoids severing very much property in crossing the point of land between miles 1.4 and 3.6. From mile 3.6 to mile 8.7, the channel crosses the open side of the embayment on which Seadrift is located. A branch channel extends from mile 7 to a commercial turning basin at the town of Seadrift. The Seadrift basin is to be designed and constructed by the local interests.

From mile 8.7 to mile 13.6, the channel is located along the bay shore line adjacent to the foot of the bluff bordering Guadalupe Bay. This location affords the adjacent high land ready access to the channel for navigation; it avoids the excessive volume of excavation that would be entailed in cutting through the bluff which reaches an elevation of about 20 ft; and it permits the construction of a spoil-bank levee along the bay side of the channel to protect navigation on the channel.

Continuing above mile 13.6, the location was determined by the crossing of Green Lake. The bed of this lake is privately owned. The owners have studied the possibility of developing Green Lake, and are considering several diverse plans. One would be to pump the lake dry so that the bed could be used for agricultural land, and another plan would be to use the lake as a storage reservoir to supply water for irrigation of agricultural land on the high ground. The navigation canal could not be coordinated functionally with any of these plans and must be separated completely from Green Lake. Locations were considered between Green Lake and the Guadalupe River and along the east shore of the lake. The former location was discarded because the protection levee would constrict excessively the flood plain of the river and result in increased flood heights in the flood plains of the San Antonio River and the Guadalupe River above Green Lake. The river lies along the right side of the flood plain in the vicinity of Green Lake and locating the channel with its river side levee between the river and the lake would reduce the flood plain width from 20,000 ft to 6,000 ft, which would seriously increase flood heights. A location along the east shore of Green Lake would require an excessive degree of curvature in the channel. Accordingly, it was decided to locate the channel across the middle of the lake. This location permits a practically straight alinement from mile 12 to mile 30.

Above Green Lake, locating the channel along the course of a bayou running through the reach from the lake to mile 30, as proposed in the project report was considered; however, there was little reduction in the quantity of excavation on this alinement and a number of curves were also introduced. The straight alinement is preferable. The first lock in the lock canal would be located at mile 29.6 and would provide a lift of 18 ft, raising the water surface above the lock to an elevation of 18 ft above mean sea level.

From mile 30 to mile 32.5, the river channel lies close to the edge of the flood plain which is against a steep hillside in this reach, and the channel and levee must be located between the toe of the slope of the bluff and the river

channel. Several spur hills, about 20 ft in height above the general elevation, must be cut by the channel. At four points in this reach, the center line of the channel is within 800 ft of the center of the river channel.

Above mile 32.5, the channel follows a generally straight alinement located so that it would not constrict the flood plain width to less than the width at valley control points. No particular alinement problems are encountered in this reach, which extends to the proposed turning basin.

Suitable sites for the turning basin are available at mile 38 and mile 35. The site at mile 38 is a wide, level area that would permit port development at an elevation of 47 ft above the water surface in a sea-level canal and about 29 ft above the water surface of a lock canal. The maximum cut for a lock canal would be about 40 ft. The site at mile 35 has an average elevation of about 30 ft and would permit port development at an elevation of 30 ft above the water surface of a sea-level canal and about 12 ft above the water surface of a lock canal. The maximum cut for a sea-level canal would be 41 ft. Both sites afford readily available access to railroad service through spur connections that could be extended to the turning basin areas with equal facilities for either site.

The location of the turning basin at these sites differs from the location given in the project document plan, which shows the turning basin further upstream above a second lock. Either of the two downstream locations would reduce the costs of the channel by eliminating one lock structure and would serve the commercial tributary areas satisfactorily.

Channel and Levee Side Slopes

Investigation of the subsurface soils was made to determine the character of materials to be excavated; to determine the side slopes of the channel and the protection levee; to determine the foundation conditions for structures and levees; and to determine the possible seepage from the canal. A total of 147 holes were drilled in these explorations, of which 122 holes were on the final channel alinement. Of these holes 107 were earth auger holes and 15 were cored holes. The holes were spaced about a half mile apart.

The investigations reveal that the subsurface materials encountered on the channel alinement are principally sands and sandy clays in the reach from the Intracoastal Waterway to about mile 15, and clays and sandy clays in the part of the canal above mile 15. A number of gravel deposits occur in the reaches above mile 25

The design of the canal slopes was based on estimates of the shearing strength of the principal types of material found in typical borings. The estimates were based on the general characteristics of the soils, and on a knowledge of the behavior of soils with these characteristics. The values of these estimated shearing strengths were checked by shear tests on samples of the weakest materials. From these strength values and the thickness of strata, weighted values for the cohesion strength c and friction angle ϕ were determined for the materials at each hole. From these values and the depth of cut, the slopes were determined by the ϕ-circle method. A safety factor of 1.3 was considered sufficient. The water level in the canal will be nearly constant and there

should be no rapid drawdown of the water surface sufficient to weaken the stability of the canal slopes.

The levee slopes were determined in a similar manner. The value of c for hydraulic fill was assumed to be 75% of the value of c for material in the borings. The value of ϕ for the angle of friction was assumed to be 25% of the value of ϕ for the material in the adjacent boring. A factor of safety of 1.3 was used also in deriving the levee slopes. These slopes were determined at each boring location. The slopes for a levee of dragline fill were considered to be the same as the canal slopes.

TABLE 1.—ESTIMATED SIDE SLOPES FOR CANAL AND LEVEE

Reach (miles)	Canal	Levee Fill	
		Dragline	Hydraulic
0 to 10.0	1 on 5	None	None
10.0 to 20.3	1 on 3	None	1 on 6
20.3 to 32	1 on 2	1 on 2	1 on 4
32.2 to 38	1 on 2	1 on 2	1 on 4

For the purposes of estimating quantities and costs the slopes of the levee and canal as determined at each boring location were then tabulated and divided into reaches of similar slopes. A constant slope for each reach was selected which was as steep as most of the individual slopes. The slopes so determined are shown in Table 1.

LEVEE GRADE

The levee along the river side of the canal would afford protection to the canal and the area between the canal and the edge of the flood plain from floods on the Guadalupe River and the San Antonio River. The levee grade above mile 12 was determined from the flood height of the maximum flood of record as increased by the backwater effect of the proposed levee. The maximum flood of record occured on July 3, 1936, and reached an elevation of 60.45 ft above mean sea level at Victoria. The peak discharge was 179,000 cu ft per sec. Backwater computations indicate that the constriction of the flood plain caused by the protection levee would increase the height of a flood of this magnitude by about 3 ft. Accordingly, the levee grade was set at about 6 ft above the high-water profile of the flood of July, 1936, which provides a freeboard of about 3 ft for the recurrence of the maximum storm of record. Profiles of the high water for the maximum flood of record and for the levee grade are shown in Fig. 2. The average levee grade is at a height of about 13 ft above the average ground surface. Actually this levee grade will be used only in the reach from mile 12 to mile 22 where levees are provided on both sides of the channel. In all other areas the quantity of excavated material will exceed the quantity of material required to construct the levee to the design grade.

Below mile 12 the riverside levee serves to reduce the maintenance of the channel and to contain the salt water in the navigation channel and prevent contamination of the fresh water supplies in the adjacent bodies of water which are used for irrigation. The levee grade is set at 6 ft in this reach. A parallel levee is required on the land side of the channel from high ground at about mile 12 below Mission Lake to high ground above Green Lake at mile 22 to prevent salt water intrusion in the adjacent lakes from high storm tides. The land side levee grade is set at 8 ft throughout. It is considered that major

storms causing tides in excess of 8 ft would be accompanied by winds and rains of such intensity that they would destroy most of the rice crop and pollute the available source of fresh water so that protection of the area from inundation by a higher levee grade, above the maximum storm tide, would not be feasible.

The spoils from channel excavation are all to be deposited in the spoil area along the levee, and it is proposed to deposit these spoils so as to constitute the required levee. It is proposed to limit the height of the spoil dump to about 25 ft above the natural ground. The spoils would be confined by a dragline fill on the canal side with slopes of 1 on 2 and allowed to flow on the river side to slopes of about 1 on 4 to 1 on 6. The spoil embankment for the 9-ft by 100-ft channel under these conditions would have bottom widths varying from 153 ft at mile 21, where the ground elevation is 5 ft, to 363 ft at mile 35, where the ground elevation is about 30 ft. The reach between mile 30 and mile 32.5 includes a short reach through a spur hill where the cut reaches a depth of 55 ft. This section is close to the river channel so that disposal of all the excavated material on the river side would not be practicable and the excess material will be spoiled on the land side of the canal. The spoil from the lock canal would be smaller in quantity and would not require as wide a spoil bank. Under both plans the large quantities of material from the turning basin would be deposited around the upstream side of the turning basin where the protection levee ties into high ground.

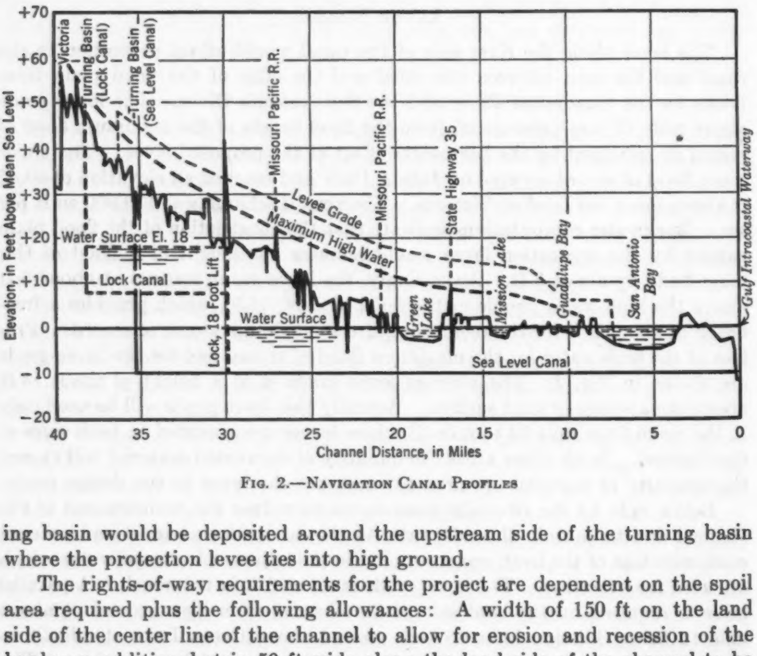

Fig. 2.—Navigation Canal Profiles

The rights-of-way requirements for the project are dependent on the spoil area required plus the following allowances: A width of 150 ft on the land side of the center line of the channel to allow for erosion and recession of the bank; an additional strip 50 ft wide along the land side of the channel to be controlled by the navigation district; a 40-ft width on the river side to provide

for future widening and deepening of the channel; a 100-ft berm from the future top of the bank to the toe of the slope of the levee or spoil embankment; and a width of 250 ft on the river side of the spoil dump to afford spoil-disposal area for future enlargement and maintenance of the channel and to provide for a large drainage ditch along the river side of the area. The total width of rights of way required for the project, in the reach above mile 22, varies from about 700 ft to 1,000 ft. Typical cross sections showing the several width requirements are depicted in Fig. 3(a).

The parallel levees across Green Lake (Fig. 3(*b*)) require more material than would be removed from the net channel section, largely because the bed of Green Lake is from 1 ft to 2 ft below mean sea level and because of the flat levee slopes in this reach. The boring samples from the bed of Green Lake show that the subsurface materials are clays and sandy clays, and no difficulty

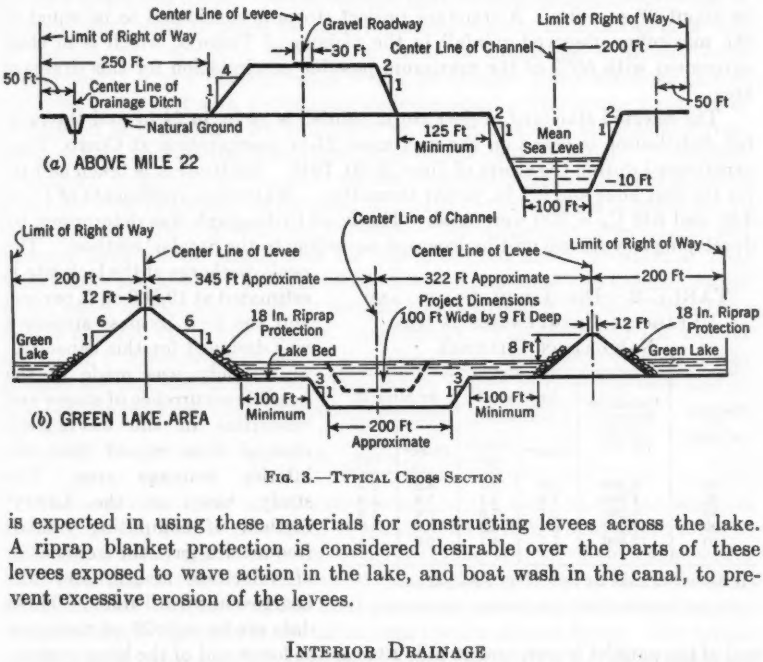

FIG. 3.—TYPICAL CROSS SECTION

is expected in using these materials for constructing levees across the lake. A riprap blanket protection is considered desirable over the parts of these levees exposed to wave action in the lake, and boat wash in the canal, to prevent excessive erosion of the levees.

INTERIOR DRAINAGE

The river side protection levee would intercept a drainage area of 73 sq miles for the sea-level canal and 86 sq miles for the lock canal. The natural drainage in this area is by a number of short streams flowing from the adjacent high ground. Above mile 30, the natural drainage is across part of the flood plain to a stream parallel to the river which collects the drainage and carries it to the Guadalupe River. In this reach the channel and levee will be generally along the land side of the drainage stream and will intercept the lateral

drainage. Between mile 30 and Green Lake, another flood plain drainage stream is intercepted by the channel and levee. All of these intercepted lateral drains would discharge directly into the channel. In the design of drainage facilities, each lateral drain was considered separately and methods were determined to discharge the drainage of the twenty-five-year frequency into the channel without erosion of the bank. Either drop-inlet structures or a paved open ditch extending down the bank of the channel is provided. Between the Green Lake area and the Mission Lake area, conduits through the land side levee into the canal would afford the necessary drainage facilities. These structures are designed to carry the estimated runoff of a storm with a frequency of about once in ten years.

Design of the by-pass facilities for the discharge of floodwaters past the lock structure in the canal required a determination of the design flood discharge. The drainage area above the lock structure and within the levee would be about 27 sq miles. A standard project storm is considered to be equal to the maximum observed rainfall in the vicinity of Victoria, which is in close agreement with 50% of the maximum possible precipitation for this drainage area.

The selected standard project storm rainfall is 16 in. in 24 hr and the rainfall distribution is based on the maximum 24-hr precipitation at Cuero, Tex., experienced during the storm of June 28-30, 1940. Infiltration is taken as 1 in. for the first hour and 0.1 in. per hr thereafter. Watershed coefficients of C_t = 3.00 and 640 C_p = 300 were used. The flood hydrograph was determined by developing a synthetic unit hydrograph according to the Snyder[2] method. The peak discharge at the lock site is estimated at 10,300 cu ft per sec. and the lock by-pass structure was designed for this capacity.

A study was made of the possible occurrence of stages and velocities in the navigation channel from run-off from the interior drainage area. The study, based on the Lowry[3] method of computing rainfall frequencies, gave the frequencies of velocities, stages, and discharges shown in Table2. These data are for mile 22, at the upper end of the parallel levees, and at mile 12 near the lower end of the levee system.

TABLE 2.—DISCHARGE, STAGE, AND VELOCITY FREQUENCIES IN THE NAVIGATION CHANNEL

Frequencies, in years	Estimated discharge (cu ft per sec)	At Mile 12		At Mile 22	
		Stage[a]	Velocity[b]	Stage[a]	Velocity[b]
10	5,500	2.6	2.7	4.2	2.3
25	7,200	3.8	3.1	5.8	2.6
50	9,200	5.1	3.6	7.4	2.9
100	11,500	6.4	3.9	9.0	3.0
140	12,800	7.1	4.1	10.0	3.1

[a] In feet above mean sea level. [b] In miles per hour.

FRESH WATER SIPHONS

Locating the channel across Green Lake posed the problem of maintaining storage capacity of the entire lake for water supply as desired by the owners.

[2] "Synthetic Unit Graphs," by Franklin F. Snyder, *Transactions* Am. Geophysical Union, Pt. 1, 1938, p. 447.

[3] "Excessive Rainfall in Texas," by Robert L. Lowry, Jr., *Bulletin No. 25*, State of Texas Reclamation Dept., November, 1934.

A siphon under the canal is proposed to connect the two parts of the lake. This siphon would serve to equalize the water storage in Green Lake and permit the use of all storage in the lake for fresh water supply. The owners of Green Lake have filed a presentation with the Texas State Board of Water Engineers to consider the diversion of 20,000 acre-ft of water per annum from the Guadalupe River into Green Lake. The capacity of a siphon to meet these requirements is 525 cu ft per sec at a head differential of 1 ft. Three 8-ft-high by 6-ft-wide box culverts are required.

A siphon under the canal at the head of Mission Lake is required to provide for the water supply of the rice irrigation system. At present, this company obtains water by two methods: (*a*) By diversion from the river through Mission Lake and a natural bayou to the pumping station and (*b*) by diversion from the Guadalupe River at River Mile 10.4, through ditches and natural bayous to the pumping station, where it is lifted to high ground for gravity delivery to the rice fields. The navigation channel crosses both delivery routes and provision must be made for their replacement as an item of rights of way for the channel. A siphon under the canal at the upper end of Mission Lake is proposed. A new delivery canal would be dredged along the river side of the levee to connect with the existing delivery canal. The intake structure of the siphon is provided with two gates so that water can be obtained from Mission Lake or from the Guadalupe River by the delivery canal. The siphon is designed to provide for the existing and proposed increased requirements of water for rice irrigation, which total 600 cu ft per sec. This is provided by three 8-ft-high by 6-ft-wide box culverts. The siphons at Green Lake and Mission Lake will be placed with the top of the box at an elevation of 21 ft below mean sea level for a length of 200 ft under the canal and thence upward to the outer levee toes, giving an over-all length of 850 ft for the Green Lake siphon and 740 ft for the Mission Lake siphon. The inverts of the siphons are set at 2 ft below mean sea level. The intake and discharge ends of the siphons are designed so that stop logs can be placed to close the ends and so that the conduits can be dewatered for cleaning and repairs.

Lock Canal Structures

The requirements of a lock canal would be the same as for the sea-level canal up to the lock at mile 29.6, at which point a lock would afford a lift of 18 ft above mean sea level. Above the lock, the bottom of the canal would be at elevation 9 ft above mean sea level. At the upper end of the lock canal, an intake with a capacity of 200 cu ft per sec at a head of 12 ft would be provided for supplying water to the canal from the Guadalupe River. The intake would consist of an open canal about 5,000 ft long with a 4-ft gate-controlled conduit under the levee. A diversion dam would be required in the Guadalupe River to direct flows into the intake canal. A concrete ogee dam is proposed, with a length of 140 ft and crest elevation of 30 ft. The bottom of the river channel at the dam site is at an elevation of 22 ft. A concrete stilling basin, concrete training walls, riprap, and steel-sheet piling protective features are provided. The structure would be founded on steel bearing piles.

The lock chamber would be 75 ft by 400 ft long with the sill at an elevation of 14 ft below mean sea level. Studies have been made of four different plans for details of the lock structure. These plans differed as to the type of gate and as to the provision for the discharge of flood waters from the local drainage area above the dam.

Plan 1.—A masonry lock structure was proposed, with a miter gate at the downstream end and a vertical slide gate at the upstream end. There would be a by-pass structure adjacent to the right lock wall with a side gate for the regulation of the upper pool and for the discharge of minor floods; major floods would be discharged through the lock chamber. The upper slide gate could be used in the lock-filling operations.

Plan 2.—As in Plan 1, this proposal was for a masonry lock structure with a miter gate at the downstream end. A tainter gate with capacity sufficient to discharge all floods is provided in the by-pass structure, and a miter gate is provided for the upstream lock gate. The upper pool would be regulated and controlled by the by-pass gate.

Plan 3.—Likewise, similar to Plan 1, a masonry lock structure was proposed, with a miter gate at the downstream end and a vertical slide gate at the upstream end. In this plan, a by-pass culvert was provided around the upper and lower gates for filling and emptying the lock, and the lock-chamber walls between the gate abutments were to be of steel-sheet piling.

Plan 4.—This proposal was exactly the same as Plan 1 except that it would have a lift 3 ft greater to reduce the excavation required above the lock.

Foundation explorations in the lock area indicated the necessity of pile foundations. The borings revealed a gravel stratum about at the floor level of the lock, which would require a steel-sheet pile cutoff wall beneath the lock structure.

Relative Costs.—The several plans were outlined by sketches sufficient to furnish data for estimating comparative costs. Plan 3 was the cheapest of the plans investigated but has an inefficient filling and emptying system and would have a higher maintenance cost. Plans 2 and 4 are of approximately the same cost, which is about $200,000 more than Plan 1. Plan 1 would cause interruption to traffic during major floods and the upstream sliding gate would be subject to excessive obstruction from silt and debris. The lock details in Plan 2 were considered to be the most desirable for the lock canal and comparative cost estimates were based on that plan.

Turning Basin and Terminal Facilities

Turning basins and terminal facilities must be furnished at Victoria and Seadrift by the local navigation districts under the terms of the authorizing act, and are of interest to the Corps of Engineers to the extent of determining the adequacy of the plans proposed by the local interests. It is considered that the turning basin should be at least 400 ft wide and that the Victoria basin should be an off-channel basin so that it will permit upstream extension of the channel. Preliminary designs for this turning basin indicated a basin

400 ft wide, at the project depth of −10 ft, and about 1,000 ft long, extending at an angle upstream from the channel. The plans provided for future enlargement of the harbor facilities by an extension of the basin and by the construction of a second basin. Designs for wharves and docks on the turning basin and for cargo-handling facilities will be made by engineers employed by the navigation district.

Bridges and Pipe Lines

The channel will be crossed by two railroad bridges and one highway bridge and by ten oil and gas pipe lines. The cost of the necessary alterations to these structures must be borne by the local interests. It is proposed that movable bridges be provided with unlimited vertical clearance and 125-ft horizontal clearance between fenders, and that pipe lines be placed at a minimum depth of 21 ft below mean sea level for a width of 125 ft under the channel.

Water Supply for the Lock Canal

The question of the adequacy of the water supply in the Guadalupe River for a lock canal required restudy because, in the interval since the project report investigations, an extensive use of the waters of the river had developed. A rice irrigation development in the vicinity of Seadrift obtained its water supply from the Guadalupe. The irrigation company has appropriations of water from the Guadalupe River for a total of 572 cu ft per sec for irrigation. The appropriations are for a total of 55,617 acre-ft of water to irrigate 27,559 acres annually with a maximum rate of withdrawal of 572 cu ft per sec. The installed capacity at the company's pumping plant is 340 cu ft per sec. The method of operation is to pump water from Mission Bay until the bay becomes salty, and then water is drawn from the river intakes. The pumps generally are operated at full capacity for about half of the time during the irrigating season, from April through September.

A second water use is for an industrial development below Victoria. The industry has appropriations for 198,000 acre-ft annually with a maximum rate of withdrawal from the river of 300 cu ft per sec. The pumping plant, with an installed capacity of 45 cu ft per sec is located opposite channel mile 31. Delivery pipes extend across the narrow flood plain at this point to a canal on high ground which carries the water to the plant. Of the total appropriations for industrial use, only 33,000 acre-ft per yr or 45 cu ft per sec is consumed and the remainder is returned to the river uncontaminated.

The consumptive appropriations of water from the Guadalupe River below Victoria total 617 cu ft per sec. In addition, two certified filings have been made with the Texas Board of Water Engineers for (*a*) appropriations of 20,000 acre-ft annually (approximately 170 cu ft per sec, maximum rate), and (*b*) water to irrigate 100,000 acres of additional land (approximately 850 cu ft per sec, maximum rate).

The water required for the operation of the navigation lock is estimated at 190 cu ft per sec. This is based on twenty lockages per day with 40% alternation; that is, lockages succeeded by lockages in the opposite direction 40% of the time. The number of twenty lockages per day is based on full develop-

ment of the estimated prospective commerce of 1,600,000 tons annually, with allowance for the lockage of single commercial and pleasure boats. The maximum possible number of lockages based on a half hour for a lockage would be forty eight per day. Allowance is made in estimating the water required for leakage through the gates and valves, seepage, evaporation, and for the excess displacement of inbound commerce. Seepage losses from the canal above the lock might be quite large, even after the provision of cutoff walls through the gravel deposits. The estimated water required for the operation of the lock is as follows:

Purpose	Demand (cu ft per sec)
Lockage	112.0
Excess inbound commerce displacement	1.3
Leakage at lock gates and valves	25.0
Leakage at by-pass gate	20.0
Seepage	30.0
Evaporation	1.9
Total	190.2

The total estimated consumptive water demand on the lower Guadalupe and San Antonio rivers, including the navigation requirements and the present appropriations of water for irrigation and industrial use, amounts to 807 cu ft per sec divided as follows:

Purpose	Demand (cu ft per sec)
Irrigation demand	572
Industrial use	45
Navigation requirement	190
Total	807

Water Supply

In order to determine the water supply available to meet this demand, a study was made of the records of flow on the Guadalupe and San Antonio rivers. The records at Victoria, mile 51 on the Guadalupe River, are available from 1904 to1949; and records at Goliad, Tex., mile 66.5 on the San Antonio River, are available from 1924 to 1928 and from 1939 to 1949. Flow-duration curves were compiled from these records for the individual and coincident combined flow of both streams for the six-month irrigation season. The curves for the Guadalupe River at Victoria and the combined curves for the Guadalupe River at Victoria and the San Antonio River at Goliad are shown in Fig. 4.

The line of the maximum demand of 807 cu ft per sec is shown on the graph. It will be noted that for 19% of the time during the six months of the irrigation season (April to September) the natural water supply in the Guadalupe and San Antonio rivers would be insufficient to meet the total demand for agricultural, industrial, and navigational purposes. There would be a deficiency of water on an average of forty-six days annually.

The authorized federal project for the Canyon Reservoir on the upper Guadalupe River would regulate the flow at the dam site to a minimum of about 165 cu ft per sec. If this flow were available on the Guadalupe River below Victoria, the period of insufficient water supply would be reduced to about 10% of the six-month irrigation system, or about eighteen days annually.

The natural water supply would be sufficient for present demand if a method could be devised to utilize the water for the operation of the lock and then make it available for irrigation. The difficulty would be to deliver the water to the irrigation pumps uncontaminated by salt water or other polution. The navigation canal below the lock would be at sea level and salt water intrusion in the canal from the Intracoastal Waterway would be a certainty, especially during periods of low flow in the rivers when all available water would be

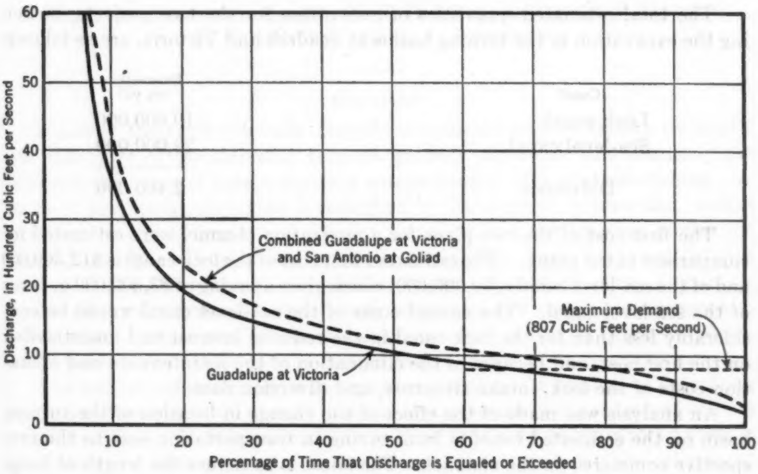

FIG. 4.—FLOW-DURATION CURVES (FOR THE IRRIGATION SEASON ONLY—APRIL TO SEPTEMBER, 1924 TO 1928 AND 1939 TO 1949)

needed to meet the demand. No plan that would insure delivery of fresh water from the navigation canal to the irrigation pumps could be devised other than one requiring an additional lock and that would increase the cost of the project.

The water supply in the Guadalupe River for operation of a navigation lock under existing conditions would be inadequate during a considerable part of the irrigation season, because of the demand for irrigation and industrial use. The expressed federal policy is to recognize the rights of local interests in water utilization and control. Therefore, operation of the lock canal would be jeopardized during periods of low flow under existing conditions. Further development of uses of water on the rivers would aggravate this situation. Canyon Reservoir, when completed, will appreciably increase the low flow on the lower river and if this flow were available for appropriation exclusively for

operation of the navigation project by the federal government, it would be sufficient to insure continuous operation as required to accommodate navigation. The authorization for Canyon Reservoir states that the storage is for development of hydroelectric power and for navigation. However, there is no assignment of specific quantities of water to navigation, and it is doubtful if, after release of water in the generation of electric power, it could be claimed for navigation on the lower river. An additional reservoir on the Guadalupe River has been found to be economicaly feasibile and has been recommended for construction, but this project has not been authorized by Congress. This reservoir would not afford a regulated water supply for operation of the navigation project below Victoria.

Comparison of the Two Plans

The total estimated quantities of excavation for the two projects, including the excavation in the turning basins at Seadrift and Victoria, are as follows:

Canal	Excavation (cu yd)
Lock canal	19,600,000
Sea-level canal	22,000,000
Difference	2,400,000

The first cost of the two plans for a navigation channel were estimated for comparison of the plans. The estimated first cost of the lock canal is $12,500,000 and of the sea-level canal is $9,000,000, which gives a saving of $3,500,000 in favor of the sea-level canal. The annual costs of the sea-level canal would be considerably less than for the lock canal in the reduced interest and amortization on the first cost, and because of the elimination of the maintenance and operation costs of the lock, intake structure, and diversion dam.

An analysis was made of the effect of the change in location of the turning basin on the estimated benefits from saving in transportation cost to the prospective commerce on the channel. The effect is to reduce the length of barge haul and increase the rail, truck, or pipe line haul in the joint movement of of commodities. The net result was to reduce the benefits of the project but the difference was not sufficient to affect the favorable ratio of benefits to costs.

In view of the reduced first cost and annual charges, and because of the probable inadequacy of the water supply for operation of the navigation lock, the sea-level canal was considered to be the more feasible project for construction. The adoption of the sea-level canal also would be in the interest of expediting construction of the channel since it would not require the use of any appreciable quantities of scarce construction materials.

Acknowledgements

The conclusions in this paper are those of the writer and are based on studies prepared by the personnel of the Galveston District, Corps of Engineers.

AMERICAN SOCIETY OF CIVIL ENGINEERS
Founded November 5, 1852

TRANSACTIONS

Paper No. 2552

RATE OF CHANGE OF GRADE PER STATION

By Clarence J. Brownell,[1] A. M. ASCE

With Discussion by Messrs. T. F. Hickerson, Robert T. Howe, E. N. Prouty, and C. J. Brownell

Synopsis

Highway engineers generally describe a vertical curve by stating its length and the rates of the adjacent tangent grades. Although this definitely establishes the curve it does not give a comprehensive idea of its sharpness. A curve in horizontal alinement is described by its angle of intersection, radius or degree of curve, length and tangent distances, and the bearings of the adjacent tangents. These data, especially the radius, convey a very definite picture of the sharpness of the circular curve. A vertical curve is part of a parabola, computed and laid out using horizontal and vertical measurements. Being a parabola, a vertical curve has no constant radius or degree of curve, which probably accounts for the lack of such a factor in its description.

The purpose of this paper is to urge the adoption of a method of describing vertical curves which will give an immediate impression of the sharpness of such a curve. The method explained herein does that very thing, and further, it provides a convenient tool for the solution of problems in vertical alinement that can otherwise be determined only by trial and error. In the coming era of divided highways and on-and-off ramps, this tool will be found most convenient.

General

The method involves the use of a factor R which can be described as the "rate of change of grade per station." In a parabolic curve, R is the percentage change in grade of the tangent to the curve in one station of distance. For instance, if the grade G_1 of the tangent is 0 at one station and $G_2 = +1\%$ at the next station, the rate of change of grade per station is $+1\%$. If the grade is $G_1 = -5\%$ at one station and $G_2 = -7\%$ at the next station, the rate of change of grade per station is $\frac{G_2 - G_1}{1} = -2\%$. Positive rates of

Note.—Published in March, 1952, as *Proceedings-Separate No. 121*. Positions and titles given are those in effect when the paper or discussion was received for publication.

[1] Associate Bridge Engr., Bridge Dept., State Div. of Highways, Sacramento, Calif.

change curve upward; negative rates of change curve downward. Vertical curves with the same rate of change of grade per station are parts of identical parabolas, regardless of their lengths or the grades of their adjacent tangents.

In Fig. 1 let: H be the difference in elevation between the beginning and the end of a vertical curve; L be the distance in stations between two points; and V be the tangent offset between the two tangents of a vertical curve. For the purpose of illustration, let $R = +1\%$ in Fig. 1(*a*) and let the grade at station 10 be $G_{10} = +1\%$. Since R is the percentage change in grade of the tangent to the curve in one station, the computed values for G for each station

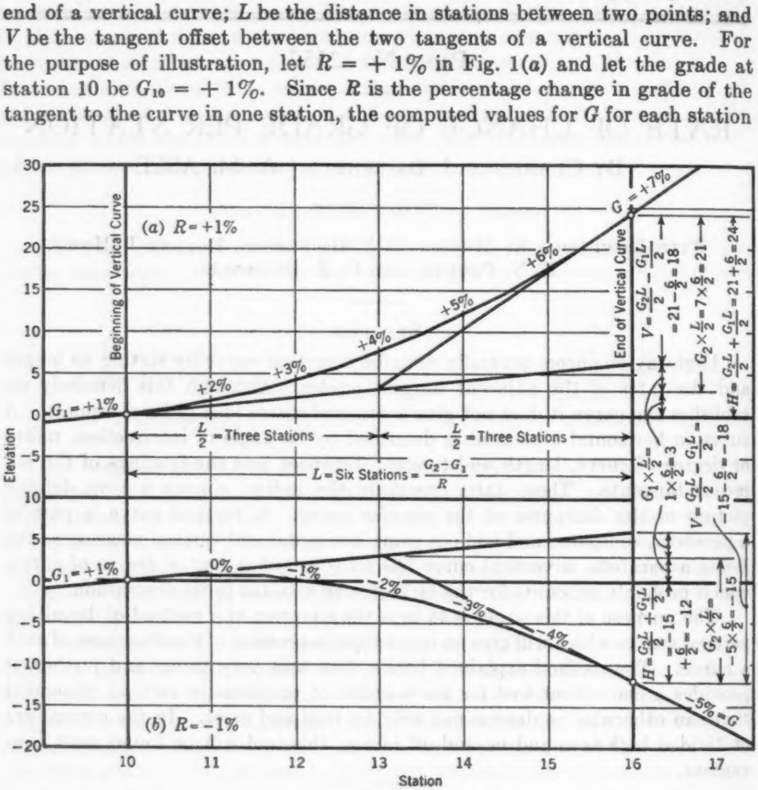

Fig. 1

are as shown directly on the curve in Fig. 1(*a*). For purposes of clarity and explanation, the curve has been drawn as a series of tangents, each one station in length. The tangents intersect at the + 50 points.

Now consider Fig. 1(*b*). Using the same grade of + 1% at station 10, but using a rate of change of grade per station of − 1%, the grade G at each station is shown along the curve. From inspection of the two curves in Fig. 1, and from the definition of R, it is apparent that the algebraic difference of the grades is equal to the length of the curve, in stations, multiplied by the rate of change of grade per station, or

$$G_2 - G_1 = L\,R \qquad (1)$$

in which G_1 is the grade at the first point on the curve; G_2 is the grade at the second point on the curve; L is the distance in stations between the two points; and R is the rate of change of grade per station. Symbols G_1 and G_2 denote the grades at the beginning and the end of the curve, or they may be the grades at any points on the curve, as long as L is the distance, in stations, between them. This distance L may be in stations of 100 ft or of any convenient length. It is suggested that "rate of change of grade per station" be abbreviated on plans as "R/C" or "Rc" in order to avoid confusing it with the abbreviation for the radius of a circular curve. The letter symbol R will be used in formulas. The tangent offset V (Fig. 1) is composed of two parts, $G_2 \frac{L}{2}$ and $G_1 \frac{L}{2}$. Keeping the direction of these values in mind, the equation for V can be written as

$$V = \frac{L}{2}(G_2 - G_1) \qquad (2)$$

Consider the difference in elevation between any two points, designated H in Fig. 1. In order to maintain the established sign notation, H must be considered as positive when measured upward and negative when measured downward. Again by inspection, watching signs, the equation for H can be written as

$$H = \frac{L}{2}(G_2 + G_1) \qquad (3)$$

Eqs. 1, 2, and 3 express the three basic principles. From them, and combinations of them, any problem in vertical curves can be solved. The reader is urged to familiarize himself thoroughly with the graphical presentation. The formulas will then become second nature, and there will be no need to memorize them. Consider the formulas merely as a concise and convenient method of expressing a thought—as engineering "shorthand."

By combining Eqs. 3 and 1 the expression,

$$H = G_1 L + \frac{R}{2} L^2 \qquad (4a)$$

can be written. This is the equation of a parabola, symmetrical about a vertical axis with its origin on the curve at a point where the tangent to the curve has a grade of G_1. Such an equation in the usual x-coordinates and y-coordinates would be written

$$y = \frac{-a_x}{p} + \frac{1}{2p} x^2 \qquad (4b)$$

in which a is the horizontal distance from the vertex to the origin of coordinates and p is the distance from the directrix to the focus of the parabola. It is apparent by comparison that $R = \frac{1}{p}$ and $G_1 = \frac{-a}{p}$, from which

$$a = \frac{-G_1}{R} \qquad (5)$$

The grade at any point on the curve may be described mathematically as the first derivative of the equation of the curve:

$$\frac{dH}{dL} = \frac{d}{dL}\left(G_1 L + \frac{R}{2} L^2\right) = G_1 + R\,L = G_2 \qquad \text{(6a)}$$

which is in agreement with Eq. 1. The rate of change of grade per station may be described mathematically as the second derivative of the equation of the curve:

$$\frac{d^2H}{dL^2} = \frac{d^2}{dL^2}\left(G_1 L + \frac{R}{2} L^2\right) = R \qquad \text{(6b)}$$

The same principle holds for parabolic curves of other than the second power; but the second derivative of such an equation is not a constant.

The statement of a $+ 10\%$ grade, immediately conjures up a very definite impression to any highway engineer. Likewise, a $- 12\%$ grade gives another immediate impression; and if a vertical curve one station long were to be placed between them it would be stated, without hesitation, to be too short. Mentally, a rate of change of grade of $- 22\%$ per station was pictured without being aware of why or how it was done. Knowingly describing vertical curves by the method of rate of change will give an immediate appreciation of their sharpness. Vertical curves occur on highways far more frequently than do horizontal curves, and they can be just as dangerous. Therefore, they should be described and analyzed every bit as completely. The factor, "rate of change," will provide that description and analysis.

Typical Examples

To illustrate the use of "rate of change," the following typical problems are presented, with a clue for their solution.

Example 1.—A common occurrence is the need for the elevation at a few intermediate points along a vertical curve, such as at the abutments and piers of a bridge. These can most readily be determined by tabulation, as in Table 1. All the necessary steps have been shown. With familiarity, the computations would probably be made on scratch paper and only Cols. (1), (2), (5), and (8) would be tabulated. The computations close on the end of the vertical curve (EVC) thereby making a definite check on all values. Instead of a tabulation of tangent elevations and corrections, which have no further value, there is a tabulation of the grade at each point, which is of inestimable value.

Example 2.—It is frequently desirable to tabulate the elevations at each station along a vertical curve. For this purpose it is convenient to consider the curve as made up of a series of chords between stations. The grade of such a chord is equal to the grade of the tangent to the curve midway between stations. For proof of this statement consider that the grade of the chord (Fig. 2) is equal to the difference in elevation (H) divided by the distance (L) between points. From a combination of Eqs. 1 and 3, $H = G_1 L + R \frac{L^2}{2}$; therefore,

$$\frac{H}{L} = G_1 + R \frac{L}{2} \qquad \text{(7)}$$

By reference to Eq. 1 the grade at $\frac{L}{2}$ can be written as $G_1 + R\frac{L}{2}$. Hence $\frac{H}{L}$ is the grade of the tangent at $\frac{L}{2}$.

TABLE 1.—COMPUTATION OF INTERMEDIATE ELEVATIONS ON A VERTICAL CURVE (Rate of Change R equals 0.4%)

Procedure:

Col. (3), the interval between stations in Col. (1).
Col. (4), the difference between grades, as given by Eq. 1, is found by multiplying Col. (3) by 0.4%.
Col. (5), $G_2 = G_1 + RL$, from Eq. 1; thus, at Sta. 12+50, $G_2 = -0.22$ from Col. (5), plus +0.12 from Col. (4), equals −0.10.
Col. (6), the average percentage grade, is the average of adjacent values in Col. (5).
Col. (7), the difference of elevation, in feet, computed by Eq. 3, is the product of Cols. (3) and (6).
Col. (8), elevation $E_2\ (= E_1 + H)$, in feet, is computed by adding the proper value from Col. (7) to the next preceding elevation (E_1) in Col. (8); thus, at Sta. 12+50, $E_2 = 98.548$, from Col. (8), plus −0.048 from Col. (7), equals 98.500.

Station	Description	Length, L	$G_2 - G_1$ (Eq. 1)	Grade, G_2	$\frac{G_2 + G_1}{2}$	H, in feet	Elevation, E_2
(1)	(2)	(3)	(4)	(5)	(6)	(7)	(8)
16+00	End of vertical curve (EVC)			+1.30			100.600
		2.80	+1.12		+0.74	+2.072	
13+20	Abutment No. 4			+0.18			98.528
		0.30	+0.12		+0.12	+0.036	
12+90	Pier No. 3			+0.06			98.492
		0.40	+0.16		−0.02	−0.008	
12+50	Pier No. 2			−0.10			98.500
		0.30	+0.12		−0.16	−0.048	
12+20	Abutment No. 1			−0.22			98.548
		2.20	+0.88		−0.66	−1.452	
10+00	Beginning of vertical curve (BVC)			−1.10			100.000

A sample tabulation with explanatory headings and side notes is shown below. In Table 2, the grade at each + 50-point is obtained by adding the rate of change to the preceding + 50-point; and the elevation at each station is found by adding the grade at the midpoint to the elevation at the preceding

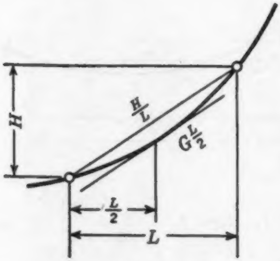

FIG. 2

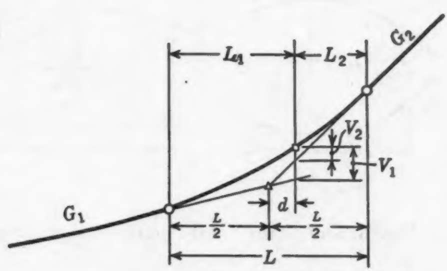

FIG. 3

station. If the elevations are desired at the + 50-points, repeat the process by writing the grades at the stations and the elevations at the + 50-points. The process can be repeated to obtain elevations at any intervals desired.

When completed there is a tabulation of grades at each point, rather than tangent elevations and curve corrections which have no meaning. Note that the computations close on the EVC, providing a positive check on the entire tabulation.

Example 3.—A problem that frequently arises is to find the curve that will pass through a known point and meet a pair of given tangents. There is only one curve that will meet this condition. Consider the curve in two parts (see Fig. 3). Since it is to be the same continuous curve, the rate of change will be the same for each part. From Eqs. 1 and 2:

$$R = \frac{2\,V}{L^2} \quad \ldots\ldots (8)$$

For the first part of the curve, $R = \frac{2\,V_1}{L^2_1}$, in which V_1 is the vertical offset from the first tangent and L_1 is the distance from the BVC to the point. For the second part of the curve, $R = \frac{2\,V_2}{L^2_2}$, in which V_2 is the vertical offset from the second tangent and L_2 is the distance from the point to the EVC. If the distance from the vertical point of intersection (VPI) to the point is designated d, Fig. 3, and if the total length of the curve is L, then $L_1 = \frac{L}{2} + d$ and $L_2 = \frac{L}{2} - d$, noting the proper sign for d. Since, then, $\frac{2\,V_1}{\left(\frac{L}{2} + d\right)^2} = \frac{2\,V_2}{\left(\frac{L}{2} - d\right)^2}$, the final step is to evaluate V_1, V_2, d, and solve for L.

TABLE 2.—COMPUTATION OF ELEVATIONS, EACH STATION ALONG A VERTICAL CURVE[a] ($R = +\,0.5\%$, Example 2)

Station[b] (1)	Grade, G_2 (5)	Elevation, E_2 (8)	Procedure[a] (2)
6+70	+1.25	100.5625	99.81+(1.075×0.70)
			+1.075+(0.5×0.35)
6+35	+1.075		−0.65+(0.5×0.85)
6+00		99.81	99.16+(+0.65×1.00)
5+50	+0.65		+0.15+(0.5×1.00)
5+00		99.16	99.01+(+0.15×1.00)
4+50	+0.15		−0.35+(0.5×1.00)
4+00		99.01	99.36+(−0.35×1.00)
3+50	−0.35		−0.80+(0.5×0.90)
3+00		99.36	100.00+(−0.80×0.80)
2+60	−0.80		−1.00+(0.5×0.40)
2+20	−1.00	100.00	Beginning vertical curve[b]

[a] The column numbers and the procedure are the same as in Table 1 and Example 1. [b] In the notes, the beginning of the vertical curve is designated BVC and the end of the vertical curve (Sta. 6+70) is designated EVC.

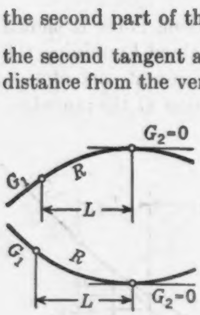

FIG. 4

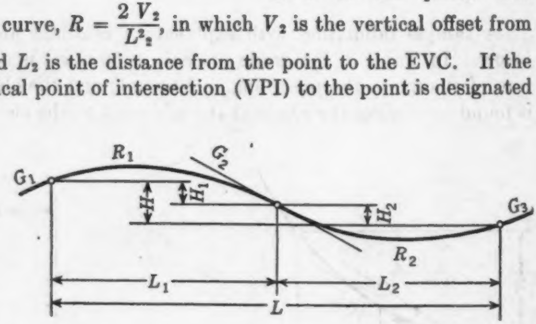

FIG. 5

Example 4.—For purposes of drainage, it is frequently desirable to find the location and elevation of the lowest or highest point on a vertical curve.

Obviously, this will be the point at which the grade of the tangent to the curve is 0%. Eq. 1, solved for L, with $G_2 = 0$, will give the distance from the BVC to the lowest or highest point. The elevation of this point (see Fig. 4) can be found from Eq. 3.

Example 5.—The determination of the vertical alinement for an interchange ramp amounts to evaluating the data for a pair of reverse curves between the two roads. The complete data (see Fig. 5) will consist of the following:

Description	Symbol
Grade of the approaching tangent	G_1
Grade of the common tangent	G_2
Grade of the receding tangent	G_3
Length of the first curve	L_1
Length of the second curve	L_2
Vertical change in the first curve	H_1
Vertical change in the second curve	H_2
Rate of change of the first curve	R_1
Rate of change of the second curve	R_2
Over-all length ($L_1 + L_2$)	L
Over-all difference in elevation ($H_1 + H_2$)	H

The solution can be divided into various cases dependent upon the known and assumed data.

Case I. Values of G_1, G_3, and L Are Known.—Assume values for R_1 and R_2. As a guide for these assumptions use the charts presented subsequently as Figs. 7, 8, and 9. The fundamental formula, Eq. 1, can be written:

$$L_1 = \frac{G_2 - G_1}{R_1} \qquad (9a)$$

and

$$L_2 = \frac{G_3 - G_2}{R_2} \qquad (9b)$$

By adding Eqs. 9,

$$L = \frac{G_2 - G_1}{R_1} + \frac{G_3 - G_2}{R_2} \qquad (10a)$$

which can be reduced to

$$G_2 = \frac{R_1 (R_2 L - G_3) + R_2 G_1}{R_2 - R_1} \qquad (10b)$$

With this value of G_2, the values of L_1 and L_2 can be found from Eqs. 9. The values of H_1 and H_2 can be found from Eqs. 3, written as

$$H_1 = \frac{L_1}{2} (G_2 + G_1) \qquad (11a)$$

and

$$H_2 = \frac{L_2}{2} (G_3 + G_2) \qquad (11b)$$

Also

$$H = H_1 + H_2 \qquad (12)$$

Case II. Values of G_1, G_3, and H Are Known.—Assume values for R_1 and R_2 using the charts for sight distance (Figs. 7, 8, and 9) as a guide. The fundamental formulas, Eqs. 1 and 3 can be combined and written:

$$H_1 = \frac{G^2_2 - G^2_1}{2\,R_1} \qquad (13a)$$

and

$$H_2 = \frac{G^2_3 - G^2_2}{2\,R_2} \qquad (13b)$$

By adding these two equations,

$$H = \frac{G^2_2 - G^2_1}{2\,R_1} + \frac{G^2_3 - G^2_2}{2\,R_2} \qquad (14a)$$

which can be reduced to

$$G_2 = \sqrt{\frac{R_1\,(2\,R_2\,H - G^2_3) + R_2\,G^2_1}{R_2 - R_1}} \qquad (14b)$$

Having determined the value of G_2, proceed as in Case I to find the other data.

Case III. Values of G_1, L, and H Are Known.—Assume values for R_1 and R_2 using the charts for sight distance (Figs. 7, 8, and 9) as a guide. Equating the expressions for G_2 as found in Cases I and II, and reducing,

$$G_3 = G_1 + R_1\,L + \sqrt{(R_1 - R_2)(R_1\,L^2 + 2\,G_1\,L - 2\,H)} \qquad (15)$$

Having the value of G_3, proceed as in Case I to find G_2 and the other data.

Case IV. Values of G_3, L, and H Are Known.—Assume Values for R_1 and R_2 using the charts for sight distance (Figs. 7, 8, and 9) as a guide. Equating the expressions for G_2 as found in Cases I and II, and reducing,

$$G_1 = G_3 - R_2\,L + \sqrt{(R_2 - R_1)(R_2\,L^2 - 2\,L\,G_3 + 2\,H)} \qquad (16)$$

Having determined the value of G_1 proceed as in Case I to find G_2 and the other data.

Case V. Values of G_1, G_3, L, and H Are Known, and the Value of R_1 Is Known or Assumed.—Equating the expressions for G_2 as found in Cases I and II, and reducing,

$$R_2 = \frac{2\,R_1\,(L\,G_3 - H) - (G_3 - G_1)^2}{L\,(R_1\,L - 2\,G_3) + 2\,H} \qquad (17)$$

Having found the value of R_2, proceed as in Case I to find G_2 and the other data.

Case VI. Values of G_1, G_3, L, and H Are Known, and the Value of R_2 Is Known or Assumed.—Equating the expressions for G_2 as found in Cases I and II, and reducing,

$$R_1 = \frac{2\,R_2\,(H - L\,G_1) - (G_3 - G_1)^2}{L\,(R_2\,L - 2\,G_3) + 2\,H} \qquad (18)$$

Having found the value of R_1 proceed as in Case I to find G_2 and the other data.

Case VII. Values of G_1, G_3, L, and H Are Known, and the Values of R_1 and R_2 Are Unknown, but the Greatest Possible Sight Distances Are Desired.—Assume values for R_1 and R_2 using the charts for sight distance (Figs. 7, 8, and 9) as a guide. Let their ratio $\frac{R_1}{R_2} = C$; then $R_1 = C\,R_2$. Equating the expressions for G_2 as found in Cases I and II but replacing R_1 with its equivalent $C\,R_2$, and reducing,

$$R_2 = \frac{1}{C\,L^2}\{\sqrt{[L\,(G_1 - C\,G_3) + H\,(C-1)]^2 - C\,L^2\,(G_3 - G_1)^2} - [L\,(G_1 - C\,G_3) + H\,(C-1)]\} \quad \text{..(19a)}$$

Find the value of R_1 from its ratio $R_1 = C\,R_2$ and determine the remaining data by the method of Case I. It may be more convenient to express the ratio as $\frac{R_2}{R_1} = K$; then $R_2 = K\,R_1$ and

$$R_1 = \frac{1}{K\,L^2}\{\sqrt{[L\,(K\,G_1 - G_3) + H\,(1-K)]^2 - K\,L^2\,(G_3 - G_1)^2} - [L\,(K\,G_1 - G_3) + \mathrm{H}\,(1-K)]\} \quad \text{..(19b)}$$

Find the value of R_2 from its ratio $R_2 = K\,R_1$ and determine the remaining data by the method of Case I.

In using these equations it is absolutely necessary that sign notations be followed strictly:

$+R$ is used for rising curves,
$-R$ is used for curves leading downward,
$+H$ indicates that the second point is higher than the first,
$-H$ indicates that the second point is lower than the first,
$+G$ indicates grades that slope upward, and
$-G$ indicates grades that slope downward.

The problem has been illustrated using R_1 as negative (summit) and R_2 as positive (sag). The same equations will hold if the problem is set up in the reverse order.

The vertical curve of a desired rate of change of grade per station can be passed through two known points by using a combination of Eqs. 1 and 3 in the form $G_1 = \frac{H}{L} - \frac{L\,R}{2}$ and $G_2 = \frac{H}{L} + \frac{L\,R}{2}$. The vertical curve that will pass through three points can be determined by using the foregoing expressions and considering the curve in two parts, with a common R and a common tangent at the intermediate point. The point on a vertical curve at which its tangent produced will pass through a given point outside the curve can be readily found using the rate of change of grade per station.

Sight Distance Over a Summit

The "passing sight distance over a summit" has been defined as the distance between points 4.5 ft vertically above the road surface, which are visible one

to the other. "Nonpassing sight distance" is defined as the distance at which an observer, with his eye 4.5 ft above the surface can see an object 4 in. above the surface of the road.[2] The sight distance, S, over a summit can be readily expressed in terms of "rate of change R."

Passing Sight Distance.—When the length of the vertical curve is equal to or greater than the sight distance, Eq. 8 can be solved for L_a. Referring to Fig. 6(*a*): $L_a = \frac{S}{2} = \sqrt{\frac{2\,(-4.5)}{R}}$; and, $S = \frac{6\sqrt{-1}}{\sqrt{R}}$. Since R is negative, the sight distance S will be equal to

$$S = \frac{6}{\sqrt{R}} \qquad (20)$$

When the sight distance S is greater than the length of the vertical curve, it will be made up of two parts (see Fig. 6(*b*)), the length of the curve and parts

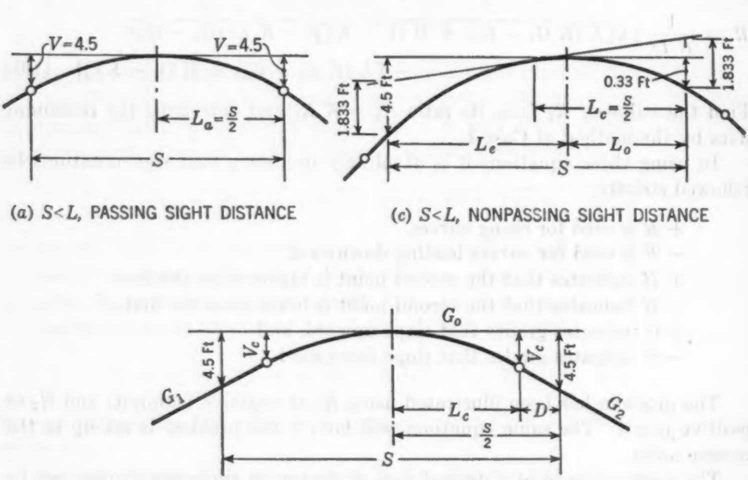

(*a*) $S<L$, PASSING SIGHT DISTANCE

(*c*) $S<L$, NONPASSING SIGHT DISTANCE

(*b*) $S>L$, PASSING SIGHT DISTANCE

FIG. 6

of the tangents at each end. It can be expressed as

$$S = 2\cdot(L_c + D) \qquad (21)$$

From Eq. 1, L_c can be expressed as

$$L_c = \frac{G_2 - G_c}{R} \qquad (22a)$$

[2] "A Policy on Sight Distance for Highways," Am. Assn. of State Highway Officials, 1940, p. 17.

The distance D along the forward tangent (Fig. 6(b)) can be expressed as

$$D = \frac{4.5 - V_c}{G_2 - G_c} \qquad (22b)$$

Substituting Eqs. 22 in Eq. 21,

$$S = 2\left(\frac{G_2 - G_c}{R} + \frac{4.5 - V_c}{G_2 - G_c}\right) \qquad (23)$$

In Eq. 23, substituting,

$$V_c = \frac{(G_2 - G_c)^2}{2\,R} \qquad (24)$$

the sight distance becomes

$$S = 2\left(\frac{G_2 - G_c}{2R} + \frac{4.5}{G_2 - G_c}\right) \qquad (25a)$$

Since G_c is the grade at the center of the curve, it can be expressed as $G_c = \frac{G_2 + G_1}{2}$, and $(G_2 - GF_c)$ becomes $\frac{G_2 - G_1}{2}$. Therefore, Eq. 25a becomes

$$S = \frac{18}{G_2 - G_1} + \frac{G_2 - G_1}{2\,R} \qquad (25b)$$

When $S = L$ (Fig. 6(c)), Eq. 1 can be written $R = \frac{G_2 - G_1}{S}$ and Eq. 25b becomes

$$S = \frac{18}{G_2 - G_1} + \frac{G_2 - G_1}{\frac{2\,(G_2 - G_1)}{S}} \qquad (26)$$

and

$$S = \frac{36}{G_2 - G_1} \qquad (27)$$

Eq. 27 must be equal to Eq. 20; therefore, if $G_2 - G_1$ in Eq. 27 is replaced by $R\,S$ then $S = \frac{36}{R\,S}$, and again $S = \frac{6}{\sqrt{R}}$.

Nonpassing Sight Distance.—For nonpassing sight distance, V has two different values—4.5 ft and 0.33 ft. By Eq. 8, $L = \sqrt{\frac{2\,V}{R}}$, $L_o = \sqrt{\frac{2(0.33)}{R}} = \frac{0.667}{R}$, and $L_e = \sqrt{\frac{2(4.5)}{R}} = \sqrt{\frac{9}{R}}$. Therefore (compare Eq. 20),

$$S = L_o + L_e = \frac{0.8165 + 3}{\sqrt{R}} = \frac{3.8165}{\sqrt{R}} \qquad (28)$$

In order to simplify the data so that the second part of the problem will be similar to the one already discussed, it is convenient to find the tangent

offset for one half the total sight distance. This can be done easily by working the foregoing data backward. Since $S = \sqrt{\frac{14.662}{R}}$, $\frac{S}{2}$ (or L_e) $= \sqrt{\frac{3.666}{R}}$; and since $L_e = \sqrt{\frac{2\,V_e}{R}}$, the tangent offset $V_e = \frac{3.666}{2} = 1.833$.

By the same reasoning as before, Eq. 25*b* becomes, for nonpassing sight distance,

$$S = \frac{7.331}{G_2 - G_1} + \frac{G_2 - G_1}{2\,R} \qquad (29a)$$

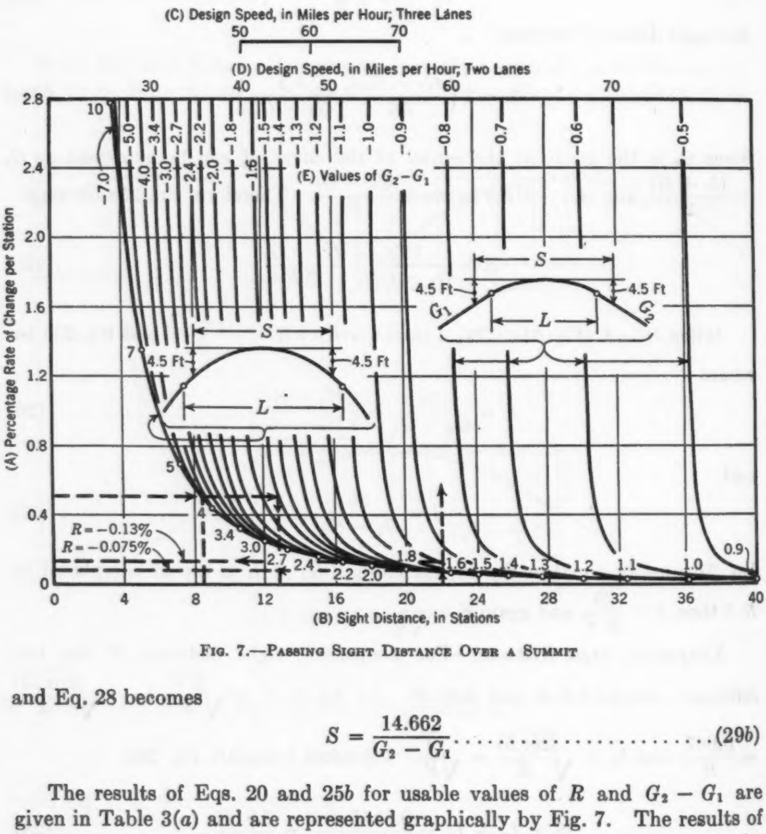

FIG. 7.—PASSING SIGHT DISTANCE OVER A SUMMIT

and Eq. 28 becomes

$$S = \frac{14.662}{G_2 - G_1} \qquad (29b)$$

The results of Eqs. 20 and 25*b* for usable values of R and $G_2 - G_1$ are given in Table 3(*a*) and are represented graphically by Fig. 7. The results of Eq. 27 are given in Table 4(*a*) and are indicated on Fig. 7 by small circles at the junction of the curves. The results of Eqs. 28 and 29*a* are given in Table 3(*b*) and are represented graphically by Fig. 8. The results of Eq. 29*b* are given in Table 4(*b*) and are indicated on Fig. 8 by small circles at the junction of the

curves. (Scale-A values are negative when applied to Figs. 7 and 8 and positive when applied to Fig. 9.)

Values of S are readable from the charts to the nearest 5 ft and values of R to the nearest 0.01% per station. Straight-line interpolation between the values given in Table 3(a) will be slightly greater than calculated values. For example at a value of $R = -1.0\%$ per station and $G_2 - G_1 = -0.55\%$, the interpolated value of S will be 27 ft greater than the calculated value. For a

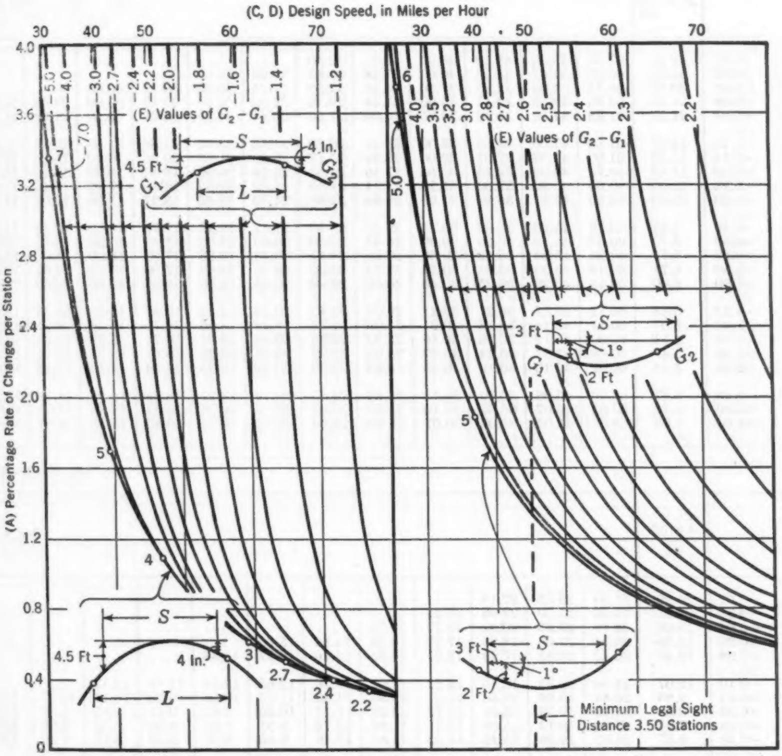

FIG. 8.—NONPASSING SIGHT DISTANCE OVER A SUMMIT

FIG. 9.—HEADLIGHT, NONPASSING SIGHT DISTANCE IN A SAG

value of $R = -1.0\%$ per station and $G_2 - G_1 = -4.5\%$, the interpolated value of S will be 5 ft greater than the computed value. An increase of 0.1 ft in the height of the driver's eye and the object above the road surface will increase the sight distance 74 ft at $R = -1.0\%$ per station and $G_2 - G_1 = -0.55\%$ and will increase the sight distance 9 ft at $R = -1.0\%$ per station and $G_2 - G_1 = -4.5\%$.

TABLE 3.—SIGHT DISTANCES (IN STATIONS) OVER

R	$S > L$	VALUES OF											
		0.3	0.4	0.5	0.6	0.7	0.8	0.9	1.0	1.1	1.2	1.3	1.4
		(a) PASSING											
	$S = \frac{6}{\sqrt{R}}$	$S < L$; S											
−0.02	42.43	67.50	55.00	48.50	45.00	43.21	42.50	....	....	....	....	....	....
−0.03	34.64	65.00	51.67	44.30	40.00	37.38	35.83	35.00	34.67	....	....	....	....
−0.04	30.00	63.75	51.00	42.25	37.50	34.46	32.50	31.25	30.50	30.11	30.00	....	....
−0.06	24.49	62.50	48.33	40.17	35.00	31.54	29.16	27.50	26.33	25.53	25.00	24.68	24.52
−0.08	21.21	61.88	47.50	39.12	33.75	30.09	27.50	25.64	24.25	23.23	22.50	21.98	21.61
−0.10	18.97	61.50	47.00	38.50	33.00	29.21	26.50	24.50	23.00	21.86	21.00	20.35	19.86
−0.15	15.49	61.00	46.33	37.67	32.00	28.04	25.17	23.00	21.33	20.06	19.00	18.20	17.52
−0.20	13.42	60.75	46.00	37.25	31.50	27.46	24.50	22.25	20.50	19.14	18.00	17.10	16.36
−0.25	12.00	60.60	45.80	37.00	31.20	27.11	24.10	21.80	20.00	18.58	17.40	16.45	15.66
−0.30	10.95	60.50	45.67	36.83	31.00	26.88	23.83	21.50	19.66	18.21	17.00	16.02	15.19
−0.40	9.49	60.38	45.50	36.62	30.75	26.59	23.50	21.12	19.25	17.75	16.50	15.48	14.61
−0.50	8.49	60.30	45.40	36.50	30.60	26.41	23.30	20.90	19.00	17.47	16.20	15.15	14.26
−0.60	7.75	60.25	45.33	36.42	30.50	26.29	23.17	20.75	18.83	17.28	16.00	14.93	14.03
−0.80	6.71	60.19	45.25	36.31	30.38	26.15	23.00	20.56	18.62	17.06	15.75	14.66	13.73
−1.00	6.00	60.15	45.20	36.25	30.30	26.06	22.90	20.45	18.50	16.91	15.60	14.50	13.56
−1.20	5.48	60.12	45.17	36.21	30.25	26.00	22.83	20.38	18.42	16.82	15.50	14.39	13.44
−1.40	5.07	60.11	45.14	36.18	30.21	25.96	22.79	20.32	18.36	16.76	15.43	14.31	13.36
−1.60	4.74	60.09	45.12	36.16	30.19	25.93	22.75	20.28	18.31	16.71	15.37	14.26	13.30
−1.80	4.47	60.08	45.11	36.14	30.17	25.91	22.72	20.25	18.28	16.67	15.33	14.21	13.25
−2.00	4.24	60.07	45.10	36.12	30.15	25.88	22.70	20.22	18.25	16.64	15.30	14.18	13.20
−2.40	3.87	60.06	45.08	36.10	30.12	25.86	22.67	20.19	18.21	16.59	15.25	14.12	13.15
−3.00	3.46	60.05	45.07	36.08	30.10	25.83	22.63	20.15	18.17	16.54	15.20	14.07	13.09
−4.00	3.00	60.04	45.05	36.06	30.07	25.80	22.60	20.12	18.12	16.40	15.15	14.01	13.03
		(b) NONPASSING											
	$S = \frac{3.8165}{\sqrt{R}}$	$S < L$; S											
−0.02	26.99	31.94	28.33	27.16	....	....	....	....	....	....	....	....	....
−0.03	22.03	29.44	25.00	22.99	22.22	....	....	....	....	....	....	....	....
−0.04	19.08	28.19	23.33	20.91	19.72	19.32	....	....	....	....	....	....	....
−0.06	15.58	26.94	21.66	18.83	17.22	16.30	15.82	15.65	....	....	....	....	....
−0.08	13.49	26.32	20.83	17.79	15.97	14.85	14.16	13.77	13.58	....	....	....	....
−0.10	12.07	25.94	20.33	17.16	15.22	13.97	13.16	12.65	12.33	12.16	12.11	....	....
−0.15	9.85	25.44	19.66	16.33	14.22	12.80	11.83	11.15	10.66	10.33	10.11	10.07	9.90
−0.20	8.53	25.19	19.33	15.91	13.72	12.22	11.16	10.40	9.83	9.41	9.11	8.89	8.74
−0.25	7.63	25.04	19.13	15.66	13.42	11.87	10.76	9.95	9.33	8.86	8.51	8.24	8.04
−0.30	6.97	24.92	19.00	15.49	13.22	11.64	10.49	9.65	8.99	8.50	8.11	7.80	7.57
−0.40	6.03	24.82	18.83	15.28	12.97	11.35	10.16	9.27	8.58	8.04	7.61	7.26	6.99
−0.50	5.40	24.70	18.73	15.16	12.82	11.17	9.96	9.05	8.33	7.76	7.31	6.94	6.64
−0.60	4.93	24.69	18.66	15.08	12.72	11.05	9.83	8.90	8.16	7.58	7.11	6.72	6.41
−0.80	4.27	24.63	18.58	14.97	12.60	10.91	9.66	8.71	7.95	7.35	6.86	6.55	6.11
−1.00	3.82	24.59	18.53	14.91	12.52	10.82	9.56	8.60	7.83	7.21	6.71	6.29	5.94
−1.20	3.48	24.57	18.50	14.87	12.47	10.76	9.49	8.52	7.75	7.12	6.61	6.18	5.82
−1.40	3.23	24.55	18.47	14.84	12.43	10.72	9.45	8.47	7.69	7.06	6.54	6.10	5.74
−1.60	3.02	24.53	18.45	14.82	12.41	10.69	9.41	8.43	7.64	7.01	6.48	6.05	5.68
−1.80	2.84	24.52	18.44	14.80	12.39	10.67	9.38	8.40	7.61	6.97	6.43	6.00	5.63
−2.00	2.70	24.51	18.43	14.78	12.37	10.64	9.36	8.37	7.58	6.94	6.41	5.96	5.58
−2.40	2.46	24.50	18.41	14.76	12.34	10.62	9.33	8.33	7.54	6.89	6.36	5.91	5.53
−3.00	2.20	24.49	18.40	14.74	12.32	10.59	9.29	8.30	7.50	6.85	6.31	5.86	5.47
−4.00	1.91	24.48	18.38	14.72	12.30	10.56	9.26	8.26	7.45	6.80	6.26	5.80	5.41

A VERTICAL CURVE WHEN L IS NOT EQUAL TO S

CHANGE IN GRADE, $G_2 - G_1$:														
1.5	1.6	1.8	2.0	2.2	2.4	2.7	3.0	3.4	4.0	5.0	7.0	10.0	12.0	R
SIGHT DISTANCE														
$= \frac{18}{G_2 - G_1} + \frac{G_2 - G_1}{2R}$														
....	....	....	....	....	....	....	....	....	....	....	....	....	....	−0.02
....	....	....	....	....	....	....	....	....	....	....	....	....	....	−0.03
....	....	....	....	....	....	....	....	....	....	....	....	....	....	−0.04
....	....	....	....	....	....	....	....	....	....	....	....	....	....	−0.06
21.38	21.25	....	....	....	....	....	....	....	....	....	....	....	....	−0.08
19.50	19.25	19.00	....	....	....	....	....	....	....	....	....	....	....	−0.10
17.00	16.58	16.00	15.66	15.51	....	....	....	....	....	....	....	....	....	−0.15
15.75	15.25	14.50	14.00	13.68	13.50	....	....	....	....	....	....	....	....	−0.20
15.00	14.45	13.60	13.00	12.58	12.30	12.07	12.00	....	....	....	....	....	....	−0.25
14.50	13.92	13.00	12.33	11.85	11.50	11.17	11.00	....	....	....	....	....	....	−0.30
13.87	13.25	12.25	11.50	10.93	10.50	10.05	9.75	9.55	....	....	....	....	....	−0.40
13.50	12.85	11.80	11.00	10.38	9.90	9.37	9.00	8.70	8.50	....	....	....	....	−0.50
13.25	12.58	11.50	10.66	10.01	9.50	8.92	8.50	8.13	7.83	....	....	....	....	−0.60
12.94	12.25	11.12	10.25	9.56	9.00	8.36	7.83	7.42	7.00	6.72	....	....	....	−0.80
12.75	12.05	10.90	10.00	9.28	8.70	8.02	7.50	7.00	6.50	6.10	....	....	....	−1.00
12.62	11.92	10.75	9.83	9.10	8.50	7.79	7.25	6.72	6.17	5.68	....	....	....	−1.20
12.53	11.82	10.64	9.71	8.97	8.36	7.63	7.07	6.51	5.93	5.39	5.07	....	....	−1.40
12.47	11.75	10.56	9.63	8.87	8.26	7.51	6.94	6.36	5.75	5.16	4.76	....	....	−1.60
12.42	11.69	10.50	9.56	8.79	8.17	7.42	6.83	6.24	5.61	4.92	4.51	....	....	−1.80
12.37	11.65	10.45	9.50	8.73	8.10	7.33	6.75	6.15	5.50	4.85	4.32	....	....	−2.00
12.31	11.58	10.38	9.42	8.64	8.00	7.23	6.63	6.01	5.33	4.64	4.03	....	....	−2.40
12.25	11.52	10.30	9.33	8.55	7.90	7.12	6.50	5.87	5.17	4.43	3.73	3.47	....	−3.00
12.19	11.45	10.22	9.25	8.45	7.80	7.00	6.38	5.73	5.00	4.22	3.44	3.05	3.00	−4.00
SIGHT DISTANCE														
$= \frac{7.331}{G_2 - G_1} + \frac{G_2 - G_1}{2R}$														
....	....	....	....	....	....	....	....	....	....	....	....	....	....	−0.02
....	....	....	....	....	....	....	....	....	....	....	....	....	....	−0.03
....	....	....	....	....	....	....	....	....	....	....	....	....	....	−0.04
....	....	....	....	....	....	....	....	....	....	....	....	....	....	−0.06
....	....	....	....	....	....	....	....	....	....	....	....	....	....	−0.08
....	....	....	....	....	....	....	....	....	....	....	....	....	....	−0.10
....	....	....	....	....	....	....	....	....	....	....	....	....	....	−0.15
8.64	8.58	....	....	....	....	....	....	....	....	....	....	....	....	−0.20
7.89	7.78	7.67	....	....	....	....	....	....	....	....	....	....	....	−0.25
7.39	7.25	7.07	6.99	....	....	....	....	....	....	....	....	....	....	−0.30
6.76	6.58	6.32	6.16	6.08	6.05	....	....	....	....	....	....	....	....	−0.40
6.39	6.18	5.87	5.66	5.53	5.45	5.42	....	....	....	....	....	....	....	−0.50
6.14	5.91	5.57	5.32	5.16	5.05	4.97	....	....	....	....	....	....	....	−0.60
5.82	5.58	5.19	4.91	4.71	4.55	4.41	4.33	4.28	....	....	....	....	....	−0.80
5.64	5.38	4.97	4.66	4.43	4.25	4.07	3.94	3.86	....	....	....	....	....	−1.00
5.51	5.25	4.82	4.49	4.25	4.05	3.84	3.69	3.57	3.51	....	....	....	....	−1.20
5.42	5.15	4.71	4.37	4.12	3.91	3.68	3.52	3.37	3.27	....	....	....	....	−1.40
5.36	5.08	4.63	4.29	4.02	3.81	3.56	3.38	3.22	3.09	....	....	....	....	−1.60
5.30	5.02	4.57	4.22	3.94	3.72	3.47	3.28	3.10	2.95	2.79	....	....	....	−1.80
5.26	4.98	4.52	4.16	3.88	3.65	3.39	3.19	3.01	2.84	2.72	....	....	....	−2.00
5.20	4.91	4.45	4.08	3.79	3.55	3.28	3.07	2.86	2.67	2.51	....	....	....	−2.40
5.14	4.85	4.37	3.99	3.70	3.45	3.17	2.94	2.72	2.53	2.30	....	....	....	−3.00
5.07	4.78	4.29	3.86	3.60	3.35	3.05	2.82	2.58	2.34	2.09	1.92	....	....	−4.00

Headlight Sight Distance in a Sag

The distance at which the headlights of a car will illuminate the road surface may be a determining factor in establishing the sharpness of a vertical curve in a sag (see Fig. 9). It is not within the province of this paper to discuss the amount of illumination necessary to make the road surface visible to the

TABLE 4.—Sight Distances on a

Symbol[a]	Values of Change											
	0.3	0.4	0.5	0.6	0.7	0.8	0.9	1.0	1.1	1.2	1.3	1.4
												(a) Passing
R	−0.0025	−0.0004	−0.0007	−0.001	−0.014	−0.018	−0.024	−0.028	−0.033	−0.040	−0.047	−0.054
S	120.00	90.00	72.00	60.00	51.40	45.00	40.00	36.00	32.73	30.00	27.69	25.71
												(b) Nonpassing
R	−0.005	−0.01	−0.02	−0.025	−0.03	−0.04	−0.055	−0.07	−0.083	−0.10	−0.115	−0.13
S	48.87	36.66	29.30	24.20	20.94	18.30	16.29	14.66	13.33	12.20	11.28	10.46

[a] The symbol R = Percentage rate of change of grade per station;

driver. The Vehicle Code of the State of California specifies certain limitations on automobile headlight equipment, as follows[3]:

> "Headlamps shall be located at a height measured from the center of the headlamps of not more than fifty-four inches nor less than twenty-four inches above the level surface upon which said vehicle stands."

Obviously, the lesser height will provide illumination at a shorter distance. Hence a height of 2 ft has been used as a condition for the following calculations. Referring to multiple-beam road-lighting equipment, the code states[4]:

> "There shall be an uppermost distribution of light, or composite beam, so aimed and of such intensity as to reveal persons and vehicles at a distance of at least 350 feet ahead for all conditions of loading. The maximum intensity of this uppermost distribution of light or composite beam one degree of arc or more above the horizontal level of the lamps when the vehicle is not loaded shall not exceed 8,000 apparent candlepower, and at no other point of the distribution of light or composite beam shall there be an intensity of more than 75,000 apparent candlepower."

An analysis of this paragraph reveals that 350 ft is established as a minimum legal sight distance and that $+1°$ is the maximum vertical angle of the effective light beam.

Distances are measured horizontally and vertically. Hence, in order to determine the true length of the sight distance in the simplest manner, the

[3] "Vehicle Code, State of California, as Amended to 1949," issued by Dept. of Motor Vehicles, Div. 10, Equipment, Chapter 2 (Required Lighting Equipment), Sect. 619, p. 253.

[4] *Ibid.*, Div. 10, Equipment, Chapter 4 (Test and Approval of Lamps, Lamp Equipment and Signal Devices), Sect. 648, Para. (a), p. 268.

light beam will be pictured as a horizontal line. The vertical angle between the road surface and the light beam is 1°, so the angle of the road surface will be 1° downward from the horizontal. The tangent of a 1° angle is 0.017455, defining a slope of 0.017455 ft per ft, or 1.7455 ft in 100 ft, which, in other conventional terms, is a grade of − 1.7455%.

Vertical Curve When L is Equal to S

in Grade, $G_2 - G_1$:														Symbol[a]
1.5	1.6	1.8	2.0	2.2	2.4	2.7	3.0	3.4	4.0	5.0	7.0	10.0	12.0	
Sight Distance, $R = \frac{(G_2 - G_1)^2}{36}$; $S = \frac{36}{G_2 - G_1}$														
−0.062 24.00	−0.07 22.50	−0.090 20.00	−0.11 18.00	−0.13 16.36	−0.16 15.00	−0.20 13.33	−0.25 12.00	−0.32 10.59	−0.44 9.00	−0.70 7.20	−1.36 5.14	−2.78 3.60	−4.00 3.00	R S
Sight Distance, $R = \frac{(G_2 - G_1)^2}{14.662}$; $S = \frac{14.662}{G_2 - G_1}$														
−0.153 9.77	−0.18 9.15	−0.22 8.14	−0.27 7.32	−0.33 6.66	−0.39 6.10	−0.50 5.42	−0.61 4.88	−0.788 4.31	−1.09 3.66	−1.70 2.93	−3.37 2.09	....	....	R S

[a] The symbol S = Sight distance, in hundreds of feet.

The headlamp height is not less than 2 ft normal to the road surface (see Fig. 10); this height, on a − 1.7455% grade, amounts to a vertical distance of 2.000304 ft. Such accuracy is not needed in this problem, and the vertical distance from the road surface to the light will be assumed as 2 ft.

The driver of a motor vehicle sits behind the headlamps an average distance of about 5 ft in most passenger cars. In trucks and buses that have the engine mounted under the seat or at the back, this distance may be as short as 2.5 ft. For purposes of calculating sight distance, a value of 3 ft will be added to the length of the light beam. Two general cases will be considered.

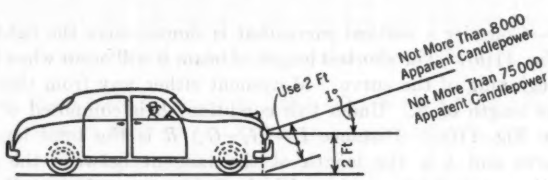

Fig. 10

Case 1.—Consider an indefinitely long curve—one in which the length of the curve is greater than the length of the light beam (see Fig. 11(a)). Designate the length of the light beam as B and the length of the part of the curve as L. The difference in elevation H between the two points on the curve is 2 ft.

The grade at the first point is $G_1 = -1.7455\%$. Eqs. 1 and 3 combined as—

$$L = \sqrt{\left(\frac{G_1}{R}\right)^2 + \frac{2H}{R}} - \frac{G_1}{R} \quad \text{(30)}$$

—fits this condition. Substituting the foregoing values, Eq. 30 becomes

$$B = \sqrt{\left(\frac{-1.7455}{R}\right)^2 + \frac{2(2)}{R}} - \frac{-1.7455}{R}$$

$$= \frac{1}{R}(\sqrt{3.0468 + 4R} + 1.7455) \quad \text{(31)}$$

—and the sight distance will be $B + 0.03$ stations, or

$$S = \frac{1}{R}(\sqrt{3.0468 + 4R} + 1.7455) + 0.03 \quad \text{(32)}$$

—from which the sight distance for any desired value of rate of change may be determined.

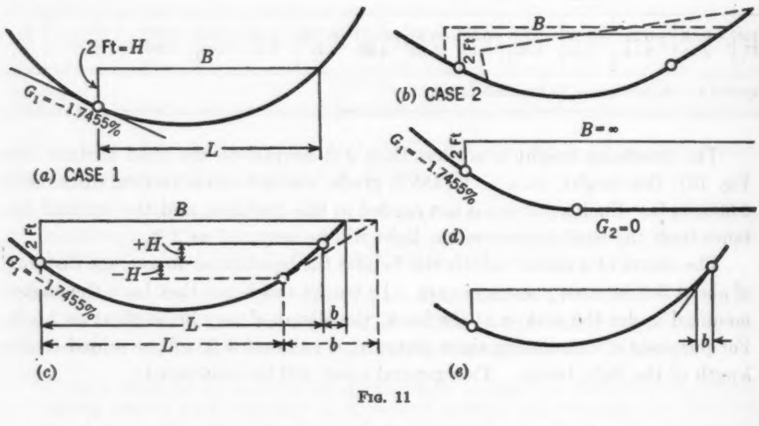

FIG. 11

Case 2.—Consider a vertical curve that is shorter than the light beam, as shown in Fig. 11(*b*). The shortest length of beam B will occur when the vehicle is at the beginning of the curve. Movement either way from this point will increase the length of B. Under this condition, B is composed of two parts L and b, in Fig. 11(*c*). Distance $L = (G_2 - G_1)/R$ is the total length of the vertical curve and b is the length of the tangent between the end of the curve and the point of intersection with the light beam. Height H is now the difference in elevation of the two ends of the curve. By inspection

$$b = \frac{2 - H}{G_2} \quad \text{(33)}$$

The elevation difference H may be positive or negative within certain limits. In the special case when H is 0, grade G_2 will be equal to $-G_1$, and b will be

2/+ 1.74455. Substituting Eq. 3 in Eq. 33,

$$b = \frac{2 - 0.5\,L\,(G_2 + G_1)}{G_2} \qquad (34)$$

In Eq. 34, substitute the value of L determined from Eq. 1, and substitute for $G_2 + G_1$ its equivalent $(G_2 - G_1) + 2\,G_1$—which is equal to $(G_2 + G_1) + 2\,(-1.7455)$ or $(G_2 - G_1) - 3.4910$. Also, substitute for G_2 its equivalent

TABLE 5.—HEADLIGHT, NONPASSING SIGHT DISTANCE IN A SAG (IN STATIONS), WHEN L IS NOT EQUAL TO S

R	S (Eq. 32, $S > L$)	Values of $G_2 - G_1$:															
		2.0	2.1	2.2	2.3	2.4	2.5	2.6	2.7	2.8	2.9	3.0	3.2	3.5	4.0	5.0	6.0
		$S < L$, S from Eq. 36															
0.1	36.05	86.47	67.87	57.68	51.34	47.09	44.10	41.93	40.31	39.10	38.36	37.50	36.61	36.08			
0.2	18.56	47.18	36.77	31.05	27.49	25.09	23.39	22.15	21.22	20.51	20.06	19.56	19.01	18.64			
0.3	12.72	34.08	26.41	22.18	19.54	17.75	16.49	15.56	14.86	14.32	13.96	13.58	13.14	12.81			
0.4	9.78	27.54	21.22	17.74	15.56	14.09	13.04	12.26	11.67	11.22	10.91	10.59	10.21	9.90			
0.5	8.01	23.61	18.11	15.08	13.18	11.89	10.96	10.28	9.76	9.36	9.08	8.72	8.45	8.15			
0.6	6.83	20.99	16.04	13.31	11.59	10.42	9.58	8.96	8.49	8.12	7.86	7.54	7.27	6.99	6.83		
0.7	5.98	19.12	14.56	12.04	10.45	9.37	8.60	7.82	7.58	7.24	6.99	6.75	6.43	6.16	5.99		
0.8	5.34	17.71	13.45	11.09	9.61	8.59	7.86	7.32	6.90	6.57	6.35	6.11	5.81	5.53	5.35		
0.9	4.83	16.62	12.58	10.35	8.94	7.98	7.28	6.77	6.37	6.06	5.83	5.61	5.32	5.05	4.86		
1.0	4.43	15.75	11.89	9.76	8.41	7.49	6.82	6.33	5.94	5.64	5.42	5.21	4.93	4.67	4.47		
1.1	4.10	15.03	11.33	9.27	7.97	6.97	6.45	5.97	5.60	5.31	5.10	4.89	4.61	4.34	4.14		
1.2	3.82	14.44	10.86	8.87	7.61	6.75	6.13	5.67	5.31	5.02	4.81	4.61	4.34	4.08	3.87		
1.3	3.58	13.93	10.46	8.53	7.31	6.47	5.87	5.44	5.06	4.79	4.58	4.38	4.11	3.86	3.65		
1.4	3.38	13.50	10.12	8.23	7.04	6.23	5.64	5.20	4.85	4.58	4.38	4.19	3.92	3.66	3.44		
1.5	3.20	13.13	9.82	7.98	6.82	6.02	5.44	5.01	4.67	4.41	4.20	4.02	3.75	3.50	3.28		
1.6	3.04	12.80	9.56	7.76	6.62	5.84	5.27	4.84	4.51	4.25	4.05	3.87	3.61	3.35	3.14		
1.7	2.90	12.51	9.33	7.56	6.44	5.67	5.12	4.70	4.37	4.11	3.92	3.73	3.48	3.21	3.00		
1.8	2.78	12.25	9.13	7.39	6.29	5.53	4.98	4.57	4.25	3.98	3.80	3.62	3.36	3.11	2.89		
1.9	2.67	12.03	8.95	7.23	6.15	5.40	4.86	4.45	4.14	3.88	3.69	3.51	3.26	3.01	2.78	2.67	
2.0	2.56	11.82	8.78	7.09	6.02	5.29	4.75	4.35	4.04	3.79	3.59	3.42	3.17	2.92	2.69	2.57	
2.2	2.39	11.46	8.50	6.85	5.81	5.06	4.56	4.17	3.86	3.62	3.43	3.26	3.01	2.76	2.53	2.39	
2.4	2.24	11.16	8.26	6.65	5.62	4.92	4.41	4.02	3.72	3.48	3.29	3.12	2.87	2.62	2.40	2.25	
2.6	2.11	10.91	8.06	6.48	5.47	4.78	4.27	3.89	3.59	3.36	3.17	3.00	2.76	2.50	2.28	2.12	
2.8	2.00	10.70	7.89	6.33	5.34	4.66	4.16	3.78	3.49	3.25	3.08	2.91	2.66	2.42	2.19	2.02	
3.0	1.91	10.51	7.75	6.21	5.23	4.55	4.06	3.69	3.40	3.17	2.98	2.82	2.58	2.33	2.10	1.93	
3.2	1.82	10.34	7.62	6.10	5.13	4.46	3.98	3.61	3.32	3.09	2.91	2.75	2.51	2.26	2.03	1.85	
3.4	1.74	10.20	7.50	6.00	5.04	4.38	3.90	3.53	3.25	3.02	2.84	2.68	2.44	2.20	1.96	1.78	
3.6	1.69	10.07	7.40	5.91	4.96	4.31	3.83	3.47	3.19	2.96	2.78	2.62	2.38	2.14	1.90	1.71	
3.8	1.61	9.96	7.31	5.83	4.89	4.24	3.77	3.41	3.13	2.91	2.73	2.57	2.33	2.09	1.85	1.66	1.61
4.0	1.56	9.85	7.23	5.76	4.83	4.19	3.72	3.36	3.08	2.85	2.68	2.52	2.29	2.04	1.80	1.61	1.56

$(G_2 - G_1) + G_1$—which is equal to $(G_2 - G_1) + (-1.7455)$ or $(G_2 - G_1) - 1.7455$. Entering these several values in Eq. 34 and reducing,

$$b = \frac{4\,R - (G_2 - G_1)\,[(G_2 - G_1) - 3.491]}{2\,R\,[(G_2 - G_1) - 1.7455]} \qquad (35)$$

From Fig. 11(*c*), $B = L + b$ and $S = B + 0.03 = L + b + 0.03$ stations. With proper substitutions,

$$S = \frac{G_2 - G_1}{R} + \frac{4\,R - (G_2 - G_1)\,[(G_2 - G_1) - 3.491]}{2\,R\,[(G_2 - G_1) - 1.7455]} + 0.03 \qquad (36)$$

Examination of Eq. 36 reveals that if $G_2 - G_1 = +1.7455$, in terms of Fig. 11(d), when $G_2 = 0$, the second term b will become infinite. Hence, the sight distance will be infinite regardless of the value of R. Also, when $H = 2$ (which is when the numerator of the second fraction in Eq. 36 equals zero), the second term, b, will be zero and the length of the curve is equal to B. In that case,

$$S = \frac{G_2 - G_1}{R} + 0.03 \qquad (37)$$

This condition will exist when

$$R = \frac{(G_2 - G_1)\,[(G_2 - G_1) - 3.491]}{4} \qquad (38)$$

—that is, when the numerator of the second fraction in Eq. 36 is zero. From Eq. 38, the values of R that will produce a curve of the same length as the light beam can be found for any desired values of $G_2 - G_1$. Conversely,

$$G_2 - G_1 = \sqrt{4R + 3.0468} + 1.7455 \qquad (39)$$

From Eq. 39 the value of $G_2 - G_1$ that will produce a curve of the same length as the light beam can be found for any desired values of R.

TABLE 6.—Headlight, Nonpassing Sight Distance in a Sag When L Is Equal to S

$G_2 - G_1$	R (Eq. 38)	S (Stations) (Eqs. 32 or 36)
3.4910	0.0000	Infinite
3.5	0.0079	403.46
4.0	0.5090	7.90
5.0	1.8862	2.68
6.0	3.7635	1.62
7.0	6.1408	1.17

For values of $G_2 - G_1$ equal to or greater than those determined by Eq. 39, the second term of Eq. 36 will be zero or negative, respectively. When negative, it indicates that b is measured backward to the stationing (Fig. 11(e)). If the expression $G_2 - G_1$ in Eq. 36 is replaced with its equivalent from Eq. 39, and reduced, it becomes identical with Eq. 32. Eqs. 32, 36, and 38 have been solved for desirable values of $G_2 - G_1$ and the results are presented in Tables 5 and 6 and Fig. 9.

The lower curve of Fig. 9 represents the relation between sight distance and rate of change when the curve is of greater length than the sight distance. When the difference of grades is such that the sight distance is greater than the length of the curve, the line labeled with the respective difference of grades applies.

DISCUSSION

T. F. HICKERSON,[11] M. ASCE.—In urging a more general adoption of "rate of change of grade" for highways, as has long been the practice for railways, this paper is timely. A clearer concept of the sharpness of the curve is obtained and, incidentally, there is provided greater facility in the solution of curve problems.

The determination of the vertical alinement for a pair of reverse curves (Example 5) is a noteworthy contribution; but it appears simpler to substitute the given data in Eqs. 9 to 12 and solve them simultaneously, rather than to use the long expressions presented in cases II to VII.

Using the author's sign convention, it follows that the rate of change of grade is positive for sags and negative for crests; hence, $R_2 - R_1$, shown in Fig. 5, is positive.

The derivation of Eq. 20 is unique. The absolute value of R must be used in this formula, otherwise it reads

$$S = \frac{6}{\sqrt{-R}} \qquad (40)$$

ROBERT T. HOWE,[12] A. M. ASCE.—The theory of vertical curves is useful to a teacher of railroad and highway surveying, as a review of one phase of analytic geometry. The topic may be introduced through the general equation of a parabola with its axis parallel to the y-axis—

$$y = A\,x^2 + B\,x + C \qquad (41)$$

in which x is the horizontal distance from the origin (selected through the BVC) to any point on the curve, and y is the elevation of that point.

Comparing the first two coefficients in Eq. 41 with those of Eq. 4a, coefficient A is found to equal $R/2$ and B is found to equal G_1. Referring to Fig. 1, it is found that C is the elevation of BVC.

Use the nomenclature of Eq. 4b, and let h equal the distance from the zero datum (usually sea level) to the directrix of the parabola. The basic properties of the parabola give the equation—

$$y - h = \sqrt{(x - a)^2 + [y - (h + p)]^2} \qquad (42)$$

—which reduces to

$$y = \frac{x^2}{2\,p} - \frac{2\,a}{2\,p}\,x + \frac{a^2 + 2\,p\,h + p^2}{2\,p} \qquad (43)$$

[11] Prof. of Applied Math., Univ. of North Carolina, Chapel Hill, N. C.
[12] Asst. Prof. of Civ. Eng., Univ. of Cincinnati, Cincinnati, Ohio.

Consider Fig. 1(a) as an example, in which the vertex is outside the vertical curve, $G_1 = +1\%$, $G_2 = +7\%$, and $L = 6$ stations, from which $R = +1\%$. Assume that the BVC is at El. 200.00 rather than at El. 0. Then, $\frac{1}{2p} = \frac{R}{2} = \frac{1}{2}$, from which $p = +1.00$, and $-\frac{2a}{2p} = G_1 = 1.00$, from which $a = -1.00$. This means that the vertex is 1 station to the left of the origin, or at station $9 + 00$. Then $\frac{a^2 + 2ph + p^2}{2p} = 200.00$, the elevation of the BVC; thus, $h = 199.00$ ft, the elevation of the directrix. Adding $\frac{p}{2}$ to h yields 199.50 ft, the elevation of the vertex of the parabola.

In Table 1, the author gives an illustration of a situation in which the vertex of the parabola is within the limits of the vertical curve. Here, $G_1 = -1.10\%$, $G_2 = +1.30\%$, and $L = 6$ stations, from which $R = +0.4\%$. The BVC is at El. 100.00. Then

$$y = 0.2\,x^2 - 1.10\,x + 100.00 \qquad (44)$$

which yields $p = +2.50$, $a = 2.75$, and $h = 97.237$ ft. The vertex and low point of the vertical curve are therefore at station $12 + 75.00$, and at El. 98.487.

TABLE 7.—COMPUTATION OF INTERMEDIATE ELEVATIONS, BASED ON EQ. 44

Station (1)	Description (2)	x, from BVC (3)	$-1.10\,x$ (4)	x^2 (5)	$0.2\,x^2$ (6)	Elevation from BVC[a] (7)	Elevation,[b] E_2 (8)
12+90	Pier No. 3	2.90	−3.19	8.41	1.68	−1.51	98.49
12+20	Abutment No. 1	2.20	−2.42	4.84	0.97	−1.45	98.55
10+00	Beginning of vertical curve (BVC)	0	0	0	0	0	100.00

[a] The values in Col. 7 are found by adding the values in Col. 4 to those in Col. 6. [b] The values in Col. 8 are found by adding 100.00 ft to the values in Col. 7.

The author's solution for the elevations of intermediate points of this curve is novel, but certainly no more direct than the tabular solution of the equation of the curve, as demonstrated in Table 7.

Should the grade at any station be desired, differentiate the equation of the curve, as in Eq. 6a, and then substitute the proper value of x.

The solution of a general equation of the form of Eq. 41 also simplifies the selection of a curve that will meet certain restrictions, such as passing through a given elevation at a specified station. For example, if it is given that $G_1 = +2.30\%$, $G_2 = +4.70\%$, the BVC is at El. 218.75, and at station $13 + 00$; and there is a fixed point at station $17 + 40$ of El. 230.13; let it be required to find the length of the vertical curve that will fit this situation. The general equation of this curve becomes

$$y = \frac{2.40}{2\,L}\,x^2 + 2.30\,x + 218.75 \qquad (45)$$

At the fixed point, $y = 230.13$ and $x = 4.40$ stations. Therefore, $L = 18.438$ stations.

Although the author's development of the rate-of-change-of-grade method is interesting, and undoubtedly has advantages in certain situations, it is perhaps a step away from the fundamentals that the colleges are so frequently urged to stress. Because this rate-of-change-of-grade method rests squarely on two of the three right-hand terms of the general equation of a parabola with its axis parallel to the y-axis, why not simply use the entire equation as illustrated herein.

E. N. Prouty,[13] A.M. ASCE.—The solution proposed in this paper can be simplified considerably. For example, in the equation for a vertical curve the elements given in any problem are G_1 and G_2, the rates of the intersecting grades to be joined. Those to be selected to satisfy the conditions of the particular location of construction and operation are L, the length, and R, the rate of change of grade per station. From these, the most rapid and simplest solution would seem to be to use Eq. 2 to get V for the chosen L; then, combining Eqs. 1 and 2 (see Eq. 8)—

$$V = L^2 \frac{R}{2} \qquad (46)$$

—from which R for that particular length L is fixed. The rate of change in grade R is constant for any curve of length L. It may be used advisedly as the nominal characteristic of that curve and must satisfy the requirements for safety and comfort of traffic under the conditions of volume and speed provided for that curve.

The ordinate from the tangent having grade G to the curve at distance x from the BVC, being $\frac{V}{L^2} x^2$, allows a quick examination of curve point elevation at any particular x without computing all consecutive chord points from the BVC. When curve elevations at selected points prove to be satisfactory, then a full tabulation, x_1, x_2, ..., of station points on the curve, where grade elevations are required to be set for construction—elevations of the tangent at G_1, x_2, x_2, ..., values of $x^2{}_1$, $x^2{}_2$, ..., values of $\frac{V}{L^2} x^2{}_1$, $\frac{V}{L^2} x^2{}_1$, ..., and grade elevations on the curve at x_1, x_2, ... x_L—is a form of record more readily adaptable for field checking and use than is Table 1.

C. J. Brownell,[14] A. M. ASCE.—In reply to Mr. Howe's suggestion concerning the fundamental equation of the parabola, the one important characteristic of a parabola is that the change of slope per unit of distance is constant. It is the rate of this change of slope that distinguishes one parabola from another. In terms of analytic geometry, this rate is expressed by the factor $1/p$. In the vernacular of the highway engineer, it is the rate of change of

[13] Engr., Clyde C. Kennedy, San Francisco, Calif.

[14] Associate Bridge Engr., Bridge Dept., State Div. of Highways, Sacramento, Calif.

grade per station—designated R in this paper. The description and solution of vertical curves by the rate of change of grade per station are steps toward the practical application of mathematical theory.

With reference to Mr. Prouty's remarks relative to Eq. 45, R is the distinguishing characteristic of a vertical curve of infinite length, and L can be any segment of the curve as illustrated in Fig. 12.

Mr. Howe's use of sea-level datum as the x-axis is an excellent way of explaining the complete problem. The use of h, the vertical distance from sea level to the directrix of the parabola, would be good for impressing the theory of the parabola on students. However, in highway practice the directrix and focus of the parabolic vertical curve are almost never referred to nor considered. The elevation E_1 expresses the distance from sea level to the first point on the curve (the intersection of the curve with the y-axis).

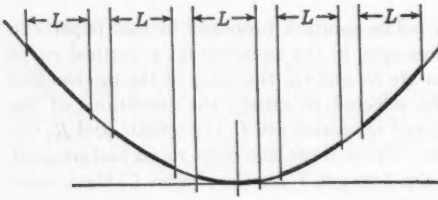

FIG. 12.

Mr. Hickerson's observation concerning the use of the absolute value of R in Eq. 20 is correct. However, a better expression would be

$$S = 6\sqrt{\frac{-1}{R}} \qquad (47)$$

in which R has its proper algebraic sign. Similarly, under the heading, "Nonpassing Sight Distance," the values of V are -4.5 ft and -0.33 ft. The subsequent expressions containing these values are changed accordingly. Eq. 28 should read

$$S = L_o + L_e = (0.8165 + 3)\sqrt{\frac{-1}{R}} = 3.8165\sqrt{\frac{-1}{R}}.$$

The signs in the ensuing expressions must be similarly changed, so that $S = \sqrt{\frac{-14.662}{R}}$ and $L_e = \sqrt{\frac{-3.667}{R}}$, and the value of V_e becomes -1.833.

For summit vertical curves, the value of V is always negative, as it is measured downward from the tangent. Figs. 7 and 8, "Sight Distance Over a Summit," would have been more appropriately drawn in the fourth quadrant.

Mr. Howe's discussion indicates the desirability of tabulating the solution in terms of the equation. In keeping with this procedure, the tabular system used in Tables 1 and 2 can be expressed as

$$\frac{G_1 + (G_1 + L\,R)}{2}\,L + E_1 = E_2 \text{ (Col. 8)}$$

in which

$$L = \text{Distance between points (Col. 3)}$$

$$L\,R = G_2 - G_1 \text{ (Col. 4)}$$

$$G_1 + L\,R = G_2 \text{ (Col. 5)}$$

$$\frac{G_1 + (G_1 + L\,R)}{2} = \frac{G_2 + G_1}{2} \text{ (Col. 6)}$$

$$\frac{G_1 + (G_1 + L\,R)}{2}\,L = H \text{ (Col. 7.)}$$

In reply to Mr. Prouty's suggestion concerning comfort and safety, reference is made to a solution of this problem by Ralph A. Moyer.[16] Converting his equation for comfort on either sag or summit vertical curves to the nomenclature of this paper, $R_{\text{comfort}} = \frac{15{,}000}{(\text{Velocity})^2}$. His expression for take-off speed reduces to $R_{\text{take-off}} = \frac{150{,}000}{(\text{Velocity})^2}$. In these expressions the velocity is in miles per hour.

TABLE 8.—COMPARISON OF COMPUTATION TIMES

Computer	Time, in Minutes: Tangent-offset method	Time, in Minutes: Rate-of-change-of-grade-per station method	Time saving, in %
	Problem 1A		
R. W. B.	19	14	26
R. P. H.	20	10	50
W. J. J.	18	17	5
C. J. B.	16	14	12
Average	18.25	13.75	24.5
	Problem 1B		
R. W. B.	18	12	33
R. P. H.	20	16	20
W. J. J.	10	10	0
C. J. B.	19	13	31
Average	16.75	12.75	23.8
Over-all average	17.5	13.25	24.3

In connection with Mr. Prouty's remarks, a brief time study was conducted among a few engineers who are familiar with both the methods of tangent offset and rate of change of grade per station for the solution of vertical curves. Two problems of the type of Case 1, having six intermediate points each, but having different stations, grades, and R-values, were used. The results of this study are tabulated in Table 8. The averages show that 24.3% less time was re-

[16] *Supplementary Notes and Typical Problems for Highway Engineering Course, Civil Engineering 106, University of California Syllabus Series, Syllabus W C,* by Ralph A. Moyer and John Hugh Jones, Univ. of California Press, Berkeley, Calif. (2d Ed. revised), 1950, p. 120.

quired by the method of rate of change of grade per station than by the method of tangent offsets for a single solution of the problem. One solution by the method of rate of change of grade per station is sufficiently accurate because the computations close on the EVC. However, a solution by tangent offsets requires a second independent calculation for a check. If the average time for a single solution by tangent offsets is doubled to account for this check, there results a net saving of 62.1% in favor of the method of rate of change of grade per station.

AMERICAN SOCIETY OF CIVIL ENGINEERS
Founded November 5, 1852

TRANSACTIONS

Paper No. 2553

VARIATION OF WIND VELOCITY AND GUSTS WITH HEIGHT

BY R. H. SHERLOCK,[1] M. ASCE

WITH DISCUSSION BY MESSRS. W. WATTERS PAGON; IRVING A. SINGER AND MAYNARD E. SMITH; PERCY H. THOMAS AND M. H. FRESEN; ROBERT A. MCCORMICK; EDWARD COHEN; AND R. H. SHERLOCK

SYNOPSIS

The flow of air in level, open country is adopted as the standard of reference in this paper, assuming that the influence of local shielding and unusual topography will be evaluated by the designer in each individual case, perhaps with suggestions in the code. Recommendations are based on velocity pressures rather than on design pressures.

The theory of the variation of wind velocity with height, based on the Ekman spiral, is first discussed. The records of a particular storm are used to validate the theory and to provide detailed information regarding gust characteristics. The duration and extent of the minimum effective gust is discussed. A recommendation is made for the variation of velocity pressure with height, to be used in obtaining the design pressure at any height. The magnitude of the design pressure will depend upon the recommended velocity pressure near the ground in each particular geographical location. A special recommendation is made for the case of guyed towers.

The one-seventh-power law is a sufficiently close approximation to the variation of 5-min wind velocity with height up to 1,000 ft above which a constant velocity is justified. Gust factors are proportional to the inverse ratio of heights raised to the power 0.0625. The combined effect gives velocity pressures which are proportional to the ratio of heights raised to the power 0.161.

INTRODUCTION

The theory of the variation of wind velocity with height is discussed in the first part of this paper. Throughout the remainder of the paper the records of

NOTE.—Published in April, 1952, as *Proceedings-Separate No. 126*. Positions and titles given are those in effect when the paper or discussion was received for publication.

[1] Prof. of Civ. Eng., Univ. of Michigan, Ann Arbor, Mich.

a particular storm are used to validate the theory further and to provide detailed information regarding gust characteristics. The duration and extent of the minimum effective gust is also discussed. A recommendation is made for the variation of velocity pressure with height to be used in obtaining the design pressure at any height. The magnitude of the design pressure will depend upon the recommended velocity pressure near the ground in each particular geographical location. A special recommendation is made for the case of guyed towers.

The subject of the variation of wind velocity with height is complicated by the highly uncertain nature of much of the available storm observations and by the high cost of setting up a station to obtain this information under proper controls. The most voluminous information is contained in the reports of the Weather Bureau, Department of Commerce. These latter data, however, are not homogeneous since the condition under which they were taken varied from time to time. This variation is chiefly the result of the first-order stations having been located, until recently, in cities where the degree of exposure was constantly changing with the erection of new, tall buildings, and where the air flow was badly distorted by the buildings upon which the anemometers were mounted.

It is desirable that code recommendations be based on some standard of reference, such as air flow in level open country, and that the influence of local shielding and unusual topography be evaluated by the designer in each individual case, perhaps with suggestions in the code.

Definitions and Notations

The letter symbols introduced in this paper are defined where they first appear, in the text or by illustrations. Essentially, they conform to American Standard Letter Symbols for Structural Analysis (ASA-Z10.8—1949). Technical terms used in the paper are defined as follows:

Wind Velocity.—Speed and direction of air movements with reference to points on the ground. Units are in miles per hour unless otherwise noted.

Five-Minute Velocity.—Average velocity V_5, during five consecutive minutes. At a height of z feet above the ground, the 5-min velocity is designated V_z.

Gust.—Localized high wind velocity lasting a short time.

Gust Factor, F.—Gust velocity divided by the 5-min velocity. At a height of z feet above the ground, the gust factor is F_z.

Eddy.—A parcel of air with components of motion transverse to the general stream.

Eddy Viscosity.—Resistance to free laminar flow which is provided by eddies in the air stream.

Jet.—Temporary stream of air that moves at a higher velocity than the surrounding air.

Surface Wind.—Wind vector on the ground.

Gradient Wind.—Wind vector at a height at which the influence of the ground friction is negligible.

Geostrophic Wind.—A first approximation to the gradient wind, in which the inertia forces due to the curvature of the wind path are neglected.

Isobar.—Locus of points of equal atmospheric pressure, as shown on weather maps.

Pressure Gradients.—Rate of change of atmospheric pressure, as shown graphically by the spacing of the isobars on weather maps.

Gradient and Geostrophic Winds

There is some height at which the influence of the ground friction, transmitted upward through eddy-viscosity, has a negligible effect on the velocity of the wind as it responds to the pressure gradient. At this height the pressure gradient is said to be dynamically balanced against two components arising from centrifugal force, one due to the rotation of the earth and the other due to the curvature of the wind path. The wind velocity computed on this basis is called the "gradient wind." If the curvature of the wind path is neglected it is called the "geostrophic wind," which is sometimes referred to as the first approximation to the gradient wind.[2]

Theory of Wind Velocity Versus Height

The factors entering into the variation of wind velocity with height are the pressure gradient, the coefficient of eddy viscosity of the air, the mass density of the air ρ, the angular velocity of the earth's rotation, the geographic latitude at which observations are made, and the curvature of the wind path. This is on the usual assumption that the eddy viscosity does not change with the height due to different degrees of vertical mixing at different heights. The relation between these factors has been expressed by Horace Lamb[3] and G. I. Taylor.[4] The equations derived by Mr. Taylor have been discussed at length by W. Watters Pagon,[5] M. ASCE.

The equations developed by V. W. Ekman,[6] originally applied to ocean drift, may be used to construct a graphical representation of this relation. W. J. Humphreys[7] states the matter thus:

> "Ekman assumed a straightaway wind blowing over an initially quiet body of water of great extent and considerable depth, and found what would be the resulting movements of the water on the attainment of a steady state."

By inverting the system of coordinates, it is possible to find the resulting movements within a body of air relative to which the underlying water, or land, is apparently moving. It can be shown that the relation between wind velocity and height is represented graphically by an equiangular (logarithmic) spiral, if the velocity vectors are projected onto the surface plane, as shown in

---

[2] "Physical and Dynamical Meteorology," by D. Brunt, Cambridge Univ. Press, Cambridge, England, 1941, pp. 189–190.

[3] "Hydrodynamics," by Horace Lamb, 5th Ed., Cambridge Univ. Press, Cambridge, England, 1924, p. 655.

[4] "Eddy Motion in the Atmosphere," by G. I. Taylor, *Philosophical Transactions*, Royal Soc. of London, England, Series A, Vol. 215, 1915, p. 14.

[5] "Wind Velocity in Relation to Height Above Ground," by Watters Pagon, *Engineering News-Record*, Vol. 114, 1935, pp. 742–745.

[6] "On the Influence of the Earth's Rotation on Ocean Currents," by V. W. Ekman, *Arkiv för matematik, astronomi ocn fysik*, Stockholm, Sweden, 1905.

[7] "Physics of the Air," by W. J. Humphreys, 3rd Ed., McGraw-Hill Book Co., Inc., New York, N. Y., 1940, p. 128.

Fig. 1. In 1934, P. O. Huss, at the University of Michigan, Ann Arbor, Mich., found that this spiral also represents the relations as given by Messrs. Lamb and Taylor, since all three equations can be reduced to the same form.

In Fig. 1 the velocity of the surface wind is given in magnitude and direction by the vector AB; that of the gradient wind by AC; and that of the drift wind by their vectorial difference, BC. The velocity of the wind at any intermediate height z is given by the vector AD and the drift wind by

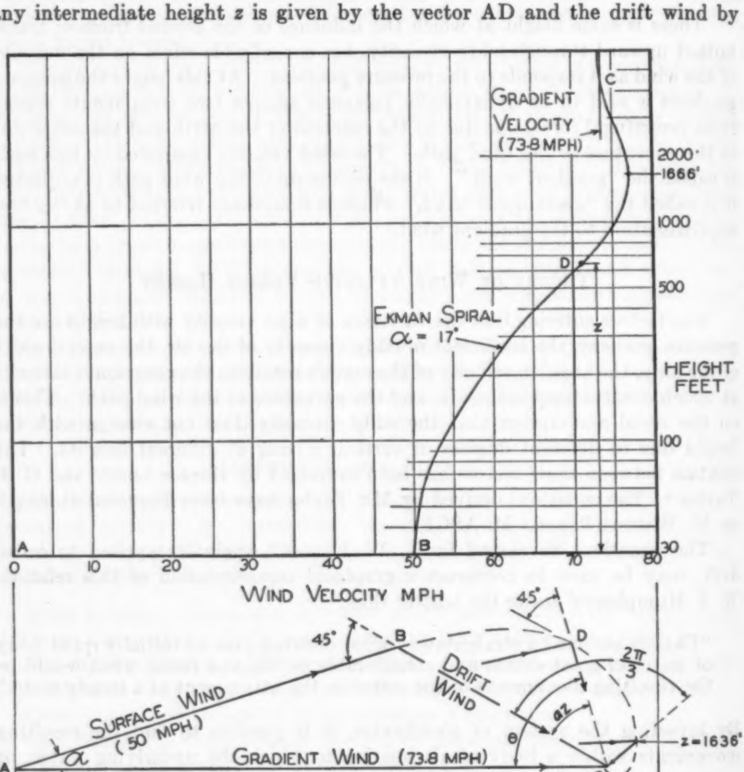

FIG. 1.—THEORETICAL VARIATION OF WIND VELOCITY WITH HEIGHT ACCORDING TO THE EKMAN SPIRAL

DC. The angle between the surface wind, and its vectorial difference from the gradient wind (drift wind), is always 45° regardless of the value of α, the angle between the surface wind and the gradient wind. Since the vector AD gives the velocity at height z it is necessary to establish the point D on the spiral in order to obtain the velocity. The velocity may be obtained by letting $\theta = 45° - \alpha + a\,z$. There are then two unknown quantities, α and a. Mr. Humphreys makes use of the assumption that the wind velocity reaches a maximum at 500 m (1666 ft) and accordingly chooses the value $a\,z = \frac{2\pi}{3}$

at that height; whence $a = \frac{2\pi}{5{,}000 \text{ ft}}$. There remains then the necessity of finding the value of α experimentally by observations during periods of strong winds.

In fitting the spiral to any set of experimental data it is necessary to choose (1) some point through which to pass the spiral at an assumed maximum value of the vector AD, as explained in the previous paragraph; and (2) an effective ground height as the value of $z = 0$ at point A, Fig. 1. The latter should be chosen at least high enough to escape the effects of small local units of roughness. The angle, α, of the spiral and its position are then chosen by trial to give the best fit to the observed points showing the relation between wind velocity and height, as in Fig. 2. The velocity at which the spiral reaches the gradient level is thus fixed automatically for each fitted spiral.

Observations during a winter storm will show that the direction of the gradient wind, as indicated by the direction of cloud movement, differs from the wind direction at the surface by a considerable angle, usually about 20° or less, but sometimes amounting to as much as 180° at the time of the wind-shift as a warm front or cold front is passing.

Storm Observations

The number of controlled experiments made for the purpose of studying the relation between wind velocity and height in open country has been very small, because of the great expense involved. On one such project[8] observations during winter wind storms were conducted over a period of seven years, and during the later phases of the project a steel tower 250 ft high was erected with a number of specially designed anemometers mounted on it. During some of the storms the spacing of the anemometers along the tower was 25 ft and the anemometers and recording oscillograph were adjusted for reading wind velocities for intervals as short as one-quarter second. The storm that was selected as being sufficiently representative to justify intensive study, and for which an unusually adequate amount of coincidental meteorological information was available, occurred on January 19, 1933. The experimental equipment for recording this storm has been reported elsewhere[9, 10, 11] together with some of the results.

Fig. 12, introduced subsequently, is a wind map showing the turbulent nature of the flow during a part of a typical run. The numbers at the bottom denote seconds, and it will be seen that this map includes a period of 39 sec; that is, seconds 210 to 249 of Run No. 026. The numbers within the map are the velocity readings in miles per hour, averaged over 0.25 sec at each station on the tower. The vertical distance between anemometer stations was either 25 ft or 50 ft. Iso-velocity contours were drawn so that a given contour line

---

[8] "Storm Loading and Strength of Wood Pole Lines and Study of Wind Gusts," by R. H. Sherlock, M. B. Stout, W. G. Dow, J. S. Gault, and R. S. Swinton, Edison Electric Institute, 1936.

[9] "Wind Structure in Winter Storms," by R. H. Sherlock and M. B. Stout, *Journal of the Aeronautical Sciences*, Vol. 5, 1937, pp. 53–61.

[10] "The Relation Between Wind Velocity and Height During a Winter Storm," by R. H. Sherlock and M. B. Stout, *Proceedings*, Fifth International Cong. for Applied Mechanics, 1938, p. 436.

[11] "An Anemometer for a Study of Wind Gusts," by R. H. Sherlock and M. B. Stout, *Engineering Research Bulletin No. 20*, Univ. of Michigan, Ann Arbor, Mich., May, 1931.

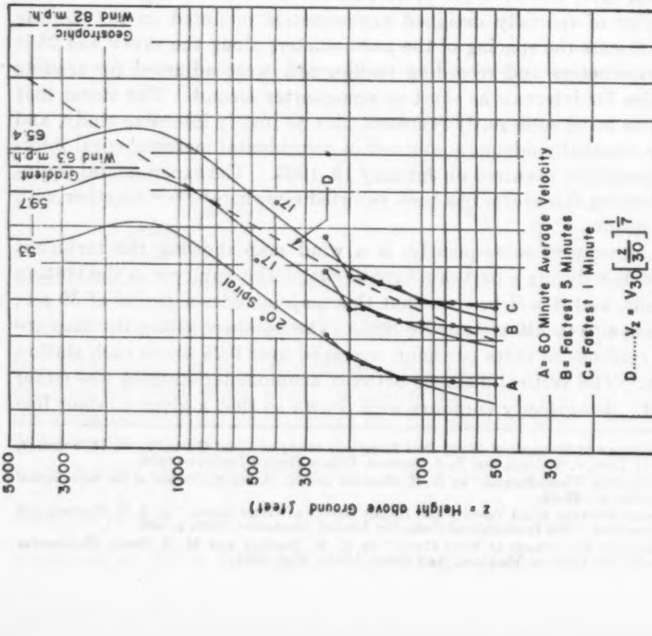

FIG. 2.—EKMAN SPIRALS FITTED TO OBSERVED WIND VELOCITIES AND COMPARED WITH COMPUTED GRADIENT WIND

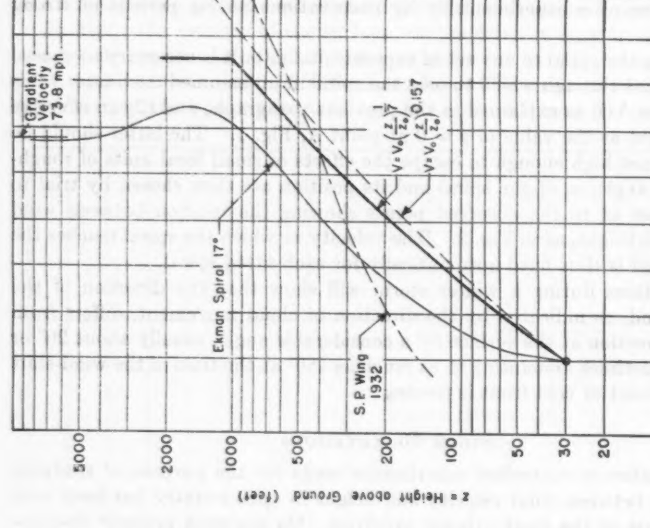

FIG. 3.—THREE CURVES COMPARED WITH AN EKMAN SPIRAL

always passes through the same velocity number. Where the contours are close together the velocity is changing rapidly.

In Fig. 2, three sets of data from this storm have been plotted. They show, respectively, the fastest one-minute velocity (Curve C), the fastest 5-min velocity (Curve B), and, finally, the fastest 60-min velocity (Curve A) within which the two shorter periods occurred. Also shown are the computed values of gradient wind and geostrophic wind.

Fortnuatley, the most intense part of the storm occurred about noon. At this time a large number of airports reported meteorological observations to the U. S. Weather Bureau. It was possible, therefore, to obtain these reports and to construct a weather map from which the pressure gradient and the curvature of the isobars could be determined. By assuming that the wind direction followed the isobars it was possible to compute the velocity of the gradient wind. There were then available two sets of independent observations, one being the variation of wind velocity with height as determined by measurements on the 250-ft tower, and the other being the computed coincidental gradient velocity. These were then used to test the validity of the Ekman spiral, and its associated theory, in representing actual conditions in the free-flowing air in fairly level, open country, during a wind storm.

The position and slope of the fitted spiral were determined primarily by those points on the tower which were above the influence of the ground topography. There was a slope of about 175 ft in 4½ miles to the southwest, which is the direction from which the wind was blowing. This 4% slope to the windward side of the tower gave an increased velocity to the lower layers of the wind. The curves show that the ground effect extended approximately to the 100-ft level and that the velocities at the 50-ft and 75-ft levels were from 1 to 2½ miles per hr higher than the fitted spiral.

At the two highest stations irregularities occurred in the 1-min and 5-min data. These have been shown[12] to depend upon temporary channels of high velocity which maintain themselves for 10 sec or 15 sec, and at times even for 1 min, and which tended to recur at the same height.

The five upper stations of the 60-min curve, however, deviated from the wind spiral by only a fraction of 1 mile per hr, whereas at the gradient level the fitted spiral was 10 miles per hr below the gradient level. It should be remembered that the pressure gradient may be changing at any given location, as the low-pressure area is passing; also, that there are local deviations not usually shown on the small-scale synoptic charts of the U. S. Weather Bureau. Therefore, it would not be surprising, if, over a period of 60 min, the average pressure gradient at this location should have changed so as to decrease the average gradient velocity from 63 to 53 miles per hr.

The fastest 1-min velocity occurred within two or three minutes of the noon hour at which the barometer readings were taken at the various airports. It would be expected that there would be better agreement between the fitted spiral and the gradient velocity for this 1 min than for the 60-min period, provided that it is assumed that the 1-min interval is a sufficiently long period of

[12] "Gust Factors for the Design of Buildings," by R. H. Sherlock, International Assn. for Bridge and Structural Eng. Publications, Zurich, Switzerland, Vol. 8, 1947, p. 209.

time for establishing compatible values between velocity and pressure gradients throughout the full depth of atmosphere below the gradient level. The average velocity within this depth was approximately 60 miles per hr and, therefore, this interval measured the passage of approximately one mile of wind. This mass of moving air, therefore, was between two and three times as long as it was deep. A closer agreement could have been obtained by giving greater weight to the five readings from 100 ft to 200 ft and less weight to the reading at 250 ft. This approach might have been justified on the grounds that the high velocity exhibited at the 250-ft level is the result of one or more of the transient "jets" previously referred to as "temporary channels." Such jets would have required a spiral of about 18° instead of 17°.

The deviations of the 5-min spiral are greater than those of the 1-min spiral. The points on the tower show less regularity, and if the same argument were used for underweighting the point at the 250-ft level, an 18° spiral could have been justified instead of the 17° spiral. This would have resulted in a still greater difference at the gradient level. However, it was felt that the points at the 200-ft and 250-ft levels should be given their full values in fitting the spiral, and this was done.

It has been seen that the computed gradient wind is about midway between the spirals for the fastest 5 min and the fastest 1 min, whereas the geostrophic wind is far faster than the fitted curves. This indicates that the curvature of the wind path, which was ignored in computing the geostrophic wind, contributed an important component to the dynamic balance. When it is considered that the curvature of the wind path was estimated from the curvature of the isobars, the fit between the spiral and the two sets of independent observations (anemometer readings and computed gradient wind) must be said to be very good indeed. The curvature of the isobars would normally be less than the curvature of the wind path and, therefore, the computed gradient wind is the lowest reasonable value. A higher value would give a better fit to the 17° curve for the fastest 1 min.

This is only one storm; but it is a typical storm, for which the coincidental meteorological characteristics[13] might well serve as textbook material illustrating severe storms in the United States. The conclusions which may be drawn from these observations are:

1. The theory expounded by Mr. Taylor[4] and others fits the experimental data for this fairly intense winter storm very well;

2. The angle between the surface wind and the gradient wind in such a storm will lie between 17° and 20° depending upon the period of time over which the velocity is averaged; and

3. The curvature of the wind path supplies an important component in establishing the gradient wind, amounting in this case, if ignored, to 30% of the gradient wind.

The Seventh-Power Law

In Fig. 2 a one-seventh power curve has been drawn so as to pass through the value of 40 miles per hr at the 50-ft level. This is a slightly higher velocity

[13] "Gust Factors for the Design of Buildings," by R. H. Sherlock, International Assn. for Bridge and Structural Eng. Publications, Zurich, Switzerland, Vol. 8, 1947, Fig. 3.

than that of the fitted curve for the fastest 5 min. The slope of the power curve between the 100-ft and 200-ft levels is remarkably similar to that of the fitted spirals. In general it gives only a small deviation from the fitted spiral below the 1000-ft level. The extent of the deviation will depend upon the level at which the power curve is started. If it were made to coincide with the spiral at the 100-ft level the deviations would be smaller than those shown in the diagram, whereas if it were made to coincide at the 30-ft level the deviations would be considerably increased. If it is desired to use a power curve as an approximation to the theoretical curve, it should be used only up to about the 1000-ft or 1500-ft level above which a constant velocity should be used.

In Fig. 3 the 17° Ekman spiral has been repeated, but this time it has been passed through the point giving 50 miles per hr at a height of 30 ft, as was done in Fig. 1. This is a point sometimes used in discussing the U. S. Weather Bureau records for the fastest daily 5-min average velocity. The one-seventh power curve has been passed through this same point, and it is seen that by lowering this "effective ground level" the deviations between the spiral and the power curve have become greater than in Fig. 2. They amount to 7 miles per hr, or about 9% of the theoretical value, at the 1000-ft level.

In his discussions of the Taylor equations, Mr. Pagon[5] has used the power 0.157, as considered by Ludwig Prandtl and O. G. Tollmien, instead of 0.143 (=1/7). This curve is likewise shown, and is obviously more conservative.

U. S. Weather Bureau Data

Fig. 3 likewise shows a curve for the maximum 5-min velocity presented by S. P. Wing[14] in 1931. This curve is based on an outstanding analysis of the U. S. Weather Bureau records for Chicago, Ill., and New York, N. Y. Because of the badly dispersed nature of the records Mr. Wing considered it necessary to use statistical methods in his analysis. It is believed that his approach to an interpretation of these results was a proper one and that the only criticism that can be raised against the curve must be based on the changing conditions of exposure, the distorted pattern of flow around the buildings on which the anemometers were mounted, and the pessimistic prediction of what the wind may be expected to do above the highest elevation available in these records—454 ft. In this latter prediction Mr. Wing was influenced at least to some extent by statements attributed to W. H. Dines and C. F. Marvin, that the wind doubled at from 1000 ft to 1500 ft above the ground. The curves proposed by Mr. Wing for the variation of 5-min velocities with height must be looked upon as ultra-conservative, but as being probably the best available analysis of the Weather Bureau records as they bear upon the question of the variation of wind velocity with height.

Gust Factors

Before the wind pressures acting on a structure can be determined it is necessary to select the maximum wind velocity that is proper for the locality and for the size and exposure of the structure. This is the design velocity.

[14] "Wind-Bracing in Steel Buildings," Second Progress Report of Sub-Committee No. 31, Committee on Steel of the Structural Division; Discussion by S. P. Wing, *Proceedings*, ASCE, August, 1932, p. 1103.

It must include an allowance for gusts which are of relatively short duration but which are of sufficient extent to envelop the structure and to permit the resulting aerodynamic pressures to develop on all sides of the structure.

The Weather Bureau records contain very little on the subject of gusts since its reports are based on 5-min average velocities. The fastest mile of passing wind can be read from the records, but this is of only limited usefulness since, in a gale, it corresponds to a period of about 1 min during which several strong fluctuations may occur. Also, the fastest mile of wind is difficult to read accurately from the type of record used in the Weather Bureau. It is necessary to supplement the Weather Bureau records of 5-min average velocity, therefore, by studies of gustiness in records from other sources.

Gustiness is accompanied by so many variations of velocity, temperature, and humidity that no comprehensive theory exists as to why it arises or how it proceeds.[15] However, it may safely be assumed that gusts are caused chiefly by the growth of eddies, local pressure differences, deflection around objects, vertical thermodynamic interchange, and by combinations of these causes. The most important cause is unquestionably vertical interchange due to thermal instability. This phenomenon is well known and has been studied extensively.[16]

When a cold air mass moves over ground that has previously been covered by a warm air mass, or when a warm air mass is overrun by a cold air mass, the temperature lapse rate is changed so that the conditions necessary for thermodynamic stability are altered. Usually, but not always, the highest velocities and the most violent gusts occur within the southwest quadrant of the low-pressure area, that is, while the highly turbulent and unstable front portion of the cold air mass is passing. In this zone of transition there is a condition of thermal instability which permits occasional and sometimes violent interchanges between the higher and lower strata. Large gusts occur near the ground because masses of air from the more rapidly moving higher strata reach the ground before losing all of their excess forward momentum. Gusts from this source may be of a violence limited only by the kinetic energy present in the high strata.

Near the ground the wind is unable to respond fully to the pressure-gradient because of friction. This retarding effect is transmitted upward through the medium of eddy-viscosity—that is, through the resistance to free laminar flow that is provided by the transverse components of motion in the eddies. However, there is some height at which the effect of ground friction is negligible, and where the air is free to respond to the pressure gradient without this retarding effect. As the warm air at the lower levels is forced upward by the heavier cold air it must be replaced by the colder, fast moving air from above. If the masses of air involved in this interchange are sufficiently large, the retardation produced upon the falling mass of air, through eddy viscosity and collision with slower moving masses, may be so small that the descending mass loses only a small part of its velocity before reaching the lower strata, and a violent gust occurs.

---

[15] "Physical and Dynamical Meteorology," by D. Brunt, Cambridge Univ. Press, Cambridge, England, 1941, p. 212.

[16] "Weather Analysis and Forecasting," by S. Pettersen, McGraw-Hill Book Co., Inc., New York, N. Y., 1940, p. 11.

The vertical speed with which this increased velocity travels downward has been shown by the wind maps to have been about 40 ft per sec, that is, about 27 miles per hr[17] in one case, and about 14 ft per sec in another.[18] These observations were on the 250-ft tower. This effect could be produced through shear between horizontal layers or through vertical displacement, as described, or through a combination of these two means. At any rate this effect of increasing velocity through falling masses of rapidly moving air have been shown to reach the ground within a few seconds after first appearing at the 250-ft level; or, to descend to a level of 200 ft or 250 ft and then to recede without having reached the ground; or to have receded and then resumed the descent within 3 sec.[18]

The rate of change of wind velocity with height has been shown to be very great during periods of temperature inversions.[19] However, such inversions do not occur in conjunction with steep pressure-gradients and, consequently, with high gradient-velocities. During those storms when high velocities occur the vertical mixing is so active as to destroy any possibility of the stability required for temperature inversion. The inversions usually occur when a warm air mass moves over ground that has previously been covered by a cold air mass, or when a warm air mass overruns a cold air mass, and this creates a condition favorable to stability and unfavorable to the gustiness of vertical interchange.

Gust factors are referred to the 5-min average velocity in this paper because that is the principal unit used in the long-time records of the U. S. Weather Bureau. The gusts that occur within such a period may have any duration up to 5 min; that is, 300 sec. The gust factor, within any 5-min interval, is defined as the ratio of the fastest gust velocity to the 5-min average velocity. Within a storm there will be 5-min intervals of many different velocities and these will be distributed in accordance with some statistical law. That 5-min interval which has the highest velocity may be looked upon as a gust within the storm. Its average velocity will approach, and through deflections may actually exceed, that which could be expected from the spiral fitted to the computed gradient velocity. It is not to be expected, then, that the gust factors in the fastest 5-min interval for a given storm will be as great as within a 5-min interval of lesser velocity.

This phenomenon is shown in Fig. 4, which is taken from a report of gustiness during the same storm for which the characteristics of the Ekman spiral were previously discussed.[20] Each point is for a particular 5-min interval whose velocity is expressed in units equal to the average velocity of the storm sample. A Pearson Type III statistical curve was used to establish an envelope for each set of points. It appears that the gust factors that occurred within the storm were greatest for those 5-min intervals which had approximately the

---

[17] "Picturing the Structure of the Wind," by R. H. Sherlock and M. B. Stout, *Civil Engineering*, June, 1932, p. 361.

[18] "Wind Structure in Winter Storms," by R. H. Sherlock and M. B. Stout, *Journal of the Aeronautical Sciences*, Vol. 5, 1937, Fig. 10.

[19] "Wind Structure Near the Ground and its Relation to Temperature Gradient," by G. S. P. Heywood, *Quarterly Journal*, Royal Meteorological Soc., Vol. 57, 1931, p. 433.

[20] "Gust Factors for the Design of Buildings," by R. H. Sherlock, International Assn. for Bridge and Structural Eng. Publications, Zurich, Switzerland, Vol. 8, 1947, Fig. 15.

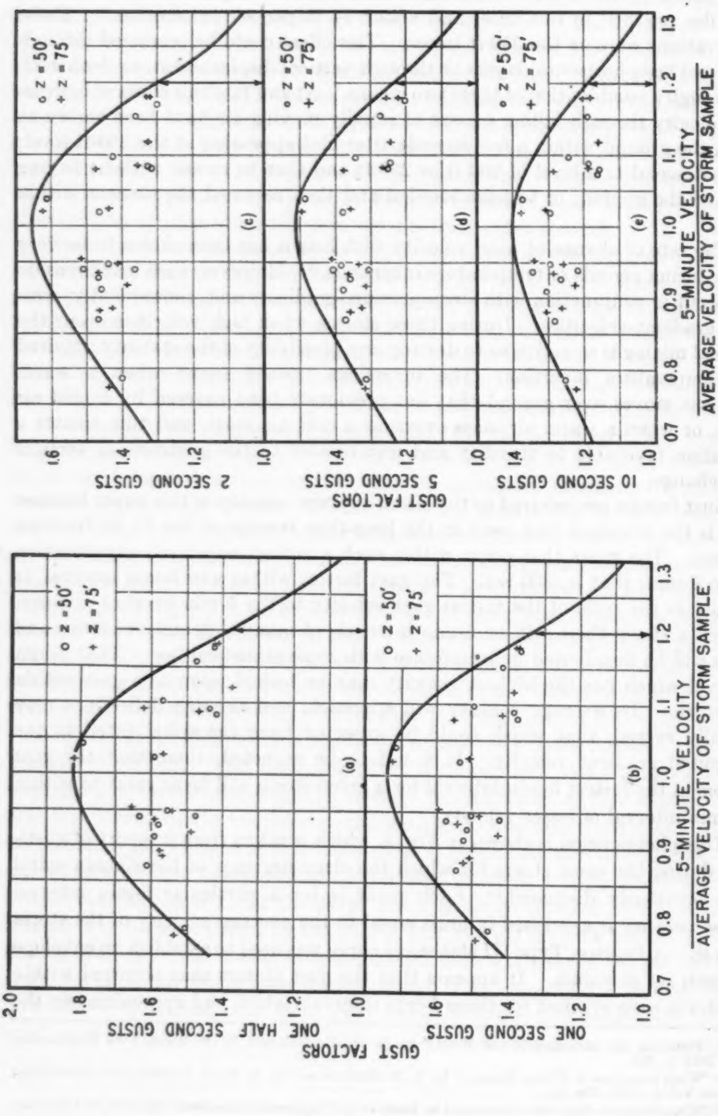

Fig. 4.—Envelopes for Observed Gust Factors of Various Gust Durations

average velocity of the storm, and were lowest for those 5-min intervals which approached the maximum for the storm. It is important to note that no 5-min velocity exceeded the storm average by more than 20%, and, as would be expected, that the gust factors were largest for the shortest gust period.

Fig. 5 illustrates a different method of showing the variation of gustiness with height. Here a total of fourteen 5-min intervals have been separated into three groups. Group 1 represents the average of six 5-min intervals for a total of 30 min. Groups 2 and 3 represent the averages of four 5-min intervals for a total of 20 min each.

Fig. 5(a) shows that Group 1 has the highest velocities, Group 2 intermediate velocities, and Group 3 the lowest velocities except at the 200-ft level. Fig. 5(b) shows the increments ΔV_5 that were added to the 5-min veloc-

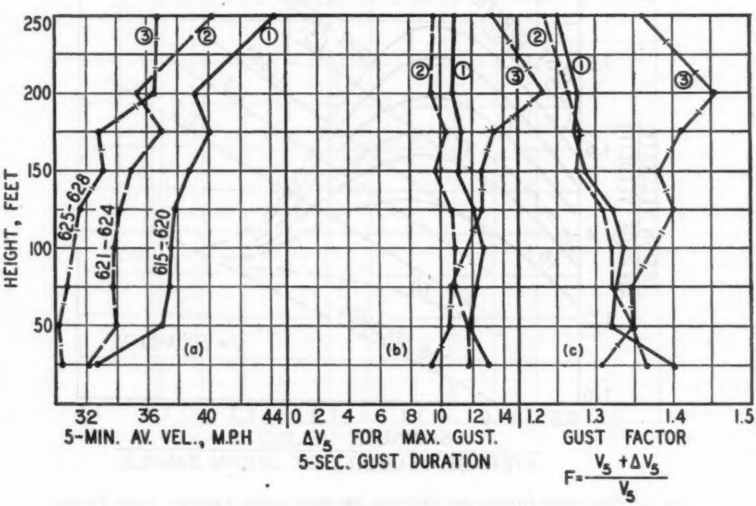

FIG. 5.—WIND VELOCITIES AND GUST FACTORS OBSERVED ON THE 250-FT TOWER

ities by the gusts of these three groups; 5-sec gusts are used for purpose of illustration. The maximum 5-sec gust was chosen for each 5-min interval and the average of all such gusts was taken for each group of intervals at each elevation. At the upper stations of the tower the largest gusts are those which occur with the lowest 5-min velocities, that is, in Group 3. In Fig. 5(*c*) are plotted the gust factors—

$$F = \frac{V_5 + \Delta V_5}{V_5} \qquad (1)$$

—for the same three groups, again computed for each 5-min interval and averaged for each group at each elevation. At all except the 25-ft elevation the largest gust factors accompany the lowest 5-min velocities.

The design velocity that must eventually be chosen will be equal, in each case, to a 5-min velocity multiplied by the proper gust factor. Therefore, the question must be answered:

> "Will the lower five-minute velocities with high gust factors ever produce a higher design velocity than that which is obtained by taking the highest five-minute velocity on record and applying to it a lower gust factor?"

Before answering this question it should be noted that, for the higher V_5-velocities (in miles per hour), ΔV_5 decreases only slightly with height, whereas V_5 increases rapidly with height. This means that the decrease in gust factors with height, which has such an important part in later discussions, is due mostly

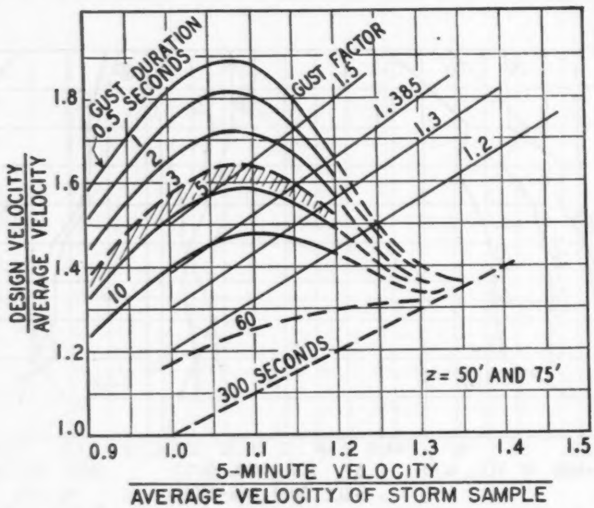

FIG. 6.—NOMOGRAM GIVING THE RELATION BETWEEN 5-MIN VELOCITY, GUST FACTOR, GUST DURATION, AND DESIGN VELOCITY (z = 50 FT AND 75 FT)

to the increasing values of V_5 rather than to the decreasing values of ΔV_5. There is a fundamental difference in interest, therefore, between the areonautical designer and the structural designer. To the former the magnitude of the gust in miles per hour is usually most important, and to the latter the most important consideration is its percentage of the steady wind to which it must be added.

In Fig. 6 the envelopes for the data in Fig. 4 have been replotted in such a way as to answer this question:

> "Which gives the higher design velocity, a high 5-min velocity with a small gust factor or a low 5-min velocity with a large gust factor?"

Since the relation between the gust factor and the 5-min average velocity depends on the position of the 5-min interval within the storm, it was decided

to use the average velocity of the storm sample as the unit of velocity. In other words, the 5-min velocity is divided by the average of the storm sample to obtain the 5-min velocity in storm units. The design velocity is plotted vertically and the 5-min velocity horizontally. Here the curves have been shown as solid lines up to a value of 1.2 for the V_5-velocity, since no 5-min interval during this storm exhibited a higher velocity. Diagonal lines are drawn to show the relation between the V_5-velocity, the gust factor F, and the design velocity.

It is readily seen that the highest design velocity does not occur either at the storm average or at the peak when $V_5 = 1.2$, except in the case of large gusts having a duration of 60 sec. In this latter case $F = 1.08$ at $V_5 = 1.2$; but at the storm average, $F = 1.17$. The corresponding design velocities,

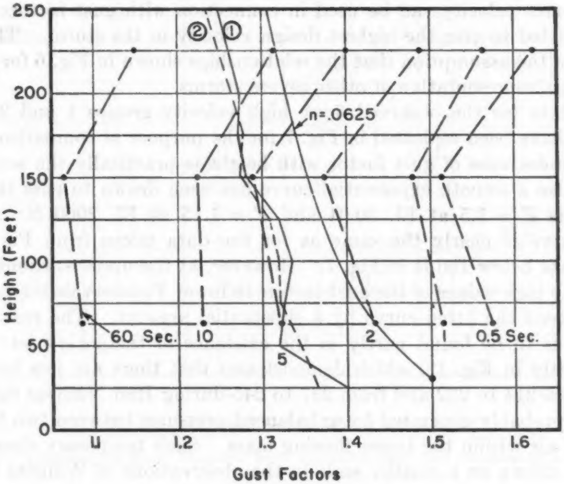

FIG. 7.—VARIATION OF GUST FACTORS WITH HEIGHT

expressed in units of the storm average, are 1.30 and 1.17, respectively. Obviously the larger design velocity will be obtained by using the highest V_5 (that is, $V_5/V_{\text{aver}} = 1.2$) with its accompanying lower gust factor in the case of 60-sec gusts. This is not always the case, however. For example, the curve for 10-sec gusts shows that the design velocity for maximum V_5 is 1.43 and for the storm average is 1.40, neither of which is the maximum. An intermediate value of V_5 gives the maximum design velocity of 1.475 with a gust factor of 1.34. The answer in this case, then, is that neither the average of the storm sample nor the maximum value of V_5 has an accompanying gust factor that gives the maximum design velocity. This condition is true for all curves shown here for gust durations of 10 sec or less.

Fig. 7 has been drawn to show the relation between gust factors and height for different gust durations from 0.5 sec to 60 sec. Dash lines are values

observed during the passage of a jet at the 225-ft level, and n is the exponent of a fitted curve. The points shown at elevation 62.5 ft are taken from Fig. 6 covering observations at 50 ft and 75 ft; those for elevation 150 ft are taken from a similar drawing covering observations at 125 ft, 150 ft, and 175 ft; and those shown at an elevation of 225 ft are from data for heights of 200 ft and 250 ft. Here the gust factors are obtained by dividing the highest design velocity by $V_5 = 1.2$ (in storm units) in order to obtain an adjusted gust factor. For example, at the elevation $z = 62.5$ ft, Fig. 6 shows that for a gust duration of 10 sec the maximum design velocity is 1.475. This occurs approximately at $V_5 = 1.1$ with a coincidental gust factor of 1.34; but the gust factor in Fig. 7 was obtained by dividing 1.475 by 1.2 instead of 1.1. This gave the adjusted gust factor of 1.23 shown in Fig. 7. This method was used for all other points in the diagram. In this manner the U. S. Weather Bureau records for the daily fastest 5-min velocity can be used in connection with gust factors that have been adjusted to give the highest design velocity in the storm. This method is valid on the assumption that the relationships shown in Fig. 6 for this storm are likewise representative of other severe storms.

The data for the observed 5-sec high velocity groups 1 and 2 shown in Fig. 5(*c*) have been replotted in Fig. 7 for the purpose of comparison. Below 150 ft the decrease of gust factor with height is practically the same in both cases. Also a smooth exponential curve has been drawn to pass through the two points $F = 1.5$ at El. 30 ft and $F = 1.15$ at El. 2000 ft. The slope of the curve is nearly the same as for the data taken from Fig. 5(*c*) and for the data below 150 ft in Fig. 7. However, at the upper stations the influence of the high values of the gust factors in lower V_5-intervals is such that the points exceed the fitted curve by a substantial amount. The reason for this variation is to be found partly in the existence of temporary jets as shown subsequently in Fig. 12, which demonstrates that there are jets lasting from Second No. 214 to 232 and from 237 to 245 during Run Number 026. These jets were probably generated by unbalanced pressures between two fairly large masses of air within the larger flowing mass. Such temporary channels have also been shown on a smaller scale in the observations of Wilhelm Schmidt.[21] It was he who first applied the expression "jets" to these phenomena.

Fig. 8 shows the variation of wind velocity with height during the passage of a jet at elevation 200 ft. A total of 30 sec is shown, divided into three periods of 10 sec each; thus (see Fig. 12, introduced subsequently):

Curve:	Shows the average of:
1	Seconds 214 to 224
2	Seconds 224 to 234
3	Seconds 236 to 246

This 32-sec period is coincident with the arrival of a gust that had been preceded by another gust whose effect had not yet disappeared entirely. The equation—

$$V \propto \left(\frac{z}{30}\right)^{0.161/2} \qquad \text{(2)}$$

[21] "Turbulence Near the Ground," by Wilhelm Schmidt, *Journal*, Royal Aeronautical Soc., London, England, May, 1935, p. 361

—which is recommended for the variation of velocity with height, including a gust factor, is representated by the heavy solid line (Curve 4). It shows that the jet at the 200-ft station establishes a velocity curve that exceeds the actual velocity at the 250-ft elevation by 7.9%, and at the 175-ft elevation by 17.9%, of the expected velocities at these points.

Since small jets of less than 1 m have been observed near the ground by Mr. Schmidt, and larger jets of 50 ft to 75 ft, with 1-min duration, and at a height of 200 ft have been observed at the University of Michigan, it is only prudent to assume that the pressure differences that gave rise to these jets can

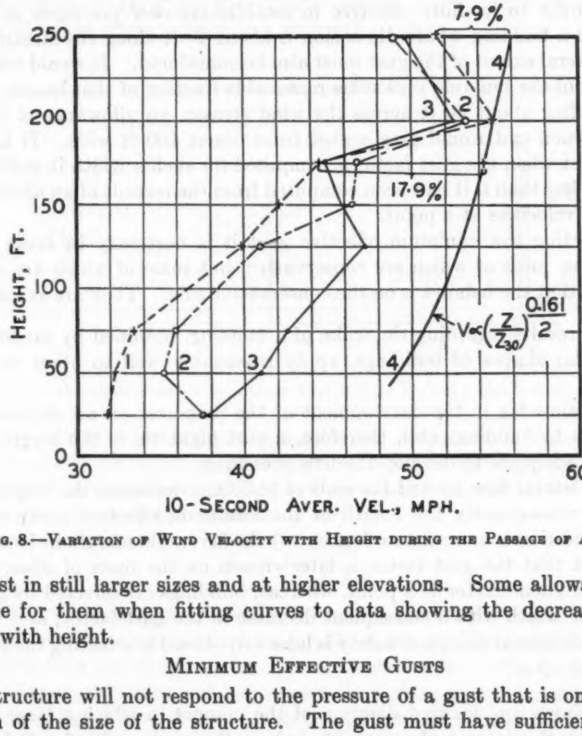

FIG. 8.—VARIATION OF WIND VELOCITY WITH HEIGHT DURING THE PASSAGE OF A JET

also exist in still larger sizes and at higher elevations. Some allowance must be made for them when fitting curves to data showing the decrease of gust factors with height.

MINIMUM EFFECTIVE GUSTS

A structure will not respond to the pressure of a gust that is only a small fraction of the size of the structure. The gust must have sufficient vertical and horizontal extent to envelop not only the structure but also those flow patterns to the windward and to the leeward which are responsible for the maximum pressures on the structure. In the case of a building, turbulence will be generated to the leeward involving a mass of air which is separated from the higher undisturbed flow by vortex layers. In front of the building, a turbulent zone is likewise formed, and it likewise is separated from the higher streamlined flow by a vortex layer. The entire flow pattern is such as to produce, within the air, a streamlined surface that offers a minimum loss of energy to the flow past the building. After the streamlined flow has been

established in the wind, there may be superimposed upon the average flow the additional velocities of a gust.

The size of the gust necessary to envelop a sufficient amount of this streamlined wind structure to transmit the corresponding changes in pressure to all sides of the building has been shown[22] to be about eight times the dimension of the building along the wind direction. This factor, eight, is based on a study of experiments[23] performed on airfoil sections. The results are adopted here because of the absence of experimental data based on sharp-edged structures, and because this procedure is believed to be conservative. Under this assumption, if a gust is traveling at 75 miles per hr it should have a duration of at least 3 sec in order to be fully effective in establishing new pressures on all the surfaces of a building whose dimension is about 40 ft along the stream.

The lateral extent of the gust must also be considered. It would need to be the length of the building plus some reasonable fraction of that length. For a small building about 50 ft across the wind stream, an allowance of half this length at each end would give a gust front about 100 ft wide. It has been shown[24] that when the gust factor is computed for such a width it will be from 3% to 8% less than if it had been computed from the records of an anemometer measuring velocities at a point.

In selecting the minimum effective gust it is necessary to make several assumptions, most of which are conservative, but some of which are not. It is believed that the balance is on the conservative side. They are as follows:

1. The results regarding the wake of a building, obtained by investigators on particular shapes of buildings, apply reasonably well to other shapes of structures;
2. The time lag in the development of the pressures on an airplane wing applies also to buildings and, therefore, a gust eight times the length of the building is adequate to develop the new pressures;
3. The lateral flow around the ends of buildings decreases the length of the wake and consequently the length of the minimum effective gust; but this adverse condition is more than offset by (*a*) the favorable margin in Item 2 and (*b*) the fact that the gust factor is later chosen on the basis of observations taken by an anemometer at a point, whereas, buildings are affected by gusts of considerable width with a consequent decrease in the gust factor; and
4. An additional margin of safety is later introduced in selecting the position of the fitted curve.

Fig. 9 shows an idealized diagram of the manner in which a large gust is generated by the descent of a mass of air from the gradient level. It has previously been mentioned that some gusts have been shown to descend with a velocity of 40 ft per sec (27 miles per hr). This descent is not uniform but is made in surges due to the unquestionably turbulent nature of the gust front.

---

[22] "Gust Factors for the Design of Buildings," by R. H. Sherlock, International Assn. for Bridge and Structural Eng. Publications, Zurich, Switzerland, Vol. 8, 1947, p. 221.

[23] Proceedings of the 3rd International Cong. for Applied Mechanics, Stockholm, Sweden, 1930, p. 329, Fig. 8.

[24] "Gust Factors for the Design of Buildings," by R. H. Sherlock, International Assn. for Bridge and Structural Eng. Publications, Zurich, Switzerland, Vol. 8, 1947, p. 220.

If it is desired to envelop the entire depth of a tall structure, such as a modern tower building, the gust would have to be of such duration that it would have proceeded at least six times the size of the building downwind from its windward face.

During the time that the minimum effective gust is being developed at the lower part of the building the gust at the top of a building 1000 ft high would have been blowing for considerably more than 30 sec. The probability that the entire height of such a tall building would be simultaneously subject to the maximum 10-sec gust is very remote. Therefore, if the 10-sec gust is taken for purpose of establishing the design velocity there would be a statistical margin of safety when applied to a very tall structure.

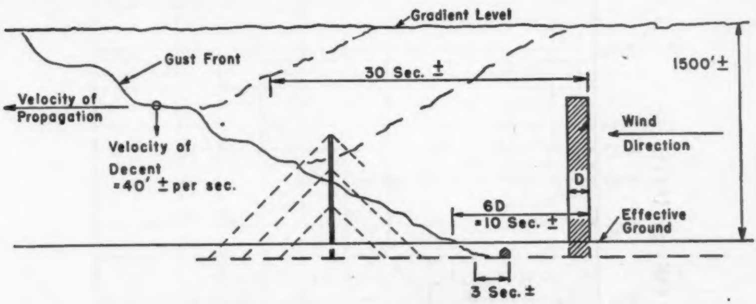

FIG. 9.—IDEALIZED PASSAGE OF A GUST PAST A HIGH BUILDING AND A GUYED TOWER

The 10-sec gust is hereby adopted for the purpose of this paper, and the corresponding gust factor is taken at $F = 1.5$ for an elevation of 30 ft and at $F = 1.15$ at an elevation of 2000 ft. The variation of gust factors with height is thus established by the equation

$$F_z = F_{30}\left(\frac{30}{z}\right)^{0.0625} \qquad \text{(3)}$$

In Fig. 7 the adopted variation of gust factors with height is shown for comparison with the data taken on the 250-ft tower. It is seen that: (*a*) Such a curve is very nearly parallel to the lines plotted from Fig. 5 based on high 5-min average velocities and 5-sec gusts; (*b*) it gives an ample margin of safety for the usual gust factors found with the adopted 10-sec gusts; (*c*) it makes an allowance for the occasional appearance of the jets which were principally responsible for the high gust factors shown at El. 225; (*d*) it gives gust factors larger than those required for the 3-sec gusts that will be necessary to envelop buildings of less than 100 ft in height; and (*e*) for very large structures, which might require gusts of from 10 sec to 60 sec, there is an ample margin of safety.

DESIGN PRESSURE

The design pressure will always be equal to some shape factor multiplied by the velocity pressure. The ASCE Structural Division Committee on Wind

Forces is currently preparing recommendations regarding the velocity pressures to be used near the ground for different parts of the United States. Therefore, it seems reasonable to express the recommendation for the variation of design pressures with height in terms of those velocity pressures which are to be adopted for use near the ground in open country. In this way, if the standard of reference is that which would prevail in open, level country, each designer can make whatever adjustments seem advisable to evaluate such influences as local shielding and unusual topography.

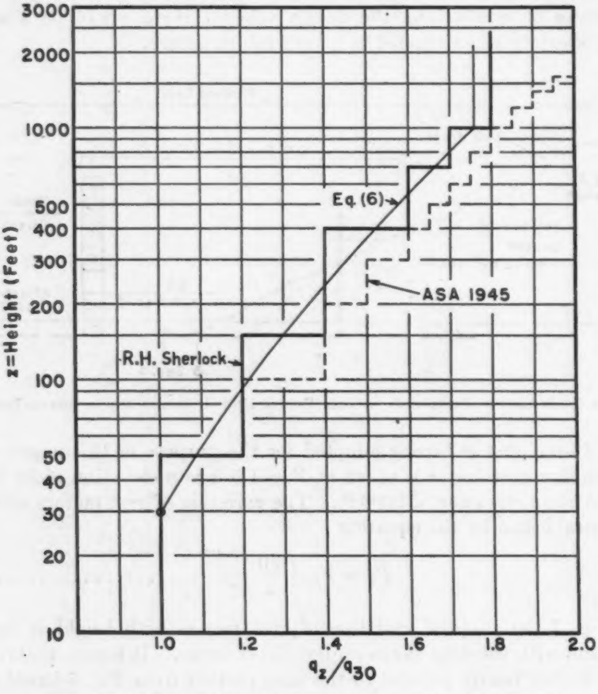

FIG. 10.—VARIATION OF DESIGN VELOCITY PRESSURE WITH HEIGHT

The relation between design pressure f, shape factor C, mass air density ρ, and wind velocity V is as follows (in pounds per square foot):

$$f = C\left(\frac{\rho V^2}{2}\right) = C\,q \qquad (4)$$

in which the velocity pressure q is expressed as:

$$q = \frac{\rho V^2}{2} \qquad (5)$$

If V_z and V_{30} are the maximum 5-min velocities at heights z and 30 ft, respectively, and if F_z and F_{30} are the corresponding gust factors:

$$\frac{q_z}{q_{30}} = \frac{\frac{1}{2}\rho V_z^2}{\frac{1}{2}\rho V_{30}^2} = \left(\frac{V_z F_z}{V_{30} F_{30}}\right)^2 = \left[\left(\frac{Z}{30}\right)^{1/7}\left(\frac{Z}{30}\right)^{-0.0625}\right]^2 = \left(\frac{Z}{30}\right)^{0.161} \quad (6)$$

Eq. 6 is valid up to $z = 1000$ ft, above which a constant value of q is to be used; that is:

$$q_z = q_{1000} \quad (7)$$

It will be seen that Eq. 6 includes the variation of both the velocity with height and the gust factor with height. It is represented in Fig. 10 by a curve, to which a stepped approximation is fitted as the recommendation of this paper

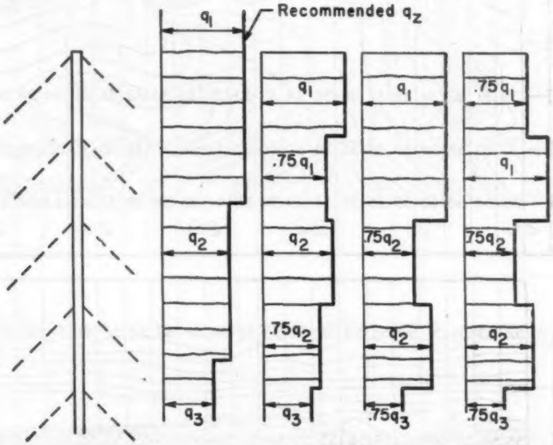

FIG. 11.—WIND LOADING VARIATIONS TO PRODUCE MAXIMUM MOMENTS AND SHEARS IN A GUYED TOWER

for the variation of velocity pressure with height. The stepped recommendations of the "American Standard Minimum Design Loads in Buildings and Other Structures" (ASA-A58.1-1945) are shown for comparison. The differences are chiefly that, in this paper (*a*) above 100 ft the velocity pressures are less; (*b*) fewer steps are used; and (*c*) a constant velocity pressure is used above 1000 ft.

GUYED TOWERS

Because of the presence of the jet type of gusts, and because the spans between the upper guys may be loaded with gusts that have not yet reached the lower spans, it is essential that deviations from the recommended variation of gust velocities with height should be taken into consideration in this type of structure. It is recommended that the velocity pressures shown in Fig. 10 should be reduced by 25% in that guyed span of a tower which would result in larger moments or shears in that span or any other span. This is shown dia-

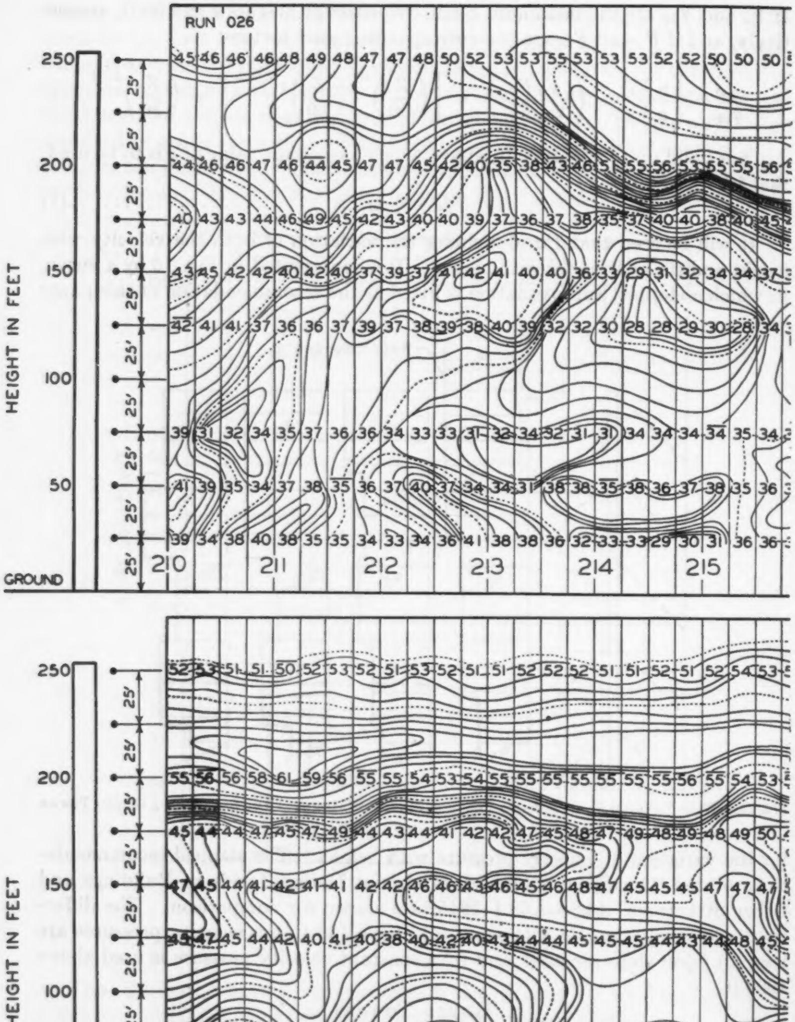

FIG. 12.—WIND MAP FOR PART OF RUN

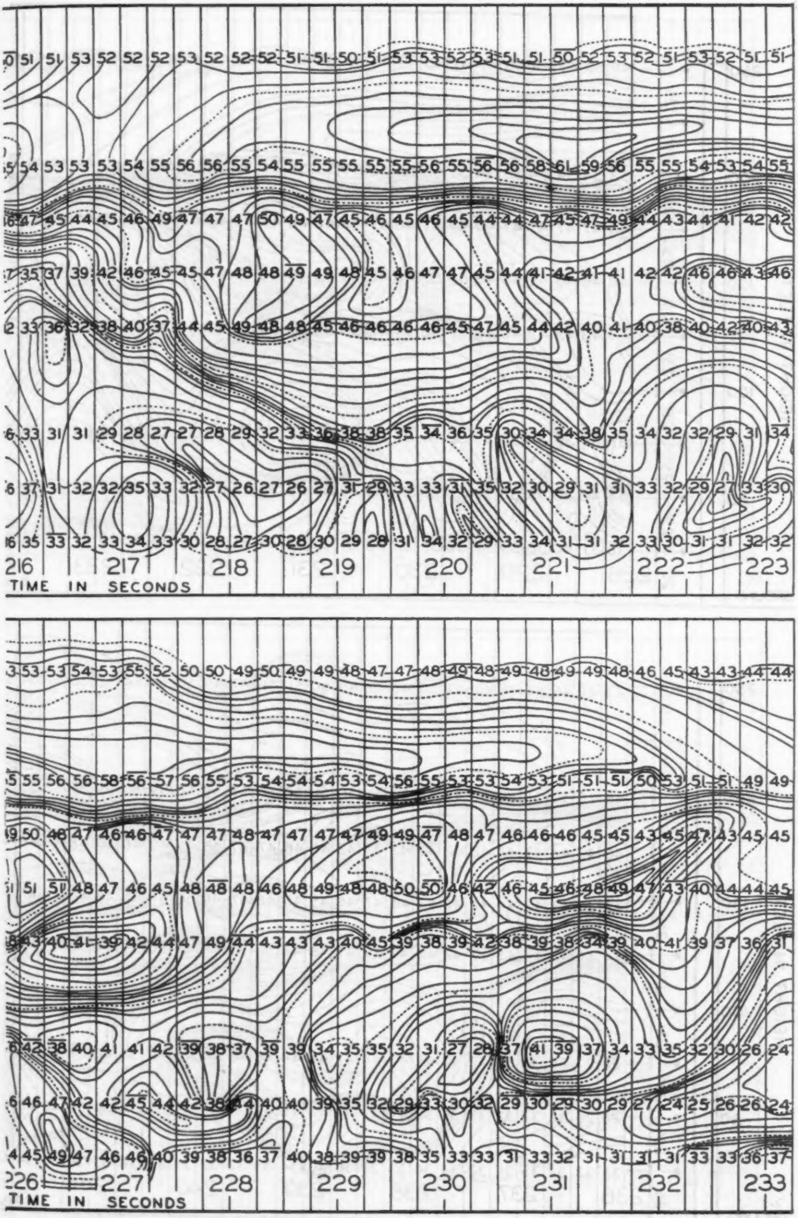

026, Study of Wood Pole Lines.

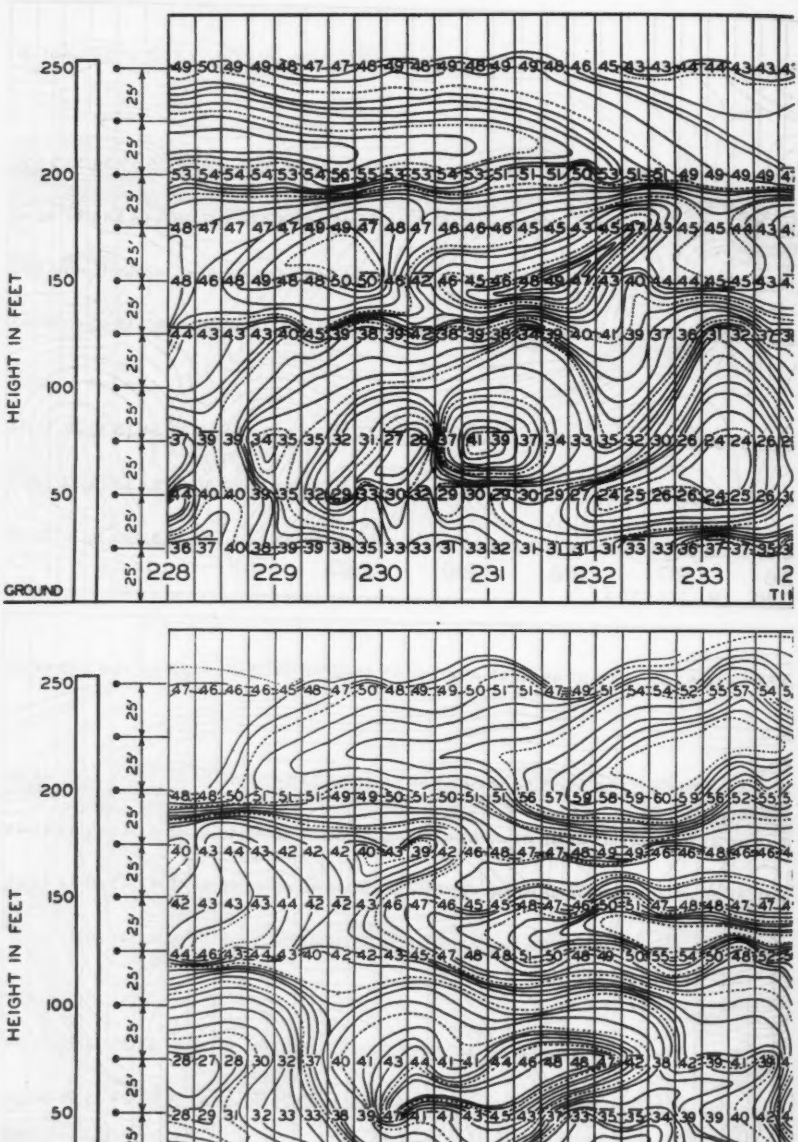
HEIGHT IN FEET
250
200
150
100
50
GROUND
25'
228
229
230
231
232
233
HEIGHT IN FEET
250
200
150
100
50
GROUND
25'
236
237
238
239
240
241

FIG. 12.—

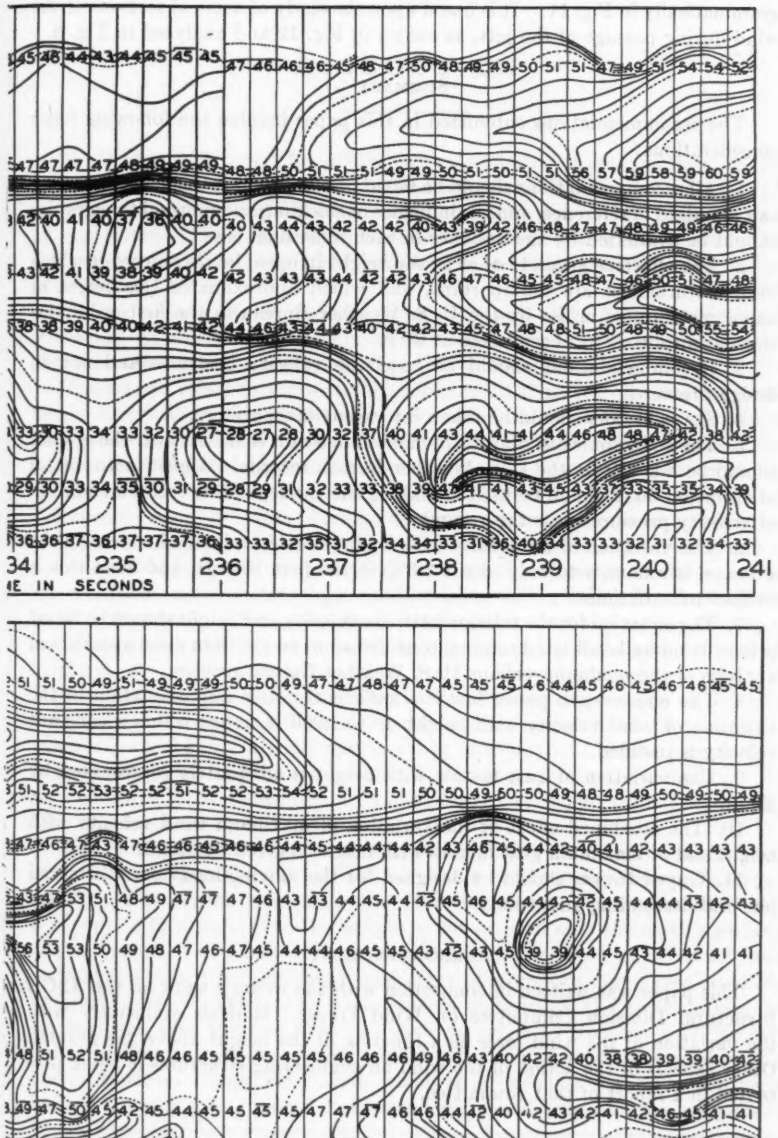
34 235 236 237 238 239 240 241
IE IN SECONDS
42 243 244 245 246 247 248 249
IE IN SECONDS

Continued

grammatically in Fig. 11. It is based upon the study of vertical sections of the wind during passage of the jets, as shown in Fig. 12 and analyzed in Fig. 8.

Summary

The recommendations submitted in this paper involve the following basic considerations:

1. All recommendations should be based on conditions in open, level country as a standard of reference, and the influence of shielding and unusual topography should be evaluated by the designer in each individual case.
2. The effective ground—that is, the height in open, level country at which local disturbances are unimportant, and which approximates the height of anemometers now in use by the U. S. Weather Bureau in the first-order stations at airports—has been taken at 30 ft.
3. Recommendations should be based on velocity pressures and not on design pressures.
4. Shape factors should be taken into account separately.
5. The geographic distribution of maximum 5-min velocities near the ground should be taken from the U. S. Weather Bureau records. A gust factor of 1.5 at elevation 30 ft should be used in making the corresponding recommendation of velocity pressures near the ground.
6. The variation of air density with height should be ignored, since, on the average, it amounts to only about 3.3% in the first 1000 ft, and even this is subject to variations.
7. The equation for the relation between velocity and height should be based primarily on well-validated rational considerations rather than upon a statistical analysis of the nonhomogeneous U. S. Weather Bureau records.
8. The one-seventh power law is a sufficiently close approximation to the variation of wind velocity with height up to 1,000 ft, above which a constant velocity is justified.
9. The variation of gust factors with height is adequately represented by Eq. 3.
10. The combined effect of the variation of maximum wind velocity with height and of maximum gust factors with height is given by Eq. 6.
11. Guyed towers should be designed for the moving-load effects of aerial jets and descending gust fronts.

Acknowledgment

This paper was written in connection with the writer's work on the ASCE Structural Division Committee on Wind Forces. It deals exclusively with the variation of the wind force as a function of the height above the ground. Other aspects of the action of the wind on engineering structures is being presented in a report of that committee.

DISCUSSION

W. Watters Pagon,[25] M. ASCE.—A vast number of detailed data on the storm depicted—and on other storms that have been recorded over a period of more than 16 years—have been collected and analyzed by Mr. Sherlock and his associates. The data and the author's analyses are of great value to the engineering profession, and Mr. Sherlock is to be highly complimented on his contribution.

The writer is in accord with the views expressed. The few comments that follow are intended to interpolate a few items of correlative interest and to give a somewhat more geographical breadth to the subject.

The author refers to the writer's use of the 0.157 power for variation with height rather than the 0.143 power (see under the heading, "The Seventh-Power Law"). There is really little choice between these two figures because in the literature on the subject there is a variation from 0.13, as recorded by Scrase[5] for zero temperature gradient, to 0.157, used by Messrs. Prandtl and Tollmien.[5] Also, in 1886, Archibald[5] experimented with anemometers on kites and found a power of 0.192 for instruments at 1,095 ft and 767 ft, and a power of 0.363 for instruments at 250 ft and 102 ft. However, no information was available on the meteorologic conditions prevailing during Mr. Archibald's tests. Nevertheless, the writer finds it interesting that the author derives a combined power of 0.161 when he brings together in Eq. 6 the added effects of height on the uniform velocity and on gusts. This power is close to that of Messrs. Prandtl and Tollmien. Despite the (possible) presence of thermal instability in the storms cited and the entire absence of it in the tests used by Messrs. Prandtl and Tollmien, may it not be possible that the macroscopic flow in the atmosphere and the microscopic flow in pipes follow the same law? If so, a choice of 0.167 is suggested by the writer as a close approximation to fact. This number lends itself to slide-rule computation.

Before utilizing the power law, the author makes an excellent application of the Ekman spirals of 20° and 17° (see under the heading, "Storm Observations"). The writer has made the following rough summarization[26]—the tendency to flow parallel to the isobars is not realized near the earth's surface due to friction. At sea the average angle of deviation is about 10° to 20°, but on land the hills, trees, buildings, and other obstructions may cause an angle as great as 45°. The author's statements concerning the surroundings of his test site, and the fact that he found an angle of from only 17° to 20° indicates that the site was fairly unobstructed. The writer has made some observations on Nantucket Island, which is 30 miles at sea. The southern half of the island is a glacial "outwash" plain and hence an almost perfect

[25] Cons. Engr., Baltimore, Md.

[26] "Vortices, Eddies and Turbulence as Experienced in Air Movements," by W. Watters Pagon, *Engineering News-Record*, Vol. 114, Part V, 1935, p. 582.

plane surface having a slope of 10 ft per mile or 20 ft per mile. Its surface has no vegetation other than a dense ground cover approximately 6 in. deep and scattered bayberry bushes not more than 4 ft high. On this plain, the writer has observed an angle of approximately 20° or 25° between the surface wind and the wind and clouds aloft during a cool, clear, northeast (hence, offshore) wind at the south shore. In such a summer wind, the sky is clear blue with scattered small clouds. In a warm, humid, but cloudless southwest wind (hence, onshore) the angle is essentially the same. However, in such a wind a "stationary cloud" hovers over the island a little downwind, continually forming upwind, and fragmenting and evaporating downwind. In the first case, the wind comes unobstructed from the Grand Banks, and in the second case, unobstructed from New Jersey; and it is strong even at El. 6 ft. The writer notes[5] that S. P. Wing made tests in Ireland in " * * * open country 65 ft. above sea level and about one-half mile from the ocean behind low rolling sand dunes 70 ft. high * * *." These tests, as well as Mr. Wing's curve, shown in Fig. 3, show a much more rapid increase in velocity with height.

The burden of this discussion thus far is that, although the use of a one-sixth power law fits the author's test data well, it is also quite likely that over large areas of water (and at cities along the oceans, the Gulf of Mexico, and the Great Lakes coasts) a more rapid increase of velocity with height at low elevations is more appropriate, so that the gradient wind is approached more rapidly at low elevations than is indicated by the sixth-power law, thus producing greater pressures on high buildings and bridges.

In the dust squall and the rain squall of a thunderstorm—especially when the storm is a part of an advancing cold front, with the horizontal wind outward from the storm area—the high horizontal velocity usually has a frontal width many times the lateral dimension of all but the very largest buildings and longest bridges. Fig. 9 apparently indicates such an attack. Therefore, it would seem that where such storms are to be anticipated it will be safer not to make the small reduction of from 3% to 8% noted by the author (see under the heading, "Minimum Effective Gusts").

Concerning the vertical distance through which a rapidly falling mass of air passes, it is the writer's recollection that the line squall that caused the destruction of the *USS Shenandoah* raised the ship at approximately 16.4 ft per sec through a height of roughly 3,000 ft, then allowed it to drop again at 25 ft per sec—at which time the altimeter ceased to function—and then raised it again. Such an atmospheric condition is somewhat similar to the breaking of a wave on the foreshore of a beach. The mass of the falling cold air, accompanied by heavy rain, is almost inconceivable, and its kinetic energy is transformed into forward horizontal velocity.

In tropical hurricanes, and typhoons of the Pacific Ocean—such as those which come ashore occasionally—the forces result from the very high horizontal and rotating velocities that are engendered, and that act on a wide front when compared with building dimensions, or even with the length of many bridges. There are no data on the variation with height of the velocity of such storms,

but it would seem reasonable to consider a rapid increase from the effective ground level.

The author properly refers his derived velocities to an "effective ground level." As yet there is no basis, except individual judgment, as to what is the height to assume, other than the 30 ft which the author cites. It would be of great value to the profession were someone to make tests on synthetic cities, composed of model individual houses, or rows of houses, in rectangular array, and of groups of "garden type" or lofty apartment buildings. Probably tests on a water table would give good basis for judgment, the flow about the buildings resembling the flow of water over stones in a rapids, with shooting flow and many eddies and suction effects on the buildings, which simulate rocks.

There are some situations in which, for economic reasons, a structure may be designed for less than the pressure resulting from the maximum recorded wind, and in which damage to person and property cannot occur. For such instances, it is helpful to have some indication as to the probabilities. The writer derived the probabilities of attaining less than absolute maximum velocities over a short period of time in years, and from this tabulated the probability of attaining a gradient wind of the following amounts:[27]

No. of years	Probable 5-min gradient wind velocities, in miles per hour
1	56
2	61
3	65
5	68
8	73
10	76
20	80
50	88
75	91
100	93

These values apply to the Baltimore (Md.) area. From these values, using the power law, the velocity for 5 min at any height can be determined, and then increased to allow for gusts. Following the author's derivation this would be increased for gusts by 50% at El. 30 (see under the heading, "Minimum Effective Gusts").

It is gratifying to have such a substantial basis for the adoption of a gust factor as that presented by the author. Heretofore, the 50% increase has been used purely on the basis of judgment.

In general, the author's treatment of his subject is outstanding.

Irving A. Singer[28] and Maynard E. Smith[29].—An improved approach to the difficult task of deriving design parameters for tall buildings from the wind data that are generally available is embodied in Mr. Sherlock's recent paper on the vertical variation of wind velocity and gusts. The most serious

[27] "Using Aerodynamic Research Results in Civil Engineering Practice," by W. Watters Pagon *Engineering News-Record*, October 31, 1935, p.601.

[28] Associate Meteorologist, Brookhaven National Lab., Upton, Long Island, N. Y.

[29] Leader, Meteorology Group, Brookhaven National Lab., Upton, Long Island, N. Y

criticism of the work is that it was based largely on data obtained at only one location (see under the heading, "Storm Observations"), giving rise to the question as to whether it is representative. It is understandable that only a single set of data was used because very few records of the proper type and quality are available, but the basic question of general applicability remains.

In view of this, studies based on data obtained by the Meteorology Group at Brookhaven National Laboratory, Upton, Long Island, N. Y., are compared with the author's results. Such comparisons, although they do not constitute full verification or disproof of the value of the original work, at least provide information from different locations.

Specifically, the study of the extremely violent coastal storm of November 25, 1950, reported by Mr. Lowry,[30] the analysis of one year of hourly wind records by H. A. Panofsky and Mr. Singer,[31] and a recent investigation of wind gustiness by the writers,[32] serve as the basis for the succeeding comments.

A brief description of the installation and terrain is necessary in view of the author's specification (see under the heading, "Summary") of "*** open, level country as a standard of reference ***." Wind measurements were made on a 410-ft meteorological tower, the installation being located near the center of Long Island. The terrain is fairly level and is uniformly covered with scrub oak and pine to a height of from 25 ft to 30 ft above ground.

TABLE 1.—Variation of Wind with Height at Brookhaven Laboratory

Height, in ft, above ground	Velocity, in Miles per Hour			Gust Factor[a]	
	Storm average	Fastest 30-min	Fastest 6-min	Observed mean value	Calculated[b] factor, F
37	29.1	33.6	35.1	1.94	1.94
75	37.4	41.2	45.2	1.70	1.86
150	44.7	49.4	53.0	1.60	1.78
410	57.3	61.1	64.2	1.41	1.67

[a] $\frac{V\text{ (peak)}}{V\text{ (6-min avg)}}$. [b] $F = F_{37}\left(\frac{37}{z}\right)^{0.0625}$.

Wind Speed Profiles.—The data for the November 25, 1950, storm were obtained with the instruments operating at normal chart speed, so that it is not possible to specify the exact duration of short-period fluctuations, although their magnitude can be determined. The comparison must therefore be restricted to averages of minutes, rather than seconds. Mr. Sherlock's contention that wind profiles under storm conditions can be described by either logarithmic or power-law approximations seems amply supported (see under the heading, "The Seventh-Power Law"). The Brookhaven data, in which the recorded velocities show even better agreement with theory than those of the author, appear in Table 1.

[30] "The Wind and Temperature Structure of the Lowest 125 Meters During the Storm of November 25, 1950, at Brookhaven National Laboratory," by P. H. Lowry, Internal Report, BNL (unpublished).

[31] "A.E.C. Air Pollution Project, Meteorological Phase," by H. A. Panofsky and I. A. Singer, New York Univ. College of Eng., Technical Information Service, Oak Ridge, Tenn., NYO-1559, June 30, 1951.

[32] "Microclimatology at Brookhaven," by I. A. Singer and M. E. Smith, *Journal of Meteorology* (publication pending).

These results can be fitted by a power-law approximation with a mean error of only 2% for the storm average, but the value of the exponent is 0.274 rather than 0.143 (the one-seventh power law). Thus, for this storm, the one-seventh power law would underestimate the steepness of the wind profile, and a calculation of the 410-ft wind based on 30 miles per hr at 37 ft would be low by 16 miles per hr. The fact that a study of thirteen recent storms indicated a mean value of the exponent of 0.250 shows that these values are typical of the profiles during strong winds in this location.

Gust Factors.—It is unfortunate that the records of the November 25, 1950, storm do not permit a firm comparison of gust factors. The best that can be accomplished is a study of the ratio of the peak speed to the 6-min average speed, without knowledge of the duration of the peaks. It may be anticipated at the outset that the F-values (defined under the heading, "Definitions and Notations") should lie near or above the 0.5-sec and 1.0-sec curves shown in Fig. 6 because the recorded peaks often may have been of very short duration, and the denominator represents a slightly longer averaging period.

The decrease of F with height, and the association of low winds with high gustiness factors and vice versa (see Fig. 5) are both reflected in the Brookhaven data. The mean gustiness factors were as shown in Table 1.

The exponent 0.0625 does not fit the Brookhaven results well. The gust factors decreased more rapidly with height, and a value of 0.147 would have resulted in a much better approximation.

The data for the November 25, 1950, storm also show that the range of speed (peak to lull) changes very little with height, so that the decrease in F is primarily a result of the increase in wind speed (see under the heading, "Gust Factors").

Recommendations.—In summary, it is felt that the author has achieved an approach to the problem that is essentially sound. However, comparison with data from another location casts doubt on the reliability of the values chosen for the parameters, both for wind speed and gust profiles. Brookhaven data indicate that the value of the power in the wind profile equation may be as high as one third. It seems clear that further investigation is necessary in order to determine the most conservative, and, therefore, the safest figures to be used.

The use of standard U. S. Weather Bureau surface observations as a basis for calculation is also an important topic (see under the heading, "Summary"). Mr. Sherlock has specified the necessity of flat terrain and a minimum of obstructions, if adequate data are to be obtained. The importance of this cannot be overemphasized. Each station should be carefully considered before the data are accepted for studies of this type. It is also important to re-emphasize the author's contention (see under the heading, "Gust Factors") that this approach is valid only for high winds (winds greater than or equal to 25 miles per hr at 30 ft). It is not valid at low wind speeds because at low velocities excessive gust factors and different speed profiles occur.

Acknowledgments.—Bendix-Friez Aerovanes were used for the wind measurements at Brookhaven National Laboratory.

PERCY H. THOMAS[33] AND M. H. FRESEN,[34] A.M. ASCE.—The variations of wind velocity and momentary pressures from gusty winds with height are of interest not only to civil and structural engineers but also to the designers of the giant wind turbines proposed for electric utilities.[35,36,37,38] The author's paper and an earlier paper[17] by Messrs. Sherlock and M. B. Stout present material that is almost unique in studies of the intimate nature of the wind and gives an invaluable and indispensable picture of the moment-to-moment behavior of high-velocity winds. The engineer's wind-turbine interest in the paper extends not only to the variation of wind velocity with height above ground, but also to other features that will be mentioned in this discussion.

Wind Velocity Variation with Height.—Table 2 presents some data illustrating the law of the variation of velocity with height that are exceptionally convincing, at least for the first few hundred feet. This table shows, for each month of the year, the average wind velocity at each of the six heights, averaged over the 5-year period from 1945 to 1949. When these data are put in the form of ratios of the velocities at the several heights to the velocity at the 100-ft height, as in Table 2, the ratios are almost identical for each of the months of the year, and their percentage differences from the 5-year averages are small.

TABLE 2.—VARIATION OF AVERAGE WIND VELOCITIES WITH HEIGHT, 1945 TO 1949

Height, in ft above ground	Wind Velocity,[a] in Miles per Hour												
	Jan.	Feb.	Mar.	Apr.	May	June	July	Aug.	Sept.	Oct.	Nov.	Dec.	Average
7	4.1 (0.58)[a]	5.2 (0.58)	6.0 (0.61)	6.7 (0.66)	6.7 (0.66)	7.4 (0.67)	6.9 (0.68)	6.1 (0.65)	5.7 (0.63)	5.1 (0.60)	5.0 (0.62)	4.4 (0.58)	5.8 (0.63)
50	5.9 (0.83)	7.4 (0.83)	8.0 (0.82)	8.4 (0.82)	8.7 (0.85)	9.4 (0.85)	8.9 (0.87)	8.2 (0.87)	7.9 (0.87)	7.4 (0.87)	6.9 (0.85)	6.5 (0.86)	7.8 (0.85)
100	7.1 (1.00)	8.9 (1.00)	9.8 (1.00)	10.2 (1.00)	10.2 (1.00)	11.1 (1.00)	10.2 (1.00)	9.4 (1.00)	9.1 (1.00)	8.5 (1.00)	8.1 (1.00)	7.6 (1.00)	9.2 (1.00)
200	8.1 (1.14)	10.2 (1.15)	11.1 (1.13)	11.4 (1.12)	11.6 (1.14)	12.5 (1.13)	11.6 (1.14)	10.6 (1.13)	10.3 (1.13)	9.6 (1.13)	9.4 (1.16)	8.9 (1.17)	10.4 (1.13)
300	8.6 (1.21)	10.9 (1.22)	11.9 (1.21)	12.4 (1.22)	12.5 (1.23)	13.6 (1.23)	12.8 (1.25)	11.9 (1.27)	11.4 (1.25)	10.4 (1.22)	10.2 (1.26)	9.3 (1.22)	11.3 (1.23)
400	9.1 (1.28)	11.3 (1.27)	12.5 (1.28)	13.0 (1.27)	13.1 (1.28)	14.5 (1.31)	13.7 (1.34)	12.5 (1.33)	12.0 (1.32)	11.1 (1.31)	10.6 (1.31)	9.7 (1.28)	11.9 (1.29)

[a] Numbers in parentheses are the ratios of the velocities to those at the 100-ft height.

The exponential equation for the relation of velocity ratios to height ratios can be determined by plotting the logarithms of the ratios on uniform scale cross section paper, or by plotting the ratios themselves on logarithmic paper. The resulting equation for the data in Table 2 was found to be

$$\frac{V}{V_{100}} = \left(\frac{z}{100}\right)^{1/5.4} = \left(\frac{z}{100}\right)^{0.185} \quad \ldots\ldots\ldots\ldots\ldots\ldots (8)$$

[33] Cons. Eng., Montclair, N. J.; formerly with Federal Power Comm., Washington, D. C.

[34] Engr., Bureau of Reclamation, U. S. Dept. of the Interior, Washington, D. C.

[35] "Power from the Wind," by Palmer C. Putnam, D. Van Nostrand Co., New York, N. Y., 1948.

[36] "Electric Power from the Wind," by Percy H. Thomas, Federal Power Comm., Washington, D. C., March, 1945.

[37] "The Wind Power Aerogenerator," by Percy H. Thomas, Federal Power Comm., Washington, D. C., March, 1946.

[38] "Aerodynamics of the Wind Turbine," by Percy H. Thomas, Federal Power Comm., Washington, D. C., January, 1949.

in which V and z designate velocity and height, respectively, and the value of the exponent is 0.185. The logarithmic tangent line from heights of 50 ft through 400 ft is very close to a straight line, the points falling on the line within a very small percentage below 50 ft. The exponent gets smaller for the heights very close to the ground surface, as would be expected. The height of 100 ft was taken as a reference point to avoid the uncertainty of measurements near the ground.

Fig. 3 shows several curves of variation of wind velocity with height, in which a value of $z_o = 30$ ft has been used as a reference height, with a corresponding wind velocity of 50 miles per hr. It can be shown that Eq. 8 can be written in the form:

$$\frac{V}{V_o} = \left(\frac{z}{z_o}\right)^{1/n} \qquad \text{(9a)}$$

or more specifically,

$$\frac{V}{V_{30}} = \left(\frac{z}{30}\right)^{1/5.4} \qquad \text{(9b)}$$

Table 3 has been computed to compare Eq. 9*b* with Fig. 3, on the basis of a wind velocity of 50 miles per hr at a 30-ft height. The author used the one-seventh power ($1/n = 0.143$) as the exponential relation between velocity and height. The writers determined the exponent as $1/n = 0.185$. Table 3 indicates that Eq. 9*b* at heights of 400 ft and 1,000 ft gives velocities 11% and 16% greater, respectively, than the author's Fig. 3 with $n = 7$.

TABLE 3.—COMPARISON OF WIND VELOCITY EQUATIONS

Height, z, in ft	$\frac{V}{V_{30}}$, from Eq. 9b	Velocity, V, in Miles per Hour		Ratio of velocities[a]
		$n = 5.4$	$n = 7$	
(1)	(2)	(3)	(4)	(5)
30	1.000	50.0	50.0	1.00
50	1.099	55.0	53.8	1.02
100	1.250	62.5	59.4	1.05
200	1.421	71.1	65.6	1.08
300	1.531	76.6	69.5	1.10
400	1.614	80.7	72.4	1.11
600	1.741	87.1	76.8	1.13
800	1.836	91.8	80.0	1.15
1,000	1.913	95.7	82.6	1.16

[a] The values in Col. 5 are the values in Col. 3 (from Eqs. 9) divided by the corresponding values in Col. 4 (from Fig. 3).

Mr. Humphreys[39] cites the equation of G. Hellmann:

$$\frac{V}{V_o} = \left(\frac{z}{z_o}\right)^{1/5} \qquad \text{(10)}$$

as applicable for heights of from 16 m (52.49 ft) to 300 m (984.25 ft) or 400 m (1,312.33 ft) above the surface, especially over open country. Table 2 and Eq. 9*b* appear to substantiate approximately Mr. Hellmann's value of $n = 5$ in Eq. 10.

[39] "Physics of the Air," by W. J. Humphreys, McGraw-Hill Book Co., Inc.,New York, N. Y., 3rd Ed., 1940, p. 140.

Peak Gust Wind Velocities.—Eq. 3 and Eq. 6 indicate that the wind velocities during gusts vary inversely with the 0.0625 power of the height. Table 4 presents a summary of peak gust velocities based on measurements for the same installation as that of Table 2. The selected 9 records in the table, for which ratios are given, are those for peak gusts occurring on the same day at the two heights of 50 ft and 400 ft. These records are believed to be based on nonsimultaneous readings, and are, therefore, not comparable to the author's data in Fig. 12. From this table, it would appear that the nonsimultaneous peak gust velocities vary approximately as the 0.10 power of height based on the average ratio of 1.23 for 9 records.

These few records could not be cited as evidence that wind velocities during gusts vary directly as some exponential power of the height, which would be in contradiction to the author's derivation of Eq. 6, and to his simultaneous velocity readings plotted in Fig. 12. However, Table 4 indicates that, even on days of extremely high wind velocities, the nonsimultaneous peak gust velocities increase as the height increases, within limits not definable from the available data.

TABLE 4.—RATIOS OF PEAK GUST VELOCITIES OF RECORD, FOR THE 7-YEAR PERIOD, 1945 TO 1951

Height, in ft	Peak Velocity, in Miles per Hour												
	Jan.	Feb.	Mar.	Apr.	May	June	July	Aug.	Sept.	Oct.	Nov.	Dec.	Year[a]
50	62	56	53	51	71	61	50	50	58	63	64	60	71
400	73	70	66	58	80	84	73	80	66	80	85	74	85
Ratio of the Peak Velocity at 400 Ft to That at 50 Ft													
	1.18	1.25	1.25	1.14	1.13	1.38	...	...	1.14	1.27	1.33	...	1.23[b]

[a] Peak. [b] Average.

Wind Velocity and Gust Considerations Affecting Wind Power.—Because the kinetic energy of the wind varies as the cube of its velocity, height is advantageous to a wind turbine tower. The advantage of height is aided by the fact that the extra cost of high towers is very modest when a design is chosen in which it is possible to increase the base with the height. Such a design is proposed for the 6-legged tower of the Federal Power Commission's 7,500 kw-aerogenerator.[37] A second interesting characteristic of the wind turbine is the fact that only the component of the wind at right angles to the plane of the wheel yields power. When an unevenness of the ground, or an obstacle, causes an upward or a sidewise diversion of the wind stream, there is a corresponding loss of the energy available to a turbine.

There are certain configurations of the ground that contribute something to the available energy of the wind, among which are the summit of a long ridge (or even the sides near the top of a mountain), a wind gap in a hill through which the wind is accelerated, the narrow point in some natural venturi-type ground formation, or the downhill face of a ridge on which the general level is lower on

the lee side of the hill. In the case of the latter the question arises as to whether or not the wind will take an accelerated pace as does the flow of water on the downstream side of a submerged weir. Some observations of Palmer C. Putnam[40] suggest that this may be an important factor. Although the potentialities of these formations are usually accepted, the writers know of no quantitative data available to assist in appraising these potentialities relatively. Any such contribution from civil engineers would be very welcome.

The wheel of the wind turbine must adjust itself automatically to the changes in the velocity of the wind. From the designer's point of view, this fact puts a limit on the danger from gusts in that any gust that takes longer to develop than the time required for the turbine to adjust itself to the changed velocity should be classed as a change in the wind velocity, not as a gust increasing the stresses. The 7,500-kw aerogenerator referred to here adjusts itself to the variations of the wind by changing its speed and overloading the generator on rising winds, which causes a waste of energy by slowing down the wheel. This process is expected to require only a few seconds to be completed, so that only gusts of shorter duration are dangerous.

As the author has pointed out under the heading, "Minimum Effective Gusts," the large blades of these giant turbines would be immune to gusts of short duration and of limited extent. Such gusts would have too little energy to bend the blade enough to reach the safety limit of the material. In large blades, an appreciable time will be so required. However, there is to be considered the extra stress caused by the overrun in a blade continuously exposed to a steady deflecting force. The opportunity and obligation of the builders of a full-sized prototype aerogenerator to resolve such matters is rather intriguing. Suggestions would be in order as to the best methods of measuring the pressure momentarily over the whole surface of a blade 75 ft by 13 ft, front and back (while operating) and for repeating this for a large number of operating conditions. Suggestions would also be in order for conveniently and quickly plotting the local air currents over each of a number of alternative sites, so that the designer of a full-sized wind turbine would have before him a complete picture, covering the various directions, velocities, and types of the prevailing winds.

Although a stationary surface normally exposed to a wind experiences a pressure proportional to the square of the wind velocity, the moving turbine blade is subjected to a unit pressure proportional to the square of the "relative velocity"—a very different matter. The relative wind is the vectorial resultant of the actual wind and the blade speed. Because the blade speed in the turbine mentioned here is thirteen times the wind velocity, the effect is clear. The pressure on the turbine blade is also proportional to the angle of attack of the relative wind against the blade surface, and this angle is nearly proportional to the actual wind speed. As a result, the relative velocity of the wind on the blade does not change with gusts, and the actual stress is increased approximately in proportion to the first power of the gust, as long as the wheel is revolving.

In a number of places in this discussion it has been mentioned that additional information would be helpful in connection with the measurement of wind

[40] "Power from the Wind," by Palmer C. Putnam, D. Van Nostrand Co., New York, N Y., 1948, pp. 80-81, Fig. 49.

velocities and pressures, and the action of wind in general, as well as that of gusts on moving wind-turbine blades and other structural components of very high aerogenerators. The author has made numerous and extensive investigations in this respect. The engineering profession would be indebted to the author for any comments he would make in this regard in his closing discussion, or to other persons who may pursue the subject further and make known their findings.

Acknowledgment.—Grateful acknowledgment is made to Donald G. Sturges (chief, Operations Division, Hanford Operations Office, United States Atomic Energy Commission (AEC)), for permission to use data (Tables 2 and 4) included herein, and to D. E. Jenne (head, Synoptic Meteorology unit of the General Electric Company), who compiled the data.

Data for Table 2 were taken from the records of wind measurements at six heights at the Hanford Works at Richland, Wash., with the permission of the AEC.

ROBERT A. McCORMICK[41].—An interesting and provocative paper on a subject for which few and limited observational data have been obtained (only a fraction of these data have been published) has been written by Mr. Sherlock. However, analysis of the data recently obtained at Brookhaven National Laboratory (Upton, N. Y.) and by Guggenheim Airship Institute (Akron, Ohio), under P. O. Huff, in cooperation with the U. S. Weather Bureau, should add considerably to the information on the subject.

The validity, for the general case, of any empirical relationship describing the structure of low-level wind in one storm sample, even a "typical" one, must be looked upon with skepticism. Granted that the theoretical relationships are most applicable for average (near neutral) stability conditions—a reasonable assumption for periods of high winds—they contain implied or expressed parameters, such as the roughness length, which must be evaluated locally. In the storm described by Mr. Lowry,[30] the variation of wind speed with height agreed very well with a 1/3.6-power law, but in the storm Mr. Sherlock describes, a fair fit was obtained with the 1/7-power law (see Fig. 2). It is possible to get a slightly better fit for Mr. Sherlock's data using the power law[42] of E. L. Deacon, assuming $\beta = 0.9$. These results are a further indication that the power-law index is quite sensitive to surface roughness under fairly similar stability conditions and serve to discourage the arbitrary application of one set of conditions to another location even when uncomplicated by "unusual" topographies.

More information can be obtained from the expression for the design velocity as a power function of height (Eq. 2), if $\left(\frac{V_z F_z}{V_{30} F_{30}}\right)^2$ from Eq. 6 is

[41] Meteorologist, Weather Bureau, U. S. Dept. of Commerce, Upton, N. Y.

[42] "Vertical Diffusion in the Atmosphere," by E. L. Deacon, *Quarterly Journal*, Royal Meteorological Soc., Vol. 75, 1949, pp. 89–103.

written

$$\left(\frac{V_z F_z}{V_{30} F_{30}}\right)^2 = \left[\frac{\bar{V}_z \dfrac{\bar{V}_z + \Delta V_z}{\bar{V}_z}}{\bar{V}_{30} \dfrac{\bar{V}_{30} + \Delta \bar{V}_{30}}{\bar{V}_{30}}}\right]^2 = \left[\frac{V_z(t)_1}{V_{30}(t)_1}\right]^2 \qquad (11)$$

in which the bars indicate maximum 5-min storm velocities and ΔV indicates the maximum 10-sec (positive) deviations from the $\bar{V}$-value. The expressions $V_z(t)_1$ and $V_{30}(t)_1$ indicate the absolute magnitudes of the 10-sec velocities at heights z and 30 ft, respectively. Thus, the $V(t)_1$-values are the highest observed 10-sec velocities at each level during the time of occurrence of the maximum 5-min velocities, which may not be simultaneous. Therefore, the curve of Eq. 2 should be compared with the variation with height of the $V(t)_1$-values. There is also a possibility that the $V(t)$-values found in 5-min periods with less than maximum mean velocity may exceed the $V(t)_1$ defined in Eq. 11.

EDWARD COHEN,[43] J. M. ASCE.—The French building code regulations for wind—adopted in 1946 by the French Ministry of Reconstruction and City Planning and currently (1952) in use—are based on a variation of velocity with height according to the rule $\left(\frac{H}{10}\right)^{1/7}$, in which 10 is the reference elevation in meters, and H is the height in meters at which the velocity is to be computed. For ease of calculation and to include the effect of gusts, the following formula was given for computing velocity pressures at different levels:

$$\frac{q_h}{q_{10}} = 2.5 \frac{H + 18}{H + 60} \qquad (12)$$

in which q_{10} and q_h are the wind pressures at heights 10 m and H m above the ground, respectively. The limiting ratio $\frac{q_h}{q_{10}} = 2.5$ is reached as H approaches infinity.

The code also specifies a maximum velocity pressure of 162 kg per sq m or approximately 35 lb per sq ft. In effect, this value reduces the difference between the basic and maximum velocity pressures for areas of more severe exposure—as, for example, along the coast line. For structures less than 10 m (32.808 ft) in height, the design may also be reduced according to Eq. 11. For a structure 15 ft high, the loading is approximately 85% of the basic value. Shielding, resonance, shape factor, and other influencing factors are considered separately.

By Eq. 11 the ratio of the pressure at the 1,000-ft level to the basic load at the 33-ft (10-m) level is 2.2, as compared to the value 1.8, the ratio recommended by the author (see Fig. 10). However, in view of the many uncertainties involved and the limited quantity of data available, the agreement appears to be satisfactory.

In writing about gust effect on structures, apparently the author has assumed that the resulting pressures may always be considered static loads. Actually, the computation of stresses resulting from gust pressures is a dy-

[43] Asst. Engr., Ammann & Whitney, Cons. Engrs., New York, N. Y.

namic problem and should be so treated. For example,[44] a gust having an instantaneous time of rise and a duration equal to one half the fundamental period of a simple structure produces an effect equal to that of a static pressure of approximately twice the intensity of the pressure rise. If the duration of the gust is less than one half the fundamental period, the response is reduced as a function of the duration. Thus, at a duration of one tenth of the natural period, the elastic stress in the structure will be approximately six tenths of that caused by a static load of the same intensity. If the gust loading takes longer than two tenths of the natural period to build up to a maximum value, the dynamic effect is also reduced. When the build-up time exceeds approximately four times the natural period, the dynamic effect disappears.

For these reasons, it would be highly desirable to relate gust effects to the dynamic characteristics of the isolated members, frameworks, and buildings subjected to such loading.

R. H. Sherlock,[45] M. ASCE.—In his discussion, Mr. Pagon refers to the fact that many of the older reports on the variation of wind velocity with height fail to include coincidental meteorological data. These data are of great importance. Wind forces acting on structures are significantly large only during strong winds, and these winds occur only during storms when the vertical mixing of the atmosphere is active, with an accompanying high value for the coefficient of eddy viscosity. At the other end of the range of possible meteorological conditions is the temperature inversion, during which the atmosphere is so stable that there is little, if any, vertical mixing, and the coefficient of eddy viscosity is correspondingly small. In the latter case there is little friction between the horizontal layers, and the velocity changes rapidly with height. The pressure gradients accompanying a temperature inversion are never large, and the gradient velocities are, therefore, never great. It is not valid to use the rapid rate of change of velocity with height which occurs in an inversion, when one is considering the matter of variation of storm winds with height. It is interesting, but not surprising, that a wide range of values has been obtained from investigations that were made under possibly various, but unrecorded, meterorological conditions.

Mr. Pagon also raises the question whether, at cities along the ocean and other large bodies of water, a more rapid increase of velocity with height is appropriate than is given by the one-seventh power law. This seems to imply a lowering of the gradient level and to be in accord with the ideas underlying the French Code of 1946, as expressed subsequently in Fig. 14. The table reproduced in Mr. Pagon's discussion indicates that the gradient wind is approached in the coastal zone of Germany at about 750 meters (2,460 ft) which is one half the height at which it occurs in middle Germany (1,500 meters). These great heights represent an average over a long period during which many degrees of stability and instability of the atmosphere may have prevailed. They should not be considered representative of storm conditions without further subdivision and study of the data for stormy parts of these periods.

---

[44] "Effects of Impact on Simple Structures," by J. N. Frankland, *Proceedings*, Soc. for Experimental Stress Analysis, Vol. VI, No. 2, pp. 9–10.

[45] Prof. of Civ. Eng., Univ. of Michigan, Ann Arbor, Mich.

The same comments apply to the angles of deviation shown in that table. Nevertheless, it is interesting to note that, in fitting curves to the Brookhaven data in Fig. 13, the Ekman spiral required an angle of about 30.5°, and the Rossby spiral required an angle of about 35°. This question is examined later in connection with the discussions by Messrs. Singer and Smith and by Mr. Cohen.

The vertical velocities of the *USS Shenandoah*, cited by Mr. Pagon, are of the same order of magnitude as, although somewhat less than, the rate at which horizontal velocities were propagated downward at the gust fronts examined in the storm quoted by the writer. Here again, the coincidental meteorological data would have a bearing on any comparison between these two cases.

The discussion by Messrs. Singer and Smith brings to the structural engineer information which has only recently become available at Brookhaven. It is fortunate indeed that this installation was ready to take records of the storm of November 25, 1950. The criticism has been raised by several writers that this paper has been based largely on data obtained at only one location and for only one storm, thus raising doubts as to whether it is representative of other storms and of locations along coastal areas rather than at inland locations. The data that Messrs. Singer and Smith present are taken from another storm, with wind from the ocean, and from a location near the coast within a network of first-order U. S. Weather Bureau stations. They thus make possible a detailed study of another storm and its coincidental meteorological information.

The data concerning the fastest 6 min of the storm, as shown in Table 1, are plotted in two different ways in Figs. 13 and 14. In Fig. 13, the wind velocity is plotted horizontally, and the height above the ground is plotted vertically. The wind velocities at the four different stations on the tower are shown by small circles. The gradient wind, between 104 miles per hr and 110 miles per hr, and the geostrophic wind, at 138 miles per hr, are shown at the upper right-hand corner of the diagram. In Fig. 13, the letter A designates the curve represented by $V_z = V_{30}\left(\frac{Z}{30}\right)^{0.25}$, the letter B designates the Ekman spiral, and the letter C designates the Rossby spiral.

The information for computing the gradient and geostrophic winds was taken from a report prepared under the direction of Ernest J. Christie.[46] In this report, synoptic maps are shown for the period from November 24, 1950, to November 27, 1950, at intervals of 6 hr. The pressure gradient in the region of Long Island appeared to be greatest on the map for the hour of 1330 Eastern Standard Time (1830 Greenwich Standard Time) on November 25, 1950. At this time the center of the storm was in southeastern Pennsylvania and was moving approximately north. The arrows show that the wind was coming from the east at Brookhaven. This is supported by the tabulations, which also show that this hour was within the period of strongest winds as given by the hourly velocities at the 37-ft level. It was assumed that the

[46] "Report on the Storm of November 25, 1950," U. S. Weather Bureau Office, New York, N. Y., December, 1950.

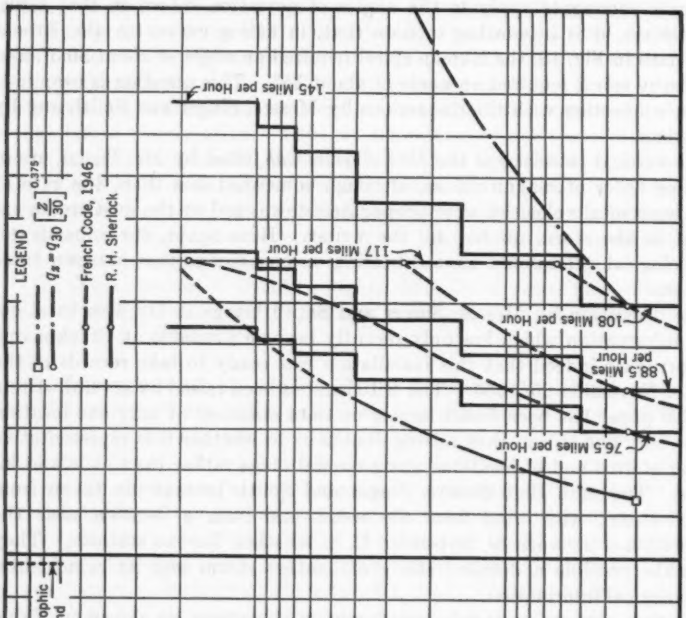
LEGEND
$q_z = q_{30}\left[\frac{z}{30}\right]^{0.375}$
French Code, 1946
R. H. Sherlock
Gradient Wind
Geostrophic Wind
Brookhaven Data,
Storm of November 25, 1950
Fastest 6-Minute Average
145 Miles per Hour
117 Miles per Hour
108 Miles per Hour
88.5 Miles per Hour
76.5 Miles per Hour
A B C
Height Above Ground, in Feet
Wind Velocity, in Miles per Hour
Velocity Pressure, q, in Pounds per Square Foot

FIG. 13

FIG. 14

pressure gradient obtained from this map was related to the fastest 6-min velocities of Table 1.

The gradient as scaled from the map was 24 millibars in 210 miles. This is equivalent to 7.1 millibars per 100 kilometers. The radius of curvature of the wind path in this area varied from 1,450 kilometers (900 miles) to 1,880 kilometers (1,170 miles), depending whether the wind direction arrows or the isobars were used as a basis of measurement. The gradient velocity based on this information and computed by standard methods for a latitude of 41°, varied from 104 miles per hr to 110 miles per hr, and the geostrophic wind was equal to 138 miles per hr. The gradient wind velocity of 104 miles per hr is considered the most reliable estimate, and this value has been used in fitting these curves.

Of the three curves used, one is an empirical exponential curve with the value of the exponent taken at 0.250. This value is referred to by Messrs. Singer and Smith as being the mean value obtained from a study of thirteen recent storms at Brookhaven. The other two curves are spirals. The one by Mr. Ekman, previously described, is based on a theory of eddy viscosity, and the other one by Mr. Rossby is based on the theory of the "mischungsweg" (mixing length).[47] The curves have been spread somewhat for the sake of clarity and, therefore, they are not exactly the best fit. For example, the Rossby curve (curve C) could be made to pass among the three upper points by changing from a velocity of 45 miles per hr at a height of 30 ft to a velocity of 42 miles per hr. However, the curves illustrate the relation between the actual observations of wind velocity and the two theories. In this case, a Rossby spiral fits the data better than does the Ekman spiral, although the difference is not great.

The two spirals reach the 1,000-ft level at approximately the same value for the wind velocity, namely, 104 miles per hr. The exponential curve, if extrapolated beyond the level of 410 ft, reaches the 1,000-ft level at a wind velocity of only approximately 82 miles per hr. Shall the velocities at higher levels be obtained by a simple extrapolation of the nontheoretical (empirical) curve, or shall the curves that represent a theoretical approach be used for purposes of extrapolation? In this connection it should be noted that the fastest 6 min, as recorded by Messrs. Singer and Smith in Table 1, did not occur simultaneously at the 4 stations on the tower, and that the individual 6-min intervals were separated by as much as 2.5 hr.

In Fig. 14, the French recommendations, as reported by Mr. Cohen in his discussion, have been superimposed upon the recommendations of this paper for further comparison. Fortunately, the effective ground level is taken at approximately the same height in both cases, being 30 ft for this paper and 10 meters (32.8 ft) in the French Code. This makes comparison relatively easy. Two curves adapted from the Brookhaven data are shown also.

It will be seen that, if the basic velocity pressure is taken at 15 lb per sq ft, the recommendations of the French Code exceed those of the writer for all heights from 10 meters to 2,000 ft, except between 50 ft and 65 ft. At

[47] "A Generalization of the Theory of the Mixing Length with Applications to Atmospheric and Oceanic Turbulence," by C. G. Rossby, *Metorological Papers*, Vol. I, No. 4, Massachusetts Inst. of Technology, Cambridge, Mass., 1932, p. 33.

1,000 ft, the French Code recommends a velocity pressure of 33 lb per sq ft, but the writer has recommended 27 lb per sq ft. For those geographical areas in which a basic velocity pressure of 15 lb per sq ft is justifiable, the French Code is more conservative, but in those areas where a basic velocity pressure of 30 lb per sq ft is justifiable, the two recommendations are substantially the same to a height of 150 ft, above which this paper is much more conservative.

The use, by the French Code, of a constant velocity pressure of 35 lb per sq ft above the height of 62 ft is probably based on two assumptions. The first of these assumptions is that, within the geographical areas served by that code, the same gradient velocity is equally probable at all locations, and that the difference between the gradient velocity and that which is experienced at the effective ground level is almost entirely due to eddy viscosity caused by the roughness of the terrain over which the wind is blowing, and only to a minor extent by the thermal mixing. The second assumption is that, at the exposed coastal areas where a basic velocity pressure of 30 lb per sq ft would be justifiable, the gradient velocity would be found at a height of 62 ft above the ground, and that at some inland location, where records call for a velocity pressure of only 15 lb per sq ft, the gradient velocity would not be found below a height of 1,850 ft.

In Fig. 14, two curves adapted from the Brookhaven data are also shown, using the form of Eq. 6. For example,

$$q_z = q_{30}\left[\left(\frac{Z}{30}\right)^{0.250}\left(\frac{Z}{30}\right)^{-0.0625}\right]^2 = q_{30}\left(\frac{Z}{30}\right)^{0.375}.$$

The exponent 0.250 for the variation of wind velocity with height (6-min average), is based on the Brookhaven data, but the exponent -0.0625 has been retained from the writer's recommendation for the variation of gust factors with height even though it seems too conservative on the basis of the observations at Brookhaven. This exponent is on the safe side. Furthermore, it makes allowance for those cases in which the strongest gust does not occur in the 5-min period having the highest average velocity. This point is discussed in connection with Figs. 5, 6, and 7. It also makes allowance for atmospheric jets. The 6-min velocity of 35.1 miles per hr at an elevation of 30 ft was multiplied by a gust factor of 1.5. This was reduced to velocity pressure by the expression, $q = 0.00255\,[35.1 \times 1.5]^2$, and the curve was drawn on the basis of the foregoing equation. The curve, if extrapolated, would reach the velocity pressure of 35 lb per sq ft at about the same elevation as the French Code, even though it started at an elevation of 30 ft with only half the pressure of the French Code. Also, when a basic velocity pressure of 30 lb per sq ft is assumed at 10 meters, the application of the equation based on the Brookhaven data yields a velocity pressure of 65 lb per sq ft at a height of only 240 ft. If extrapolated to a height of 1,000 ft, it would yield a velocity pressure of 111.5 lb per sq ft. These values are entirely out of agreement with any existing practices and seem much too conservative. It seems that the curve based on the Brookhaven data is, while more conservative, not far out of agreement with the recommendations of this paper when applied to the variation of wind velocity with height accompanying fairly low basic velocities at 30 ft. How-

ever, when the same equation is applied to the higher velocity pressures, such as 30 lb per sq ft, which are justified in exposed coastal areas subject to the hurricane type of storm, the curve yields velocity pressures that are far too conservative.

When dealing with the higher ranges of velocity pressures, it seems that the truth must lie somewhere between the very optimistic requirements of the French Code and the extremely pessimistic predictions based upon the Brookhaven data. It may well be that the writer's recommendations, which lie between the French requirements and the predictions based on the Brookhaven data, are not the best that could be obtained for exposed coastal areas subject to hurricanes. However, the writer is not familar with any storm observations that would justify the assumption that the gradient velocity may be found at an elevation of only 62 ft above the ground anywhere in the United States. Of course, during periods of deep temperature inversions, the gradient velocity might very well be found at low elevations—but this would involve little or no vertical mixing and would occur when the wind velocity was so small that it would have no significance in the design of structures. Furthermore, eddy viscosity, which has such an important part in fixing the height of the gradient level, is not caused entirely by ground roughness but is caused likewise by thermal instability of the air and this may also occur over large bodies of water. Thus, it seems better to assume that, during periods of strong storms when vertical mixing in the atmosphere is extremely active, there is no lowering of the height at which the gradient velocity is reached. No justification is evident for the adoption of a constant velocity pressure of 35 lb per sq ft above 62 ft anywhere in the United States, especially considering the uncertainties that exist in regard to the variation of velocity with height under hurricane conditions. On the other hand, the adoption of a purely empirical curve based on the Brookhaven data, as a guide in choosing a variation of velocity with height, would lead to results implying that gusts exist having a velocity of 158 miles per hr at 240 ft, and of 210 miles per hr at 1,000 ft. These values would be true velocities reduced to standard atmosphere at sea level, not velocities from the old 4-cup anemometers that "overshot" the true velocities by about 40%.

Messrs. Thomas and Fresen introduce a subject that at first sight may seem unrelated to the work of structural engineers—namely, the subject of power from the wind. However, a little consideration convinces one that the wind loading of structures incident to the support of such generating stations cannot be dismissed as being trivial. This part of their discussion will undoubtedly prove a worthwhile contribution in this unusual field.

The velocities listed by Messrs. Thomas and Fresen in Table 2 are the averages over a considerable period of time. No doubt, they include velocities occurring during every conceivable degree of stability and instability, and these would include the very rapid increase of velocity with height during periods of temperature inversions. Therefore, it is questionable whether or not the exponent 0.185, which they obtained, should be used for storm periods in that area without separating the data on that basis. The tendency would be for their data to show a higher exponential value than the data taken during

storm periods. Nevertheless, their data constitute a contribution and will undoubtedly be taken into consideration by the ASCE Structural Division Committee on Wind Forces.

The exponent −0.0625, which was used by the writer in Eq. 6 to describe the variation of gust factors with height, cannot be compared with the ratio of peak gust velocities at two different heights. This is because the gust factors must necessarily be used with some average velocity, either coincidental or adjusted so as to be applicable in the use of the Weather Bureau records for the daily fastest 5-min velocity. This point is explained in connection with Figs. 6 and 7. For example,

$$\frac{\text{Peak velocity at } Z}{\text{Peak velocity at } 30} = \frac{V_z\,F_z}{V_{30}\,F_{30}} \neq \frac{F_z}{F_{30}}.$$

Messrs. Thomas and Fresen present an interesting but different scheme for describing gusts.

Mr. McCormick describes a method for taking care of those cases in which the highest peak velocity occurs within a 5-min interval that does not have the highest average velocity of the storm sample, thus making possible the use of the Weather Bureau records of the daily fastest 5-min velocity. His point is an important one, as described and provided for in connection with Figs. 6 and 7.

Mr. McCormick's pessimism regarding the transfer of empirical information from one location to another is understandable, but this should not be taken as a prohibition against the attempt to find improved engineering solutions for difficult problems. For several generations, engineers have been designing and constructing wind-loaded structures on the basis of even more meager empirical information than now exists. One of the novel features of the data presented in this paper and of the data from Brookhaven is that in each case it has been possible to supplement the empirical information from the towers with theoretical interpretations based on coincidental observations of pressure gradients. It is hoped that the meteorological towers at Brookhaven and at Hanford, Wash., will provide additional storm information supplementing the rather limited empirical data available to the engineer. It is further hoped that these installations may some day be equipped with more sensitive anemometers that will yield more refined information as to wind structure. Because of the high cost of such installations, perhaps it is too much to hope that additional installations such as this will be built in other parts of the country and thus provide data for other locations and types of storms.

It is gratifying to note that Mr. Cohen is drawing attention to the dynamic response of gust-loaded structures. It was not the intention of the writer to imply that this dynamic response might be ignored. It is generally recognized that the dynamic response of a structure to a gust will sometimes involve stresses considerably in excess of those that would exist if the stresses had been computed on the basis of static loads. Perhaps one reason for the increased interest in this matter is the recent necessity for investigating the

effects of bomb blasts. Another reason may be the more frequent use of tall flexible towers and steel chimneys.

The mechanics of computing a structure's elastic response to fluctuating or suddenly applied loads have been well established and accepted by engineers. However, there is an aerodynamic time-lag between the passage of a gust front and the response of the structure, and this fact has not been generally recognized by structural engineers. This time-lag is not dependent upon the elastic properties of the structure but upon its aerodynamic properties. It is obvious that, aerodynamically, a structure will not be fully affected by a gust that is only a small fraction of the size of the structure. A gust must have sufficient vertical and horizontal extent to envelop not only the structure but also those flow patterns to the windward and to the leeward that are responsible for the maximum pressures upon the structure. This matter is discussed under the heading, "Minimum Effective Gusts" and in other publications.[22,23,24] Relative to Mr. Cohen's mention of "* * * a gust having an instantaneous time of rise and a duration equal to one-half the fundamental period of a simple structure * * *," it must be explained that there is no such thing as an instantaneous gust when one speaks of the applied forces on the structure. The gust must have a length of several times the size of the structure before the pressures incident to that gust have been completely established on all sides of the structure. Unfortunately, this aerodynamic time-lag has not been experimentally evaluated for sharp-edged bodies. The only experiments known to the writer are those performed by W. S. Farren on airfoils, as discussed under the heading, "Minimum Effective Gusts," and referred to elsewhere.[22] The evaluation of the aerodynamic time-lag on sharp-edged structures awaits further experimental evidence. Such experiments are now being undertaken at the University of Michigan in Ann Arbor.

The question raised by Mr. Cohen deserves further consideration in a separate paper devoted to that subject. However, a complete treatment of this subject would require (*a*) that the gust be separated from the average velocity upon which it is superimposed, (*b*) that the aerodynamic time-lag for that particular type of structure be known, (*c*) that a minimum effective gust be properly chosen, and (*d*) that the elastic response of the structure be computed.

Summary of Closing Remarks.—In closing, the writer wishes to express his thanks to those who have participated in the discussion of this paper. He feels that the future work of the ASCE Committee on Wind Forces Acting on Structures has been more clearly indicated in so far as the variation of velocity with height is concerned.

Some of the items in the writer's "Summary" are in need of modification. Item 8 should read: The one-seventh power law is a sufficiently close approximation to the variation of wind velocity with a height up to 1,000 ft, above which a constant velocity is justified. An exception should be made in coastal areas exposed to hurricane conditions and in other areas in which the records justify a basic velocity pressure above 20 lb per sq ft. Recommendations for

such areas should await further study by the ASCE Structural Division Committee on Wind Forces. Item 9 should read: The variation of gust factors with height is adequately represented by Eq. 3, except for the areas mentioned in Item 8. Item 10 should read: The combined effect of the variation of maximum wind velocity with height and of maximum gust factors with height is given by Eq. 6, except for the areas mentioned in Item 8.

AMERICAN SOCIETY OF CIVIL ENGINEERS
Founded November 5, 1852

TRANSACTIONS

Paper No. 2554

IRRIGATION WATER RIGHTS IN THE HUMID AREAS

By Howard T. Critchlow,[1] M. ASCE

With Discussion by Messrs. Harold E. Gray, and Howard T. Critchlow

Synopsis

In the eastern part of the United States, and especially in New Jersey, the practice of supplemental irrigation has been growing, resulting in increased competition for the use of water for all purposes in large centers of population and industrial development. To deal with this subject, the paper is divided into two parts—(1) general description of present practice; and (2) water rights.

Introduction

The information used has been obtained through a brief questionnaire sent to thirty-seven agencies in fourteen northeastern states, extending south and west to include Virginia, West Virginia, and Ohio. The agencies contacted were the state departments of agriculture, the agricultural experiment stations, and the farm bureaus. Replies have been received from all these states and most of their bureaus. All have reported the use of supplemental irrigation to some degree, varying from a maximum of about 50,000 acres in New York State (largely on Long Island and Staten Island), 25,000 acres in New Jersey, to a minimum of 250 acres in West Virginia.

Generally the areas are near centers of large populations, and the crops are raised as produce to be delivered to local markets and not essentially for canning. The principal crops irrigated are vegetables, potatoes, and hay, with occasional applications to fruit and nursery products, to cranberries in Massachusetts and New Jersey, and tobacco in Massachusetts and Connecticut.

Supplemental irrigation is practiced to save special crops from loss due to deficient rainfall in the growing season and also in order to increase the yield. A relatively small percentage of the total agricultural land is irrigated, generally limited to small units of area, rarely more than 50 acres in extent. The practice is due not to any lack of rainfall throughout the year but to its

Note.—Published in July, 1952, as *Proceedings-Separate No. 140.* Positions and titles given are those in effect when the paper or discussion was received for publication.

[1] Director and Chf. Engr., Div. of Water Policy and Supply, New Jersey Dept. of Conservation and Economic Development, Trenton, N. J.

distribution during the growing season. For example, in 1949 the average rainfall in the State of New Jersey in June was less than one-quarter inch.

There are two principal kinds of irrigation systems used in the east, the permanent or oscillating type, and the portable or rotary-head type. Only a few surface or flooding installations through ditches are found, as practiced in the arid west. A fourth or permanent type, with distribution mains on the ground connected to overhead sprinkling systems, is used on relatively small areas, generally for truck gardening. The portable type has been developed largely since World War II and makes use of lightweight pipe and sprinkler heads that can be moved easily from one area to the next. This type is economical to use, where the more permanent types may be prohibitive in cost. Irrigation is predominantly from surface waters, ground waters being estimated at less than 10% in all cases except New Jersey (10% to 40%) and New York—Long Island (50% to 90%).

The impetus in this irrigation practice seems to be quite generally due to the drought of 1948-1950, and in New Jersey is thought to be primarily for preventing loss rather than for increasing yield. In no case, however, has irrigation practice reached such proportions as to have necessitated state control over irrigation as such. New York requires permits for water used for irrigation from the Barge Canal, which may be considered a special case. Maryland requires permits for well drilling, and a permit from the state to use both surface and underground waters for any purpose except domestic and farming uses. New Jersey also requires permits for well drilling and is concerned with the use of water for industrial purposes, including irrigation, but only in certain areas threatened with overdraft and salt water intrusion. The State of New York controls ground water in Long Island for all uses except for agriculture. In all the other states surveyed, water rights apparently are governed by common law precepts, and approximately one third of the states replying reported cases of establishment of water rights by litigation and court decisions in individual cases.

1. Impetus to Irrigation Practice

A general description of present practice is afforded by brief reports from ten stations.

Connecticut Experiment Station.—The 1949 drought increased irrigation practice by thousands of dollars worth of equipment. The 1950 season was comparatively wet and did not require much increase. Twenty-five farmers interviewed stated that irrigation "paid," and many were able to pay off the cost of equipment in one year.

Delaware Department of Agriculture.—Irrigation developed mostly within the years 1948-1950, primarily on potatoes. Increased use is expected.

Maine Experiment Station.—Particular interest is being shown in pasture irrigation due to drought conditions.

Massachusetts Experiment Station.—Particular interest is shown in the development of water rights, since in the past priority was given to the use of water for power development.

New Jersey Experiment Station.—Irrigation nearly doubled during and after the 1949 dry season.

New York State Experiment Station.—Considerable increase in the building of farm ponds due to drought has been noted. Farm ponds, 10 ft or more in height, are subject to state control as to the stability and safety of the dam or embankment constructed to impound the water. A similar law also obtains in New Jersey and Pennsylvania.

Ohio Department of Agriculture.—The high price of farm products during and since World War II, and the introduction of lightweight portable pipe and rotary sprinklers, have done much to increase the practice of irrigation.

Vermont Department of Agriculture.—The value of irrigation for truck gardening has been established, but not as yet for pasture lands.

Virginia Extension Service.—Irrigation has only begun. The number of installations and the acreage will increase with continued profitable prices for farm products. Crops watered are Irish potatoes, tomatoes, beans, strawberries, eggplants, squash, hay, and pastures. One of the pioneers in the use of liquid fertilizer with irrigation water states that he has secured a yield of three hundred 100-lb bags of potatoes per acre whereas his neighbor obtained only from forty to sixty bags on similar land and under the same condition except for the application of water and ammonium nitrate.

West Virginia Experiment Station.—Several new installations have been made in 1950 on truck farms and one on grass land.

2. Legal Control of Water Rights

In most of the fourteen states surveyed the riparian doctrine of the common law controls rights to water use, especially surface waters. Some control of ground waters is exercised in a few states, including Maryland, New Jersey, New York, and Pennsylvania.

A summary of the comments on the legal control of water for irrigation or other private use from the several states follows, with the source of the information as noted parenthetically.

General.—The riparian doctrine gives owners along the bank of a stream certain rights to the natural flow of the water. Each owner is entitled to have the water in the watercourse flow by his land in its natural channel unobstructed, unpolluted, and free from unreasonable diminution. This rule applies only to water flowing in a watercourse. "Watercourse" is defined by the courts as a stream of water usually flowing in a definite channel and having a bed and sides or banks, and discharging itself into some other stream or body of water. "Diffused surface waters" have been classified as all waters flowing over the surface of the land for a short duration, which are not running in a natural watercourse, and which have yet been concentrated in lakes or ponds. This water belongs to the owner across whose land it flows and may be collected for irrigation without infringing on the legal rights of his neighbors.

Two general uses of water are recognized under the common law doctrine of water rights. They are: (1) Domestic use and (2) extraordinary use. The courts have expressed the view that the domestic uses of water—such as for drinking, household purposes, and watering stock—are its natural and

primary ones. After all domestic needs of the proprietor have been fulfilled, the surplus water must be returned to the stream and allowed to run its ordinary course. The use of water for irrigation is an extraordinary use. It has nevertheless been declared a lawful use by the courts.

Connecticut.—No permit is required for irrigation use. One lawsuit in 1949 was for the establishment of water rights (George W. Crowther, extension agricultural engineer).

Delaware.—As of 1950, there had been no occasion for the state to establish any law to govern irrigation (Ralph R. Peters, executive secretary, Delaware Farm Bureau).

Maine.—Water rights are governed by common law precepts (F. W. Peikert, University of Maine, Orono).

Maryland.—The water resources law of 1933 declares it to be the policy of the state to control the appropriation and use of both surface and underground waters and makes it unlawful to appropriate or use any waters without a permit. The use of water for domestic and farming purposes is exempted from this control.

Massachusetts.—There is considerable interest in the future development of irrigation water rights and this phase of the question is being investigated along with irrigation research. Water rights have been established by litigation in only a few cases and these have been with respect to water power rights (Karol J. Kucinski, University of Massachusetts at Amherst). The principles of law under riparian rights govern the quantity of water used by riparian owners. Ground water is under the control of the land owner. Common law precepts are mingled with some statutory provisions in determining water rights. Water cannot be diverted from the stream for irrigation purposes to the injury of ancient mill owner or the destruction of the stream for the purpose of quenching thirst (Daniel J. Curran, agriculturalist and legal counsel, Massachusetts Department of Agriculture).

New England.—The present right to apply water to purposes of irrigation depends for the most part on the riparian rights of the owner of land bordering on a stream, and on the right to the common use of the water found beneath the surface of the earth. Since it has been established that the riparian owner has a right to use the water for irrigation purposes, it becomes necessary to determine the extent of that right. The only rule that can be adopted under the principles of the common law, which recognizes no favoritism, is that the use made by each owner after the necessities of life are satisfied must be such as to be reasonable under all circumstances, with no priority in favor of any interest. This rule gives every owner the right to use the water for any purpose as long as his use is reasonable in view of the other interests which attach to the stream (Daniel J. Curran).

New Hampshire.—Irrigation is so limited in its size and volume that the use of water is no problem. The state pays no attention to it (Alfred L. French, secretary, New Hampshire Farm Bureau Federation).

New Jersey.—The riparian doctrine governs the private use of surface waters by owners of land along natural watercourses. Surface and ground waters for public and potable use are subject to legal control under legislation

passed in 1907 and 1910. In 1947 a law was enacted (Chapter 375) giving authority to regulate the diversion of subsurface waters of the state for domestic, industrial, and other uses including irrigation. This law requires divertors to obtain permits to use in excess of 100,000 gal daily in certain areas of the state.[2]

New York.—The control of surface waters is under the common law. Some farmers utilize water from the Barge Canal. Although there is a right to the use of such water in most deeds to the land, a permit is required for irrigation uses. On Long Island most of the water for irrigation is obtained from wells. A permit is required to drill wells on Long Island and also for the diversion of water in excess of 100,000 gal a day for all uses except agricultural uses.

Ohio.—Since no permits are required for irrigation in Ohio, it is difficult to give an accurate appraisal of the extent of irrigation. It is estimated at 16,000 acres, 25% of which is supplied with ground water and 75% from surface sources (Virgil Overholt, extension agricultural engineer).

Pennsylvania.—Irrigation is a new use for water in Pennsylvania. Although some litigation involves disputes over irrigation as contained in the Pennsylvania court records of more than a century ago, this agricultural practice has been nearly nonexistent until recently. Humid irrigation is designed to supplement rainfall by providing water to crops, pastures, and orchards in dry periods occurring during the growing season.

> "The law of water rights in Pennsylvania is based upon the common law doctrine that the upper owner of land on a stream may use as much water as needed for domestic purposes; but that for non domestic purposes, such as irrigation, he may not materially diminish the stream. The extensive use of water for purposes of irrigation is a new problem. Consequently, there are no statutory laws or legal decisions as to the right to appropriate overflow waters by impounding in reservoirs, or the right of an irrigation company to use the power of eminent domain as a public water agency. By legislative action or by court decision, the existing law of riparian rights can be adapted to cope with the problem of irrigation by giving land owners along streams the right to capture overflow waters, authorize irrigation companies to use the power of eminent domain so that owners whose land lies beyond the stream may obtain water as well as those owners along the stream, and by applying the principle of prior appropriation to navigable streams under the jurisdiction of the Commonwealth. [W. C. Anderson and F. H. Cook]."

Rhode Island.—Water rights are governed by common law precepts only (T. E. Odland, Department of Agronomy).

Vermont.—There are many rulings of the Vermont Supreme Court concerning water rights which are interpretations of the common law. Although the rights to water are based on the common law concept of reasonable use, the definition of "reasonable use" has had to be decided many times by the courts. Should irrigation become a widely accepted practice in Vermont there might very well be need to overhaul and clarify the laws with respect to water rights (L. J. Peet, state conservationist, U. S. Soil Conservation Service).

---

[2] "Policies and Problems in Controlling Ground Water Resources," by H. T. Critchlow, *Journal, A.W.W.A.*, Vol. 40, July, 1948, p. 775.

Virginia.—The state has no legal control over the use of water for irrigation. With the growing scarcity of water suitable for irrigation purposes, a source of water satisfactory in quality and quantity is the first consideration. The present practice takes practically all the water from surface sources by impounding waters behind earth dams. It is the opinion of informed people that the use of irrigation in Virginia has only begun (J. A. Waller, Jr., extension agricultural engineer, Agricultural Extension Service).

West Virginia.—There is no legal control over the use of water for irrigation. Known litigation in connection with water rights generally deals with pollution and not with use for irrigation (S. L. Galpin, hydrologist, Agricultural Experiment Station).

Summary and Conclusions

Undoubtedly there is a growing need for investigation in the field of supplemental irrigation to determine its benefits and the best practices to be followed for the conservation of the available water supplies. As the demand for this and other uses increases, the question of control by states will have to be considered and legislation enacted to meet the needs of the several states. The effect of the mineral content of the water on crops and soils—particularly from wells—may need to be investigated if the practice of irrigation becomes more general and continues year after year. Government regulations should be designed to obtain the greatest use to the greatest number. The effect on users of water for other purposes, particularly in industry, air conditioning, and other essential private uses, as well as the larger public use of waters, must be given due consideration in the development of irrigation practice.

It is evident from this brief survey that supplemental irrigation is growing in the humid areas. Where properly planned it is economically sound. Legal control of both surface and ground waters for all uses will undoubtedly be necessary, particularly in states with large populations and large demands for water for municipal, domestic, and industrial uses. It is doubtful whether uniform laws can be used.

In closing, another quotation Mr. Curran of (Massachusetts Department of Agriculture) is pertinent:

> "If we give attention to the results attained in successful irrigation projects in New England during the summer of 1949 the facts all seem to point to one conclusion, and that is, that the agriculture of the future must, if the population of the world continues to increase, be rescued from uncertain dependence upon natural rainfall, and be brought under the influence of a controlled water supply."

Acknowledgments

Many public officials and individuals, in letters to the writer, have furnished information about irrigation practice and laws governing the use of water in their states. Special mention should be made of Daniel J. Curran, W. C. Anderson, A. M. ASCE, F. H. Cook, and James A. Waller, Jr.

DISCUSSION

HAROLD E. GRAY[3].—A problem which has confronted many farmers and other workers in the field of supplemental irrigation in the northeast, and which will continue to increase as the practice of irrigation spreads, has been presented by the author.

An indication of the magnitude of the problem can be obtained from information on the amount of irrigation being practiced in New York State. This information is based on the results of a survey conducted in 1950 by Harry A. Kerr. Reports from fifty-two counties in the state showed nearly two thousand farmers using supplemental irrigation in 1950. Although over one half of these were concentrated in the two counties on Long Island (New York), forty-nine of the fifty-two counties reported the use of irrigation. The rapid growth is indicated by the fact that this same survey showed that slightly more than one thousand farmers were using irrigation 5 yr prior to the time of survey and that only six hundred and fifty were using it 10 yr before. Furthermore, there were six hundred and fifty farmers who indicated that they were planning to install irrigation systems in the immediate future, probably by 1952. Unfortunately, no figures are available to confirm this last statement.

At present, irrigation is practiced on nearly all vegetables grown commercially and for home consumption. Small berries, strawberries in particular, have responded to the addition of supplemental water. There is an increasing interest in the use of irrigation on pasture by dairy farmers.

The general feeling among farmers who have used irrigation is that it will save a crop 1 yr out of 5, give increased yields 2 or 3 yr out of 5, and that it is useless the other 1 or 2 yr. However, much more information is necessary concerning the consumptive use of water for different crops in humid climates, and concerning drought frequency expectancy, before this condition can be stated as a fact.

On Long Island, where there are heavy concentrations of irrigated areas, the need for the control of water has already become apparent and steps have been taken to insure this control. A similar need has not been recognized in other parts of the state. It is conceivable that, with the increased use of water for irrigation, the situation will become critical. This problem needs considerable study so that a workable system of legally-controlled water rights can be established. No one can argue against the advantage of establishing such a control to forestall a critical situation, as opposed to the establishment of the control to correct a critical situation after it has occurred.

There has been considerable interest in new sources of water supply for irrigation. The author indicated the increase in the building of farm ponds in New York State as a result of drought. However, caution must be observed in recommending farm ponds as ready and economical sources of water for

[3] Prof., Dept. of Agri. Eng., N. Y. State College of Agri., Cornell Univ., Ithaca, N. Y.

irrigation. A few figures will serve to emphasize this face. The farm pond of average size probably will hold 500,000 gal. It takes more than 27,000 gal to apply 1 in. of water on 1 acre of ground. A 1-in. application on 10 acres of ground would take more than one half the capacity of this average-sized pond. When the pond depends upon runoff for replenishment, especially during dry periods when the need for irrigation water is greatest, the supply of water may not meet the demand. Furthermore, this example makes no provision for pond losses, such as evaporation, seepage, and other uses of water.

The writer does not intend to assert that farm ponds cannot be used for irrigation. His intent was to indicate that, if ponds are to be used for irrigation, careful planning and design are essential to their success, so that an adequate supply of water will be available at the time of greatest demand.

In conclusion, it is repeated that, with increased demand for water for irrigation in the humid regions, a thorough study of the problem is essential in order to derive a workable system of legal control of water rights.

HOWARD T. CRITCHLOW,[4] M. ASCE.—Since preparing the original paper, the writer has participated in a survey of ground-water supplies for the United States. This survey was made in connection with a conference on water resources in Urbana-Champaign, Ill., in October, 1951. The significant fact disclosed by the survey, with relation to irrigation in humid areas, is that, of the twelve states having legal control over the allocation and use of ground water, New Jersey is the only state in which such control applies to irrigation and agricultural use. This law requires that diverters obtain permits from the state water control agency to use ground water in excess of 100,000 gal daily in certain areas of the state. To date (1952) this control has not restricted the development of supplemental irrigation, but there are indications that the extent of such irrigation may be limited by the availability of ground water.

The discussion by Mr. Gray indicates a rapid growth of supplemental irrigation in New York, largely from wells on Long Island and from surface supplies in up-state regions. One important fact emphasized by Mr. Gray is the danger of failure of the source of water supply from small ponds in drought, unless ample provision is made for evaporation, seepage, and other losses of water from such sources. Several cases have occurred in New Jersey, where irrigators have depended upon surface streams and ponds for irrigation use, only to have these sources fail in drought periods, with a resultant loss of valuable crops. The development of well supplies has resulted from such experiences. Good agricultural engineering practice is the only cure and guarantee that will assure successful irrigation, even in normally humid areas.

---

[4] Director and Chf. Engr., Div. of Water Policy and Supply, New Jersey Dept. of Conservation and Economic Development, Trenton, N. J.

AMERICAN SOCIETY OF CIVIL ENGINEERS
Founded November 5, 1852

TRANSACTIONS

Paper No. 2555

HORIZONTALLY CURVED BOX BEAMS

By Charles E. Cutts,[1] A. M. ASCE

With Discussion by Messrs. A. George Mallis, DeForest A. Matteson, Jr., and Charles E. Cutts

Synopsis

A beam curved horizontally through an angle of 90° and resting on four supports is analyzed for maximum torque, shear, moment, deflection, and rotation when the beam carries a uniform load. Three types of curved box beams were fabricated and tested with five concentrated loads placed symmetrically on the curved part of the beam to assimilate uniform loading. Unit strains were measured at critical points on the beam by means of SR-4 electrical strain gages.

A new method of design for closed section curved beams and a theoretical development for determining rotation and longitudinal warping stresses are included herein.

Introduction

The shape of the cross section of rolled steel sections, such as the I-sections and channel sections, have been designed for maximum resistance of the section to bending moment. These sections do not resist torsion well and do not utilize the material economically for this purpose. Inge Lyse and Bruce G. Johnston (11*a*)[2] have indicated the relative torsional rigidity and torsional strength of various sections (see Fig. 1.)

Since closed steel sections have such large values of torsional rigidity and strength, appreciable reduction in shearing stresses and rotation due to torsion can be obtained by building up a closed section member. Fig. 2 indicates the three types of closed sections tested—(*a*) consisting of two channels; (*b*) consisting of four plates; and (*c*) consisting of an I-beam with side plates. The two-channel section (Fig. 2(*a*)) was joined by intermittent butt welds and the other two sections by intermittent fillet welds. The welding consisted of 7-in. welds with 3 in. clear distances between them.

Fig. 3 illustrates one of the uses of the horizontally curved beam. In this building the corner column has been eliminated and the horizontally curved

Note.—Published in May, 1952, as *Proceedings-Separate No. 128*. Positions and titles given are those in effect when the paper or discussion was received for publication.

[1] Associate Prof. of Civ. Eng., Univ. of Florida, Gainesville, Fla.

[2] Numerals in parentheses, thus: (11*a*), refer to corresponding numbers in the bibliography, Appendix I.

beam spans the gap. The curved corner in this illustration is believed to be supported by cantilever construction as noted at the top of the building. This corner could be designed by using a closed-section beam continuous past the first columns from the corner and held down at the second columns, eliminating the supporting cantilever construction.

SECTIONS	RIGIDITY	STRENGTH
(a)	100.0	100.0
(b)	637.0	332.0
(c)	5.5	18.0
(d)	70.0	62.0
(e)	88.0	74.0
(f)	341.0 (Approx.)	280.0 (Approx.)
(g)	9.9 (Nearly Exact)	22.2 (Approx.)
(h) $r = w = \frac{2}{3}n$	11.6 (Nearly Exact)	22.8 (Approx.)
(i) Fixed Ends; 6.5 In.; 1.5 Ft	78.1 (Approx.)	38.3 (Approx.)

FIG. 1

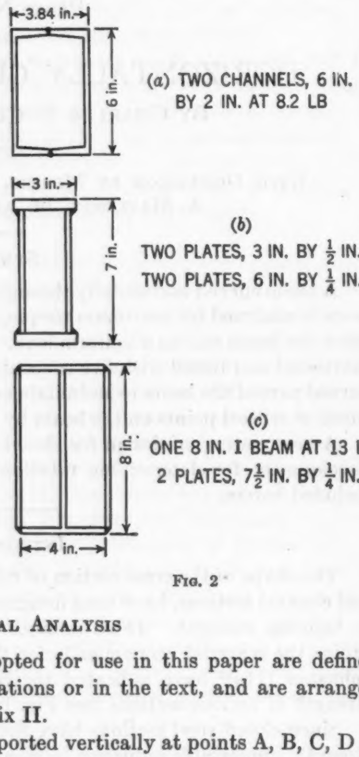

FIG. 2

THEORETICAL ANALYSIS

Notation.—The letter symbols adopted for use in this paper are defined where they first appear, in the illustrations or in the text, and are arranged alphabetically for reference in Appendix II.

The beam is continuous, and is supported vertically at points A, B, C, D as shown in Fig. 4. These four supports remain at the same elevation and offer no resistance to flexural or torsional rotation. The section is assumed to be compact, and secondary effects are omitted from the general equilibrium equations. The secondary effects are considered separately in the second part of this analysis.

The uniform load of w lb per ft is distributed from point A to point B on the curved part of the beam. Because of the symmetry of the beam and loading, by the law of statics $\Sigma V = 0$, and shears at reactions A and B are equal to one half of the load on the beam:

$$V_A = V_B = \frac{w \pi r}{4} \qquad (1)$$

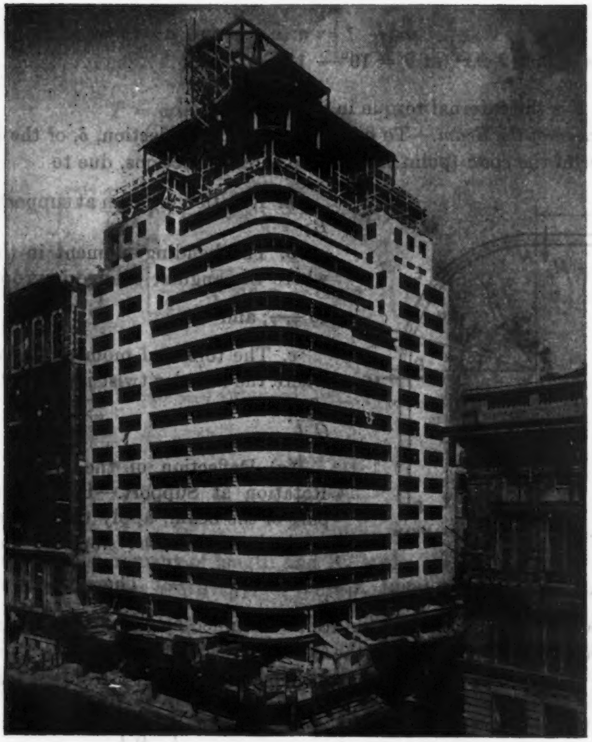

FIG. 3

Taking $\Sigma M = 0$ about the axis BD:

$$M_A = -\frac{\pi r^2}{4} w + \int_0^{\pi/2} w\, r^2 (1 - \cos \alpha)\, d\alpha = -\left(1 - \frac{\pi}{4}\right) w\, r^2 \qquad (2a)$$

$$M_A = M_B = -\,0.2146\, w\, r^2 \qquad (2b)$$

$$M_\theta = -\left(1 - \frac{\pi}{4}\right) w\, r^2 \cos \theta + \frac{w\, \pi\, r}{4} \times r \sin \theta - \int_0^\theta w\, r^2 \sin \alpha\, d\alpha \qquad (2c)$$

$$M_\theta = w\, r^2 \left(\frac{\pi}{4} \sin \theta + \frac{\pi}{4} \cos \theta - 1\right) \qquad (2d)$$

$$M_E = +\, w\, r^2 \left(\frac{\sqrt{2}\, \pi}{4} - 1\right) = +\, 0.1107\, w\, r^2 \qquad (2e)$$

$$T_\theta = M_B \sin \theta + \frac{w\, \pi\, r^2}{4} (1 - \cos \theta) - \int_0^\theta w\, r^2\, d\alpha\, (1 - \cos \alpha) \qquad (2f)$$

$$T_\theta = w\, r^2 \left[\frac{\pi}{4} (1 + \sin \theta - \cos \theta) - \theta\right] \qquad (2g)$$

$$T = 0 \text{ (at points A, B, and E)} \qquad (2h)$$

and

$$T_{max} = 0.03312\, w\, r^2 \text{ (at } \theta = 19° - 12') \qquad (2i)$$

in which T is the external torque in inch-pounds.

Deflection of the Beam.—To find the maximum deflection, δ, of the beam at the center of the span (point E) add the three deflections, due to

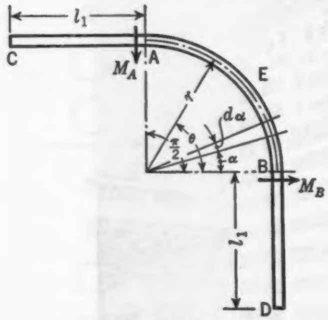

FIG. 4.—PLAN VIEW OF BEAM

a. Rotation of beam at supports A and B;

b. The bending moment in the beam where the angular change is proportional to $\frac{M}{E\,I}$; and

c. The torsional moment in the beam where the angular twist is proportional to $\frac{T}{G\,J}$.

(*a*) Deflection of the Beam Due to Rotation at Support.—For the straight part of the beam, apply the moment-area method to find the slope at the inner supports. The slope at point A $= -\,0.0715 \frac{w\, r^2\, l_1}{E\, I}$. The deflection at the center (point E) is equal to this rotation multiplied by the distance $r \sin 45°$.

(*b*) Deflection of the Beam at the Center of Span Due to Bending Moment.—Applying the moment-area method, the deflection of point E from the tangential plane to the elastic curve at point A is equal to $\int \frac{M\, ds}{E\, I}$ multiplied by the tangential distance $r \sin\left(\frac{\pi}{4} - \alpha\right)$:

$$M = w\, r^2 \left[\frac{\pi}{4}(\sin\alpha + \cos\alpha) - 1\right] \qquad (3a)$$

$$\delta \text{ (center)} = \int_0^{\pi/4} \frac{M\, ds}{E\, I}\left[r \sin\left(\frac{\pi}{4} - \alpha\right)\right] \qquad (3b)$$

$$\delta \text{ (center)} = \frac{w\, r^4}{\sqrt{2}\, E\, I}\int_0^{\pi/4}\left[\frac{\pi}{4}(\sin\alpha + \cos\alpha) - 1\right](\cos\alpha - \sin\alpha)\, d\alpha \qquad (3c)$$

and

$$\delta \text{ (center)} = \frac{w\, r^4}{\sqrt{2}\, E\, I}\left(\frac{\pi}{8} - \sqrt{2} + 1\right) = -\,0.015212 \frac{w\, r^4}{E\, I} \text{ (downward)} \qquad (3d)$$

(*c*) Deflection of the Beam at the Center of Span Due to Torque.—The deflection of point E from the tangential plane to the elastic curve is equal

to $\int \frac{T\,ds}{G\,J}$ multiplied by the torque arm $r\left[1 - \cos\left(\frac{\pi}{4} - \alpha\right)\right]$; thus,

$$T = w\,r^2\left[\frac{\pi}{4}(1 + \sin\alpha - \cos\alpha) - \alpha\right] \quad (4)$$

and

$$\delta\,(\text{center}) = \int_0^{\pi/4} \frac{T\,ds}{G\,J}\,r\left[1 - \cos\left(\frac{\pi}{4} - \alpha\right)\right] \quad (5a)$$

$$\delta\,(\text{center}) = \frac{w\,r^4}{G\,J}\int_0^{\pi/4}\left[\frac{\pi}{4}(1 + \sin\alpha - \cos\alpha)\right]\left[1 - \cos\left(\frac{\pi}{4} - \alpha\right)\right]d\alpha \quad (5b)$$

and

$$\delta\,(\text{center}) = -\,0.0016845\,\frac{w\,r^4}{G\,J}\,(\text{upward}) \quad (5c)$$

in which (10)

$$J = \frac{4\,A^2_s}{\oint \frac{ds}{t}} \quad (6)$$

and ds is a short increment of length and A_s is the shear area.

Rotation and Stresses Resulting from Warping of the Section Due to Torsion.—In this development, the beam is analyzed for one half of its curved length since symmetrical stress conditions exist in the two 45° halves of the curved part. This solution is approximate in that an equivalent length of straight beam is analyzed and that the variation in torque is assumed to be a function of the sine curve.

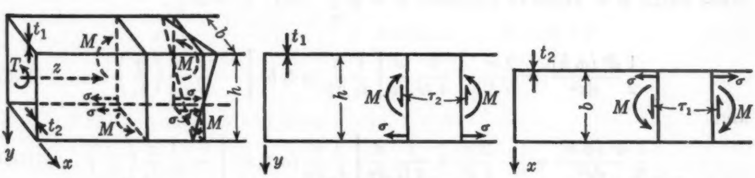

(*a*) (*b*) ELEVATION VIEW (*c*) PLAN VIEW

FIG. 5

When torque is applied to a section as shown in Fig. 5, in addition to shearing stresses, τ, resisting the torque there appear longitudinal stresses as well. These longitudinal stresses are caused by the warping of the section and are related in part to the wall thicknesses and side dimensions. By the double integration method (16),

$$\frac{d^2x}{dz^2} = \frac{M_y}{E\,I_y} - \frac{1}{G}\frac{d\tau_1}{dz} \quad (7a)$$

and

$$\frac{d^2y}{dz^2} = -\frac{M_x}{E\,I_x} - \frac{1}{G}\frac{d\tau_2}{dz} \qquad (7b)$$

Since the unit bending stress $\sigma = \frac{M_c}{I}$,

$$\frac{d^2x}{dz^2} = \frac{2\,\sigma}{b\,E} - \frac{1}{G}\frac{d\tau_1}{dz} \qquad (8a)$$

$$\frac{d^2y}{dz^2} = -\frac{2\,\sigma}{h\,E} - \frac{1}{G}\frac{d\tau_2}{dz} \qquad (8b)$$

$$q = \tau_1\,t_1 = \tau_2\,t_2 \qquad (8c)$$

$$t_1\,\tau_1 = \frac{d}{dz}\left(\frac{2\,\sigma}{b}\,Q_1\right) \qquad (8d)$$

and

$$t_2\,\tau_2 = -\frac{d}{dz}\left(\frac{2\,\sigma}{h}\,Q_2\right) \qquad (8e)$$

in which q denotes shear flow and Q is the statical moment of area about the neutral axis. The maximum values of shear flow become

$$t_1\,\tau_1 = \frac{1}{4}\frac{d}{dz}(\sigma\,t_1\,b) + q \qquad (9a)$$

and

$$t_2\,\tau_2 = -\frac{1}{4}\frac{d}{dz}(\sigma\,t_2\,h) + q \qquad (9b)$$

Since (with ϕ = angle of rotation) $x = \phi\frac{h}{2}$ and $y = \phi\frac{b}{2}$,

$$\frac{1}{2}\frac{d^2(\phi\,h)}{dz^2} = \frac{2\,\sigma}{b\,E} - \frac{1}{4\,G}\frac{d}{dz}\left[\frac{1}{t_1}\frac{d}{dz}(\sigma\,t_1\,b)\right] - \frac{1}{G}\frac{d}{dz}\left(\frac{q}{t_1}\right) \qquad (10a)$$

and

$$\frac{1}{2}\frac{d^2(\phi\,b)}{dz^2} = -\frac{2\,\sigma}{h\,E} + \frac{1}{4\,G}\frac{d}{dz}\left[\frac{1}{t_2}\frac{d}{dz}(\sigma\,t_2\,h)\right] - \frac{1}{G}\frac{d}{dz}\left(\frac{q}{t_2}\right) \qquad (10b)$$

and equating these expressions,

$$\frac{4\,\sigma}{E\,h\,b} - \frac{\sigma''\,b}{2\,G\,h} - \frac{2\,q'}{G\,t_1\,h} = -\frac{4\,\sigma}{E\,h\,b} + \frac{\sigma''\,h}{2\,G\,b} - \frac{2\,q'}{G\,t_2\,b} \qquad (11a)$$

$$\frac{\sigma''}{2\,G}\left(\frac{h}{b} + \frac{b}{h}\right) - \frac{8\,\sigma}{E\,h\,b} - \frac{2\,q'}{G}\left(\frac{1}{t_2\,b} - \frac{1}{t_1\,h}\right) = 0 \qquad (11b)$$

$$T = 2\left(\int_{-b/2}^{b/2}\tau_1\,t_1\frac{h}{2}\,dx + \int_{-h/2}^{h/2}\tau_2\,t_2\frac{b}{2}\,dy\right) \qquad (11c)$$

and

$$T = 2\,q\,b\,h + \frac{\sigma'\,b\,h}{6}\,(b\,t_1 - h\,t_2) \qquad (11d)$$

Solving for q,

$$q = \frac{T}{2\,b\,h} - \frac{\sigma'}{12}\,(b\,t_1 - h\,t_2) \qquad (12)$$

Since the torque varies in a manner similar to the function $\sin \frac{\pi z}{l}$,

$$T = T_{\max} \sin \frac{\pi z}{l} \qquad (13)$$

in which l is one half the span length and the following differential equation is obtained:

$$\sigma'' - a^2\sigma + C \cos \frac{\pi z}{l} = 0 \qquad (14)$$

in which

$$a^2 = \frac{\dfrac{48\,G}{E}}{b\,h\left[3\left(\dfrac{h}{b} + \dfrac{b}{h}\right) + \left(\dfrac{1}{t_2\,b} - \dfrac{1}{t_1\,h}\right)\left(b\,t_1 - h\,t_2\right)\right]} \qquad (15a)$$

and

$$C = \frac{-\dfrac{6\,\pi\,T_{\max}}{l}\left(\dfrac{1}{t_2\,b} - \dfrac{1}{t_1\,h}\right)}{b\,h\left[3\left(\dfrac{h}{b} + \dfrac{b}{h}\right) + \left(\dfrac{1}{t_2\,b} - \dfrac{1}{t_1\,h}\right)\left(b\,t_1 - h\,t_2\right)\right]} \qquad (15b)$$

The general solution to Eq. 14 becomes

$$\sigma = \frac{C}{\dfrac{\pi^2}{l^2} + a^2} \cos \frac{\pi z}{l} + A \sinh a\,z + B \cosh a\,z \qquad (16)$$

If $\sigma = 0$ at the center of the span where, $z = 0$,

$$B = -\frac{C}{\dfrac{\pi^2}{l^2} + a^2} \qquad (17)$$

and, since $\sigma' = 0$ at $z = l$,

$$A = \frac{C}{\dfrac{\pi^2}{l^2} + a^2}\left(\frac{e^{al} + e^{-al}}{e^{al} - e^{-al}}\right) \qquad (18)$$

By substituting Eq. 16 in

$$\phi'' = \frac{4\,\sigma}{b\,h\,E} - \frac{b}{2\,G\,h}\,\sigma'' - \frac{2}{G\,t_1\,h}\,q' \qquad (19)$$

and integrating,

$$\phi' = \frac{4}{E\,h\,b}\left(\frac{\frac{l}{\pi}C}{\frac{\pi^2}{l^2}+a^2}\sin\frac{\pi z}{l} + \frac{A}{a}\cosh a z + \frac{B}{a}\sinh a z\right)$$

$$- \frac{b}{2\,G\,h}\left(\frac{-\frac{\pi}{l}C}{\frac{\pi^2}{l^2}+a^2}\sin\frac{\pi z}{l} + A\,a\cosh a z + B\,a\sinh a z\right)$$

$$- \frac{2}{G\,t_1\,h}q + D \quad \text{..(20)}$$

Since $\phi' = 0$ at $z = 0$,

$$D = -\frac{4\,A}{E\,h\,b\,a} + \frac{a\,b\,A}{2\,G\,h} \quad \text{.....................(21)}$$

Integrating again,

$$\phi = \frac{4}{E\,h\,b}\left(-\frac{\frac{l^2}{\pi^2}C}{\frac{\pi^2}{l^2}+a^2}\cos\frac{\pi z}{l} + \frac{A}{a^2}\sinh a z + \frac{B}{a^2}\cosh a z\right)$$

$$- \frac{b}{2\,G\,h}\left(\frac{C}{\frac{\pi^2}{l^2}+a^2}\cos\frac{\pi z}{l} + A\sinh a z + B\cosh a z\right)$$

$$- \frac{2}{G\,t_1\,h}\left[-\frac{T_{\max}\frac{l}{\pi}\cos\frac{\pi z}{l}}{2\,b\,h} - \frac{\sigma}{12}(b\,t_1 - h\,t_2)\right] + D\,z + E \quad \text{..(22)}$$

when $z = l$ and $\phi = 0$:

$$E = -\frac{4}{E\,h\,b}\left[\frac{\frac{l^2}{\pi^2}C}{\frac{\pi^2}{l^2}+a^2} + \frac{A}{a^2}\left(\frac{e^{al}-e^{-al}}{2}\right) + \frac{B}{a^2}\left(\frac{e^{al}-e^{-al}}{2}\right)\right]$$

$$+ \frac{b}{2\,G\,h}\left[-\frac{C}{\frac{\pi^2}{l^2}+a^2} + A\left(\frac{e^{al}-e^{-al}}{2}\right) + B\left(\frac{e^{al}-e^{-al}}{2}\right)\right]$$

$$+ \frac{2}{G\,t_1\,h}\left\{\frac{T_{\max}\frac{l}{\pi}}{2\,b\,h} - \left(\frac{b\,t_1 - h\,t_2}{12}\right)\left[-\frac{C}{\frac{\pi^2}{l^2}+a^2} + A\left(\frac{e^{al}-e^{-al}}{2}\right)\right.\right.$$

$$\left.\left. + B\left(\frac{e^{al}+e^{-al}}{2}\right)\right]\right\} - D\,l \quad \text{....(23)}$$

and

$$\phi \text{ (center)} = \frac{4}{E\,h\,b}\left(-\frac{\frac{l^2}{\pi^2}C}{\frac{\pi^2}{l^2}+a^2}+\frac{B}{a^2}\right)-\frac{b}{2\,G\,h}\left(\frac{C}{\frac{\pi^2}{l^2}+a^2}+B\right)$$

$$-\frac{2}{G\,t_1\,h}\left(-\frac{T_{max}\,l/\pi}{2\,b\,h}\right)+E \ldots (24)$$

The hyperbolic functions cancel out for the ordinary span lengths used in building construction, thus greatly simplifying these expressions. A numerical example illustrating the application of the foregoing theory is presented in Appendix III.

Experimental Procedure and Results

Fig. 6 indicates the plan and side views of the typical specimen tested in this experiments. Section A-A, Fig. 6(*a*) refers to either of the three sections in Fig. 2. The cost of the members varied from $126 to $170. Welding the

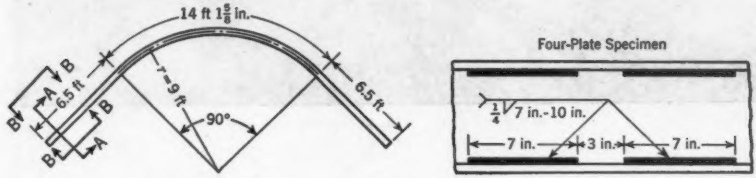

(*a*) PLAN VIEW (*b*) SIDE VIEW B-B

Fig. 6

members together provided considerable saving in cost compared to that of members joined by riveting.

Fig. 7 shows the layout plan for testing in which the box beams were supported by 3-in. square bearing plates at the intermediate supports and held down at the ends by loaded platforms. The curved beam was divided into six equal parts, and five equal concentrated loads were applied at 15° intervals. The loading was applied by means of lever arms with a platform carrying sacks of shot suspended from the outer end of each lever arm. Rotation at the center of the beam was measured by means of an optical lever. Vertical deflection of the beam was measured by Ames dials. A-1 and AR-1 (rosette type) electrical strain gages were located at twenty-two points to measure the unit strains. Fig. 8 shows the wiring arrangement with leads attached to a switching control near the K-box.

The total loading on the beams varied as indicated in line 2, Table 1. These loadings were calculated to produce a unit bending stress over the supports of 20,000 lb per sq in.

It is interesting to compare the unit stresses in flexure and shear with those calculated by the theory (lines 3, 4, and 5, Table 1).

The measured deflections of the beams varied from 0.40 in. to 0.55 in., and measured rotations at the center of the beam varied from 1.1° to 1.3°. The

computed deflections varied from 0.33 in. to 0.48 in. and the computed rotations at the center of beam varied from 0.64° to 0.99°.

The measured warping stress at the support for the two-channel section (Fig. 2(*a*)) varied from σ = 145 to 690 lb per sq in.; for the four-plate section

FIG. 7

FIG. 8

(Fig. 2(*b*)) from σ = 1628 to 2698 lb per sq in.; and for the I-section with side plates (Fig. 2(*c*)) from σ = 710 to 1508 lb per sq in. The calculated values of this secondary effect (pounds per square inch) are 266, 620, and 220, respectively. The poor comparison between calculated and test results for rotation

and the secondary warping stress may be due to the intermittent welding of test members, slight resistance to torsional rotation at the supports, and inability of one section to retain its rectangular shape. In this latter respect it is noted that the largest warping stresses occurred in the four-plate section which offered the least resistance to change of cross section and the smallest

TABLE 1.—COMPARISON OF OBSERVED AND COMPUTED UNIT STRESSES (UNITS, POUNDS PER SQUARE INCH)

Item	Description	Two Channels		Four Plates		I-Beam	
		Measured	Computed	Measured	Computed	Measured	Computed
(1)	(2)	(3)	(4)	(5)	(6)	(7)	(8)
1	Reference to Fig. 2	Fig. 2(a)		Fig. 2(b)		Fig. 2(c)	
2	Loading on the beams, in pounds	9,900		13,510		16,430	
	Longitudinal stress due to bending:						
3	End gages, 6 in. from support	13,041	16,495	17,181	16,513	14,750	16,477
4	Central gages, 6 in. from center of span	8,124	10,443	9,599	10,455	11,192	10,432
	Maximum shearing stress at outside face:						
5	19°21.69′ from the supports	4,772	4,710	6,450	6,462	4,411	3,788

warping stresses occurred in the two-channel section which was welded at the center of the top and bottom.

Thus, by using this arrangement of continuing the beam over the supports, and by using a closed section, the warping stress is minimized to that of a secondary effect and the bending stresses at the support control the design. This condition is to be contrasted with the case of an I-beam curved horizontally through 120° and fixed at the supports, in which the stresses due to this effect are equal to, or larger than, the bending stresses (14).

CONCLUSIONS

From the analysis of the experimental data taken on the testing of box sections, the following conclusions are offered for discussion:

1. Box sections are recommended for use in the design of beams subjected to torsion and bending, since they provide much greater torsional rigidity than the open section.
2. The design of a box section for a curved corner unsupported between column supports is recommended and is indicated in Appendix III.
3. The secondary effect (called "warping of the section") can be reduced by selecting dimensions such that the ratio of the thickness of the sides to their lengths are equal—that is, $t_1/b = t_2/h$.
4. Use of the section made up of two channels (Fig. 2(*a*)) is recommended over the section composed of four plates (Fig. 2(*b*)), since the two-channel section has greater resistance to change of cross-sectional shape.
5. The section consisting of an I-beam with side plates (Fig. 2(*c*)) may be reduced in cost by discontinuing the side plates over a part of the straight

section of beam on each end—the portion of beam being the length over which the required section modulus is smaller than that provided by the I-beam.

ACKNOWLEDGMENTS

The writer wishes to acknowledge the assistance and guidance rendered him by Joseph Alexander Wise, M.ASCE; also to the St. Paul Structural Steel Company and the American Institute of Steel Construction for furnishing the test members. Copy for Fig. 3 was supplied by Bethlehem Steel Company, Bethlehem, Pa.

APPENDIX I. BIBLIOGRAPHY ON HORIZONTALLY CURVED BOX BEAMS

(1) **"Zur Berechnung gekrümmter Träger,"** by W. L. Andree, *Der Eisenbau*, Vol. 9, 1918, pp. 184–190.

(2) **"Bethlehem Manual of Steel Construction,"** Bethlehem Steel Co., Bethlehem, Pa., 1934, pp. 279–289.

(3) **"Berechnung des senkrecht zu seiner Ebene Belastiten Bogenträgers,"** by Karl Federhofer, *Zeitschrift für Mathematik und Physik*, 1914, Vol. 62, pp. 40–63.

(4) **"Beitrag zur Berechnung gekrümmter Träger,"** by J. Hailer, *Die Bautechnik*, 1932, Vol. 10, p. 372.

(5) **"Der Kontinuierliche, halbkreisförmig gebogene und gleichmässig belastete Eisenbetonträger mit rechteckigem Querschnitt auf drei und vier gleich weit enfernten Stützen,"** by S. Hessler, *Beton und Eisen*, Vol. 29, 1930, pp. 149–154.

(6) **"Torsion of Flanged Members with Cross-Sections Restrained Against Warping,"** by H. M. Hill, *Technical Note No. 888*, National Advisory Committee for Aeronautics, March, 1943.

(7) **"Torsion of Rectangular Tubes,"** by William Hovgaard, *Journal of Applied Mechanics*, Vol. 4, No. 3, September, 1937, pp. 131–135.

(8) **"Zur Theorie Torsionfester Ringe,"** by B. G. Kannenberg, *Der Eisenbau*, Vol. 4, 1913, pp. 329–334.

(9) **"A Recurrence Formula for Shear-Lag Problems,"** by Paul Kuhn, *Technical Note No. 739*, National Advistory Committee for Aeronautics, December, 1939.

(10) **"Some Elementary Principles of Shell Stress Analysis with Notes on the Use of the Shear Center,"** by Paul Kuhn, *Technical Note No. 691*, National Advisory Committee for Aeronautics, March, 1939.

(11) **"Structural Beams in Torsion,"** by I. Lyse and B. G. Johnston, *Transactions*, ASCE, Vol. 101, 1936, p. 857. (a) Fig. 8, p. 865.

(12) **"Über Elastizität und Stabilität des geschlossen und offenen Kreisbogens,"** by R. Mayer, *Zeitschrift für Mathematik und Physik*, Vol. 61, 1913, pp. 302–308.

(13) **"Stresses in a Curved Beam Under Loads Normal to the Plane of Its Axis,"** by Robert B. B. Moorman, *Iowa State College Bulletin No. 145*, Iowa State College, Ames, Iowa, March, 1940.

(14) "Stresses in a Uniformly Loaded Circular Arc I-Beam," by Robert B. B. Moorman, Vol. 48, No. 27, *Engineering Series No. 36*, University of Missouri, Columbia, Mo., 1947.

(15) "The Stress Analysis of Bow Girders," by A. J. S. Pippard and F. L. Barrow, Department of Scientific and Industrial Research, *Building Research Board Technical Paper No. 1*, His Majesty's Stationery Office, London, 1926.

(16) "Neure Probleme aus der Flugzeugstatik," by H. Reissner, Vol. 18, 1926, p. 384.

(17) "The Torsion of Members Having Sections Common in Aircraft Construction," by George W. Trayer and H. W. March, *Technical Report No. 334*, National Advisory Committee for Aeronautics, March, 1930.

(18) "Der Kreistrager," by G. Unold, *Forschungsarbeiten auf dem gebiete des Ingenieurwesens*, No. 255, Verein Deutscher Ingenieure, Berlin, Germany, 1922.

(19) "Circles of Strain," by Joseph A. Wise, *Journal of the Aeronautical Sciences*, Vol. 7, No. 10, August, 1940, p. 438.

(20) "Torsional Strength of Steel I-Sections," by C. R. Young and C. A. Hughes, *Bulletin 4*, School of Engineering Research, University of Toronto, Toronto, Ont., Canada, 1924, pp. 131–144.

Appendix II.—Nomenclature

The following symbols, adopted for use in the paper and for the guidance of discussers, conform essentially with "American Standard Letter Symbols for Structural Analysis" (ASA-Z10.8–1942), prepared by a committee of American Standards Association with ASCE participation, and approved by the Association in 1942:

A = a mathematical coefficient defined by Eq. 18.
A_s = shear area, in square inches. $(b \times h.)$
a = a substitution factor defined by Eq. 15*a*.
b = width of section (center to center of side walls), in inches.
B = a mathematical coefficient defined by Eq. 17.
C = a substitution factor defined by Eq. 15*b*.
D = a mathematical coefficient defined by Eq. 21.
E = modulus of elasticity in pounds per square inch.
E = a mathematical coefficient defined by Eq. 23.
e = base of natural logarithms.
f_b = allowable stress in bending.
G = modulus of elasticity in shear, in pounds per square inch.
h = depth of section (center to center of top and bottom thicknesses of the section), in inches.
I = moment of inertia, in inches^4.
J = torsional rigidity of section, in inches^4.
l = length of beam from center of span to the support, in inches.
M = resisting bending moment in beam, in inch-pounds.
Q = statical moment of area about the neutral axis, in inches^3.

q = shear flow, in pounds per inch.
r = radius of curvature of the beam, in feet.
S = section modulus, in inches^3.
s = distance; ds = small increment of length.
T = external torque in inch-pounds; T_{max} = maximum torque.
t = thickness, in inches.
t_1 = top and bottom walls of sections.
t_2 = side walls of section.
V = vertical shear, in pounds.
w = uniform load, in pounds per foot of beam.
x, y, and z = coordinate axes and corresponding distances.
α = angle measured in the horizontal plane.
δ = deflection, in inches.
σ = unit stress due to bending, in pounds per square inch.
θ = angle measured in the horizontal plane.
τ = unit stress in shear, in pounds per square inch.
ϕ = angle of rotation, in radians.

Appendix III.—Proposed Method of Design

Statement of Problem.—Design a horizontally curved beam as shown in Fig. 4 with a radius of curvature r = 12 ft, w = 600 lb per ft over the entire length from point C to point D, and l_1 = 12 ft. The maximum bending moments in the beam occur at the supports A and B. From Fig. 9(*a*) and Eq. 2(*b*): $M_A = M_B = -0.2146\, w\, r^2$ = 222,497.28 in.-lb. The maximum torques occur at $\theta = 19°12'$ from supports A and B on the curved length of the beam as shown in Fig. 9(*c*) and by Eq. 2(*i*): $T_{max} = 0.03312\, w\, r^2$ = 34,338.82 in.-lb. The vertical shear at point of maximum torque may be taken from the diagram in Fig. 9(*b*), or computed, thus, for $\theta = 19°12'$: $V = 0.7854\, w\, r - \frac{19.2}{180}\pi\, w\, r$ = 2431.62 lb.

The stress that approaches the allowable unit stress first is the unit stress created by bending at supports A and B. This stress will be increased by the warping of the section. Selection of the section will be based on the required section modulus as determined by M_A and by keeping the term $\frac{1}{t_2 b} - \frac{1}{t_1 h}$ to a minimum. The required section modulus is $S = \frac{M}{f_b} = \frac{222{,}497.28}{20{,}000} = 11.1249$ in^3. (The 1946 specifications of the American Institute for Steel Construction, AISC, gives f_b = 20,000 lb per sq in.)

Try two channels, 6 in. by 2 in. by 13.0 lb, with dimensions as shown in Fig. 10, and other characteristics as follows: S = 11.6 in.^{3}; I = 34.6 in.^{4}; b = 4.314 − 0.437 = 3.877 in.; h = 6.000 − 0.343 = 5.657 in.; and $A_s = b\,h$ = 3.877 × 5.657 = 21.9322 sq in. The relations $\tau = \frac{T}{2\,A_s\,t_2}$ and $J = \frac{4\,A_s^2}{\oint \frac{ds}{t}}$ have been devel-

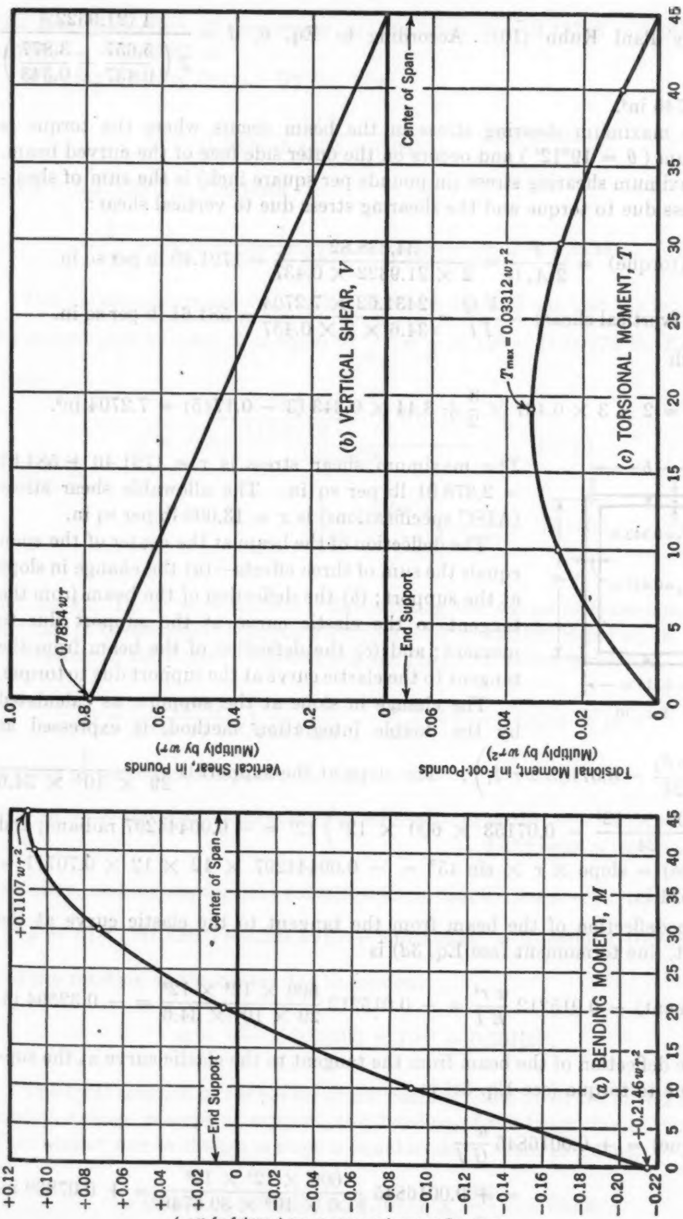

FIG. 9.—VARIATIONS IN MOMENT AND SHEAR OVER THE CURVED LENGTH OF THE BEAM, UNIFORMLY LOADED (LENGTH AB, FIG. 4)

oped by Paul Kuhn (10). According to Eq. 6, $J = \dfrac{4\,(21.9322)^2}{2\left(\dfrac{5.657}{0.437} + \dfrac{3.877}{0.343}\right)}$ $= 39.6746$ in^4.

The maximum shearing stress in the beam occurs where the torque is maximum ($\theta = 19°12'$) and occurs on the outer side face of the curved beam. The maximum shearing stress (in pounds per square inch) is the sum of shearing stress due to torque and the shearing stress due to vertical shear:

$$\tau(\text{torque}) = \frac{T}{2\,A_s\,t_2} = \frac{34{,}338.82}{2 \times 21.9322 \times 0.437} = 1791.40 \text{ lb per sq in.}$$

$$\tau\ (\text{vertical shear}) = \frac{V\,Q}{I\,t} = \frac{2431.62 \times 7.2704}{34.6 \times 2 \times 0.437} = 584.61 \text{ lb per sq in.}$$

in which

$$Q = 2 \times 3 \times 0.437 \times \frac{3}{2} + 3.44 \times 0.343\,(3 - 0.1715) = 7.2704 \text{ in}^3.$$

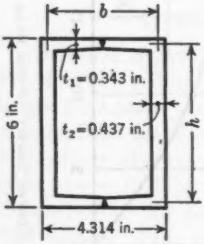

FIG. 10

The maximum shear stress is $\tau = 1791.40 + 584.61 = 2{,}376.01$ lb per sq in. The allowable shear stress (AISC specifications) is $\tau = 13{,}000$ lb per sq in.

The deflection of the beam at the center of the span equals the sum of three effects—(*a*) the change in slope at the support; (*b*) the deflection of the beam from the tangent to the elastic curve at the support due to moment; and (*c*) the deflection of the beam from the tangent to the elastic curve at the support due to torque.

The change in slope at the support, as calculated by the double integration method, is expressed as $\dfrac{1}{E\,I}\left(\dfrac{w\,l^3_1}{24} - 0.07153\,w\,r^2\,l_1\right)$. The slope at the support is $\dfrac{1}{29 \times 10^6 \times 34.6} \times \left(\dfrac{600 \times 12^3}{24} - 0.07153 \times 600 \times 12^3\right) 12^2 = -\,0.00444297$ radians; and δ (slope) = slope $\times\, r \times \sin 45° = -\,0.00444297 \times 12 \times 12 \times 0.70711 = -\,0.4524$ in.

The deflection of the beam from the tangent to the elastic curve at the support, due to moment (see Eq. 3*d*) is

$$\delta\ (\text{moment}) - 0.015212\,\frac{w\,r^4}{E\,I} = -\,0.015212\,\frac{600 \times 12^4 \times 12^3}{29 \times 10^6 \times 34.6} = -\,0.32594 \text{ in.}$$

The deflection of the beam from the tangent to the elastic curve at the support due to torque (see Eq. 5*c*) is

$$\delta\ (\text{torque}) = +\,0.0016845\,\frac{w\,r^4}{G\,J}$$

$$= +\,0.0016845\,\frac{600 \times 12^4 \times 12^3}{11.6 \times 10^6 \times 39.6746} = +\,0.07869 \text{ in.}$$

The total deflection at the center of the span is $-0.45240 - 0.32594 + 0.07869 = -0.69965$ in.

Warping Effect of Beam.—By Eq. 15*a*,

$$a^2 = \frac{19.2}{21.9322\,(6.4334 - 0.0855)} = 0.13790843$$

and $a = 0.3713602$. The term

$$\frac{1}{t_2 b} - \frac{1}{t_1 h} = \frac{1}{0.437 \times 3.877} - \frac{1}{0.343 \times 5.657} = 0.07486.$$

The maximum torque $T_{\max} = 34{,}338.82$ in.-lb; and one half the length of the curved part of beam, l, is equal to $\frac{\pi}{4} r = \frac{\pi}{4} \times 12^2 = 113.0972$ in. Eq. 15*b* yields

$$C = -\frac{\dfrac{6\pi \times 34{,}338.816}{113.0972} \times 0.07486}{139.2228} = -3.0774.$$

By Eq. 17,

$$B = -\frac{C}{\dfrac{\pi^2}{l^2} + a^2} = \frac{3.0774}{0.000772 + 0.137908} = 22.1905$$

and, by Eq. 18, $A = -22.1905$. Substituting the values of these constants into Eq. 16 to determine warping σ (support): $B = 22.1905$ lb per sq. in.

Rotation of the Beam.—Substituting the foregoing values in Eq. 21,

$$D = \frac{22.1905}{5.657 \times 10^6}\left(\frac{4}{41.7531} - \frac{1.43976}{23.2}\right) = 0.13236 \times 10^{-6}.$$

Making proper substitutions in Eq. 23,

$$E = 10^{-6}\,(+\,180.8642 + 2506.4437 + 0.6555 - 14.3976) = 2{,}672.9938 \times 10^{-6} \text{ radians.}$$

Similarly, making appropriate substitutions in Eq. 24, for $z = 0$:

$$\phi = 10^{-6}\,(181.8762 + 2{,}504.1913 + 2{,}672.9938) = 5.35906 \times 10^{-3} \text{ radians}$$

and the rotation at the center due to torsion:

$$\phi = \frac{180}{\pi} \times 5.35906 \times 10^{-3} = 0.30705^\circ.$$

The total rotation of the center of the beam is made up of the effects due to torsion, change in slope of support, and bending of the beam due to moment. The rotation due to change in slope is equal to slope $\times \sin 45^\circ$; thus,

$$\phi\ (\text{slope}) = 0.004443 \times 0.70711 \times \frac{180}{\pi} = 0.18000^\circ.$$

The rotation due to the effect of bending the beam from the support to the center of span equals the expression for deflection due to moment with r^3 instead of r^4:

$$\phi \text{ (moment)} = 0.015212 \frac{w\,r^3}{E\,I} = 0.015212 \frac{600 \times 12^3}{29 \times 10^6 \times 34.6}$$

$$= 0.00226 \text{ radians} = 0.00226 \times \frac{180}{\pi} = 0.12969°.$$

The total rotation of the beam at the center of the span equals the sum of the three effects:

$$\phi \text{ (total)} = 0.30705° + 0.18000° + 0.12969° = 0.61674°.$$

Welding of Channels.—The two channels are connected by intermittent butt welds. The allowable unit stress for shear on throat area of butt welds (AISC Specifications) = 13,000 lb per sq in. The maximum shear flow $q = \dfrac{T_{\max}}{2\,A_s}$ = 782.84 lb per linear in. The capacity of a $\frac{3}{16}$-in. weld = $\frac{3}{16} \times 13{,}000 = 2438$ lb per linear inch of weld. Use an intermittent weld of 4 in. with 6-in. spaces between welds.

DISCUSSION

A. GEORGE MALLIS[3], M. ASCE.—A curved profile has been a favorite design pattern of architects in the past decade, particularly in cantilevered canopies. Structural engineers have thus been faced with a problem that all too often has been completely ignored in textbooks used in undergraduate study and appears rather sparingly in graduate or advanced mechanics of materials. Practicing structural engineers have more often overcome this problem by applying empirical methods of design used in the particular design office in which they happened to be working. Mr. Cutts has done a creditable piece of work in his presentation, and his proposed method of design is certainly worthy of serious consideration for standard use in design offices.

However, as a practicing structural engineer, the writer must take serious exceptions to the author's design procedures. For example, Appendix III presents a typical design problem based on a loading of w equals 600 lb per sq ft. After a statement of the problem, the author proceeds to develop moments of 222,497.22 in.-lb, a torque of 34,338.82 in.-lb, and shear to a value of 2431.62 lb. To the writer a design analysis with computations extended to five or six significant figures, based on assumptions of two significant figures, is decidedly improper. It would have been better if the moments had been given to 223,000 in.-lb, torque to 34,300 in.-lb, and shear to 2430 lb. The same comment would apply to the determination of the required section modulus of 11.1249. The handbook of the American Institute for Steel Construction (AISC) gives section moduli to three figures, indicating that $S = 11.1$ in., cubed, would have been adequate.

DEFOREST A. MATTESON, JR.,[4] J.M. ASCE.—Engineers abroad used the cellular section in concrete work long before World War II, because of the high specific strength of this section in flexure and compression. Additional useful qualities have caused increasing use of the hollow girder in heavy construction in the United States. It is adapted easily to prestressed concrete construction of the precast, standardized type. Box beams are well adapted to welded steel construction, as in the author's specimens. "Locked-up" stresses in welded box beams have been studied. The flexural strength of such sections about two axes facilitates bridge construction. Box sections are valuable for resisting lateral buckling.

The torsional rigidity of the cellular section has been long realized, particularly by aircraft designers. Its value is indicated for use in girders of a straight bridge under a loading that is markedly antisymmetrical about the center line of the roadway. Straight spandrels of buildings also must resist applied torque.

---

[3] Senior Engr., Charles A. Maguire & Associates, Providence, R. I.

[4] Associate Editor, Technical Publications, ASCE, New York, N. Y

More important in this respect are the curved highway ramp, the sharply-skewed rigid frame, and the curved spandrel illustrated in the paper.

Because of the inadequate development of applicable analysis and design procedures, box sections for beams have usually been designed on a simplified basis. For concrete work, the assumptions and coefficients applicable to T-beam design have been used, giving a safe but unrealistic answer (21).[4a] The assumptions used in designing sheet metal aircraft sections may not apply to heavier structural shapes.

Commendably, the author presents a numerical example. A complete study of the horizontally curved beam must include such a test of the engineering applicability of the theory. It is the purpose of this discussion to examine some of the pitfalls that may face the designer when translating theory into a physical picture of structural behavior.

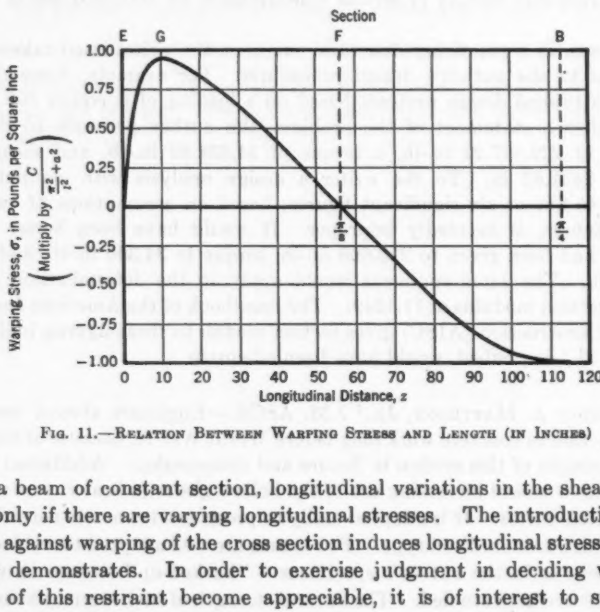

FIG. 11.—RELATION BETWEEN WARPING STRESS AND LENGTH (IN INCHES)

In a beam of constant section, longitudinal variations in the shear flow, q occur only if there are varying longitudinal stresses. The introduction of restraint against warping of the cross section induces longitudinal stresses, as the author demonstrates. In order to exercise judgment in deciding when the effects of this restraint become appreciable, it is of interest to study the variation of σ with z.

The author has shown the secondary nature (for the curved box beam) of the longitudinal stresses resisting warping. However, some useful information may be obtained from Fig. 11, which is a sketch of the variation in σ (see Eq. 16), using the constants expressed in Eqs. 17 and 18, and the physical quantities in the example of Appendix III.

The shape of the curve of σ-values in Fig. 11 is dependent on three conditions stated by the author: (a) It is assumed that the torque varies in a manner simi-

lar to the function $\sin \frac{\pi z}{l}$; (b) it is asserted that σ equals zero at midspan; and (c) it is asserted that $\sigma' = 0$ at $z = l$.

Because T varies sinusoidally—according to condition (a)—the stress follows a pure cosine curve except for nearly 15 in. on each side of section E. The downward deviation near E reflects the influence of the second and third terms on the right-hand side of Eq. 16. The values of these terms depend on condition (b). The author has not explained the basis for this condition.

The fact that there is no warping at section E is caused by symmetry of geometry and loading, and cannot form a basis for asserting that longitudinal stresses vanish at that section.

Fig. 11 shows that zero longitudinal stress does not necessarily accompany zero torque. When T is zero, σ equals either zero or σ_{max}, and when σ is zero, T equals either zero or T_{max}.

Eqs. 8 explain the situation clearly. If both the change in torsional warping and the change in torsional shear deformation are zero, σ must vanish, as at section E. If neither the warping nor the shear deformation becomes constant, but if the angle change of warping equals the negative of the angle change of shear deformation (neither of these is ϕ), σ becomes zero. Accordingly, torsional shear without restraint against torsional warping occurs at the quarter points, where T reaches its maximum value. Of course, there are additional effects caused by ordinary bending of the beam.

Therefore, it is true that σ is zero where z is zero; but the designer may also need to remember that σ reaches a peak for small values of z near section E, as shown in Fig. 11.

Because the stress σ reaches a maximum at supports A and B (see Fig. 4), condition (c) is reasonable. However, the symmetry of loading and geometry used by the author seems essential to his derivations. It is possible for warping of the cross section to occur at cross sections C and D. Therefore, it must be assumed that the straight parts of the beam are long and of equal stiffness, so that this warping becomes negligible in deflection computations.

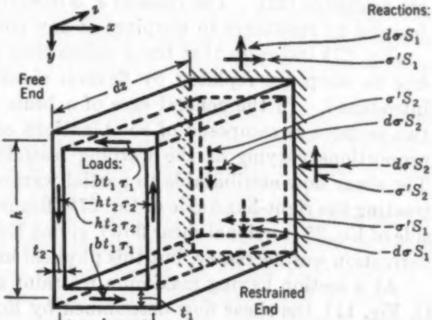

Fig. 12.—Cantilever Box Beam Under Torsional Load

If span BD were removed (see Fig. 4), leaving beam CAB on three supports, the structure would be stable under the author's loading. Clearly, the value of σ at the supports depends on the ability of the straight parts to develop resistance to warping. If span BD were shorter or of smaller section (less stiff) than the rest of the beam, the σ-value at point A would exceed that at point B. The section at which σ equals zero would have shifted to one side of section

E and the solution of Eq. 16 would require the knowledge of additional conditions.

Under the author's heading, "Conclusions," number five seems to be a good suggestion, but it might cause the values of σ to be altered.

Variation in Shear Flow.—The writer believes that Eqs. 8 would be better presented if static equilibrium were more carefully indicated in Fig. 5.

Fig. 12 shows a straight cantilever box beam of length dz, free to warp at one end and perfectly restrained against warping at the other end. Shear values are positive downward and to the reader's right. Moment vectors follow the right-hand rule and are positive upward or to the right. The loads are based on the relationship:

$$q = \frac{T}{2\,b\,h} \qquad (25)$$

which gives

$$b\,t_1\,\tau_1 = \sigma'\,S_1 \qquad (26a)$$

and

$$h\,t_2\,\tau_2 = -\,\sigma'\,S_2 \qquad (26b)$$

Eqs. 26 are comparable to Eqs. 8*d* and 8*e*.

Substituting Eq. 8*c* into Eqs. 26, and solving Eqs. 26 simultaneously,

$$2\,q = \sigma'\left(\frac{2\,I_1}{b^2} - \frac{2\,I_2}{h^2}\right) \qquad (27a)$$

and

$$q = \frac{\sigma'}{12}\,(b\,t_1 - h\,t_2) \qquad (27b)$$

Eq. 25 was used by the author to determine torsional shear in Appendix III. This expression usually is derived on the assumption that longitudinal stresses are negligible (22). The value of σ' is directly proportional to the flexural shear (caused by resistance to warping) at any point along the beam.

Eq. 27*b* indicates that the q-values that would exist at a section originally free to warp are replaced by flexural shear stresses, as warping restraint is introduced. In the general case of a beam under torsion only, shear at any two sections is composed of combinations of torsional and flexural shear, the proportions varying as the warping restraint σ varies between the sections. The shear flow attributable to partial warping of the section is found by subtracting the right-hand side of Eq. 27*b* (flexural shear flow) from the right-hand side of Eq. 25 (torsional shear flow), giving Eq. 12. The author's mathematical derivation was necessary, but this physical interpretation seems helpful.

At a section having maximum restraint against torsional warping (section G, Fig. 11), the shear flow determined by Eq. 27*b* vanishes at the section and Eq. 12 reduces to Eq. 25. The opposite extreme case occurs if σ' is a maximum, in which case Eq. 12 reduces to Eq. 27*b*, even though there is no warping restraint.

Eq. 25 is often considered applicable only where there is negligible restraint. The author has made an important contribution by showing that, in the general case, Eq. 25 holds at sections on which the warping-restraint stress σ is constant in the z-direction (it may be either a maximum or a minimum), and that it is

least valid at sections where σ' is a maximum—as at section F, on which σ is zero but not constant along the beam. The case of pure torsion is thus a special (and somewhat misleading) one.

Torsional Shearing Stress.—The author's example in Appendix III has not considered the implications of Eq. 12 in the determination of the shear stress. The torsional shear is more properly determined by Eqs. 9, in which q is defined by Eq. 12.

Fig. 11 is proportional to the curve of moments produced by restraint against warping. The curve of σ'-values (the shear accompanying these moments) has its maximum value adjacent to midspan. Eq. 9a reduces to

$$\tau_1 = \sigma' \left(\frac{b}{\sigma} + \frac{h\, t_2}{12\, t_1} \right) \ldots\ldots\ldots\ldots\ldots\ldots\ldots (28)$$

if z equals zero. For the example in Appendix III, this yields τ_1 (torque) = -10.3 lb per sq in. at midspan. This value indicates that, for the beam used in the author's example, the shear effects caused by restraint against warping are negligible. Therefore, Eq. 25 is applicable as used by the author.

Under the author's heading, "Conclusions," the third conclusion is interesting when applied to the effect that warping restraint has on shear stresses. Examination of Eqs. 15 and 16 shows that the proportion suggested by the author also causes Eq. 12 to reduce to Eq. 25.

Angle of Twist.—The writer questions the importance of considering longitudinal stresses when computing ϕ. The twist per unit length ds of a hollow member that is not restrained against warping, and that is subjected to pure torque, is expressed as $\frac{T\, ds}{G\, J}$. Therefore, the angle of twist for such a member is

$$\phi = \int \frac{T\, ds}{G\, J} \ldots\ldots\ldots\ldots\ldots\ldots\ldots\ldots (29)$$

in which J is given by Eq. 6. However, the derivation of Eq. 6 is commonly based on the assumption that the longitudinal stresses equal zero everywhere n the beam (22)—a stress condition that actually occurs only at a few sections in the author's specimens.

Mr. Kuhn has warned that, for thin-walled cylinders having restraint against warping, Eq. 6 may be safely used to compute the angle of twist per unit of length only at a "considerable distance" from the section that remains plane—that is, from the section on which σ is the maximum (10).

The author's derivation of Eq. 24 for expressing ϕ is to be commended because it takes under consideration the warping stresses. Frequently, methods have been presented for analyzing curved beams, in which knowledge of a geometrical factor K (indicating the relationship between T and ϕ) has been presupposed; but the writer has seen few explanations as to how K is to be evaluated when warping stresses are present. The author indicates the complexity of the problem.

However, neglecting the effects of restraint against warping, Eq. 29 yields

$$\phi_{\max} = \int_0^{\frac{\pi}{4}} \frac{T_{\max}\, r}{G\, J} \sin \frac{\pi\, r\, \alpha}{l}\, d\alpha = - \frac{T_{\max}\, l}{G\, J\, \pi} \left(\cos \frac{\pi^2\, r}{4\, l} - 1 \right).$$

For the example in Appendix III, this equation yields ϕ_{max} (torsion) = 5.370 $\times 10^{-3}$, as compared with the value $\phi = 5.359 \times 10^{-3}$ yielded by Eq. 24. The error is approximately 0.2%, which is negligible. Thus, for this particular example, ϕ may be found by neglecting the effect of warping stresses and by using Eq. 29.

The values of both ϕ and δ are affected by the sum of the work done by the longitudinal stresses which resist warping in both the curved and straight parts of the beam. However, the work done by the beam is proportional to the sum of the squares of the various stresses. Therefore, the fact that the author's example involves a maximum value of τ (torque), which is approximately eighty times as great as the maximum σ-value, suggests that the effect of warping restraint on the twist and deflections of the curved box beam may be negligible.

Deflections.—Strictly speaking, Eq. 6 applies only to a thin-walled cylinder in torsion without end restraint. The moments $d\sigma\ S$ in Fig. 12 tend to reduce ϕ and δ. A superficial study of Eqs. 5, on the basis of the conservation of energy, indicates that to produce the same deflection value—δ at a specific z-value or s-value—a smaller applied load (therefore, less external work) will be required if there are only torsional shear stresses than if both transverse shear and longitudinal stresses are produced by the torsional loads. Therefore, the correct value of δ (torque) in the example in Appendix III should be smaller than the value given by Eq. 5 because of an increase in J based on the geometry of the section. Consideration of the energy concept indicates that knowledge of only those longitudinal stresses existing at or near the section under investigation is not a wise basis for judging the applicability of Eq. 6 in the calculation of δ.

The author has provided expressions that may be combined to form an equation expressing deflection, in which the effects of restraint against warping have been taken into account. However, in the example in Appendix III, the author has not used this mathematical tool.

The change in the angle of twist in a unit of length dz is $\phi'\ dz$, and may be expressed by substituting Eq. 21 into Eq. 20. If this angle is multiplied by the torque arm, $r\left[1 - \cos\left(\frac{\pi}{4} - \alpha\right)\right]$, and integrated between the appropriate limits, the expression for deflection will result. This expression differs from Eq. 5*b* in that the effects of warping restraint have been considered. A form of this relationship is

$$\delta\ (\text{center}) = \int_0^{\frac{\pi}{4}} \phi'\ r^2 \left[1 - \cos\left(\frac{\pi}{4} - \alpha\right)\right] d\alpha \ldots\ldots\ldots\ldots (30)$$

The right-hand side of Eq. 30, when integrated between limits, yields an unwieldy expression having more than thirty terms. The writer has not thoroughly computed ϕ by Eq. 30, but the evaluation of a few of the significant terms suggests that very little difference may exist between the author's value for δ(torque) in Appendix III and the value obtained by use of Eq. 30 in the

same example. Possibly, mathematical or numerical procedures can be devised for simplifying the evaluation of Eq. 30. Although, for large values of r, a small error in ϕ may accompany a large error in δ, the writer feels that the value yielded by Eq. 5b may be sufficiently accurate for most cases and that the evaluation in Appendix III is correct.

Experimental Results.—As mentioned by the author, torsion experiments have been conducted by others (see under the heading, "Introduction"). These tests have determined a constant of proportionality, K, such that $T = K\,G\,\frac{d\phi}{dz}$, for various structural sections. The constant K is a measure of torsional stiffness, which finds various applications in structural analysis. In the absence of warping restraint, $K = J$ for the closed hollow section. It might be possible for the author to study the effects of the warping stresses on this constant by tests on a curved box beam.

The author suggests that factors such as the ability of the cross section to retain its shape add greatly to the complexity of the problem. This condition indicates the importance of further testing and the possible establishment of empirical constants. The writer believes that a hollow triangular section composed of three plates, or a rectangular section to which a diagonal plate had been added, would hold its shape well, and might have some practical application.

Conclusions.—The author seems to have illustrated a fact not previously emphasized in structural engineering literature because he not only indicates that a beam that is of closed hollow section and that is continuous over the supports is highly resistant to torque (a well-known fact), but his example also suggests that for this beam the effects of restraint may be neglected in design calculations.

Neglecting secondary effects, the writer finds that the same torsion equations seem to apply to the curved box beam as those that apply to a circular tube in torsion. This fact is particularly true if $t_1/b = t_2/h$. Thus, some of the author's mathematical development becomes primarily of academic interest, and the process of design is greatly simplified.

The writer has suggested in this discussion that the expression relating shear flow and applied torque (Eq. 25) applies, regardless of the magnitude of any warping restraint existing at the section on which q is evaluated, if the restraining stresses are constant with respect to z at that section.

Charles E. Cutts,[5] A. M. ASCE.—The author agrees with Mr. Mallis regarding the number of significant places in carrying out design computations.

Mr. Matteson is to be commended for his extensive study of the paper and for his clarification of several relationships. He has indicated additional uses of the curved box beam and the comparative advantages of the box section for developing flexural and torsional strength. In regard to restraint, it should be reiterated that the supports in this problem offer no resistance to flexural or

[5] Associate Prof. of Civ. Eng., Univ. of Florida, Gainesville, Fla.

torsional rotation. The inner supports react vertically upward and the outer supports, vertically downward, permitting lateral as well as longitudinal rotation of the member at all supports. Structural designers are cautioned that imposing torsional restraint at any of the supports will increase the longitudinal stress produced by warping. In the experimental studies on the three types of closed sections, the reactions were transmitted to the member by steel bearing plates. Slight lateral rotation of the curved beam caused the beam to bear more on the outside section than on the inside section of the bearing plates at A and B in Fig. 4, thus creating a small torsional restraint. Because this arrangement would be used in practice, it was felt that stress studies of this nature would be more valuable than the use of ball-and-socket bearing arrangements to match the theoretical development.

Fig. 11 illustrates the variation of warping stress over the length of the beam from the center of the curved span where $z = 0$ to the inner support where $z = 113$ in. The maximum value of warping stress σ occurring 10 in. from the center of the span is only slightly less than the maximum value of warping stress σ at the support. However, the effect on design is not altered because the warping stress near the center of the span is added to a bending stress less than one half as great as the bending stress at the support. The critical design sections occur at the inner supports.

In the analysis it was assumed that $\sigma = 0$ at the center of the span at section E. However, the experimental studies indicated longitudinal warping stresses at the center of the span. The magnitude of these stresses was smaller than those at the supports A and B (23). Mr. Matteson has sought justification of this assumption by using Eqs. 8.

In comparing Eq. 26*a* and Eq. 8*d*, Mr. Matteson's value of $t_1 \tau_1$ is only 50% of the writer's value. The writer used the relationship:

$$V_1 = \frac{dM_1}{dz} \quad \text{(31)}$$

for the flexural shear flow, in which V_1 is the vertical shear in one side, and M_1 is the bending moment in one side. For the top or bottom side of thickness t_1 and width b, this equation becomes

$$\frac{t_1 \tau_1 I_1}{Q_1} = \frac{d}{dz}\left(\frac{\sigma I_1}{\frac{b}{2}}\right) \quad \text{(32)}$$

in which I_1 is the moment of inertia of the side about its neutral axis perpendicular to the plane of bending. The symbol Q_1 is the statical moment of inertia for a side about the same axis and is a variable quantity. This equation reduces to Eq. 8*d*, which represents the flexural shear flow. The derivation of Eqs. 8 is included in this discussion. The expressions for Q are $Q_1 = \frac{t_1}{2}\left(\frac{b^2}{4} - x^2\right)$ and $Q_2 = \frac{t_2}{2}\left(\frac{h^2}{4} - y^2\right)$ in which x and y are measured from the centers of the plates to express the variation of the flexural shearing stress. The total shear flow is equal to the sum of the flexural shear flow plus

the torsional shear flow:

$$t_1\,\tau_1 = \frac{d}{dz}\left[\frac{\sigma\,t_1}{b}\left(\frac{b^2}{4} - x^2\right)\right] + q \quad\ldots\ldots\ldots\ldots\ldots\ldots(33a)$$

$$t_2\,\tau_2 = -\frac{d}{dz}\left[\frac{\sigma\,t_2}{h}\left(\frac{h^2}{4} - y^2\right)\right] + q \quad\ldots\ldots\ldots\ldots\ldots\ldots(33b)$$

The maximum values of the total shear flow are indicated by Eqs. 9. The variation of the flexural shear flow is parabolic across the side; thus, the flexural shear force on one side is

$$b\,t_1\,\tau_1 = \tfrac{2}{3}\,b\left[\tfrac{1}{4}\,\frac{d}{dz}\left(\sigma\,t_1\,b\right)\right] = \frac{\sigma'\,t_1\,b^2}{6} = \sigma'\,S_1 \quad\ldots\ldots\ldots\ldots(34)$$

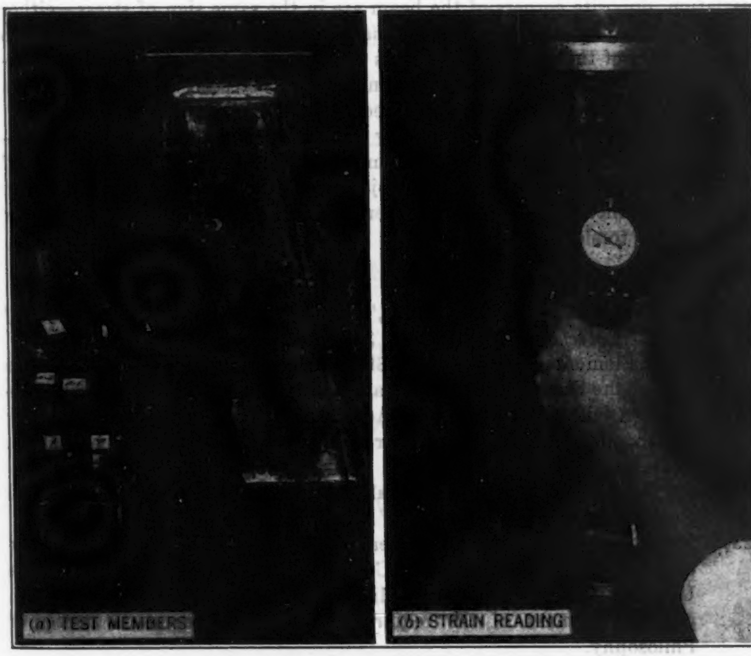

FIG. 13.—BOX BEAM TORSION TEST

Eq. 34 is identical with Mr. Matteson's Eq. 26*a* and substantiates his work. His development in expressing Eq. 25 through Eq. 27*b* checks the writer's Eq. 12 and directs attention to the two types of shear flow, namely, flexural and torsional.

With reference to Mr. Matteson's conclusions, the writer has not intended in his example to suggest that the effects of restraint may be neglected in design—rather, that longitudinal warping stresses associated with restraint may be

reduced by proper selection of box-beam proportions indicated in Conclusion 3. The writer agrees with Mr. Matteson's conclusion that Eq. 25 applies when the longitudinal warping stresses are constant. This may be shown by Eq. 12, when σ = constant, then $\sigma' = 0$ and $q = \frac{T}{2\,b\,h}$.

Mr. Matteson has suggested studies of the effect of warping stresses on the torsional stiffness constant K. In this regard, Charles R. Burke and the writer have conducted laboratory research on the torsional properties of closed box sections. Fig. 13(a) illustrates some of the test members composed of two structural steel angles welded together to form a box beam. Measurements of strain variations and stiffness were made on these test members. The variation of longitudinal stress in the sides of box beams has been assumed to be a straight-line relationship in this paper, as indicated in Fig. 5(a). With this variation, opposite corners of the beam are in the same sign of stress—either tension or compression. This means that the stress distribution is sensitive to reorientation of the axes and questions the linear variation of stress distribution. Fig. 13(b) shows the box beam in the torsion testing machine, in which the longitudinal strain is being measured by a 2-in. Whittemore strain gage.

Two areas of interest not touched by the discussion are the stress concentration at reentrant corners (7) and the limitations of wall thickness in the use of the thin-shell analysis methods. A projection of the present studies may be of further assistance to structural designers in determining the behavior of box beams under torsional loads.

Bibliography:—

(7) "Torsion of Rectangular Tubes," by William Hovgaard, *Journal of Applied Mechanics*, Vol. 4, No. 3, September, 1937, pp. 131-135.

(10) "Some Elementary Principles of Shell Stress Analysis with Notes on the Use of the Shear Center," by Paul Kuhn, *Technical Note No. 691*, National Advisory Committee for Aeronautics, March, 1939.

(21) "Continuous Hollow Girder Concrete Bridges," Portland Cement Assn., Chicago, Ill., 1949.

(22) "Advanced Mechanics of Materials," by Glenn Murphy, McGraw-Hill Book Co., Inc., New York, N. Y., 1946, Chapter VII.

(23) "Stress Analysis of Curved Box Beams Subjected to Loads Perpendicular to the Plane of Curvature," by Charles E. Cutts, thesis presented to the University of Minnesota, at Minneapolis, Minn., in April, 1949, in partial fulfilment of the requirements for the degree of Doctor of Philosophy.

AMERICAN SOCIETY OF CIVIL ENGINEERS

Founded November 5, 1852

TRANSACTIONS

Paper No. 2556

ENGINEERING ASPECTS OF WATER WAVES

A SYMPOSIUM

PAGE

Surface Water Wave Theories
By Martin A. Mason, M. ASCE 546

Characteristics of the Solitary Wave
By James W. Daily, A. M. ASCE, and Samuel C. Stephan, Jr., J. M. ASCE 575

Long-Period Waves or Surges in Harbors
By John H. Carr 588

Engineering Aspects of Diffraction and Refraction
By J. W. Johnson, M. ASCE 617

Wave Forces on Breakwaters
By Robert Y. Hudson, M. ASCE 653

SURFACE WATER WAVE THEORIES

By Martin A. Mason,[1] M. ASCE

Synopsis

The formation and action of surface water waves is a subject of vital concern to a large proportion of the engineering profession, and yet little is actually known regarding these phenomena. This paper discusses the characteristics of oscillatory surface waves and summarizes the development of pertinent theory. The more important equations that characterize wave formation and movement are presented.

The method by which waves are believed to be generated is described, and a theory of the growth of waves is formulated. Several charts provide convenient means of determining wave characteristics and wave effects from a knowledge of the limiting factors. Other subjects, including wave refraction, diffraction, and reflection, are also briefly treated.

Several formulas are available for determining the action of waves on structures. Although these formulas are not perfect they offer convenient design criteria when used intelligently and carefully.

The paper reviews available knowledge on transportation of beach and bottom material and makes recommendations for likely fields of future research. A brief summary of the use of models in the study of wave problems is also included.

Introduction

The theories and discussions presented in this paper are based on both hypothesis and analysis of observed physical phenomena. They should be considered as representing the best concepts of the present (1950) subject to modification, or even major revision, as more is learned about a complex natural phenomenon that has not yet been completely defined.

The waves to be considered are the surface waves usually observed on large bodies of water. They are periodic disturbances of the surface layers of the water, generated by wind and moving under the control of gravity and inertia. They induce a steady state of oscillation in the water over whose surface they move and are of such height and period as to break, forming surf, on a sloping shore. They occur on oceans, lakes, reservoirs, rivers, or any body of water in which they can be formed by the action of wind blowing over the water surface. They are not tidal waves, surge waves, ripples, or waves of translation.

Note.—Published in March, 1952, as *Proceedings-Separate No. 120.* Positions and titles given are those in effect when the paper was received for publication.

[1] Dean of Eng., The George Washington Univ., Washington, D. C.

The water surface pattern at any time may be the result of a single series of waves of approximately uniform character (rarely) or (usually) of one or more series of waves of varying character. In general, the most obvious characteristic of the water surface under wave action is confusion. In contrast, the waves to be discussed in this paper are assumed to be orderly arrays of uniform character, each wave following another in mathematical precision.

It will be apparent to the most casual reader that the waves to be discussed probably never occur in nature as they will be described. Not only do uniform individual waves of unlimited lateral extent probably not occur but neither do single trains or series of waves of uniform character and appearance occur. This very complexity has forced students of oscillatory wave phenomena to attempt simplification of the problem, leading obviously to the basic hypothesis that any wave situation is the result of the simultaneous existence of one or more series of waves whose character may be considered to be uniform over short intervals of time but variable over long intervals. In this simplified situation the various component wave systems each can be studied as a series, or train, of waves of uniform characteristics.

No methods are known by which the components of a natural wave situation may be separated or assumed uniform wave systems combined to simulate natural conditions. Nevertheless, it is believed that an arbitrary uniform wave system can be defined such that its effects, insofar as engineering problems are concerned, approximate closely those of the natural wave system. This arbitrary system is considered to be composed of waves having a height equal to the average height of the one-third highest natural waves present and a period equal to the average period of the most prominently defined waves present.

This stratagem has produced satisfactory results in the solution of several engineering problems, but care must be exercised in any specific case to insure its admissibility as an adequate method of analysis.

The reader will be warned by these preliminary words that no formalized solutions of engineering problems involving waves should be expected and that the uninformed and indiscriminate use of the information that follows may lead to wholly erroneous solutions.

Characteristics of Oscillatory Waves

Definitions of Wave Characteristics.—Oscillatory waves can be defined by certain measurable characteristics (Fig. 1). The length of the wave, L, is the linear distance in the direction of wave travel between any two identical elements of the wave surface, for instance, crest to crest, or trough to trough. The crest length of the wave, or linear distance measured along the crest of the wave, is a measure of the extent of the wave; it is the width or lateral extent of the wave. The height of the wave, H, is the vertical difference in elevation between the highest and lowest parts of the wave surface, or, more simply, the vertical distance from trough to crest. The period of the wave, T, is the time interval required for passage of a single wave past a fixed point; it may be measured by a variety of obvious means.

The shape of the wave is the geometry of a single wave surface that is usually measured as an instantaneous section of the surface. No adequate

definition of wave shape in the form of a shape factor has been developed. The steepness of the wave is defined by usage, but incorrectly, as the ratio of the length to the height of the wave, or its reciprocal. This ratio has little physical significance; but it is convenient since wave height and length are measured easily, and the ratio has been found useful in defining certain effects of waves. The velocity of the wave, C, or wave celerity, is the rate of travel of any element of the wave surface in the direction of travel of the wave. It can be measured by several methods, the most popular of which is the timing of passage of a wave crest over a known distance.

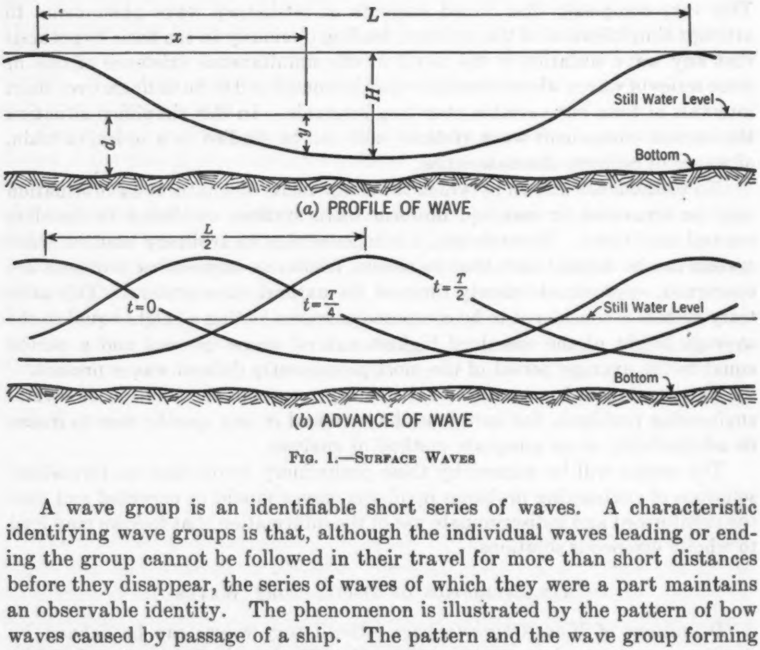

(a) PROFILE OF WAVE

(b) ADVANCE OF WAVE

FIG. 1.—SURFACE WAVES

A wave group is an identifiable short series of waves. A characteristic identifying wave groups is that, although the individual waves leading or ending the group cannot be followed in their travel for more than short distances before they disappear, the series of waves of which they were a part maintains an observable identity. The phenomenon is illustrated by the pattern of bow waves caused by passage of a ship. The pattern and the wave group forming the pattern is discerned easily as the waves break on shore. A wave train is any series of waves, which may include one or more wave groups, all travelling in the same direction.

Certain other features of oscillatory waves are of importance in engineering and will be mentioned without extensive discussion. The movement of oscillatory waves past a fixed point entails periodic variations in the motion of the water particles, in the water pressure at any point affected by the motion, and in the surface elevations, each quantity passing through a continuous series of values and returning to its initial value at regular intervals of time equal to the wave period.

Particular note should be made of the fact that only the wave form shows continuous movement in the direction of wave travel, the water particles them-

selves being moved in a cyclic fashion but not transported continuously with the wave. In fact, except for a small secondary transportation effect known as mass transport, the water particles remain in their original area, although the wave form passes on to ultimate dissipation.

Development of Theory of Progressive Oscillatory Wave Motion

The study of oscillatory wave motion can be traced through scientific literature to Leonardo da Vinci and beyond. However, in this discussion it is sufficient to remark that these early students were led to their theoretical concepts by observation of some of the now more obvious characteristics of wave motion.

F. V. Gerstner is usually credited as being the first, in 1802, to formulate a general theory of oscillatory waves without, however, specifying the applicable field of the theory. This deficiency was supplied by the experimentation of E. Weber and W. Weber, who demonstrated some ingenuity by employing water, mercury, and brandy to study the effects of liquid specific weight. Although Mr. Gerstner postulated a theory of oscillatory wave motion, his theory is based on observations of the characteristics of solitary waves; therefore, the theory's applicability to the progressive oscillatory wave regimen is subject to some doubt.

Early theories did not adequately define observed wave motion and were in themselves conflicting. The state of knowledge in the early 1800's may be described by the reported pungent observation of Lord Rayleigh, who said that it might be possible to devise more elaborate mathematical theories that would not conflict with physical laws but that it would not be certain that waves so described actually occurred in nature!

The accepted basic theory of oscillatory wave motion was developed by G. B. Airy, G. G. Stokes, J. W. S. Rayleigh, T. Levi-Civita, D. J. Struik, and others. These students started from the same observed characteristics as did Mr. Gerstner but their philosophy differed. All the theories are based, in the first instance, on the observation that the water particles involved in oscillatory wave motion move up and down, as well as to and fro.

Mr. Gerstner sought to determine if the simplest form of harmonic motion, that is, the uniform movement of particles in a circular path or orbit, was consistent with the dynamic and continuity equations; thus he arrived at his so-called "trochoidal theory." Stokes criticized this theory on two points; first, the limiting shape of the crest of a Gerstner wave would be that of a razor edge of infinitely small curvature; second, the Gerstner wave contains vortices—an impossible condition under natural circumstances. Experiments and observations made in recent years support the theory developed by Stokes following his critique of Gerstner's theory. The Stokes theory, as modified by other contributors, is accepted thus far as the best theoretical solution of the problem.

The Stokes theory is based in a mathematical sense on the Euler equations of motion and the concept that there exists a velocity potential satisfying the Laplace equation for certain boundary conditions. For the purposes of this

paper the elegant mathematics of the development of the theory will be neglected, and only the expressions defining the wave characteristics of interest to engineers will be stated.

The form of the wave in water deeper than one half the wave length is given by the expression

$$y = \frac{H}{2} \cos \frac{2 \pi x}{L} + \frac{\pi H^2}{4 L} \cos \frac{4 \pi x}{L}$$

$$\frac{(e^{2\pi d/L} + e^{-2\pi d/L})\,(e^{4\pi d/L} + e^{-4\pi d/L} + 4)}{2\,(e^{2\pi d/L} - e^{-2\pi d/L})^3} \qquad (1a)$$

and in water depths less than one half the wave length by

$$y = \frac{H}{2} \cos \frac{2 \pi x}{L} - \frac{\pi H^2}{2 L} \cos \frac{4 \pi x}{L}$$

$$\times \frac{(e^{2\pi d/L} + e^{-2\pi d/L})\,(e^{4\pi d/L} + e^{-4\pi d/L} + 4)}{(e^{2\pi d/L} - e^{-2\pi d/L})^4} + \frac{\pi^2 H^3}{8 L^2} \cos \frac{6 \pi x}{L}$$

$$\times \frac{5\,(e^{12\pi d/L} + e^{-12\pi d/L}) + 14\,(e^{8\pi d/L} + e^{-8\pi d/L}) + 19\,(e^{4\pi d/L} + e^{-4\pi d/L}) + 32}{(e^{2\pi d/L} - e^{-2\pi d/L})^6} \qquad (1b)$$

In these expressions d is the water depth, H is the wave height, L is the wave length, y is the distance of surface above or below still water level, and x is the distance along the wave length in the direction of wave motion. Actual wave shapes agree with these theoretical shapes sufficiently well to constitute confirmation of the expressions.

The velocity of travel of the wave form (wave velocity in common terminology) in water of any depth is expressed as:

$$C = \left[\frac{g L}{2 \pi} \frac{e^{2\pi d/L} - e^{-2\pi d/L}}{e^{2\pi d/L} + e^{-2\pi d/L}}\right]^{\frac{1}{2}} = \sqrt{\frac{g L}{2 \pi} \tanh \frac{2 \pi d}{L}} \qquad (2)$$

A higher degree of approximation to the theoretical true velocity is possible by the addition of terms involving the wave height, but the improvement of accuracy obtained does not justify the use of the longer form for most engineering purposes.

It should be noted that as the depth increases the value of Eq. 2 approaches $\left(\frac{g L}{2 \pi}\right)^{\frac{1}{2}}$. As the depth decreases $\tanh 2 \pi d/L$ approaches $2 \pi d/L$ in value and Eq. 2 takes the form $C = \sqrt{g d}$. This is the well-known equation for velocity of long waves of small amplitude. Fig. 2 is a useful graphical representation of Eq. 2. The applicability of Eq. 2 to actual conditions has been confirmed satisfactorily by observations and experiment.

A word of explanation may not be amiss here. The velocity defined by Eq. 2 is the rate of travel of an individual wave form over the water surface. This velocity does not represent the speed of travel of the water itself; neither does it represent the speed of a series of waves except under certain circum-

stances. The velocity of the water is that of the water particles participating in the wave motion. These particles follow orbits that vary in shape from essentially circular paths for wave motion in deep water to flat elliptical paths for wave motion in shallow water. Typical paths of water particles are shown on

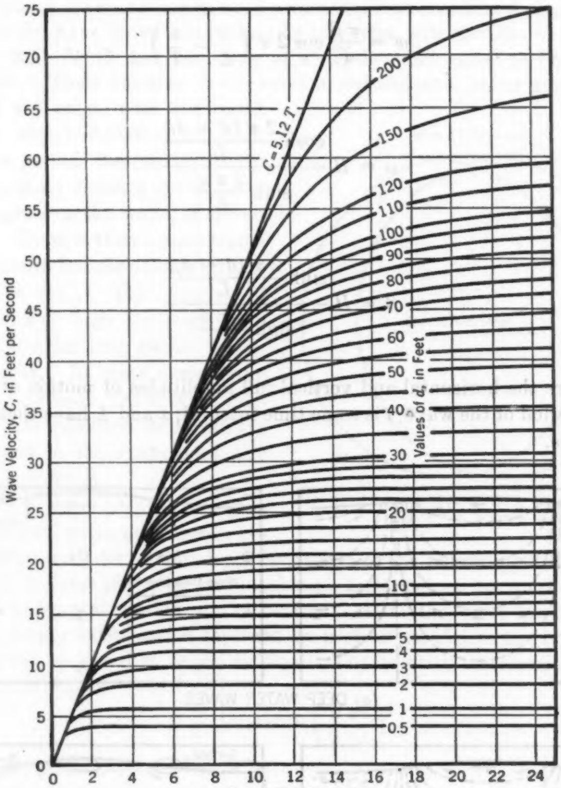

FIG. 2.—CHARACTERISTIC CURVES OF WAVE VELOCITY

Fig. 3. The dashed lines in the left section of Fig. 3 are the streamlines, that is, lines everywhere parallel to the flow. The direction and length of the arrows indicate direction and velocity of orbital motion. The right section of Fig. 3 shows the particle trajectories (the paths described by individual particles of fluid).

The expressions for the horizontal and vertical components of velocity of the water particles occupying an average position at depth d_i below the surface are:

(*a*) **Horizontal component:**

$$u = \frac{\pi\,\alpha}{T} \sin 2\,\pi \left(\frac{x}{L} - \frac{t}{T}\right) \qquad \text{(3a)}$$

(*b*) **Vertical component:**

$$w = \frac{\pi\,\beta}{T} \cos 2\,\pi \left(\frac{x}{L} - \frac{t}{T}\right) \qquad \text{(3b)}$$

in which

$$\alpha = H \frac{\cosh \dfrac{2\,\pi\,(d - d_i)}{L}}{\sinh \dfrac{2\,\pi\,d}{L}}$$

and:

$$\beta = H \frac{\sinh \dfrac{2\,\pi\,(d - d_i)}{L}}{\sinh \dfrac{2\,\pi\,d}{L}}$$

α and β are the horizontal and vertical full amplitudes of motion at depth d_i; T is the period of the wave; t is some time interval; x and L have their previous significance.

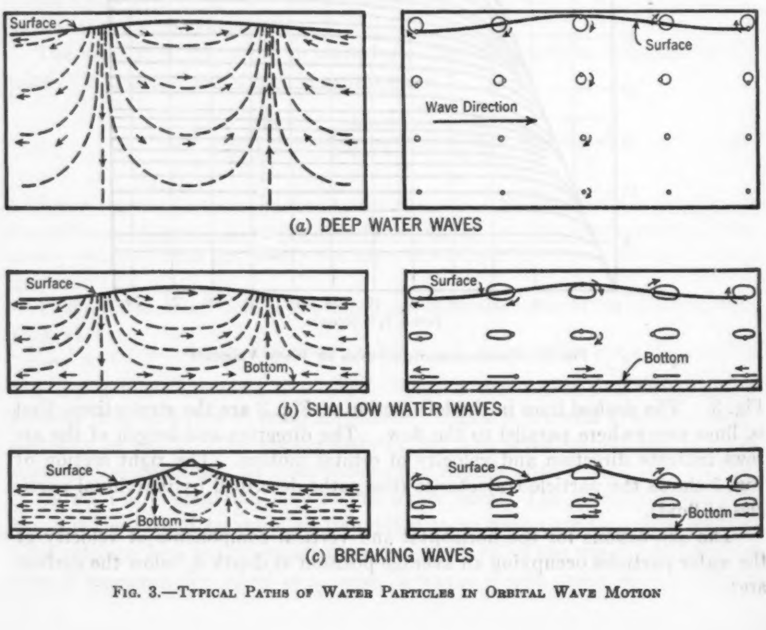

FIG. 3.—TYPICAL PATHS OF WATER PARTICLES IN ORBITAL WAVE MOTION

It is apparent that these are the velocities defining the dynamics of the wave, rather than the wave velocity as given by Eq. 2. An important characteristic of oscillatory surface waves is that the orbital velocities decrease with increasing depth and disappear at depths below about one half the wave length.

When waves are travelling in deep water (depths exceeding $L/2$), the water particles in the wave move approximately in circles, with the size of the circles decreasing with depth and vanishing at a depth about equal to one half the wave length. Their velocity in the orbit is not uniform, being greatest near the top of the orbit, with the result that with the completion of each cycle (wave period) the particles have advanced a short distance in the direction of progress of the wave, as shown in Fig. 4. There is thus a mass transport of water in the direction of travel of the wave (16).[2] The velocity of the transport is high for steep high waves and low for long period waves of low height. In most engineering problems mass transport may be neglected, but its existence must always be recognized in the analysis of any wave action problem.

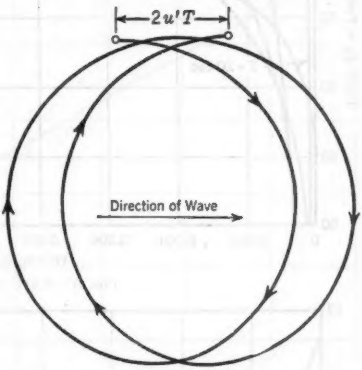

FIG. 4.—ORBITAL MOTION OF A WATER PARTICLE IN A DEEP WATER WAVE

In shallow water (depths less than $L/2$) the orbital paths are ellipses, becoming flatter with decreasing depth by reason of the reduction of the vertical motion of the water particles, and reaching a limit, before the wave breaks, of to-and-fro horizontal motion at the bottom. After the wave breaks, orbital motion no longer exists and is replaced by motion parallel to the bottom of a nature similar to variable, reversing flow. The velocity distribution of mass transport is given by

$$\bar{U} = H^2 e^{4\pi d_i/L} \left(\frac{g\,\pi^3}{2\,L^3}\right)^{\frac{1}{2}} \dots\dots\dots\dots\dots\dots (4)$$

and is shown graphically on Fig. 5.

The total volume of transport per unit width of wave crest is

$$G = H^2 \left(\frac{g\,\pi}{32\,L}\right)^{\frac{1}{2}} \dots\dots\dots\dots\dots\dots (5)$$

Experiments confirm the existence and most details of the orbital motion required by theory.

It will be noted that wave motion involves differences in elevation of the water surface, or potential energy, and motion of the water particles, or kinetic energy. Mathematical studies, confirmed in gross by experiment, lead to the conclusion that the potential and kinetic energies are equal. The energy in a

[2]Numerals in parentheses, thus: (16), refer to corresponding items in the Bibliography (see Appendix).

wave at any instant (per unit crest length, or width) is then the sum of the kinetic and potential energies of the wave. The kinetic energy is the summation of the individual kinetic energies appertaining to the orbital velocities discussed above; the potential energy is computed from the elevation or depression

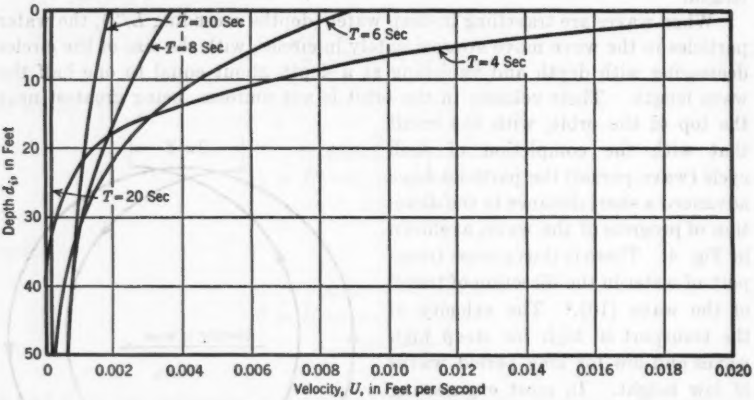

FIG. 5.—RATE OF MASS TRANSPORT

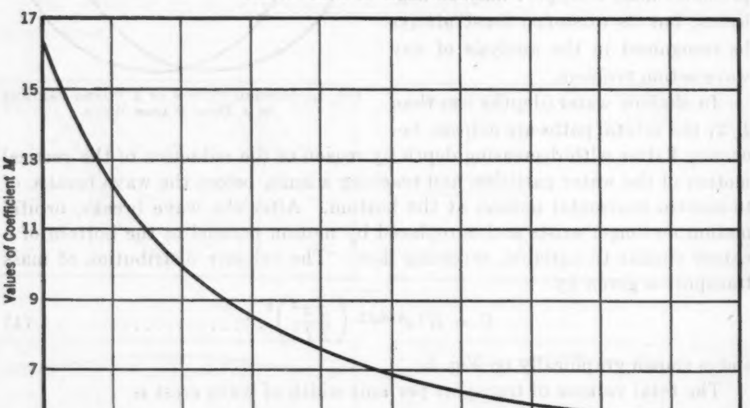

FIG. 6.—VALUES OF COEFFICIENT M

of the water surface from the still water surface. The total energy can be expressed by

$$E = \frac{w\,L\,H^2}{8}\left(1 - M\,\frac{H^2}{L^2}\right) \qquad (6)$$

in which w is the specific weight of water, and M is a number depending in value upon some function of the ratio d/L (see Fig. 6).

The total energy defined by Eq. 6 is available for the application of forces to engineering structures only as the wave is destroyed by action on the structure. For example, all the wave energy is destroyed when a wave breaks and rushes up on a shore; whereas, when a wave breaks offshore in whitecaps, only a portion of the energy is lost and the wave continues its advance.

A graph showing the energy content per foot of crest width of waves of various heights and lengths is shown as Fig. 7.

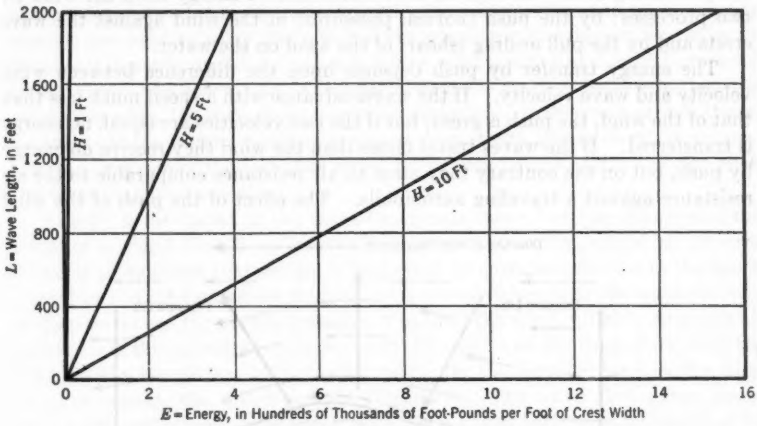

FIG. 7.—GRAPH OF DEEP WATER WAVE ENERGY

The partition, or distribution, of energy in the wave should be considered when designing works to resist wave action; yet little is known of the time rate of transformation of wave energy during destruction of wave action. Although studies of this matter have been made, no conclusive results are available. For the solution of important problems of this type, recourse to models appears to offer a satisfactory approach.

OSCILLATORY WAVE GENERATION

Perhaps the greatest deficiency in wave knowledge confronting engineers concerned with wave problems is the lack of information on the wave action to be expected at any given locality and time. Very few observations of wave action in nature have been made, although a few wave observation stations providing continuous measurement over limited periods of time have been established. Data available from these stations can be obtained from the Waves Project, University of California, at Berkeley, Calif., or the Beach Erosion Board (Corps of Engineers, United States Army) at Washington, D. C. Wave measurement stations are difficult and expensive to install and maintain. Furthermore, the time schedule of many engineering works will not permit the long delay required to obtain observational data. Attempts have been made, for these and other reasons, to develop methods of predicting wave conditions from easily available synoptic weather charts, or similar data from which wind

movement over the water area concerned may be determined. These prediction methods are based on two slightly different hypotheses. Both hypotheses presume the transfer of energy from the wind to the water and some initial roughness of the water surface (see Fig. 8). The hypothesis of H. U. Sverdrup and W. H. Munk will be discussed first, in essentially the words of the originating authors.

The Sverdrup-Munk Theory.—The area in which waves are formed is called the generating area. In such an area waves receive energy from the wind by two processes: by the push (normal pressures) of the wind against the wave crests and by the pull or drag (shear) of the wind on the water.

The energy transfer by push depends upon the difference between wind velocity and wave velocity. If the waves advance with a speed much less than that of the wind, the push is great; but if the two velocities are equal, no energy is transferred. If the waves travel faster than the wind they receive no energy by push, but on the contrary they meet an air resistance comparable to the air resistance against a traveling automobile. The effect of the push of the wind

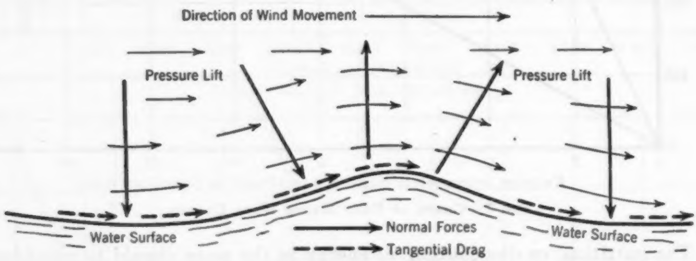

Fig. 8.—Schematic Representation of Wind System and Forces Generating Oscillatory Waves

or of the air resistance against the wave depends on the wave form. There enters, therefore, a fundamental coefficient that is related to the degree to which the wave is streamlined and which is called the "sheltering coefficient." The determination of this coefficient is necessary for the exact evaluation of energy transfer by push, that is, by normal pressures.

The pulling force of the wind is analogous to the shear of skin or pipe friction and always acts in the direction of the wind. It is the same at the wave crest and the wave trough, but the effect differs. Energy is transferred from the air to the water (the movement of the surface is speeded up) if the surface water moves in the direction of the wind; but energy is given off from the water to the air. (The movement of the surface water is slowed down) if the surface water moves against the wind. When wind and waves move in the same direction, the water particles at the crest move in the direction of the wind drag, while those in the trough move against the drag (see Figs. 3 and 8). In the absence of a mass transport velocity, the particle velocities at the crest and the trough are equal but in opposite directions, so that the effect of the pulling force of the wind at the wave crest is exactly balanced by the effect at the wave trough. However, in the presence of a mass transport velocity, the forward motion at

the crest is greater than the backward motion in the trough, and a net amount of energy is transferred to the water. No satisfactory explanation of the growth of waves can be given without assuming a transfer of energy because of the wind pulling at the water particles; and this fact is the best argument for the presence of a mass transport velocity in ocean waves.

The pulling force, or shear, of the wind over the ocean can be determined by methods used in meterology, and then the energy transfer from the air to the water by wind drag can be computed with considerable accuracy, using the theoretical values for mass transport velocity. Even when the wave velocity exceeds the wind velocity, the effect of the wind drag remains nearly the same because it depends on the difference between wind velocity and particle velocity in the water. In general, the water particles move much more slowly than the wind even when the wave form moves much faster. If the wind cannot transfer energy to the water by pulling at the water particles, no satisfactory explanation can be given of the fact that waves frequently have a higher velocity than the wind that produces them.

Energy is dissipated in the wave by viscous shear, but the viscosity of the water is so slight that these losses can be neglected in the generating process. There is no evidence that energy is dissipated by turbulent motion in the wave. Therefore the chief processes that can alter the wave height or the wave velocity in deep water are the normal pressure or push of the wind, which becomes an air resistance if the wave travels faster than the wind, and the drag or shear of the wind on the sea surface (which adds energy to the wave so long as the wind velocity exceeds the water particle velocities). The wave thus grows larger until a balance is reached between the energy added by shear and that lost by air resistance.

Knowing the rate of energy transfer from the wind and the rate at which the wave energy advances, it is possible to establish a differential equation from which the relationships between the waves and wind velocity, fetch, and duration are obtained as special solutions. The equation contains three numerical constants (including the "sheltering coefficient") that have to be determined in such a manner that nine empirical relationships are satisfied. This has been accomplished, and at the same time discrepancies between existing empirical relationships have been accounted for.

The maximum wave that can be generated is thus determined by: (1) the wind velocity; (2) the interval of time during which that wind velocity exists, or the wind duration; and (3) the distance over which the wind blows with that velocity, or the fetch.

The Jeffreys Theory.—The second hypothesis, formulated by H. Jeffreys, is similar to the first in its major concepts, except that it is assumed that energy transfer takes place by normal pressures (push) only. Therefore no net transfer of energy can occur once the wave speed equals the wind speed, and no wave can travel faster than the wind that generated the wave.

Analysis of Hypotheses.—The relatively meagre amount of observational data available to confirm the hypotheses does not permit an absolute confirmation of either; however, what is available appears to show the Sverdrup-Munk hypothesis in closer agreement with the data than the Jeffreys hypothesis.

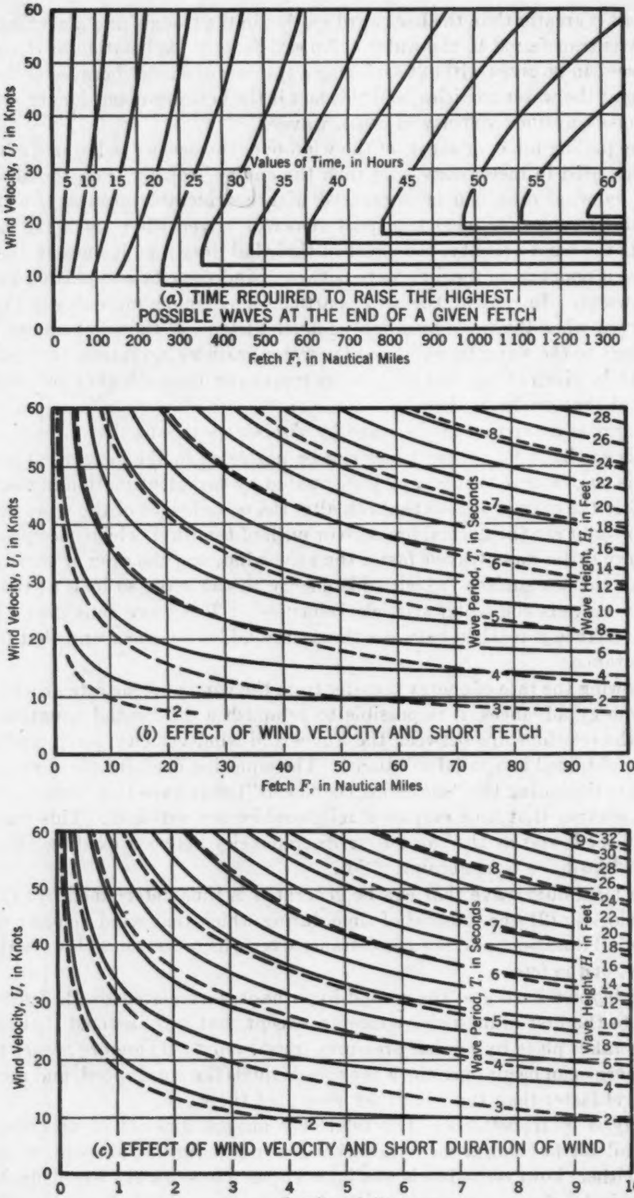

FIG. 9.—SHORT-TERM GROWTH OF WIND WAVES

Speaking generally, the hypothesis of Messrs. Sverdrup-Munk leads to agreement of the order of $\pm 25\%$ with observed data, but there is as yet no confirmation of their concept of the details of the generation process.

It should be noted that the hypotheses discussed involve the concept of an area in which the waves are being generated and have not reached a stable form. They involve also the concurrent concept of a decay area, outside the generating area, in which the waves are of stable form but losing energy, slowly by air resistance, and very slowly by internal friction, as they travel away from the generating area. It is apparent that any single wave or series of waves in the ocean may travel through one or more generating and decay areas in its course toward a shore. In a lake, a reservoir, or another body of water of limited extent, the wave is probably always in its generating area and may not attain a stable maximum form before reaching shore. Many engineering problems of wave action involve the latter situation and justify extensive further study of waves within a generating area.

Messrs. Sverdrup and Munk have prepared useful charts for the prediction of wave heights and periods. The reliability of this data for situations of limited fetch and duration times, for instance, in the case of lakes or reservoirs, is open to question. However, tests have shown a fair agreement between observed and computed wave characteristics (see Fig. 11). The empirical formulas of T. Stevenson, D. A. Molitor, and W. P. Creager, and others do not yield results comparable in accuracy of agreement with observation to those obtained from the Sverdrup-Munk formula. Therefore, it must be concluded that they are inferior to that formula for engineering purposes. The growth of waves in terms of the wind velocity, the fetch, and the time required to generate the highest possible waves is shown in Fig. 9(*a*). This chart is used to determine the minimum length of time (duration) the wind must blow at a given velocity and over a given fetch to generate the highest possible waves that can be generated under those conditions of velocity and fetch.

Figs. 9(*b*) and 10(*a*) show the relationships between wave period or wave height, wind velocity, and fetch. Fig. 9(*b*) is the short fetch portion of Fig. 10(*a*) reproduced to a larger scale. These figures are used to determine the height and period of the wave generated.

Since either fetch or wind duration may be the controlling factor in wave generation, the relations shown in Figs. 9(*c*) and 10(*b*) between wave height or period, wind velocity, and wind duration have been prepared.

The use of these graphs can be illustrated by a simple example. Let it be supposed that a wind of 30 knots velocity blows over a fetch of 450 nautical miles for a period of 30 hr. Fig. 9(*a*) is used to determine whether fetch or duration is the limiting factor in the wave generation. The graph shows that the highest possible wave that can be generated under these conditions will be generated, since a 30-knot wind blowing over a 450-mile fetch requires just 30 hr. to generate the maximum wave. Fig. 10 is now used to determine the height and period of the generated wave. Entering Fig. 10(*a*) on the left at a wind velocity of 30 knots and moving to the intersection of this line with 450-mile fetch, a wave height of 19.5 ft is found with a corresponding wave period of 9 sec.

Suppose, however, that the wind blows for a time of only 20 hr. Fig. 9(*a*) then shows that wind duration is the control and that Fig. 10(*b*) must be used to determine the wave characteristics. Entering Fig. 10(*b*) on the left at a wind

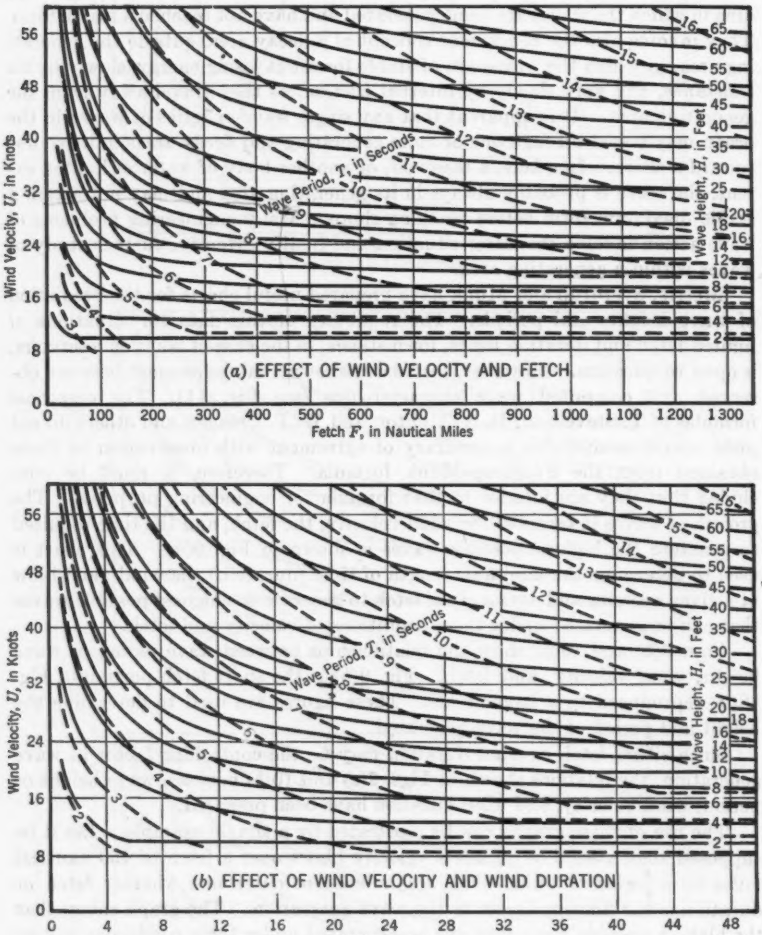

FIG. 10.—LONG-TERM GROWTH OF WIND WAVES

velocity of 30 knots and moving to the intersection with 20 hr a wave height of 16.5 ft and a wave period of 7.6 sec is found.

Fig. 11 shows a comparison between wave heights and periods as predicted by the Sverdrup-Munk method and as observed in tests at Abbotts Lagoon.

In this figure, T is the wave period; H is the wave height; F is the fetch; and u is the wind speed 8 meters above water surface. The data apply to short fetches and are presented in dimensionless form for convenience of comparison. Fig. 12 is presented primarily to show the observations of waves whose velocity exceeds that of the generating wind (values of wave age in excess of one) supporting the Sverdrup-Munk hypothesis of wave generation.

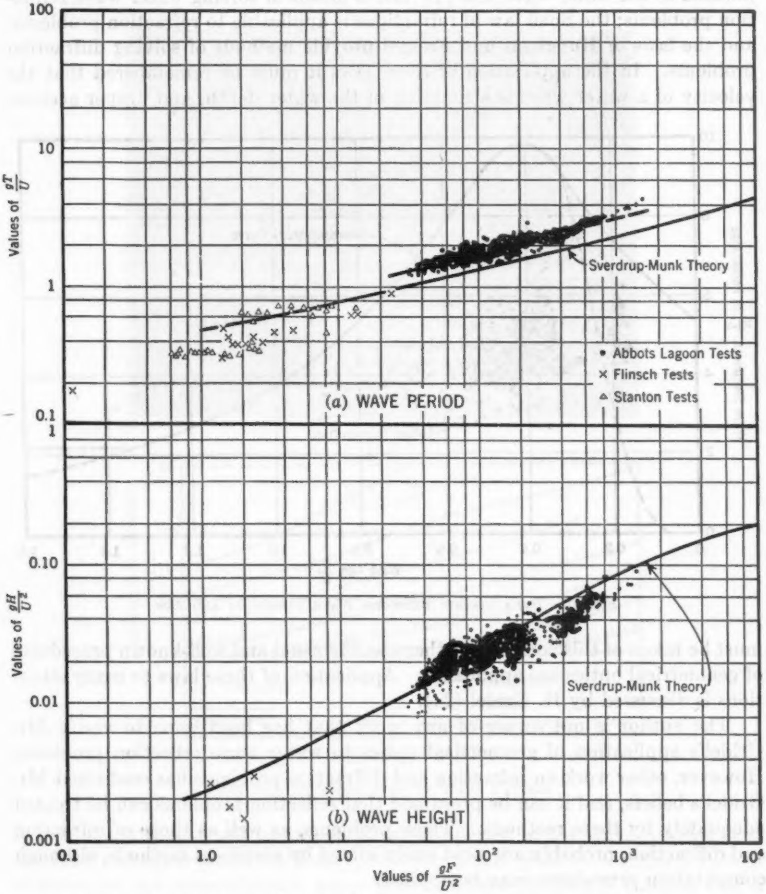

Fig. 11.—Comparison Between Theoretical and Experimental Results

Wave Refraction, Diffraction, and Reflection.—From the engineering viewpoint the problems of wave reflection, refraction, and diffraction are probably of more interest than any others, except those involving wave forces. Observation of wave behavior in nature and in the laboratory has led to the conclusion

that progressive oscillatory waves in water behave in a manner similar to light, thus leading to the use of geometrical optics and the wave theory of light to solve water wave problems. There is presumed to be an analogy between the individual water wave and the light wave, as well as between direction of travel of the water wave and light rays. If this presumption is true, then Descarte's law stating that the angle of incidence is equal to the angle of reflection is applicable to the water wave and provides a means of solving water wave refraction problems; the Snell law of refractions is applicable to refraction problems; and the laws of Huyghens and Fresnel provide methods of solving diffraction problems. In the application of these laws it must be remembered that the velocity of a water wave is a function of the water depth, and proper account

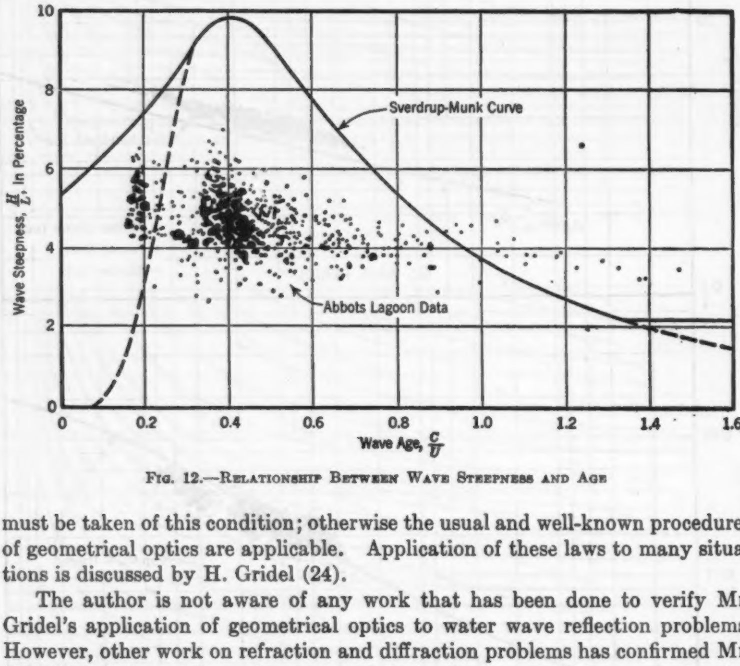

FIG. 12.—RELATIONSHIP BETWEEN WAVE STEEPNESS AND AGE

must be taken of this condition; otherwise the usual and well-known procedures of geometrical optics are applicable. Application of these laws to many situations is discussed by H. Gridel (24).

The author is not aware of any work that has been done to verify Mr. Gridel's application of geometrical optics to water wave reflection problems. However, other work on refraction and diffraction problems has confirmed Mr. Gridel's beliefs, and it can be presumed that reflection problems can be treated adequately by these methods. These problems, as well as those of refraction and diffraction, probably are most easily solved by graphical methods, although computation procedures may be applied.

In view of the large number of possible engineering problems involving wave reflection, refraction, and diffraction and the high development of methods of geometrical optics, no discussion will be included in this paper of specific applications. The reader is referred to the "Appendix-Bibliography on Wave Theories" and to a paper by J. W. Johnson for information on the details of applicable laws and methods available for solution of such water wave problems.

It must be stated that few problems of this type have been solved for engineering purposes, but the theoretical concepts are available and merely await application.

Recapitulating, it was noted previously in discussion of the characteristics of oscillatory waves that water depth affected the height, length, and velocity of a wave whenever the depth was less than about one-half the wave length.

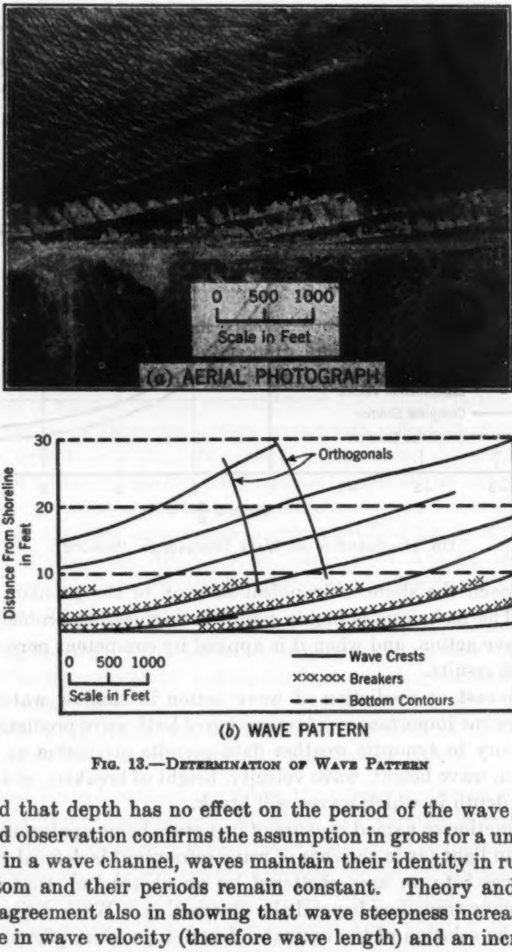

FIG. 13.—DETERMINATION OF WAVE PATTERN

It is believed that depth has no effect on the period of the wave; further it is assumed, and observation confirms the assumption in gross for a uniform system of waves, as in a wave channel, waves maintain their identity in running over a sloping bottom and their periods remain constant. Theory and observation are in close agreement also in showing that wave steepness increases by reason of a decrease in wave velocity (therefore wave length) and an increase in wave height. The dissipation of energy by internal and bottom friction has been assumed to be negligible for engineering purposes, and the assumption is confirmed in gross by experiment.

A typical example of wave refraction is illustrated in Fig. 13, which is an aerial photograph of swell, breakers, and surf north of Oceanside, Calif. Since the wave velocity decreases with a decrease in water depth, the inshore end of the wave travels at a slower rate than the offshore end, thus bending (or refracting) the wave and causing its direction of approach to tend more and more toward a perpendicular to the shore. It is evident that analogous sections of each wave in the series pass through the same sequence of angles and velocities

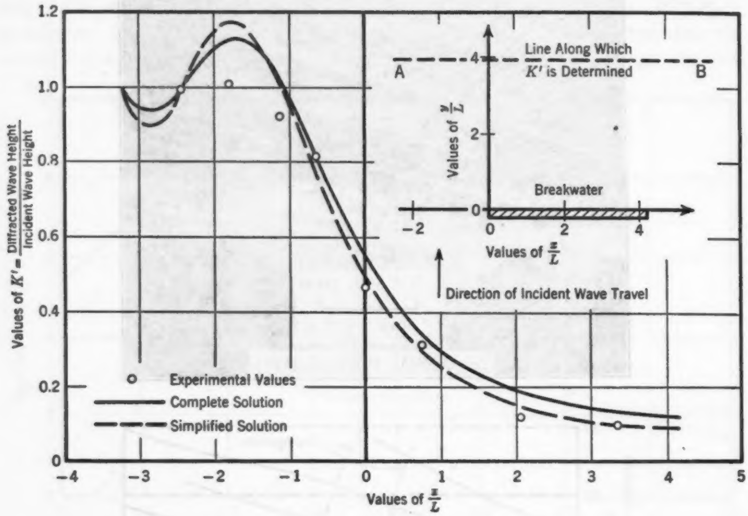

FIG. 14.—SOLUTION OF WAVE DIFFRACTION PROBLEM

as they approach the shore. Graphical solution of the problem is indicated (27), (32). The technique is highly useful in engineering problems involving oscillatory wave action, and when it is applied by competent personnel it gives quite accurate results.

In the forecast or prediction of wave action in shallow water, refraction effects are of prime importance. Application of both wave prediction and wave refraction theory to synoptic weather data permits prediction at the shore of wave direction, wave height, wave velocity, height of breakers, character of the surf, and the depth in which waves will break.

Wave diffraction so named because of its nature being analogous to the same phenomenon in light (as in the case of wave refraction) is defined as the propagation of waves into an area sheltered by an obstruction that interrupts a portion of a wave travelling beyond the obstruction. Wave diffraction theory is similar to the solution of the optical diffraction problem offered by A. Sommerfeld (34), and is described in detail by J. A. Putnam (35), R. S. Arthur, and others (36, 37). The theory assumes unnatural conditions, but agreement with observation in nature is good nonetheless. The solution of a typical case in-

volving a harbor breakwater is shown in Fig. 14, as an illustration of the application of the method.

Discussion of oscillatory wave reflection phenomena is required to be unsatisfactory, since little study has been devoted to the subject. Students of wave theory appear to be in accord generally that the analogy to light reflection is applicable in this case, as in the cases of refraction and diffraction. Mr. Gridel states that the analogy is complete and gives several illustrative examples to prove the validity of his opinion without, however, the proof of experimental evidence. There is certainly little, if any, evidence available to contradict his treatment of the problem. Studies have been made by Joseph M. Caldwell (39), Assoc. M. ASCE, of the reflection of solitary waves, and the results are believed to be applicable to oscillatory waves. The engineer concerned with such problems is referred to the bibliography of this paper for sources of detailed information, but he is warned that stock solutions of his problems probably will not be found. However, as Mr. Gridel states, he probably will find that application of the methods of optics will permit the solution of problems for which there does not appear now to be any other satisfactory method of solution.

Wave Action on Structures

Development of the theory of wave action on structures is incomplete, and consequently available knowledge is both limited and somewhat uncertain by reason of lack of verification of theoretical concepts.

Two cases of wave action on structures are recognized: In the first the waves act on a structure as unbroken surface waves with reflection of the waves being minor to an extent permitting its neglect; in the second the waves are (essentially) totally reflected by the structure and may approach as unbroken waves, or as surf (that is, during or following breaking).

Typical of the first case is the problem studied by J. R. Morison (43), Morrough P. O'Brein (M. ASCE), J. W. Johnson (M. ASCE), and S. A. Schaaf, who state that the force exerted by unbroken surface waves on a cylindrical object is made up of two components:

1. A drag force proportional to the square of the particle orbital velocities, which may be represented by a drag coefficient having substantially the same value as for steady flow;
2. A force proportional to the horizontal component of the accelerative force exerted on the mass of water displaced by the object.

Since both these forces are caused by the orbital motion in wave action, the forces are oscillatory, reversing in direction and varying in magnitude during the wave cycle. Laboratory investigations lead to the recommendation of the following expressions as sufficiently accurate for design purposes, pending the completion of more extensive development. Mr. Morison and his associates propose as the expression for the maximum force exerted at any particular depth z:

$$\left(\frac{dF}{dz}\right)_{max} = \frac{\pi^2 \rho D H^2}{2 T^2}\left(f_d + \frac{f^2_m}{f_d}\right) \dots\dots\dots\dots\dots (7)$$

in which ρ is the water mass density, in slugs per cu ft; D is the pile diameter, in feet; H is the wave height, in feet; T is the wave period, in seconds; $f_d =$ (1.626 ± 0.414)

$$\left[\frac{\cosh \frac{2\,\pi\,(d+z)}{L}}{\sinh \frac{2\,\pi\,d}{L}}\right]^2; \text{ and } f_m = (1.508 \pm 0.197)\,\frac{\pi\,D}{H}\left[\frac{\cosh \frac{2\,\pi\,(d+z)}{L}}{\sinh \frac{2\,\pi\,d}{L}}\right].$$

Their expression for the moment about the bottom of the pile caused by wave force is:

$$M = \frac{\rho\,D\,H^2\,L^2}{T^2}\left(-\frac{D\,\pi}{4\,H}\,C_m\,K_1 \sin\theta \pm C_d\,K_2 \cos^2\theta\right) \quad \ldots\ldots\ldots (8)$$

in which

$C_m = 1.508 \pm 0.197$; $C_D = 1.626 \pm 0.414$; $\sin\theta = f_m/2\,f_d$; $\cos^2\theta$

$$= \frac{4\,f_d^2 - f_m}{4\,f_d^2};\ K_1 = \frac{1 + \frac{2\,\pi\,d}{L}\sinh\frac{2\,\pi\,d}{L} - \cosh\frac{2\,\pi\,d}{L}}{2\sinh\frac{2\,\pi\,d}{L}};\ \text{and } K_2$$

$$= \frac{1 + \frac{1}{2}\left(\frac{4\,\pi\,d}{L}\right)^2 + \frac{4\,\pi\,d}{L}\sinh\frac{4\,\pi\,d}{L} - \cosh\frac{4\,\pi\,d}{L}}{64\left(\sinh\frac{2\,\pi\,d}{L}\right)^2}.$$

Mr. Munk has treated the same problem on the theoretical concept that only the drag forces need be considered, arriving at the maximum force expression

$$F = C_D\,D\,H^2\,K_f \quad \ldots\ldots\ldots (9)$$

in which C_D depends upon the object shape and Reynolds number ($C_D = 0.33$ for a cylindrical pile), and $K_f = \frac{g}{8}\left[1 + \frac{\frac{4\,\pi\,d}{L}}{\sinh\frac{4\,\pi\,d}{L}}\right]$.

His expression for the moment about the bottom of the pile caused by wave force is

$$M = C_D\,D\,H^2\,d\,K_m \quad \ldots\ldots\ldots (10)$$

in which

$$K_m = \frac{g}{8}\left[1 + \frac{\frac{2\,\pi\,d}{L}}{\sinh\frac{4\,\pi\,d}{L}} - \frac{\tanh\frac{2\,\pi\,d}{L}}{\frac{4\,\pi\,d}{L}}\right].$$

Neither of the theories noted has received confirmation from actual observations of forces or moments; however the Morison theory shows close agreement with laboratory observations.

The second case of wave action on structures, involving reflection of the waves in an unbroken or broken state, has received considerable attention by foreign students. Their interest was aroused by a number of failures of vertical face breakwaters under the stress of wave action, and their theories are concerned primarily with such situations. The most generally accepted theory is that developed by G. Sainflou in 1928 from earlier studies by M. Benezit in 1923. In the Sainflou theory it is considered that essentially total reflection of the wave occurs, giving rise to a clapotis (standing wave), and the resulting pressures and forces are computed from standing wave theory.

The expression for maximum pressure at any depth d_i is

$$P = d + H\left[\frac{\cosh \dfrac{\pi (d - d_i)}{L}}{\cosh \dfrac{\pi d}{L}} - \frac{\sinh \dfrac{\pi (d - d_i)}{L}}{\sinh \dfrac{\pi d}{L}}\right] \quad \text{(11)}$$

in which d is the water depth, in feet; H is the wave height, in feet; and d_i is the depth to any point, in feet.

The maximum moment referred to the base of the structure is

$$M = \frac{\left(d + \dfrac{\pi H^2}{2L}\coth\dfrac{\pi d}{L} + H\right)^3}{6} \frac{\left(d + \dfrac{H}{\cosh \pi d/L}\right)}{\dfrac{\pi d}{L}} - \frac{d^3}{6} \quad \text{(12)}$$

in which d is the still water depth, in feet; H is the wave height, in feet; and L is the wave length, in feet.

It should be noted that for complete design analysis both maximum and minimum pressures should be computed, as well as the distribution of pressures (45).

The problem of the size of stone and side slopes to be used in the construction of breakwaters, sea walls, or revetments to resist wave action has been treated as a special problem by R. Iribarren (42). The Iribarren theory presumes that disintegration or failure of the structure occurs by reason of displacement of the individual stones of the structure. This displacement is caused by resultant forces on the faces of the stone, due to wave action, exceeding the weight and keying forces associated with the stone size, shape, and position. The theory does not lead to a rigorous solution; however, Mr. Iribarren has derived the following empirical relationship that is being used increasingly for design purposes:

$$P = \frac{K A^3 \rho}{(\cos \alpha - \sin \alpha)^3 (\rho - 1)^3} \quad \text{(13)}$$

in which P is the weight of stone, in kilograms; A is the height of wave acting on the structure, in meters; ρ is the density of stone, in tons per cubic meter;

α is the side slope of dike, angle with horizontal; and K is the coefficient, having a value of 15 for natural rock shapes and 19 for artificial blocks.

Although several structures in the United States are understood to have been designed according to the Iribarren criterion, there is not sufficient confirmation of the formula available to obviate the need for further study and test. The author is aware that Spanish, Portugese, and French engineers also are using the Iribarren formula, and it appears that it enjoys the confidence of many engineers engaged in the design of maritime structures.

Transportation of Beach and Bottom Material

A phenomenon of engineering importance involving wave action is that of the movement of beach and bottom material by waves. No complete and adequate theory of transportation by waves has been developed; however, there has been much research on the problem. Available concepts of the transportation phenomena are included in the following description of what has been observed or is believed to occur.

As noted previously, there is a motion of water particles associated with wave action, the motion being a maximum at the surface and decreasing to zero at a depth approximately half the wave length. As a wave progresses into shallow water, this water motion approaches the bottom; beginning at a depth of about $L/2$ there exists a velocity field contiguous to the bottom. As the wave moves shoreward, the velocities at the bottom increase until they are sufficiently high to induce creep, saltation, and suspension of the bottom material. However the velocities are not uniform or steady but periodic and reversing. Experiments at the Beach Erosion Board and elsewhere have confirmed that movement of bottom material in this region does occur and that it is frequently accompanied by sand ripple formation on the bottom. Farther shoreward the wave breaks, rushes up the beach, pauses for an instant, and then flows back down the beach slope. Experiments have shown highly turbulent flow conditions and a very high percentage of suspended material to exist in the breaker region. The Beach Erosion Board is engaged in making high speed photographic studies of this region in an effort to define its behavior.

The material thus stirred up and placed in suspension is carried by the uprush of the wave onto and along the beach, and to some extent seaward. Laboratory tests have shown the transportation to be related in some fashion to the wave steepness, net movement to the beach being associated with low steepness, net movement seaward accompanying waves of high steepness. It is believed that as much as 80% of the material moved by wave action is moved in the area from the point of breaking waves to the limit of uprush of the waves on the beach, as shown in Fig. 15. In this figure, sand movement is given in zones parallel to the shore.

Hydraulic Models of Waves

As stated previously, perhaps the most obvious characteristic of wave motion in nature is its apparent confusion. This inherent variability makes study of waves in nature an expensive and difficult task, with the result that most developments in wave study have been dependent on model experimentation.

It is almost certain that this situation will continue. It is then pertinent to examine the possibilities of hydraulic wave model experimentation and the reliability of such results.

As a general requirement it can be stated that an hydraulic model of a wave situation requires complete geometric similitude; that is, no model distortion is permissible. The requirement arises from the fact that the characteristics of the wave, other than period, are functions of the water depth, and can be relaxed only for wave problems that do not involve waves in shallow water, that is depths less than $L/2$.

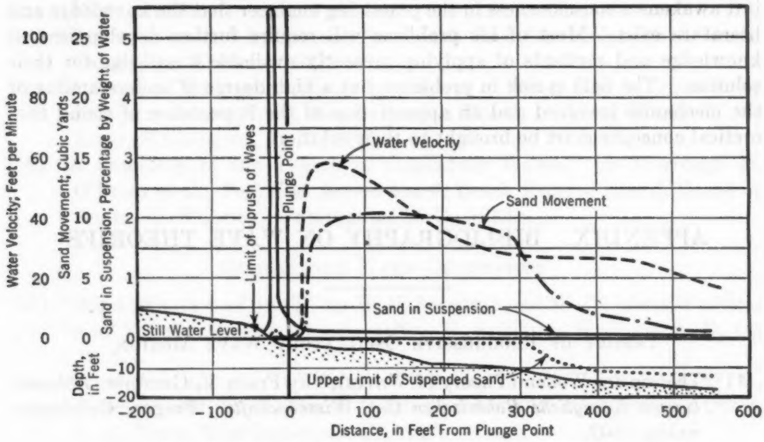

FIG. 15.—SAND MOVEMENT AT LONG BRANCH, NEW JERSEY

Mr. Johnson (66) has summarized the various instances in which wave theories have been verified experimentally and in which wave models at several scales have permitted an evaluation of the scale effect in the application of data from hydraulic wave models. He states that, in general, basic wave theory has been confirmed independently both in nature and in model, this confirmation in itself furnishing the strongest proof that hydraulic wave models can be made. Experiments on models of various scales and in nature have shown similar characteristics of wave action in the surf zone insofar as these characteristics can be observed, of longshore currents, and of beach profiles. Model tests at various scales have shown that breakwater stability can be studied by model experimentation based on the Froude law.

It is the author's belief that model experimentation is an admissible and powerful tool for the study of wave action and many related phenomena, but that an understanding of the physics of the situation to be studied in model is a necessary requisite to its successful use. The most certain procedure available is the application of classical model theory to the equations defining the dynamics of the wave situation. When such equations do not exist or when departures from established laws are required, confirmation of the model results should be considered as a necessary part of the study.

Conclusion

The hydraulic engineer who finds himself concerned with oscillatory wave problems should consider this paper as but a very brief introduction to a body of knowledge and literature that has grown at an astonishing rate since 1940. It will be apparent to him relatively soon in his studies that, although much progress has been made, there remain multitudes of unsolved problems of both a theoretical and a practical nature. The purpose of this paper will be served if it awakens a consciousness in the practicing engineer that the knowledge and literature exist. Most of his problems will require further development of knowledge and methods of applying presently available knowledge for their solution. The field is rich in problems, but a high degree of understanding of the mechanics involved and an appreciation of the importance of sound theoretical concepts must be brought to their solution.

APPENDIX. BIBLIOGRAPHY ON WAVE THEORIES

Theory of Progressive Oscillatory Wave Motion

(1) "Theorie der Wellen (Theory of Waves)," by Franz V. Gerstner, *Abhandlungen Königliche Bohmischen Ges. Wissenschaften*, Prague, Czechoslovakia, 1802.

(2) *Annalen der Physik*, edited by Ludwig Wilhelm Gilberts, Leipzig, Germany, Vol. XXXII, 1809.

(3) "Wellenlehre auf Experimente Gegrundet (Experimental Studies of Waves)," by Ernst Weber und Wilhelm Weber, Gerhard Fleischer, Leipzig, Germany, 1825.

(4) "On Tides and Waves," by Sir. G. B. Airy, *Encyclopedia Metropolitana*, Vol. 5, 1845, p. 241.

(5) "Periodic Irrotational Waves of Finite Height," by E. T. Havelock, *Proceedings*, Royal Society of London, Series A, Vol. 95, 1918, p. 38.

(6) "On The Theory of Oscillatory Waves," by George Gabriel Stokes, *Mathematical and Physical Papers*, Cambridge Univ. Press, Cambridge, England, Vol. I, 1880, p. 197.

(7) "On Periodic Irrotational Waves at the Surface of Deep Water," by Lord Rayleigh, *Philosophical Magazine*, Sixth Series, Vol. XXXIII, 1917, p. 381.

(8) "On Progressive Waves," by Lord Rayleigh, *Proceedings*, London Mathematical Society, Vol. IX, 1877, p. 21.

(9) "On Waves," by Lord Rayleigh, *Philosophical Magazine*, Fifth Series, Vol. I, 1876, p. 257.

(10) "Détermination Rigoureuse des Ondes Permanentes d'Ampleur Finie (Rigorous Determination of Permanent Waves of Finite Amplitude)," by T. Levi-Civita, *Annales Mathématiques*, Vol. XCIII, 1925, p. 264.

(11) "Détermination Rigoureuse des Ondes Irrotationelles Périodiques dans un Canal à Profondeur Finie (Rigorous Determination of Periodic Irrotational Waves in a Canal of Finite Depth)," by D. J. Struik, *Mathematical Annales,* Vol. XCV, 1926, p. 595.

(12) "Probleme der Wasserwellen," by H. Thorade, H. Grand, Hamburg, Germany, 1931.

(13) "On the Exact Form of Waves near the Surface of Deep Water," by W. J. M. Rankine, *Philosophical Transactions,* Royal Society of London, 1863, p. 127.

(14) "Hydrodynamics," by Horace Lamb, 6th Ed., Cambridge Univ. Press, Cambridge, England, 1932.

(15) "A Study of Progressive Oscillatory Waves in Water," by M. A. Mason, *Technical Report No. 1,* Beach Erosion Board, Corps of Engrs., U. S. Army, Washington, D. C., 1942.

(16) "A Summary of the Theory of Oscillatory Waves," by Morrough P. O'Brien et al., *Technical Report No. 2,* Beach Erosion Board, Corps of Engrs., U. S. Army, Washington, D. C., 1942.

Oscillatory Wave Generation

(17) "Wind, Waves, and Swell," by H. U. Sverdrup and W. H. Munk, *Publication No. 11275,* Hydrographic Office, U. S. Navy, Washington, D. C., 1945.

(18) "Wind, Sea, and Swell: Theory of Relations for Forecasting," by H. U. Sverdrup and W. H. Munk, *Publication No. 601,* Hydrographic Office, U. S. Navy, Washington, D. C., 1947.

(19) "An Experimental Investigation of Wind-Generated Surface Waves," by H. V. N. Flinsch, dissertation submitted to the University of Minnesota, at Minneapolis, Minn., in June, 1946, in partial fulfilment of the requirements for the degree of Doctor of Philosophy.

(20) "The Growth of Waves on Water Due to the Action of the Wind," by Sir Thomas Stanton, Dorothy Marshall, and R. Houghton, *Proceedings,* Royal Society of London, Series A, Vol. 137, 1932, p. 283.

(21) "Relationships Between Wind and Waves, Abbotts Lagoon, California," by J. W. Johnson, *Transactions,* Am. Geophysical Union, Vol. 31, p. 386.

(22) "The Characteristics of Wind Waves on Lakes and Protected Bays," by J. W. Johnson, *Transactions,* Am. Geophysical Union, Vol. 29, 1948, p. 671.

(23) "The Forecasting of Sea and Swell Waves," H. N. Suthons, Naval Meteorological Branch, British Admiralty, London, England, 1945.

Wave Refraction, Diffraction, and Reflection

(24) "Essai d'Application des Résultats de la Physique Ondulatoire à l'Etude des Phénomènes de Propagation de la Houle (Application of Wave Physics to Study of Wave Propagation Phenomena)," by H. Gridel, *Annales des Ponts et Chaussees,* Vol. 116, 1946, pp. 77–105, 330–351.

(25) "Refraction of Shallow Water Waves: The Combined Effect of Currents and Underwater Topography," by R. S. Arthur, *Wave Report No. 91*, Scripps Institution of Oceanography, La Jolla, Calif., March, 1950.
(26) "The Refraction of Surface Waves by Currents," by J. W. Johnson, *Transactions*, Am. Geophysical Union, Vol. 28, 1947, p. 867.
(27) "Graphical Construction of Wave Refraction Diagrams," by J. W. Johnson, M. P. O'Brien, and J. D. Isaacs, *Publication No. 605*, Hydrographic Office, U. S. Navy, Washington, D. C., 1948.
(28) "Refraction of Ocean Waves: A Process Linking Underwater Topography to Beach Erosion," by Walter H. Munk and Melvin A. Traylor, *The Journal of Geology*, Vol. 55, 1947, p. 1.
(29) "The Interpretation of Crossed Orthogonals in Wave Refraction Phenomena," by W. J. Pierson, Jr., *Technical Memorandum No. 21*, Beach Erosion Board, Corps. of Engrs., U. S. Army, Washington, D. C., 1951.
(30) "The Application of Conformal Transformations to Ocean Wave Refraction Problems," by L. S. Pocinki, Research Div., New York Univ., New York, N. Y., April, 1950 (unpublished).
(31) "Refraction of Water Waves by Islands and Shoals with Circular Bottom-Contours," by Robert S. Arthur, *Transactions*, Am. Geophysical Union, Vol. 27, 1946, p. 168.
(32) "Graphical Construction of Refraction Diagrams Directly by Orthogonals," *Technical Report HE-116-273*, Univ. of California, Berkeley, Calif., November, 1947.
(33) "Note sur la Diffraction de la Houle en Incidence Normale (Note on the Diffraction of a Normally Incident Wave)," by H. Lacombe, Extract from *Annales Hydrographiques*, No. 1363, Imprimerie Nationale, Paris, France, 1949.
(34) "Théorie Mathématique de la Diffraction (Mathematical Theory of Diffraction)," by A. Sommerfeld, *Mathematical Annales*, Vol. XLVII, 1895, p. 317.
(35) "Diffraction of Water Waves by Breakwaters," by J. A. Putnam and R. S. Arthur, *Transactions*, Am. Geophysical Union, Vol. 29, 1948, p. 481.
(36) "Diffraction of Sea Waves by Breakwaters," by W. G. Penney and A. T. Price, *Technical History No. 26*, Artificial Harbors, Sec. 3D, Directorate of Miscellaneous Weapons Development, London, England, 1944.
(37) "Diffraction of Water Waves Passing Through a Breakwater Gap," by Frank L. Blue, Jr., and J. W. Johnson, *Transactions*, Am. Geophysical Union, Vol. 30, 1949, p. 705.
(38) "Reflection of Tsunamis," by D. Cochrane and R. S. Arthur, *Journal of Marine Research*, Vol. VII, 1948, p. 239.
(39) "Reflection of Solitary Waves," by J. M. Caldwell, *Technical Memorandum No. 11*, Beach Erosion Board, Corps of Engrs., U. S. Army, Washington, D. C., November, 1949.
(40) "De la Houle et du Clapotis (Swell and Clapotis)," by Barre de St. Venant, *Annales des Ponts et Chaussees*, Vol. 58, 1888, p. 33.

WAVE ACTION ON STRUCTURES

(41) "Engineering Aspects of Diffraction and Refraction," by J. W. Johnson, *Proceedings-Separate*, 122, ASCE, 1952.

(42) "A Formula for the Calculation of Rock Fill Dikes," by R. Iribarren, *Bulletin*, Beach Erosion Board, Corps of Engrs., U. S. Army, Washington, D. C., Vol. 3, No. 1, January, 1949.

(43) "The Force Exerted by Surface Waves on Piles," by J. R. Morison, M. P. O'Brien, J. W. Johnson, and S. A. Schaaf, *Petroleum Transactions*, Am. Inst. of Mining and Metallurgical Engrs., Vol. 189, 1950, p. 149.

(44) "Wave Action on Structures," by Walter H. Munk, *Technical Publication No. 2322*, Am. Inst. of Mining and Metallurgical Engrs., March, 1948.

(45) "Essai sur les Digues Maritimes Verticales (Study of Maritime Dikes)," by G. Sainflou, *Annales des Ponts et Chaussees*, Partie Technique, Vol. 98, Fasc. IV, 1928, p. 5. (Translation available at Beach Erosion Board, Corps of Engrs., U. S. Army, Washington, D. C.)

(46) "The Problems of Wave Action on Earth Slopes," by Martin A. Mason, *Transactions*, ASCE, Vol. 116, 1951, p. 1398.

(47) "Wave Action in Relation to Engineering Structures," by D. D. Gaillard, Professional Papers of the Corps of Engineers, U. S. Army, Washington, D. C., 1904.

(48) "Wave Impact on Engineering Structures," by Arnold Hartley Gibson, *Minutes of Proceedings*, The Inst. of Civ. Engrs., London, England, Vol. 187, 1912, p. 274.

(49) "Wave Pressures on Sea-Walls and Breakwaters," by David A. Molitor, *Transactions*. ASCE, Vol. 100, 1935, p. 984.

(50) "Experimental Investigation of Dynamic Action of Waves on Hydro-Maritime Structures" (in Russian, with English summary), by W. E. Timonoff, *Transactions*, Central Research Inst. of Water Transportation, Moscow, Russia, 1934.

(51) "Wave Forces on Breakwaters," by Robert V. Hudson, *Proceedings-Separate No. 113*, ASCE, January, 1952.

TRANSPORTATION OF BEACH AND BOTTOM MATERIAL

(52) "The Prediction of Longshore Currents," by J. A. Putnam, W. H. Munk, and M. A. Traylor, *Transactions*, Am. Geophysical Union, Vol. 30, 1949, p. 337.

(53) "The Formation and Movement of Sand Bars by Wave Action," by C. A. M. King and W. W. Williams, *The Geographical Journal*, Vol. CXIII, 1949, p. 70.

(54) "Sorting of Sediments in the Light of Fluid Mechanics," by D. L. Inman, *Journal of Sedimentary Petrology*, Vol. 19, No. 2, 1949, p. 51.

(55) "Waves as a Sand-Transporting Agent," by U. S. Grant, *American Journal of Science*, Vol. 241, 1943, p. 117.

(56) "Interim Report," Beach Erosion Board, Corps of Engrs., U. S. Army, Washington, D. C., 1933.

(57) "Applied Sedimentation" edited by Parker D. Trask, John Wiley & Sons, Inc., New York, N. Y., 1950 (see "Geology in Shore-Control Problems," by Martin A. Mason), p. 276.

(58) "Shore Processes and Beach Characteristics," by W. C. Krumbein, *Technical Memorandum No. 3*, Beach Erosion Board, Corps of Engrs., U. S. Army, Washington, D. C., May, 1944.

(59) "Shore Currents and Sand Movement on a Model Beach," by W. C. Krumbein, *Technical Memorandum No. 7*, Beach Erosion Board, Corps of Engrs., U. S Army, Washington, D. C., September, 1944.

(60) "An Experimental Study of Submarine Sand Bars," by Garbis H. Keulegan, *Technical Report No. 3*, Beach Erosion Board, Corps of Engrs., U. S. Army, Washington, D. C., 1948.

(61) "Longshore-Bars and Longshore-Troughs," by Francis P. Shepard, *Technical Memorandum No. 15*, Beach Erosion Board, Corps of Engrs., U. S. Army, Washington, D. C., January, 1950.

(62) "Report on Beach Study in the Vicinity of Mugu Lagoon, California," by D. L. Inman, *Technical Memorandum No. 14*, Beach Erosion Board, Corps. of Engrs., U. S. Army, Washington, D. C., March, 1950.

(63) "Test of Nourishment of the Shore by Offshore Deposition of Sand," by J. V. Hall and W. J. Herron, *Technical Memorandum No. 17*, Beach Erosion Board, Corps of Engrs., U. S. Army, Washington, D. C., June, 1950.

(64) "Movement of Beach Sands by Water Waves," by Hans Albert Einstein, *Transactions*, Am. Geophysical Union, Vol. 29, 1948, p. 653.

HYDRAULIC MODELS OF WAVES

(65) "Conformity Between Model and Prototype: A Symposium," *Transactions*, ASCE, Vol. 109, 1944, p. 1.

(66) "Scale Effects in Hydraulic Models Involving Wave Motion," by J. W. Johnson, *Transactions*, Am. Geophysical Union, Vol. 30, 1949, p. 517.

(67) "Empirical Verification of Transference Equations in Laboratory Study of Breakwater Stability," *Bulletin No. 31*, U. S. Waterways Experiment Station, Vicksburg, Miss., April, 1948.

(68) *Hydraulics Bulletin*, U. S. Waterways Experiment Station, Vicksburg, Miss., Vol. 3, No. 1, 1940.

CHARACTERISTICS OF THE SOLITARY WAVE

By James W. Daily,[1] A. M. ASCE, and Samuel C. Stephan, Jr.,[2] J. M. ASCE

Synopsis

The existence of the solitary wave was first reported by J. Scott Russell in 1838. This wave consists of a single elevation that seems to be propagated at constant velocity and unaltered in form. The solitary wave has assumed importance because of the occurrence under a variety of natural circumstances of solitary-like waves whose behavior apparently approximates that of the solitary wave. This similarity suggests the possibility of predicting the effects of these waves through knowledge of the characteristics of the solitary wave. For the purpose of such predictions, there is available a fund of theoretical treatments with some experimental confirmation, mostly based on very early investigations. There has been some renewed interest in checking experimentally the preciseness of the theory to describe certain of the characteristics, and a program of research has been undertaken by the Massachusetts Institute of Technology (MIT), in Cambridge, Mass. The purpose of this paper is to describe the solitary wave and the range of its occurrence and to summarize its theoretically determined characteristics and the status of their experimental verification.

Description of the Solitary Wave

Gravity waves can be broadly classified as either oscillatory or translatory. Oscillatory waves are periodic in character, imparting to the liquid an undulating motion with both horizontal and vertical components without causing appreciable permanent displacement. Translatory waves, on the contrary, cause a net displacement (translation) of the liquid in the direction of the wave motion. Oscillatory waves may occur in either relatively deep water affecting only the liquid near the surface, or in relatively shallow water affecting the liquid over the full depth. A characteristic of translatory waves is that the fluid is set in motion over the full depth (with nearly constant velocity over any cross section at any instant). Thus translatory waves are, relatively speaking, shallow water waves. Oscillatory waves can be created by a periodic disturbance; translatory waves by a sudden permanent displacement (addition or subtraction) of a mass of liquid.

Note.—Published in December, 1951, as *Proceedings-Separate No. 107*. Positions and titles given are those in effect when the paper or discussion was received for publication.

[1] Associate Prof. of Hydraulics, Massachusetts Inst. of Technology, Cambridge, Mass.

[2] Research Asst., Hydr. Civ. Engr., Massachusetts Inst. of Technology, Cambridge, Mass.

The solitary wave is a translation wave. Included in this classification are tidal waves, seismic waves, bore waves and other channel surges, and flood waves. Each of these several types of wave occurs under different circumstances and is propagated with different characteristics, depending on the relative importance of the gravity, friction, and inertia forces. For the flood wave, friction is predominant in controlling the motion. Tidal wave motion is essentially irrotational, with frictional damping producing only a secondary effect. Solitary wave motion also is essentially irrotational. Between these extremes, the several intermediate types form a continuous transition.

Translation waves of finite height or amplitude are in general propagated with a celerity that depends on height and with a wave form that changes with time. This continuous deformation of the wave form is independent of any simultaneous effect of friction in absorbing energy and changing the form. The solitary wave is an exception in that it is apparently a wave of permanent form and constant celerity so long as friction effects can be ignored. It consists of a single elevation of liquid above the level of the originally undisturbed surface, as shown in Fig. 1. Theoretically, the wave extends to infinity on either side of the crest, but practically its length is limited. A passing wave accelerates the liquid from zero to a maximum velocity as the crest passes and then allows a deceleration to zero again, causing a horizontal displacement by an amount proportional to the wave volume. The major portion of the wave energy is concentrated within a narrow zone straddling the crest.

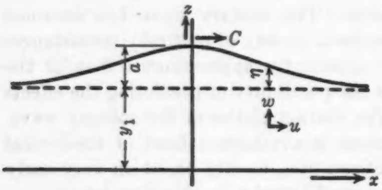

FIG. 1.—THE SOLITARY WAVE

Although the shape and other characteristics of oscillatory waves depend on wave length (the distance between two crests) as well as the wave height and the liquid depth,[3] the solitary wave characteristics are described completely by the wave height and liquid depth.

RANGE OF APPLICATION OF SOLITARY WAVE CHARACTERISTICS

J. Scott Russell[4,5] was responsible for calling attention to the solitary wave, in 1838, and for making the first investigations of its characteristics during the period from 1838 to 1845. He observed that acceleration or deceleration of ships in navigation channels sometimes set up a wave with a solitary crest that then traversed the length of the channel, essentially unaltered in form and at constant velocity of propagation. He also observed that tidal waves behaved similarly in traversing the channels. The field observations were then supple-

[3] "A Summary of the Theory of Oscillatory Waves," *Technical Report No. 2*, Beach Erosion Board, Corps of Engrs., U. S. Army, Washington, D. C., 1942.

[4] "Report of the Committee on Waves," by J. Scott Russell, Seventh Meeting of the British Association for the Advancement of Science, 1838, p. 417.

[5] "Report on Waves," by J. Scott Russell, Fourteenth Meeting of the British Association for the Advancement of Science, 1845, p. 311.

mented with laboratory experiments that were undertaken primarily in consequence of an interest in waves as affecting navigation, although a broader significance was recognized at the time.

In the following fifty years, the solitary wave was the subject of considerable academic interest and theoretical study, with some additional experimental research. Then interest lagged until the growing concern over beach erosion and other shore-line problems, flood routing, and wave action in navigation inlets led to the application of the accumulated theoretical results to several practical problems.

Aside from the more obvious cases, such as tidal waves or artificially produced solitary crests traversing a channel, river, or canal, perhaps the most interesting application of knowledge of solitary wave characteristics is to the approximation of the behavior of periodic waves of long wave length in relatively shallow water. As oscillatory waves enter into shallow water, the crest increases in height and curvature, the trough becomes flatter, and the behavior of the individual crests becomes nearly independent of the wave length. This independence, as well as an observed physical similarity between the resulting crest and the solitary wave crest, led to the application of the characteristics of the solitary wave to the transformation and breaking of waves in shallow water, the rise of the sea surface accompanying high surf, the refraction of waves, the establishment of longshore currents, and the transport of sand in the surf zone. Walter H. Munk[6] has summarized the procedures and progress made along these lines.

Characteristics of the Solitary Wave

The key characteristics of the solitary wave are the wave celerity, wave form, and liquid particle velocities. With these known, the wave volume, wave energy, and amount of displacement of liquid can be determined as functions of depth and of the ratio of amplitude to depth. In addition the manner of energy loss through friction is an important consideration.

All theoretical solutions for the behavior of the solitary wave are based on the common conditions of irrotational two-dimensional motion of a liquid that satisfies the following boundary conditions: (1) The wave form is permanent; (2) the pressure over the free surface is constant; (3) the motion vanishes at infinity in both directions; and (4) the vertical motion vanishes at the channel bottom. Using the dynamical equations of motion, the velocity potential function can be expressed by an infinite series. Existing theories differ as to the type of series to be employed and the degree of approximation imposed by limiting the number of terms in the series when calculating each of the several characteristics. An exact solution has not been reported. This situation has resulted in certain differences in published formulas for celerity, profile shape, and other characteristics. These differences have been only partially reconciled by comparison with experimental evidence.

[6] "The Solitary Wave Theory and its Application to Surf Problems," by Walter H. Munk, *Annals of the New York Academy of Science*, Vol. 51, 1949, p. 376.

The most important results in this field are attributed to J. Boussinesq,[7] Lord Rayleigh,[8] and J. McCowan.[9] Rayleigh and Boussinesq employed a first approximation using only a few terms to establish expressions for the various characteristics. Mr. McCowan discussed solutions to a higher approximation with significant difference from the previous results in that the expressions for particle motion are more reasonable. In the excellent summary by Mr. Munk[6] the results of Boussinesq and Mr. McCowan were employed. From time to time, improvements in the theory have been suggested. Thus, A. Weinstein[10] proposed an expression for celerity carried to a higher approximation, and Joseph B. Keller[11] published a method of analysis in which the degree of approximation was more easily established and more easily extended, if desired. Garbis H. Keulegan and George Patterson[12] have reviewed the theory in detail and Mr. Keulegan[13] has discussed the effect of friction on damping.

This paper will summarize the most important of the theoretical principles and comment on their agreement with experimental results. For experimental confirmation, theoretical investigators have relied primarily upon the initial measurements of Mr. Russell and other measurements made a short time later by H. Bazin.[14] Generally this confirmation was restricted to the expression for celerity, the empirical form of which was similar to that obtained by Boussinesq and Rayleigh. The renewal of interest in the solitary wave has led to a reexamination of its characteristics in the laboratory in regard to agreement with theory and the effects of friction. Results of a program of research in the Hydrodynamics Laboratory at MIT will be used in this paper for comparison with the theory.

The laboratory program at MIT included measurements of celerity, wave form, particle motion, and the effects of channel surface friction in both horizontal and shoaling channels. However, data used for illustrations in the following sections include only measurements of celerity and profile shapes with a horizontal bottom. These experiments were made in a transparent walled channel 16.5 in. wide and 32 ft long. Waves were generated by a plunger that displaced a certain definite volume of liquid to cause the solitary elevated wave. The wave as initially generated is very close to the solitary form, and, after a travel of about 16 ft, it ceases to deform perceptibly, apparently reaching its final stable form. Celerity measurements are then made by timing the passage of the crest between two stations. The corresponding wave profile is obtained

---

[7] "Theorie Des Onde Et De Remous Qui Se Propagent Le Long D'un Canal Rectangulaire Horizontal, en Communiquant Au Liquide Contenn Dans Ce Canal Des Vitesses Sensiblement Parielles de La Surface Au Fond," by J. Boussinesq, *Journal of Mathematics*, Liouvilles, France, Vol. 17, 1872, p. 55.

[8] "On Waves," by Lord Rayleigh, *The London, Edinburgh, and Dublin Philosophical Magazine and Journal of Science*, Vol. 1, 1876, p. 257.

[9] "On the Solitary Wave," by J. McCowan, *The London, Edinburgh, and Dublin Philosophical Magazine and Journal of Science*, Vol. 32 (5), 1891, p. 45.

[10] "Sur La Vitesse De Propagation De L'onde Solitaire," by A. Weinstein, *Comptes Rendus*, Accademia del Lincei, Vol. 3, No. 8, 1926, p. 463.

[11] "The Solitary Wave and Periodic Waves in Shallow Water," by Joseph B. Keller, *Communications on Applied Mathematics*, Institute of Mathematics and Mechanics, New York University, New York, N. Y., Vol. I, No. 3, 1948, p. 286.

[12] "Mathematical Theory of Irrotational Translation Waves," by Garbis H. Keulegan and George W. Patterson, *Journal of Research*, National Bureau of Standards, Vol. 24, 1940, p. 47.

[13] "Gradual Damping of Solitary Waves," by G. H. Keulegan, *Journal of Research*, National Bureau of Standards, Vol. 40, 1948, p. 487.

[14] "Recherches Experimentales Sur La Propagation Des Ondes," by H. Bazin, Memoires Divers Savants a l'Academie des Sciences, Vol. 19, 1865, p. 495.

photographically. These preliminary measurements show considerable scatter that is caused by lack of precision in making these measurements rather than by any systematic error. Thus, despite this experimental scatter, certain trends are indicated that are felt to be reliable enough to justify discussion.

Celerity.—Mr. Russell reported that the velocity of wave propagation could be expressed by the relation

$$C = \sqrt{g(y_1 + a)} = \sqrt{g\, y_1}\left(1 + \frac{a}{y_1}\right)^{\frac{1}{2}} \qquad (1)$$

in which C is the celerity of the wave, g is the acceleration of gravity, y_1 is the depth of the undisturbed water, and a is the wave amplitude (elevation of the crest above y_1). Later, Boussinesq, Rayleigh, and Mr. McCowan each obtained this equation theoretically as a "first approximation," as previously mentioned. In addition, Mr. McCowan pointed out that with slightly higher degrees of approximation, there could be obtained

$$C = \sqrt{g\, y_1}\left(1 + \frac{a}{y_1 + a}\right)^{\frac{1}{2}} \qquad (2)$$

$$C = \sqrt{g\, y_1}\left(1 + \frac{a}{y_1 + \frac{19}{12}\, a}\right)^{\frac{1}{2}} \qquad (3)$$

Mr. Weinstein obtained, by a different method, the same equation carried to a higher degree of approximation

$$C = \sqrt{g\, y_1}\left[1 + \frac{a}{y_1} - \frac{21}{20}\left(\frac{a}{y_1}\right)^2\right]^{\frac{1}{2}} \qquad (4)$$

This equation is intended to apply for ratios of a/y_1 less than 0.2 whereas no such limit was specified for the previous equations. Eq. 1 indicated a linear relation between C^2 and the depth of liquid at the wave crest, while Eqs. 2, 3, and 4 each give increasingly large departures from the linear relation, as the ratio of a/y_1 increases.

The results of the early experiments of Mr. Bazin as well as those of Mr. Russell supported Eq. 1 to within an error of about 1%. The results of the measurements at MIT are shown in Fig. 2. In Fig. 2 observed celerities of a series of measurements are compared with the celerities as given by Eq. 1. This comparison indicates that the observed celerities are slightly less than the theoretical celerities. The total mass of this MIT data tends to substantiate this indication, as is shown by the center of gravity of the band of points in Fig. 2(*b*). None of the Eqs. 2, 3, or 4 appears to follow exactly the trend of experimental data although for values of a/y_1 less than 0.2 these equations each provide corrections in the right direction. For values of the term above 0.2 all the equations indicate increasingly large deviations from the measured values. For the full range of amplitude up to the point of breaking (important in surf problems), Eq. 1, possibly with a correction of about 0.5%, remains the best expression for the celerity.

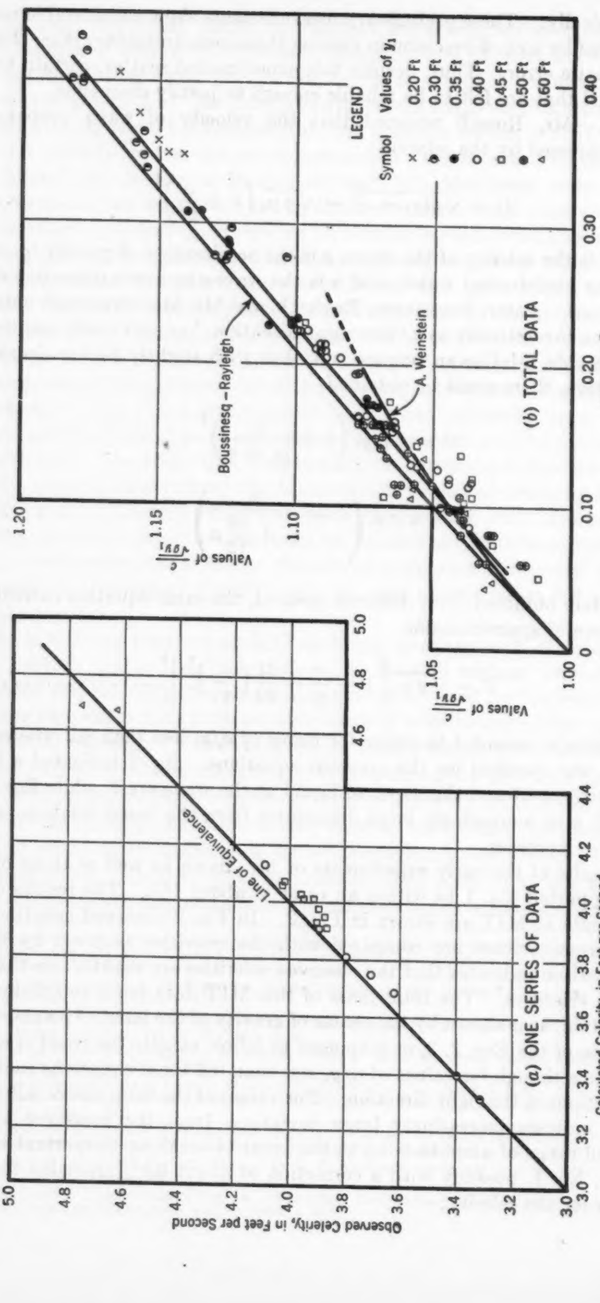

FIG. 2.—COMPARISON OF WAVE CELERITIES

Surface Profile.—The second report by Mr. Russell[5] contained traces of surface profiles that were described by a curve of versed sines. All theoretical solutions have indicated that the profile should be described by a hyperbolic secant curve. Mr. McCowan gave the solution as

$$\eta = a \operatorname{sech}^2 \left(\frac{m\, x}{2} \right) \qquad (5)$$

in which η is the surface elevation above the undisturbed water level, a is amplitude as described, x is the horizontal distance measured from the crest

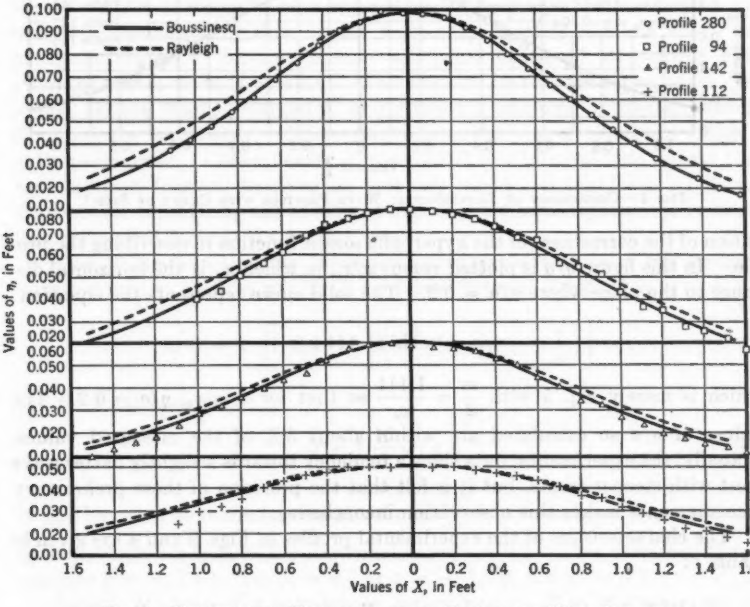

FIG. 3.—COMPARISON OF EXPERIMENTAL AND THEORETICAL WAVE PROFILES

position, and m is an expression that depends on the type of solution and degree of approximation. This value has been determined by various investigators, as follows:

Investigator	Value of m	
J. Boussinesq	$\sqrt{\dfrac{3\,a}{y^3_1}}$	(6a)
Lord Rayleigh	$\sqrt{\dfrac{3\,a}{y^2_1\,(y_1 + a)}}$	(6b)
J. McCowan	$\sqrt{\dfrac{3\,a}{y^2_1 \left(y_1 + \dfrac{19}{12}\,a\right)}}$	(6c)

With each successive modification, the steepness of the wave front varies downward from the steepest form as given by Boussinesq. This is evidenced by the comparison between the plotted Boussinesq and Rayleigh equations in Fig. 3.

Actual waves should be expected to differ from these theoretical profiles in that the elevated surface will extend for only a finite distance from the crest. Practically, the degree of agreement near the crest is more important since the wave volume and energy are primarily concentrated there. Fig. 4 gives an indi-

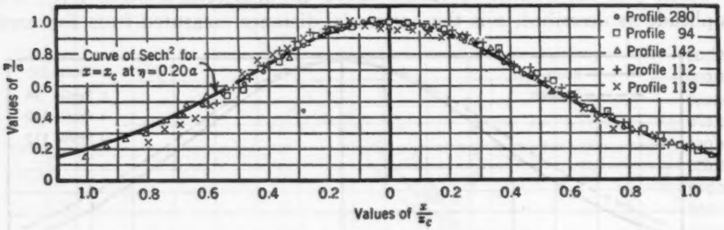

FIG. 4.—COMPARISON OF EXPERIMENTAL WAVE PROFILES WITH CURVE OF SECH²

cation of the correctness of the hyperbolic secant function in describing the profile. In this figure η/a is plotted versus x/x_c, in which x_c is the horizontal distance to the place where $\eta/a = 0.2$. The solid curve represents the equation

$$\eta/a = \text{sech}^2\,(1.444\,x/x_c)$$

which is merely Eq. 5 with $\frac{m}{2} = \frac{1.444}{x_c}$ so that for $x = x_c$, $\eta/a = 0.2$. The values of η/a so calculated are within about 5% of the measured values. Actually, the experimental data show a tendency towards a slightly flatter wave crest with steeper fronts, but it is felt that the precision of these preliminary measurements makes this observation inconclusive.

The characteristics of the experimental profiles in Figs. 3 and 4 are given in Table 1:

TABLE 1.—CHARACTERISTICS OF EXPERIMENTAL WAVE PROFILES

Profile number	Depth y_1 feet	Amplitude a feet	Ratio a/y_1	Distance x_c to $\eta/a = 0.2$ feet
(1)	(2)	(3)	(4)	(5)
280	0.4311	0.0992	0.230	1.505
94	0.4409	0.0804	0.180	1.653
142	0.3766	0.0604	0.160	1.487
112	0.4377	0.0503	0.115	1.925
119	0.4367	0.0351	0.080	1.940

In Fig. 3 the same data are compared with the Boussinesq and the Rayleigh theoretical profiles. Substantial agreement with the Boussinesq form is obtained. The Rayleigh profiles fall ouside the range covered by scatter and other deviations in the measured data. These curves cover the range of values

of the ratio a/y_1 below 0.23. There is evidence to indicate that at higher ratios of a/y_1, the actual profiles may be more peaked than the Boussinesq relation would indicate. The traces obtained by Mr. Russell showed this in some instances and occasional profiles published subsequently, such as those of J. M. Caldwell[15] have indicated the same characteristics. However, the exact deviation is not yet established so that the continued use of the simpler Boussinesq equation seems justified.

In the laboratory there is always some question as to whether the generated waves have attained a final permanent form as postulated in developing the theory. First, as the wave form approaches the permanent form, the deformation rate becomes very slow or the wave may possibly oscillate about the permanent shape.[12] Second, friction will cause continual attenuation even after the stable form is attained. Fortunately, in the oscillating stage, the profile cannot change markedly, and frictional damping ultimately should eliminate the oscillations. Before this occurs, the rate of change of shape is quite perceptible. Consequently, if the rate of loss in amplitude is near that expected from friction, the wave has probably reached its final form. This was the basis for considering the profiles of Figs. 3 and 4 to be representative of the true permanent form of the solitary wave.

Wave Volume.—Using the Boussinesq profile, the volume of the elevated wave per unit of crest length (ΔQ) contained between limits of $+x$ to $-x$ is

$$\Delta Q = 2 \int_0^x \eta \, dx = \left[\left(\frac{16}{3} y_1^3 \, a \right) \left(1 - \frac{\eta}{a} \right) \right]^{\frac{1}{2}} \qquad (7)$$

and the total volume (Q) is

$$Q = \left(\frac{16}{3} y_1^3 \, a \right)^{\frac{1}{2}} \qquad (8)$$

It will be noted that the fractional volume $\frac{\Delta Q}{Q}$ is a function of η/a. For the zone in which $\eta/a \geq 0.19$ the fractional volume is 0.9. This corresponds to a distance $x = \pm 2.4 \, y_1$ if $a/y_1 = 0.5$ or $x = \pm 3.8 \, y_1$ if $a/y_1 = 0.2$.

Particle Motion.—The solution as determined by Mr. McCowan for the horizontal and vertical components of the local liquid velocities induced by the wave's passage are given by Mr. Munk in the form

$$\frac{u}{C} = N \frac{1 + \cos\left(M \frac{z}{y_1}\right) \cosh\left(M \frac{x}{y_1}\right)}{\left\{ \cos\left(M \frac{z}{y_1}\right) + \cosh\left(M \frac{x}{y_1}\right) \right\}^2} \qquad (9)$$

$$\frac{w}{C} = N \frac{\sin\left(M \frac{z}{y_1}\right) \sinh\left(M \frac{x}{y_1}\right)}{\left\{ \cos\left(M \frac{z}{y_1}\right) + \cosh\left(M \frac{x}{y_1}\right) \right\}^2} \qquad (10)$$

[15] "Reflection of Solitary Waves," by J. M. Caldwell, *Technical Memorandum No. 11*, Beach Erosion Board, Corps of Engrs., U. S. Army, Washington, D. C., 1949.

in which u and w are the horizontal and vertical components of the velocity, and the parameters, M and N are functions of the ratio a/y_1 (Fig. 5) according to the equations

$$a/y_1 = \frac{N}{M} \tan \tfrac{1}{2} [M (1 + a/y_1)] \text{.................(11)}$$

$$N = \frac{2}{3} \sin^2 \left[M \left(1 + \frac{2\,a}{3\,y_1} \right) \right] \text{.................(12)}$$

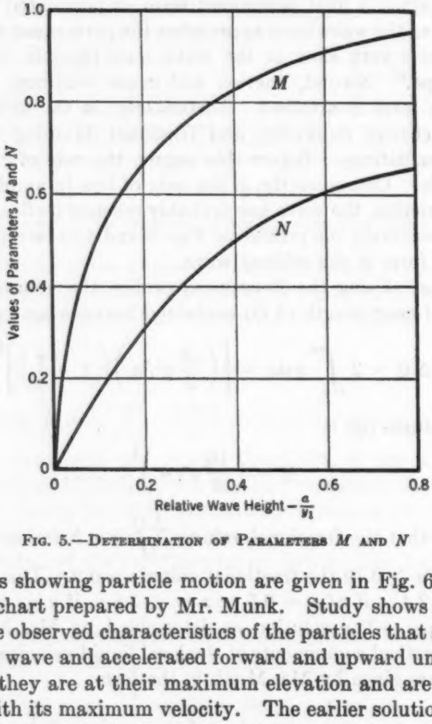

FIG. 5.—DETERMINATION OF PARAMETERS M AND N

Typical diagrams showing particle motion are given in Fig. 6 which has been adapted from a chart prepared by Mr. Munk. Study shows that these equations describe the observed characteristics of the particles that are set in motion by the oncoming wave and accelerated forward and upward until at the instant of crest passage they are at their maximum elevation and are all moving horizontally, each with its maximum velocity. The earlier solutions of Boussinesq were inaccurate to the extent of indicating finite vertical (downward) velocities beneath the crest.

After the crest passes, the particles gradually return to rest at their original elevation but displaced in the direction of motion by a certain amount, the surface liquid being displaced farther than the bottom liquid. The average value of this horizontal displacement (or mass transport) is

$$\Delta x = \frac{Q}{y_1} \text{.........................(13)}$$

These particle motions and displacements have been confirmed only qualitatively. Mr. Russell approximated the orbits of particles by a curve of

versed sines, as he did the surface profile. The velocities are low, and the motions of short duration, making measurements difficult. Since these internal motions are important in the discussion of sediment transportation and of other phenomena associated with shoreward transport, return flow and drift in the surf, a more exact verification is likely to be required.

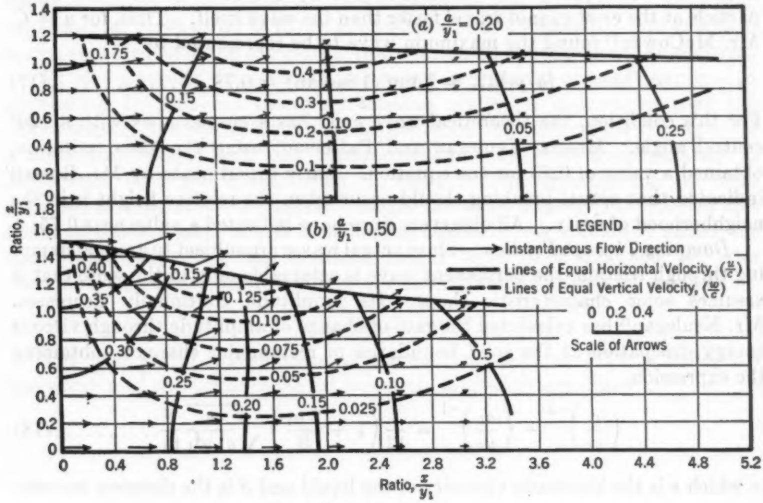

FIG. 6.—SURFACE PROFILES AND ORBITAL MOTIONS

Wave Energy.—The potential and kinetic energies of the elevated wave are approximately equal.[11] Therefore, the energy per unit length of crest (ΔE) of the liquid contained between $+x$ and $-x$ becomes

$$\Delta E = \Delta E_p + \Delta E_k = 2\,\rho\,g \int_0^x \frac{\eta^2}{2}\,dx \ldots\ldots\ldots\ldots\ldots(14)$$

in which the subscripts p and k denote potential and kinetic, respectively, and ρ is the density of the liquid. Using Eqs. 5 and 6*a*,

$$E = \frac{4}{3\sqrt{3}}\,\rho\,g\,a^{\frac{3}{2}}\,y^{\frac{3}{2}}_1\,(2 + \eta/a)\,(1 - \eta/a)^{\frac{1}{2}} \ldots\ldots\ldots\ldots(15)$$

and the total energy (and hence the work necessary to generate the wave)

$$E = E_p + E_k = \frac{8}{3\sqrt{3}}\,\rho\,g\,a^{\frac{3}{2}}\,y^{\frac{3}{2}}_1 \ldots\ldots\ldots\ldots\ldots(16)$$

As observed for the fractional volume, the fractional energy $\frac{\Delta E}{E}$ is a function of η/a (and in turn of x, y_1, and a). For $\eta/a \geq 0.19$, the fractional energy is 0.99 compared with 0.90 for the fractional volume within the same limits.

Ninety percent of the energy is contained within the limits described by $\eta/a \geq 0.46$.

The Limiting Wave.—It should be noted that a limit exists as to the amount of energy that can be propagated with a solitary wave, since in a liquid of given depth y_1, the wave will break at a certain maximum height. This limiting height can be approximated theoretically using the criterion that the liquid particle at the crest cannot travel faster than the wave itself. Thus, for $u = C$, Mr. McCowan[16] found the maximum wave to be represented by

$$(a/y_1)_{max} = \tfrac{1}{2} \tan (1 \text{ radian}) = 0.78 \ldots\ldots\ldots\ldots\ldots (17)$$

For this condition, the theoretical wave crest has a cusped apex with a 120° central angle. Messrs. Keulegan and Patterson, using the same criterion, obtained a value of 0.73 for the equation. Early experiments by Mr. Russell indicated that actual breaking should occur when the relative height is in the neighborhood of unity. All observers since have indicated a value near 0.75.

Damping Through Friction.—Since actual waves are subject to gradual damping through friction, the permanent wave is attainable only in the sense that it assumes some characteristic shape. Its amplitude continually decreases. Mr. Keulegan[13] has calculated the rate of change of amplitude through viscous energy dissipation at the solid boundaries of rectangular channels, obtaining the expression

$$\left(\frac{a}{y_1}\right)^{-\frac{1}{4}} - \left(\frac{a_0}{y_1}\right)^{-\frac{1}{4}} = \frac{1}{12}\left(1 + \frac{2\,y_1}{B}\right)\sqrt{\frac{\nu}{g^{\frac{1}{2}}\,y_1^{\frac{3}{2}}}}\,\frac{S}{y_1} \ldots\ldots\ldots (18)$$

in which ν is the kinematic viscosity of the liquid and S is the distance traveled by a wave in a rectangular channel of width B as the wave amplitude changes from a_0 to a. For a wide channel or two-dimensional case this equation reduces to

$$\left(\frac{a}{y_1}\right)^{-\frac{1}{4}} - \left(\frac{a_0}{y_1}\right)^{-\frac{1}{4}} = \frac{1}{12}\sqrt{\frac{\nu}{g^{\frac{1}{2}}\,y_1^{\frac{3}{2}}}}\,\frac{S}{y_1} \ldots\ldots\ldots\ldots\ldots (19)$$

Using values of temperature (and hence viscosity) estimated from weather records, the original attenuation data compiled by Mr. Russell checks Eq. 18. These measurements were made by allowing the waves to undergo repeated reflections from the plane ends of a 20-ft laboratory channel until the length of travel was several hundred feet. Negligible loss during reflection is assumed. This is the most extensive data available for substantiating theoretical results.

CONCLUSIONS

The extensive measurements by Mr. Russell as well as further experiments have reasonably well verified the Boussinesq-Rayleigh celerity equation. The Boussinesq profile appears to agree best with experimental results but the supporting evidence is not extensive. Efforts are underway to obtain more refined profile measurements, but major differences from the present conclusions are not expected. The expressions derived by Mr. McCowan for internal motions are

[16] "On the Highest Wave of Permanent Type," by J. McGowan, *The London, Edinburgh, and Dublin Philosophical Magazine and Journal of Science*, Vol. 38, 1894, p. 351.

yet to be verified and should be given attention, particularly in view of their application to sediment transportation problems. Data on damping should also be verified and extended.

The actual need for precise verification of theoretical wave motions may be questioned since natural waves seldom, if ever, conform exactly to the pure waves discussed theoretically or investigated in the laboratory. However, experimental verification in fixing knowledge of the phenomenon will establish the reasonableness of the calculating procedures and approximations employed.

All of the results discussed are for waves in water of constant depth. In application to problems involving shoaling water, it is assumed that the characteristics at a particular still water depth are the same on the sloping as on a horizontal bottom and that transformations take place approximately in accordance with the conservation of energy. The investigation of these premises is important. Strangely enough, the work done by Mr. Russell also included a few measurements in a sloping channel. As previously noted, his observations regarding the breaking height have been modified by later observers, suggesting the desirability of checking and extending his results.

ACKNOWLEDGMENT

The program of investigation of the solitary wave at MIT is under the sponsorship of the Office of Naval Research, United States Navy.

LONG-PERIOD WAVES OR SURGES IN HARBORS

By John H. Carr[1]

With Discussion by Messrs. John S. McNown, B. W. Wilson, and John H. Carr

Synopsis

The topic of long-period waves is of importance in the design and construction of harbor facilities, since these waves affect floating objects within the confines of the harbor.

This paper reports the results of field and model studies of the sources and characteristics of long-period waves in harbors and analyzes the subjects of basin resonance and water motions induced by the waves. The particular adaptability of models to this type of study is discussed, and examples of the use of models in the design of harbor facilities are given.

Long-period waves are known to affect the motion of moored ships, and a discussion of this phenomenon is given.

Introduction

Long-period waves are of importance in harbor operations because of the effect of their associated water motions on floating objects. Like all other waves, long-period waves are characterized by oscillatory horizontal and vertical water motions, and these motions cause all floating objects to oscillate at the wave frequency and with amplitudes comparable to the water motion amplitude, unless the objects are restrained. However, for waves of the same height, the horizontal amplitude of the water motion increases linearly with the wave period. Thus long-period waves of relatively low wave height can induce greater amplitude motions of a nonrigidly moored ship than those induced by high storm waves of the usual 8-sec to 15-sec periods.

The Hydraulic Structures Laboratory of the California Institute of Technology, at Pasadena, has conducted investigations of long-period wave disturbances in connection with two studies made for the Bureau of Yards and Docks, United States Department of the Navy. This paper utilizes three of the topics of those investigations:

Note.—Published in April, 1952, as *Proceedings-Separate No. 123.* Positions and titles given are those in effect when the paper or discussion was received for publication.

[1] Senior Research Engr., Hydrodynamics Lab., California Inst. of Technology, Pasadena, Calif.

1. A review of the characteristics of long-period waves in harbors, including an analysis of the phenomena of basin resonance, an analysis of the wave-induced water motions, and some postulations concerning the sources of long-period waves;

2. A discussion of the particular usefulness of model studies for the solution of problems of harbor design arising from long-period wave phenomena; and

3. A discussion of an important engineering problem associated with long-period wave disturbances, namely, the motion of moored ships under the influence of this type of excitation.

Characteristics of Long-Period Waves in Basins

Standing Wave Pattern.—An important factor affecting long-period wave motion in harbors is the possibility of these long-period waves exciting an oscillation of the harbor basin, with resulting build-up of wave height (hence water motion) as a result of resonant amplification, in a manner analogous to a mechanical vibrating system.

The oscillation of a basin is a special case of a standing wave pattern and is best considered in that light. When a wave train encounters a reflecting shore line, the reflected wave passes through and interferes with the oncoming one. The effect of this interference is reinforcement where incident and reflected motions coincide and cancellation where the motions are opposed. Since the lengths of the incident and reflected wave lengths are the same, the points of reinforcement and cancellation are fixed in space; and a standing wave pattern, with stationary positions of maximum and minimum motion, or loops and nodes, is produced. For the special case in which the direction of incident wave travel is normal to a straight reflecting surface, the standing wave pattern will take the form of a series of straight crests and troughs parallel

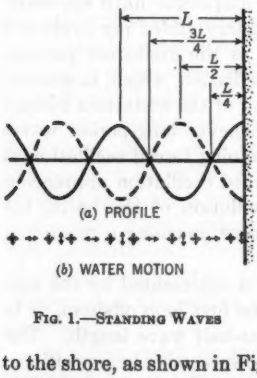

Fig. 1.—Standing Waves

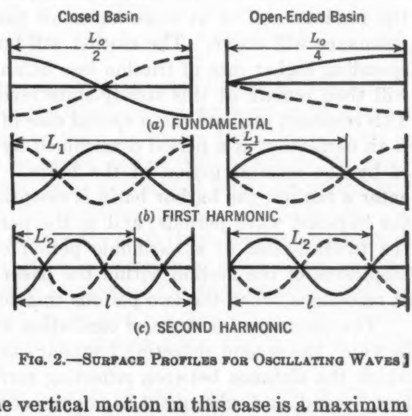

Fig. 2.—Surface Profiles for Oscillating Waves

to the shore, as shown in Fig. 1. The vertical motion in this case is a maximum at the reflecting surface and at 1/2, 1, 3/2, 2, and so on, wave lengths offshore (or at integer multiples of half the wave length offshore) and zero at distances of 1/4, 3/4, 5/4, and so on, wave lengths offshore. The horizontal motion is

zero at the boundary and at the other loop positions and a maximum at the nodal positions.

These results may be derived simply in analytical form as follows: The profile of the incident and reflected wave trains may be expressed in terms of their vertical amplitudes, η_1 and η_2, and of the two variables of time (t) and horizontal distance (x). The equations expressing this relationship are:

$$\eta_1 = a \sin 2\pi \left(\frac{t}{T} - \frac{x}{L}\right) \qquad \text{(1a)}$$

$$\eta_2 = a \sin 2\pi \left(\frac{t}{T} + \frac{x}{L}\right) \qquad \text{(1b)}$$

in which a is the maximum wave amplitude; T is the wave period; and L is the wave length. The resultant water surface profile is given by the sum of η_1 and η_2, or

$$\eta_1 + \eta_2 = 2\, a \sin 2\pi \frac{t}{T} \cos 2\pi \frac{x}{L} \qquad \text{(2)}$$

from which the values of $\frac{x}{L}$ listed previously for maximum and zero vertical motion may be readily verified.

If a second reflecting boundary occurs at a loop position, the basin so bounded constitutes a system capable of executing free vibrations, or oscillation. In the absence of damping, the standing wave pattern or its equivalent, a progressive wave travelling back and forth between the boundaries will persist with the initial amplitude. If energy losses do occur, as in any actual physical system, the basin oscillation is a typical damped free vibration, and the wave amplitude decreases exponentially with time. If, instead of only an initial excitation, the harbor is subject to a periodic addition of energy at the fundamental or at some harmonic period of free oscillation of the basin, resonance will occur. The motion will build up in amplitude until the corresponding higher rate of friction loss balances the energy added per cycle and will then remain at this steady-state level as long as the excitation persists. This resonant oscillation is a special case of forced oscillation, which, in general, is an oscillation at a period determined by the period of the excitation instead of by the natural period of the basin. Thus, whenever long-period waves enter a harbor, the harbor basin is essentially undergoing forced oscillation at the imposed wave periods; and as the period of forced oscillation approaches the fundamental or a harmonic period of free oscillation of the basin, the amplitude of the motion within the basin will increase, reaching a maximum at resonance, when the two periods coincide.

The fundamental mode of oscillation of a basin is represented by the case in which the second reflecting boundary occurs at the first loop offshore, or in which the distance between reflecting surfaces is one-half wave length. The first, second, and subsequent harmonics correspond to successive loop positions, or to basin lengths of 1, 1½, 2, and so on, wave lengths and subsequent integer multiples of half the wave length as shown in Fig. 2(a). The fundamental period (T_o) of the oscillation is, therefore, the period of a wave whose length

is twice the distance between reflecting boundaries. The harmonic period corresponding to the harmonic modes of oscillation are 1/2, 1/3, 1/4, and so on, of the fundamental, or

$$T_n = \frac{2\,l}{(n+1)\,C} \qquad (3)$$

in which n is the order (1st, 2nd, and so on) of the harmonic, $n = o$ corresponding to the fundamental period, C is the wave velocity, and l is the distance between boundaries.

A second type of basin oscillation is possible if, instead of a reflecting surface located at a loop, an opening across which flow may occur is located at a node and connects the basin to a relatively large body of water. The fundamental mode of oscillation for such a configuration is that for the case of the opening at the first node position (or 1/4 wave length offshore). Harmonic modes are represented by the location of the opening at successive nodal positions as shown in Fig. 2(*b*). Except for the shape of the water surface, the oscillation proceeds in the same manner as previously discussed, and it is readily apparent that the periods of the oscillation are given by

$$T_n = \frac{4\,l}{(n+1)\,C} \qquad (4)$$

The application of these equations to the computation of the natural periods of oscillation of a harbor is simplified by the fact that the long-period waves considered are always shallow-water waves in typical harbor-water depths. Hence, their velocity is given by

$$C = \sqrt{g\,d} \qquad (5)$$

in which d is the water depth. The average value of C and the length l between oppositely disposed reflecting surfaces, or reflecting surface and opening, can be computed readily from harbor charts and a close approximation of the natural periods thus arrived at.

It may be noted that the apparent damping is much higher for the higher harmonics of basin oscillation than for the fundamental, so much so that basin oscillation at higher than the second or third harmonic is seldom observed. This is not because of the friction losses associated with the water motion, since this energy loss is independent of wave period, but is caused by the loss of energy by imperfect reflection at the basin boundaries. The quality of a reflecting surface is a function of the magnitude of its irregularities with respect to the wave length reflected. Thus, the same stretch of shore line may be a very good reflector for the long wave lengths of the fundamental mode of oscillation and a rather poor reflector, scattering a large part of the imposed energy out of the path of oscillation, for the shorter wave lengths of the higher harmonics.

As a final word on the theoretical aspects of basin oscillation, it may be remarked that in a typical harbor basin there may be several possible modes of oscillation. If the fundamental or harmonic periods of two or more of these modes are the same, both modes will be excited by an exciting wave of this

period. In this case, the energy of the forcing wave is split between the two modes of oscillation and their resulting amplitudes will be less than when excited separately.

Water Motion.—The motion of the water in the long-period, shallow-water waves considered in this paper is very closely represented by the classical wave theory of G. B. Airy.[2] The particles may be considered to be travelling in elliptical orbits whose horizontal major diameter is nearly of constant magnitude from the surface to the bottom and whose vertical minor diameter varies linearly from a maximum at the surface (where it is equal to the wave height in magnitude) to zero at the bottom. The magnitude of the horizontal diameter is a function of the wave length or period, the wave height, and the water depth; and it is very much larger than the surface value of the vertical diameter.

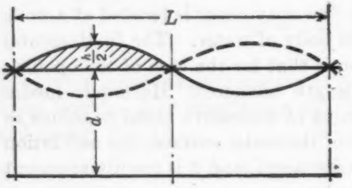

FIG. 3.—HORIZONTAL VELOCITY

The horizontal water particle velocities may be calculated by assuming a sinusoidal wave profile and considering the flow across nodal sections as the wave form progresses (Fig. 3). The volume of water (V_w) that must flow across nodal sections is

$$V_w = \int_0^{L/2} \frac{h}{2} \sin \frac{2\pi x}{L} \, dx = \frac{h L}{2 \pi} \qquad (6)$$

in which h is the vertical height of the wave. Hence, the average flow rate (Q) across the nodal section in one half the wave period is

$$Q = \frac{V_w}{\frac{T}{2}} = \frac{h L}{\pi T} \qquad (7)$$

The average horizontal velocity across the nodal section is, therefore,

$$V_{av} = \frac{Q}{A} = \frac{h L}{\pi d T} \qquad (8)$$

in which V is the horizontal velocity and A is the cross-sectional area. The amplitude of a water particle will be

$$a = V \frac{T}{2} = \frac{h L}{2 \pi d} \qquad (9)$$

Since $\frac{L}{T} = C$, and $C = \sqrt{g\,d}$ for these shallow-water waves,

$$V_{av} = \frac{\sqrt{g}}{\pi} \frac{h}{\sqrt{d}} \qquad (10)$$

The maximum horizontal velocity, being $\frac{\pi}{2}$ times the average velocity for

---

[2] "A Summary of the Theory of Oscillatory Waves," by Morrough P. O'Brien, *Technical Report No. 2*. Beach Erosion Board, Corps of Engrs., U. S. Dept. of the Army, Washington, D. C., 1942.

sinusoidal motion, is

$$V_{\max} = \frac{\sqrt{g}}{2} \cdot \frac{h}{\sqrt{d}} \quad \ldots\ldots\ldots\ldots\ldots\ldots\ldots (11)$$

Thus the horizontal water velocities associated with long-period wave motion are independent of wave period or length but are directly proportional to the wave height and inversely proportional to the square root of the water depth. This latter factor is of special interest since it indicates that shallow areas of a harbor will be more active than deeper regions under the same wave conditions.

To translate these equations into numerical values of water particle amplitude and velocity that may be experienced in typical harbors during typical surge conditions, it is necessary to estimate the height of the imposed waves. The amplitudes of long-period waves in the ocean are very small compared to ordinary wind waves, usually being considerably less than 1 ft in height. For example, the largest amplitude long-period waves recorded at Terminal Island, Los Angeles, Calif.,[3] were those due to the Alaskan earthquake of April 1, 1946, and on this occasion 12-min period wave trains 1 ft in height and 6-min period wave trains ½ ft in height were measured at the outer breakwater. With a resonant amplification factor between 1 and 2, which appears to be an average range for typical harbors, such a strong surge might produce a vertical water motion of 1 ft inside the harbor. The resulting average horizontal velocity would be 0.266 ft per sec at a nodal section in a harbor with 45-ft water depth and the corresponding displacement of the water particles would be 0.133 times the wave period in seconds, or 48 ft, for example, if this period were 6 min. At the other extreme, a low surge of 3-min period and 0.2 ft height would produce average horizontal velocities of 0.053 ft per sec with horizontal displacements of nearly 5 ft.

It should be emphasized that, since large amplitude surge motion will usually be the result of resonant amplification, the water motions are the result of a standing wave pattern and the vertical motion is a maximum at the loops, as at the reflecting boundaries, although the horizontal motion is zero there. Conversely, the vertical motion is zero, and the horizontal motion is a maximum at nodal positions, such as ¼ wave length offshore of the reflecting boundary. Thus, there are alternate active and quiet zones in the harbor, their size and distribution being a function of the period of oscillation of the harbor.

Sources of Long-Period Disturbances.—Although the presence of long-period waves in harbors have occasionally been ascribed to local phenomena such as earthquakes, local winds, and atmospheric pressure anomalies, it is fairly certain that in practically all cases the source of the disturbance is a long-period wave train arriving from the open sea.

One clearly recognized source of such waves are seismic disturbances, an example of which was the Alaskan earthquake of April 1, 1946.[3] Waves caused by this disturbance were observed along nearly the entire western coast of

[3] "Memorandum on Waves in the Los Angeles Harbor Associated with the Alaskan Earthquake of April 1, 1946," by Robert T. Knapp and Robert E. Carr, Report to the Bureau of Yards and Docks (Contract No. y-13116), U. S. Dept. of the Navy, Washington, D. C., April, 1947.

North and South America, and persisted for approximately 24 hr. In the southern California region this disturbance included a wave period spectrum of from 1 to 60 min, with 6-min and 12-min period waves predominating. Fig. 4 is a reproduction of a marigram from a tide gage station in Los Angeles outer harbor for this occasion.

FIG. 4.—MARIGRAM RECORD OF LONG-PERIOD WAVES IN LOS ANGELES (CALIF.) HARBOR

The infrequency of large-scale submarine earthquakes indicates that some other mechanism of long-period wave generation must be responsible for the relatively frequent occurrences of harbor surging. An attractive hypothesis of such a mechanism is contained in the theory of surf beats. The theory of beats in the case of the superimposing of two waves of nearly the same period is well known, especially in acoustics. The familiar result is a wave form consisting of a long-period modulation of the short-period interfering elements as shown in Fig. 5. For the case of interference of water wave trains in an ocean basin, the result is a water surface profile that may appear to be the superposition of long- and short-period components, but, in fact, is not. Although this process produces a long-period vertical water motion, the really important factor of long-period horizontal water motion is lacking, since there is no actual long-period component present in the wave system.

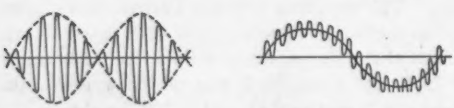

(a) INTERFERENCE OF TWO WAVE TRAINS OF SLIGHTLY DIFFERENT PERIODS (BEATS)

(b) SUPERPOSITION OF LONG AND SHORT PERIOD WAVE COMPONENTS

FIG. 5.—WATER SURFACE PROFILES

However, theoretical and experimental evidence[4] indicates that, in the presence of the nonlinear boundary conditions of the surf zone, the effect of the inherent variability of wave trains (with respect to period, and especially with respect to height) is to produce a true long-period wave train. Thus, it is estimated that beaches may reflect approximately 1% of the energy incident on them in the form of long-period waves. This phenomenon has been repeatedly observed in small bays and coves along the California and Oregon coasts, where it has been interpreted as the local cause of local surging. The reporters of these observations have tended to discount the theory of the existence of long-period wave trains as a general condition throughout large ocean areas.

Evidence that the latter theory is an important aspect of the long-period wave picture is given by the several years of observations at Terminal Island[5]

---

[4] "Surf Beats," by W. H. Munk, *Transactions*, Am. Geophysical Union, Vol. 30, 1949, p. 849.

[5] "Wave and Surge Study for the Naval Operating Base, Terminal Island, California," *Hydrodynamics Laboratory Publication No. 55*, California Inst. of Technology, Pasadena, Calif., 1945.

where on many occasions the most severe surging conditions corresponded to an otherwise calm sea. This is a condition not compatible with the local surf beat. Further evidence has been obtained in the form of simultaneous tide gage records (marigrams) from San Diego, San Pedro, Catalina Island, and Port Hueneme, Calif., showing identical long-period wave activity at these locations. Since these locations span a 200-mile stretch of the southern California coastline, such records are convincing evidence that long-period wave trains do exist from time to time as a general ocean condition and that the search for the source of excitation for harbor surging cannot be confined to local phenomenon. Therefore, it is suggested that, in general, long-period waves are due to surf beat, but surf beat occurring at some distant part of an oceanic basin instead of in the immediate vicinity of the observing station.

Model Studies

The Hydraulic Structures Laboratory has had the opportunity of investigating long-period wave phenomena in harbors in connection with two research contracts with the Bureau of Yards and Docks. Each of these contracts has involved both field and model studies, and together they have served to illustrate the importance of long-period waves in harbor design and the utility of model studies in the solution of such problems.

Reasons for Model Studies.—The principal reason for the usefulness of model studies in harbor design is that, whereas the amount of energy entering the harbor can be accurately calculated for a given wave height and direction if the breakwater gate alinement is fixed, the energy level inside the harbor is a function of these known factors plus the unknown factors of basin configuration and damping capacity. Since the frictional damping loss which must equal the rate of energy input in the steady-state condition increases with increasing energy level, a harbor acts as an energy reservoir, storing up wave energy until a level is reached at which the rate of energy loss balances the input. The factors that determine the damping capacity of a harbor are not only difficult to evaluate by analytical methods, but in a typical harbor design study it may be necessary to consider the effect of a number of possible development plans, each of which imply a change in the basin damping capacity. Since the factors that affect the damping capacity may be accurately reproduced in a properly designed model, such a model is more than an empirical testing device. It may be likened to a computing machine into which a large number of variables can be introduced and by which the net result of these variables can be given in a form suitable for use in engineering design.

For the particular case of long-period wave disturbances, the resultant water motion in particular areas within a basin is the result of the sum of incident and reflected waves. Since the standing wave pattern is determined by the configuration of the reflecting boundaries, the harbor shape will have an important bearing on the water motion within the basin. The particular utility of model studies in such problems is caused by the fact that in actual harbors there are a multiplicity of reflecting surfaces, each of which is responsible for a different standing wave pattern for each imposed wave period. Hence, it is a practical impossibility to compute the net effect in a particular

area. A model, however, gives the integrated effect of all of these standing wave patterns at each point.

Examples of Model Studies.—Brief descriptions of the model studies conducted under the research program mentioned above are given in the following sections.

Terminal Island.—The first of the model studies was in connection with harbor improvements at the Naval Operating Base (NOB), Terminal Island. The presence of long-period waves in the ocean regions adjacent to southern California have long been known; the surge conditions in Los Angeles harbor, in particular, were noted in the *United States Coast Pilot* since 1914. The very low level of pre World War II harbor activity accounted for the fact that this condition was largely ignored. With the tremendously increased wartime activities, the surge problem became more serious, and steps for its alleviation in the NOB area were taken. A proposed solution—the construction of an impervious mole to protect the area—was accordingly initiated, and at the same time (December, 1943) the Hydraulic Structures Laboratory was requested to study the problem and to assist in the mole design.

In the first stage of the study, efforts were made to determine the nature of the damaging ship motions and of any correlation between ship motion and observable water motions. These investigations indicated that during periods of damage the longitudinal and transverse ship motions were of high amplitude and long period (on the order of 4 to 10 ft and 2 to 3 min), whereas the vertical ship motion was of short period (10 to 15 sec), corresponding to the period of the prevailing wind waves. Modified tide gages were established in the NOB area, and from these it was determined that during periods of damage, low amplitude waves with periods corresponding to the long-period ship motion were present.

The Los Angeles harbor outer breakwater, which forms the primary protective barrier for the NOB area, contains two gates approximately 2,000 ft wide, and terminates about 2½ miles offshore at its eastern end, leaving the east side of the harbor area unprotected. These openings provide a direct path for wave energy to enter the harbor; and, in addition, field studies showed the outer breakwater to be sufficiently porous to admit a small fraction of the typical short-period wind waves into the harbor. Since the breakwater is even more "transparent" for long-period waves than it is for short, it is apparent that such long-period motion can enter the harbor area from any direction, with the most severe conditions being those in which the waves are directed through one of the gaps in the breakwater. These field studies verified the existence of long-period waves in the NOB area and demonstrated the relationship between the ship surging and these waves. These conclusions served to define the requirements of the proposed mole; that is, to eliminate as much as possible of both the short- and long-period wave motion and insofar as possible to define a basin whose natural periods would not be in the range of probable exciting wave periods.

The orientation of the mole gate was fixed by the necessity that it be centered on the existing dredged ship channel. The approximate over-all dimensions of the mole basin were fixed by minimum basin area requirements and

funds available. Proceeding within the framework of these limitations, the model study investigated the nature of the water surface disturbances within the basin for 14 mole configurations. The comparison of effectiveness of the various role configurations was based on the measured wave disturbances in the vicinity of the dry docks and piers, since this area had been defined by NOB authorities as the critical area that was to receive the best possible protection. This study considered the effect of both 15-sec period wind waves and 2-min, 3-min, and 4-min surges.

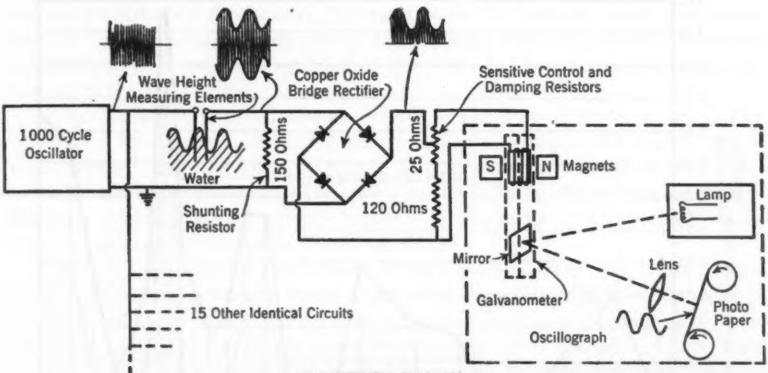

(a) SCHEMATIC DIAGRAM

(b) CONDUCTIVITY ELEMENTS

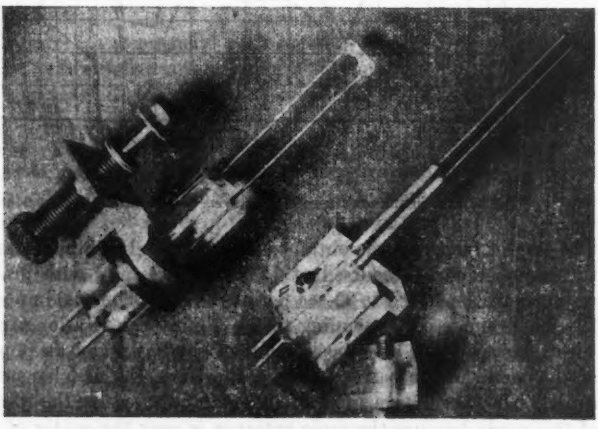

FIG. 6.—LABORATORY WAVE HEIGHT MEASURING SYSTEM

Wave heights were measured by electrical conductivity elements, consisting of a pair of spaced wires projecting into the water. A constant alternating voltage is applied across the two wires of an element. The resulting current flow depends on the immersion of the element and hence is a function of the wave height at any instant. The current signal, representative of the vertical

water motion at the element location, is recorded on a galvanometer oscillograph (Fig. 6).

This study fixed the choice of the optimum mole alinement, and further studies were made to completely determine the water motion in the mole basin so defined. A frequency response study, in which the maximum vertical water motion anywhere within the basin was plotted against imposed wave period, was carried out for a range of wave periods from 10 sec to 15 min (Fig. 7).

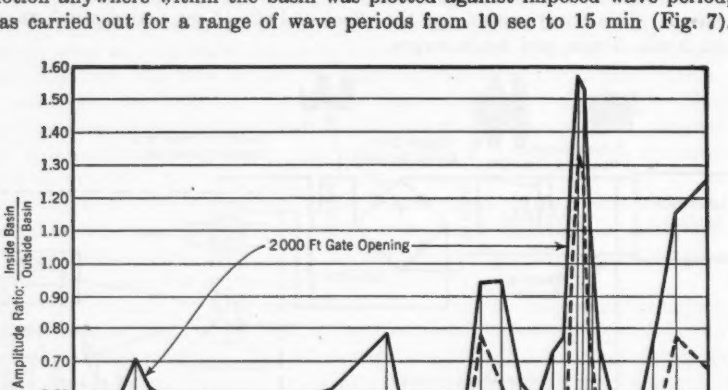

FIG. 7.—FREQUENCY RESPONSE ANALYSIS FOR TERMINAL ISLAND MOLE BASIN

The largest response was obtained with a period of 6 min, and lesser peaks in the response curve occurred at 12, 3, and 1½ min, with practically uniform response in the 10-sec to 20-sec period range of the usual imposed ocean waves. The basin mode corresponding to the 6-min peak is a longitudinal oscillation with in-phase loops at opposite ends of the basin and an opposite-phase loop at the center of the basin. This is, therefore, the first harmonic of the longitudinal basin oscillation and is of higher amplitude than the 12-min fundamental of this mode because the mole entrance is near the center of the longitudinal dimension of the basin. The entering wave spreads out as it passes through the gate and starts a wave crest travelling towards each end of the basin, thus exciting the symmetrical first harmonic of the longitudinal mode. A 12-min wave also spreads and sends disturbances travelling toward each end of the basin, but since the mode of oscillation for the 12-min fundamental is antisymmetrical, this oscillation is not as strongly excited. The 3-min oscillation

is composed of several modes, the most prominent being the fundamental of a path across the width of the basin, with the third harmonic of the longitudinal mode being excited also. Since the pattern is more complicated and the incoming energy more subdivided, the maximum amplitudes are lower than those for the 6-min period. This same reason explains the continual reduction in observed amplitudes at still lower periods, the number of possible modes becoming increasingly large and the amplitudes correspondingly lower.

Further studies were made to determine the contours of vertical water surface disturbance throughout the mole basin for various wave and surge periods. Such measurements served to delineate the characteristic modes of oscillation of the basin and established the regions of maximum and minimum motion in the mole basin.

Apra Harbor, Guam, Marianne Islands.—The second study in which the Hydraulic Structures Laboratory has investigated long-period waves was a model investigation of Apra Harbor.[6] In this case there were no field data available dealing with long-period waves in the vicinity, since shipping activities were practically nil until the harbor's development by the United States Navy in the closing phases of World War II.

Because the potential importance of long-period waves was realized as a result of the Terminal Island studies, part of the program of field measurements was devoted to the investigation of the inclusion of long-period components in the wave trains in the ocean areas surrounding Apra Harbor. Laboratory measurements were made with a harbor model to determine the possible modes of oscillation within the harbor and the resulting horizontal and vertical water motions.

The field measurements were made with specially modified recording tide gages, the float-well orifices being proportioned to exclude the obscuring effects of normal surface waves, but to permit the recording of waves with periods longer than 1 min. The recording speed was increased to 30 in. per hr to give good time resolution of the shortest effective wave. Five of these gages were installed, three in the harbor and two in the adjacent ocean areas, and were operated for a period of several months. During this time no evidence of persistent trains of long-period waves of the type found in the Terminal Island study were observed, only very long-period, low amplitude wave trains with periods of about 45 and 90 min being recorded. Although this is a somewhat sterile result, it may be remarked that it does not furnish conclusive evidence that the Apra Harbor area is never visited by waves in the period range from 1 to 6 min, since the observations at Terminal Island indicate that the frequency of occurrence of such wave trains is very irregular and long intervals may elapse between successive strong surge conditions. The measurements at Apra Harbor were necessarily of limited duration because of schedules and funds.

Apra Harbor is an even more complicated basin than the NOB mole basin at Terminal Island, and the number of possible paths or modes of oscillation is therefore greater. In spite of this complication, an effort was made

[6] "Model Studies of Apra Harbor, Guam, M. I.," *Hydrodynamics Laboratory Report No. N-63*, California Inst. of Technology, Pasadena, Calif., 1949.

to predict the modes and periods of resonant oscillation of the harbor; subsequent model experiments showed that this could be done with fair success, as evidenced by Table 1. For the Apra Harbor study, the frequency response

TABLE 1.—PREDICTED AND OBSERVED MODES OF APRA HARBOR OSCILLATION (WAVE PERIOD OF GUAM, IN MINUTES)

Mode number	Direction[a]	Location	Predicted			Observed				
			Fundamental	Harmonic		Fundamental	Harmonic			
				1st	2nd		1st	2nd	3rd	4th
1	E-W	Basin[b] to open harbor entrance[c]	29.0	9.5	5.8	31.5[d]	10.5	6.5	4.6	3.6
1?	E-W	Basin[b] to breakwater near entrance	12.5	6.3	4.2	...	...	...	...	...
2	E-W	LST landing[e] to harbor entrance[c]	...	...	...	20.0[d]	6.7	4.0	2.9	...
3	E-W	Inner breakwater[f] to harbor entrance[c]	15.0	5.0	3.0	15.0[d]	5.0	3.0	...	...
3?	E-W	Breakwater[f] near harbor entrance	6.5	3.2	2.2	...	...	...	...	...
4	N-S	Gab-Gab Beach to outer breakwater	4.4	2.2	1.4	4.4[d]	2.2	1.5[d]	1.1	...
5	E-W	Basin[b] to inner breakwater[f]	5.8	2.9	1.9	5.7	2.9	1.9	...	...
6	N-S	In repair basin	3.2	1.6	1.1	3.8	1.9	1.3	...	...
7	N-S	South end to Dock N-1[g]	6.9	3.4	2.3	6.4	...	...	...	...
8	NE-SW	Dry dock to Dock W-1[g]	...	...	...	5.0	...	...	...	...
9	NW-SE	Dock Z-1 to southeast shore[g]	...	...	...	3.8	1.9	...	...	...
10	E-W	Dry dock to Dock Y[g]	...	...	...	3.8	1.9	...	...	...
11	E-W	Dry dock to Dock Q[g] [h]	4.5	2.2	1.5	4.4	2.2	...	...	...

[a] The letters N, E, W, and S denote "north," "east," "west," and "south," respectively. [b] East end of repair basin. [c] Open harbor entrance, Mode 2 with an inner breakwater and Mode 1 observation without an inner breakwater. [d] Calculated, not observed. [e] "LST" denotes "Landing Ship Troops." [f] Predicted for shoals or inner breakwater. Mode 3 observed from the south leg of the inner breakwater to the harbor entrance. [g] In inner harbor. [h] Predicted for the north half of the inner harbor.

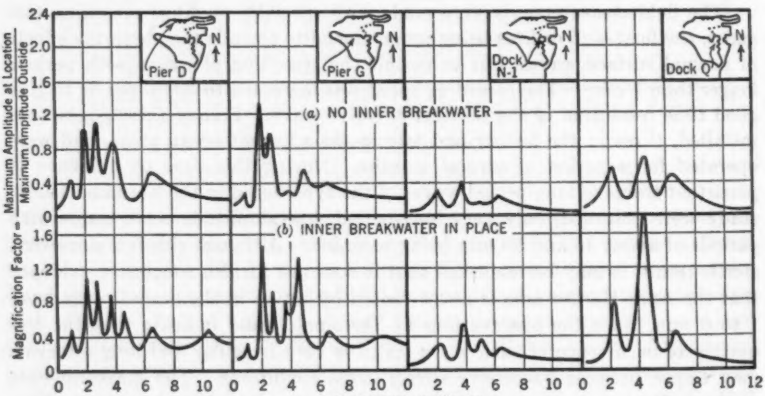

FIG. 8.—FREQUENCY RESPONSE ANALYSIS FOR REPRESENTATIVE LOCATIONS IN APRA HARBOR, GUAM

analysis took the form of measuring the vertical water motion as a function of incident wave period at a number of points in the harbor, most of which points were in operationally important docking areas, as shown in Fig. 8. An additional variation in this study was the determination of the effect of adding

a breakwater to an existing group of shoals that separate the outer harbor and repair basin.

Measurements of the horizontal water motion at resonant periods were obtained by photographing the movement of reflector floats drifting on the water surface. These observations assisted in the identification of modes of oscillation by defining nodal zones in which the horizontal motion is a maximum and permitted the determination of water velocities to be expected in the various docking areas as the result of a given surge condition.

The results of these studies indicate that Apra Harbor is subject to resonant oscillation, with amplification factors as high as two, for at least five surge periods in the range from 1 to 6 min. Horizontal water velocities as high as 0.25 knots per ft of imposed wave height may result in various docking areas as the result of such oscillations. The effect of adding a breakwater to the existing shoals is to increase their efficiency as a reflecting surface, especially for waves of longer than 3-min period, and to slightly restrict the excitation entering the repair basin and inner harbor areas.

Effects on Harbor Operations

Although the importance of long-period waves in harbors is entirely the result of the effect they may have on harbor operations, such as ship mooring and outfitting, this phase of the problem has been least studied. This deficiency did not come about because of lack of interest or misdirection of effort but because of the fact that, during World War II and during the immediate postwar period when funds for this necessarily expensive research were available, time was available only for the solution of the immediate problem of reducing the known bad excitation conditions. Since that time the level of activity has been greatly reduced because of the curtailment of funds. The only field observations available on which to base a few tentative conclusions are those made at Terminal Island, and the following discussion is limited to that extent.

Ship Mooring.—The most striking example of the importance of long-period waves or surges has been in connection with the mooring of ships to piers at the NOB. Even when restrained by very heavy tackle and sometimes even when the water surface appeared glassy, these moored ships have displayed longitudinal and transverse drift amplitudes of up to 10 ft, snapping mooring lines, breaking piles, and damaging the ships themselves.

The recorded experience at Terminal Island prior to the mole construction had shown the period of these damaging ship motions to be in the range from 2 to 3 min, corresponding to the observed ocean surge conditions. As a result of the model study, it was expected that 3-min surges would still be felt in the pier area but with lessened severity and that the most severe conditions within the mole could be expected with the arrival of 6-min period excitation. No persistent wave trains with periods in the 6-min range were recorded at Terminal Island until April 1, 1946. On this date a wave spectrum containing all periods from 1 min to 60 min, but with a large part of the energy contained in 6-min and 12-min period waves, arrived as the result of the Alaskan earthquake of that same date.

Records obtained from tide gages installed throughout the harbor, and, particularly in the NOB area, confirmed the predicted large amplitude water motions within the mole basin as a result of the 6-min excitation. Sufficient instruments were not available to map the motion of the water in the mole basin completely, but records from two significant stations—the pier area and the northwest corner of the basin—showed regular trains of 6-min waves with heights as great as 0.8 ft to 1 ft. The inference from these records is that the mole basin oscillated in the predicted mode with an amplification factor (ratio of maximum amplitude at location to maximum amplitude outside) of 1.5 or 2. However, an additional and surprising observation on this occasion was that, despite the relatively large amplitude, long-period water motion in the mole basin, no cases of unusual ship motion or damage were officially reported.

This evidence has led to the hypothesis that the motion of moored ships is a dynamic problem, with the possibility that a resonant period may exist that is a function of the mass of the ship and the elasticity of the mooring system. This theory offers a satisfactory explanation for the limited observed phenomena since approximate calculations show that the natural period of lateral oscillation of a typical ship-mooring line system is in the 2-min to 3-min range. Hence, it is in resonance with the usual type of long-period disturbances observed at Terminal Island and relatively unresponsive for either the 6-min or 15-sec excitation. In addition, it should be noted that the NOB was alerted for high waves from the Alaskan earthquake, and extra lines were added and moorings tightened on all ships. The effect of this precaution would be to stiffen the system and thus to reduce the natural period of oscillation, moving the resonant point even farther from the 6-min forcing period. The problem of the effect of ship mooring still is not settled but obviously warrants further investigation.

Ship Outfitting.—The problems peculiar to ship outfitting operations are a special case of shop mooring in which any appreciable motion is undesirable, even though it be much less than those that cause ship and pier damage. Thus, if heavy equipment must be hoisted from pier to ship and lowered accurately into position, either horizontal or vertical motions of fractions of a foot may be intolerable.

If, as seems clear from the Terminal Island study, the horizontal motion is the result of long-period waves and the vertical motion is the result of short-period waves, a theoretical solution would be to locate the outfitting dock at a point in the harbor where a node of the short-period standing wave pattern and a loop of the long-period standing wave pattern coincide. This combination would assure minimum values of horizontal and vertical water motion. At least part of this solution may be practical if the long-period excitation is fairly constant as to period, since the standing wave patterns are quite well defined for these long waves and may be determined analytically for simple harbors or may be determined for complicated harbors by model studies or field observations with suitable instruments.

Since the wave length of the standing wave pattern caused by the usual ocean waves is of the same order as the length of a ship, it is, of course, impossible to position the ship at a point of minimum vertical motion. However,

within a harbor there are always areas in which the ocean wave amplitudes are a minimum because of refractive and diffractive effects. By combining this fact with the previous observation of the practical possibilities of allowing for long-period standing waves, a rational choice of the quietest location in the harbor can be made.

Conclusions

The experience at Terminal Island has shown that the presence of long-period waves in harbors can constitute an important technical and economic problem. The possible extent of this problem is indicated by the fact that surge motion similar to that studied intensively at Terminal Island has been observed along the entire Pacific coast and at Hilo harbor in Hawaii. It is a fair assumption that these conditions exist in many parts of the world and go unreported, either because the lack of harbor developments prevent the occurrence of a problem or because many places that have a problem tolerate it through ignorance of possible remedial measures.

There are two fundamental aspects of this subject, on which additional information would be applicable to any particular problem. These are: (1) The cause and characteristics of long-period waves in the sea; and (2) the behavior of moored ships and other nonrigid structures under the influence of surge excitation. Future investigations of the harbor surge problem should certainly seek to expand the knowledge of these questions. Some particular suggestions for such a program are: (a) To test the theory of distant surf beat as a source of long-period waves by "hind casts"—determination of surf conditions from past meteorological records and subsequent refraction diagrams to project the long-period wave fronts from possible generating areas to areas in which long-period waves were observed; and (b) the accurate determination of the natural period of oscillation of moored ships by exact analytical methods or by experiment, using a large mechanical oscillator as the periodic driving force, as has been done for the determination of the critical periods of bridges and other large structures.

For any particular harbor, a model study is the best means to determine the location and magnitude of the standing wave patterns associated with any given excitation, permitting the design of harbor configurations to minimize surge motion and to accurately define optimum areas within the harbor for specified types of operational activity.

DISCUSSION

JOHN S. MCNOWN,[7] M. ASCE.—In his study of long-period waves in harbors, Mr. Carr calls attention to a factor in harbor design that is both important and very little understood. Such waves are commonly referred to by the French word, "seiche," in publications from England and from the European continent, and the writer recommends its adoption in American publications. The author's title serves to emphasize the need for such a term. The term, "wave," invariably requires a modifier, and the term, "surge," is frequently reserved for the moving hydraulic jump or tidal bore. A seiche can be defined as a periodic disturbance in a partly or completely enclosed body of water, the entire volume being put in motion (rather than just that portion at or near the surface), and the characteristics of the motion being closely related to the geometry of the containing basin.

Because the writer had already made theoretical and laboratory studies of seiche, he found particularly enlightening the author's discourse concerning field observations and the probable origin of disturbances having periods much greater than those of ordinary sea waves. Under the heading, "Characteristics of Long-Period Waves in Basins," the author writes about the simplest forms of two-dimensional wave patterns for rectangular basins only. Because a more general statement of the problem can be made, and because specific solutions are available for other simplified harbor forms, the writer would like to present a brief summary of this topic. In addition to the writer's work on the subject,[8,9] Lord Rayleigh,[10] H. Lamb,[11] and H. Bouasse[12] have written about seiche or mass oscillation in enclosed basins of regular shape. The problem of the two-dimensional seiche in lakes was ably treated by G. Chrystal,[13] and other papers have been written on calculations and observations for various lakes.

In common with many types of wave motion, seiche is essentially irrotational, and the motion can therefore be defined in terms of a velocity potential. The essential boundary conditions can be stated as follows: (1) The normal component of the velocity, $\partial\phi/\partial n$, must be zero at the solid boundaries; (2) the familiar free surface condition must be satisfied—namely, that the normal component of the velocity of a particle at the free surface must equal the normal velocity of the surface itself; and (3) a special boundary condition is hypothesized for the opening or entrance. In addition, the usual first ap-

[7] Prof. of Mechanics and Hydraulics, and Associate Director, Iowa Inst. of Hydr. Research, State Univ. of Iowa, Iowa City, Iowa.

[8] "Sur l'entretien des eaux portuaires sous l'action de la haute-mer," by J. S. McNown, *Comptes Rendus de l'Académie des Sciences*, Paris, France, May 28, July 2, and July 27, 1951.

[9] "Waves and Seiche in Idealized Ports," by J. S. McNown, National Bureau of Standards, Washington, D. C. (publication pending).

[10] "On Waves," by Lord Rayleigh, *Philosophical Magazine*, Vol. V, 1876, pp. 257-279.

[11] "Hydrodynamics," by H. Lamb, Dover Publications, New York, N. Y., 1945, pp. 282-290

[12] "Houle, rides, seiche et marées," by H. Bouasse, Delagrave, Paris, France, 1924, pp. 92-145.

[13] "On the Hydrodynamical Theory of Seiches," by G. Chrystal, *Transactions*, Royal Soc. of Edinburgh, Vol. 46, No. 20, Part III, 1908.

proximation to the actual occurrence is made by assuming that the amplitudes of the vertical motion are small. As the details of the development, starting from this point, have been presented elsewhere,[8,10] an expression for the surface displacement η is written directly:

$$\eta = \frac{k\,T}{2\,\pi} \sin\left(\frac{2\,\pi\,t}{T}\right) F(x,y) \qquad (12)$$

in which k is a dimensional constant related to the mode of the motion, t is time, T is the period of the occurrence, and $F(x,y)$ is a function of horizontal position.

For the definition of the unknown spatial function, F, and the third boundary condition, the geometry of both the harbor and the entrance must be known or assumed. Only geometrically simple harbor forms can be analyzed without elaborate calculations. Harbor plans that are circular or rectangular can be solved in terms of ordinary functions. Additional prerequisites of a straightforward analysis are the assumption of constant depth, and walls that are vertical and totally reflecting. Although these restrictions are somewhat extreme, complete analysis of any one port form provides an insight into the characteristics of such a phenomenon. In problems as complex as this one, it is natural to work from the particular toward the general solution.

Also, a distinction must be made between two types of motion. One, which has been designated as resonant, is any one of the discrete natural motions that could be excited in the harbor even if it were enclosed on all sides. These can be likened to the various discrete modes of a taut membrane, each having a characteristic frequency. Because the frequency of the wave—or of the exciting force—can differ from any of the resonant frequencies of the harbor, another class of motions (designated as nonresonant) can also occur. For resonant motions, the component of velocity normal to the plane of the entrance is zero, so that the entrance is, in effect, a continuation of the solid boundary. The other type of motion is nonresonant, in which a periodic flow into and out of the port takes place. This latter condition is considerably more difficult to fulfil, and the characteristics of the velocity at the entrance must be assumed so as to be an acceptable approximation of the actual occurrence in the laboratory or in nature.

For circular cylindrical basins, F is directly expressible in terms of Bessel functions. A general resonant motion is characterized by the expression:

$$F_n(r, \theta) = \cos(n\,\theta)\, J_n(k\,r) \qquad (13)$$

in which r and θ are spatial coordinates in the plane of the undisturbed surface, n is any integer, $J_n(k\,r)$ is a Bessel function, and the dimensional constant, k, is any one of the values that make the velocity normal to the vertical walls equal to zero. In mathematical terms, k is selected so that $\left.\frac{\partial J_n(k\,r)}{\partial r}\right|_{r=R} = 0$, R being the radius of the circular harbor. The period of such motions is given by the relationship,

$$\left(\frac{2\,\pi}{T}\right)^2 = g\,k \tanh(k\,h) \qquad (14)$$

in which h is the depth of the water. Thus, once a mode of motion has been selected, the corresponding value of $k R$ can be determined from a table of Bessel functions, and T can then be calculated for known values of g, R, and h.

For nonresonant motions, a summation of all possible particular solutions must be made so that a complete solution with a realistic boundary condition at the entrance can be obtained. Hence, F is written in general form as an infinite series of terms like the one in Eq. 13.

$$F(r, \theta) = \sum_{n=0}^{\infty} A_n \cos(n\,\theta)\, J_n(k\,r) \qquad (15)$$

The coefficients A_n can then be evaluated by means of a Fourier expansion so that the boundary condition assumed for the entrance is satisfied. Fortunately, for most motions of practical importance, the first ten terms are dominant. Therefore, an approximation can be made, if necessary, for all terms that remain after a certain number of terms have been evaluated. As they are available elsewhere, the details of such calculations are less important to this discussion than is the experimental justification of the importance and applicability of the results obtained therefrom.

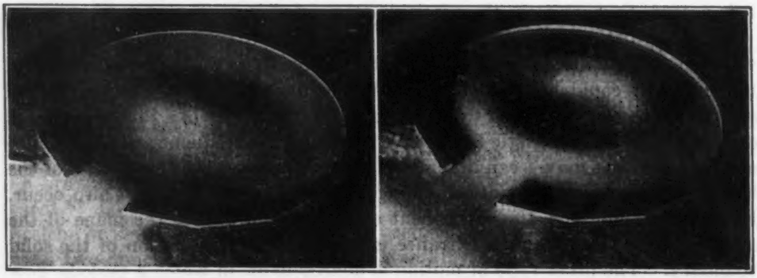

FIG 9.—RESONANT SEICHE IN A CIRCULAR HARBOR

In an experiment conducted by the writer at the Neyrpic Hydraulics Laboratory in Grenoble, France, harbors of simple geometry were constructed and a series of observations were made. Initially, a circular harbor was constructed with a radius of 1.60 m (5.25 ft) and a water depth of 16 cm (6.3 in.) was maintained. Waves were produced at one end of a channel, in which the structure had been placed; and the waves, acting through a symmetrically placed opening of one sixteenth of the circumference, produced motion within the harbor. Wave filters were used to refine the wave forms, and a beach on either side of the harbor entrance effectively eliminated the reflection of energy. Observations of the wave amplitude were made at various points inside and outside the model harbor with a specially-designed point gage.

One particularly impressive motion is shown in Fig. 9, the water having been made somewhat opaque by a suspension of starch. In this case, the Bessel function of zero order with two nodal circles was selected for the mode, the value of $k R$ being 7.015, so that $k = 7.015/1.60 = 4.38$ meters^{-1} (1.34

ft^{-1}), and, from Eq. 14, $T = 1.23$ sec. The theoretical profiles of maximum displacement are compared with the observed values in Fig. 10. The remarkable features of these results are the relatively large amplitudes observed and computed for the center of the harbor, and the close correspondence between the two results. For these measurements, the amplitude at the center was 3.3 times that at the wall and entrance; and—because a clapotis tends to form at the entrance—the amplitude there is nearly double that of the incident wave. For this study, the amplitude at the entrance was approximately 1 cm (0.4 in.). Other modes were perhaps less impressive but were found to possess similar characteristics.

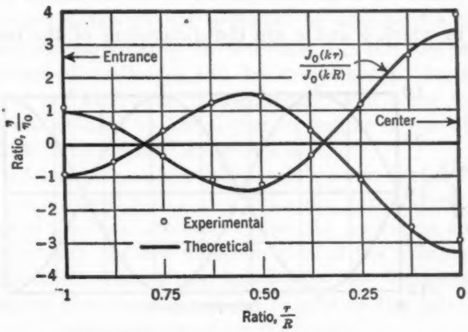

FIG. 10.—COMPARISON OF THEORETICAL AND OBSERVED AMPLITUDES FOR RESONANT MOTION IN A CIRCULAR HARBOR

Besides visual comparisons for many typical resonant motions and detailed measurements for a few, observations and calculations were made of one nonresonant motion. The value $k R = 6$ was chosen, both because it was convenient for the laboratory arrangement and because there were no resonant values near this value. The comparison between the series calculations and the measurements are shown for one half the circumference (along the boundary) in Fig. 11. The reference amplitude was computed from the characteristics of the incident wave, including its phase at the entrance. If it is considered that several approximations and assumptions had necessarily been made in obtaining the calculated curve, its correspondence with the measured

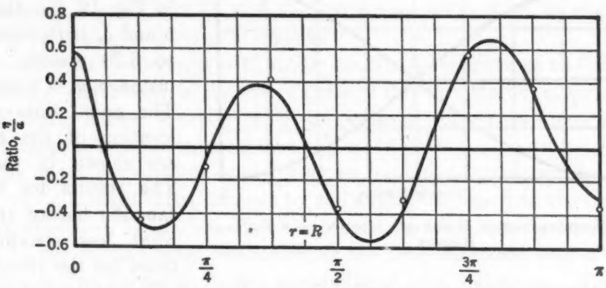

FIG. 11.—COMPARISON OF THEORETICAL AND OBSERVED AMPLITUDES FOR NONRESONANT MOTION IN A CIRCULAR HARBOR

values seems quite close. Surely the trend or mode of motion is clearly and correctly defined.

Resonant motions were also investigated for a rectangular port, the *F*-function in Eq. 12 being

$$F\,(x,y) = B \cos \frac{\pi\, m\, x}{b} \cos \frac{\pi\, n\, y}{c} \qquad (16)$$

in which b and c are the dimensions of the rectangle in the x-direction and y-direction, respectively. The coefficient k, and hence the period, can be determined from the relationship:

$$\left(\frac{k}{\pi}\right)^2 = \left(\frac{m}{b}\right)^2 + \left(\frac{n}{c}\right)^2 \qquad (17)$$

Such motions are more general than the two-dimensional waves described by Mr. Carr, but are still restricted to discrete periods for which m and n are integers. Measurements taken for a representative motion are shown in Fig. 12, the dimensions b and c, both being equal to 3.20 meters. In this instance, $m = 2$ and $n = 5$. The nodal lines and the location of the entrance are shown in the inset. The results for the rectangular harbor are somewhat less striking than those for the circular harbor, but they are evidently as well defined. Because the positions of the nodal lines and the location of the entrance are not necessarily reconcilable, the motions in the rectangular harbor are seen to have one more degree of freedom than those in the circular harbor. This is reflected in the fact that a double summation would be necessary for the nonresonant motions in rectangular harbors.

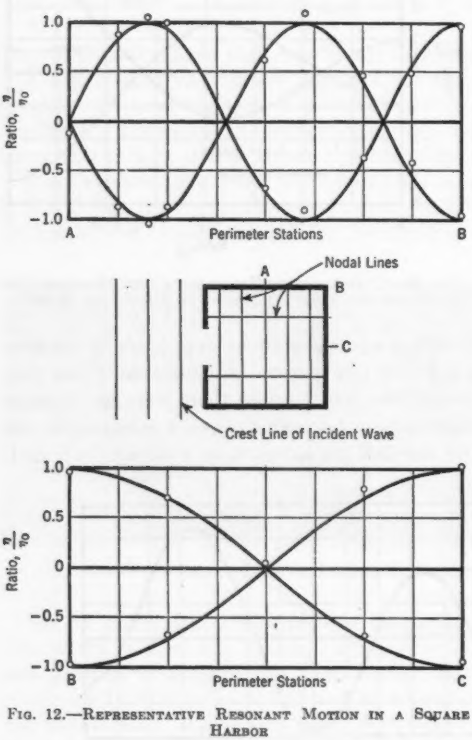

FIG. 12.—REPRESENTATIVE RESONANT MOTION IN A SQUARE HARBOR

Several characteristics of seiche in harbors having engineering importance were clarified in this somewhat idealized study. Clearly demonstrated was the

fact that seiche patterns that are characteristic of a given harbor exist, and that they can be excited as the result of a periodic disturbance at the entrance. In the absence of sufficient dissipation within the harbor, the amplitudes of these disturbances can even exceed those of the incident wave, and the disturbances will not necessarily be reduced by a reduction in the width of the harbor opening. Because the nature or mode of the motion is extremely variable with the period, harbor models should probably be studied for a considerable range of frequencies, particularly in the light of Mr. Carr's indications that very long-period disturbances can be troublesome. It is probable that the amplitude of a disturbance varies greatly from place to place in a harbor such as the one studied by the author as well as in one of simplified geometry such as those depicted in this discussion.

These studies, made in what has been called "the world's worst harbor," were obviously not intended as a model study of a proposed harbor form. Rather, insight into the nature of the basic problem was sought, as well as an evaluation of the analytical approach and the determination of the primary characteristics of seiche in harbors. The writer hopes that the foregoing definition and description of this phenomenon will be helpful in the interpretation of practical studies such as that presented by the author.

Acknowledgment.—The experiment described in this discussion was performed at the suggestion of P. Danel, A. M. ASCE, director of the Neyrpic Hydraulics Laboratory.

B. W. WILSON,[14] A. M. ASCE.—A welcome contribution has been made by the author to the literature of a subject which, from the engineering point of view, has hitherto received rather meagre attention. However, it is now blossoming out with great rapidity, largely, it would seem, as a result of the experiences of World War II and the gathering momentum in engineering opinion of the value of hydraulic models.

The writer was concerned with rather similar investigations to those cited by the author—involving, in the writer's case, Table Bay Harbor at Cape Town, Union of South Africa. A few parallel comparisons where they hinge upon the author's paper may be of interest here.

At the onset, perhaps the writer may be pardoned for correcting what he believes to be a slight misstatement by the author in regard to the harmonics of a standing-wave oscillation. He believes that it is accepted scientific usage to refer to the fundamental oscillation as the first harmonic with a nodality of one, the second harmonic having a nodality of two, and so on. This would amend the author's Eq. 3 to

$$T_n = \frac{2\,l}{n\,C} \qquad (18)$$

in which $n = 1, 2, 3, \cdots$ represents both the harmonic order and the nodality; thus, $n = 1$ would correspond to the fundamental oscillation or first harmonic.

[14] Formerly Asst. Research Engr., Chf. Civ. Engr.'s Office, South African Railways & Harbours, Johannesburg, Union of South Africa.

Eq. 18 is attributed to J. R. Merian[15] (1828). In terms of Eq. 18, the author's left-hand Figs. 2(*b*) and 2(*c*) strictly should read "Second" and "Third" harmonics, respectively, and the statements made in the text below Fig. 7 would need a corresponding correction.

For a basin opening upon a larger body of water, such as the sea, the author's Eq. 4 should, on the same basis, read

$$T_m = \frac{4\,l}{m\,C} \qquad (19)$$

where the harmonic order, m, in this case, has the values $m = 1, 3, 5$.[16] The circumstances of this state of oscillation permit only the odd harmonics to exist, the true second, fourth, and other even-numbered harmonics being entirely suppressed. The right-hand part of Fig. 2(*b*) is thus correctly the third harmonic, and that of Fig. 2(*c*), the fifth harmonic. The right-hand part of Fig. 2(*a*) is in effect one half of the left-hand part of Fig. 2(*a*), and the right-hand part of Fig. 2(*b*) is one half of the left-hand part of Fig. 2(*c*). It is suggested that the captions for Figs. 2(*a*), (*b*), and (*c*) might better have been written "Fundamental (or First) Mode," "Second Mode," and "Third Mode," respectively, the use of the word "mode" implying essentially the manner of oscillation.

The author mentions that a resonant amplification factor between 1 and 2 for long waves appears to be an average for typical harbors. This statement seems to be based on the relation between the wave-heights just outside the confines of a harbor, and those within, but the writer would point out that the wave-heights of long waves, when measured anywhere near a linear boundary, are themselves increased by the wave reflections. It is virtually impossible to judge the original heights of long waves at, or near, a boundary, because the long wave can exist in that region only as a standing-wave system, whose theoretical amplification factor (assuming no energy loss on reflection) is 2. Thus, by the time a disturbance has produced resonance inside a harbor (and here the author's amplification factor of 1 to 2 enters) the true amplification of the original wave may be anything from 2 upwards.

At Table Bay Harbor, it can be shown that just outside the harbor no less than six systems of standing waves, formed by incident waves and first reflections, can coexist as a result of the ingress into Table Bay of a single train of long waves from the outer ocean. The incoming waves divide around Robben Island (which is some 3 miles offshore in the approach to Table Bay), and converge on the harbor from two directions; when the external swell direction is favorable, the three standing-wave systems induced by each set of incident waves come into phase to give a theoretical amplification factor of 6 outside the harbor. Each set of three standing waves involves the incident waves and two reflections (shoreline and harbor) twice over. Hence, the theoretical magnification of [(3 × 2) + (3 × 2)] is halved to yield 6. The writer cites this behavior outside the harbor to illustrate the probability that the true resonant

[15] "The Oceans," by Sverdrup, Johnson, and Fleming, Prentice-Hall, Inc., New York, N. Y., 1942, p. 539.

[16] "Hydrodynamics," by Horace Lamb, University Press, Cambridge, England, 1932, p. 267.

amplification factor for the interiors of most harbors, referred to a point reasonably remote from the harbor, exceeds 2.

The term "seiche," not used by the author, denotes resonance or near-resonance oscillations (both forced and free) in a basin, as distinct from non-resonant oscillations (such as individual standing waves), and the writer would emphasize the advantage of its adoption in the terminology of this subject.

The author's statements concerning the large horizontal displacements of the water particles possible at the nodes of long-period seiches in harbor basins can be confirmed from the experience in Table Bay Harbor in 1940, when a large ship displacing 42,000 tons, tied at the center berth along the short side of a long rectangular basin, broke all her moorings and ranged to and fro through approximately 20 ft (according to report). At the time, the ship was lying in a depth of 43 ft of water at the node of the fundamental transverse oscillation for the dock, which has a period of about 1.8 min. A tide gage at the antinode of this transverse seiche registered a height range (h) for this periodicity of 18 in. Calculation shows that the maximum water particle displacement in a 1.8-min seiche of this magnitude is about 11 ft, which would account for the major part of the movement of the ship; the remainder probably derived from the influences of superposed second and third harmonic transverse oscillations, which commonly occur.

The writer strongly supports the author in his belief that long-period wave trains, as distinct from surf beats, are a frequent cause of harbor surging. The Munk theory of surf beats has now received additional support from British investigators,[17] and it would appear that this form of surge must be considered a reality unless the phenomenon is in some way merely a manifestation of an underlying series of long waves which are part of the short-period, high-amplitude wave group, but which lag the latter in the manner found for surf beats. The possibility of this being true is at least suggested by the theoretical digressions of Lord Kelvin[18] on the form of the front and rear of a free procession of waves in deep water. Fig. 13, which is reproduced from Lord Kelvin's paper,[18] but in which the underlying long-wave system was inserted by the writer, indicates that a procession of waves having a surface profile at both front and rear similar to Fig. 13(a), would at a time 25 wave-periods later, assuming progression to the right, have the front and rear configurations shown respectively by Figs. 13(b) and 13(c). In Fig. 13(b), which shows the attenuation of the group in long waves, point A has advanced from the origin at the full wave velocity; point B has advanced from the origin at only half the wave velocity. In Fig. 13(c), point C has advanced from the rear origin at the full wave velocity; point D has advanced at half the wave velocity. The comparison between front and rear is illuminating; the undulating effect in the latter is found to reside in the expansion through the wave group from the rear (dash-line curve, Fig. 13(c)) of the underlying "push-pull" wave, P-Q, which initially defines the junction of the wave group with still water (see Fig. 13(a)). The underlying wave of Fig. 13(c) was obtained by "residuating" the surface

[17] "Surf Beats: Sea Waves of 1 to 5-Minute Period," by M. J. Tucker, *Transactions*, Royal Soc. of London, Series A, Vol. 202, August, 1950, pp. 565–573.

[18] "On the Front and Rear of a Free Procession of Waves in Deep Water," by Lord Kelvin, *Mathematical and Physical Papers*, Cambridge, England, Vol. IV, No. 36, 1910, pp. 351–367.

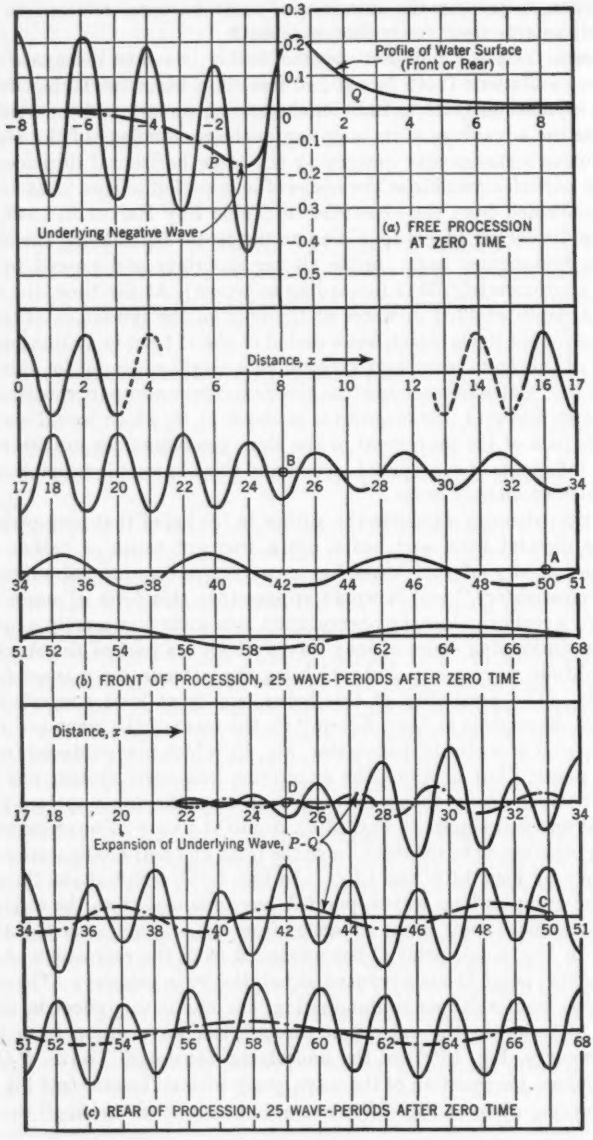

FIG. 13.—THE FORM OF THE FRONT AND REAR OF A FREE PROCESSION OF SINUSOIDAL WAVES IN DEEP WATER

profile with respect to the main sinusoidal wave, the residual being found similar in all respects to Lord Kelvin's separate analysis of the expansion of a single "push-pull" wave.

With respect to the incidences of surging in Table Bay Harbor, there is now clear evidence of association with traveling depressions of the South Atlantic Ocean, which skirt the coast of the Cape of Good Hope on southeasterly courses. Although harbor surging is always accompanied by swell conditions, many cases were recorded at Cape Town in which prominent swells failed to produce surging. This condition would seem to suggest that the surf beat alone cannot explain the phenomenon in the general case.

At Cape Town, it has been proved repeatedly that small barometric fluctuations in the overlying atmosphere—in generally calm and clear weather, but with a winddrift from the open sea (northwest)—are capable of exciting strong oscillations in Table Bay with consequent powerful surging through the harbor entrances. Fig. 14 is furnished in evidence of this and shows the obvious dependence of the sea oscillation upon the barometric disturbance.

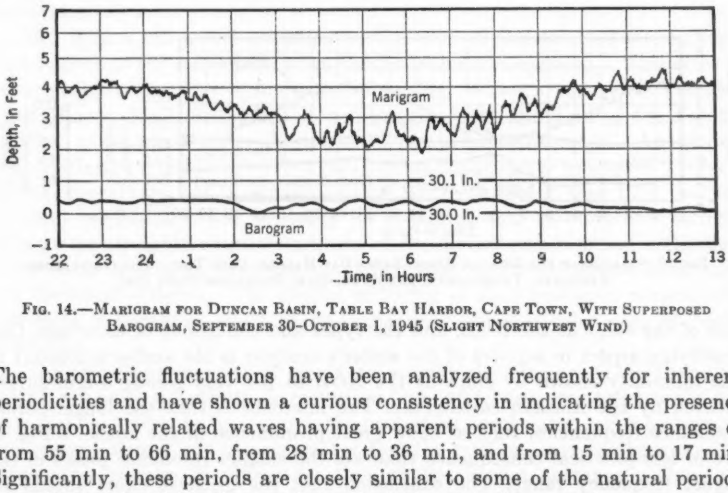

FIG. 14.—MARIGRAM FOR DUNCAN BASIN, TABLE BAY HARBOR, CAPE TOWN, WITH SUPERPOSED BAROGRAM, SEPTEMBER 30–OCTOBER 1, 1945 (SLIGHT NORTHWEST WIND)

The barometric fluctuations have been analyzed frequently for inherent periodicities and have shown a curious consistency in indicating the presence of harmonically related waves having apparent periods within the ranges of from 55 min to 66 min, from 28 min to 36 min, and from 15 min to 17 min. Significantly, these periods are closely similar to some of the natural periods of oscillation for Table Bay, as determined theoretically, graphically, and from marigram analyses.

Range action at Cape Town, as affecting ships at their berths (which the surging shown in Fig. 14 does not do), is characterized by a different sort of trace on the tide gage of which Fig. 15 is a typical example. The absence of much local wind or barometric fluctuation in this case shows that the disturbances must have come from far away. The wide range of resonant periodicities normally found in different parts of the harbor on an occasion such as this would seem to indicate that exciting ground swells of many periods usually accompany the visible swells. Just as local barometric fluctuations are capable of inducing coastal seiches, so must distant meteorological disturbances

(particularly the barometric oscillations near the centers and along the cold fronts of the traveling depressions) be capable of exciting long ground swells in addition to the high surface waves which the strong winds in these distant areas tend to generate. A want of space precludes presentation of the many other arguments and supporting facts that justify the view that long waves have a real identity in the undulations of the sea.

The author has concluded by recommending a program of investigation directed toward defining the critical periods of the resonance of moored ships under the stimulus of seiches. It would appear that at the time of writing he was unaware that this study, to some extent at least, had already been begun.[19] It is therefore interesting to find that the author's and the writer's observations on this subject led to parallel conclusions regarding the importance of the ship's mooring-line system.

It appears that the likelihood of oscillations with periods as great as 3 min being really critical for moored ships at the NOB, is debatable in the light of the writer's analysis (which indicated that critical periodicities could generally be expected in a range less than 2 min). However, much could depend on the

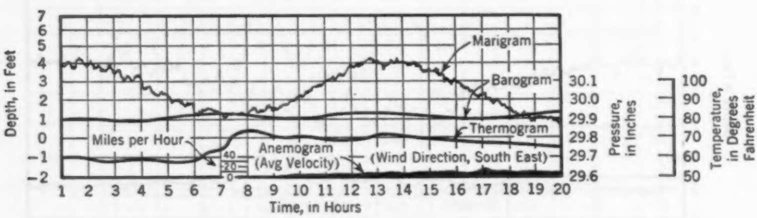

FIG. 15.—MARIGRAM FOR DUNCAN BASIN, TABLE BAY HARBOR, CAPE TOWN, WITH SUPERPOSED BAROGRAM, THERMOGRAM, AND ANEMOGRAM, DECEMBER 17–20, 1946

size of the ships at the NOB, and the types and conditions of moorings. One gratifying aspect in support of the writer's analysis is the author's account of the immunity shown by ships at the NOB to the very strong 6-min surges created by the Alaskan earthquake. The inference is that the longer-period resonance frequencies, such as show great prominence in the author's Fig. 7, are of less practical consequence than are the smaller resonance peaks in the higher frequency range. The conclusion that the greatest effort should be concentrated upon reducing the magnitudes of seiches having periods less than 2 min, and to a lesser extent those with periods from 2 to 4 min, has been the guiding principle adopted in seeking a solution to the Cape Town problem.

One other conclusion reached at Cape Town is borne out by Fig. 7 of the author's paper. This pertains to the fact, shown by the Terminal Island model studies, that the effectiveness of restricting the gate opening is usually least for long wave periods. It is an inescapable fact that narrowing a basin entrance will be of very little help in controlling long-period surging, especially of the type shown in the writer's Fig. 14, and these surges, in general, must be tol-

[19] "Ship Response to Range Action in Harbor Basins," by B. W. Wilson, *Transactions*, ASCE, Vol. 116, 1951, pp. 1129–1157.

erated. The earlier statement that they are of less practical consequence than the periodicities below, for example, 4 min, is only partly true, because certain of the long-period surges (depending on the seiches in the outer embayment) cause such strong reversal currents through the basin entrances that they constitute a potential danger to the navigation of large ships.

JOHN H. CARR[20].—An interesting addition to the paper has been made by Mr. McNown in his indications of the extent to which mathematical analysis may be applied to the problem of basin oscillation. It is unfortunate that the typical complicated geometry and appreciable damping of harbors preclude the immediate applications of such analysis to many practical problems. The growing evidence that the effect of long-period waves is most serious for the period range of from 1 min to 2 min indicates that analytical work should be directed at harbor response to waves of this period. Consideration of harbor depth and size then will indicate which harmonics of basin oscillation are most significant; in typical cases these will be the third, fourth, or higher harmonics.

Mr. Wilson has called attention to the writer's nonstandard terminology with respect to the numbering of harmonic modes of oscillation. This error is acknowledged, and the writer concurs in Mr. Wilson's suggested changes. Both Messrs. McNown and Wilson recommend the adoption of the French "seiche" to designate the oscillation of a basin in a natural mode. At the risk of appearing provincial, the writer still prefers the phrases "long-period wave" for the general case, and "basin oscillation" for the particular case; first, because resonant oscillation is not necessary for damaging ship motions, and, second, because the straightforward description of the motion as a resonant oscillation of the water mass immediately recalls similar behavior in mechanical, acoustical, and electrical systems. The mental picturing of such analogies cannot help but have a beneficial effect in understanding the particular case of basin oscillation.

The writer's observation of maximum amplification factors of less than two is with reference to harbors characterized by a large basin connected to the sea by a small opening, as by a gap in the protecting breakwater. For harbors of this general plan, it will be appreciated that the exciting wave height is greatly attenuated because of diffraction through the harbor entrance. Thus, an amplification factor of one, with reference to the height of the exciting wave outside the harbor entrance, may still represent a very large increase in the height of waves incident on a reflecting boundary within the harbor.

Mr. Wilson's remarks on the subject of the origin of long-period waves in the sea are of great interest. It is to be hoped that this phenomenon will be further explored by meteorologists and oceanographers, and will eventually become subject to accurate forecasting.

The writer is especially gratified by Mr. Wilson's comments on the importance of the ship mooring system in determining the engineering significance of long-period wave motion in harbors. The writer is currently (1952) engaged

[20] Senior Research Engr., Hydrodynamics Lab., California Inst. of Technology, Pasadena, Calif.

in a study for the Bureau of Yards and Docks of the Department of the Navy, in which a continuously recording direct measurement system is being used to determine the forces in a ship's mooring lines. This study is directed primarily at the development of information on loading conditions for the structural design of mooring structures, but it also may be expected to yield further data on the response of moored ships to periodic water forces.

ENGINEERING ASPECTS OF DIFFRACTION AND REFRACTION

By J. W. Johnson,[1] M. ASCE

With Discussion by Messrs. M. E. Stelzriede, and J. W. Johnson

Synopsis

The design, construction, and operation of many coastal engineering works is considerably dependent on the principles of wave refraction and diffraction. This paper develops and illustrates principles that enable the estimation of wave conditions at specified points in shallow water or at the shore line. The wave characteristics can be developed from weather observations or forecasts, or from wave recorders.

The phenomenon of wave refraction on a shoaling bottom, together with its companion effects such as littoral currents, is discussed. Refraction of waves by currents is also considered, and formulas are developed that make possible the measurement of this effect under various conditions. Wave diffraction by breakwaters is an important consideration in the engineering design of harbor facilities. Means of measuring and locating the area in which the phenomenon will occur are given for conditions of semi-infinite breakwaters and also for breakwater gaps.

An appendix presents a summary of the basic theory of wave diffraction and illustrates the computations necessary for the construction of a diffraction diagram.

Introduction

The extensive research on the problems of waves, surf, and related phenomena that has been completed since the start of World War II, has yielded valuable design data for the practicing engineer. These extensions of the understanding of wave motion have, in many instances, replaced empirical methods dating back to the 1870's, in other instances, they have permitted the analytical solution of problems that were still solved primarily by rather expensive hydraulic model studies. Results obtained from some of these analyses are frequently only qualitative in character, but even so, they provide a rational

Note.—Published in March, 1952, as *Proceedings-Separate No. 122*. Positions and titles given are those in effect when the paper or discussion was received for publication.

[1] Associate Prof. of Mech. Eng., Univ. of California, Berkeley, Calif.

basis for planning shore protection and improvement. Additional research and its correlation with field observations are necessary; however, sufficient progress has been made so that the compilation of wave data for design purposes and wave refraction and diffraction analyses are approaching the status of a standard component of shore-line investigations. The application of these principles are of basic importance to the design engineer. In some instances these principles also have permitted the analytical reconstruction and explanation of unusual phenomena observed in the past.

Estimation of Wave Characteristics

In the design, construction, and operation of structures exposed to wave action, adequate information is necessary on the height and period of the waves that might be expected to occur in the locality under study. The waves most commonly considered are those generated by wind. The characteristics of such waves can be predicted with reasonable accuracy from known meteorological conditions. Other waves of importance in the design of structures in certain localities are harbor surges and tsunamies. The problem of surging[2] is not considered in this paper. Tsunami waves, like earthquakes, are as yet impossible to predict but are capable of causing considerable damage to shore-line structures in certain localities. Although brief reference to tsunami waves is made in this paper, wind-generated waves are considered of primary importance. Unless otherwise noted, this paper will be confined to a discussion of wind-generated waves.

Wave Characteristics from Weather Observations or Forecasts.—Workable relationships[3] between the characteristics of waves and a generating wind appear to be fairly well established. These relationships between the height and period of waves, the fetch, and the velocity and duration of the wind have been presented in convenient graphical form[4] and can be used with confidence in estimating wave heights. (Wave heights refer to the "significant" height; that is, the average of the highest one third of the waves.) Continuing observations, however, indicate that wave periods obtained by these graphs are generally lower than has been observed,[5,6] and therefore, these graphs have been revised.[7]

The estimation of wave conditions may be made on the basis of either a forecast or a hindcast. If wind velocities and the fetch are estimated from a weather chart, then an estimate of the wave conditions at a given locality at sea or at a coastal point also can be made. Such estimates usually are made

---

[2] "Long-Period Waves in Harbors," by John H. Carr, *Proceedings-Separate No. 123*, ASCE, April, 1952.

[3] "Wind, Sea and Swell; Theory of the Relations for Forecasting," by H. U. Sverdrup and W. H. Munk, *Technical Report in Oceanography No. 1, H. O. Publication No. 601*, Hydrographic Office, U. S. Navy, Washington, D. C., 1947.

[4] "Oscillatory Waves, Diagrams and Tables of Relationships Commonly Used In Investigations of Surface Waves," by R. L. Wiegel, *Bulletin*, Special Issue No. 1, Beach Erosion Board, Corps of Engrs., U. S. Army, Washington, D. C., July 1, 1948.

[5] "Comparison Between Recorded and Forecast Waves on the Pacific Coast," by J. D. Isaacs, and Thorndike Savelle, Jr., *Annals*, New York Academy of Science, Vol. 51, 1949, pp. 502–510.

[6] "Relationships Between Wind and Waves, Abbotts Lagoon, California," by J. W. Johnson, *Transactions*, Am. Geophysical Union, Vol. 31, 1950, p. 386.

[7] "Revised Forecasting Relationships," by C. L. Bretschneider, *Proceedings*, Second Conference on Coastal Eng., Council on Wave Research, The Eng. Foundation, 1952, pp. 1–5.

where large-scale wind patterns are involved, such as in ocean areas. Wave forecasts are of particular importance to construction engineers when reliable information must be available on the wave and weather conditions that are likely to exist in a few hours. Such data are vital to the efficient planning of operations involving expensive construction equipment.

From the design engineer's point of view, a knowledge of the expected climate of a given location and a statistical summary of the height and period of waves from various directions is necessary. For localities along an open coast such summaries of wave conditions can be compiled by using the forecasting principles in a hindcasting procedure.[8] In this procedure the wave conditions for the winds and fetches, obtained from past weather charts, are estimated by use of the forecasting graphs previously mentioned and "roses" of wave heights and period are prepared.[9] In lakes and protected bays, it is usually unnecessary to resort to weather charts for past wind conditions, and local wind records of magnitude, duration, and direction are sufficient for estimating the wave conditions that might be expected to occur at any particular locality for various seasons of the year.[9]

The waves estimated from the foregoing procedures refer to deep-water conditions. For a shore point at which the waves must move through shallow water, considerable change in the wave characteristics might take place as a result of refraction and diffraction. Energy losses caused by bottom friction and flow in the permeable bed are of importance only in localities in which the waves must move for relatively long distances over a gently sloping bottom,[10, 11] such as on the Atlantic and the northwest Pacific coasts of the United States. In estimating wave conditions on lakes and bays, the variability of wave direction assumes considerable importance, since within the limits of the 30° angle of wave propagation a large range in fetch (and thus height and period) might be possible.[12] The variability of wave direction also is of importance since it materially affects the refraction of waves in passing an island or headland.

Wave Characteristics From Wave Recorders.—In addition to the forecasting method of compiling statistical data on wave conditions, recorders have been installed at numerous localities on the Atlantic, Gulf, and Pacific coasts.[13, 14, 15, 16] The data from the recorders also provide a means of checking the forecasting

---

[8] "Hindcasting Technique Provides Statistical Wave Data," by W. V. Burt and J. F. T. Saur, Jr., *Civil Engineering*, Vol. 18, 1948, pp. 47–49.

[9] "Action and Effect of Waves," by J. W. Johnson and J. D. Isaacs, *Western Construction News*, Vol. 23, 1948, pp. 97–102.

[10] "Loss of Wave Energy Due to Percolation in a Permeable Sea Bottom," by J. A. Putnam, *Transactions*, Am. Geophysical Union, Vol. 30, 1949, pp. 349–356.

[11] "Dissipation of Wave Energy by Bottom Friction," by J. A. Putnam and J. W. Johnson, *Transactions*, Am. Geophysical Union, Vol. 30, 1949, pp. 67–74.

[12] "Variability in Direction of Wave Travel," by R. S. Arthur, *Annals*, New York Academy of Sciences, Vol. 51, 1949, pp. 511–521.

[13] "Ocean Wave Measuring Instrument," by Joseph M. Caldwell, *Technical Memorandum No. 6*, Beach Erosion Board, Corps of Engrs., U. S. Army, Washington, D. C., October, 1948.

[14] "Measurement of Ocean Waves," by R. G. Folsom, *Transactions*, Am. Geophysical Union, Vol. 30, 1949, pp. 691–699.

[15] "Details of Shore-Based Wave Recorder and Ocean Wave Analyzer," by A. A. Klebba, *Annals*, New York Academy of Sciences, Vol. 51, May, 1949, pp. 533–544.

[16] "Wave Recorders," by Frank E. Snodgrass, *Proceedings*, First Conference on Coastal Eng., Council on Wave Research, Engineering Foundation, 1951.

technique previously discussed. The use of recorders in compiling statistical data on the frequency of wave occurrence of various heights and periods has the disadvantage that several years of records are necessary before average conditions may be determined. Even so, a year of record at a given station is of considerable value in giving important data for the design engineer.[17] Although the accuracy of the forecasting technique may be improved, recorders at certain key stations should always be maintained for checking purposes and for giving a record of the waves existing at any given instant. A forecaster benefits greatly, particularly, if a wave recorder is in operation in the forecasting office at the time the analysis is made. It is important to note that not all oceans are covered by weather maps; therefore, the hindcast procedure alone is insufficient. An example of this deficiency is evident along the coast of southern California, where, during a large percentage of time, waves reach the coast from generating areas to the south for which weather charts are not available. Wave recorders provide the only means of supplying complete data on wave conditions in this locality.

Wave Refraction on a Shoaling Bottom

General.—When waves move into shallow water, important transformations of all wave characteristics, except probably the wave period, take place. Waves approaching a shore line at an angle are bent, or refracted, because the inshore portion of the wave front travels at a lower velocity than does the portion in deeper water; consequently, the waves tend to swing around and conform to the bottom contours as shown in Fig. 1. The characteristics of the bottom topography, the wave period, and the wave direction in deep water determine the pattern of the wave crests in shallow water.[18, 19] The result of refraction is a change in the height and direction of the waves. With very irregular bottom conditions the heights may differ greatly between closely adjacent points along a coast.

The magnitude of the height and direction changes resulting from refraction can be estimated by use of a refraction diagram. Such a diagram may be considered to be a map showing the successive positions of a particular wave crest as it moves shoreward. If no energy flows laterally along the wave crest, then, in a steady state of wave motion, the same amount of energy should flow past all positions between any two sets of lines (orthogonals) that are everywhere perpendicular to the wave crests (Fig. 2). The power P transmitted by a train of sinusoidal waves is

$$P = C_g \times \frac{w}{8} \times b\, H^2 \ldots\ldots\ldots\ldots\ldots\ldots\ldots (1)$$

in which C_g = velocity of energy transmission; w = unit weight of water; b = length of crest; and H = wave height. Indicating the conditions in deep

[17] "Analysis of Data from Wave Recorders on the Pacific Coast of the United States," by R. L. Wiegel, *Transactions*, Am. Geophysical Union, Vol. 30, 1949, pp. 700–704.

[18] "Graphical Construction of Refraction Diagrams," by J. W. Johnson, M. P. O'Brien, and J. D. Isaacs, *H.O. Publication No. 605.*, Hydrographic Office, U. S. Navy, Washington, D. C., February, 1948.

[19] "Refraction of Ocean Waves: A Process Linking Underwater Topography to Beach Erosion," by W. H. Munk and M. A. Traylor, *Journal of Geology*, Vol. 55, 1947, pp. 1–26.

water by the subscript zero,

$$P = P_0 \ldots\ldots\ldots\ldots\ldots\ldots\ldots\ldots (2a)$$

or

$$H = H_0 \sqrt{\frac{C_{g0}}{C_g}} \sqrt{\frac{b_0}{b}} \ldots\ldots\ldots\ldots\ldots\ldots (2b)$$

The quantity $\sqrt{b_0/b}$ is termed the refraction coefficient and usually is designated as K_d. The quantity $\sqrt{C_{g0}/C_g}$ represents the effect of a change in depth

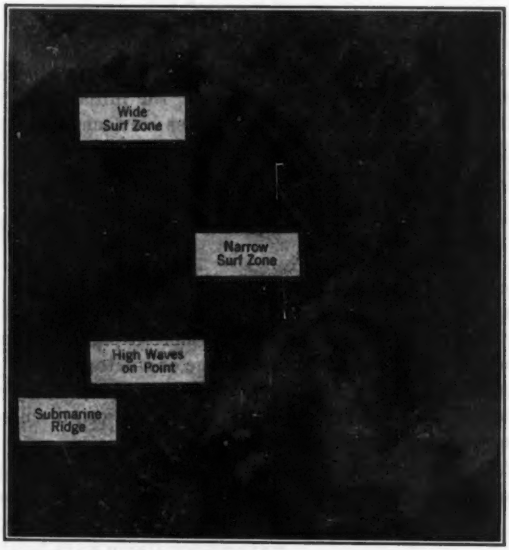

Fig. 1.—Refraction Effects of Waves on a Shoaling Bottom

on the wave height and is designated as D.[20] Then the wave height in any depth of water, may be written as:

$$H = H_0 \, D \, K_d \ldots\ldots\ldots\ldots\ldots\ldots\ldots\ldots (3)$$

The values of the factors D and K_d depend on the depth and wave length and usually are opposite in effect. Refraction commonly tends to increase the length of the wave crest and to reduce the height, while the effect of D is to increase the height. With d representing the water depth, values of D for various values of relative depth (d/L_0) are available in published form.[4] In general, the D term is neglected in refraction studies. The values of K_d, on the other hand, can be determined from refraction diagrams for any given wave direction

[20] "Surface Water Wave Theories," by Martin A. Mason, *Proceedings-Separate No. 120*, ASCE, March, 1952.

and period. As illustrated by Fig. 3, the initial form of the wave is a straight line in the deep-water area. This figure shows that the graphical construction of a refraction diagram for a specified wave period consists simply of moving each point of the wave crest a distance perpendicular to the crest, equal to the wave velocity and multiplied by a convenient time interval.

The wave velocity for each depth is computed by the common wave equations:

$$L = C\,T \qquad (4)$$

and

$$C = \sqrt{\frac{g\,L}{2\,\pi}\tanh\frac{2\,\pi\,d}{L}} \qquad (5)$$

in which C = wave velocity; L = wave length; T = wave period; and d = depth. When the wave crests are completed, the initial wave crest in deep water is divided into equal increments, and lines are then drawn perpendicular to all intermediate crests from these division points to the shore as shown in Fig. 3. Refraction coefficients for any points in shallow water can be calculated by the equation $K_d = \sqrt{\frac{b_0}{b}}$ from orthogonal spacings measured on the diagram.

In addition to the wave-front method described briefly in the previous sections, refraction coefficients can be obtained by a method of drawing orthogonals directly. This latter method requires more experienced personnel than does the former; however, it has the advantage of greater speed of construction than the wave-front method, and a greater degree of accuracy is obtained in many instances. The details of both methods have been discussed elsewhere and, therefore, need not be considered in this paper.[18]

Refraction coefficients afford a convenient method of comparing wave heights at various localities. It is of interest to note that a convergence of orthogonals indicates a concentration of wave energy (large wave heights), whereas a divergence of orthogonals indicates a spreading out of energy, or low wave heights (Fig. 1). Thus, swell coming over a submarine valley usually experiences a decrease in height, and swell passing over a submarine ridge usually will be increased in height. Often the submarine topography is a continuation of the shore line and a submarine ridge frequently extends seaward at a point or headland. Similarly, a submarine valley often exists offshore of a bight or indentation in the coast line.

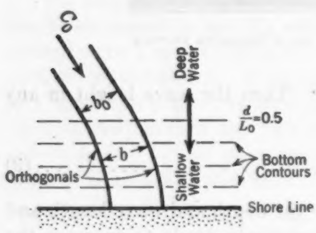

FIG. 2.—WAVE REFRACTION ASSUMING GRADUAL WAVE VELOCITY CHANGE

Of great importance in the refraction of waves around headlands and islands is the variability of wave direction. Although waves are considered to be progressing in a certain direction, actually individual waves will be found

travelling in directions up to 30° either side of the average direction. This means that the penetration of waves to the lee of an island or headland may be much greater than that predicted from a refraction diagram based on the average direction of travel. A complete discussion of this phenomena has been presented by R. S. Arthur.[21]

Refraction diagrams are used primarily in connection with two types of investigation: (1) In the hindcasting and forecasting of wave or surf conditions; and (2) in the analysis and explanation of unusual wave conditions observed in the past. Depending on the use for which refraction diagrams are prepared, the coefficients usually are summarized in convenient tabular or graph form.

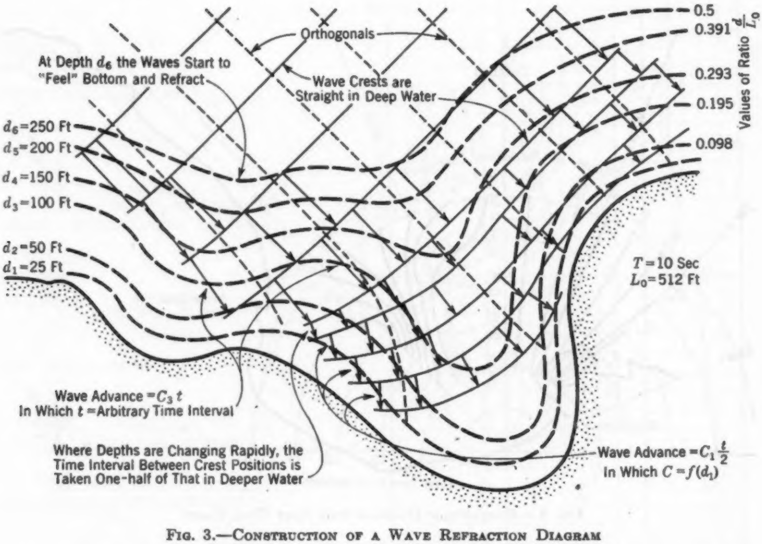

FIG. 3.—CONSTRUCTION OF A WAVE REFRACTION DIAGRAM

Some of the common uses of refraction diagrams and the presentation of pertinent data are presented in succeeding sections as well as elsewhere.[22]

Forecasting and Hindcasting of Wave Characteristics.—The technique of estimating wave conditions from synoptic weather charts has been discussed elsewhere.[20, 23] Such estimates pertain to deep-water conditions, but the transmission of these estimates into shallow water requires the use of refraction coefficients. The coefficients obtained from measurements made on refraction diagrams usually are summarized in graphical form. For example, when forecasts (or hindcasts) are being made for a single point on shore, a polar plot of

[21] "Variability in Direction of Wave Travel," by R. S. Arthur, *Annals*, New York Academy of Sciences, Vol. 51, Article 3, May, 1949, pp. 511–522.

[22] "Refraction and Diffraction Diagrams," by James W. Dunham, *Proceedings*, First Conference on Coastal Eng., Council on Wave Research, Engineering Foundation, 1951, pp. 33–49.

[23] "Wind Waves and Swell, Principles of Forecasting," by H. U. Sverdrup and W. H. Munk, *H. O. Publication 11,275*, Hydrographic Office, U. S. Navy, Washington, D. C., 1944.

K_d as a function of wave direction and period affords a rapid and convenient method of estimating wave heights at shore for any deep-water conditions, as indicated by Fig. 4. If forecasts are being made for several points along a coast, a convenient means of summarizing the data is a graph that shows K_d values plotted against distance along the shore for various wave periods. As shown in the typical example in Fig. 5, a separate curve for each wave direction is necessary. The basic data for plotting such summary diagrams, as illustrated by Fig. 4 and Fig. 5, are obtained most expeditiously by the method of plotting orthogonals directly, instead of by use of the wave-front method. It should be recognized that for those localities in which the tidal range is large, it may be necessary to construct separate refraction diagrams for different

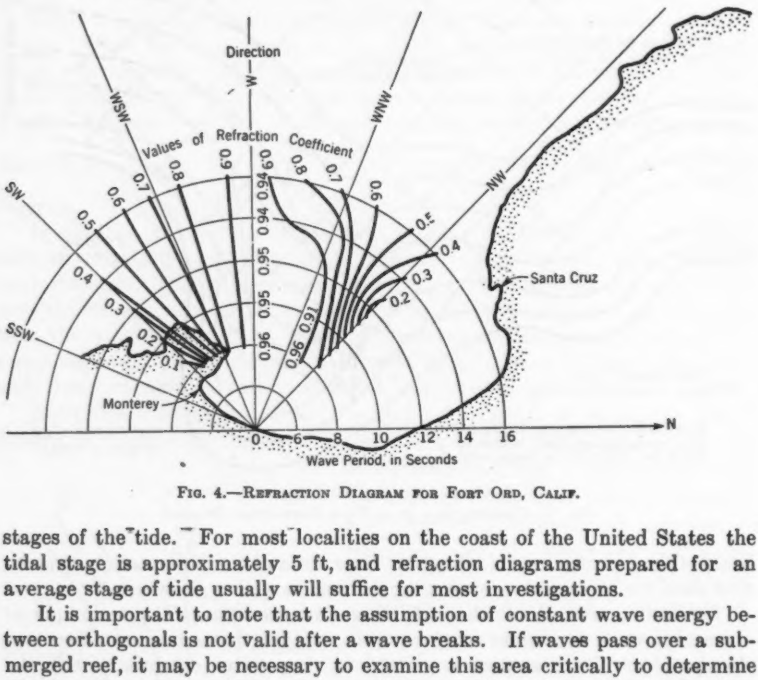

FIG. 4.—REFRACTION DIAGRAM FOR FORT ORD, CALIF.

stages of the tide. For most localities on the coast of the United States the tidal stage is approximately 5 ft, and refraction diagrams prepared for an average stage of tide usually will suffice for most investigations.

It is important to note that the assumption of constant wave energy between orthogonals is not valid after a wave breaks. If waves pass over a submerged reef, it may be necessary to examine this area critically to determine whether the wave breaks at some, or all, stages of the tide. Should breaking occur, wave heights beyond the reef would be lower than that determined by the use of K_d factors from a refraction diagram. As a wave passes over a reef, whether breaking occurs or not, the crest may divide into several crests, as shown in Fig. 6. Thus, the further refraction of the wave may be complex.

Littoral Currents.—When waves approach a shore line at an angle and then break upon the beach, a certain longshore component of the breaker velocity exists. Consequently, a littoral or longshore current is established in the direction of this component. It is this littoral current, combined with the

agitating action of the breaking waves, that is the primary factor in causing a movement of sand along a coast line. For a long straight beach the strength of the littoral current has been found by laboratory studies, supplemented by field observations,[24] to be

$$V = \frac{e}{z}\left[\sqrt{1 + \frac{3.45\, H^{3/2}_b}{e}\sin \alpha_b} - 1\right] \qquad (6)$$

in which $e = \dfrac{2.61\, m\, H_b \cos \alpha_b}{K\, T}$; V = littoral velocity in feet per second; m =

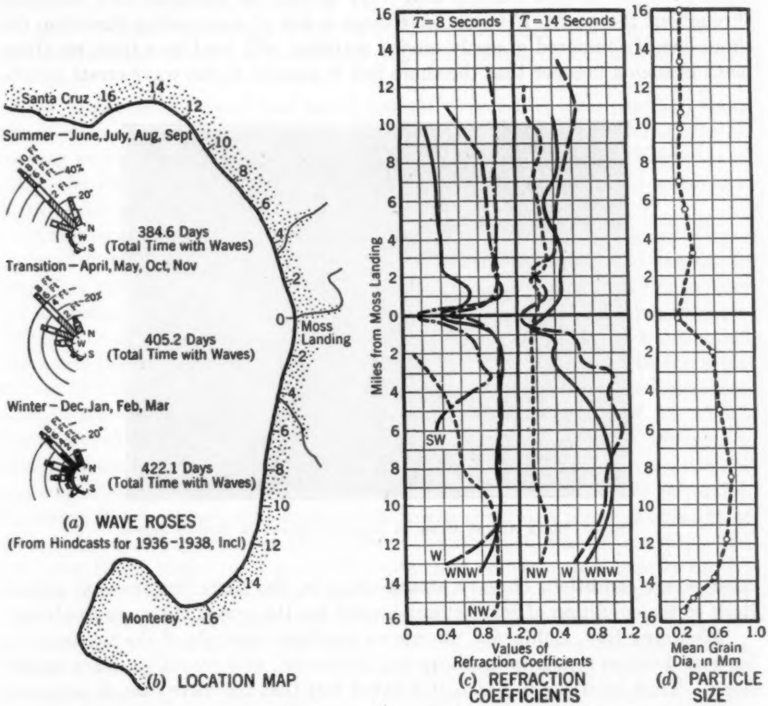

FIG. 5.—VARIATION OF REFRACTION COEFFICIENT AND SIZE OF BEACH MATERIAL ALONG SHORE LINE OF MONTEREY BAY

average beach slope; H_b = breaker height in feet; α_b breaker angle; T = wave period in seconds, and K = a dimensionless friction parameter depending on the hydraulic roughness of the bottom.[25, 26]

---

[24] "Prediction of Longshore Currents," by J. A. Putnam, W. H. Munk, and M. A. Traylor, *Transactions*, Am. Geophysical Union, Vol. 30, 1949, pp. 337–345.

[25] "Nearshore Circulation," by F. P. Shepard and D. L. Inman, *Proceedings*, First Conference on Coastal Eng., Council on Wave Research, Engineering Foundation, 1951, pp. 50–59.

[26] "Prediction and Variability of Longshore Currents," by D. L. Inman and W. H. Quinn, Second Conference on Coastal Eng., Houston, Tex., November, 1951.

For a given beach with a known slope, the strength of the littoral current can be estimated by first making a forecast (or hindcast) of deep-water wave conditions. The breaker height and angle can be determined from a refraction diagram constructed to show wave fronts up to the point of breaking. Knowing the period and deep-water height, the refraction diagram permits an estimate of the wave height at the breaker line as well as the measurement of the breaker angle. With these variables known the strength of the littoral current, therefore, can be calculated by using Eq. 6.

For a shore line that is subjected to waves of various periods from various directions, the littoral current may vary greatly in strength and direction throughout the year. If waves have more or less of a prevailing direction, the shore line, if composed of easily eroded material, will tend to adjust its alinement in such a manner that the shore line is parallel to the wave crests for the

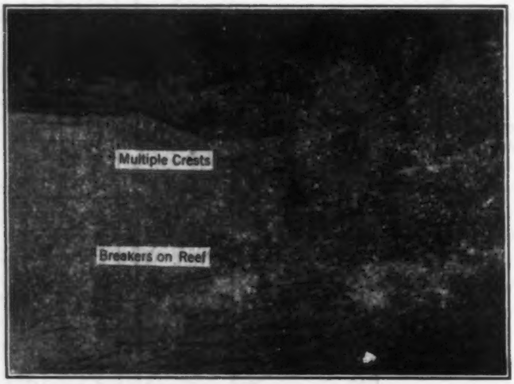

FIG. 6.—WAVE ACTION OVER AN ABRUPT CHANGE IN BOTTOM SLOPE

most severe conditions of wave attack—that is, the shore line tends to adjust itself to the condition of zero littoral current for the prevailing wave condition.

Monterey Bay, California, affords an excellent example of the relationship between bottom topography, shore-line alinement, and prevailing wave conditions. Thus, referring to Fig. 5, it is noted first that the wave rose, as prepared by the hindcasting technique,[8] shows a prevailing wave direction from the northwest. Refraction coefficients for waves of low period (8 sec) and high period (14 sec) from this direction were computed and plotted for various points along the shore line and are shown in Fig. 5. Also plotted in this diagram is the value of the mean grain diameter of the beach sand at various points along the shore line. The fact that the point of maximum values of K_d (mile 8–9 from Moss Landing) coincides with the point of maximum grain size is a significant factor and may be explained by recognizing that at those points along a shore line at which the refraction coefficient is high the littoral current is low, and vice versa. That is, the greater the refraction of the waves the

smaller is the refraction coefficient but the greater is the breaker angle and hence the larger the littoral current. The existence of a region of little or no littoral current, therefore, is a point of desposition and also a point of relatively large wave attack. Applying this reasoning to the southern half of Monterey Bay, it appears that at the section of the coast between miles 8 and 9 below Moss Landing, at which point the wave attack is the greatest, the littoral current is relatively weak. This reach is, therefore, a point of sand deposition from which the prevailing on shore winds remove material and build sand dunes along the back beach. The relatively large extent of wave attack is responsible for causing considerable sorting of the beach material by moving the finer sediment fractions into deep water and leaving the larger sizes on the shore. The relationship between sand size and degree of wave attack is well illustrated by Fig. 5.

To recognize that sand may move generally to certain localities on a shore line is of importance to construction engineers seeking a source of sand supply. As long as the removal of sand from such a source does not exceed the rate of supply by littoral drift, the shore line will remain stable with no serious erosion to adjacent beaches by such sand removal.

Analysis of Past Events.—On numerous occasions in the past, instances have occurred in which unusual wave conditions caused large amounts of damage to shore-line structures. At the time of occurrence of these conditions data were not available, in most instances, to explain completely the events that were observed to have occurred; however, with the increase in knowledge of wave action and related phenomena, many of these events have been explained to the satisfaction of those familiar with the problem. For example, from the knowledge of wave forecasting and wave refraction, Morrough P. O'Brien,[9, 27] M. ASCE has analyzed the occurrence in 1930 in which heavy wave action damaged a portion of the breakwater at Long Beach, Calif. At the time no wave action of unusual intensity was observed in adjacent areas. With the aid of refraction diagrams, it was shown that high-period waves generated many thousands of miles to the south (possibly in the southern hemisphere) must have approached the Long Beach area over a submarine ridge and concentrated directly on the breakwater. Because the submarine ridge was deeply submerged, it affected only waves of unusually long period, which thereby accounts for the fact that the phenomenon was a rare occurrence. In the case of wave damage at Long Beach, the serious beach erosion occurring at Santa Barbara, Calif., following the construction of the breakwater[27, 28] and other instances, refraction diagrams have played an important part in providing a rational basis for reasoning about the causes of damage and means of improvement.

Another example of the value of refraction diagrams in reconstructing and explaining past events is the tsunami wave of April 1, 1946, that caused considerable damage in the Hawaiian Islands and portions of the California coast. This wave resulted from an earthquake on the north face of the Aleutian trench, south of Unimak Island at latitude 53½° *N*, longitude between 163° and 164°.

---

[27] "Wave Refraction at Long Beach and Santa Barbara, California," by M. P. O'Brien, *Bulletin, No. 1*, Beach Erosion Board, Corps of Engrs., U. S. Army, Washington, D. C., January, 1950, p. 2.

[28] "Model Studies Made at the University of California River and Harbor Laboratory," by J. W. Johnson, *Transactions*, Am. Geophysical Union, Vol. 29, 1948, pp. 107–116.

The time of origin was 12:20.9 Greenwich civil time on April 1, 1946. The wave was observed at numerous points along the entire North and South American west coast, in the Hawaiian Islands, Tuamotu Archipelago, and at Bikini Atoll. Data on this wave, obtained from various sources, include information on arrival times from recording tide gages and the visual and photographic

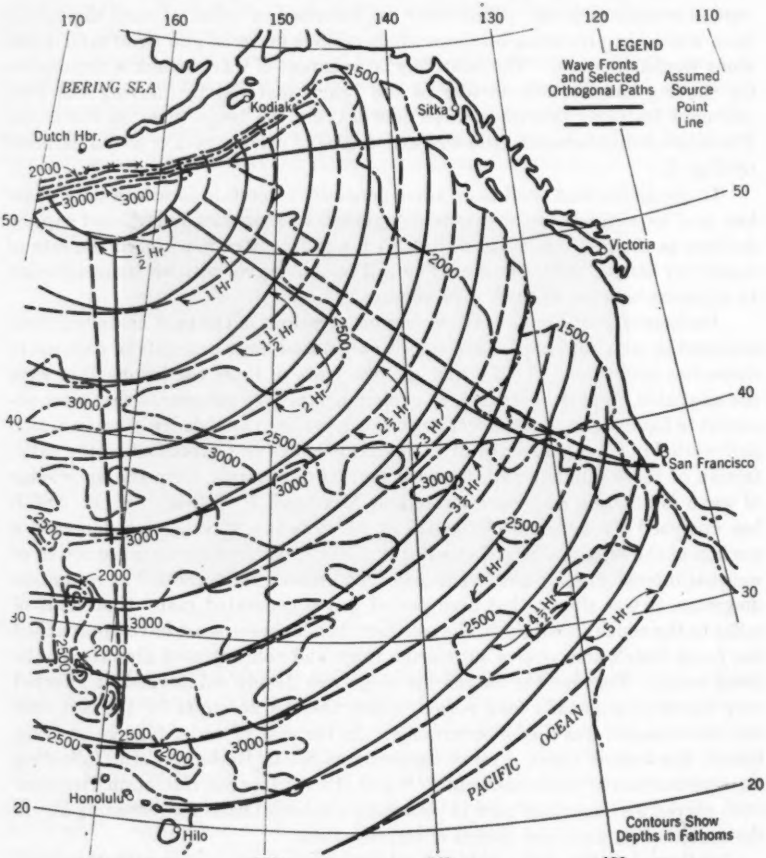

FIG. 7.—WAVE-FRONT DIAGRAM FOR SEISMIC SEA WAVE, APRIL 1, 1946

observations of wave heights and damage. The tide gage data, in particular, afford an opportunity for checking the shallow-water wave theory by comparing observed wave travel times to various points with those times calculated from a refraction diagram. In this instance, the basic theory for the construction of a refraction diagram is founded on the assumption that the waves are long

enough to conform to the shallow-water law for wave velocity ($C = \sqrt{g\,d}$). Thus, the velocity of propagation is independent of wave period. It is, therefore, evident that for a given seismic generating area, only one wave-front diagram is required to obtain the travel time to any point, and the results are applicable even in the absence of exact knowledge of the period or periods of the waves present in the generated train. The only point of uncertainty in the construction of a wave refraction diagram is the extent and shape of the initially generated wave front surrounding the disturbed area at the time of the earthquake. The location of the epicenter and the time of the first shock, however, are known with reasonable accuracy from seismographic data. Assuming both a point source and a line source at the epicenter, refraction diagrams were prepared by the wave-front method [29] and are shown in Fig. 7. The diagram for the line source was constructed on the arbitrary assumption that the source was approximately 168 nautical miles long and parallel to the face contours of the Aleutian Trench. The travel times for each position of the wave fronts are indicated in Fig. 7. A complete tabulation of travel times for those stations for which there was no circumstance casting any doubt on either the observed or computed results is given in Table 1. It is noted from this table that a maximum difference in travel time using the two types of epicenter was 19 min. This difference in travel time, when considered in the light of the total observed travel time (for example, the total observed time to San Francisco, Calif., was 5 hr 31 min) indicates a fair degree of accuracy.

TABLE 1.—DISCREPANCIES BETWEEN OBSERVED AND PREDICTED TRAVEL TIMES FOR SELECTED STATIONS

STATION	TRAVEL TIME DIFFERENCES IN MIN[a]	
	Point source	Line source
Honolulu, Hawaii	−7	−5
Sitka, Alaska	−21	−5
Clayoquot, British Columbia	−18	−2
Crescent City, Calif.	−19	−1
San Francisco, Calif.	−14	+4
Half Moon Bay, Calif.	+2	+20
Avila, Calif.	−7	+12
Port Hueneme, Calif.	−6	+11
La Jolla, Calif.	−14	−5

[a] Negative values indicate observed arrival in advance of theoretical indication.

Within practical limits it appears that the preceding analysis is valid as to travel time calculations and that the assumed line source gives results fitting the observations to within the order of accuracy of the analysis. It is of importance to recognize, however, that the waves as generated in a seismic disturbance constitute a wave group in which the first wave generated becomes progressively smaller with distance from the source and may even vanish, thus making the discrepancy between theoretical and observed arrival times even greater than that shown in Table 1. An examination of tide gage records[30] that recorded the tsunami of April 1, 1946, show that the wave of maximum

[29] "A Study Relating Data from the Seismic Sea Wave of April 1, 1946 to the Theory of its Propagation," by F. C. Roop, *Report HE-116-215*, Inst. of Eng. Research, Univ. of California, Berkeley, Calif., July 11, 1946 (unpublished).

[30] "Seismic Sea Wave of April 1, 1946, as Recorded on Tide Gages," by C. K. Green, *Transactions*, Am. Geophysical Union, Vol. 27, 1946, pp. 490–500.

height is, in general, the third or fourth wave in the group, and thus indicating that a group of waves did exist. The characteristic of a wave group is that the first wave eventually disappears and that the maximum wave height moves progressively back through the group.

Sufficient data are not available to make a comparison of measured and observed wave heights; however, it is perhaps reasonable to assume that, if the wave theory applies to estimates of travel time from refraction diagrams, then reasonably accurate estimates of relative wave heights at various points also could be made by determining refraction coefficients from these diagrams. In such estimates, however, the shoaling factor D in Eq. 3 undoubtedly should be considered.

Although the time and location of the source of tsunami waves are unpredictable, certain of the Pacific islands and parts of the Pacific coast of the United States have felt the damaging effects of such waves in the past, and there is no reason to expect that such effects will not be felt again in the future. A consideration of the basic principles of refraction permits an engineer to estimate the relative vulnerability of various localities along a given coast line to destruction by tsunami waves. Historically, it is known that certain cities have been greatly damaged several times by tsunami waves despite the fact that the waves originated in entirely different regions. Other near-by regions have never suffered damage. Hence, it appears that local underwater topography is particularly important in arriving at an evaluation of the safety of various localities against destructive action from tsunami sea waves coming from all possible directions. Such information is of importance in the orientation of breakwaters and other shore-line improvements, as well as in the structural design of the installations themselves. Actual damage at points at which the potential damage is great obviously will occur only if improvements of a character that waves can damage are in existence.

Refraction by Currents

When waves moving through still water encounter a current moving with, against, or at an angle to the wave direction, the waves undergo a change in length and steepness. In the case in which the waves meet a current at an angle, the waves also change their direction. In the forecasting of wave conditions there are two situations in which the refraction of waves by currents may be of practical importance. At tidal entrances, ebb currents run counter to the waves and increase the wave height and steepness, thereby adding to the hazards of navigation, while flood currents flatten out the waves. Large-scale ocean currents, such as the Gulf Stream, may have great effect on the height, length, and direction of the waves approaching the current discontinuity. In some instances, almost complete reflection of waves of certain periods will occur. In other instances, the waves have been forced by refraction to exceed their critical steepness and then to break.

The principal application of refraction methods is to predict the occurrence and height of breakers around a tidal entrance. The direction, height, and period of the waves in deep water are variable, the bottom contours usually are irregular, and the currents are variable throughout the tidal cycle. Under such

conditions quantitative forecasting by the purely analytical approach probably is not reliable, but a combination of theory and observation would be adequate for making forecasts of probable wave conditions at harbor entrances. In other instances the engineer might use the general principles of refraction by currents to design the shape of dredged tidal channels such that wave action within the channel will be reduced in magnitude.[31]

Surface waves in deep or shallow water are refracted by currents to an extent that depends on the initial wave velocity and direction and the strength of the current. Two common conditions are treated in the subsequent section which, for simplicity, is concerned only with deep-water waves.

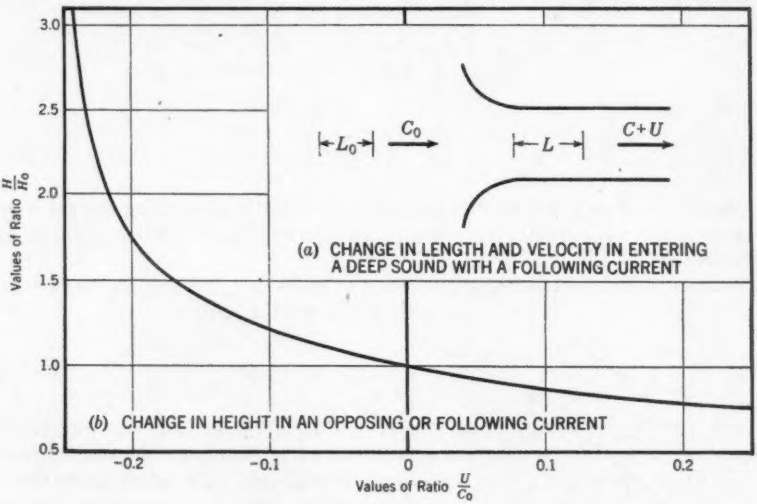

FIG. 8.—CHANGE IN WAVE CHARACTERISTICS

Waves Meeting or Following a Current.—When waves proceed from still, deep water into a deep sound in which a current runs directly with or against the advancing waves, the wave period remains constant, but the wave length, velocity, and height change.[32] Thus, referring to Fig. 8(*a*), if L_0 and C_0 represent the deep-water wave length and velocity, respectively, the wave length in the sound will be changed to a new value L. The wave velocity (relative to the water) corresponding to this wave length is $C^2 = \frac{(g\ L)}{(2\ \pi)}$; thus,

$$\frac{L}{L_0} = \left(\frac{C}{C_0}\right)^2 \qquad (7)$$

[31] "The Refraction of Surface Waves by Currents, A Discussion," by J. D. Isaacs, *Transactions*, Am. Geophysical Union, Vol. 29, 1948, pp. 739–742.

[32] "On Wave Heights in Straits and Sounds When Incoming Waves Meet a Strong Tidal Current," by H. U. Sverdrup, Scripps Inst. of Oceanography, La Jolla, Calif., April 20, 1944 (unpublished).

The wave velocity over the ground is equal to $(C + U)$, in which U is the velocity of the current in the sound. For constant period,

$$T = \frac{L_0}{C_0} = \frac{L}{(C + U)} \quad \text{(8)}$$

From Eqs. 7 and 8,

$$\frac{C}{C_0} = \frac{1}{2}\left[1 \pm \sqrt{1 + 4\frac{U}{C_0}}\right] \quad \text{(9a)}$$

Here the plus sign must be taken since C must equal C_0 where $U = 0$. Thus, if it is assumed that $\sqrt{1 + 4\frac{U}{C_0}} = a$,

$$\frac{C}{C_0} = \frac{1}{2}(1 + a) \quad \text{(9b)}$$

and

$$\frac{L}{L_0} = \left(\frac{1 + a}{2}\right)^2 \quad \text{(10)}$$

Considering Eqs. 7 and 9a it is seen that the effect of a following current is to increase the wave length, whereas the opposite effect results from an opposing current.

From a consideration of the advance of wave energy it can be shown that the ratio of the wave heights is

$$\frac{H}{H_0} = \sqrt{\frac{2}{a(1 + a)}} \quad \text{(11)}$$

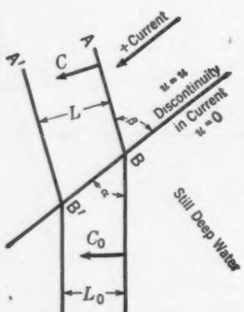

Fig. 9.—Relative Positions of Wave Crests Before and After Refraction by a Current

A plot of this equation showing the change in wave height in an opposing or following current is presented in Fig. 8(*b*). The effect on the wave steepness is obtained from a combination of Eqs. 10 and 11. Thus,

$$\frac{H}{L} = \frac{H_0}{L_0}\sqrt{\frac{2}{a(1 + a)}}\left[\frac{2}{(1 + a)}\right]^2 \quad \text{(12)}$$

in which the wave steepness H/L in the sound is seen to depend on the initial steepness H_0/L_0 and on the ratio U/C_0. The waves in the sound will break when the value of H/L reaches the critical value of 1/7. As is apparent from Fig. 8(*b*), this condition takes place only when the waves meet an opposing current; that is, it is in this type of current that the height in the sound is increased over the deep-water height H_0.

Waves at an Angle to a Current.—Referring to Fig. 9, when a wave crest progresses from the position A B C in deep, still water across a current discontinuity to a position A′ B′ C′, changes in the wave length, height, and stepeness

occur. This refraction by currents has two effects on the wave steepness. One effect is on the change in the wave length and the other is on the stretching or compressing of the wave crest. These effects may oppose or add, depending on whether the current direction is plus or minus. A treatment of the general

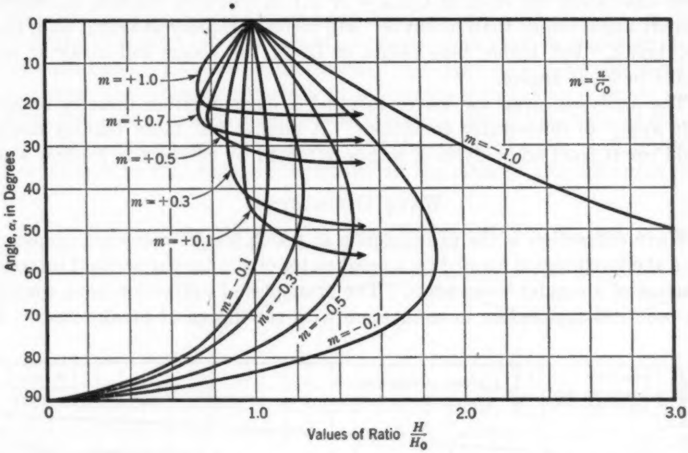

FIG. 10.—EFFECT OF REFRACTION BY CURRENTS ON WAVE HEIGHT

condition sketched in Fig. 9 shows[33] that the effect on wave length is

$$\frac{L}{L_0} = \frac{1}{\left(1 - \frac{U}{C_0 \sin \alpha}\right)^2} \quad \text{(13)}$$

and the effect on wave steepness is

$$\frac{H}{L} = \frac{H_0}{L_0} \sqrt{\frac{\cos \alpha}{\cos \beta} \left[\frac{\left(1 - \frac{U}{C_0 \sin \alpha}\right)^6}{\left(1 + \frac{U}{C_0 \sin \alpha}\right)}\right]} \quad \text{(14)}$$

or

$$\frac{H}{L} = \frac{H_0}{L_0} \ (m) \quad \text{(15a)}$$

This can be rewritten in the form,

$$\frac{H}{H_0} = \left(\frac{L}{L_0}\right) m \quad \text{(15b)}$$

This combination of Eqs. 13 and 14 permits the preparation of a diagram (Fig. 10) that gives the change in wave height as a function of the strength and

[33] "The Refraction of Surface Waves by Currents," by J. W. Johnson, *Transactions*, Am. Geophysical Union, Vol. 28, 1947, pp. 867–874.

direction of the current compared to that of the incident wave. The most interesting feature of the curves presented in Fig. 10 is that, whether the waves enter an oncoming or a following current, they may increase in height (and, therefore, steepness) and then break. As an example, examination of Fig. 10 shows that when the value of $U/C_0 = +0.1$ (a following current) all waves of incident angle larger than about 58° will increase rapidly in height and, therefore, break. For higher plus values of U/C_0, the waves will break at much smaller incident angles.

The analyses given for waves meeting a current either directly or at an angle apply to deep-water conditions. A similar but more tedious analysis would result from an analysis of waves refracted by currents in shallow water.

Wave Diffraction

Wave diffraction is the phenomenon in which water waves are propagated into a sheltered region formed by a breakwater or similar barrier that interrupts a portion of a regular wave train. The principles of diffraction have considerable practical application in connection with the design of breakwaters. The

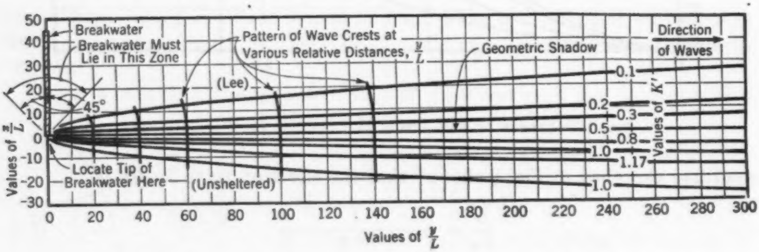

Fig. 11.—Generalized Diffraction Diagram for Tip of Breakwater

phenomenon is analogous to the diffraction of light, sound, and electromagnetic waves, and theories for breakwater diffraction have been adapted from the theory of these phenomena. Two general types of diffraction problems usually are encountered: (*a*) The passage of waves around the end of a semi-infinite impermeable breakwater; and (*b*) the passage of waves through a gap in a breakwater. The complete theory for these two conditions appears to have been first developed during World War II.[34] These theories later were reworked and verified experimentally by model studies.[34, 35, 36] It appears, however, that the theory for the case of a semi-infinite breakwater was developed independently in France as early as 1942 and checked by field observations.[37] It also appears that simultaneously with these other studies, R. Iribarren in

[34] "Diffraction of Water Waves by Breakwaters," by J. A. Putnam and R. S. Arthur, *Transactions*, Am. Geophysical Union, Vol. 29, 1948, pp. 481–490.

[35] "Diffraction of Water Waves Passing Through a Breakwater Gap," by F. L. Blue, Jr., and J. W. Johnson, *ibid.*, Vol. 30, 1949, pp. 705–718.

[36] "Diffraction of Water Waves by Breakwaters," by J. H. Carr and M. E. Stelzriede, Circular 521, National Bureau of Standards, U. S. Dept. of Commerce, Washington, D. C., November 28, 1952.

[37] "La deformation ondulatoire des jetees verticales," by M. J. Larras, *Travaux*, Vol. 26, June, 1942, pp. 167–170.

Spain,[38] and J. Thysse and J. B. Schijf [39] made experimental studies on diffraction and applied the results to practical design problems. More recently, M. H. Lacombe[40] has made a comparison between the classical hydrodynamic methods of studying wave diffraction and the optical methods of C. Huyghens. In general, the theoretical solutions have been found to apply with conservative results—that is, the predicted wave heights in the lee of a breakwater are found to be slightly larger than the height of waves that may be expected under actual conditions. The use of the diffraction theory in breakwater design is made convenient when summarized in a diagram with curves of equal values of diffraction coefficients on a coordinate system in which the origin of the system is at the tip of a single breakwater or at the center of a gap.[41] The diffraction coefficient in this instance is defined as the ratio of the diffracted wave

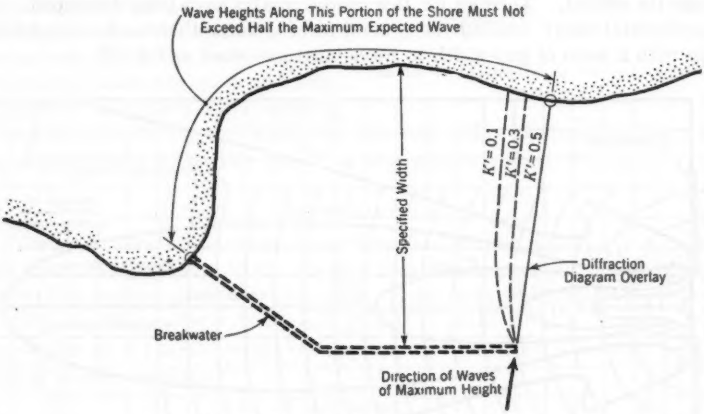

Fig. 12.—Use of a Diffraction Diagram

height to the incident wave height and is usually designated by the symbol K'. The procedure to be followed in preparing diffraction diagrams appears in the Appendix.

Semi-Infinite Breakwater.—The generalized diffraction diagram shown in Fig. 11 can be applied to a particular breakwater problem once the characteristics of the design wave have been selected—that is, the height, period, and direction of the incident wave from which protection is to be provided. For example, Fig. 12 shows a map of a harbor for which protection is desired for a specified reach of the shore line for waves approaching from the critical direction.

[38] "Protection des Ports," by R. C. Iribarren and C. O. Nogales, XVII International Congress, Section II, Communication 4, Lisbon, Portugal, 1949, pp. 31–79.

[39] "Penetration of Waves and Swells into Harbors," by J. Thysse and J. B. Schijf, VII International Navigation Congress, Section II, Communication 4, Lisbon, Portugal, 1949, pp. 151–171.

[40] "Note sur la diffraction de la Houle en incidence normal," by M. H. Lacombe, *Annales Hydrographiques, Separate No. 1363*, Paris, France, 1949, pp. 1–49.

[41] "Generalized Wave Diffraction Diagrams," by J. W. Johnson, *Proceedings*, Second Conference on Coastal Eng., Council on Wave Research, Eng. Foundation, 1952, pp. 6–23.

For the given wave period (or length) a diagram similar to Fig. 11 is plotted on transparent paper to the same length scale as the map of the harbor area. This transparent overlay then is moved over the map, keeping the geometric shadow parallel to the direction of travel until the desired degree of protection for the selected reach of the shore line is obtained. The location of the tip of the breakwater thus is obtained as illustrated by the final location of the overlay shown in Fig. 12.

Diffraction at a Breakwater Gap.—The treatment of diffraction problems, as discussed in the preceding section, is concerned with waves moving past a breakwater tip with an infinite expanse of water existing away from the tip. In many harbors, however, waves move through a relatively narrow gap in a breakwater, hence, diffraction occurs at the two sides of the gap and changes in wave height in the lee of the breakwater; hence, it will be different than if a single tip existed. Theories for this condition also have been developed. An experimental study verified the general form of these theories for breakwater gaps with a ratio of gap-width to wave length as small as 0.5.[35,36]

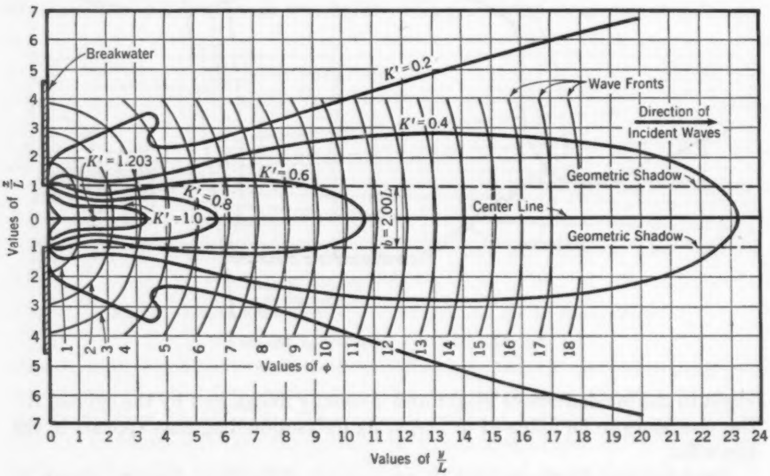

FIG. 13.—GENERALIZED DIFFRACTION DIAGRAM FOR A BREAKWATER GAP

As an illustration of a generalized diagram that gives diffraction coefficients to the lee of a breakwater gap, Fig. 13 shows a diagram for the case in which the gap is two wave lengths in width. The method of making the necessary computations of these diffraction coefficients as well as the computations for the position of the wave fronts are shown in the Appendix. These generalized diagrams,[41] when used as transparent overlays, can be moved over a map of a locality to obtain the most desirable protection, similar to the procedure described for the single breakwater.

When the gap width is in excess of about five wave lengths, the diffraction patterns at each side of the opening are more or less independent of each other.

In such cases, the pattern given by Fig. 11 for a semi-infinite breakwater can be used to estimate the height and direction of waves on the leeward side. For these relatively large gap openings the direction of the incident waves with respect to the breakwater alinement can lie anywhere within the zone indicated in Fig. 11 without the diffraction pattern being appreciably affected.

For relatively narrow gaps the experimental work[42] has been concerned with the case in which the angle between the incident wave and the breakwater is less than 20°. Until more experimental data are available, however, it is believed that useful approximations can be made for cases of oblique incidence by drawing a line through the gap center and normal to the incident wave direction, and then computing diffraction coefficients as though the breakwater were along this line—the end of the imaginary gap being at the projections on this line of the true gap ends (Fig. 14).

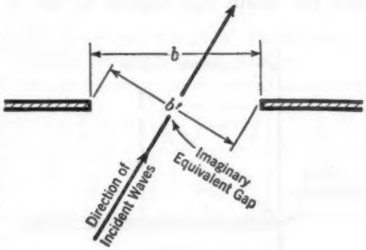

FIG. 14.—WAVE INCIDENCE OBLIQUE TO BREAKWATER GAP

SUMMARY

The application of the principles of refraction and diffraction is of considerable practical importance in the design, construction, operation, and maintenance of many coastal engineering works. These principles permit the estimate of wave conditions at specified points in shallow water or at a shore line from deep-water wave characteristics that are known from either a forecast, a hindcast, or a wave recorder.

APPENDIX

The basic theory of diffraction has been presented elsewhere[34] and need not be discussed in detail in this paper. Basically, the theory assumes: (1) That the waves are of small amplitude compared to the wave length; and (2) that the water is of uniform depth. The first assumption covers the range of wave steepness up to that of storm waves—that is, $H_0/L_0 = 0.03$.

Diffraction by a Vertical Impermeable Semi-Infinite Breakwater.—As mentioned previously, the diffraction coefficient K' is defined as the ratio of diffracted wave height to incident wave height. The value of K' is a function of position with respect to the breakwater, that is,

$$K' = f(u_1) \qquad (16)$$

In this equation

$$u_1 = \sqrt{\frac{4}{L}\left[\sqrt{(x^2 + y^2)} - y\right]} \qquad (17a)$$

[42] "Diffraction of Water Waves Passing Through a Breakwater Gap," by F. L. Blue, Jr., thesis presented to the University of California, at Berkeley, Calif., in 1948, in partial fulfilment of the requirements for the degree of Doctor of Philosophy.

or

$$\frac{x}{L} = \pm \frac{u_1}{\sqrt{2}} \sqrt{\frac{y}{L} + \frac{u^2{}_1}{8}} \quad \text{(17}b\text{)}$$

Referring to Fig. 15, the plus sign in Eq. 17*b* applies to the region of $-(x/L)$ and the minus sign applies to the $+(x/L)$ region. The evaluation of $K' = f(u_1)$ is obtained from a projection of the Cornu spiral. The values of the factor u_1 for various values of K' are given in Table 2.

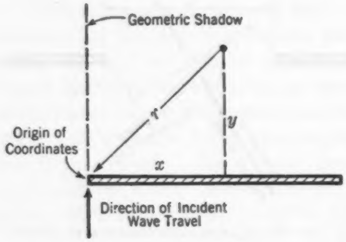

FIG. 15.—WAVE DIFFRACTION ANALYSIS AT BREAKWATER TIP

Eq. 17*b*, used in conjunction with Table 2, permits the construction of a diffraction diagram that shows parabolas of the constant K'. For example, to plot the curve of $K' = 0.2$, the following calculations are made: From Table 2, with $K' = 0.2$, find $u_1 = -1.02$. From Eq. 17*b*, compute $x/L = (-)\ (0.707)\ (-1.02)\ \sqrt{y/L + (0.125)\ (-1.02)}$ $= +\ 0.722\ \sqrt{y/L + 0.13}$. The plus sign indicates the region in the lee of the breakwater. The values of x/L now can be computed for various assumed values of relative distance (y/L) using a computation form similar to that outlined in Table 3.

TABLE 2.—VALUES OF THE TERM u_1

Diffraction coefficient K'	Factor u_1	Crest lag in percentage of wave length L
(a) LEE REGION $(+x/L)$		
0.1	−2.25	140
0.15	−1.44	60
0.2	−1.02	33
0.3	−0.528	13
0.4	−0.225	6
(b) GEOMETRIC SHADOW REGION		
0.5	0.000	0
(c) UNSHELTERED REGION $(-x/L)$		
0.6	0.184	−3
0.7	0.341	−5
0.8	0.486	−6
0.9	0.631	−5
1.0	0.779	−5
1.17	1.218	0
1.0	1.610	0
0.88	1.878	−3
1.0	2.124	...

Complete plotting data for various constant values of diffraction coefficients are summarized in Table 4 and plots of these data are shown in Fig. 11. As previously discussed, this figure is a generalized diagram that shows curves of equal values of diffraction coefficients on a coordinate system in which the origin is at the breakwater tip. It is of interest to note on this diagram that along the geometric shadow the wave heights are one half of the height of the incident waves and that waves slightly greater in height than the incident waves are possible beyond the breakwater. This diagram is applicable for a

uniform depth with either deep-water or shallow-water waves, provided that the proper wave length is used in the particular case. It also applies for conditions in which the angle between the incident wave and the breakwater is other than 90°, as shown by Fig. 11.

In addition to the plot of diffraction coefficients shown in Fig. 11, a plot of wave patterns is desirable in certain investigations. Data for plotting wave patterns are presented in the last column of Table 2, where the lag or lead of the wave front is given. Thus, along the parabola $K' =$ constant, at the corresponding value of (y/L) and (x/L) the wave front will lag (or lead) by the given percentage of the wave length, that portion of the front of the same wave that is at the geometric shadow. It should be recognized that the wave patterns plotted by this method apply only if the water is of uniform depth. Should

TABLE 3.—COMPUTATION FORM FOR DIFFRACTION COEFFICIENTS

$\left(\frac{y}{L}\right)$	$\left(\frac{y}{L}+0.13\right)$	$\sqrt{\left(\frac{y}{L}+0.13\right)}$	$\frac{x}{L}$
5	5.13	2.27	1.64
10	10.13	3.18	2.30
15	15.13	3.89	2.80

TABLE 4.—VALUES OF COORDINATE $\frac{x}{L}$ FOR DIFFRACTION AT THE END OF A SEMI-INFINITE BREAKWATER

Coordinate y/L	Diffraction Coefficient K'						
	Lee or + Values		Geometric Shadow	Unsheltered or − Values			
	0.1	0.2	0.5	0.8	1.0	1.17	1.0
5	3.78	1.64	0.00	0.77	1.24	1.96	3.54
10	5.19	2.30	0.00	1.09	1.75	2.75	4.89
15	6.29	2.80	0.00	1.33	2.14	3.36	5.93
20	7.23	3.23	0.00	1.54	2.47	3.87	6.82
30	8.81	3.95	0.00	1.88	3.02	4.74	8.31
40	10.13	4.56	0.00	2.17	3.49	5.46	9.58
50	11.31	5.10	0.00	2.43	3.90	6.11	10.68
60	12.38	5.59	0.00	2.66	4.27	6.68	11.70
70	13.37	6.04	0.00	2.87	4.61	7.22	12.62
80	14.28	6.46	0.00	3.07	4.93	7.71	13.48
90	15.14	6.85	0.00	3.26	5.23	8.18	14.30
100	15.91	7.22	0.00	3.44	5.51	8.62	15.03
120	17.43	7.90	0.00	3.76	6.04	9.44	16.47
140	18.83	8.53	0.00	4.07	6.52	10.20	17.79
160	20.13	9.13	0.00	4.34	6.97	10.90	19.03
180	21.35	9.68	0.00	4.61	7.40	11.55	20.16
200	22.50	10.20	0.00	4.86	7.80	12.18	21.24
220	23.59	10.70	0.00	5.10	8.18	12.78	22.27
240	24.64	11.18	0.00	5.32	8.54	13.34	23.27
260	25.66	11.63	0.00	5.54	8.89	13.89	24.21
280	26.62	12.07	0.00	5.75	9.23	14.42	25.13
300	27.56	12.50	0.00	5.95	9.55	14.92	26.01

these waves, after passing the breakwater, move into shoaling water in which the bottom contours are not normal to the wave directions, refraction as well as diffraction must be considered; in fact, after a few wave lengths beyond the

barrier, refraction may be more important than diffraction if the depth is changing rapidly. One possible method for treating such problems has been suggested,[42] but further experimental studies in this field appear desirable.

Diffraction at a Breakwater Gap.—A theory for this problem has been discussed elsewhere,[35] and only a summary and an illustrated example need be presented herein. For any position (x, y) as illustrated in Fig. 16, the diffraction coefficient is given by the expression:

$$K' = [F\,(x, y)] \qquad (18)$$

and

$$\text{Phase Difference} = \arg\,(F \text{ for diffracted wave} + k\,y) \qquad (19)$$

in which arg denotes argument and $k = 2\,\pi/L$.

In Eq. 18, for $x \leqq b/2$,

$$F\,(x, y) = e^{-i\,k\,y} - f_1 + g_1 - f_2 + g_2 \qquad (20a)$$

and for $x \geqq b/2$ and $y \geqq 0$,

$$F\,(x, y) = f_1 + g_1 - f_2 + g_2 \qquad (20b)$$

At $x = b/2$ (geometric shadow) these expressions, of course, are identical. The factors in Eqs. 20 are computed in terms of real and imaginary components, each of which are added arithmetically and combined into a resultant $F\,(x, y)$. The terms f and g in Eq. 20 are defined as follows:

$$f = f\,(r, y) = e^{-i\,k\,y} \times f\,(-\,u) \qquad (21)$$

and

$$g = f\,(r, -\,y) = e^{i\,k\,y} \times f\,(-\,u) \qquad (22)$$

in which

$$f\,(-\,u) = S + i\,w$$

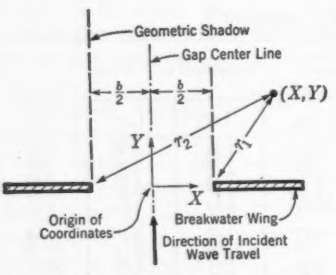

FIG. 16.—WAVE DIFFRACTION ANALYSIS FOR BREAKWATER GAP

S and w are, respectively, the real and imaginary components of $f\,(-\,u)$ and $i = \sqrt{-\,1}$. The term u is defined by the expression,

$$u = \sqrt{\frac{4\,(r - y)}{L}} \qquad (23)$$

Values of S and w[42] as functions of the quantity u^2 are shown in Fig. 17.

The diffraction coefficient and phase difference at any point (x, y) for a particular breakwater gap of width b are computed by using Eqs. 20 in the following steps. Values of r_1 and r_2 are first obtained from relationships that are

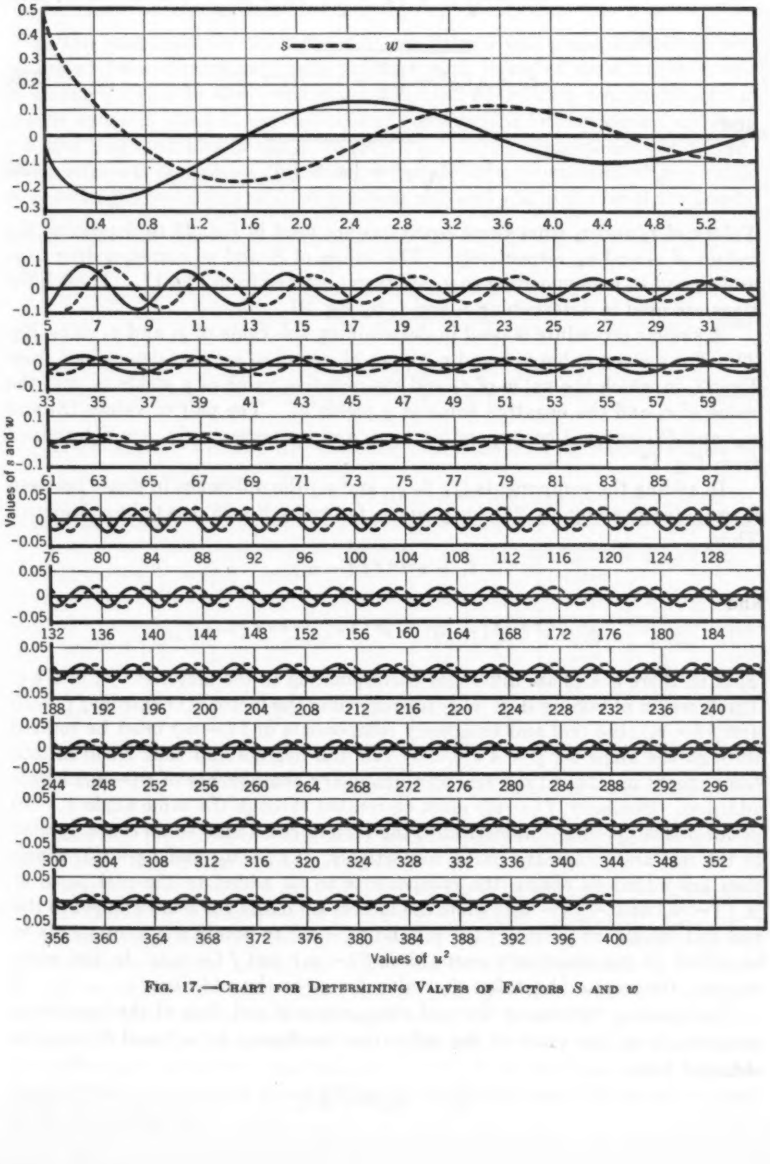

FIG. 17.—CHART FOR DETERMINING VALVES OF FACTORS S AND w

readily derived from the geometry of the system shown in Fig. 16. These are:

$$r_1 = \sqrt{y^2 + \left(x - \frac{b}{2}\right)^2} \text{ for } x \geqq \frac{b}{2} \quad \text{(24a)}$$

$$r_1 = \sqrt{y^2 + \left(\frac{b}{2} - x\right)^2} \text{ for } x \leqq \frac{b}{2} \quad \text{(24b)}$$

and

$$r_2 = \sqrt{y^2 + \left(x + \frac{b}{2}\right)^2} \quad \text{(25)}$$

Values of r_1 and r_2 from these equations are used in Eq. 23 to determine the values of u_1 and u_2, respectively. The values of S_1 and w_1 corresponding to u_1 and S_2 and w_2 corresponding to u_2 are then obtained from Fig. 17. These functions are used in determining f_1 and f_2 by Eq. 21.

A similar procedure is used in determining the value of g_1 and g_2 using Eq. 22. For a given value of x and y, values of u_3 and u_4 are first determined from Eq. 23, in which the value of r_1 and the negative value of y yields u_3, and the value of r_2 and the negative value of y yields u_4. The pair of values (S_3 and w_3) and (S_4 and w_4) corresponding to u_3 and u_4, respectively, are determined from Fig. 17.

In adding the components (f_1, f_2, g_1, and g_2) the difference in phase between f_1 and f_2 (as given by Eq. 21) and g_1 and g_2 (given by Eq. 22) has to be considered. Thus,

$$f_1 = e^{-i\,k\,y} f\,(-\,u_1)$$

and

$$g_1 = e^{i\,k\,y} f\,(-\,u_3) = e^{2\,i\,k\,y}\left[e^{-i\,k\,y} f\,(-\,u_3)\right]$$

That is, there is a phase difference corresponding to the factor $e^{2\,i\,k\,y}$, or $2\,k\,y$. Therefore, in obtaining $\pm f_1 + g_1$ (disregarding the factor $e^{-i\,k\,y}$) from $f\,(-\,u_1)$ and $f\,(-\,u_3)$, the real and imaginary components of $f\,(-\,u_3)$ must be rotated through the angle $2\,k\,y = 4\,\pi\,y/L = 720\;y/L$ degrees and then resolved into components parallel to the real and imaginary components of $f\,(-\,u_1)$ before addition. Similarly, $f\,(-\,u_4)$ must be rotated through the same angle α. To perform this operation numerically, the factors $\cos\alpha$ and $-\sin\alpha$ are applied to the real and imaginary parts, respectively, of $f\,(-\,u_3)$ and $f\,(-\,u_4)$, which then are added to obtain the components to be added to the real parts of $\pm f\,(-\,u_1)$ and $-f\,(-\,u_2)$; while the factors $\sin\alpha$ and $\cos\alpha$ are applied to the real and imaginary parts of $f\,(-\,u_3)$ and $f\,(-\,u_4)$ to obtain the components to be added to the imaginary parts of $\pm f\,(-\,u_1)$ and $f\,(-\,u_2)$. In the same manner, the term $e^{-i\,k\,y}$, takes the value $1 + io$ in the addition.

Designating the sum of the real components S and that of the imaginary components w, the value of the diffraction coefficient $K' = [\text{mod}\,F\,(x, y)]$ is obtained from

$$K' = \sqrt{w^2 + S^2} \quad \text{(26)}$$

and the phase difference caused by diffraction is

$$\text{phase difference} = \tan^{-1}\left(\frac{w}{S}\right) \qquad (27)$$

In the practical case the diffraction coefficients and phase differences are calculated for a breakwater gap of width b with waves of wave length L approaching parallel to the breakwater. Instead of making computations for specific values of b and L, the results can be generalized by considering values of b, x, and y as multiples of the wave length L. Thus, computations of diffraction coefficients and phase differences are made for a given ratio of gap-width to wave length at various relative positions x/L and y/L in the lee of the breakwater. For convenience in computations, Eq. 24 and Eq. 25 with $x \geqq \frac{b}{2}$ are written:

$$\frac{r_1}{L} = \sqrt{\left(\frac{y}{L}\right)^2 + \left(\frac{x}{L} - \frac{b}{2L}\right)^2} \qquad (28a)$$

$$\frac{r_2}{L} = \sqrt{\left(\frac{y}{L}\right)^2 + \left(\frac{x}{L} + \frac{b}{2L}\right)^2} \qquad (28b)$$

Values u_1^2, u_2^2, u_3^2, and u_4^2, therefore, are computed for various values of $\frac{x}{L}$ and $\frac{y}{L}$ from Eq. 23 transformed as follows:

$$u_1^2 = 4\left(\frac{r_1}{L} - \frac{y}{L}\right) \qquad (29a)$$

$$u_2^2 = 4\left(\frac{r_2}{L} - \frac{y}{L}\right) \qquad (29b)$$

$$u_3^2 = 4\left(\frac{r_1}{L} + \frac{y}{L}\right) \qquad (29c)$$

$$u_4^2 = 4\left(\frac{r_2}{L} + \frac{y}{L}\right) \qquad (29d)$$

TABLE 5.—COMPUTATION OF ANGLE α

Assumed value of n	y/L	$y/L - n/2$	$\alpha = 720(y/L - n/2)$ degrees	Sin α	Cos α
(1)	(2)	(3)	(4)	(5)	(6)
1	0.6	0.1	72	+0.951	+0.309
3	1.8	0.3	216	−0.588	−0.809
5	3.0	0.5	360	0	+1.000
7	4.2	0.7	144[a]	+0.588	−0.809
10	6.0	1.0	—	0	+1.000
20	12.0	2.0	—	0	+1.000
30	18.0	3.0	—	0	+1.000
50	30.0	5.0	—	0	+1.000

[a] 504° = 144°.

From Fig. 17, values of S and w are obtained, and the diffraction coefficients and phase differences are then computed.

Numerical Example.—A generalized diagram is to be drawn for diffraction at a breakwater gap whose width is two wave lengths. Thus, $b/L = 2$.

As an illustration, Tables 5 and 6 give a typical setup for computation of diffraction coefficients and phase differences at various positions y/L ranges 0, 1, 2, and 3 from the gap. The positions y/L have been arbitrarily assumed to be multiples "m" of an initial value of $y/L = 0.6$. The sequence of the steps in the calculation process in Tables 5 and 6 is self explanatory. A plot of the diffraction coefficients can be made directly from the data shown in Table 6, from which contours of equal diffraction coefficients can then be constructed, as shown in Fig. 13.

TABLE 6.—CALCULATION OF DIFFRACTION COEFFICIENT FOR BREAKWATER GAP

Assumed Value of n	y/L	$\frac{r_1}{L}$ [a]	u_1^2 [b]	f_1 [c]		u_2^2 [d]	g_1 [c]		$\frac{r_2}{L}$ [a]	u_3^2 [f]	f_2 [c]		u_4^2 [g]	g_2 [c]		M [h, i]
				S_1	w_1		S_2	w_2			S_3	w_3		S_4	w_4	
(1)	(2)	(3)	(4)	(5)	(6)	(7)	(8)	(9)	(10)	(11)	(12)	(13)	(14)	(15)	(16)	(17)
(a) $x/L = 2$ $(K' = f_1 + g_1 - f_2 + g_2)$																
1	0.6	1.166	2.26	−0.069	+0.131	7.06	+0.062	+0.062	3.06	9.84	−0.065	+0.035	14.64	+0.015	+0.057	+0.077
3	1.8	2.06	1.04	−0.116	−0.158	15.44	+0.054	+0.008	3.50	6.80	+0.038	+0.080	21.2	−0.042	−0.025	+0.012
5	3.0	3.16	0.64	+0.013	−0.235	24.6	−0.006	−0.043	4.24	4.96	−0.061	−0.076	29.0	−0.028	−0.029	−0.034
7	4.2	4.32	0.48	+0.096	−0.245	34.1	−0.022	+0.032	5.16	3.84	+0.103	−0.049	37.4	−0.033	−0.006	−0.055
10	6.0	6.08	0.32	+0.175	−0.230	48.3	+0.010	−0.030	6.71	2.84	+0.055	+0.120	50.8	+0.015	+0.030	+0.025
20	12	12.04	0.16	+0.282	−0.184	96.2	+0.010	−0.021	12.37	1.48	−0.169	−0.034	97.5	−0.021	−0.001	−0.011
30	18	18.028	0.112	+0.327	−0.156	144.1	+0.011	−0.014	18.25	1.00	−0.106	−0.167	145.0	−0.013	−0.012	−0.002
50	30	30.017	0.068	+0.365	−0.126	240.1	+0.008	−0.012	30.15	0.60	+0.031	−0.239	240.6	−0.002	−0.014	+0.006
(b) $x/L = 1 = \frac{b}{2}$ Geometric Shadow $(K' = f_1 + g_1 - f_2 + g_2)$																
1	0.6	0.600	0.000	+0.500	0.000	4.80	−0.042	−0.091	2.09	5.96	−0.074	+0.059	10.76	+0.026	+0.053	−0.016
3	1.8	1.800	0.000	+0.500	0.000	14.40	−0.011	+0.057	2.69	3.56	+0.119	0.000	17.96	−0.037	+0.034	−0.048
5	3.0	3.00	0.000	+0.500	0.000	24.0	+0.034	−0.032	3.61	2.44	−0.028	+0.140	26.44	−0.005	+0.040	+0.029
7	4.2	4.20	0.000	+0.500	0.000	33.6	−0.038	+0.006	4.65	1.80	−0.149	+0.054	35.4	+0.032	+0.007	−0.006
10	6.0	6.00	0.000	+0.500	0.000	48.0	+0.023	−0.024	6.33	1.32	−0.161	−0.081	49.3	−0.029	−0.008	−0.006
20	12	12.00	0.000	+0.500	0.000	96.0	+0.017	−0.017	12.17	0.68	−0.012	−0.230	96.7	−0.006	−0.022	+0.011
30	18	18.00	0.000	+0.500	0.000	144.0	+0.013	−0.012	18.11	0.44	+0.106	−0.244	144.4	+0.003	−0.018	+0.016
50	30	30.00	0.000	+0.500	0.000	240.0	+0.011	−0.011	30.07	0.28	+0.197	−0.233	240.3	+0.005	−0.015	+0.016
(c) $x/L = 0$ $(K' = e^{-iky} - f_1 + g_1 - f_2 + g_2)$																
1	0.6	1.166	2.26	−0.069	+0.131	7.06	+0.062	+0.062	1.116	2.26	−0.069	+0.131	7.06	+0.062	+0.062	+0.124
3	1.8	2.06	1.04	−0.116	−0.158	15.44	+0.054	+0.008	2.06	1.04	−0.116	−0.158	15.44	+0.054	+0.008	+0.108
5	3.0	3.16	0.64	+0.013	−0.235	24.6	−0.006	−0.043	3.16	0.64	+0.013	−0.235	24.6	−0.006	−0.043	−0.012
7	4.2	4.32	0.48	+0.086	−0.245	34.1	−0.022	+0.032	4.32	0.48	+0.086	−0.245	34.1	−0.022	+0.032	−0.044
10	6.0	6.08	0.32	+0.175	−0.230	48.3	+0.010	+0.030	6.08	0.32	+0.175	−0.230	48.3	+0.010	−0.030	+0.020
20	12	12.04	0.16	+0.282	−0.184	96.2	+0.010	−0.021	12.04	0.16	+0.282	−0.184	96.2	+0.010	−0.021	+0.020
30	18	18.028	0.112	+0.327	−0.156	144.1	+0.011	−0.014	18.028	0.112	+0.327	−0.156	144.1	+0.011	−0.014	+0.022
50	30	30.017	0.068	+0.365	−0.126	240.1	+0.008	−0.012	30.017	0.068	+0.365	−0.126	240.1	+0.008	−0.012	+0.016
(d) $x/L = 3$ $(K' = f_1 + g_1 - f_2 + g_2)$																
1	0.6	2.09	5.96	−0.074	+0.059	10.76	+0.025	+0.063	4.045	13.78	−0.057	+0.025	18.58	+0.007	+0.024	+0.032
3	1.8	2.69	3.56	+0.119	0.000	17.96	−0.038	+0.034	4.39	10.36	−0.018	+0.066	24.76	−0.015	−0.041	−0.053
5	3.0	3.61	2.44	−0.028	+0.140	26.44	−0.005	+0.040	5.00	8.00	+0.060	−0.053	32.00	+0.027	−0.026	+0.022
7	4.2	4.65	1.80	−0.149	+0.054	35.4	+0.032	+0.007	5.80	6.40	−0.019	+0.086	40.0	+0.026	+0.023	+0.058
10	6.0	6.33	1.32	−0.161	−0.081	49.3	−0.029	−0.008	7.21	4.84	−0.043	−0.089	52.89	−0.014	−0.028	−0.043
20	12	12.166	0.66	+0.004	−0.233	96.7	−0.005	−0.022	12.65	2.60	+0.006	+0.138	98.6	+0.003	+0.023	−0.002
30	18	18.111	0.44	+0.106	−0.244	144.4	+0.003	−0.018	18.44	1.76	−0.153	+0.044	145.8	−0.016	+0.009	−0.013
50	30	30.067	0.27	+0.202	−0.220	240.3	+0.005	−0.015	30.266	1.064	−0.123	−0.150	241.1	−0.011	−0.007	−0.006

[a] Eq. 28a. [b] Eq. 29a. [c] Fig. 17. [d] Eq. 29c. [e] Eq. 28b. [f] Eq. 29b [g] Eq. 29d. [h] $M = S_2 + S_4$. [i] Continued in Col. 18 to 32.

TABLE 6.—(*Continued*)

Assumed Value of n (1)	N[j,k] (18)	$M \cos \alpha$[l] (19)	$-N \sin \alpha$[l] (20)	$S_1 - S_2$ (21)	ΣS (22)	$M \sin \alpha$[l] (23)	$N \cos \alpha$[l] (24)	$w_1 - w_2$ (25)	Σw (26)	w^2 (27)	S^2 (28)	K'[m] (29)	$\frac{w}{S}$ (30)	Phase[n] difference, degrees (31)	$\frac{y}{L}$ (32)
(a) $x/L = 2$ $(K' = f_1 + g_1 - f_2 + g_2)$															
1	+0.119	+0.024	−0.113	−0.004	−0.093	+0.073	+0.037	+0.096	+0.206	0.0424	0.0086	0.226	− 2.215	+114.3	0.6
3	−0.017	−0.009	−0.010	−0.154	−0.173	−0.007	+0.014	−0.238	−0.231	0.0534	0.0299	0.289	+ 1.335	−126.8	1.8
5	−0.072	−0.034	0.000	+0.074	+0.040	0.000	−0.072	−0.159	−0.231	0.0534	0.0016	0.235	− 5.675	− 80.2	3.0
7	+0.026	+0.045	−0.015	−0.017	+0.013	−0.032	−0.021	−0.196	−0.249	0.0620	0.0002	0.249	−19.15	− 87.0	4.2
10	0.000	+0.025	0.000	+0.120	+0.145	0.000	0.000	−0.350	−0.350	0.1225	0.0210	0.379	− 2.414	− 67.5	6.0
20	−0.022	−0.011	0.000	+0.451	+0.440	0.000	−0.022	−0.150	−0.172	0.0296	0.1936	0.472	− 0.3909	− 21.4	12
30	−0.026	−0.002	0.000	+0.433	+0.431	0.000	−0.026	+0.011	−0.015	0.0002	0.1858	0.431	− 0.0348	− 2.0	18
50	−0.026	+0.006	0.000	+0.334	+0.340	0.000	−0.026	+0.113	+0.087	0.0076	0.1156	0.351	+ 0.2559	+ 14.4	30
(b) $x/L = 1 = \frac{b}{2}$ Geometric Shadow $(K' = f_1 + g_1 - f_2 + g_2)$															
1	−0.038	−0.005	+0.036	+0.574	+0.605	−0.015	−0.012	−0.059	−0.086	0.0074	0.3660	0.611	− 0.1421	− 8.1	0.6
3	+0.091	+0.039	+0.053	+0.381	+0.473	+0.028	−0.074	0.000	−0.046	0.0021	0.2237	0.475	− 0.0973	− 5.6	1.8
5	+0.008	+0.029	0.000	+0.528	+0.577	0.000	+0.008	−0.140	−0.132	0.0174	0.3102	0.572	− 0.2370	− 13.3	3.0
7	+0.013	+0.005	0.000	+0.649	+0.646	−0.004	−0.011	−0.054	−0.069	0.0048	0.4173	0.650	− 0.1068	− 6.1	4.2
10	−0.032	−0.006	0.000	+0.661	+0.655	0.000	−0.032	+0.081	+0.049	0.0024	0.4290	0.657	+ 0.0748	+ 4.3	6.0
20	−0.039	+0.011	0.000	+0.512	+0.523	0.000	−0.039	+0.230	+0.191	0.0365	0.2735	0.557	+ 0.3652	+ 20.1	12.
30	−0.030	+0.016	0.000	+0.394	+0.410	0.000	−0.030	+0.244	+0.214	0.0458	0.1681	0.463	+ 0.5220	+ 27.6	18
50	−0.026	+0.016	0.000	+0.303	+0.319	0.000	−0.026	+0.223	+0.197	0.0388	0.1018	0.375	+ 0.6176	+ 31.7	30
(c) $x/L = 0$ $(K' = e^{-iky} - f_1 + g_1 - f_2 + g_2)$															
1	+0.124	+0.038	−0.118	+1.138[o]	+1.058	+0.118	+0.038	−0.262[p]	−0.106	0.0112	1.1194	1.063	− 0.1002	− 5.7	0.6
2	+0.016	−0.087	+0.009	+1.232	+1.154	−0.063	−0.013	+0.316	+0.240	0.0576	1.3317	1.179	+ 0.2080	+ 11.8	1.8
5	−0.086	−0.012	0.000	+0.974	+0.962	0.000	−0.086	+0.470	+0.384	0.1475	0.9254	1.036	+ 0.3992	+ 21.8	3.0
7	+0.064	+0.036	−0.038	+0.828	+0.826	−0.026	−0.042	+0.490	+0.412	0.1697	0.6823	0.923	+ 0.4998	+ 26.5	4.2
10	−0.060	+0.020	0.000	+0.650	+0.670	0.000	−0.060	+0.460	+0.400	0.1600	0.4489	0.780	+ 0.5970	+ 30.8	6.0
20	−0.052	+0.020	0.000	+0.436	+0.456	0.000	−0.042	+0.363	+0.326	0.1063	0.2074	0.561	+ 0.7149	+ 35.6	12
30	−0.028	+0.022	0.000	+0.346	+0.368	0.000	−0.028	+0.312	+0.284	0.0807	0.1354	0.465	+ 0.7717	+ 37.7	18
50	−0.024	+0.016	0.000	+0.270	+0.286	0.000	−0.024	+0.252	+0.228	0.0520	0.0818	0.366	+ 0.7972	+ 38.6	30
(d) $x/L = 3$ $(K' = f_1 + g_1 - f_2 + g_2)$															
1	+0.087	+0.010	−0.083	−0.017	−0.090	+0.030	+0.027	+0.034	+0.091	0.0083	0.0081	0.128	− 1.0111	+134.7	0.6
3	−0.007	+0.043	−.0004	+0.137	+0.176	+0.031	+0.006	−0.066	+0.029	0.0008	0.0310	0.178	− 0.1648	− 9.4	1.8
5	+0.014	+0.022	0.000	−0.088	−0.066	0.000	+0.014	+0.193	+0.207	0.0428	0.0044	0.217	− 3.1364	+107.7	3.0
7	−0.016	−0.047	+0.009	−0.130	−0.168	+0.034	+0.013	−0.032	+0.015	0.0002	0.0282	0.169	− 0.0892	+174.9	4.2
10	−0.036	−0.043	0.000	−0.118	−0.161	0.000	−0.036	+0.008	+0.028	0.0008	0.0259	0.163	+ 0.1739	−170.1	6.0
20	+0.001	−0.002	0.000	−0.002	−0.004	0.000	+0.001	−0.371	+0.370	0.1369	0.0000	0.370	+92.50	− 90.6	12
30	−0.009	−0.013	0.000	+0.259	+0.246	0.000	−0.009	−0.288	−0.297	0.0882	0.0605	0.386	− 1.2073	− 50.4	18
50	−0.022	−0.006	0.000	+0.325	+0.319	0.000	−0.022	−0.070	−0.092	0.0085	0.1018	0.332	− 0.2884	− 16.1	30

[j] $N = w_3 + w_4$. [k] Continued from Col. 1 to 17. [l] Sin α and Cos α from Table 5. [m] $K' = \sqrt{w^2 + s^2}$. [n] Eq. 27. [o] Values in this section of Col. 21 are computed using $1 - S_1 - S_2$. [p] Values in this section of Col. 25 are computed using $-w_1 - w_2$.

A plot of the wave patterns in the lee of the breakwater gap involves additional computations. The "phase difference," as computed in Table 6, is that of Eq. 19, with complete cycles omitted. To express this phase difference in terms of complete cycles, it must be divided by 360°. To obtain the complete phase, the phase of the incident wave must be added to the phase difference.

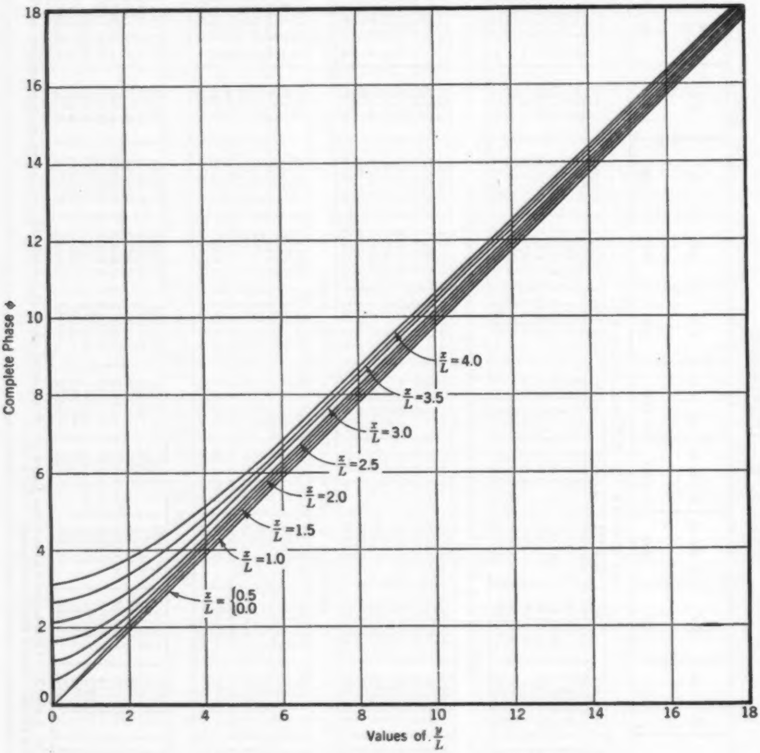

FIG. 18.—BREAKWATER DIFFRACTION FOR GAP WIDTH $b/L = 2$

The phase of the incident wave also is expressed in cycles, that is $\frac{-y}{L+m}$, in which m is an integer. The whole cycles are omitted, both phases being expressed as negative angles, thus indicating a decrease in phase as y increases. In the computations for complete phase for various positions (x/L, y/L) it is usually convenient to make a plot of the phase, ϕ. against values of y/L, as shown in Fig. 18. Since the curve for $x/L = 0$ rises at slightly less than 45°, a 45° line is first drawn lightly on the plot, thus making clear the value of the integer m (or the whole number of cycles) to be added to the phase difference. The computation procedure in arriving at the complete phase is illustrated in

Table 7. Thus, for various of y/L and x/L the corresponding values of phase difference (PD), as computed and shown in col. 31 of Table 6 were first tabulated (minus values of phase difference were subtracted from 360° before tabulation in Table 7. These values of PD were next divided by 360°. Referring to Fig. 18, the integer m was obtained for each value of y/L (for example, for $y/L = 3$, the value of m is equal to the first integer below the $x/L = 0$ line, which is 2). Values of m for the various values of y/L are shown in Table 7.

TABLE 7.—TYPICAL COMPUTATION FOR COMPLETE PHASE

m	y/L	Phase difference, degrees	Col. 3 ÷ 360	Complete phase[a]	Phase difference, degrees	Col. 3 ÷ 360	Complete phase[a]	Phase difference, degrees	Col. 3 ÷ 360	Complete phase[a]
(1)	(2)	(3)	(4)	(5)	(3)	(4)	(5)	(3)	(4)	(5)
		(a) $x/L = 0$			(b) $x/L = 1$			(c) $x/L = 2$		
1	0	360	1.000	0	360	1.000	0	319.7	0.888	0.112
−1	0.6	354.3	0.984	0.616	352.2	0.978	0.622	114.3	0.318	0.282
1	1.8	11.8	0.033	0.767	354.4	0.984	0.816	232.9	0.647	0.153
2	3.0	21.8	0.061	0.939	346.7	0.963	0.037	279.8	0.777	0.223
4	4.2	26.5	0.074	0.126	353.9	0.983	0.217	273.0	0.758	0.442
5	6.0	30.8	0.086	0.914	4.3	0.012	0.988	292.5	0.813	0.187
8	9.0	33.9	0.094	0.906	15.3	0.042	0.958	320.5	0.890	0.110
11	12	35.6	0.099	0.901	20.1	0.056	0.944	338.6	0.941	0.059
14	15	36.9	0.102	0.898	23.4	0.065	0.935	352.0	0.978	0.022
17	18	37.7	0.105	0.895	27.6	0.077	0.923	358.0	0.994	0.006

[a] $-\frac{PD}{360} + \frac{y}{L} - m.$

TABLE 8.—BREAKWATER DIFFRACTION TABULATION

Values of ϕ	Values of y/L								
	0	0.5	1.0	1.5	2.0	2.5	3.0	3.5	4.0
0	0	0	0	—	—	—	—	—	—
1	1.00	1.00	0.95	0.75	—	—	—	—	—
2	2.05	2.05	1.95	1.90	1.65	1.10	—	—	—
3	3.10	3.10	3.00	2.90	2.75	2.50	2.05	1.30	—
4	4.05	4.05	4.00	3.90	3.75	3.65	3.35	3.00	2.45
5	5.05	5.05	5.00	4.85	4.75	4.70	4.50	4.25	3.85
6	6.10	6.10	6.00	5.90	5.80	5.70	5.50	5.35	5.05
7	7.10	7.10	7.00	6.95	6.85	6.70	6.55	6.40	6.20
8	8.10	8.10	8.05	7.95	7.85	7.75	7.60	7.45	7.20
9	9.10	9.10	9.05	8.95	8.90	8.80	8.65	8.50	8.25
10	10.10	10.10	10.05	10.00	9.90	9.80	9.70	9.55	9.30
11	11.10	11.10	11.05	11.00	10.95	10.85	10.75	10.60	10.40
12	12.10	12.10	12.05	12.00	11.95	11.85	11.75	11.60	11.45
13	13.10	13.10	13.05	13.00	12.95	12.90	12.80	12.65	12.50
14	14.10	14.10	14.05	14.00	13.95	13.90	13.80	14.70	13.55
15	15.10	15.10	15.05	15.00	15.00	14.90	14.80	14.70	14.60
16	16.10	16.10	16.05	16.05	16.00	15.95	15.85	15.75	15.60
17	17.10	17.10	17.05	17.05	17.00	16.95	16.85	16.75	16.65
18	—	—	—	—	18.00	17.95	17.85	17.75	17.65

The remaining steps consist of the summation of the terms $(-\overline{\mathrm{PD}}/360)$, (y/L) and $-m$, for each value of x/L, using

$$\frac{-\mathrm{PD}}{360} + \frac{y}{L} - m = \text{complete phase} \quad \text{..............(30)}$$

The remaining curves of phase (for x/L = constant) now may be drawn by starting at $x/L = 0$ with phases taken from Table 7, due allowance being made for the value of m, or the complete cycles. Each curve of (x/L = constant) lies above and approximately parallel to the preceding curve as higher values of y/L are used.

Points for the wave pattern are computed by noting from the curves shown in Fig. 18 the values of y/L at which the phases for x/L = constant reached integral values. These points are tabulated in Table 8. Wave patterns now may be drawn as curves joining the points having the same integral phases. The patterns for the gap width of 2 L are shown in Fig. 13, together with the contours of equal diffraction coefficients.

DISCUSSION

M. E. STELZRIEDE[43].—The impetus provided by World War II and the post-war interest in harbor design have resulted in a number of analytical solutions of the diffraction problem as related particularly to water waves. Three of these solutions appear to lend themselves most readily to a study of this hydrodynamic phenomenon. One theoretical approach is demonstrated by Mr. Johnson. A second is adapted from the work of P. M. Morse and P. J. Rubinstein,[44] and a third was developed by Mr. Lacombe.[45] The close agreement between the results of these independent methods is significant.

The diffraction-diagram approach illustrated by Mr. Johnson is especially useful when it is desirable to predict wave patterns over large areas of a harbor. These diagrams represent graphically the solution of W. G. Penney and A. T. Price,[46] as refined and simplified by J. A. Putnam and R. S. Arthur,[34] and by F. L. Blue, Jr., and the author.[35] The approximations applied in constructing the diagrams for the semi-infinite breakwater impose certain limitations on the use of the diagram which are generally not severe. One of these restrictions relates to the angle between the breakwater and the diffraction axis, which (as Mr. Johnson shows) should lie somewhere between the limits of 45° and 135°. The deviation of this simplified solution from the complete Penney-Price solution at short distances from the terminus is discussed by the Scripps Institution of Oceanography.[47] A good minimum limit of distance appears to be about three wave lengths; and, even at this distance, the error may become large, percentagewise, at points that lie at a large angular distance from the diffraction axis. The energy level in that area, fortunately, is very low in any case so the error in terms of absolute wave height is small.

The diffraction diagram for a breakwater gap is constructed by superposing complete Penney-Price solutions for two semi-infinite breakwaters separated by a gap of the desired width. The composite solution so obtained is no longer exact because of the influence of one arm of the breakwater on the diffractive function performed by the other. For very small openings the error in boundary conditions becomes infinite; but when the gap size is about two wave lengths or more, this error is not excessive, and, for very large openings, it is insignificant. It is interesting to note that, although Mr. Johnson's diffraction diagram is for a breakwater opening that is toward the lower limit of the acceptable

[43] Research Engr., Hydr. Structures Lab., California Inst. of Technology, Pasadena, Calif.

[44] "The Diffraction of Waves by Ribbons and by Slits," by P. M. Morse and P. J. Rubinstein, *The Physical Review*, December 1, 1938, Vol. 54, pp. 895-898.

[45] "Diffraction de la Houle par une Breche," by Henri Lacombe, *Bulletin d'Information du Comité d'Océanographie et d'Etude des Côtes, No. 2*, 4th Year, February, 1952 (published by Service Hydrographique de la Marine).

[46] "Diffraction of Sea Waves by Breakwaters," by W. G. Penney and A. T. Price, Directorate of Miscellaneous Weapons Development History No. 26, Artificial Harbors, Sec. 3D, London, England, 1944.

[47] "Application of a Solution of the Water Wave Diffraction Problem," *Wave Project Report No. 42*, Scripps Inst. of Oceanography, La Jolla, Calif., 1945.

range, the curves agree remarkably well with those obtained from other solutions.

The Morse-Rubinstein approach to the diffraction problem was originally developed for the diffraction of electromagnetic waves by ribbons and by slits in an infinite plane,[44] and the theory has been substantially verified in the wave basin at the Hydraulic Structures Laboratory of the California Institute of Technology in Azusa. Although the solution is difficult to compute manually because of the series of Mathieu functions involved, it possesses several valuable features. The solution is exact, for example, for openings of any size, although the series converge best for very small gaps. The solution applies directly to oblique angles of approach as low as zero degrees, as well as to the condition of normal wave approach. This method determines the energy distribution leeward of the breakwater in terms of an intensity factor proportional to the square of the wave height. To find the intensity at a point whose polar coordinates are (R, ϕ) with respect to the center of a gap of given width B/L and an approach angle θ find the intensity factor corresponding to the direction of the point in question. The intensity at (R, ϕ) as a fraction of the incident wave intensity, then, is this intensity factor divided by R/L. Intensity factors have been computed and plotted[48] for openings 0.5 L, 1.0 L, 2.0 L, and 3.0 L, and for approach angles of 0°, 15°, 30°, 45°, 60°, 75°, and 90°.

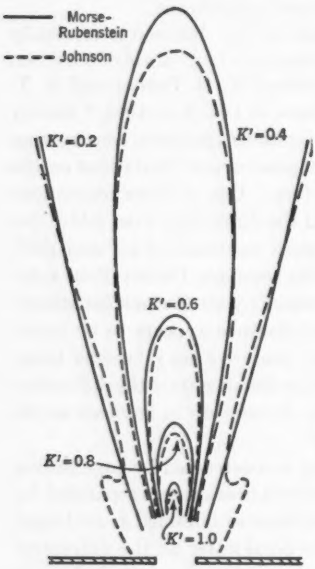

FIG. 19.—COMPARISON OF DIFFRACTION DIAGRAMS

Fig. 19 shows a comparison on a wave height basis of Mr. Johnson's diffraction diagram for a gap of 2.0 L and a similar one is derived from the Morse-Rubinstein equations. It is encouraging to note that the maximum distance between corresponding curves using the two methods is of the order of but 7% or 8% of the distance to the origin. The secondary lobes near the base of the Johnson curves appear also on the Morse-Rubinstein curves in a somewhat different direction, although they are not shown in Fig. 19.

The Lacombe solution, derived directly from Huyghens' principle and expressed in terms of trigonometric functions, appears to be easiest of all to compute. Mr. Lacombe's paper (referred to in this discussion) demonstrates the striking similarity between the Morse-Rubinstein polar intensity curves for various openings and for various approach angles, and those obtained by the Lacombe equations. For approach angles of 45° or greater the two solutions

[48] "Diffraction of Water Waves by Breakwaters," by John H. Carr and M. E. Stelzriede, *Circular 521*, National Bureau of Standards, U. S. Dept. of Commerce, Washington, D. C., November 28, 1952, pp. 109–125.

produce almost identical results. The similarity breaks down somewhat for very small approach angles and for very small gaps, but these energy curves, as Mr. Lacombe shows, exaggerate the real differences in wave height predicted by the two methods.

In the experience of the Hydraulic Structures Laboratory, it has been found that, at nominal distances from the center of a gap, five wave lengths or more in width, wave heights (as Mr. Johnson suggest) may be determined simply by the application of the diffraction diagram for the semi-infinite breakwater to each of the two arms of the breakwater. At distances very large compared to the gap width, however, the two diffraction patterns appear to be no longer independent of each other. It then becomes advisable to construct a diffraction diagram for a gap as in Fig. 13, or to use some method that will achieve the same purpose.

In this connection, a modified Morse-Rubinstein curve may be used, in which the curve for the proper approach angle and for a gap of 3.0 L (the largest for which the curves are plotted) is used with only its scale altered. This adoption is made because the curves for intensity distribution for very large openings change but little in geometrical form from the long, slim loops of the curves of 3.0 L. The new scale is such that the maximum intensity factor is equal to the square of the gap width in wave lengths. When incidence is oblique. the opening size to be squared is the projected gap width, or—as Mr. Johnson refers to it—the "imaginary equivalent gap." With this modified curve, the wave height at a particular point is computed in the usual manner, and the method has been found satisfactory for all except the very acute approach angles.

J. W. Johnson,[49] M. ASCE.—In the short time since the writer's paper was submitted for publication additional research and study have been made on many of the problems presented in the paper. A brief summary of these developments is presented here.

The theory and extent of field observations on the generation and decay of wind waves have been extended, with the result that wave characteristics can be estimated with a much better degree of accuracy than was previously possible.[50] For the benefit of the practicing engineer these data have been summarized in convenient charts which permit the making of rapid estimates of wave characteristics from wind data.[7] Special problems, such as the forecasting of waves generated by near-coastal storms, have been discussed in detail in the literature.[51]

In connection with wave refraction on a shoaling bottom, considerable progress has been made in the improvement of the orthogonal method for the preparation of refraction diagrams. This work has been directed toward

[49] Prof. of Hydr. Eng., Univ. of California, Berkeley, Calif.

[50] "The Generation and Decay of Wind Waves in Deep Water," by C. L. Bretschneider, *Transactions*, Am. Geophysical Union, Vol. 33, No. 3, June 1952, pp. 381-389.

[51] "Near-Coastal Storms and Associated Waves," by D. K. Todd and R. L. Wiegel, *Transactions*, Am. Geophysical Union, Vol. 33, No. 2, April, 1952, pp. 217-225.

drawing orthogonals seaward from the shore[52,53] as well as deriving refraction coefficients directly from a single orthogonal.[54] Some work has been done on the comparison of observed wave directions with those obtained by means of a refraction diagram.[55] Besides the study of refraction caused by underwater topography, both theoretical and experimental work has been completed on refraction by currents.[56,57] The problem of wave reflection—both at structures[58] and in the surf zone[59]—has been investigated. To a varying extent, wave reflection is involved in those problems that are concerned with the damping action when waves pass over a submerged barrier[60] or through a pile structure.[61]

The more recent work on wave diffraction at breakwater gaps has been presented by Mr. Stelzriede. Little can be added to his discussion other than to point out that wave diffraction diagrams for breakwater gaps of various widths have been prepared and assembled into convenient form for the design engineer.[41] These diagrams were computed by the method of John H. Carr, J.M. ASCE, and Mr. Stelzriede[36] for relatively narrow gaps and by the procedure of F. L. Blue, Jr., and the writer[35] for the wider gaps. These diagrams pertain to gaps ranging in width from ½ wave length to 5 wave lengths, with the direction of wave approach normal to the gap. Diagrams also are provided to permit the preparation, by interpolation, of diffraction diagrams for any specific width. This simplified procedure for constructing diffraction diagrams is acceptable in the majority of design problems in which the accuracy with which the design wave data are known usually does not justify great refinement.

---

[52] "A Method for Drawing Orthogonals Seaward from Shore," by Thorndike Saville, Jr., *Bulletin*, Beach Erosion Board, Corps of Engrs., Washington, D. C., Vol. 5, No. 4, October 1, 1951, pp. 1–6.

[53] Discussion by Kenneth Kaplan of "A Method for Drawing Orthogonals Seaward from Shore," by Thorndike Saville, Jr., *ibid.*, Vol. 6, No. 1, January 1, 1952, pp. 18–21.

[54] "Wave Intensity Along a Refracted Ray," by W. H. Munk and R. S. Arthur, *Wave Report No. 95*, Scripps Inst. of Oceanography, La Jolla, Calif., June 1, 1951 (publication pending).

[55] "Comparison of Observed Wave Direction with a Refraction Diagram," by D. R. Forrest, *Bulletin*, Beach Erosion Board, Corps of Engrs., Washington, D. C., Vol. 5, No. 2, April 1, 1951, pp. 24–25.

[56] "Refraction of Shallow Water Waves: The Combined Effect of Currents and Underwater Topography," by R. S. Arthur, *Transactions*, Am. Geophysical Union, Vol. 31, No. 4, August, 1950, pp. 549–552.

[57] "Breaking of Waves by an Opposing Current," by Y-Yuan Yu, *ibid.*, Vol. 33, No. 1, February, 1952, pp. 39–41.

[58] "Reflection of Solitary Waves," by J. M. Caldwell, *Technical Memorandum No. 11*, Beach Erosion Board, Corps of Engrs., Washington, D. C., 1949.

[59] "Total Reflection of Surface Waves by Deep Water," by J. D. Isaacs, E. A. Williams, and C. Eckart, *Transactions*, Am. Geophysical Union, Vol. 32, No. 1, February, 1951, pp. 37–40.

[60] "The Damping Action of Submerged Breakwaters," by J. W. Johnson, R. A. Fuchs, and J. R. Morison, *ibid.*, Vol. 32, No. 5, October, 1951, pp. 704–718.

[61] "Damping of Water Waves by Vertical Circular Cylinders," by R. D. Costello, *ibid.*, Vol. 33, No. 4, August, 1952, pp. 513–519.

WAVE FORCES ON BREAKWATERS

By Robert Y. Hudson,[1] M. ASCE

With Discussion by Messrs. Kenneth Kaplan, R. G. Hennes and C. E. Leonoff, and Robert Y. Hudson

Synopsis

This paper reviews the common theories for determining the magnitude and distribution of wave forces on vertical walls and sloping, rubble-mound breakwaters and compares these theories, selecting the best available for use. The results of the better theories are compared with experimental data, and an outline is given of experimental investigations considered necessary to obtain data sufficient for the design of economical and safe breakwaters.

Introduction

The two principal types of breakwaters are: (*a*) Vertical-wall structures; and (*b*) those with sloping faces constructed of rubble. Each of these types offers certain advantages, depending primarily on location and exposure to wave action. Because of the complexity of the phenomena, whereby waves exert forces on breakwaters, it is difficult to arrive at a rational basis for determining the magnitude and distribution of forces with sufficient accuracy to insure that both safe and economical designs are obtained. Design engineers make use of theoretical and empirical formulas, several of which are explained in this paper, but there is no formula available that has won the complete confidence of the engineering profession. It has become possible to calculate with reasonable accuracy the height, length, and direction of design waves as a function of fetch and wind velocity, duration, and direction.[2] It has also become possible to chart selected design waves from deep water into shallow water and determine wave characteristics at the location of proposed breakwaters.[3] There is an urgent need for methods by which breakwaters may be designed with an accuracy compatible with the accuracy with which

Note.—Published in January, 1952, as *Proceedings-Separate No. 113*. Positions and titles given are those in effect when the paper or discussion was received for publication.

[1] Hydr. Engr.; Chf., Wave Action Section, Waterways Experiment Station, Vicksburg, Miss.

[2] "Wind, Sea, and Swell: Theory of Relations for Forecasting," by H. U. Sverdrup and W. H. Munk, Hydrographic Office, U. S. Navy, Washington, D. C., 1947.

[3] "Breakers and Surf, Principles in Forecasting," Hydrographic Office, U. S. Navy, Washington, D. C., 1944.

design-wave characteristics can be determined. Although the science of waves and wave action on breakwaters is not exactly in its infancy (some of the best mathematicians and engineers having worked on it since about 1800), the design of breakwaters is yet to be placed on a sound scientific basis in which known safety factors can be selected. The purpose of this paper, therefore, is threefold: (1) To review the most important theories pertaining to wave forces on breakwaters; (2) to compare these theories and select the best available for use at the present time; and (3) to compare the results of the better theories with experimental data and point out the type of additional information required to satisfy the demands of design engineers.

Notation.—Letter symbols are defined where they first appear and are assembled alphabetically for convenience of reference in Appendix I.

Vertical-Wall Breakwaters

Vertical-wall breakwaters are usually considered most efficient when the structure is to be situated in water of considerable depth or when stone for construction of a rubble mound is not available at economical prices. If water is of sufficient depth to prevent the breaking of waves (that is, the depth of water below still-water level (d) is greater than the wave height (H) from trough to crest) and if wave heights are relatively small, standing waves are formed with accompanying pressures for which fairly accurate theoretical formulas exist giving their overturning effect on the structure. However, as the waves increase in magnitude, available evidence indicates that pressures become larger than predicted by available theory. Also, if waves break on a vertical wall, localized pressures may be produced that are several times greater than those resulting from nonbreaking waves.

Wave Theories.—The bases upon which some of the most important theories of wave force on vertical breakwaters are founded are the mathematical works of Franz V. Gerstner,[4] and Barre de St. Venant and A. Flamant.[5] Mr. Gerstner, in 1802, obtained an exact solution of the equations of motion for deep-water waves. However, his solution is based on geometrical considerations rather than the fundamental equations of motion. Also, the motion is rotational, and the waves cannot be generated by natural forces. The parametric equations that define the Gerstner wave form referred to rectangular axes x and y, and in terms of the parameter x_o, are:

$$x = x_o - r \sin \frac{2 \pi x_o}{L} \qquad (1a)$$

$$y = y_o + h_s + r \cos \frac{2 \pi x_o}{L} \qquad (1b)$$

in which x is the abscissa and y is the ordinate of a particle in wave motion; x_o and y_o are the abscissa and ordinate, respectively, of a particle at rest; r is the horizontal radius of the orbital ellipse; L is the wave length; and h_s is the distance of a particle's orbital axis above the plane of rest.

[4] "Theorie der Wellen," by Franz V. Gerstner, *Abhandlungen der königlichen Bohmischen Gesellschaft der Wissenschaften*, Prague, Czechoslovakia, 1802.

[5] "De la Houle et du Clapotis," by Barre de St. Venant and A. Flamant, *Annales des ponts et chaussées*, Paris, France, 1888.

These equations define trochoids with the y-axis through a crest and the x-axis on the still-water level (SWL). The curves are generated by a point P that lies at a distance r from the center of a circle of circumference L that rolls on a line at a distance $L/(2\pi)$ above the orbital axis. The tracing point P describes a wave form with the orbital axis $y = y_o + h_z$. The undisturbed level of this wave form is $y = y_o$. The term y_o is always negative or equal to zero. The method by which the wave form may be determined geometrically and the relations between the variables described are shown by Fig. 1.

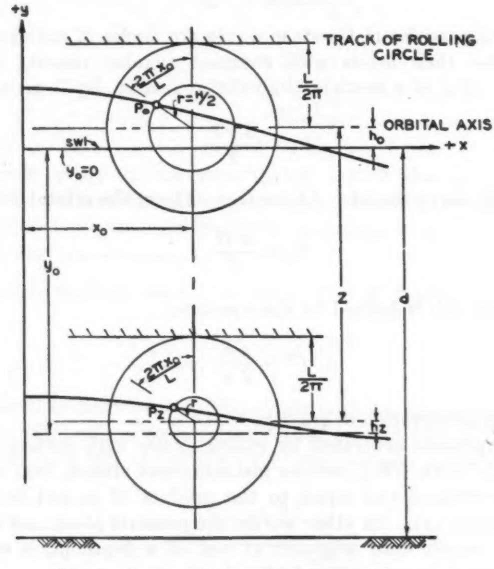

FIG. 1.—GEOMETRICAL DETERMINATION OF WAVE FORM

The following relations are in strict accord with the general equations of hydrodynamics:

$$h_s = \frac{\pi r^2}{L} \quad \text{(2a)}$$

When $y_o = 0$, radius $r = H/2$, and Eq. 2a becomes:

$$h_o = \frac{\pi H^2}{4L} \quad \text{(2b)}$$

in which h_o is the distance of the surface particles' orbital axis above SWL. Eq. 2b is the value of h_s corresponding to the free surface. Also:

$$r = \frac{H}{2} e^{2\pi z/L} \quad \text{(3a)}$$

in which e is the base of natural logarithms and z, as defined in Fig. 1, is:

$$z = y_o + h_s - h_o \qquad (3b)$$

Eq. 3a is not an explicit formula for r, since the value of h_s in Eq. 3b depends on r, but it can be solved by successive approximations. However, since the term $h_s - h_o$ in Eq. 3b is small, approximately:

$$r = \frac{H}{2} e^{2\pi y_o / L} \qquad (4)$$

The orbits of particles in Gerstner waves are circles of radius r, and these particles describe their orbits with constant angular velocity $2\pi/T$. The orbital velocity (V_s) of a particle originally at rest at depth y_o is:

$$V_s = \frac{2\,\pi\, r}{T} \qquad (5a)$$

in which T is the wave period. At the free surface, the orbital velocity V_o is:

$$V_o = \frac{\pi\, H}{T} \qquad (5b)$$

The wave celerity (C) is defined by the equation:

$$C^2 = \frac{g\, L}{2\, \pi} \qquad (6)$$

in which g is the acceleration of gravity.

All of the trochoids generated by rolling circles with centers at different depths ($y_o + h_s$) below SWL become instantaneous stream lines along which the pressure is constant and equal to the product of y_o and to the specific weight of the liquid (γ). In other words, the pressure along any stream line, the particles of which were originally at rest at a depth y_o, is equal to the hydrostatic pressure corresponding to the depth y_o.

Although the Gerstner theory affords a mathematically exact solution to a type wave that approximates observed wave characteristics in deep water, it does not describe the characteristics of waves in shallow water. In 1888 Mr. de St. Venant and Mr. Flamant[5] generalized the Gerstner theory of the orbital motion by assuming the particle orbits to be ellipses. They obtained the following equations for the wave form:

$$x = x_o - r \sin \frac{2\,\pi\, x_o}{L} \qquad (7a)$$

and

$$y = y_o + h_s + r' \cos \frac{2\,\pi\, x_o}{L} \qquad (7b)$$

in which r' is the vertical radius of orbital ellipse (in deep water $r = r'$). For these waves,

$$h_s = \frac{\pi\, r\, r'}{L} \qquad (8)$$

The stream lines described by Eq. 7 have been called elliptical trochoids, although the curves cannot be determined by a rolling motion as in the case of simple trochoids. The orbital motion defined by these equations does not conform exactly to the continuity equation, as do those for the Gerstner waves. However, the following equations, which define orbital radii, are approximate solutions of the continuity equation:

$$r = (H/2)\,\frac{\cosh \frac{2\,\pi}{L}\,(d + y_o)}{\sinh \frac{2\,\pi\,d}{L}} \qquad (9a)$$

$$r' = (H/2)\,\frac{\sinh \frac{2\,\pi}{L}\,(d + y_o)}{\sinh \frac{2\,\pi\,d}{L}} \qquad (9b)$$

These equations satisfy the condition that $r' = H/2$ when $y_o = 0$, and $r' = 0$ when $y_o = -d$. Other relations between the variables of the elliptical trochoid theory for waves in water of finite depth, according to Messrs. de St. Venant and Flamant, are:

a. At the free surface, when $y_o = 0$ and $r' = H/2$, Eq. 8 becomes

$$h_o = \frac{\pi\,H^2}{4\,L}\coth\frac{2\,\pi\,d}{L} \qquad (10)$$

b. The particles describe elliptical orbits with an angular velocity that is not constant. The orbital crest velocity at any depth (V_c) is $2\,\pi\,r/T$, and for a particle initially at rest at depth y_o, the crest velocity of the particle is

$$V_{sc} = \frac{\pi\,H}{T}\,\frac{\cosh \frac{2\,\pi}{L}\,(d + y_o)}{\sinh \frac{2\,\pi\,d}{L}} \qquad (11a)$$

At the free surface $y_o = 0$, and $V_{oc} = \frac{\pi\,H}{T}\coth\frac{2\,\pi\,d}{L}$ (11b)

c. The wave celerity is $C^2 = \frac{g\,L}{2\,\pi}\tanh\frac{2\,\pi\,d}{L}$ (12)

which becomes $C^2 = \frac{g\,L}{2\,\pi}$ as d/L approaches infinity, and $C^2 = g\,d$ as d/L approaches zero.

d. The pressure along any elliptically trochoidal stream line is approximately constant and is equal to:

$$\frac{p}{\gamma} = z + \frac{g\,T^2}{2\,L^2}\left[\frac{H^2}{4} - \left(\frac{2\,\pi\,r\,L}{g\,T^2}\right)^2\right] - \left(\frac{2\,\pi\,L}{g\,T^2} - r'\right)\cos\frac{2\,\pi\,x_o}{L} \qquad (13)$$

in which p is the pressure intensity.

Wave-Pressure Theories.—Thomas Stevenson (1842–1858)[6] and D. D. Gaillard (1890–1903)[7] made extensive dynamometer measurements of wave forces on breakwaters and shoreline structures. However, the accuracy of their measuring equipment was not adequate, and the manner in which the data were obtained did not permit accurate determination of the magnitude and distribution of the pressures or the correlation of pressures with wave dimensions.

In 1890 Mr. L. d'Auria[8] calculated the pressure of waves on a vertical wall by applying the principle of "quantity of motion" (momentum). Dividing the quantity of motion, $H\,L\,C/(2\,g)$, by the duration of motion, $L/(2\,C)$, he obtained the mean pressure,

$$\frac{p}{\gamma} = \frac{H\,C^2}{g} \qquad (14)$$

that was assumed to be equally distributed over the height of the wave, presumably about the SWL. To this pressure was added the hydrostatic pressure corresponding to the depth of water at the crest position of the wave. The sum of these pressures was taken as the maximum on the structure acting shoreward. If there is water on both seaward and shoreward sides of the structure and if there exists no wave action on the shoreward side, the net unbalanced overturning pressure is obtained by subtracting from the sum of the two pressures mentioned the hydrostatic pressure corresponding to the SWL depth.

A method somewhat similar to that of Mr. d'Auria but utilizing to some extent the wave theories of Messrs. Gerstner and de St. Venant and Mr. Flamant, was proposed in 1926 by Jorge Lira Orrego.[9] The Lira theory is explained as follows: At the instant when the highest point of the wave crest comes in contact with the vertical wall, there is a pressure of the static type because of the height of the wave crest above SWL, and a dynamic pressure, extending from the wave crest to the bottom, caused by the wave particles that at this instant are at the upper part of their elliptical orbits and have the corresponding orbital velocities given by Eq. 11. Mr. Lira assumes the height of the wave crest above SWL to be $H/2 + h_o$, in which from Eqs. 2 and 9*a*,

$$h_o = \frac{\pi\,H^2}{4\,L} \coth^2 \frac{2\,\pi\,d}{L} \qquad (15)$$

The hydrostatic SWL pressure is deducted from the sum of the static and dynamic pressures to obtain the net pressure acting shoreward if the structure has water on its inner side without wave action. The dynamic pressure created by the cresting wave, according to Mr. Lira, is given by the equation:

$$\frac{p_s}{\gamma} = \frac{k\,V_c^2}{2\,g} \qquad (16)$$

[6] "The Design and Construction of Harbours," by Thomas Stevenson, Adam Black, and Charles Black, 3rd Ed., Edinburgh, Scotland, 1886.

[7] "Wave Action in Relation to Engineering Structures," by D. D. Gaillard, U. S. Govt. Printing Office, Washington, D. C., 1904.

[8] "On the Force of Impact of Waves and the Stability of the Superstructure of Breakwaters," by L. d'Auria, *Journal*, Franklin Inst., Vol. 130, 1890, p. 373.

[9] "Breakwaters or Jetties in Tideless Seas," by Jorge Lira Orrego, *Report No. 29*, XIVth International Cong. of Navigation, Cairo, Egypt, 1926.

The coefficient k was assumed to have a value of 4. By substituting this value and the expression for V_e (Eq. 11) in Eq. 16, the equation for dynamic pressure is obtained:

$$\frac{p_e}{\gamma} = \frac{2\,\pi^2\,H^2}{g\,T^2} \frac{\cosh^2 \frac{2\,\pi}{L}(d + y_o)}{\sinh^2 \frac{2\,\pi\,d}{L}} \quad \text{(17a)}$$

When $y_e = 0$, at the free surface,

$$\frac{p_o}{\gamma} = \frac{2\,\pi^2\,H^2}{g\,T^2} \coth^2 \frac{2\,\pi\,d}{L} \quad \text{(17b)}$$

When $y_e = -d$, at the bottom,

$$\frac{p_d}{\gamma} = \frac{2\,\pi^2\,H^2}{g\,T^2 \sinh^2 \frac{2\,\pi\,d}{L}} \quad \text{(17c)}$$

In 1938 Ramon Iribarren Cavanilles[10] modified portions of the de St. Venant and Flamant theory and obtained equations for the static and dynamic pressures caused by waves on a vertical wall. The static pressures were calculated, based on those in a trochoidal movement at any depth, and are less than those of Mr. Lira. The Iribarren dynamic-pressure equations introduce the wave celerity instead of orbital velocity, as did those of Mr. d'Auria, and the resulting pressures are greater than those found by the Lira formula. Mr. Iribarren determines the height of the wave axis above SWL (h_o) to be the same as that given by Messrs. de St. Venant and Flamant (Eq. 10). The dynamic pressures $\left(\frac{p}{\gamma}\right)_{dy}$ assumed to act at orbital crests at distances from the SWL of

$$y = y_e + h_o + H \frac{\sinh \frac{2\,\pi}{L}(d + y_o)}{\sinh \frac{2\,\pi\,d}{L}} \quad \text{(18)}$$

are given by the equation:

$$\left(\frac{p}{\gamma}\right)_{dy} = \left(\frac{H}{2}\right) \frac{\cosh \frac{2\,\pi}{L}(d + y_o)}{\cosh \frac{2\,\pi\,d}{L}} \quad \text{(19)}$$

The corresponding static pressures, acting at depths y_o, are

$$\left(\frac{p}{\gamma}\right)_s = \left(\frac{p}{\gamma}\right)^2_{dy} \frac{\pi}{L} \coth \frac{2\,\pi\,d}{L} + \left(\frac{p}{\gamma}\right)_{dy} \quad \text{(20)}$$

If y is positive, the crest considered is above SWL and, therefore, becomes an additional component of the static pressure to be added to that given by Eq. 20.

[10] "Diques de Abrigo en Puertos," by Marciano Martinez Catena, *Revista de Obras Públicas, No. 2715*, July, 1941. (*Translation No. 44-1*, Waterways Experiment Station, Corps of Engrs., U. S. Army, Vicksburg, Miss., 1944.)

The d'Auria, Lira, and Iribarren solutions have been called the static-dynamic methods. The principal objections to these methods are: (*a*) They are based on the calculation of particle velocities at the crest of their elliptical orbits, which orbits cannot be followed at a vertical wall. (In other words, the methods assume that the breakwater does not disturb the wave movement, and the pressures are those that would be produced against a plane suddenly inserted at a wave crest); and (*b*) the theories do not explain observed phenomena at vertical breakwaters, such as the large quantities of water that pass over them without spray, and the considerable velocities that obtain at the base of vertical walls during wave attack.

In 1923 Victor Benezit[11] introduced a method that was the first to consider the effects of standing waves, or clapotis, on a vertical wall. The Benezit calculations were based upon the Gerstner theory.

"Clapotis" is a French term that refers to the phenomenon in which a series of progressive waves is reflected by a vertical surface perpendicular to the advancing waves and produces standing waves seaward of the structure. The equations of motion were obtained by superimposing opposite trains of progressive deep-water waves. The wave height of the clapotis was found to be $2\,H$, and the height of the orbital axis of these waves above SWL was assumed to be the same as that of the unobstructed waves (Eq. 2*b*). The pressure at a depth $d = L/2$ was assumed to be $\gamma d = \gamma L/2$. The derived pressure equation is

$$\frac{p}{\gamma} = z + \frac{\pi H^2}{2\,L} \left(e^{4\pi z/L} - \tfrac{1}{2}\right) \dots\dots\dots\dots\dots\dots (21)$$

These pressures are applied at distances r above and below the orbital axes, where

$$r = H\, e^{2\pi z/L} \dots\dots\dots\dots\dots\dots\dots\dots (22)$$

This is twice the radius of the orbits described by particles of the unobstructed wave, as given by Eq. 3. The resulting pressure curves give the pressures on the seaward side of the breakwater for the crest and trough positions of the clapotis. If still water exists on the shoreward side of the structure, the net unbalanced pressure is obtained for both the crest and trough positions of the wave by subtracting the SWL hydrostatic pressure. Mr. Benezit assumed that $d = L/2$ regardless of the actual depth in which the breakwater was situated.

In 1928 George Sainflou[12] published a theory for calculating pressures on vertical breakwaters in finite depths. Mr. Sainflou superimposed two opposite trains of progressive elliptically trochoidal waves to obtain standing elliptically trochoidal waves, which type of motion, according to him, occurs in front of a vertical wall. The superimposing of elliptically trochoidal waves is not possible, rigorously, and further approximations other than those inherent in the progressive, shallow-water wave theory were necessary. In the resulting

[11] "Les digues maritimes verticales," by Victor Benezit, *Annales des Ponts et Chaussées*, Paris, France, 1923.

[12] "Essai sur les digues maritimes verticales," by George Sainflou, *ibid*, 1928. (Translated copy on file in the office of the Div. Engr., Great Lakes Div., Corps of Engrs., U. S. Army, Chicago, Ill., 1938.)

wave movement (clapotis) a particle with coordinates (x_o, y_o) at rest describes an orbit represented by the equations

$$x = x_o + 2\,r \sin\frac{2\,\pi\,t}{T}\cos\frac{2\,\pi\,x_o}{L} \quad \text{(23a)}$$

and

$$y = y_o + \frac{4\,\pi\,r\,r'}{L}\sin^2\frac{2\,\pi\,t}{T} + 2\,r'\sin\frac{2\,\pi\,t}{T}\sin\frac{2\,\pi\,x_o}{L} \quad \text{(23b)}$$

The maximum and minimum ordinates of the particle initially at rest at point x_o, y_o differ by the amount $4\,r'\cos\frac{2\,\pi\,x_o}{L}$. Hence, the wave height of the clapotis is $4\,r'$, or twice the height of the unobstructed wave. The crests of the clapotis orbits stand at a height $\frac{4\,\pi\,r\,r'}{L} + 2\,r'$ above the level y_o. The first term of this expression represents the maximum value of the mean level of the particle orbit above the particle at rest, or

$$h_s = \frac{4\,\pi\,r\,r'}{L} \quad \text{(24a)}$$

For the free surface, $y_o = 0$, $r' = \frac{H}{2}$, and $r = \frac{H}{2}\coth\frac{2\,\pi\,d}{L}$ (from Eq. 9), and

$$h_o = \frac{\pi\,H^2}{L}\coth\frac{2\,\pi\,d}{L} \quad \text{(24b)}$$

This is four times the corresponding value of h_o for the unobstructed wave, as given by Eq. 10. The Sainflou expression for pressure on a vertical wall is

$$\frac{p}{\gamma} = y_o \pm H\sin\frac{2\,\pi\,t}{T}\left[\frac{\cosh\frac{2\,\pi}{L}(d + y_o)}{\cosh\frac{2\,\pi\,d}{L}} - \frac{\sinh\frac{2\,\pi}{L}(d + y_o)}{\sinh\frac{2\,\pi\,d}{L}}\right] \quad \text{(25a)}$$

When $\sin\frac{2\,\pi\,t}{T} = \pm 1$, Eq. 25a gives pressures for points situated a distance $2\,r'$ above and below the orbital axis $y_o + h_s$. When the clapotis is in a crest position on the wall, this equation represents a curve with a pressure of zero at height $H + h_o$ above SWL, and a pressure at the bottom $(y_o = -d)$ of

$$\frac{p}{\gamma} = d + \frac{H}{\cosh\frac{2\,\pi\,d}{L}} \quad \text{(25b)}$$

When the clapotis is in a trough position, Eq. 25a represents a curve with a pressure of zero at a distance $(H - h_o)$ below SWL, and a pressure at the bottom of

$$\frac{p}{\gamma} = d - \frac{H}{\cosh\frac{2\,\pi\,d}{L}} \quad \text{(25c)}$$

The resulting pressure curves can be approximated with an added factor of safety by straight lines, which makes for a very simple calculation of pressures on a vertical wall. In case still water exists on the shoreward side of the structure, the net unbalanced pressure is obtained, as mentioned previously, by subtracting the SWL hydrostatic pressure. If wave action exists on both sides of the breakwater simultaneously, the pressures are calculated for both sides of the structure and the more unfavorable algebraic combination of the two sets of pressures determines the net overturning moment.

In 1935, M. Gourret[13] published an interesting paper dealing with the clapotis in water of finite depth, in which he analyzed the approximations introduced by Messrs. Benezit and Sainflou. Mr. Gourret stressed the point that his method, as well as those of Messrs. Benezit and Sainflou, was applicable, theoretically, for waves of small height only, and that the approximations introduced became less allowable with decreasing depths. The equations derived by Mr. Gourret give results that are in fair agreement with those of Mr. Sainflou. The wave height of the clapotis was given as $2\,H$, as in the Sainflou method, and at the free surface, the height of the orbital axis above SWL was given as

$$h_o = \frac{\pi\,H^2}{L}\left(\tanh\frac{2\,\pi\,d}{L} - \coth\frac{4\,\pi\,d}{L}\right) + \frac{\pi\,H^2}{2\,L}\,\frac{\coth\dfrac{4\,\pi\,d}{L}}{\sinh^2\dfrac{2\,\pi\,d}{L}} \ldots\ldots (26)$$

which gives values less than that obtained by the Sainflou method except for small values of d/L. Mr. Gourret determined the pressure on a vertical wall for the crest and trough positions of the clapotis. The resulting pressure curves can be replaced with straight lines without appreciable error. The pressure is zero at a height $(H + h_o)$ above SWL for the crest position, and zero at a distance $(H - h_o)$ below SWL for the trough position. The pressure at the bottom, at depth d, is

$$\frac{p}{\gamma} = d - \frac{\pi\,H^2}{L}\tanh\frac{2\,\pi\,d}{L} \pm \frac{H}{\cosh\dfrac{2\,\pi\,d}{L}} \ldots\ldots\ldots\ldots (27)$$

the last term of Eq. 27 is positive when the clapotis is at the crest position and negative for the trough position.

In 1934 David A. Molitor[14] developed an empirical method of computing wave pressures on vertical breakwaters. By supplementing the wave-pressure data recorded by Mr. Gaillard,[7] he obtained a pressure curve the shape of which conforms to the envelope of maximum pressures at different elevations. According to the Molitor envelope curve, the pressure is zero at a height $H + \frac{4\,H^2}{L}$ above SWL and at a distance $H - \frac{2\,H^2}{L}$ below SWL. The maximum pressure, which was assumed to act at a height $h_o = \frac{2\,H^2}{L}$ above SWL,

[13] "Sur un movement approche de clapotis, application en calcul des digues maritimes verticales," by M. Gourret, *Annales des Ponts et Chaussées*, Paris, France, 1935.

[14] "Wave Pressure on Sea-Walls and Breakwaters," by David A. Molitor, *Proceedings*, ASCE, Vol. 60, May, 1934, p. 653

was given as

$$\frac{p_m}{\gamma} = \frac{k}{2g}(C + V_{oc})^2 \ldots\ldots\ldots\ldots\ldots\ldots (28)$$

in which C and V_{oc} are given by Eqs. 12 and 11*b*, respectively. Mr. Molitor evaluated the factor k from Gaillard's observations on the Great Lakes and arrived at values for k ranging from 1.3 for a 30 miles per hr wind to 1.7 for a 70 miles per hr wind. For ocean storms, Mr. Molitor suggested a k-value of 1.8. These pressures and corresponding elevations, together with a pressure $p = 0.72\, p_m$ located at a distance $\frac{H}{4} - \frac{2H^2}{L}$ below SWL, determine the Molitor pressure curve. Mr. Molitor does not admit that there is pressure below the trough of the wave, which premise is contrary to both theory and experiment. The method by which he determined values for the empirical coefficient (k) is obscure.

Selection of Design Method (Nonbreaking Waves).—The results obtained using the different methods of computing wave pressures on vertical breakwaters, except the d'Auria method that was omitted, are shown in Table 1. The d'Auria theory is an oversimplification of the phenomena involved, and the overturning moments obtained are considerably higher than are obtained by the other theories. The values shown in Table 1 are calculated from the simplified versions of the various theories as shown in Fig. 2. The derivation of the pressure equations presented in Fig. 2 was based on the assumption that the theoretical pressure curves were straight lines in each case. Although liberties were taken with the original theories in devising the simplified methods of calculation, these curves are of sufficient accuracy for comparing the different methods, and, in so far as the original theories are adequate, the simplified methods are believed to give results within the range of accuracy required for actual design of vertical breakwaters. The diagrams of Fig. 2 show the magnitude and distribution of wave pressures from which the maximum (wave at crest) net overturning moments shoreward can be calculated, assuming SWL hydrostatic pressure on the shoreward side. For all methods based upon the formation of the clapotis, similar diagrams could be prepared to show net pressures seaward when the wave was at a trough position, and for net unbalanced pressures when wave action existed on both sides of the breakwater. The methods explained in preceding paragraphs can be placed in three categories: (1) The static-dynamic d'Auria, Lira, and Iribarren methods; (2) the standing-wave or clapotis methods of Messrs. Benezit, Sainflou, and Gourret; and (3) the Molitor empirical method. Recalling the objections to the static-dynamic theories in general, and to the d'Auria method in particular, and noting from Table 1 that the Lira method gives overturning moments much smaller than any other method, it is seen that the Iribarren method is the only one of this type that could be considered for use. In the standing-wave methods, that of Mr. Benezit should be discarded, although it gives pressures nearly as large as the Sainflou method, since it deals only with waves in deep water. By the process of elimination the conclusion has been reached that the Iribarren, Sainflou, and Gourret methods are the theories that should be considered for use in calculating wave forces on vertical breakwaters. Until

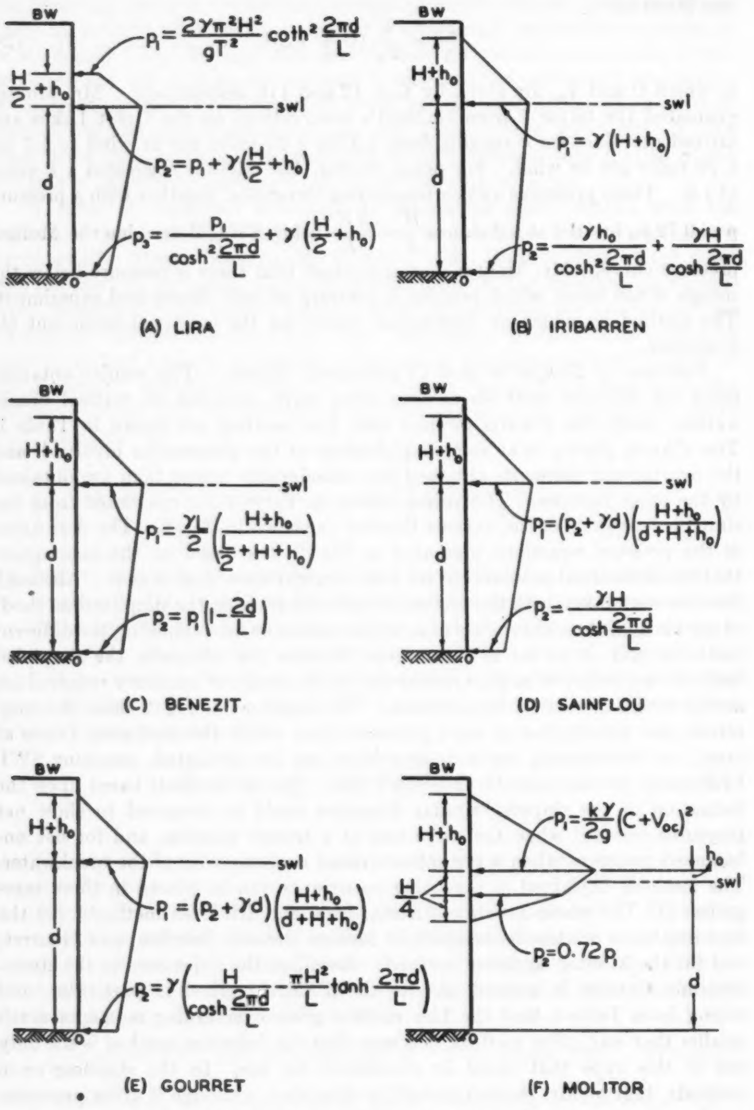

FIG. 2.—WAVE PRESSURE DIAGRAMS, MODIFIED THEORIES

TABLE 1.—WAVE PRESSURE THEORIES—COMPARISON OF RESULTS

Item					
Ratio H/L	Ratio d/L	h_o (ft)	Crest above still water level (ft)	Pressure per unit length P_t (lb per ft)	Overturning moment M_o (ft lb per ft)
(*a*) J. LIRA (1926)					
0.057	0.252	0.6	6.6	28,700	855,000
0.057	0.143	1.0	7.0	20,300	362,900
0.020	0.088	0.7	6.7	28,700	826,200
0.020	0.050	2.0	8.0	22,800	401,900
(*b*) R. IRIBARREN (1938)					
0.057	0.252	0.6	12.6	33,700	1,168,000
0.057	0.143	0.8	12.8	25,200	494,600
0.020	0.088	0.4	12.4	42,800	1,306,500
0.020	0.050	0.6	12.6	28,000	518,500
(*c*) V. BENEZIT (1923)					
0.057	0.252	0.5	12.5	32,100	1,067,000
0.057	0.143	0.5	12.5	22,300	434,400
0.020	0.088	0.2	12.2	39,800	1,218,500
0.020	0.050	0.2	12.2	25,300	469,800
(*d*) G. SAINFLOU (1928)					
0.057	0.252	2.3	14.3	33,600	1,174,000
0.057	0.143	3.0	15.0	25,800	528,000
0.020	0.088	1.5	13.5	43,800	1,366,000
0.020	0.050	2.5	14.5	29,400	571,900
(*e*) M. GOURRET (1935)					
0.057	0.252	0.0	12.0	25,400	901,000
0.057	0.143	0.4	12.4	20,600	406,000
0.020	0.088	0.8	12.8	41,700	1,291,000
0.020	0.050	5.5	17.5	33,000	686,900
(*f*) D. MOLITOR (1934)					
0.057	0.252	1.4	14.7	18,300	1,036,600
0.057	0.143	1.4	14.7	16,800	565,000
0.020	0.088	0.5	13.0	28,100	1,563,000
0.020	0.050	0.5	13.0	20,700	673,300
(*g*) MODEL DATA (*a*) (1945)					
0.057	0.252.	−3.0	9.0	25,600	821,700
0.057	0.143	2.5	14.5	24,500	500,000
0.020	0.088	4.0	16.0	52,500	1,670,900
0.020	0.050	16.0	28.0	50,100	1,185,400

(*a*) Waterways Experimentation Station, Vicksburg, Miss.

such time when the science of wave action has been placed on a sounder basis, it is believed that the Sainflou and Gourret methods should be used to calculate moments, and the one adopted that shows the worse effects on stability. Also, these methods should be used to obtain the crown height of the wall, adopting the one that gives the maximum value. The Iribarren method is very good, but it is rather complicated in application, and, too, one or the other of the methods selected gives results greater than that of the Iribarren formula in all cases. The empirical method of Mr. Molitor gives results in fair agreement with the better theories, but the value of this method for design depends on a judicious selection of coefficients corresponding to different wind velocities and durations. (Values of k used for purposes of comparing the Molitor method with the other wave-pressure theories were 1.3, 1.4, 1.5, and 1.6 for wave periods of 6.7, 7.6, 15.2, and 19.7 sec, respectively. These wave periods correspond to the d/L ratios in Table 1 of 0.252, 0.143, 0.088, and 0.05.) The Molitor method should be used with caution and only in locations for which accurate coefficients have been established.

Adequacy of Methods Selected.—E. Coen-Cagli,[15] in 1936, criticized the methods of Mr. Sainflou and others adhering to the clapotis theory, on the basis that standing waves are not formed at a vertical wall unless wave heights are small. The clapotis theories assumed small wave heights, yet it was claimed that reasonably accurate results were obtained by application of these theories when wave heights became appreciable. Mr. Coen-Cagli declared that natural storm waves retain the essential characteristics of unobstructed trochoidal waves and, consequently, cause pressures greater than the clapotis, and that the ratio of pressures that actually obtain, to the pressures calculated from the clapotis theories, increases with decreasing d/L-ratios. In proving his contentions Mr. Coen-Cagli cited prototype and model investigations of wave action on breakwaters in the ports of Genoa, Italy, and Algiers, Algeria. From these experiments the following conclusions were drawn and represent the ideas of Mr. Coen-Cagli as to the magnitude and distribution of pressures on vertical breakwaters: (*a*) The larger storm waves are not transformed in the clapotis movement, but retain the essential characteristics of unobstructed waves although the orbital motion is changed; (*b*) the total force exerted is greater than that of the clapotis; (*c*) the maximum pressure is near and slightly below SWL and is approximately equal to γH; and (*d*) pressure decreases linearly from SWL to a point about $\frac{2}{3} H$ above SWL, whereas, below SWL the pressure decreases slowly with depth, the rate of decrease becoming less with smaller values of H/L. Mr. Coen-Cagli did not present a mathematical expression for wave force, but recommended that model tests be conducted for each breakwater problem. His conclusions were based on prototype observation and model tests and are borne out by the results of his experiments. In the model tests, however, waves were used that formed a clapotis, as well as others of the same dimensions that did not. The manner whereby the latter feat was accomplished is not understood. Furthermore, if the Sainflou equations are used to calculate pressures, using the same dimensions of H, L,

[15] "L'action des lames de tempête sur les digues maritimes à paroi verticale," by E. Coen-Cagli, *Le Génie Civil*, Vol. 109, No. 9, August, 1936. (*Translation No. 43-36*, Waterways Experiment Station, Corps of Engrs., U. S. Army, Vicksburg, Miss., 1943.)

and *d* as were used by Mr. Coen-Cagli in his model tests, the calculated pressures agree more closely with the results of tests in which the waves did not form a clapotis. Therefore, the conclusions of Mr. Coen-Cagli can be viewed with some suspicion. On the other hand, model tests conducted at the Waterways Experiment Station,[16] Corps of Engineers, United States Army, Vicksburg, Miss. (hereinafter called the Waterways Experiment Station), seem to bear out the contentions of Mr. Coen-Cagli. The results of Waterways Experiment Station tests are shown in Table 1, and Fig. 3 shows a comparison of the test results with overturning moments about the base calculated from the Sainflou

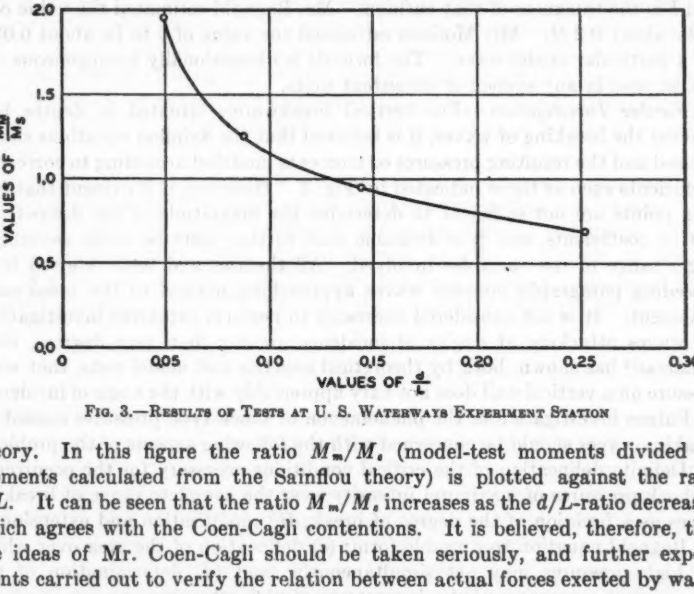

Fig. 3.—Results of Tests at U. S. Waterways Experiment Station

theory. In this figure the ratio M_m/M_s (model-test moments divided by moments calculated from the Sainflou theory) is plotted against the ratio d/L. It can be seen that the ratio M_m/M_s increases as the d/L-ratio decreases, which agrees with the Coen-Cagli contentions. It is believed, therefore, that the ideas of Mr. Coen-Cagli should be taken seriously, and further experiments carried out to verify the relation between actual forces exerted by waves on vertical walls and those calculated by the Sainflou theory. If a simple relation between theoretical and actual forces (as indicated by Fig. 3) could be proven, it is believed that the design of vertical breakwaters situated in depths of water sufficient to prevent breaking waves would be possible within the degree of accuracy of design wave selection.

Pressures Due to Breaking Waves.—If vertical breakwaters are situated where the bottom slopes seaward, and in depths approximately equal to the wave height, the waves are no longer reflected but are orbitally destroyed and break on the structure with resulting shock pressures much larger in magnitude than those of the clapotis-type waves. This phenomenon has been studied by Ralph A. Bagnold[17] in 1939 and by J. R. Morison[18] in 1948, but their analysis and experiments were not sufficiently extensive to furnish final solution

[16] "Model Tests of Portable Breakwaters for D-Day Invasion Harbors," by Robert Y. Hudson, *Civil Engineering*, Vol. 15, 1945, p. 405.

[17] "Interim Report on Wave-Pressure Research," by Ralph Alger Bagnold, *Journal*, Inst. C. E., Vol. 12, 1939, p. 202.

[18] "Wave Pressures on a Vertical Wall," by J. R. Morison, *Technical Report-HE-116-298*, Dept. of Eng., Univ. of California, Berkeley, Calif., December, 1948.

to the problem. Mr. Bagnold found that all breaking waves do not result in shock pressures, because a critical system of conditions is necessary before the phenomenon of high shock pressures can occur. According to Mr. Bagnold, the critical condition necessary is the trapping of a thin cushion of air between the folding front of a breaking wave and the wall. The formula he proposed for the maximum pressure developed by a breaking wave is

$$\frac{p_m}{\gamma} = \frac{2.7}{g} C^2 \frac{m}{b} \qquad (29)$$

in which m is the length of water column brought to rest by the air cushion and b is the thickness of that cushion. Mr. Bagnold estimated the value of m to be about $0.2\,H$. Mr. Morison estimated the value of b to be about 0.02 ft for a particular model wave. The formula is dimensionally homogeneous and can be used in any system of consistent units.

Further Investigation.—For vertical breakwaters situated in depths that prevent the breaking of waves, it is believed that the Sainflou equations should be used and the resulting pressures or moments modified according to corrective coefficients such as those indicated by Fig. 3. However, it is evident that four data points are not sufficient to determine the magnitude of the desired corrective coefficients, and it is desirable that further tests be made covering a larger range of the variables involved. All theories and tests referred to in preceding paragraphs concern waves approaching normal to the breakwater alinement. It is not considered necessary to perform extensive investigations for waves attacking at angles of incidence greater than zero degrees, since J. Larras[19] has shown, both by theoretical analysis and model tests, that wave pressure on a vertical wall does not vary appreciably with the angle of incidence.

Future investigation of the phenomenon of shock-type pressures caused by breaking waves should be concerned with the following aspects of the problem: (*a*) Definite delineation of the critical conditions necessary for the occurrence of shock pressures of maximum intensity over the complete range of breaking waves as a function of the degree of break; (*b*) modification and extension of the Bagnold equation to a usable form; (*c*) delineation of the area over which the high pressures may act simultaneously; and (*d*) determination of the frequency of occurrence of shock pressures of high intensity.

Rubble-Mound Breakwaters

The use of rubble breakwaters for protecting harbors and shore-line structures is indicated for localities in which the water is not very deep and an adequate quantity of suitable rock is available at reasonable cost. Although a greater volume of rock is required to construct a rubble breakwater than is required for construction of a vertical-wall, gravity-type structure, the unit cost of placing the rubble is less, and, if a good quarry is available in the vicinity of the site, the unit cost of material is less. A rubble mound never fails completely under the attack of waves greater than the selected design wave. As rocks are displaced from a rubble mound by wave action, the breakwater tends to become more stable. Also, repair of the damage is relatively cheap. On

[19] "La résistance des jettées veriticles aux houles obliques," by J. Larras, *Annales des Ponts et Chaussées*, August, 1937. (Translated copy on file in the Office of the Chief of Engrs., Dept. of the Army, Washington, D. C.)

the other hand, the failure of a vertical-wall breakwater is usually conclusive and entails more expensive reconstruction.

Design Methods.—Rubble breakwaters are usually designed by rule-of-thumb based upon past experience. One philosophy of design, by no means without merit, is to obtain the largest rock available at a reasonable price and construct the breakwater with the steepest slope possible using available equipment. If and when rocks are displaced from the section by waves, the structure is repaired by dumping more rock. This method takes advantage of the fact that the removal of rock by wave action from the upper portions of a rubble mound results in flatter slopes and a more stable section. If it were not for the understandable reluctance of engineers to approve the design of a structure that is expected to fail before a successful design is obtained, it is believed that this method of designing rubble breakwaters would be more prevalent. What is needed, of course, is a method of design that allows the use of known factors of safety in order that the most economical type breakwater can be selected.

Some use is made of semirational and empirical formulas, but there is no formula available for the design of rubble breakwaters that can be used with assurance. Mr. Iribarren[20] developed a formula for the design of rubble-mound breakwaters in 1938. Harris Epstein and F. C. Tyrrell, M. ASCE, derived a formula similar to that of Mr. Iribarren, although developed from different concepts, in 1949.[21] The formula proposed by Mr. Iribarren is

$$W = \frac{K\,\gamma_r\,H^3}{(\gamma_r - 1)^3(\cos\alpha - \sin\alpha)^3}, \qquad (30)$$

in which W is the weight of individual cap rock in kilograms; K is a coefficient = 15 and 19 for natural and artificial rock, respectively; H is wave height in meters; γ_r is the specific weight of cap rock in metric tons per cubic meter; and α is the angle, measured from horizontal, of the breakwater slope. The coefficient of friction between rock was assumed to be unity. In this formula K is not dimensionless. The values of K given above were determined by Mr. Iribarren from observations of actual breakwaters. A more general form of Eq. 30, which is dimensionally homogeneous and includes the coefficient of friction, is

$$W = \frac{K'\,\gamma_r\,\gamma_f^3\,\mu^3\,H^3}{(\gamma_r - \gamma_f)^3(\mu\cos\alpha - \sin\alpha)^3}, \qquad (31)$$

in which K' is an undetermined dimensionless coefficient, γ_r is the specific weight of cap rock, γ_f is the specific weight of liquid in which the rock is submerged, and μ is the effective coefficient of friction between rock. Since Eq. 31 is dimensionally correct, it is equally valid for any system of units. By comparison of Eqs. 30 and 31, and by dimensional considerations, it can be shown that the values of K' corresponding to $K = 15$ and $K = 19$ are $K' = 0.015$ and $K' = 0.019$, respectively.

[20] "Translation of a Formula for the Calculation of Rock-Fill Dikes," by Ramon Iribarren Cavanilles, *Technical Report-HE-116-295*, Dept. of Eng., Univ. of California, Berkeley, Calif., August, 1948.

[21] "Design of Rubble-Mound Breakwaters," by Harris Epstein and F. C. Tyrrell, Section 2, Communication 4, XVIIth International Cong. of Navigation, Lisbon, Portugal, 1949.

Derivation of the original Iribarren formula and that of Eq. 31 was based upon the assumption that dynamic forces tending to displace rock from the breakwater slope are proportional to wave height, area of rock over which the forces act, and the specific weight of the liquid ($F_{dy} = k\, A\, \gamma_f\, H$). Also, the analysis is based on an assumed force diagram for a single rock, as shown in Fig. 4. For equilibrium, the friction force R must balance the down-slope component of the submerged rock weight W'. The dynamic force (F_{dy}) is assumed to act upward, perpendicular to the breakwater slope. This assumption is based on the premises that: (1) The waves break on the structure and

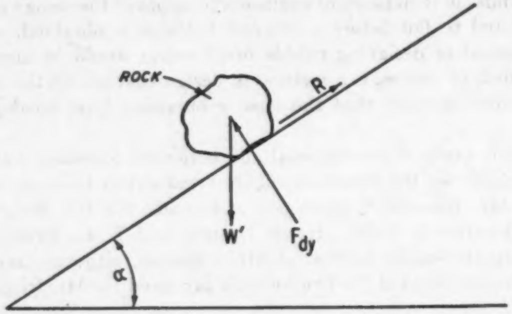

FIG. 4.—FORCE DIAGRAM FOR RUBBLE-MOUND BREAKWATER

direct jets of water downward perpendicular to the slope; and (2) at the beginning and end of the splashes the jets create forces opposite in direction to the flow of water in the jets. Although the latter premise is probably correct generally, the assumption that a wave makes a complete break and directs a jet downward perpendicular to the slope is open to criticism. Experiments at the Waterways Experiment Station indicate that waves at a breakwater tend to do one of three things: (*a*) They may execute a complete break with the direction of the jet approximately perpendicular to the slope; (*b*) they may be reflected and establish a standing wave system seaward of the structure; or (*c*) they may execute a partial break, with the resulting jet action poorly defined, and with a portion of the wave energy reflected. The formula can also be questioned because it does not take into account the inherent stability or instability of the attacking waves (which is a function of H, L, and d), voids in the rubble, width of breakwater near SWL, and rock shape and effective roughness. The effects of these variables, which are not included in the formula, and the effects of inaccuracies in the basic assumptions must be contained in the coefficient K'. If the Iribarren formula is to be made sufficiently accurate for design purposes, over the range of variables met in practice, it will be necessary to determine, either experimentally or from a large number of prototype observations, the important variables contained in K', and variations of K' with variations of these important variables.

The formula proposed by Messrs. Epstein and Tyrrell is

$$W = \frac{R_t\, \gamma_r\, \gamma^2_f \cos^3 \alpha\, H^3}{(\gamma_r - \gamma_f)^3 (\mu \cos \alpha - \sin \alpha)^3} \qquad (32)$$

in which R_t is an undetermined coefficient. Derivation of this formula was based on a force diagram similar to that of Mr. Iribarren (Fig. 4), except that a tangential force, attributed to movement of the water, was added. It was assumed that the vertical component of the dynamic pressure on the rock is proportional to the square of the vertical component of the orbital velocity of the wave motion, and that the horizontal component of dynamic pressure is proportional to the product of the wave celerity and the horizontal component of the orbital velocity. Also, the formula was derived assuming that the waves at the breakwater do not break. Although it is difficult to interpret rationally the assumptions upon which the Epstein-Tyrrell formula is based, surprisingly, the formula obtained is the same as that of Iribarren if $R_t = \frac{K'\, \mu^3\, \gamma_f}{\cos^3 \alpha}$. Messrs. Epstein and Tyrrell also developed a formula for R_t in terms of α, μ, and the d/L ratio, but the formula is rather complicated and involves three additional unknown coefficients, some of which are probably variables. Evaluation of the coefficients in R_t, therefore, would involve about the same amount of work as that in evaluating the coefficient K' of the Iribarren formula.

Model Tests in Progress (1950).—Tests of small-scale rubble breakwaters were being conducted in 1950 by the Waterways Experiment Station for the Bureau of Yards and Docks, Department of the Navy, in which the coefficients of the Iribarren and Epstein-Tyrrell formulas are being evaluated. Tests completed (1950) have been concerned with evaluating the variables contained in K' of the Iribarren formula. The testing program will provide data for cap rock of three sizes and corresponding void ratios, one shape factor, and four specific gravities. One depth of water and three wave periods are being used, corresponding to d/L ratios of 0.16 to 0.38. Although the testing program is incomplete, the results obtained to date are instructive and indicate the type and extent of experiments needed to furnish adequate coefficients for the Iribarren formula. Some of the test results are shown in Fig. 5, in which K' is plotted against the d/L ratio, with breakwater slope as a parameter. The coefficient of friction (μ) used in calculating K' was obtained by taking an average of the angles of repose determined by dumping the rock under water and placing the rock by hand. When dumped, the angle of repose was found to be 45°. When placed by hand, as was done for the model tests, the rock could be made to stand at an angle slightly greater than 50°. The coefficient used (1.09) is the tangent of a 47° 30′ angle. It can be seen that K' is not constant but varies with both d/L and α. The testing program had not advanced sufficiently at the time of preparation of this paper to show whether these are the two most important of the variables contained in K'.

Further Investigations.—Other experiments that are thought necessary to complete the testing program relative to the Iribarren formula are indicated by the dashed lines of Fig. 5. The range of d/L-ratios should be extended to

include a minimum value of the ratio of about 0.05 and a maximum value of 0.5. Tests to date have been performed with the waves approaching normal to the structure. Tests using other angles of incidence should be made and are included in the testing program authorized by the Bureau of Yards and Docks. The tests in 1950 were conducted in such a manner that no overtopping of the breakwater crown by attacking waves was permitted, and the greatest wave height that would not cause displacement of rock from the face

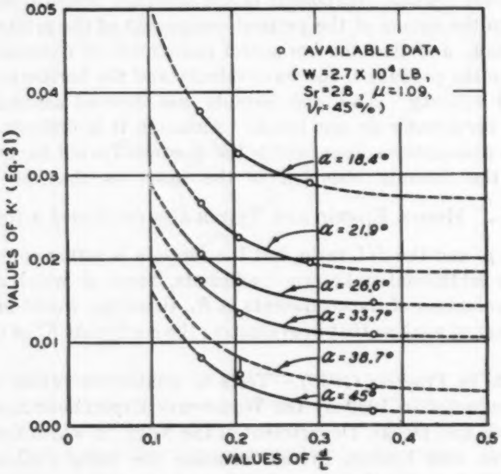

FIG. 5.—VALUES OF COEFFICIENT K'

slope was determined. It has been found, however, that if a slight amount of damage, insufficient to reduce appreciably the efficiency of the breakwater, is allowed, the design waves can be increased several feet in height. Therefore, compilation of data showing the effects on K' of allowing slight overtopping of, and damage to, the breakwater crown should prove invaluable to the design engineer, giving him considerably more latitude in selecting the most economical breakwater for a given degree of exposure to wave action. Tests should also be performed to isolate the effects of rock shape factor.

The outlined testing program is very general in character and is designed primarily to evaluate the coefficient K' in the Iribarren formula. There are many questions of design that are left unanswered by these experiments. However, tests of rubble breakwaters, even with small-scale models, are very expensive and time consuming. It is believed, therefore, that the general testing program should be completed first, leaving tests of particular breakwater types and problems of a less general nature for future study.

CONCLUSIONS

Vertical-Wall Breakwaters.—Until the science of wave action on vertical walls has been placed on a sound basis, the theories of Messrs. Sainflou and

Gourret should be utilized for the design of breakwaters situated in depths that do not cause breaking waves. Experiments should be performed to obtain coefficients that will bring calculated pressures in line with actual measured values. Experiments should also be performed to determine the magnitude, distribution and frequency of occurrence of shock-type pressures caused by breaking waves.

Rubble-Mound Breakwaters.—Because of the complexity of the phenomena whereby waves attack a mound of rock, and the many variables involved in waves and in the characteristics of rock and rock mounds, it is not believed necessary to develop a more accurate theoretical basis than that of the Iribarren formula. However, before rubble breakwaters can be designed with known factors of safety, further experimental data will be required to evaluate the coefficient (K') of this formula.

Acknowledgments

Grateful acknowledgment is hereby made of the Bureau of Yards and Docks, Department of the Navy, Washington, D. C., and the Waterways Experiment Station, Corps of Engrs., U. S. Army, Vicksburg, Miss., for permission to use the model test data from which Figs. 3 and 5 were prepared. Special acknowledgment is due the late Harris Epstein, consultant, Bureau of Yards and Docks, who conceived the testing program on rubble breakwaters at the Waterways Experiment Station, and under whose general supervision most of the tests were conducted. Acknowledgment is also made L. Frank Moore, hydraulic engineer, Waterways Experiment Station, for his aid in the preparation of material and review of the paper.

APPENDIX. LIST OF SYMBOLS

The following letter symbols introduced in this paper are assembled for the convenience of the discussers:

- b = thickness of air cushion, in Eq. 29
- C = wave celerity
- d = depth of water measured from SWL
- e = 2.3183, base of natural logarithms
- F_{d_y} = dynamic force
- g = gravitation acceleration
- γ = specific weight (wt/unit volume)
- h_s = distance of a particle's orbital axis above its plane of rest
- h_o = distance of a surface particle's orbital axis above SWL
- H = wave height, trough to crest
- k = cofficient in Eqs. 16 and 28
- K = coefficient in Iribarren's original formula (Eq. 30)
- K' = dimensionless coefficient in the generalized form of Iribarren's formula (Eq. 31)
- L = wave length
- m = length of water column brought to rest by air cushion (Eq. 29)
- M = net overturning moment (shoreward) about the base
- p = pressure intensity

P_t = total pressure per unit length of breakwater
r = horizontal radius of orbital ellipse
r' = vertical radius of orbital ellipse (in deep water $r = r'$; that is the orbits are circles)
SWL = still-water level, level of free surface at rest
T = wave period
t = time elapsed by a particle in wave motion
μ = effective coefficient of friction, rock on rock
V = orbital velocity of a particle
W = weight of individual cap rock in Eqs. 30, 31, and 32
x = abscissa of particle in wave motion
x_0 = abscissa of particle at rest
y = ordinate of particle in wave motion
y_0 = ordinate of particle at rest
z = distance from orbital axis of surface particle to orbital axis of particle originally at rest at depth y_0
α = angle measured from horizontal of rubble breakwater slope on sea or lake side of the structure

DISCUSSION

KENNETH KAPLAN.[22]—The basic homogeneous Eq. 31 for the determination of stable slopes and stone sizes of rubble-mound breakwaters, $W = \frac{K' \gamma_r \gamma_f \mu^3 H^3}{(\gamma_r - \gamma_f)^3 (\mu \cos \alpha - \sin \alpha)^3}$, may be put in the form,

$$\frac{W}{K H^3} = \frac{K'}{f(\alpha)} \qquad (33)$$

in which K is a constant for any one condition of rock and fluid and $f(\alpha) = (\mu \cos \alpha - \sin \alpha)^3$. In this manner, the variation in stone weight with stable

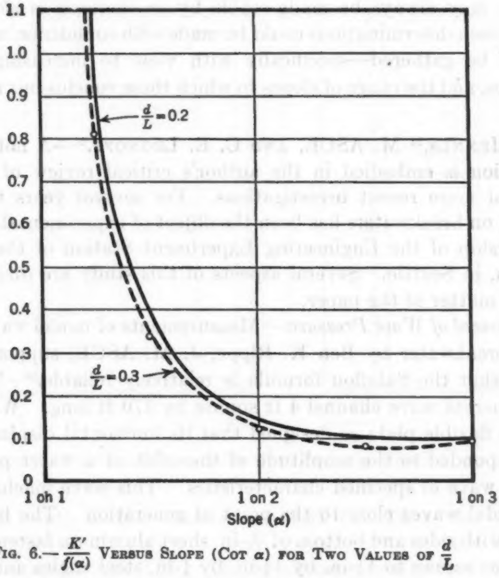

FIG. 6.—$\frac{K'}{f(\alpha)}$ VERSUS SLOPE (COT α) FOR TWO VALUES OF $\frac{d}{L}$

breakwater slope may be found for a particular value of wave height. From the curves of Fig. 5, for any value of $\frac{d}{L}$ additional curves may be drawn showing the variation of $\frac{K'}{f(\alpha)}$ with values of α or slope. This has been done in Fig. 6 for $\frac{d}{L}$-values of 0.2 and 0.3.

---

[22] Hydraulic Engr., Beach Erosion Board, Corps of Engrs, U. S. Dept. of the Army, Washington, D. C.

The most noticeable characteristics of these curves is that $\frac{K'}{f(\alpha)}$ approaches a limiting value at an approximate slope of 1 on 2.5. This would indicate that, for any given stone weight and wave attack, there exists an optimum slope that would limit the effectiveness of a breakwater. That is, if a breakwater were built with (say) a 1 on 5 slope, it would be no more stable than one built of the same materials with a 1 on 2.5 slope.

If these conclusions are substantially correct, they could be of great value to a breakwater designer. It would be possible, for example, to determine the ultimate effectiveness of a contemplated rubble-mound breakwater in terms of the maximum stone size available at the site. Eventually it may be possible, with further study, to develop criteria for the extent of maintenance that would be required if available quarry stone is not of sufficient size to be entirely stable under expected wave attack.

Determinations such as these would be impossible if the original works of R. Iribarren and C. Nogales were to be applied, since these suggest that a breakwater may always be made stable by an increase in slope. However, before any such determinations could be made with confidence, many additional data must be gathered—specifically with view to increasing the range of (d/L)-values, and the range of slopes to which these conclusions may be applied.

R. G. Hennes,[23] M. ASCE, and C. E. Leonoff.[24]—A notable service to the profession is embodied in the author's critical review of classical wave theories and more recent investigations. For several years the problem of wave forces on breakwaters has been the object of experimental research under the sponsorship of the Engineering Experiment Station of the University of Washington, in Seattle. Several aspects of this study are directly related to the subject matter of the paper.

Measurement of Wave Pressure.—Measurements of model wave pressures on a vertical breakwater by Ben K. Rippe, J. M. ASCE, support the author's contention that the Sainflou formula is relatively reliable.[25] The tests were run in a concrete wave channel 4 ft square by 170 ft long. Waves were generated by a flexible plate so designed that its horizontal displacement at any point corresponded to the amplitude of the orbit of a water particle at that depth for a wave of specified characteristics. This wave machine,[26] produced true trochoidal waves close to the point of generation. The breakwater was a bulkhead with sides and bottom of $\frac{3}{16}$-in. sheet aluminum fastened by countersunk machine screws to $1\frac{1}{2}$-in. by $1\frac{1}{2}$-in. by $\frac{1}{8}$-in. steel angles and caulked with rubber or other type gasket material. Two separate trusses were later added to increase the rigidity. The breakwater was placed across the channel and equipped with nine pressure cells dispersed along the vertical center line, as

[23] Prof. of Civ. Eng., Univ. of Washington, Seattle, Wash.

[24] Research Fellow, Eng. Experiment Station, Univ. of Washington, Seattle, Wash.

[25] "Wave Pressures on Vertical Bulkheads," by Ben K. Rippe, thesis presented to the Univ. of Washington, at Seattle, Wash., in 1951, in partial fulfilment of the requirements for the degree of Master of Science.

[26] "Laboratory Control of Ocean Waves," by F. J. Sines, *Engineering News-Record*, Vol. 141, No. 24, December 9, 1948, pp. 96–97.

shown in Fig. 7. The cell openings are $\frac{3}{8}$ in. in diameter and well rounded on the upstream face. Rubber diaphragms about 0.03 in. thick and 2 in. square were fastened with rubber cement directly to the aluminum. Each pressure cell consisted of a $\frac{1}{2}$-in. brass disk mounted behind a rubber membrane and bolted to a thin brass beam to which were cemented two SR–4 strain gages. The cells and their electrical hookup are shown in Figs. 8 and 9. In Fig. 9, the letter A marks the position of the signal generator, B is the bridge balancing unit, C represents the pressure cell strain gages, D is a basic amplifier, E is a diode rectifier, and F is a brush magnetic recorder of two channels. The model waves had a height of 0.5 ft, a length of 7.1 ft, and a period of 1.18 sec.

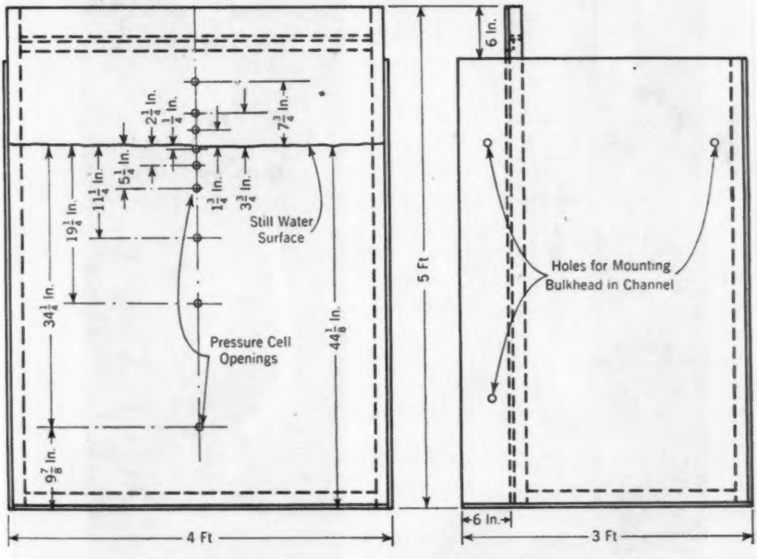

FIG. 7.—VERTICAL BULKHEAD FOR WAVE PRESSURE MEASUREMENT

The still-water depth in the channel was 3.67 ft. Thus, the $\frac{H}{L}$-ratio was 0.071 and the $\frac{d}{L}$-ratio was 0.52. The breakwater was placed at a distance of twelve wave lengths from the wave generator.

In these experiments, clapotis waves appeared at the breakwater with the arrival of the twelfth or thirteenth wave of a train. The amplitude of the ensuing waves varied over a wide range, which is contrary to the Sainflou assumption that, once formed, clapotis waves will continue to form with the same height and period, provided the generated deep-water wave does not vary.[12] Many of these waves rose considerably above the height $H + h$,

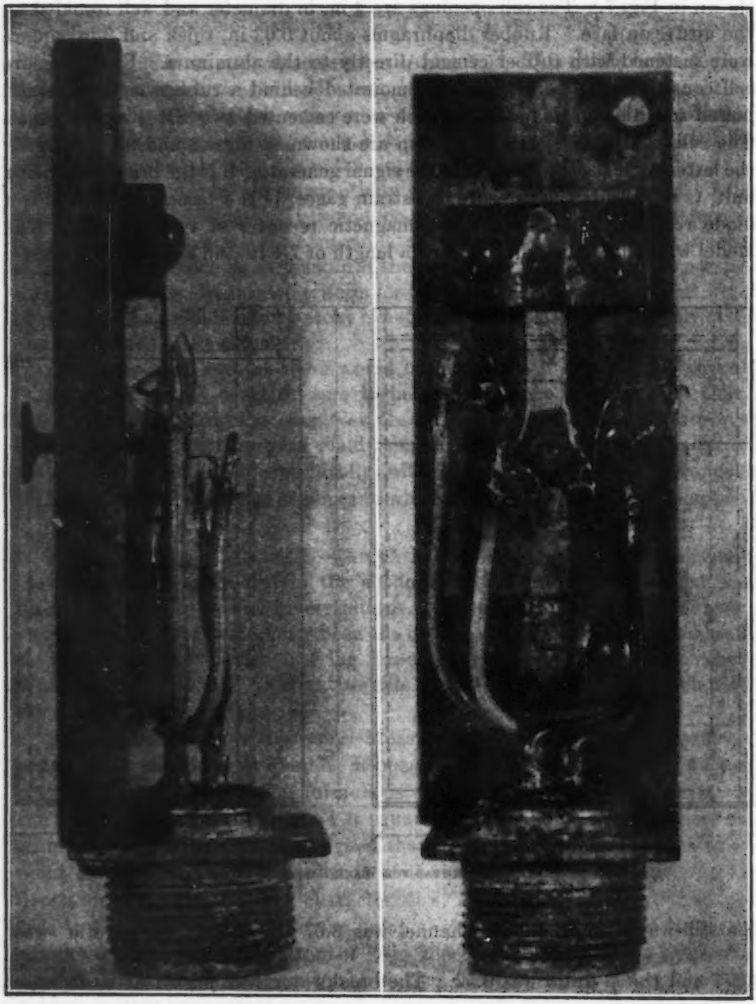

FIG. 8.—PRESSURE CELL

stipulated by Mr. Sainflou, but without any corresponding increase in maximum pressure. In fact, maximum pressure did not accompany maximum rise at the face of the breakwater. However, the evidence of these tests is that the Sainflou equation does yield the proper value for maximum pressure. This may be shown by comparing the Rippe test results with corresponding values

of unbalanced pressure (the excess of the total pressure over the static still-water pressure) obtained from the Sainflou equation (Eq. 25*a*) and the other modified wave pressure equations presented by the author (Fig. 2). Table 2 gives unbalanced pressures for a wave having the $\frac{H}{L}$ -ratios and $\frac{d}{L}$ -ratios of 0.071 and 0.52, respectively (used by Mr. Rippe), and a wave height of 12 ft, which seems to be the value used by the author in Table 1.

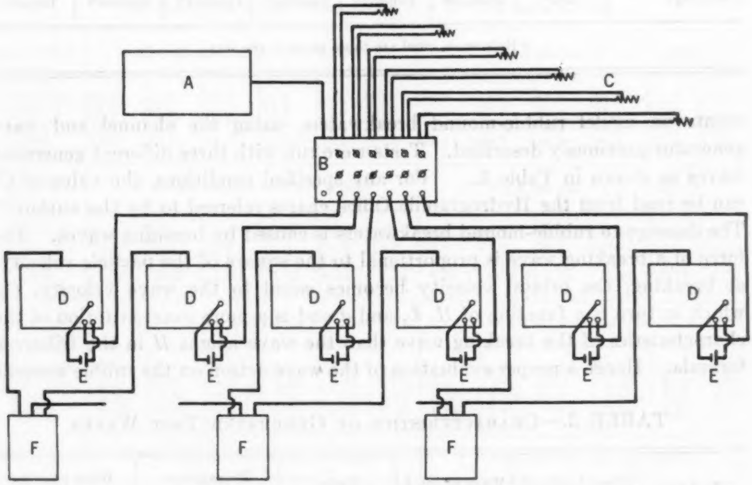

FIG. 9.—BLOCK DIAGRAM OF ELECTRICAL SYSTEM

Experiments on Rubble-Mound Breakwaters.—After reviewing the rather complex theories for computing wave pressures on vertical-wall breakwaters, the author presents the simpler Iribarren equation (Eq. 31) as a sufficiently accurate theoretical basis for the design of rubble-mound breakwaters. The anomaly of this situation is best exemplified by comparing the Iribarren formulas involving both vertical walls and rubble mounds. Although Eqs. 18, 19, and 20 require full knowledge of the wave characteristics, Eq. 30 involves no other property of the wave except its height, which is by no means an adequate recognition of the factors involved. The author did well to note that the Iribarren equation involving rubble mounds does not take into account the stability or instability of the attacking waves and to emphasize the need for further experimental data to evaluate the modified coefficient K'. (See text, under the heading, "Rubble-Mound Breakwater: Design Methods.") This is illustrated by Fig. 5, which shows that K' responds so importantly to moderate variations in the $\frac{d}{L}$-ratio. It would thus seem more appropriate to use a formula that directly recognizes wave characteristics other than H alone. In an attempt to reach this objective, the writers have conducted experi-

TABLE 2.—COMPARISON OF VARIOUS METHODS OF COMPUTING UNBALANCED WAVE PRESSURES (IN POUNDS PER SQUARE FOOT)

Depth	Pressures Corresponding to the Following Values of h_o (in Feet)						
	0.67	0.67	0.67	2.7	0	1.7	0.80
Still-water level	585	789	688	794	660	1,880	720
Mid-depth, $d/2$	501	423	344	426	330	0	174
Authority[a]	Lira[9]	Iribarren	Benezit[11]	Sainflou[12]	Gourret[13]	Molitor[14]	Rippe[26]

[a] References cited are those given in the text.

ments on model rubble-mound breakwaters, using the channel and wave generator previously described. Tests were run with three different generated waves as shown in Table 3. For any specified conditions, the value of C_b can be read from the Hydrographic Office charts referred to by the author.[2,3] The damage to rubble-mound breakwaters is caused by breaking waves. The force of a breaking wave is proportional to the square of the particle velocity; at breaking, the orbital velocity becomes equal to the wave velocity, C_b, which in turn is a function of H, L, and d and is a more exact criterion of the characteristics of the breaking wave than the wave height H in the Iribarren formula. Hence a proper evaluation of the wave action on the rubble mounds

TABLE 3.—CHARACTERISTICS OF GENERATED TEST WAVES

Test run	Wave height H, in ft	Wave length L, in ft	Ratio, H/L	Propagation velocity C, in ft per sec	Wave velocity at breaking C_b, in ft per sec
1	0.5	7.1	0.071	6.02	5.12
2	0.333	4.72	0.071	4.92	4.18
3	0.333	7.1	0.047	6.02	4.21

should be based on C_b rather than on H. Only in recent years has this development been made possible through the Hydrographic Office publications. Now that maximum values of C_b can be predicted nearly as well as values of H for all practical purposes, it seems timely to abandon the Iribarren equation, which was handicapped by the limitations of a more primitive stage of the science, rather than to attempt to correct its defects by additional coefficients.

Beginning with a force diagram somewhat similar to that in Fig. 4, the writers developed a formula that was modified, after a study of the test data, into the equation:

$$D = \frac{0.00633\, C^2_b}{(G - 1)(\tan\phi - \tan\alpha)} \quad \text{(34)}$$

in which D is the required diameter of a spherical rock, in feet; C_b is the velocity of the design wave at breaking; G is the specific gravity of the rock; $\tan\phi$ is the

TABLE 4.—Diameter of Rock (in Feet) Required for Stability Under Wave Attack—Comparison of Formulas

Side slopes	Experimental	Iribarren		de Castro y Briones	Mathews	Rodolf	Experimental	Iribarren		de Castro y Briones	Mathews	Rodolf
		Revised	Original					Revised	Original			
	(1)	(2)	(3)	(4)	(5)	(6)	(1)	(2)	(3)	(4)	(5)	(6)
(a) Prototype Waves (Assumptions: G = 2.70 and $\tan \phi$ = 1.09)												
H_o = 50 ft	T = 14 sec and H_o/L_o = 0.0497						T = 11.7 sec and H_o/L_o = 0.0712					
1 on 1.25	35.0	43.3	57.7	21.2	19.2	18.7	34.0	43.3	57.7	21.2	18.1	17.6
1 on 1.5	24.0	27.8	32.4	18.4	15.9	16.8	23.3	27.8	32.4	18.4	15.0	15.8
1 on 2	17.2	18.6	20.1	15.0	13.1	14.5	16.7	18.6	20.1	15.0	12.3	13.7
1 on 3	13.4	13.7	14.3	11.3	11.1	12.5	13.0	13.7	14.3	11.3	10.5	11.7
H_o = 35 ft	T = 13.8 sec and H_o/L_o = 0.0359						T = 9.8 sec and H_o/L_o = 0.0710					
1 on 1.25	24.6	30.4	40.3	14.8	15.1	14.7	23.4	30.4	40.3	14.8	13.5	13.1
1 on 1.5	16.9	19.5	22.7	12.9	12.5	13.2	16.0	19.5	22.7	12.9	11.1	11.8
1 on 2	12.1	13.0	14.3	10.5	10.3	11.4	11.5	13.0	14.3	10.5	9.15	10.2
1 on 3	9.42	9.56	9.96	7.86	8.66	9.76	8.97	9.56	9.96	7.86	7.78	8.71
H_o = 25 ft	T = 11.8 sec and H_o/L_o = 0.0351						T = 8.0 sec and H_o/L_o = 0.0762					
1 on 1.25	18.0	21.7	28.8	10.6	11.5	11.1	17.4	21.7	28.8	10.6	10.1	9.76
1 on 1.5	12.3	13.9	16.2	9.22	9.46	9.98	12.0	13.9	16.2	9.22	8.31	8.76
1 on 2	8.87	9.31	10.1	7.50	7.78	8.66	8.58	9.31	10.1	7.50	6.83	7.58
1 on 3	6.90	6.84	7.11	5.61	6.62	7.40	6.68	6.84	7.11	5.61	5.81	6.51
H_o = 15 ft	T = 10.8 sec and H_o/L_o = 0.0251						T = 6.2 sec and H_o/L_o = 0.0761					
1 on 1.25	10.6	13.0	17.3	6.34	7.91	7.67	10.0	13.0	17.3	6.34	6.56	6.38
1 on 1.5	7.27	8.36	9.70	5.54	6.53	6.89	6.88	8.36	9.70	5.54	5.42	5.74
1 on 2	5.22	5.59	6.04	4.50	5.37	5.96	4.94	5.59	6.04	4.50	4.46	4.96
1 on 3	4.06	4.11	4.26	3.38	4.57	5.12	3.85	4.11	4.26	3.38	3.79	4.26
H_o = 10 ft	T = 9.2 sec and H_o/L_o = 0.0230						T = 5.1 sec and H_o/L_o = 0.0752					
1 on 1.25	6.84	8.67	11.5	4.22	5.73	5.55	6.60	8.67	11.5	4.22	4.69	4.56
1 on 1.5	4.68	5.58	6.48	3.69	4.72	4.99	4.52	5.58	6.48	3.69	3.88	4.06
1 on 2	3.37	3.72	4.02	3.00	3.88	4.32	3.25	3.72	4.02	3.00	3.19	3.54
1 on 3	2.62	2.73	2.84	2.25	3.30	3.70	2.53	2.73	2.84	2.25	2.72	3.04
H_o = 5 ft	T = 6.5 sec and H_o/L_o = 0.0232						T = 3.5 sec and H_o/L_o = 0.0797					
1 on 1.25	3.63	4.33	5.77	2.12	3.21	3.12	3.25	4.33	5.77	2.12	2.61	2.54
1 on 1.5	2.49	2.78	3.24	1.84	2.65	2.80	2.23	2.78	3.24	1.84	2.16	2.28
1 on 2	1.79	1.86	2.01	1.50	2.18	2.42	1.60	1.86	2.01	1.50	1.77	1.97
1 on 3	1.39	1.37	1.43	1.13	1.85	2.08	1.25	1.37	1.43	1.13	1.51	1.69
H_o = 2 ft	T = 4.7 sec and H_o/L_o = 0.0177						T = 2.3 sec and H_o/L_o = 0.0738					
1 on 1.25	1.51	1.74	2.31	0.846	1.57	1.52	1.35	1.74	2.31	0.846	1.23	1.20
1 on 1.5	1.03	1.11	1.30	0.738	1.29	1.37	0.925	1.11	1.30	0.738	1.02	1.08
1 on 2	0.741	0.745	0.806	0.601	1.06	1.18	0.663	0.745	0.806	0.601	0.837	0.931
1 on 3	0.577	0.548	0.570	0.450	0.901	1.01	0.517	0.548	0.570	0.450	0.712	0.797

TABLE 4.—(*Continued*)

Side slopes	Experimental	Iribarren		de Castro y Briones	Mathews	Rodolf	Experimental	Iribarren		de Castro y Briones	Mathews	Rodolf
		Revised	Original					Revised	Original			
	(1)	(2)	(3)	(4)	(5)	(6)	(1)	(2)	(3)	(4)	(5)	(6)
(*b*) Model Waves (Assumptions: $G = 2.70$ and $\tan\phi = 1.171$)												
$H_o = 0.5$ ft	$T = 1.176$ sec and $H_o/L_o = 0.0707$						...	...	...	...	...	...
1 on 1.25	0.263	0.364	0.577	0.212	0.391	0.380	...	...	...	...	...	...
1 on 1.5	0.193	0.252	0.324	0.184	0.322	0.341	...	...	...	...	...	...
1 on 2	0.145	0.179	0.201	0.150	0.266	0.295	...	...	...	...	...	...
1 on 3	0.116	0.132	0.142	0.113	0.226	0.253	...	...	...	...	...	...
$H_o = 0.333$ ft	$T = 1.176$ sec and $H_o/L_o = 0.0471$						$T_o = 0.96$ sec and $H_o/L_o = 0.0706$					
1 on 1.25	0.178	0.243	0.384	0.141	0.298	0.290	0.176	0.243	0.384	0.141	0.278	0.271
1 on 1.5	0.130	0.168	0.217	0.123	0.246	0.260	0.129	0.168	0.217	0.123	0.230	0.244
1 on 2	0.0978	0.119	0.134	0.0997	0.202	0.226	0.0968	0.119	0.134	0.0997	0.189	0.210
1 on 3	0.0787	0.0884	0.0947	0.0746	0.172	0.193	0.0778	0.0884	0.0947	0.0746	0.161	0.180

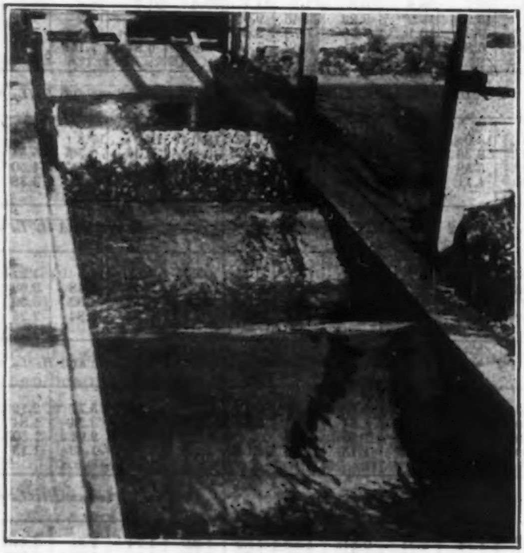

Fig. 10.—Model Wave Channel and Breakwater

coefficient of friction, rock on rock; and α is the angle made by the breakwater side slope with the horizontal. Table 4 presents a comparison of this formula with other published equations over a considerable range of wave heights. The revised Iribarren formula (Col. 3, Table 4) is Eq. 31. The testing program included four side slopes: 1 on 1.25, 1 on 1.5, 1 on 2, and 1 on 3. The breakwater model was constructed using crushed rock, with 71% passing the standard 1-in. sieve and retained on the $\frac{3}{4}$-in. sieve. The mean diameter of the particles was 0.925 in. This size was selected to insure turbulent seepage velocities without precluding some readjustment of the slopes. The

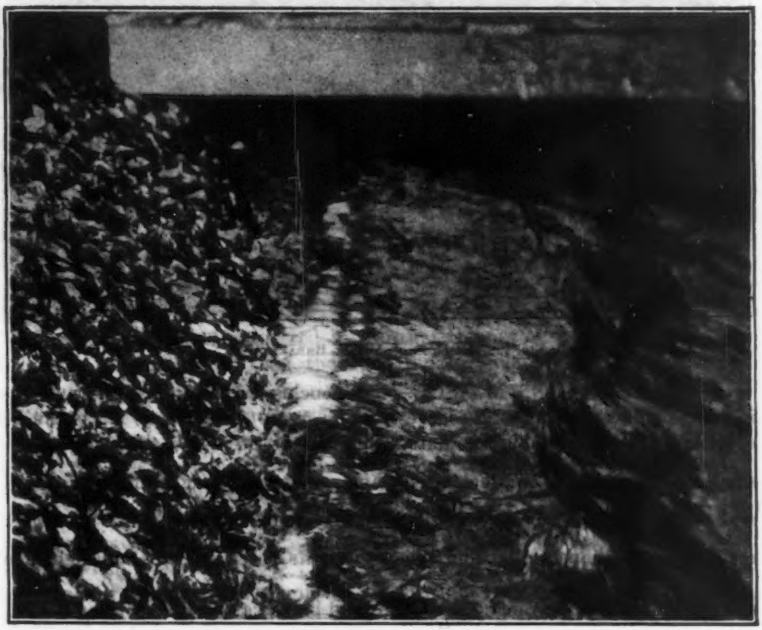

FIG. 11.—BREAKING WAVE

coefficient of friction of the crushed rock, determined by means of triaxial compression tests, was 1.171. Figs. 10, 11, and 12 provide further information on the nature of the experiment.

The author also states that tests should be performed to determine the effects of the rock shape factor, including rock shape and effective roughness. (See text, under the heading, "Rubble-Mound Breakwaters: Further Investigations.") At the University of Washington Engineering Experiment Station, a large number of direct shear tests were made on rounded river gravel and angular crushed rock, chosen to give a maximum of contrast in surface texture and angularity. The results indicate that the coefficient of friction for these two greatly diverse rock surfaces does not vary by more than about 0.035

for grain sizes between ¼ in. and ¾ in.[27,28] It would appear, therefore, that, for the type of rock normally used in rubble-mound breakwater construction, the effect of surface shape and roughness on the coefficient of friction would be insignificant in comparison to the other variables.

FIG. 12.—EROSION OF MODEL BREAKWATER

ROBERT Y. HUDSON,[29] M. ASCE.—The conclusions of Mr. Kaplan, concerning the significance of the K'-curves in Fig. 5, are correct in so far as can be determined from available test data. The curves of Fig. 5 show data from small-scale tests using one rock size, shape and specific weight, three $\frac{d}{L}$ -ratios, and six side slopes. Tests completed subsequently provide data for three rock sizes, one shape factor, four specific weights, three $\frac{d}{L}$-ratios, and eight side slopes. However, the range of $\frac{d}{L}$ -ratios and breakwater slopes have not been increased since 1950. It is planned to perform tests for $\frac{d}{L}$ -ratios of 0.05 and 0.10 and breakwater slopes of 1 on 4 and 1 on 5.

The test data obtained since 1950 did not change the K'-curves appreciably from those shown in Fig. 5. Therefore, it is recommended that these curves be used for designing rubble breakwaters until more accurate and extensive information becomes available. The coefficient of friction of the rock used

[27] "Indicator Tests for Shear Resistance of Soils," by G. B. Bennett, thesis presented to the University of Washington, in Seattle, Wash., in 1949, in partial fulfilment of the requirements for the degree of Master of Science, p. 28.

[28] "The Determination of Indicative Tests for Internal Friction of Granular Soils," by H. G. Mason, thesis presented to the University of Washington, in Seattle, Wash., in 1950, in partial fulfilment of the requirements for the degree of Master of Science, p. 31.

[29] Hydr. Engr.; Chf., Wave Action Section, U. S. Waterways Experiment Station, Corps of Engrs., Dept. of the Army, Vicksburg, Miss.

in the investigation at the Waterways Experiment Station varied from about 1.01 to 1.10.

The tests performed by Messrs. Hennes and Leonoff relative to wave pressures on a vertical wall were not sufficiently extensive to determine the accuracy of the Sainflou theory. Test data for the complete ranges of the $\frac{H}{L}$-ratios and $\frac{d}{L}$-ratios possible in nature are required. Despite the statements of Messrs. Hennes and Leonoff to the contrary, the writer is still of the opinion that the generalized Iribarren formula (Eq. 31) will be sufficiently accurate for designing rubble breakwaters, when K'-curves which cover the complete range of variables encountered in actual practice are made available. It should be sufficient to determine K'-curves for $\frac{H}{L}$-ratios from 0.01 to 0.10; $\frac{d}{L}$-ratios from 0.05 to 0.50; breakwater slopes (α) from 1 on 1 to 1 on 5; and specific gravities of cap rock, relative to pure water, from 2.0 to 3.0. The writer agrees with Messrs. Hennes and Leonoff that, for the type of rock normally used in rubble-mound breakwater construction, the effects of surface shape and roughness on the coefficient of friction are insignificant in comparison with the other variables. This applies, however, only to ordinary dumped rubble obtained from quarries. More stable breakwaters can be obtained with masonry blocks especially shaped and placed. However, this type breakwater may seldom be feasible economically.

The design formula suggested by Messrs. Hennes and Leonoff can never be made more accurate than the Iribarren formula because the principal assumption upon which it was derived is in error. Messrs. Hennes and Leonoff state: "The damage of rubble-mound breakwaters is caused by breaking waves." It was also concluded that the velocity of the wave at breaking (C_b) " * * * is a more exact criterion of the characteristics of the breaking wave than the wave height [H] of the Iribarren formula." As was explained in the paper, waves at a rubble breakwater do not necessarily break. Mr. Iribarren made an erroneous assumption similar to that of Messrs. Hennes and Leonoff when he stated that "* * * the waves break on the structure and direct jets of water downward perpendicular to the slope." This is one of the reasons K'-curves similar to those in Fig. 5 are necessary if the Iribarren formula is to be made sufficiently accurate for design purposes. A similar set of corrective coefficient curves would be necessary if Eq. 34 were to be made usable over the complete range of variables met in practice.

AMERICAN SOCIETY OF CIVIL ENGINEERS
Founded November 5, 1852
TRANSACTIONS

Paper No. 2557

STRESSES IN DEEP BEAMS

By Li Chow,[1] Harry D. Conway,[2] and George Winter,[3] M. ASCE

With Discussion by Messrs. Arturo M. Guzmán and Cesar J. Luisoni; William A. Conwell; and Harry D. Conway and George Winter

Synopsis

Beams whose depths are comparable to their spans are used in a variety of structures. The distribution of bending and shear stresses in such deep beams departs radically from that given by the ordinary, simple formulas for shallow members. Information on the stresses in continuous, deep beams is available elsewhere, and corresponding information for single-span beams is presented in this paper. Five cases of loading are studied, and, for four of these cases, three different span-to-depth ratios are examined. Distributions and magnitudes of bending and shear stresses are given in graphical and tabular form suitable for direct use in design. Although this information is directly applicable to structures made of homogeneous material, such as steel, their use in connection with reinforced concrete requires some special considerations that are briefly outlined.

Introduction

A deep beam may be defined as one whose depth is comparable to its span. Beams of this type, both in steel and in reinforced concrete, often arise in the construction of bins, hoppers, or similar structures, as well as in more ordinary construction in foundation walls or in cases in which walls are supported on individual columns or footings. The horizontal or vertical diaphragms used to transmit wind forces in buildings (floors or walls) are frequently of such dimensions as to represent deep beams. In reinforced concrete hipped-plate construction[4] the plates of the structure proper or the supporting diaphragms often fall into this category.

In all these cases, design based on the ordinary, straight-line distribution of bending stresses in shallow beams may be seriously in error, since the simple

Note.—Published in May, 1952, as *Proceedings-Separate No. 127.* Positions and titles given are those in effect when the paper or discussion was received for publication.

[1] Graduate student at Cornell Univ., Ithaca, N. Y.

[2] Prof. of Applied Mech., Cornell Univ., Ithaca, N. Y.

[3] Prof. and Head, Dept. of Structural Eng., Cornell Univ., Ithaca, N. Y.

[4] "Hipped Plate Construction," by G. Winter and M. Pei, *Journal*, Am. Concrete Inst., Vol. 18, No. 5, 1947, pp. 505-531.

theory of flexure (according to Navier's hypothesis) takes no account of the effect of the normal pressures on the top and bottom edges of the beam caused by the loads and reactions. The effect of these normal pressures on the stress distribution in deep beams is such that the distribution of bending stresses on vertical sections is not linear and the distribution of shear stresses is not parabolic. Consequently, a transverse section which is plane before bending does not remain approximately plane after bending and the neutral axis does not usually lie at the mid-depth, its position being variable in a span-wise direction.

Since information on the stresses in continuous deep beams have already been made available[5] as a result of the work of F. Dischinger,[6] the purpose of this paper is to present the stresses in single-span beams under various types of loading and to indicate how they differ in distribution and magnitude from those predicted by the ordinary beam formulas. It is assumed that the beam material is homogeneous and isotropic. The beams are analyzed as problems in plane stress, using the finite difference method to solve the differential equation for the stress function. The complete details of these solutions have been given by Mr. Chow,[7] while the finite difference method itself has been fully described and discussed in a previous paper by two of the present writers and G. W. Morgan.[8] For this reason, the method proper will not be described in any detail although the results obtained from it are given in full. Although most of these results are new, some obtained previously by H. Bay[9] have been included for completeness and are so indicated on the corresponding distribution charts.

Formulas of the Finite Difference Method

The area enclosed by the four edges of a deep beam is designated as the x–y plane, and this plane is divided into a network of equal divisions by lines parallel to the edges; h and k are the lengths of divisions in the x and y directions, respectively. Furthermore, $Z_{x,y}$ denotes the ordinate at each net-point (x,y) to a curved surface representing G. B. Airy's stress function $Z = f(x,y)$. Then, the biharmonic differential equation that Airy's stress function must satisfy is equivalent to the following linear equation in terms of Z:

$$Z_{x,y}\left\{6\left(\lambda + \frac{1}{\lambda}\right) + 8\right\} - 4\left\{(1+\lambda)(Z_{x-h,y} + Z_{x+h,y}) + \left(1 + \frac{1}{\lambda}\right)(Z_{x,y-k} + Z_{x,y+k})\right\} + 2(Z_{x-h,y-k} + Z_{x-h,y+k} + Z_{x+h,y-k} + Z_{x+h,y+k}) + \lambda(Z_{x-2h,y} + Z_{x+2h,y}) + \frac{1}{\lambda}(Z_{x,y-2k} + Z_{x,y+2k}) = 0 \quad (1)$$

in which $\lambda = (k/h)^2$.

[5] "Design of Deep Girders," *Pamphlet No. ST 66*, Concrete Information, Structural Bureau, Portland Cement Assn., Chicago, Ill.

[6] "Beitrag zur Theorie der Halbscheibe und des wandartigen Trägers," by F. Dischinger, *Publications*, International Assn. for Bridge and Structural Eng., Zurich, Switzerland, Vol. 1, 1932, pp. 69–93.

[7] "Stresses in Deep Beams," by Li Chow, thesis presented to Cornell University, at Ithaca, N. Y., in 1951, in partial fulfilment of the requirements for the degree of Doctor of Philosophy.

[8] "Analysis of Deep Beams," by H. D. Conway, L. Chow, and G. W. Morgan, *Journal of Applied Mechanics*, ASME, Vol. 18, No. 2, June, 1951, pp. 163–172.

[9] "Uber den Spannungszustand in hohen Trägern und die Bewehrung von Eisenbetontragwänden," by H. Bay, Stuttgart, Germany, 1931, p. 64.

The unknown Z-values are determined by solving the set of simultaneous linear equations obtained from the application of Eq. 1 to each net-point. The normal stress σ at any point (x,y) can then be calculated by means of the following formula,

$$\sigma_x = \frac{\partial^2 Z}{\partial y^2} = \frac{Z_{x,y-k} - 2\,Z_{x,y} + Z_{x,y+k}}{k^2} \quad \text{(2a)}$$

$$\sigma_y = \frac{\partial^2 Z}{\partial x^2} = \frac{Z_{x-h,y} - 2\,Z_{x,y} + Z_{x+h,y}}{h^2} \quad \text{(2b)}$$

The shear stress τ at the point is

$$\tau_{xy} = -\frac{\partial^2 Z}{\partial x\,\partial y} = \frac{(Z_{x-h/2,y+k/2} + Z_{x+h/2,y-k/2}) - (Z_{x-h/2,y-k/2} + Z_{x+h/2,y+k/2})}{h\,k} \quad \text{(3)}$$

It should be noticed that Eqs. 2(*a*) and 2(*b*) give the normal stresses on the sections along the lines of division of the network, whereas Eq. 3 gives the shear stresses on sections midway between the lines of division, due to the presence of $h/2$ and $k/2$ in the subscripts of Z.

Types of Loading

Five types of loading have been analyzed by the finite difference method and are indicated in Fig. 1. These loadings were chosen to represent, in a general manner, the most common types occurring in practice. Each of the first four types (Fig. 1(*a*) to Fig. 1(*d*)) were investigated for three values of the height-to-span ratio, namely, $H/L = \frac{1}{2}$, 1, and 2. The results presented herein utilizing the loading of Fig. 1(*a*) (with $H/L = \frac{1}{2}$ and 1) and Fig. 1(*c*) (with $H/L = 1$ and 2) are taken from the analyses made by Mr. Bay, who also used the finite difference method.

For the loading of Fig 1(*e*), the central portion of the beam is subject to pure bending, and the simple flexure theory predicts zero shear stresses throughout this portion. However, this is not true for deep beams, except for the midspan section in which the shear stresses are zero by symmetry. The case of $H/L = 1$ was, therefore, analyzed to show this deviation from the usual assumption.

For all the cases presented in this paper, $h = L/6$ and $k = H/6$ were used in constructing the network of divisions. However, Mr. Bay used $h = L/4$ and $k = H/4$ for the case of $H/L = \frac{1}{2}$ under the loading of Fig. 1(*a*) and $h = L/6$ and $k = H/5$ for the case of $H/L = 2$ under the loading of Fig. 1(*c*). A somewhat better accuracy was, thereby, achieved in the writers' solutions than in those of Mr. Bay.

Results and Discussion

Figs. 2(*a*), 3(*a*), 4(*a*), and 5(*a*) show the bending stress distributions at the midspan section of a beam under the loadings of Fig. 1(*a*) to Fig. 1(*d*). The stress shown is unit stress, being in terms of beam width, *b*. The midspan section was chosen for consideration since it is the section of maximum bending

moment. It is seen that, for all types of loading, when $H/L = \frac{1}{2}$ the stress curve agrees reasonably well with the linear distribution of the simple flexure theory. The deviation of the curves from the linear distribution becomes increasingly pronounced as the height-to-span ratio increases. The maximum

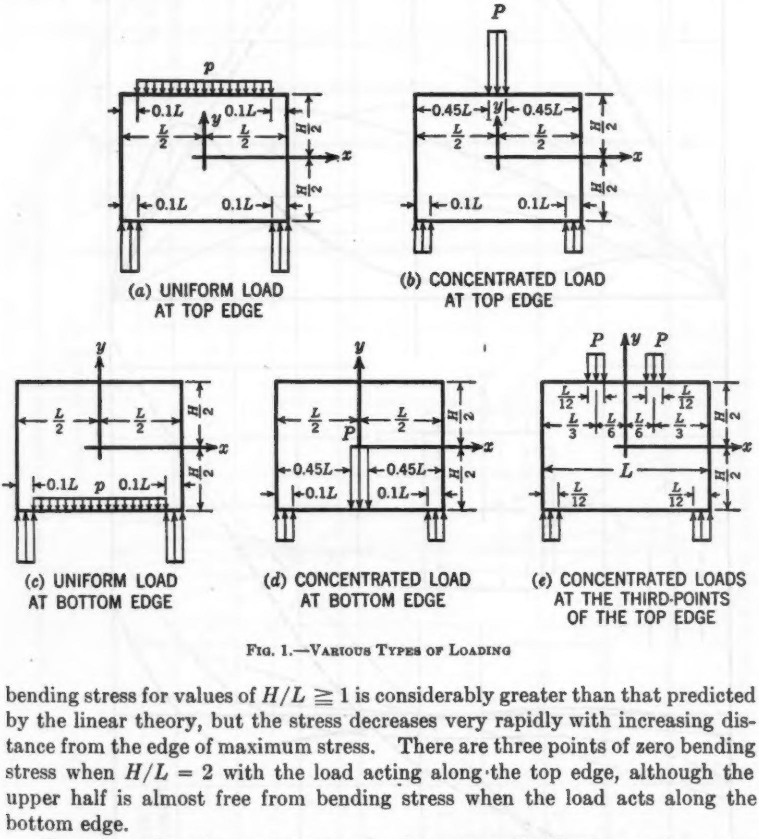

FIG. 1.—VARIOUS TYPES OF LOADING

bending stress for values of $H/L \geqq 1$ is considerably greater than that predicted by the linear theory, but the stress decreases very rapidly with increasing distance from the edge of maximum stress. There are three points of zero bending stress when $H/L = 2$ with the load acting along the top edge, although the upper half is almost free from bending stress when the load acts along the bottom edge.

Figs. 2(*b*), 3(*b*), 4(*b*), and 5(*b*) give the shear stress distributions at the section $x = L/4$ under the loading shown in Fig. 1(*a*) to Fig. 1(*d*). The total shear force at this transverse section is a maximum for the cases shown in Fig. 1(*b*) and Fig. 1(*d*), but it is less than the maximum value that occurs at the section $x = 0.4\,L$, for the cases shown in Fig. 1(*a*) and Fig. 1(*c*). Deviations from the simple theory are always present for sections near the loads and reactions, no matter what value the height-to-span ratio may be. These variations are the result of the local influence of the loading and occur also in shallow beams. For this reason, it is preferable to consider a section that is at some distance from the supports for investigating the validity of the simple theory. Moreover, the

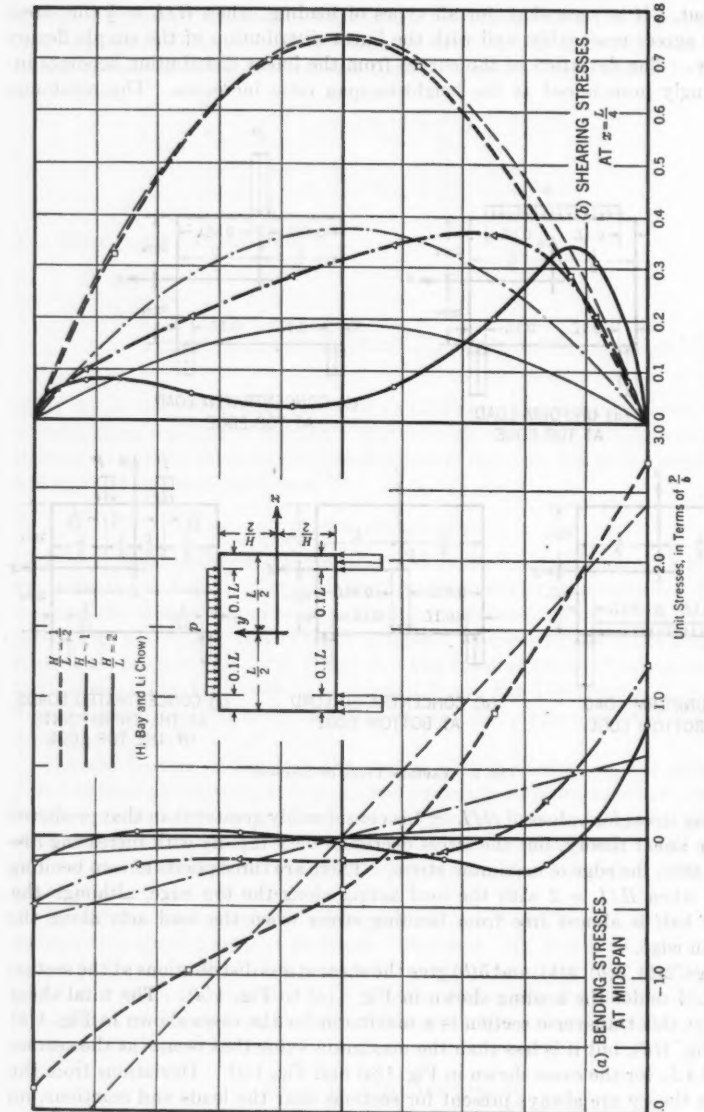

FIG. 2.—STRESSES IN BEAMS HAVING UNIFORM LOADING AT THE TOP EDGE

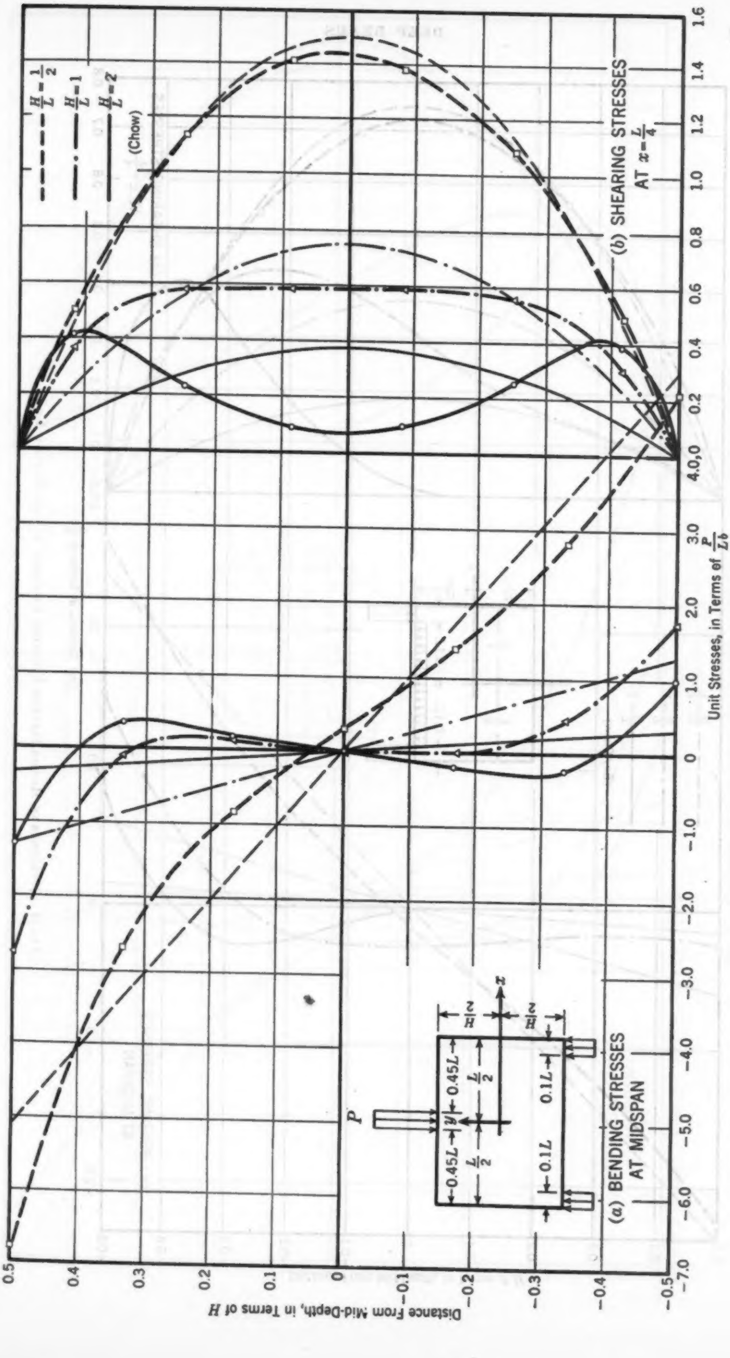

FIG. 3.—STRESSES IN BEAMS HAVING CONCENTRATED LOADING AT THE TOP EDGE

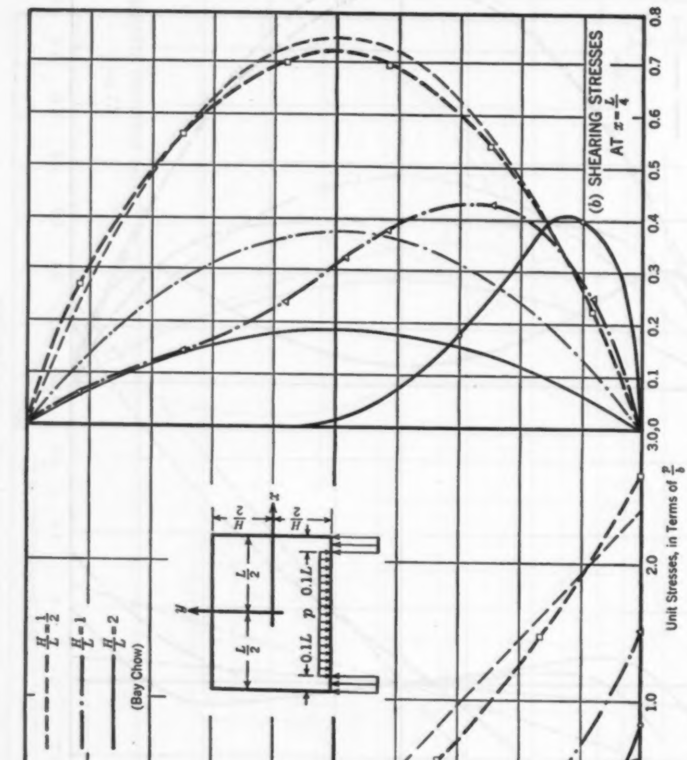

Fig. 4.—Stresses in Beams Having Uniform Loading at the Bottom Edge

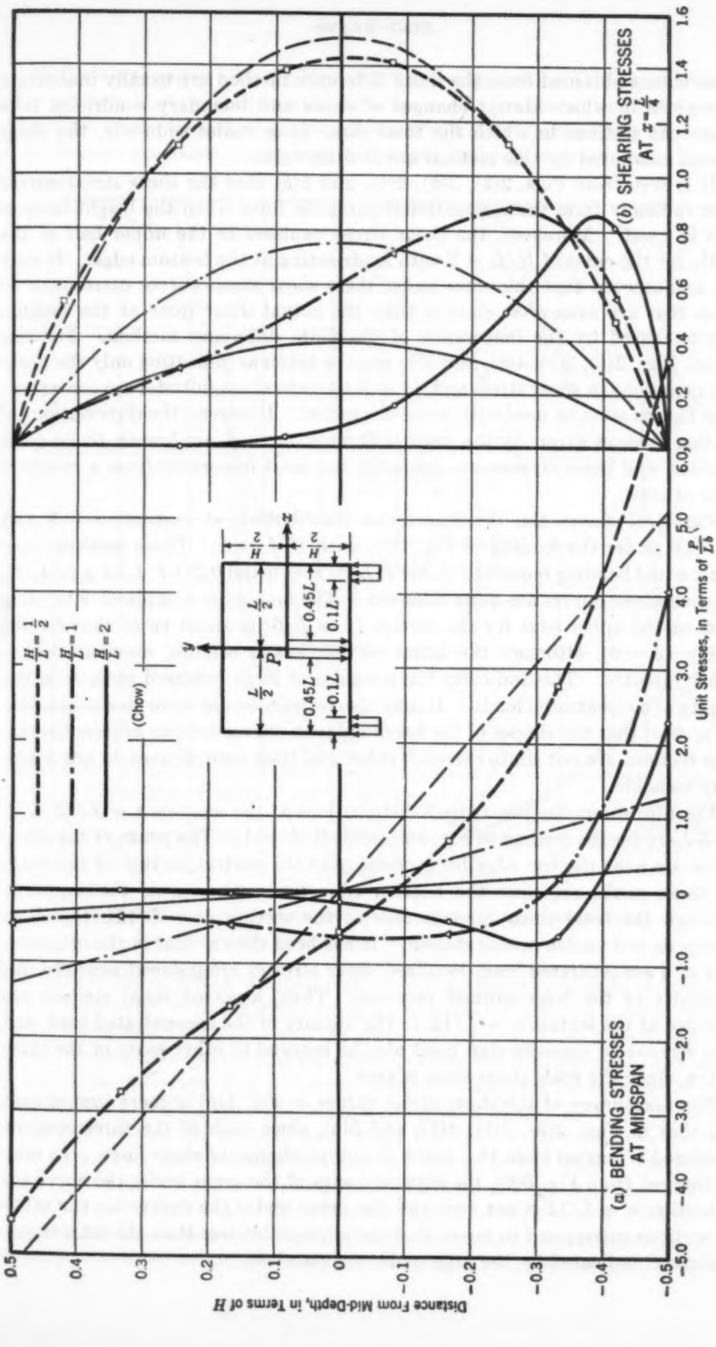

FIG. 5.—STRESSES IN BEAMS HAVING CONCENTRATED LOADING AT THE BOTTOM EDGE

stress values obtained from the finite difference method are usually inaccurate for regions in which abrupt changes of stress and boundary conditions take place. At sections in which the total shear force varies suddenly, the shear stresses computed by this method are of little value.

It is seen from Figs. 2(*b*), 3(*b*), 4(*b*), and 5(*b*) that the shear stress curves differ radically from the conventional parabolic form when the height-to-span ratio is great. Moreover, the shear stress vanishes in the upper half of the depth, for the cases of $H/L = 2$ with loads acting at the bottom edge. It may also be observed that the areas under these shear stress curves correspond to forces that are somewhat smaller than the actual shear force at the section. This is caused by the inaccuracy of the finite difference method. For this reason, Figs. 2(*b*), 3(*b*), 4(*b*), and 5(*b*) may be taken as indicating only the probable variations in shear stress and, in so far as actual magnitudes are concerned, these figures must be used with some discretion. However, the distributions of bending stresses given by the finite difference method are known to be quite accurate, and these stresses are probably the most important from a practical point of view.

Fig. 6(*a*) shows the bending stress distribution at sections $x = 0$ and $x = L/6$ under the loading of Fig. 1(*e*), with $H/L = 1$. These sections have nearly equal bending moments ($0.292\, P\, L$ for $x = 0$ and $0.281\, P\, L$ for $x = L/6$), but their stress curves are quite different. The maximum compressive bending stress at the upper edge for the section ($x = L/6$) is about twice that for the section ($x = 0$), although the latter section has a bending moment that is slightly greater. This indicates the presence of large localized stresses in the vicinity of concentrated loads. It may also be pointed out from an examination of Fig. 6(*a*) that the shapes of the bending stress curves for two adjacent transverse sections are not similar to each other and their neutral axes do not necessarily coincide.

Fig. 6(*b*) shows the shear stress distributions at the sections $x = L/12$, $L/4$, and $5\, L/12$ for the loading of Fig. 1(*e*), with $H/L = 1$. The peaks of the stress curves are near the top edge for sections near the central portion of the span, but these peaks are near the bottom edge for sections near the supports. Although the total shear force is zero at the section ($x = L/12$), the shear stresses do not vanish in this section. It has been shown[7] that in the neighborhood of a concentrated load, localized shear stresses are induced near the discontinuity of the large normal pressure. Thus, localized shear stresses are produced at the section $x = L/12$, in the vicinity of the concentrated load, and shear stresses of opposite sign must also be induced in other parts of the same section, since the total shear force is zero.

The inaccuracy of the shear stress values in Fig. 6(*b*) is more pronounced than that in Figs. 2(*b*), 3(*b*), 4(*b*), and 5(*b*), since each of the three sections considered is located close to a point of sudden change of shear force. As may be observed from Fig. 6(*b*), the algebraic sum of the areas under the curve for the section $x = L/12$ is not zero and the areas under the curves for the other two sections correspond to forces that are appreciably less than the total shearing force P indicated by the area under the parabola.

All the stress values given in Figs. 2 to 6 are either in terms of p/b, in which p is the uniform load per unit length of the beam and b is the width of the beam, or in terms of $P/(L\,b)$, in which P is the concentrated load and L is the length of the beam—according to the type of loading indicated in each of the figures.

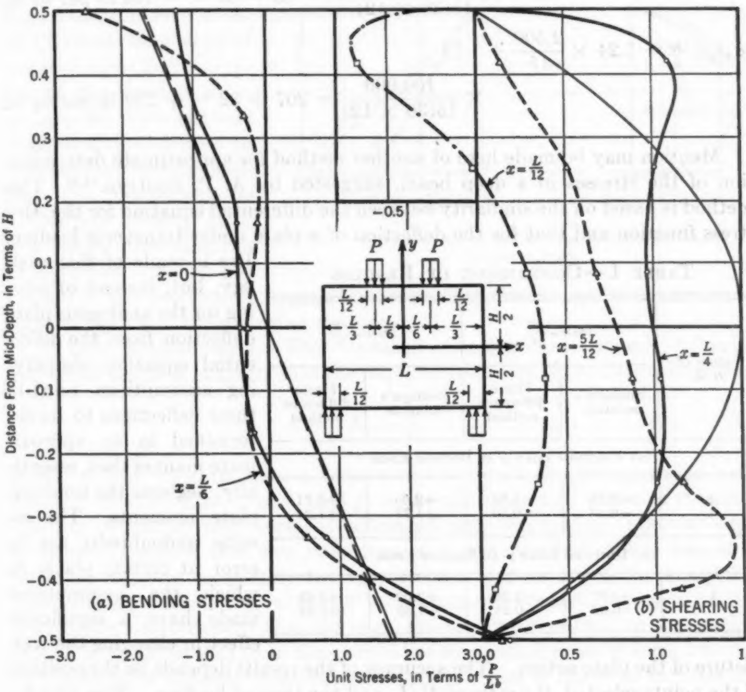

FIG. 6.—STRESSES FOR BEAMS WITH $\frac{H}{L} = 1$ AND HAVING CONCENTRATED LOADS AT THE THIRD POINTS OF THE TOP EDGE

By means of the principle of superposition, it is possible to compute the stresses for any combination of the given loadings, such as for uniform loading with a concentrated load at the center of the span. For example, let it be required to find the extreme fiber stresses at the midspan section of a single-span deep beam for which the following data are given: Length of support for reaction or concentrated load = 3 ft; span (L) = 30 ft; height of beam (H) = 30 ft; width of beam (b) = 1.25 ft; uniform load along top edge = 30,000 lb per lin ft = 2,500 lb per in.; and concentrated load at center of top edge = 100,000 lb. Since $H/L = 1$, the stress coefficients selected from Figs. 2(a) and 3(a) are $-$ 0.50 and $+$ 1.24 for the uniform loading and $-$ 2.74 and $+$ 1.74 for the concentrated load. The plus sign indicates tension and the minus sign, compression. The maximum and minimum bending stresses in pounds per square

inch for the combined loading are then

$$(\sigma_x)_{y=+\frac{H}{2}} = (-\,0.50) \times \frac{2{,}500}{15} + (-\,2.74) \times \frac{100{,}000}{15(30 \times 12)} = -\,83 - 51 = -\,134 \text{ lb per sq in.}$$

$$(\sigma_x)_{y=-\frac{H}{2}} = 1.24 \times \frac{2{,}500}{15} + 1.74 \times \frac{100{,}000}{15(30 \times 12)} = 207 + 32 = +\,239 \text{ lb per sq in.}$$

Mention may be made here of another method for approximate determination of the stresses in a deep beam, suggested by A. P. Sinitsyn.[10,11] This method is based on the similarity between the differential equation for the Airy stress function and that for the deflection of a plate under transverse loading. Use is made of this analogy, but, instead of solving for the analogous plate deflection from the differential equation, simplifying assumptions enable these deflections to be determined in an approximate manner that, essentially, neglects the torsional plate moments. The results undoubtedly are in error at certain places in which the assumptions made have a significant effect in changing the true picture of the plate action. The accuracy of the results depends on the position of the points selected, the ratio of H/L, and the type of loading. This may be seen from the following comparison between the results of Sinitsyn's method and those given by the finite difference method. The discrepancy is substantial in certain cases. Stresses in Table 1 are in units of p/b and the midspan section of a beam is considered.

TABLE I.—COMPARISON OF RESULTS

Values of H/L	$(\sigma_x)_{y=+\frac{H}{2}}$		$(\sigma_x)_{y=-\frac{H}{2}}$	
	Sinitsyn's solution	Finite difference method	Sinitsyn's solution	Finite difference method
(a) UNIFORM LOAD p AT BOTTOM EDGE				
$\frac{1}{2}$	−2.38	−1.82	+2.69	+2.71
1	−0.53	−0.50	+1.77	+1.24
(b) UNIFORM LOAD p AT BOTTOM EDGE				
$\frac{1}{2}$	−2.33	−2.26	+2.62	+2.65
1	−0.32	−0.24	+1.52	+1.53

APPLICATION TO THE DESIGN OF REINFORCED CONCRETE STRUCTURES

For beams of homogeneous material, a determination of the bending and shear stresses by means of Figs. 2 to 6 gives sufficient information for design purposes. Reinforced concrete, on the other hand, is not a homogeneous material, so that one of the basic assumptions of the preceding data is not satisfied. The additional fact that the tension zone of reinforced concrete beams must be considered cracked, modifies the stress distribution even in shallow beams

[10] "Approximate Analysis of Beam-Walls" (in Russian), by A. P. Sinitsyn, *Proyect y Standart*, No. 5, 1935, p. 21.

[11] *Ibid.*, No. 10, p. 24.

(Fig. 7). The analysis is simplified for such beams, however, by the reasonable validity of the assumption that plane cross sections remain plane despite cracking. For deep beams, on the other hand, this assumption cannot be made. The stress distribution in such reinforced concrete members must be expected to differ from that given by Figs. 2 to 6 on two counts: (1) The nonhomogeneity of material; and (2) the cracking of the tension zone. A rigorous, theoretical analysis of the stresses in such beams is hardly feasible. For this reason, no unique and strictly justified design procedure can be proposed. Some discussion of this problem and suggestions regarding tension and shear reinforcement are given in the following sections.

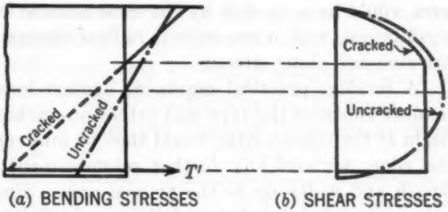

(a) BENDING STRESSES (b) SHEAR STRESSES

FIG. 7.—EFFECT OF CRACKING ON STRESS DISTRIBUTIONS IN A SHALLOW BEAM

Tensile Reinforcement.—The Portland Cement Association,[5] following European practice, suggests that the required steel area A_s be determined from

$$A_s = \frac{T}{f_s} \quad \text{(4)}$$

in which T is the total tension force computed from the homogeneous beam analysis (that is, Figs. 2 to 6) and f_s is the allowable unit stress of the steel. The entire tension reinforcement is located near the tension (bottom) edge. It must be realized that this procedure, although possibly safe in regard to strength, destroys completely the very assumptions on which the analysis is based and from which the value of T is determined. Indeed, by concentrating the tension reinforcement near the edge, the total tension force in the cracked section is forced to shift from the centroid of the tension areas of Figs. 2 to 6 to the centroid of the reinforcement (Fig. 8(*a*)). This is likely to increase the

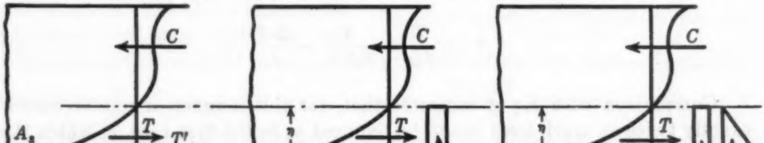

FIG. 8.—PROPOSED ARRANGEMENTS OF TENSILE REINFORCEMENT

effective internal lever arm although such a statement cannot be made with certainty for lack of rigorous, analytical support. If such increase does occur, it implies, of course, a decrease of the actual force T' in the reinforcement as compared to its computed value T and a corresponding decrease of the total compression force, since the couple formed by these forces equals the given

static moment. As a consequence, the resulting distribution of both normal and shear stresses is likely to be entirely different from that obtained from the analysis of the homogeneous beam. Even if a change of lever arm would not occur, the stress distribution would still be strongly affected by the forced shift of the tensile force to the edge since, in this case, the centroid of the compression area would have to shift by the same amount in the same direction to maintain equilibrium, with a consequent radical change in the distribution of the compression and shear stresses.

A further, practical argument against locating the reinforcement in this manner concerns the type and extent of cracking likely to occur. Cracks that begin at the tension edge would then be intercepted by reinforcement only near the edge, without any further reinforcement counteracting their growth in length and width up to the neutral axis. Since this axis, even in the homogeneous beam, is located at a distance from the tension edge varying from one half to one ninth of the depth—and likely to be larger yet in the nonhomogeneous, cracked beam—cracks of very considerable extent and width result in large, wall-like beams. To reduce these cracks additional distributed reinforcement at least of the amount usually prescribed against shrinkage would be called for over the entire tension zone.

Another scheme of reinforcing that could be rationally justified is one that would convert the beam as nearly as possible into a homogeneous beam. This can be achieved by distributing horizontal reinforcement uniformly throughout the tension zone to provide equal resistance and rigidity for every unit of depth throughout that zone, which is the essential prerequisite of "nearly homogeneous action." It is obvious that such distributed reinforcement would minimize cracking and would result in a location of the resultant of the steel stresses very close to, if not coincident with, that of the theoretical location of T (Fig. 8(*b*)).

To determine the amount of reinforcement required in this case, use can be made of the fact that from Figs. 2 to 6 the tensile stresses are seen to be nearly linearly distributed. Hence, with uniform steel distibution, the average steel stress for all practical purposes equals half that in the bar closest to the edge. The latter, as usual, must be limited to the allowable steel stress f_s. Hence

$$A_s = \frac{T}{f_{av}} = \frac{T}{0.5 f_s} = \frac{2\,T}{f_s} \qquad (5)$$

Comparison with Eq. 4 indicates that, for this manner of reinforcement, exactly twice as much steel would be required as in the first case, in which the entire steel was concentrated near the tension edge. It is likely, therefore, that such uniform reinforcement is overconservative and uneconomical, since the part of the steel near the neutral axis is stressed very little.

For an apparently sensible compromise between these conflicting requirements a different approach suggsets itself.

The total required steel area may be determined from

$$A_s = \frac{1.5\,T}{f_s} \qquad (6)$$

Half of this area is uniformly distributed throughout the tension zone, while for the other half the spacing between rods is increased linearly with increasing distance from the tension edge, as schematically indicated in Fig. 8(*c*). Such distribution evidently provides sufficient steel at all levels to counteract excessive cracking and to secure at least some measure of homogeneous action. It can also be shown that the outermost rods of this arrangement will not be overstressed. Indeed, the arrangement of Fig. 8(*b*), which provides for the required stress f_s in the outer rods, results in an amount of steel per vertical inch at the tension edge, equal to

$$a_s = \frac{2\,T}{f_s\,\eta} \quad \ldots\ldots\ldots (7)$$

in which η is the distance to the neutral axis from the tension edge (see Fig. 8). For the arrangement of Fig. 8(*c*) and Eq. 6, the amount of reinforcement per vertical inch at the tension edge, where tensile stresses are highest, is easily computed from the separate contributions of the two total areas $\frac{A_s}{2}$ each, and equals

$$a_s = \frac{0.75\,T}{f_s\,\eta} + \frac{2 \times 0.75\,T}{f_s\,\eta} = \frac{2.25\,T}{f_s\,\eta} \quad \ldots (8)$$

Comparison of Eqs. 7 and 8 shows that this arrangement provides a steel density 12.5% larger than that required in scheme Fig. 8(*b*) to insure the edge steel against overstressing. (If this suggested scheme is followed, obviously no actual distinction need be made between the rods of the two differently distributed areas $\frac{A_s}{2}$. Since, at the neutral axis, $a_s = \frac{0.75\,T}{f_s\,\eta}$, comparison with Eq. 8 shows that such a steel distribution is achieved if the total area A_s is so arranged that the area per vertical inch or foot at the tension edge is three times that at the neutral axis, with reasonably linear transition between these two extremes.) It is not likely that the steel area required by this alternative is significantly larger than that for Eq. 4 and for Fig. 8(*a*), if, for the latter arrangement, the required additional shrinkage steel is added to the computed reinforcement A_s.

Since the use of any of these formulas for A_s requires that the magnitude of the total tensile force T and the location of the neutral axis be known, these values, measured from the stress curves, are given in Table 2.

TABLE 2—TOTAL TENSILE FORCE T AND DISTANCE η OF THE NEUTRAL AXIS FROM THE TENSION EDGE FOR SECTION $x=0$

Types of loading	$\frac{H}{L}$	T	$\frac{\eta}{H}$
Uniform load p at top edge (Fig. 1(*a*))	½	$0.510\ pH$	0.400
	1	$0.131\ pH$	0.255
	2	$0.010\ pH$ $0.045\ pH$	$\left\{\begin{matrix}0.890\\0.583\end{matrix}\right.$ 0.111
Concentrated load P at top edge (Fig. 1(*b*))	½	$1.125\ PH/L$	0.547
	1	$0.022\ PH/L$ $0.196\ PH/L$	$\left\{\begin{matrix}0.820\\0.495\end{matrix}\right.$ 0.336
	2	$0.085\ PH/L$ $0.047\ PH/L$	$\left\{\begin{matrix}0.900\\0.505\end{matrix}\right.$ 0.117
Uniform load p at bottom edge (Fig. 1(*c*))	½	$0.549\ pH$	0.467
	1	$0.161\ pH$	0.228
	2	$0.060\ pH$	0.125
Concentrated load P at bottom edge (Fig. 1(*d*))	½	$1.097\ PH/L$	0.418
	1	$0.353\ PH/L$	0.186
	2	$0.146\ PH/L$	0.115
Two loads P at third points of top edge (Fig. 1(*e*))	1	$0.359\ PH/L$	0.278

It is seen from the stress distribution graphs that in some cases a second tensile region exists in addition to the bottom one. The stresses in these regions are often too small to cause cracks, making reinforcement unnecessary. If these stresses exceed the tensile strength of concrete, the steel area required can be easily computed from the corresponding value of T.

Shear Reinforcement.—The question of shear reinforcement is rather involved, even for shallow beams. The conventional procedure of designing for shear reinforcement is not theoretically exact, since it is merely an approximate means of accounting for the inclined principal tensile stresses in the concrete. In fact, beams do not fail by direct shear but by inclined tension induced by shear and normal stresses. The allowable shear stress v_c for concrete is determined empirically in such a manner that the value is low enough to insure against failure by inclined tension. Therefore, the allowable values of v_c are known to be considerably below the safe working stress of concrete in direct shear.[12]

For shallow, homogeneous beams in which the effect of σ_y is customarily neglected, the principal tensile stress σ_1 is expressed by

$$\sigma_1 = \frac{\sigma_x}{2} + \tfrac{1}{2}\sqrt{\sigma^2{}_x + 4\,\tau^2{}_{xy}} \qquad (9)$$

and the angle of inclination θ between σ_1 and σ_x is given by

$$\tan 2\,\theta = \frac{2\,\tau_{xy}}{\sigma_x} \qquad (10)$$

At the neutral axis $\sigma_x = 0$ so that $\sigma_1 = \tau_{xy}$ and $\theta = 45°$. The same condition is assumed to be true in a reinforced concrete beam for any point below the neutral axis since, in view of cracking, σ_x is assumed to be zero throughout the tension part of the beam. Thus, the maximum inclined tension is, with sufficient accuracy, equal to the maximum shear stress, and web reinforcement is designed to resist the difference between this maximum shear stress and the amount of shear assigned to the concrete. It is well known that this method is a somewhat crude approximation and even slightly contradictory in itself, but it leads to a workable and safe design method for shallow beams.

However, even for shallow beams, Mr. Bay[13,14,15] has shown that the customary shear investigation leads to an overestimate of the magnitude of the maximum principal tensile stress and that the critical section for inclined tension is not at the support but at a distance of approximately 0.65 H from the support. This is true since, near a support, the values of the vertical compressive stresses σ_y are large and cannot be neglected. Therefore, Eqs. 9 and

---

[12] "Design of Concrete Structures," by L. C. Urquhart and C. E. O'Rourke, McGraw-Hill Book Co., Inc., New York, N. Y., 4th Ed., 1940, p. 104.

[13] "Die schiefen Hauptzugspannungen beim Eisenbetonbalken," by H. Bay, *Ingenieur-Archiv*, Vol. 4, 1933, p. 244.

[14] "Scherbeanspruchung und Scherfestigkeit beim Beton," by H. Bay, *ibid.*, Vol. 14, 1943, pp. 267–276.

[15] "Der Einfluss der lotrechten Pressungen auf die Hauptzugspannungen beim Eisenbetonträger," by H. Bay, *Beton und Eisen*, Vol. 22, 1933, pp. 239–241.

10 are replaced by

$$\sigma_1 = \frac{\sigma_x + \sigma_y}{2} + \tfrac{1}{2}\sqrt{(\sigma_x - \sigma_y)^2 + 4\,\tau^2_{xy}} \qquad (11)$$

$$\tan 2\,\theta = \frac{2\,\tau_{xy}}{\sigma_x - \sigma_y} \qquad (12)$$

As seen from these equations, the presence of the compressive stress σ_y in the vicinity of the supports will reduce the magnitude of σ_1 and also make θ considerably less than 45°.

The principal tensile stresses are, therefore, nearly horizontal and may be carried by the logitudinal steel. Mr. Bay confirmed his analysis by tests that showed that the vicinity of the supports was free from cracks at loads far greater than those that had caused inclined cracks to occur in the same beams at points farther removed from the supports. The value of σ_y decreases with increasing distance from the support, so its effect on σ_1 becomes negligible at a distance of about 0.65 H from the support. Hence, σ_1 reaches a maximum at this point. The tests by Mr. Bay also showed that the first inclined crack actually appeared at this place at which σ_1 was a maximum.

The foregoing discussion is presented for the purpose of illustrating some of the difficulties involved in obtaining a logically consistent procedure for designing shear reinforcement. It is obvious that the conventional, semi-empirical method for shallow beams cannot be applied to deep beams in which the magnitude of σ_1 is greatly affected by the presence of σ_y throughout the beam, in a manner similar to that just discussed for the vicinity of the supports of shallow beams. For these reasons the shear stress cannot be regarded as a reliable measure of inclined tension in deep beams, and accurate information could be obtained only by actually computing principal tension stresses. Since such a procedure would be extremely involved, the approximate method for shear in deep beams, proposed by the Portland Cement Association,[5] appears sensible. It is suggested that, for $H/L > 0.4$, the allowable shear stress for deep beams be increased to $\dfrac{v_c\left(1 + 5\dfrac{H}{L}\right)}{3}$ in which v_c is the value allowed for shallow beams. This accounts for the fact that, because of the presence of vertical compression σ_y, the inclined tension σ_1 is smaller than the maximum shear τ_{max}. Instead of computing this lower inclined tension and comparing it with v_c, the Portland Cement Association method proposes raising the allowable shear stress and comparing it with τ_{max}. The effect is identical, of course, at least qualitatively.

It is further recommended in the previously mentioned publication that the maximum shear be computed from $\tau_{max} = \dfrac{8\,V}{7b\,H}$, that is, from the usual, approximate formula for shallow beams. This procedure may be justifiable for lack of better information if the beam is reinforced according to Fig. 8(*a*) (with reinforcement at the tension edge) since, in that case, the actual stress distribution is highly uncertain. However, if reinforcement is arranged to approach more closely the condition of homogeneity (such as in Fig. 8(*b*) or 8(*c*)), the shear distribution can be assumed to be fairly close to that in a homogeneous beam, and τ_{max} can then be taken from the appropriate curves of Figs. 2 to 6.

In many cases τ_{max} will be found to be smaller than the shear value assigned to concrete in deep beams, so that shear reinforcement is not required. If this is not the case such reinforcement must be provided primarily by inclined bars or by a network of horizontal and vertical bars. In contrast to shallow beams, cracks in deep beams are nearly vertical (since principal tensions are nearly horizontal) so that vertical shear reinforcement, such as stirrups, is largely ineffective.

This brief discussion of the questions involved in correctly reinforcing deep concrete beams is not meant to be either exhaustive or authoritative. It is merely intended to point up some of the differences in approach required in designing deep as compared to shallow concrete beams and to suggest methods that seem reasonable to the authors. Experimental investigations in this field would do more to settle the question of the most desirable arrangement of reinforcement than any amount of theorizing.

Conclusions

For shallow beams, the normal pressures on the longitudinal edges have little effect on the stress distributions at sections a small distance from supports or concentrated loads. The stresses at these sections depend only on the bending moment and shear force, and the values computed by the ordinary beam formulas are accurate for practical purposes. The stresses in deep beams, however, depend not only on the bending moment and shear force at a section but also on the variation of normal pressures along the loaded edges. The greater the height-to-span ratio, the more significant becomes the latter factor. Thus, for deep beams in which the load is applied to the bottom edge, the stress distributions are quite different from those caused by the same loading applied at the top edge. In general, the ordinary beam formulas may be considered as valid for computing stresses in beams whose height-to-span ratio is less than one half and in which the sections under study are not too near to loads and reactions.

Analytical results for the stresses in deep beams of homogeneous material are presented and can be applied directly to the design of structures made of such material. The design of deep reinforced concrete beams, on the other hand, involves the difficulty of dealing with a slightly cracked, nonhomogeneous material. A rigorous theoretical analysis of this situation is hardly possible. The stresses obtained from analyses based on the assumption of homogeneity may serve as a reasonable guide for estimating the actual stresses in the cracked state of the nonhomogeneous beam, provided the beam is so reinforced as to approach homogeneous performance. Suggestions regarding tensile and shear reinforcement have been presented to achieve such performance and to limit the extent of cracking.

Acknowledgment

The need for more detailed data for the design of deep beams was established in discussions of the Subcommittee on Hipped Plate Structures (Committee on Masonry and Reinforced Concrete, ASCE Structural Division), of which two of the writers are members.

DISCUSSION

ARTURO M. GUZMÁN[16] AND CESAR J. LUISONI[17].—Special interest has been aroused by the subject because of the importance of the deep beam as a strong structural element in reinforced concrete industrial buildings and in large residential blocks. In France, numerous detailed specifications have been issued by the government on this matter.[18]

The analysis of a single-span deep beam is particularly difficult. For their calculations, the authors use the method of finite differences, and the agreement of the approximation depends, of course, on the density of the network that has been adopted. For the case $H = L$ with supporting width 0.1 L and the load on the top edge, there exist complete photoelastic tests using the very exact, purely optical, Favre method.[19] In the central section, for the maximum bending stress, σ_x, the difference is 20% at the bottom edge; and the finite differences method, with the network width as indicated by the authors, yields smaller values than the experimental method.

A more accurate approximation, involving less calculation,[20,21] is possible by using fifth-degree polynomials for the Airy stress function and, therefore, third-degree polynomials for σ_x, the coefficients for the polynomials being determined by the Galerkin variational method. This solution has then been extended to several cases of load,[22,23] with tabular data being given for each. In the case analyzed by the authors, using finite differences, fifteen equations with as many unknowns must be solved, whereas with the Galerkin variational method used by the writers, only four equations with as many unknowns are required, the agreement with the photoelastic test being very good.

For the case $H = 1.5\,L$, uniformly loaded, the writers have used the finite differences method with a very dense network, $h = k = L/8$ or 44 points, solving the equations by the Southwell relaxation method[22,23] and using the so-called block relaxation to speed up the convergence; even so, however, the calculation work is considerable. Nevertheless, differences of about 10% to 20% as compared with experimental values[24] always arise. The rectangular network used by Mr. Bay[9] and the authors is not to be recommended as it

---

[16] Prof., Facultad de Ciencias Fisico-matemáticas, Ciudad Eva Perón (Ex-La Plata), Argentina.

[17] Prof., Facultad de Ciencias Fisico-matemáticas, Ciudad Eva Perón (Ex-La Plata), Argentina.

[18] "Traité de Beton Armé," by A. Guerrin, *Règles B. A. 45 du Ministère de la Reconstruction et de l'Urbanisme (1945–1948)*, Paris, France, Vol. II, 1951, pp. 208–216.

[19] "Ensayo fotoelástico de una viga de gran altura," by C. A. Sciammarella and M. A. Palacio, *Ciencia y Técnica*, Buenos Aires, Argentina, Vol. 113, No. 569, 1949.

[20] "Solución variacional del problema de la viga rectangular simplemente apoyada de gran altura," by A. M. Guzmán and C. J. Luisoni, *ibid.*, Buenos Aires, Argentina, Vol. 111, No. 555, 1948.

[21] *Applied Mechanics Reviews*, ASME, Vol. 1, November, 1948, Revs. 1608.

[22] "Sobre la viga simplemente apoyada de gran altura. Teoria y experimentación," by A. M. Guzmán and C. J. Luisoni, *Ciencia y Técnica*, Buenos Aires, Argentina, Vol. 114, No. 576, 1950.

[23] *Applied Mechanics Reviews*, ASME, Vol. 3, October, 1950, Revs. 1867.

[24] "Ensayo fotoelástico de una viga de gran altura," by C. A. Sciammarella and M. A. Palacio, *Ciencia y Técnica*, Buenos Aires, Argentina, Vol. 117, No. 588, 1951.

increases the error. This defect is discernible in Fig. 4 for $H = 2\,L$, in which the surface of the compression zone is about 70% superior to the tension zone for σ_x, whereas both must be equal for calculation control and static conditions.

For uniform load, the maximum bending stress at the bottom edge does not occur in the middle but on the sides. This fact cannot appear in finite differences, but is revealed in the variational method, and has been confirmed by photoelastic tests.

The behavior of tensile reinforcement, for single-span or two-span reinforced concrete deep beams, has not been studied extensively. Special mention should be made of a contribution by H. Nylander and H. Holst[25] that is not sufficiently known, and a recent discussion in which experiments by Garcia Olano-Fliess[26] are cited. The Swedish authors[25] give interesting conclusions regarding the cracking mechanism of deep beams with a load on the top edge, which can be forecast by studying theoretically derived isostatics or by photoelasticity. Messrs. Nylander and Holst[27] state:

> "* * * after the formation of tensile cracks the member acts as a straining trestle-work provided with tension rods, and the load-bearing capacity is therefore dependent on the anchorage of the bending tensile reinforcement. For this reason, the shear reinforcement should be proportioned so as to provide safety against the formation of detrimental cracks."

Tests[26] for a single-span deep beam with a load at the top edge, and for $H = 1.5\,L$, reveal that the failure occurs when the member has lost its resistance to compression in the supports and that the tension in the reinforcement at failure is very low. The cracks always start on the interior supporting edge and spread upward, tending to form arches. The function of the reinforcement is then to act as a tension rod, and under these conditions the required section seems to be very much smaller than the one calculated by prior methods. Special reinforcement should be provided at the supports, taking into account the local concentration of stress. The usual criterion seems then to be uneconomical. The proposed criteria have been applied in recently-constructed industrial buildings in Argentina,[24] and a satisfactory behavior has been observed, with a considerable saving of steel.

William A. Conwell,[28] M. ASCE.—The authors are to be commended for bringing to the publications of the ASCE the results of problems of great interest to the structural engineer. However, a real appreciation of what has been done requires reference to the work of two of the present authors and Mr. Morgan,[8] in which they outline their methods. The writer believes that only with this work as a background can one assess the value of this paper. It would have been most fortuitous had both works been published under one cover.

---

[25] "Några Undersökningar Rörande Skivor Och Höga Balkar Av Armerad Betong," by H. Nylander and H. Holst, *Transactions*, Royal Technical Univ., Stockholm, Sweden, No. 2, 1946.

[26] "Vigas de gran altura: Algunos criterios para su cálculo y disposición de la armadura," by C. A. Sciammarella, *Hormigón Elástico*, Buenos Aires, Argentina, December, 1951.

[27] "Några Undersökningar Rörande Skivor Och Höga Balkar Av Armerad Betong," by H. Nylander and H. Holst, *Transactions* Royal Technical Univ., Stockholm, Sweden, No. 2, 1946, pp. 51–52.

[28] Gen. Engr., Structural Eng. and Design Dept., Duquesne Light Co., Pittsburgh, Pa.

There are two distinct goals in this type of work. They are: (1) To provide methods with which the engineer can obtain, quickly, approximate solutions which are an aid to his judgment and better than rule-of-thumb procedures; and (2) to give the engineer data, based on rigorous research, upon which he can base his designs. The paper, with its predecessor,[8] accomplishes the first end. Although it may not fully attain the second, particularly in the field of shear stresses (which can be important), it certainly indicates the direction in which considerably more work is needed.

One of the striking results of the paper is the close agreement between the authors' diagrams for shear and bending stresses for $\frac{H}{L} = \frac{1}{4}$, and those stresses obtained by the usual theory of flexure (see Figs. 2, 3, 4, and 5). It should serve to indicate that subsequent work might be directed toward problems having values of $\frac{H}{L}$ greater than $\frac{1}{2}$.

The authors indicate that the "*** shear stress curves correspond to forces that are somewhat smaller than the actual shear force at the section" (see under the heading, "Results and Discussion"). By reading values from the shear curves for $\frac{H}{L} = 2$, the writer found errors in total shear of 8.4%, 11.8%, 15.2%, and 9.2% for Figs. 2(*b*), 3(*b*), 4(*b*), and 5(*b*), respectively. These percentages of error in total shear indicate that there are probably still greater errors in the shear stress at any point. Although the errors may seem large, the data remain valuable as an aid to judgment; and, although the authors charge the errors to the "*** inaccuracy of the finite difference method" (see under the heading, "Results and Discussion"), there is no reason why the errors cannot be reduced substantially by using the finite difference method with a finer net. It may be necessary to introduce the finer net only in a part of the beam by methods developed by George H. Shortley, Royal Weller, and Bernard Fried.[29] The finer net would seem to be worthwhile in the region of sharp curvature of the shear stress curve, for example, in the region from $-0.3\,H$ to $-0.5\,H$.

A valuable addition to the paper (perhaps it could be included in the closing discussion) would be a contour plot of the principal stresses for at least one of the examples. Engineers are familiar with such plots, based on the usual theory of flexure and made in elementary strength of materials courses. A comparison with a contour plot obtained by the authors' method would be interesting.

It might be questioned whether, in the use of an expression as involved as Eq. 1, the authors have not lost some of the advantages usually attributed to the physical significance of the finite difference method. It is believed that considerable simplification would result in taking $\lambda = 1$, and treating with a special equation any rectangular net elements that might appear at the bound-

[29] "Numerical Solutions of LaPlace's and Poisson's Equations," by George H. Shortley, Royal Weller, and Bernard Fried, *Bulletin No. 107*, Eng. Experiment Station, Ohio State Univ., Columbus, Ohio, September, 1940.

aries.[29] Still further, Eq. 1 is the difference equation equivalent to a fourth-order differential equation. The physical concept of such an equation often staggers the mind of an engineer who finds second-order equations (including partial derivatives) well within his grasp. Furthermore, the equation does not readily lend itself to the use of the numerical methods which can be very powerful in these problems.

The writer suggests the inclusion of a function,

$$u = \frac{\partial^2 Z}{\partial x^2} + \frac{\partial^2 Z}{\partial y^2} \qquad (13)$$

The resulting difference equations would be

$$u_{x,y} = \frac{u_{x-\Delta,y} + u_{x+\Delta,y} + u_{x,y-\Delta} + u_{x,y+\Delta}}{4} \qquad (14)$$

$$Z_{x,y} = \frac{Z_{x-\Delta,y} + Z_{x+\Delta,y} + Z_{x,y-\Delta} + Z_{x,y+\Delta} + u_{x,y}\,\Delta^2}{4} \qquad (15)$$

in which $h = k = \Delta$. The writer cannot say that it would be easier to solve simultaneously twelve equations of the type of Eqs. 14 and 15, rather than six of the more involved type of Eq. 1. However, it is apparent that Eqs. 14 and 15 lend themselves more readily to numerical computations.

As for physical significance, because $\nabla^2 Z = u$ and $\nabla^2 u = 0$, the sum of the angle changes in the x-direction and y-direction on the Z-surface equals u, and the sum of the angle changes in the x-direction and y-direction on the u-surface equals zero.

As an indication of the relative simplicity of the procedure which involves writing difference equations at two levels, the writer has selected from the previous paper by Messrs. Conway, Chow, and Morgan[8] the array of Z-values for the problem treated there, which would go into Eq. 1.

		6.038		
	5.440	4.754	2.778	
3.500	4.000	3.500	2.000	−0.500
	2.560	2.246	1.222	
		0.962		

This array is composed of Z-values in terms of $\frac{P\,a^2}{32}$.

The corresponding sets of values for the two-level procedure at the same point are

Values of Z			Values of $u\,\Delta^2$		
	4.754			1.260	
4.000	3.500	2.000	1.000	1.000	1.000
	2.246			0.740	

All values in these two arrays are expressed in terms of $\frac{P\,a^2}{32}$. In each array, the value at the point being considered is the average of the four adjacent points—adjusted, in the case of Z, by the value $\frac{u\,\Delta^2}{4}$.

The writer considers it a privilege to discuss a paper into which the authors have put so much effort. He hopes that they will be able to continue the work they have begun so ably so that the profession will have the full benefit of their special talents.

HARRY D. CONWAY[30] AND GEORGE WINTER,[31] M. ASCE.—The writers wish to thank Messrs. Guzmán, Luisoni, and Conwell for their discussions. These contributions add materially to the worth of the paper.

The references to theoretical and experimental researches made in Argentina and Sweden are particularly interesting because they indicate the considerable practical importance of the subject. In so far as experimental research is concerned, the difficulty in obtaining a close approximation to uniform loading is considerable. As mentioned in the paper, theory shows that singularities exist in the shearing stresses at points on the boundary where the loading is discontinuous. In practice, the stress gradients are quite likely to be large at these points but they are hardly likely to be infinite. These and other practical considerations must be borne in mind when comparing theory with experiment, and may account for some apparent discrepancies.

The use of the Galerkin variational method by Messrs. Guzmán and Luisoni [20,21] indicates an increase in accuracy with a decrease in labor. However, it is a little surprising to find that, in a later paper,[22,23] they have reverted to the finite difference method. While on this subject, the writers would like to draw attention to a further method presented in the paper by two of the present authors and Mr. Morgan.[8] An extension of this last method to beams of orthotropic material has been presented in a recent paper by one of the writers.[32]

Mr. Conwell's summary, as well as his suggestions for increasing the accuracy of the shear stresses and possibly simplifying the numerical procedures, is valuable. These factors will be carefully considered when making further calculations.

The writers are not familiar with the Swedish[25] and Argentine[26] publications quoted by Messrs. Guzmán and Luisoni in spite of their extensive search of foreign literature. In addition, the second of these[26] was published subsequent to the writing of the present paper. The quotation from the paper by Messrs. Nylander and Holst reinforces the writers' contention that reinforcement should be arranged to counteract cracking, which cannot be achieved by concentrating tension reinforcement at the edge. If the latter is done, cracking converts the structure into an arch-like member whose action is entirely different from that predicted by deep-beam analysis. This, too, seems to be confirmed in the summary by Messrs. Guzmán and Luisoni of the Argentine[26] test results. Even though such arch action subsequent to extensive cracking is stated to require less reinforcement than computed by previous methods, the control over crack formation, possibly even at design loads, seems to be lost

---

[30] Prof. of Applied Mech., Cornell Univ., Ithaca, N. Y.

[31] Prof. and Head, Dept. of Structural Eng., Cornell Univ., Ithaca, N. Y.

[32] "Some Problems in Orthotropic Plane Stress," by Harry D. Conway, Paper No. 52-A-4, *Journal of Applied Mechanics*, ASME (publication pending).

in the process—a circumstance which is considerably more serious in deep beams than in shallow beams.

Also, because Messrs. Guzmán and Luisoni state that in these tests " *** failure occurs when the member has lost its resistance to compression in the supports ***" it seems evident that, in view of this extraneous type of failure, full deep-beam (or arch) stresses leading to failure could not have been developed and, therefore, conclusions regarding them must be taken with reservations. The concentration of compression at, and near, the supports may require special measures in the form of reinforcement or even thickening of the section. Only when such local crushing has been eliminated will it be possible, in tests, to determine the effects of various types of reinforcement. Until such more extensive test evidence is available, the indication by Messrs. Guzmán and Luisoni of the importance of compression at the supports should be heeded in design.

In conclusion, attention may be drawn to another paper on this problem, which contains information supplementing in part that presented by the writers.[33]

[33] "The Theory of Girder Walls with Special Reference to Reinforced Concrete Design," by H. L. Uhlmann, *The Structural Engineer*, Vol. XXX, No. 8, London, England, August, 1952, p. 172.

AMERICAN SOCIETY OF CIVIL ENGINEERS
Founded November 5, 1852

TRANSACTIONS

Paper No. 2558

THE VALUE AND ADMINISTRATION OF A ZONING PLAN

BY HUBER EARL SMUTZ,[1] A. M. ASCE

WITH DISCUSSION BY MESSRS. HENRY HOROWITZ, AND HUBER EARL SMUTZ

SYNOPSIS

The first half of the twentieth century has witnessed many outstanding and phenomenal developments and probably more beneficial progress than any other given period in the history of civilization. Undoubtedly the outstanding civic development during this half century has been the remarkable development and spread of city planning and zoning in American cities, particularly comprehensive zoning.

NEED FOR ZONING

The old adage that "necessity is the mother of invention" certainly holds true in relation to the advancement of this new technique in public administration. Prior to the marked increase in the population of urban areas during this half century, and before the urban life sprouted four new extremities in the form of wheels, cities were more or less zoned by natural boundaries. Industries were forced to locate near the railroads or water front, commercial activities sought the center of accessibility and stayed there, and residential districts sought the higher rolling ground or developed beyond the commercial areas. The increased use of the motor truck and other modern conveniences made it possible for warehouses and industries to leave the railroad and water front for other locations which too frequently proved to be in an established residential district. The great increase and concentration of population in cities also made it possible and profitable for business enterprises to locate in residential areas. The development of the skyscraper concurrently with this rapid urban growth brought with it uneconomic land overcrowding, traffic congestion, inadequate light and air, additional fire hazards and health menaces, and increased problems of many types. The general detrimental result

NOTE.—Published in July, 1952, as *Proceedings-Separate No. 138*. Positions and titles given are those in effect when the paper or discussion was received for publication.

[1] Zoning Administrator, City of Los Angeles, Calif.

(and even more so the direct cost to property owners and to the community as a whole) of the misuse of land and urban deterioration produced a growing social consciousness and led to more critical examination of the social and economic adequacy of cities. It was ascertained that conflicting uses of land and haphazard development (1) impair property values and destroy neighborhood character; (2) tend toward the stagnation of property that would otherwise be beneficially used in an orderly manner; and (3) result ultimately in spreading areas of obsolescence, deterioration, and decay, which are costly to maintain, economically unproductive, and socially detrimental. These factors combined to produce a necessity for and an insistence on public regulation of the use of land to obtain orderliness in urban development in the future and correction of the results of haphazard urban growth in the past. The answer to this necessity and insistence has been the development of comprehensive zoning and its validation by the highest courts in the land as a proper use of the police power.

Economic Losses

Thomas Adams, the eminent planner who directed the development of the Plan for Greater New York and Its Environs, once stated:

> "If we penetrate deep enough into the cause of the most and worst of the evils that affect urban communities, we will find that they are rooted in the false economic standards that have been applied to the development of lands. Although some owners of property gain from overcrowding, owners as a whole over wide areas do not gain and the community always loses."

The total economic loss that has occurred in cities through causes which could have been largely prevented by early effective comprehensive zoning is enormous and must reach several billion dollars. Many of these losses are traceable to the premature obsolescence of good buildings and reduction of property values caused by blighted districts. Other losses arise from the stifling effect of congestion, the destruction of good buildings by fire, the increased cost of fire insurance, the high taxes needed to furnish municipal and public utility services made inefficient by the disorderly and haphazard location of various uses, and the greater original or replacement cost of installing streets, sewers, and other public utilities (which ultimately is paid for by the public) because of the inability to ascertain in advance the ultimate capacity or use of such utilities. The statement has been made, and with just reason, that

> "It is remarkable that property owners, industrialists, business men, taxpayers and voters should so long have permitted their interests to go unguarded. For there is no citizen who does not stand to profit in the long run from an orderly and conveniently planned community; there is no one who does not stand to lose from the waste of a city which sprawls haphazard at its outskirts and which decays from congestion at its heart."

That zoning served a definite need and was at least a partial answer to the dilemma in which cities found themselves at the turn of the century is attested by its phenomenally rapid spread. Although the City of Los Angeles, Calif., adopted its first zoning ordinance in 1904, it was not until 1915, when a supplement of that early ordinance was upheld by the United States Supreme Court

in the now famous Hadacheck Case,[2] that impetus was given to the zoning movement. Since that time, and particularly after the second "shot in the arm" provided when the Supreme Court upheld comprehensive zoning in the often cited Euclid Village Case,[3] zoning has spread until approximately three fourths of the urban population of the United States in more than 1700 cities and towns (including every large city except Houston, Tex.) now live under the protection of zoned communities.

The aforementioned phenomenal growth indicates the strong appeal which zoning has to the hearts of the people, particularly in urban communities. There has been no other advancement in public administration which has equaled zoning in popularity among the rank and file of the citizenry. It is the best example of democracy and the capacity for self-government at work, with the prime consideration being the general public welfare. There is a feeling (*a*) on the part of the home owner that in no other way can ample protection be provided; (*b*) on the part of the realtor that wise and sane development can take place; (*c*) on the part of mortgage lending and insurance companies, that stability and safety for investments will be brought about; and (*d*) on the part of city engineers, planners, and municipal officials that only in this way can the future development and needs of a city, with the necessary improvements and utilities, be provided without waste and with prudent expenditure of public funds. In 1926 the National Association of Real Estate Boards issued the following statement:

> "Zoning gives the poor man such security from nuisance and invasion as the rich may secure for themselves at great expense. The property owner is beginning to realize at last that by zoning he can secure for nothing even better protection against the selfish use of neighboring property, than he had ever been able to secure previously even by paying a fancy price for property in a highly restricted private development or by buying up property around him, so as to prevent it being used harmfully."

Advancement from Nuisance to Planning Theory

The technique and benefits of zoning have progressed immeasurably since the early concepts which were designed primarily to prevent the encroachment of nuisances into residential areas (now known as "the nuisance theory of zoning"). The City of Los Angeles, although originating modern zoning, lagged behind other cities in applying comprehensive zoning such as was developed in New York, N. Y., in 1916, and which embodied height and area regulations as well as use regulations. Los Angeles was the first city, however, to answer the home owners' insistence upon protected single-family residence districts. The first Los Angeles ordinance embodying this type of zone, an interim ordinance adopted in 1920, was upheld by the California Supreme Court in one of the landmark decisions in the progress of zoning.[4] This decision, which the United States Supreme Court on appeal refused to review, not only sustained the validity of single-family residence zones from which even two-family dwellings were excluded and in strong language removed all doubt as to the

[2] Hadacheck vs Sebastian (1915) 239 U. S. 394.
[3] Euclid vs Ambler Realty Co. (1926) 272 U. S. 365.
[4] Miller vs Board of Public Works (1925) 195 Cal. 477.

constitutionality of zoning regulations, but marked an appreciable change in judicial thinking from the nuisance to the planning theory of zoning.

Zoning Part of Comprehensive Planning

Since the Miller and Euclid decisions, zoning techniques and concepts as a part of comprehensive city planning have advanced immeasurably as has also the general acceptance, by the courts, of the planning theory of zoning. It is now well recognized that zoning can neither be completely comprehensive nor permanently effective unless undertaken as part of a comprehensive city plan. If not so undertaken, the zoning ordinance becomes only an instrument of expediency, subject to constant and often whimsical change. This leads to instability, uncertainty, and ineffectiveness. Comprehensive zoning must be an honest effort to control the growth of a city as an entity in an orderly, intelligent manner. Areas sufficient for each class of use must be deliberately planned for, with ample room for each to expand as reasonable growth may be anticipated, each in appropriate locations. There must be a study of quantity and of balance and of the relationship of the various uses and population densities allowed, to other features and details of the master plan.

Los Angeles, Zoning Laboratory

Los Angeles has been an outstanding zoning laboratory and the experiences and experiments there demonstrate the value that can be derived from zoning activities. It is the largest city in area within the nation (453.51 sq miles) and the fourth largest in population—1,969,264. It has a north and south dimension of 45 miles, and an east and west dimension of 30 miles, but has an irregular shape with some areas only one half mile in width. It rises from sea level to an elevation of 5,053 ft at Mt. Lukins in the Tujunga section, with consequent varied topography ranging from sandy beach lots to rugged hillside lots, inaccessible mountain areas, and flat valley agricultural sections. The northerly part of the city (known as the San Fernando Valley, containing more than 200 sq miles, and until 1930 largely agricultural in nature) is separated from Hollywood and the central section of the city by the Santa Monica Mountains. The southerly part, known as the Harbor District, is connected with the central section by a strip only one half mile in width and approximately 10 miles in length. Nearly every conceivable problem can be found within the city limits—summer beach homes, week-end mountain cabins, palatial estates, dude ranches, blighted districts, farm land, grazing land, orchards, oil fields, quarries, mines, international airport, shipping harbor, pleasure craft harbor, Hollywood, and, combined with all this, the usual residential, business and industrial development of a metropolitan city. To the physical problems must be added the many social problems produced by unprecedented growth.

While Los Angeles was doing its first basic zoning, between 1920 and 1930, the population increased 114.7% by addition of 661,375 persons, with consequent phenomenal building construction, land subdivision, and real estate speculation activity. In one year (1923), 62,548 building permits were issued and 43,842 dwelling units were constructed. An average of more than 23,200 dwelling units were constructed during each year of the ten-year period.

During this hectic decade it was not possible to zone the entire city comprehensively but only to give some protection to the rapidly developing urban area. This was done by spreading the detailed use regulations over about 50% of the area of the city. At that time little was known about the economic factors of zoning. The same mistakes were made as in every other city and, even in compromises with the real estate interests, their optimism was reflected, and entirely too much property was classified in the business and unlimited residential zones. The ordinance at that time had no density controls or varying height limits and it was only the fortunate city charter height limit of thirteen stories that prevented disastrous overloading of the land.

Problem in Land Economics

Experiences during the 1920's in administering the zoning plan demonstrated the necessity of a more realistic and scientific approach to the problem. Those concerned became convinced that zoning was nothing more or less than a problem in land economics, and that the laws of supply and demand and marginal utility were particularly pertinent and must be considered. The engineers called upon to design the public utility systems to serve the phenomenally growing city found the zoning extremely useful and beneficial; but they emphasized that the lack of density controls, and particularly the great gap between the single-family zone and the multiple-family zone which permitted thirteen-story apartment houses, prevented a scientific approach and the most efficient and economical designing of these facilities. Property owners and realtors also demanded more protection for areas building up with small multiple dwelling against the encroachment of the occasional large apartment house and hotel with their monopoly of light, air, public utilities, and onstreet parking space.

In 1930 a new zoning ordinance was adopted in Los Angeles which, although not entirely comprehensive in nature, contained four residential zones, some height, area, and density regulations, and many refinements and improvements. This ordinance (for the first time in the United States) made a move in the direction of solving the increasing onstreet parking problem by requiring every apartment house containing more than twenty dwelling units to provide garage space on the premises for one automobile for each unit. This requirement was sponsored and insisted on by the realty board. The wisdom of regulation became so apparent, and the results so beneficial, that in 1935 the city expanded the regulation to require a garage space for each dwelling unit in connection with every multiple-family use of a lot. In 1935, a supplement to the zoning regulations, called the *Comprehensive Yard Ordinance*, was adopted which required front, side, and rear yards in the various residential zones and loading space in the business and industrial zones adjoining public alleys. The benefits and value of these yard regulations were so evident and popular that about a year later an endeavor to repeal the ordinance was promptly defeated. Organizations that came to the support of the ordinance and vigorously opposed its repeal included the Chamber of Commerce, Realty Board, Apartment House Owners' Association, American Institute of Architects, Federal Housing Administration (which had relied on the regulations for

protection in insuring mortgages), the Fire Insurance Underwriters' Association, and the Fire Department. The Los Angeles Fire Chief and the Fire Insurance Underwriters' Association both emphasized the benefits of the regulations in fire-fighting activities and in preventing the spread of fire, and the tremendous saving resulting from reduced fire insurance rates. Incidentally, Los Angeles has the lowest fire insurance rates of any large city, which is partly due to its excellent fire department and the results of the early zoning and planning activities in producing a more orderly growth and securing more open space about buildings, particularly in residential districts. The yearly rate per $100 valuation on a frame dwelling with composition roof prior to 1935 was 45¢. In 1951 the rate was 16¢, which amounts to a saving of about $20 per year to the average home owner.

Need for Improved Administration

The next major change in the evolution of the zoning regulations in Los Angeles involved a movement to improve administration. The California State Zoning Enabling Act, adopted in 1917 (among the first adopted by any state in the United States), made no provision for boards of zoning adjustment such as were later incorporated in the Standard State Zoning Enabling Act recommended by the United States Department of Commerce and adopted by most of the other states. Since no specific provision was included in the statute for the appointment of boards of zoning adjustment, the early legal opinions were to the effect that there was no authority for such boards in California. As a result California cities and counties had to devise some other method of providing a safety valve in zoning ordinances for the granting of variances or adjustments of zone. Until about 1941 practically all cities and counties in California, including Los Angeles, followed the method of granting variances or special exceptions by ordinances adopted by the legislative body after hearings had been conducted and recommendations made by the planning commission. This method proved unsatisfactory in several respects:

1. The planning commission's time was consumed with zoning administrative details and little could be accomplished toward the important task of completing the master plan.
2. The City Council and mayor were bothered with minor zoning quarrels which involved only administrative rather than legislative problems.
3. Too frequently political favors in the nature of so-called "spot zones" were granted by the City Council over the planning commission denial.
4. No one person or group of persons had direct authority; hence, it was difficult to maintain any consistency of action or policy.
5. Entirely justifiable minor variances were unnecessarily delayed due to the time required to enact an ordinance and due to the thirty-day referendum period before an ordinance became effective.

Office of Zoning Administrator Created

The situation became so unsavory in Los Angeles that a citizens' committee was proposed and a charter amendment was adopted in 1941 creating the

Office of Zoning Administrator and vesting him with the authority to hear and determine all applications for variances from the zoning regulations. The charter amendment also gave the director of planning and the City Planning Commission specific duties and more power with respect to preparation and administration of the master plan, and created a three-man citizen Board of Zoning Appeals to whom appeals can be taken from actions and decisions of the zoning administrator. The zoning administrator is essentially a full-time one-man board of zoning adjustments similar to those functioning in most other states, whereas the Board of Zoning Appeals is essentially a court of review which, on appeal, reviews the administrator's decisions. The actions and decisions of the administrator are final, unless an appeal is taken to the board within ten days. The board is subject to the same limitations as those placed on the administrator, and has no more delegated authority than he; but, after hearing the appeal, the board may affirm, change, or modify the ruling or determination of the administrator subject to the same limitations placed on the administrator by the charter. The administrator does not have full discretion; the charter provides that he may grant applications for variances only if he finds:

a. That the strict application of the provisions of the zoning ordinance would result in practical difficulties or unnecessary hardships inconsistent with the general purpose and intent of the ordinance;

b. That there are exceptional circumstances or conditions applicable to the property involved or to the intended use or development of the property that do not apply generally to other property in the same zone or neighborhood;

c. That the granting of a variance will not be materially detrimental to the public welfare or injurious to the property or improvements in such zone or neighborhood in which the property is located; and

d. That the granting of a variance will not be contrary to the objectives of the master plan.

In granting a variance the zoning administrator may impose such conditions as are necessary to protect the public health, safety, or welfare, in accordance with the purpose and intent of the zoning ordinance.

The zoning administrator not only has considerable authority, but also is assigned tremendous responsibilities, particularly in the matter of granting or denying requests for zone variances and conditional uses. Under this system, however, there is definite fixed responsibility and a better chance of following consistent policies than under the former system requiring legislative enactment, where politics could enter into the situation and matters were shunted back and forth between the commission and the City Council. Zone variances are now made administrative quasi-judicial matters handled by a full-time administrator, protected by civil service regulations. The administrator is thus able to act impartially on the facts and merits of a case and to maintain consistent policies. Although the procedure for appeal to the Board of Zoning Appeals does not relieve the administrator of any of his responsibility, it does

provide a method of review and a safety valve which prevents criticism to the effect that the administrator is vested with too much authority.

The City Planning Commission and the City Council have no jurisdiction to consider or grant any type of zoning variance. Zone changes, however, still require a legislative enactment, and are first heard and considered by the City Planning Commission and then by the City Council, if recommended by the commission, or if an appeal is taken from the commission's disapproval.

Zone Variances

The zoning administrator is fully aware of dangers to the effectiveness of the zoning plan inherent in the improper use of the power to grant variances. He is constantly confronted by some of the sadly misplaced buildings or uses that were allowed by the old council "spot zone" practices. Improperly allowed variances can soon puncture the zoning plan and start disintegration, which undermines confidence in its integrity. On the other hand, the zone variance was devised and is necessary as a safety valve to adjust unequal and unnecessarily restrictive application of the regulations in specific situations which are certain to arise. There has to be some flexibility to accommodate changing methods and designs in building construction and improved operations of certain types of uses, particularly in some of the formerly considered nuisance industries which, under modern methods, can be operated without objection in light industrial areas. It is not the administrator's function to correct improper zoning by indirectly changing the zone map by the granting of variances for buildings or uses which do not conform with the plan. There are many situations, however, at the boundaries between zones, where transitions are desirable or where adjustments are necessary to permit a building or use to extend a limited distance from the less restricted zone into the more restricted zone. Special uses such as offstreet parking lots adjoining business zones are about the only type of use variance ever granted in residential zones, except an occasional temporary use in undeveloped territory such as a real estate subdivision sales office. Most of the requests for variances involve adjustments in the various yard, area, or building-line regulations or modification of some specific regulation. A few variances involve limited manufacturing in commercial zones, such as motion picture studios or small precision instrument, garment, or handicraft type industries or limited food or drug products processing. Occasionally an application is received for variance to permit an M–3 heavy industrial use in an M–2 light industrial zone where the contention is made that the type of machinery used and methods employed eliminate all nuisance features. A number of such variances have been granted, but only under specific conditions which specify the methods of operation and type of machinery or equipment to be employed such as installation of efficient dust collecting systems or soundproofing of certain rooms. Frequently, the administrator reserves the right to impose additional conditions or require corrective measures if the use proves to be objectionable or detrimental to the adjacent property owners. Practically no difficulty has been encountered in Los Angeles with uses that have been established under such variances.

Zoning Enforcement

The original charter amendment adopted in 1941 also gave the administrator control of, and responsibility for, the administration and enforcement of the zoning ordinances. To accomplish its purpose and be most effective, the ordinance must be strictly enforced. Minor violations should not be "winked at," since infractions soon lead to disrespect for the law and soon encourage major violations. Many violations, however, are innocently created, and the administrator has followed the practice of giving a zone violator reasonable opportunity to discontinue the violation before prosecuting him. The city attorney has always insisted that the ordinance be so worded that violations can be prosecuted as misdemeanors, rather than by injunction methods as used in some cities.

A later charter amendment, adopted in 1947, transferred the responsibility of enforcing the zoning ordinance to the Department of Building and Safety, and empowered the zoning administrator to hear and determine appeals from any order, requirement, decision, or determination made by said department in its zoning enforcement activities.

New Comprehensive Zoning Ordinance

The next and latest step in the evolution of the zoning system in Los Angeles was the adoption, in 1946, of a new entirely comprehensive zoning ordinance, with accompanying maps, which for the first time precisely zoned all parts of the city. Some features of the new ordinance and its correlation with other phases of the master plan are worth emphasis.

The San Fernando Valley section of the city contains about 212 sq miles in the northern part. The problems incident to preparing an intelligent master plan for this rapidly growing section of the city and implementing such a plan with proper land use control, were probably the chief motivating influences in the preparation and adoption of the new ordinance. It was found that the then existing zoning regulations were not adequate to accomplish the type of land use control necessary. The major part of the valley was essentially agricultural in nature and some type of zone was necessary that would protect and encourage the use and retention of large areas in the valley for agricultural pursuits. It was particularly necessary to have legislation on the books which could be used in connection with land subdivision control to prevent the premature division, into urban town lots, of large sections of agricultural land in areas that were not properly served with public utilities.

Quantitative Subdivision Control Problems

The subdivision control ordinance adopted for Los Angeles, pursuant to authority of state law and policies of the City Planning Commission and the City Council thereunder, required all new recorded subdivisions to install public utilities and improve all dedicated streets. The cost of these improvements somewhat deterred premature land subdivision. Nevertheless, the absorption of subdividable land in other sections of the city and the pressure of a housing shortage for additional homes, coupled with the activities of large-

scale home building concerns, were resulting in the premature subdivision of farms and citrus groves in isolated sections of the valley. The cost to the general taxpayer of extending public utility lines, building new schools, and providing other urban services to these isolated subdivisions, and the fact that some of the areas were not served or servable with trunk-line sewers, and that cesspool or septic tanks might pollute the underground water supply which comes from this area and augments other water supplies—pointed up the necessity of additional zoning regulations for this area. Furthermore, the competition among land developers for the purchase of subdividable acreage in this area and the high prices paid for agricultural land were being reflected in assessed valuations which considered most agricultural property as potential subdivisions with a resulting tax rate that made the continued use of the property for agricultural pursuits entirely unprofitable.

Therefore, the new comprehensive zoning ordinance was devised not only to solve the problems in the rapidly developing San Fernando Valley but to modernize the entire zoning system for the remainder of the city, using density regulations throughout and several new devices for more effective land use control. The ordinance included for the first time agricultural zones which, in addition to controlling the size of parcels of land, liberalized former protective regulations in the agricultural areas by automatically permitting dairies, horse raising ranches, and other animal husbandry pursuits in some of the agricultural zones if sufficient land area were utilized. The A–1 zone requires a minimum five-acre area, the A–2 zone a minimum two-acre area, and the R–A zone a minimum area of 20,000 sq ft. In all other zones a minimum lot area of 5000 sq ft was required for any residential use.

Agricultural Zones Effective in San Fernando Valley

The agricultural zones, with their area requirements as applied to the San Fernando Valley, have proved indispensable in controlling the phenomenal subdivision activities that have occurred in that district since 1946. In 1950 alone, 3,622 acres were subdivided. The urbanization of this area has even exceeded the expectations of the planning department in the original allocation of urban types of residential zones and it has been necessary, on application, to reclassify some of the areas from the A–2 or R–A zones to an R–1 zone in order to permit town lot subdivisions and the construction of badly needed low-cost homes for veterans. Each of these requests, however, has been correlated with the subdivision control activities and the practicability of serving the area with public utilities. Most of the requested changes which were approved carried a stipulation that the ordinance would not be adopted until a subdivision plan for the area had been approved and was ready for recordation. The Health Department and the Water Department have been brought into the picture, and those subdivisions which could not be served with sewers and which otherwise might contaminate the underground water supply have been rejected. Although the new zoning ordinance contained, when adopted, a total of sixteen different zone classifications, the aforementioned land subdivision and rezoning activity emphasized the desirability of still another zone between the R–A with its 20,000-sq-ft lot area and the R–1 with its 5000-sq-ft

lot area. This resulted in the creation of a new R–S zone which has a minimum lot area of 7500 sq ft.

The provisions of the zoning ordinance which preclude the selling or creation of parcels of land below the minimum lot widths and areas specified in the particular zone have already been the subject of an important court decision in which the California Supreme Court sustained the validity of the ordinance.[5] This case involved selling units of a bungalow court with only 900 sq ft of lot area for each unit instead of the 5,000-sq-ft minimum required by the ordinance.

New Innovations

Several innovations were included in the zoning ordinance. The requirements for offstreet parking or garage space in connection with all multiple dwellings, which formerly applied only in the residential zones, were expanded to apply to residential uses in any zone and were also expanded to include offstreet parking space for all types of uses that might create an on-street parking problem. Churches, schools, theaters, auditoriums, stadiums, and other places of public assemblage are required to provide parking space for one automobile for each ten seats. All commercial and industrial buildings having more than 7,500 sq ft of floor area are required to provide one parking space for each 1,000 sq ft of floor area in the building. The ordinance goes back to the principle sustained in the Hadacheck Case by employing a type of retroactive zoning. Nonconforming uses of land, where no main buildings are concerned, as well as nonconforming billboards and outdoor advertising structures and nonconforming uses of conforming buildings were required to be removed in five years. Nonconforming business and industrial buildings in all residential zones are required to be removed within a stated period of years depending on the type of construction of the building and its age. This provision does not become operative for twenty years from the effective date of the ordinance in order to permit a reasonable amortization period for these nonconforming buildings. It provides that these buildings shall be removed or converted to conforming buildings within a period dated from the time the building was erected—forty years for class I and II buildings, thirty years for class III and IV buildings, and twenty years for class V buildings, as such classes of buildings are defined in the building code. The ordinance for the first time recognizes the need for affording better protection to industrial districts from the harassment of residential uses located therein and also of removing the unhealthful, hazardous, and blighting effect of heavy industry on such residential uses by prohibiting further residential development in the M–3 heavy industrial zone. A new P or parking zone has been established which is combined with residential zone classification on certain strategic areas adjoining business sections, and under proper controls permits offstreet automobile parking in addition to the permitted residential uses.

Oil Drilling and Rock and Gravel Extraction

The important oil drilling activities and rock and gravel extracting enterprises which occur in several sections of the city are recognized and properly controlled by the creation of special oil drilling districts and rock and gravel

[5] Clemons vs City of Los Angeles (1950) 36 Cal. 2d 95.

districts which overlap the other precise zoning classifications. These districts do not automatically permit oil drilling or rock and gravel extracting but require that applications in each instance be submitted for determination of conditions and methods of operation to be employed in the particular location in question. The City Planning Commission determines the conditions and methods of operation for rock and gravel extraction and the zoning administrator determines the conditions and methods of operation in connection with each oil drilling enterprise within an oil drilling district. Some of the newer oil fields in residential sections are scarcely discernible since conditions require that the derricks must be removed on completion of the well and the property landscaped around the low electric-powered pumping unit.

Conditional Uses

It has long been recognized that there are certain problem type and community service uses which require special types of locations that cannot always be anticipated or provided for in the zoning plan and which, if located in residential zones, are difficult to justify as a zone variance or a change of zone. The new ordinance covers this problem by enumerating these uses which may be located in certain zones only if their location is first approved by the City Planning Commission in some instances and by the zoning administrator in other instances. These uses are called "conditional uses," and the procedure for processing requests for such uses is very similar to the procedure used in other jurisdictions for handling so-called use permits or special zoning exceptions. The type of uses over which the City Planning Commission has jurisdiction are those which essentially might have some bearing on the master plan or overall land use pattern such as cemeteries, airports, full-time schools and universities, churches, hospitals with more than a hundred beds, governmental enterprises, and public utility and public service uses or structures. The type of conditional uses which the administrator has authority to process include such matters as philanthropic and correctional institutions, private schools without a full curriculum, private clubs, privately operated recreational facilities, motion picture studios, radio or television transmitters, columbariums and mausoleums, mortuaries or funeral parlors and trailer camps in commercial zones, and tourist courts or trailer camps on property abutting federal or state highways. Appeals from the zoning administrator's decisions on conditional use requests may be taken to the Board of Zoning Appeals in the same manner as appeals concerning zone variance requests. Appeals from the City Planning Commission's decisions on those conditional uses over which they have jurisdiction may be taken to the City Council. A California Supreme Court dedecision concerning a cemetery which the City Council authorized in a residential district, after disapproval by the City Planning Commission, has sustained the conditional use procedure contained in the Los Angeles zoning ordinance.[6]

Zoning No Hindrance to Rapid Growth

The zoning regulations in Los Angeles have never interfered with its expansion but have only served to make its development more healthy and

[6] Essick vs City of Los Angeles (1950) 34 Cal. 2d 614.

orderly. The most rapid growth in both the 1920's and again in the 1940's was experienced after the adoption of new zoning ordinances.

In the ten-year period between 1940 and 1950 the population of Los Angeles increased by 455,000. During 1950 alone a total of 66,444 building permits was issued at a valuation greater than $407,178,693, and 32,579 dwelling units were constructed. An average of 25,756 dwelling units have been constructed in each of the five years from 1946 through 1950.

Conclusion

Experience has demonstrated that in this modern age no city of any size can afford to permit its citizens to be "rugged individualists" and to develop their property without the guiding influence and protection of a well-conceived comprehesive zoning plan. City planning cannot be effective—it cannot accomplish its purpose—without implementation of reasonable land use control provided through zoning. Zoning need no longer be thought of in terms of negative legislation—that which prohibits. It should be used and thought of as a positive instrument to effectuate the master plan by directing and molding growth along orderly lines. Zoning should be administered in close coordination with strict control over land subdivisions—both quantitative and qualitative. Without complete and early establishment of both of these forms of control, reasonable regulation of land use becomes difficult and ineffective. Zoning is a present means of avoiding future city problems.

DISCUSSION

HENRY HOROWITZ,[7] J. M. ASCE.—An excellent explanation of the administration of the Los Angeles zoning ordinance is presented by Mr. Smutz.

The zoning administrator is given original jurisdiction to hear and determine all applications for variances from the zoning regulations; original jurisdiction to approve the location of certain conditional uses; and appellate jurisdiction to hear and determine appeals from any order, requirement, decision, or determination made by the Department of Building and Safety. On the administrator's shoulders rests a burden of no small weight.

In an action before a judicial body, the opposing parties are usually in disagreement as to the true facts; and, when the court has determined the true conditions, a correct solution will usually follow. In a proceeding before a quasi-judicial body, such as the office of zoning administrator, the parties usually are in agreement as to the facts, but conflict regarding the proper answer. It is noted at once that in the discretion of the administrator lies the granting or denial of the petitioner's request.

Under the heading, "Office of Zoning Administrator Created," it is stated that "* * * The administrator does not have full discretion * * *" because the charter requires four specific findings before a variance may be granted. Actually, these findings present no limitation because they are of such a nature that should they be disregarded there would be an abuse of discretion even if the charter did not expressly require that they be present before a variance is granted.

This writer feels that the granting of variances is too important a power to rest with a one-man administrative board. It is suggested that the method employed for the establishment of conditional uses be adopted for the granting of variances—that is, to allow the administrator to grant deviations from the zoning regulations when such deviations are of minor importance. The variances which involve large land area or pecuniary interest should be left for the City Planning Commission.

It is true that, under the present system, the decisions of the zoning administrator are subject to review by the Board of Zoning Appeals. This fact adds no sanction to the handling of important variance problems by the zoning administrator because hearings before administrative boards are time-consuming and expensive.

HUBER EARL SMUTZ,[8] A. M. ASCE.—The remarks and comments expressed by Mr. Horowitz are greatly appreciated. He makes an interesting comment that the findings specified in the Los Angeles City Charter, as a prerequisite to the granting of a variance, present no limitation on the zoning administrator, since they are of such a nature that, should they be disregarded, there would

[7] Asst. Civ. Engr., Dept. of City Planning, New York, N. Y.

[8] Zoning Administrator, City of Los Angeles, Calif.

be an abuse of discretion. Theoretically, this is a correct statement. However, the findings are a device with which to measure each requested variance in considering the application of discretion. They are particularly necessary as a guide for the lay members of the Board of Zoning Appeals who cannot be expected to have the experience and knowledge of zoning principles which might enable a qualified zoning administrator to use discretion. The findings are also valuable in explaining to lay applicants why there would be an abuse of discretion from a zoning standpoint in granting a particular request. The zoning administrator, despite an attempt to maintain a quasi-judicial approach toward each application, is frequently subjected to strong pressures with respect to a particular application. It is most helpful to the administrator to be able to use the measuring devices prescribed by the city charter for judging applications, and to challenge those applying pressure or criticism to explain how the application fits the prescribed measurements.

Mr. Horowitz' statement that "* * * the granting of variances is too important a power to rest with a one-man administrative board" deserves comment. This is an opinion usually expressed by uninformed disgruntled applicants or politicians. Planning experts and authorities on zoning administration and practice, after a study of the operation of zoning adjustment boards or planning commissions, agree that in most instances these agencies do not properly exercise their authority to grant variances and are too liberal in the delicate adjustments which they have the power to grant. This is substantiated by many court decisions overruling such boards for overstepping the boundaries of the zoning variance. A study of the actions taken by the Board of Zoning Appeals of Los Angeles on appeals from decisions of the zoning administrator, which are the only cases it considers, will confirm this opinion. This situation is partly understandable since the appointed lay personnel on such boards and commissions are frequently changed. Because of this turnover no member has time enough to obtain from experience, or from study and review, the knowledge of zoning law and techniques which is desirable for proper performance of his duties.

There is merit in Mr. Horowitz' opinion, if the zoning administrator is a political appointee who might change with each administration. This possibility was carefully guarded against, in Los Angeles, by the requirement that the administrator come under civil service provisions and be chosen by examination based on experience and ability. An impartial survey will reveal that the administrator has maintained far more consistent policies and a more impartial approach to applications than could be obtained through any other method. Persons who have had applications processed under both the old and new methods have stated that the impartial, informed, quasi-judicial approach and consistent policies of the zoning administrator are preferred to the approach of a politically appointed board or commission

Few people question the judicial system under which judges in the lower courts sit as individuals and render decisions and pronounce sentences on far more weighty problems than most zone variance requests. Many such judges are appointed or elected under political consideration rather than for their abilities or qualifications for the office. The zoning administrator, however,

is selected for his office by examination which tests both his abilities and qualifications for the position. Why then is the granting of variances a power too important to be vested in the zoning administrator?

Mr. Horowitz seems not to realize the effect of the right of appeal from decisions of the administrator to the Board of Zoning Appeals. He feels that such a right lends no sanction to the zoning administrator and is both "time-consuming and expensive." The right of appeal provides a system of checks and balances which protects citizens from dictatorial and arbitrary public officials. The appeal was instituted to prevent the administrator from becoming too liberal and granting unjustified variances. The reverse has proved to be the result since the Board of Zoning Appeals, in the few cases in which it has reversed the decision of the administrator, has rarely denied a variance which the zoning administrator granted, but too often has granted variances over his denial or has relaxed his conditions.

In the only case under the Los Angeles system to be adjudicated, the feeling that the board has been too liberal has been affirmed. The case involved a request for variance to erect and maintain an automobile service station in a multiple-family residential zone. The variance was denied by the administrator but was granted by the Board of Zoning Appeals. Adjacent homeowners took the matter to court where the trial judge, in a memorandum ruling, affirmed the administrator's denial of the request and cited the administrator for "a keen sense of the requirements of the law and his duty." The court denounced the board's action and findings with a decision which included the following:[9]

> "If the Board of Appeals is to be permitted to operate, as it has in this instance, the quicker the City of Los Angeles junks the entire Comprehensive Zoning Plan the better for all concerned, as in the long run it will be but an aching memory."

This decision, added to similar decisions of the courts in other jurisdictions, serves to justify further the thoroughly tested system which utilizes a full-time, qualified, one-man board of zoning adjustments, called a "Zoning Administrator," to hear and decide on all applications for variances from the zoning regulations.

[9] Beloin et al vs Blankenhorn & Board of Zoning Appeals, Superior Court Case 560,288.

AMERICAN SOCIETY OF CIVIL ENGINEERS

Founded November 5, 1852

TRANSACTIONS

Paper No. 2559

ANALYSIS OF ARCH DAMS OF VARIABLE THICKNESS

By W. A. Perkins,[1] M. ASCE

With Discussion by Messrs. Alfred L. Parme; L. J. Mensch; Fairfax D. Kirn and Gurmukh S. Sarkaria; A. C. Josephs; George E. Goodall; and W. A. Perkins

Synopsis

The advantage that can frequently be gained by increasing the thickness of arch dams toward the abutments in order to allow for the larger moments has made it desirable to find a workable expression for such thickening. This expression must be sufficiently flexible to permit any degree of thickening and, in addition, should be adaptable to mathematical analysis. These criteria were found to be satisfied by the law of variation of thickness that was made the basis for the formulas and curves presented in this paper.

The developed formulas are long and complex, but their use has been made practical by a series of curves and abbreviated formulas in which values from the curves are to be substituted. These formulas (Table 1) and curves and an example of their use are given following the development of the general formulas. By the use of the simplified formulas and curves, stresses and deflections can be computed analytically with a slide rule, without the aid of tables or a computing machine. This simple procedure permits, much more readily, the selection of an arch of the most economical dimensions to fit given conditions.

Introduction

Notation.—The letter symbols introduced in this paper are defined where they first appear, in the text, or by illustration, and are assembled alphabetically in the Appendix for convenience of reference.

Summary of Theory.—Solution of the problem of finding a workable expression for the thickening of arch dams toward the abutments is based on the method of analysis used by the late William Cain,[2] M. ASCE. In so far as

Note.—Published in May, 1952, as *Proceedings-Separate No. 129.* Positions and titles given are those in effect when the paper or discussion was received for publication.

[1] Cons. Engr., Sacramento, Calif.

[2] "The Circular Arch Under Normal Loads," by William Cain, *Transactions*, ASCE, Vol. LXXXV, 1922, p. 233.

possible the nomenclature and solutions of this paper are in accordance with those used by Mr. Cain, to facilitate understanding by those familiar with the Cain formula.

The law of variation of thickness of the arch is

$$t = \frac{t_o}{\cos (a\,\phi)} \qquad (1)$$

in which t is the thickness at angular distance ϕ from the crown; t_o is the thickness at the crown; and a is a factor (usually varying from 0 to 1) by which the angle ϕ is multiplied before taking the cosine. For example, if $t_o = 30$ ft, $a = 0.5$, and $\phi = 40°$,

$$t = \frac{30}{\cos (0.5 \times 40)} = \frac{30}{\cos 20} = \frac{30}{0.94} = 31.9$$

When $a = 0$, t at any point $= t_o/1 = t_o$ which represents an arch of uniform thickness. The moment of inertia I at any point ϕ is

$$I = \frac{t_o^3}{12 \cos^3 a\,\phi} \qquad (2)$$

Fig. 1 represents an arch ring, 1 ft in depth, perpendicular to the plane of the paper, that varies in thickness in accordance with the law previously stated.

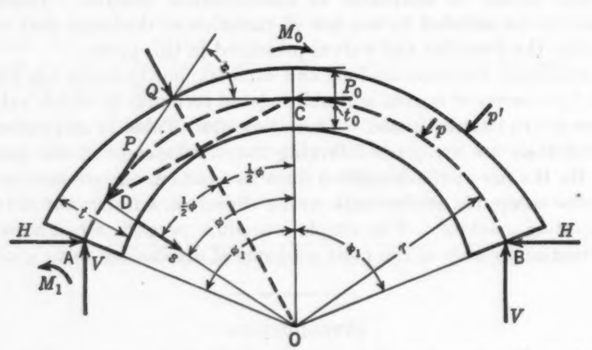

Fig. 1.—Elements of the Arch Ring

Throughout this paper the subscript e will indicate the extrados location, i the intrados, o the crown, 1 the abutment, and t the temperature.

Moment Thrust and Shear

Using Fig. 1 to define the symbols, the equations derived by Mr. Cain are summarized here. The values of V_e and H_e are determined at the abutments,

but the other equations give values at any point D whose coordinates are (r, ϕ)

$$Q_c = p \times 2\,r \sin\frac{\phi}{2} \qquad (3)$$

$$V_c = p\,r \sin\phi_1 \qquad (4)$$

$$H_c = p\,r \cos\phi_1 - (p\,r - P_o) \qquad (5)$$

$$M = M_o + (p\,r - P_o)\,r\,(1 - \cos\phi) \qquad (6)$$

$$P = p\,r - (p\,r - P_o)\cos\phi \qquad (7)$$

$$S = (p\,r - P_o)\sin\phi \qquad (8)$$

$$t = \frac{t_o}{\cos a\,\phi} \qquad (9)$$

Determination of Substitution Factors.—Taking the partial derivatives of Eqs. 6, 7, and 8,

$$\frac{dM}{dM_o} = 1 \qquad (10a)$$

$$\frac{dM}{dP_o} = -\,r\,(1 - \cos\phi) \qquad (10b)$$

$$\frac{dP}{dM_o} = 0 \qquad (11a)$$

$$\frac{dP}{dP_o} = \cos\phi \qquad (11b)$$

$$\frac{dS}{dM_o} = 0 \qquad (12a)$$

$$\frac{dS}{dP_o} = -\sin\phi \qquad (12b)$$

The internal elastic work, L, of the semi-arch is

$$L = \frac{r}{2}\int_0^{\phi_1}\frac{M^2\,d\phi}{E\,I} + \frac{r}{2}\int_0^{\phi_1}\frac{p^2\,d\phi}{E\,t} + 2.88\,\frac{r}{2}\int_0^{\phi_1}\frac{S^2\,d\phi}{E\,t} \qquad (13)$$

By the theorem of Alberto Castigliano,[3] the values of the unknowns, M_o and P_o, can be found by letting $dL/dM_o = 0$ and $dL/dP_o = 0$ and solving. Since the shear at the crown is 0, these are the only unknowns to be found.

Differentiating Eq. 13, dividing the result by dM_o, and remembering that $dM/dM_o = 1$, $dP/dM_o = 0$, and $dS/dM_o = 0$, the simplified result is

$$\frac{dL}{dM_o} = r\int_0^{\phi_1}\frac{M\,d\phi}{I} = 0 \qquad (14)$$

[3] "Systèmes Élastiques," by Alberto Castigliano, p. 265.

now,

$$I = \frac{t^3_o}{12 \cos^3 a \phi} \qquad (15)$$

and

$$M = M_o + (p\,r - P_o)\,r\,(1 - \cos\phi)$$
$$= M_o + r\,(p\,r - P_o) - r\,(p\,r - P_o)\cos\phi \qquad (16)$$

Substituting the values of Eqs. 15 and 16 in Eq. 14, the expanded expression is

$$\frac{12\,r}{t^3_o}\left[M_o + (p\,r - P_o)\,r\right]\int_0^{\phi_1} \cos^3 a\,\phi\,d\phi - \frac{12\,r}{t^3_o}(p\,r^2 - P_o\,r)\int_0^{\phi_1}\cos\phi\cos^3 a\,\phi\,d\phi = 0 \qquad (17)$$

Let

$$\frac{12\,r}{t^3_o}\left[M_o + (p\,r - P_o)\,r\right] = U \qquad (18)$$

and

$$\frac{12\,r}{t^3_o}(p\,r^2 - P_o\,r) = W \qquad (19)$$

Note that

$$\cos^3 a\,\phi = \tfrac{1}{4}(\cos 3\,a\,\phi + 3\cos a\,\phi) \qquad (20)$$

Substituting Eqs. 18, 19, and 20 in Eq. 17,

$$\frac{U}{4}\int_0^{\phi_1}(\cos 3\,a\,\phi\,d\phi + 3\cos a\,\phi\,d\phi) - \frac{W}{4}\int_0^{\phi_1}(\cos\phi\cos 3\,a\,\phi\,d\phi + \cos\phi\,3\cos a\,\phi\,d\phi) = 0 \qquad (21)$$

Multiply this integral expression by 4 and integrate to obtain

$$U\left[\left(\frac{\sin 3\,a\,\phi_1}{3\,a}\right) + \left(\frac{3\sin a\,\phi_1}{a}\right)\right] - \frac{W}{2}\left[\left(\frac{\sin(1+3\,a)\,\phi_1}{(1+3\,a)}\right) + \left(\frac{\sin(1-3\,a)\,\phi_1}{(1-3\,a)}\right) + \left(\frac{3\sin(1+a)\,\phi_1}{(1+a)}\right) + \left(\frac{3\sin(1-a)\,\phi_1}{(1-a)}\right)\right] = 0 \qquad (22)$$

If the expression in brackets after U is designated C and that after $W/2$ is called B, Eq. 22 becomes

$$U\,C - \frac{W\,B}{2} = 0 \qquad (23)$$

Dividing the differential of Eq. 13 by dP_o gives

$$\frac{dL}{dP_o} = \int_0^{\phi_1}\frac{M\,dM\,d\phi}{I\,dP_o} + \int_0^{\phi_1}\frac{P\,dP\,d\phi}{t\,dP_o} + 2.88\int_0^{\phi_1}\frac{S\,dS\,d\phi}{t\,dP_o} = 0 \qquad (24)$$

Substituting in Eq. 24 the values of dM/dP_o, dP/dP_o, and dS/dP_o from Eqs. 10*b*, 11*b*, and 12*b*, respectively, and utilizing Eq. 14,

$$r \int_0^{\phi_1} \frac{M \cos\phi \, d\phi}{I} + \int_0^{\phi_1} \frac{P \cos\phi \, d\phi}{t} - 2.88 \int_0^{\phi_1} \frac{S \sin\phi \, d\phi}{t} = 0 \ldots (25)$$

In the first integral term of Eq. 25 the values of M and I from Eqs. 15 and 16 are substituted. This term becomes

$$\frac{12\,r}{t^3_o}(M_o + p\,r^2 - P_o\,r) \int_0^{\phi_1} \cos\phi \cos^3 a\,\phi \, d\phi$$
$$- \frac{12\,r}{t^3_o}(p\,r^2 - P_o\,r) \int_0^{\phi_1} \cos^2\phi \cos^3 a\,\phi \, d\phi \,.. (26)$$

Noting that $\cos^2\phi = \frac{1}{2}(1 + \cos 2\,\phi)$ and substituting the equivalent values of U and W as given by Eqs. 18 and 19 and also the value for $\cos^3 a\,\phi$, Eq. 26 becomes

$$\frac{U}{4} \int_0^{\phi_1} \cos\phi \cos 3\,a\,\phi \, d\phi + 3 \cos\phi \cos a\,\phi \, d\phi$$
$$- \frac{W}{8} \int_0^{\phi_1} [(1 + \cos 2\,\phi) \cos 3\,a\,\phi \, d\phi + (1 + \cos 2\,\phi)\, 3 \cos a\,\phi \, d\phi] \,.. (27a)$$

The expression after $U/4$ is the same as that after $W/4$ in the integral expression in Eq. 21. Integration of this term gives $U\,B/8$. Integration of the second term of Eq. 27*a* gives

$$- \frac{W}{8} \left[\frac{\sin 3\,a\,\phi_1}{3\,a} + \frac{\sin (2 + 3\,a)\,\phi_1}{2\,(2 + 3\,a)} + \frac{\sin (2 - 3\,a)\,\phi_1}{2\,(2 - 3\,a)} \right.$$
$$\left. + \frac{3 \sin a\,\phi_1}{a} + \frac{3 \sin (2 + a)\,\phi_1}{2\,(2 + a)} + \frac{3 \sin (2 - a)\,\phi_1}{2\,(2 - a)} \right] \,.. (27b)$$

The expression in brackets is now designated A. The simplified form of the first term of Eq. 25 after integration is

$$\frac{U\,B}{8} - \frac{W\,A}{8} \ldots\ldots\ldots\ldots\ldots\ldots (28)$$

In the second term of Eq. 25 the value of P, given in Eq. 7, and the value of t, given in Eq. 9, are substituted. The resulting integral expression is

$$\int_0^{\phi_1} \frac{P \cos\phi \, d\phi}{t} = \frac{1}{t_o} \int_0^{\phi_1} p\,r \cos\phi \cos a\,\phi \, d\phi$$
$$- \frac{1}{t_o} \int_0^{\phi_1} (p\,r - P_o) \cos^2\phi \cos a\,\phi \, d\phi \,.. (29)$$

The integral of this expression is

$$\frac{p\,r}{2\,t_o}\left[\frac{\sin(1+a)\,\phi_1}{(1+a)}+\frac{\sin(1-a)\,\phi_1}{(1-a)}\right]$$
$$-\frac{(p\,r-P_o)}{2\,t_o}\left[\frac{\sin a\,\phi_1}{a}+\frac{\sin(2+a)\,\phi_1}{2\,(2+a)}+\frac{\sin(2-a)\,\phi_1}{2\,(2-a)}\right]\ldots(30)$$

The expression in the first set of brackets is designated K and that in the second set is designated F. The simplified form of Eq. 30 then becomes

$$\frac{p\,r}{2\,t_o}K-\frac{(p\,r-P_o)}{2\,t_o}F\ldots\ldots\ldots\ldots\ldots\ldots\ldots(31)$$

In the third term of Eq. 25 the values of S and t from Eqs. 8 and 9 are substituted, and for the resulting $\sin^2\phi$ the term $(1-\cos 2\,\phi)/2$ is used

$$2.88\int_0^{\phi_1}\frac{S\sin\phi\,d\phi}{t}=\frac{2.88\,(p\,r-P_o)}{2\,t_o}\int_0^{\phi_1}(1-\cos 2\,\phi)\cos a\,\phi\,d\phi\ldots(32)$$

The integral of this expression is

$$2.88\,\frac{(p\,r-P_o)}{2\,t_o}\left[\frac{\sin a\,\phi}{a}-\frac{\sin(2+a)\,\phi_1}{2\,(2+a)}-\frac{\sin(2-a)\,\phi_1}{2\,(2-a)}\right]\ldots(33)$$

If the expression in brackets is designated J, Eq. 33 becomes

$$\left[\frac{2.88\,(p\,r-P_o)}{2\,t_o}\right]J\ldots\ldots\ldots\ldots\ldots\ldots\ldots(34)$$

After integration of Eq. 25 the complete simplified form is

$$\frac{U\,B}{8}-\frac{W\,A}{8}+\frac{p\,r\,K}{2\,t_o}-\frac{(p\,r-P_o)\,F}{2\,t_o}-\frac{2.88\,(p\,r-P_o)\,J}{2\,t_o}=0\ldots(35)$$

The values of M_o and P_o are determined by simultaneous solution of Eqs. 23 and 35. Eq. 23 is multiplied by $B/4$:

$$\frac{U\,B\,C}{4}-\frac{W\,B^2}{8}=0\ldots\ldots\ldots\ldots\ldots\ldots\ldots(36)$$

Eq. 35 is multiplied by $2C$:

$$\frac{U\,B\,C}{4}-\frac{W\,A\,C}{4}+\frac{p\,r\,C\,K}{t_o}-\frac{(p\,r-P_o)\,C\,F}{t_o}-\frac{2.88\,(p\,r-P_o)\,C\,J}{t_o}=0\ldots(37)$$

Subtracting Eq. 37 from Eq. 36,

$$\frac{W}{8}(2\,A\,C-B^2)+[p\,r-P_o]\left[\frac{(C\,F+2.88\,C\,J)}{t_o}\right]=\frac{p\,r\,C\,K}{t_o}\ldots(38)$$

The value $\frac{12 r^2}{t^3_o}(p r - P_o)$ is substituted for W:

$$(p r - P_o)\left[\frac{F C}{t_o} + \frac{1.5 r^2}{t^3_o}(2 A C - B^2) + \frac{2.88 C J}{t_o}\right] = \frac{p r C K}{t_o} \quad (39a)$$

Rearranging,

$$(p r - P_o) = \frac{p r K}{\frac{r^2}{t^2_o}\left[1.5\left(2 A - \frac{B^2}{C}\right)\right] + F + 2.88 J} \quad (39b)$$

Summary of Substitution Factor.—For convenience, the expressions for which the factors A, B, C, K, F, and J have been substituted are listed as Eqs. 40 to 45:

$$\frac{\sin 3 a \phi_1}{3 a} + \frac{\sin (2 + 3 a)\phi_1}{2(2 + 3 a)} + \frac{\sin (2 - 3 a)\phi_1}{2(2 - 3 a)} + \frac{3 \sin a \phi_1}{2} + \frac{3 \sin (2 + a)\phi_1}{2(2 + a)} + \frac{3 \sin (2 - a)\phi_1}{2(2 - a)} = A \quad (40)$$

$$\frac{\sin (1 + 3 a)\phi_1}{(1 + 3 a)} + \frac{\sin (1 - 3 a)\phi_1}{(1 - 3 a)} + \frac{3 \sin (1 + a)\phi_1}{(1 + a)} + \frac{3 \sin (1 - a)\phi_1}{(1 - a)} = B \quad (41)$$

$$\left(\frac{\sin 3 a \phi_1}{3 a}\right) + \left(\frac{3 \sin a \phi_1}{a}\right) = C \quad (42)$$

$$\frac{\sin a \phi_1}{a} + \frac{\sin (2 + a)\phi_1}{2(2 + a)} + \frac{\sin (2 - a)\phi_1}{2(2 - a)} = F \quad (43)$$

$$\frac{\sin (1 + a)\phi_1}{1 + a} + \frac{\sin (1 - a)\phi_1}{1 - a} = K \quad (44)$$

and

$$\frac{\sin a \phi_1}{a} - \frac{\sin (2 + a)\phi_1}{2(2 + a)} - \frac{\sin (2 - a)\phi_1}{2(2 - a)} = J \quad (45)$$

It will be noted that the terms in factor C are the same as the first and fourth in factor A; the terms in factor F are one third the value of the last three terms in factor A; the terms of factor K are one third the value of the last two terms in factor B; and factor J is the same as factor F, except that the signs of the last two terms are minus instead of plus.

Derivation of Simplified Equations.—In Eq. 23 the values of factors U and W are substituted, giving

$$\frac{12 r}{t^3_o}[M_o + (p r - P_o) r]\frac{2 C}{2} - \frac{12 r}{t^3_o}(p r - P_o) r \frac{B}{2} = 0 \quad (46a)$$

Clearing terms,

$$2 C M_o = (p r - P_o) r (B - 2 C) \quad (46b)$$

Simplifying,

$$M_o = (p\,r - P_o)\,r\left(\frac{B}{2\,C} - 1\right) \qquad (46c)$$

Also, from Eq. 6,

$$M = M_o + (p\,r - P_o)\,r\,(1 - \cos\phi) = (p\,r - P_o)\,r\left(\frac{B}{2\,C} - \cos\phi\right) \qquad (47)$$

From Eq. 7,

$$P_o = p\,r - (p\,r - P_o) \qquad (48)$$

and

$$P = p\,r - (p\,r - P_o)\cos\phi \qquad (7)$$

Using Eqs. 7, 8, 39*b*, 46*c*, and 47, the moment, thrust, and shear at any point in the arch can be determined.

Unit stresses are determined by the formula,

$$s = \left(\frac{p}{t}\right) \pm \left(\frac{6\,M}{t^2}\right) \qquad (49)$$

Radial Deflection, n, of the Crown

The integral expression for finding the coefficient of deflection,[4] in terms of the nomenclature adapted, is

$$\frac{E\,n}{r} = \int_0^{\phi_1} \frac{M\,r\sin\phi\,d\phi}{I} + \int_0^{\phi_1} \frac{P\sin\phi\,d\phi}{t} + \int_0^{\phi_1} \frac{2.883\cos\phi\,d\phi}{t} \qquad (50)$$

In the first term of Eq. 50 equivalent values are substituted for M and I, using for $\cos^3 a\,\phi$ the expression $\frac{1}{4}(\cos 3\,a\,\phi + 3\cos a\,\phi)$.

The transformed expression for the first term of Eq. 50 becomes

$$\int_0^{\phi_1} \frac{12\,r}{t^3_o}\left[(p\,r^2 - P_o\,r)\left(\frac{B}{2\,C} - \cos\phi\right)\frac{\sin\phi}{4}(\cos 3\,a\,\phi + 3\cos a\,\phi)\right]d\phi \qquad (51a)$$

A more convenient form for integration of Eq. 51 is

$$\frac{W\,B}{8\,C}\int_0^{\phi_1}[\sin\phi\cos 3\,a\,\phi\,d\phi + \sin\phi\,3\cos a\,\phi\,d\phi]$$
$$- \frac{W}{4}\int_0^{\phi_1}[\sin\phi\cos\phi\cos 3\,a\,\phi\,d\phi + \sin\phi\cos\phi\,3\cos a\,\phi\,d\phi] \qquad (51b)$$

In the second term of Eq. 50 equivalent values are substituted for P and t

$$\int_0^{\phi_1} \frac{[p\,r - (p\,r - P_o)\cos\phi]\sin\phi\cos a\,\phi\,d\phi}{t_o} \qquad (52a)$$

[4] "The Circular Arch Under Normal Loads," by William Cain, *Transactions*, ASCE, Vol. LXXXV, 1922, p. 270.

Simplifying,

$$\int_0^{\phi_1}\left[\frac{p\,r\sin\phi\cos a\,\phi\,d\phi}{t_o}-\frac{(p\,r-P_o)}{t_o}\sin\phi\cos\phi\cos a\,\phi\,d\phi\right]\ldots(52b)$$

In the third term of Eq. 50 the equivalent values of S and t are substituted:

$$2.88\,\frac{(p\,r-P_o)}{t_o}\int_0^{\phi_1}\sin\phi\cos\phi\cos a\,\phi\,d\phi\ldots\ldots\ldots\ldots(53)$$

Eqs. 51b, 52b, and 53 are now integrated between the limits 0 and ϕ_1, remembering that for $\phi = 0$, $\cos\phi = 1$,

$$\begin{aligned}
n = \frac{r}{E\,t_o}\Bigg\{&\frac{12\,r^2}{t_o^2}(p\,r-P_o)\\
&\times\Bigg[\frac{B}{16\,C}\left(\frac{1-\cos(1+3\,a)\,\phi_1}{1+3\,a}+\frac{1-\cos(1-3\,a)\,\phi_1}{1-3\,a}\right)\\
&+\frac{3\,B}{16\,C}\left(\frac{1-\cos(1+a)\,\phi_1}{1+a}+\frac{1-\cos(1-a)\,\phi_1}{1-a}\right)\\
&-\frac{1}{16}\left(\frac{1-\cos(2+3\,a)\,\phi_1}{2+3\,a}+\frac{1-\cos(2-3\,a)\,\phi_1}{2-3\,a}\right)\\
&-\frac{3}{16}\left(\frac{1-\cos(2+a)\,\phi_1}{2+a}+\frac{1-\cos(2-a)\,\phi_1}{2-a}\right)\Bigg]\\
&+\frac{P\,r}{2}\left(\frac{1-\cos(1+a)\,\phi_1}{1+a}+\frac{1-\cos(1-a)\,\phi_1}{1-a}\right)\\
&+0.47\,(p\,r-P_o)\left(\frac{1-\cos(2+a)\,\phi_1}{2+a}+\frac{1-\cos(2-a)\,\phi_1}{2-a}\right)\Bigg\}\ldots(54)
\end{aligned}$$

in which n is the radial deflection of the crown.

Integrating the second half of Eqs. 52b and 53 gives $-\frac{p\,r-P_o}{4}$ and $\frac{2.88\,(p\,r-P_o)}{4}$ times the expression in brackets in the last term of Eq.54. Combining, $\frac{2.88}{4}-\frac{1}{4}=0.47$.

The values of $(p\,r-P_o)$ and B/C have been determined in finding the stresses in the arch. Therefore Eq. 54 is simplified by introducing these values instead of their complex equivalents.

For convenience, let

$$\frac{1-\cos(1+3\,a)\,\phi}{1+3\,a}+\frac{1-\cos(1-3\,a)\,\phi}{1-3\,a}=N\ldots\ldots\ldots(55a)$$

$$\frac{1-\cos(1+a)\,\phi}{1+a}+\frac{1-\cos(1-a)\,\phi}{1-a}=Q\ldots\ldots\ldots(55b)$$

$$\frac{1-\cos(2+3\,a)\,\phi}{2+3\,a}+\frac{1-\cos(2-3\,a)\,\phi}{2-3\,a}=R\ldots\ldots\ldots(55c)$$

$$\frac{1-\cos(2+a)\,\phi}{2+a}+\frac{1-\cos(2-a)\,\phi}{2-a}=V\ldots\ldots\ldots(55d)$$

Substituting the symbols, N, Q, R, and V in Eq. 54,

$$n = \frac{r}{E\,t_o}\left[(p\,r - P_o)\frac{3}{4}\left(\frac{B}{C}(N + 3\,Q) - (R + 3\,V)\right)\right.$$
$$\left. + 0.47\,V\,(p\,r - P_o) + \frac{p\,r}{2}\,Q\right] \quad \ldots (56)$$

Letting

$$\frac{3}{4}\left(\frac{B}{C}(N + 3\,Q) - (R + 3\,V)\right) = Z \quad \ldots\ldots\ldots\ldots\ldots (57)$$

Eq. 56 becomes

$$n = \frac{r}{E\,t_o}\left[\left(\frac{r^2}{t_o^2}\,Z + 0.47\,V\right)(p\,r - P_o) + \frac{P\,r\,Q}{2}\right] \quad \ldots\ldots\ldots (58)$$

Temperature Stresses

Letting e equal the change in length per foot for a rise or fall of one degree in temperature, letting T be the number of degrees change in temperature, and letting E be the modulus of elasticity, $E\,e\,T\,t$ will then represent the force exerted by a change of temperature of T degrees.

Mr. Cain[5,6] gives the method for determining the temperature stresses and deflections caused by temperature changes. Since the procedure is almost identical with that used in developing the stresses caused by water load, it is unnecessary to extend this paper by a repetition of the process.

The functions resulting from stresses are proportional to those caused by water pressure, with a ratio of proportionality equal to $\frac{E\,e\,T\,t'}{p\,r}$. It should be noted that H in Mr. Cain's study corresponds to the term $(p\,r - P_o)$ in the development of stresses caused by water load.

Having computed in a given problem the values of P, M, S, and n for water pressure, the temperature stresses can be determined from the following ratios:

$$\frac{H_t}{(p\,r - P_o)} = \frac{M_t}{M} = \frac{S_t}{S} = \frac{n_t}{n} = \frac{E\,e\,T\,t'}{p\,r} \quad \ldots\ldots\ldots\ldots (59a)$$

$$[P_t = H_t \cos\phi] \quad \ldots\ldots\ldots\ldots\ldots\ldots\ldots (59b)$$

The signs, indicating the direction of action, are omitted in the ratios and can be determined by the application of the following set of rules: For a rise in temperature, the thrust is in the same direction as that resulting from the water load, but the moments and deflections have signs opposite to those caused by the water load. For a fall in temperature, these conditions are reversed.

Mr. Cain[7] gives ratios similar to the foregoing except for the ratio P_t/P. The average thickness, t', is used in determining temperature stresses because

[5] "The Circular Arch Under Normal Loads," by William Cain, *Transactions*, ASCE, Vol. LXXXV, 1922, p. 245.

[6] Discussion by William Cain of "Stresses in Thick Arches of Dams," by B. F. Jakobsen, *ibid.*, Vol. 90, 1927, p. 542.

[7] *Ibid.*, p. 543.

it greatly simplifies the procedure, and the error is within the limits of accuracy of the determination of temperature changes.

The average thickness is found by first determining the area A of the arch ring.

$$A = t\,r\,\phi \qquad (60)$$

Differentiating, then integrating between the limits zero and ϕ_1,

$$A = \frac{t_o\,r}{a}\left[\log_e \tan\left(\frac{\pi}{4} + \frac{a\,\phi_1}{2}\right)\right] \qquad (61)$$

Using common logs,

$$A = \frac{2.3026\,t_o\,r}{a}\left[\log \tan\left(45^\circ + \frac{a\,\phi_1}{2}\right)\right] \qquad (62)$$

Since the average thickness, t', $= \dfrac{A}{\text{length}} = \dfrac{A}{r\,\phi}$,

$$t' = \frac{2.3026\,t_o}{a\,\phi_1}\left[\log \tan\left(45^\circ + \frac{a\,\phi_1{}^\circ}{2}\right)\right] \qquad (63)$$

in which the term $a\,\phi_1$ is expressed in radians, except in the last parenthesis.

Proof of Formulas

The formulas derived can be proved by letting $a = 0$ and comparing with Mr. Cain's original formulas. For simplicity, comparison is made of the values of the deflection coefficient n, since this coefficient includes the term $(p\,r - P_o)$ or its equivalent, and thus the formulas for $(p\,r - P_o)$ and for n are proved simultaneously.

It is first necessary to determine the values of the terms A, B, C, and the other factors when $a = 0$. The first term of A, $\dfrac{\sin 3\,a\,\phi}{3\,a}$ becomes $0/0$ when $a = 0$ and must be evaluated. Taking the differential of the numerator and denominator, with a as the variable,

$$\frac{d(\sin 3\,a\,\phi)}{d(3\,a)} = \frac{3\,\phi\cos 3\,a\,\phi\,da}{3\,da} = \phi\cos 3\,a\,\phi \qquad (64)$$

When $a = 0$, $\cos 3\,a\,\phi = 1$ and $\dfrac{\sin 3\,a\,\phi}{3\,a} = \phi$. By similar reasoning the fourth term of A is equal to $3\,\phi$.

When $a = 0$, the terms of this paper assume the following values:

$$A = 4\,\phi + 2\sin 2\,\phi \qquad (65a)$$

$$B = 8\sin\phi \qquad (65b)$$

$$C = 4\,\phi \qquad (65c)$$

$$F = \phi + \frac{\sin 2\phi}{2} \ldots\ldots\ldots\ldots\ldots\ldots\ldots (65d)$$

$$K = 2 \sin \phi \ldots\ldots\ldots\ldots\ldots\ldots\ldots\ldots\ldots (65e)$$

$$J = \phi - \frac{\sin 2\phi}{2} \ldots\ldots\ldots\ldots\ldots\ldots\ldots (65f)$$

$$N \text{ and } Q = 2\,(1 - \cos \phi) \ldots\ldots\ldots\ldots\ldots\ldots (65g)$$

$$R \text{ and } V = (1 - \cos 2\phi) \ldots\ldots\ldots\ldots\ldots\ldots (65h)$$

In Eq. 58 substitute for Z, V, Q, and $(p\,r - P_o)$ their values in terms of the factors A, B, C, and so on, when $a = 0$, and remembering that $0.47 = 2.88 - 1/4$, the formula takes the form:

$$n = \frac{r}{E\,t_o}\left\{\frac{p\,r\,2 \sin \phi_1\left[\frac{0.75\,r^2}{t^2_o}\left(\frac{8 \sin \phi_1}{4\,\phi_1} \times 8\,(1 - \cos \phi_1) - 4\,(1 - \cos \phi_1)\right) + \frac{2.88 - 1}{4}\,(1 - \cos 2\,\phi_1)\right]}{\phi_1 + \frac{\sin 2\,\phi_1}{2} + \frac{1.5\,r^2}{t^2_o}\,(8\,\phi_1 + 4 \sin 2\,\phi_1) - \frac{64 \sin^2 \phi_1}{4\,\phi_1} + 2.88\left(\phi_1 - \frac{\sin 2\,\phi_1}{2}\right)} + p\,r\,(1 - \cos \phi)\right\} \quad (66a)$$

Place $p\,r$ outside the brackets, simplify the numerator and denominator, multiply each by $\frac{t^2_o}{12\,r^2}$, and multiply the term $(1 - \cos \phi_1)$ by the denominator in order to combine with the numerator to give

Numerator.—

$$n = \frac{p\,r^2}{E\,t_o}\left\{\frac{2 \sin^2 \phi_1}{\phi_1}\,(1 - \cos \phi_1) - \left(1 + \frac{t^2_o}{12\,r^2}\right) 2 \sin \phi_1 \frac{(1 - \cos 2\,\phi_1)}{4}\right.$$
$$+ 2.88\,\frac{t^2}{12\,r^2}\,2 \sin \phi_1 \frac{(1 - \cos 2\,\phi_1)}{4} + (1 - \cos \phi_1)\left[\left(1 + \frac{t^2_o}{12\,r^2}\right)\right.$$
$$\left.\left.\times\left(\phi_1 + \frac{\sin 2\,\phi_1}{2}\right) - \frac{2 \sin^2 \phi_1}{\phi_1} + 2.88\,\frac{t^2_o}{12\,r^2}\left(\phi_1\,\frac{\sin 2\,\phi_1}{2}\right)\right]\right\}.$$

Denominator.—

$$\left(1 + \frac{t^2_o}{12\,r^2}\right)\left(\phi_1 + \frac{\sin 2\,\phi_1}{2}\right) - \frac{2 \sin^2 \phi_1}{\phi_1} + 2.88\,\frac{t^2_o}{12\,r^2}\left(\phi_1 - \frac{\sin 2\,\phi_1}{2}\right).$$

Combining, with $2 \sin^2 \phi = 1 - \cos 2\,\phi = 2\,(1 + \cos \phi)\,(1 - \cos \phi)$ and $\sin 2\,\phi = 2 \sin \phi \cos \phi_1$, the reduced formula becomes

$$n = \frac{p\,r^2}{E\,t_o}\left\{\frac{(1 - \cos \phi_1)\left[\left(1 + \frac{t^2}{12\,r^2}\right)(\phi_1 - \sin \phi_1) + 2.88\,\frac{t^2}{12\,r^2}\,(\phi_1 + \sin \phi_1))\right]}{\left(1 + \frac{t^2_o}{12\,r^2}\right)\left(\phi_1 + \frac{\sin 2\,\phi_1}{2}\right) - \frac{1 - \cos 2\,\phi_1}{\phi_1} + 2.88\,\frac{t^2_o}{12\,r^2}\left(\phi_1 - \frac{\sin 2\,\phi_1}{2}\right)}\right\} \ldots (66b)$$

This is identical with the formula for n, as derived by Mr. Cain, except that $\frac{t^2_o}{12\,r^2}$ is used in place of k^2/r^2.

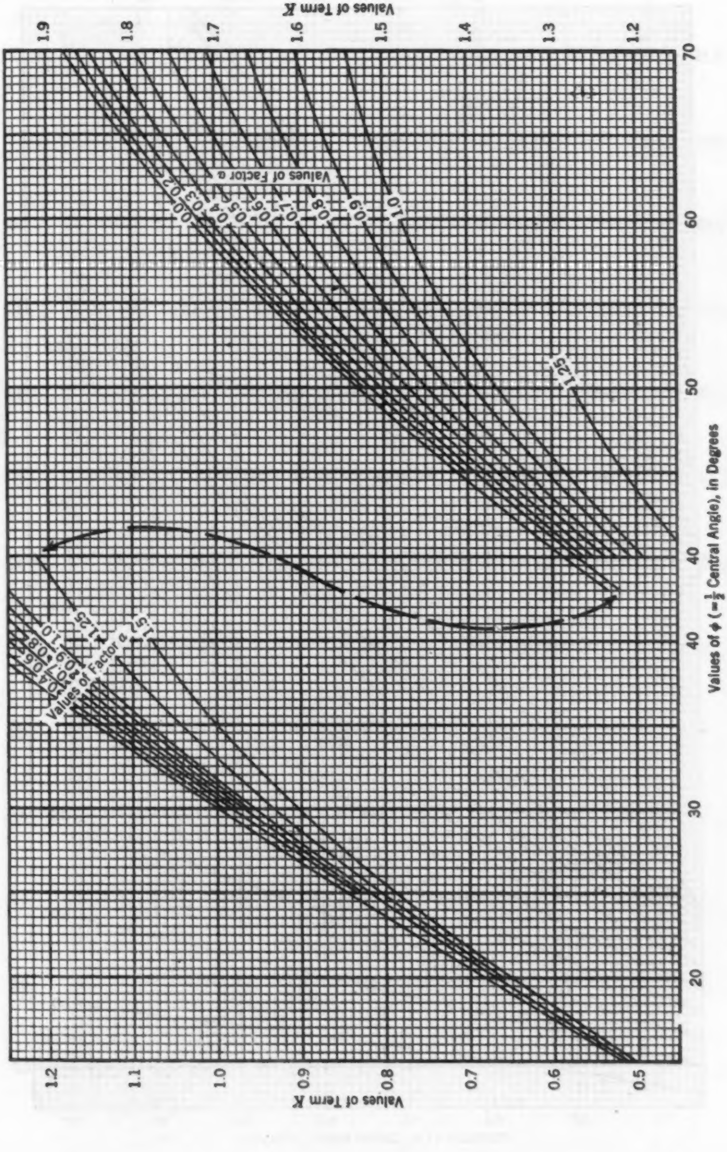

FIG. 2.—VALUES OF THE TERM K

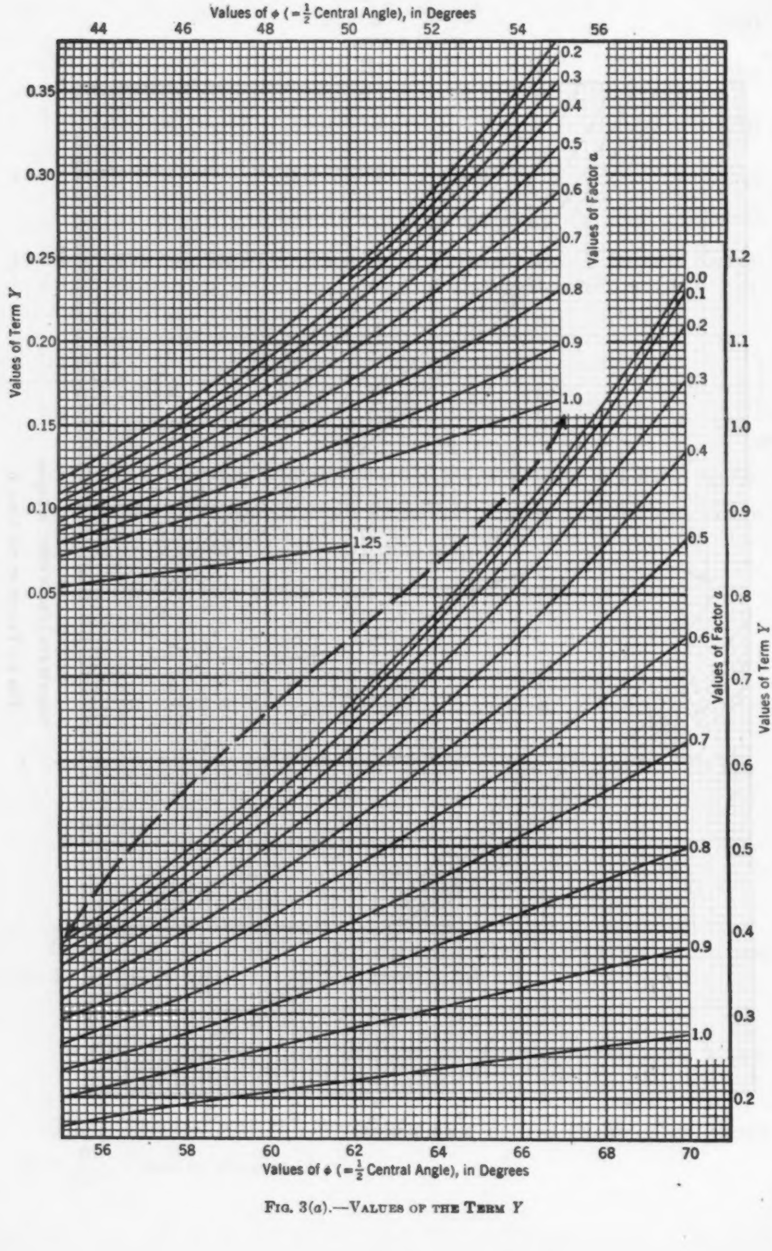

FIG. 3(a).—VALUES OF THE TERM Y

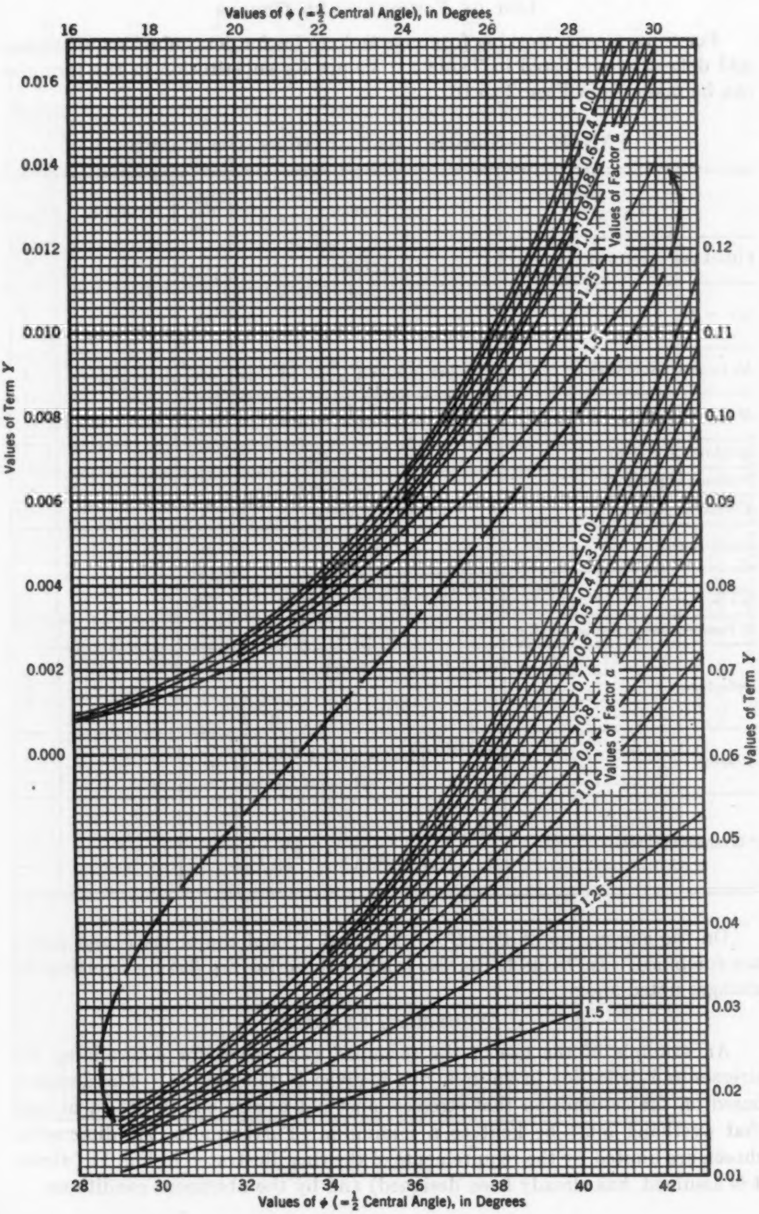

FIG. 3(b).—VALUES OF THE TERM Y

List of Formulas and Curves

For convenience, working formulas and curves for determination of stresses and deflection are listed in Table 1. Values for substitution in the formulas can be taken from Figs. 2 to 10.

TABLE 1.—Summary of Equations and Curves

Term	Equation	Equation No.	Function	Figure
t (thickness at point ϕ)	$\frac{t_o}{\cos a\,\phi}$	...	a	9
$(p\,r - P_o)$	$\frac{p\,r\,K}{\frac{r^2}{t_o^2}Y + (F + 2.88\,J)}$	39c	$\begin{cases} K \\ Y \\ (F + 2.88\,J) \end{cases}$	2 3 4
M_o (moment at crown)	$(p\,r - P_o)\,r\left(\frac{B}{2\,C} - 1\right)$	46c	$\frac{B}{2\,C}$	5
M (moment at point ϕ)	$(p\,r - P_o)\,r\left(\frac{B}{2\,C} - \cos\phi\right)$	47	...	...
P_o (thrust at crown)	$p\,r - (p\,r - P_o)$	...	...	...
P (thrust at point ϕ)	$p\,r\,(p\,r - P_o)\cos\phi$	7	...	...
S (shear at point ϕ)	$(p\,r - P_o)\sin\phi$	8	...	...
s (unit stress)	$\frac{P}{t} \pm \frac{6\,M}{t^2}$	49	...	...
$\frac{H_t}{(p\,r - P_o)}$	$\frac{M_t}{M} = \frac{S_t}{S} = \frac{n_t}{n} = \frac{E\,e\,T\,t'}{p\,r}$	59a	...	...
P_t (temperature thrust at point ϕ)	$H_t\cos\phi$	...	...	...
Deflection, n	$\frac{r}{E\,t_o}\left[\left(\frac{r^2}{t_o^2}Z + 0.47\,V\right) \times (p\,r - P_o) + \frac{p\,r\,Q}{2}\right]$	58	$\begin{cases} Z \\ 0.47\,V \\ Q \end{cases}$	6 7 8
A (area)	$\frac{2.3026\,t_o\,r}{a}\left[\log\tan\left(45° + \frac{a\,\phi_1}{2}\right)\right] = t'\,r\,\phi_1$ in radians	62	...	...
t' (average thickness)	$\frac{2.3026\,t_o}{a\,\phi_1 \text{ (in radians)}} \times \left[\log\tan\left(45° + \frac{a\,\phi_1}{2}\right)\right]$	63	t'	10

On the curves, $1.5\,(2\,A - B^2/C)$ is called Y, and the terms F and $2.88\,J$ are combined. In Table 1, Eq. 39c is substituted for Eq. 39b by inserting the changes noted above.

Numerical Example

An example of the use of the formulas and curves for determining the stresses and deflection in an arch ring is given in this section. The design is based on the assumption that stresses must not exceed 800 lb per sq in. and that overhang must be kept to a minimum. Furthermore, the dimensions chosen are limited by the requirements of the ring illustrated in Fig. 11 (which, it is assumed, has already been designed) and by the abutment conditions.

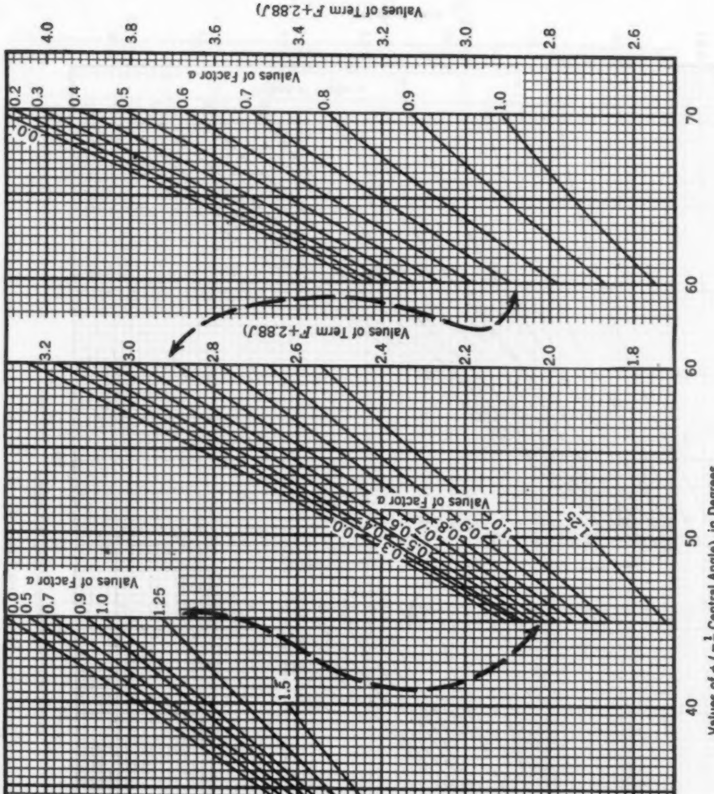

FIG. 4.—VALUES OF THE TERM $(F + 2.88\,J)$

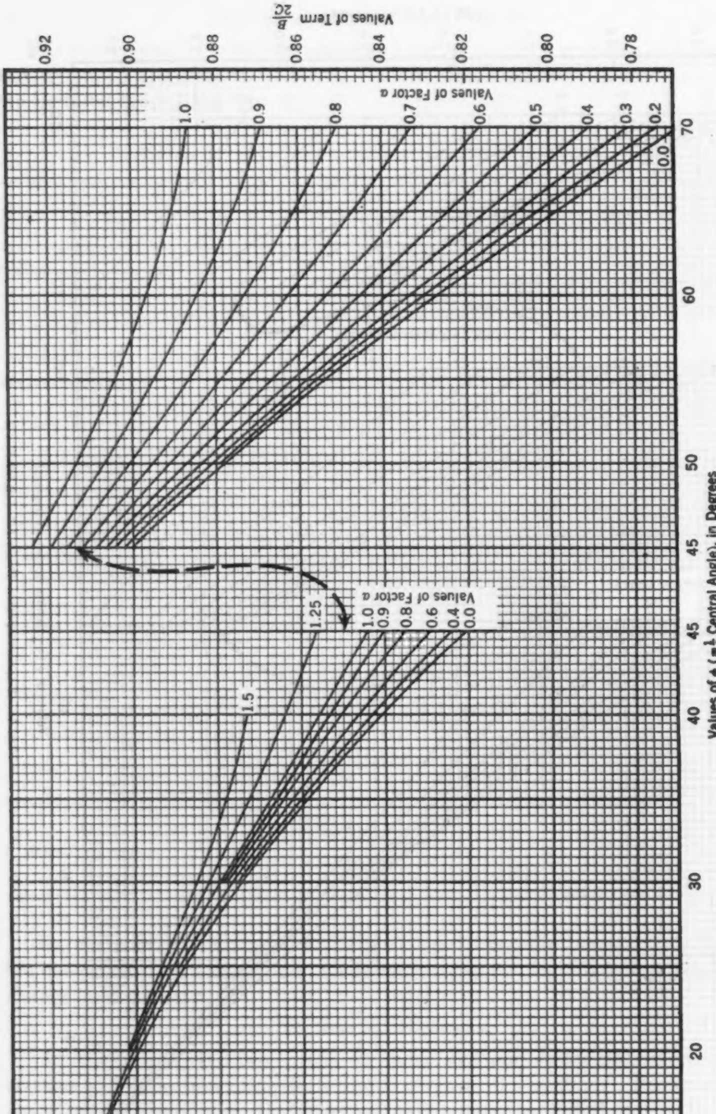

FIG. 5.—VALUES OF THE TERM $B/2C$

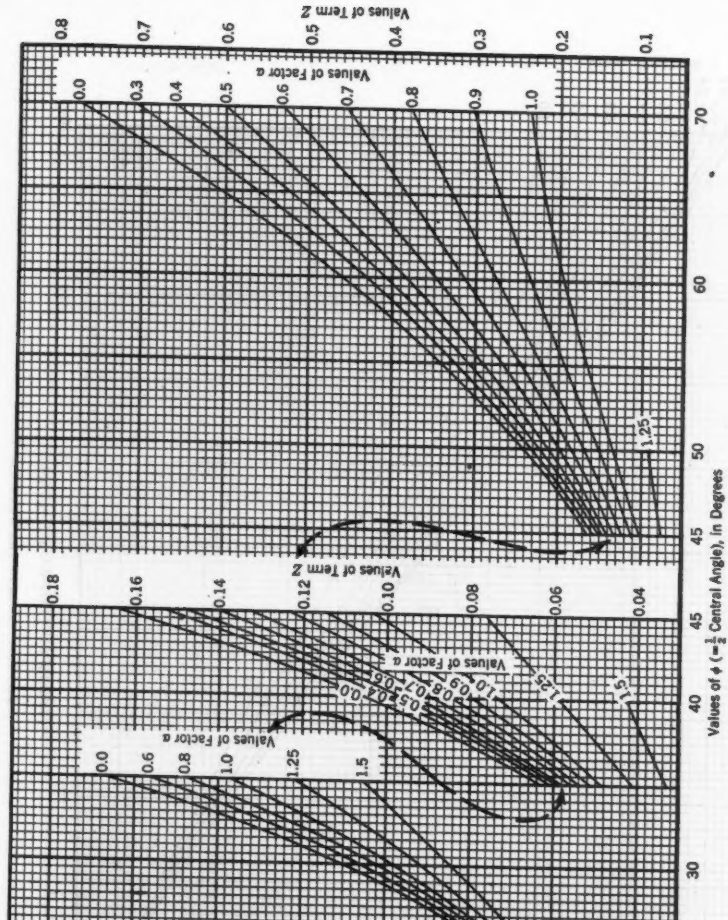

FIG. 6.—VALUES OF THE TERM Z

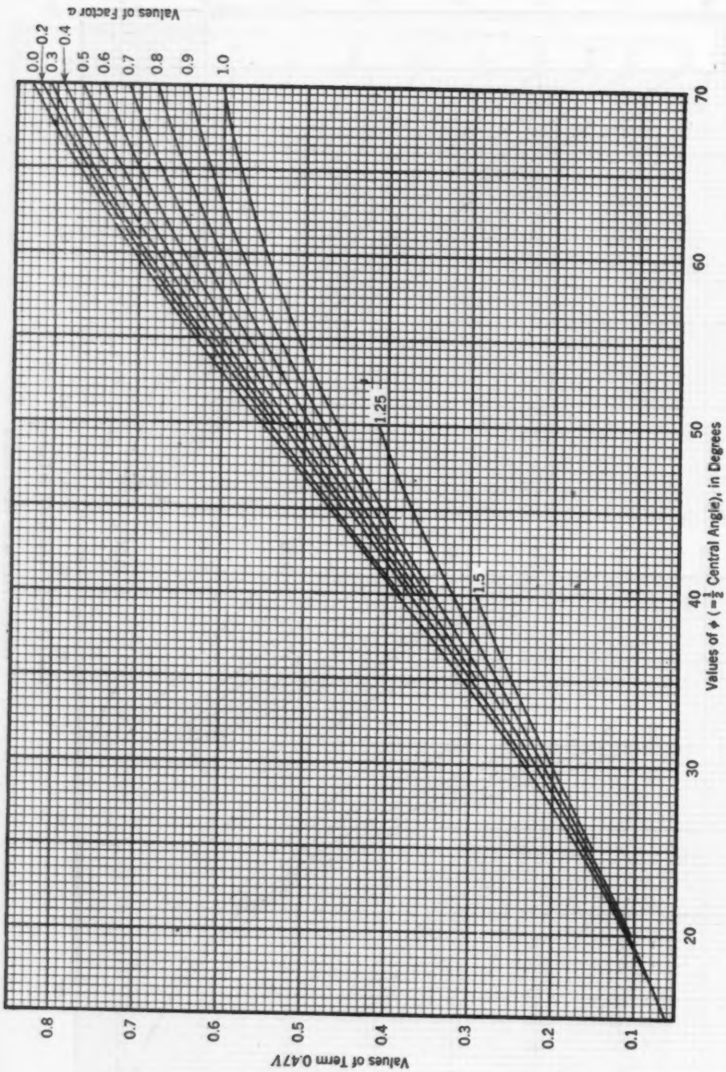

FIG. 7.—VALUES OF THE TERM 0.47 V

FIG. 7.—VALUES OF THE TERM 0.47 V

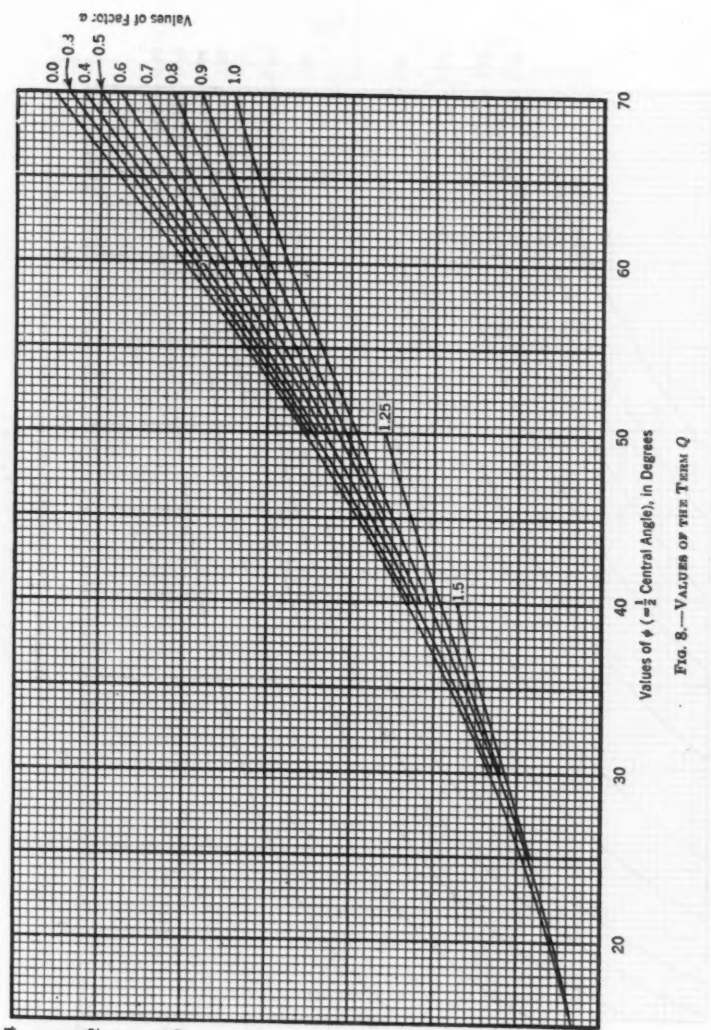

FIG. 8.—VALUES OF THE TERM Q

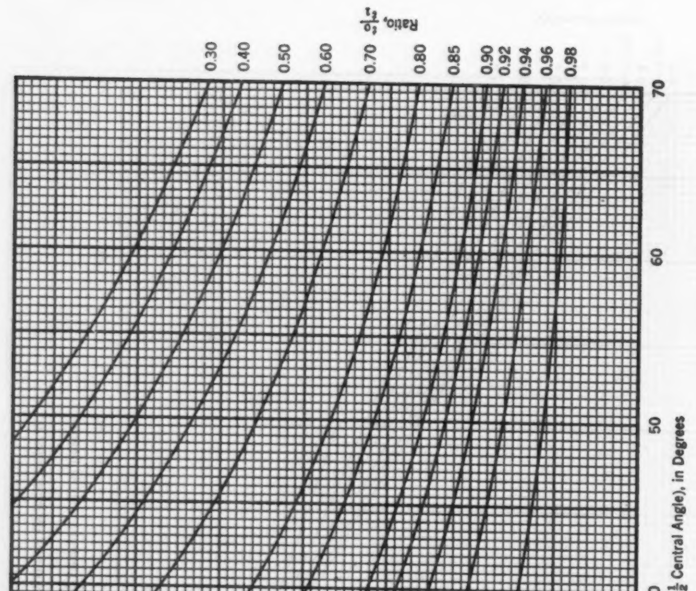

FIG. 9.—VALUES OF THE FACTOR a

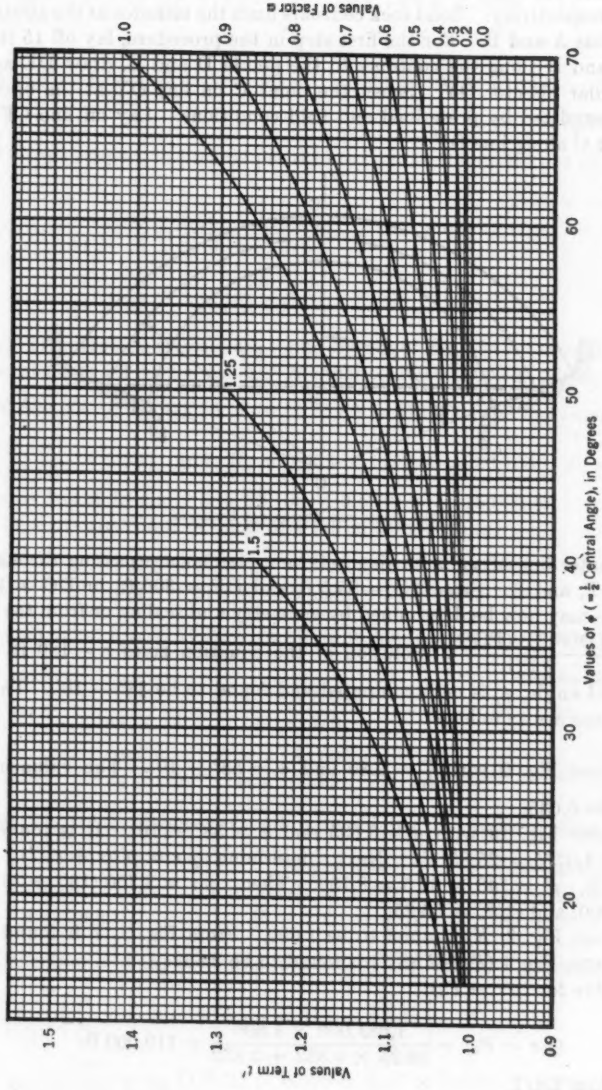

FIG. 10.—VALUES OF AVERAGE THICKNESS

Dimensions of previously designed adjacent rings and a water head of 140 ft indicate that the respective crown and abutment thicknesses should be 24 ft and 30 ft, respectively. Solid rock contours limit the intrados at the abutments to the points A and B. For the first step in the procedure, lay off 15 ft from points A and B along the contours to the points D and E, draw DE and its perpendicular bisector OY. Select the point C on line OY at the upstream position permitted by prescribed and field conditions. Lay off line CF 12 ft from point C along line OY.

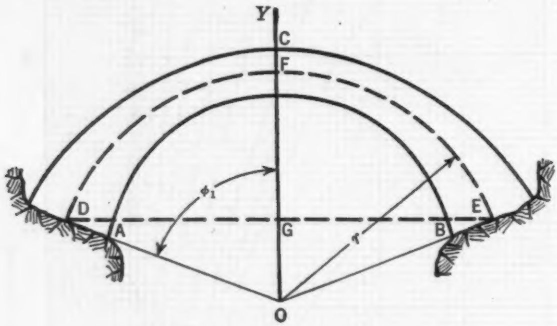

FIG. 11.—ARCH FOR NUMERICAL EXAMPLE

The center line of the arch ring will be a circular arc passing through the points D, F, and E. Scale FG = 85.5 ft and DE = 306 ft, or DG = 153 ft. The radius may now be determined by geometry and scaling or from the equation $r = \dfrac{(DG^2) + (FG^2)}{2\,FG}$. Solution of the equation gives r = 180 ft. The half central angle, ϕ, is next computed and found to be $58° - 10'$. The succeeding steps are as follows:

(1) Enter Fig. 9 with $\dfrac{t_o}{t_1} = 0.80$ and $\phi = 58° - 10'$. The value of a is found to be 0.635.

(2) Enter Fig. 10 with $a = 0.635$ and $\phi = 58° - 10'$. It is found that $t' = 24 \times 1.0775 = 25.85$ ft. Next, determine $p\,r = p'\,(r + t'/2)$. With $h = 140$ ft, $p' = 140 \times 62.5 = 8{,}750$. Then, $p\,r = 8{,}750\,(180 + 25.85/2) = 1{,}687{,}000$, and $r^2/t^2_o = 56.25$.

(3) From Fig. 2, K is found to be 1.600. From Fig. 3, Y is found to be 0.352. From Fig. 4 $(F + 2.88\,J)$ is found to be 2.832.

(4) Solve for $(p\,r - P_o)$:

$$(p\,r - P_o) = \frac{1{,}687{,}000 \times 1.600}{56.25 \times 0.352 + 2.832} = 119{,}000 \text{ lb.}$$

(5) From Eq. 7,

$$P_o = p\,r - (p\,r - P_o) = 1{,}687{,}000 - 119{,}000 = 1{,}568{,}000 \text{ lb}$$
$$P_1 = p\,r - (p\,r - P_o)\cos\phi = 1{,}687{,}000 - 119{,}000 \times 0.5275 = 1{,}624{,}000 \text{ lb.}$$

(6) From Eqs. 46*c* and 47 and Fig. 5,

$$M_o = (p\,r - P_o)\,r\left(\frac{B}{2\,C} - 1\right) = 119{,}000 \times 180 \times (0.8632 - 1)$$
$$= -\,2{,}930{,}000 \text{ ft-lb.}$$

$$M_1 = (p\,r - P_o)\,r\left(\frac{B}{2\,C} - \cos\phi\right) = 119{,}000 \times 180 \times (0.8632 - 0.5270)$$
$$= 7{,}200{,}000 \text{ ft-lb.}$$

(7) Unit stresses in pounds per square inch are found by use of Eq. 49,

		Extrados	Intrados
$s_o = \dfrac{1{,}568{,}000}{144 \times 24} \pm \dfrac{6 \times -2{,}930{,}000}{144 \times 576}$	$= 454 \pm 212 =$	666	242
$s_a = \dfrac{1{,}624{,}000}{144 \times 30} \pm \dfrac{6 \times 7{,}200{,}000}{144 \times 900}$	$= 376 \pm 333 =$	43	709

(8) Temperature stresses are found by use of Eq. 59*a* by assuming a fall in temperature of 10° and a value of E equal to 360,000,000 lb per sq ft, $E\,e\,T\,t'$ $= 360{,}000{,}000 \times 0.0000055 \times 10 \times 25.86 = 512{,}000$ lb. The ratio of $\dfrac{E\,e\,T\,t'}{p\,r}$ $= \dfrac{513{,}000}{1{,}687{,}000} = 0.303$, and $H_t = 0.303 \times 119{,}000 = 36{,}100$. $P_t = H_t \cos\phi$. $P_{to} = -\,36{,}100$ lb and $P_{t1} = 36{,}100 \times 0.5270 = -\,19{,}000$ lb.

The signs are minus because of a fall in temperature.

$$M_{to} = 0.303 \times -\,2{,}930{,}000 = -\,888{,}000.$$
$$M_{t1} = 303 \times 7{,}200{,}000 = 2{,}180{,}000.$$

Again using Eq. 49 to find the stress in pounds per square inch,

		Extrados	Intrados
$s_{to} = -\,\dfrac{36{,}400}{144 \times 24} \pm \dfrac{6 \times -\,888{,}000}{144 \times 576}$	$= -\,10 \pm 64$	54	−74
$s_{ta} = -\,\dfrac{19{,}000}{144 \times 30} \pm \dfrac{6 \times 2{,}180{,}000}{144 \times 900}$	$= -\,4 \pm 101$	−105	97

(9) The total stresses are found by combining the results of steps (7) and (8).

	Extrados stress	Intrados stress
Crown	$666 + 54 = 720$	$242 - 74 = 168$
Abutment	$43 - 105 = -\,62$	$709 + 97 = 806$

Deflection n of the arch ring is found by Eq. 58 and Figs. 6, 7, and 8:

$$n = \frac{r}{E\,t_o}\left[\left(\frac{r^2}{t_o^2}\,Z + 0.47\,V\right)(p\,r - P_o) + \frac{p\,r\,Q}{2}\right]$$

$$n = \frac{180}{360{,}000{,}000 \times 24}\,[(56.25 \times 0.308 + 0.47 \times 0.618)\,(119{,}000)]$$
$$+ (1{,}687{,}000 \times 0.426)$$

$n = 0.0586$ ft $= 0.704$ in. water pressure only.

Deflection for temperature = 0.303 times that for water. Therefore, total deflection = 1.303 × 0.704 = 0.915 in.

In a U-shaped canyon, where the arch rings near the base are long, a deflection of this amount will cause very heavy shear and compression stresses at the foundation. To avoid this contingency, several arch dams in California have been built with a slip joint just above the foundation, permitting the upper portion of the dam to deflect freely over the base. The writer first suggested the use of this device in 1930 to avoid excessive local stresses at points where there was a very abrupt change in the profile of one of the abutments of a dam under construction. Since then it has been used in several dams to avoid excessive foundation stresses due to large deflections.

The Value of p r.—The method given for determining the value of $p\,r$ is not strictly correct, but the error is very small and well within the limits of determinate values of other factors, such as $2\,\phi$ and the effects of vertical beam or so-called "cantilever action."

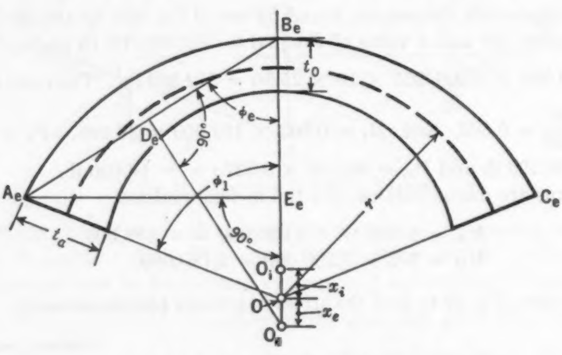

FIG. 12.—SIMPLIFIED ARCH LAYOUT

At the crown, the use of the average thickness, t', gives a value of $p\,r$ slightly in excess of the true value, while at the abutment the reverse is true. Also, true radial pressure exists only at the crown, but the neglected component at the abutment, if it were used, would slightly reduce the values of unit stresses since it would reduce the moment at that point. In the example given, the error in the values of the unit stresses is less than 0.50%, and this error will be less than 1% in all but very extreme cases.

For simplicity of construction it may be desirable to use true circles for the extrados and intrados. The locations of the centers and length of the radii are shown in Fig. 12 and Eqs. 67 to 74.

$$\overline{A_e\,E_e} = (r + \tfrac{1}{2}\,t_a)\sin\phi_1 \qquad \text{(67a)}$$

$$\mathrm{O}\,E_e = (r + \tfrac{1}{2}\,t_a)\cos\phi \qquad \text{(67b)}$$

$$\theta_e = \tan^{-1}\left(\frac{\overline{A_e\,E_e}}{(r + \frac{1}{2}\,t_o) - \mathrm{O}\,E_e}\right) = \left(\frac{(r + \frac{1}{2}\,t_a)\sin\phi_1}{(r + \frac{1}{2}\,t_o) - (r + \frac{1}{2}\,t_a)\cos\phi_1}\right) \qquad \text{(68)}$$

$$\overline{B_e D_e} = \frac{1}{2}\,\frac{\overline{A_e E_e}}{2 \sin \theta_e} \qquad (69a)$$

$$\overline{B_e O_e} = \frac{\overline{B_e D_e}}{\cos \theta_e} = \frac{(r + \frac{1}{2} t_a) \sin \phi_1}{2 \sin \theta_e \cos \theta_e} \qquad (69b)$$

$$X_e = \overline{B_e O_e} - (r + \tfrac{1}{2} t_o) = \frac{r + \frac{1}{2} t_a \sin \phi_1}{\sin 2\,\theta_e} - (r + \tfrac{1}{2} t_o) \qquad (70)$$

and

$$r_e = r + \tfrac{1}{2} t_o + X_e \qquad (71)$$

In a similar manner,

$$\theta_i = \tan^{-1} \frac{(r - \frac{1}{2} t_a) \sin \phi_1}{(r - \frac{1}{2} t_o) - (r - \frac{1}{2} t_a) \cos \phi_1} \qquad (72)$$

$$X_i = (r - \tfrac{1}{2} t_o) - \frac{(r - \frac{1}{2} t_a) \sin \phi_1}{\sin 2\,\theta_i} \qquad (73)$$

$$r_i = r - \tfrac{1}{2} t_o - X_i \qquad (74)$$

An arch laid out in this manner would require a slight increase in the amount of concrete, as it is slightly thicker at the quarter points than one laid out in accordance with the formula $t = \frac{t_o}{\cos a\,\phi}$, but the difference is not enough to affect materially the stresses determined from the curves and formulas of this paper. Eqs. 62 and 63 are not applicable for determining the area and thickness unless allowance is made for the additional thickening at the quarter points.

SUMMARY

The formulas and curves presented in this paper are for the determination of stresses resulting from uniform radial loading in horizontal arch rings of variable thickness. The loads may be modified somewhat by the vertical beam or so-called "cantilever action" of the dam, but, if the arch is designed to take full water and temperature loads, there need be no concern about the cantilever action.

For any given site, the arch dam with the minimum volume of concrete will be of the variable radius type. This will have a considerable overhang at the abutments on the upstream side, but, if the rock topography permits, the amount of this overhang can be reduced by placing the upper arch rings downstream with respect to the lower rings, resulting in a portion of the overhang being at the crown on the downstream side. If necessary, concrete supports can be placed under the upstream overhang, and these can be so designed that they will not interfere with arch action. This has been done in several cases in California. In such a design as this, it will be found that very little, if any, saving can be made in the thickness of the arches by attempting to give credit to the work done by cantilever action. In this connection it should be pointed out that in several published articles, for ease of computation, the vertical beams have been assumed to have parallel faces, giving undue credit to the

stiffness of the cantilevers. If the ratio of t/r is 0.3, the thickness of the downstream face of a vertical slice is only 74% of the thickness at the upstream face, and the relative stiffness, compared with a rectangular beam, is 86%. If t/r is 0.5, the corresponding values are 60% and 78%.

By a few simple computations it will be found that the controlling height of an arch dam, within the limits of practical dimensions and of allowable unit stresses and without excessive tensile stresses at the extrados near the abutments, is between 300 ft and 400 ft. However, by use of the sliding joint with a gravity section below that elevation, the total height of a dam is not limited; and with the aid of the formulas and curves presented, a structure with a minimum volume of concrete can be designed.

Acknowledgment

The writer gratefully acknowledges the valuable assistance of Joseph G. Bastow, M. ASCE, in the development of the basic formulas during the early stages of the preparation of the paper. Credit is also due to Clifford J. Cortright and Carl L. Stetson, J. M. ASCE, for their valuable aid in the preparation of the curves.

Appendix—Notation

The following letter symbols, adopted for use in the paper and for the guidance of discussers, conform essentially with "American Standard Letter Symbols for Structural Analysis" (ASA—Z10.8—1942), prepared by a committee of American Standards Association with ASCE participation, and approved by the Association in 1942.

$A, B, C, F, K, J, N, Q, R, V, R, W, Y, Z$ are abbreviations for mathematical expressions.

a = the factor in the expression $t = t_o/\cos(a\,\phi)$;

E = modulus of elasticity of arch, in pounds per square foot;

e = change of length per unit length for a change of one degree in temperature;

H_t = thrust due to temperature and corresponds to the expression $(p\,r - P_o)$ for water pressure;

H_e and V_e = respectively, the horizontal and vertical components of the loads at the abutment;

M, P, and S = respectively, the moment, tangential component of the thrust, and shear at $D(r, \phi)$;

M_o = moment at the crown, taken positive clockwise;

P_o = thrust at the crown, in pounds per square foot;

p = radial pressure in pounds per square foot, on center line $p = p'\dfrac{\left(r + \dfrac{t'}{2}\right)}{r}$ for use in formulas;

p' = radial pressure, in pounds per square foot, on extrados;

Q_c = the component of the arch loads on the segment CD $= p \times 2\,r \sin\dfrac{\phi}{2}$;

r = radius of center line of arch, in feet;
l = length of arc, CD, $= r\,\phi$ and $dl = r\,d\phi$;
s = unit stress;
T = total number of degrees change;
t = thickness, in feet, at any point, D;
t_o = radial thickness, in feet, of arch at the crown;
t' = average thickness in feet;
ϕ = angle between radius at crown and any point, D; and
ϕ_1 = the half central angle of the arch.

(Subscripts used are "e" for extrados, "i" for intrados, "o" for crown, 1 for abutment and "t" for temperature.)

DISCUSSION

Alfred L. Parme,[8] A. M. ASCE.—The merits of arch dams with arches of variable thickness have been brought to the forefront once again in the author's excellent paper. Not only does the arch of variable thickness result in a more well-balanced stress condition than does an arch of constant thickness, but such arches simplify the task of satisfying stress requirements in the lower regions of a dam. For a given chord width, rise, and abutment thickness, the flexural stresses in an arch of variable thickness are less than those in an arch of constant thickness. Consequently, the avoidance or minimization of tension in an arch dam formed with such arches is much less of a problem than it is in one built of arches of constant thickness.

The mathematical solution presented by the author is a considerable improvement over lengthy arithmetical summations. More than this, however, the thickness relationship introduced in the paper indicates that an exact expression for the variation in thickness is not required in the elastic equations. In a published paper[9] the writer presented a similar solution for dams with symmetrical arches of variable thickness. The outline of the arches treated by the writer was composed of two circular arcs struck from different centers. The variation in thickness for these arches was shown to be given closely by the expression:

$$t = \frac{1}{1 - \cos\phi_1}\left[k - \cos\phi_1 - (k - 1)\cos\phi\right] t_o \quad \text{..........(75)}$$

in which k equals the ratio of the abutment thickness to the crown thickness. Also, the analysis was made on the basis that the water load was acting on the extrados face. In spite of these two noticeable differences, it is quite surprising to find that the values computed by means of Mr. Perkins' graphs agree remarkably well with values taken from the charts previously prepared by the writer.[9] For example, values interpolated from the writer's charts for $k = 1.2$ and $k = 1.3$, $\frac{t_o}{r} = \frac{24}{180} = 0.133$, and $\phi_1 = 58°\ 10'$ yield, for a 10-ft head, the following stresses:

Stressed fiber	Stress, in pounds per square inch
Crown extrados	47.5
Crown intrados	17.0
Abutment extrados	3.1
Abutment intrados	50.5

[8] Structural Engr., Portland Cement Assn., Chicago, Ill.

[9] "Arch Dams with Arches of Variable Thickness," by A. L. Parme, in "Modern Developments in Reinforced Concrete," Portland Cement Assn., Chicago, Ill., 1947.

Hence, for a 140-ft head, the stresses are as follows:

Stressed fiber	Stress, in pounds per square inch
Crown extrados	665
Crown intrados	238
Abutment extrados	43
Abutment intrados	710

A comparison of these values with those shown under the heading, "Numerical Example," step (7), reveals only minor differences.

This favorable agreement also applies to an arch having a small central angle, a large value of k, and relatively great thickness. As evidence of this,

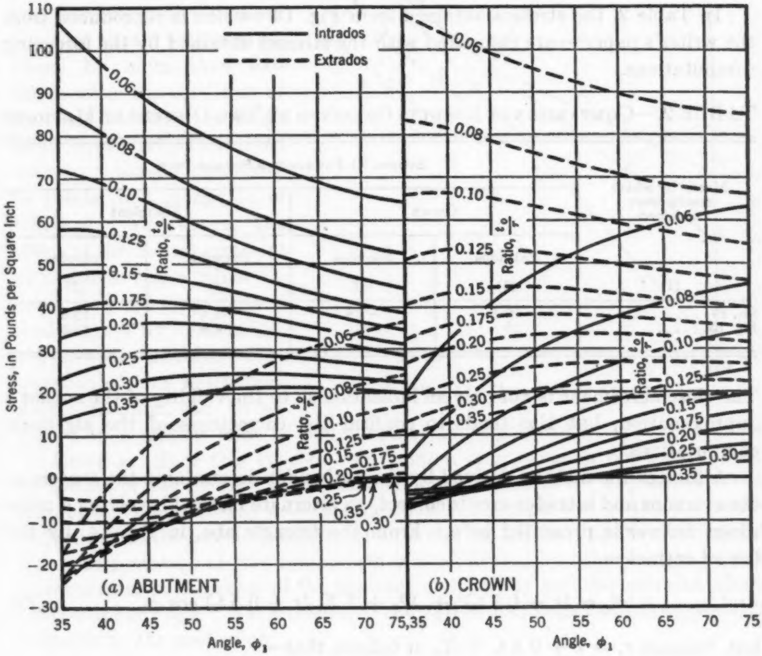

FIG. 13.—STRESSES, FOR $k = 1.5$

the stresses caused by a 10-ft head obtained by the author and previously by the writer[9] for an arch in which $\phi_1 = 35°$, $k = 1.5$, and $t_o/r = 0.35$ or $r/t_o = 2.86$.

Following the procedure outlined by the author (see under the heading, "Numerical Example"):

(1) Enter Fig. 9 with values of $t_o/t_1 = 0.667$ and $\phi = 35°$. The value of a is found to be 1.38.

(2) From Fig. 10, $t' = 1.15\, t$.

(3) Fig. 2 yields a value of K equal to 1.023. From Fig. 3, $Y = 0.0220$ and from Fig. 4, $(F + 4J)$ is found to equal 1.295.

(4) Consequently, $p\,r - P_o = \dfrac{p\,r \times 1.023}{2.862 \times 0.0220 + 1.295} = 0.694\,p\,r.$

(5) Hence, $P_o = 0.306\,p\,r$ and $P_1 = p\,r - (0.694 \times 0.819)\,p\,r = 0.432\,p\,r.$

(6) Also, by means of Fig. 5 with $B/2C = 0.956$: $M_o = 0.694\,p\,r^2\,(0.956 - 1) = -0.031\,p\,r^2$, and, similarly, $M_1 = 0.694\,p\,r^2\,(0.956 - 0.819) = 0.095\,p\,r^2$.

(7) With $p = 625/144 = 4.34$ lb per sq in. and $r/t_o = 2.86$, the unit stress at the crown is $s_c = 4.34 \times 2.86\,(0.306 \pm 0.031 \times 6 \times 2.86) = 3.8 \pm 6.6.$ At the abutment, $s_a = 4.34 \times \dfrac{2.86}{1.5}\left(0.432 \pm \dfrac{0.95 \times 6 \times 2.86}{1.5}\right) = 3.6 \pm 9.0.$

In Table 2, the stresses obtained from Fig. 13—which is reproduced from the writer's paper[9]—are compared with the stresses obtained by the foregoing computations.

TABLE 2.—COMPARISON OF RESULTS OBTAINED BY TWO DIFFERENT METHODS

Means by which results were obtained	Stress, in Pounds per Square Inch			
	Crown		Abutment	
	Extrados	Intrados	Extrados	Intrados
(1)	(2)	(3)	(4)	(5)
Eq. 49	10.4	−2.8	−5.4	12.6
Fig. 13	10	−3	−4.8	13.2

The close agreement is not only an indication as to the validity of the author's approximation, but also tends to confirm the correctness of the algebraic computations.

Although the method derived by the author for determining the centers of the extrados and intrados arcs is correct, an alternate method involving a more direct answer is presented here. From the triangle abc, in Fig. 14, by the law of cosines—

$$r_e^2 = (r + 0.5\,t_1)^2 + X_e^2 + 2\,X_e\,(r + 0.5\,t_1)\cos\phi_1 \quad\text{.......(76)}$$

but, because $r_e = r + 0.5\,t_o + X_e$, it follows that—

$$(r + 0.5\,t_o)^2 + X_e^2 + 2\,X_e\,(r + 0.5\,t_o) = (r + 0.5\,t_1)^2 + X_e^2 + 2\,X_e\,(r + 0.5\,t_1)\cos\phi_1.$$

Therefore,

$$X_e = \frac{(2\,r + t_1)^2 - (2\,r + t_o)^2}{4\,[(2\,r + t_o) - (2\,r + t_1)\cos\phi_1]} \quad\text{.............(77)}$$

and, in a similar manner,

$$X_i = \frac{(2\,r - t_1)^2 - (2\,r - t_o)^2}{4\,[-(2\,r - t_o) + (2\,r - t_1)\cos\phi_1]} \quad\text{...........(78)}$$

The brief reference to the use of slip or sliding joints at the base of an arch dam is of considerable interest (see under the heading, "Numerical Example") There is no doubt that this type of construction reduces considerably the cantilever action occurring in the lower region of an arch dam. Even if friction caused by the weight of the dam is sufficient to prevent sliding, the absence of flexural restraint greatly reduces cantilever action. In several examples investigated, the magnitude of the load carried in the vertical direction (beam action) is reduced by more than two thirds when the condition of restraint at the base is altered from a fully restrained base to a hinged base (free to rotate but incapable of sliding). Therefore, the effect of horizontal restraint at the base has a minor influence on the proportion of load carried by vertical and horizontal action. The question of how much horizontal freedom can be expected in a sliding joint is therefore not too significant.

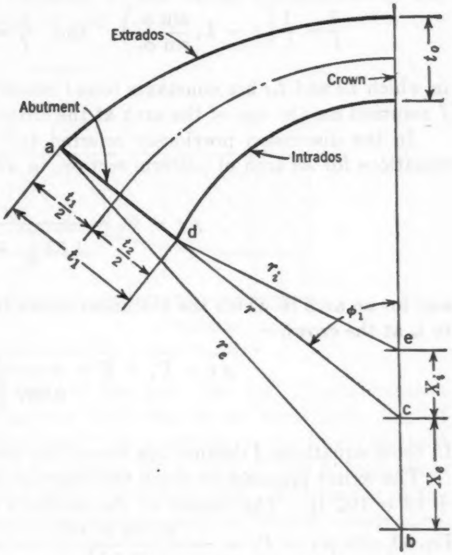

FIG. 14.—GEOMETRY OF THE ARCH

However, since this type of construction is growing in popularity, some indication of the efficacy of the sliding joint is desirable. A procedure that might yield some insight into this question is a comparison of the theoretical deflections to the actual deflection of an arch ring adjacent to the sliding joint. The interpretation of this comparison is complicated by other factors such as uncertainties in the value of the modulus of elasticity and the restraint offered by the upper rings. Nevertheless, if the author had such data, they would be valuable to the profession.

L. J. MENSCH,[10] M. ASCE.—Many years of experience have borne out the writer's repeated assertions that the solution of hydrostatic structures is more of an art than a science, and it will be shown presently that this is so in this case.

This paper treats only the case of an ideal horizontal arch slice, unaffected by its own weight, shrinkage and flow of concrete, the effect of Poisson's ratio, or the influence of adjoining arch slices.

Eqs. 40 through 45 and Eqs. 54 through 56 would have been considerably shorter if the author had selected with greater art such functions of the varia-

[10] Gen. Contractor, Evanston, Ill.

bility of t and I as to facilitate the work of integration of the differential equations. The same problem has been treated by the writer in the discussion of a paper on the same subject.[11] The writer selected in place of the author's Eqs. 1 and 2 the function:

$$\frac{1}{t} = \frac{1}{t_o}\left(1 - L_t \frac{\sin\phi}{\sin\phi_1}\right); \text{ and } \frac{1}{I} = \frac{1}{I_o}\left(1 - L_I \frac{\sin\phi}{\sin\phi_1}\right) \dots\dots (79)$$

in which L_t and L_I are constants found immediately from the values of t and I assumed for the size of the arch at the crown and abutments.

In the discussion previously referred to,[11] the writer gave the following equations for an arch of uniform section, in which $\phi_1 = 60°$:

$$p\,r - P_o = \frac{p\,r}{1.33\,\frac{f^2}{t_o^2} + 1.92} \dots\dots\dots\dots\dots\dots (80)$$

and for an arch in which the thickness varies from $t_I = 1.5\,t_o$ at the abutment to t_o at the crown—

$$p\,r - P_o = T = \frac{p\,r}{0.707\,\frac{f^2}{t_o^2} + 1.81} \dots\dots\dots\dots\dots (81)$$

In these equations, f denotes the rise of the arch.

The writer proposes to check the example of the author, in which $r = 180 + 12 = 192$ ft. The values of the author's example, when substituted in Eq. 80, give $p\,r - P_o = \frac{8{,}750 \times 192}{1.33\left(\frac{85.5}{24}\right)^2 + 1.92} = 89{,}000$ lb and, similarly, Eq. 81, $p\,r - P_o = 154{,}000$ lb. The correct value for the author's example should be approximately the average of 89,000 lb and 154,000 lb because $\frac{t_1}{t_o} = 1.25$ is the average of $\frac{t_1}{t_o} = 1$ and $\frac{t_1}{t_o} = 1.50$. The mean value is $\frac{89{,}000 + 154{,}000}{2} = 122{,}000$ lb, which varies from the author's value by 2%. Therefore, it can be concluded that the equations suggested by the writer yield results that agree with those of the author.

FAIRFAX D. KIRN[12] AND GURMUKH S. SARKARIA,[13] J. M. ASCE.—An interesting graphical solution of an elastic, variable-thickness arch that conforms to a certain law of variation of thickness, has rigid abutments, and is subjected to uniform radial loads acting along its assumed circular center line has been presented by the author. However, it would not be technically correct to designate the method presented in this paper as "an analysis of arch dams of variable thickness." The limited scope of this graphical solution—and hence

[11] Discussion by L. J. Mensch of "Analysis of Arch Dams by the Trial Load Method," by C. H. Howell and A. C. Jaquith, *Transactions*, ASCE, Vol. 93, 1929, p. 1250.

[12] Head, Trial Load Analysis Group, U. S. Bureau of Reclamation, Denver, Colo.

[13] Asst. Design Engr., Punjab Irrig. Branch, Simla, India.

its restricted applicability to stress analysis of arch dams—is evident from the assumptions made by the author regarding the shape of the arch ring, the rigidity of the abutments, and the characteristics of the load on the arch. Some of these assumptions are discussed here with reference to the practice of the Bureau of Reclamation (USBR), United States Department of the Interior, for the design and analysis of arch dams.

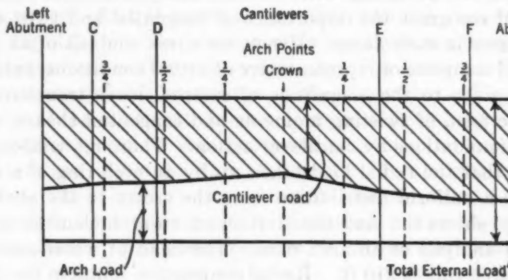

FIG. 15.—LOAD DISTRIBUTION ON AN ARCH ELEMENT

The law of variation of thickness of the arch (see Eq. 1) establishes a so-called equivalent arch for the true arch ring in an ideal arch dam of variable thickness. This equivalent arch with a circular center line is assumed to have the same properties and to behave (as a part of the homogeneous structure) in the same manner as does the true arch ring. The results of the analyses of the two arch rings, appearing subsequently in Table 3, clearly show

FIG. 16.—ARCH RING

that the equivalent arch ring cannot be substituted for the true arch ring of a variable-thickness arch dam. Also, the writers feel that it would be nearly impossible to lay out an arch dam composed of arch rings with circular center lines but with noncircular extradosal and intradosal faces. From the viewpoints of construction, form-work economy, and appearance, the upstream and downstream faces of the arch dam should each have a smooth and uniform

variation in vertical, as well as horizontal, curvature; and, above all, the surface should be easy to lay out at the site. Except for arches of uniform thickness, the most suitable type of arch dam from the construction standpoint has circular extradosal and intradosal faces, and has arches that vary in thickness from their crowns to their abutments. However, in many cases a dam with fillet arches will be found to be the most economical of the variable-thickness types.

Engineers who are proficient with detailed analysis of arch dams by the trial-load method recognize the importance of tangential and twist effects for determining stresses in such dams. Hence, no stress analysis of an arch dam can be considered complete or representative of actual conditions, unless proper consideration is given to the magnitude of external loads transferred to the abutments in the form of twisting moments and tangential shears, as well as vertically to the foundations by cantilever action. Thorough trial-load analyses also indicate that the radial load taken up by an arch ring of a dam does not usually have a uniform distribution from the crown to the abutments of the arch. Fig. 15 shows the load distribution on an arch element determined from a trial-load analysis of an arch dam. The head of water acting at the elevation of the arch ring is 210 ft. Radial contraction joints in the dam were assumed to be grouted, and the analysis included the effects of tangential shear and twist action, horizontal earthquake, yielding abutments, and temperature changes. Inspection of the load diagram shows that the major portion of the total load is carried by cantilever action, not by arch action, and that the load carried by the arch ring is not uniform from its crown to the abutments.

The arch ring analyzed by the author is assumed to have rigid abutments, with no consideration given the effects on the stresses in the arch produced by the yielding of the abutments or by the value of the modulus of elasticity of the abutment rock. The trial-load method of analysis recognizes and takes into consideration the effects of elastic abutments and foundations.

Fig. 16 shows one of the variable-thickness arch rings of the arch dam mentioned herein. This arch has been analyzed for the following three conditions: (*a*) As an equivalent arch ring, using the assumptions and method given in the paper under discussion; (*b*) as a true variable-thickness arch ring, assuming rigid abutments and uniform application of the water load at the extrados of the arch; and (*c*) as a true variable-thickness arch ring with the effects of abutment yielding included, and with uniform application of the water load at the extrados of the arch. (Dimensions, radii, and the central angle of the arch are shown in Fig. 16.)

From the dimensions of the variable-thickness arch as built, the dimensions for the author's equivalent arch obtained by the procedure described in his paper are as follows: r is the radius of the center line of the arch, equal to 1,129.5 ft and a is the factor used in the expression for the law of variation of thickness, equal to 0.995. This equivalent arch, when analyzed by the author's method for a water load of 13,125 lb per sq ft, assumed to be acting uniformly at the circular center line, yielded the results listed in Table 3.

In Table 3 results obtained by the author's method are compared with the stresses found by analyzing the arch shown in Fig. 16 by the method used by

the USBR for computing moments, thrusts, shears, and stresses in any arch ring.[14]

For the case of yielding abutments, the sustained modulus of elasticity of abutment rock in compression or tension was assumed to be equal to that of the concrete used in the arch dam.

A study of the results in Table 3 indicates that: (*a*) The equivalent arch designed by the author's method will have higher stresses on both façes—at the crown as well as at the abutments—than will the variable-thickness arch shown in Fig. 16. (*b*) The stresses show a general tendency to decrease for the case assuming yielding abutments. (*c*) The influence of the yielding of abutments is appreciable on stresses at the abutments. The tensile stress at the extrados of the abutment shows a decrease of 25.6% for the case assuming yielding abutments below the corresponding stress for the case of the true variable-thickness arch with rigid abutments. This decrease is 35.3%, when compared to results for the equivalent arch. (*d*) An arch of these dimensions will not be safe from the viewpoint of stresses, if it is designed to take the entire water load. The stresses obtained in all the three cases discussed here

TABLE 3.—COMPARISON OF STRESSES FOUND BY DIFFERENT METHODS[a]

Method	Crown Stresses, s_0, in Pounds per Square Inch		Abutment Stresses, s_1, in Pounds per Square Inch	
	Intrados	Extrados	Intrados	Extrados
That of the author	−269	+1,057	+1,560	−785
That of the USBR, for arch rings:				
(*a*) Assuming rigid abutments	−216	+1,001	+1,456	−683
(*b*) Assuming yielding abutments	−200	+1,046	+1,327	−508
The trial-load method	+ 88	+ 311	+ 290	+125

[a] Plus signs indicate compression; minus signs indicate tension.

are too high to be permissible in a safe structure, and indicate thickening of the arch to lower the stresses.

To clarify this last point, and to show the significance of vertical cantilever action as emphasized in the trial-load method of analysis, the stresses in this arch obtained by such an anlysis are shown in the last line of Table 3.

Fig. 15 shows the distribution of external loads between the arch and cantilever elements at this particular elevation. An examination of these results, and a comparison of them with the results of the three arch analyses described before, clearly indicate the fallacy of designing an arch dam based on the analysis of arch rings alone. The stresses obtained by trial-load analysis are within permissible limits, indicating a safe and stable structure.

In his summary, the author asserts:

> "The [arch] loads may be modified somewhat by the vertical beam or so-called 'cantilever action' of the dam, but, if the arch is designed to take full water and temperature loads, there need be no concern about the cantilever action."

[14] "Trial Load Method of Analyzing Arch Dams," *Bulletin No. 1*, Pt. V, Boulder Canyon Project Final Reports, U. S. Bureau of Reclamation, Denver, Colo., 1938.

Actual model tests[15] have shown that the so-called "cantilever action" exists in every arch dam, and that the water load carried by any arch element of the dam is not uniform from the crown to its abutments. The magnitude of cantilever action, or the portion of the water load that is carried by a cantilever at a certain section depends on the shape of the canyon, the location of the cantilever, and the stiffness of the cantilever concerned. An arch dam with grouted contraction joints is a homogeneous structure. Therefore, wishful thinking will not prevent the vertical cantilevers from transferring part of the external load to the foundation by cantilever action. The division of load between the two systems of elements must be such as to maintain continuity of deformation and rotation throughout the structure. In any case, if the arches in an arch dam are designed to resist the full water load, temperature effects, and other stresses, with no consideration being given to the cantilever action, the arch rings will be unnecessarily oversafe and uneconomically designed. Also, the computed stresses will be incorrect. Even the provision of a horizontal sliding joint at the base of the arch dam cannot completely nullify the vertical cantilever action because the vertical elements will still transfer a part of the external load to its base by horizontal shears acting at the sliding joint. Therefore, it is difficult to understand how a complete stress picture can be obtained for any arch dam by neglecting cantilever action and by using the author's method of arch ring analysis.

Although it is true (as the author states) that in several published articles, for ease of computation, the vertical beams have been assumed to have parallel faces—thus giving undue credit to stiffness of the cantilevers—this statement does not apply to the trial-load method of analysis as used by the USBR in the design of arch dams. In this method of analysis, the vertical cantilever elements are assumed to have radial sides (not parallel sides); and all computations are based on this assumption.

The trial-load method makes it possible to analyze load distributions, deflections, and stresses in curved concrete or masonry dams of all sizes and shapes—whether of the massive arch gravity type, the thin arch type, or the cupola-shaped design. This method considers the deformation of the abutments and foundation, the shape of the canyon in which the dam is to be built, and the construction program planned for grouting any contraction joints in the dam. Furthermore, the trial-load method includes the effects of tangential shear and twist action that exist in every dam. These cannot be determined by the author's method of analysis. Also, the correctness of the trial-load method has been substantiated by tests on models[15] as well as the Stevenson Creek Test Dam[16] in California.

In defense of the trial-load method of analysis—if understood, this method is not unduly cumbersome, nor is the length of time required to make an analysis unreasonable. High concrete dams are costly structures; and their structural behavior is too complicated to be interpreted and analyzed by over-simplified short-cut methods. The sum of money that can often be saved by determining the true picture of stresses in such a structure by using a thorough

[15] "Model Tests of Boulder Dam," *Bulletin No. 3*, Part V, Boulder Canyon Project Final Reports, U. S. Bureau of Reclamation, Denver, Colo., 1939.

[16] "Arch Dam Investigation," Vol. I and Vol. II, The Eng. Foundation, New York, N. Y., 1934.

and complete method of analysis (such as the trial-load method), and the evolution of a safe and satisfactory design, are two important factors in favor of comparatively lengthy but more thorough analyses. Simplified and abbreviated methods based on drastically limiting assumptions, such as the author's method, have a definite value in the preliminary design of arch dams. However, such methods should not be used as the final analyses for the design of high arch dams.

A. C. Josephs,[17] A. M. ASCE.—The use of design curves, pattern loads, tables of constants, and other labor-saving aids has become necessary for the analysis of most arch dams if the engineer is to have any time available to make the necessary design studies. The mechanics in the analysis of the elements of the dam have received considerable attention; actual design has been dictated by, or limited to, forms for which simple methods of analysis are available. As a result, there has been little or no progress made in the art of design of this structure since about 1932. The writer will confine his discussion to a few brief comments on some aspects of design.

In the "Summary," the author states: "For any given site, the arch dam with the minimum volume of concrete will be of the variable radius type." If this statement is presumed to mean that the horizontal arch elements are essentially circular and that the radii vary with the elevation, this generalization does not seem to be justified. This criterion for minimum volume has wide acceptance and would probably be correct if each arch ring were free to carry its load by deflecting independently of its neighbors. The arch rings are not free to deflect in such a manner, and the restraining influence of the adjacent rings and of the mass forces causes a "redistribution" of the load between the various arch elements. The shape of the redistributed load is a function of the shape or profile of the dam site.

Designers who have had the experience of analyzing arch dams by the "trial-load method"[18] are aware that once an approximate agreement between the deflections of the arch and gravity elements is reached, changing the volume or shape of the dam within practical limits does not appreciably alter the shape of this redistributed load. Very rarely will the load distribution between arch rings result in a load that is uniform along any horizontal arch ring, and in the case of sites which are irregular or unsymmetrical, the load will not even approximate that condition—whether or not the mass forces are considered. One of the rewards of the long and tedious effort of a trial-load analysis is the insight gained by the designer into the individual characteristics of that particular site. If the dam is shaped to conform to this loading, there will be a minimum of load transfer between the arch rings, and an economical design that conforms to the restraint characteristics of the site will result. An irregular or unsymmetrical site will normally require arch rings of compound curvature. The writer made preliminary studies[19] of a design along

[17] Vice Pres., Zalk-Josephs Co., Duluth, Minn.

[18] "Analysis of Arch Dams by the Trial Load Method," by C. H. Howell and A. C. Jaquith, *Transactions*, ASCE, Vol. 93, 1929, p. 1191.

[19] "Ueber den Entwurf gewölbte Mauern," Technische Hochschule Vienna, Austria, 1933.

this line about 1933, but had neither the staff nor the time to bring it to its logical conclusion—that is, the complete analysis of a dam so designed.

In the writer's opinion, an arch dam of minimum volume will result if the arch rings carry their load with a minimum of restraint. In all cases known by the writer where the design investigation has been thorough, the inclusion of the gravity effect in the design calculations has always resulted in a very substantial increase in the volume of the dam because the gravity element restrains the arch and prevents it from carrying its load effectively. The gravity or mass effect does exist and the designer must take it into consideration. For arch dams of moderate height, located on favorable sites, the experienced designer can, and should, design the dam for maximum economy, as outlined in the summary of Mr. Perkins' paper. However, to insure a safe and economical design, major structures and those at "unfavorable" sites should have the benefit of a detailed study of the effects of restraint.

George E. Goodall,[20] M. ASCE.—Without having checked the derivation of the various formulas in this paper, the writer can testify, nevertheless, to the accuracy of the results that they yield. In 1946, an existing arch dam was investigated to determine the feasibility of raising it. The thickness toward the abutment was increased by shifting the center of curvature of the intrados upstream from the center that was used for the extrados along the symmetry of the ring. The arch thus constructed is a close approximation of the arch envisioned by "the law of variation of thickness" (Eq. 1).

TABLE 4.—Comparison of Unit Arch Stresses, in Pounds per Square Inch

Surface	Abutment*			Crown		
	Perkins	Goodall	Vogt	Perkins	Goodall	Vogt
Intrados..........	456	452	562	24	64	57
Extrados.........	−96	−78	−16	440	414	382

* Minus sign indicates tension.

For example, consider an arch ring with thicknesses of 40 ft and 60 ft at the crown and abutment, respectively. Radii r_e and r_i were 240.0 ft and 148.9 ft; $2\phi_1$ was 106° 46′, and the design head was 135 ft. In 1946 the writer applied the methods of A. Floris[21] to this arch, and later compared the results by Mr. Perkins' procedure. Table 4 indicates that stresses computed by either method are sufficiently accurate for design purposes and that Figs. 4 to 10 reduce the work to a minimum for this type of arch. Both methods of analysis disregard the effects of the displacement of the neutral axis, Poisson's ratio, and deformation of the abutments. Some approximate calculations of stresses where moments and thrusts are referred to the neutral axis instead of the gravity axis indicate that disregard of the true location of the neutral axis is of minor

[20] Cons. Engr., Sacramento, Calif.

[21] Discussion by A. Floris of "Analysis of Arch Dams by the Trial Load Method," by C. H. Howell and A. C. Jaquith, *Transactions*, ASCE, Vol. 93, 1929, p. 1296.

importance as compared to the effects of lateral strains and deformation of the abutments. This fact has been well illustrated by Fredrik Vogt,[22] M. ASCE.

As a matter of fact, an arch with a uniform thickness of 40 ft, having the same inside radius and central angle as the foregoing, and under the same head, has 562 lb per sq in. and −16 lb per sq in. at the abutment intrados and extrados, respectively, and 57 lb per sq in. and 382 lb per sq in. for the corresponding values at the crown (Table 4), when analyzed by the Vogt formulas, which include the effects omitted by Mr. Perkins. A very small increase in either thickness or central angle would eliminate the tensile stress, and the maximum compressive stress would still be low.

It has been the writer's practice to include these effects in the design of arch dams. By taking advantage of the known effects of the lateral strains and abutment yield, it is possible to design a much more economical arch dam for a given site, within allowable stresses, than by increasing abutment thickness, as proposed by the author.

In the closing paragraph of the paper the author states:

> "* * * the controlling height of an arch dam, within the limits of practical dimensions and of allowable unit stresses and without excessive tensile stresses at the extrados near the abutments, is between 300 ft and 400 ft."

It is suggested that the author give his thoughts on what maximum unit compressive stresses should be allowed in the arches of dams built with good concrete on sound rock. The writer contends that no tensile stresses should be permitted in arch dams. Every practical arch dam of which the writer has any knowledge was constructed with a number of contraction joints. If tension is permitted at the extrados near the abutments of the arches, there is certain to be some place along the profile where this tensile stress would be indicated across a contraction joint which obviously can transmit no tensile stress. Furthermore, the writer does not place any reliance in the tensile stress that can be developed between the concrete of the arch and the rock abutment against which it has been placed.

With the invention of the vibrator and the development of modern weigh-batching plants, it has been demonstrated repeatedly that concretes having a twenty-eight-day crushing strength of 4,000 lb per sq in. are readily attained. Since the lower parts of an arch dam will generally have aged six months or more prior to loading, it would seem that compressive stresses of 1,000 lb per sq in. in compression are conservative. However, no tensile stresses should be permitted. If the effects of lateral strains and deformation of abutments are included in the arch analysis, the limiting height, as determined by the writer, can be greatly exceeded. In the design of an arch dam to be constructed in California to a height of nearly 480 ft above its foundation, all arch rings have been analyzed by the Vogt formulas. They were shaped so as to have no tensile stresses; yet the maximum compressive stress is slightly less than 850 lb per sq in. However, this result would have been impossible had the effects of lateral strains and deformation of the abutments been neglected.

[22] Discussion by Fredrik Vogt of "Stresses in Thick Arches of Dams," by B. F. Jakobsen, *Transactions*, ASCE, Vol. 90, 1927, p. 561.

Acknowledgment.—The writer acknowledges the assistance of Jack S. Barrish, A. M. ASCE, and Klyne G. Beaumont, J. M. ASCE, who made and checked some of the computations entering into this discussion.

W. A. PERKINS,[23] M. ASCE.—In order to provide a ready means of analyzing stresses caused by water load and temperature changes in a horizontal slice of an arch dam of varying thickness, and to determine the deflection at the crown, this paper was written. As it would be of little practical value without the curves, it was not presented for publication until these curves could be completed. During the interval an excellent treatise was published by Mr. Parme.[9] Since this paper did not make provision for determining temperature stresses, and since the method of approach was different, the writer concluded that, for the benefit of those familiar with Mr. Cain's paper, and to determine the effects of temperature, publication of this paper was justified.

The writer questions Mr. Parme's reference to the "author's approximation." The formulas were developed in accordance with the principle of least work, which is an exact, and not an approximate, principle. The only approximation made is in assuming that the load P_0 acts radially on the center line of the dam, which is not exactly true, as was explained in the paper.

Mr. Parme inquired about the sliding joint referred to in the paper. At the Matilija Dam in Ventura County, California, one of these joints was placed 4 ft above the base at the center line. This dam is in a U-shaped canyon, and at the elevation of the joint the dam is approximately 200 ft long. The arch deflection at this height, 154 ft below the crest, would be about ¾ in. without restraint. Such a condition would develop very high shear stresses at the foundation contact and introduce indeterminate stresses.

The joint was constructed by carefully leveling and finishing the surface at the joint level. This was then covered with a layer of a commercial, highly compressed, graphite-impregnated, asbestos planking. The planking was covered with a thin coating of graphite that, in turn, was covered with paper, and the upper layers of concrete were poured thereon. Leakage was prevented by a copper water stop bolted to the upstream face of the dam and this, in turn, was protected by a steel plate.

This reservoir filled for the first time in the fall of 1952, and there was opportunity for observing the behavior of the joint. It was found that at the crown the deflection was 1.02 in. and at the quarter points, 0.59 in. and 0.73 in., respectively. The deflection of 1.02 in. instead of ¾ in. occurred because the ¾-in. deflection did not include temperature effects and, also, there is probably some abutment yield.

The joint installed in 1930 was observed by the writer from 1930 to 1950, and it was found to act according to expectations. This joint is at approximately mid-height of the dam, at which the head is 50 ft. It was installed at the elevation where the right abutment changed from approximately vertical to approximately horizontal, and conditions made it necessary to extend the arch for a considerable distance along this bench to a point where it was

---

[23] Cons. Engr., Sacramento, Calif.

feasible to construct a gravity thrust block. A movement of about 3/8 in. has been observed, and a larger movement is not expected. The use of these joints, with gravity sections below, will be found very advantageous in the design and construction of arch dams.

It is interesting to observe the variety of opinions among engineers regarding the merits of the trial load method for the analysis of dams. This can be noted in the discussions of this paper, some of which advocate exclusive use of this method, whereas others ignore it. This same divergency of opinion will be found among engineers in general who have given this subject careful attention

This divergency results from two different approaches to the problem. One approach is to assume that the arch should be designed to take full water load, the other, that the cantilever take the major portion. Designs which attempt to divide the load between arch and cantilever action frequently result in structures that show high tensile stresses both in the arches and at the base of the cantilever.

At a site that is suitable for an arch, it will be found that a thin arch designed to take the full water load without tension will require much less concrete than a structure that is designed to carry a part of the load by gravity action. Such an arch, if of considerable height, or if the site is irregular, or if there are abrupt breaks in the profile of the abutments, should be investigated for vertical beam action so as to determine the stresses at the foundation and the load on the mid-arches in the vicinity of the breaks. In some cases, it has been found that under such conditions the arches were carrying a load in excess of the direct water load.

For dams of heights of from 300 ft to 400 ft, analysis by the trial load method is an expensive diversion. For extremely high dams, such as Hoover Dam, on the Colorado River in Arizona and Nevada, all precautions of design should be utilized. Hoover Dam, however, is essentially a gravity structure as its base thickness is approximately 90% of its height. Because of its height it is estimated, without any study, that the deflection of the crest under full load is approximately 3 in. or 4 in., which would produce considerable arch resistance in the upper section since it is curved in plan. Terming such curved gravity dams "arch dams" is a misnomer and is probably the chief reason for disagreement among engineers regarding the methods of an analysis to be used for true arches.

With reference to Fig. 16, in the discussion submitted by Messrs. Kirn and Sarkaria, the dam depicted is termed an arch—but it will be noted that the crown thickness is 141 ft, or 67% of the height to the crest, and at the abutments it is 159.74 ft, or 76% of the height. Such measurements would classify this dam as a gravity section. The section shown in Fig. 16 could be replaced by a true arch with a crown thickness of approximately 90 ft, an abutment thickness of 120 ft, a radius of 595 ft, a central angle of 125°, and an average thickness of approximately 98 ft. The difference in thickness is approximately 50 ft from that proposed by Messrs. Kirn and Sarkaria, allowing for a large saving in concrete.

The comparison of stresses in Table 3 is of little value since no one would think of designing a true arch of the dimensions shown. From their remarks about construction, it would appear that Messrs. Kirn and Sarkaria did not read the last part of the paper embracing Eq. 67 to Eq. 74.

Inclusion of tangential and twist effects in the analysis of an arch dam will cause a reduction of stresses below those found when these are not included. Their inclusion would add two more terms to the right side of Eq. 13, thus reducing the amount of work done by each of the three terms used therein. The tangential and twist effects are relatively small, however, and in moderate size dams will not indicate any appreciable saving in the quantity of concrete in the dam.

Messrs. Kirn and Sarkaria and Mr. Goodall have stressed the importance of abutment yield. Little is known about the true behavior of the abutments and foundations of dams. Therefore, in order to evaluate the results of this part of the stress analysis of dams, it is necessary to investigate the validity of the assumptions that are made concerning this behavior. In this closure, the remarks will be confined to arch dams, but the same general principles apply to gravity dams.

It may be logically assumed that elastic yield is the only type of yield that may be mathematically analyzed. The arch action ends at the contact with the abutment at the termination of the section where the value of the moment of inertia used in the arch analysis is applicable. Abutment yield can best be divided into two parts—translation and rotation. Translation consists o the elastic yield of the abutment caused by pressure on the rock throughout the width of the concrete contact, equal to the pressure at the extrados. Rotation is the yield caused by the additional stress at the intrados.

The yield of translation will have the same effect as a drop in temperature. The amount of this yield will be $\frac{s_e\, l}{2\, E_r}$, in which s_e is the unit stress at the extrados, l is the distance to the point of no yield in the rock, and E_r is the modulus of elasticity of the rock. In the arch a drop of t degrees will cause a shortening equal to $0.0000055\ t\, r\, \phi$. To determine the arch stresses, it is necessary to find a value of t equivalent to the amount of abutment yield. From the equation,

$$t = \frac{s_e\, l}{(2\, E_r\, r\, \phi)\ 0.0000055} \qquad (83)$$

t can be determined and the stresses can be found with the aid of Eq. 59*a* and Eq. 59*b*.

Rotation at the abutment will cause a tendency for rotation of the crown, and the resistance to this rotation, by equal and opposite reactions from the other half arch, causes stresses, induced by moment, which act in the same direction as those resulting from water loading. These stresses, however, cause a resistive moment at the abutment which increases the compressive stress at the extrados and decreases it at the intrados.

A method for determining the moments and stresses caused by the rotation due to abutment yield will be presented. This method is an approximation, but, since the stresses involved are not large, the results should be made within the limits of basic assumptions. The yield of the rock y_r equals $\frac{(s_i - s_e)\, l}{2\, E_r}$ as in translation. The yield of the concrete at the crown will be

$$y_c = \left[\frac{(s_i - s_e)\, l}{2\, E_r} \times \frac{t_o}{2\, t_1}\right] = \frac{s_c\, r\, \phi}{E_c} \qquad (84)$$

Since the rotation at the crown produces both compression and tension, the ratio of stresses at the abutment and crown is $\frac{t_o}{2\, t'}$,

$$s_c = \frac{E_c}{2\, E_r}\,(s_i - s_e)\,\frac{l\, t_o}{r\, \phi\, 2\, t} \qquad (85)$$

and

$$M = \frac{s_c}{2} \times \frac{4\, t_o}{3} = \frac{E_c}{6\, E_r}\,(s_i - s_e)\,\frac{l\, t_o}{r\, \phi\, t_1} \qquad (86)$$

This moment acts at the crown in the same direction as the moment due to water load, but at the abutment it acts in the opposite direction so as to reduce the moment and stresses at that point. These moments are combined with the load moments to find the unit stresses.

Mr. Goodall made a comparison of stresses in an arch of varying thickness as computed by his and the writer's methods. However, the studies were not carried far enough to reveal the advantages of an arch of varying thickness as indicated by the following example: An arch slice was computed lying entirely within the area embraced in the 40-ft constant thickness design suggested by Mr. Goodall, with these assumptions and results: Abutment at intrados and crown at extrados coincident with like points in design; t_o = 24 ft, t_1 = 32 ft, a = 0.67, t' = 26.33 ft, $2\,\phi$ = 121° 54′, and r = 151.22 ft. The stresses were as follows: Extrados—crown stress, 556 lb per sq in., and abutment stress, 10 lb per sq in.; intrados—crown stress, 175 lb per sq in., and abutment stress, 565 lb per sq in. The close balance between the maximum compressive stresses at the crown and at the abutment indicates the most economical use of concrete in the arch. The maximum stresses in the two arches are almost identical; yet the average thickness of this arch is less than two thirds of the 40-ft uniform thickness arch recommended by Mr. Goodall, and there is no tension at the abutment.

Mr. Goodall inquires about the controlling height of arch dams and the assumed allowable stress. Permissible stress depends as much on the quality of the abutments as on that of the concrete. With a good quality of concrete mixed from good materials in a modern mixing plant, a compressive stress of 1,000 lb per sq in. is a conservative value. However, this value is too high for the quality of many of the abutments that are encountered. Since the design is usually completed before the abutments are uncovered, the limiting stress must be a matter of judgment.

With respect to the limiting height of dams, reference is made to a frequently used curve.[24] Assuming the condition of an arch with zero stress at the extrados of the abutments, and a unit stress limit of 1,000 lb per sq in., the average stress is 500 lb per sq in. By the cylinder formula, $t = \frac{p\,r}{s}$, or $p = \frac{t\,s}{r}$; so in order to avoid tension at the extrados of the abutment, with a value of $\frac{t}{r} = 0.3$, the central angle must equal 140°, an extremely high value. Solving with these values, $p = 150$ lb per sq ft and the head is equal to 345 ft. Use of the cylinder formula is a close approximation since $P_1 = p\,r - (p\,r - P_0) \cos \phi$ and $(p\,r - P_0) \cos \phi$ is only a small percentage of $p\,r$.

The discussions by Mr. Josephs and Mr. Mensch are constructive and helpful and do not call for extended comment by the writer except in the use of the sliding joint. The sliding joint is used since it will greatly aid in minimizing the restraint mentioned by Mr. Josephs.

[24] "Stresses in Thick Arches of Dams," by B. F. Jakobsen, *Transactions*, ASCE, Vol. 90, 1927, p. 511.

AMERICAN SOCIETY OF CIVIL ENGINEERS

Founded November 5, 1852

TRANSACTIONS

Paper No. 2560

TORSION OF I-TYPE AND H-TYPE BEAMS

BY JOHN E. GOLDBERG,[1] M. ASCE

WITH DISCUSSION BY MESSRS. KURT H. GERSTLE, AND JOHN E. GOLDBERG

SYNOPSIS

Beginning with a review of pure torsion and torsion bending of I-type and H-type sections, the basic differential equation is obtained for the twisting of such sections. The stresses resulting from twist—namely, the simple torsional stresses and longitudinal and shearing stresses due to warping restraints—are discussed from the engineering viewpoint. Particular solutions of the differential equation are obtained for various warping conditions at the ends, and it is shown how these solutions are combined to formulate and analyze various problems, including that of a framed floor panel. The concept of the warping angle is introduced in the belief that its easily visualized character leads to a simpler formulation of problems lying within the scope of this theory.

INTRODUCTION

In certain important cases of twisting of I-beams and similar types of beams, the bending stiffness of the flanges in their respective planes and any possible additional restraints against warping at any of the cross sections have a significant influence upon the manner in which the torsional load is resisted, and upon the over-all torsional stiffness of the beam.

Consider an I-beam (Fig. 1(*a*)), simply supported at its ends with respect to lateral bending of its flanges, which is subjected to an external torque T applied at the midspan. Each cross section rotates through an angle ϕ varying along the length of the beam. Also, by virtue of symmetry, there is absolutely no warping of the cross section at the midspan, whereas at each end there is no restraint against warping. Assuming that the web has been removed (Fig. 1(*b*)), the torque T is imposed as a pair of equal and opposite forces $P = T/h$ upon the respective flanges; and, if the beam is not excessively long, the flanges alone are quite capable of supporting the applied torque by virtue of their bending stiffness in their own planes.

NOTE.—Published in August, 1952, as *Proceedings-Separate No. 145*. Positions and titles given are those in effect when the paper or discussion was received for publication.

[1] Associate Prof. of Structural Eng., Purdue Univ., Lafayette, Ind.

Returning to the whole beam of Fig. 1(a), the elementary theory of torsion of prismatic bars reveals that at each section some quantity, C, times $d\phi/dx$, of the applied torque is resisted as "simple torsion." The factor C is a property of the cross section and is therefore constant along the beam. Obviously,

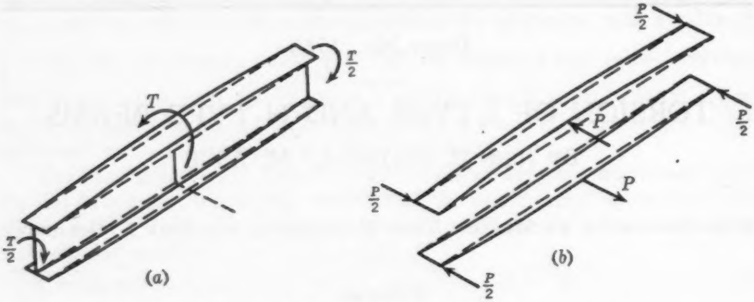

FIG. 1.—RESISTANCE OF COMPLETE BEAM AND OF FLANGES ALONE TO TORSIONAL LOAD APPLIED AT MIDSPAN

$d\phi/dx$ is not constant along the beam but varies from a maximum at the ends to zero at the midspan where the warping is also zero. The net torque at every section, however, has the constant magnitude $T/2$. Therefore, some additional resisting torque must be provided, presumably by the shearing couples in the flanges, so that, at each section, the sum of this resisting torque plus the "simple" torsional resistance, $C\,d\phi/dx$, has the constant total magnitude $T/2$. It may be shown that similar considerations govern the behavior of I-type beams when a torque is applied at any intermediate point. Moreover, any end conditions, symmetrical or unsymmetrical, can be imposed on the beam without annulling the restraint against warping which necessarily exists at the point of application of the torque.

DISPLACEMENT-LOAD RELATIONSHIPS

(a) *Simple Torsion.*—In so far as "simple torsion" is concerned, the web and each of the two flanges of, say, a wide flange beam behave very much like three independent narrow rectangular bars. For such a bar, of width b and thickness t, the resisting torque is approximately[2]

$$T = \frac{G}{3}\, b\, t^3 \left(1 - 0.630\,\frac{t}{b}\right)\frac{d\phi}{dx} \qquad \text{(1a)}$$

Considering the ensemble of the web and the two flanges, this portion of the resisting torque may be expressed as

$$T_s = C\,\frac{d\phi}{dx} \qquad \text{(1b)}$$

The following formulas for C are suggested because of their simplicity and as

[2] "Theory of Elasticity," by S. Timoshenko, McGraw-Hill Book Co., Inc., New York, N. Y., 1st Ed., 1934, p. 249.

they are sufficiently accurate for practical purposes: For beams with parallel-sided flanges—

$$C = \frac{G}{3}\left[d t^3_w + 2\,b\,t^3_f\right] \ldots\ldots\ldots\ldots\ldots\ldots (2a)$$

For beams with tapered flanges—

$$C = \frac{G}{3}\left[d t^3_w + 2\,b\,(t_1 + t_2)\,(t^2_1 + t^2_2)\right] \ldots\ldots\ldots\ldots (2b)$$

Since d is the total depth of the beam, Eqs. 2 give consideration to the added stiffness developed at the junctions of the web and the flanges by considering the mutual areas twice, and thus tend to compensate for the omission of the correction term 0.630 t/b. More accurate formulas for C have been presented by A. A. Griffith and G. I. Taylor,[3,4] by G. W. Trayer and H. W. March,[5] by Inge Lyse, A.M. ASCE, and Bruce G. Johnston,[6] M. ASCE, and by others.

(*b*) *Torsion Bending.*—As noted previously, the twisting of the beam results in lateral displacement of the flanges. Assuming that the displacements are small and that there is no appreciable distortion in the plane of the cross sections, the lateral displacement w of each flange is (see Fig. 2)

$$w = \phi\left(\frac{h}{2}\right) \ldots\ldots\ldots\ldots\ldots\ldots (3)$$

in which ϕ is the angular displacement of the cross section and $h/2$ is the distance of the flange centroid from the axis of twist—that is, from the center

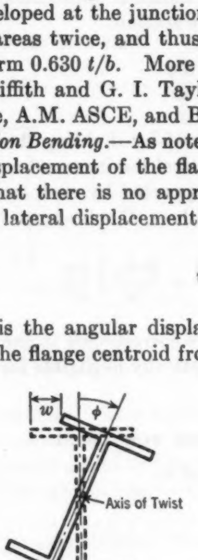

Fig. 2.—Rotational Displacement of Cross Section

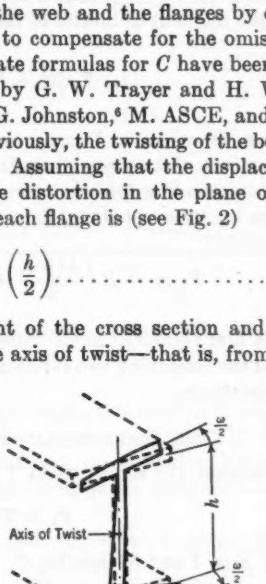

Fig. 3.—Principal Warping of Cross Section

of the cross section. The elementary theory of bending shows that the bending moment and transverse shear in each flange are

$$M = E\,I_f\,\frac{d^2w}{dx^2} \cong E\,I_f\,\frac{h}{2}\,\frac{d^2\phi}{dx^2} \ldots\ldots\ldots\ldots\ldots\ldots (4a)$$

[3] "The Use of Soap Film in Solving Torsion Problems," by A. A. Griffith and G. I. Taylor, *Reports and Memoranda No. 333*, British Air Ministry, June, 1917.

[4] "The Determination of the Torsional Stiffness and Strength of Cylindrical Bars of Any Sections," by A. A. Griffith and G. I. Taylor, *Reports and Memoranda No. 334*, British Air Ministry, June, 1917.

[5] "The Torsion of Members Having Sections Common in Aircraft Construction," by G. W. Trayer and H. W. March, *Report No. 334*, National Advisory Committee for Aeronautics, Washington, D. C., 1929.

[6] "Structural Beams in Torsion," by Inge Lyse and Bruce G. Johnston, *Transactions*, ASCE, Vol. 101, 1936, pp. 857–896.

and

$$S = E\,I_f \frac{d^3w}{dx^3} \cong E\,I_f \frac{h}{2} \frac{d^3\phi}{dx^3} \qquad (4b)$$

in which I_f is the moment of inertia of one flange about the centroidal axis normal to the flange. The corresponding torque is

$$T_b \cong -S\,h = -E\,I_f \frac{h^2}{2} \frac{d^3\phi}{dx^3} \qquad (5a)$$

Noting that the moment of inertia of one flange is approximately equal to one half of the moment of inertia of the entire section,

$$T_b \cong -E\,I_y \frac{h^2}{4} \frac{d^3\phi}{dx^3} \qquad (5b)$$

A more precise value for T_b may be obtained by dividing the section into horizontal laminae and subsequently into vertical laminae and evaluating the shear and corresponding torsional moment supported by each lamina. Upon integration in the case of parallel-flanged members, this leads to

$$T_b = -E\left(\frac{h^2\,b^3\,t_f}{24} + \frac{b^3\,t^3 f}{36} + \frac{h^3\,t^3_w}{72}\right)\frac{d^3\phi}{dx^3} \qquad (5c)$$

In Eq. 5*c* the first term within the parentheses corresponds to the value given in Eq. 5*a* and the remaining two terms are practically negligible for members of ordinary proportions.

The Differential Equation for Twist

At any section, the total torsion T is equal to

$$T_s + T_b = T \qquad (6)$$

Substituting[7] Eqs. 1 and 5*b* into Eq. 6,

$$C\frac{d\phi}{dx} - E\,I_y \frac{h^2}{4} \frac{d^3\phi}{dx^3} = T \qquad (7)$$

If T, the applied torque at the section, is constant in an interval, the general solution of Eq. 7 for that interval is

$$\phi = A_1 \sinh\frac{x}{a} + A_2 \cosh\frac{x}{a} + \frac{T\,x}{G} + A_3 \qquad (8)$$

in which

$$a = \sqrt{\frac{E\,I_y\,h^2}{4\,C}} \qquad (9)$$

and A_1, A_2, and A_3 are arbitrary constants.

[7] See "Strength of Materials," by S. Timoshenko, D. Van Nostrand Co., Inc., New York, N. Y., Part II, 2d Ed., 1941, p. 285.

ANGLE OF WARP

Consider a given cross section of the beam and imagine a pair of transverse lines (that is, lines parallel to the upper surface) passing through the centroids of each flange (see Fig. 3). Under zero load, these two lines are parallel. Under the action of a torsional moment, however, an angle, ω, will exist

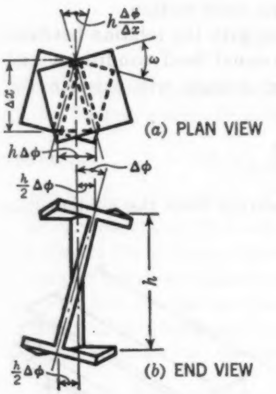

FIG. 4.—RELATION BETWEEN WARPING ANGLE ω AND TWISTING ANGLE ϕ

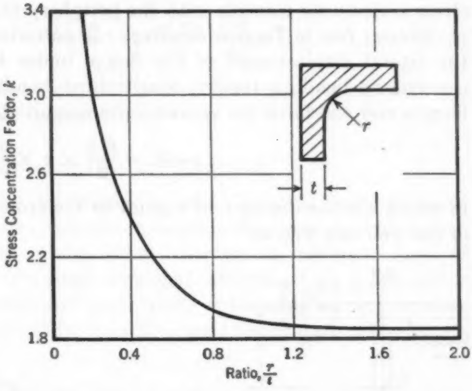

FIG. 5.—STRESS CONCENTRATION FACTORS FOR A FILLET IN SINGLE TORSION

between these lines. This angle, ω, the "angle of warp," is indeed a measure of the major nonplanarity or warping of the cross section. Fig. 4 shows that ω is substantially equal to the angle between corresponding edges of the two flanges. Although not rigorous, this definition is adequate for most structural problems.

A value for ω is obtained from the geometrical relationships of Fig. 4:

$$\omega = h\frac{d\phi}{dx} \quad \text{(10)}$$

STATE OF STRESS IN TORSION

The stresses induced by twisting of I-type sections consist primarily of

1. Shearing stresses due to simple torsion; and
2. Bending and shearing stresses, primarily in the flanges, which are related to the warping resistance.

Shearing Stresses Due to Simple Torsion.—Except for a stress concentration that occurs in the region of the web-to-flange junction, the maximum values of the simple torsional stresses at any cross section occur at the periphery of the section and have the value—

$$\tau_0 = G\,t\,\frac{d\phi}{dx} \quad \text{(11)}$$

—in which t is the local thickness. In the fillet region, this maximum stress is increased to

$$\tau_{max} = k\,\tau_0 \qquad (12)$$

—in which k is an empirical stress-concentration factor. A generally conservative value of k may be obtained[8] from Fig. 5. It will be remembered that this maximum occurs at the edge of the fillet and that the maximum shearing stress trajectories coincide with the periphery of the cross section.

Stresses Due to Torsion Bending.—In accordance with the relation between the lateral displacement of the flange under torsional load conditions and elementary bending theory, longitudinal bending stresses will exist in the flanges and will have the approximate magnitude—

$$\sigma_b \cong -\frac{E\,h}{2} \times z \times \frac{d^2\phi}{dx^2} \qquad (13a)$$

in which z is the distance of a point in the cross section from the median line of the web (see Fig. 6).

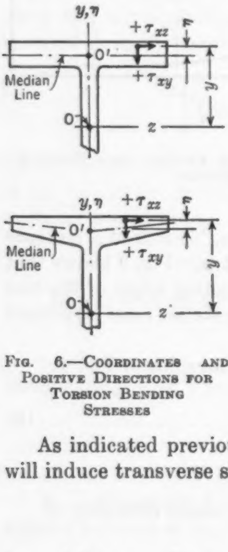

FIG. 6.—COORDINATES AND POSITIVE DIRECTIONS FOR TORSION BENDING STRESSES

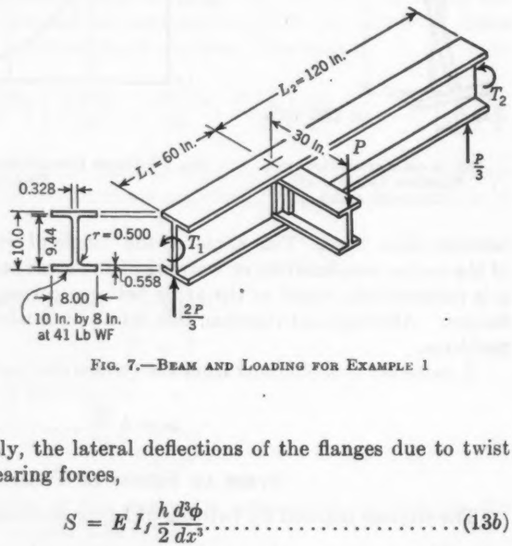

FIG. 7.—BEAM AND LOADING FOR EXAMPLE 1

As indicated previously, the lateral deflections of the flanges due to twist will induce transverse shearing forces,

$$S = E\,I_f\,\frac{h}{2}\frac{d^3\phi}{dx^3} \qquad (13b)$$

in each flange. The corresponding shearing stresses may be assumed to be distributed across the width of the flange in accordance with elementary theory. Thus, for parallel flanges, this distribution will be parabolic and will vary from zero at the edges of the flange to a maximum at the center line of the section ($z = 0$):

$$(\tau_{xz})_b = -\frac{E\,b^2\,t_f\,h}{16}\left(1 - \frac{4\,z^2}{b^2}\right)\frac{d^3\phi}{dx^3} \qquad (14a)$$

[8] See "Structural Beams in Torsion," by Inge Lyse and Bruce G. Johnston, *Transactions*, ASCE, Vol. 101, 1936, p. 865.

with a maximum value—

$$(\tau_{xy})_b = -\frac{E\,b^3\,t_f\,h}{16}\frac{d^3\phi}{dx^3} \quad \text{(14b)}$$

It may be shown that small additional shearing stresses, τ_{yz}, will also exist in the flanges (see Fig. 6):

$$(\tau_{xy})_b = -\frac{E\,t^3{}_f\,z}{8}\left(1 - \frac{4\,\eta^2}{t^2{}_f}\right)\frac{d^3\phi}{dx^3} \quad \text{(15)}$$

Small shearing stresses will also exist in the web, but these, along with τ_{xy} in the flanges, generally may be neglected.

Fundamental Cases of Twisting

The general solution of the differential equation (Eq. 8) contains three arbitrary constants that must be evaluated in terms of the prescribed boundary conditions for a given segment of the beam. Certain fundamental cases of beams or segments subjected to a single torsional moment which is applied at one end and resisted at the other are particularly interesting since a number of practical problems may be solved by the subsequent application of the results of these fundamental studies.

Case I. Flanges Pinned at Each End, Constant Torsion.—In this well-known case, since there can be no restraint against warping at the ends of the beam, the bending moments in the flanges must be zero at these points. The boundary conditions are, therefore, at $x = 0$—$\phi = 0$ and $\frac{d^2\phi}{dx^2} = 0$; and at $x = L$—$\frac{d^2\phi}{dx^2} = 0$. Applying these conditions to the general solution serves to verify the formula for simple twisting of a prismatic bar; thus,

$$\phi = \frac{T}{C}x \quad \text{(16a)}$$

Since the second and third derivatives of ϕ are zero, it follows from Eqs. 13 and 14 that there are no torsion bending stresses at any section. The total twist is

$$\phi_{(x=L)} = \frac{T\,L}{C} \quad \text{(16b)}$$

Case II. Arbitrary Warping Angle at One End, Flanges Not Restrained at Other End, Constant Torsion.—Let ω_0 be the prescribed warping angle at $x = 0$. Then the boundary conditions for this important case are at $x = 0$—$\phi = 0$ and $\frac{d\phi}{dx} = \frac{\omega_0}{h}$; and at $x = L$—$\frac{d^2\phi}{dx^2} = 0$. These conditions are satisfied when

$$\phi = a\left(\frac{T}{C} - \frac{\omega_0}{h}\right)\left(\tanh\frac{L}{a}\cosh\frac{x}{a} - \sinh\frac{x}{a} - \tanh\frac{L}{a}\right) + \frac{T}{C}x \quad \text{(17a)}$$

The total twist is

$$\phi_{(x=L)} = \frac{T}{C}\left(L - a\tanh\frac{L}{a}\right) + a\frac{\omega_0}{h}\tanh\frac{L}{a} \qquad (17b)$$

For subsequent use in the calculation of stresses, the necessary derivatives are

$$\frac{d\phi}{dx} = \left(\frac{T}{C} - \frac{\omega_0}{h}\right)\left(\tanh\frac{L}{a}\sinh\frac{x}{a} - \cosh\frac{x}{a}\right) + \frac{T}{C} \qquad (18a)$$

$$\frac{d^2\phi}{dx^2} = \frac{1}{a}\left(\frac{T}{C} - \frac{\omega_0}{h}\right)\left(\tanh\frac{L}{a}\cosh\frac{x}{a} - \sinh\frac{x}{a}\right) \qquad (18b)$$

and

$$\frac{d^3\phi}{dx^3} = \frac{1}{a^2}\left(\frac{T}{C} - \frac{\omega_0}{h}\right)\left(\tanh\frac{L}{a}\sinh\frac{x}{a} - \cosh\frac{x}{a}\right) \qquad (18c)$$

At $x = 0$, the derivatives have the values,

$$\left(\frac{d\phi}{dx}\right)_{(x=0)} = \frac{\omega_0}{h} \qquad (18d)$$

$$\left(\frac{d^2\phi}{dx^2}\right)_{(x=0)} = \frac{1}{a}\left(\frac{T}{C} - \frac{\omega_0}{h}\right)\tanh\frac{L}{a} \qquad (18e)$$

$$\left(\frac{d^3\phi}{dx^3}\right)_{(x=0)} = \frac{1}{a^2}\left(\frac{\omega_0}{h} - \frac{T}{C}\right) \qquad (18f)$$

The case of a beam which is built-in at $x = 0$ and has unrestrained flanges at the opposite end may be obtained directly from Eqs. 17 and 18 merely by setting $\omega_0 = 0$.

Case III. Prescribed Warping Angles at Both Ends, Constant Torsion.— The boundary conditions for this case are at $x = 0$—$\phi = 0$ and $\frac{d\phi}{dx} = \frac{\omega_0}{h}$; and at $x = L$—$\frac{d\phi}{dx} = \frac{\omega_L}{h}$. The particular solution becomes

$$\phi = a\left(\frac{\omega_0}{h} - \frac{T}{C}\right)\sinh\frac{x}{a} + \frac{a\cosh\frac{a}{x}}{\sinh\frac{L}{a}}\left[\frac{\omega_L}{h} - \frac{T}{C} - \left(\frac{\omega_0}{h} - \frac{T}{C}\right)\cosh\frac{L}{a}\right]$$
$$+ \frac{Tx}{C} - \frac{a}{\sinh\frac{L}{a}}\left(\frac{\omega_L}{h} - \frac{T}{C}\right) + \frac{a\cosh\frac{L}{a}}{\sinh\frac{L}{a}}\left(\frac{\omega_0}{h} - \frac{T}{C}\right) \qquad (19)$$

The total twist is obtained by setting $x = L$ in Eq. 19:

$$\phi_{(x=L)} = \frac{2T}{C}\left(\frac{L}{2} - a\tanh\frac{L}{2a}\right) + (\omega_0 + \omega_L)\frac{a}{h}\tanh\frac{L}{2a} \qquad (20)$$

For use in the calculation of stresses, the derivatives are

$$\frac{d\phi}{dx} = \left(\frac{\omega_0}{h} - \frac{T}{C}\right)\cosh\frac{x}{a} + \frac{\sinh\frac{x}{a}}{\sinh\frac{L}{a}}\left[\frac{\omega_L}{h} - \frac{T}{C} - \left(\frac{\omega_0}{h} - \frac{T}{C}\right)\cosh\frac{L}{a}\right] + \frac{T}{C} \quad \text{(21}a\text{)}$$

$$\frac{d^2\phi}{dx^2} = \frac{1}{a}\left(\frac{\omega_0}{h} - \frac{T}{C}\right)\sinh\frac{x}{a} + \frac{\cosh\frac{x}{a}}{a\sinh\frac{L}{a}}\left[\frac{\omega_L}{h} - \frac{T}{C} - \left(\frac{\omega_0}{h} - \frac{T}{C}\right)\cosh\frac{L}{a}\right] \quad \text{(21}b\text{)}$$

and

$$\frac{d^3\phi}{dx^3} = \frac{1}{a^2}\left(\frac{\omega_0}{h} - \frac{T}{C}\right)\cosh\frac{x}{a} + \frac{\sinh\frac{x}{a}}{a^2\sinh\frac{L}{a}}\left[\frac{\omega_L}{h} - \frac{T}{C} - \left(\frac{\omega_0}{h} - \frac{T}{C}\right)\cosh\frac{L}{a}\right] \quad \text{(21}c\text{)}$$

At $x = 0$, the derivatives have the values:

$$\left(\frac{d\phi}{dx}\right)_{(x=0)} = \frac{\omega_0}{h} \quad \text{(21}d\text{)}$$

$$\left(\frac{d^2\phi}{dx^2}\right)_{(x=0)} = \frac{1}{a\sinh\frac{L}{a}}\left[\frac{\omega_L}{h} - \frac{T}{C} - \left(\frac{\omega_0}{h} - \frac{T}{C}\right)\cosh\frac{L}{a}\right] \quad \text{(21}e\text{)}$$

and

$$\left(\frac{d^3\phi}{dx^3}\right)_{(x=0)} = \frac{1}{a^2}\left(\frac{\omega_0}{h} - \frac{T}{C}\right) \quad \text{(21}f\text{)}$$

By setting the corresponding values of ω equal to zero, Eqs. 19 to 21 may be reduced to those for beams with one or both ends built-in.

The Fundamental Problem

The stresses and deflections that result from the application of a single torsional load at some point between its two ends constitute the basic problem in the twisting of an I-type beam. Three methods of solution are discussed.

Method I. Indeterminate Analysis.—A uniform beam of length L (see Fig. 7) is subjected to a torsional load T applied at distances L_1 and L_2, respectively, from the ends. The solution is obtained by imagining the beam to be cut at the section where the load is applied. The conditions of equilibrium and continuity at the cut faces are then formulated in four steps: (1) The

warping angles must be consistent; (2) the angular displacements must be equal; (3) the longitudinal fiber stresses must be equal; and (4) the sum of the two resisting torsions must equal the applied torsion.

The method of solution is essentially the same whether the ends of the beam are pinned, built-in, or arbitrarily warped. In fact, the method may be extended to the case where the rotational and warping restraints at the ends of the beam are elastic. The case of a beam with warping angles ω_1 and ω_2 at the ends is considered first and, to make the solution more general, a known difference ϕ_e is assumed to exist between the angular positions at the two ends of the beam—that is, $\phi_2 = \phi_1 + \phi_e$.

It is convenient to take the origin at the cut section for each of the two sublengths, L_1 and L_2, and to take the positive direction for each part as going from the cut section to the respective ends of the beam. Let ω_0 be the warping angle at the cut section associated with the sublengths L_1. Then condition (1) is satisfied, in view of the indicated sign convention, if the warping angle at the cut section associated with L_2 is taken as $-\omega_0$.

Eq. 20 is applied to each sublength to formulate condition (2). Since I_f has the same value at each face of the cut section, condition (3) is formulated by direct application of Eq. 21*e* to both sublengths. The resulting equations are

$$\frac{2\,T_1}{C}\left(\frac{L_1}{2} - a\tanh\frac{L_1}{2\,a}\right) + (\omega_0 + \omega_1)\,\frac{a}{h}\tanh\frac{L_1}{2\,a} + \phi_e$$

$$= \frac{2\,T_2}{C}\left(\frac{L_2}{2} - a\tanh\frac{L_1}{2\,a}\right) + (-\,\omega_0 + \omega_2)\,\frac{a}{h}\tanh\frac{L_2}{2\,a} \quad \text{..(22a)}$$

$$\frac{1}{\sinh\frac{L_1}{a}}\left[\frac{\omega_1}{h} - \frac{T_1}{C} - \left(\frac{\omega_0}{h} - \frac{T_1}{C}\right)\cosh\frac{L_1}{A}\right]$$

$$= \frac{1}{\sinh\frac{L_2}{a}}\left[\frac{\omega_2}{h} - \frac{T_2}{C} - \left(\frac{\omega_0}{h} - \frac{T_2}{C}\right)\cosh\frac{L_1}{a}\right] \quad \text{..(22b)}$$

and

$$T_1 + T_2 = T \quad \text{.......................(22c)}$$

The simultaneous solution of Eqs. 22 yields values of T_1, T_2, and ω_0 which, by means of Eqs. 18 or Eqs. 21, will determine the shearing and bending stresses throughout the beam.

For the case of a beam with pin-ended flanges, Eqs. 17*b* and 18*e* are used instead of Eqs. 20 and 21*e* to formulate conditions (2) and (3). If $\phi_e = 0$ in the pin-ended case, it will be found that T_1 and T_2 are in inverse proportion to the respective sublengths L_1 and L_2. Thus, ω_0 is the only unknown and this may be determined by either condition (2) or condition (3) using only one equation. The case where L_1 and L_2 are dissimilar beams, joined integrally, can be handled merely by modifying Eq. 22*b*. If the two segments have the same depth, one needs only to multiply each member of Eq. 22*b* by the corresponding value of $E\,I_f$.

The case of applied flange warping moments is also handled by modification of Eq. 22*b*. This case arises, for example, where the flanges of a floor beam are welded directly to the flanges of the girder. If M_f is the value of each of the two equal and opposite warping moments applied, respectively, to the two flanges, one merely writes

$$E\,I_f\,\frac{h}{2}\left[\left(\frac{d^2\phi}{dx^2}\right)_1 - \left(\frac{d^2\phi}{dx^2}\right)_2\right] = M_f \quad \text{(23)}$$

in which the subscripts indicate evaluation immediately to the left and to the right of the point of application of the external moments, and in which Eq. 18*e* or Eq. 21*e* is used in the formulation.

Method II. Superposition.—Superposition methods have the advantage of avoiding simultaneous equations, but frequently are more time-consuming than direct methods. A typical superposition procedure consists of six steps, as follows:

1. Assume the beam to be cut at the point of application of the torsional load; pick convenient values T'_1 and T'_2 such that $T'_1 + T'_2 = T$.
2. Applying Eq. 18*e* or Eq. 21*e* to each of the two sublengths (note that ω'_0 for one sublength requires $-\omega'_0$ for the other) and equating the results, solve for ω'_0.
3. Using T'_1, T'_2, and ω'_0, calculate the total twist of each segment using Eq. 17*b* or Eq. 19. In general, these twists will not satisfy the condition $\phi_2 = \phi_1 + \phi_e$. Therefore, calculate $\Delta\phi = \phi_2 - \phi_1 - \phi_e$, the error in the total twist.
4. Using either Eq. 16*b* for a pin-ended beam or Eq. 20 for a restrained beam, determine the torsion ΔT that must be applied to the unloaded whole beam of length $L = L_1 + L_2$ to obtain a twist of $-\Delta\phi$.
5. Calculate ω''_0, the correction to ω'_0 due to the added twist $-\Delta\phi$. Note that, in the case of a pin-ended beam, $\omega''_0 = -h\,(\Delta\phi/L)$. In the case of a restrained beam, Eq. 21*a* may be used with $x = L_1$ and $L = L_1 + L_2$.
6. For $T_1 = T'_1 + \Delta T$ and $\omega_0 = \omega'_0 + \omega''_0$, determine stresses and deflections where desired in the first segment; calculate stresses and deflections in the second segment using the corresponding values of torsion and warping.

Method III. Trigonometric Series.—In the case of a pin-ended beam to which a torsional load is applied at $x = c$ (the origin being taken at one end), the angular displacement at any point x may be represented by the series[9]

$$\phi = \sum_{n=1}^{\infty} a_n \sin\frac{n\,\pi\,x}{L} \quad (n = 1, 2, 3, \cdots) \quad \text{(24)}$$

in which

$$a_n = \frac{2\,T\sin\dfrac{n\,\pi\,c}{L}}{C\,\dfrac{n^2\,\pi^2}{L} + \dfrac{E\,I_y\,h^2\,n^4\,\pi^4}{4\,L^3}} \quad \text{(25)}$$

[9] "On the Application of Trigonometric Series to the Twisting of I-Type Beams," by John E. Goldberg, *Proceedings*, First U. S. National Cong. of Applied Mech., Chicago, Ill., June, 1951.

Because of the powers of n in the denominator, this series converges with reasonable rapidity and only a few terms are required, in general, to obtain satisfactory values for the angular deflections. The series may be differentiated to obtain the functions necessary to the calculation of stresses:

$$\frac{d\phi}{dx} = \sum_{n=1}^{\infty} a_n \frac{n\,\pi}{L} \cos \frac{n\,\pi\,x}{L} \qquad (26a)$$

and

$$\frac{d^2\phi}{dx^2} = -\sum_{n=1}^{\infty} a_n \frac{n^2\,\pi^2}{L^2} \sin \frac{n\,\pi\,x}{L} \qquad (26b)$$

The case of several torsional loads may be obtained from Eqs. 26 by superposition. For cases in which restraints against warping exist at the ends of the beam, the final solution may be obtained by superimposing upon the results of Eq. 24 a residual solution from Case III which cancels the untenable part of the warping displacements at the ends of the beam.

In the case of a pair of equal and opposite warping moments M_f applied to the flanges of a pin-ended beam at $x = c$, the corresponding series are

$$\phi = \sum_{n=1}^{\infty} b_n \sin \frac{n\,\pi\,x}{L} \quad (n = 1, 2, 3, \cdots) \qquad (27a)$$

$$\frac{d\phi}{dx} = \sum_{n=1}^{\infty} b_n \frac{n\,\pi}{L} \cos \frac{n\,\pi\,x}{L} \qquad (27b)$$

$$\frac{d^2\phi}{dx^2} = -\sum_{n=1}^{\infty} b_n \frac{n^2\,\pi^2}{L^2} \sin \frac{n\,\pi\,x}{L} \qquad (27c)$$

in which

$$b_n = \frac{M_f \dfrac{h\,n\,\pi}{L} \cos \dfrac{n\,\pi\,c}{L}}{C \dfrac{n^2\,\pi^2}{L} + E\,I_y \dfrac{h^2}{4} \dfrac{n^4\,\pi^4}{L^3}} \qquad (27d)$$

Unlike the previous methods, the series method does not require decomposition of the beam into two sublengths.

Illustrative Examples

Example 1. Pin-Edged Beam with Torsion Applied at Intermediate Point of Span (Fig. 7).—As indicated previously, it can be shown that an applied torsional load is distributed to the two ends of a uniform pin-ended beam in inverse proportion to the sublengths. Thus, T_1 and T_2 are immediately known:

$$T_1 = \frac{T\,L_2}{L_1 + L_2} = \frac{T\,L_2}{L} = \frac{2\,T}{3} \qquad (28a)$$

and

$$T_2 = \frac{T\,L_1}{L} = T - T_1 = \frac{T}{3} \qquad (28b)$$

Therefore, it is necessary to determine only, say, the warping angle at the point of loading. For the beam in Fig. 7: $I_y = 47.7$ in.^{4}; $E = 29 \times 10^6$ lb per sq in., $G = 11 \times 10^6$ lb per sq in.; $C = G/3\ (2 \times 8.00 \times 0.558^3 + 10.00 \times 0.328^3) = 11.484 \times 10^6$ lb-in.^{2}; and $a = \frac{9.44}{2}\sqrt{\frac{29 \times 10^6 \times 47.7}{11.484 \times 10^6}} = 51.80$ in. Finally,

$$L_1 = 60 \text{ in.};\ \tanh\frac{L_1}{a} = 0.8202;\ a\tanh\frac{L_1}{a} = 42.49 \text{ in.};\ L_1 - a\tanh\frac{L_1}{a} = 17.51 \text{ in.}$$

and

$$L_2 = 120 \text{ in.};\ \tanh\frac{L_2}{a} = 0.9808;\ a\tanh\frac{L_2}{a} = 50.80 \text{ in.};\ L_2 - a\tanh\frac{L_2}{a} = 69.20 \text{ in.}$$

Noting that $+\ \omega_0$ to the left of the load implies $-\ \omega_0$ to the right (if x is positive both directions from the load) and applying Eq. 17*b* to each sublength and equating the total twists,

$$\frac{T_1}{C}(17.51) + 42.49\frac{\omega_0}{h} = \frac{T_2}{C}(69.20) - 50.80\frac{\omega_0}{h} \qquad \text{(29)}$$

Since $T_1 = 2\ T_2 = 2\ T/3$, Eq. 29 yields

$$\frac{\omega_0}{h} = 0.1221\frac{T}{C} \qquad \text{(30)}$$

Eq. 18*e* may be used instead of Eq. 17*b*:

$$\frac{1}{a}\left(\frac{T_1}{C} - \frac{\omega_0}{h}\right)0.8202 = \frac{1}{a}\left(\frac{T_2}{C} + \frac{\omega_0}{h}\right)0.9808$$

which yields the same value of ω_0/h.

By Eq. 17*b* the angular displacement at the point of loading is

$$\phi = \frac{2}{3}\frac{T}{C}(17.51) + 42.49\left(0.1221\frac{T}{C}\right) = 16.86\frac{T}{C} \qquad \text{(31)}$$

For the calculation of stresses in the shorter span adjacent to the load (that is, at $x = 0$), the following derivatives are required: By Eqs. 18—

$$\frac{d\phi}{dx} = 0.1221\frac{T}{C} \qquad \text{(32a)}$$

$$\frac{d^2\phi}{dx^2} = \frac{1}{51.80}\left(\frac{2}{3}\frac{T}{C} - 0.1221\frac{T}{C}\right)0.8202 = 0.00866\frac{T}{C} \qquad \text{(32b)}$$

and

$$\frac{d^3\phi}{dx^3} = \frac{1}{(51.80)^2}\left(0.1221\frac{T}{C} - \frac{2}{3}\frac{T}{C}\right) = -0.000204\frac{T}{C} \qquad \text{(32c)}$$

and by Eq. 6—

$$T_b = T_1 - T_s = \frac{2\,T}{3} - C\frac{d\phi}{dx} = 0.5446\ T \quad\text{(33a)}$$

Check of Eq. 33a by Eq. 5b:

$$T_b = -\,E\,I_y\frac{h^2}{4}\frac{d^3\phi}{dx^3}$$

$$= -\,29 \times 10^6 \times 47.7 \times \frac{9.44^2}{4}\left(-\,\frac{0.000204\ T}{11.484 \times 10^6}\right) = 0.547\ T \quad\text{(33b)}$$

Stresses in the flange immediately to the left of the applied load are determined, as follows, by Eq. 11:

$$\tau_0 = G\,t\frac{d\phi}{dx} = 11 \times 10^6 \times 0.558 \times 0.1221\,\frac{T}{11.484 \times 10^6} = 0.0652\ T \quad\text{(34)}$$

The effect of the stress concentration at the fillet is determined as follows: $r/t = 0.93$; $k = 1.92$ (from Fig. 5); and $\tau_{s(\max)} = 1.92 \times 0.0652\ T = 0.125\ T$. The shear per flange is

$$S = \frac{T_b}{h} = \frac{0.5446\ T}{9.44} = 0.0577\ T \quad\text{(35a)}$$

and

$$\tau_{b(\max)} = \frac{3\,S}{2\,A_f} = \frac{3 \times 0.0577\ T}{2 \times 0.558 \times 8.00} = 0.0194\ T \quad\text{(35b)}$$

The longitudinal fiber stresses at the edges of the flanges are by Eq. 13a

$$\sigma_b \cong 29 \times 10^6 \times \frac{9.44}{2} \times 4.00 \times \frac{0.00866\ T}{11.484 \times 10^6} = 0.413\ T \quad\text{(35c)}$$

Thus, if $P = 2{,}000$ lb, then for the beam in Fig. 7, $T = 60{,}000$ lb-in., and (in pounds per square inch): $\tau_{s(\max)} = 7{,}500$; $\tau_b = 1{,}164$; and $\sigma_b = 24{,}780$.

These stresses, of course, are to be added to the stresses due to vertical shear and bending.

In this example, the total deformations are small and, therefore, the change in the applied torsion is practically negligible. Likewise, if P remains vertical, its component in the lateral direction of the beam is also negligible. Such effects, however, should be checked in general and, if necessary, corrections can be introduced on the basis of the deformed geometry.

In addition to the foregoing procedure, Example 1 can be solved by the method of superposition or by the trigonometric series method. Two terms of the series Eq. 26 gives $\phi = \dfrac{16.64\ T}{C}$ at the load point.

Example 2. Beam with Prescribed Warping Angles at Ends, Torsion Applied at Intermediate Point.—A beam similar to that of Example 1, but with prescribed warping angles, ω_1 and ω_2, at the left and right ends, respectively, is analyzed. The distribution of the applied torsion to the two sublengths of the

beam is not a direct function of the lengths as in the case of the pin-ended beam; thus,

$$\tanh \frac{L_1}{2a} = \tanh \frac{60}{103.6} = 0.5221; \text{ and } a \tanh \frac{L_1}{2a} = 27.05$$

$$\tanh \frac{L_2}{2a} = \tanh \frac{120}{103.6} = 0.8202; \text{ and } a \tanh \frac{L_2}{2a} = 42.49 \text{ in.}$$

$$\left(\frac{L_1}{2} - a \tanh \frac{L_1}{2a}\right) = 2.96 \text{ in.; and } \left(\frac{L_2}{2} - a \tanh \frac{L_2}{2a}\right) = 17.51 \text{ in.}$$

$$\sinh \frac{L_1}{a} = 1.4354; \text{ and } \cosh \frac{L_1}{a} = 1.7494$$

$$\sinh \frac{L_2}{a} = 5.0223; \text{ and } \cosh \frac{L_2}{a} = 5.1209.$$

Let ω_0 be the warping angle for segment L_1 immediately to the left of the applied load. Then, taking x as also positive in L_2, the warping angle for this sublength at the load ($x = 0$) is $-\omega_0$.

Eqs. 22, which equate the angular displacements of the two sublengths and the flange bending stresses at the load point, and insure equilibration of the applied load, become

$$\frac{2T_1}{C} 2.96 + \frac{\omega_0 + \omega_1}{h} 27.05 + \phi_e = \frac{2T_2}{C} 17.51 + \frac{-\omega_0 + \omega_2}{h} 42.49 \quad (36a)$$

$$\frac{1}{1.4354}\left(\frac{\omega_1}{h} - 1.7494 \frac{\omega_0}{h} + 0.7494 \frac{T_1}{C}\right)$$
$$= \frac{1}{5.0223}\left(\frac{\omega_2}{h} + 5.1209 \frac{\omega_0}{h} + 4.1209 \frac{T_2}{C}\right) \quad (36b)$$

and

$$\frac{T_1}{C} + \frac{T_2}{C} = \frac{T}{C} \quad (36c)$$

The simultaneous solution of Eqs. 36 yields

$$\frac{T_1}{C} = 0.732 \frac{T}{C} - 0.589 \frac{\omega_1}{h} + 0.589 \frac{\omega_2}{h} - 0.01210 \phi_e \quad (37a)$$

$$\frac{T_2}{C} = 0.268 \frac{T}{C} + 0.589 \frac{\omega_1}{h} - 0.589 \frac{\omega_2}{h} + 0.01210 \phi_e \quad (37b)$$

and

$$\frac{\omega_0}{h} = 0.726\, T - 0.042 \frac{\omega_1}{h} + 0.264 \frac{\omega_2}{h} - 0.0073 \phi_e \quad (37c)$$

For the case of the beam with built-in ends, it is necessary only to set ω_1 and ω_2 equal to zero.

This problem can be solved by a method of superimposing a residual solution for the proper end conditions upon the solution for the pin-ended case which was obtained in Example 1. By substituting the values of T_1 and ω_0 into Eq. 18b and evaluating at $x = L_1$, it is found that $\omega/h = 0.3491\ T/C$ at

the left end of the pin-ended beam. Similarly, using T_2 and $-\omega_0$ with $x = L_2$, it is found that $\omega/h = 0.2444\ T/C$ at the right end. Therefore, in order to adapt the pin-ended solution to the prescribed end conditions, the designer must impose additional warping angles ω_l and ω_r at the left and right ends of the beam such that

$$\frac{\omega_l}{h} = \frac{\omega_1}{h} - 0.3491\frac{T}{C} \quad \text{(38a)}$$

and

$$\frac{\omega_r}{h} = \frac{-\omega_2}{h} + 0.2444\frac{T}{C} \quad \text{(38b)}$$

The additional torque ΔT induced by imposing these angles along with the prescribed differential displacement of the ends, ϕ_e, is determined by Eq. 20:

$$\phi_{(x=L)} = \frac{2\,\Delta T}{C}\left(\frac{L}{2} - a\tanh\frac{L}{2a}\right) + (\omega_l + \omega_r)\frac{a}{h}\tanh\frac{L}{2a} \quad \text{(39a)}$$

or

$$-\phi_e = \frac{2\,\Delta T}{C}\left(\frac{180}{2} - 51.80\tanh\frac{180}{103.60}\right)$$
$$+\left(\frac{\omega_1}{h} - 0.3491\frac{T}{C} - \frac{\omega_2}{h} + 0.2444\frac{T}{C}\right)51.80\tanh\frac{180}{103.60} \quad \text{(39b)}$$

Eq. 39 yields

$$\frac{\Delta T}{C} = 0.0617\frac{T}{C} - 0.589\frac{\omega_1}{h} + 0.589\frac{\omega_2}{h} - 0.0121\,\phi_e \quad \text{(40a)}$$

Adding and subtracting to $\frac{T_1}{C}$ and $\frac{T_2}{C}$ for the pin-ended case results in

$$\frac{T_1}{C} = \frac{2\,T}{3\,C} + \frac{\Delta T}{C} = 0.729\frac{T}{C} - 0.589\frac{\omega_1}{h} + 0.589\frac{\omega_2}{h} - 0.0121\,\phi_e \quad \text{(40b)}$$

and

$$\frac{T_2}{C} = \frac{T}{3\,C} - \frac{\Delta T}{C} = 0.272\frac{T}{C} + 0.589\frac{\omega_1}{h} - 0.589\frac{\omega_2}{h} + 0.0121\,\phi_e \quad \text{(40c)}$$

—which agree substantially with the simultaneous equation solution.

Example 3. Floor Panel Framing Problem (Fig. 8).—Problems involving interaction of spandrel or floor girders and floor beams may be solved by any one of several procedures. For example, appropriate equations of Cases II and III can be applied to the beam and to each segment of the girder, writing the conditions of twisting and warping equilibrium for each girder-beam junction in terms of the angular and warping displacements, and using the slope deflection equation to express the end moment of the floor beam. Indeed, if the floor beam flanges are rigidly attached to the girder flanges, thus forcing the beam to assume the same warping angle as the girder at the junction, it may be necessary to use this procedure. For example, if the beam and girder have the same depth, the equilibrium condition for flange warping moments

consists of multiplying Eq. 18e or Eq. 21e by the corresponding $(E I_f)$-values and setting the sum of the three values thus obtained at each joint equal to zero.

In general, however, the connections between beam and girder will be such that the beam is free to warp at the junction, and the following simple pro-

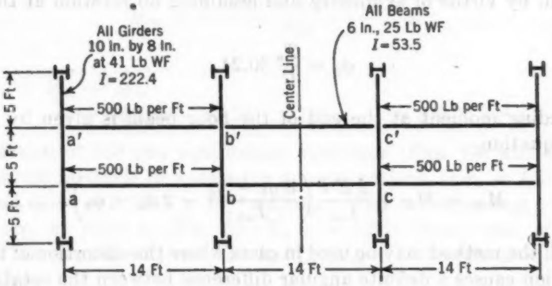

FIG. 8.—FLOOR FRAMING PLAN FOR EXAMPLE 3

cedure will be adequate. This procedure requires knowledge of the angle of twist of the girder at each junction for unit torques applied at these points. The data are obtained by preliminary solutions for the girder for a series of unit torques, following the method of Example 1 or by the series method. Thus, using the results of Example 1, a torque T_a applied at the third-point results in a rotation at that point having a value

$$\phi'_a = \frac{T_a}{C} 16.86 \qquad \text{(41a)}$$

This torque also induces a rotation at point b which is obtained by evaluating Eq. 17a at $x = 60$ in. in the 120-in. sublength:

$$\phi'_{a'} = \frac{T_a}{C} 16.86 - \left[a\left(\frac{T_2}{C} - \frac{\omega_0}{h}\right)\left(\tanh\frac{L_2}{a}\cosh\frac{x}{a} - \sinh\frac{x}{a} - \tanh\frac{L_2}{a}\right) + \frac{T_2}{C}x\right] \qquad \text{(41b)}$$

Substituting the values $\frac{\omega_0}{h} = -0.1221\frac{T_a}{C}$, $T_2 = \frac{T_a}{3}$, $\cosh\frac{x}{a} = 1.7494$, $\sinh\frac{x}{a} = 1.4354$, and $\tanh\frac{L_2}{a} = 0.9808$, gives

$$\phi'_{a'} = \frac{T_a}{C} 13.38 \qquad \text{(41c)}$$

It may be noted that using only two terms of the series of Eq. 24 gives $\phi'_{a'} = 13.48\ T/C$. By Maxwell's theorem, the total angular displacement at

$x = a$ is

$$\phi_a = \frac{T_a}{C} 16.86 + \frac{T_{a'}}{C} 13.38 \qquad (41d)$$

In the general case, it is necessary to obtain similar expressions for each junction and to adjust for relative rotation at the ends of the girders. In the panel shown, by virtue of symmetry and assuming no rotation at the ends of the girders,

$$\phi_a = \frac{T_a}{C} 30.24 \qquad (41e)$$

The bending moment at the end of the floor beam is given by the slope deflection equation,

$$M_{ab} = M_F + \frac{2\,E\,I}{L_{ab}}\left(\frac{3\,y_b - y_a}{L_{ab}} - 2\,\phi_a - \phi_b\right) \qquad (42)$$

Although the method may be used in cases where the distortion of the beam-girder junction causes a definite angular difference between the rotation of the girder and the end slope of the beam, in this example it is assumed that $\theta_a = \phi_a$, and similarly at other junctions.

To include the vertical deflections, y_a and y_b, as unknowns would require several additional simultaneous equations. From a practical standpoint, of course, it is desirable to avoid the added complications of the additional equations. Fortunately, because of the torsional flexibility of the girder and the relative insensitivity of the beam reactions to the end moments, it is generally possible to treat the vertical deflections as known quantities that have been determined previously by estimate or by preliminary analysis.

Thus, for the loading of Fig. 8, one may estimate that beam ab is pin-ended at point a and is approximately 50% restrained at point b (primarily by span bc). Comparing with the case of a beam fully restrained at point b and hinged at point a, for which the end shears are 5 $W/8$ and 3 $W/8$, a reasonable estimate of the end shears in this problem would be 9 $W/16$ and 7 $W/16$. The difference, $W/8 = 875$ lb, would cause a differential vertical deflection of the girders (assuming fixed-end conditions), $y_b - y_a = 0.0047$ in. The contribution of this term to the end moments is $\frac{2\,E\,I}{L_{ab}}\left(3\,\frac{y_b - y_a}{L_{ab}}\right) = \frac{2 \times 30 \times 10^6 \times 53.5}{168} \times 3 \times \frac{0.0047}{168} = +\,1{,}605$ lb-in. at each end of the beam.

The moments at joint a are

$$T_a = (C/30.24)\,\phi_a = -\,(11.484 \times 10^6/30.24)\,\phi_a = -\,0.3798 \times 10^6\,\phi'_a \qquad (43a)$$

and

$$M_{ab} = \frac{500 \times 14^2 \times 12}{12} + 1{,}605 - \frac{2 \times 30 \times 10^6 \times 53.5}{168}(2\,\phi_a + \phi_b) \qquad (43b)$$

and, since the joint is in equilibrium,

$$\sum M_a = T_a + M_{ab} = 99{,}605 - 38.594 \times 10^6\,\phi_a - 19.107 \times 10^6\,\phi_b = 0 \qquad (43c)$$

At joint b, since $\phi_c = -\phi_b$,

$$T_b \doteq -(C/30.24)\,\phi_b = -0.3798 \times 10^6\,\phi_b \qquad (44a)$$

$$M_{ba} = -\frac{500 \times 14^2 \times 12}{12} + 1{,}605 - \frac{2 \times 30 \times 10^6 \times 53.5}{168}(2\,\phi_b + \phi_a) \qquad (44b)$$

$$M_{bc} = \frac{2 \times 30 \times 10^6 \times 53.5}{168}\,\phi_b \qquad (44c)$$

and

$$\begin{aligned}\sum M_b &= T_b + M_{ba} + M_{bc}\\ &= -96{,}395 - 57.701 \times 10^6\,\phi_b - 19.107 \times 10^6\,\phi_a = 0 \qquad (44d)\end{aligned}$$

The solution of the two equilibrium equations (Eqs. 43*c* and 44*d*), using either algebraic methods or successive approximations, is $\phi_a = 4.0761 \times 10^{-3}$ radians; and $\phi_b = -3.0203 \times 10^{-3}$ radians. The corresponding torques and moments are, at joint a (Fig. 8)—$T_a = -1{,}550$ lb-in.; and $M_{ab} = 1{,}550$ lb-in.; and at joint b—$T_b = 1{,}150$ lb-in.; $M_{ba} = -58{,}860$ lb-in.; and $M_{bc} = 57{,}710$ lb-in.

In place of the estimated difference of 875 lb in the end shears of beam ab, the corrected value is $\dfrac{2(58{,}860 - 1{,}550)}{168} = 684$ lb which would cause a differential vertical deflection of 0.0037 in. in the girders. If the slope deflection analysis were carried through, the error of 0.0010 in., in turn, would cause $\Delta T_a = 3$ lb-in.; $\Delta M_{ab} = -3$ lb-in.; $\Delta M_{ba} = -70$ lb-in.; $\Delta M_{bc} = +68$ lb-in.; and $\Delta T_b = +2$ lb-in. These results are sufficiently small to require no further correction, and, therefore, $T_a = -1{,}547$ lb-in.; $M_{ab} = +1{,}547$ lb-in.; $T_b = 1{,}152$ lb-in.; $M_{ba} = -58{,}930$ lb-in.; and $M_{bc} = +57{,}768$ lb-in.

It will be noted that the analysis could be made by the moment distribution method instead of the slope deflection procedure. It will be noted also that a separate analysis for the effects of a unit differential vertical deflection of the girders would be helpful in some cases, particularly if several successive corrections to the vertical deflections are required.

For the case in which beams bc are also loaded with a distributed load of 500 lb per ft, the designer can take three eighths of the total load on span ab as an initial estimate for the girder load at point a, whereas the girder load at point b is estimated at five eighths of the load on span ab plus one half of the load on span bc. The difference between these reactions is 5,250 lb, which causes a differential vertical deflection of 0.0283 in. Carrying through the procedure as before, $T_a = -1{,}230$ lb-in.; $M_{ab} = 1{,}230$ lb-in.; $T_b = 343$ lb-in.; $M_{ba} = -115{,}625$ lb-in.; and $M_{bc} = 115{,}282$ lb-in.

The corrected difference between reactions at points b and a is 4,864 lb. The reduction—5,250 − 4,864 = 386 lb—results in the following corrections: $\Delta T_a = +5$; $\Delta M_{ab} = -5$; $\Delta T_b = +3$; $\Delta M_{ba} = -145$; and $\Delta M_{bc} = +142$ lb-in. Obviously, further corrections are negligible.

Conclusion

The principles of a linear torsion bending theory for I-type and H-type sections have been reviewed and have been applied to certain idealized forms

of problems which occur in structural practice. Although a small deflection theory, it is felt that this viewpoint is valid for most cases that occur in practice. The extent to which the actual problem may be formulated directly in terms of this theory depends on such physical factors as the true continuity and rigidity of connections and the restraints imposed by slabs, walls, and fireproofing. The evaluation of these factors and the determination of the extent to which the idealized solution is valid are the functions of the engineer.

The concept of the warping angle ω has been introduced as a tangible parameter in the belief that its easily visualized physical character leads to a clearer understanding of the mode of deformation and hence a simpler formulation of the problems lying within the scope of this theory.

Several simple problems have been solved to illustrate the basic principles. By no means do these cover the field of applicability of these principles. Many additional types of problems can be solved by this procedure and, indeed, all such problems must satisfy these basic equations.

In these equations, the end conditions have been prescribed arbitrarily and may therefore be expressed in terms of elastic parameters which will then represent the coupling or interaction forces between the twisted member and adjacent parts of the frame. The possibility of working this concept into the slope deflection or moment distribution procedure is obvious.

DISCUSSION

KURT H. GERSTLE,[10] J. M. ASCE.—Engineers concerned with the analysis of members that resist an applied torque by both twisting and bending of the fibers will find this paper of interest and value. The outline of the stress analysis, as well as the summary of expressions for the twisting of beams subject to various boundary conditions, will facilitate the application to practical cases of the theory of torsional bending.

The writer believes that the main obstacle to the widespread use of the method is the time consuming indeterminate solution of the beam with restrained ends subject to a torque applied at an intermediate point. Obviously, the author has realized this fact and, therefore, has presented three different methods of solution for this fundamental problem. The application of the Müller-Breslau principle would greatly simplify this solution, and, therefore, might help in the application of the torsional bending theory to practical design work. The writer will demonstrate the application of this principle.

According to the Müller-Breslau principle, the influence line for a certain stress element will be proportional to the deflected shape of the structure which results when the stress element desired is replaced by a displacement in the sense and direction of this stress element.[11] The value of the influence ordinate at any point then will be given by the negative ratio of the deflection at that point to the displacement induced.

The problem at hand is the determination of the influence line for a reactive torque at one end produced by a torque applied at any point of the member. Therefore, the induced displacement will be an angle of twist at one end, and the deflection proportional to the influence ordinate will be given by the corresponding angle of twist at any section. Accordingly, solving for the reactive torque $T_{(x=L)}$ due to an applied torque T—and using Eq. 8—

$$T_{(x=L)} = \frac{\phi}{\phi_{(x=L)}} T = \frac{A_1 \sinh \frac{x}{a} + A_2 \cosh \frac{x}{a} + \frac{T}{C} x + A_3}{A_1 \sinh \frac{L}{a} + A_2 \cosh \frac{L}{a} + \frac{T}{C} L + A_3} T \ldots . (45)$$

For a beam with both ends rigidly fixed against twisting, $\omega_0 = 0$, and $\omega_L = 0$. In this case, the constants A_1, and A_2, and A_3 are

$$A_1 = - a \frac{T}{C}; \qquad A_2 = \frac{T a}{C} \tanh \frac{L}{2 a}; \qquad A_3 = - \frac{T a}{C} \tanh \frac{L}{2 a}$$

Putting these constants into Eq. 45,

$$T_{(x=L)} = - \frac{\frac{x}{a} - \sinh \frac{x}{a} + \tanh \frac{L}{2 a} \left(\cosh \frac{x}{a} - 1 \right)}{\frac{L}{a} - \sinh \frac{L}{a} + \tanh \frac{L}{2 a} \left(\cosh \frac{L}{a} - 1 \right)} T \ldots \ldots . (46)$$

---

[10] Instructor in Civ. Eng. Univ. of Colorado, Boulder, Colo.

[11] "Elementary Structural Analysis," by J. B. Wilbur and C. H. Norris, McGraw-Hill Book Co., Inc., New York, N. Y., 1948, p. 450.

This expression represents the influence line for the reactive torque at the end where x equals L produced by a torque T applied to any point x of the fixed-ended beam.

Substituting values for the beam of the author's first example (see under the heading, "Illustrative Examples") in Eq. 46,

$$\left.\begin{aligned} T_2 &= \frac{\frac{60}{51.80} - \sinh \frac{60}{51.80} + \tanh \frac{180}{103.60}\left(\cosh \frac{60}{51.80} - 1\right)}{\frac{180}{51.80} - \sinh \frac{180}{51.80} + \tanh \frac{180}{103.60}\left(\cosh \frac{180}{51.80} - 1\right)} T = 0.268\, T \\ &\text{Similarly,} \\ T_1 &= 0.732\, T \end{aligned}\right\} \ldots (47)$$

If, in addition to the restraint produced by the fixed-ended condition, prescribed warping angles ω_1 and ω_2 and a differential displacement ϕ_e are imposed, their effect on the reactive torques can be computed by the procedure implied in Eq. 39:

$$-\phi_e = \frac{2\,T}{C}\left(\frac{L}{2} - a \tanh \frac{L}{2\,a}\right) + \left(\frac{\omega_1 - \omega_2}{h}\right) a \tanh \frac{L}{2\,a};$$

or

$$\frac{T_1}{C} = -\frac{T_2}{C} = \frac{-\phi_e - \left(\frac{\omega_1 - \omega_2}{h}\right) 48.6}{2\,(90 - 48.6)}$$

$$= \mp 0.0121\, \phi_e \pm 0.589 \left(\frac{\omega_2 - \omega_1}{h}\right) \ldots (48)$$

Superposing the effects shown in Eqs. 47 and 48 leads to Eqs. 37. In the writer's opinion, the foregoing computations involve considerably less time and effort than the methods demonstrated by the author.

JOHN E. GOLDBERG,[12] M. ASCE.—The writer is grateful for Mr. Gerstle's appraisal of his paper and for the interest which has moved him to suggest an additional method for applying Eq. 8 to the solution of the basic type of problem. The writer believes that the obstacle to widespread use of the theory is not, as Mr. Gerstle feels, the time involved, but rather an unawareness of the existence of the actual problem and of the method of formulation. A primary purpose of the paper was to stimulate interest in, and to cause a wider understanding of, the phenomenon of warping. The methods of solution which were presented were not presumed to constitute a complete and closed group of procedures since the basic equations may be combined in several ways to devise various alternative methods.

Mr. Gerstle's suggested use of the Müller-Breslau principle, in conjunction with the given equations, to obtain an influence line for reactive torque at the

[12] Associate Prof. of Structural Eng., Purdue Univ., Lafayette, Ind.

end of the member is quite correct and useful. However, what is required is not only the reactive torque, but also the warping moments, the flange shears, and the various stresses. This means that warping conditions must be evaluated at a sufficient number of points, so as to particularize the arbitrary constants of Eq. 8. Alternatively, Eq. 18 or Eq. 21 may be used in the computation of stresses. Since ω_0 is treated as one of the unknowns in Eq. 22, this approach yields the necessary data for completing the stress analysis. The trigonometric series procedure has the advantage of not requiring explicit computation of intermediate warping.

AMERICAN SOCIETY OF CIVIL ENGINEERS

Founded November 5, 1852

TRANSACTIONS

Paper No. 2561

STEADY-STATE FORCED VIBRATION OF CONTINUOUS FRAMES

BY C. T. G. LOONEY,[1] A. M. ASCE

WITH DISCUSSION BY MESSRS. E. F. MASUR, A. S. VELETSOS, WILLIAM A. CONWELL, AND C. T. LOONEY

SYNOPSIS

The analysis of the vibration of continuous frames subjected to a periodic force is important in the study of the design of structures that support machinery. The motion of the machinery produces a force that is usually small, but which, because of its periodic nature, sometimes causes large deflections to develop. Analyses have been made of the forced vibrations of simple systems—that is, a spring supporting a mass, and a simply supported beam. The study of simply supported beams by means of harmonic analysis is particularly congruous in the relation of the mathematics to the nature of the physical phenomena.

The theory presented in this paper makes it possible to analyze continuous frames, utilizing the system of harmonic analysis as it is applied to simple beams. The structure will here be treated as a series of simply supported members with periodic end moments which will provide continuity.

1. THEORY

The application of this analysis to continuous frames reveals an interesting phenomenon. In order to attain the greatest deflection due to a periodic force, the continuous frame must behave as a series of simply supported members with very small end moments. The deflection of each member must be, very closely, the shape of one of the normal modes of a simply supported beam Therefore, the proposed method is particularly adapted to the analysis of these conditions.

It will first be necessary to describe the vibration of a simply supported member due to a uniformly distributed or a concentrated periodic force, with special attention to the determination of the end slopes. This will be followed

NOTE—Published in June, 1952, as *Proceedings-Separate No. 136*. Positions and titles given are those in effect when the paper or discussion was received for publication.

[1] Associate Prof. of Civ. Eng., Yale Univ., New Haven, Conn.

by an analysis of the vibration of a simply supported beam due to a periodic end moment, and finally, a description of the method used to determine the magnitude and phase of the end moments required to provide continuity.

The equation for the forced vibration of a beam with damping proportional to the velocity is

$$E I \frac{d^4 y}{dx^4} + m \frac{d^2 y}{dt^2} + 4 \pi \delta m \frac{dy}{dt} = w \ldots\ldots\ldots\ldots\ldots (1)$$

in which E is the modulus of elasticity; I is the rectangular moment of inertia; m is the mass per unit of length; δ is the damping constant; y is the deflection of the beam at a distance x from the left end (y is positive downward); w is the load per unit of length; and t is the time. In Eq. 1 the damping force is considered to be a distributed force of $4 \pi m \delta$ times the velocity of the beam at any point. The steady-state vibrations of a simply supported beam due to several different periodic forces are, for a uniformly distributed load $w \sin 2 \pi f t$ (w positive downward),

$$y = \frac{4 w l^4}{\pi^5 E I} \left[\frac{1}{1^5} \beta_1 \sin \frac{\pi x}{l} + \frac{1}{3^5} \beta_3 \sin \frac{3 \pi x}{l} \cdots + \frac{1}{n^5} \beta_n \sin \frac{n \pi x}{l} \right] \sin (2 \pi f t - \alpha_n) \ldots (2a)$$

and

$$\theta = \frac{dy}{dx} = \frac{4 w l^3}{\pi^4 E I} \left[\frac{1}{1^4} \beta_1 \cos \frac{\pi x}{l} + \frac{1}{3^4} \beta_3 \cos \frac{3 \pi x}{l} \cdots + \frac{1}{n^4} \beta_n \cos \frac{n \pi x}{l} \right] \sin (2 \pi f t - \alpha_n) \ldots (2b)$$

in which β_n is the dynamic magnification factor; n is a series of integers, in this case odd, 1, 3, 5 . . . ; f is the frequency of the periodic force; α is the phase angle; and l is span length.

For a concentrated load $P \sin 2 \pi f t$ at the center (P positive downward):

$$y = \frac{2 P l^3}{\pi^4 E I} \left[\frac{1}{1^4} \beta_1 \sin \frac{\pi x}{l} - \frac{1}{3^4} \beta_3 \sin \frac{3 \pi x}{l} \cdots \pm \frac{1}{n^4} \beta_n \sin \frac{n \pi x}{l} \right] \sin (2 \pi f t - \alpha_n) \ldots (3a)$$

and

$$\theta = \frac{dy}{dx} = \frac{2 P l^2}{\pi^3 E I} \left[\frac{1}{1^3} \beta_1 \cos \frac{\pi x}{l} - \frac{1}{3^3} \beta_3 \cos \frac{3 \pi x}{l} \cdots \pm \frac{1}{n^3} \beta_n \cos \frac{n \pi x}{l} \right] \sin (2 \pi f t - \alpha_n) \ldots (3b)$$

For a concentrated load $P \sin 2 \pi f t$ at a distance a from the left end (P positive downward):

$$y = \frac{2 P l^3}{\pi^4 E I} \left[\frac{1}{1^4} \beta_1 \sin \frac{\pi a}{l} \sin \frac{\pi x}{l} + \frac{1}{2^4} \beta_2 \sin \frac{2 \pi a}{l} \sin \frac{2 \pi x}{l} \cdots + \frac{1}{n^4} \beta_n \sin \frac{n \pi a}{l} \sin \frac{n \pi x}{l} \right] \sin (2 \pi f t - \alpha_n) \ldots (4a)$$

and

$$\theta = \frac{dy}{dx} = \frac{2\,P\,l^2}{\pi^2\,E\,I}\left[\frac{1}{1^3}\beta_1 \sin\frac{\pi\,a}{l}\cos\frac{\pi\,x}{l} + \frac{1}{2^3}\beta_2 \sin\frac{2\,\pi\,a}{l}\cos\frac{2\,\pi\,x}{l}\cdots + \frac{1}{n^3}\beta_n \sin\frac{n\,\pi\,a}{l}\cos\frac{n\,\pi\,x}{l}\right]\sin\,(2\,\pi\,f\,t - \alpha_n)\,..(4b)$$

For a periodic moment $M \sin 2\,\pi\,f\,t$ at the left end (M positive clockwise):

$$y = \frac{2\,M\,l^2}{\pi^3\,E\,I}\left[\frac{1}{1^3}\beta_1 \sin\frac{\pi\,x}{l} + \frac{1}{2^3}\beta_2 \sin\frac{2\,\pi\,x}{l}\cdots + \frac{1}{n^3}\beta_n \sin\frac{n\,\pi\,x}{l}\right]\sin\,(2\,\pi\,f\,t - \alpha_n)\,..(5a)$$

and

$$\theta = \frac{dy}{dx} = \frac{2\,M\,l}{\pi^2\,E\,I}\left[\frac{1}{1^2}\beta_1 \cos\frac{\pi\,x}{l} + \frac{1}{2^2}\beta_2 \cos\frac{2\,\pi\,x}{l}\cdots + \frac{1}{n^2}\beta_n \cos\frac{n\,\pi\,x}{l}\right]\sin\,(2\,\pi\,f\,t - \alpha_n)\,..(5b)$$

In Eqs. 2 to 5, the dynamic magnification factor β_n, and the phase angle α_n, are to be defined as follows:

$$\beta_n = \frac{1}{\sqrt{\left(1 - \frac{f^2}{f^2_n}\right)^2 + \left(2\,\frac{\delta}{f_n} \times \frac{f}{f_n}\right)^2}} \quad \ldots\ldots\ldots\ldots\ldots (6)$$

$$\tan \alpha_n = \frac{2\,\frac{\delta}{f_n} \times \frac{f}{f_n}}{1 - \frac{f^2}{f^2_n}} \quad \ldots\ldots\ldots\ldots\ldots\ldots\ldots (7)$$

in which f_n, the natural frequency, is

$$f_n = \frac{1}{2\,\pi}\sqrt{\frac{n^4\,\pi^4\,E\,I}{m\,l^4}} \quad \ldots\ldots\ldots\ldots\ldots\ldots (8)$$

The total deflection, y, in Eqs. 2 to 5 is the sum of several deflection curves, $\sin\frac{\pi\,x}{l}$, $\sin\frac{2\,\pi\,x}{l}\cdots\sin\frac{n\,\pi\,x}{l}$. These curves have the same shapes as the modes of free vibration for a simply supported beam. The dynamic magnification factor β_n determines the amplitude of each mode. A large amplitude occurs when the frequency of the periodic force f is equal to the natural frequency of one of the modes, f_1, f_2, $f_3\cdots f_n$. When $f = f_n$ the dynamic magnification factor β_n, for that mode, is a maximum and is large as compared with the values of β for the other modes. For this condition (called "synchronism") the total deflection, y, will consist of a large deflection having the shape of the mode for which $f = f_n$, plus some very minor deflections corresponding to the other modes.

The phase angle α_n is a convenient method of representing a time lag of from zero ($\alpha = 0°$) to one-half period ($\alpha = 180°$). The deflection y always

lags behind the periodic force by the phase angle α_n. In a study of vibrations the analyst is chiefly interested in the large deflection that occurs when the frequency of the periodic force is equal to one of the natural frequencies.

A study of the values of β_n, α_n, f_n, and δ shows that Eqs. 6 and 7 can be simplified considerably, when f equals f_1, f_2, f_3, or f_n; and $\delta < 0.1 f_1$. Then

$$\left.\begin{aligned} \beta_n &= \frac{1}{2}\frac{f_n}{\delta} \text{ (for } f = f_n) \\ \beta_n &\cong \frac{1}{1 - \dfrac{f^2}{f^2{}_n}} \text{ (for } f \neq f_n) \end{aligned}\right\} \quad \text{(9)}$$

and

$$\left.\begin{aligned} \alpha_n &= 90^\circ \text{ (for } f = f_n) \\ \alpha_n &= 0^\circ \text{ or } 180^\circ \text{ } (\tan \alpha < 0.05) \text{ (for } f \neq f_n) \end{aligned}\right\} \quad \text{(10)}$$

In this analysis of continuous frames the following conditions will be used:

$$\left.\begin{aligned} &\text{When } \frac{f}{f_n} < 1 \text{ —} \\ &\qquad \alpha_n = 0^\circ \text{ and } \sin(2\,\pi\,f\,t - \alpha_n) = \sin 2\,\pi\,f\,t \\ &\text{When } \frac{f}{f_n} = 1 \text{ —} \\ &\qquad \alpha_n = 90^\circ \text{ and } \sin(2\,\pi\,f\,t - \alpha_n) = \sin(2\,\pi\,f\,t - 90^\circ) \\ &\text{When } \frac{f}{f_n} > 1 \text{ —} \\ &\qquad \alpha_n = 180^\circ \text{ and } \sin(2\,\pi\,f\,t - \alpha_n) = -\sin 2\,\pi\,f\,t \end{aligned}\right\} \quad \text{(11)}$$

2. General Method of Analysis

Large dynamic deflections in a continuous frame occur when the frequency of the periodic force coincides with the natural frequency of one of the modes of the loaded member. The members immediately adjacent to the loaded member must also have one natural frequency which coincides with the frequency of the periodic force. The continuous members must behave as simply supported members and the large deflections must coincide with the modes of a simply supported member.

The end slopes established by the periodic force are first determined. These will henceforth be called "free-end slopes." The geometric discontinuity that results from these free-end slopes is corrected by periodic end moments with the same frequency as the periodic force. The correction is made by a distribution procedure that corrects the end slopes joint by joint. The periodic moments applied to the ends meeting at a joint have a zero resultant. Thus, statics and dynamics are not affected while the geometry is being corrected. This distribution procedure requires the development of the stiffness of a member. The stiffness is defined as the periodic moment necessary to produce a slope of one (+1) at the end at which the moment is applied. Carry-over slopes are incurred, and these can best be described subsequently in Section 4.

3. Free-End Slopes

Eqs. 2, 3, and 4 are used to compute the free-end slopes. Consider, for example, a periodic force $P \sin 2\pi f t$ at the center of a beam for which $f_1 = 5$, $f = f_1$, and $\delta = 0.1$. The free-end slopes are given by Eq. 3*b*, which yields

$$\theta_{x=0} = -\theta_{x=l} = \frac{2 P l^2}{\pi^3 E I}\left[\frac{1}{1^3}\beta_1 - \frac{1}{3^3}\beta_3 \cdots \pm \frac{1}{n^3}\beta_n\right] \sin(2\pi f t - \alpha_n) \quad (12a)$$

Since α_n can be taken as 0°, 90°, or 180°,

$$\theta_{x=0} = \frac{2 P l^2}{\pi^3 E I}\Bigg[\underbrace{\frac{1}{1^3}\beta_1 \sin(2\pi f t - 90°)}_{\left(\frac{f}{f_n} = 1 \text{ and } \alpha_n = 90°\right)} + \underbrace{\left(-\frac{1}{3^3}\beta_3 + \frac{1}{5^3}\beta_5 \cdots \pm \frac{1}{n^3}\beta_n\right)\sin 2\pi f t}_{\left(\frac{f}{f_n} < 1 \text{ and } \alpha_n = 0°\right)}\Bigg] \quad (12b)$$

For convenience in computing, let $\beta_n = \gamma_n + 1$, thus separating θ into static and dynamic parts:

$$\begin{aligned}\theta_{x=0} = {} & \underbrace{\frac{2 P l^2}{\pi^3 E I}\left[\frac{1}{1^3} - \frac{1}{3^3} + \frac{1}{5^3} \cdots \pm \frac{1}{n^3}\right]\sin 2\pi f t}_{\text{(Static)}} \\ & + \underbrace{\frac{2 P l^2}{\pi^3 E I} \times \frac{1}{1^3}\beta_1 \sin(2\pi f t - 90°)}_{\text{(Dynamic)}} - \underbrace{\frac{2 P l^2}{\pi^3 E I} \times \frac{1}{1^3}\sin 2\pi f}_{\text{(Dynamic)}} \\ & + \underbrace{\frac{2 P l^2}{\pi^3 E I}\left[-\frac{1}{3^3}\gamma_3 + \frac{1}{5^3}\gamma_5 \cdots \pm \frac{1}{n^3}\gamma_n\right]\sin 2\pi f t}_{\text{(Dynamic)}} \quad (12c)\end{aligned}$$

The series for the static part is equal to $\frac{1}{16}\frac{P l^2}{E I}\sin 2\pi f t$; and data used in computing the dynamic part are presented in Table 1. Selecting values from this table for substitution in Eq. 12*c*,

$$\begin{aligned}\theta_{x=0} = {} & \underbrace{\frac{1}{16}\frac{P l^2}{E I}\sin 2\pi f t}_{\text{(Static)}} \\ & + \underbrace{\frac{2 P l^2}{\pi^3 E I} \times \frac{1}{1^3} 25.00 \sin(2\pi f t - 90°)}_{\text{(Dynamic)}} - \underbrace{\frac{2 P l^2}{\pi^3 E I} \times \frac{1}{1^3}\sin 2\pi f t}_{\text{(Dynamic)}} \\ & + \underbrace{\frac{2 P l^2}{\pi^3 E I}\left[-\frac{1}{3^3} \times 0.01250 + \frac{1}{5^3} \times 0.00160 \cdots\right]\sin 2\pi f t}_{\text{(Dynamic)}} \quad (13)\end{aligned}$$

—from which

$$\theta_{x=0} = \frac{P\,l^2}{E\,I}\left[-\,0.00203 \sin 2\,\pi f t + 1.6126 \sin (2\,\pi f t - 90^\circ)\right] \ldots (14a)$$

and

$$\theta_{x=l} = \frac{P\,l^2}{E\,I}\left[+\,0.00203 \sin 2\,\pi f t - 1.6126 \sin (2\,\pi f t - 90^\circ)\right] \ldots (14b)$$

Fig. 1 represents the end slopes by means of vectors; they are shown in relation to the force P for $t = \frac{1}{4\,f}$ (one fourth of period) when P is a maximum downward. The projection of the slope vectors on the vertical axis will be equal to $\theta_{x=0}$ and $\theta_{x=l}$. These vectors rotate clockwise with an angular velocity of $2\,\pi f$.

In this position P is used as a reference for all slopes and end moments. Statics and dynamics have been satisfied for the periodic force $P \sin 2\,\pi f t$. The free-end slopes constitute a geometrical discontinuity with the adjacent members at the joints. This discontinuity must be corrected by periodic end moments.

TABLE 1.—DATA REQUIRED TO COMPUTE THE DYNAMIC PARTS OF EQ. 12c

n	f_n	f/f_n	β_n	γ_n	*Tan α_n
1	5	5/5 = 1	25.0	....	(90°)
2	20	5/20 = 1/4	1.06667	0.06667	0.00267
3	45	5/45 = 1/9	1.01250	0.01250	0.00050
4	80	5/80 = 1/16	1.00392	0.00392	0.000157
5	125	5/125 = 1/25	1.00160	0.00160	0.000064

* Values of tan α_n are listed to show that $\alpha = 0°$ can be used when $f \neq f_n$.

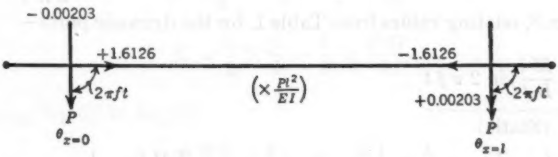

FIG. 1.—FREE-END SLOPES

4. STIFFNESS

The periodic moment required to produce a unit end slope is computed by Eq. 5. In this example the periodic moment $M \sin 2\,\pi f t$ is applied at the left end of a span for which $f_1 = 5$, $f = f_1$, and $\delta = 0.1$ (the same data as in Section 3); thus,

$$\theta_{x=0} = \frac{2\,M\,l}{\pi^2\,E\,I}\left[\frac{1}{1^2}\beta_1 + \frac{1}{2^2}\beta_2 \cdots \frac{1}{n^2}\beta_n\right] \sin (2\,\pi f t - \alpha_n) \ldots\ldots (15a)$$

and

$$\theta_{x=l} = \frac{2\,M\,l}{\pi^2\,E\,I}\left[-\frac{1}{1^2}\beta_1 + \frac{1}{2^2}\beta_2 \cdots \pm \frac{1}{n^2}\beta_n\right] \sin (2\,\pi f t - \alpha_n) \ldots (15b)$$

Since α_n can be taken as 0°, 90°, or 180°,

$$\theta_{x=0} = \frac{2\,M\,l}{\pi^2\,E\,I}\Bigg[\underbrace{\frac{1}{1^2}\beta_1 \sin(2\,\pi\,f\,t - 90°)}_{\left(\frac{f}{f_n} = 1 \text{ and } \alpha = 90°\right)} + \underbrace{\left(\frac{1}{2^2}\beta_2 + \frac{1}{3^2}\beta_3 \cdots + \frac{1}{n^2}\beta_n\right)}_{\left(\frac{f}{f_n} < 1 \text{ and } \alpha = 0°\right)} \sin 2\,\pi\,f\,t\Bigg] \quad (16)$$

Introducing $\beta_n = \gamma_n + 1$ as in Eq. 12*c*,

$$\theta_{x=0} = \underbrace{\frac{2\,M\,l}{\pi^2\,E\,I}\left[\frac{1}{1^2} + \frac{1}{2^2} + \frac{1}{3^2} \cdots \frac{1}{n^2}\right]\sin 2\,\pi\,f\,t}_{\text{(Static)}}$$
$$+ \underbrace{\frac{2\,M\,l}{\pi^2\,E\,I} \times \frac{1}{1^2}\beta_1 \sin(2\,\pi\,f\,t - 90°)}_{\text{(Dynamic)}} - \underbrace{\frac{2\,M\,l}{\pi^2\,E\,I} \times \frac{1}{1^2}\sin 2\,\pi\,f\,t}_{\text{(Dynamic)}}$$
$$+ \underbrace{\frac{2\,M\,l}{\pi^2\,E\,I}\left[+\frac{1}{2^2}\gamma_2 + \frac{1}{3^2}\gamma_3 \cdots \frac{1}{n^2}\gamma_n\right]\sin 2\,\pi\,f\,t}_{\text{(Dynamic)}} \quad (17)$$

The series for the static part is equal to the static-end slope $\frac{1}{3}\frac{M\,l}{E\,I}\sin 2\,\pi\,f\,t$. As in Section 3, relating values from Table 1, for the dynamic parts—

$$\theta_{x=0} = \underbrace{\frac{1}{3} \times \frac{M\,l}{E\,I}\sin 2\,\pi\,f\,t}_{\text{(Static)}}$$
$$+ \underbrace{\frac{2\,M\,l}{\pi^2\,E\,I} \times \frac{1}{1^2} \times 25.00 \sin(2\,\pi\,f\,t - 90°)}_{\text{(Dynamic)}} - \underbrace{\frac{2\,M\,l}{\pi^2\,E\,I} \times \frac{1}{1^2} \times \sin 2\,\pi\,f\,t}_{\text{(Dynamic)}}$$
$$+ \underbrace{\frac{2\,M\,l}{\pi^2\,E\,I}\left[\frac{1}{2^2} \times 0.06667 + \frac{1}{3^2} \times 0.01250 + \frac{1}{4^2} \times 0.00392\right]\sin 2\,\pi\,f\,t}_{\text{(Dynamic)}} \quad (18)$$

—from which

$$\theta_{x=o} = \frac{M\,l}{E\,I}\Big[0.134 \sin 2\,\pi\,f\,t + 5.07 \sin(2\,\pi\,f\,t - 90°)\Big] \quad (19a)$$

and

$$\theta_{x=l} = \frac{M\,l}{E\,I}\Big[0.0396 \sin 2\,\pi\,f\,t - 5.07 \sin(2\,\pi\,f\,t - 90°)\Big] \quad (19b)$$

The end moment required to produce a unit end slope, defined as stiffness, S, is $\frac{1}{5.07} \times \frac{E\,I}{l}$ and for this moment θ becomes

$$\theta_{x=0} = [0.0265 \sin 2\,\pi\,f\,t + 1 \sin (2\,\pi\,f\,t - 90°)] \qquad (20a)$$

and

$$\theta_{x=l} = [0.00782 \sin 2\,\pi\,f\,t - 1 \sin (2\,\pi\,f\,t - 90°)] \qquad (20b)$$

In Eq. 20a the +1 is the required unit end slope, and the remaining numerical values in Eqs. 20, +0.0265, +0.00782, and the −1, are all carry-over slopes. Fig. 2 shows the vector diagram for the stiffness and carry-over slopes. Eqs. 20 are used also for a clockwise moment on the right end, but with $\theta_{x=0}$ and $\theta_{x=l}$ interchanged.

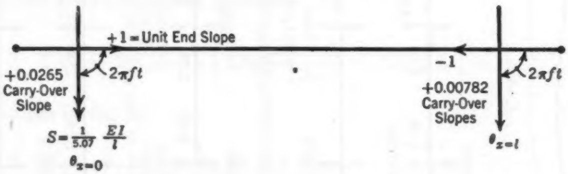

FIG. 2.—STIFFNESS AND CARRY-OVER SLOPES

A study of this analysis shows that, when the frequency of the periodic force is equal to one of the natural frequencies $f_1, f_2 \cdots f_n$, the stiffness is

$$S = \frac{\pi^2}{2} \times \frac{E\,I}{l} \times \frac{n^2}{1} \times \frac{1}{\beta_n} \qquad (21)$$

in which

$$\beta_n = \frac{1}{2} \times \frac{f_n}{\delta} = \frac{1}{2} \times \frac{n^2 f_1}{\delta} \qquad (22)$$

Substituting Eq. 22 in Eq. 21,

$$S = \frac{\pi^2\,E\,I}{l} \times \frac{\delta}{f_1} \text{ or } S \propto \frac{E\,I}{e} \times \frac{\delta}{f_1} \qquad (23)$$

The horizontal carry-over slope is always −1 for odd modes and +1 for even modes. The vertical carry-over slopes are plus or minus, but small as compared to 1.

5. Method for Correcting the Free-End Slopes by Periodic End Moments

Fig. 3(a) shows three members meeting at a joint with three end slopes $\Delta\theta_1$, $\Delta\theta_2$, and $\Delta\theta_3$, which are not equal. Periodic moments with the same frequency as the periodic force $P \sin 2\,\pi\,f\,t$ are applied at the ends meeting at the joint. These moments must make the three horizontal components of the end slopes equal, and the moments must have a resultant of zero. The stiffness and carry-over slopes for each member are shown in Fig. 3(b). The relative stiff-

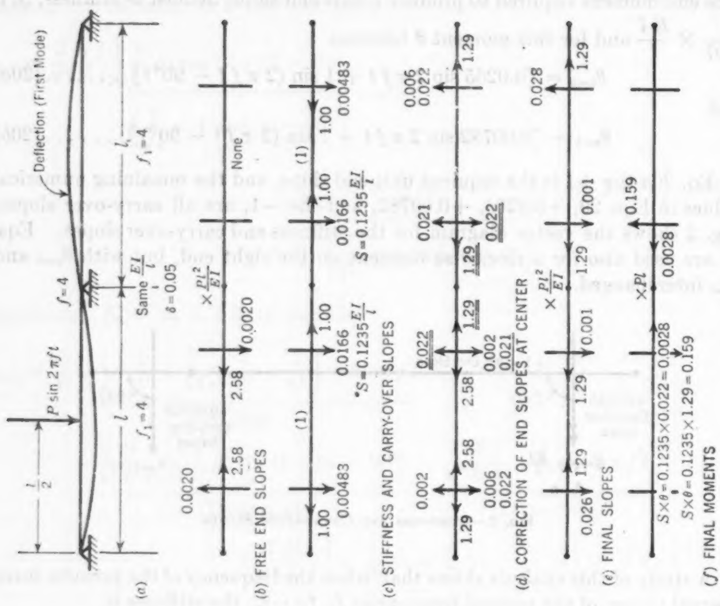

FIG. 4.—END MOMENTS AND SLOPES FOR TWO CONTINUOUS SPANS

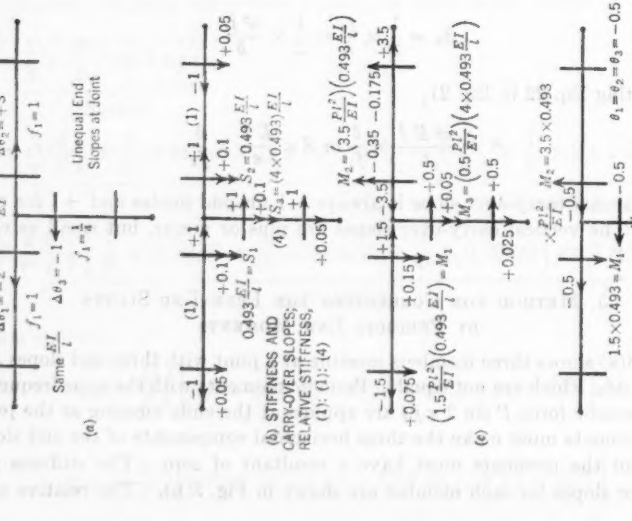

FIG. 3.—CORRECTION OF FREE-END SLOPES

nesses (assuming EI/l the same for each member) are 1, 1, and 4. The formula for the end slope, resulting from the end moments required to equalize the slopes for each member, is as follows:

$$\left.\begin{aligned} \theta_1 &= \frac{\Sigma S_n\,\Delta\theta_n}{\Sigma S_n} - \Delta\theta_1 \\ \theta_2 &= \frac{\Sigma S_n\,\Delta\theta_n}{\Sigma S_n} - \Delta\theta_2 \\ \theta_3 &= \frac{\Sigma S_n\,\Delta\theta_n}{\Sigma S_n} - \Delta\theta_3 \end{aligned}\right\} \quad \ldots\ldots\ldots\ldots\ldots\ldots(24)$$

Then $\theta_n + \Delta\theta_n = \dfrac{\Sigma S_n\,\Delta\theta_n}{\Sigma S_n}$ (the same slope for each member). The end moments will have a zero resultant because—

$$\Sigma M_n = \Sigma S_n\,\theta_n = \left[\Sigma S_n \frac{\Sigma S_n\,\Delta\theta_n}{\Sigma S_n} - \Sigma S_n\,\Delta\theta_n\right] = 0 \ldots\ldots\ldots(25)$$

For the example in Fig. 3,

$$\frac{\Sigma S_n\,\Delta\theta_n}{\Sigma S_n} = \frac{S_1\,\Delta\theta_1 + S_2\,\Delta\theta_2 + S_3\,\Delta\theta_3}{S_1 + S_2 + S_3}\left(\frac{P\,l^2}{E\,I}\right)$$

$$= \frac{[1 \times (-2)] + [1 \times (+3)] + [4 \times (-1)]}{[1 + 1 + 4]}$$

$$= \frac{-3}{6} = -0.5\,\frac{P\,l^2}{E\,I} \,..(26)$$

Then

$$\left.\begin{aligned} \theta_1 &= -0.5 - (-2) = 1.5\,\frac{P\,l^2}{E\,I} \\ \theta_2 &= -0.5 - (+3) = -3.5\,\frac{P\,l^2}{E\,I} \\ \theta_3 &= -0.5 - (-1) = 0.5\,\frac{P\,l^2}{E\,I} \end{aligned}\right\} \quad \ldots\ldots\ldots\ldots(27)$$

Multiply all quantities in Fig. 3(*b*) by the corresponding value θ_1, θ_2, and θ_3 and the results shown in Fig. 3(*c*) are obtained. The moments have a resultant of zero and the slopes are equal:

$$\left.\begin{aligned} \theta_1 + \Delta\theta_1 &= -0.5\,\frac{P\,l^2}{E\,I} \\ \theta_2 + \Delta\theta_2 &= -0.5\,\frac{P\,l^2}{E\,I} \\ \theta_3 + \Delta\theta_3 &= -0.5\,\frac{P\,l^2}{E\,I} \end{aligned}\right\} \quad \ldots\ldots\ldots\ldots\ldots\ldots\ldots(28)$$

The vertical end slopes at the joint are corrected in the same way. The general procedure for the analysis consists of the following steps; illustrative examples will be explained: (1) Find free-end slopes; (2) find stiffness and carry-over

slopes for all members; (3) correct horizontal slopes and vertical slopes; (4) carry over the slopes; and (5) repeat steps (3) and (4).

6. Examples

The following examples illustrate the application of this analysis and demonstrate, to a limited extent, the nature of the behavior of continuous frames subjected to a periodic forced vibration. Fig. 4 shows a two-span continuous beam with a periodic force at the center of the left span. The free-end slopes, the stiffnesses, and carry-over slopes are given. Since the spans are identical they have a relative stiffness of 1:1. The analysis for the horizontal correction of the free-end slope at the center support is as follows:

$$\frac{\Sigma S_n \,\Delta\theta_n}{\Sigma S_n} = \frac{1 \times (-2.58)}{1+1} = -1.29$$

$$\theta_1 = -1.29 - (-2.58) = +1.29$$

$$\theta_2 = -1.29 - (0.0) = -1.29.$$

These values of θ_1 and θ_2 are shown with a double underline in Fig. 4(*d*). The carry-over slopes are obtained by multiplying the factors in the diagram by θ_1 and θ_2. For the left span the carry-over slopes are

$$\begin{array}{lll} 0.0166 \times 1.29 = +0.021 & \text{(center)} \\ 0.00483 \times 1.29 = +0.006 & \text{(left end)} \\ -1.00 \times 1.29 = -1.29 & \text{(left end)} \end{array}$$

and for the right span,

$$\begin{array}{ll} 0.0166 \times -1.29 = -0.021 & \text{(center)} \\ 0.00483 \times -1.29 = -0.006 & \text{(right end)} \\ -1.00 \times -1.29 = +1.29 & \text{(right end).} \end{array}$$

For the vertical correction:

$$\frac{\Sigma S_n \,\Delta\theta_n}{\Sigma S_n} = \frac{[1 \times (+0.023)] + [1 \times (-0.021)]}{1+1} = +0.001$$

$$\theta_1 = 0.001 - (+0.023) = -0.022$$

$$\theta_2 = 0.001 - (-0.021) = +0.022$$

These values of θ are shown with a double underline in Fig. 4(*d*). The carry-over slopes for the left span are, for the left end—

$$\begin{array}{l} 0.0166 \times -0.022 = -0.000365 \\ 0.00483 \times -0.022 = -0.000106 \\ -1.00 \times -0.022 = +0.022 \end{array}$$

and, for the right span (right end)—

$$\begin{array}{l} 0.0166 \times 0.022 = +0.000365 \\ 0.00483 \times 0.022 = +0.000106 \\ -1.00 \times 0.022 = -0.022. \end{array}$$

Only the 0.022 quantities appear in Fig. 4, the other quantities being a remainder that is very small. There is a small difference of slope at the center equal to $2 \times 0.000365 = 0.00073$ which is not corrected.

The final slopes at the ends are obtained by adding, algebraically, the horizontal and vertical slope vectors. The final moments at the center are obtained by multiplying the θ-values at the center (these have a double underline in Fig. 4(*d*)) by the stiffness, S. The frequency of the periodic force P is equal to the natural frequency of the first mode of these beams. Therefore the deflection has the shape of the first mode (see Fig. 4). There are some minor deflections of the shape of the other modes.

The bending moment and shear diagrams are derived from Eqs. 3 and 5 for the deflections. Eq. 5*a*, for a periodic moment on the left end of a simply supported beam, becomes the following equation for a periodic moment on the right end (M positive clockwise):

$$y = -\frac{2\,M\,l^2}{\pi^3\,E\,I}\left[\frac{1}{1^3}\beta_1 \sin\frac{\pi\,x}{l} - \frac{1}{2^3}\beta_2 \sin\frac{2\,\pi\,x}{l}\cdots \pm \frac{1}{n^3}\beta_n \sin\frac{n\,\pi\,x}{l}\right]\sin\,(2\,\pi\,f\,t - \alpha_n) \quad (29)$$

The bending moment for the left span can be written in the following manner, similar to the derivation for determining the free-end slopes, from Eq. 3*a*:

$$M_P = \underbrace{\frac{2\,P\,l}{\pi^2}\left[\frac{1}{1^2}\sin\frac{\pi\,x}{l} - \frac{1}{3^2}\sin\frac{3\,\pi\,x}{l}\cdots \pm \frac{1}{n^2}\sin\frac{n\,\pi\,x}{l}\right]\sin\,(2\,\pi\,f\,t)}_{\text{(Static)}}$$

$$+ \underbrace{\frac{2\,P\,l}{\pi^2}\frac{1}{1^2}\beta_1 \sin\frac{\pi\,x}{l}\sin\,(2\,\pi\,f\,t - 90^\circ)}_{\text{(Dynamic)}} - \underbrace{\frac{2\,P\,l}{\pi^2}\frac{1}{1^2}\sin\frac{\pi\,x}{l}\sin 2\,\pi\,f\,t}_{\text{(Dynamic)}}$$

$$+ \underbrace{\frac{2\,P\,l}{\pi^2}\left[-\frac{1}{3^2}\gamma_3 \sin\frac{3\,\pi\,x}{l} + \frac{1}{5^2}\gamma_5 \sin\frac{5\,\pi\,x}{l}\cdots \pm \frac{1}{n^2}\gamma_n \sin\frac{n\,\pi\,x}{l}\right]\sin 2\,\pi\,f\,t}_{\text{(Dynamic)}} \quad (30)$$

and from Eq. 29, for a periodic moment, M_m, on the right end:

$$M_m = \underbrace{-\frac{2\,M}{\pi}\left[\frac{1}{1}\sin\frac{\pi\,x}{l} - \frac{1}{2}\sin\frac{2\,\pi\,x}{l}\cdots \pm \frac{1}{n}\sin\frac{n\,\pi\,x}{l}\right]\sin 2\,\pi\,f\,t}_{\text{(Static)}}$$

$$\underbrace{-\frac{2\,M}{\pi}\frac{1}{1}\beta_1 \sin\frac{\pi\,x}{l}\sin\,(2\,\pi\,f\,t - 90^\circ)}_{\text{(Dynamic)}} - \underbrace{\frac{2\,M}{\pi}\left(-\frac{1}{1}\sin\frac{\pi\,x}{l}\right)\sin 2\,\pi\,f\,t}_{\text{(Dynamic)}}$$

$$\underbrace{-\frac{2\,M}{\pi}\left[-\frac{1}{2}\gamma_2 \sin\frac{2\,\pi\,x}{l} + \frac{1}{3}\gamma_3 \sin\frac{3\,\pi\,x}{l}\cdots\frac{1}{n}\gamma_n \sin\frac{n\,\pi\,x}{l}\right]\sin 2\,\pi\,f\,t}_{\text{(Dynamic)}} \quad (31)$$

In this latter equation $M = 0.159\,P\,l$ (from Fig. 4).

The bending moment diagram for part of Eq. 30 is a diagram with the same shape as that of the diagram for the static simple-beam bending moment for concentrated load, P. The ordinates vary, periodically, with the bending moment under the load equal to $\frac{P\,l}{4}\sin 2\,\pi\,f\,t$.

The static part of Eq. 31 is a diagram with the same shape as that of the diagram for the static bending moment with a moment on the end. The ordinates vary periodically with the end moment, which is $0.159\,P\,l\sin 2\,\pi\,f\,t$. The bending-moment diagrams for the terms marked "dynamic" are sine curves, as shown, with ordinates that vary periodically.

The terms that contain β_1 are so much larger than all the other terms that only these need be considered. There are two terms which contain β_1:

$$\frac{2\,P\,l}{\pi^2}\times\frac{1}{1^2}\,\beta_1\sin\frac{\pi\,x}{l}\sin(2\,\pi\,f\,t-90°)$$

and

$$-\frac{2\,M}{\pi}\times\frac{1}{1}\,\beta_1\sin\frac{\pi\,x}{l}\sin(2\,\pi\,f\,t-90°).$$

The bending-moment diagram for the left span is essentially a sine curve with ordinates that vary periodically. The center ordinate is $\left[\left(\frac{2\,P\,l}{\pi^2}\times\frac{1}{1^2}\,\beta_1\right)-\left(\frac{2\,M}{\pi}\times\frac{1}{1}\,\beta_1\right)\right]\sin(2\,\pi\,f\,t-90°)$. Since $\beta_1=\frac{1}{2}\frac{f_1}{\delta}=\frac{1}{2}\times\frac{4}{0.05}=40$ and $M=0.159\,P\,l$; the center ordinate is $(8.10\,P\,l-4.04\,P\,l)\sin(2\,\pi\,f\,t-90°)$ or $4.06\,P\,l\sin(2\,\pi\,f\,t-90°)$.

A comparison of the dynamic and static moments is interesting. Over the center support the dynamic is only 1.5 times the static, whereas, at the middle of the left span, the dynamic is twenty times the static. Therefore, as previously stated, the continuous beam behaves as two simply supported beams.

The shear diagrams are obtained from Eqs. 30 and 31. As before the congruous shear diagram for the static part of the equation for the bending moment M_P derived from Eq. 3 is a diagram with the same shape as that of the diagram for the simple beam shear diagram for a concentrated load, P. The ordinates vary periodically, equal to $\frac{P}{2}\sin 2\,\pi\,f\,t$. The congruous shear diagram for the static part of Eq. 31 is a diagram with the same shape as that of the diagram for the static shear diagram for a moment on the end. The ordinates vary periodically, equal to $-0.159\,P\sin 2\,\pi\,f\,t$. The shear diagrams for the terms marked "dynamic" are obtained by differentiation. These shear diagrams are cosine curves with ordinates that vary periodically.

The terms that contain β_1 are so much larger than all the other terms that only these need be considered. These same terms for the bending moment, on differentiation, become

$$\frac{2\,P}{\pi}\,\frac{1}{1}\,\beta_1\cos\frac{\pi\,x}{l}\sin(2\,\pi\,f\,t-90°)$$

and

$$-\frac{2M}{l}\beta_1 \cos\frac{\pi x}{l}\sin(2\pi f t - 90°).$$

The shear diagram, then, is a cosine curve with a value at the left end of

$$12.76\, P \sin(2\pi f t - 90°).$$

Fig. 5 shows the results of several analyses of the previous example, with some variations. The results shown in Fig. 5(a) are for the same data as those in

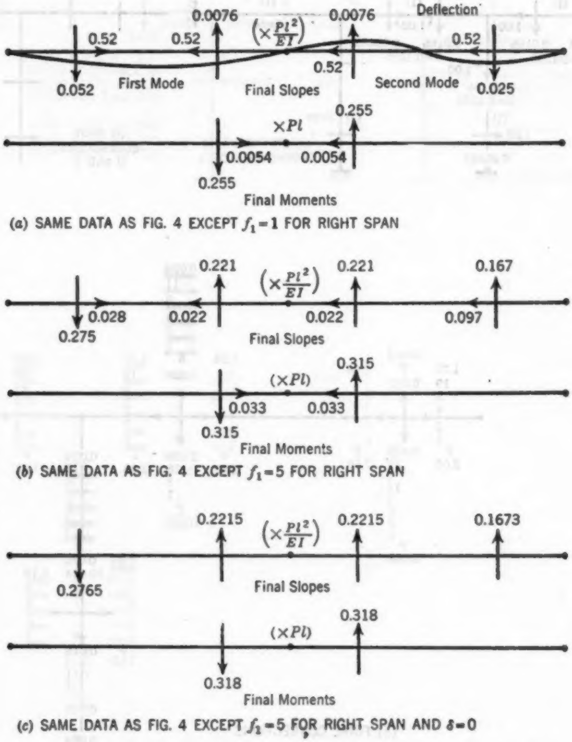

FIG. 5.—END MOMENTS AND SLOPES FOR TWO CONTINUOUS SPANS

Fig. 4 with the exception that the fundamental frequency of the right span was changed from 4 to 1. Then $f_2 = 4$ for the right span and the second mode was excited by the periodic force. The first mode of the left span and the second mode of the right span comprise the deflection (Fig. 5(a)). This change of frequency increased the stiffness of the right span and this, in turn, reduced the end slope (and deflection) from that obtained in Fig. 4; and it increased the

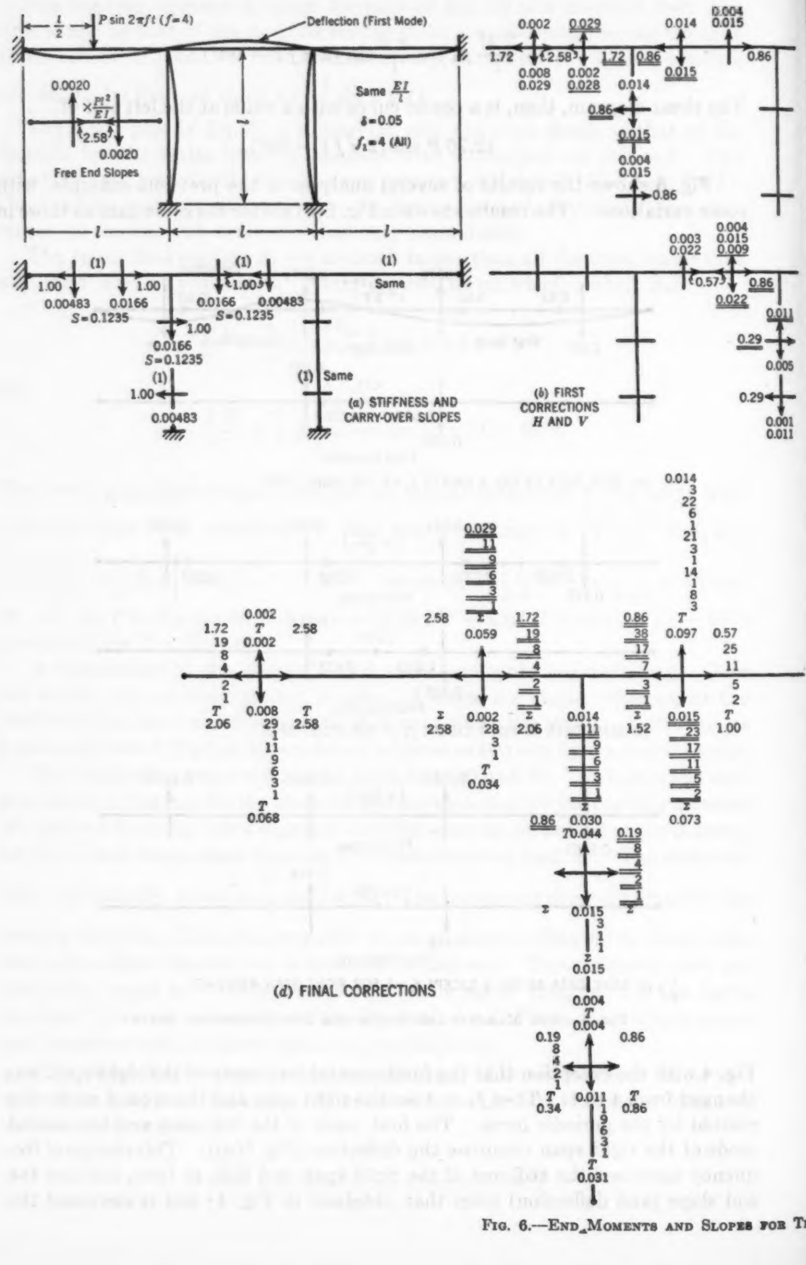

FIG. 6.—END MOMENTS AND SLOPES FOR TH

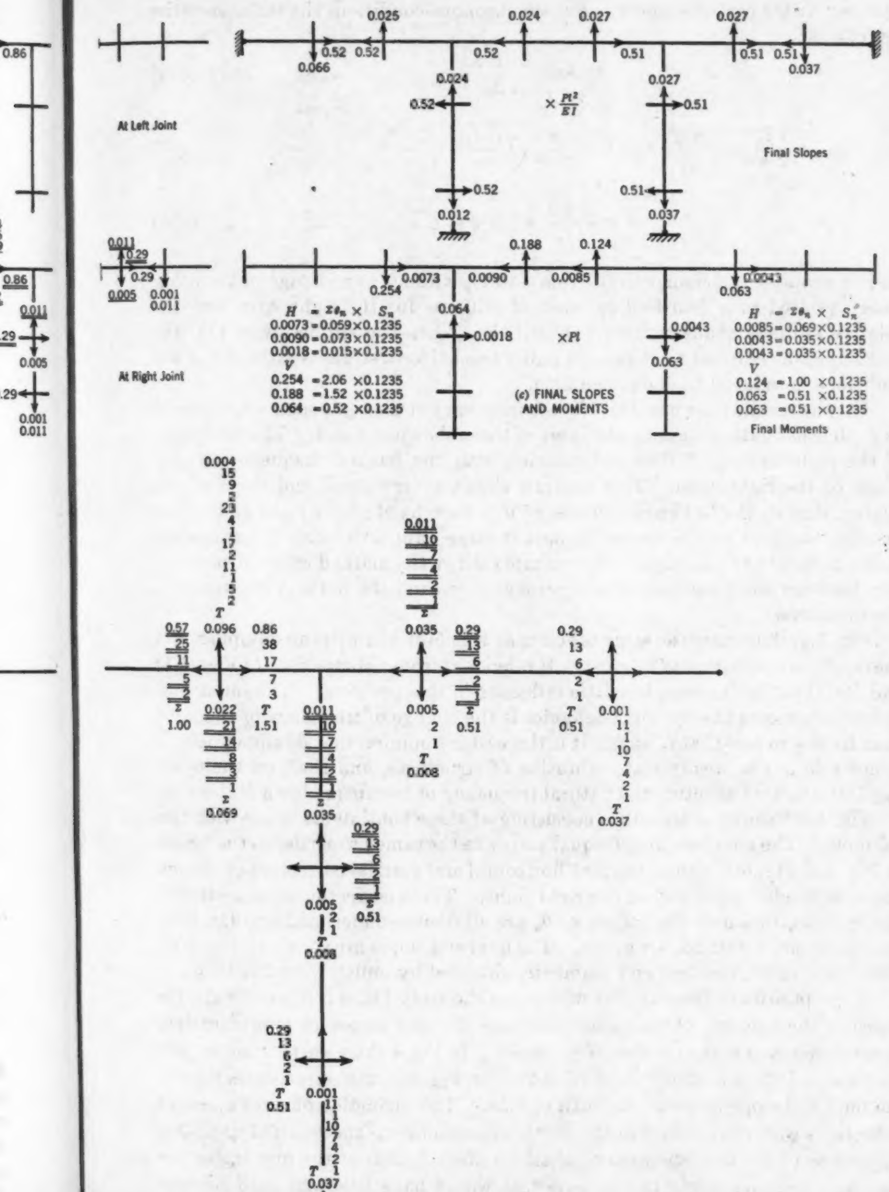

s FOR TH REE CONTINUOUS SPANS WITH TWO COLUMNS

moment at the center support. For synchronous conditions the stiffness varies as follows:

$$S \propto \frac{n^2 E I}{l \beta_n} \qquad (32a)$$

Since $\beta_n = \frac{1}{2}\frac{f_n}{\delta} = \frac{1}{2}\frac{n^2 f_1}{\delta}$ and $f_1 = \frac{\pi^2}{2 l^2}\sqrt{\frac{E I}{m}}$,

$$S \propto \frac{E I \delta}{l f_1} \propto l \delta \sqrt{m E I} \qquad (32b)$$

In this example the change in f_1 (from 4 to 1), without any change in the other data, resulted in a four-fold increase of stiffness for the right span and the relative stiffness changed from 1:1 to 1:4. When the stiffness was 1:1, the end slope was reduced to about one half whereas, for a stiffness ratio of 1:4 the end slope is reduced to about one fifth.

For the results shown in Fig. 5(*b*) the frequency of the right span was changed to 5, all other data remaining the same as those shown in Fig. 4. The frequency of the periodic force P does not coincide with the natural frequency of any mode of the right span. This analysis shows a very small end slope at the center; that is, the left span behaves as if it were fixed at the right end. The bending moment at the center support is large—approximately 3.5 times the static moment at this point. The example shows the marked effect of the relation between the frequency of the periodic force and the natural frequency of the members.

Fig. 5(*c*) illustrates the same problem as Fig. 5(*b*) but with no damping, and the results are of particular interest. It is evident from a comparison of Figs. 5(*b*) and 5(*c*) that the damping has little influence in this problem. The important factor influencing the dynamic behavior is the change of frequency of the right span from 4 to 5 so that $f_n \neq f$. It is the writer's opinion that damping plays a minor role in the steady-state vibration of structures, and that, on the other hand, the factors affecting the natural frequency of members play a major role.

Fig. 6(*a*) shows a structure consisting of three continuous spans with two columns. The members are all equal and have the same properties as the beams in Fig. 4. Fig. 6(*b*) shows the first horizontal and vertical correction of the end slopes at the left joint and at the right joint. These corrections are continued in Fig. 6(*d*), in which the values of θ_n are all double-underlined and the total change of slope and $\Sigma\theta_n$ are given. The final end slopes are shown in Fig. 6(*c*), which also shows the final end moments, obtained by multiplying $\Sigma\theta_n$ by S_n.

A comparison of these results with those shown in Fig. 4 is interesting. Increasing the number of members decreases the end slopes in approximately direct proportion to the number of members. In Fig. 4 there are two beams and the final end slope is about one half of 2.58; in Fig. 6(*c*) there are five beams and the final end slope is about one fifth of 2.58. This reduction of end slopes and deflections with the increase in the number of members is the result of damping. The shape of the deflection curve of all members is that of the first mode (see Fig. 5). Approximately the same results would have been obtained by con-

sidering the structure in Fig. 6(a) as a simply supported beam with five times the damping ($\delta = 0.25$ instead of 0.05).

7. Supplementary Procedure for Lateral Displacement

In the analysis that has been presented, all the joints were fixed against displacement. In most cases the effect of joint displacement is negligible, but it is possible to assign conditions that will magnify lateral displacement of joints. In Fig. 7, which illustrates displacement of joints, conditions have been chosen which magnify this effect. The bent has a periodic force at the quarter point with a frequency equal to the natural frequency of the second mode of the horizontal member and equal to the natural frequency of the first mode of the legs. Under these conditions both legs deflect in the same direction (see Fig. 7) and, as a result, will have a large unbalanced horizontal shear.

The following procedure was used in analyzing the effect of lateral displacement. An analysis was first made with the joints fixed against lateral displacement, and the restraining force was found. Then an analysis was made for a periodic lateral displacement in phase with force P, and the force necessary to produce this lateral displacement was determined.

The lateral displacement caused by a force equal and opposite to the restraining force can be found by proportion and by changing the phase of the displacement relative to P. Fig. 7 shows the results of such an analysis. On the left is the analysis for the bent restrained from lateral displacement. The figure shows the moment at the top of the legs and the shears. The sum of the shears is the total restraining force. On the right are shown the results of an analysis for a periodic lateral displacement in phase with the force P. The moments and shears at the top of the legs are shown. The total force is equal to the shear plus a force necessary to give a periodic displacement to the horizontal member.

A periodic lateral displacement, as shown at the bottom of the figure, would require a force equal and opposite to the restraining force. Therefore an analysis that includes lateral displacement of the joints involves the addition of the effect of a periodic lateral displacement to the effect of the periodic forced vibration restrained against lateral displacement.

In the application of this analysis to engineering structures it may be necessary to take into account the effect of a concentrated mass on the structure. Fig. 8(a) shows a beam with a mass $[M]$ associated with a periodic force $P \sin 2\pi f t$. First, make an analysis for a periodic force $P' \sin 2\pi f t$, the force between the mass and the beam, as yet unknown. The rotating vector diagram shows P', α', and y_a; and a vector $[M]\ddot{y}_a$ opposite to y_a. This latter vector represents the force on the mass $[M]$ and is equal to $P \sin 2\pi f t - P' \sin 2\pi f t$. The known periodic force $P \sin 2\pi f t$ is the resultant of $P' \sin 2\pi f t$ and $[M]\ddot{y}_a$, and determines the magnitude of P', y_a, and α. If a mass $[M_b]$ is at a point other than that where the periodic force is located, as shown Fig. 8(b), first make an analysis for the force $P \sin 2\pi f t$ and determine the deflection and acceleration of point B neglecting the mass $[M_b]$. Make a second analysis for a force $P' \sin 2\pi f t$ at point B, the force between the mass $[M_b]$ and the beam, as yet unknown. Since a reciprocal relation exists between points A and B,

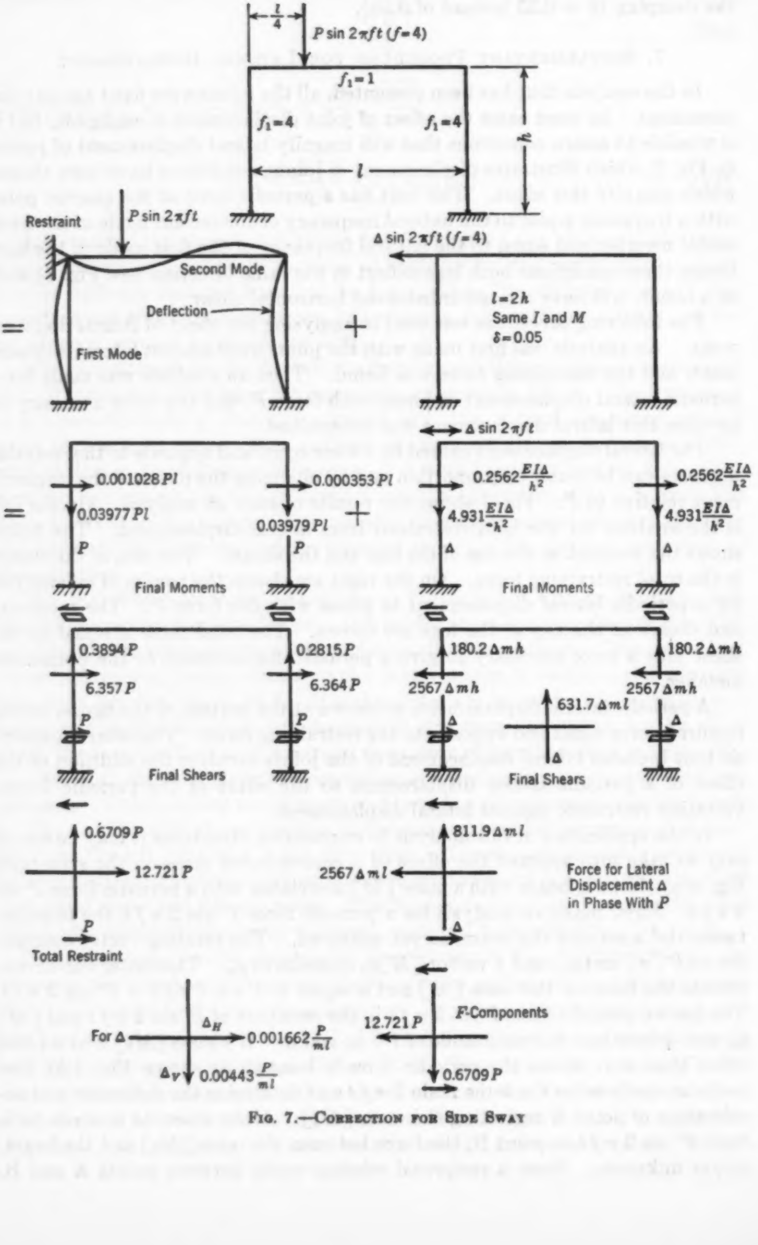

FIG. 7.—CORRECTION FOR SIDE SWAY

Fig. 8(*b*), the first analysis will give the relative proportions of these vectors and the phase angles. Combine the two acceleration vectors at point B—$\ddot{y}_{ba}$ due to P at point A, and $\ddot{y}_{bb}$ due to P' at point A, so that the resultant acceleration $\ddot{y}_b$ is in line with P' and $P' = M_b\ddot{y}_b$. The force on the beam, P', will then be equal and opposite to the force on the mass $[M_b]\ddot{y}_b$. The total deflection will be the vector sum of that due to P and that due to P', the phase relation with P as shown.

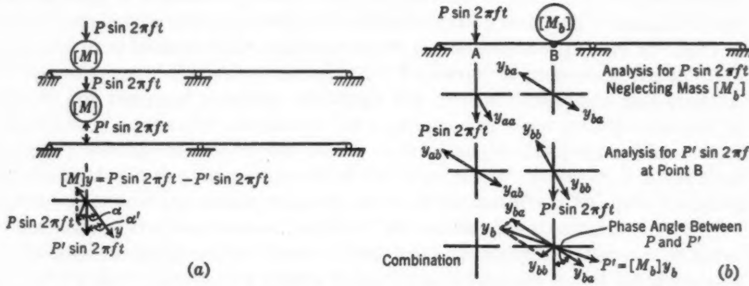

FIG. 8.—EFFECT OF CONCENTRATED MASS

The effect of several periodic forces may need to be considered. If the several forces have the same frequency, the vector sum of the several solutions with proper regard to phase relations will result in a steady-state periodic forced vibration. If the several forces have different frequencies separate analyses can be made and added vectorially.

8. SUMMARY

The analysis described in this paper is designed as a practical method for studying the vibration of civil engineering structures. The assumptions are those commonly used in structural analysis and in the analysis of the vibrations of simple systems. The distribution procedure adapted to this analysis is an analytical tool familiar to most structural engineers. Distribution of the end slopes rather than of the end moments was chosen because initial conditions more closely approximate the final conditions, and therefore there is less correction by distribution. Experience in the behavior of structures for static loads is of little value to the understanding of the vibration of structures. A practical analytical procedure has been lacking, and this paper supplies the necessary equipment to study the vibration of structures.

In conclusion a few statements will be added to supplement the analysis described:

1. This method of analysis is not restricted to the conditions $f = f_1, f_2 \cdots f_n$ and $\delta < 0.1 f_1$;

2. Several periodic forces with the same frequency can be analyzed simultaneously;

3. Several periodic forces at different frequencies must be analyzed separately and the solutions added;
4. The use of modified stiffnesses is of particular value because of the large carry-over slopes; and
5. Free vibrations with velocity damping can be added to the steady-state vibrations to obtain the initial vibrations. Consequently an analysis for transients can be made.

DISCUSSION

E. F. Masur[2].—Except for a few relatively simple types of continuous structures, formidable numerical difficulties are involved in the determination of the natural frequencies and modes of vibration of continuous frames and the response of these structures to applied periodic forces. The author should be commended for applying successive approximation methods in the solution of such problems because most engineers are now conversant with such methods as far as problems of statics are concerned. However, as presented, the solution ignores the transient response, although the critical deflections and stresses, which are of particular interest to the engineer, are often greatly affected by transient vibrations, especially in the case of slight damping. The author alludes to this in the last paragraph of the "Summary"; however, it is not clear to the writer how the author proposes to apply his method to the determination of the natural frequencies and modes of the continuous structure.

It is the writer's opinion that a great deal of computing labor can be saved in finding the response of a simple beam by avoiding the use of infinite series. This suggestion is particularly true for the calculation of the stiffness factor and the carry-over factor (see Eq. 5b). In what follows, it will be assumed that the beam is undamped, although the effect of damping can be included with little additional labor.

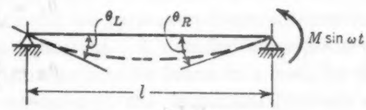

Fig. 9.

If the beam shown in Fig. 9 is subjected to a periodic couple at the right end as shown, the deflection $y(x, t)$ satisfies the differential equation:

$$E\,I\,\frac{\partial^4 y}{\partial x^4} + m\,\frac{\partial^2 y}{\partial t^2} = 0 \quad \text{(33)}$$

Letting the steady-state solution be of the type—

$$y\,(x, t) = Y\,(x) \sin \omega\, t = Y\,(x) \sin 2\,\pi\, f\, t \quad \text{(34)}$$

in which $Y(x)$ denotes the mode of vibration, and considering the boundary conditions,

$$y\,(0, t) = \left.\frac{\partial^2 y}{\partial x^2}\right|_{(0,\ t)} = y\,(l, t) = 0 \quad \text{(35a)}$$

$$E\,I \left.\frac{\partial^2 y}{\partial x^2}\right|_{(l,\ t)} = -\,M \sin \omega\, t \quad \text{(35b)}$$

the deflection function is obtained

$$Y(x) = \frac{M\,l^2}{2\,E\,I}\,\frac{1}{\phi^2}\left(\frac{\sin \frac{\phi x}{l}}{\sin \phi} - \frac{\sinh \frac{\phi x}{l}}{\sinh \phi}\right) \quad \text{(36)}$$

[2] Associate Prof. of Civ. Eng., Illinois Inst. of Technology, Chicago, Ill.

in which $\phi = \sqrt[4]{\frac{m\,\omega^2\,l^4}{E\,I}} = \pi\,\sqrt{\frac{\omega}{\omega_1}} = \pi\,\sqrt{\frac{f}{f_1}}$, with ω_1, representing the fundamental frequency of the simple beam, so that $\omega_1 = \sqrt{\frac{\pi^4\,E\,I}{m\,l^4}} = 2\,\pi\,f_1$. By differentiation, it follows from Eq. 36 that—

$$\theta_L = \left.\frac{dY}{dx}\right|_{(0)} = \frac{M\,l}{2\,E\,I\,\phi}\,(\csc\phi - \operatorname{csch}\phi) \qquad (37a)$$

and that—

$$\theta_R = -\left.\frac{dY}{dx}\right|_{(l)} = \frac{M\,l}{2\,E\,I\,\phi}\,(\coth\phi - \cot\phi) \qquad (37b)$$

Introducing the notation,

$$s = \tfrac{1}{2}\,(s' + s'') \qquad (38a)$$

and

$$c = \tfrac{1}{2}\,(c' + c'') \qquad (38b)$$

in which $s' = \frac{1}{\phi^2}\,(\phi\csc\phi - 1)$, $s'' = \frac{1}{\phi^2}\,(1 - \phi\operatorname{csch}\phi)$, $c' = \frac{1}{\phi^2}\,(1 - \phi\cot\phi)$, and $c'' = \frac{1}{\phi^2}\,(\phi\coth\phi - 1)$, Eqs. 37 can be written in the form:

$$\theta_L = \frac{M\,l}{E\,I}\,s \qquad (39a)$$

$$\theta_R = \frac{M\,l}{E\,I}\,c \qquad (39b)$$

The expressions, $\frac{E\,I}{l}\,\frac{1}{c}$ and $\frac{s}{c}$, represent, respectively, the stiffness and carry-over factors for the beam.

The quantities c', c'', s', and s'' are identical with the coefficients of the moments appearing in the familiar four-moment equations of continuous beam-columns; the single primes refer to members in compression and the double primes to those in tension. These coefficients have been tabulated and are available in several textbooks, such as the one by the late Friedrich Bleich,[3] M. ASCE. Thus, the problem at hand has been reduced to a similar and more familiar one of analyzing a structure consisting of continuous beam-columns, in which the coefficients of the moments in the continuity equations are the mean between the coefficients for tension members and those for compression members.

In closing, the writer would like to point out that the problem under consideration, for the undamped case, has been treated previously in a similar manner.[4] In that paper, the steady-state response of a continuous structure was obtained by both the successive removal of angular discontinuities and moment distribution. It was found that convergence of the latter process is assured only when the applied frequency is less than the fundamental frequency

[3] "Buckling Strength of Metal Structures," by Friedrich Bleich, McGraw-Hill Book Co., Inc., New York, N. Y., 1952, p. 204.

[4] "On Moment Balancing in Structural Dynamics," by R. E. Gaskell, *Quarterly of Applied Mathematics*, Vol. 1, 1943, pp. 237–249.

of the continuous structure. To the writer's knowledge, the convergence of the method of removing angular discontinuities has not been investigated analytically; however, it is apparent that its range of convergence is also limited.

A. S. VELETSOS[5].—An extension of the method of L. E. Grinter, M. ASCE, of balancing end angle changes[6] has been presented by the author for the determination of the steady-state response of continuous beams and frames subjected to harmonically varying forces, such as those resulting from rotating machinery. This paper is of considerable significance in that it brings to the attention of the profession an important engineering problem which, unfortunately, has not been discussed sufficiently in the engineering literature of the United States.

The problem considered in this paper has been treated by a number of investigators in Europe. The pioneering work in this field was done by W. L. Cowley and H. Levy[7] who, as early as 1918, investigated the dynamic response of continuous beams. The first practical method for analyzing the steady-state forced vibrations of continuous beams and frames was presented in 1930 by W. Prager,[8] M. ASCE. Mr. Prager developed equations analogous to the three-moment and four-moment equations and applied them in the analysis of several practical cases. To facilitate the application of this method, S. Gradstein and Mr. Prager[9] later published a tabulation of the various coefficients appearing in the three-moment and four-moment equations. A detailed description of the results of these and of other investigations is to be found in a book by K. Hohenemser and Mr. Prager[10]. The extension to the dynamical problem of the modern distribution procedures of indeterminate stress analysis was first presented in 1943 by R. E. Gaskell,[4] who generalized the concepts of stiffness and carry-over factors to include the dynamic effect, developed the appropriate analytical expressions in terms of the functions tabulated by Messrs. Hohenemser and Prager [10] and showed the application of both the method of moment distribution developed by Hardy Cross,[11] Hon. M. ASCE, and the method of distributing angle changes of Mr. Grinter. In this, as in all previous investigations, the effect of damping on the steady-state forced vibration was assumed to be negligible.

The two distinguishing features of the author's work are: (*a*) The effect of damping, which was neglected in previous investigations, was considered;

---

[5] Research Associate in Civ. Eng., Univ. of Illinois, Urbana, Ill.

[6] "Analysis of Continuous Frames by Balancing Angle Changes," by L. E. Grinter, *Transactions*, ASCE, Vol. 102, 1937, pp. 1020-1036.

[7] "Vibration and Strength of Struts and Continuous Beams Under End Thrusts," by W. L. Cowley and H. Levy, *Proceedings*, Royal Soc. of London, Vol. 95, 1918, pp. 440-457.

[8] "Die Beanspruchung von Tragwerken durch schwingende Lasten," by W. Prager, *Ingenieur-Archiv*, Vol. 1, 1930, pp. 527-532.

[9] "Beanspruchung und Formanderung von Stabwerken bei erzwungenen Schwingungen," by S. Gradstein and W. Prager, *ibid.*, Vol. 11, 1932, pp. 622-650.

[10] "Dynamik der Stabwerke," by K. Hohenemser and W. Prager, Julius Springer, Berlin, Germany, 1933, Chapter IV, pp. 238-289.

[11] "Analysis of Continuous Frames by Distributing Fixed-End Moments," by Hardy Cross, *Transactions*, ASCE, Vol. 96, 1932, pp. 1-10.

and (*b*) the solution of the governing differential equation was obtained in an infinite series form, whereas in previous studies it was obtained in a closed form. In the steady-state response of continuous systems, damping seems to be of importance only for frequencies of vibration equal to, or very nearly equal to, one of the natural frequencies of the system. The effect of damping at these frequencies is to prevent the stresses and the deflections from attaining infinitely large values. For exciting frequencies sufficiently removed from the critical frequencies of the system, the effect of damping is fairly small; and for all practical cases it can be safely disregarded.

Two of the principal reasons why the Cross method of distributing fixed-end moments and the alternate Grinter method of distributing end angle changes have found such widespread application in the analysis of frames subjected to static loads are as follows: (*a*) These methods, if carried through a sufficiently large number of cycles, will always converge to a unique and correct answer, and (*b*) the rate of convergence of these methods is fairly rapid so that, in general, a small number of distributions will yield answers of satisfactory engineering accuracy. It is to be emphasized that this statement is concerned with static loads. Unfortunately, when applied to the analysis of the steady-state response of systems subjected to pulsating forces, the Cross and Grinter methods will not always converge to the true answer; and for those cases for which the successive approximation procedures do converge, their rate of convergence may be extremely slow. It is beyond the scope of this discussion to define the conditions under which the Cross and Grinter methods will converge when extended to the analysis of systems subjected to pulsating loads. It is sufficient to state that Mr. Gaskell has proved that, for an undamped system, convergence of these procedures can be insured only if the frequency of the pulsating force is below the fundamental or first natural frequency of the system. Under certain conditions, these methods may converge for frequencies of vibration above the first natural frequency of the system; however, lack of convergence is a definite possibility which should not be overlooked.

The author is aware of the possibility of slow convergence, and in the "Summary" he points out the desirability of using modified stiffnesses. It is the opinion of the writer that, except for frequencies of vibration that are below the gravest natural frequency of the system, the use of those methods of indeterminate stress analysis which do not involve problems of convergence is in general more efficient than any of the distribution procedures previously referred to. To those for whom modern methods of analysis are more appealing than the use of the three-moment equation, the method of direct moment distribution[12] of T. Y. Lin, M. ASCE, provides a very efficient alternative. One could also develop an alternate method of direct angle-change distribution. Of course, these methods are effective only for structures that do not involve closed figures. For frames, in general, one must use other more appropriate techniques. Because the choice of an analytical procedure is, to a large extent, a question of personal preference, it does not seem desirable to elaborate further on this point. It is important to state, however, that the most ap-

[12] "A Direct Method of Moment Distribution," by T. Y. Lin, *Transactions*, ASCE, Vol. 102, 1937, pp. 561–571.

parent need at the present stage of engineering knowledge is a detailed tabulation of such quantities as dynamic fixed-end moments or free end slopes, dynamic stiffnesses, and dynamic carry-over factors. In a dynamical problem, the laws of statics alone are not sufficient for evaluating the moments and shears at the interior of a span from the known moments and shears at the end of the member. Additional influence coefficients are needed for this purpose. A considerable quantity of valuable information can be derived from tabulated values.[10] However, there are several gaps that remain to be filled.

Two relationships that are of extreme usefulness in a study of the dynamics of frameworks are presented herein. The author refers to one of them but does not elaborate on it. It has been proved[13] that Maxwell's law of reciprocity is valid in the steady-state forced vibration of systems subjected to pulsating loads. This relationship may be stated as follows: The generalized dynamic displacement (linear or angular) at a point A of a structure due to a harmonically varying generalized load (force or moment) at point B is equal to the displacement at B due to the same load applied at A. This relationship can be used to prove that the principle of Müller-Breslau is also applicable. According to this principle: The influence line for a dynamic effect (moment or shear) at some point A of a structure due to a harmonically varying load can be obtained as the deflected shape of the structure due to a very small unit dynamic distortion (rotation or deflection) introduced at point A.

The writer cannot agree with the statement made repeatedly in the paper that a continuous system behaves dynamically very nearly as a series of simply supported beams. This statement is valid only for a few particular cases such as some of the illustrative examples considered in the paper. In a continuous system, the restraint exerted at the ends of a span by the members on either side of it may be of such magnitude that the span may essentially behave as a clamped-ended member. In such cases the moments at the supports can be several times larger than the moments below the concentrated pulsating force. The degree of restraint exerted at the ends of a span depends not only on the mass per unit of length, the span length, and the flexural rigidity of cross section of the adjoining members, but also, to a very large extent, on the frequency of the disturbing force. Because the final moments at the joints of a continuous system may be fairly large, in general, the method of distributing end slopes is not superior to the equivalent method of distributing end moments.

In the analysis and design of structures supporting machinery, the determination of the stresses and deformations of the structure are, of course, of considerable importance. However, the fact should not be overlooked that mere knowledge of these stresses and deformations is not sufficient to insure a satisfactory design. Of equal (and probably of much greater) importance is a knowledge of the natural frequencies of the system. It is the writer's opinion

[13] "The Theory of Sound," by Lord Rayleigh, Vol. 1, Dover Publications, New York, N. Y., 1945, pp. 150–157.

that the first step in the analysis of frames supporting machinery should be to evaluate the natural frequencies of the system and to compare these frequencies with the operating frequencies of the machinery. If the latter are found to be in resonance with, or sufficiently close to, any one of the natural frequencies of the system, the design should be modified. Having eliminated the undesirable possibility of resonance, it would then be necessary to compute the maximum stresses and deformations to ascertain that allowable design limits have not been exceeded.

Acknowledgments.—The writer gratefully acknowledges the benefit that he has derived from discussing problems of the dynamic response of structures with N. M. Newmark, M. ASCE, and L. E. Goodman, A. M. ASCE, both of the University of Illinois, at Urbana. The writer is also indebted to J. G. Sutherland, J. M. ASCE, for calling his attention to Mr. Gaskell's paper.[4]

WILLIAM A. CONWELL,[14] M.ASCE.—An approach to an important problem in the field of structural engineering has been presented by the author. He has done a particularly good job of cataloging for the profession, in one place, the expressions for the forced vibration of a simple beam resulting from periodic concentrated and uniform loads and from periodic end moments (Eqs. *2a* to *5b*, inclusive).

However, some clarification seems necessary for the statements made in the first paragraph under the heading, "1. Theory," and in the first paragraph under the heading, "2. General Method of Analysis." There is no question concerning the application of the statements regarding small end moments and the resulting approximate behavior as simple spans, when the simply supported members have equal natural frequencies of vibration. Similarly, there seems to be some justification for the author's statements when the natural frequencies of the members and their location in a structure permit them to vibrate in such a way that nodes will occur and end moments will be small. There may be structures for which these two conditions do not obtain, with the result that end moments of sufficient magnitude will develop and vibrations of the members will have characteristics other than those for simple beams. Furthermore, even when the second condition holds, the mode of vibration of the structure will not necessarily correspond to that which gives maximum deflections. Larger amplitudes are characteristic of structural vibrations in which the number of nodes is a minimum.

The author states, in the "Synopsis," that "Analyses have been made of the forced vibrations of simple systems—that is, a spring supporting a mass ***." He might have added that valuable lessons may be learned from the study of these simple systems. Such study is indispensable to the practicing engineer applying judgment in the design and analysis of continuous frames. At the risk of being elementary, the writer would like to report the results of one such study of a simple system.

In Fig. 10 is shown a system consisting of two "members." The first member with a weight $W_1 = 1$ lb and a spring with constant $K_1 = 4{,}419$ lb per

[14] Gen. Engr., Structural Eng. and Design Dept., Duquesne Light Co., Pittsburgh, Pa.

ft would, if supported rigidly at the base of its spring, have a frequency, f_1, equal to 60 cycles per sec for its one mode of free vibration. The second member with a weight $W_2 = 2$ lb and a spring with constant $K_2 = 35{,}353$ lb per ft would, alone, have a frequency, f_2, equal to 120 cycles per sec for its one mode of free vibration. When the system as shown is acted upon by a periodic force $P = 100 \sin 2\pi ft$ resonance will occur, not at the natural frequency of vibration of the individual members (60 cycles per sec and 120 cycles per sec), but at a value of f_1 equal to 55.9 cycles per sec, and a value of f_2 equal to 129.1 cycles per sec. These latter figures represent the frequencies of the first and second principal modes of the free vibration of the system. The effects of the individual members are shown in the results, but they are effects only. The principal contributor to the system's first principal mode of vibration is the first member. Its support is less rigid than when it is considered individually, so it tends to vibrate freely at a lower frequency—55.9 cycles per sec. The second member, with a spring above and below it, is more rigidly supported than when it is considered alone and, therefore, its contribution is to the second, higher frequency of 129.1 cycles per sec.

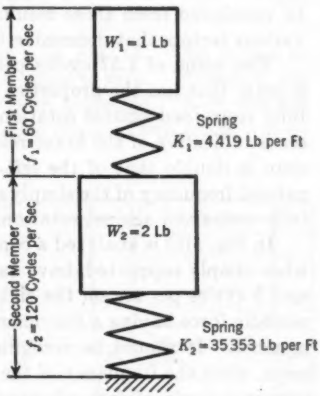

FIG. 10

A similar phenomenon occurs in the study of the vibration of continuous beams. In Fig. 4(*a*) the author shows a two-member system, the first mode of vibration of which will be that shown, with $f_1 = 4$, the natural frequency of vibration of the individual members. In Fig. 5(*a*) there is shown a mode of vibration of the two-beam system corresponding to the natural frequency $f_1 = 4$ in the left member and in each half of the right member, where a node occurs. This mode of vibration is actually the second principal mode of vibration of the two-beam system. The first mode of vibration is characterized by a nodeless span with correspondingly higher deflections than in the second mode, end moments in both spans at the center support, and a lower natural frequency of vibration. Could the closing discussion include an analysis of this first mode of vibration which is usually the most important to the engineer?

There is an implication in Figs. 5, 6, and 7 that the behavior of one member of a vibrating system may be determined if one knows its natural frequency of vibration and that of the other members of the system. It is evident from Eq. 8 that a natural frequency of vibration of 1 cycle per sec for the right-hand span in Fig 5(*a*), treated as a simple span, may be obtained by taking its span as twice that of the left beam and using m and I with the same values as the left span. An approximation to the natural frequency of the first mode of vibration of a system so constructed is 1.29 cycles per sec. If, however, one

chooses to establish a natural frequency for the right span, simply supported, of 1 cycle per sec by holding the span and mass the same as the left span while taking $I_R = I_L/16$, the natural frequency of the system becomes, roughly, 1.57 cycles per sec. Here, the subscripts R and L indicate the right-hand span and left-hand spans, respectively, of a two-span continuous beam. It must be concluded from these results that the behavior is not independent of the various factors that determine the natural frequency.

The value of 1.57 cycles per sec is approximately the natural frequency of a beam that has the properties of the right-hand span of Fig. 5(*a*) but that is fully restrained against rotation at one support. The value of 1.29 cycles per sec is indicative of the lower relative stiffness of the right-hand beam when its span is double that of the left-hand span. This frequency lies between the natural frequency of the simply supported beam and that for which one end is fully restrained against rotation.

In Fig. 5(*b*) is analyzed a continuous two-span beam in which the members, when simply supported, have natural frequencies of 4 cycles per sec on the left and 5 cycles per sec on the right. The paper deals with the case in which a periodic force having a frequency of 4 cycles per sec is applied to the left-hand member. It should be recognized, however, that maximum deflections will occur when the frequency of the applied force equals the frequency of the first principal mode of free vibration of the two-beam system, which is roughly 4.41 cycles per sec ($m_L = m_R$; $I_L = I_R$; and $L_R = 0.894\ L_L$). Would it not be appropriate for the author to make some reference to the methods for determining natural frequencies of frames as a means for finding the frequency of the periodic load which will produce maximum deflections?

In posing these questions, the writer's only purpose is to clarify parts of the paper that may be puzzling to readers. If, in the closure or in the other discussions, the questions are answered, the author can be credited with having brought into sharp focus an important problem in dynamics. The civil engineer, faced with the design of supports for expensive, high-speed machinery and equipment, is becoming increasingly interested in problems of this type.

C. T. LOONEY,[15] A.M. ASCE.—The important and interesting problem of the behavior of structural frames subjected to a steady-state forced vibration has been introduced by Mr. Conwell. This behavior is dependent upon the natural frequencies and modes of vibration of the structure, and the method of analysis presented in the paper can be used to determine these natural frequencies and modes of vibration.

To use the writer's method of investigation, it is necessary to introduce a hinge at the end of a member in the structure. An analysis is then made of the end slopes adjacent to the hinge due to equal and opposite periodic end moments. The end slopes will be equal when the frequency of the end moments is equal to a natural frequency of the structure. The natural frequencies of the structure are approximate in value to the natural frequencies of the individual members. The frequencies of the structure are found by a trial-

[15] Associate Prof. of Civ. Eng., Yale Univ., New Haven, Conn.

and-error method, using appropriate curves. These curves relate a (a measure of the end slopes due to a periodic end moment of a simply supported beam) to the ratio of the frequency of the end moment to the fundamental frequency of the beam. The value of a is obtained from the equation,

$$\theta|_{x=0} = a \frac{M L}{E I} \sin 2 \pi f t \ldots\ldots\ldots\ldots\ldots\ldots (40)$$

Such a set of curves is identified by the letter A in Fig. 11. The curves in Fig. 11 were obtained by use of Eq. 5*b*, with α_n equal to zero. Therefore, the damping effect on the natural frequency has been neglected. With the aid of Fig. 11, the natural frequencies of a continuous beam of two spans will be investigated.

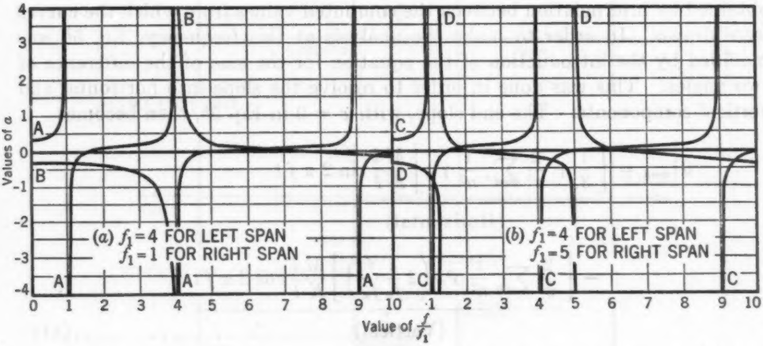

FIG. 11.—THE RELATIONSHIP BETWEEN END SLOPES AND THE RATIO OF THE FREQUENCY OF THE END MOMENT TO THE FUNDAMENTAL FREQUENCY OF THE BEAM

When the two spans have the same frequency, as in Fig. 4(*a*), the structure will have natural frequencies corresponding to $\frac{f}{f_1} = 1, 4, 9, \ldots$, equal to those of the individual members. There are also natural frequencies at points where $\theta = 0$, for which $\frac{f}{f_1} = 1.57, 5.07, \ldots$, as shown in Fig. 11(*a*). At these frequencies, the two members act as if their ends were fixed at the center support. For both spans, m, L, E, and I can be varied in any way since, as long as their fundamental frequencies are equal, the natural frequencies of the structure will remain the same.

In Fig. 5(*a*), $f_1 = 4$ for the left span and $f_1 = 1$ for the right span. In Fig. 11(*a*), the curves A represent the slope at the center support of the right span due to a moment equal to $M \sin 2 \pi f t$, and the curves B represent the slope at the center support of the left span due to a moment equal to $- M \sin 2 \pi f t$. The curves B are equal to the curves A with the horizontal scale of B four times greater than that of A. The curves are inverted with respect to each other because of the negative moment. The horizontal scale $\frac{f}{f_1}$ is drawn

with reference to the fundamental frequency of the right span, which in this case is equal to one. The vertical scale for both sets of curves is the same because $E\,I/l$ is the same for both spans. Where these curves intersect, the end slopes, due to an equal and opposite periodic moment at the center support, will be equal. These values of $\frac{f}{f_1}$ are approximately equal to 1.2, 6.4, and 9.6, and, since $f_1 = 1$, these are natural frequencies of the structure. These values of $\frac{f}{f_1}$ are not independent of l, E, and I which determine the vertical scale. In addition, there are natural frequencies for the structure when the natural frequencies of the members coincide. This occurs at $\frac{f}{f_1} = 4, 16, 36, \ldots$.

An accurate determination of the first natural frequency is 1.189. This is obtained by interpolation between the computed values from which the curves were drawn. In order to make the analysis at this frequency, Eq. 5*b* was modified by the introduction of the equation for the sine of the difference of two angles. This was done in order to resolve the slope into horizontal and vertical components. The end slope, with $x = 0$ in Eq. 5*b*, then becomes

$$\theta|_{x=0} = \underbrace{\left[\frac{1}{3} + \frac{2}{\pi^2}\sum_n \frac{1}{n^2}\gamma'_n\right]\frac{M\,l}{E\,I}\sin 2\,\pi\,f\,t}_{\text{(Horizontal)}}$$

$$-\underbrace{\left[\frac{2}{\pi^2}\sum_n \frac{1}{n^2}\beta^2_n\left(2\,\frac{\delta}{f_n}\frac{f}{f_n}\right)\right]\frac{M\,l}{E\,I}\cos 2\,\pi\,f\,t}_{\text{(Vertical)}} \qquad \text{(41a)}$$

in which

$$\beta^2_n\left(1 - \frac{f^2}{f^2_n}\right) = 1 + \gamma'_n \qquad \text{(41b)}$$

and $n = 1, 2, 3, \ldots$.

For the left span, $f_1 = 4$, $f = 1.189$, and $\delta = 0.05$, from which Eq. 41*a* becomes

$$\theta|_{x=0} = \frac{M\,l}{E\,I}(0.353 \sin 2\,\pi\,f\,t - 0.001838 \cos 2\,\pi\,f\,t) \qquad \text{(42a)}$$

For the right span, $f_1 = 1$, $f = 1.189$, and $\delta = 0.05$, and Eq. 41*a* becomes

$$\theta|_{x=0} = \frac{M\,l}{E\,I}(-\,0.316 \sin 2\,\pi\,f\,t - 0.1305 \cos 2\,\pi\,f\,t) \qquad \text{(42b)}$$

The end slopes $0.353 \sin 2\,\pi\,f\,t$ and $-\,0.316 \sin 2\,\pi\,f\,t$ were made equal by an additional moment of $-\,0.279\,M \cos 2\,\pi\,f\,t$. Eqs. 42 then become

$$\theta|_{x=0} = \frac{M\,l}{E\,I}(0.353 \sin 2\,\pi\,f\,t - 0.1003 \cos 2\,\pi\,f\,t) \qquad \text{(43a)}$$

and

$$\theta|_{x=0} = \frac{M\,l}{E\,I}(-\,0.353 \sin 2\,\pi\,f\,t - 0.0423 \cos 2\,\pi\,f\,t) \qquad \text{(43b)}$$

From Eqs. 43, the stiffness and carry-over slopes were obtained, and used in the analysis in Fig. 12. For the determination of the final moments, the end moment has two components. For the left span, $S = 1/0.1003 = 9.97$ as

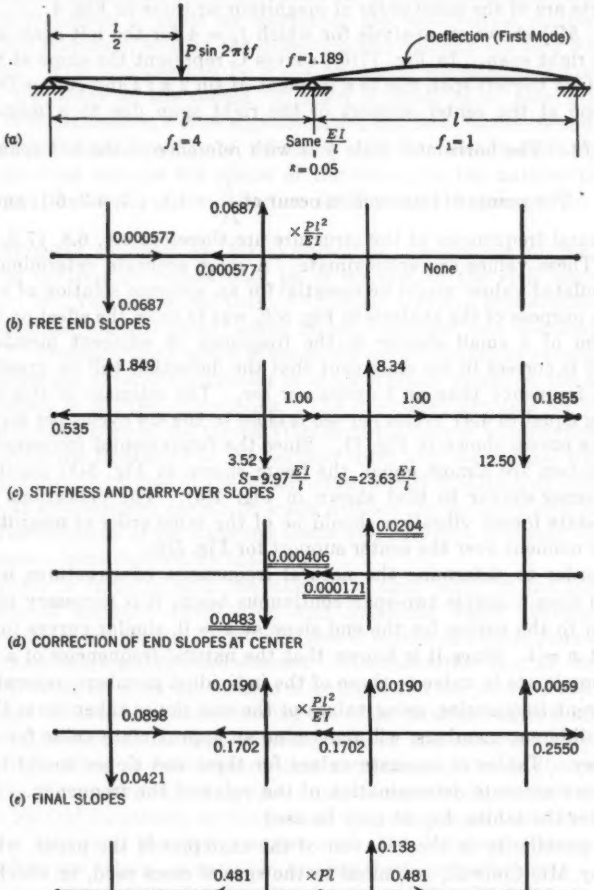

FIG. 12.—END MOMENTS AND SLOPES FOR TWO CONTINUOUS SPANS

shown and $S = 0.279/0.1003 = 2.78$. For the right span, $S = 1/0.0423 = 23.63$ as shown and $S = 0.279/0.0423 = 6.60$. A comparison of the final slopes with the slopes in Fig. 4 indicates that the new slopes are approximately

0.13. A comparison of values of the final moments with the moments in Fig. 4 illustrates that the new moments are 3.1 times greater than those in Fig. 4. The deflection obtained in Fig. 12 is similar to that in Fig. 4 and is proportional to the end slopes; however, neither the deflection nor the moments are of the same order of magnitude as those in Fig. 4.

Fig. 5(*b*) shows an analysis for which $f_1 = 4$ for the left span and $f_1 = 5$ for the right span. In Fig. 11(*b*), curves C represent the slope at the center support for the left span due to a moment $M \sin 2\pi f t$ and curves D represent the slope at the center support of the right span due to a moment $-M \sin 2\pi f t$. The horizontal scale $\frac{f}{f_1}$ is with reference to the left span in which $f_1 = 4$. The points of intersection occur at $\frac{f}{f_1} = 1.1$, 1.7, 4.3, 6.1, and 9.4, and the natural frequencies of the structure are therefore 4.4, 6.8, 17.2, 24.4, and 37.6. These values are approximate. A more accurate determination from the tabulated values would be essential for an accurate solution of a problem.

The purpose of the analysis in Fig. 5(*b*) was to show the effect on the forced vibration of a small change in the frequency of adjacent members. Mr. Conwell is correct in his statement that the deflection will be greater at the natural frequency than at 4 cycles per sec. The estimate of this frequency as being equal to 4.41 cycles per sec is close to the 4.4 cycles per sec obtained from the curves shown in Fig. 11. Since the fundamental frequencies of the two members are almost equal, the beam shown in Fig. 5(*b*) should behave in a manner similar to that shown in Fig. 4(*a*). The deflections due to a steady-state forced vibration should be of the same order of magnitude, with a larger moment over the center support for Fig. 5(*b*).

In order to determine the natural frequencies of structures more complicated than a simple two-span continuous beam, it is necessary to have, in addition to the curves for the end slope at $x = 0$, similar curves for the end slope at $x = l$. Since it is known that the natural frequencies of a structure are approximate in value to those of the individual members, several analyses at different frequencies, using values of the end slopes taken from the curves for the different members, will determine an approximate value for a natural frequency. Tables of accurate values for these end slopes would be helpful for a more accurate determination of the value of the frequency. As a substitute for the tables, Eq. 5*b* may be used.

The peculiarity in the behavior of the examples in the paper, which were noted by Mr. Conwell, is limited to the special cases used, in which $E\,I/l$ is the same for all members, and limited also to the frequency chosen.

Mr. Masur's suggestion for the computation of stiffness and carry-over factors is a useful addition to the writer's method of analysis. The writer derived the same results by using a finite expression for the deflection of a simply-supported beam due to a periodic end moment, as developed in a paper by R. D. Mindlin, A.M. ASCE, and Mr. Goodman.[16] Values of the functions

[16] "Beam Vibration with Time-Dependent Boundary Conditions," by R. D. Mindlin and L. E. Goodman, *Journal of Applied Mechanics, Paper No. 49—A-19*, ASME.

used were obtained from tables by Keiichi Hayashi.[17] However, these tables require the use of involved methods of interpolation, which outweigh their time-saving value.

The method of analysis described in the paper can be used to determine natural frequencies and modes of vibration for a continuous structure. The analysis for transients is made by combining the steady-state solution with modes of free vibration, so that the deflection and velocity are zero when the time is zero. This analysis can be made by use of simultaneous equations. When the frequency of the forced vibration is equal to or near a natural frequency of the structure, a close approximation can be obtained by combining judiciously the natural modes of vibration with the steady-state solution. This can be done because the shape of the curve for the natural mode of vibration and the steady-state deflection for the same frequency are almost identical.

The references supplied by Mr. Veletsos on the subject of the forced vibration of continuous frames may be of interest to the civil engineering profession. Mr. Veletsos states that "* * * in all previous investigations, the effect of damping on the steady-state forced vibration was assumed to be negligible." Damping has a minor effect on the forced vibrations at frequencies removed from the natural frequencies of the structure; however, the analysis of this problem is of little importance. The important problem for the civil engineer is the analysis of the forced vibrations that occur when synchronism exists between the frequency of the periodic force and the natural frequency of the structure. Analyses of the steady-state forced vibration of continuous structures at synchronism cannot be made without the inclusion of a damping factor. The inclusion of the damping factor and examples of forced vibration at synchronism were covered by the writer.

The writer is familiar with the difficulties that occur in the successive convergence of moment distribution and balancing angle changes. Two familiar examples are the static-load analyses of arches on elastic piers and of a building frame subjected to wind stresses. The realization that an important relationship exists between the method of analysis and the physical behavior of the structure will lead to a discriminating use of the analysis rather than merely automatic application. A discriminating use of the analysis will likewise solve the difficulties of convergence that sometimes occur in the problems described in this paper. In the paper, analyses were made without difficulty, below the natural frequency, at the natural frequency, and above the natural frequency. However, the writer agrees with Mr. Veletsos' statement that tabular values are helpful as an aid in making these computations.

Mr. Veletsos' mention of the writer's statement that "* * * a continuous system behaves dynamically very nearly as a series of simply supported beams" requires comment since this statement was qualified under the heading, "1. Theory," by the words, "In order to attain the greatest deflection due to a periodic force * * *." The properties of the structures and the frequencies used in the examples were chosen so that they behaved in this fashion. If the

[17] "Sieben-und mehrstellige Tafeln der Kreis-und Hyperbelfunktionen und deren Produkte sowie der Gammafunktion," by Keiichi Hayashi, Julius Springer, Berlin, Germany, 1926.

properties and frequencies are such that this behavior does not exist, the deflection will not be so great as that encountered. Mr. Veletsos also states that "* * * the method of distributing end slopes is not superior to the equivalent method of distributing end moments." The writer states (under the heading, "8. Summary") that

> "Distribution of the end slopes rather than of the end moments was chosen because initial conditions more closely approximate the final conditions, and therefore there is less correction by distribution."

If initial fixed-end conditions more closely approximated the final conditions, the distribution of end moments would entail less work and would therefore be preferable.

AMERICAN SOCIETY OF CIVIL ENGINEERS
Founded November 5, 1852
TRANSACTIONS

Paper No. 2562

TOPOGRAPHIC MAPPING IN KENTUCKY

By Phil M. Miles[1]

With Discussion by Mr. Herbert Milwit

Synopsis

The purpose of this paper is to present the experiences of one state in obtaining and utilizing modern topographic data and to direct attention to a few of the uses of the published maps and by-product materials. This involves the history of the mapping program in Kentucky; the general specifications for such mapping, techniques, and equipment used; the progress of the program; the state's facilities for distribution and filing of topographic data; and the outlook for the completion of the program. Good maps are invaluable to the efficient development of the United States, and it is hoped that this paper may be useful to others for initiating or expanding "topo" activities.

History

The Topographic Division of the United States Geological Survey (USGS), of the Department of the Interior, is responsible for domestic topographic mapping. Usually, the cost of such mapping is divided equally between the USGS and the states, the mapping being done by the USGS. The Kentucky mapping program described herein is operating under such an arrangement. The USGS has a long record of topographic mapping in Kentucky, beginning in 1882. Cooperative state-federal mapping in Kentucky began in 1903 and grew to a substantial program in the 1920's, but was terminated in 1929. No cooperative mapping was accomplished within the state between 1929 to 1948. The year 1948 marks the beginning of the second cooperative program, with mapping (covering Jefferson County) sponsored by the City of Louisville, Jefferson County, the Louisville Area Development Association, and the Kentucky departments of Highways and of Revenue.

In the period of no mapping, state agencies, individuals, and private organizations advocated the resumption of cooperative mapping, but they lacked the support necessary to put the program into effect. Principal

Note.—Published in September, 1952, as *Proceedings-Separate No. 151*. Positions and titles given are those in effect when the paper or discussion was received for publication.

[1] Chf., Maps and Minerals Div., Kentucky Agri. and Industrial Development Board, Frankfort, Ky.

agencies that now (1952) advocate topographic mapping are the Kentucky Geological Survey, the Kentucky Department of Highways, and the Kentucky Department of Conservation. The Postwar (World War II) Advisory Planning Commission of Kentucky recommended that topographic mapping be completed within the state by the earliest possible date. The great emphasis that was placed upon maps during World War II, and the fact that many agencies are affected by the availability of good maps, contributed to a favorable atmosphere for inaugurating a new mapping program.

The Kentucky Chamber of Commerce became actively interested in the state mapping problem in this post-war period and provided some of the basic planning for the reactivation of the program in Kentucky. The fact that the Kentucky Chamber of Commerce, various state organizations, and many business organizations were behind the program was undoubtedly a convincing argument to state administrators. The Kentucky Department of Revenue also is believed to have been a major factor in the revival of interest, since it is vitally concerned with adequate base maps for property surveys. With much of the groundwork laid, the Kentucky Agricultural and Industrial Development Board (AIDB) at Frankfort, Ky., provided the necessary coordination, administration, and technical direction to formulate concrete plans, with the USGS for a complete five-year mapping program.

Kentucky Map Status in 1947.—In devising a plan of action, the first step was to review the status of mapping. A study made in 1947 disclosed that approximately 35% of the state's 40,500 sq miles had never been mapped topographically. Approximately 20% of the area of the state was covered by topographic maps which were made in the period from 1882 to 1910, many of which were to a scale of 1:125,000, and could only be considered useful for reconnaissance purposes. This area required remapping under any mapping program then contemplated. It was found that approximately 30% of the state was covered by $\frac{1}{62{,}500}$-scale maps, made in the period from 1910 to 1930. These maps required cultural revision and partial resurvey, which would include additional control and aerial photography. About 5% of the state was covered by good $\frac{1}{62{,}500}$-scale topographic maps which would require only cultural revision. Fortunately, about 10% of the state was in the process of being remapped by modern methods by the Tennessee Valley Authority (TVA) and the Army Map Service (AMS), United States Corps of Engineers, using $\frac{1}{24{,}000}$ and $\frac{1}{25{,}000}$ scales, respectively.

Choice of Scale.—Approximately 55% of the state required complete remapping under any circumstances. The question was raised as to the advisability of trying to complete and bring up to date the old $\frac{1}{62{,}500}$-scale topographic cover instead of remapping at a scale of 1:24,000. The USGS informed state officials concerned with the new topographic mapping that $\frac{1}{24{,}000}$-scale maps were becoming more popular and that the USGS had

adopted such a scale as a standard for a new map series based on $7\frac{1}{2}$-minute sheet lines. However, it was explained that it was the state's decision as to whether cooperative work would be done a scale of 1:24,000 or 1:62,500.

In examing the problem as to the relative merits of the two scales, it is patently true that greater detail and more accuracy are obtainable with the larger scale and that the cost would be considerably greater.

As a rule of thumb, it is believed by the writer that the usefulness of a basic topographic map (other qualities being considered constant) varies as the square of the map scale. This is merely an application of the area relationship to scale.

In studying the history of mapping programs for large areas, such as a state, it is apparent that a given map series designed for a particular time becomes obsolete, and the area must be remapped at a larger scale. The USGS first began topographic mapping in about 1875 and the standard scale was $\frac{1}{250,000}$. In about 1880 the standard scale was changed to $\frac{1}{125,000}$. In about 1900 the scale was changed again to $\frac{1}{62,500}$. In the late 1920's and early 1930's there was a definite trend to the $\frac{1}{31,680}$ scale, and just before World War II maps were being produced by the USGS on a scale of $\frac{1}{24,000}$. The trend is always to a larger scale, so in considering a modern mapping program it appeared that mapping on the $\frac{1}{62,500}$-scale basis could result in maps that might soon become obsolete for many purposes. The use of the word "obsolete" here refers to inadequate scale, since modern engineering requires ground information as accurate as is practicable to obtain. The recognition of such a trend pointed to the desirability of adopting the $\frac{1}{24,000}$ scale and completely remapping the state. Of course, this concept fitted well with new mapping already under way by the TVA and the AMS. The army standard large-scale topographic series is to a $\frac{1}{25,000}$ scale, since the army is on the metric system, into which such a scale fits readily. Of course, the $\frac{1}{24,000}$ scale is convenient in the English system since 1 inch is equal to 2,000 feet on this scale.

When it was decided that a $\frac{1}{24,000}$-scale program would be considered, estimates were obtained from the USGS as to the minimum time required to remap completely the state and the cost of doing so. It was estimated that the state (some 36,000 sq miles after deducting TVA and AMS areas) could be completely mapped for about \$7,000,000 (total federal-state cost) and that the work could be accomplished in five years. These estimates of cost and time caused eyebrows to be raised by various geologists and engineers who had been familiar with the previous topographic mapping in the state. The fact was emphasized that topographic mapping is relatively cheaper and much faster than it was

twenty years ago. It was also estimated that the $\frac{1}{62{,}500}$-scale mapping could be completed and brought up to date for about $6,000,000.

With only about 18% difference in cost between $\frac{1}{62{,}500}$-scale mapping and $\frac{1}{24{,}000}$-scale mapping, it was not difficult to conclude that the large-scale mapping would be the best choice.

Allocation of Funds.—By June 30, 1950, the state had expended $180,000 on co-op mapping on a $\frac{1}{24{,}000}$ scale. This left $3,320,000 of state funds required to complete the program, which was estimated at $7,000,000 total. The USGS and the state agreed that the money could be expended most efficiently and economically as follows:

Year ending June 30	State	Federal
1951	$332,000	$332,000
1952	830,000	830,000
1953	830,000	830,000
1954	830,000	830,000
1955	498,000	498,000
Total	$3,320,000	$3,320,000

This program was approved by the state Budget Commission and by the governor and the 1950 state legislature provided funds for the first two years.

In summary: The most important factors in this phase of the mapping activities in Kentucky were to formulate a complete, comprehensive plan, and to present the facts as to utilization and cost of good maps to the public and to the authorities. This is essentially what was done in Kentucky, and it resulted in the inauguration of the largest cooperative mapping program ever undertaken by the USGS.

General Specifications

At the beginning of this project, the general specifications for the mapping in Kentucky had already been established by the USGS. The standard coverage of the $\frac{1}{24{,}000}$-scale maps is 7½ minutes of latitude and 7½ minutes of longitude. This gives a sheet size of 22 in. by 27 in. over all, covering about 59 sq miles. Neat-line size at the middle latitude of the state is 18.125 in. by 22.875 in.

Accuracy.—Standard map accuracy, as developed by the United States Bureau of the Budget, is required. The horizontal accuracy requirement for maps on publication scales smaller than 1:20,000 is that not more than 10% of the points tested shall be in error by more than 0.02 in. at publication scale. Points selected for testing are to be plottable to 1:100 in. at map scale. This means that on $\frac{1}{24{,}000}$-scale maps, horizontal positioning is accurate to within 40 ft. The vertical accuracy standard requires that not more than 10% of

the elevations tested shall be in error by more than one half of a contour interval for all scales of maps. The apparent vertical error of a test elevation may be decreased by assuming a horizontal displacement of the point within the permissible horizontal error for a map of that scale. The contour interval for the Kentucky $\frac{1}{24,000}$-scale maps is variously 10 ft, 20 ft, and 40 ft, depending on the terrain. The standard accuracy is 5 ft, 10 ft, and 20 ft, respectively, for such maps. The vertical accuracy of USGS mapping is actually much better than this, as is shown by test profiles. Profiles usually disclose vertical error of the order of 2 ft or 3 ft for 10-ft contour intervals and many profiles show that errors may not exceed 1 ft.

Contour Intervals.—A plan indicating the contour interval for each 7½-minute quadrangle was set up early in the five-year program, providing for 10-ft and 20-ft intervals. This was based upon an examination of existing topographic map coverage, at scales of 1:62,500 and 1:125,000, and field reconnaissance by federal and state engineers. As the mapping progressed, it developed that contour intervals had to be altered in order to portray adequately relief features and to prevent congestion of contours. In some areas where 20-ft contours were selected, 10-ft supplemental contours were added in the valley flats. Similar treatment was also given to a few areas where 10-ft and 40-ft contours were adopted. The USGS had strongly recommended that the rugged terrain in southeast Kentucky be mapped with a 40-ft contour interval. This recommendation was finally accepted by the state.

Under the state rectangular coordinate system devised by the United States Coast and Geodetic Survey (USCGS), all horizontal control run is computed in terms of the state grid and the state grid is shown on published $\frac{1}{24,000}$-scale maps by 10,000-ft ticks along the neat line. This is to insure that if any company or agency desires to use a rectangular coordinate system, the basic element for a universal state system will already be established and thereby greatly facilitate any such operations. The trend toward the use of rectangular coordinates is well-established and it is believed to offer the only practicable solution to some problems, such as adequate property descriptions.

Priority Requirements.—Priority areas for new mapping were established by mutual agreement between the state and federal officials. It was agreed at the outset that, if the mapping was to be completed in five years, operational considerations would dictate priority areas. The priority requirements of various state and federal agencies received secondary consideration. However, a survey was made of the desires of various state and federal agencies and secondary priorities were established. Several areas which were in line with operational priorities have been expedited in order that good map information might be available to the Kentucky Highway Department for road relocation problems. The primary priority areas proved to be areas that had never been mapped topographically before or were covered with the old $\frac{1}{125,000}$-scale reconnaissance maps.

Technique and Equipment

The general techniques for the type of mapping done in Kentucky have been well perfected during a twenty-year period. These involve the use of aerial photography and special photogrammetric equipment which can be used in various combinations or in connection with ground survey methods—that is, the plane table.

Aerial Photography and Ground Control.—Aerial photography is used to map all areas, with the scale of the photographs varying from about 1:14,000 to 1:35,000, depending on the terrain and the type of equipment to be used. Such photography is of precision type and is done with special cameras which must be submitted to the National Bureau of Standards for checking and calibration.

Even with the high degree of development in the use of aerial photographs, it is still necessary to obtain a fair amount of vertical and horizontal ground control consisting of position and elevation determinations of a number of points. For the horizontal control, the initial phase is accomplished by the USCGS and consists of first-order and second-order triangulation. The practice is to limit triangulation legs to about 6 or 8 miles, if possible. Thus a good density of first-order and second-order horizontal control is available. In the second phase, the USGS begins at a primary triangulation point and, in general, runs a third-order transit traverse around the border of each 15-minute quadrangle.

The first-order, vertical control is run by the USCGS and provides a primary net for the use of the USGS in establishing additional control which is third order. If practicable the level lines and transit traverse lines coincide. This procedure provides the net for the establishment of supplemental (or what is sometimes known as photo) control. This supplemental control consists of obtaining at least four points per "stereo" pair (aerial photographs) to an accuracy of at least one tenth of the contour interval.

The general practice followed with control and photogrammetric work is that horizontal control can be more sparse than vertical control because the horizontal scaling can be held more rigidly than can the vertical scaling.

Compilation.—Stereoscopic compilation follows the establishment of control and is the photogrammetric machine stage, which consists of drawing the contours and all planimetric detail to be shown on the final map, plus fence lines and all rural buildings. In some cases where the contouring is to be completed in the field by plane table methods, only planimetric detail is compiled by stereoscopic methods.

Various methods of compilation are utilized, involving several types of photogrammetric equipment in combination with the plane table. The principal types of photogrammetric equipment used by the USGS in the Kentucky work include the Multiplex Aero-projector, the Kelsh Plotter, the Zeiss Stereoplanigraph, and the Wild A5 and A6 stereoscopic plotting machines. All these machines, as in the case of engineering equipment in general, have their advantages and disadvantages. It is believed, however, that the USGS has assembled the most modern and efficient photogrammetric equipment, permitting great flexibility in mapping operations.

Different types of plotting equipment produce different manuscript (original map drawing) scales, depending on the flight height of photography, which in turn is determined primarily by the contour interval on the final map. The following manuscript scales have been used: 1:6,000, 1:7,200, 1:10,000, 1:12,000, 1:15,000, 1:15,840, and 1:20,000. This range of scales includes manuscripts compiled by the TVA and the AMS.

Final Operations.—After "stereo" compilation is complete, the map is sent to the field for checking and completion. The field check includes tests for position accuracy and completeness of detail. Field completion may consist of the addition of contours in flat areas: For example, 5-ft supplementals may be added on a 10-ft interval map where it is considered that the 10-ft interval does not adequately show relief features. Also, in the field check and field completion phase, cultural and drainage names are determined and checked and political boundaries are plotted.

After field check and completion, the map is returned to the office where all information pertaining to the quadrangle is assembled and color-separation drafting is accomplished. For color separation a separate drawing is prepared on a stable medium for each color to be printed on the final map. The standard colors for the 1:24,000 series "topo" sheets are green for woods, brown for contours, blue for drainage and water features, and black for cultural features.

Following color-separation drafting, a composite is made of the various drawings and this map is subjected to a thorough editing. Composite prints are sent to state and local agencies for a final check. After a reasonable length of time, the composite map is given a final editing and correcting. When this editing is complete, the reproduction copy is given to the reproduction section and the final map is printed by photolithographic processes.

The final reproduction run is usually approximately 5,000 copies, of which 80% are with green woods overprint.

State Files of Topographic Data

At the outset of this program, it was decided that a state depository and distribution center should be established for topographic maps and allied data. It is not generally appreciated, but many useful by-products come from modern topographic mapping program. The by-products are aerial photographs, vertical and horizontal control data, copies of map manuscripts, and blueline prints.

The sponsoring agency (AIDB) has established files for all of the aforementioned by-products and maintains stocks of all published topographic maps of Kentucky. Files of aerial photography consists of one set for the permanent file and one set for lending purposes. Copies are filed of mimeographed lists of the unadjusted field values of horizontal and vertical control points. It is the standard policy of the USGS to publish all such control data after the final adjustment. Since this may be several years after field work, unadjusted field data are made available.

The advisability of filing copies of map manuscripts may well be questioned. However, if it is considered that the manuscripts are to a considerably larger scale, generally, than the final published maps, that they are available from

one year to two years before them, and that they contain information concerning fence lines and buildings that is not shown on the final published maps, it can be seen that such material will serve many useful purposes during the interim between compilation and publication. Also, they are useful after publication for purposes requiring detail and large scale.

Blueline prints also serve as interim and detail maps and have special uses since they are printed on scales of 1:20,000 and 1:24,000.

All the materials available as a result of the mapping program are put to use. An increasing number of requests have been received by the AIDB as more topographic data have become available. Aerial photography is used in coal land surveys, mineral tax appraising projects, highway drainage problems, waterway development projects, flood control projects, and industrial site planning. "Bluelines," copies of manuscripts, and published maps are also used for the aforementioned purposes, plus farm planning, geologic mapping, and special oil field surveys. The uses for maps and topographic data mentioned herein are only a few which have been brought to the attention of AIDB in the distribution of the material. Undoubtedly, there are many other applications. For example, an order for twelve copies of a blueline sheet was received from an undertaker, for some unexplained reason.

In order to keep interested parties informed as to the progress of the program and the availability of material, a progress map is published and distributed every three months by the AIDB.

Progress in the Kentucky Program

The program sponsored by the AIDB was begun in a small way on January 1, 1949. Full-scale operations on the complete program did not begin until January, 1950. Including TVA and AMS work, approximately 38,740 sq miles of mapping were under way or complete as of July 1, 1952, and can be broken down into the principal phases as follows (area of Kentucky—40,360 sq miles):

Subdivision	Square miles
Aerial photography	38,740
Ground control	29,100
Manuscripts and "bluelines"	17,660
Published	4,160

Outlook for the Completion of the Kentucky Program

State appropriations covering the biennium, July 1, 1952, to July 1, 1954, along with previous appropriations, provide for approximately 85% of the entire program. It remains to be seen whether or not the state legislature will appropriate the funds required to complete the mapping. As the mapping has been scheduled, suitable appropriations by one more general assembly would provide for completion of the program.

There are several powerful arguments in favor of completing the Kentucky mapping. The fact that much money has already been invested and that much of it would be lost if operations were terminated on June 30, 1954, is certainly to be considered. The opinion, held by businessmen and industrial-

ists who have studied the mapping question, that the value of the maps greatly exceeds their cost, is certainly a sound argument. Also, it has been demontrated with "topo" material previously completed that the arguments for large-scale topographic mapping are well-founded.

Every effort has been made by the AIDB to advise potential map users of the availability of topographic data and to assist them in proper utilization. These efforts have met with success. Even with all this in favor of good maps, a program such as the Kentucky one requires the active support of public and private organizations.

DISCUSSION

HERBERT MILWIT.[2]—In describing the evolution of the topographic mapping program in Kentucky, Mr. Miles has made a worthy contribution to the systematic and economical development of the United States. Progress in the sensible exploitation of the nation's natural resources will be increased materially, duplication of effort in mapping and allied activities will be reduced, costly errors in the siting of the works of man will be minimized, the entire national economy will be benefited by longer range planning made possible by the more exact knowledge of what there is to work with, and many times the investment will be saved if other states and the federal government follow the example set by the enlightened program undertaken by the State of Kentucky.

Mr. Miles shows very clearly the difficulties encountered in securing the wide base of support needed to sustain a mapping program. This is a common experience the world over, and in practically every case the governing body itself has had to step in to do the job for the very many users who could not get together to do the job as a private venture.

The United States lags far behind every enlightened country in its topographic mapping program, and its lack of foresight in failing to provide suitable map coverage well in advance of the pressing needs of today has already handicapped the orderly exploitation of resources and the expansion of agricultural and industrial facilities. Mr. Miles' contribution should be taken as a timely aid to other states which are "dragging their heels" on their own programs or are not adequately supporting the federal effort.

It should be borne in mind that what the State of Kentucky is doing in this program is simply to provide a minimum basic topographic mapping coverage without which no government can effectively administer its jurisdiction or plan for its growth. There will still remain the task of producing larger scale maps or plans which can be true to scale and serve for detail structure planning and cadastral needs.

The methods followed in the topographic mapping of the State of Kentucky are modern and economical, and the program is considered a reasonable one, certain to return great dividends to the state and to the nation.

[2] Colonel, Corps of Engrs., Eng. Research and Development Labs., Fort Belvoir, Va.

AMERICAN SOCIETY OF CIVIL ENGINEERS
Founded November 5, 1852

TRANSACTIONS

Paper No. 2563

EAST ST. LOUIS VETERANS MEMORIAL BRIDGE

BY A. L. R. SANDERS,[1] M. ASCE

WITH DISCUSSION BY MESSRS. W. H. JAMESON, JOSEPH SORKIN, AND A. L. R. SANDERS

SYNOPSIS

Many of the important problems that were encountered in the design of the East St. Louis Veterans Memorial Bridge—said to be the longest cantilever span across the Mississippi River—are described in this paper. Solutions evolved by the engineering consultants and steel fabricators are discussed and described.

Specifications governing the design of the structural members on the bridge superstructure are given to indicate a number of modifications in the standard design code. Various design details, such as shoes, floor beam hangers, anchorages, lateral bending in floor beams, and trestle construction are described and illustrated.

INTRODUCTION

Although the East St. Louis Veterans Memorial Bridge is believed to be the longest cantilever span crossing the Mississippi River, it is the intent of this paper to emphasize a few of the important details of the bridge, rather than the routine engineering involved in the design and supervision of construction of a cantilever highway bridge.

The project, consisting essentially of a river crossing connected to a grade separation by a hydraulic fill embankment 1,700 ft long, is approximately 1.5 miles long. The river crossing (see Fig. 1) consists of one 964-ft channel span, two 470-ft anchor spans, two 213-ft deck truss spans, two 120-ft girder spans, 1,440 ft of steel trestle and, at the western end, a 160-ft paved approach fill within retaining walls. The 964-ft channel span includes a 324-ft suspended span.

The grade separation consists of one 250-ft through truss span, 1,000 ft of steel trestle, and, at the eastern end, a 550-ft paved approach fill. The three main river spans required 5,150 tons of fabricated steel, and have a total length of 1,904 ft.

NOTE.—Published in September, 1952, as *Proceedings-Separate No. 150.* Positions and titles given are those in effect when the paper or discussion was received for publication.

[1] Partner and Chf. Engr., Hazelet & Erdal Cons. Engrs., Chicago, Ill.

Substructure

Design of the substructure offered no particular problems since all main piers are founded on limestone rock. Pier No. 9 (Fig. 1) was constructed inside a steel sheet-pile cofferdam. Caissons, sunk by dredging through wells in the caissons, were used in the construction of Pier Nos. 10 and 11. It was necessary to sink the caisson at Pier No. 11 through 28 ft of water and 65 ft of coarse river sand containing some silt and gravel. The caissons were finally seated and

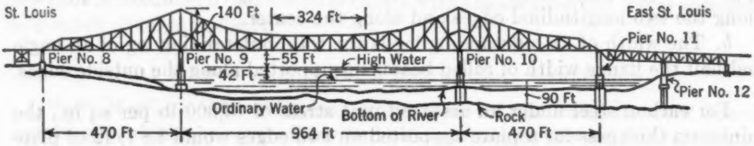

Fig. 1.—Elevation of East St. Louis (Ill.) Veterans Memorial Bridge

sealed under air. The deepest pier (Pier No. 11) required 48 lb-pressure, which is nearly the maximum pressure under which men are permitted to work. Twin circular caissons were used in constructing Pier No. 11, which was designed for much lighter loads than Pier No. 10, where a single caisson was used.

Superstructure Specifications

The design of the span was based on the specifications of the American Association of State Highway Officials (AASHO),[2] except for certain modifications, the most significant of which are concerned with (1) the design of the main compression members and (2) wind loads.

1. *Design of Main Compression Members.*—To provide adequate local buckling strength in main compression members, the recommendations of L. T. Wyly, M. ASCE, in regard to plate thickness,[3] were adopted in lieu of the requirements of the AASHO.

The thicknesses (t) of plates and outstanding flanges and legs of angles were limited to not less than—

$$t_a = \frac{b}{\sqrt{\frac{26,250,000}{s}}} \qquad \text{(1a)}$$

—for the case of plates supported on two edges, such as webs and cover plates of truss members, and to—

$$t_w = \frac{b}{\sqrt{\frac{2,187,500}{s}}} \qquad \text{(1b)}$$

—for the case of plates supported on one edge, such as the section of perforated cover plates along the perforation and for the case of outstanding legs of angles. On main members and bracing members having low unit stresses, the minimum

[2] "Standard Specifications for Highway Bridges," adopted by the Am. Assn. of State Highway Officials, Washington, D. C., 1944.

[3] "Rational Design of Sections for Short Compression Members of Steel," by L. T. Wyly, *Bulletin No. 467*, Am. Ry. Eng. Assn., Chicago, Ill., June-July, 1947, p. 3.

thickness was set at $b/60$ for plates supported on two edges and $b/16$ for plates supported on one edge.

In Eqs. 1, s is the computed axial unit stress in a member and b is the width, defined as follows:

a. Plate width is the distance from the unsupported edge (the edge of a hole in a perforated plate) to the supported edge for plates supported at one edge only, the total width between edges for plates supported along two opposite edges only, and half the width between edges for plates supported along the two longitudinal edges and along the center.

b. The width of an outstanding leg is the total outstanding leg of an angle and half the flange width of rolled beams unsupported along the outside edges.

For carbon steel under an assumed unit stress of 15,000 lb per sq in., the minimum thickness for a plate supported on two edges would be 1/42 of plate width. For silicon steel at 20,000 lb per sq in., the ratio would be 1/36 of plate width. In the case of plates supported at one edge and in the case of the outstanding legs of angles, the minimum thickness at 15,000 lb per sq in. and 20,000 lb per sq in. would be 1/12 and 1/10.5, respectively.

The "width of plate" intended under the design specifications is the total width. The AASHO specification requires the thickness of plates making up the section to be a function of the distance between the nearest rivet lines, or the roots of flanges of rolled sections. In the case of main webs, the function is 1/32 for carbon steel and 1/28 for silicon steel; for solid cover plates and diaphram plates, the functions are 1/40 and 1/36, respectively, and in the case of perforated cover plates, the function is 1/50 for carbon steel and 1/45 for silicon steel.

In general, the web plates on the East St. Louis Veterans Memorial Bridge were 26 in. wide and the rivet lines were 18½ in. on center. The design specification would require 0.62-in. web plates, if carbon steel were used at 15,000 lb per sq in., whereas the AASHO specifications would require 0.58-in. plates. Generally, the solid cover plates and the perforated cover plates were 22½ in. wide with rivets at 16 in. on center. The design specifications would require 0.54-in. cover plates, if carbon steel were used at 15,000 lb per sq in., whereas the AASHO specifications would require 0.40-in. plates.

The design specifications, however, permit a reduction in plate thickness with a reduction in unit stress, and all plates entering into the make-up of the member are treated on the same basis, which seems to be the logical procedure. In most of the chord and web compression members, the loads were so large that the sections chosen were well above the minimum thickness.

2. *Wind Loads.*—The following requirements for wind loads were substituted for those specified by the AASHO in those spans that were more than 250 ft long, all wind loads being considered horizontal:

Transverse Wind Loads, Bottom Laterals.—A moving horizontal load equal to 30 lb per sq ft on 1½ times the area of the structure as seen in elevation, plus 200 lb per lin ft with 25% increase in normal unit stresses.

Transverse Wind Loads, Top Laterals.—Top laterals shall be designed for a moving wind load of 30 lb per sq ft at normal unit stresses.

Transverse Wind Loads, Chord Members.—When chord members are part of the portal system, they shall be designed for dead load plus live load plus impact, plus a moving horizontal load of 30 lb per sq ft with 25% increase in normal unit stresses. All other chord members shall be designed for dead load plus live load plus impact, plus a moving horizontal load of 15 lb per sq ft with a 25% increase in normal unit stresses.

Longitudinal Wind Loads.—Longitudinal wind loads equal to 70% of the specified transverse wind load shall be applied to the bridge. Such wind load shall not be assumed to act simultaneously with the longitudinal forces specified as a result of braking loads.

Design and Details of the Superstructure

Main Members.—All elements, except most of the hangers, were boxed members in which the cover plates had oblong cutouts, at regular intervals, to provide access for riveting and painting. These holes were 10 in. by 20 in., except at panel points, where in some cases it was necessary to make them 12 in. by 24 in. to allow a man to enter the member during riveting. In the latter case the member was reinforced to compensate for the additional sectional area removed.

The AASHO specification requires the removal of at least $\frac{1}{4}$ in. of metal by milling, chipping, or grinding in the case of flame-cut edges of silicon steel. This is an extremely costly requirement.

The fabricator was permitted to flame-cut the holes, providing the edges were annealed simultaneously by a gas flame. This procedure had previously been used on two other large bridges in which extensive tests were made before the procedure was adopted by the engineers.

Bridge Shoes.—On the main piers at panel point L14, the original design contemplated the use of a shoe in which the members entering the joint were joined by large pins. A study indicated that the bearing pressure on these pins would be so great that rotation could hardly be expected to take place. Jonathan Jones, Hon. M. ASCE, suggested the use of a rocker type of shoe. Study of this problem by both the Bethlehem Steel Company, in Bethlehem, Pa., and the consultants resulted in the development of the rocker shown in Fig. 2. This shoe is subjected to a total load of 4,840,000 lb. The radius and face width were proportioned on the basis of a formula for large rollers proposed by Wilbur M. Wilson, Hon. M. ASCE—

$$w = (12{,}000 + 80\,D)\,\frac{s_y - 13{,}000}{23{,}000} \quad\ldots\ldots\ldots\ldots\ldots(2)$$

in which w is the allowable load per linear inch; D is the diameter of the roller, in inches; and s_y is the yield point of material in pounds per square inch.

"Mayari R" steel was used for the $7\frac{1}{2}$-in. slab on the top of the bearing and the 9-in. slab and $1\frac{1}{2}$-in. sole plate on the truss. The material conformed to the American Society for Testing Materials (ASTM) specification A242, except that it had a specimen yield point of about 45,000 lb per sq in.

The remainder of the shoe was fabricated from material meeting ASTM specification A7, except that physical tests were waived and the carbon and

manganese contents were specified to lie within the range of from 0.15 to 0.25 and 0.40 to 0.60, respectively, by ladle analysis. Killed steel was used. The physical tests were waived since it is known that specimens cut from thick slabs will not test as high as those from ordinary structural shapes. Lower designing unit stresses were used to compensate for the lower yield point.

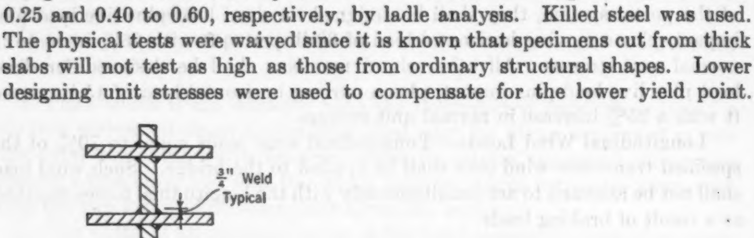

FIG. 2.—DETAIL OF ROCKER BEARING AT PANEL POINT L14

For material having a yield point of 45,000 lb per sq in., a 70-ft-diameter roller would have a permissible line bearing of 110,000 lb per lin in. The actual line bearing, based on a net width of 40.375 in., is 120,000 lb per lin in. Tests conducted by Mr. Wilson indicated that the critical load was 50% greater than the permissible load given by Eq. 2, and for the case considered here would be approximately 165,000 lb per lin in.

The width (b_c) of the area in contact, as a result of flattening, can be determined by the Hertz formula:

$$b_c = 0.0004 \sqrt{w \times D} \quad \text{.......................} \quad (3)$$

in this case b_c is 4 in. On that basis, the average unit pressure is approximately 30,000 lb per sq in. The natural tendency in constructing the shoe would be to place one main web transverse to the center line of the truss. To do so, however, would require excessively large welds attaching the longitudinal stiffening plates to the web. The shoes were constructed using three 3-in. longitudinal webs with short transverse sections of 5-in. material between the webs. This arrangement greatly reduced the shear on the vertical welds.

The shoes, upon completion of the welding, were normalized in accordance with the 1946 American Society of Mechanical Engineers (ASME) code for the fusion welding of unfired pressure vessels.

Floor Beam Hangers.—Considerable time was devoted to the design ot the floor beam connections and to the design of those truss members commonly called floor beam hangers. The rotation of the ends of floor beams (particularly in structures having wide roadways) caused by the deflection of the beams under the dead load of the floor system, plus live and impact loads, produce high bending stresses in the floor beam hangers.

Mr. Wyly shows[4] that, unless a correction is made in the usual analysis of the frame formed by a floor beam, the floor beam hangers, and the top strut or portal frame, stresses considerably in excess of those calculated by the usual analysis should be anticipated.

Hangers in the plane under discussion are displaced laterally at the top of the floor beam, as well as rotated through the same angle as the end rotation of the floor beam since floor beams are usually relatively deep compared to the width of floor beam hangers. The stress resulting from this translation might readily be overlooked in the design of the hanger. The end connections of all floor beams were canted out at the top through an angle approximately equal to the end rotation of the floor beam caused by full dead load plus one-half live load and impact. This induced an erection stress of opposite sign in the hanger, as a result of bending, approximately equal to that resulting from full dead, live, and impact loads.

Anchorage.—Short links were used at the ends of the anchor spans to transmit the end reactions to the anchor piers. Short links, 2 ft 9 in. center to center of pins, were not objectionable since an overlapping finger type of joint was used across the roadway and no harm would be done by a slight unevenness caused by the rise and fall resulting from the rotation of the short links as the anchor spans expanded and contracted.

Lateral Bending in Floor Beams.—The steel company fabricated the stringers to the theoretical panel length and cambered the trusses so that, under full dead load, the trusses would assume the design proportion—that is, have the grade and panel length shown on the stress sheet. During erection, the ends of the floor beams in many cases must be bent laterally, in order to connect them to the trusses because of the change in length of the bottom chord members in cambering. This bending was relieved to a considerable extent by resting the stringers on shelves provided on occasional floor beams, rather than framing them into the floor beam. For the concrete floor slab a pour sequence was selected that would not aggravate the lateral bending in the floor beams. It was also realized that, after all construction was finished, the lateral bending in the floor beams would be produced by the passage of live load over the structure. The lateral flexibility of the top flanges of the floor beams was increased by painting their top surfaces with an asphalt paint (so that there would be no bond between concrete and steel) from the truss connection to the

[4] "Two Problems in Bridge Design," by L. T. Wyly, *Bulletin No. 454*, Am. Ry. Eng. Assn., Chicago, Ill., September-October, 1945, p. 27.

first interior stringer. The concrete slab was carefully formed to permit lateral bending for the length thus painted.

Trestle Construction.—Many engineers visiting the project were interested in the trestle construction. In general, the trestles were a series of four continuous spans separated by braced tower spans. In order to reduce to a minimum the moment in the longitudinal direction on the pedestal piers, the bents were constructed with rockers at the base of the columns and under each stringer, where they passed over the floor beams. Thus, each bent between braced towers was free to rock back and forth. One end of the continuous construction was fixed to a braced tower and the other end was left free to slide on the next braced tower.

Acknowledgments

The engineering board charged with the bridge design consisted of the late Charles A. Ellis, M. ASCE, and the late George A. Maney, M. ASCE; Mr. Wyly; and Hymen Shifrin, M. ASCE, of the firms of Horner & Shifrin and Hazelet & Erdal, consultants. The three main spans were fabricated and erected by the Bethlehem Steel Company.

The writer is indebted to Mr. Wyly for his review of the design and his helpful suggestions.

DISCUSSION

W. H. Jameson,[5] M. ASCE.—This discussion presents, from the viewpoint of a member of the engineering staff of the fabricator, some of the problems that were encountered in the long-span cantilever crossing the Mississippi River at East St. Louis, Ill. Also the writer will comment on the modification in (b/t)-ratios for components of compression members as used for this structure.

In the case of Mr. Wyly's formula for plate thickness in compression members, there are two points of deviation from standard specifications such as those of the AASHO and the American Railway Engineering Association (AREA) which deserve further study on the part of specification writers. The first is the question as to whether b should be the full width of the plate, or the distance between the nearest lines of connecting rivets. Mr. Wyly has based his decision to use the full width on the test reports on compression plates for the Delaware River Bridge at Philadelphia, Pa.; the writer believes that there is so much scatter in these test results that either value of b could be used logically, and he recommends that further testing should be carried out, probably in connection with the program of the Column Research Council.

The other question involves the use of a formula that omits all consideration of the allowable unit stress. The allowable unit stress determined by any usual column formula is supposed to be that average unit stress on the section which will keep the maximum unit stress on the extreme fiber within the stress determined by dividing the yield point of the material by the factor of safety. Therefore, in the case of a member with an actual unit stress and an allowable unit stress of the same value, no change in the (b/t)-ratio should be permitted—no matter how small this unit stress may be—because a plate situated at the extreme fiber may be considered already stressed to the maximum. It is only when the actual unit stress is less than the allowable unit stress that a change should be permitted, and the method used in the AREA specifications is the theoretically correct method. In the AREA specifications, the (b/t)-ratio for carbon webs is 32 and for carbon cover plates it is 40, but these ratios may be increased by the ratio $(s_{allow}/s_{actual})^{\frac{1}{2}}$. However, the writer agrees with Mr. Wyly's basic requirement that the same limits for b/t should apply to both the webs and the cover plates.

The discourse in the paper concerning the welded shoes at the main piers is an indication of the close cooperation that existed between the consulting engineers and the engineering staff of the fabricator; and it indicates how such cooperation can result in a better structure, usually with a saving in cost. At the main pier of a large cantilever there is always the possibility of developing severe secondary stresses—caused by the rotation of the span as a whole as the live loading moves from main span to anchor arm and by the deformations of the members themselves. After considerable discussion between the consulting engineers and the fabricator's engineers it was decided that it was better to provide for span rotation by using an articulated shoe, as

[5] Asst. Chf. Engr., Bethlehem Steel Co., Fabricated Steel Constr., Bethlehem, Pa.

shown in Fig. 2, than to attempt to reduce secondary stresses by using pin-ended members at a shoe that could not rotate. Mr. Wyly's measurements, on which the author has provided a preliminary report, but which were not available when this discussion was prepared, should prove whether this procedure has tended to minimize the secondary stresses, and whether rotation of the span as a whole with respect to the pier actually has occurred during erection and concreting and subsequent to completion of the bridge.

Another example of the close cooperation between the consulting engineers and the fabricator's engineers is in the design of the main truss members. For complex reasons, it had been necessary to design these members in a very short time, and without complete study as to how they could be fitted together satisfactorily. After the award of the contract, the members were re-designed to the satisfaction of all parties concerned, and a better structure, with consistent details throughout, was the result. Attention is called to the use of 5-in. by 5-in. angles as the corner angles for nearly all box members. When 4-in. by 4-in. angles, or 6-in. by 6-in. angles with double gages are used, there is always difficulty at chord splices in getting rivets through outstanding 4-in. legs, or through outstanding 6-in. legs on the inner gage line, because of the packing out of splice plates over the web legs of the angles. The use of 5-in. by 5-in. angles, with single gages in each leg, greatly facilitates field riveting and consequently results in better rivets. Some concern was expressed that there would be a tendency for the heel of these 5-in. by 5-in. angles with rivets on a single gage line to pull away from the edge of the web or cover plates. Close inspection of the members revealed no such difficulty, and no special care had to be exercised by the fabricating shop to guard against this.

The design of the floor steel presented some difficulties to the erector, and the solution described here was greatly facilitated by the close cooperation of the consulting engineers. The stringers framed to the floor beam web, in some cases between floor beam stiffeners, and the outstanding legs of these stiffeners made it impossible to erect the stringers by swinging them in. One framing angle for the stringer to the floor beam connection was shop riveted to the floor beam web, and the other was loose. It was decided, therefore, to eliminate vertical stiffeners on one side of the floor beam web, and to use a single longitudinal stiffener on that otherwise plain side. This longitudinal stiffener was located below the stringers, and thus the stringers could be swung in freely without interference at that end away from the outstanding legs of the vertical stiffeners.

The main structure, as now standing, is a prime example of teamwork between designer and fabricator. The result proves that such cooperation, which modifies the construction to utilize most effectively the available fabricating and erecting facilities, pays real dividends in a better structure and, usually, in a financial saving.

Joseph Sorkin,[8] M. ASCE.—Among the topics in this paper is a discussion of the modification of AASHO specifications as regards the design of main compression members. These specifications, as well as other standard design

[8] Partner, Howard, Needles, Tammen & Bergendoff, Cons. Engrs. Kansas City Mo.

specifications, are intended for relatively short spans. In the design of longer spans it behooves one to explore the fundamental concepts regarding the stability of thin plates in compression. The importance of the structure under consideration fully justifies the more thorough and accurate approach to the problem from the standpoint of safety as well as economy. The designers of the bridge are to be commended for that reason.

For relatively heavy reactions of a long span of the magnitude of the Veterans Memorial Bridge, a line bearing is definitely preferable to the conventional shoes in which pins transfer the loads to the supports. Forces

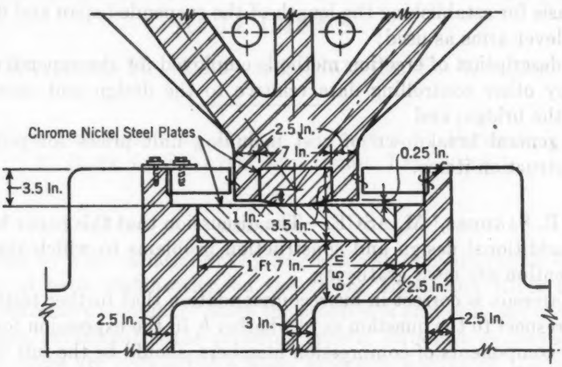

FIG. 3.—Bearing Surfaces.

engendered by pin-type shoes, in the frictional resistance to articulation, may cause significant secondary stresses in the truss members in the immediate vicinity of the bearing, as well as adversely affecting the supporting piers. The type of shoe used for the Veterans Memorial Bridge has been used in several long-span bridges. Instead of special alloys for the bearing slabs, it has been found advantageous to provide inserts of chrome nickel alloys into slabs made of ordinary cast steel. The inserts, made of alloy with a high elastic modulus, may be subjected to considerably higher bearing concentrations. Fig. 3 shows the details of this arrangement. The chrome nickel plates are press fitted into the shoes, the bearing surface of the upper plate having a radius of 8 ft. Incidentally, the same type of bearing may also be used for expansion shoes by setting the lower casting on alloy rollers.

Vertical dimensions of the truss framework at the ends of the 470-ft end spans are not given. As shown in Fig. 1, it appears that the inclination of the end posts is at an unusually acute angle. In certain instances it has been that with end posts sharply inclined there is a tendency toward considerable vibration of the span under live load. This condition apparently results from the fact that the framework in the immediate vicinity is subjected to bending moments analogous to a rigid frame, thus resulting in correspondingly greater deflections.

Details of structures are important and their description is of interest. However, the writer is of the opinion that a recorded history of the principal

aspects of planning and construction of projects of this magnitude is of even greater importance and interest. Thus, the value of the paper could be greatly enhanced if, in addition to the details described by the author, information were furnished as regards other basic problems related to the project. It is hoped that in the closing discussion the author will present the following data:

1. Conditions dictating the lengths of spans;
2. Other types of structures considered and the reasons for adopting cantilever trusses;
3. Basis for establishing the length of the suspended span and of the cantilever arms as used;
4. A description of erection methods employed for the superstructure;
5. Any other controlling data relative to the design and construction of the bridge; and
6. A general breakdown of cost including unit prices for principal construction items.

A. L. R. Sanders,[7] M. ASCE.—The discussion that this paper has received and the additional design and construction problems to which the discussers draw attention are most gratifying.

Mr. Jameson is correct in his recommendation that further tests be carried out with respect to the question as to whether b, in the expression for the (b/t)-ratios for components of compression members, should be the full width of the plate or the distance between the nearest lines of connecting rivets.

The type of shoe shown in Fig. 3 is an interesting variation from that shown in the paper. The writer believes that Mr. Sorkin's design would show greater economy as the load to be carried increases, when compared with that used at East St. Louis. Mr. Sorkin's remarks with respect to the inclination of the end post drew attention to an error in the proportions of Fig. 1. The end post has a rise of 45 ft in a distance of 50 ft, and the depth of the center span is 50 ft.

For complex reasons, as stated by Mr. Jameson, the selection of the type of structure, the determination of the span lengths, the relative length of the suspended span and the cantilever arms, and the design of the main members had to be accomplished in a short period of time. Studies made by the designing engineers indicated that a cantilever structure having the ratios (anchor span to center span) finally adopted would be the most economical.

The length of the center span and the location of Piers No. 9 and 10 were conditions established by the United States War Department in the issuance of the permit for the construction of the bridge. The span length and pier location were affected materially by the Eads Bridge, which spans the Mississippi River approximately 800 ft downstream from the site of the East St. Louis Veterans Memorial Bridge. The project was constructed with a lump sum type of contract, and unit prices for the various construction items are not available.

[7] Partner and Chf. Engr., Hazelet & Erdal Cons. Engrs., Chicago, Ill.

AMERICAN SOCIETY OF CIVIL ENGINEERS
Founded November 5, 1852

TRANSACTIONS

Paper No. 2564

BANK STABILIZATION BY REVETMENTS AND DIKES

By Raymond H. Haas[1] and Harvill E. Weller[2]

With Discussion by Messrs. Harrison V. Pittman, E. R. de la Sayette, and Serge Leliavsky

Synopsis

Aggravated by wide variations of hydrographic and physiographic elements, the problem of bank stabilization on the Lower Mississippi River has been found to be extremely complex. Since the problem is primarily one of arresting bank recession, revetment is the principal type of structure employed; dikes, retards, and groins are installed to a lesser extent depending on the particular situation encountered. These bank protection structures have been developed by theory and experience since the early 1880's. For the most part, the details of their design are peculiar to the lower river alone. The protection of the banks is progressing in a systematic manner, with a view to modifying the primitve stream artificially for the purpose of securing effective flood control and navigation.

Introduction

The problem of stabilizing the Lower Mississippi River is not wholly a matter of applying known hydraulic formulas; nor is it simply a proposition of adopting structural design that has proved successful elsewhere. Details of the protective structures in use are peculiar, for the most part, to the lower river alone. These structures, revetments, dikes, groins, and retards are designed to fit conditions not only in the lower river generally, but also those conditions prevailing in a particular reach at the time they are to be used.

***Instability of the River Banks.*—The Lower Mississippi River, because of its wide variations in depth and width, volume and velocity, direction of flow, slope and water surface, and conditions of bed and banks presents an extremely difficult problem of stabilization. These factors all contribute to the erosion of the banks and consequent formation of bars. The river banks are inherently**

Note.—Published in September, 1952, as *Proceedings-Separate No. 148*. Positions and titles given are those in effect when the paper or discussion was received for publication.

[1] Chf., Bank Protection Branch, Mississippi River Comm., Vicksburg, Miss.

[2] Chf., Dikes Section, Mississippi River Comm., Vicksburg, Miss.

unstable, being composed of finely divided clays and silts overlying easily erodible sands. Bank recession may vary from a few feet annually to more than 1,500 ft in some isolated cases. It has been computed that the caving banks between Cairo, Ill., and Donaldsonville, La., yield annually about 1,000,000 cu yd of material per mile. The silt in colloidal suspension, however, is of secondary importance since, although it has been variously estimated as being between 300,000,000 cu yd and 400,000,000 cu yd annually, it is probably transported in one continuous journey from its source to the Gulf of Mexico. The major part of the material from a caving bank forms an accretionary deposit immediately below its source. As the bank in a concave bend continues to recede, the point bar below enlarges and consequently aggravates the bank caving conditions in the next bend downstream.

Therefore, the basic difficulty to be overcome by bank stabilization on the Lower Mississippi River is the instability of the river itself.

History of Bank Stabilization Efforts.—Prior to the creation of the Mississippi River Commission (hereinafter called the "Commission") in 1879, a board of engineers concluded that the greatest obstacle to navigation improvement and levee maintenance was bank caving. In its first preliminary report, submitted in 1880, the Commission called for navigation improvement by regulation of the river channel and by protection of its banks.[3] The improvement was to be accomplished by the construction of permeable contraction works that would limit the width of the low-water channel to 3,000 ft, and by bank revetments that would arrest recession in the concave bends. Late in 1881 the Commission initiated operations for the stabilization of Plum Point reach, about 130 miles above Memphis, Tenn., and in the Lake Providence reach in northern Louisiana. It was not until the passage of the Flood Control Act of December 22, 1944, which authorized completion of the stabilization program on the Lower Mississippi River, that adequate funds, plants, and equipment were made available to prosecute the work in a systematic manner. As planned, bank revetment will be the principal structure in the program because the problem is mainly one of arresting bank recession in concave bends in which depths are too great for any other known device to be constructed economically. Dikes, retards, and groins will be used where feasible, to prevent bank caving, but to a greater extent for supplementary works.

Revetments

Design of Revetments.—A revetment is a structure designed to protect the river banks directly. It consists of two distinct parts: The section below normal low water, known as the "mattress," and the part extending from the mattress to the top of bank, called "bank paving." The mattress work comprises roughly three fourths to four fifths of the entire structure.

Experience has shown that, to be effective, a revetment must be sufficiently long to protect the entire concave bend from the upper to the lowermost points of caving at all stages. It must extend from the top of the bank to the toe of the underwater slope, a vertical distance of from 80 ft to 150 ft. It should

[3] "Annual Report of the Chief of Engineers 1880," Appendix SS, pp. 2733–2736, U. S. Govt. Printing Office, Washington, D. C.

be flexible so that it can mold itself to irregular surfaces; it must have sufficient strength to remain intact in the event of uneven slope settlement or scour. It should be relatively impermeable and continuous in order to prevent fine soil particles from leaching out through the mattress under the action of current that may reach a maximum velocity of 12 ft per sec. Also, as far as practicable, the revetment material should be indestructible in air or water.

Construction.—Construction normally follows a sequence of bank clearing and grubbing, clearing of the underwater slope of snags, bank grading, mattress sinking, and, finally, bank paving.

The bank in a concave bend is typically very steep above the water surface and, consequently, is unstable. Therefore, grading to a stable slope, initially, is necessary. The slope required for stability is determined by an analysis of the soil from representative borings taken at close intervals along the bank on which the revetment is to be constructed. Bank slopes varying between the limits of 1 ft vertical to from 3 ft to 5 ft horizontal are usually required to insure stability.

In the earlier days of construction, banks were usually graded after the sinking of the subaqueous mattresses; but the availability of equipment to do this part of the work, without delaying progress on the work as a whole, was often the determining factor. Usually the bank was graded after the mattress was in place because it was thought that the waste material from the bank-grading operations was beneficial for filling or loading the mattress. Bank-grading operations today are prosecuted in advance of sinking operations because of operational considerations and because the modern mattress has sufficient body and weight to eliminate the requirement for filling and loading.

Development of Materials.—Soon after the initiation of work by the Commission at Plum Point and Lake Providence, it became apparent that the light, flexible, and comparatively inexpensive structures of poles and brush being used were inadequate to cope with the conditions prevailing on the lower river. Between 1882 and 1893 numerous mattress types of willow, lumber, and other native materials were designed and tested. Two of the types developed during this period, the framed willow and willow fascine mattresses, were used extensively until about 1930. Because of the scarcity of willows, the short construction season, the relatively slow production rate, and the greater cost of construction only a limited number of these types of revetments have been constructed since 1930. The most recent examples of the use of these types were a willow fascine mattress placed in Memphis harbor in 1948, and a framed willow mattress constructed in New Orleans (La.) harbor in 1949.

Articulated Concrete Mattress.—During the thirty-year period between 1914 and 1944, four distinct types of concrete mattresses and one compacted asphalt mattress were developed. Of these types (the monolithic concrete, the articulated concrete, the lapped and butt slab, the compacted asphalt, and the flexible roll type concrete) only the articulated concrete mattress proved to be satisfactory in respect to production, cost, and service.

The articulated concrete mattress originated with experiments, begun in 1915, to develop a flexible and permanent underwater mattress. After many trials and alterations, the present forms of mattress and sinking mechanism

were evolved. The mattress is composed of precast units 25 ft long by 4 ft wide and 3 in. thick. Each unit has twenty individual blocks, 14 in. wide, spaced approximately 1 in. apart, on heavy corrosion-resisting reinforcing fabric that is continuous throughout the unit. The precast units are assembled on the sloping deck of a launching barge where they are united to each other and to launching cables by wire rope clips and twist wires. The launching cables are fastened ashore to anchors embedded in the bank. The barge is then moved riverward 25 ft, allowing the joined units to slide off the curved launching apron and hang suspended in the water on the launching cables. This launching process is repeated until a complete mattress of any desired width has been constructed. The cables are then cut at the outstream end and the plant moved upstream into position for laying the next mattress. Details of the placement operation are shown in Figs. 1 and 2.

The articulated concrete mattress is the best type of revetment devised, and the only type that can be placed at the rate required for the proper prosecution of the stabilization program. Three complete revetment construction plants, especially designed to place the articulated concrete mattress, are

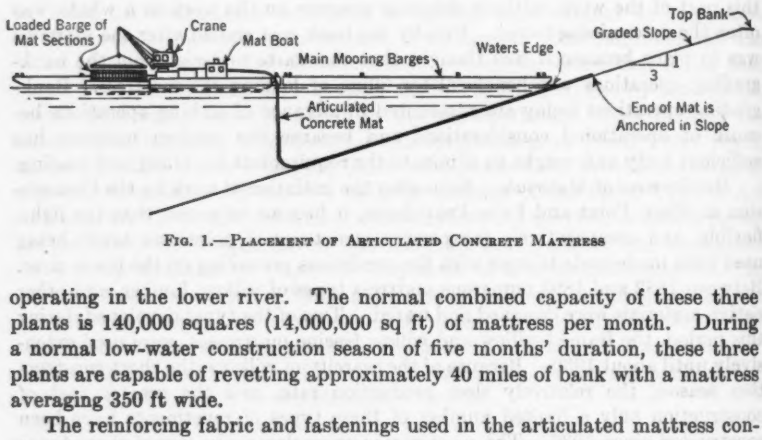

Fig. 1.—Placement of Articulated Concrete Mattress

operating in the lower river. The normal combined capacity of these three plants is 140,000 squares (14,000,000 sq ft) of mattress per month. During a normal low-water construction season of five months' duration, these three plants are capable of revetting approximately 40 miles of bank with a mattress averaging 350 ft wide.

The reinforcing fabric and fastenings used in the articulated mattress construction are made of corrosion-resisting metal. Copper-coated, high-tension steel, or stainless steel wires, each having a breaking strength of 4,000 lb, are used. This fabrication makes the mattress as indestructible as possible in air and water.

Since complete flexibility is not compatible with a concrete product, the necessary articulation produces interstices through which bank fines can be drawn by the current. Since 1948, a less permeable modification of the articulated concrete mattress, a so-called V-type mattress, has been developed. Only small test installations have been made, but during the 1950 construction season a test section of considerable size was constructed using this mattress. The V-type mattress has open areas of 3% as compared to about 8% in the conventional mattress.

Asphaltic Mixes.—Experiments with nonreinforced asphaltic mixtures are now being made in the form of plastic masses or blocks. For mass placement, the heated mixture is placed in bottom dump barges, towed to the site, and released. The plastic mass spreads and congeals to cover the subaqueous slope. When used in the form of blocks, the asphalt mix is cast in water-cooled forms at the site and subsequently released through wells in the barge to cover the underwater slope. This method has not been very successful for new construction, but is usually effective for repair of damaged work, especially in the less turbulent reaches of the lower river.

Bank Pavements.—After a mattress is in place, the graded bank above the water surface is paved to prevent erosion by river currents, which would result in bank instability and consequent loss of the subaqueous mattress.

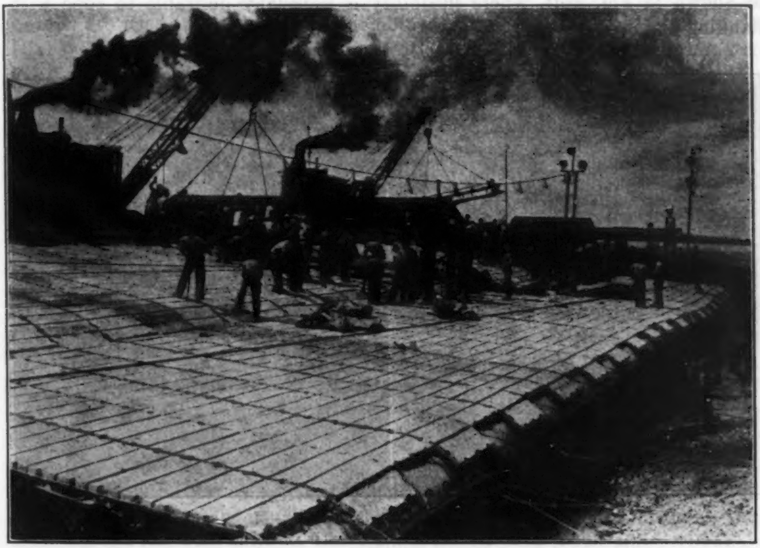

FIG. 2.—CONSTRUCTION PLANT FOR PLACEMENT OF ARTICULATED CONCRETE MATTRESS

Bank pavements of the earlier revetments were generally constructed with the same material as the mattress but experience with brush or fascines and wire netting proved that, when subjected to alternate wetting and drying, the wood soon decayed and the metal parts corroded rapidly. Consequently, stone was adopted as the standard material for bank paving.

Riprap on a 4-in. gravel blanket is considered the most effective pavement yet constructed but, because of the local unavailability of stone, it is rarely used below Memphis. A 10-in. riprap paving can adjust itself faithfully to irregularities in the slope; and it can reform and continue to give protection in the event of minor bank subsidence and sloughing. A pavement that cannot

accommodate such settlements fails locally and requires costly maintenance.

In an attempt to find durable substitutes for riprap, pavements of monolithic concrete, articulated concrete, asphalt, and manufactured blocks have been constructed with varying degrees of success. Of these types only the articulated concrete and noncompacted asphalt pavements remain in general use.

The articulated concrete pavement is identical to the mattresses of the same material but differs in the detail of placement. It is placed on a 4-in. gravel blanket that permits relatively free drainage of ground water but retains the bank fines. Although the articulated concrete bank paving is relatively simple to place, it is comparatively expensive. Therefore, its use is generally limited to connections between the subaqueous mattress and other types of paving. It is also used extensively at the upper and lower ends of revetments, as shown in Fig. 3(*a*), where flexibility is especially desirable to cope with flanking action.

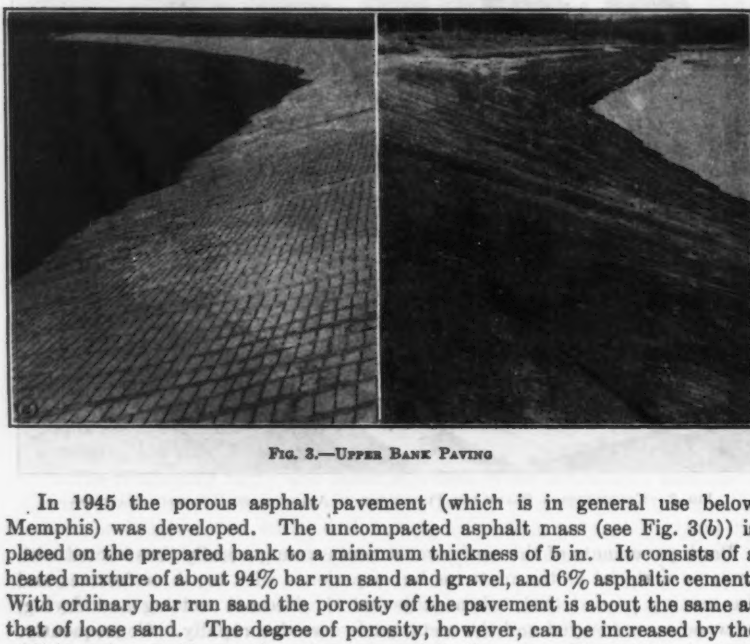

FIG. 3.—UPPER BANK PAVING

In 1945 the porous asphalt pavement (which is in general use below Memphis) was developed. The uncompacted asphalt mass (see Fig. 3(*b*)) is placed on the prepared bank to a minimum thickness of 5 in. It consists of a heated mixture of about 94% bar run sand and gravel, and 6% asphaltic cement. With ordinary bar run sand the porosity of the pavement is about the same as that of loose sand. The degree of porosity, however, can be increased by the addition of a small quantity of pea gravel in the mix. The relatively free-draining feature of the uncompacted asphalt makes it superior to either a monolithic concrete or compacted asphalt pavement.

Pavements composed of ordinary concrete blocks or tetrahedral-shaped blocks show little, if any, advantage over stone. In addition, their high initial cost prohibits general use.

Dikes, Groins, and Retards

Dikes, groins, and retards are intermittent structures that may be permeable or impermeable, according to the function performed and the materials of which they are constructed. Pile dikes and triangular-framed retards are permeable, whereas groins are impermeable. In the past these structures have been used on the Mississippi River below Cairo, mainly as contraction works and as a method of closing secondary channels. Because of the excessive depths and the large amounts of drift present during rising stages, only limited use has been made of pile dikes as bank protection on the Lower Mississippi River. On the Red and Arkansas rivers, however, pile dikes have been used extensively for bank protection with considerable success. A limited use has also been made of retards, groins, and stone dikes on these rivers.

In the plan of stabilization adopted by the Commission, pile dikes and retards are used independently or combined: First, as bank protection works in concave bends; second, as flank protection when a revetment is terminated in an exposed flank; third, to control flow in secondary channels; and, fourth, to deflect or train the channel into a more favorable alinement. Groins may be used for the same purposes, but, because of comparatively higher construction costs, their use is not always justifiable.

As bank protection structures, dikes and groins are designed to defend the banks by holding destructive currents well offshore, but the manner in which this is accomplished differs with the type of the structure. The success of permeable types depends on their ability to trap material moving as bed load or in suspension. The impermeable types fend off current without dependence on accretionary deposits. As in the layout for revetment, the dike system should extend the entire length of the concave bend. When constructed, the outboard ends of the dikes should lie in a smooth curve to minimize turbulent flow, and should extend at least to, and preferably past, the thalweg of the river.

Dikes are used at the lower end of revetments to prevent loss of the revetment by flanking and to provide a directive into the crossing below. The ends of the dikes should lie along a curve of a sharper radius than that obtaining in the bend immediately above. When used to control the flow in secondary channels, the dikes are usually placed at the lower end of the channel, thus trapping the bed load entering the channel through the upper end. Dikes are used to train the river into a more favorable alinement in locations in which it is shallow and has a tendency to meander. Dikes designed to promote growth or downstream migration of bars are examples of this type of construction.

Pile Dikes.—The first pile dike constructed on the Mississippi River consisted of a double row of single piles with the tops pulled together and wired, and the structure wattled with brush. No foundation mattress was provided. This construction proved too light and the dikes were gradually strengthened, the wattling was eliminated, and a mattress was provided along the axis of the dike at the bottom of the river. The common pile dike as shown in Fig. 4, consists of two or more, up to a maximum of seven, rows of pile clumps, three piles constituting a clump. The rows are spaced approximately 5 ft apart,

with pile stringers placed between each row. Clumps are spaced from 15 ft to 20 ft apart depending on the number of rows in the dike. Piles and stringers are secured with several turns of $\frac{3}{8}$-in. galvanized wire strand fastened with boat spikes. The pile penetration varies from 20 ft to 30 ft below the river bed. Each dike is constructed on a woven willow or lumber mattress, as shown in Fig. 5, extending from the water's edge from 45 ft to 75 ft beyond the channelward end of the dike proper. Mattress widths vary from 77 ft to 100 ft. The mattress is ballasted with 15 lb of stone per sq ft and an additional 500 lb of stone per row, per lin ft, are placed in the dike line to fill holes torn in the mattress by pile driving.

The crest elevation of the pile dike is usually set at mid-bank stage, which is from 15 ft to 17 ft above the low-water plane. There are two reasons for choosing this elevation. First, pile lengths would become excessive if the top

Fig. 4.—Pile Dike Systems

of the dike were raised substantially above this elevation, and, second, the most severe current impingement on the bank in a bend usually occurs between the low and mid-bank stages. After the latter stage is exceeded, the river has inundated the bar opposite the bend and the flow becomes more or less axial.

Bank protection dikes are spaced from $1\frac{1}{2}$ times to $2\frac{1}{2}$ times the length of the upstream dike, depending on the radius of curvature of the bend and the angle and intensity of the current attack. The upstream dike of a system is inclined downstream at a small angle with the bank and extends to the rectified channel line. This upstream structure is designed to turn the current slightly offshore. The remaining dikes in a system are placed normal to the bank line or angled approximately 15° downstream from normal.

When used to control flow in secondary channels, the height of the dike is raised, where feasible, to the top of bank elevation and the dike is extended completely across the channel.

Dikes placed on the convex side of the river to promote bar growth are spaced about 2½ times the length of the upstream dike up to a dike length of 1,000 ft. For longer dikes, the relation between length of dike and spacing is less. All dikes are normally angled slightly downstream.

After the mattress has been constructed and pile driving has begun, the bank head is graded to a stable slope. The width of the bank head is equal to the width of the mattress. The graded slope is then dressed and paved with a 10-in. stone pavement. When necessary, a gravel blanket is placed under the stone to prevent loss of bank fines. The dike is extended landward to the top

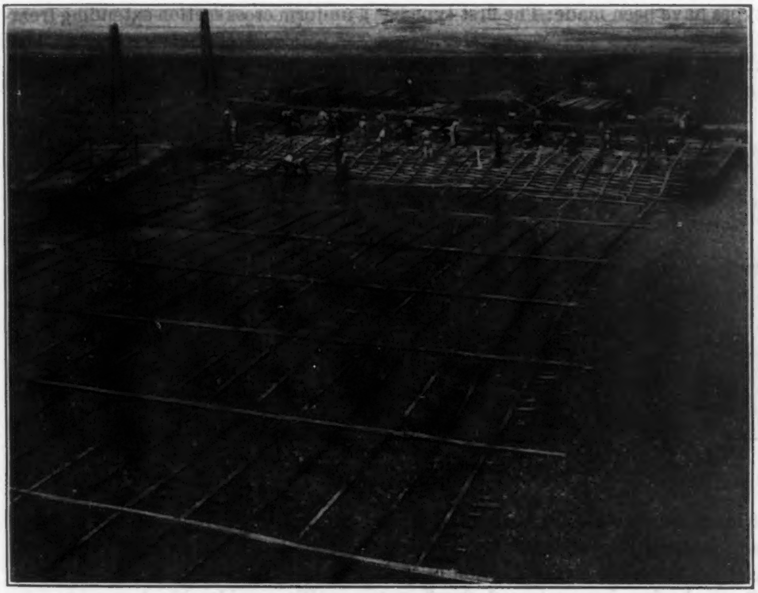

FIG. 5.—LUMBER MATTRESS UNDER CONSTRUCTION

of the graded slope by a root section of single piles spaced 6 ft apart. Root piles are staggered in two rows in order to permit the placement of stringers.

Abatis Retard.—The abatis retard, first constructed in 1898, is a forerunner of the triangular-framed retard, which consists of a triangular prism of lumber frames with a covering of screen poles on the upstream face. A willow pole mattress 26 ft wide is an integral part of the structure. The retard is constructed on barges in lengths up to 98 ft. In order to facilitate sinking, ballast stone in an amount of 500 lb per lin ft is placed on the upstream 8 ft of the mattress. After assembling a section on a barge and ballasting, anchors leading upstream are attached and the section is sunk to the river bed as shown

in Fig. 6. By placing multiple sections, the retard can be made to extend any desired length. When in place, the tips of the screen poles are about 20 ft above the river bed. Unless the retard is placed as an extension to pile dikes, the bank is graded and paved, and a pile root is constructed in the same manner as for the pile clump dike. Retards are usually built in pairs normal to the current, the individual retards being from 200 ft to 500 ft apart and the pairs, from 1,000 ft to 1,500 ft apart.

Groins.—Groins are in the experimental stage on the Lower Mississippi River, although several rock groin installations have been successful on the Arkansas and Red rivers (Fig. 7). On the Lower Mississippi River groins have commonly been constructed with mass asphalt. Experiments with three types have been made: The first type has a uniform cross section extending from the bank to the deep water; the second has a level crown elevation; and the third type is merely a flexible blanket about 200 ft wide, extending from the top of the bank to the thalweg. In an experiment with the latter type, a series

FIG. 6.—LAUNCHING OF TRIANGULAR-FRAMED RETARD

of blankets were placed in a concave bend and, as the current scoured out the sand between the blankets (the blankets being more resistant to scour), a relatively superior crest elevation to the intervening area was maintained, thus effectively forming groins of the first type with considerably less material. Although results have not been evaluated, considerable weakness has been indicated at the shore connections that are vulnerable to destruction by eddy action both from upstream and downstream.

Stone and asphalt dikes serve the same function as groins but differ in construction detail. The crown is kept at a constant elevation, usually equal to the top of the bank. Excessive quantities of materials are required for these structures and the consequent high cost prohibits their use except in rare cases.

PROBLEM OF BANK STABILIZATION

As of January, 1950, there were approximately 170 miles of stabilized banks on the Lower Mississippi River between Cairo and Baton Rouge, La. Approximately 255 miles of caving bank remained to be stabilized. The greater

part of this mileage will be protected by articulated concrete revetment and a lesser part by dikes, retards, and groins.

Causes of Failure.—The design of articulated concrete mattresses is being modified from time to time as improvements are evolved. Although the primary purpose of a revetment is to stabilize the banks, a revetment is not a retaining wall; hence, effectiveness is lost whenever the bank loses its equilibrium. A bank may become unstable, after revetting, from numerous causes. Excessive scour that undermines the revetment along the toe may steepen the slope to such an extent that it is no longer stable and the bank sloughs, moving the revetment with it. Intensive and prolonged attack may disarrange parts

FIG. 7.—STONE GROINS

of the mattress and leave the bank vulnerable to attack, or the bank may slide because of hydrostatic pressures or an inherently unstable condition.

There is much speculation as to whether the weight of the revetment is sufficient to prevent disarrangement by river currents with velocities in excess of 5 ft per sec. It has been suggested that vibration of the slabs would destroy the integrity of the revetment, in time, and thus subject the bank to slides by scour. A theoretical investigation of the extent and consequences of such action is being made in the laboratory. Because of the great depths, swift currents, and opaqueness of the water, determinations from subaqueous examinations of mattress work by divers have not been entirely satisfactory.

Dikes and other timber structures are ordinarily satisfactory when material deposits from within three to four years. Until such deposits form, the dikes

are subject to destruction by drift, ice, and vibration. If no accretion forms, the dikes are subjected to deterioration by decay. Experience indicates that no accretionary deposit is more permanent than the structure that produces it; therefore, retards and dikes are constructed principally of creosoted timbers to give longer life.

Many of the recorded failures of revetments and dikes on the lower river cannot be ascribed to the material used or to the type of structure built but to the inability to complete the works as conditions required. Many losses result from the flanking action of river currents when the demand for work at other critical locations makes it impossible to complete the work to the full extent of the caving bank. Most of the critical situations will be ameliorated and the work contemplated by the stabilization project can then be vigorously prosecuted in a systematic manner. Although so far first consideration has been given to the correction of especially troublesome reaches involving levee locations, stabilization of the reach from Helena, Ark., to the mouth of the Arkansas River is almost completed.

Experimental Work.—Work of an experimental nature has also been progressing in selected reaches. Three revetments were installed during the 1949 construction season to support revetments in the opposite bends immediately below. The proposed function of these supporting revetments, in addition to maintaining a favorable channel alinement, is to reduce, radically, the volume of material normally contributed to the point bars opposite the lower revetment. In these three particular instances, encroachment of the point bar is believed to be the principal cause of considerable destruction to the lower revetment. Studies of the reaches were made for considerable distances upstream and downstream to determine the effect of these revetments on bar building and silt movement.

Conclusion

Many theoretical data are being developed by the laboratories of the United States Waterways Experiment Station at Vicksburg, Miss., and the engineering staff of the Commission, but corroboration and the final value of the theory must be determined by actual installations in the prototype. In cases of uncertainty, especially troublesome reaches of the river are chosen to serve as pilot models for testing new ideas and improved structures. Thus, the stabilization of the Lower Mississippi River is following a plan based on both theory and experience, especially the latter. The river flow is not being radically interfered with but its lateral movement and, consequently, the material contributed to the stream by bank erosion are being controlled in order to (1) preserve the benefits of lower flood heights previously obtained by the cutoff program, (2) direct the river energy in deepening the channel for navigation, and (3) eliminate the necessity for continually retiring the levees.

Acknowledgment

The photographs reproduced in this paper were supplied by the Mississippi River Commission.

DISCUSSION

HARRISON V. PITTMAN,[4] M. ASCE.—Timely and interesting is this description of bank stabilization along the Lower Mississippi River, presented in the interest of both navigation and flood control. However, the paper omits the many interesting details of the historical development of the various plans, types of structures, devices, and materials that have been either tried and abondoned or else adopted and improved upon during the many years of effort to stabilize and control the Mississippi River. Statements concerning their abandonment or adoption, together with the specific reasons for such decisions, would be valuable and enlightening contributions to a study of this river. For example, an asphaltic type mattress was once developed and used experimentally by the New Orleans District, Corps of Engineers, United States Department of the Army. This project showed great promise and received world-wide publicity, but eventually it was abandoned.

A paper by Charles Senour, M. ASCE., gives an excellent presentation of the historical and physical sequences of flood control and channel regulation in the Lower Mississippi River valley.[5] Mr. Senour's paper serves as a valuable reference for a fuller understanding of the subject matter of the authors' paper.

The problem of bank stabilization and the improvement of the navigable channel of the Mississippi River is an old one. There was on file in the Office of the District Engineer, St. Louis, Mo. (about 1911), a drawing which bore the signature of Robert E. Lee, First Lieutenant, Corps of Engineers, U. S. Army, and was dated 1835.. It depicted a design for a number of spur dikes, consisting of stone and brush, which were installed along the waterfront of St. Louis to improve navigation. These dikes probably were among the very first regulatory structures to be installed on the Mississippi River. Throughout succeeding years various plans have been tried, and experimentation and studies in field and office will be continued in order to improve methods and materials for a more satisfactory and permanent control of the river.

Records show that the Mississippi is a river with caving banks and shifting bottom. No other river under improvement for purposes of navigation equals it in the magnitude of its bed disturbance. This is particularly true of the Lower Mississippi River, although partly applicable to the Middle Mississippi River.

The nearest approach to completion of open river regulation on the Mississippi River, by means of contraction works for rectifying and deepening the channel and by revetments for stabilizing the banks, is that which has been accomplished between St. Louis and Cairo. However, the plan of improvement, alike in principle to that now in use on the Lower Mississippi River, makes no provision for the rectification and stabilization of the uncontrolled, erosive alluvium bed of the river with its variable slopes, velocities, pools, and

[4] Engr., Special Asst., Little Rock Dist., Corps of Engrs., Little Rock, Ark.

[5] "New Project for Stabilizing and Deepening Lower Mississippi River," by Charles Senour, *Transactions*, ASCE, Vol. 112, 1947, p. 277.

shoals. It is this lack of complete control over the entire cross section of the river that causes much of the severe damage to (or the destruction of) many of the stabilization structures. The lack of bed control constitutes the major part of the complex and difficult problem of permanently stabilizing the river at the present time.

In the writer's opinion, the only feasible plan that has been proposed for the complete regulation of the Mississippi River was that developed by the late W. M. Penniman, M. ASCE.[6]

This plan proposed three forms of permanent construction: (1) The necessary side contraction, (2) the stabilizing of all concave bends, and (3) the regulation of the entire bed of the stream by fixation of the crests of the controlling bars. This fixation of natural or artificial bars would equalize the fall of the river and preserve the required cross section for complete regulation. Sill dams or cross weirs would regulate the flow, thus maintaining the desired depth of channel obtained by side contraction and bank protection.

Two forms of construction that were in use at the time Mr. Penniman's plan was proposed were considered to be standard. These were side contraction and the stabilization of concave bends. The third form of construction mentioned in the plan remains untried on any major stream in the United States.

Instability of the River Banks.—The different types of caving banks encountered on the Mississippi River which are of constant concern to engineers, have been classified and described.[7] Following surveys and field observations extending over a period from about 1877 to 1908, it was decided to classify caving banks as eroding banks, slumping banks, sinking banks, and sliding or slipping banks.

An eroding bank is one in which the whole side of the river bank, from the water surface to the foot of the bank on the river bottom, is gradually wearing away under the scour of the moving water. Its soil is not cohesive enough to withstand the attack of the ordinary currents natural to the mean-water and low-water stages of the river. The bank becomes undercut and the upper parts break away. Stopping the erosion below the low-water line is of major importance. The slumping bank is usually steep and perhaps vertical on the side next to the river. It becomes dry and perhaps cracked by evaporation during a continued low-water season and becomes thoroughly soaked and filled with water during high waters. As the water falls and the temporary support given it by the water pressure is taken away, the front breaks off from the dryer or tougher sections of the bank behind, and it slides down into the bed of the river. The sinking bank is one in which a large mass of earth material rests upon a layer of very soft material which may be squeezed out by pressure of the overlying earth or washed out. In such cases, the entire river bank may settle uniformly, or nearly so, for any depth from a few inches to many feet, its top surface remaining nearly horizontal. The stratum of quicksand or other soft material may be many feet below the ordinary water

[6] *House Document No. 50*, 61st Cong., 1st Session, 1909, Appendix No. 5.
[7] *House Document No. 50*, 61st Cong., 1st Session, 1909, Appendix No. 1.

surface of the river, and such sinking banks are therefore liable to be developed at any stage of water.

The sliding or slipping bank is one where a large mass of material slides down the bank into the river. Usually, the slide results from the fact that material of considerable weight rests upon a smooth inclined surface of slippery material, and under the influence of heavy rainfall the earth mass slides as a unit until its foot reaches some solid point of support farther down the bank. Slides are usually entirely independent of high water and dependent almost entirely on heavy rainfall and poor runoff back of the river bank.

As explained, sinking banks and sliding banks are mainly independent of river conditions, and slumping banks occur only intermittently at high water, but eroding banks, especially below low water, are constantly in action and, therefore, are to be feared the most. These different types of caving banks must be considered individually when designing works for their most effective and permanent stabilization.

The authors state, under the heading, "Revetments: Design of Revetments," that "Experience has shown that, to be effective, a revetment***must extend from the top of the bank to the toe of the underwater slope***." Normally, it should extend a short distance beyond the thalweg of the stream.

Under the heading, "Dikes, Groins, and Retards," no mention is made as to whether these structures are now used for the contraction of the river to some predetermined width for increasing the low-water navigable depths over the bars or crossings to 12 ft, or as training works for guiding the flow into the next bend below.

The statement that "Bank protection dikes are spaced from 1½ times to2½ times the length of the upstream dike * * *" (see under the side heading, "Pile Dikes") is not quite clear. Referring to Fig. 4, the distance of the second dike downstream from the first dike does not conform to this rule. The rule of thumb in general use would be to locate the second dike downstream from the "foot" of the first dike, a distance of from 1½ times to 2½ times the distance between the foot of the first dike and the high bank, measured on a line perpendicular to the bank. Then, the third dike would likewise be located with reference to the second dike, and so on for the remaining dikes in the system. This fact applies to all dikes inclined downstream and is based on the effectiveness of dikes in deflecting the currents away from the bank. Should the dikes be placed perpendicular to the bank, the spacing of each succeeding dike applies to the actual length of the preceding dike.

The authors state, under the heading, "Problem of Bank Stabilization: Causes of Failure," that

> "As of January, 1950, there were approximately 170 miles of stabilized banks on the Lower Mississippi River between Cairo and Baton Rouge, La. Approximately 255 miles of caving banks remain to be stabilized."

Mr. Senour[5] writes that

> "The study developed that, in the 737 miles between Cairo and Baton Rouge, 97½ miles of effective bank revetment were already in place, and indicated that, to stabilize the banks between the two points, about 230 additional miles would be required***."

A comparison of these two statements indicates that between February, 1946, and January, 1950, an additional 72½ miles of bank were stabilized, but there still remained 255 miles to be stabilized—25 miles more than was required in 1946. At this rate, it is rather difficult to estimate just when this project will be completed and what the cost will be.

Under the heading, "Problem of Bank Stabilization: Causes of Failure," the authors state that .

> "Because of the great depths, swift currents, and opaqueness of the water, determinations from subaqueous examinations of mattress work by divers have not been entirely satisfactory."

This is a questionable statement since, in 1932, a diver was employed to determine the condition of the thirty-year-old willow fascine mattress placed along the waterfront at Helena (Ark.). The diver's examination showed that the mattress soon would reach the limit of its effectiveness, although no serious scouring action or caving had as yet developed. Samples of the tie wires appeared to be of bronze, still intact, and effective. The top poles, cribbing, almost all the stone ballast, and the greater part of the brush composing the facines had disappeared. The brush that remained in the fascines had been eroded to about the size of a finger. As a result of these observations, a new willow fascine mattress was installed within a short time.

The authors assert, under the heading, "Problem of Bank Stabilization: Causes of Failure," that

> "Dikes and other timber structures are ordinarily satisfactory when material deposits from within three to four years. Until such deposits form, the dikes are subject to destruction by drift, ice, and vibration. If no accretion forms, the dikes are subjected to deterioration by decay. Experience indicates that no accretionary deposit is more permanent than the structure that produces it; therefore, retards and dikes are constructed principally of creosoted timbers to give longer life."

These statements are concurred in as they call attention to the temporary nature of these wood structures even when they have been creosoted and the required deposit has been obtained. It continues to be necessary to maintain effectively these structures in order to hold the artificial accretion, or else to place revetments along the river face of such an accretion so as to insure its permanency. The use of concrete piles would appear to bear investigation because of the relative permanency of the concrete, the ease of manufacture and placing, and the possible economy. The writer knows of no instance where concrete piles have been used or even considered in works for open river regulation on the Mississippi River.

The placement of revetments in isolated localities for the purpose of safeguarding front-line levees from destruction by caving banks has always been an expedient of a temporary nature. Rarely can such work be depended on to fit in with, and become an integral part of, the continuous, systematic, and more permanent stabilization works. Their cost constitutes a continued expenditure, in excess of the funds normally required for the comprehensive plan of improvement of the river for navigation and flood control, and prolongs the time for its completion.

Reference is made (under the heading, "Problem of Bank Stabilization: Experimental Work") to the three experimental revetments installed in 1949, "***to support revetments in the opposite bends immediately below." Information is desired as to whether any training works were installed below the foot of the upstream revetment so as to direct the low-stage and mid-stage flows over the crossing between the upper and lower revetments. This installation would bring about a deepening and a fixation of such crossing and would establish a satisfactory approach flow into, and a parallel flow along side of, the downstream revetment. Such treatment is imperative to avoid downstream migration of both bar and crossing, to maintain a navigable depth, and to insure the integrity of the mattress in the bend immediatley below by preventing masking or destruction by shifting attacks of flow.

E. R. DE LA SAYETTE,[8] J.M. ASCE.—In their interesting paper, Messrs. Haas and Weller state, under the heading, "Revetments: Articulated Concrete Mattress," that "***a less permeable modification of the articulated concrete mattress, a so-called V-type mattress***," has been developed. It might be of interest to American civil engineers to know that this type of revetment, which has not been used extensively in the United States, is now being used in France on two bank stabilization projects.

FIG. 8.—REVETMENT ALONG THE DONZÈRE-MONDRAGON CANAL IN FRANCE

The first of these is shown in Fig. 8. This is the revetment on part of the 17-mile Donzère-Mondragon Canal, one of the main features of the Rhône River development. The second is the revetment on the Randens Canal, the tailrace channel of the Isère-Arc hydroelectric project in the French Alps.

These two enterprises illustrate that articulated concrete mats can be an economical solution for the revetment of canal banks of small area, as well as the large bank areas of the Mississippi River.

[8] Head Engr., Société du Vacuum Concrete, Paris, France.

The solution to the bank stabilization problem, as described by the authors, has been carefully studied by the writer, who paid a valuable visit to the Memphis District of the Corps of Engineers, United States Department of the Army, in 1951. However, solutions must be chosen according to the scale of the individual project. At Donzère, France, the project involves 6,000,000 sq ft of revetment. Each revetment unit, called a "square," is 3 ft wide by 24 ft long; it is composed of 22 individual blocks, 3$\frac{3}{16}$ in. thick. At Randens, France, the area covered is 250,000 sq ft, the total length of the canal being only 1,500 yds. The square in this case is 3 ft wide and 18 ft long, made up of 14 blocks, 4¾ in. thick.

The casting and handling methods are similar for the two projects, both making use of vacuum concrete processes. The concrete is poured on concrete casting beds. For each square the side form is composed of a concrete curb with steel angles set in the casting bed to obtain the bevel at the bottom of the V-shape. The fresh concrete is screeded and the upper bevel of the V is obtained by stamping this concrete (under vibration) with steel angles protruding from the bottom of the semi-rigid vacuum mat. The fresh concrete is then vacuum processed and the mat immediately re-used on the next square.

Unmolding, placing in stock, removing from stock, and even the placing on canal banks is done by using a flexible vacuum lifter, invented by K. P. Billner and experimented with by the Memphis District of the Corps of Engineers.

It should be noted, however, that a huge floating construction plant such as that used on the Mississippi River, or even a smaller but similar machine, could not be operated economically on small jobs. The squares described were placed one at a time at Randens, and two at a time at Donzère. The lifter used on these projects was found to be quite adaptable for placing the squares, since it can be used under water with minor adjustments to the equipment.

Serge Leliavsky,[9] M. ASCE.—Credit is due the authors of this interesting paper for having re-opened discussion on some vital problems of river-training engineering—such as the old debate between the defenders of the "passive" revetments system and those who favor the "active" spur, or groin, system. These problems were once in the forefront of progressive hydraulic interest, but they were subsequently eclipsed by the spectacular applications of the Prandtl-von Kármán turbulence theory, which monopolized attention for many years. This trend resulted in the almost complete neglect of the three-dimensional aspects of the sediment transportation problem as evolved by the river-training experts of the first decades of the twentieth century. Instead, a characteristically two-dimensional approach became prevalent, marked by a galaxy of brilliant attempts to find new significant parameters correlating the turbulence theory with the results of laboratory tests on sediment transportation, instead of paying more attention to the three-dimensional velocity observations in natural rivers.

[9] Civ. & Hydr. Engr., Maadi, Cairo, Egypt.

It is true that these two-dimensional attempts may clarify a number of problems relevant to sediment transportation in general. However, they will not yield the basis for solving the problem of sediment regimen in rivers because, as the ratio of channel width to channel depth begins to increase, the water flow and sediment movement—even in the rigid flume of a laboratory experiment[10]—cease to follow routes that are even approximately parallel, and become distinctly helicoidal; that is, basically three-dimensional. The well-known experiments of Vito A. Vanoni,[10] M. ASCE, are a case in point. In spite of all the precautions taken to produce parallel flow, in the experiments, the water would not spread the sediment uniformly over the width of the steel flume, but, instead, transported it in the form of three clouds or ribbons, parallel to the flow, which settled in three clearly defined streaks when the flow was stopped. This result could be explained only by the action of secondary circulation—that is, four helicoidal currents.

If conditions such as these prevail in an artificially-built, rigid, rectangular channel, the three-dimensional effect in a naturally winding river must be much greater. The classical theory[11] of James Thomson, accepted subsequently by Hubert Engels, Max Möller, and others, lends support to the foregoing statement by showing that the meanders themselves, and the shape of the channel in them, are consequences of a naturally created three-dimensional current.

Therefore, the advantages of a group of spurs or groins, as opposed to those of a revetment for an equal length of bank—and the optimum layout for the former system—must be judged by the effect on the flow lines, particularly the helicoidal current, controlling the formation of the earthen channel.

Gerard H. Matthes,[12] Hon. M. ASCE, states that he was unable to observe the helicoidal current in the Lower Mississippi River, but this statement must have resulted from his method of observation. One would not expect the three-dimensional effect in a river the size of the Mississippi to be so obvious and easily observed by the naked eye as were the sediment ribbons in Mr. Vanoni's trough. Conclusions on the existence and effect (if any) of the helicoidal current in a river of this size must be based on instrumental observations of the direction of the flow, at different stations along the channel, and at various depths.

Therefore, a rational reply to the main problem in the authors' paper—that of the relative advantages of spurs as opposed to revetments—must be based on observations of the regimen of velocities in the zone affected.

As to the writer's knowledge, two different apparatuses have been used for this purpose—a rather light instrument applied by B. O. Hellstrom to the study of helicoidal flow in small canals,[12] and a much larger, more advanced device used by Nicolas de Leliavsky,[13,14] in the design of training works on the Dnieper River.

[10] "Transportation of Suspended Sediment by Water," by Vito A. Vanoni, *Transactions*, ASCE, Vol. 111, 1946, p. 67.

[11] *Proceedings*, Royal Soc. of London, Vol. 25, 1877, p. 6.

[12] "Macroturbulence in Natural Stream Flow," by Gerard H. Matthes, *Transactions*, Am. Geophysical Union, Vol. 28, Pt. 2, 1947.

[13] "Des Courants Fluviaux et de Formation du Lit Fluvial," by Nicolas de Leliavsky, *Proceedings*, Sixth International Navigation Cong., The Hague, Holland, 1894.

[14] "Résultats obtenus par le Dragage sur les Seuils des Rivières," by Nicolas de Leliavsky, *Proceedings*, Eighth International Navigation Cong., Milan, Italy, 1905.

As seen from Fig. 9, the apparatus of Mr. de Leliavsky consisted of a float built of two barges about 56 ft in length, with a tripod that rested on the bed of the river during the observations. A current meter of the Amsler type, with a tail extension similar to the tail of an airplane, was attached by means of a universal articulation to the tripod, and connected with indicators that could be read from an overhead platform. The tower and tripod were mounted amidships and the winch for raising the tripod and meter was near the stern. The barges were securely anchored before the tripod was lowered. It is essential to realise that in spite of the turbulent fluctuations, the apparatus yielded consistent average velocities for all the points observed. An example of a set of such observations is given in Fig. 10.

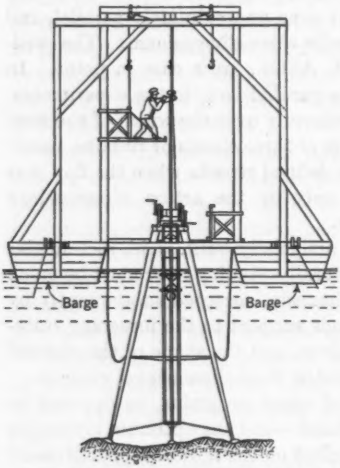

FIG. 9.—FRONT VIEW OF THE CURRENT MEASURING APPARATUS OF MR. DE LELIAVSKY

The empirical law derived by Mr. de Leliavsky from a large number of such observations correlated the depth with the convergency of the flow lines.

Considering these results, uniformity of river flow is but an academic assumption, which is true in the statistical sense only—that is, from the standpoint of over-all averages such, for instance, as the total discharge of the river. In nature, however, a river channel is a mosaic composed of individual small spots in which the flow is either permenently accelerated or permanently decelerated. This condition does not interefere with statistical over-all bulk

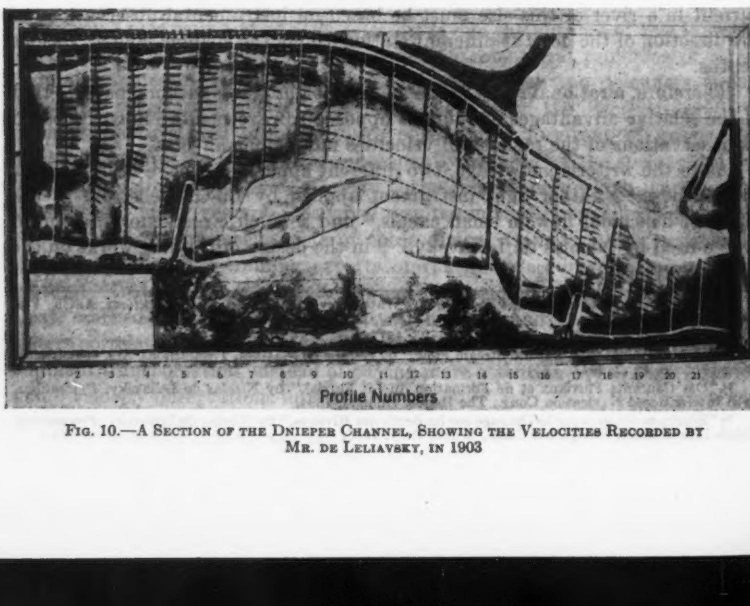

FIG. 10.—A SECTION OF THE DNIEPER CHANNEL, SHOWING THE VELOCITIES RECORDED BY MR. DE LELIAVSKY, IN 1903

uniformity because in the first case the flow lines are convergent and in the second case they diverge. Since scour always accompanies acceleration, and deceleration causes the sediment carried by the water to be deposited, it follows that convergent flow must occur in deep spots, and divergent velocities must be correlated with shoals. In fact this was proved by Mr. de Leliavsky's observations and might therefore be taken as the basic empirical law of the natural channel formation in general.

An analogy exists between this reasoning and that which explains the correlation between perpendicular velocity fluctuations in the Prandtl turbulent shear mechanism.[15]

Applying the results of his observations to river-training design, Mr. de Leliavsky found that the groin alternative, wherever applicable, yielded the more satisfactory solution. After his death in 1905 Mr. de Leliavsky's work was continued for some time by I. A. Rosoff, C. A. Akouloff, and N. V. Terpougoff, but results of their work have not been made generally available (1953).

A few words must be added about the constructional merits of the articulated reinforced concrete bank protection described in the paper, and its substitute, the willow fascine mattress with broken stone as ballast, which was popular in pre-revolutionary Russia.

The latter had a willow skeleton, resembling in shape the inverted ribbed slab of a reinforced concrete floor. This mattress had the advantage of being capable of erection on the surface of the ice in winter, in the immediate neighborhood of the spot where it was to be finally placed. The ice was then removed from this spot, and the completely erected willow structure of the mattress was dragged into the hole thus created and was sunk by loading it with the broken-stone ballast. Surprisingly vast areas could be thus covered in a single operation. Success depended on completion of the sinking within a few hours, thereby preventing water from eroding a hole beneath the partly sunk mattress.

The willow fascine mattress does not belong to either the permeable class or the impermeable class described by the authors, but it is an intermediate, semi-permeable subclass. Its limited capacity to resist percolation of water can be estimated from the fact that 7 in. of head were allowed as a maximum for dams built in this manner.

The great advantage of the willow mattress was that above water level it could rest on almost vertical slopes because the willows soon began to grow and their roots contributed materially to the strengthening of the earthern bank beneath it.

Recent research conducted by the Grenoble (France) laboratory appears to explain from an hydraulic standpoint the structural advantages of such a continuous semi-permeable revetment, as compared with the articulated type that consists of solid elements separated by open articulation joints.

The research at Grenoble was conducted by means of motion-picture studies of reduced scale models of various types of revetments used in North

[15] "The Mechanics of Turbulent Flow," by Boris A. Bakhmeteff, Princeton Univ. Press, Princeton, N. J., 1936, Fig. 30.

African ports. In Fig. 11, let MNP and mnp represent, respectively, the curves of the free wave, and of the forced wave in the granular soil beneath the revetment. The less the permeability of the protection, the greater the difference between the curves.

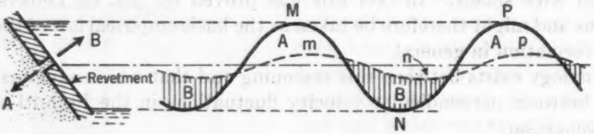

FIG. 11.—FREE WAVES AND FORCED WAVES ACTING ON THE SOIL BENEATH A REVETMENT

From the results of such tests one may possibly conclude that whenever curve MNP lies above curve mnp, clear water is forced into the joint, as shown by the arrow, A. Under reversed conditions (arrow, B) soil-laden water is pumped out of the joint. Thus, the balance of the soil movements in the vicinity of such a joint is always negative, and eventually this may cause trouble.

The important factor in the design of groins is whether they are built to the high water level, or only to the normal low water level.

AMERICAN SOCIETY OF CIVIL ENGINEERS
Founded November 5, 1852

TRANSACTIONS

Paper No. 2565

RICE IRRIGATION IN LOUISIANA

BY E. E. SHUTTS,[1] M. ASCE

WITH DISCUSSION BY MESSRS. LLOYD E. MYERS, JR., AND E. E. SHUTTS

SYNOPSIS

Rice is the principal energy food of the population of the world and is the main staple food for China, India, Japan, Indo-China, Siam, the Dutch East Indies, the Philippines, Malaya, and Madagascar. More than 96% of the world's annual rice crop is produced in the Far East. The principal production countries in the temperate region are Italy, the United States, Spain, Brazil, and Egypt. The consumption of rice in the Far East ranges from 200 lb per capita per year in India, China, Java, and the Philippines to from 300 lb to 400 lb per capita per year in Japan and Siam. The consumption in the United States is only between 5 lb and 6 lb per capita per year.

The culture of rice in all countries is dependent on irrigation, as approximately 3 tons of water are required to produce 1 lb of rice. The scope of this paper, and of its discussion, is confined to experience with the irrigation of rice in the United States.

HISTORY OF RICE CULTURE AND IRRIGATION

Rice ranks among the oldest staple crops in the world. Its cultivation and irrigation probably originated in the area of South India and spread northeastward to China about 3000 B. C. From there rice culture moved through India to Persia, Arabia, Egypt, and ultimately to Europe and the United States. Rice was first produced in the American colonies in 1685, near Charleston, S.C. From North Carolina and Georgia, its production spread to the Mississippi River and Louisana during the Civil War period. By 1890, Louisiana became (and still is) the leading producer of rice. The gradual shift of the rice production areas in the United States from the South Atlantic states to Louisiana, Texas, Arkansas, and California is shown in Table 1. At present,

NOTE.—Published in October, 1952, as *Proceedings-Separate No. 156*. Positions and titles given are those in effect when the paper or discussion was received for publication.

[1] Cons. Civ. Engr., F. Shutts' Sons, Lake Charles, La.

TABLE 1.—RICE PRODUCTION IN THE UNITED STATES,[a] 1839 - 1945 (THOUSANDS OF BUSHELS)

State	1839	1849	1859	1869	1879	1889	1899	1909	1919	1929	1939	1945[a]
Ark.		2	1	3				1,264	7,600	7,956	8,550	14,612
Calif.									9,300	5,719	9,000	14,520
Fla.	17	39	8	14	47	36	81	20	33			
Ga.	445	1,401	1,889	801	913	524	402	139	58			
La.	130	159	228	570	834	2,721	6,213	12,617	19,005	18,832	21,340	23,028
Miss.	28	98	29	13	62	24	27					
N. C.	101	197	273	74	202	210	284	22				
S. C.	2,180	5,753	4,284	1,162	1,873	1,091	1,704	528	131			
Tex.		3	1	2	2	4	259	8,996	6,784	7,027	15,172	18,000
Others[b]	7	93	20	10	29	16	33					
Total	2,908	7,745	6,733	2,649	3,962	4,626	9,003	23,586	42,911	39,534	54,062	70,160

[a] Bureau of the Census, U.S. Dept. of Commerce, except that the statistics for 1945 are estimates of the Bureau of Agri. Economics, U.S. Dept. of Agri. [b] All the remaining states.

the four principal rice producing states in the United States and the acreage and production in barrels (1 barrel equals 162 lb) are as follows:

State	Acres	Barrels
Louisiana	638,516	6,950,282
Texas	524,068	6,762,550
Arkansas	360,064	5,029,716
California	223,385	3,968,173
Total	1,746,033	22,710,721

It is the intent of this paper to deal primarily with the irrigation of rice in the State of Louisiana.

History of Irrigation.—The development of rice as a staple crop has gone hand in hand with the development of irrigation, as it is primarily a water crop. In ancient times, rice was grown in low, flat areas which were irrigated by "providence" methods—that is, by flooding during high water in rivers or impounding either tides or rainfall in low places and later drawing that water on to lower ground for irrigation purposes. Rice was thus grown in the Carolinas by the providence method. High water in streams was impounded by levees. After the rice matured, the water was drawn off for the harvesting of the rice.

After the Civil War, farmers in Louisiana began to consider growing rice on low prairie land in southwest Louisiana and also in southeast Texas—by providence irrigation. In wet seasons this worked fairly well, but dry seasons caused the loss of crops and money invested.

In 1885, J. B. Watkins of the North American Land and Timber Company, working mostly with English capital, attempted a large-scale reclamation and irrigation project using the same general method of the early rice culture in the Carolinas. A 4,000-acre area of coastal marsh on the east bank of Calcasieu Lake, some 30 miles below Lake Charles, was levied off with low levees about 4 ft above the surface of the marsh. The marsh was flat, with a surface elevation of about 1 ft to 1.5 ft above mean low Gulf elevation. Mr. Watkins cut this area east and west with small canals, spaced 0.5 mile apart, using

floating dredges for this work. The water in Calcasieu Lake normally stands at an elevation of about 6 in. above the ground surface, and his idea was to flood this marsh at high tide from the lake, to hold the water on the area with the protection levees, and to pump off prior to the harvest season.

A. Thomson and P. H. Philbrick designed a system of pumps to be used in controlling the water flow. They developed a method for cultivating this marshland by building small steam-driven winch or winding barges, which they placed in the east-west canals. Thus, they plowed the marshland by winching the plow back and forth across these half-mile strips. They encountered a dry season during which the water for irrigation became salty by infiltration from the Gulf. A very wet autumn, with high water outside the protection levees, and the failure of the primitive drainage pumps, caused the loss of the crop.

In 1898, Mr. Watkins undertook the irrigation of rice on high land prairies with construction of the Farmers Canal. A year later the Louisiana Canal was constructed and is still (1952) in operation. Both canals drew water from the Calcasieu River upstream from Lake Charles. Prior to this time, the Riverside Canal, utilizing water from the Mermentau River in the Crowley rice area, was built.

All of the first canals were wide and shallow, built above the surface of the ground and above the layer of impervious clay hardpan of southwest Louisiana and southeast Texas. The hardpan prevented much loss through seepage. Levees were spaced 100 ft apart and earth used in construction of the levees was taken from borrow pits.

The most westerly part of the rice producing area shown in Fig. 1, and lying between the Calcasieu River and the Sabine River, is irrigated from the Sabine River. The large Sabine canal system and the Krause and Managan irrigation canal serve this area. These canals are considered the safest system, from a salt-water-pollution standpoint, in this entire area, as they draw their waters from the Sabine River, which has a large water shed.

Size of Irrigation Systems.—For many years the rice farmer would cultivate a particular field 1 year and let it lie fallow 1 year. As the fertility of the land was exhausted, it became the practice to farm it 1 year and rest it 2 years. It is now the best practice to farm it 2 years and rest it 3 years; and the 3 years that the land is not farmed are used in planting lespedeza and white dutch clover for grazing beef cattle. By working a combination of rice farming and cattle raising, farmers have been able to increase their revenue tremendously and improve their lands. For this reason, canal systems must be designed large enough to serve several times the actual acreage planted to rice in any 1 year.

The first canals constructed were given very little or no slope leading away from the pumping plants toward the end of the system. Most of these early canals were built with pumping plants on the north end and with their system extending toward the south, following the natural slope of the land. Later, it was discovered that prevailing winds from the south tended to back the water up and prevent its proper movement out through the system. Old canals were largely rebuilt and new canals were given a slope of approximately 0.5 ft per mile to overcome this difficulty.

The irrigation season lasted from 100 to 150 days, after which these canals were allowed to dry out. This practice, and the fact that canals were very shallow, caused dense growth of marsh grass and water weeds to choke the flow of water. It is now the accepted procedure to squeeze in the levees and to dig the channels deep, using material for levees taken from the inside of these canals.

Irrigation waters were originally taken over natural drainage through long wooden flumes—some of the flumes being more than 1,000 ft long. Common practice today is to take natural surface drainage under these canals through concrete boxes or large pipe siphons.

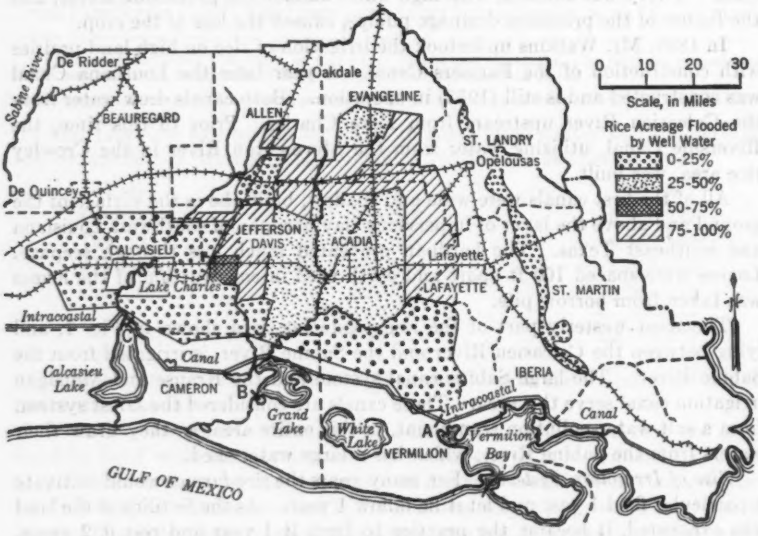

FIG. 1.—SOUTHWESTERN LOUISIANA SHOWING RICE AREA, BY IRRIGATION WATER SOURCE, IN 1947

Irrigation Pumps.—By 1900 sufficient pioneer work had been done in raising irrigated rice crops to indicate the need for larger central pumping plants which could supply water to large acreages. The rice farmers paid for this water either on the basis of acreage water rental or on a share crop basis, thus eliminating the need for individual farmers maintaining a separate small pumping plant. A number of so-called irrigation canal companies were formed and pumping plants of corresponding size were required.

At this time, the centrifugal pump was available as a vertical box type or horizontal pump, built in comparatively small sizes so that pumps of 25,000 gal per min or 30,000 gal per min were considered very large. The vertical pumps at that date were usually unsuited to anything but quite low lifts, and the horizontal pump, equally inefficient, was adapted to higher heads and was made of cast iron.

Several types of large-capacity pumps were tried. At least one triple expansion pumping unit was used and a number of rotary pumps of the conoidal type were installed. The latter pumps were suprisingly efficient and some of them are still in use (1952), but slow speed and costly construction make them uneconomical as compared with the centrifugal pump. The need for large efficient centrifugals prompted the pump manufacturers to improve their product. Pump designers from Europe were imported to design more efficient pumps. By 1910 pumping units as large as 48 in. and with capacities of from 50,000 to 60,000 gal per min each were in use.

The period from 1920 to 1930 saw many important changes. The diesel engine with its superior fuel economy reached the United States and many diesel-driven pumping units were installed. Inasmuch as the speed of all prime movers, including diesel engines, had gradually increased, pumps of higher speed design were a parallel development to permit direct connection.

An equally important development was the general use of electric current. There was a period of great expansion of the electric high lines at this time and the "electric people," needing load, welcomed the large motors needed for these pumping plants, particularly as the pump load came at a season (although only about 100 days duration corresponding to the rice growing season) when the electric loads were low.

Progressive pump manufacturers developed a type of pump impeller combining the characteristics of the centrifugal and axial flow units which resulted in a nearly flat horsepower curve at all pumping heads. Practically all large units built since the late 1920's have had this mixed flow type of impellers.

The history of pumping units since 1930 has been one of steady application of new prime movers combined with increased pump efficiency. Fortunately, the mixed flow unit readily lends itself to higher speeds than previous types.

Because of the widespread availability of cheap gas fuel, most new pumping plants use gas engine drive. These drives have paralleled the development of the gas engine, including the conventional low compression spark ignition engine, the high compression gas diesel and dual fuel diesel engines, and also the latest type of high compression spark ignition engines.

The size of individual units can be increased to whatever the irrigation companies deem necessary. No unit larger than 125,000 gal per min is in actual use as the question of flexibility and dependability indicate the need of multiple units beyond this capacity.

Distribution of Water from Main Canals.—Southwest Louisiana's flat prairie land was cut up into rectangular fields by the building of earth levees approximately 1.5 ft high. These fields were flooded 1 ft deep on one side and only several inches on the high side. Large volumes of water were required for unequal flooding. The method of contour leveeing was then developed and the first levees of this type were constructed on 0.5-ft intervals and were about 1 ft high. The water was led from the main canals through smaller laterals, following in general the crest of the ridges. It was then let out through wooden gates into the high points of the rice field. From here it gravitated down from one field to another through small cuts open in the levees until the entire field was flooded. Better results were obtained from this type of irrigation, and the

interval between contour levees was gradually decreased from 0.5 ft to 0.3 ft, then to 0.25 ft and to 0.2 ft; and, in some instances, these contour levees have been run on as little as 0.15-ft intervals. It is now the general practice to make these levees low and flat, to plow over them, to drill or seed over them, and later to harvest over them.

Much less water is required with the contour levees on smaller intervals. It also has a distinct advantage when one considers the increased use of the airplane in agricultural work. It would be impossible to leave the levees unplanted and unfertilized when planting and fertilizing from the air.

In addition to the marked improvement in the system of leveeing rice for irrigation, since 1951 the farmers have developed a method of land leveling. All of the prairie land in southwest Louisiana is "peppered" with small mounds or knolls spread at close intervals. These knolls are from 1 ft to 3 ft high and constitute a hinderance to irrigation. A method has been developed for removing the soil from the tops of the knolls, grading down the subsoil and replacing the top soil.

Quantities of Water Required for Irrigation

The quantity of rainfall occurring during the growing season, the temperature, and the humidity—all affect the quantity of water required for pumpage. Years ago, when most of the large irrigation systems were designed, the design factor used was for a pump and canal capacity of 10 gal per acre per min. Through the years most of the canal operators found, by actual experience, that the customary pumpage varied from 5 gal per min to 7 gal per min. The modern trend in design is to provide more pump capacity for quicker initial flooding of the fields. A rate as much as 12 gal per acre per min is recommended. Various losses occur in handling irrigation water which affect the volume pumpage required. These principal losses are evaporation and leakage. Until recently no real data were collected on either the supply or the demand of irrigation water in southwest Louisiana. The United States Geological Survey (USGS) and the State of Louisana, Department of Public Works, are now (1952) engaged in an extensive study of this problem. Research has been done by the Rice Experimental Station located at Crowley, La., and preliminary reports are available.

In 1949 the USGS and the State of Louisana determined that the pumpage required on an area of 254,000 acres of rice was 381,000 acre-ft; that is, sufficient water was pumped to flood 254,000 acres approximately 1.5 ft deep. The total acreage irrigated for rice in this area is about 600,000 acres of which 300,000 acres are irrigated from surface water. Fig. 1 shows areas of southwest Louisana irrigated by wells, and Fig. 2 shows the total acreages harvested by years since 1904. The remainder of this acreage is watered from deep wells or from a combination of surface water and ground water. Considerable variations occurred from year to year, and, whereas the year 1949 required 1.5 acre-ft per acre, the year 1948 on the same area required 2.3 acre-ft, and the year 1947 required 1.6 acre-ft. It was determined that the average pumpage used for the irrigation of each deep well in 1949 was 356 acre-ft compared with 598 acre-ft in 1948 and 393 acre-ft in 1947; and 307 acre-ft were produced by

the average well for the year 1946. Where irrigation is done by a combination of surface water and ground water, it is difficult to determine the exact proportion of water used or produced from each source as farmers normally do not keep such records. They naturally use surface water, which is cheaper to pump, as long as possible or until the supply becomes contaminated with salt water, and they then begin to use their wells or reduce the contamination of the surface water by mixing it with well water.

When the rice is young, it is affected by even small amounts of chlorides. It builds up resistance to salt with age and stands more salt in its maturity. Table 2, by B. M. Sturgis, agronomist, gives the commonly accepted tolerance of rice to salt water.

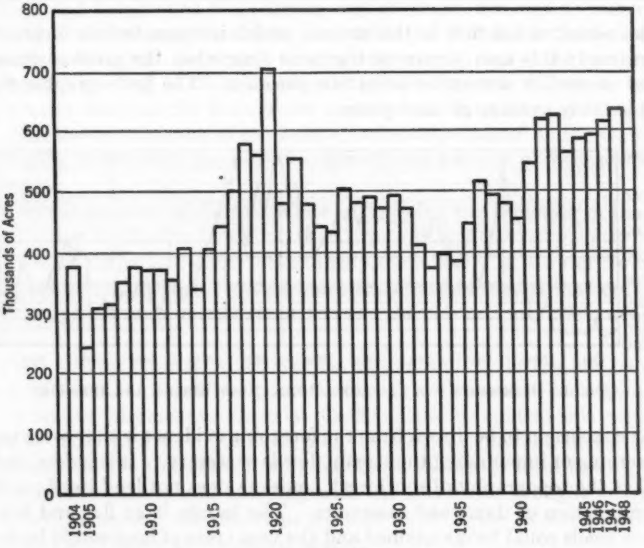

Fig. 2.—Total Acreage of Rice Harvested Annually in Louisiana

Stream Flows and Seasonal Demands for Irrigation.—The State of Louisana has been blessed naturally with one of the highest rainfalls of any state in the union—the average yearly rainfall since 1900 being about 56.4 in. Because of the hot climate, evaporation is also very high. Unfortunately for the rice industry, the maximum rainfall and attendant stream flow do not occur during the irrigation season. In the Calcasieu River at Kinder, La., the USGS has established a gaging station and Fig. 3 is a copy of their hydrographic chart of the Calcasieu River flow at this station during the year 1948-1949. The runoff in the stream at this station reaches a peak of more than 12,000 cu ft per sec on December 1, maintaining a high average until May 1. In the period from June to October the flow is well below 1,000 cu ft per sec and drops to a minimum of 400 cu ft per sec.

TABLE 2.—COMMONLY ACCEPTED TOLERANCE OF RICE TO SALT WATER

Concentration of Salts as NaCl, in Water			Relative Tolerance at Various Stages
Grains[a]	Ppm	Pressure[b]	
35	600	0.50	Tolerable at all stages; not harmful.
75	1,300	1.09	Tolerable from tillering on to heading. Rarely harmful, and only to seedlings after the soil is dry enough to crack.
100	1,700	1.42	Harmful before tillering; tolerable from jointing to heading.
200	3,400	2.84	Harmful before booting; tolerable from booting to heading.
300	5,100	4.27	Harmful to all stages of growth. This concentration stops growth and can only be used at the heading stage when the soil is saturated with fresh water.

[a] Grains per gallon. [b] Osmotic pressure, in atmospheres.

The period of low flow in this stream, which is characteristic of practically all streams in this area, occurs at the same time when the greatest demand is thrown on surface waters for irrigation purposes. The hydrographic chart in Fig. 3 is fairly average of most years.

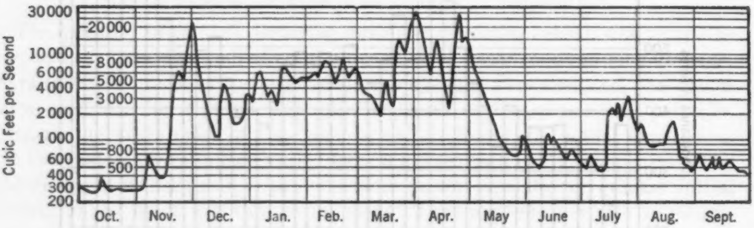

FIG. 3.—HYDROGRAPH FOR CALCASIEU RIVER, NEAR KINDER, LA., 1948–1949

The conclusion to be drawn from the foregoing evidence is that some method of conserving or impounding the stream flow is necessary. It is indeed unfortunate that the topography of southwest Louisana does not lend itself readily to the construction of dams and reservoirs. The terrain is so flat and low that only low heads could be maintained and the vast areas of land would be flooded in any impounding project. For instance, a plan to dam the Calcasieu River has been considered for many years. It is feasible to impound only 25 ft in depth, and if such a dam were constructed, only about 200,000 acre-ft could be impounded.

Salt-Water Menace.—Strange as it may seem, with the high rainfall rate in Louisana, the fresh-water situation for irrigation is becoming critical. The denuding of timber land in the upper areas of the stream basins in the state, the completion of numerous extensive drainage ditches throughout the agricultural areas, and the improvement of the lower reaches of most of the streams for navigation—have all combined to increase runoff during the heavy rainy season. They have also drained the fresh-water coastal marshes, which in the past have acted as fresh-water reservoirs. Most of the coastal streams in Louisana are deep, with large cross-sectional areas and sluggish currents. Normally these streams enter the Gulf through shallow passes. Upstream from these

passes there are usually some large shallow lakes, or some bodies of water, into which the fresh water from the streams flow before entering the Gulf. For example, the Calcasieu River has a depth of from 35 ft to 60 ft, maintaining these depths for some 50 miles above the Gulf. However, 20 miles above the Gulf this river spreads out into Calcasieu Lake with an average depth of less than 4 ft, and a width of from 10 miles to 12 miles. Originally, the pass into the Gulf maintained a depth of about 7 ft. In 1940, a 30-ft channel was dug into this lake and out into the Gulf for deep-sea navigation. The water level in this stream, even 50 miles above the Gulf, normally stands at about 1.5 ft above sea level.

The Mississippi River Commission and the United States Corps of Engineers in their laboratory at Vicksburg, Miss., constructed a model of this river about 250 ft long, and determined that, during normal times, a wedge of salt water from the Gulf moved upstream along the bottom of the channel and river at the same time that fresh water was flowing out over the top of the salt water. The hydraulic grading of these streams is so low that the difference in the specific gravity between the fresh water and the salt water creates this condition. Since the construction of the Lake Charles ship channel to the Gulf, the lower 40 miles of this river has ceased to function as a source of fresh water for rice irrigation.

Plan for Conservation of Surface Water.—Realizing the depletion of the surface fresh-water supplies in Louisana, the Corps of Engineers have constructed a series of three major salt-water locks to stop the inflow of salt water from the Gulf through the intracoastal system (and the natural streams that cross it), and to recharge the large marsh areas between the rice belt and the coast with fresh water.

The first lock on the east, which is at the eastern limit of the rice belt, is what is known as Vermilion Lock (see point A, Fig. 1). The second lock (point B, Fig. 1) is on the Mermentau River at Catfish Lake to control salt water at this point. The third lock (point C, Fig. 1) is at the junction of the intracoastal canal and the Calcasieu River, and keeps the water from flowing west into the Calcasieu River and mingling with the salt water brought in by the Calcasieu ship channel. It also stops the salt water in the ship channel from flowing eastward during the pumping season.

It has also been proposed to construct two or more dams on the upper Calcasieu—one near Kinder and one farther north. A study has also been made of the possibility of constructing skimmer locks or gates across the Calcasieu River and its tributaries above the head of the deep-sea navigation at Lake Charles. These gates or locks would not raise any appreciable head in the river, and the crest of these dams would be sufficiently below the surface to allow small boats to navigate over them. They would allow fresh water to flow over the top but would stop salt-water movement upstream along the bottom.

Ground-Water Sources

The Use of Ground Water for Irrigation.—Nature has provided the State of Louisiana with a bountiful rainfall. She has also provided a large storage

capacity for underground water, found in thick aquifers or water-bearing sands. The location of nine test wells is shown in Fig. 4, and a vertical section through these wells, prepared from electric well survey logs, is shown in Fig. 5. Paul

FIG. 4.—PART OF SOUTHWEST LOUISIANA SHOWING THE POSITION OF THE GEOLOGICAL SECTION IN FIG. 5

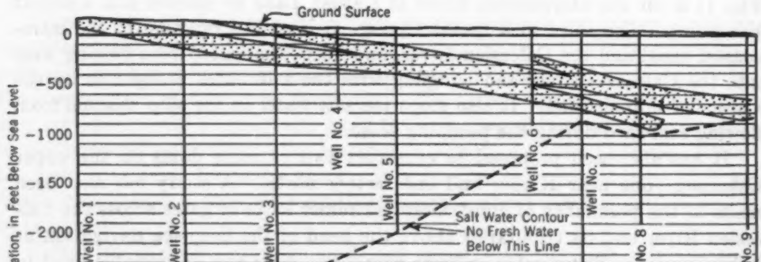

FIG. 5.—NORTH-SOUTH GEOLOGICAL SECTION SHOWING FRESH-WATER SANDS OF THE PLEISTOCENE AGE FROM ELECTRIC WELL SURVEY LOGS ON THE NINE WELLS LOCATED IN FIG. 4

H. Jones, in charge of ground-water resources surveys in this area for the USGS, reports (unpublished paper, "Depth of occurrence of Fresh Ground Water in Southwest Louisiana," January, 1950) as follows on ground waters:

"Most fresh ground water originates as precipitation entering the aquifer in the area in which it crops out and percolating through the aquifer in the direction of the hydraulic gradient. Salty water, which may have saturated the aquifer at the time of its deposition, or subsequent to it, is flushed from the updip part of the aquifer by recharge and sub-surface flow."

"Rainfall is evenly distributed by seasons in the outcrop areas of the aquifers and ranges from fifty to sixty inches a year. The rate of precipitation generally is in excess of the rate at which the aquifers can transmit the water down the dip, under existing hydraulic gradients. There is, therefore, throughout the year local ground-water discharge 'rejected recharge,' into the streams that cross the outcrop areas."

It would appear from this statement that there would always be an ample supply of ground water for every need in southwest Louisiana. The pollution of the surface streams has now increased the irrigation demands on ground water. The pumpage for rice irrigation in 1949, to irrigate 254,000 acres of rice, was about 381,000 acre-ft. Inasmuch as the demands on ground waters for rice irrigation are seasonal, nature has given an opportunity to recharge the aquifers during the 8-month period in which no pumping is done. Fig. 6 is

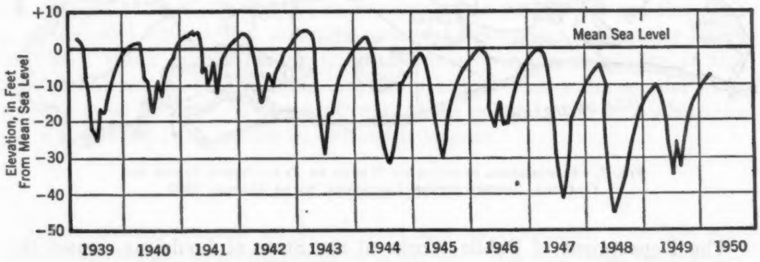

FIG. 6.—FLUCTUATION OF WATER LEVEL IN OBSERVATION WELL JD-9, THREE MILES EAST OF WELCH, LA.

a hydrograph showing the fluctuation of the water level in one well located 3 miles east of Welch, La., and covering an 11-year period. This hydrograph clearly indicates the recovery of the ground-water level when pumping ceases and also shows the maximum pull-down when pumping is in progress. It reflects a gradual lowering in the water level in the aquifers at this point from 4 ft above sea level to 10 ft below sea level after recovery has occurred.

Other Demands on Ground Water.—With the completion of the Port of Lake Charles for deep-sea navigation, a heavy industrial development of this area has occurred. These industries use large quantities of ground water for cooling and other purposes. It is estimated that during the 1949 season, the maximum industrial pumpage of ground water in the Lake Charles area was about 58,000,000 gal per day. This a constant demand and gives no opportunity for recovery of the water level in the aquifers. In the entire area surrounding Lake Charles, there has been a continuous and rapid drop in this water level with no recovery.

Fig. 7 is a map of southwest Louisiana showing the piezometric surface of the water and the pleistocene sands and gravels as of March, 1950. The fresh-water surface in the sands in the vicinity of Lake Charles has been pulled down below 50 ft. At one point in September, 1950, it was reported as low as 70 ft. Deep well pumps in this area are now (1952) being set as low as 300 ft below ground surface.

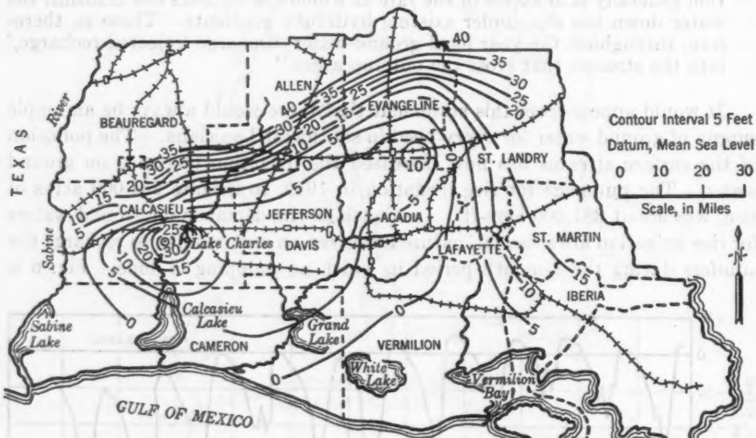

Fig. 7.—Piezometric Surface of Water in Pleistocene Sands and Gravels, Southwestern Louisiana, as of March, 1950

The Department of Public Works of the State of Louisiana, issued the following statement:[2]

"It is of grave significance that these withdrawals have resulted in an intrusion of salt water from the Gulf into the aquifers. Withdrawals of ground water for irrigation purposes have been of such magnitude and intensity that the ground water elevations along the lower limits of the rice area is lower than Gulf level during the irrigation season. This condition, aggravated by occasional dry periods such as occurred in 1924 and again in 1930, may result in salt water intrusion to the extent that a large portion of the rice producing area will have to be abandoned unless an adequate supply of surface water is made available."

The foregoing statement does not take into consideration the tremendous constant demand on underground waters for heavy industrial uses.

Protection and Conservation of Ground-Water Supplies.—From the statement quoted in the preceding section, and from a study of the piezometric surface of underground water, it is apparent that Southwest Louisiana is in need of some immediate solution of this problem and of an active conservation

[2] "Summary of Improvements Necessary for Navigation; Flood Control; Drainage; Irrigation and Alleviation of Stream Pollution in South West Louisiana," by Dewitt L. Pyburn and Leo M. Odom, Dept. of Public Works, State of Louisiana, May, 1947.

program. It has been suggested that this underground reservoir of fresh water be recharged or supercharged in some manner. The construction of a series of small impounding areas along the outcropping of the aquifers is being studied. Also some method of surcharging is needed, drilling large shallow wells for recharging these aquifers with water that is now allowed to run off as surface water during the rainy season. The lowering of the water levels in these sands from 50 ft to 70 ft below sea level, at a point only 30 miles above the Gulf coast line, creates an interesting question. Will the hydraulic pressure differences between the salt waters in the Gulf and the water pressure in the fresh-water sands now at − 50 ft cause some break-through or leakage back from the Gulf? Mr. Jones has stated that these water-bearing sands must be fairly well sealed off by a bending down of the formations along the coastal shelf and possibly a sealing off of these sands with impervious clay deposited on the Gulf floor.

In addition to the danger expressed in the foregoing paragraph, there is another source of possible pollution of these aquifers. Fig. 5 shows the contour line between salt water and fresh water in the vertical section. This is the point below which no fresh water is found in this area. This salt-water line, as plotted from the electric survey logs, rises rapidly toward the Gulf shore line, and wells drilled along the coast for fresh water are usually found brackish. There exists a grave question concerning the possibility of this underground salt water intruding into the principal fresh-water aquifer at or near the coast line and flowing northward, thus polluting the area where the heavy agricultural and industrial demand is located.

Conclusion

In his steady progress for betterment and improvement, man has constantly depleted the bountiful resources of nature. Has southwest Louisiana—by denuding its forests, by improving its surface-water runoff through improved drainage, by the construction of deep-sea and barge navigation channel and river improvements for marine traffic, by its successful bid for heavy industrial development, and by its increased agricultural activities—endangered its supply of the most necessary resource for human existence, namely, fresh water?

If this is the fact, man must bestir himself to conserve and to replenish this resource in order to maintain his supply of fresh water and food upon which life is dependent.

Source of Information

The information contained in this paper has been drawn from the following sources and the writer is indebted to these sources for most of the statistics given: The USGS—Mr. Jones, geologist in charge of ground-water investigation, and E. L. Hendricks (A. M. ASCE), hydraulic engineer in charge of surface-water investigation; the Louisiana Department of Conservation; the Department of Public Works; the Louisiana State Rice Experimental Station of which Rufus K. Walker, agronomist, is the director; John Welsh, general manager of the Sabine Canal system; Frank Everett, chief engineer of the

Acadia-Vermilion irrigation system; H. G. Chalkley, president of the North American Land Company; S. Arthur Knapp, manager of Walker Calcasieu Properties; John E. Jackson, county agent, Calcasieu Parish; the Corps of Engineers, from their Hydraulic Experimental Station at Vicksburg; F. Shutts' Sons, Consulting Civil Engineers of Lake Charles; J. Mitchell Jenkins, agronomist and retired superintendent, Rice Experimental Station; and B. S. Nelson, consultant on irrigation pumps.

DISCUSSION

LLOYD E. MYERS, JR.,[3] J. M. ASCE.—The large quantities of water required for rice irrigation are a cause for great concern in any water-deficient area in which rice irrigation is practiced. The quantity of water used for rice production in any given field is governed by a number of factors, including the cultural practices utilized by the rice grower concerned. Two factors mentioned by Mr. Shutts are land leveling and spacing of contour levees. A third factor worthy of mention is the practice of draining certain rice fields, at some time subsequent to the initial flooding, and reflooding those fields after accomplishing the purpose for which drainage was done. Although this practice is not followed by every rice grower, and in certain areas, may not be used at all, it is commonly utilized in enough areas within the United States to make it of general interest and concern. Such flood-drain-reflood cycles not only result in an increased use of irrigation water, but also have a detrimental effect on human health, comfort, and economy by increasing the production of pest mosquitoes. The importance of water conservation is common knowledge. The importance of rice-field mosquitoes may not be so well-known.

Rice fields, because of their ordinarily intense production of mosquitoes, are of considerable concern to the public health. Malaria and rice growing have been synonymous throughout history. The near-elimination of malaria in the United States has reduced the danger of anopheline malaria vector mosquitoes; but (1953), the problem of encephalitis (sleeping sickness) and the mosquito *Culex tarsalis*, which is the principal vector of this disease in the United States, has not yet been conquered. Also of concern are the pestiferous *Aedes* and *Psorophora* mosquitoes, which fly long distances and bite viciously, and thus seriously interfere with the comfort and mental health of both workers and residents in the rice growing areas. Livestock and poultry production are often reduced by these pest mosquitoes. There are records of cattle deaths which resulted from attacks by swarms of *Psorophora* mosquitoes.

Because *Anopheles* and *Culex* mosquitoes lay their eggs directly on the water, production of these mosquitoes may be slightly reduced by the flood-drain-reflood cycles. *Aedes* and *Psorophora* mosquitoes, however, lay their eggs on moist soil. The eggs usually are laid on recently drained soil and then hatch when the soil is reflooded. Each cycle of draining and flooding ordinarily produces a huge brood of these mosquitoes. The mosquitoes whose numbers may possibly be slightly reduced by the flood-drain-reflood cycles fly relatively short distances, usually less than one mile, whereas the mosquitoes whose numbers are greatly increased by the cycles fly relatively long distances. The net result is an increase in the number of mosquitoes produced in the rice fields involved, and an increase in the distance from those fields that man, livestock, and poultry will be subject to attack by mosquitoes. This result is highly undesirable.

[3] Asst. San. Engr. (R), Communicable Disease Center, Public Health Service, U. S. Dept. of Health, Education, and Welfare, Atlanta, Ga.

There are a number of reasons for the use of the flood-drain-reflood cycle, all of them based on benefits to rice production. The principal reasons are as follows:

1. Certain rice-damaging aquatic insects are not easily controlled by chemical means. When a rice field becomes infested with these insects, control is often accomplished by draining the field. The field is reflooded after the ground surface has dried enough to eliminate the insects.

2. Some rice growers believe that rice seedlings develop best in a moist, nonflooded soil, and use the flood-drain-reflood cycle for planting. The soil is thoroughly moistened by flooding the field before planting, the seed is sown by airplane in the flooded field, and the field is drained shortly after planting to permit optimum development of the rice seedlings. The field is reflooded after the seedlings are well established.

3. Rice fields are sometimes drained to check the excessive growth of rice plants which occurs under certain conditions. Such growth may result in a late crop which will not fill well, or mature. Excessive growth can be checked by draining the affected field, and drying it until the rice plants actually suffer from a lack of moisture. The field is reflooded after the growth has been checked.

Regardless of any undesirable results of the flood-drain-reflood cycle, from the standpoints of water conservation and public health, the practice is justified by the benefits to rice production. Reduction in the use of the cycle can be brought about only by the development of alternate means of accomplishing the purposes for which the cycle is used.

The flood-drain-reflood cycle is but one example of a situation associated with rice irrigation which creates problems in water conservation and public health; there are many others. Unfortunately, answers have not yet been found for most of these problems and much work remains to be done. It is hoped that investigations will develop practical answers. The relationships between water conservation, public health, and rice-cultural practices create a definite need for cooperative action on the part of the various groups concerned. Each group should become familiar with the interests and activities of the other groups. Joint interest and efforts will result in more rapid and effective solution of mutual problems than will uncoordinated and independent efforts.

E. E. Shutts,[4] M. ASCE.—Sixty-six years of rice-irrigation experience in southwest Louisiana leads to the observation that mosquitoes normally do not breed or concentrate in large quantities in irrigated rice fields. This is caused by the fact that the water in the rice fields is not stagnant, but constantly replenished and circulated. The water containing fish life is pumped from surface streams through the canal system and into the fields themselves. The fish destroy the mosquito eggs and prevent their breeding.

Sea Marshes.—What has been previously stated concerning mosquito breeding in rice fields also applies to the band of deep sea marsh extending along the entire coast of southwest Louisiana. A heavy concentration of mos-

[4] Cons. Civ. Engr., F. Shutts' Sons, Lake Charles, La.

quitoes is always found on the ridges along the marsh and in the short grass marshes that are alternately wet and dried. In the middle of the deep sea marsh, small fish life prevents the breeding or concentration of mosquitoes. During the years when the mosquito plague is greatest, mosquitoes are found in the high places in the marshes and in the prairie grass where rice is not cultivated.

Rice is not grown in water-short areas; it is only cultivated where water is abundant. However, water is never wasted as the pumping and the handling of it is too costly. Irrigation water is taken from streams or is a mixture of well and stream water. Rice plants consume water constantly until ready to head, some water evaporates, and a very minute quantity of water seeps through the ground despite the shallow hardpan. Rice irrigation aids rivers and bayous in draining land, and drainage is necessary to remove stagnant water in order to overcome mosquito plagues.

From 1913 to 1953, either as a result of natural causes or from the benefits of public health services, rice areas in southwest Louisiana and Arkansas were free of malaria and sleeping sickness. There were only a few scattered cases of malaria in southwest Louisiana during 1953, whereas fifty years previously, before the land was extensively cultivated for rice, malaria was very common. In these early days of rice culture in this area, when rice was irrigated by the Providence system (using stagnant water), rice culture may have contributed to the breeding of mosquitoes. At the present time (1953) there are no epidemics of malaria and there is a very high standard of public health in southwest Louisiana. A publication concerned with the life history of mosquitoes states that:[5]

> "The necessity of a low oxygen concentration for the hatching of 'Aedes' mosquito eggs was reported by C. M. Gjullin, C. P. Hegarty and W. M. Bollen in 1941. They found that any method, chemical or physical, caused hatching when the oxygen content of the water was reduced. They concluded that bacteria or other organisms stimulated 'Aedes' eggs to hatch by reducing the oxygen content of the water flooding 'Aedes' eggs, which are normally layed on 'dry' ground. This contradicts the early belief that heat, cold, or drying, by causing a so-called conditioning or incubation period, was a necessary prelude to hatching."

The method of irrigation used in southwest Louisiana actually increases the oxygen content in the water. If this were not so, fish life would not abound in the irrigation canals and rice fields, and this accounts for finding mosquitoes concentrated largely on marsh ridges and in prairie grass rather than in the irrigated rice fields.

[5] "Insects," *The Year Book of Agriculture*, U. S. Dept. of Agri., Washington, D. C., 1952, pp. 476–486.

AMERICAN SOCIETY OF CIVIL ENGINEERS

Founded November 5, 1852

TRANSACTIONS

Paper No. 2566

DEVELOPMENT OF A FLOOD-CONTROL PLAN FOR HOUSTON, TEX.

By Ellsworth I. Davis,[1] A. M. ASCE

Synopsis

In 1940 a detailed plan for the control of floods on Buffalo Bayou, which traverses Houston, Tex., was formulated by the Corps of Engineers, United States Army. Under this plan, two upstream detention reservoirs were constructed and some channel rectification was accomplished. Construction delays occasioned by World War II and the phenomenal growth of Houston have rendered the 1940 plan infeasible. Accordingly, the United States Congress in 1948 directed the chief of engineers to review the existing project and develop a new plan.

This paper describes the element of the 1940 Project Plan, the derivation of a new standard project flood, and two basic plans that were considered in the investigations. One basic plan provides for the diversion of most of the floodwaters into another watershed—the Brazos River. The other plan relies on rectification of the principal channels in the Buffalo Bayou watershed to pass peak discharges without appreciable damage. As a result of the investigation, it was concluded that the channel rectification plan was economically more justified.

The Flood-Control Problem at Houston

The New Orleans Flood Problem.—The two principal cities on the coast of the Gulf of Mexico, New Orleans (La.) and Houston, have one problem in common—floods—although the causes and characteristics of their floods have nothing in common. People in the United States are somewhat familiar with the problem confronting New Orleans. The Mississippi River, draining approximately 1,244,000 sq miles (or 40% of the United States), from the Alleghenies to the Rockies, flows past its door. The runoff from a storm on a

Note.—Published in December, 1952, as *Proceedings-Separate No. 159.* Positions and titles given are those in effect when the paper or discussion was received for publication.

[1] Colonel, Corps of Engrs., U. S. Army War College, Carlisle Barracks, Pa.

tributary watershed 1,000 miles away will finally make its way past New Orleans, and if superimposed upon flood runoffs from other tributary streams, creates a flood condition at New Orleans. The floods are slow to rise and slow to fall, and their crests are predictable days and even weeks in advance. Since the record flood of 1927, the city has been further protected by the raising and strengthening of its levees, by the construction of floodways to divert floodwaters to the Gulf through Lake Pontchartrain and through the Atchafalaya Basin, and by the construction of reservoirs on the headwaters of tributary rivers. In short, the flood problem at New Orleans is national in character. The flood discharges are enormous, but predictable so that ample time is provided for placing into effect the required components of its flood-control system.

The Houston Flood Problem.—On the other hand, Houston's flood problem, although just as acute, is very local in character. Buffalo Bayou, a small stream virtually unknown outside of Harris County, Texas, is the offender. Its drainage area just below its confluence with Brays Bayou is only 626 sq miles. Houston floods, therefore, are the result of local storms. These storms are of high intensity and are unpredictable. Since the topography is flat and there are few adequate natural drainage channels, the essential ingredients of a flood are constantly present.

Buffalo Bayou is important to Houston not only because it is the principal drainage channel, but also because the lower reaches, above the junction with the San Jacinto River, have been dredged to form the upper portion of the Houston Ship Channel and the turning basin of the Port of Houston. Floods on Buffalo Bayou, therefore, can inconvenience and delay shipping by causing excessive current velocities and depositing silt in the ship channel and turning basin. Any plan for the control of floods in Houston and its environs consequently must consider these current velocities and silt deposits.

Description of Buffalo Bayou Watershed

Buffalo Bayou (Fig. 1) rises in eastern Waller County and western Harris County, flows generally eastward in a narrow and tortuous channel 75 miles long, passes through the City of Houston, and enters the San Jacinto River 9 miles above Galveston Bay. The lower reaches of the bayou, as previously mentioned, have been improved as a part of the Houston Ship Channel, which affords deep draft ocean navigation to extensive terminal developments in and below Houston. The authorized project depth of the channel is 36 ft, through Galveston Bay to the Gulf.

The watershed of Buffalo Bayou lies entirely within a broad, almost featureless plain that rises gently toward the northwest with a slope of about 3 to 7 ft per mile. Surface soils consist essentially of fine sand loam and clay that are poorly drained and do not permit much percolation of surface water.

The streams in the Buffalo Bayou watershed have little or no flow during a considerable portion of the year, but are subject to high flood stages resulting from surface runoff during storms. The stream channels are small and the divides between drainage areas are not clearly defined. Consequently, during

heavy rainstorms, the streams overflow their banks and push generally southward across the divides from one watershed to the next.

Buffalo Bayou is joined in the commercial district of Houston by White Oak Bayou. Brays and Sims bayous, which pass through residential areas,

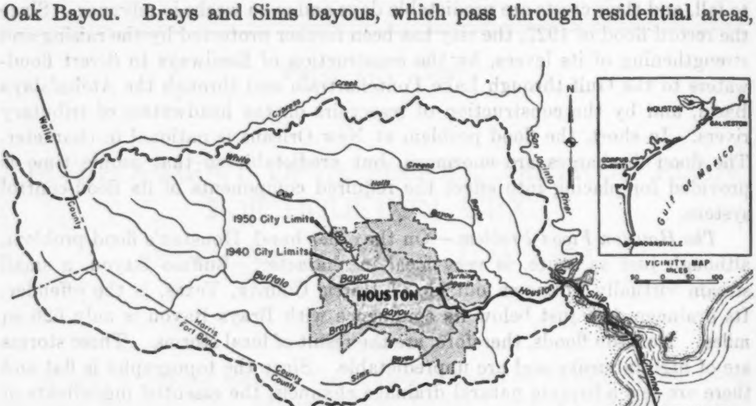

Fig. 1.—Map of Buffalo Bayou Watershed

also enter the main stream within the city. The increasing value of lands in the commercial area of the city has resulted in encroachment upon the flood plain of Buffalo Bayou by building adjacent to the channel and even over it.

Authorization of 1940 Flood-Control Plan for Buffalo Bayou

Following the disastrous Buffalo Bayou flood of December, 1935, Congress directed the chief of engineers to investigate and submit a report on a plan to improve the Houston Ship Channel, to protect it from siltation, and to provide flood control on Buffalo Bayou and its tributaries. This report was prepared by the Galveston District of the Corps of Engineers and was submitted in April, 1937. The project as proposed in the report was authorized by Congress in 1938 and modified as to terms of local cooperation in 1939. Based on this authorization, the Galveston District, in 1940, prepared a more detailed plan for flood control on Buffalo Bayou and its tributaries above the turning basin. This plan constitutes the authorized project plan.

Selection of Design Storm for the 1940 Project Plan

In order to determine the most severe storm to be expected in the basin, fifty-two storms in central and coastal Texas were investigated. Of these, three storms were selected in the development of a design storm for the project. These storms were as follows:

Storm of June 27 to July 1, 1899.—This storm, which centered at Hearne, Tex., produced greater depths over a larger area than any other storm of record

in the United States (see Fig. 2). The maximum depth of this storm was 31.4 in. in a period of three days, and the average depth over an area of 1,000 sq miles was 25.8 in.

Storm of September 6 to 10, 1921.—According to the United States Weather Bureau, the greatest 24-hr rainfall ever recorded in the United States occurred at Taylor, Tex., September 9 to 10, 1921, when 23.11 in. fell in 24 hr. In many

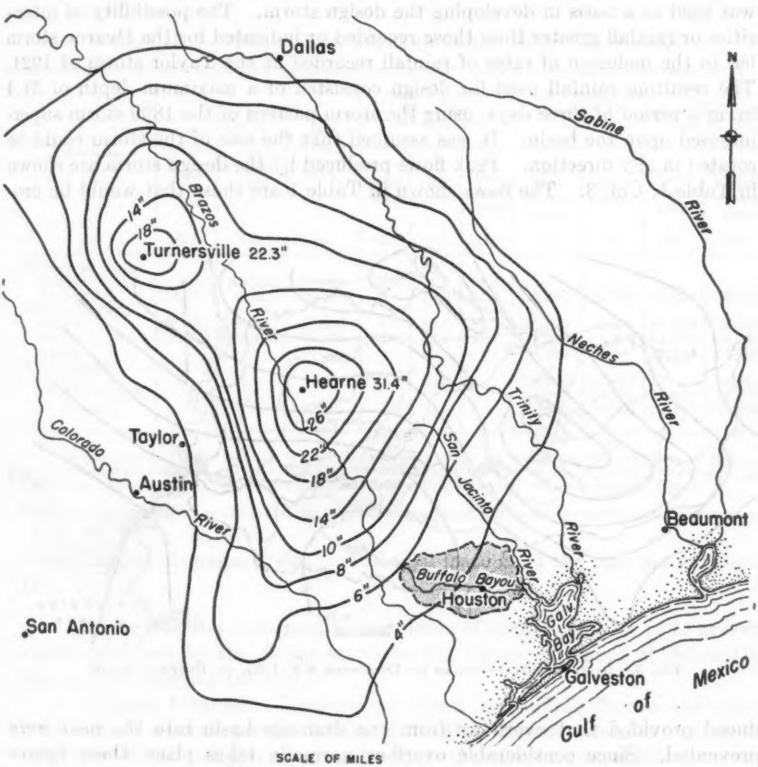

FIG. 2.—ISOHYETAL MAP—STORM OF JUNE 27–JULY 1, 1899, AT HEARNE, TEX.

places, 30 in. of rain fell in 15 hr, and in a small area north and east of Taylor, the total rainfall exceeded 36 in. Whereas the area covered by this storm was not as large as that of the 1899 Hearne storm, the depths over a basin as small as Buffalo Bayou would be considerable.

Storm of December 6 to 8, 1935.—This storm produced the maximum flood of record on Buffalo Bayou (Fig. 3). The flood caused the loss of eight lives, property damage estimated at $2,529,000, and the stoppage of traffic to the

Port of Houston for three days because of excessive currents in the ship channel. The storm produced an average rainfall depth of 14.8 in. on the watershed above the confluence of Buffalo and White Oak bayous, and resulted in the peak flows shown in Table 1, Col. 2. During this flood some overflow occurred from White Oak Bayou into Buffalo Bayou, and considerable overflow occurred from Buffalo Bayou into Brays Bayou.

The Hearne storm of 1899, which centered only 90 miles from Houston, was used as a basis in developing the design storm. The possibility of intensities or rainfall greater than those recorded or indicated for the Hearne storm led to the inclusion of rates of rainfall recorded at the Taylor storm of 1921. The resulting rainfall used for design consisted of a maximum depth of 31.4 in. in a period of three days, using the storm pattern of the 1899 storm superimposed upon the basin. It was assumed that the axis of the storm could be rotated in any direction. Peak flows produced by the design storm are shown in Table 1, Col. 3. The flows shown in Table 1 are those that would be pro-

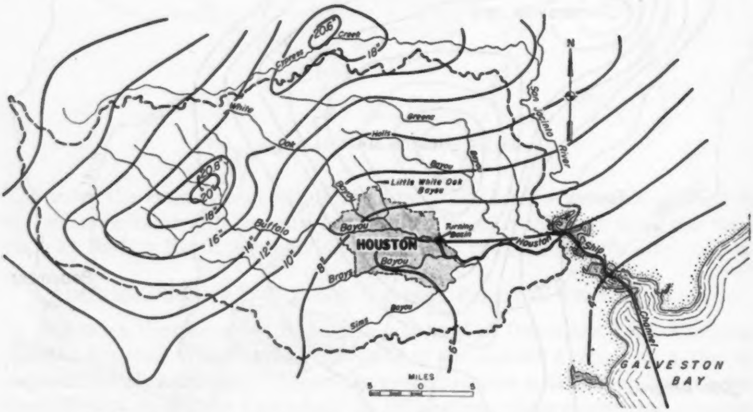

FIG. 3.—ISOHYETAL MAP—STORM OF DECEMBER 6–8, 1935, ON BUFFALO BAYOU

duced provided that overflows from one drainage basin into the next were prevented. Since considerable overflow normally takes place, these figures represent potential flows.

Local interests stated that, although ultimate protection against the design storm was desirable, they would be satisfied initially with construction that would provide protection against a lesser flood. They expressed satisfaction with protection against a storm that would develop runoffs 50% greater than those following the 1935 storm. For purposes of computation, the Corps of Engineers used the design storm for the design of the reservoirs of the flood-control plan and the storm of 1935 increased 50%, for the design of the portion of the system below the reservoirs. The 1935 storm increased 50% was transposed to critical locations in order to determine the worst flood conditions for

this rainfall. The peak flows that would be produced by this storm are shown in Table 1, Col. 4.

Development of the 1940 Project Plan

In the development of the 1940 Project Plan for flood control of Buffalo Bayou, plans for channel rectification and enlargement, regulation, and diversion were investigated. The plan as finally evolved consisted essentially of a

TABLE 1.—Peak Flow Data in Cubic Feet per Second

Location	Storm of Dec. 6–8, 1935	Design storm for 1940 Project Plan	1935 storm increased 50%	1940 Project Plan in Operation[a]			Conditions Existing in 1951		New Project Flood Plans[c]	
				1935 storm	1935 storm[b]	Design storm	Standard project storm	1935 storm[b]	Diversion plan	Channel rectification plan
(1)	(2)	(3)	(4)	(5)	(6)	(7)	(8)	(9)	(10)	(11)
White Oak Bayou										
Above[d]	...	22,700	19,300	2.6	7.4	8.5	...	...	...	...
At mouth	16,750	27,600	23,500	5.6	14.8	17.5	25,200	24,700	12,400	25,200
Buffalo Bayou										
Above[e]	40,000	84,700	60,000	8.4	19.5	24.3	26,400	22,500	27,600	26,400
Below[e]	53,000	104,400	79,500	13.6	32.8	40.7	49,200	46,200	34,300	49,200
Below[f]	...	...	...	...	...	...	74,000	70,700	52,700	74,000
Brays Bayou										
Below[g]	...	...	...	...	...	...	16,200	17,800	0	16,200
At USGS Gage	...	...	...	...	...	...	25,000	24,600	15,800	25,000
At mouth	...	...	...	...	...	...	31,200	30,700	23,000	31,200

[a] In thousands of cubic feet per second. [b] Increased 50%. [c] Comparison of peak flows of standard project flood with diversion and channel rectification plans in operation. [d] Above Little White Oak Bayou. [e] Above or below mouth of White Oak Bayou. [f] Below Brays Bayou. [g] Below Kegans Bayou.

detention and diversion system. Principal features of the plan are as follows (Fig. 4):

1. White Oak Reservoir.—A storage basin of such magnitude as to prevent runoff produced by the design storm on the upper watershed of White Oak Bayou from entering the city.

2. By-pass Channel.—Designed to divert to Buffalo Bayou the runoff produced on a small portion of the White Oak Bayou watershed, which lies outside of White Oak Reservoir and would otherwise be undrained.

3. North Canal.—A waterway to divert the floodwaters entering White Oak Reservoir into the San Jacinto River.

4. Addicks and Barker Reservoirs.—On Buffalo Bayou and tributaries, detention basins of such magnitude as to limit the runoff produced by the design storm to a maximum total regulated discharge of about 15,000 cu ft per sec.

5. Cypress Creek Levee.—To prevent overflow into Addicks Reservoir.

6. Rectification of Buffalo Bayou.—From Addicks and Barker reservoirs to the entrance of South Canal, to accommodate the maximum outflow from these reservoirs.

7. **Interception Dam on Buffalo Bayou.**—West of the city limits, to divert flood flows from this bayou into South Canal.

8. **South Canal.**—A channel of sufficient capacity to divert to Galveston Bay the regulated discharge from Addicks and Barker reservoirs, and a large portion of the flows from the uncontrolled areas west and south of them.

9. **Removal of Encroachments in Buffalo Bayou.**—Within the city, to provide protection against the runoff that would be produced below White Oak Reservoir and the interception dam on Buffalo Bayou by a storm as large as the 1935 storm increased 50%.

The peak flows (with all the features of the 1940 Project Plan in operation) that would be produced with a recurrence of the 1935 storm, the 1935 storm increased 50%, and the design storm are shown in Table 1, Cols. 5, 6, and 7. The latter two storms are centered in positions below Addicks and Barker reservoirs to produce maximum peak flows.

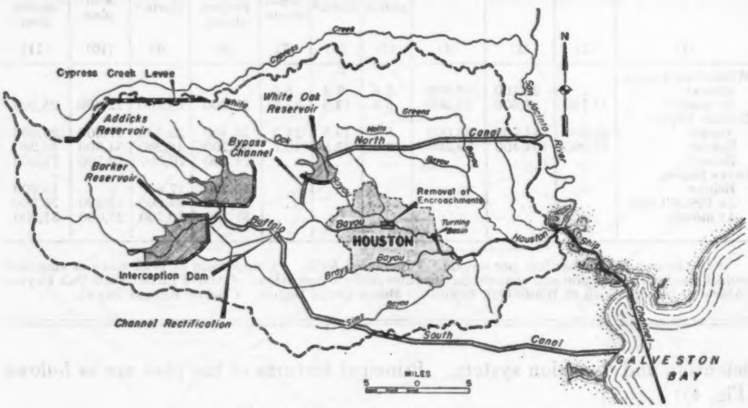

FIG. 4.—MAP OF 1940 FLOOD-CONTROL PROJECT PLAN

The only items of the 1940 Project Plan that have been completed are: (*a*) Addicks Reservoir, increased in size to eliminate the need for the Cypress Creek Levee; (*b*) Barker Reservoir; and (*c*) rectification of Buffalo Bayou downstream from the two reservoirs for a distance of 6.2 miles. These projects were completed in 1948.

NEED FOR A NEW PROJECT PLAN

Growth of Area.—The project plan was drawn up in 1940. Since that time World War II has been fought and new industries, based on newly discovered petroleum and natural gas supplies, have been developed in the Houston area. Houston, by virtue of its near-by and easily developed natural resources, its accessibility to markets through an extensive rail network, the Houston Ship Channel, and the Gulf Intracoastal Waterway, has grown vigorously. Its population increased 54% from approximately 385,000 in 1940 to 594,000 in 1950. The site selected for the White Oak Reservoir is now within the city

limits and is in a residential area. Residential areas also cover considerable portions of the rights of way of the proposed North and South canals. Furthermore, the original plan provided for protection of only that portion of the watershed above the turning basin of the Houston Ship Channel. Since the war, there has been extensive development along the ship channel below the turning basin and also along Brays Bayou, which was not considered in the initial report because it enters Buffalo Bayou below the turning basin. Brays Bayou has been the site of one of the greatest concentrations of residential and hospital development within the city. As a consequence, it is no longer feasible to complete the remaining elements of the original project plan.

In view of the foregoing facts, Congress, in 1948, directed the chief of engineers to review the 1940 authorized project and to develop a comprehensive plan for the control of floods throughout the entire Buffalo Bayou watershed. The Galveston District of the Southwestern Division of the Corps of Engineers made this review examination and survey.

Determination of Standard Project Flood for New Project Plan

Definition of Terms.—As the result of additional experience and study since 1940, and in order to achieve more uniform results in the hydrological investigations of its field agencies, the Corps of Engineers has developed the concept of a standard project storm and a standard project flood for its flood-control investigations. A standard project storm for a particular drainage area is the most severe flood-producing rainfall quantity-intensity sequence relationship and areal distribution of any storm that is considered reasonably characteristic of the region in which the drainage basin is located.

The standard project flood is the runoff from the standard project storm. The standard project flood represents a practical measure of the "flood potentiality" of a particular drainage basin, corresponding to storms and runoff conditions observed in the region on a sufficient number of occasions to demonstrate that a distinct danger exists of such a flood occurrence. The standard project flood reflects a generalized analysis of flood potentialities in a region, as contrasted to an analysis of limited flood records at the specific locality that may be misleading because of the inadequacies of records or abnormal sequences of hydrologic events. The statistical probability of occurrence of this standard project flood is not of primary importance. The principal purposes of the standard project flood are to: (*a*) Serve as a "standard" against which the degree of protection finally selected for the project may be judged and compared with protection provided at other projects of a similar nature; and (*b*) represent the flood discharge that should be selected as the design flood for the project, or approached as nearly as practicable in consideration of economic or other governing limitations, if an unusually high degree of protection is justified by hazards to life and high property values within the area to be protected.

Basis of Standard Project Flood.—The standard project flood used in the 1951 investigation of Buffalo Bayou is derived from an over-all study, by the Corps of Engineers, of all recorded major storms in the United States east of the 105th meridian for small drainage basins of 1,000 sq miles or less. The 105th meridian crosses the extreme western tip of the State of Texas and

Buffalo Bayou therefore falls within the area encompassed by this study. The rainfall criteria used in the over-all study are based primarily on an analysis of major convective-type storms and relate to a total storm duration period of 24 hr. The average depth over an area of 200 sq miles for a duration period of 24 hr was used as the unit for comparing and correlating the storms.

The average depths of 24-hr rainfall over an area of 200 sq miles for all storms that have been investigated to date were plotted in their geographical positions. Generalized isohyets representing maximum possible 24-hr rainfall over 200 sq miles were obtained from the Weather Bureau and superimposed over this map. Studies of the relationship between maximum possible rainfall and the major storms of record indicated that, in general, 50% of maximum possible rainfall includes all but about 15% of the major storms of record. Accordingly, 50% of the maximum possible rainfall in the vicinity under consideration was adopted for the standard project storm.

Selection of Rainfall Pattern.—The areal distribution of the standard project storm is determined by selecting one of four typical rainfall isohyetal patterns:

Pattern	Shape
A	Ellipse
B	Pear or tear shaped
C	Elongated and flattened ellipse
D	Similar to Pattern B except that it is elongated and flattened

The pattern is selected that gives the greatest yield when "fitted" over the watershed under investigation. Pattern B was selected for application to the Buffalo Bayou watershed since it created the greatest peak runoff. These patterns all have the same isohyetal depth values for corresponding isohyetal lines, varying from a maximum of 12 in. downward, and are adjusted to the standard project storm pattern by a constant additive value. For the Buffalo Bayou standard project storm, this value is 9.0 in. Fig. 5 shows the standard project storm as thus determined, fitted over the Buffalo Bayou watershed below Addicks and Barker reservoirs.

After fitting the standard project storm over the section of the watershed being studied, to give the maximum peak discharges, the total 24-hr storm volume is determined in the usual way, by planimetering the isohyetal patterns and determining the average depth of storm rainfall. This storm rainfall depth is then divided into four 6-hr periods in accordance with percentages determined in the over-all study. The Buffalo Bayou standard project storm has an average depth of 19 in. over 200 sq miles in 24 hr. For this depth, the time distribution of rainfall for the four 6-hr periods is as follows:

Period	Percentage of rainfall
First	9.5
Second	20.1
Third	56.7
Fourth	13.7

Infiltration losses of 1.0 in. for the first 6-hr period, and 0.6 in. for each of the three remaining 6-hr periods were then subtracted to obtain the rainfall excess. The rainfall excess was then developed into the standard project flood by means of the Snyder unit hydrograph method.[2] The coefficients used in this formula were determined from the reproduction of actual floods on Buffalo Bayou and tributaries.

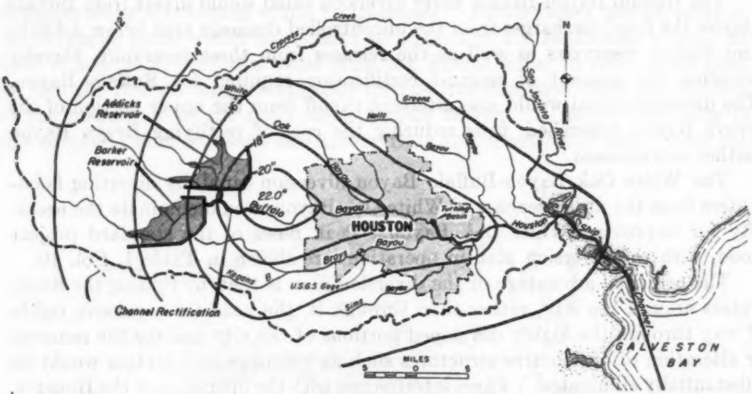

FIG. 5.—ISOHYETAL MAP OF STANDARD PROJECT STORM

The peak flows that would be produced by the standard project storm fitted over the principal parts of the Buffalo Bayou watershed, under conditions existing in 1951, with Addicks and Barker reservoirs in operation, are shown in Table 1, Cols. 8 and 9. For comparison, the peak flows that would be produced by the 1935 storm increased 50% are also shown.

PLANS OF IMPROVEMENT CONSIDERED

In an endeavor to expedite the preparation of a report that would provide a solution for the most pressing flood problems of Houston, consideration of the flood problems on the tributary streams that do not appreciably affect Houston, such as Sims, Halls, and Greens bayous was postponed. The resultant interim report consequently covers only Buffalo Bayou itself and its two principal tributaries, White Oak Bayou and Brays Bayou.

Of the numerous general plans of improvement considered, two have shown the greatest possibilities of providing flood protection at a justifiable cost. The first of these plans calls for the diversion of the bulk of the floodwaters to the Brazos River; the second provides for rectification of existing channels to pass the standard project flood safely.

DIVERSION PLAN

The basic aspect of the diversion plan (Fig. 6) is the routing of floodwaters from the upper reaches of Buffalo and Brays bayous through an artificial

[2] "Synthetic Unit Graphs," by Franklin F. Snyder, *Transactions*, Am. Geophysical Union, Part IV, 1939, pp 725–738.

channel to the Brazos River. The plan utilizes the storage effects of Addicks and Barker reservoirs, which were constructed under the 1940 Project Plan. Its main features are as follows: Addicks Reservoir; Barker Reservoir; diversion canal from Buffalo Bayou to the Brazos River, 18 miles long; diversion canal from White Oak Bayou to Buffalo Bayou, 7 miles long; rectification of Brays Bayou; and rectification of Buffalo Bayou.

The Buffalo Bayou-Brazos River diversion canal would divert from Buffalo Bayou the flood discharges from the uncontrolled drainage area below Addicks and Barker reservoirs as well as the releases from these reservoirs, thereby reducing the amount of channel rectification required for Buffalo Bayou. The diversion canal would also intercept runoff from the upper portion of the Brays Bayou watershed, thus reducing the cost of rectifying Brays Bayou farther downstream.

The White Oak Bayou-Buffalo Bayou diversion canal, by diverting floodwaters from the upper reaches of White Oak Bayou, would eliminate the necessity for improving White Oak Bayou. Peak flows of the standard project flood, with the diversion plan in operation, are shown in Table 1, Col. 10.

The principal advantage of the diversion plan is that, by routing the floodwaters around the city, rather than through it, the need for expensive rights of way through the highly developed portions of the city and for the removal or alteration of obstructive structures such as buildings and bridges would be substantially eliminated. Flood interference with the operation of the Houston Ship Channel would be reduced, but would be so very infrequent, after the channel has been enlarged to its authorized dimensions, that this advantage is relatively unimportant.

FIG. 6.—MAP OF DIVERSION PLAN

Opposed to these advantages are the difficulty and expense of maintaining two artificial diversion canals having a combined length of 25 miles. Experience has shown that, with the high annual rainfall in the area and the long growing season, channels are quickly grown up in weeds which, of course,

effectively reduce channel discharge capacity. The diversion canals would also necessitate the construction of several highway and railroad bridges, pipe-line crossings, and siphons for irrigation ditches. Another disadvantage of the diversion plan is that the Brazos River could be in flood at the same time that floodwaters from the Buffalo Bayou watershed were being discharged through the diversion canal to the Brazos River. In such an event flood damages along the Brazos would be increased. Furthermore, the capacity of the diversion canal would be reduced as a result of the backwater effect. In fact, it is possible that the water from the Brazos River in flood could back up into the Buffalo Bayou watershed through the diversion canal thus adding to the magnitude of the flood along Buffalo Bayou. A further difficulty of this proposed plan is a legal one arising from the diversion of water from one

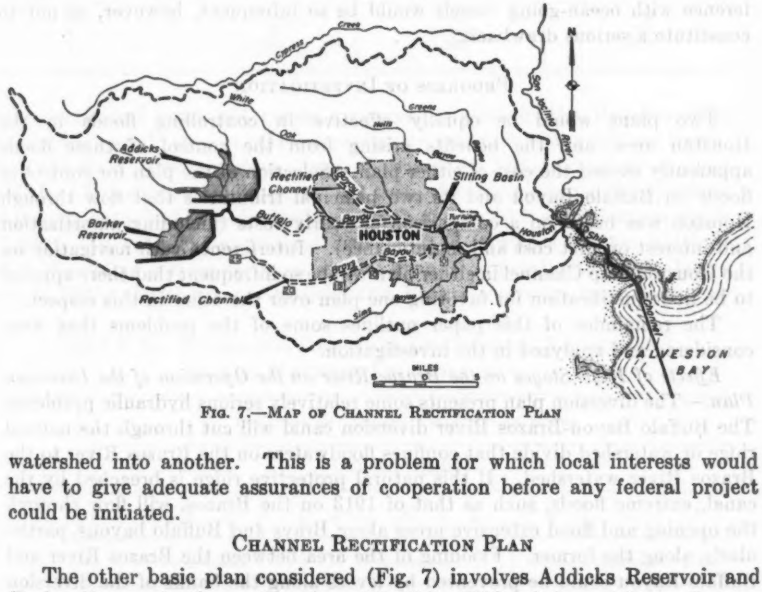

Fig. 7.—Map of Channel Rectification Plan

watershed into another. This is a problem for which local interests would have to give adequate assurances of cooperation before any federal project could be initiated.

Channel Rectification Plan

The other basic plan considered (Fig. 7) involves Addicks Reservoir and Barker Reservoir, the rectification of Buffalo, White Oak, and Brays Bayous so they would carry within their banks the runoff from the standard project storm as regulated by Addicks and Barker reservoirs, and the dredging of a silting basin immediately upstream of the turning basin to reduce the amount of silt deposit in the turning basin and the ship channel. Peak flows of the standard project flood with this plan in operation are compared with those of the diversion plan in Table 1, Cols. 10 and 11.

The principal advantage of this plan is the elimination of the two artificial diversion canals required by the diversion plan. The elimination of these channels would result in a substantial reduction in maintenance since only the rectified natural channels would have to be maintained. The legal complica-

tions of diverting water from one watershed to another would also be eliminated.

Disadvantages of the plan are that it would necessitate the removal or alteration of a substantial number of existing installations, including buildings and bridges, and would require very costly rights of way, particularly through the highly developed commercial and residential portions of the city. Another problem is that of disposing of approximately 8,100,000 cu yd of material excavated from within the city. The foregoing disadvantages could be overcome to a large extent by lining the channels to permit the use of smaller cross sections having the same discharge capacities. Comparison of the over-all costs of channel rectification, with and without lining, show that on White Oak Bayou and portions of Brays Bayou, channel lining is justified.

Flood discharges would interfere with barge navigation on the Houston Ship Channel somewhat more frequently than with the diversion plan. Interference with ocean-going vessels would be so infrequent, however, as not to constitute a serious drawback.

Progress of Investigation

Two plans would be equally effective in controlling floods in the Houston area, and the benefits arising from the control of these floods apparently exceed the cost of either plan. Selection of the plan for control of floods on Buffalo Bayou and its two principal tributaries that flow through Houston was based on a comparison of yearly costs (including amortization and interest on first cost and maintenance). Interference with navigation on the Houston Ship Channel in either plan will be so infrequent that there appears to be little justification for favoring one plan over the other in this respect.

The remainder of this paper outlines some of the problems that were considered and analyzed in the investigation.

Effects of High Stages on the Brazos River on the Operation of the Diversion Plan.—The diversion plan presents some relatively serious hydraulic problems. The Buffalo Bayou-Brazos River diversion canal will cut through the natural ridge or watershed divide that confines floodwaters on the Brazos River to the Brazos River watershed. If this natural protective ridge is breached by the canal, extreme floods, such as that of 1913 on the Brazos, will flow through the opening and flood extensive areas along Brays and Buffalo bayous, particularly along the former. Flooding of the area between the Brazos River and Buffalo Bayou could be prevented by levees along the banks of the diversion canal and along upper Brays and Buffalo bayous, with outlet structures for minor tributaries. However, if the upper reaches of Brays Bayou or Buffalo Bayou were in flood, the resulting flooding in those areas would be considerably more severe since the flows would be affected by the Brazos River backwater in the diversion canal.

Examination of past rainfall over the Buffalo Bayou watershed in the area above the diversion canal to the Brazos River, and of coincident past floods on the Brazos River, reveals that once in about every 3 to 5 years Brays and Buffalo bayous would be discharging into the Brazos River when the Brazos River is above flood stage, resulting from either runoff from its own watershed or in combination with discharge from Brays and Buffalo bayous. The average

annual damage on Buffalo and Brays bayous because of backwater from the Brazos River, and the damage to the Brazos River watershed as a result of discharges from the diversion canal would be subtracted from the benefits arising from the diversion plan.

Effects on Navigation in the Houston Ship Channel of the Diversion and Channel Rectification Plans.—Any plan for the control of floods in the Buffalo Bayou watershed must not create excessive currents in the Houston Ship Channel that would stop or otherwise seriously interfere with maritime traffic. The 1935 flood (the maximum flood of record on Buffalo Bayou) stopped traffic for three days. However, at that time, the channel immediately below the turning basin had been dredged to a depth of only 30 ft and a bottom width of 150 ft. In 1951, the authorized depth was 36 ft with a bottom width of 300 ft, providing a cross-sectional area of channel approximately 84% larger than in 1935. Furthermore, Addicks and Barker reservoirs have been constructed and they reduce the discharge and consequently the velocities through the ship channel.

TABLE 2.—ESTIMATED FREQUENCY OF CURRENT VELOCITIES IN THE HOUSTON SHIP CHANNEL

Current velocity (miles per hr)	Frequency of Current Velocities in Years		
	1951 conditions	Diversion plan	Channel rectification plan
2	3	43	8
4	37	1,000	500
7	1,000	1,000	1,000

TABLE 3.—ESTIMATED DURATION OF CURRENT VELOCITIES IN THE HOUSTON SHIP CHANNEL

Frequencies (years)	Duration of Current Velocities in Hours								
	Current Velocities								
	2	4	7	2	4	7	2	4	7
	1951 conditions			Diversion plan			Channel rectification plan		
5	33	0	0	0	0	0	0	0	0
10	43	0	0	0	0	0	17	0	0
25	55	0	0	0	0	0	31	0	0
50	62	14	0	6	0	0	39	0	0
100	67	23	0	16	0	0	45	0	0

Table 2 shows the estimated frequency at which current velocities in the Houston Ship Channel could be expected to occur under 1951 conditions and with the diversion and channel rectification plans in effect. Frequencies shown for diversion and channel rectification plans are based on the assumption that

the channel has been dredged to authorized dimensions. Frequencies shown under "1951 Conditions" are based on actual channel dimensions at that time.

Table 3 shows the estimated duration, in hours, of current velocities, in the Houston Ship Channel, through a frequency range of from 5 yr to 100 yr, under 1951 conditions and with the diversion and channel rectification plans in effect.

From Tables 2 and 3 it may be seen that under either plan interference with ocean-going ship traffic would be negligible. Since the tow boats used for barge transportation along the Texas Gulf Coast usually have less than 400 hp, interference with barge traffic would be somewhat greater. However, this traffic is more flexible because of its shorter haul distances, and its fixed operating expenses are less than for ocean traffic. Consequently, interference with barge traffic would be relatively insignificant under either plan.

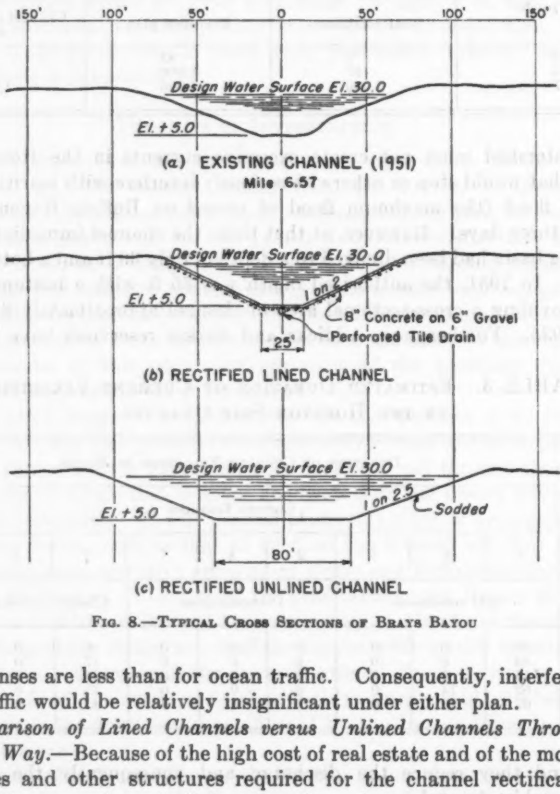

FIG. 8.—TYPICAL CROSS SECTIONS OF BRAYS BAYOU

Comparison of Lined Channels versus Unlined Channels Through Costly Rights of Way.—Because of the high cost of real estate and of the modifications to bridges and other structures required for the channel rectification plan, consideration was given to lining the channels to reduce the channel cross section, and consequently the requirements for real estate, bridge widening, and modifications to structures. Lined channels have the further advantage of lowering annual channel maintenance costs. In addition, channel lining of Buffalo and White Oak bayous would largely eliminate the scouring effects of

the floodwaters and make unnecessary the silting basin upstream from the turning basin of the ship channel.

The effectiveness of channel lining in reducing the width of the rectified channel of Brays Bayou is shown in Figs. 8 and 9. It may be seen from Fig. 9 that, for the channel rectification plan, the reduction in top width varies from approximately 100 ft near the upper end of the project to approximately

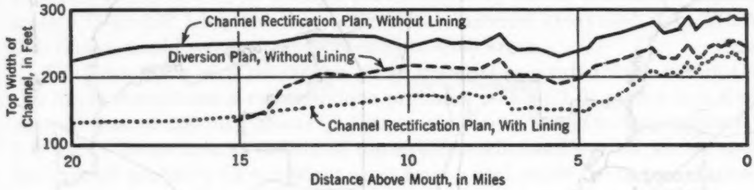

FIG. 9.—PROFILE OF BRAYS BAYOU

50 ft near the mouth of the bayou. In fact, as shown in Fig. 9, Brays Bayou, if lined for the channel rectification plan, is narrower than the unlined rectified channel of the diversion plan.

The studies of costs of several plans of channel rectification showed that partial lining of the bottom and lower portions of the sides of Brays Bayou would retain most of the advantages of full channel lining and would, of course, be more economical.

There are fewer advantages for lining Buffalo Bayou than for Brays Bayou. Between the turning basin and the mouth of White Oak Bayou, only 1,800,000 cu yd of material would have to be removed. The channel section in this

TABLE 4.—ESTIMATED EXCAVATION QUANTITIES FOR CHANNEL RECTIFICATION PLAN

Channel	Channel Excavation, in Cubic Yards	
	Capable of being disposed of alongside channel	Requiring transportation to spoil areas
Buffalo Bayou	5,300,000	1,800,000
Brays Bayou	5,300,000	6,300,000
White Oak Bayou	2,100,000	0
Totals	12,700,000	8,100,000
Total excavation	20,800,000	

reach is generally adequate, the required work consisting essentially of trimming occasional restrictions and providing bulkheads or retaining walls for the local treatment of encroaching structures and improvements. Above the mouth of White Oak Bayou, the channel of Buffalo Bayou is adequate. Rectification in this area would consist of cutting through circuitous bends in the channel. The 5,300,000 cu yd of material so removed would be placed in the abandoned

river bends. Channel lining is not economically justified, therefore, on Buffalo Bayou.

White Oak Bayou, on the other hand, requires lining because of its steep slope, which averages 3.7 ft per mile on the rectified alinement. For the standard project flood, velocities as high as 10 ft per sec in an unlined rectified

FIG. 10.—POTENTIAL SPOIL DISPOSAL AREAS

channel would result. These velocities would cause excessive scour unless the channel were lined.

Disposition of Large Amounts of Spoil Excavated Within City Limits.—Under the channel rectification plan, assuming that Buffalo and Brays bayous are not lined, approximately 20,800,000 cu yd of material would have to be ex-

cavated in widening, deepening, and straightening Buffalo, Brays, and White Oak bayous. From Table 4 it may be seen that of this amount 12,700,000 cu yd could be deposited alongside the bayous or in bends that have been cut off and abandoned as a result of channel straightening. The disposal of this material could be done with conventional, heavy earth-moving equipment and, consequently, creates no unusual problem. The remaining 8,100,000 cu yd, however, would have to be transported through city streets to suitable disposal areas. It should be noted that none of the material excavated from White Oak Bayou would require transportation to spoil areas.

The disposition of 8,100,000 cu yd of material excavated from within the city limits constitutes a rather unique problem. This fill, if placed in a spoil disposal area of 250 city blocks (2.5 acres per block), would be approximately 8 ft high. In an area as devoid of topographic relief as Houston, such a spoil bank would probably be a distinct asset from a real estate development viewpoint. The possibilities of this, however, cannot be explored until the excavation is actually made. Consequently, unit costs used in estimates do not include any credit for such land enhancement.

The development of reasonably accurate unit costs for the excavation of 8,100,000 cu yd of material and its removal by truck from the vicinity of the channels is dependent on locating adequate spoil disposal areas in or near the city. Reconnaissances on the ground, supplemented by the use of aerial photographs, disclosed suitable areas, as shown in Fig. 10, with capacities exceeding the requirements. Use of these areas has not been confirmed at this stage of the investigation, nor do the areas indicate all the possible ones. Furthermore, it is quite possible that a substantial portion of the 8,100,000 cu yd could be deposited locally in low spots or in old bayou bends that are cut off in the channel straightening. However, reconnaisances do indicate generally the availability of adequate disposal areas.

The maximum length of haul to the areas shown in Fig. 10 is 2.5 miles. However, to provide for the possibility that all the areas might not be available when the project is under construction, an average haul of 5 miles was used in the estimates.

As a result of these studies and investigations, it was concluded that the channel rectification plan would be more economically justified to provide for the control of floods on Buffalo Bayou and its two principal tributaries that flow through the City of Houston, than would the diversion plan.

Acknowledgments

The writer, as district engineer of the Galveston District, Corps of Engineers, under whom the investigation was conducted, had general supervision over the project. Information and data used in this paper were derived largely from the following:

Kenneth Heagy (M.ASCE), chief, Engineering Division, Galveston District; E. A. Weiser, chief of the Buffalo Bayou Report Section, and E. H. Brown, chief of the Hydraulics and Hydrology Section, both being under the

general supervision of A. B. Davis, Jr., chief of the Planning and Reports Branch, Engineering Division, Galveston District; K. V. Speeg (A.M.ASCE), Fort Worth District, Corps of Engineers; and Albert L. Cochran (M. ASCE), Office, Chief of Engineers. In addition, information was obtained from Howard Jensen, engineer for the Harris County Flood Control District, and Henry R. Norman (M.ASCE), consultant to the Harris County Flood Control District.

AMERICAN SOCIETY OF CIVIL ENGINEERS
Founded November 5, 1852

TRANSACTIONS

Paper No. 2567

CHARACTERISTICS OF FIXED-DISPERSION CONE VALVES

By Rex A. Elder,[1] A. M. ASCE, and Gale B. Dougherty,[2] J. M. ASCE

With Discussion by Messrs. Edwin W. Murphy; Rodolfo E. Ballester; T. T. Siao; Verne Gongwer; and Rex A. Elder and Gale B. Dougherty

Synopsis

The Tennessee Valley Authority (TVA) has installed and operated five fixed-dispersion cone valves at the Chatuge, Fontana, Nottely, and Watauga projects. The hydraulic laboratory of the TVA has been closely associated with the design of the dissipating structures which were placed around these valves (known as "Howell-Bunger" valves) and has therefore made prototype observations of their performance. The Fontana and Watauga installations were made in enclosed conduits so that all air drawn into the valve area must be supplied through long air passages. Although the air demand is a function of the structure surrounding the valve, observations have been made at these installations to yield an indication of the air demand conditions. Correlation of the observations of operation of the dissipating structures and the air demand quantities have led to the formulation of ideas as to the mechanics of the air demand.

In addition to the prototype observation studies made by the hydraulic laboratory, the staff was also delegated to prepare accurate ratings of these valves for use in operating them as integrated parts of the TVA multipurpose water system. These valves were rated by field measurement of the discharge, and of the differential pressures in the conduit upstream from the valve. Sufficient data were obtained, also, to allow calculation of the discharge coefficients. These tests were run on valves with diameters of 78 in., 84 in., and 96 in., and covered gross heads from 26 ft to 296 ft.

Introduction

Essentially the valve analyzed in this paper is a cylindrical gate mounted with the axis horizontal. When open, the flow is deflected by a conical end

Note.—Published in September, 1952, as *Proceedings-Separate No. 153*. Positions and titles given are those in effect when the paper or discussion was received for publication.

[1] Head, Hydr. Lab. Section, TVA, Norris, Tenn.

[2] Hydr. Engr., TVA Hydr. Lab., Norris, Tenn.

piece mounted with the apex upstream and issues from the valve as a diverging hollow conical jet. Fig. 1 shows a typical valve and valve installation. The deflector cone is connected to the valve body by vanes that connect the two parts and act as guides to the external sleeve. The external sleeve, which controls the valve opening, seats against the cone and retracts over the outside of the valve body. The sleeve is moved by means of screws, connected by shafting and gearing to the operating motor and controls. The position of this sleeve is shown on an indicator dial which is directly connected to the driving mechanism. With the dial properly graduated and calibrated, the valve can be set readily and accurately to any desired discharge. Since the sleeve does not operate against water pressure, the force required to open or close the valve is only that necessary to overcome the frictional resistances of

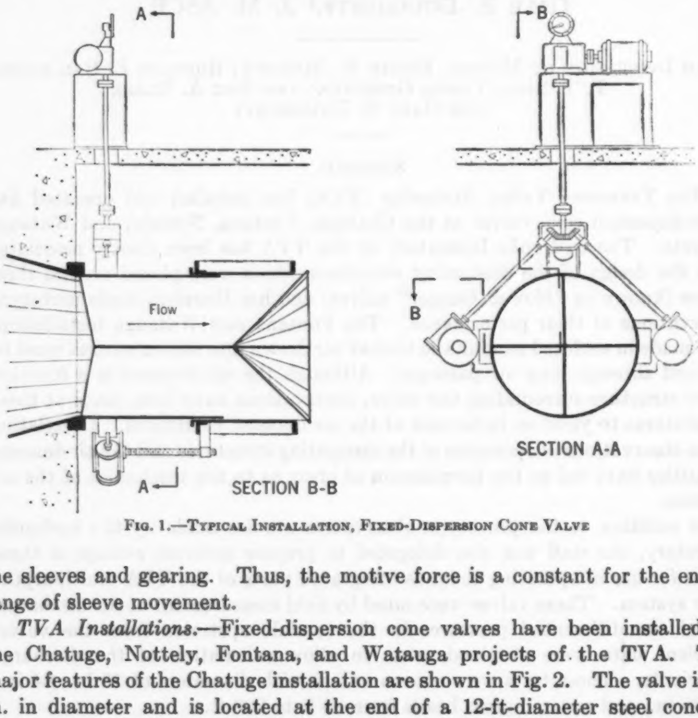

FIG. 1.—TYPICAL INSTALLATION, FIXED-DISPERSION CONE VALVE

the sleeves and gearing. Thus, the motive force is a constant for the entire range of sleeve movement.

TVA Installations.—Fixed-dispersion cone valves have been installed at the Chatuge, Nottely, Fontana, and Watauga projects of the TVA. The major features of the Chatuge installation are shown in Fig. 2. The valve is 78 in. in diameter and is located at the end of a 12-ft-diameter steel conduit 769.5 ft long. The valve discharges into an open-type energy dissipating structure. Two rings of piezometers are provided in the transition section immediately upstream from the valve for flow metering purposes. This valve operates between heads of 59 ft and 128 ft with a maximum expected head of 133.3 ft. The Chatuge Reservoir stores water during the wet season and releases it through the valve during low-water periods. The project was

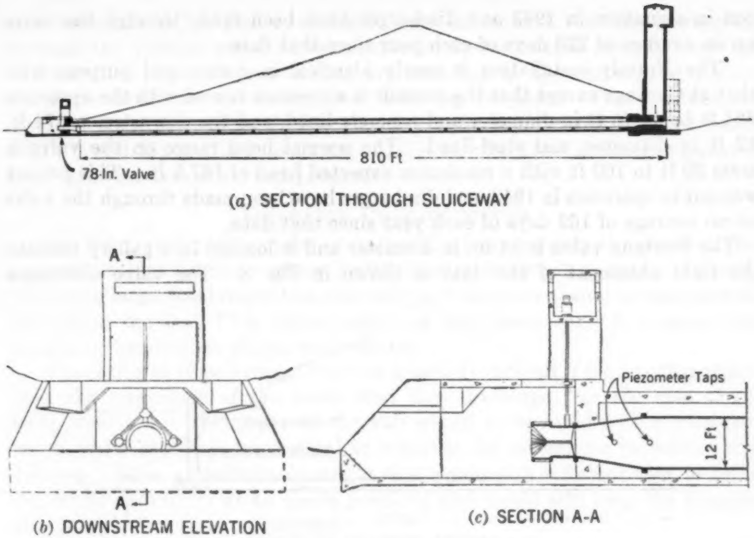

Fig. 2.—Valve Installation, Chatuge Project

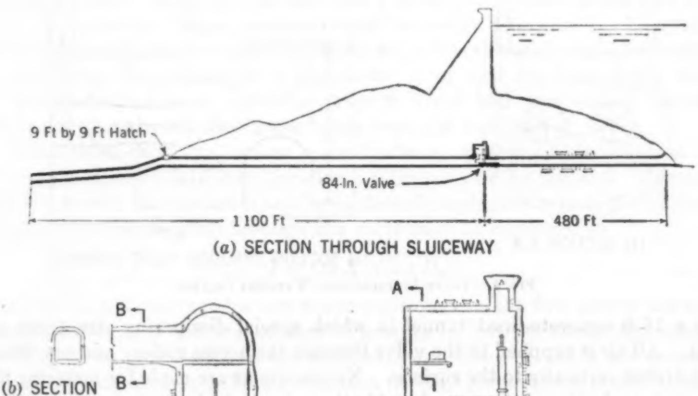

Fig. 3.—Valve Installation, Fontana Project

put in operation in 1943 and discharges have been made through the valve on an average of 223 days of each year since that date.

The Nottely installation is nearly identical in design and purpose with that at Chatuge except that the conduit is a pressure tunnel with the upstream 364 ft being 15 ft in diameter and concrete-lined, and the downstream 374 ft, 12 ft in diameter, and steel-lined. The normal head range on the valve is from 20 ft to 160 ft with a maximum expected head of 167.9 ft. This project was put in operation in 1943, and discharges have been made through the valve on an average of 162 days of each year since that date.

The Fontana valve is 84 in. in diameter and is located in a gallery beneath the right abutment of the dam as shown in Fig. 3. The valve discharges

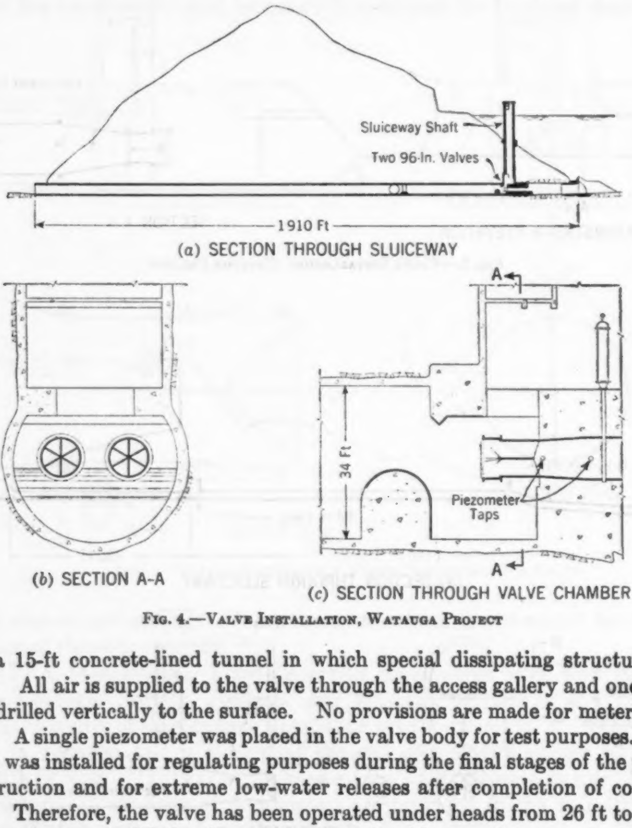

FIG. 4.—VALVE INSTALLATION, WATAUGA PROJECT

into a 15-ft concrete-lined tunnel in which special dissipating structures are built. All air is supplied to the valve through the access gallery and one 36-in. vent drilled vertically to the surface. No provisions are made for metering the flow. A single piezometer was placed in the valve body for test purposes. This valve was installed for regulating purposes during the final stages of the project construction and for extreme low-water releases after completion of construction. Therefore, the valve has been operated under heads from 26 ft to 346 ft. The maximum possible head would be 382.1 ft with a maximum operating head of 373 ft.

The Watauga installation consists of two 96-in. valves located in a tunnel, 34 ft in diameter, beneath the right abutment of the dam. Special dissipating

structures, shown in Fig. 4, are built into the tunnel. All air is supplied through the vertical access tower (diameter, 25 ft) located directly over the valves. Two rings of piezometers are installed in the rectangular section upstream from the valves for flow metering purposes. These valves are installed for reservoir regulation purposes and are operated between heads of 109 ft and 253 ft with a maximum of 275.4 ft. To date (1952) they have not been operated except for test purposes.

Discharge Characteristics

The integrated multipurpose operation of a large number of projects makes accurate ratings for the various hydraulic structures a necessity. Accurate ratings for large, fixed-dispersion cone valves at all sleeve positions were unavailable when the first TVA valves were put into operation. A program was initiated, therefore, to obtain such ratings.

The rating of large hydraulic valves is usually difficult if for no other reason than the magnitude of the water that they discharge. In the case of the tests presented in this paper all the valves had to be rated with a minimum use of water as it was impractical to schedule the ratings for periods of high releases. Thus, a method was sought that would give sufficient data to define the rating accurately at all sleeve positions and would still keep the quantity of water discharged at a minimum.

At all installations a means was found for measuring, in the conduit immediately upstream from the valve, a differential pressure proportional to the discharge. These differential pressures could be measured quickly with only a small usage of water and thus a value, proportional to the discharge, for a large number of sleeve positions could be readily determined. In addition to the differential pressures, the hydraulic grade-line elevation could be obtained by measuring the pressure at a piezometer at or near the base of the valve. All installations were at operating projects which had permanently installed headwater recorders so that gross heads were also available.

With these data and one or more discharge measurements taken at any gate position and headwater elevation a rating can be determined. Assuming that the flow in the conduit is near or in the fully turbulent region, the discharge (in cubic feet per second) through the valve may be expressed as

$$Q = C_G A \sqrt{2 g H_G} \qquad (1)$$

in which C_G is a constant for any sleeve position; A is the flow area of the valve in square feet; g is the acceleration of gravity in feet per second per second; and H_G is the gross head on the valve in feet. Since A and g are constants for any given valve and C_G is a constant for any given sleeve position, transposition of the terms to—

$$\frac{Q}{\sqrt{H_G}} = C_G A \sqrt{2 g} \qquad (2a)$$

—gives an equation which has the variables on the left and a constant, f, for each sleeve position on the right, thus:

$$\frac{Q}{\sqrt{H_G}} = f \qquad (2b)$$

Assuming that fully developed turbulent flow exists in the conduit leading to the valve, the discharge may be expressed as

$$Q = K \sqrt{\Delta P} \qquad (3)$$

in which ΔP is the pressure difference between two points in the conduit expressed in feet of water and K is a constant for the particular conduit. Combining Eqs. 1 and 3 the equation—

$$C_G A \sqrt{2 g H_G} = K \sqrt{\Delta P} \qquad (4)$$

—will result, from which by transposition,

$$K \sqrt{\frac{\Delta P}{H_G}} = C_G A \sqrt{2 g} \qquad (5)$$

As the right-hand terms of Eqs. 2*a* and 5 are identical,

$$\frac{Q}{\sqrt{H_G}} = K \sqrt{\frac{\Delta P}{H_G}} \qquad (6)$$

Since in Eq. 2*b* $\frac{Q}{\sqrt{H_G}}$ is a function of the sleeve position, the quantity $\sqrt{\frac{\Delta P}{H_G}}$ in Eq. 6 must also be a function of a sleeve position with the numerical values differing by the factor K. Thus, a semi-log plotting of $\sqrt{\frac{\Delta P}{H_G}}$ versus sleeve position will give a curve of the same shape as the curve of a semi-log plotting of $\frac{Q}{\sqrt{H_G}}$ versus sleeve position. Since values of ΔP and H_G were readily obtainable for each sleeve position, the shape of the curve would be established. With one or more points on the $\frac{Q}{\sqrt{H_G}}$-curve, the entire curve could then be drawn by fitting the $\sqrt{\frac{\Delta P}{H_G}}$-curve through these points. Actually, in practice, the plots were made as $\frac{\Delta P}{H_G}$ versus sleeve position and $\frac{Q^2}{H_G}$ versus sleeve position because of the ease of computing these values. Since the semi-logarithmic plot was used, the computation of the square of both log terms was permissible.

The definition of the curve for $\frac{Q}{\sqrt{H_G}}$ versus sleeve position is all that is required to rate any given valve installation. However, for future design purposes and for comparison of results from the several valves tested, the discharge coefficient is desirable.

The discharge coefficient for a fixed-dispersion cone valve can be defined in terms of net head at the base of the valve and an area which, for the purposes defined herein, can be taken as the net flow area in the valve body, thus:

$$C = \frac{Q}{A \sqrt{2 g H}} \qquad (7)$$

in which C is the coefficient of discharge for a given sleeve position and H is the net head at the base of the valve.

The flow Q could be determined from the curves of $\frac{Q}{\sqrt{H_G}}$ versus sleeve position, and the area A was obtained by actual measurement of the valve; H, however, could not be measured directly in the field but could be computed since the pressure head at or near the base of the valve was obtained by field measurement and the velocity head could be computed after the discharge was determined.

Rating of the Fontana Valve.—The application of these methods can be illustrated best by describing the Fontana rating. To obtain the discharge rating, only the differential pressures between two points in the closed conduit above the valve for known sleeve position and headwater elevations, and one or more discharge measurements for known sleeve positions and headwater elevations, were required. The computation of the discharge coefficient required, in addition, the measurement of the pressure head at or near the base of the valve, the area of the conduit at the point of pressure head measurement, and the measurement of the flow area in the valve body.

Differential Pressures.—The differential pressures were measured between the downstream end of a 3-in. by-pass line around the vertical slide gate, which is just upstream from the valve, and a piezometer which was drilled into the body of the valve. The connection to the downstream side of the by-pass line could be readily made in the valve chamber, as a flushing arrangement which opened into the valve chamber had been provided in the piping. The piezometer in the valve body was specially placed for these tests.

The range of heads tested and the type of equipment available at the laboratory at the time of the various tests were such that no set method was used in making these measurements. Six series of tests were made with one or more of the following methods being used during each test:

1. Measurement of the hydraulic grade-line pressure with water, mercury, and bourdon gages, and a special electrical recorder which used a bourdon tube pickup. The differentials were then determined by taking the difference in hydraulic grade-line elevations.
2. Measurement of the differential pressures by air-water or water-mercury differential gages and by the special electrical recorder with a differential bellows-type pickup.

Sleeve Positions.—For rating purposes, the sleeve position as given by the indicator dial on the driving mechanism was all that was required. The indicator dial was divided into one hundred divisions. The pointer was fairly rough but the divisions were large enough in comparison with the pointer to make the estimation of 0.1-division positions possible. The indicator read 0.75 when the sleeve was closed and 98.5 when opened as far as the limit switches would allow. For comparison of the results with other valves, the actual sleeve travel was necessary. The travel was measured with a steel tape, and a comparison between indicated sleeve position and the actual travel was thus determined.

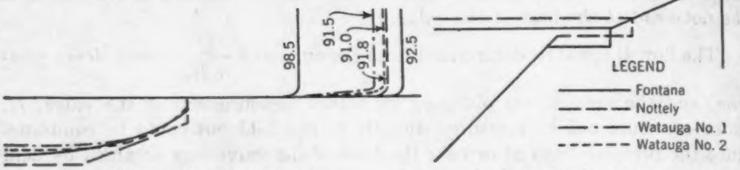

(*a*) COMPARISON OF LIP SHAPES (*b*) SLEEVE SEAL COMPARISON

FIG. 5.—COMPARISON OF FLOW AREAS, FIXED-DISPERSION CONE VALVES

Headwater Elevation.—The headwater elevations were obtained from the chart of the water-stage recorder near the center of the dam. The instrument was checked against the actual water surface after each test and the error, if any, was subsequently removed from the data.

Discharge Measurements.—Opportunities for making field measurements of discharge were infrequent because of the necessity for generating power as a war emergency measure and the fact that the valve discharge could not be separated from the turbine discharge in the river below. Five tests were made during periods when the turbines were shut down and sufficient time and water were available to allow the river flow to stabilize before the measure-

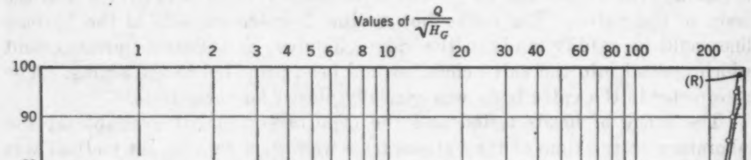

FIG. 6.—SLEEVE POSITION IN RELATION TO $\sqrt{\frac{\Delta P}{H_G}}$ AND $\frac{Q}{\sqrt{H_G}}$ AT FONTANA DAM

ments were started. The discharges for these tests were obtained from current meter measurements made in the river channel. These measurements were made by personnel of the United States Geological Survey (USGS) with selected meters and using the best techniques known for this type of measurement.

Six discharge values were obtained from a stage-discharge curve that had been prepared by the USGS for a temporary channel through the construction area. These values were taken for periods when the turbines were not discharging and when the valve was held at a constant discharge for sufficient time for the stage to stabilize. One extremely low discharge measurement was made by calculating the flow over the weir on the outlet structure.

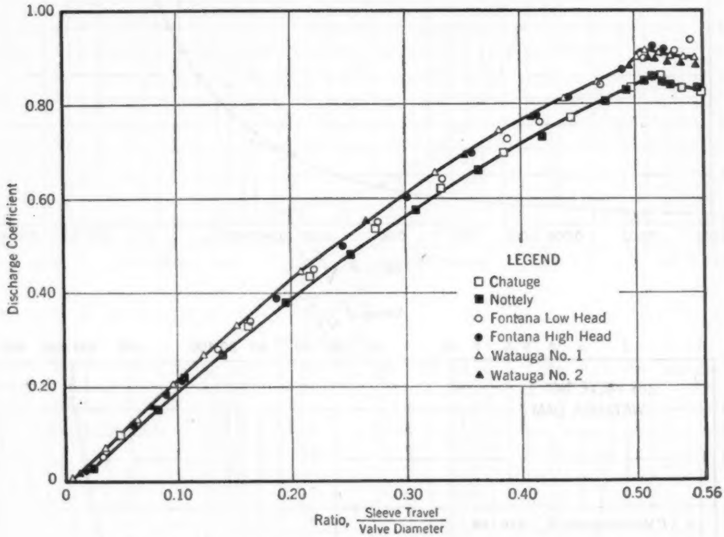

FIG. 7.—DISCHARGE COEFFICIENTS, FIXED-DISPERSION CONE VALVES

Pressure Head.—The pressure head was measured at the base of the valve by use of the special piezometer placed there for differential pressure measuring purposes. The pressures were obtained by water, mercury, or bourdon gages, or by a special electrical recorder which used a bourdon-type pickup.

Flow Area of Body.—On the Fontana project there was a difference between the flow area of the body and the area at the point of pressure head measurement. The actual dimensions of the valve necessary for computing this area were obtained by field measurement. The shape of the outlet end of the body and the seal area of the cone were also determined (Fig. 5).

Test Procedure.—In general, the test procedure was to set the valve sleeve at about ten different positions during the opening cycle and then to set positions midway between each of these on the closing cycle. If any

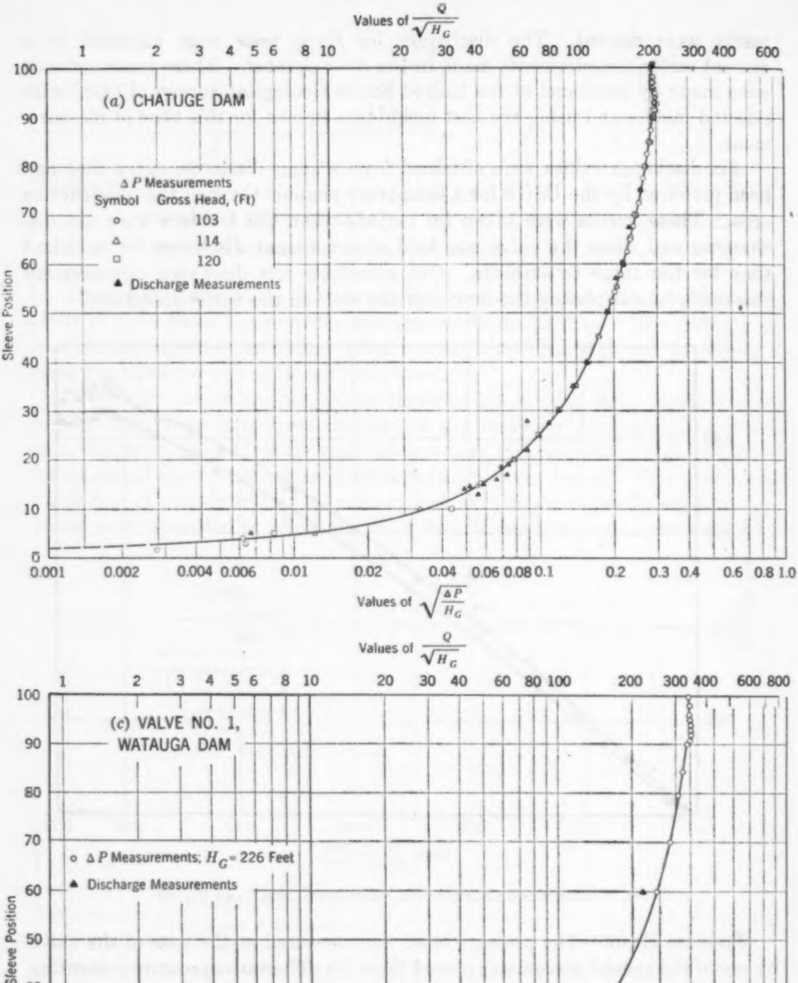

FIG. 8.—SLEEVE POSITION IN RELATION TO $\sqrt{\frac{\Delta P}{H_G}}$

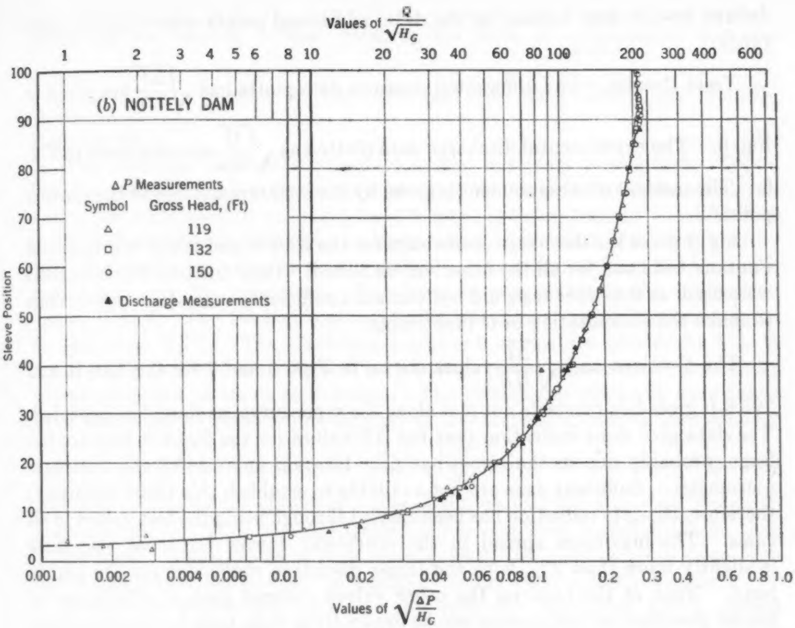

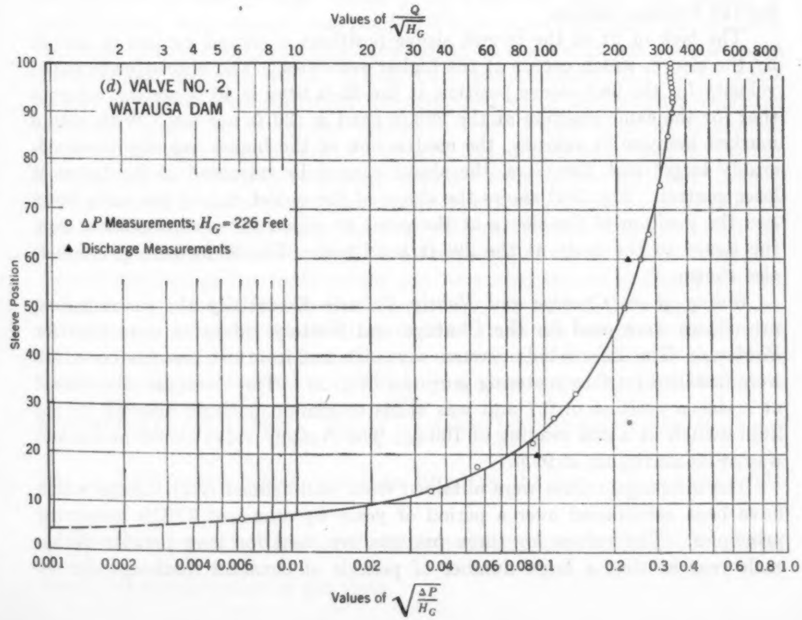

AND $\frac{Q}{\sqrt{H_G}}$, FIXED-DISPERSION CONE VALVES

definite breaks were noticed in the data, additional points were taken in that range.

Tests Results.—The differential pressure data plotted as $\sqrt{\frac{\Delta P}{H_G}}$ are given in Fig. 6. The experimental discharge data plotted as $\sqrt{\frac{Q}{H_G}}$ are also given in Fig. 6. The method of measurement is given by the letters appended to the plotted points.

Fig. 7 gives the discharge coefficients for the 32.0-ft and 295.8-ft gross-head Fontana tests and for all the other valves tested. Only the two Fontana tests were used, as the other tests did not contain a sufficient range of sleeve positions to make the computation of C practicable.

The C-values and $\sqrt{\frac{\Delta P}{H_G}}$-values shown in Figs. 6 and 7 for the 32.0-ft and 295.8-ft gross-head tests do not plot along the same curve, as should be expected. The data give some indication that the ΔP-values for the 295.8-ft test are too large, probably due to the somewhat poor location and size of the upstream piezometer. Sufficient data are not available to establish this point definitely; therefore, the data reduction has been carried through using the test values in all cases. The maximum spread in the coefficient curves for these two tests is slightly more than 2%, with the larger discharge coefficient for the higher head. None of the tests on the other valves covered such a wide range of heads; therefore, no conclusions can be drawn from these tests to aid in evaluating the Fontana results.

The lack of fit at the largest sleeve positions is caused by loss of control by the sleeve, which occurs at the higher velocities. The approximate outlet velocity for the 98.5 sleeve position at the 32-ft head is 40 ft per sec, whereas that for the same position at the 296-ft head is 120 ft per sec. With such a marked increase in velocity, the contraction at the higher velocity is considerably larger and, therefore, the sleeve cannot be retracted as far before it loses control. Fig. 5(*a*) shows the shape of the outlet end of the valve body and the position of the sleeve at the point at which the control shifted from the sleeve to the body at the 296-ft head test. The 98.5-sleeve position is also shown.

Rating of the Chatuge and Nottely Valves.—Essentially the same testing procedures were used for the Chatuge and Nottely valves as were used for Fontana. The differential pressures were obtained from two piezometers which were installed for flow metering purposes (Fig. 2). The Chatuge valve closed at a sleeve position of 0.7 and was at its maximum position allowed by the limit switch at a dial reading of 100.5. The Nottely valve closed at 0.9 and was at its maximum at 99.6.

The discharge values were obtained from well-defined river ratings which have been established over a period of years by standard USGS measuring principles. The valves for these projects are used for long periods during each year so that a large number of periods of constant discharge can be

found in the records. These data, in the form of $\frac{Q}{\sqrt{H_G}}$-points and the $\sqrt{\frac{\Delta P}{H_G}}$-points, are plotted in Figs. 8(*a*) and 8(*b*) for Chatuge and Nottely, respectively.

The pressure head was measured at the upstream piezometer. Therefore, the pressure head at the base of the valve for use in the coefficient determination was computed by reducing the measured pressure head by the difference in the velocity heads at the two sections, and a friction loss was computed by Manning's equation using an n-value of 0.011. Average values of the hydraulic radius and velocity were used. No allowance was made for the contraction losses, if any. The friction loss correction was almost negligible, being equal to less than 0.3%. The discharge coefficient values are plotted in Fig. 7.

Rating of the Watauga Valve.—The Watauga valves were rated by essentially the same means as those at Fontana. The differential pressures were taken from two rings of piezometers located in the transition section immediately upstream from the valve (Fig. 4). The $\sqrt{\frac{\Delta P}{H_G}}$-values are plotted in Figs. 8(*c*) and 8(*d*). The valves closed at a sleeve position of 3.0 and were tested to positions above 100 as the limit switches had not been installed at the time of the tests. Since the tests were made (1950), the limit switches have been set at the 92 position so that "overgating" of the valve could not occur.

These two valves are used for any reservoir regulation which cannot be supplied by the turbines. Since 1949, when the valves were placed in operation, the water supply has been such that valve regulation has not been required. Therefore, the ratings have had to be made with but one discharge measurement for each valve. These two measurements had to be made at a river section that contained the combined valve and turbine discharge and which was affected by the backwater from Wilbur Dam in Tennessee. Since Wilbur Lake contains only 72 acres, it was impossible to hold the pool at a constant level during the discharge period. Because the Watauga turbines were not rated at the time of these measurements, two discharge measurements had to be made for each test, the first with the turbine and valve and the second with the turbine alone. As a consequence of the poor measuring conditions, the ratings for these valves can be considered as preliminary only, and the data are included in this report solely to extend the range of valve sizes tested. Although the accuracy of the data is not comparable with that for the Fontana, Nottely, and Chatuge valves, the observations should be usable for design purposes and will give a close approximation for valves that cannot be rated easily. The $\sqrt{\frac{\Delta P}{H_G}}$-values for both valves were combined into a single curve, which was then fitted to the two $\frac{Q}{\sqrt{H_G}}$-values. The $\sqrt{\frac{\Delta P}{H_G}}$-values for each valve have been plotted separately in Figs. 8(*c*) and 8(*d*) merely for simplification of the plots.

The pressure head was measured at the downstream piezometer, which is located 8 in. upstream from the base of the valve. The pressure head at the base of the valve was computed by subtracting the difference in velocity heads at the two sections from the measured value. Because of the short length between sections no allowance was made for friction or other losses. The discharge coefficients are plotted in Fig. 7.

Comparison of Results.—The results of these discharge rating tests can best be observed in Fig. 7. In general, the coefficient of discharge increases for any given ratio of sleeve travel to body diameter as the body diameter increases. The Fontana data indicate an increase in C with an increase in head but (see under the heading, "Rating of the Fontana Valve; Test Results") this may be explained by possible incorrect differential pressure values.

Each of the valves had a definite break in the curve at a sleeve position of about 90 to 95. This break is caused by the loss of control by the sleeve as it is retracted past a certain position. The point at which this occurs probably is a function of the valve body outlet shape and the velocity of the water through the valve. The Fontana, Nottely, and Watauga valves have been measured. The shapes of the outlet end of the body and the position of the sleeve at the break point in the curve are shown in Fig. 5. Fig. 5(b) shows the shape of the seal part of the cone for Fontana and Nottely. Justification of the theory that the velocity of the jet controls the position of sleeve for the break point is shown in Fig. 5(a). The slope of a line tangent to the body and to the sleeve, at the position for the break in the curve, increases as the velocity decreases. The Fontana valve, which was tested at a 296-ft gross head, has the flattest slope; the Watauga valves, which were tested at a 226-ft head, have the next flattest slope; the Nottely valve which was tested at heads of from 120 ft to 150 ft was next, and the 32-ft Fontana test did not exhibit a break at the maximum gate position. Naturally a decrease in discharge coefficient means a decrease in discharge; therefore, the maximum discharge for these valves does not necessarily occur at maximum gate position.

Operational Characteristics of Valves.—The TVA has experienced no operational troubles with any of the valves it has in service. They do exhibit two definite characteristics of operation, neither of which is of importance if the valve is operated properly. At settings of 3 to 5 on the dial above the closed position a loud, piercing howl develops. If the valve were to be operated for any length of time at such a position, the noise would be annoying to any personnel close at hand. The existence of the noise indicates a vibration phenomenon that could be harmful to the valve if operated at such a position for extended periods of time. There is some indication that, on the same valve, the noise occurs at smaller openings for low heads than it does for higher heads.

The second operational characteristic of these valves is the vibration that occurs after the break point in the discharge curve is reached. The vibration is worse just beyond the break point and decreases as the sleeve is further retracted. This is undoubtedly explained by a continual shift of control between the sleeve and the body. There is no reason to open the sleeve past the break point. Therefore, once the break point is determined, the limit switches can be set to cut off at that point and this vibration thus cannot occur.

Characteristics of Associated Structures

The associated structures for the fixed-dispersion cone valves used on TVA projects have been built to satisfy two requirements: (1) The energy of the jet must be dissipated sufficiently to prevent channel erosion and to provide for suitable downstream velocities; and (2) the air demand of the valve should be satisfied and kept to a minimum. These requirements have been met in the TVA installations under two different conditions: (*a*) The installation of the valve at the end of a sluice and discharging into the river channel; and (*b*) the installation of the valve in a chamber and discharging into a conduit.

Chatuge and Nottely Projects.—The open discharge type of installation has been used at Chatuge and Nottely dams. The Chatuge installation will be described because the two projects differ in only minor details, and what is true of one is true of the other. Because the valve was placed at a very low level it was necessary to protect the stream channel from erosion at the point of impact of the lower part of the jet. It was also necessary to limit the horizontal spread of the jet and confine it to the stream channel. These requirements were met by combining, into one structure, a short stilling basin to absorb the energy and deflect the lower part of the jet, and a box-type deflector placed downstream from the valve to deflect the diverging jet into the channel. The details of the structure at Chatuge can be seen in Fig. 2. The deflected jet is confined to the stream channel. The operation has been very satisfactory and only minor erosion has occurred downstream from the structure after several years of use. The air required by the jet is drawn through an opening 12 ft by 16 ft directly over the valve. There is a perceptible movement of air toward this opening when the valve is discharging. No measurements of air demand have been made on this installation because of the adequacy of the supply and the difficulty of isolating the flow.

Fontana Project.—An enclosed valve has been used at Fontana (North Carolina), and at Watauga, and South Holston (both in Tennessee). In these installations, air demand was an important consideration in the selection of the type of energy dissipators or velocity reducers to be used.

The 78-in. valve installed at the Fontana project controls the low-level outlet. The valve discharges into a tunnel (diameter, 15 ft) leading to the river channel downstream from the dam. The energy-dissipating structure was required to reduce the downstream velocities and was built as shown in Fig. 3. When the valve is opened the upper part of the jet strikes the roof, is broken up by the two projecting fingers, and is deflected by the wall back onto the tunnel invert. The air required by the jet is drawn through the 8-ft by 8-ft access gallery and an overhead air vent 3 ft in diameter.

Model tests had indicated that slight changes in deflector structures greatly changed the air demand. A model design that produced minimum air demand was developed and used. However, even with a minimum demand, it was recognized that large quantities of air would be required although quantitative values were unobtainable from the model tests. The somewhat oversize access gallery was constructed to meet this anticipated air requirement. Because of the unknown quantitative value, a prototype check program was scheduled

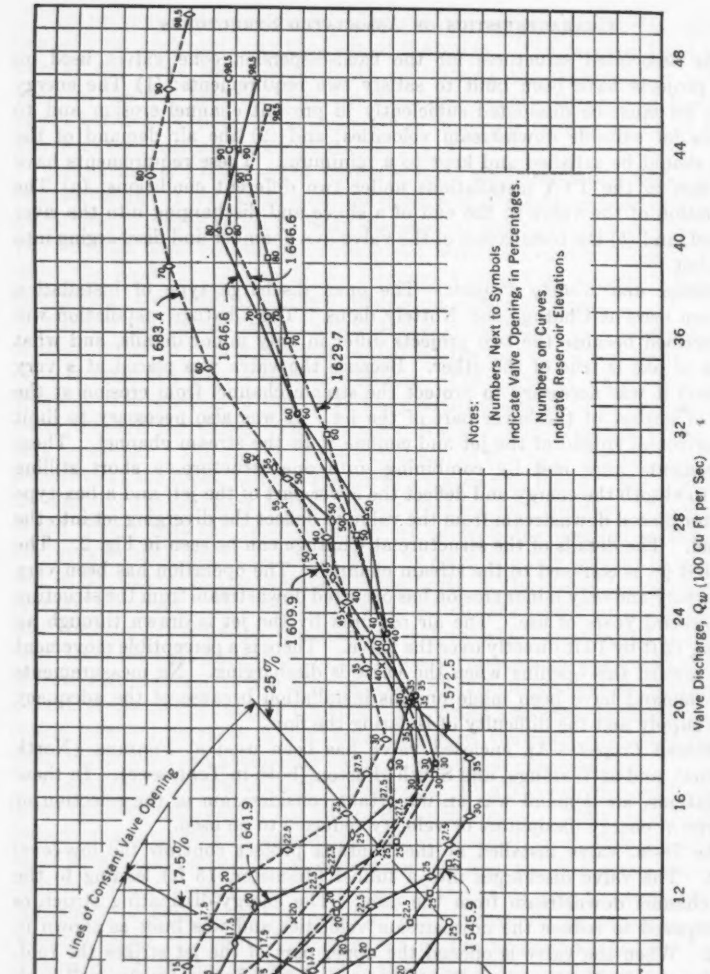

FIG. 9.—PROTOTYPE PERFORMANCE; AIR DEMAND FOR VALVE ON THE FONTANA PROJECT

to determine the air demand for various operating heads and sleeve positions. The air velocity was measured in the 8-ft by 8-ft gallery with an anemometer held at various points in the cross section. The readings were averaged and recorded to the nearest mile per hour. The air supplied by the 3-ft vent could not be measured because of the drip pan installed beneath it, and it could not be plugged because of the inaccessibility of the upper end. Therefore, the data apply only to the air drawn through the gallery. The quantity of air required was computed as the product of measured average wind velocity and the cross-sectional area of the gallery. The gallery is 8 ft by 8 ft with 2-ft fillets in the upper two corners resulting in an area of 60 sq ft. The valve discharge was determined from the valve rating table for the sleeve position

TABLE 1.—AIR-WATER RATIO, FONTANA PROJECT (TVA)

Sleeve Position	Gross Head, H_G, in Feet										
	168.0	188.6	208.8	235.4	272.8	292.6	304.8	309.5	309.5	346.3	Average
2	...	...	...	...	...	...	...	...	...	62.4	62.4
2.5	43.3	41.7	...	...	...	...	...	...	...	...	42.5
3	...	...	34.2	38.6	36.2	...	33.3	...	...	40.8	36.6
4	...	24.0	...	...	...	...	...	...	...	...	24.0
5	16.0	15.2	15.5	15.7	15.8	15.5	14.9	...	...	15.9	15.56
6	...	11.2	11.4	11.9	11.5	...	11.7	...	10.6	10.4	11.24
7.5	8.39	6.83	...	...	...	...	...	...	...	...	7.61
8	...	...	6.93	6.65	7.53	...	7.13	...	6.66	6.80	6.95
10	4.88	4.60	4.70	4.74	4.78	4.29	4.88	...	4.29	4.50	4.63
12.5	3.58	3.05	3.38	3.26	3.37	...	3.20	...	...	3.17	3.29
15	2.42	...	2.36	2.41	2.52	2.19	2.44	...	...	2.42	2.39
17.5	1.79	...	1.87	1.82	1.92	...	1.95	...	...	1.96	1.885
20	1.338	...	1.383	1.435	1.535	1.308	1.604	...	1.270	1.605	1.435
22.5	...	...	1.053	1.143	1.241	...	1.140	...	...	1.217	1.159
25	0.888	...	0.868	0.818	0.918	0.839	0.959	...	...	0.915	0.887
27.5	...	...	0.720	0.679	0.773	...	0.759	...	...	0.775	0.741
30	...	...	...	0.565	0.656	0.592	0.695	0.576	0.576	0.664	0.618
35	...	...	...	0.486	0.587	...	0.556	0.539	0.539	0.611	0.553
40	...	...	...	0.557	0.578	0.547	0.565	0.533	0.533	0.575	0.555
45	...	...	...	...	0.591	...	0.577	...	...	0.550	0.573
50	...	...	...	...	0.590	0.498	0.527	0.470	0.501	0.563	0.525
55	...	...	...	...	0.591	...	0.574	...	...	...	0.582
60	...	...	...	...	0.594	0.472	...	0.500	0.500	0.588	0.531
70	...	...	...	...	...	0.468	...	0.491	0.480	0.566	0.501
80	...	...	...	...	...	0.448	...	0.490	0.480	0.535	0.488
90	...	...	...	...	...	0.432	...	0.431	0.442	0.473	0.444
98.5	...	...	...	...	...	0.386	...	0.384	0.412	0.425	0.402

at the time of velocity measurement. The air demand versus the water discharge is plotted in Fig. 9. As the valve opened, the air demand increased rapidly to a maximum at a sleeve position of 8. As the sleeve was opened farther, the air demand decreased until a sleeve position of 30 was reached. Beyond this point, the air demand increased slowly but never was as large as it was at sleeve position 8. Fig. 9 indicates that the air demand increased with increased head.

A fairly definite relationship was found for the air-water ratio at each sleeve position for the range of heads tested. Table 1 gives the ratios for each test point and Fig. 10 is a curve based on the average of all test points. From Fig. 10 it will be noted that the air-to-water ratio decreased rapidly until a

sleeve position of 35 was reached, after which little effective change in ratio occurred. To illustrate the magnitude of the air requirement problem, Fig. 11 has been prepared from the curve in Fig. 10. These two curves give the velocity of the air through the access gallery for the maximum demand and for full-valve opening demand.

The model tests proved definitely that the air requirements are a function of the deflector structure design. Therefore the data that have been presented are only applicable for a structure identical to that built at Fontana. The operation of the valve caused water to splash into the rear of the chamber. Splashing began at a sleeve position of about 15. At a sleeve position of 25 the splash reached to the top rear of the operating chamber, a distance of about 45 ft. There was a definite relation between the amount of splashing and the air demand; that is, as the splashing increased the air demand decreased.

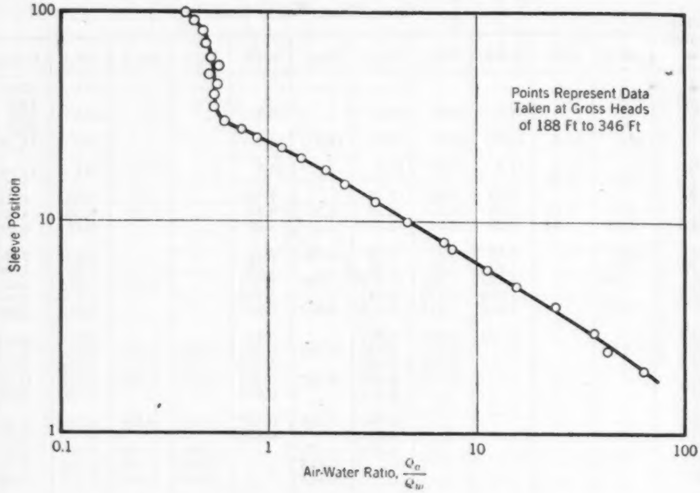

FIG. 10.—SLEEVE POSITION IN RELATION TO $\frac{Q_a}{Q_w}$, FONTANA LOW-LEVEL OUTLET

Watauga Project.—The two 96-in. valves at Watauga, like Fontana, are built to discharge into a tunnel. The design for this installation was developed by means of model studies (Fig. 4). The two valves are set side by side. A 15-ft-high by 15-ft-thick weir is placed 11.5 ft downstream from the valve to absorb the energy of the lowermost part of the jet. The upper part of the jet strikes the roof deflector and is deflected down beyond the weir. These structures provided proper flow conditions in the tunnel downstream.

The air supply is drawn down the tower through a 10-ft by 12-ft grated opening at the top. Prototype tests to determine the air demanded by this installation were made at the same time as the preliminary rating measurements. Since a very minimum volume of water had been made available for the rating

tests, it was not possible to secure readings at sufficiently close intervals to define the air-demand curves fully or to obtain data for dual valve operation.

The air demand was measured during the rating tests by using the open grate as an orifice. A micrometer, zero-reading, differential manometer was constructed to measure the pressure drop through this grate. The air demand was pulsating; therefore it was necessary to set the micrometer at an average setting. The air volumes were calculated using an orifice coefficient of 0.61 and the net area of the intake opening as 110.3 sq ft (Fig. 12). The air demand for single valve operation reaches a maximum at a sleeve position of 20 and decreases gradually to a maximum valve discharge. The air pulsations are very noticeable, not only because of the rattling of the doors but also because of the aural discomfort to personnel in the shaft. An aneroid barometer placed in the operating chamber pulsated over a range of 0.2 in. of mercury at a frequency of about 50 cycles per min.

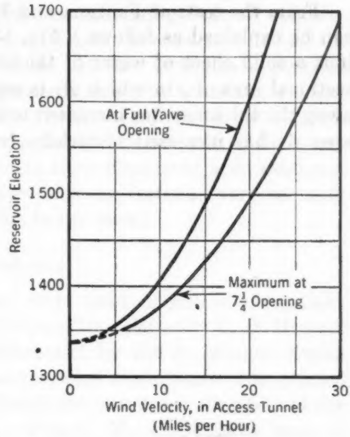

FIG. 11.—WIND VELOCITIES IN THE ACCESS TUNNEL (PROTOTYPE PERFORMANCE), FONTANA PROJECT

As a single valve was opened, splashing over or behind the valves began at about sleeve position 10. The first splashing was in the form of a backward jet of water which was directed across and over the adjacent valve. Further sleeve movement pulled this jet over until it struck the wall between the valves with a sound similar to several rivet hammers. With further opening,

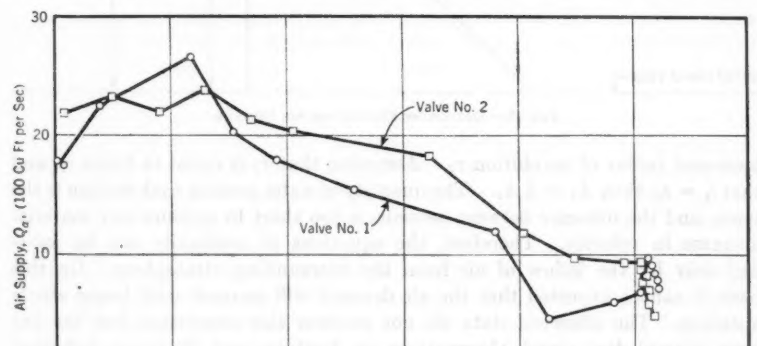

FIG. 12.—AIR DEMAND, FIXED-DISPERSION CONE VALVE AT WATAUGA PROJECT (GROSS HEAD H_G, 226.6 FT)

a swirling motion was imparted to the water which caused it to follow the tunnel walls passing under the valves and splashing it back over the top of them. This splashing finally covered the valves completely. As at Fontana, correlation of the measured air demand and the observed flow conditions indicated that the greater the splash the smaller the air demand would be.

From the tests at Fontana and Watauga the air demand and its variation can be explained as follows. Fig. 13 shows that, as the jet leaves the valve, it is a solid sheet of water of thickness t_1, radius of revolution r_1, and cross-sectional area A_1, in which A_1 is equal to t_1 times $2\,\pi\,r_1$. At some distance away the thickness has increased to t_2 due to the expansion of the jet, and the area A_2 has increased materially because of the increase in t and also the

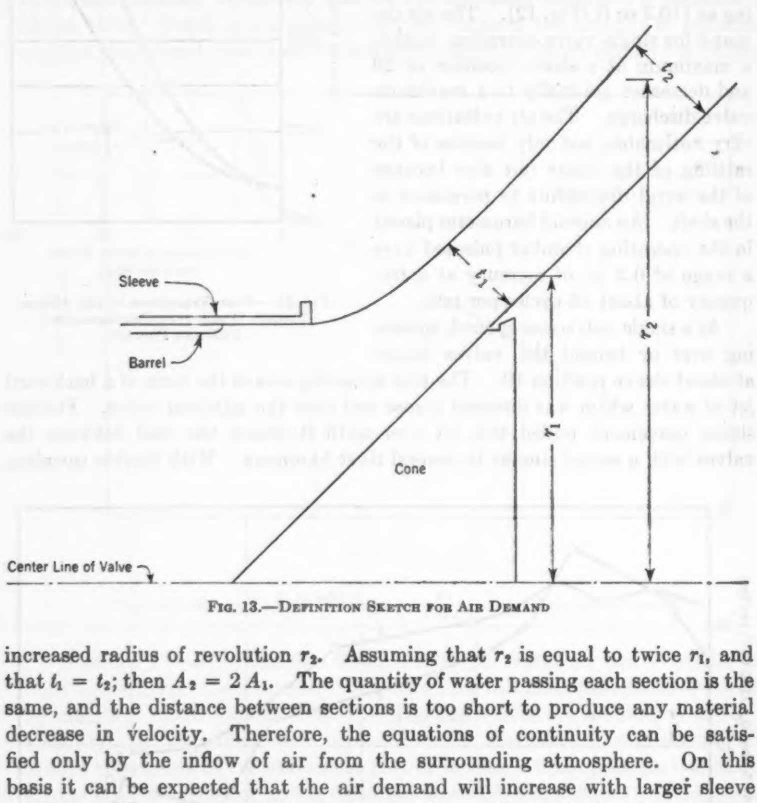

FIG. 13.—DEFINITION SKETCH FOR AIR DEMAND

increased radius of revolution r_2. Assuming that r_2 is equal to twice r_1, and that $t_1 = t_2$; then $A_2 = 2\,A_1$. The quantity of water passing each section is the same, and the distance between sections is too short to produce any material decrease in velocity. Therefore, the equations of continuity can be satisfied only by the inflow of air from the surrounding atmosphere. On this basis it can be expected that the air demand will increase with larger sleeve openings. The observed data do not confirm this conclusion but (as has been shown) the visual observations at Fontana and Watauga indicated that the secondary back flow and splash tended to form a curtain that reduced, materially, the flow of air into the jet from the upstream direction. Without a heavy back flow the spray that developed behind the

valves was carried directly into the sides of the discharging water jets. As a curtain of back splash formed, this spray was drawn into any openings in the curtain and directly toward the discharging jets. When (as occurred at Watauga at the higher sleeve positions) the valves were completely smothered, the air demand was reduced to a minimum.

The air data, therefore, can be interpreted as indicating that air requirements greatly in excess of any measured by the TVA can be expected if a curtain of water does not form over the air entrance. It also indicates a possible approach to future designs of low air requirements in which a curtain is deliberately formed. Observations of the results of the action of the back splash on auxiliary equipment placed near the valves and within the path of the spray have indicated that thought must be given to their placement and fastening. Such items as access ladders and grease lines must be fastened very securely to resist the forces exerted upon them by the heavy spray.

ACKNOWLEDGMENTS

The fixed-dispersion cone valves which were used in the investigations reported are known as "the Howell-Bunger Valves," developed by C. H. Howell, M. ASCE, and H. P. Bunger, and manufactured by the S. Morgan Smith Company. The investigations of performance were made under the general direction of Albert S. Fry, M. ASCE, and under the immediate direction of the TVA Hydraulic Laboratory staff. G. H. Hickox, M. ASCE, was head of the laboratory during the time when the first measurements on the Fontana, Chatuge, and Nottely valves were being made and was primarily responsible for the methods of analysis used in obtaining the discharge ratings.

DISCUSSION

Edwin W. Murphy[3].—Two 48-in. valves of the type discussed in this paper were installed by Messrs. Howell and Bunger, at El Vado Dam in Chama, N. Mex., in 1935. They are now operating under a load of 140 ft. Since that time valves have been developed in sizes ranging from 4 in. to 108 in. in diameter and for heads varying from 55 ft to 700 ft.

Hydraulic engineers who are faced with the problem of controlling discharge of sluice water under head need information from field tests. The data presented in this paper, therefore, are of great value to designers.

Observations from several installations are reported, and the results compared so that the conclusions drawn from these data do not represent an isolated condition meeting only specific requirements. With tests conducted on five valves, whose sizes range from 78 in. to 96 in., the findings in this paper present a general picture of performance.

The designers and manufacturers of any new product must depend first on their calculations, and next on results of model tests to evaluate the finished article and to predict its performance. Reports of tests from the field under actual working conditions are needed to compare with the original assumptions so that proper correction factors may be determined. A concise method of calibrating the actual discharge of the valve under varying head and gate openings is included in the paper. Eq. 7 gives the discharge coefficient for any condition of head. Fig. 7 illustrates how the discharge coefficient varies from the closed position to the maximum open position of the valve. The efficiency of the valves is shown to increase as the size of the valves increases although all designs are homologous.

The point of maximum discharge for the valve (Fig. 7) is not at its full open position but at a point slightly ahead of it. When the valve was first being developed, the stroke was made slightly longer than was believed necessary. This was done because many installations are made to control discharge of waters impounded during flood stage and gradually discharged later so as not to cause property damage downstream. Under these circumstances, the valve must be used to draw down the reservoir level from a maximum head to the zero point. Under conditions of extreme low head this additional stroke was to provide more opening and to discharge faster. The Fontana valve, when tested under a gross head of 295.8 ft, reached its point of maximum discharge with the gate opened at 92.5% of its full stroke (Fig. 7, Fontana high head). When tested under a gross head of 32.0 ft, this valve shows its best discharge at 98.5% of its full stroke (Fig. 7, Fontana low head). These results indicate that the valve stroke should be made sufficiently long to take care of all conditions. In the field, the maximum desired open position can be easily determined, and through a simple adjustment of a limit switch the operating mechanism will limit the travel of the gate to that point. A vibration is set up by the discharge when the cylinder gate is opened beyond the

[3] Head Structural Engr., S. Morgan Smith Co., York, Pa.

point where the lip of the sleeve is in contact with the jet (see under the heading, "Discharge Characteristics: Operational Characteristics of Valves.") When the lip is moved beyond this point there is a "make and break" action between it and the jet. This action is believed to cause the vibration. Since opening the valve wider will eliminate this action and the vibration, but will add nothing to its discharge, the logical solution is to limit travel to a point just ahead of the spot where the discharge lip is clear from the discharge jet.

The valve under discussion was designed primarily as an energy dissipater and free-discharge valve. Through its action of throwing its jet out in a hollow, cone-shaped, expanding spray, the valve obtains the maximum resistance from the air and thus dissipates a large part of the energy carried in the water. Consider the figures for the Fontana valve when operating under a head of 295.8 ft and at its point of maximum discharge: Under these conditions it is spilling 4,600 cu ft of water every second. In terms of hydraulic energy—

$$HP = 0.1134\, Q\, H \qquad (8)$$

—it is found that 155,000 horsepower (HP) of energy is to be controlled. This energy, unless dissipated at once, would destroy anything in its path. To visualize this enormous force, consider a 12-in. valve discharging under an 850-ft head. This valve throws out a mountain of spray approximately 40 ft in diameter. The air resistance encountered absorbs nearly all energy and dissipates it. The large spread of the jet eliminates any necessity of digging a huge pothole at the base of the dam for an energy absorber.

Many locations do not have an unlimited space for the valve jet to spread out and be broken up by air resistance as does the one already described. It is necessary then to provide some means of controlling the spread of the jet and restricting the air resistance. Although this action does defeat the energy dissipater function, it is possible to reach a compromise. The first attempt to do this was to place a separate cylinder, or hood, around the valve. This has been done on an installation in South America in which an 8-in. valve is discharging through such a hood and operating under a 700-ft head. This valve shows a marked decrease in the spread of the discharge jet. However, the water has considerable energy remaining in it as it leaves the end of the hood, and could seriously erode the tailrace were the channel not properly protected.

The Fontana installation (Fig. 3) is a further development of this principle, in that it discharges into a tunnel 15 ft in diameter, leading to the river downstream from the dam. Baffles are placed in the tunnel to break up the jet and to destroy part of the energy. It is evident that, when the free expansion of the jet is restricted in this manner, large quantities of air will be drawn into the tunnel along with discharge from the valve. In the early development stages some method was needed to determine how large an air inlet should be to admit sufficient air to supply this demand. With what information was then available, and by studies from a laboratory test model, the manufacturers suggested that the vent area be made at least equal to the square of the diameter of the valve. From the field tests on Fontana project it is illustrated that the wind velocity through the access tunnel at full valve open position is slightly less than 20 miles per hr. The access tunnel provides a

total vent area of 60 sq ft. A vent 3 ft in diameter furnishes an additional area of 7 sq ft. Assuming that the velocity through this vent will be the same as through the tunnel, the valve is drawing air at approximately 2,000 cu ft per sec. The maximum discharge does not require as much air as other gate positions. The addition of baffles in the path of the valve jet also modifies the air requirements.

To engineers who are studying proposed installations, and to the manufacturers and designers of this type of valve, the presentation of these findings provides a means for studying and comparing the results with the assumed design and to base calculations on a somewhat sounder footing. These findings were based on a particular case and, unless all features are duplicated, the same results cannot be expected in other cases. When test data become available from the field operation of a piece of equipment, comparison with original model tests is imperative. Through such a comparison it is possible to obtain new correction factors through which a proper step-up between model and prototype can be made.

Laboratory tests do not always present a true picture of how the prototype will perform. Many engineers hold differing opinions as to proper coefficients to use in rating a model test against expected field performance. This difference in opinion applies in many fields other than the study of hydraulics. It appears that much research work remains to be done along these lines.

The valve under discussion is of a very simple construction, with only one moving part contacting the water. Its construction eliminates, almost entirely, the effects of water load or hydraulic unbalance in opening or closing the cylinder gates. Almost all the operating force required is needed to overcome the mechanical friction of the stuffing box and necessary gearing. On one installation, where the valve discharges downward at a 30° angle and with cylinder sleeve operated by an oil pressure servomotor, the operator found that slightly less pressure, as calculated, was required to close against full head than to open. This observation indicates that a fraction of weight of the moving parts is greater than hydraulic unbalance.

With the elimination of moving parts, sources of vibration are not present, and the entire valve operates smoothly without any of the destructive vibrations set up in most free-discharge controlling devices—a spouting jet of water under high head can be throttled without disturbing a coin balanced edgewise on the body of the valve.

Rodolfo E. Ballester[4].—In Argentina there have been installed six fixed-dispersion cone valves of the same type as the valve described by the authors. However, the valves in Argentina differ from Howell-Bunger valves in that they are operated by levers instead of screws.

Table 2 lists the installations. There are two valves at each dam. All the valves discharge into the open air, making unnecessary any air-demand provisions in the surrounding structures, such as those described by the authors under the heading, "Characteristics of Associated Structures."

[4] Prof. of Applied Hydraulics, Univ. of Buenos Aires, Buenos Aires, Argentina.

TABLE 2.—FIXED-DISPERSION CONE VALVES INSTALLED IN ARGENTINA

Dams	Valve Diameter		Minimum Head		Maximum Head	
	Meters	Inches	Meters	Feet	Meters	Feet
San Roque........	1.524	60.0	3.0	10	28.0	92
La Viña........	1.100	43.3	3.0	10	56.0	184
Cruz del Eje......	1.100	43.3	3.0	10	22.5	74

In order to control the spreading and direction of the jets, deviations from the standard valve design have been used successfully at two dams. The first of these adaptations is the reduction of the central angle of the cone valve; the other is the introduction of an angle between the axis of the valves and the axis of the conduits. The authors may be able to add information or opinions concerning similar unusual installations.

The results of model tests using a scale of 1:10 have been described by the writer,[5] and some comparisons might be made with the results given by the authors. From the results of these tests, a table and a graph were prepared for the operation of the prototype valves. This procedure is in contrast to the method of field observation and prototype study used by the authors.

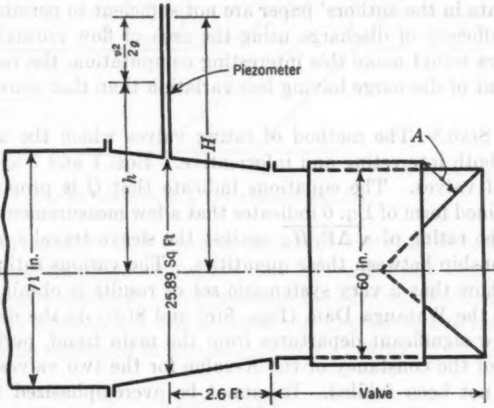

FIG. 14.—FIXED-DISPERSION CONE VALVE

The discharge into the conduit at a short distance upstream of the valve is given by Eq. 7. During the model tests, the discharge Q and the static pressure h were measured for different positions of the sleeve. The cross section of flow A seems to have been taken by the authors as the cylindrical opening left by the sleeve. However, in the tests described by the writer, a section was selected normal to the surface of the cone and bounded by the edge of the sleeve, and A was defined as this area. This section shows contraction along

[5] "Válvulas para la regulación de la descarga de los embalses de San Roque, La Viña y Cruz del Eje," by R. E. Ballester, *La Ingeniería*, Buenos Aires, Argentina, *No. 856*, February, 1946, pp. 91–101.

the sleeve and no contraction along the cone. Fig. 14 illustrates the meanings of symbols used in the computations.

If the area of the cross section at the piezometer is w, and v is the velocity, $\frac{v^2}{2g} = \frac{Q^2}{2g\,w^2}$ and the final equation is

$$Q = \frac{1}{\sqrt{1 - \frac{C^2}{w^2} A^2}}\; CA\sqrt{2\,g\,h} \quad \text{.............(9)}$$

The coefficient of discharge for openings of from 22% to 79% of the sleeve course was nearly constant and equal to 0.79. For an opening of 88% of the course, C increases to 0.81. For small openings of 12% of the sleeve course, the coefficient increases to 0.85. This peculiar result may have been the result of an observational error, because an error of 0.2 millimeter (0.008 in.) in the measure of the depth of the normal opening in the model causes an error of 3.9% in the computation of the area of flow.

The valves have been in operation since 1943, and no troubles have been recorded. Unfortunately, no special measurements have been made in the prototypes to check the model experiments, and the graph that was prepared has been used for regulating the discharges. Procedures such as the authors describe would be of value in checking this graph.

The data in the authors' paper are not sufficient to permit the computation of the coefficient of discharge using the area of flow normal to the cone. If the authors would make this interesting computation, the results should yield a coefficient of discharge having less variation than that shown in Fig. 7.

T. T. Siao.[6]—The method of rating valves which the authors have presented is both interesting and informative. Eqs. 1 and 3 are fundamental to a study of valves. The equations indicate that Q is proportional to $\sqrt{\Delta P}$. The combined form of Eq. 6 indicates that a few measurements of Q will suffice, through the rating of $\sqrt{\Delta P/H_G}$ against the sleeve travel s, so as to establish the relationship between these quantities. The various rating curves in Figs. 6 and 8 show that a very systematic set of results is obtained. Only in the curves for the Watauga Dam (Figs. 8(*c*) and 8(*d*)) do the discharge measurements show significant departures from the main trend, perhaps because the condition of the constancy of the K-value for the two valves at the Watauga Dam has not been fulfiled. It cannot be overemphasized that, in order to yield a constant K-value, the two piezometer taps must be located far enough from the valve opening so that the flow pattern between and around the taps will undergo practically no change due to alteration of valve opening. The two taps can actually be located anywhere, in so far as the K-value obtained is constant and the value of ΔP is sufficiently large.

The coefficient of discharge used by the authors varies considerably with the valve opening, as seen in Fig. 7, because the area A in Eq. 7 is not the effective area of efflux. A discharge coefficient based on the area of the opening would be more significant. It is possible to derive, by analytical means, a coefficient of discharge of the latter type for comparison with the observed results.

[6] Research Associate, Iowa Inst. of Hydraulic Research, State Univ. of Iowa, Iowa City, Iowa.

The hydraulician has found that a special type of flow embodied in the formation of a jet from a container of simple geometric form can be analyzed by the method of conformal mapping. Although this method has been developed for two-dimensional flow only, the work of Hunter Rouse, M. ASCE, and A. Abul-Fetouh[7] and J. S. McNown, M. ASCE, and E. Y. Hsu,[8] A. M. ASCE, among others, shows that the results obtained for two-dimensional flows can often be applied with good accuracy to the corresponding three-dimensional flows—at least for a bulk characteristic such as the discharge coefficient. According to Mr. McNown, the discharge coefficient of a cone valve is subject to this type of analysis, and a comparison between the results obtained with those observed by the authors in Fig. 7 is relevant to the authors' purpose in presenting the study.

Fig. 15 is a definition sketch of the comparable two-dimensional flow. Revolution of the boundaries EAB and DC about AB gives the boundaries of

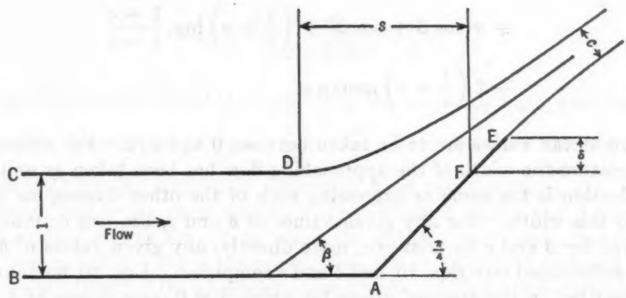

FIG. 15.—SKETCH OF A TWO-DIMENSIONAL JET

a cone valve. It is assumed that there is no loss of energy. By means of a series of mathematical transformations, the flow is changed into that resulting from an idealized source and sink. The relationships between the final width c, the ultimate angle of deflection β, the dimension δ, and the sleeve travel s for the plane flow may be expressed in two equations, as follows:

$$-\frac{\pi\,\delta}{c} = (\cos\beta - \sin\beta)\log_e\left[\tan\frac{1}{2}\left(\frac{\pi}{4}+\beta\right)\right] + (\cos\beta + \sin\beta)\log_e\left[\tan\frac{1}{2}\left(\frac{\pi}{4}-\beta\right)\right] + \pi\cos\beta + \frac{1}{2}\left(c+\frac{1}{c}\right)\log_e\frac{1+\sqrt{2}\,c+c^2}{1-\sqrt{2}\,c+c^2} + \left(\frac{1}{c}-1\right)\arctan\frac{\sqrt{2}\,c}{1-c^2} \ldots (10a)$$

[7] "Characteristics of Irrotational Flow Through Axially Symmetric Orifices," by Hunter Rouse and A. Abul-Fetouh, *Transactions*, ASME, Vol. 17, 1950, p. 421.

[8] "Application of Conformal Mapping to Divided Flow," by J. S. McNown and E. Y. Hsu, *Proceedings*, Midwest Conference on Fluid Dynamics, J. W. Edwards, Ann Arbor, Mich., 1951.

TABLE 3.—CHARACTERISTICS OF THE TWO-DIMENSIONAL

Characteristic	Sleeve Travel s						
	0	0.0944	0.1889	0.3778	0.5680	0.7619	0.9655
Flow width c	0	0.05	0.1	0.2	0.3	0.4	0.5
Ratio $\frac{c}{s}$	0.530	0.530	0.529	0.529	0.528	0.525	0.518
Angle β, in degrees	42.04	42.04	42.04	42.02	41.99	41.92	41.79
Ratio $\frac{s}{D}$	0	0.0472	0.0945	0.1889	0.2840	0.3810	0.4828
Coefficient C_1	0	0.1	0.2	0.4	0.6	0.8	1.0
Coefficient C_2	0.530	0.530	0.529	0.529	0.528	0.525	0.518

and

$$\frac{\pi s}{c} = 2 \cos \beta \log_e \tan \frac{\beta}{2} + 2 \sin \beta \log_e \left[\tan \frac{1}{2} \left(\frac{\pi}{4} - \beta \right) \right]$$

$$+ \pi(\cos \beta + \sin \beta) + \left(\frac{1}{c} + c \right) \log_e \frac{1 + c}{1 - c}$$

$$+ 2 \left(\frac{1}{c} - c \right) \arctan c \ldots\ldots\ldots\ldots (10b)$$

The two arctan values are to be taken between 0 and $\pi/2$. For simplicity of nomenclature the width of the approaching flow has been taken as unity; this simplification is the same as expressing each of the other dimensions in their ratio to this width. For any given values of δ and s, the two equations can be solved for β and c by trial—or, more directly, any given values of β and c can be substituted into Eqs. 10, and δ and s computed. Eqs. 10, for the special case described in the authors' study for which $\delta = 0$, give values of s, c, c/s, and β, as arranged in Table 3. The discharge coefficient is obtained by dividing the discharge Q by the product of the flow area A and $\sqrt{2\, g\, H}$. Evidently, A can be taken either as the cross-sectional area in the valve body, as the authors have done, or as the area uncovered by the sleeve travel; the corresponding coefficients of discharge are quite different, since A is constant in the former case and variable in the latter. For the two-dimensional flow the two coefficients of discharge are simply c and c/s, provided there is no loss of energy.

A logical approach to the adaptation of these results to the determination of the discharge coefficient for the corresponding three-dimensional flow is to assume that corresponding ratios between the initial and the final area of the jet are the same in each case (as was found for the orifice[7]); that is,

$$\frac{c}{s} = \frac{[w(2\,\pi\, r)]_{ult}}{s(2\,\pi\, \overline{BC})} \ldots\ldots\ldots\ldots (11)$$

in which w is the thickness of the three-dimensional jet at a certain point; r is the distance from the point to the axis AB; $\overline{BC}$ is the width of the approaching flow; and $[w(2\,\pi\, r)]_{ult}$ is the ultimate value of $w(2\,\pi\, r)$. The two coeffi-

Jet and the Corresponding Cone Valve

Sleeve Travel s						Characteristic
1.1880	1.4490	1.7887	2.3290	2.8369	∞	
0.6	0.7	0.8	0.9	0.95	1.0	Flow width c
0.505	0.483	0.447	0.386	0.335	0	Ratio $\frac{c}{s}$
41.62	41.30	40.82	40.11	39.66	39.19	Angle β, in degrees
0.5940	0.7245	0.8944	1.1645	1.4185	∞	Ratio $\frac{s}{D}$
1.2	1.4	1.6	1.8	1.9	2.0	Coefficient C_1
0.505	0.483	0.447	0.386	0.335	0	Coefficient C_2

cients of discharge, from Eq. 11, are

$$C_1 = \frac{[w(2\,\pi\,r)]_{\text{ult}}}{\pi\,\overline{\text{BC}}^2} = 2\,c \qquad (12a)$$

and

$$C_2 = \frac{[w(2\,\pi\,r)]_{\text{ult}}}{s(2\,\pi\,\overline{\text{BC}})} = \frac{c}{s} \qquad (12b)$$

Table 3 also contains, for the cone valve, the values C_1, C_2, β, and the sleeve travel-valve diameter ratio $\frac{s}{D} = \frac{s}{2\,\overline{\text{BC}}} = \frac{s}{2}$. The C_1-values are comparable to those used by the authors in presenting their test results in Fig. 7, since both are defined in the same manner. The values of C_1, C_2, and β have been plotted against s/D in Fig. 16, in which the authors' test results for C_1, from Fig. 7, are included. Since the assumption shown in Eq. 11 is based on the similarity of pattern of the axially symmetrical flow to that of the corresponding plane flow, it is expected that the smaller the ratio s/D the better the assumption will be, and vice versa. For large values of s/D, Eq. 11 becomes absurd; in fact, it cannot be valid at all for $c > 0.5$, since C_1 cannot be greater than unity. For this reason, only values corresponding to $C_1 < 1.0$ are plotted. It can be seen that there is close agreement between the test results and the analysis for s/D up to 0.25. For $(s/D) > 0.25$ the test results start to fall below, as this type of analysis of the axisymmetric flow can no longer be expected to be accurate for large values of s/D. The true C_1-curve must be tangential to the horizontal line $C_1 = 1$ at $(s/D) = \infty$, and also to the curve $C_1 = 2\,c$ at $(s/D) = 0$.

Even for $(s/D) < 0.25$ the test results are systematically slightly smaller than those computed. The explanation could be that the boundary layer which develops along the valve wall causes the total discharge under a certain head to be less than that which would be attained under the same head if the velocity of approach were truly constant. In contrast to C_1, C_2 varies only slightly with s/D. It is of interest to note that, for the valid range $0 < (s/D) < 0.25$, a constant theoretical value of $C_2 = 0.530$ can be adopted. As to the practical values of C_2, converted from the test results for C_1 by dividing the latter by $4\,s/D$, it can safely be regarded as a constant equal to 0.521 for

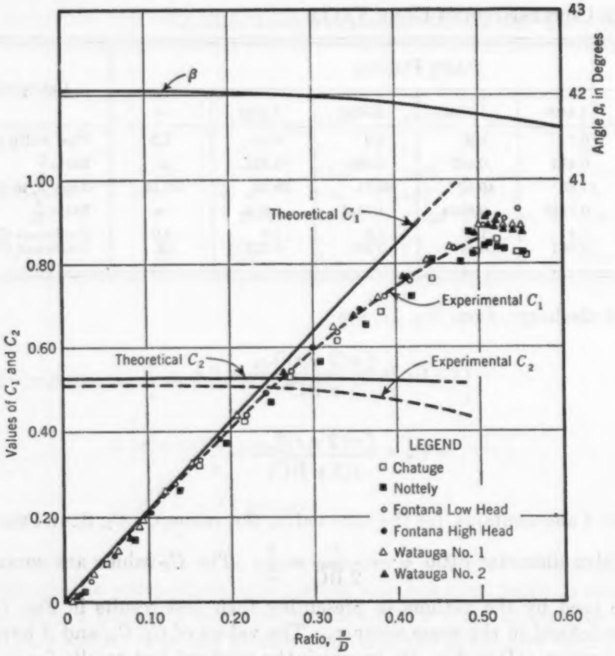

FIG. 16.—CHARACTERISTIC CURVES FOR A CONE VALVE

$(s/D) < 0.25$. Therefore, the discharge coefficient C_2, in comparison to C_1, has certain merits in so far as it not only is conventional, but also remains practically constant for small (s/D)-ratios.

Regarding the deflection angle β, the writer would like to point out that Fig. 13 does not seem to be accurate, since it shows the jet to follow the 45° direction throughout its course. Actually, there will always be some difference between the angle of the cone and that of the jet. For the corresponding two-dimensional jet, the final angle of deflection is between 39.19° and 42.04° for all possible sleeve travels. Even though it is impossible to predict the exact value of β for the cone valve, the range is likely to be approximately the same.

It has been shown that the results of theoretical analysis are directly useful for values of s/D less than approximately 0.25. The theoretical method is also applicable for cone valves of angles other than 45°. Modifications of the design of the angle of the cone valve could therefore be studied analytically. The discharge coefficient and the final angle of deflection β, which give an immediate evaluation of the force exerted on the cone, should be among the primary considerations. Although experimental research would be necessary, a theoretical analysis would undoubtedly provide, at very little cost, a basis for a comparison of the significant characteristics. A judicious combination of both theory and experiment provides the required results.

VERNE GONGWER,[9] M. ASCE.—In view of the scarcity of published data on the subject, from both a theoretical and an operational point of view, the authors should be commended for an interesting and substantial contribution to the literature.

In 1941, with only meager data available, the writer adopted and installed two 66-in. fixed-dispersion cone valves with hoods at Alder and La Grande dams, on the Nisqually River in Washington. In the subsequent testing, gaging, and operation of these valves, some of the data and characteristics which were reported by the authors were independently discovered and verfied. Some of these characteristics were also verified in model tests on this type of valve conducted in the hydraulic laboratory of the Corps of Engineers, United States Department of the Army, at Bonneville, Ore.

The Valve at La Grande Dam.—Fig. 17 shows a 66-in. valve (during construction) in the base of La Grande Dam. The valve is located below the

FIG. 17.—LA GRANDE DAM (WASHINGTON) VALVE DURING CONSTRUCTION

bucket of the overflow "ski-jump" spillway, and is fitted with a steel hood. Originally, it was intended to surround the valve with a concrete, steel-lined box, or to confine it with concrete "side-blinders." However, the manufacturer suggested a simple conical-cylindrical hood of unstiffened ¾-in. plate, 8 ft in diameter, bolted directly to the valve sleeve. Model tests were performed which gave apparently satisfactory results. This valve was identical with the Alder Dam valve but was to operate under less maximum head (187 ft). There is no air venting of the valve or hood.

The Valve at Alder Dam.—As at La Grande Dam, this valve was intended to supply water intermittently to the next powerhouse downstream in case of outage of the turbines. However, owing to the restricted availability of

[9] Construction Engr., U.S.N., Civ. Engr. Corps, Twenty Nine Palms, Calif; Formerly Chf. Engr., Construction, Dept. of Public Utilities, Tacoma, Wash.

materials and equipment during World War II, only the 40,000-kw unit was released for the La Grande powerhouse and the two Alder Dam units were withheld for more than 18 months. As a consequence, the Alder Dam valve had to operate constantly for more than two years, at heads up to a maximum of 265 ft, whenever the reservoir level was below the lip of the spillway.

Starting with a full reservoir, as the dry season approached and the storage level dropped slowly toward the lip of the spillway, some pitting of the ½-in. steel hood developed just below the 30° angle, where the conical frustrum was bolted to the end of the valve sleeve, and one small pinhole went entirely through the steel. Failure of the hood would have been very serious since the spreading jet could not have been permitted, and the new 40,000-kw La Grande unit might have been forced to run on very low stream flow, with a 200,000-acre-ft reservoir standing full but useless. After hurried studies, and notices to the manufacturer, regarding either alterations to the hood or a new

FIG. 18.—ALDER DAM (WASHINGTON) VALVE OPERATING UNDER FULL HEAD

type of hood, the writer determined, by crude means, that a cylinder with both ends open and one diameter in length beyond the point of impingement of the jet would transform the free-spreading jet into a cylindrical shape. The manufacturer expedited laboratory check tests while the fixed cylinder hood design was prepared and the steel liner was ordered.

Fig. 18 shows the new, 14-ft diameter, cylindrical hood at full discharge. Fig. 18(*b*) indicates the tailwater depressor effect of approximately 4 ft produced by the valve. The pronounced flattening or inward depressing of the jet on both sides, on the top, and on the bottom, which is believed to indicate self-venting of the interior of the jet, is shown in these photographs.

The movable hoods were abandoned because in tests of the Alder Dam valve, at full open position, the motor stalled in closing and the valve had to be closed by hand to a one-half opening before the motor could close it completely. After some investigation, from which it was noted that the flare of the jet was greater than that of the conical frustrum, observations with 3 pressure gages, tapped into the frustrum, disclosed an upstream component too great for the motor to overcome.

Air Demand.—The authors' statement (in the "Synopsis") that "*** the air demand is a function of the structure surrounding the valve ***" appears to be verified by experience and observation of the Alder Dam valve and others. In the first movable hoods at Alder and La Grande dams—the first such hoods ever used, in so far as is known—no air was admitted, either in the model which the manufacturer arranged to be made and tested at a government laboratory, or in the prototypes. Nevertheless, this combination of valve and hood operated with no sensible vibration. The observer's teeth could be placed against the flanges between sleeve and hood with very little unpleasant sensation.

Had the motor and operating gear been designed to overcome the upstream thrust safely, the pitting might have been obviated at slight maintenance expense by periodic welding or by the application of a welded circumferential facing of stainless steel approximately 12 in. wide. Sufficient air possibly to eliminate pitting might have been admitted at this point by the simple expedient of drilling a ring of closely spaced holes, provided the situation had been fully understood at the time. However, much air might have been required to satisfy the demand and the discharge coefficient might have been greatly reduced, or other difficulties resulted.

Negative pressures and cavitation undoubtedly occurred at the extreme upper end of the conical frustrum at certain gate openings, however, the available gages could not indicate them. Readings were taken at each one-tenth gate opening up to five-tenths, at which point the gages were wrecked internally by the rapid pressure variations. It was noted that the pressure curves plotted from these crude experiments, with the three gages tapped in along the top element of the frustrum, reversed themselves between the upstream and downstream gages.

For the 14-ft-diameter, fixed-cylinder, Alder Dam valve hood, an air inlet area of approximately 50 sq ft was provided above the upstream end of the cylinder, based on the manufacturer's model tests. At the smaller gate openings air rushed through the gratings at relatively high velocity. There was no back-lash of spray at these openings, and the slots cut in the conical jet by the horizontal and vertical diaphragms could be observed readily. It is probable that the air passed downstream through these slots. Part of it may also have passed through the aerated outer periphery of the jet itself.

Where there is no surrounding structure it is apparent that, were it not for impedence of the atmosphere, the conical jet would spread to infinity, with infinite diameter and, if conceivable, zero density. Actually, in this case, the air may be considered to be the surrounding structure, which impedes as well as aerates the jet, both from within and from without. Assuming that the thickness of the jet is constant, with a valve diameter of 66 in., expanding to the limit of the 14-ft-diameter hood, the density of the solid jet must be reduced in the ratio 66:168, or to approximately 40%, as it strikes the 14-ft-diameter hood. The percentage of water content is further reduced by the slight increase in the thickness of the expanding jet, which must obtain this air, as found by the authors.

As the Alder Dam valve opening increased from about one-half gate to full gate, the air drawn through the grill progressively decreased to zero, and the back-lash of spray increased considerably. However, this back-lash was not sufficient, as a water curtain, to cause the observed decrease in the air intake or demand. The upper part of the valve was still visible since the spray fell and was ejected by the bottom of the jet. This characteristic of the air demand appears to be similar to that indicated in Figs. 10 and 12.

From the experiences with the Alder Dam valve, the writer formed the conclusion that a hood of the Alder Dam type does not actually require any air upstream from the jet because the jet can procure the necessary air through the sides of the already aerated cylindrical jet. This is believed to be indicated by the depression in the sides and on the top and bottom of the jet (Figs. 18 and 19). The reason for the flattening of the jet, occurring at the top, the sides, and the bottom, rather than elsewhere, may be the influence of the "fins" of water which appear downstream of the diaphragms or vanes when the jet is not confined, as has been observed in some model tests.

It is suggested that, where the spreading jet is discharged into a tunnel, or into a chamber with baffles or dissipators—so that it may be difficult for the downstream air to balance the reduced pressures—the installation may act on the "ejector" principle. The valve then takes great quantities of upstream air, depending on the efficiency of the combination as an ejector, and that demand or need for upstream air may be eliminated, or greatly reduced, by omitting the baffles, unless these are an absolute necessity for dissipating the energy at that point. The Alder Dam installation contains no baffles, and the hollow jet is directed down the solid rock stream bed. Excess energy is absorbed by aeration and by water-cushioning in the small depression dug by the jet in the rock channel. There is very little solid rock into which such a jet will not dig to some extent.

Discharge Coefficients.—Difficulties similar to those described by the authors were encountered in gaging the discharge of the Alder Dam valve. Fig. 19 shows the discharge coefficients for the Alder Dam valve computed from the gaging results by Mr. Hickox, plotted on curves for the Chatuge, Fontana, and Nottely installations (Tennessee Valley Authority). The data were given to Mr. Hickox by H. Wiersema and Mr. Fry. The coefficient at the 50%-valve-opening was obtained from measurements taken with the original movable hood in place and conforms closely to the curve of all other coefficients that were obtained with the fixed hood, open at both ends. Apparently neither type of hood, nor the Fontana Dam dissipators, impaired the coefficient of discharge.

From Fig. 5, the lip of the end of the Alder Dam pipe (within the valve) was shaped like that at Fontana Dam, but if, as is apparent, the upstream position of the end of the valve sleeve at Fontana Dam was nearer the lip than the others, it invalidates the writer's previous impression that the "falling off" of the coefficients in the Chatuge and Notteley valves was caused by overtravel of the sleeves. In the Bonneville tests it was found that the maximum discharge of the models occurred at about 0.94 gate, as the control changed from

the end of the sleeve to the end of the pipe. The curves of the Alder and Fontana dams do not fall off at about 0.90 gate as do the others.

The limit switches at Alder Dam were set so that the indicator read exactly 0 and 1.00 in fully closed and fully opened positions, respectively. Not having the opportunity, subsequent to the Bonneville tests, to investigate this feature at Alder Dam, the writer assumed that the Alder Dam sleeve did

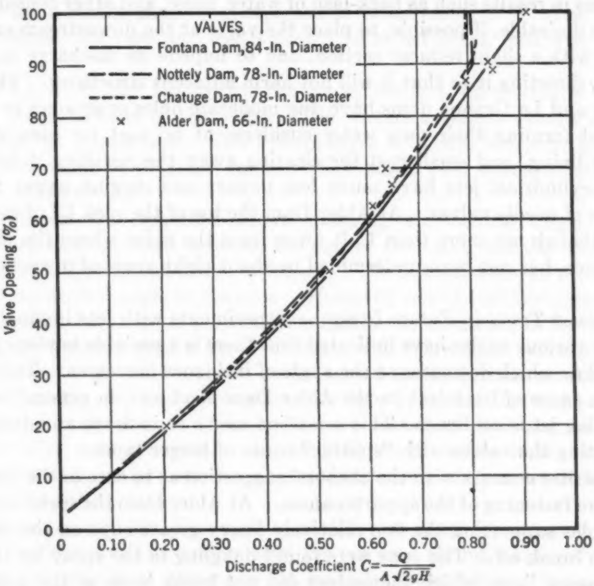

FIG. 19.—COMPARISON OF DISCHARGE COEFFICIENTS FOR SEVERAL FIXED-DISPERSION CONE VALVES

not overtravel or that the control change from sleeve to pipe. This appeared to be a proper assumption since there was no pitting of the ends of either sleeve or pipe after several years of operation, as might be expected from the negative pressures found in the Bonneville models under the end of the sleeve with the latter in the wide open position. There seems, therefore, as suggested by the authors, little point in having the sleeves overtravel, or the indicators register other than 0.0 and 1.00 in closed and open positions.

Vibration and Noise.—There is no sensible vibration at any gate opening of the Alder Dam valve or hood, and no loud noise at any critical opening, such as is described by the authors. There is a slight "wire drawing" sound at the last "pinch off" in seating the valve in closed position, which is neither annoying nor detrimental. It is conjectured whether the "howl" mentioned by the authors is a matter of acoustics and reverberation, rather than harmful vibration. In the silent Alder Dam powerhouse, a slight acoustic effect from the valve initially caused some head shaking of experienced operators and en-

gineers. However, this was quickly forgotten and overshadowed by the much higher noise levels caused by the generators when the latter were in operation.

Necessity for Energy Absorption and River-Bed Protection.—Where design conditions require that valves be located in tunnels or chambers, the problems of directing the jets; supplying sufficient air; and, possibly, dissipating some of the energy are recognized. Such requirements evidently introduce many variations in results such as back-lash of water, noise, and other considerations. It seems desirable, if possible, to place the valve at the downstream end of the conduit with a slight reducer section, and to impede its discharge as little as possible, directing it so that it will not harm adjacent structures. The valves at Alder and La Grande dams have dug moderate holes or grooves in the rock river bed forming their own water cushions, at no cost for excavations or concrete lining, and small cost for clearing away the resulting debris. The aerated cylindrical jets have much less impact and digging power than the solid jets of needle valves. At Alder Dam the toe of the rock fill of the service road, although not more than 15 ft away from the point where the jet strikes the tailrace, has not been undermined in about eight years of operation of the valve.

Suggested Trend in Future Design.—Experiments with jets impinging upon plates at various angles have indicated that there is a variable tendency toward reverse flow which decreases as the angle of incidence decreases. This may be the basic cause of back-lash in the Alder Dam hood and, in general, wherever a spreading jet is confined. This condition seems to indicate an advantage in constructing the valves with "splitter" cones of longer taper.

The writer concurs with the authors' suggestion as to care in the placement and secure fastening of the appurtenances. At Alder Dam the spray caused the frail nipples supporting the two relatively heavy grease cups on the operating screws to break off. The cups were found dangling in the spray by the small copper grease lines, which themselves did not break loose at the upper end. The grease lines were removed and separate alemite fittings were installed. Certain other bolts and fastenings of the ladders also became loose and were welded. There is no loud noise, and the spray is of insufficient force to remove paint from the shafts or grease from the exposed operating screws or large bronze sleeve.

The differences in the behavior of the several installations suggest the advantage of studies toward the development of a separate chamber or discharge outlet for each valve, and toward the elimination of all possible baffles or obstructions that would impede air supply from downstream, thereby reducing upstream air demand. An attempt should be made to develop a light, movable, vented or unvented hood similar to the original hoods at Alder and La Grande dams, with the exception that the hoods and water passages be streamlined, and that the motors and operating gear be designed for those conditions. Having all moving parts exposed would facilitate inspection and maintenance, unhampered by back-lash of spray.

REX A. ELDER,[10] M. ASCE, and GALE B. DOUGHERTY,[11] A.M. ASCE.—The reception given this paper by the discussers and the diversity of phases of the subject discussed have been highly gratifying. Each discussion has added to the total value of the paper and thus to the fund of engineering knowledge.

Mr. Murphy wrote in reference to the air-demand results that "*** These finding were based on a particular case and, unless all features are duplicated, the same results cannot be expected in other cases. ***" The writers heartily endorse this view and feel it should be noted by all who wish to use the data.

The TVA hydraulic laboratory has never made a model study of the operating characteristics of the valve. The writers therefore cannot make a model-prototype comparison. The writers agree with Mr. Murphy that such a comparison could be of great value. They hoped that others might have made such studies.

Mr. Ballester has inquired about changing the central angle of the deflector cone and the angle between the axis of the valve and the conduit in order to change the size and shape of the jet. The authors know of no data on changes in the central angle of the cone. However, recent (1952) studies at the TVA hydraulic laboratory on proposed changes in valve location at the Nottely and Chatuge projects might be of interest with respect to valve location. At these projects, the valves are to be connected to the turbine scroll case as shown in Fig. 20. In this illustration, the heavy broken line indicates the limits of the jet impact area. The tailwater elevation is 1612 and the center line of the valve is at El. 1613.5. In studying the jet action in the model, it was found that the jet pattern was unsymmetrical, having heavier flow on the right side (Fig. 20).

Mr. Ballester and Mr. Siao each used different areas for determining the discharge coefficient. The writers used the net area through the body of the valve—not the cylindrical opening as Mr. Ballester understood. This measurement was selected in preference to the others because (1) it provided the simplest and easiest approach for a designer concerned with determining the proper valve size and (2) it provided the simplest computation approach for preparing a table of discharges for various gate openings. In response to Mr. Ballester's suggestion, however, the discharge coefficients for one test each from the Nottely and Fontana data have been computed using his definition of area. The results are shown in Fig. 21 and compared with Mr. Ballester's results.

Mr. Siao's approach is very interesting, and within the limits he defined could probably be used by the maunfacturer's designers in studying the effect of changes in their cone dimensions.

Mr. Siao calls attention to the shape of the issuing jet shown in Fig. 13. This sketch was intended to show not basic shapes but merely general nomenclature. The writers agree with Mr. Siao that the jet shape probably is not exactly as shown, but they do not have any data.

[10] Head, Hydr. Lab. Sections, TVA, Norris, Tenn.

[11] Hydr. Engr., TVA Hydr. Lab., Norris, Tenn.

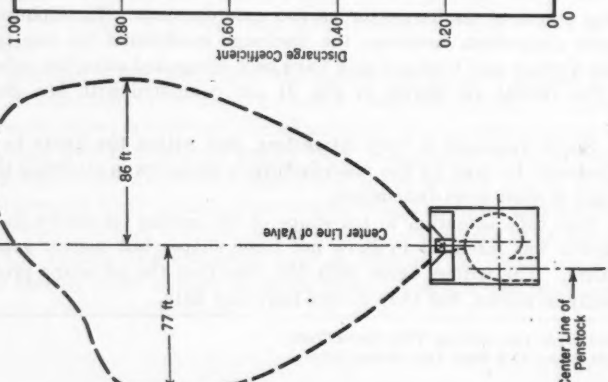

FIG. 20.—JET PATTERN OF A MODEL

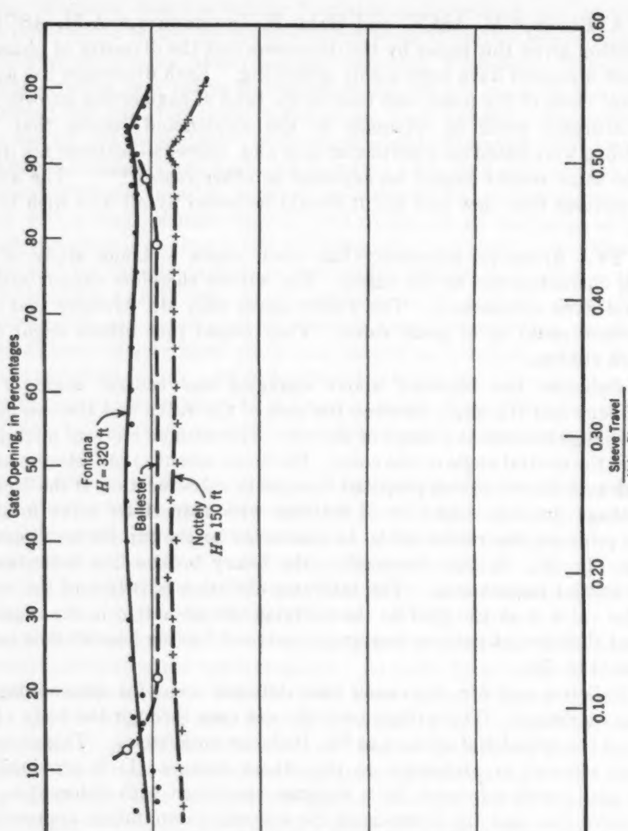

FIG. 21.—DISCHARGE COEFFICIENTS

Mr. Gongwer's observations at Alder Dam are interesting and informative. When sleeve positions based on an indicator reading of 1.00 at a fully opened position are used, the question arises as to where that actual position is located. Because of this uncertainity, the writers chose to present the coefficient data in Fig. 7 plotted against the ratio of sleeve travel divided by the valve diameter. If homologous valves are used, this system should yield definable results.

AMERICAN SOCIETY OF CIVIL ENGINEERS
Founded November 5, 1852

TRANSACTIONS

Paper No. 2568

METHOD FOR MAKING HIGHWAY SOIL SURVEYS

By K. B. Woods,[1] M. ASCE

With Discussion by Messrs. George F. Sowers, and K. B. Woods

Synopsis

Rapid developments in the field of soil mechanics since about 1927, combined with improvements in the methods of design of bases and pavements, have led to other important developments and refinements in methods for making highway soil surveys.

Established procedures for making these surveys include the use of test pits, core drilling, and auger borings to obtain samples for the determination of the engineering characteristics of the materials in the various layers and horizons of the soil profile. These procedures are costly, tedious, and somewhat slow. As a result, the engineer has been interested in refining these procedures and in developing new methods for making soil surveys.

Rapid advancements have been made in the use of agricultural soil-survey maps and certain types of geologic maps for soils engineering purposes. Methods of interpreting this information have enhanced the value of these maps for use in many sections of the United States. The development of airphoto interpretation techniques for bounding areas of soils of like engineering characteristics and for making engineering soil maps has led to the rather wide use of this tool. Resistivity methods and seismic methods for locating buried channels and for obtaining information on the depth of rock under a soil cover have had increased use, particularly in the New England states.

Introduction

For many years, highway engineers have used various procedures for obtaining information concerning the soils encountered in construction projects.[2,3]

Note.—Published in September, 1952, as *Proceedings-Separate No. 152*. Positions and titles given are those in effect when the paper was received for publication.

[1] Associate Director, Joint Highway Research Project, and Prof. of Highway Eng., Purdue Univ., Lafayette, Ind.

[2] "Soil Surveys for Highways in New Hampshire," by J. O. Norton, *Engineering News-Record*, Vol. 114, 1935, pp. 706–709.

[3] "Soil Survey Practice in the United States," by Levi Muir and William F. Hughes, *Proceedings*, Highway Research Board, National Research Council, Vol. 19, 1939, pp. 467–483.

Increased use of highways by both passenger cars and trucks has created a need for better alinement, flatter grades, and wider and thicker pavements and base courses. These changes, in turn, have emphasized soil problems in drainage, foundations for embankments, landslides, and subgrade effects such as frost action and pavement pumping. The solution to most of these problems requires complete information on the engineering characteristics of the soils that are to be encountered during the construction process.

Some highway departments, including those of North Carolina, Missouri, and particularly Michigan, have used agricultural soil-survey techniques to develop soils maps for highway engineering use. The fact that these states continued to use these methods in lieu of more recently-developed ones attests to the soundness of the procedures. The slowness of other states to "borrow" from the related science of agriculture is probably caused, in part, by the complicated terminology used and by the lack of understanding of the concepts of pedology.

Geologic maps have long been of great value in many highway departments, particularly where the soil cover over rock is relatively shallow and the bedrock itself is the major material. Certain types of glacial maps have proved exceptionally useful for the compilation of general soils information, whereas new procedures in geologic mapping bear promise of contributing to that phase of soil mechanics concerned with the engineering characteristics of the immediate surface materials.

The aerial photograph is a more recent tool, used by highway engineers for obtaining information on soils. This technique has three direct uses—(*a*) in conjunction with field surveys for making large-scale engineering soil maps on a county basis or even on a state basis, (*b*) in gathering information concerning relatively unmapped areas through the fundamental principles of airphoto interpretation, and (*c*) in obtaining boundary information on materials of unlike characteristics and thus provide a method for predetermining the places where field data should be obtained.

Seismic methods and resistivity methods have not been universally accepted by highway engineers, although their use in the New England states has increased. However, these techniques have possible application in certain types of foundation problems and particularly in determining the elevation of bedrock buried under deep soil cover such as drift and wind-blown silt.

Highway Soil-Survey and Mapping Techniques

The purpose of the highway soil survey is to furnish information on the engineering characteristics of soils and rocks, for use by the design engineer in (*a*) the establishment of the final location of the road—both grade and alinement; (*b*) the selection of fill materials that will have optimum usefulness in embankments and subgrades; (*c*) the obtaining of subgrade information with respect to drainage requirements, possible frost action, the pumping of rigid pavements, and the rutting of flexible pavements; and (*d*) the location

of borrow material and of granular material for possible use as sub-bases and bases.[4,5,6]

The standard method used in developing information for the highway soil surveys includes the auger boring and test pits to determine the soil profile.[7,8] Particular attention is directed to the location of water-bearing strata. Samples are obtained that give information on texture, color, soil structure, consistency, compactness, cementation, and—in many situations—chemical composition. In the latter instance, emphasis is placed on the determination of organic matter and salts of the alkalies, and horizons with lime carbonate accumulations. In situations where foundations must carry heavy embankment loads, test pits are frequently used to obtain undisturbed samples for use in determining consolidation, shear, and permeability characteristics. Core drilling is common in bedrock country.

In almost all situations some field work is desirable. However, there is hardly a spot on the surface of the earth that has not been described sufficiently to afford some information on the character of the soil. The accuracy will vary, of course, but important data can usually be developed by a careful search of the existing information. Some of the most important material to be checked are geologic, pedologic, and topographic maps and aerial photographs.

Use of Geologic Maps for Highway Soil-Survey Purposes.—Utilization of geologic maps to assist the engineering soil surveyor depends greatly on the type of terrain involved and on the orignal purpose assigned to the development of the geologic map. In terrain where the overburden is shallow and residual soils have been developed from bedrock in place, the engineer will frequently find that geologic maps are almost indispensable for the economical collection of engineering data for a given road project.

For those who have an interest in working with generalized information, the 1933 edition of the Geological Map of the United States, published by the United States Geological Survey (USGS), is recommended. This map has some use for regional planning and for an over-all understanding of the bedrock geology of the United States. Its limitations with regard to soil-survey work include (*a*) an almost complete lack of information on glacial deposits and loessial deposits, and (*b*) a geolgoic time concept in place of a rock-texture concept. Most of the states of the United States have "geologic surveys" and through these facilities, or through the facilities of the USGS, geological maps of individual states are frequently available. Of course, such maps are more useful than the Geological Map of the United States because of their increased scale, but their limitations when used for engineering work are similar to those of the USGS map.

---

[4] "Classification and Identification of Soils," by Arthur Casagrande, *Transactions*, ASCE, Vol. 113, 1948, p. 901.

[5] "Report of Committee on Classification of Materials for Subgrades and Granular Type Roads," *Proceedings*, Highway Research Board, National Research Council, Vol. 25, 1945, pp. 375–392.

[6] "Standard Methods of Surveying and Sampling Soils for Highway Subgrades," A.A.S.H.O. Designation: T 86–42, *Highway Materials*, Part II, Tests, Am. Assn. of State Highway Officials, 1947, p. 178.

[7] "Soil Mechanics Applied to Highway Engineering in Ohio," by K. B. Woods and R. R. Litehiser, *Engineering Bulletin No. 99*, Ohio State Univ., Columbus, Ohio, Vol. 7, No. 2, July, 1938.

[8] "Subgrade Soil Practices," by Tilton E. Shelburne, from "Report of Committee on Concrete Pavement Design," *Technical Bulletin No. 121*, Am. Road Builders' Assn., 1947, pp. 3–27.

Geologic reports and accompanying maps, made on a quadrangle basis, or even on a county basis, are useful for highway soil-survey purposes. Such reports and maps usually contain detailed information about bedrock and all surficial deposits.[9,10,11] Geologic reports and maps of this type include rather detailed information on the nature of terrace deposits and the textures of upland soils; and emphasis is placed on the location and engineering characteristics of select materials of construction. The ultimate potential of this type of geologic presentation has not been fully realized, not only in highway engineering but also in airport work, site selection, ground-water study, and general engineering.

A third type of geologic presentation is the report (accompanied by maps) that is frequently available for glacial areas. The glacial maps of Maine,[12] Minnesota,[13] and other states are well done and they have wide application for engineering soil-survey purposes. The terminology is different from that used by the engineer and some effort must be devoted to obtaining background with respect to the methods employed in mapping and to the terminology used. Such terms as "kames," "eskers," "drumlins," "outwash plains," "till plains," "moraines," and "lacustrine deposits" are the word tools used by the geologist in presenting his information concerning glacial areas.

Use of Agricultural Soil-Survey Maps.—Procedures for making agricultural soil maps have been evolved during the 50 years or more since the beginning of the century. The oldest maps contain boundary information similar, in many respects, to certain types of geologic boundaries. Over a 25-year period (since about 1927) these procedures have been refined to include the climatic aspects of soil development as one of the major variables. Constant research and many years of experience have enabled the pedologist to improve his mapping procedures so that the modern soil-survey map includes not only parent material and climate as variables, but also vegetation, slope, and age of the material.[14]

Because these maps are prepared on a local political boundary basis—a county basis, for instance—it is frequently true that the variations of climate, parent material, vegetation, and length of the weathering time within the given political unit are either insignificant or their influence on the soil properties cannot be determined within the limits of the one map. This leaves topography as the major variable. The nomenclature used to designate the various soils includes geographical names that refer to the type of locality where the soil was first mapped. Soils differing primarily in slope variations are grouped together as a "catena." Descriptions of various horizons or

---

[9] "Geology and Mineral Resources of the Cleveland District, Ohio," by H. P. Cushing, Frank Leverett, and Frank R. Van Horn, *Geological Survey Bulletin 818*, U. S. Dept. of the Interior, 1931.

[10] "Maps of Construction Materials," by Frank E. Byrne, from "Soil Exploration and Mapping," *Bulletin No. 28*, Highway Research Board, National Research Council, 1950, p. 63.

[11] "Preparation of an Engineering Geologic Map of the Homestead Quadrangle, Montana," by Clifford A. Kaye, from "The Appraisal of Terrain Conditions for Highway Engineering Purposes," *Bulletin No. 13*, Highway Research Board, National Research Council, 1948, p. 48.

[12] "A Survey of Road Materials and Glacial Geology of Maine," by H. Walter Leavitt and Edward H. Perkins, *Bulletin No. 30*, Vol. II, Maine Technology Experiment Station, Orono, Maine, 1935.

[13] "Quaternary Geology of Minnesota and Parts of Adjacent States," by Frank Leverett and Frederick W. Gardeson, *Professional Paper No. 161*, U. S. Geological Survey, Washington, D. C., 1932.

[14] "Soils of the United States," by C. F. Marbut, from "Atlas of American Agriculture," Part III, Bureau of Chemistry and Soils, USDA (Advance Sheets, No. 8), July, 1935.

layers of the soil profile include detailed information such as the color, texture, structure, and compactness. Unfortunately, actual laboratory tests have not been reported extensively and the reader must obtain his knowledge of the soils from the word picture developed in the report accompanying the soil-survey map.

Most of the information shown on the agricultural soil-survey map can be used for engineering soil-survey purposes.[15,16] However, the information presented on these maps is frequently given in considerable detail; thus it is often desirable to regroup the soils shown on the agricultural soil map in the construction of the engineering soil map.

The pedological method of soil survey has been utilized in two general ways. In states such as Michigan,[17] Missouri,[18] and North Carolina the soil-survey terminology is used with very little change by the soils engineer and any

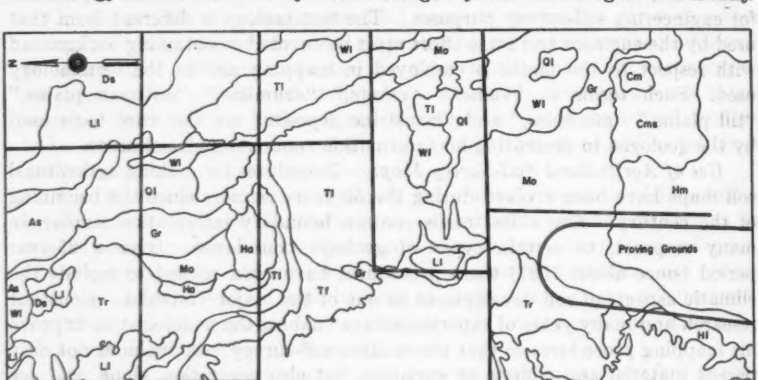

FIG. 1.—PART OF AN AGRICULTURAL SOIL-SURVEY MAP OF ST. JOSEPH COUNTY, INDIANA

new maps that must be prepared for a given highway project embody the basic principles used by the pedologist in the preparation of this soil-survey map. In Michigan (for example), the soils engineer who prepares the soils

[15] "Longitudinal Cracking of Concrete Pavements on State Highway 12 in Clark and Taylor Counties, Wisconsin," by H. F. Janda, *Proceedings*, Highway Research Board, National Research Council, Vol. 15, 1935, pp. 157–169.

[16] "Engineering Use of Agricultural Soil Maps," *Bulletin No. 22*, Highway Research Board, National Research Council, 1949.

[17] "Field Manual of Soil Engineering," Michigan State Highway Dept., Lansing, Mich., February, 1946.

[18] "Soils Manual," Missouri State Highway Comm., Bureau of Materials, Jefferson City, Mo., 1948.

map for the location survey aids in the preparation of plans and specifications and makes field inspections during the construction period. In contrast, states such as New York,[19] Indiana,[20] and many others use the available agricultural soil-survey maps for determining the general characteristics of the area in question and for locating important areas for field sampling. These data are then supplemented by actual laboratory tests on carefully selected soil samples. Both field and laboratory work can be reduced materially by the employment of either of these two processes.

Seismic and Electrical Resistivity Methods.—Since the early 1930's, the United States Bureau of Public Roads and some state highway departments have experimented with geophysical methods of subsurface exploration.[21] R. Woodward Moore[22] and E. Raymond Shepard[23] have published much information concerning these methods.

The seismic procedure consists of creating waves by exploding small charges of dynamite buried near the surface of the soil and "measuring the time of travel of these waves from their point of origin to each of several detectors placed at small distances from the source."[22] The mechanical energy picked up by the detectors is converted into electrical energy and a record is made of the time required for the wave to be transmitted from its source to any given pickup. An analysis is made of the data thus collected at the several pickups, and predictions are made with respect to the nature and depth of the various layers of material. The method has particular application in finding rock lines under buried soils and in evaluating foundation problems, especially in peat bogs and in swampy areas.

In the electrical resistivity method, the resistance to the flow of an electric current through the subsurface materials is measured at certain intervals of the ground surface. Because many rocks and soils have differences in resistivities, it is often possible to develop a general idea of subsurface conditions. The method has particular application to geological work in bedrock areas. However, the method has been used for solving foundation problems, and particularly for finding rock lines under deep soil cover, for mapping buried channels, and for obtaining information on the characteristics of rock and soil materials in highway cut sections.

Use of Aerial Photographs in Soil Surveying.—In the late 1920's, aerial photographs were first used in the preparation of agricultural soil-survey maps.[24] All agricultural soil-survey maps in Indiana are now (1952) made with the aid of airphotos.

---

[19] "An Engineering Grouping of New York State Soils: Geology of New York, Engineering Grouping of Soils, Production of Area Soil Maps, Use of Engineering Soil Maps," by Earl F. Bennett and George W. McAlpin, from "The Appraisal of Terrain Conditions for Highway Engineering Purposes," *Bulletin No. 13*, Highway Research Board, National Research Council, 1948, pp. 55–63.

[20] "Distribution, Formation, and Engineering Characteristics of Soils," by D. J. Belcher, L. E. Gregg, and K. B. Woods *Engineering Bulletin*, Purdue Univ., Lafayette, Ind., *Research Series No. 87*, Vol. 27, January, 1943.

[21] "Application of Geology and Seismology to Highway Location and Design in Massachusetts," from "The Appraisal of Terrain Conditions for Highway Engineering Purposes," *Bulletin No. 13*, Highway Research Board, National Research Council, 1948, pp. 66–90.

[22] "Development of Geophysical Methods of Subsurface Exploration in the Field of Highway Construction," by R. Woodward Moore, from "Soil Exploration and Mapping," *Bulletin No. 28*, Highway Research Board, National Research Council, 1950, p. 73.

[23] "Subsurface Explorations by Geophysical Methods," by E. Raymond Shepard, *Proceedings*, ASTM, Vol. 49, 1949, pp. 993–1009.

The adaptation of this technique to engineering soil surveys has been pursued at Purdue University, at Lafayette, Ind.,[20,25] and at other institutions. The aerial photograph has three distinct applications with respect to the highway soil survey. In the first place, the airphoto can be used advantageously

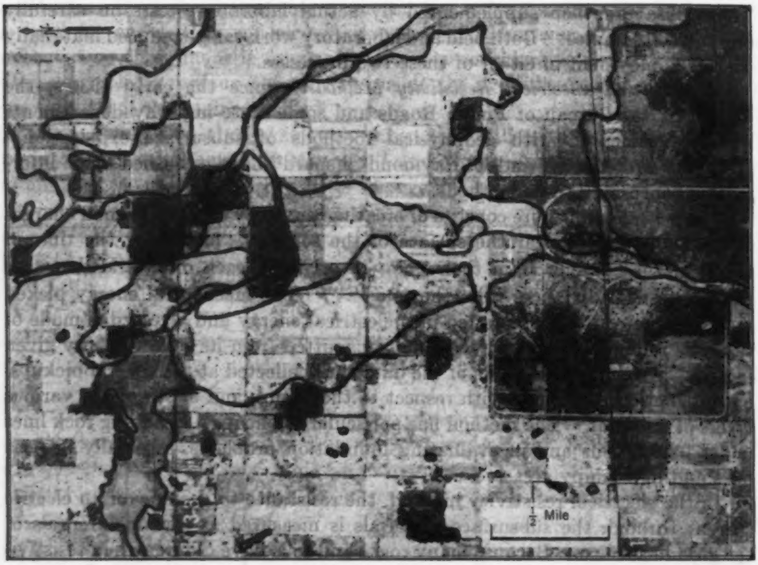

Fig. 2.—Contact Aerial Photograph of Area Shown in Fig. 1.

for locating the boundaries between soils of unlike characteristics and from this information a generalized engineering soils map can be prepared.[26] Carefully planned field checks constitute an essential part of this type of program and the precision of airphoto interpretation depends on the quantity of detail desired in the finished map. Secondly, the aerial photograph is used in unmapped areas, in particular, to predict the engineering characteristics of soils.[27] The processes involved in this type of work require considerable study and training on the part of the interpreter, and moderately rigid photographic specifications must be used with respect to scale, quality of paper, and climatic influence at the time of flight. The third, and perhaps most practical, use of the aerial photograph is for locating field-sampling areas in connection with the

[24] "The Story of Indiana Soils," by T. M. Bushnell, *Special Circular 1*, Agri. Experiment Station, Purdue Univ., Lafayette, Ind., June, 1944.

[25] "The Origin, Distribution and Airphoto Identification of United States Soils," by D. S. Jenkins, D. J. Belcher, L. E. Gregg, and K. B. Woods, *Technical Development Report No. 52*, Civ. Aeronautics Administration, May, 1946.

[26] "The Engineering Significance of Airphoto Patterns of Northern Indiana Soils," by Pacifico Montano, thesis presented to Purdue University at Lafayette, Ind., in June, 1946, in partial fulfilment of the requirements for the degree of Master of Science in Civil Engineering.

[27] "The Development of Engineering Soils Maps," by D. J. Belcher, *Proceedings*, Twenty-ninth Annual Purdue Road School, *Engineering Bulletin*, Purdue Univ., Lafayette, Ind., *Extension Series No. 55*, Vol. 27, No. 2, March, 1943, pp. 86–92.

development of the engineering soil-survey strip map for a given highway project.[28,29] These photographs, used either alone or in conjunction with geologic, pedologic, or even topographic maps, have wide application in this type of survey. The Sonne, strip-film method (low altitude, continuous strip) has possibilities, not only for soil survey but also for use in pavement performance surveys, in topographic and property line surveying, and even for location work.[30]

Regardless of the intended use of the aerial photograph in connection with the soil-survey work, it is important that the soils engineer have some general background in the methods involved. He should have a good concept of pedological and geological methods of mapping, including the basic concepts

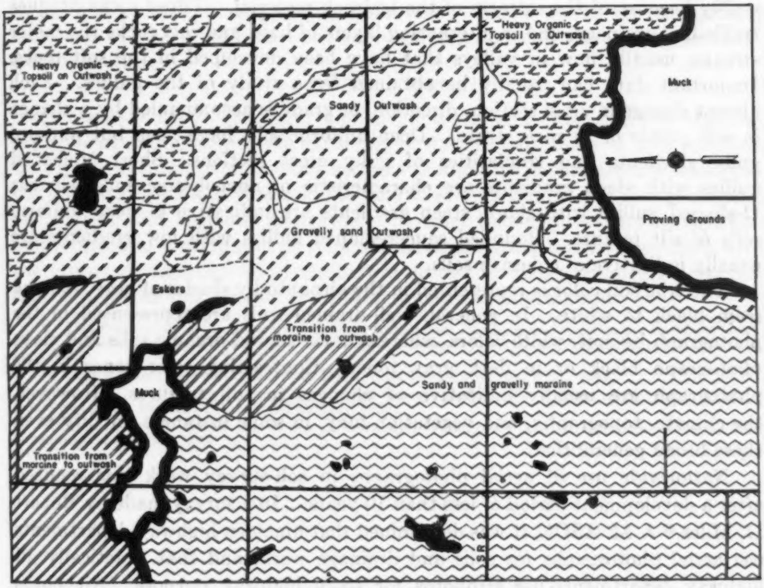

FIG. 3.—AN ENGINEERING SOILS MAP OF THE AREA SHOWN IN FIGS. 1 AND 2

from which these sciences have been developed; and he should have some background in airphoto interpretation techniques.

Through research, airphoto interpretation techniques have been developed that have resulted in the definition of certain so-called "elements of the

[28] "The Use of Aerial Maps in Soil Studies and in the Location of Borrow Pits," by R. E. Frost, *Proceedings*, Kansas State Highway Eng. Conference, July 1, 1946, pp. 58–82.

[29] "Airphoto Interpretation of Soils and Drainage of Parke County, Indiana," by Merle Parvis, thesis presented to Purdue University at Lafayette, Ind., in June, 1946, in partial fulfilment of the requirements for the degree of Master of Science in Civil Engineering.

[30] "Application of Aerial Strip Photography to Highway and Airport Engineering," by J. E. Hittle, *Proceedings*, Highway Research Board, National Research Council, Vol. 26, 1946, pp. 226–235.

pattern."[31] These elements include the "landform" or "topographic expression," the "drainage pattern," the "color tones," "erosional characteristics," and "land use." Of all these elements, perhaps the most important with respect to the identification of the textures of soil and rock materials is that of the topographic expression. Such glacial forms as kames, eskers, and terraces—which in turn suggest soil textures—are easily identified. In bedrock regions, the character of the rock can usually be predicted on the basis of certain landform elements. For example, flat-lying soluble limestones contain sinkholes; and alternate beds of shale and sandstone, outcropping in a tilted position, appear in the airphoto as valleys and ridges.

Drainage and erosional features are important elements of the airphoto pattern. In shale areas, for example, channels and gullies meander considerably because of the softness of the bedrock material. Tilted rocks produce trellis-like drainage, and in alternating layers of hard and soft rocks the major streams usually flow in valleys that have been developed in the soft rocks. Important data can usually be obtained by a study of the gullies. Each abrupt change in cross section, direction, or grade is accompanied by a change in soil profile or in rock strata. Deep uniform soils have deep but uniform gully gradients and similarities of gully cross sections. Short V-shaped gullies with steep gradients are characteristic of noncohesive soils whereas U-shaped gullies with short, steep gradients are indicative of deep uniform soils of silt texture. Rounded saucer-shaped gullies with low gradients are usually indicative of cohesive soils.

The true soil color is represented in the airphoto by shades of gray, ranging from black to white. In general, well-drained soils are represented in the photograph by soft, white colors, whereas dark-colored organic soils and clays photograph black or in dark gray tones. Contrasting color tones in the photograph are usually indicative of changes in soil textures. However, the climate, topography, and vegetation may, in some instances, modify even these broad generalities.

Nationwide use of aerial photographs in soil-survey work was realized after a development period of less than 10 years. In a survey made by Robert D. Miles,[32] J. M. ASCE, it was determined that nineteen highway departments use aerial photographs for soils and drainage work, and that practically all highway departments use airphotos for some highway purpose. Airphotos have been used for site selection by the Civil Aeronautics Administration[20] and later by the Corps of Engineers, United States Department of the Army.[33] It seems safe to assume that this tool will find increased use as interpretation techniques are developed and as more soils engineers become familiar with these techniques.

---

[31] "Aerial Photographs Used for an Engineering Evaluation of Soil Materials," by R. E. Frost and K. B. Woods, *Proceedings*, Second International Conference on Soil Mechanics and Foundation Eng., Rotterdam, Holland, 1948, pp. 324–330.

[32] "Procedures for Making Preliminary Soils and Drainage Surveys from Aerial Photographs," by Robert D. Miles, thesis presented to Purdue University at Lafayette, Ind., in June, 1951, in partial fulfilment of the requirements for the degree of Master of Science in Civil Engineering.

[33] "Correlation Between Permafrost and Soils as Indicated by Aerial Photographs," by K. B. Woods, Jean E. Hittle, and R. E. Frost, *Proceedings*, Second International Conference on Soil Mechanics and Foundation Eng., Rotterdam, Holland, 1948, pp. 321–324.

Combined Use of Several Methods.—The modern highway soils engineer is finding that the most economical procedure to be followed in developing the highway soils survey is to utilize all the various types of maps and information available.[34,35,36,37] These include topographic maps, agricultural soil-survey maps, various types of geologic maps, and contact airphoto prints. Illustrations of the combined use of various available maps are shown in Figs. 1, 2, and 3.

Fig. 1 represents a part of an agricultural soil-survey map from St. Joseph County, Indiana, in the glacial drift region. The nomenclature at the bottom of this figure indicates the typical method of naming soils. Fig. 2 is an aerial photograph made to approximately the same scale as the soil-survey map, and it was selected to cover approximately the same area. The boundary information shown is that which usually would be established for the development of a generalized engineering soils map. Fig. 3 shows the engineering soils map as interpreted from the aerial photograph and the agricultural soil-survey map.

Conclusion

Because geology, pedology, and airphotos offer a vast store of data to supplement and minimize the gathering of data for soil surveys, it is probable that in the future the larger soils sections of highway departments will employ not only engineers well versed in the field of soil mechanics, but also geologists, pedologists, and airphoto interpreters, in order that highway soil surveys can be produced in a minimum of time and at a reasonable cost. Specialists with the proper background and training are needed to help engineering organizations realize the full benefits from these sources of information.

[34] "The Preparation of Engineering Soil Maps from Aerial Photographs," by Charles R. McCullough, *Proceedings*, Third Annual Florida Highway Conference, *Bulletin Series No. 31*, Vol. 4, No. 1, January, 1950, pp. 42–53.

[35] "Soils Manual," Wyoming Highway Dept., Soils Div., Cheyenne, Wyo., 1949.

[36] "State-Wide Highway Planning Survey Soil Study," *Bulletin No. 6*, State of Nebraska, Dept. of Roads and Irrig., Bureau of Roads and Bridges, 1939.

[37] "Soils of Iowa," *Special Report No. 3*, Iowa Agri. Experiment Station, Agronomy Section, Soils Subsection, November, 1936.

DISCUSSION

GEORGE F. SOWERS,[38] A.M. ASCE.—Highway planners and designers, as well as soils engineers, will find the information which Mr. Woods has presented to be of great value. It is the writer's opinion, however, that a mere description of the methods of exploration that are in use is not sufficient. Most engineers are familiar with the well-established procedures for making soil surveys, however, techniques such as the use of pedological data and geophysical methods are not so clearly understood. Unfortunately, the enthusiasm with which these methods have been advocated and adopted has not always been accompanied by a thorough consideration of what information these methods can and cannot supply

In making soil surveys the engineer has depended on direct methods, such as borings and test pits. Newer fields of science have made available both ready-made data on soil conditions and indirect techniques of making soil surveys. These approaches have the important advantage of providing extensive data at a lower cost than do the older methods, but they do have inherent shortcomings which should be clearly understood by the engineers who use them.

Geological and Pedological Data.—The geological and pedological surveys, mentioned by Mr. Woods, classify soils primarily on the basis of genealogy (including the age of the deposit), its method of formation, and the type of soil (usually based on texture or mineralogy) of which it is composed. This information is helpful, but it does not supply the answers to specific engineering problems.

These questions may be answered in one of two ways. In some states the different geologic and pedologic groups are correlated with soil performance. The design problems affected by the soil are then solved by empirical relationships. Unfortunately, the basic geologic and pedologic classifications ignore many of the pertinent soil properties. Consequently, the correlations between performance and soil group are often rather crude and sometimes little better than guesswork. If, in the design, the average correlation of values is used, occasional failures must be expected; if the correlation is conservative, there will be many cases of overdesign. The writer believes that such an empirical approach is fundamentally unsound. It encourages shortsighted designers to follow a set rule without the need for determining the best design for each set of soil conditions. Furthermore, this approach tends to stifle productive research for better methods of correcting difficult situations, since it concentrates attention on methods of classifying soils rather than on methods of evaluating the physical properties of a soil.

The second approach described by Mr. Woods is to use the pedological and geological data to define areas in which the soil conditions are likely to be homogeneous. Representative samples from each area are tested to deter-

[38] Associate Prof. of Civ. Eng., Georgia Inst. of Technology, Atlanta, Ga.; Cons. Engr., Law-Barrow-Agee Labs., Atlanta, Ga.

mine the soil properties and the range of these properties. The design can then be based on actual test results rather than on some empirical correlation. If the range of the properties within any one area is so great that a safe, economical design cannot be had, all that is necessary is to increase the amount of sampling and testing so as to secure more extensive data. The use of this approach stimulates research into the causes and cures of highway difficulties, since the engineers deal with the physical properties of the soil in their everyday problems.

Geophysical Methods.—As Mr. Woods states, the geophysical methods of exploration have been used in highway work to some extent since 1930. In more recent years, the development of more compact equipment by organizations engaged in mineral exploration has resulted in increased interest and more extensive use of geophysical exploration in all civil engineering site investigations. The author does not point out, however, that geophysical exploration has limitations which can discredit its use if those limitations are not clearly understood.

The geophysical methods do not directly determine the locations of soil and rock strata. Instead, they measure changes in effects of a force such as an electric current or a shock wave on the earth. These changes, in many cases, can be interpreted so as to obtain an estimate of the soil and rock conditions.

Seismic Method as Applied to Civil Engineering.—The seismic method utilizes the different velocities of a shock wave in soils and rocks to determine the thicknesses of the strata. The ideal situation for the application of seismic exploration consists of horizontal, well-defined strata in which the velocity of sound becomes greater in each deeper stratum. When underground conditions resemble the ideal, the seismic method yields accurate, dependable information, but if the underground conditions differ from the ideal, the results may be far from reliable.

One application in which the method has proved useful is in the determination of the thickness of unconsolidated mantle overlying bedrock. It has been particularly useful in the preliminary studies for bridge and dam foundations where sound rock may be covered by several hundred feet of boulder-filled materials. It may also be used when the ground surface is covered with water. In some cases it has been possible to use this method for determining the thickness of different strata of unconsolidated materials. Unfortunately, however, the velocities in unlike soil strata may be so nearly alike that the method is of little value for this purpose.

In many cases it has been possible to identify consolidated and unconsolidated materials from the velocities of wave travel in them. It has been possible in some areas to correlate the engineering properties, such as strength, with the velocities so that the seismic data can be used to predict the structural capabilities of the materials. However, such relations apply only to the materials of a restricted group and should not be used indiscriminately.

When the rock surface is very irregular or deeply weathered, the seismic refraction method is of doubtful value. So many different interpretations of the data are possible that the results are of little use to either the planner or

the designer. When the velocities within the strata decrease with increasing depth, or when the velocities vary erratically, the results of the method may be of little value. The water table often confuses seismic data so that rational interpretation is impossible.

Electrical Resistivity Methods.—The electrical resistivity methods are based on the fact that different soils and rocks offer different resistances to the passage of an electric current. Two methods are commonly used. In the first, the soil resistivity is measured at one location between two electrodes whose spacing is increased by increments. A graph showing resistivity as a function of electrode spacing is prepared and the curve is analyzed to determine the depth of strata having different resistances.

The first method is well-suited to the determination of the depth and thickness of soil strata having great differences in resistance. Since electrical resistance depends largely on the degrees of ionization, materials that differ greatly in water content, porosity, and chemical composition are likely to have different resistances. Moist clays and silts ordinarily have low resistances whereas sands, gravels, dry soils, and rocks have high resistances.

This method has proved particularly useful for locating sound rock when the rock lies at depths of less than 75 ft. This makes it adaptable to preliminary surveys for highway location where the possibility of rock excavation is an important factor in the determination of the final design. The method has also been successful in locating the water table in sands and gravels and other soils which have high resistances when dry. In areas where the soil profile consists of alternate strata of dry sands and gravels and moist clays, it has been possible to identify the depth and thickness of each stratum, and in a few instances it has been possible to identify the materials by their resistances. Such identifications must be confirmed by borings before they can be used for engineering purposes.

The second method, often termed the "constant-depth traverse," or "resistivity traverse," uses a constant electrode spacing and requires measurements at many different locations over the project site. From these data "contour" maps of resistivity are prepared which show areas of high and low values. Since dry sands and gravels have high resistivities, this method is particularly useful for locating such deposits and for showing the location at which the deposit is likely to be the thickest. It also could be used in preliminary studies of marsh areas to locate sand bars and similar soils of relatively high bearing capacity. This method might also be used to trace the beds of buried glacial streams for ground-water supplies. In areas where the rock is deep and foundations must extend down to it, the method can define the areas where rock lies closest to the ground surface.

Value of Geophysical Methods.—The geophysical methods of exploration are indirect means of identifying marked differences in the electrical resistance or wave velocities of the underground materials. The methods are useful only if these differences can be accurately interpreted in terms of engineering data, and if the data can be secured as easily and as economically as similar data obtained by other methods of exploration.

The depth and thickness of the strata can be estimated with an accuracy of about 1 ft or 2 ft, if the underground conditions approach the ideal of horizontal well-defined strata. Unfortunately, there have been instances in which the data indicate that the conditions are ideal and the measurements of depth and thickness have been 50% in error. When the underground conditions are far from ideal, such as when the upper surface of bedrock is very irregular or badly weathered, the results may be inaccurate and misleading. On one project, in North Carolina during 1951, the seismic refraction records indicated that sound rock was at a uniform depth of 30 ft and was overlain by unconsolidated materials. When the site was excavated, however, rock was found at a depth of 15 ft, but was somewhat irregular.

TABLE 1.—RELATIVE MERITS OF GEOPHYSICAL METHODS AND COMPARABLE BORING METHODS

Method	Equipment cost (in dollars)	Typical weight (in lb)	Minimum crew	Cost per ft of depth[a] (in dollars)	Advantages	Disadvantages and limitations
Hand auger.....	10	10	1	0.50–1.00	Soil samples	Limited by gravel and ground-water table, 30-ft maximum depth.
Two-man powered auger	500	80	2	0.25–0.50	Soil samples	Limited to from 6-ft to 8-ft depth. Cannot bore coarse gravel.
Jeep-mounted powered auger	3,500	3,000	1	0.30–1.00	Soil samples	Limited by boulders and ground water.
Wash boring....	500	200	2	0.30–1.00	Washed "samples"	Cannot bore gravel.
Seismic........	4,000	150	3 to 4	0.25–0.50	Not hampered by boulders	Boring confirmation necessary. Unreliable if rock surface is irregular. Estimated soil character only. Requires explosives.
Resistivity......	500	25	2 to 3	0.25–0.50	Not hampered by boulders	Boring confirmation necessary. Estimated soil character only. Affected by strong electric current.

[a] Commercial cost including overhead and reporting of data.

A resistivity survey of a building site in Georgia during 1952 was used to establish the depth to rock. Subsequent borings indicated that the minimum error of the actual depth to rock was 40% and the average error was 160%.

In some cases the geophysical methods suffer from outside limitations. For example, the seismic method often cannot be used in cities because of restrictions on explosives. In 1952 the electrical resistivity method was used to determine the depth of an old rubbish dump in Altanta, Ga. The measurements were completely obscured by electrical currents generated by the action of acid-forming cinders and metal in the fill.

The geophysical data only indicate the engineering characteristics of the materials. In any one area it is sometimes possible to establish an empirical correlation between resistivity of wave velocity and properties such as strength. However, such relationships are crude at best and furnish only limited infor-

mation for the planning stages of a project. Since the relationships are empirical, it is dangerous to apply the experience gained in one region to materials from another region with different geologic characteristics.

The information obtained by geophysical exploration is in many ways comparable to that obtained by wash boring, hand auger boring, or power auger boring. The decision of whether to use the geophysical methods or the direct methods depends largely on convenience and cost. In general, the geophysical equipment is expensive and relatively fragile and requires trained personnel and experienced supervision in order to obtain even passable results. On the other hand, a well-trained crew is able to secure considerable data in a short time. The comparable simple boring methods (except power augers) require relatively inexpensive, easily portable equipment and do not necessarily require trained personnel to obtain good results. In some situations, such as with irregular rock, the geophysical methods may prove useless, whereas in other situations, such as with a boulder-filled deposit, the simple boring methods are useless.

Table 1 shows some of the relative merits of geophysical methods compared with the more common direct method.

K. B. Woods,[39] M. ASCE.—Mr. Sowers, in his discussion of the original paper, has supplied some additional and important data in the field of explorations, particularly with respect to geophysical methods. The research of C. R. Lennertz, J. M. ASCE, in the field of electrical resistivity exploration, supports Mr. Sowers' observation as to the dependability and need of collaborating information. Experiments to date (1953) indicate the need of some type of control data when exploring alluvial deposits and locating bedrock that is covered with glacial and alluvial sediments. However, many highway departments are finding the electrical resistivity technique an economic and useful tool to supplement many of their exploratory programs.[40]

---

[39] Associate Director, Joint Highway Research Project, and Prof. of Highway Eng., Purdue Univ., Lafayette, Ind.

[40] "Soil Investigation Employing a New Method of Layer-Value Determination for Earth Resistivity Interpretation," by H. E. Barnes, *Bulletin No. 65*, Highway Research Board, National Research Council, 1952, pp. 26–36.

AMERICAN SOCIETY OF CIVIL ENGINEERS

Founded November 5, 1852

TRANSACTIONS

Paper No. 2569

ELECTRICAL ANALOGIES AND ELECTRONIC COMPUTERS

A SYMPOSIUM

PAGE

Surge and Water Hammer Problems
By Henry M. Paynter, J.M. ASCE 962

Application to an Hydraulic Problem
By R. E. Glover, M. ASCE, D. J. Hebert, and C. R. Daum 1010

Application to Stream-Flow Routing
By M. A. Kohler, A.M. ASCE 1028

Hydrodynamic Problems in Three Dimensions
By P. G. Hubbard, J.M. ASCE, and S. C. Ling 1046

Pipe Networks Studied by Nonlinear Resistors
By Malcolm S. McIlroy 1055

SURGE AND WATER HAMMER PROBLEMS

By Henry M. Paynter,[1] J. M. ASCE

With Discussion by Messrs. E. B. Strowger, George R. Rich, Donald R. F. Harleman and Edward N. Rein, and Henry M. Paynter

Synopsis

In the course of extensive investigations in the fields of speed and pressure regulation at the Massachusetts Institute of Technology (M.I.T.), at Cambridge, use has been made of certain electrical-fluid analogies. Also, as an aid to obtaining direct solutions while retaining the basically nonlinear features in the components of the systems being studied, an electronic computer has been found useful.

This paper describes the foundation for these techniques, the types of analogies, methods developed, and equipment employed, together with a few representative results and conclusions drawn from these studies. The particular cases of pressure transients in a uniform pipe and surges in a simple tank have been selected for discussion. However, no such restrictions are inherent in the methods developed.

Emphasis has been placed on the utilization of analog techniques to extend, refine, and clarify analytical procedures to secure a more thorough understanding of the basic hydraulic phenomena and to furnish results that are generally useful and accessible. Brief mention is made of some improved analytical procedures developed in connection with these studies.

Introduction

The interconnection of hydraulic and steam power plants within modern electric power networks gives rise to numerous complex problems concerning both the influence of load fluctuations and frequency control equipment on the stable operation of the generating units, and, conversely, the effects of the transient behavior of the hydraulic and mechanical components of the units on the performance of the electrical network. A representative hydroelectric system is shown schematically in Fig. 1, in which B is the gate opening, H is the head, P is the power, N is the speed, and Q is the discharge. As subscripts, c denotes "conduit," l denotes "transmission line," r denotes "reservoir," and

Note.—Published in August, 1952, as *Proceedings-Separate No. 146.* Positions and titles given are those in effect when the paper or discussion was received for publication.

[1] Asst. Prof. of Hydr. Eng., Dept. of Civ. and San. Eng., Massachusetts Inst. of Technology, Cambridge, Mass.

t denotes "surge tank." In the course of this paper, use will be made of dimensionless incremental variables—the "per-unit" variables familiar to electrical engineers. These will generally be denoted by the lower case letters corresponding to the physical variables; thus, $b = \frac{\Delta B}{B_0}, h = \frac{\Delta H}{H_0}, p = \frac{\Delta P}{P_0}, n = \frac{\Delta N}{N_0}$, $q = \frac{\Delta Q}{Q_0}$, in which the numerators in each case represent changes from a refer-

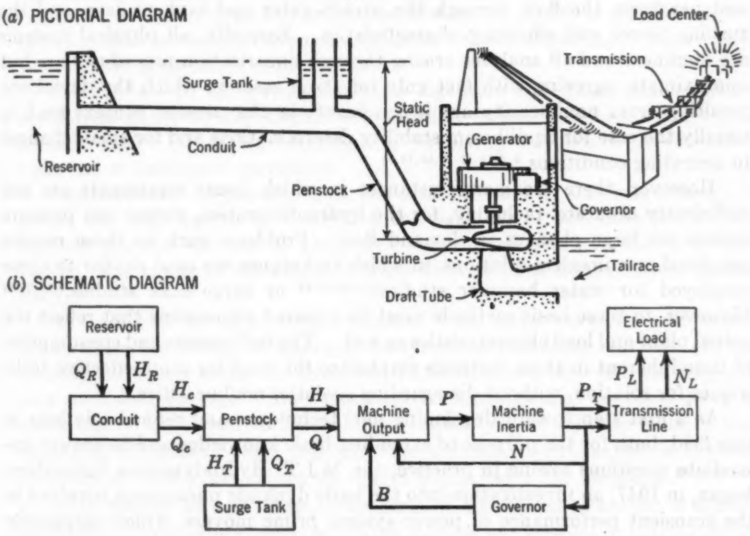

FIG. 1.—TYPICAL HYDROELECTRIC INSTALLATION

ence condition and the denominators correspond to this reference or index condition, denoted by the subscript zero.

Most earlier investigations in the regulation field were not extended much beyond the point at which immediate and practical questions were answered. Thus, the classical researches into water hammer and surge phenomena that formed the subject of many pioneering investigations[2,3,4,5,6,7] remained adequate as long as the various generating stations were loosely tied and operated in

[2] "Über den hydraulischen Stoss in Wasserleitungsrohren," by N. Joukowsky, *Memoires de l'Academie du Sciences de St. Petersbourg*, Vol. 9, 8th Serie, 1898.

[3] "Théorie générale du mouvement varié de l'eau dans les tuyaux de conduite," by L. Allievi, *Revue de Mecanique*, Janvier et Mars, 1904.

[4] "Teoria del colpo d'ariete," by L. Allievi, *Reale Academia dei Lincei*, Anno CCCIX, 1912.

[5] "The Surge Tank in Water Power Plants," by R. D. Johnson, *Transactions*, ASME, Vol. 30, 1908, p. 443.

[6] "Pressures in Penstocks Caused by Gradual Closing of Turbine Gates," by N. R. Gibson, *Transactions*, ASCE, Vol. 83, 1920, p. 707.

[7] "Sur Théorie des Wasserschlosses bei selbstatig geregelten Turbinenanlagen," by D. Thoma, Oldenburg, Munchen, Germany, 1910.

relative isolation. However, with the growth of interconnection to the level at which nearly all the plants in a particular system and even entire systems are coupled together, these earlier methods of analysis and special solutions have become inadequate.

Straightforward extension and generalization of the pioneer studies are hampered by the presence of inescapable nonlinearities in the various physical components of the problem. These nonlinearities occur in the hydraulic elements of a hydroelectric plant, for example, in the friction loss in the conduit and penstock, the flow through the wicket gates and tank orifices, and the turbine power and efficiency characteristics. Basically, all physical systems are nonlinear and all analyses arising through linearization procedures are but approximate, agreeing with fact only for those cases in which the deviations resulting from nonlinearity are insignificant; in the present context such is usually the case for equilibrium stability determinations and for small changes in operating conditions.[8,9,10,11,12,13,14,15]

However, there are many instances in which linear treatments are not sufficiently accurate, including, for the hydraulic system, surges and pressure swings for large changes in demand flow. Problems such as these require graphical or numerical solutions, in which techniques are used similar to those employed for water hammer studies[4,6,16,17,18] or surge tank studies.[5,19,20,21] However, to these basic methods must be annexed expressions that reflect the actual plant and load characteristics as well. The tediousness and consumption of time inherent in these methods emphasize the need for more effective techniques for solution, without disregarding essential nonlinearities.

As a first step toward developing new techniques and refined solutions in this field, both for the purpose of extending basic knowledge and to answer immediate questions arising in practice, the M.I.T. Hydrodynamics Laboratory began, in 1947, an investigation into the basic dynamic phenomena involved in the transient performance of power system prime movers, which necessarily

---

[8] "Contribution à l'étude des régulateurs de vitesse. Considerations sur le problème de la stabilité," by D. Gaden, Editions La Concorde, Lausanne, Switzerland, 1945.

[9] "Étude de la stabilité d'un réglage automatique de vitesse par des diagrammes vectoriels," by D. Gaden, *Informations Techniques Charmilles No. 2*, Geneve, Switzerland, 1946.

[10] "Influence de certaines caractéristiques intervenant dans la condition de stabilité. À propos du réglage automatique de vitesse des turbines hydrauliques," by D. Gaden, Editions La Concorde, Lausanne, Switzerland, 1949.

[11] "Influence de l'inertie de l'eau sur la stabilité d'un groupe hydroelectrique," by P. Almeras, *La Houille Blanche*, Novembre, 1945.

[12] "Influence des phénomènes de coup de pélier sur le réglage de la vitesse des turbines hydrauliques," by M. Cuenod, *ibid.*, Mars-Avril, 1949.

[13] "La regolazione delle turbine idrauliche," by G. Evangelisti, Zanichelli, Bologna, 1947.

[14] "Sulla stabilità di regolazione nelle installazioni idroelettriche," by G. Evangelisti, *L'Energia Elettrica*, 1946.

[15] "Sulla validità della regola di Thoma per le vasche di oscillazione degli impianti idroelettrici," by E. Scimemi, *ibid.*, 1947.

[16] "Methode graphique génèrale de calcul des propagations d'ondes planes," by L. Bergeron, *Memoires de la Societé des Ingenieurs Civils de France*, 1937.

[17] "Water Hammer in Pipes, Including Those Supplied by Centrifugal Pumps," by R. W. Angus, *Proceedings*, Inst. of Mech. Eng., Vol. 136, 1937, p. 245.

[18] "Druckstösse in Pumpensteigleitungen," by O. Schnyder, *Schweizerische Bauzeitung*, Vol. 94, Nos. 22 and 23, 1929.

[19] "Théorie de chambres d'équilibre," by J. Calame and D. Gaden, Gautier-Villars, Paris, France, and La Concorde, Lausanne, Switzerland, 1926.

[20] "The Surge Chamber in Hydroelectric Installations," by R. S. Cole, *Selected Engineering Papers, No. 55*, Inst. C. E., London, England, 1927.

[21] "Zur Berechnung von Wasserschlössern," by E. Braun, *Schweizerische Bauzeitung*, Band 86, 1925.

required research into the field of hydraulic transients. Certain of these studies are outlined here as well as in a related paper by the author.[22]

Analogs and Computers

One fruitful approach toward understanding these problems has been found in the use of electrical analogs and computers, by means of which solutions may be obtained rapidly and in immediately useful form. These devices fall naturally into two classes,[23,24,25] analogs and computers.

Analogs.—In analogs the prototype system, in effect, is duplicated by a model system whose equivalent components behave according to laws analogous to those governing the prototype.

Computers.—In computers the basic algebraic and differential equations are solved either by (*a*) Digital computation (numerical calculation by discrete steps) or (*b*) analog computation (involving calculation by continuous variation of analogous variables).

Comparisons.—Generally, then, the establishment of a formal analogy between the basic equations describing the behavior of two different physical systems permits the use of previously determined solutions for new cases. Indeed, this is one of the major benefits derived from mathematical analysis itself.

As problems become more complex, with more variables and system parameters, the utility of analog techniques becomes more marked. In particular, most mechanical (or dynamical) problems can be represented by suitable electrical analogs. Since electrical terminology and concepts have become highly developed in the fields of unsteady and periodic motion, these analogies will usually prove fruitful. For a detailed introduction to the basic structure of analog techniques the reader is referred to the literature.[26,27,28,29,30]

With respect to computers, some form of high-speed computer is useful if the system under study involves a large number of variables or many different solutions for varying parameters and conditions. Even linear analyses became awkward for these cases. Computers are also helpful if the system possesses one or more significant nonlinear features that render analytic solutions impossible.

Many problems in the field of speed and pressure regulation possess both of these attributes. In this paper the latter aspect has been emphasized, especially since a number of novel results have been obtained.

---

[22] "Methods and Results from M.I.T. Studies in Unsteady Flow," by H. M. Paynter, *Journal*, Boston Soc. of Civ. Engrs., VXXXIX, No. 2, April, 1952.

[23] "High Speed Computing Devices," Eng. Research Associates, McGraw-Hill Book Co., Inc., New York, N. Y., 1950.

[24] "Calculating Instruments and Machines," by D. R. Hartree, Univ. of Illinois Press, Urbana, Ill., 1949.

[25] "Theory of Mathematical Machines," by F. J. Murray, Kings Crown Press, New York, N. Y., 1947.

[26] "Transients in Linear Systems," by M. F. Gardner and J. L. Barnes, John Wiley & Sons, Inc., New York, N. Y., 1942.

[27] "Applied Mathematics for Engineers and Physicists," by L. A. Pipes, McGraw-Hill Book Co., Inc., New York, N. Y., 1946, Chapter VIII.

[28] "Mathematical Methods in Engineering," by T. von Kármán and M. Biot, McGraw-Hill Book Co., Inc., New York, N. Y., 1940, Chapter VI.

[29] "Dynamical Analogies," by H. F. Olson, D. Van Nostrand, Inc., New York, N. Y., 1943.

[30] "Similitude in Engineering," by Glenn Murphy, Ronald Press, New York, N. Y., 1950.

Some Physical Concepts

All continuous devices to transport energy over distances possess many features in common. Such mechanisms may be mechanical shafts, electrical transmission lines, pressure pipe lines, or open channels, all of which can be conceived of as a series of inertial elements linked together by elastic or flexible couplings capable of storing potential energy. In other words, these systems may be visualized in terms of a simple dynamical model consisting of mass cars

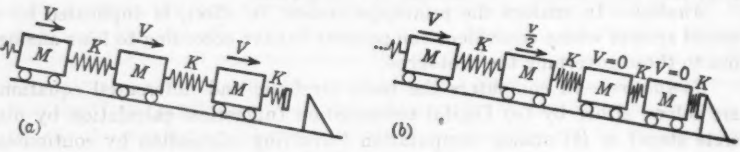

Fig. 2.—Mass-Spring Model

M and coupling springs K, as shown in Fig. 2. The energy terms associated with these elements are

$$\mathrm{KE} = \tfrac{1}{2} M V^2 \qquad (1a)$$

and

$$\mathrm{PE} = \tfrac{1}{2} K X^2 \qquad (1b)$$

in which KE is kinetic energy and PE is potential energy when the cars are moving with a velocity V and the springs are compressed a distance X.

If the leading car is suddenly stopped, the springs must each in turn absorb the kinetic energy of the adjacent car, and convert it into potential energy. Furthermore, a definite time delay occurs at each unit, in order to decelerate the mass and build up the compression. These two features may be obtained from the conservation of energy and momentum principles as follows:

Energy—

$$\mathrm{KE} = \mathrm{PE} \qquad (2a)$$

$$\tfrac{1}{2} M V^2_{\max} = \tfrac{1}{2} K X^2_{\max} \qquad (2b)$$

or

$$X_{\max} = \sqrt{\frac{M}{K}}\, V_{\max} = Z_0\, V_{\max} \qquad (3)$$

in which Z_0 = surge impedance = $\sqrt{\frac{M}{K}}$.

Momentum—

$$\mathrm{M}\, \Delta V = F\, \Delta T \text{ gives } M\, V_{\max} \sim K\, X_{\max}\, \Delta T \qquad (4)$$

From which

$$\text{delay } \Delta T \sim \frac{M\, V_{\max}}{K\, X_{\max}} = \frac{M}{Z_0\, K} = \sqrt{\frac{M}{K}} \qquad (5)$$

and

$$c \sim \frac{1}{\Delta T} \sim \sqrt{\frac{K}{M}} \qquad (6)$$

in which c is the propagation velocity. In the case of elastic pressure waves, the corresponding values for the surge impedance Z_0 and propagation velocity c become

$$Z_0 = \frac{c}{g} = \frac{\Delta H}{\Delta V} \qquad (7)$$

in which g is the acceleration due to gravity, and for unbounded fluid,

$$c = \sqrt{\frac{E_b}{\rho}} \qquad (8)$$

in which ρ is the density, with Z_0 relating the change in head to the change in velocity. These concepts prove generally useful for all types of transmission problems.

Electrical Analogy

It is demonstrated in Table 1 that a uniform, frictionless pipe line is formally analogous to a uniform, dissipationless electrical transmission line. Thus the

TABLE 1.—Electrical-Hydraulic Analogy

Line	(a) Hydraulic System: Uniform frictionless pipe line	(b) Electrical System: Uniform lossless transmission line
	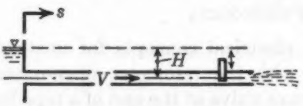	
1	Inertia equation: $-\frac{\partial H}{\partial s} = \frac{1}{g}\frac{\partial V}{\partial t}$	Voltage drop: $-\frac{\partial E}{\partial s} = L\frac{\partial I}{\partial t}$
2	Continuity equation: $-\frac{\partial V}{\partial s} = \frac{w}{E_b}\left(1 + \frac{E_b}{E_y}\frac{D}{e}\right)\frac{\partial H}{\partial t}$	Line charging: $-\frac{\partial I}{\partial s} = C\frac{\partial E}{\partial t}$
3	Wave equations: $\frac{\partial^2 H}{\partial t^2} = c^2\frac{\partial^2 H}{\partial s^2}$	Wave equations: $\frac{\partial^2 E}{\partial t^2} = c^2\frac{\partial^2 E}{\partial s^2}$
4	$\frac{\partial^2 V}{\partial t^2} = c^2\frac{\partial^2 V}{\partial s^2}$	$\frac{\partial^2 I}{\partial t^2} = c^2\frac{\partial^2 I}{\partial s^2}$
5	Propagation velocity: $c = \sqrt{\frac{E_b/\rho}{1 + \frac{E_b}{E_y}\frac{D}{e}}}$	Propagation velocity: $c = \sqrt{\frac{1}{LC}}$
6	Surge impedance: $Z_0 = \frac{c}{g}$	Surge impedance: $Z_0 = \sqrt{\frac{L}{C}}$
	Reflections:	Reflections:
7	Open end: Pressure node: $\Delta H = 0$	Grounded end: Voltage node: $\Delta E = 0$
8	Reflection factor: $r = -1$	Reflection factor: $r = -1$
9	Closed end: Velocity: $\Delta V = 0$	Open end: Current node: $\Delta I = 0$
10	Reflection factor: $r = +1$	Reflection factor: $r = +1$

ANALOGY

Head $H \longleftrightarrow$ Voltage E
Velocity $V \longleftrightarrow$ Current I

water hammer waves and surges of the hydraulic engineer became the traveling waves, electrical surges, and switching transients of the electrical engineer. The fruits of this analogy are (1) the ability to make use of the many useful tools and concepts developed by the electrical engineer since 1900 and (2) the realization that, when viewed in this light, hydraulic and electrical engineers have similar problems and a common language.

In short, velocity V is analogous to current I, and head H is analogous to voltage E.

As long as dissipation phenomena are negligible in both systems these analogies are strictly valid. Nevertheless, in the practical case resistance and losses must be taken into account. For the complex forms of pipe networks, even in steady flow, computers are useful. With steady flow one successful method of making friction proportional to an exponential power of the flow is embodied in the pipe flow analyzer.[31] For unsteady flow problems, using electronic computers, it is possible to account for this frictional effect satisfactorily through special components described subsequently.

However, even in the loss-free form, many concepts of electrical engineering have direct application to problems of unsteady flow. For example, the ordinary alternating-current vector diagrams furnish valuable clues to the behavior of pipe lines subjected to alternations of flow and pressure. Moreover, the use of surge impedance and the other generalized circuit constants can be extremely profitable.

Resonance Phenomena

An excellent example of the use of electrical concepts for unsteady flow problems can be shown in connection with the resonance phenomena associated with the rhythmic motion of a gate or valve at the end of a pipe line. In such cases, the resultant pressure fluctuations along the pipe may often be substantially in excess of the maximum at the valve for the full gate stroke, for which the governor or gate mechanism timing is usually specified and adjusted. It will also be of interest to compare the results obtained by these techniques with those obtained by following the classical methods.

The solutions of the electrical wave equations for long alternating-current transmission lines, as derived in any standard work on power transmission,[32,33,34] may be put in the form:

$$\vec{E}_x = \vec{E}_s \cosh(\overrightarrow{\alpha x}) - \vec{I}_s \vec{Z}_0 \sinh(\overrightarrow{\alpha x}) \qquad (9)$$

and

$$\vec{I}_x = \vec{I}_s \cosh(\overrightarrow{\alpha x}) - \left(\frac{\vec{E}_s}{\vec{Z}_0}\right) \sinh(\overrightarrow{\alpha x}) \qquad (10)$$

in which x is the distance along the transmission line from the sending end; $\vec{E}_x$ is the voltage vector at point x; $\vec{E}_s$ is the voltage vector at the sending end;

[31] "Nonlinear Electrical Analogy for Pipe Networks," by Malcolm S. McIlroy, *Transactions*, ASCE, Vol. 118, 1953, p. 1055.

[32] "Principles of Electric Power Transmission," by L. F. Woodruff, John Wiley & Sons, Inc., New York, N. Y., 1938.

[33] "Power System Interconnection," by H. Rissik, Pitman, London, England, 1940.

[34] "Standard Handbook for Electrical Engineers," edited by A. E. Knowlton, McGraw-Hill Book Co., Inc., New York, N. Y., 1941, Sect. 13.

$\vec{I}_x$ is the current vector at point x; $\vec{I}_s$ is the current vector at the sending end; $\vec{\alpha}$ is the vector propagation constant; and $\vec{Z}_0$ is the vector surge impedance.

If the line is short-circuited (analogous to open reservoir) at $x = L$, then $E_L = 0$, and the sending end voltage and current are related by the expression,

$$\vec{E}_s = \vec{I}_s \vec{Z}_0 \tanh(\overline{\alpha L}) \qquad (11)$$

Furthermore, if the line resistance is negligible (analogous to the frictionless pipe), the propagation constant $\vec{\alpha}$ is given by

$$\vec{\alpha} = \vec{j}\,\frac{\omega}{c} \qquad (12)$$

in which ω is the angular frequency of transmission; c is the propagation velocity; and $j = \sqrt{-1}$.

By the analogy between flow velocity $\longleftrightarrow$ current, and head $\longleftrightarrow$ voltage, one may rewrite this expression directly in hydraulic terms, to obtain corresponding values for head and velocity at the gate, thus:

$$\vec{h} = -2\,K\,\vec{v}\,\vec{j}\tan\left(\frac{\pi}{2}\frac{T_n}{T_0}\right) \qquad (13)$$

and

$$\vec{v} = +\frac{\vec{h}}{2\,K}\,\vec{j}\cot\left(\frac{\pi}{2}\frac{T_n}{T_0}\right) \qquad (14)$$

in which $T_n = \frac{4\,L}{c}$ equals natural period of pipe; T_0 is the period of gate oscillation; $K = \frac{c\,V_0}{2\,g\,H_0}$ equals the Allievi parameter; $h = \frac{\Delta H}{H_0}$ equals the relative head change; and $v = \frac{\Delta V}{V_0}$ $\left(\text{numerically equal to } \frac{\Delta Q}{Q_0}\right)$ equals the relative velocity (or flow) change.

Eqs. 13 and 14 demonstrate that the head variation will always lag behind the flow variation by an angle of 90° and that the amplitude ratio of head relative to flow is given by the expression:

$$\left[\frac{h}{v}\right] = 2\,K\tan\left(\frac{\pi}{2}\frac{T_n}{T_0}\right) \qquad (15)$$

For small variations, however, the normalized flow v may also be found from the expression:

$$(1 + v) = (1 + b)\sqrt{1 + h} \qquad (16)$$

in which $b = \Delta B/B_0 =$ relative gate opening, or, approximately

$$v = b + (\tfrac{1}{2})\,h \qquad (17)$$

Combining Eqs. 15 and 17,

$$\left[\frac{h}{b}\right] = -2\cos\phi_h \text{ (with } h \text{ lagging } b \text{ by angle } \phi_h) \qquad (18)$$

and

$$\tan \phi_h = -\frac{1}{K} \cot \left[\frac{\pi}{2} \frac{T_n}{T_0} \right] \quad \text{.................... (19)}$$

A graphical representation of these expressions is shown in Figs. 3 and 4. These results were first obtained by D. Gaden[8] using interval equations derived by L. Allievi.

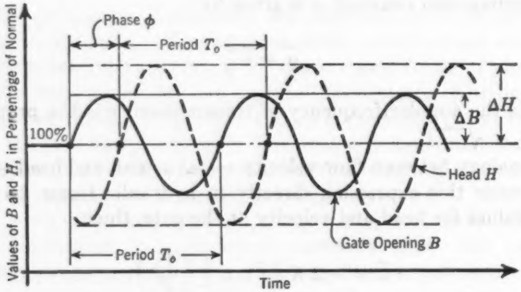

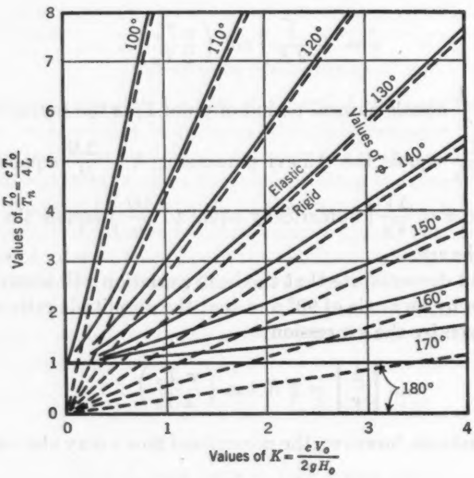

FIG. 3.—WATER HAMMER RESONANCE

For example, in Fig. 4 assume $K = 5$ and $\frac{T_0}{T_n} = 2.5$ to locate the point A; then extend a line OB through point A to point B on the semicircle. The values $\frac{h}{b} = 1.92$ and $\phi_h = 164°$ are read directly. The significance of these curves arises from a consideration of the variations in velocity (or flow) and input torque (or power) caused by oscillations of gate opening. The velocity and

input torque in the normalized (or per-unit) dimensionless form may be expressed by the equations:

Flow—

$$(1 + v) = (1 + b)\sqrt{1 + h} \quad \text{(20)}$$

and power—

$$(1 + p) = (1 + h)(1 + v) = (1 + b)\sqrt{(1 + h)^3} \quad \text{(21)}$$

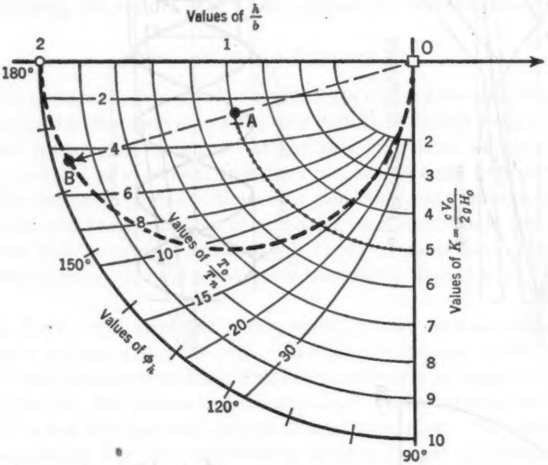

FIG. 4.—RESONANCE DIAGRAM

For small increments Eqs. 20 and 21 become

$$v = b + (\tfrac{1}{2})\, h \quad \text{(22)}$$

and

$$p = b + (\tfrac{3}{2})\, h \quad \text{(23)}$$

These sinusoidally varying increments can be conceived as rotating vectors (as illustrated in Fig. 5) and the resulting amplitude ratios, making use of the previously determined expressions, become

$$\left[\frac{v}{b}\right] = \sin\phi \quad \text{(24)}$$

and

$$\left[\frac{p}{b}\right] = \sqrt{\tfrac{1}{2}(5 + 3\cos 2\phi)} = \sqrt{1 + 3\cos^2\phi} \quad \text{(25)}$$

with $\phi = \phi_h$, the lagging angle between the gate vector b and the head vector h, as before, increasing from 90° (for $T_0/T_n \rightarrow \infty$) up to 180° (for $T_0/T_n = 1$). Thus, both the velocity v and the power p always lag behind the gate b, as demonstrated in Fig. 5, in which it should be noted that the tips of the v-vector and p-vector, as well as the multiples of h, all execute circular loci as the frequency increases.

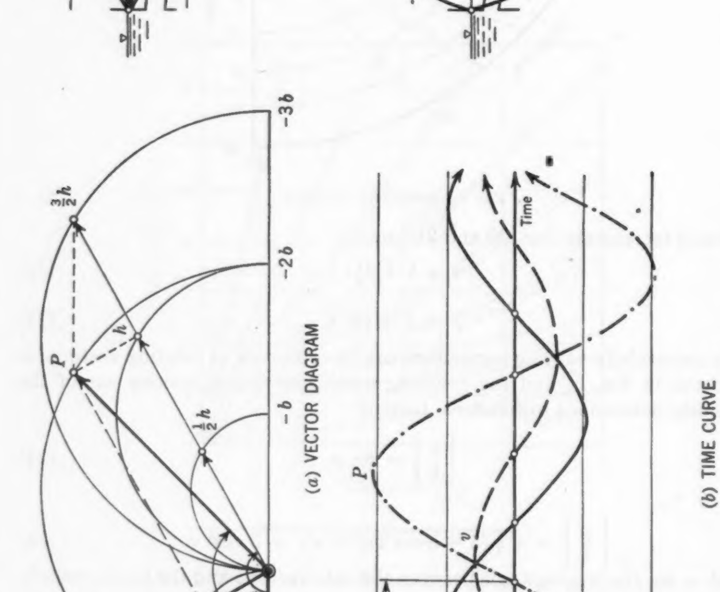

FIG. 5.—RESPONSE CURVES

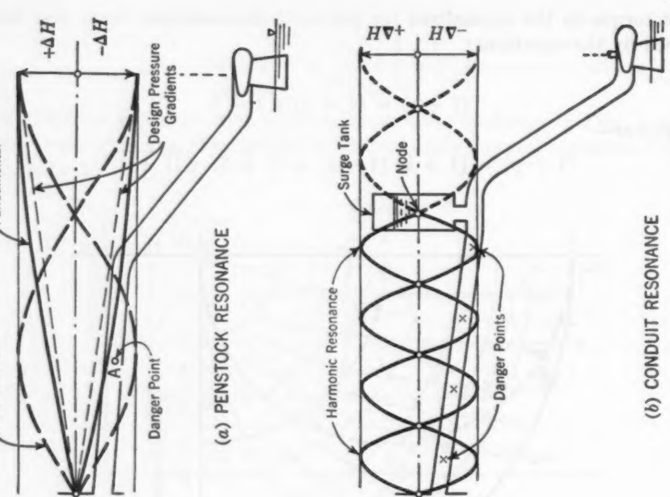

FIG. 6.—CASES OF RESONANCE

It may be concluded from these analyses that the input power to the prime mover inherently lags behind the gate opening, no matter how slowly the gate is moved, with increasing phase shift ϕ_p for higher frequencies; this circumstance is critical in determining the transient performance of hydroelectric units and clearly indicates one of the fundamental limitations of such units for participation in system load and frequency control programs.

In the Appendix, a numerical example is given showing the use of Figs. 3, 4, and 5 and comparing the results with those obtained by conventional methods.

Application of Results

From the foregoing it is evident that oscillations of the gate or valve produce standing waves in the pipe or systems of pipes with the familiar loops and nodes of all vibratory continuous systems. At the gate end there will usually be a pressure loop, and at the upstream end there is a node at the free surface.

From purely intuitive considerations it is clear that only resonances of the fundamental and odd harmonics can occur under such conditions; but for all of these cases, the full pressure variation will occur at each loop, making the resonance of the harmonics, in general, more dangerous than that of the fundamental.

Moreover, it can be shown that it is possible, under certain conditions, to produce pressure swings along the pipe (through oscillations of the gate that are consistent with the governor timing and stroke) nearly as large as the design values established by the conventional methods. These extreme fluctuations can exist both for the fundamental and the lower harmonics. For example, the pipe line illustrated in Fig. 6(*a*) would be in serious danger of bursting or collapse near point A under the conditions shown.

Another dangerous case of simultaneous resonance can arise between the gate, penstock, and conduit as shown in Fig. 6(*b*). In this case, the surge tank will not serve to trap the elastic waves since a node exists at its base, and, therefore, renders the tank inoperative. Failure resulting from excessive positive or negative pressures may occur at the loops.

Useful Surge Concepts

Considerable insight into the analysis and behavior of simple surge tanks can be gained through consideration of the energy principles involved in the elementary problem of sudden, full-load rejection with a cylindrical tank. The basic dimensions and physical constants of such a tank are indicated in Fig. 7.

For the limiting case of a frictionless conduit, the conservation of energy may be expressed in the form:

$$KE + PE = \text{constant} = (KE)_0 \qquad (26)$$

or, specifically,

$$\tfrac{1}{2} M_c V^2 + M_t g h = \tfrac{1}{2} M_c V_0^2 \qquad (27)$$

with M_c and M_t being the mass of water in the conduit and tank, respectively.

With the data of Fig. 7 there results

$$\frac{1}{2}\left(\frac{w}{g}A_c L_c\right) V^2 + (w\, A_t\, Y)\,\frac{Y}{2} = \frac{1}{2}\left(\frac{w}{g}A_c L_c\right) V^2_0 \quad \text{(28)}$$

or

$$\alpha\, V^2 + \beta\, Y^2 = \alpha\, V^2_0 \quad \text{(29)}$$

in which α and β are constants.

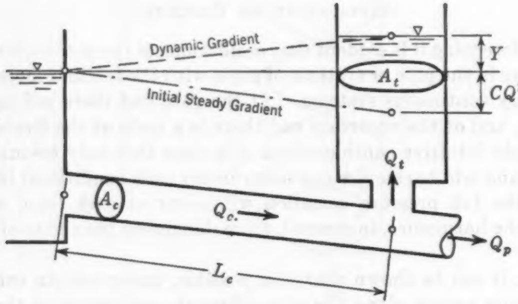

FIG. 7.—SURGE TANK ELEMENTS

This expression is therefore the equation of an ellipse which can be always transformed into a circle by the process of normalization, that is, by making horizontal and vertical scales homogeneous. Thus, dividing through by the term ($\alpha\, V^2_0$),

$$\frac{\alpha\, V^2}{\alpha\, V^2_0} + \frac{\beta\, Y^2}{\alpha\, V^2_0} = 1 \quad \text{(30)}$$

$$\left(\frac{V}{V_0}\right)^2 + \left(\frac{Y}{Y_0}\right)^2 = 1 \quad \text{(31)}$$

in which

$$Y_0 = V_0\sqrt{\frac{A_c\, L_c}{A_t\, g}} = V_0\, Z_0 \quad \text{(32)}$$

with $Z_0 = \sqrt{\frac{A_c\, L_c}{A_t\, g}}$ defined as the surge impedance of the tank. This situation is sketched in Fig. 8(a), in which it is seen that a maximum positive surge occurs at point 2, for which

$$Y_{\max} = Y_0 \quad \text{(33)}$$

or

$$Y_{\max} = V_0\sqrt{\frac{A_c\, L_c}{A_t\, g}} = \text{“free” surge} \quad \text{(34)}$$

From Fig. 8(a) it is also clear that the tank will oscillate indefinitely as a result of continuous interchange of energy without dissipation.

In the practical case, however, conduit friction will modify the basic energy expression into the form:

$$PE = KE + (\text{work done against friction}) \ldots\ldots\ldots\ldots (35)$$

Thus the total change of water level in the tank will be increased by the presence of friction, although the surges will dampen out successively as a result of dissipation, as shown in Fig. 8(*b*).

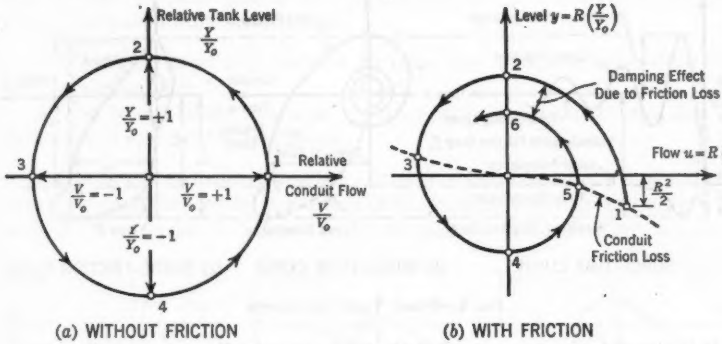

FIG. 8.—SURGE ENERGY DIAGRAMS

The effect of friction, for any given transient, can be measured if the ratio of friction loss to free surge is known. Thus the parameter may be defined as

$$R = \frac{2\,H_f}{Y_0} = \frac{2\,H_f}{V_0}\sqrt{\frac{A_t\,g}{A_c\,L_c}} \ldots\ldots\ldots\ldots (36)$$

in which H_f is the rated conduit friction loss. For a particular value of R the surge oscillations would be modified as shown. It should be noted that the initial friction loss relative to Y_0 is given by $R/2$.

It has been found useful and convenient to multiply both the horizontal (conduit flow = u) and vertical (tank level = y) scales by the constant factor R, to obtain the normalized plots shown in Fig. 9.

Further analysis will show that in terms of the notation used in the diagram—

$$PE = KE + (\text{work done}) \ldots\ldots\ldots\ldots (37)$$

becomes—

$$\frac{z^2}{2} = \frac{u^2}{2} + \int f\,dz \ldots\ldots\ldots\ldots (38)$$

Eq. 38 resolves the problem of computing surges into the evaluation of the work integral on the right-hand side, corresponding to the areas A and B in Fig. 9. This can be done by several different procedures and has been successfully achieved using the electronic computer.

The value of the particular formulation of the problem as implied by Eqs. 37 and 38 lies in the considerable precision that may be derived using even approximate methods of integration. Employing such techniques, tables of surges that are accurate to four significant figures have been prepared for the normal range of tank design. Similar procedures have been developed for restricted orifice and differential tanks.

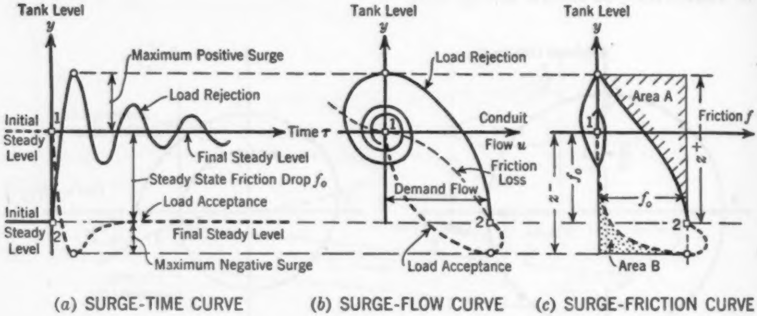

FIG. 9.—SURGE TANK TRANSIENTS

It is also of interest to note that the tank constant R serves as a dimensionless hydraulic similitude index similar to the Reynolds, Froude, and Mach numbers. In other words, two simple surge tanks A and B will be dynamically similar if

$$R_a = R_b \qquad (39)$$

or

$$\frac{2\,H_{fa}}{V_a\sqrt{\dfrac{A_{ca}\,L_{ca}}{A_{ta}\,g}}} = \frac{2\,H_{fb}}{V_b\sqrt{\dfrac{A_{cb}\,L_{cb}}{A_{tb}\,g}}} \qquad (40)$$

This conclusion agrees with the tank similitude analyses of A. H. Gibson[35,36] and W. F. Durand.[37]

SURGE TANK PROBLEMS

The excellent early studies of R. D. Johnson[5] were essentially limited only to establishing design constants and dimensions for fixed positive and negative surge heights. Mr. Johnson did not attempt the determination of the various relationships between diverse values of the many system constants, but rather established working design values for a particular choice of these constants; these restrictions appreciably simplified the analysis of performance, leading directly to the type of results that Mr. Johnson sought.

[35] "The Investigation of the Surge Tank Problem by Model Experiments," by A. H. Gibson, *Proceedings*, Inst. C. E., London, England, 1924–1925.

[36] "A Comparison of Observations on Surge Tank Installations and on Their Scale Models," by A. H. Gibson, *ibid.*, 1932–1933.

[37] "Application of the Law of Kinematic Similitude of the Surge-Chamber," by W. F. Durand, *Transactions*, ASME, Vol. 43, 1921, p. 1177.

However, many tanks now installed are often required to operate under conditions quite different from those selected for design, and the behavior under these conditions has sometimes been unfavorable and unexpected. The problem of determining the response of tanks under all reasonable disturbances that might be encountered has been neglected in the past, largely because of the altogether forbidding length of time required by even the most elementary investigations using conventional methods.

With these needs in view, the research efforts reported in this paper have been devoted, in the surge tank field, to the following problems concerning present and proposed tank installations:

1. The behavior of tank systems for operating conditions other than those used for design; and
2. The true stability margins for surge tanks subjected to specified disturbances of appreciable magnitude.

It has long been realized that the actual transient behavior of surge tanks is considerably influenced by the action of the turbine governor and other plant and load characteristics. However, the magnitude of this effect depends on the

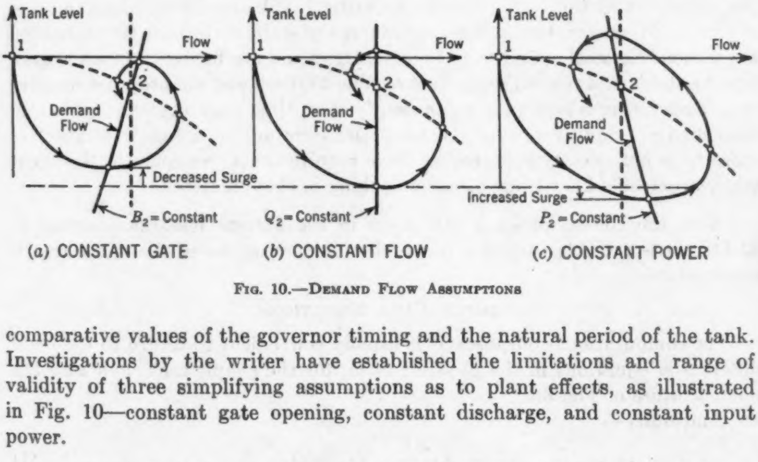

FIG. 10.—DEMAND FLOW ASSUMPTIONS

comparative values of the governor timing and the natural period of the tank. Investigations by the writer have established the limitations and range of validity of three simplifying assumptions as to plant effects, as illustrated in Fig. 10—constant gate opening, constant discharge, and constant input power.

1. Constant Gate Opening (B_2 = Constant) at the Final Steady-State Value.—This is the situation most representative of a unit under manual control by the operator, and produces the least surge, under otherwise comparable conditions, as a result of increased positive damping action.

2. Constant Discharge (Q_2 = Constant) at the Final Steady-State Value.—This was the basis of the methods of Mr. Johnson and most other investigators and produces a greater surge than assumption 1.

3. Constant Input Power (P_2 = Constant) to the Runner at the Final Steady-State Value.—This assumes that efficiency changes are small and the turbine regulates over a time that is very short compared to the tank period. This

assumption gives materially greater surges, and can even lead to instability, as explained subsequently in Fig. 14.

This method, when suitably linearized, was the basis of the classical tank stability analyses[7] that have been modified by later work[38,39,13] of J. Calame and D. Gaden, G. Evangelisti, and the writer.[39]

In addition to the conventional problem of a sudden or step-change in demand conditions, the electronic computer has been applied successfully in the examination of two other types of problems—synchronous or resonant load changes and true static and dynamic stability margins.

4. Synchronous or Resonant Load Changes, of the Pulsing and Oscillatory Type.—Such a loading program may result in abnormally high surges and pressure swings as the period of the disturbance approaches the natural period of the tank. Previously, this problem had been investigated only for a handful of cases.[40]

5. True Static and Dynamic Stability Margins for Tanks Operating Both Under Steady-Load Conditions and Under Appreciable Changes in Demand.—The simplified techniques of the linear stability theory, for example, cannot account for the known augmentation to stability through the differential principle, giving rather the same value for the critical tank area for all common types of tank. Moreover, the engineering concept of stability implies far more than the various classical definitions of mathematics and mechanics. If a surge tank is to be stable in a real sense, it must be able to reach and maintain an effective steady operating condition in a sufficiently short time after any reasonable load disturbance. Simply having the oscillations die out in a time just short of eternity is not adequately meeting these requirements, yet quantitative, generally applicable knowledge has been lacking in these matters.

With the conclusion of a first stage in the current research program at M.I.T., it is possible to give a few preliminary examples of the many results obtained.

Simple Tank Equations

For computational purposes, it is usually convenient to return to the basic differential equations in the physical form; for the simple tank, following the nomenclature of Fig. 6(*b*),

Continuity—

$$- A_t \frac{dY}{dt} = Q_p - Q_c \qquad (41)$$

Acceleration—

$$- \frac{Lc}{A_c\, g} \frac{dQ_c}{dt} = Y + C\, Q^2_c \qquad (42)$$

Assuming a uniform conduit and tank, with square law friction, these may be

[38] "De la stabilité des instalations hydrauliques munies des chambres d'equilibre," by J. Calame and D. Gaden, *Schweizerische Bauzeitung*, Band 90, 1927.

[39] "The Stability of Surge Tanks," by H. M. Paynter, thesis presented to Massachusetts Institute of Technology, at Cambridge, Mass., in 1949, in partial fulfilment of the requirements for the degree of Master of Science.

[40] "The Differential Surge Tank," by R. D. Johnson, *Transactions*, ASCE, Vol. 78, 1915, p. 760.

normalized to the form:

Continuity—

$$-\frac{dy}{d\tau} = v - u \qquad (43)$$

Acceleration—

$$-\frac{du}{d\tau} = y + \tfrac{1}{2}u^2 \qquad (44)$$

in which $y = R\,(Y/Y_0)$; $u = R\,(Q_c/Q_0)$; $\tau = 2\,\pi\,t/T_{ct}$; $v = R\,(Q_v/Q_0)$; $R = 2\,H_f/Y_0$; and $T_{ct} = 2\,\pi\sqrt{\dfrac{A_t\,L_c}{A_c\,g}}$ = free period. As a particular case one

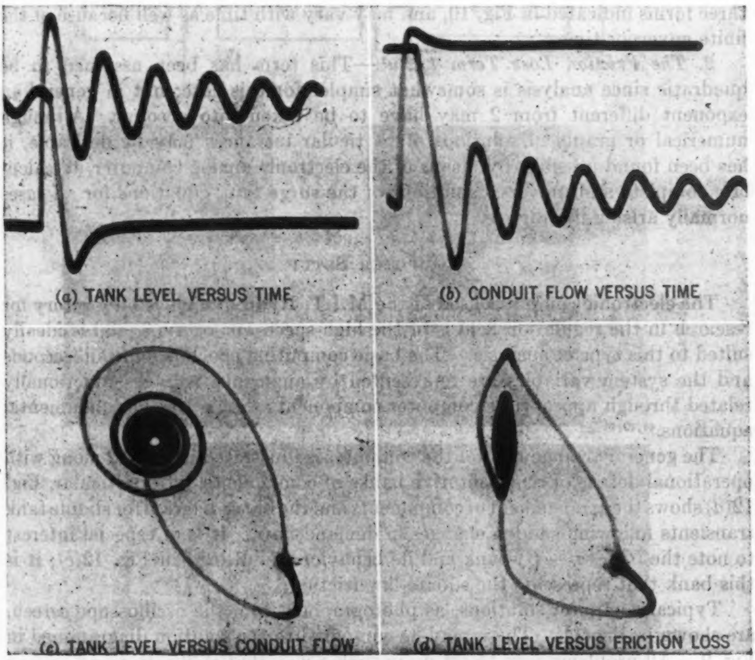

FIG. 11.—REPRESENTATIVE COMPUTER SOLUTIONS OF SURGE TANK TRANSIENTS

might take the transient from an initial steady state $v_1 = R_1 = 1.7$ to a final steady state $v_2 = R_2 = 0$ that might be either full or partial rejection to zero for a great number of practical instances. This transient is indicated in Figs. 9 and 11.

Thus, any given plant can be specified by the value of the parameter R for rated conditions, and the particular transients are specified by the initial and final steady states $u_1 = v_1 = R_1$ and $u_2 = v_2 = R_2$, respectively.

The work of W. E. Milne in this field[41,42,43] involved a complete investigation by numerical methods of the system of Eqs. 43 and 44. Mr. Milne also described the general case of a quadratically damped vibration; but his solutions were only for a step change in demand flow, assumption 2. Nevertheless, his tables use the identical normalized variables as outlined in this paper and it is hoped that this paper may serve as another introduction to Mr. Milne's valuable work.

Nonlinear Features

The two principal nonlinearities of the simple surge tank equations, as outlined, lie in the demand flow characteristic v and the friction loss term $u^2/2$.

1. The Demand Flow Characteristic v.—This factor may have any of the three forms indicated in Fig. 10, and may vary with time as well because of the finite governor time.

2. The Friction Loss Term 1/2 u^2.—This term has been assumed to be quadratic since analysis is somewhat simpler for this case; but in general an exponent different from 2 may have to be taken into account. Although numerical or graphical solutions of particular instances may be desirable, it has been found possible, by means of the electronic analog computer, to calculate complete and universal solutions of the surge tank equations for all cases normally arising in practice.

Computer Setup

The electronic computer used at the M.I.T. Hydrodynamics Laboratory for research in the regulation field is of the high-speed analog type, and is ideally suited to this type of analysis. The basic computing epoch is four milliseconds and the system variables are represented by analogous voltages functionally related through appropriate computer components that solve the fundamental equations.[44,45,46]

The general arrangement of the computer is illustrated in Fig. 12 along with operational details of representative banks of components. In particular, Fig. 12(*d*) shows the arrangement of components and the block diagram for simple tank transients following sudden changes in demand flow. It is of especial interest to note the ($C - \sigma - C$)-bank and its behavior as outlined in Fig. 12(*c*); it is this bank that represents the square-law friction.

Typical computer solutions, as photographed from the oscilloscope screen, are shown in Fig. 11. These may be compared to the solution diagrammed in Fig. 9. All problems may be set up in such a way that calibration and scaling can be made directly from the final photographic records. This arrangement

[41] "Damped Vibrations: General Theory Together with Solutions of Important Special Cases," by W. E. Milne, Univ. of Oregon Publications, Eugene, Ore., August, 1923.

[42] "Tables of Damped Vibrations," by W. E. Milne, Univ. of Oregon Publications, Eugene, Ore., March, 1929.

[43] "Tables of Derivatives for Damped Vibrations," by W. E. Milne, Oregon State College Monographs, Corvallis, Ore., December, 1935.

[44] "The Study of Oscillatory Circuits by Analog Computer Methods," by H. Chang, R. C. Lathrop, and J. C. Rideout, *Proceedings*, National Electronic Conference, 1950.

[45] "Catalog and Manual," G. A. Philbrick Researches Inc., Boston, Mass., 1950.

[46] "The Electronic Analog Computer as a Laboratory Tool," by G. A. Philbrick and H. M. Paynter, *Industrial Laboratories*, May, 1952.

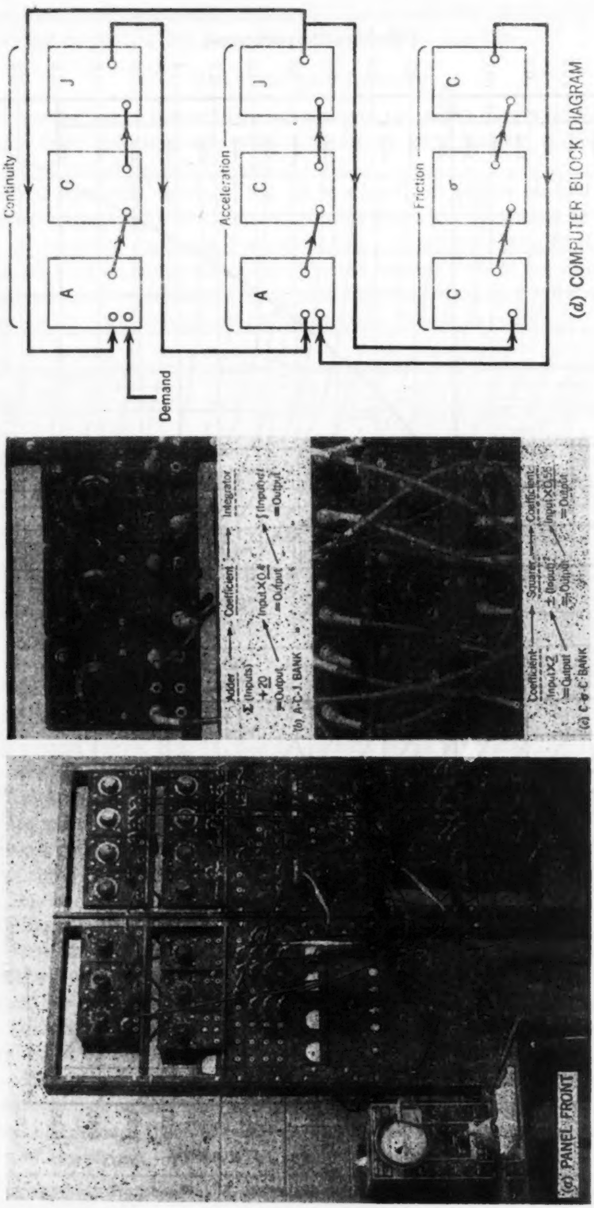

FIG. 12.—ARRANGEMENT OF COMPUTER

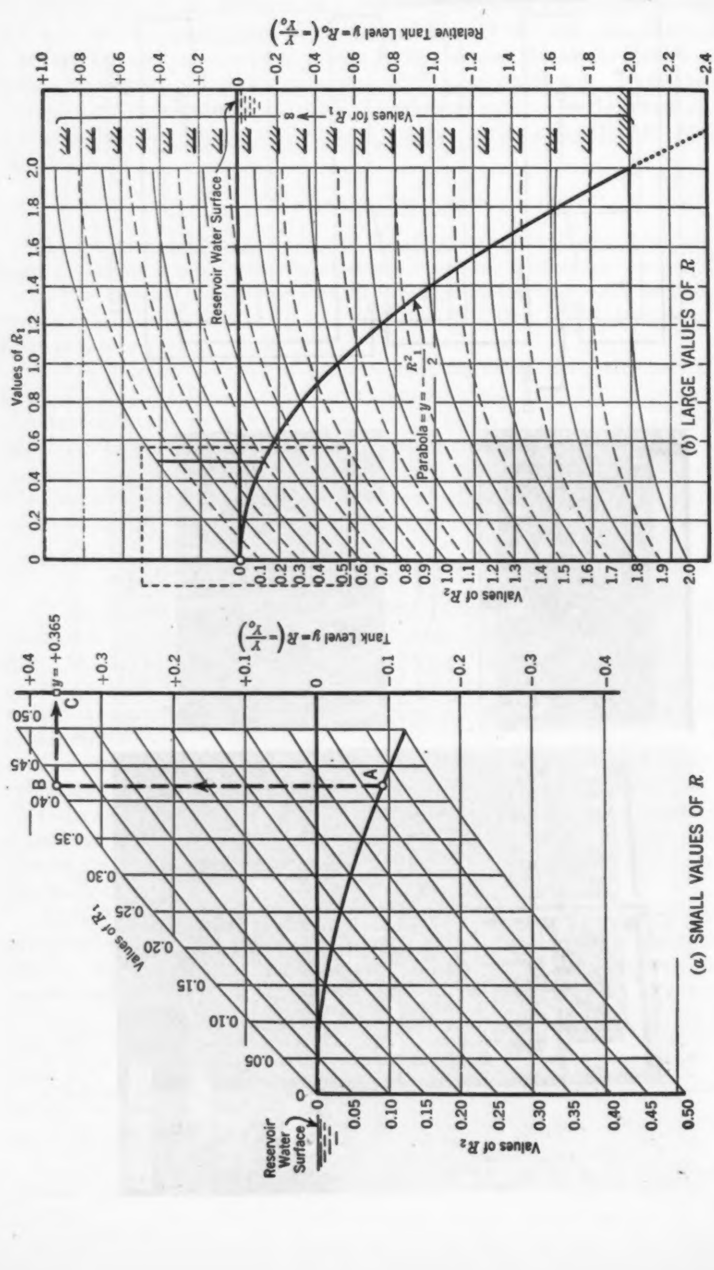

FIG. 13.—SIMPLE TANK SURGE CURVES

has been found very successful in practice and constitutes another strong argument for the normalization procedures that make it possible.

Analysis and Results

It is worthwhile to present two examples of the many charts that have been assembled from the computer studies on simple surge tanks. Similar curves have been obtained for other types of tanks.

The first specimen, shown in Fig. 13, is a family of curves, plotted similar to the method indicated by Mr. Durand,[37] from which the maximum or minimum tank level resulting from any load acceptance or rejection transient with any simple tank may be computed, subject to the assumptions of constant demand flow and square-law friction. This plot may be compared with the earlier Johnson plot.[47] An example of its use is given in the Appendix.

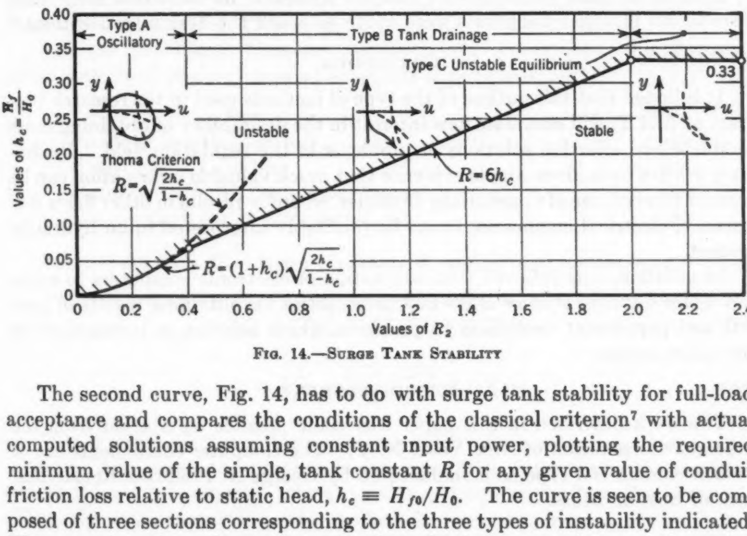

FIG. 14.—SURGE TANK STABILITY

The second curve, Fig. 14, has to do with surge tank stability for full-load acceptance and compares the conditions of the classical criterion[7] with actual computed solutions assuming constant input power, plotting the required minimum value of the simple, tank constant R for any given value of conduit friction loss relative to static head, $h_c \equiv H_{f0}/H_0$. The curve is seen to be composed of three sections corresponding to the three types of instability indicated. There are, in order—the oscillatory region, the drainage region, and the region of unstable steady state.

1. Oscillatory Region (Small Frictional Effect).—In this range stable response (below the curve) is indicated by damped oscillations and unstable behavior is evidenced by oscillations of growing magnitude.

2. Drainage Region (Medium Frictional Effect).—For this region satisfactory behavior results in rapidly damped return to full-load gradient conditions. However, if the tank is of insufficient size, the conduit flow would fail to accelerate as fast as the tank was being drained, and, in the practical case, the unit would evidence instability by failure to deliver the required power at the bottom of the swing. This might result in loss of synchronism.

[47] "Hydroelectric Handbook," by W. P. Creager and J. D. Justin, John Wiley & Sons, Inc., New York, N. Y., 1950, Chapter XXV.

FIG. 13.—SIMPLE TANK SURGE CURVES

3. Region of Unstable Steady State (High Frictional Effect).—When $h_c > 1/3$, the static equilibrium is unstable and the slightest disturbance would result in unstable response. Stating the fact another way, if the rated friction loss H_{f0} is greater than one third the static head H_0, stable regulation is impossible regardless of the presence or size of the tank.

Comments.—Of course, all these conclusions are based on the assumption of constant power input to the prime mover (case 3). However, the effect of the finite time taken by the governor to respond to the changes of head as well as the effects of interconnected generating units usually are such as to ameliorate these conditions. Nevertheless, the curves serve the useful purpose of design limitations and it should be noted that the conventional allowance for drooping efficiency curves applied to the Thoma criterion may still be inadequate for the larger values of h_c.

The use of these curves is shown in the Appendix for an actual surge tank installation in which field tests were made to check the design assumptions.[48]

Conclusion

It is hoped that this outline of the type of methods used in the research program at M.I.T. will stimulate new interest in the desirability of obtaining more complete and effective solutions of problems in the regulation field. Preliminary results have given ample evidence that much valuable information can be derived through use of appropriate analogies, whereby results in other fields (for instance, electrical engineering) may be profitably interpreted in an hydraulic context.

In addition, it is believed that adaptation of electronic computers to surge and water hammer studies offers new possibilities for obtaining results of general and permanent usefulness to problems whose solution is impractical by any other means.

Acknowledgment

The work described in this paper was made possible by a grant from the Research Corporation of New York, N. Y. The computer components are of a stock commercial type as manufactured by George A. Philbrick Researches, Inc., of Boston, Mass.

APPENDIX. TYPICAL EXAMPLES

Explanatory Notes.—The following two examples have been included primarily to demonstrate the use and limitations of the design curves presented in the paper. In particular, the second example, treating surges in the simple surge tank at Tallulah Falls, Ga., was chosen from among the many field test results principally because the deviations from computed studies (obtained by electronic computer or any other means) represent the typical range of uncertainty encountered in practice.

[48] "Tests Check Computed Values of Surges," by Eugene Lauchli, *Engineering Record*, Vol. 71, 1915, p. 378.

It is not intended that the very brief exposition of methods presented be considered complete in itself, but it is outlined only to demonstrate the value of generalized curves and formulas for rapid approximate computations.

The material in Example 1 is drawn from the curves presented in Figs. 3 and 4. A complete explanation and theoretical treatment of water hammer resonance have been presented by Mr. Gaden[8] and Mr. Evangelisti.[13] The confirmation of these results by a graphical solution follows well-known methods.[16,17,18]

However, in Example 2, in addition to the use of the surge diagram of Fig. 13, certain approximate formulas for times and alternate surges have been employed that were not described in the text of the paper. These rough formulas have been found to give good results when checked against both the writer's theoretical studies and field tests, and are similar to certain expressions proposed in the work of Mr. Milne.[41] An explanation of the nature and use of diagrams similar to Fig. 13 is given in the paper of Mr. Durand.[37]

Example 1. Water Hammer Resonance.—A hypothetical hydroelectric plant with the following physical constants is to be analyzed:

Factor	Value
Penstock length L, in feet	1288
Rated head H_0, in feet	200
Rated velocity V_0, in feet per second	10
Wave velocity a, in feet per second	3220

From these data the elastic constants K and μ may be obtained. Thus,

$$K = \frac{c\,V_0}{g\,H_0} = \frac{3220 \times 10}{32.2 \times 200} = 5 \quad \text{(45)}$$

$$\mu = \frac{2\,L}{c} = \frac{2 \times 1288}{3220} = 0.8 \text{ sec} \quad \text{(46)}$$

If it is assumed that gate oscillations exist with a period of 4.8 sec and a swing of 20% range, the problem is concerned with determining the resultant head swings in the penstock, where the natural frequency is $T_n = 2\,\mu = 1.6$ sec. Thus, the data, concerning gate oscillations, required for using the resonance diagram are: The oscillations are assumed sinusoidal about a 100% gate opening, in a range of $\pm 10\%$. The relative period $T_0/T_n = 4.8/1.6 = 3$.

Referring to the resonance diagram (Fig. 4), $\phi_h = 161°$ and $h/b = 1.90$. The head oscillations are thus found to range over $(1.90 \times 20 =)$ 38%, the period for this case being $3\,T_n = 6\,\mu = 4.8$ sec, with a phase lag ϕ of 161°.

The foregoing determination can be checked graphically by reference to Fig. 15. Thus, for a gate swing of 20% and a period (as before) of $T_0 = 3\,T_n = 6\,\mu = 4.8$ sec, the head range is found to be 38% with a phase lag of 165°.

Although the resonance diagrams presented were derived on the basis of small changes, the agreement with conventional computations for large changes is satisfactory for most purposes. However, the upward shift in the head variation curve should be noted, since this assymmetry may reach substantial proportions in particular cases.

Example 2. Surge Tank at Tallulah Falls.[48]—The design data and general computations in Table 2 are self-explanatory. The use of these preliminary data is demonstrated for three cases.

Case A, $R_1 = 0.425$ and $R_2 = 0$.—Enter Fig. 13(*a*) at $R_1 = 0.425$ (point A), read vertically upward to intersect at $R_2 = 0$ (point B). From this point, read

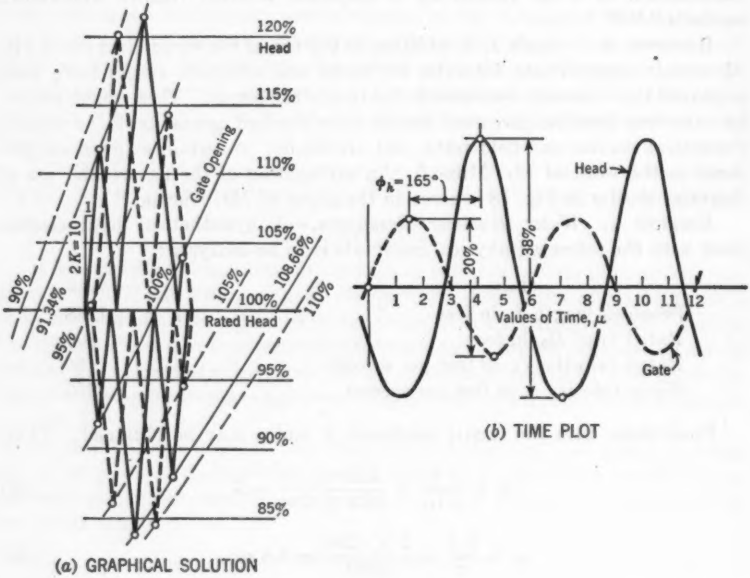

FIG. 15.—EXAMPLE OF RESONANCE

horizontally to point C on the scale at the right, obtaining $y_A = +0.365$. The initial friction drop may be evaluated as $f_A = \frac{1}{2} R_1^2 = 0.091$, or may be read directly from the chart at point A.

Thus, in summary,

Relative surge y_A, in feet above the reservoir surface	+0.365
Relative friction drop f_A, in feet below reservoir surface	0.091
Relative level change from the initial level $z_A = y_A + f_A$	0.456

These values can be converted to physical magnitudes most easily through the proportional relationship:

$$\frac{\text{Level change (in feet)}}{\text{Friction drop (in feet)}} = \frac{\text{relative change }(z)}{\text{relative friction }(f)} \qquad (47)$$

TABLE 2.—DESIGN OF SURGE TANK AT TALLULAH FALLS, GA. (EXAMPLE 2)

Case	DESIGN DATA[a]		OBSERVED DATA			COMPUTATIONS		
	Velocity, ΔV (ft per sec)	Friction loss (ft)	Velocity increment (ft per sec)	Level change (ft)	Time to maximum change (sec)	Free surges[b] $Y_0 = \Delta V \times Z_0$ (ft)	Transients[c] $R = \frac{2H_f}{Y_0}$: R_1	R_2
	(1)	(2)	(3)	(4)	(5)	(6)	(7)	(8)
A	6.13	5.0	6.13→0	23.6	120	6.13×3.83 = 23.5	2×5/23.5 = 0.425	0
B	3.18	1.5	3.18→0	11.9	80	3.18×3 83 = 12.2	0.425×3.18/6.13 = 0.222	0
C	0.16	(0.2)	0.16→1.6	−6.65	100	−1.44×3.83 = −5.52	0.425×0.16/6.13 = 0.011	..[d]

[a] The tank in this example has a rectangular section, 30 ft by 71 ft, with a cross section area of (A_t = 30 × 71 =) 2,131 sq ft. The length L_c of the conduit is 6,666 ft and its area A_c is 151 sq ft. The observed friction measurements are given in Cols. 1 and 2.

[b] Surge impedance Z_0 (Eqs. 32 and 34) $= \sqrt{\frac{L_c\, A_c}{g\, A_t}} = \sqrt{\frac{6{,}666 \times 151}{32.2 \times 2{,}130}} = 3.83$ sec

Free period $T_0 = 2\pi \sqrt{\frac{L_c\, A_t}{g\, A_c}} = 2\pi \sqrt{\frac{6{,}666 \times 2{,}130}{32.2 \times 151}} = 342$ sec.

[c] See Eq. 36. [d] In case C, R_2 (Col. 8) = 0.425 × 1.6/6.13 = 0.111.

or

$$\text{Level change (in feet)} = \left(\frac{z}{f}\right) \times \text{friction drop (in feet)} \qquad (48)$$

Thus, level change $= \left(\frac{0.456}{0.091}\right) \times 5.0 = 25.0$ ft; and time to maximum—

$$T_m = \frac{T_0}{4}\left(1 + \frac{2\,R_1}{\pi}\right) = 85\left(1 + \frac{0.85}{3.14}\right) = 108 \text{ sec}$$

alternate surges for corresponding surge numbers (i):

$$\left|\frac{1}{y_{i+1}}\right| = \left|\frac{1}{y_i}\right| + \frac{2}{3};\ T_{i+1} = T_m + i\,\frac{T_0}{2} = 108 + i\,170.$$

The computation of surge time for $i = 1$ to 5 is listed in Table 3(a).

Case B. $R_1 = 0.222$ *and* $R_2 = 0$.—Enter Fig. 13(a) at $R_1 = 0.222$, read vertically upward to intersect at $R_2 = 0$. From this point, read horizontally to the scale at the right, obtaining $y_B = +0.207$. As in case A, the initial friction drop may be evaluated as $f_B = \frac{1}{2} R^2_1 = 0.022$, or may be read directly from Fig. 13(a). In other words,

Relative surge y_B, in feet above the reservoir surface	+0.207
Relative friction drop f_B, in feet below reservoir surface	0.022
Relative level change from the initial level	0.229

Again, applying the relationships expressed by Eqs. 47 and 48,

TABLE 3.—COMPUTATIONS OF SURGE TIME

Surge number i	(a) Case A				(b) Case B				(c) Case C		
	y_i	$\frac{1}{y_i}$	Surge (ft)	Time (sec)	y_i	$\frac{1}{y_i}$	Surge (ft)	Time (sec)	y_i	Surge (ft)	Time (sec)
	(1)	(2)	(3)	(4)	(5)	(6)	(7)	(8)	(9)	(10)	(11)
1	0.365	2.740 +0.667	+20.0	108 +170	0.207	4.831 +0.667	+11.0	97 +170	−0.100	−5.5	92
2	0.293	3.407 +0.667	−16.1	278 +170	0.182	5.498 +0.667	− 9.7	267 +170	+0.069	+3.8	262
3	0.245	4.074 +0.666	+13.4	448 +170	0.162	6.165 +0.666	+ 8.6	437 +170	−0.073	−4.0	432
4	0.211	4.740 +0.667	−11.6	618 +170	0.146	6.831 +0.667	− 7.8	607 +170	+0.047	+2.6	602
5	0.185	5.407	+10.1	788	0.134	7.498	+ 7.1	777	...	...	

Time to first maximum—

$$T_m = \frac{T_0}{4}\left(1 + \frac{2 R_1 + R_2}{\pi}\right) = 85\left(1 + \frac{0.444}{3.14}\right) = 97 \text{ sec}$$

Alternate surges—

$$\text{(Amplitude)} \quad \frac{1}{y_{i+1}} = \frac{1}{y_i} + \frac{2}{3}$$

$$\text{(Time)} \quad T_{i+1} = T_m + i\frac{T_0}{2} = 97 + 170\,i$$

The remaining steps in the computation of surge time are entered in Table 3(*b*).

Case C. $R_1 = 0.011$ and $R_2 = 0.111$.—Following the same procedure as in cases A and B,

Relative surge y_c, in feet above the reservoir surface	−0.100
Relative friction drop f_C, in feet below reservoir surface	0.000
Relative level change from the initial level	−0.100

Eqs. 47 and 48 yield:

Time to first maximum—

$$T_m = \frac{T_0}{4}\left[1 + \frac{2\,(R_1 + R_2)}{\pi}\right] = 85\left[1 + \frac{0.244}{3.14}\right] = 92 \text{ sec.}$$

Alternate Surges (amplitudes as in Fig. 16)—

$$\text{(Time)} \quad T_{i+1} = 92 + 170\,i.$$

The computations for the remainder of case C are shown in Table 3(*c*).

Plots.—The values of surge heights for the three cases given are plotted in Fig. 16, for comparison with the actual test records plotted as the smooth curves. The divergences for the load rejection cases are caused primarily by the slow rate at which the demand flow was reduced. On the other hand, for

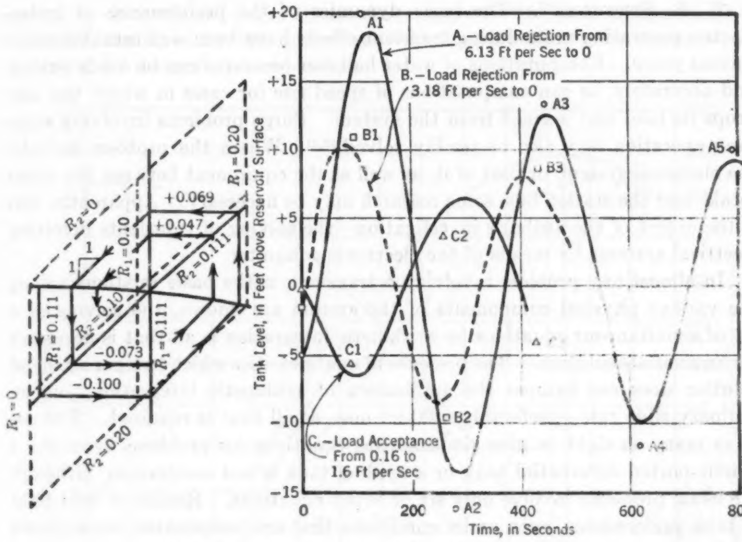

FIG. 16.—TRANSIENTS OF TALLULAH (GA.) TANK

the load-acceptance case, the actual curves may be expected to be in excess of the constant demand-flow results because of the effort of the governor to preserve constant power.

DISCUSSION

E. B. Strowger[49].—The basic dynamics of the performance of hydroelectric generating units during transient effects have been well established for several years. Computations of water hammer pressures can be made quickly and accurately, as can computations of speed rise for cases in which the unit drops its load and is freed from the system. Surge problems involving surge tank operation may also be readily solved.[50,51] Where the problem includes the electrical system, or part of it, as well as the equipment between the water intake and the station bus, some research may be necessary. Apparently, this is the object of the author's investigation—the solving of transients involving electrical systems by means of the electronic computer.

In almost any problem involving a transient, if the basic relations among the various physical components of the system are known, the solving of a set of simultaneous equations by arithmetic integration is all that is necessary for an accurate solution. The presence of nonlinearities which hamper a general solution does not hamper the application of arithmetic integration, and an ordinary slide rule—preferably a 20-in. one—is all that is required. The use of as many as eight or nine simultaneous equations for problems involving a double-ported differential tank or a spilling tank is not uncommon, although the usual problems involve only six or seven equations. Results of field tests of tank performance, even under conditions that are complicated, have shown good agreement with computed performance curves. The design of the surge tank installation at Fort Peck Dam in Montana included three interconnected orifice-type tanks, one on each of the three 14-ft penstocks that in turn were supplied by a tunnel 24.67 ft in diameter. In addition, there was a control shaft (or simple tank) of 50-ft diameter on the supply tunnel, half way between the powerhouse and the intake. Computations by arithmetic integration of the effect of the control shaft on the functioning of the surge tanks were checked by model tests that showed very satisfactory agreement.[52]

To the writer's knowledge, the simple surge tank is no longer used in new installations and he assumes that the author has used it to insure simplicity in his example. For this purpose, the author has selected the Tallulah Falls tank described by E. Lauchli.[48] Fig. 17 reproduces the experimental surge curve given by Mr. Lauchli as the test record for a change in velocity of from 6.13 ft per sec to zero ft per sec caused as follows:

---

[49] Chf. Hydr. Engr., Niagara Mohawk Power Corp., Buffalo, N. Y.

[50] "Speed Changes of Hydraulic Turbines for Sudden Changes of Load," by E. B. Strowger and S. Logan Kerr, *Transactions*, ASME, Vol. 48, 1926, p. 209.

[51] "Arithmetic Integration Applied to Surge Tank Problems," by E. B. Strowger, Chapter 35 B in "Hydroelectric Handbook," by W. P. Creager and J. D. Justin, John Wiley & Sons, Inc., New York, N. Y., 1950.

[52] "Model Study of Hydraulic Characteristics of Power Tunnel, Fort Peck Dam," *Technical Memorandum No 185-1*, U. S. Waterways Experiment Station, Vicksburg, Miss.

"The relief valves of the turbine were held open with chain blocks and at a given time they were left to close rapidly. The average total closure of the valves took place in less than 40 seconds, the relief valves closing rapidly first during the first 25 to 30 seconds and then more slowly *** ."[48]

Point A1 in Fig. 17 represents the surge height at the end of a quarter period as determined by the electronic computer. The lack of agreement of results is explained by the author as "*** caused primarily by the slow rate at which the demand was reduced."

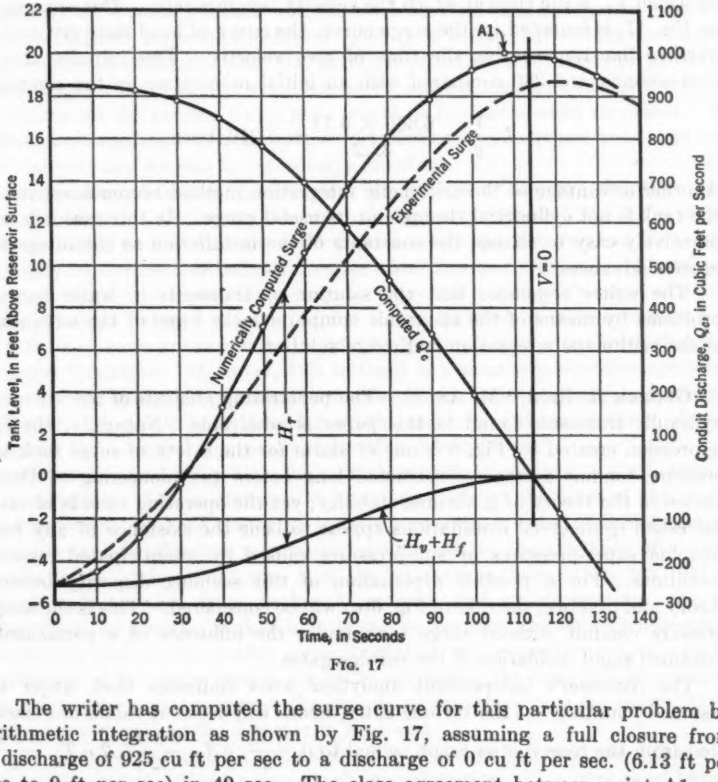

FIG. 17

The writer has computed the surge curve for this particular problem by arithmetic integration as shown by Fig. 17, assuming a full closure from a discharge of 925 cu ft per sec to a discharge of 0 cu ft per sec. (6.13 ft per sec to 0 ft per sec) in 40 sec. The close agreement between point A1 and the maximum surge of the numerically computed curve is apparent. The small differences between the computed results and the test results suggest a slight change in the initial discharge, final discharge, or load-rejection time. In Fig. 17, H_v represents velocity head, H_f is friction loss, and H_r designates the retarding head.

One advantage of arithmetic integration as a method of computation is that it produces the complete surge curve which may be used as a check on the

over-all solution. This check is made by plotting the relationship between retarding head and time, and measuring the area under the curve from zero time to the point at which the velocity of the conduit becomes zero. This area, in units of foot-seconds, should equal the initial momentum of the water in the conduit, $\frac{L_c V}{g}$ in foot-seconds. The area of the retarding head-time curve is

$$\int_{t=0}^{t=T_m} H_r \, dt \ldots\ldots\ldots\ldots\ldots\ldots (49)$$

in which T_m is the time at which the velocity becomes zero. This area, shown in Fig. 17, is bounded by the surge curve, the curve of head recovery, and the vertical line representing the time of zero velocity. This impulse area, in foot-seconds, is 1,280 compared with an initial momentum in the conduit of

$$L_c \frac{V}{g} = \frac{6{,}666 \times 6.13}{32.2} = 1{,}270 \text{ ft-sec} \ldots\ldots\ldots\ldots (50)$$

Another advantage of the arithmetic integration method becomes apparent if the tank is not cylindrical throughout its useful range. In this case it is comparatively easy to change the constants of the installation as the integration process advances.

The writer concludes that the solution of transients in water hammer problems by means of the electronic computer lacks some of the advantages of the arithmetic integration method of solution.

George R. Rich,[53] M. ASCE.—The penetrating analysis of the science of hydraulic transients found in this paper is admirable. Naturally, the first impression created by Fig. 6 is one of alarm for the safety of surge tank and pressure conduit systems constructed long before the pioneering of Daniel Gaden in the theory of governing stability; yet the operating records of many successful commercial installations appear to belie the existence of any catastrophic super-pressures or sub-pressures caused by unanticipated resonant conditions. For a possible explanation of this seeming disparity between theory and practice, the case of Fig. 6(*a*) will be considered. This is the simple pressure conduit without surge tank under the influence of a permanently sustained small oscillation of the turbine gates.

The discusser's independent analytical work indicates that, under the assumed "hunting" of the turbine gates, nodes will occur at values of x (measured from the reservoir as origin) equal to 0, $\frac{a\,T_0}{2}$, $a\,T_0$, $\frac{3\,a\,T_0}{2}$, $2\,a\,T_0$, $\frac{5\,a\,T_0}{2}$, ... $\frac{n\,a\,T_0}{2}$; and maxima (and minima) may be expected at x equal to $\frac{a\,T_0}{4}$, $\frac{3\,a\,T_0}{4}$, $\frac{5\,a\,T_0}{4}$, $\frac{7\,a\,T_0}{4}$, . . . $\frac{(2\,n-1)\,a\,T_0}{4}$—in which a is the velocity of propagation of the water hammer wave in feet per second; and T_0 is the period of oscillation of the turbine gates, in seconds.

[53] Cons. Engr., Director, Charles T. Main, Inc., Boston, Mass.

In practice, the value of T_0 will of course have been predetermined by governing stability computations and corresponding selection of physical elements, so as to be far removed from the zone of resonance. However, preserving the original thesis, the lowest conceivable practicable minimum value of $T_0 = 5$ sec and a low value of $a = 3{,}000$ ft per sec will be considered. The first node will occur at a distance $x = \frac{a\,T_0}{2}$ from the reservoir or $x = \frac{3{,}000\ (5)}{2} = 7{,}500$ ft. Consequently, there appears to be no practicable possibility of a node between the reservoir and turbine unless the pressure conduit (without surge tank) exceeds 7,500 ft in length. If so long a conduit were employed without a tank, the governor period would necessarily be made much longer than 5 sec to avoid excessive water hammer; and the value of x required for the existence of a node would be proportionately increased. It is therefore concluded that in practice the likelihood of a second node between the reservoir and turbine is exceedingly remote.

By analogous reasoning, the peak pressure will decrease steadily (not linearly) from the turbine to the reservoir, unless x exceeds 3,750 ft (without a surge tank); and, if a longer conduit were employed, the value of T_0 would probably be increased as before to reduce water hammer pressures. Therefore, in the majority of cases, there may be expected a steady decrease of peak water hammer values from the turbine to the reservoir in actual commercial installations, even in the event of a hunting governor that actually reaches the resonant condition. However, this in itself is a remote probability, because even in the 1920's no practical operator would have tolerated a swinging governor. He would have slowed down the response of the governor to obtain stability and accepted the resultant sacrifice in regulation.

With reference to Fig. 6(*b*), the writer's investigations lead to the following interpretation. The existence of a complete node at the base of the surge tank indicates not that the surge tank is inoperative, but it definitely shows that the tank is affording maximum benefit—just as the existence of a node at the reservoir does not mean that the reservoir is inoperative, but that it affords infinite relief from both sub-pressures and super-pressures. As an illustration, let a simple tank of infinite size be installed; the tank then becomes a reservoir that (as the author correctly states) will certainly produce a node. If the size of the surge tank is gradually decreased, the node will be replaced by a dip in the pressure curves, the amount of departure from the perfect node being proportional to the decrease in tank size.

An alternative approach is illustrated by the strictly hypothetical case of a very long conduit without a surge tank in conjunction with a very short period of oscillation of the turbine gates—a combination not at all likely to occur for the reasons already given. Under this admittedly artificial system, several nodes could occur in the conduit. If a surge tank of liberal size were then placed over the node nearest the turbine, the author reasons that there would be no effect on the system. The writer's investigations indicate the contrary. The addition of the tank would cause a considerable change in the reflection of the increments generated at the turbine subsequent to the addition of the

tank. Also—(1) The intensity of pressures in the section between the tank and turbine would be greatly reduced; (2) the pressures upstream of the surge tank would be much less in magnitude than those in the downstream penstock; (3) there would be a depression that would at least approach a node at the tank; and (4) the location and number of nodes in the entire system would be changed. In summary, it is contended that the existence of a node at the surge tank is not a detriment or an abnormality; but that it is a benefit that is present, at least in partial form, as a pronounced dip at every tank of adequate size.

To clarify the issues raised by this discussion, it is suggested that the author organize an extensive series of investigations by the electronic computer (using a wide range of values of conduit length and period of gate oscillation) because this topic is of the utmost importance to designers of tanks and conduits.

Regarding surge tank stability, the ambiguity depicted by Fig. 12 applies only to the application of preliminary trial devices such as the Thoma formula. It is the writer's practice always to verify the stability of the tank selected by arithmetic integration, placing a relatively small load on the turbine and making certain that the resultant damping of the surge oscillations is sufficiently rapid—or, in technical language, that the logarithmic decrement is sufficiently large. In such integration, the port or orifice area participates to the correct extent (even though small) and exact account is taken of the shape of the turbine efficiency curve.

In the arithmetic integration for the case of load demand, the turbine gates are always blocked to avoid operation on the rapidly falling part of the efficiency curve. In the writer's experience, it has never been found economical to make the tank or turbine large enough to maintain instantaneous full-load power at the extreme low point of the riser drop curve.

The casual reader will interpret Fig. 14 as a sweeping condemnation of the Thoma formula; although as a matter of fact the Thoma expression was never intended for use except in the zone labeled "Type A—Oscillatory." In this, its intended field of application, there is a remarkable agreement with results obtained by the electronic computer. Zones indicated as "Type B" and "Type C" of the author's Fig. 14 are not usually classified under the heading of stability at all; but are commonly called "draining the tank" and are handled very accurately by arithmetic integration, as well as with good accuracy even by the load-demand charts of R. D. Johnson.[40] Under Zone B, with $\phi < 0.33$ it will be found theoretically possible (perhaps not economical) always to carry full power demand, without draining the tank, by increasing the tank diameter, if the turbine that is purchased is large enough to permit the discharge so required at the reduced head.

In zone "Type C," the conduit friction is so large that the tank action is "dead beat" at the quarter-cycle, so that the tank will drain under full power demand no matter how large the tank is made. In this zone, the gradient change increases more rapidly than the discharge at the constantly dropping head. The standard practice in making arithmetic integration studies in this zone is to block the turbine at about 80% gate, to purchase the turbine only

slightly (if any) larger than necessary to meet the power required at the rated head, and to accept whatever power the turbine can develop under the gradient for the new demanded load at minimum reservoir elevation.

Nevertheless, it would be a great advantage to designing engineers if a more comprehensive and accurate trial chart for preliminary stability tests were made available. Therefore, it is suggested that the author conduct extensive research culminating in a chart similar to Fig. 14. Such a chart would not presuppose constant gate, constant flow, or constant power but would reflect the actual response of the gate and governing mechanism as faithfully as would the arithmetic integration for load demand. In the latter case, the turbine gate openings do not remain constant but move on and off the blocked position in response to head and discharge changes.

As a practicing engineer in the analytical field, the writer can hardly be expected to agree (under the heading, "Surge Tank Problems") that:

> "***The problem of determining the response of tanks under all reasonable disturbances that might be encountered has been neglected in the past, largely because of the altogether forbidding length of time required by even the most elementary investigations using conventional methods."

With twenty or thirty years of background experience with surge problems, most engineers in this field can accomplish a very sizable volume of computation in one or two weeks, for which the consulting costs would be far from forbidding.

In conclusion, it is the opinion of the discusser that the electronic computer can be used to the greatest advantage in pioneering research to provide more incisive tools for the rapid preparation of trial design charts. Such work should be financed by the existing agencies that are organized expressly for the purpose of promoting worthwhile research. This would benefit a broad segment of practicing engineers who are not necessarily specialists in the final surge design, but who nevertheless must always bear the responsibility for the economic coordination of entire projects in which regulation is one component feature. This feature is adjusted by the project engineer in proper economic relation to the other constituent features.

DONALD R. F. HARLEMAN[54] AND EDWARD N. REIN,[55] JUNIOR MEMBERS, ASCE.—The principal aim of this discussion is to emphasize, further illustrate, and extend the remarks which Mr. Paynter has made about the effect of demand flow characteristics on surge computations. Some additional developments by the author have been utilized to obtain simplified computational procedures for the case of simple surge tanks.[22,56,57] The writers show a comparison of the results of these procedures with some experimental investiga-

[54] Asst. Prof. of Hydraulics, Dept. of Civ. and San. Eng., Massachusetts Inst. of Technology, Cambridge, Mass.

[55] Teaching Asst., Dept. of Civ. and San. Eng., Massachusetts Inst. of Technology, Cambridge, Mass.

[56] "Regulation of Hydroelectric Plants," by A. T. Gifford and H. M. Paynter (mimeographed notes), 1952.

[57] "New Relationships for the Analysis of Surge Tank Transients," by A. T. Gifford and H. M. Paynter, *Proceedings of the MIT Hydrodynamics Symposium*, Massachusetts Inst. of Technology, Cambridge, Mass., June, 1951.

tions on the surge tank equipment in the M.I.T. Hydrodynamics Laboratory. The Tallulah Falls example is also included for direct comparison with the computer solution.

General Tank Level Equation for Constant Flow.—When Eq. 43 and Eq. 44 are combined, by eliminating the common time variable, the resulting equation is known as the phase or energy equation—

$$\frac{du}{dy} = \frac{y + \frac{1}{2} u^2}{v - u} \qquad (51)$$

which may be rewritten as

$$\frac{dw}{dz} = \frac{z - f}{\Delta R - w} \qquad (52)$$

in which $z \equiv y + \frac{R^2{}_1}{2}$, $w \equiv u - R_1$, $f \equiv \frac{R^2{}_1}{2} + \frac{u}{2}\left|u\right|$, and $\Delta R \equiv R_2 - R_1$. These substitutions and $\Sigma R \equiv R_2 + R_1$, $f_0 \equiv \frac{R^2{}_1}{2} - \frac{R^2{}_2}{2}$, and $R_2 = v$ (constant demand flow) are shown in Fig. 18.

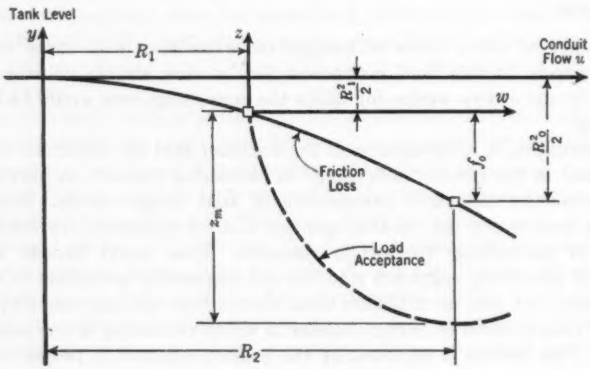

FIG. 18.—PHASE DIAGRAM

The solution of Eq. 52 can be obtained by separating variables and integrating, as follows,

$$\frac{z^2}{2} - \int_0^z f\,dz = \frac{(\Delta R)^2}{2} \qquad (53a)$$

in which the value of $\int_0^z f\,dz$ is the area under the surge-friction curve of Fig. 9(*c*). This integral also can be written as

$$\int_0^z f\,dz = K\,z\,f_0 = -K\,z\,\frac{\Sigma R\,\Delta R}{2} \qquad (53b)$$

in which K depends only upon the shape of the curve.

Using Eq. 53*b* and solving the resulting quadratic equation for z, the general surge formula for the case of constant demand flow, assuming square-law friction for the simple surge tank, is

$$z_m = -\Delta R \left[\frac{K\,\Sigma R}{2} + \sqrt{1 + \left(\frac{K\,\Sigma R}{2}\right)^2} \right] \dots\dots\dots (54)$$

To determine values of K, Eq. 53*a* can be solved for z graphically or by the use of the computer. The value of z then can be substituted into Eq. 4, leaving K as the only unknown. Tables of values of K are available.[22]

It has been found that, in the region where R_1 and R_2 approach zero, K approaches a limiting value K_0 which can be expressed as

$$K_0 = \frac{0.33\,R_1 + 0.10\,R_2}{\Sigma R} \dots\dots\dots (55)$$

Modification of this result, to give values of K that are valid in the range from $R_1 = R_2 = 0$ to $R_1 = R_2 = 1$, leads to the following expression that closely approximates the relationship between K and R:

$$K = K_0\,(1 + 0.1\,\Sigma R) \dots\dots\dots (56)$$

Translating the general surge formula (Eq. 54) into physical terms, the first extremum level change for either load acceptance or load rejection may be expressed as

$$\text{Level change} = K\,\Delta H_f + \sqrt{(\Delta Y_0)^2 + (K\,\Delta H_f)^2} \dots\dots\dots (57)$$

in which $\Delta H_f \equiv |H_{f1} - H_{f2}| = C\,|Q^2{}_2 - Q^2{}_1|$; and $\Delta Y_0 \equiv |Y_{02} - Y_{01}| = |Q_2 - Q_1| \sqrt{\frac{L_c}{g\,A_c\,A_t}}$.

Surges and Times for Full Load Rejection.—For the computation of the subsequent surge heights, in the case of full load rejection, the phase equation with $v = 0$ becomes

$$\frac{du}{dy} = \frac{y + \frac{1}{2}\,u|u|}{-\,u} \dots\dots\dots (58a)$$

for which an approximate solution in physical terms is

$$Y_{i+1} = \frac{\dfrac{3\,Y_0}{2\,R_0}}{\dfrac{3\,Y_0}{2\,R_0\,Y_m} + i} \dots\dots\dots (58b)$$

in which $i = 1, 2, 3, \dots$. The sign of the surge alternates appropriately.

The time to the first extreme surge may be computed by using the generalized results of many graphical, computer, and analytical solutions, which are presented in Table 4.

TABLE 4.—TIME TO FIRST EXTREME FOR LOAD REJECTION IN SIMPLE SURGE TANK

Tank parameter, R	0.0	0.2	0.4	0.6	0.8	1.0	1.2	1.4	1.6	1.8	2.0
$\tau_m = t_m/T_{CT}$	0.25	0.26	0.27	0.29	0.30	0.32	0.33	0.35	0.37	0.39	0.41

The period for the subsequent surges of the load rejection case can be assumed to be equal to the free period because of the small effect of friction at low flows. The time between surges can be taken as $t = T_{CT}/2$.

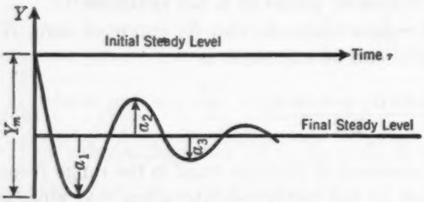

FIG. 19.—SURGE-TIME CURVE

Surges and Times for Load Acceptance, Constant Demand Flow.—The first extreme change in level can be computed from the general surge formula. However, computation of the subsequent surges requires a slightly different technique from that used for the case of load rejection. This is because no generalization can be applied until after the first positive surge has been reached, since quadratic damping has so large an effect. The ratio of the first positive surge to the first extreme surge, in which the symbol a denotes amplitude measured from the final steady level, can be expressed as

$$\frac{a_2}{a_1} = \frac{\dfrac{a_i}{a_{i-1}}}{1 + \dfrac{2}{3}\,a_1} \qquad (59)$$

Eq. 59 is shown graphically in Fig. 19. The remaining surges may be computed directly from $\frac{a_i}{a_{i-1}}$ which is the ratio that any subsequent surge bears to the surge immediately preceding it. This amplitude ratio is computed by assuming that over a small range of flow near the final steady state, the friction characteristic, is linear. Table 5 shows these amplitude ratios and applies to

TABLE 5.—SURGE AMPLITUDE RATIOS AND HALF PERIODS FOR LOAD ACCEPTANCE IN A SIMPLE SURGE TANK

R_2	0	0.2	0.4	0.6	0.8	1.0	1.2	1.4	1.6	1.8	2.0
$\frac{a_i}{a_{i-1}}$	1.000	0.728	0.527	0.373	0.254	0.164	0.095	0.046	0.016	0.002	0.0
$\bar{\tau}_p$	0.500	0.502	0.510	0.524	0.546	0.578	0.625	0.700	0.834	1.148	∞

all surges following the first positive surge for the case of load acceptance and constant demand flow. The half period $\bar{\tau}_p$ is equal to $t_{\frac{1}{2}\,\text{period}}/T_{CT}$.

The time to the first extreme surge for the case of load acceptance and constant demand flow can be computed from the generalized results presented in Table 6, which gives values of $\bar{\tau}_m$. The half periods of the subsequent surges may be computed from Table 5.

TABLE 6.—TIME TO FIRST EXTREME SURGE FOR LOAD ACCEPTANCE

R_2	Q_1/Q_2					
	0.0	0.2	0.4	0.6	0.8	1.0
0.0	0.25	0.25	0.25	0.25	0.25	0.25
0.2	0.26	0.26	0.26	0.26	0.26	0.27
0.4	0.26	0.27	0.27	0.28	0.28	0.29
0.6	0.27	0.27	0.28	0.29	0.30	0.31
0.8	0.28	0.29	0.30	0.31	0.32	0.34
1.0	0.29	0.31	0.32	0.34	0.36	0.39
1.2	0.30	0.32	0.34	0.37	0.40	0.44
1.4	0.31	0.34	0.38	0.42	0.47	0.52
1.6	0.32	0.37	0.42	0.48	0.57	0.66
1.8	0.34	0.40	0.48	0.60	0.76	0.98
2.0	0.37	0.46	0.57	0.73	0.96	∞

Surges and Times for Load Acceptance, Constant Gate Flow.—The surge amplitude that results from constant gate demand flow regulation is less than the surge of a comparable constant demand flow. The gate characteristics, in effect, introduce additional damping into the system. This effect is best

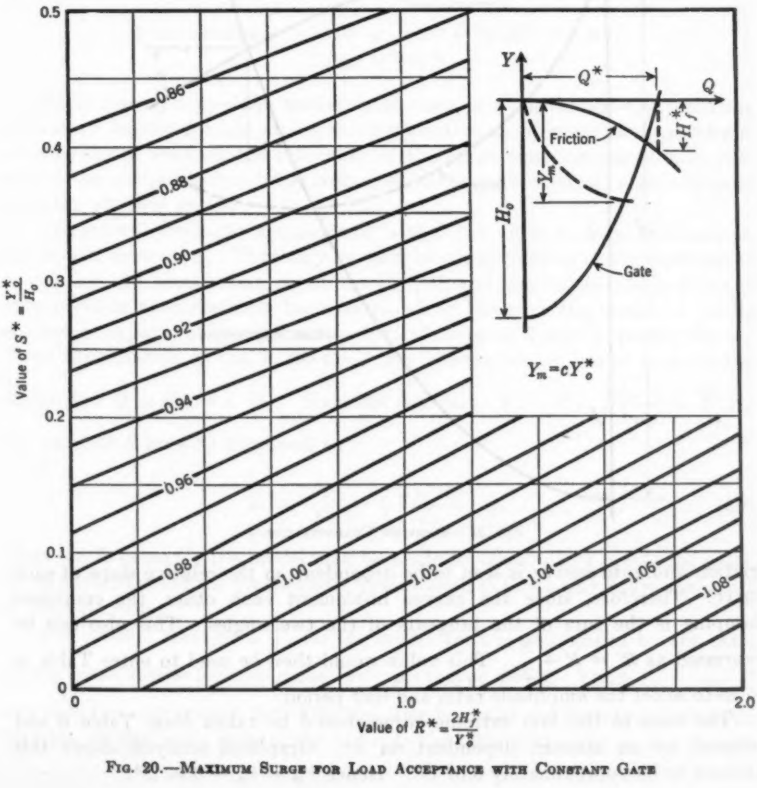

FIG. 20.—MAXIMUM SURGE FOR LOAD ACCEPTANCE WITH CONSTANT GATE

treated by graphical analysis and the results presented in Fig. 20 permit the computation of the first extreme surge. To account for the gate flow characteristics, a new parameter is introduced and is defined as the ratio of the free surge to the index head. The free surge, in this case, is based on the gate flow that would be obtained under the index head in the absence of friction loss (see Fig. 20). The parameter R^*also is based on this flow. The index head is the total headwater-to-tailwater difference in elevation. The factor obtained from Fig. 20 is then multiplied by the free surge Y^* to obtain the actual surge.

The subsequent surges can be computed in the same manner as those accompanying constant demand flow. However, it is necessary to account for the additional damping. From Fig. 21, the damping action of both

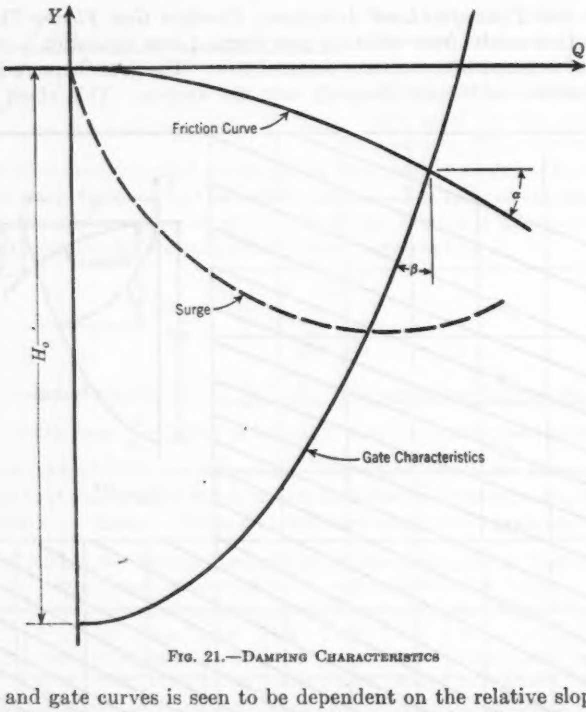

FIG. 21.—DAMPING CHARACTERISTICS

friction and gate curves is seen to be dependent on the relative slope of each curve. Therefore, since the curves implement each other, the combined damping is the sum of the tangents of the two angles. This also can be expressed as $R' = R + \frac{S}{2}$. This value would then be used to enter Table 5, so as to select the amplitude ratio and half period.

The time to the first extreme surge should be taken from Table 6 and reduced by an amount dependent on S^*. Graphical analysis shows this amount to be approximately 0.07 S^*. Hence $\bar{\tau}'_m = \bar{\tau}_m - 0.07\ S^*$.

Tallulah Falls Plant, Constant Flow Regulation Assumed.—

Case A.—Load rejection $R_1 = 0.425$ and $R_2 = 0$

$$\text{Level change} = K\,\Delta H_f + \sqrt{(\Delta Y_0)^2 + (K\,\Delta H_f)^2}$$

$$\Delta H_f = 5.0 - 0 = 5.0 \text{ ft } K_0 = \frac{0.33\,R_1 + 0.10\,R_2}{\Sigma R} = 0.33$$

$$\Delta Y_0 = 23.5 - 0 = 23.5 \text{ ft } K = 0.33\,(1 + 0.0425) = 0.344$$

$$\text{Level change} = 0.344 \times 5 + \sqrt{(23.5)^2 + (0.344 \times 5.0)^2} = 25.3 \text{ ft}$$

$$\text{Surge } Y_m = 25.3 - 5.0 = 20.3 \text{ ft}$$

Case B.—Load rejection $R_1 = 0.246$ and $R_2 = 0$

$$\text{Level change} = 0.52 + \sqrt{(12.2)^2 + (0.52)^2} = 12.7 \text{ ft}$$

$$\text{Surge} = 12.7 - 1.5 = 11.2 \text{ ft}$$

Case C.—Load acceptance $R_1 = 0.011$ and $R_2 = 0.111$

$$\text{Level change} = 0.10 + \sqrt{(5.5)^2 + (0.10)^2} = 5.6 \text{ ft}$$

$$\text{Surge} = 5.6 \text{ ft}$$

Model Description.—The model surge tank is a convenient and accurate laboratory facility for the study and demonstration of surge tank problems. As a means of showing the reliability of the surge equations previously presented, the computed results are compared to the experimental values obtained from the physical system.

The general similarity requirement is that the value of R be the same in model and prototype. This may be seen by an inspection of the normalized continuity and acceleration equations (Eq. 43 and Eq. 44) in which R is the only variable characterizing the system. The basis for the design of model equipment capable of simulating all practical values of R may be readily shown. Using the notation of Fig. 7, the head loss between reservoir and tank for the design flow Q_0 is $H_{f0} = C\,Q^2{}_0$. Since the free surge $Y_0 = V_0 \sqrt{\dfrac{A_c\,L_c}{A_t\,g}} = \dfrac{Q_0}{A_c} Z_0$, the value of R may be expressed as

$$R = \frac{2\,H_{f0}}{Y_0} = \left(\frac{2\,C\,A_c}{Z_0}\right) Q_0 \ldots\ldots\ldots\ldots\ldots\ldots (60)$$

Thus the R-value for the model may be made to agree with a prototype value by an adjustment of the conduit flow Q_0 inasmuch as C, A_c, and Z_0 are constants of the equipment.

The vertical scale ratio Y_r for the model tank is determined by the ratio of the head losses for the model and prototype flows. Thus $Y_r = \dfrac{(H_{f0})_m}{(H_{f0})_p}$ and from the requirement that R be the same in model and prototype, it follows that the vertical scale ratio is also equal to the ratio of the free surge in model

and prototype or $Y_r = \frac{(Y_0)_m}{(Y_0)_p}$. The corresponding time ratio for surges is then equal to the ratio of the free periods, $t_r = \frac{(T_{CT})_m}{(T_{CT})_p}$.

At the M.I.T. Hydrodynamics Laboratory, the model surge tank consists of a rectangular reservoir having a surface area of 14 sq ft, a conduit 49 ft long and 2 in. in diameter, connected to a lucite surge tank 3 in. in diameter and 6 ft high. The penstock, below the surge tank connection, contains the discharge-regulating valve followed by a quick-acting gate valve at the end where the penstock discharges into a sump. From the sump, water is pumped back into the reservoir with provision for matching conduit flow rate and pumping rate in order that a constant total head can be maintained on the system. Data are recorded by marking and timing the surge heights on a paper strip attached to the lucite tank.

Assuming the three types of demand flow shown in Fig. 10, it is seen that the case of load acceptance in the model surge tank is one of constant gate regulation. Therefore, the computations of the performance of this tank include the gate discharge characteristics using the equations and tables presented by the writers under the heading, "Surges and Times for Load Acceptance, Constant Gate Flow."

These conditions are typical of model studies of surge tanks. Since the practical regulation of most actual hydroelectric plants is necessarily for constant power, an inherent error exists when such conditions are present and this error is on the unsafe side. Model indications are for a surge that is smaller than the surge that will appear in the prototype tank.

Computations for Model Surge Tank.—

Load Acceptance.—$Q_1 = 0.0042$ cu ft per sec and $Q_2 = 0.0410$ cu ft per sec

First extreme surge $R^* = \frac{2\,H^*_f}{Y^*_0} = \frac{2\,(0.65)}{1.14} = 1.14$,

and $S^* = \frac{Y^*_0}{H_0} = \frac{1.76}{3.53} = 0.50$

For 90% load acceptance and from Fig. 20, $Y_m = 0.90 \times 1.76 \times 0.87 = 1.38$ ft

Subsequent surges $R' = R + S/2 = 1.0 + 0.22 = 1.22$,

and from Table 5, $\frac{a_i}{a_{i-1}} = 0.090$

$$\begin{aligned} a_1 &= 1.38 - 0.77 = 0.61 & Y_1 &= 1.38 \text{ ft} \\ a_2 &= 0.61 \times 0.090 = 0.055 & Y_2 &= 0.77 - 0.06 = 0.71 \text{ ft} \\ a_3 &= 0.055 \times 0.090 = 0.005 & Y_3 &= 0.77 + 0.005 = 0.78 \text{ ft} \end{aligned}$$

Time of surge $R_2 = 1$, $\frac{Q_1}{Q_2} = 0.102$, and $T_{CT} = 11.6$ sec

From Table 6, $\bar{\tau}_m = 0.30 - 0.08\,(0.50) = 0.26$, and $t_m = 0.26 \times 11.6 = 3.0$ sec

From Table 5, $\bar{\tau}_p = 0.625$, $t_p = 0.578 \times 11.6 = 6.7$ sec,

and $t_2 = 3.0 + 6.7 = 9.7$ sec

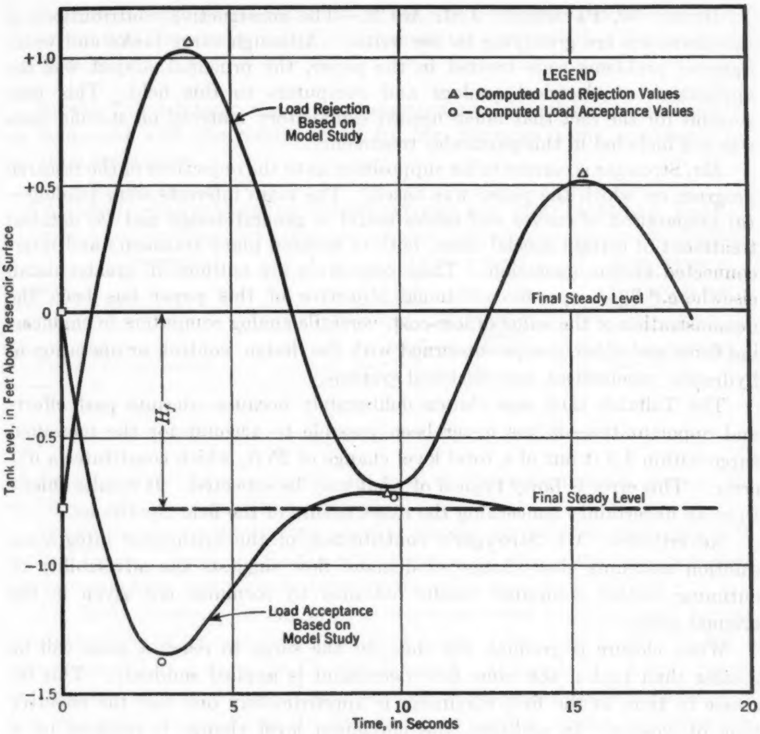

FIG. 22.—TRANSIENTS IN MODEL OF SIMPLE SURGE TANK

Load Rejection.—$R_1 = 1$, $R_2 = 0$, and $Y_0 = 1.54$ ft

First extreme surge

$$\Delta H_f = 0.77 \text{ ft} \qquad K_0 = 0.33$$
$$\Delta Y_0 = 1.54 \text{ ft} \qquad K = 0.33\,(1.1) = 0.364$$

$$\text{Level change} = 0.364 \times 0.77 + \sqrt{(1.54)^2 + (0.364 \times 0.77)^2} = 1.83 \text{ ft}$$

$$\text{Surge} = 1.83 - 0.77 = 1.06 \text{ ft}$$

$$\text{Subsequent surges } Y_{i+1} = \frac{2.30}{2.17 + i},\; Y_2 = -0.725, \text{ and } Y_3 = +0.55$$

Time of surge

From Table 4, $\bar{\tau}_m = 0.32$, $t_m = 0.32 \times 11.6 = 3.7$ sec,

$$t_p = \frac{11.6}{2} = 5.8 \text{ sec},\; t_2 = 9.5 \text{ sec, and } t_3 = 15.3 \text{ sec}$$

Fig. 22 shows a comparison between the surge tank experimental data and the values computed from the formulas.

Henry M. Paynter,[58] J.M. ASCE.—The constructive contributions of the discussers are gratifying to the writer. Although surge tanks and water hammer problems were treated in the paper, the principal subject was the application of electrical analogs and computers to this field. This may account for the fact that much needed explanatory material on specific cases was not included in this particular treatment.

Mr. Strowger is correct in his supposition as to the objectives of the research program on which the paper was based. The main interests were twofold—(*a*) preparation of curves and tables useful in general design and (*b*) detailed treatment of certain special cases, both of isolated plant transients and interconnected system operation. These objectives are outlined in greater detail elsewhere.[59,57] A specific additional objective of this paper has been the demonstration of the value of low-cost, versatile analog computers to engineering firms and other groups concerned with the design, control, or operation of hydraulic, mechanical, and electrical systems.

The Tallulah tank was chosen deliberately because—despite past efforts and opportunities—it has never been possible to account for the measured surge within 1.5 ft out of a total level change of 25 ft, which constitutes a 6% error. This error is fairly typical of what may be expected. It results chiefly from an uncertainty concerning the exact nature of the field conditions.

Nevertheless, Mr. Strowger's contribution of the arithmetic integration solution assuming slow change of demand flow suggests the advisability of outlining certain computed results obtained by formulas not given in the original paper.

When closure is gradual, the time for the surge to reach a peak will be greater than that if the same flow decrement is applied suddenly. This increase in time to the first maximum is approximately one half the effective time of closure. In addition, the maximum level change is reduced by a normally small amount, which varies with the square of the closure time. These two approximations, made through analysis of computed and experimental results, may be expressed as the following equations:

Gradual Closure.—(1) The time to the first maximum is

$$T_{ms} - T_{m0} + 0.5\, T_d \qquad (61)$$

in which T_{ms} is the time to the first maximum for a slow change, T_{m0} represents the time to the first maximum for a sudden change, and T_d is the effective closure time.

(2) The reduction in the surge is

$$\Delta Y = 1.65\, Y_0 \left(\frac{T_d}{T_{ct}}\right)^2 \qquad (62)$$

[58] Asst. Prof. of Hydr. Eng., Dept. of Civ. and San. Eng., Massachusetts Inst. of Technology, Cambridge, Mass.

[59] "Methods and Results from M.I.T. Studies in Unsteady Flow," by H. M. Paynter, *Journal*, Boston Soc. of Civ. Engrs., VXXXIX, No. 2, April, 1952, pp. 120–163.

in which ΔY equals the reduction in the surge height, Y_0 is the free surge for the flow decrement, and T_{et} represents the free period of the tank and conduit.

For the Tallulah tank, the appropriate numerical calculations (see Table 7) are compared with the results found by Mr. Strowger using arithmetic integration techniques.

TABLE 7.—SLOW-CLOSURE COMPUTATIONS FOR THE TALLULAH TANK

Description	Levels, in feet	Time, in seconds
Constants	$Y_0 = 23.5$	$T_{et} = 342$; $T_d = 40$
Surge, for sudden closure	$Y_{m0} = 20.0$[a]	$T_{m0} = 92.0$[b]
Corrections	$Y = 1.65 \times 23.5 \times \left(\frac{40}{342}\right)^2 = 0.6$	$\Delta T = 0.5 \times 40 = 20$
Surge, for final closure	$Y_{ms} = 20.0 - 0.6 = 19.4$	$T_{ms} = 92 + 20 = 112$
Mr. Strowger's computations[c]	$Y_{ms} = 19.8$	$T_{ms} = 114$

[a] Above the reservoir water surface. [b] Based on Table 4. [c] See Fig. 17.

Simple corrections may thus be made to the basic formulas to account for significant effects encountered in practice.

Moreover, the computer may account for the variation in tank area with vertical height. Solutions for the most common of these situations have been put into graphical and formula form by the writer and A. T. Gifford.[56]

Mr. Rich questions the engineering importance and physical basis for the examples of elastic resonance outlined in the paper. The cases depicted in Fig. 6 were suggested by a paper by Charles Jaeger.[60] Although Mr. Jaeger asserts at the outset that most cases of resonance occur because of small increments of flow and pressure, for which the flow line is adequately strong, he cites in this reference eleven specific cases in which resonance effects produced serious troubles. In particular, Mr. Jaeger writes:[61]

> "***Resonance is dangerous not only for the pipeline, but sometimes also for the tunnel upstream from the surge tank. It can be theoretically proved that harmonics can penetrate far into a tunnel, in spite of the presence of a surge tank.
>
> "***We have had the opportunity of investigating such a case very thoroughly. Within a long period of operation, extending over many years, fissures had developed three times in a certain tunnel, each time at the same place. Horizontal, parallel fissures, which measured more than 60 feet in length indicated the presence of water hammer. A further examination revealed more fissures at equal distance from one another, and a study of the system showed that there had been a resonance of the eleventh harmonic inside the tunnel.***"

The disturbance producing this frequency was found to be a faulty air valve in the penstock.

[60] "Water Hammer Effects in Power Conduits," by Charles Jaeger, *Civil Engineering and Public Works Review*, Vol. 43, Nos. 500-503, London, England, February-May, 1948.

[61] *Ibid.*, p. 61.

Perhaps the discrepancy between the statements of the writer and the comments of Mr. Rich can be resolved by an examination of the essential behavior of surge tanks, and particularly the difference between (on one extreme) the large surge chamber, forebay, or equalizing reservoir, which completely isolates the conduit from the penstock—thus serving as a wave trap—and in contrast, the ordinary elevated surge tank, stand pipe, or chamber connected to the flow line through a base pipe or riser. In the first case the tank serves as a nodal clamp since the nearly constant pressure condition extends over a length comparable to the wave lengths of all disturbances traveling up the penstock. However, in the second case the tank serves more nearly as a nodal point (rather than a nodal clamp), and the pressure influence is imposed only over a small distance compared to the wave length. Any reader who has had the opportunity to play a stringed instrument (an Hawaiian guitar in particular) will recognize this difference. The tank of the second case may act exactly like the steel bar of the Hawaiian guitar, which serves as a node but permits vibrations of the string on each side.

This description may avoid possible misunderstanding, since the writer had in mind the conditions of the second case whereas Mr. Rich may have been referring to the wave-trap tank of the first type. The writer believes that the analogous situation of capacitor-loaded electrical transmission lines commonly found in practice renders any hydraulic verification of these principles unnecessary; however, systematic analysis and computational research may be in order.

The purpose of Fig. 14 was to emphasize the significance of the Thoma tank-stability criterion for the region of oscillatory instability—both for large load changes in which nonlinear effects are important, and for the small increments that provide the basis for the linear analysis from which the Thoma formula is obtained. The demonstration and proof of this single fact are significant because the required tank diameter for stability as computed by the uncorrected Thoma formula,

$$A_t > A_{thoma}$$

$$A_{thoma} = A_c \left(\frac{V^2{}_0/2\,g}{H_f} \right) \frac{L_c}{H_n}$$

in which H_n is the rated net head equal to $H_0 - H_f$, for all installations in which the friction drop is less than 7% of the static head, can produce at most an error of 7% in the required diameter. In other words, for this oscillatory region, Mr. Rich seems to consider the linear Thoma area (when suitably increased to provide sufficient damping) to be an adequate basis for trial design figures. Nevertheless, if more reliable figures are desired for cases in which the tank will be subjected to large load increments (such as might occur during power-system emergency conditions), the writer suggests his own curve based on analysis and precise computer solutions, in the following form,

$$A_t > A_{0sc}$$

in which $A_{0sc} = \left(1 + \frac{H_f}{H_0}\right)^2 A_{thoma}$ since the Thoma area always errs on the low side.

By contrast, for those fairly uncommon, but nonetheless important, installations in which the value of $\dot{h}_c$ is greater than 7% but less than 33%, the Thoma formula is entirely misleading for all but the smallest load increments, since a tank based on the Thoma size always will have an incipient tendency to drain for the larger changes in load. Whereas, as Mr. Rich remarks, it may not be economical to design a tank large enough to prevent drainage tendencies for large load increments, the writer would ask only that this situation be appreciated both at the time of design and under operating conditions. For those who may wish to know this drainage limitation, the writer's approximate expression,

$$A_{drain} = 18\, A_c \frac{V^2{}_0}{2\, H_0} \frac{L_c}{H_0} \qquad (63)$$

indicates the required minimum area to avoid drainage tendencies (or power drop) for the region of h_c between 0.07 and 0.33. It is interesting to note that Eq. 63 does not contain a term representing the conduit friction loss. The two tank areas A_{thoma} and A_{drain} may be compared in computations for a typical hypothetical installation in this range. Data for this example are $L_c = 8{,}000$ ft, $V_0 = 8$ ft per sec, $h_c = 0.20$, $H_f = 20$ ft, $H_0 = 100$ ft, and $V^2{}_0/2\,g = 1$ ft. Computations for the Thoma area are

$$\frac{A_{thoma}}{A_c} = \frac{L_c}{H_n} \frac{V^2{}_0}{2\,g\,H_f} = \frac{8{,}000 \times 1}{80 \times 20} = 5.0$$

whereas those for the required minimum area to avoid drainage are

$$\frac{A_{drain}}{A_c} = 18\, \frac{L_c}{H_0} \frac{V^2{}_0}{2\,g\,H_0} = 18\, \frac{8{,}000 \times 13}{100 \times 100} = 14.4.$$

From these numbers it is clear that the Thoma area, even if augmented by a considerable allowance, may not satisfy the drainage criterion.

The writer's remarks under the heading, "Surge Tank Problems," were perhaps unfortunately worded. The intent of the paragraph, rather than to disparage the fine work of Mr. Rich, Mr. Strowger, and others in this field, was to affirm the indisputable point that hand-calculation methods of any type are not practically suited to general studies—such as those of the effects of a fluctuating rolling-mill load on the generating units of an interconnected system, and in particular the effects on the level swings of a certain surge tank whose natural period is approximately resonant with the load pulses. Such studies had not been made, to the writer's knowledge, prior to his use of the electronic computer for research of this type. This area of design solutions and exploratory studies is where the newer machine computations and analog methods seem most promising.

The writer wishes to thank Messrs. Harleman and Rein for contributing additional material of later origin, arising from the M.I.T. researches. The bulk of the specific material concerning surge tanks has been placed on a more substantial basis since the original writing of the paper in 1950. Use of these better results for rapid prediction is demonstrated by the discussers. Also, the value of the M.I.T. model tank and its role in the program of computation and analysis is described.

Of particular importance to the hydraulic designer are the specified limitations of the model technique as used at MIT and elsewhere. To overcome the limitations of constant gate operation of the model, a controlled regulating valve can be constructed in order to permit programming any desired relation between demand flow Q_p, total head $H = H_0 + Y$, gate opening B, and time t during a model study. In this way, regulating performance of an actual hydroelectric plant may be simulated by the model tank, in a manner similar to that used with the electronic computer.

Several points in the discussion by Messrs. Harleman and Rein might be clarified herein in order that the data presented may be applied correctly, and that earlier formulas may be appropriately amended.

The expression for the full-rejection surge amplitudes given by Eq. 58*b* corresponds identically to the computational procedure indicated in Table 3, Cols. 1, 2, 3, 5, 6, and 7. Table 4 replaces the formula used to compute the time to the first maximum as given in Table 3, Cols. 4 and 8.

For load acceptance (assuming constant demand flow, which is realistic only if h_e is very small), Eq. 59 and Table 5 replace the graphical procedure indicated in the left-hand part of Fig. 16. The time to the first minimum, as indicated by the first entry in Table 3, Col. 11, may be computed more accurately using Table 6. The remaining time values in this column should be computed from the half-periods given in Table 5.

Fig. 20, which gives values of $c = Y_m/Y^*$, was originally constructed from the results of the electronic computer solutions, and later checked by graphical methods and against model studies. This curve is similar to one provided in the book of J. Calame and D. Gaden.[19] For small values of R^* and S^* these curves may be approximated by

$$c = 1.0 + 0.05\, R^* - 0.35\, S^* \qquad (64)$$

For those who wish to see a graphic comparison of actual water behavior as compared to the performance of the electronic computer, contrasting the model tank level measurements of Fig. 22 with the computer oscilloscope photograph of Fig. 11(*a*) may be convincing. Of course, the conditions (the values of R) are different.

In conclusion, the writer wishes to express his opinion as to the importance of finding and using practical methods of analysis and computation in solving engineering problems. In order for any method to qualify as practical for use by the engineer, it must be (*a*) simple and readily understood, (*b*) applicable to varied problems, (*c*) fast, (*d*) inexpensive, (*e*) available, (*f*) adaptable to the use of experimental data, (*g*) free as possible from manipulative errors, (*h*) easily checked, and (*i*) designed to give direct, easily-read results. Of the many tools to which these tests may be applied, three which pass with distinction are numerical methods, graphical methods, and analog methods.

Both Mr. Strowger and Mr. Rich have asserted in their discussions and have demonstrated in their many other writings that any problem involving hydraulic (or other) transients can be solved with simple techniques of arithmetic integration. For the same type of problem, the writer has developed what he considers to be an excellent method of graphical analysis. The

paper attempted to outline the potentialities of analog concepts and analog computers, not only for schools and abstract analysts, but also for operating companies, equipment manufacturers, and consulting firms who have down-to-earth problems in design and development. In both these areas the commercially available, low-cost analog computer can play an important role. However, analog concepts, as distinguished from the actual computers, cost only the time to be learned but may reward the "investor" beyond his expectations.

APPLICATION TO AN HYDRAULIC PROBLEM

By R. E. Glover,[1] M. ASCE, D. J. Hebert,[2] and C. R. Daum[3]

With Discussion by Messrs. J. van Veen; W. Douglas Baines; T. Blench; and R. E. Glover, D. J. Hebert, and C. R. Daum

Synopsis

This paper discusses the general conditions of the problem of flow distribution in a network of estuarine channels to which an analog computer model was applied. After developing the analog requirements, the model is described, with emphasis on the electronic circuit that provides the required square-law resistance. The equations correlating electrical and hydraulic quantities are developed from the basic electrical and hydraulic relationships. Finally, the methods by which the required boundary conditions were duplicated are discussed.

Introduction

The Delta area of California is a roughly triangular tract of land lying just to the east of Suisun Bay. This area, extending for a distance of about 50 miles north and south with a maximum width of about 25 miles, was originally a marsh with a network of channels threading through it. At the present time this area is agricultural land which has been reclaimed from the marshes by constructing dikes along the old channels to inclose areas that can be pumped out and farmed.

The Delta is traversed by the Sacramento River, entering from the north, by the San Joaquin River, entering from the south, and by the north and south forks of the Mokelumne River that come in from the east. The old network of channels, effectively preserved and stabilized by the process of reclamation, still carries the flow of these streams through the Delta.

Tides coming into San Francisco Bay from the Pacific Ocean propagate themselves through Suisun Bay and enter the Delta channels. Since the tidal currents generally exceed the currents resulting from stream flow, the direction of flow in the channels is periodically reversed and the resulting movement and mixing of fresh and saline waters provides a mechanism capable of propagating ocean salinity into the Delta channels. The salinity encroachment is held in

Note.—Published in June, 1952, as *Proceedings-Separate No. 134*. Positions and titles given are those in effect when the paper or discussion was received for publication.

[1] Engr., Bureau of Reclamation, U. S. Dept. of the Interior, Denver, Colo.

[2] Engr., Bureau of Reclamation, U. S. Dept. of the Interior, Denver, Colo.

[3] Physicist, Bureau of Reclamation, U. S. Dept. of the Interior, Denver, Colo.

check by stream flow that tends to flush the salinity out of the channels. In times of flood the salinity is driven back but in times of low stream flow the tidal ebb and flow succeeds in carrying some salt water into the channels.

Construction of Shasta Dam on the upper Sacramento River has made available a water supply intended for use on some of the lands in the San Joaquin Valley. To supply this demand, the Tracy pumping plant will lift water out of the channels at the south end of the Delta. This water must be brought across the Delta through its channels.

The problem to be solved is how to bring the Sacramento River water across the Delta to the San Joaquin side while maintaining a pattern of flow in the channels which will hold the intrusion of ocean salinity in check and thereby permit the transfer to be made without danger of contamination.

Reasons for Use of an Analog

With the Tracy pumps in operation, it will be necessary to increase the natural transfer of water from the Sacramento channel to the San Joaquin channel in order to replenish the water supply of the southern part of the Delta and thereby maintain a proper balance of flow. A tidal phase difference exists at one of the sites where a channel could be cut through to increase the transfer, and since gates would be necessary in any case for protection during floods, it would be possible to open the gates when the tidal currents were favorable and to close them when the currents were adverse to increase the net flow. Good

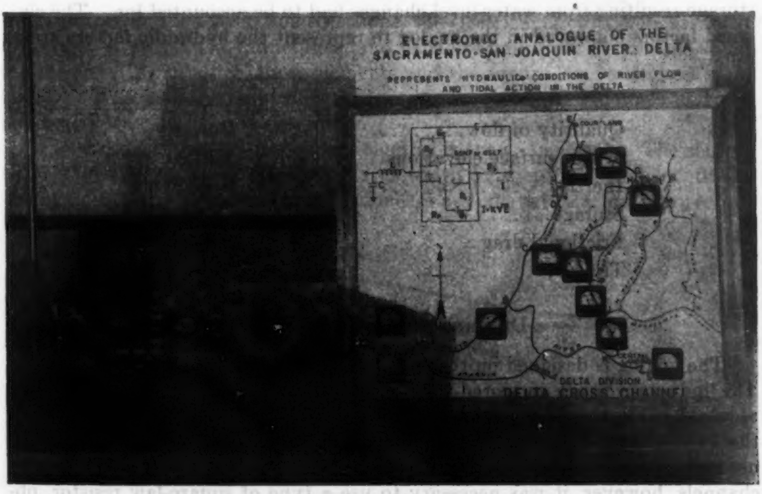

Fig. 1.—External Appearance of Electronic Analog

progress had previously been made for estimating flow patterns by model testing and by use of the procedure of Hardy Cross,[4] Hon. M. ASCE, but the

[4] "Analysis of Flow in Networks of Conduits or Conductors," by Hardy Cross, *Bulletin No. 286*, Univ. of Illinois Eng. Experiment Station, Urbana, Ill., November, 1936.

complexities introduced by the tidal factor made it desirable to seek some new method of solution.

The electronic analog computer, built to expedite these computations, was successful for this purpose. The appearance of the completed analog is shown in Fig. 1.

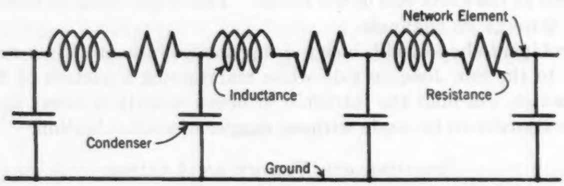

Fig. 2.—Basic Analog Circuit

Design Requirements

In order to solve the Delta problem, it was required that the analog be able to reproduce the square-law relation between friction and velocity that is characteristic of fluid flow. In addition, it was required to represent the wave motion associated with the tides. To do this, the factors of inertia and of storage resulting from water level changes had to be accounted for. The electrical factors employed in the analog to represent the hydraulic factors are as follows:

Hydraulic	Electrical
Quantity of flow	Current
Water surface elevations	Voltage
Inertia	Inductance
Storage	Capacity
Frictional drag	Resistance
Time	Time

Description of the Analog

The analog is designed on the basis of circuits of the type shown in Fig. 2. The inductances are air-cored coils of commercial types or were wound as required. The condensers are commercial units of the paper or mica type. In the large channels having very low frictional resistance, linear resistors were used with appropriate average values for the currents flowing. In the smaller channels, however, it was necessary to use a type of square-law resistor, obtained by taking advantage of certain vacuum tube characteristics that have approximately the required form of variation. These tubes were used with resistors in parallel and in series to obtain the desired characteristic. A biasing voltage was also required in this adjustment. The circuit used in such cases is shown in Fig. 3.

A dual triode tube with sections connected in parallel, opposing, is used to permit current to flow in either direction. This type of resistor is not wholly satisfactory since the tubes show variations that make it necessary to adjust each section separately. The current carrying capacity is restricted within narrow limits, and it is necessary, therefore, to design the analog around these elements. Net current flows were read on direct current milliammeters and tidal amplitudes and phase differences were read on a cathode-ray oscilloscope. The gate keeper was represented by a rectifier circuit that was also found to have some shortcomings near the zero point, introducing an effect analogous to gate leakage. In spite of these minor difficulties, the analog operates in a very satisfactory manner. Some idea of the speed with which the device works may be obtained from the fact that the analog runs through about 500 days of actual tidal changes in each second of operating time.

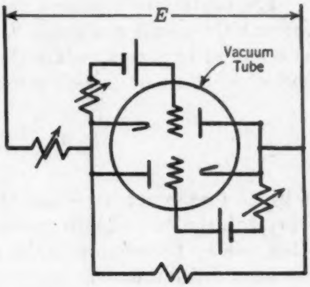

FIG. 3.—SQUARE-LAW RESISTOR

BASIC EQUATIONS

In setting up the correlation equations, the electrical circuits were assumed to have their resistance, inductance, and capacity uniformly distributed along their length. In practice, these elements and the square-law resistances were lumped. The inertia and storage factors were considered together, and the resistances were considered separately.

A longitudinal section of a stream channel is shown in Fig. 4. The shaded element in Fig. 4 represents a lamina of width b_w, depth H, and length dx. For analytical purposes the actual channel is assimilated to a uniform rectangular channel that has the same top width and cross-sectional area as the actual channel. As stated previously, frictional forces are not introduced into the dynamical equations, but are treated separately. Since x represents a distance measured along the stream from some fixed point on the bank, the planes

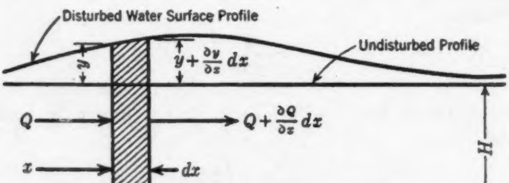

FIG. 4.—LONGITUDINAL SECTION OF A CHANNEL

defined by x and $x + dx$ do not change position with time. It is assumed that y, the surface elevation above sea level, is small compared to H, the depth of the stream.

The continuity condition requires that, if the quantities of water flowing through the planes x and $x + dx$ differ, the surface elevation must rise or fall as required to accommodate the changes of volume. If small quantities are neglected, this requirement is expressed by the equation:

$$b_w\, dx \frac{\partial y}{\partial t} = + Q - \left(Q + \frac{\partial Q}{\partial x} dx\right) \quad \text{.......} (1)$$

in which t represents time and Q represents flow. If a surface gradient $\partial y/\partial x$ is present, the water depth on one side of the lamina will be greater than on the other side by the amount $(\partial y/\partial x)\, dx$ and the additional pressure resulting from this head differential will cause the water within the lamina to be accelerated. Thus, the requirements of Newton's law are expressed to a first order of approximation by

$$\frac{\gamma\, b_w H}{g} dx \frac{\partial}{\partial t}\left(\frac{Q}{b_w H}\right) = - \gamma\, b_w H \frac{\partial y}{\partial x} dx \quad \text{.......} (2)$$

in which γ represents the weight of water per unit volume and g represents the acceleration of gravity. Eqs. 1 and 2 can be simplified by canceling common terms and collecting. Then the equation of continuity becomes

$$\frac{\partial Q}{\partial x} + \frac{b_w \partial y}{\partial t} = 0 \quad \text{.......} (3)$$

and Newton's law takes the form:

$$\frac{\partial y}{\partial x} + \frac{1}{g\, H\, b_w} \frac{\partial Q}{\partial t} = 0 \quad \text{.......} (4)$$

It is of interest to note that, if Q is eliminated from Eqs. 3 and 4, the wave equation is obtained:

$$\frac{\partial^2 y}{\partial x^2} = \frac{1}{g\, H} \frac{\partial^2 y}{\partial t^2} \quad \text{.......} (5)$$

The relation between flow and gradient for the hydraulic channel can be expressed in the form:

$$Q = M \sqrt{\frac{\partial y}{\partial x}} \quad \text{.......} (6)$$

in which M is a constant of the channel specifying its flow resistance. Eq. 6 may be recognized as a form of the Chezy formula. In the electrical circuits let C represent the capacity per unit length of circuit; E the potential with respect to ground; I the current; K a constant applying to a circuit; r the resistance per unit length of circuit; η the time in the analog; λ the inductance per unit length of circuit; and ξ the distance along a circuit.

Then, the equations for the idealized electrical circuits[5] that correspond to Eqs. 3 and 4 for the hydraulic channels are

$$\frac{\partial I}{\partial \xi} + C\frac{\partial E}{\partial \eta} = 0 \quad \text{.......................(7)}$$

$$\frac{\partial E}{\partial \xi} + \lambda\frac{\partial I}{\partial \eta} = 0 \quad \text{.......................(8)}$$

From Eqs. 7 and 8, there is obtained, on elimination of I,

$$\frac{\partial^2 E}{\partial \xi^2} = \lambda\, C\frac{\partial^2 E}{\partial \eta^2} \quad \text{.......................(9)}$$

For the circuits provided with an electronic resistor to represent hydraulic resistances of the type expressed by Eq. 6

$$I = K\sqrt{\frac{\partial E}{\partial \xi}} \quad \text{.......................(10)}$$

or, if the circuit has a linear resistance,

$$I = \frac{1}{r}\frac{\partial E}{\partial \xi} \quad \text{.......................(11)}$$

Correlation Equations

The electronic analog operates at a frequency of 1,000 cycles per sec. The sinusoidal variations imposed on the analog approximately represent tidal oscillations having a frequency of about 2 cycles per day. The correlation equations that were found suitable for use with the available electrical components are as follows:

$$y = 0.1\,E \quad \text{.......................(12a)}$$

$$Q = 10{,}000{,}000\,I \quad \text{.......................(12b)}$$

$$x = 10{,}000\,\xi \quad \text{.......................(12c)}$$

$$t = 45{,}000{,}000\,\eta \quad \text{.......................(12d)}$$

Other applications would, of course, require other constants. An analogous electrical quantity is obtained by substituting the foregoing relations into the hydraulic equations. For example, Eq. 6, on substitution becomes

$$10{,}000{,}000\,I = M\sqrt{\frac{0.1\,\partial E}{10{,}000\,\partial \xi}} \quad \text{..............(13a)}$$

or

$$I = \frac{M}{3.2 \times 10^9}\sqrt{\frac{\partial E}{\partial \xi}} \quad \text{.......................(13b)}$$

[5] "The Theory of Sound," by Lord Rayleigh, Dover Publications, London, England, 1945, Vol. 1, p. 467, paragraph 235.

Then, the quantity $\frac{M}{3.2 \times 10^9}$ is the K-value in Eq. 10. By this choice of constants the electrical circuit is given resistance characteristics that are analogous to the friction in the corresponding hydraulic channel. The other relations are treated in a similar way.

Boundary Conditions

To account for the stream flow it was necessary to introduce direct currents of specified amounts at certain points in the analog and to take them out at certain other points. In general, the currents fed into the network represent river flows entering the Delta area, while currents leaving the network represent the draft of the Tracy pumps and the flow from the Delta area into Suisun Bay. To simulate these currents, voltages of controllable magnitude were introduced between the network and the ground wire (see Fig. 2). Control of the currents was obtained by variable resistors located at the points at which the currents enter and leave the network.

The tides were represented by alternating voltages of specified magnitude applied between the network and the ground wire at the point on the analog representing the entrance to Suisun Bay. A blocking condenser was used here to prevent the flow of direct current through the transformer windings. The actual tides occurring at this point vary somewhat from day to day because of varying phase relations between the lunar and solar components. In the analog, these tidal variations were replaced by a single sinusoidal variation of average amplitude. The connections arranged for introducing the direct currents representing stream flow would permit the alternating currents representing the tides to pass into the ground wire at other points than that representing the entrance to Suisun Bay. Since this would introduce errors, inductive blocking impedances were placed in the direct current circuit wherever necessary to confine the alternating currents to the proper network circuits. At points where stream channels continued beyond the area represented by the analog, lumped impedances were introuced in the circuit to represent those portions beyond the analog area. In most cases these impedances were determined by trial, so that known tidal behavior would be properly represented.

In order to protect the direct current meters from loss of field caused by the alternating current components, these meters were shunted by condensers having impedances to alternating current that were low compared to the resistance of the meter.

Conclusions

An analog of the type described in this paper is an effective means of expediting the work of finding flow distribution patterns in a network of channels. It is particularly effective when tidal effects must also be included in addition to gravity flows. The results obtained have checked well with those obtained by other means.

DISCUSSION

J. VAN VEEN[6].—Tidal flow in estuaries, with which this paper is concerned, is a problem in which the Dutch engineers have been much interested for a long time. It may be worthwhile to mention some Dutch practices.

For deltaic schemes, such as for the making of new tidal channels or improving them by dredging (that is, narrowing or widening them), making new open harbors, closing inlets, and other similar projects, Dutch engineers use three different methods to check one another and to enhance results. They are: (1) Mathematical methods, (2) hydraulic laboratory methods, and (3) electrical methods. These methods give nearly the same results when handled well, but each has a point of advancement over the other. (1) Mathematical research is very satisfactory except in the amount of work that has to be put into the calculations. (2) Hydraulic laboratory tests give quick results, but they may be somewhat lacking in exactness, mainly because of the difficulties arising in reproducing the right amount of friction; baffles must be used, which (produced on the prototype scale) would be enormous structures in the bed of the river, taking perhaps 10% or 20% of the width. (3) Electrical imitation of the tides is essentially the same as the mathematical method because this imitation is a calculating machine, or electronic computer, based on the mathematical formulas. Although the results can be obtained very quickly and accurately, the computer needs much supervision, and none of the many electronic tubes should show deterioration.

The three methods can be coordinated very well. It became possible by taking the average of 2 or 3 runnings of the model to reach an accuracy of about plus and minus 3% in the normal vertical tide on an hydraulic model of the estuary of the Rhine-Maas (the vertical scale was 1:64 and the horizontal scale was 1:2400) when the results of that model were compared with those of accurate measurement data. The accuracy of the data given by the electrical model and by the mathematical computations may be as great. The accuracy of the data for the currents, obtained by electrical models, may be much greater than that obtained by an hydraulic model.

Electrical imitation can do much work alone—namely, the work of determining the water levels and water currents in the channels of an estuary, but not the determination of the sand movements, scouring, and siltations. Those problems are for hydraulic models and mathematics. The literature shows that it took engineers a long time to solve the electrical imitation problems wholly, or at least to great perfection, partly because the intricate details of mathematics had to be solved first. There resulted three different mathematical methods to solve the quadratic tidal formulas: (*a*) Harmonic method, using sinusoids; (*b*) Taylor series development; and (*c*) the method of charac-

[6] Chf. Engr., Research Dept., Governmental Tidal Waters Dept., The Hague, Holland.

teristic wave components. Without the knowledge of these methods, good results cannot be obtained by electrical computers.

Although giving practically the same results, all three mathematical methods are extremely unwieldy to handle—so much so that for a certain proposed project only a few calculations could be made per year (using about ten calculators), although the results of scores of calculations were needed. Often fifty equations had to be solved each time—hence the need of hydraulic or electrical models. H. A. Lorentz, of Leiden University, initiated the modern method of tidal calculations in 1918 when calculating the Zuider-Zee enclosure scheme. He used formulas of the linear type that (after a slight modification) electrical engineers are accustomed to call the telegraph equation. It would have been easy to imitate electrically the tides in the Zuider-Zee channels according to these linear formulas, and the solution would have been simple. It is the quadratic law of resistance of water movement that necessitates the use of highly complex mathematics and electronics. It increases difficulties a hundredfold. Of course, neither the electrical computers nor the hydraulic models of greatly reduced scale are able to deal with sand movements and salt problems.

Thus, the principle of the computer described by the authors offers the advantage of speed and accuracy, and there are no limitations as to its ability to imitate purely hydraulic phenomena except the great practical and theoretical difficulties of construction of the computer. Some difficulties that were encountered by Dutch engineers in their 30 years of practice may also have been experienced by the authors and are described here.

The accuracy of the electrical method depends mainly on the accuracy, flexibility, and reliability of the elements of self-inductance, capacity, and resistance; on the number of sinusoids used for the boundary conditions; and also on the length of a river section. Engineers of the Dutch Government take these sections no longer than 5 km. The accuracy of the electrical measurements is about 1%. In Holland engineers use a period of $\frac{1}{1{,}000}$ sec for a tidal period. Cathode-ray tubes are used as indicators only, not for measurements.

Of course, the elements of self-inductance, capacity, and resistance must change with the tidal depths and tidal widths of each section. This caused great difficulties in the construction of the Dutch electrical computer. The authors have not mentioned that problem, therefore, their computer will be fit for small tidal ranges only, say, 1 ft or 2 ft. Another difficulty was the inability of the factories to make special electronic tubes having the desired variable quadratic accuracy. The electrical computers for engineering purposes do not use exact "quadratical"-tubes in great quantities so that the manufacture of these special tubes is costly. When these "quadratical law"-computers become numerous, manufacture of these special electronic tubes may become economically feasible. However, some other electrical design has been evolved which gives good results, although it is not so elegant as the use of special electronic tubes would be.

All sections of the Dutch computer are constructed for universal use; they may be used for channels of any width, depth, and tide within wide ranges. One hundred sections, or elements, or more are needed to imitate the main networks of the Dutch tidal channels. A rather large room is needed to house this computer although each element is contained in a box 1 ft $\times 1\frac{1}{2}$ ft $\times 1\frac{1}{2}$ ft. There are auxiliary instruments for the boundary conditions and for measurements. The universal characteristics of each section imply that any existing or future network and any tide can be imitated with those sections. The exact imitation of tides by electrical gadgets is difficult. Although, under the heading, "Conclusions," the authors assert that they have found their computer particularly effective for their purpose; great difficulties arise when more detail is wanted. The imitation of currents in a network of pipes is not so involved. Water currents in soils, or in dams, can be imitated easily because they are linear. Also, the air currents in an underground railroad system or in a mine can be imitated easily by means of electricity. It has become a general practice in the past few years in Holland.

If the engineers would unite in their efforts to induce electronic tube factories to produce the required kind of electronic tube (especially a tube with a variable quadratic characteristic), this would mean a simplifying and refining of electrical computers. The Dutch engineers would welcome any suggestion as to how to obtain the special variable quadratic valve-tubes.

Reading References.—The following literature is pertinent to the subject of this paper: "Verslag van de Staatscommissie Zuiderzee," by H. A. Lorentz, Algemene Landsdrukkerij, The Hague, Holland, 1918–1926; "l'Influence de la fermeture du Zuiderzee sur le régime des marées le long des côtes neérlandaises," by J. Th. Thijsse, *Bulletin de l'Association permanente des Congrès de Navigations*, No. 15, 1933; "Een getijberekening voor benedenrivieren" (Taylor series development), by J. J. Dronkers, *De Ingenieur*, The Hague, Holland, 1935; "De berekening van getijden en stormvloeden op benedenrivieren," by J. P. Mazure, Drukkerij Gerretsen, The Hague, Holland, 1937; "Getijstroomberekeningen met behulp van wetten analoog aan die van Ohm en Kirchhoff" ("Tidal Calculation with Laws Analogous to Those of Ohm and Kirchhoff"), by J. van Veen, *De Ingenieur*, No. 3, 1937; "Tidal Hydraulics," by G. B. Pillsbury, Govt. Printing Office, Washington, D. C., 1940; "Electrische nabootsing van getijden" ("Electrical Imitation of Tides"), by J. van Veen, *De Ingenieur*, No. 3, 1946; "The Calculation of Tides in New Channels," by J. van Veen, *Transactions*, Am. Geophysical Union, Vol. 28, No. 6, December, 1947, p. 861; "Analogie entre marées et courants alternatifs," by J. van Veen, *La Houille Blanche*, No. 5, September-October, 1947; "Methoden van getijberekening" ("Methods of tidal calculation"), by J. J. Dronkers, *De Ingenieur*, No. 45, 1947; "Een bijdrage tot de kennis van de getij beweging op benedenrivieren," ("How to Improve on Tidal Calculation"), by H. J. Stroband, *De Ingenieur*, No. 36, 1947; "De voortplanting van het getij bepaald met behulp van de electrotechniek met inachtneming weerstandswet" ("Propagation of the Tide Determined with the Aid of Electrotechnique"), by H. J. Stroband, *Polytechnisch Tijdschrift*, The Hague, Holland, November 18 and November 30, 1948; "Aperçu des méthodes pour la détermination du mouvement de

marée dans les embouchures et les fleuves à marée neérlandais," by J. J. Dronkers and J. van Veen, *Rapport 17e*, Congrès International de Navigation Lisbon, Portugal, 1949, Section 2, Question 1, p. 159; "An Electrical Analogue for Mine Ventilation and Its Application to Ventilation Planning," by W. Maas, *Geologie en Mijnbouw*, The Hague, Holland, April, 1950, p. 117; "Het bepalen van drukverliezen in leidingnetten met behulp van een electrisch model" ("Determination of Press Losses in Water Works with the Aid of an Electric Model"), by Th. G. van Zoest, *Tijdschrift "Water,"* The Hague, Holland, 1951; "Le calcul du mouvement non-permanent dans les rivières par la méthode dite des lignes d'influence," by H. Holsters, *Revue Général de l'Hydraulique*, Brussels, Belgium, 1947; "Propagation of Tides and Similar Waves," by J. C. Schönfield, Delft, Holland, 1950; and "Determination of Flows in Estuarine Channels," by Fr. E. Swain, *Transactions*, Am. Geophysical Union, Vol. 32, No. 5, October, 1951, pp. 653–672.

W. Douglas Baines,[7] J. M. ASCE.—The representation of a physical phenomenon by another physical phenomenon, its analog, can be divided into two distinct steps. The first step is the accurate mathematical description of the first phenomenon step and the second is the representation of this mathematical description by the second phenomenon. In general, it can be stated that, if the two phenomena are described by the same mathematical equations (with corresponding boundary conditions), the second phenomenon is a perfect analog of the first. In the authors' attempt to make an electrical analog of unsteady flow in a natural river system, they have written sets of mathematical equations to describe the flow in the river channels and the electrical properties of the analog circuit. The mathematical equations are identical—hence, the electrical analog can be expected to solve the equations which are set up for the flow. However, the authors have not clearly explained how the mathematical equations describe the physical aspects of the flow. They have asserted that they are using the first approximation to the complete flow equations, but they have not shown to what extent this approximation describes the flow as it occurs in the natural river channels. The writer's criticism is limited to a discussion of this approximation.

The equations of motion for unsteady flow in an open channel are[8] the continuity equation:

$$\frac{\partial Q}{\partial x} + b_w \frac{\partial Y}{\partial t} = 0 \qquad (14)$$

and Newton's second law:

$$S_o - S_f = \left(1 - \frac{Q^2}{b^2_w\, g\, Y^3}\right) \frac{\partial Y}{\partial x} + \frac{2\,Q}{b_w\, g\, Y^2} \frac{\partial Q}{\partial x} + \frac{1}{b_w\, g\, Y} \frac{\partial Q}{\partial t} \qquad (15)$$

in which S_o equals the river bed slope, S_f equals the friction slope, and Y equals $y + H$, thus representing the instantaneous water stage. The equation of continuity (Eq. 3), used by the authors, can be seen to be the exact equation,

[7] Research Officer, National Research Council, Div. of Mech. Eng., Univ. of British Columbia, Vancouver, B. C., Canada.

[8] "Flood Routing," by B. R. Gilcrest, in "Engineering Hydraulics" (edited by H. Rouse), John Wiley & Sons, Inc., New York, N. Y., 1950, p. 640.

but several terms have been dropped from Newton's second law as can be observed by comparing Eq. 15 with Eq. 4. In obtaining their first approximation, the authors must, therefore, have made the following assumptions:

1. The tide height disturbance, y, is small as compared to the mean depth, H. It is not clear how small y must be in comparison to H for this condition to be true, but it seems that, if y/H had a maximum value of about 0.1, such an assumption would be justified.

2. The depth H is not a function of x. This is tantamount to assuming that the natural river channel has a uniform cross section and is straight. This assumption may, or may not, be correct and can be checked only by a close examination of the river. Judging that these two assumptions are satisfied, Eq. 15 reduces to

$$S_o - S_f = \left(1 - \frac{Q^2}{b_w\, g\, H^3}\right)\frac{\partial y}{\partial x} + \frac{2\,Q}{b_w\, g\, H^2}\frac{\partial Q}{\partial x} + \frac{1}{b_w\, g\, H}\frac{\partial Q}{\partial t} \qquad (16)$$

3. It is assumed that $\frac{Q^2}{b_w\, g\, H^3} \ll 1$. Examination of the small amount of field data at the writer's disposal[9] shows that this assumption is justified. For August 23, 1929, the flow in the San Joaquin River, at Antioch, Calif., has the maximum value for $\frac{Q^2}{b_w\, g\, H^3}$ of $\frac{Q^2}{b_w\, g\, H^3} = F^2 = \frac{(2.5)^2}{32.2 \times 40} = 0.00475 \ll 1$, in which F equals the Froude number of the flow.

4. The term $\frac{2\,Q}{b_w\, g\, H^2}\frac{\partial Q}{\partial x}$ is much smaller than the terms $\frac{\partial y}{\partial x}$ and $\frac{1}{b_w\, g\, H}\frac{\partial Q}{\partial t}$. Again, the only way these terms can be checked is by an examination of field data from the river. The writer does not have enough data available to verify this assumption, and so is unable to decide whether or not it is justified. However, in the case of the Fraser River (in British Columbia, Canada) and other streams which the writer has examined in detail, it has been found that $\frac{2\,Q}{b_w\, g\, H^2}\frac{\partial Q}{\partial x}$ is of the same order as the other terms in the equation. Accepting the contention that the term is negligible for the San Joaquin River, then Eq. 16 is simply

$$S_o - S_f = \frac{\partial y}{\partial x} + \frac{1}{b_w\, g\, H}\frac{\partial Q}{\partial t} \qquad (17)$$

5. It is assumed that $S_o - S_f = 0$. It is most common in the analysis of unsteady flow to use Chezy's form for the expression of friction slope, S_f, so that this assumption gives the following equation, which must be satisfied by the discharge:

$$Q = M\,\sqrt{S_o} \qquad (18)$$

It is easily seen that Eq. 18 is not physically correct because of the fact that S_o

---

[9] "On the Nature of Estuarine Circulation," by H. Stommel and H. G. Farmer, Woods Hole Oceanographic Inst., Woods Hole, Mass., August, 1952.

is a constant, requiring Q to be constant. The authors have side-stepped this difference by replacing S_o with $\frac{\partial y}{\partial x}$, the instantaneous water surface slope, in obtaining Eq. 6. The reason for the choice of $\frac{\partial y}{\partial x}$ is not clear because it produces a condition that is not physically correct. For example, near local high or low tide—$\left(\text{when } \frac{\partial y}{\partial x} = 0\right)$ $Q = 0$ by Eq. 6. It is demonstrated subsequently that this fact is contrary both to the general solution of Eqs. 3 and 4 and to the observed facts. The exact relation between flow and friction is found by solving Eq. 17 for Q, which yields

$$Q = M \sqrt{S_o - \frac{\partial y}{\partial x} - \frac{1}{b_w \, g \, H} \frac{\partial Q}{\partial t}} \qquad (19)$$

It may be true that the expression under the square root sign in Eq. 19 is a good approximation of $\frac{\partial y}{\partial x}$ in this particular case, thereby justifying the authors' assumption. This would be fortuitous indeed.

It becomes clear that there is an inconsistency in the authors' assumptions. If it is accepted that they are using Eqs. 3 and 4 to describe the flow, the complete solution to the problem is defined, and this solution cannot satisfy any other condition except boundary or initial conditions. The general solutions of Eqs. 3 and 4 are[10]

$$\frac{y}{H} = F_1 (x - t \sqrt{g H}) + F_2 (x + t \sqrt{g H}) \qquad (20)$$

and

$$\frac{Q}{b_w \, H \sqrt{g H}} = F_1 (x - t \sqrt{g H}) - F_2 (x + t \sqrt{g H}) \qquad (21)$$

in which F_1 and F_2 are arbitrary functions. These two equations describe a pair of waves, one moving in the positive x-direction, and the other moving in the negative direction. Each element of the profile for these waves moves with the same celerity, and, consequently, the profile is unchanged in shape and amplitude. If it is assumed that $x = 0$ on the ocean end of the tidal river, $F_2 = 0$ for the region of interest, and the following simple relationship between y and Q must hold:

$$\frac{Q}{b_w \, H \sqrt{g H}} = \frac{y}{H} \qquad (22)$$

The form of the function F_1 is determined by boundary or initial conditions which, for tidal-influenced flow, are of the form:

$$y\,(a, t) = \sum_{k=1}^{n} A_k \sin \frac{k \pi t}{T} \qquad (23)$$

---

[10] "Wave Motion," by G. H. Kuelegan, in "Engineering Hydraulics" (edited by H. Rouse), John Wiley & Sons, Inc., ew York, N. Y., 1950, p. 718.

in which a equals a fixed value of x, A_k is a series of constants, and T is the tidal cycle period. If the differential equation for friction (Eq. 6) is combined with Eq. 22, having boundary conditions of the form of Eq. 23, a redundant condition is obtained which cannot be satisfied.

It is easy to demonstrate that Eq. 6 imposes a condition on Eqs. 3 and 4 which it is impossible to satisfy for the sinusoidal type of boundary condition. Eliminating $\frac{\partial y}{\partial x}$ from Eqs. 4 and 6 produces a differential equation:

$$M^2\, g\, H\, b_w\, Q^2 = -\frac{\partial Q}{\partial t} \qquad (24)$$

which has the general solution:

$$Q = [M^2\, g\, H\, b_w\, t + c_1(x)]^{-1} \qquad (25)$$

in which $c_1(x)$ equals a function of x. This solution, when inserted in Eq. 3, yields the following differential equation:

$$\frac{c'_1(x)}{[M^2\, g\, H\, b_w\, t + c_1(x)]^2} = b_w \frac{\partial y}{\partial t} \qquad (26)$$

which has the general solution:

$$b_w\, y = -\frac{c'_1(x)}{M^2\, g\, H\, b_w [M^2\, g\, H\, b_w\, t + c_1(x)]} + c_2(x) \qquad (27)$$

Eq. 27 is a hyperbola expressed in terms of the variable, t, and, as a result, it is impossible to satisfy boundary conditions of the type illustrated by Eqs. 23 and 27. The writer is thus forced to conclude that the authors have not described the flow by Eqs. 3, 4, and 6, but have used other unstated equations. The writer is at a loss to explain how these other equations were obtained because of the meager amount of information contained in the paper.

In spite of the uncertainties in the foregoing assumptions, the electrical analog may be a good representation of the flow in a tidal river; and, if so, it would prove to be valuable to engineers who must plan structures that disturb the natural regime of the river.

It would be interesting to know whether or not the peculiarities of the tidal effects in rivers are demonstrated by the electrical analog. In particular, the change of the shape of the curve relating stage and time at any station should be produced. At the river mouth, this curve resembles a sine curve with rounded peaks and a constantly changing slope on both ebb and flood tides. In the upstream reaches, it is usually observed that the curve relating the stage and the time approaches a saw-toothed shape, with sharp peaks and a linear rise and fall.

Another factor in evaluating the electrical analog is whether or not it produces the correct phase difference between the stage and the velocity. In most rivers, the maximum inflow or outflow velocity precedes the maximum or minimum stage, respectively, by about 3 hours. This factor is very important when sediment transport must be considered because the rate of bed movement depends on both the depth and velocity of flow. The wave equation predicts

no phase difference between the stage and the current, and Eq. 6 predicts approximately a 6-hour difference. Thus, neither of these solutions describes the actual physical conditions.

Other investigators have studied the possibility of the electrical analog in tides, particularly A. T. Doodson,[11] but none has been able to produce an analog of practical value. If the authors can show that their analog is a good representation of the actual flow in natural rivers, they are to be commended for a very valuable contribution to engineering science.

T. Blench,[12] M. ASCE.—An analog of the type described by the authors was designed by Mr. van Veen[11,13] who shunted the resistance across the capacitance instead of placing it in series with the inductance. The consequence was that the electric current represented the tidal displacement and the voltage represented the fluid discharge. The technical difficulties of representing branching channels with tidal displacement at the joint may be

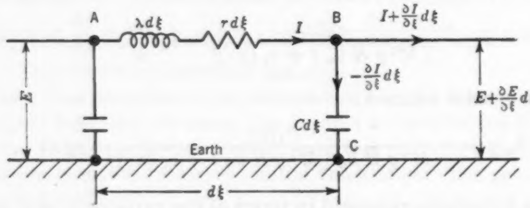

Fig. 5.—Basic Analog Circuit

imagined, and the authors are to be commended for their ingenuity in removing the difficulty; however, the derivations of both the hydraulic and the electric equations seem to be incorrect. Fig. 5 is Fig. 2 with the relevant electrical data inserted. In Fig. 5, from A to B—

$$-\frac{\partial E}{\partial \xi}\,d\xi = r\,d\xi\,I + \lambda\,d\xi\,\frac{\partial I}{\partial \eta}$$

and from B to C—

$$-\frac{\partial I}{\partial \xi}\,d\xi = C\,d\xi\,\frac{\partial E}{\partial \eta}$$

from which

$$\frac{\partial I}{\partial \xi} + C\,\frac{\partial E}{\partial \eta} = 0 \ldots\ldots\ldots\ldots\ldots\ldots\ldots\ldots(7)$$

and

$$\frac{\partial E}{\partial \xi} + \lambda\,\frac{\partial I}{\partial \eta} + r\,I = 0 \ldots\ldots\ldots\ldots\ldots\ldots\ldots(28)$$

of which Eq. 28 contradicts Eq. 8.

---

[11] "Tide Models," by A. T. Doodson, *Dock and Harbour Authority No. 339*, Vol. 29, January, 1949.

[12] Cons. Eng., Associate Prof. of Civ. Eng., Univ. of Alberta, Edmonton, Alt., Canada.

[13] "Coasts, Estuaries and Tidal Hydraulics," by J. van Veen, from "Civil Engineering Reference Book," Butterworths, London, England, 1951.

The dynamical error seems to be in writing Eq. 4 without friction and then applying Eq. 6 separately, as if it were related to the total unsteady nonuniform flow. The writer feels that the method of Mr. van Veen is correct; that is, to write Eq. 4 as

$$\frac{\partial y}{\partial x} + \frac{1}{g\,H\,b_w}\,\frac{\partial Q}{\partial t + F} = 0 \qquad (29)$$

in which F is a friction term whose expression depends on the individual's preference in flow formulas. It is worthwhile to note that Eq. 4 omits convective acceleration and, therefore, does not apply to tides of high amplitude; that is, y/H greater than 0.25. The form of F used by Mr. Doodson, who accepted the Chezy formula, is tantamount to

$$F = \frac{K\,Q\,|Q|}{g\,b^2_w\,H^3} \qquad (30)$$

in which k is a coefficient, $|Q|$ means "absolute value of Q," and there is zero flow at half tide. The writer had occasion to try to extend the theory to the case of a half-tide flow of velocity U, and to replace the Chezy formula by a more realistic expression. This substitution yielded

$$F = \frac{Q\,|Q|}{c\,b^2_w\,H^{3.5}} = \frac{U\,|U|}{c\,H^{1.5}} \qquad (31)$$

in which c is a friction coefficient. The continuity equation (Eq. 3) remains unchanged.

The comparison of Eq. 7 and Eq. 28 with Eq. 3 and Eq. 29 shows that the authors' analog still holds, but a question arises as to whether the conversion factors may not need some numerical modification, and a comparison of predicted results with prototype results would be interesting.

R. E. GLOVER,[14] M.ASCE, D. J. HEBERT,[15] AND C. R. DAUM[16].—Mr van Veen describes the experiences of Dutch engineers who have had to deal with hydraulic problems where tidal influences are a factor. His remarks are of interest because they are based on these experiences, and also because they make the results of Dutch research available to American engineers. It is regrettable that the statement that cathode-ray tubes are not used for measurement in Holland was not amplified. It has been the writers' experience that the high speed at which electronic analogs work usually makes oscillograph recording difficult unless the working speed is reduced by use of iron-core inductances. Such expedients usually result in a loss of accuracy.

The difficulties introduced by changes in water-surface areas and hydraulic resistance brought about by changes in depth are real ones. The presence of levees along the channels and the limited variations of depth in the Delta minimized these troubles in the case described by the writers.

[14] Engr., Bureau of Reclamation, U. S. Dept. of the Interior, Denver, Colo.
[15] Engr., Bureau of Reclamation, U. S. Dept. of the Interior, Denver, Colo.
[16] Physicist, Bureau of Reclamation, U. S. Dept. of the Interior, Denver, Colo.

Mr. Baines and Mr. Blench subjected the analytical aspects of the work to a searching scrutiny. The questions they ask are of a type which should be considered whenever an electronic analog is to be used for solving any specific hydraulic problem. The Delta channels are of nearly constant cross section for great distances. Furthermore, the presence of levees holds the changes of width of the water surface to values that are small compared to the original top widths and, since the changes of level to be accounted for were small compared to the original water depths, the difficulties produced by variations of top width and cross section were small enough to be ignored in the construction of the Delta analog. In the case of the problem of routing a flood down a river, cross-sectional areas and top widths would ordinarily be subject to large variations, and an analog of the type described would not be suitable.

Although it is certainly desirable to obtain a highly accurate representation of the hydraulic conditions, electrical difficulties often make compromises necessary. The development of a tube having adjustable characteristics would greatly facilitate overcoming some of these difficulties. Mr Blench comments on the neglect of the convective acceleration term. Although his purpose was to emphasize the limitations of the analog, it may be added that electrical devices to represent the convective acceleration term in an analog would be difficult to devise. The writers would prefer to replace the linear resistance term in Eq. 28, as presented by Mr. Blench, with a term of the form I^2/K^2 obtained from the relations expressed by Eq. 10. Such a replacement would lead to an effective procedure for selecting the square-law resistor to represent hydraulic friction in the analog. Suppose the friction term in Eq. 17 of Mr. Baines' discussion had been expressed explicitly in the form Q^2/M^2 obtained by squaring Eq. 18, after replacing the quantity S_o by S_f. Since, in the writers' application S_o could be set equal to zero, Mr. Blench's electrical equation and Mr. Baines' hydraulic equation would become analogous and the constants for the square-law resistor could be selected with the use of the correlation equations. Such a procedure should also answer Mr. Baines' question in connection with Eq. 19 because it is a modified form of Eq. 17 which would then be exactly satisfied. This procedure would lead to the same choice of friction constants as were obtained by the writers. The choice of constants for square-law resistors is more readily understood when the friction term is included in the original equations as suggested by Mr. Baines and Mr. Blench. The limitations expressed in assumption No. 2, as listed by Mr. Baines, may be present when lumped electrical components are used to represent a channel, as in the Delta analog. This limitation can be removed by using several electrical components to represent a channel. As many changes of section can then be represented as there are components in the circuit.

Some changes in wave shape are produced in the Delta analog. These probably result from the action of the square-law resistors. The types of wave profile changes occurring in hydraulic channels as the result of the increase of the celerity of wave propagation with depth will not be produced by an analog of the type described, because the analog contains no electrical counterpart of the hydraulic factors that will produce changes of wave propagation speeds with changes of voltage.

Field data are available that make possible evaluation of the success attained by the analog in spite of the difficulties mentioned. The Walnut Grove channel has now been constructed to increase the flow of water in the lower Mokelumne channel and thereby compensate for the flow changes which result from operation of the Tracy pumping plant. Analog readings indicated that, with 10,000 cu ft per sec flowing in the Sacramento River at Sacramento, a total of 5,200 sec-ft should be transferred to the lower Mokelumne channel by the Walnut Grove cut and the Georgina slough. Field measurements indicate that with a flow of 10,600 cu ft per sec at Sacramento, the total transfer is 5,470 sec-ft.

In closing, the writers wish to express their appreciation to those who have contributed discussions to this paper.

APPLICATION TO STREAM-FLOW ROUTING

By Max A. Kohler,[1] A. M. ASCE

With Discussion by Messrs. Alfred J. Cooper, C. O. Clark, and Max A. Kohler

Synopsis

Late in 1948, the Weather Bureau, United States Department of Commerce, developed an electronic device for stream-flow routing[2,3] that has proved to be highly effective in the preparation of river stage forecasts. Although originally designed for routing flows from point to point along a stream, subsequent studies indicate that the equipment is equally applicable to the direct routing of effective rainfall (runoff) over relatively large basins. This application of the flow analog and the conditions under which the original circuit fails to provide a satisfactory reproduction of the outflow hydrograph are discussed in this paper. The basis for the circuit employed in the analog and the method of operating the equipment are also discussed briefly.

Introduction

Basis of the Analog.—Stream-flow routing is usually accomplished through the simultaneous solution of two equations—one equation relating storage to the instantaneous flow in the reach and the other an equation of continuity. In the Muskingum method[4] of routing, storage is assumed to be directly proportional to a weighted value of the flow within the reach, that is,

$$S = K\left[x\,I + (1 - x)\,O\right] \qquad (1)$$

in which S is the storage; I is the inflow; O is the outflow; and K and x are constants for the reach. It can be shown that the circuit of Fig. 1(a) satisfies this equation, provided the resistances R_1 and R_3 are equal and the capacitance

Note.—Published in June, 1952, as *Proceedings-Separate No. 133.* Positions and titles given are those in effect when the paper or discussion was received for publication.

[1] Chf. Research Hydrologist, Weather Bureau, U.S. Dept. of Commerce, Washington, D.C.

[2] "Applied Hydrology," by R. K. Linsley, M. A. Kohler, and J. L. H. Paulhus, McGraw-Hill Book Co., Inc., New York, N. Y., 1949, pp. 537-541.

[3] "Electronic Device Speeds Flood Routing," by R. K. Linsley, L. W. Foskett, and M. A. Kohler, *Engineering News-Record,* Vol. 141, 1948, pp. 64-66.

[4] "Engineering Construction—Flood Control," by G. T. McCarthy, The Engineer School, Ft. Belvoir, Va., 1940, pp. 147-156.

of condensers C_1 and C_2 are equivalent. In this case,

$$K = 2\,(R_1\,C_1 + R_2\,C_1) \qquad (2)$$

and

$$x = \frac{R_1}{2\,(R_1 + R_2)} \qquad (3)$$

Thus, by using fixed capacitance the circuit can be adjusted to any paired values of K and x if the proper values of resistance are set at three points in the circuit.

Circuits.—This is the basic circuit used in the flow analog. In practice, however, it is modified as shown in Fig. 1(*b*), to facilitate controlling the inflow current and observing both the inflow and outflow values. Moreover, there are two identical circuits feeding to a common outflow potentiometer, making it possible to derive the outflow graph from two sources of inflow undergoing different storage characteristics. Actually, three, four, or more inflow sources can be treated in a similar manner by simply increasing the number of circuits. Self-balancing potentiometers are inserted in the circuit, across pick-up resistors, to record the inflow and outflow currents. The pick-up resistances are very small compared to the values of R_1, R_2, R_3 and, consequently, have no significant effect on the characteristics of the circuit. To control the inflow current a photo-tube is inserted in the circuit and the light intensity activating this tube is regulated by a hand wheel.

Fig. 2 is a photograph of the analog as assembled. In operation, the plotted inflow graph is placed on the drum and the proper resistance values set on the panel. The inflow and outflow drums are synchronized and rotate

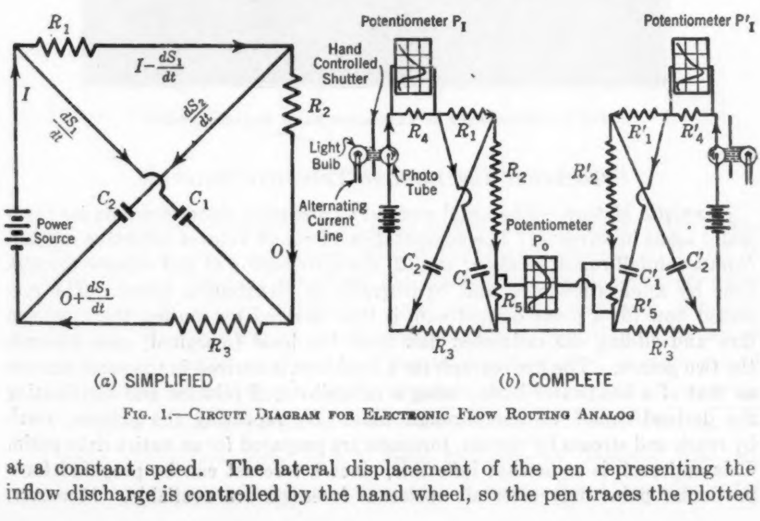

FIG. 1.—CIRCUIT DIAGRAM FOR ELECTRONIC FLOW ROUTING ANALOG

at a constant speed. The lateral displacement of the pen representing the inflow discharge is controlled by the hand wheel, so the pen traces the plotted

hydrograph, thus maintaining the inflow current in the circuit in identical ratio with the discharge. Simultaneously, the pen on the center potentiometer records the routed outflow hydrograph.

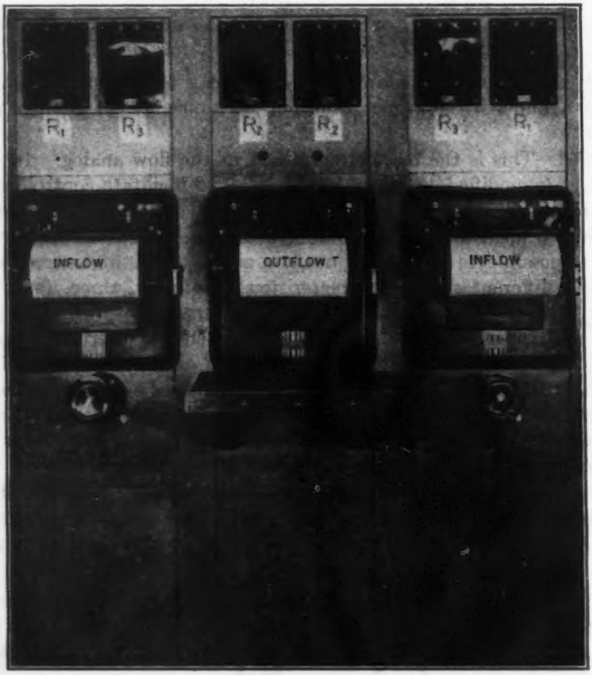

FIG. 2.—PHOTOGRAPH OF ELECTRONIC FLOW ROUTING ANALOG

PROCEDURE FOR ROUTING EFFECTIVE RAINFALL

Analytic Method.—The usual method of preparing flood forecasts for headwater areas involves: (1) The computation of runoff volume (effective rainfall) from a rainfall-runoff relation; and (2) the distribution of this volume through time by application of a unit hydrograph or distribution graph. The predicted flow for a point downstream is then derived by routing the upstream flow and adding the estimated flow from the local (marginal) area between the two points. The hydrograph for a local area is derived in the same manner as that of a headwater basin, using a rainfall-runoff relation and distributing the derived runoff volume through time. By repeating the process, reach by reach and stream by stream, forecasts are prepared for an entire river basin. This approach is somewhat inflexible, since a forecast can be prepared for a particular point only after all upstream forecasts are available. Moreover,

keeping the reaches of optimum length frequently makes it necessary to predict the hydrograph for points at which the forecasts are of little or no value. By routing the effective rainfall, however, a priority system can be used, preparing first the forecasts for those areas in which the flood threat is the most serious.

Use of the Analog.—The concept of simulating the hydrograph at a point by routing effective rainfall over the area above the point is not new. It is essentially the approach described by C. O. Clark,[5] A. M. ASCE, and has been considered by numerous other hydrologists.[6,7] The assumed inflow hydrograph is derived by lagging effective rainfall over various sub-areas in pro-

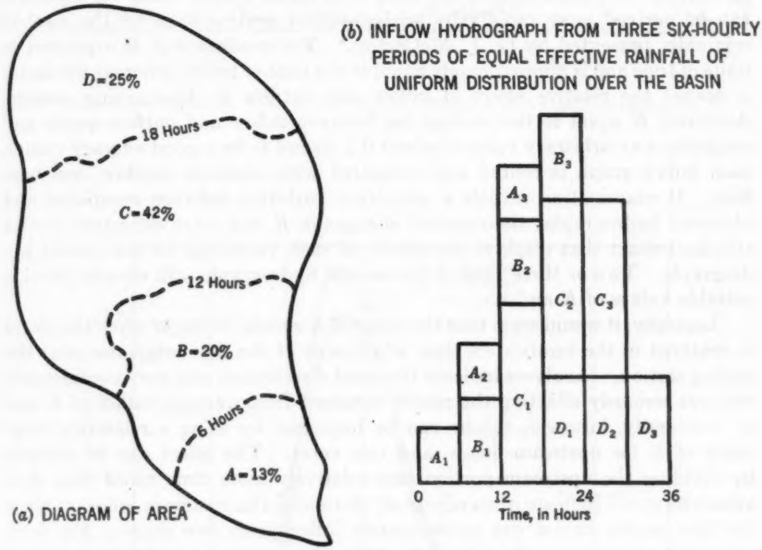

FIG. 3.—DERIVATION OF INFLOW GRAPH OF EFFECTIVE RAINFALL

portion to the travel time above the gaging station. Thus, in Fig. 3, the blocks A_1, B_1, C_1, and D_1 are in direct proportion to the areas of zones A, B, C, and D, respectively, and therefore constitute the inflow graph for one 6-hr period of effective rainfall, evenly distributed over the basin. Similarly, elements labeled with subscripts 2 and 3 are the result of rainfall occurring in the second and third 6-hr periods, respectively. The total inflow graph of storm runoff is thus derived by taking 6-hourly increments of effective rainfall over the

[5] "Storage and the Unit Hydrograph," by C. O. Clark, *Transactions*, ASCE, Vol. 110, 1945, pp. 1419–1488.

[6] "Virtual Channel-Inflow Graphs," by R. E. Horton, *Transactions*, Am. Geophysical Union, 1941, pp. 811–819.

[7] "The Flood Hydrograph," by H. M. Turner and A. J. Burdoin, *Journal*, Boston Soc. of Civ. Engrs., Vol. XXVIII, July, 1941, p. 232.

various zones, converting to mean cubic feet per second, and lagging to the outflow point.

Inflow graphs of effective rainfall can be converted to simulated outflow hydrographs by one of a number of routing techniques. Since storage is appreciably influenced by inflow, results are generally not satisfactory if storage is assumed to be a function of outflow only. Since the flow analog assumes storage to be a function of both inflow and outflow, it provides an efficient means of routing effective rainfall.

Determination of Factors.—Having derived inflow hydrographs for a number of past storms, the next step in the development of the procedure is the determination of the most suitable values of K and x (in Eq. 1) for the basin. In all routing with the analog, it has been found that proper values of K and x can be derived more rapidly by trial-and-error routing than by the method originally presented by G. T. McCarthy.[4] The coefficient K is expressed in units of time and is approximately equal to the time of travel, whereas the factor x defines the relative effect of inflow and outflow in determining storage. Assuming K equal to the average lag between inflow and outflow peaks and assigning x an arbitrary value of about 0.2 (found to be a good average value), each inflow graph is routed and compared with observed outflow, less base flow. If examination reveals a consistent variation between computed and observed hydrographs, the required changes in K and x are estimated from a standard chart that displays the effects of such variations on the routed hydrograph. Two or three runs of the several hydrographs will usually provide suitable values of K and x.

Logically, it would seem that the value of K should be larger when the storm is centered in the headwaters than when most of the flow originates near the gaging station. Analyses indicate the areal distribution can vary considerably without seriously affecting the results obtained from average values of K and x. Generally, however, results can be improved by using a relatively large value of K for upstream floods, and vice versa. This effect can be reduced by dividing the upstream portion into relatively more time zones than flow velocities would indicate, thus effectively flattening the upstream inflow. Since the flow analog in use can accommodate inflow from two sources, the most efficient approach is a division of the inflow into two parts. In this manner, the upstream and downstream flows can be routed with different storage factors and, if necessary, the analog can be expanded to provide for three or more sources of inflow.

Potomac River Study.—A rather thorough analysis has been made for the Potomac River Basin in which average values of K and x were determined for six sub-basins having a drainage area ranging from 1,470 to more than 11,000 sq miles. Fig. 4 shows typical results for the lowermost gaging station on the Potomac. The inflow graphs to be routed were constructed by connecting the mid-points of the 6-hourly mean flows. The values of K and x used in these cases are the best over-all values derived for a series of storms. The April, 1937, flood was definitely an upstream flood and the agreement between routed and observed flows is improved by using divided inflows, as demonstrated in Fig. 5. This figure shows the comparative results for Point of Rocks, Md., the first gaging point above the Washington station.

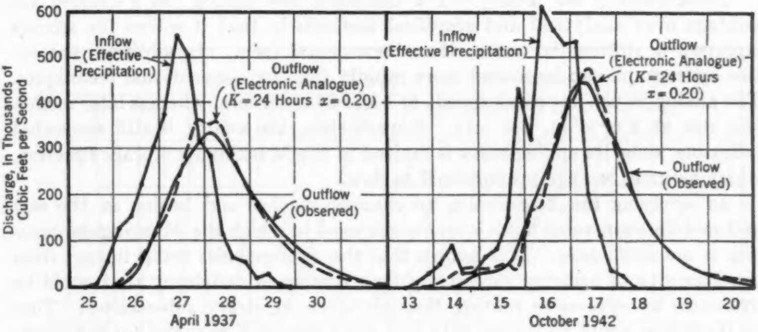

FIG. 4.—ROUTED AND OBSERVED HYDROGRAPHS FOR THE POTOMAC RIVER NEAR WASHINGTON, D. C.

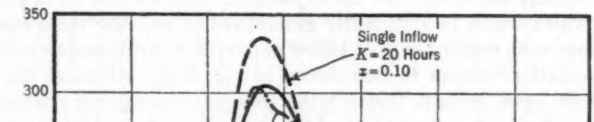

FIG. 5.—COMPARATIVE RESULTS USING SINGLE AND DIVIDED INFLOW (EFFECTIVE PRECIPITATION)

Applicability of Muskingum Equation

Limitations of the Analog.—The electronic flow analog has a decided advantage over analytical and graphical methods in that it solves the storage equation in differential rather than incremental form. In addition, the entire hydrograph can be routed more rapidly than by conventional techniques. The analog in use has chart speeds of 1 and 2 in. per min, whereas later models will run at 2 or 4 in. per min. Nevertheless, the analog is still somewhat inflexible, since its applicability is limited to the Muskingum storage function, which assumes storage proportional to flow.

In applying the flow analog to channel reaches and basins in the east and middle west, cases have been encountered in which the Muskingum equation is not applicable. It is known that the discrepancies result in part from the necessity of utilizing excessively long reaches, a deficiency that could be overcome by successive routing through short, arbitrary sub-reaches. That is, the inflow could be routed with half the value of K required for the reach, and the resulting flow routed again to obtain the outflow hydrograph. This approach would, however, greatly increase the time required to prepare forecasts.

Cumberland River Study.—Those cases in which the analog did not yield satisfactory reproduction of the outflow hydrograph were analyzed to determine the storage function, with the expectation that another circuit might be designed which would be sufficiently generalized to embrace these exceptions. Storage data were computed from inflow and outflow hydrographs and plotted to derive relations similar to that shown in Fig. 6(*a*). Although the plotted data in some cases indicate that a rather complex, curvilinear relation exists, the function does not appear to be of the generally accepted form:

$$S = K\left[x\, I^m + (1 - x)\, O^m\right] \qquad (4)$$

in which the exponent, m, is assumed to be positive and constant for a particular reach.

In the case of the Cumberland River from Wolf Creek Dam (Kentucky) to Celina (Tenn.), a family of curves was first constructed to fit the data best and a number of inflow graphs routed. Then the data were fitted to a relatively simple function of the form:

$$S = a\, I + b\, O + c\, I\, O \qquad (5)$$

in which a, b, and c are constants as shown in Fig. 6(*b*). The inflow graphs were then routed again.

This function was tested because it seemed plausible that an electrical circuit could be designed for the function and because the plotted data indicated it was the simplest equation that could be expected to yield satisfactory duplication of the outflow hydrograph. An examination of the equation will reveal the fact that it is identical with the Muskingum equation, except for the added term involving the product of inflow and outflow. This term, however, introduces curvature in the storage-flow relation. That is,

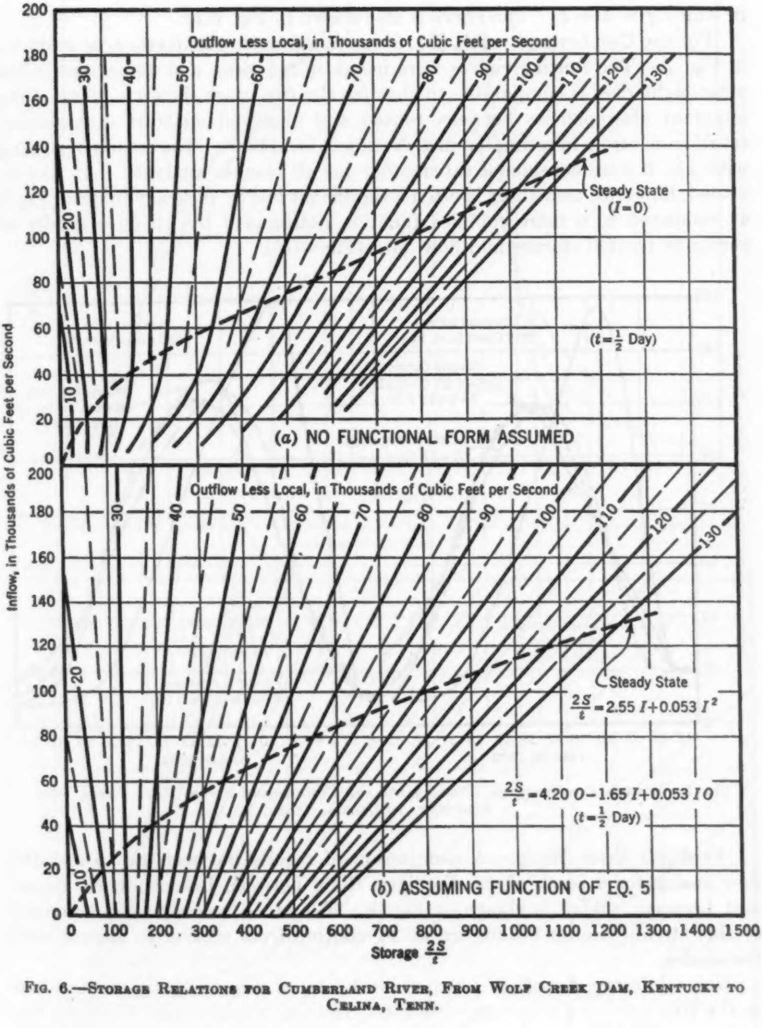

FIG. 6.—STORAGE RELATIONS FOR CUMBERLAND RIVER, FROM WOLF CREEK DAM, KENTUCKY TO CELINA, TENN.

for steady-flow conditions ($\dot{I} = 0$), Eq. 5 becomes

$$S = g\,I + c\,I^2 = g\,O + c\,O^2 \qquad (6)$$

in which $g = a + b$. The curve is also shown in Fig. 6(*b*).

For the Cumberland reach, Eq. 5 was found quite satisfactory, as is shown in Fig. 7. The routing curves were based on ten rises, and agreement in the other eight rises is comparable to that for the two cases shown. Some of the apparent discrepancies between routed and observed outflows undoubtedly result from errors in estimated distribution of local flow. The results of routing with Eq. 5 were considered satisfactory for all reaches analyzed. It was revealed, however, that there is often a significant loss in accuracy in using Eq. 5 as compared to a more complex function determined by fitting a family of curves to plotted storage and flow data (Fig. 6(*a*)).

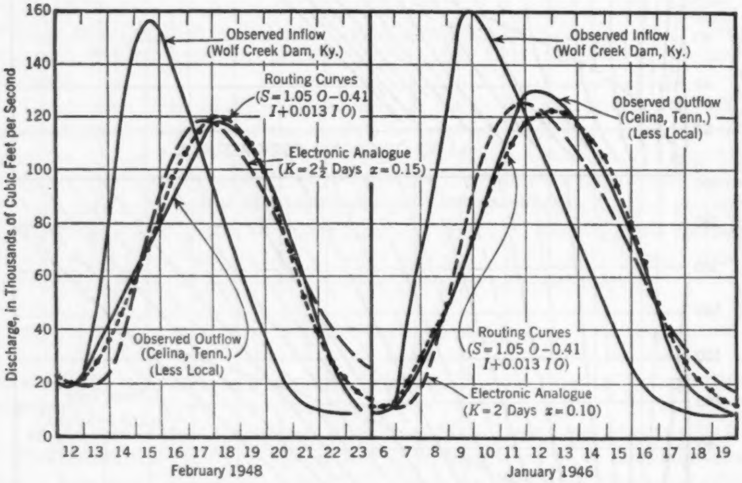

FIG. 7.—ROUTED AND OBSERVED HYDROGRAPHS FOR CUMBERLAND RIVER, WOLF CREEK DAM, KENTUCKY, TO CELINA, TENN.

Verdigris River Study.—A comparison of results between Eq. 5 and the flow analog for a reach of the Verdigris River between Independence, Kans., and Lenapah, Okla., is shown in Fig. 8. The steep recession characteristic of this stream cannot be duplicated by routing from station to station with the analog.

General Storage Equation.—As previously stated, Eq. 4 is generally accepted as the true form of the storage equation. In those cases studied for which the analog was not satisfactory, however, this equation did not appear to be materially better. The equation that appears to be most generally applicable (Fig. 9) is of the form:

$$S = a\,I + b\,O^n + c\,I\,O^n \qquad (7)$$

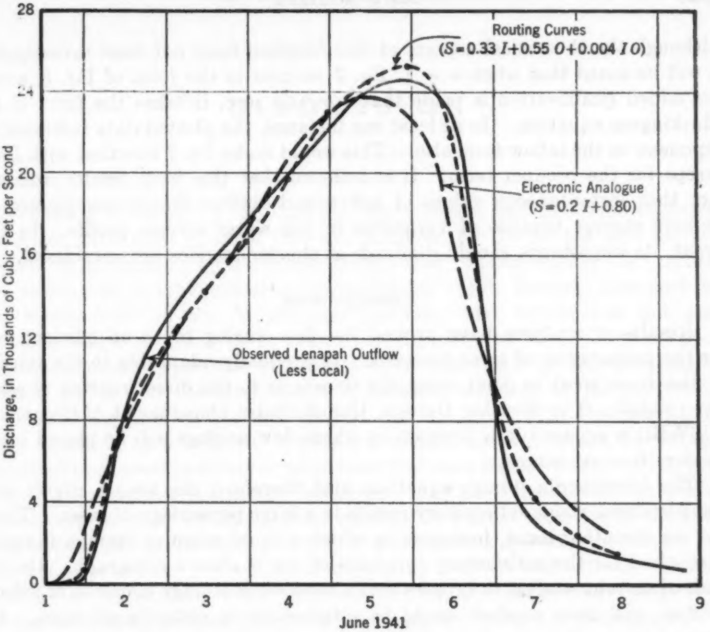

FIG. 8.—ROUTED AND OBSERVED HYDROGRAPHS FOR VERDIGRIS RIVER, FROM INDEPENDENCE, KANS., TO LENAPAH, OKLA.

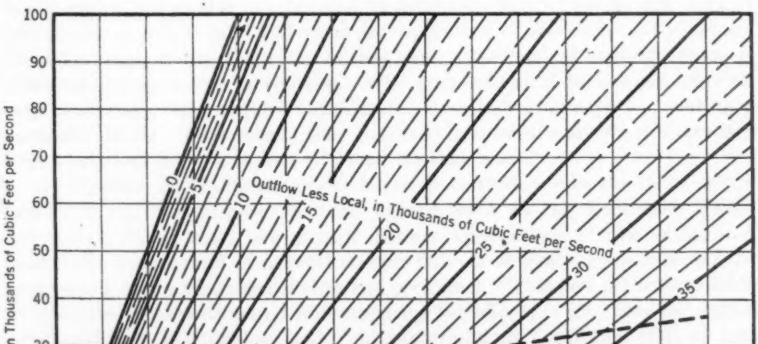

FIG. 9.—STORAGE FUNCTION FOR VERDIGRIS RIVER ABOVE INDEPENDENCE, KANS.

Although the theoretical aspects of this function have not been investigated, it will be noted that when $n = 1$, Eq. 7 reduces to the form of Eq. 5, and if the added qualification is made that c equals zero, it takes the form of the Muskingum equation. In at least one instance, the plotted data indicated an exponent on the inflow term also. This would make Eq. 7 identical with Eq. 4 except for the product term. It is believed that this term results from the fact that instantaneous values of inflow and outflow do not completely determine storage because of variations in the water surface profile. In this event, its importance should diminish as shorter reaches are considered.

Conclusions

Results of analyses have proved the flow analog to be an efficient tool for the preparation of river forecasts. It is equally adaptable to the routing of flow from point to point along the stream or to the direct routing of effective rainfall. The Weather Bureau, United States Department of Commerce (USWB), is engaged in a program in which flow analogs will be placed in all its river forecast centers.

The Muskingum storage equation, and, therefore, the analog circuit now being utilized, yields satisfactory results in a large percentage of cases. There are, on the other hand, instances in which a more complex storage function is required for the satisfactory synthesis of the outflow hydrograph. On the basis of current studies, it appears that a three-term storage equation of inflow, outflow, and their product would be satisfactory in virtually all cases. Attempts are now being made to design a corresponding circuit and thus enhance the utility of the flow analog.

DISCUSSION

Alfred J. Cooper,[8] A. M. ASCE.—Hydrologists and hydraulic engineers concerned with open channel flow are indebted to the author and his colleagues for developing an electronic stream-flow routing analog that utilizes the well-known mathematical relationship for reach storage expressed by Mr. McCarthy[9,4] in the Muskingum method. Mr. Kohler has indicated that the design of this type of router can probably be modified to adapt it to more complex equations of storage than that used in the Muskingum method. This fact should make it a valuable addition to the profession.

Considering this device for what it can do, even with the deficiencies of the equation upon which it is based, it reveals certain distinct advantages compared to present methods of analytically routing stream flows. Analytical routing procedures are extremely laborious. Any simplification of the mathematical approach, as by an electrical analogy, is a great economy in time and labor. In addition, the analog is simple in design and operation, relatively low in cost, and produces results faster than existing methods and with an accuracy equal to, or better than, other methods. It has the distinct advantage over routing by certain periods of time in producing a continuous hydrograph. It is better than other routing devices in that adjustments for the major variables of different reaches or basins are simple to make—merely by the turning of dials. Furthermore, the analog can be used to determine reach flow-storage data, if desired, by a simple trial-and-error determination of K-values and x-values. The advantage of the electronic analog over a mechanical routing analog is in its ease of preparation for routing. Whereas mechanical devices can function very accurately, they require considerable time in preparation for routing a particular reach. As a result, they become economical only when there is a large volume of routing to be performed for that reach.

Applications to Multiple-Purpose Reservoir Operation.—In the daily operation of a multiple-purpose reservoir system such as the Tennessee Valley Authority (TVA), there are certain distinct applications of this analog. A continuous hydrograph of natural stream flow at several key points can be maintained with a minimum of time and personnel. This flow is then available for guidance in operation and for comparing the effects of alternate regulation combinations. The analog could aid materially in predicting inflows into tributary reservoirs and runoff from local areas between main river projects by the routing of effective rainfall. It could solve the problem of predicting crest flows and stages at critical points such as towns and cities on small creeks and rivers which are unregulated by the reservoir system, yet present flood problems. Such streams require a warning system that is rapid enough

[8] Head, Procedures Development Sect., Hydr. Data Branch, TVA, Knoxville, Tenn.

[9] "The Unit Hydrograph and Flood Routing," by G. T. McCarthy, unpublished manuscript presented at the Conference of the North Atlantic Div., Corps of Engrs., War Dept., June, 1938.

to be useful, needs the minimum of personnel and money for its execution, and yet should not interfere materially with the main task for the river-control organization—that is, the water-control operations of the reservoir system. A further use could be the determination of the transformation of waves generated by fluctuations of discharges at dams. This use would permit chronological forecasts of flows and stages downstream to serve as the basis of water-supply purification, and it would furnish minor navigation information such as the accessibility of islands.

Deficiencies of Router in Multiple-Purpose Reservoir Operations.—From a water-control point of view, the TVA is singularly in a situation in which, eventually, the entire United States will find itself with the trend toward regulation of rivers for single or multiple purposes. The TVA is faced with the necessity of operating a regulated stream in which many critical river points do not have a simple stage-discharge relation. In its present design, this analog is not adaptable to the solution of problems involving more than the three variables of inflow, outflow, and storage. With controlled outflow a fourth variable appears in the picture—backwater, or slope, effect. This variable occurs also in natural streams affected by backwater, as in the Tennessee River below Pickwick Landing Dam even prior to the impoundment of Kentucky Reservoir, in the reach below Kentucky Dam, and in the Ohio River. The graphical and analytical routing procedures presently used by the TVA involve these four variables.

It is desirable that a circuit be devised in which some of the factors now used as constants could be varied during the operation of the analog to simulate the conditions found in open channel flow. Even with the present circuit applicable to most cases of uncontrolled outflow, it would increase the accuracy of the results if the factors K and x could be varied since these items, usually, do not remain constant throughout the range from low to flood flows. Investigations reported in 1944[10] indicated clearly that there are different times of wave travel; hence there is a variation in K-value over a wide range of stage in a given reach. Preliminary studies of the value of x for the mid-August and late August, 1940, floods on the Holston and French Broad rivers just above Knoxville indicate that a variation of x is encountered, which is not only dependent on the distribution of runoff in the area but also, to a minor degree, in the range of flows occurring in the mid-August flood.

The use of an empirical function such as Eq. 5 to define the storage, in the cases where the Muskingum equation apparently did not serve to evaluate it, seems to be the reversal of a modern trend in the field of hydraulics—that is, finding a mathematical relation for a theoretical analysis developed from basic physical principles and observations. In the selection of such a function, there is no assurance that it will apply in any other instance since there is no theoretical basis for its selection. The only attribute of this alternate equation is that it does provide a function of higher degree and possibly can be used as the basis for designing an electrical circuit. Inasmuch as routing is an approximation, it is likely that, where the data indicated that a rather complex curvilinear

[10] "Translatory Waves in Natural Channels," by J. H. Wilkinson, *Transactions*, ASCE, Vol. 110, 1945, p. 1203.

relation existed, the relation could be simulated by a series of connected straight lines. Such an assumption would necessitate a change in the value of K, and possibly x, at each break, that would hold to the next break. If these discontinuity points occur at about the same flow values for a given reach or basin, the instrument could be stopped when those points are reached, as indicated by some index such as weighted flow. Then the new K-values and x-values could be placed on the circuit, and routing could be continued.

It is quite likely that the effect of slope in the Wolf Creek Dam to Celina reach will explain one of the reasons why the Muskingum equation is not satisfactory for this reach. The discharge ratings for the ends of this reach are rate-of-change ratings which, in themselves, are tacit admissions of the slope effect of the reach and typify, to a lesser degree, conditions in many reaches in the Tennessee Valley.

Mr. Kohler is to be commended because he has found instances where the original circuit did not provide the accuracy desired; he has taken steps to find the cause, and has offered a solution rather than make a broad claim that the present circuit will apply anywhere.

Opportunity for Future Research.—In June, 1951, the USWB established an electronic stream-flow routing analog, with its operators, near the central offices of the TVA water-control staff in Knoxville, Tenn. In the continued excellent cooperative program which has been in existence since early 1940 between the TVA and the USWB, this analog is being utilized wherever applicable. It is hoped that the experience with the stream flows and characteristics of the TVA system will serve as a basis for future research to expand the usefulness of this type of analog beyond its present capabilities.

This instrument marks another milestone in the progress of developing a rapid and accurate river forecasting system. It is now produced at a relatively small cost by an instrument manufacturer. Therefore, it is not untimely to suggest that much testing of it beyond the available time, personnel, and funds of the USWB could be undertaken by other federal and state agencies and private concerns engaged in water utilization. Inasmuch as there is no large monetary return for those who develop instruments of this nature, it is unlikely that they will be developed or experimented with other than by those engaged in related work. Within these various organizations are personnel who have also the talents and experience to add to the usefulness of such instruments. These investigations would be analogous to discussions of technical papers. Some may result in modifications of the original ideas which would be definite improvements. An example is the distribution graph proposed by the late Merrill Bernard,[11] M. ASCE, which was a variation on the unit hydrograph proposed by LeRoy K. Sherman,[12] Hon. M. ASCE.

Those who persist in regarding with skepticism the analogy of flow of a true fluid and that of an electrical current should note that, even as only a first trial, the similarity of relations will accelerate many exploratory investigations, and at a reduced cost. Then, the final result can be tested under actual flow conditions.

[11] "An Approach to Determinate Stream Flow," by Merrill Bernard, *Transactions*, ASCE, Vol. 100, 1935, p. 347.

[12] "Streamflow from Rainfall by the Unit-graph Method," by LeRoy K. Sherman, *Engineering News-Record*, Vol. 108, 1932, p. 501.

C. O. Clark,[13] A. M. ASCE.—In applying an electrical circuit to the problem of flood routing, Mr. Kohler demonstrates again that much of the mechanics of hydraulic flow is similar to the mechanics of electrical flow, and, therefore, that an electrical model may indicate the answers to problems which might otherwise be sought in a hydraulic model. His electronic analog is an electrical model; he has applied it to part of the hydraulic problem of flow in open channels. His electrical model, besides being cheap enough to use where a hydraulic model would be prohibitively costly, is clean, dry, compact, and silent. Thus, it is usable in an office instead of a laboratory.

The results appear promising. The possibilities outlined, of applying the electrical model to two or more sources of inflow, are even more promising because, in these fields, manually applied mathematics fails for lack of time and labor, and taxes the mental capacity of those who try it.. However, the electric analog solves only a part of the physical problem. The entire hydraulic problem may have an analog both in an hydraulic model and in an electrical one, but the physical significance, or the physical prototype, of that portion of the flow problem solved by the electrical device is not yet recognizable in nature—that is, both the hydrograph transposition with respect to time. which Mr. Kohler calls "lagging effective rainfall," and the subsequent hydrograph attenuation accomplished by the electrical circuit, are aspects of the same physical phenomenon. In nature the physical division of the two aspects does not exist. In his logical process, a man is able to simulate what does happen by two simple logical steps. One of the steps is transposition, translation, or lagging—that is, change with respect to time but without change in form or shape. The second step is attenuation, that is, flattening and lengthening—a definite change in form.

By trial and error it has been shown that a proper combination of these two steps can be satisfactory for many computational purposes. It is important, however, to recognize that both transposition and attenuation are manifestations of the existence of storage capacity (volume) along a waterway which has flow-carrying capacity (discharge), and that, for some physical reason, the waterway and the storage space are associated in such a way that when one increases so does the other.

There appears to be an appreciable time lag, or delay in flow, only because there is storage capacity. There is storage capacity in a very tangible form, in which the water which has not been passed is being stored at any given moment. Much of this storage capacity is in the channels themselves; but much of it is also in the swamps and low ground that has overflowed adjacent to the waterway. Changes in this volume are continually being made as men build levees around (or drain) the flood plain areas, either decreasing the storage capacity, or increasing the flow capacity, and thereby decreasing the combination which shows itself as a time delay in flow.

To illustrate: In Fig. 3, the "time of concentration" of this area is portrayed as 24 hr. This means that, when a steady flow rate is established from one end of the watershed to the other, there are 2 acre-ft of water in storage in the waterway, and along it, for every unit of flow of 1 cu ft per sec;

[13] Hydr. Engr., Corps of Engrs., Southwestern Div., Tulsa, Okla.

or, if the flow is steady from each point in the watershed to the outlet, there is about 1 acre-ft of water in storage in the waterways of that watershed for each unit of flow at the outlet point.

This much storage was accounted for by the transposition, "lagging of effective rainfall," in Mr. Kohler's presentation. A much smaller amount of storage is then accounted for by the electrical machine in the routing process of attenuation. Mr. Kohler has indicated that some of the precedent for these two processes of modification, or flood routing, was in the work of the writer[5]; the writer found it in much older work. The logical ease with which one can comprehend transposition of flow will always be an adequate reason for thinking in terms of "time of concentration." Experience built up in these terms can thus be the yardstick for thinking and remembering about what really happens.

This yardstick has two corrections: (1) For the flattening or attenuation effect of storage with which the author deals, and which is computed by the machine, and (2) for the fact that the time elements are not altogether constant. Thinking about storage capacity along the stream helps to make the second correction. If the relation of that storage to the channel is such that, at all stages, there is a constant ratio of stored water to the flow capacity, there can be nearly constant time elements in small and large floods. If the capacity is always available and remains the same, it may produce the same time elements from year to year.

Although these time elements may appear to be constant (and most engineers assume they are), it is a convenient approximation of what is not exactly true. The channel flow capacity can be changed; it frequently is. The storage capacity can be changed, by either scouring the bed or breaking levees during a given flood, or by erecting levees between floods. The constant relationship between storage and discharge capacities, essential to the Muskingum theory of routing (Eq. 4), to "time of concentration" concepts, to unit hydrograph, and to many seasoned mathematical devices for understanding flood flow, does not exist in any natural channel; but, in many cases, it is a surprisingly good approximation of the composite of valley sections and of the heterogeneous obstructions which all together make up many flow channels.

However, the fact is that large floods sometimes move with unanticipated speed, also, that second floods on top of earlier large ones move even more rapidly in channels already full. Streams that increase their flow capacity by bottom scour, instead of by rising in the channel, store so little water as they change flow that the time of travel is always less than anticipated by those educated in the writings about more orthodox waterways. Finally, some streams have their storage capacity distributed in such odd ways that the net result is not to flatten the wave peak, but to build it up—not to flatten the recession part of the hydrograph, but to steepen it.

What the phenomena are, and how they are changing, can be known from the storage and discharge relationships that exist along the channel. If the conditions that exist do fit (and continue to fit) the mathematics set forth for the solution, the electronic computing device will be of inestimable aid to routine computations. Woe be to anyone who believes, without investigation,

that these relationships are inherent, universal, unchanging, or unchangeable! Woe be, also, to the rising group of nontechnical managers who accept from a machine the mechanical solutions to equations they would not understand as answers to problems that even the maker of the machine could not know!

Mr. Kohler has made an outstanding contribution in developing the principle that an electric circuit can be devised to solve the simpler calculation problems of flood prediction. It opens a wide door. Through that door may very soon walk the man who will model an entire river system, with wire conduits for channels, resistances, and capacitances combining to synthesize the frictional factors and flood plain storage in whatever relation fits a particular river system. The flood hydrographs will be predicted by operating such a model forward from runoff that has been estimated from rainfall. Then, running the model backward from the early parts of the developing hydrographs, it is possible to determine more closely the real volume of runoff that appears to be causing the floods, and thereby to improve the predictions. Each of the foregoing steps can be made with a speed and precision not possible with currently available mechancial computing machines. A new day is dawning in the mechanics of nonsteady flow in open channels.

MAX A. KOHLER,[14] A. M. ASCE.—It is agreed, as Mr. Cooper states (under the heading, "Deficiencies of Router in Multiple-Purpose Reservoir Operations") that

> "*** it would increase the accuracy of the results if the factors K and x could be varied since these items, usually, do not remain constant throughout the range from low to flood flows."

Such variations would, in many cases, overcome the deficiencies of the Muskingum equation. Although the values of K and x can be changed at any time during a routing operation with the analog, by simply changing the resistances, surges of current will cause minor discontinuities in the outflow hydrograph which then must be smoothed by sketching. The use of Eq. 5 yields results similar to the varying of K and x. This is demonstrated by the fact that for steady-state conditions—that is, with $I=0$—the storage-flow relationship is curvilinear, as shown in Fig. 6(b).

Another technique has been developed for applying the analog to areas in which the Muskingum equation is not completely applicable. This technique involves a separation of the inflow into two parts—one representing within-bank flows, and the other, over-bank flows. In this manner, proper values of K and x for each type of flow can be used. This technique becomes even more applicable if the value of either K or x, or both, used for the over-bank flow, is made a function of the inflow peak.

As stated in the paper, apparent deficiencies in the results obtained by using the Muskingum equation occasionally occur, since the extent of the application is excessively long. Under these circumstances, multiple routing will improve the results, but the time required for the operation will be increased accordingly. Similar results can be obtained in a shorter period of

[14] Chf., Research Hydrologist, Weather Bureau, U. S. Dept. of Commerce, Washington, D. C.

time by lagging the inflow hydrograph and then by routing it with appropriate values of K and x.

Mr. Clark states that both the Muskingum equation and the unit hydrograph concept assume constant time elements; that is, a constant relation between storage and discharge capacity had been assumed. The simulation of the hydrograph by routing effective rainfall, as described in the paper, is based on this premise. This simulation can be used to develop unit hydrographs for any specified runoff distribution, or even for partial area unit hydrographs.

Flow routing analogs have been installed in each of the river forecast centers of the USWB. Forecasting procedures utilizing the analogs are being developed as rapidly as possible. The unit at Knoxville, is prepared to make forecasts of natural flow at selected points in the Tennessee River Basin. This unit is also engaged in further development work.

The officials of the USWB still hold the opinion that more accurate forecasts can be made in less time if the circuit of the analog can be modified to accommodate a more complex storage-flow function. To study this modification, a cooperative project is now (1953) being undertaken at Stanford University, at Stanford, Calif. This investigation is under the direction of Ray K. Linsley, A. M. ASCE.

HYDRODYNAMIC PROBLEMS IN THREE DIMENSIONS

BY P. G. HUBBARD,[1] J. M. ASCE, AND S. C. LING[2]

SYNOPSIS

The rather familiar analog utilizing an electrolytic bath to represent potential fluid motion has been refined and thoroughly tested in connection with fundamental investigations of fluid flow. Principles and techniques of the investigations are fully presented in this paper with emphasis on the general approach for three-dimensional flow and typical results. Solution of a representative problem is given.

INTRODUCTION

The particular electrical analogy with which this paper is concerned fits within the rather broad classification frequently referred to as the "electrolytic-tank method." In common with several other analogs, it represents potential motion in the prototype—that is, motion that may be described by a velocity potential with respect to the axes of motion $\phi\ (x, y, z)$ such that

$$\frac{\partial^2\phi}{\partial x^2} + \frac{\partial^2\phi}{\partial y^2} + \frac{\partial^2\phi}{\partial z^2} = 0 \qquad (1)$$

The motion also possesses the property that the gradient of the scalar field described by ϕ is the velocity vector,

$$v_x = \frac{\partial\phi}{\partial x};\ v_y = \frac{\partial\phi}{\partial y};\ v_z = \frac{\partial\phi}{\partial z} \qquad (2)$$

in which v is the velocity. Electric field theory includes a similar concept for voltage E, with a scalar field $E(x, y, z)$ that also satisfies the Laplace equation:

$$\frac{\partial^2 E}{\partial x^2} + \frac{\partial^2 E}{\partial y^2} + \frac{\partial^2 E}{\partial z^2} = 0 \qquad (3)$$

and whose gradient is the vector representing ϵ, the electric field strength,

$$\epsilon_x = \frac{\partial E}{\partial x};\ \epsilon_y = \frac{\partial E}{\partial y};\ \epsilon_z = \frac{\partial E}{\partial z} \qquad (4)$$

NOTE.—Published in August, 1952, as *Proceedings-Separate No. 143*. Positions and titles given are those in effect when the paper was received for publication.

[1] Research Engr., Iowa Inst. of Hydr. Research, State Univ. of Iowa, Iowa City, Iowa.

[2] Research Associate, Iowa Inst. of Hydr. Research, State Univ. of Iowa, Iowa City, Iowa.

This mathematical similarity forms the basis for the analogy, and the application of the electrolytic-tank method involves the exploration of a conductor geometrically similar to the corresponding flow system. The application of a voltage $(E_1 - E_2)$ across the conductor, between zones representing the entrance and exit of the fluid in the system, establishes within the conductor a potential field similar to that of its fluid prototype. The potential pattern is obtained by means of electrodes in contact with the conductor, using standard electrical potentiometer systems. The details of the particular method described in this paper have been presented previously.[3]

Experimental Techniques

The conductor representing the flow system in the analog is usually an electrolytic solution, and it is held to the proper form by nonconductors, representing flow boundaries (or planes of flow symmetry), and by metal anodes representing equipotential surfaces at the extremities of the system. In constructing the plastic forms representing flow boundaries, extreme care must be exercised to hold tolerances within close limits, especially at points of curvature at which the pressure gradients would be relatively great. The models should be made on as large a scale as is convenient, of course, but the size limitations usually encountered cause the errors from small deviations to be greatly magnified. For the same reason, the electrodes used to measure potential differences should be quite small in area, and their spacing should be measured with high precision. Fixed electrodes flush with the surface of the models can usually be located with greater accuracy than a movable probe, and fixed electrodes also present less disturbance to the flow. Since the most extreme conditions must occur at the boundary, the absence of any measurement in the fluid interior is not important.

The electrical potentiometers employed should be capable of measuring potential differences with a precision at least equal to that with which electrode spacings are measured. The potentiometers used in all tests at the Iowa Institute of Hydraulic Research, State University of Iowa, in Iowa City, measured the potential at each point with an accuracy of 0.01% of the total applied potential. The only instruments needed were a four-dial decade potentiometer and a sensitive vacuum-tube millivoltmeter. The latter was necessary because of the low applied potential (6 volts) and the need for a high-impedance null detector. The millivoltmeter internal impedance of 5 megohms (see Fig. 1) assures negligibly small currents through the electrodes even when the system is far from balance, thus avoiding distortion of the potential pattern. The sensitivity of 0.0003 volt of the millivoltmeter assures adequate response for the detection of the smallest change on the decade potentiometer. Miniature tubes and battery supply were used to keep size and capacitance to ground at a minimum. In use, the potentiometer was simply connected in parallel with the power supply to the anodes, while the millivoltmeter was connected between the movable tap on the po-

[3] "Application of the Electrical Analogy in Fluid Mechanics Research," by P. G. Hubbard, *Review of Scientific Instruments*, November, 1949.

tentiometer and an electrode. The dials were then adjusted until the voltage difference was a minimum, using a modified Wagner ground (a second potentiometer with movable tap connected to ground through a 0.05 microfarad condenser) to increase the sharpness of the null if necessary. The readings of the four dials thus gave the relative potential directly, and no other electrical quantity was required.

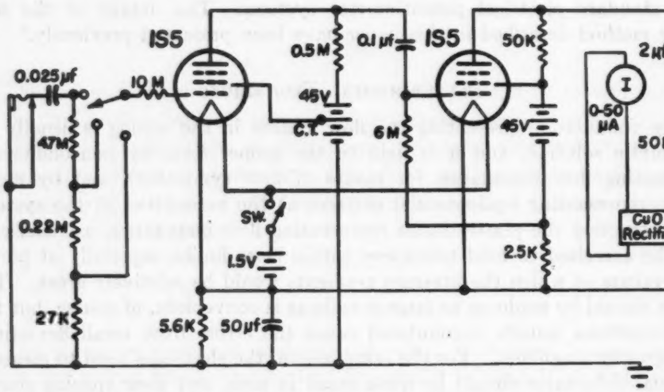

FIG. 1.—VACUUM-TUBE MILLIVOLTMETER USED AS NULL DETECTOR

The direction of the streamlines (except for their tangency to the boundary surface) will not be known in advance in the general case, and this fact must be considered in locating electrodes and computing velocity or pressure distributions. To facilitate the determination of the resultant velocity vector, it is convenient to place electrodes in an orthogonal (x, y) pattern on the developed boundary, with electrode spacings Δx and Δy maintained small relative to the radius of curvature. Then, since the boundary is a stream surface, the resultant velocity v_s may be computed from Δx, Δy, and the corresponding potential difference $\Delta\phi$ between any pair,

$$v_s = \frac{\partial\phi}{\partial s} \doteq \frac{\Delta\phi}{\Delta s} = \sqrt{\left(\frac{\Delta\phi}{\Delta x}\right)^2 + \left(\frac{\Delta\phi}{\Delta y}\right)^2} \quad \cdots\cdots\cdots (5)$$

The corresponding piezometric head h may be obtained from the Bernoulli relationship:

$$\frac{h - h_0}{\dfrac{V^2_0}{2g}} = 1 - \left(\frac{v}{V_0}\right)^2 \doteq 1 - \frac{(\Delta\phi/\Delta x)^2 + (\Delta\phi/\Delta y)^2}{(\Delta\phi/\Delta x)^2_0 + (\Delta\phi/\Delta y)^2_0} \quad \cdots\cdots (6)$$

The quantities $(\Delta\phi/\Delta x)_0$ and $(\Delta\phi/\Delta y)_0$ are obtained from measurements between electrodes placed in a region of uniform flow at velocity V_0 and piezo-

metric head h_0. Pressure distributions are obtained by plotting points from Eq. 6 approximately midway between the corresponding electrodes and then adjusting the curves so that the area under the curve is equal to that beneath a bar graph drawn through individual points.

Evaluation of Earlier Tests

The method described was first used at the Iowa Institute of Hydraulic Research in 1945, and has undergone a continuous modification since that time, being used for both research and design in three-dimensional problems. Until the initiation of the tests described in this paper, however, its use was limited to axially symmetrical flow systems because of the desire to check thoroughly and continually on its accuracy before presenting it as a reliable tool. Many of the results were verified either analytically, using the potential concept, or experimentally, using a water tunnel.

These earlier tests,[3,4,5,6] fell naturally into two classifications based on the relationship of the fluid to the associated boundary: (1) Those in which the flow is external to the boundary, such as various head forms for submerged bodies; and (2) those in which the flow is internal such as conduit inlets and contractions or a free liquid jet impinging upon a plane normal to its axis. The nature of these systems demonstrates the basic requirements involved in the use of the analogy, namely, that viscous effects must be negligible and that the flow pattern must be determined solely by the boundary geometry. Thus, decelerating flow around tail forms, or through expansions or outlets that involve boundary-layer separation, cannot be represented by this electrical analog. Moreover, the analog may not represent the actual pattern ever for generally accelerating flow if regions of local deceleration exist that tend to cause local separation. The analog will indicate the existence of such conditions, however, and one of its most valuable uses is in testing and modifying designs to obtain the most economical separation-free form.

The analogy has proved useful—particularly for extensive exploratory surveys—because of its flexibility, its economy of time compared with analytical methods in general, and its economy of equipment compared with hydrodynamic or aerodynamic models. These virtues will become apparent as the description of a particular series proceeds. In most tests, the accuracy has been sufficient for design purposes, indicating velocities that deviate by less than 1% from those determined by other methods. In one particular test reported earlier,[5] however, an inadequate length of uniform section led to over-optimistic conclusions concerning circular inlets. The error was not discovered until the new series of tests described in this paper was completed, indicating results incompatible with the former. When careful checking and reconstruction of the analog continued to disprove the earlier

[4] "Use of the Three-Dimensional Electrical Analogy in the Design of Conduit Contractions," by M. M. Hassan, dissertation presented to the State University of Iowa, at Iowa City, Iowa, in August, 1948, in partial fulfilment of the requirements for the degree of Doctor of Philosophy.

[5] "Cavitation-Free Inlets and Contractions," by H. Rouse and M. M. Hassan, *Mechanical Engineering*, March, 1949.

[6] "Deflection of a Liquid Jet by a Perpendicular Boundary," by A. Leclerc, thesis presented to the State University of Iowa, at Iowa City, Iowa, in August, 1948, in partial fulfilment of the requirements for the Degree of Master of Science.

conclusions, a mathematical check, using the relaxation method, was made. The results were in accordance with those presented in the final section of this paper. If proper care is given to all phases of construction, measurement, and interpretation, results of any desired accuracy should be obtainable.

Use of the Analog

Typical Tests.—Having established the accuracy of the method by experiments on several analogs of axially symmetrical flow systems in which a comparison could be made with analytical methods, it appears safe to use the electrical analogy to represent a design problem in which the absence of an axis of symmetry makes a mathematical analysis impractical or virtually impossible. Such problems naturally represent one of the most valuable applications of the electrical analogy since the only alternative method of solution is a series of expensive models. One system of practical importance is that of the transition, using cylindrical sections, from a reservoir of fluid to a conduit of square cross section. This configuration appears frequently in the design of hydraulic inlet works, in which the prediction of low-pressure zones is important because of the danger of cavitation. Since a study to minimize the tendency toward separation in an inlet is well-suited to the capabilities of the electrical analogy and is of practical importance, it has been chosen to demonstrate the application of this method.

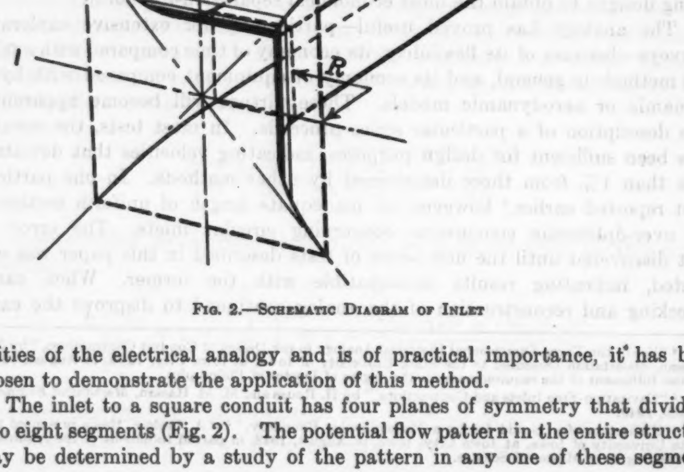

Fig. 2.—Schematic Diagram of Inlet

The inlet to a square conduit has four planes of symmetry that divide it into eight segments (Fig. 2). The potential flow pattern in the entire structure may be determined by a study of the pattern in any one of these segments

bounded by two adjacent planes of symmetry and a section of the transition boundary. In the electrical analog (Fig. 3), a sheet of plate glass inclined at an angle of 45° to the horizontal represents a plane passing through the center lines of opposite sides of the conduit, and the sections representing the

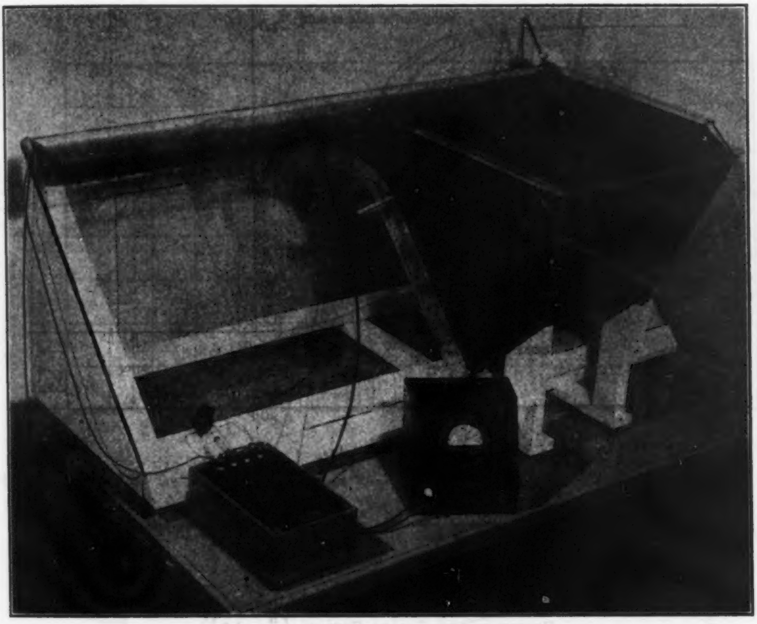

FIG. 3.—ELECTRICAL ANALOG FOR SOLUTION OF INLET PROBLEM

transition boundary are formed of lucite sheets and a section of a lucite cylinder. At zones corresponding to equipotential surfaces in the conduit and reservoir, respectively, anodes of sheet copper and copper screen are placed. Small electrodes inserted in an orthogonal pattern in the lucite sections complete the form without the use of precision machine tools. When the copper sulfate solution (approximately 0.016 molar) is poured into this form, its free surface intersects the glass along a line representing the center line of the transition, while its intersection with the lucite boundary represents the juncture of the conduit sides. Although the radius R of the cylindrical section (Fig. 2) remains fixed, its ratio to the conduit width B may be varied at will over a wide range simply by adjusting the elevation of the free surface. In this manner a single inexpensive form is used to represent an infinite number of circular transitions with varied curvature. This extreme flexibility is possibly the most important advantage the analog has over other methods.

Results.—The results of measurements on this model are summarized here. In Fig. 4, isobars (or isovels) estimated from the potential measurements have been drawn, together with curves showing the pressure distributions along the center of a side and along the juncture between two sides, for one

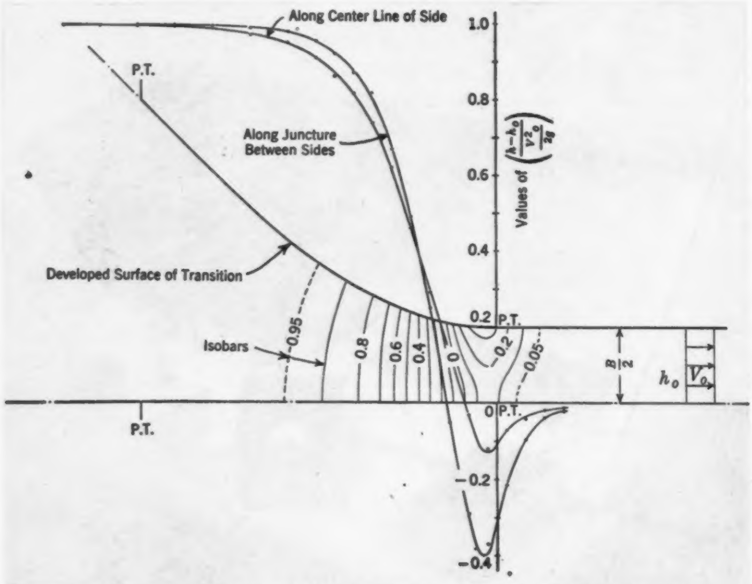

FIG. 4.—PATTERN OF PRESSURES ALONG BOUNDARY OF ROUNDED TRANSITION FROM A RESERVOIR TO A SQUARE CONDUIT $\left(\frac{R}{B} = 1.5\right)$.

particular relative radius of curvature. The curves show quite clearly that the most critical region is along the juncture, just upstream from the point at which the transition curve becomes tangent to the straight conduit. However, pressures below that in the conduit prevail in a small region completely across the side at this zone. It should be noted again that the measurements are taken only at the boundary (where the most extreme conditions always occur) and that pressures away from the boundary will behave differently. In particular, it should be expected that the pressure along the center line of the conduit will decrease uniformly from the reservoir to the conduit with no underpressure. For prediction of cavitation or over-all forces, however, only boundary pressures are of interest.

In Fig. 5, a family of curves shows the variation in pressure distribution along the juncture (which includes the most critical point) for various relative radii of curvature. This figure indicates quantitatively the benefits achieved from decreasing the curvature. The trend with decreasing curvature is indicated more clearly by the curves of Fig. 6, in which the minimum pressures

along the juncture and along the center line of a side are plotted against the relative radius of curvature.

As an aid in applying the results of these tests, it may be noted that the values of $\frac{(h - h_0)}{\frac{V^2_0}{(2g)}}$ presented in this paper probably represent actual condi-

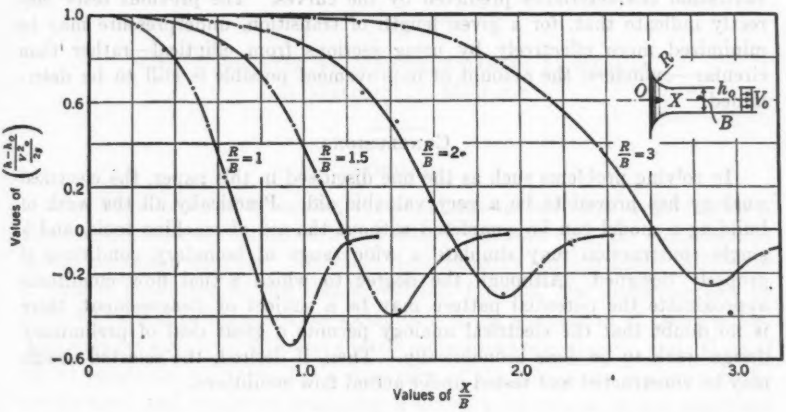

FIG. 5.—EFFECT OF RELATIVE CURVATURE ON PRESSURE DISTRIBUTION ALONG JUNCTURE OF SIDES

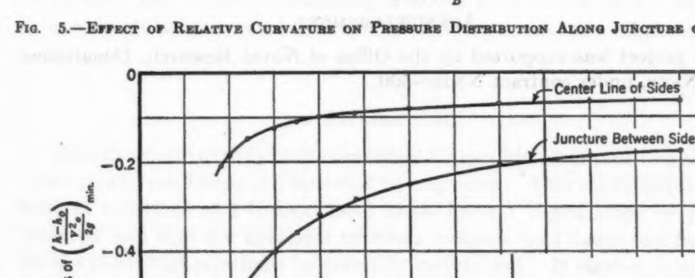

FIG. 6.—MINIMUM PRESSURE AS A FUNCTION OF RELATIVE CURVATURE

tions within a few percent, except where local deceleration will lead to separation. Since, contrary to the conclusions of other research workers,[5] the tendency toward cavitation decreases indefinitely with increasing radius of curvature, the design radius should be made as large as is consistent with con-

struction requirements. Other factors will influence the value chosen, of course, such as slope, roughness and length of the conduit, and the hydrostatic pressure at the outlet. Downward slopes, smooth surfaces, and short lengths of conduit will increase the easement of curvature necessary to achieve a given condition. The turbulent boundary layer of the prototype will decrease the tendency toward separation, but will not appreciably influence the cavitation characteristics predicted by the curves. The previous tests[5] correctly indicate that, for a given length of transition, underpressure may be minimized more effectively by using sections from elliptical—rather than circular—cylinders; the amount of improvement possible is still to be determined.

Conclusions

In solving problems such as the one discussed in this paper, the electrical analogy has proved to be a very valuable aid. Practically all the work of building a model can be completed without the aid of machine tools, and a single construction may simulate a wide range of boundary conditions if properly designed. Although the degree to which actual flow conditions approximate the potential pattern may be a subject of disagreement, there is no doubt that the electrical analogy permits a great deal of preliminary design work to be done economically. Then, if desired, the selected design may be constructed and tested under actual flow conditions.

Acknowledgment

The project was supported by the Office of Naval Research, Department of the Navy, under contract N8onr-500.

PIPE NETWORKS STUDIED BY NONLINEAR RESISTORS

By Malcolm S. McIlroy[1]

With Discussion by Messrs. Charles L. Barker, and Malcolm S. McIlroy

Synopsis

The labor involved in solving the simultaneous head-loss equations for a pipe-line network is eliminated by an electric network analyzer comprised of special nonlinear resistors. Although these resistors automatically perform in a manner analogous to the Hazen-Williams formula, the procedure can be modified readily to represent the Colebrook-White adaptation of Darcy's law. Analogies between hydraulic and electric quantities are explained, and values of useful constants are tabulated. Accuracy of the procedure is shown to be satisfactory, and results of analyzing a network by means of the nonlinear electric circuit are compared with results of rigorous algebraic solutions.

Introduction

The quantitative study of the operating characteristics of pipe-line networks under steady conditions is important to engineers. This study requires that flows at junctions and friction head losses around closed loops be properly balanced, and that the nonlinear relations between head losses and flow rates for the individual pipe lines be correctly maintained. If algebra is employed in the study, these restrictions are expressed by a set of nonlinear simultaneous equations. Since the solution of these equations involves tedious successive approximations,[2,3,4] engineers have often thought of using electric circuits to provide solutions for pipe-line network problems by analogy. This paper describes a method of evaluating flows and head losses in pipe-line networks by means of analogous electric circuits that employ special nonlinear resistors to

Note.—Published in July, 1952, as *Proceedings-Separate No. 139.* Positions and titles given are those in effect when the paper or discussion was received for publication.

[1] Prof. of Electrical Eng., Cornell Univ., Ithaca, N. Y.; and Consultant to the Standard Electric Time Co., Springfield, Mass.

[2] "Analysis of Flow in Networks of Conduits or Conductors," by Hardy Cross, *Bulletin 286*, Univ. of Illinois Eng. Experiment Station, Urbana, Ill., 1936.

[3] "A Rapid Method of Analyzing Flow in Water Distribution Systems," by T. Francis O'Connor, *Proceedings*, Maryland-Delaware Water and Sewerage Assn., 1943, p. 61.

[4] "Pipeline Network Flow Analysis Using Ordinary Algebra," by Malcolm S. McIlroy, *Journal*, A.W.W.A.. Vol. 41, May, 1949, p. 422.

represent the pipe lines. When this method of analysis is used, no algebraic solution is required. Readings of electric instruments furnish directly the desired information concerning the performance of the pipe-line network.

Electrical Analogy Method

Two fundamental analogies exist between the performance of an incompressible fluid in a pipe-line network and of electricity in a resistive circuit. With electric current representing flow, the total current approaching a terminal equals the total current leaving it, just as fluid flows balance at a pipe-line junction. With voltage drop representing friction head loss, total clockwise voltage drop around any circuit loop equals total counterclockwise voltage drop, just as fluid head losses balance around a pipe-line loop.

If an electric circuit is connected to simulate a pipe-line network, and suitable conversion factors are used to relate electric and hydraulic quantities, the performance of the pipe-line network is indicated by conditions in the electric circuit. Complete proportionality of corresponding quantities does not occur, however, unless the voltage drop across each resistor in the electric circuit is related to the current through it in a manner analogous to the nonlinear relation between head loss and flow rate for the pipe line that it represents. Two general methods have been developed previously for satisfying this nonlinear relation. The first method[5,6,7] is a direct analogy that involves one or more successive approximations, between which the settings of ordinary linear resistors must be changed in the direction indicated by the preceding trial. The second method[8] employs a modified analogy that leads indirectly to the desired results. Both methods involve computations for corrections of the settings of all resistors in the circuit between successive traverses.

The following presentation describes the analysis of pipe-line networks by means of electric circuits whose resistors automatically represent an accepted relation between head loss and flow rate. This method gives the desired values of flow rates and head losses directly, without successive approximations or the computation of corrected settings of resistors. The method has been used successfully in analyses of distribution systems for water, steam, and illuminating gas at low and high pressures, with accuracy well within the limits of reasonable knowledge of the condition of the internal surface of pipe lines. Since the application of the method to water distribution systems has been described in detail previously,[9] the ensuing discussion is limited to the basic principles of the procedure and accuracy of results.

---

[5] "Hydraulic Analysis of Water Distribution Systems by Means of an Electric Network Analyzer," by Thomas R. Camp and Harold L. Hazen, *Journal*, New England Water Works Assn., Vol. 48, December, 1934, p. 383.

[6] "Solution of Hydraulic Flow Distribution Problems Through Use of the Network Calculator," by L. M. Haupt, *Research Report No. 18*, Texas Eng. Experiment Station, College Station, Tex., September, 1950.

[7] "Use of A-C Network Calculator in Distribution System Design," by M. V. Suryaprakasam, G. W. Reid, and J. C. Geyer, *Journal*, A.W.W.A., Vol. 42, December, 1950, p. 1154.

[8] "Network Flow Analysis Speeded by Modified Electrical Analogy," by H. A. Perry, Jr., D. E. Vierling, and R. W. Kohler, *Engineering News-Record*, Vol. 143, No. 12, September, 1949, p. 19.

[9] "Direct-Reading Electric Analyzer for Pipeline Networks," by Malcolm S. McIlroy, *Journal*, A.W.W.A., Vol. 42, 1950, p. 347.

PROPERTIES OF NONLINEAR RESISTORS

A nonlinear resistor that is to represent a pipe line in an analogous electric circuit must perform so that a rational law or acceptable empirical formula relating head loss to flow rate is properly simulated by the relation between voltage across the resistor and current through it. Flow rate, rather than velocity, is the fundamental variable in network analysis because flow rates balance at pipe-line junctions, whereas velocities, in general, do not. At a given flow rate, the rate of change of head loss with flow differs for pipes of different diameters and surface conditions. In one pipe, the head loss may vary nearly as the 1.8 power of flow rate, if the flow rate is low; in another it may vary nearly as the second power of flow rate, and all intermediate values of the exponent are possible. To design a type of nonlinear resistor that can accommodate all possible values of the exponent, as affected by the Reynolds number and the relative roughness of a pipe, appears economically unjustified because the cost of incorporating allowances for all the variables involved, if they could be achieved physically, would undoubtedly be prohibitive. A compromise is sought that meets the requirements of the great mass of network-analysis problems with satisfactory accuracy, and is acceptable from a cost standpoint.

Hydraulic engineers concerned with networks of pipes often find that an empirical formula relating head loss to flow gives results sufficiently accurate for most engineering work, with a saving of effort compared with that involved in employing the Colebrook-White adaptation of Darcy's law.[10] The search for a useful expression led A. Hazen and G. S. Williams to their well-known formula, which can be expressed in the form,

$$H = A\,k_p\,Q^{1.85} \qquad (1)$$

in which H is the head loss along a pipe line; A is a scale factor related to units used; k_p is a constant, called the head-loss coefficient of the pipe line (a function of length, diameter, and condition); and Q is the flow rate in the pipe line.

The evaluation of the head-loss coefficient, k_p, and of the scale factor A, corresponding to several systems of units, is described in the Appendix.

In order that a nonlinear resistor may operate in a manner analogous to Eq. 1, the voltage across its terminals must be related to the current in its filament according to the expression,

$$V = k\,I^{1.85} \qquad (2)$$

in which V is the voltage drop across the resistor, proportional to H; k is a constant, called the coefficient of the resistor, proportional to $A\,k_p$; and I is the current through the resistor, proportional to Q.

Eq. 2 satisfies the requirements previously stated for the economical design of a series of nonlinear resistors. In order to perform in accordance with Eq. 2, the resistance of a nonlinear resistor must vary automatically as the positive 0.85 power of the current through the resistor. Ordinary linear

[10] "Turbulent Flow in Pipes, with Particular Reference to the Transition Region Between the Smooth and Rough Pipe Laws," by C. F. Colebrook, *Journal*, Inst. C. E., London, England, Vol. 11, 1938–1939, p. 133.

resistors and the many types of negative-exponential resistors cannot automatically represent this equation.

The positive variation of resistivity of tungsten with temperature, and therefore with resistor current, is employed in the nonlinear resistors used in the direct electrical analogy method of pipe-line network analysis. With the proper combination of dimensions of the diameter and length of a tungsten filament and its supporting leads, a tungsten filament mounted in a vacuum can be made to operate according to Eq. 2 over a useful range of voltage. At about 1 volt, the filaments of all the special resistors, regardless of the values of their coefficients, barely glow, with a dull red color. At 4.6 volts, they operate at the normal temperature of incandescent lamps, with a bright whitish-yellow glow. The filaments fail at approximately 12 volts. To avoid continued operation above 4.6 volts, the nonlinear resistors are used in series to represent pipe lines with unusually large head losses.

Since voltage drop is proportional to head loss, and filament temperature depends on the voltage across the filament, the relative brilliances of the filaments of the resistors in an analysis indicate roughly the relative head losses of the pipe lines, and serve as a quick guide to the portions of the network that require improvement. At less than about 1 volt, the filaments are not incandescent, and the percentage accuracy of representation is somewhat impaired. Since these low voltage situations correspond to low head losses, this reduction in accuracy has a negligible effect on total network head loss.

To represent the range of pipe-line length, diameters, and conditions to be expected in a pipe-line network analysis, the nonlinear resistors are constructed in a series of approximately 200 designs. The value of each coefficient in this series is about 1.05 times that of the next smaller coefficient. The head-loss coefficient of a pipe line may usually be represented, therefore, with an error within $\pm$ 2.5%. Studies show that the effect of this error in coefficient values, randomly distributed over a network, is very small.

Equipment Needed for an Analysis

A problem of pipe-line network analysis usually concerns a definite plan of pipe lines with specified physical properties. For any known set of operating conditions, the purpose of the analysis is to evaluate the unknown conditions. For example, with values and locations of input heads and output discharges known, values of head losses and flow rates for all or part of the network pipe lines may be found; or for a minimum permissible head at some critical discharge point, the maximum possible discharge rate may be determined. To permit the representation of a great variety of network maps and the proper control of the fundamental variables, a device called a pipe-line network analyzer has been developed and installed at the College of Engineering, Cornell University, Ithaca, N. Y. The analyzer was constructed by the Standard Electric Time Company of Springfield, Mass., and the nonlinear resistors were manufactured by Sylvania Electric Products, Incorporated, of Salem, Mass. Fig. 1 is a photograph of the operating side of a network panel of this analyzer. The circuit arrangement in a grid of squares representing pipe-line

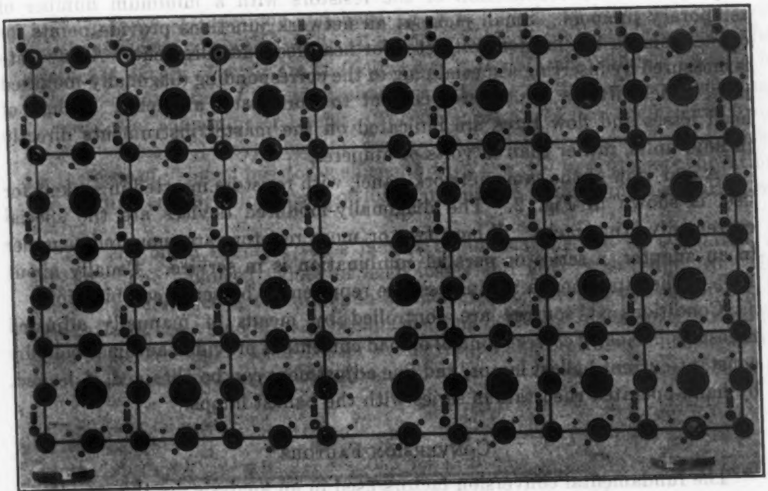

Fig. 1.—Operating Panel of Pipe-Line Network Analyzer

Fig. 2.—Rear View of Pipe-Line Network Analyzer

loops permits interconnection of the resistors with a minimum number of temporary jumpers. Small jacks at all network junctions provide points for connections to the master voltmeter for head-loss measurement. A flow rate is measured by inserting a special plug in the corresponding diagonally-mounted jack, which diverts the resistor current to the master ammeter. Values of head losses and flow rates are indicated on the master instruments directly in fluid units, rather than in volts or amperes.

A rear view of the same network panel, with resistors inserted in sockets for use, is shown in Fig. 2. The diagonally-mounted devices are the special current-diverting jacks. Where two or more resistors are mounted together in an adapter, a series or parallel combination is in service. Usually about 10% of the pipe lines in an analysis are represented by series combinations.

Conditions at sources are controlled by means of manually adjusted rheostats. Nearly correct control of load currents is provided automatically by constant-current ballast lamps, and fine adjustment can be obtained, if desired, by hand-operated rheostats in series with the ballast lamps.

Conversion Factors

The fundamental conversion factors used in an analysis are the ratio,

$$B = \frac{V}{H} \quad \text{(3)}$$

between the voltage (V) and head loss (H) across any corresponding pair of points in the electric circuit and the pipe-line network that it simulates, and the ratio,

$$G = \frac{I}{Q} \quad \text{(4)}$$

between current (I) and flow rate (Q) in any corresponding elements of the electric circuit and the pipe-line network. Values of the basic conversion factors are selected to be appropriate for the capacity of the available source of power supply, the ratings of the load devices, and the safe operation of the resistors.

The conversion factor,

$$\theta = \frac{k}{k_p} \quad \text{(5)}$$

that relates the coefficient of every resistor in an analysis (k) to the head-loss coefficient of the corresponding pipe line (k_p) has the value,

$$\theta = \frac{A\ B}{G^{1.85}} \quad \text{(6)}$$

The proper value of any single-unit resistor coefficient, or resultant coefficient of a series or parallel group of resistors, is found by multiplying the value of the head-loss coefficient of the pipe line it represents by the constant θ.

ACCURACY

Since flows at junctions and head losses around loops inherently balance nearly perfectly when the electrical analogy method of analysis is used, the significant causes of error are the following, if the Hazen-Williams formula is considered correct: (1) Circuit resistances external to the resisters, including resistances of the ammeter circuit; (2) differences of resistor coefficients from desired values; (3) deviations of resistor characteristics from desired form; (4) increase of value of resistor coefficients with age; (5) instrument calibration and reading errors; (6) changes of load currents or source voltages during an analysis.

The combined effect of these factors in an analysis can be evaluated, if desired. The balanced values of head losses and flow rates found from the analysis give values of the pipe-line coefficients, k_p, through the use of Eq. 1. The ratio of the value of each coefficient thus derived, to the specified value, leads to a correction in head loss for the corresponding pipe line. The algebraic sum of all head-loss corrections divided by the sum of all head losses found in

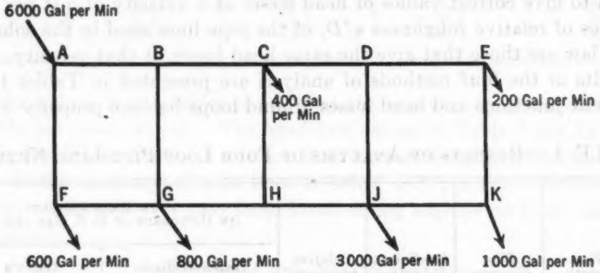

FIG. 3.—PIPE-LINE NETWORK FOR TYPICAL ANALYSIS

the analysis is a fair measure of the over-all error. This error has not exceeded 3% in all the analyses made at Cornell University for which error studies have been made. The error has always been conservative because of the dominant effect of resistances of the conductors that interconnect the nonlinear resistors.

If the Colebrook-White adaptation of Darcy's law is taken as the standard for evaluating errors, rather than the Hazen-Williams formula, additional small errors in head losses and flow rates occur for individual pipe lines, because the head-loss-flow characteristic curves of the two expressions coincide at only one flow rate. The characteristic curves are very close, however, for a large range of flow rates on either side of the intersection. For flow rates below the intersection of the two curves, the Hazen-Williams formula gives a higher head loss, and for flow rates above the intersection, Darcy's law gives a higher head loss. The tendency for these differences to compensate over a large network makes the Hazen-Williams formula very useful in network-analysis work. Furthermore, the Hazen-Williams formula may readily be applied in the pipe-line network analyzer to give an excellent representation of Darcy's law. For this purpose, the nonlinear resistors are first chosen as previously

described, without regard to Darcy's law, and the analyzer is then operated for a trial run under the given conditions. Flow rates are read for the resistors that glow brightly, indicating significant head losses. A correction curve similar to one previously published[11] is consulted to determine the values of factors by which the resistor coefficient should be multiplied to make their performance agree closely with Darcy's law for flow rates near those found from the trial. The resistors are then replaced with others having suitably altered coefficients, and the complete analysis may then be conducted in close conformance with Darcy's law.

Comparison of Actual Analyses

As an example of the results obtained from different methods of analysis, the four-loop pipe-line network shown schematically in Fig. 3 has been analyzed, first by rigorous algebraic solutions obtained from the linear-approximation method, and then by the pipe-line network analyzer, using both the Hazen-Williams formula and the Colebrook-White adaptation of Darcy's law. The values of the Hazen-Williams smoothness coefficient C, given in Table 1, are assumed to give correct values of head losses at a velocity of 5 ft per sec and the values of relative roughness η/D, of the pipe lines used in the solution by Darcy's law are those that give the same head losses at that velocity.

Results of the four methods of analysis are presented in Tables 1 and 2. All flows at junctions and head losses around loops balance properly when the

TABLE 1.—Results of Analysis of Four Loop Pipe-Line Network

Pipe-line	Pipe length (ft)	Pipe diameter (in.)	Coefficient of friction C	Relative roughness η/D	Flow Rate Results (in Hundreds of U. S. Gal per Min): Hazen-Williams, Rigorous algebraic solution	Hazen-Williams, Network analyzer solution	Darcy's Law, Rigorous algebraic solution	Darcy's Law, Network analyzer solution
(1)	(2)	(3)	(4)	(5)	(6)	(7)	(8)	(9)
AB	2510	20	120	0.001	50.12	50.40	50.03	50.22
BC	1450	20	120	0.001	42.02	42.30	41.92	42.20
CD	2430	16	110	0.0021	24.11	23.80	24.69	23.90
DE	2230	8	100	0.0062	6.74	6.70	6.70	6.90
AF	1940	10	100	0.0055	9.88	9.96	9.97	9.88
BG	2105	10	100	0.0055	8.10	8.10	8.11	8.02
CH	2010	12	110	0.0032	13.91	14.10	13.23	14.20
DJ	2580	12	110	0.0032	17.37	17.10	17.99	17.00
EK	1630	8	100	0.0062	4.74	4.60	4.70	4.84
FG	1430	8	100	0.0062	3.88	3.92	3.97	3.98
GH	1940	10	100	0.0055	3.98	4.10	4.08	4.10
HJ	2230	12	110	0.0032	17.89	18.20	17.31	18.30
JK	2120	8	100	0.0062	5.26	5.20	5.30	5.10

values of individual flows and head losses listed in the tables occur. For the algebraic solutions, the relations between head losses and flows agree either with the Hazen-Williams formula or with Darcy's law, as indicated by the column headings. For the solutions conducted on the analyzer, the values

[11] "Direct-Reading Electric Analyzer for Pipeline Networks," by Malcolm S. McIlroy, *Journal*, A.W.W.A., Vol. 42, 1950, p. 363, Fig. 13.

listed are those read from the analyzer, slightly adjusted in the third decimal place to provide perfect balances. The total input flow used in the analyzer was 6,036 gal per min for the Hazen-Williams solution and 6,010 gal per min for the Darcy solution, instead of the specified value of 6,000 gal per min. Inspec-

TABLE 2.—COMPARISON OF HEAD LOSSES

Junction point	TOTAL LOSS IN FEET OF HEAD FROM INPUT AT POINT A			
	Hazen-Williams Formula		Darcy's Law	
	Rigorous algebraic solution	Network analyzer solution	Rigorous algebraic solution	Newtork analyzer solution
(1)	(2)	(3)	(4)	(5)
B	12.2	12.8	12.3	12.5
C	17.3	18.1	17.3	17.5
D	28.0	28.8	28.0	28.3
E	59.8	60.9	58.8	60.9
F	19.1	20.0	18.8	19.7
G	26.6	28.0	25.9	27.5
H	30.1	31.5	29.1	30.9
J	52.8	55.5	51.6	54.9
K	72.0	74.0	70.1	72.5

tion of the values in the tables shows that the analyzer solutions are entirely acceptable for practical use. The head-loss values in Table 2 are, in general, higher for the Hazen-Williams solution than for the Darcy solution because the velocity in the majority of pipe lines is below 5 ft per sec. Both solutions conducted on the analyzer gave head losses erring slightly on the conservative side, as usual.

ADVANTAGES AND DISADVANTAGES

The advantages of the direct-analogy process of pipe-line network analysis are as follows:

a. No computations involving the configuration of the network are needed.

b. No guesses of values of flow rates or head losses, followed by successive approximations, are involved.

c. Only those values actually needed are recorded.

d. Changes to represent alternative plans of constructing or operating a network can be made readily, and their effects quickly visualized and evaluated.

e. Solutions automatically balance with accuracy suitable for engineering work.

f. Solutions are rapid, and the probability of human error is minimized.

g. The glowing resistor filaments direct attention to parts of the network in which head losses are greatest, without the necessity of reading any instruments.

h. A network of almost any size and degree of complexity can be analyzed without any fundamental difficulty.

The disadvantages of the method are the investment cost of installing the analyzer, a small maintenance cost, the use of floor space, and the need to

exert reasonable care in operating the analyzer to avoid subjecting the resistors to voltages above their safe working range. Since learning to operate the analyzer takes no longer than learning to carry out an algebraic solution, the training required for using the analyzer is not a significant disadvantage.

Conclusion

The electric analyzer employing special nonlinear resistors provides an automatic analogy to a network of pipe lines. Desired results of an analysis are given quickly and directly in terms of fluid quantities. Values of important quantities, such as total head loss between remote junctions or flow rates in principal pipe lines can be found immediately without any need to find values of head losses or flow rates for other pipe lines. The method provides ready visualization and evaluation of the effects of alternative plans for network construction or operation.

TABLE 3.—Values of Constant A

(a) American and British Units

Units used for flow Q	Units Used for Head Loss, H	
	Feet of water	Lb per sq in
United States gallons per minute	10^{-5}	4.34×10^{-6}
Hundreds of United States gallons per minute	0.0501	0.0217
United States million gallons per day	1.807	0.783
Imperial gallons per minute	1.401×10^{-5}	6.07×10^{-6}
Hundreds of Imperial gallons per minute	0.0702	0.0304
Imperial million gallons per day	2.53	1.098

(b) Metric Units

Units used for flow Q	Meters of water	Kg per sq cm
Liters per second	10^{-3}	10^{-4}
Kiloliters per minute	0.182	0.0182
Million liters per day	9.29×10^{-2}	9.29×10^{-3}

APPENDIX. VALUES OF CONSTANTS

Constants in United States and British Units..—The value of the head-loss coefficient, k_p, for a pipe line that is described physically in units employed in the United States or the British Commonwealth, is expressed in the form,[12]

$$k_p = M\,l \qquad (7a)$$

and

$$M = \frac{5830}{d^{4.87}\,C^{1.85}} \qquad (7b)$$

in which l is the length of pipe in thousands of feet; d is the diameter of pipe in feet; and C is the Hazen-Williams smoothness coefficient, usually in the range of 90 to 130.

[12] "Direct-Reading Electric Analyzer for Pipeline Networks," by Malcolm S. McIlroy, *Journal*, A.W.W.A., Vol. 42, 1950, p. 366.

A table that gives values of M for a range of values of C from 20 to 140 and for standard pipe diameters from 4 in. to 72 in. is available. Values of constant A in Eqs. 1 and 3 are listed in Table 3(a).

Constants in Metric Units.—For pipe lines described in the metric system of units, the value of k_p is

$$k_p = P\,l \qquad (8a)$$

$$P = \frac{29.6}{d^{4.87}\,C^{1.85}} \qquad (8b)$$

in which l is the length of pipe in kilometers; d is the diameter of pipe in meters; and C is the Hazen-Williams smoothness coefficient, usually in the range of 90 to 130. Values of constant A in Eqs. 1 and 3, for problems in which the metric system is employed, are listed in Table 3(b).

DISCUSSION

CHARLES L. BARKER,[13] A. M. ASCE.—The theory and principles of operation for a new engineering tool are presented in this paper—a tool that will become of increasing value as engineers become aware of its usefulness and capabilities. The author has not mentioned the many applications of the network analyzer. Perhaps he left this phase to the imagination of the reader.

At the State College of Washington, at Pullman, problems of air, gas, oil, and water have been worked on it, and, as is the case in many new tools, the analyzer has been able to do many things that were not even considered in the original planning.

On a problem of a distribution system for a city of about 50,000, extensive changes were contemplated. These involved increasing pipe sizes in the present system to meet heavier loads, extension of present mains to take care of population growth, and, finally, studying the effect of additional sources. Added to these was the problem of adequate fire protection. In 21 hr of analyzer operation, twenty-four pressure contour maps were prepared presenting the various combinations of the foregoing problems. The expected pressure for the given flow conditions was given on each map. This pressure was equivalent to a solution of a thirty-five-loop system by the Hardy Cross method twenty-four times. In fact, the work was more than that because when each study was started, preliminary tests of pressure were made for the flow conditions assumed. If the pressures were unsatisfactory, pipe changes were made by changing the nonlinear resistors, and then the test began again.

In another study it was planned to remove an undesirable source from the system and to supply the system from a reservoir to be filled in off-peaks operation. The system was placed on the analyzer, pipes were changed to give adequate pressure and fire protection, and, finally, the height of the reservoir was determined. The analyzer time was 8 hr.

One problem of maximum fire flow on a system was studied. A load representing a fire load was placed at different points in the system. The size of this load was increased until the pressure at the outlet was as low as was felt to be satisfactory, thus giving the maximum fire load possible.

Studies of the effect of pipe roughness on system-pumping costs can be made easily, and the effect of changing the roughness value is thus made immediately apparent. All the foregoing comments refer to the flow of water. Similar studies can be made on other fluids.

Mr. McIlroy has given the engineer a new tool—one that he must learn to use before its value can be fully appreciated—and engineers owe him a vote of thanks.

---

[13] Prof. of Civ. Eng., College of Eng., State College of Washington, Pullman, Wash.

MALCOLM S. MCILROY[14].—The description, by Mr. Barker, of the solution of four problems by use of the nonlinear analyzer at the State College of Washington, constitutes a valuable addition to the paper. Similar studies of distribution systems for water, steam, and gas have been conducted on the analyzers at the Midwest Research Institute, in Kansas City, Mo., and at Cornell University, at Ithaca, N. Y. Studies have also been made of the performance of a storm sewer system and of the circulation of ventilating air in a coal mine. Investigations in the field of gas distribution, by use of large nonlinear analyzers, will be undertaken at Columbus, Ohio, St. Louis, Mo., and Newark, N. J.

As Mr. Barker indicates, the use of the analyzer as an aid to design can best be appreciated after actual experience. If various conditions are imposed on a network in a logical sequence, the results of each test suggest alternatives that may be investigated at once, leading to a judicious solution to the problem. The elimination of extensive computations greatly extends the possibility of undertaking investigations that might otherwise be prohibited by cost and time requirements.

Since the original paper was written, extensions of the method to satisfy square-law fluid-flow equations have been published.[15] This method has also been used to investigate the flow of compressible fluids.[16] Convenient tables of constants applying to water-distribution have also been made available.[17]

---

[14] Prof. of Electrical Eng., Cornell Univ., Ithaca, N. Y.; and Consultant to the Standard Electric Time Co., Springfield, Mass.

[15] "Gas Pipe Networks Analyzed by Direct-Reading Electric Analogue Computer," by Malcolm S. McIlroy, *Publication DMC-52-10*, Am. Gas Assn., April, 1952.

[16] "Steam-Distribution Systems Analyzed by Nonlinear Electrical-Analogy Method," by Malcolm S. McIlroy and Chao K. Chow, *Proceedings*, National District Heating Assn., Vol. XLIII, 1952.

[17] "Water-Distribution Systems Studied by a Complete Electrical Analogy," by Malcolm S. McIlroy, *Journal*, New England Water Works Assn., Vol. LXV, No. 4, 1951, p. 299.

AMERICAN SOCIETY OF CIVIL ENGINEERS
Founded November 5, 1852
TRANSACTIONS

Paper No. 2570

EFFECT OF ENTRANCE CONDITIONS ON DIFFUSER FLOW

By J. M. Robertson,[1] M. ASCE, and Donald Ross[2]

With Discussion by Messrs. Steponas Kolupaila, Arthur L. Collins, R. M. Olson, and J. M. Robertson and Donald Ross

Synopsis

An experimental investigation was made of the flow conditions in conical diffusers when preceded by relatively short lengths of straight pipe and a well-faired, large area-ratio contraction. Diffusers having total angles of 5°, 7.5°, and 10° were studied when preceded by 2-diameter, 5-diameter, and 9-diameter lengths of straight pipe. The experimental measurements included pressure distributions along the diffusers and velocity traverses at three or more stations. It was found that the area-ratio of the diffuser is the major geometric parameter governing the shape and extent of the boundary layer. The extent of the boundary layer at the entrance to the diffuser, given indirectly by the length-diameter ratio of the preceding straight pipe, is as important a factor in determining the flow as is the diffuser angle. Within the range tested, the pressure efficiency was found to be a function of the product of diffuser angle and effective entrance length; and the energy efficiency, although decreasing with increasing area-ratio, is practically independent of the angle and entrance conditions. It was concluded that the only consideration which should affect the choice of diffuser geometry is the desired factor of safety with regard to separation. As a few of the velocity traverses taken in the experimental program indicated or suggested the occurrence of separation near the end of the diffuser, it was possible to determine the critical values of two velocity-profile form parameters. Methods for estimating the values of these parameters in any diffuser were developed. Thus, this study allows the prediction of the mean flow conditions in conical diffusers, at least within the range of the test variables.

Note.—Published in July, 1952, as *Proceedings-Separate No. 141.* Positions and titles given are those in effect when the paper or discussion was received for publication.

[1] Prof. of Eng. Research, Ordnance Research Lab., The Pennsylvania State College, State College, Pa.

[2] Associate Prof. of Eng. Research, Ordnance Research Lab., The Pennsylvania State College, State College, Pa.

Introduction

A diffuser is a common hydraulic component in which the flow expands and the kinetic energy of a high-velocity stream is converted into potential or pressure energy. A well-designed diffuser can have a fairly high efficiency, whereas one poorly designed will not only have a lower efficiency but also may introduce deleterious flow conditions into the following sections of the system. The type of diffuser flow with which this paper is concerned is that in which the diffuser is preceded by a nozzle or contraction and a relatively short length of straight pipe, as in a venturi meter. Thus, the velocity profile at the start of the diffuser is characterized by a uniform central core and a thin boundary layer at the edges. As the flow proceeds down the diffuser, the boundary layer grows rapidly in thickness until it reaches the center, and the "fully-developed" diffuser flow occurs.

The prediction of the flow conditions in diffusers has long been a major unsolved problem in fluid mechanics. The chief complicating effect is the presence of the large adverse pressure gradient, whose exact influence on the velocity distribution has defied mathematical analysis. Although many investigators have studied the flow of air or water in expanding pipes and channels, some of the basic questions remain unanswered. In most cases, the entrance conditions were either poor, unknown, or otherwise of such a nature as to make the resulting data of doubtful value. Usually, the range of Reynolds numbers was too small to allow scaling of the data, and often certain basic quantities were not even measured. In many cases two-dimensional diffusers, in which the flow is affected by the secondary currents at the corners, were studied.

The present study of diffuser flow was supplemented by a thorough review of the literature (1)[3]. In the well-known, early experimental work of A. H. Gibson (2) (3) the minimum head loss was found to occur for about 5½° (total angle) for circular and square pipes and about 11° for rectangular conduits. The German studies (4) (5) (6) (7) on the flow of air and water in rectangular channels, with diffusion in one plane only, culminated in the work of J. Nikuradse (8). His measurements resulted in the most thorough study of diffuser flow yet reported. Unfortunately, Mr. Nikuradse only presents velocity traverses taken at one station where the flow was "fully developed." He found instability and separation for total angles between 8° and 10°. He presented a semi-rational treatment of the results, which implies that the higher the Reynolds number, the smaller the angle will be at which separation occurs. Experiments similar to the German work were reported by A. M. Vedernikoff (9) who noted instability at the end of his 12° diffuser.

George E. Lyon (10) found the maximum efficiency at 8° for conical draft tubes in which the entering flow was uniform with only a thin boundary layer. In a continuation of Mr. Gibson's work, H. Peters (11) found that for angles less than 30° the efficiency is several percent greater with the nearly flat entering velocity profile than with the fully-developed flow. Neither of these studies reveals much about the details of the flow conditions. Other studies

[3] Numerals in parentheses, thus: (1), refer to corresponding items in Appendix I.

of the flow in conical diffusers, with fully-developed entrance flow, are those of G. A. Gourzhienko (12) and A. A. Kalinske, M. ASCE (13).

Other researchers have studied the rate of growth and velocity profile of a boundary layer in an increasing pressure. A. Buri (14) developed a method of analysis based on an approximation to certain terms in the momentum equation of Theodor von Kármán, Hon. M. ASCE. E. Gruschwitz (15) (16) and A. Kehl (17) evolved an empirical method of analysis based on studies in special channels. The work reported by R. C. Binder (18) in 1947 contains some truly two-dimensional diffuser studies analyzed in a fashion similar to those analyzed by Mr. Buri. A. E. von Doenhoff and N. Tetervin (19) (20) (21) and H. C. Garner (22) have developed semi-empirical methods of analysis which appear to be of limited usefulness (1). A more fundamental approach in terms of the turbulence mechanism has been initiated by K. Fediaevsky (23) (24) and improved by the writers (25).

There appears to be a need for more information on the action of a boundary layer under an adverse pressure gradient. More pressure and velocity measurements, as well as more information on turbulence, are needed. Certainly, the effects of entrance conditions on diffuser flow are not well defined, and the conclusions implied by the Nikuradse analysis need confirmation. This need for more information for use in design analysis was the reason for the tests reported in this paper.

Apparatus and Procedure

Notation.—The letter symbols adopted for use in this paper are defined where they first appear, in the text or by illustration, and are assembled alphabetically for convenience of reference in Appendix II.

Test Facility.—The measurements of the flow in diffusers were obtained in the experimental water tunnel located in the Hydraulics Laboratory of The Pennsylvania State College at State College. This facility, described elsewhere (26), consists of a system in which water flows as great as 10 cu ft per sec can be pumped through aluminum test sections simulating a nozzle, cylindrical pipe section, diffuser, and turn. Fig. 1 shows a typical test setup in which the flow from the 18-in. pipe on the left is accelerated by a nozzle with a discharge diameter of 6 in. A cylindrical pipe section 2 diameters long is separated from the 7.5° diffuser by a gradual transition. The diffuser is followed by a miter turn 12 in. in diameter containing rough turning vanes. The rate of flow through the experimental tunnel was measured by means of a calibrated rectangular weir. The pressure drop across the nozzle was calibrated by comparison with this weir and was then used as a secondary flow standard. The pressure distributions along the walls of the various diffusers were measured by wall piezometer holes connected to differential manometers. Velocity distributions were measured at several cross sections using a cylindrical pitot tube.

Diffuser Test Program.—The nature of the flow in the diffuser is a function of the diffuser angle, the velocity distribution at the entrance, and the Reynolds number of the flow. Diffusers of 5° and 7½° total angle were tested,

preceded by straight pipe-entrance lengths of 2, 5, and 9 diameters, over a pipe Reynolds number—

$$\mathrm{R}_o = \frac{U_o D_o}{\nu} \qquad \text{(1)}$$

—range of 0.5×10^6 to 2.5×10^6. (In Eq. 1, U_o is the average velocity in the pipe at the entrance to the diffuser; D_o is the diameter of the pipe at that point; and ν is the kinematic viscosity of the fluid.) A 10° diffuser was tested with 2-diameter and 5-diameter lengths of pipe preceding it. The use of the different entrance pipe lengths gave different boundary-layer thicknesses at the diffuser entrance. The effective entrance length L was greater than the nominal length because the boundary layer had an appreciable thickness at the end of the nozzle (27) and because it continued to grow in the transition section before the effective start of the diffuser. Correcting the nominal lengths for these two factors yielded the values of the effective entrance lengths listed in Table 1.

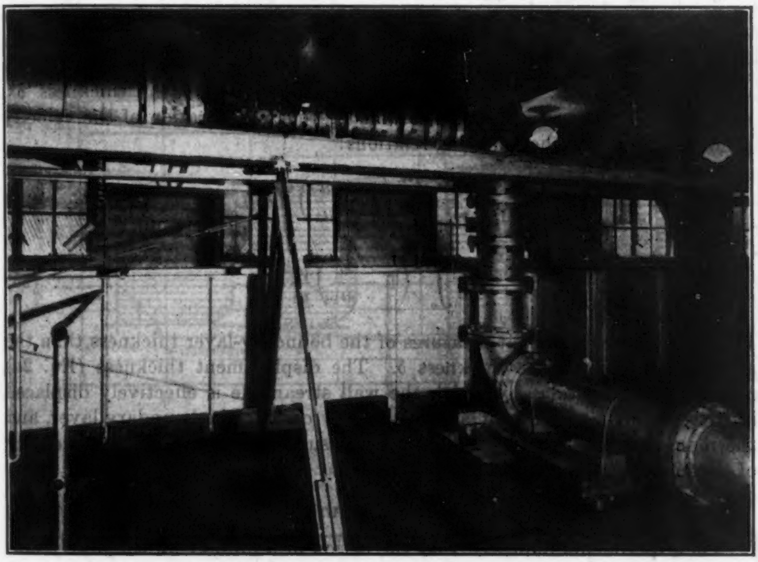

FIG. 1.—EXPERIMENTAL WATER TUNNEL

The pressures were measured throughout the length of the diffuser, over the entire range of Reynolds numbers, and velocity traverses were taken at three or five stations at about three different Reynolds numbers.

Procedure.—The raw experimental data consisted of readings of differential manometers connected between wall piezometers or between the static and dynamic holes of a pitot tube. The wall-pressure distribution data were handled by converting them into pressure coefficients (differences in pressure

between a piezometer and a standard reference piezometer divided by the straight pipe velocity pressure) which were then grouped according to the Reynolds number range in which they were obtained. This procedure yielded average values of the pressure coefficients C_p at various locations in the diffuser for certain Reynolds numbers. Because the data were grouped, these coefficients have an accuracy somewhat greater than that of any individual test reading. The velocity traverse data yielded values for the maximum velocity u_1, the estimated disturbance thickness δ and the displacement thickness δ^*, and the momentum thickness θ, obtained through integration of the velocity profile according to the following relations:

TABLE 1.—EFFECTIVE ENTRANCE LENGTHS (IN DIAMETERS)

Length[a]	5°	7½°	10°
2	3.3	3.5	3.6
5	6.2	6.4	6.4
9	10.1	10.4	....

[a] Nominal length, in diameters.

$$\delta^* = \int_o^\delta \left(1 - \frac{u}{u_1}\right) dy \quad \text{(2a)}$$

and

$$\theta = \int_o^\delta \left(1 - \frac{u}{u_1}\right) \frac{u}{u_1} dy \quad \text{(2b)}$$

Eqs. 2 are more significant measures of the boundary-layer thickness than the apparent or disturbance thickness δ. The displacement thickness (Eq. 2*a*) represents the distance by which the wall streamline is effectively displaced into the fluid in so far as it affects the flow outside the boundary layer, and the momentum thickness (Eq. 2*b*) is a measure of the momentum deficiency of the boundary layer.

TEST RESULTS

The experiments indicated that the action of a diffuser on the nearly uniform entering flow is to increase the rate of growth of the boundary layer and to change the form of the velocity distributions, while lowering the velocity in the uniform central core. This action is illustrated in Fig. 2, which shows velocity and pressure changes for a typical diffuser.

Pressure Variations.—All the diffuser-pressure measurements were made with reference to a piezometer near the downstream end of the working section. These measurements were reduced to pressure coefficients—

$$C_p = \left(\frac{\Delta p}{\frac{1}{2}\,\rho\, U^2_o}\right) \quad \text{(3)}$$

—and handled in the semi-statistical method previously referred to. For a fundamental presentation, the pressures should be referred to that at the actual or geometric start of the diffuser, defined as the location in the transition section where the projection of the cylindrical entrance pipe wall intersects the projection of the conical diffuser wall. Therefore, the pressure coefficients were corrected for the pressure loss between the reference piezometer and the

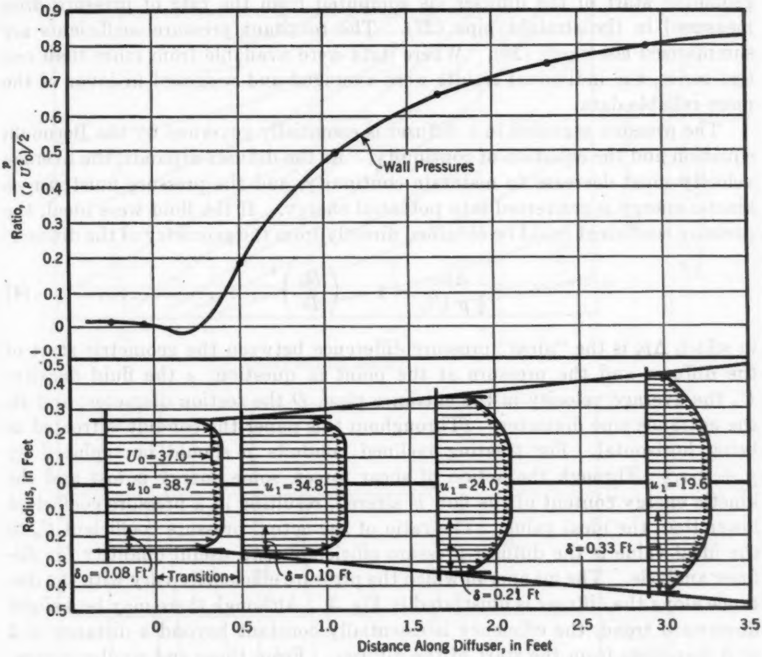

FIG. 2.—FLOW CONDITIONS IN A 7.5° DIFFUSER (FIVE DIAMETERS OF STRAIGHT SECTION PRECEDING THE TRANSITION; $R_e = 2 \times 10^6$)

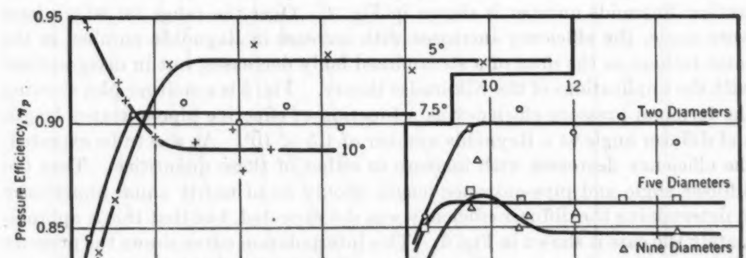

FIG. 3.—PRESSURE EFFICIENCIES ALONG SEVERAL DIFFUSERS

geometric start of the diffuser, as computed from the rate of pressure drop measured in the straight pipe (27). The resultant pressure coefficients are summarized elsewhere (28). Where data were available from more than one test series, the individual results were averaged and weighted in favor of the more reliable data.

The pressure regained in a diffuser is essentially governed by the Bernoulli equation and the equation of continuity. As the diffuser expands, the average velocity must decrease to maintain continuity, and the pressure must rise as kinetic energy is converted into potential energy. If the fluid were ideal, the pressure coefficient could be obtained directly from the geometry of the diffuser:

$$\frac{\Delta p_i}{\frac{1}{2}\rho U^2_o} = 1 - \left(\frac{D_o}{D}\right)^4 \qquad (4)$$

in which Δp_i is the "ideal" pressure difference between the geometric start of the diffuser and the pressure at the point in question; ρ the fluid density; U_o the average velocity in the entrance pipe; D the section diameter; and D_o the entrance pipe diameter. (Throughout this paper the conduit is treated as being horizontal. For treating inclined conduits p should be replaced by $p + \gamma z$.) Through the action of shear forces, some energy is lost and the kinetic energy content of the flow is altered, resulting in a pressure coefficient lower than the ideal value. The ratio of the actual pressure coefficient C_p to the ideal value is the diffuser-pressure efficiency η_p, a useful quantity for diffuser analysis. The manner in which the pressure efficiencies vary with the distance along the diffuser is illustrated in Fig. 3. Although there may be a slight downward trend, the efficiency is essentially constant beyond a distance of 2 or 3 diameters from the start of the diffuser. From these and similar curves, terminal values of diffuser-pressure efficiency were evaluated for each of the eight test setups and for each Reynolds number.

The manner in which diffuser-pressure efficiencies vary with the working-section Reynolds number is shown in Fig. 4. Over the range for which tests were made, the efficiency increases with increase in Reynolds number in the same fashion as the drag of a streamlined body decreases, but in disagreement with the implications of the Nikuradse theory. Fig. 5 is a contour plot showing the terminal pressure efficiency as a function of effective pipe-entrance length and diffuser angle at a Reynolds number of 1.5×10^6. As was to be expected, the efficiency decreases with increase in either of these quantities. That the diffuser angle and pipe-entrance length should be of nearly equal importance in determining the diffuser efficiency was not expected, but that this is approximately the case is shown in Fig. 6. This interpolation curve shows the pressure efficiency plotted against the product of diffuser angle β and the effective pipe-entrance length, L/D_o. All the experimental points lie close to a single curve, and this curve may be used to predict the diffuser efficiency for a diffuser, between the limits: $5° < \beta < 12°$; $2 < \frac{L}{D_o} < 12$; $12 < \beta \frac{L}{D_o} < 60$—and at a Reynolds number of 1.5×10^6.

The pressure efficiency data obtained with the experimental water tunnel established the importance of the entrance conditions on a par with the diffuser

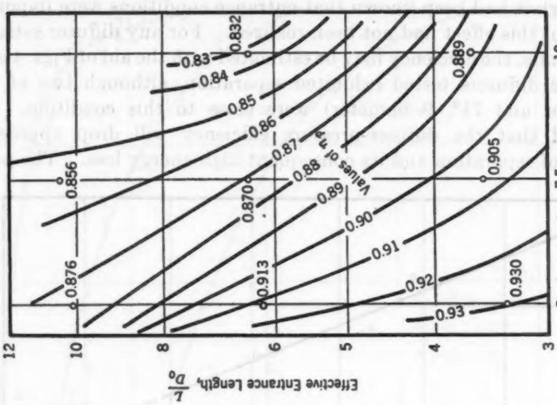

FIG. 5.—PRESSURE EFFICIENCIES AS A FUNCTION OF PIPE-ENTRANCE LENGTH AND DIFFUSER ANGLE ($R_o = 1.5 \times 10^6$)

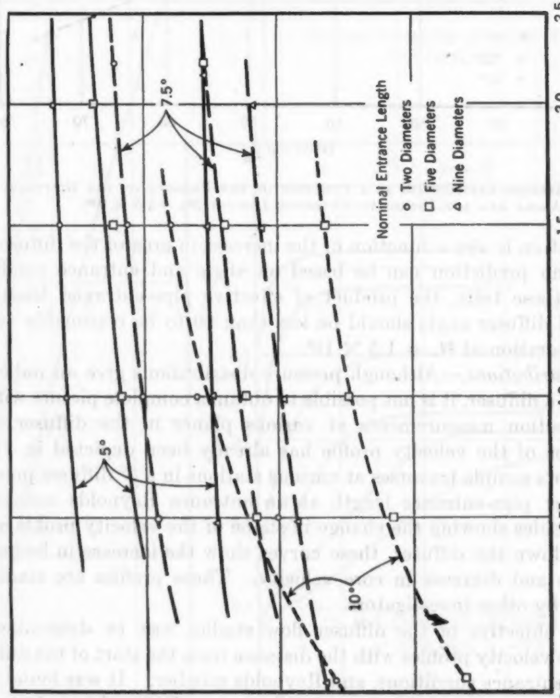

FIG. 4. TERMINAL PRESSURE EFFICIENCIES AS A FUNCTION OF REYNOLDS NUMBER

angle. Although it had been known that entrance conditions were important, the full extent of this effect had not been realized. For any diffuser satisfying the foregoing limits, the efficiency may be estimated with the aid of Figs. 4 and 6.

None of the diffusers tested exhibited separation, although two of them (10°, 5-diameter and $7\frac{1}{2}$°, 9-diameter) were close to this condition. It is to be expected that the diffuser-pressure efficiency will drop appreciably with the onset of separation and its consequent high energy loss. The proba-

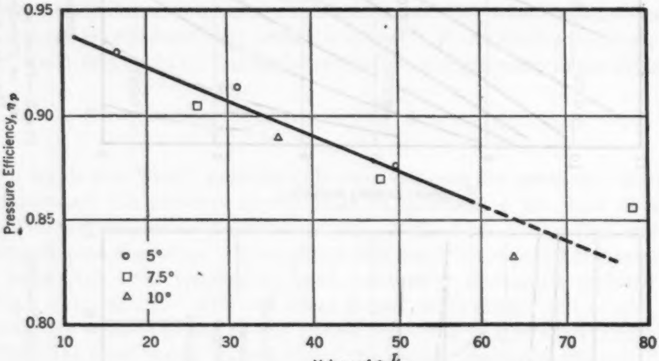

FIG. 6.—PRESSURE EFFICIENCIES AS A FUNCTION OF THE PRODUCT OF THE DIFFUSER ANGLE AND THE EFFECTIVE ENTRANCE LENGTH ($\mathbf{R}_o = 1.5 \times 10^6$)

bility of separation is also a function of the increase in area of the diffuser and consequently no prediction can be based on angle and entrance conditions alone. From these tests, the product of effective pipe-entrance length (in diameters) and diffuser angle should be less than 60 to be reasonably certain of avoiding separation at $\mathbf{R}_o = 1.5 \times 10^6$.

Velocity Distributions.—Although pressure distributions give an indication of the action of a diffuser, it is not possible to obtain a complete picture without velocity-distribution measurements at various planes in the diffuser. The change in shape of the velocity profile has already been depicted in Fig. 2. Fig. 7(*b*) presents sample traverses at various stations in a 5° diffuser preceded by a 5-diameter pipe-entrance length at an entrance Reynolds number of 1.5×10^6. Besides showing the change in shape of the velocity profile as the flow proceeds down the diffuser, these curves show the increase in boundary-layer thickness and decrease in core velocity. These profiles are similar to those reported by other investigators.

The major objective of the diffuser flow studies was to determine the variation of the velocity profiles with the distance from the start of the diffuser, diffuser angle, entrance conditions, and Reynolds number. It was found that, within the accurary of the experiments, the effect of the Reynolds number on the shape of the velocity distributions was negligible. This is illustrated by the data presented in Fig. 7(*a*) for three locations in a 7.5° diffuser. The scatter is typical of the velocity measurements.

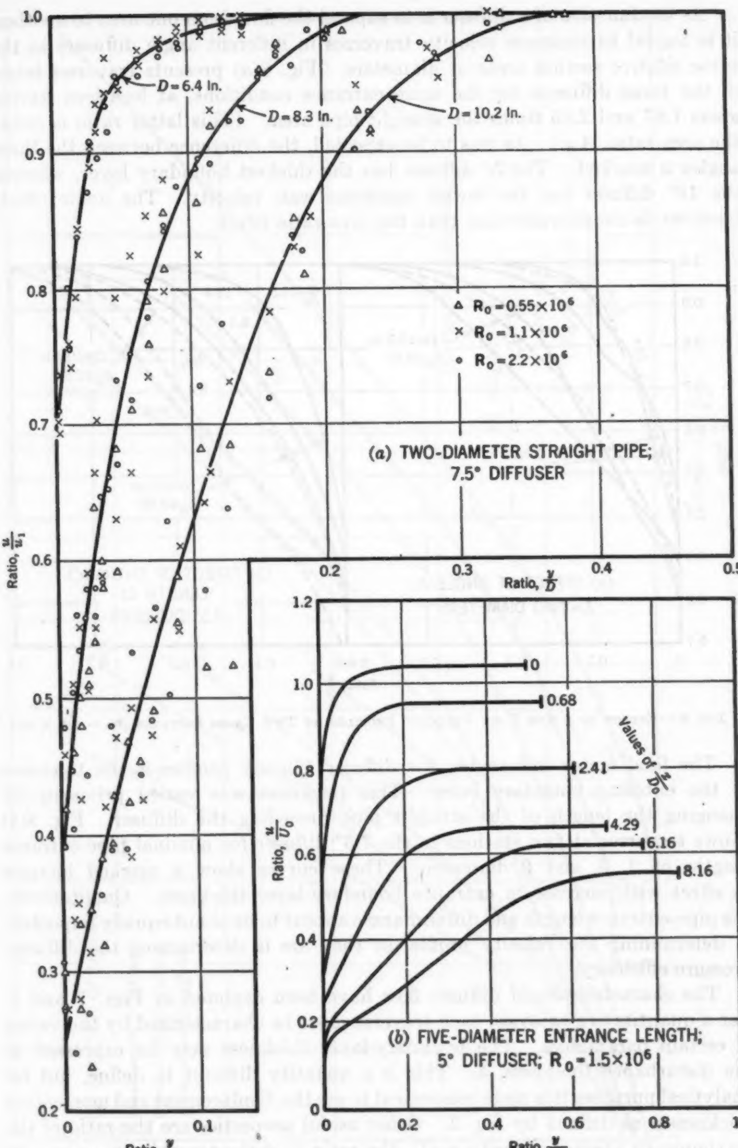

Fig. 7.—Velocity Profiles in two Diffusers

As the function of a diffuser is to expand the flow from one area to another, it is logical to compare velocity traverses in different angle diffusers at the same relative section areas or diameters. Fig. 8(a) presents traverses taken in the three diffusers for the same entrance conditions, at locations having areas 1.87 and 2.85 times the straight pipe area. (This latter ratio is called the area-ratio, A_R.) As was to be expected, the difference between the three angles is marked. The 5° diffuser has the thickest boundary layer, whereas the 10° diffuser has the lowest apparent wall velocity. The angle effect, however, is considerably less than the area-ratio effect.

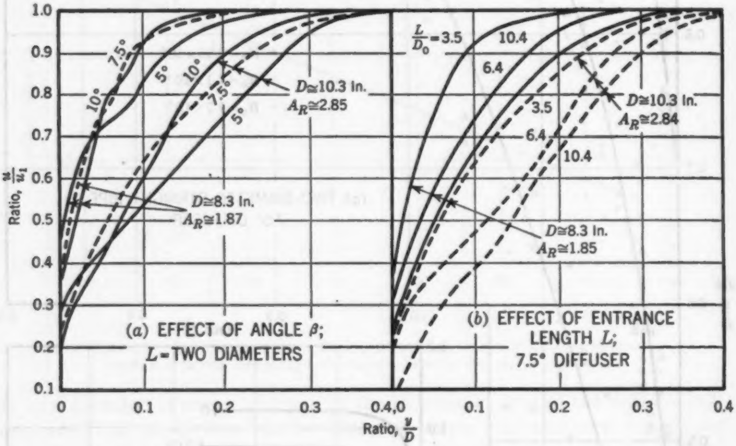

FIG. 8.—EFFECT OF β AND L ON VELOCITY PROFILES AT TWO CROSS SECTIONS ($R_e = 1.5 \times 10^5$)

The final factor influencing the diffuser velocity profiles is the thickness of the entering boundary layer. This thickness was varied primarily by changing the length of the straight pipe preceding the diffuser. Fig. 8(b) shows traverses at two stations in the 7.5° diffuser for nominal pipe-entrance lengths of 2, 5, and 9 diameters. These curves show a marked increase in effect with increase in entrance boundary-layer thickness. Qualitatively, the pipe-entrance length and diffuser angle appear to be about equally important in determining the velocity profile, as they are in determining the diffuser-pressure efficiency.

The characteristics of diffuser flow have been depicted in Figs. 7 and 8. For a quantitative analysis, each traverse must be characterized by the values of certain parameters. The boundary-layer thickness may be expressed as the disturbance thickness, δ. This is a quantity difficult to define, but for analytical purposes it is more convenient to use the displacement and momentum thicknesses as defined by Eq. 2. Other useful properties are the ratio of the maximum to average velocity u_1/U, the ratio α of the true kinetic energy to that based on the average velocity, and some parameter characteristic of the shape of the velocity distribution. Other researchers (18) have found that the

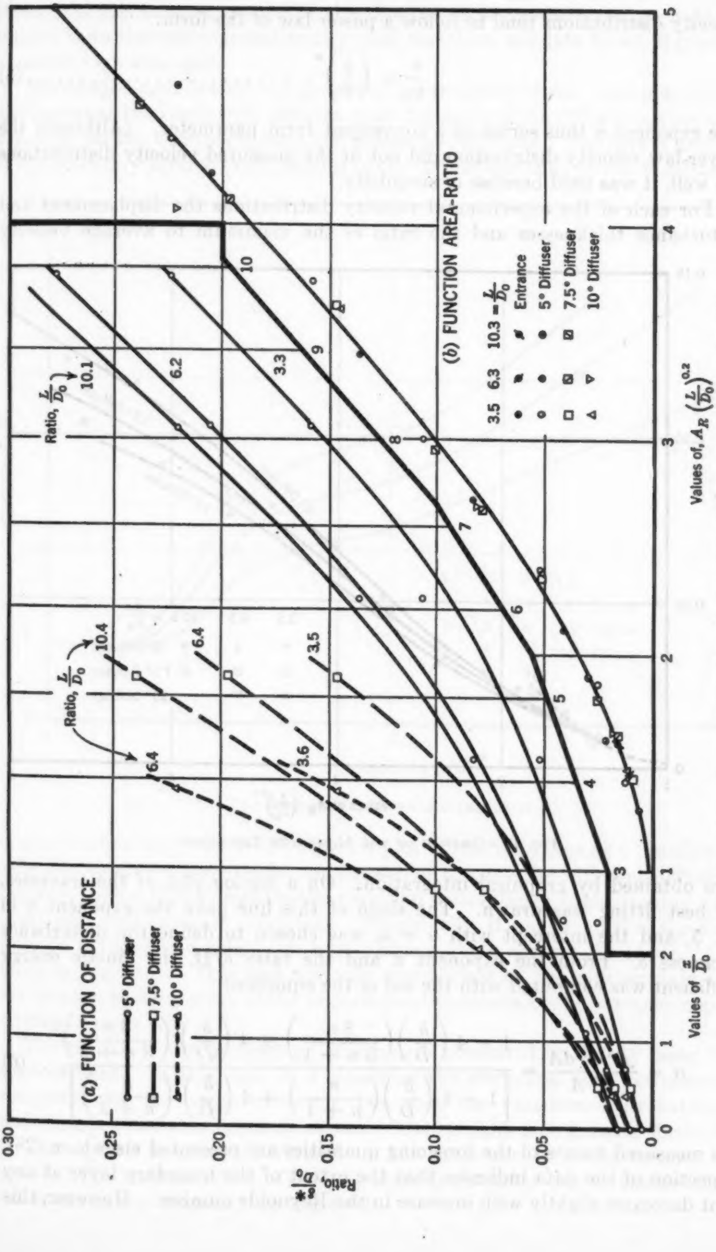

FIG. 9.—DISPLACEMENT THICKNESS AS FUNCTIONS OF DISTANCE AND AREA-RATIO

velocity distributions tend to follow a power law of the form:

$$\frac{u}{u_1} = \left(\frac{y}{\delta}\right)^n \qquad (5)$$

The exponent n thus serves as a convenient form parameter. (Although the power-law velocity distribution did not fit the measured velocity distributions too well, it was used because of simplicity.)

For each of the experimental velocity distributions the displacement and disturbance thicknesses and the ratio of the maximum to average velocity

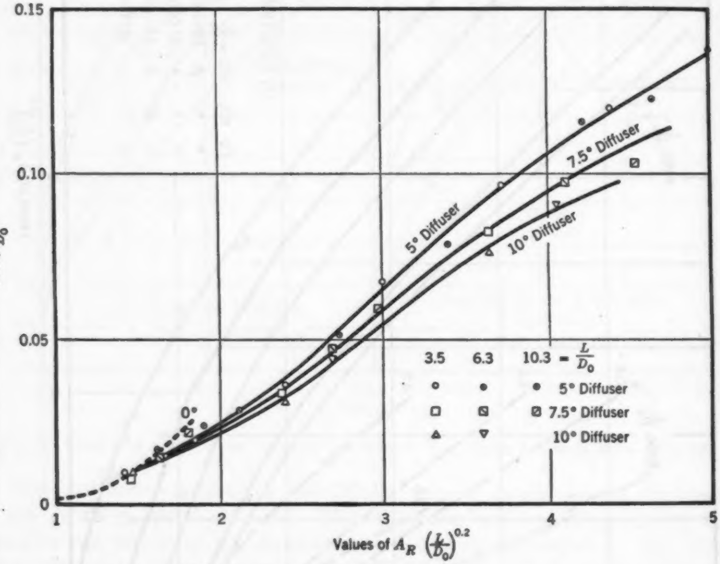

Fig. 10.—Growth of the Momentum Thickness

were obtained by graphical integration. On a log-log plot of the traverses, the best fitting was drawn. The slope of this line gave the exponent n in Eq. 5, and the intercept with $u = u_1$ was chosen to define the disturbance thickness δ. From the exponent n and the ratio δ/D, the kinetic energy coefficient was computed with the aid of the equation:

$$\alpha = \frac{\int^A u^3\, dA}{U^3 A} = \frac{1 - 4\left(\frac{\delta}{D}\right)\left(\frac{3\,n}{3\,n + 1}\right) + 4\left(\frac{\delta}{D}\right)^2\left(\frac{3\,n}{3\,n + 2}\right)}{\left[1 - 4\left(\frac{\delta}{D}\right)\left(\frac{n}{n + 1}\right) + 4\left(\frac{\delta}{D}\right)^2\left(\frac{n}{n + 2}\right)\right]^3} \qquad (6)$$

The measured values of the foregoing quantities are presented elsewhere (28). Inspection of the data indicates that the extent of the boundary layer at any point decreases slightly with increase in the Reynolds number. However, this

effect, which is in agreement with the upward trend in the pressure data, is smaller than the experimental scatter, and, therefore, the data for all Reynolds numbers were averaged.

Boundary-Layer Growth.—A graphical presentation of the variation of the displacement thickness with distance from the start of the diffuser is shown in Fig. 9(a), for the various diffusers and entrance conditions. The rate of growth of the boundary layer is much greater in the 10° diffuser than in the 5° diffuser.

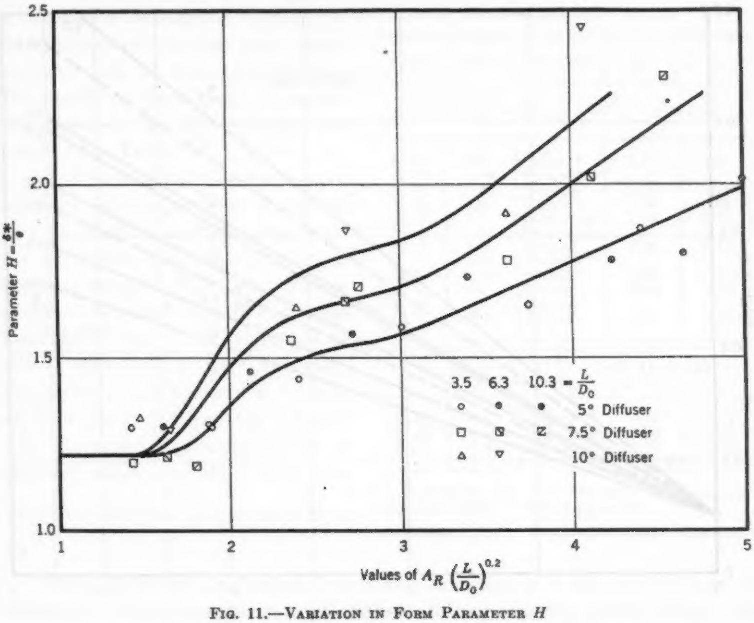

FIG. 11.—VARIATION IN FORM PARAMETER H

As noted previously, one would expect a plot of this thickness as a function of area-ratio to give a more useful comparison of the data for different diffusers. Actually, such a plot eliminates the variation with diffuser angle, leaving only a variation with entrance conditions. Empirically, it was found that the data could be reduced to a single curve by plotting δ^*/D_o against $A_R\ (L/D_o)^{0.2}$ as shown in Fig. 9(b). This plot not only summarizes all the diffuser data but also represents the growth of the displacement thickness in the entrance region of straight pipes ($A_R = 1$).

The growth of the momentum thickness is presented in Fig. 10 using the same abscissa. In this case, it is seen that the area-ratio does not account completely for the angle variation, but that the variation with entrance conditions is satisfactorily compensated. The straight pipe growth, shown by the dashed line, is seen to diverge from the other curves in the manner expected. The residual effect of diffuser angle is probably due to the effect of wall shear on the boundary-layer growth.

The ratio H of the displacement thickness δ^* to the momentum thickness θ is a common form parameter used to characterize the velocity profile and to indicate the proximity to separation. This is easily computed from the data presented in Fig. 9(b) and Fig. 10, and the resulting values are plotted in Fig. 11. The scatter of these data is so large that it is difficult to define average curves. However, the trend-curves shown in this figure were obtained from the average curves in Fig. 9(b) and Fig. 10. These curves are reasonably good for values

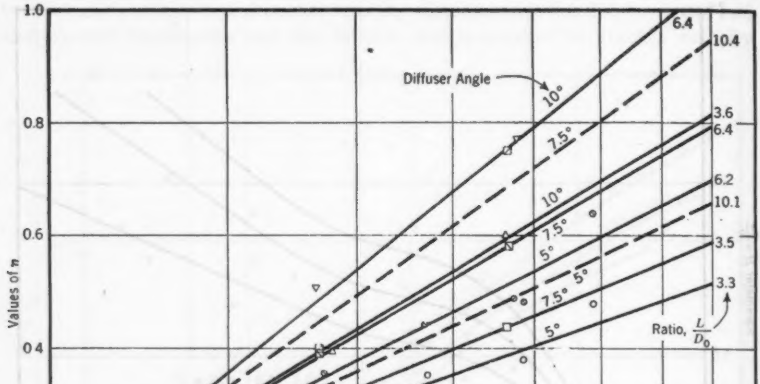

FIG. 12.—VARIATION IN THE POWER-LAW EXPONENT n

of H less than 2. As might be expected, the 10° diffuser has the highest H-value, and hence is nearer separation, at any given station for specific entrance conditions.

The results of the power-law analysis of the diffuser velocity profiles are shown in Fig. 12, in which the exponent n is plotted as a function of the area-ratio. Beginning with the value of n which occurs at the end of the straight pipe, the exponent increases directly with log A_R. This logarithmic variation applies to a developing boundary layer, but probably does not hold when the boundary layer completely fills the diffuser. The variation of n with diffuser angle and entrance conditions is not definite, although the product $\frac{L}{D_o}\,\beta$ seems to determine the position of the curves up to moderate values $\frac{L}{D_o} = 8$ and $\beta = 8°$.

Occurrence of Separation.—Some of the velocity traverses taken near the downstream end of the 7.5° diffuser preceded by a 9-diameter pipe-entrance section and the 10° diffuser with a 5-diameter entrance section suggested that separation was occurring at or near these stations. This condition was indicated by flow asymmetries or zero velocities at or near the wall. In an attempt to establish the conditions under which separation occurs, a large number of traverses were taken near the end of the 7.5° diffuser. The results of these tests, together with those in the 10° diffuser, are presented in Table 2.

TABLE 2.—VELOCITY TRAVERSES INDICATING INCIPIENT SEPARATION

Run	$\mathbf{R}_o$[a]	Comments	H	n
(a) 7.5°; $\frac{L}{D_o} = 10.4$; $\frac{D}{D_o} = 1.68$; $A_R = 2.83$				
M 93	0.8	Unsym.[b]	2.43	0.81
M 70	0.85	Separated	....	....
D 73	1.2	Normal	2.29	0.66
M 90	1.2	Unsym.[b]	2.09	0.59
M 71	1.5	Separated[c]	2.34	0.76
P 1	1.5	Separated	....	....
P 2	1.5	Normal	2.30	0.77
P 5	1.5	Normal	....	....
D 74	1.95	Normal	2.24	0.71
P 3	2.0	Normal	2.35	0.78
P 6	2.0	Normal	....	....
M 91	2.05	Normal	2.42	0.85
(b) 10°; $\frac{L}{D_o} = 6.4$; $\frac{D}{D_o} = 1.68$; $A_R = 2.83$				
E 39	0.5	Normal	2.34	0.70
E 40	0.5	Separated[d]	2.52	0.76
E 41	0.85	Separated[c]	2.57	0.85

[a] Multiply by 10^5. [b] Slightly unsymmetrical. [c] Just separated. [d] Almost separated.

At these two stations, the occurrence of separation was noted in only a fraction of the tests, with the probability seemingly greater at the lower Reynolds numbers. Values of the form parameters H and n are listed in Table 2 for those cases where they could be evaluated. Separation seems to occur for values of H of about 2.4 and for n about 0.8. As noted in the discussion of pressure efficiency, separation can occur for values of $\frac{L}{D_o}\beta$ greater than 60.

Energy Relations in Central Core.—The existence of a flat central core in diffuser flow has been shown in all plots of diffuser velocity distributions. In this region, outside of the wall boundary layer, the transverse velocity gradient is zero, and there are no shear stresses. It follows that there is no energy loss in this region, and that the sum of the static pressure and core-velocity pressure must be a constant. Table 3 gives the static and velocity-pressure coefficients and their sum for the 7.5° diffuser tests. Within experimental accuracy the specific energy of the core is constant, a fact which is of value in relating the velocity distributions to the pressure coefficients in diffuser flow.

Diffuser Energy Efficiency.—The pressure efficiency η_p used in this paper is the ratio of the diffuser-pressure rise to the ideal value for a frictionless diffuser. This efficiency is a simple measure of the effectiveness of the diffuser, as the ideal pressure coefficient is determined solely by the diffuser area-ratio. However, this does not take into account the changes in the kinetic energy of the flow and hence is not a true efficiency. The efficiency of a diffuser as a circuit element is the ratio of the discharge energy flux to the input energy flux, or the

TABLE 3.—ENERGY RELATION IN THE CORE OF A 7.5° DIFFUSER ($R_o = 1.2 \times 10^6$)

$\frac{D}{D_o}$	(a) PIPE-ENTRANCE LENGTH, 3.5				(b) PIPE-ENTRANCE LENGTH, 6.4				(c) PIPE-ENTRANCE LENGTH, 10.4			
	Pressure coefficient (1)	$\left(\frac{u_1}{U_o}\right)^2$ (2)	Bernoulli constant (3)	Difference[a] (4)	Pressure coefficient (1)	$\left(\frac{u_1}{U_o}\right)^2$ (2)	Bernoulli constant (3)	Difference[a] (4)	Pressure coefficient (1)	$\left(\frac{u_1}{U_o}\right)^2$ (2)	Bernoulli constant (3)	Difference[a] (4)
1.000	0	1.049	1.049	....	0	1.090	1.090	....	0	1.135	1.135	....
1.061	0.179	0.845	1.024	−0.025	0.179	0.898	1.077	−0.013	0.178	0.952	1.130	−0.005
1.362	0.642	0.392	1.034	−0.015	0.615	0.461	1.076	−0.014	0.605	0.528	1.133	−0.002
1.684	0.792	0.250	1.042	−0.007	0.759	0.326	1.085	−0.005	0.749	0.407	1.156	+0.021

[a] Difference from initial value (Col. 3 for $D/D_o = 1.000$).

entering energy minus the energy losses divided by the entering energy:

$$\eta_e = \frac{\alpha_o \frac{\rho\, U_o^2}{2} - \text{losses}}{\alpha_o \frac{\rho\, U_o^2}{2}} \dots\dots\dots\dots\dots\dots (7)$$

The pressure p is not included in the expression for the entering energy because in itself it does not represent a capacity to do work (29). Therefore, the only entering energy is the kinetic energy. Determining the losses from the Bernoulli theorem, the efficiency is

$$\eta_e = \frac{p - p_o + \alpha \frac{\rho\, U^2}{2}}{\alpha_o \frac{\rho\, U_o^2}{2}} = \frac{C_p}{\alpha_o} + \frac{\alpha}{\alpha_o}\left(\frac{D_o}{D}\right)^4 \dots\dots\dots\dots (8a)$$

in which the subscript o refers to the entrance conditions. The energy efficiency is related to the pressure efficiency by the formula,

$$\eta_e = \frac{\eta_p}{\alpha_o} + \frac{\alpha - \eta_p}{\alpha_o}\left(\frac{D_o}{D}\right)^4 \dots\dots\dots\dots\dots\dots (8b)$$

From Eq. 8b it may be seen that for a large area-ratio diffuser, the energy efficiency becomes less than the pressure efficiency. For small area-ratios, η_e is greater than η_p and close to unity.

Values of the energy efficiency have been computed from the diffuser measurements using Eq. 8b. The variation in η_e with the Reynolds number was found to be less than the variation in η_p because of the slight decrease in α with an increase in Reynolds number. For an average test Reynolds number the energy efficiencies, at an area-ratio of about 3, are listed in Table 4 together with the corresponding values of the pressure efficiency. The energy efficiency is seen to be a more constant factor than the pressure efficiency. A reasonable value for a diffuser efficiency at an area-ratio of three, without separation, is 0.95.

The energy efficiency is higher than the pressure efficiency. Neither of these terms, as measured, completely accounts for the action of the diffuser as a circuit element. These efficiencies are for stations at the end of a diffuser, but the diffuser has an effect on the flow in the following section. Determination of the true diffuser efficiency must include an analysis of the energy changes introduced into the following sections by the diffuser. Thus, if the diffusers in Table 4 were followed by straight pipe, there would be some additional pressure increase and energy loss resulting from the redistribution in the velocities. The resulting pressure efficiency would be higher, whereas the final energy efficiency would be lower.

TABLE 4.—DIFFUSER EFFICIENCIES AT $R_o = 1.2 \times 10^6$ ($A_R = 3$)

L/D_o	η_p	η_e
$\beta = 5°$:		
3.3	0.93	0.965
6.2	0.91	0.955
10.1	0.875	0.915
$\beta = 7.5°$:		
3.5	0.90	0.95
6.4	0.865	0.94
10.4	0.85	0.95
$\beta = 10°$:		
3.6	0.88	0.945
6.4	0.835	0.94

A common parameter introduced by Mr. Peters (11), and used by other authors, is the diffuser energy conversion efficiency. This is the ratio of the increase in potential energy to the decrease in kinetic energy. This efficiency was not used in analyzing the present data because it is not suitable as a circuit parameter. For a large area-ratio diffuser, the energy conversion efficiency is only slightly less than the energy efficiency. However, for small area-ratios, this efficiency becomes indeterminate.

SUMMARY

The analysis of the diffuser test data obtained in the experimental water tunnel has revealed eight general properties for the flow in the entrance region of a conical diffuser:

1. The effect of the Reynolds number on the flow is small, there being a slight increase in the pressure efficiency and a slight decrease in the extent of the boundary layer with increase in the entrance pipe Reynolds number. There is even less variation in the energy efficiency.

2. The area-ratio of the diffuser is the major geometric parameter governing the shape and extent of the boundary layer.

3. The extent of the boundary layer at the entrance to the diffuser, given indirectly by L/D_o, is as important a factor in determining the diffuser flow as is the diffuser angle β. Within certain limits, the pressure efficiency and the velocity profile are functions of the product of L/D_o times β.

4. The Bernoulli energy (total head) is constant in the uniform central core.

5. Although it decreases with an increase in area-ratio, the energy efficiency is practically independent of angle and entrance conditions, having a value of 0.95 at an area-ratio of three.

6. The boundary-layer displacement thickness is a unique function of $A_R (L/D_o)^{0.2}$, the relation also being applicable in a straight pipe. The momentum thickness is a function of the same parameter and of the angle β.

7. Separation occurs for values of H greater than 2.4 and n greater than 0.8. Neither of these form parameters can be correlated too well with geometric parameters near separation. If the product $\frac{L}{D_e}\beta$ is less than 60, separation should not occur for area-ratios up to about 4.

8. The diffuser efficiency is practically constant as long as separation does not occur; therefore, the only factor affecting the choice of diffuser geometry is the desired factor of safety with regard to separation.

The results presented in this paper should enable the design of diffusers for the conditions encountered in water and air tunnel practice and in other large structures in which the type of entrance conditions studied occur.

The manner in which this information would be applied to the design of a diffuser is illustrated in Appendix III where the design analysis is given of the diffuser for the large high-speed water tunnel (30) built at The Pennsylvania State College for underwater ordnance research.

ACKNOWLEDGMENT

The tests and analyses herein described were conducted as part of the design research for the water tunnel built at The Pennsylvania State College by the United States Navy for the use of the Ordnance Research Laboratory (Contract No. NOrd 7958). The project received the active support of H. P. Hammond, M. ASCE, dean of the School of Engineering; Eric A. Walker, director of the Ordnance Research Laboratory; and R. B. Power, project engineer in charge of the engineering and construction of the 48-in. water tunnel. The writers wish to acknowledge the assistance of the personnel of the Ordnance Research Laboratory and of the Hydraulics Laboratory of the Civil Engineering Department, and specifically: A. J. Turchetti, Alfred M. Feiler, A. M. ASCE, P. M. Kendig, W. M. Wachter, A. M. ASCE., Mrs. Irene Sebring, Mrs. Rosemary Schaver, H. W. Bennett, F. E. Shuster, and D. H. Ruhl.

APPENDIX I. LIST OF REFERENCES

(1) "Water Tunnel Diffuser Flow Studies, Part I—Review of Literature," *Report No. NOrd 7958–139*, Ordnance Research Lab., The Pennsylvania State College, State College, Pa., May 16, 1949.

(2) "On the Flow of Water Through Pipes Having Converging or Diverging Boundaries," by A. H. Gibson, *Proceedings*, Royal Soc. of London, Series A, Vol. 83, 1910, p. 366.

(3) "Conversion of Kinetic to Potential Energy in the Flow of Water Through Passages Having Divergent Boundaries," by A. H. Gibson, *Engineering*, Vol. 93, 1912, p. 205.

(4) "Versuche über die Unsetzung von Wassergeschwindigkeit in Druck," by K. Andres, *Forschungsarbeiten des Vereines Deutscher Ingenieure*, Heft 76, 1909.

(5) "Versuche über die Stromungsvorgange in Erweiterten und Verengten Kanalen," by H. Hochschild, *ibid.*, Heft 114, 1912.

(6) "Versuche über Stromungen in Stark Erweiterten Kanalen," by R. Kroner, *ibid.*, Heft 222,1920.

(7) "Divergente und Konvergente Turbulente Strömung mit Kleinen Offnungswinkeln," by F. Donch, *ibid.*, Heft 282, 1926.

(8) "Untersuchungen über die Strömung des Wassers in Konvergenten und Divergenten Kanalen," by J. Nikuradse, *ibid.*, Heft 289, 1929.

(9) "An Experimental Investigation of the Flow of Air in a Flat Broadening Channel," by A. M. Vedernikoff, *Report No. 21*, Central Aero-Hydrodynamical Inst., Moscow, U.S.S.R., 1928 (also *Zeitschrift für Agnewandte Mathematik und Mechanik*, 1927, translated in *Technical Memorandum No. 1059*, National Advisory Committee for Aeronautics, 1944).

(10) "Flow in Conical Draft Tubes of Varying Angles," by George E. Lyon, *Mechanical Engineering*, Vol. 44, 1922, pp. 177–180.

(11) "Conversion of Energy in Cross-sectional Divergences under Different Conditions of Inflow," by H. Peters, *Ingenieur-Archiv*, Vol. II, 1931 (translated in *Technical Memorandum No. 737*, National Advisory Committee for Aeronautics, 1934).

(12) "Turbulent Flow in Diffusers of Small Divergence Angle," by G. A Gourzhienko, *Report No. 462*, Central Aero-Hydrodynamical Inst., Moscow, U.S.S.R., 1939 (translated in *Technical Memorandum No. 1137*, National Advisory Committee for Aeronautics, 1947).

(13) "Conversion of Kinetic to Potential Energy in Flow Expansions," by A. A. Kalinske, *Transactions*, ASCE, Vol. 111, 1946, pp. 355–390.

(14) "A Method of Calculation of the Turbulent Boundary Layer with Accelerated and Retarded Basic Flow," by A. Buri, Thesis 652, Eidgenossiche Technische Hochschule, Institut fur Aerodynamic, Zurich, Switzerland, 1931 (translated in *RTP Translation No. 2073*, British Ministry of Aircraft Production).

(15) "Die Turbulente Reibungschicht in Ebener Strömung bei Druckabfall und Druckanstieg," by E. Gruschwitz, *Ingenieur-Archiv*, Vol. 2, 1931, pp. 321-346.

(16) "The Process of Separation in the Turbulent Friction Layer," by E. Gruschwitz, *Zeitschrift fur Flugtechnick und Motorluftschiffart*, Vol. 23, No. 11, June, 1932 (translated in *Technical Memorandum No. 699*, National Advisory Committee for Aeronautics, 1933).

(17) "Investigations on Convergent and Divergent Turbulent Boundary Layers," by A. Kehl, *Ingenieur-Archiv*, Vol. 13, 1943, pp. 293, 329 (translated in *RTP Translation No. 2035*, British Ministry of Aircraft Production).

(18) "Calculation of Diffuser Efficiency for Two-Dimensional Flow." by R. C. Binder, *Journal of Applied Mechanics*, A.S.M.E., Vol. 69, 1947, p. A-213.

(19) "Determination of General Relations for the Behavior of Turbulent Boundary Layers," by A. E. von Doenhoff and N. Tetervin, *Report No. 772*, National Advisory Committee for Aeronautics, 1943.

(20) *Wartime Report ACR No. 3G13*, National Advisory Committee for Aeronautics, July, 1943.

(21) *Wartime Report L382*, National Advisory Committee for Aeronautics, July, 1943.

(22) "The Development of Turbulent Boundary Layers," by H. C. Garner, *Reports and Memoranda No. 2133*, British Aeronautical Research Committee, 1944.

(23) "Turbulent Boundary Layer of an Airfoil," by K. Fediaevsky, *Report No. 282*, Central Aero-Hydrodynamical Inst., Moscow, U.S.S.R., 1936 (translated in *Technical Memorandum No. 822*, National Advisory Committee for Aeronautics, 1937).

(24) "Turbulent Boundary Layer of an Airfoil," by K. Fediaevsky, *Journal of the Aeronautical Sciences*, Vol. 4, 1937, pp. 491-498.

(25) "Shear Stress in a Turbulent Boundary Layer," by Donald Ross and J. M. Robertson, *Journal of Applied Physics*, June, 1950, pp. 557-561.

(26) "The Experimental Water Tunnel at The Pennsylvania State College," *Report No. NOrd 7958–89*, Ordnance Research Lab., The Pennsylvania State College, State College, Pa., July 8, 1949.

(27) "Water Tunnel Working Section Flow Studies," *Report No. NOrd 7958–97*, Ordnance Research Lab., The Pennsylvania State College, State College, Pa., June 15, 1948.

(28) "Water Tunnel Diffuser Flow Studies, Part II—Experimental Research," *Report No. NOrd 7958–143*, Ordnance Research Lab., The Pennsylvania State College, State College, Pa., July 8, 1949.

(29) "Elementary Mechanics of Fluids," by Hunter Rouse, John Wiley & Sons, Inc., New York, N. Y., 1946, p. 114.

(30) "Hydrodynamic Design of the 48-Inch Water Tunnel at the Pennsylvania State College," by Donald Ross, J. M. Robertson, and R. B. Power, *Transactions*, Soc. of Naval Archts. and Marine Engrs., Vol. 56, 1948, pp. 5–29. (*a*) p. 18.

(31) "Model Experiments for the Design of a Sixty-Inch Water Tunnel, Part IV—Diffuser Studies," by J. S. Holdhusen, *Project Report No. 13*, St. Anthony Falls Hydraulic Lab., Univ. of Minnesota, Minneapolis, Minn., September, 1948.

(32) "Model Studies for the Design of an Open- or Closed-Jet Water Tunnel," by J. S. Holdhusen, *Project Report No. 22*, St. Anthony Falls Hydraulic Lab., Univ. of Minnesota, Minneapolis, Minn., June, 1950.

(33) "Design Studies for a Closed-Jet Water Tunnel," by J. F. Ripken, *Technical Paper No. 9, Series B*, St. Anthony Falls Hydraulic Lab., Univ. of Minnesota, Minneapolis, Minn., August, 1951.

(34) "Model Studies of a Water Tunnel with an Air-Bubble Resorber," by R. M. Olson, *Project Report No. 29*, St. Anthony Falls Hydraulic Lab., Univ. of Minnesota, Minneapolis, Minn., February, 1952.

APPENDIX II. LIST OF SYMBOLS

The following letter symbols, adopted for use in this paper and its discussion, conform essentially with American Standard Letter Symbols for Hydraulics

(ASA–Z10.2–1942), prepared by a committee of the American Standards Association, with ASCE participation and approved by the Association in 1942:

A = area;
A_R = area-ratio;
C = coefficient;
C_p = a pressure coefficient defined by Eq. 3;
D = diameter; section diameter;
D_e = diameter of the pipe at the entrance to the diffuser;
H = boundary-layer form parameter; ratio of displacement thickness to momentum thickness;
L = length; effective length of pipe entrance;
n = exponent of velocity distribution power law;
p = pressure per unit area; static pressure intensity (for nonhorizontal conduits p should be replaced by $p + \gamma h$):
Δp = pressure difference measured from the start of the diffuser;
Δp_i = ideal pressure difference between the geometric start of the diffuser and the pressure at a given point in question;
R = Reynolds number;
R_e = pipe Reynolds number at entrance of the diffuser (Eq. 1);
U = average velocity, ratio of discharge to area;
U_e = average value of U in the pipe at the entrance to the diffuser;
u = temporal mean velocity at a point in the direction of the tunnel axis;
u_1 = velocity u outside the boundary layer;
x = distance in the direction of flow;
y = transverse distance measured from the surface;
z = elevation above arbitrary datum;
α = kinetic energy coefficient; ratio of the true kinetic energy to that based on the average velocity;
α_e = kinetic energy coefficient at the entrance to the diffuser;
β = total angle of the diffuser;
γ = specific weight of fluid;
δ = boundary-layer disturbance thickness;
δ^* = boundary-layer displacement thickness, Eq. 2a;
η = efficiency:
η_e = energy efficiency;
η_p = pressure efficiency; ratio of the diffuser-pressure rise to the ideal value for a frictionless diffuser;
θ = boundary-layer momentum thickness, Eq. 2b;
ν = kinematic viscosity of the fluid; and
ρ = fluid density.

APPENDIX III. WATER TUNNEL DIFFUSER DESIGN

The manner in which the information obtained in this study would be applied to the design of a large structure is illustrated in the design of the diffuser of the 48-in. high-speed water tunnel for which these tests were run.

The water tunnel is shown in Fig. 13, from which it can be seen that the structure is of considerable size, being nearly 100 ft long. The principal diffuser in the circuit is that which extends from the 4-ft-diameter working or test section (in middle of upper leg) to the turn immediately preceding the propeller pump (in the right-hand part of the lower leg) (30). It is divided into two parts by the first miter turn. The analysis of the experimental studies of

FIG. 13.—CONSTRUCTION VIEW OF THE GARFIELD THOMAS WATER TUNNEL

diffuser flow presented in this paper indicates three methods of determining the diffuser angle from knowledge of the area-ratio and the entrance conditions. In each case, the analysis is based on the avoidance of separation in the diffuser.

The area-ratio of this diffuser was fixed at $A_R = 4.2$ by the working section diameter of 4 ft and the diameter at the second turn of 8 ft 2 in. The equivalent or pipe-entrance length was computed by adding to the 3.5 diameters (14 ft) of the actual working section 2 diameters for the equivalent lengths added by the nozzle and transition sections. Adding an additional diameter, to allow for possible effects of models, gave a total effective working section length of 6.5 diameters.

The three methods of diffuser design were based on the exponent n, the form parameter H, and the analysis of the pressure efficiency. The critical value of the power-law exponent n for the occurrence of separation was found to be approximately 0.8. Taking 0.75 as the maximum design value of n, Fig. 12 shows that at an area-ratio of $A_R = 4.2$ and a ratio L/D_o close to 6.5 the angle should be slightly less than 7.5°. The value of H for separation was found to be 2.4, and 2.3 was taken as a design value. Extrapolating the curves in Fig. 12, and interpolating between 5° and 7.5° angles for $A_R\ (L/D_o)^{0.2} = 6.1$,

yields an angle of about 6°. The third way of obtaining the design angle makes use of the fact that separation occurs for values of $\frac{L}{D_o} \beta$ greater than 60, as noted in the discussion of pressure efficiency. Taking the value of 50 as a safe value, the diffuser angle for L/D_o of 6.5 was 7.7°.

The three methods all yield values of the diffuser angle approximating 7°. Each of these analyses included a small margin of safety to account for various possible disturbing factors, such as the effect of the first turn between the two parts of this diffuser. As the H-analysis was inaccurate, less weight was placed on it, and an angle of 7° was chosen for the water tunnel design.

Besides yielding a design for the water tunnel diffuser, the analysis enables a prediction of the flow conditions in the diffuser. The two points of interest are the stations immediately preceding the first and second turns. For these stations the boundary-layer thicknesses and velocity-form parameters, as well as the pressure and energy efficiencies, were computed. The displacement and momentum thicknesses are obtained from Fig. 9(b) and Fig. 10. The power-law exponent n can be estimated from Fig. 12 to be 0.60 and 0.68 at the two locations. The pressure efficiency is given by Fig. 6 with a Reynolds number correction based on Fig. 4. The kinetic energy coefficient α is computed from Eq. 6, yielding values of 1.65 and 1.85. The energy efficiency from Eq. 8b is 0.95 with a pressure efficiency of 0.905 at a Reynolds number of 12×10^6 (U_o = 30 ft per sec). The computations show that at both stations the boundary layer is not fully developed, there is little danger of separation (although at the second station the H-prediction does not agree on this), the pressure and energy efficiencies are constant, and only 5% of the entering kinetic energy is lost. Although the power law is known to be inexact, it was used to predict the approximate velocity distributions at the two stations. These are shown in Fig. 14. Obviously it is expected that the sharp breaks at the outer edge of the boundary layer will be rounded.

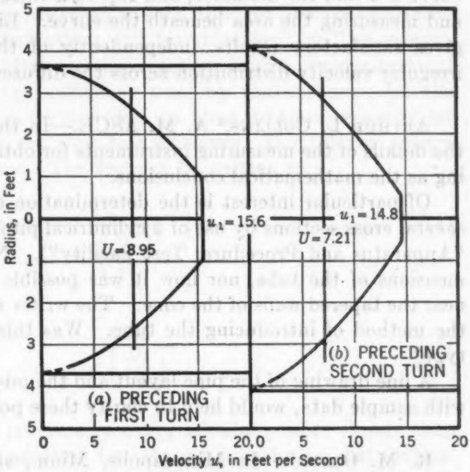

Fig. 14.—Predicted Water Tunnel Diffuser Velocity Profiles, for a Test Section Velocity of 30 Ft per Sec

DISCUSSION

STEPONAS KOLUPAILA[4].—For the computation of the kinetic energy coefficient, the authors have developed a complicated formula (Eq. 6), based on the power law of velocity distribution, Eq. 5. Since the power-law velocity distribution admittedly does not fit measured velocity distributions too well, the writer suggests a direct procedure based on the integration of

$$\int^{A} u^3\, dA = 2\,\pi \int_0^r u^3\, x\, dx \qquad (9)$$

or

$$\int^{A} u^3\, dA = \pi \int_0^{r^2} u^3\, d(x^2) \qquad (10)$$

Eq. 9 is integrated by the planimetering of the area enclosed between the curve $u^3\,x$ and the diameter; and Eq. 10 is integrated by plotting u^3 against x^2 and measuring the area beneath the curve. Either integration is simple and gives satisfactory results, independently of the assumed law, even for an irregular velocity distribution across the diffuser.

ARTHUR L. COLLINS,[5] A. M. ASCE.—In the presentation of this subject the details of the measuring instruments for obtaining the data are as interesting as the mathematical conclusions.

Of particular interest is the determination of the velocity distribution at several cross sections by use of a cylindrical pitot tube (see under the heading, "Apparatus and Procedure: Test Facility"). No mention is made of the dimensions of the tube, nor how it was possible to take satisfactory readings near the tapered walls of the cone. The writer would also appreciate knowing the method of introducing the tube. Was this tube of the stub or through type?

A line drawing of the pipe layout and the pitot tube dimensions, submitted with sample data, would help to clarify these points.

R. M. OLSON[6].—In Minneapolis, Minn., studies of diffuser design and performance have been made at the St. Anthony Falls Hydraulic Laboratory. Fig. 2 indicates that the length of the transition between the straight pipe and the diffuser was about one pipe diameter for the 7.5° diffuser. The transition length for the other two divergence angles is not stated. Radial pressure gradients as well as longitudinal wall-pressure gradients in the transition region are both quite sensitive to changes in the length of this transition. The writer used a parabolic curve; but the difference between this curve and

[4] Prof., College of Eng., Univ. of Notre Dame, Notre Dame, Ind.

[5] Cons. Engr., Berkeley, Calif.

[6] Research Associate, St. Anthony Falls Hydr. Lab., Univ. of Minnesota, Minneapolis, Minn.

others is usually less than allowable machining tolerances. The effect of these variations on diffuser efficiency has not been studied systematically. The studies have been concerned primarily with the flow quality upstream from the diffuser, and, secondarily, with the diffuser performance. (Reports of these studies (31) (32) (33) (34) are available on interlibrary loan at the University of Minnesota Library, Minneapolis 14, Minn.)

The velocity profiles shown in Figs. 2, 7, and 8 are representative of diffusers with no obstructions in the entrance. This condition would exist for a venturi tube or for a bare water tunnel. However, experimental studies in water tunnels usually require the insertion of a test body and supports. The velocity profiles in the diffuser were quite dependent on the presence and location of even very small obstructions a short distance upstream from the diffuser. As an example, a faired probe, occupying less than 0.2% of the cross-sectional area of a 6-in. diameter test section, affected the flow in such a way as to change the core velocity at the end of the diffuser from 1.6 times the mean to less than the mean velocity when the probe was moved from the center to a point halfway to the wall. In each instance, the profiles were different from that for a bare diffuser entrance. No measurements of diffuser efficiency were made during any of these tests.

It is unfortunate that diffusers are rated on such different bases of efficiency. Hydraulic literature contains derivations and formulas for: (*a*) The energy-conversion efficiency, based on ideal pressure recovery from a one-dimensional analysis (this is the pressure (η_p) efficiency used by the authors); (*b*) the actual energy-conversion efficiency (η), based on ideal pressure recovery for the actual flow conditions; (*c*) the form-loss efficiency; and (*d*) the energy efficiency, as used by the authors. The first can be written as

$$\eta_p = \frac{C_p}{1 - \left(\frac{D_o}{D}\right)^4} \qquad (11)$$

and the second as

$$\eta = \frac{C_p}{\alpha_o - \alpha\left(\frac{D_o}{D}\right)^4} \qquad (12)$$

Eq. 12 seems to represent the pressure recovery efficiency more closely than Eq. 11 because it takes into account the change in velocity distribution. It would be of interest to know why the authors consider the second definition "* * * not suitable as a circuit parameter" (see the paragraph preceding "Summary").

At the St. Anthony Falls Hydraulic Laboratory, the measured efficiencies have consistently been about 3% less than those indicated in Fig. 6 and Table 4. This may be illustrated by citing tests conducted at R_o equal to 1×10^6 to 2.4×10^6, with a diffuser that had an area ratio of approximately 4, and angle of 6°40′, and a galvanized surface throughout most of its length. The acual entrance lengths were increased by one half an entrance diameter for the effect of the nozzle upstream, and by one half the length of the parabolic

transition to obtain the effective length. The measured pressure coefficients were also corrected to refer to the geometric beginning of the diffuser. Typical results are as follows:

β L/D.	Measured pressure efficiency	Pressure efficiency from Fig. 6
7.7	0.91	0.94
19.8	0.89	0.925

Similar differences exist between the measured energy efficiencies and those indicated in Table 4. It is indicated in Fig. 3 that the differences in area ratio should not account for the differences in efficiency. Perhaps they are caused by a difference in diffuser wall roughness.

J. M. Robertson,[7] M. ASCE, and Donald Ross.[8]—A specific study made for a certain design need was the basis for this paper on diffuser flow. From this study was extracted information of a basic nature which could be applied to similar problems; hence, the paper involved a compromise between the engineering and scientific approaches and is an attempt to condense a fifty-page report (28). The comments of the discussers are appreciated, as they indicate regions in which this condensation was excessive, in addition to supplementing the paper.

The pitot tube, about which Mr. Collins inquires, was a ⅛-in. monel tube (0.028-in. wall) spanning the section, with an impact hole pointing upstream, and with the static pressure obtained from wall piezometers in the same plane as the front of the tube. With a small correction for the effect of the tube on the pressures at the wall piezometers, such a transverse pitot tube was found to give integrated discharges in excellent agreement with other flow measurements. Detailed checks with hypodermic-type pitot tubes showed the resultant velocity data to be satisfactory for the type of analysis presented in the paper, although not precise enough for a detailed study of the velocity profiles near the walls. Fig. 7(*a*) shows the scatter in the data. It is not felt that any other presentation of sample data would be of value. Fig. 15 is a line drawing of one of the test setups, which indicates the locations of the piezometer and pitot-tube stations. Details of the experimental techniques including all measuring instruments were presented in another report (26).

The writers agree with Mr. Kolupaila as to the desirability of obtaining the kinetic-energy coefficient by direct integration rather than by substitution into a formula of doubtful validity. Since a precise value of this factor was not necessary and Eq. 6 was quickly determined, engineering expediency prevailed over scientific thoroughness. The writers would like to point out, however, that the greatest error from use of the power profiles occurs near the walls. The profiles were nonetheless neither accurate nor symmetrical enough to warrant detailed integration.

Mr. Olson's discussion is welcome because it is based on a similar research study. The writers have studied the water tunnel investigations at the Univers-

[7] Prof. of Eng. Research, Ordnance Research Lab., The Pennsylvania State College, State College, Pa.

[8] Associate Prof. of Eng. Research, Ordnance Research Lab., The Pennsylvania State College, State College, Pa.

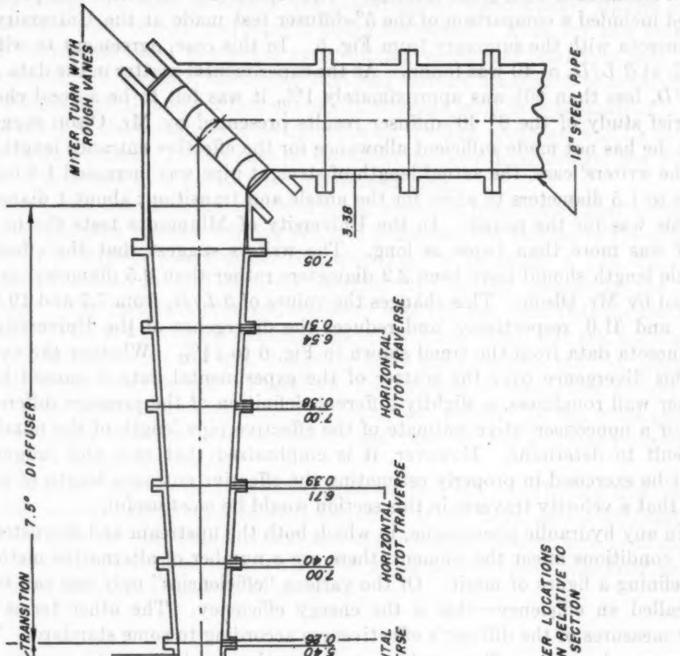

FIG. 15.—INSTRUMENTATION FOR A TEST SERIES

ity of Minnesota with great interest. The report (28) on which this paper is based included a comparison of the 5°-diffuser test made at the University of Minnesota with the summary from Fig. 6. In this case, agreement to within 0.8% at $\beta\ L/D_o$ of 40 was found. As the experimental scatter in the data (for $\beta\ L/D_o$ less than 60) was approximately 1%, it was felt to be a good check. A brief study of the 6° 40′ diffuser results presented by Mr. Olson suggests that he has not made sufficient allowance for the effective entrance length, L. In the writers' case, the actual length of straight pipe was increased 1.3 diameters to 1.5 diameters to allow for the nozzle and transition; about 1 diameter of this was for the nozzle. In the University of Minnesota tests the nozzle used was more than twice as long. The writers suggest that the effective nozzle length should have been 2.2 diameters rather than 0.5 diameter, as assumed by Mr. Olson. This changes the values of $\beta\ L/D_o$ from 7.7 and 19.8 to 19.4 and 31.0, respectively, and reduces the divergence of the University of Minnesota data from the trend shown in Fig. 6 to $1\frac{1}{2}$%. Whether the excess of this divergence over the scatter of the experimental data is caused by a higher wall roughness, a slightly different definition of the pressure difference Δp, or a nonconservative estimate of the effective pipe length of the nozzle is difficult to determine. However, it is emphasized that care and judgment must be exercised in properly estimating the effective entrance length of pipe, and that a velocity traverse in this section would be most useful.

In any hydraulic phenomena, in which both the upstream and downstream flow conditions affect the element, there are a number of alternative methods of defining a figure of merit. Of the various "efficiencies" only one can truly be called an efficiency—this is the energy efficiency. The other terms are only measures of the diffuser's effectiveness according to some standard. The writers used pressure efficiency because it was the simplest possible measure of diffuser effectiveness, in so far as this efficiency refers the regained pressure to a quantity uniquely determined by the diffuser geometry. It was for this reason that the variation in this factor was correlated with other geometric terms. The suitability of any such factor as a circuit parameter is based on the needs in circuit analysis. Given the initial conditions—pressure, velocity distribution, and total energy at the start of the element, it is desired to compute the terminal conditions. The pressure efficiency, which is a function of the entrance conditions, determines the pressure at the discharge end, whereas the energy efficiency determines the losses. The discharge-velocity distribution is described by the factor α, or by the boundary-layer thickness and velocity-profile shape parameter. The only factor of importance to circuit analysis not covered in the paper is the energy change occurring downstream from the diffuser, where in straight pipe the velocity profile eventually returns to that of normal pipe flow.

The writers' objections to the conversion efficiency (Eq. 12) were based on its lack of suitability when applied to elements other than diffusers. The true energy efficiency seemed more appropriate because it is as meaningful for a straight pipe or a pipe bend as it is for a diffuser.

The writers agree with Mr. Olson concerning the importance of having the diffuser preceded by an adequate transition. For the results reported in the paper the transition was about 1 diameter long and the contour was a modified

cubic (30a). In other phases of the experimental water-tunnel studies other transitions were tested, including a sharp transition. Even for this extreme case, no serious effect was noted on a diffuser which was relatively safe from separation. It appears, therefore, that any curved transition is satisfactory for diffuser flow if it is gradual enough to prevent local flow separation. The chief effect of the transition is its influence on the flow upstream and its cavitation potentialities. In the case of the 48-in. water-tunnel design, the 7° diffuser is preceded by a transition 1.5 diameter long.

Mr. Olson discusses the effects of a test model or other small obstruction in the straight pipe (test or working section) preceding the diffuser in the diffuser flow. The writers also studied this question, by inserting a 1-in.-diameter simulated model in a 3-diameter straight-pipe section preceding the 7.5° diffuser. The resultant pressure efficiency was 1% less than that for the bare tunnel. Velocity traverses indicated an appreciable effect, but the body wake did not interact with the wall boundary layer until an area ratio of approximately three was reached. Therefore, the chances of separation should not have been appreciably altered. The maximum velocity in the cross section was naturally increased and the center-line velocity was decreased over that obtained without the model.

The paper reports on research completed in 1948. Following this, many papers have appeared on turbulent boundary-layer flows, and additional detailed studies of both an analytical and experimental nature have been made. The interim conclusions reported in the paper are of value primarily to designers of diffusers similar to those tested.

AMERICAN SOCIETY OF CIVIL ENGINEERS

Founded November 5, 1852

TRANSACTIONS

Paper No. 2571

UNCONFINED GROUND-WATER FLOW TO MULTIPLE WELLS

By Vaughn E. Hansen,[1] J. M. ASCE

With Discussion by Messrs. Ahmed Shukry; Carl Rohwer; David K. Todd and Lloyd C. Fowler; and Vaughn E. Hansen

Synopsis

The purpose of this paper is to clarify the nature of unconfined flow to single and multiple wells, and to present a method of solving problems associated with this type of flow. The effect of the capillary fringe on the location of the free surface and the form of the flow patterns, the zone of validity of the Dupuit equation, the shape of the free surface near the well, and the variation in the stream surface spacing are all discussed. A functional relationship independent of the radius of influence is established, relating the variables at the well; this relationship applies to both single and multiple wells. A fundamental dimensionless parameter consisting of a ratio of the Froude number to the Reynolds number is formulated that characterizes the shape of the cone of depression around a well. The concepts of well efficiency and effectiveness are clarified and guides are presented for their correct use.

Introduction

Notation.—The letter symbols introduced in this paper are defined where they first appear and are assembled alphabetically in the Appendix for convenience of reference.

The need for a clearer understanding of the flow to unconfined wells and for better methods of solving the problems arising from this flow has arisen as a result of extensive pumping of ground water and the demand for a more economical use of the water. The investigation reported in this paper was undertaken in an effort to contribute further knowledge to both the nature of the flow and the method of solution.

Flow into wells can be divided into two broad classifications, depending on the boundary conditions. The first classification is confined flow, in which

Note.—Published in August, 1952, as *Proceedings-Separate No. 142.* Positions and titles given are those in effect when the paper or discussion was received for publication.

[1] Irrig. Engr. Irrig. Div., SCS; and Asst. Prof. of Research, Utah State Agri. College, Logan, Utah.

the water is restricted under pressure between two rather impermeable layers. The second classification is unconfined flow, the upper surface of which is at atmospheric pressure.

Since confined flow occurs between fixed boundaries, it is susceptible to rather complete analysis based on relatively few approximations and assumptions, with the result that the theoretical solutions conform very closely to the observed conditions. Consequently, considerable knowledge is available regarding the theory and practical aspects of such flow.

Unconfined flow is much more involved, however, because of the existence of an unbounded water surface. Since the shape of the surface is not known, an approximate analysis based on extensive assumptions must be made, thus imposing rather severe limitations on the resulting solution. The general acceptance of the solution, without understanding the inherent limitations, has produced a certain degree of complacency among many practical ground-water engineers, as well as a tendency to disregard any observations at variance with the expected solution. It is important, also, that the theoretician clearly appraise the limitations imposed by nature on the too extensive application of equations of ground-water flow; nature rarely provides the idealized case assumed in most theoretical developments. However, the simplified situation must remain the basis of study, with the knowledge that it does not occur, and the results must be modified accordingly.

In this study, the usual assumptions of steady flow through a homogeneous porous medium have been made. For the confined flow, the bounding surfaces are assumed to be parallel, horizontal, impermeable layers; for the unconfined flow, the wells are assumed to penetrate completely the homogeneous medium overlying an impermeable, horizontal bed.

General Flow Analysis

A general analysis of flow through porous media has been extensively covered by several writers.[2,3] The essentials of these analyses, as applied to the case of steady flow into wells, will be summarized in order to interpret the significance of the experimental results.

Darcy's law is

$$v = K \frac{dh}{ds} \qquad (1)$$

in which v is velocity, K is the coefficient of permeability, h is the piezometric head, and s is the length along a stream line. When Eq. 1 is combined with partial differential equation of continuity $\nabla v = 0$ for confined flow, the Laplace equation ($\nabla^2 h = 0$) is obtained. When the boundary conditions for confined radial flow are applied and the differential equation is integrated, the following equation for the shape of the piezometric surface of a single artesian well is obtained:

$$h - h_1 = \frac{Q}{2 \pi K t} \log_e \frac{r}{r_1} \qquad (2)$$

[2] "Flow of Ground Water," by C. E. Jacob, "Engineering Hydraulics," John Wiley & Sons, Inc., New York, N. Y., 1950, Chapter 5.

[3] "The Flow of Homogeneous Fluids Through Porous Media," by M. Muskat, McGraw-Hill Book Co., Inc., New York, N. Y., 1946.

in which Q is the total discharge, t is the thickness, and r is the radius of the well. Since the Laplace equation is linear in h, the solution for multiple wells is simply the sum of the solutions for each individual well.

As was previously stated, the existence of a free surface greatly complicates the analysis. One writer has gone so far as to claim that the problem cannot be solved with the present knowledge of mathematics. This, of course, is an extreme statement of the complexity of the problem, for through the use of simplifying assumptions, clearly understood, a solution may be obtained that will be of considerable value. The failure to understand these assumptions and their effect upon the solution has been the root of a great deal of confusion in the minds of many practical as well as theoretical investigators.

The classical analysis of this problem was presented by Jules Dupuit in 1863. He assumed horizontal flow throughout a homogeneous material underlain by an impermeable stratum with a well completely penetrating the permeable material. Necessarily, then, the flow occurred through concentric cylinders of a variable height h that were potential surfaces, the last and smallest cylinder having a height equal to the depth of the water in the well. The result of an analysis based on these assumptions is the formula commonly known as the Dupuit equation:

$$h^2 - h_1^2 = \frac{Q}{\pi K} \log_e \frac{r}{r_1} \quad \text{.......................(3)}$$

Limitations of the Dupuit Equation.—Since the free surface approaches the horizontal at a considerable distance from the well, it can be seen that the assumption of horizontal flow through vertical potential surfaces will become more accurate as the radius increases, with a resulting increase in the accuracy of the Dupuit equation.

The surface given by the Dupuit equation intersects the well at the level of the water in the well, whereas it is a known fact that the free surface intersects the well above this point, giving rise to what is commonly referred to as a zone of seepage that increases in extent as the drawdown increases. Moreover, as the fluid approaches the well, the free-surface slope increases, causing the potential surfaces (that must be normal to the flow surfaces) to depart more and more from the cylindrical form assumed in the derivation. For these reasons the actual free surface would be above that calculated by the Dupuit equation, the difference being greatest at the edge of the well.

Effect of a Capillary Zone.—In addition to the flow conditions already mentioned, the effect of the capillary zone must be considered. This is especially true for model studies wherein the capillary rise may be an appreciable percentage of the depth of flow. Ordinarily it is sufficiently accurate to state that the free surface is the surface below which the voids are saturated with fluid. However, when a capillary zone becomes important because of its relative size, this definition is no longer sufficient and the free surface can best be defined as the surface of atmospheric pressure. R. D. Wyckoff, H. G. Botset, and M. Muskat,[4] and others have found that the potential distribution extends

[4] "Flow of Liquids Through Porous Media Under the Action of Gravity," by R. D. Wyckoff, H. G Botset, and M. Muskat, *Physics*, Vol. 3, 1932, pp. 90–114.

across the atmospheric-pressure surface into the capillary zone. This potential distribution in the capillary zone will give rise to additional flow that cannot be neglected.

Experimental Studies

Several investigators, recognizing the limitations of the Dupuit equation, have conducted model tests to ascertain closely the true nature of the complex problem of unconfined flow. In 1932, Messrs. Wyckoff, Botset, and Muskat[4] constructed a 15° sand sector with glass sides and piezometers connected to the bottom. They found that the base piezometric heads, rather than the free surface, were given by the Dupuit equation. By injecting dye into the sand at the inflow face and tracing its movement to the well, they found that the capillary zone contributed a sizable discharge. These measurements were used to substantiate a modification of the Dupuit equation that allows for the increased flow resulting from capillarity. Apparently no attempt was made to determine the effect of the capillary flow on the free surface.

Harold E. Babbitt, M. ASCE, and David H. Caldwell,[5] A.M. ASCE, have undertaken a very extensive three-phase study of unconfined flow. The first phase of the study was a series of electrical-analogy tests on a thin carbon wedge representing a single well. In addition to verifying the previously mentioned limitations of the Dupuit equation, they developed an equation for the free surface near the well.

The second phase of the investigation was the construction of a 15° sand sector 100 in. long and 16 in. high having a single well located at the apex. Along one of the sides the piezometric head was measured and the free surface determined. The discharges were compared with those given by the equation developed by the electrical-analogy method and were found to be in good agreement.

A study of multiple wells comprised the third phase. A 13-ft square container was filled to a depth of 13 in. with ordinary building sand. Water was admitted through screens located at the corners and flowed toward various combinations of 5 wells placed near the center. The discharges were compared with those computed from a multiple-well analysis based on certain simplifying assumptions. A fair agreement was secured.

Since the study by Messrs. Babbitt and Caldwell represents the most exhaustive investigation of unconfined flow known to the writer, it has been used as the starting point for the experiments reported herein. For that reason an appraisal of the results of the Babbitt and Caldwell tests is needed at this point to understand clearly the objectives of this investigation.

First of all, with regard to the electrical-analogy study, it is felt that the resulting free surface is a good representation of the true free surface. However, caution should be used near the well, since the wedge was very thin and any small cracks or lack of homogeneity as well as improper electrode contact would be more noticeable in this region. Moreover, the range of variables

[5] "The Free Surface Around, and Interference Between, Gravity Wells," by Harold E. Babbitt and David H. Caldwell, *Bulletin Series No. 374*, Eng. Experiment Station, Univ. of Illinois, Urbana, Ill., January 7, 1948.

studied was rather small. For example, the maximum external radius was only 25 well radii and varied from 3.2 to 6.5 times the maximum depth of flow.

The formula proposed by Messrs. Babbitt and Caldwell was presented in the form:

$$h_e - h = \frac{2.3\, Q\, C_x}{\pi\, K\, h_e} \log \frac{r_e}{0.1\, h_e} \quad \text{(4)}$$

in which the subscript *e* refers to the external boundary, and the coefficient C_x is defined by a curve relating the drawdown to the radius. Of extreme interest is the fact that when C_x is plotted against the logarithm of the quantity (r/r_e), a straight line results to a value of $r/r_e = 0.05$. Since the minimum value of r/r_e in the electrical-analogy experiments was only 0.04 and the maximum 0.087, the logarithmic relation holds essentially true to the edge of the well.

When the approximation ($C_x = 0.3 \log r/r_e$) is substituted in Eq. 4, the following formula results:

$$h_e - h = \frac{0.69\, Q}{\pi\, K\, h_e} \log \frac{r_e}{0.1\, h_e} \log \frac{r_e}{r} \quad \text{(5)}$$

Noteworthy is the fact that the elevation of the free surface is expressed as a linear function of the radius in a manner very similar to that for artesian wells, whereas the Dupuit equation is not a linear function.

Model Studies of Unconfined Flow

Equipment for Model Studies.—The sand-model studies described herein were undertaken at the laboratory of the Iowa Institute of Hydraulic Research, principally for the purpose of gaining further information about the free surface near the well. A 90° sector containing sand (Fig. 1) was constructed, in which the inflow screen was 120 in. from a central well having a radius of 1.2 in. The depth of inflow was maintained at approximately 24 in. in 30 in. of sand. Two other wells, each of 1.2-in. radius, were located 36 in. from the apex. The wells were placed along planes of symmetry so that by the principle of images the full pattern of wells would be in the center of a circular confining boundary. One of the planes of symmetry was made of plexiglas, containing 174 piezometer connections. The inflow face was formed of two layers of copper screen supported by 1-in. by 4-in. timber ribs. The base of the model was constructed of concrete and the sides, exclusive of the plexiglas, were of ½-in. plywood. Two layers of copper screen, soldered to ½-in. hardware cloth, formed the well face. Water entered the sand through the screen at the outer periphery and flowed toward the wells, at which point the water surface was maintained at the required level by an overflow control. The discharge was measured by weighing the water flowing from the wells.

The sand used in the model was graded Iowa River mason's sand, with most of the fines removed by washing. To reduce the amount of trapped air, which has a considerable and variable effect on the permeability,[6] the sand was placed under water. Each layer was approximately 1-in. thick and was raked

[6] "Effect of Entrapped Air upon the Permeability of Soils," by J. E. Christiansen, *Soil Science*, Vol. 58, No. 5, November, 1944.

thoroughly with a leaf rake to free any additional air. Moreover, the raking reduced the horizontal stratification as well as the orientation of the grains.

Procedure for Model Studies.—The sequence of operations in the series of tests was determined by the criterion that the water level in the sand should

FIG. 1.—PHOTOGRAPH OF SAND MODEL

not be raised after it was once lowered. By raising the level, even though slowly, air would be trapped in the pores and the permeability would thus be reduced. This effect could very well be serious near the well at which point the drawdown is a maximum.

The water surface in the central well was lowered to 18.3 in. and the reservoir level to approximately 24 in., which was maintained during the remainder of the tests. Since the sand was 30 in. deep, this differential allowed for the expected maximum capillary rise of 6 in. to be completed near the outer periphery. The piezometric heads, together with the discharge, were used in determining when an equilibrium condition was approached.

Triple-strength red food coloring was placed in all piezometer tubes. This dye served two very useful purposes in addition to functioning as the piezometer fluid. The dye could be made to enter the flow and trace out the stream lines (Fig. 2) by either placing additional dye in the tubes or simply compressing the rubber tube leading to the piezometer connection. Moreover, when the

tubes were given an initial compression, the velocity of the resulting dye front could be determined. The piezometer readings were corrected for the increase in specific gravity resulting from the coloring.

Experimental Tests on Model.—Seven complete tests were made. The central well, referred to hereafter as well 1 (Figs. 1 and 3), was operated at four

FIG. 2.—DYE FRONTS TRACING OUT STREAM LINES

levels: 18.3 in., 12.3 in., 6.3 in., and complete drawdown. (All elevations were measured above the base of the model.) A typical result is shown in Fig. 4.

The fifth test setup consisted of 3 wells in a straight line with the central well maintained at full drawdown and the outside wells at 12.9 in. elevation.

The potential distribution for this case was obtained in two steps. In the first step well 1 was at full drawdown and well 3 at 12.9 in. The flow pattern thus determined along the plexiglas boundary was then at right angles to the line of wells. The second step was to close well 3 completely and lower the water sur-

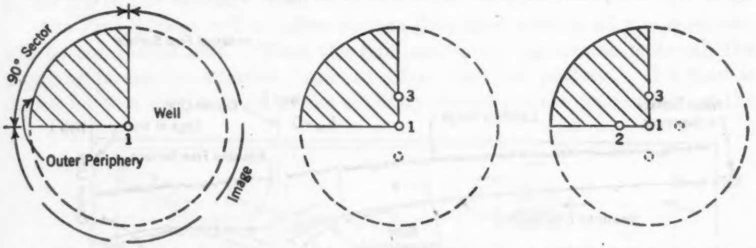

FIG. 3.—PLAN OF WELL LAYOUT FOR MODEL TESTS

face in well 2 to 12.9 in. In this manner the flow pattern along the line of wells was determined. It will be observed that it was necessary to raise the water surface over a portion of the flow area, but the tests were arranged so that this fluctuation always occurred at well 3, the farthest from the line of piezometers. In this way it was hoped to minimize the effect of trapped air.

The sixth test was made with 4 wells in a square and the fifth well in the center. The pattern consisted of 3 of the wells in a line along a diagonal operat-

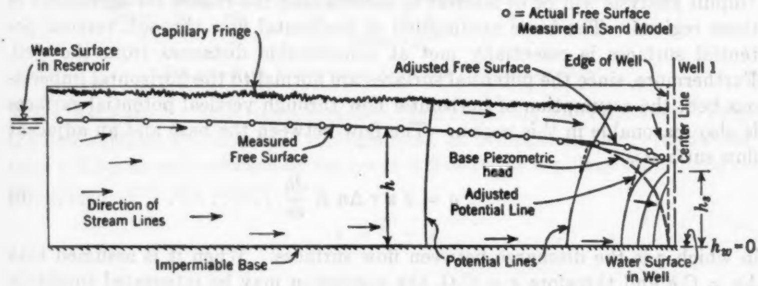

FIG. 4.—FLOW PATTERN FOR TEST NUMBER 4

ing at full drawdown, and the remaining 2 operating at 12.9 in. The first stage was obtained with wells 1 and 3 at full drawdown and well 2 at 12.9 in. The flow pattern thus obtained was at right angles to the line of 3 wells at full drawdown. When well 2 was lowered to full drawdown and well 3 was raised to 12.9 in., the flow pattern along the line of the 3 wells was obtained.

The last test, number seven, was with all 3 wells at full drawdown, resulting in a pattern of 5 wells under full operation; the results of this test are shown in Fig. 5.

Analysis of Test Results.—The discussion of the sand-model tests will be separated into four categories—the Dupuit analysis, the capillary zone, the free surface, and the boundary conditions at the well.

The Dupuit Analysis.—The Dupuit equation has been shown previously to agree with the piezometric heads measured along the bottom of the permeable

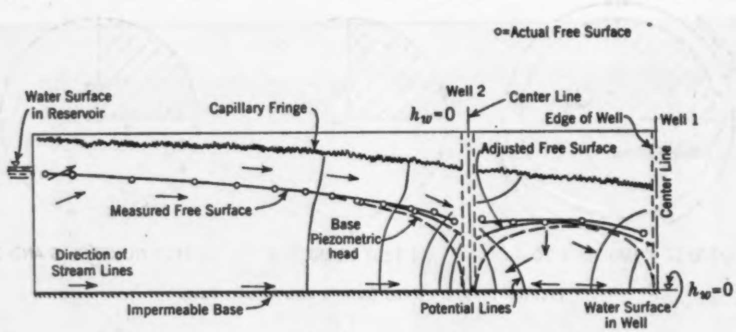

FIG. 5.—FLOW PATTERN FOR TEST NUMBER 7

stratum. Additional experimental verification is shown in Fig. 6, in which the Dupuit equation is the best fit curve for the experimental data obtained from tests one to four. With the experimental tests indicating that the Dupuit equation accurately gives the free surface at considerable distances from the well and also the piezometric head along the entire base, a re-examination of the Dupuit analysis will be of interest in ascertaining the reason for agreement in these regions. The basic assumption of horizontal flow through vertical potential surfaces is essentially met at considerable distances from the well. Furthermore, since the potential surfaces are normal to the horizontal impervious bed, the assumption of horizontal flow through vertical potential surfaces is also reasonable in this region. The flow between the base and an adjacent flow surface is

$$q = 2\,\pi\,r\,\Delta n\,K\,\frac{dh}{dr} \qquad (6)$$

in which q is the discharge between flow surfaces. When it is assumed that $\Delta n = C\,h$ and therefore $q = C\,Q$, the expression may be integrated to obtain the Dupuit equation. Since the resulting equation is verified experimentally, the assumption is evidently sound, and can therefore be used in further defining the pattern of flow. In brief, this analysis means that the normal distance between stream surfaces immediately adjacent to the impermeable base remains a constant fraction of the piezometric head above the impervious base as the fluid approaches the well.

Effect of the Capillary Zone.—The capillary zone had considerable effect on the results, as its relative magnitude would indicate—the inflow depth being approximately 24 in. and the average capillary rise being 5 in. From Figs. 4 and 5, the potentials can be seen to extend across the free surface and

well into the capillary zone. This, of course, should be expected since the flow of the fluid depends on the gradient and not the absolute magnitude of the piezometric head. The potential pattern is modified to some extent, however, by the difference in permeability that occurs in the fringe itself. In any graded granular material, a fringe rather than a definite clear-cut line will exist at the top of the capillary zone.

The Free Surface.—The inflow surface that must exist in all model studies will be considered first. When the fluid enters the permeable material, the capillary forces immediately begin to affect the flow pattern. The fluid is drawn up to a height equal to the capillary rise above the free surface of the

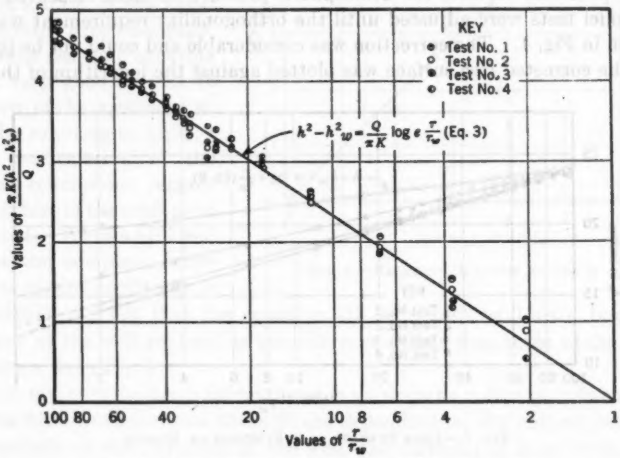

FIG. 6.—BASE PIEZOMETRIC HEAD FOR UNCONFINED FLOW

water in the sand. This rise is completed in a relatively short distance. Since the flow surfaces and potential surfaces must be orthogonal, the potential surfaces will be moved rearward by the upward flow to the capillary zone. Hence, at a given point, the potential,

$$h = \frac{p}{\gamma} + z \quad \text{(7)}$$

(in which γ is the weight per unit volume and z is the elevation) will decrease, and since the elevation z remains constant, the pressure p must decrease. Consequently, the atmospheric-pressure surface, or what is hereafter referred to as the free surface, is lowered slightly as a result of this upward flow. Once the capillary zone is fully developed, the location of the free surface is not affected until the flow reaches the vicinity of the well. Throughout the central portion of the flow, the free surface is a stream surface above which the fluid within the capillary zone is flowing at less than atmospheric pressure. In order for the fluid to enter the well that is at atmospheric pressure, the pressure in the fluid must be increased until it is equal or above atmospheric pressure by a decrease

in elevation. The resulting flow across the atmospheric-pressure line near the well causes the potential surfaces to lower in order that the potential and stream surfaces remain normal. Hence, at a given point the potential ($h = p/\gamma + z$) is increased by an increase in pressure, resulting in a higher atmospheric-pressure line. Thus, the capillary flow has lowered the free surface when the flow is established at the periphery, and raised the free surface in the vicinity of the well, as can be seen from Figs. 4 and 5.

The flow-net principles were used to estimate the extent to which the free surface was altered by the downward capillary flow near the well. Since the free surface unaffected by capillary flow is a stream surface that must be normal to each potential surface, the atmospheric-pressure surfaces measured in the sand-model tests were adjusted until the orthogonality requirement was met, as shown in Fig. 4. The correction was considerable and could not be ignored. When the corrected free surface was plotted against the logarithm of the term

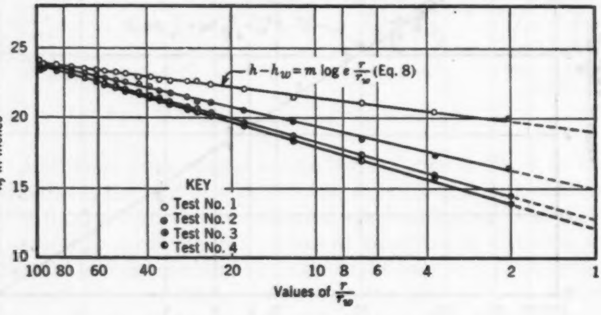

FIG. 7.—FREE SURFACE AS A FUNCTION OF RADIUS

r/r_w (Fig. 7), an essentially straight line was obtained, giving a linear logarithmic function of the form:

$$h - h_1 = m \log_e \frac{r}{r_1} \qquad (8)$$

in which m is the slope and has the dimension of a length.

Since a similar equation was obtained by the writer from a re-examination of the Babbitt-Caldwell data, sufficient experimental confirmation of the linear logarithmic nature of the free surface near the well is available to justify an analysis of the flow pattern to learn the implication of such a relation. Consider the differential flow ($q = C_1 Q$) occurring between the free surface and an adjacent stream surface. By assuming that the vertical distance between stream surfaces remains constant ($\Delta z = C_2$) as the flow approaches the well, the following linear logarithmic equation is obtained by combining the Darcy and continuity equations, and integrating

$$h - h_1 = \frac{Q\, C_1}{2\,\pi\, K\, C_2} \log_e \frac{r}{r_1} \qquad (9)$$

Data obtained from a sufficient range of the controlling variables are not available to enable the establishment of the parameters involved in the constants C_1 and C_2. Additional data should aid materially in defining these terms. However, from Fig. 8, in which m is plotted against Q for the single well tests, it can be seen that Q is the primary variable. Hence, the assumption that the vertical distance between the free surface and an adjacent flow surface remains constant, not only results in a form of the equation verified experimentally, but also the resulting equation gives a very good clue as to the nature of the coefficient m. Again, by referring to Eq. 5, a further confirmation of the foregoing conclusions regarding the nature of the coefficient is obtained. When additional data for the complete determination of the coefficient m are available, it is felt that the equation will be more useful if the boundary conditions at the well are used as the reference rather than those at the radius of influence, as in Eq. 5.

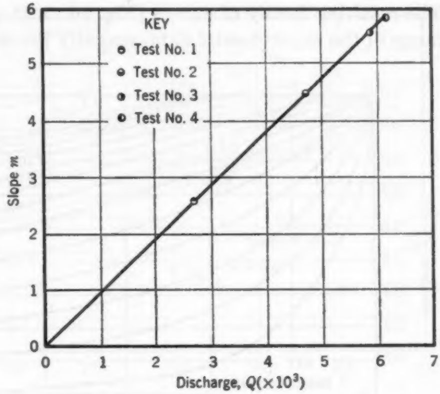

Fig. 8.—Relation Between m and Q

Under ordinary field conditions there is no definite radius of influence because the conditions far from the well are dependent on the natural recharge, so an analysis of the variables at the well was undertaken in an attempt to define the flow conditions. When the variables Q, K, r_w, h_w, and h_s at the well are combined to form dimensionless parameters, the following functional relationship is obtained:

$$\frac{Q}{K\,r_w^2} = f\left(\frac{h_w}{h_s}, \frac{h_w}{r_w}\right) \quad \text{(10)}$$

in which h_s is the height of the intercept of the free surface with the edge of the well.

Boundary Conditions.—Using the results of Messrs. Babbitt and Caldwell's electrical-analogy tests and the writer's data from the sand-model tests, the parameters were plotted as shown in Fig. 9, thereby obtaining the discharge for unconfined well flow in terms of the boundary conditions at the well. Because of the nature of the dimensionless parameters, a family of curves was quite accurately obtained from the available experimental data. However, such a presentation fails to give the values of h_s for the important case of complete drawdown, h_w/h_s being zero for all values of $\frac{Q}{K\,r_w^2}$. For this reason the vari-

ables at the well were grouped into the dimensionless form,

$$\frac{Q}{K\,r_w^2} = f\left(\frac{h_s}{r_w}, \frac{h_w}{r_w}\right) \ldots\ldots\ldots\ldots\ldots\ldots\ldots\ldots (11)$$

The resulting family of curves (Fig. 10), although less accurate because of the range of the experimental data, magnify the relationships when $h_w \rightarrow 0$.

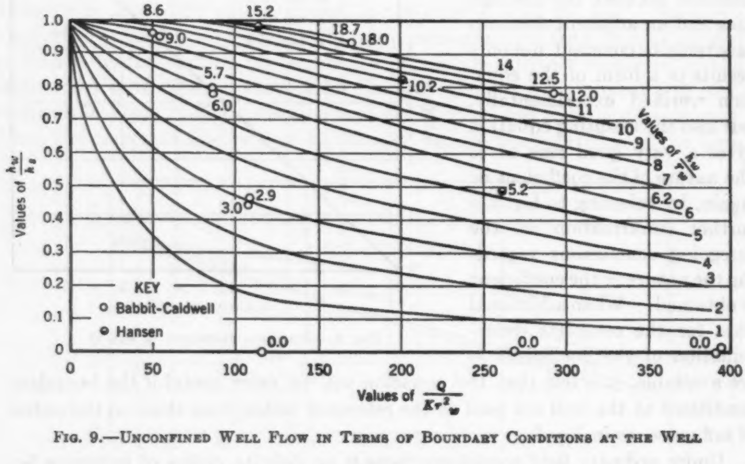

FIG. 9.—UNCONFINED WELL FLOW IN TERMS OF BOUNDARY CONDITIONS AT THE WELL

To verify this functional relation further, the values obtained from the plots were compared with the results for the multiple-well tests and found to be in good agreement. This means that unconfined flow to either single or multiple wells in any arrangement can be defined in terms of the boundary conditions at the well, and hence, the vague quantity—radius of influence—can be avoided.

It should be remembered that both dimensionless plots are based on limited data. Consequently, the results should be taken as a positive indication of the possibilitites of such an analysis, and not as the final answer. When the results of other experimental work are available, the usefulness of the plots can then be extended.

Since the free surface next to the well is not only hard to measure, but is also affected considerably by the entrance conditions, the intercept at the well was obtained by plotting the free-surface elevations against the logarithm of the term r/r_w and extending the essentially straight line to the well (Fig. 7). A similar procedure is recommended when field data are used to relate the boundary conditions at the well.

The fundamental nature of the dimensionless parameter $\frac{Q}{K\,r_w^2}$ should not be overlooked. This parameter is an index of the shape of the cone of depression of the water table around the well, large values being characteristic of the deep cones, small values characterizing shallow depressions.

An analysis will show that this parameter, fundamental in all well flow, is nothing more than the ratio of the Froude and Reynolds numbers, which is the ratio of the viscous to the gravity forces; the inertial forces cancel because of their minor importance in comparison to the viscous and gravity forces.

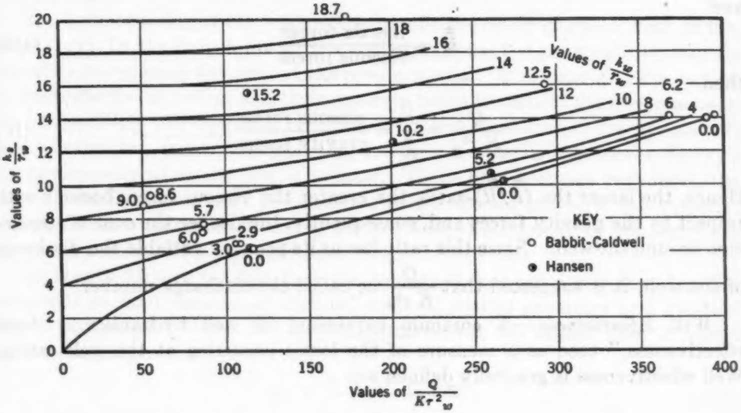

FIG. 10.—UNCONFINED WELL DISCHARGE AS A FUNCTION OF DRAWDOWN AND FREE SURFACE INTERCEPT

When into the basic well parameter, $\frac{Q}{K r^2_w}$, the coefficient of permeability $K = \frac{C d^2 \gamma}{\mu}$ (in which μ is the viscosity) is substituted, the following results:

$$\frac{Q}{K r^2_w} = \frac{Q \mu}{C d^2 \gamma r^2_w} \quad \text{.......................(12)}$$

Considering $C d^2$ as a representative area characterizing the porous media through which the flow occurs, the quotient $\frac{Q}{C d^2}$ has the dimensions of velocity that could be considered as characteristic of a flow produced by a given boundary condition. Substituting v' for $\frac{Q}{C d^2}$, together with $\gamma = \rho g$, into the well parameter, the following equation is obtained:

$$\frac{Q}{K r^2_w} = \frac{v' \mu}{\rho g r^2_w} \quad \text{.......................(13)}$$

When numerator and denominator are multiplied by v',

$$\frac{Q}{K r^2_w} = \frac{\dfrac{(v')^2}{g r^2_w}}{\dfrac{\rho v' r_w}{\mu}} \quad \text{.......................(14a)}$$

or

$$\frac{Q}{K r^2_w} = \frac{\bar{\bar{F}}}{\bar{\bar{R}}} \quad \text{.......................(14b)}$$

in which $\tilde{\tilde{F}}$ and $\tilde{\tilde{R}}$ are the Froude and Reynolds numbers, respectively. However, since

$$\tilde{\tilde{F}} = \frac{\text{inertia forces}}{\text{gravity forces}} \qquad (15a)$$

and

$$\tilde{\tilde{R}} = \frac{\text{inertia forces}}{\text{viscous forces}} \qquad (15b)$$

then

$$\frac{Q}{K\, r^2_w} = \frac{\tilde{\tilde{F}}}{\tilde{\tilde{R}}} = \frac{\text{viscous forces}}{\text{gravity forces}} \qquad (16)$$

Hence, the larger the $(\tilde{\tilde{F}}/\tilde{\tilde{R}})$-ratio, the greater the viscous forces become with respect to the gravity forces and, consequently, the deeper the cone of depression around the well. Since this ratio has as its primary variable the discharge of the well, it is suggested that $\frac{Q}{K\, r^2_w}$ be called the discharge number.

Well Effectiveness.—A common expression in well hydraulics is "well effectiveness," used as a measure of the losses occurring at the well casing. Well effectiveness is generally defined as

$$E_W = \frac{h_e - h_s}{h_e - h_w} \qquad (17)$$

or the ratio between the drawdown measured outside and inside the well.

If the piezometric heads in Eq. 17 are measured in the zone in which Dupuit's equation applies, the results are indicative of the losses occurring at the well casing. However, when the piezometric heads are measured outside the Dupuit region and in particular at or near the free surface, the definition given is not only erroneous but grossly misleading. In fact, from Fig. 9 it is seen that h_w/h_s varies from 0 to 1.0, depending on the values of h_w/r_r and $\frac{Q}{K\, r^2_w}$. When the possible extremes of h_w/h_s of 0 and 1.0 are substituted into Eq. 17, it is seen that the value of E_W can be varied over the entire range from 0 to 1.0 without any loss occurring at the well.

Too often these basic principles are ignored, with the result that the seepage face that must accompany this type of flow is considered as well loss caused by poor design or poor development of the well. When subsequent extensive development fails to alter the flow pattern materially, the premature conclusion is too often reached that either the driller does not know his profession or the formulas are of no value.

If the free surface near the well is observed, the piezometric heads should be plotted against the logarithm of the radius and the resulting straight line extrapolated to its intersection with the well casing. The losses occurring at the well casing can then be determined by comparing the extrapolated value of h_s with the value calculated by the use of Fig. 9 or Fig. 10. The ratio between these two values is a measure of well efficiency. When the square of the piezometric heads plotted against the logarithm of the radius results in a straight line, the

indication is that the measurements were taken in the Dupuit zone. The intersection of the resulting straight line extrapolated to the well casing, when compared to the depth of the water in the well, will also be a measure of well efficiency. The loss occurring at the well will be the difference between these two values.

The loss occurring at the well casing may be the result of one or both of two factors: (1) In the derivation of the well equations, the permeability was assumed to be constant throughout the porous media. If silt and clay are carried by the water to the casing and their presence tends to restrict the flow passages, the permeability will decrease, resulting in an increased loss of energy, and (2) in the derivation, it was assumed that Darcy's law applied; however, Darcy's law applies only when the flow is laminar. If the flow becomes turbulent, the loss of head is more nearly proportional to the second power of the velocity. Hence, the two factors responsible for low well effectiveness or efficiency are decreased permeability and turbulent flow.

To clarify further the fact that the seepage face is not a well loss, the discharges from unconfined and confined wells of similar geometry and location will be compared. When the Dupuit equation for unconfined flow is solved for the discharge,

$$Q_u = \frac{\pi K (h^2 - h^2_w)}{\log_e \frac{r}{r_w}} \qquad (18)$$

Likewise, the confined discharge is

$$Q_c = \frac{2 \pi K t (h - h_w)}{\log_e \frac{r}{r_w}} \qquad (19)$$

The value of h represents some peripheral boundary condition in each case, so that the depth of water in each well (h_w), in addition to K, r, and r_w, are equal; then by dividing the unconfined discharge (Q_u) by the confined discharge (Q_c) an interesting equation is obtained:

$$\frac{Q_u}{Q_c} = \frac{h + h_w}{2 t} \qquad (20)$$

Since t must be less than h_w, which must likewise be less than h ($t < h_w < h$), the unconfined discharge must always be greater than the confined discharge ($Q_u > Q_c$) for comparable boundary conditions. Consequently, the existence of the seepage face does not result in a less efficient well system.

Conclusions

The potential distribution for unconfined flow was found, by model experiments on single and multiple wells, to extend essentially unaltered across the atmospheric-pressure surface and completely through the capillary zone into the capillary fringe. In model studies in which the height of the capillary rise is a significant fraction of the model size, the effect of the capillary flow on the shape of the free surface cannot be ignored. However, when the free surface

for a single well under various drawdowns is corrected for the effect of the capillary flow, the shape of the free surface near the well can be closely approximated by a linear logarithmic function. The free surface in unconfined well flow must always intersect the well casing above the water surface in the well, resulting in a zone of seepage that increases as the drawdown increases. The free surface, consequently, is above that calculated by the Dupuit equation, the difference being greatest at the edge of the well.

Measurements of the base piezometric head show a good agreement with the Dupuit equation; analysis indicates that this equation should not only accurately describe the base piezometric head distribution but also describe the free surface with increasing accuracy as the radius increases. Over the zone in which the Dupuit equation applies, the stream-surface spacing is proportional to the piezometric head. Very near the free surface, at which the linear logarithmic solution applies, the vertical distance between stream surfaces remains essentially constant as the flow approaches the well.

Based upon experimental data, functional relationships (Figs. 9 and 10) between the variables at the well have been developed for unconfined flow. These relationships apply to the solution of either single or multiple systems. The dimensionless parameter $\frac{Q}{K\,r^2_w}$ characterizes the shape of the cone of depression occurring around a well. This parameter, fundamental in all well flow, is nothing more than the ratio of the Froude and Reynolds numbers or the ratio of the viscous to the gravity forces. Since this ratio has as its primary variable the discharge of the well, it is suggested that $\frac{Q}{K\,r^2_w}$ be called the discharge number.

The commonly used term "well effectiveness" is grossly misleading for unconfined flow unless piezometric heads are measured in the zone in which the Dupuit equation applies. When the square of the piezometric heads plotted against the logarithm of the radius results in a straight line, the indications are that the measurements were taken in the Dupuit zone. The intersection of the resulting straight line, extrapolated to the well casing, when compared to the depth of the water in the well, will be a measure of well efficiency. The loss occurring at the well will be the difference between these two values. If the free surface near the well is observed, the piezometric head should be plotted against the logarithm of the radius and the resulting straight line extrapolated until it intersects the well casing. The losses occurring near the well casing can then be determined by comparing the extrapolated value of h_s with that calculated from the curves of Fig. 9 or Fig. 10. The ratio between these two values is also a measure of well efficiency. Well losses can be attributed to either a decrease in permeability near the well or to turbulent flow. The zone of seepage is not a well loss.

Acknowledgments

This paper is based on a dissertation entitled "Evaluation of Unconfined Flow to Multiple Wells by the Membrane Analogy" submitted by the author in partial fulfilment of the requirements for the degree of Doctor of Philosophy, to

the Department of Mechanics and Hydraulics, of the Graduate College of the State University of Iowa, in Iowa City, June, 1949. The research was conducted at the Iowa Institute of Hydraulic Research, with the wholehearted financial assistance of the Department of Mechanics and Hydraulics of the university.

Appreciation for his cooperation is extended to Hunter Rouse, M. ASCE, under whose direction this study was made. To Emmett M. Laursen, A.M. ASCE, the author gives very sincere thanks for his many helpful suggestions.

APPENDIX. NOTATION

a = flow area;

C_z = Babbitt-Caldwell dimensionless, variable coefficient relating the draw-down to the radius;

E_W = well effectiveness;

h = piezometric head, $p/\gamma + z$:

- h_e = piezometric head at the radius of influence;
- h_s = height of the intersection of the free surface with the edge of the well;
- h_w = piezometric head in the well;

K = coefficient of permeability having the dimension of velocity;

m = slope of the linear logarithmic equation representing the free surface near the well;

p = unit pressure;

q = discharge between flow surfaces;

Q = total discharge;

r = radial distance from axis of well:

- r_e = radius of influence;
- r_w = radius of the well;

s = length along a stream line;

t = thickness;

v = velocity in Darcy's equation;

z = elevation; and

γ = weight per unit volume.

DISCUSSION

Ahmed Shukry,[7] A. M. ASCE.—The deviation of the free surface, in the vicinity of an unconfined well, from that computed by the Dupuit equation has long been recognized, although it is still ignored by some engineers. This deviation is generally attributed to the following two causes:

(1) The flow of water through porous soils obeys the Darcy law if the slope is less than $\frac{dh}{ds}$. For greater slopes, actual velocities will be smaller than those computed by this law. The limiting slope for the application of the Darcy law was found to depend on the permeability coefficient: According to E. Prinz,[8] this slope does not exceed 1 on 1 in ordinary sand.

(2) Two approximate assumptions that are used in the Dupuit equation produce deviation. They are the assumption that the slope of the free surface is $\frac{dh}{dr}$ instead of $\frac{dh}{ds}$, and the assumption that the potential surfaces are vertical cylindrical surfaces. Both assumptions nearly represent the actual conditions at some distance from the well and, for this reason, the measured seepage discharges agree closely with those computed according to the Dupuit equation. This agreement has been confirmed by different authors adopting diverse methods of investigation such as mathematical analysis,[3] electric analogy,[5] sand model tests,[5,9] and the relaxation method.[9]

Leo Casagrande,[10] when applying the Dupuit equation to seepage through earth dams, assumed the slope of the water surface to be $\frac{dh}{ds}$ instead of $\frac{dh}{dx}$. Applying the same modification for the case of the flow of unconfined ground water toward a single well, the basic differential equation becomes

$$Q = K\, 2\, \pi\, r\, h \frac{dh}{ds} \qquad (21)$$

The slope of the water surface in Eq. 6 may be modified accordingly, so that the equation may represent more closely the actual conditions near the well.

Relative to the distribution of pressures at the impermeable base, the author's results confirm those obtained by Messrs. Wyckoff, Botset, and Muskat[4] who referred to the Dupuit equation as the "base-pressure equation." This conclusion was also checked by Messrs. Babbitt and Caldwell, who performed tests on electric and sand models.[5] On the other hand, using the relaxation method, S. T. Yang[11] found that the Dupuit equation does not

---

[7] Prof. of Irrig., Faculty of Eng., Alexandria Univ., Alexandria, Egypt.

[8] "Hydrologie," by E. Prinz, J. Springer, Berlin, Germany, 2d Ed., 1920.

[9] "The Flow Pattern Near a Gravity Well in a Uniform Water-Bearing Medium," by Norman Savage Boulton, *Journal*, Inst. of C.E., London, England, December, 1951, pp. 534–550.

[10] "Naeherungsmethoden zur Bestimmung von Art und Menge der Sickerung durch geschuettete Daemme," by Leo Casagrande, Technische Hochschule, Vienna, Austria, July, 1932. (Translated into English by staff, U. S. Waterways Experiment Station, Vicksburg, Miss.)

[11] "Seepage Toward a Well Analyzed by the Relaxation Method," by S. T. Yang, thesis presented to Harvard Univ., at Cambridge, Mass., in 1949, in partial fulfilment of the requirement for the degree of Doctor of Science.

yield the correct distribution of pressures along the impermeable base. In the writer's opinion, the agreement between the Dupuit equation and the piezometric base pressures is valid only at some distance from the well; but in the region where the free surface is sharply curved, a marked discrepancy should be expected between the two values. The writer checked this point from a pattern of flow toward an unconfined well, solved by Mr. Boulton[9] using the relaxation method (Fig. 11).

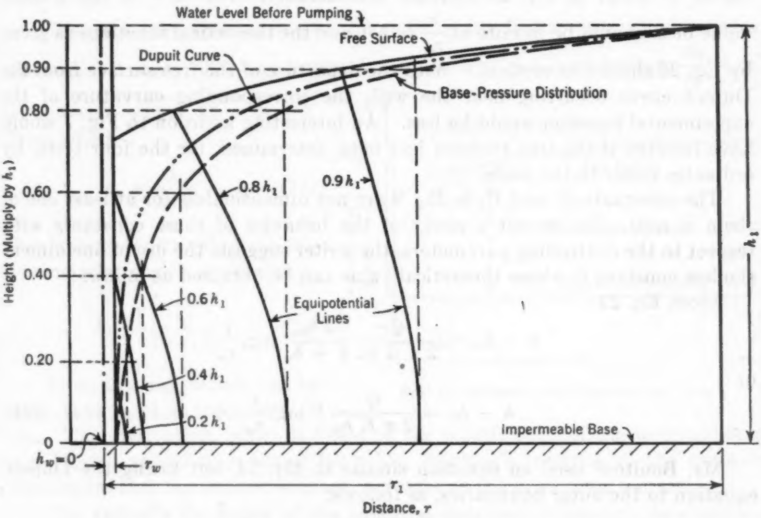

Fig. 11.—The Pressure Distribution at the Impermeable Base as Obtained from a Flow Pattern Solved by the Relaxation Method

Eq. 8 is in an empirical form. To enable a clear study of the slopes of the experimental functions shown in Fig. 7, it is suggested to derive this equation from the Dupuit equation as follows:

$$h^2 - h^2{}_1 = \frac{Q}{\pi K} \log_e \frac{r}{r_1} \qquad (3)$$

Therefore,

$$h - h_w = \frac{Q}{\pi K \, (h + h_w)} \log_e \frac{r}{r_w} \qquad (22)$$

Therefore, the theoretical values of the slopes in Eq. 8, according to the Dupuit assumptions, would be given by

$$m = \frac{Q}{\pi K \, (h + h_w)} \qquad (23)$$

In this form, the experimental values of m can be compared with the Dupuit values. It has been stated that the free surface profile of the flow

agrees favorably with the Dupuit equation, at long distances from the well. According to Messrs. Babbitt and Caldwell[5] and Mr. Boulton,[9] this distance is approximately 1.5 h. Because the Dupuit value of the slope m as given by Eq. 23 is not constant, it follows that the logarithmic functions shown in Fig. 7 cannot be straight lines. However, they may be considered, approximately, as such for large values of r because of the flatness of the free surface. In the vicinity of the well, where the free surface curves down sharply, the values $(h + h_w)$ in Eq. 23 decrease considerably. For $h_w = 0$, the Dupuit value of m should be infinite at $\frac{r}{r_w} = 1.0$, and the theoretical functions as given by Eq. 22 should be vertical. With the departure of the free surface from the Dupuit curve occurring near the well, the corresponding curvature of the experimental function would be less. An interesting addition to Fig. 7 would have resulted if the free surfaces had been determined, for the four tests, by ordinates closer to the wells.

The constants C_1 and C_2 in Eq. 9 are not dimensionless (or at least one of them is not). To permit a study of the behavior of these constants with respect to the controlling parameters, the writer suggests the use of one dimensionless constant C whose theoretical value can be obtained as follows:

From Eq. 22,

$$h - h_w = \frac{Q}{2\,\pi\,K\,h_w}\,\frac{2\,h_w}{h + h_w}\log_e\frac{r}{r_w}$$

or

$$h - h_w = \frac{Q}{2\,\pi\,K\,h_w}\,C\log_e\frac{r}{r_w}\ldots\ldots\ldots\ldots\ldots\ldots(24)$$

Mr. Boulton[9] used an equation similar to Eq. 24, but fitting the Dupuit equation to the outer boundaries, as follows:

$$h_e - h = \frac{Q}{2\,\pi\,K\,h_e}\,\frac{2\,h_e}{h_e + h}\log_e\frac{r_e}{r}\ldots\ldots\ldots\ldots\ldots\ldots(25)$$

and writing—

$$\frac{2\,\pi\,K\,h_e\,(h_e - h)}{Q} = \xi$$

Eq. 25 becomes

$$\xi = \frac{2\,h_e}{h_e + h}\log_e\frac{r_e}{r}\ldots\ldots\ldots\ldots\ldots\ldots(26)$$

If r equals r_w, it follows that $h = h_s$ and $\xi = \xi_s$. Mr. Boulton investigated the experimental and the relaxation values of the dimensionless number ξ_s with respect to both the dimensionless parameters $\frac{r_w}{h_e}$ and $\frac{h_w}{h_e}$, which define the conditions at the well. An important finding of Mr. Boulton's work is that ξ_s, or rather the drawdown $(h_e - h_s)$ at the well, is practically independent of the water level in the well for ranges of $\frac{h_w}{h_e}$ between zero and 0.40. It would be interesting if the author would check this important conclusion, which can be proved also as follows:

From Eq. 21, $\frac{ds}{dh} = \frac{2\,\pi\,K}{Q}\,r\,h$. Assuming that $(ds)^2 = (dh)^2 + (dr)^2$ and referring to Fig. 12, $1 + \left(\frac{dr}{dh}\right)^2 = \frac{4\,\pi^2\,K^2}{Q^2}\,r^2\,h^2$. Letting $\frac{2\,\pi\,K}{Q} = b$, the equation can be written as follows:

$$\frac{dh}{dr} = \frac{1}{\sqrt{b^2\,r^2\,h^2 - 1}} \qquad (27)$$

Using the theoretical value of the slope of the free surface where it joins the well,[12] namely, 90°, and letting h equal h_s at $r = r_w$ and because $\frac{dh}{dr} = \infty$ at the well, $\sqrt{b^2\,r^2_w\,h^2_s - 1} = 0$, from which

$$h_s = \frac{1}{b\,r_w} \qquad (28)$$

Replacing b by its value, the following relationship is obtained:

$$h_s = \frac{Q}{2\,\pi\,K\,r_w} \qquad (29)$$

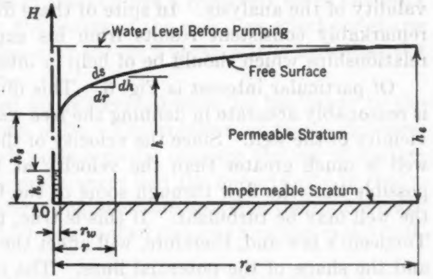

FIG 12.—FLOW TO AN UNCONFINED WELL

From this equation it can be seen that h_s is independent of h_w. This derivation, which is based on the modification of the water slope in the Dupuit equation, confirms both Mr. Boulton's results and the author's conclusion that the zone of seepage increases as the drawdown increases.

The author's discussion of the potential distribution through the capillary zone of a sand model is illuminating (see under the heading, "Model Studies of Unconfined Flow"). The main disadvantage of sand model tests which caused some investigators to recommend relaxation[9,11,12] methods or iteration[13] methods was the difficulty in locating the exact position of the free water surface.

The author should be complimented for developing functional relationships between the variables at the well. His statement (see under the heading, "Model Studies of Unconfined Flow," the paragraph preceding Eq. 10) that "Under ordinary field conditions there is no definite radius of influence because the conditions far from the well are dependent on the natural recharge ***" should be considered carefully by future investigators in their attempts to provide fruitful results for use by the practical engineering profession.

[12] "Relaxation Methods Applied to Engineering Problems," by F. S. Shaw and R. V. Southwell, Chapter VII of "Problems Relating to Percolation of Fluids Through Porous Materials," *Proceedings*, Royal Soc. of London, Series A, No. 972, Vol. 178, May, 1941.

[13] "Numerical Solutions of Steady-State and Transient Flow Problems; Artesian and Water-Table Wells," by A. A. I. Kashef, Y. S. Toulouklan, and R. E. Fadum, *Research Series No. 117*, Purdue Eng. Experiment Station, Lafayette, Ind., 1952.

CARL ROHWER,[14] M. ASCE.—Problems involving confined or unconfined flow of water through porous media are complicated in that, even in the laboratory, it is almost impossible to obtain a truly homogeneous material. This is because of the effect of entrapped air and the difficulty in getting uniformly compacted material. Another difficulty is encountered if the water passing through the material being tested is increasing in temperature. This results in the air in solution being liberated, causing a reduction in the effective pore space. Likewise, if the water temperature is reduced as it passes through the material, air will be absorbed and the permeability of the media increased.

Furthermore, the application of the hydraulic principles governing the flow of water into wells involves mathematical problems, the solution of which cannot even be approximated without making assumptions which affect the validity of the analysis. In spite of these difficulties, the author has obtained remarkably consistent results from his experiments and has obtained new relationships which should be of help in interpreting well-flow phenomena.

Of particular interest is Fig. 6. This illustrates that the Dupuit equation is reasonably accurate in defining the free water surface beyond the immediate vicinity of the well. Since the velocity of the water through the sand near the well is much greater than the velocity at the periphery of the model, it is possible that the flow through some of the larger interstices of the sand near the well may be turbulent. If this is true, this portion of the flow will follow Torricelli's law and, therefore, will affect the position of the free water surface and the shape of the potential lines. The curvature of the potential lines in the area near the well, as shown in Fig. 5, results in the development of the seepage face; and, since the seepage face is affected by the nature of the flow in this region, the change from laminar flow to turbulent flow will affect its height. However, this effect may be so small that it may not be possible to detect it in a model study.

According to Fig. 7, the plot of the adjusted free water surface, with h as the ordinate and $\log_e \left(\frac{r}{r_w}\right)$ as the abscissa, is a straight line for values of $\frac{r}{r_w}$ greater than 2. The author concludes from this fact that this line may be extended to the well to determine the elevation of the free water surface at the well. This procedure may give the correct result, but extrapolation is usually an unsound expedient. This is particularly true in the case under discussion because of the many uncertainties as to the nature of the flow in the zone adjacent to the well. It would have been helpful if the author had shown the actual elevation of the free surface at the well, as determined by the model study, even though precise readings at this point were difficult to obtain.

This comment is not intended to minimize the importance of the author's results, since Eq. 8 should be useful in checking the accuracy of piezometer readings and in locating the free water surface at the well. In field studies where the free water surface is at a considerable depth below the ground surface, the free surface near the well is difficult to determine because the location of the piezometer with reference to the well is uncertain. Eq. 8 provides a

[14] Senior Irrig. Engr., Div. of Irrig. Eng., SCS, U. S. Dept. of Agriculture, Ft. Collins, Colo.

means of obtaining the elevation of the free surface in this zone if the elevations of points removed from this zone are known.

The author states that the dimensionless parameter, given in Eq. 11, indicates whether the well has a deep or shallow cone of depression. This statement conforms with the writer's experience. As Q increases, the cone of depression is deepened. Similarly, if the radius of the well is decreased and Q remains constant, the cone of depression is deepened. The effect of K on the cone of depression is well known. It is probably the most important factor in determining the well characteristics. An interesting feature of this parameter is that the shape of the cone of depression is a function of the reciprocal of the square of the radius of the well. This seems unusual because it is usually believed that the radius of the well has a relatively small effect on the well characteristics. However, the radius of the well does affect the shape of the cone of depression in the zone near the well because it is here that the slope of the free surface is greatest.

The author is to be commended for the contribution he has made to the knowledge of the flow of water into wells. The solution of many problems involving the flow of water through porous media requires the use of mathematical techniques which older engineers never had the opportunity to study. It is gratifying to note that the younger engineers are applying their knowledge to the solution of these problems which have defied rigorous analysis in the past.

DAVID K. TODD[15] AND LLOYD C. FOWLER,[16] JUNIOR MEMBERS, ASCE.—The problem of finding an accurate and rational solution for gravity flow into a well has been of interest to engineers for many years. The model studies and analytic studies reported by Mr. Hansen are valuable contributions to this field. This discussion embodies a suggestion to extend the method of analysis developed by the author.

The interpretation of the dimensionless parameter, in terms of the ratio of the Froude number to the Reynolds number, indicates certain inconsistencies in the interpretation of the definitions involved in these dimensionless quantities. The Reynolds number, which is commonly used to define the influence of viscosity on the flow pattern, is normally expressed as

$$\mathsf{R} = \frac{\rho\, v\, l}{\mu} \qquad (30)$$

in which ρ is the density, v the velocity, μ the viscosity of the fluid, and l is a characteristic linear dimension. For flow in pipes, the diameter of the pipe is used for l, and for flow in a porous medium, some measure of the pore openings or grain size is used.[17]

The author defines v' as $\left(\frac{Q}{C\, d^2}\right)$. If d represents a characteristic grain size or pore size of the porous medium, and if the dimensionless constant C combines the geometrical shape factor of the internal structure of the porous

[15] Lecturer in Civ. Eng. and Irrig., Univ. of California, Berkeley, Calif.

[16] Lecturer in Civ. Eng. and Irrig., Univ. of California, Berkeley, Calif.

[17] "The Flow of Homogeneous Fluids Through Porous Media," by M. Muskat, McGraw-Hill Book Co., Inc., New York, N. Y., 1946, p. 56.

medium with the number of interstices through which flow is occurring, then v' is the mean microscopic velocity of flow through the aquifer.[18] The combination of this velocity with the well radius as the characteristic length in the Reynolds number, as done in Eq. 14*a*, has no relation to defining the flow conditions. To illustrate this, two horizontal pipes, filled with sand under identical conditions, are assumed to be connected, at the same elevation, to a constant-head tank. According to the definition of the Reynolds number, as given in Eq. 14*a*, for the first pipe,

$$\mathbf{R}_a = \frac{\rho_a\, v_a\, r_a}{\mu_a} \qquad (31)$$

and for the second pipe,

$$\mathbf{R}_b = \frac{\rho_b\, v_b\, r_b}{\mu_b} \qquad (32)$$

in which r_a and r_b are the radii of the first and second pipes, respectively. Under any given temperature conditions, $\rho_a = \rho_b$ and $\mu_a = \mu_b$, and, since both pipes are under the same pressure head, $v_a = v_b$ by the Darcy law. Dividing $\mathbf{R}_a$ by $\mathbf{R}_b$, and canceling terms, the ratio of the two Reynolds numbers is

$$\frac{\mathbf{R}_a}{\mathbf{R}_b} = \frac{r_a}{r_b} \qquad (33)$$

If the first pipe has twice the radius of the second pipe, this does not mean that $\mathbf{R}_a = 2\,\mathbf{R}_b$, but it does signify that the flow conditions are identical in the two pipes, and, hence $\mathbf{R}_a$ must equal $\mathbf{R}_b$. This result can be achieved only by replacing the pipe radii with the characteristic pore or grain sizes of the sand. These sizes will necessarily be equal for the same sand and packing conditions.

The same reasoning can be applied to the Froude number to show that r_w is not the characteristic length used to determine v'. To obtain the author's ratio, it would be necessary to express $\frac{Q}{K\, r^2_w}$ as $\frac{Q}{K\, d^2}$. The variable d does not depend on the well characteristics, but is a property of the porous medium only. Thus, in Eq. 12, K is defined in terms of d.

The author's statement that the parameter $\frac{Q}{K\, r^2_w}$ is "an index of the shape of the cone of depression around the well" can be illustrated by reference to Eq. 6. Rewriting this equation as

$$Q = 2\,\pi\, r\, h\, K \frac{dh}{dr} \qquad (34)$$

and substituting the parameter yields

$$\frac{Q}{K\, r^2_w} = 2\,\pi \left(\frac{h_s}{r_w}\right)\left(\frac{dh}{dr}\right) \qquad (35)$$

in which $r = r_w$ and $h = h_s$. This may be stated as follows:

$$\frac{Q}{K\, r^2_w} = C\left(\frac{h_s}{r_w}\right) \tan \alpha \qquad (36)$$

---

[18] "The Theory of Ground-Water Motion," by M. K. Hubbert, *Journal of Geology*, Vol. 48, 1940, p. 816.

in which C is a constant, and α is the angle between the horizontal and the free water surface at the well. The value $\frac{h_s}{r_w}$ may vary from zero to twenty-five, as shown in Fig. 13, whereas tan α may vary from zero to infinity. Thus, the slope governs the magnitude of the parameter, a large value indicating a deep cone and a small value indicating a shallow cone.

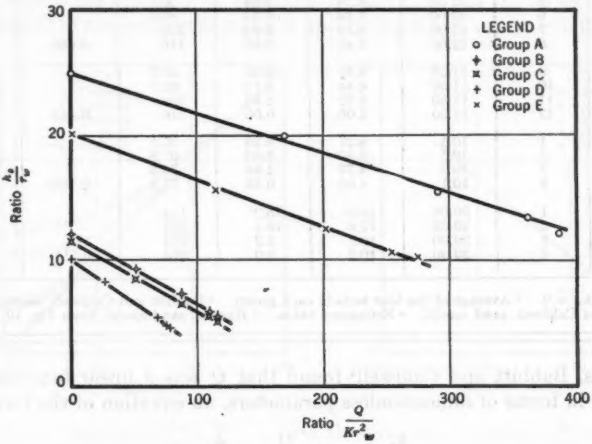

FIG. 13.—RELATION OF $\frac{h_s}{r_w}$ TO $\frac{Q}{K r_w^2}$

Because of a typographical error in the paper by Messrs. Babbitt and Caldwell,[5] Mr. Hansen's statement that their "* * * maximum external radius was only 25 well radii * * *" is in error. The actual maximum external radius can be found from the values, obtained by Messrs. Babbitt and Caldwell, for $\frac{h_e}{r_e}$ and $\frac{r_w}{h_e}$ as follows:

$$\frac{h_e}{r_e} \times \frac{r_w}{h_e} = \frac{r_w}{r_e} = 0.155 \times 0.040 = 0.0062 \qquad (37)$$

This relationship yields

$$r_e = 161.3\, r_w \qquad (38)$$

An examination of the author's analysis of gravity flow into a well and of data presented by the author and Messrs. Babbitt and Caldwell (tabulated in Table 1) indicates that it may be possible to extend the relationships involved by introducing two new symbols. The first symbol is the variable h_s, denoting the piezometric head at the well when there is no drawdown, and a β-factor, which is a measure of the resistance to flow at or near the well face.

TABLE 1.—SUMMARY OF DATA FROM MODEL TESTS

Group	Test No.	$\frac{h_e}{r_w}$	$\frac{h_s}{r_w}$	$\frac{h_w}{r_w}$	$\frac{Q}{K\,r^2_w}$	$\frac{h_s}{h_e}$[a]	Factor[b]
A[c]	1	25.00	20.00	18.75	169		0.0317
	2	25.00	15.62	12.50	290		
	3	25.00	13.50	6.25	362		
	4	25.00	12.25	0.00	386	0.490	
B[c]	5	12.06	9.28	9.04	50.9		0.0566
	6	12.06	7.28	6.03	86.9		
	7	12.06	5.79	3.02	109		
	8	12.06	5.43	0.00	116	0.450	
C[c]	9	11.50	8.51	8.62	50.7		0.0565
	10	11.50	6.44	5.75	87.1		
	11	11.50	5.52	2.88	109		
	12	11.50	5.06	0.00	116	0.440	
D[d]	1	10.1	8.27	8.23	26.1		0.0706
	5	10.1	5.40	3.60	67.8		
	7	10.1	4.73	1.66	75.5		
	8	10.1	4.60	0.28	77.4	0.455[e]	
E[f]	1	20.00	15.6	15.2	115		0.0367
	2	20.00	12.6	10.2	202		
	3	20.00	10.7	5.2	254		
	4	20.00	10.3	0.0	273	0.515	

[a] When $h_w = 0$. [b] Average of the four tests in each group. [c] Babbitt and Caldwell, electrical model. [d] Babbitt and Caldwell, sand model. [e] Estimated value. [f] Hansen, sand model, from Fig. 10.

Messrs. Babbitt and Caldwell[5] found that Q was a linear function of h_s; therefore, in terms of dimensionless parameters, an equation of the form:

$$\frac{h_s}{r_w} = -\beta\,\frac{Q}{K\,r^2_w} + \frac{h_e}{r_w} \qquad (39)$$

may be used to relate these parameters. The constant term $\frac{h_e}{r_w}$ appears on the right side of the equation so that when $Q = 0$, indicating no drawdown at the well, Eq. 39 becomes $h_s = h_e$. The negative sign is inserted in the equation because of the inverse relation of Q to h_s. To verify Eq. 39, values of $\frac{h_s}{r_w}$ and $\frac{Q}{K\,r^2_w}$ were plotted in Fig. 13. These points were fitted by straight lines having an intercept value of $\frac{h_e}{r_w}$, and it is seen that these lines fit closely the observed data, thus verifying the findings of Messrs. Babbitt and Caldwell. The slopes of these five lines, represented by the β-factor in Eq. 39, are tabulated in Table 1. If the β-factor were increased for any one of the sets of data, the slope of the line through the fixed intercept would be increased negatively; hence, for a given value of $\frac{Q}{K\,r^2_w}$, $\frac{h_s}{r_w}$ would be less. This means that a greater drawdown would be required to obtain the same discharge since K and r^2_w are constant. Thus, the β-factor is directly proportional to flow resistance. More extensive data may make it possible to relate the β-factor to types of well screens or perforation, to gravel packing conditions, or to the degree of clogging of the openings in the well face. The deterioration of a well with age might be expressed in terms of increasing values of the β-factor.

Completion of the analysis necessitates relating $\frac{h_s}{r_w}$ to $\frac{h_w}{r_w}$, as is done in Fig. 14, based on data from Table 1. The curves through these points extend from the line having the equation,

$$\frac{h_s}{r_w} = \frac{h_w}{r_w} \qquad (40)$$

when $Q = 0$ to the line $h_w = 0$, when Q is a maximum. It can be seen that the curves are all of the same general form, indicating that a general mathematical

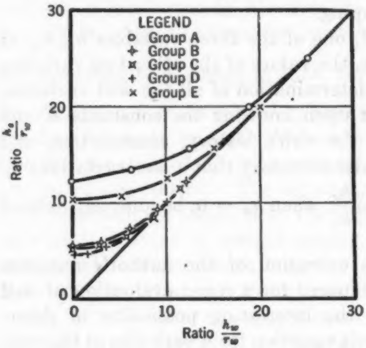

FIG. 14.—RELATION OF $\frac{h_s}{r_w}$ TO $\frac{h_w}{r_w}$

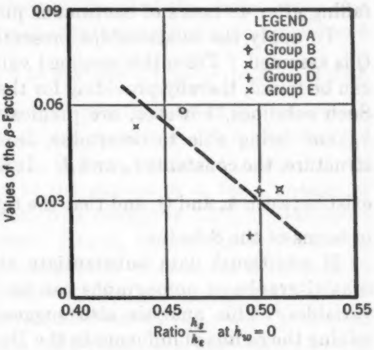

FIG. 15.—RELATION OF β-FACTOR TO $\frac{h_s}{h_e}$, WHEN $h_w = 0$

relationship can be developed for the family of curves if the end points are known. The end point on the line of Eq. 40 is readily obtainable because at this point

$$\frac{h_s}{r_w} = \frac{h_w}{r_w} = \frac{h_e}{r_w} \qquad (41)$$

and $\frac{h_e}{r_w}$ is known. To find the value of $\frac{h_s}{r_w}$ when $\frac{h_w}{r_w} = 0$, requires another step. A solution can be obtained if the relative drawdown outside the well, when $h_w = 0$, is assumed to be some function of the resistance to flow in the vicinity of the well face. In Fig. 15, the β-factor, expressing this flow resistance, is plotted against the dimensionless parameter $\frac{h_s}{h_e}$ using the data recorded when $h_w = 0$. The curve through the plotted points indicates a monotonic relationship, so that as the β-factor increases, the ratio $\frac{h_s}{h_e}$ decreases. Therefore, a well with a great flow resistance will have a larger relative drawdown, and a smaller discharge, when $h_w = 0$, than will a well with a small resistance. Using the relationships of Figs. 14 and 15, it is thus possible to relate $\frac{h_s}{r_w}$ to $\frac{h_w}{r_w}$. No attempt has been made to derive a general equation for this rela-

tionship because of the limited amount of data available. Since the data in Table 1 are from laboratory experiments on electrical and sand models, additional field data are necessary to verify, refine, and extend the relationships presented.

It has been assumed throughout this discussion that the relationships apply only to steady-state flow conditions. Under field conditions, the time lag between the initiation of pumping and the development of steady-state conditions may amount to several days. L. K. Wenzel[19] has shown that the drawdown curve in a pumping test in the Platte River Valley, in Nebraska, was still falling after 48 hours of continuous pumping.

To apply the relationships presented, one of the three variables h_s, h_w, or Q is assumed. From this assumed value, the values of the other two variables can be found, thereby providing for the determination of all the well variables. Such solutions, however, are predicated upon knowing the constants K and h_e, and being able to determine, from the well's history, construction, and structure, the constants r_w and β. It is also necessary that a linear relationship exist between h_s and Q, and that the ratio $\frac{h_s}{h_e}$, when $h_w = 0$, be uniquely defined in terms of the β-factor.

If additional data substantiate this extension of the author's analysis, coaxial graphs or nomographs can be prepared for a rapid evaluation of well variables. This analysis also suggests the interesting possibility of determining the radius of influence in the Dupuit equation from variables at the well.

VAUGHN E. HANSEN,[20] J.M. ASCE.—The writer wishes to express his sincere appreciation to the discussers. They have strengthened many of the concepts presented in the paper by adding their experience and analysis. The science of the flow of water into unconfined wells is such that engineers must work together, each contributing a segment to the whole, in order to arrive at a valid solution.

The discussion of the limitation of the Darcy law, presented by Mr. Shukry, is not clear. It is general practice to consider the validity of the Darcy law in terms of the Reynolds number of the flow that encompasses implicitly the gradient and permeability referred to by Mr. Shukry. Mr. Muskat[3] defines this limit as follows:

> "* * * it will suffice to accept as a safe lower limit where deviations from Darcy's law will become appreciable as given by a Reynolds number of 1, with d chosen as any reasonable average diameter of the sand grains."

Mr. Shukry states that

> "Because the Dupuit value of the slope m as given by Eq. 23 is not constant, it follows that the logarithmic functions shown in Fig. 7 cannot be straight lines."

Such is not the case because the piezometric heads in Eqs. 3 and 8 are not the same. The same symbols are used to avoid a complex symbol notation, but

[19] "Specific Yield Determined from a Thiem's Pumping-Test," by L. K. Wenzel, *Transactions*, Am. Geophysical Union, Vol. 14, 1933, p. 475.

[20] Irrig. Engr., Irrig. Div., SCS; and Associate Prof. of Research, Utah State Agri. College, Logan, Utah.

the reader should note carefully that for the Dupuit equation (Eq. 3) to be valid, the measurements of piezometric head (h) should be made in zones of essentially horizontal flow, whereas Eq. 8 applies to measurements taken in the curvilinear zone at or near the free surface. Such limitations result in Eq.23 being an approximation that consequently affects the conclusions drawn therefrom.

Mr. Boulton's finding that "* * * the drawdown ($h_e - h_s$) at the well, is practically independent of the water level in the well for ranges of h_w/h_e between zero and 0.4" is mentioned by Mr. Shukry, who suggests that the writer check this conclusion. Fig. 10 shows that, even for a change in values of h_w/r_w from 0 to 6 corresponding to a change of h_w/h_e from 0 to 0.37 for a $\left(\frac{Q}{K\,r^2_w}\right)$-value of 250, the change in h_s/r_w is relatively small, being approximately 12%. However, the drawdown continued to increase until h_w was equal to 0. A further insight into the variation of h_s with a variation in h_w is given in Fig. 14 in which h_s/r_w and h_w/r_w are plotted. The significance of the change in h_s for a change of h_w/h_e from 0 to 0.4 depends on the application; a change of 12% in drawdown may be important in certain applications. Hence, the writer would prefer stating that the drawdown does not increase greatly when h_w/h_e is reduced to less than 0.4. However, the drawdown does continue to increase until $h_w = 0$.

Eq. 27, solved for the proper boundary conditions, should yield the desired solution to the shape of the free surface. However, the application of the proper boundary conditions is a complex problem. The simplified boundary conditions applied by Mr. Shukry (at $r = r_w$, $h = h_s$ and $dh/dr = \infty$) to obtain Eqs. 28 and 29 are boundary conditions at a point and not the boundary conditions that apply to Eq. 21. Since Eq. 21 involves the total flow, the applied boundary conditions must be those governing the total flow. The solution obtained, as represented by Eq. 29, is a solution for a well having Mr. Shukry's boundary conditions along the entire inner boundary. A detailed discussion of the boundary conditions at an unconfined well has been presented by Chong-Hung Zee[21] in a doctoral dissertation at the Utah State Agricultural College, in Logan.

Further proof that Eq. 29 is incorrect is obtained when both sides of the equation are divided by r_w:

$$\frac{h_s}{r_w} = \frac{1}{2\,\pi}\left(\frac{Q}{K\,r^2_w}\right) \qquad (42)$$

This equation is seen to lack the term h_w/r_w of Eq. 11. Reference to Fig. 10, in which the parameters of Eq. 11 are plotted, shows a family of curves designated as h_w/r_w. Hence, both Eq. 11 and Fig. 10 prove that h_s is not independent of h_w as claimed by Mr. Shukry.

Mr. Rohwer, in discussing the effect of the discharge number, $\frac{Q}{K\,r^2_w}$ (and particularly the radius of the well, r_w) on the cone of depression, comments that it is surprising

[21] "The Use of Combined Electrical and Membrane Analogies to Investigate Unconfined Flow into Wells," by Chong-Hung Zee, thesis presented to the Irrig. and Drainage Dept., Utah State Agri. College, in Logan, Utah, in 1952, in partial fulfilment of the requirements for the degree of Doctor of Philosophy.

"* * * that the shape of the cone of depression is a function of the reciprocal of the square of the radius of the well. This seems unusual because it is usually believed that the radius of the well has a relatively small effect on the well characteristics."

The discharge number is deceiving in that one may be tempted to state that the discharge will vary as the square of the radius. However, observing Eq. 11, it will be seen that the radius also appears on the right side of the functional relationship. To clarify the effect of a change of radius on the discharge of the well, Fig. 16 has been prepared from theoretical Eqs. 2and 3 for flow into both confined and unconfined wells. A family of curves exists since a change in well radius will usually produce a change in external boundary conditions.

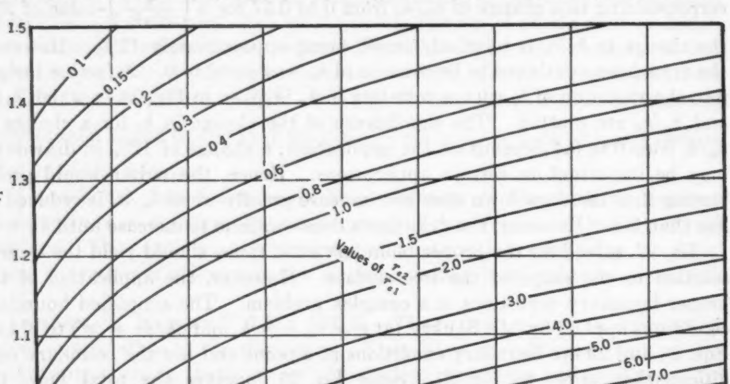

FIG. 16.—RELATIONSHIP BETWEEN DISCHARGE AND WELL RADIUS FOR EITHER CONFINED OR UNCONFINED FLOW.

However, if the external conditions remain the same, an increase of 100% in well radius only produces an increase of approximately 11% in the well discharge. Hence, as far as the general hydraulics of the flow are concerned, Mr. Rohwer is correct in feeling that the radius of the well has a relatively small effect on the well characteristics—particularly on the discharge. However, practical considerations not encompassed by the theoretical formula often play an important part in the relation between the discharge and the well radius. Since factors affecting loss of energy at and in a well are more important in a small well than in a larger one, losses at the well frequently reduce the discharge materially. Fig.16 summarizes the effect produced by a change of well radius on the discharge from an ideal well in which the losses at and in the well are negligible.

The writer disagrees with Messrs. Todd and Fowler in their discussion of definitions of the Froude and Reynolds numbers involved in the discharge number. Those discussers assert that combining the mean microscopic velocity of the flow "* * * with the well radius as the characteristic length in the

Reynolds number, as done in Eq. 14*a*, has no relation to defining the flow conditions." The mean grain diameter, or some other representative cross-sectional measure of the flow path, is generally used to evolve a Reynolds number that is characteristic of the flow through porous media. Flow to a well is certainly flow through porous media, but one subtle difference becomes apparent as one carefully analyzes the implication of the discharge number. This number is a characteristic of flow into a well, not flow through porous media; consequently, the characteristic length in the Reynolds number should be related to the geometry of the well—otherwise the derived Reynolds number will have no relation to the well. The writer's analogy, as involved in Eqs. 31, 32, and 33, is correct and sound for flow in porous media. Such a discussion has no bearing, however, on flow into a well if the cone of depression is quantitatively described by the discharge number (which in effect is the ratio of the viscous forces to the gravity forces involved in the phenomona of water entry into the well). The well is the internal boundary condition controlling the drawdown phenomona, and hence its geometry determines the length criterion in both the Reynolds and Froude numbers.

Eq. 38 extends the range to which the linear logarithmic relationship (Eq. 8) fits the free surface with reasonable accuracy.

Eq. 39 is not fundamentally sound in that h_e can be varied without affecting h_s. To illustrate, reference is made to Fig. 4 in which h_e can be considered the water surface in the reservoir. The values of h_s/r_w and $\frac{Q}{K\,r^2_w}$ in Eq. 39 would not change if h_e were reduced by removing the left half of the sand model, shaping the interface between the reservoir and model to conform to the shape of the original potential surface, and lowering the water level in the reservoir to the original height of the measured free surface at the new external radius. A correct functional relationship is obtained if h_w is combined with h_s, Q, K, and r_w as shown in Eq. 11 and as plotted in Fig. 10. Note that the coordinates of Fig. 10 are identical to those of Fig. 13.

It is questionable whether the β-factor suggested by Messrs. Todd and Fowler is a measure of the resistance to flow at or near the well face and hence indicative of the type of well screen, perforation, gravel pack, or degree of clogging, as they suggest. Analysis of the β-factor in Table 1 and in Fig. 15 indicates that it is a direct function of the applied boundary condition and consequently will not be a function of well resistance or well losses. It appears that the points are plotted incorrectly in Fig. 15. This error may be easily rectified by reference to Table 1 in which the correct values are listed.

The results of the North Platte River Valley (Nebraska) pumping tests[19] were pointed out by Messrs. Todd and Fowler to show that generally steady-state flow conditions are not reached for several days. Actually, steady-state conditions are never reached unless the water table is sloping, or unless vertical recharge is involved. Modifications of steady-state flow formulas to the cases of sloping water tables and vertical recharge are presented by Dean F. Peterson, Jr., Orson W. Israelsen, Members, ASCE, and the writer.[22] Steady-state flow formulas also can be applied to unsteady horizontal flow. The interested

[22] "Hydraulics of Wells," by Dean F. Peterson, Jr., Orson W. Israelsen, and Vaughn E. Hansen, *Technical Bulletin No. 351*, Agri. Experiment Station, Utah State Agri. College, Logan, Utah, March, 1952.

reader can use the Nebraska tests, referred to by Messrs. Todd and Fowler, to verify the contentions that follow.

The analysis of unsteady unconfined flow involves two types of problems. The first type of problem applies to measurements of piezometric head taken in the zone where the Dupuit equation applies ($h^2 \approx \log r$). In this case the square of the piezometric head (h^2) should be plotted against the logarithm of the radius of the well. The second type of problem applies to measurements taken in the zone of curvilinear flow near the free surface where the linear logarithmic relation applies ($h \approx \log r$). This second case also applies to the analysis of unsteady confined flow to wells. Making the appropriate semi-logarithmic graph will show the plotted data adjacent to the well lying in a straight line regardless of the time since pumping began. The extent of the straight line will increase as the pumping test continues. The slope of the resulting straight line, regardless of its radial extent, will be a valid index to the discharge and coefficient of permeability. Note that Eq. 3 for unconfined flow can be written as

$$\frac{h^2 - h^2_1}{\log_e \frac{r}{r_1}} = \frac{Q}{\pi K} \quad \text{(43)}$$

whereas Eq. 8 can be written as

$$\frac{h - h_1}{\log_e \frac{r}{r_1}} = m \quad \text{(44)}$$

Also, Eq. 2 for confined flow is

$$\frac{h - h_1}{\log_e \frac{r}{r_1}} = \frac{Q}{2 \pi K t} \quad \text{(45)}$$

The left sides of Eqs. 43, 44, and 45 are the slopes of the straight lines resulting from the appropriate semi-logarithmic plotting.

A further extension of the foregoing analysis will provide a sound quantitative evaluation of the radius of influence. It is suggested that the radius of influence be considered as the radial distance to the intersection between the straight line as described and the original water table, or piezometric surface, before pumping was begun.

Additional experimental data concerning flow to unconfined wells can be found in Mr. Zee's dissertation which analyzes the free surface in terms of the dimensionless parameters presented herein by combining his own data with those of Messrs. Babbitt and Caldwell,[5] Yang,[11] Zee[21] and that of the writer.[23] Mr. Zee obtained his results by combining the electrical analogy with the membrane analogy suggested by the witer.[24] Using the data of these same men, a further extension of well hydraulics has been made by Messrs. Peterson, Israelesen, and the writer.[22]

---

[23] "Evaluation of Unconfined Flow to Multiple Wells by the Membrane Analogy," by Vaughn E. Hansen, thesis presented to the State University of Iowa, at Iowa City, Iowa, in 1949, in partial fulfilment of the requirements for the degree of Doctor of Philosophy.

[24] "Complicated Well Problems Solved by the Membrane Analogy," by Vaughn E. Hansen, *Transactions*, Am. Geophysical Union, Vol. 33, No. 6, December, 1952, p. 912.

AMERICAN SOCIETY OF CIVIL ENGINEERS
Founded November 5, 1852
TRANSACTIONS

Paper No. 2572

FIELD STUDY OF A SHEET-PILE BULKHEAD

By C. Martin Duke,[1] A. M. ASCE

With Discussion by Messrs. Gregory P. Tschebotarioff; Walter C. Boyer; Paul Baumann; S. Packshaw; W. F. Way; J. Owen Lake; K. Terzaghi; D. P. Krynine; Trent R. Dames and David C. Liu; Roy W. Carlson; and C. Martin Duke

Synopsis

Methods and results of a field study of the structural performance of a flexible anchored bulkhead are presented in this paper. The bulkhead retains a 55-ft height of fine sand hydraulic fill in Long Beach Harbor, California. A coarse granular dike extends for half the height on both inside and outside. Instrumentation was provided for the measurement of soil pressure, pore pressure, tie-rod tension, and deflection during and after the filling operation.

During filling, the lateral soil pressure distribution was approximately in proportion to the weight of the overlying fill, with a lateral pressure coefficient of approximately 0.7. After the completion of filling, the lateral pressures above the wale increased sharply and those below decreased. This change is attributed to the settlement of fill and the accompanying partial support of fill on the tie rods and wale.

The inner dike was effective in reducing outward soil pressures on the bulkhead. The outer dike provided some passive resistance to deflection and served to confine the bulkhead foundation.

Introduction

The anchored flexible bulkhead presents an example of the group of problems in foundations and earth structures that are not amenable to accurate analysis because of insufficient understanding of the performance of the prototype system. Performance of such bulkheads is poorly understood for the following reasons:

1. The bulkhead, the backfill, and the supports at the anchor and the toe all deform in accordance with as yet unformulated functions of soil and bulkhead load-deformation characteristics;

Note.—Published in October, 1952, as *Proceedings-Separate No. 155*. Positions and titles given are those in effect when the paper or discussion was received for publication.

[1] Associate Prof. of Eng., Univ. of California, Los Angeles, Calif.

2. The factors determining relations between lateral and vertical soil pressures even under idealized conditions are still incompletely understood; and

3. The influences on lateral pressures of such prototype phenomena as tide fluctuation, pore pressure, settlement of fill, and construction irregularities are not quantitatively known.

Efforts toward a determination of the fundamental parameters of bulkhead performance have led (as with many other soil problems) to the conclusion that further advance must lean heavily on experimental scientific studies of actual engineering structures. An opportunity for an investigation of this type arose when the Port of Long Beach, Calif., as part of its development program, planned the construction of two large hydraulically-filled piers bordered by anchored steel sheet-pile quay walls. This project led to the cooperative program of investigations which is the subject of this paper.

The structural performance of the east bulkhead of Pier C, Long Beach Harbor (Fig. 1), during and after hydraulic filling of the pier, was investigated

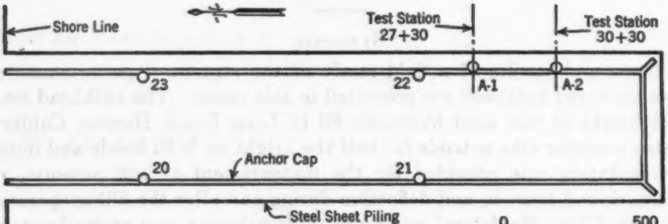

FIG. 1.—PIER C, LONG BEACH HARBOR, CALIFORNIA

by instruments installed at two test stations. The pier was filled to El. +17 and has an outboard bottom elevation of −38 at the test locations. A coarse granular dike was placed on both sides of the bulkhead to El. −10 prior to filling. The fill material consisted predominately of a fine sand containing varying amounts of silt.

Provision was made at the principal test station for the measurement of total deflection of bulkhead and anchor, relative deflection at various elevations on the bulkhead, bending strain in the bulkhead, tension in tie rods, soil pressures at various elevations, and water pressures at significant locations in the fill. These measurements, except for soil and water pressure, were duplicated at another test station. Observations were made over a period of eight months, from February to October, 1949, with principal activity during the filling operation from February to June.

The investigation probed the distribution and magnitude of soil pressure against the bulkhead and its variation with height and age of fill. Also studied were the effectiveness of the dike in carrying a part of the lateral pressure and the pore pressure phenomena in the fill and dike. Special emphasis was

given to those aspects of the study that would yield information not obtainable quantitatively from laboratory, model, or theoretical analyses.

Structure and Materials

The Pier C quay wall (Fig. 2) consists of a bulkhead of 78-ft steel sheet piles (MZ-38) anchored by 3-in. tie rods at 6-ft intervals to a concrete-capped batter-pile anchor set 62 ft back of the bulkhead center line. A continuous wale consisting of two 15-in. channels is bolted to the inside of the wall. Tie rods are set on a slope of 1 on 27. The timber anchor piles are 3 ft, center to center, in two rows battered each way from the anchor center line. Tide range in Long Beach Harbor is about 8 ft between annual extremes; there are two high tides and two low tides each day.

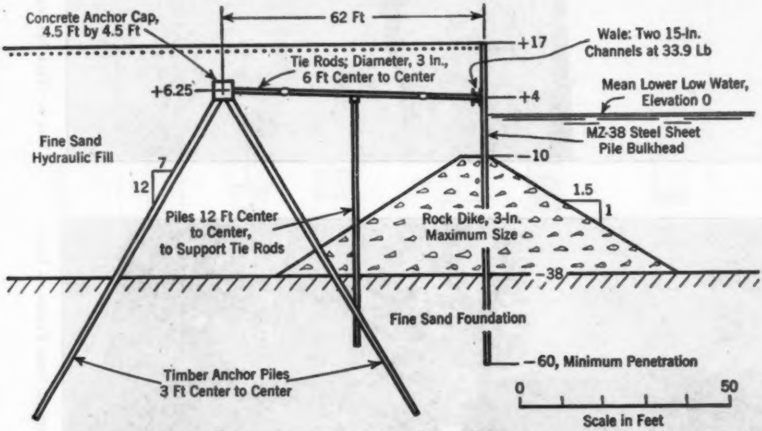

Fig. 2.—Design Features, Pier C Bulkhead

After the completion of pile driving, installing wale and tie rods, and concreting the anchor cap, the rock dike was placed by clamshell buckets on both sides of the wall, sloping at its natural angle of repose. The rock used in the dike was a partly decomposed diabase obtained from a quarry west of near-by San Pedro. The larger particles are angular and fairly hard (Fig. 3). Mechanical analyses showed 90% passing the 3-in. sieve and 15% passing the ¼-in. sieve. The angle of repose measured from the dike profiles was 32°.

Hydraulic filling from dredges working in the vicinity of the Los Angeles River delta was begun in mid-December, 1948, at the north or shore end of the pier and progressed seaward. Overflow was at the seaward end, first through the unclosed southeast corner of the pier and later through a sea-level spillway in the center of the south bulkhead. This procedure tended to produce a characteristic fill profile, grading from silty clay at the bottom to coarse sand at the top. In mid-February, 1949, deposition began at Test Station 27 + 30, and by mid-June, 1949, filling had been substantially completed at both test stations. Fig. 4 is a typical view of the fill.

FIG. 3.—DIKE MATERIAL AS DEPOSITED ON WALE AND DETAIL OF TYPICAL PORE PRESSURE POINT

FIG. 4.—FILL MATERIAL SHOWING CRACK OVER ANCHOR CAP DUE TO FILL SETTLEMENT

Samples were studied from sixty-nine borings in the harbor area. Four of the borings, numbers 20, 21, 22, 23, Figs. 1 and 5, were made in Pier C prior to filling, and extended to about El. −100. "Undisturbed" samples, 3 in. in diameter, were taken at 3-ft intervals in twenty three of the borings, including those in Pier C, and classification samples were taken in the remainder. Laboratory density, mechanical analysis, "quick" triaxial compression, permeability, and consolidation tests were made on a large number of samples representing all soil types encountered. Approximate tests were made to estimate maximum and minimum void ratios, and Atterberg limits were established for the few plastic soil types encountered. After completion of

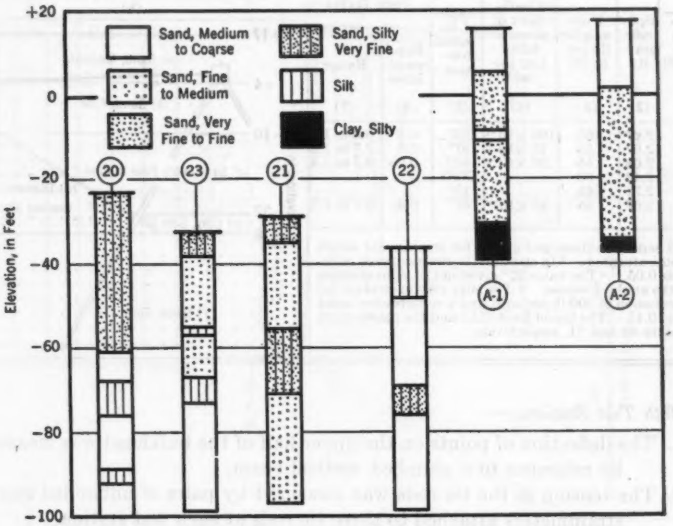

FIG. 5.—LOGS OF BORINGS

filling, borings A-1 and A-2, Figs. 1 and 5, were made through the fill opposite the test stations.

Soil property and stratification data as they pertain to Pier C at the test stations are summarized in Table 1, where data on dike properties also are included. The compressive index (decrease in void ratio per tenfold increase in pressure on a preconsolidated specimen) for strata (b) and (d) were obtained from tests on similar soils in other parts of the harbor. Grain size limits are those of the United States Bureau of Chemistry and Soils.[2] For the fine sands of the fill, the permeability coefficient ranged between 10 and 35×10^{-4} cm per sec, and the percentage of the material passing sieve No. 200 ranged

[2] "Soil Mechanics," by D. P. Krynine, McGraw-Hill Book Co., Inc., New York, N. Y., 1947, p 17.

between 5 and 15, approximately. Lenses of silt and of coarse and medium sands and occasional lumps of organic clay were present.

Instrumentation

Scheme of Instrumentation.—Much study was given to the problem of how best to observe the behavior of the soil and bulkhead. General features of instrumentation are shown in Fig. 6. Measurements consisted of the following:

TABLE 1.—Summary of Soil Properties at Test Stations

Stratum (see Col. 8)	Specific gravity	Unit weight[a] (lb per cu ft)	Coefficient of permeability (cm per sec)	Angle of internal friction	Void Ratio: Representative	Void Ratio: Range
(1)	(2)	(3)	(4)	(5)	(6)	(7)
(a)	2.67	105	100×10^{-4}	38°	0.8	0.6 to 1.1
(b)[b]	2.67	55	25×10^{-4}	37°	0.8	0.7 to 1.2
(c)	2.68	55	20×10^{-4}	34°	0.95	0.7 to 1.3
(d)[c]	2.42	60	....	(32°)	....	....
(e)[d]	2.72	48	....	13°	....	....
(f)	2.67	55	25×10^{-4}	37°	0.8	0.7 to 1.2

[a] All samples submerged except for stratum (a) which was semisaturated. [b] In stratum (b) the compressive index was 0.05. [c] The value 32° given in Col. 5 for stratum (d) is the angle of repose. [d] The silty clay in stratum (e) has a cohesion of 900 lb per sq ft and a compressive index value of 0.15. The liquid limit (LL) and the plastic limit (PL) were 48 and 31, respectively.

Description of Strata (See Col. 1)
(8)

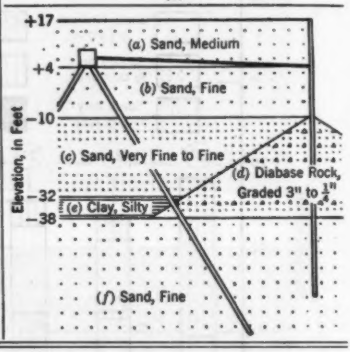

At Both Test Stations.—

1. The deflection of points on the upper half of the bulkhead was measured by reference to a plumbed vertical beam.
2. The tension in the tie rods was measured by pairs of unbonded electric strainmeters attached to three tie rods at each test station.
3. Fill settlement was determined by indirect methods.

At Station 27 + 30 Only.—

4. Pressure of the soil against the bulkhead was obtained with nine electric stressmeters. Four of these instruments were installed in the fill above the dike. Five were installed in the dike—three inside, and two outside, the bulkhead.
5. Water pressure on stressmeters and on the inside of the bulkhead, and pore pressure in the fill, were measured with six standpipe piezometers.

In addition, at both test stations, measurements were undertaken of the bulkhead bending moment by a mechanical strain gage and of the total deflection of bulkhead and anchor by transit. The precision and consistency of these measurements was so poor that they have been disregarded. Water and fill elevations were referred directly to points on the bulkhead in order to

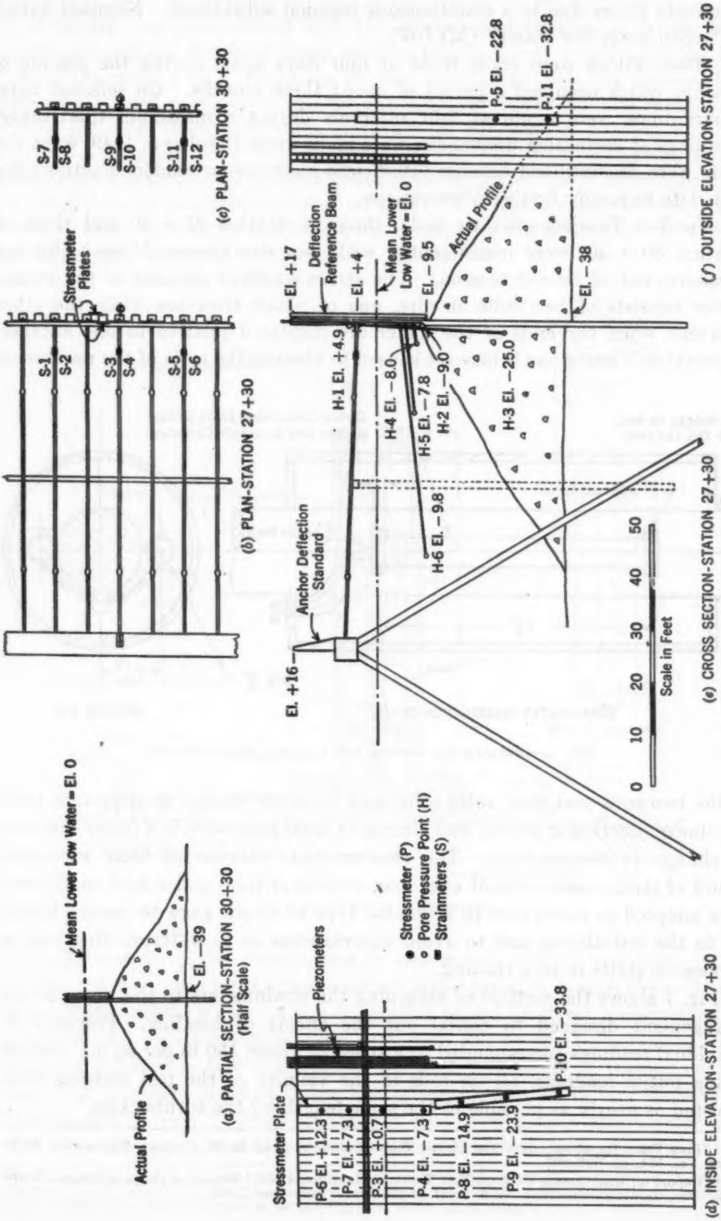

FIG. 6.—INSTRUMENTATION LAYOUT

eliminate errors due to a simultaneous regional subsidence. Nominal datum is "mean lower low water" (MLLW).

Observations were made three or four days apart during the placing of the fill, which occupied a period of about three months. On selected days, observations were made at 2-hr intervals during a maximum tidal range. Readings at decreasing frequencies were made up to October 5, 1949, when the tests were discontinued because insufficient instruments remained active after this date to justify further observations.

Tie-Rod Tension.—Six tie rods, three at Station 27 + 30 and three at Station 30 + 30, were instrumented with two strainmeters,[3,4] each, for the measurement of tie-rod tension. The strain-sensitive element of the strainmeter consists of two coils of wire, one of which stretches while the other shortens when the ends of the meter are displaced relative to one another. A portable Wheatstone bridge set is used to observe the ratio of the resistances

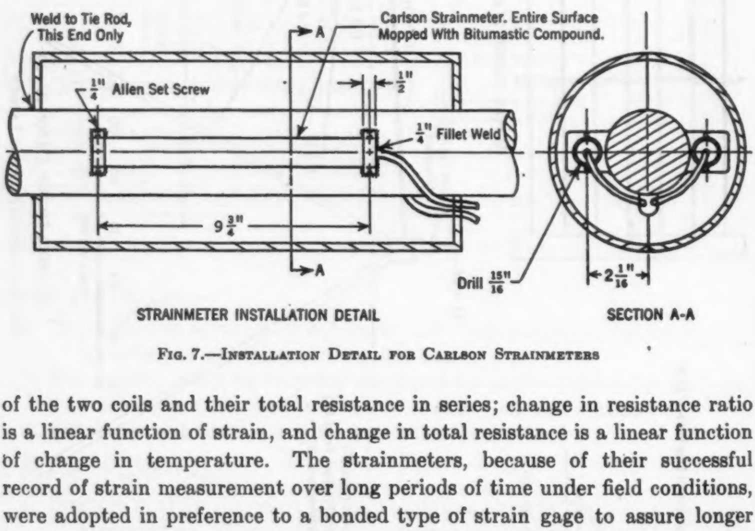

FIG. 7.—INSTALLATION DETAIL FOR CARLSON STRAINMETERS

of the two coils and their total resistance in series; change in resistance ratio is a linear function of strain, and change in total resistance is a linear function of change in temperature. The strainmeters, because of their successful record of strain measurement over long periods of time under field conditions, were adopted in preference to a bonded type of strain gage to assure longer life to the installation and to avoid uncertainties as to waterproofing and as to possible shifts in zero reading.

Fig. 7 shows the method of attaching the strainmeters to the tie rods—an arrangement designed to cancel out the effects of bending. Precision of individual readings corresponded to a stress of about 150 lb per sq in. Before taking initial readings, all tie rods in the vicinity of the test stations were adjusted as nearly as possible to the same length by the turnbuckles.

[3] "Five Years Improvement of the Elastic Wire Strainmeter," by R. W. Carlson, *Engineering News-Record*, Vol. 114, pp. 696–697.

[4] "Report on Instruments Used on Test Track at Hamilton Field," Report of Corps of Engrs., South Pacific Div., San Francisco Dist., U. S. Dept. of the Army, December, 1946.

Difficulty was encountered with the strainmeters because of failure adequately to protect the lead wires against tensile forces resulting from the drag of the settling fill. When the fill level reached El. +8, the strainmeters began to become inoperative one by one until, when the fill had reached its full height there were only three strainmeters left—one at Station 27 + 30 and two at Station 30 + 30. Fortunately, the loss of strainmeters was a gradual process and it was possible to continue computations of tie-rod tensions by using data from one strainmeter on a rod. For these computations it was assumed that any strains resulting from bending in the horizontal plane were not significant except under the lower tensions.

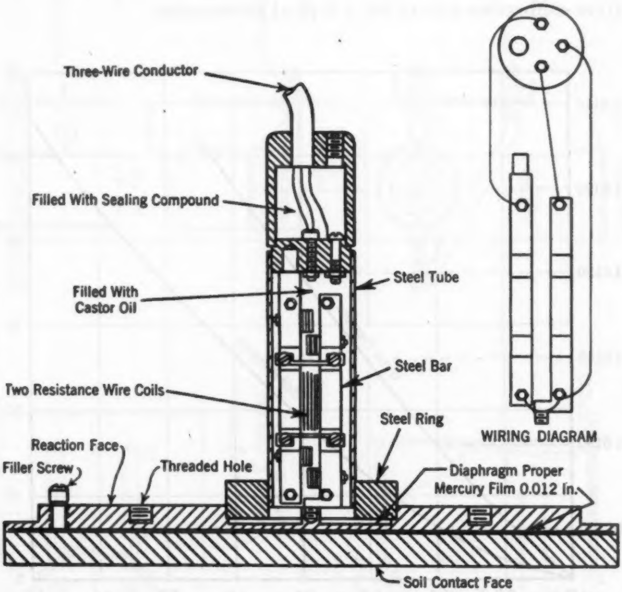

FIG. 8.—CARLSON STRESSMETER

Soil Pressure.—Nine stressmeters,[4,5] with ranges of 20 lb per sq in. and 40 lb per sq in. were used for the measurement of soil pressure against the bulkhead. These instruments, which have a successful record of stress measurement in concrete, and previously have been used with soil on several occasions, were specially adapted to this soil pressure problem. Pressure on the soil contact face (Fig. 8) causes pressure in the film of mercury which in turn deflects the "diaphragm proper." This deflection is measured with a strainmeter unit. The least reading corresponds to a pressure of less than 50 lb per sq ft.

[5] "Development and Analysis of a Device for Measuring Compressive Stress in Concrete," by Roy W. Carlson, thesis presented to the Massachusetts Institute of Technology, at Cambridge, Mass., in 1939, in partial fulfilment of the requirements for the degree of Doctor of Science.

The stressmeters were calibrated for soil pressure in a testing machine using a stiff rubber pad[4] about 1 in. thick between the soil contact face and the testing machine weighing table. Load was uniformly distributed over the "reaction face" (Fig. 8). Calibration for water pressure was carried out at the test site by suspending the stressmeters in a cloth bag at measured distances below the water surface; fluid pressure then acted uniformly over the entire outside surface of the stressmeter. Four or five corresponding values of pressure and resistance ratio were determined in each case. Loading and unloading portions of the calibration cycles checked closely. Recalibrations checked to about 1% for soil pressure and to about 2% for water pressure. Fig. 9 gives calibration curves for a typical stressmeter.

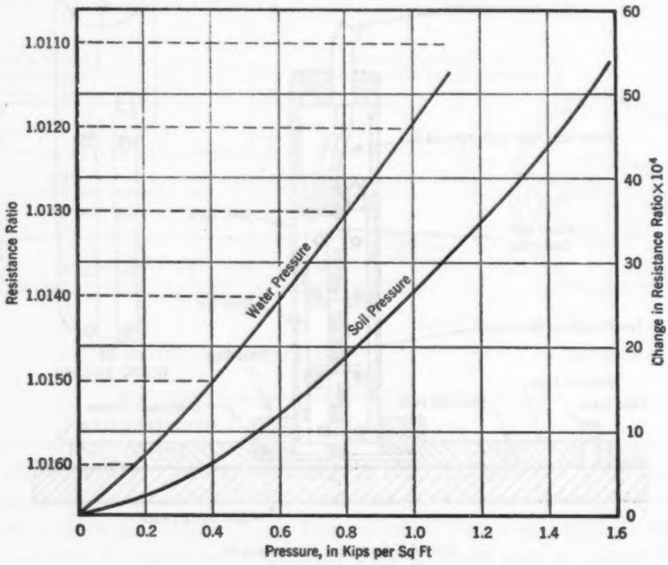

Fig. 9.—Typical Stressmeter Calibration Curves (Stressmeter P-4)

The stressmeters were mounted in 22-in. steel plates as shown in Fig. 10. Reaction for the pressure was provided by two steel bars which also served to stiffen the plate; because of the considerable stiffness of the reaction face of the stressmeter, these bars were considered to provide the same support as used in the soil pressure calibration. The steel plates were held in the bulkhead troughs by spring friction clips. After the stressmeters had been installed, the steel plates (Fig. 6) were lowered into position, pressed into the bulkhead troughs by a diver, and securely welded to the bulkhead at their tops only.

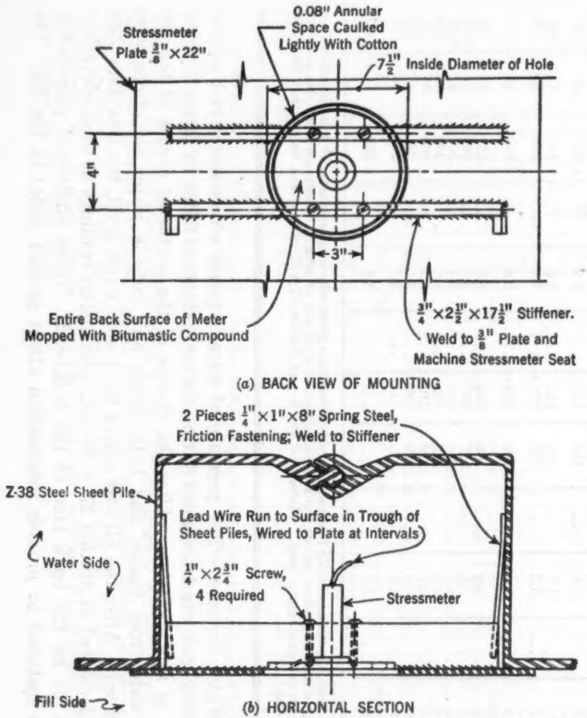

FIG. 10.—INSTALLATION DETAIL FOR CARLSON STRESSMETER

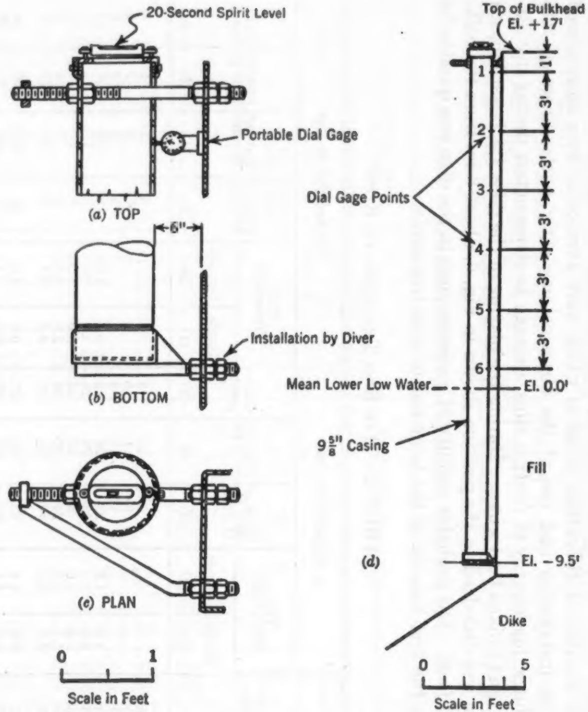

FIG. 11.—DEFLECTION MEASURING SYSTEM

A number of difficulties (most of which were overcome) were encountered in the installation and use of the stressmeters—early unsteadiness of zero readings, inadequacy of friction clips, damage to stressmeters during installation, and broken lead wires. During the placing of the dike, the lower inboard plate was dislodged to the position shown in Fig. 6, about 6 in. from the bulkhead face. The probable validity of measurements in the dike was questioned from the first because of the large size of dike fragments.

TABLE 2.—TIE-ROD TENSIONS, IN KIPS

Date (1949)	(a) STATION 27 + 30					(b) STATION 30 + 30					
	Tide Elevation[a]		Station[b] 27 + 18	Station[b] 27 + 42	Composite	Tide Elevation[a]		Station[b] 30 + 18	Station[b] 30 + 30	Station[b] 30 + 42	Composite
	Inside	Outside				Inside	Outside				
	(1)	(2)	(3)	(4)	(5)	(1)	(2)	(3)	(4)	(5)	(6)
April—											
15	....	....	6	10	8	....	....	−5	5	1	0
19	....	....	6	11	8	....	....	−7	2	2	0
19	....	....	4	11	8	....	....	−5	3	2	0
23	4.2	1.7	22	24	23	5.1	1.9	8	22	7	12
26	5.0	2.0	28	24	26	5.0	2.0	3	17	11	10
26	5.3	4.0	18	25	22	5.0	3.0	9	21	13	14
26	5.5	6.0	24	27	26	5.6	5.6	3	7	0	3
29	5.6	3.9	30	23	26	5.2	3.1	4	26	21	17
May—											
3	5.5	4.4	32	30	31	5.5	4.5	19	33	26	26
6	6.6	4.4	46	42	44	6.6	3.7	11	40	34	28
10	8.2	2.5	30	53	42	8.2	3.7	33	48	41	41
14	10.5	3.7	....	62	58	10.5	3.7	49	122	62	78
17	....	4.8	72	76	74	....	4.7	48	109	....	73
20	....	4.0	138	97	118	....	4.0	63	162	67	97
24	....	4.4	....	155	155	....	5.0	73	183	63	106
June—											
3	....	5.7	....	182	182	....	6.0	71	194	55	107
11	....	0.5	....	205	205	....	1.0	....	266	76	153
July—											
12	....	3.6	....	209	209	....	3.8	....	255	49	135
August—											
5	....	8.0	....	198	198	....	8.0	....	257	55	139
5	....	5.5	....	197	197	....	5.5	....	265	57	143
5	....	4.0	....	214	214	....	3.7	....	267	62	147
6	....	2.0	....	212	212	....	1.6	....	269	64	149
6	....	0.7	....	219	219	....	0.7	....	269	66	150
17	....	6.0	....	229	229	....	5.6	....	291	83	169
24	....	2.8	....	....	....	....	3.7	....	297	92	176
October—											
5	....	3.0	....	....	....	....	3.2	....	293	....	172

[a] Both inside and outside free water levels (in feet) are given where appropriate. [b] A horizontal rule in a column indicates where one of the two strainmeters went out of action. Increases from this point are based on one strainmeter only. Meters S-3 and S-4 at Station 27 + 30 gave erratic values that have been discarded.

Water Pressure.—The pressure of water against stressmeters and against the bulkhead was determined during the early stages of filling by direct observation of tide elevation. After the closure of the southeast corner of the pier the water rose inside, and both inside and outside water elevations were observed. After the fill rose above the inside water level, the tide data were supplemented at Station 27 + 30 with piezometer readings at three elevations (Fig. 6) on the back face of the bulkhead. Three additional piezometers were installed to provide information about ground water in the fill. The

piezometers consisted of pipes running to simple filter-type pore pressure points (Fig. 3).

Bulkhead Deflection.—Deflection of bulkhead points was determined by the vertical reference beam shown in Figs. 7 and 11. The beam was plumbed by a precise level tube mounted at the top. Relative deflection measurements

TABLE 3.—SUMMARY OF MEASUREMENTS, STATION 27 + 30

Date (1949)	ELEVATIONS,[a] IN FEET			Stress[b] σ_v at El. −10	Tie-rod tension (kips)	Horizontal deflection at El. −9.5 (in.)	SOIL PRESSURE IN KIPS PER SQUARE FOOT						
	Fill	Tide					Inside Face					Outside Face	
		Inside	Outside				El. +12.3	El. +7.3	El. +0.7	El. −7.3	El. −14.9	El. −22.8	El. −32.8
(1)	(2)	(3)	(4)	(5)	(6)	(7)	(8)	(9)	(10)	(11)	(12)	(13)	(14)
February—													
17	−32	....	....	0	....	....	....	....	....	....	0.00	0.00	0.00
25	−30	....	....	0	....	....	....	....	....	....	0.00	0.56	0.38
March—													
1	−29	....	....	0	....	....	....	....	....	....	0.22	0.70	0.26
4	−27.5	....	....	0	....	....	....	....	....	....	0.40	0.69	0.27
8	−27	....	....	0	....	....	....	....	....	....	0.50	....	....
13	−26	....	....	0	....	....	....	....	....	....	0.73	0.86	0.36
17	−22	....	....	0	....	0.02	....	....	....	....	0.77	0.84	0.38
22	−22	....	....	0	....	0.05	....	....	....	....	1.40	0.94	0.50
26	−21	....	....	0	....	0.00	....	....	....	....	1.00	0.99	0.33
29	−21	....	....	0	....	0.00	....	....	....	....	0.96	1.15	0.30
April—													
2	−18	....	....	0	....	0.11	....	....	....	....	0.80	0.98	0.31
6	−17.5	....	....	0	....	0.02	....	....	....	....	0.80	1.03	0.28
9	−14	....	....	0	....	0.04	....	....	....	....	0.90	1.02	0.40
12	−11	....	1.2	0	....	0.09	....	....	....	....	1.20	1.32	0.53
15	− 8.5	....	2.7	0.08	8	0.42	....	....	....	....	1.10	1.22	0.42
19	− 7	....	3.5	0.17	8	0.52	....	....	....	0.00	1.06	1.20	0.45
23	− 1	4.2	1.7	0.50	23	0.82	....	....	....	0.17	1.33	1.47	0.60
26	3.2	5.3	4.0	0.73	25	1.89	....	....	0.00	0.55	1.19	1.61	1.05
29	5.8	5.6	3.9	0.88	26	2.15	....	....	0.11	0.50	1.06	1.38	1.27
May—													
3	7.5	5.5	4.4	1.00	31	2.48	....	0.00	0.00	0.76	1.06	2.40	1.12
6	7.8	6.6	4.4	1.07	44	2.57	....	0.08	0.00	0.55	1.00	1.47	0.87
10	9.4	8.2	2.5	1.17	42	2.78	....	0.08	0.26	0.86	0.98	1.90	1.04
14	12.0	10.5	3.7	1.42	58	....	0.00	0.38	0.56	1.04	1.62	2.30	1.12
17	12.1	....	4.8	1.52	74	3.39	....	0.73	0.68	1.25	1.84	1.98	0.98
20	13.1	....	4.0	1.59	118	3.33	....	0.26	0.85	1.48	1.59	1.60	0.96
24	16.0	....	4.4	1.94	155	3.42	....	0.55	0.23	1.14	1.70	1.58	0.95
June—													
3	16.3	....	5.7	2.01	182	3.36	....	0.67	1.30	1.04	1.74	1.35	0.60
11	16.5	....	0.5	2.14	205	3.40	....	0.70	1.18	0.71	2.52	1.88	0.85
July—													
12	16.5	....	3.6	2.07	209	3.46	....	1.28	0.00	0.58	2.53	1.58	....
August—													
5	16.5	....	8.0	1.96	198	3.37	....	1.79	0.00	0.68	2.79	0.80	0.6
6	16.5	....	0.7	2.09	219	3.37	....	1.85	0.00	0.24	2.33	0.95	....
17	20.5	....	6.0	2.43	229	3.37	2.70	2.36	0.00	0.55	1.62	0.69	1.07
24	20.5	....	2.8	2.49	....	3.41	2.85	2.60	0.00	0.48	1.30	0.87	....
October—													
5	20.5	....	3.0	2.48	....	3.63	....	....	0.00	0.57	1.85	0.74	....

[a] Both inside (Col. 3) and outside (Col. 4) free water levels are given where appropriate. [b] In Col. 5, σ_v is the computed vertical soil pressure, in kips (thousands of pounds) per square foot.

were made to the nearest 0.01 in. with a portable dial gage. Although provision was made for transit observations of anchor deflection using a special fin (Fig. 4) bolted to the cap and projecting up through the fill, these were insufficiently precise; thus in the calculations it has been necessary to neglect deflection of the anchor and wale.

Data Presentation

Data on Bulkhead Performance.—Results of measurements are presented in Tables 2 through 5 and in Fig. 12. Tie-rod tension measurements at both test stations are given in Table 2 and are summarized in Tables 3 and 4. Because of the successive breaking of strainmeter leads, the composite values in Table 2 become gradually more approximate with the passage of time, beginning about May 6.

TABLE 4.—Summary of Measurements, Station 30 + 30

Date (1949)	Elevations, in Feet			Stress[b] σ_v at El. −10	Tie-rod tension (kips)	Horizontal deflection at El. −9.5 (in.)
	Fill	Tide[a]				
		Inside	Outside			
(1)	(2)	(3)	(4)	(5)	(6)	(7)
March—						
1	−35	....	....	0	....	....
17	−30.5	....	....	0	....	0.00
22	....	....	....	0	....	0.02
26	....	....	....	0	....	0.13
29	....	....	....	0	....	0.08
April—						
2	....	....	....	0	....	0.17
6	−28.5	....	....	0	....	0.13
9	−26	....	....	0	....	0.14
12	−25	....	....	0	....	0.10
15	−23	....	....	0	0	0.14
19	−22	....	....	0	0	0.16
23	−20	5.1	1.9	0	12	0.86
26	−14.5	5.0	3.0	0	10	1.16
29	− 6	5.2	3.1	0.22	17	1.60
May—						
3	− 3	5.5	4.5	0.38	26	2.02
6	0.5	6.6	3.7	0.58	28	2.28
10	4.5	8.2	3.7	0.80	41	2.58
14	9.0	10.5	3.7	1.05	78	....
17	10.2	....	4.7	1.38	73	3.57
20	12.0	....	4.0	1.62	97	3.66
24	12.7	....	5.0	1.63	106	3.69
June—						
3	12.5	....	6.0	1.56	107	3.86
11	15.5	....	1.0	2.13	153	....
July—						
12	15.5	....	3.8	1.99	135	....
August—						
5	16.0	....	8.0	1.83	139	3.69
6	16.0	....	0.7	2.20	150	3.69
17	21.5	....	5.6	2.53	169	3.67
24	21.5	....	3.7	2.62	176	3.67
October—						
5	21.5	....	3.2	2.65	172	3.92

[a] Both inside and outside free water levels are given where appropriate. [b] In Col. 5, σ_v is the computed vertical soil pressure, in kips per square foot.

Tables 3, 4, and 5 summarize all measurements at the two stations. Free body diagrams of the bulkhead at Station 27 + 30 on 19 dates through August 17 are drawn in Fig. 12. Tie-rod tension values have been divided by six for these diagrams to give anchor pull per linear foot of bulkhead. Measurements of water pressure by piezometers have been used in computing soil pressures from stressmeter readings. Hydrostatic excess, which was small in

general, and therefore has not been shown in Fig. 12, can be computed from data in Table 5.

Data on Settlement.—Unfortunately, direct measurements of fill settlement as a function of time and of position in fill were omitted. Sufficient indirect data are available, however, to permit approximate quantitative determinations. Measurement of movements of piezometer pipes showed settlements adjacent to the bulkhead ranging up to 0.6 ft for piezometer H-6; this amount apparently occurred below El. −9 where the horizontal pipe to H-6 left the bulkhead, Fig. 6. Cracks of considerable magnitude occurred in the fill over the anchor caps, as illustrated in Fig. 4, which indicate sizable settlements.

TABLE 5.—PIEZOMETER READINGS, STATION 27 + 30
(FEET ABOVE MEAN LOWER LOW WATER)

Date (1949)	Time	Tide[a]	Piezometer						Inside water level	Fill elevation (ft)
			H-1	H-2	H-3	H-4	H-5	H-6		
(1)	(2)	(3)	(4)	(5)	(6)	(7)	(8)	(9)	(10)	(11)
April—										
19	3:00 p.m.	4.2 (r)	....	4.0	4.4	4.1	4.0	4.0	Tide	−7
23	12:00 p.m.	1.5 (f)	....	3.3	2.8	2.2	4.8	3.8	3.4	−1
May—										
3	3:00 p.m.	4.4 (r)	6.5	4.3	4.2	4.5	4.5	4.5	5.5	7.5
6	3:30 p.m.	4.6 (r)	5.8	4.5	4.9	5.1	5.1	4.9	6.6	7.8
10	2:30 p.m.	2.7 (r)	7.1	4.4	2.3	4.4	5.7	5.5	8.2	9.4
14	3:15 p.m.	3.7 (f)	7.5	5.4	3.0	5.2	5.6	5.4	10.5	12.0
17	3:20 p.m.	4.8 (r)	5.8	5.8	4.5	5.7	6.3	5.7	....	12.1
20	2:10 p.m.	3.8 (r)	7.1	5.2	3.7	5.0	5.9	5.8	....	13.1
24	3:15 p.m.	4.2 (r)	5.6	4.6	3.7	4.9	5.9	5.6	....	16.0
June—										
3	3:30 p.m.	5.9 (r)	<5.4	5.0	5.6	6.3	6.3	5.1	....	16.3
11	5:30 a.m.	0.9 (r)	<5.4	2.6	1.0	2.3	2.6	4.6	....	16.5
July—										
12	4:30 p.m.	3.7 (r)	<5.4	4.1	3.5	3.5	3.8	3.8	....	16.5
August—										
5	7:10 p.m.	8.0 (f)	5.4	6.2	7.0	6.4	5.9	5.5	....	16.5
5	10:00 p.m.	4.8 (f)	5.5	6.0	5.1	5.3	5.6	5.6	....	16.5
5	10:40 p.m.	4.0 (f)	5.5	5.5	3.9	4.4	5.4	5.4	....	16.5
6	12:05 a.m.	2.0 (f)	<5.4	4.6	2.3	3.3	4.0	4.2	....	16.5
6	2:00 a.m.	0.7 (f)	<5.4	3.5	1.2	2.5	3.0	3.1	....	16.5
17	4:40 p.m.	6.0 (f)	<5.4	5.3	5.3	5.3	5.5	5.0	....	20.5
17	5:45 p.m.	5.2 (f)	<5.4	5.3	5.2	....	....	....	....	20.5
24	4:00 p.m.	3.4 (r)	<5.4	4.1	3.3	3.4	3.8	4.1	....	20.5
October—										
5	3:00 p.m.	3.0 (r)	<5.4	4.3	4.6	4.5	4.7	4.2	....	20.5

[a] (r) denotes rising tide and (*f*) denotes falling tide.

Breakage of strainmeter leads seems attributable only to such a cause. Usual experience of the Long Beach Harbor Department with similar fills obtained from the same Los Angeles River delta soils has indicated settlements of the order of from 2% to 3% over periods of from six months to eighteen months; this would correspond to about 1 ft in six months at the Pier C test stations at locations away from the bulkhead and anchor.

No doubt the greater part of the differential settlement of fill with respect to the bulkhead is seated in the lower fill strata (Table 1) of very fine sand and silty clay, and in the silty upper stratum (Fig. 5) of the foundation soil. Rough computation using the compressibility data of Table 1 yields a value of about 1 ft for the differential settlement due to these strata.

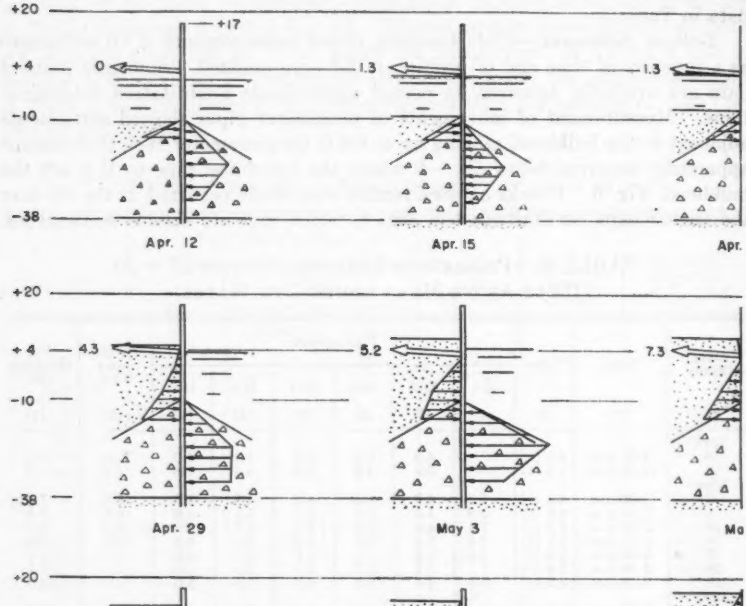

FIG. 12.—BULKHEAD FREE BODY

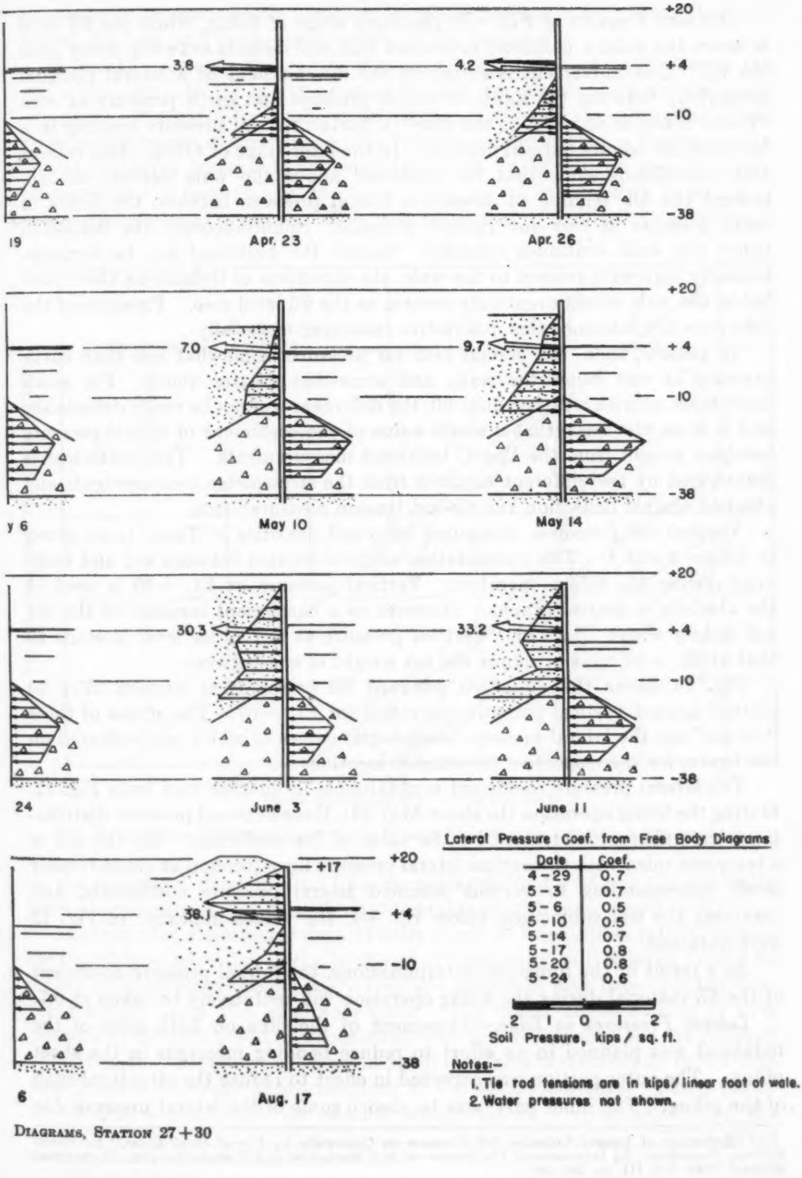

DIAGRAMS, STATION 27+30

Bulkhead Performance During Filling

Outward Pressure of Fill.—In the early stage of filling, while the fill level is below the wale, a bulkhead in contact with soil deflects outward, away from the fill. This movement is suited to the development of a lateral pressure somewhere between the limits of active pressure and earth pressure at rest. "Earth pressure at rest," is the state of horizontal soil pressure existing in a horizontally infinite natural deposit. In the later stage of filling, observations and calculations show that the bulkhead above the wale deflects inward, toward the fill, tending to develop a lateral pressure between the limits of earth pressure at rest and passive pressure. Simultaneously the deflection below the wale continues outward. Should the bulkhead top be unprecedentedly high with respect to the wale, the directions of deflections above and below the wale would eventually reverse as the fill level rose. Presence of the dike does not influence this qualitative reasoning materially.

In general, then, one should look for pressures somewhat less than earth pressure at rest below the wale, and somewhat greater above. For small deflections, or with a rather fluid fill, the difference will not be easily detectable, and it is on this basis that a single value of the coefficient of lateral pressure has been sought from the Pier C bulkhead measurements. This coefficient is determined by two different methods from the stressmeter measurements and checked against deflection and tie-rod tension measurements.

Vertical soil pressures, computed from soil densities in Table 1, are given in Tables 3 and 4. This computation neglects friction between soil and bulkhead during the filling operation. Vertical pressure at El. −10 is used as the abscissa in several graphs. It serves as a convenient measure of the net soil weight above El. −10. Vertical pressure at any other level is equal to that at El. −10, plus or minus the net weight of soil between.

Fig. 13 shows the measured outward fill pressures at Station 27 + 30 plotted against vertical pressure computed for El. −10. The slopes of these "curves" are the lateral pressure coefficients, values of which are indicated on the figure, for the respective stressmeter locations.

The lateral pressure coefficient is obtainable in another way from Fig. 12. During the filling operation (to about May 24), these outward pressure distributions have shapes determined by the value of the coefficient. By the use of a template ruled with theoretical lateral pressure lines (broken at ground-water level) corresponding to various assumed lateral pressure coefficients, and assuming the soil submerged below El. +4, the values indicated in Fig. 12 were obtained.

As a result of the foregoing determinations, the lateral pressure coefficient of the fill material during the filling operation will tentatively be taken at 0.7.

Lateral Pressures in Dike.—Placement of the dike on both sides of the bulkhead was planned in an effort to reduce bending moments in the sheet piling. The outer portion was expected in effect to reduce the structural span of the piling. The inner part[6] was to absorb some of the lateral pressure due

[6] "Reduction of Lateral Cohesive Soil Pressure on Quaywalls by Use of Sand Dikes," by Harris Epstein, *Proceedings*, 2d International Conference on Soil Mechanics and Foundation Eng., Rotterdam, Holland, 1948, Vol. III, pp. 291–296.

to the rather fluid fill. The inner dike could not have been placed more strategically to perform this function, for the deposition of sediments (Table 1) placed the finer and more plastic strata at the bottom.

The dike exerted a theoretical initial lateral pressure on both sides of the wall about equal to the active pressure since it was placed at its natural angle of repose. Theoretically, again, as the fill rose in the pier, the outer dike lateral pressures increased in accordance with increasing deformation. The inner dike lateral pressures increased, corresponding with rising fill, to greater active pressures at the base and, in the upper part, to values probably in excess of active dike-material pressure. This is an extension of findings[7,8] and theory,[6]

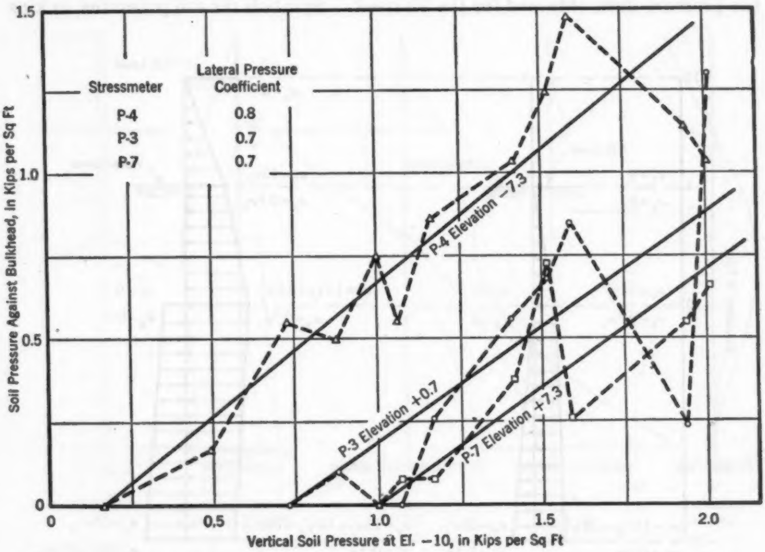

FIG. 13.—LATERAL PRESSURE COEFFICIENTS, DURING FILLING, FROM INDIVIDUAL STRESSMETERS

on the subject of dikes in fluid fills, necessitated for Pier C by the gradually increasing thickness of dike with depth combined with large depth of fill.

Because dike stressmeter data (Tables 3 and 4) were not as satisfactory as for the fill (probably due to the large size of fragments), full reliance cannot be placed on these observations in arriving at a picture of dike behavior; the foregoing theory must also be drawn upon. The initial measurements of dike pressure in the bulkhead are inconsistent with active pressures and are believed to be in error. However, subsequent small increases in stressmeter indications may possibly be rough approximations to the actual increases. Based partly on the theory and partly on rational interpretation of stressmeter data, the

[7] "Soil Mechanics, Foundations, and Earth Structures," by Gregory P. Tschebotarioff, McGraw-Hill Book Co., Inc., New York, N. Y., 1951, pp. 293–303.
[8] *Ibid.*, pp. 510–514.

following idealizations are made tentatively to facilitate checking the various types of measurements against one another:

1. For the inner dike, the lateral pressure at the base was taken as active with a coefficient of 0.3; the lateral pressure at the top was taken as that due to fill, with a coefficient of 0.7; and a straight-line variation of pressure was assumed between.

2. For the outer dike, the lateral pressure was taken as active, with a coefficient of 0.3, until the fill reached El. +4 (see Table 3); for the fill above El. +4, the lateral pressure was taken as active, plus a uniform 0.5 kips per sq ft.

These idealizations are given in Fig. 14 for two levels of fill to supplement the pressure data obtained for the fill itself. Symbols for soil pressures, in kips

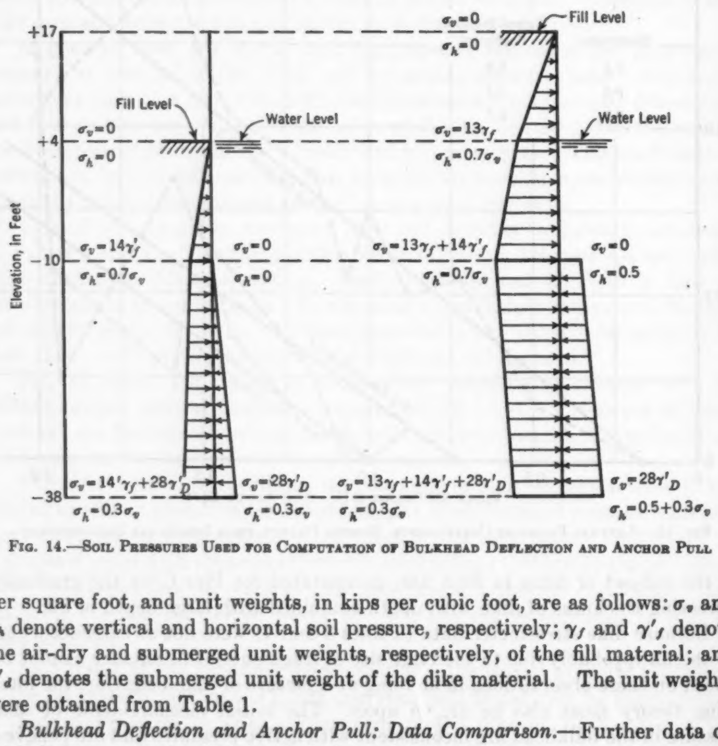

FIG. 14.—SOIL PRESSURES USED FOR COMPUTATION OF BULKHEAD DEFLECTION AND ANCHOR PULL

per square foot, and unit weights, in kips per cubic foot, are as follows: σ_v and σ_h denote vertical and horizontal soil pressure, respectively; γ_f and γ'_f denote the air-dry and submerged unit weights, respectively, of the fill material; and γ'_d denotes the submerged unit weight of the dike material. The unit weights were obtained from Table 1.

Bulkhead Deflection and Anchor Pull: Data Comparison.—Further data on lateral pressure are implicit in the bulkhead deflection and anchor pull measurements, which are of special importance because results are available from both of the test stations. These are now to be compared with the direct pressure measurements at Station 27 + 30, which are summarized in Fig. 14 for two levels of fill.

The method of computing deflections and tie-rod tensions from soil pressure measurements is shown in Fig. 15. It is idealized that the bulkhead is fixed against rotation at El. −38; confinement due to the dike and rigidity of the natural ground tend to provide this restraint. The statically indeterminate free body thus obtained has been analyzed according to the conventional theory of flexure, and curves of shear, moment, and deflection are given.

The first comparison is given in Fig. 16, where representative observed and computed profiles of the deflected bulkhead are superposed. The shapes of the curves, in so far as they correspond, are in fair agreement, but computed values are less than those directly observed.

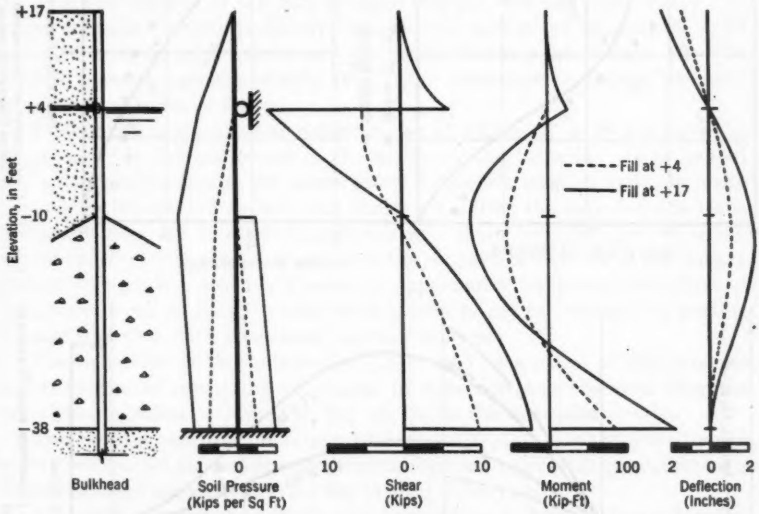

FIG. 15.—BULKHEAD DEFLECTION AND ANCHOR PULL COMPUTED FROM MEASURED SOIL PRESSURES

The most significant comparison is shown in Fig. 17, in which the results of Fig. 15 have been amplified slightly to give theoretical plots against vertical soil pressure at El. −10. Reasonable agreement between computed and measured tie-rod tensions is indicated for the period here considered—that is, during the filling operation. The large tensions at Station 30 + 30 in the early stages are attributed to the high inside water level during that period (Table 4). This influence is also felt in the observed deflections at Station 30 + 30. The hinge at the bottom of the deflection reference beam (El. −9.5) deflects about 25% less by computation than in fact, as shown by the upper curves of Fig. 17. Shapes of both computed curves compare reasonably well with the observed.

It is considered that these comparisons of data obtained during the filling operation are acceptably good. The check between tie-rod tensions and soil pressures (Fig. 17) is further evidence of the correctness of the previously

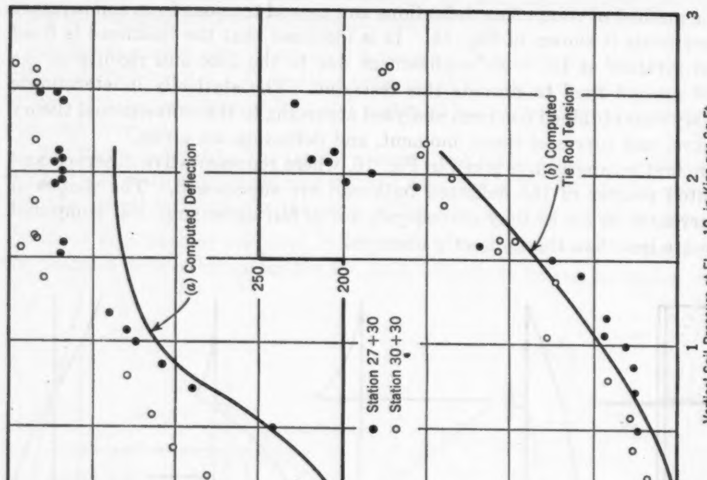

Fig. 17.—Comparison of Measured Deflections and Anchor Pulls with Values Computed from Measured Soil Pressures

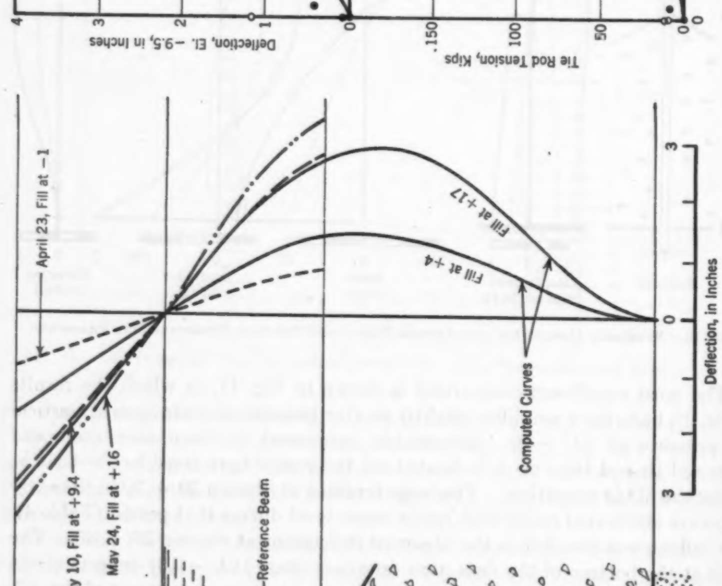

Fig. 16.—Measured Deflection Profiles Versus Those Computed from Measured Soil Pressures, Station 27 +30

deduced lateral pressure coefficient of 0.7 and to a degree validates the assumptions relating to the dike and to the condition of base support. The 25% discrepancy of the deflections computed from soil pressures (Figs. 16 and 17) relative to those observed directly may quite possibly be due to a small outward deflection of the bottom of the bulkhead.

Other Pressure Distributions

Nonproportional Pressure Distribution After Filling.—Beginning on about June 11, the lateral pressure distribution curve at Station 27 + 30 began to assume a significantly different shape (Fig. 12). Lateral pressure was no longer directly proportional to the weight of the overlying fill. Pressures between the wale and the top of the dike dropped sharply, whereas those above this region increased. Simultaneously, the tie-rod tension at Station 27 + 30 increased considerably. However, the tie-rod tension at Station 30 + 30 did not increase correspondingly (Fig. 17). Deflections remained constant after the completion of filling.

Explanation of the pressure redistribution at Station 27 + 30 is believed to lie primarily in the settlement of the fill below the tie rods. As estimated above, the compression of the strata below the tie-rod level, at locations away from the bulkhead and anchor, was about 1 ft during the period of the tests. Settlement adjacent to the bulkhead was only about half this distance which was due partly to the dike, but largely to the supporting capacity of the tieback system. There is a relative absence of opportunity for lateral deflection at the tie-rod level, so that the rods were caused to act as "cables" supporting a transverse load, with a resultant increase in stress.

The deflection of the bulkhead is discounted as a cause of this pressure redistribution, as essentially no change in deflection was observed after the completion of filling. Curve (*a*), Fig. 17, shows this condition clearly.

This result is new in so far as quantitative observation is concerned although experience has led at least one progressive engineer[9] to provide special features in his bulkhead design to prevent the loading of tie rods.

A tentative design consideration of importance is that maximum bending moment and tie-rod tension probably do not occur simultaneously in any filled anchored bulkhead. The former occurs between the wale and the ground during filling, and results from the high lateral pressure coefficient which is approximately uniform before settlement of the upper fill. The latter occurs after the settlement of the fill due to the supporting, on the tieback system, of a part of the weight of fill above the tie rods. Conceivably, with the passage of years, the pressure distribution might trend toward a proportional one once more, although with a smaller lateral pressure coefficient.

The seeming absence of this interesting finding at Station 30 + 30 could be related to the high inside water level during the early stages of filling at that station.

Surcharge.—The effect of a 4-ft surcharge close to the bulkhead at Station 27 + 30 on pressure distribution is seen by comparison of the August 5 and

---

[9] "Soil Mechanics, Foundations, and Earth Structures," by Gregory P. Tschebotarioff, McGraw-Hill Book Co., Inc., New York, N. Y., 1951, p. 514.

August 17 free body diagrams (Fig. 12). Increase in pressure above the wale, and in the tie-rod tension, indicates that this surcharge has been carried essentially by the wale-and-tie-rod system. Increase in tie-rod tension due to this action of the tie rods as "cables" is directly related to the increase in lateral pressure. This finding is checked qualitatively by the measurements at Station 30 + 30, where tie-rod tension increased slightly (Tables 3 and 4) due to a 5.5-ft surcharge. This is significant for design purposes as it indicates that surcharge should be especially investigated for its effect on tie-rod tension.

Tide Fluctuation.—Table 5 yields some results regarding water pressure fluctuations in the dike and the fill. Noting the close comparison of readings of piezometer H-3 (which was in the dike) with the tide levels, it is seen that the combination of dike and sheet piles was pervious. The dike pore pressures were nearly equal to the free outside water pressure at all times, even when a high inside free water level prevailed, as on May 10 and 14.

The August 5 and 6 readings (Table 5) are most descriptive of the effect of tide variation on pore pressures. Piezometer readings in the fill were roughly the same regardless of location, and ranged from about +6 to about +3 while the tide dropped from +8.0 to +0.7.

Changes in bulkhead loading due to this same large range of tide are given for a typical case in Fig. 12, August 5 and 6, at Station 27 + 30. Hydrostatic excess, which acts inward on August 5 and outward on August 6, is not shown in Fig. 12 but may be obtained from data in Table 5. Tie-rod tension increases about 15 kips (averaging Stations 27 + 30 and 30 + 30) with falling tide, while the changes in hydrostatic excess roughly balance those in soil pressure. The indicated changes, although appreciable, are small in comparison with total pressures and tie-rod tensions. For construction of the type at Pier C it would be overconservative to design in the usual fashion for the low tide condition, assuming water behind the bulkhead to be at high tide level.

Summary of Test Results

During the filling operation the pressure of fill against the bulkhead was approximately in proportion to the weight of the overlying fill. The proportionality constant, or coefficient of lateral pressure, was found to be about 0.7 for this predominately fine sand material. Internal pressure distribution not in proportion to the weight of overlying fill developed after the completion of filling. Pressures above the wale increased sharply while those below decreased. This condition is attributed mainly to the approximately 1-ft settlement of the fill and accompanying partial support of the upper part of the fill on wale and tie rods. This result was obtained at the primary test station only.

Maximum deflections were approximately 3.6 in. outward at the top of the dike and 3.9 in. inward at the top of the bulkhead, assuming no deflection of the wale. No reversal in direction of the deflections occurred at any time. Deflection changes ceased upon completion of filling. Observed deflections at the two test stations agreed reasonably closely. Predictions of deflections, based on soil pressure measurements and a structural analysis of the bulkhead, agreed qualitatively but were about 25% low.

Maximum tie-rod tension was about 200 kips. This occurred near the end of the tests, under maximum influence of pressure redistribution. Observed tie-rod tensions agreed reasonably closely at the two test stations. They agreed well with values predicted from measured soil pressures and bulkhead structural analysis.

The part of the dike inside the bulkhead was effective in reducing outward pressures. Its vertical position is such as to be of maximum efficiency, since the finer fill strata are in the lower depths. The part of the dike outside the bulkhead provided some passive resistance and served to confine the bulkhead foundation.

The surcharge piled close to the bulkhead after completion of filling was carried principally by the tieback system, pressures below the wale being not much affected.

Pore pressures in both inner and outer dikes were nearly equal to the free outside water pressures at all times. The extreme range of pore pressure fluctuation in the fill was about 3 ft of water and was roughly the same at all locations. Tie-rod tension increased about 15 kips in one case due to a 7-ft drop of tide.

Suggestions for Future Bulkhead Field Studies

Experience with the conduct and interpretation of the Pier C bulkhead tests has led to nine suggestions to future field investigators of anchored bulkheads, as follows:

1. An adequate system of survey control should be established, with better provision for observing total horizontal and vertical deflections.

2. Fill settlement should be observed with permanent reference points established both in and on the various soil strata.

3. Borings should be made in the fill and at intervals during fill deposition and "undisturbed" samples taken to determine density and shear strength.

4. Test stations, both with and without a dike, should be included.

5. Special attention should be given to tie-rod tension measurement, as this simple and inexpensive determination is probably the most significant of the various indicators of anchored bulkhead performance. Lead wires should be run in pipe, or otherwise protected from the settling fill.

6. Bulkhead bending strains could be remotely measured by a technique similar to that used for tie-rod tension.

7. The sensitivity and reliability of soil pressure measurements could be improved by a new design of the stressmeter mounting. A large plate in contact with the soil or the dike could be used to transmit force to one or more stressmeters. A simple inexpensive soil pressure cell would be a boon to the progress of soil mechanics.

8. Special attention to insuring long life to the instrumentation would make possible the study of the permanence of observed pressure distributions and of such influences as static and moving surcharge, impact, and seismic loadings. The changes accompanying passage of time, up to several years, are little known. The electric instruments used in these tests are suited to such long-time studies.

9. Creative thought is needed on the problem of the difficult and probably expensive quantitative observation of passive resistance phenomena at the base of a bulkhead.

Acknowledgment

The Long Beach Harbor Department designed the quay wall and purchased and installed the instruments. R. R. Shoemaker, M. ASCE, chief harbor engineer, jointly with the writer, conceived the test program. B. N. Hoffmaster, A. M. ASCE, and T. J. Thorley supervised the installation of instruments and contributed to the planning and execution. Exploration and testing of soils was carried out by L. T. Evans, A. M. ASCE, consultant to the harbor department.

The Department of Engineering, University of California, in Los Angeles, planned the instrumentation and conducted the tests and analyses. D. P. Krynine, M. ASCE, visiting professor, advised in the planning. The writer was in immediate charge. Students in engineering who participated were D. L. Wheeler, E. R. Hallett, V. S. Peterson, R. J. Reich, and E. Carlson, J. M. ASCE. The methods of attaching the strainmeters to the tie rods and of mounting the stressmeters were developed in consultation with Roy W. Carlson, M. ASCE, the inventor, and with David Pirtz, J. M. ASCE.

The Soil Mechanics Committee, Los Angeles Section, ASCE, gave considerable study to the planning of the test program and made numerous valuable suggestions. Committee members were T. R. Dames, M. ASCE (Chairman); F. J. Converse, M. ASCE; Mr. Evans; S. S. Green, M. ASCE; T. M. Leps, A. M. ASCE; D. F. Warren, J. M. ASCE; and the writer.

Interpretation of test results has benefited materially as a result of discussions with Mr. Krynine and with G. P. Tschebotarioff, M. ASCE.

To all these engineers, and to the many who helped in other ways, the writer extends his sincere thanks.

DISCUSSION

Gregory P. Tschebotarioff,[10] M.ASCE.—The great practical and theoretical value of studies of the type performed at Long Beach cannot be exaggerated, and all participants in this work and the sponsors of it deserve the highest commendation. A wealth of data has been obtained by such studies that could not be obtained by any other means. In the past there has been reluctance among practicing engineers to perform such measurements and, especially, to make their results public for fear of criticisms of their previous designs. The Board of Harbor Commissioners of the City of Long Beach is to be commended highly for taking a different attitude in this matter. The observations made should permit design improvements, not only at Long Beach, but in many other harbors, which otherwise could not have been accomplished. The author and his staff at the University of California are to be complimented highly for having performed this work, as is the Committee on Soil Mechanics of the Los Angeles Section, ASCE, for having sponsored it, and for having encouraged the publication and discussion of the results.

In order to facilitate the following discussion, four of the nineteen test stages reported in Fig. 12 by Mr. Duke have been selected as most significant. They are replotted at a larger scale in Fig. 18. The anchor forces are in kips per foot, and the bulkhead pressures are in kips per square foot.

The author has estimated that, during backfilling, the average lateral pressure coefficients varied from $K=0.7$ to $K=0.8$ (Fig. 13). This average value is, roughly, 60% higher than the value $K=0.44$, obtained by the writer under static conditions during a model test with silty sand at Princeton University, at Princeton, N. J. It is approximately 190% higher than the average value of 0.24 obtained during the several model tests with clean sand.[11] However, strong vibration was found, at Princeton, to increase the above static lateral pressure coefficients by 227% for silty sand and by from 58% to 111% for clean sand.[11]

Therefore, it is possible that the high K-values recorded by the author were caused by continued slight vibrations of the type produced by wave action, which caused the sand fill to "wedge itself in" behind the bulkhead while consolidating during the backfilling.

However, another explanation is also possible. It will be noted from Fig. 18, stage 1, that the pressure distribution was not entirely hydrostatic—the K-values increasing from $K=0.4$ above the anchor level to almost $K=1.00$ near the top of the rock dike. The latter high values may have been caused by "true arching" in the sand in a horizontal direction between the rock dike and the closely spaced batter piles of the anchorage, as shown by the arrows (II) in Fig. 19. This illustration is from a previous work by the writer.[12] No such batter piles were present during the Princeton model tests.

[10] Prof. of Civ. Eng., Princeton Univ., Princeton, N. J.

[11] "Final Report. Large Scale Earth Pressure Tests with Model Flexible Bulkheads," by Gregory P. Tschebotarioff, submitted to Bureau of Yards and Docks, Dept. of the Navy, Princeton Univ., Princeton, N. J., January, 1949.

[12] "Einfluss der Gewölbebildung auf die Erddruckverteilung," by Gretory P. Tschebotarioff, *Bautechnik-Archiv*, Heft 8, W. Ernst and Son, Berlin, Germany, 1952.

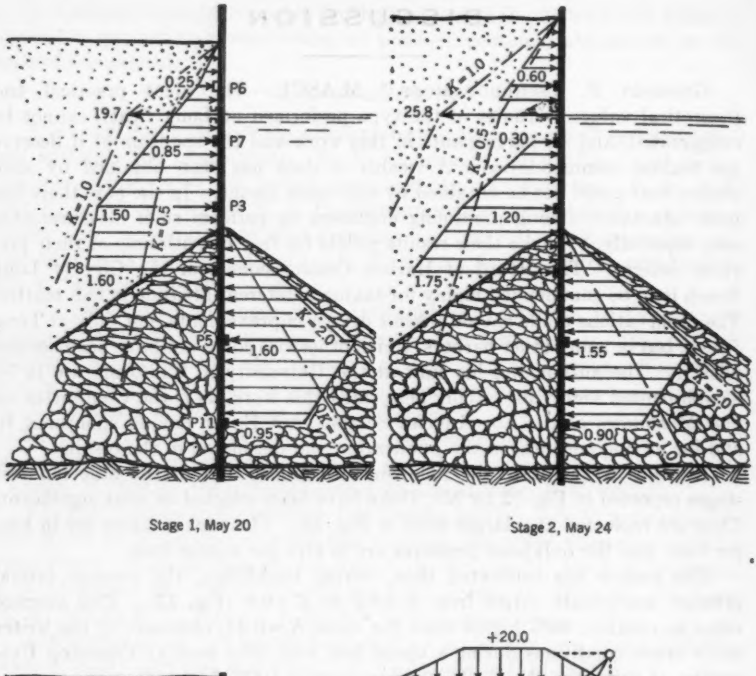

FIG. 18.—ANALYSIS OF THE LONG BEACH PIER C BULKHEAD TEST DATA 1949

The term "true arching" means a condition under which the sand grains wedge themselves between unyielding supports in such a manner as to form sand "arches" which can carry part, or all, of their own weight in addition to superimposed loads. Lateral pressures can be increased appreciably thereby.

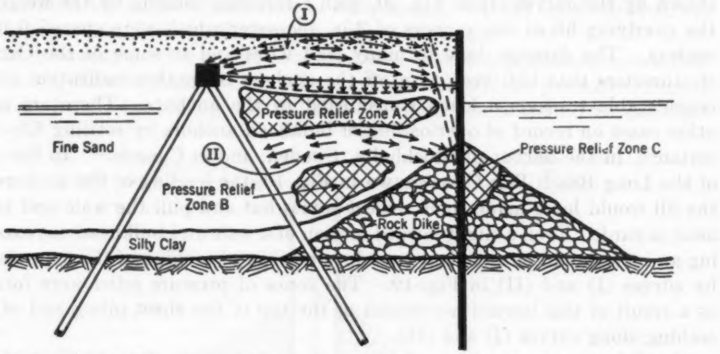

FIG. 19.—ZONES OF "TRUE ARCHING" AND OF PRESSURE RELIEF IN THE SOIL, LONG BEACH PIER C

Their estimation becomes possible from the theory of solid arches.[12,13] "True arching" in sand is facilitated by the yielding of underlying layers. Therefore, the consolidation of the freshly deposited layer of silty clay may have provoked, at first, partial arching of the "true" type above the clay, as shown by the curves (II) in Fig. 19, which arching caused the temporary high pressures recorded by the cell P-4 during stage 1, Fig. 18.

However, it should be noted that "true arching" is a relatively unstable phenomenon in dry, or in submerged, sand. Capillary saturation lends it stability.[12] Therefore, further consolidation of the silty clay layer is likely to have caused the complete redistribution of pressures recorded during the subsequent stages (stage 2, stage 3, and stage 4), shown in Fig. 18.

The shape of lateral earth pressure curves during stages 2 through 4 has only a superficial resemblance to the shape of the theoretical curves proposed by some engineers[14,15] and attributed to the deflection of the sheet piling. There is a fundamental difference. Whereas both the Danish rules[14] and Karl Terzaghi,[15] Hon. M. ASCE, indicate a maximum pressure immediately under the anchor and a minimum at midspan further down, exactly the reverse was observed at Long Beach during stages 2 through 4, Fig. 18. The pressure under the anchor was zero, and increased from there on downward. Thus, this redistribution was produced by causes other than "vertical arching," induced by the deflection of the piling between the level of the anchor and the level of its lower support near the dredge line.

The suggested explanation seems to agree with the views expressed by the author. All hydraulic fills tend to settle somewhat. At Long Beach, the

[13] "Soil Mechanics, Foundations and Earth Structures," by Gregory P. Tschebotarioff, McGraw-Hill Book Co., Inc., New York, N. Y., 1951, p. 274.

[14] "Normer for Vandbygings-Konstruktioner," *Udgivet af Dansk Ingeniorforening*, Copenhagen, Denmark, 1937.

[15] "Theoretical Soil Mechanics," by Karl Terzaghi, John Wiley and Sons, Inc., New York, N. Y., 1943.

settlement of the upper layers of the fill must have been accentuated by the presence of a layer of silty clay from 5 ft to 6 ft thick, which was deposited ahead of the advancing sand fill proper. This settlement of the fill after placing must have produced some transverse horizontal arching of the type shown by the curves (I) in Fig. 20, with a resulting loading by the weight of the overlying fill of the anchors of 3-in. diameter which were spaced 6 ft on centers. The damage done to many lead wires and to some of the Carlson strainmeters that had been torn off the anchors is another indication of the considerable transverse loads transmitted to the anchors. There are some other cases on record of overloading of bulkhead anchors by settling fills—for instance, in the harbor of Stockholm, Sweden, and in Canada.[16] In the case of the Long Beach Pier C, as shown in Fig. 19, the loading of the anchors by the fill would have made them deflect somewhat and pull the wale and bulkhead inward. Even a slight inward motion of a wale and bulkhead not exceeding an inch should be sufficient to induce horizontal arching of the type shown by curves (I) and (II) in Fig. 19. The zones of pressure relief were formed as a result of this inward movement of the top of the sheet piling and of the arching along curves (I) and (II).

Special attention is drawn to the fact that a progressive decrease of the passive resistance pressures of the outer rock dike against cell P-5 was observed during stages 1 through 4 (Fig. 18), indicating a zone of pressure relief (zone C) which is shown in Fig. 19. This observation is in direct contradiction to any possible assumption of arching in the vertical direction because the outer dike would then have had to act as an outer abutment to any such vertical arches, and to provide part of the necessary increased resistance to their load. However, the observed decrease of passive resistance is entirely consistent with the explanation of horizontal arching above the anchor level which followed the loading and pulling in of the anchor, and through it, of the bulkhead. This movement decreased the passive resistance pressures of the outer dike but increased them on the inner dike. The great increase of the anchor pulls themselves (42% between stages 2 and 3, and 85% between stages 1 and 3) provides further support to the explanation proposed.

Thus, the findings of the Princeton tests concerning the absence of vertical arching behind backfilled bulkheads[11,17] have been confirmed fully by the Long Beach field observations, just as the writer's Princeton tests have been confirmed further by model tests of a somewhat different type in England.[18,19] New important data have been obtained at Pier C, which emphasize the need for the protection of anchors by special measures, such as hollow pipes.[20]

Further field observations are essential. However, such observations alone cannot form the basis for a rapid advance of knowledge concerning the

[16] "Soil Mechanics, Foundations and Earth Structures," by Gregory P. Tschebotarioff, McGraw-Hill Book Co., Inc., New York, N. Y., 1951, pp. 511-516.

[17] "Soil Mechanics, Foundations and Earth Structures," by Gregory P. Tschebotarioff, McGraw-Hill Book Co., Inc., New York, N. Y., 1951.

[18] "Anchored Sheet-Pile Walls," by Peter W. Rowe, *Proceedings*, Inst. of C. E., Pt. 1, London, England, January, 1952, pp. 27-70.

[19] Discussion by Gregory P. Tschebotarioff of "Anchored Sheet-Pile Walls," by Peter W. Rowe, *ibid.*, September, 1952.

[20] "Soil Mechanics, Foundations and Earth Structures," by Gregory P. Tschebotarioff, McGraw-Hill Book Co., Inc., New York, N. Y., 1951, Figs. 16-29, and 16-30.

actual performance of earth-retaining structures. The number of factors that affect the performance of such structures is so great that, in accordance with the theory of probability, little possibility exists of variation of these factors among observed structures in a manner permitting rapid numerical evaluation of the separate influence of each factor. Model tests, checked by, and correlated to, field studies are essential to that end.[21]

The following further suggestions are made concerning possible future field studies: (*a*) The formation of a silty clay layer should be prevented during future hydraulic backfilling. (*b*) Reliable reference points should be provided

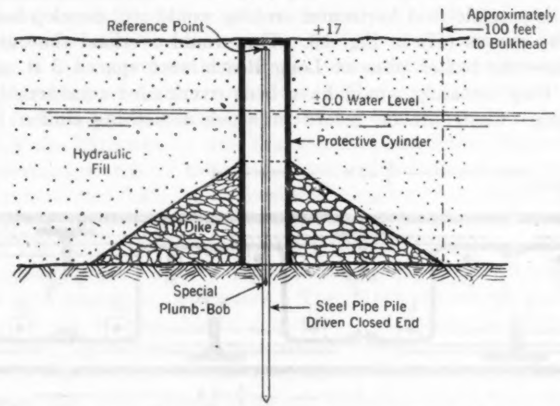

FIG. 20.—POSSIBLE METHOD OF PROVIDING REFERENCE CONTROL POINTS FOR BULKHEAD DISPLACEMENT MEASUREMENTS

for displacement measurements. (*c*) The effects of possible overloading of the anchor piles should be considered. (*d*) Pressure cells might be placed in groups to obtain more accurate measurements.

Prevention of a silty clay layer, mentioned as condition (*a*), may not be easy, but the objective may possibly be attained by providing overflows at regular intervals along the pier to shorten the path of flow of water laden with silt and clay over the pier areas to be backfilled. Relative to suggestion (*b*), the difficulties encountered on this particular job seem to duplicate difficulties encountered elsewhere, when it usually proved impossible to obtain sufficiently accurate displacement measurements by sighting over considerable distances. Therefore, it is suggested that some arrangement, such as that shown by Fig. 20, might be attempted. A steel pipe pile driven closed end into the underlying sand layer would be left unfilled to permit pumping out. An outer protective cylinder—made, for instance, of concrete pipe having a 10-ft diameter—would be placed around it. A conical rock dike could be used to protect the outer cylinder and the soil around the pipe pile from displacements that might be caused later by temporary one-sided loading by the

[21] "Some Unsolved Problems of Importance for the Design of Earth Retaining Structures," by Gregory P. Tschebotarioff, *Bulletin No. 33*, Permanent International Assn. of Navigation Congress, 1950.

hydraulic fill. If any such displacements did occur later, they should involve a tilting of the pipe pile but not a displacement of its lower end. Any such tilting could be measured by a specially designed plumb bob. Two reference points of this type, placed approximately 100 ft from the bulkhead, could be used to check each other and should permit quite accurate displacement measurements of the bulkhead. Regarding deflection measurements themselves, the use of stainless steel strips fixed to the bulkhead sheet piling might serve to decrease some of the corrosion difficulties encountered at Pier C.

Suggestion (*c*) involves possible overloading of the anchor piles. If the anchors were protected by concrete pipes, as the writer has described elsewhere,[20] it is possible that horizontal arching would still develop below them, as shown by curves (II) in Fig. 19. This would overload the outer row of timber piles—the batter piles at Long Beach were spaced 3 ft on centers. Therefore, they certainly would have been overloaded considerably by any such arching. Cases are on record in which something similar happened.

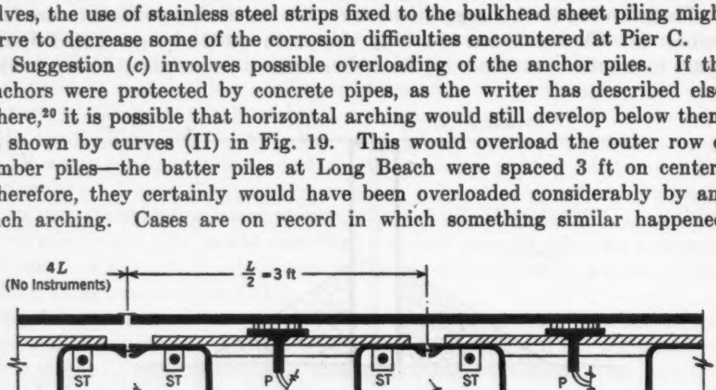

FIG. 21.—SKETCH SHOWING POSSIBLE METHOD OF MOUNTING THE CARLSON STRESSMETERS (P) AND THE CARLSON STRAINMETERS (ST)

Therefore, the question arises as to whether or not it would be advantageous to use a different system of anchorage—such as is illustrated elsewhere by the writer. Precast reinforced concrete anchor blocks might be dropped to the harbor bottom and anchored to the wale by steel anchors. The slope of the inner rock dike might be made to coincide with the slope of the anchors in order to avoid the loading of the latter by the settlement of any underlying fill. The outer rock dike might possibly be omitted entirely under such conditions.

The difficulties encountered during the earth-pressure measurements made by means of pressure cells at Long Beach Pier C seem to indicate that this type of measurement does not have all the advantages sometimes attributed to it. It is not enough just to measure a pressure directly—one has to get an accurate value and that is far from easy. As stated in suggestion (*d*), a possible improvement might consist in using pressure cells in groups, as shown by Fig. 21, so that the cells P would receive much greater total pressures from the individual steel plates that they supported. Similar arrangements have been successfully used in Germany on massive retaining walls. The same general arrangement might be used to make bending strain measurements on the sheet piles by means of Carlson strainmeters, marked ST in Fig. 21. The writer

believes that the strain measurements are more important than the direct pressure measurements because the bending strain readings can be taken all along the depth of the bulkhead down to the original ground level. A bending moment curve thus obtained clearly indicates whether or not there is fixation at the ground level and where the point of contraflexure actually lies. No definite conclusions on this essential point can be made on the strength of the pressure measurements at Pier C described by the author.

All the suggestions in this discussion would require greater sums of money than were available in the case of the author's studies. The writer hopes that this type of work will not only be continued but will be developed.

One reason why research has not yet been developed in civil engineering as much as in some other branches of technology (for instance, in electrical engineering) is the fact that there are no comparably large concerns in the civil engineering industry which could bear the high cost of continued organized research. In Europe, the construction industry contributes to research. The Laboratoires du Bâtiment et des Travaux Publics, Paris, France, perform civil engineering research for the entire construction industry in France, which in return contributes 0.3% of its business turnover. Of course, in Europe the institution of consulting engineers is not so developed as it is in the United States, and most general civil engineering contractors make their own designs, thereby having a greater direct interest in the results of related research than is the case with American contractors. The extent of centralization found in France would not be desirable in a country as large as the United States. Several cooperating, but independent, research centers would produce a valuable spirit of competition. Their location at universities should safeguard their independence from harmful pressures by vested interests of all types.

WALTER C. BOYER,[22] A.M. ASCE.—Those engineers interested in the design of flexible sheet-pile bulkheads should study carefully this paper by Mr. Duke. This report verifies important concepts that have been proposed by other engineers and gives quantitative evidence of factors such as the effect of settlement on tie-rod tension.

It is hoped that this paper will provide the impetus for a series of tests on similar installations that pose a variety of problems. The writer concurs in the statement by Mr. Duke that the problems must be investigated in the field. The bulkhead selected for this test was an excellent choice in one respect and an unfortunate choice in another. The bulkhead provided valuable field evidence of the value of a rock dike in reducing pressures on the wall, but correspondingly reduced the possibility of detecting passive resistance values. This difficulty could have been eliminated, to some degree, by taking strain measurements on the sheet pile. The correlation of pressure readings with strain measurements would, in itself, constitute an interesting study. Although this does not constitute a criticism of the investigation, it adds emphasis to the writer's contention that field investigation is a source of much needed data for the designer of flexible bulkheads retaining cohesive backfill and anchored in cohesive material.

---

[22] Asst. Prof., The Johns Hopkins Univ., Baltimore, Md.

The clear description of the instrumentation utilized for this program of study is a welcome contribution—it should serve as a valuable guide to future investigators. There appears to be no unanimity of agreement that the answer to such field investigation lies in electrically controlled equipment. A number of failures, while attempting to utilize such equipment, have been reported. Hence the methods used are worthy of detailed study. However, with the realization that a large financial burden is involved in test programs of this character, duplicate mechanical strain equipment should be utilized wherever possible. Therefore, it would appear that an access well to the tie rod could have been installed and waterproofed, without great expense. This would permit a method of taking periodic tie-rod tension readings for an indefinite length of time.

The development of wall pressures, as presented in Fig. 12, appears to agree with the distribution predicted by the Rankine theory. The deviation from predicted values, after May 24, becomes quite pronounced. The redistribution has been attributed to a settlement of the fill below the tie rods. The development of high tensile stresses, as a result of fill settlement, including actual anchorage failures, have been reported, but no data permitting a quantitative measure have been available. It would be of interest to investigate the loadings which can produce such tension increases.

The steel sheet piles shown in Fig. 6(*e*) are 78 ft long and are anchored by 3-in. tie rods on 6-ft. centers. The tie rods may be taken as 62 ft in length, with a tie-rod support system dividing this span in half. If the rod is considered as a flexible member of little rigidity, the change in length under uniform loading may be determined from the expression:

$$\Delta l = \tfrac{1}{2} \int_0^l \left(\frac{dy}{dx}\right)^2 dx \quad \text{.......................(1)}$$

in which l is half of the tie-rod length, y is the deflection, and x is the distance from the center support—the coordinate system origin assumed to be at the center support. If the tie rod is taken as a beam, with hinged ends, and supported at the center, the deflection is

$$y = \left(\frac{5}{48}\, w\, l\, x^3 - \frac{w\, l^2\, x^2}{16} - \frac{w\, x^4}{24}\right) \frac{1}{E\, I} \quad \text{..............(2)}$$

in which w is the uniform load, E is the modulus of elasticity, and I is the moment of inertia of the bulkhead section.

From Eqs. 1 and 2,

$$\Delta l = \frac{1}{2} \int_0^l \left[\left(\frac{5}{16}\, w\, l\, x^2 - \frac{w\, l^2\, x}{8} - \frac{w\, x^3}{6}\right) \frac{1}{E\, I}\right]^2 dx \quad \text{.........(3)}$$

The tie-rod tension has been determined by Joel I. Abrams, J. M. ASCE, by equating Δl to the change in length caused by P, the change in axial force.

This is expressed as

$$\frac{P\,l}{A\,E} = \frac{1}{2}\int_0^l \left[\left(\frac{5}{16}\,w\,l\,x^2 - \frac{w\,l^2\,x}{8} - \frac{w\,x^3}{6}\right)\frac{1}{I\,\mathrm{E}}\right]^2 dx \quad \text{..........(4)}$$

in which A is the area of the section.

For the problem under consideration, Eq. 4 reduces to

$$w = 0.22\,\sqrt{P} \quad \text{..........(5)}$$

and if some yielding of the anchorage or wall is to be considered, Eq. 5 becomes

$$w = 0.22\,\sqrt{\frac{100\,P}{Y}} \quad \text{..........(6)}$$

in which Y is the yield defined as a percentage of Δl.

These relationships neglect the moment caused by original tie-rod tension and the moment developed by an increase in tie-rod tension. However, for a member as flexible as a tie rod, such an assumption should not influence the results greatly. The resulting load on the tie rod, due to settlement, is not considered to be uniform, but this assumption leads to an indication of the loading requirements to produce increases of tie-rod tension as reported in the paper.

By use of Eq. 6, the values for uniform loading to produce changes in tie-rod tension as given in Table 6 may be computed. It is noted that a yield of 50% does not alter the values greatly.

TABLE 6.—Tie-Rod Tension Developed Under Uniform Loading, Tie Rod Acting as a Beam

Date	Tie-rod tension T, in kips	Change in axial force P, from May 24, in kips	Uniform load w, in lb per ft, Eq. 5	Uniform load w, in lb per ft, for $Y = 50\%$, Eq. 6
May 24	155	...	0	0
June 3	182	37	36	51
June 11	205	50	49	69
July 12	209	54	51	73
August 5	214	59	54	76
August 6	219	64	56	79
August 17	229	74	60	85

For a tie-rod spacing of 6 ft, the tributary overburden is approximately 8,800 lb per ft of tie-rod length. It is not implied that a substantial percentage of this loading could act on the cable under settlement conditions, but the values as given in Table 6 are feasible.

If the tie rods are considered to act as flexible cables under an initial tension T_0, the change in length under uniform loading may be determined by the expression[23]:

$$\Delta l = \frac{1}{2}\int_0^l \frac{w^2}{T^2}\left(x - \frac{l}{2}\right)^2 dx \quad \text{..........(7)}$$

[23] "Statistically Indeterminate Structures," by L. C. Maugh, John Wiley & Sons, Inc., New York, N. Y., 1946, p. 261.

The final tie-rod tension T can be determined by equating Δl to the change in length due to axial force. This is expressed as

$$\frac{(T - T_0)\, l}{A\, E} = \frac{1}{2} \int_0^l \frac{w^2}{T^2} \left(x - \frac{l}{2}\right)^2 dx \ldots\ldots\ldots\ldots\ldots\ldots (8)$$

For the problem under consideration Eq. 8 becomes

$$w = \frac{T}{92{,}500} \sqrt{T - T_0} \ldots\ldots\ldots\ldots\ldots\ldots\ldots\ldots (9)$$

By use of Eq. 9 the values for uniform loading to produce tie-rod tensions as given in Table 7 may be computed. It is noted that the uniform loadings required are considerably greater than those for the condition of the tie rod acting as a flexible beam (Table 6).

TABLE 7.—TIE-ROD TENSION DEVELOPED UNDER UNIFORM LOADING, TIE ROD ACTING AS A CABLE

Date	Tie-rod tension T, in kips	Change in tie-rod tension $T - T_0$ from May 24, in kips	Uniform load w, in lb per ft	Tie-rod tension T', in kips[a]
May 24	155[b]	...	0	155
June 3	182	27	326	163
June 11	205	50	497	172
July 12	209	54	525	174
August 5	214	59	562	176
August 6	219	64	600	179
August 17	229	74	675	183

[a] T' is the tie-rod tension for the tie-rod supports placed at 15 ft 6 in. on centers. [b] This value is the initial tie-rod tension, that is, T_0 = 155 kips.

The values presented in Tables 6 and 7 probably bracket the actual loading that was developed because of the settlement of the bulkhead under consideration. The placement of turnbuckles between the supporting piles probably reduces the action of the tie rod to a case intermediate between the case of a flexible beam and a cable.

Although the preceding analyses are admittedly rational, they lead to interesting conclusions relative to the spacing of tie-rod support systems. In the bulkhead design under consideration, the tie rod had an unsupported length of 31 ft (not considering earth support). If this spacing is reduced to 15 ft 6 in., the increase in tie-rod tension is markedly reduced.

For the case of the tie rod acting as a flexible beam,

$$w^2 \propto \frac{P}{l^6} \ldots\ldots\ldots\ldots\ldots\ldots\ldots\ldots\ldots (10)$$

Hence, if the spacing of tie-rod supports is reduced to $l/2$,

$$w^2 \propto \frac{64\, P}{l^6} \ldots\ldots\ldots\ldots\ldots\ldots\ldots\ldots\ldots (11)$$

Thus, for the existence of uniform loads as previously computed, P would develop values of less than 2% of those measured in the study.

For the case of the tie rod acting as a cable,

$$w^2 \propto \frac{T^2 (T - T_0)}{l^2} \qquad (12)$$

Hence, if the spacing of tie-rod supports is reduced to $l/2$,

$$w^2 \propto \frac{4 (T')^2 (T' - T_0)}{l^2} \qquad (13)$$

Thus, for the existence of uniform loads as previously computed, the value of T' computed in accordance with Eq. 13 is given in Table 7. The values of T' are less than 38% of those measured in the study.

This indicates the importance of the spacing of tie-rod supports to insure tension values consistent with the design considerations. Unfortunately, these calculations are possible only as a result of the values developed in the study. It is not possible to estimate, during the design stage, even by rational methods, the uniform loads on the tie rods which may exist under conditions of fill settlement. This problem is worthy of continued study and research. It is important in a number of design problems other than the one under consideration.

In view of the uncertainty of such estimates, it would appear that the tie rods should be placed in conduits which would prevent development of uniform loadings due to the soil overburden. This would be necessary for conditions where relatively large settlements are likely to occur. However, this solves the problem by avoiding it, and it certainly is not the most economically advantageous method. It would appear from the results of the study that the spacing of tie-rod supports at 31 ft, for a fill where settlement is likely to occur, is excessive, and therefore should be reduced to 15 ft.

PAUL BAUMANN,[24] M. ASCE.—Valuable information concerning active and passive earth pressures on a steel sheet-pile bulkhead of unusual height is presented in this paper. Great care and attention to details were given to the planning and installation of the measuring instruments and to the arrangement of the facilities for measuring tie-rod tension and wall deflections. However, a number of features concerning the active and passive pressures remained vague and elusive.

A test on a steel sheet-pile bulkhead was conducted by the writer in the area described by Mr. Duke.[25] Although the two tests have much in common, the principal purpose is different. The writer's test was conducted to ascertain passive pressure or resistance in relation to safe anchorage, whereas the determination of active and passive pressures during, and subsequent to, the fill operation was the principal objective of the test described by Mr. Duke.

In the writer's test the active pressure was created by use of sea water. The active pressure was known above the ground surface and was known approximately below the surface, whereas the magnitude and the distribution

[24] Asst. Chf. Engr., Los Angeles County Flood Control Dist., Los Angeles, Calif.

[25] "Analysis of Sheet-Pile Bulkheads," by Paul Baumann, *Transactions*, ASCE, Vol. 100, 1935, p. 707.

of the passive resistance were determined from observed deflections and equilibrium conditions. The free height of the bulkhead, over which the active pressure was exactly known and the deflections were precisely measured, was 15 ft and the penetration was 12 ft. Hence, deformations for approximately 56% of the sheet-pile wall could be observed. In Mr. Duke's test the free height of the bulkhead above the top of the rock-fill dike was 26.5 ft, the penetration into the dike was 28.5 ft, and the penetration below the floor of the harbor was a minimum of 22.0 ft. Hence, the exposed length of sheet-pile wall which lent itself to direct observation was approximately one third of the total length.

It is regrettable that pressure cells on the active-pressure side were not extended so far down as on the passive-pressure side prior to the placing of the dike and that the number of cells on the passive-pressure side had to be limited to two, 10 ft apart vertically. This latter limitation caused straight lines to be drawn between the measuring points and the top of the dike as shown in Fig. 12 which, therefore, does not represent the true distribution of passive pressure. In all probability, a curve drawn through the respective three points would have been a better approximation of the pressure distribution. The writer showed [26] the actual distribution of passive pressure for homogeneous, granular materials, based on large-scale tests.

A number of the features shown in Fig. 12 are rather difficult to understand. Among them is the acute increase in active pressure, starting on June 11 below an approximate elevation of -8, accompanied by a decrease in the passive pressure in the four subsequent drawings. On July 12 and August 6 the lowest passive pressure cell either was not read or perhaps it showed erratic readings which had to be ignored. Such mishaps seem to be the rule rather than the exception where earth pressure cells are involved. However, the response of the pressure cells to tidal changes—that is, changes in external water pressure—is remarkable. A rise in tide generally caused an increase in active pressure associated, paradoxically, with a decrease in tie-rod tension and passive resistance. The active pressure, therefore, was actually in part passive pressure.

The writer's statement[27] regarding the impossibility of securing an exact, analytical solution so long as the active loading could not be expressed as a steady function of the height appears to have been confirmed by Mr. Duke. The close spacing of the tie rods, for instance, gave rise to a vertical arching and thereby an approach to the effect of a relieving platform.

In the study of the deflections of the sheet-pile wall, Mr. Duke assumed no deflection at El. -38, the surface of the soil in situ. No support is offered for this assumption and, on the basis of Fig. 12, its validity must be doubted. Indication of the author's own doubt appears evident in item 9 (under the heading, "Suggestions for Future Bulkhead Field Studies")—

> "Creative thought is needed on the problem of the difficult and probably expensive quantitative observation of passive resistance phenomena at the base of a bulkhead."

This is a sound suggestion.

---

[26] "Analysis of Sheet-Pile Bulkheads," by Paul Baumann, *Transactions*, ASCE, Vol. 100, 1935, p. 728.
[27] *Ibid*, p. 738.

It would be interesting if tests similar to those conducted by Mr. Duke and the writer could be broadened so as to include sheet-pile bulkheads of at least two greatly differing rigidities. On the basis of the statically indeterminate solution applied to two such bulkheads—a steel sheet-pile wall and a reinforced concrete sheet-pile wall—the writer showed[28, 29] that the latter, because of its greater rigidity, may require a penetration approximately 20% greater than that of the former. It is well to recall that bulkhead failures have, almost without exception, been associated with faulty anchorage rather than deficient structural qualities.

S. Packshaw,[30] M. ASCE.—Opportunities for studying the behavior of retaining walls constructed of sheet-steel piling are rather rare. The new wall is frequently driven in front of an existing structure, which has an unknown effect on the earth pressures and the stresses which the piling has to withstand. It may also be difficult to determine the properties of the soil and of the backfilling with enough accuracy to assess their precise active and passive pressures. The conditions at the Long Beach Harbor bulkhead were ideal for a field study such as that undertaken by Mr. Duke, and some valuable deductions can certainly be made. A study of the results indicates, however, that the information yielded by the tests is applicable primarily to bulkheads tied to anchorages on closely spaced raking piles; it would be misleading to apply the author's conclusions to sheet-pile retaining walls in general.

It is assumed that the soil properties given in Table 1 were determined by the usual soil mechanics procedures. The properties are fairly typical of materials used for backfilling a wall and of fine sand into which piling is driven. The corresponding Rankine or Coulomb active pressure coefficients for the sand strata (neglecting friction between the soil and the wall) vary from approximately 0.24 to approximately 0.28, as compared to the lateral pressure coefficient of 0.7 suggested by Mr. Duke. Many designers would use the Rankine coefficients, or values close to them, as a basis for the computation of a retaining wall for similar conditions. The corresponding pressure diagram, which incorporates some minor approximations and assumes that an angle of wall friction of 20° is developed on the passive side, is shown in Fig. 22(*a*). The dotted lines superimposed on the conventional pressure diagram serve as a comparison to the author's measurements shown in Fig. 12. The difference between the lines is too great to be accounted for merely by errors in ascertaining the soil properties and earth pressure coefficients. The explanation must lie elsewhere.

Fig. 12 shows a gradual, although not very regular, increase in active pressure until May 20, when backfilling was nearly complete. After that date, the pressure above the tie rods continued to increase throughout the period of observation, but below the tie rods the pressures fell off sharply. It is probable that the increase in pressure above the tie rods and the reduction in pressure below the tie rods were caused primarily by horizontal arching within the soil between the bulkhead and the anchor piles. Measurement of the tie-rod loads

[28] "Analysis of Sheet-Pile Bulkheads," by Paul Baumann, *Transactions*, ASCE, Vol. 100, 1935, p. 794.

[29] *Ibid.*, p. 795.

[30] Director, British Steel Piling Co., Ltd., London, England.

shows them to be about three times as great as might be expected from the conventional "fixed-earth support" computation of Fig. 22(*a*). Abnormal stresses were developed when the fill under the tie rods consolidated, thus leaving the tie rods with little or no support for carrying the weight of the fill above them. The tie rods should have been laid along the inverts of concrete pipes, the diameter of the pipes being large enough to take up any settlement of the fill, thus protecting the rods from vertical loads for which they were not

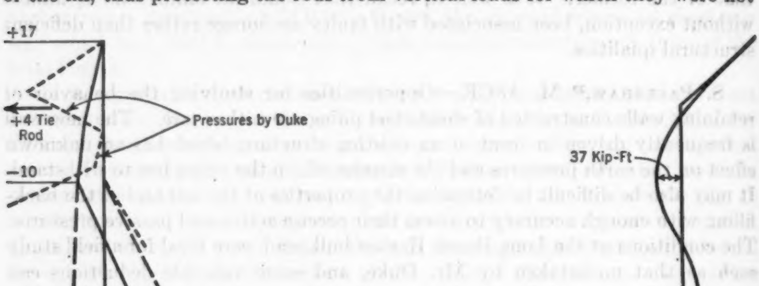

FIG. 22.—PRESSURES AND MOMENTS, STATION 27 +30

designed. This simple method has been adopted elsewhere and is quite effective. The tie rods, however, are too small and too far apart to act as a relieving platform, even though the observations on and after July 12 showed that the pressure immediately below the ties had been reduced to zero—a condition typical of pressure diagrams for walls with relieving platforms.

It seems more likely that this reduction to zero pressure was caused by arching within the wedge-shaped soil mass contained between the bulkhead and the forward raking piles, because these piles are so close together that they can be regarded as a continuous wall. European practice rarely utilizes this type of construction, but when it does, the piles are more heavily loaded and consequently spaced wider apart. If the backfill does not permit the use of a normal type of anchorage, such as concrete blocks, groups of short vertical sheet piles, or an anchor wall, it is usual to secure the wall to a relieving platform on raking piles.

It is regrettable that the mechanical strain gages for measuring the bulkhead bending moment proved to be unreliable and that no observations of the stress in the sheet piles were obtained. The conventional method of analysis, shown in Fig. 22(*b*), is to assume that the waling load is approximately 9,400 lb per ft of wall and that the bending moment is approximately 37 kip-ft when

the backfill is level with the top of the wall. In designing the wall, allowance must be made for the surcharge caused by filling to El. +20 and for the ground-water level remaining 2 ft or 3 ft higher than the harbor water level at low tide. When all this is taken into consideration the bending moment and waling load make necessary the choice of a section of steel piling and size of tie rods in accordance with those selected by the designer of the bulkhead. Innumerable retaining walls have been designed on the same basis, which, for all its short-comings, has been proved in practice to be satisfactory for normal conditions. Mr. Duke's observations do not appear conclusive enough to warrant the general use of the lateral pressure coefficient of 0.7 instead of the Rankine coefficients corresponding to the soil properties, or of the two rules which are listed under the heading, "Bulkhead Performance During Filling: Lateral Pressures in Dike."

The large deflections which were observed are approximately three times greater than would be expected, but they may have been influenced by the elastic extension of the tie rods (about $\frac{3}{4}$ in. under maximum load) and by the probably even greater movement caused by the consolidation of the ground at the anchorage. However, the wedging and arching of the soil mass between the wall and the front raker piles, and the consequent concentrations of pressure, are likely to be the main reason for the large deflections.

Researches on model flexible walls by Mr. Tschebotarioff,[31] and P. W. Rowe[18] have done much to advance the knowledge of the behavior of these walls. Mr. Rowe's research led to the result that fixity can be expected to develop when the ground below the dredging level is composed of dense sand or similar material, with an angle of internal friction approximately equal to 40°. This appears to justify the conventional method of Fig. 22(*b*). Mr. Rowe also showed that, with all but the more rigid sections of sheet piling, the actual bending moment is less than that computed directly from the earth pressures on the wall. He also obtained the quantitative relation between the bending moment, the flexural properties of the material, and the section of the sheet piling.

If, for example, the calculation for the Long Beach Harbor bulkhead showed that the stress in the MZ-38 section, which has a section modulus of 46.8 in. cubed per ft of wall, is 16,000 lb per sq in., then the stress in the more flexible MZ-32 section will not be 19,500 lb per sq in., because of its section modulus of 38.3 in. cubed per ft of wall, but some substantially lower figure. If Mr. Rowe's method is compared with the conventional fixed earth-support procedure, it is found that the maximum bending moment may be greater or smaller, depending on the ground conditions and the type of piling. The difference between methods is frequently small, but one of the advantages of Mr. Rowe's method is that it clearly demonstrates the effect of varying the section of piling and using steels with different permissible stresses.

The results of Mr. Duke's research do not lend themselves to universal use in the design of sheet-pile retaining walls. However, two vaulable deductions can be made: First, the tie rods are subjected to large stresses if they

[31] "Large-Scale Model Earth Pressure Tests on Flexible Bulkheads," by Gregory P. Tschebotarioff, *Transactions*, ASCE, Vol. 114, 1949, p. 415.

have to carry the weight of the superimposed fill caused by the settlement of the ground below them; and second, the unpredictable concentrations of pressure may result from the effect of wedging and arching of the soil between the wall and the closely-spaced raking anchor piles.

W. F. WAY,[32] M. ASCE.—Worthwhile research can be successfully performed in the field, as is shown by the useful results of an interesting test by Mr. Duke.

The specific tests were well planned, executed, and presented. All that was planned did not work out as was desired and this is to be expected. In the test, the planners were pioneering in the sense that they did not have the benefit of the results of similar tests which might highlight the important features to be considered. Engineers interested in and conversant with problems peculiar to sheet-pile bulkhead design should find much of interest in this paper. Engineers who are to design a sheet-pile bulkhead will find much help, even though the design in question might be substantially different from that of the test. A study of the tests and their results will assist the designer to "feel" his way to a better design.

Mr. Duke's "Suggestions for Future Bulkhead Field Studies" is a well-considered listing of important items. Item 8 is very important and especially true because it includes tests which cannot be made in the laboratory. Since the function of a bulkhead is to retain a fill on which a live load can be carried, it is impossible to overemphasize the need for study of the effect of surcharge. The pressures and stresses in the structure caused by a surcharge load will vary in accordance with the lateral pressure coefficient of the fill behind the bulkhead. The first application of a surcharge load will increase the tie-rod stresses; after removal of the surcharge, there will be a removal of most of the stress, but a residual stress will remain in the tie rods. Subsequent loadings and removals will follow the same cycle. Studies to determine the increased stresses, rebounds, and residual stresses caused by these successive loadings would be valuable.

Field tests to check design assumptions have not been extensively included in engineering research. There seems to be hesitancy among designers to promote field tests such as those described by Mr. Duke. The reasons for this attitude are:

1. The designer is not equipped for testing, nor, perhaps, has he had the experience to enable him to undertake such tests.

2. Almost any field test would interfere with the progress in construction, which would adversely influence construction personnel.

3. Tests require funds, and finding someone to furnish these funds requires both time and patience.

4. There is a feeling among many designers that the tests apply only to a few particular sections, and the results obtained are not representative, and therefore not worthwhile.

---

[32] Vice-Pres., Frederic R. Harris, Inc., New York, N. Y.

With the knowledge of these objections to field tests, the writer feels that there are instances when the reasons for making the tests outweigh the objections. Advantage should be taken of these favorable instances as they occur, and Mr. Duke is to be commended for having the interest and energy necessary to see this interesting field test made.

J. Owen Lake,[33] A. M. ASCE.—The opportunity for scientific study of the structural performance of full-size anchored sheet-pile bulkheads is rare. It is therefore regrettable that Mr. Duke was prevented from obtaining unqualified data by the doubtful validity of the readings obtained from the stressmeters located in the dike and by the progressive failures in the lead wires to the strainmeters. The author stated, under the heading, "Instrumentation: Soil Pressure," that "The probable validity of measurements in the dike was questioned from the first because of the large size of dike fragments." Therefore, cannot the authenticity of the free body diagrams in Fig. 12 be doubtful below El. + 0.7? The stressmeters were installed only at Station 27 + 30 and were vertically disposed in a single line, and from these few measurements the distribution and intensity of the lateral earth pressure was deduced. However, reference to the tie-rod tensions listed in Table 2 indicates a wide scattering of values which could mean a variation of pressure in a horizontal direction at the face of the bulkhead, although a large part of this variation in the tie-rod loading is probably due to the differential yield of the closely spaced ties combined with the continuity of the wale. Nevertheless, considerable local variation of pressure is expected behind bulkheads and this necessitates the averaging of readings from a substantial number of stressmeters if a representative diagram of pressure distribution is to be obtained.

In Fig. 5 it is shown that silty clay existed below El. − 35 in borings A-1 and A-2, which were sunk after the filling operation was complete. These borings were adjacent to the test stations, and this silty clay stratum may not have been entirely displaced by the deposition of the rock dike. Because of the low cohesion of silty clay in the initial stages of filling, there would be a horizontal plane of low shear resistance at El. − 35 which would allow appreciable forward deflection of the bulkhead during the early stages of filling. This is especially true since there is a large tidal lag. For example, on April 23 at Station 30 + 30, with a fill increase of only 2 ft, the bulkhead deflection increased from 0.16 in. to 0.86 in., an unexplained increase unless the significance of the tide at El. 5.1 on the inside and El. 1.9 on the outside is acknowledged. The measured deflection profiles were obtained only to El. − 9.5, and it is noted that they could easily approximate computed deflection curves if the bulkhead had been displaced forward at El. − 38 during the earlier stages of filling. If such movement had taken place, the assumption that the bulkhead is fixed against rotation at El.-38 would be incorrect. Some confirmation of a lower point of "fixity" is possibly indicated since the predictions of the deflections based on the soil pressure measurements were 25% too low. The increase of pressure above the wale and the decrease of pressure below the wale have been attributed mainly to the settlement of the fill, but it is suggested that if forward

[33] Cons. Engr., Toronto, Ont., Canada.

movement at El. − 38 occurred with time, caused by soil creep on the passive side, the bulkhead would tend to rotate about the tie-rod level and would result in the variation of pressure that was observed at Station 27 + 30 without any appreciable alteration to the deflection curve above the reference level of El. − 9.5. Variability of strata below the harbor bed level of El. − 38 could then account for the absence of pressure variation at Station 30 + 30.

The phenomena of decreased lateral pressures on the bulkhead below the tie rods could also be associated with the reduction of excess pore-water pressures as consolidation proceeded. Such excess hydrostatic pressures would be unlikely to occur appreciably above the tie rods where the sand is of medium particle size. However, below the ties the sand is fine and contains a proportion of silt, and such a soil would undoubtedly be in a loose state just after deposition. During deposition, by hydraulic fill, the soil mass acts as a viscous fluid and therefore exerts relatively high lateral pressures that approach a lateral pressure coefficient of unity. Thereafter the effective stress develops as the pore-water pressure falls and the lateral earth pressure coefficient also is reduced. Thus, as further hydraulic fill is deposited on the soil already in position, the bulkhead tends to deflect and inevitably brings into effect the reduced lateral earth pressure coefficient which is operative in the lower regions of the fill where the "effective" stress has developed appreciably. In Table 3 it can be seen that the stressmeters at El. − 7.3 and El. − 14.9 did not indicate a linear increase of pressure as the fill rose from El. − 7.0 to El. + 5.8.

A further factor which could undoubtedly contribute to the relatively high lateral pressure coefficient of 0.7, deduced from the observations, is the tidal lag which occurred frequently during the filling operations. During periods of tidal lag the deflection of the bulkhead would be increased and the sand fill would move forward correspondingly. As the tidal lag reduced, the bulkhead would be left in a prestressed condition, resulting in a tendency toward the development of passive resistance in the fill immediately behind the bulkhead. If the tidal lag had been large enough, actual passive pressure would have been obtained after the tidal lag had been dissipated. Therefore, if after the fill was complete, the nuts of the tie rods were slackened to allow the bulkhead to move forward slightly at the waling level, the relatively high lateral earth pressure would be reduced. This expedient is worthwhile, as the load of 200 kips in some of the ties appears to give a factor of safety only slightly greater than unity when referred to the yield stress.

Under the heading, "Summary of Test Results," Mr. Duke states that

> "The surcharge piled close to the bulkhead after completion of filling was carried principally by the tieback system, pressures below the wale being not much affected."

It is suggested that precisely this appearance of no increase in lateral pressure below the wale could occur because of a prestressed condition of the bulkhead caused by tidal lag during filling operations and resulting in a lateral pressure coefficient considerably above the normal active value for sand. Such a condition is then obtained whereby a certain degree of surcharge can be added without a noticeable change in the lateral pressure below the wale until the

intensity of the surcharge results in lateral pressures greater than the pressures arising from the restitutional force of the prestressed condition of the bulkhead.

It is agreed that settlement of the fill and the partial support of the upper part of the fill on the tie rods is always an important consideration. It may be that this condition had an appreciable influence on the field study under discussion. However, the complexity of the subject is perhaps further exemplified by the existence of the factors mentioned by the writer.

K. TERZAGHI,[34] HON. M. ASCE.—Observations such as those described in the paper are urgently needed and their merits are too obvious to require special emphasis. Therefore, this discussion deals exclusively with the controversial aspects of some of the findings.

Coefficient of Lateral Earth Pressure.—Of the author's conclusions, the most startling is contained in a statement under the heading, "Summary of Test Results," that: "The proportionality constant, or coefficient of lateral pressure, was found to be about 0.7 ***." Previously, it has been assumed that the coefficient of lateral sand pressure K on bulkheads, like that of the sand pressure on retaining walls, is slightly greater than that of the coefficient K_A of active earth pressure; and all the experimental investigations made prior to publication of this paper are in accordance with this assumption. The value of K_A is less than 0.3. If a bulkhead were exceptionally rigid and the anchorage did not yield at all, the value of K could conceivably increase to 0.4 or 0.45. The author's statement that K was equal to 0.7 would imply that the value K of the coefficient of lateral earth pressure of sand may range between the wide limits of less than 0.3 (coefficient of active earth pressure) and as much as 0.7. If K could, in fact, assume any value within this range, the attempts of engineers to establish rational methods for bulkhead design might as well be abandoned as hopeless. Considering this serious implication of the author's findings concerning the value of K, it is of utmost importance to ascertain to what extent the value 0.7 can be relied upon.

The author's evaluation of K is based on two independent sets of data, the results of pressure cell readings and those of the measurement of the sheet-pile deflections. He states that both sets of data lead to the same conclusion, that K equals 0.7.

The reliability of the pressure cell data depends on the accuracy of the calibration curve. A description of the procedure for calibrating the cells can be found under the heading, "Instrumentation." The results of the calibration are indicated in Fig. 9. In Fig. 23(*a*), which is a slightly modified replica of Fig. 9, the water pressure curve is labeled W and the soil pressure curve, S. The abscissas represent the unit pressure on the contact face of the cell, and the ordinates, the change in the resistance ratio.

Curve W shown in Fig. 23(*a*) represents the relation between the change in the resistance ratio and the pressure exerted by water on the contact face, whereas curve S represents the relation between change in the resistance ratio and the soil pressure. The position of curve S with reference to curve W depends on the calibration procedure. Since it cannot be taken for granted that

[34] Prof., Civ. Eng., Div. of Eng. Sciences, Harvard Univ., Cambridge, Mass.

the author's test arrangement represents a satisfactory equivalent for the field conditions, it is necessary to inquire whether or not his calibration curve S is compatible with the operation of the cells attached to the bulkhead.

The position of the soil pressure curve, S, in Fig. 23(*a*), with reference to the water pressure curve W has the following physical meaning. If the contact face of the cell were acted upon, for instance, by a water pressure of 0.8 kips per

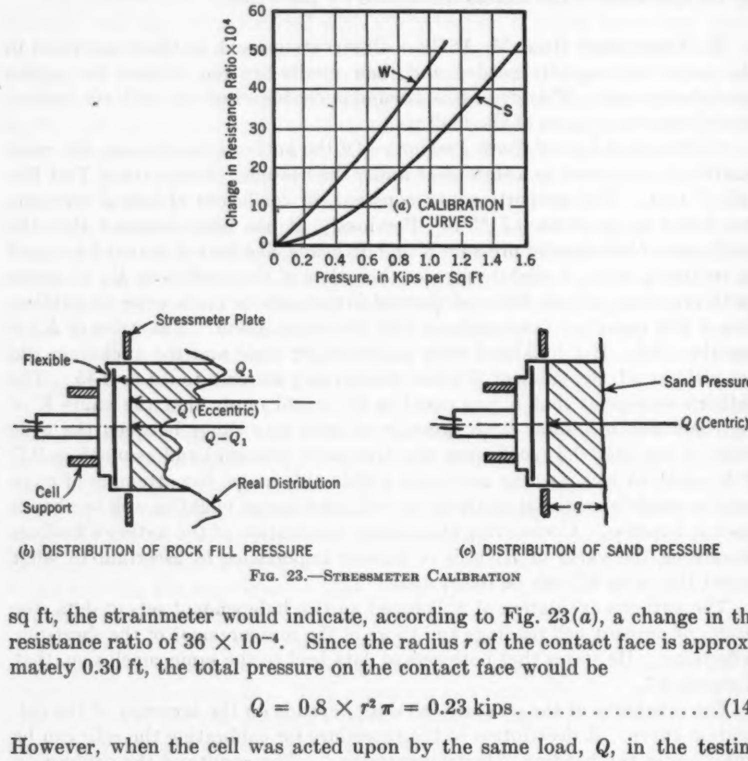

FIG. 23.—STRESSMETER CALIBRATION

sq ft, the strainmeter would indicate, according to Fig. 23(*a*), a change in the resistance ratio of 36×10^{-4}. Since the radius r of the contact face is approximately 0.30 ft, the total pressure on the contact face would be

$$Q = 0.8 \times r^2 \pi = 0.23 \text{ kips} \ldots\ldots\ldots\ldots\ldots\ldots (14)$$

However, when the cell was acted upon by the same load, Q, in the testing machine, during the test that was supposed to simulate the loading conditions in the field, the change in resistance ratio was only 18×10^{-4}, corresponding to a water pressure of only 0.46 kips per sq ft and to a value of $Q' = 0.46 \times r^2 \pi = 0.13$ kips.

The resistance ratio increases approximately in direct proportion to the deflection of the membrane shown in Fig. 8, which in turn increases in direct proportion to the pressure q_m in the mercury film contained in the cell. If the contact face of the cell is acted upon by water under a pressure of 0.8 kips per sq ft, the pressure in the mercury film is approximately equal to the water pressure,

$$q_m \approx 0.8 \text{ kips per sq ft} = \frac{Q}{r^2 \pi} = \frac{0.23}{r^2 \pi} \ldots\ldots\ldots\ldots\ldots (15)$$

yet the same load Q, applied to the cell by the testing machine, produced (in the mercury film) a pressure of not more than

$$q'_m = 0.46 \text{ kips per sq ft} = \frac{Q'}{r^2 \pi} = \frac{0.13}{r^2 \pi} \ldots\ldots\ldots\ldots (16)$$

This pressure is equal to the water pressure corresponding to a change in resistance ratio of 18×10^{-4}.

The importance of the difference between the values q_m (Eq. 15) and q_m (Eq. 16) indicates that the pressure cells had some defects. The disks on both sides of the mercury film were not rigid enough to prevent disturbing deformations, and part of the space between the disks was probably filled with gas—not with liquid mercury. Because of these defects of the cells the method used for calibrating the cells was not appropriate, since the readings on the cells depend largely on the type and magnitude of the cell deformations produced by the application of the test load. If the thickness of the rubber pad had been increased, or if the pad had been made of a softer or stiffer rubber, contrastingly different calibration curves would have been obtained.

The conditions under which the cells operate in the field are illustrated in Figs. 23(*b*) and 23(*c*). Fig. 23(*b*) shows a cell in contact with the rock fill. The rock fill contains 10% of stones larger than 3 in. and the diameter of the cells is approximately 7 in. The distribution of the pressure of a rock fill over an area with a diameter of 7 in. is inevitably nonuniform and involves eccentric loading of the contact face. Because of this loading condition, the inner face of the outer disk of the cell bears at some point against the outer edge of the inner disk. Hence, one part Q_1 of the total load Q acting on the contact face will be transmitted directly onto the inner disk which rests on the stiffeners, and the pressure in the mercury film will be (Eq. 15) $q'_m = \frac{Q - Q_1}{r^2 \pi} < \frac{Q}{r^2 \pi}$. The value Q_1 depends on the eccentricity of the load, which is different for every cell. This fact excludes the possibility of determining the lateral pressure of rock fill by means of small pressure cells such as those used on Pier C.

Fig. 23(*b*) shows a cell in contact with fine to medium sand deposited by sluicing. The distribution of pressure exerted by such a sand can be assumed almost perfectly uniform over the contact face. The increase with depth of the lateral pressure of the sand is much smaller than the increase of the pressure in the mercury film because of the weight of the mercury. In the writer's opinion there seems to be no reason why the relation between the same pressure of a given intensity and the mercury pressure should be different from the relation between water pressure of the same intensity and the mercury pressure. Hence, the calibration curve for the sand pressure should be practically identical with the calibration curve for water pressure, W in Fig. 23(*a*). If the author had evaluated the strainmeter readings on the basis of curve W in Fig. 23(*a*), he would have obtained a K-value of approximately 0.4. Since he used curves S, he obtained $K = 0.7$.

Whichever calibration curve is used, the interpretation of the strainmeter reading is based on the assumption that the unit pressure on the contact face of the cell is equal to the average unit pressure on the bulkhead at

the elevation of the cell. If the plane of the contact face would yield under the influence of the lateral sand pressure without warping, this assumption would be justified. However, while the sand fill is being placed, the plane recedes slightly between the flanges of the sheet piles and it also yields on both sides of the rigid bridges that support the cells. The consequences of this condition are illustrated in Fig. 24.

Fig. 24(*a*) is a vertical section through the center line of a cell. Since the cell is mounted on a relatively rigid bridge, the stressmeter plate yields above and below the cell under the influence of the increasing lateral sand pressure, with reference to the cell. Fig. 24(*b*) represents the plane B-B of Fig. 24(*c*), in

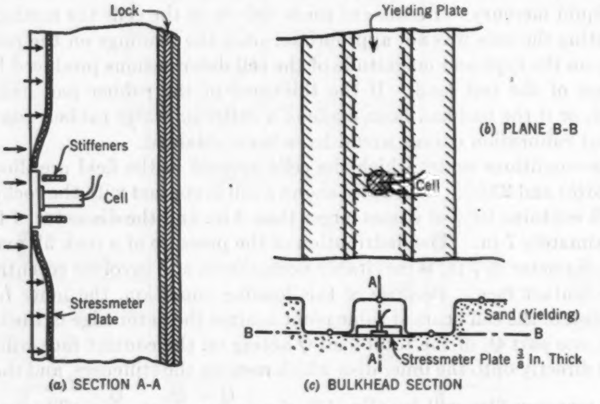

FIG. 24.—WARPING OF THE PLANE CONTAINING THE SOIL CONTACT FACE OF THE PRESSURE CELLS (BLANK AREAS YIELD WITH REFERENCE TO SHADED AREAS)

which the stressmeter plates lie. The shaded areas indicate the relatively unyielding areas of this plane. The yield of the lateral support between the shaded areas involves an increase of the unit pressure on the shaded areas and a decrease of the pressure on the blank areas, with reference to the average unit pressure q on the bulkhead, at the elevation of the cell. The cell is located in a shaded area. Therefore, the unit pressure on the cell will exceed q. The evalualtion of the strainmeter readings by means of the calibration curve W in Fig. 23(*a*) furnishes the value for the pressure on the cell and not the average value q of the pressure on the wall. Since the evaluation of the cell readings by means of curve W (Fig. 23(*a*)) leads to a K-value of approximately 0.4, the real value of K should be expected to be between 0.3 and 0.4.

The uncertainties involved in the interpretation of Mr. Duke's cell readings could have been avoided by reinforcing the stressmeter plates by means of closely-spaced steel ribs to a distance of several feet above and below each cell. Such reinforcement would have eliminated the yield of the stressmeter plate above and below each cell, and, as a consequence, an evaluation of the strainmeter readings by means of curve W in Fig. 23(*a*) would have furnished reasonably accurate results.

On the basis of his value $K = 0.7$, the author computed the deflections of the bulkhead and found that the computed deflections are approximately equal to the measured ones. Therefore, he concluded that the value $K = 0.7$ must approximate the real one. The computation was based on the assumption that the distribution of the earth pressure on the two sides of the bulkhead is that shown in Fig. 14. However, it is no exaggeration to say that the assumed pressure distributions are fictitious. The real distribution of the passive earth pressure over the outer face of the buried parts of the sheet pile depends entirely on the flexural rigidity of the piles and the compressibility of the adjacent soil; consequently the deflection of the piles at a given intensity and distribution of the active earth pressure can vary between wide limits. This has been demonstrated by a long series of very instructive bulkhead tests performed by P. W. Rowe.[18,35] These tests disclosed the fact that if the flexural rigidity of the sheet piles is increased, the maximum bending moment in the piles may increase by as much as 300% with no alteration in the active earth pressure on the inner face of the bulkhead. The increase of the maximum bending moment is almost exclusively the result of the influence of the flexural rigidity on the distribution of the passive earth pressure over the outer face of the buried part of the sheet piles, and on the location of the center of pressure. This fact invalidates the results of Mr. Duke's interpretation of the deflection data. The data are theoretically compatible with any value of K between 0.3 and 0.7, depending on the assumptions made regarding the distribution of the passive earth pressure.

The preceding discussion leads to the following conclusions: (*a*) The pressure cells used for determining the soil pressure on the contact face of the cells had some defects that precluded reliable calibration; (*b*) because of the flexibility of the stressmeter plates, the unit pressure on the contact face of the cells was considerably greater than the average unit pressure on the bulkhead at the elevation of the cells and this fact has not been considered; (*c*) the cells in contact with rock fill were subject to eccentric loading and, as a consequence, there is no definite relationship between the pressure on these cells and the cell readings; and (*d*) the determination of the K-value of the backfill on the basis of the results of the deflection observations on the bulkhead involves serious errors caused by the uncertainties associated with the assumptions concerning the distribution of the passive earth pressure over the face in contact with rock fill.

Because of these facts, the observational data contained in the paper do not permit a reliable evaluation of the K-value of the backfill of the Long Beach bulkhead. They do not, therefore, justify the conclusion that this value is greater than 0.4, which is the upper limiting value compatible with the present (1953) knowledge of the mechanical properties of sand. The value of K for this backfill may even be smaller than 0.4.

Piezometric Data.—Table 5 contains the results of piezometric readings. A digest of the data contained in the table may produce very instructive results. For example, Fig. 25(*a*) represents the hydraulic conditions that prevailed in the fill on June 11, 1949, at 5:30 a.m. The tide was rising and the tide level was still very low (+0.9 ft). The hydrostatic pressures in the pore water of the

[35] Discussion of "Anchored Sheet-Pile Walls," by Peter W. Rowe, *Proceedings*, Inst. of C. E., Vol. I, Pt. 1, September, 1952, pp. 616–647.

fill are determined by the readings on the piezometric tubes H-1 to H-6. At the tip of every piezometric tube the hydraulic head is equal to the difference between the elevation of the water in the tube and the elevation of the tip of the tube. The location of the tips of the tubes is shown in Fig. 25(*b*). In Fig. 25(*a*) the readings on the gages H-1 to H-4 are indicated by small circles and those on gage H-6 by a cross. The increase of the hydraluic head with depth is shown in Fig. 25(*a*) by the broken line A B C. The position of the section BC of the line with reference to the vertical axis shows that the pore water in the rock fill behind the bulkhead communicated almost freely with the open water

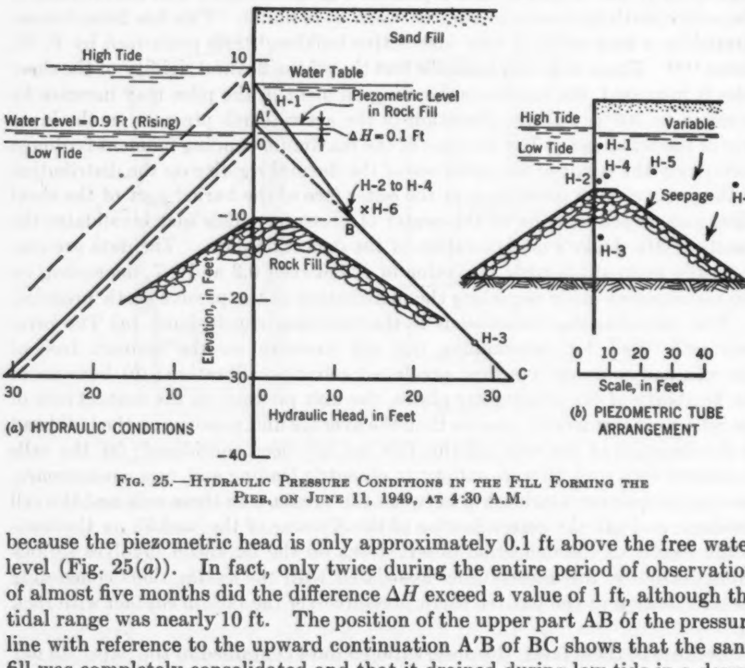

FIG. 25.—HYDRAULIC PRESSURE CONDITIONS IN THE FILL FORMING THE PIER, ON JUNE 11, 1949, AT 4:30 A.M.

because the piezometric head is only approximately 0.1 ft above the free water level (Fig. 25(*a*)). In fact, only twice during the entire period of observation of almost five months did the difference ΔH exceed a value of 1 ft, although the tidal range was nearly 10 ft. The position of the upper part AB of the pressure line with reference to the upward continuation A′B of BC shows that the sand fill was completely consolidated and that it drained during low tide in a downward direction toward the rock fill. In Fig. 25(*b*) the direction of the flow of seepage is indicated by arrows. In order to get a clear conception of this process it would have been necessary to make at least one piezometric reading per hour over a period of twenty-four hours, supplemented by simultaneous determination of the elevation of the free water level in the harbor, on two or three different days. Considering the importance of this information and its bearing on the earth pressure conditions, it is suggested that such observations be made. The results might be published by the author in the closure to the discussion, together with information concerning the tidal characteristics of the harbor. It also would be useful to the readers to know the inner diameter of the piezometric tubes, because this diameter and the coefficient of permeability of the fill

determine the time lag between the change in the pore-water pressure and the corresponding change of the water level in the tube.

Performance of Tie Rods.—The bottom set of diagrams in Fig. 12 shows that the major part of the fill above the tie-rod level is carried by the tie rods and that it acts on the tie rods as an ice load does on an electric conduit suspended between transmission towers. This loading condition invalidates the design assumptions for the tie rods and is inevitable if the tie rods are buried in a backfill that rests on a subsoil containing highly compressible layers. Elimination of this condition by installing the tie rods on the bottoms of conduits allows the fill to subside and the conduits to settle without affecting the rods.

Soil Test Data.—Under the heading, "Structure and Materials," Mr. Duke describes the laboratory tests that have been performed on many samples from twenty borings. Unfortunately, the most important property of the fill material—its relative density—has not received any consideration. If the fill material is dense, its angle of internal friction ϕ is great and a slight yield of the lateral support is sufficient to reduce the lateral pressure exerted by the fill to its minimum value. However, if the fill is loose, its ϕ-value is small and the lateral pressure decreases at a slow rate, while the bulkhead yields. The ϕ-values of 38° and 37° appearing in Table 1 for the upper strata *a* and *b* of the hydraulic fill are ϕ-values for a sand in a dense state, but it is unlikely that the fill really is dense. Considering the large quantities of time and money that have been invested in the study, it would certainly be justified to make one more exploratory boring through the fill material, combined with standard penetration tests, to secure reasonably reliable information concerning the relative density of the sand fill. Accurate information conceivably could be obtained by laboratory tests on undisturbed samples, but the recovery of such samples from sand strata is impracticable unless elaborate and expensive precautions are taken, such as chemical solidification or the freezing of a plug at the lower end of the sample.

Extensive testing has been performed in the laboratory, and valuable information can be extracted from these data by constructing soil profiles showing curves of equal effective grain size for both the fill and the natural ground. There is an urgent need for reliable information concerning the pattern of stratification of both hydraulic fills and natural sand deposits. Profiles of this kind would be a valuable and appreciated addition if added to the closure. If the borings are combined with standard penetration tests, the soil profiles should be supplemented by others showing curves of equal numbers of blows, which furnish approximate information concerning the variation of the relative density within the strata. The opportunity for securing such profiles should never be missed.

Uncertainties Involved in Bulkhead Design.—According to a statement in the "Introduction," anchored flexible bulkheads are not yet amenable to accurate analysis "*** because of insufficient understanding of the performance of the prototype system." In the writer's opinion the reason is a different one. Knowledge of the performance of bulkheads in general has already advanced to a state which leaves little to be desired (1953). However, as knowledge of the subject increased, engineers realized that some of the most

important factors on which the performance depends—such as the pattern of the variation of the compressibility of the soil in contact with the buried part of the sheet piles—cannot reliably be determined by any practicable means. Hence, the major uncertainties associated with bulkhead design are not caused by broad gaps in the knowledge of bulkhead performance. They result from the fact that the time and money that reasonably can be spent on subsoil exploration are limited, and this condition will never cease, irrespective of what engineers may learn.

Practical Value of the Investigation.—In spite of his objections to some of Mr. Duke's statements, the writer feels that the results of the investigation fully justify the work and expenditures involved. These results demonstrated emphatically the effect of a subsidence of the fill on the performance of the tie rods. They showed that the recession of the tide may be associated with a flow of seepage through the fill material involving a temporary increase of the effective weight of the fill. They also call attention to the inevitable uncertainties involved in bulkhead design. Hence, investigations of this kind certainly should be encouraged, whatever their shortcomings may be, because their results are the only source of information concerning the inevitable errors involved in the application of theoretical procedures of any kind to bulkhead design. It is always possible somehow to "extract the gold from the gravel." The Long Beach Harbor Department deserves the gratitude of the profession for having sponsored and financed the investigation.

D. P. Krynine,[36] M. ASCE.—Members of the engineering profession are always interested in the proper approach to the design and construction of water-front structures such as bulkheads, and important results of laboratory work on bulkhead models have been published. Although these findings were widely publicized, practical engineers are doubtful as to the unquestionable validity of this model research unless the results of such research are checked by observations on the prototypes under actual in-service conditions. It is difficult to reproduce storms and tides, or even hydraulic-fill construction. Wave action is a common phenomenon in the ocean and is apparently responsible for some of the features involved in bulkhead performance, which escape or are misinterpreted by a laboratory investigator.

The paper tends to fill the existing gap, but it was impossible to cover the whole field and to answer all pertinent questions. The writer was present at the initial stages of Mr. Duke's work. There was simplicity and efficiency in the instrumentation, combined with energy and a wide outlook, for the performance of this pioneer work. The writer has no doubt as to the correctness of the reported data, but merely wishes to revise the general opinion on the subject matter in the light of Mr. Duke's findings.

Action of the Dike.—The horizontal pressures exerted by the outer part of the dike on the sheet piling (shown in Fig. 6 and termed passive resistance) equal the horizontal stress components at the outside face of the sheet piling. The horizontal pressures exerted by the inner part of the dike on the sheet piling (active pressure) equal the horizontal stress components at the inside

[36] Cons. Engr., San Francisco, Calif.

face of the sheet piling. If the sheet piling were a thin, stressless membrane, horizontal pressures on both sides of the membrane would be equal. In this case, the horizontal pressure diagrams on both faces of the sheet piling would be identical. Because of the relative stiffness of the sheet piling, the numerical values of the abscissas of these diagrams would be different on both faces of the sheet piling.

As a rough approximation, assuming that the diagrams in question are identical, and using the outside horizontal pressures from Fig. 12 and Table 3 for plotting the inside horizontal pressures, the diagrams for active pressures

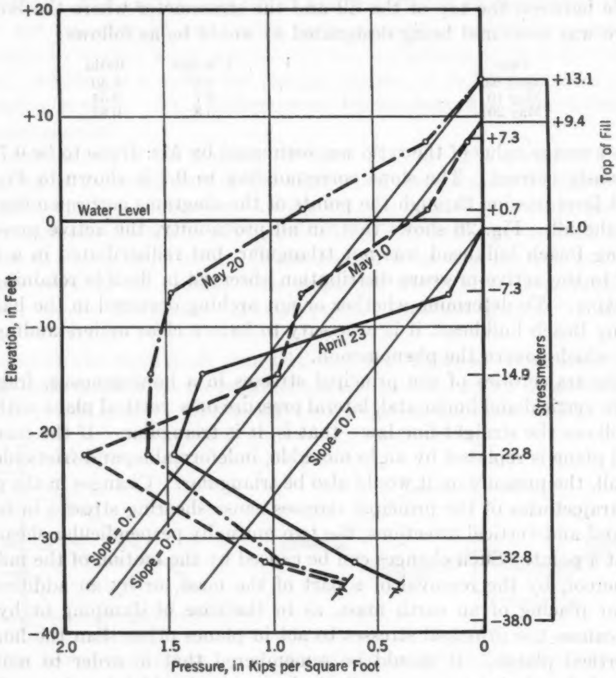

FIG. 26.—ACTIVE-PRESSURE DIAGRAMS AT STATION 27 + 30

acting on the bulkhead may be plotted, as in Fig. 26. In using this figure, it should be remembered that all abscissas above El.-14.9 are measured values, whereas those below El.-14.9 are assumed values which are fair approximations.

Field Active-Pressure Diagrams.—In Fig. 26, three field active-pressure diagrams are superimposed. They were drawn on the basis of research data obtained during the filling operations.

These three diagrams have been chosen at random from Fig. 12, and they can be considered as representative samples of the active-pressure distribution before changes caused by the settlement of the fill occurred on June 11. Con-

sidering the upper part of Fig. 26 (above El.-14.9), the writer believes that the first sentence under the heading, "Summary of Test Results," should read as follows:

> During the filling operation, the pressure of fill against the bulkhead in the upper part of the latter increased as the weight of the overlying fill was increasing.

It should be noted that, at the top of the April 23 curve in Fig. 26, the ratio between the horizontal pressure and the weight of the overlying fill is smaller than in the underlying layers located above El.-14.9. In fact, this ratio (the distance between the top of the fill and the stressmeter where the horizontal pressure was measured being designated h) would be as follows:

Date	h, in feet	Ratio
April 23	6.3	0.50
May 10	8.7	0.54
May 20	5.8	0.82

The average value of the ratio was estimated by Mr. Duke to be 0.7, which is obviously correct. The slope corresponding to 0.7 is shown in Fig. 26 as straight lines passing through the points of the diagrams corresponding to the top of the fill. Fig. 26 shows that, in all probability, the active pressure on the Long Beach bulkhead was not triangular, but redistributed in a manner similar to the active-pressure distribution observed in flexible retaining walls.

Arching.—To determine whether or not arching occurred in the backfill of the Long Beach bulkhead, it is necessary to have a clear understanding of the factors which govern the phenomenon.

If the trajectories of the principal stresses in a homogeneous, fragmental mass are vertical and horizontal, lateral pressure on a vertical plane within that mass follows the straight-line law—that is, it is triangular. If the imaginary, vertical plane is replaced by an immovable, indeformable, and frictionless vertical wall, the pressure on it would also be triangular. Changes in the position of the trajectories of the principal stresses cause shearing stresses in both the horizontal and vertical directions, the two mutually perpendicular shears being equal at a point. Such changes can be caused by the motion of the mass, or a part thereof, by the removal of a part of the mass, or by an addition to it. Irregular placing of an earth mass, as in the case of dumping or hydraulic filling, causes the principal stresses to act in planes other than the horizontal and vertical planes. It should be remembered that in order to mobilize a system of shearing stresses a small displacement should take place. Thus, if a homogeneous, fragmental mass is bounded by an immovable, vertical plane which is prevented from sufficient bending by its rigidity, the trajectories of the principal stresses in this mass would remain horizontal and vertical, and the active-pressure distribution would be triangular.

Shearing stresses of a certain magnitude, developed horizontally and vertically on the trajectories of principal stresses of a homogeneous fragmental mass, cause a shifting of these trajectories. At all points through which the new trajectories pass, the state of stress changes, since all shears at these points vanish. The adjacent particles are thus given an opportunity to press against one other without any disturbance or tendency toward lateral displacement

caused by shears. If pressed from both ends, this trajectory may stretch or arch; hence, the most probable arching curves in a sand mass are the trajectories of the principal stresses. Stretching or arching along a trajectory of principal stresses can occur only if there are two relatively immovable points at the ends of that trajectory. Presumably, the arch thus formed should also satisfy the requirements of stability—and if one of the abutments moves, the stretching loosens, and the arch breaks. Since major principal stresses generally begin at the free surface of the earth mass (the backfill, in the case of a bulkhead), arching along the trajectory of the major principal stress may be expected only occasionally. The arches into which the trajectories of the minor principal stresses are transformed are loaded (not necessarily uniformly) along their total length by normal loads provided by the trajectories of the major principal stresses. Arching is a particular case of transfer or redistribution of pressure by shearing stresses. This difference in terminology has been indicated by Mr. Tschebotarioff.

An examination of the diagram for April 12 (Fig. 12) shows that the stress distribution in the outer part of the dike, when there was no fill above the top of the dike, was not triangular. In the writer's opinion, the outer part of the dike was arched, one of the abutments of the arch being at the bulkhead and the other at the ground level. If the ground level was too soft to offer the resistance required for arching, this resistance would have been provided by the lower layers of diabase particles pressed into the ground, as shown in Fig. 27.

Engineers who have dealt with settlements of highway embankments know that the settlement of an embankment is a maximum either at its center line, or at two points on both sides of the center line, as indicated in Fig. 28. The

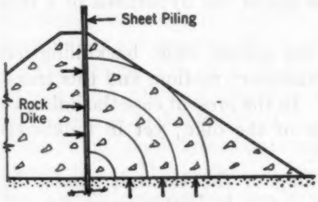

FIG. 27.—ARCHING IN THE DIKE

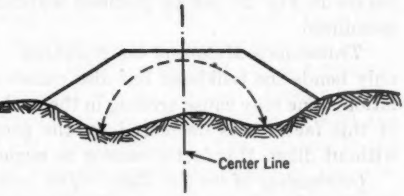

FIG. 28.—SETTLEMENT OF A ROADWAY EMBANKMENT

latter case is a result of an arching with redistribution of the pressure on the ground and a relief of pressure at the center. This analogy is mentioned in order to support the opinion concerning the arching in the Long Beach dike. Arching similar to that shown in Fig. 28 requires a favorable background, such as (1) firm support at two places on both sides of the center line and (2) earthwork by dumping rather than by compacting regularly-placed thin lifts.

A movement of the wall away from the earth mass it supports causes horizontal arching in the latter, as first shown by Mr. Terzaghi. In fact, one abutment of the arch is on the wall, and the other is on the potential shearing surface which is a physical reality such as the wall itself. It is clear that terms such as vertical or horizontal arching, often used in describing certain

arching phenomena, are inadequate and should be eliminated from soil mechanics nomenclature. The arching shown in Fig. 27, which took place along the trajectories of the minor principal stresses, was neither vertical nor horizontal.

Arching of the Backfill of the Long Beach Bulkhead.—It is difficult to answer categorically whether or not there was arching of the backfill behind the Long Beach bulkhead. Possibilities for arching did exist there. For example, a trajectory of the minor principal stress, with one abutment at the tie rods and the other on or next to the heel of the dike, was in a condition to cause arching under the action of a convenient system of forces. Such an arching would have decreased the bending moment in the span below the tie rods. In work similar to hydraulic filling, the trajectories of principal stresses shift their location continually, and arches are formed and broken. In this connection, irregular, so-called "erratic" readings may be obtained. An example is the excessively protruding abscissa of the diagram for April 23 in Fig. 26. These erratic readings are quite correct if the instrumentation works properly; however, the pressures are erratic.

In the case of the Long Beach bulkhead, the fact that the active-pressure distribution on the bulkhead was not triangular, but was redistributed by shearing stresses was important. Because of the physical nature of shearing stresses, they cannot create pressure, but can only redistribute or transfer it; that is, they are self-balanced. In the upper part of the curves of Fig. 26 there is an excess of pressure (in comparison with the triangular distribution) which is being caused by horizontal shears acting toward the bulkhead. Since these shears should be balanced, the logical conclusion is that, at the lower part of the bulkhead, there should be shearing stresses acting in the opposite direction—that is, decreasing the pressures. This means that the general shape of the curves in Fig. 26 can be justified without the use of the hypothesis of a thin membrane.

Translatory Motion of the Bulkhead.—In the general case, backfilling not only bends the bulkhead but also causes a translatory motion, and this translation alone may cause arching in the backfill. In the present case the influence of this factor was decreased by the presence of the dike; yet in bulkheads without dikes, this factor cannot be neglected.

Overloading of the Tie Rods.—The overloading of the tie rods cannot be explained by arching from tie rod to tie rod, since, in such a case, the soil material above the tie rods would not move downward, being supported by the arches. This would cause the material below the tie-rod level to settle away from the tie rods; but such a phenomenon did not take place.

A probable explanation consists in the formation of shearing surfaces above each tie rod. Such shearing surfaces would be closed surfaces, and if there is not enough vertical distance for their development, they would intersect the surface of the backfill. Soil material enclosed by these shearing surfaces was supported by the tie rods and made them sag. In addition, there was drag (negative pressure) on the shearing surfaces.

In connection with the overloading of the tie rods, there should have been back motion of the bulkhead. The upper abutment of the arches, shown in Fig. 27, then moved toward the inside of the backfill, and the arches loosened

and broke. This is represented by the diagrams of August 5 and the following days (Fig. 12).

Suggestions for Future Research.—Mr. Duke is to be commended for presenting suggestions to future field investigators of anchored bulkheads. The writer wishes to add to item 3 of these suggestions that, if the soil material at a given project is more or less uniform, moisture content at different elevations could be calibrated against density and shearing strength. Thus, in addition to a relatively limited number of undisturbed sample testings, a large number of moisture-content determinations could be made, thus giving a number of approximate density and shearing-strength values.

TRENT R. DAMES,[37] M. ASCE, AND DAVID C. LIU.[38]—New techniques in field instrumentation and new information on bulkhead behavior are presented by the author. The paper represents the first important published result of a careful study of an anchored bulkhead. He is to be complimented for successfully accomplishing this study in such a careful manner. The engineering profession also owes much to the Long Beach Harbor Department for cooperating in this research. The writers hope that similar studies will be made often, in order to furnish field evidence for comparison with classical methods of analysis and laboratory experimental data.

The writers will discuss (*a*) the design of the Long Beach bulkhead, (*b*) the reported pressure observations, (*c*) the author's suggestions concerning future research, and (*d*) possible additional study of the Long Beach bulkhead.

(*a*) The use of a granular dike to reduce the pressure from the more fluid hydraulic fill at the lower elevations is commendable. Having the rock dike on both sides of the bulkhead not only provides the effect of a reduction of the pressure acting on the inside of the dike but also a considerable increase in the resisting pressure on the outside. Using this construction, it might have been possible to have reduced the length of the sheet piling from that shown in Fig. 2.

The anchor piles (with 40-ft penetration into natural sand and 3-ft spacing) have much batter and therefore are comparatively unyielding. Even with the high stress of 32,000 lb per sq in. observed in the tie rods at Station 27 + 30, the sheet piling could deflect outward by only approximately $\frac{3}{4}$ in. relative to the anchor cap. This deflection, together with the small movement of the relatively unyielding anchor cap, is quite insignificant in terms of soil deformation behind bulkheads; and, therefore, the soil pressure near the wale should be close to the "at-rest" value.

It is conceivable that a more flexible system of anchorage, together with the use of ties protected from sagging caused by settlement of fill, would have resulted in lower tie-rod tensions.

(*b*) The information presented by the author concerning observed soil pressures is of great interest and importance because the observed values exceed normal assumptions by more than 100%.

To explain this difference, it is necessary to consider the pressure-deformation relationship of soils. It is not possible to establish quantitative relationships for any soil without extensive experimentation, but it is safe to say that,

[37] Executive Partner, Dames and Moore, Los Angeles, Calif.

[38] Eng.-Analyst, Dames and Moore, New York, N. Y.

when a bulkhead moves away from the soil, the pressure against the bulkhead will be reduced. It is possible that the high pressures reported in this paper were caused, at least in part, by the lack of appreciable outward deformation of the wale—it is doubtful whether the wale actually moved outward after the completion of filling early in June. The tie-rod tension increased approximately 25% between June and October at Station 27+30, indicating an elongation of approximately $\frac{1}{8}$ in. In the meantime, the fill settled and caused the tie rod to sag. This sag would tend to pull the wale and the anchor cap together, probably by an amount greater than the elongation of the tie rods. Thus, there was never sufficient outward movement of the bulkhead to reduce the lateral soil pressures to values normally assumed.

(*c*) The author's nine suggestions under the heading, "Suggestions for Future Bulkhead Field Studies," are of particular value to anyone who may perform field studies of earth structures. The experiences in instrumentation reported in this paper should prove invaluable as background for planning future field studies. It might be desirable, relative to suggestions 6, to install gages measuring strain in a vertical direction on both sides of a bulkhead in order to detect any appreciable friction on the inside. The gages could be protected by pieces of channel sections covering the gages and welded to the bulkhead on one flange immediately above the gage.

(*d*) At present (1953), it is understood that the Long Beach bulkhead will be extended upward and that the stresses in the tie rods will be relieved by excavation of fill from around the rods and loosening of the turnbuckles. In an operation of this type on any similar bulkhead, the change in tie-rod tension accompanying the loosening of the turnbuckles might be determined by pulling the tie rod on the outboard side of the bulkhead, holding the wall, and finding the pull on the tie rod necessary to separate the rod from the wall. Strain gages can be attached to tie rods with known stresses, and the subsequent changes in stresses determined. To avoid local horizontal redistribution of pressure, at least three adjacent tie rods should be released at the same time; observations should be made on all three. Perhaps observations of this nature would be of value in determining a proper range of elongations for all the ties. It might be well to protect the gaged rods, and possibly all the rods, against subsequent fill settlement by enclosing them in boxes.

Roy W. Carlson,[39] A.M. ASCE.—Some caution is suggested in accepting the author's finding that the horizontal pressure against the bulkhead is approximately 70% of the vertical load. The lateral pressures were determined by use of stressmeters and checked by tie-rod tensions measured by strainmeters. The certainty of the results is doubtful because of the peculiar characteristics of the particular stressmeters used. Furthermore, the check by measurement of the tie-rod tensions was not exact; it was dependent on assumptions concerning the pressure distribution at lower levels. The exact method of determining pressures from the stressmeters must therefore be investigated.

The calibration curves for one stressmeter (Fig. 9) shows that the response was nonlinear and was markedly different for water pressures and soil pressures.

---

[39] Cons. Engr., Berkeley, Calif.

After the Long Beach study was completed, the writer secured several similar stressmeters. These meters were found to have a high and nonlinear compressibility, indicating the presence of air entrapped with the mercury. This indication was confirmed by the fact that the response became linear when the meters were refilled with mercury. High compressibility would allow a large part of the load to be carried by the metal rim—especially under types of

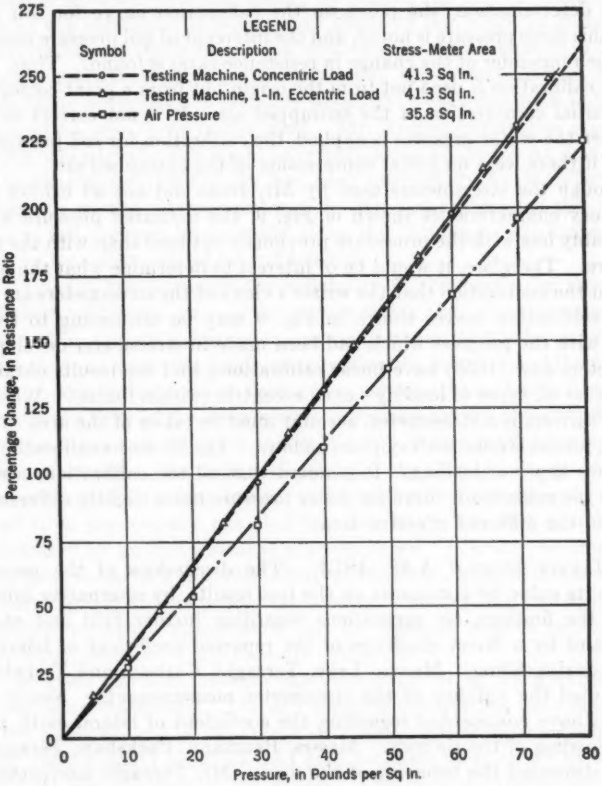

FIG. 29.—STRESSMETER CALIBRATION

loading where the plates of the stressmeter were not free to "dish." The response should be greatest with water loading, since the plates could dish and most of the pressure would be applied to the mercury film. At low pressures the response is only partial with soil pressure loading when the rim carries much of the load; the response is more nearly normal at high pressures, when the entrapped air is highly compressed. The calibration curves of Fig. 9 are in accordance with such reasoning.

If the stressmeters have these characteristics, a modified manner of using the calibration curves is necessary. Where both water pressure and soil pressure are acting, it is not correct to use both the calibration curves for water and soil, respectively, from the origin. A more correct procedure would be as follows: Since there was an initial water pressure, the calibration curve for water pressure should be used to determine what part of the observed change in resistance ratio of the stressmeter was caused by the water pressure. Following this determination, the point on the calibration curve for soil pressure having this same pressure is noted, and the intercept of soil pressure corresponding to the remainder of the change in resistance ratio is found. Thus, the soil-pressure calibration is used not from the origin but from a point corresponding to the initial compression of the entrapped air. It is not correct to assume that, after the water pressure is applied, the calibration for soil pressure is the same as if there were no initial compression of the entrapped air.

Although the stressmeters used by Mr. Duke did not all exhibit the unsatisfactory characteristics shown in Fig. 9, the indicated pressure would be considerably less with the procedure previously outlined than with the author's procedure. Therefore, it would be of interest to determine what the pressures were—on the assumption that the writer's views of the stressmeters are correct.

The calibration curves shown in Fig. 9 may be misleading to those unfamiliar with the progress which had been made in stressmeter development.[40] Stressmeters now (1953) have linear calibrations, and the results obtained are the same for all types of loading—even eccentric (within limits). When water pressure surrounds a stressmeter, account must be taken of the area subject to pressure, just as is done with sylphon bellows. Fig. 29 shows calibration curves for various types of loading. It is noted that all the calibrations are linear, and that the calibration curve for water pressure has a slightly different slope, ecause of the different effective area.

C. Martin Duke,[41] A.M. ASCE.—The discussions of the paper have added to its value by comments on the test results, by alternative interpretations of the findings, by suggestions regarding further field and analytical studies, and by a direct challenge of the reported coefficient of lateral earth pressure during filling. Messrs. Lake, Terzaghi, Carlson, and Tschebotarioff have studied the validity of the stressmeter measurements. Nearly all the discussers have commented regarding the coefficient of lateral earth pressure and the loading of the tie rods. Messrs. Baumann, Packshaw, Terzaghi, and Krynine discussed the behavior of the dike. Mr. Terzaghi interpreted some of the pore pressure measurements. Several of the discussers made suggestions for additional field research on anchored bulkheads. Messrs. Boyer, Way, and Terzaghi commented on the philosophy of the field study approach. Mr. Packshaw and Messrs. Dames and Liu gave special attention to the subject of design of flexible bulkheads as influenced by the Pier C test findings.

Validity of Stressmeter Measurements.—The values of soil pressure as computed from the readings of the stressmeters were questioned on the bases that

[40] "Development of a Device for the Direct Measurement of Compressive Stress," by R. W. Carlson and David Pirtz, *Journal*, A. C. I., November, 1952.

[41] Associate Prof. of Eng., Univ. of California, Los Angeles, Calif.

(1) the diameter of the stressmeter contact face was too small, and not enough of these instruments were used; (2) the method by which the stressmeter calibrations were utilized was incorrect; and (3) the method of mounting the stressmeters used was questionable.

The number of stressmeters used was limited by economic circumstances. In planning the test program it was therefore hoped to obtain an over-all indirect determination of soil pressure by measuring tie-rod tensions. The diameter of the individual cells was only about $7\frac{1}{2}$ in., which as stated in the paper is certainly too small for reliable quantitative measurements in the dike. Considering the nature of all soils, especially those deposited in full-scale hydraulic filling operations, it certainly would have been desirable to have had a larger contact area, even in the sand. Mr. Tschebotarioff has suggested a device (Fig. 21) whereby this might have been accomplished. An arrangement similar to that shown in Fig. 21 was used successfully by Mr. Terzaghi in measurements on the Chicago subway.[42] Mr. Lake indicates the apparent variation of soil pressure horizontally along the bulkhead as indicated by the variation in measurements of tie-rod tension.

Mr. Terzaghi has discussed the reliability of the particular stressmeters used, of their calibration, and of the way in which they were mounted on the bulkhead. Mr. Carlson's discussion answers some of the questions raised by Mr. Terzaghi and also gives an opinion regarding the proper use of the particular soil pressure and water pressure calibration curves obtained. It is clear that the mercury chamber of the stressmeters contained air, which accounts for the nonlinearity of the two curves shown in Fig. 9. Presence of this nonlinearity was most unfortunate; the writer is happy for the sake of future users of the stressmeters that Mr. Carlson has devised a method[40] of permanently eliminating all air from the mercury chamber (see Fig. 29). The Pier C stressmeters were fabricated by an inexperienced manufacturer. If it is to be emphasized, however, that the actual calibration curves obtained, both with soil and with water, were reproducible to a fully satisfactory accuracy, the particular curves used for the respective stressmeters can be expected to give reliable values of either water pressure or soil pressure acting alone.

Fig. 30 gives the soil pressure calibration curves of all stressmeters for which results are presented. The soil pressure calibrations were made in the laboratory as shown in Fig. 29, except that the stressmeters were bedded on a firm, stiff rubber pad 1 in. thick and of a hardness of from 60 to 70 Shore, and the load was centered on the meters. Choice of the rubber bedding was based on a series of experiments conducted at the University of California at Berkeley in 1944 and subsequently substantiated by field measurements at an airport pavement test program[4] where satisfactory checks were obtained between the readings of stressmeters beneath the pavement and loads applied on the surface of the pavement.

The fact that the calibration curves for both soil pressure and water pressure for the Pier C stressmeters were nonlinear and were different from one another

[42] "Liner-Plate Tunnels on the Chicago (Ill.) Subway," by Karl Terzaghi, *Transactions*, ASCE, Vol. 108, 1943, p. 991.

gave the writer considerable concern during the test program and the subsequent analysis of data. To solve the problem of finding the soil pressure from a stressmeter reading by utilizing a known water pressure and the two nonlinear calibration curves is not easy. Messrs. Terzaghi and Carlson very properly call attention to this characteristic of the instruments and challenge

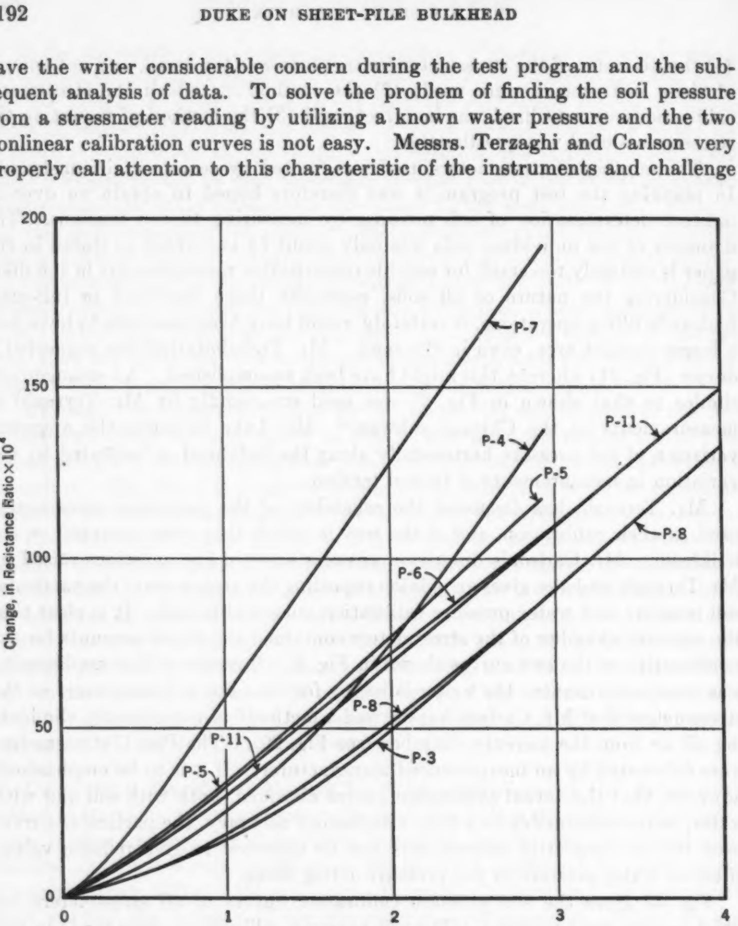

FIG. 30.—SOIL-PRESSURE CALIBRATION OF STRESSMETERS

the writer's use of the two curves. Mr. Carlson explains clearly why the nonlinearities exist. He also explains (in terms of the presence of air in the mercury layer) why the water-pressure calibration curve should lie above the soil pressure calibration curve (Fig. 9). The procedure adopted in the paper was, in effect, to use the parts of the two curves near the origin. The writer has discussed this subject with Messrs. Carlson and Terzaghi and agrees with Mr. Carlson that a better procedure would have been as follows: The calibration curve for water pressure should be used to determine what part of the observed change in the resistance ratio resulted from water pressure; the reader should then move vertically to a point on the calibration curve for soil pressure and

use the remaining amount of resistance-ratio change to move to a higher point on the soil pressure curve; the horizontal intercept between the latter two points should be taken as the recorded soil pressure. This procedure is preferred to that (suggested by Mr. Terzaghi) of using the water pressure calibration curve for both water and soil because (as explained by Mr. Carlson) the shapes of the two calibration curves theoretically should be different. The effect of the revised (Carlson) procedure is to reduce appreciably the values of soil pressure indicated by the stressmeters having the more nonlinear soil pressure calibration curves. The nature and extent of this reduction will be considered subsequently. The writer agrees with Mr. Terzaghi that the stressmeter mounting plates were too flexible at points away from the meters and that this tends to cause recorded pressures to be too great (Fig. 24).

Behavior of Dike.—The writer agrees with Messrs. Baumann, Terzaghi, and Krynine that the lack of adequate data on the behavior of the bulkhead below the top of the dike is regrettable. The difficulty of obtaining quantitative pressure measurements in the dike has been emphasized by several of the discussers. Probably some qualitative information can be gleaned from the Pier C measurements. Two stressmeters in addition to P-8 (Fig. 6) were placed in the dike on the inner side of the bulkhead, but these were damaged during the placing of the fill and no measurements were made with them.

Messrs. Terzaghi and Packshaw have commented on the assumptions regarding pressure distribution between the dike and the bulkhead, on which the partial check between tie-rod tension and soil pressure measurements was based. There are several possible assumptions about the dike pressure distribution; the check of tie-rod tension against soil pressure is therefore only partial. The writer does not in any sense advance the procedures he used in producing Fig. 14 as desirable design practice.

Mr. Krynine has suggested an ingenious scheme for using the measured pressures in the outer dike to approximate those in the inner dike, on the assumption that the stiffness of the sheet-pile wall is negligible. Qualitatively, at least, this gives a result (Fig. 26) consistent with the assumption of Fig. 14. The concept of membrane action would be most valid at places where the shear in the bulkhead is small (see Fig. 15). The upper two lines labeled "Slope = 0.7" in Fig. 26 should be broken to show a flatter slope at the groundwater level.

Messrs. Tschebotarioff and Krynine have given considerable attention to the subject of "arching." The writer agrees with Mr. Tschebotarioff's deduction from the test data that there was no evidence of arching caused by deflection of the bulkhead. No observable change in deflection occurred at any point on the bulkhead during the pressure redistribution of Fig. 12. Mr. Krynine's general discussion of the subject of arching with application to the situation at the Pier C bulkhead (Figs. 27 and 28) should be read as an aid to understanding the basic mechanism of the arching phenomenon. In the opinion of the writer, the shear-stress concept is the only rational approach that can be made to this complex phenomenon.

Messrs. Dames and Liu comment on the function of the dike and rightly explain that the designer should take full advantage of its structural characteristics.

The silty clay found in borings A-1 and A-2 and shown in Table 1 was laid down during the filling process, which postdated the placing of the rock dike. Except for this fact, Mr. Lake's suggestion for a possible rotation with respect to the tie-rod level of the lower part of the bulkhead, including the dike, would be feasible.

Earth Pressure Against Bulkhead During Filling.—Most discussers noted the magnitude and distribution of lateral earth pressure against the bulkhead during the filling operation. Mr. Terzaghi challenged the validity of the reported coefficient of lateral earth pressure (K equals 0.7) on the bases of the stressmeter calibration and reliability and the experiences of previous investigators with determinations of earth pressure at rest. Messrs. Tschebotarioff, Lake, and Packshaw, and Messrs. Dames and Liu observed the unexpectedly high value of this coefficient and offered possible explanations for it. Messrs. Krynine and Tschebotarioff have correctly pointed out that the concept of a single-valued coefficient is fallacious. The value of K probably varies both with time and with elevation on the bulkhead.

Based on the preceding discussion of the stressmeter calibration curves, the writer has recomputed some of the soil pressures obtained with those stressmeters having the more nonlinear calibrations and has found that this appreciably reduces the coefficient of lateral pressure during filling. Such a reduction occurs because the more nonlinear the stressmeters used (P-3, P-4, P-8) all happened to be located where they had a strong influence on the computation of the value of K.

Mr. Tschebotarioff suggested that the high value of K reported for Pier C by the writer may have been caused by vibration accompanying wave action on the bulkhead. Mr. Lake suggested that the water-level differential between the inside and the outside of the bulkhead during three weeks of the filling operation (Table 3) could be responsible for a value of K that was higher than normal. The high inside water level could easily have caused large bulkhead deflections that could not subsequently reverse against the passive soil resistance. Mr. Packshaw suggests that the high value of K may result from arching of the soil between the forward-raking batter piles and the bulkhead wall during the filling operation. Messrs. Dames and Liu observe that the deflection of the bulkhead probably was not sufficient to cause appreciable reduction of the lateral earth pressures to less than the value of earth pressure at rest.

The writer's conclusion with regard to the lateral earth pressure, after study of the discussions and re-evaluation of the data, is that the coefficient of lateral earth pressure during filling was smaller than that reported in the paper. However, the errors and uncertainties discussed herein make it unwise to assign a numerical value to the coefficient.

Loading of Tie Rods.—In general, the discussers concurred with the writer's interpretation of the redistribution of soil pressure and the change in tie-rod tension following the completion of filling. That this tension change was

caused by the loading of the tie rods as a result of fill settlement is fairly well established. Practical remedies suggested included the placing of the tie rods inside concrete pipes and the provision of additional vertical supports along the length of the tie rods. Mr. Krynine rightly contends that complete soil arches in the architectural sense could not have developed between the tie rods, but rather that the drag of the tie rods with respect to the settling fill produces shear stresses without causing appreciable discontinuity in the soil.

Messrs. Tschebotarioff and Packshaw explain that the redistribution of pressure might logically be attributed to other causes of shear-stress distribution or arching. One of these causes is the presence of the rigidly supported anchor cap. Another is the presence of the closely spaced batter piles of the anchorage and the possibility of developing arch abutments on the batter piles and on the dike.

Mr. Boyer makes a strong contribution in computing the drag force that the fill would have to transmit to the tie rods in order to produce the tension increases observed subsequent to the completion of the filling operation. His computations indicate that a reasonable composite value for probable drag would be of the order of magnitude of 300 lb per lin ft of rod. He also shows that closer supports for the tie rods would greatly reduce the excessive tensions.

Pore Pressures.—Mr. Terzaghi reached essentially the same conclusions (Fig. 25) with regard to the effect of tide fluctuation on the pore pressures as were expressed by the writer under the heading, "Other Pressure Distributions." Direct use was made of the data of Table 5 in correcting stressmeter readings for water pressure and in computing those values of vertical soil pressure which required an allowance for seepage force.

The piezometer tubes were of $\frac{3}{4}$-in. inside diameter. Unfortunately, construction operations and the forces of nature have so damaged the instrumentation that it is no longer feasible to obtain additional data on pore pressures (as was suggested by Mr. Terzaghi). However, the data for August 5 and 6, Table 5, partly satisfy his request.

General Comments.—Most discussers made valuable suggestions for future field research on bulkheads. The comments of Mr. Packshaw and Messrs. Dames and Liu should be helpful to those interested in the design of bulkheads.

Although the quantity of information obtained from soil explorations and tests immensely exceeded that which the writer chose to include in the paper, the sixty-nine borings in the harbor area were too widely spaced to permit the construction of soil profiles as suggested by Mr. Terzaghi. Table 1 gives the general soil characteristics at Pier C on a quasi-statistical basis; the void ratio data permit computation of relative densities for the various strata. The actual void ratios (based on 3-in. Shelby tube push samples) are relatively low. Time did not permit the performance of Mr. Terzaghi's suggestion of making penetration tests in the fill.

Field studies in soil mechanics would benefit from a statistical approach. Although detailed study of specific earth structures of various types is necessary, much is lacking in such an approach that could be obtained by observations of only a few fundamental parameters at a large number of similar installations. For example, in a bulkhead study there might be measured at

twenty stations the tie-rod tension and the deflections at the wale, maximum bulge, and toe.

In closing, the writer desires to make clear certain limitations of the Pier C bulkhead tests.

1. The reported value of the coefficient of lateral pressure during the filling operation has not been determined with precision. The value reported in the paper, K equals 0.7, is too great. It is unlikely that this "coefficient" is constant; it probably varies both with time and with elevation on the bulkhead.
2. No quantitative conclusions are offered regarding the behavior of the dike or the passive resistance phenomena at the base of the bulkhead.
3. Important atypical features of the test were: The closely spaced batter piles; the silt layer at the bottom of the fill; the large differential between inside and outside water levels during an important part of the test; and the presence of the rock dike having a 3-in. maximum diameter.

The writer wishes to thank very sincerely the discussers, all of whom have made important additions to the value of the paper. Only a fraction of their many contributions could be considered in detail in this closure.

AMERICAN SOCIETY OF CIVIL ENGINEERS
Founded November 5, 1852
TRANSACTIONS

Paper No. 2573

FLEXURE OF DOUBLE CANTILEVER BEAMS

BY F. E. WOLOSEWICK,[1] M. ASCE

WITH DISCUSSION BY MESSRS. LU-SHIEN HU, LEWIS SCHNEIDER, RAY W. CLOUGH, WILLIAM A. CONWELL, AND F. E. WOLOSEWICK

SYNOPSIS

A cantilever beam is a simple structural element. When two cantilever beams at right angles to each other are joined rigidly, a complicated structure results. Each cantilever beam is subject to torsion and bending.

Construction of this type is becoming more frequent in buildings, water works, power plants, and industrial works. The elimination of the corner caisson and the supporting columns is an invitation to economy. Frequently such supporting members cannot be provided because of physical restrictions and architectural requirements.

Since concrete is weak in torsion, and existing steel shapes are unsuitable for resisting high torsional stresses, it is important to determine the correct magnitudes of torsional moments in such supporting members.

Conventional supporting members have average height-to-depth ratios. For such sections the elastic functions (identified as A, B, and C) are small. Consequently, torsional moments will be high and must require careful consideration. As these elastic functions increase numerically, torsional moments have secondary effects.

The resulting equations have been arranged in such a manner that, for any loading conditions, forces can be evaluated by direct substitution and by simultaneous solutions of necessary equations.

INTRODUCTION

Two cantilever beams, at right angles to each other, having their free ends connected either rigidly, or by a universal joint, form a double cantilever system. Such systems are shown isometrically in Fig. 1. Under normal construction procedure, either in concrete or steel, ends C would be joined

NOTE.—Published in November, 1952, as *Proceedings-Separate No. 158*. Positions and titles given are those in effect when the paper or discussion was received for publication.

[1] Structural Engr., Sargent & Lundy, Chicago, Ill.

together. When so constructed, resistance to rotation would be developed by both beams. Torsional moments would then be transferred from one beam to the other. When rotations would be allowed at joint C, torsional moments would not exist, and both cantilevers would be subject to bending moments.

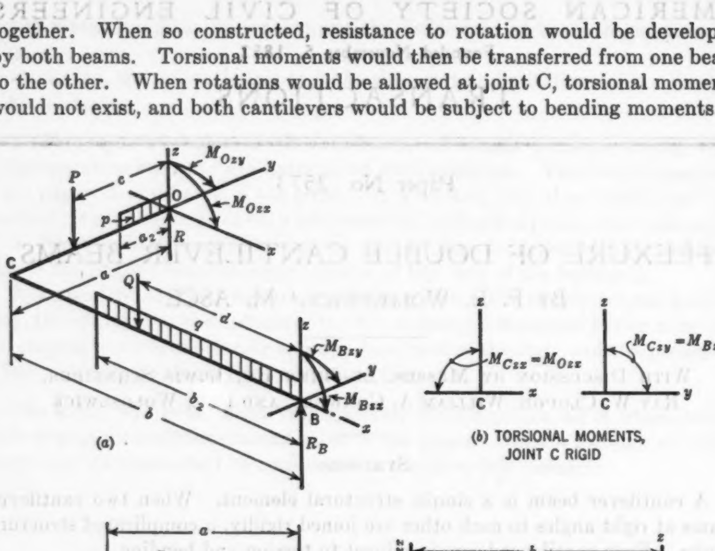

(a) (b) TORSIONAL MOMENTS, JOINT C RIGID

(c) BENDING MOMENTS, JOINT C RIGID

(d) BENDING MOMENTS, JOINT C HINGED

FIG. 1.—DOUBLE CANTILEVERS WITH FIXED AND RIGID JUNCTION POINTS

In the analysis and discussions which follow, point O is assumed as the origin. The reaction at point O is called R, and is positive if acting as shown in Fig. 1. The bending moment M_{Ozy} is positive when rotating clockwise in Fig. 1(a). Torsional moment M_{Ozx} is considered positive if acting as shown in Fig. 1(a). It may have zero value or be negative, depending on the ratios of lengths, elastic and torsional properties of the cantilever beams defined by functions A, B, and C, and the magnitudes of applied loads. In discussions of right-angle cantilevers, the observer is assumed to be standing at four o'clock, and looking toward point O.

All moments are defined by subscripts designating the planes in which they rotate. A subscript preceding a plane designation would define the point where rotations are occurring. This designation is easier to visualize than rotations about an axis.

With the forces at the origin known, the bending and torsional moments can be determined at any point in both spans by statics. Torsional moments do not enter into the equation for flexure on any point in member a, and must therefore be treated independently. Similarly, bending moments are not affected by torsional moments, and as such must be treated independently. This would be true, of course, as long as both cantilevers are at right angles to each other. With an angle other than 90°, components of torsional and bending moments must be considered in determining the resultant effect. At point C the torsional moment of one span becomes the bending moment for the other span, at right angles to the one considered. Likewise at point C, the bending moment of one span becomes the torsional moment for the other span, at right angles to the one considered.

General Case of Continuity

The most general case of a system of restraining forces is shown in Fig. 1(a). There are six restraining forces in the system, three at point O and three at point B. Since three forces, located correctly, preserve equilibrium, the remaining unknowns must be determined from continuity. These unknowns can be obtained most conveniently by the theory of least work. Special cases frequently occur in which it is inconvenient or impossible to

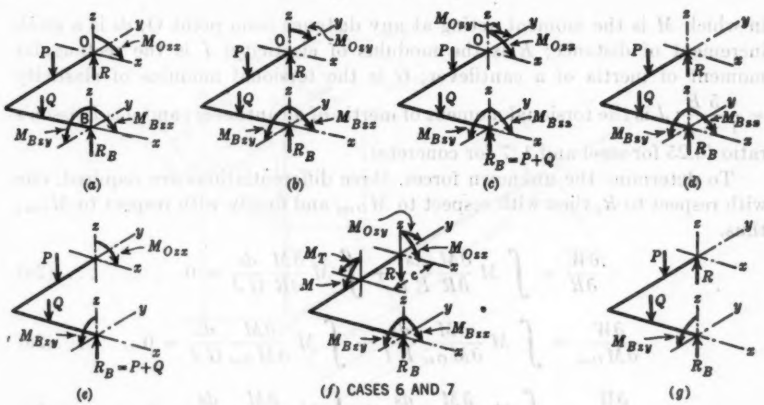

Fig. 2

develop all restraining forces at point O or point B. These cases are shown isometrically in Fig. 2.

Thus in Fig. 2(a), there are two restraining forces at point O, (M_{Oxz} and R) and in Fig. 2(b) there are two forces, M_{Oxy} and R at point O. Fig. 2(c) is a special case of a guided cantilever at point O, with restraining moments

M_{Oxz} and M_{Oxy}, without reaction R. Fig. 2(d) is a special case of double cantilever, where resisting moments cannot be developed, and only reaction R is available.

Further specialized cases of a double cantilever can be developed. Thus at point O either one of the two moments can be acting without the benefit of reaction R. All such cases of guided cantilevers are of limited usefulness structurally, but may have considerable applications in instrumentation engineering. Fig. 2(g) shows an unstable structure. Although three forces are shown acting, which numerically satisfy the equation of stability, a little study will show instability. Thus, it is not possible to have two reactions, and a single moment to preserve equilibrium. Equilibrium can only be preserved when one of the reactions is replaced by a moment, rotating in the plane at 90° to the other moment.

This brief summary indicates that location of restraining moments and reactions can be made dependent on the physical conditions affecting the design.

Development of General Equations

The most general case of a system of restraining forces at the origin is shown in Fig. 1(a), with three forces at points O and B. Such a system is indeterminate to the third degree. For any manner of loading on spans a or b, the equation expressing work for the entire system is

$$W = \int \frac{M^2\, ds}{2\, E\, I} + \int \frac{M^2\, ds}{2\, G\, J} \ldots\ldots\ldots\ldots\ldots\ldots (1)$$

in which M is the moment acting at any distance from point O; ds is a small increment of distance; E is the modulus of elasticity; I is the rectangular moment of inertia of a cantilever; G is the torsional modulus of elasticity $= \dfrac{0.5\, E}{1 + \mu}$; J is the torsional moment of inertia of a cantilever; and μ is Poisson's ratio (0.25 for steel and 1/7 for concrete).

To determine the unknown forces, three differentiations are required, one with respect to R, then with respect to M_{Oxz}, and finally with respect to M_{Oxy}; thus,

$$\frac{\partial W}{\partial R} = \int M \frac{\partial M}{\partial R} \frac{ds}{E\, I} + \int M \frac{\partial M}{\partial R} \frac{ds}{G\, J} = 0 \ldots\ldots\ldots\ldots (2a)$$

$$\frac{\partial W}{\partial M_{Oxz}} = \int M \frac{\partial M}{\partial M_{Oxz}} \frac{ds}{E\, I} + \int M \frac{\partial M}{\partial M_{Oxz}} \frac{ds}{G\, J} = 0 \ldots\ldots\ldots (2b)$$

$$\frac{\partial W}{\partial M_{Oxy}} = \int M \frac{\partial M}{\partial M_{Oxy}} \frac{ds}{E\, I} + \int M \frac{\partial M}{\partial M_{Oxy}} \frac{ds}{G\, J} = 0 \ldots\ldots\ldots (2c)$$

Integrations of Eqs. 2 lead to solutions listed as Eqs. 3 to 17, in Table 1. These equations contain three unknown forces which can be evaluated algebraically. The formal solutions of Eqs. 2 have been deleted from this paper because of their length. For certain loading conditions and boundary conditions they become somewhat unmanageable.

In Table 1, the subscripts a and b refer to the beams having those lengths (see Fig. 1). The symbols p and q are the uniform loads on cantilevers of lengths a and b, respectively. In Table 1, I is the moment of inertia of a cantilever, P equals the concentrated load on length a, and Q equals the concentrated load on length b. The symbol i is the ratio, I_a/I_b; m denotes the ratio, q/p; r is the ratio b/a; A is the dimensionless quantity, $\dfrac{E\,I_a}{G\,J_b}$; B is the dimensionless quantity, $\dfrac{E\,I_b}{G\,J_a}$; C is a dimensionless quantity, $\dfrac{E\,I_a}{G\,J_a}$; and S is the normal cross-sectional area of a beam. The Greek letters are defined as follows: The ratio, a_2/a is expressed as α_2; β_2 is the ratio, b_2/b; γ is the ratio, c/a; δ is the ratio, d/b; Δz is the deflection, in the z-direction, of point O; θ_{yz} equals the angular rotation of point O in the yz-plane, in radians; and θ_{zx} equals the angular rotation of point O in the zx-plane, in radians.

Particular Solutions

From general solutions for any loading conditions, a series of special equations can be developed, dependent solely on the boundary conditions at points O and B.

As a specific illustration, assume that M_{Ozx} cannot be developed, but that R and M_{Ozy} can be resisted. To determine forces from this boundary condition, use equations a and c in Table 1, with M_{Ozx} being set equal to zero. Simultaneous solutions will determine the unknown forces.

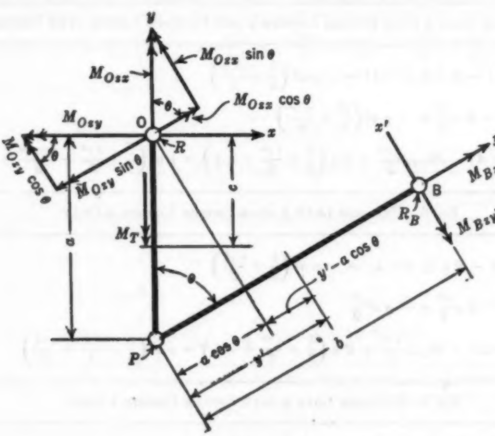

Fig. 3

When both moments at point O cannot be resisted, but only the reaction R is available to resist vertical shears, its magnitude can be determined from Eq. c of any loading condition in Table 1. This equation is the only one containing values of M_{Ozx} and M_{Ozy}, both of which can be equated to zero and still offer a solution for R. For a condition of a guided cantilever, reaction R

is zero, and moments M_{Osz} and M_{Osy} are assumed to be acting. The values of these moments can be determined by combining Eqs. *a* (Table 1) with Eqs. *b* and solving simultaneously with Eqs. *c*, with R in all three being set to zero. A special case of a guided cantilever would be one in which only moment M_{Osy} is acting. The value of this moment can be determined from Eqs. *a*, with R being zero. Similarly when only M_{Osz} is required, Eqs. *b* will furnish the required answer.

TABLE 1.—EQUATIONS FOR VARIOUS LOADING CONDITIONS [a]

	EQ. 3—CONCENTRATED LOAD P ON SPAN a
a	$M_{Osy}(1 + rA) - Ra(\tfrac{1}{2} + rA) = Pa(\gamma - \tfrac{1}{2}\gamma^2 - \tfrac{1}{2} - rA + \gamma rA)$
b	$M_{Osz}(r + B) - Ra\frac{r^2}{2} = -Pa\frac{r^2}{2}$
c	$-M_{Osy}(\tfrac{1}{2} + rA) - M_{Osz}\frac{ir^2}{2} + Ra\left(\frac{1}{3} + \frac{ir^3}{3} + rA\right) = Pa\left(\frac{1}{3} + \frac{\gamma^3}{6} - \frac{\gamma}{2} + \frac{ir^3}{3} + rA - \gamma rA\right)$
	EQ. 4—CONCENTRATED LOAD Q ON SPAN b
a	$M_{Osy}(1 + rA) - Ra(\tfrac{1}{2} + rA) = 0$
b	$M_{Osz}(r + B) - Ra\frac{r^2}{2} = -Q\frac{ar^2\delta^2}{2}$
c	$-M_{Osy}(\tfrac{1}{2} + rA) - M_{Osz}\frac{ir^2}{2} + Ra\left(\frac{1}{3} + \frac{ir^3}{3} + rA\right) = Qair^3\left(\frac{1}{3} - \frac{(1-\delta)}{2} + \frac{(1-\delta)^3}{6}\right)$
	EQ. 5—UNIFORM LOAD p OVER ENTIRE LENGTH a AND UNIFORM LOAD q OVER ENTIRE LENGTH b
a	$M_{Osy}(1 + rA) - Ra(\tfrac{1}{2} + rA) = -pa^2\left(\frac{1}{6} + \frac{rA}{2}\right)$
b	$M_{Osz}(r + B) - Ra\frac{r^2}{2} = -pa^2\left(\frac{r^2}{2} + \frac{mr^3}{6}\right)$
c	$-M_{Osy}(\tfrac{1}{2} + rA) - M_{Osz}\frac{ir^2}{2} + Ra\left(\frac{1}{3} + \frac{ir^3}{3} + rA\right) = pa^2\left(\frac{1}{8} + \frac{ir^3}{3} + \frac{imr^4}{8} + \frac{rA}{2}\right)$
	EQ. 6—UNIFORM LOAD p OVER ENTIRE LENGTH a ONLY
a	$M_{Osy}(1 + rA) - Ra(\tfrac{1}{2} + rA) = -pa^2\left(\frac{1}{6} + \frac{rA}{2}\right)$
b	$M_{Osz}(r + B) - Ra\frac{r^2}{2} = -pa^2\frac{r^2}{2}$
c	$-M_{Osy}(\tfrac{1}{2} + rA) - M_{Osz}\frac{ir^2}{2} + Ra\left(\frac{1}{3} + \frac{ir^3}{3} + rA\right) = pa^2\left(\frac{1}{8} + \frac{ir^3}{3} + \frac{rA}{2}\right)$
	EQ. 7—UNIFORM LOAD q OVER ENTIRE LENGTH b ONLY
a	$M_{Osy}(1 + rA) - Ra(\tfrac{1}{2} + rA) = 0.$
b	$M_{Osz}(r + B) - Ra\frac{r^2}{2} = -q\frac{b^2r}{6}$
c	$-M_{Osy}(\tfrac{1}{2} + rA) - M_{Osz}\frac{ir^2}{2} + Ra\left(\frac{1}{3} + \frac{ir^3}{3} + rA\right) = qb^3\frac{ir^2}{8}$

[a] Equation numbering is in sequence with the numbering in the text.

TABLE 1.—(*Continued*)

Eq. 8—Torsional Moment M_T Acting at Any Point, Distance c from Point O

a $\quad M_{Osy}(1 + rA) - Ra(\tfrac{1}{2} + rA) = 0$

b $\quad M_{Osz}(r + B) - Ra\frac{r^2}{2} = M_T(\beta - \gamma\beta + r)$

c $\quad -M_{Osy}(\tfrac{1}{2} + rA) - M_{Osz}\frac{ir^2}{2} + Ra\left(\frac{1}{3} + \frac{ir^3}{3} + rA\right) = -M_T\frac{ir^2}{2}$

Eq. 9—Bending Moment M Acting at Any Distance c from Point O

a $\quad M_{Osy}(1 + rA) - Ra(\tfrac{1}{2} + rA) = M(1 - \gamma + rA)$

b $\quad M_{Osz}(r + B) - Ra\frac{r^2}{2} = 0$

c $\quad M_{Osy}(\tfrac{1}{2} + rA) - M_{Osz}\frac{ir^2}{2} + Ra\left(\frac{1}{3} + \frac{ir^3}{3} + rA\right) = M\left(\frac{1}{2} - \frac{\gamma^2}{2} + rA\right)$

Eq. 10—Uniform Load q over Distance b_2. Length b_2 Measured from Point B to End of Load

a $\quad M_{Osy}(1 + rA) - Ra(\tfrac{1}{2} + rA) = 0$

b $\quad M_{Osz}(r + B) - Ra\frac{r^2}{2} = -q\frac{b^2 r}{2}\left[\tfrac{1}{3} - (1 - \beta_2) + \tfrac{1}{2}(1 - \beta_2)^2 + (1 - \beta_2)^2\beta_2\right]$

c $\quad -M_{Osy}(\tfrac{1}{2} + rA) - M_{Osz}\frac{ir^2}{2} + Ra\left(\frac{1}{3} + \frac{ir^3}{3} + rA\right)$

$$= q\,b^2 i r^2\left[\frac{1}{8} - \frac{1}{3}(1 - \beta_2) + \frac{1}{4}(1 - \beta_2)^2 - \frac{1}{24}(1 - \beta_2)^4\right]$$

Eq. 11—Uniform Load p over Distance a_2. Length a_2 Measured from Point O

a $\quad M_{Osy}(1 + rA) - Ra(\tfrac{1}{2} + rA) = -pa^2\left[\frac{1}{6}\alpha_2^3 - \frac{\alpha_2^2}{2} + rA\left(\alpha_2 - \frac{\alpha_2^2}{2}\right) + \frac{\alpha_2}{2}\right]$

b $\quad M_{Osz}(r + B) - Ra\frac{r^2}{2} = -pa^2\frac{r^2\alpha_2}{2}$

c $\quad -M_{Osy}(\tfrac{1}{2} + rA) - M_{Osz}\frac{ir^2}{2} + Ra\left(\frac{1}{3} + \frac{ir^3}{3} + rA\right)$

$$= pa^2\left\{\frac{\alpha_2^4}{8} + \alpha_2\left[\frac{(1 - \alpha_2^2)}{3} - \frac{\alpha_2(1 - \alpha_2^2)}{4} + \frac{(2 - \alpha_2)\,rA}{2} + \frac{r^3 i}{3}\right]\right\}$$

Eq. 12—Forces and Moments May Be Determined When Support O Settles or Rotates

a $\quad M_{Osy}(1 + rA) - Ra(\tfrac{1}{2} + rA) = \Theta_{sy}EI_a/a$

b $\quad M_{Osz}(r + B) - Ra\frac{r^2}{2} = \Theta_{sz}EI_b/a$

c $\quad -M_{Osy}(\tfrac{1}{2} + rA) - M_{Osz}\frac{ir^2}{2} + Ra\left(\frac{1}{3} + \frac{ir^3}{3} + rA\right) = \Delta Z\,EI_a/a^2$

Eq. 13—Uniform Load p over Spans a and b Taking Shear Distortion into Consideration

a $\quad M_{Osy}(1 + rA) - Ra(\tfrac{1}{2} + rA) = -pa^2\left(\frac{1}{6} + \frac{rA}{2}\right)$

b $\quad M_{Osz}(r + B) - Ra\frac{r^2}{2} = -pa^2\left(\frac{r^2}{2} + \frac{r^3}{6}\right)$

c $\quad -M_{Osy}(\tfrac{1}{2} + rA) - M_{Osz}\frac{ir^2}{2} + Ra\left[\frac{1}{3} + \frac{ir^3}{3} + rA + \underline{\frac{EI_a}{a^2GS_a}\left(1 + r\frac{S_a}{S_b}\right)}\right]$

$$= pa^2\left[\frac{1}{8} + \frac{ir^3}{3} + \frac{1}{8}ir^4 + \frac{rA}{2} + \underline{\frac{EI_a}{a^2GS_a}\left(\frac{1}{2} + r\frac{S_a}{S_b}\right) + \frac{r^2}{2}\frac{S_a}{S_b}}\right]$$

TABLE 1.—(*Continued*)

Eq. 14—Load P at Distance a from Point O Taking Shear Distortions into Consideration

$$a \quad M_{Osy}(1 + r\,A) - R\,a\left(\tfrac{1}{2} + r\,A\right) = 0$$

$$b \quad M_{Osz}(r + B) - R\,a\frac{r^2}{2} = -P\,a\frac{r^2}{2}$$

$$c \quad -M_{Osy}\left(\tfrac{1}{2} + r\,A\right) - M_{Osz}\frac{i\,r^2}{2} + R\,a\left[\frac{1}{3} + \frac{i\,r^3}{3} + r\,A + \underline{\frac{E\,I_a}{G\,S_a\,a^2}\left(1 + r\frac{S_a}{S_b}\right)}\right] = P\,a\left(\frac{i\,r^3}{3} + r\,\underline{\frac{E\,I_a}{a^2\,G\,S_b}}\right)$$

Eq. 15—Uniform Load p on Spans a and b for Any Variable Angle θ Between Cantilevers

$$a \quad M_{Osy}(1 + i\,r\cos^2\theta + r\,A\sin^2\theta) + M_{Osz}\left(\frac{i\,r\sin 2\theta}{2} - \frac{r\,A\sin 2\theta}{2}\right) + R\,a\left(\frac{i\,r^2\cos\theta}{2} - i\,r\cos^2\theta - \frac{1}{2} - r\,A\sin^2\theta\right) = -p\,a^2\left(\frac{1}{6} - \frac{i\,r^2\cos\theta}{2} + \frac{i\,r\cos^2\theta}{2} - \frac{i\,r^3\cos\theta}{6} + \frac{r\,A\sin^2\theta}{2}\right)$$

$$b \quad M_{Osy}\left(\tfrac{1}{2}r\,i\sin 2\theta - \tfrac{1}{2}r\,A\sin 2\theta\right) + M_{Osz}(C + r\,i\sin^2\theta + r\,A\cos^2\theta) + R\,a\left(\tfrac{1}{2}r^2\,i\sin\theta - \tfrac{1}{2}r\,i\sin 2\theta + \tfrac{1}{2}r\,A\sin 2\theta\right) = p\,a^2\left(\frac{1}{2}r^2\,i\sin\theta - \frac{1}{4}r\,i\sin 2\theta + \frac{r^3\,i\sin\theta}{6} + \frac{1}{4}r\,A\sin 2\theta\right)$$

$$c \quad -M_{Osy}\left(\tfrac{1}{2} + r\,i\cos^2\theta - \tfrac{1}{2}r^2\,i\cos\theta + r\,A\sin^2\theta\right) + M_{Osz}\left(\frac{r^2\,i\sin\theta}{2} - \frac{1}{2}r\,i\sin 2\theta + \frac{1}{2}r\,A\sin 2\theta\right) + R\,a\left(\frac{1}{3} + \frac{i\,r^3}{3} - r^2\,i\cos\theta + r\,i\cos^2\theta + r\,A\sin^2\theta\right) = p\,a^2\left(\frac{1}{8} + \frac{1}{3}i\,r^3 - \frac{1}{2}r^2\,i\cos\theta - \frac{r^2\,i\cos\theta}{4} + \frac{r\,i\cos^2\theta}{2} + \frac{r^4\,i}{8} - \frac{r^3\,i\cos\theta}{6} + \frac{r\,A\sin^2\theta}{2}\right)$$

Eq. 16—Concentrated Load P at Distance a from Point O for Any Variable Angle θ Between Cantilevers

$$a \quad M_{Osy}(1 + i\,r\cos^2\theta + r\,A\sin^2\theta) + M_{Osz}\left(\frac{i\,r\sin 2\theta}{2} - \frac{r\,A\sin 2\theta}{2}\right) + R\,a\left(\frac{i\,r^2\cos\theta}{2} - i\,r\cos^2\theta - \frac{1}{2} - r\,A\sin^2\theta\right) = \tfrac{1}{2}P\,a\,i\,r^2\cos\theta$$

$$b \quad M_{Osy}\left(\tfrac{1}{2}r\,i\sin 2\theta - \tfrac{1}{2}r\,A\sin 2\theta\right) + M_{Osz}(C + r\,i\sin^2\theta + r\,A\cos^2\theta) + R\,a\left(\tfrac{1}{2}r^2\,i\sin\theta - \tfrac{1}{2}r\,i\sin 2\theta + \tfrac{1}{2}r\,A\sin 2\theta\right) = \tfrac{1}{2}P\,a\,i\,r^2\sin\theta$$

$$c \quad -M_{Osy}\left(\tfrac{1}{2} + r\,i\cos^2\theta - \tfrac{1}{2}r^2\,i\cos\theta + r\,A\sin^2\theta\right) + M_{Osz}\left(\frac{r^2\,i\sin\theta}{2} - \frac{1}{2}r\,i\sin 2\theta + \frac{1}{2}r\,A\sin 2\theta\right) + R\,a\left(\frac{1}{3} + \frac{i\,r^3}{3} - r^2\,i\cos\theta + r\,i\cos^2\theta + r\,A\sin^2\theta\right) = P\,a\left(\frac{i\,r^3}{3} - \frac{r^2}{2}i\cos\theta\right)$$

Eq. 17—Torsional Moment M_T Acting at Distance c from Point O on Span a for Any Variable Angle θ Between Cantilevers

$$a \quad M_{Osy}(1 + i\,r\cos^2\theta + r\,A\sin^2\theta) + M_{Osz}\left(\frac{i\,r\sin 2\theta}{2} - \frac{r\,A\sin 2\theta}{2}\right) + R\,a\left(\frac{i\,r^2\cos\theta}{2} - i\,r\cos^2\theta - \frac{1}{2} - r\,A\sin^2\theta\right) = M_T\left(\tfrac{1}{2}i\,r\sin 2\theta - \tfrac{1}{2}r\,A\sin 2\theta\right)$$

$$b \quad M_{Osy}\left(\tfrac{1}{2}r\,i\sin 2\theta - \tfrac{1}{2}r\,A\sin 2\theta\right) + M_{Osz}(C + r\,i\sin^2\theta + r\,A\cos^2\theta) + R\,a\left(\tfrac{1}{2}r^2\,i\sin\theta - \tfrac{1}{2}r\,i\sin 2\theta + \tfrac{1}{2}r\,A\sin 2\theta\right) = M_T(C - \gamma C + i\,r\sin^2\theta + r\,A\cos^2\theta)$$

$$c \quad -M_{Osy}\left(\tfrac{1}{2} + r\,i\cos^2\theta - \tfrac{1}{2}r^2\,i\cos\theta + r\,A\sin^2\theta\right) + M_{Osz}\left(\frac{r^2\,i\sin\theta}{2} - \frac{1}{2}r\,i\sin 2\theta + \frac{1}{2}r\,A\sin 2\theta\right) + R\,a\left(\frac{1}{3} + \frac{i\,r^3}{3} - r^2\,i\cos\theta + r\,i\cos^2\theta + r\,A\sin^2\theta\right) = M_T\left(\tfrac{1}{2}i\,r^2\sin\theta - \tfrac{1}{2}i\,r\sin 2\theta + \tfrac{1}{2}r\,A\sin 2\theta\right)$$

General Case for a Variable Angle

Two cases will be evaluated for this condition, one for a uniform load on both spans, the other for a torque M_T acting at a distance of c from point O.

With restraining forces at point O, the cantilever of length b at an angle θ will be acted upon by components of bending and torsional moments, to be combined vectorially. These are shown in Fig. 3.

In the vectorial system, sense and direction of moments can be determined readily by visualizing vectors as arrows. If one were to grasp the arrow with the right hand (the thumb pointing toward the head of the arrow), the direction in which the fingers wrap themselves around the shaft will indicate the direction in which the moments rotate. The right-hand system of rotations is used throughout. General equations for moments are not stated in this paper because of their length. The pattern in general is the same as for Eq. 1. Partial differentials are similar to Eqs. 2. Angle θ is constant. Final solutions are shown in Table 1.

When angle θ is 0°, cantilevers a and b are parallel to each other. When θ is 90°, the conditions are identical for the right-hand cantilever. At angle θ equals 180°, the double cantilever becomes a beam with fixed ends, assuming that restraining moments would be acting. When these moments are zero, a simple beam will result.

A word of caution is necessary. These equations were developed in terms of distance a. Thus, when the angle is 180°, M_{O_y} is expressed as $\frac{p\,a^2}{3}$ when both cantilevers of the same length carry uniformly distributed load. The conventional manner of indicating this moment is in terms of the entire length. Hence, if $L = 2\,a$, the bending moment M_{O_y} will be equal to $\frac{p\,L^2}{12}$.

Effect of Shear

It is generally assumed by structural engineers that shear distortions produce minor additive forces to reactions, and a slight reduction to bending moments in conventional indeterminate structures, when the ratio of length to depth of beam is greater than four. Consequently, the shear effect is ignored, as a differential of a higher order. In order to investigate shear effects on a 90° double cantilever, two cases were studied, and equations for both are shown in Table 1.

The first case considered is one in which both cantilevers were loaded with uniformly distributed load p, the second, with a concentrated load P, at point O.

The general equation of work considering shear is

$$W = \int \frac{M^2\,ds}{2\,E\,I} + \int \frac{M^2\,ds}{2\,G\,J} + \int \frac{V^2\,ds}{2\,G\,A} \qquad (18)$$

The first two parts of Eq. 18 have been solved for a number of loading conditions. The third is a corrective factor due to shear, and is additive to Eqs. c, Table 1. These corrective factors have been underscored in respective equations where they appear.

Settlements of Supports and Rotations of End Tangents

It may be necessary to determine the effects of settlement of end supports and rotations of end tangents. The three equations expressing vertical displacements and end rotations at point O, for a right-angle cantilever, are listed in Table 1. Their application is simple. The only precaution necessary is to determine consistent signs for displacements and angular rotations.

Practical Considerations

To simplify calculations, equations have been reduced into a series of dimensionless quantities. Terms on the left of the equality sign contain functions of elastic properties of the double cantilever and are invariants. On the right of the equality sign, the functions depend on the applied loads, and on the elastic and torsional properties of sections.

It has been found from actual calculations that these equations do not lend themselves readily to slide-rule calculations. In many instances, slide-rule calculations differed as much as from 100% to 200% from true values. The reasons for these discrepancies are the small differences of large quantities, which cannot be estimated closely on a 10-in. slide rule. In order to determine satisfactory values, calculations should be carried to three or four significant figures.

Variations in Moments and Shears

To show the effects of torsional stiffness on moments and shears, Table 2 has been prepared for a uniformly distributed load over both lengths of the right-angle cantilever, and also for a concentrated load P acting at point C. Both cantilevers have the same physical dimensions—that is, $A = B$, and variations are assumed from one to fifty.

TABLE 2.—Effects of Torsional Stiffness on Moments and Shears

$A\ (= B)$	(a) Concentrated Load, P ($c = a = b$ and $R = P/2$)		(b) Uniform Load, p ($a_2 = a = b = b_2$ and $R = p\,a$)	
	M_{Oxy}	M_{Oxz}	M_{Oxy}	M_{Oxz}
1	$3\,P\,a/8$	$-P\,a/8$	$5\,p\,a^2/12$	$-p\,a^2/12$
5	$11\,P\,a/24$	$-P\,a/24$	$17\,p\,a^2/36$	$-p\,a^2/36$
10	$21\,P\,a/44$	$-P\,a/44$	$32\,p\,a^2/66$	$-p\,a^2/66$
50	$101\,P\,a/204$	$-P\,a/204$	$152\,p\,a^2/306$	$-p\,a^2/306$

Applications to Continuous Structures

An isolated double cantilever is rarely encountered in practice. It is generally a segment of a continuous structure extending beyond points O and B. When ratios of A and B are reasonably large, it is convenient to treat resulting moments as moments due to cantilevers, and then distribute the resulting moments to the contiguous parts of the structure according to conventional methods of analysis. This procedure is not quite correct, but it should give workable results. Special situations may arise in the more im-

portant structures where beams at the ends of the cantilevers must be included in resisting both torsion and flexure. Formal methods of attack, using the theory of least work, would be quite involved, but not too difficult to solve. Because of the considerable length of time necessary to determine correct values, such procedures would be viewed unfavorably in most engineering offices.

Conclusions

It is unfortunate that the equations in this paper cannot be plotted to cover practical ranges met in daily practice. Some plots were attempted, but since they covered a very narrow range, they were omitted. It is important to observe that, when ratios of A, B, and C are small, torsional moments begin to have considerable importance in these structures, and should be taken into consideration. When the values of A, B, and C are large, torsional moments are of secondary importance as compared with bending moments.

Acknowledgment

Suggestions for this study were made by J. R. Arena, M. ASCE, who has reviewed this paper, checked the equations, prepared the necessary table, and made valuable suggestions which were incorporated in the preparation of this paper. Source material used as reference was taken from the published works of C. M. Spofford,[2,3] M. ASCE, and J. B. Wilbur, M. ASCE, and W. M. Fife,[4] A.M. ASCE.

[2] "Theory of Structures," by C. M. Spofford, McGraw-Hill Book Co., Inc., New York, N. Y., 1928.

[3] "Theory of Continuous Structures and Arches," by C. M. Spofford, McGraw-Hill Book Co., Inc., New York, N. Y., 1937.

[4] "Theory of Statically Indeterminate Structures," by J. B. Wilbur and W. M. Fife, McGraw-Hill Book Co., Inc., New York, N. Y., 1937.

DISCUSSION

LU-SHIEN HU,[5] J.M. ASCE.—In the analysis of double cantilever beams, the method of moment distribution can readily be applied. The final end moments, both bending and torsional, can be obtained in two steps. The first step is to supply a temporary support to point C, the intersection point of the two cantilevers (Fig. 1). The reaction at C is then computed from the end moments obtained by the application of the method of moment distribution. Secondly, the reaction at C is removed and a specific displacement is introduced. The difference between the application of the method of moment distribution to this particular spatial frame from that of its application to ordinary plane frames is the separate recording of both bending and torsional moments at the ends of each member.

To apply the method of moment distribution the following must be known—fixed-end moments, distribution factors, and carry-over factors. In double cantilever beams, the fixed-end moments and the carry-over factors for bending are the same as for a straight beam. The carry-over factors for torsion are unity. The distribution factors for perpendicular double cantilever beams have been used in various problems.[6,7]

The distribution factors for double cantilever beams intersecting at an angle θ can be derived by considering continuity and equilibrium at point C. The result is as follows:

$$M_{CA} = \frac{1}{D} \quad K_{CA} \left(K'_{CA} + K_{CB} \sin^2\theta + K'_{CB} \cos^2\theta\right) \times M_1 - \frac{1}{D} K_{CA} \left(K_{CB} - K'_{CB}\right) \sin\theta \cos\theta\, M_2 \quad (19a)$$

$$M'_{CA} = \frac{1}{D} K'_{CA} \left(K_{CB} - K'_{CB}\right) \sin\theta \cos\theta\, M_1 + \frac{1}{D} K'_{CA} \times \left(K_{CA} + K_{CB} \cos^2\theta + K'_{CB} \sin^2\theta\right) M_2 \quad (19b)$$

$$M_{CB} = -\frac{1}{D} K_{CB} \left(K'_{CA} + K'_{CB}\right) \cos\theta\, M_1 - \frac{1}{D} K_{CB} \times \left(K_{CA} + K'_{CB}\right) \sin\theta\, M_2 \quad (20a)$$

$$M'_{CB} = \frac{1}{D} K'_{CB} \left(K_{CB} + K'_{CA}\right) \sin\theta\, M_1 - \frac{1}{D} K'_{CB} \times \left(K_{CA} + K_{CB}\right) \cos\theta\, M_2 \quad (20b)$$

in which

$$D = K_{CA} K'_{CA} + K_{CB} K'_{CB} + \left(K_{CA} K_{CB} + K'_{CA} K'_{CB}\right) \times \sin^2\theta + \left(K_{CA} K'_{CB} + K_{CB} K'_{CA}\right) \cos^2\theta \quad (21)$$

in which M represents the bending end moment, and M' represents the torsional end moment. These moments are positive if acting as shown in Fig. 4, in

[5] Designer, Howard, Needles, Tammen & Bergendoff, New York, N. Y.

[6] "Reinforced Concrete Structures," by Dean Peabody, John Wiley & Sons, Inc., New York, N. Y., 1946.

[7] "Deflections in Gridworks and Slabs," by Walter W. Ewell, Shigeo Okubo, and Joel I. Abrams, *Transactions*, ASCE, Vol. 117, 1952, p. 869.

which they are represented by vectors of right-hand rule. In Eqs. 19, 20, and 21 flexural rigidity is represented by K, and K' denotes torsional rigidity—that is, the moment required to produce a unit rotation. For prismatic straight members with the far end fixed, $K = \frac{4\,E\,I}{L}$ and $K' = \frac{G\,J}{L}$. The expressions for J of various sections can be found elsewhere.[6,8,9,10]

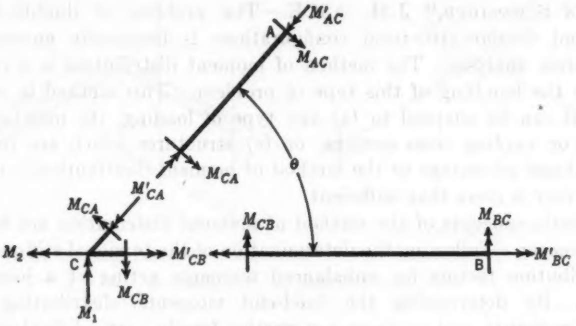

FIG. 4

Special cases can be derived from Eqs. 19, 20, and 21. When $\theta = 180°$, $\sin\theta = 0$, and $\cos\theta = 1$, the distribution factors for continuous beams are

$$M_{CA} = \frac{K_{CA}}{K_{CA} + K_{CB}} M_1 \qquad (22a)$$

$$M'_{CA} = \frac{K'_{CA}}{K'_{CA} + K'_{CB}} M_2 \qquad (22b)$$

$$M_{CB} = \frac{K_{CB}}{K_{CA} + K_{CB}} M_1 \qquad (23a)$$

$$M'_{CB} = \frac{K'_{CB}}{K'_{CA} + K'_{CB}} M_2 \qquad (23b)$$

When $\theta = 90°$, $\sin\theta = 1$, and $\cos\theta = 0$, the distribution factors for perpendicular double cantilever beams are

$$M_{CA} = \frac{K_{CA}}{K_{CA} + K'_{CB}} M_1 \qquad (24a)$$

$$M'_{CA} = \frac{K'_{CA}}{K_{CB} + K'_{CA}} M_2 \qquad (24b)$$

$$M_{CB} = -\frac{K_{CB}}{K_{CB} + K'_{CA}} M_2 \qquad (25a)$$

$$M'_{CB} = \frac{K'_{CB}}{K_{CA} + K'_{CB}} M_1 \qquad (25b)$$

---

[8] "Strength of Materials," by S. Timoshenko, D. Van Nostrand Co., New York, N. Y., 1947.

[9] "Structural Beams in Torsion," by Inge Lyse and Bruce G. Johnston, *Transactions*, ASCE, Vol. 101, 1936, p. 857.

[10] "Torsion of Plate Girders," by F. K. Chang and Bruce G. Johnston, *ibid.*, Vol. 118, 1953, p. 337.

The method of moment distribution can be applied to double cantilever beams with end conditions other than fixed, provided that the flexural rigidity K is derived for the actual end conditions.

In the paper the sign of the term M_{Ozx} in all formulas in Table 1 seems inconsistent with the sign conventions adopted by the author.

LEWIS SCHNEIDER,[11] J.M. ASCE.—The problem of double cantilever beams and similar structural configurations is frequently encountered in piping stress analysis. The method of moment distribution is a convenient device in the handling of this type of problem. This method is convenient because it can be adapted to (a) any type of loading, (b) members having different or varying cross sections, or (c) structures which are continuous. An additional advantage to the method of moment distribution is that slide-rule accuracy is more than sufficient.

The basic concepts of the method of moment distribution are familiar to most engineers. Following the determination of the torsional stiffness factors, the distribution factors for unbalanced moments acting at a joint can be obtained. By determining the fixed-end moments, distributing the unbalanced moments, and applying a correction for the vertical displacements of unsupported joints (analogous to the sidesway correction for bents), it is possible to obtain the end reactions for a structure having any degree of indeterminacy.

By applying arbitrary couples at the points of support and determining the resulting angular deflection at the joint under consideration (by the application of the slope-deflection equations), it is possible to determine both the stiffness and carry-over moments for the complete structure. For example, if in the system OCB (Fig. 1(*a*)), an arbitrary moment M_{Ozy} is applied at O and moment distribution is performed, the resulting moments M_{Ozx}, M_{Bzy}, and M_{Bzx}, can be determined. This establishes a relationship that shows what magnitude of moments are produced at O and B by the application of a unit moment at O in the *yz*-plane. By writing the slope-deflection equation for the member OC, a solution for the rotation of O, caused by the application of the unit moment, is obtained. By direct proportion, the moment corresponding to a rotation of one radian can be obtained and this moment is, by definition, the stiffness factor S_{OB}. Similarly, the torsional stiffness and carry-over moments for a twisting moment at O are established. These factors can be used to acquire a solution when full fixity is not obtainable at the points of support. An illustrative problem is shown in Figs. 5 and 6, which show the sequence of operations.

In the second term of the right-hand side of Eq. 1, the term J, generally used to represent the polar moment of inertia of a section, is used to define the ratio of proportionality between the torsional moment and the angular deflection of a member. This definition is correct for circular shafts only. Another symbol would have been a more proper choice. If this symbol were T,

[11] Design Engr., Arthur G. McKee, Co., Union, N. J.

for a rectangular member, then

$$T = \frac{b^3 d^3}{3.58 (b^2 + d^2)} \quad \text{(26)}$$

in which d would represent the greatest dimension of the rectangle.[12] For rolled steel sections, values of T have been tabulated as "K-values."[13]

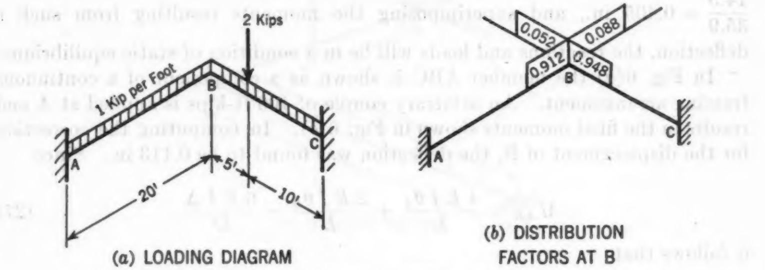

FIG. 5.—DOUBLE CANTILEVER CONCRETE BEAM

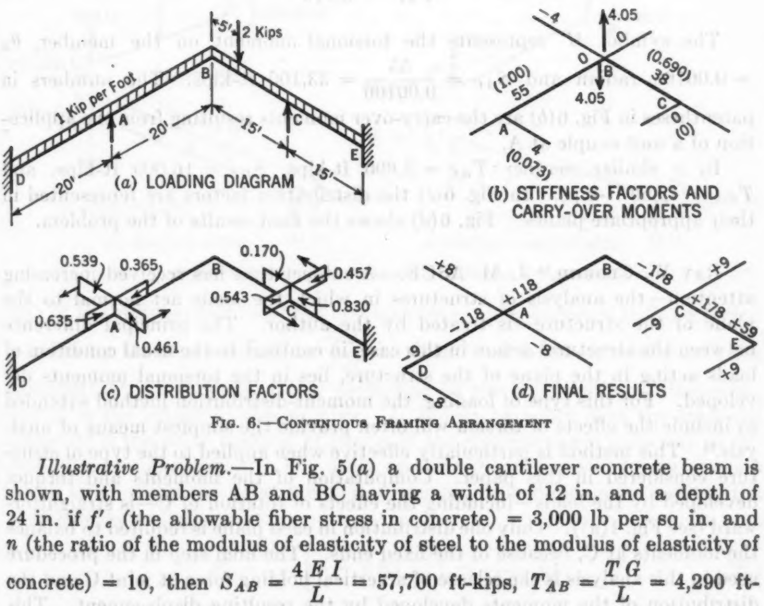

FIG. 6.—CONTINUOUS FRAMING ARRANGEMENT

Illustrative Problem.—In Fig. 5(a) a double cantilever concrete beam is shown, with members AB and BC having a width of 12 in. and a depth of 24 in. if f'_c (the allowable fiber stress in concrete) = 3,000 lb per sq in. and n (the ratio of the modulus of elasticity of steel to the modulus of elasticity of concrete) = 10, then $S_{AB} = \frac{4\,E\,I}{L} = 57{,}700$ ft-kips, $T_{AB} = \frac{T\,G}{L} = 4{,}290$ ft-kips, $S_{BC} = 76{,}800$ ft-kips, and $T_{BC} = 5{,}710$ ft-kips. In Fig. 5(b) the distribution factors at B are represented in their appropriate planes.

[12] "Design of Reinforced Concrete in Torsion" by Paul Andersen, *Transactions*, ASCE, Vol. 103, 1938, p. 1503.

[13] "Torsional Stresses in Structural Beams," Bethlehem Steel Co., Bethlehem, Pa., 1950, pp. 5–8.

To determine the vertical deflection correction, point B is deflected 1 in. and the unbalanced fixed-end moments are distributed. By the use of statics it is found that a force of 35.9 kips will produce this 1-in. deflection. The fixed-end moments resulting from the applied loads are then distributed. It is found, by the use of the principles of statics, that a force of 14.5 kips is required at B to prevent that joint from deflecting downward. By allowing a deflection $\frac{14.5}{35.9} = 0.405$ in., and superimposing the moments resulting from such a deflection, the reactions and loads will be in a condition of static equilibrium.

In Fig. 6(*a*) the member ABC is shown as a component of a continuous framing arrangement. An arbitrary couple of 100 ft-kips is applied at A and results in the final moments shown in Fig. 6(*b*). In computing the correction for the displacement of B, the deflection was found to be 0.113 in. Since

$$M_{AB} = \frac{4\,E\,I\,\theta_A}{L} + \frac{2\,E\,I\,\theta_B}{L} - \frac{6\,E\,I\,\Delta}{L^2} \quad \text{(27)}$$

it follows that

$$\theta_B = \frac{M'_{CB}}{T_{BC}} = \frac{0}{5{,}710} = 0 \quad \text{(28)}$$

The symbol M' represents the torsional moment on the member, $\theta_A = 0.00166$ radian and $S_{AC} = \frac{55}{0.00166} = 33{,}100$ ft-kips. The numbers in parentheses in Fig. 6(*b*) are the carry-over moments resulting from the application of a unit couple at A.

In a similar manner $T_{AC} = 3{,}690$ ft-kips, $S_{CA} = 16{,}000$ ft-kips, and $T_{CA} = 4{,}850$ ft-kips. In Fig. 6(*c*) the distribution factors are represented in their appropriate planes. Fig. 6(*d*) shows the final results of the problem.

RAY W. CLOUGH,[14] J. M. ASCE.—A subject that has received increasing attention—the analysis of structures in which the loads act normal to the plane of the structure—is treated by the author. The principal difference between the structural action in this case, in contrast to the usual condition of loads acting in the plane of the structure, lies in the torsional moments developed. For this type of loading, the moment-distribution method extended to include the effects of torsion will often provide the simplest means of analysis.[15] This method is particularly effective when applied to the type of structure considered in this paper. Computation of the moments and torques developed by the loads—including the effects of rotation of C—is straightforward (see Fig. 1(a)). Only one distribution in each plane is required to balance the moments at C, because of the fixed ends. The final step in the procedure used in this analysis is the release of a vertical holding force at joint C and the distribution of the moments developed by the resulting displacement. This computation is most readily made by computing the moments associated with

[14] Asst. Prof. of Civ. Eng., Univ. of California, Berkeley, Calif.

[15] "The Design of Reinforced Concrete Structure," by Dean Peabody, John Wiley & Sons, Inc., New York, N. Y.; 1946, p. 419.

an arbitrary magnitude of the holding force. The moments that would be developed by releasing the actual holding force are determined by proportion.

As an example of the procedure, the double cantilever structure shown in Fig. 7 (*a*) is analyzed in Table 3. The first step in the analysis is the determina-

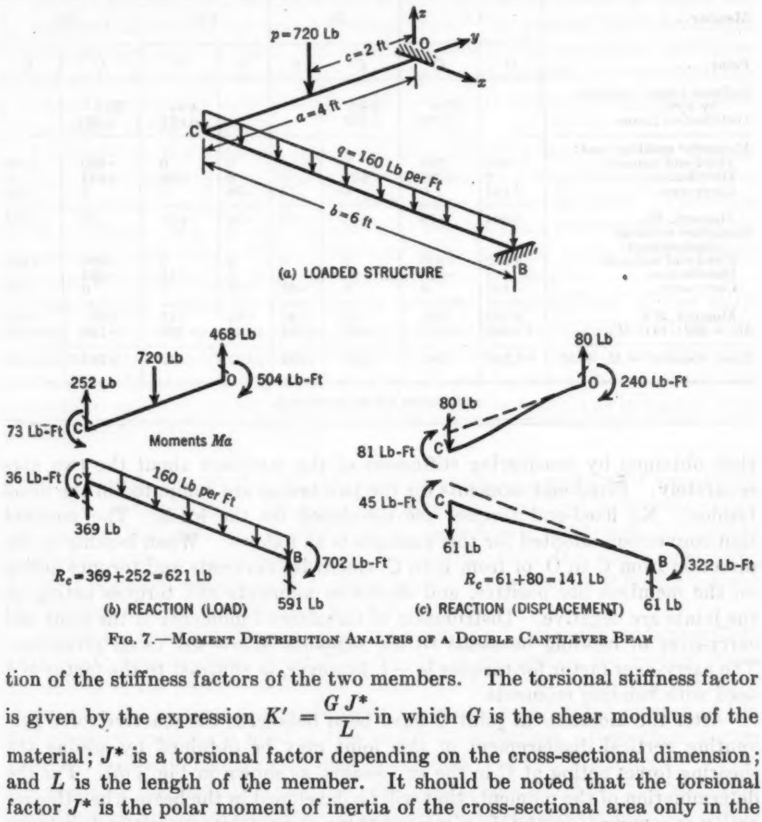

FIG. 7.—MOMENT DISTRIBUTION ANALYSIS OF A DOUBLE CANTILEVER BEAM

tion of the stiffness factors of the two members. The torsional stiffness factor is given by the expression $K' = \frac{G\,J^*}{L}$ in which G is the shear modulus of the material; J^* is a torsional factor depending on the cross-sectional dimension; and L is the length of the member. It should be noted that the torsional factor J^* is the polar moment of inertia of the cross-sectional area only in the case of a circular section. For other sections it is less—and in many cases much less[16]—than the polar moment of inertia. For rectangular sections the torsional factor is given by

$$J^* = \frac{d\,b^3}{3}\left[1 - 0.63\,\frac{b}{d}\left(1 - \frac{b^4}{12\,d^4}\right)\right] \qquad (29)$$

in which b is the width of the section, and d the depth.

In the moment-distribution solution, moments in the zx-plane and the zy-plane are considered separately. The distribution factors at joint C are

[16] "Formulas for Stress and Strain," by R. J. Roark, McGraw-Hill Book Co., Inc., New York, N. Y., 1943, p. 169.

TABLE 3.—MOMENT DISTRIBUTION FOR THE LOADED STRUCTURE OF FIG. 7

PROCEDURE	MOMENTS IN THE *xy*-PLANE[a]				MOMENTS IN THE *xz*-PLANE[a]			
Member	CO		BC		CO		BC	
Point	O	C	C	B	O	C	C	B
Stiffness factor (multiply by 10^6)		27.0	6.86			4.94	60.7	
Distribution factor		0.797	0.203			0.075	0.925	
Moments[a] resisting load:								
Fixed-end moment	+360	−360	0	0	0	0	−480	+480
Distribution	0	+287	+73	0	0	+36	+444	0
Carry-over	+144	0	0	−73	−36	0	0	+222
Moment, M_a	+504	−73	+73	−73	−36	+36	−36	+702
Moments[a] resisting displacement:								
Fixed-end moment	+400	+400	0	0	0	0	+600	+600
Distribution	0	−319	−81	0	0	−45	−555	0
Carry-over	−160	0	0	+81	+45	0	0	−278
Moment, M'_b	+240	+81	−81	+81	+45	−45	+45	+322
$M_b = (621/141)\, M'_b$	+1,059	+357	−357	+357	+198	−198	+198	+1,420
Total Moment $= M_a + M_b$	+1,563	+284	−284	+284	+162	−162	+162	+2,122

[a] All values are in pound-feet.

thus obtained by considering stiffnesses of the members about the two axes separately. Fixed-end moments for the two beams are computed in the usual fashion. No fixed-end torques are developed by the loads. The moment sign convention adopted for this example is as follows: When looking in the direction from C to O, or from B to C, clockwise moments and torques acting on the members are positive, and clockwise moments and torques acting on the joints are negative. Distribution of unbalanced moments at the joint and carry-over of bending moments to the supports follow the usual procedure. The carry-over factor for torques is −1, however, in contrast to the factor of ½ used with bending moments.

After the moments at joint C have been balanced, the reactive force preventing vertical displacement of this joint may be obtained by adding the shearing forces acting at C in the two beams, as shown in Fig. 7(*b*). For the determination of the moments that will be developed in the beam when this reaction is removed, joint C is displaced through an arbitrary vertical distance Δ_c without rotation. Because of this displacement, fixed-end moments will be developed in the beams, equal to $\frac{6\,E\,I}{L^2}\,\Delta_c$. In this example, the deflection Δ_c was chosen to develop moments in member CO of 400 lb-ft. The corresponding moments in member BC are given by the relationship $\frac{M_{C\,B}}{M_{C\,O}} = \frac{(I/L^2)_{C\,B}}{(I/L^2)_{C\,O}}$ because the same deflection applies to each beam.

The reactive force at C associated with the resulting end moments (M'_b) is determined by summing shears in the beams at joint C as shown in Fig. 7(*c*). The moments and torques (M_b) that would be developed in the beams by re-

moving the actual holding force may then be computed by proportion (Table 3). The final values of end moments and torques in the beams are obtained by adding the moments produced by the loads (M_a) to the moments resulting from the displacements (M_b).

As this example demonstrates, the stresses in double cantilever beams can be determined quickly by moment distribution. In general, the advantages making the method of moment distribution popular for the analysis of structures loaded in their own planes (principally avoiding the solution of simultaneous equations) are equally beneficial for cases in which the loads are applied normal to the plane of the structure.

Contrary to the author's statement, the structure shown in Fig. 2(*g*) is stable. The reactions R and R_B are equivalent to a vertical force and a couple. This couple has components in both the *zx*-plane and the *zy*-plane. The three given reactions—M_{By}, R, and R_B can thus provide three independent reaction components (moments in the *zx*-plane and in the *zy*-plane, and a vertical force) sufficient for equilibrium in the given condition of loading.

The double cantilever structure is actually indeterminate to the sixth degree, but for the special type of structure (composed of members of which a principal axis lies in the plane of the structure) and the special case of loading (normal to the plane of the structure) considered by the author, three of the redundant reactions vanish, and the structure may be treated as though it were indeterminate to the third degree.

William A. Conwell,[17] M. ASCE.—An intriguing problem is treated by the author in this paper. The type of construction described is becoming more prevalent (1953) and has a wide field of application. Although the double cantilever beam is more complicated to analyze than the single cantilever beam, it is simple enough to be a valuable step in engineering thinking toward the solution of more complicated space structures.

Under the heading, "General Case of Continuity," the author indicates that, in general, three reactions occur at each point of support for the vertical loads considered in the paper. A further observation might be made that, for loads inclined to the vertical, three additional reactions would occur at each of the two supports, making a total of twelve for the structure. Inspection shows, however, that any inclined load may be resolved into two components—one in the plane of the structure and the other perpendicular to it. The structure may then be analyzed separately for each of the components and the results superimposed for the final solution of the problem.

The writer prefers to think of moments acting in a plane, about or along an axis rather than "rotating," as in the author's terminology.

In preliminary preparation of this discussion the writer independently checked the values given in Table 2 for $A = 1$ and $A = 10$. Although the writer's results agreed in magnitude with the moments shown, the conclusion was reached that all signs for M_{Osz} should be plus instead of minus. It is believed that one can arrive at the proper direction of the moments from several independent considerations of the structural action involved. There should

[17] Gen. Engr., Structural Eng. and Design Dept., Duquesne Light Co., Pittsburgh, Pa.

be, however, no more convincing proof than the laws of statics. Referring to Fig. 1, if one considers the case of the load P at point C of a structure for which $A = 1$ and assumes the author's value of $M_{Ozy} = 3\ P\ a/8$ to be correct, application of symmetry and summation of moments about the axis of member OC yields a clockwise direction, and hence, a positive sign, for M_{Ozz} (see Fig. 8(*a*)). A similar observation for the uniform load p requires that the signs for M_{Ozz} be positive.

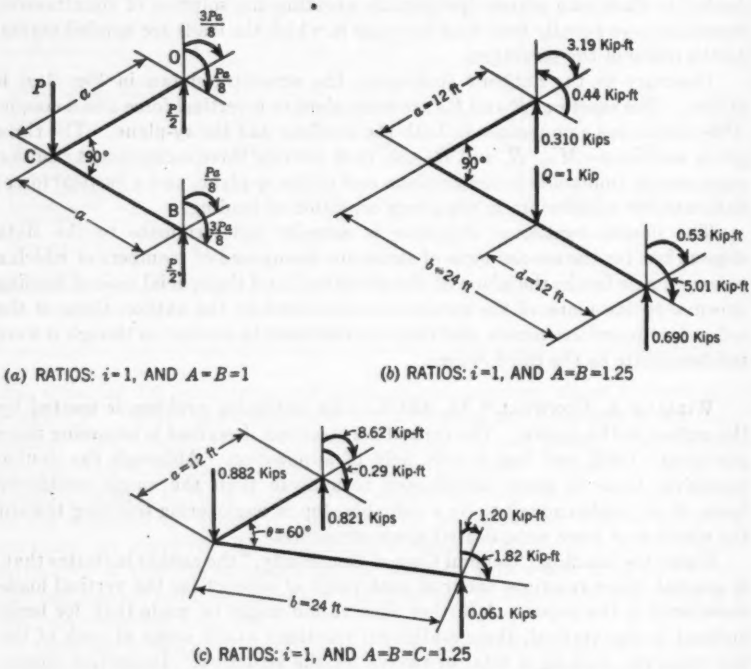

FIG. 8.—REACTIONS, CONCENTRATED LOAD

The writer did not attempt to check the derivation of the author's equations, but instead applied certain equations to specific cases for which solutions could be obtained by an independent method. Applications of Eqs. 3 and 4 yielded correct values for the reactions at O, but not the correct sign for M_{Ozz}. Fig. 8(*b*) shows what the writer believes to be the correct solution to a particular problem. Eqs. 4, applied to this problem, yield the value $M_{Ozz} = +0.44$ kip-ft, a direction opposite to that shown in Fig. 8(*b*). It is evident that this reversed value of M_{Ozz} would affect the value of M_{Bzz}—making it 4.13 kip-ft instead of 5.01 kip-ft—revealing a considerable error in a major moment. The writer has reluctantly reached the conclusion that, if the definition of positive moment, as illustrated in Fig. 1(*a*), is to be retained, the signs of the terms containing M_{Ozz} in Eqs. 3 and 4 should be reversed. Because the left-

hand terms of Eqs. 3 to 12, inclusive, are identical (Eq. 9c, which has a different sign for the M_{Ozy}-term, is probably in error), it is believed that this conclusion applies to all the aforementioned equations and should be extended to Eqs. 13 and 14, whose terms are somewhat different.

With the thought of confirming Eqs. 16, an independent analysis was made of a problem to which they would apply. The result of the analysis is shown in Fig. 8(*c*). Before making the substitutions in Eqs. 16 it was decided to test them. The test applied was the reduction of the terms of Eqs. 16, for the special case of $\theta = 90°$, to identity with the terms of Eqs. 3, for the special case of $\gamma = 1$. The reduced terms were identical with those for the special case of Eqs. 3. However, the M_{Ozz}-terms from Eqs. 16 had signs opposite to those of Eqs. 3, which confirmed the writer's opinion of the signs. Substitution of the values shown in Fig. 8(*c*) showed that Eqs. 16 would have yielded correct results if they had been applied to this problem.

Experience with the equations indicates that they need a thorough checking before being applied to any problem.

Under the heading, "Development of General Equations," the author rightly explains that for "*** certain loading conditions and boundary conditions formal solutions of Eqs. 2 become somewhat unmanageable." Under the heading, "Practical Considerations," he emphasizes, again correctly, the futility of attempting to solve simultaneous equations of this type with a small slide rule. Under the heading, "Applications to Continuous Structures," he suggests an approximation for solution of the most usual case which occurs when the double cantilevers are not isolated. These observations are those which are almost invariably associated with the classical methods of analysis—the only ones available before Hardy Cross, Hon. M. ASCE, revolutionized the analysis of statically indeterminate structures. The question arises as to whether the disadvantages of the classical methods might in this instance be overcome by the application of moment distribution. The answer is "yes." The independence of the torsional and bending moments in either of the beams of a right-angle double cantilever (mentioned by the author in the "Introduction") makes possible an "exact" solution in only one cycle of distribution and carry-over.

Mr. Cross had written[18] that

> "It is a simple matter to include the effect of torsion of connecting members in frame analyses provided we know the torsional properties of the members. Evidently the carry-over factor for torsion is unity, by statics."

One can see what Mr. Cross had in mind when one applies his method to the problem of this paper. In moment-distribution computations such as those that produced the results shown in Fig. 8(*b*), not only have the disadvantages of the classical method been overcome but all the advantages of moment distribution are gained. The procedure used by the writer involves the distribution of moments for no vertical deflection of C, and the distribution of arbitrary moments associated with a vertical movement at C, followed by a pro-

[18] "Continuous Frames of Reinforced Concrete," by Hardy Cross and Newlin Dolbey Morgan, John Wiley & Sons, Inc., New York, N. Y., 1932.

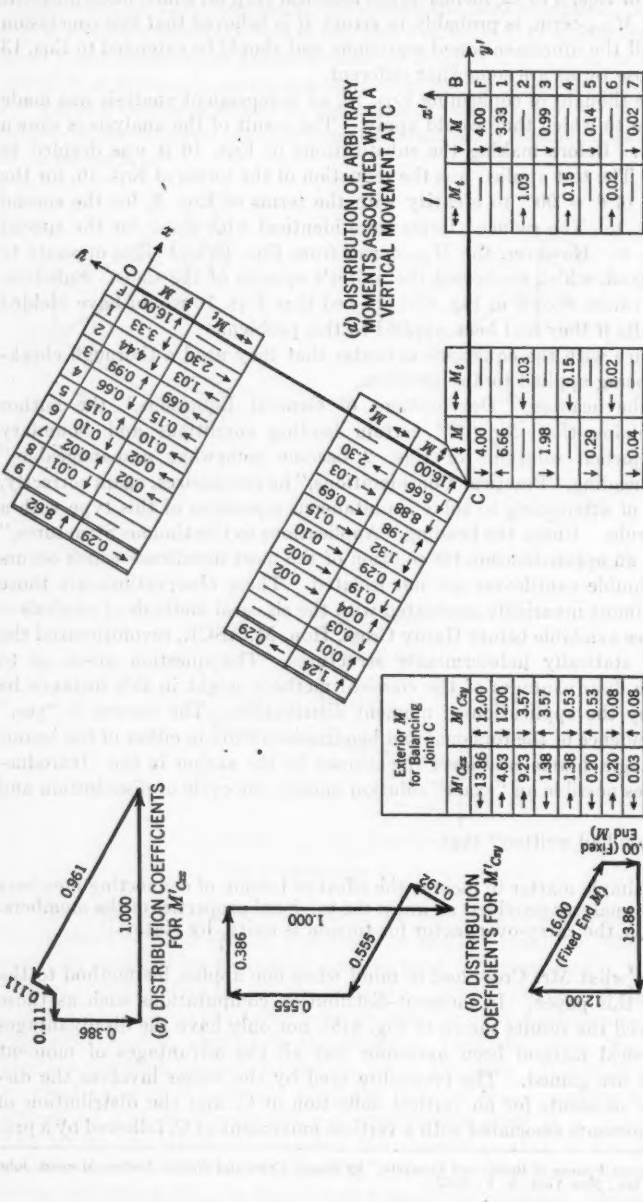

FIG. 9.—MOMENTS IN KIP-FEET, CORRESPONDING TO THE REACTIONS OF FIG. 8(c)

portional correction of these moments which reduces the reaction at point C to zero.

Fig. 9 shows the computations that produced the results of Fig. 8(c). In this instance several cycles were required and the distribution was vectoral rather than numerical. There was, however, no question but that reasonably accurate results could be obtained with a slide rule. The author's suggestion of applying a right-hand rule for designation of moments was most valuable in this analysis (see Fig. 9). In this illustration, M denotes flexural moments, and M_t symbolizes torsional moments. In this particular set of computations, M'_{Cxz} is defined as an exterior moment about the y'-axis, and M'_{Cxy} is defined as an exterior moment about the x'-axis, both moments acting at C.

The writer feels that the profession is indebted to the author for his contribution.

F. E. Wolosewick,[19] M. ASCE.—The writer is pleased that his paper has stimulated interest in the analysis of double cantilever beams. The use of other methods for solving such problems, in lieu of the classical methods, should lead to more intensive studies of similar structures and more precise evaluations of their behavior.

As mentioned by Messrs. Conwell and Hu, the signs of the torsional moments shown in Table 2 are at variance with restraining torsional moments at the support. In the initial derivations, the internal torsional moment in the cantilever was used instead of the restraining couple at the support. This was done intentionally to indicate the direction of the angular rotation that the bending part of the structure would exert on the torsional part. The fact that the resulting answer is negative indicates that the internal torsional moment acts in an opposite sense to the external couple at the support.

The internal torsional moment was used in developing Eqs. 3 to 14, and the external torsional moment was used in Eqs. 15 to 17.

These equations were developed to solve complex cantilevers encountered in actual practice, with various combinations of loads. It was also considered important to take the effect of shear into consideration. In every instance in which these equations were applied, bending and torsional moments were checked from one support to the other. Deflected structures were similarly evaluated showing the torsional rotations and displacements produced by the applied loads.

Drawing the deflected structure in its entirety helps in applying the solution of a double cantilever. To a practicing engineer, no solution would be acceptable unless the geometry of the deflected structure could be clearly pictured and analytically checked for proper signs. It is especially important to know the variation of tensile and shear forces in concrete structures, in order to reinforce properly for these stresses.

Mr. Clough is correct in his analysis of the stability of Fig. 2(g). It is interesting to note, that for cantilevers of equal length, with load P at the apex, R_B is zero, R_A is equal to P, and the torsional moment at B is equal to P_a, and clockwise.

The writer wishes to express his thanks to the various commentators for the interest shown.

[19] Structural Engr., Sargent & Lundy, Chicago, Ill.

AMERICAN SOCIETY OF CIVIL ENGINEERS

Founded November 5, 1852

TRANSACTIONS

Paper No. 2574

REVIEW OF FLOOD FREQUENCY METHODS

FINAL REPORT OF THE SUBCOMMITTEE OF THE JOINT DIVISION COMMITTEE ON FLOODS

SYNOPSIS

This report summarizes the available methods of predicting flood frequencies. It considers the factors affecting the accuracy of such predictions and gives the limitations of the various approaches to the problem.

INTRODUCTION

The report gives consideration to definitions of flood probability in common use. It describes the several methods used to construct flood frequency curves including the "basic stage" and the "yearly flood" methods. Particular attention is given to the extrapolation of such curves to indicate the probability or average return period of floods of exceptional magnitude.

The committee concludes that present (1951) methods of determining flood probabilities are suitable for use in connection with cofferdams, highways, and other minor structures, but believes that existing methods which use solely extrapolations of frequency plotting of existing flood records are to be condemned for the determination of the probable frequency of floods for which major structures should be designed, the failure of which would result in a calamity.

FLOOD FREQUENCY

Definition.—Flood frequency has been variously defined as "percent chance"[1] and "future frequency"[2,3,4] and has been related to probability,[5] recurrence interval,[6] and return period[5] of a given flood. Most people are apt to consider

NOTE.—Published in December, 1951, as *Proceedings-Separate No. 110*.

[1] "Flood Flows," by Allen Hazen, John Wiley & Sons, Inc., New York, N. Y., 1930.

[2] "Hydroelectric Handbook," by William P. Creager and Joel D. Justin, John Wiley & Sons, Inc., New York, N. Y., 1927 and 1950.

[3] "Engineering for Dams," by William P. Creager, Joel D. Justin, and Julian Hinds, John Wiley & Sons, Inc., New York, N. Y., 1945.

[4] "A Simple Method of Estimating Flood Frequency," by Ralph W. Powell, *Civil Engineering*, Vol. 13, 1943, p. 105.

[5] "Floods Estimated by Probability Method," by E. J. Gumbel, *Engineering News-Record*, Vol. 134, 1945, p. 833.

[6] "Floods in Ohio, Magnitude and Frequency," by W. P. Cross, *Bulletin No. 7*, Ohio Water Resources Board, Columbus, Ohio, 1946.

that a maximum yearly flood, estimated to have a 1% chance of occurring, or a probability of occurrence of once in 100 years, or a frequency of occurrence corresponding to a recurrent interval (or return period) of 100 years, will occur exactly once each 100 years; and that, having occurred, it will not occur again for another 100 years. This opinion is, of course, entirely wrong.

In order to remove this confusion of thought, the following definitions and limitations are suggested:

The percentage frequency of a given flood may be defined as the percent of observed floods that were equal to, or larger than, a given flood within the period of records under observation. It also may be used as the estimated percent of floods that will be equal to, or larger than, a given flood. It corresponds to the percent chance.

The recurrence interval and return period of a given flood may be defined as the average interval of time within which the flood will be equaled or exceeded once in the mean. It must be understood that, when the frequency of a given flood magnitude is expressed by the return period, the computed period is solely an average, and the next such period may experience none, one, or more than one flood equal to or greater than the given flood.

As a matter of theory, if the basic data are truly representative, a flood having a return period of 100 years will be equaled or exceeded in a great length of time, on an average of once in 100 years. With 10,000 years of record there would be 10,000/100, or 100 such floods. However, if these 10,000 years were divided into 100 periods of 100 years each, about 37% of such periods would not experience that flood; about 37% of the periods would experience one such flood; about 18% would experience 2; about 6% would experience 3; about 1.5% would experience 4; and about 0.5% would experience 5 or more such floods.

Flood Frequency in General.—Methods have been devised for the determination of the probable frequency of floods based on records of stream flow. Such methods ordinarily make use of frequency curves that have been well described in the literature.[6,7,8] They are applicable to the determination of the frequency of floods for cofferdams, highways, and other minor structures (in which flood damage would entail a financial loss and inconvenience but would not be classed as a calamity) and to the solution of the problem of economic justification of flood control programs. However, in the United States and some other countries there is a lack of records of stream flow covering a period of sufficient length; hence, such methods are not applicable to the determination of the probable frequency of floods for which major structures should be designed and whose failure would be classed as a calamity.

This subcommittee has devoted much time to the question of the frequency of such large floods. As a result of such studies the conclusion reached was that no method has yet been devised that can be used to indicate the probable frequency of such floods. It is the consensus among those who have given considerable study to the subject that existing methods depending only on

[7] "Hydrology Handbook," *Manual No. 28*, ASCE, 1949.

[8] "Floods of May-June, 1948 in Columbia River Basin," *Water Supply Paper No. 1080*, U. S. G. S., U. S. Govt. Printing Office, Washington, D. C., 1949.

extrapolations of frequency plotting of existing flood records are inadequate for use in determining flood frequencies. However, these methods are still being used by some engineers in the United States and abroad.

Flood Frequency Curves.—In the process of collecting flood data on a river many ordinary floods are recorded during a long period of time during which occasional extreme high floods will be recorded. The resulting series of flood events is analyzed by the application of the theory of probability. This consists of calculating and plotting the percentage chance (or the return period) of all the floods in the series, and by eye or by a mathematical process, drawing a regular curve or, in special cases, a straight line through such plotted points. Such a curve is a frequency curve and is usually well defined in its central portion but is likely to be poorly defined at the upper end. This condition often prevents extension of the curve with a dependable degree of accuracy.

The calculation for plotting the points for the frequency curve can be made by either the annual flood method (sometimes called the yearly flood method) or the basic flood method (sometimes called the basic stage method or partial duration series). The fundamental principles of analysis in each of these methods are the same. In the annual flood method only the maximum flood during each year of record is used and the advantage of the method lies in the fact that statistical analysis can be used. In the basic flood method all floods of record that exceeded a given base flow are used. This involves many more floods and therefore is more tedious to use than the annual flood method. The base flow for the basic flood method is usually taken approximately equal to the lowest annual flood. Each flood to be listed should be the peak of a flood resulting from an independent hydrologic event. Both the annual flood and basic flood methods have their utility, as explained in the following sections of this paper.

In order to derive a general equation for estimating flood frequency, all the floods of record using either the yearly flood or basic flood methods should be listed in the order of decreasing magnitude, and each should be given a number, M, in a consecutive series. The number M then indicates the number of times that a given flood was equaled or exceeded during the period of records. For the maximum flood of record, therefore, $M = 1$.

If N equals the number of years of record, the estimated return period (T) of a given flood, in years, may be expressed as

$$T = \frac{N + 1}{M} \quad \text{(1)}$$

If a structure, such as a temporary bridge or a cofferdam, is to be designed to withstand a flood not exceeding one having a return period of about 10 years, the basic stage method of flood prediction should be used. On the other hand, if an extrapolation is to be made as far as possible, such as for the determination of the economic justification for flood control or the elevation of an important building, the yearly stage method involves less work and may be used.

In many instances in studies of flood frequencies one or more floods, either modern or historical, is found to be of much greater magnitude than the

rest. If this flood is given its normal position in the usual probability plotting, the result is a probability curve that, if obtained by any mathematical method, lies below the outstanding flood and considerably higher than all other floods of record. The accuracy of this curve is open to question. There is a divergence of opinion as to the proper method of treatment of these great floods. In drawing the curves these floods may be given only little weight by raising the curve according to judgment, but this provides no specific basis for the location of the curve, and each investigator would draw a different curve. A more logical practice is to recognize that these great floods have a return period much longer in years than the length of record and to draw the curve without regard to them. Points representing these floods would then be plotted on an extension of the frequency curve, and the indicated return period would show the most probable frequency of that flood. It is believed by some that such outstanding floods follow some law of their own that comes into operation at very long intervals. Whether or not they follow their own or the usual laws, it would seem obvious that they cannot be assumed to have a return period equal to the length of the records.

Extrapolation of Frequency Curves.—If the floods are plotted on rectangular coordinate paper, a frequency curve drawn through them may show exceeding curvature and be difficult to extrapolate by eye. Such interpolation is necessary in order to estimate the frequency of floods having a return period considerably greater than the length of record. If plotted on some form of probability paper, or on semilog or log-log paper, the curvature will be more moderate.

If the plotted points are not too scattered and a line drawn through them is not too curved, a moderate extrapolation of the line can be made by eye, within the accuracy of available data. If the line is quite curved when plotted on probability or log paper, it still can be used.[9] By trial a constant q must be determined that is added to or subtracted from all the ordinates of the curve. The new curve so obtained will approach a straight line that can be more accurately extrapolated. If the points are quite scattered, or if a more precise extrapolation is desired, there are available many mathematical procedures, based on the different laws of probabilities, for plotting the probability curve and its extrapolation. A historical review of the many different methods suggested for the determination of flood frequency may be found in publications of the United States Geological Survey (USGS).[10,8]

It is not within the scope of this report to describe concisely the methods proposed for calculating mathematically the probability curve of floods. The procedure recommended by A. Hazen,[1] based on the method proposed by H. Alden Foster, M. ASCE,[11] is still in use. E. J. Gumbel[6] has devised a probability paper adaptable only to the annual flood method on which the frequency curve theoretically will be a straight line.

---

[9] "Straight Line Plotting of Skew Frequency Data," by R. D. Goodrich, *Transactions*, ASCE, Vol. 91, 1927, p. 1.

[10] "Floods in the United States, Magnitude and Frequency," *Water Supply Paper No. 771*, U. S. G. S., U. S. Govt. Printing Office, Washington, D. C., 1936.

[11] "Theoretical Frequency Curves and Their Application to Engineering Problems," by H. Alden Foster, *Transactions*, ASCE, Vol 87, 1924, p. 142.

There is a practical limit to the extent to which a simple frequency curve can be extrapolated with reasonably accurate results. The extreme limit of extrapolation for frequency curves in modern practice is that required for determining the economic justification of flood control projects. In such cases there arises the necessity for estimating the magnitude of a flood that has a return period of 100 or 200 years, and extrapolations to 3 or 4 times the period of record have been required. This is justified only where there is no other method of analysis.

In Massachusetts, a process of analysis applicable to rivers in that area has been made by H. B. Kinnison, M. ASCE, and B. R. Colby.[12] This process provides the means of extending frequency curves to a computed maximum possible flood arbitrarily plotted at a return period of 100,000 years. Intermediate points on the frequency curve for major and rare floods (for convenience called the 100-year and 1,000-year floods, respectively) are computed from a frequency study of great storms combined with a study of rainfall-runoff relations and the application of the unit hydrograph. The maximum possible flood is likewise computed by the application of the unit hydrograph to the maximum possible precipitation, determined by the application of physical laws to the atmosphere and computed and published by the Weather Bureau, United States Department of Commerce.[13] By passing the frequency curve through the points plotted at the lower end of each curve and thence through the computed points for the major, rare, and maximum possible floods, a complete frequency curve is prepared that, it is claimed, makes it possible to estimate the frequency of all floods. The results of this work are applicable only to the area studied, and the accuracy is limited by incomplete data and short records.

Use of Historic Floods

Properly authenticated historic floods, antedating periods of consecutive records, can be used to widen immeasurably the horizon in regard to the frequency of occurrence of floods. The first systematic effort at authentication of historic floods was undertaken by the State Water Supply Commission of Pennsylvania in 1913.[14] Since that time good progress on the compilation of historic floods has been made by federal agencies and Army district engineers in connection with studies on flood control projects. Other researches are referred to in the literature[15,16,17,18] and in various flood control reports of the

---

[12] "Flood Formulas Based on Drainage Basin Characteristics," by H. B. Kinnison and B. R. Colby, *Transactions*, ASCE, Vol. 110, 1945, p. 849.

[13] "Generalized Estimates, Maximum Possible Precipitation Over the United States, East of the 105th Meridian," *Hydrometeorological Report No. 23*, Weather Bureau, U. S. Dept. of Commerce, Washington, D. C., June, 1947.

[14] "Floods," *Water Resources Inventory Report*, Water Supply Commission of Pennsylvania, Pt. VIII, 1917.

[15] "The Floods of March 1936," *Water Supply Papers Nos. 798, 799, and 800*, U. S. G. S., U. S. Govt. Printing Office, Washington, D. C., 1937.

[16] "The Floods of Ohio and Mississippi Rivers, January–February, 1937," *Water Supply Paper No. 838*, U. S. G. S., U. S. Govt. Printing Office, Washington, D. C., 1938.

[17] "Stages and Flood Discharges of the Connecticut River at Hartford, Conn.," by H. B. Kinnison, L. F. Conover, and B. L. Bigwood, *Water Supply Paper No. 836-A*, U. S. G. S., U. S. Govt., Printing Office, Washington, D. C., 1938.

[18] "Statistical Forecast of Floods," by E. J. Gumbel, *Bulletin No. 15*, Ohio Water Resources Board, 1949.

War Department published in House Documents. Historic floods have also been recorded in the USGS Water Supply Papers for particular drainage areas.

In the course of time, the value of data of this kind has become recognized, and former skepticism has given way to extended research. Therefore, many of the older records that have ceased to supply usable flood data as the result of artificial regulation have now become enhanced in value by revision to include historic floods. Estimated discharge based on authenticated stages of historic floods that occurred prior to a period of continuous records may be used in connection with the continuous records to obtain a more accurate probability curve.

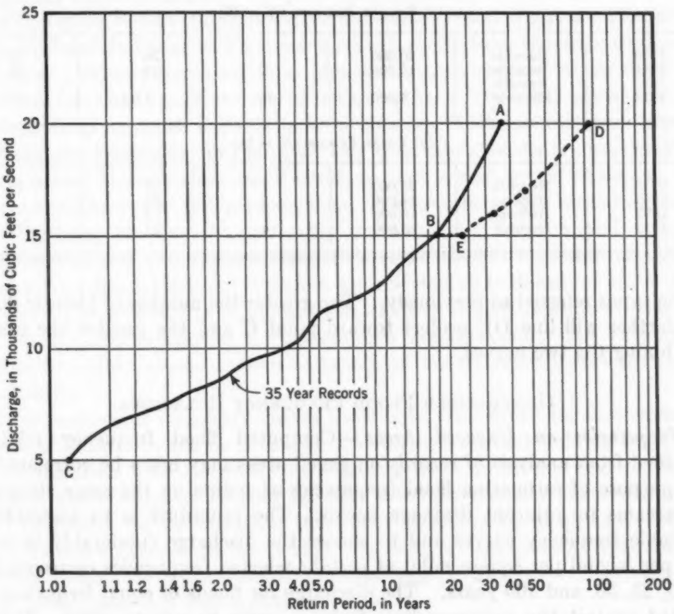

FIG. 1.—USE OF HISTORIC FLOODS

Assume that 35 years of flood records for a stream are available from 1910 to 1944. Line ABC in Fig. 1 indicates the frequency curve for that period of records obtained by usual methods. Assume now that the total number of occurrences of all floods equal to or exceeding a given flood (say, 15,000 cu ft per sec) for the 95-year period preceding 1944 has been definitely established from flood marks on buildings or other conclusive evidence. The upper section of a 95-year frequency curve can then be established enveloping all floods equal to or exceeding 15,000 cu ft per sec. This part of the 95-year frequency curve is just as accurate as though all the floods during the 95 years were known. It is calculated in the following table and is plotted in Fig. 1 as line DE.

The flood of 15,000 cu ft per sec is common to both the 95-year and the 35-year frequency curves and is represented by line EB. It now remains to smooth out line DEBC for extrapolation by eye (not shown) to determine the frequency of floods larger than that indicated by point D. This method is purely empirical and cannot be incorporated in strictly mathematical analyses of the types referred to previously. The greater the number of historic floods, the farther will line DE project toward point C and the greater the ease of combining the two curves.

TABLE 1.—CALCULATION FOR HISTORIC FLOODS

Year	Designation	Discharge (cu ft per sec)	Order of magnitude (M)	Return period (T) (yr)	Point, Fig. 1
(a) RECENT RECORDS ($N = 35$)					
1933	Records	20,000	1	36	A
1915	Records	15,000	2	18	B
etc.	Records				
1912	Records	5,000	35	1.03	C
(b) TOTAL FLOODS ($N = 95$)					
1933	Records	20,000	1	96	D
1850	Historic	17,000	2	48	...
1882	Historic	16,000	3	32	...
1915	Records	15,000	4	24	E

GENERALIZED FLOOD FREQUENCY RELATIONS

Frequencies on Ungaged Areas.—Computed flood frequency relations obtained from analysis of records on gaged areas may often be correlated for the purpose of estimating flood frequencies at points on the same stream or on streams in adjacent drainage basins. The procedure is to assemble all available frequency curves and to choose the discharge (preferably in cubic feet per second per square mile) at certain selected frequencies corresponding to 10, 25, 50, and 100 years. The discharge for floods of equal frequency are plotted against the corresponding drainage areas in square miles. The resulting plot will produce a family of generally parallel curves, establishing a relationship between discharge and drainage area with frequency as a parameter. The estimated frequency of floods on an ungaged area may be obtained by entering the plot at the proper drainage area and picking off the discharges at the selected frequencies. The interpolated data can then be used to plot a continuous curve of estimated frequencies for the ungaged area. The curves can also be used to determine the probable reliability of a frequency curve obtained from a very short record on a gaged area. In plotting and utilizing such generalized relations it should be reasonably certain that all the gaged and ungaged areas under consideration have similar hydrologic, topographic, and geologic characteristics; otherwise the procedure can lead to very unreliable results.

Volume Frequency.—The frequency with which various volumes of flood runoff (expressed in cubic feet per second per day, acre-feet, or inches of runoff) are equaled or exceeded is important in analyzing the future operation of dams when appreciable volumes of flood runoff are to be stored temporarily, or in flood control studies in which a reservoir is required to control a flood of specified frequency. An approach to the volume frequency can be made by probability curves plotted in accordance with methods previously described for flood peak flows. Methods such as these have been used.

The volume of runoff for each flood, analyzed with respect to duration as described hereinafter, can be determined and plotted on probability paper and a frequency curve obtained. It is therefore possible to determine the return period of a given flood volume as well as the return period of a given flood peak, but the volume and peak of a known flood will rarely have the same computed frequency. Volume frequency data obtained without regard to the duration of the various floods analyzed are of limited value. The most useful analysis approach is to establish the relationship between the three variables (depth, duration, and frequency) in the same way that rainfall data are analyzed for use in urban storm-water runoff studies. For example, in analyzing the records of a number of independent flood hydrographs over a period of years, all the greatest one-day (or preferably the maximum 24-hr) runoff volumes are tabulated and a frequency relation is established. Then the maximum two-day (and the subsequent) volumes are selected up to durations of ten days or more. The selection of significant durations of runoff depends on the size and runoff characteristics of the areas under consideration. For very small areas perhaps the volumes should be tabulated for intervals of less than one-day duration.

After a series of frequency curves have been established for flow volumes of various durations, the data can be cross-plotted so that volume is plotted against duration with frequency as a parameter. As in the case of depth, duration, and frequency data for rainfall, it is very unlikely that volumes of equal frequency for all durations will occur in the same flood, but such an assumption is on the conservative side. In fact, for estimates of frequency of reservoir filling, the volume-duration curve can be used as a mass curve of inflow to the reservoir with satisfactory results.

If the storage behind a dam or above a spillway crest is sufficient to materially modify the peak discharge of a flood, the shape of the inflow hydrograph becomes less important than the volume of the flood, and hence the question of the frequency of the peak discharge is not important. However, in low dams with no appreciable storage, the peak discharge governs the ultimate height to which the water will rise. The probable relation between the frequencies of flood volumes and the frequencies of peak discharges can be determined approximately by computing flood volumes for smaller and smaller units of time and comparing the resulting volume frequency curves with available discharge frequency curves. Identical frequency relations should be obtained if volume frequency and discharge frequency are obtained for identical units of time, such as 1 day.

In a search for data on record volumes, it must be remembered that the maximum flood volume discharge in any year may not be concurrent with the maximum peak discharge in that year and that all floods must be examined for maximum volume. For the large floods of rare occurrence it is no easier to determine frequency of flood volume than to determine frequency of flood peak flow, although an adaption of the Kinnison-Colby method, explained previously, might be used with limitations for determination of volume frequency but not for the shape of the hydrograph.

Effect of Available Period of Records on Flood Frequency Curves.—Minor periodical fluctuations (with periods varying from 10 to 25 years) in average annual temperature, river discharge, maximum yearly floods, and other meteorological conditions have occurred in the past and will occur in the future. Therefore, in each study of flood frequency, a careful inspection should be made to determine if the period of records covered a valley or a peak in such fluctuations. Analyses have been made of long records of floods to determine whether component periods within the long record produce similar flood frequency curves. In most cases the shorter periods do not give the same result as the total record but the difference is not necessarily due to the difference in the lengths of record but rather to the concentration of major floods in certain periods. For example, there were many major floods in the United States in the periods: 1820–1834, 1842–1854, 1861–1875, 1881–1896, 1902–1909, 1913–1922, 1926–1938, and 1942–1949.

If an available record of runoff happened to fall between these periods or includes these periods but not the periods without major floods, the resulting flood frequency curves will be distorted either above or below a curve derived from a record including both wet and dry periods. Thus, it is known that flood records of less than possibly 50 years in length are not, as a rule, true samples of much longer records. It is possible that floods occur in an irregular cyclical pattern instead of in accordance with the laws of pure chance. In that case much of the precise mathematical and statistical analysis that has been recommended for flood frequency determinations will only produce a false impression of accuracy. The purpose of this report is to warn engineers to be cautious in applying flood frequency studies and to make sure that an available record is a good representation of the flood history of the general region.

Flood Frequency by Seasons.—Some interest is attached to the knowledge of flood frequency by seasons. Farmers, for instance, are interested in the possibility of floods occurring during the planting and growing season of crops. Contractors are interested in the frequency of floods during the construction season. If the damage done by one flood cannot be remedied until the following year, the yearly stage method of prediction may be used, recording, however, not the yearly maximum flood but the maximum yearly flood occurring during the season in question. If two or more floods in a given season would do more damage than just one flood, the basic stage method should be used, recording not only the maximum yearly seasonal flood but all other seasonal floods that could cause damage.

Errors in Statistical Methods

In preparing graphs for frequency of flood recurrence in the manner herein described, it is assumed that the record information of floods is truly representative and that each point on the graph represents the most common occurrence for the frequency as shown (modal value). If the record information covers a sufficient period of time it is possible to construct control curves indicating the limits of variation from the modal figures within any chosen probability. Such statistical control curves have been published.[19] Another procedure starts from the parameters and gives their limits within any chosen probability. Such limiting values, however, will not embrace all probabilities as there is still a chance that floods will occur beyond such limiting values. (The computations for limiting value are made on the assumption that Poisson's approximation to the binomial expansion is applicable to the distribution of flood frequencies.)

Changing Conditions on Watershed

Present and possible future changing conditions on the watershed should be given careful consideration in the determination of flood frequencies. It is evident that any such changes that result in a greater percentage or more rapid rate of runoff will tend to increase the flood of a given frequency. Among other things, such changed conditions may be due to the removal of forests, and for the smaller drainage areas, the conversion of land to urban uses.

Climatic Changes.—There have been basic climatic changes during the geologic periods, perhaps to a lesser extent during the past 1,000 years.

J. B. Kincer[20] has shown that there has been an over-all trend toward rising temperatures for the last century, but no correlation between mean annual temperature and flood magnitude has been found, nor is such a relationship considered probable. In the United States during the period from 1932 to 1944 there occurred an exceptional number of large floods. This gave rise to the thought that meteorological conditions had changed.

Based on studies by the Subcommittee and on the opinions of the best authorities on the subject, it is believed that these phenomena are actually part of a relatively short-term periodical fluctuation in meteorological conditions. It would seem that no permanent climatic changes are taking place which would in any way affect basic engineering assumptions based on the statistical treatment of climatological data.

Relation of Flood Peaks to Average Daily Discharge.—In the early days of stream gagings, the rates of flow were published for the average calendar day, determined very largely from readings of staff or chain gages, often with only one or two observations a day. It is obvious that this method not only often gave incorrect average calendar day flow, but also was far removed from recording accurately the momentary peak of floods. The momentary peak in some cases is in excess of ten times the average calendar day for small watersheds with rapid runoff characteristics. Similar records are published today,

[19] "On the Plotting of Flood-Discharges," by E. J. Gumbel, *Transactions* Am. Geophysical Union, Vol. 24, Pt. II, 1943, pp. 699–716.

[20] "Our Changing Climate," by J. B. Kincer, *ibid.*, Vol. 27, 1946, pp. 342–347.

although the greatly increasing use of gaging stations equipped with water-stage recorders provides for the determination of the momentary peak as well as a continuous hydrograph of the flood.

The derivation of the peak discharge from records of the average daily discharge, when continuous recording records are not available, can be obtained by a method[11] that consists of plotting the average calendar day flow for each day of the flood as bar ordinates of a width equal to the day interval. The approximate mid-points of the bars, except for the peak of the flood, are connected by lines to represent a continuous hydrograph that contains, as nearly as possible, the same volume for each daily runoff as that recorded. The upward and downward limbs of the hydrograph are then extended to such an intersection on the day of peak flow as will give results for that day consistent with the known average daily flow.

Weston E. Fuller[21] proposed an equation that has been frequently used to convert maximum average 24-hr flood discharge to peak discharge. It is also used to convert calendar day average flow to peak. This equation is

$$Q = Q_{24} (1 + 2 A^{-0.3})^2 \qquad (2)$$

in which Q is the momentary peak discharge, Q_{24} is the maximum average 24-hr discharge, and A is the drainage area.

Studies of many more records than were available at the time of preparation of this formula have indicated that the use of this equation will give results that will be far from correct, for the reason that it does not include consideration of all the factors governing the shape of the hydrograph.

Respectfully submitted,

Subcommittee, Review of Flood Frequency Methods, of the Joint Division Committee on Floods.

William P. Creager, Joint Committee Chairman
Harvey B. Kinnison, Representing the Sanitary Engineering Division
Hymen Shifrin, Representing the City Planning Division
Franklin F. Snyder, Representing the Waterways Division
Gordon R. Williams, Representing the Hydraulics Division
E. J. Gumbel, G. H. Matthes } Collaborators

---

[21] "Flood Flows," by Weston E. Fuller, *Transactions*, ASCE, Vol. 77, 1914, p. 564.

MEMOIRS OF DECEASED MEMBERS

FRANKLIN THOMAS, PAST-PRESIDENT, ASCE[1]

DIED AUGUST 27, 1952

Franklin Thomas, the son of the Rev. Thomas D. and Eleanor (Jones) Thomas, was born near Red Oak, Iowa, on May 19, 1885. He was graduated with the degree of Bachelor of Engineering from the State University of Iowa, at Iowa City, in 1908, and did graduate work at McGill University, in Montreal, Que., Canada, the following year. In 1913, the State University of Iowa granted him the degree of Civil Engineer. In June, 1949, he received the honorary degree of Doctor of Engineering from the University of Southern California, at Los Angeles.

Between 1909 and 1913, Mr. Thomas was, successively, construction foreman for one year with the Mines Power Company, at Cobalt, Ont., Canada; instructor for two years in the Engineering Department at the University of Michigan, at Ann Arbor; and designer for a year for the Alabama Power Company.

In 1913, Mr. Thomas began an association with the California Institute of Technology, at Pasadena, that was to continue until the end of his life. His first task was the establishment of a department of civil engineering. He became professor of civil engineering in 1915, and during 1917, and again in 1920 and 1921, he served as chairman of the administrative committee of the faculty during the absence of the president. From 1924 until 1944, he was chairman of the division of civil and mechanical engineering, aeronautics, and meteorology, and from 1944 until his death was dean of students.

Through thirty-nine years of effort, Dean Thomas contributed his full share to the establishment of "Cal-Tech's" enviable reputation as one of the great scientific schools of the world. More than that was his contribution, through example and precept, to the idealism of the many students who came his way.

Dean Thomas' useful activities were not confined to the institute. Worthy of special note was his service to the Metropolitan Water District of Southern California, the instrumentality which constructed the great aqueduct from the Colorado River into the Southern California coastal area. Dean Thomas was a member of the inner council during the conception and planning of this district. At the inaugural meeting, held on December 29, 1928, he was the official representative of the City of Pasadena, and from that date until his death he served continuously as a director of the district. Subsequent to the completion of the aqueduct, his interests were particularly devoted to including, within the scope of the Colorado River Aqueduct project, all sections of Southern California to which benefits could properly and economically be extended.

NOTE.—Complete manuscripts have been deposited in the Engineering Societies' Library, 29 West 39 St., New York, N. Y., and are available for consultation. Many of these memoirs have been abbreviated for printing in *Transactions*.

[1] Memoir prepared by Julian Hinds, M. ASCE.

In 1947, Earl Warren, Governor of California, appointed him to the Colorado River Board of California, and, in 1948, he was elected chairman of that board. Dean Thomas also served as a consultant on flood control and sanitation projects for the City of Los Angeles, for Los Angeles and Orange counties, and for other agencies.

Long interested in civic affairs, Dean Thomas was a member and vice-chairman of the board of directors of the City of Pasadena from 1921 to 1927. He was also president of the Pasadena Chamber of Commerce, the Pasadena Community Chest, and the Civic Orchestra Association. For "distinguished service to the city," he was awarded the Arthur Noble Medal for 1939.

In addition to the Society, his affiliations included membership in Sigma Tau, Tau Beta Pi, Sigma Xi, Kiwanis, the American Water Works Association, the California Sewage Works Association, the American Society for Engineering Education, and the International Commission on large dams.

On September 20, 1910, he was married to Marie Planck in Red Oak, Iowa. He is survived by his widow; two daughters, Eleanor (Mrs. Lee Champion) and Katherine (Mrs. Donald Langille); two sons, Richard and William; and fifteen grandchildren.

He served the Society as Vice-President from Zone IV in 1944 and 1945. He was a member of the special Committee on Irrigation Hydraulics from 1922 to 1933, and chairman of the Committee on Accredited Schools in 1937.

Dean Thomas was elected a Junior of the American Society of Civil Engineers on December 3, 1912; an Associate Member on October 10, 1916; and a Member on October 15, 1923. He served as Director from 1930 to 1933, and as President in 1949.

FRANK REA ALLEN, A. M. ASCE[1]

DIED MAY 29, 1952

Frank Rea Allen, the son of Benjamin F. and Fannie Elizabeth (Snyder) Allen, was born in Tiro, Ohio, on May 30, 1887. He was educated at Ohio Northern University, at Ada, and received the Degree of Bachelor of Science in Civil Engineering from that university.

Mr. Allen had varied experience in railroad construction in the west. In 1909, he moved to Arkansas, where he maintained his home and practiced his profession for the remainder of his life except for the time spent in military service. Mr. Allen first made his home in Pine Bluff, Ark., and was appointed its city engineer in 1911.

At the outbreak of World War I, Mr. Allen was commissioned a Captain in the Corps of Engineers, United States Army. His service in France and Germany with the 603rd Engineers was the beginning of a long and distinguished career as a civilian soldier. He was commissioned in the reserve at the end of World War I, and he advanced progressively to the rank of Colonel in the Corps

---

[1] Memoir prepared by John E. Buxton, A. M. ASCE, and Leonard N. White, M. ASCE.

of Engineers. He was graduated from the Command and General Staff School at Fort Leavenworth, Kans., in 1932.

On his return to civilian life after World War I, Mr. Allen resumed his position as city engineer of Pine Bluff. He was also engaged in the general engineering practice. He served as state director of flood relief in 1927, and in 1931 and 1932 he was director of drought relief for the American Red Cross. Later he became state director of research and statistics.

After his return to active duty in 1941, and his attendance at the School of Military Government at the University of Virginia, at Charlottesville, Colonel Allen was ordered to the Tunisian front. He was later appointed Governor of Tunisia, and was awarded by the French government the decoration of Commandeur du Nicham Iftikhar, for

> "***directing successfully and against many handicaps and frequently under enemy fire, the relief of the civilian peoples in the zone of combat, during the Tunisian campaign, AND, following the end of hostilities, for directing and executing the operations for relief of the European and Native populations of Tunisia and for the establishing of outstanding friendships conducive to the better relations of France and her Allies."

On completion of his overseas service, and after a five-month lecture tour of northern and eastern universities, Colonel Allen was made Commandant of the Army and Navy School of Military Government of Stanford University, at Palo Alto, Calif., and professor of military science and tactics. This was his last active duty assignment. In Little Rock, Ark., he was engaged in consulting practice with the firm of Buxton and Allen until his death.

Colonel Allen was a member of the Presbyterian Church, Masonic Bodies, American Legion, and other veteran organizations. He also held membership in the Society of Military Engineers and in the National Society of Professional Engineers.

On September 17, 1913, Mr. Allen was married to Jeannette Lloyd in Pine Bluff. He is survived by his widow; two sons, Frank Rea Allen, Jr., and Lloyd Allen; a daughter, Mrs. R. J. Mackin, Jr.; and five grandchildren.

Colonel Allen was elected an Associate Member of the American Society of Civil Engineers on October 9, 1917.

GEORGE DOUGLAS ANDREWS, M. ASCE[1]

DIED JANUARY 9, 1952

George Douglas Andrews was born in Coatesville, Pa., on February 12, 1890. He was the fifth son of James Walkenshaw and Mary Elizabeth (Carmichael) Andrews.

He attended the elementary schools in Harrisburg, Pa., and Montreal, Que., Canada. His higher education was received at the United States Military

---

[1] Memoir prepared by Arthur G. van Reuth, A.M. ASCE.

Academy, at West Point, N. Y.; Lafayette College, at Easton, Pa.; and The Johns Hopkins University, in Baltimore, Md.

Mr. Andrews was a commissioned officer in World War I, and served in the Engineers' Reserve Corps until 1935. After World War I, he became associated with the Pennsylvania Department of Health, from 1924 to 1933, later going to Easton, where he made studies of the sewerage system and the sewage treatment works and also of the Delaware Watershed (at Easton and Bethlehem, Pa.). During the same period he completed the studies and design for the Metropolitan District Water Supply, Sewerage and Sewage Treatment Works for the entire Lehigh Valley of Pennsylvania. During the period from 1933 to 1935, he served as engineer-officer, United States Army, in responsible charge of the Civilian Conservation Corps (CCC) program in Pennsylvania, and was later called to Washington, D. C., as associate engineer of public works and as liaison officer to the White House.

In 1936, Franklin D. Roosevelt, then President of the United States, appointed Mr. Andrews federal administrator of all public works in Pennsylvania, where he administered a construction program of approximately $313,000,000.00 under the late Harold Ickes. This program encompassed filtration plants, waterworks, sewerage systems, and sewage treatment plants.

After finishing this work, which was rated first among all the states under the federal program, Mr. Andrews opened his own offices in New York, N. Y., as a consulting engineer and contractor under the name of Andrews and Andrews, Incorporated. He completed design and construction projects for the rehabilitation of the Consolidated Shipbuilding Company, for the Pennsylvania Turnpike, and for two Veterans Hospitals on Staten Island, N. Y., for the New York State Department of Public Works.

From 1941 to 1944, in association with F. H. McGraw and Company, he served as project manager on the construction of the Jayhawk Ordnance Works, in Kansas, and directed the completion of a $31,000,000.00-ammonia-nitrate plant for the federal government. This project received the first "Army-Navy E" Award for excellence in wartime. Upon completing this work, he went to Brazil for principal operations in Central and South America during World War II.

In 1944, he became chief engineer of the Metropolitan District of Baltimore County, Maryland, in complete charge of the design and construction of water and sewerage projects. He made studies and investigations incidental to the adoption of a comprehensive plan for the conveyance and disposal of sewage, commonly known as the "Andrews Report." In 1948, he opened his own offices in Towson, Md., as an engineering consultant, and was maintaining this business at his death.

Mr. Andrews is survived by his widow, Alma Reinsch Andrews; four daughters by a previous marriage (to Helen Shaver), Mrs. George Fanning, Mrs. Richard Ronaldson, and the Misses Margaret and Marjorie Andrews; one brother, Robert M. Andrews; and a sister, Katherine S. Andrews.

Mr. Andrews was elected an Associate Member of the American Society of Civil Engineers on March 7, 1921, and a Member on April 18, 1927.

DAVID MAURICE BERRY, A.M. ASCE[1]

DIED MAY 8, 1952

David Maurice Berry, the son of Renis S. and Eva (Maurice) Berry, was born on June 24, 1907, in Los Angeles, Calif. He received his engineering education from courses at the International Correspondence Schools and also at the Extension Division of the University of California, at Berkeley.

In Los Angeles, he began his engineering career as a draftsman with a local architectural firm in 1923. Five years later he widened his experience by working in California and Oregon on field surveys for power, railroad, and reclamation projects.

In the period from 1929 to 1933, Mr. Berry was employed by the California Division of Highways. His work consisted of making highway location and construction surveys in Districts III, V, VII, and VIII. Then in 1934 and 1935, as instrumentman, he did the surveying for various elements of the San Francisco-Oakland Bay Bridge, which was under construction by the California Department of Public Works.

In April, 1936, Mr. Berry began a career, which was to last sixteen years, with the Bridge Department of the California Division of Highways when he accepted the position of junior bridge construction engineer. He progressed steadily with the organization through the various civil service positions to that of associate bridge engineer. His assignments as assistant resident engineer and resident engineer on bridge construction projects carried him to many parts of the state. After 1946, he was a bridge designer in the organization's headquarters at Sacramento. Just prior to his death he passed the examination for senior bridge engineer and was on the promotional list for that position. This is particularly creditable since his formal engineering education was obtained mainly through university extension and correspondence courses. As a student, he was the envy of his contemporaries.

From November, 1942, to November, 1945, he served with the Civil Engineering Corps of the United States Navy, advancing from Petty Officer, Second Class, to Chief Warrant Officer. After training at Camp Davis, Rhode Island, he saw duty in the Aleutians, Hawaii, and the Philippines. After World War II, he was active in Naval Reserve work and was a training officer for Organized Construction Battalion No. 12-8 in Sacramento.

Mr. Berry was a licensed civil engineer in California and was active in the Masonic Lodge, being a Past-Master of Athens Lodge No. 228, Free and Accepted Masons.

In May, 1933, Mr. Berry was married. He is survived by his widow.

Mr. Berry was elected a Junior of the American Society of Civil Engineers on January 13, 1936, and an Associate Member on May 13, 1940.

[1] Memoir prepared by a Committee of the Sacramento Section consisting of Wayne J. Deady, Theodore W. Rodgers, and James G. Standley, Jr., Associate Members, ASCE.

ALEXANDER BONNYMAN, M. ASCE[1]

Died April 15, 1953

Alexander Bonnyman, the son of George and Sarah (Toner) Bonnyman, was born in Edinburgh, Scotland, on December 8, 1868. The family moved during his childhood to Lexington, Ky., where he was educated. In 1885 he entered the University of Kentucky, in Lexington, taking courses in civil engineering until 1888. He was later (1950) to be awarded the honorary degree of Doctor of Laws by this university.

Mr. Bonnyman began his career in 1888 with what is now part of the Louisville & Nashville Railroad, and during the following twenty years, was associated with other railroads. He culminated his railroad work as chief engineer and general manager of the Atlanta, Birmingham, and Atlantic Line, now part of the Atlantic Coast Line System.

In November, 1912, Mr. Bonnyman entered the coal mining business in Kentucky and Tennessee. He was later to become president of the Blue Diamond Coal Company.

Mr. Bonnyman held membership in the American Geographical Society; Academy of Political Science in the City of New York (N. Y.); Association of Master Knights of Sovereign Military Order of Malta, in the United States; American Institute of Mining and Metallurgical Engineers; Society of American Military Engineers; American Ordnance Association; Kentucky Society of Professional Engineers; American Academy of Political and Social Science; Scottish-American Memorial Association; Cherokee Country Club of Knoxville; and Princeton Engineering Association.

On November 12, 1906, Mr. Bonnyman was married to Frances Berry, in Rome, Ga. He is survived by his widow; two daughters, Mrs. Margot McKeon and Mrs. Anne Atkinson; and a son, Gordon Bonnyman. His other son, Alexander Bonnyman, Jr., died in World War II and was awarded posthumously the Congressional Medal of Honor.

Mr. Bonnyman was elected a Member of the American Society of Civil Engineers on November 4, 1908. He became a Life Member in January, 1940.

CHARLES FREDERICK CAPES, M. ASCE[2]

Died January 30, 1953

Charles Frederick Capes, the son of Horace and Margaret (Berry) Capes, was born on May 24, 1891, in Lincoln, Nebr. He was only seven when he, his parents, and sister arrived in Boulder, Colo., by covered wagon, to make their home.

[1] Memoir prepared by Julian R. Fleming, A. M. ASCE.
[2] Memoir prepared by Clyde E. Learned, M. ASCE.

Mr. Capes received his elementary education in Boulder, and attended the Boulder State Preparatory School for four years. After completing his education, he undertook ranching and stock raising for about three years. In 1915, he accepted a position with the United States Forest Service as a forest guard in Routt County, Colorado.

He transferred in 1916 to the United States Bureau of Public Roads at Denver, Colo., and worked continuously (except for one year—1918—when he resigned to undertake ranching and stock raising near Denver) until June, 1952, when he retired. After retiring from government service he accepted the position of road supervisor of Boulder County, the position he held at the time of his death. His entire government service covered thirty-six years.

His first position with the Bureau of Public Roads was as a surveyor's chainman. He worked his way upward in the Public Roads organization, and for fifteen years was resident engineer in charge of highway construction in Yellowstone National Park, Wyoming. During 1942–1943 he was construction engineer in charge of the southern sector of 600 miles of the Alcan Highway, with headquarters at Fort St. John, B. C., Canada. With the completion of the highway, Mr. Capes returned to his former headquarters at Denver, as construction engineer in charge of forest and park highways.

In 1949, he accepted a two-year assignment from the Bureau of Public Roads to supervise work on the Pan-American Highway and others in Ecuador and Colombia, South America. In 1951, he again returned to Denver, where he was appointed division staff officer in charge of construction, the position he held at the time of his retirement.

Particularly noteworthy was his assignment to the Alcan Highway, a project which was constructed through pioneer country under adverse conditions. Mr. Capes also had to his credit many outstanding contributions to highway construction in the Rocky Mountain region, particularly in Yellowstone National Park.

He was a member of Southgate Lodge 138, Free and Accepted Masons of Denver, and was active in the local branch of the Izaak Walton League.

In 1914, Mr. Capes was married to Etta Clark, a classmate during his school days in Boulder. He is survived by his widow; four children—Mary (Mrs. Russell Lambert), Montie Capes, James Capes, and William Capes; five grandchildren; and his mother, Mrs. Margaret Capes.

Mr. Capes was elected a Member of the American Society of Civil Engineers on August 13, 1945.

CHARLES STUART CLARK, M. ASCE[1]

Died April 6, 1952

Charles Stuart Clark was born on November 2, 1880, at Fort Worth, Tex. When he was a child, he moved to Albany, N. Y., and there received his elementary and high school education.

[1] Memoir prepared by Trigg Twichell, A.M. ASCE.

After four years at Texas A&M College, at College Station, he began his professional career as a civil engineer in railroad construction work for the Southern Pacific Railroad. Later, he assisted in the location and construction of the St. Louis, Brownsville and Mexico Railroad from Houston, Tex., to the Rio Grande Valley.

While working in the valley, he began a private practice in land subdivision and drainage work and later added irrigation and its related problems. He also, at various times, was engineer for the Rio Grande Construction Company, the Alamo Land and Sugar Company, and the Hildago County Drainage District, and was chief engineer and general manager of the Donna Irrigation District.

Mr. Clark was appointed a member of the Texas Board of Water Engineers on December 1, 1917, and served until his resignation in 1948, immediately after he had been appointed and confirmed for a sixth consecutive six-year term. He was chairman of the board from 1936 to 1948. Following his resignation from the Texas Board of Water Engineers, Mr. Clark acquired a financial interest in the Calhoun County Canal Company and was vice-president and general manager of that enterprise at the time of his death.

He held membership in the National Society of Professional Engineers, the Scottish Rite Masonic bodies of Austin, Tex., and the Shrine.

On April 2, 1906, Mr. Clark was married to Bertha McClellan in Brownsville, Tex. He is survived by his widow.

Mr. Clark was elected a Member of the American Society of Civil Engineers on October 15, 1923. He became a Life Member in January, 1951.

WALTER WILLIAM COLPITTS, M. ASCE[1]

DIED DECEMBER 23, 1951

Walter William Colpitts, the son of Henry Herbert and Lucy Anne (Bissett) Colpitts, was born in Moncton, New Brunswick, Canada, on September 17, 1874. He attended the local schools and after graduation gained considerable experience in railroad work before entering McGill University in Montreal, Quebec, in 1895.

He was graduated in 1899 with the degree of Bachelor of Science and was the valedictorian of his class. During each year of his course he was the winner of the British Association Medal, awarded to the highest ranking pupil. In 1901, he received from McGill University the degree of Master of Science, and, in 1921, in recognition of his contribution to the engineering profession, he was awarded the honorary degree of Doctor of Laws by McGill University.

After working as chief clerk to the president of the Canadian Pacific Railway Company, Mr. Colpitts came to the United States, in 1901, as assistant chief engineer of the Kansas City, Mexico & Orient Railway Company (later part of the Atchison, Topeka & Santa Fe), which was then in the process of construction between Witchita, Kans., and Mexico. While he was still assistant chief engineer,

[1] Memoir prepared by George W. Burpee, M. ASCE.

his versatility and ingenuity in engineering constructon were well demonstrated in the methods which he adopted in the building of a 900-foot bridge over the Rio Conchos in Mexico. The construction of this bridge by conventional methods was started in 1907, and by May, 1908, was half finished. It became evident that different measures would be necessary to complete this bridge before the August, 1908, deadline, which was set because of the necessary hauling of fall crops. Because the Conchos River is subject to sudden rises and to an annual freshet in late August, it was necessary to complete the pier construction in the stream bed before the freshet. Mr. Colpitts planned a method of attack based on the very limited amount of equipment available, and successfully completed the program within four months,[3] before the freshet and in time to enable the railroad to handle the fall crops.

In 1909, Mr. Colpitts was appointed chief engineer of the "Orient." During this period he became greatly interested in the use of reinforced concrete. The results of his studies were the first to be published in the English language.

During 1912, Mr. Colpitts met William H. Coverdale, M. ASCE, when the latter was engaged by a group of security holders to make a study of the "Orient." The mutual esteem that arose from their working together resulted in an invitation from Mr. Coverdale that Mr. Colpitts associate himself with him in his consulting engineering business in New York, N. Y. Late in 1913 began the association which continued until Mr. Coverdale's death in August, 1949. From early in 1916 the business was carried on under the firm name of Coverdale & Colpitts.

During his association with the firm, Mr. Colpitts was responsible for conducting numerous important engagements related to the management, reorganization, and financing of railway properties. The method of attacking the complex problems incident to the reorganization of one railroad in particular, the Missouri-Kansas-Texas, was hailed at the time as original and epoch-making in railroad reorganization. From 1938 to 1943, he was chairman of the Reorganization Committee of the Minneapolis & St. Louis Railroad and acted for the firm of Coverdale & Colpitts as reorganization manager.

At the time of his death he was a director of the The Budd Company, the Carriers & General Corporation, The Celotex Corporation, and the Pepsi-Cola Company; a trustee of the Bank of New York and of the Fifth Avenue Bank; and, until recently, a governor of McGill University. In the past he served as a director of the Chicago, Milwaukee, St. Paul & Pacific Railroad; the Père Marquette Railway; the Seaboard Air Line Railway; the Autocar Company; the Pierce Petroleum Corporation; the Bullock Fund, Limited; the Nation-Wide Securities Company; and the Central National Corporation.

He belonged to the Alpha Delta Phi Fraternity; the Lawyers Club; the Canadian Club, of which he was a past-president; the Recess Club; the Economic Club (New York); Nassau and Tiger Inn (Princeton, N. J.); the Chicago Club (Chicago, Ill.); and the Faculty Club (Montreal). He was a member and past-president of the American Institute of Consulting Engineers, and was a member of the American Railway Engineering Association and the Engineering Institute of Canada.

---

[3] *Railroad Age Gazette*, January 22, 1909.

On October 15, 1907, Mr. Colpitts was married to Florence Rossington of Topeka, Kans. Mrs. Colpitts died at Naples, Italy, on August 27, 1952. He is survived by a daughter, Lucy (Mrs. Howard Menand); a son, Jeremy; a sister, Mrs. A. Ross Smith; a brother, Charles B. Colpitts; and six grandchildren.

Mr. Colpitts was elected a Member of the American Society of Civil Engineers on November 1, 1905. He became a Life Member in January, 1940.

RALPH STEPHENSON CORLEW, M. ASCE[1]

DIED SEPTEMBER 26, 1952

Ralph Stephenson Corlew, the son of John S. and Amy (Stephenson) Corlew, was born on December 3, 1884, in Ogden, Utah. After being graduated from the Ogden high school in 1902, he studied civil engineering through the International Corrspondence School, and later took a course in higher mathematics at the University of Colorado, at Boulder.

From 1906 to 1908 Mr. Corlew was employed by L. B. Spencer & Company. He performed land irrigation and mineral surveys in Utah and Nevada.

The following two years he was associated with the city engineering department in Ogden. A major part of his work during this period was the development of dam sites and storage reservoir facilities.

From 1910 until 1919 he held various positions in the engineering department of Weber County, in Utah, including those of assistant county surveyor, county surveyor, county engineer, and road commissioner. His duties included land, irrigation, and drainage surveys; location, construction, and maintenance of highways; and bridge design and construction.

In May, 1919, Mr. Corlew began an association with the United States Bureau of Public Roads which was to last for thirty-three years until his death. From 1920 to 1938 he was engaged on federal-aid construction inspection work in Colorado and Wyoming, and in 1939 he became district maintenance engineer and handled federal-aid work in Colorado, New Mexico, and Wyoming. In 1948 Mr. Corlew was promoted to the position of division construction and maintenance engineer, with headquarters in Denver, Colo. He supervised the construction and maintenance work on forest and national park highways and was in charge of inspection work on federal-aid construction and maintenance in the states of Colorado, New Mexico, South Dakota, Utah, and Wyoming. His vast knowledge of highway work made him a most successful member of the Public Roads' organization.

In 1921, Mr. Corlew moved to Lakewood, Colo., a suburb of Denver. In Lakewood, he was very active in civic affairs and served on the school board and on the Board of Directors of the Water Company for several years.

In 1909, Mr. Corlew was married to Bertha L. Price of Ogden. He is

---

[1] Memoir prepared by Clyde E. Learned, M. ASCE.

survived by his widow; three sons, Ralph P. Corlew, Jack S. Corlew, and W. L. Corlew; and seven grandchildren.

Mr. Corlew was elected a Member of the American Society of Civil Engineers on March 12, 1945.

GEORGE THOMAS DEAN, A.M. ASCE[1]

DIED MAY 30, 1952

George Thomas Dean, the son of George Adam and Mineria (Blachley) Dean, was born at Manhattan, Kans., on March 29, 1908. He received his early training in the Manhattan public schools and completed his professional training at Kansas State College, in Manhattan. In May, 1930, he was awarded the degree of Bachelor of Science in Civil Engineering, and, in May, 1941, the degree of Master of Science in Civil Engineering. His scholastic record was most commendable and he was elected a member of Chi Epsilon and an associate member of Sigma Xi.

Mr. Dean began his professional career in 1927, when he was employed by the Kansas State Highway Commission. He worked during college vacation periods with the commission until 1930. After being graduated from Kansas State College, he joined the Missouri Highway Department and continued in this employment until early in 1939, when he again became associated with the Kansas State Highway Commission as an associate civil engineeer. It was during this period that Mr. Dean found time to devote to graduate studies.

In the latter part of 1941, he joined the faculty of the Alabama Polytechnic Institute at Auburn, and served as assistant professor of civil engineering until May, 1943. While employed at the institute, Mr. Dean also served as city engineer of Auburn.

In May, 1943, Mr. Dean became a Lieutenant in the Civil Engineering Corps of the United States Navy. He served mainly with a civil engineering construction battalion, and, in May, 1945, he was wounded by enemy mortar fire on Okinawa. He was subsequently decorated for bravery.

After the war, in August, 1946, Mr. Dean was employed by the Veterans Administration and served as supervisor of the Buildings and Grounds Unit for the western states and Hawaii. In May, 1949, he transferred to the Veterans Administration Center at Reno, Nev., where he served as chief of the engineering division in charge of utilities and maintenance. He held this position at his death.

He is survived by his parents, three sisters, and a brother.

Mr. Dean was elected an Associate Member of the American Society of Civil Engineers on February 10, 1941.

---

[1] Memoir prepared by Howard B. Blodgett, M. ASCE, and Elwood T. Rose, A.M. ASCE.

FRANK HOLLIDAY DERBY, M. ASCE[1]

DIED FEBRUARY 8, 1951

Frank Holliday Derby, the son of Minot F. and M. Elizabeth Derby, was born in Revere, Mass., on May 11, 1885. He was graduated with a degree in civil engineering from the University of Maine, at Orono, in 1911, and he received the professional degree of Civil Engineer from his alma mater in 1923.

His early engineering experience included positions as junior engineer and surveyor with the Bureau of Reclamation, United States Department of the Interior, and as an aide to the valuation corps of the Pennsylvania Railroad Company. He served his country in World War I as a Lieutenant in the Field Artillery.

Following the war, Mr. Derby joined the engineering faculty of Washington University, in St. Louis, Mo. He taught there as an associate professor of civil engineering until 1941.

In that year he resigned from Washington University and joined the Tennessee Valley Authority at Wilson Dam, in Alabama, as a design engineer in the chemical engineering office.

During the ten years he spent in the Wilson Dam area, Mr. Derby was unquestionably the most faithful supporter that the Muscle Shoals Subsection of the Tennessee Valley Section of the Society had, staying with it even during the period when the organization was inactive because of a dearth of members. His loss is keenly felt by the Muscle Shoals Subsection, Tennessee Valley Section, and by a host of friends.

While a student at the University of Maine, Mr. Derby became a member of Tau Beta Pi, the national engineering honor society, and Alpha Tau Omega, the national social fraternity. He was a member of the Free and Accepted Masons (Fourteenth Degree) and was a member of the Engineers Club of St. Louis and the American Society for Engineering Education. Stamp collecting was a particular hobby of his over many years, and gardening also occupied his interests.

On January 30, 1914, he was married to Vivian A. Page, in Boston, Mass. He is survived by his widow, who resides in Clayton, Mo.

Mr. Derby was elected a Member of the American Society of Civil Engineers on August 15, 1938.

JOHN RALPH DOBBIN, A.M. ASCE[2]

DIED NOVEMBER 1, 1952

John Ralph Dobbin, the son of Stewart and May (Graham) Dobbin, was born at Viola, Kans., on October 15, 1911. He attended Northwestern Teachers Col-

[1] Memoir prepared by B. E. Cherry, A.M. ASCE.

[2] Memoir prepared by Clare R. Van Orman, M. ASCE.

lege, in Oklahoma, for approximately two years and Kansas State College of Agriculture and Applied Science, at Manhattan. He was graduated with the degree of Bachelor in Civil Engineering in 1937.

Subsequently, his work with the Kansas State Highway Department took him to various division points throughout the state. In 1942, after a short period with a private consulting firm, he entered government service with the Corps of Engineers.

During World War II he served in field offices as control chief, and in the district office at Kansas City as chief of the schedules and progress branch, both positions being concerned with military construction. After the war Mr. Dobbin progressively advanced through key positions in the construction division of the Kansas City District until, at the time of his death, he was serving as deputy chief for all flood control and military construction.

Throughout his very active life, Mr. Dobbin was constantly in search of the right way to do the job. He held tenaciously to what he believed to be the terms of a contract, the performance required, or the payment due. He was liked and respected by contractor and engineer alike—by employee and supervisor.

On December 18, 1938, in Conway Springs, Kans., Mr. Dobbin was married to Aline M. Ogden. He is survived by his widow.

Mr. Dobbin was elected a Junior of the American Society of Civil Engineers on November 22, 1937, and an Associate Member on April 14, 1947.

JOHN NORTH EDY, M. ASCE[1]

DIED MAY 10, 1952

John North Edy was born in Kimwick, Mo., on November 21, 1883. He was awarded two degrees in civil engineering from the University of Missouri, at Columbia, in 1905 and 1909, and he received the master's degree in political science from the University of California, at Berkeley, in 1927. Mr. Edy continued his studies at Stanford University, at Stanford, Calif., from 1928 to 1930.

In 1905, he began his civil engineering career and continued in this field until he became city manager of Berkeley, in 1923. In 1930, he was appointed city manager of Flint, Mich., and after a year he was called to Dallas, Tex., where he served as city manager from 1931 to 1935.

After a brief period as assistant director of the United States Bureau of the Budget, he became city manager of Toledo, Ohio, in 1936. In 1939, he again worked with the federal government, this time as executive assistant and budget officer of the Federal Works Agency.

In January, 1943, Mr. Edy became the first city manager of Houston, Tex. He served as Houston's chief executive until December, 1945, when he resigned to enter private business.

[1] Memoir prepared by T. Spence Love, M. ASCE.

Mr. Edy was elected a Junior of the American Society of Civil Engineers on October 31, 1911; and Associate Member on April 2, 1913; and a Member on September 9, 1919. He became a Life Member in January, 1948.

JOSEPH WILTON ELLMS, M. ASCE[1]

Died February 7, 1950

Joseph Wilton Ellms, the son of Almoran and Julia Elizabeth (Marston) Ellms, was born in Ayer, Mass., on October 4, 1867. He was graduated from Framingham Academy and High School in 1886 and received his technical education at the Massachusetts Institute of Technology, at Boston, from 1890 to 1892.

Following a three-year period with the Massachusetts State Board of Health, Mr. Ellms participated in the basic water purification studies at Louisville, Ky. (1896); in the work of the Brooklyn, N. Y., Department of Health (1897); and, in 1898, in the water purification experiments at Cincinnati, Ohio. He remained in Cincinnati for nine years as engineer of tests and research at the time the new water works were built, and for another ten years he was in charge of operations of the new plant.

The early experiments at Louisville and Cincinnati marked the beginning of rapid sand filtration on a large scale and of present-day water purification practices, and also of controls over typhoid and other water-borne diseases. In his work at Cincinnati, Mr. Ellms developed many basic improvements in mixing devices, filter strainer systems, and other important elements of water purification plants. He also conducted the initial studies of water pollution in the Ohio River at Cincinnati during 1911, with particular regard to the possible effects of the sewage discharged into the river on the Cincinnati waterworks intake as a result of the construction of Fernbank Dam below the city.

Mr. Ellms served as consultant on many water supply projects, notably those for Dayton, Ohio; Bay City, Mich.; Milwaukee, Wis.; Baltimore, Md.; St. Paul, Minn.; and Cleveland, Ohio. He came to the Department of Public Utilities of the City of Cleveland, in 1916, to place the division filtration plant into operation and to act as design consultant for the Baldwin Filtration Plant, and he remained as active consultant on all phases of Cleveland's water supply and sanitation problems since that date. He applied the hydraulic jump to the application of chemicals in water purification. Since 1937 he had been Commissioner of Sewage Disposal for Cleveland and completely supervised the operation of three large modern sewage treatment plants, known as the Westerly, Southerly, and Easterly plants.

As Cleveland's sewage treatment plants were expanded Mr. Ellms devoted all his time to the newly formed Division of Sewage Disposal. He was very active

[1] Memoir prepared by George W. Hamlin, William L. Havens, and Frederick H. Waring, Members, ASCE.

in setting the pattern for the new division to follow and in establishing a rate system for collecting sewage service charges, based on the amount of water used by each consumer. The determination of these rates and the negotiation of service contracts with the various municipalities involved required much time.

In addition to being the author of "Water Purification," one of the most important books in the field,[2] he prepared more than forty published papers and more than that number of unpublished reports all dealing with various phases of sanitary engineering. In 1941 he was awarded the Rudolph Hering Medal for his outstanding work as chairman of the Committee on Water Practice and for formulation of the Society's *Manual No. 19*.[3]

Mr. Ellms was a fellow of the American Association for the Advancement of Science and of the American Public Health Association. He belonged to the American Water Works Association, the American Chemical Society, the Federation of Sewage and Industrial Wastes Association, and the National Society of Professional Engineers. He was a member of the Free and Accepted Masons. In 1942, the Case School of Applied Science (later Case Institute of Technology), at Cleveland, awarded him the honorary degree of Sanitary Engineer.

On February 23, 1897, Mr. Ellms was married to Geneva Eunice Conradt, in Baltimore. Four children survive—Esther Geneva, Elizabeth Conradt (Mrs. H. D. Bogart), Helen Taylor (Mrs. R. C. Wahl), and Robert Wilton.

Mr. Ellms was elected a Member of the American Society of Civil Engineers on April 2, 1913. He became a Life Member in January, 1938.

EDMUND BURKE FELDMAN, M. ASCE[1]

DIED SEPTEMBER 11, 1952

Edmund Burke Feldman, the son of Ephraim and Eva Feldman, was born in Cincinnati, Ohio, on December 17, 1894. He studied civil engineering at the University of Cincinnati, receiving the degree of Bachelor of Civil Engineering in 1916. Mr. Feldman did post-graduate work in indeterminate structures at the University of Minnesota, at Minneapolis.

From September, 1920, until June, 1921, he was an instructor in civil engineering at the University of Minnesota.

He was associate professor of civil engineering at the University of Utah, at Salt Lake City, from July, 1921, until July, 1929. During his spare time he completed a course in geology, irrigation, and drainage, and in 1928 was given the degree of Master of Science from the same university.

[2] "Water Purification," by Joseph W. Ellms, McGraw-Hill Book Co., Inc., New York, N. Y., 1918.

[3] "Water Treatment Plant Design," *Manual No. 19*, ASCE, 1940.

[1] Memoir prepared by Frank A. Schilling, A. M. ASCE.

Following his scholastic work, Mr. Feldman became associated with a large construction firm in Salt Lake City as engineer and superintendent of construction. After this he was employed by the Idaho State Highway Department, at Boise, as assistant bridge engineer.

From August, 1933, until October, 1937, he acted as chief engineer for the Public Works Administration, in Utah. Here he reveiwed and examined applications, approved contracts, and inspected projects amounting to more than $20,000,000 per year. He was then transferred to Region No. 6 (PWA), acting as an assistant to the regional engineer in the direction of a staff of more than three hundred office engineers and fieldmen.

In April, 1940, Mr. Feldman entered business for himself in Salt Lake City, designing many reinforced concrete structures, and estimating work for various contractors. In July, 1941, Mr. Feldman became associated with the Federal Works Agency, as regional engineer of Region No. 9, at Denver, Colo., where he was in charge of all activities of the engineering section of the regional office.

Mr. Feldman entered military service in 1943, and studied at the School of Military Government, at Fort Custer, in Michigan. He subsequently continued his schooling in military government at Yale University, in New Haven, Conn. His first assignment was at Palermo, Sicily, with the rank of Captain, United States Army, where he served from October 15, 1943, until December 31, 1943, in the public works and utilities sub-commission of the Allied Military Government. In January, 1944, he was transferred to Naples, Italy, where he fulfiled a dual responsibility as liaison officer for both the Fifth Army Engineer Section and Engineer Service Peninsular Base Section and the Azienda Autonoma Stradale della Stato.

In January, 1945, Captain Feldman was ordered to Leghorn, Italy, to join the Allied Military Government public works program. He was confronted with many grave problems resulting from the destruction of Leghorn by allied bombings. His efforts as liaison officer between the Engineer Service and local public utilities and governmental agencies secured much cooperation between military and civilian agencies.

His excellent record with the Allied Military Government led to Captain Feldman's assignment to a similar mission in Verona, Italy. There he exercised the same efficiency in enabling the city officials to restore public utilities.

In recognition of Captain Feldman's services, he was promoted to the rank of Major on March 27, 1945. On November 1, 1945, Major Feldman was awarded the Legion of Merit.

At the time of his death, Major Feldman was employed by the Hayden-Lee Development Company, as chief engineer. He had served in this capacity almost three years, during which time he designed nearly fifty buildings, the largest being more than 90,000 square feet in area. Most of these buildings were of the tilt-up concrete type of construction, remarkable for its simplicity and economy. Many improvements in design were incorporated into the plans under Major Feldman's direction, and he became known as an authority on this type of construction.

On August 18, 1936, in Salt Lake City, he was married to Hattie Soble. He is survived by his widow.

Major Feldman was elected an Associate Member of the American Society of Civil Engineers on August 28, 1922, and a Member on July 8, 1941.

EDWIN CLIFFORD FINLEY, M. ASCE[1]

DIED JULY 20, 1951

Edwin Clifford Finley was born on May 13, 1866, in Lee County, Mississippi. He was graduated from the University of Mississippi, at University, in 1889.

Except for one year, 1895, when he worked for the United States Geological Survey, his early experience was with surveys, construction, and maintenance of way for the following railroads: Cincinnati and Lenoir City Railroad; Mobile and Ohio Railroad; Kansas City, Memphis and Birmingham Railroad; and Southern Pacific Railroad. After three years as engineer of railroads for the Louisiana Purchase Exposition in St. Louis, Mo., he served two years, 1904–1905, as superintendent of the railroad exhibits.

Between 1905 and 1908 he was engineer for the Mississippi Railroad Commission, and from 1905, president and engineer of the Itawamba Engineering Company of St. Louis. Beginning in 1911 he was appointed chief engineer of the Manufacturers Railway of St. Louis but transferred in 1913 to the San Antonio and Arkansas Pass Railroad as superintendent of maintenance of way.

In 1919 Mr. Finley was assistant advisory engineer of roads and railroads in the Construction Division of the War Department. During the 1920's he worked as a consulting engineer in St. Louis as well as in Tupelo, Miss.—with the exception of 1927 when he was resident engineer on the St. Louis and Sante Fe Railroad and was stationed in Columbus, Miss.

Mr. Finley spent the next few years in Florida working as a civil and structural engineer in Bradenton and Tampa. For two years, 1935–1936, he worked for the Fuller Earth Company in Midway, Fla.

From 1937 until his retirement, he was a civil and structural engineer in Tupelo, specializing in the design and construction of reinforced concrete structures. Following his retirement, he made his home in Tupelo.

Mr. Finley was elected an Associate Member of the American Society of Civil Engineers on April 5, 1905, and a Member on November 30, 1909. He became a Life Member in January, 1937.

[1] Memoir prepared by S. W. Chandler, M. ASCE.

GLENN FREDERICK FINNER, J.M. ASCE[1]

Died February 17, 1949

Glenn Frederick Finner, the son of Fred F. and Luella (Wolfe) Finner, was born on December 7, 1919, at New Holstein, Wis. He attended high school in Sheboygan Falls, Wis., and entered the University of Wisconsin, at Madison, in 1937. He was graduated in 1941 with the degree of Bachelor of Science in Civil Engineering. While attending the university, Mr. Finner was elected to membership in Tau Beta Pi and Chi Epsilon, national honor societies.

After graduation, he worked for the Hydraulic Data Branch of the Tennessee Valley Authority at Knoxville, Tenn., for about two years. From 1943 to 1945, he was a technical supervisor with the Tennessee Eastman Corporation at Oak Ridge, Tenn. Following this work, he returned to the Tennessee Valley Authority and to Knoxville.

Mr. Finner taught engineering drawing at the University of Tennessee (at Knoxville) from 1946 to 1948, leaving the university in June, 1948, to join the Wilson-Weesner-Wilkinson Company of Knoxville as a structural steel designer.

On December 4, 1945, he was married to Pauline Simmons. He is survived by his widow and parents.

Mr. Finner was elected a Junior of the American Society of Civil Engineers on October 9, 1941.

JOSEPH WATSON GROSS, M. ASCE[2]

Died April 29, 1952

Joseph Watson Gross, the son of Lee N. and Anna W. Gross, was born on September 13, 1884, at Mitchell, S. Dak. In 1894 the family moved to Oakland, Calif., where Mr. Gross was educated, being graduated from high school in 1903.

He entered the University of California, at Berkeley, and was graduated in the class of 1907 with the degree of Bachelor of Science in Civil Engineering. After graduation, Mr. Gross took an active part in all phases of civil engineering —surveying, drafting, estimating, planning, and supervising construction.

Always advancing, he was in charge, as chief deputy county engineer of Sacramento County, in California, of the construction of the first bascule bridge across the Sacramento River. As chief deputy city engineer of Sacramento, he was responsible for the planning and construction of a program of sewer, dock, wharf, and flood control work, estimated at $3,000,000.

During two years' work with the newly organized California State Highway Commission, Mr. Gross gained experience in highway and bridge engineering,

[1] Memoir prepared by C. R. Ownbey, A.M. ASCE.

[2] Memoir prepared by Norwood Silsbee and Walter E. Stoddard, Associate Members, ASCE, and Fred J. Grumm, M. ASCE.

and, as assistant examiner with the State Civil Service Commission, he widened his circle of friends.

During World War I, he was assistant to the chief engineer representing Monks and Johnson, of Boston, Mass., and was in charge of much of the designing and construction of Liberty Yard, at Alameda, Calif., a ship-building plant of an estimated cost of $25,000,000.

In 1920, he opened his own office in Sacramento, specializing in municipal and agricultural engineering. Thereafter, he was closely identified with water problems in northern California and was in demand as an expert witness. His clients had implicit confidence in his judgment and integrity.

Mr. Gross was instrumental in organizing the first University Club in Sacramento, which was disbanded during World War I when most of its members entered the armed services, and also in organizing the Sacramento Engineers Club, disbanded when the Sacramento Section of the Society was formed in 1922. Mr. Gross was a charter member of the Sacramento Section, its first Secretary, and, in 1929, President.

Always active in Local Section affairs, he was particularly interested in the University of Nevada Student Chapter, at Reno, and in junior member activities. During the depression years, much of his time was devoted to finding or helping to "make" temporary jobs for unemployed engineers. Through his efforts, the Sacramento Section built up an "unemployment fund," now known as the "Joseph W. Gross Relief Fund," from which small loans were made which accomplished much good. Most of these loans were eventually repaid.

He was a member of Sacramento Lodge No. 40, Free and Accepted Masons, of the Scottish Rite Bodies of Sacramento, and of Ben Ali Temple, Ancient Arabic Order of Nobles of the Mystic Shrine. He belonged to the American Society of Agricultural Engineers, the American Geophysical Union, and the Commonwealth Club. Mr. Gross' professional specialty was agricultural engineering, his avocation was California engineering history. His collection of original reports, maps, and plans of the great flood of 1862, and of the Central and Southern Pacific Railroads is priceless.

He was married to Marjory May in Sacramento, on May 5, 1917. He is survived by his widow; three children: Joseph W. and twins, Richard S. and Barbara (Mrs. W. T. Hume); and three grandchildren.

Mr. Gross was elected a Junior of the American Society of Civil Engineers on September 1, 1908; an Associate Member on October 1, 1913; and a Member on October 14, 1929. He became a Life Member in 1948.

MARVIN FURR HARTSFIELD, A.M. ASCE[1]

Died January 14, 1953

Marvin Furr Hartsfield, was born at Oxford, Miss., on November 14, 1913. He received his engineering education at the University of Mississippi, at Oxford, being graduated in 1937.

[1] Memoir prepared by C. M. DuBois, A.M. ASCE.

After two years' experience at the university, with the Mississippi State Highway Department, and with the Corps of Engineers, United States Army, he was employed by the Tennessee Valley Authority on Guntersville Dam in November, 1939, and later worked at Pickwick Landing Dam.

In October, 1941, Mr. Hartsfield left the employ of the Tennessee Valley Authority to accept an appointment with the Special Engineering Division for the Panama Canal. This work involved engineering studies for the Third Locks project.

Between September, 1943, and May, 1946, he served in New Guinea and the Philippine Islands as a Lieutenant (j.g.) in the Civil Engineer Corps, United States Navy. On his return to civilian life he resumed his work with the Panama Canal. Later he became associated with the J. A. Jones Construction Company on the expansion of the facilities of the Atomic Energy Commission, at Hanford, Wash.

In May, 1949, Mr. Hartsfield became a partner in the general contracting firm of Berg-Hartsfield of Lincoln, Nebr. He was re-employed by the Tennessee Valley Authority in June, 1951, and was engaged on the Kingston Steam Plant project at the time of his death.

He was a member of the Delta Tau Delta fraternity and was a registered professional engineer in the State of Mississippi.

On July 23, 1948, in Hanford, he was married to Mary Wright. In addition to his widow and a son, Marvin Furr, Mr. Hartsfield is survived by his parents; three brothers, William L., James C., and John E.; and two sisters, Mrs. Robert K. McClain and Miss Clyde Little.

Mr. Hartsfield was elected a Junior of the American Society of Civil Engineers on February 14, 1938, and an Associate Member on July 6, 1948.

WILLIAM SHERMAN HEWETT, M. ASCE[1]

DIED NOVEMBER 20, 1951

William Sherman Hewett, the son of William and Elizabeth (Payson) Hewett, was born in South Hope, Me., on October 27, 1864. He received his education at the Normal School in Castine, Me.

In 1887, Mr. Hewett went to Minneapolis, Minn., and started work for his uncle, Seth Maurice Hewett, in the construction of highway bridges. Although he never had any formal technical training, he had a thorough and complete training in the fundamentals of stress analysis by the practical application of these fundamentals.

Mr. Hewett began his own bridge contracting business under the name of the William S. Hewett Bridge Company in March, 1897. He built many of the early steel highway bridges throughout Minnesota, the Dakotas, and Montana, and pioneered in reinforced concrete construction. He is credited with building

[1] Memoir prepared by Maurice W. Hewett, M. ASCE.

the first, or one of the first, reinforced concrete bridges in the United States, and he also constructed a very early Melan type arch bridge. During the period from about 1900 to 1910, all bridges built for the Twin City Rapid Transit Company and for the Minneapolis Park Department were planned and built by Mr. Hewett. Two notable projects of this period were the strengthening of two existing bridges over the Mississippi River—one was at Washington Avenue in Minneapolis and the other was the Lake Street-Marshall Avenue Bridge between Minneapolis and St. Paul, carrying street railway traffic.

In about 1903, he and his cousin, Arthur Hewett, formed the Security Bridge Company and constructed many bridges over the Missouri, the Yellowstone, and many other streams in the Dakotas, Montana, and Minnesota. At one time, he was associated with A. Y. Bayne of Minneapolis in the construction of a bridge over Minnehaha Glen in Minneapolis and the bridge over the Mississippi River from Fort Snelling to St. Paul.

During this period Mr. Hewett developed and patented a type of precast concrete culvert of rectangular sections with pipe inserts near the four corners that engaged the adjacent section. He termed this culvert the Security Culvert.

In the 1920's, he added irrigation work to his bridge activities. Many of the structures on the Milk River irrigation project in Montana were built by him. As most of his work was now being done in this area, he severed his connections with the Security Bridge Company and set up a new company under his own name.

After World War I, his son, Maurice, joined the company. One project that was undertaken by the company in 1919–1920, the water tower and tank at Brainerd, Minn., was to open up another field of engineering for him. His experiences with the Brainerd water tank led to the development of a pioneer method of constructing prestressed concrete tanks. Many notable tanks were subsequently built by Mr. Hewett using this method and under his own specifications.

A second very important contribution to structural engineering by Mr. Hewett was his method of concrete dome construction. Examples of his work can be found throughout the United States. A detailed description of the construction procedure was published in *Concrete*.[3]

From 1924 to 1929, Mr. Hewett spent time in Colorado, California, and Idaho, promoting the construction of prestressed tanks. In 1930, he opened an office in Chicago, Ill., as a consulting engineer specializing in reinforced concrete tank and dome construction. He maintained this office until 1946. The last years of his life were spent in retirement in Florida.

In 1887, Mr. Hewett was married to Helen Mar Obert. He is survived by two sons, Maurice (M. ASCE) and Harold; and three daughters, Agnes Carvill, Pauline Paine, and Elizabeth Addington.

Mr. Hewett was elected a Member of the American Society of Civil Engineers on June 1, 1909. He became a Life Member in January, 1935.

---

[3] *Concrete*, February, 1939.

GEORGE PERCIVAL HOLLAND, A.M. ASCE[1]

Died October 30, 1950

George Percival Holland, was born on July 22, 1897, in Shelby County, Kentucky. His boyhood was spent in Louisville, Ky.

In 1912, at the age of fifteen, he began his engineering career with the Southern Railway Company. From 1912 until 1918 he worked for various railroads in Kentucky.

During World War I, Mr. Holland served in the United States Army as a Sergeant in the Field Artillery and as an officer candidate at Camp Zachary Taylor in Kentucky. On receiving his discharge from the service on January 17, 1919, he returned to railroad engineering work. He continued in this field until 1920 when he became associated with the North Carolina State Highway Department. In 1924, he joined the Tennessee Highway Department as resident engineer on construction of many of the first primary highways built in that state.

From 1941 to 1946, when World War II sharply curtailed state highway construction, Mr. Holland worked for the Highway and Railroad Division of the Tennessee Valley Authority on relocation work incident to the construction of dams and reservoirs.

In 1946, he returned to the Tennessee Highway Department as senior resident engineer. Among other projects, Mr. Holland supervised the construction of the six-lane Magnolia Avenue Parkway in Knoxville, Tenn.

Mr. Holland belonged to that fast-disappearing group of engineers who acquired their knowledge of engineering the hard way—by experience, correspondence courses, and midnight oil. He possessed a tremendous enthusiasm for his profession and a devotion to duty and hard work.

In addition to his work in the Society, Mr. Holland was also an active member of the Knoxville Technical Society. He was a devoted Mason, belonging to Woodward Lodge No. 737, Free and Accepted Masons; Paxton Chapter No. 184, Royal Arch Masons; Knoxville Council No. 75, Royal and Select Masters; Couer de Lion Commandery No. 9, Knights Templar; and others.

On June 11, 1921, he was married to Letitia Wiseman, of Plumtree, N. C. He is survived by his widow.

Mr. Holland was elected an Associate Member of the American Society of Civil Engineers on December 21, 1943.

CLEMENT JOHN HOWARD, M. ASCE[2]

Died July 11, 1952

Clement John Howard, the son of the Rev. Henry A. and Emma (Skipp) Howard, was born in Maple Valley, Ont., Canada, on June 23, 1882. He moved

[1] Memoir prepared by C. R. Ownbey, A.M. ASCE.

[2] Memoir prepared by Robert J. Cummins, M. ASCE.

with his family to Texas as a child and was educated in the public schools of Texas. In 1899, he entered the University of Texas, at Austin, receiving the civil engineering degree in 1903.

Following graduation he became identified with the Corps of Engineers, United States Army, and was engaged in river and harbor improvement work, being stationed at Galveston, Tex. From 1905 to 1907, he worked for the Santa Fe Railroad and supervised the construction of part of the interurban line from Sherman to Dallas, in Texas. In 1908, he joined the Fred A. Jones Company, Consulting Engineers, of Dallas, specializing in bridge construction. From 1910 to 1912, he was with the Texas Company.

Mr. Howard moved to Corpus Christi, Tex., in 1912, and became a member of the engineering staff of that municipality. He was made city engineer in 1919. In 1923, he resigned to join the consulting engineering firm of Robert J. Cummins, M. ASCE, of Houston, Tex. During the almost thirty years he was associated with Mr. Cummins he planned and supervised the following projects: The construction of the original and most of the subsequent developments of the Port of Corpus Christi; the reconstruction of the LaFruta Dam on the Nueces River, designed to impound a water supply for the City of Corpus Christi; and the construction of the original harbor improvements of the Port of Brownsville, Tex., together with most of the subsequent additions to that port. In addition, he supervised the construction of the following: The municipally owned and operated $1,500,000 Recreation Pier at Galveston; the steel sheet pile wharf and bulkhead for the Sheffield Steel Company, on the Houston Ship Channel; the eighteen-story Oil & Gas Building in Fort Worth, Tex., and the adjoining 600-car parking garage; and the six-story garage for the National Bank of Commerce, in Houston, costing $1,500,000.

In 1914, Mr. Howard was married to Nell Kathleen Smith of Corpus Christi. He is survived by his widow; a son, Walter; and a daughter, Kathleen. Mr. Howard's brother, Ernest Howard, was a Past-President of the Society.

Mr. Howard was elected a Junior of the American Society of Civil Engineers on September 6, 1904; an Associate Member on September 3, 1912; and a Member on October 11, 1920. He became a Life Member in January, 1947.

GEORGE WILLIAM HOWSON, M. ASCE[1]

Died August 7, 1952

George William Howson, the son of George and Mary Howson, was born in Sacramento, Calif., on September 26, 1883. He was graduated from the University of California, at Berkeley, in 1909.

After his graduation, during 1909 and 1910, he was employed on the design and construction of buildings and roads at the University of California. This work was followed by service with the Sierra and San Francisco Power Company

[1] Memoir prepared by Carl B. Meyer, David S. Stoner, and Donald S. Hays, Associate Members, ASCE.

for nearly ten years, from 1910 to 1920. The early part of this service was spent on the construction of dams, ditches, and transmission lines for the power company. Included was the construction of the rock-fill Strawberry Dam, on the south fork of the Stanislaus River, in California. The latter part of his service with this company was spent as division manager in charge of the operations of the company's mountain property, including reservoirs, powerhouses, and transmission lines.

In 1920, Mr. Howson then served as one of four members of a commission reporting on a suitable water supply for the City of Athens, in Greece. The report of the commission resulted in the construction of a project, a few years later, at an estimated cost of $23,000,000.

In 1921 and 1922, Mr. Howson was in charge of the civil engineering design of the California Memorial Stadium at the University of California, a concrete structure seating 85,000 people. Following this, he was employed by the contractor as assistant superintendent on the construction of the stadium.

Service then followed in Kentucky, from 1924 to 1934: First, as resident engineer on Dix Dam, the highest rock-fill dam constructed prior to 1925; second, for a period of more than ten years, as superintendent of operations of the Kentucky Utilities Company, and later, also, for the Lexington Utilities Company.

During the period from 1935 to 1940, Mr. Howson was engaged by the Public Works Administration and the National Resources Planning Board in the investigation of projects where special construction or engineering problems were involved.

He was employed by the United States Bureau of Reclamation, at Sacramento, from 1941 to 1947, spending the last few years as field coordinator of the Central Valley Project problem studies. In the Central Valley Project problem studies, committees were appointed from personnel of the U. S. Bureau of Reclamation and other interested agencies to survey and recommend solutions to problems which were expected to be encountered upon the completion of the Central Valley Project, such as the disposal of the water and power which would be produced by the project. There were some twenty-four problems of this type, and it was the duty of Mr. Howson to coordinate the efforts of the committees investigating them.

After 1947, Mr. Howson was employed by the Division of Water Resources of the State of California on the state-wide water resources investigation. This investigation is intended to determine the present water utilization and water requirements under conditions of ultimate development for the entire state. Recently, Mr. Howson was employed in determining the number and location of the multitude of agencies presently supplying water for domestic and irrigation purposes throughout the state.

In 1910, in San Rafael, Calif., he was married to Gertrude Meyers. He is survived by his widow, a son, two daughters, and six grandchildren.

Mr. Howson was elected a Junior of the American Society of Civil Engineers on October 5, 1909; an Associate Member on January 6, 1915; and a Member on June 11, 1945.

WILLIAM HENRY HUNT, M. ASCE[1]

DIED JUNE 30, 1952

William Henry Hunt, the son of William H. and Amelia F. Hunt, was born in New York, N. Y., on December 15, 1872. He received his engineering education at The Cooper Union in New York.

Mr. Hunt began his engineering career in 1897 with the Hay Foundry & Iron Works and was employed as a structural designer for Milliken Brothers until 1900. He then served for two years as an assistant subway design engineer with the Rapid Transit Commission.

From 1903 until 1910, he was associated with the late G. K. Hooper as chief engineer on the design and construction of large industrial projects. The following four years, from 1911 until 1914, he was employed by the American Cement & Tile Company.

Then, from 1915 to 1924, Mr. Hunt was sales engineer for the Pittsburgh Bridge & Iron Works, the Lehigh Structural Steel Company, and the Bethlehem Steel Company. Later, he became associated with the Frank M. Weaver Company, Incorporated, of Lansdale, Pa., as sales engineer and manager of the New York office. In 1950, Mr. Hunt retired because of ill health.

He had many admirable traits that attracted and retained his friends. As an engineer, he was earnest, intelligent, and possessed sound judgment. For his recreation, he was intensely interested in classical music, having been a fine pianist.

Mr. Hunt was married in 1908. His wife died during the same year. There are no survivors.

Mr. Hunt was elected a Member of the American Society of Civil Engineers on June 30, 1911. He became a Life Member in January, 1943.

GEORGE WASHINGTON KELLY, A.M. ASCE[2]

DIED JULY 7, 1952

George Washington Kelly, the son of Michael J. and Mollie J. Kelly, was born in Baltimore, Md., on February 22, 1891. He was educated in the parochial schools of Baltimore and completed his schooling at the Baltimore Polytechnic Institute in 1911.

He was first employed as a draftsman with the Baltimore and Ohio Railroad. He then transferred his interests to the City of Baltimore, where he was employed in 1912 by the Annex Improvement Commission as a draftsman, preparing paving plans.

---

[1] Memoir prepared by John B. Stein, A.M. ASCE.
[2] Memoir prepared by Bernard F. Suwall, A.M. ASCE.

In 1917, he was promoted to principal draftsman with the Bureau of Drafting and was placed in charge of a group of draftsmen preparing drawings in connection with traffic maintenance and the establishment of street grades.

In World War I, Mr. Kelly was called to the service of his country and served with distinction in the Ordnance Department at Aberdeen, Md.

After being discharged from the United States Army in March, 1919, he entered the employ of the Bethlehem Steel Company, preparing plans for the construction of concrete foundations, cooling systems, water supply systems, and sewerage and drainage structures that were required in the modernization of their tin mill plant.

In August, 1920, Mr. Kelly again entered the employment of the Baltimore and Ohio Railroad, in the cost engineer's office, where he prepared estimates of costs of improvements under the Valuation Act of the Interstate Commerce Commission.

He re-entered the employ of the City of Baltimore in April, 1921, as a junior civil engineer in the Sewerage Division of the Highways Department. He remained with the Sewer Department, later known as the Bureau of Sewers, and, successively, held the positions of assistant civil engineer and designing engineer of sewers. He also made extensive valuation estimates regarding the inclusion of various privately-owned sewerage systems into the municipal system.

In March, 1942, Mr. Kelly was promoted to chief designing engineer in charge of the Division of Surveys and Design of the Bureau of Sewers, and he continued in this capacity until failing health caused his retirement from active service early in 1951.

While he was in charge of the Designing Division of the Bureau of Sewers, notable extensions to the sewerage system were made, among which were the provision of sewerage and drainage systems for many new highways required by the defense program of World War II and the provision of the sanitary sewer to serve the Jones Falls Valley area at a construction cost of several million dollars.

Mr. Kelly was a registered professional engineer.

On May 28, 1919, he was married to Ella L. Bochardy. He is survived by his widow and their two children, Donald and Katherine.

Mr. Kelly was elected an Associate Member of the American Society of Civil Engineers on February 14, 1944.

CLYDE CHARLES KENNEDY, M. ASCE[1]

Died April 25, 1952

Clyde Charles Kennedy, the son of Robert and Mary (Barnes) Kennedy, was born in Rushville, Ind., on April 1, 1881. Mr. Kennedy attended Friends Academy at Spiceland, Ind., and Earlham College in Richmond, Ind.

[1] Memoir prepared by H. C. Vensano, M. ASCE.

Following his graduation from Earlham College in 1904, Mr. Kennedy served as way engineer for the Pennsylvania Railroad. In 1907, he was elected county surveyor for Rush County, in Indiana, and while so employed became interested in sanitation and public health. With this interest he came to California to study in the new School of Public Health and Sanitary Engineering at the University of California, at Berkeley, from which he received the degree of Master of Science in 1911. His studies led to the appointment as assistant city engineer, and later, as city engineer of the City of Berkeley, in which position he served until 1919.

In 1919, he opened his own engineering office which specialized in municipal problems. Many of the major water and sewerage works in the west were designed under his direction. Prominent among these are the City of San Francisco's Richmond-Sunset Sewage Treatment Plant, built in 1939, and the North Point and Southeast plants of the same city, built 1949–1952. Other sewage treatment plants were designed for the cities of Sacramento, Pittsburg, San Leandro, and Stockton (in California); Tacoma, Wash.; and Phoenix, Ariz.

The water supply projects on which he was engaged include the supply for Fairbanks, Alaska; Phoenix; and, in California, supplies for Calistoga and the City of Eureka. The latter project included the design and construction of the Sweasy Dam on the Mad River.

Mr. Kennedy was commissioned a Captain in the Sanitary Corps, United States Army, in World War I. In World War II, his experience in railroad work helped to expedite expansion of Benicia Arsenal, in California, and Sierra Ordnance Depot, near Honey Lake, Calif.

His office also provided facilities for numerous air fields, army camps, and navy installations in the west, including the design of the Naval Supply Depot at Clearfield, Utah. At the time of his death, Mr. Kennedy was a senior partner, in business with his sons.

He was a member of the American Water Works Association, the California Sewage Works Association, the American Association for the Advancement of Science, and a fellow in the American Public Health Association. In addition, he was a founding member of the Federation of Sewage Works Associations from June, 1928, and was active in that organization until his death, serving as national director from 1944 to 1947. Through the League of California Cities (later the League of California Municipalities) he helped to develop the improvement acts now used in the State of California. He was technical editor of *Western Construction News* for many years, and a contributor to various technical journals.

On January 20, 1907, in Noblesville, Ind., Mr. Kennedy was married to Mabel Roberts. He is survived by his widow and two sons, Richard and Robert Kennedy.

He was elected a Member of the American Society of Civil Engineers on June 1, 1920.

KARL QUILL KIRK, A.M. ASCE[1]

DIED JANUARY 26, 1953

Karl Quill Kirk, the son of William Addison and Augusta Eliza (Potter) Kirk, was born in Chattanooga, Tenn., on July 11, 1877, and spent most of his life there. He was graduated an engineer from the International Correspondence Schools.

Mr. Kirk was resident engineer on the construction of the Memorial Auditorium and the Clemens Brothers Building in Chattanooga. For the last twenty-nine years of his life he was chief estimator for this company and helped construct the Medical Arts Building and the new Interstate Life and Accident Insurance Company Building in Chattanooga. The latter structure was erected on the site of the home in which he and his wife had lived for many years.

Mr. Kirk was a registered engineer in Tennessee and a member of the National Society of Professional Engineers.

On May 10, 1919, in Chattanooga he was married to Theresa de Georges. He is survived by eleven nieces and nephews.

Mr. Kirk was elected an Associate Member of the American Society of Civil Engineers on April 12, 1943.

ALPHONSUS PAUL McBRADY, A. M. ASCE[2]

DIED DECEMBER 25, 1951

Alphonsus Paul McBrady, the son of Robert and Bridget (Hurley) McBrady, was born in Graceville, Minn., on January 9, 1886. He received his education in the Graceville public schools; the University of Minnesota, at Minneapolis; and the University of Dublin in Ireland as an United States Army student.

His professional career began with railroad building and canal and irrigation work in Idaho, North Dakota, and Montana with the Chicago, Milwaukee & St. Paul Railway and Soo Lines. In 1911, he went to Fort Worth, Tex., and became associated with Stone and Webster, Engineers.

When the United States entered World War I, he volunteered and was assigned to the 23rd Engineers, United States Army, in France. After his return from military service he was a county surveyor in McCone and Garfield counties in Montana, and, from 1921 to 1923, was project engineer for the Missouri State Highway Department, stationed in Jefferson City. For the next eight years Mr. McBrady was associated with the Don Hall Construction Company, in Houston, Tex.

---

[1] Memoir prepared by Robert H. Nagel, A.M. ASCE.

[2] Memoir prepared by T. Spence Love, A.M. ASCE.

He served the public at three different periods, once with the Public Works Administration from 1935 to 1940, and twice with the Federal Housing Authority from 1941 to 1945 and from 1946 to 1947. After four years of retirement, he returned to engineering work with the Hubbard Construction Company at Houston in 1951, and was associated with that firm at the time of his death.

In Texarkana, Ark., on April 24, 1924, he was married to Agnes M. Donohue. He is survived by his widow; a brother, Robert S. McBrady; and two nieces and two nephews.

Mr. McBrady was elected an Associate Member of the American Society of Civil Engineers on March 10, 1930.

DONALD HULL McCREERY, M. ASCE[1]

DIED JUNE 11, 1951

Donald Hull McCreery, the son of Rollo and Blanche (Hull) McCreery, was born in Denver, Colo., on June 12, 1899. He grew up in Pasadena, Calif., where he received his elementary and high school education, and for two years attended the California Institute of Technology before transferring to the Massachusetts Institute of Technology, at Cambridge. He was graduated from this institution, in 1922, with the degree of Bachelor of Science.

Within a year after graduation, Mr. McCreery was employed by the Richards-Neustadt Construction Company in Los Angeles, Calif. He rose to the position of general superintendent after several years. While he served in this capacity, the most noteworthy structure built under his supervision was the First Congregational Church in Los Angeles, completed in 1933, at an estimated cost of $750,000.

From 1936 to 1940, Mr. McCreery was self-employed as a general contractor on residential and small commercial projects in the Los Angeles area. In 1940, he served as senior office engineer for Leeds Hill Barnard & Jewett, Consulting Engineers, completing the company's engineering contract for Camp San Luis Obispo, in California.

In 1941, he was chief engineer on the design and construction of Camp Cooke at Santa Maria, Calif. Continuing as chief engineer for Leeds Hill Barnard & Jewett, from 1942 until 1945, he supervised several major contracts. They were the Second Division Cantonment at Del Rio, Ariz.; the conversion of the Vista Del Arroyo Hotel to a general hospital (McCormack); the design of the Birmingham General Hospital at Van Nuys (Calif.), as well as the Santa Maria and Blythe air bases.

With the organization of Quinton Engineers, Limited, of Los Angeles, in 1945, Mr. McCreery became its vice-president and general manager, and in 1947, its president. During these years (until 1951), this company, under his administrative direction, successfully completed plans and specifications for all types of

---

[1] Memoir prepared by C. M. Corbit, M. ASCE.

sanitary engineering structures—airports, industrial buildings, and school buildings, and prepared master plans for airports and municipal utilities.

A few months before his death, Mr. McCreery resigned from Quinton Engineers, Limited, to accept an assignment as director of engineering for Homes and Narver, Incorporated, Consulting Engineers, of Los Angeles.

Throughout his engineering life he was actively interested in the affairs of the Society, serving as President of the Los Angeles Section in 1944. From time to time, he contributed articles to several construction and engineering magazines, of which the most outstanding [2] was his article "Organizational Set-Up of an 'Architect-Engineer.'"

He actively participated in civic affairs, serving on several committees of the Los Angeles Chamber of Commerce. He was also a member of the American Society for Testing Materials, the Economic Round Table, and the Los Angeles University Club.

On June 12, 1929, Mr. McCreery was married to Eleanor Burdorf in Fullerton, Calif. He is survived by his widow and his mother, Mrs. Blanche Hull McCreery.

Mr. McCreery was elected a Junior of the American Society of Civil Engineers on October 2, 1922; an Associate Member on October 24, 1932; and a Member on January 11, 1943.

ANDREW JACKSON McKENZIE, A.M. ASCE[3]

Died October 1, 1952

Andrew Jackson McKenzie, the son of James and Jemima (Jackson) McKenzie, was born in Marshall, Mo., on February 6, 1883. Mr. McKenzie entered the University of Missouri, at Columbia, and, in 1907, was graduated with the degree of Bachelor of Science in Civil Engineering.

After working with a survey party for the Frisco Railway Company, he became city engineer for Webb City, Mo. Mr. McKenzie resigned in 1912 to organize the McKenzie Construction Company which, since that time, has completed more than 350 large construction projects, totaling more than $100,000,000. Some of the larger projects are as follows: The Smith-Young Tower Building, the Plaza Hotel and Annex, the Alamo National Bank Building, and the Bell Telephone Building in San Antonio, Tex.; the Driscoll Hotel in Corpus Christi, Tex.; and the Hilton Hotel in Dallas, Tex.

During both World War I and World War II the McKenzie Construction Company was awarded numerous large United States War Department contracts, including extensive military construction and camp construction at Fort Sam Houston, Camp Travis, and Paulex Ordnance Plant at Amarillo, Tex. The company also completed the Marshall Ford Dam as a joint venture with Brown & Root, Incorporated.

[2] "Organizational Set-Up of an 'Architect-Engineer,'" by Donald H. McCreery, *Civil Engineering*, October, 1943, p. 477.

[3] Memoir prepared by O. H. Koch, M. ASCE.

Mr. McKenzie was always very active in the civic affairs of his community. He served as president of the Rotary Club of San Antonio, Potentate of Alzafar Shrine, president of the San Antonio Chamber of Commerce, and president of the Texas Branch of Associated General Contractors of America.

On December 25, 1911, he was married to Eulah Smith of Webb City. He is survived by his widow; a son, Andrew Jackson, Jr.; two daughters, Christine and Mary Jane; and five grandchildren.

Mr. McKenzie was elected an Associate Member of the American Society of Civil Engineers on December 5, 1911, and a Member on October 15, 1923.

JOHN OWEN MILLER, M. ASCE[1]

DIED MARCH 7, 1952

John Owen Miller was born in Bakersfield, Calif., on August 19, 1886. He entered Stanford University at Stanford, Calif., in 1904, and was graduated in 1912 with the degree of Bachelor of Arts in Civil Engineering.

While attending Stanford University, he was employed as an engineer and superintendent of construction for railroad location, and on the construction of streets, water and sewer systems, and sea walls. In college he was an outstanding athlete in track and football and one of the greatest trackmen in the history of Stanford University.

After graduation, Mr. Miller worked on the American-Cosumnes section of John R. Freeman's "Water Supply Report for the City of San Francisco" and on the design of the distribution system of the South San Joaquin Irrigation District in California. The following four years, he was employed on reinforced concrete construction work for the City of Palo Alto, the County of Santa Clara, Stanford University, the South San Joaquin Irrigation District, and the Shell Oil Company—all of California. He also was employed on the construction of the Carriso Gorge Section of the San Diego and Arizona Eastern Railroad in San Diego County.

During War I, Mr. Miller served as First Sergeant in the 345th Machine Gun Battalion, 91st Division, and as Lieutenant, United States Army, Corps of Engineers, instructing at the Engineers' Officer Training Camp at Camp Humphrey, Virigina. After receiving his discharge, Mr. Miller worked for seven years as assistant engineer for the Department of Public Works in Norfolk, Va., where he was engaged in a variety of engineering projects.

From 1926 through 1932, he specialized in the field of sanitary engineering. For a time he worked as a sanitary engineer in the cities of Richmond and Woodland in California, and later entered private practice in Woodland.

His next employment, from 1933 to 1938, was as director for the Civil Works Administration in Yolo County and as engineer for the Works Progress Adminis-

---

[1] Memoir prepared by a committee of the Sacramento Section consisting of Gerald H. Jones, Percy H. Van Etten, and Asa G. Proctor, Members, ASCE.

tration in northern California. In April, 1938, he entered the service of the State of California as associate hydraulic engineer, Division of Water Resources. Mr. Miller served as engineer on numerous flood damage repair projects, and, in July, 1946, became senior hydraulic engineer on the development and maintenance of various features of the Sacramento River Flood Control Project. In August, 1950, he was advanced to the position of supervising hydraulic engineer on flood control, the position he held at the time of his death.

Mr. Miller was a member and past-commander of Yolo Post No. 77, American Legion, and a member of various masonic bodies in Virginia and California, including the orders of Knights Templar and the Mystic Shrine.

He took an active part in the affairs of the Sacramento Section, which he served as Program Committee Chairman in 1945 and First Vice-President in 1950.

He was married to Aleene Bradford Edwards. Mrs. Miller died on August 14, 1952. He is survived by two brothers, Thomas Miller and Harry Miller, and a sister, Mary Ashe Miller.

Mr. Miller was elected a Junior of the American Society of Civil Engineers on July 2, 1913; an Associate Member of January 14, 1918; and a Member on January 18, 1926.

FRANZ MARTIN MISCH, A.M. ASCE[1]

DIED DECEMBER 1, 1952

Franz Martin Misch, the son of Franz and Annie May (Christian) Misch, was born at Dos Palos, Calif., on December 3, 1907. After attending Dos Palos and Berkeley high schools, he entered the University of California, at Berkeley. He was graduated *cum laude* with the degree of Bachelor of Science in Civil Engineering in 1928.

Mr. Misch began his engineering career in 1928 with the American Toll Bridge Company. He was assistant engineer on the construction of the Carquinez Bridge, between Crockett and Vallejo, in California.

In April, 1929, he became associated with the Southern Pacific Company as junior engineer and inspector on the construction of the Martinez-Benicia Railroad Bridge across Carquinez Straits. He transferred, in 1933, to the Bridge and Building Department, and held positions in the system steel bridge gang until 1936 when he was appointed bridge and building inspector on the San Joaquin Division. Two years later, in February, 1938, he was promoted to assistant bridge and building supervisor of that division.

From February, 1939, to March, 1943, Mr. Misch was head inspector of bridge and tunnel construction on the new main line railroad being built around Shasta

[1] Memoir prepared by E. E. Mayo, M. ASCE.

Dam Reservoir between Redding and Delta, in California. This work comprised thirty miles of new railroad and involved very heavy construction, including eight high steel viaduct bridges and twelve tunnels.

On March 24, 1943, Mr. Misch was appointed general bridge and building supervisor of the Pacific Lines of the Southern Pacific Company. He held this position at the time of his death.

Mr. Misch, through his experience and individual effort, contributed greatly in the supervision of many large programs and emergency reconstruction projects of the Bridge and Building Department. Included among these was the reconstruction of tunnels damaged by the Tehachapi earthquake in July, 1952.

Mr. Misch was a member of Chi Epsilon and Tau Beta Pi, honorary engineering fraternities; the University of California Alumni Association; Scabbard and Blade; and the Pacific Railway Club. In addition, he was a past-director of the American Railway Bridge and Building Association.

On November 4, 1933, in Berkeley, Mr. Misch was married to Daisy L. Millican. He is survived by his widow; a son, Franz H. Misch; and two daughters, Sonya and Kathryn Misch.

Mr. Misch was elected a Junior of the American Society of Civil Engineers on November 12, 1928, and an Associate Member on October 9, 1940.

JOHN EARL MORELOCK, M. ASCE[1]

DIED DECEMBER 26, 1951

John Earl Morelock, the son of John H. and Ethel (Leonard) Morelock, was born on October 3, 1887, at Birchwood, Tenn. Mr. Morelock's engineering training consisted of two years' study at the University of Tennessee, at Knoxville, and a short term at the University of Washington, at Seattle, between 1906 and 1909. In 1920, he completed the course in civil engineering of the International Correspondence Schools.

Except for the following sequence of service—eight months as deputy county engineer for Snohomish County in Washington, in 1909; eight months as structural draftsman for the American Bridge Company at Gary, Ind., in 1914; and two years of military service as a Second Lieutenant, United States Army, from 1917 to 1919, on active duty in the United States and France—Mr. Morelock practiced his profession in Chattanooga, Tenn. In this practice he rose to a place of high prestige and responsibility and was regarded as a structural engineer of greatest competence.

Between 1909 and 1917, Mr. Morelock was chief draftsman for the Chattanooga Iron & Wire Works, draftsman for the Hamilton County Tennessee Road

[1] Memoir prepared by Lewis A. Schmidt, Jr., M. ASCE.

Commission, structural draftsman and structural engineer for the Converse Bridge and Steel Company, and inspector in the Chattanooga city engineer's office. Each of these assignments was in Chattanooga.

After his tour of duty with the U. S. Army, Mr. Morelock became chief engineer of the Converse Bridge and Steel Company in Chattanooga in 1919, a position which he held until 1937. In 1922 he also assumed the added duties of plant manager, and, in 1937, in addition to being plant manager, he was elected secretary of the company. Mr. Morelock became vice-president of the Converse Bridge and Steel Company in 1939 and held this office until his retirement in 1948.

Many structures built by Mr. Morelock are evidence of his outstanding specialized training and experience in the structural field. Among these are a very large acid chamber for the Tennessee Copper Company at Copperhill, Tenn.; the steel framework of the Chattanooga Municipal Auditorium; the Lenoir Car Works Shop at Lenoir City, Tenn.; the Gulf States Steel Company rolling mill at Anniston, Ala.; and numerous highway and railroad bridges and mill buildings throughout the Southeast.

He belonged to the Episcopal Church and was a member of the Free and Accepted Masons. After retirement he busied himself about his home at Hixson, Tenn., and, in 1951, moved to Parker, Fla.

On April 6, 1911, Mr. Morelock was married to Edith Miller. He is survived by his widow and his mother.

Mr. Morelock was elected an Associate Member of the American Society of Civil Engineers on June 11, 1917, and a Member on October 15, 1923.

CHARLES FREDERICK PARKER, M. ASCE[1]

Died May 22, 1952

Charles Frederick Parker, the son of Jared and Mary (Cruttenden) Parker, was born in Meridan, Conn., on November 15, 1874. He received his engineering education at the Sheffield Scientific School of Yale University, at New Haven, Conn., and was graduated in 1898 with the degree of Bachelor of Arts.

After graduation, Mr. Parker went to Mexico and spent thirteen years on railway location and construction work, as a mining engineer and superintendent, and as a railroad contractor.

In 1912 he moved to San Antonio, Tex., where he established an engineering office and then entered the building materials business, in which he was to continue for the remainder of his active life, specializing in contractors' and builders' specialties and equipment. He also did considerable contracting in the comparatively new field of concrete construction. For many years he was recognized in San Antonio as the leading specialist on waterproofing of basements.

[1] Memoir prepared by Terrell Bartlett, M. ASCE.

Mr. Parker was a leader in the affairs of the local Builders Exchange and at the time of his death was the sole honorary member of that organization. Despite a progressively serious physical condition he maintained an active participation in business, professional, and soceal activities.

He was married to Helen Sill Woodrow.

Mr. Parker was elected a Junior of the American Society of Civil Engineers on June 5, 1900; an Associate Member on September 2, 1903; and a Member on April 2, 1912. He became a Life Member in January, 1938.

WILLIAM ALLEN POE, A. M. ASCE[1]

Died September 25, 1952

William Allen Poe, the son of William P. and Mary (Ritchie) Poe, was born at Belle, Mo., on August 29, 1883. He was educated in the public schools of Belle. He had no formal engineering education, but he studied engineering under M. M. Hollenbeck, at Springfield, Mo., while working as draftsman and instrumentman. Through self-help and conscientious effort he became a competent design and construction engineer.

From 1906 to 1908 Mr. Poe was resident engineer for the Chicago, Milwaukee and St. Paul Railway. In 1911, he became manager of the McMillan Construction Company, doing general construction work, which included an important concrete viaduct in Kansas City, Mo.

From 1919 to 1921 he was with the List Construction Company on highway work in Kansas.

From 1921 to 1927 he was general manager of a narrow gage railway which served five strip coal mining operations near Branch, Ark. For the next two years he was field engineer and assistant district engineer for District No. 8 of the Arkansas State Highway Department. After his transfer to the Bridge Division of the Arkansas State Highway Department in 1929, Mr. Poe became assistant bridge engineer in charge of location and surveys and in general charge of construction. He continued his association with the Bridge Division until 1950, at which time, in a rearrangement of the Bridge Department, he became assistant construction engineer. He held this position at the time of his death.

On November 1, 1908, Mr. Poe was married to Nettie Lou Anderson, in Kansas City. He is survived by his widow; a daughter, Mrs. Jack C. Hammett; and one grandson.

Mr. Poe was elected an Associate Member of the American Society of Civil Engineers on November 10, 1930.

[1] Memoir prepared by Neal B. Garver, M. ASCE.

FREMONT EMERSON ROPER, M. ASCE[1]

DIED MAY 2, 1952

Fremont Emerson Roper, the son of the Rev. C. Fremont and Bertha (Robertson) Roper, was born in West Concord, N. H., on October 9, 1889. After being graduated from high school he attended Brown University, at Providence, R. I., and was awarded the degree of Bachelor of Science in Civil Engineering in June, 1911.

From September, 1911, until June, 1912, Mr. Roper was a transitman in the coal and copper mines of Utah and Nevada. In July, 1912, he was employed by the Standard Oil Company of California as a field engineer in the Portland (Ore.) sales district and by 1915 rose to the position of division superintendent of construction in Seattle, Wash.

In 1917, he enlisted in the United States Army at Vancouver Barracks, Washington Training Camp, where he was commissioned First Lieutenant, Corps of Engineers, in December. He went overseas with Company C, 319th Regiment Engineers, 8th Division, American Expeditionary Forces, and in May, 1919, became Captain of D Company. On his return to the United States, in September, 1919, he was honorably discharged.

In November, 1919, when Mr. Roper returned to the Standard Oil Company of California, he was appointed superintendent of construction and in 1924 he became assistant manager of all marketing construction and maintenance work within the company. In 1928, the Construction and Maintenance Department was formed with Mr. Roper as manager. The Engineering Division of the Marketing Department was reorganized in 1944 and he was designated assistant chief engineer, the position he held at his death.

Mr. Roper's responsibilities included the supervision of the preparation of plans for the construction of all the retail and wholesale marketing outlets of the company. Probably the most significant activity under his supervision was the development of the "service station" from the crude early design to the streamlined functional design of the present.

For many years he was secretary-treasurer of the Brown Alumni Club of Alta California, and he also took an active part in the affairs of the 319th Engineers Veterans Association. He belonged to the First Congregational Church of Berkeley, Calif., and was most active in church affairs and with the Boy Scouts of America as well.

In September, 1930, Mr. Roper was married to Myrtis Eddy. He is survived by his widow; a daughter, Ann Louise; a son, John Charles; his mother, Mrs. C. Fremont Roper; a sister, Mrs. J. E. Capps; and a brother, F. R. Roper.

[1] Memoir prepared by J. Marshall Evans, M. ASCE, and Paul L. Fahrney, A.M. ASCE.

He was licensed professional engineer in the states of California, Oregon, Washington, New Mexico, and Utah, and was a member of the San Francisco Post of The Society of American Military Engineers, the Engineers Club of San Francisco, and the Commonwealth Club of California.

Mr. Roper was elected an Associate Member of the American Society of Civil Engineers on June 1, 1925, and a Member on October 8, 1951.

PHILIP TUSTIN SAMUEL, AFFILIATE, ASCE[1]

DIED DECEMBER 26, 1952

Philip Tustin Samuel, the son of William B. and Mary (Tustin) Samuel, was born on October 13, 1883, in Knoxville, Tenn. He attended the University of Tennessee at Knoxville from 1898 to 1901.

His first positions were as draftsman, clerk, and salesman, successively, in Knoxville, and Nashville, Tenn. Mr. Samuel spent thirty years with the Corps of Engineers, United States Army, beginning in 1918. During World War II, from 1942 to 1943, he had the rank of Lieutenant-Colonel and was in charge of the Marine Division of the Corps at Philadelphia, Pa.

Later, Mr. Samuel supervised the Defense Plant Corporation tug and barge program, and he also directed the training of military crews for the port repair of ships. He directed the design and construction of four sea-going hopper dredges.

At the time of his death, Mr. Samuel was procurement director for the Maxon Construction Company, Incorporated, of Dayton, Ohio. He was engaged in building additions to the Atomic Energy Commission plant at Oak Ridge, Tenn.

In addition to the Society, Mr. Samuel was a member of the American Society of Military Engineers, the Society of Naval Architects and Marine Engineers, and the American Section of the Permanent International Navigation Congress. He belonged to the American Legion and was active in its affairs, and he held membership in the Military Order of the World Wars.

Mr. Samuel had been married to Lieze Marshall Sharp, who died in June, 1927, in Florence, Ala. On January 14, 1929, in Florence, he was married to Mary Porter. He is survived by his widow; one sister, Mrs. Emily S. Gehry; and two brothers, David B. Samuel and Joseph B. Samuel.

Mr. Samuel was elected an Affiliate of the American Society of Civil Engineers on December 14, 1925.

---

[1] Memoir prepared by Joseph P. Laws and Robert H. Nagel, Associate Members, ASCE.

ROYAL UPSON ST. JOHN, A.M. ASCE[1]

DIED JULY 31, 1952

Royal Upson St. John, the son of Benjamin and Louise (Upson) St. John, was born in Des Moines, Iowa, on September 10, 1889. In 1904 the family moved to California, where he was educated, receiving the degree of Bachelor of Arts in Civil Engineering in 1911 from Stanford University, at Stanford, Calif.

While still in college, he served as an instrumentman and as an inspector on street paving and sewer construction in Benicia, Calif. For three years after graduation he was engaged on bridge construction for Solano County (California) and topographic surveying for Solano Irrigated Farms, Incorporated, and for the Waterford Irrigation District.

In 1914 Mr. St. John began his career with the Standard Oil Company of California, designing and superintending construction of oil storage and distributing stations on the Pacific Coast. He enlisted in the United States Air Service as a Second Lieutenant in 1917, and for eighteen months he served in France as a combat pilot, advancing to First Lieutenant and receiving a citation.

Returning to California, and to the Standard Oil Company, Mr. St. John became district engineer and settled in Sacramento. Always interested in aviation, he was instrumental in selecting the site of Sacramento Airport and he designed the original field. This work led to his being appointed designer and construction supervisor of the San Francisco Bay Airdrome, in Alameda, Calif. He was its first and only manager.

Following the entry of the United States into World War II the government assumed control of the Bay Airdrome, and for a time Mr. St. John was in charge of the Civil Air Patrol. In June, 1942, he entered the Army Air Force, this time as a Major, and saw active service with the 12th Bomber Command and later with the 15th U. S. Air Force in England, North Africa, and Italy. Returning to the United States, to Chanute Field, in Illinois, he was retired as a Colonel, and was awarded the Bronze Star.

Mr. St. John returned to Contra Costa County, California, and from 1947 until his death was associated with the county engineer.

While living in Alameda, Mr. St. John was a member of the Rotary Club, from 1930 to 1941; president of the San Francisco Bay Chapter, National Aeronautical Association, in 1934; and president of the Alameda Chamber of Commerce, in 1936.

Mr. St. John was active in Society affairs. He was a charter member of the Sacramento Section and Vice-President of the section in 1926 and 1927.

On September 15, 1920, Mr. St. John was married to Gail Casad. He is survived by his widow.

Mr. St. John was elected a Junior of the American Society of Civil Engineers on July 9, 1912, and an Associate Member on June 1, 1920.

[1] Memoir prepared by Norwood Silsbee, A.M. ASCE, and Frederick E. Eastman, Affiliate, ASCE.

WILLIAM HATFIELD SEARS, M. ASCE[1]

Died April 20, 1951

William Hatfield Sears, was born on March 8, 1874, at Fabius, N. Y. He attended Colgate Academy at Hamilton, N. Y., and, in 1904, was graduated from the College of Architecture of Columbia University, at New York, N. Y.

In 1906, Mr. Sears joined the R. H. Hunt Company, an architectural firm in Chattanooga, Tenn., and, in 1908, had established a private practice there with the firm of Huntington and Sears. He began an individual practice in 1913, and, in 1920, Percy B. Shepherd joined him as an associate. In 1937, the firm became known as Sears & Shepherd and remained so until the death of Mr. Sears.

Among the local works of architecture for which Mr. Sears will be remembered are Science Hall and the dining room of the University of Chattanooga, T. C. Thompson Children's Hospital, Erlanger Hospital, Elbert Long School, Chambliss Detention Home, American Lava Corporation, East Lake Courts Housing Project, a number of other schools, and an uncounted number of fine residences. Away from Chattanooga, the First Baptist Church of Oklahoma City, Okla., was designed by Mr. Sears, and, during World War II, he served the Holston Ordnance Works at Kingsport, Tenn., in an achitectural capacity.

With the establishment of the Tennessee State Board of Architectural and Engineering Examiners in 1920, Mr. Sears was appointed as one of the three architect members of this board and he served in this position continuously until his resignation in 1948. His twenty-seven years of voluntary service in that post were stated to have been equaled by only one other architect in the nation. As if this service were not sufficient, Mr. Sears also served for twenty-two years on the National Council of State Boards of Architectural and Engineering Examiners.

Mr. Sears, with two other prominent Chattanoogans, founded and helped finance, often from his own resources, the Chattanooga Council of the Boy Scouts of America in 1910, the year scouting came to the United States. For thirty-five years, this organization enjoyed Mr. Sears' sponsorship, and for his service, he was presented with scouting's highest honor, the Silver Beaver Award.

He was a member of the First Baptist Church of Chattanooga and served on the board of deacons for a number of years. He was also a director of the Young Men's Christian Association, and for many years was active in the construction, maintenance, and operation of the T. C. Thompson Children's Hospital of Chattanooga. Also, he was a prominent member of the Civitan Club of Chattanooga.

The Chattanooga Engineers Club was founded in 1924 and listed Mr. Sears among its charter members. In 1935, he was president of this organization. He was also a member of the American Institute of Architects.

In 1903, Mr. Sears was married to Florence Burgwin. Two sons, Howard and Robert, survive.

[1] Memoir prepared by Lewis A. Schmidt, Jr., M. ASCE.

Mr. Sears was elected an Associate Member of the American Society of Civil Engineers on April 18, 1916, and a Member on March 11, 1919. He became a Life Member in January, 1946.

GEORGE DAVID SHANNAHAN, A. M. ASCE[1]

Died August 19, 1952

George David Shannahan, the son of Maurice and Ovanda (Sutherlin) Shannahan, was born at Ritchey, Mo., on May 16, 1908. He was graduated from the University of Southern California, in Los Angeles, in June, 1932, with the degree of Bachelor of Science in Civil Engineering.

After being graduated from the university, Mr. Shannahan joined the firm which later became Shannahan, Incorporated. His entire professional life was centered in the activities of this firm. For many years he was chief engineer in charge of heavy construction throughout Southern California and Arizona. The company specialized in railroad construction and maintenance; pile driving, dredging, pier construction, and other harbor work; rock quarrying; and bridge work. During World War II, the firm was actively engaged in various important defense projects in California and Arizona.

Mr. Shannahan was a registered professional engineer in both California and Arizona. He was past-president of the Engineering Alumni Association of the University of Southern California, and also of Alpha Alumni of Sigma Phi Delta, international engineering fraternity. He was active in civic and church organizations and was a member of the Free and Accepted Masons.

On October 21, 1933, Mr. Shannahan was married to Erline Pearl Duncan. He is survived by his widow and a daughter, Erline Carolyn Mae.

Mr. Shannahan was elected a Junior of the American Society of Civil Engineers on November 28, 1932, and an Associate Member on September 8, 1941.

JOSIAH ROSCOE SHARP, A.M. ASCE[2]

Died November 14, 1950

Josiah Roscoe Sharp, the son of Josiah B. and Rebecca (Ward) Sharp, was born in Vineland, N. J., on April 21, 1891. He received his early education in Vineland and Ocean City, N. J., being graduated from the Ocean City high school. Later he attended Drexel Institute in Philadelphia, Pa.

From 1908 to 1917, Mr. Sharp worked as an architectural draftsman and specifications writer with Otis M. Townsend, an architect of Ocean City. From 1917 to 1919, he was with the Pennsylvania Railroad Company in Philadelphia

[1] Memoir prepared by David M. Wilson, M. ASCE.
[2] Memoir prepared by Clifton W. Bolleau, A.M. ASCE.

as an architectural designer and inspector of contract work in the maintenance-of-way department. Mr. Sharp then worked for the Stone and Webster Corporation in Baltimore, Md., as general foreman and inspector, from 1920 to 1922. Following this employment, he was office and erecting engineer with the United Gas and Electric Company and the United Engineers and Contractors. Mr. Sharp entered the employ of the Tennessee Valley Authority in April, 1935, and was assigned as field mechanical engineer on the construction of Wheeler Dam in Alabama. After two years in the field he was transferred to the mechanical design branch in Knoxville, Tenn., where his major responsibility was the preparation of specifications and the procurement of mechanical equipment and piping.

One of Mr. Sharp's hobbies was music. He was a charter member of the Knoxville Male Chorus and for twelve years was one of its most faithful and enthusiastic members.

In addition to the Society, Mr. Sharp held membership in the Society of American Military Engineers.

In 1944, Mr. Sharp was married to Mrs. Golda (Susong) Forgey. He is survived by his widow and two sisters, Myrtle Sharp and Mrs. James N. Weber.

Mr. Sharp was elected an Associate Member of the American Society of Civil Engineers on November 12, 1928.

JOSEPH WAGONER SHEPPARD, J.M. ASCE[1]

Died March 1, 1951

Joseph Wagoner Sheppard was born at Louisville, Ky., on March 22, 1919. He received his elementary and high school education in Louisville, and, in 1937, entered the Speed Scientific School, University of Louisville, as a cooperative student.

While in college he worked alternately with the Mammoth Cave National Park, the Kosmos Portland Cement Company, the Independent Oil Producers of Kentucky, and the Louisville District, United States Engineer Department. After graduation, in May, 1940, Mr. Sheppard began his full-time engineering career with the Louisville Cement Corporation.

In January, 1942, he left his native Louisville to join the engineering staff of the Tennessee Valley Authority as a junior structural engineer.

During World War II he entered military service as an electronic technician's mate with the United States Naval Reserve and spent considerable time in Panama in the defense of the canal.

In March, 1946, Mr. Sheppard returned to the staff of the Tennessee Valley Authority. He was employed by this organization at the time of his death.

He was very active in civic matters and played an important role in the affairs of the Town of Norris, Tenn., when the town was incorporated and released from

[1] Memoir prepared by F. E. Bosland, A.M. ASCE.

government ownership. His work in the civic and religious affairs of this community stand as a monument to his memory.

He was married to Helyn Hudson. Surviving are his widow; a son, William; and a daughter, Susan.

Mr. Sheppard was elected a Junior of the American Society of Civil Engineers on October 9, 1940.

JOHN DOLSON SLYE, M. ASCE[1]

DIED JANUARY 15, 1953

John Dolson Slye, the son of Luman and Elizabeth (Williamson) Slye, was born in Independence, Iowa, on March 27, 1886. When he was a young boy his family moved from Iowa to Boulder, Colo. He attended school at Boulder and was graduated from the University of Colorado College of Engineering, at Boulder, in 1914 with a Bachelor of Science degree.

His first employment after graduation was with several railroad evaluation projects in Nebraska and other states for the Interstate Commerce Commission. With the advent of World War I, he was commissioned a First Lieutenant and was stationed at Camp Humphries, in Virginia. After World War I he accepted a commission in the Engineer Section, Officers' Reserve Corps.

In April, 1919, Mr. Slye was employed by the Bureau of Public Roads (then in the United States Department of Agriculture) as transitman on the Monarch Pass forest highway construction project, in Colorado. The following year he was promoted to chief of a road survey party on the Crested Butte-Somerset forest highway project in Colorado. Following that assignment, he was engaged in supervising construction on the Durango-Silverton forest highway project in Colorado; the Dayton-Kane forest highway project in Wyoming; and several other forest highway projects.

Mr. Slye received and accepted a fellowship in highway engineering and received his master's degree in Highway Engineering at the University of Michigan, at Ann Arbor, in June, 1923. On his return to duty with the Bureau of Public Roads, he was promoted to the position of associate highway engineer. He was assigned to federal-aid work and was active principally in Wyoming, making federal-aid highway inspections from 1924 to 1926. From July, 1926, to the end of 1933, he was in charge of field work in Wyoming, as a representative of the Bureau of Public Roads.

On January 1, 1934, he was placed in charge of the branch office of the Bureau of Public Roads in Santa Fe, N. Mex., where he handled all federal-aid work in the state and represented the bureau in all local contacts. On January 1, 1935, he was promoted to highway engineer in charge of federal and national park highway work, with headquarters in Santa Fe. Later, forest highway

[1] Memoir prepared by Albert C. Spann, M. ASCE.

construction and development of roads on Indian lands were added to his responsibilities.

Mr. Slye's acumen and general engineering ability won him the position of district engineer for Wyoming when the Bureau of Public Roads established that office in August, 1945. He served in this capacity until his retirement in August, 1952, when he moved to Mesa, Ariz.

He was also a member of the American Planning and Civic Association, the First Presbyterian Church of Cheyenne, Wyo., and the Masonic Lodge. In 1951, he served as President of the Wyoming Section of the Society.

On December 18, 1920, Mr. Slye was married to Ursula Patton, of Boulder. He is survived by his widow and two sons, John Marshall and Edwin Bartlett.

Mr. Slye was elected a Member of the American Society of Civil Engineers on December 25, 1944.

JOHN GODFREY SPIELMAN, M. ASCE[1]

DIED JANUARY 3, 1951

John Godfrey Spielman, the son of John A. and Christina (Hershberger) Spielman, was born at Germanville, Iowa, on January 2, 1863. His father, a Captain in the Union Army, established his home in the near-by town of Fairfield, Iowa, on returning from the Civil War.

After completing his elementary education at Fairfield, Mr. Spielman attended Carthage College in Illinois for a year and then, the State University of Iowa, at Iowa City, for three years, from 1883 to 1886. He left college before graduation to begin his career on railroad location in western Kansas. Starting as a draftsman, he progressed in one year through the positions of instrumentman and bridge engineer to that of division engineer on location of the Chicago, Kansas and Nebraska Railway (Rock Island) in Kansas and Colorado.

In 1888 he was chief engineer on irrigation projects for C. J. (Buffalo) Jones in western Kansas, and in 1889 returned to Fairfield as city engineer. The following year he went east to work for the Union Bridge Company of New York (N. Y.) and Pittsburgh (Pa.) and later became associated with the Pittsburgh Bridge Company, holding, successively, the positions of chief draftsman, chief engineer, and general manager. In 1902, he was transferred to Chicago (Ill.) by the United States Steel Corporation as chief draftsman for the Illinois Steel Company at the North Works. His work there included the preparation of plans for the initial plant constructed by the Steel Corporation at Gary, Ind. (which ranks as one of the leading steel mills in the United States), as well as for those constructed at South Chicago, Ill., and for the cement mills of the Universal Portland Cement Company of Buffington, Ind.

In 1911, Mr. Spielman was loaned by the Steel Corporation to the Chicago Harbor and Subway Commission as chief office engineer. It was under his supervision that plans and specifications for the North Shore Recreation Pier

[1] Memoir prepared by John V. Spielman, A.M. ASCE, and Charles T. Leeds, M. ASCE.

(4,000 ft by 300 ft) at an estimated $4,000,000 were prepared. He also directed the physical valuation of Chicago's four elevated railways (total valuation $63,000,000). In 1912, the State University of Iowa conferred upon him the Honorary Degree of Civil Engineer.

Because of poor health, in 1913, he moved his family to Long Beach, Calif., where he was engaged in commercial and maunfacturing interests until 1922. He became quite active in community affairs, being a member of the Chamber of Commerce, and was elected president of the Long Beach Businessmen's Association.

Returning to professional engineering, from 1922 to 1927, Mr. Spielman did consulting work, particularly on property appraisals, and, in 1927, was appointed city assessor of Long Beach, partly for the purpose of making a uniform reappraisal of the entire city.

After his retirement in 1932, Mr. Spielman continued to take an extremely active part in community affairs. He was for many years an active member of the Iowa Association of Southern California. Until the time of his death, he was active in the Sons of Union Veterans of the Civil War and served as Commander, Department of California and the Pacific. He was officially named "Chief Engineer" of the G.A.R. Highway, which is U.S. Route 6, from Cape Cod, Massachusetts, to Long Beach (Calif.).

Mr. Spielman was president of the University Club of Long Beach in 1941, and, in 1950, was made the first honorary member of the club. He was a member of the Delta Tau Delta fraternity.

In 1892, at Fairfield, he was married to Kathryn Aletha Voorhies. Mrs. Spielman died in 1936. He is survived by a daughter, Dorothea, and a son, John.

Mr. Spielman was elected a Junior of the American Society of Civil Engineers on March 4, 1891; an Associate Member on May 1, 1895; and a Member on October 14, 1930. He became a Life Member in January, 1930.

JOHN EDWARD STIRLING THORPE, A.M. ASCE[1]

Died February 24, 1950

John Edward Stirling Thorpe, the son of John and Elizabeth (Stirling) Thorpe, was born in Cheshire, England, on January 29, 1885. When he was about six years of age his family moved to America. He attended the public schools in Baltimore, Md., and received his engineering degree from Johns Hopkins University, also in that city. In addition, he was awarded a certificate in business law from Columbia University in New York, N.Y.

After completing his education, Mr. Thorpe did construction and operational work for hydroelectric companies in Puerto Rico for several years, and he spent three years in the same type of work in Mexico. He first went to North Carolina

[1] Memoir prepared by Thomas G. Johnson, A.M. ASCE.

in 1915 where he was responsible for the construction of the Aluminum Company of America's plant at Badin. In 1922, he moved to Niagara Falls, N. Y., and was head of the power plant there until 1924 when he became vice-president of the C. P. Hawley Engineering Company in Washington, D. C.

In 1926 and 1927, Mr. Thorpe did research work in Russia for the Aluminum Company. The following year, he was in charge of the construction of the company's new plant in Calderwood, Tenn., and he remained there until he was named president of the Nantahala Power Company in July, 1929. At that time he moved to Franklin, N. C., where he maintained headquarters until 1937.

On July 14, 1951, a large power development was dedicated at Tuckasegee, N. C., to the memory of Mr. Thorpe. The ten-year-old Glenville Development of the Nantahala Power and Light Company was renamed the Thorpe Development.

In the past, Mr. Thorpe was president of the Southeastern Electrical Exchange, a member of the Board of Directors of the Aluminum Company plant at Badin, and, at the time of his death, chairman of the North Carolina State Board of Registration for Engineers and Land Surveyors. He was a former vice-president of the Tennessee Valley Section of the Society and was a member of the American Institute of Electrical Engineers. His clubs were the Biltmore Forest Country Club in Asheville, N. C.; the Cosmos and Metropolitan clubs in Washington, D. C.; the Duquesne Club in Pittsburgh, Pa.; and the Niagara Club of Niagara Falls. He was a member of the Masonic Lodge in Badin and of the St. Agnes Episcopal Church in Franklin.

On January 11, 1911, he was married to Olivia Brown. In addition to his widow, the survivors include one son, Foster, and two sisters, the Misses May and Nora Thorpe.

Mr. Thorpe was elected an Associate Member of the American Society of Civil Engineers on May 31, 1916.

EUGENE TRUE THURSTON, JR., M. ASCE[1]

DIED MAY 3, 1952

Eugene True Thurston, Jr., the son of Eugene True and Anna Zarissa (Morse) Thurston, was born in Oakland, Calif., on April 24, 1873. After being graduated from Oakland High School, he attended the University of California, at Berkeley, and was awarded the degree of Bachelor of Science in Civil Engineering in 1895.

After graduation, he worked with a survey crew in the San Joaquin Valley (California) for the San Francisco and San Joaquin Valley Railroad, which afterward became the Los Angeles-San Francisco branch of the Sante Fe Railroad. Mr. Thurston advanced to the position of estimator in the chief engineer's office in San Francisco, Calif., and then was put in charge of the construction of the Sante Fe Terminal, in San Francisco. He worked successively in the office of

[1] Memoir prepared by Walter N. Frickstad, M. ASCE, and Earl M. Buckingham, A. M. ASCE.

J. D. Galloway, M. ASCE; for three years as assistant to the chief engineer of the Southern Pacific Railroad; assistant engineer for a contracting firm; and as chief engineer for another firm.

In 1906, he became assistant chief engineer of the Syndicate Water Company, which then planned to absorb and expand the water supply system of the eastern side of San Francisco Bay. In 1907 he formed a partnership with Maurice C. Couchot, M. ASCE, as engineers and contractors. Mr. Thurston was in business for himself, from 1910 to 1917, as a general contractor.

During World War I, he was a Captain in the Corps of Engineers, United States Army. From 1919 to 1924, he was consulting engineer on building and construction operations and also secretary-manager of the General Contractors Association of San Francisco; from 1924 to 1936, he acted as consulting engineer on public and private buildings and as resident representative of foreign contractors in San Francisco. Thereafter, until the time of his retirement in 1943, he was superintendent of buildings for the City of Oakland.

Mr. Thurston was active in the civic affairs of Oakland. From 1905 to 1907 he served on the city council; he was secretary of the San Francisco Section of the American Society of Civil Engineers from 1908 to 1917, and thereafter, member or chairman of numerous committees of the Society; he was a member of the Engineers Club of San Francisco, the Sons of the American Revolution, the Oakland Masonic Bodies, and the Sierra Club; he devoted the most time to the Commonwealth Club of California. Mr. Thurston became secretary of this club in 1923, then vice-president, and in 1927–1928 president. For twenty-nine years he was a member of its board of governors.

On October 15, 1922, he was married to Mary Ella Robinson, in Fresno, Calif. He is survived by his widow and a daughter, Emily Anne.

Mr. Thurston was elected an Associate Member of the American Society of Civil Engineers on March 6, 1907, and a Member on February 28, 1911. He became a Life Member in 1942.

GEORGE NEVILLE WHEAT, M. ASCE[1]

DIED JUNE 22, 1952

George Neville Wheat, the son of Ira L. and Nancy (Carothers) Wheat, was born in Atascosa County near San Antonio, Tex., on April 14, 1878. He attended the Agricultural and Mechanical College of Texas, at College Station, from which he was graduated in 1897 with the degree of Bachelor of Science in Civil Engineering. He also studied architectural engineering for two years at the Massachusetts Institute of Technology, in Boston, Mass.

Mr. Wheat was employed successively by the Gulf, Colorado, Sante Fe Railway and the International and Great Northern Railroad in Texas on location and construction work. Following his years in Boston he was engaged in struc-

[1] Memoir prepared by Terrell Bartlett, M. ASCE.

tural design work in Pittsburgh, Pa., Martins Ferry, Ohio, and Detroit, Mich., from 1903 to January, 1908. He returned to the Agricultural and Mechanical College of Texas to design its reinforced concrete buildings. During the period from 1908 to 1917 he designed buildings and bridges, in Houston and San Antonio (both in Texas), and architectural flat slab buildings and steel and reinforced concrete structures for the Kansas Terminal Railway.

In 1917, Mr. Wheat became a Captain of Engineers with the American Expeditionary Forces in France. On his return to civilian life in 1919 his career led him from the position as designer of highways in Edwards County, Texas, to checker and estimator on bridges and buildings in the vicinity of Chicago, Ill., where he remained as structural designer for various railways and architects until 1931. During the 1930's he was engaged with the United States Forest Service on soil erosion control work, and in the latter part of the year, 1935, he accepted a position with the Veterans Bureau in Washington, D. C., designing hospitals and their appurtenances until his retirement in 1948.

In 1910, Mr. Wheat was married to Maud Mihills, in Houston. He is survived by his widow; three daughters, Mrs. James H. Hale, Mrs. Harry E. Houston, and Mrs. Victor E. Ferlazzo; and nine grandchildren.

Mr. Wheat was elected an Associate Member of the American Society of Civil Engineers on January 4, 1910, and a Member on September 12, 1921. He became a Life Member in January, 1945.

ROBERT LEWIS WING, A.M. ASCE[1]

DIED APRIL 30, 1952

Robert Lewis Wing was born on September 10, 1896, at Palo Alto, Calif. He was the son of the late Charles B. Wing, professor emeritus of civil engineering at Stanford University, at Stanford, Calif., a pioneer professor at the university. His brother was the late Sumner P. Wing, a civil engineer, with the United State Bureau of Reclamation for twenty-one years and recently in charge of the foreign activity programs of the bureau.

Mr. Wing was graduated with a degree in civil engineering from Stanford University in 1921, and was a charter member and president of the first Student Chapter of the American Society of Civil Engineers, which was established at Stanford University.

After graduation, Mr. Wing served as engineer for Santa Clara County, in California. From 1922 to 1924, he was an assistant engineer for the Southern Pacific Railroad Company on the construction of the second track over the Sierra Nevada. His next position, from 1924 to 1927, was as assistant hydraulic engineer for the California State Division of Engineering and Irrigation on water resources investigations, with special work on the flood studies of California

[1] Memoir prepared by a Committee of the Sacramento Section consisting of Theodore Neuman, *Chairman*, C. B. Meyer, and William L. Berry, Associate Members, ASCE.

streams. The following year he served as assistant engineer for the Orange County Flood Control District on the formulation of a flood control plan for that county.

From 1929 until his death, he served with the California State Division of Water Resources, advancing from associate hydraulic engineer to supervising hydraulic engineer. During most of that period he had an active part in the investigations of the water resources of California, and, recently, in the preparation of the California Water Plan. He made hydrographic studies for spillway capacities of most of the constructed dams in the state. For several years, he was the state's representative on work involving the mapping of California. He was one of the veterans in the formulation of the State Water Plan for California which led to the construction of the Central Valley Project. Mr. Wing was a civil engineer of great professional ability.

During World War I, he saw service in France with the 23rd Engineers. He was a member and a director of the American Congress on Surveying and Mapping; a past-president of the Northern California Section of the American Society of Photogrammetry; a past-president of the Sacramento Chapter of the California Society of Professional Engineers; and was state director from the Sacramento Chapter. He belonged to the Chi Psi Fraternity and was a member of the University Club of Sacramento (Calif.).

On April 17, 1927, in Oroville, Calif., he was married to Dorothy Steadman. He is survived by his mother; his widow; two children, David and Teresa; two brothers, Winchester and Carl; a step-brother, Ashley Browne; and a step-sister, Mrs. Robert Wenzel.

Mr. Wing was elected an Associate Member of the American Society of Civil Engineers on October 1, 1926.

WALTER FERRELL WINTON, AFFILIATE, ASCE[1]

DIED MAY 12, 1952

Walter Ferrell Winton, the son of George and Jessie (McClair) Winton, was born in Santa Rosa, Calif., on October 11, 1886. He was educated in Mexico and the United States, and, in 1907, was graduated from Vanderbilt University, in Nashville, Tenn., with the degree of Bachelor of Arts in Civil Engineering.

Mr. Winton was resident engineer in the Durango sector for Ferrocarriles Nacionales de Mexico until late in 1911, when he joined the United States Army as a Second Lieutenant in the Cavalry. He was active in the Philippine Pacification, the Pershing Expedition into Mexico, and World War I.

Following World War I, he was military attaché to Peru and Bolivia and was awarded the Peruvian government's highest order, Knight Commander of the

---

[1] Memoir prepared by Donald S. Tedford and William F. Turney, M. ASCE.

Order of the Sun. Just before the outbreak of World War II, he was stationed at Fort Bliss, in Texas, in command of the 82nd Field Artillery Regiment of the First Cavalry Division. Later he was transferred to Fort Collins, in Colorado, as professor of military science and tactics and commander of the Army Specialist Training Program at Colorado A & M College, at Fort Collins.

In 1945, Colonel Winton retired from the army after thirty-four years of service. He held the degree of Master of Arts from the University of Toulouse (Toulouse, France) and belonged to the Phi Kappa Sigma Fraternity, the American Society for the Advancement of Science, and the National Geographic Society. Colonel Winton was also a member of the Free and Accepted Masons.

In 1884 he was married to Maria Calhoun in Nashville. He is survived by his widow; two sons, Lt.-Col. Walter F. Winton, Jr., U.S.A., and Tyler C. Winton, U. S. Border Patrol; two brothers, Will M. Winton and Col. George P. Winton, U.S.A. (retired); a sister, Dorothy Winton; and five grandchildren.

Colonel Winton was elected a Junior of the American Society of Civil Engineers on October 31, 1911, and an Affiliate on January 14, 1918.

CLEMENT TEHLE WISKOCIL, M. ASCE[1]

DIED OCTOBER 21, 1952

Clement Tehle Wiskocil, the son of Augustine Vincent and Elizabeth (Tehle) Wiskocil, was born in Milwaukee, Wis., on August 24, 1889. His early education was received in the public schools of Milwaukee. He was awarded the degree of Bachelor of Science in 1912 and the degree of Civil Engineering in 1913 from the University of Wisconsin, at Madison, where he then served as a research assistant until 1914. He was active in athletics and received letters in track and crew.

Mr. Wisckocil joined the Department of Civil Engineering of the University of California, at Berkeley, in 1914, and became widely known as an outstanding teacher of structural engineering and engineering ethics. He was co-author of the book,[2] "Testing and Inspection of Engineering Materials," and for some years was the head of the Civil Engineering Materials and Testing Laboratory. He served the university for thirty-eight years, and during these many years he retained a sympathetic and understanding interest in students and gave unstintingly of his time and energy to their problems and their activities. He was revered by students for his teaching and wise counseling.

For many years Professor Wiskocil was faculty advisor to student organizations—among them Chi Epsilon, Tau Beta Pi, and the Student Chapter of the Society. In January, 1952, the Student Chapter of the Society honored him for the contributions he had made to the chapter during the twenty-five years he was the faculty advisor.

---

[1] Memoir prepared by Raymond E. Davis and Morrough P. O'Brien, Members, ASCE.

[2] "Testing and Inspection of Engineering Materials," by H. E. Davis, G. E. Troxell, and C. T. Wiskocil, McGraw-Hill Book Co., Inc., New York, N. Y., 1941.

In his teaching and in his counseling he particularly stressed ethics and the relationships and duty of the engineer in practice to the public, civic bodies, and others in the profession. For seven years students who had been taught, counseled, and guided directly by Professor Wiskocil won the national Daniel W. Mead Prize awarded annually for the best student paper on a subject in the field of engineering ethics.

Professor Wiskocil was a leader in the engineering profession and in educational activities. He was President of the San Francisco Section of the Society in 1951, president of the Structural Engineers Association of California, and of the Structural Engineers of Northern California in 1941, and from 1941 to 1945 he was chairman of the Pacific Southwest Section of the American Society for Engineering Education. In addition, he was active in the American Society of Testing Materials and the American Concrete Institute.

In 1914, Professor Wiskocil was married to Olga E. Reiner. He is survived by his widow; a daughter, Patricia (Mrs. H. Gregg Hodes); a son, John Clement; and four grandchildren.

Professor Wiskocil was elected a Member of the American Society of Civil Engineers on November 18, 1935.

WILLIAM CLAYTON WITT, JR., J.M. ASCE[1]

Died August 24, 1952

William Clayton Witt, the son of William Clayton and Maurine (Pickard) Witt, was born in Dallas, Tex., on August 9, 1927. He was educated at the Highland Park High School and at Southern Methodist University (both in Dallas), receiving the degree of Bachelor of Science in Civil Engineering from the university in May, 1949. He also earned a degree in business administration from Tulane University, in New Orleans, La.

From February, 1946, to May, 1947, Mr. Witt served in the United States Army at Fort Lewis in Washington and in the Edgewood Arsenal in Maryland. After being graduated from Tulane University he entered the Atlantic Refining Company Training Program, and was employed by the company in Corpus Christi, Aransas Pass, Longview, Midland, and Odessa, in Texas. At the time of his death, he was a junior engineer with the Atlantic Refining Company in Odessa and Midland.

Mr. Witt was elected a Junior of the American Society of Civil Engineers on September 6, 1949.

---

[1] Memoir prepared by I. W. Santry, Jr., A.M. ASCE.

BYRLE BURTON WOMBLE, A.M. ASCE[1]

DIED MAY 24, 1952

Byrle Burton Womble, the son of G. H. and Delia (Cassels) Womble, was born at Wildorado, Tex., on November 24, 1913. He received his elementary and high school education in Hume, Mo., and was graduated in 1944 from Kansas State College of Agriculture and Applied Science, at Manhattan, with the degree of Bachelor of Science in Civil Engineering.

During the interim of his university work he was employed by the Engineering Department of Sedgwick County, Kansas, at Wichita, in various positions from instrumentman to office engineer and resident engineer.

After being graduated in 1944 he was employed by Howard, Needles, Tamman & Bergendoff in Kansas City, Mo., as draftsman and detailer on the design of bridges, highways, viaducts, and floodwalls, and later as designer of steel and reinforced concrete structures.

In April, 1946, Mr. Womble joined J. W. Shikles & Company, also of Kansas City, as assistant engineer, working on basic surveys and designs of sewage treatment works and water supply systems.

From August, 1946, to February, 1948, he was resident engineer in charge of construction of a lake project and filtration plant for the City of Pleasant Hill, Mo., amounting to approximately $200,000.

From February, 1948, to May, 1948, he did basic survey and design work. Following this period, he was resident engineer, supervising the construction of the Kirksville (Mo.) Sewer Treatment Works and the Spring Lake project from May, 1948, to September, 1949.

From September, 1949, to January, 1950, Mr. Womble worked on basic surveys and designs of various projects. Then, for two and a half years, until May, 1952, he was employed as resident engineer in charge of construction of the Big Creek Impounding Reservoir and Pump Station. These Kirksville projects amounted to approximately $1,250,000, and the last of these was nearly completed at the time of his fatal illness.

Mr. Womble was married on May 19, 1938, to Lillian Wharton at Powhattan, Kans. He is survived by his widow; two children, Janice Louise and Judice Lillian; his mother, Mrs. G. H. Womble; one brother, G. H. Womble, Jr.; and four sisters: Mrs. C. B. Courtney, Mrs. L. L. Bishop, Mrs. R. V. Hays, and Mrs. H. B. Ryder.

Mr. Womble was elected a Junior of the American Society of Civil Engineers on October 16, 1944, and an Associate Member on February 14, 1949.

[1] Memoir prepared by J. W. Shikles, M. ASCE.

BYRLE BURTON WOMBLE, A.M. ASCE[1]

Died May 25, 1952

Byrle Burton Womble, the son of [illegible] and [illegible] Womble, was born at [illegible], Tex., on November 24, [illegible]. He received his elementary and high school education in [illegible], and was graduated in [illegible] from Oklahoma State College of Agriculture and [illegible] at Stillwater, with the degree of Bachelor of Science in Civil Engineering.

During the [illegible] work he was employed by the [illegible] Department of [illegible] County, [illegible], in [illegible] information [illegible].

After being graduated in [illegible] he was employed by [illegible] & [illegible], on [illegible] as [illegible] of [illegible], and [illegible] structures.

In April, [illegible], Mr. Womble joined [illegible] & Company, [illegible] City, as [illegible] engineer, working on [illegible] and [illegible].

From August, [illegible], to [illegible], he was resident engineer in charge of construction [illegible] Mr. [illegible] approximately [illegible].

From [illegible] to May, [illegible], he [illegible] following [illegible] the construction of the [illegible] and the [illegible] from May, [illegible] to September, [illegible].

From September, [illegible], to [illegible], Mr. Womble worked on field surveys and designs of [illegible]. [illegible] May, [illegible] he [illegible] of the [illegible] Creek Engineering [illegible] projects amounted to approximately [illegible] and [illegible] at the time of his fatal illness.

Mr. Womble was married on May [illegible] to [illegible] Kans. He is survived by his widow; [illegible]; his mother, Mrs. [illegible] Womble; [illegible] Womble; [illegible] sisters, Mrs. [illegible], Mrs. [illegible], Mrs. [illegible] and Mrs. [illegible].

Mr. Womble was elected a Junior of the American Society of Civil Engineers on October [illegible], 1944, and an Associate Member on February [illegible].

[1] Memoir prepared by [illegible], M. ASCE.

TRANSACTIONS

OF THE

AMERICAN SOCIETY OF CIVIL ENGINEERS

INDEX

VOLUME 118

1953

SUBJECT INDEX, PAGE 1284

AUTHOR INDEX, PAGE 1346

Titles of papers are in quotation marks when given with the author's name.

VOLUME 118

SUBJECT INDEX

ABUTMENTS

See DAMS, ARCH

ACCIDENTS

See HIGHWAYS AND ROADS—Safety; *see also* FAILURES . . .

ACCOUNTS AND ACCOUNTING

See COSTS . . . ; *also* subheading Financing under relative subject

ADDRESSES

See AMERICAN SOCIETY OF CIVIL ENGINEERS—Addresses

AERIAL . . .

See also AIR . . .

AERIAL MAPS AND MAPPING

See MAPS AND MAPPING, AERIAL

AERIAL PHOTOGRAPHY

See SURVEYS AND SURVEYING, AERIAL

AERIAL SURVEYS AND SURVEYING

See SURVEYS AND SURVEYING, AERIAL

AERODYNAMICS

See also AIR FLOW; *also* under relative subject

Theory of wind velocity versus height as based on the Ekman spiral, 463, 465, 468, 489, 503.

AGGREGATES AND AGGREGATION

Aggregate breakdown findings in water spreading research project in San Joaquin Valley, in California, 212.

"Flocculation Phenomena in Turbid Water Clarification," W. F. Langelier, Harvey F. Ludwig and Russell G. Ludwig, 147.

Properties of synthetic turbid waters, 150.

AGREEMENTS

See CONTRACTS

AGRICULTURE

See DRAINAGE; IRRIGATION; LAND . . . ; SOILS; WATER RIGHTS

AIR . . .

See also AERIAL . . . ; AERO- . . .

AIR DEMAND

See VALVES

AIR ENTRAINMENT

See WATER, FLOW OF . . .

AIR FLOW

"Variation of Wind Velocity and Gusts with Height," R. H. Sherlock (with discussion), 463.

AIR POLLUTION

See AIR SANITATION

AIRPORTS (structures and localities)

See COSTS, AIRPORT

AIR SANITATION

"The Allegheny Conference—Planning in Action," Park H. Martin (with discussion), 235.

AIR TUNNELS

See TUNNELS, AIR

ALINEMENT CURVES

See CURVES (alinement curves)

ALLUVIATION

See BARS (alluvia); EROSION . . . ; GEOLOGY; RIVER DELTAS; SEDIMENT AND SEDIMENTATION; SILT AND SILTING, CHANNEL

ALUM

See WATER TREATMENT

AMERICAN SOCIETY OF CIVIL ENGINEERS

Addresses

1953—*See* Vol. CT (Centennial Transactions)

Committee Reports—Floods

"Review of Flood Frequency Methods": Final Report of the Subcommittee of the Joint Division Committee on Floods, William P. Creager, Harvey B. Kinnison, Hymen Shifrin, Franklin F. Snyder, Gordon R. Williams, E. J. Gumbel, G. H. Matthes, 1220.

ANALOGS AND ANALOGIES

See under relative subject, e.g., HYDRAULICS; STRUCTURES, THEORY OF; *see also* ELECTRIC ANALOGY (cross reference thereunder)

ANALYSIS, DESIGN

See under relative subject, e.g., STRUCTURES, THEORY OF

ANALYSIS OF DATA

See EQUATIONS; GRAPHICAL CHARTS; MATHEMATICS; PROBABILITY, THEORY OF; STRUCTURES, THEORY OF; *also* under relative subject, e.g., BEAMS

ANALYSIS, STRUCTURAL

See EQUATIONS; STRUCTURES, THEORY OF

ANALYSIS, WATER

See WATER ANALYSIS

ANCHORAGES, BRIDGE
See BRIDGE ANCHORAGES

APPARATUS
See under relative subject, e.g., TUNNELS, WATER; *also* cross references under INSTRUMENTS

APPARATUS, TRIAXIAL COMPRESSION
See SOILS—Tests and Testing

AQUEDUCTS
See TUNNELS, WATER; WATER DIVERSION

AQUIFERS
See WELLS

ARCH DAMS
See DAMS, ARCH

ARCHES
See DAMS, ARCH

ARCHITECTURE
See type of structure or structural part

ASSOCIATIONS
See SOCIETIES, TECHNICAL (cross reference thereunder)

ATMOSPHERIC CORROSION
See CORROSION AND PROTECTION OF METALS

ATMOSPHERIC POLLUTION
See AIR SANITATION

ATMOSPHERIC PRESSURE
"Unconfined Ground-Water Flow to Multiple Wells," Vaughn E. Hansen (with discussion), 1098.

AUTHORITIES
See RIVER VALLEY AUTHORITIES

AUTOMOBILE ACCIDENTS
See HIGHWAYS AND ROADS—Safety

AUTOMOBILE LIGHTING
"Rate of Change of Grade per Station," Clarence J. Brownell (with discussion), 437.

AUTOMOBILE PARKING
See also COSTS, AUTOMOBILE PARKING
"The Allegheny Conference—Planning in Action," Park H. Martin (with discussion), 235.

BACKWATER
"Graphical Solution of Hydraulic Problems," Kenneth E. Sorensen, 61.

BANKS AND BANK PROTECTION, CHANNEL
See CHANNEL BANKS AND BANK PROTECTION (cross references thereunder)

BANKS AND BANK PROTECTION, RIVER

See RIVER BANKS AND BANK PROTECTION (cross references thereunder)

BANK STABILIZATION, RIVER

See RIVER BANKS AND BANK PROTECTION (cross references thereunder)

BARGE CANALS

See CANALS

BARS (alluvia)

See also RIVER DELTAS

"Bank Stabilization by Revetments and Dikes," Raymond H. Haas and Harvill E. Weller (with discussion), 849.

BASINS (depression in earth's surface)

See DRAINAGE; RAINFALL; RESERVOIRS . . . ; RIVER VALLEY AUTHORITIES; VALLEYS

BASINS, HARBOR

See HARBORS

BEACHES

See EROSION, BEACH; SHORES AND SHORE PROTECTION

BEAMS (General)

See also FLANGES; GIRDERS; STRESS AND STRAIN—Beams (General); STRUCTURES, THEORY OF—Beams and Girders (General); TORSION

Equations for various loading conditions of double cantilever beams, 1202.

"Flexure of Double Cantilever Beams," F. E. Wolosewick, 1197. *Discussion:* Lu-Shien Hu, Lewis Schneider, Ray W. Clough, William A. Conwell, and F. E. Wolosewick, 1208.

Formulas of and computation by the finite difference method, for deep beams, 687, 703.

"Stresses in Deep Beams," Li Chow, Harry D. Conway and George Winter (with discussion), 686.

"Thin-Walled Members in Combined Torsion and Flexure," Warner Lansing, 128.

"Torsion of I-Type and H-Type Beams," John E. Goldberg (with discussion), 771.

BEAMS, CONTINUOUS

See also BRIDGES; COSTS, BEAM (CONTINUOUS BEAMS); STRESS AND STRAIN—Beams, Continuous; STRUCTURES, THEORY OF—Beams and Girders, Continuous; STRUCTURES, THEORY OF—Frames, Continuous

Design of bridge floor beam hangers and lateral bending in floor beams, 843.

"Flexure of Double Cantilever Beams," F. E. Wolosewick (with discussion), 1197.

"Horizontally Curved Box Beams," Charles E. Cutts, 517. *Discussion:* A. George Mallis, DeForest A. Matteson, Jr., and Charles E. Cutts, 535.

"Steady-State Forced Vibration of Continuous Frames," C. T. G. Looney (with discussion), 794.

Bibliography

Horizontally curved box beams, 528, 544.

BEARING CAPACITY (foundations, rocks, soils)

For more general interpretation *see* cross references under LOAD

"Control of Embankment Material by Laboratory Testing," F. C. Walker and W. G. Holtz (with discussion), 1.

Determination of compaction effect of sheepsfoot rollers, 1.

BED LOAD DISPOSAL

See SILT AND SILTING . . .

BENDING

See MOMENTS; STRESS AND STRAIN; *also* relative structure, structural part or material, e.g., BEAMS

BIBLIOGRAPHY

See subheading Bibliography under relative subject. (Comprehensive bibliographical footnotes existing in individual papers in which books and other material are cited)

BIOGRAPHIES OF DECEASED MEMBERS

See cross reference under MEMOIRS OF DECEASED MEMBERS

BOLTS

See JOINTS

BORINGS

See also DRILLS AND DRILLING

"Field Study of a Sheet-Pile Bulkhead," C. Martin Duke (with discussion), 1131.

Relative merits of geophysical methods and comparable boring methods, 959.

BOUNDARIES (land ownership)

See CITY PLANNING; SURVEYS AND SURVEYING

BOX BEAMS

See BEAMS

BRACING

See TRUSSES . . . ; WIND BRACING

BREAKWATERS

See also SHORES AND SHORE PROTECTION; WATER PRESSURE; WAVES

Usage advantages of vertical wall breakwaters and those with sloping faces constructed of rubble, 653, 654, 668, 672, 673.

BRIDGE ANCHORAGES

"The Delaware Memorial Bridge": A Symposium, Homer R. Seely, Charles H. Clarahan, Jr. and Elmer K. Timby, 397.

BRIDGE CABLES

"The Delaware Memorial Bridge": A Symposium, Homer R. Seely, Charles H. Clarahan, Jr. and Elmer K. Timby, 397.

BRIDGE FLOORS AND FLOORING

"The Delaware Memorial Bridge": A Symposium, Homer R. Seely, Charles H. Clarahan, Jr. and Elmer K. Timby, 397.

BRIDGE LAW

1945–1946 federal and state enabling legislation pertaining to erection of Delaware Memorial Bridge, 399.

BRIDGE PIERS

"The Delaware Memorial Bridge": A Symposium, Homer R. Seely, Charles H. Clarahan, Jr., and Elmer K. Timby, 397.

"East St. Louis Veterans Memorial Bridge," A. L. R. Sanders (with discussion), 838.

BRIDGES (General)

See also BEAMS; CAISSONS; COLUMNS; COSTS, BRIDGE; FOUNDATIONS, BRIDGE; GIRDERS; TRUSS . . . ; VIBRATION; WIND . . .

BRIDGES, CANTILEVER

"East St. Louis Veterans Memorial Bridge," A. L. R. Sanders, 838. *Discussion:* W. H. Jameson, Joseph Sorkin and A. L. R. Sanders, 845.

Specifications governing design of structural members on superstructure, 839.

BRIDGE SHOES

See BRIDGES

BRIDGES, SUSPENSION

"The Delaware Memorial Bridge": A Symposium, Homer R. Seely, Charles H. Clarahan, Jr. and Elmer K. Timby, 397.

BRIDGE TOWERS

"The Delaware Memorial Bridge": A Symposium, Homer R. Seely, Charles H. Clarahan, Jr. and Elmer K. Timby, 397.

BUILDING (process)

See CONSTRUCTION (cross references thereunder)

BUILDING MATERIALS

See MATERIALS OF CONSTRUCTION

BUILDINGS

See COSTS . . . ; FLOORS AND FLOORING; FOUNDATIONS . . . ; MATERIALS OF CONSTRUCTION; STRESS AND STRAIN . . . ; STRUCTURES, THEORY OF; VIBRATION; WIND . . . ; *also* under type of building

BULKHEADS

See also FOUNDATIONS, BULKHEAD; RETAINING WALLS; SHORES AND SHORE PROTECTION; STRESS AND STRAIN—Bulkheads; WAVES

"Field Study of a Sheet-Pile Bulkhead," C. Martin Duke, 1131. *Discussion:* Gregory P. Tschebotarioff; Walter C. Boyer; Paul Baumann; S. Packshaw; W. F. Way; J. Owen Lake; K. Terzaghi; D. P. Krynine; Trent R. Dames and David C. Liu; Roy W. Carlson; and C. Martin Duke, 1157.

Suggestions for future field studies of anchored bulkheads, 1155, 1161, 1168, 1172, 1187, 1188.

Tie rod tension measurements, 1131.

BULKHEAD WALLS

See RETAINING WALLS

CABLES, BRIDGE

See BRIDGE CABLES

CAISSONS

"The Delaware Memorial Bridge": A Symposium, Homer R. Seely, Charles H. Clarahan, Jr. and Elmer K. Timby, 397.

"East St. Louis Veterans Memorial Bridge," A. L. R. Sanders (with discussion), 838.

CANALS (General)

See also CHANNELS; COSTS, CANAL; EROSION, STREAM; IRRIGATION CANALS; LOCKS; SILT AND SILTING, CHANNEL; SIPHONS; WATER, FLOW OF, IN OPEN CHANNELS; WATER TRANSPORTATION: WATERWAYS; WAVE . . .

"A Navigation Channel to Victoria, Tex.," Albert B. Davis, Jr., 420.

The navigation channel to Victoria, Texas, as a means of barge transportation, 420.

CANALS (Geographical)

Texas

"Development of a Flood-Control Plan for Houston, Tex.," Ellsworth I. Davis, 888.

CANALS, IRRIGATION

See IRRIGATION CANALS

CANTILEVER BEAMS

See BEAMS (General)

CANTILEVER BRIDGES

See BRIDGES, CANTILEVER

CAPILLARITY

See SOILS

CARRIERS

See MOTOR . . . ; TRANSPORTATION (cross references thereunder)

CARS

See AUTOMOBILE . . . ; MOTOR . . .

CEMENT

See also AGGREGATES AND AGGREGATION; CLAY; GROUTING

Grouting cement used at Hoover Dam, near Las Vegas, Nevada, 90.

CHANNEL BANKS AND BANK PROTECTION

See WATER, FLOW OF, IN OPEN CHANNELS; WAVES

CHANNEL BEAMS

See BEAMS

CHANNEL LININGS

Comparison of lined versus unlined channels, 902.

CHANNEL RECTIFICATION

See BARS (alluvia); CHANNELS; DIKES; IRRIGATION CANALS; WATER DIVERSION; WATER, FLOW OF, IN OPEN CHANNELS

CHANNELS (waterways)

See also EROSION, STREAM; RIVERS; SILT AND SILTING, CHANNEL; SLUICES; WATER DIVERSION; WATER, FLOW OF, IN OPEN CHANNELS; WATER POLLUTION

Buffalo Bayou as a flood menace to Houston, Texas, 888.

"Development of a Flood-Control Plan for Houston, Tex.," Ellsworth I. Davis, 888.

"Diversions from Alluvial Streams," C. P. Lindner (with discussion), 245.

"Electrical Analogies and Electronic Computers": A Symposium, Henry M. Paynter; R. E. Glover, D. J. Hebert and C. R. Daum; M. A. Kohler; P. G. Hubbard and S. C. Ling; and Malcolm S. McIlroy (with discussion), 961.

Methods in locating buried channels, 946.

"A Navigation Channel to Victoria, Tex.," Albert B. Davis, Jr., 420.

Tidal flow in estuarine channels in Delta area of California, 1010.

CHARTS

See GRAPHICAL CHARTS; HYDROGRAPHS; *also* MAPS AND MAPPING; *see also* under relative subject, e.g., WAVES

CHEMISTRY

See under relative technical subject, e.g., CORROSION AND PROTECTION OF . . .

CITIES

See AIRPORTS (cross reference thereunder); AUTOMOBILE PARKING; BUILDINGS (cross references thereunder); CITY PLANNING; COSTS . . . ; DOCKS AND WHARVES; ELECTRIC POWER; INDUSTRIAL . . . ; PARKS; SEWAGE . . . ; WATER FRONT (cross references thereunder); WATER SUPPLY (cross references thereunder); ZONING; *also* geographical subheading under relative subject, e.g., HARBORS—California

CITY PLANNING (General)

See also PARKS; ZONING

"The Value and Administration of a Zoning Plan," Huber E. Smutz (with discussion), 709.

CITY PLANNING (Geographical)

Pittsburgh, Pa.

"The Allegheny Conference—Planning in Action," Park H. Martin, 235. *Discussion:* Louis P. Blum, and Park H. Martin, 243.

CITY PLANNING LAW

"The Allegheny Conference—Planning in Action," Park H. Martin (with discussion), 235.

CIVIL ENGINEERS AND ENGINEERING

See AMERICAN SOCIETY OF CIVIL ENGINEERS; ENGINEERS AND ENGINEERING

CLARIFICATION, WATER
See WATER TREATMENT

CLASSIFICATION OF SOILS
See SOILS—Classification

CLAY
See also SOILS
"Flocculation Phenomena in Turbid Water Clarification," W. F. Langelier, Harvey F. Ludwig and Russell G. Ludwig, 147.
Geological formation known as Beaumont clay as it exists in Guadalupe River valley in Texas, 422.

COAGULANTS AND COAGULATION
See WATER TREATMENT

COAST
See SEACOAST (cross references thereunder)

COATINGS, PROTECTIVE
See CORROSION AND PROTECTION OF METALS

COLUMNS
"Torsion of Plate Girders," F. K. Chang and Bruce G. Johnston (with discussion), 337.

COMMERCE
See AIRPORTS (cross reference thereunder); CHANNELS; CITIES (cross references thereunder); DOCKS AND WHARVES; HARBORS; LAKES; RIVERS; TRANSPORTATION (cross references thereunder); WATERWAYS; *also* under other relative subject headings

COMMITTEE REPORTS
See AMERICAN SOCIETY OF CIVIL ENGINEERS—Committee Reports; *see also* under subject of report

COMPACTION
See BEARING CAPACITY

COMPRESSION MEMBERS
See COLUMNS

COMPUTERS, ELECTRONIC
See ELECTRONIC INSTRUMENTS

CONCRETE (General)
See also CEMENT; PAVEMENT AND PAVING, CONCRETE; SAND; STRESS AND STRAIN—Concrete; *also* under special structure or structural part, e.g., DAMS, MASONRY AND CONCRETE

Construction
"Bank Stabilization by Revetments and Dikes," Raymond H. Haas and Harvill E. Weller (with discussion), 849.

Mattresses
Method of placing articulated concrete mattress in bank stabilization work, 851.

Temperature
Temperature conditions at Shasta Dam, in California, as related to vertical stress, 305.

CONCRETE DAMS
See DAMS, MASONRY AND CONCRETE

CONCRETE PAVEMENT AND PAVING
See PAVEMENT AND PAVING, CONCRETE

CONCRETE, REINFORCED
See CONCRETE

CONDUITS
See also FLUMES; PENSTOCKS; PIPE LINES; TUNNELS . . .
"Characteristics of Fixed-Dispersion Cone Valves," Rex A. Elder and Gale B. Dougherty (with discussion), 907.
"Electrical Analogies and Electronic Computers": A Symposium, Henry M. Paynter; R. E. Glover, D. J. Hebert and C. R. Daum; M. A. Kohler, P. G. Hubbard and S. C. Ling; and Malcolm S. McIlroy (with discussion), 961.

CONES, FIXED DISPERSION
See VALVES

CONICAL DIFFUSERS
See DIFFUSER . . . (cross reference thereunder)

CONNECTORS AND CONNECTIONS
See JOINTS

CONSERVATION
See GROUND WATER; WATER CONSERVATION (cross references thereunder)

CONSOLIDATION TESTS, SOIL
See SOILS—Tests and Testing

CONSTRUCTION
See BUILDINGS (cross references thereunder); CONTRACTS; COSTS . . . ; CURVES (alinement curves); FAILURES; MATERIALS OF CONSTRUCTION; SPECIFICATIONS (cross references thereunder); STRESS AND STRAIN; STRUCTURES, THEORY OF; *also* under type of construction, e.g., BRIDGES, SUSPENSION; CONCRETE—Construction

CONSTRUCTION CURVES
See CURVES (alinement curves)

CONSTRUCTION MATERIALS
See MATERIALS OF CONSTRUCTION

CONTAMINATION, STREAM
See WATER POLLUTION

CONTINUOUS BEAMS
See BEAMS, CONTINUOUS

CONTINUOUS FRAMES
See STRUCTURES, THEORY OF—Frames, Continuous

CONTINUOUS GIRDERS
See STRUCTURES, THEORY OF—Beams and Girders, Continuous

CONTINUOUS STRUCTURES
See STRUCTURES, THEORY OF

CONTINUOUS TRUSSES
See TRUSSES, CONTINUOUS

CONTRACTS
See also SPECIFICATIONS (cross references thereunder)
Delaware Memorial Bridge contract awards, 410.

CONVENTIONS (American Society of Civil Engineers)
See AMERICAN SOCIETY OF CIVIL ENGINEERS—Addresses

CORROSION AND PROTECTION OF . . .
See also COSTS, CORROSION CONTROL

CORROSION AND PROTECTION OF METALS
Selection of materials of construction in relation to underground and atmospheric corrosion resistance, 167.
"Underground Corrosion of Piping," R. A. Brannon, 165. *Discussion:* Lyle R. Sheppard, and R. A. Brannon, 177.

COSTS (of work)
See COSTS

COSTS, AIRPORT
Costs of Greater Pittsburgh Airport, 238.

COSTS, AUTOMOBILE PARKING
Pittsburgh, Pennsylvania parking improvement costs, 239.

COSTS, BEAM (CONTINUOUS BEAMS)
Welding of members compared with riveting, 525.

COSTS, BRIDGE
Cost of bridges across Monongahela River and Allegheny River in Pittsburgh area, in Pennsylvania, 238.
Delaware Memorial Bridge cost financing and itemized cost estimates, 399, 410.

COSTS, CANAL
"A Navigation Channel to Victoria, Tex.," Albert B. Davis, Jr., 420.

COSTS, CORROSION CONTROL
Protective coatings in relation to their relative costs, 170, 171, 172, 173, 174, 175, 176.

COSTS, DAM MAINTENANCE
Hoover Dam penstock painting and seepage water pumping costs, 97.

COSTS, DRAINAGE
Hoover Dam foundation grouting and drainage costs, 97, 105.

COSTS, FLOOD
Buffalo Bayou, Texas, 1935 flood damage estimate, 891.

COSTS, FOUNDATION (DAM FOUNDATIONS)
Hoover Dam foundation grouting and drainage costs, 97, 105.

COSTS, GROUTING

Hoover Dam foundation grouting and drainage costs, 97, 105.

COSTS, HIGHWAY AND ROAD

Penn-Lincoln Highway estimated and actual costs, 237, 238.

COSTS, INDUSTRIAL PROPERTY

Allegheny Conference on Community Development projects in Pittsburgh, Pennsylvania area, 240, 241.

COSTS, MAP AND MAPPING

Cost distribution in the Topographic Division of the United States Geological Survey, 829, 831, 832, 837.

COSTS, PIPE LINE

Network analyzer cost, 1063.

COSTS, RESERVOIR

Yield and cost of surface reservoirs (1950), in Southern California, 228, 230, 231.

COSTS, SOIL TESTING

Variance of costs to comply with United States Bureau of Reclamation compaction requirements, 36.

COSTS, SPREADING (WATER SPREADING)

Suggested means of alleviating high cost of spreading, 215.

COSTS, WATER CONSERVATION

Utilization of underground storage reservoirs as a means of achieving maximum salvage, at minimum cost, of water now lost through natural causes, 220, 233, 234.

COSTS, WATER POLLUTION CONTROL

Estimate of cost of Allegheny County, Pennsylvania, water pollution control works, 238.

COSTS, WAVE DAMAGE

Corps of Engineers' report on wave damage of United States shore lines, 57.

CREEP

See STRESS AND STRAIN

CURRENT METERS

See METERS AND METERING, CURRENT

CURRENTS

See ELECTRIC POWER; OCEAN CURRENTS (cross references thereunder); WATER . . . ; WAVES

CURVED STRUCTURES

See STRUCTURES, THEORY OF—Curved Structures

CURVES (alinement curves)

"Rate of Change of Grade per Station," Clarence J. Brownell (with discussion), 437.

CURVES (backwater)

See BACKWATER

CURVES (construction curves)

See CURVES (alinement curves)

CURVES (vertical curves)
See CURVES (alinement curves)

CURVES, FREQUENCY
See under topic, e.g., FLOODS

CUTOFFS (General)
See DAMS

DAMPING
See STRUCTURES, THEORY OF

DAMS (General)
See also COSTS, DAM MAINTENANCE; STRUCTURES, THEORY OF—Dams; WATER DIVERSION; WATER PRESSURE
"Characteristics of Fixed-Dispersion Cone Valves," Rex A. Elder and Gale B. Dougherty (with discussion), 907.

DAMS, ARCH
See also STRESS AND STRAIN—Dams, Arch
"Analysis of Arch Dams of Variable Thickness," W. A. Perkins, 725. *Discussion:* Alfred L. Parme; L. J. Mensch; Fairfax D. Kirn and Gurmukh S. Sarkaria; A. C. Josephs; George E. Goodall; and W. A. Perkins, 754.
"The Development of Stresses in Shasta Dam," J. M. Raphael (with discussion), 289.

DAMS, CONCRETE
See DAMS, MASONRY AND CONCRETE

DAMS, EARTH
See also SEEPAGE; WAVES
"Control of Embankment Material by Laboratory Testing," F. C. Walker and W. G. Holtz (with discussion), 1.

DAMS, GRAVITY
See DAMS, MASONRY AND CONCRETE

DAMS, MASONRY AND CONCRETE
See also FOUNDATIONS, DAM; SEEPAGE; STRESS AND STRAIN—Dams, Masonry and Concrete; WATER PRESSURE
"The Development of Stresses in Shasta Dam," J. M. Raphael (with discussion), 289.
"Final Foundation Treatment at Hoover Dam," A. Warren Simonds (with discussion), 78.
Plan of Hoover Dam and appurtenant works, 79.

DEFINITIONS
See TERMINOLOGY

DEFLECTIONS
See DEFORMATION (cross references thereunder); MOMENTS; STRESS AND STRAIN; STRUCTURES, THEORY OF; *also* under relative structure or structural part, e.g., BEAMS; BULKHEADS

DEFORMATION

See FAILURES; STRESS AND STRAIN; STRUCTURES, THEORY OF; *also* under specific type of stress, e.g., TORSION; *also* under type of material

DELTAS

See RIVER DELTAS

DESIGN

See under relative subject, e.g., HIGHWAYS AND ROADS—Planning and Design; *see also* SPECIFICATIONS (cross references thereunder)

DESIGN ANALYSIS

See under relative subject, e.g., STRUCTURES, THEORY OF

DIAGRAMS

See under relative subject

DIFFUSER FLOW

See TUNNELS, WATER; WATER, FLOW OF, THROUGH ORIFICES

DIKES

See also FAILURES, DIKE; EMBANKMENTS; LEVEES

"Bank Stabilization by Revetments and Dikes," Raymond H. Haas and Harvill E. Weller, 849. *Discussion:* Harrison V. Pittman, E. R. de la Sayette, and Serge Leliavsky, 861.

"Field Study of a Sheet-Pile Bulkhead," C. Martin Duke (with discussion), 1131.

DISCHARGE

See GROUND WATER; SLUICES; WATER, FLOW OF, IN OPEN CHANNELS

DISCHARGE COEFFICIENTS

See under relative subject

DISEASE

See PUBLIC HEALTH

DISINTEGRATION OF MATERIALS

See CORROSION AND PROTECTION OF METALS; *also* under type of material

DISPERSION CONES, FIXED

See FIXED DISPERSION CONES (cross reference thereunder)

DISTORTION

See STRESS AND STRAIN; TORSION

DIVERSION

See WATER DIVERSION

DIVERSION CANALS

See CANALS

DOCKS AND WHARVES

See also BULKHEADS; HARBORS; WATER FRONT (cross references thereunder)

Long period waves and their motion effect upon ships moored to piers, 588, 601, 611, 614.

DOMES AND VAULTS

See WIND . . .

DRAFT TUBES

"Effect of Entrance Conditions on Diffuser Flow," J. M. Robertson and Donald Ross (with discussion), 1068.

DRAINAGE

See also COSTS, DRAINAGE; DAMS; PIPES AND PIPING; RAINFALL; RUNOFF

Description of Buffalo Bayou watershed in Texas, 889.

DRAWDOWN

See RESERVOIRS, WATER SUPPLY; WELLS

DRAWINGS

See under relative subject

DRIFT, LITTORAL

See SHORES AND SHORE PROTECTION

DRILLS AND DRILLING

See also BORINGS

"Final Foundation Treatment at Hoover Dam," A. Warren Simonds (with discussion), 78.

DYNAMICS OF . . .

See also STATICS OF . . . (cross reference thereunder)

DYNAMICS OF FLUIDS

See HYDRODYNAMICS

DYNAMICS OF GASES

See AERODYNAMICS

DYNAMICS OF STRUCTURES

See STRUCTURAL DYNAMICS (cross references thereunder)

EARTH . . .

See also GROUND . . . ; LAND . . . ; SOIL . . .

EARTH DAMS

See DAMS, EARTH

EARTH MOVEMENTS

See EARTHQUAKES

EARTH PRESSURE

"Field Study of a Sheet-Pile Bulkhead," C. Martin Duke (with discussion), 1131.

Phenomenon of arching in lateral pressure, 1159, 1184, 1193.

EARTHQUAKES

See also TSUNAMIES (cross reference thereunder); VIBRATION

Long period waves caused by seismic disturbances, 593.

EARTHS

See SOILS

EARTHWORK

See also DAMS, EARTH; EMBANKMENTS; FOUNDATIONS . . . ; LEVEES; REVETMENT

Suggestions for future field studies of anchored bulkheads and any earth structure, 1155, 1161, 1168, 1172, 1187, 1188.

ECONOMICS

See also CONTRACTS; COSTS . . . ; *also* under relative subject, subheading Financing

"The Value and Administration of a Zoning Plan," Huber E. Smutz (with discussion), 709.

ELASTICITY

See STRESS AND STRAIN

ELECTRIC ANALOGY

See WATER PRESSURE

ELECTRIC ENGINEERS AND ENGINEERING

See under relative subject, e.g., LIGHTING (cross reference thereunder)

ELECTRIC MODELS

See MODELS, ELECTRIC

ELECTRIC POWER (General)

"Electrical Analogies and Electronic Computers": A Symposium, Henry M. Paynter; R. E. Glover, D. J. Hebert and C. R. Daum; M. A. Kohler; P. G. Hubbard and S. C. Ling; and Malcolm S. McIlroy, 961. *Discussion:* E. B. Strowger; George R. Rich; Donald R. F. Harleman and Edward N. Rein; and Henry M. Paynter; J. van Veen; W. Douglas Baines; T. Blench; and R. E. Glover, D. J. Hebert and C. R. Daum; Alfred J. Cooper; C. O. Clark; and Max A. Kohler; Charles L. Barker; and Malcolm S. McIlroy, 990.

Vacuum tube millivoltmeter used as null detector, 1047, 1048.

ELECTRIC TRANSMISSION

See ELECTRIC POWER

ELECTRONIC COMPUTERS

See ELECTRONIC INSTRUMENTS

ELECTRONIC INSTRUMENTS

"Electrical Analogies and Electronic Computers": A Symposium, Henry M. Paynter; R. E. Glover, D. J. Hebert and C. R. Daum; M. A. Kohler; P. G. Hubbard and S. C. Ling; and Malcolm S. McIlroy (with discussion), 961.

EMBANKMENTS

See also DAMS, EARTH; FOUNDATIONS, EMBANKMENT; LEVEES; ROCK; SOILS

"Control of Embankment Material by Laboratory Testing," F. C. Walker and W. G. Holtz, 1. *Discussion:* George F. Sowers, D. P. Krynine, D. F. Glynn, and F. C. Walker and W. G. Holtz, 26.

ENERGY

See AERODYNAMICS; ELECTRIC POWER; HYDRODYNAMICS; POWER; STRUCTURES, THEORY OF; WATER, FLOW OF, IN OPEN CHANNELS; WATER POWER

ENERGY, LOSS OF

See FRICTION; VALVES; WATER, FLOW OF . . .

ENGINEERING

See ENGINEERS AND ENGINEERING

ENGINEERING BIBLIOGRAPHY

See BIBLIOGRAPHY (cross references thereunder)

ENGINEERING GLOSSARIES

See TERMINOLOGY

ENGINEERING SOCIETIES

See AMERICAN SOCIETY OF CIVIL ENGINEERS

ENGINEERS AND ENGINEERING (General)

See also AMERICAN SOCIETY OF CIVIL ENGINEERS (for memoirs of deceased members *see* name of member in Author Index); CONTRACTS; RESEARCH; TERMINOLOGY

Present and Future Trends

The need of specialists in the field of corrosion control, 176.

ENGINES

See TURBINES

ENTRAINMENT, AIR

See WATER, FLOW OF . . .

EQUATIONS

See also relative subject, e.g., WATER, FLOW OF, IN PIPES

Applicability of Muskingum equation in flow routing, 1034, 1038, 1039.

"Flexure of Double Cantilever Beams," F. E. Wolosewick (with discussion), 1197.

"Rate of Change of Grade per Station," Clarence J. Brownell (with discussion), 437.

Solutions of the differential equations for various warping conditions, 771, 774, 777.

EROSION, BEACH

"Lake Michigan Erosion Studies," John R. Hardin and William H. Booth, Jr., 39. *Discussion:* Thomas B. Casey, Charles E. Lee, and John R. Hardin and William H. Booth, Jr., 51.

Transportation of beach and bottom material due to wave action, 568.

EROSION, STREAM

"Bank Stabilization by Revetments and Dikes," Raymond H. Haas and Harvill E. Weller (with discussion), 849.

"Diversions from Alluvial Streams," C. P. Lindner (with discussion), 245.

ESTIMATES

See COSTS

ESTUARIES

See MODELS . . . ; RIVERS

EXCAVATION (General)

See under specific substructure

EXPERIMENTS

See LABORATORIES (cross reference thereunder); MODELS . . . ; TESTS AND TESTING (cross references thereunder); *also* under material, structure or structural part tested

EXPLORATION

See BORINGS; FOUNDATIONS; PILES AND PILE DRIVING

FACT FINDING

See RESEARCH

FAILURES (General)

See also BEARING CAPACITY; SAFETY (cross reference thereunder); STRESS AND STRAIN; STRUCTURES, THEORY OF

FAILURES, DIKE

Causes of failure, 859, 863.

FAILURES, REVETMENT

Causes of failure, 859, 863.

FATIGUE

See under relative subject; *see also* FAILURES

FILL, SETTLEMENT OF

See HYDRAULIC FILLING

FILTERS AND FILTRATION, SEWAGE

See also SEWAGE DISPOSAL

"Industrial Waste Treatment in Iowa," Paul Bolton, 322.

FINANCE

See COSTS . . . ; ECONOMICS; *see also* subheading Financing under relative subject

FIXED DISPERSION CONES

See VALVES

FLANGES

"Torsion of Plate Girders," F. K. Chang and Bruce G. Johnston (with discussion), 337.

FLEXURE

See STRESS AND STRAIN

FLOCS AND FLOCCULATION

See AGGREGATES AND AGGREGATION

FLOOD CONTROL

See FLOOD ROUTING; FLOODS; RESERVOIRS, FLOOD CONTROL

FLOOD FORECASTING

See FLOODS

FLOOD HYDROGRAPHS

See HYDROGRAPHS, STREAM FLOW

FLOOD ROUTING

See also WATER DIVERSION

"Development of a Flood-Control Plan for Houston, Tex.," Ellsworth I. Davis, 888.

"Electrical Analogies and Electronic Computers": A Symposium, Henry M. Paynter; R. E. Glover, D. J. Hebert and C. R. Daum; M. A. Kohler; P. G. Hubbard and S. C. Ling; and Malcolm S. McIlroy (with discussion), 961.

"Graphical Solution of Hydraulic Problems," Kenneth E. Sorensen, 61.

United States Weather Bureau development of electronic device for stream flow routing and flow analog program, 1028, 1038, 1041, 1045.

FLOODS (General)

See also COSTS, FLOOD; HYDROGRAPHS, STREAM FLOW; RAINFALL; RESERVOIRS, FLOOD CONTROL; RUNOFF

Flood frequency curves and their extrapolation, 1220.

Method of preparing flood forecasts for headwater areas, 1028, 1030.

"Review of Flood Frequency Methods": Final Report of the Subcommittee of the Joint Division Committee on Floods, William P. Creager, Harvey B. Kinnison, Hymen Shifrin, Franklin F. Snyder, Gordon R. Williams, E. J. Gumbel, G. H. Matthes, 1220.

FLOODS (Geographical)

Buffalo Bayou, Tex.

"Development of a Flood-Control Plan for Houston, Tex.," Ellsworth I. Davis, 888.

Houston, Tex.

"Development of a Flood-Control Plan for Houston, Tex., Ellsworth I. Davis, 888.

New Orleans, La.

"Development of a Flood-Control Plan for Houston, Tex.," Ellsworth I. Davis, 888.

Pittsburgh, Pa.

"The Allegheny Conference—Planning in Action," Park H. Martin (with discussion), 235.

Report of Flood Commission of Pittsburgh, Pennsylvania to Pittsburgh Chamber of Commerce, 1911, regarded as earliest American proposal for controlling river floods, 243.

FLOOR BEAMS

See BEAMS . . .

FLOORS AND FLOORING

See also BRIDGE FLOORS AND FLOORING

"Torsion of I-Type and H-Type Beams," John E. Goldberg (with discussion), 771.

FLOW

See AIR FLOW; DIFFUSER FLOW (cross references thereunder); FLOODS; GROUND WATER; RUNOFF; SEEPAGE; SEWAGE . . . ; TURBULENCE; VALVES; WATER, FLOW OF . . .

FLOW METERS

See METERS AND METERING

FLOW OF FLUIDS

See PIPES AND PIPING; WATER, FLOW OF . . .

FLOW OF SOLIDS

See PIPE LINES; PUMPS AND PUMPING; SEDIMENT AND SEDIMENTATION; SILT AND SILTING; WATER, FLOW OF, IN OPEN CHANNELS; WATER, FLOW OF, IN PIPES

FLOW OF WATER

See WATER, FLOW OF . . .

FLOW, SHEAR

See SHEAR

FLUIDS, DYNAMICS OF

See HYDRODYNAMICS

FLUIDS, FLOW OF

See PIPES AND PIPING; WATER, FLOW OF . . .

FLUMES

See also SLUICES; WATER, FLOW OF, IN OPEN CHANNELS

Sand bed flume with diversion channel to illustrate diversion of sediments, 281.

FLUVIAL MODELS

See MODELS, HYDRAULIC

FORMULAS

See under relative subject, e.g., GROUND WATER; WAVES

FOUNDATIONS (General)

See also ABUTMENTS (cross reference thereunder); BEARING CAPACITY; BORINGS; BRIDGE PIERS; CAISSONS; COSTS, FOUNDATION . . . ; EARTHWORK; EXCAVATION (cross reference thereunder); GROUTING; PILES AND PILE DRIVING; SEEPAGE; SOILS; WATER PRESSURE; *also* under special material, e.g., SAND

"Analysis of Ground-Water Lowering Adjacent to Open Water," Stuart B. Avery, Jr. (with discussion), 178.

FOUNDATIONS, BRIDGE

"The Delaware Memorial Bridge": A Symposium, Homer R. Seely, Charles H. Clarahan, Jr. and Elmer K. Timby, 397.

FOUNDATIONS, BULKHEAD

"Field Study of a Sheet-Pile Bulkhead," C. Martin Duke (with discussion), 1131.

FOUNDATIONS, DAM

See also COSTS, FOUNDATION (DAM FOUNDATIONS)

"Final Foundation Treatment at Hoover Dam," A. Warren Simonds, 78. *Discussion:* James B. Hays, V. L. Minear, Byram W. Steele, William H. McAlpine, Fred H. Lippold, O. E. Boggess, H. Cambefort, and A. Warren Simonds, 100.

FOUNDATIONS, EMBANKMENT

"Control of Embankment Material by Laboratory Testing," F. C. Walker and W. G. Holtz (with discussion), 1.

FOUNDATIONS, PILE

See PILES AND PILE DRIVING

FOUNDATIONS, UNDERWATER

See PILES AND PILE DRIVING

FRAMES (General)
See BEAMS; COLUMNS; GIRDERS
FRAMES, CONTINUOUS
See STRUCTURES, THEORY OF—Frames, Continuous
FRAMES, RIGID
See STRUCTURES, THEORY OF—Frames, Rigid
FRAMEWORKS
See STRUCTURES, THEORY OF
FREQUENCY CURVES
See under topic, e.g., FLOODS
FRICTION
"Electrical Analogies and Electronic Computers": A Symposium, Henry M. Paynter; R. E. Glover, D. J. Hebert and C. R. Daum; M. A. Kohler; P. G. Hubbard and S. C. Ling; and Malcolm S. McIlroy (with discussion), 961.
GAGES (General)
See also METERS AND METERING . . . ; *also* cross references under INSTRUMENTS
GAGES, STRAIN
Data and installation detail for Carlson strainmeter and stressmeter, 1131, 1138, 1139, 1156, 1162, 1173.
Usage of Carlson elastic-wire strain meter for measuring mass concrete deformations in Shasta Dam, in California, 289.
GASES, DYNAMICS OF
See AERODYNAMICS
GATES
See under type of gate
GAUGES (measuring instruments)
See GAGES
GEOGRAPHY
See under relative technical subject
GEOLOGY
Geological sections of Louisiana, 880.
"Method for Making Highway Soil Surveys," K. B. Woods (with discussion), 946.
GEOMETRY
See under relative subject, e.g., MOMENTS
GIRDERS (General)
See also BEAMS; CONNECTORS AND CONNECTIONS (cross reference thereunder); FLANGES; STRESS AND STRAIN—Girders; STRUCTURES, THEORY OF—Beams and Girders (General)
"Torsion of Plate Girders," F. K. Chang and Bruce G. Johnston (with discussion), 337.
GIRDERS, CONTINUOUS
See STRUCTURES, THEORY OF—Beams and Girders, Continuous
GLOSSARIES
See TERMINOLOGY

GOVERNMENT

See PUBLIC . . . ; *also* LAW subject heading under related topic, e.g., IRRIGATION LAW

GRADES

See HIGHWAYS AND ROADS—Grades

GRAPHICAL CHARTS

See also HYDROGRAPHS . . . ; *also* under relative subject

"Graphical Solution of Hydraulic Problems," Kenneth E. Sorensen, 61.

GRAVEL

See SAND; SEEPAGE; SOILS

GRAVITY DAMS

See DAMS, MASONRY AND CONCRETE

GRAVITY WELLS

See WELLS

GROINS

"Bank Stabilization by Revetments and Dikes," Raymond H. Haas and Harvill E. Weller (with discussion), 849.

GROUND . . .

See also EARTH . . . ; LAND . . . ; SOIL . . . ; UNDERGROUND (cross references thereunder)

GROUND WATER

See also SEEPAGE; WATER SUPPLY (cross references thereunder)

"Analysis of Ground-Water Lowering Adjacent to Open Water," Stuart B. Avery, Jr., 178. *Discussion:* Matthew I. Rorabaugh, S. J. Johnson, and Howard P. Hall, 194.

"Research in Water Spreading," Dean C. Muckel, 209.

"Rice Irrigation in Louisiana," E. E. Shutts (with discussion), 871.

Salt water invasion in Central Coastal Plain area of California, 232.

"Unconfined Ground-Water Flow to Multiple Wells," Vaughn E. Hansen (with discussion), 1098.

"Utilization of Underground Storage Reservoirs," Harvey O. Banks, 220.

GROUND WATER SPREADING

See SPREADING, WATER

GROUNDWORK

See EARTHWORK; FOUNDATIONS

GROUTING

See also COSTS, GROUTING

"Final Foundation Treatment at Hoover Dam," A. Warren Simonds (with discussion), 78.

GROYNES

See GROINS

GUSTS

See WIND . . .

HARBORS (General)

See also BREAKWATERS; BULKHEADS; CHANNELS; DOCKS AND WHARVES: JETTIES (cross references thereunder); RETAINING WALLS; SHORES AND SHORE PROTECTION; WATER FRONT (cross references thereunder); WATER POLLUTION; WATER TRANSPORTATION

Characteristics of long period waves in basins, 589, 598.

Engineering aspects of diffraction and refraction, 617.

Long period waves or surges in harbors, 588.

HARBORS (Geographical)

California

Long period waves or surges in harbors of California, 588.

HEAD, LOSS OF

See WATER, FLOW OF . . .

HEALTH, PUBLIC

See PUBLIC HEALTH

HIGHWAY BRIDGE FLOORS

See BRIDGE FLOORS AND FLOORING

HIGHWAY BRIDGES

See BRIDGES

HIGHWAY CURVES

See CURVES (alinement curves)

HIGHWAY GRADES

See HIGHWAYS AND ROADS—Grades

HIGHWAYS AND ROADS (General)

See also BRIDGE FLOORS AND FLOORING; BRIDGES; COSTS, HIGHWAY AND ROAD; CURVES (alinement curves); MOTOR . . . ; PAVEMENT AND PAVING; TRAFFIC . . . (cross references thereunder); VEHICLES (cross references thereunder)

Sight distance over a summit, 445, 460.

Construction

"Method for Making Highway Soil Surveys," K. B. Woods (with discussion), 946.

Costs. *See* COSTS, HIGHWAY AND ROAD

Grades

"Rate of Change of Grade per Station," Clarence J. Brownell, 437. ***Discussion:*** T. F. Hickerson, E. N. Prouty and C. J. Brownell, 457.

Planning and Design

"The Allegheny Conference—Planning in Action," Park H. Martin (with discussion), 235.

"Method for Making Highway Soil Surveys," K. B. Woods (with discussion), 946.

Roadbeds. *See* SOILS

Safety

"Rate of Change of Grade per Station," Clarence J. Brownell (with discussion), 437.

HISTORY, ENGINEERING

See under relative subject, e.g., FLOODS; IRRIGATION

HOWELL–BUNGER VALVES

See VALVES

HURRICANES

See WIND PRESSURE

HYDRAULIC FILLING

"Field Study of a Sheet-Pile Bulkhead," C. Martin Duke (with discussion), 1131.

HYDRAULIC MACHINERY

See under type of machinery, e.g., PUMPS AND PUMPING

HYDRAULIC MODELS

See MODELS, HYDRAULIC

HYDRAULICS

See also BREAKWATERS: BULKHEADS; CANALS; CHANNELS; CONDUITS; COSTS . . . ; DAMS; DIKES; DOCKS AND WHARVES; DRAINAGE; EROSION . . . ; FAILURES . . . ; FILTERS AND FILTRATION . . . ; FLOOD . . . ; FLOW . . . (cross references thereunder); FLUIDS (cross references thereunder); FLUMES; FOUNDATIONS . . . ; GROUND WATER; GROUTING; HARBORS; HYDRAULIC . . . ; HYDRO– . . . ; IRRIGATION; JETTIES (cross references thereunder); LAKES; LEVEES; LOCKS; METERS AND METERING; MODELS, HYDRAULIC; PENSTOCKS; PILES AND PILE DRIVING; PIPE . . . ; POWER PLANTS; PROBABILITY, THEORY OF; PUMPS AND PUMPING; RAINFALL; RESERVOIRS . . . ; RETAINING WALLS; RIVER . . . ; RUNOFF; SEA . . . ; SEACOAST (cross references thereunder); SEDIMENT AND SEDIMENTATION; SEEPAGE; SEWAGE . . . ; SHORES AND SHORE PROTECTION; SILT AND SILTING . . . ; SIPHONS; SLUICES; SPREADING, WATER; STRESS AND STRAIN; STRUCTURES, THEORY OF; TANKS; TERMINOLOGY; TIDES; TUNNELS, WATER; TURBINES, WATER; TURBULENCE; VALLEY . . . ; VALVES; WATER . . . ; WAVES; WELLS

Arithmetic integration method of solving water hammer problems compared with electronic computer solutions, 990.

"Effect of Entrance Conditions on Diffuser Flow," J. M. Robertson and Donald Ross (with discussion), 1068.

"Electrical Analogies and Electronic Computers": A Symposium, Henry M. Paynter; R. E. Glover, D. J. Hebert and C. R. Daum; M. A. Kohler; P. G. Hubbard and S. C. Ling; and Malcolm S. McIlroy, 961. *Discussion:* E. B. Strowger; George R. Rich; Donald R. F. Harleman and Edward N. Rein; and Henry M. Paynter; J. van Veen; W. Douglas Baines; T. Blench; and R. E. Glover, D. J. Hebert, and C. R. Daum; Alfred J. Cooper; C. O. Clark; and Max A. Kohler; and Charles L. Barker; and Malcolm S. McIlroy, 990.

"Engineering Aspects of Water Waves": A Symposium, Martin A. Mason; James W. Daily and Samuel C. Stephan, Jr.; John H. Carr, J. W. Johnson, and Robert Y. Hudson (with discussion), 545.

"Graphical Solution of Hydraulic Problems," Kenneth E. Sorensen, 61.

"Unconfined Ground-Water Flow to Multiple Wells," Vaughn E. Hansen (with discussion), 1098.

HYDRAULIC STRUCTURES

See also under type of structure, e.g., DAMS

"Control of Embankment Material by Laboratory Testing," F. C. Walker and W. G. Holtz (with discussion), 1.

HYDRAULIC TURBINES

See TURBINES, WATER

HYDRODYNAMICS

See also HYDROSTATICS

"Electrical Analogies and Electronic Computers": A Symposium, Henry M. Paynter; R. E. Glover, D. J. Hebert and C. R. Daum; M. A. Kohler; P. G. Hubbard and S. C. Ling; and Malcolm S. McIlroy (with discussion), 961.

"Engineering Aspects of Water Waves": A Symposium, Martin A. Mason; James W. Daily and Samuel C. Stephan, Jr.; John H. Carr; J. W. Johnson; and Robert Y. Hudson (with discussion), 545.

Hydrodynamic problems in three dimensions, 1046.

HYDROELECTRIC PLANTS

See POWER PLANTS

HYDROELECTRIC POWER

See WATER POWER

HYDROGRAPHS, RIVER

See HYDROGRAPHS, STREAM FLOW

HYDROGRAPHS, RUNOFF

Annual runoff in Sespe and Piru Creeks, tributaries of Santa Clara River, in Southern California, 225.

HYDROGRAPHS, STREAM FLOW

"Diversions from Alluvial Streams," C. P. Lindner (with discussion), 245.

Hydrograph for Calcasieu River, near Kinder, Louisiana, 1948-1949, 878.

Routed and observed hydrographs for the Potomac River, near Washington, D. C., and other specified rivers in Tennessee, Kansas and Oklahoma, 1033, 1036, 1037.

Routed outflow and inflow hydrographs, 1028.

HYDROLOGY

See also DRAINAGE; FLOODS; GROUND WATER; HYDROGRAPHS; INFILTRATION (cross references thereunder); LAKES; OCEAN . . . (cross references thereunder); RAINFALL; RIVERS; RUNOFF; SEA WATER; WATER . . .

Hydrology of ground water basins, 221, 224.

HYDROMETRY

See WATER, FLOW OF . . .

HYDROSTATIC PRESSURE

See HYDROSTATIC UPLIFT (cross reference thereunder)

HYDROSTATICS

See also HYDRODYNAMICS; WATER PRESSURE

"Analysis of Arch Dams of Variable Thickness," W. A. Perkins (with discussion), 725.

HYDROSTATIC UPLIFT
See WATER PRESSURE

IMPOUNDING, WATER
See WATER STORAGE

INDUSTRIAL PLANTS
See under specific type of plant, e.g., PACKING HOUSES; POWER PLANTS

INDUSTRIAL PROPERTY
See also COSTS, INDUSTRIAL PROPERTY
"The Allegheny Conference—Planning in Action," Park H. Martin (with discussion), 235.

INDUSTRIAL WASTE
See SEWAGE DISPOSAL; WATER POLLUTION—Industrial Waste Pollution

INDUSTRIAL WATER SUPPLY
See IRRIGATION; RESERVOIRS . . . ; WATER SUPPLY (cross references thereunder)

INDUSTRY
See under relative technical classification; *see also* under type of industry or industrial plant

INFILTRATION
See FLOODS; GROUND WATER; LAND . . . ; RUNOFF; SEEPAGE

INFLUENCE LINES
See MOMENTS

INSTRUMENTS
See GAGES; METERS AND METERING; *also* under general types of instruments, e.g., ELECTRONIC INSTRUMENTS; *also* under usage; *see also* cross references under specific type of instrument, e.g., STRESSMETERS

INSURANCE
"The Value and Administration of a Zoning Plan," Huber E. Smutz (with discussion), 709.

IRON
See CORROSION AND PROTECTION OF METALS; STEEL (cross references thereunder); *also* under structure or structural part

IRRIGATION (General)
History of rice culture in its relation to irrigation, 871.

IRRIGATION (Geographical)

Louisiana
Methods used to prevent salt water pollution in rice fields in Louisiana, 871.
"Rice Irrigation in Louisiana," E. E. Shutts, 871. *Discussion:* Lloyd E. Myers, Jr., and E. E. Shutts, 885.

New Jersey
"Irrigation Water Rights in the Humid Areas," Howard T. Critchlow (with discussion), 509.

United States
Irrigation Water Rights in the Humid Areas," Howard T. Critchlow, 509. *Discussion:* Harold E. Gray, and Howard T. Critchlow, 515.

IRRIGATION CANALS

"Control of Embankment Material by Laboratory Testing," F. C. Walker and W. G. Holtz (with discussion), 1.

Usage of canals in Louisiana to prevent salt water invasion from Gulf of Mexico, 871.

IRRIGATION LAW

"Irrigation Water Rights in the Humid Areas," Howard T. Critchlow (with discussion), 509.

JETS

See WATER, FLOW OF, THROUGH ORIFICES

JETTIES

See SHORES AND SHORE PROTECTION; *see also* BREAKWATERS; WAVES

JOINTS (General)

See also RIVETS AND RIVETING; STRESS AND STRAIN—Joints; WELDS AND WELDING

"Torsion of Plate Girders," F. K. Chang and Bruce G. Johnston (with discussion), 337.

LABORATORIES

See under relative subject

LAKES (General)

See also SHORES AND SHORE PROTECTION; WATER . . .

LAKES (Geographical)

Lake Michigan

"Lake Michigan Erosion Studies," John R. Hardin and William H. Booth, Jr. with discussion), 39.

Recommended improvements which would provide beach space for recreational use, 47.

LAND . . .

See also EARTH . . . ; GROUND . . . ; INDUSTRIAL PROPERTY; MAPS AND MAPPING; SOIL . . . ; SURVEYS AND SURVEYING

LAND RECLAMATION

See IRRIGATION; RIVER DELTAS; WATER RIGHTS

LAND SUBMERGENCE

See SPREADING, WATER

LATERAL PRESSURE

See DIKES; EARTH PRESSURE

LAW

See LAW subject heading under related topic, e.g., CITY PLANNING LAW; IRRIGATION LAW; *see also* WATER RIGHTS

LEGISLATION

See under relative subject (under the subject law heading, e.g., BRIDGE LAW)

LEVEES

See also DIKES; EMBANKMENTS

"A Navigation Channel to Victoria, Tex.," Albert B. Davis, Jr., 420.

LIGHTING

See AUTOMOBILE LIGHTING

LININGS

See under relative type, e.g., CHANNEL LININGS

LIQUIDS, FLOW OF . . .

See VALVES; WATER, FLOW OF . . .

LIQUIDS, FLOW OF, THROUGH ORIFICES

See WATER, FLOW OF, THROUGH ORIFICES

LITTORAL DRIFT

See SHORES AND SHORE PROTECTION

LOAD

See BEARING CAPACITY; BUILDINGS (cross references thereunder); FAILURES; STRESS AND STRAIN; VIBRATION; WATER PRESSURE; WIND PRESSURE; *also* under structure, structural member or part, e.g., BEAMS

LOAD, SUSPENDED

See SEDIMENT AND SEDIMENTATION; SILT AND SILTING . . .

LOCKS

"A Navigation Channel to Victoria, Tex.," Albert B. Davis, Jr., 420.

LOSS OF ENERGY

See FRICTION; VALVES; WATER, FLOW OF . . .

LOSS OF HEAD

See WATER, FLOW OF . . .

MACHINERY

See under general types of machinery; *also* under specific type of machine, e.g., TURBINES; *also* under usage

MAPS AND MAPPING (General)

See also COSTS, MAP AND MAPPING; SURVEYS AND SURVEYING; *also* under relative subject

Agricultural soil survey and geologic maps, 946.

"Topographic Mapping in Kentucky," Phil M. Miles, 829. *Discussion:* Herbert Milwit, 837.

MAPS AND MAPPING, AERIAL

"Method for Making Highway Soil Surveys," K. B. Woods (with discussion), 946.

MARINE . . .

See SEA . . .

MASONRY

See CEMENT; DAMS, MASONRY AND CONCRETE; FOUNDATIONS

MASONRY DAMS

See DAMS, MASONRY AND CONCRETE

MATERIALS OF CONSTRUCTION

See also CEMENT; CLAY; CONCRETE; CORROSION AND PROTECTION OF . . . ; EARTHWORK; EROSION . . . ; PERMEABILITY OF MATERIALS (cross references thereunder); SAND; SEEPAGE; SOILS; STRESS AND STRAIN; *also* under usage

"Control of Embankment Material by Laboratory Testing," F. C. Walker and W. G. Holtz (with discussion), 1.

MATERIALS, STRENGTH OF

See STRENGTH OF MATERIALS (cross references thereunder)

MATERIALS, TESTING OF

See TESTS AND TESTING (cross references thereunder)

MATHEMATICS

See also EQUATIONS; GRAPHICAL CHARTS; PROBABILITY, THEORY OF; *also* under relative subject

"Unconfined Ground-Water Flow to Multiple Wells," Vaughn E. Hansen (with discussion), 1098.

MEANDERS AND MEANDERING

See RIVERS

MECHANICAL ENGINEERS AND ENGINEERING

See under relative subject, e.g., AUTOMOBILE . . . ; MACHINERY (cross references thereunder); MOTOR . . . ; TURBINES . . .

MECHANICS (General)

See DYNAMICS (cross references thereunder); MATHEMATICS; STRUCTURAL . . . ; STRUCTURES, THEORY OF; TESTS AND TESTING (cross references thereunder)

MECHANICS, SOIL

See SOILS

MEMBERS (ASCE)

For memoirs of deceased members, *see* name of member in Author Index

MEMBERS, COMPRESSION

See COLUMNS

MEMBERS, STRUCTURAL

See BEAMS . . . ; COLUMNS; GIRDERS . . . ; STRUCTURES, THEORY OF; *also* under structure, e.g., BRIDGES; *also* under material

MEMOIRS OF DECEASED MEMBERS

See name of member in Author Index

METALLURGY

See under specific metal

METAL PROTECTION

See CORROSION AND PROTECTION OF METALS

METALS

See REINFORCED CONCRETE (cross reference thereunder); STRESS AND STRAIN—Steel; WELDS AND WELDING; *also* under specific metal or its alloy

METEOROLOGY

See also ATMOSPHERIC . . . ; RAINFALL

"Engineering Aspects of Water Waves": A Symposium, Martin A. Mason; James W. Daily and Samuel C. Stephan, Jr.; John H. Carr; J. W. Johnson, and Robert Y. Hudson (with discussion), 545.

"Variation of Wind Velocity and Gusts with Height," R. H. Sherlock (with discussion), 463.

METERS AND METERING (General)

See also GAGES; INSTRUMENTS (cross references thereunder)

METERS AND METERING, CURRENT

Pitot tubes used in determining diffuser flow velocity measurements, 1070, 1092, 1094.

METERS AND METERING, VENTURI

"Effect of Entrance Conditions on Diffuser Flow," J. M. Robertson and Donald Ross (with discussion), 1068.

METERS AND METERING, WATER (stream velocity)

See METERS AND METERING, CURRENT

MILITARY ENGINEERS AND ENGINEERING

See under relative technical subject, e.g., AIRPORTS (cross references thereunder); BRIDGES

MODELS, ELECTRIC

Hydraulic and electric model comparison for a normal vertical tide in an estuary, 1010, 1017.

MODELS, HYDRAULIC

"Characteristics of Fixed-Dispersion Cone Valves," Rex A. Elder and Gale B. Dougherty (with discussion), 907.

Description of surge tank model, 1001.

"Diversions from Alluvial Streams," C. P. Lindner (with discussion), 245.

Electric and hydraulic model comparison for a normal vertical tide in an estuary, 1010, 1017.

"Engineering Aspects of Water Waves": A Symposium, Martin A. Mason, James W. Daily, Samuel C. Stephan, Jr., John H. Carr, J. W. Johnson and Robert Y. Hudson (with discussion), 545.

Hydraulic inlet work design problems, 1050.

"Unconfined Ground-Water Flow to Multiple Wells," Vaughn E. Hansen (with discussion), 1098.

Bibliography

Hydraulic models of waves, 574.

MODELS, STRUCTURAL

Model tests to determine torsional rigidity and stress distribution in suspended structure of a suspension bridge, 418.

MOISTURE

See SOILS

MOMENT DISTRIBUTION

See MOMENTS; STRUCTURES, THEORY OF

MOMENTS

See also STRESS AND STRAIN; STRUCTURES, THEORY OF; *also* under specific type of stress, e.g., TORSION

"Flexure of Double Cantilever Beams," F. E. Wolosewick (with discussion), 1197.

"Horizontally Curved Box Beams," Charles E. Cutts (with discussion), 517.

"Influence Lines by Corrections to an Assumed Shape," James P. Michalos and Edward N. Wilson, 113.

"Steady-State Forced Vibration of Continuous Frames," C. T. G. Looney (with discussion), 794.

MOORINGS AND MOORAGES, SHIP

See DOCKS AND WHARVES

MOSQUITOES

See PUBLIC HEALTH

MOTIVE POWER

See ELECTRIC POWER; WATER POWER

MOTOR BUSES

See MOTOR VEHICLES; TRAFFIC . . . (cross references thereunder)

MOTOR CARS

See AUTOMOBILE . . . ; MOTOR VEHICLES; TRAFFIC . . . (cross references thereunder)

MOTOR TRAFFIC

See TRAFFIC . . . (cross references thereunder)

MOTOR TRUCKS

See MOTOR VEHICLES; TRAFFIC . . . (cross references thereunder)

MOTOR VEHICLE ACCIDENTS

See HIGHWAYS AND ROADS—Safety

MOTOR VEHICLES

"Rate of Change of Grade per Station," Clarence J. Brownell (with discussion), 437.

MOTORWAYS

See HIGHWAYS AND ROADS

MULTIPLE PURPOSE RESERVOIRS

See RESERVOIRS, MULTIPLE PURPOSE

MUNICIPAL ENGINEERS AND ENGINEERING

See BRIDGES; CITIES (cross references thereunder); CITY PLANNING; COSTS . . . ; DRAINAGE; ELECTRIC POWER; FILTERS AND FILTRATION . . . ; HARBORS; PAVEMENT AND PAVING; POWER; SANITATION (cross references thereunder); SEWAGE . . . ; WATER . . . ; and similar relative subjects

MUNICIPALITIES
See CITIES (cross references thereunder)

NAVIGATION
See CANALS; CHANNELS; DAMS; FLOODS; HARBORS; LAKES; LOCKS; RIVERS; RIVER VALLEY AUTHORITIES; TIDES; WATER TRANSPORTATION; WATERWAYS

NAVIGATION LOCKS
See LOCKS

NETWORKS
See PIPE LINES

NOMENCLATURE
See TERMINOLOGY

NUISANCES, ABATEMENT OF
See SMOKE ABATEMENT (cross reference thereunder); *see also* PUBLIC HEALTH

OBITUARIES OF MEMBERS
See name of member in Author Index

OCEAN . . .
See also SEA . . . ; TIDES; WAVES

OCEAN BEACHES
See EROSION, BEACH; SHORES AND SHORE PROTECTION

OCEAN CURRENTS
See EROSION, BEACH; TIDES; WAVES

OCEAN WAVES
See WAVES

OPEN CHANNELS
See CHANNELS; WATER, FLOW OF, IN OPEN CHANNELS

ORGANIZATIONS
See SOCIETIES, TECHNICAL (cross reference thereunder)

ORIFICES
See SIPHONS; WATER, FLOW OF, THROUGH ORIFICES

OSCILLATION
See VIBRATION; WAVES

OSCILLOGRAPHS
See VIBRATION RECORDING APPARATUS

PACKING HOUSES
Treatment of packing house wastes in Iowa, 323.

PAINTS AND PAINTING
See CORROSION AND PROTECTION OF METALS

PARKING REGULATIONS
See AUTOMOBILE PARKING

PARKS
"The Allegheny Conference—Planning in Action," Park H. Martin (with discussion), 235.

PAVEMENT AND PAVING (General)
"Bank Stabilization by Revetments and Dikes," Raymond H. Haas and Harvill E. Weller (with discussion), 849.

PAVEMENT AND PAVING, CONCRETE
"The Delaware Memorial Bridge": A Symposium, Homer R. Seely, Charles H. Clarahan, Jr. and Elmer K. Timby, 397.

PEDOLOGY
See SOILS—Classification

PENSTOCKS
See also PIPE LINES; TANKS, SURGE
"Electrical Analogies and Electronic Computers": A Symposium, Henry M. Paynter; R. E. Glover, D. J. Hebert and C. R. Daum; M. A. Kohler; P. G. Hubbard and S. C. Ling; and Malcolm S. McIlroy (with discussion), 961.

PERCOLATION
See GROUND WATER; SEEPAGE; SEWAGE DISPOSAL

PERMEABILITY OF MATERIALS
See CORROSION AND PROTECTION OF . . . ; SEEPAGE; *see also* under type of material, e.g., SAND; SOILS

PHOTOGRAMMETRY
See MAPS AND MAPPING, AERIAL

PHOTOGRAPHY, AERIAL
See SURVEYS AND SURVEYING, AERIAL

PIERS (waterway structures)
See DOCKS AND WHARVES

PIERS, BRIDGE
See BRIDGE PIERS

PILES AND PILE DRIVING
See also BEARING CAPACITY
"Bank Stabilization by Revetments and Dikes," Raymond H. Haas and Harvill E. Weller (with discussion), 849.
"Field Study of a Sheet-Pile Bulkhead," C. Martin Duke (with discussion), 1131.

PIPES LINES
See also COSTS, PIPE LINE; PENSTOCKS; PIPES AND PIPING; PUMPS AND PUMPING; WATER, FLOW OF, IN PIPES
Advantages and disadvantages of direct analogy method of network analysis, 1063.
"Electrical Analogies and Electronic Computers": A Symposium, Henry M. Paynter; R. E. Glover, D. J. Hebert and C. R. Daum; M. A. Kohler; P. G. Hubbard and S. C. Ling; and Malcolm S. McIlroy (with discussion), 961.
Increase in pipe line usage in relation to need for greater interest in underground corrosion, 177.
Properties of nonlinear resistors and network analyzers, representing pipe lines, 1057, 1058.

PIPES AND PIPING (fluid conveyance)

See also AQUEDUCTS (cross references thereunder); CONDUITS; CORROSION AND PROTECTION OF METALS; PENSTOCKS; PIPE LINES; SIPHONS; TUNNELS, WATER; WATER, FLOW OF, IN PIPES; WATER HAMMER

"Electrical Analogies and Electronic Computers": A Symposium, Henry M. Paynter; R. E. Glover, D. J. Hebert and C. R. Daum; M. A. Kohler; P. G. Hubbard and S. C. Ling; and Malcolm S. McIlroy (with discussion), 961.

PITOT TUBES

See METERS AND METERING, CURRENT

PLANNING

See CITY PLANNING; HIGHWAYS AND ROADS—Planning and Design; ZONING

PLANTS (industrial buildings and equipment)

See under type of plant, e.g., PACKING HOUSES; POWER PLANTS

PLATE GIRDERS

See GIRDERS

PLATES

See also JOINTS

"Torsion of Plate Girders," F. K. Chang and Bruce G. Johnston (with discussion), 337.

POLLUTION, AIR

See AIR SANITATION

POLLUTION, STREAM

See WATER POLLUTION

PORE WATER PRESSURE

See WATER PRESSURE

POROSITY

See SEEPAGE

PORTS

See AIRPORTS (cross reference thereunder); HARBORS

POWER (General)

See also BEARING CAPACITY; DAMS; DYNA- . . . (cross references thereunder); ELECTRIC POWER; PUMPS AND PUMPING; TOWERS; TURBINES . . . ; WATER HAMMER; WATER POWER

"Electrical Analogies and Electronic Computers": A Symposium, Henry M. Paynter; R. E. Glover, D. J. Hebert and C. R. Daum; M. A. Kohler; P. G. Hubbard and S. C. Ling; and Malcolm S. McIlroy (with discussion), 961.

POWER PLANTS (General)

See also PENSTOCKS; TANKS, SURGE; TURBINES . . .

"Electrical Analogies and Electronic Computers": A Symposium, Henry M. Paynter; R. E. Glover, D. J. Hebert and C. R. Daum; M. A. Kohler; P. G. Hubbard and S. C. Ling; and Malcolm S. McIlroy (with discussion), 961.

PRECIPITATION

See RAINFALL

PRESERVATION OF . . .

See CORROSION AND PROTECTION OF . . .

PRESIDENTIAL ADDRESSES (AMERICAN SOCIETY OF CIVIL ENGINEERS)

See AMERICAN SOCIETY OF CIVIL ENGINEERS—Addresses; *see also* under subject of address

PRESSURE

See ATMOSPHERIC PRESSURE; EARTH PRESSURE; HYDROSTATIC UPLIFT (cross reference thereunder); PUMPS AND PUMPING; STRESS AND STRAIN; WATER HAMMER; WATER PRESSURE; WAVES; WIND PRESSURE

PRESSURE TRANSMISSION THROUGH SOLIDS

See EARTH PRESSURE

PRESSURE TUNNELS

See TUNNELS, WATER

PRIME MOVERS

See ENERGY (cross references thereunder); POWER

PRINCIPLE OF SUPERPOSITION

See STRUCTURES, THEORY OF

PROBABILITY, THEORY OF

Analysis of flood frequency by theory of probability, 1222.

PROPERTY (landed property)

See INDUSTRIAL PROPERTY; LAND . . . (cross references thereunder); SURVEYS AND SURVEYING

PROTECTIVE COATINGS

See CORROSION AND PROTECTION OF METALS

PROTECTIVE WORKS

See under relative type, e.g., GROINS

PROTOTYPES AND MODELS

See MODELS

PUBLIC HEALTH

See also SANITATION (cross references thereunder)

Mosquitoes, malaria and rice fields, 885, 886.

PUBLIC SERVICES

See CITIES (cross references thereunder); GOVERNMENT (cross references thereunder); *see also* under type of service, e.g., SEWAGE DISPOSAL

PUBLIC UTILITIES

See ELECTRIC POWER; POWER; POWER PLANTS; WATER POWER

PUBLIC WORKS

See RIVER VALLEY AUTHORITIES; *also* under type of structure or project

PUMPS AND PUMPING (General)

"Analysis of Ground-Water Lowering Adjacent to Open Water," Stuart B. Avery, Jr. (with discussion), 178.

Development of irrigation pumps and their usage in Louisiana rice fields, 874.

PURIFICATION

See AIR SANITATION; WATER TREATMENT

RAILROAD BRIDGES

See BRIDGES . . .

RAILROAD CURVES

See CURVES (alinement curves)

RAILROADS (General)

See BRIDGES . . . ; CURVES (alinement curves); PUBLIC UTILITIES (cross references thereunder)

RAILROAD TRACKS

See CURVES (alinement curves); EARTHWORK; EMBANKMENTS; PAVEMENT AND PAVING

RAINFALL (General)

See also DRAINAGE; FLOODS; HYDROLOGY; PROBABILITY, THEORY OF; RUNOFF; SEEPAGE

Procedure for routing effective rainfall, 1028, 1030.

RAINFALL (Geographical)

Buffalo Bayou, Tex.

"Development of a Flood-Control Plan for Houston, Tex.," Ellsworth I. Davis, 888.

Hearne, Tex.

"Development of a Flood-Control Plan for Houston, Tex.," Ellsworth I. Davis, 888.

Louisiana

Average yearly rainfall since 1900, 877, 881.

Texas

Maximum observed rainfall in vicinity of Victoria, Texas, in relation to design of navigation channel, 420.

RECLAMATION, LAND

See LAND RECLAMATION (cross references thereunder)

RECLAMATION, SEWAGE

See SEWAGE DISPOSAL

RECORDING APPARATUS

See under general types of apparatus, e.g., VIBRATION RECORDING APPARATUS; *see also* under relative subject

RECORDING INSTRUMENTS

See under relative subject

RECORD KEEPING

See GRAPHIICAL CHARTS; HYDROGRAPHS; *also* cross references under RECORDING . . . ; *also* under relative subject

RECREATIONAL FACILITIES

See CITY PLANNING; LAKES; PARKS

REGIONAL PLANNING

See HIGHWAYS AND ROADS—Planning and Design; ZONING

REINFORCED CONCRETE

See CONCRETE

REPORTS OF COMMITTEES

See AMERICAN SOCIETY OF CIVIL ENGINEERS—Committee Reports; *see also* under subject of report

RESEARCH

See also AMERICAN SOCIETY OF CIVIL ENGINEERS; LABORATORIES (cross reference thereunder); MODELS . . . ; PROBABILITY, THEORY OF; STRUCTURES, THEORY OF; TESTS AND TESTING (cross references thereunder); *see also* under relative subject, e.g., SPREADING, WATER

Lack of development of organized research in civil engineering and its causes, 1163.

RESERVOIRS (General)

See also COSTS, RESERVOIR; DAMS; WATER DIVERSION; WATER STORAGE; WAVES

RESERVOIRS, FLOOD CONTROL

"Graphical Solution of Hydraulic Problems," Kenneth E. Sorensen, 61.

RESERVOIRS, MULTIPLE PURPOSE

Electronic stream flow routing analog application to reservoir operation, 1039.

RESERVOIRS, WATER SUPPLY

"Utilization of Underground Storage Reservoirs," Harvey O. Banks, 220.

RESONANCE

See VIBRATION; WATER HAMMER; WAVES

RETAINING WALLS

See also BULKHEADS; EARTH PRESSURE; EARTHWORK; EMBANKMENTS; REVETMENT; SEA WALLS (cross references thereunder)

Behavior of retaining walls of sheet steel piling, 1169.

RETARDS

"Bank Stabilization by Revetments and Dikes," Raymond H. Haas and Harvill E. Weller (with discussion), 849.

REVETMENT

See also FAILURES, REVETMENT; DIKES; LEVEES; RETAINING WALLS; WAVES

"Bank Stabilization by Revetments and Dikes," Raymond H. Haas and Harvill E. Weller, 849. *Discussion:* Harrison V. Pittman, E. R. de la Sayette, and Serge Leliavsky, 861.

Rhone River development work in France, 865.

RIGID FRAMES

See STRUCTURES, THEORY OF—Frames, Rigid

RIPARIAN RIGHTS

"Irrigation Water Rights in the Humid Areas," Howard T. Critchlow (with discussion), 509.

RIVER BANKS AND BANK PROTECTION

See DIKES; EROSION, STREAM; FLOODS; GROINS; RETARDS; REVETMENT; SEDIMENT AND SEDIMENTATION

RIVER BANK STABILIZATION

See RIVER BANKS AND BANK PROTECTION (cross references thereunder)

RIVER BASINS

See DRAINAGE; RAINFALL; RESERVOIRS . . . ; RIVER VALLEY AUTHORITIES; VALLEYS

RIVER CHANNELS

See CHANNELS

RIVER DELTAS

Hydraulic problems in Delta area of California, 1010.

RIVER DIVERSION

See WATER DIVERSION

RIVER POLLUTION

See WATER POLLUTION

RIVER RECTIFICATION

See RIVER REGULATION (cross references thereunder) ; *see also* other related RIVER . . . subject headings

RIVER REGULATION

See BARS (alluvia) ; DIKES; FLOOD ROUTING; IRRIGATION CANALS; REVETMENT; RIVERS; RIVER VALLEY AUTHORITIES; WATER DIVERSION; WATER, FLOW OF, IN OPEN CHANNELS

RIVERS (General)

See also BARS (alluvia) ; BRIDGES; DIKES; DRAINAGE; EROSION, STREAM; FLOOD ROUTING; FLOODS; HARBORS; HYDROGRAPHS, STREAM FLOW; HYDROLOGY; LEVEES; LOCKS; MODELS, HYDRAULIC; RAINFALL; RESERVOIRS . . . ; RETAINING WALLS; RUNOFF; SEDIMENT AND SEDIMENTATION; SILT AND SILTING, CHANNEL; TIDES; VALLEYS; WATER . . . ; WAVES

"Diversions from Alluvial Streams," C. P. Lindner (with discussion), 245.

Paths of sand travel in meandering rivers, 260.

RIVERS (Geographical)

California

Tidal flow in estuarine channels in Delta area, 1010.

Guadalupe River, Tex.

"A Navigation Channel to Victoria, Tex.," Albert B. Davis, Jr., 420.

Iowa

"Industrial Waste Treatment in Iowa," Paul Bolton, 322.

Mississippi River

"Bank Stabilization by Revetments and Dikes," Raymond H. Haas and Harvill E. Weller (with discussion), 849.

East St. Louis Veterans Memorial Bridge longest cantilever span across Mississippi River, 838.

Southern California

"Utilization of Underground Storage Reservoirs," Harvey O. Banks, 220.

RIVER TIDES

See TIDES

RIVER VALLEY AUTHORITIES

"Characteristics of Fixed-Dispersion Cone Valves," Rex A. Elder and Gale B. Dougherty (with discussion), 907.

Tennessee Valley Authority usage of electronic stream flow routing analog, 1039.

RIVER VALLEYS

See VALLEYS

RIVETS AND RIVETING

"Torsion of Plate Girders," F. K. Chang and Bruce G. Johnston (with discussion), 337.

RIVET SPACING

See RIVETS AND RIVETING

ROADBEDS

See EARTHWORK; RAILROAD TRACKS (cross references thereunder); *also* under specific type, e.g., HIGHWAYS AND ROADS—Roadbeds (cross reference thereunder)

ROADS

See HIGHWAYS AND ROADS

ROCK

See also BEARING CAPACITY; EARTH PRESSURE; FOUNDATIONS . . .

"Method for Making Highway Soil Surveys," K. B. Woods (with discussion), 946.

RODS, TIE

See BULKHEADS

ROLLED-FILL DAMS

See DAMS, EARTH

ROUTING, FLOOD

See FLOOD ROUTING

RUNOFF (General)

See also FLOODS; HYDROGRAPHS, RUNOFF; RAINFALL

Flood frequencies as related to changing conditions of watershed, 1229.

"Review of Flood Frequency Methods": Final Report of the Subcommittee of the Joint Division Committee on Floods, William P. Creager, Harvey B. Kinnison, Hymen Shifrin, Franklin F. Snyder, Gordon R. Williams, E. J. Gumbel, G. H. Matthes, 1220.

SAFETY

See HIGHWAYS AND ROADS—Safety

SALT WATER

See SEA WATER

SALT WATER INVASION

See GROUND WATER; IRRIGATION; WATER, FLOW OF, IN OPEN CHANNELS

SAND

See also BARS (alluvia); GRAVEL (cross references thereunder); GROUTING; SEDIMENT AND SEDIMENTATION; SEEPAGE; SILT AND SILTING . . . ; SOILS; WATER, FLOW OF, THROUGH SAND (cross references thereunder)

"Field Study of a Sheet-Pile Bulkhead," C. Martin Duke (with discussion), 1131.

Graded mason's sand with fines removed used in testing unconfined flow to multiple and single wells, 1102.

"Unconfined Ground-Water Flow to Multiple Wells," Vaughn E. Hansen (with discussion), 1098.

SAND BARS

See BARS (alluvia)

SAND SCREENS

See WATER, FLOW OF, IN OPEN CHANNELS

SANITATION

See AIR SANITATION; DRAINAGE; FILTERS AND FILTRATION . . . ; INDUSTRIAL WASTE (cross references thereunder); PIPES AND PIPING (cross references thereunder); PUBLIC HEALTH; SEWAGE DISPOSAL; SMOKE ABATEMENT (cross reference thereunder); TANKS . . . ; WASTE DISPOSAL (cross references thereunder); WATER . . .

SCIENCE

See under specific science, e.g., ECONOMICS

SCIENTIFIC SOCIETIES

See AMERICAN SOCIETY OF CIVIL ENGINEERS

SCOUR

See EROSION . . .

SCREENS, SAND

See WATER, FLOW OF, IN OPEN CHANNELS

SEA . . .

See also OCEAN . . . (cross references thereunder)

SEACOAST

See HARBORS; OCEAN CURRENTS (cross references thereunder); SHORES AND SHORE PROTECTION; TIDES; WAVES

SEAPORTS

See HARBORS

SEASHORE

See SHORES AND SHORE PROTECTION

SEA WALLS

See SHORES AND SHORE PROTECTION; WATER PRESSURE; WAVES

SEA WATER

Accepted tolerance of rice to salt water in relation to irrigation needs, 878.

SEA WATER INTRUSION

See SALT WATER INVASION (cross references thereunder)

SEAWAYS

See WATERWAYS

SEDIMENT AND SEDIMENTATION
See also SILT AND SILTING; TURBULENCE; WATER DIVERSION
"Diversions from Alluvial Streams," C. P. Lindner (with discussion), 245.

SEEPAGE
See also GROUND WATER
"Analysis of Ground-Water Lowering Adjacent to Open Water," Stuart B. Avery, Jr. (with discussion), 178.
"Control of Embankment Material by Laboratory Testing," F. C. Walker and W. G. Holtz (with discussion), 1.
"Final Foundation Treatment at Hoover Dam," A. Warren Simonds (with discussion), 78.
"Research in Water Spreading," Dean C. Muckel, 209.
"Unconfined Ground-Water Flow to Multiple Wells," Vaughn E. Hansen (with discussion), 1098.

SEISMOLOGY
See EARTHQUAKES

SETTLEMENT OF FILL
See HYDRAULIC FILLING

SETTLEMENT OF STRUCTURES
See EARTH PRESSURE; EMBANKMENTS; FOUNDATIONS . . . ; SOIL . . .

SEWAGE DISPOSAL
See also FILTERS AND FILTRATION, SEWAGE; PIPES AND PIPING
Utilization of underground reservoirs in reclamation of water from sewage, 233.

SEWAGE RECLAMATION
See SEWAGE DISPOSAL

SEWAGE TREATMENT
See SEWAGE DISPOSAL

SHEAR
"Analysis of Arch Dams of Variable Thickness," W. A. Perkins (with discussion), 725.
"Control of Embankment Material by Laboratory Testing," F. C. Walker and W. G. Holtz (with discussion), 1.
"The Development of Stresses in Shasta Dam," J. M. Raphael (with discussion), 289.
"Flexure of Double Cantilever Beams," F. E. Wolosewick (with discussion), 1197.
"Horizontally Curved Box Beams," Charles E. Cutts (with discussion), 517.
"Influence Lines by Corrections to an Assumed Shape," James P. Michalos and Edward N. Wilson, 113.
"Stresses in Deep Beams," Li Chow, Harry D. Conway and George Winter (with discussion), 686.
"Thin-Walled Members in Combined Torsion and Flexure," Warner Lansing, 128.
"Torsion of I-Type and H-Type Beams," John E. Goldberg (with discussion), 771.
"Torsion of Plate Girders," F. K. Chang and Bruce G. Johnston (with discussion), 337.

SHEAR FLOW

See SHEAR

SHEARING STRESS

See SHEAR

SHEET PILING

See PILES AND PILE DRIVING

SHELL STRUCTURES

See DOMES AND VAULTS (cross reference thereunder); FLUMES; PIPE LINES; PIPES AND PIPING

SHIP MOORINGS AND MOORAGES

See DOCKS AND WHARVES

SHIPS AND SHIPPING

See WATER TRANSPORTATION

SHORES AND SHORE PROTECTION (lands adjacent to lake, ocean or sea water)

See also BREAKWATERS; EROSION, BEACH; RETAINING WALLS; WAVES; *also* cross references under RIVER BANKS AND BANK PROTECTION

"Engineering Aspects of Water Waves": A Symposium, Martin A. Mason; James W. Daily and Samuel C. Stephan, Jr.; John H. Carr; J. W. Johnson; and Robert Y. Hudson (with discussion), 545.

"Lake Michigan Erosion Studies," John R. Hardin and William H. Booth, Jr. (with discussion), 39.

SIGHT DISTANCE

See HIGHWAYS AND ROADS

SILT AND SILTING (General)

See also AGGREGATES AND AGGREGATION; RIVER DELTAS; SEDIMENT AND SEDIMENTATION

"Engineering Aspects of Water Waves": A Symposium, Martin A. Mason; James W. Daily and Samuel C. Stephan, Jr.; John H. Carr; J. W. Johnson; and Robert Y. Hudson (with discussion), 545.

Bibliography

Transportation of beach and bottom material, 573.

SILT AND SILTING, CHANNEL

See also RIVER DELTAS

"Diversions from Alluvial Streams," C. P. Lindner, 245. *Discussion:* T. Blench, Serge Leliavsky Bey, A. R. Thomas, D. C. Bondurant, and C. P. Lindner, 270.

SIPHONS

See also WATER, FLOW OF, THROUGH ORIFICES

Fresh water siphons proposed to provide proper water supply conditions in Victoria, Texas region, 430.

SLUICES

See also FLUMES; PENSTOCKS

"Characteristics of Fixed-Dispersion Cone Valves," Rex A. Elder and Gale B. Dougherty (with discussion), 907.

SMOKE ABATEMENT
See AIR SANITATION

SOCIETIES, TECHNICAL
See AMERICAN SOCIETY OF CIVIL ENGINEERS; *see also* ENGINEERS AND ENGINEERING

SOIL . . .
See also EARTH . . . ; GROUND . . . ; LAND . . .

SOIL CORROSION
See CORROSION AND PROTECTION OF METALS

SOIL MECHANICS
See SOILS

SOIL PRESSURE
See EARTH PRESSURE

SOILS (General)
See also BEARING CAPACITY; CLAY; COSTS, SOIL . . . ; DRAINAGE; EROSION, BEACH; FOUNDATIONS . . . ; FRICTION; GRAVEL (cross references thereunder); GROUND . . . ; LAND . . . ; PAVEMENT AND PAVING; SAND; SEDIMENT AND SEDIMENTATION; SEEPAGE; SILT AND SILTING . . . ; *also* under name of soil structure, e.g., DAMS, EARTH

Classification
"Method for Making Highway Soil Surveys," K. B. Woods, 946. *Discussion:* George F. Sowers, and K. B. Woods, 956.
Use of aerial photographs in soil surveying, 951.

Compaction. *See* BEARING CAPACITY

Construction
"Field Study of a Sheet-Pile Bulkhead," C. Martin Duke (with discussion), 1131.

Tests and Testing. *See also* COSTS, SOIL TESTING
Apparatus and procedure used by United States Bureau of Reclamation in the development of the triaxial shear test, 1.
"Control of Embankment Material by Laboratory Testing," F. C. Walker and W. G. Holtz (with discussion), 1.
"Field Study of a Sheet-Pile Bulkhead," C. Martin Duke (with discussion), 1131.
"Method for Making Highway Soil Surveys," K. B. Woods (with discussion), 946.

SOIL TRANSPORTATION
See SEDIMENT AND SEDIMENTATION; SILT AND SILTING

SOLIDS, FLOW OF
See FLOW OF SOLIDS (cross references thereunder)

SOLIDS, PRESSURE TRANSMISSION THROUGH
See EARTH PRESSURE

SPACE STRUCTURES
See STRUCTURES, THEORY OF; TOWERS; WIND . . .

SPECIFICATIONS

See under relative subject, e.g., BRIDGES; *see also* CONTRACTS

SPREADING, WATER

See also COSTS, SPREADING (WATER SPREADING)

First large scale usage of water spreading as a means of conservation, 210.

"Research in Water Spreading," Dean C. Muckel, 209.

STABILITY

See AERODYNAMICS (cross reference thereunder); HYDRODYNAMICS

STATICALLY INDETERMINATE STRUCTURES

See STRUCTURES, CONTINUOUS (cross reference thereunder)

STATICS OF . . .

See also DYNAMICS OF . . . (cross references thereunder)

STATICS OF FLUIDS

See HYDROSTATICS

STATISTICS

See relative subject

STEEL

See CORROSION AND PROTECTION OF METALS; REINFORCED CONCRETE (cross reference thereunder); STRESS AND STRAIN—Steel; WELDS AND WELDING; *also* under special structure or structural part, e.g., BRIDGES

STIFFENING TRUSSES

See TRUSSES, STIFFENING

STIFFNESS

"Flexure of Double Cantilever Beams," F. E. Wolosewick (with discussion), 1197.

"Steady-State Forced Vibration of Continuous Frames," C. T. G. Looney (with discussion), 794.

"Torsion of I-Type and H-Type Beams," John E. Goldberg (with discussion), 771.

"Torsion of Plate Girders," F. K. Chang and Bruce G. Johnston (with discussion), 337.

STONE

See ROCK

STORAGE

See RESERVOIRS . . . ; WATER STORAGE

STORMS

See RAINFALL; WAVES; WIND

STORM WATER

See DRAINAGE; SEWAGE DISPOSAL

STRAIN

See STRESS AND STRAIN

STRAIN GAGES

See GAGES, STRAIN

STRAINMETERS

See GAGES, STRAIN

STREAM CONTAMINATION

See WATER POLLUTION

STREAM EROSION

See EROSION, STREAM

STREAM FLOW

See WATER, FLOW OF, IN OPEN CHANNELS and cross references thereunder

STREAMS

See RIVERS and cross references thereunder

STREETS

See BRIDGES; CITIES (cross references thereunder); CITY PLANNING; CONDUITS; CURVES (alinement curves); HIGHWAYS AND ROADS; MOTOR . . . ; PIPES AND PIPING; TRAFFIC, STREET (cross reference thereunder); VEHICLES (cross references thereunder); ZONING

STRENGTH OF MATERIALS

See STRESS AND STRAIN; *also* under specific material (*see* list of materials under MATERIALS OF CONSTRUCTION); *also* under fabricated structure or structural part

STRESS AND STRAIN (General)

See also CONCRETE—Temperature; EARTH PRESSURE; FAILURES; GAGES, STRAIN; MOMENTS; STIFFNESS; STRENGTH OF MATERIALS (cross references thereunder); STRUCTURES, THEORY OF; TEMPERATURE; VIBRATION; WATER PRESSURE; WAVES; WIND . . . ; *also* under specific type of stress, e.g., SHEAR; TORSION

Beams (General). *See also* SHEAR; TORSION

"Flexure of Double Cantilever Beams," F. E. Wolosewick (with discussion), 1197.

"Stresses in Deep Beams," Li Chow, Harry D. Conway and George Winter, 686. *Discussion:* Arturo M. Guzman and Cesar J. Luisoni; William A. Conwell; and Harry D. Conway and George Winter, 703.

"Thin-Walled Members in Combined Torsion and Flexure," Warner Lansing, 128.

Beams, Continuous

"Horizontally Curved Box Beams," Charles E. Cutts (with discussion), 517.

Relation between warping stress and length, 536, 542.

Bulkheads

"Field Study of a Sheet-Pile Bulkhead," C. Martin Duke (with discussion), 1131.

Concrete

"Stresses in Deep Beams," Li Chow, Harry D. Conway and George Winter (with discussion), 686.

Dams, Arch

"Analysis of Arch Dams of Variable Thickness," W. A. Perkins (with discussion), 725.

"The Development of Stresses in Shasta Dam," J. M. Raphael (with discussion), 289.

Dams, Masonry and Concrete

Creep properties as determined by tests at Shasta Dam, in California, 289.

"The Development of Stresses in Shasta Dam," J. M. Raphael, 289. *Discussion:* Ross M. Riegel, Roy W. Carlson, J. Laginha Serafim, A. D. Ross, J. A. Hanson, A. Warren Simonds, and J. M. Raphael, 310.

Girders. *See also* TORSION

"Torsion of Plate Girders," F. K. Chang and Bruce G. Johnston (with discussion), 337.

Joints

"Analysis of Arch Dams of Variable Thickness," W. A. Perkins (with discussion), 725.

Materials of Construction

"Control of Embankment Material by Laboratory Testing," F. C. Walker and W. G. Holtz (with discussion), 1.

Steel

"Stresses in Deep Beams," Li Chow, Harry D. Conway and George Winter (with discussion), 686.

STRESSMETERS

See GAGES, STRAIN

STRUCTURAL ANALYSIS

See EQUATIONS; STRUCTURES, THEORY OF

STRUCTURAL DYNAMICS

See AERODYNAMICS; EARTHQUAKES; VIBRATION

STRUCTURAL MATERIALS

See MATERIALS OF CONSTRUCTION

STRUCTURAL MEMBERS

See BEAMS . . . ; COLUMNS; GIRDERS . . . ; STRUCTURES, THEORY OF; *also* under structure, e.g., BRIDGES; *also* under material

STRUCTURAL MODELS

See MODELS, STRUCTURAL

STRUCTURES (General)

See also BUILDINGS (cross references thereunder); CONSTRUCTION (cross references thereunder); FOUNDATIONS . . . ; MATERIALS OF CONSTRUCTION; MODELS, STRUCTURAL; STRESS AND STRAIN . . . ; STRUCTURES, THEORY OF; VIBRATION; WIND . . . ; *also* under specific type of structure or related subject, e.g., WAVES; *also* under general types of structures, e.g., HYDRAULIC STRUCTURES

"Thin-Walled Members in Combined Torsion and Flexure," Warner Lansing, 128.

STRUCTURES, CONTINUOUS

See STRUCTURES, THEORY OF

STRUCTURES, CURVED

See CURVED STRUCTURES (cross reference thereunder)

STRUCTURES, HYDRAULIC

See HYDRAULIC STRUCTURES

STRUCTURES, SETTLEMENT OF

See EARTH PRESSURE; EMBANKMENTS; FOUNDATIONS . . . ; SOIL . . .

STRUCTURES, SHELL

See SHELL STRUCTURES (cross references thereunder)

STRUCTURES, SPACE

See SPACE STRUCTURES (cross references thereunder)

STRUCTURES, STATICALLY INDETERMINATE

See STRUCTURES, CONTINUOUS (cross reference thereunder)

STRUCTURES, THEORY OF (General)

Advantages of analysis by superposition methods, 781.

Beams and Girders (General)

Analogy existing in investigation for thin-walled open section beams loaded in a manner that produces combined torsion and flexure, 128.

"Stresses in Deep Beams," Li Chow, Harry D. Conway and George Winter (with discussion), 686.

"Thin-Walled Members in Combined Torsion and Flexure," Warner Lansing, 128.

"Torsion of I-Type and H-Type Beams," John E. Goldberg (with discussion), 771.

Beams and Girders, Continuous

"Horizontally Curved Box Beams," Charles E. Cutts (with discussion), 517.

"Influence Lines by Corrections to an Assumed Shape," James P. Michalos and Edward N. Wilson, 113.

Continuous Structures

Flexure of double cantilever beams when a segment of a continuous structure, 1206, 1217.

Curved Structures

"Horizontally Curved Box Beams," Charles E. Cutts (with discussion), 517.

Dams

"Analysis of Arch Dams of Variable Thickness," W. A. Perkins (with discussion), 725.

Comparison of stresses found by different methods, emphasizing trial-load analysis, 725, 760, 761, 762, 763, 767.

Frames, Continuous

An analytical procedure which can be used to determine displacements in continuous frames, 127.

"Flexure of Double Cantilever Beams," F. E. Wolosewick (with discussion), 1197.

"Steady-State Forced Vibration of Continuous Frames," C. T. G. Looney, 794. *Discussion:* E. F. Masur, A. S. Veletsos, William A. Conwell and C. T. G. Looney, 815.

Frames, Rigid

"Influence Lines by Corrections to an Assumed Shape," James P. Michalos and Edward N. Wilson, 113.

Girders (General). *See* Beams and Girders (General) (hereunder)

Girders, Continuous. *See* Beams and Girders, Continuous (hereunder)

STRUCTURES, UNDERGROUND

See UNDERGROUND STRUCTURES (cross references thereunder)

STRUTS

See COLUMNS

SUB– . . .

See also UNDER– . . .

SUBMERGENCE, LAND

See LAND SUBMERGENCE (cross reference thereunder)

SUBSTRUCTURES

See CONCRETE; EARTHWORK; EXCAVATION (cross reference thereunder); FOUNDATIONS; MASONRY (cross references thereunder); *also* under type of substructure, e.g., TUNNELS . . .

SUPERPOSITION, PRINCIPLE OF

See STRUCTURES, THEORY OF

SURGES (water surface)

See WAVES

SURGE TANKS

See TANKS, SURGE

SURVEYING

See SURVEYS AND SURVEYING

SURVEYS (research data)

See under relative subject, e.g., CITY PLANNING; *see also* RESEARCH

SURVEYS AND SURVEYING (General)

See also MAPS AND MAPPING; PROPERTY (landed property) (cross references thereunder); TRIANGULATION

"Method for Making Highway Soil Surveys," K. B. Woods (with discussion), 946.

"Rate of Change of Grade per Station," Clarence J. Brownell (with discussion), 437.

SURVEYS AND SURVEYING, AERIAL

See also MAPS AND MAPPING, AERIAL

Aerial photography usage in mapping Kentucky, 834.

SUSPENDED LOAD

See SEDIMENT AND SEDIMENTATION; SILT AND SILTING . . .

SUSPENSION BRIDGES

See BRIDGES, SUSPENSION

SYMBOLS

See relative subject, e.g., HYDRAULICS; MATHEMATICS; STRUCTURES, THEORY OF

SYPHONS

See SIPHONS

TANKS (General)

See also WATER, FLOW OF, IN OPEN CHANNELS; WATER STORAGE

"Electrical Analogies and Electronic Computers": A Symposium, Henry M. Paynter; R. E. Glover, D. J. Hebert and C. R. Daum; M. A. Kohler; P. G. Hubbard and S. C. Ling; and Malcolm S. McIlroy (with discussion), 961.

TANKS, SURGE

See also PENSTOCKS

"Electrical Analogies and Electronic Computers": A Symposium, Henry M. Paynter; R. E. Glover, D. J. Hebert and C. R. Daum; M. A. Kohler; P. G. Hubbard and S. C. Ling; and Malcolm S. McIlroy (with discussion), 961.

"Graphical Solution of Hydraulic Problems," Kenneth E. Sorensen, 61.

TECHNICAL SOCIETIES

See AMERICAN SOCIETY OF CIVIL ENGINEERS; *see also* ENGINEERS AND ENGINEERING

TEMPERATURE

See also CONCRETE—Temperature

"Analysis of Arch Dams of Variable Thickness," W. A. Perkins (with discussion), 725.

TENNESSEE VALLEY AUTHORITY

See RIVER VALLEY AUTHORITIES

TENSILE STRESS

See STRESS AND STRAIN

TENSION

See STRESS AND STRAIN

TERMINOLOGY (Arranged hereunder by specific or comprehensive subject word when possible)

Analog as defined in relation to hydraulic problems, 1020.

Arch dam usage for curved gravity dams regarded a misnomer, 767.

Beams. (A deep beam defined), 686.

Beams. (Angle of warp as applied to warping of a cross section), 775.

Bed load and suspended load as terms describing material movement in streams, 286.

Earth pressure. (True arching as a term used in relation to lateral pressures), 1159.

Flood frequency, probability, and similar definitions in common use, 1220.
Flood project terms, 895.
Highways and roads. (Passing sight distance over a summit and nonpassing sight distance differentiated), 445, 446.
Mastics in protective coatings, 172.
Oscillatory waves defined by their measurable characteristics, 547.
Revetment as a term in river bank protection, 850.
Silt and silting. (Exchange capacity as a term in soil technology), 150.
Soils. (Terms used by geologists for glacial areas), 949.
Soil stress as related to protective coatings of underground structures, 169.
Synchronism defined, 796.
Watercourse, and diffused surface waters, as defined by the courts, 511.
Water diversion. (Angle of twist and angle of diversion compared), 273.
Water flow. (Diffuser flow in water tunnels), 1069.
Water rights and "reasonable use" as used under common law doctrine, 511, 513.
Water spreading as used in some localities, 209.
Water supply. (Safe yield as defined in relation to underground storage), 223.
Waves. (Seiche recommended for American usage), 604, 611, 615.
Waves. (Usage of French term clapotis in relation to wave movement), 660.
Wind velocity and terms related to air flow, 464, 465.

TESTING MACHINES

See under use, material, structure or structural part tested, e.g., TORSION

TESTS AND TESTING

See FAILURES; LABORATORIES (cross reference thereunder); MODELS . . . ; SHEAR; STRENGTH OF MATERIALS (cross references thereunder); STRESS AND STRAIN; STRUCTURES, THEORY OF; TORSION; WATER ANALYSIS; *also* under material, structure or structural part tested, e.g., DAMS, EARTH; SOILS—Tests and Testing

THEORIES

See cross references hereunder and under ANALYSIS OF DATA; *see also* under relative subject or its relative science, e.g., HYDRAULICS; WAVES

THEORY OF PROBABILITY

See PROBABILITY, THEORY OF

THEORY OF STRUCTURES

See STRUCTURES, THEORY OF

THEORY OF SUPERPOSITION

See STRUCTURES, THEORY OF

THRUST

See relative structure, structural part or material.

TIDAL POWER

See WATER POWER

TIDES

See also OCEAN CURRENTS (cross references thereunder); WAVES

"Electrical Analogies and Electronic Computers": A Symposium, Henry M. Paynter; R. E. Glover, D. J. Hebert and C. R. Daum; M. A. Kohler; P. G. Hubbard and S. C. Ling; and Malcolm S. McIlroy (with discussion), 961.

Tide fluctuations as related to water pressure in dike and fill of sheet pile bulkhead, 1145, 1154, 1195.

Bibliography

Flow calculating in tidal hydraulics, 1019.

TIE RODS

See BULKHEADS

TOOLS

See under general types of tools or usage; *also* cross references under APPARATUS; INSTRUMENTS; MACHINERY

TOPOGRAPHIC MAPS AND MAPPING

See MAPS AND MAPPING (General)

TORNADOES

See WIND PRESSURE

TORSION

"Flexure of Double Cantilever Beams," F. E. Wolosewick (with discussion), 1197.

"Horizontally Curved Box Beams," Charles E. Cutts (with discussion), 517.

Procedure of analysis embodying the principles of a linear torsion bending theory for I-type and H-type sections, 789.

"Thin-Walled Members in Combined Torsion and Flexure," Warner Lansing, 128.

"Torsion of I-Type and H-Type Beams," John E. Goldberg, 771. *Discussion:* Kurt H. Gerstle and John E. Goldberg, 791.

"Torsion of Plate Girders," F. K. Chang and Bruce G. Johnston, 337. *Discussion:* Arthur P. Jentoft, Richard W. Mayo and E. Russell Johnston, Jr.; and F. K. Chang and Bruce G. Johnston, 383.

Torsion testing machine for plate girder specimens, 363.

TOWERS

See also BRIDGE TOWERS; WIND . . .

Wind bracing of guyed towers, 463, 483.

TRACKS

See under type of track, e.g., RAILROAD TRACKS (cross references thereunder)

TRACTION

See CONDUITS; ELECTRIC POWER

TRAFFIC ACCIDENTS

See HIGHWAYS AND ROADS—Safety

TRAFFIC, HIGHWAY AND ROAD

See HIGHWAYS AND ROADS—Safety

TRAFFIC, STREET

See AUTOMOBILE PARKING

TRANSMISSION LINES

See ELECTRIC POWER

TRANSMISSION, PRESSURE, THROUGH SOLIDS

See EARTH PRESSURE

TRANSPORTATION

See CANALS; LAKES; PIPE LINES; RAILROADS (cross references thereunder); RIVERS; SOIL TRANSPORTATION (cross references thereunder); WATER TRANSPORTATION; WATERWAYS

TRIANGULATION

See also SURVEYS AND SURVEYING

Triangulation system required to locate piers and preliminary system set up for locating borings for Delaware Memorial Bridge, 400.

TRIAXIAL COMPRESSION APPARATUS

See SOILS—Tests and Testing

TRUCKS

See MOTOR TRUCKS (cross references thereunder)

TRUSSES, CONTINUOUS

An analytical procedure which can be used to obtain preliminary influence lines for design purposes, 127.

TRUSSES, STIFFENING

"The Delaware Memorial Bridge": A Symposium, Homer R. Seely, Charles H. Clarahan, Jr. and Elmer K. Timby, 397.

TSUNAMIES (seismic sea waves)

See WAVES

TUBES

See CONDUITS; DRAFT TUBES; PIPE LINES; PITOT TUBES (cross reference thereunder); SHELL STRUCTURES (cross references thereunder); SIPHONS; TUNNELS; WATER, FLOW OF, IN PIPES

TUNNELS, AIR

"Effect of Entrance Conditions on Diffuser Flow," J. M. Robertson and Donald Ross (with discussion), 1068.

Bibliography

Diffuser flow, 1086.

TUNNELS, WATER

Apparatus and procedure for flow in diffusers, 1070.

"Effect of Entrance Conditions on Diffuser Flow," J. M. Robertson and Donald Ross, 1068. *Discussion:* Steponas Kolupaila, Arthur L. Collins, R. M. Olson, and J. M. Robertson and Donald Ross, 1092.

Bibliography

Diffuser flow, 1086.

TURBINES, WATER

See also DRAFT TUBES; PENSTOCKS

Early researches not adequate in solving the problems of widely interconnected generating station systems, 963.

"Electrical Analogies and Electronic Computers": A Symposium, Henry M. Paynter; R. E. Glover, D. J. Hebert and C. R. Daum; M. A. Kohler; P. G. Hubbard and S. C. Ling; and Malcolm S. McIlroy (with discussion), 961.

TURBULENCE (water agitation)

See also FRICTION; WATER, FLOW OF . . .

"Effect of Entrance Conditions on Diffuser Flow," J. M. Robertson and Donald Ross (with discussion), 1068.

Bibliography

Diffuser flow, 1086.

TURBULENCE, WIND

See WIND . . .

TWISTING

See TORSION; *also* under relative material, structure or structural part, e.g., BEAMS

UNDER- . . .

See also SUB- . . .

UNDERFLOW

See SEEPAGE

UNDERGROUND CORROSION

See CORROSION AND PROTECTION OF METALS

UNDERGROUND STRUCTURES

See under type of structure, e.g., CONDUITS; PIPES AND PIPING (cross references thereunder); *also* under related subject, e.g., SOILS

UNDERGROUND WATER

See GROUND WATER

UNDERGROUND WATER STORAGE

See WATER STORAGE

UNDERWATER FOUNDATIONS

See FOUNDATIONS, UNDERWATER (cross reference thereunder)

UNITED STATES WEATHER BUREAU

See under relative subject, e.g., FLOOD ROUTING; WIND

UPLIFT, HYDROSTATIC

See WATER PRESSURE

URBAN . . .

See CITIES (cross references thereunder)

UTILITIES

See PUBLIC UTILITIES (cross references thereunder)

VALLEY AUTHORITIES

See RIVER VALLEY AUTHORITIES

VALLEYS (Geographical)

Potomac River Basin

Potomac River Basin inflow and outflow flood routing study, 1032.

San Joaquin Valley, Calif.

"Research in Water Spreading," Dean C. Muckel, 209.

Southern California

"Utilization of Underground Storage Reservoirs," Harvey O. Banks, 220.

Tennessee River Valley. *See* RIVER VALLEY AUTHORITIES

VALVES

"Characteristics of Fixed-Dispersion Cone Valves," Rex A. Elder and Gale B. Dougherty, 907. *Discussion:* Edwin W. Murphy; Rodolfo E. Ballester; T. T. Siao; Verne Gongwer; and Rex A. Elder and Gale B. Dougherty, 928.

"Electrical Analogies and Electronic Computers": A Symposium, Henry M. Paynter; R. E. Glover, D. J. Hebert and C. R. Daum; M. A. Kohler; P. G. Hubbard and S. C. Ling; and Malcolm S. McIlroy (with discussion), 961.

Howell-Bunger valves, 907, 928.

Mechanics of air demand in relation to fixed dispersion cone valves, 907.

VAULTS

See DOMES AND VAULTS (cross reference thereunder)

VEHICLES

See under general types of vehicles, e.g., MOTOR VEHICLES; *also* under specific type of vehicle, e.g., AUTOMOBILE . . .

VEHICULAR TRAFFIC

See TRAFFIC . . . (cross references thereunder)

VELOCITY DISTRIBUTION

See WATER, FLOW OF . . .

VENTURI METERS

See METERS AND METERING, VENTURI

VERTICAL CURVES

See CURVES (alinement curves)

VESSELS

See cross references under SHIP . . .

VIBRATION

Resonance phenomena, 968.

"Steady-State Forced Vibration of Continuous Frames," C. T. G. Looney (with discussion), 794.

VIBRATION RECORDING APPARATUS

Galvanometer oscillograph for measuring water motion, 597, 598.

WALLS

See under relative structure or type of wall, e.g., BREAKWATERS; JETTIES (cross references thereunder); RETAINING WALLS; SEA WALLS (cross references thereunder); TANKS; *see also* WIND . . .

WAR AND ENGINEERING

See cross references under MILITARY ENGINEERS AND ENGINEERING

WASTE DISPOSAL

See INDUSTRIAL WASTE (cross references thereunder); SANITATION cross references thereunder); SEWAGE DISPOSAL; WATER POLLUTION

WASTE OF WATER

See WATER CONSERVATION (cross references thereunder)

WASTE WATER

See SEWAGE DISPOSAL; WATER POLLUTION

WATER . . .

See also AQUEDUCTS (cross references thereunder); BACKWATER; CAPILLARITY (cross reference thereunder); CONDUITS; COSTS . . . ; DAMS; DRAINAGE; DRAWDOWN (cross references thereunder); EROSION; FILTERS AND FILTRATION; FLOODS; FLUMES; FOUNDATIONS, UNDERWATER (cross reference thereunder); GROUND WATER; HYDRAULIC . . . ; HYDRO– . . . ; IRRIGATION; LAND RECLAMATION (cross references thereunder); METERS AND METERING; MODELS, HYDRAULIC; OCEAN . . . (cross references thereunder); PIPE LINES; PIPES AND PIPING; RAINFALL; RESERVOIRS; RUNOFF; SALT WATER INVASION (cross references thereunder); SANITATION (cross references thereunder); SEA WATER; SEEPAGE; SEWAGE DISPOSAL; SPREADING, WATER; STORM WATER (cross references thereunder); TANKS . . . ; TERMINOLOGY; TUNNELS, WATER; TURBULENCE; WAVES; WELLS

WATER ANALYSIS

See also WATER TREATMENT

Treatment of test ponds used in water spreading project in San Joaquin Valley, in California, 213.

WATER CLARIFICATION

See WATER TREATMENT

WATER COLLECTION

See INFILTRATION (cross references thereunder); WELLS

WATER CONSERVATION

See COSTS, WATER CONSERVATION; RESERVOIRS, WATER SUPPLY; RIVER VALLEY AUTHORITIES; SPREADING, WATER; WATER STORAGE

WATER DISTRIBUTION

See AQUEDUCTS (cross references thereunder); CANALS; CONDUITS; IRRIGATION; PIPES AND PIPING

WATER DIVERSION

See also CANALS; FLOOD ROUTING

"Diversions from Alluvial Streams," C. P. Lindner (with discussion), 245.

"A Navigation Channel to Victoria, Tex.," Albert B. Davis, Jr., 420.

WATER, FLOW OF (General)

See also FLOODS; FLUMES; FRICTION; GROUND WATER; HYDRAULICS; MODELS, HYDRAULIC; TURBULENCE; VALVES; WATER HAMMER

"Engineering Aspects of Water Waves": A Symposium, Martin A. Mason; James W. Daily and Samuel C. Stephan, Jr.; John H. Carr; J. W. Johnson; and Robert Y. Hudson (with discussion), 545.

Velocity distribution as it relates to varied types of water waves, 545.

WATER, FLOW OF, FRESH WATER WITH SALT WATER

See WATER, FLOW OF, IN OPEN CHANNELS

WATER, FLOW OF, FROM DRAINAGE BASINS

See DRAINAGE

WATER, FLOW OF, IN FLUMES

See WATER, FLOW OF, IN OPEN CHANNELS

WATER, FLOW OF, IN OPEN CHANNELS

See also BACKWATER; FLOODS; HYDROGRAPHS, STREAM FLOW; METERS AND METERING, CURRENT; METERS AND METERING, VENTURI; RUNOFF; SEDIMENT AND SEDIMENTATION; SILT AND SILTING, CHANNEL; WAVES

"Diversions from Alluvial Streams," C. P. Lindner (with discussion), 245.

"Effect of Entrance Conditions on Diffuser Flow," J. M. Robertson and Donald Ross (with discussion), 1068.

"Electrical Analogies and Electronic Computers": A Symposium, Henry M. Paynter; R. E. Glover, D. J. Hebert and C. R. Daum; M. A. Kohler; P. G. Hubbard and S. C. Ling; and Malcolm S. McIlroy (with discussion), 961.

Estimated frequency and duration of current velocities in the Houston Ship Channel, 901.

"Graphical Solution of Hydraulic Problems," Kenneth E. Sorensen, 61.

Mixing of fresh and saline waters in Delta channels of California, 1010.

Sand screens used in water diversion in alluvial streams, 274, 275.

WATER, FLOW OF, IN PIPES

See also PIPE LINES; PIPES AND PIPING; PUMPS AND PUMPING; WATER HAMMER; WATER PRESSURE

"Effect of Entrance Conditions on Diffuser Flow," J. M. Robertson and Donald Ross (with discussion), 1068.

"Electrical Analogies and Electronic Computers": A Symposium, Henry M. Paynter; R. E. Glover, D. J. Hebert and C. R. Daum; M. A. Kohler; P. G. Hubbard and S. C. Ling; and Malcolm S. McIlroy (with discussion), 961.

Usage of nonlinear resistors versus simultaneous equations in study of loss of head and flow rate in pipe line networks, 1055.

WATER, FLOW OF, THROUGH DIFFUSERS
See WATER, FLOW OF, THROUGH ORIFICES

WATER, FLOW OF, THROUGH ORIFICES
See also SIPHONS
"Characteristics of Fixed-Dispersion Cone Valves," Rex A. Elder and Gale B. Dougherty (with discussion), 907.
"Effect of Entrance Conditions on Diffuser Flow," J. M. Robertson and Donald Ross (with discussion), 1068.

WATER, FLOW OF, THROUGH SAND
See GROUND WATER; SPREADING, WATER

WATER, FLOW OF, THROUGH SHORT TUBES AND NOZZLES
See WATER, FLOW OF, THROUGH ORIFICES

WATER FRONT
See BREAKWATERS; BULKHEADS; DOCKS AND WHARVES; HARBORS; JETTIES (cross references thereunder); PILES AND PILE DRIVING; WATER TRANSPORTATION

WATER HAMMER
See also WATER PRESSURE
"Electrical Analogies and Electronic Computers": A Symposium, Henry M. Paynter; R. E. Glover, D. J. Hebert and C. R. Daum; M. A. Kohler; P. G. Hubbard and S. C. Ling; and Malcolm S. McIlroy (with discussion), 961.

WATER IMPOUNDING
See WATER STORAGE

WATER INSTRUMENTS
See METERS AND METERING

WATER LAW
See WATER RIGHTS

WATER LEVEL CONTROL
See SIPHONS

WATER MAINS
See PIPES AND PIPING

WATER METERS AND METERING (stream velocity)
See METERS AND METERING, CURRENT

WATER PIPES AND PIPING
See PIPES AND PIPING

WATER POLLUTION (General)
See also COSTS, WATER POLLUTION CONTROL; SALT WATER INVASION (cross references thereunder); SEWAGE DISPOSAL; WATER TREATMENT
"The Allegheny Conference—Planning in Action," Park H. Martin (with discussion), 235.
Industrial Waste Pollution
"Industrial Waste Treatment in Iowa," Paul Bolton, 322.

WATER POWER (General)

See also DAMS; ELECTRIC POWER; POWER PLANTS; RIVER VALLEY AUTHORITIES; TURBINES, WATER

"Electrical Analogies and Electronic Computers": A Symposium, Henry M. Paynter; R. E. Glover, D. J. Hebert and C. R. Daum; M. A. Kohler; P. G. Hubbard and S. C. Ling; and Malcolm S. McIlroy (with discussion), 961.

"Graphical Solution of Hydraulic Problems," Kenneth E. Sorensen, 61.

WATER PRESSURE

See also HYDROSTATICS; WATER HAMMER; WAVES

"Analysis of Arch Dams of Variable Thickness," W. A. Perkins (with discussion), 725.

"Characteristics of Fixed-Dispersion Cone Valves," Rex A. Elder and Gale B. Dougherty (with discussion), 907.

"Control of Embankment Material by Laboratory Testing," F. C. Walker and W. G. Holtz (with discussion), 1.

"Effect of Entrance Conditions on Diffuser Flow," J. M. Robertson and Donald Ross (with discussion), 1068.

"Electrical Analogies and Electronic Computers": A Symposium, Henry M. Paynter; R. E. Glover, D. J. Hebert and C. R. Daum; M. A. Kohler; P. G. Hubbard and S. C. Ling; and Malcolm S. McIlroy (with discussion), 961.

"Field Study of a Sheet-Pile Bulkhead," C. Martin Duke (with discussion), 1131.

"Final Foundation Treatment at Hoover Dam," A. Warren Simonds (with discussion), 78.

"Unconfined Ground-Water Flow to Multiple Wells," Vaughn E. Hansen (with discussion), 1098.

WATER PURIFICATION

See WATER TREATMENT

WATER RIGHTS

"Irrigation Water Rights in the Humid Areas," Howard T. Critchlow (with discussion), 509.

WATER, SEA

See SEA WATER

WATERSHEDS

See DRAINAGE; HYDROGRAPHS, RUNOFF; RAINFALL; RUNOFF

WATER SPREADING

See SPREADING, WATER

WATER STORAGE

See also RESERVOIRS . . . ; WATER CONSERVATION (cross references thereunder)

Supply and disposal from water table as affected by man's activities, 222.

"Utilization of Underground Storage Reservoirs," Harvey O. Banks, 220.

WATER, STORM

See DRAINAGE; SEWAGE DISPOSAL

WATER SUPPLY

See AQUEDUCTS (cross references thereunder); DAMS . . . ; FLOOD . . . ; GROUND WATER; IRRIGATION . . . ; METERS AND METERING; PIPE LINES; PIPES AND PIPING (cross references thereunder); PUMPS AND PUMPING; RAINFALL; RESERVOIRS . . . ; SILT AND SILTING (cross references thereunder); SPREADING . . . ; TANKS . . . ; TUNNELS, WATER; WATER . . . (related subject headings thereunder); WELLS

WATER SURFACE SURGES

See WAVES

WATER TABLE

See WATER STORAGE

WATER THROW

See JETS (cross reference thereunder)

WATER TRANSPORTATION

See also CANALS; CHANNELS; DOCKS AND WHARVES; HARBORS; LAKES; LOCKS; RIVERS; WATER FRONT (cross references thereunder); WATERWAYS

"A Navigation Channel to Victoria, Tex.," Albert B. Davis, Jr., 420.

WATER TREATMENT

See also AGGREGATES AND AGGREGATION; WATER ANALYSIS; WATER POLLUTION

"Flocculation Phenomena in Turbid Water Clarification," W. F. Langelier, Harvey F. Ludwig and Russell G. Ludwig, 147.

Usage of alum as a hydrolyzing coagulant chemical in flocculation process, 147.

WATER TUNNELS

See TUNNELS, WATER

WATER TURBINES

See TURBINES, WATER

WATER, UNDERGROUND

See GROUND WATER

WATER VELOCITY METERS

See METERS AND METERING, CURRENT

WATER, WASTE

See SEWAGE DISPOSAL; WATER POLLUTION

WATER, WASTE OF

See WATER CONSERVATION (cross references thereunder)

WATER, WASTE, UTILIZATION OF

See WATER STORAGE

WATER WAVES

See WAVES

WATERWAYS (General)

See also CANALS; CHANNELS; DOCKS AND WHARVES; HARBORS; LAKES; OCEAN . . . (cross references thereunder); RIVERS; SEA-COAST (cross references thereunder); WATER DIVERSION; WATER TRANSPORTATION

WATERWAYS (Geographical)

Gulf Intracoastal Waterway

"A Navigation Channel to Victoria, Tex.," Albert B. Davis, Jr., 420.

WATERWAY TRANSPORTATION

See WATER TRANSPORTATION

WATERWORKS (General)

See DAMS; METERS AND METERING, VENTURI; PIPE LINES; PIPES AND PIPING; PUBLIC UTILITIES (cross references thereunder); PUMPS AND PUMPING; RESERVOIRS; SEDIMENT AND SEDIMENTATION; TUNNELS, WATER; WATER STORAGE; WATER SUPPLY (cross references thereunder); WATER TREATMENT; WATER, WASTE OF (cross reference thereunder); WELLS

WAVE RECORDING AND RECORDING APPARATUS

Wave characteristics from wave recorders, 619, 623, 637.

WAVES

See also BREAKWATERS; COSTS, WAVE DAMAGE; EROSION, BEACH; JETTIES (cross references thereunder); OCEAN CURRENTS (cross references thereunder); RETAINING WALLS; SEA WALLS (cross references thereunder); SHORES AND SHORE PROTECTION; TIDES; WATER PRESSURE

Computation of diffraction coefficient for breakwater gaps, 644, 645.

"Electrical Analogies and Electronic Computers": A Symposium, Henry M. Paynter; R. E. Glover, D. J. Hebert and C. R. Daum; M. A. Kohler; P. G. Hubbard and S. C. Ling; and Malcolm S. McIlroy (with discussion), 961.

"Engineering Aspects of Water Waves": A Symposium, Martin A. Mason; James W. Daily and Samuel C. Stephan, Jr.; John H. Carr; J. W. Johnson; and Robert Y. Hudson, 545. *Discussion:* John S. McNown, B. W. Wilson and John H. Carr; M. E. Stelzriede and J. W. Johnson; Kenneth Kaplan, R. G. Hennes and C. E. Leonoff, and Robert Y. Hudson, 588.

Geometrical determination of wave form, 655.

Gerstner's trochoidal theory of progressive oscillatory wave motion, and other related theories, 549, 654, 656.

Massachusetts Institute of Technology research program in solitary wave theory, 575, 578, 579.

Simplified versions of wave pressure theories with tabulated comparison of results, 663, 664, 665.

Tsunamies in their relation to structure design in some localities, 618, 629, 630.

Wave action on structures, 545, 618, 627.

Wind velocity and duration as they relate to wave theories in their engineering aspects, 545.

Bibliography

Classified bibliography on wave theories, 570.

WEATHER

See ATMOSPHERIC . . .; FLOODS; HYDROLOGY; METEOROLOGY; RAINFALL; WIND . . .

WEATHER BUREAU, UNITED STATES

See under relative subject, e.g., FLOOD ROUTING; WIND

WEATHERPROOFING

See CORROSION AND PROTECTION OF . . .

WEBS

See BEAMS; GIRDERS

WELDS AND WELDING

"Torsion of Plate Girders," F. K. Chang and Bruce G. Johnston (with discussion), 337.

WELLS

See also GROUND WATER

Analysis of an actual installation of wellpoints adjacent to open water, 191.

"Analysis of Ground-Water Lowering Adjacent to Open Water," Stuart B. Avery, Jr. (with discussion), 178.

"Unconfined Ground-Water Flow to Multiple Wells," Vaughn E. Hansen, 1098. *Discussion:* Ahmed Shukry; Carl Rohwer; David K. Todd and Lloyd C. Fowler; and Vaughn E. Hansen, 1116.

Usage of aquifers in rice irrigation in Louisiana, 871.

"Utilization of Underground Storage Reservoirs," Harvey O. Banks, 220.

WHARVES

See DOCKS AND WHARVES

WIND

See also EROSION, BEACH; WAVES

U. S. Weather Bureau most voluminous information source for wind velocity variations, 464, 471, 472, 473, 488.

"Variation of Wind Velocity and Gusts with Height," R. H. Sherlock (with discussion), 463.

WIND BRACING

"The Delaware Memorial Bridge": A Symposium, Homer R. Seely, Charles H. Clarahan, Jr. and Elmer K. Timby, 397.

WIND PRESSURE

See also AERODYNAMICS

"East St. Louis Veterans Memorial Bridge," A. L. R. Sanders (with discussion), 838.

"Variation of Wind Velocity and Gusts with Height," R. H. Sherlock, 463. *Discussion:* W. Watters Pagon; Irving A. Singer and Maynard E. Smith; Percy H. Thomas and M. H. Fresen; Robert A. McCormick; Edward Cohen; and R. H. Sherlock, 489.

WIRE TRANSMISSION

See ELECTRIC POWER; POWER

WORK, COST OF

See COSTS

WORKS (industrial buildings and equipment)

See under general types of works, e.g., PUBLIC WORKS (cross references thereunder); *also* under specific type of works, e.g., WATERWORKS (cross references thereunder); *see also* cross references under PLANTS

ZONING

See also BUILDINGS (cross references thereunder); CITIES (cross references thereunder); CITY PLANNING; INDUSTRIAL PROPERTY; PROPERTY (landed property) (cross references thereunder); PUBLIC UTILITIES (cross references thereunder); REGIONAL PLANNING (cross references thereunder)

Los Angeles, California, a pioneer in residential zoning, 709.

"The Value and Administration of a Zoning Plan," Huber E. Smutz, 709. *Discussion:* Henry Horowitz and Huber E. Smutz, 722.

ZONING LAW

Los Angeles, California and its administration of zoning ordinances, 709.

ZONING OF CITIES

See ZONING

AUTHOR INDEX

ALLEN, FRANK REA
Memoir of, 1232.

ANDREWS, GEORGE DOUGLAS
Memoir of, 1233.

AVERY, STUART B., JR.
"Analysis of Ground-Water Lowering Adjacent to Open Water," 178.

BAINES, W. DOUGLAS
Hydraulic problems, 1020.

BALLESTER, RODOLFO E.
Fixed dispersion cone valves, 930.

BANKS, HARVEY O.
"Utilization of Underground Storage Reservoirs," 220.

BARKER, CHARLES L.
Pipe networks, 1066.

BAUMANN, PAUL
Sheet pile bulkheads, 1167.

BERRY, DAVID MAURICE
Memoir of, 1235.

BLENCH, T.
Diversions from alluvial streams, 270.
Hydraulic problems, 1024.

BLUM, LOUIS P.
Allegheny Conference on Community Development, 243.

BOGGESS, O. E.
Hoover Dam foundation treatment, 106.

BOLTON, PAUL
"Industrial Waste Treatment in Iowa," 322.

BONDURANT, D. C.
Diversions from alluvial streams, 278.

BONNYMAN, ALEXANDER
Memoir of, 1236.

BOOTH, WILLIAM H., JR.
"Lake Michigan Erosion Studies," 39.

BOYER, WALTER C.
Sheet pile bulkheads, 1163.

BRANNON, R. A.
"Underground Corrosion of Piping," 165.

BROWNELL, CLARENCE J.

"Rate of Change of Grade per Station," 437.

CAMBEFORT, H.

Hoover Dam foundation treatment, 107.

CAPES, CHARLES FREDERICK

Memoir of, 1236.

CARLSON, ROY W.

Shasta Dam stresses, 310.

Sheet pile bulkheads, 1188.

CARR, JOHN H.

"Engineering Aspects of Water Waves (symposium): Long-Period Waves or Surges in Harbors," 588.

CASEY, THOMAS B.

Shore erosion, 51.

CHANG, F. K.

"Torsion of Plate Girders," 337.

CHOW, LI

"Stresses in Deep Beams," 686.

CLARAHAN, CHARLES H., JR.

"The Delaware Memorial Bridge (symposium): Design Problems," 411.

CLARK, C. O.

Flow routing, 1042.

CLARK, CHARLES STUART

Memoir of, 1237.

CLOUGH, RAY W.

Cantilever beams, 1212.

COHEN, EDWARD

Wind velocity, 499.

COLLINS, ARTHUR L.

Diffuser flow, 1092.

COLPITTS, WALTER WILLIAM

Memoir of, 1238.

CONWAY, HARRY D.

"Stresses in Deep Beams," 686.

CONWELL, WILLIAM A.

Cantilever beams, 1215.

Deep beams, 704.

Forced vibration, 820.

COOPER, ALFRED J.

Flow routing, 1039.

CORLEW, RALPH STEPHENSON
Memoir of, 1240.

CREAGER, WILLIAM P.
"Review of Flood Frequency Methods": Final Report of the Subcommittee of the Joint Division Committee on Floods, 1230.

CRITCHLOW, HOWARD T.
"Irrigation Water Rights in the Humid Areas," 509.

CUTTS, CHARLES E.
"Horizontally Curved Box Beams," 517.

DAILY, JAMES W.
"Engineering Aspects of Water Waves (symposium): Characteristics of the Solitary Wave," 575.

DAMES, TRENT R.
Sheet pile bulkheads, 1187.

DAUM, C. R.
"Electrical Analogies and Electronic Computers (symposium): Application to an Hydraulic Problem," 1010.

DAVIS, ALBERT B., JR.
"A Navigation Channel to Victoria, Tex.," 420.

DAVIS, ELLSWORTH I.
"Development of a Flood-Control Plan for Houston, Tex.," 888.

DEAN, GEORGE THOMAS
Memoir of, 1241.

de la SAYETTE, E. R.
Bank stabilization, 865.

DERBY, FRANK HOLLIDAY
Memoir of, 1242.

DOBBIN, JOHN RALPH
Memoir of, 1242.

DOUGHERTY, GALE B.
"Characteristics of Fixed-Dispersion Cone Valves," 907.

DUKE, C. MARTIN
"Field Study of a Sheet-Pile Bulkhead," 1131.

EDY, JOHN NORTH
Memoir of, 1243.

ELDER, REX A.
"Characteristics of Fixed-Dispersion Cone Valves," 907.

ELLMS, JOSEPH WILTON
Memoir of, 1244.

FELDMAN, EDMUND BURKE
Memoir of, 1245.

FINLEY, EDWIN CLIFFORD
Memoir of, 1247.

FINNER, GLENN FREDERICK
Memoir of, 1248.

FOWLER, LLOYD C.
Multiple wells, 1121.

FRESEN, M. H.
Wind velocity, 494.

GERSTLE, KURT H.
Torsion of beams, 791.

GLOVER, R. E.
"Electrical Analogies and Electronic Computers (symposium): Application to an Hydraulic Problem," 1010.

GLYNN, D. F.
Embankments and foundations, 33.

GOLDBERG, JOHN E.
"Torsion of I-Type and H-Type Beams," 771.

GONGWER, VERNE
Fixed dispersion cone valves, 937.

GOODALL, GEORGE E.
Arch dams, 764.

GRAY, HAROLD E.
Irrigation water rights, 515.

GROSS, JOSEPH WATSON
Memoir of, 1248.

GUMBEL, E. J.
"Review of Flood Frequency Methods": Final Report of the Subcommittee of the Joint Division Committee on Floods, 1230.

GUZMAN, ARTURO M.
Deep beams, 703.

HAAS, RAYMOND H.
"Bank Stabilization by Revetments and Dikes," 849.

HALL, HOWARD P.
Ground water lowering, 204.

HANSEN, VAUGHN E.
"Unconfined Ground-Water Flow to Multiple Wells," 1098.

HANSON, J. A.
Shasta Dam stresses, 315.

HARDIN, JOHN R.
"Lake Michigan Erosion Studies," 39.

HARLEMAN, DONALD R. F.
Electronic computers, 995.

HARTSFIELD, MARVIN FURR
Memoir of, 1249.

HAYS, JAMES B.
Hoover Dam foundation treatment, 100.

HEBERT, D. J.
"Electrical Analogies and Electronic Computers (symposium): Application to an Hydraulic Problem," 1010.

HENNES, R. G.
Wave forces, 676.

HEWETT, WILLIAM SHERMAN
Memoir of, 1250.

HICKERSON, T. F.
Rate of change of grade for highways, 457.

HOLLAND, GEORGE PERCIVAL
Memoir of, 1252.

HOLTZ, W. G.
"Control of Embankment Material by Laboratory Testing," 1.

HOROWITZ, HENRY
Zoning plans, 722.

HOWARD, CLEMENT JOHN
Memoir of, 1252.

HOWE, ROBERT T.
Rate of change of grade for highways, 457.

HOWSON, GEORGE WILLIAM
Memoir of, 1253.

HU, LU-SHIEN
Cantilever beams, 1208.

HUBBARD, P. G.
"Electrical Analogies and Electronic Computers (symposium): Hydrodynamic Problems in Three Dimensions," 1046.

HUBER, WALTER L.
For address at the Annual Convention, San Francisco, Calif., March 4, 1953 *see* Vol. CT

HUDSON, ROBERT Y.
"Engineering Aspects of Water Waves (symposium): Wave Forces on Breakwaters," 653.

HUNT, WILLIAM HENRY
Memoir of, 1255.

JAMESON, W. H.
East St. Louis Veterans Memorial Bridge, 845.

JENTOFT, ARTHUR P.
Plate girders, 383.

JOHNSON, J. W.
"Engineering Aspects of Water Waves (symposium): Engineering Aspects of Diffraction and Refraction," 617.

JOHNSON, S. J.
Ground water lowering, 199.

JOHNSTON, BRUCE G.
"Torsion of Plate Girders," 337.

JOHNSTON, E. RUSSELL, JR.
Plate girders, 383.

JOSEPHS, A. C.
Arch dams, 763.

KAPLAN, KENNETH
Wave forces, 675.

KELLY, GEORGE WASHINGTON
Memoir of, 1255.

KENNEDY, CLYDE CHARLES
Memoir of, 1256.

KINNISON, HARVEY B.
"Review of Flood Frequency Methods": Final Report of the Subcommittee of the Joint Division Committee on Floods, 1230.

KIRK, KARL QUILL
Memoir of, 1258.

KIRN, FAIRFAX D.
Arch dams, 758.

KOHLER, MAX A.
"Electrical Analogies and Electronic Computers (symposium): Application to Stream-Flow Routing," 1028.

KOLUPAILA, STEPONAS
Diffuser flow, 1092.

KRYNINE, D. P.
Embankments and foundations, 29.
Sheet pile bulkheads, 1182.

LAKE, J. OWEN
Sheet pile bulkheads, 1173.

LANGELIER, W. F.
"Flocculation Phenomena in Turbid Water Clarification," 147.

LANSING, WARNER
"Thin-Walled Members in Combined Torsion and Flexure," 128.

LEE, CHARLES E.
Shore erosion, 55.

LELIAVSKY, SERGE
Bank stabilization, 866.
Diversions from alluvial streams, 272.

LEONOFF, C. E.
Wave forces, 676.

LINDNER, C. P.
"Diversions from Alluvial Streams," 245.

LING, S. C.
"Electrical Analogies and Electronic Computers (symposium): Hydrodynamic Problems in Three Dimensions," 1046.

LIPPOLD, FRED H.
Hoover Dam foundation treatment, 105.

LIU, DAVID C.
Sheet pile bulkheads, 1187.

LOONEY, C. T. G.
"Steady-State Forced Vibration of Continuous Frames," 794.

LUDWIG, HARVEY F.
"Flocculation Phenomena in Turbid Water Clarification," 147.

LUDWIG, RUSSELL G.
"Flocculation Phenomena in Turbid Water Clarification," 147.

LUISONI, CESAR J.
Deep beams, 703.

MALLIS, A. GEORGE
Curved box beams, 535.

MARTIN, PARK H.
"The Allegheny Conference—Planning in Action," 235.

MASON, MARTIN A.
"Engineering Aspects of Water Waves (symposium): Surface Water Wave Theories," 546.

MASUR, E. F.
Forced vibration, 815.

MATTESON, DeFOREST A., JR.
Curved box beams, 535.

MATTHES, G. H.
"Review of Flood Frequency Methods": Final Report of the Subcommittee of the Joint Division Committee on Floods, 1230.

MAYO, RICHARD W.
Plate girders, 383.

McALPINE, WILLIAM H.
Hoover Dam foundation treatment, 104.

McBRADY, ALPHONSUS PAUL
Memoir of, 1258.

McCORMICK, ROBERT A.
Wind velocity, 498.

McCREERY, DONALD HULL
Memoir of, 1259.

McILROY, MALCOLM S.
"Electrical Analogies and Electronic Computers (symposium): Pipe Networks Studied by Nonlinear Resistors," 1055.

McKENZIE, ANDREW JACKSON
Memoir of, 1260.

McNOWN, JOHN S.
Surges in harbors, 604.

MENSCH, L. J.
Arch dams, 757.

MICHALOS, JAMES P.
"Influence Lines by Corrections to an Assumed Shape," 113.

MILES, PHIL M.
"Topographic Mapping in Kentucky," 829.

MILLER, JOHN OWEN
Memoir of, 1261.

MILWIT, HERBERT
Mapping in Kentucky, 837.

MINEAR, V. L.
Hoover Dam foundation treatment, 101.

MISCH, FRANZ MARTIN
Memoir of, 1262.

MORELOCK, JOHN EARL
Memoir of, 1263.

MUCKEL, DEAN C.
"Research in Water Spreading," 209.

MURPHY, EDWIN W.
Fixed dispersion cone valves, 928.

MYERS, LLOYD E., JR.
Rice irrigation, 885.

OLSON, R. M.
Diffuser flow, 1092.

PACKSHAW, S.
Sheet pile bulkheads, 1169.

PAGON, W. WATTERS
Wind velocity, 489.

PARKER, CHARLES FREDERICK
Memoir of, 1264.

PARME, ALFRED L.
Arch dams, 754.

PAYNTER, HENRY M.
"Electrical Analogies and Electronic Computers (symposium): Surge and Water Hammer Problems," 962.

PERKINS, W. A.
"Analysis of Arch Dams of Variable Thickness," 725.

PITTMAN, HARRISON V.
Bank stabilization, 861.

POE, WILLIAM ALLEN
Memoir of, 1265.

PROUTY, E. N.
Rate of change of grade for highways, 457.

RAPHAEL, J. M.
"The Development of Stresses in Shasta Dam," 289.

REIN, EDWARD N.
Electronic computers, 995.

RICH, GEORGE R.
Electronic computers, 992.

RIEGEL, ROSS M.
Shasta Dam stresses, 310.

ROBERTSON, J. M.
"Effect of Entrance Conditions on Diffuser Flow," 1068.

ROHWER, CARL
Multiple wells, 1120.

ROPER, FREMONT EMERSON
Memoir of, 1266.

RORABAUGH, MATTHEW I.
Ground water lowering, 194.

ROSS, A. D.
Shasta Dam stresses, 313.

ROSS, DONALD
"Effect of Entrance Conditions on Diffuser Flow," 1068.

ST. JOHN, ROYAL UPSON
Memoir of, 1268.

SAMUEL, PHILIP TUSTIN
Memoir of, 1267.

SANDERS, A. L. R.
"East St. Louis Veterans Memorial Bridge," 838.

SARKARIA, GURMUKH S.
Arch dams, 758.

SCHNEIDER, LEWIS
Cantilever beams, 1210.

SEARS, WILLIAM HATFIELD
Memoir of, 1269.

SEELY, HOMER R.
"The Delaware Memorial Bridge (symposium): Planning and Construction," 398.

SERAFIM, J. LAGINHA
Shasta Dam stresses, 311.

SHANNAHAN, GEORGE DAVID
Memoir of, 1270.

SHARP, JOSIAH ROSCOE
Memoir of, 1270.

SHEPPARD, JOSEPH WAGONER
Memoir of, 1271.

SHEPPARD, LYLE R.
Underground corrosion, 177.

SHERLOCK, R. H.
"Variation of Wind Velocity and Gusts with Height," 463.

SHIFRIN, HYMEN
"Review of Flood Frequency Methods": Final Report of the Subcommittee of the Joint Division Committee on Floods, 1230.

SHUKRY, AHMED
Multiple wells, 1116.

SHUTTS, E. E.
"Rice Irrigation in Louisiana," 871.

SIAO, T. T.
Fixed dispersion cone valves, 932.

SIMONDS, A. WARREN
"Final Foundation Treatment at Hoover Dam," 78.
Shasta Dam stresses, 316.

SINGER, IRVING A.
Wind velocity, 491.

SLYE, JOHN DOLSON
Memoir of, 1272.

SMITH, MAYNARD E.
Wind velocity, 491.

SMUTZ, HUBER E.
"The Value and Administration of a Zoning Plan," 709.

SNYDER, FRANKLIN F.
"Review of Flood Frequency Methods": Final Report of the Subcommittee of the Joint Division Committee on Floods, 1230.

SORENSEN, KENNETH E.
"Graphical Solution of Hydraulic Problems," 61.

SORKIN, JOSEPH
East St. Louis Veterans Memorial Bridge, 846.

SOWERS, GEORGE F.
Embankments and foundations, 26.
Soil surveys, 956.

SPIELMAN, JOHN GODFREY
Memoir of, 1273.

STEELE, BYRAM W.
Hoover Dam foundation treatment, 103.

STELZRIEDE, M. E.
Diffraction and refraction, 649.

STEPHAN, SAMUEL C., JR.
"Engineering Aspects of Water Waves (symposium): Characteristics of the Solitary Wave," 575.

STROWGER, E. B.
Electronic computers, 990.

TERZAGHI, K.
Sheet pile bulkheads, 1175.

THOMAS, A. R.
Diversions from alluvial streams, 276.

THOMAS, FRANKLIN
Memoir of, 1231.

THOMAS, PERCY H.
Wind velocity, 494.

THORPE, JOHN EDWARD STIRLING
Memoir of, 1274.

THURSTON, EUGENE TRUE, JR.
Memoir of, 1275.

TIMBY, ELMER K.
"The Delaware Memorial Bridge (symposium): Design Problems," 411.

TODD, DAVID K.
Multiple wells, 1121.

TSCHEBOTARIOFF, GREGORY P.
Sheet pile bulkheads, 1157.

van **VEEN, J.**
Hydraulic problems, 1017.

VELETSOS, A. S.
Forced vibration, 817.

WALKER, F. C.
"Control of Embankment Material by Laboratory Testing," 1.

WAY, W. F.
Sheet pile bulkheads, 1172.

WELLER, HARVILL E.
"Bank Stabilization by Revetments and Dikes," 849.

WHEAT, GEORGE NEVILLE
Memoir of, 1276.

WILLIAMS, GORDON R.
"Review of Flood Frequency Methods": Final Report of the Subcommittee of the Joint Division Committee on Floods, 1230.

WILSON, B. W.
Surges in harbors, 609.

WILSON, EDWARD N.
"Influence Lines by Corrections to an Assumed Shape," 113.

WING, ROBERT LEWIS
Memoir of, 1277.

WINTER, GEORGE
"Stresses in Deep Beams," 686.

WINTON, WALTER FERRELL
Memoir of, 1278.

WISKOCIL, CLEMENT TEHLE
Memoir of, 1279.

WITT, WILLIAM CLAYTON, JR.
Memoir of, 1280.

WOLOSEWICK, F. E.
"Flexure of Double Cantilever Beams," 1197.

WOMBLE, BYRLE BURTON
Memoir of, 1281.

WOODS, K. B.
"Method for Making Highway Soil Surveys," 946.